Scientific and Technical Aerospace Reports

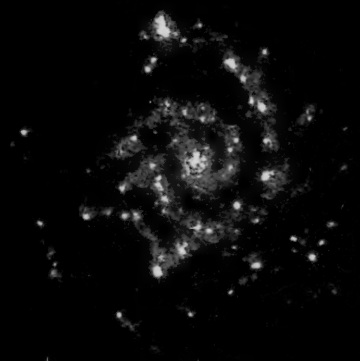

An Abstract Journal

Volume 32, Number 9
September 1994
N94-30981 to N94-33356

The NASA STI Program ... in Profile

Since its founding, NASA has been dedicated to the advancement of aeronautics and space science. The NASA Scientific and Technical Information (STI) Program plays a key part in helping NASA maintain this important role.

The NASA STI Program provides access to the NASA STI Database, the largest collection of aeronautical and space science STI in the world. The Program is also NASA's institutional mechanism for disseminating the results of its research and development activities.

Specialized services that help round out the Program's diverse offerings include creating custom thesauri, translating material to or from 34 foreign languages, building customized databases, organizing and publishing research results ... even providing videos.

For more information about the NASA STI Program, you can:

- **Phone** the NASA Access Help Desk at (301) 621-0390
- **Fax** your question to the NASA Access Help Desk at (301) 621-0134
- **E-mail** your question via the **Internet** to help@sti.nasa.gov
- **Write** to:

NASA Access Help Desk
NASA Center for AeroSpace Information
800 Elkridge Landing Road
Linthicum Heights, MD 21090-2934

Scientific and Technical Aerospace Reports

Scientific and Technical Aerospace Reports (STAR), is published each month as a major product of the NASA Scientific and Technical Information (STI) Program.

Inside this issue you will find:

- **Front Matter** containing a typical citation and abstract sample explaining the standard format, including codes for ordering reports
- **An Abstract Section** containing citations and abstracts of reports and publications that provide comprehensive coverage of worldwide aerospace-related topics including aeronautics and space science technology. *STAR* lists published and publicly available reports entered into the NASA STI Database during the four weeks preceding publication of this issue. These citations and abstracts are listed by subject categories.
- **An Index Section**
  - Subject
  - Personal author
  - Corporate source
  - Contract number
  - Report number
- **An Appendix** containing a guide for ordering cited reports, registering with the NASA STI Program, and using the available products and services. Additionally, price schedules, phone numbers, and addresses are included in this information packed section.

NASA also sponsors the companion journal, *NASA Open Volumes on Aerospace (NOVA)*, which lists abstracts of the open literature on aerospace subjects available worldwide. *NOVA* is for internal NASA use only, available from the NASA Center for AeroSpace Information (CASI).

Entries found in *STAR* are available through the NASA online retrieval service, RECON, and through DIALOG as the Aerospace Database.

The NASA STI Program gathers information through national and international agreements and exchanges and makes this information available to the NASA community and to the public in many forms through various outlets.

For additional information on the NASA STI Program, call the NASA Access Help Desk at (301) 621-0390, or write to:

NASA Center for AeroSpace Information
800 Elkridge Landing Road
Linthicum Heights, Maryland 21090-2934

US ISSN 0036-8741

This publication was prepared by the NASA Center for AeroSpace Information,
800 Elkridge Landing Road, Linthicum Heights, MD 21090-2934, (301) 621-0390.

Volume 32 Number 9 / September 1994

TABLE OF CONTENTS

AERONAUTICS For related information see also *Astronautics.*

01 AERONAUTICS (GENERAL) **3565**

02 AERODYNAMICS **3567**
Includes aerodynamics of bodies, combinations, wings, rotors, and control surfaces; and internal flow in ducts and turbomachinery. For related information see also *34 Fluid Mechanics and Heat Transfer.*

03 AIR TRANSPORTATION AND SAFETY **3574**
Includes passenger and cargo air transport operations; and aircraft accidents. For related information see also *16 Space Transportation* and *85 Urban Technology and Transportation.*

04 AIRCRAFT COMMUNICATIONS AND NAVIGATION **3576**
Includes digital and voice communication with aircraft; air navigation systems (satellite and ground based); and air traffic control. For related information see also *17 Space Communications, Spacecraft Communications, Command and Tracking* and *32 Communications and Radar.*

05 AIRCRAFT DESIGN, TESTING AND PERFORMANCE **3578**
Includes aircraft simulation technology. For related information see also *18 Spacecraft Design, Testing and Performance* and *39 Structural Mechanics.* For land transportation vehicles see *85 Urban Technology and Transportation.*

06 AIRCRAFT INSTRUMENTATION **3581**
Includes cockpit and cabin display devices; and flight instruments. For related information see also *19 Spacecraft Instrumentation* and *35 Instrumentation and Photography.*

07 AIRCRAFT PROPULSION AND POWER **3583**
Includes prime propulsion systems and systems components, e.g., gas turbine engines and compressors; and onboard auxiliary power plants for aircraft. For related information see also *20 Spacecraft Propulsion and Power, 28 Propellants and Fuels,* and *44 Energy Production and Conversion.*

08 AIRCRAFT STABILITY AND CONTROL **3585**
Includes aircraft handling qualities; piloting; flight controls; and autopilots. For related information see also *05 Aircraft Design, Testing and Performance.*

09 RESEARCH AND SUPPORT FACILITIES (AIR) **3586**
Includes airports, hangars and runways; aircraft repair and overhaul facilities; wind tunnels; shock tubes; and aircraft engine test stands. For related information see also *14 Ground Support Systems and Facilities (Space).*

ASTRONAUTICS For related information see also *Aeronautics.*

12 ASTRONAUTICS (GENERAL) **3591**
For extraterrestrial exploration see *91 Lunar and Planetary Exploration.*

13 ASTRODYNAMICS **3601**
Includes powered and free-flight trajectories; and orbital and launching dynamics.

14 GROUND SUPPORT SYSTEMS AND FACILITIES (SPACE) **3602**
Includes launch complexes, research and production facilities; ground support equipment, e.g., mobile transporters; and simulators. For related information see also *09 Research and Support Facilities (Air).*

15 LAUNCH VEHICLES AND SPACE VEHICLES **3602**
Includes boosters; operating problems of launch/space vehicle systems; and reusable vehicles. For related information see also *20 Spacecraft Propulsion and Power.*

16 SPACE TRANSPORTATION **3608**
Includes passenger and cargo space transportation, e.g., shuttle operations; and space rescue techniques. For related information see also *03 Air Transportation and Safety* and *18 Spacecraft Design, Testing and Performance.* For space suits see *54 Man/System Technology and Life Support.*

17 SPACE COMMUNICATIONS, SPACECRAFT COMMUNICATIONS, COMMANDAND TRACKING....N.A.
Includes telemetry; space communications networks; astronavigation and guidance; and radio blackout. For related information see also *04 Aircraft Communications and Navigation* and *32 Communications and Radar.*

N.A.—No abstracts were assigned to this category for this issue.

18 SPACECRAFT DESIGN, TESTING AND PERFORMANCE **3609**
Includes satellites; space platforms; space stations; spacecraft systems and components such as thermal and environmental controls; and attitude controls. For life support systems see *54 Man/System Technology and Life Support.* For related information see also *05 Aircraft Design, Testing and Performance, 39 Structural Mechanics,* and *16 Space Transportation.*

19 SPACECRAFT INSTRUMENTATION **3613**
For related information see also *06 Aircraft Instrumentation* and *35 Instrumentation and Photography.*

20 SPACECRAFT PROPULSION AND POWER **3613**
Includes main propulsion systems and components, e.g., rocket engines; and spacecraft auxiliary power sources. For related information see also *07 Aircraft Propulsion and Power, 28 Propellants and Fuels, 44 Energy Production and Conversion,* and *15 Launch Vehicles and Space Vehicles.*

CHEMISTRY AND MATERIALS

23 CHEMISTRY AND MATERIALS (GENERAL) **3616**

24 COMPOSITE MATERIALS **3617**
Includes physical, chemical, and mechanical properties of laminates and other composite materials. For ceramic materials see *27 Nonmetallic Materials.*

25 INORGANIC AND PHYSICAL CHEMISTRY **3631**
Includes chemical analysis, e.g., chromatography; combustion theory; electrochemistry; and photochemistry. For related information see also *77 Thermodynamics and Statistical Physics.*

26 METALLIC MATERIALS **3640**
Includes physical, chemical, and mechanical properties of metals, e.g., corrosion; and metallurgy.

27 NONMETALLIC MATERIALS **3648**
Includes physical, chemical, and mechanical properties of plastics, elastomers, lubricants, polymers, textiles, adhesives, and ceramic materials. For composite materials see *24 Composite Materials.*

28 PROPELLANTS AND FUELS **3666**
Includes rocket propellants, igniters and oxidizers; their storage and handling procedures; and aircraft fuels. For related information see also *07 Aircraft Propulsion and Power, 20 Spacecraft Propulsion and Power,* and *44 Energy Production and Conversion.*

29 MATERIALS PROCESSING **3667**
Includes space-based development of products and processes for commercial application. For biological materials see *55 Space Biology:*

ENGINEERING For related information see also *Physics.*

31 ENGINEERING (GENERAL) **3668**
Includes vacuum technology; control engineering; display engineering; cryogenics; and fire prevention.

32 COMMUNICATIONS AND RADAR **3670**
Includes radar; land and global communications; communications theory; and optical communications. For related information see also *04 Aircraft Communications and Navigation* and *17 Space Communications, Spacecraft Communications, Command and Tracking.* For search and rescue see *03 Air Transportation and Safety,* and *16 Space Transportation.*

33 ELECTRONICS AND ELECTRICAL ENGINEERING **3686**
Includes test equipment and maintainability; components, e.g., tunnel diodes and transistors; microminiaturization; and integrated circuitry. For related information see also *60 Computer Operations and Hardware* and *76 Solid-State Physics.*

34 FLUID MECHANICS AND HEAT TRANSFER **3699**
Includes boundary layers; hydrodynamics; fluidics; mass transfer and ablation cooling. For related information see also *02 Aerodynamics* and *77 Thermodynamics and Statistical Physics.*

35 INSTRUMENTATION AND PHOTOGRAPHY **3711**
Includes remote sensors; measuring instruments and gauges; detectors; cameras and photographic supplies; and holography. For aerial photography see *43 Earth Resources and Remote Sensing.* For related information see also *06 Aircraft Instrumentation* and *19 Spacecraft Instrumentation.*

36 LASERS AND MASERS **3714**
Includes parametric amplifiers. For related information see also *76 Solid-State Physics.*

37 MECHANICAL ENGINEERING **3722**
Includes auxiliary systems (nonpower); machine elements and processes; and mechanical equipment.

38 QUALITY ASSURANCE AND RELIABILITY **3730**
Includes product sampling procedures and techniques; and quality control.

39 STRUCTURAL MECHANICS **3732**
Includes structural element design and weight analysis; fatigue; and thermal stress. For applications see *05 Aircraft Design, Testing and Performance* and *18 Spacecraft Design, Testing and Performance.*

GEOSCIENCES For related information see also *Space Sciences.*

42 GEOSCIENCES (GENERAL) **3741**

43 EARTH RESOURCES AND REMOTE SENSING **3741**
Includes remote sensing of earth resources by aircraft and spacecraft; photogrammetry; and aerial photography. For instrumentation see *35 Instrumentation and Photography.*

44 ENERGY PRODUCTION AND CONVERSION **3758**
Includes specific energy conversion systems, e.g., fuel cells; global sources of energy; geophysical conversion; and windpower. For related information see also *07 Aircraft Propulsion and Power, 20 Spacecraft Propulsion and Power,* and *28 Propellants and Fuels.*

45 ENVIRONMENT POLLUTION **3763**
Includes atmospheric, noise, thermal, and water pollution.

46 GEOPHYSICS **3770**
Includes aeronomy; upper and lower atmosphere studies; ionospheric and magnetospheric physics; and geomagnetism. For space radiation see *93 Space Radiation.*

47 METEOROLOGY AND CLIMATOLOGY **3776**
Includes weather forecasting and modification.

48 OCEANOGRAPHY **3787**
Includes biological, dynamic, and physical oceanography; and marine resources. For related information see also *43 Earth Resources and Remote Sensing.*

LIFE SCIENCES

51 LIFE SCIENCES (GENERAL) **3792**

52 AEROSPACE MEDICINE **3794**
Includes physiological factors; biological effects of radiation; and effects of weightlessness on man and animals.

53 BEHAVIORAL SCIENCES **3798**
Includes psychological factors; individual and group behavior; crew training and evaluation; and psychiatric research.

54 MAN/SYSTEM TECHNOLOGY AND LIFE SUPPORT **3802**
Includes human engineering; biotechnology; and space suits and protective clothing. For related information see also *16 Space Transportation.*

55 SPACE BIOLOGY **3806**
Includes exobiology; planetary biology; and extraterrestrial life.

MATHEMATICAL AND COMPUTER SCIENCES

59 MATHEMATICAL AND COMPUTER SCIENCES (GENERAL) **3806**

60 COMPUTER OPERATIONS AND HARDWARE **3806**
Includes hardware for computer graphics, firmware, and data processing. For components see *33 Electronics and Electrical Engineering.*

61 COMPUTER PROGRAMMING AND SOFTWARE **3808**
Includes computer programs, routines, algorithms, and specific applications, e.g., CAD/CAM.

62 COMPUTER SYSTEMS **3823**
Includes computer networks and special application computer systems.

63 CYBERNETICS **3828**
Includes feedback and control theory, artificial intelligence, robotics and expert systems. For related information see also *54 Man/System Technology and Life Support.*

64 NUMERICAL ANALYSIS **3839**
Includes iteration, difference equations, and numerical approximation.

65 STATISTICS AND PROBABILITY **3850**
Includes data sampling and smoothing; Monte Carlo method; and stochastic processes.

66 SYSTEMS ANALYSIS **3852**
Includes mathematical modeling; network analysis; and operations research.

67 THEORETICAL MATHEMATICS **3855**
Includes topology and number theory.

PHYSICS For related information see also *Engineering.*

70 PHYSICS (GENERAL) **3858**
For precision time and time interval (PTTI) see *35 Instrumentation and Photography*; for geophysics, astrophysics or solar physics see *46 Geophysics, 90 Astrophysics*, or *92 Solar Physics.*

71 ACOUSTICS **3859**
Includes sound generation, transmission, and attenuation. For noise pollution see *45 Environment Pollution.*

72 ATOMIC AND MOLECULAR PHYSICS **3862**
Includes atomic structure, electron properties, and molecular spectra.

73 NUCLEAR AND HIGH-ENERGY PHYSICS **3875**
Includes elementary and nuclear particles; and reactor theory. For space radiation see *93 Space Radiation.*

74 OPTICS **3877**
Includes light phenomena and optical devices. For lasers see *36 Lasers and Masers.*

75 PLASMA PHYSICS **3885**
Includes magnetohydrodynamics and plasma fusion. For ionospheric plasmas see *46 Geophysics.* For space plasmas see *90 Astrophysics.*

76 SOLID-STATE PHYSICS **3894**
Includes superconductivity. For related information see also *33 Electronics and Electrical Engineering* and *36 Lasers and Masers.*

77 THERMODYNAMICS AND STATISTICAL PHYSICS **3910**
Includes quantum mechanics; theoretical physics; and Bose and Fermi statistics. For related information see also *25 Inorganic and Physical Chemistry* and *34 Fluid Mechanics and Heat Transfer.*

SOCIAL SCIENCES

80 SOCIAL SCIENCES (GENERAL) **3913**
Includes educational matters.

81 ADMINISTRATION AND MANAGEMENT **3914**
Includes management planning and research.

82 DOCUMENTATION AND INFORMATION SCIENCE **3915**
Includes information management; information storage and retrieval technology; technical writing; graphic arts; and micrography. For computer documentation see *61 Computer Programming and Software.*

83 ECONOMICS AND COST ANALYSIS **3924**
Includes cost effectiveness studies.

84 LAW, POLITICAL SCIENCE AND SPACE POLICY **3924**
Includes NASA appropriation hearings; aviation law; space law and policy; international law; international cooperation; and patent policy.

85 URBAN TECHNOLOGY AND TRANSPORTATION **3924**
Includes applications of space technology to urban problems; technology transfer; technology assessment; and surface and mass transportation. For related information see *03 Air Transportation and Safety, 16 Space Transportation,* and *44 Energy Production and Conversion.*

SPACE SCIENCES For related information see also *Geosciences.*

88 SPACE SCIENCES (GENERAL) ..... **N.A.**

89 ASTRONOMY **3924**
Includes radio, gamma-ray, and infrared astronomy; and astrometry.

90 ASTROPHYSICS **3927**
Includes cosmology; celestial mechanics; space plasmas; and interstellar and interplanetary gases and dust. For related information see also *75 Plasma Physics.*

91 LUNAR AND PLANETARY EXPLORATION **3939**
Includes planetology; and manned and unmanned flights. For spacecraft design or space stations see *18 Spacecraft Design, Testing and Performance.*

92 SOLAR PHYSICS **3952**
Includes solar activity, solar flares, solar radiation and sunspots. For related information see also *93 Space Radiation.*

93 SPACE RADIATION **3954**
Includes cosmic radiation; and inner and outer earth's radiation belts. For biological effects of radiation see *52 Aerospace Medicine.* For theory see *73 Nuclear and High-Energy Physics.*

GENERAL

Includes aeronautical, astronautical, and space science related histories, biographies, and pertinent reports too broad for categorization; histories or broad overviews of NASA programs.

99 GENERAL **3956**

SUBJECT INDEX **I-1**

PERSONAL AUTHOR INDEX **I-161**

CORPORATE SOURCE INDEX **I-179**

CONTRACT NUMBER INDEX **I-207**

REPORT NUMBER INDEX **I-213**

APPENDIX **A-1**

TYPICAL CITATION AND ABSTRACT

NASA SPONSORED — ON MICROFICHE

ACCESSION NUMBER → **N94-12270*#** United Technologies Corp., West Palm Beach, FL. ← CORPORATE SOURCE
Pratt and Whitney.

TITLE → **ADVANCED CONTROL FOR AIRBREATHING ENGINES, VOLUME 1: PRATT AND WHITNEY**

AUTHOR → J. A. Ralph Jul. 1993 83 p ← PUBLICATION DATE

CONTRACT OR GRANT → (Contract NAS3-25952; RTOP 505-62-61)

REPORT NUMBERS → (NASA-CR-189203; E-8006; NAS 1.26:189203) Avail: CASI HC A05/MF A01 ← AVAILABILITY SOURCE AND PRICE CODE

The application of advanced control concepts to air breathing engines may yield significant improvements in aircraft/engine performance and operability. Screening studies of advanced control concepts for air breathing engines were conducted by three major domestic aircraft engine manufacturers to determine the potential impact of concepts on turbine engine performance and operability. The purpose of the studies was to identify concepts which offered high potential yet may incur high research and development risk. A target suite of proposed advanced control concepts was formulated and evaluated in a two phase study to quantify each concept's impact on desired engine characteristics. To aid in the evaluation specific aircraft/engine combinations were considered: a Military High Performance Fighter mission, a High Speed Civil Transport mission, and a Civil Tiltrotor mission. Each of the advanced control concepts considered in the study are defined and described. The concept potential impact on engine performance was determined. Relevant figures of merit on which to evaluate the concepts are determined. Finally, the concepts are ranked with respect to the target aircraft/engine missions. A final report describing the screening studies was prepared by each engine manufacturer. Volume 1 of these reports describes the studies performed by Pratt & Whitney. Author (revised)

VOLUME 32 NUMBER 9 / September 1994

Scientific and Technical Aerospace Reports

A Monthly Publication of the National Aeronautics and Space Administration

01 AERONAUTICS (GENERAL)

N94-31332# Naval Postgraduate School, Monterey, CA.
AN ANALYSIS OF THE MAINTENANCE PERFORMANCE MEASUREMENT SYSTEM FOR LAMPS MK 3 HELICOPTER SQUADRONS M.S. Thesis
Richard K. Fawcett Dec. 1993 212 p
(AD-A276421) Avail: CASI HC A10/MF A03

With the current downsizing of the United States military and the defense budget, the diminishing availability of resources has increased the focus on the need for effective management. This thesis discusses several factors affecting performance improvement (effectiveness, efficiency, quality, productivity, budgetability, quality of work life, and innovation) for LAMPS MK 3 helicopter squadrons. Current non-financial measures for monitoring the performance of maintenance are examined and evaluated. Alternative maintenance performance measures are described and discussed. The alternative measures for which source data is available are analyzed. A new performance measurement model, the Multi-Criteria Performance/Productivity Measurement Technique, and the Objectives Matrix, is described and recommended for measuring LAMPS MK 3 helicopter squadron maintenance performance. DTIC

N94-31342* National Aeronautics and Space Administration, Washington, DC.
AERONAUTICAL ENGINEERING: A CONTINUING BIBLIOGRAPHY WITH INDEXES (SUPPLEMENT 302)
Mar. 1994 69 p
(NASA-SP-7037(302); NAS 1.21:7037(302)) Avail: CASI HC A04

This bibliography lists 152 reports, articles, and other documents introduced into the NASA scientific and technical information database. Subject coverage includes: design, construction and testing of aircraft and aircraft engines; aircraft components, equipment, and systems; ground support systems; and theoretical and applied aspects of aerodynamics and general fluid dynamics. Author

N94-31362# Air Force Inst. of Tech., Wright-Patterson AFB, OH.
AN EVALUATION OF AIRCRAFT MAINTENANCE PERFORMANCE FACTORS IN THE OBJECTIVE WING M.S. Thesis
Mark A. Gray and Margaret M. Ranalli Sep. 1993 152 p
(AD-A276010; AFIT/GLM/LA/93S-22) Avail: CASI HC A08/MF A02

Prior to 1992, organizational maintenance was aligned under a separate maintenance organization. In 1992, the Air Force restructured into objective wings with organizational maintenance aligned under the flying squadrons. This study looks at the impact of this reorganization on maintenance performance factors. The researchers developed maintenance performance models using regression and principal component analysis. Mission capable rate and total not mission capable maintenance rate are used as dependent variables. A comparison of key maintenance performance indicators and model predictions before and after the reorganization is accomplished. Based on the results of this analysis, the researchers conclude that there is significant improvement in all dependent variables, model predictions of these dependent variables, and some of the independent variables. Improvement occurred after organizational structure changed; however, other factors not included in the models such as the stand-down of the alert force may also contribute to this improvement. DTIC

N94-31367# Wright Lab., Wright-Patterson AFB, OH.
THE MAINTENANCE OF OPERATIONAL FLIGHT PROGRAM Final Report, 5-8 Oct. 1992
Charles P. Satterthwaite Jan. 1994 10 p
(AF Proj. 9994)
(AD-A276363; WL-TR-94-1009) Avail: CASI HC A02/MF A01

The process of maintaining Operational Flight Programs (OFP's) is discussed so that interested individuals can understand (1) how OFP's work, (2) how OFP's are changed, (3) how OFP's are tested, (4) how OFP's are documented, (5) how to train OFP maintainers, and (6) how to measure OFP's. DTIC

N94-31381* National Aeronautics and Space Administration, Washington, DC.
AERONAUTICAL ENGINEERING: A CONTINUING BIBLIOGRAPHY WITH INDEXES (SUPPLEMENT 303)
Apr. 1994 89 p
(NASA-SP-7037(303); NAS 1.21:7037(303)) Avail: CASI HC A05

This bibliography lists 211 reports, articles, and other documents introduced into the NASA scientific and technical information database. Subject coverage includes: design, construction, and testing of aircraft and aircraft engines; aircraft components, equipment, and systems; ground support systems; and theoretical and applied aspects of aerodynamics and general fluid dynamics. CASI

N94-31830# Robbins-Gioia, Inc., Alexandria, VA.
INITIAL ESTIMATES OF INTEGRATED MAINTENANCE INFORMATION SYSTEM (IMIS) COSTS AND BENEFITS, VOLUME 1 Final Report, Jul. - Sep. 1993
Robert J. Tomasetti, A. B. Calogero, Charlie E. Jones, Charles L. Hanna, and Thomas J. Guarino Oct. 1993 53 p
(Contract F33600-85-D-7002)
(AD-A276144; AL/HR-TR-1993-0178-Vol-1) Avail: CASI HC A04/MF A01

This report analyzes the system-wide costs and benefits of implementing the Integrated Maintenance Information System (IMIS) for the F-16. The Human Resources Directorate of the Armstrong Laboratory has undertaken IMIS as an Advanced Technology Transition Demonstration (ATTD) effort. ATTD efforts provide proof-of-principle demonstrations conducted at the system or major subsystem level in an operational environment. They demonstrate the potential of new technologies to provide significant improvements in cost-effectiveness. IMIS has the potential to provide major improvements in the efficiency of aircraft maintenance processes. This report documents the initial effort to develop a rough order of magnitude estimate of the functional costs and benefits of implementing the IMIS technology. Estimates are developed for the Base Case and two IMIS implementation alternatives. The alternatives are analyzed, results identified, and conclusions reached. DTIC

N94-31959 Rand Graduate Inst. for Policies Study, Santa Monica, CA.
PROSPECTS FOR THE FRENCH FIGHTER INDUSTRY IN A POST-COLD WAR ENVIRONMENT: IS THE FUTURE MORE THAN A MIRAGE? Ph.D. Thesis
Yolande Marie Simon 1993 344 p
Avail: Univ. Microfilms Order No. DA9327555

Since withdrawing from NATO's integrated military structure in 1966, France has striven for self-sufficiency in the defense sector. A major component of this policy has been to maintain an independent arms

manufacturing capability, particularly a fighter industry. The small size of the domestic market has necessitated an aggressive export policy, which met with considerable success under the guidance of French aviation industrialist Marcel Dassault. France found a niche in marketing midrange, moderately priced fighters (the Mirage series) known for their simplicity, reliability, and excellent performance. This strategy was altered in the early 1980s with the design of the Rafale multirole fighter, which will directly compete with American or Soviet fighters. This new strategy comes at a time when a variety of factors have been threatening France's arms export policy: shrinking international arms market, increasing cost of weapons, and intensified competition. The collapse of the Soviet Union, compounded with economic recession, has led to the slowing or elimination of aircraft modernization programs. In this changing environment, is the concept of an independent French fighter industry more than a mirage? This report sheds new light on the prospects for the French fighter industry. It seeks to estimate the potential export sales of the Rafale over the next twenty years, to offer an independent estimate of the cost of the Rafale program and to compare it with published cost estimates, and to explore the viability of the Rafale program in light of these two estimates. To these ends, this paper considers both the demand for and the cost of the Rafale. Part 1 describes the inception of the Rafale program, the controversies which have surrounded it, and those aircraft which will compete most directly with it. Part 2 probes the potential global demand for fighters over the next two decades and estimates the future demand for French fighters. Part 3 analyzes the cost of the Rafale, using DAPCA, a cost analysis model created at RAND. Finally, this paper considers the implications of these assessments for the future of the Rafale program and the French fighter industry. Dissert. Abstr.

N94-32157# Federal Aviation Administration, Atlantic City, NJ. Technical Center.

SHEAROGRAPHIC INSPECTION OF A DEHAVILLAND DHC-7

Stephen N. Bobo Dec. 1993 24 p

(AD-A276716; DOT/FAA/CT-TN92/39) Avail: CASI HC A03/MF A01

Under a Cooperative Research and Development Agreement between the Volpe National Transportation Systems Center (VNTSC) and Henson Aviation, Inc., operator of USAir Express, a shearographic demonstration inspection of the fuselage of a DeHavilland DHC-7 aircraft was performed at a US Air repair station at Norfolk, VA, on August 8, 1992. The inspection compared the effectiveness of shearography with currently mandated methods in detecting disbonds in the fuselage. Adhesive bonding is utilized in modern aircraft fuselages, frequently in combination with rivets. As aircraft age, bond failure becomes a major problem, since it may promote fatigue cracking, moisture intrusion, and subsequent corrosion. Any of these events may cause cabin pressure loss and, sometimes, catastrophic fuselage failure. The shearographic method of detecting disbonds depends on the deformation of the aircraft skin under mechanical stimulus. When illuminated by coherent light, the phase relationship and intensity of the light reflected from any two points of the skin changes as a result of this deformation. Surface changes down to 0.00025 millimeter can be detected and displayed as a real-time image of the field of view. Comparison of successive images as the deformation changes permits interpretation of the condition of a bond. In addition, other selected areas of the aircraft suspected to contain disbonds were inspected. No disbonds were found either by shearography or confirming ultrasound readings. Shearography was clearly able to identify the presence of waffle doublers wherever drawings of the aircraft indicated that they should exist. DTIC

N94-32254# Aerospace Medical Research Labs., Wright-Patterson AFB, OH. Human Resources Directorate.

HUMAN COMPUTER INTERFACE SPECIFICATIONS (HCIS) FOR THE INTEGRATED MAINTENANCE INFORMATION SYSTEM (IMIS)

Jeffrey L. Wampler, David R. Gunning, Cher E. Wynkoop, Laurie L. Quill, and Laura L. Moorman Oct. 1993 145 p

(Contract F33615-88-C-0024)

(AD-A277184; AL/HR-TP-1993-0035) Avail: CASI HC A07/MF A02

The Armstrong Laboratory Logistics Research Division (AL/HRG) is developing a proof-of-concept Integrated Maintenance Information System (IMIS). The IMIS will demonstrate the capability to access and integrate maintenance information from multiple sources and present the information to technicians and maintenance personnel through hand-held and workstation computers. A significant part of IMIS is the user interface. Current practices in the DoD procurement process do not emphasize the specification of a system's user interface as requirements. Instead, the user interface is often designed as the system develops. This paper documents a baseline user interface specification for all IMIS applications and a detailed user interface specification for an interactive electronic technical manual (IETM) presentation system. DTIC

N94-32793*# National Aeronautics and Space Administration, Washington, DC.

AIRBORNE TRAILBLAZER: TWO DECADES WITH NASA LANGLEY'S 737 FLYING LABORATORY

Lane E. Wallace 1994 193 p *Its* NASA History series Original contains color illustrations

(NASA-SP-4216; NAS 1.21:4216; LC-94-5874) Avail: CASI HC A09/MF A03; SOD HC; 76 functional color pages

This book is the story of a very unique aircraft and the contributions it has made to the air transportation industry. NASA's Boeing 737-100 Transport Systems Research Vehicle started life as the prototype for Boeing's 737 series of aircraft. The airplane was acquired by LaRC in 1974 to conduct research into advanced transport aircraft technologies. In the twenty years that followed, the airplane participated in more than twenty different research projects, evolving from a research tool for a specific NASA program into a national airborne research facility. It played a critical role in developing and gaining acceptance for numerous significant transport technologies including 'glass cockpits,' airborne windshear detection systems, data links for air traffic control communications, the microwave landing system, and the satellite-based global positioning system (GPS). Author (revised)

N94-32853* National Aeronautics and Space Administration, Washington, DC.

AERONAUTICAL ENGINEERING: A CONTINUING BIBLIOGRAPHY WITH INDEXES (SUPPLEMENT 304)

May 1994 158 p

(NASA-SP-7037(304); NAS 1.21:7037(304)) Avail: CASI HC A08

This bibliography lists 453 reports, articles, and other documents introduced into the NASA scientific and technical information system in May 1994. Subject coverage includes: design, construction and testing of aircraft and aircraft engines; aircraft components, equipment, and systems; ground support systems; and theoretical and applied aspects of aerodynamics and general fluid dynamics. Author

N94-33016# Federal Aviation Administration, Washington, DC. Office of Aviation Policy and Plans.

FAA AVIATION FORECASTS, FISCAL YEARS 1994-2005

Mar. 1994 194 p

(AD-A277808; FAA-APR-94-1) Avail: CASI HC A09/MF A03

This report contains the Fiscal Years 1994-2005 Federal Aviation Administration (FAA) forecasts of aviation activity at FAA facilities. These include airports with FAA control towers, air route traffic control centers, and flight service stations. Detailed forecasts were made for the major users of the National Aviation System: air carriers, air taxi/commuters, military, and general aviation. The forecasts have been prepared to meet the budget and planning needs of the constituent units of the FAA and to provide information that can be used by state and local authorities, the aviation industry, and the general public. The slow pace of the economic recovery in United States and economic recessions in several of the major world trade areas have caused the aviation industry to experience continued slow traffic growth. However, the outlook for the 12-year forecast period is for moderate economic growth, stable real fuel prices, and modest inflation. Based on these assumptions, aviation activity for fiscal year 2005 is forecast to increase by 22.6 percent at towered airports and 24.0 percent at air route traffic control centers. The general aviation active fleet is forecast to decline by 3.8 percent during the forecast period but increased utilization (hours flown by aircraft) results in a 12.0 percent increase in general aviation hours flown during the same period. Scheduled domestic revenue passenger miles (RPM's) are forecast to increase 55 percent, scheduled international RPMS are forecast to increase by 108 percent, and regional/commuter RPM's are forecast to increase by 166 percent. DTIC

N94-33046*# National Aeronautics and Space Administration. Lewis Research Center, Cleveland, OH.
RESEARCH AND TECHNOLOGY, 1993
1993 176 p
(NASA-TM-106376; E-8187; NAS 1.15:106376) Avail: CASI HC A09/MF A02

This report selectively summarizes the NASA Lewis Research Center's research and technology accomplishments for the fiscal year 1993. It comprises approximately 200 short articles submitted by the staff members of the technical directorates. The report is organized into seven major sections: Aeronautics, Aerospace Technology, Space Flight Systems, Space Station, Engineering and Computational Support, Lewis Research Academy, and Technology Transfer and Utilization. A table of contents by subject has been developed to assist the reader in finding articles of special interest. This report is not intended to be a comprehensive summary of all research and technology work done over the past fiscal year. Most of the work is reported in Lewis-published technical reports, journal articles, and presentations prepared by Lewis staff members or by contractors. In addition, university grants have enabled faculty members and graduate students to engage in sponsored research that is reported at technical meetings or in journal articles. For each article in this report a Lewis contact person has been identified, and where possible, reference documents are listed so that additional information can be easily obtained. The diversity of topics attests to the breadth of research and technology being pursued and to the skill mix of the staff that makes it possible. Author

N94-33064*# National Aeronautics and Space Administration. Lewis Research Center, Cleveland, OH.
VIBRATION ISOLATION TECHNOLOGY (VIT) ATD PROJECT Final Report
Joseph F. Lubomski, Carlos M. Grodsinsky, Kirk A. Logsdon, Douglas A. Rohn, and N. Ramachandran Mar. 1994 36 p
(RTOP 694-03-0C)
(NASA-TM-106496; E-8487; NAS 1.15:106496) Avail: CASI HC A03/MF A01

A fundamental advantage for performing material processing and fluid physics experiments in an orbital environment is the reduction in gravity driven phenomena. However, experience with manned spacecraft such as the Space Transportation System (STS) has demonstrated a dynamic acceleration environment far from being characterized as a 'microgravity' platform. Vibrations and transient disturbances from crew motions, thruster firings, rotating machinery etc. can have detrimental effects on many proposed microgravity science experiments. These same disturbances are also to be expected on the future space station. The Microgravity Science and Applications Division (MSAD) of the Office of Life and Microgravity Sciences and Applications (OLMSA), NASA Headquarters recognized the need for addressing this fundamental issue. As a result an Advanced Technology Development (ATD) project was initiated in the area of Vibration Isolation Technology (VIT) to develop methodologies for meeting future microgravity science needs. The objective of the Vibration Isolation Technology ATD project was to provide technology for the isolation of microgravity science experiments by developing methods to maintain a predictable, well defined, well characterized, and reproducible low-gravity environment, consistent with the needs of the microgravity science community. Included implicitly in this objective was the goal of advising the science community and hardware developers of the fundamental need to address the importance of maintaining, and how to maintain, a microgravity environment. This document will summarize the accomplishments of the VIT ATD which is now completed. There were three specific thrusts involved in the ATD effort. An analytical effort was performed at the Marshall Space Flight Center to define the sensitivity of selected experiments to residual and dynamic accelerations. This effort was redirected about half way through the ATD focusing specifically on the sensitivity of protein crystals to a realistic orbital environment. The other two thrusts of the ATD were performed at the Lewis Research Center. The first was to develop technology in the area of reactionless mechanisms and robotics to support the eventual development of robotics for servicing microgravity science experiments. This activity was completed in 1990. The second was to develop vibration isolation and damping technology providing protection for sensitive science experiments. In conjunction with the this activity, two workshops were held. The results of these were summarized and are included in this report. Author

N94-33338 Alberta Research Council, Edmonton. Dept. of Advanced Computing Engineering.
THE CF-18 DIAGNOSTIC AND MAINTENANCE EXPERT SYSTEM PROJECT
J. B. Tubman, M. D. Brinsmead, C. C. Lumb, M. M. Mendoza, and I. S. L. Tan *In* Royal Military Coll. of Canada, Proceedings of the Symposium/Workshop on Applications of Expert Systems in DND Apr. 1992 p 74-92 (For primary document see N94-33335 09-66)
Avail: Issuing Activity (Royal Military Coll. of Canada, Vimy Post Office, Kingston, ON K7K 5L0 Canada)

02 AERODYNAMICS

Includes aerodynamics of bodies, combinations, wings, rotors, and control surfaces; and internal flow in ducts and turbomachinery.

For related information see also *34 Fluid Mechanics and Heat Transfer.*

N94-31180 National Aerospace Lab., Amsterdam (Netherlands). Fluid Dynamics Div.
CFD-BASED DRAG PREDICTION: STATE-OF-THE-ART, THEORY, PROSPECTS
J. vanderVooren and J. W. Slooff 15 Sep. 1992 75 p Presented at the AIAA Professional Studies Series, Course on Drag-Prediction and Measurement, Portland, OR, 23-24 Aug. 1990 Limited Reproducibility: More than 20% of this document may be affected by microfiche quality
(AD-B179297; NLR-TP-90247-U; ETN-94-95974) Avail: CASI HC A04

An overview of the state of the art and the theory of Computational Fluid Dynamics (CFD) based drag prediction, with some emphasis on transport aircraft, is presented. The entire field, ranging from potential codes to Reynolds averaged Navier-Stokes codes is covered. Only steady flow, in the absence of propulsion, is discussed. It is concluded that, although CFD based drag prediction can be viewed with 'cautious optimism', it still has a long way to go; research and development in CFD post processing routines for drag prediction purposes is required for many years to come. ESA

N94-31204 Rensselaer Polytechnic Inst., Troy, NY.
AN ADAPTIVE FINITE ELEMENT METHOD FOR UNSTEADY COMPRESSIBLE ROTOR AIRFOIL AERODYNAMICS Ph.D. Thesis
Bruce Eugene Webster 1993 199 p
Avail: Univ. Microfilms Order No. DA9325276

The accurate treatment of unsteady compressible rotor airfoil aerodynamic flows requires the capability to efficiently resolve the widely varying length scales of the flow physics as they evolve temporally. An adaptive finite element methodology suitable for this type of problem is developed in this thesis. It is based upon an automated adaptive environment consisting of the Finite Quadtree automatic mesh generator, a time-discontinuous Galerkin Least Squares finite element flow solver, an error indicator based upon interpolation estimates, and a mesh enrichment procedure. The time-discontinuous Galerkin Least Squares finite element flow solver is particularly well suited to handle problems with multiple relative motion. A linear space-time wedge element formulation was developed and implemented which is suitable for two dimensional problems with relative body motion. The mesh enrichment procedure developed to enable the solution process to be spatially adaptive (h-refinement) is edge based and stores no mesh enrichment history. Steady and unsteady transonic airfoil calculations show good correlation with other experimental and numerical data. Based upon these results it is concluded that this type of automated adaptive CFD technique is a viable computational tool capable of accurately resolving unsteady compressible flow features and should be developed further to handle three dimensional problems where multiple relative motion is important, i.e. the flow field around an entire helicopter. Dissert. Abstr.

N94-31216 Michigan Univ., Ann Arbor.
CONTROL OF HYPERSONIC AERODYNAMIC FORCES WITH SURFACE

BLOWING Ph.D. Thesis
Michael David Matarrese 1993 156 p
Avail: Univ. Microfilms Order No. DA9319582

Aerodynamic forces are obtained for laminar flow past a slender wedge at high Mach number and high Reynolds number, with a cool inert gas injected at the surface. Mass-flow rates are taken to be large enough to blow the boundary layer away from the wall as a free shear layer, but small enough that the effective body remains thin. Cases studied include distributed blowing where the wall mass flux is proportional to a power of the streamwise coordinate, uniform blowing from a strip located downstream from the wedge vertex, and various examples of time-dependent mass injection. For power-law blowing, self-similar solutions are obtained in the strong- and weak-interaction limits for the layer of blown gas adjacent to the surface, for the viscous shear layer, and for the outer inviscid-flow region between the shear layer and the shock wave. Formulas are derived which relate the surface pressure and surface shear stress to the mass flow, and the behavior of the pressure force and drag are examined for a range of parameter values, for different injectants, and for various distributions of the injected mass. Equilibrium dissociation of oxygen and other real-gas effects are included in part of the analysis. For strip blowing on a cool wall, mass flows are chosen such that the flow separates upstream of the slot leading edge in a hypersonic free interaction. The pressure force as a function of mass-flow rate is obtained for various slot geometries, including an example with two slots. For unsteady distributed blowing, time histories of the pressure force are computed for various cases where the shear layer may be neglected and the time rate of change of the wall boundary conditions is small compared to the residence time in the outer flow. Dissert. Abstr.

N94-31220# Aeronautical Research Inst. of Sweden, Stockholm. Aerodynamics Dept.
PREDICTION OF TRANSONIC POTENTIAL FLOW WITH SLIPSTREAMS AROUND CONFIGURATIONS
Wang Dieqian and Sven G. Hedman Feb. 1993 58 p Sponsored by Aeronautical Research Inst. of Sweden
(Contract NUTEK-5623-92-01540)
(FFA-TN-1992-15; ETN-94-95879) Avail: CASI HC A04/MF A01

A potential flow code was developed for the simulation of transonic flow around wing/body/nacelle configurations and for the prediction of propeller/airframe interference. The propeller is modeled as an actuator disk, and the effect of the slipstream is considered in an approximate way. The wing/body/nacelle flow solver and the grid generator were developed from earlier codes for wing/body cases. The computational space is divided into two blocks, with one block inboard and one outboard of the nacelle. The algorithm for the two block case is fully implicit not only in all the three coordinate directions but also between the two blocks. It is uniformly stable for all regions in the field. The method uses almost the same CPU (Central Processing Unit) time as the one block solver does for wing/body configurations. Hence, it is a very robust algorithm and the method is cost effective. Applications are shown for three cases simulating propeller driven airplanes in subsonic climb and transonic cruise. Comparisons are made with data from Euler code calculations and also with results from wind tunnel tests. In general the obtained agreement is very good. ESA

N94-31287 Old Dominion Univ., Norfolk, VA.
GRID SENSITIVITY FOR AERODYNAMIC OPTIMIZATION AND FLOW ANALYSIS Ph.D. Thesis
Ideen Sadrehaghighi 1993 119 p
Avail: Univ. Microfilms Order No. DA9319038

An algorithm is developed to obtain the grid sensitivity with respect to design parameters for aerodynamic optimization. Two distinct parameterization procedures are developed for investigating the grid sensitivity with respect to design parameters of a wing section as an example. The first procedure is based on traditional (physical) relations defining NACA four-digit wing sections. The second is advocating a novel (geometrical) parameterization using spline functions such as NURBS (nonuniform rational b-splines) for defining the wing section geometry. An interactive algebraic grid generation technique, known as two-boundary grid generation (TBGG), is employed to generate C-type grids around wing sections. The grid sensitivity of the domain with respect to design and grid parameters has been obtained by direct differentiation of the grid equations. A hybrid approach is proposed for more geometrically complex configurations. A comparison of the sensitivity coefficients with those obtained using a finite difference approach is made to verify the feasibility of the approach. The aerodynamic sensitivity coefficients are obtained using the compressible, two dimensional, thin-layer Navier-Stokes equations. An optimization package has been introduced into the algorithm in order to optimize the wing section surface using both physical and geometric parameterization. Results demonstrate a substantially improved design, particularly in the geometric parameterization case. Dissert. Abstr.

N94-31421# Office National d'Etudes et de Recherches Aerospatiales, Paris (France).
EXPERIMENTAL AND NUMERICAL SIMULATION OF HELICOPTER ROTOR FUSELAGE INTERACTION Ph.D. Thesis - Aix-Marseille Univ. [SIMULATION EXPERIMENTALE ET NUMERIQUE DE L'INTERACTION ROTOR-FUSELAGE D'HELICOPTERE]
Roland Hanotel 1993 141 p In FRENCH Original contains color illustrations
(ISSN 0078-3781)
(ONERA-NT-1993-8; ETN-94-96063) Avail: CASI HC A07/MF A02

A Computational Fluid Dynamics (CFD) method for prediction of helicopter/fuselage interactions is proposed. The main rotor blades are modeled using lifting line theory, with the rotor wake discretized using a lattice of radial and tangential elements. The fuselage is modeled by a surface distribution of sources and doublets. The interaction is computed by balancing out iteratively the influence of the rotor and that of the fuselage. The latter was analyzed by means of isolated rotor and coupled fuselage/rotor computations. Induced velocities from two different data banks were used to validate this method. ESA

N94-31578# Sandia National Labs., Albuquerque, NM.
A NOVEL CFD/STRUCTURAL ANALYSIS OF A CROSS PARACHUTE
R. A. LaFarge, J. M. Nelsen, and K. W. Gwinn 1993 11 p Presented at the 32nd Aerospace Sciences Meeting and Exhibit, Reno, NV, 11-14 Jan. 1994
(Contract DE-AC04-94AL-85000)
(DE94-005271; SAND-93-3895C; CONF-940152-1) Avail: CASI HC A03/MF A01

A novel CFD/structural analysis was performed to predict functionality of a cross parachute under loadings near the structural limits of the parachute. The determination of parachute functionality was based on the computed structural integrity of the canopy and suspension lines. In addition to the standard aerodynamic pressure loading on the canopy, the structural analysis considered the reduction in fabric strength due to the computed aerodynamic heating. The intent was to illustrate the feasibility of such an analysis with the commercially available software PATRAN. DOE

N94-31734# Toronto Univ. (Ontario). Dept. of Aerospace Science and Engineering.
HEAVE DYNAMICS OF AN AIR CUSHION VEHICLE BAG AND FINGER SKIRT M.S. Thesis
Joon Chung 1993 114 p
(ISBN-0-315-87053-2; CTN-94-61242) Copyright Avail: Micromedia Ltd., Technical Information Centre, 240 Catherine Street, Suite 305, Ottawa, Ontario, K2P 2G8, Canada HC/MF

A theoretical analysis of the heave dynamics of an air cushion vehicle bag and finger skirt is presented. The dynamic response of the skirt was predicted using a simplified model derived from Lagrange's equations. The skirt mass is lumped in the finger, and the fingers are modelled as rigid bodies having both mass and moment of inertia. The equations governing the dynamics of the bag and finger system and its interaction with cushion and craft systems are then derived. The theoretical model uses a simplified geometry and has two degrees of freedom. It is further developed to explore its ability to predict dynamic skirt responses. A system of nonlinear differential equations is solved by integration using Gear's method. The assumptions related to the fluid mechanics, skirt material properties, and skirt geometry used in the analysis are presented and the reasons for their choice are discussed. The theoretical results of the nonlinear heave response and the effect of both the skirt mass and changing skirt geometry on frequency response are detailed. Simulation results show that though air cushion dynamics are nonlinear as a whole, there are distinct segments which may be predicted by linear analysis. Author (CISTI)

N94-31759 Colorado Univ., Boulder.
NUMERICAL SIMULATION OF COMBINED EXTERNAL/INTERNAL TRANSONIC FLOW ON THE FOREBODY/INLET OF THE AV-8B HARRIER 2 Ph.D. Thesis
Stephen John Mysko, III 1993 117 p
Avail: Univ. Microfilms Order No. DA9320457

In this work, the computation of combined external/internal transonic flow on the complex forebody/inlet configuration of the AV-8B Harrier 2 is performed. The actual aircraft has been measured and its surface and surrounding domain have been defined using computational structured grids. The thin-layer Navier-Stokes equations were used to model the flow along with the Chimera overlaid multiblock technique. A fully conservative, alternating direction implicit (ADI), approximately-factored (two factors), partially flux-split algorithm was employed to perform the computation. Comparisons to some experimental data yielded good agreement for the simplifications incorporated into the analysis. The aim of the dissertation is to provide a methodology or computational tool for the numerical solution of complex flows, specifically combined external/internal flows. The use of embedded multiblocks enables easier definition of the geometry and also allows for single surfaces to be defined by more than one grid. The unique grid system must account for a geometry which has a fuselage and inlet which share a wall, and at the same time be able to model both external and internal flow. An existing code was altered to conform with the needs of the study, and a special boundary condition was developed and is presented. This boundary condition was used near the inlet engine face to improve the accuracy of the numerical model. The algorithm incorporates the Chimera technique and an algebraic turbulence model in order to deal with the overlaid multiblocks and viscous governing equations. The TFFS (two-factor, flux-split) scheme was applied to solve steady flows using the CRAY Y-MP supercomputer. The general flow quality was discussed and evaluated and any problem areas were expanded upon. The results for flow at zero incidence and angle of attack compared favorably with the experimental data both for local surface pressure data and globally over the entire engine face. In addition, the inlet back pressure boundary condition was employed to generate off-design flow characteristics. The results indicate the methodology used here is a viable tool for aircraft modeling. Dissert. Abstr.

N94-31822# Groningen Rijksuniv. (Netherlands). Dept. of Mathematics.
ON AN ADAPTATION METHOD FOR 2-DIMENSIONAL C-TYPE GRIDS
P. W. J. vanHengel and M. A. Vis 1993 12 p Presented at ISNaS Symposium, Emmeloord, Netherlands, 19-20 Sep. 1991 Prepared in cooperation with National Aerospace Lab.
(W-9322; ETN-94-96183) Avail: CASI HC A03/MF A01

A practical application of an adaptive grid method for two dimensional C type grids around aerofoils is presented. The method was applied to adapt grids used for the simulation of inviscid flow (NACA 0012 aerofoil) and viscous flow (RAE 2822 aerofoil). It is concluded that the method is very well suited for grids with moderate aspect ratios as used for inviscid flow computations. High aspect ratio grids, as used for viscous flow computations, require more careful tuning of the parameters in the adaptation algorithm. ESA

N94-31828 Colorado Univ., Boulder.
A NEW INVERSE METHOD FOR GENERATING HIGH-SPEED AERODYNAMIC FLOWS WITH APPLICATION TO WAVERIDER DESIGN Ph.D. Thesis
Kevin Daniel Jones 1993 172 p
Avail: Univ. Microfilms Order No. DA9320435

The design of efficient high-speed aircraft is of considerable interest for use in a multitude of applications including civil transport, access to low earth orbit, and aeroassisted orbital transfer. The design of such vehicles is often accomplished with the aid of numerical methods. A new, numerical inverse-design method is developed for the principle lifting surface of such vehicles. Here the compressible three dimensional Euler equations are marched spatially away from a prescribed shock surface in a cross-stream direction to define the post-shock flowfield. The general three dimensional problem is mathematically ill-posed; however, by marching within the local osculating plane, accurate and stable solutions are obtained. The algorithm is applied to the design of a class of hypersonic vehicles called waveriders. The waverider's lower surface is defined as a stream surface carved from the post-shock flowfield computed by this marching procedure. The waverider's upper surface is a parametrically defined expansion surface, and the flowfield there is predicted by an approximation of the axisymmetric method of characteristics. Comparisons with exact theory and direct Euler simulations demonstrate the validity and accuracy of the method. The algorithm's application to waverider design affords much greater flexibility in the choice of shock shapes than any previous studies, including here the possibility of nonaxisymmetric shocks with nonconstant shock strengths. Dissert. Abstr.

N94-31879 Texas Univ., Arlington.
SHOCK IMPINGEMENT NEAR MILD HYPERSONIC EXPANSION CORNERS Ph.D. Thesis
Kung-Ming Chung 1992 151 p
Avail: Univ. Microfilms Order No. DA9315977

Experiments were performed in the UTA shock tunnel at Mach 8 and a Reynolds number of 10.2 million/m. A cold-wall, turbulent boundary layer developed along a long flat plate installed in the test section. An expansion corner of 2.5 deg or 4.25 deg was located at 0.77 meters (30.25 inches) from the leading edge of the flat plate. The test surface was instrumented for surface pressure measurement using flush-mounted, fast-response pressure transducers. Interactions were generated by full-span external shock generation in the form of a 2 deg or 4 deg sharp wedge. A hypersonic similarity parameter was identified which scaled the downstream influence of an expansion corner, indicating that the flow can be treated as primarily rotational and inviscid. The surface pressure fluctuations were severely damped by the expansion. The pressure distributions with shock impingement were strongly influenced by the presence of the expansion corners. The upstream influence scale decreased as the shock impinged further downstream of the corner. The unsteadiness of the shock wave/boundary layer interactions was characterized by an intermittent region together with a local rms pressure peak near the upstream influence line. Also, the peak rms pressure fluctuations increased with a larger overall inviscid pressure ratio. Dissert. Abstr.

N94-31880 Ohio State Univ., Columbus.
DESIGN AND INITIAL TESTING OF A FACILITY TO MEASURE UNSTEADY PRESSURES ON AN OSCILLATING CASCADE WITH SUPERSONIC LEADING EDGE LOCUS Ph.D. Thesis
Daniel Eugene Erwin 1993 156 p
Avail: Univ. Microfilms Order No. DA9316150

The development of analytical codes to predict the lift and moment coefficients on an airfoil in an oscillating cascade with a supersonic leading edge locus (SLEL) has generated a need to obtain unsteady experimental pressure data to validate the codes. A facility to gather such data was designed and constructed at the Ohio State University Aeronautical and Astronautical Research Laboratory, and unsteady pressure data was collected for a cascade oscillating at zero stagger angle. Unsteady pressures were measured for reduced frequencies ranging from .025 (26 Hz) to .159 (166 Hz), based on half chord. An experimental influence coefficient technique originally developed for subsonic and transonic cascades was extended to the case of a cascades with a SLEL. This technique was developed to obtain the unsteady pressure difference coefficient on an airfoil in a cascade of airfoils, all of which were executing constant amplitude oscillations at a constant interblade phase angle. This influence coefficient technique allowed the measurement of the pressures by oscillating one airfoil at a time. In order to extend the influence coefficient technique to the measurement of unsteady pressures on a cascades with a SLEL, it was first necessary to derive the equations applicable to a SLEL cascade. The unsteady pressure on a reference airfoil due to all of the airfoils oscillating was then the sum of the influence coefficients from each airfoil. Dissert. Abstr.

N94-31882 North Carolina State Univ., Raleigh.
BOUNDARY LAYER STUDY ON NOZZLE WALL AT HYPERSONIC VELOCITIES Ph.D. Thesis
Kenneth Morris Jones 1993 151 p
Avail: Univ. Microfilms Order No. DA9316605

The boundary layer on the wall of Naval Surface Warfare Center (NSWC) Hypervelocity Tunnel 9 has been investigated with pitot pressure and total temperature measurements. Experimental results are presented for standard Mach 14 runs and supercooled Mach 14 and Mach 18 runs. The experimental results are compared to numerical predictions made with

a modified Navier-Stokes algorithm including vibrational nonequilibrium and intermolecular force effects. The code uses the Cebeci-Smith turbulence model, which has real gas terms incorporated, to model the boundary layer. For standard Mach 14 conditions, the numerical solutions agree very well with experimental data. For the supercooled cases, the numerical code predicts the total temperature well; however, it over-predicts the pitot pressure. In all cases, the turbulence model significantly underestimated the boundary layer thickness and displacement thickness. A study of the method of characteristics/boundary layer technique to design hypersonic nozzles was also carried out. A Mach 18 nozzle was designed with this method and analyzed with the same Navier-Stokes code used to analyze the experimental data. The numerical analysis revealed that the nozzle generated a uniform, disturbance free core flow. Dissert. Abstr.

N94-31907 California Inst. of Tech., Pasadena.
TIP EFFECTS ON THE VORTEX WAKE OF AN AXISYMMETRIC BODY AT ANGLE OF ATTACK Ph.D. Thesis
David Henry Bridges 1993 186 p
Avail: Univ. Microfilms Order No. DA9316833

Experiments on the effects of conditions at the tip of an axisymmetric body on the vortex wake of the body at large angle of attack in incompressible flow have been performed. The separation patterns that occur at the nose of a cone with a hemispherical tip have been documented for ranges of Reynolds number based on tip radius and of relative angle of attack. Tips with cross sections that vary smoothly from elliptic to circular have been designed and tested on a cone. The effectiveness of the tips in varying the cone side force coefficient as the tip is rotated has been demonstrated. The relation between tip roll angle and side force coefficient has been shown to be essentially independent of Reynolds number, for the range of Reynolds number tested, as well as cone base conditions and roll direction. The relation between tip roll angle and side force coefficient has been shown to be a strong function of angle of attack. The reasons for nonsmooth variation of side force coefficient with tip roll angle at higher angles of attack have been determined by examinations of the vortex wake geometry. Peaks in the magnitude of the side force coefficient after zero crossings have been shown to be caused by a rapid shift in the wake vortices away from a symmetric configuration as the tip rotates away from a symmetry condition. Reductions in magnitude of the ride force coefficient between magnitude peaks have been demonstrated to be a result of the near vortex crossing over the cone centerline. This vortex crossover has been shown to occur near and after the breakaway from the cone of the far vortex. The ability of one of the elliptic cross section tips to produce smooth variations of side force coefficient with roll angle ahead of vortex breakaway has been demonstrated, suggesting that the tip might be an effective yaw control device for aircraft at high angle of attack. Dissert. Abstr.

N94-31958 Stanford Univ., CA.
VIBRATIONAL ENERGY TRANSFER OF DIATOMIC GASES IN HYPERSONIC EXPANDING FLOWS Ph.D. Thesis
Stephen Merrick Ruffin 1993 196 p
Avail: Univ. Microfilms Order No. DA9326551

In high temperature flows related to vehicles at hypersonic speeds significant excitation of the vibrational energy modes of the gas can occur. Accurate predictions of the vibrational state of the gas and the rates of vibrational energy transfer are essential to achieve optimum engine performance, for design of heat shields, and for studies of ground based hypersonic test facilities. The Landau-Teller relaxation model is widely used because it has been shown to give accurate predictions in vibrationally heating flows such as behind forebody shocks. However, a number of experiments in nozzles have indicated that it fails to accurately predict the rate of energy transfer in expanding, or cooling, flow regions and fails to predict the distribution of energy in the vibrational quantum levels. The present study examines the range of applicability of the Landau-Teller model in expanding flows and develops techniques which provide accurate predictions in expanding flows. In the present study, detailed calculations of the vibrational relaxation process of N2 and CO in cooling flows are conducted. A coupled set of vibrational transition rate equations and quasi one dimensional fluid dynamic equations is solved. Rapid anharmonic vibration translation transition rates and vibration-vibration exchange collisions are found to be responsible for vibrational relaxation acceleration in situations of high vibrational temperature and low translational temperature. The predictions of the detailed master equation solver are in excellent agreement with experimental results. The exact degree of acceleration is cataloged in this study for N2 and is found to be a function of both the translational temperature (T) and the ratio of vibrational to translational temperatures (T(sub vib)/T). Non-Boltzmann population distributions are observed for values of T(sub vib)/T as low as 2.0. The local energy transfer rate is shown to be an order of magnitude or more faster than the Landau-Teller model for more extreme cases of thermal nonequilibrium. However, these large degrees of local acceleration are difficult to observe in gas dynamic flows because the vibrational energy becomes frozen in rapid expansions. The Landau-Teller model fails to predict non-Boltzmann population distributions for even moderate degrees of thermal nonequilibrium but only fails to accurately predict the overall amount energy in vibration for flows which both have high values of T(sub vib)/T and are not vibrationally frozen. A simplified relaxation model is developed which allows both non-Boltzmann population distributions and includes anharmonic transition rates and energy transfer. Although the simplified anharmonic model requires significantly less computational time than the master equation solver it gives good agreement with the detailed solver and with experimental test results. Dissert. Abstr.

N94-31971 Notre Dame Univ., IN.
A STUDY OF THE DEVELOPMENT AND ATTENUATION OF WING-GENERATED, VORTICAL WAKES Ph.D. Thesis
Vojin Rade Nikolic 1993 255 p
Avail: Univ. Microfilms Order No. DA9319292

Lift-generated wake vortices trailing behind present-day heavy aircraft are of great concern to the aviation community, because they can pose a hazard to a following aircraft that inadvertently penetrates the wake. In order to address the problem of wake-vortex alleviation in a systematic way, an inviscid three dimensional model for calculation of the roll up of wing vortex wakes was developed. The code was extensively tested and validated using a large body of theoretical, computational, and experimental results. During the validation, it was shown that the second moment of vorticity, heretofore assumed to be constant, not only changes as the wake evolves, but must do so in order to conserve energy. Further, the second moment of vorticity has been shown to be a reliable measure of the completeness of the wake roll up process. Found efficient and reliable, the computer code has been applied to computationally investigate some alleviation schemes suggested in the literature as well as some original concepts. It was demonstrated that tailoring the wing spanwise load distribution by use of flaps modifies the resulting wake in terms of making it both more diffuse and, by mooring the primary vortices closer together, renders it more susceptible to the 'Crow' far field instability. Although injection of counter-rotating (with respect to the wing tip vortex) vortices showed little merit, injection of corotating discrete midspan vortices both changes the roll up pattern and hastens the far field instability (from a separation point of view), but causes induced drag penalties. As a completely new idea, excitation of the far field instability of the main wing-vortex pair by injecting relatively weak, intermediate-span, discrete vortices was investigated. During the course of this last investigation, a new method of determining the character of vortex entrainment was developed and shown to be viable. The result of this excitation investigation showed that injection of single, relatively weak, corotating discrete vortices near 0.5 semispans on the left and right side of the wing effectively excited the far field, most-unstable wavelength. The optimal wing location for vortex injection was shown to be only weakly dependent on vortex strength. These findings appear to be compatible with some experimental results from the literature, although the authors of the article containing these results offer an alternative explanation for the mechanism responsible for their results. In fact, the work of this dissertation shows that the alternative explanation appears to be incorrect. Additionally, in an unrelated investigation performed as part of this dissertation research, it was confirmed that the wake roll up can be disorganized by implementing positive bound-circulation gradients near wing tips; however, this benefit was offset by high drag and weight penalties.
Dissert. Abstr.

N94-32027 George Washington Univ., Washington, DC.
SHOCK-DEPENDENT, OPTIMUM THRUST WINGS IN SUPERSONIC FLOW Ph.D. Thesis
James Lee Pittman 1993 141 p
Avail: Univ. Microfilms Order No. DA9318335

This study proposes a new wing concept that reduces the inviscid drag of a wing in supersonic flow. This wing concept contours the surface of each streamwise airfoil aft of the maximum thickness location to produce a significant thrust force thereby reducing the inviscid drag of the wing. The effectiveness of the thrust-wing concept is dependent upon the occurrence of a secondary shock on the wing surface. The secondary shock is clearly identified and exploited herein for the first time. The thrust-wing concept was evaluated on delta wing planforms and compared with delta wings using modified NACA 4-digit airfoils at M(sub infinity) = 1.60. The basic wing camber surface is a spanwise circular arc. The primary figure of merit for the evaluation was the inviscid drag coefficient as computed by a full-potential flow solver for supersonic flow, NCOREL. A design procedure was developed to calculate a feasible, optimum thrust wing at a specified Mach number and lift coefficient for a given planform. The optimization algorithm was the Method of Feasible Directions as found in the CONMIN program. The optimization for a 60 degree delta wing at M(sub infinity) = 1.60 yielded a thrust wing with 17 percent lower inviscid drag at CL = 0.1 compared to the corresponding wing that utilized a modified NACA 4-digit airfoil. At C(sub L) = 0.3, a 9 percent inviscid drag reduction was obtained. Dissert. Abstr.

N94-32063*# National Aeronautics and Space Administration. Ames Research Center, Moffett Field, CA.

A CRITICAL ASSESSMENT OF UH-60 MAIN ROTOR BLADE AIRFOIL DATA

Joseph Totah Sep. 1993 24 p Presented at the 11th Annual Applied Aerodynamics Meeting, Monterey, CA, 9-13 Aug. 1993 See also A93-47210

(RTOP 505-59-36)

(NASA-TM-103985; A-93004; NAS 1.15:103985) Avail: CASI HC A03/MF A01

Many current comprehensive rotorcraft analyses employ lifting-line methods that require main rotor blade airfoil data, typically obtained from wind tunnel tests. In order to effectively evaluate these lifting-line methods, it is of the utmost importance to ensure that the airfoil section data are free of inaccuracies. A critical assessment of the SC1095 and SC1094R8 airfoil data used on the UH-60 main rotor blade was performed for that reason. Nine sources of wind tunnel data were examined, all of which contain SC1095 data and four of which also contain SC1094R8 data. Findings indicate that the most accurate data were generated in 1982 at the 11-Foot Wind Tunnel Facility at NASA Ames Research Center and in 1985 at the 6-inch by 22-inch transonic wind tunnel facility at Ohio State University. It has not been determined if data from these two sources are sufficiently accurate for their use in comprehensive rotorcraft analytical models of the UH-60. It is recommended that new airfoil tables be created for both airfoils using the existing data. Additional wind tunnel experimentation is also recommended to provide high quality data for correlation with these new airfoil tables. Author (revised)

N94-32475*# Illinois Univ., Urbana.

AN EXPERIMENTAL STUDY OF THE FLOWFIELD ON A SEMISPAN RECTANGULAR WING WITH A SIMULATED GLAZE ICE ACCRETION Ph.D. Thesis, 1993 Final Report

Abdollah Khodadoust Cleveland, OH NASA Apr. 1994 249 p Original contains color illustrations

(Grant NAG3-1134; RTOP 505-68-10)

(NASA-CR-195301; E-8693; NAS 1.26:195301) Avail: CASI HC A11/MF A03; 7 functional color pages

Wind tunnel experiments were conducted in order to study the effect of a simulated glaze ice accretion on the flowfield of a semispan, reflection-plane, rectangular wing at Re = 1.5 million and M = 0.12. A laser Doppler velocimeter was used to map the flowfield on the upper surface of the model in both the clean and iced configurations at alpha = 0, 4, and 8 degrees angle of attack. At low angles of attack, the massive separation bubble aft of the leading edge ice horn was found to behave in a manner similar to laminar separation bubbles. At alpha = 0 and 4 degrees, the locations of transition and reattachment, as deduced from momentum thickness distributions, were found to be in good agreement with transition and reattachment locations in laminar separation bubbles. These values at y/b = 0.470, the centerline measurement location, matched well with data obtained on a similar but two dimensional model. The measured velocity profiles on the iced wing compared reasonably with the predicted profiles from Navier-Stokes computations. The iced-induced separation bubble was also found to have features similar to the recirculating region aft of rearward-facing steps. At alpha = 0 degrees and 4 degrees, reverse flow magnitudes and turbulence intensity levels were typical of those found in the recirculating region aft of rearward-facing steps. The calculated separation streamline aft of the ice horn at alpha = 4 degrees, y/b = 0.470 coincided with the locus of the maximum Reynolds normal stress. The maximum Reynolds normal stress peaked at two locations along the separation streamline. The location of the first peak-value coincided with the transition location, as deduced from the momentum thickness distributions. The location of the second peak was just upstream of reattachment, in good agreement with measurements of flows over similar obstacles. The intermittency factor in the vicinity of reattachment at alpha = 4 degrees, y/b = 0.470, revealed the time-dependent nature of the reattachment process. The size and extent of the separation bubble were found to be a function of angle of attack and the spanwise location. Three dimensional effects were found to be strongest at alpha = 8 degrees. The calculated separation and stagnation streamlines were found to vary little with spanwise location at alpha = 0 degrees. The calculated separation streamlines at alpha = 4 degrees revealed that the bubble was largest near the centerline measurement plane, whereas the tip-induced vortex flow and the model root-tunnel wall boundary-layer interaction reduced the size of the bubble. These effects were found to be most dramatic at alpha = 8 degrees. Author (revised)

N94-32476*# Analytical Methods, Inc., Redmond, WA.

A NOVEL POTENTIAL/VISCOUS FLOW COUPLING TECHNIQUE FOR COMPUTING HELICOPTER FLOW FIELDS Final Report, 16 Mar. 1990 - 26 May 1993

J. Michael Summa, Daniel J. Strash, and Sungyul Yoo 21 Jun. 1993 89 p

(Contract NAS2-13194; SBIR-02.09-9090)

(NASA-CR-193272; NAS 1.26:193272; AMI-9304) Avail: CASI HC A05/MF A01

The primary objective of this work was to demonstrate the feasibility of a new potential/viscous flow coupling procedure for reducing computational effort while maintaining solution accuracy. This closed-loop, overlapped velocity-coupling concept has been developed in a new two-dimensional code, ZAP2D (Zonal Aerodynamics Program - 2D), a three-dimensional code for wing analysis, ZAP3D (Zonal Aerodynamics Program - 3D), and a three-dimensional code for isolated helicopter rotors in hover, ZAPR3D (Zonal Aerodynamics Program for Rotors - 3D). Comparisons with large domain ARC3D solutions and with experimental data for a NACA 0012 airfoil have shown that the required domain size can be reduced to a few tenths of a percent chord for the low Mach and low angle of attack cases and to less than 2-5 chords for the high Mach and high angle of attack cases while maintaining solution accuracies to within a few percent. This represents CPU time reductions by a factor of 2-4 compared with ARC2D. The current ZAP3D calculation for a rectangular plan-form wing of aspect ratio 5 with an outer domain radius of about 1.2 chords represents a speed-up in CPU time over the ARC3D large domain calculation by about a factor of 2.5 while maintaining solution accuracies to within a few percent. A ZAPR3D simulation for a two-bladed rotor in hover with a reduced grid domain of about two chord lengths was able to capture the wake effects and compared accurately with the experimental pressure data. Further development is required in order to substantiate the promise of computational improvements due to the ZAPR3D coupling concept. Author

N94-32491 Waterloo Univ. (Ontario).

AERODYNAMIC DRAG OF DROPLETS IN TURBULENT FLOW FIELDS Ph.D. Thesis

William David Warnica 1992 166 p

(ISBN-0-315-75827-9) Avail: Univ. Microfilms Order No. DANN75827

The primary objectives of this research were to design, construct, and test an experimental apparatus which introduces liquid droplets into co-flowing, turbulent, gaseous fields under controlled and measurable conditions and to measure the drag of nonevaporating droplets in turbulent flow fields and parametric ranges relevant to spray combustion, as characterized by the Reynolds number, and the intensity and spatial scales of turbulence. Measured drag coefficients are required for use in computational models of equipment such as gas-turbine combustion

chambers where flame characteristics and combustion performance are strongly dependent on the manner in which droplets are transported and evaporated. Current computational models use drag coefficients of solid spheres in a quiescent field because the effects of turbulence on drag are not well defined, especially at Reynolds numbers characteristic of spray combustion. The experimental apparatus comprised a wind tunnel and a unique piezoelectric droplet generator. The experimental procedure was to inject water droplets of uniform size co-currently and continuously with vertical turbulent air flows while droplet velocities were measured at different elevations using laser Doppler velocimetry. Turbulence was characterized using hot-wire anemometry prior to droplet injection. Drag coefficients were calculated using these main measurements and the law of conservation of mechanical energy. This experimental methodology provided an effective means of determining the drag of droplets. There was no experimental evidence that the drag of droplets in turbulent fields is significantly different than that of solid spheres in a quiescent field at the same Reynolds number. The total measurement uncertainty of this result was approximately 30 percent. Reynolds numbers were investigated in the range 10 to 100, in terms of the equivalent spherical diameter of a droplet, and the mean relative velocity between the ambient gaseous field and droplets. Weber numbers were much less than unity so that droplets were effectively spherical. Relative intensities of turbulence were investigated in the range 0 to 100 percent, in terms of the mean relative velocity. Spatial scales of turbulence were large in comparison to the droplets so that the ratio between the spatial integral scale and droplet diameter was in the range 4 to 20. Dissert. Abstr.

N94-32714 Cincinnati Univ., OH.

STUDY OF DYNAMIC STALL PHENOMENON AND ITS CONTROL USING VORTICITY, STREAM FUNCTION AND CIRCULATION FORM OF THE UNSTEADY NAVIER-STOKES EQUATIONS Ph.D. Thesis

Junho Yang 1993 156 p

Avail: Univ. Microfilms Order No. DA9319276

An unsteady Navier-Stokes (NS) analysis is developed for studying flow past a maneuvering body. The present inclusion of circulation in the vorticity-stream function formulation of the unsteady NS analysis makes it feasible, for the first time, to correctly simulate the asymptotic far-field boundary condition. In the overall analysis, a clustered conformal mesh with C-grid topology is used, with the governing differential equations being solved using the implicit ADI-BGE technique. The effects of grid size and clustering on the flow solution, and the effect of grid stretching on the far-field solution, are studied using the flow configuration with Re = 45,000 and constant-rate pitch-up motion, with dot-alpha(exp +) = 0.2. The influence of the various initial states considered on this flow field is also carefully examined. The results obtained for this case compare very satisfactorily with the available experimental data. Other numerical results are also used to carefully validate the analysis developed here. An active control strategy in terms of modulated suction/injection (MSI) applied at the airfoil surface and its effect on the aerodynamic forces are studied and extended to various dot-alpha(exp +) motions, and, to some extent, different Re flows. Finally, an MSI control law for a constant-rate pitch-up motion is developed. The results obtained using this control law provide very optimal control of the unsteady separation process and subsequent formation of the dynamic-stall vortex and leads to an increase in lift and reduction in drag. Dissert. Abstr.

N94-32865*# National Aeronautics and Space Administration. Langley Research Center, Hampton, VA.

A FINITE-DIFFERENCE APPROXIMATE-FACTORIZATION ALGORITHM FOR SOLUTION OF THE UNSTEADY TRANSONIC SMALL-DISTURBANCE EQUATION

John T. Batina Jan. 1992 38 p

(RTOP 505-63-50-12)

(NASA-TP-3129; L-16781; NAS 1.60:3129) Avail: CASI HC A03/MF A01

A time-accurate approximate-factorization (AF) algorithm is described for solution of the three-dimensional unsteady transonic small-disturbance equation. The AF algorithm consists of a time-linearization procedure coupled with a subiteration technique. The algorithm is the basis for the Computational Aeroelasticity Program-Transonic Small Disturbance (CAP-TSD) computer code, which was developed for the analysis of unsteady aerodynamics and aeroelasticity of realistic aircraft configurations. The paper describes details on the governing flow equations and boundary conditions, with an emphasis on documenting the finite-difference formulas of the AF algorithm. Author

N94-32873*# National Aeronautics and Space Administration. Langley Research Center, Hampton, VA.

USER'S GUIDE FOR A FLAT WAKE ROTOR INFLOW/WAKE VELOCITY PREDICTION CODE, DOWN

John C. Wilson Nov. 1991 28 p

(RTOP 505-59-36-01)

(NASA-TM-104139; NAS 1.15:104139; AVSCOM-TR-91-B-016; AD-B161021L) Avail: CASI HC A03/MF A01

A computer code named DOWN was created to implement a flat wake theory for the calculation of rotor inflow and wake velocities. A brief description of the code methodology and instructions for its use are given. The code will be available from NASA's Computer Software Management and Information Center (COSMIC). Author

N94-32880*# National Aeronautics and Space Administration. Hugh L. Dryden Flight Research Facility, Edwards, CA.

FLIGHT TEST RESULTS OF RIBLETS AT SUPERSONIC SPEEDS

Fanny A. Zuniga, Bianca T. Anderson, and Arild Bertelrud Jun. 1992 37 p

(RTOP 505-60-21)

(NASA-TM-4387; H-1774; NAS 1.15:4387) Avail: CASI HC A03/MF A01

A flight experiment to test and evaluate the skin friction drag characteristics of a riblet surface in turbulent flow at supersonic speeds was conducted at NASA Dryden. Riblets of groove sizes 0.0030 and 0.0013 in. were mounted on the F-104G flight test fixture. The test surfaces were surveyed with boundary layer rakes and pressure orifices to examine the boundary layer profiles and pressure distributions of the flow. Skin friction reductions caused by the riblet surface were reported based on measured differences of momentum thickness between the smooth and riblet surfaces obtained from the boundary layer data. Flight test results for the 0.0030 in. riblet show skin friction reductions of 4 to 8 % for Mach numbers ranging from 1.2 to 1.6 and Reynolds numbers ranging from 2 to 3.4 million per unit foot. The results from the 0.0013 in. riblets show skin friction reductions of 4 to 15 % for Mach 1.2 to 1.4 and Reynolds numbers ranging from 3.6 to 6 million per unit foot. Author

N94-32926*# Sverdrup Technology, Inc., Brook Park, OH.

AN ANALYSIS OF SUPERSONIC FLOWS WITH LOW-REYNOLDS NUMBER COMPRESSIBLE TWO-EQUATION TURBULENCE MODELS USING LU FINITE VOLUME IMPLICIT NUMERICAL TECHNIQUES Final Report

J. Lee Apr. 1994 15 p Presented at the 32nd Aerospace Sciences Meeting and Exhibit, Reno, NV, 10-13 Jan. 1994; sponsored by AIAA

(Contract NAS3-25266; RTOP 505-62-40)

(NASA-CR-195302; E-8701; NAS 1.26:195302; AIAA Paper 94-0193)

Avail: CASI HC A03/MF A01

A generalized flow solver using an implicit Lower-upper (LU) diagonal decomposition based numerical technique has been coupled with three low-Reynolds number kappa-epsilon models for analysis of problems with engineering applications. The feasibility of using the LU technique to obtain efficient solutions to supersonic problems using the kappa-epsilon model has been demonstrated. The flow solver is then used to explore limitations and convergence characteristics of several popular two equation turbulence models. Several changes to the LU solver have been made to improve the efficiency of turbulent flow predictions. In general, the low-Reynolds number kappa-epsilon models are easier to implement than the models with wall-functions, but require much finer near-wall grid to accurately resolve the physics. The three kappa-epsilon models use different approaches to characterize the near wall regions of the flow. Therefore, the limitations imposed by the near wall characteristics have been carefully resolved. The convergence characteristics of a particular model using a given numerical technique are also an important, but most often overlooked, aspect of turbulence model predictions. It is found that some convergence characteristics could be sacrificed for more accurate near-wall prediction. However, even this gain in accuracy is not sufficient to model the effects of an external pressure gradient imposed by a shock-wave/ boundary-layer interaction. Additional work on turbulence models, especially for

compressibility, is required since the solutions obtained with base line turbulence are in only reasonable agreement with the experimental data for the viscous interaction problems. Author

N94-32950*# National Aeronautics and Space Administration. Langley Research Center, Hampton, VA.
FOURTH-ORDER 2N-STORAGE RUNGE-KUTTA SCHEMES
Mark H. Carpenter and Christopher A. Kennedy Jun. 1994 26 p
(RTOP 505-70-62-13)
(NASA-TM-109112; NAS 1.15:109112) Avail: CASI HC A03/MF A01

A family of five-stage fourth-order Runge-Kutta schemes is derived; these schemes required only two storage locations. A particular scheme is identified that has desirable efficiency characteristics for hyperbolic and parabolic initial (boundary) value problems. This scheme is competitive with the classical fourth-order method (high-storage) and is considerably more efficient and accurate than existing third-order low-storage schemes. Author

N94-32974 Department of the Navy, Washington, DC.
ACTIVE VORTEX CONTROL FOR A HIGH PERFORMANCE WING Patent
Marvin M. Walters, inventor (to Navy) and Steven B. Kern, inventor (to Navy) 1 Feb. 1994 12 p Filed 21 Dec. 1992
(AD-D016140; US-Patent-5,282,591; US-Patent-Appl-SN-994229; US-Patent-Class-244-199) Avail: US Patent and Trademark Office

An on-demand wing vortex control system includes a pair of retractable panels which extend forward through slots in the leading edges of the strake and main wing at their junction. When not in use, the device is retracted in a stowed position, thus having zero impact on the cruise efficiency and observability characteristics designed into the aircraft. The panels extend forward from the strake and wing, providing an added leading edge airfoil surface when in the deployed position. Both panels are slideably and rotatably affixed to the aircraft. A front panel is affixed to and supported within the strake, while a rear panel is affixed and supported within the main wing. The planform of each panel is symmetrically identical, and the movements of the panels are mechanically coordinated. DTIC

N94-32984*# National Aeronautics and Space Administration. Lewis Research Center, Cleveland, OH.
USE OF NAVIER-STOKES METHODS FOR THE CALCULATION OF HIGH-SPEED NOZZLE FLOW FIELDS
Nicholas J. Georgiadis and Dennis A. Yoder Jun. 1994 20 p Proposed for presentation at the 30th Joint Propulsion Conference, Indianapolis, IN, 27-29 Jun. 1994; sponsored by AIAA, ASME, SAE, and ASEE
(RTOP 537-02-23)
(NASA-TM-106551; E-8703; NAS 1.15:106551; AIAA Paper 94-3212)
Avail: CASI HC A03/MF A01

Flows through three reference nozzles have been calculated to determine the capabilities and limitations of the widely used Navier-Stokes solver, PARC. The nozzles examined have similar dominant flow characteristics as those considered for supersonic transport programs. Flows from an inverted velocity profile (IVP) nozzle, an under expanded nozzle, and an ejector nozzle were examined. PARC calculations were obtained with its standard algebraic turbulence model, Thomas, and the two-equation turbulence model, Chien k-epsilon. The Thomas model was run with the default coefficient of mixing set at both 0.09 and a larger value of 0.13 to improve the mixing prediction. Calculations using the default value substantially underpredicted the mixing for all three flows. The calculations obtained with the higher mixing coefficient better predicted mixing in the IVP and underexpanded nozzle flows but adversely affected PARC's convergence characteristics for the IVP nozzle case. The ejector nozzle case did not converge with the Thomas model and the higher mixing coefficient. The Chien k-epsilon results were in better agreement with the experimental data overall than were those of the Thomas run with the default mixing coefficient, but the default boundary conditions for k and epsilon underestimated the levels of mixing near the nozzle exits. Author (revised)

N94-33071*# Old Dominion Univ., Norfolk, VA.
CONTROL OF LOW-SPEED TURBULENT SEPARATED FLOW OVER A BACKWARD-FACING RAMP Ph.D. Thesis - Old Dominion Univ.
John C. Lin May 1992 204 p
(NASA-TM-109740; NAS 1.15:109740) Avail: CASI HC A10/MF A03

The relative performance and flow phenomena associated with several devices for controlling turbulent separated flow were investigated at low speeds. Relative performance of the devices was examined for flow over a curved, backward-facing ramp in a wind tunnel, and the flow phenomena were examined in a water tunnel using dye-flow visualization. Surface static pressure measurements and oil-flow visualization results from the wind tunnel tests indicated that transverse grooves, longitudinal grooves, submerged vortex generators, vortex generator jets (VGJ's), Viets' fluidic flappers, elongated arches at positive angle of attack, and large-eddy breakup devices (LEBU's) at positive angle of attack placed near the baseline separation location reduce flow separation and increase pressure recovery. Spanwise cylinders reduce flow separation but decrease pressure recovery downstream. Riblets, passive porous surfaces, swept grooves, Helmholtz resonators, and arches and LEBU's with angle of attack less than or = 0 degrees had no significant effect in reducing the extent of the separation region. Wall-cooling computations indicated that separation delay on a partially-cooled ramp is nearly the same as on a fully-cooled ramp, while minimizing the frictional drag increase associated with the wall cooling process. Dry-flow visualization tests in the water tunnel indicated that wishbone vortex generators in the forward orientation shed horseshoe vortices; wishbone vortex generators oriented in the reverse direction and doublet vortex generators shed streamwise counterrotating vortices; a spanewise cylinder located near the wall and LEBU's at angle of attack = -10 degrees produced eddies or transverse vortices which rotated with the same sign as the mean vorticity in a turbulent boundary layer; and the most effective VGJ's produced streamwise co-rotating vortices. Comparative wind-tunnel test results indicated that transferring momentum from the outer region of a turbulent boundary layer through the action of embedded streamwise vortices is more effective than by transverse vortices for the separation control application studied herein. Author

N94-33108# Naval Postgraduate School, Monterey, CA.
THE ANALYSIS OF WAKE-INDUCED UNSTEADY AERODYNAMICS RELATED TO HIGHER HARMONIC CONTROL Ph.D. Thesis
Ahmed A. Abourahma Dec. 1993 165 p
(AD-A277914) Avail: CASI HC A08/MF A02

Performance data from the NASA-Army OH-6A higher harmonic control (HHC) flight test program showed significant reductions in main rotor shaft torque and engine power in hover and forward flight 1. The unsteady aerodynamics with the higher harmonic control system application, including wake effects. were considered to study whether such power reductions are feasible. An airfoil oscillating in pure plunge can achieve propulsive force (Katzmayr effect), as in the case of birds' wings flapping in flight. Here it will be shown that this effect can be enhanced in the presence of layers of shed vorticity with the proper phasing. In addition, while it is known that an airfoil oscillating in pitch, will typically produce drag at most values of reduced frequency, it is found that the presence of another layer of shed vorticity of the proper phase, can reduce the drag on the pitching airfoil depending upon wake spacing reduced frequency, and phase. Under some conditions the added layer or layers of shed vorticity will even result in propulsive force acting on the pitching airfoil similar to the Katzmayr effect for the plunging case. It was found, for the OH-6A helicopter, that the measured reductions in main rotor shaft torque and engine power are feasible when evaluated with respect to the Katzmayr effect and the additional drag reduction or propulsive force obtained due to pitch and plunge oscillations with the effect of adjacent wake layers of shed vorticity. DTIC

N94-33119*# Sverdrup Technology, Inc., Brook Park, OH.
INSTALLED F/A-18 INLET FLOW CALCULATIONS AT 30 DEGREES ANGLE-OF-ATTACK: A COMPARATIVE STUDY Final Report
C. Frederic Smith and Steve D. Podleski Cleveland, OH NASA Apr. 1994 51 p
(Contract NAS3-25266; RTOP 505-68-30)
(NASA-CR-195297; E-8678; NAS 1.26:195297) Avail: CASI HC A04/MF A01

NASA Lewis is currently engaged in a research effort as a team member of the High Alpha Technology Program (HATP) within NASA. This program utilizes a specially equipped F/A-18, the High Alpha Research Vehicle (HARV), in an ambitious effort to improve the maneuverability of high-performance military aircraft at low subsonic speed, high angle of attack conditions. The overall objective of the Lewis effort is to develop

inlet technology that will ensure efficient airflow delivery to the engine during these maneuvers. One part of the Lewis approach utilizes computational fluid dynamics codes to predict the installed performance of inlets for these highly maneuverable aircraft. Full Navier-Stokes (FNS) calculations on the installed F/A-18 inlet at 30 degrees angle of attack, 0 degrees yaw, and a freestream Mach number of 0.2 have been obtained in this study using an algebraic turbulence model with two grids (original and revised). Results obtained with the original grid were used to determine where further grid refinements and additional geometry were needed. In order to account properly for the external effects, the forebody, leading edge extension (LEX), ramp, and wing were included with inlet geometry. In the original grid, the diverter, LEX slot, and leading edge flap were not included due to insufficient geometry definition, but were included in a revised grid. In addition, a thin-layer Navier-Stokes (TLNS) code is used with the revised grid and the numerical results are compared to those obtained with the FNS code. The TLNS code was used to evaluate the effects on the solution using a code with more recent CFD developments such as upwinding with TVD schemes versus central differencing with artificial dissipation. The calculations are compared to a limited amount of available experimental data. The predicted forebody/fuselage surface static pressures compared well with data of all solutions. The predicted trajectory of the vortex generated under the LEX was different for each solution. These discrepancies are attributed to differences in the grid resolution and turbulence modeling. All solutions predict that this vortex is ingested by the inlet. The predicted inlet total pressure recoveries are lower than data and the distortions are higher than data. The results obtained with the revised grid were significantly improved from the original grid results. The original grid results indicated the ingested vortex migrated to the engine face and caused additional distortions to those already present due to secondary flow development. The revised grid results indicate that the ingested vortex is dissipated along the inlet duct inboard wall. The TLNS results indicate the flow at the engine face was much more distorted than the FNS results and is attributed to the pole boundary condition introducing numerical distortions into the flow field. Author (revised)

N94-33263 Naval Surface Warfare Center, Dahlgren, VA.
A NEW METHOD FOR CALCULATING WING ALONG AERODYNAMICS TO ANGLE OF ATTACK 180 DEG
Roy M. McInville and Frank G. Moore Mar. 1994 65 p Limited Reproducibility: More than 20% of this document may be affected by microfiche quality
(AD-A277965; NSWCDD/TR-94/3) Avail: CASI HC A04

A new semiempirical method has been developed to estimate wing alone aerodynamics at all Mach numbers and angles of attack (AOA) encountered in flight. The method utilizes the slender body or linearized theories at low AOA and several wing alone data bases at higher AOA. In areas where data is not available, extrapolations and interpolations are used with existing data. The new method is shown to be more accurate than the second-order technique developed for the 1993 version of the NSWCDD Aeroprediction Code (AP93) over the AOA range of 0 to 30 degrees where that technique is applicable. More importantly, however, is the fact that the new method allows AOA to 180 deg. As a result, this new wing alone method forms the first step in expanding the AP93 to higher AOA than 30 degrees. DTIC

03 AIR TRANSPORTATION AND SAFETY

Includes passenger and cargo air transport operations; and aircraft accidents.

For related information see also *16 Space Transportation* and *85 Urban Technology and Transportation.*

N94-31230# Office National d'Etudes et de Recherches Aerospatiales, Paris (France).
DEVELOPMENT OF A THREE-DIMENSIONAL ICING MODEL FOR PREDICTING ICE ACCRETION ON AIRCRAFT Ph.D. Thesis - Clermont-Ferrand II Univ. [MODELISATION TRIDIMENSIONNELLE DES DEPOTS DE GIVRE SUR LES VOILURES D'AERONEFS]
Thierry Hedde 1993 148 p In FRENCH
(ISSN 0078-3781)
(ONERA-NT-1993-5; ETN-94-95874) Avail: CASI HC A07/MF A02

The development of a three dimensional icing code is described. Nonviscous flows may be calculated using either the Euler method, especially in the transonic domain, or the panel method, mainly for multistep ice accretion calculations. A Van Driest roughness model was implemented in the turbulent boundary layer calculation, and yields realistic values of the heat transfer coefficient. The estimation of the runback equation terms shows that the air/water interface shear stress is the leading one. A new grid built up along the runback paths can be used to establish the thermodynamic balance and calculate the ice thickness. The qualities of the model at high velocities (150 to 300 m/s) can be seen by comparison of the simulated ice shapes with the experimental shapes obtained on a parabolic rotor blade tip. Comparison with 'lobster tails' ice shapes grown on a swept NACA 0012 airfoil at low speed (70 m/s) shows the model's limits. The 'lobster tails' accretion is explained by way of droplet scale shadowing phenomena, and by local variation of the heat transfer coefficient. A ballistic model simulates the lobster tail accretion well, although only qualitatively, due to lack of experimental data. ESA

N94-31246# Galaxy Scientific Corp., Pleasantville, NJ.
ROTORCRAFT DITCHINGS AND WATER-RELATED IMPACTS THAT OCCURRED FROM 1982 - 1989, PHASE 2 Final Report
Mark Muller and Lindley W. Bark Oct. 1993 43 p
(Contract DTFA03-89-C-00043)
(AD-A276473; DOT/FAA/CT-92/14) Avail: CASI HC A03/MF A01

This report documents Phase II of a two-phase effort to examine rotorcraft ditchings and water-related impacts for rotorcraft, that occurred between the years 1982 through 1989. The main tasks performed for this phase of the investigation were assessment of the effects of structure on occupant injury, determination of the specific modes of structural failure, identification of the potential means to alleviate injury, and evaluation of available analytical methods for modeling rotorcraft water impacts. The Phase II analysis examined specific aspects of the Phase I data for accidents that fulfilled the criteria for the three impact scenarios. The main impact injuries were from flailing and excessive acceleration and resulted from occupant interaction with the rotorcraft interior and insufficient energy absorption. Drowning and exposure were found to be the main post-impact hazards and other post-impact injuries were minor in severity. Structural failures of the rotorcraft are identified and discussed as they affected occupant injury. The performance and adequacy of rotorcraft flotation equipment is discussed. Means of alleviating occupant injury in rotorcraft water impacts are identified and discussed. An analytical method for modeling the water impact of a rotorcraft is evaluated. DTIC

N94-31678# Gates Learjet Corp., Wichita, KS.
AIRCRAFT ICING HANDBOOK (UPDATE) Final Report
1993 436 p Revised Sponsored by FAA
(AD-A276499) Avail: CASI HC A19/MF A04

The first update of the Aircraft Icing Handbook does not change the organization of the handbook into volumes and chapters as delineated on page 7. However, new sections have been added to Chapter 3: ice protection methods. Section 1.0 no longer contains information on pneumatic impulse deicing and has therefore been retitled: Section 1.0 - Conventional pneumatic boot deicing systems. Three new sections have been added: Section 1A.0 - pneumatic impulse deicing systems; Section 4A.0 - electro-explusive deicing systems; and Section 4B.0 - eddy current deicing systems. DTIC

N94-31803* National Aeronautics and Space Administration. Lewis Research Center, Cleveland, OH.
WHIPICE (Videotape)
1992 Videotape: 8 min. 30 sec. playing time, in color, with sound
(NASA-TM-109749; NONP-VT-94-9949) Avail: CASI VHS A01/BETA A22

This video documents efforts by NASA Lewis Research Center researchers to improve ice protection for aircraft. A new system of deicing aircraft by allowing a thin sheet of ice to develop, then breaking it into particles, is being examined, particularly to determine the extent of shed ice ingestion by jet engines that results. The process is documented by a high speed imaging system that scans the breakup and flow of the ice particles at 1000 frames per second. This data is then digitized and analyzed using a computer program called WHIPICE, which analyzes grey scale images of the ice particles. Detailed description of the operation of this computer program is provided. CASI

N94-31902 Communications Research Centre, Ottawa (Ontario). Mobile Satellite Communications.
SATCOM FEASIBILITY STUDY FOR SEARCH AND RESCUE AIRCRAFT Final Report
John Sydor and Jack Rigley Jan. 1993 131 p
(DSIS-94-01083; CTN-94-61214) Avail: CASI HC A07/MF A02

The feasibility of using satellite communications to improve the reliability of communications to search and rescue (SAR) aircraft throughout the Canadian SAR regions is examined. The primary satellite communications media considered are MSAT and Inmarsat. The main communications requirement for SAR aircraft operations is reliable voice communications throughout the SAR regions. Secondary or desirable requirements include global operations and security of voice and data communication. Both Inmarsat and MSAT systems were found capable of meeting the prime requirement. The differences between those two systems is most evident in the avionics and antennas required to access them. Inmarsat equipment is much larger and more expensive than the equivalent MSAT equipment, since the MSAT system (to become operational by 1995) will be more powerful and sensitive. However, MSAT aeronautical satcom terminals are not yet available and would have to be developed, most likely as a derivative of MSAT land mobile terminals. Analysis of Satcom installations for CC-130 and CH-113 SAR aircraft was completed for both Inmarsat and MSAT compatible avionics and antennas. Most currently available Inmarsat compatible equipment is feasible for the CC-130, while only the smaller sized MSAT antenna is feasible for the CH-113. Author (CISTI)

N94-32168# Industrial Coll. of the Armed Forces, Washington, DC.
A COMPARISON OF MILITARY AND COMMERCIAL AIRCRAFT DEVELOPMENT Report, Aug. 1992 - Apr. 1993
Michael S. Mutty Apr. 1993 37 p
(AD-A276830; NDU/ICAF-93-F3) Avail: CASI HC A03/MF A01

When compared to the commercial sector, it takes the military almost four times longer to develop an aircraft. For example, Boeing Company developed the 767 jetliner in about four years whereas the Navy's next generation tactical aircraft, the AX, is expected to take 15 years to develop. This research paper examines both commercial and military approaches to aircraft development. The paper focuses on establishing whether or not commercial practices, where more cost effective, can be incorporated into the military acquisition system. The paper illustrates that aircraft development in the commercial and military are different for two fundamental reasons. First, military aircraft development exploits the latest untested developments in technology where the commercial sector relies only on existing technologies. Second, a commercial aircraft is developed for the single mission of ferrying passengers and cargo. Military aircraft are required to perform far more varied and different missions with each parameter driving its own unique challenge for design and testing. This research paper concludes that without similar mission requirements, there are few commercial applications that can be applied to military aircraft development. DTIC

N94-32363# Army Aeromedical Research Lab., Fort Rucker, AL.
ESTIMATING THE IMPACT OF CRASHWORTHINESS STANDARDS ON MORTALITY AND MORBIDITY EVENTS IN THE US ARMY ROTARY-WING AIRCRAFT MISHAPS Final Report
Samuel G. Shannon and Dennis F. Shanahan Sep. 1993 49 p
(DA Proj. 3M1-62787-A-878)
(AD-A277121; USAARL-93-37) Avail: CASI HC A03/MF A01

It is desirable to provide modern military helicopters with the maximum crashworthiness that is practical in order to reduce injury in helicopter crashes. Although crashworthy design features have been proven to be extremely effective in reducing morbidity and mortality, a penalty of increased weight and added procurement cost must be paid. Consequently, the degree of crashworthiness designed into an aircraft must be a tradeoff between economics, aircraft performance, and the perceived risk of injury. To help these judgments, it would be useful to develop a mathematical model capable of predicting morbidity outcomes for a given aircraft design. All crashes of five types of U.S. Army helicopters occurring between 1 Oct. 1979 and 30 Sep. 1991 were examined to determine crash conditions and morbidity and mortality outcomes. Analyses were conducted with logistic regression (LOGISTIC) for mortality, and the fit of the model was considered. DTIC

N94-32405 Naval Research Lab., Washington, DC.
GLUTINOUS WATER: PROTECTING VERTICAL AND OVERHEAD SURFACES FROM FIRE SPREAD
Homer W. Carhart 28 Feb. 1994 12 p Limited Reproducibility: More than 20% of this document may be affected by microfiche quality
(AD-A277280; NRL/MR/6180-94-7431) Avail: Issuing Activity (Defense Technical Information Center (DTIC))

Most of the water used in firefighting is not only wasted, it also contributes extensively to total damage. Water is an unusual chemical in that, due to hydrogen bonding, it is a liquid at room temperature and it also has a very high heat of evaporation. So, if one could make water adhere significantly to vertical and overhead surfaces, a great deal of fire protection could be bought because such surfaces could not get hotter than the boiling point of water (100 C) and a great deal of heat energy would be required to evaporate it. This can be accomplished by making water glutinous, either by making a foam (e.g. shaving cream) or by thickening it (e.g. gravy), or both. Calculations and experiment show that up to at least ten times greater fire protection could be achieved with only about 1/20 to 1/50 the amount of water. DTIC

N94-32620# Mitre Corp., McLean, VA.
THE 1993 AVIATION SYSTEM CAPACITY PLAN
1993 367 p Prepared in cooperation with MiTech, Inc., Rockville, MD and JIL Systems, Inc., Arlington, VA
(AD-A276958; DOT/FAA/ASC-93-1) Avail: CASI HC A16/MF A03

This is a comprehensive review of the Federal Aviation Administration's program to improve the capacity of the National Air Transportation System. The Plan identifies the causes and extent of capacity and delay problems currently associated with air travel in the U.S. and outlines various planned and ongoing FAA projects that will reduce the severity of the problems in the future. The major areas of discussion are: airport development, airport and airspace capacity, technology for capacity improvement, and marketplace solutions. DTIC

N94-32925# National Transportation Safety Board, Washington, DC.
ANNUAL REVIEW OF AIRCRAFT ACCIDENT DATA: US AIR CARRIER OPERATIONS, CALENDAR YEAR 1991
15 Apr. 1994 74 p
(PB94-158847; NTSB/ARC-94/01) Avail: CASI HC A04/MF A01

This publication presents the record of aviation accidents involving revenue operations of U.S. Air Carriers including Commuter Air Carriers and On Demand Air Taxis for calendar year 1991. The report is divided into three major sections according to the federal regulations under which the flight was conducted - 14 CFR 121, 125, 127, Scheduled 14 CFR 135, or Nonscheduled 14 CFR 135. In each section of the report tables are presented to describe the losses and characteristics of 1991 accidents to enable comparison with prior years. Author

N94-32927*# National Aeronautics and Space Administration. Ames Research Center, Moffett Field, CA.
AVIATION HUMAN FACTORS RESEARCH IN US UNIVERSITIES: POTENTIAL CONTRIBUTIONS TO NATIONAL NEEDS
R. Key Dismukes Mar. 1994 21 p
(RTOP 505-64-13)
(NASA-TM-108814; A-94060; NAS 1.15:108814) Avail: CASI HC A03/MF A01

Universities can and should make vital contributions to national needs in aviation human factors. However, to guide and utilize university research effectively we must understand what types of expertise and facilities universities can bring to bear on aviation problems. We should be aware of where relevant research is already underway and where untapped potential exists. How does the character of research in universities differ from and complement research in government and industry laboratories? What conditions would encourage universities to focus on national priorities and would promote high quality, relevant research? This paper attempts to address these issues. It is based on a survey conducted by the author, which included site visits to several universities, telephone interviews with faculty members at other universities, and a search of the aviation human factors research literature. Author

N94-32938# National Transportation Safety Board, Washington, DC.
AIRCRAFT INCIDENT REPORT: IN-FLIGHT TURBULENCE ENCOUNTER AND LOSS OF PORTIONS OF THE ELEVATORS, CHINA AIRLINES FLIGHT CI-012, MCDONNELL DOUGLAS MD-11-P, TAIWAN REGISTRATION B-150 ABOUT 20 MILES EAST OF JAPAN, 7 DECEMBER 1992
15 Feb. 1994 58 p
(PB94-910403; NTSB/AAR-94/02) Avail: CASI HC A04/MF A01

This report explains the in-flight turbulence encounter of China Airlines flight CI-012, an MD-11 airplane, which subsequently departed controlled flight and sustained damage to the outboard elevators, portions of which separated from the airplane, on 7 Dec. 1992, about 20 miles east of Japan. The safety issues discussed in the report include the design and certification of the MD-11. Safety recommendations concerning these issues were made to the Federal Aviation Administration. Author (revised)

N94-32955# Federal Aviation Administration, Atlantic City, NJ. Technical Center.
CIVIL TILTROTOR MARKET PENETRATION: EFFECTS ON NORTHEAST CORRIDOR AIRPORT DELAY
Anny S. Cheung and Douglas Baart Feb. 1994 38 p
(AD-A277534; DOT/FAA/CT-TN94/1; FAA-AOR-100-94-001) Avail: CASI HC A03/MF A01

This report addresses the delay impacts resulting from replacing conventional aircraft services with civil tiltrotor (CTR) operations in the Northeast corridor at four CTR service levels. This analysis was conducted by using the National Airspace System performance analysis capability (NASPAC) simulation modeling system (SMS). Cost of delay savings were derived by using the cost of delay module. The result of this study will be used by the Vertical Flight Program Office (ARD-30) in assessing the benefits of the CTR operations in the Northeast corridor. DTIC

N94-33063*# San Jose State Univ., CA.
THREE DIMENSIONAL AUDIO VERSUS HEAD DOWN TCAS DISPLAYS
Durand R. Begault and Marc T. Pittman Mar. 1994 14 p
(Contract NCC2-327)
(NASA-CR-177636; A-94066; NAS 1.26:177636) Avail: CASI HC A03/MF A01

The advantage of a head up auditory display was evaluated in an experiment designed to measure and compare the acquisition time for capturing visual targets under two conditions: Standard head down traffic collision avoidance system (TCAS) display, and three-dimensional (3-D) audio TCAS presentation. Ten commercial airline crews were tested under full mission simulation conditions at the NASA Ames Crew-Vehicle Systems Research Facility Advanced Concepts Flight Simulator. Scenario software generated targets corresponding to aircraft which activated a 3-D aural advisory or a TCAS advisory. Results showed a significant difference in target acquisition time between the two conditions, favoring the 3-D audio TCAS condition by 500 ms. Author

N94-32454*# Axiomatics Corp., Woburn, MA.
CONTINUOUS MEASUREMENT OF AIRCRAFT WING ICING
Stephen S. C. Yao *In* NASA, Washington, Technology 2003: The Fourth National Technology Transfer Conference and Exposition, Volume 2 Feb. 1994 p 295-300 (For primary document see N94-32420 09-99)
Avail: CASI HC A02/MF A04

04 AIRCRAFT COMMUNICATIONS AND NAVIGATION

Includes digital and voice communication with aircraft; air navigation systems (satellite and ground based); and air traffic control.

For related information see also *17 Space Communications, Spacecraft Communications, Command and Tracking* and *Communications and Radar.*

N94-31080# Army Topographic Engineering Center, Fort Belvoir, VA.
RESULTS OF REAL-TIME TESTING AND DEMONSTRATION OF THE US ARMY CORPS OF ENGINEERS REAL-TIME ON-THE-FLY POSITIONING SYSTEM
Sally L. Frodge, Benjamin W. Remondi, and Dariusz Lapucha Feb. 1994 12 p
(AD-A276160; TEC-R-215) Avail: CASI HC A03/MF A01

The U.S. Army Corps of Engineers has been developing a GPS carrier phase based positioning system for hydrographic surveying and dredging since 1988. This system provides real-time three dimensional positions with horizontal and vertical accuracies better than one decimeter over ranges up to 20 kilometers from a single reference station without static initialization. The project has passed from concept development through feasibility studies, system analysis, resolution of carrier ambiguities on-the-fly (OTF), and on to final system integration. The real-time testing of the system began in Mar. of 1993 and public demonstrations of the system began in Oct. 1993. Testing of the system has been performed under varying operating conditions to evaluate the limits of OTF ambiguity resolution for precisely positioning moving platforms. Tests have shown that this system is capable of 1-3 centimeters in all three dimensions. This paper will discuss the results of the testing to date and briefly describe the OTF system. DTIC

N94-31306# Sandia National Labs., Albuquerque, NM.
AN INVESTIGATION OF AIRBORNE GPS/INS FOR HIGH ACCURACY POSITION AND VELOCITY DETERMINATION
H. Sun (Calgary Univ., Alberta.), M. E. Cannon (Calgary Univ., Alberta.), T. E. Owen, and M. A. Meindl 1993 9 p Presented at the Institute of Navigation National Technical Meeting, San Diego, CA, 24-26 Jan. 1994
(Contract DE-AC04-94AL-85000)
(DE94-006139; SAND-93-2413C; CONF-940158-1) Avail: CASI HC A02/MF A01

An airborne test using a differential GPS-INS system in a Twin Otter was conducted by Sandia National Laboratories to assess the feasibility of using the integrated system for cm-level position and cm/s velocity. The INS is a miniaturized ring-laser gyro IMU jointly developed by Sandia and Honeywell while the GPS system consists of the NovAtel GPSCard(trademark). INS position, velocity and attitude data were computed using Sandia's SANDAC flight computer system and logged at 4 Hz and GPS data was acquired at a 1 Hz rate. The mission was approximately 2.5 hours in duration and the aircraft reached separations of up to 19 km from the base station. The data was post-processed using a centralized Kalman filter approach in which the double differenced carrier phase measurements are used to update the INS data. The INS position is in turn used to detect and correct GPS carrier phase cycle slips and also to bridge GPS outages. Results are presented for the GPS-only case and also for integrated GPS/INS. DOE

N94-31680 Federal Aviation Administration, Cambridge, MA.
FLIGHT TECHNICAL ERROR FOR CATEGORY B NON-PRECISION APPROACHES AND MISSED APPROACHES USING NON-DIFFERENTIAL GPS FOR COURSE GUIDANCE Final Report, Apr. 1992 - Mar. 1993
M. S. Huntley, J. W. Turner, and R. Palmer Nov. 1993 67 p Limited Reproducibility: More than 20% of this document may be affected by microfiche quality
(PB94-142734; DOT-VNTSC-FAA-93-17; DOT/FAA/RD-93/17) Avail: CASI HC A04

The report documents and discusses the performance of twelve general aviation pilots who used nondifferential global positioning system (GPS) in a Beechcraft Baron to fly 93 category B approaches defined by GPS waypoints. The research reported here was part of the U.S. Federal Aviation Administration (FAA) GPS Overlay Project and provided the data required by the agency to implement phase 1 of the GPS satellite operational plan for category B nonprecision approaches. The data collection and analysis procedures described herein were developed with and approved by the FAA's Satellite Operations Implementation Team. It should be noted, however, that additional work would be required to prepare the data for use in the development of GPS TERPS. NTIS

N94-31845 Colorado Univ., Boulder.
ERROR ANALYSIS OF REAL-TIME AND POST-PROCESSED ORBIT DETERMINATION FOR THE GEOSAT FOLLOW-ON ALTIMETRIC SATELLITE USING GPS TRACKING Ph.D. Thesis
William Steven Schreiner 1993 145 p
Avail: Univ. Microfilms Order No. DA9320477

The global positioning system (GPS) has the capability to supply real-time and post-processed positioning of unprecedented accuracy for low earth orbiting (LEO) satellites. This thesis has evaluated the expected orbit accuracy of the U.S. Navy's Geosat Follow-On (GFO) altimetric satellite for real-time and post-processed modes of operation when using GPS tracking. There is an interest in using orbit solutions that are generated by an onboard GPS navigation processor to compute altimetric ocean surface heights for near real-time mesoscale studies. Numerical simulations were performed to evaluate the on-board GFO radial orbit error and demonstrated that the spectral content of the orbit error contained significant power at mesoscale frequencies. However, it was demonstrated that a fitting process utilizing analytical J2 orbit theory can remove this mesoscale frequency content and provide an ephemeris adequate for real-time mesoscale oceanographic studies. This fitting procedure was verified by processing on-board GPS orbit and altimeter data from the TOPEX/POSEIDON mission. Processing GPS pseudorange and carrier phase measurements in a post-processed mode will allow precise orbit determination based on dynamics, kinematics, and a combination of the two. However, when the Department of Defense (DoD) enables their policy of selective availability/anti-spoof (SA/A-S), this positioning precision will be degraded for non SA/A-S capable receivers because they will no longer be able to use a dual frequency mode of ionospheric calibration. There does exist a less precise single frequency mode of ionospheric calibration called differenced range versus integrated Doppler (DRVID). The DRVID technique has been studied through equation development and data analysis. The method of covariance analysis was used to determine the expected radial orbit accuracy of GFO for both dual and single frequency (DRVID) GPS receiver configurations when using dynamic, kinematic, and reduced dynamic tracking. These analyses showed that the GFO orbit can be determined to an accuracy below the decimeter level in the radial direction if a dual frequency GPS receiver is used with reduced dynamic tracking. A single frequency (DRVID) low data noise receiver configuration also showed the potential to reach decimeter level tracking of the radial height of GFO when reduced dynamic tracking is employed. Dissert. Abstr.

N94-32505 Artificial Intelligence Management and Development Corp., Toronto (Ontario).

PLAN RECOGNITION FOR AN AIR TRAFFIC CONTROL SIMULATION Interim Report

Sep. 1993 102 p

(DSIS-94-01221; CTN-94-61217) Copyright Avail: CASI HC A06/MF A02

Experiments were conducted in which human subjects performed an air traffic control simulation. Based on the results of that experimental study, work was then started on designing and developing a system for recognizing and predicting the subjects' plans for the aircraft as they fly through the simulation airspace. In designing the experimental study, results were used from pilot research which suggested that it would be possible to bring naive subjects to a level of play so that their results could be used in the development of a system to predict reliably the plans of other future subjects in the simulation. The pilot research results were used to design an experiment to collect data for use in developing the plan recognizer. The experimental design and procedure used are described, as well as the simulation airspace and its properties. The highest level of decomposition of the plan recognizer is reviewed with respect to four elements of the system's architecture: an air traffic control simulation; a database of session statistics, initial information about aircraft and airports, interface action information, and abstract plans for aircraft; a Nexpert Object expert system, which operates in the background to access database information and infer plans; and a Hypercard display component.

Author (CISTI)

N94-32864*# Draper (Charles Stark) Lab., Inc., Cambridge, MA.

PERFORMANCE ANALYSIS OF AN INTEGRATED GPS/INERTIAL ATTITUDE DETERMINATION SYSTEM M.S. Thesis - MIT

Wendy I. Sullivan May 1994 91 p

(Contract NAS9-18426)

(NASA-CR-188289; NAS 1.26:188289; CSDL-T-1227) Avail: CASI HC A05/MF A01

The performance of an integrated GPS/inertial attitude determination system is investigated using a linear covariance analysis. The principles of GPS interferometry are reviewed, and the major error sources of both interferometers and gyroscopes are discussed and modeled. A new figure of merit, attitude dilution of precision (ADOP), is defined for two possible GPS attitude determination methods, namely single difference and double difference interferometry. Based on this figure of merit, a satellite selection scheme is proposed. The performance of the integrated GPS/inertial attitude determination system is determined using a linear covariance analysis. Based on this analysis, it is concluded that the baseline errors (i.e., knowledge of the GPS interferometer baseline relative to the vehicle coordinate system) are the limiting factor in system performance. By reducing baseline errors, it should be possible to use lower quality gyroscopes without significantly reducing performance. For the cases considered, single difference interferometry is only marginally better than double difference interferometry. Finally, the performance of the system is found to be relatively insensitive to the satellite selection technique. Author (revised)

N94-32961 Department of the Navy, Washington, DC.

RELATIVE MOTION PINWHEEL Patent

Gary E. Streimer, inventor (to Navy) and Leslie P. Benda, inventor (to Navy) 30 Nov. 1993 6 p Filed 5 Oct. 1991

(AD-D016107; US-Patent-Appl-SN-956327; US-Patent-Class-33-1-SB)

Avail: US Patent and Trademark Office

An apparatus for visualizing relative motion between two moving objects in a two-dimensional plane is provided. A planar base has a first compass rose printed thereon. Rotatably attached to the center of the first compass rose is a means for indicating a present course of a first moving object relative to a true bearing indication on the first compass rose. A second moving object assembly consists of a second compass rose rotatably attached to a means for indicating a present course of the second moving object relative to a true bearing indication on the second compass rose. The true bearing indication on the second compass rose is aligned to be equivalent to the true bearing indication on the first compass rose. Attached at the centers of the first and second compass roses is a means for tethering the second moving object assembly to the first compass rose. The second compass rose is free to rotate about its center, and the second moving object assembly is free to revolve in a single plane around the center of the first compass rose. The tethering means indicates a lint of relative bearing from the first moving object to the second moving object. DTIC

N94-33095# Army Topographic Engineering Center, Fort Belvoir, VA.

REAL-TIME CENTIMETER POSITIONING WITH GPS: A SYSTEM DEVELOPED BY THE US ARMY CORPS OF ENGINEERS

Sally L. Frodge, Benjamin Remondi, and Dariusz Lapucha 11 Apr. 1994 11 p

(AD-A278152; R-223) Avail: CASI HC A03/MF A01

The United States Army Corps of Engineers has been developing a Global Positioning System (GPS) carrier phase based positioning system for hydrographic surveying and dredging since 1988. This system provides real-time three-dimensional positions with horizontal and vertical accuracies better than 1 decimeter over ranges up to 20 kilometers from a single reference station without static initialization. The project has passed from concept development through feasibility studies, system analysis, resolution of carrier ambiguities on-the-fly (OTF), to final system integration which is nearing completion. The real-time testing of the system began in March of 1993. This testing was performed under varying operating conditions to evaluate the limits of OTF ambiguity resolution for precisely positioning moving platforms. This paper summarizes the results of those tests. Early real-time tests performed have shown 1-3 centimeters in all three dimensions. The final design of the real-time system and its integration to hydrographic survey platforms are also discussed. DTIC

N94-33253 Naval Command, Control and Ocean Surveillance Center, San Diego, CA. RDT and E Div.

AN EVALUATION OF THREE GPS RECEIVERS FOR USE IN THE GPS SOUNDER Final Report, period ending Oct. 1993

K. D. Anderson Apr. 1994 53 p Limited Reproducibility: More than 20% of this document may be affected by microfiche quality

(ONR Proj. R035S83)

(AD-A278157; NCCOSC/RDT/E-TR-1637) Avail: CASI HC A04

Three high performance, geodetic quality, Global Positioning System (GPS) receivers were tested at the Naval Command, Control and Ocean Surveillance Center RDT and E Division to evaluate their use in supporting

the GPS Sounder. These tests are focused on comparisons of the signal-to-noise ratio (SNR) of the GPS satellite is either rising or setting on the ocean horizon. Of primary interest is the ability of the receiver to lock onto and track the GPS signals when the satellite is at elevation angles of less than 1 degree. This requirement is unique to the GPS Sounder and is one of the most stressful conditions for receiving processing. In most applications, GPS signals never examined at ground-to-satellite elevation angles of less than about 15 degrees because of multipath effects on signal reception. However, the ability to lock onto and track the GPS signals in the presence of severe multipath conditions is crucial to the success of the GPS Sounder. DTIC

05 AIRCRAFT DESIGN, TESTING AND PERFORMANCE

Includes aircraft simulation technology.

For related information see also *18 Spacecraft Design, Testing and Performance* and *39 Structural Mechanics*.For land transportation vehicles see *85 Urban Technology and Transportation.*

N94-31078# Little (Arthur D.), Inc., Cambridge, MA.
A LABORATORY STUDY OF MULTIPLE SITE DAMAGE IN FUSELAGE LAP SPLICES Final Report, Nov. 1989 - Feb. 1992
R. Mayville and M. Sigelmann Dec. 1993 107 p Sponsored by FAA
(AD-A276151; DOT-VNTSC-FAA-93-12; DOT/FAA/CT-93/74) Avail: CASI HC A06/MF A02

This report details an experimental study that was conducted to explore the causes of fuselage lap splice multiple site damage (MSD), which has been observed in several aging aircraft. MSD was partially responsible for the 1988 Aloha Airlines accident. A specimen was designed and tests were conducted to investigate the effects on MSD and fatigue of: (1) a terminating action repair; (2) simultaneous tension and shear; and (3) stress and several lap splice configurations. The results of over 120 tests were supported by finite element analysis, strain gage studies and statistics. DTIC

N94-31387# Wright Lab., Wright-Patterson AFB, OH.
TESTING OPERATIONAL FLIGHT PROGRAMS (OFP'S) Final Report, 10 - 13 May 1993
Charles P. Satterthwaite Feb. 1994 13 p
(AF Proj. 9994)
(AD-A276361; WL-TR-94-1007) Avail: CASI HC A03/MF A01

Operational Flight Programs are the software programs of avionics embedded computer systems. Not only is it desirable to be able to test and model Operational Flight Programs, it is essential. The consequences of not performing accurate Operational Flight Program testing can be devastating. Some of these include premature weapon releases, erroneous flight instrument displays, and complete system failure. In order to test Operational Flight Programs, there are several things one must know about the Operational Flight Program, its weapon system host, its support environment, and how to generate and perform its test. This paper will address these issues as it develops a strategy to test an Operational Flight Program. DTIC

N94-31442# Naval Postgraduate School, Monterey, CA.
UNMANNED AIR VEHICLE/REMOTELY PILOTED VEHICLE ANALYSIS FOR LETHAL UAV/RPV M.S. Thesis
Burke R. Kaltenberger Sep. 1993 83 p
(AD-A276052) Avail: CASI HC A05/MF A01

An investigation was conducted to provide a comprehensive evaluation of current unmanned aircraft vehicle/remotely piloted vehicle (UAV/RPV) system and its applicability as a lethal weapon system. Numerous systems were evaluated while concentrating on the Department of Defense's more prominent programs, the Pioneer UAV, vertical takeoff and landing (VTOL) UAV, and BQM-147A (EXDRONE) UAV. Israel has proven time and time again that UAVs/RPVs, when properly integrated into the combat arena as a lethal weapon system, can contribute significantly at a lower cost with less risk to an aircrew man in a manned aircraft system. In general the thesis shows many capable UAV/RPV systems designs are available in the market place today. These systems are assessed to determine their viability in the ever changing combat environment. DTIC

N94-31674# Technische Univ., Delft (Netherlands). Structures and Materials Lab.
DAMAGE TOLERANCE ASPECTS OF A FULL COMPOSITE AIRPLANE FUSELAGE: REQUIREMENTS, MODELLING, PREDICTIONS, EXPERIMENTS
M. N. vanBeijnen, M. J. L. vanTooren, T. deJong, and A. Beukers Jul. 1993 176 p
(LR-728; ETN-94-96138) Avail: CASI HC A09/MF A02

Composite fuselage structures are described, design concepts are mentioned, airworthiness rules for fuselage structures are discussed, and the loads on a fuselage structure and impact characteristics of composite materials are addressed. A theory for strength prediction, based on fracture mechanics and the stress intensity factor, under the presence of cracks is presented. Results of tests on stiffened panels are discussed. A stiffened panel which may improve the damage tolerance capabilities of the given composite sandwich fuselage structure is designed. A stiffened panel is produced and tested to check the predicted residual strength behavior of the panel. ESA

N94-31675# Technische Univ., Delft (Netherlands). Faculty of Aerospace Engineering.
MULTIPLE-SITE DAMAGE IN AIRCRAFT FUSELAGE STRUCTURES
J. Schijve Jul. 1993 29 p
(LR-729; ETN-94-96139) Avail: CASI HC A03/MF A01

Since the Aloha accident, the MSD (Multiple Site Damage) problem of riveted lap joints in aircraft fuselages has drawn much attention. The failure scenarios for a lead crack and more small MSD cracks as discussed by Broek and Swift are summarized, including results of relevant test series of Broek. Small MSD cracks are shown to possibly significantly reduce the load for unstable crack extension. Prevention of catastrophic consequences requires crack arresting capability of the structure. Related aspects of the problem setting are discussed with reference to failure criteria for ligament failure, the MSD problem for existing and new aircraft, and different options for crack stopper bands. Recommendations for future research are made. ESA

N94-31881 Virginia Polytechnic Inst. and State Univ., Blacksburg.
MULTIDISCIPLINARY OPTIMIZATION OF HIGH-SPEED CIVIL TRANSPORT CONFIGURATIONS USING VARIABLE-COMPLEXITY MODELING Ph.D. Thesis
Matthew Gerry Hutchison 1993 157 p
Avail: Univ. Microfilms Order No. DA9318184

An approach to aerodynamic configuration optimization is presented for the high speed civil transport (HSCT). Methods to parameterize the wing shape, fuselage shape, and nacelle placement are described. Variable complexity design strategies are used to combine conceptual and preliminary level design approaches, both to preserve interdisciplinary design influences and to reduce computational expense. The preliminary design level analysis methods used to estimate aircraft performance are described. Conceptual design level (approximate) methods are used to estimate aircraft weight, supersonic wave drag and drag due to lift, and landing angle of attack. The methodology is applied to the minimization of the gross weight of an HSCT that flies at Mach 2.4 with a range of 5500 n.mi. Results are presented for wing planform shape optimization and for combined wing and fuselage optimization with nacelle placement. Case studies include both all-metal wings and advanced composite wings. The results indicate the beneficial effect of simultaneous design of an entire configuration over the optimization of the wing alone and illustrate the capability of the optimization procedure. Dissert. Abstr.

N94-31957 Utah Univ., Salt Lake City.
EFFECTS OF FREQUENCY AND AMPLITUDE VARIATIONS OF SUPERIMPOSED MINOR LOADING SEQUENCES ON THE CORROSION FATIGUE BEHAVIOR OF AIRCRAFT STRUCTURAL ALUMINUM ALLOYS Ph.D. Thesis
Andrew Danton Paulson 1993 219 p
Avail: Univ. Microfilms Order No. DA9327339

Economic considerations have forced users of commercial jet transports to retain the services of aircraft that have surpassed the designed lifetime

of structural components of the aircraft. With the increased service time that these aircraft are experiencing, many of the aircraft are becoming increasingly susceptible to corrosive attack. Additionally, the increased public awareness of commercial aircraft incidents has mandated that the behavior of so called 'aging' aircraft structures be better understood. Fatigue crack growth tests were conducted using four aluminum alloys that are commonly used in the structural components of commercial jet transports. Two of these materials represented materials that were commonly used in the construction of the what are now termed 'aging' aircraft. The other two materials are typically used in the new commercial transports. These materials were subjected to trapezoidal loading cycles with superimposed minor loading cycles. The amplitude and frequency of the minor loading cycles were varied in order to determine the effects of such loading variations on the corrosion fatigue behavior of the alloys. It was determined that the minor cycles did not influence the crack growth rate of the material below some specific minor cycle amplitude. Indications were seen that the amplitude at which the minor cycles become active may be influenced by the presence of the corrosive environment. The effect of the active minor cycles on the fatigue crack growth process could be seen in the crack growth rate curves and also in the fractographic analysis of the specimen surfaces. The combined influence of the frequency and environment on the fatigue behavior of the alloys was noted. Once the minor cycles had become active, a lower minor cycle frequency led to a larger impact of the corrosive environment. It is believed that the identification of the activity or inactivity of minor cycle loading will aid in the development of spectrum loading determined from actual components. The actual spectrums may be simplified based on the fact that specific minor cycles are known to be inactive, due to insufficient amplitude to effect the fatigue crack growth process.

Dissert. Abstr.

N94-32015# Foster-Miller Associates, Inc., Waltham, MA.
FRACTURE AND FATIGUE STRENGTH EVALUATION OF MULTIPLE SITE DAMAGED AIRCRAFT FUSELAGES - CURVED PANEL TESTING AND ANALYSIS Final Report, Aug. 1989 - Mar. 1991
G. Samavedam and D. Hoadley Jan. 1994 171 p
(Contract DTRS57-89-D-0009)
(AD-A277100; DOT-VNTSC-FAA-93-8; DOT/FAA/CT-94/10) Avail: CASI HC A08/MF A02

As the fleet of commercial passenger aircraft is utilized beyond their design lives, flaws have developed at the rivet holes of fuselage lap joints on some aircraft which can grow and link up into cracks of significant length. Understanding, predicting, and controlling this crack growth and the ensuing linkup requires analysis and evaluation of the structural parameters in concert with confirmation by testing representative models of the fuselage. A dedicated test facility has been designed, built, and tested for this purpose. Seven full-sized curved fuselage panels have been built and tested. This report describes the design rationale for the facility, the details of its construction and performance and the design and testing of compatible panels which simulate fuselage structural details. Data on basic material properties of interest to the aging aircraft issue have been compiled from existing Literature and from R-curve testing and rivet stiffness testing performed as part of the effort. Analytic techniques have been developed to evaluate stress distributions and to estimate elastic stress intensity factors for flat and curved test panels. A flat test panel has been designed that demonstrates hoop stress equivalence to the curved fuselage. A 3-D FE mesh of a riveted lap joint is also presented. DTIC

N94-32058# Industrial Coll. of the Armed Forces, Washington, DC.
V-22: DUAL-USE TECHNOLOGY OR RED HERRING? Research Report, Aug. 1993
William H. Round Apr. 1993 43 p
(AD-A276577; NDU-ICAF-93-F39) Avail: CASI HC A03/MF A01

The V-22 Osprey has been a pawn in the battle between requirements and costs almost from its inception. The major factors with regard to the future of the V-22 are a combination of economic, political and military considerations. It is well known that a coalition of industry, congress and covertly the Marine Corps are on one side of the argument facing the administration and the Office of the Secretary of Defense (OSD) on the other. Each side has invoked arguments either for or against the program in the areas of economics (cost) and utilization (need) requirements.

DTIC

N94-32062 Aeronautical Systems Div., Wright-Patterson AFB, OH.
AIRCRAFT WEIGHT PREDICTION CAPABILITY. VOLUME 1: WEIGHT STUDY AND RESULTS Final Report, 1 Jan. - 30 May 1993
Thomas E. Oole May 1993 65 p Limited Reproducibility: More than 20% of this document may be affected by microfiche quality
(AD-A277206; ASC-TR-93-5022-Vol-1) Avail: Issuing Activity (Defense Technical Information Center (DTIC))

This report presents the study results, conclusions and recommendation of the application of various weight prediction methodologies to three modern aircraft that are representative of low observable (LO) and/or advanced technologies. In the continuous effort of the Mass Properties Group of the Flight Systems Engineering Division to improve the correlation of predicted weight to actual weight, this report and the corresponding study are intended to serve as a guide to the strength and weaknesses of current available prediction methodologies, identification of technical areas for which methodology is either lacking or inadequate, and recommendations to enhance our capability. Volume 1 of this report documents the background of the study, the weight estimation process of this office, the approach to the study, general results, conclusions, and recommendations to correct deficiencies and improve the Air Force capability. The following volumes will document the methodologies used and the detailed results for the aircraft analyzed. DTIC

N94-32232# Industrial Coll. of the Armed Forces, Washington, DC.
ARMY SCOUT/RECONNAISSANCE HELICOPTERS VERSUS UNMANNED AERIAL VEHICLES Report, Aug. 1992 - Apr. 1993
Dennis A. Williamson Apr. 1993 19 p
(AD-A276902; NDU-ICAF-93-S83) Avail: CASI HC A03/MF A01

All armies have long recognized the importance of reconnaissance in the successful accomplishment of their mission. Operations Desert Shield/Storm were no exceptions and, once again, proved that knowing the location of the enemy ground forces is paramount to achieving a decisive victory. However, with the reduction of the defense budget, the U.S. Army needs to relook how best to meet its future aerial scout/reconnaissance requirements. To solve the unarmed reconnaissance deficiency, there is a joint program to develop a new family of unmanned aerial vehicles (UAV's) underway. Likewise, to solve the armed reconnaissance deficiency, the Army is developing a new reconnaissance, attack helicopter. In this paper, I review some of our experiences in the Persian Gulf War with using both UAV's and helicopters. Also discussed are some of the costs associated with each system and its organizational structure. In addition, I outline the major advantages and disadvantages related to the systems. Finally, I provide recommendations on how the Army can best accomplish its reconnaissance mission with these two new systems. DTIC

N94-32242 Army Aeromedical Research Lab., Fort Rucker, AL.
TECHNICAL EVALUATION OF THE UH-60Q: MEDICAL OXYGEN SYSTEM
James E. Bruckart and Joseph R. Licina Jan. 1994 21 p Limited Reproducibility: More than 20% of this document may be affected by microfiche quality
(AD-A276983; USAARL-94-9) Avail: CASI HC A03

The UH-60Q prototype MEDEVAC Black Hawk is configured to provide day/night, adverse weather, emergency movement of patients. The objective of this report is to describe the results of performance tests on the medical oxygen system installed on the prototype aircraft. The medical oxygen system in the aircraft consists of a molecular sieve oxygen generating system (MSOGS) and support equipment. The MSOGS uses bleed air to produce high concentration oxygen. The MSOGS in the prototype aircraft is capable of producing 15 to 20 lpm of 94% oxygen and storing 163 l of oxygen in the backup oxygen supply (BOS). Lower bleed air pressures in ground tests may account for some decrement in performance of the MSOGS when compared to laboratory testing. Inflight testing is required. The support equipment, including oxygen concentration analyzer, BOS pressure monitor, and oxygen flowmeter do not function properly. The regulated oxygen pressure is too low to allow proper operation of the oxygen flow selectors. The oxygen analyzer is redundant and can be eliminated; the flowmeter could be eliminated if the oxygen flow selectors function properly. DTIC

N94-32263 Electronics Research Lab., Adelaide (Australia).
REAL TIME CHARACTER RECOGNITION FOR F-111C VIDEO TAPE RECORDS
Stephen Bourn Nov. 1993 28 p Limited Reproducibility: More than 20% of this document may be affected by microfiche quality
(AD-A277061; ERL-0593-RN; DODA-AR-006-924) Avail: Issuing Activity (Defense Technical Information Center (DTIC))

For evaluation purposes it is often necessary to reconstruct the tracks of F-111C aircraft participating in Australian Defense Force Exercises. The necessary information can be obtained from a video tape recording of one of the aircraft's displays. An image processing system has been developed to automatically extract this data. DTIC

N94-32264 Aeronautical Research Labs., Melbourne (Australia).
FINITE ELEMENT ANALYSIS OF MB326H MACCHI WING LOWER SPAR CAP FATIGUE CRACKS
D. Rees Dec. 1993 30 p Limited Reproducibility: More than 20% of this document may be affected by microfiche quality
(AD-A277062; ARL-TN-63; DODA-AR-008-410) Avail: Issuing Activity (Defense Technical Information Center (DTIC))

A three dimensional finite element analysis of cracks in the MB326H Macchi wing lower spar cap is presented. The case of cracks emanating from the intersection of a wing attachment fitting bolt hole and a web attachment fastener hole at wing station Y900 is considered. Stress intensity factors for two proposed crack geometries and the residual strength of the ligament above the web attachment fastener hole in the spar cap flange are calculated. DTIC

N94-32362 Aeronautical Research Labs., Melbourne (Australia).
SIX DEGREE OF FREEDOM FLIGHT DYNAMIC MODEL OF A Mk-82 STORE
M. A. Shilo Jan. 1994 45 p Limited Reproducibility: More than 20% of this document may be affected by microfiche quality
(AD-A277065; ARL-TN-25; DODA-AR-006-666) Avail: Issuing Activity (Defense Technical Information Center (DTIC))

A six degree of freedom, flight dynamic model incorporating an aerodynamic database derived from DSTO wind tunnel data was developed for the Mk-82 store. The model can be linked with aircraft flight dynamic models, and it forms part of a general program to model aircraft carriage and delivery, weapon release, and store ballistics. A rudimentary ejection model was also incorporated to represent the forces and moments experienced by the store at the point of release. The model is valid for free stream flight only, and ignores the effects of aircraft-store interaction. DTIC

N94-32378 Materials Research Labs., Ascot Vale (Australia).
IMPROVED RESEALING PROCEDURES FOR THE SECOND DESEAL/RESEAL PROGRAM IN RAAF F111 AIRCRAFT FUEL TANKS
S. Batten, R. H. Huang, and L. V. Wake Jan. 1994 33 p Limited Reproducibility: More than 20% of this document may be affected by microfiche quality
(AD-A277069; MRL-TR-93-64; DODA-AR-008-616) Avail: Issuing Activity (Defense Technical Information Center (DTIC))

A high temperature-resistant polyester sealant was originally employed to seal faying surface grooves in F-111 fuselage fuel tanks as well as structural voids and aerodynamic surfaces. Chemical hydrolysis of this material was detected in March 1974 and led to its replacement by a polysulfide sealant in the late 70's and early 80's. Where possible, the polyester was removed, however much of it remained inaccessibly located between the overlapping panels. It was found that the continued hydrolysis of this residual polyester generated sufficient pressure to penetrate the polysulfide sealant resulting in fuel leaks as well as appearing externally in trails along the skin of the aircraft. To protect the polysulfide from penetration, a mechanical barrier was applied in the form of a layer of epoxy polyamide between the polysulfide and the polyester. This system was successful for some years, however the occurrence of fuel leaks had become unacceptable by 1987. All F-111 aircraft suffered numerous fuel leaks over the period 1988-91 including a number of safety-of-flight (SOF) incidents. A detailed investigation was therefore requested to identify the cause(s) of sealant failures. This investigation found that the sealant and the underlying epoxy barrier coating could be manually peeled from the painted tank surface when prepared by the recommended methods and that two procedures were responsible for the poor adhesion. One of the procedures involved application of the barrier coating over incomplete cure priming paint resulting in solvent attack of the barrier. The second procedure, involving the use of a so-called titanate adhesion promoter, significantly reduced peel strength of the barrier coating to the paint. DTIC

N94-32658 Lawrence Livermore National Lab., CA.
DUAL-BAND INFRARED IMAGING TO DETECT CORROSION DAMAGE WITHIN AIRFRAMES AND CONCRETE STRUCTURES
N. K. DelGrande and P. F. Durbin Jan. 1994 10 p Presented at the 16th SPIE Thermosense: International Conference on Thermal Sensing and Imaging and Diagnostic Applications, Orlando, FL, 4-8 Apr. 1994 Limited Reproducibility: More than 20% of this document may be affected by microfiche quality
(Contract W-7405-eng-48)
(DE94-006047; UCRL-JC-115950; CONF-940483-1) Avail: CASI HC A02

We are developing dual-band infrared (DBIR) imaging and detection techniques to inspect air frames and concrete bridge decks for hidden corrosion damage. Using selective DBIR image ratios, we enhanced surface temperature contrast and removed surface emissivity noise associated with clutter. Our surface temperature maps depicted defect sites, which heat and cool at different rates than their surroundings. Our emissivity-ratio maps tagged and removed the masking effects of surface clutter. For airframe inspections, we used time-resolved DBIR temperature, emissivity-ratio, and composite thermal inertia maps to locate corrosion-thinning effects within a flash-heated Boeing 737 airframe. Emissivity-ratio maps tagged and removed clutter sites from uneven paint, dirt, and surface markers. Temperature and thermal inertia maps characterized defect sites, types, sizes, thicknesses, thermal properties and material-loss effects from air frame corrosion. For concrete inspections, we mapped DBIR temperature and emissivity-ratio patterns to better interpret surrogate delamination sites within naturally-heated, concrete slabs and remove the clutter mask from sand pile-up, grease stains, rocks, and other surface objects. DOE

N94-33056# Naval Postgraduate School, Monterey, CA.
DESIGN AND MONTE CARLO ANALYSIS OF AN UNMANNED AERIAL VEHICLE M.S. Thesis
Joseph P. Fordham Dec. 1993 88 p
(AD-A277648) Avail: CASI HC A05/MF A01

In the last several years, software innovations and the increasing speed and availability of microcomputers and workstations have made the dynamic simulation of complex systems more practical. One such system, a short-range Unmanned Aerial Vehicle called Bluebird, was previously modeled on Simulink, a commercial software package. The high fidelity model includes six degree of freedom nonlinear equations of motion with onboard sensors and a Global Positioning System and inertial navigation system. Because of interest expressed by the Unmanned Aerial Vehicle Joint Program Office in how accurately a UAV could identify a target's geographical coordinates, the Bluebird model, with an added guidance and control system, was evaluated as to its navigational and attitudinal accuracy in a dynamic simulation using Monte Carlo techniques. Because of the modular nature of the simulation, future evaluations of manned or unmanned aircraft and avionics will involve relatively uncomplicated changes to the existing model. DTIC

N94-33107 Wright Lab., Wright-Patterson AFB, OH.
RESPONSE OF A CANTILEVERED PLATE IN SUPERSONIC FLOW Interim Report, Jan. 1993 - Feb. 1994
Mark A. Hopkins Feb. 1994 54 p Limited Reproducibility: More than 20% of this document may be affected by microfiche quality
(AF Proj. 2401)
(AD-A277487; WL-TM-94-3031) Avail: Issuing Activity (Defense Technical Information Center (DTIC))

The response of a thin rectangular panel to supersonic flow over its upper surface is investigated. The panel is fabricated of an isotropic material and has a constant thickness. The panel is fixed along one side such that the flow passes over its freely supported leading and trailing edges parallel to the fixed edge. A Rayleigh-Ritz method is applied to determine the in-plane and transverse response of the panel. The panel deflections either decay to a zero equilibrium or grow to a limited amplitude oscillation once the transients have decayed depending on the panel and flow parameters.

At some combination of panel and flow parameters, the panel will begin to oscillate harmonically about a buckled state. Further increasing the flow conditions will cause the panel to either oscillate periodically about a buckled state or nonperiodically. The steady state response is dependent on the flow conditions and the initial deflections and velocity profiles of the panel. The flow Mach number and panel length-to-width ratios were varied. The cantilevered panel response is compared to previous research. A simply supported panel is briefly discussed and its response is also compared to previous work. DTIC

N94-33329 RAND Corp., Santa Monica, CA.
THE NATIONAL AEROSPACE PLANE (NASP): DEVELOPMENT ISSUES FOR THE FOLLOW-ON VEHICLE
B. W. Augenstein and E. D. Harris 1993 47 p Limited Reproducibility: More than 20% of this document may be affected by microfiche quality
(AD-A278417; R-3878/1-AF; ISBN-0-8330-1842-4) Avail: Issuing Activity (Defense Technical Information Center (DTIC))

This executive summary presents the final results of a project Air Force study on development issues for follow on systems for the National Aerospace Plane (NASP). It provides an independent overview assessment of the NASP program, which is currently in phase 2 of a three-phase research, development, test, and evaluation (RDT&E) program. The project was to aid the NASP Joint Program Office (JPO) and others directly concerned with NASP in two major areas: to assist in efforts to define and validate the utility of potential missions in support of the phase 3 decision milestone and to conduct an integrated system overview of NASP and NASP-derived systems that considers enabling technologies, logistic support, military missions, economics, and political implications. CASI

06 AIRCRAFT INSTRUMENTATION

Includes cockpit and cabin display devices; and flight instruments.

For related information see also *19 Spacecraft Instrumentation* and *35 Instrumentation and Photography.*

N94-31368# Wright Lab., Wright-Patterson AFB, OH.
TECHNOLOGIES FOR AVIONICS EMBEDDED COMPUTER SYSTEMS Final Report, period ending 17 Feb. 1993
Charles P. Satterthwaite Feb. 1994 15 p
(AF Proj. 9994)
(AD-A276364; WL-TR-94-1010) Avail: CASI HC A03/MF A01

Avionics embedded computer systems are an important part of the United States Air Force's plans for using advanced technologies to keep their aircraft highly capable and superior. Highly desirable features such as reconfigurability, rapid turnaround, expandability, and testability are made increasingly available through the use of these embedded systems. This paper discusses avionics embedded computer systems primarily through a discussion of their Operational Flight Programs (OFP's), near and far term requirements of OFP maintainers, and current technologies being developed for OFP maintenance. DTIC

N94-31458# Wright Lab., Wright-Patterson AFB, OH.
ANALYSIS OF THE EFFECT OF ROUTING STRATEGIES FOR PARALLEL IMPLEMENTATIONS OF A SELECTED AVIONICS APPLICATION Interim Report, 1 Feb. 1992 - 1 Sep. 1993
Jason L. Carter and Stephen L. Hary Dec. 1993 72 p
(AF Proj. 2003)
(AD-A276069; WL-TR-93-1173) Avail: CASI HC A04/MF A01

The purpose of this study is to evaluate the Texas Instruments TMS32OC40 (C40) digital signal processor for a selected avionics application. In this effort, the C40's on-chip communication ports are benchmarked to give indications of the amount of overhead involved in initiating a message transfer and the data throughput rates of the network. A network of C40's is compared to an iwarp parallel processor to compare the processing capabilities between the C40's store-and-forward router and the iWarp's wormhole router. Several network topologies that can easily be constructed from C40's are described, along with ways of partitioning an image processing task across each of them. Performance measurements of both the C40's and iWarp's performance on parallelized implementations of the image processing algorithm are detailed, along with estimated measurements for large-scale arrays of C40's. Finally, the C40's computing power is compared with an avionics hardware program being developed at wright Laboratories, System Avionics Division, Information Processing Technology Branch. DTIC

N94-31903 Canadian Marconi Co. Ltd., Kanata (Ontario).
STUDY OF VIRTUAL PROTOTYPING OF AIRCRAFT INSTRUMENTS Concluding Report
Peter M. Wells, R. D. Kobierski, and Gordon Youngson 9 Aug. 1993 204 p
(CMC-0687-1090; DSIS-94-01381; CTN-94-61215) Copyright Avail: CASI HC A10/MF A03

A project was initiated to identify the methodology, cost parameters, and data structure required to create a taxonomy of Canadian Forces aircraft cockpit representations using the Virtual Applications Prototyping System (VAPS). The cockpit panels of the CC-130H Hercules were selected for prototyping as they provide a convenient and timely test case for this process. During the data collection process required to support generation of the VAPS prototypes, a number of lessons were learned regarding both aircraft cockpit preparation and photographic techniques. A VAPS prototype library has been designed which utilizes the capacity of VAPS to create composite prototypes by loading reference components from other files. This effort resulted in generation of significantly more complex VAPS prototypes than those previously used. The variety of options used to improve performance, including hardware and software based approaches, are discussed. A VAPS component inventory database was created for systematic organization of information on components of VAPS prototypes. Efforts were made to establish links between the VAPS and other applications, and to develop software tools to enable the VAPS prototype library to support systems engineering tasks. A low-cost cockpit demonstration system that would maximize the utility of VAPS prototypes is also proposed. Author (CISTI)

N94-31977 Advisory Group for Aerospace Research and Development, Neuilly-Sur-Seine (France).
AEROSPACE SOFTWARE ENGINEERING FOR ADVANCED SYSTEMS ARCHITECTURES
Nov. 1993 248 p Limited Reproducibility: More than 20% of this document may be affected by microfiche quality
(AD-A277101; AGARD-CP-545) Avail: Issuing Activity (Defense Technical Information Center (DTIC))

During the past decade, many avionics functions which have traditionally been accomplished with analog hardware technology are now being accomplished by software residing in digital computers. Indeed, it is clear that in future avionics systems, most of the functionality of an avionics system will reside in software. In order to design, test, and maintain this software, software development/support environments will be extensively used. The significance of this transition to software is manifested in the fact that 50 percent or more of the cost of acquiring and maintaining advanced weapons systems is directly related to software considerations. It is also significant that this dependence on software provides an unprecedented flexibility to quickly adapt avionics systems to changing threat and mission requirements. Because of the crucial importance of software to military weapons systems, all NATO countries are devoting more research and development funds to explore every aspect of software science and practice. The purpose of this symposium was to bring together military aerospace software experts from all NATO countries to share the results of their software research and development and virtually every aspect of software was considered with the following representing a partial set of topics: aerospace electronics software specification, software design, programming practices and techniques, software validation and testing, software management, and software environments. DTIC

N94-32055# Wright Lab., Wright-Patterson AFB, OH.
GETTING A HANDLE ON DESIGNING FOR AVIONICS SOFTWARE SUPPORTABILITY AND MAINTAINABILITY Final Report, 18 - 22 May 1992
Charles P. Satterthwaite Feb. 1994 10 p See also A93-42862
(AF Proj. 9994)
(AD-A276362; WL-TR-94-1008) Avail: CASI HC A02/MF A01

The engineering design issues of supportability and maintainability are expanded upon so that interested individuals can understand (1) how these

issues impact a modern weapon system, (2) what impact the lack of concern for these issues is having on today's weapon systems, and (3) how these issues might be better considered and implemented in future weapon system designs. DTIC

N94-32223# Logicon Technical Services, Inc., Dayton, OH.
ASSESSMENT OF INTERIOR MODIFICATIONS IN C-130 AND C-141 AIRCRAFT FOR NIGHT VISION GOGGLE OPERATIONS Final Report, Mar. - Dec. 1992
Jeffrey L. Craig May 1993 20 p
(Contract F33615-89-C-0532)
(AD-A276843; AL/CF-TR-1993-0095) Avail: CASI HC A03/MF A01

An evaluation was conducted to examine the effects of interior paint scheme modifications to C-130 and C-141 aircraft on night vision goggle (NVG) operations. The evaluation consisted of direct measurement of aircraft interior radiance levels, calculation of surface reflectivities, and a human factors assessment of effects on aircrew NVG performance. The data were collected for both modified and original interior scheme C-130 and C-141 aircraft at Pope AFB and Charleston AFB, respectively. Reflectance values were determined for various flight deck and cargo bay surfaces. The reflectance values were calculated from the radiance levels within the sensitivity range of the NVG's. The results indicated that the reflectances were higher in modified aircraft for the majority of surfaces measured, but well within the specifications set by the relevant military standard. The human factors evaluation indicated that the vast majority of aircrew responding experienced no adverse effect on NVG performance attributable to the new interior scheme. In general, it was concluded that the modified interior scheme should not interfere with NVG operations. DTIC

N94-32328 Air Force Occupational Measurement Center, Randolph AFB, TX.
AIRCRAFT COMMUNICATION AND NAVIGATION SYSTEMS AND COMMUNICATION AND NAVIGATION SYSTEMS Occupational Survey Report
Jan. 1994 151 p Limited Reproducibility: More than 20% of this document may be affected by microfiche quality
(AD-A277309; AFPT-90-455-876) Avail: CASI HC A08

This report presents the results of a detailed Air Force (AF) occupational survey of the communication and navigation systems career ladder Air Force Specialty Codes (AFSCs) 2A4X2 and 2A1X3 (formerly 453X2 and 455X2, respectively). Authority for conducting occupational surveys is contained in AFR 35-2. DTIC

N94-32909# Wright Lab., Wright-Patterson AFB, OH.
A FRAMEWORK FOR DEVELOPING AND MANAGING REUSABLE AVIONICS SOFTWARE Final Report, 1 May - 1 Sep. 1993
Raghava G. Gowda Sep. 1993 24 p
(AF Proj. 9994)
(AD-A276846; WL-TR-94-1033) Avail: CASI HC A03/MF A01

Developing reusable software for avionics systems is a challenge to software engineers. The task involves foreseeing future applications, modeling real-world events, using appropriate CASE tools throughout the development life cycle, and providing for storage and retrieval of reusable software components. This report presents a model for developing and managing reusable software components, briefly describes the software process maturity model and the integration of CASE tools with the process maturity model. It also identifies tools/techniques and methodologies for real-time systems development, examines the critical issues in managing software projects, and offers the management a set of guidelines to introduce software engineering methodologies and CASE tools within the organization through a model project which may enforce standards for new projects. Author

N94-33076# Federal Aviation Administration, Washington, DC. Synthetic Vision Program Office.
SYNTHETIC VISION TECHNOLOGY DEMONSTRATION. VOLUME 1: EXECUTIVE SUMMARY Final Report
Malcolm A. Burgess, Terence Chang, Dale E. Dunford, Roger H. Hoh, Walter F. Horne, and Richard F. Tucker Dec. 1993 111 p
(DOT/FAA/RD-93/40-Vol-1) Avail: CASI HC A06/MF A02

This report contains the description and results of a Synthetic Vision technology demonstration program conducted jointly by the Federal Aviation Administration, the Department of Defense and industry. The relevant technologies including millimeter wave radar sensors, infrared sensors, head-up displays, and computer processing were developed and tested in static tower tests and in flight tests in which the weather conditions were carefully measured and documented. The purpose of the program was to evaluate and demonstrate the performance of the imaging sensors and of the complete imaging system during aircraft approaches and landings in low-visibility conditions. The static tower test facility used was the Avionics Tower Test Facility, located at Wright Patterson AFB, in which candidate sensors were set up at approximately 260 feet overlooking a nearby runway. The runway scene imaged by the sensors was instrumented to carefully measure the characteristics of fog, rain and snow as those conditions occurred in 1991-1992. Sensor performance and phenomenology was then fully characterized to provide a basis for further sensor development and for selection of sensors with which to proceed to flight test. The test aircraft used was a Gulfstream II configured with a comprehensive data collection system and instrumentation to permit measurement of fog and precipitation through which the aircraft was flown as well as system and pilot performance during those operations. Millimeter wave sensors and an infrared sensor were used to provide an electronic image of the runway on both head-up and head-down displays during approach, landing and takeoff. Test and demonstration flights were flown into 27 different airports in a wide variety of rain, fog and snow conditions during the period of May through December, 1992. This first volume is an executive summary containing an overview of the work from a management perspective. Author

N94-33077# Federal Aviation Administration, Washington, DC. Synthetic Vision Program Office.
SYNTHETIC VISION TECHNOLOGY DEMONSTRATION. VOLUME 2: SENSOR TOWER TESTING Final Report
Brian H. Hudson (Georgia Tech Research Inst., Atlanta.), Molly J. Gary (Georgia Tech Research Inst., Atlanta.), Malcolm A. Burgess, and J. Allen Zak Dec. 1993 293 p
(DOT/FAA/RD-93/40-Vol-2) Avail: CASI HC A13/MF A03

This report contains the description and results of a Synthetic Vision technology demonstration program conducted jointly by the Federal Aviation Administration, the Department of Defense and industry. The relevant technologies including millimeter wave radar sensors, infrared sensors, head-up displays, and computer processing were developed and tested in static tower tests and in flight tests in which the weather conditions were carefully measured and documented. The purpose of the program was to evaluate and demonstrate the performance of the imaging sensors and of the complete imaging system during aircraft approaches and landings in low-visibility conditions. The static tower test facility used was the Avionics Tower Test Facility, located at Wright Patterson AFB, in which candidate sensors were set up at approximately 260 feet overlooking a nearby runway. The runway scene imaged by the sensors was instrumented to carefully measure the characteristics of fog, rain and snow as those conditions occurred in 1991-1992. Sensor performance and phenomenology was then fully characterized to provide a basis for further sensor development and for selection of sensors with which to proceed to flight test. The test aircraft used was a Gulfstream II configured with a comprehensive data collection system and instrumentation to permit measurement of fog and precipitation through which the aircraft was flown as well as system and pilot performance during those operations. Millimeter wave sensors and an infrared sensor were used to provide an electronic image of the runway on both head-up and head-down displays during approach, landing and takeoff. Test and demonstration flights were flown into 27 different airports in a wide variety of rain, fog and snow conditions during the period of May through December, 1992. This is volume 2 of a four volume final report on the Synthetic Vision Technology Demonstration Program. This volume documents the tower tests performed in the program. Author (revised)

N94-33078# Federal Aviation Administration, Washington, DC. Synthetic Vision Program Office.
SYNTHETIC VISION TECHNOLOGY DEMONSTRATION. VOLUME 3: FLIGHT TESTS Final Report
Malcolm A. Burgess, Terence Chang, Dale E. Dunford, Roger H. Hoh, Walter F. Horne, Richard F. Tucker, and J. Allen Zak Dec. 1993 398 p
(DOT/FAA/RD-93/40-Vol-3) Avail: CASI HC A17/MF A04

This report contains the description and results of a Synthetic Vision technology demonstration program conducted jointly by the Federal Aviation Administration, the Department of Defense and industry. The relevant technologies including millimeter wave radar sensors, infrared sensors, head-up displays, and computer processing were developed and tested in static tower tests and in flight tests in which the weather conditions were carefully measured and documented. The purpose of the program was to evaluate and demonstrate the performance of the imaging sensors and of the complete imaging system during aircraft approaches and landings in low-visibility conditions. The static tower test facility used was the Avionics Tower Test Facility, located at Wright Patterson AFB, in which candidate sensors were set up at approximately 260 feet overlooking a nearby runway. The runway scene imaged by the sensors was instrumented to carefully measure the characteristics of fog, rain and snow as those conditions occurred in 1991-1992. Sensor performance and phenomenology was then fully characterized to provide a basis for further sensor development and for selection of sensors with which to proceed to flight test. The test aircraft used was a Gulfstream II configured with a comprehensive data collection system and instrumentation to permit measurement of fog and precipitation through which the aircraft was flown as well as system and pilot performance during those operations. Millimeter wave sensors and an infrared sensor were used to provide an electronic image of the runway on both head-up and head-down displays during approach, landing and takeoff. Test and demonstration flights were flown into 27 different airports in a wide variety of rain, fog and snow conditions during the period of May through December, 1992. This is the third of four volumes and it documents the flight tests performed in the program, incorporating reports from all of the participants. Author (revised)

N94-33079# Federal Aviation Administration, Washington, DC. Synthetic Vision Program Office.

SYNTHETIC VISION TECHNOLOGY DEMONSTRATION. VOLUME 4: APPENDICES Final Report

Malcolm A. Burgess, Terence Chang, Dale E. Dunford, Roger H. Hoh, Walter F. Horne, Richard F. Tucker, and Brian H. Hudson Dec. 1993 317 p

(DOT/FAA/RD-93/40-Vol-4) Avail: CASI HC A14/MF A03

This report contains the description and results of a Synthetic Vision technology demonstration program conducted jointly by the Federal Aviation Administration, the Department of Defense and industry. The relevant technologies including millimeter wave radar sensors, infrared sensors, head-up displays, and computer processing were developed and tested in static tower tests and in flight tests in which the weather conditions were carefully measured and documented. The purpose of the program was to evaluate and demonstrate the performance of the imaging sensors and of the complete imaging system during aircraft approaches and landings in low-visibility conditions. The static tower test facility used was the Avionics Tower Test Facility, located at Wright Patterson AFB, in which candidate sensors were set up at approximately 260 feet overlooking a nearby runway. The runway scene imaged by the sensors was instrumented to carefully measure the characteristics of fog, rain and snow as those conditions occurred in 1991-1992. Sensor performance and phenomenology was then fully characterized to provide a basis for further sensor development and for selection of sensors with which to proceed to flight test. The test aircraft used was a Gulfstream II configured with a comprehensive data collection system and instrumentation to permit measurement of fog and precipitation through which the aircraft was flown as well as system and pilot performance during those operations. Millimeter wave sensors and an infrared sensor were used to provide an electronic image of the runway on both head-up and head-down displays during approach, landing and takeoff. Test and demonstration flights were flown into 27 different airports in a wide variety of rain, fog and snow conditions during the period of May through December, 1992. This is the final volume of the report. It is a compilation of appendices containing additional detail pertaining to the flight tests. Author (revised)

N94-33280# Federal Aviation Administration, Cambridge, MA. National Transportation Systems Center.

COCKPIT ELECTRONIC DISPLAY WORKSHOP: A SYNOPSIS Final Report, Apr. - Oct. 1993

M. S. Huntley, Jr. and Rowena Morrison Dec. 1993 25 p Workshop held in Cambridge, MA, 7-9 Apr. 1993

(AD-A277728; DOT-VNTSC-FAA-93-21; DOT/FAA/RD-93/42) Avail: CASI HC A03/MF A01

Thirty-six government, academic, and industry human factors professionals participated in a workship convened at the Volpe National Transportation Systems Center to identify human factors issues associated with depicting terminal area operations information on electronic cockpit displays. Two working groups, formed from the meeting attendees, identified a variety of research issues associated with the identification, distribution, and electronic presentation of terminal area information to flight crews. This document presents a summary of the proceedings produced by that meeting and an edited list of research issues derived from those proceedings. The summary document also includes two disks containing the original workshop proceedings. These disks were formatted in Microsoft Word 5.1 for Macintosh. Please refer to the Read me file for further instructions. DTIC

N94-32457*# National Aeronautics and Space Administration. Lyndon B. Johnson Space Center, Houston, TX.

MICROWAVE SENSOR FOR ICE DETECTION

G. D. Arndt, A. Chu, L. G. Stolarczyk, and G. L. Stolarczyk *In* NASA, Washington, Technology 2003: The Fourth National Technology Transfer Conference and Exposition, Volume 2 Feb. 1994 p 318-325 (For primary document see N94-32420 09-99)

Avail: CASI HC A02/MF A04

07 AIRCRAFT PROPULSION AND POWER

Includes prime propulsion systems and systems components, e.g., gas turbine engines and compressors; and onboard auxilliary power plants for aircraft.

For related information see also *20 Spacecraft Propulsion and Power, 28 Propellants and Fuels,* and *44 Energy Production and Conversion.*

N94-31290# Naval Postgraduate School, Monterey, CA.

AN ANALYSIS OF NON-INTEGERIZING THE AIRCRAFT ENGINES COST EFFECTIVENESS ANALYSIS SPREADSHEET MODEL (CEAMOD VERSION 2.0) M.S. Thesis

Karl F. Rau Dec. 1993 114 p

(AD-A276251) Avail: CASI HC A06/MF A02

This thesis investigated the effect of integerization in the Cost Effectiveness Analysis Spreadsheet Model (CEAMOD Version 2.0) used by the Navy and the Air Force for decision-making in their aircraft engine Component Improvement Programs (CIP). A non-integerized model was developed and sensitivity analysis was performed to determine the cost drivers of the revised model. Three major cost drivers were then utilized as sensitivity analysis tools for comparing the decision values obtained from the current model with those obtained from the revised model. The author concluded that while the non-integerized CEAMOD is more theoretically correct, it would not lead to different decisions than CEAMOD Version 2.0. DTIC

N94-31931 Pennsylvania State Univ., University Park. Applied Research Lab.

SOLUTION OF THE AVERAGE-PASSAGE EQUATIONS FOR THE INCOMPRESSIBLE FLOW THROUGH MULTIPLE-BLADE-ROW TURBOMACHINERY

J. J. Dreyer and W. C. Zierke Feb. 1994 125 p Limited Reproducibility: More than 20% of this document may be affected by microfiche quality

(Contract N00039-92-C-0100)

(AD-A276515; PSU/ARL-TR-94-05) Avail: CASI HC A06

A system of equations governing the incompressible flow through a multiple-blade-row turbomachine is presented. These equations basically form the pseudo-compressible analog to the equations derived by Admaczyk 1984 for compressible, average-passage flow. The methodology behind the derivation is outlined, including a closure model for the time-averaged form of the equations. The equations are then preconditioned to facilitate numerical treatment. An explicit numerical procedure based on Runge-Kutta time stepping for cell-centered, hexahedral finite volumes is outlined for the approximate solution of the governing equations. Convergence

acceleration techniques, boundary conditions, and closure issues are also addressed for the numerical scheme. Finally, results are presented for a simulation of the high Reynolds number flow through a two-blade-row, axial-flow pump. These comparisons suggest that the pseudo-compressible average-passage equations can make reasonable predictions. DTIC

N94-31967 Stevens Inst. of Tech., Hoboken, NJ.
COMPUTATIONAL PREDICTION OF STALL FLUTTER IN SPANWISE-FINITE BLADE CASCADES Ph.D. Thesis
Tsong-Hsin Chen 1993 160 p
Avail: Univ. Microfilms Order No. D/ 9328508

Aeroelastic instabilities in turbomachinery are of great importance in practice and in the design process. Stall flutter is one of the important off-design phenomena at which airfoils experience flow separation with propagating stall cells. Prediction to prevent the onset of stall for given blade geometry and material properties is necessary. In this study, the unsteady aeroelastic behavior of the turbomachinery blade cascades is analyzed. A 'pseudo-three-dimensional' approach based on the well-tested vortex method is employed for the unsteady aerodynamics of spanwise-finite turbomachine blade cascades. The cascaded airfoils are modeled structurally using discretized beam theory and coupled with the unsteady aerodynamics algorithm for simultaneous solution by a time-marching technique. Before performing these computations, the static blade deflections and natural frequencies with/without rotation are all compared with the available experimental and analytical works to ensure the reliability of the structure dynamics algorithm. A six-element blade is proposed in order to reduce the CPU time and yet maintain acceptable accuracy. The mutual interaction of the structural dynamic displacement and the unsteady aerodynamic loading is effectively captured by this algorithm. The pseudo-three-dimensional results for the spanwise-finite airfoil cascades are shown to compare well with those for infinite linear cascades modeled by a two-dimensional characteristic section with a single degree-of-freedom in either bending or torsion. The computational results for a cascade of compressor blades with pretwist show that the bending motion normal to the chord dominates blade displacement for stall flutter in the fundamental frequency mode. The results also indicate that while entrainment or frequency synchronization may occur over a certain interval of frequency, the spanwise behavior of the cascade can exhibit considerable variations. The possibility of the second harmonic of the stall frequency exciting the blade at its natural frequency is uncovered. As to a lower stiffness blade, the torsional motion is found to dominate the whole motion and evoke a similar entrainment response like pure torsional motions in two-dimensional cascades. Finally, the chaotic behavior of nonlinear systems is observed in the aerodynamics of airfoil cascades when a coherent vibration is not present in coupled mode flutter. However, the limit cycle behavior is shown to be present in pure torsional or bending mode flutter. Dissert. Abstr.

N94-32026 Naval Postgraduate School, Monterey, CA.
DEVELOPMENT OF A CASCADE SIMULATION OF FAN-PASSAGE FLOW M.S. Thesis
Eric A. Tapp Dec. 1993 139 p Limited Reproducibility: More than 20% of this document may be affected by microfiche quality
(AD-A277234) Avail: CASI HC A07

A small-scale blowdown wind tunnel apparatus was developed to investigate techniques to alleviate the negative effects of shock-boundary layer interaction in the blading of aircraft engine fans. Using shadowgraph and surface injection techniques, probe surveys, and static pressure measurements, it was shown that acceptable periodicity and repeatability could be obtained in a two-passage cascade model at M = 1.4 if air supply pressure, back pressure, and porous-wall bleed pressures were properly controlled. It was also shown that local separation due to shock boundary layer interaction was present at the design flow incidence of 1.15 deg, but not at 0.85 deg. Complete data are reported for the design condition to serve as a baseline for separation alleviation experiments. Necessary hardware and software developments are also documented. DTIC

N94-32075*# Case Western Reserve Univ., Cleveland, OH.
ANTIWINDUP ANALYSIS AND DESIGN APPROACHES FOR MIMO SYSTEMS Final Report
Vincent R. Marcopoli and Stephen M. Phillips Apr. 1994 8 p See also A93-51403
(Grant NAG3-1232; RTOP 505-62-50)
(NASA-CR-195304; E-8706; NAS 1.26:195304) Avail: CASI HC A02/MF A01

Performance degradation of multiple-input multiple-output (MIMO) control systems having limited actuators is often handled by augmenting the controller with an antiwindup mechanism, which attempts to maintain system performance when limits are encountered. The goals of this paper are: (1) To develop a method to analyze antiwindup systems to determine precisely what stability and performance degradation is incurred under limited conditions. It is shown that by reformulating limited actuator commands as resulting from multiplicative perturbations to the corresponding controller requests, mu-analysis tools can be utilized to obtain quantitative measures of stability and performance degradation. (2) To propose a linear, time invariant (LTI) criterion on which to base the antiwindup design. These analysis and design methods are illustrated through the evaluation of two competing antiwindup schemes augmenting the controller of a Short Take-Off and Vertical Landing (STOVL) aircraft in transition flight. Author

N94-32238 Naval Postgraduate School, Monterey, CA.
ANALYSIS OF NAVY AIRCRAFT ENGINE AND ENGINE COMPONENT WARRANTIES M.S. Thesis
Melissa S. Andrews and Suzanne C. Hickey Dec. 1993 136 p Limited Reproducibility: More than 20% of this document may be affected by microfiche quality
(AD-A276936) Avail: CASI HC A07

Since the enactment of Title 10, Section 2403 of the United States Code in 1985, written warranty clauses have been mandated for the procurement of all major weapon systems. This thesis discusses the aircraft engine warranty program established by the Naval Air Systems Command in response to that warranty legislation. Warranty procedures and issues are examined during procurement, contract negotiations, and in the daily operations of the fleet. The aircraft engine warranty program of a major commercial airline (United Airlines) is presented to allow the reader to form a basis from which to make program comparisons. Those areas in which a commercial warranty may be applicable to a military environment are described and analyzed. Conclusions are drawn concerning the effectiveness of the Navy's warranty program and recommendations are suggested for improvements and/or follow on studies. DTIC

N94-32859*# United Technologies Corp., Windsor Locks, CT.
IN FLIGHT MEASUREMENT OF STEADY AND UNSTEADY BLADE SURFACE PRESSURE OF A SINGLE ROTATION LARGE SCALE ADVANCED PROP-FAN INSTALLED ON THE PTA AIRCRAFT Final Report
D. Parzych, L. Boyd, W. Meissner, and A. Wyrostek Sep. 1991 188 p Original contains color illustrations
(Contract NAS3-23051; RTOP 535-03-10)
(NASA-CR-187096; NAS 1.26:187096) Avail: CASI HC A09/MF A02; 42 functional color pages

An experiment was performed by Hamilton Standard, Division of United Technologies Corporation, under contract by LeRC, to measure the blade surface pressure of a large scale, 8 blade model prop-fan in flight. The test bed was the Gulfstream 2 Prop-Fan Test Assessment (PTA) aircraft. The objective of the test was to measure the steady and periodic blade surface pressure resulting from three different Prop-Fan air inflow angles at various takeoff and cruise conditions. The inflow angles were obtained by varying the nacelle tilt angles, which ranged from -3 to +2 degrees. A range of power loadings, tip speeds, and altitudes were tested at each nacelle tilt angle over the flight Mach number range of 0.30 to 0.80. Unsteady blade pressure data tabulated as Fourier coefficients for the first 35 harmonics of shaft rotational frequency and the steady (non-varying) pressure component are presented. Author

N94-33035*# Massachusetts Inst. of Tech., Cambridge. Dept. of Aeronautics and Astronautics.
INLET DISTORTION IN ENGINES ON VSTOL AIRCRAFT Final Technical Report, Oct. 1989 - Dec. 1993
Choon S. Tan and Edward M. Greitzer May 1994 61 p
(Grant NAG3-1567)
(NASA-CR-195841; NAS 1.26:195841) Avail: CASI HC A04/MF A01

This report presents the results of a research program on inlet distortion in engines on VSTOL aircraft carried out at the MIT Gas Turbine Laboratory

during the period Oct. 1989 - Dec. 1993. The program focused on the development of three dimensional flow computational methodology for predicting the effects of nonuniform flow on the performance of aircraft engines in VSTOL aircraft, the development of a three dimensional instability analysis of flow in multistage axial compressors, and the preliminary applications of these newly developed methodologies for elucidating the effects of flow three dimensionality. The accomplishments of the program are brought out when the current status of predictive capabilities for three dimensional flow instabilities in compressors is assessed against that in 1989. Author (revised)

N94-33266 Naval Postgraduate School, Monterey, CA.
A USER'S MANUAL FOR THE COST EFFECTIVENESS ANALYSIS SPREADSHEET MODEL FOR AIRCRAFT ENGINES (CEAMOD VERSION 2.0) M.S. Thesis
Ross R. Reeves Dec. 1993 364 p Limited Reproducibility: More than 20% of this document may be affected by microfiche quality
(AD-A278042) Avail: CASI HC A16

This thesis provides a comprehensive procedures manual and user's guide which will enable both current users and beginners to understand and employ Version 2.0 of the Cost Effectiveness Analysis model (CEAMOD), which is written in EXCEL spreadsheet software, in their service's aircraft engine Component Improvement Programs (CIP). The purpose of the CEAMOD is to project the possible savings which would be achieved from an Engineering Change Proposal's (ECP) implementation. The thesis begins by describing the model's background, basic assumptions, and format. Next, a detailed description of each page and the cell formulas used in each column of the spreadsheet are provided. A 'getting started' user's guide was also created to provide the user with the basic information necessary to actually use the CEA Deck/EXCEL spreadsheet software. An example of each page of the CEA model is provided as well as the Standard History File fleet input pages. DTIC

N94-33283 Naval Postgraduate School, Monterey, CA.
ANALYSIS OF INTERMEDIATE LEVEL MAINTENANCE FOLLOWING F404-GE-400 ENGINE COMPONENT LIFE REDUCTIONS M.S. Thesis
Jeri S. King and William M. Tooker Dec. 1993 85 p Limited Reproducibility: More than 20% of this document may be affected by microfiche quality
(AD-A277918) Avail: CASI HC A05

This thesis is an analysis of the effect that component life limit reductions of the F404-GE-400 engine have on AIMD Lemoore Power Plants Division operations. Estimations of fleet impact due to F404 component life limit reductions did not include the affect on production work centers. This thesis used simulation modeling of the F404 engine repair process at AIMD Lemoore to investigate the impact of these reductions. The simulation model outcomes provide strong indications that AIMD Power Plants Division operations will not be substantially altered by F404 component life limit reductions. However, there will be a significant impact on engine turn around time and the number of aircraft grounded awaiting engines. Recommendations to reduce the impact of component life limit reductions include improved logistical support in long-lead repair items. Additionally, the researchers recommend greater use of simulation modeling in future planning and analysis of significant logistics support changes. DTIC

N94-33339 Canadian Forces Base Trenton, Astra (Ontario).
AN EXPERT SYSTEM APPLICATION FOR TROUBLESHOOTING THE CF18 F404 ENGINE
W. D. E. Allan and R. C. Best *In* Royal Military Coll. of Canada, Proceedings of the Symposium/Workshop on Applications of Expert Systems in DND Apr. 1992 p 93-101 (For primary document see N94-33335 09-66)
Avail: Issuing Activity (Royal Military Coll. of Canada, Vimy Post Office, Kingston, ON K7K 5L0 Canada)

08 AIRCRAFT STABILITY AND CONTROL

Includes aircraft handling qualities; piloting; flight controls; and autopilots.

For related information see also *05 Aircraft Design, Testing and Performance.*

N94-31203*# California Polytechnic State Univ., San Luis Obispo.
CONTROLS DESIGN WITH CROSSFEEDS FOR HOVERING ROTORCRAFT USING QUANTITATIVE FEEDBACK THEORY
Semiannual Progress Report, Nov. 1993 - Mar. 1994
Daniel J. Biezad 15 Apr. 1994 30 p
(Contract NCC2-833)
(NASA-CR-195765; NAS 1.26:195765) Avail: CASI HC A03/MF A01

This work is extending the research accomplished on project NCC2-751. A newly implemented helicopter model has been used to simulate 25 flight configurations near hover for the UH-60 RASCAL aircraft. A new engine model has been installed in the FORECAST simulation (alias UMGENHEL) for the better prediction of the yaw and heave responses. By applying the decoupling metric from project NCC 751 it was determined that the aileron to pitch and the elevator to yaw responses do not indicate the need for crossfeeds since both of them have a decoupling metric value over 20 dB (less than 10 percent coupling). In the case of the aileron to heave and the elevator to heave responses, the large size and the overlapping of the templates indicate that a low-order dynamic crossfeed cannot be found. The low-order dynamic crossfeed selection is proceeding, however, for the remaining eight crossfeeds. Note that most of them have successfully decoupled the system by 20 dB or more, except for the rudder to heave crossfeed (18.2 dB). It is probable that the engine model needs more accuracy to further improve the heave to yaw crossfeed decoupling metric value. To see how the new low-order dynamic crossfeeds perform, a simulation was accomplished using MATLAB SIMULINK. Author (revised)

N94-31677# Ecole Centrale de Lyon (France). Lab. de Mecanique des Solides.
AEROELASTIC VIBRATIONS OF LIFTING SURFACES Ph.D. Thesis [VIBRATIONS AEROELASTIQUES DES SURFACES PORTANTES]
Cosmas PanditPagwiwoko 1991 159 p In FRENCH
(ECL-91-01; ETN-94-95985) Avail: CASI HC A08/MF A02

Work to establish calculation methods for solving aeroelastic problems is presented. The software developed is listed, and calculations were carried out for a hypothetical missile. A calculation method for unsteady aerodynamic loads in the subsonic and supersonic regimes modeling the lifting surface by singularities is presented. The problem of aeroservoelasticity is addressed. Flutter forces are presented in the form of a V-g diagram and by the place of the dynamic system transfer function roots. Aeroelastic responses of the nonlinear system and the control system are observed in the time domain. During numerical simulation, the gust effect and noise in the aeroelastic behavior are taken into account. ESA

N94-31837# Toronto Univ. (Ontario). Flight Simulator Lab.
DEVELOPMENT OF A RECONFIGURABLE HELICOPTER FLIGHT CONTROL SYSTEM M.S. Thesis
Pavan Rajagopal 1992 342 p
(ISBN-0-315-87218-7; CTN-94-61256) Copyright Avail: Micromedia Ltd., Technical Information Centre, 240 Catherine Street, Suite 305, Ottawa, Ontario, K2P 2G8, Canada HC/MF

A helicopter response type is a description of the coupling between the cockpit controls and the flight characteristics of the helicopter. A helicopter can be used to perform several different tasks, each requiring a different response type. During a given mission, it may be necessary to execute several tasks and therefore there is a requirement to be able to change the control configuration, or to reconfigure the control, while in flight. A study was conducted to examine the possibility of switching between configurations during flight and to determine the best way to achieve a control transition. An automatic control system was implemented on a helicopter simulator and a set of control algorithms was obtained which implemented seven response types. Most of these algorithms used proportional feedback. Two attempts were made to develop a control reconfiguration strategy. It was found that the most critical factor is the minimization of a control discontinuity over a transition. A method was developed to achieve such a minimization by setting the reference or

initial control deflection equal to the current or final control deflection of the old configuration. The tests performed on the reconfiguration algorithms show that smooth transitions are achievable between all response types in the appropriate channels. CISTI

N94-32217# Army Aeromedical Research Lab., Fort Rucker, AL.
TECHNICAL EVALUATION OF THE UH-60Q: AIRCRAFT IN TYPICAL AEROMEDICAL EVACUATION MISSIONS
James E. Bruckart and Joseph R. Licina Feb. 1994 37 p
(AD-A276944; USAARL-94-10) Avail: CASI HC A03/MF A01

The UH-60Q prototype MEDEVAC Black Hawk is configured to provide day/night, adverse weather, emergency movement of patients. The objective of this report is to describe the ability of the prototype aircraft to perform typical aeromedical evacuation missions. The prototype aircraft performed five simulated day and night medical evacuation missions as described in the Materiel Need Statement for the Dustoff UH-60Q. Medical aidmen and aviators rated the medical interior and avionics systems and provided comments on their in-flight experiences. The prototype UH-60Q Black Hawk is capable of performing the typical MEDEVAC missions. Nondevelopmental components of the medical interior require some refinements including improved vertical clearance for litters, improved durability, and environmental tolerance. Communications and cabin lighting require additional study to refine these requirements. DTIC

N94-32224# RANN, Inc., Palo Alto, CA.
ACTIVE CONTROL FOR FIN BUFFET ALLEVIATION Final Report, Jun. 1992 - Jun. 1993
Holt Ashley, Stephen M. Rock, Ramarao Digumarthi, Kenneth Chaney, and Alfred J. Eggers, Jr. Jan. 1994 142 p
(Contract F33615-92-C-3605)
(AD-A276844; WL-TR-93-3099) Avail: CASI HC A07/MF A02

A one year program of research for fighter aircraft with twin vertical stabilizers and which operate at high angles of attack was undertaken the following objective: to examine the possibility that active control can alleviate the response to buffeting and enhance fatigue life of the structure. Although there is no way that the phenomenon could have been anticipated during the initial phases of their design, 'fin buffeting' as a consequence of high-alpha maneuvers has been encountered on several military aircraft with such twin tails. Other affected fighters include the F-14 and the F/A-18. Future designs for which some level of buffeting is anticipated are the F-22. Measurements on a wind-tunnel model have already reported fin buffeting. Although they have single, center-line, vertical stabilizers, similar phenomena have occurred at high alpha on the X-29 and the X-31. DTIC

N94-32713 Colorado Univ., Boulder.
NUMERICAL ANALYSIS OF TRANSONIC WING BUFFET Ph.D. Thesis
Shen-Jwu Su 1992 151 p
Avail: Univ. Microfilms Order No. DA9318138

Transonic wing buffet is caused by shock-induced boundary layer separation on the wing. The inherent fluctuating buffet force can significantly reduce the flight performance of an airplane. An analysis of transonic wing buffet phenomena using modern numerical techniques is described here. The numerical tool developed for this purpose can accurately compute the solution for turbulent flow over a wing at high Reynolds numbers and at fairly high angles of attack. The computer code consists of two major parts: a three dimensional multiple block grid generation package, and an implicit finite difference code for solving the thin-layer compressible Navier-Stokes equations. Wind tunnel data for transonic flow past a swept ONERA M6 wing were used for code validation. The computed pressure distributions compared favorably with measurements. The buffet boundaries were predicted for the M6 wing, and the corresponding shock boundary-layer interaction during buffet onset was described. In order to avoid the separation penalties and to raise the buffet boundaries in the transonic speed regime, two types of wing designs, namely the twisted wing and step wing concepts, have been studied here. They were implemented separately by modifying the M6 wing geometry. The results indicate that both types of wing modifications can significantly alter the shock-wave and boundary-layer characteristics in a favorable way to reduce the rise of shock-induced separation on the wing and thus efficiently raise the buffet onset boundary. To examine the complex separated flow pattern obtained from numerical simulation, the concept of envelope of limiting streamlines and topology of phase plane was discussed. This provides a generalized approach to the classification of three dimensional separated flow patterns defined by streamlines for flow at or away from a solid surface. Dissert. Abstr.

N94-32951*# National Aeronautics and Space Administration. Langley Research Center, Hampton, VA.
MODELING OF AIRCRAFT UNSTEADY AERODYNAMIC CHARACTERISTICS. PART 1: POSTULATED MODELS
Vladislav Klein (George Washington Univ., Hampton, VA.) and Keith D. Noderer (George Washington Univ., Hampton, VA.) May 1994 26 p
(RTOP 505-64-52-01)
(NASA-TM-109120; NAS 1.15:109120) Avail: CASI HC A03/MF A01

A short theoretical study of aircraft aerodynamic model equations with unsteady effects is presented. The aerodynamic forces and moments are expressed in terms of indicial functions or internal state variables. The first representation leads to aircraft integro-differential equations of motion; the second preserves the state-space form of the model equations. The formulations of unsteady aerodynamics is applied in two examples. The first example deals with a one-degree-of-freedom harmonic motion about one of the aircraft body axes. In the second example, the equations for longitudinal short-period motion are developed. In these examples, only linear aerodynamic terms are considered. The indicial functions are postulated as simple exponentials and the internal state variables are governed by linear, time-invariant, first-order differential equations. It is shown that both approaches to the modeling of unsteady aerodynamics lead to identical models. Author

N94-33086# Naval Postgraduate School, Monterey, CA.
FAULT DETECTION AND ISOLATION FOR THE BLUEBIRD TEST BED AIRCRAFT M.S. Thesis
Mario J. Levesque Dec. 1993 117 p
(AD-A277979) Avail: CASI HC A06/MF A02

A Fault Detection and Isolation (FDI) algorithm design is presented using the Multiple Model algorithm technique for the Bluebird aircraft being developed at the Naval Postgraduate School. The requirement to maintain high performance in the dynamic system of the aircraft necessitates the use of FDI techniques to detect and isolate malfunctions in the sensors and actuators of the aircraft without using hardware redundancy. The solution presented makes use of analytical redundancy in a bank of Kalman filters. Statistical tests using Bayesian theory are applied on the filter's innovations to perform the task of detection and isolation. The algorithm was developed using MATLAB software from The Math Works, Inc. The work presented in this thesis is related only to the task of FDI. The remaining task of the monitoring system, reconfiguration and continued operation by the observed plant after a failure detection, will not be addressed. DTIC

09 RESEARCH AND SUPPORT FACILITIES (AIR)

Includes airports, hangars and runways; aircraft repair and overhaul facilities; wind tunnels; shock tubes; and aircraft engine test stands.

For related information see also *14 Ground Support Systems and Facilities (Space).*

N94-31058# Dayton Univ. Research Inst., OH.
VARIABLE-RESOLUTION IMAGERY FOR FLIGHT SIMULATION Final Report, Jun. 1989 - Jun. 1993
George A. Geri, Yehoshua Y. Zeevi, and Craig A. Vrana Jan. 1994 100 p
(Contract F33615-90-C-0005)
(AD-A276199; AL/HR-TR-1993-0180) Avail: CASI HC A05/MF A02

A position-varying, low-pass filter was used to produce variable-resolution images whose spatial frequency content varies as a function of distance from their center. Such images can be matched in some sense to the spatial inhomogeneities of the human visual system, and thus, they may be visually acceptable even though they contain less information than an unprocessed version of the same image. Following a discussion of image representation with nonuniform sampling and of the concept of locally bandlimited spaces, two experiments were performed to visually assess variable-resolution images. In Experiment 1, images were generated using a series of distortion functions (differing in central blur, peripheral blur, and blur gradient) chosen to approximate cortical magnification functions

(CMFN's) derived from existing anatomical and psychophysical data. The distortion functions, corresponding to the images that were just discriminable from an unprocessed image, were used to define the wide-field CMFN associated with changes in blur discrimination across the visual field. In Experiment 2, blur thresholds were measured using apertures in the form of either circles or 3 deg-wide angular segments centered in either 15 deg or 30 deg eccentricity. Differences in blur discrimination for the two stimulus configurations, matched in area, suggest that the spatial organization of the visual mechanisms underlying blur discrimination changes with eccentricity. Finally, the perceptual data obtained here were used to efficiently sample and represent a variable-resolution image. DTIC

N94-31179# National Aerospace Lab., Amsterdam (Netherlands). Flight Div.

AIRCRAFT SIMULATION AND PILOT PROFICIENCY: FROM SURROGATE FLYING TOWARDS EFFECTIVE TRAINING

P. G. A. M. Jorna, E. R. A. vanKleef, and W. P. Boer 30 Jul. 1992 32 p Presented at the AGARD Conference on Piloted Simulation Effectiveness, Brussels, Belgium, 1992

(AD-B179300; NLR-TP-91489-U; ETN-94-95973) Avail: CASI HC A03/MF A01

Experiences with the application of simulators in military flight training are reviewed and research strategies like the development of objective performance measures in support of validation trials and future simulator development are reported. It is proposed to prototype simulator concepts before implementing them and relevant research initiatives in this area are reviewed. The credibility of simulators is assessed from a pilot's perspective. It is noted that a missing link between simulator and real flight is the obvious absence of physical danger. Safety serves to reduce anxiety and influences the pilot strategies for task execution: who is afraid of crashing a simulator. Effects of anxiety on performance could be demonstrated and interactions with high workload conditions occurred. Coping with the mental perils of flight is an important component of pilot proficiency and simulating such an environment, or at least its impact on performance, is one of the many challenges for the training community. ESA

N94-31295# TeSCO, Inc., Tullahoma, TN.

MODEL BORNE DATA MANAGEMENT SYSTEM FOR WIND TUNNEL TESTING, PHASE 2 Final Report, 1 Oct. 1991 - 1 Oct. 1993

Lee F. Webster and T. S. Paige Nov. 1993 37 p

(Contract F33615-91-C-3007)

(AD-A276296; TESCO-TR-93-1-Phase-2; WL-TR-93-3125-Phase-2) Avail: CASI HC A03/MF A01

This report covers the development of a modern model mounted wind tunnel data acquisition and processing system called MDARS, short for Modular Data Acquisition and Recording System. During this Phase, prototypes of the model borne components and the pc interface were developed. The system was then installed in a HP-MaRV model for demonstration testing in AEDC's wind tunnel B. Following these tests the performance and durability of the system was analyzed and lessons learned were identified and incorporated into a production version of the system. These activities resulted in a proven data system, ready for marketing. The MDARS uses modern high density surface mount components in a compact modular/bus arrangement which allows a size which can be accommodated by most wind tunnel models. It also allows the system to be controlled and data to be acquired by a modern personal computer thus decreasing or eliminating dependence on facility data systems. The system multiplexes all data channels and converts all analog signals digital. The remote system communicates with the Control Personal Computer by fiber optic cable. The use of MDARS will reduce facility data system dependence while reducing test set up costs and schedule delays. DTIC

N94-31318 Naval Surface Weapons Center, Silver Spring, MD.

HYPERVELOCITY TUNNEL 9 MACH 10/14 CALIBRATION

Dan Marren 31 Jan. 1994 65 p Limited Reproducibility: More than 20% of this document may be affected by microfiche quality

(AD-A275960; NSWCDD/TR-92/160) Avail: CASI HC A04

This report documents the Tunnel 9 Mach 10/14 Calibration test program (WTR 1608) performed at the Naval Surface Warfare Center, White Oak, Maryland. This effort was sponsored by the National Aerospace Plane Joint Program Office (NASP JPO). Free stream flow field parameter distributions were obtained for both the Mach 10 and 14 nozzles spanning the Reynolds number range. A total of four Mach 10, and ten Mach 14 runs were performed during this test program. The test period was 7 to 22 May 1991. Results from this test entry were combined with previous test data in the final analysis. Data from the test reveal that high quality uniform flow exists and that deviations in core flow field parameters are comparable with the calibration data taken in the past. DTIC

N94-31346# IBM Federal Systems Div., Gaithersburg, MD.

CLEANROOM ENGINEERING HANDBOOK. VOLUME 6: CERTIFICATION TEAM PRACTICES

31 Jul. 1993 54 p

(Contract F19628-88-D-0032)

(AD-A275951) Avail: CASI HC A04/MF A01

This is one of a series of six engineering handbooks prepared for and used by the engineering staff at Picatinny Arsenal for the STARS technology transfer demonstration. The handbooks define the engineering process and algorithms that will be used in Cleanroom projects. They are designed to provide support to trained engineers using Cleanroom engineering, not to substitute for training. This volume describes the activities of Cleanroom software certification for each increment/accumulation of project development. Process P5.j.2, preparation for certification of accumulation j, and process P6.j, software certification for accumulation j, are expanded into engineering subprocesses (i.e., tasks) for execution by Cleanroom-trained software engineers. These tasks result in the preparation for and performance of the certification of developed software. DTIC

N94-31356# IBM Federal Systems Div., Gaithersburg, MD.

CLEANROOM ENGINEERING HANDBOOK. VOLUME 1: CLEANROOM ENGINEERING PROCESS INTRODUCTION AND OVERVIEW

31 Jul. 1993 46 p

(Contract F19628-88-D-0032)

(AD-A275949) Avail: CASI HC A03/MF A01

This is one of a series of six engineering handbooks prepared for and used by the engineering staff at Picatinny Arsenal for the STARS technology transfer demonstration. The handbooks define the engineering process and algorithms that will be used in Cleanroom projects. They are designed to provide support to trained engineers using Cleanroom Engineering, not to substitute for training. This handbook, Volume 1, presents an introduction to the Cleanroom engineering process model and is recommended for all software planning and development participants. It defines the Cleanroom process in light of the project organization which consists of: The Specification Team; The Development Team; The Certification Team; and the software transformations which are: Specification Development - To define the software system to be developed and record the definition in the specification document; and Software Development and Certification - To develop and certify software in the target language that runs on the target processor and exhibits the same behavior described in the specification. DTIC

N94-31710# Royal Military Coll. of Canada, Kingston (Ontario). Dept. of Civil Engineering.

DETERMINING THE BEARING CAPACITY OF FLEXIBLE AIRFIELD PAVEMENTS USING A HEAVY WEIGHT DEFLECTOMETER M.S. Thesis

R. E. Fenton Sep. 1992 173 p

(ISBN-0-315-86210-6; CTN-94-61186) Copyright Avail: Micromedia Ltd., Technical Information Centre, 240 Catherine Street, Suite 305, Ottawa, Ontario, K2P 2G8, Canada HC/MF

In 1985, increasing costs and the inconvenience associated with conducting plate bearing tests prompted Transport Canada to investigate the feasibility of replacing the controlled rate of loading (CROL) test with falling weight deflectometer testing for determining the standard surface bearing strength Pstd of flexible airfield pavements. In summer 1990, 180 heavy weight deflectometer (HWD) and CROL tests were conducted at eight Transport Canada airfields in central Canada. The Pstd determined from the CROL test, Pcrol, was compared to the HWD deflection at the center of the HWD loading plate, the radius of curvature of the HWD deflection bowl, and the area of the HWD deflection bowl at loads of 60, 120, 180, and 240 kilonewtons. A relationship between the slope and intercept of the deflection bowl area versus HWD load plots and Pcrol with a correlation coefficient of about 0.84 was developed. This relationship is considered to be a viable method of estimating the Pstd from HWD data for airfields located in central Canada. Author (CISTI)

N94-31747# Laval Univ. (Quebec). Faculte des Sciences et Genie.
DEVELOPMENT OF A ROBOTIC SIMULATOR FOR STUDYING INTERFERENCE AND CONTACT PROBLEMS M.S. Thesis [DEVELOPPEMENT D'UN SIMULATEUR ROBOTIQUE POUR L'ETUDE DES PROBLEMES D'INTERFERENCE ET DE CONTACT]
Gaetan Michaud Sep. 1993 97 p In FRENCH
(ISBN-0-315-86705-1; CTN-94-61224) Copyright Avail: Micromedia Ltd., Technical Information Centre, 240 Catherine Street, Suite 305, Ottawa, Ontario, K2P 2G8, Canada HC/MF

Novel algorithms for studying the contact interference problem in robotics are developed with the objective of introducing them into a new approach for analyzing contact forces during grasping operations. A new approach for analyzing mechanical contacts is utilized for validation. With the aid of Winkler's method and interference algorithms, an analysis of two objects in contact is presented under three different conditions with respect to the types of surfaces which are in contact: a pointed object contacting a plane surface, an edge contacting another edge, and a cylinder contacting a plane surface. The study is based on one of the necessary conditions of the Winkler method, i.e. the analogy to volumetric interference, related to a material interpenetration between two objects. To incorporate the previous elements, a simulator and a data structure are developed. The simulator is used to validate the algorithm of detection of interference between a plane surface and a cylinder. CISTI

N94-32009 Arnold Engineering Development Center, Arnold AFS, TN.
DEVELOPMENT OF HIGH-PRESSURE DIAPHRAGMS FOR THE AEDC IMPULSE TUNNEL Final Report, 1 Oct. 1991 - 1 Oct. 1993
J. R. DeWitt Feb. 1994 29 p Prepared in cooperation with Calspan Corp., Arnold AFS, TN Limited Reproducibility: More than 20% of this document may be affected by microfiche quality
(AD-A277053; AEDC-TR-93-28) Avail: CASI HC A03

Operation of the AEDC Impulse Tunnel at high stagnation conditions will require diaphragm burst pressures up to approximately 6,900 bars. A hemispherically shaped diaphragm design made of high-strength material has been developed and tested in a test rig for the pressure range from 1,400 to 6,800 bars. Flat diaphragms have been developed and used in the Impulse Tunnel at pressures up to 1,400 bars. A nearly linear relationship between the burst pressure and the ratio of remaining metal thickness to the radius of the cavity into which the diaphragm opens allows linear scaling to different size facilities. DTIC

N94-32014# Boeing Defense and Space Group, Huntsville, AL. Simulation and Training Systems.
MODULAR SIMULATOR SYSTEM (MSS) MANAGEMENT GUIDE Final Report
K. Kelly, J. Brown, G. Kamsickas, and W. Tucker 20 Aug. 1993 48 p
(Contract F33657-86-C-0149)
(AD-A277098; S495-10459-1; ASC-TR-94-5008) Avail: CASI HC A03/MF A01

This document provides guidance and reference information for management personnel in the use of the Modular Simulator System (MSS) design principles. It identifies those unique management considerations required when employing the modular simulator design to a simulation and/or training device. This guide serves as both an educational and decision tool for the manager. The guide will educate the manager in the basic concepts of the modular simulator design and its basis for development. Key program decisions and considerations that must be made when using the modular simulator design are identified and discussed. The advantages and disadvantages of using the modular simulator design along with associated cost/risk analysis, logistics impacts, management implications, lessons learned and basis for invoking the modular simulator design on a procurement/program are provided. DTIC

N94-32120# Federal Aviation Administration, Atlantic City, NJ. Technical Center.
EVALUATION FOR THE DEVELOPMENT OF TAXIWAY LIGHTING INTENSITY STANDARDS
Keith W. Bagot Feb. 1994 15 p
(AD-A276706; DOT/FAA/CT-TN93/50) Avail: CASI HC A03/MF A01

The purpose of this evaluation was to gather data to produce taxiway lighting intensity standards to be incorporated into DOT/FAA Order 7110.65H, Air Traffic Control. Currently, there are no tables of standard intensity settings for taxiway lighting systems. Air traffic controllers are only instructed to operate the taxiway lights between sunset and sunrise and at other times they consider it necessary. DTIC

N94-32241 Boeing Defense and Space Group, Huntsville, AL. Simulation and Training Systems.
MODULAR SIMULATOR SYSTEM (MSS). EXECUTIVE REPORT Final Report
K. Kelly, J. Brown, G. Kamsickas, and W. Tucker 20 Aug. 1993 72 p
Limited Reproducibility: More than 20% of this document may be affected by microfiche quality
(Contract F33657-86-C-0149)
(AD-A276966; S495-10441-1; ASC-TR-94-5006) Avail: CASI HC A04

This report provides an executive overview and top level presentation materials for the Modular Simulator System (MSS). It provides a brief overview of the MSS project, system architecture and design, and application alternatives for employing the design to a simulation and/or training device. This report serves as both an educational and decision tool for all levels of management and engineering personnel. This report describes the basic concept of the MSS design and its basis for development. The intent is to support informed decisions regarding the application of the MSS approach to a specific training system development. Additional sources for detailed MSS data are also provided for further reference. DTIC

N94-32311 Boeing Defense and Space Group, Huntsville, AL. Simulation and Training Systems.
MODULAR SIMULATOR SYSTEM (MSS). INTERFACE REQUIREMENTS SPECIFICATION FOR THE GENERIC MSS Final Report
K. Kelly, J. Brown, G. Kamsickas, and W. Tucker 20 Aug. 1993 61 p
Limited Reproducibility: More than 20% of this document may be affected by microfiche quality
(Contract F33657-86-C-0149)
(AD-A276965; S495-10734-1; ASC-TR-94-5005) Avail: CASI HC A04

This document describes the interface requirements for the Modular Simulator System. Tailoring will be necessary to meet specific training system requirements. Specific tailoring instructions are included for each paragraph. It is suggested that the user read the 'Modular Simulator Engineering Design Guide' and the 'Modular Simulator Management Guide' prior to tailoring this specification. DTIC

N94-32312 Boeing Defense and Space Group, Huntsville, AL. Simulation and Training Systems.
MODULAR SIMULATOR SYSTEM (MSS). SYSTEM/SEGMENT SPECIFICATION FOR THE GENERIC MSS-SYSTEM INTEGRATION, VOLUME 1 Final Report
K. Kelly, J. Brown, G. Kamsickas, and W. Tucker 20 Aug. 1993 86 p
Limited Reproducibility: More than 20% of this document may be affected by microfiche quality
(Contract F33657-86-C-0149)
(AD-A276968; S495-10400D-Vol-1; ASC-TR-94-5010) Avail: CASI HC A05

This is the System Integration portion of the generic Modular Simulator System (MSS) specification. It is designed to be tailored to specify the requirements for a specific aircraft training device or family of aircraft training devices. This specification contains specific tailoring instructions for each paragraph. When the tailoring process is complete, the italicized tailoring instructions should have been replaced by application specific text or deleted from the specification. It is suggested that the user read the 'Modular Simulator Engineering Guide' and the 'Modular Simulator Management Guide' prior tailoring this volume. DTIC

N94-32313 Boeing Defense and Space Group, Huntsville, AL. Simulation and Training Systems.
MODULAR SIMULATOR SYSTEM (MSS). SYSTEM/SEGMENT SPECIFICATION FOR THE GENERIC MODULAR SIMULATOR SYSTEM-FLIGHT STATION MODULE, VOLUME 2 Final Report
K. Kelly, J. Brown, G. Kamsickas, and W. Tucker 20 Aug. 1993 36 p
Limited Reproducibility: More than 20% of this document may be affected by microfiche quality
(Contract F33657-86-C-0149)
(AD-A276969; S495-10400D-Vol-2; ASC-TR-94-5011) Avail: CASI HC A03

This is the Flight Station portion of the generic Modular Simulator System (MSS) specification. It is designed to be tailored to specify the requirements for a specific aircraft training device or family of aircraft training devices. This specification contains specific tailoring instructions for each paragraph. When the tailoring process is complete, the italicized tailoring instructions should have been replaced by application specific text or deleted from the specification. It is suggested that the user read the 'Modular Simulator Engineering Guide' and the 'Modular Simulator Management Guide' prior to this volume. DTIC

N94-32314# Boeing Defense and Space Group, Huntsville, AL. Simulation and Training Systems.

MODULAR SIMULATOR SYSTEM (MSS). SYSTEM/SEGMENT SPECIFICATION FOR THE GENERIC MODULAR SIMULATOR SYSTEM-RADAR MODULE, VOLUME 8 Final Report

K. Kelly, J. Brown, G. Kamsickas, and W. Tucker 20 Aug. 1993 34 p
(Contract F33657-86-C-0149)
(AD-A276975; S495-10400D-Vol-8; ASC-TR-94-5018) Avail: CASI HC A03/MF A01

This is the Radar portion of the generic Modular Simulator System (MSS) specification. It is designed to be tailored to specify the requirements for a specific aircraft training device or family of aircraft training devices. This specification contains specific tailoring instructions for each paragraph. When the tailoring process is complete, the italicized tailoring instructions should have been replaced by application specific text or deleted from the specification. It is suggested that the user read the 'Modular Simulator Engineering Guide' and the 'Modular Simulator Management Guide' prior to tailoring this volume. DTIC

N94-32315 Boeing Defense and Space Group, Huntsville, AL. Simulation and Training Systems.

MODULAR SIMULATOR SYSTEM (MSS). SYSTEM/SEGMENT SPECIFICATION FOR THE GENERIC MODULAR SIMULATOR SYSTEM-ELECTRONIC WARFARE MODULE, VOLUME 9 Final Report

K. Kelly, J. Brown, G. Kamsickas, and W. Tucker 20 Aug. 1993 33 p
Limited Reproducibility: More than 20% of this document may be affected by microfiche quality
(Contract F33657-86-C-0149)
(AD-A276976; S495-10400D-Vol-9; ASC-TR-94-5019) Avail: CASI HC A03

This is the Electronic Warfare portion of the generic Modular Simulator System (MSS) specification. It is designed to be tailored to specify the requirements for a specific aircraft training device or family of aircraft training devices. This specification contains specific tailoring instructions for each paragraph. When the tailoring process is complete, the italicized tailoring instructions should have been replaced by application specific text or deleted from the specification. It is suggested that the user read the 'Modular Simulator Engineering Guide' and the 'Modular Simulator Management Guide' prior to tailoring this volume. DTIC

N94-32316 Boeing Defense and Space Group, Huntsville, AL. Simulation and Training Systems.

MODULAR SIMULATOR SYSTEM (MSS). SYSTEM/SEGMENT SPECIFICATION FOR THE GENERIC MODULAR SIMULATOR SYSTEM-PHYSICAL CUES MODULE, VOLUME 10 Final Report

K. Kelly, J. Brown, G. Kamsickas, and W. Tucker 20 Aug. 1993 33 p
Limited Reproducibility: More than 20% of this document may be affected by microfiche quality
(Contract F33657-86-C-0149)
(AD-A276977; S495-10400D-Vol-10; ASC-TR-94-5020) Avail: CASI HC A03

This is the Physical Cues portion of the generic Modular Simulator System (MSS) specification. It is designed to be tailored to specify the requirements for a specific aircraft training device or family of aircraft training devices. This specification contains specific tailoring instructions for each paragraph. When the tailoring process is complete, the italicized tailoring instructions should have been replaced by application specific text or deleted from the specification. It is suggested that the user read the 'Modular Simulator Engineering Guide' and the 'Modular Simulator Management Guide' prior to tailoring this volume. DTIC

N94-32317 Boeing Defense and Space Group, Huntsville, AL. Simulation and Training Systems.

MODULAR SIMULATOR SYSTEM (MSS). SYSTEM/SEGMENT SPECIFICATION FOR THE GENERIC MODULAR SIMULATOR SYSTEM-VISUAL MODULE, VOLUME 11 Final Report

K. Kelly, J. Brown, G. Kamsickas, and W. Tucker 20 Aug. 1993 55 p
Limited Reproducibility: More than 20% of this document may be affected by microfiche quality
(Contract F33657-86-C-0149)
(AD-A276978; S495-10400D-Vol-11; ASC-TR-94-5021) Avail: CASI HC A04

This is the Visual portion of the generic Modular Simulator System (MSS) specification. It is designed to be tailored to specify the requirements for a specific aircraft training device or family of aircraft training devices. This specification contains specific tailoring instructions for each paragraph. When the tailoring process is complete, the italicized tailoring instructions should have been replaced by application specific text or deleted from the specification. It is suggested that the user read the 'Modular Simulator Engineering Guide' and the 'Modular Simulator Management Guide' prior to tailoring this volume. DTIC

N94-32318# Boeing Defense and Space Group, Huntsville, AL. Simulation and Training Systems.

MODULAR SIMULATOR SYSTEM (MSS). SYSTEM/SEGMENT SPECIFICATION FOR THE GENERIC MODULAR SIMULATOR SYSTEM-INSTRUCTOR/OPERATOR STATION MODULE, VOLUME 12 Final Report

K. Kelly, J. Brown, G. Kamsickas, and W. Tucker 20 Aug. 1993 42 p
(Contract F33657-86-C-0149)
(AD-A276979; S495-10400D-Vol-12; ASC-TR-94-5022) Avail: CASI HC A03/MF A01

This is the Instructor/Operator Station portion of the generic Modular Simulator System (MSS) specification. It is designed to be tailored to specify the requirements for a specific aircraft training device or family of aircraft training devices. This specification contains specific tailoring instructions for each paragraph. When the tailoring process is complete, the italicized tailoring instructions should have been replaced by application specific text or deleted from the specification. It is suggested that the user read the 'Modular Simulator Engineering Guide' and the 'Modular Simulator Management Guide' prior to tailoring this volume. DTIC

N94-32319 Boeing Defense and Space Group, Huntsville, AL. Simulation and Training Systems.

MODULAR SIMULATOR SYSTEM (MSS). SYSTEM/SEGMENT SPECIFICATION FOR THE GENERIC MODULAR SIMULATOR SYSTEM-ENVIRONMENT MODULE, VOLUME 13 Final Report

K. Kelly, J. Brown, G. Kamsickas, and W. Tucker 20 Aug. 1993 34 p
Limited Reproducibility: More than 20% of this document may be affected by microfiche quality
(Contract F33657-86-C-0149)
(AD-A276980; S495-10400D-Vol-13; ASC-TR-94-5023) Avail: CASI HC A03

This is the Environment portion of the generic Modular Simulator System (MSS) specification. It is designed to be tailored to specify the requirements for a specific aircraft training device or family of aircraft training devices. This specification contains specific tailoring instructions for each paragraph. When the tailoring process is complete, the italicized tailoring instructions should have been replaced by application specific text or deleted from the specification. It is suggested that the user read the 'Modular Simulator Engineering Guide' and the 'Modular Simulator Management Guide' prior to tailoring this volume. DTIC

N94-32394# Boeing Defense and Space Group, Huntsville, AL. Simulation and Training Systems.

MODULAR SIMULATOR SYSTEM (MSS). ENGINEERING DESIGN GUIDE Final Report

K. Kelly, J. Brown, G. Kamsickas, and W. Tucker 20 Aug. 1993 86 p
(Contract F33657-86-C-0149)
(AD-A276967; S495-10440-1; ASC-TR-94-5007) Avail: CASI HC A05/MF A01

This document is intended as an engineering guide for designing a modular simulator. This guide addresses the definition, history, and

characteristics of a modular simulator. Systems and software engineering activities are defined, and modular simulator segment specific and networking design considerations are discussed. This document discusses the modular simulator program design goals and rationale, design rules and guidelines, and lessons learned that have evolved through the program's demonstration phase. The effective use of this guide, in conjunction with the modular simulator architecture documents referenced herein, can substantially reduce the cost, schedule, and risk involved in developing a modular simulator.
DTIC

N94-32395# Boeing Defense and Space Group, Huntsville, AL. Simulation and Training Systems.
MODULAR SIMULATOR SYSTEM (MSS). SYSTEM/SEGMENT SPECIFICATION FOR THE GENERIC MODULAR SIMULATOR SYSTEM-FLIGHT CONTROLS MODULE, VOLUME 3 Final Report
K. Kelly, J. Brown, G. Kamsickas, and W. Tucker 20 Aug. 1993 41 p
(Contract F33657-86-C-0149)
(AD-A276970; S495-10400D-Vol-3; ASC-TR-94-5013) Avail: CASI HC A03/MF A01

This is the flight controls portion of the generic Modular Simulator System (MSS) specification. It is designed to be tailored to specify the requirements for a specification aircraft training device or family of aircraft training devices. This specification contains specific tailoring instructions for each paragraph. When the tailoring process is complete, the italicized tailoring instructions should have been replaced by application specific text or deleted from the specification. It is suggested that the user read the 'Modular Simulator Engineering Guide' and the 'Modular Simulator Management Guide' prior to tailoring this volume. DTIC

N94-32396# Boeing Defense and Space Group, Huntsville, AL. Simulation and Training Systems.
MODULAR SIMULATOR SYSTEM (MSS). SYSTEM/SEGMENT SPECIFICATION FOR THE GENERIC MODULAR SIMULATOR SYSTEM-FLIGHT DYNAMICS MODULE, VOLUME 4 Final Report
K. Kelly, J. Brown, G. Kamsickas, and W. Tucker 20 Aug. 1993 36 p
(Contract F33657-86-C-0149)
(AD-A276971; S495-10400D-Vol-4; ASC-TR-94-5014) Avail: CASI HC A03/MF A01

This is the flight dynamics portion of the generic Modular Simulator System (MSS) specification. It is designed to be tailored to specify the requirements for a specific aircraft training device or family of aircraft training devices. This specification contains specific tailoring instructions for each paragraph. When the tailoring process complete, the italicized tailoring instructions should have been replaced by application specific text or deleted from the specification. It is suggested that the user read the 'Modular simulator Engineering Guide' and the 'Modular Simulator Management Guide' prior to tailoring this volume. DTIC

N94-32397# Boeing Defense and Space Group, Huntsville, AL. Simulation and Training Systems.
MODULAR SIMULATOR SYSTEM (MSS). SYSTEM/SEGMENT SPECIFICATION FOR THE GENERIC MODULAR SIMULATOR SYSTEM-PROPULSION MODULE PROPULSION MODULE, VOLUME 5 Final Report
K. Kelly, J. Brown, G. Kamsickas, and W. Tucker 20 Aug. 1993 41 p
(Contract F33657-86-C-0149)
(AD-A276972; S495-10400D-Vol-5; ASC-TR-94-5015) Avail: CASI HC A03/MF A01

This is the propulsion portion of the generic Modular Simulator System (MSS) specification. It is designed to be tailored to specify the requirements for a specific aircraft training device or family of aircraft training devices. This specification contains specific tailoring instructions for each paragraph. When the tailoring process is complete, the italicized tailoring instructions should have been replaced by application specific text or deleted from the specification. It is suggested that the user read the 'Modular Simulator Engineering Guide' and the 'Modular Simulator Management Guide' prior to tailoring this volume. DTIC

N94-32398# Boeing Defense and Space Group, Huntsville, AL. Simulation and Training Systems.
MODULAR SIMULATOR SYSTEM (MSS). SYSTEM/SEGMENT SPECIFICATION FOR THE GENERIC MODULAR SIMULATOR SYSTEM-NAVIGATION/COMMUNICATION MODULE, VOLUME 6 Final Report
K. Kelly, J. Brown, G. Kamsickas, and W. Tucker 20 Aug. 1993 34 p
(Contract F33657-86-C-0149)
(AD-A276973; S495-10400D-Vol-6; ASC-TR-94-5016) Avail: CASI HC A03/MF A01

This is the navigation/communication portion of the generic Modular Simulator System (MSS) specification. It is designed to be tailored to specify the requirements for a specific aircraft training device or family of aircraft training devices. This specification contains specific tailoring instructions for each paragraph. When the tailoring process is complete, the italicized tailoring instructions should have been replaced by application specific text or deleted from the specification. It is suggested that the user read the 'Modular Simulator Engineering Guide' and the 'Modular Simulator Management Guide' prior to tailoring this volume. DTIC

N94-32399# Boeing Defense and Space Group, Huntsville, AL. Simulation and Training Systems.
MODULAR SIMULATOR SYSTEM (MSS). SYSTEM/SEGMENT SPECIFICATION FOR THE GENERIC MODULAR SIMULATOR SYSTEM-WEAPONS MODULE, VOLUME 7 Final Report
K. Kelly, J. Brown, G. Kamsickas, and W. Tucker 20 Aug. 1993 38 p
(Contract F33657-86-C-0149)
(AD-A276974; S495-10400D-Vol-7; ASC-TR-94-5017) Avail: CASI HC A03/MF A01

This is the weapons portion of the generic Modular Simulator System (MSS) specification. It is designed to be tailored to specify the requirements for a specific aircraft training device or family of aircraft training devices. This specification contains specific tailoring instructions for each paragraph. When the tailoring process is complete, the italicized tailoring instructions should have been replaced by application specific text or deleted from the specification. It is suggested that the user read the 'Modular Simulator Engineering Guide' and the 'Modular Simulator Management Guide' prior to tailoring this volume. DTIC

N94-32403 Boeing Defense and Space Group, Huntsville, AL. Simulation and Training Systems.
MODULAR SIMULATOR SYSTEM (MSS): INTERFACE DESIGN DOCUMENT FOR THE GENERIC MSS Final Report
K. Kelly, J. Brown, G. Kamsickas, and W. Tucker 20 Aug. 1993 474 p
Limited Reproducibility: More than 20% of this document may be affected by microfiche quality
(Contract F33657-86-C-0149)
(AD-A277270; S495-10735-1; ASC-TR-94-5009) Avail: CASI HC A20

This document describes the detailed design for the interfaces associated with the Modular Simulator System. Tailoring will be necessary to meet specific training system requirements. Specific tailoring instructions are included for each paragraph. It is suggested that the user read the 'Modular Simulator Engineering Design Guide' and the 'Modular Simulator Management Guide' prior to tailoring this document. DTIC

N94-33139 Naval Postgraduate School, Monterey, CA.
AN EVALUATION FRAMEWORK FOR DESIGNING A NIGHT VISION, COMPUTER-BASED TRAINER M.S. Thesis
Eric W. Caudle Dec. 1993 63 p Limited Reproducibility: More than 20% of this document may be affected by microfiche quality
(AD-A278005) Avail: CASI HC A04

The mission requirement of low-level, nightime navigation employing night vision goggles has expanded. This has led to a greater demand for training NVG skills and initiated a requirement for a low-cost, desktop, computer-based trainer (CBT). A framework is presented in this thesis that includes a review of the technology available for designing a night vision CBT. System attributes and constraints are identified and analyzed; and evaluation criteria developed to allow for examination of alternative system configurations. Two configurations are developed one PC-based and one workstation-based. These configurations present different cost/benefit components. A sample in graphics capabilities, processor performance and

peripheral support is provided for the two configurations. In addition, cost range estimates are included and possible baseline capabilities established to assist in the determination process. DTIC

N94-33167 Calspan-Buffalo Univ. Research Center, NY.
CALIBRATION AND VALIDATION STUDIES IN THE LENS FACILITY Final Report, 10 Aug. 1991 - 9 Feb. 1994
Michael Holden 9 Feb. 1994 60 p Limited Reproducibility: More than 20% of this document may be affected by microfiche quality
(Contract F49620-91-C-0085)
(AD-A278403; AFOSR-94-0161TR) Avail: Issuing Activity (Defense Technical Information Center (DTIC))

This report describes recent developments in the LENS facility, flow field calibration studies, and aerothermal and aero-optical measurements to evaluate the turbulent flow field characteristics of seeker head configurations in hypervelocity airflow. The development of the LENS facility to run at pressure levels up to 30,000 psi and temperatures up to 14,000 degrees R are reviewed. Issues associated with diaphragm performance, reservoir configuration, throat melting and burning, and modifications to the facility for large recoil loads at high pressure operation are briefly reviewed. Flow field measurements made during calibration studies are compared with computer predictions. Validation studies with simple seeker head aperture configurations in high enthalpy flows are then discussed. The models and aerothermal and aero-optical instrumentation used in these studies are described. The measurements obtained in flows up to 12,000 ft/sec are compared with similar measurements at lower velocities, simple correlation techniques, and detailed computer simulations. DTIC

N94-32473*# National Aeronautics and Space Administration. Langley Research Center, Hampton, VA.
HIGH PERFORMANCE REAL-TIME FLIGHT SIMULATION AT NASA LANGLEY
Jeff I. Cleveland, II *In* NASA, Washington, Technology 2003: The Fourth National Technology Transfer Conference and Exposition, Volume 2 Feb. 1994 p 456-462 (For primary document see N94-32420 09-99)
Avail: CASI HC A02/MF A04

N94-32474*# ECC International Corp., Orlando, FL.
THE EFFECTS OF ABOVE REAL-TIME TRAINING (ARTT) IN AN F-16 SIMULATOR
Dutch Guckenberger, Kay Stanney, and Norman E. Lane *In* NASA, Washington, Technology 2003: The Fourth National Technology Transfer Conference and Exposition, Volume 2 Feb. 1994 p 463-470 (For primary document see N94-32420 09-99)
Avail: CASI HC A02/MF A04

12 ASTRONAUTICS (GENERAL)

For extraterrestrial exploration see *91 Lunar and Planetary Exploration.*

N94-31012*# National Aeronautics and Space Administration. Marshall Space Flight Center, Huntsville, AL.
LDEF MATERIALS RESULTS FOR SPACECRAFT APPLICATIONS
Ann F. Whitaker, comp. and John Gregory, comp. Dec. 1993 533 p Conference held in Huntsville, AL, 27-28 Oct. 1992; sponsored by NASA, Univ. of Alabama, Huntsville, Alabama Space Grant Consortium, and SAMPE
(NASA-CP-3257; M-742; NAS 1.55:3257) Avail: CASI HC A23/MF A04

These proceedings describe the application of LDEF data to spacecraft and payload design, and emphasize where space environmental effects on materials research and development is needed as defined by LDEF data. The LDEF six years of exposure of materials has proven to be by far the most comprehensive source of information ever obtained on the long-term performance of materials in the space environment. The conference provided a forum for materials scientists and engineers to review and critically assess the LDEF results from the standpoint of their relevance, significance, and impact on spacecraft design practice. The impact of the LDEF findings on materials selection and qualification, and the needs and plans for further study, were addressed from several perspectives. Many timely and needed changes and modifications in external spacecraft materials selection have occurred as a result of LDEF investigations. For individual titles, see N94-31013 through N94-31051.

N94-31013*# National Aeronautics and Space Administration. Marshall Space Flight Center, Huntsville, AL.
THE PERFORMANCE OF THERMAL CONTROL COATINGS ON LDEF AND IMPLICATIONS TO FUTURE SPACECRAFT **c27**
Donald R. Wilkes (AZ Technology, Huntsville, AL.), Edgar R. Miller (AZ Technology, Huntsville, AL.), Richard J. Mell (AZ Technology, Huntsville, AL.), Paul S. LeMaster (AZ Technology, Huntsville, AL.), and James M. Zwiener *In its* LDEF Materials Results for Spacecraft Applications Dec. 1993 p 3-20 (For primary document see N94-31012 09-12)
Avail: CASI HC A03/MF A04

The stability of thermal control coatings over the lifetime of a satellite or space platform is crucial to the success of the mission. With the increasing size, complexity, and duration of future missions, the stability of these materials becomes even more important. The Long Duration Exposure Facility (LDEF) offered an excellent testbed to study the stability and interaction of thermal control coatings in the low-Earth orbit (LEO) space environment. Several experiments on LDEF exposed thermal control coatings to the space environment. This paper provides an overview of the different materials flown and their stability during the extended LDEF mission. The exposure conditions, exposure environment, and measurements of materials properties (both in-space and postflight) are described. The relevance of the results and the implications to the design and operation of future space vehicles are also discussed. Author (revised)

N94-31014*# Boeing Defense and Space Group, Seattle, WA.
PERFORMANCE OF SILVERED TEFLON (TRADEMARK) THERMAL CONTROL BLANKETS ON SPACECRAFT **c27**
Gary Pippin, Wayne Stuckey, and Carol Hemminger *In* NASA. Marshall Space Flight Center, LDEF Materials Results for Spacecraft Applications Dec. 1993 p 21-30 (For primary document see N94-31012 09-12)
Avail: CASI HC A02/MF A04

Silverized Teflon (Ag/FEP) is a widely used passive thermal control material for space applications. The material has a very low alpha/e ratio (less than 0.1) for low operating temperatures and is fabricated with various FEP thicknesses (as the Teflon thickness increases, the emittance increases). It is low outgassing and, because of its flexibility, can be applied around complex, curved shapes. Ag/FEP has achieved multiyear lifetimes under a variety of exposure conditions. This has been demonstrated by the Long Duration Exposure Facility (LDEF), Solar Max, Spacecraft Charging at High Altitudes (SCATHA), and other flight experiments. Ag/FEP material has been held in place on spacecraft by a variety of methods: mechanical clamping, direct adhesive bonding of tapes and sheets, and by Velcro(TM) tape adhesively bonded to back surfaces. On LDEF, for example, 5-mil blankets held by Velcro(TM) and clamping were used for thermal control over 3- by 4-ft areas on each of 17 trays. Adhesively bonded 2- and 5-mil sheets were used on other LDEF experiments, both for thermal control and as tape to hold other thermal control blankets in place. Performance data over extended time periods are available from a number of flights. The observed effects on optical properties, mechanical properties, and surface chemistry will be summarized in this paper. This leads to a discussion of performance life estimates and other design lessons for Ag/FEP thermal control material. Author (revised)

N94-31015*# National Aeronautics and Space Administration. Marshall Space Flight Center, Huntsville, AL.
SPACE ENVIRONMENT DURABILITY OF BETA CLOTH IN LDEF THERMAL BLANKETS **c27**
Roger C. Linton, Ann F. Whitaker, and Miria M. Finckenor *In its* LDEF Materials Results for Spacecraft Applications Dec. 1993 p 31-45 (For primary document see N94-31012 09-12)
Avail: CASI HC A03/MF A04

Beta cloth performance for use on long-term space vehicles such as Space Station Freedom (S.S. Freedom) requires resistance to the degrading effects of the space environment. The major issues are retention of thermal insulating properties through maintaining optical properties, preserving mechanical integrity, and generating minimal particulates for contamination-sensitive spacecraft surfaces and payloads. The longest in-flight test of beta cloth's durability was on the Long Duration Exposure

Facility (LDEF), where it was exposed to the space environment for 68 months. The LDEF contained 57 experiments which further defined the space environment and its effects on spacecraft materials. It was deployed into low-Earth orbit (LEO) in Apr. 1984 and retrieved Jan. 1990 by the space shuttle. Among the 10,000 plus material constituents and samples onboard were thermal control blankets of multilayer insulation with a beta cloth outer cover and Velcro attachments. These blankets were exposed to hard vacuum, thermal cycling, charged particles, meteoroid/debris impacts, ultraviolet (UV) radiation, and atomic oxygen (AO). Of these space environmental exposure elements, AO appears to have had the greatest effect on the beta cloth. The beta cloth analyzed in this report came from the MSFC Experiment S1005 (Transverse Flat-Plate Heat Pipe) tray oriented approximately 22 deg from the leading edge vector of the LDEF satellite. The location of the tray on LDEF and the placement of the beta cloth thermal blankets are shown. The specific space environment exposure conditions for this material are listed. Author (revised)

N94-31016*# McDonnell-Douglas Aerospace, Huntington Beach, CA.
SPACE STATION WP-2 APPLICATION OF LDEF MLI RESULTS **c27**
Charles A. Smith, Mark M. Hasegawa, and Cherie A. Jones *In* NASA. Marshall Space Flight Center, LDEF Materials Results for Spacecraft Applications Dec. 1993 p 47-60 (For primary document see N94-31012 09-12)
Avail: CASI HC A03/MF A04

The Cascaded Variable Conductance Heat Pipe Experiment, which was developed by Michael Grote of McDonnell Douglas Electronic Systems Company, was located in Tray F-9 of the Long Duration Exposure Facility (LDEF), where it received atomic oxygen almost normal to its surface. The majority of the tray was covered by aluminized Kapton polyimide multilayer insulation (MLI), which showed substantial changes from atomic oxygen erosion. Most of the outermost Kapton layer of the MLI and the polyester scrim cloth under it were lost, and there was evidence of contaminant deposition which discolored the edges of the MLI blanket. Micrometeoroid and orbital debris (MM/OD) hits caused small rips in the MLI layers, and in some cases left cloudy areas where the vapor plume caused by a hit condensed on the next layer. The MLI was bent gradually through 90 deg at the edges to enclose the experiment, and the Kapton that survived along the curved portion showed the effects of atomic oxygen erosion at oblique angles. In spite of space environment effects over the period of the LDEF mission, the MLI blanket remained functional. The results of the analysis of LDEF MLI were used in developing the standard MLI blanket for Space Station Work Package-2 (WP-2). This blanket is expected to last 30 years when exposed to the low Earth orbit (LEO) environment constituents of atomic oxygen and MM/OD, which are the most damaging to MLI materials. The WP-2 standard blanket consists of an outer cover made from Beta-cloth glass fiber fabric which is aluminized on the interior surface, and an inner cover of 0.076-mm (0.003-in) double-side-aluminized perforated Kapton. The inner reflector layers are 0.0076-mm (0.0003-in) double-side aluminized, perforated Kapton separated by layers of Dacron polyester fabric. The outer cover was selected to be resistant to the LEO environment and durable enough to survive in orbit for 30 years. This paper describes the analyses of the LDEF MLI results, and how these results contributed to the selection of the WP-2 MLI blanket materials and configuration.
Author (revised)

N94-31017*# Boeing Defense and Space Group, Seattle, WA.
ANODIZED ALUMINUM ON LDEF **c26**
Johnny L. Golden *In* NASA. Marshall Space Flight Center, LDEF Materials Results for Spacecraft Applications Dec. 1993 p 61-71 (For primary document see N94-31012 09-12)
(Contracts NAS1-19247; NAS1-18224)
Avail: CASI HC A03/MF A04

A compilation of reported analyses and results obtained for anodized aluminum flown on the Long Duration Exposure Facility (LDEF) was prepared. Chromic acid, sulfuric acid, and dyed sulfuric acid anodized surfaces were exposed to the space environment. The vast majority of the anodized surface on LDEF was chromic acid anodize because of its selection as a thermal control coating for use on the spacecraft primary structure, trays, tray clamps, and space end thermal covers. Reports indicate that the chromic acid anodize was stable in solar absorptance and thermal emittance, but that contamination effects caused increases in absorptance on surfaces exposed to low atomic oxygen fluences. There were some discrepancies, however, in that some chromic acid anodized specimens exhibited significant increases in absorptance. Sulfuric acid anodized surfaces also appeared stable, although very little surface area was available for evaluation. One type of dyed sulfuric acid anodize was assessed as an optical baffle coating and was observed to have improved infrared absorptance characteristics with exposure on LDEF. Author (revised)

N94-31018*# European Space Agency. European Space Research and Technology Center, ESTEC, Noordwijk (Netherlands).
FOLLOW-UP ON THE EFFECTS OF THE SPACE ENVIRONMENT ON UHCRE THERMAL BLANKETS **c27**
Francois Levadou and Marc vanEesbeek *In* NASA. Marshall Space Flight Center, LDEF Materials Results for Spacecraft Applications Dec. 1993 p 73-84 (For primary document see N94-31012 09-12)
Avail: CASI HC A03/MF A04

An overview of the effects of the space environment on the thermal blanket of the UHCRE experiment is presented with an emphasis on atomic oxygen (AO) erosion. A more accurate value for FEP Teflon reaction efficiency is given and corresponds, at normal incidence, to 3.24 10(exp -25) cu cm/atomic, therefore, the FEP Teflon erosion corresponding to the Long Duration Exposure Facility (LDEF) total mission is 29.5 microns. A power 1.44 of the cosine of the incident angle of the oxygen atoms is found. It is shown that this value is not far from the power found using Fergusson's relationship between efficiency and energy of the O-atoms. An hypothesis concerning the effect of oxygen ions (O(+)) is also presented. The presence of oxygen ions may explain the different results obtained from different flights and from laboratory tests. Finally an XPS analysis of Chemglaze Z306(tm) black paint demonstrates the presence of silicone in the paint which may explain part of the contamination found on LDEF.
Author (revised)

N94-31019*# National Aeronautics and Space Administration. Marshall Space Flight Center, Huntsville, AL.
MODELING OF LDEF CONTAMINATION ENVIRONMENT **c18**
M. Ralph Carruth, Jr., Ray Rantanen, and Tim Gordon *In its* LDEF Materials Results for Spacecraft Applications Dec. 1993 p 87-95 (For primary document see N94-31012 09-12)
Avail: CASI HC A02/MF A04

The Long Duration Exposure Facility (LDEF) satellite was unique in many ways. It was a large structure that was in space for an extended period of time and was stable in orientation relative to the velocity vector. There are obvious and well documented effects of contamination and space environment effects on the LDEF satellite. In order to examine the interaction of LDEF with its environment and the resulting effect on the satellite, the Integrated Spacecraft Environments Model (ISEM) was used to model the LDEF-induced neutral environment at several different times and altitudes during the mission. Author

N94-31020*# Boeing Defense and Space Group, Seattle, WA.
SPACECRAFT CONTAMINATION ISSUES FROM LDEF: ISSUES FOR DESIGN **c18**
Gary Pippin and Russ Crutcher *In* NASA. Marshall Space Flight Center, LDEF Materials Results for Spacecraft Applications Dec. 1993 p 97-103 (For primary document see N94-31012 09-12)
(Contracts NAS1-19247; NAS1-18224)
Avail: CASI HC A02/MF A04

Many contamination sources have been identified on the Long Duraticn Exposure Facility (LDEF). Effects of contamination from these sources are being quantified and have been reported on in several papers. For a designer, the essential question is how much contamination from all sources can be tolerated without causing a given spacecraft system to degrade below a critical performance level, or fail altogether. Even a rudimentary knowledge of the mechanisms by which molecular and particulate contamination can occur will allow simple design options to be chosen to circumvent potential contamination problems and reduce contamination levels. Because of the varied nature and condition of hardware used on LDEF experiments, examples of many types of contamination were seen and these provide a useful guide to expected performance of many types of materials in space environments. Author

N94-31021*# Boeing Defense and Space Group, Seattle, WA.
MODEL OF SPACECRAFT ATOMIC OXYGEN AND SOLAR EXPOSURE MICROENVIRONMENTS **c90**
R. J. Bourassa and H. G. Pippin *In* NASA. Marshall Space Flight Center, LDEF Materials Results for Spacecraft Applications Dec. 1993 p 105-114 (For primary document see N94-31012 09-12)
(Contract NAS1-19247)
Avail: CASI HC A02/MF A04

Computer models of environmental conditions in Earth orbit are needed for the following reasons: (1) derivation of material performance parameters from orbital test data, (2) evaluation of spacecraft hardware designs, (3) prediction of material service life, and (4) scheduling spacecraft maintenance. To meet these needs, Boeing has developed programs for modeling atomic oxygen (AO) and solar radiation exposures. The model allows determination of AO and solar ultraviolet (UV) radiation exposures for spacecraft surfaces (1) in arbitrary orientations with respect to the direction of spacecraft motion, (2) overall ranges of solar conditions, and (3) for any mission duration. The models have been successfully applied to prediction of experiment environments on the Long Duration Exposure Facility (LDEF) and for analysis of selected hardware designs for deployment on other spacecraft. The work on these models has been reported at previous LDEF conferences. Since publication of these reports, a revision has been made to the AO calculation for LDEF, and further work has been done on the microenvironments model for solar exposure. Author

N94-31022*# National Aeronautics and Space Administration. Marshall Space Flight Center, Huntsville, AL.
ATOMIC OXYGEN EROSION CONSIDERATIONS FOR SPACECRAFT MATERIALS SELECTION **c27**
Ann F. Whitaker and Rachel R. Kamenetzky *In its* LDEF Materials Results for Spacecraft Applications Dec. 1993 p 117-123 (For primary document see N94-31012 09-12)
Avail: CASI HC A02/MF A04

The Long Duration Exposure Facility (LDEF) satellite carried 57 experiments that were designed to define the low-Earth orbit (LEO) space environment and to evaluate the impact of this environment on potential engineering materials and material processes. Deployed by the Shuttle Challenger in April of 1984, LDEF made over 32,000 orbits before being retrieved nearly 6 years later by the Shuttle Columbia in January of 1990. The Solar Array Passive LDEF Experiment (SAMPLE) AO171 contained approximately 300 specimens, representing numerous material classes and material processes. AO171 was located on LDEF in position A8 at a yaw of 38.1 degrees from the ram direction and was subjected to an atomic oxygen (AO) fluence of 6.93 x 10(exp 21) atoms/sq cm. LDEF AO171 data, as well as short-term shuttle data, will be discussed in this paper as it applies to engineering design applications of composites, bulk and thin film polymers, glassy ceramics, thermal control paints, and metals subjected to AO erosion. Author

N94-31023*# National Aeronautics and Space Administration. Langley Research Center, Hampton, VA.
PERFORMANCE OF SELECTED POLYMERIC MATERIALS ON LDEF **c27**
Philip R. Young, Wayne s. Slemp, and Bland A. Stein *In* NASA. Marshall Space Flight Center, LDEF Materials Results for Spacecraft Applications Dec. 1993 p 125-142 (For primary document see N94-31012 09-12)
Avail: CASI HC A03/MF A04

The NASA Long Duration Exposure Facility (LDEF) provided a unique environmental exposure of a wide variety of materials for potential advanced spacecraft application. This paper examines the molecular level response of selected polymeric materials which flew onboard this vehicle. Polymers include epolyimide, polysulfone, and polystyrene film and polyimide, polysulfone, and epoxy matrix resin/graphite fiber reinforced composites. Several promising experimental films were also studied. Most specimens received 5.8 years of low Earth orbital (LEO) exposure on LDEF. Several samples received on 10 months of exposure. Chemical characterization techniques included ultraviolet-visible and infrared spectroscopy, thermal analysis, x-ray photoelectron spectroscopy, and selected solution property measurements. Results suggest that many molecular level effects present during the first 10 months of exposure were not present after 5.8 years of exposure for specimens on or near Row 9. Increased AO fluence near the end of the mission likely eroded away much environmentally induced surface phenomena. The objective of this work is to provide fundamental information for use in improving the performance of polymeric materials for LEO application. A secondary objective is to gain an appreciation for the constraints and limitations of results from LDEF polymeric materials experiments. Author

N94-31024*# National Aeronautics and Space Administration. Lewis Research Center, Cleveland, OH.
ATOMIC OXYGEN INTERACTION AT DEFECT SIGHTS IN PROTECTIVE COATINGS ON POLYMERS FLOWN ON LDEF **c27**
Bruce A. Banks, Kim K. deGroh, Bruce M. Auer, Linda Gebauer, and Cynthia LaMoreaux *In* NASA. Marshall Space Flight Center, LDEF Materials Results for Spacecraft Applications Dec. 1993 p 143-158 (For primary document see N94-31012 09-12)
Avail: CASI HC A03/MF A04

Although the Long Duration Exposure Facility (LDEF) has exposed materials with a fixed orientation relative to the ambient low-Earth-orbital environment, arrival of atomic oxygen is angularly distributed as a result of the atomic oxygen's high temperature Maxwellian velocity distribution and the LDEF's orbital inclination. Thus, atomic oxygen entering defects in protective coatings on polymeric surfaces can cause wider undercut cavities than the size of the defect in the protective coating. Because only a small fraction of atomic oxygen reacts upon first impact with most polymeric materials, secondary reactions with lower energy thermally accommodated atomic oxygen can occur. The secondary reactions of scattered and/or thermally accommodated atomic oxygen also contribute to widening the undercut cavity beneath the protective coating defect. As the undercut cavity enlarges, exposing more polymer, the probability of atomic oxygen reacting with underlying polymeric material increases because of multiple opportunities for reaction. Thus, the effective atomic oxygen erosion yield for atoms entering defects increases above that of the unprotected material. Based on the results of analytical modeling and computational modeling, aluminized Kapton multilayer insulation exposed to atomic oxygen on row 9 lost the entire externally exposed layer of polyimide Kapton, yet based on the results of this investigation, the bottom surface aluminum film must have remained in place, but crazed. Atomic oxygen undercutting at defect sites in protective coatings on graphite epoxy composites indicates that between 40 to 100 percent of the atomic oxygen thermally accommodates upon impact, and that the reaction probability of thermally accommodated atomic oxygen may range from 7.7 x 10(exp -6) to 2.1 x 10(exp -3), depending upon the degree of thermal accommodation upon each impact. Author

N94-31025*# National Aeronautics and Space Administration. Marshall Space Flight Center, Huntsville, AL.
FLUORESCENCE OBSERVATIONS OF LDEF EXPOSED MATERIALS AS AN INDICATOR OF INDUCED MATERIAL REACTIONS **c25**
Roger C. Linton, Ann F. Whitaker, and Rachel R. Kamenetzky *In its* LDEF Materials Results for Spacecraft Applications Dec. 1993 p 159-178 (For primary document see N94-31012 09-12)
Avail: CASI HC A03/MF A04

Observations and measurements of induced changes in the fluorescent emission of materials exposed to the space environment on the Long Duration Exposure Facility (LDEF) have revealed systematic patterns of material-dependent behavior. These results have been supplemented by inspection of similar materials exposed on previous Space Shuttle Missions and in laboratory testing. The space environmental factors affecting the fluorescence of exposed materials have been found to include (but are not necessarily limited to) solar ultraviolet (UV) radiation, atomic oxygen (AO), thermal vacuum exposure, and synergistic combinations of these factors. Observed changes in material fluorescent behavior include stimulation, quenching, and spectral band shifts of emission. For example, the intrinsic yellow fluorescence of zinc oxide pigmented thermal control coatings undergoes quenching as a result of exposure, while coloration is stimulated in the fluorescent emission of several polyurethane coating materials. The changes in fluorescent behavior of these materials are shown to be a revealing indicator of induced material reactions as a result of space environmental exposure. Author

N94-31026*# Southwest Research Inst., San Antonio, TX.
LASER-INDUCED FLUORESCENCE OF SPACE-EXPOSED POLYURETHANE **c27**

Ralph H. Hill, Jr. *In* NASA. Marshall Space Flight Center, LDEF Materials Results for Spacecraft Applications Dec. 1993 p 179-192 (For primary document see N94-31012 09-12)
Avail: CASI HC A03/MF A04

The object of this work was to utilize laser-induced fluorescence technique to characterize several samples of space-exposed polyurethane. These samples were flown on the Long Duration Exposure Facility (LDEF), which was in a shuttle-like orbit for nearly 6 years. Because of our present work to develop laser-induced-fluorescence inspection techniques for polymers, space-exposed samples and controls were lent to us for evaluation. These samples had been attached to the outer surface of LDEF; therefore, they were subjected to thermal cycling, solar ultraviolet radiation, vacuum, and atomic oxygen. It is well documented that atomic oxygen and ultraviolet exposure have detrimental effects on many polymers. This was a unique opportunity to make measurements on material that had been naturally degraded by an unusual environment. During our past work, data have come from artificially degraded samples and generally have demonstrated a correlation between laser-induced fluorescence and tensile strength or elasticity. Author

N94-31027*# Alabama Univ., Huntsville. Dept. of Chemistry.
ON THE LINEARITY OF FAST ATOMIC OXYGEN EFFECTS **c18**
J. C. Gregory *In* NASA. Marshall Space Flight Center, LDEF Materials Results for Spacecraft Applications Dec. 1993 p 193-198 (For primary document see N94-31012 09-12)
Avail: CASI HC A02/MF A04

The effect of bombardment of 8 km per second atomic oxygen (AO) experienced by exposed surfaces of satellites in low Earth orbit must be considered in the selection of materials to be used in instruments and functional systems on these satellites. The degree of importance of the effects varies widely depending on the material, the application, and the exposure (fluence of atoms) to which it is to be subjected. Some highly erodible thin polymer film materials might be considered unacceptable on a long-lived space station, but may be perfectly serviceable on a normal shuttle flight. In order to determine the acceptability of a material for a particular environment, a designer must know the relationship between the magnitude of the effect (for example, mass-loss) and the magnitude of the fluence. To determine this relationship, we need data over a useful range of fluence. Until the return of the Long Duration Exposure Facility (LDEF), the bulk of the data on materials effects was obtained from a few shuttle flights, and the bulk of that data from the flight of experiment Evaluation of Oxygen Interaction with Materials (EOIM-2) on STS-8 in 1983. EOIM-2 obtained a fluence of 3.5 x 10(exp 20) atoms cm(exp -2), while the LDEF fluence approached 10(exp 22) atoms cm(exp -2), or about 30 times greater. Although other flight exposures had been obtained with lower fluences, considerable uncertainty was attached to these results because of the possibility of large relative systematic errors and of other factors such as sweeping angle of attack. In the future, it is hoped that simulation facilities in the laboratory will allow testing of materials without the necessity of flying them in space. In addition, if the relationship of effect with oxygen fluence is well determined, it should not be necessary to expose a material for an entire mission fluence. In this paper, we shall avoid a comparison of flight data with results from simulators, though that comparison is important for the materials community. The present discussion is limited to flight data only. Author

N94-31028*# National Aeronautics and Space Administration. Marshall Space Flight Center, Huntsville, AL.
IMPACT OF LDEF PHOTOVOLTAIC EXPERIMENT FINDINGS UPON SPACECRAFT SOLAR ARRAY DESIGN AND DEVELOPMENT REQUIREMENTS **c44**
Leighton E. Young *In its* LDEF Materials Results for Spacecraft Applications Dec. 1993 p 201-215 (For primary document see N94-31012 09-12)
Avail: CASI HC A03/MF A04

Photovoltaic cells (solar cells) and other solar array materials were flown in a variety of locations on the Long Duration Exposure Facility (LDEF). With respect to the predicted leading edge, solar array experiments were located at 0 degrees (row 9), 30 degrees (row 8) and 180 degrees (row 3). Postflight estimates of location of the experiments with respect to the velocity vector add 8.1 degrees to these values. Experiments were also located on the Earth end of the LDEF longitudinal axis. Types and magnitudes of detrimental effects differ between the locations with some commonality. Postflight evaluation of the solar array experiments reveal that some components/materials are very resistant to the environment to which they were exposed while others need protection, modification, or replacement. Interaction of materials with atomic oxygen (AO), as an area of major importance, was dramatically demonstrated by LDEF results. Information gained from the LDEF flight allows array developers to set new requirements for on-going and future technology and flight component development. Author

N94-31029*# Georgia Tech Research Inst., Atlanta.
DEGRADATION OF OPTICAL COMPONENTS IN SPACE **c74**
M. D. Blue *In* NASA. Marshall Space Flight Center, LDEF Materials Results for Spacecraft Applications Dec. 1993 p 217-226 (For primary document see N94-31012 09-12)
Avail: CASI HC A02/MF A04

This report concerns two types of optical components: multilayer filters and mirrors, and self-scanned imaging arrays using charge coupled device (CCD) readouts. For the filters and mirrors, contamination produces a strong reduction in transmittance in the ultraviolet spectral region, but has little or no effect in the visible and infrared spectral regions. Soft substrates containing halides are unsatisfactory as windows or substrates. Materials choice for dielectric layers should also reflect such considerations. Best performance is also found for the harder materials. Compaction of the layers and interlayer diffusion causes a blue shift in center wavelength and loss of throughput. For sensors using CCD's, shifts in gate voltage and reductions in transfer efficiency occur. Such effects in CCD's are in accord with expectations of the effects of the radiation dose on the device. Except for optical fiber, degradation of CCD's represents the only ionizing-radiation induced effect on the Long Duration Exposure Facility (LDEF) optical systems components that has been observed. Author

N94-31030*# Vanderbilt Univ., Nashville, TN.
PHYSICAL PROPERTIES OF GLASSES EXPOSED TO EARTH-FACING AND TRAILING-SIDE ENVIRONMENTS ON LDEF **c27**
David E. Wiedlocher, Donald L. Kinser, Robert A. Weller, Robert A. Weeks, and Marcus H. Mendenhall *In* NASA. Marshall Space Flight Center, LDEF Materials Results for Spacecraft Applications Dec. 1993 p 227-243 (For primary document see N94-31012 09-12)
(Contracts NAG8-156; NAS8-32695; L-17761D)
Avail: CASI HC A03/MF A04

The exposure of 108 glass samples and 12 glass-ceramic samples to Earth-orbit environments permitted measurements which establish the effects of each environment. Examination of five glass types and one glass ceramic located on both the Earth-facing side and the trailing edge revealed no reduction in strength within experimental limits. Strength measurements subjected less than 5 percent of the sample surface area to stresses above 90 percent of the glass's failure strength. Seven micrometeorite or space debris impacts occurred on trailing edge samples. One of those impacts occurred in a location which was subjected to 50 percent of the applied stress at failure. Micrometeorite or space debris impacts were not observed on Earth-facing samples. The physical shape and structure of the impact sites were carefully examined using stereographic scanning electron microscopy. These impacts induce a stress concentration at the damaged region which influences mechanical strength. The flaw size produced by such damage was examined to determine the magnitude of strength degradation in micrometeorite or space-debris impacted glasses. Scanning electron microscopy revealed topographical details of impact sites which included central melt zones and glass fiber production. The overall crater structure is similar to much larger impacts of large meteorite on the Moon in that the melt crater is surrounded by shocked regions of material which fracture zones and spall areas. Residual stresses arising from shock compression and cooling of the fused zone cannot currently be included in fracture mechanics analyses based on simple flaw size examination. Author

N94-31031*# Auburn Univ., AL. Mechanical Engineering.
MORPHOLOGY CORRELATION OF CRATERS FORMED BY HYPERVELOCITY IMPACTS **c39**
Gary D. Crawford, M. Frank Rose, and Ralph H. Zee *In* NASA. Marshall Space Flight Center, LDEF Materials Results for Spacecraft Applications

Dec. 1993 p 245-257 (For primary document see N94-31012 09-12)
Avail: CASI HC A03/MF A04

Dust-sized olivine particles were fired at a copper plate using the Space Power Institute hypervelocity facility, simulating micrometeoroid damage from natural debris to spacecraft in low-Earth orbit (LEO). Techniques were developed for measuring crater volume, particle volume, and particle velocity, with the particle velocities ranging from 5.6 to 8.7 km/s. A roughly linear correlation was found between crater volume and particle energy which suggested that micrometeoroids follow standard hypervelocity relationships. The residual debris analysis showed that for olivine impacts of up to 8.7 km/s, particle residue is found in the crater. By using the Space Power Institute hypervelocity facility, micrometeoroid damage to satellites can be accurately modeled. Author

N94-31032*# National Aeronautics and Space Administration. Marshall Space Flight Center, Huntsville, AL.
MICROMETEOROID/SPACE DEBRIS EFFECTS ON MATERIALS c39
James M. Zwiener and Miria M. Finckenor *In its* LDEF Materials Results for Spacecraft Applications Dec. 1993 p 259-279 (For primary document see N94-31012 09-12)
Avail: CASI HC A03/MF A04

The Long Duration Exposure Facility (LDEF) micrometeoroid/space debris impact data has been reduced in terms that are convenient for evaluating the overall quantitative effect on material properties. Impact crater flux has been evaluated as a function of angle from velocity vector and as a function of crater size. This data is combined with spall data from flight and ground testing to calculate effective solar absorption and emittance values versus time. Results indicate that the surface damage from micrometeoroid/space debris does not significantly affect the overall surface optical thermal physical properties. Of course the local damage around impact craters radically alter optical properties. Damage to composites and solar cells on an overall basis was minimal. Author

N94-31033*# Toronto Univ., North York (Ontario). Inst. for Aerospace Studies.
THERMAL-VACUUM RESPONSE OF POLYMER MATRIX COMPOSITES IN SPACE c24
R. C. Tennyson and R. Matthews *In* NASA. Marshall Space Flight Center, LDEF Materials Results for Spacecraft Applications Dec. 1993 p 283-299 (For primary document see N94-31012 09-12)
Avail: CASI HC A03/MF A04

This report describes a thermal-vacuum outgassing model and test protocol for predicting outgassing times and dimensional changes for polymer matrix composites. Experimental results derived from 'control' samples are used to provide the basis for analytical predictions to compare with the outgassing response of Long Duration Exposure Facility (LDEF) flight samples. Coefficient of thermal expansion (CTE) data are also presented. In addition, an example is given illustrating the dimensional change of a 'zero' CTE laminate due to moisture outgassing. Author

N94-31034*# Aerospace Corp., El Segundo, CA.
THE IMPACT OF LDEF RESULTS ON THE SPACE APPLICATION OF METAL MATRIX COMPOSITES c24
Gary L. Steckel and Tuyen D. Le *In* NASA. Marshall Space Flight Center, LDEF Materials Results for Spacecraft Applications Dec. 1993 p 301-318 (For primary document see N94-31012 09-12)
(Contract F04701-88-C-0089)
Avail: CASI HC A03/MF A04

Over 200 graphite/aluminum and graphite/magnesium composites were flown on the leading and trailing edges of LDEF on the Advanced Composites Experiment. The performance of these composites was evaluated by performing scanning electron microscopy and x-ray photoelectron spectroscopy of exposed surfaces, optical microscopy of cross sections, and on-orbit and postflight thermal expansion measurements. Graphite/aluminum and graphite/magnesium were found to be superior to graphite/polymer matrix composites in that they are inherently resistant to atomic oxygen and are less susceptible to thermal cycling induced microcracking. The surface foils on graphite/aluminum and graphite/magnesium protect the graphite fibers from atomic oxygen and from impact damage from small micrometeoroid or space debris particles. However, the surface foils were found to be susceptible to thermal fatigue cracking arising from contamination embrittlement, surface oxidation, or stress risers. Thus, the experiment reinforced requirements for carefully protecting these composites from prelaunch oxidation or corrosion, avoiding spacecraft contamination, and designing composite structures to minimize stress concentrations. On-orbit strain measurements demonstrated the importance of through-thickness thermal conductivity in composites to minimize thermal distortions arising from thermal gradients. Because of the high thermal conductivity of aluminum, thermal distortions were greatly reduced in the LDEF thermal environment for graphite/aluminum as compared to graphite/magnesium and graphite/polymer composites. The thermal expansion behavior of graphite/aluminum and graphite/magnesium was stabilized by on-orbit thermal cycling in the same manner as observed in laboratory tests. Author

N94-31035*# Auburn Univ., AL. Materials Engineering Program.
SPACE ENVIRONMENTAL EFFECTS ON POLYMER COMPOSITES: RESEARCH NEEDS AND OPPORTUNITIES c24
Bor Z. Jang, J. Bianchi, Y. M. Liu, and C. P. Chang *In* NASA. Marshall Space Flight Center, LDEF Materials Results for Spacecraft Applications Dec. 1993 p 319-333 (For primary document see N94-31012 09-12)
Avail: CASI HC A03/MF A04

The long-term performance of polymer-based composites in the space environment is discussed. Both thermoset and thermoplastic matrix composites are included in this discussion. Previous efforts on the space environmental effects on composites are briefly reviewed. Focus of this review is placed on the effects of hygrothermal stresses, atomic oxygen, ultraviolet (UV), and space debris/micrometeoroid impacts along with the potential synergism. Potential approaches to estimating the residual strength of polymer composites after exposure to atomic oxygen erosion or space debris/micrometeoroid impact are evaluated. New ground-based data are then utilized to illustrate the effects of atomic oxygen and thermal cycling on the failure behavior of polymer composites. Finally, research needs, challenges, and opportunities in the field of space environmental effects on composite materials are highlighted. Author

N94-31036*# Boeing Defense and Space Group, Seattle, WA.
LOW-EARTH ORBIT EFFECTS ON ORGANIC COMPOSITE MATERIALS FLOWN ON LDEF c24
Pete E. George and Harry W. Dursch *In* NASA. Marshall Space Flight Center, LDEF Materials Results for Spacecraft Applications Dec. 1993 p 335-354 (For primary document see N94-31012 09-12)
(Contracts NAS1-18224; NAS1-19247)
Avail: CASI HC A03/MF A04

Over 35 different types of organic matrix composites were flown as part of 11 different experiments onboard the NASA Long Duration Exposure Facility (LDEF) satellite. This materials and systems experiment satellite flew in low-earth orbit (LEO) for 69 months. For that period, the experiments were subjected to the LEO environment including atomic oxygen (AO), ultraviolet (UV) radiation, thermal cycling, microvacuum, meteoroid and space debris (M&D), and particle radiation. Since retrieval of the satellite in January of 1990, the principal experiment investigators have been deintegrating, examining, and testing the materials specimens flown. The most detrimental environmental effect on all organic matrix composites was material loss due to AO erosion. AO erosion of uncoated organic matrix composites (OMC) facing the satellite ram direction was responsible for significant mechanical property degradations. Also, thermal cycling-induced microcracking was observed in some nonunidirectional reinforced OMC's. Thermal cycling and outgassing caused significant but predictable dimensional changes as measured in situ on one experiment. Some metal and metal oxide-based coatings were found to be very effective at preventing AO erosion of OMC's. However, M&D impacts and coating fractures which compromised these coatings allowed AO erosion of the underlying OMC substrates. The findings for organic matrix composites flown on the LDEF are summarized and the LEO environmental factors, their effects, and the influence on space hardware design factors for LEO applications are identified. Author (revised)

N94-31037*# National Aeronautics and Space Administration. Langley Research Center, Hampton, VA.
SUMMARY OF MATERIALS AND HARDWARE PERFORMANCE ON LDEF c27
Harry Dursch (Boeing Defense and Space Group, Seattle, WA.), Gary Pippin (Boeing Defense and Space Group, Seattle, WA.), and Lou Teichman *In*

NASA. Marshall Space Flight Center, LDEF Materials Results for Spacecraft Applications Dec. 1993 p 355-369 (For primary document see N94-31012 09-12)
(Contracts NAS1-18224; NAS1-19247)
Avail: CASI HC A03/MF A04

A wide variety of materials and experiment support hardware were flown on the Long Duration Exposure Facility (LDEF). Postflight testing has determined the effects of the almost 6 years of low-earth orbit (LEO) exposure on this hardware. An overview of the results are presented. Hardware discussed includes adhesives, fasteners, lubricants, data storage systems, solar cells, seals, and the LDEF structure. Lessons learned from the testing and analysis of LDEF hardware is also presented.
Author (revised)

N94-31038*# National Aeronautics and Space Administration. Marshall Space Flight Center, Huntsville, AL.
LDEF MATERIALS SPECIAL INVESTIGATION GROUP'S DATA BASES **c82**
John W. Strickland (BAMSI, Inc., Huntsville, AL.), Joan G. Funk (National Aeronautics and Space Administration. Langley Research Center, Hampton, VA.), and John M. Davis *In its* LDEF Materials Results for Spacecraft Applications Dec. 1993 p 371-376 (For primary document see N94-31012 09-12)
Avail: CASI HC A02/MF A04

The Long Duration Exposure Facility (LDEF) was composed of and contained a wide array of materials, representing the largest collection of materials flown for space exposure and returned for ground-based analyses to date. The results and implications of the data from these materials are the foundation on which future space missions will be built. The LDEF Materials Special Investigation Group (MSIG) has been tasked with establishing and developing data bases to document these materials and their performance to assure not only that the data are archived for future generations but also that the data are available to the space user community in an easily accessed, user-friendly form. The format and content of the data bases developed or being developed to accomplish this task are discussed. The hardware and software requirements for each of the three data bases are discussed along with current availability of the data bases.
Author (revised)

N94-31039*# National Aeronautics and Space Administration. Lyndon B. Johnson Space Center, Houston, TX.
GROUND-BASED SIMULATION OF LEO ENVIRONMENT: INVESTIGATIONS OF A SELECT LDEF MATERIAL: FEP TEFLON (TRADEMARK) **c27**
Jon B. Cross (Los Alamos National Lab., NM.) and Steven L. Koontz *In* NASA. Marshall Space Flight Center, LDEF Materials Results for Spacecraft Applications Dec. 1993 p 379-389 (For primary document see N94-31012 09-12)
Avail: CASI HC A03/MF A04

The Long Duration Exposure Facility (LDEF) has produced a wealth of data on materials degradation in the low earth orbit (LEO) space environment and has conclusively shown that surface chemistry (as opposed to surface physics-sputtering) is the key to understanding and predicting the degradation of materials in the LEO environment. It is also clear that materials degradation and spacecraft contamination are closely linked and that the fundamental mechanisms responsible for this linking are in general not well understood especially in the area of synergistic effects. The study of the fundamental mechanisms underlying materials degradation in LEO is hampered by the fact that the degradation process itself is not observed during the actual exposure to the environment. Rather the aftermath of the degradation process is studied, i.e., the material that remains after exposure is observed and mechanisms are proposed to explain the observed results. The EOIM-3 flight experiment is an attempt to bring sophisticated diagnostic equipment into the space environment and monitor the degradation process in real time through the use of mass spectrometry. More experiments of this nature which would include surface sensitive diagnostics (Auger and photoelectron spectroscopes) are needed to truly unravel the basic chemical mechanisms involved in the materials degradation process. Since these in-space capabilities will most likely not be available in the near future, ground-based LEO simulation facilities employing sophisticated diagnostics are needed to further advance the basic understanding of the materials degradation mechanisms. The LEO simulation facility developed at Los Alamos National Laboratory has been used to investigate the atomic oxygen/vacuum ultraviolet (AO/VUV) enhanced degradation of FEP Teflon. The results show that photo-ejection of polymer fragments occur at elevated temperature (200 C), that VUV synergistic rare gas sputtering of polymer fragments occur even at 25 C, and that combined OA/VUV interaction produces a wide variety of gas phase reaction products. Author (revised)

N94-31040*# National Aeronautics and Space Administration. Lyndon B. Johnson Space Center, Houston, TX.
AN OVERVIEW OF THE EVALUATION OF OXYGEN INTERACTION WITH MATERIALS-THIRD PHASE (EOIM-3) EXPERIMENT: SPACE SHUTTLE MISSION 46 **c25**
Lubert J. Leger, Steven L. Koontz, James T. Visentine, and Donald Hunton *In* NASA. Marshall Space Flight Center, LDEF Materials Results for Spacecraft Applications Dec. 1993 p 391-417 (For primary document see N94-31012 09-12)
Avail: CASI HC A03/MF A04

The interaction of the atomic oxygen (AO) component of the low earth orbit (LEO) environment with spacecraft materials has been the subject of several flight experiments over the past 11 years. The effect of AO interactions with materials has been shown to be significant for long-lived spacecraft such as Space Station Freedom and has resulted in materials changes for externally exposed surfaces. The data obtained from previous flight experiments, augmented by limited ground-based evaluation, have been used to evaluate hardware performance and select materials. Questions pertaining to the accuracy of this data base remain, resulting from the use of long-term ambient density models to estimate the O-atom fluxes and fluences needed to calculate materials reactivity in short-term flight experiments. The EOIM-3 flight experiment was designed to produce benchmark AO reactivity data and was carried out during STS-46. Ambient density measurements were made with a quadrupole mass spectrometer which was calibrated for AO measurements in a unique ground-based test facility. The combination of these data with the predictions of ambient density models allows an assessment of the accuracy of measured reaction rates on a wide variety of materials, many of which had never been tested in LEO before. The mass spectrometer is also used to obtain a better definition of the local neutral and plasma environments resulting from interaction of the ambient atmosphere with various spacecraft surfaces. In addition, the EOIM-3 experiment was designed to produce information on the effects of temperature, mechanical stress, and solar exposure on the AO reactivity of a wide range of materials. An overview of the EOIM-3 methods and results are presented. Author (revised)

N94-31041*# Rome Lab., Griffiss AFB, NY.
ANALYSIS OF LEADING EDGE AND TRAILING EDGE COVER GLASS SAMPLES BEFORE AND AFTER TREATMENT WITH ADVANCED SATELLITE CONTAMINATION REMOVAL TECHNIQUES **c27**
S. P. Hotaling *In* NASA. Marshall Space Flight Center, LDEF Materials Results for Spacecraft Applications Dec. 1993 p 419-436 (For primary document see N94-31012 09-12)
Avail: CASI HC A03/MF A04

Two samples from Long Duration Exposure Facility (LDEF) experiment M0003-4 were analyzed for molecular and particulate contamination prior to and following treatment with advanced satellite contamination removal techniques (CO2 gas/solid jet spray and oxygen ion beam). The pre- and post-cleaning measurements and analyses are presented. The jet spray removed particulates in seconds. The low energy reactive oxygen ion beam removed 5,000 A of photo polymerized organic hydrocarbon contamination in less than 1 hour. Spectroscopic analytical techniques were applied to the analysis of cleaning efficiency including: Fourier transform infrared, Auger, x ray photoemissions, energy dispersive x ray, and ultraviolet/visible. The results of this work suggest that the contamination studied here was due to spacecraft self-contamination enhanced by atomic oxygen plasma dynamics and solar UV radiation. These results also suggest the efficacy for the jet spray and ion beam contamination control technologies for spacecraft optical surfaces. Author (revised)

N94-31042*# Alabama Univ., Huntsville. Surface Science Labs.
PRELIMINARY RESULTS FROM THE CONCAP-2-01 AND EIOM-3 EXPERIMENTS ON STS-46 **c27**
John C. Gregory and Ganesh N. Raikar *In* NASA. Marshall Space Flight

Center, LDEF Materials Results for Spacecraft Applications Dec. 1993 p 439-453 (For primary document see N94-31012 09-12)
Avail: CASI HC A03/MF A04

CONCAP-2-01 (complex autonomous payload, first flight) was the maiden flight of 'CONCAP-2,' a secondary payload, utilizing the get-away special (GAS) carrier system, sponsored by the Consortium for Materials Development in Space (CMDS) at the University of Alabama in Huntsville (UAH). A host of materials such as high-T(sub c) superconductor samples, metal films, polymers, carbons, and semiconducting materials were exposed to a low earth orbit (LEO) environment. We have also measured on orbit the changes in the electrical resistance of some of the high-T(sub c) materials plus carbon and silver dosimeters exposed to the space environment. The preliminary results of this experiment are compared with those from EOIM-3, both of which flew on STS-46. Author (revised)

N94-31043*# Marquette Univ., Milwaukee, WI. Dept. of Mechanical and Industrial Engineering.

EFFECTS OF ORBITAL EXPOSURE ON RTV DURING THE LDEF MISSION **c25**

William E. Brower, Jr., S. V. Golub, and Robert A. Bauer *In* NASA. Marshall Space Flight Center, LDEF Materials Results for Spacecraft Applications Dec. 1993 p 455-463 (For primary document see N94-31012 09-12)
Avail: CASI HC A02/MF A04

Thermomechanical analysis (TMA), differential scanning calorimetry (DSC), and thermogravimetric analysis (TGA) were performed on samples of RTV 511 exposed on the Long Duration Exposure Facility (LDEF) mission for 6 years in orbit and unexposed RTV 511 control samples. Slices 20- to 400-microns thick were removed from the exposed surface down to a depth of 1,500 microns through the 3-mm thick samples. The TMA and DSC results, which arise from the entire slice and not just its surface, showed no significant differences between the LDEF exposed and the control samples. TMA scans were run from ambient to 500 C; results were compared by a tabulation of the onset temperatures for flow. DSC scans were run from ambient to 600 C; no endotherms or exotherms occurred over the range observed. What appear to be glass transition temperatures were compared for the samples as a function of section depth within the sample and between the exposed and control samples. The TGA scans from 25 to 900 C, which arise from the surface of the sample initially, showed a slight increase in the top most 105-micron slice (the exposed, discolored side) in the weight loss at 600 C in oxygen. This weight loss dropped to bulk values at the next slice below the top section, a mean depth of 258 microns. The control sample also showed an increase in weight loss as the top surface was approached, but the 600 C weight losses were very inconsistent. The LDEF RTV sample appears to be mechanically undamaged, with a surface layer which oxidizes slightly faster as a result of orbital exposure. Author

N94-31044*# National Aeronautics and Space Administration, Washington, DC.

NASA'S SPACE PLATFORM TECHNOLOGY PROGRAM AND PLANNING

Gary L. Bennett and Russell C. Cykoski *In* NASA. Marshall Space Flight Center, LDEF Materials Results for Spacecraft Applications Dec. 1993 p 467-484 (For primary document see N94-31012 09-12)
Avail: CASI HC A03/MF A04

As part of the Civil Space Technology Initiative, NASA has established a space platform technology program which encompasses two ongoing programs as well as active planning for new platform initiatives in such areas as advanced heat rejection technologies, advanced space suits, advanced life support, and better support equipment (refrigerators, furnaces, etc.). Platform technology is extremely important because it provides both the basis for future missions and enhanced national competitiveness in space. Author

N94-31045*# Centre National d'Etudes Spatiales, Toulouse (France).

SPACECRAFT MATERIALS: COMPARISON BETWEEN FLIGHT RESULTS OBTAINED ON LDEF AND MIR **c18**

Jean-Claude Guillaumon and Alain Paillous *In* NASA. Marshall Space Flight Center, LDEF Materials Results for Spacecraft Applications Dec. 1993 p 485-498 (For primary document see N94-31012 09-12)
Avail: CASI HC A03/MF A04

Two flight experiments dedicated to the study of the performance of materials in space have been carried out. Material samples have been exposed passively to low-Earth orbit (LEO) environment, then retrieved for laboratory study. The first experiment was conducted in the framework of the FRECOPA project and was flown on the trailing edge of the Long Duration Exposure Facility (LDEF) (exposure to vacuum and ultraviolet (UV) radiation for 5.5 years). The experiment COMES was installed outside of the MIR space station during an extravehicular activity; it was exposed to vacuum, O-atoms, and UV radiation for 1.1 year; and it was brought back to Earth by cosmonauts. The difference in exposure conditions and the use of transparent filters protecting some samples of COMES enable to differentiate the effects of UV radiation and oxygen atoms. The degradations of several thermal control coatings (paints, metalized polymeric films with and without ITO), structural materials, and optical components have been observed, measured, and compared after these two flight experiments. This paper summarizes various 'lessons learned' that can be used to identify aspects of space aging, to orient future research in this field, and to assist in spacecraft design. Author

N94-31046*# National Aeronautics and Space Administration. Ames Research Center, Moffett Field, CA.

CHARACTERIZATION OF POLYMER DECOMPOSITION PRODUCTS BY LASER DESORPTION MASS SPECTROMETRY **c27**

Joan B. Pallix, Kenneth A. Lincoln, Charles J. Miglionico, Robert E. Roybal, Charles Stein, and Jon H. Shively *In* NASA. Marshall Space Flight Center, LDEF Materials Results for Spacecraft Applications Dec. 1993 p 499-509 (For primary document see N94-31012 09-12)
Avail: CASI HC A03/MF A04

Laser desorption mass spectrometry has been used to characterize the ash-like substances formed on the surfaces of polymer matrix composites (PMC's) during exposure on LDEF. In an effort to minimize fragmentation, material was removed from the sample surfaces by laser desorption and desorbed neutrals were ionized by electron impact. Ions were detected in a time-of-flight mass analyzer which allows the entire mass spectrum to be collected for each laser shot. The method is ideal for these studies because only a small amount of ash is available for analysis. Three sets of samples were studied including C/polysulfone, C/polyimide and C/phenolic. Each set contains leading and trailing edge LDEF samples and their respective controls. In each case, the mass spectrum of the ash shows a number of high mass peaks which can be assigned to fragments of the associated polymer. These high mass peaks are not observed in the spectra of the control samples. In general, the results indicate that the ash is formed from decomposition of the polymer matrix. Author

N94-31047*# Boeing Defense and Space Group, Huntsville, AL.

DESIGN APPLICATION AND DEVELOPMENT OF SPACECRAFT IN LEO UTILIZING LDEF RESULTS **c18**

George B. Rauch, Jr. and Richard D. Sudduth *In* NASA. Marshall Space Flight Center, LDEF Materials Results for Spacecraft Applications Dec. 1993 p 511-523 (For primary document see N94-31012 09-12)
Avail: CASI HC A03/MF A04

In general, the results from the Long Duration Exposure Facility (LDEF) have provided much useful information on material sensitivity in the low-Earth orbit (LEO) environment. This is particularly true for selected materials such as thermal control coatings, composites, polymers, fasteners and solar cells. However, LDEF material sensitivity data for other materials like glasses, glass coatings, lubricants, adhesives and seal materials were limited. Some of this important LDEF material sensitivity data has not yet been addressed in detail at the LDEF meetings. The type of material information needed in the design and development of a new spacecraft in LEO depends to a large extent on program phase. In early program phases it is only necessary to have material sensitivity data to determine what materials may or may not work. Later program phases require details on the material strength, optical properties, and/or other long term survivability requirements for materials in LEO. Unfortunately, documentation of exposure results for many materials sensitivity experiments that flew on LDEF has not yet been summarized in a convenient form for use by multiple users. Documentation of this data in a form convenient for scientists, engineers as well as technicians remains a significant area of concern for the aerospace industry. Many of the material experiments that flew on LDEF were only designed to measure material sensitivity for one year in an LEO environment. However, some materials expected to survive one year simply did not survive the 5.8 years that LDEF eventually remained in orbit. Therefore

the survivability of several materials in an LEO environment was determined by default. Most of the LDEF materials experiments were not designed to establish long term material survivability data. This long term material survivability data is particularly useful in later program phases of spacecraft development. The lack of more controlled materials experiments to determine long term material survivability was one of the major limitations of many LDEF experiments. The identified need for this critical information on the long term survivability offers a challenge to possible future LDEF type experiments. Author

N94-31048*# National Aeronautics and Space Administration. Marshall Space Flight Center, Huntsville, AL.

MSFC ORBITAL SPACECRAFT DEVELOPMENT EMPHASES FOR THIS DECADE **c18**

Robert J. Schwinghamer *In its* LDEF Materials Results for Spacecraft Applications Dec. 1993 p 525-531 (For primary document see N94-31012 09-12)

Avail: CASI HC A02/MF A04

Historically, the Marshall Space Flight Center (MSFC) has been responsible for significant accomplishments in the area of developing both manned and unmanned spacecraft. MSFC is presently involved in many of NASA's largest and most prominent programs, with some operational, others being readied for flight, and still others in various stages of design and development. Examples of MSFC programs being designed or developed are Space Station Freedom (S.S. Freedom), the Advanced X-Ray Astrophysics Facility (AXAF) which includes imaging and spectroscopy facilities, the Laser Atmospheric Wind Sounder (LAWS), and the Lunar Ultraviolet Telescope Experiment (LUTE), with Spacelab and Tethered Satellite System (TSS) as examples of current operational MSFC spacecraft. The information obtained from the Long Duration Exposure Facility (LDEF) will aid the design process and life predictions for these and all future spacecraft. A second LDEF is presently being considered. All of these projects will be briefly described in this paper. Author

N94-31049*# Aerospace Corp., El Segundo, CA.

AN OVERVIEW OF THE ON-ORBIT CONTAMINATION OF THE LONG DURATION EXPOSURE FACILITY (LDEF) **c18**

W. K. Stuckey *In* NASA. Marshall Space Flight Center, LDEF Materials Results for Spacecraft Applications Dec. 1993 p 533-539 (For primary document see N94-31012 09-12)

Avail: CASI HC A02/MF A04

Contamination that leads to degradation of critical surfaces becomes a vital design issue for many spacecraft programs. One of the processes that must be considered is the on-orbit accumulation of contaminants. The Long Duration Exposure Facility (LDEF) has presented an opportunity to examine the deposits on surfaces returned from orbit in order to help in understanding the deposition processes and the current models used to predict spacecraft contamination levels. The results from various investigators on the contamination of LDEF have implications for material selection, contamination models, and contamination control plans for the design of future spacecraft. Author

N94-31050*# National Aeronautics and Space Administration. Marshall Space Flight Center, Huntsville, AL.

WHAT LDEF MEANS FOR DEVELOPMENT AND TESTING OF MATERIALS **c25**

Ann F. Whitaker, Wayne K. Stuckey, and Bland A. Stein *In its* LDEF Materials Results for Spacecraft Applications Dec. 1993 p 541-546 (For primary document see N94-31012 09-12)

Avail: CASI HC A02/MF A04

The Long Duration Exposure Facility (LDEF) served as the ultimate laboratory to provide combined space environmental effects on materials. The LDEF structure and its 57 experiments contained an estimated 12,000 to 14,000 specimens of materials and materials processes. It not only provided information about the resistance of these materials to the space environment but gives us direction into future needs for spacecraft materials development and testing. This paper provides an overview of the materials effects observed on the satellite and suggests recommendations for the future work in space-qualified materials development and space environmental simulation. Author

N94-31051*# Wales Univ., Swansea. Dept. of Physics.

ATOMIC OXYGEN DAMAGE CHARACTERIZATION BY PHOTOTHERMAL SCANNING **c25**

A. W. Williams, N. J. Wood, and A. B. Zakaria *In* NASA. Marshall Space Flight Center, LDEF Materials Results for Spacecraft Applications Dec. 1993 p 547-553 (For primary document see N94-31012 09-12)

Avail: CASI HC A02/MF A04

In this paper we use a photothermal imaging technique to characterize the damage caused to an imperfectly coated gold-coated Kapton sample exposed to successively increased fluences of atomic oxygen in a laboratory atomic source. Author

N94-31208 National Aerospace Lab., Amsterdam (Netherlands). Space Div.

DEVELOPMENT CONCEPT FOR DUTCH USER SUPPORT

C. N. A. Pronk, N. Koopman, and D. deHoop 25 Jun. 1992 15 p Presented at the International Astronautical Federation 43rd Congress, Washington, DC, 28 Aug. - 5 Sep. 1992 See also A92-57139 Limited Reproducibility: More than 20% of this document may be affected by microfiche quality

(PB94-125523; NLR-TP-92272-U; ETN-94-95588) Avail: CASI HC A03

The main development approaches and some technologies developed in support of the different objectives of the Dutch Utilization Center (DUC) are reported. The DUC acts as a point of coordination of Dutch user support activities. The support needs of the user are analyzed and from there the required support efforts of the entities in the Dutch User Support Organization (DUSO) are activated. The main objectives of the DUSO are to promote the availability of the Columbus Space Station infrastructure among potential Dutch users, and to assist the users during the process of experiment definition, development, execution, and results evaluation. The DUSO support activities cover promotion and familiarization, and administrative, scientific, technical, and operational support to microgravity and space experimentation. The DUC developmental approaches consist of two approaches: a top down or formal approach; and a bottom up approach. ESA

N94-31425*# National Aeronautics and Space Administration. Marshall Space Flight Center, Huntsville, AL.

THE SECOND ANNUAL INTERNATIONAL SPACE UNIVERSITY ALUMNI CONFERENCE

Les Johnson, comp. and Paul A. Robinson, comp. Washington Feb. 1994 151 p Conference held in Huntsville, AL, 6 Aug. 1993; sponsored by International Space Univ., Inc.

(NASA-CP-3253; M-738; NAS 1.55:3253) Avail: CASI HC A08/MF A02

The papers presented at the conference reflect the multidisciplinary nature of the International Space University (ISU) and its alumni. The first papers presented hold special relevance to the design projects, and cover such topics as lunar-based astronomical instrumentation, solar lunar power generation, habitation on the moon, and the legal issues governing multinational astronauts conducting research in space. The next set of papers cover various technical issues such as project success assessment, satellite networks and space station dynamics, thus reflecting the diverse backgrounds of the ISU alumni. For individual titles, see N94-31426 through N94-31438.

N94-31426*# National Aeronautics and Space Administration. Marshall Space Flight Center, Huntsville, AL.

MITIGATION OF ADVERSE ENVIRONMENTAL EFFECTS ON LUNAR-BASED ASTRONOMICAL INSTRUMENTS **c89**

Les Johnson, Kurtis L. Dietz, T. W. Armstrong, and B. L. Colborn *In its* The Second Annual International Space University Alumni Conference Feb. 1994 p 1-7 (For primary document see N94-31425 09-12)

Avail: CASI HC A02/MF A02

The galactic cosmic-ray flux incident on the Moon was examined for its potential adverse impact on the performance of the large lunar telescope (LLT) proposed as a part of NASA's Space Exploration Initiative (SEI). Noise produced by the cosmic-ray flux in the charge coupled devices (CCD's) to be used as the primary photodetector in the telescope was estimated. It was calculated that approximately 2.5 m of regolith would provide the shielding necessary to reduce the noise to an acceptable level. Dust is an omnipresent environmental concern for any human-assisted or robotic scientific instruments deployed on the Moon. The degree to

which dust poses an operational risk to the telescope was examined. Three potential methods for reducing this risk were identified: locating scientific instruments at remote locations; utilizing a prepared, dust-free site for all rocket activities; and covering the optics during high-risk times. Author

N94-31427*# National Aeronautics and Space Administration. Lewis Research Center, Cleveland, OH.

SOLAR LUNAR POWER **c44**

Sheila G. Bailey and Geoffrey A. Landis *In* NASA. Marshall Space Flight Center, The Second Annual International Space University Alumni Conference Feb. 1994 p 8-25 (For primary document see N94-31425 09-12)

Avail: CASI HC A03/MF A02

Current and projected technology is assessed for photovoltaic power for a lunar base. The following topics are discussed: requirements for power during the lunar day and night; solar cell efficiencies, specific power, temperature sensitivity, and availability; storage options for the lunar night; array and system integration; the potential for in situ production of photovoltaic arrays and storage medium. Author

N94-31428*# Jet Propulsion Lab., California Inst. of Tech., Pasadena.

CHANNEL AND TERMINAL DESCRIPTION OF THE ACTS MOBILE TERMINAL **c32**

B. S. Abbe, M. J. Agan, C. C. Girardey, and T. C. Jedrey *In* NASA. Marshall Space Flight Center, The Second Annual International Space University Alumni Conference Feb. 1994 p 26-33 (For primary document see N94-31425 09-12)

Avail: CASI HC A02/MF A02

The Advanced Communications Technology Satellite (ACTS) Mobile Terminal (AMT) is a proof-of-concept K/Ka-band mobile satellite communications terminal under development by NASA at JPL. Currently the AMT is undergoing systems integration and testing in preparation for a July 1993 ACTS launch and the subsequent commencement of mobile experiments in the fall of 1993. The AMT objectives are presented, followed by a discussion of the AMT communications channel and the mobile terminal's design and performance. Author (revised)

N94-31429*# University of Southern California, Los Angeles. Inst. of Aerospace Systems Architecture and Technology.

THE NOMAD EXPLORER ASSEMBLY ASSIST VEHICLE: AN ARCHITECTURE FOR RAPID GLOBAL EXTRATERRESTRIAL BASE INFRASTRUCTURE ESTABLISHMENT **c54**

Madhu Thangavelu (Rockwell International Corp., Downey, CA.) *In* NASA. Marshall Space Flight Center, The Second Annual International Space University Alumni Conference Feb. 1994 p 34-56 (For primary document see N94-31425 09-12)

Avail: CASI HC A03/MF A02

Traditional concepts of lunar bases describe scenarios where components of the bases are landed on the lunar surface, one at a time, and then put together to form a complete stationary lunar habitat. Recently, some concepts have described the advantages of operating a mobile or 'roving' lunar base. Such a base vastly improves the exploration range from a primary lunar base. Roving bases would also allow the crew to first deploy, test, operationally certify, and then regularly maintain, service, and evolve long life-cycle facilities like observatories or other science payload platforms that are operated far apart from each other across the extraterrestrial surface. The Nomad Explorer is such a mobile lunar base. This paper describes the architectural program of the Nomad Explorer, its advantages over a stationary lunar base, and some of the embedded system concepts which help the roving base to speedily establish a global extraterrestrial infrastructure. A number of modular autonomous logistics landers will carry deployable or erectable payloads, service, and logistically resupply the Nomad Explorer at regular intercepts along the traverse. Starting with the deployment of science experiments and telecommunication networks, and the manned emplacement of a variety of remote outposts using a unique EVA Bell system that enhances manned EVA, the Nomad Explorer architecture suggests the capability for a rapid global development of the extraterrestrial body. The Moon and Mars are candidates for this 'mission oriented' strategy. The lunar case is emphasized in this paper. Author (revised)

N94-31430*# Max-Planck-Inst. fuer Extraterrestrische Physik, Garching (Germany).

MULTIWAVELENGTH SEARCH FOR PROTOPLANETARY DISKS **c89**

Ralph Neuhaeuser and Theodor Schmidt-Kaler *In* NASA. Marshall Space Flight Center, The Second Annual International Space University Alumni Conference Feb. 1994 p 57-65 Sponsored by Hanns-Seidel-Stiftung and BMFT (For primary document see N94-31425 09-12)

Avail: CASI HC A02/MF A02

Infrared emission of circumstellar dust was observed for almost one hundred T Tauri stars. This dust is interpreted to be part of a protoplanetary disk orbiting the central star. T Tauri stars are young stellar objects and evolve into solar type stars. Planets are believed to form in these disks. The spectral energy distribution of a disk depends on its temperature profile. Different disk regions emit at different wavelengths. The disk-star boundary layer is hot and emits H(alpha) radiation. Inner disk regions at around 1 AU with a temperature of a few hundred Kelvin can be probed in near infrared wavelength regimes. Outer disk regions at around 100 AU distance from the star are colder and emit far infrared and sub-millimeter radiation. Also, X-ray emission from the stellar surface can reveal information on disk properties. Emission from the stellar surface and the boundary layer may be shielded by circumstellar gas and dust. T Tauri stars with low H(alpha) emission, i.e. no boundary layer, show stronger X-ray emission than classical T Tauri stars, because the inner disk regions of weak emission-line T Tauri stars may be clear of material. In this paper, first ROSAT all sky survey results on the X-ray emission of T Tauri stars and correlations between X-ray luminosity and properties of T Tauri disks are presented. Due to atmospheric absorption, X-ray and most infrared observations cannot be carried out on Earth, but from Earth orbiting satellites (e.g. IRAS, ROSAT, ISO) or from lunar based observatories, which would have special advantages such as a stable environment. Author (revised)

N94-31431*# Instituto Tecnologico de Aeronautica, Sao Paulo (Brazil).

LEGAL REGIME OF HUMAN ACTIVITIES IN OUTER SPACE LAW **c84**

Carlo Golda *In* NASA. Marshall Space Flight Center, The Second Annual International Space University Alumni Conference Feb. 1994 p 66-75 (For primary document see N94-31425 09-12)

Avail: CASI HC A02/MF A02

Current developments in space activities increasingly involve the presence of humans on board spacecraft and, in the near future, on the Moon, on Mars, on board Space Stations, etc. With respect to these challenges, the political and legal issues connected to the status of astronauts are largely unclear and require a new doctrinal attention. In the same way, many legal and political questions remain open in the structure of future space crews: the need for international standards in the definition and training of astronauts, etc.; but, first of all, an international uniform legal definition of astronauts. Moreover, the legal structure for human life and operations in outer space can be a new and relevant paradigm for the definition of similar rules in all the situations and environments in which humans are involved in extreme frontiers. The present article starts from an overview on the existing legal and political definitions of 'astronauts', moving to the search of a more useful definition. This is followed by an analysis of the concrete problems created by human space activities, and the legal and political responses to them (the need for a code of conduct; the structure of the crew and the existing rules in the US and ex-USSR; the new legal theories on the argument; the definition and structure of a code of conduct; the next legal problems in fields such as privacy law, communications law, business law, criminal law, etc.). Author (revised)

N94-31432*# Hong Kong Univ. Dept. of Civil and Structural Engineering.

EVALUATING SUCCESS LEVELS OF MEGA-PROJECTS **c66**

Mohan M. Kumaraswamy *In* NASA. Marshall Space Flight Center, The Second Annual International Space University Alumni Conference Feb. 1994 p 76-91 (For primary document see N94-31425 09-12)

Avail: CASI HC A03/MF A02

Today's mega-projects transcend the traditional trajectories traced within national and technological limitations. Powers unleashed by internationalization of initiatives, in for example space exploration and environmental protection, are arguably only temporarily suppressed by narrower national, economic, and professional disagreements as to how best they should be harnessed. While the world gets its act together there is time to develop the technologies of such supra-mega-project management

that will synergize truly diverse resources and smoothly mesh their interfaces. Such mega-projects and their management need to be realistically evaluated, when implementing such improvements. This paper examines current approaches to evaluating mega-projects and questions the validity of extrapolations to the supra-mega-projects of the future. Alternatives to improve such evaluations are proposed and described. Author

N94-31433*# Telstra Corp. Ltd., Sydney (Australia).
HUBLESS SATELLITE COMMUNICATIONS NETWORKS **c32**
Peter Alan Robinson *In* NASA. Marshall Space Flight Center, The Second Annual International Space University Alumni Conference Feb. 1994 p 92-95 (For primary document see N94-31425 09-12)
Avail: CASI HC A01/MF A02

Frequency Comb Multiple Access (FCMA) is a new combined modulation and multiple access method which will allow cheap hubless Very Small Aperture Terminal (VSAT) networks to be constructed. Theoretical results show bandwidth efficiency and power efficiency improvements over other modulation and multiple access methods. Costs of the VSAT network are reduced dramatically since a hub station is not required. Author

N94-31434*# Wright Lab., Wright-Patterson AFB, OH. Flight Dynamics Directorate.
A STUDY OF THE SPACE STATION FREEDOM RESPONSE TO THE DISTURBANCE ENVIRONMENT **c18**
Afzal Suleman (National Research Council of Canada, Vancouver, British Columbia.), V. J. Modi (British Columbia Univ., Vancouver.), and V. B. Venkayya *In* NASA. Marshall Space Flight Center, The Second Annual International Space University Alumni Conference Feb. 1994 p 96-111 (For primary document see N94-31425 09-12)
Avail: CASI HC A03/MF A02

A relatively general formulation for studying the dynamics and control of an arbitrary spacecraft with interconnected flexible bodies has been developed. This self-contained and comprehensive numerical algorithm using system modes is applicable to a large class of spacecraft configurations of contemporary and future interest. Here, versatility of the approach is demonstrated through the dynamics and control studies aimed at the evolving Space Station Freedom. Author (revised)

N94-31435*# Rutgers Univ., Piscataway, NJ. Center for Computer Aids for Industrial Productivity.
APPLICATION OF THE WAVELET TRANSFORM FOR SPEECH PROCESSING **c32**
Stephane Maes (Belgian National Foundation for Scientific Research, Brussels.) *In* NASA. Marshall Space Flight Center, The Second Annual International Space University Alumni Conference Feb. 1994 p 112-120 (For primary document see N94-31425 09-12)
Avail: CASI HC A02/MF A02

Speaker identification and word spotting will shortly play a key role in space applications. An approach based on the wavelet transform is presented that, in the context of the 'modulation model,' enables extraction of speech features which are used as input for the classification process.
Author (revised)

N94-31436*# International Space Univ., Inc., Toronto (Ontario).
AN INNOVATIVE APPROACH TO SPACE EDUCATION **c80**
Christine Marton, Alain B. Berinstain, and John Criswick *In* NASA. Marshall Space Flight Center, The Second Annual International Space University Alumni Conference Feb. 1994 p 121-125 (For primary document see N94-31425 09-12)
Avail: CASI HC A01/MF A02

At present, Canada does not have enough scientists to be competitive in the global economy, which is rapidly changing from a reliance on natural resources and industry to information and technology. Space is the final frontier and it is a multidisciplinary endeavor. It requires a knowledge of science and math, as well as non-science areas such as architecture and law. Thus, it can attract a large number of students with a diverse range of interests and career goals. An overview is presented of the space education program designed by Canadian Alumni of the International Space University (CAISU) to encourage students to pursue studies and careers in science and technology and to improve science literacy in Canada.
Author (revised)

N94-31437*# Tsukuba Space Center (Japan).
MULTISATELLITE CONSTELLATION CONFIGURATION SELECTION FOR MULTIREGIONAL HIGHLY ELLIPTICAL ORBIT CONSTELLATIONS **c32**
Mark G. Matossian (Colorado Univ., Boulder.) *In* NASA. Marshall Space Flight Center, The Second Annual International Space University Alumni Conference Feb. 1994 p 126-136 Sponsored by NASDA; Science and Technology Agency; and NSF (For primary document see N94-31425 09-12)
Avail: CASI HC A03/MF A02

The Archimedes Project is a joint effort of the European Space Agency (ESA) and the National Space Development Agency of Japan (NASDA). The primary goal of the Archimedes project is to perform a technical feasibility analysis and preliminary design of a highly inclined multisatellite constellation for direct broadcast and mobile communications services for Europe, Japan and much of North America. This report addresses one aspect of this project, specifically an analysis of continuous satellite coverage using multiregional highly elliptical orbits (M-HEO's). The analysis methodology and ensuing software tool, named SPIFF, were developed specifically for this project by the author during the summer of 1992 under the STA/NSF Summer Institute in Japan Program at Tsukuba Space Center. Author

N94-31438*# George Washington Univ., Washington, DC. Space Policy Inst.
ISU IN AN ERA OF PARTIAL RECONVERGENCE M.S. Thesis
Douglas M. Messier *In* NASA. Marshall Space Flight Center, The Second Annual International Space University Alumni Conference Feb. 1994 p 137-145 (For primary document see N94-31425 09-12)
Avail: CASI HC A02/MF A02

The International Space University (ISU) was founded in 1987 to provide young space professionals with an international, multi-disciplinary approach to space education. The organization has held six 10-week summer sessions at which students from throughout the world have studied space. In 1995, ISU plans to begin a one-year Ph.D.-level program in space studies. This paper examines the educational goals of ISU in the context of current education trends. It discusses how trends toward internationalism and interdisciplinary studies are reshaping both education and the aerospace field. The tensions that exist between ISU's conflicting goals are discussed in the context of these prevailing currents. Author

N94-31820* National Aeronautics and Space Administration, Washington, DC.
APOLLO 11 HIGHLIGHTS (Videotape)
1969 Videotape: 26 min. 37 sec. playing time, in color, with sound (NASA-TM-109763; NONP-VT-94-9963) Avail: CASI VHS A01/BETA A22

This video recounts the Apollo 11 Mission which took ten years of preparation and the work of over a half a million people, culminating in the first manned lunar landing on July 20, 1969. Historical footage is accompanied by a narrated account of the mission. The footage includes preparation for launch, takeoff, stage separation, docking in space the Eagle Lunar Lander, shots of the Earth and Moon from space, Michael Collins orbiting the Moon in the Columbia Orbiter, Edwin Aldrin and Neil Armstrong walking on the Moon, setting up a Solar Wind experiment, collecting lunar samples, shots aboard the U.S.S. Hornet, retrieval of the astronauts after splashdown, and the parade given in honor of the astronauts. CASI

N94-32126# Industrial Coll. of the Armed Forces, Washington, DC.
CIM IN SPACE: CORPORATE INFORMATION MANAGEMENT (CIM) IMPLICATIONS FOR SPACE-BASED INFORMATION SYSTEMS Report, Aug. 1992 - Apr. 1993
Richard V. Mock Apr. 1993 48 p
(AD-A276882; NDU-ICAF-93-F22B) Avail: CASI HC A03/MF A01

This paper describes the DOD corporate information management (CIM) initiative, space forces, and space-based information systems used by the DOD. It then describes implications of CIM in the space industry. CIM is defined as a philosophy which has management and technical components. The CIM management philosophy includes concepts for standardization, system engineering, and the use of commercial systems and technology. The technical component uses the information engineering discipline to

improve business processes. The paper provides examples of the CIM management philosophy in operation as well as opportunities for CIM application. Information engineering is described as it applies to space-based information systems. The appendix includes an illustrative example of the integrated definition (IDEF) methodology applied to the tactical warning/attack assessment mission. DTIC

N94-32211 Industrial Coll. of the Armed Forces, Washington, DC.
DOD SPACE BASED REQUIREMENTS: INCREASING DOD ACCESS TO SPACE Research Report, Aug. 1992 - Apr. 1993
Mary D. Kelly Apr. 1993 39 p Limited Reproducibility: More than 20% of this document may be affected by microfiche quality
(AD-A276874; NDU-ICAF-93-S40) Avail: CASI HC A03

This paper concerns itself with an examination of DOD's need to expand space based capabilities to support military operations while focusing on the current launch environment as the greatest limiting factor to achieving expanded exploitation of space for DOD requirements. There is a discussion of existing launch systems, facilities, and capacity as well as current and experimental efforts in both payload and launch vehicle technology. A description of commercial practices regarding payload and launch vehicle utilization is contrasted with DOD's approach, and a projection of demand for launch access is compared against launch availability. An examination of certain technical, procedural, and acquisition alternatives for improving launch capacity is presented. This concludes with selected low cost recommendations for achieving the objective of increasing the ability to access space. DTIC

N94-32870*# National Aeronautics and Space Administration. Langley Research Center, Hampton, VA.
RESULTS FOR THE HYBRID LAMINAR FLOW CONTROL EXPERIMENT CONDUCTED IN THE NASA LANGLEY 8-FOOT TRANSONIC PRESSURE TUNNEL ON A 7-FOOT CHORD MODEL
Percy J. Bobbitt, James C. Ferris, William D. Harvey, and Suresh H. Goradia Mar. 1992 18 p
(RTOP 505-69-20-01)
(NASA-TM-107582; NAS 1.15:107582) Avail: CASI HC A03/MF A01

A description is given of the development of, and results from, the hybrid laminar flow control (HLFC) experiment conducted in the NASA LaRC 8 ft Transonic Pressure Tunnel on a 7 ft chord, 23 deg swept model. The methods/codes used to obtain the contours of the HLFC model surface and to define the suction requirements are outlined followed by a discussion of the model construction, suction system, instrumentation, and some example results from the wind tunnel tests. Included in the latter are the effects of Mach number, suction level, and the extent of suction. An assessment is also given of the effect of the wind tunnel environment on the suction requirements. The data show that, at or near the design Mach number, large extents of laminar flow can be achieved with suction mass flows over the first 25 percent, or less, of the chord. Top surface drag coefficients with suction extending from the near leading edge to 20 percent of the chord were approximately 40 percent lower than those obtained with no suction. The results indicate that HLFC can be designed for transonic speeds with lift and drag coefficients approaching those of LFC designs but with much smaller extents and levels of suction. Author (revised)

13 ASTRODYNAMICS

Includes powered and free-flight trajectories; and orbital and launching dynamics.

N94-31298# Naval Postgraduate School, Monterey, CA.
AIR FORCE SPACE COMMAND SATELLITE ORBIT PREDICTOR USING PARALLEL VIRTUAL MACHINES M.S. Thesis
Susan K. Brewer Dec. 1993 104 p
(AD-A276316) Avail: CASI HC A06/MF A02

Parallel computing is the wave of the future. As the need for computational power increases, one processor is no longer sufficient to achieve the speed necessary to solve today's complex problems. The Air Force Space Command (AFSPACEOM) tracks approximately 8000 satellites daily; the model used by the AFSPACECOM, SGP4, (Simplified General Perturbation Model Four), has been the operational model since 1976. This thesis contains a detailed discussion of the mathematical theory of the SGP4 model. The tracking of a satellite requires extensive calculations. The satellite can be tracked more efficiently with parallel processing techniques. The principles developed are applicable to a Naval ship tracking multiple incoming threats; the increase in the speed of processing incoming data would result in personnel being informed faster and thus allow more time for better decisions during combat. Three parallel algorithms applied to SGP4 for implementations on a Parallel Virtual Machine (PVM) are developed. PVM is a small software package that allows a network of computer workstations to appear as a single large distributed-memory parallel computer. This thesis contains a description of several algorithms for the implementation on PVM to track satellites, the optimal number of workstations, and methods of distributing data. DTIC

N94-31769# Institut des Hautes Etudes Scientifiques, Bures-sur-Yvette (France).
GENERAL-RELATIVISTIC CELESTIAL MECHANICS. 4: THEORY OF SATELLITE MOTION
T. Damour (Observatoire de Paris, France.), M. Soffel (Tuebingen Univ., Germany.), and C. Xu (Tuebingen Univ., Germany.) Sep. 1993 36 p See also PB93-162527
(PB94-147782; IHES/P/93/47) Avail: CASI HC A03/MF A01

The basic equations needed for developing a complete relativistic theory of artificial Earth satellites are explicitly written down. These equations are given both in a local, geocentric frame and in the global, barycentric one. They are derived within our recently introduced general-relativistic celestial mechanics framework. Our approach is more satisfactory than previous ones, especially with regard to its consistency, completeness, and flexibility. In particular, the problem of representing the relativistic gravitational effects associated with the quadrupole and higher multipole moments of the moving Earth, which caused difficulties in several other approaches, is easily dealth with in our approach, thanks to the use of previously developed tools: definition of relativistic multipole moments and transformation theory between reference frames. With this last paper in a series, we hope to indicate the way of using our formalism in specific problems in applied celestial mechanics and astrometry. NTIS

N94-31802 California Univ., Los Angeles.
ATTITUDE DYNAMICS OF SPINNING ROCKETS IN SPACE WITH INTERNAL MASS MOTION Ph.D. Thesis
Brian Douglas Staunton 1993 193 p
Avail: Univ. Microfilms Order No. DA9320374

Models of spinning rockets in space with internal mass motion are developed and analyzed. Three of the models use simple combinations of particle masses and springs to represent the internal mass motion. Two more models use fluid mechanical representations. One fluid model uses inviscid fluid assumptions and has no damping in the resulting equations, while the other includes viscous effects. The research is motivated by nutation instabilities observed in a class of orbit transfer vehicles. It is hypothesized that the instability mechanism relies on the motion of liquid inside the vehicle. A linear stability analysis is used to evaluate each model. Sets of model parameters which permit instabilities are identified. While all models can exhibit instabilities, it was not possible to confirm an instability for parameters consistent with the flight data. Two of the particle models reproduce some aspects of the data. Additional findings include the identification of an equivalent particle representation for one of the fluid models. The equations governing the third particle model closely resemble those of the fluid models. Also, a degenerate case of the viscous fluid model provides a new approach for representing a class of spacecraft nutation dampers. Dissert. Abstr.

N94-32388*# Draper (Charles Stark) Lab., Inc., Cambridge, MA.
A SIX DEGREE OF FREEDOM, PLUME-FUEL OPTIMAL TRAJECTORY PLANNER FOR SPACECRAFT PROXIMITY OPERATIONS USING AN A* NODE SEARCH M.S. Thesis - MIT
Mark Charles Jackson May 1994 147 p
(Contract NAS9-18426)
(NASA-CR-188285; NAS 1.26:188285; CSDL-T-1221) Copyright Avail: CASI HC A07/MF A02

Spacecraft proximity operations are complicated by the fact that exhaust plume impingement from the reaction control jets of space vehicles can cause structural damage, contamination of sensitive arrays and instruments,

or attitude misalignment during docking. The occurrence and effect of jet plume impingement can be reduced by planning approach trajectories with plume effects considered. An A* node search is used to find plume-fuel optimal trajectories through a discretized six dimensional attitude-translation space. A plume cost function which approximates jet plume isopressure envelopes is presented. The function is then applied to find relative costs for predictable 'trajectory altering' firings and unpredictable 'deadbanding' firings. Trajectory altering firings are calculated by running the spacecraft jet selection algorithm and summing the cost contribution from each jet fired. A 'deadbanding effects' function is defined and integrated to determine the potential for deadbanding impingement along candidate trajectories. Plume costs are weighed against fuel costs in finding the optimal solution. A* convergence speed is improved by solving approach trajectory problems in reverse time. Results are obtained on a high fidelity space shuttle/space station simulation. Trajectory following is accomplished by a six degree of freedom autopilot. Trajectories planned with, and without, plume costs are compared in terms of force applied to the target structure.

Author (revised)

14 GROUND SUPPORT SYSTEMS AND FACILITIES (SPACE)

Includes launch complexes, research and production facilities; ground support equipment, e.g., mobile transporters; and simulators.

For related information see also *09 Research and Support Facilities (Air).*

N94-31814* National Aeronautics and Space Administration. Lewis Research Center, Cleveland, OH.

AEROSPACE TEST FACILITIES AT NASA LERC PLUMBROOK (Videotape)

Oct. 1992 Videotape: 10 min. 30 sec. playing time, in color, with sound (NASA-TM-109755; NONP-VT-94-9955) Avail: CASI VHS A01/BETA A22

An overview of the facilities and research being conducted at LeRC's Plumbrook field station is given. The video highlights four main structures and explains their uses. The Space Power Facility is the worlds largest space environment simulation chamber, where spacebound hardware is tested in simulations of the vacuum and extreme heat and cold of the space plasma environment. This facility was used to prepare Atlas 1 rockets to ferry CRRES into orbit; it will also be used to test space nuclear electric power generation systems. The Spacecraft Propulsion Research Facility allows rocket vehicles to be hot fired in a simulated space environment. In the Cryogenic Propellant Tank Facility, researchers are developing technology for storing and transferring liquid hydrogen in space. There is also a Hypersonic Wind Tunnel which can perform flow tests with winds up to Mach 7. CASI

N94-32333 Range Commanders Council, White Sands Missile Range, NM. Range Safety Group.

DESIGN, PERFORMANCE, AND TEST STANDARDS FOR FLIGHT TERMINATION RECEIVERS/DECODERS. VOLUME 1: DESIGN AND PERFORMANCE REQUIREMENTS

Feb. 1994 23 p See also AD-A209644 Limited Reproducibility: More than 20% of this document may be affected by microfiche quality (AD-A277245; RCC/RSG-313-94-Vol-1) Avail: Issuing Activity (Defense Technical Information Center (DTIC))

This standard provide the minimum electrical design and performance requirements for range safety flight termination receivers (FTR). The electrical design and performance requirements contained in this standard apply to all range safety FTR's. When the procurement specifications require the FTR's to have a special or peculiar feature that is not addressed in this standard, the design of that feature shall permit the feature to be tested.

DTIC

15 LAUNCH VEHICLES AND SPACE VEHICLES

Includes boosters; operating problems of launch/space vehicle systems; and reusable vehicles.

For related information see also *20 Spacecraft Propulsion and Power.*

N94-31891 Stanford Univ., CA.

ON-LINE PHYSICAL PARAMETER IDENTIFICATION AND ADAPTIVE CONTROL OF A LAUNCH VEHICLE Ph.D. Thesis

Brian Scott Keller 1993 203 p

Avail: Univ. Microfilms Order No. DA9317778

Physical parameter identification is useful in many applications, especially in aerospace where much analysis goes into developing accurate physical system models for control. A number of off-line physical parameter identification methods exist; however, the choice of on-line methods is more limited. On-line identification methods are required for adaptive control. New on-line physical parameter identification methods are developed in this work as motivated by the problem of launch vehicle adaptive control. Launch vehicles vary from launch to launch due to differences in payloads and fuel loading. Based on the known variations, launch vehicle control laws are reanalyzed and modified if necessary; this process is expensive and adds to recurring launch vehicle costs. This reanalysis is performed despite the fact that changes in the launch vehicle are relatively minor. A trustworthy adaptive control system could eliminate this expensive redesign cycle. An adaptive control system could also provide better performance than a controller redesigned off-line. However, adaptive control is still considered too risky to use with unstable systems, primarily due to limitations in the identification methods currently available for use in adaptive control. This problem is addressed with the development of new identification algorithms. A philosophy of identification is described which uses physical parameters for identification. A technique is developed to convert existing on-line methods to a form capable of identifying physical parameters. New methods include physical parameter versions of normalized least mean squares (NLMS), research least squares (RLS), extended least squares (ELS), recursive maximum likelihood (RML), and the extended Kalman filter (EKF). Compared to transfer function identification, physical parameter identification reduces the order of the problem and speeds up convergence. Compared to the extended Kalman filter, the new methods have a faster iteration time. The use of physical parameters also allows bounding based on expected parameter variations. The new identification methods are compared with existing methods and demonstrated in simulations of a two-mass/spring system, an OH-6A helicopter near hover, and the National Launch System 1.5-stage launch vehicle. Dissert. Abstr.

N94-32288 Washington Univ., Seattle. Aerospace and Energetics Research Program.

BASIC AND APPLIED STUDIES OF THE RAM ACCELERATOR AS A HYPERVELOCITY PROJECTILE LAUNCHER Annual Report, 1 Jul. 1992 - 30 Jun. 1993

Adam P. Bruckner and Carl Knowlen 10 Dec. 1993 98 p Limited Reproducibility: More than 20% of this document may be affected by microfiche quality

(Contract F49620-92-J-0375)

(AD-A277392; AFOSR-94-0100TR) Avail: CASI HC A05

The potential of using ram accelerator technology for an impulsive launcher of autonomously guided interceptors, such as the LEAP, has been studied during this contract period. In addition, fundamental investigations on some of the engineering issues which must be addressed for enabling ram accelerator propulsive modes to operate at 4 km/sec have been undertaken. An experimental investigation of the gas dynamic limits of ram accelerator operation has demonstrated the existence of two distinct limiting mechanisms that must be accounted for when designing projectiles for these launchers. Other experiments were conducted to make detailed pressure measurements of the flow fields at the tube walls to study the effects of projectile canting. Results from this LEAP launcher study and the experimental investigations indicate that the ram accelerator technology is well suited for applications as a transportable launcher capable of meeting the needs of theater ballistic missile defense missions. DTIC

N94-32494*# Dimensions International, Inc., Alexandria, VA.
SPACE FLIGHT RISK DATA COLLECTION AND ANALYSIS PROJECT: RISK AND RELIABILITY DATABASE Final Report
11 May 1994 137 p Prepared in cooperation with Science Applications International Corp., New York, NY
(Contract NASw-4776)
(NASA-CR-195879; NAS 1.26:195879) Avail: CASI HC A07/MF A02

The focus of the NASA 'Space Flight Risk Data Collection and Analysis' project was to acquire and evaluate space flight data with the express purpose of establishing a database containing measurements of specific risk assessment - reliability - availability - maintainability - supportability (RRAMS) parameters. The developed comprehensive RRAMS database will support the performance of future NASA and aerospace industry risk and reliability studies. One of the primary goals has been to acquire unprocessed information relating to the reliability and availability of launch vehicles and the subsystems and components thereof from the 45th Space Wing (formerly Eastern Space and Missile Command -ESMC) at Patrick Air Force Base. After evaluating and analyzing this information, it was encoded in terms of parameters pertinent to ascertaining reliability and availability statistics, and then assembled into an appropriate database structure. Derived from text

N94-32671# Sandia National Labs., Albuquerque, NM.
DESIGN AND EVALUATION OF COILS FOR A 50 mm DIAMETER INDUCTION COILGUN LAUNCHER
R. J. Kaye, I. R. Shokair, R. W. Wavrik, J. F. Dempsey, W. E. Honey, K. J. Shimp, and G. M. Douglas 1993 15 p Presented at the 7th Symposium on Electromagnetic Launch Technology, San Diego, CA, 20-24 Apr. 1994
(Contract DE-AC04-94AL-85000)
(DE94-005244; SAND-93-0092C; CONF-940481-1) Avail: CASI HC A03/MF A01

Coilguns have the ability to provide magnetic pressure to projectiles which results in near constant acceleration. However, to achieve this performance and control projectile hearing, significant constraints are placed on the design of the coils. We are developing coils to produce an effective projectile base pressure of 100 MPa as a step toward reaching base pressures of 200 MPa. The design uses a scalable technology applicable to the entire range of breech to muzzle coils of a multi-stage launcher. This paper presents the design of capacitor-driven coils for launching nominal 50 mm, 350 gram projectiles. Design criteria, constraints, mechanical stress analysis, launcher performance, and test results are discussed. DOE

N94-33291*# National Aeronautics and Space Administration. Lewis Research Center, Cleveland, OH.
THE 28TH AEROSPACE MECHANISMS SYMPOSIUM
Douglas A. Rohn, comp. May 1994 440 p Symposium held in Cleveland, OH, 18-20 May 1994; sponsored by NASA and Lockheed Missiles and Space Co.
(RTOP 506-43-41)
(NASA-CP-3260; E-8667; NAS 1.55:3260) Avail: CASI HC A19/MF A04

The proceedings of the 28th Aerospace Mechanisms Symposium, which was hosted by the NASA Lewis Research Center and held at the Cleveland Marriott Society Center on May 18, 19, and 20, 1994, are reported. Technological areas covered include actuators, aerospace mechanism applications for ground support equipment, lubricants, pointing mechanisms joints, bearings, release devices, booms, robotic mechanisms, and other mechanisms for spacecraft. For individual titles, see N94-33292 through N94-33323.

N94-33292*# Lockheed Missiles and Space Co., Sunnyvale, CA.
SPACE STATION FREEDOM SOLAR ARRAY CONTAINMENT BOX MECHANISMS **c44**
Mark E. Johnson, Bert Haugen, and Grant Anderson *In* NASA. Lewis Research Center, The 28th Aerospace Mechanisms Symposium May 1994 p 1-16 (For primary document see N94-33291 09-15)
Avail: CASI HC A03/MF A04

Space Station Freedom will feature six large solar arrays, called solar array wings, built by Lockheed Missiles & Space Company under contract to Rockwell International, Rocketdyne Division. Solar cells are mounted on flexible substrate panels which are hinged together to form a 'blanket.' Each wing is comprised of two blankets supported by a central mast, producing approximately 32 kW of power at beginning-of-life. During launch, the blankets are fan-folded and compressed to 1.5 percent of their deployed length into containment boxes. This paper describes the main containment box mechanisms designed to protect, deploy, and retract the solar array blankets: the latch, blanket restraint, tension, and guidewire mechanisms. Author

N94-33293*# ISRO Satellite Centre, Peenya, Bangalore (India). Spacecraft Mechanisms Group.
INSAT-2A AND 2B DEVELOPMENT MECHANISMS **c44**
M. N. Sathyanarayan, M. Nageswara Rao, B. S. Nataraju, N. Viswanatha, M. Laxmana Chary, K. S. Balan, V. Sridhara Murthy, Raju Aller, and H. N. Suresha Kumar *In* NASA. Lewis Research Center, The 28th Aerospace Mechanisms Symposium May 1994 p 17-34 (For primary document see N94-33291 09-15)
Avail: CASI HC A03/MF A04

The Indian National Satellite (INSAT) 2A and 2B have deployment mechanisms for deploying the solar array, two C/S band antenna reflectors and a coilable lattice boom with sail. The mechanisms have worked flawlessly on both satellites. The configuration details, precautions taken during the design phase, the test philosophy, and some of the critical analysis activities are discussed. Author

N94-33294*# Honeywell, Inc., Phoenix, AZ. Satellite Systems Operation.
ROLL RING ASSEMBLIES FOR THE SPACE STATION **c20**
J. Batista, J. Vise, and K. Young *In* NASA. Lewis Research Center, The 28th Aerospace Mechanisms Symposium May 1994 p 35-50 (For primary document see N94-33291 09-15)
Avail: CASI HC A03/MF A04

Space Station Freedom requires the transmission of high power and signals through three different rotational interfaces. Roll ring technology was baselined by NASA for rotary joints to transfer up to 65.5 kW of power for 30 years at greater than 99 percent efficiency. Signal transfer requirements included MIL-STD-1553 data transmission and 4.5 MHz RS250A base and color video. A unique design for each rotary joint was developed and tested to accomplish power and signal transfer. An overview of roll ring technology is presented, followed by design requirements, hardware configuration, and test results. Author

N94-33295*# Rockwell International Corp., Canoga Park, CA. Rocketdyne Div.
INTERNATIONAL SPACE STATION ALPHA'S BEARING, MOTOR, AND ROLL RING MODULE DEVELOPMENTAL TESTING AND RESULTS **c20**
David L. OBrien *In* NASA. Lewis Research Center, The 28th Aerospace Mechanisms Symposium May 1994 p 51-61 (For primary document see N94-33291 09-15)
Avail: CASI HC A03/MF A04

This paper presents the design and developmental testing associated with the bearing, motor, and roll ring module (BMRRM) used for the beta rotation axis on International Space Station Alpha (ISSA). The BMRRM with its controllers located in the electronic control unit (ECU), provides for the solar array pointing and tracking functions as well as power and signal transfer across a rotating interface. Author

N94-33296*# National Aeronautics and Space Administration. Lewis Research Center, Cleveland, OH.
DESIGN, CHARACTERIZATION AND CONTROL OF THE UNIQUE MOBILITY CORPORATION ROBOT **c37**
Virgilio B. Velasco, Jr. (Case Western Reserve Univ., Cleveland, OH.), Wyatt S. Newman (Case Western Reserve Univ., Cleveland, OH.), Bruce Steinetz, Carlo Kopf, and John Malik *In its* The 28th Aerospace Mechanisms Symposium May 1994 p 63-78 (For primary document see N94-33291 09-15)
(Contract NAS3-26285)
Avail: CASI HC A03/MF A04

Space and mass are at a premium on any space mission, and thus any machinery designed for space use should be lightweight and compact, without sacrificing strength. It is for this reason that NASA/LeRC contracted Unique Mobility Corporation to exploit their novel actuator designs to build a robot that would advance the present state of technology with respect to these requirements. Custom-designed motors are the key feature of this

robot. They are compact, high-performance dc brushless servo motors with a high pole count and low inductance, thus permitting high torque generation and rapid phase commutation. Using a custom-designed digital signal processor-based controller board, the pulse width modulation power amplifiers regulate the fast dynamics of the motor currents. In addition, the programmable digital signal processor (DSP) controller permits implementation of nonlinear compensation algorithms to account for motoring vs. regeneration, torque ripple, and back-EMF. As a result, the motors produce a high torque relative to their size and weight, and can do so with good torque regulation and acceptably high velocity saturation limits. This paper presents the Unique Mobility Corporation robot prototype: its actuators, its kinematic design, its control system, and its experimental characterization. Performance results, including saturation torques, saturation velocities and tracking accuracy tests are included. Author

N94-33297*# Maryland Univ., College Park.
DEVELOPMENT OF AN INTERCHANGEABLE END EFFECTOR MECHANISM FOR THE RANGER TELEROBOTIC VEHICLE **c37**
Robert Cohen and David L. Akin *In* NASA. Lewis Research Center, The 28th Aerospace Mechanisms Symposium May 1994 p 79-89 (For primary document see N94-33291 09-15)
Avail: CASI HC A03/MF A04

The Ranger program at the Space Systems Laboratory (SSL) at the University of Maryland is a demonstration of an extremely low cost, space flight experiment. The Ranger vehicle is designed to perform teleoperated spacecraft maintenance. Completing the various tasks included in spacecraft maintenance requires several specific tools. This paper describes the Ranger interchangeable end effector mechanism (IEEM). Its design allows Ranger to change end effectors to utilize the appropriate tool for the various tasks. The Ranger vehicle is designed with four manipulators. A seven degree-of-freedom (DOF) grappling manipulator securely attaches the vehicle to the work site. A 6 DOF camera positioning manipulator allows the operator to position a stereo pair of video cameras for visual feedback. The two remaining manipulators are the 7 DOF dexterous arms. They are the primary means by which Ranger accomplishes its required tasks. At the end of each of these dexterous manipulators is an IEEM. This paper begins with a brief overview of the Space Systems Laboratory and the Ranger program. The constraints leading to the requirements for an IEEM are described. The following section then describes the design strategies and the down selection process resulting in two candidate designs, taper and pneumatic connector type. Next, the leading candidate design is described in detail, followed by a preliminary discussion of failure modes and planned testing. The paper concludes with a brief review and a section discussing future work. Author

N94-33298*# National Aeronautics and Space Administration. Marshall Space Flight Center, Huntsville, AL.
DIAMOND TURNING IN THE PRODUCTION OF X RAY OPTICS **c74**
Steven C. Fawcett *In* NASA. Lewis Research Center, The 28th Aerospace Mechanisms Symposium May 1994 p 91-105 (For primary document see N94-33291 09-15)
Avail: CASI HC A03/MF A04

A demonstration x-ray optic has been produced by diamond turning and replication techniques that could revolutionize the fabrication of advanced mirror assemblies. The prototype optic was developed as part of the Advanced X-ray Astrophysics Facility - Spectrographic project (AXAF-S). The initial part of the project was aimed at developing and testing the replica technique so that it could potentially be used for the production of the entire mirror array comprised of up to 50 individual mirror shells. Author

N94-33299*# National Aeronautics and Space Administration. John F. Kennedy Space Center, Cocoa Beach, FL.
INNOVATIVE MECHANISM FOR MEASURING THE MASS PROPERTIES OF AN OBJECT **c37**
Kedron R. Wolcott (I-NET, Inc., Cocoa Beach, FL.), Todd A. Graham, and Keith L. Doty *In* NASA. Lewis Research Center, The 28th Aerospace Mechanisms Symposium May 1994 p 107-121 (For primary document see N94-33291 09-15)
Avail: CASI HC A03/MF A04

The Kennedy Space Center Robotics Group recently completed development and testing on a novel approach to measure the mass properties of a rigid body. This unique design can measure the payload's weight, mass center location, and moments of inertia about three orthogonal axes. Furthermore, these measurements only require a single torque sensor and a single angular position sensor. Author

N94-33300*# Lockheed Missiles and Space Co., Sunnyvale, CA.
SPACE STATION FREEDOM SOLAR ARRAY TENSION MECHANISM DEVELOPMENT **c37**
Curtis Allmon and Bert Haugen *In* NASA. Lewis Research Center, The 28th Aerospace Mechanisms Symposium May 1994 p 123-128 (For primary document see N94-33291 09-15)
Avail: CASI HC A02/MF A04

A tension mechanism is used to apply a tension force to the Space Station Freedom Solar Array Blanket. This tension is necessary to meet the deployed frequency requirement of the array as well as maintain the flatness of the flexible substrate solar cell blanket. The mechanism underwent a series of design iterations before arriving at the final design. This paper discusses the design and testing of the mechanism. Author

N94-33301*# TRW Systems Group, Redondo Beach, CA.
LEVERAGING METAL MATRIX COMPOSITES TO REDUCE COSTS IN SPACE MECHANISMS **c24**
Ted Nye, Rex Claridge, and Jim Walker *In* NASA. Lewis Research Center, The 28th Aerospace Mechanisms Symposium May 1994 p 129-134 (For primary document see N94-33291 09-15)
(Contracts F33615-90-C-3200; F33733-89-C-1011)
Avail: CASI HC A02/MF A04

Advanced metal matrix composites may be one of the most promising technologies for reducing cost in structural components without compromise to strength or stiffness. A microlight 12.50 N (2.81 lb), two-axis, solar array drive assembly (SADA) was made for the Advanced Materials Applications to Space Structures (AMASS) Program flight experiment. The SADA had both its inner and outer axis housings fabricated from silicon carbide particulate reinforced alumimun. Two versions of the housings were made. The first was machined from a solid billet of material. The second was plaster cast to a near net shape that required minimal finish machining. Both manufacturing methods were compared upon completion. Results showed a cost savings with the cast housing was possible for quantities greater than one and probable for quantities greater than two. For quantities approaching ten, casting resulted in a reduction factor of almost three in the cost per part. Author

N94-33302*# Naval Research Lab., Washington, DC.
DESIGN, DEVELOPMENT, AND TESTING OF A LIGHTWEIGHT OPTICAL SENSOR COVER SYSTEM **c18**
Mike Hurley and Scott Christiansen *In* NASA. Lewis Research Center, The 28th Aerospace Mechanisms Symposium May 1994 p 135-140 (For primary document see N94-33291 09-15)
Avail: CASI HC A02/MF A04

This paper discusses aspects of the design, development, and testing of the sensor cover on the Clementine (DSPSE) spacecraft. Particular attention is given to defining the typically ambiguous issue of cleanliness. To characterize performance with respect to these requirements, a simple and effective method for testing prototype seals was developed. This testing was useful for comparing various types of seals as well as for providing information about achievable cleanliness levels. The results were invaluable input for defining a realistic final cleanliness requirement that satisfied everyone from mechanisms to sensor engineers. Balancing torque margins (reliability) versus cost and/or weight of the system can be significantly influenced by the choice of seal type. Several seal types are discussed in terms of both cleanliness and ease of implementation. These design issues influence the actuator selection and structural integrity of the door. The cover system designed and fabricated as described above was thoroughly tested both on a component level and on the Clementine system level. Testing included characterization, vibration, pyro-shock, life, and thermal/vacuum. The extensive testing identified problems early enough that they could be resolved prior to integration and launch. Author (revised)

N94-33303*# Lockheed Engineering and Sciences Co., Houston, TX.
ENERGY ABSORBER FOR THE CETA **c18**
Clarence J. Wesselski *In* NASA. Lewis Research Center, The 28th

Aerospace Mechanisms Symposium May 1994 p 141-145 (For primary document see N94-33291 09-15)
Avail: CASI HC A01/MF A04

The energy absorber that was developed for the CETA (Crew Equipment and Translation Aid) on Space Station Freedom is a metal on metal frictional type and has a load regulating feature that prevents excessive stroking loads from occurring while in operation. This paper highlights some of the design and operating aspects and the testing of this energy absorber.
Author (revised)

N94-33304*# National Aeronautics and Space Administration. Lewis Research Center, Cleveland, OH.
DESIGN, CHARACTERIZATION, AND CONTROL OF THE NASA THREE DEGREE OF FREEDOM REACTION COMPENSATION PLATFORM c18
Craig Birkhimer (Case Western Reserve Univ., Cleveland, OH.), Wyatt Newman (Case Western Reserve Univ., Cleveland, OH.), Benjamin Choi, and Charles Lawrence *In its* The 28th Aerospace Mechanisms Symposium May 1994 p 147-152 (For primary document see N94-33291 09-15)
Avail: CASI HC A02/MF A04

Increasing research is being done into industrial uses for the microgravity environment aboard orbiting space vehicles. However, there is some concern over the effects of reaction forces produced by moving objects, especially motors, robotic actuators, and astronauts. Reaction forces produced by the movement of these objects may manifest themselves as undesirable accelerations in the space vehicle making the vehicle unusable for microgravity applications. It is desirable to provide compensation for such forces using active means. This paper presents the design and experimental evaluation of the NASA three degree of freedom reaction compensation platform, a system designed to be a testbed for the feasibility of active attenuation of reaction forces caused by moving objects in a microgravity environment. Unique 'linear motors,' which convert electrical current directly into rectilinear force, are used in the platform design. The linear motors induce accelerations of the displacer inertias. These accelerations create reaction forces that may be controlled to counteract disturbance forces introduced to the platform. The stated project goal is to reduce reaction forces by 90 percent, or -20 dB. Description of the system hardware, characterization of the actuators and the composite system, and design of the software safety system and control software are included.
Author (revised)

N94-33305*# Lockheed Engineering and Sciences Co., Houston, TX.
PIP PIN RELIABILITY AND DESIGN c37
Lane P. Skyles *In* NASA. Lewis Research Center, The 28th Aerospace Mechanisms Symposium May 1994 p 153-158 (For primary document see N94-33291 09-15)
Avail: CASI HC A02/MF A04

Pip pins are used in many engineering applications. Of particular interest to the aerospace industry is their use in various mechanism designs. Many payloads that fly aboard our nation's Space Shuttle have at least one actuated mechanism. Often these mechanisms incorporate pip pins in their design in order to fasten interfacing parts or joints. Pip pins are most often used when an astronaut will have a direct interface with the mechanism. This interfacing can be done during Space Shuttle mission EVA's (ExtraVehicular Activity). The main reason for incorporating pip pins is convenience and their ability to provide a quick release for interfacing parts. However, there are some issues that must be taken into account when using them in a design. These issues include documented failures and quality control problems when using substandard pip pins. A history of pip pins as they relate to the aerospace industry as well as general design features is discussed.
Author (revised)

N94-33306*# National Aeronautics and Space Administration. Lewis Research Center, Cleveland, OH.
INTELLIGENT CONTROL OF A MULTI-DEGREE-OF FREEDOM REACTION COMPENSATING PLATFORM SYSTEM USING FUZZY LOGIC c63
Benjamin B. Choi, Charles Lawrence, and Yueh-Jaw Lin *In its* The 28th Aerospace Mechanisms Symposium May 1994 p 159-165 (For primary document see N94-33291 09-15)
Avail: CASI HC A02/MF A04

This paper presents the development of a general-purpose fuzzy logic (FL) control methodology for isolating the external vibratory disturbances of space-based devices. According to the desired performance specifications, a full investigation regarding the development of an FL controller was done using different scenarios, such as variances of passive reaction-compensating components and external disturbance load. It was shown that the proposed FL controller is robust in that the FL-controlled system closely follows the prespecified ideal reference model. The comparative study also reveals that the FL-controlled system achieves significant improvement in reducing vibrations over passive systems.
Author (revised)

N94-33307*# Dornier System G.m.b.H., Friedrichshafen (Germany).
HIGH PRECISION MOVING MAGNET CHOPPER FOR VARIABLE OPERATION CONDITIONS c74
Winfried Aicher and Manfred Schmid *In* NASA. Lewis Research Center, The 28th Aerospace Mechanisms Symposium May 1994 p 167-181 (For primary document see N94-33291 09-15)
Avail: CASI HC A03/MF A04

In the context of an ESTEC technology contract, a Chopping Mechanism was developed and built with the Far Infrared and Submillimeter Telescope (FIRST) astronomy mission as a reference. The task of the mechanism is to tilt the subreflector of the telescope with an assumed mass of 2.5 kg about one chopping axis at nominal frequencies of up to 5 Hz and chopping angles of up to +/- 11.25 mrad with high efficiency (minimum time for position change). The chopping axis is required to run through the subreflector vertex. After performing a concept trade-off also considering the low operational temperatures in the 130 K range, a design using moving magnet actuators was found to be the favorite one. In addition, a bearing concept using flexible pivots was chosen to meet the high chopping accuracy required. With this approach, a very reliable design could be realized, since the actuators work without any mechanical contact between its moving and fixed parts, and the only bearings used are two flexible pivots supporting the subreflector mounting interface. The mechanism was completely built in titanium in a lightweight and stiff design. The moving magnet actuators were designed to meet the stringent requirements for minimum risetime (time necessary to move from one angular position to a new one) in the 20 msec range. The angular position and the corresponding chopping frequency as well can be arbitrarily selected by the user.
Author (revised)

N94-33308*# Space Systems/Loral, Palo Alto, CA.
TWO-AXIS ANTENNA POSITIONING MECHANISM c37
Michelle Herald and Leilani C. Wai *In* NASA. Lewis Research Center, The 28th Aerospace Mechanisms Symposium May 1994 p 183-197 (For primary document see N94-33291 09-15)
Avail: CASI HC A03/MF A04

The two-axis antenna positioning mechanism (TAAPM) is used to position three Ku-band and one C-band spot antennas on the INTELSAT 7 (I-7) spacecraft, which is a commercial telecommunications satellite purchased and operated by INTELSAT, an international consortium. The first I-7 was successfully launched on 22 Oct. 1993 from French Guiana on an Ariane launch vehicle. The TAAPM's on the first I-7 satellite successfully completed their in-orbit functional testing. The TAAPM was an entirely new design for Space Systems/Loral. This paper will describe the spacecraft/system requirements and application of the TAAPM and present the technical findings of TAAPM qualification and protoflight testing. Author (revised)

N94-33309*# California Univ., Berkeley. Space Sciences Lab.
DESIGN AND PERFORMANCE OF THE TELESCOPE AND DETECTOR COVERS ON THE EXTREME ULTRAVIOLET EXPLORER SATELLITE c18
James L. Tom *In* NASA. Lewis Research Center, The 28th Aerospace Mechanisms Symposium May 1994 p 199-209 (For primary document see N94-33291 09-15)
(Contract NAS5-29298)
Avail: CASI HC A03/MF A04

Two cover mechanisms were designed and developed for the Extreme Ultraviolet Explorer (EUVE) science payload to keep the EUVE telescope mirrors and detectors sealed from the atmospheric environment until the spacecraft was placed into orbit. There were four telescope front covers and seven motorized detector covers on the EUVE science payload. The EUVE satellite was launched into orbit in June 1992 and all the covers

operated successfully after launch. This success can be attributed to high design margins and extensive testing at each level of assembly. This paper described the design of the telescope front covers and the motorized detector covers. This paper also discusses some of the many design considerations and modifications made as performance and reliability problems became apparent from each phase of testing. Author

N94-33310*# MATRA Marconi Space, Toulouse (France). Automatic Control Systems and Propulsion Div.

POINTING AND TRACKING SPACE MECHANISM FOR LASER COMMUNICATION **c32**

A. Brunschvig and M. deBoisanger *In* NASA. Lewis Research Center, The 28th Aerospace Mechanisms Symposium May 1994 p 211-228 (For primary document see N94-33291 09-15)

Avail: CASI HC A03/MF A04

Space optical communication is considered a promising technology regarding its high data rate and confidentiality capabilities. However, it requires today complex satellite systems involving highly accurate mechanisms. This paper aims to highlight the stringent requirements which had to be fulfilled for such a mechanism, the way an existing design has been adapted to meet these requirements, and the main technical difficulties which have been overcome thanks to extensive development tests throughout the C/D phase initiated in 1991. The expected on-orbit performance of this mechanism is also presented. Author (revised)

N94-33311*# European Space Tribology Lab., Risley (England).

A COMPARISON OF THE PERFORMANCE OF SOLID AND LIQUID LUBRICANTS IN OSCILLATING SPACECRAFT BALL BEARINGS **c27**

S. Gill *In* NASA. Lewis Research Center, The 28th Aerospace Mechanisms Symposium May 1994 p 229-244 (For primary document see N94-33291 09-15)

Avail: CASI HC A03/MF A04

The European Space Tribology Laboratory (ESTL) has been engaged in a program to compare the performance of oscillating ball bearings when lubricated by a number of space lubricants, both liquid and solid. The results have shown that mean torque levels are increased by up to a factor of five above the normal running torque, and that often torque peaks of even greater magnitudes are present at the ends of travel. It is believed that these effects are caused by a build-up of compacted debris in the contact zone, thus reducing the ball/race conformity ratio. Author (revised)

N94-33312*# European Space Tribology Lab., Risley (England).

DEVELOPMENT OF LONG-LIFE, LOW-NOISE LINEAR BEARINGS FOR ATMOSPHERIC INTERFEROMETRY **c37**

E. W. Roberts, R. B. Watters, S. Gill, R. Birner, G. Lange, and W. Posselt *In* NASA. Lewis Research Center, The 28th Aerospace Mechanisms Symposium May 1994 p 245-264 (For primary document see N94-33291 09-15)

Avail: CASI HC A03/MF A04

This paper describes the development of dry-lubricated linear bearings for use on the Michelson interferometer for passive atmospheric sounding (MIPAS). Two candidate bearing systems were developed and tested. In the first, use was made of linear roller (needle) bearings equipped with a pulley-and-cable arrangement to prevent cage drift and to minimize roller slip. The second design was of a roller-guided bearing system in which guidance was provided by all bearings rolling along guide rods. The paper focuses on the development of these linear bearings systems and describes the approach taken in terms of bearing design, lubrication methods, screening programs, and thermal-vacuum testing. Development difficulties are highlighted and the solutions ultimately adopted are described. Author (revised)

N94-33313*# National Aeronautics and Space Administration. Lewis Research Center, Cleveland, OH.

THE PRELIMINARY EVALUATION OF LIQUID LUBRICANTS FOR SPACE APPLICATIONS BY VACUUM TRIBOMETRY **c27**

W. R. Jones, Jr., S. V. Pepper, P. Herrera-Fierro, D. Feuchter, T. J. Toddy, D. T. Jayne, D. R. Wheeler, P. B. Abel, E. Kingsbury, and W. Morales et al *In its* The 28th Aerospace Mechanisms Symposium May 1994 p 265-277 (For primary document see N94-33291 09-15)

Avail: CASI HC A03/MF A04

Four different vacuum tribometers for the evaluation of liquid lubricants for space applications are described. These range from simple ball-on-flat sliders with maximum in-situ control and surface characterization to an instrument bearing apparatus having no in-situ characterization. Thus, the former provides an abundance of surface chemical information but is not particularly simulative of most triboelements. On the other hand, the instrument bearing apparatus is completely simulative, but only allows post-mortem surface chemical information. Two other devices, a four-ball apparatus and a ball-on-plate tribometer, provide varying degrees of surface chemical information and tribo-simulation. Examples of data from each device are presented. Author

N94-33314*# Draper (Charles Stark) Lab., Inc., Cambridge, MA.

DESIGN OF A HIGH-SPEED RELIABLE BALL BEARING **c37**

Herbert B. Singer and Erik Gelotte *In* NASA. Lewis Research Center, The 28th Aerospace Mechanisms Symposium May 1994 p 279-283 (For primary document see N94-33291 09-15)

Avail: CASI HC A01/MF A04

A high-speed, reliable ball bearing has been designed for at least fifteen years of operation in space effectors, MWA's, and RWA's. Advanced bearing concepts have been used in this design, such as: no ball retainer, which eliminates all retainer-related problems; an external lubricazing system that will supply the lubricant at a specified flow rate; and a cartridge assembly that will allow the instrument user to purchase a ready to use bearing assembly, with lubricator. Currently, two assemblies are on life test at 12,000 RPM and have accumulated over 20,000 hours each, with consistent low-torque losses. This paper will describe each of the salient features. Author (revised)

N94-33315*# Lockheed Missiles and Space Co., Sunnyvale, CA.

MSAT BOOM JOINT TESTING AND LOAD ABSORBER DESIGN **c37**

D. H. Klinker, K. Shuey, and D. R. St.Clair *In* NASA. Lewis Research Center, The 28th Aerospace Mechanisms Symposium May 1994 p 285-302 (For primary document see N94-33291 09-15)

Avail: CASI HC A03/MF A04

Through a series of component and system-level tests, the torque margin for the MSAT booms is being determined. The verification process has yielded a number of results and lessons that can be applied to many other types of deployable spacecraft mechanisms. The MSAT load absorber has proven to be an effective way to provide high energy dissipation using crushable honeycomb. Using two stages of crushable honeycomb and a fusible link, a complex crush load profile has been designed and implemented. The design features of the load absorber lend themselves to use in other spacecraft applications. Author (revised)

N94-33316*# Lockheed Missiles and Space Co., Sunnyvale, CA.

SPECIAL TEST EQUIPMENT AND FIXTURING FOR MSAT REFLECTOR ASSEMBLY ALIGNMENT **c37**

Jeffrey A. Young, Michael R. Zinn, and David R. McCarten *In* NASA. Lewis Research Center, The 28th Aerospace Mechanisms Symposium May 1994 p 303-322 (For primary document see N94-33291 09-15)

Avail: CASI HC A03/MF A04

The MSAT Reflector Assembly is a state of the art subsystem for Mobile Satellite (MSAT), a geosynchronous-based commercial mobile telecommunication satellite program serving North America. The Reflector Assembly consisted of a deployable, three-hinge, folding-segment Boom, deployable 5.7 x 5.3-meter 16-rib Wrap-Rib Reflector, and a Reflector Pointing Mechanism (RPM). The MSAT spacecraft was based on a Hughes HS601 spacecraft bus carrying two Reflector Assemblies independently dedicated for L-band transmit and receive operations. Lockheed Missiles and Space Company (LMSC) designed and built the Reflector Assembly for MSAT under contract to SPAR Aerospace Ltd. Two MSAT satellites were built jointly by SPAR Aerospace Ltd. and Hughes Space and Communications Co. for this program, the first scheduled for launch in 1994. When scaled for wavelength, the assembly and alignment requirements for the Reflector Assembly were in many instances equivalent to or exceeded that of a diffraction-limited visible light optical system. Combined with logistical constraints inherent to large, compliant, lightweight structures; 'bolt-on' alignment; and remote, indirect spacecraft access; the technical challenges were formidable. This document describes the alignment methods, the special test equipment, and fixturing for Reflector Assembly assembly and alignment. Author

N94-33317*# Astro Aerospace Corp., Carpinteria, CA.
DEPLOYABLE AND RETRACTABLE TELESCOPING TUBULAR STRUCTURE DEVELOPMENT **c37**
M. W. Thomson *In* NASA. Lewis Research Center, The 28th Aerospace Mechanisms Symposium May 1994 p 323-338 (For primary document see N94-33291 09-15)
Avail: CASI HC A03/MF A04

A new deployable and retractable telescoping boom capable of high deployed stiffness and strength is described. Deployment and retraction functions are controlled by simple, reliable, and fail-safe latches between the tubular segments. The latch and a BI-STEM (Storable Tubular Extendible Member) actuator work together to eliminate the need for the segments to overlap when deployed. This yields an unusually lightweight boom and compact launch configuration. An aluminum space-flight prototype with three joints displays zero structural deadband, low hysteresis, and high damping. The development approach and difficulties are discussed. Test results provide a joint model for sizing flight booms of any diameter and length. Author

N94-33318*# Jet Propulsion Lab., California Inst. of Tech., Pasadena.
LESSONS LEARNED FROM SELECTING AND TESTING SPACEFLIGHT POTENTIOMETERS **c19**
T. Iskenderian *In* NASA. Lewis Research Center, The 28th Aerospace Mechanisms Symposium May 1994 p 339-358 (For primary document see N94-33291 09-15)
Avail: CASI HC A03/MF A04

A solar array drive (SAD) was designed for operation on the TOPEX/POSEIDON spacecraft that was launched in August, 1992. The experience gained in selecting, specifying, testing to failure, and redesigning its position sensor produced valuable lessons for future component selection and qualification. Issues of spaceflight heritage, cost/benefit/risk assessment, and component specification are addressed. It was found that costly schedule and budget overruns may have been avoided if the capability of the candidate sensors to meet requirements had been more critically examined prior to freezing the design. The use of engineering models and early qualification tests is also recommended. Author

N94-33319*# Jet Propulsion Lab., California Inst. of Tech., Pasadena.
THE GALILEO HIGH GAIN ANTENNA DEPLOYMENT ANOMALY **c32**
Michael R. Johnson *In* NASA. Lewis Research Center, The 28th Aerospace Mechanisms Symposium May 1994 p 359-377 (For primary document see N94-33291 09-15)
Avail: CASI HC A03/MF A04

On April 11, 1991, the Galileo spacecraft executed a sequence that would open the spacecraft's High Gain Antenna. The Antenna's launch restraint had been released just after deployment sequence, the antenna, which opens like an umbrella, never reached the fully deployed position. The analyses and tests that followed allowed a conclusive determination of the likely failure mechanisms and pointed to some strategies to use for recovery of the high gain antenna. Author

N94-33320*# TiNi Alloy Co., San Leandro, CA.
IMPLEMENTATION OF HEATERS ON THERMALLY ACTUATED SPACECRAFT MECHANISMS **c18**
John D. Busch and Michael D. Bokaie *In* NASA. Lewis Research Center, The 28th Aerospace Mechanisms Symposium May 1994 p 379-393 (For primary document see N94-33291 09-15)
Avail: CASI HC A03/MF A04

This paper presents general insight into the design and implementation of heaters as used in actuating mechanisms for spacecraft. Problems and considerations that were encountered during development of the Deep Space Probe and Science Experiment (DSPSE) solar array release mechanism are discussed. Obstacles included large expected fluctuations in ambient temperature, variations in voltage supply levels outgassing concerns, heater circuit design, materials selection, and power control options. Successful resolution of these issues helped to establish a methodology which can be applied to many of the heater design challenges found in thermally actuated mechanisms. Author

N94-33321*# G and H Technology, Inc., Camarillo, CA.
PAYLOAD HOLDDOWN AND RELEASE MECHANISM **c37**
Dale Chaput, Mark Visconti, Michael Edwards, and Tom Moran *In* NASA. Lewis Research Center, The 28th Aerospace Mechanisms Symposium May 1994 p 395-411 (For primary document see N94-33291 09-15)
Avail: CASI HC A03/MF A04

A payload holddown and release mechanism, designated the Model 1172, was designed and built at G&H Technology during the winter of 1992/1993. The mechanism is able to restrain and release a 45-pound payload with minimal tipoff. The payload is held in place by a stainless steel band and released using electrically triggered non-explosive actuators. These actuators provide reliable operation with negligible shock and no special handling requirements. The performance of the mechanism was demonstrated in two flight tests. Data showed pitch and yaw tipoff rates of less than 0.07 radian (4 degree) per second. The Model 1172 design is an efficient replacement for conventional payload deployment devices, especially where low transmitted shock is required. Author

N94-33322*# Naval Research Lab., Washington, DC.
ADVANCED RELEASE TECHNOLOGIES PROGRAM **c37**
Bill Purdy *In* NASA. Lewis Research Center, The 28th Aerospace Mechanisms Symposium May 1994 p 413-427 (For primary document see N94-33291 09-15)
Avail: CASI HC A03/MF A04

The objective of the ARTS program was to develop lighter and less expensive spacecraft ordnance and release systems that answer to the requirements of a wide variety of spacecraft applications. These improvements were to be evaluated at the spacecraft system level, as it was determined that there were substantial system-level costs associated with the present ordnance and release subsystems. New, better devices were to be developed, then flight qualified, then integrated into a flight experiment in order to prove the reliability required for their subsequent use on high-reliability spacecraft. The secondary goal of the program was to quantify the system-level benefits of these new subsystems based upon the development program results. Three non-explosive release mechanisms and one laser-diode-based ordnance system were qualified under the program. The release devices being developed were required to release high preloads because it is easier to scale down a release mechanism than to scale it up. The laser initiator developed was required to be a direct replacement for NASA Standard Initiators, since these are the most common initiator in use presently. The program began in October, 1991, with completion of the flight experiment scheduled for February, 1994. This paper provides an overview of the ARTS program, discusses the benefits of using the ARTS components, introduces the new components, compares them with conventional systems and each other, and provides recommendations on how best to implement them. Author

N94-33323*# National Aeronautics and Space Administration. Lyndon B. Johnson Space Center, Houston, TX.
LOAD-LIMITING LANDING GEAR FOOTPAD ENERGY ABSORPTION SYSTEM **c16**
Chris Hansen and Ted Tsai *In* NASA. Lewis Research Center, The 28th Aerospace Mechanisms Symposium May 1994 p 429-441 (For primary document see N94-33291 09-15)
Avail: CASI HC A03/MF A04

As a precursor to future manned missions to the moon, an inexpensive, unmanned vehicle that could carry small, scientific payloads to the lunar surface was studied by NASA. The vehicle, called the Common Lunar Lander, required extremely optimized structural systems to increase the potential payload mass. A lightweight energy-absorbing system (LAGFEAS), which also acts as a landing load-limiter was designed to help achieve this optimized structure. Since the versatile and easily tailored system is a load-limiter, it allowed for the structure to be designed independently of the ever-changing landing energy predictions. This paper describes the LAGFEAS system and preliminary verification testing performed at NASA's Johnson Space Center for the Common Lunar Lander program. Author

16 SPACE TRANSPORTATION

Includes passenger and cargo space transportation, e.g., shuttle operations; and space rescue techniques.

For related information see also *03 Air Transportation and Safety* and *18 Spacecraft Design, Testing and Performance.* For space suits see *54 Man/System Technology and Life Support.*

N94-32020 Naval Postgraduate School, Monterey, CA.
THEORETICAL BASIS FOR STATE VECTOR COMPARISON, RELATIVE POSITION DISPLAY, AND RELATIVE POSITION/RENDEZVOUS PREDICTION M.S. Thesis
Lester B. Makepeace, III Dec. 1993 94 p Limited Reproducibility: More than 20% of this document may be affected by microfiche quality
(AD-A277216) Avail: CASI HC A05

This thesis outlines the theoretical underpinnings used for the software designed to meet Detailed Technical Objectives 700-6 and 700-7 for the Space Shuttle Discovery mission STS-51. The primary goal was to compare state vector information produced by an onboard GPS receiver and Discovery's computers and provide real time display of the results. Because state vector information for the ORFEUS/SPAS payload was also available, relative position and rendezvous information between Discovery and ORFEUS/SPAS was made possible. Analysis of the various state vectors was used to produce a graphical display, in an operationally meaningful format, to the flight crew of Discovery. DTIC

N94-32190# Industrial Coll. of the Armed Forces, Washington, DC.
ACCESS TO SPACE: THE SPACE SHUTTLE'S EVOLVING ROLEE Report, Aug. 1992 - Apr. 1993
Steven R. Duttry Apr. 1993 44 p
(AD-A276785; NDU-ICAF-93-F27) Avail: CASI HC A03/MF A01

Access to space is of extreme importance to our nation and the world. Military, civil, and commercial space activities all depend on reliable space transportation systems for access to space at a reasonable cost. The Space Transportation System or Space Shuttle was originally planned to provide transportation to and from a manned Earth-orbiting space station. To justify the development and operations costs, the Space Shuttle took on other space transportation requirements to include DoD, civil, and a growing commercial launch market. This research paper or case study examines the evolving role of the Space Shuttle as our nation's means of accessing space. The case study includes a review of the events leading to the development of the Space Shuttle, identifies some of the key players in the decision-making process, examines alternatives developed to mitigate the risks associated with sole reliance on the Space Shuttle, and highlights the impacts of this national space policy following the Challenger accident. DTIC

N94-32295 George Washington Univ., Washington, DC.
COMPUTATIONAL METHODS FOR FRICTIONAL CONTACT WITH APPLICATIONS TO THE SPACE SHUTTLE ORBITER NOSE-GEAR TIRE Ph.D. Thesis
John A. Tanner 1993 210 p
Avail: Univ. Microfilms Order No. DA9313716

A computational procedure has been presented for the solution of frictional contact problems for aircraft tires. The Space Shuttle nose gear tire was modeled using a two-dimensional laminated anisotropic shell theory with the effects of variation in material and geometric parameters, transverse-shear deformation, and geometric nonlinearities included. The contact conditions were incorporated into the formulation by using a perturbed Lagrangian approach with the fundamental unknowns consisting of the stress resultants, the generalized displacements, and the Lagrange multipliers associated with the contact and friction conditions. The contact-friction algorithm was based on a modified Coulomb friction law. The elemental arrays were obtained by using a modified two-field, mixed variational principle. The modification consisted of augmenting the functional of that principle by two terms: the Lagrange multiplier vector associated with nodal normal and tangential contact load intensities and a regularization term which was quadratic in the Lagrange multiplier vector. Experimental measurements were made to define the response of the Space Shuttle nose-gear tire to inflation pressure loads and to combined inflation pressure loads and static normal loads against a rigid flat plate. These experimental results describe meridional growth of the tire cross section due to inflation loading, the static load-deflection characteristics of the tire, the geometry of the tire footprint under the static loading conditions, and the normal and tangential load intensity distributions in the tire footprint for the various static vertical loading conditions. Numerical results were obtained for the Space Shuttle nose-gear tire subjected to inflation pressure loads and combined inflation pressure and contact loads against a rigid flat plate. Comparisons were made between the experimental measurements and the numerical results. Dissert. Abstr.

N94-33100*# Rockwell International Corp., Huntsville, AL. Space Systems Div.
ADVANCED TRANSPORTATION SYSTEM STUDY: MANNED LAUNCH VEHICLE CONCEPTS FOR TWO WAY TRANSPORTATION SYSTEM PAYLOADS TO LEO Final Report, 15 Feb. 1992 - 15 Dec. 1993
James B. Duffy 1993 589 p
(Contract NAS8-39207)
(NASA-CR-193951; NAS 1.26:193951; SSD93M0025-1) Avail: CASI HC A25/MF A06

The purpose of the Advanced Transportation System Study (ATSS) task area 1 study effort is to examine manned launch vehicle booster concepts and two-way cargo transfer and return vehicle concepts to determine which of the many proposed concepts best meets NASA's needs for two-way transportation to low earth orbit. The study identified specific configurations of the normally unmanned, expendable launch vehicles (such as the National Launch System family) necessary to fly manned payloads. These launch vehicle configurations were then analyzed to determine the integrated booster/spacecraft performance, operations, reliability, and cost characteristics for the payload delivery and return mission. Design impacts to the expendable launch vehicles which would be required to perform the manned payload delivery mission were also identified. These impacts included the implications of applying NASA's man-rating requirements, as well as any mission or payload unique impacts. The booster concepts evaluated included the National Launch System (NLS) family of expendable vehicles and several variations of the NLS reference configurations to deliver larger manned payload concepts (such as the crew logistics vehicle (CLV) proposed by NASA JSC). Advanced, clean sheet concepts such as an F-1A engine derived liquid rocket booster (LRB), the single stage to orbit rocket, and a NASP-derived aerospace plane were also included in the study effort. Existing expendable launch vehicles such as the Titan 4, Ariane 5, Energia, and Proton were also examined. Although several manned payload concepts were considered in the analyses, the reference manned payload was the NASA Langley Research Center's HL-20 version of the personnel launch system (PLS). A scaled up version of the PLS for combined crew/cargo delivery capability, the HL-42 configuration, was also included in the analyses of cargo transfer and return vehicle (CTRV) booster concepts. In addition to strictly manned payloads, two-way cargo transportation systems (CTRV's) were also examined. The study provided detailed design and analysis of the performance, reliability, and operations of these concepts. The study analyzed these concepts as unique systems and also analyzed several combined CTRV/booster configurations as integrated launch systems (such as for launch abort analyses). Included in the set of CTRV concepts analyzed were the medium CTRV, the integral CTRV (in both a pressurized and unpressurized configuration), the winged CTRV, and an attached cargo carrier for the PLS system known as the PLS caboose. Author (revised)

N94-33323*# National Aeronautics and Space Administration. Lyndon B. Johnson Space Center, Houston, TX.
LOAD-LIMITING LANDING GEAR FOOTPAD ENERGY ABSORPTION SYSTEM
Chris Hansen and Ted Tsai *In* NASA. Lewis Research Center, The 28th Aerospace Mechanisms Symposium May 1994 p 429-441 (For primary document see N94-33291 09-15)
Avail: CASI HC A03/MF A04

17 SPACE COMM., SPACECRAFT COMM., COMMAND & TRACKING

Includes telemetry; space communications networks; astronavigation and guidance; and radio blackout.

For related information see also *04 Aircraft Communications and Navigation* and *32 Communications and Radar.*

No abstracts in this category.

18 SPACECRAFT DESIGN, TESTING AND PERFORMANCE

Includes satellites; space platforms; space stations; spacecraft systems and components such as thermal and environmental controls; and attitude controls.

For life support systems see *54 Man/System Technology and Life Support.* For related information see also *05 Aircraft Design, Testing and Performance, 39 Structural Mechanics,* and *16 Space Transportation.*

N94-31292# Environmental Research Inst. of Michigan, Ann Arbor.
SATELLITE DIRECT READOUT: OPPORTUNITIES FOR SCIENCE EDUCATION
Thomas W. Wagner Feb. 1994 42 p
(Contract DLA900-88-D-0392)
(AD-A276257; ERIM-253860-1-X(R)) Avail: CASI HC A03/MF A01

This report describes the technology associated with direct reception and analysis of environmental (weather) satellite data and the opportunities it offers to educators for enhancing mathematics, science, and technology education in the United States. With newly available capabilities, direct readout is applicable to a wide range of environmental assessments, information networking, and modelling applications, in addition to the learning opportunities in K-16 education. This report describes the institutional, technical, and pedagogical obstacles to widespread use of this technology and suggests approaches to overcoming these obstacles. DTIC

N94-31382# Sandia National Labs., Albuquerque, NM.
USING MONTE CARLO TECHNIQUES AND PARALLEL PROCESSING FOR DEBRIS HAZARD ANALYSIS OF ROCKET SYSTEMS
R. A. LaFarge Feb. 1994 56 p
(Contract DE-AC04-94AL-85000)
(DE94-007250; SAND-93-2073) Avail: CASI HC A04/MF A01

Sandia National Laboratories has been involved with rocket systems for many years. Some of these systems have carried high explosive onboard, while others have had FTS for destruction purposes whenever a potential hazard is detected. Recently, Sandia has also been involved with flight tests in which a target vehicle is intentionally destroyed by a projectile. Such endeavors always raise questions about the safety of personnel and the environment in the event of a premature detonation of the explosive or an activation of the FTS, as well as intentional vehicle destruction. Previous attempts to investigate fragmentation hazards for similar configurations have analyzed fragment size and shape in detail but have computed only a limited number of trajectories to determine the probabilities of impact and casualty expectations. A computer program SAFETIE has been written in support of various SNL flight experiments to compute better approximations of the hazards. SAFETIE uses the AMEER trajectory computer code and the Engineering Sciences Center LAN of Sun workstations to determine more realistically the probability of impact for an arbitrary number of exclusion areas. The various debris generation models are described. DOE

N94-31470 Stanford Univ., CA.
PHASE-LOCK ROLL CONTROL OF INERTIALLY POINTING SPACECRAFT Ph.D. Thesis
Jeffrey Roger Crerie 1993 203 p
Avail: Univ. Microfilms Order No. DA9326452

The spacecraft which houses the Stanford Relativity Gyroscope Experiment (GP-B) is designed to roll with a 10 minute period about its pointing axis. A precise measurement of roll phase is needed to demodulate the two relativity effects being measured by GP-B. Optimally, the spacecraft will be flown with no rotating machinery on board, so it is desired to control roll without the use of conventional rate gyros. A new technique has been devised to achieve highly accurate roll control without a rate gyro. This is done by employing one or more slit star sensors which rotate with the spacecraft, and correlate their output with a known reference to produce a measurement of roll offset. The technique developed to control roll phase and rate mimics those used in pseudorandom noise telecommunication. The algorithm regards the intensity pattern of the surrounding star field as pseudorandom noise which repeats every 360 degrees, and sets up a 'phase-locked' loop to align the pattern with a stored reference pattern. Single-axis simulations confirm that such a device, combined with a steady-state Kalman estimator, can control roll position to an accuracy of 20 arcsec RMS, and roll rate to an accuracy of 0.92 arcsec/sec RMS, even when the star sensor output and reference values are encoded with one bit and disturbance torques are very large. A hardware simulation was useful in demonstrating the capabilities of this simple, low-cost system and in determining the noise characteristics of the combined sensor and electronics. A laboratory-based hardware simulation was achieved by modeling the intensities of stars located within the relevant band on a NeXT graphics monitor and then animating this image at a rate governed by the plant dynamics model. This 'scrolling star field' is imaged onto a high-speed, high-sensitivity photodiode whose output undergoes a one-bit discretization before correlation with the stored reference. The correlation scheme, subsequent filtering, and updates to the dynamics model all occur within the Motorola DSP56001 which comes installed on the NeXT computer. This hardware-in-the-loop test validates the theory previously described.
Dissert. Abstr.

N94-31564 Texas Univ., Austin.
ADAPTIVE NONLINEAR CONTROL OF SPACECRAFT Ph.D. Thesis
Jyh-Jong Sheen 1993 139 p
Avail: Univ. Microfilms Order No. DA9323547

The feedback linearization technique is applied to the problem of spacecraft attitude control and momentum management with control moment gyros (CMG's). The feedback linearization consists of a coordinate transformation and a nonlinear state feedback to cancel the nonlinear dynamics. These two steps result in a linear system equivalent to the original nonlinear system. Pole placement techniques are then used to place the closed-loop poles. Stability in a neighborhood of a controllable torque equilibrium attitude (TEA) is guaranteed. The nonlinear control law developed via feedback linearization is simplified by a standard linearization technique. The linearized nonlinear controller provides a natural way to select control gains for the multiple-input, multiple-output spacecraft system. Simulation results using the linearized nonlinear controller show good performance relative to the nonlinear controller in the neighborhood of the TEA. A chief limitation of the feedback linearization technique is that it requires an exact cancellation of nonlinear terms in order to obtain linear input-output behavior. As a consequence, if there are uncertainties in parameters, the cancellation is no longer exact and the linear behavior can not be obtained. Adaptive control of linearizable systems is used to overcome this restriction and to achieve asymptotic linear behavior. Two adaptive control laws are developed. One is based on a tracking error model. The other utilizes both the tracking error and the prediction error. The convergence properties of the adaptive algorithms are proved. The adaptive nonlinear control laws are applied to the problem of spacecraft attitude control and momentum management, assuming uncertainties in the spacecraft principal inertias. The combined tracking and prediction-error based adaptive controller is shown to have improvement on the performance of the tracking-error based adaptive controller. Both algorithms are also tested under the circumstance of unmodeled dynamics with the cross-product inertias neglected. The adaptive tracking algorithm results in better estimation errors and state response. Dissert. Abstr.

N94-31705# Technische Univ., Delft (Netherlands). Faculty of Aerospace Engineering.
THE INFLUENCE OF THE DEORBIT-BURN MANOEUVRE ON THE FOOTPRINT OF A RE-ENTRY CAPSULE
E. Mooij Jul. 1993 96 p

(LR-727; ISBN-9-06-275906-8; ETN-94-96137) Copyright Avail: CASI HC A05/MF A01

The implementation of the deorbit-burn maneuver in the entry simulation software START (Simulation Tool for Atmospheric Re-entry Trajectories) is presented. Two models are derived. The first model assumes an impulsive Delta(v), in which the (inertial) velocity change is vectorially added to the velocity of the spacecraft. The second model takes the finite time of the maneuver into account and the maneuver is a thrusted one. The two models are evaluated and the differences in flight time, entry conditions and entry path are shown to be substantial. The impulsive model is used to do a sensitivity analysis for the Assured Crew Return Vehicle (ACRV). The influence of initial height, magnitude and direction of the burn on the footprint of the vehicle is shown and discussed. ESA

N94-31723 Toronto Univ. (Ontario).
CHAOTIC ATTITUDE MOTION OF SATELLITES IN THE CENTRAL GRAVITATIONAL FIELD Ph.D. Thesis
Xiaohua Tong 1992 176 p
(ISBN-0-315-78768-6) Avail: Univ. Microfilms Order No. DANN78768

New developments in nonlinear dynamics in the last two decades, especially chaos theory, make it possible to study various dynamic phenomena of nonlinear systems. In the present thesis, the nonlinear attitude motion of a satellite consisting of a single rigid body, or of two rigid bodies in gyrostat configuration, in a central gravitational field, on a circular or an elliptic orbit, is studied with particular attention given to the understanding of long-time dynamic behavior for a wide range of parameters. For the attitude motion of satellites in their orbital plane, it is shown that there exists chaotic motion for satellites with or without internal damping, in an elliptic orbit. It is shown that the system which describes the dynamic behavior of satellites without internal damping is nonintegrable. Thus chaotic motion and regular motion coexist. The connection between periodic motion and chaotic motion for satellites without internal damping is investigated numerically by studying the local bifurcations of periods motion. For satellites with internal damping, analytic criteria based on the Melnikov method are presented to determine whether chaotic motion might occur, and to reveal the connection between periodic motion and chaotic motion. The transition from periodic motion to chaotic motion for satellites with internal damping is studied by three means: phase planes, Poincare maps, and Lyapunov exponents. For the attitude motion of spinning axisymmetric single-body satellites or spinning axisymmetric gyrostat satellites without internal damping in a circular orbit, the Hamiltonians for the attitude motion are established and then used to reveal the characteristics of different types of motion, i.e. periodic motion, quasiperiodic motion, and chaotic motion. It is shown that except for the integrable cases where the attitude motion is either confined to small attitude angles around the equilibrium attitude positions, or the satellites are free of external torques, regular (periodic and quasiperiodic) and chaotic motion coexist depending on initial conditions, and the transition between the two types of motion is complicated. The global characteristics of the chaotic motion are obtained via the Poincare map technique. It is found that for gyrostat satellites with the axes of symmetry of the platform and the rotor coinciding, the rotor has a significant effect not only on the stability of equilibrium attitude positions, but also on the general dynamic behavior of the motion, e.g. a chaotic motion will become more and more regular as the spin velocity of the rotor increases. This is obviously of great importance in the design of gyrostat satellites.
Dissert. Abstr.

N94-31771 Institut des Hautes Etudes Scientifiques, Bures-sur-Yvette (France).
TESTING FOR PREFERRED-FRAME EFFECTS IN GRAVITY WITH ARTIFICIAL EARTH SATELLITES
T. Damour (Observatoire de Paris, France.) and G. Esposito-Farese (Centre National de la Recherche Scientifique, Marseilles, France.) Oct. 1993 30 p Submitted for publication Limited Reproducibility: More than 20% of this document may be affected by microfiche quality
(PB94-148459; IHES/P/93/48) Avail: CASI HC A03

As gravity is a long-range force, one might a priori expect the Universe's global matter distribution to select a preferred rest frame for local gravitational physics. At the post-Newtonian approximation, two parameters suffice to describe the phenomenology of preferred-frame effects. It is pointed out that the observation of particular orbits of artificial Earth satellites has the potential of improving the alpha sub 1 limits by a couple of orders of magnitude, thanks to the appearance of small divisors which enhance the corresponding preferred-frame effects. There is a discrete set of inclinations which lead to arbitrarily small divisors, while, among zero-inclination (equatorial) orbits, geostationary ones are near optimal. The main alpha sub 1 - induced effects are: (1) a complex secular evolution of the eccentricity vector of the orbit, describable as the vectorial sum of several independent rotations; and (2) a yearly oscillation in the longitude of the satellite.
NTIS

N94-31910# Montreal Univ. (Quebec). Dept. de Genie Physique.
ELECTRICAL PROPERTIES OF DOUBLE LAYER DIELECTRIC STRUCTURES FOR SPACE TECHNOLOGY Ph.D. Thesis
Anqing Lian Apr. 1993 160 p
(ISBN-0-315-86547-4; CTN-94-61211) Copyright Avail: Micromedia Ltd., Technical Information Centre, 240 Catherine Street, Suite 305, Ottawa, Ontario, K2P 2G8, Canada HC/MF

Polymeric films such as polyimide (PI) and polyethylene terephthalate (PET) are used in space technology as thermal blankets. Thin SiO2 and SiN coatings plasma deposited onto PI and PET surfaces were proposed to protect the blanket materials against the space environment. The electrical properties of this kind of dual layer dielectric structure were investigated to understand the mechanisms for suppressing charge accumulation and flashover. Bulk and surface electrical conductivities of thin single-layer PI and PET samples and of the dual layer SiO2 and SiN combinations with PI and PET were measured in a range of applied electrical fields. The capacitance voltage (CV) technique was used for analyzing charge transport and distribution in the structures. The electric current in the bulk of the SiO2/PI and SiN/PI samples was found to depend on the polarity of the electric field. Other samples did not exhibit any such polarity effect. The polarity dependence is attributed to charge trapping at the PI/plasma deposit interface. The CV characteristics of the Al-PI-SiO2-Si structure confirm that charges which can modify the local electric field can be trapped near the interface. A model is proposed to interpret the properties of the currents in dual layer structures. This model can semi-quantitatively explain all the observed results. Author (CISTI)

N94-32010 Arnold Engineering Development Center, Arnold AFS, TN.
PRE-FLIGHT TESTING OF THERMOELECTRIC QUARTZ CRYSTAL MICROBALANCES (TQCM) FOR MIDCOURSE SPACE EXPERIMENT (MSX) SPACECRAFT Final Report, 15 Dec. 1992 - 10 May 1993
R. J. Bryson, F. L. Seiber, W. T. Bertrand, J. H. Jones, and B. E. Wood Feb. 1994 98 p Prepared in cooperation with Calspan Corp., Arnold AFS, TN Limited Reproducibility: More than 20% of this document may be affected by microfiche quality
(AD-A277054; AEDC-TR-93-24) Avail: Issuing Activity (Defense Technical Information Center (DTIC))

Testing of six Midcourse Space Experiment (MSX) satellite thermoelectric quartz crystal microbalances (TQCM) was completed. These will be used to monitor contamination at various locations on the spacecraft. The tests included a 3-week drift test, power on/off tests; temperature cycling of TQCM crystals, mounting base, and flight electronics box; and deposition of carbon dioxide gas. The data obtained will be used for analyzing MSX satellite flight contamination data. DTIC

N94-32039# Industrial Coll. of the Armed Forces, Washington, DC.
SATELLITE COMMUNICATIONS INDUSTRY Research Report, Aug. 1992 - Apr. 1993
Mark S. Maranville Apr. 1993 54 p
(AD-A276685; NDU-ICAF-93-DIS) Avail: CASI HC A04/MF A01

This paper documents a baseline assessment of the Satellite Communications Industry which is defined as companies that do the following: (1) build communications satellites; (2) build communications satellite earth terminals; and (3) provide satellite communications services. The assessment uses the standard analysis tools of Structure, Conduct, and Performance to evaluate the current health of the industry and includes a discussion of the outlook for the industry, the industry's strategy for survival, and government policy recommendations. DTIC

N94-32208# Naval Postgraduate School, Monterey, CA. Dept. of Mathematics.
SEMIANALYTIC SATELLITE THEORY (SST): MATHEMATICAL

ALGORITHMS Report, Jul. 1992 - Jan. 1994
D. A. Danielson, B. Neta, and L. W. Early Jan. 1994 106 p
(AD-A276836; NPS-MA-94-001) Avail: CASI HC A06/MF A02

Modern space surveillance requires fast and accurate orbit predictions for myriads of objects in a broad range of Earth orbits. Conventional Special Perturbations orbit propagators, based on numerical integration of the osculating equations of motion, are accurate but extremely slow. Conventional General Perturbations orbit propagators, based on fully analytical theories like those of Brouwer, are faster but contain large errors due to inherent approximations in the theories. New orbit generators based on Semianalytic Satellite Theory have been able to approach the accuracy of Special Perturbations propagators and the speed of General Perturbations propagators. Semianalytic Satellite Theory has been originated by P.J. Cefola and his colleagues, but the theory is scattered throughout the published and unpublished literature. In this document the theory is simplified, assembled, unified, and extended. DTIC

N94-32369 Naval Postgraduate School, Monterey, CA.
TRAJECTORY PLANNING FOR SPACE MANIPULATORS M.S. Thesis
Mary M. Zurowski Dec. 1993 74 p Limited Reproducibility: More than 20% of this document may be affected by microfiche quality
(AD-A277229) Avail: CASI HC A04

The angular momentum of a free-flying multibody system in space is a conserved quantity. This conservation law acts as a nonholonomic constraint and manifests itself when cyclic motion of the articulated joints of an on board manipulator produces a net change in the orientation of the whole system. This poses two important and coupled problems: (1) the motion planning problem of the manipulator for attitude reorientation of the space structure using internal motion of the joints, and (2) planning the manipulator joint trajectories that produce repeatable motion of all the configuration variables. We have adopted a surface integral approach to come up with algorithms for these nonholonomic motion planning problems. DTIC

N94-32502 British Columbia Univ., Vancouver.
DYNAMICS AND CONTROL OF ORBITING FLEXIBLE SYSTEMS: A FORMULATION WITH APPLICATIONS Ph.D. Thesis
Chun-Ki Alfred Ng 1992 312 p
(ISBN-0-315-75390-0) Avail: Univ. Microfilms Order No. DANN75390

A relatively general formulation for studying the nonlinear dynamics and control of spacecraft with interconnected flexible members in a tree-type topology is developed. The distinctive features of the formulation include the following: (1) It is applicable to a large class of present and future spacecraft with flexible beam and plate type appendages, arbitrary in number and orientation. (2) The members are free to undergo predefined slewing maneuvers to facilitate modelling of sun tracking solar panels and large angle maneuvers of space based robots. (3) Solar radiation induced thermal deformations of flexible members are incorporated in the study. (4) The governing equations of motion are highly nonlinear, nonautonomous and coupled. They are programmed in a modular fashion to help isolate the effects of flexibility, librational motion, thermal deformations, slewing maneuvers, shifting center of mass, higher modes, initial conditions, etc. The first chapter of the thesis presents a general background to the subject and a brief review of the relevant literature on multibody dynamics. This is followed by the kinematics and kinetics of the problem leading to the Lagrangian equations of motion. The third chapter focuses on methodology and development of the computer code suitable for parametric dynamical study and control. Next versatility of the general formulation is illustrated through the analysis of five spacecraft configurations of contemporary interest the next generation of multi-purpose communications spacecraft represented by the INdian SATellite II (IN-SAT II): the First Element Launch (FEL) and the Permanently Manned Configuration (PMC) of the proposed Space Station Freedom; the Mobile Servicing System (MSS) to be developed by Canada for operation on the Space Station; and the Space Flyer Unit (SFU) to be launched by Japan in mid-nineties. In the FEL study, the attention is directed towards interactions between the librational and vibrational dynamics. During the PMC investigation, effects of the thermal deformation and orbital eccentricity are introduced and the microgravity environment around the station center of mass explored. The MSS study assesses pointing errors arising from inplane and out-of-plane maneuvers of the robotic arms. The SFU represents a challenging configuration to assess deployment and retrieval dynamics associated with a solar array. Parameters considered here include symmetry, orientation, and duration of the deployment/retrieval maneuvers. Results of the dynamical study clearly shows that, under critical combinations of parameters, the systems can become unstable. Obviously, the next logical step is to explore control strategies to restore equilibrium. To that end, feasibility of the nonlinear control based on the Feedback Linearization Technique (FLT) is explored with reference to the INSAT II and the MSS. Results show the procedure to be quite promising in controlling the INSAT II over a range of disturbances, including the thermal effects. Application of the control to the MSS reduced the pointing error induced by robotic arm maneuvers significantly. The amount of information obtained through a planned parametric analysis of the system dynamics and control is indeed enormous. More significant results are summarized in the concluding chapter together with a few recommendations for future study. Dissert. Abstr.

N94-32667# Oak Ridge National Lab., TN.
VULNERABILITY ASSESSMENT OF A SPACE BASED WEAPON PLATFORM ELECTRONIC SYSTEM EXPOSED TO A THERMONUCLEAR WEAPON DETONATION
C. L. Perez (North Carolina Univ., Chapel Hill.) and J. O. Johnson 1994 9 p Presented at the 8th International Conference on Radiation Shielding, Arlington, TX, 24-27 Apr. 1994
(Contract DE-AC05-84OR-21400)
(DE94-007229; CONF-940424-16) Avail: CASI HC A02/MF A01

Rapidly changing world events, the increased number of nations with inter-continental ballistic missile capability, and the proliferation of nuclear weapon technology will increase the number of nuclear threats facing the world today. Monitoring these nation's activities and providing an early warning and/or intercept system via reconnaissance and surveillance satellites and space based weapon platforms is a viable deterrent against a surprise nuclear attack. However, the deployment of satellite and weapon platform assets in space will subject the sensitive electronic equipment to a variety of natural and man-made radiation environments. These include Van Allen Belt protons and electrons; galactic and solar flare protons; and neutrons, gamma rays, and x-rays from intentionally detonated fission and fusion weapons. In this paper, the MASH vl.0 code system is used to estimate the dose to the critical electronics components of an idealized space based weapon platform from neutron and gamma-ray radiation emitted from a thermonuclear weapon detonation in space. Fluence and dose assessments were performed for the platform fully loaded, and in several stages representing limited engagement scenarios. The results indicate vulnerabilities to the Command, Control, and Communication bay instruments from radiation damage for a nuclear weapon detonation for certain source/platform orientations. The distance at which damage occurs will depend on the weapon yield (n,(gamma)/kiloton) and size (kilotons). DOE

N94-32813 Los Alamos National Lab., NM.
THE ALEXIS MISSION RECOVERY
J. Bloch, T. Armstrong, B. Dingler, D. Enemark, D. Holden, C. Little, C. Munson, B. Priedhorsky, D. Roussel-Dupre, and B. Smith et al 1994 17 p Presented at the 17th Annual American Astronomical Society (AAS) Guidance and Control Conference, Keystone, CO, 2-6 Feb. 1994 Limited Reproducibility: More than 20% of this document may be affected by microfiche quality
(Contract W-7405-eng-36)
(DE94-007549; LA-UR-94-503; CONF-940259-1) Avail: CASI HC A03

The authors report the recovery of the ALEXIS small satellite mission. ALEXIS is a 113-kg satellite that carries an ultrasoft x-ray telescope array and a high-speed VHF receiver/digitizer (BLACKBEARD), supported by a miniature spacecraft bus. It was launched by a Pegasus booster on 1993 April 25, but a solar paddle was damaged during powered flight. Initial attempts to contact ALEXIS were unsuccessful. The satellite finally responded in June, and was soon brought under control. Because the magnetometer had failed, the rescue required the development of new attitude control-techniques. The telemetry system has performed nominally. They discuss the procedures used to recover the ALEXIS mission. DOE

N94-32898*# Boeing Defense and Space Group, Huntsville, AL. Space Station Freedom Applications Group.
SPACE STATION EVOLUTION STUDY Final Report, 1993
David B. Evans Sep. 1993 85 p
(Contract NAS8-38783)

(NASA-CR-193937; NAS 1.26:193937; D495-69756-1) Avail: CASI HC A05/MF A01

This is the Space Station Freedom (SSF) Evolution Study 1993 Final Report, performed under NASA Contract NAS8-38783, Task Order 5.1. This task examined: (1) the feasibility of launching current National Space Transportation System (NSTS) compatible logistics elements on expendable launch vehicles (ELV's) and the associated modifications, and (2) new, non-NSTS logistics elements for launch on ELV's to augment current SSF logistics capability. Author

N94-33115*# Virginia Polytechnic Inst. and State Univ., Blacksburg. Dept. of Engineering Science and Mechanics.
IDENTIFICATION AND CONTROL OF STRUCTURES IN SPACE Final Technical Report, 31 Jan. 1992 - 15 Aug. 1993
Leonard Meirovitch 19 May 1994 86 p
(Grant NAG1-225)
(NASA-CR-195910; NAS 1.26:195910) Avail: CASI HC A05/MF A01

During the last phase of the project, emphasis has changed to flexible space robotics, by mutual agreement between Dr. R. C. Montgomery, NASA Technical Officer, and the Principal Investigator. Significant advances have been achieved over the period covered by this report. Research has been concerned with two main subjects: (1) the maneuvering and control of freely floating flexible space robots, and (2) the development of a theory for the motion of flexible multibody systems. Work on the first subject has resulted in two papers, both of them concerned with planar maneuvers. The first is concerned with the maneuvering and delivery of a payload to a certain point and in a certain orientation in space. The second is concerned with the docking maneuver with a target whose motion is not known a priori. Both papers will appear in the 'Journal of Guidance, Control, and Dynamics.' The second subject is concerned with the development of hybrid (ordinary and partial) differential equations for the three dimensional motion of flexible multibody systems, a subject of vital interest in flexible space robotics. The paper will appear in the 'Journal of Guidance, Control and Dynamics' in an issue dedicated to the memory of Lawrence W. Taylor, Jr. Abstracts and copies of the papers are hereby included. Author

N94-33262 Aerospace Corp., El Segundo, CA. Technology Operations.
SPACECRAFT ENVIRONMENTAL ANOMALIES EXPERT SYSTEM
Harry C. Koons and David J. Groney 23 Feb. 1994 107 p Limited Reproducibility: More than 20% of this document may be affected by microfiche quality
(Contract F04701-93-C-0094)
(AD-A277962; TR-93(3940)-11; SMC-TR-94-07) Avail: CASI HC A06

An expert system has been developed by The Aerospace Corporation, Space and Environment Technology Center for use in the diagnosis of satellite anomalies caused by the space environment. The expert system is designed to determine the probable cause of an anomaly from the following candidates: surface charging, bulk charging, single-event effects, total radiation dose, and space-plasma effects. Such anomalies depend on the orbit of the satellite, the local plasma and radiation environment (which is highly variable), the satellite-exposure time, and the hardness of the circuits and components in the satellite. The expert system is a rule-based system that uses the Texas Instrument's Personal Consultant Plus expert-system shell. The expert system's knowledgebase includes about 200 rules, as well as a number of databases that contain information on spacecraft and their orbits, previous spacecraft anomalies, and the environment. DTIC

N94-31019*# National Aeronautics and Space Administration. Marshall Space Flight Center, Huntsville, AL.
MODELING OF LDEF CONTAMINATION ENVIRONMENT
M. Ralph Carruth, Jr., Ray Rantanen, and Tim Gordon *In its* LDEF Materials Results for Spacecraft Applications Dec. 1993 p 87-95 (For primary document see N94-31012 09-12)
Avail: CASI HC A02/MF A04

N94-31020*# Boeing Defense and Space Group, Seattle, WA.
SPACECRAFT CONTAMINATION ISSUES FROM LDEF: ISSUES FOR DESIGN
Gary Pippin and Russ Crutcher *In* NASA. Marshall Space Flight Center, LDEF Materials Results for Spacecraft Applications Dec. 1993 p 97-103 (For primary document see N94-31012 09-12)
(Contracts NAS1-19247; NAS1-18224)
Avail: CASI HC A02/MF A04

N94-31027*# Alabama Univ., Huntsville. Dept. of Chemistry.
ON THE LINEARITY OF FAST ATOMIC OXYGEN EFFECTS
J. C. Gregory *In* NASA. Marshall Space Flight Center, LDEF Materials Results for Spacecraft Applications Dec. 1993 p 193-198 (For primary document see N94-31012 09-12)
Avail: CASI HC A02/MF A04

N94-31045*# Centre National d'Etudes Spatiales, Toulouse (France).
SPACECRAFT MATERIALS: COMPARISON BETWEEN FLIGHT RESULTS OBTAINED ON LDEF AND MIR
Jean-Claude Guillaumon and Alain Paillous *In* NASA. Marshall Space Flight Center, LDEF Materials Results for Spacecraft Applications Dec. 1993 p 485-498 (For primary document see N94-31012 09-12)
Avail: CASI HC A03/MF A04

N94-31047*# Boeing Defense and Space Group, Huntsville, AL.
DESIGN APPLICATION AND DEVELOPMENT OF SPACECRAFT IN LEO UTILIZING LDEF RESULTS
George B. Rauch, Jr. and Richard D. Sudduth *In* NASA. Marshall Space Flight Center, LDEF Materials Results for Spacecraft Applications Dec. 1993 p 511-523 (For primary document see N94-31012 09-12)
Avail: CASI HC A03/MF A04

N94-31048*# National Aeronautics and Space Administration. Marshall Space Flight Center, Huntsville, AL.
MSFC ORBITAL SPACECRAFT DEVELOPMENT EMPHASES FOR THIS DECADE
Robert J. Schwinghamer *In its* LDEF Materials Results for Spacecraft Applications Dec. 1993 p 525-531 (For primary document see N94-31012 09-12)
Avail: CASI HC A02/MF A04

N94-31049*# Aerospace Corp., El Segundo, CA.
AN OVERVIEW OF THE ON-ORBIT CONTAMINATION OF THE LONG DURATION EXPOSURE FACILITY (LDEF)
W. K. Stuckey *In* NASA. Marshall Space Flight Center, LDEF Materials Results for Spacecraft Applications Dec. 1993 p 533-539 (For primary document see N94-31012 09-12)
Avail: CASI HC A02/MF A04

N94-31434*# Wright Lab., Wright-Patterson AFB, OH. Flight Dynamics Directorate.
A STUDY OF THE SPACE STATION FREEDOM RESPONSE TO THE DISTURBANCE ENVIRONMENT
Afzal Suleman (National Research Council of Canada, Vancouver, British Columbia.), V. J. Modi (British Columbia Univ., Vancouver.), and V. B. Venkayya *In* NASA. Marshall Space Flight Center, The Second Annual International Space University Alumni Conference Feb. 1994 p 96-111 (For primary document see N94-31425 09-12)
Avail: CASI HC A03/MF A02

N94-33302*# Naval Research Lab., Washington, DC.
DESIGN, DEVELOPMENT, AND TESTING OF A LIGHTWEIGHT OPTICAL SENSOR COVER SYSTEM
Mike Hurley and Scott Christiansen *In* NASA. Lewis Research Center, The 28th Aerospace Mechanisms Symposium May 1994 p 135-140 (For primary document see N94-33291 09-15)
Avail: CASI HC A02/MF A04

N94-33303*# Lockheed Engineering and Sciences Co., Houston, TX.
ENERGY ABSORBER FOR THE CETA
Clarence J. Wesselski *In* NASA. Lewis Research Center, The 28th Aerospace Mechanisms Symposium May 1994 p 141-145 (For primary document see N94-33291 09-15)
Avail: CASI HC A01/MF A04

N94-33304*# National Aeronautics and Space Administration. Lewis Research Center, Cleveland, OH.
DESIGN, CHARACTERIZATION, AND CONTROL OF THE NASA THREE DEGREE OF FREEDOM REACTION COMPENSATION PLATFORM
Craig Birkhimer (Case Western Reserve Univ., Cleveland, OH.), Wyatt Newman (Case Western Reserve Univ., Cleveland, OH.), Benjamin Choi, and Charles Lawrence *In its* The 28th Aerospace Mechanisms Symposium May 1994 p 147-152 (For primary document see N94-33291 09-15)
Avail: CASI HC A02/MF A04

N94-33309*# California Univ., Berkeley. Space Sciences Lab.
DESIGN AND PERFORMANCE OF THE TELESCOPE AND DETECTOR COVERS ON THE EXTREME ULTRAVIOLET EXPLORER SATELLITE
James L. Tom *In* NASA. Lewis Research Center, The 28th Aerospace Mechanisms Symposium May 1994 p 199-209 (For primary document see N94-33291 09-15)
(Contract NAS5-29298)
Avail: CASI HC A03/MF A04

N94-33320*# TiNi Alloy Co., San Leandro, CA.
IMPLEMENTATION OF HEATERS ON THERMALLY ACTUATED SPACECRAFT MECHANISMS
John D. Busch and Michael D. Bokaie *In* NASA. Lewis Research Center, The 28th Aerospace Mechanisms Symposium May 1994 p 379-393 (For primary document see N94-33291 09-15)
Avail: CASI HC A03/MF A04

N94-33345 Air Transport Group Headquarters, Astra (Ontario).
A NEURAL NETWORK APPLICATION TO SEARCH AND RESCUE SATELLITE AIDED TRACKING (SARSAT)
Ivan W. Taylor and Michel O. Vigneault *In* Royal Military Coll. of Canada, Proceedings of the Symposium/Workshop on Applications of Expert Systems in DND Apr. 1992 p 189-201 (For primary document see N94-33335 09-66)
Avail: Issuing Activity (Royal Military Coll. of Canada, Vimy Post Office, Kingston, ON K7K 5L0 Canada)

19 SPACECRAFT INSTRUMENTATION

For related information see also *06 Aircraft Instrumentation* and *35 Instrumentation and Photography.*

N94-32924*# National Aeronautics and Space Administration. Langley Research Center, Hampton, VA.
OARE FLIGHT MANEUVERS AND CALIBRATION MEASUREMENTS ON STS-58
Robert C. Blanchard, John Y. Nicholson, James R. Ritter, and Kevin T. Larman Apr. 1994 53 p
(RTOP 237-02-02-11)
(NASA-TM-109093; NAS 1.15:109093) Avail: CASI HC A04/MF A01

The Orbital Acceleration Research Experiment (OARE), which has flown on STS-40, STS-50, and STS-58, contains a three axis accelerometer with a single, nonpendulous, electrostatically suspended proofmass which can resolve accelerations to the nano-g level. The experiment also contains a full calibration station to permit in situ bias and scale factor calibration. This on-orbit calibration capability eliminates the large uncertainty of ground-based calibrations encountered with accelerometers flown in the past on the orbiter, thus providing absolute acceleration measurement accuracy heretofore unachievable. This is the first time accelerometer scale factor measurements have been performed on orbit. A detailed analysis of the calibration process is given along with results of the calibration factors from the on-orbit OARE flight measurements on STS-58. In addition, the analysis of OARE flight maneuver data used to validate the scale factor measurements in the sensor's most sensitive range is also presented. Estimates on calibration uncertainties are discussed. This provides bounds on the STS-58 absolute acceleration measurements for future applications. Author (revised)

N94-33289*# National Aeronautics and Space Administration. Goddard Space Flight Center, Greenbelt, MD.
MODIS. VOLUME 2: MODIS LEVEL 1 GEOLOCATION, CHARACTERIZATION AND CALIBRATION ALGORITHM THEORETICAL BASIS DOCUMENT, VERSION 1
John L. Barker, Joann M. K. Harnden, Harry Montgomery, Paul Anuta, Geir Kvaran, Ed Knight, Tom Bryant, Al McKay, Jon Smid, and Dan Knowles, Jr. May 1994 184 p
(Contract NAS5-31331; RTOP 920-00-00)
(NASA-TM-104594-Vol-2; Rept-94B00069-Vol-2; NAS 1.15:104594-Vol-2)
Avail: CASI HC A09/MF A02

The EOS Moderate Resolution Imaging Spectrometer (MODIS) is being developed by NASA for flight on the Earth Observing System (EOS) series of satellites, the first of which (EOS-AM-1) is scheduled for launch in 1998. This document describes the algorithms and their theoretical basis for the MODIS Level 1B characterization, calibration, and geolocation algorithms which must produce radiometrically, spectrally, and spatially calibrated data with sufficient accuracy so that Global change research programs can detect minute changes in biogeophysical parameters. The document first describes the geolocation algorithm which determines geodetic latitude, longitude, and elevation of each MODIS pixel and the determination of geometric parameters for each observation (satellite zenith angle, satellite azimuth, range to the satellite, solar zenith angle, and solar azimuth). Next, the utilization of the MODIS onboard calibration sources, which consist of the Spectroradiometric Calibration Assembly (SRCA), Solar Diffuser (SD), Solar Diffuser Stability Monitor (SDSM), and the Blackbody (BB), is treated. Characterization of these sources and integration of measurements into the calibration process is described. Finally, the use of external sources, including the Moon, instrumented sites on the Earth (called vicarious calibration), and unsupervised normalization sites having invariant reflectance and emissive properties is treated. Finally, algorithms for generating utility masks needed for scene-based calibration are discussed. Eight appendices are provided, covering instrument design and additional algorithm details. Author

N94-30997 Centre National d'Etudes Spatiales, Toulouse (France).
SPACE EQUIPMENT FOR EARTH OBSERVATIONS [LES INSTRUMENTS SPATIAUX D'OBSERVATION DE LA TERRE]
Marc Leroy *In its* Subtropical Climates and Their Evolution: From Space-Based Observation to Modelling Oct. 1993 p 329-38 In FRENCH (For primary document see N94-30981 09-47)
Copyright Avail: Issuing Activity (CEPADUES-Editions, 111, rue Nicolas-Vauquelin, 31100 Toulouse, France)

N94-33318*# Jet Propulsion Lab., California Inst. of Tech., Pasadena.
LESSONS LEARNED FROM SELECTING AND TESTING SPACEFLIGHT POTENTIOMETERS
T. Iskenderian *In* NASA. Lewis Research Center, The 28th Aerospace Mechanisms Symposium May 1994 p 339-358 (For primary document see N94-33291 09-15)
Avail: CASI HC A03/MF A04

20 SPACECRAFT PROPULSION AND POWER

Includes main propulsion systems and components, e.g., rocket engines; and spacecraft auxilliary power sources.

For related information see also *07 Aircraft Propulsion and Power, 28 Propellants and Fuels, 44 Energy Production and Conversion,* and *15 Launch Vehicles and Space Vehicles.*

N94-31265# Sandia National Labs., Albuquerque, NM.
UTILIZING A RUSSIAN SPACE NUCLEAR REACTOR FOR A UNITED STATES SPACE MISSION: FLIGHT QUALIFICATION ISSUES
G. F. Polansky, G. L. Schmidt, E. L. Reynolds, and E. D. Schaefer 1993 8 p Presented at the 11th Symposium on Space Nuclear Power Systems, Albuquerque, NM, 9-13 Jan. 1994
(Contract DE-AC04-94AL-85000)
(DE94-004674; SAND-93-2204C; CONF-940101-28) Avail: CASI HC A02/MF A01 (US Sales Only)

Space nuclear power and nuclear electric propulsion are considered important technologies for planetary exploration, as well as selected earth

orbit applications. The Nuclear Electric Propulsion Space Test Program (NEPSTP) could provide an early flight demonstration of these technologies at relatively low cost through extensive use of existing Russian technology. The key element of Russian technology employed in the program is the Topaz II reactor. This space nuclear power system was built and flight qualified, though never tested in space, by the former Soviet Union. The NEPSTP is faced with many unique flight qualification issues. In general, the launch of a spacecraft employing a nuclear reactor power system will complicate many spacecraft qualification activities. However, the NEPSTP activities are further complicated because the reactor power system is a Russian design. Therefore, this program must deal not only with the unique flight qualification issues associated with space nuclear power, but also with differences between Russian and United States flight qualification procedures. This paper presents an overview of the NEPSTP. The program goals, the proposed mission, the spacecraft, and the Topaz II space nuclear power system are described. The subject of flight qualification is then examined. The inherent difficulties in qualifying a space reactor are described. The differences between United States and Russian flight qualification procedures are explored. A plan is then described to determine an appropriate flight qualification program for the Topaz II reactor to support a possible NEPSTP launch. DOE

N94-31423# Office National d'Etudes et de Recherches Aerospatiales, Paris (France).
THE PREDICTION OF CONVECTIVE TRANSFER ON THE THERMAL INSULATION OF A SOLID-PROPELLANT ROCKET MOTOR Ph.D. Thesis - Inst. National Polytechnique de Toulouse [PREVISION DES TRANSFERS CONVECTIFS SUR LES PROTECTIONS THERMIQUES D'UN PROPULSEUR A PROPERGOL SOLIDE]
Franck Nicoud 1993 268 p In FRENCH
(ISSN 0078-3781)
(ONERA-NT-1993-15; ETN-94-96067) Avail: CASI HC A12/MF A03

The internal aerodynamics of a solid propellant rocket motor is studied. Cold gas simulation setups are reviewed. The analysis of numerical approximations used for modeling such setups has led to the adoption of a k-L type description of turbulence. The numerical simulations of two cold flow setups enable the computer code to be checked in purely aerodynamic terms. The experimental subscale setup which allowed the construction of a database regarding the quasi steady heat exchanges generated on an inert wall within the combustion chamber of a rocket motor is described. The computations show that an approximation which does not require the use of a very fine grid at the wall is sufficient to reproduce the measured flux levels. A law of the wall is proposed which takes account of the effect of the steep temperature gradients and allows a better description of the measurements made. The evaluation of the ablation of a thermal insulation material placed in the combustion chamber of the test rocket motor is described. Teflon was employed in view of the simplicity of its degradation mechanisms. In terms of measurements, the difficulties inherent in the use of an ultrasonic method are shown. The dimensional measurements made constitute reference data through which it will be possible to check future computer codes for the ablation of thermal insulation. The validity of coupling an aerothermodynamic computer code and a module for evaluating the response of an insulation material is discussed. A full temporal numerical simulation of the tests is presented. ESA

N94-31618*# Aerojet Solid Propulsion Co., Sacramento, CA.
THE 7.5K LBF THRUST ENGINE PRELIMINARY DESIGN FOR ORBIT TRANSFER VEHICLE Final Report
Warren R. Hayden, Ralph Sabiers, and Judy Schneider Jan. 1994 365 p
(Contract NAS3-23772; RTOP 593-12-21)
(NASA-CR-189175; E-8401; NAS 1.26:189175) Avail: CASI HC A16/MF A03

This document summarizes the preliminary design of the Aerojet version of the Orbit Transfer Vehicle main engine. The concept of a 7500 lbf thrust LO2/GH2 engine using the dual expander cycle for optimum efficiency is validated through power balance and thermal calculations. The engine is capable of 10:1 throttling from a nominal 2000 psia to a 200 psia chamber pressure. Reservations are detailed on the feasibility of a tank head start, but the design incorporates low speed turbopumps to mitigate the problem. The mechanically separate high speed turbopumps use hydrostatic bearings to meet engine life requirements, and operate at sub-critical speed for better throttling ability. All components were successfully packaged in the restricted envelope set by the clearances for the extendible/retractable nozzle. Gimbal design uses an innovative primary and engine out gimbal system to meet the +/- 20 deg gimbal requirement. The hydrogen regenerator and LOX/GH2 heat exchanger uses the Aerojet platelet structures approach for a highly compact component design. The extendible/retractable nozzle assembly uses an electric motor driven jack-screw design and a one segment carbon-carbon or silicide coated columbium nozzle with an area ratio, when extended, of 1430:1. A reliability analysis and risk assessment concludes the report. Author

N94-31818* National Aeronautics and Space Administration. Lewis Research Center, Cleveland, OH.
SOLAR CONNECTION (Videotape)
1992 Videotape: 14 min. 18 sec. playing time, in color, with sound
(NASA-TM-109761; NONP-VT-94-9961) Avail: CASI VHS A01/BETA A22

This video explains the Work package 4, an electrical power system being developed by NASA Lewis Research Center, for use on the Space Station Freedom. It shows footage and explains steps in building and testing of actual flight hardware for Space Station Freedom. Details are given of the threat that plasma poses on cells. CASI

N94-31908 Pennsylvania State Univ., University Park.
PERFORMANCE EVALUATION AND OPERATING CHARACTERISTICS OF A WAVEGUIDE MICROWAVE APPLICATOR FOR SPACE PROPULSION APPLICATIONS Ph.D. Thesis
Juergen Mueller 1993 311 p
Avail: Univ. Microfilms Order No. DA9326908

A new electrothermal space propulsion concept using waveguide heated plasmas was investigated. Attention was focused on the understanding of basic operational characteristics of this thruster concept. To this end, experimental testing of various waveguide applicator configurations was conducted. Waveguide-heated plasmas are not stable but tend to propagate toward the microwave power source due to heat conduction or radiative processes. A rectangular waveguide applicator was used to measure plasma propagation velocities. Plasma velocities in nitrogen were found to be around 10 cm/s. In helium two propagation modes were observed, one ranging in plasma velocities between 10 and 90 cm/s while the faster mode showed propagation velocities up to 2000 to 3000 cm/s. Inserting a bluff body made from boron nitride material into the gas flow enabled stabilization of the microwave discharge over given power ranges depending on mass flow rates and gas pressure. For the stabilized plasma in the rectangular guide up to 90 percent coupling efficiency, i.e. absorbed over total incident microwave power, were measured. However, it was observed that a rectangular waveguide plasma sustained in a TE(sub 10) electromagnetic field pattern touches the waveguide walls at two locations, possibly resulting in problems of thruster erosion and efficiency loss. Therefore a circular TM(sub 01) mode applicator was investigated. The microwave discharge in this applicator could be sustained well separated from the waveguide walls at coupling efficiencies up to 96 percent. For a simple converging conical nozzle arrangement, using measured data on power, pressure and mass flow rate and quasi-one dimensional nozzle flow theory, values for such rocket performance parameters as thruster efficiency, specific impulse and thrust were estimated to be 40 percent, 350 sec and 0.4 N, respectively. Dissert. Abstr.

N94-32071# Naval Postgraduate School, Monterey, CA.
COMBUSTOR AND NOZZLE EFFECTS ON PARTICULATE BEHAVIOR IN SOLID ROCKET MOTORS M.S. Thesis
Bulent Yakin Dec. 1993 61 p
(AD-A277304) Avail: CASI HC A04/MF A01

An investigation was conducted using a subscale solid rocket motor to measure the effect of nozzle residence time on the behavior of Al2O3 particles to assess the applicability of subscale motor data to full-scale motors and to measure the effects of nozzle entrance particle size distribution on the slag accumulated with submerged nozzles. Although particles as large as 140 micrometers were present at the nozzle entrance, most of the particulate mass was contained in much smaller particles. This observation is in good agreement with the small mass that accumulated above the submerged nozzle. It was found that both particle breakup and collision coalescence occurred across the exhaust nozzle, with a significant

increase in the mass fraction of small (less than 2 micrometers) particles. Increasing the nozzle residence time enhanced particle breakup but did not affect the maximum plume particle size. Thus, full-scale motors are expected to have a higher percentage of mass in particles less than 2 micrometers than subscale motors but with similar diameters of the largest particles. DTIC

N94-32182# Naval Postgraduate School, Monterey, CA.
DESIGN OF A COLD-FLOW TEST FACILITY FOR THE HIGH PRESSURE FUEL TURBOPUMP TURBINE OF THE SPACE SHUTTLE MAIN ENGINE M.S. Thesis
Colin C. Studevan Dec. 1993 52 p
(AD-A276743) Avail: CASI HC A04/MF A01

The design and installation at the Naval Postgraduate School of a cold-flow test facility for the turbine of the high-pressure fuel turbopump of the Space Shuttle Main Engine, is reported. The specific article to be tested is the 'Alternate Development Model' designed and manufactured by Pratt & Whitney. The design of individual components is documented. The installation of the facility subsystem is described in detail. A preliminary estimation of turbine performance is made. DTIC

N94-32266 Brookhaven National Lab., Upton, NY.
SUMMARY OF PARTICLE BED REACTOR DESIGNS FOR THE SPACE NUCLEAR THERMAL PROPULSION PROGRAM
J. R. Powell, H. Ludewig, and M. Todosow et al Sep. 1993 185 p
Limited Reproducibility: More than 20% of this document may be affected by microfiche quality
(Contract DE-AC02-76CH-00016)
(DE94-007434; BNL-52408) Avail: CASI HC A09 (US Sales Only)

A summary report of the Particle Bed Reactor (PBR) designs considered for the space nuclear thermal propulsion program has been prepared. The first chapters outline the methods of analysis, and their validation. Monte Carlo methods are used for the physics analysis, several new algorithms are used for the fluid dynamics heat transfer and engine system analysis, and commercially available codes are used for the stress analysis. A critical experiment, prototypic of the PBR was used for the physics validation, and blowdown experiments using fuel beds of prototypic dimensions were used to validate the power extraction capabilities from particle beds. In all four different PBR rocket reactor designs were studied to varying degrees of detail. They varied in power from 400 MW to 2000 MW. These designs were all characterized by a negative prompt coefficient, due to Doppler feedback, and the feedback due to moderator heat up varied from slightly negative to slightly positive. In all practical cases, the coolant worth was positive, although core configurations with negative coolant worth could be designed. In all practical cases the thrust/weight ratio was greater than 20. DOE

N94-32500 Rensselaer Polytechnic Inst., Troy, NY.
THE EFFECT OF DUCTILE PHASE (Nb) REINFORCEMENT MORPHOLOGY ON THE MECHANICAL BEHAVIOR OF AN INTERMETALLIC MATRIX (MoSi2) Ph.D. Thesis
David E. Alman 1992 190 p
Avail: Univ. Microfilms Order No. DA9314339

This thesis was undertaken to determine the effect of a ductile reinforcement phase (Nb) morphology on the mechanical behavior of an intermetallic matrix (MoSi2). Twenty volume percent Nb was incorporated into MoSi2 in the form of particles, short fibers, aligned fibers, and with fibers of two different diameters (800 and 400 microns). Bend tests, comprehension tests and fractography were used to determine the role that Nb morphology plays on the fracture behavior of these composites. It was found that the morphology of the Nb incorporated into MoSi2 affected the fracture mechanism, hence toughness, of the composites. The addition of random short fiber or particles deflected cracks that propagated through the matrix. However, the Nb in these forms were not effective in improving the toughness via a crack deflection mechanism. The addition of continuous Nb fibers aligned perpendicular to the direction of crack propagation enhanced the toughness of MoSi2, as these fibers deformed and fractured prior to composite failure, however, there was an effect of fiber diameter. The larger diameter Nb fibers imparted the greatest toughness improvements, as these fibers deformed prior to fracture. The smaller diameter Nb did not deform prior to fracture, in fact they failed in a brittle manner. Fractography revealed that the larger diameter fibers had separated (or delaminated) from the matrix. The fiber/matrix separation relaxed the matrix constraint acting on the fiber and allowed for the fiber to undergo plastic deformation. The delamination was found to occur after the matrix had fractured and prior to deformation of the fibers. This would indicate that the delamination occurs by a pull-out mechanism. The diameter effect exhibited by the composites was attributed to the well known effect of fiber aspect ratio (l/d) on fiber pull-out. It was concluded that maximum toughness of a Nb fiber reinforced MoSi2 matrix will occur when the value of the fiber aspect ratio is within a critical range. The upper limit must not be exceeded to ensure fiber pull-out will occur; and the lower limit must be exceeded to ensure that matrix cracks do not deflect around the fiber. Dissert. Abstr.

N94-32669 Sandia National Labs., Albuquerque, NM.
INTEGRATED SAFETY PROGRAM FOR THE NUCLEAR ELECTRIC PROPULSION SPACE TEST PROGRAM
A. C. Marshall, W. F. Mehlman, and G. Kompanietz 1993 10 p Presented at the 11th Symposium on Space Nuclear Power Systems, Albuquerque, NM, 9-13 Jan. 1994 Limited Reproducibility: More than 20% of this document may be affected by microfiche quality
(Contract DE-AC04-94AL-85000)
(DE94-004670; SAND-93-2124C; CONF-940101-29) Avail: CASI HC A02 (US Sales Only)

The Nuclear Electric Propulsion Space Test Program (NEPSTP) is sponsored by the Ballistic Missile Defense Office (BMDO) to demonstrate and evaluate the Russian-built TOPAZ 2 nuclear reactor as a power source for an electric propulsion system in space. From its inception, safety has been a central feature of the NEPSTP program. This paper addresses the work done to define the safety organizational relationships, responsibilities, management, engineering requirements, and documentation to assure an integrated safety program that coordinates the various safety activities in Mission Safety, Range Safety and Nuclear Safety. Because the United States has not launched a nuclear reactor since 1965, much of the focus of the safety program has been directed toward the unique safety considerations of using a nuclear reactor in space. Our preliminary findings indicate that the safe use of the TOPAZ 2 for the NEPSTP space mission is feasible. DOE

N94-32742*# National Aeronautics and Space Administration. Lewis Research Center, Cleveland, OH.
SIMULATION OF LOW-DENSITY NOZZLE PLUMES IN NON-ZERO AMBIENT PRESSURES
Chan-Hong Chung (Toledo Univ., OH.), Kenneth J. DeWitt (Toledo Univ., OH.), Robert M. Stubbs, and Paul F. Penko Feb. 1994 10 p Presented at the 32nd Aerospace Sciences Meeting and Exhibit, Reno, NV, 10-13 Jan. 1994; sponsored by AIAA
(Contract NCC3-171; RTOP 505-62-52)
(NASA-TM-106501; E-8514; NAS 1.15:106501; AIAA Paper 94-0357)
Avail: CASI HC A02/MF A01

The direct simulation Monte-Carlo (DSMC) method was applied to the analysis of low-density nitrogen plumes exhausting from a small converging-diverging nozzle into finite ambient pressures. Two cases were considered that simulated actual test conditions in a vacuum facility. The numerical simulations readily captured the complicated flow structure of the overexpanded plumes adjusting to the finite ambient pressures, including Mach disks and barrel shaped shocks. The numerical simulations compared well to experimental data of Rothe. Author

N94-32792*# SunPower, Inc., Athens, OH.
OSCILLATING-FLOW LOSS TEST RESULTS IN RECTANGULAR HEAT EXCHANGER PASSAGES Final Report
J. Gary Wood Sep. 1991 78 p
(Contract NAS3-23885; RTOP 590-13-11)
(NASA-CR-185297; NAS 1.26:185297) Avail: CASI HC A05/MF A01

Test results of oscillating flow losses in rectangular heat exchanger passages of various aspect ratios are given. This work was performed in support of the design of a free-piston Stirling engine (FPSE) for a dynamic space power conversion system. Oscillating flow loss testing was performed using an oscillating flow rig, which was based on a variable stroke and variable frequency linear drive motor. Tests were run over a range of oscillating flow parameters encompassing the flow regimes of the proposed

engine design. Test results are presented in both tabular and graphical form and are compared against analytical predictions. Author

N94-32866*# SunPower, Inc., Athens, OH.
A 1050 K STIRLING SPACE ENGINE DESIGN Final Report
L. Barry Penswick Nov. 1988 48 p
(Contract NAS3-23885; RTOP 586-01-11)
(NASA-CR-182149; NAS 1.26:182149) Avail: CASI HC A03/MF A01

As part of the NASA CSTI High Capacity Power Program on Conversion Systems for Nuclear Applications, Sunpower, Inc. completed for NASA Lewis a reference design of a single-cylinder free-piston Stirling engine that is optimized for the lifetimes and temperatures appropriate for space applications. The NASA effort is part of the overall SP-100 program which is a combined DOD/DOE/NASA project to develop nuclear power for space. Stirling engines have been identified as a growth option for SP-100 offering increased power output and lower system mass and radiator area. Superalloy materials are used in the 1050 K hot end of the engine; the engine temperature ratio is 2.0. The engine design features simplified heat exchangers with heat input by sodium heat pipes, hydrodynamic gas bearings, a permanent magnet linear alternator, and a dynamic balance system. The design shows an efficiency (including the alternator) of 29 percent and a specific mass of 5.7 kg/kW. This design also represents a significant step toward the 1300 K refractory Stirling engine which is another growth option of SP-100. Author

N94-32970*# Los Alamos National Lab., NM.
PERFORMANCE OF A QUASI-STEADY, MULTI MEGAWATT, COAXIAL PLASMA THRUSTER Final Report
Jay T. Scheuer, Kurt F. Schoenberg, Ivars Henins, Richard A. Gerwin, Ronald W. Moses, Jr., Jose A. Garcia, Robert F. Gribble, Robert P. Hoyt, Dorwin C. Black, and Robert M. Mayo Apr. 1994 84 p
(NASA Order C-30065-A; RTOP 506-42-31)
(NASA-CR-195311; E-8723; NAS 1.26:195311) Avail: CASI HC A05/MF A01

The Los Alamos National Laboratory Coaxial Thruster Experiment (CTX) has been upgraded to enable the quasisteady operation of magnetoplasmadynamic (MPD) type thrusters at power levels from 2 to 40 MW for 10 ms. Diagnostics include an eight position, three axis magnetic field probe to measure magnetic field fluctuations during the pulse; a triple Langmuir probe to measure ion density, electron temperature, and plasma potential; and a time-of-flight neutral particle spectrometer to measure specific impulse. Here we report on the experimental observations and associated analysis and interpretation of long-pulse, quasisteady, coaxial thruster performance in the CTX device. Author

N94-33059# Walter Reed Army Inst. of Research, Washington, DC. Medical Detachment.
EXPOSURE ASSESSMENT OF JAVELIN MISSILE COMBUSTION PRODUCTS Technical Report, 1987 - 1992
Donald O. Lundy and Roland E. Langford 14 Feb. 1994 63 p
(AD-A278128; TR-94-0002) Avail: CASI HC A04/MF A01

Characterization and analysis of combustion products resulting from firing the JAVELIN missile were performed. Of those combustion products analyzed, it was determined that airborne lead concentrations exceeded the OSHA PEL of 50 micrograms each time the missile was fired while in the enclosure. Since the OSHA PEL standard is based upon a continuous rather than a short-term exposures blood lead concentrations were sought to ascertain the relationship between a short duration airborne exposure and its physiological effect on the body. Blood lead levels were taken on 49 test subjects prior to various JAVELIN missile test firings. Of those 49, 21 were outfitted With personal sampling equipment to determine airborne concentrations at the Assistant Gunner and Gunner positions. Periodic blood sampling after a single exposure showed an average increase of 2.27 micrograms/dL for all test subjects. Recommendations were made to consider changes in the positioning of the enclosure inhabitants to minimize airborne lead concentrations, to limit the number of missiles fired (situation dependent), and replacement of the lead B-resorcyolate with a non-lead containing burn rate modifier for the launch motor. DTIC

N94-33094# Aerospace Corp., El Segundo, CA. Technology Operations.
POSSIBLE EFFECT OF THE CHLORINE OXIDE DIMER ON TRANSIENT OZONE LOSS IN ROCKET PLUMES
L. R. Martin 15 Mar. 1994 16 p
(Contract F04701-93-C-0094)
(AD-A278135; TR-94(4231)-1; SMC-TR-94-14) Avail: CASI HC A03/MF A01

Understanding transient, local ozone holes that may be produced by solid rocket boosters in the stratosphere puts special demands on models. One must consider the time scales as well as the rates for all of the pertinent chemical reactions involved in the destruction of ozone. In this report, we show that consideration of the existence of the chlorine oxide dimer, Cl2O2, and consideration of the necessary time scale for ozone loss are essential for prediction of a transient ozone hole. We argue that photolysis of this species is the major source of atomic chlorine in the plume at 20 km, and the ClO + O reaction is the major source at 30 km, although both processes play a role at the higher altitude. Inclusion of the chlorine oxide dimer ozone destruction cycle, which has not been considered in any of the full-scale models to date, predicts substantial ozone destruction on a scale of about 12-km diameter at 20-km altitude and the ClO cycle produces a 49-km-diameter hole at 30-km altitude. This analysis also suggests that the size of the hole at 20 km may be highly variable since it is sensitive to the variable ozone-to-methane ratio at that altitude. DTIC

N94-33099*# GenCorp Aerojet, Sacramento, CA. Aerojet Propulsion Div.
REAL-TIME SENSOR DATA VALIDATION Final Report
Timothy W. Bickmore Apr. 1994 74 p
(Contract NAS3-25883; RTOP 584-03-11)
(NASA-CR-195295; E-8672; NAS 1.26:195295) Avail: CASI HC A04/MF A01

This report describes the status of an on-going effort to develop software capable of detecting sensor failures on rocket engines in real time. This software could be used in a rocket engine controller to prevent the erroneous shutdown of an engine due to sensor failures which would otherwise be interpreted as engine failures by the control software. The approach taken combines analytical redundancy with Bayesian belief networks to provide a solution which has well defined real-time characteristics and well-defined error rates. Analytical redundancy is a technique in which a sensor's value is predicted by using values from other sensors and known or empirically derived mathematical relations. A set of sensors and a set of relations among them form a network of cross-checks which can be used to periodically validate all of the sensors in the network. Bayesian belief networks provide a method of determining if each of the sensors in the network is valid, given the results of the cross-checks. This approach has been successfully demonstrated on the Technology Test Bed Engine at the NASA Marshall Space Flight Center. Current efforts are focused on extending the system to provide a validation capability for 100 sensors on the Space Shuttle Main Engine. Author

N94-33294*# Honeywell, Inc., Phoenix, AZ. Satellite Systems Operation.
ROLL RING ASSEMBLIES FOR THE SPACE STATION
J. Batista, J. Vise, and K. Young *In* NASA. Lewis Research Center, The 28th Aerospace Mechanisms Symposium May 1994 p 35-50 (For primary document see N94-33291 09-15)
Avail: CASI HC A03/MF A04

N94-33295*# Rockwell International Corp., Canoga Park, CA. Rocketdyne Div.
INTERNATIONAL SPACE STATION ALPHA'S BEARING, MOTOR, AND ROLL RING MODULE DEVELOPMENTAL TESTING AND RESULTS
David L. OBrien *In* NASA. Lewis Research Center, The 28th Aerospace Mechanisms Symposium May 1994 p 51-61 (For primary document see N94-33291 09-15)
Avail: CASI HC A03/MF A04

23 CHEMISTRY AND MATERIALS (GENERAL)

N94-32038 Hebrew Univ., Jerusalem (Israel).
THE SOL-GEL-XEROGEL TRANSITION
D. Avnir Nov. 1993 56 p Limited Reproducibility: More than 20% of

this document may be affected by microfiche quality
(Contract DAJA45-89-C-0024)
(AD-A276647; R/D-5548-MS-01) Avail: CASI HC A04

This contract supported the development of the technology of trapping of organic molecules and enzymes in porous sol-gel matrices. Our work led to the preparation and design of a wide range of novel optical materials. We summarize past achievements and recent progress made in the development of several classes of these materials representing the diversity that the trapping approach allows: chemical sensors, enzymatic sensors, electrooptical liquid crystal materials, luminescent materials, and photochromic materials. Emphasis in this Report is given to our own results, and in addition, results from other laboratories, which are based on our developments and which are of high relevance to the topic of the Project (e.g., liquid crystal sol-gel displays), are summarized as well. We regard these other technological fruits a direct outcome of our sol-gel research. DTIC

N94-32941*# National Aeronautics and Space Administration. Lewis Research Center, Cleveland, OH.
THE EFFECT OF PROLONGED EXPOSURE TO 750 C AIR ON THE TRIBOLOGICAL PERFORMANCE OF PM212
Kirk Bernis (Case Western Reserve Univ., Cleveland, OH.), Michael S. Bogdanski (Case Western Reserve Univ., Cleveland, OH.), Christopher DellaCorte, and Harold E. Sliney Feb. 1994 27 p Presented at the STLE Annual Meeting, Pittsburgh, PA, 2-5 May 1994; sponsored by the Society of Tribologists and Lubrication Engineers
(Contract DE-A101-91CE-50306)
(NASA-TM-106472; E-8341; NAS 1.15:106472; DOE/NASA/50306-4)
Avail: CASI HC A03/MF A01

The effect of prolonged exposure to 750 C air on the tribological performance and dimensional stability of PM212, a high temperature, self-lubricating composite, is studied. PM212, by weight, contains 70 percent metal-bonded Cr3C2, 15 percent BaF2/CaF2 eutectic, and 15 percent silver. Rub blocks were fabricated from PM212 by cold isostatic pressing followed by sintering. Prior to tribo-testing, the rub blocks were exposed to 750 C air for periods ranging from 100 to 1000 hours. Then, the rub blocks were slid against nickel-based superalloy disks in a double-rub-block tribometer in air under a 66 N load at temperatures from 25 to 750 C with a sliding velocity of 0.36 m/s. Unexposed rub blocks were tested for baseline comparison. Friction coefficients ranged from 0.24 to 0.37 for the unexposed rub blocks and from 0.32 to 0.56 for the exposed ones. Wear for both the composite blocks and superalloy disks was typically in the moderate to low range of 10(exp -5) to 10(exp -6) mm(exp 3)/N-m. Friction and wear data were similar for the rub blocks exposed for 100, 500, and 1000 hours. Prolonged exposure to 750 C air increased friction and wear of the PM212 rub blocks at room temperature, but their triboperformance remained unaffected at higher temperatures, probably due to the formation of lubricious metal oxides. Dimensional stability of the composite was studied by exposing specimens of varying thicknesses for 500 hours in air at 750 C. Block thicknesses were found to increase with increased exposure time until steady state was reached after 100 hours of exposure, probably due to oxidation. Author (revised)

N94-33021*# National Aeronautics and Space Administration. Lewis Research Center, Cleveland, OH.
PERFLUOROPOLYALKYLETHER DECOMPOSITION ON CATALYTIC ALUMINAS
Wilfredo Morales Apr. 1994 60 p
(RTOP 505-63-5A)
(NASA-TM-106547; E-8697; NAS 1.15:106547) Avail: CASI HC A04/MF A01

The decomposition of Fomblin Z25, a commercial perfluoropolyalkylether liquid lubricant, was studied using the Penn State Micro-oxidation Test, and a thermal gravimetric/differential scanning calorimetry unit. The micro-oxidation test was conducted using 440C stainless steel and pure iron metal catalyst specimens, whereas the thermal gravimetric/differential scanning calorimetry tests were conducted using catalytic alumina pellets. Analysis of the thermal data, high pressure liquid chromatography data, and x-ray photoelectron spectroscopy data support evidence that there are two different decomposition mechanisms for Fomblin Z25, and that reductive sites on the catalytic surfaces are responsible for the decomposition of Fomblin Z25. Author

N94-33022*# National Aeronautics and Space Administration. Lewis Research Center, Cleveland, OH.
COMBINED CONTAMINATION AND SPACE ENVIRONMENTAL EFFECTS ON SOLAR CELLS AND THERMAL CONTROL SURFACES
Joyce A. Dever, Eric J. Bruckner, David A. Scheiman, and Curtis R. Stidham May 1994 13 p Proposed for presentation at the 18th AIAA Aerospace Ground Testing Conference, Colorado Springs, CO, 20-23 Jun. 1994; sponsored by AIAA
(Contract NAS3-27186; RTOP 474-46-10)
(NASA-TM-106592; E-8859; NAS 1.15:106592; AIAA Paper 94-2627)
Copyright Avail: CASI HC A03/MF A01

For spacecraft in low Earth orbit (LEO), contamination can occur from thruster fuel, sputter contamination products and from products of silicone degradation. This paper describes laboratory testing in which solar cell materials and thermal control surfaces were exposed to simulated spacecraft environmental effects including contamination, atomic oxygen, ultraviolet radiation and thermal cycling. The objective of these experiments was to determine how the interaction of the natural LEO environmental effects with contaminated spacecraft surfaces impacts the performance of these materials. Optical properties of samples were measured and solar cell performance data was obtained. In general, exposure to contamination by thruster fuel resulted in degradation of solar absorptance for fused silica and various thermal control surfaces and degradation of solar cell performance. Fused silica samples which were subsequently exposed to an atomic oxygen/vacuum ultraviolet radiation environment showed reversal of this degradation. These results imply that solar cells and thermal control surfaces which are susceptible to thruster fuel contamination and which also receive atomic oxygen exposure may not undergo significant performance degradation. Materials which were exposed to only vacuum ultraviolet radiation subsequent to contamination showed slight additional degradation in solar absorptance. Author

N94-33117*# National Aeronautics and Space Administration. Ames Research Center, Moffett Field, CA.
DEVELOPMENT OF LIGHTWEIGHT CERAMIC ABLATORS AND ARC-JET TEST RESULTS
Huy K. Tran Jan. 1994 27 p
(RTOP 506-46-31)
(NASA-TM-108798; A-94017; NAS 1.15:108798) Avail: CASI HC A03/MF A01

Lightweight ceramic ablators (LCA's) were recently developed at Ames to investigate the use of low density fibrous substrates and organic resins as high temperature, high strength ablative heat shields. Unlike the traditional ablators, LCA's use porous ceramic/carbon fiber matrices as substrates for structural support, and polymeric resins as fillers. Several substrates and resins were selected for the initial studies, and the best performing candidates were further characterized. Three arcjet tests were conducted to determine the LCA's thermal performance and ablation characteristics in a high enthalpy, hypersonic flow environment. Mass loss and recession measurements were obtained for each sample at post test, and the recession rates were determined from high speed motion films. Surface temperatures were also obtained from optical pyrometers. Author

24 COMPOSITE MATERIALS

Includes physical, chemical, and mechanical properties of laminates and other composite materials.

For ceramic materials see *27 Nonmetallic Materials.*

N94-31215 Washington Univ., Seattle.
AN EFFICIENT HIGHER ORDER THEORY FOR LAMINATED COMPOSITE PLATES AND A FINITE ELEMENT IMPLEMENTATION
Ph.D. Thesis
Maeng-Hyo Cho 1993 209 p
Avail: Univ. Microfilms Order No. DA9326349

An efficient higher order plate theory for laminated composites is developed. A composite plate theory for symmetric and general lamination configurations is obtained by superposing a cubic varying displacement field on a piecewise linearly varying displacement. The theory has the same number of dependent unknowns as first-order shear deformation theory, and the number of unknowns is independent of the number of

layers. The displacement satisfies transverse shear stress continuity conditions at the interface between layers as well as shear free surface conditions. Thus an artificial shear correction factor is not needed. To demonstrate and compare with other theories, the analytical solution for cylindrical bending is obtained. To solve problems of more general engineering interest, a triangular finite element based on an efficient higher order plate theory (EHOPT) is developed for symmetric laminated composites. The nonconforming element has 5 degrees of freedom in each node. It passes proper bending and shear patch tests in arbitrary meshes in isotropic materials. Thus it converges to the exact solution. To demonstrate and compare with other theories, the finite element solutions for a static bending problem under sinusoidal loading is obtained. The present finite element result gives deflections and stresses which agree very well with 3 dimensional elasticity solutions. However, it suffers from transverse shear locking in thin plates. For the complete elimination of the locking behavior, a modified formulation of the EHOPT (MEHOPT) is proposed. These EHOPT and MEHOPT elements provide an efficient and accurate tool for the analysis of thick multilayered composite plates.
Dissert. Abstr.

N94-31225# Office National d'Etudes et de Recherches Aerospatiales, Paris (France).
MICROMECHANICAL ANALYSIS OF THE INTERFACE AND BASIC DAMAGE MODES IN GLASS FIBER/EPOXY RESIN MODEL COMPOSITES Ph.D. Thesis - Inst. National des Sciences Appliquees de Lyon [CONTRIBUTION A L'ETUDE MICROMECANIQUE DE L'INTERFACE ET DES PHENOMENES ELEMENTAIRES D'ENDOMMAGEMENT DANS DES COMPOSITES MODELES FIBRE DE VERRE/RESINE EPOXYDE]
Pascal Feillard 1993 137 p In FRENCH Original contains color illustrations
(ISSN 0078-3781)
(ONERA-NT-1993-4; ETN-94-95873) Avail: CASI HC A07/MF A02

A micromechanical study of the interface in glass fiber/epoxy matrix model composites was carried out using pull out, fragmentation and microindentation tests. Focus was on the two first tests due to the particular case of glass/epoxy systems of microindentation. The influence of the fiber silane size on the load transfer and on the damage elementary modes was studied. The experimental fragmentation processes were compared with those obtained from an analytical simulation of the fragmentation test and it was proved that one dimensional load transfer models did not allow a satisfactory description of the fragmentation process in glass/epoxy systems. Bidimensional models are more suitable for the analysis of the experimental data because they give an account of the multiaxial aspect of the fiber/matrix load transfer. However, some experimental phenomenon such as debonding interfacial plasticization and fiber/matrix friction are difficult to take into account in such bidimensional models. Moreover, a thorough examination of load transfer models recently developed for the pull out test showed that they cannot lead to a precise mechanical analysis and that a bidimensional load transfer should be envisaged. Accordingly, the mechanical analysis of these micromechanical tests has to be improved in order to take into account more precisely the local stress concentrations in the fiber/matrix system and the real mechanical behavior of the matrix. ESA

N94-31232# Office National d'Etudes et de Recherches Aerospatiales, Paris (France).
UNIDIRECTIONAL COMPOSITES COMPRESSIVE BEHAVIOUR: TEST METHODS AND MICROMECHANICAL APPROACH Ph.D. Thesis - Ecole Normale Superieure, Cachan, France [COMPRESSION DES COMPOSITES UNIDIRECTIONNELS: METHODES D'ESSAI ET APPROCHE MICROMECANIQUE]
Isabelle Grandsire-Vincon 1993 192 p In FRENCH Original contains color illustrations
(ISSN 0078-3781)
(ONERA-NT-1993-10; ETN-94-95876) Avail: CASI HC A09/MF A02

A study to better understand compressive behavior of composites is reported. The comparison of composite compression test methods and the development of a micromechanical test on a single filament specimen to characterize the carbon fiber compressive behavior are presented. The macroscopic approach points out the major effect of structural parameters when compared to materials characteristics. It appears indeed that the composite failure in compression depends strongly on the loading mode (axial compression or bending) as well as on the type of lay up. Micromechanical tests were interpreted with the help of an analytical model of fiber microbuckling. The results emphasize the high strain capability of the carbon fiber in compression. Accordingly, the compressive failure of composites is due to a combined fibers/matrix effect: the fiber cooperative microbuckling and the weaker antibuckling support of the matrix in the composite lead to a premature failure when compared to the single filament specimen case. ESA

N94-31261# California Univ., Los Angeles.
PERFORMANCE PREDICTIONS FOR COMPOSITE MATERIALS Final Report
William M. Gelbart, Shechao Feng, Howard Reiss, and Daniel Kivelson 31 Dec. 1993 7 p
(Contract DAAL03-89-K-0144)
(AD-A276451; ARO-26891.7-MS-A) Avail: CASI HC A02/MF A01

This project has initiated and brought to completion several novel microscopic approaches to the prediction of material response to applied stress. In a series of several papers we worked out a systematic formulation of failure under load as a homogeneous nucleation process, simulating the process via mean-field, Monte Carlo and molecular dynamics methods, for both model and semi-empirical interatomic potentials. We also developed a biased-random-walk description of microcrack propagation which incorporated for the first time the effects of surface reconstruction. Finally we extended multiple scattering analyses of composite and concrete materials to the limit of high crack density, allowing for new nondestructive evaluations of this important class of materials. DTIC

N94-31285 Virginia Univ., Charlottesville.
INELASTIC DEFORMATION OF METAL MATRIX COMPOSITES Ph.D. Thesis
Clifford Jesse Lissenden 1993 209 p
Avail: Univ. Microfilms Order No. DA9327902

A theoretical model capable of predicting the thermomechanical response of continuously reinforced metal matrix composite laminates subjected to multiaxial loading has been developed. A micromechanical model is used in conjunction with nonlinear lamination theory to determine inelastic laminate response. Matrix viscoplasticity, residual stresses, and damage to the fiber/matrix interfacial zone are explicitly included in the model. The representative cell of the micromechanical model is considered to be in a state of generalized plane strain, enabling a quasi two dimensional analysis to be performed. Constant strain finite elements are formulated with elastic-viscoplastic constitutive equations. Interfacial debonding is incorporated into the model. Nonlinear interfacial constitutive equations relate interfacial tractions to displacement discontinuities at the interface. Theoretical predictions are compared with the results of an experimental program conducted on silicon carbide/titanium (SiC/Ti) unidirectional, (O(sub 4)), and angle-ply, (+/- 45)(sub s), tubular specimens. Multiaxial loading included increments of axial tension, compression, torque, and internal pressure. Loadings were chosen in an effort to distinguish inelastic deformation due to damage from matrix plasticity and separate time-dependent effects from time-independent effects. Results show that fiber/matrix debonding is nonuniform throughout the composite and is a major factor in the effective response. Also, significant creep behavior occurs at relatively low applied stress levels at room temperature.
Dissert. Abstr.

N94-31313# Oak Ridge National Lab., TN.
EFFECTS OF OXIDATION AND CREEP DAMAGE MECHANISMS ON CREEP BEHAVIOR IN HIPed SILICON NITRIDES
A. A. Wereszczak, M. K. Ferber, and T. P. Kirkland 1994 8 p Presented at the 18th Annual Conference on Composites and Advanced Ceramics, Cocoa Beach, FL, 9-14 Jan. 1994
(Contract DE-AC05-84OR-21400)
(DE94-006559; CONF-940135-3) Avail: CASI HC A02/MF A01

The creep resistance of hot-isostatically pressed (HIPed) silicon nitride materials is ultimately dictated by its susceptibility to creep enhanced damage (e.g. cavitation) and oxidation induced damage. The evolution of these simultaneously occurring events has been examined in several HIPed silicon nitrides which were tested in tension at elevated temperatures. The activity and extent of each have found to be functions of several variables. These

parameters and their roles are discussed and include the following: initial alpha/beta ratio of silicon nitride grains, reaction of stable/unstable phases in the as-received material, percentage and type of sintering aid, and grain boundary crystallinity, impurity content, and viscosity. DOE

N94-31377# Ecole Centrale de Lyon (France). Dept. Materiaux-Mecanique Physique.
DEVELOPMENT AND CHARACTERIZATION OF INTERMEDIARY LAYERS ALLOWING THE BOND BETWEEN A METAL ALLOY AND A PLASMA SPRAYED CERAMIC Ph.D. Thesis [MISE AU POINT ET CARACTERISATION DE COUCHES INTERMEDIAIRES PERMETTANT L'ACCROCHAGE ENTRE UN ALLIAGE METALLIQUE ET UNE CERAMIQUE PROJETEE PLASMA]
Gausseem Saif 1991 195 p In FRENCH
(ECL-91-39; ETN-94-95909) Avail: CASI HC A09/MF A03

The resolution of three problems related to the principle of atmospheric plasma spraying usually used for realizing thermal barriers consisting of a zirconium layer sprayed on metallic substrate is reported. The problems concern: substrate corrosion through deposit porosities; residual constraints due to differences of the metal and ceramic thermal dilation coefficients; lack of adherence between the metal and the ceramic. These problems were resolved by the development of aluminide intermediary layers realized by interdiffusion of aluminum with the metallic substrate (steel or cast). Optimization of these layers was done by the use of thermomechanical characterizations (traction, thermal fatigue) associated to controls by ultrasonic mapping. The particularly favorable role of additions of silicon and above all yttrium and existence of an optimal torch/piece relative speed are shown. The results obtained are better than those given by classical solutions. ESA

N94-31444# Virginia Polytechnic Inst. and State Univ., Blacksburg.
STUDY OF WAVE PROPAGATION AND DYNAMIC RESPONSE OF LAMINATED COMPOSITE STRUCTURES Final Report, Jun. 1990 - Nov. 1993
Rakesh K. Kapania and J. N. Reddy 24 Jan. 1994 17 p
(Contract DAAL03-90-G-0134)
(AD-A276123; ARO-26908.14-EG) Avail: CASI HC A03/MF A01

We conducted a fundamental study to investigate the dynamic behavior of laminated structures. Both finite element and analytical solutions were developed. Using a 48 degree of freedom shell finite element (FE) developed by Kapania and coworkers, the effect of arbitrary inplane and out-of-plane loads on the transverse vibrations of thin arbitrarily laminated panels with or without geometric imperfections was analyzed. The element was used to investigate the effect of geometric imperfections on geometrically nonlinear impact response of thin laminated plates and cylindrical panels using reduced basis methods. A FE model was also developed to study the linear and geometrically nonlinear transient behavior of laminated beams. A postprocessor was developed that can use the transverse displacements from a classical laminated plate theory (CLPT) or a first order shear deformation theory (FSDT) to determine the transverse normal and shear stresses. The nonlinear dynamic equations of the first-order shear deformation theory and the third-order shear deformation plate theory of Reddy was reformulated to describe the interior and edge zone problems of rectangular plates. A three dimensional elasticity solution for the free vibration analysis of general cross-ply laminated plates has been carried out by combining Fourier series solution with a state space representation and the transfer matrix approach. A close theoretical examination has clarified the accuracy of the various single layer theories and a layerwise theory with the exact elasticity solution. DTIC

N94-31478# Office National d'Etudes et de Recherches Aerospatiales, Paris (France).
EVOLUTION OF THE INTERFACE PROPERTIES WITH TEMPERATURE IN THE T800H/ BISMALEIMIDE COMPOSITES Ph.D. Thesis - Paris 13 Univ. [EVOLUTION AVEC LA TEMPERATURE DES PROPRIETES DE L'INTERFACE DANS LES COMPOSITES T800H/BISMALEIMIDE]
Perrine Cheneau-Henry 1993 160 p In FRENCH Sponsored by EEC, and Service Technique des Programmes Aeronautiques Original contains color illustrations
(ISSN 0078-3781)
(ONERA-NT-1993-14; ETN-94-96066) Avail: CASI HC A08/MF A02

A study whose aim is to evaluate the interface influence on carbon/bismaleimide composites properties for temperature as high as 250 C is reported. The interface is characterized at different temperatures by pull out test and at room temperature by fragmentation and impregnated tow tensile tests. For the pull out test, the interfacial shear strength variation with temperature comes from matrix properties evolution and residual thermal stresses modification as well. The residual stresses, evaluated by finite elements, are modified by temperature and the coefficient of thermal expansion of the specimen holder. For the fragmentation test, an attempt is made to obtain a good 'coaxial' specimen which can lead to a mechanical analysis and determination of the mean shear stress. In a fragmentation test simulation, the 'coaxial' geometry in the specimen stress calculation and the pull out test results for debonding stress choice are taken into account. For the impregnated tow tensile test, a statistical analysis of debonding length distribution from the fracture surface observation is made. With a model which gives the mean debonding length, a link is established between these results and the fragmentation results. This study is a step beyond the understanding of composite properties evolution with temperature. ESA

N94-31481 Northwestern Univ., Chicago, IL.
ON THE MECHANICS OF STRESS ANALYSIS OF FIBER-REINFORCED COMPOSITES Ph.D. Thesis
Ven-Gen Lee 1993 132 p
Avail: Univ. Microfilms Order No. DA9327240

A general mathematical formulation is developed for the three-dimensional inclusion and inhomogeneity problems, which are practically important in many engineering applications such as fiber pullout of reinforced composites, load transfer behavior in the stiffened structural components, and material defects and impurities existing in engineering materials. First, the displacement field (Green's function) for an elastic solid subjected to various distributions of ring loading is derived in closed form using the Papkovich-Neuber displacement potentials and the Hankel transforms. The Green's functions are used to derive the displacement and stress fields due to a finite cylindrical inclusion of prescribed dilatational eigenstrain such as thermal expansion caused by an internal heat source. Unlike an elliptical inclusion, the interior stress field in the cylindrical inclusion is not uniform. Next, the three-dimensional inhomogeneity problem of a cylindrical fiber embedded in an infinite matrix of different material properties is considered to study load transfer of a finite fiber to an elastic medium. By using the equivalent inclusion method, the fiber is modeled as an inclusion with distributed eigenstrains of unknown strength, and the inhomogeneity problem can be treated as an equivalent inclusion problem. The eigenstrains are determined to simulate the disturbance due to the existing fiber. The equivalency of elastic field between inhomogeneity and inclusion problems leads to a set of integral equations. To solve the integral equations, the inclusion domain is discretized into finite number of sub-inclusions with uniform eigenstrains, and the integral equations are reduced to a set of algebraic equations. The distributions of eigenstrains, interior stress field and axial force along the fiber are presented for various fiber lengths and the ratio of material properties of the fiber relative to the matrix. The approach is applied to two specific problems: the load transfer of a finite cylindrical fiber into a semi-infinite matrix and the fiber with protective coating embedded in an elastic half-space. Finally, the displacement field due to a stationary dislocation loop in an elastic half-space is obtained using the Green's functions derived previously. With constant discontinuity of displacement prescribed along the circumference of a cylindrical inclusion, the results can be used to model the interfacial sliding between fiber and matrix in fiber-reinforced composites. Dissert. Abstr.

N94-31555 Northwestern Univ., Chicago, IL.
ON THE CONSTITUTIVE RESPONSE OF TRANSVERSELY LOADED FIBER COMPOSITES WITH COMPLIANT INTERPHASES Ph.D. Thesis
Michael Richard Gosz 1993 127 p
Avail: Univ. Microfilms Order No. DA9327199

The nature of fiber/matrix interphases in unidirectional fiber reinforced composites is known to significantly affect the overall behavior, especially the transverse behavior and the progressive failure under axial loading. However, there is still a lack of understanding of the local interphase behavior at the microscopic level and how this behavior influences the overall mechanical behavior and fracture at the macroscopic level. The present investigation addresses this issue from a mechanics perspective and attention is focused on the transverse behavior, where the loading is

applied perpendicular to the fiber direction. The phase geometry of the composite is modeled by a regular hexagonal array of circular fibers in a matrix. The interphase is described by a spring-layer model which permits jumps in displacement across a representative interface and assumes that the jumps are proportional to the conjugate tractions transmitted across that interface. Finite element calculations are carried out over a representative cell to obtain the mechanical response of the composite. The finite element method is then used an iterative mode to obtain the interphase properties given measured values of the composite's effective elastic constants. A modification to the spring-layer model which prevents a physically unrealistic radial overlap between the fiber and matrix phases has been recently proposed. A combined analytical and numerical method is developed to study the effect of the constraint on the response of the composite under general in-plane loading conditions. It is demonstrated that the transverse response is load-dependent and anisotropic under certain combinations of applied loading. The validity of the methodology and numerical results is established by invoking a new result in two-dimensional elasticity called the CLM theorem. In order to investigate the role of interphases in the transverse failure of fiber composites, a variationally coupled finite element - boundary element method is developed. After demonstrating the effectiveness of the method through examples in fracture mechanics and micromechanics, the method is employed to obtain the mechanical response, including the overall cracking patterns, of a hexagonal representative cell containing a center fiber and parts of surrounding fibers. It is shown that the interfacial stiffness and strength significantly affect the overall transverse stiffness and strength of the composite. Dissert. Abstr.

N94-31565 Oklahoma Univ., Norman.
ULTRASONIC TOMOGRAPHY IN FIBER-REINFORCED COMPOSITE MATERIALS Ph.D. Thesis
Yuqin Wang 1993 169 p
Avail: Univ. Microfilms Order No. DA9322515

In this work two approaches to tomographic imaging in fiber composite materials are introduced. The objective is to image the inhomogeneities of matrix properties while the source of anisotropy is known (the reinforcing fibers for fiber composites). For one approach, which is based on a simple geometric ray analysis, the traditional ART (Algebraic Reconstruction Technique) reconstruction algorithm is modified so that it accommodates the directional dependence of material properties and beam skewing due to the reinforcing fibers. In order to improve the reconstruction accuracy, a ray tracing technique based on the variational formulation of Fermat's principle is incorporated in the modified ART. It has been found that good agreement can be achieved for both synthetic and experimental data when the straight-ray-path assumption is applied to specimens with small inhomogeneities. It is also found that the iterative ray tracing technique is capable of finding 'shorter time' ray paths in most cases and reducing errors in the reconstructed images especially when relatively large inhomogeneities exist and velocity (or material property) profiles are relatively simple. In the alternative approach based on the field theory of wave propagation, one numerically solves the governing equations for wave propagation using a finite difference method. A finite difference scheme valid for the general case of a heterogeneous, anisotropic medium is used. It is shown that by directly solving the wave equation with proper boundary conditions, one can solve both the direct problems and the inverse problems. In the direct problems, the material properties are assumed to be known and the task is to compute the field variables in wave propagation or to predict various wave phenomena such as reflection, refraction, etc. or to quantitatively estimate the time of propagation and other experimentally measurable quantities. In the inverse problem, the material properties are reconstructed from experimentally measured data. In solving the travel time tomography problem, an iterative algorithm similar to the traditional ART technique is developed. The iterative process is based on evaluation of the sensitivity factors by perturbing the material properties. Using this reconstruction approach, the ray tracing problem and energy deviation problem associated with the conventional imaging algorithms are automatically solved. In this project, the finite difference approach has been applied to both direct problems and inverse problems. Results for simulations of wave fields are obtained. Material properties have also been successfully reconstructed from the time delay data for both isotropic and anisotropic media. Dissert. Abstr.

N94-31688 Technische Univ., Delft (Netherlands). Div. of Heat Treatment Science and Technology.
POWDER METALLURGICAL PROCESSING OF FIBRE REINFORCED ALUMINIUM COMPOSITES Ph.D. Thesis
J. H. terHaar 25 Jun. 1993 183 p Sponsored by Stichting voor de Technische Wetenschappen Limited Reproducibility: More than 20% of this document may be affected by microfiche quality
(PB94-148285) Avail: CASI HC A09

The thesis presents a part of the work on powder metallurgical processing of Al-matrix composites, conducted in the frame of a research program of the Foundation for Fundamental Research of Matter with financial support from the Foundation for Technological Sciences. This thesis is based on a collection of papers and follows the chronology of powder metallurgy (P/M) processing steps up to the evaluation of the semifinished product. The knowledge gathered during the several processing stages of mixing, compaction, degassing, extrusion, and evaluation provides valuable insight in the nature of problems one may be confronted with in working these materials. NTIS

N94-31706# Montreal Univ. (Quebec). Dept. de Genie Metallurgique.
CHARACTERIZATION AND GROWTH MECHANISMS OF THE MgAl2O4 PHASE IN Al2O3-REINFORCED Al-Mg COMPOSITES Ph.D. Thesis [CARACTERISATION ET MECHANISMES DE CROISSANCE DE LA PHASE MGAL2O4 DANS LES COMPOSITES AL-MG RENFORCES AVEC AL2O3]
Gianluigi Botton Dec. 1992 475 p In FRENCH
(ISBN-0-315-86531-8; CTN-94-61208) Copyright Avail: Micromedia Ltd., Technical Information Centre, 240 Catherine Street, Suite 305, Ottawa, Ontario, K2P 2G8, Canada HC/MF

Metal matrix composites reinforced with ceramics are of interest to the aerospace and auto industries. Studies have shown Al2O3 has promise as a component of those materials. The formation of Al2O4 in Al-Mg composites reinforced with Al2O3 was studied using electron energy loss spectroscopy. In studies conducted on composites processed in the liquid state, it is noted that nucleation at low temperature (700 C) is initially produced at secondary heterogeneous sites. At low and high (800 C) temperature, nucleation times correspond to formation of MgAl2O4 on the reinforcement surfaces which act as a substrate. A phenomenological model of MgAl2O4 growth is proposed in which the elements needed for forming MgAl2O4 from the liquid phase come from the Al-Mg alloy and from Al2O3 in an intermediate reaction. Experiments were conducted to identify the influence of the crystallography on the morphology of the MgAl2O4 phase, the reaction kinetics, and the nucleation and growth at 700 and 800 C. From the results, a model for the atomic structure configuration between the Al2O3 and MgAl2O4 lattices during the growth of (111) planes on alumina surfaces with (0001) orientation is proposed. The substrate orientation that retards MgAl2O4 formation is identified. The contribution of an anisotropic mechanical elastic energy was evaluated for a nucleus precipitated on a (0001) surface. Author (CISTI)

N94-31716# Montreal Univ. (Quebec). Dept. de Genie Mecanique.
OPTIMIZATION OF THE FORMING PARAMETERS OF PEEK/CARBON FIBER COMPOSITE M.S. Thesis [OPTIMISATION DES PARAMETRES DE MISE EN FORME DU COMPOSITE PEEK/FIBRE DE CARBONE]
Hachmi BenDaly Jun. 1993 208 p In FRENCH
(ISBN-0-315-86410-9; CTN-94-61192) Copyright Avail: Micromedia Ltd., Technical Information Centre, 240 Catherine Street, Suite 305, Ottawa, Ontario, K2P 2G8, Canada HC/MF

The effects of processing conditions on the crystallization kinetics and fiber/matrix interactions in polyether ether ketone (PEEK)/carbon fiber composite were investigated. The molding cycle was simulated by differential scanning calorimetry. Simulation results show that increasing the cooling rate affects the crystallization parameters. Increasing the residence time at the molding temperature results in a significant decrease in the overall rate of crystallization. The activation energy related to the crystallization process depends on the cooling rate. A study of the PEEK crystalline structure shows that a rise in the cooling rate increases the number of nucleation sites and decreases the size of the crystalline entities; longer residence time at molding temperature increases the size of those entities. The interfacial strength in the composite, evaluated by a short beam shear test, was also significantly influenced by molding parameters. An increase in molding temperature and residence time at this temperature augments

the interfacial strength, while an increase in the cooling rate significantly reduces it. Improvement in fiber/matrix interaction occurs only for laminates in which strong fiber/matrix interaction is created during the molding process. The rupture mode is ductile before annealing, while it becomes fragile afterwards. Author (CISTI)

N94-31719# Montreal Univ. (Quebec). Dept. de Genie Mecanique.
FATIGUE BEHAVIOR OF UNIDIRECTIONAL PULTRUDED COMPOSITE MATERIALS M.S. Thesis [COMPORTEMENT EN FATIGUE DE MATERIAUX COMPOSITES UNIDIRECTIONNELS PULTRUDES]
Mohamed Reda Adimi Dec. 1992 150 p In FRENCH
(ISBN-0-315-86425-7; CTN-94-61195) Copyright Avail: Micromedia Ltd., Technical Information Centre, 240 Catherine Street, Suite 305, Ottawa, Ontario, K2P 2G8, Canada HC/MF

The interlaminar shear fatigue behavior of unidirectional pultruded half-round composite rods is examined. Four materials were subjected to three-point load-controlled bending tests under a triangular waveform loading signal. The fatigue test results show that the two glass fiber reinforced epoxy materials performed better than a polyester or a vinylester reinforced by glass fibers. For all tests undertaken, a transition from interlaminar shear failure to flexural failure was observed when the stress went from high values to low values. Between these limits, there is a mixed mode of fracture. This behavior is explained qualitatively based on geometric considerations. This was confirmed by additional tests using trapezoidal cross section beams and on a specimen subjected to a four point bending test where no shear/tension transition was noted from high to low stress fatigue. For a given stress amplitude, the failure mode can be predicted from the flexural bending tests with a large span to depth ratio. With that test, it is also possible to determine the stress amplitude corresponding to the transition point in the failure mode. The fatigue tests performed using different loading waveforms show that the lifetime decreases when passing from a triangular to a square waveform. Fatigue life is reduced by a factor of 1,000 when temperature is increased from 27 C to 100 C.
Author (CISTI)

N94-31793 Utah State Univ., Logan.
EVALUATING IN-PLANE ELASTIC CONSTANTS OF DAMAGED CARBON-EPOXY LAMINATES USING A QUANTITATIVE ULTRASONIC TECHNIQUE Ph.D. Thesis
Kenneth G. Kellogg 1992 174 p
Avail: Univ. Microfilms Order No. DA9316773

To fully utilize an engineering material, it is necessary to know and understand the total mechanical behavior of the material, both damaged and undamaged. This paper addresses the effect of impact damage on the tensile properties of a laminated carbon-epoxy angle-ply composite and its relationship to ultrasonic scanning data. Numerous coupons at various orientations were fabricated and impacted. These coupons were then ultrasonically scanned for damage assessment and comparisons were made. In addition, each coupon underwent a tensile failure test to determine the principal elastic constants and failure strengths. During the tensile tests, acoustic emission data were also collected to determine when load redistribution occurs. All of the collected data were then analyzed and discussed. From the collected data it was determined that ultrasonic wave speed measurements, in conjunction with Christoffel's equation, can be used to check the calculated extensional stiffnesses for laminated composites. In addition, the mechanical failure tests reveal that the use of classical lamination theory to determine the major and minor Young's moduli and Poisson's ratios of a laminate is very accurate provided good constituent property values are known initially. In terms of ultrasonic C-scans, it was concluded that through-the-thickness information can be obtained by utilizing a focussing transducer at oblique incidence. The wave forms obtained in this way must then be carefully scrutinized to determine what part of the waveform is essential. The comparison of damaged to undamaged strengths revealed that the tensile properties of the laminate were not noticeably affected at the impact energy levels used in this research. It was concluded that for tensile properties to be affected, considerable fiber damage must be present. Dissert. Abstr.

N94-31835# Toronto Univ. (Ontario). Dept. of Metallurgy and Materials Science.
INTERFACIAL BEHAVIOUR: WETTABILITY IN SiC(SUB p) METAL MATRIX COMPOSITES M.S. Thesis
James Hwang 1993 74 p
(ISBN-0-315-87206-3; CTN-94-61254) Copyright Avail: Micromedia Ltd., Technical Information Centre, 240 Catherine Street, Suite 305, Ottawa, Ontario, K2P 2G8, Canada HC/MF

The final properties of metal matrix composites, if estimated by considering the properties of their components, do not conform to the composites' actual properties. This is attributed to reinforcement degradation and poor bonding between matrix and reinforcement. It is well-accepted that the key to maximizing interfacial bond strength is to promote wetting at the metal/ceramic interface. A study was conducted on ways of enhancing this wetting, on methods of quantifying wetting, and on the relation between interfacial wetting and final composite strength. An apparatus was designed that employs the classical sessile drop technique to determine contact angles while taking into consideration the ease of surface oxidation of molten pure Al. The effects of SiC oxidation and Mg addition on the wettability of SiC by molten Al were then studied experimentally. It was found that Al tends to wet SiC to a greater degree in the presence of a thin oxidation layer of silica, and that Mg added to the Al melt in quantities of 1 and 3 mass percent, significantly improves its wetting on SiC.
Author (CISTI)

N94-31836# Toronto Univ. (Ontario). Dept. of Aerospace Science and Engineering.
OPTIMIZATION OF COMPOSITE MATERIAL FAILURE LOADS M.S. Thesis
Aloysius Wong 1993 186 p
(ISBN-0-315-87214-4; CTN-94-61255) Copyright Avail: Micromedia Ltd., Technical Information Centre, 240 Catherine Street, Suite 305, Ottawa, Ontario, K2P 2G8, Canada HC/MF

Composite laminates are optimized in order to maximize failure loads. In the optimization procedure, the effects of lamina orientation and lamina orientation with stiffness constraints are considered for laminates constructed of different numbers of lamina. Optimal failure characteristics are determined by systematically considering all possible lamina orientations in the laminate; thus, the optima determined are global optima. In the failure analysis, the quadratic tensor polynomial failure criterion is used for most of the investigations. However, some calculations are also performed for comparison using the maximum stress and maximum strain failure criteria. It is found that, for some biaxial applied load ratios, the optimized first ply failure is unaffected by a single stiffness constraint. Furthermore, it is shown that increasing the number of lamina in a laminate may or may not increase the maximum failure load per unit thickness. In most biaxial load cases, four-layer balanced laminates are shown to be optimal.
Author (CISTI)

N94-31892 Diffracto Ltd., Windsor (Ontario).
LOCATION OF IMPACT DAMAGE SITES IN COMPOSITE AIRCRAFT STRUCTURES, TASK 3.4.1 Final Report
Frank Karpala and Omer L. Hageniers Dec. 1992 19 p
(DSIS-94-01590; CTN-94-61258) Avail: CASI HC A03/MF A01

A portable field-level inspection system called D Sight was developed to isolate areas of a composite aircraft structure that may have been damaged by low-energy impact. An extensive laboratory program was set up to determine factors which influence the correlation between D Sight indication and subsurface delamination. The program also demonstrated the applicability of D Sight to the wide range of materials, lay-ups, coatings, and structures that are potentially inspectable. The D Sight concept was tested on CF-18 composite structures under in-service conditions, including a study of various paint schemes. A second phase of the project addressed the development and evaluation of an advanced development model leading to the definition of those factors important in a commercial product. The project verified that D Sight can detect low-energy impact damage in aircraft structures at a level below that detectable by normal human visual inspection. The project also resulted in a D Sight Aircraft Inspection System that can be used in field evaluations for further definition of the design needs of a field deployable impact damage inspection system. CISTI

N94-31901 Virginia Univ., Charlottesville.
AN APPROXIMATE SOLUTION FOR INTERLAMINAR STRESSES IN LAMINATED COMPOSITES Ph.D. Thesis
Cheryl Angeline Rose 1992 193 p
Avail: Univ. Microfilms Order No. DA9316921

An approximate solution for interlaminar stresses in finite width laminated composites subjected to uniform extensional and bending loads is presented. The solution is based upon the principle of minimum complementary energy and an assumed, statically admissible stress state, derived by considering local material mismatch effects and global equilibrium requirements. The stresses in each layer are approximated by polynomial functions of the thickness coordinate, multiplied by combinations of exponential functions of the in-plane coordinate, expressed in terms of fourteen unknown decay parameters. Imposing the stationary condition of the laminate complementary energy with respect to the unknown variables yields a system of fourteen nonlinear algebraic equations for the parameters. Newton's method is implemented to solve this system. Once the parameters are known, the stresses can be easily determined at any point in the laminate. Results are presented for through-thickness and interlaminar stress distributions for angle-ply, cross-ply (symmetric and unsymmetric laminates), and quasi-isotropic laminates subjected to uniform extension and bending. It is shown that the solution compares well with existing finite element solutions and represents an improved approximate solution for interlaminar stresses, primarily at interfaces where global equilibrium is satisfied by the in-plane stresses, but large local mismatch in properties requires the presence of interlaminar stresses. Further, the contributions of both global equilibrium and local material mismatch effects to the stress field are clearly delineated. The results indicate that the significance of local mismatch effects is dependent on laminate stacking sequence. The demonstrated accuracy and efficiency of the solution make it ideally suited for parametric studies. Dissert. Abstr.

N94-31909# Montreal Univ. (Quebec). Dept. de Genie Mecanique.
LOW VELOCITY IMPACT DAMAGE IN CARBON FIBER/PEEK COMPOSITE LAMINATES Ph.D. Thesis
Hao Wang Mar. 1993 206 p
(ISBN-0-315-86546-6; CTN-94-61210) Copyright Avail: Micromedia Ltd., Technical Information Centre, 240 Catherine Street, Suite 305, Ottawa, Ontario, K2P 2G8, Canada HC/MF

Low velocity impact damage in carbon fiber polyether ether ketone (PEEK) thermoplastic composites was studied. The focus of the study was on the material properties that may control the extension of impact induced delamination (IID) and transverse cracks. The strength of materials (SoM) approach to predict the damage extension was evaluated by dynamic finite element analysis. A fracture mechanics approach is proposed to characterize the crack growth behavior of IID. Predicting delamination size is discussed using the concept of crack arrest toughness. In the crossply laminates studied, it was found that the PEEK exhibits the same damage modes as seen in thermoset epoxy composites. Considering the thermal residual stress and the crack constraining mechanism, the SoM approach could not predict extension of transverse cracks nor IID results from a Mode 2 dominated unstable fracture. IID occurs under displacement controlled conditions and seems to be arrested at constant interlaminar fracture energy. The strain energy release rate and the delamination arrest toughness of the material control the delamination extension. The end-loaded split fracture test was conducted to measure Mode 2 delamination toughness of the composite. Large deflection effects on toughness measurement were studied by nonlinear beam theory. The test was also used to measure Mode 2 crack arrest toughness. Author (CISTI)

N94-31943 Lehigh Univ., Bethlehem, PA.
TOUGHENING MECHANISMS IN FIBER-REINFORCED CERAMIC-MATRIX COMPOSITES Ph.D. Thesis
Elizabeth Patricia Butler 1993 242 p
Avail: Univ. Microfilms Order No. DA9325936

A single fiber bridging a crack at an angle of 90 degrees resulted in an increased fracture toughness of the composite over and above the intrinsic fracture resistance of the glass matrix of at least eight percent. The fracture resistance rose with increasing crack length, saturating at long crack lengths, indicating classic T-curve behavior arising from the mechanism of crack-wake bridging in which the predominant energy dissipation mechanism is frictional sliding of the fiber within the matrix. For high composite toughness the important interfacial properties are the interfacial toughness, G(sib IC), and the frictional shear resistance, tau (tau = q(sub 0) mu). A novel approach to interfacial property measurement allowed these factors to be deconvoluted for the first time. Independent measurements of the clamping stress and the friction coefficient verified these results. These interfacial parameters were found to be sensitive to composite processing; acid etching the carbon coating on the outer surface of the fiber before incorporation into the glass matrix doubled the steady maximum fracture toughness. Composites reinforced with an oxidized SiC fiber resulted in a maximum fracture resistance of 50 percent greater than that for the unreinforced glass matrix. These increases in interfacial shear resistance were due to an increase in the sliding friction coefficients; the clamping stresses were unchanged within experimental error. The effectiveness of ductile metal coatings for enhanced toughness was demonstrated using 6 micron and 19 micron copper fiber coatings. The copper coated fiber composites showed extensive T-curve behavior with a steady state toughness being reached that was 25 percent greater than the toughness of the unreinforced glass, independent of coating thickness. A new technique for measuring the interfacial shear resistances for fiber coatings sliding with respect to both the fiber and the matrix has been developed. This is the only experimental method available for such measurements. A procedure using classical fracture mechanics analysis has been developed in which the constitutive relationship for fiber bridging was deconvoluted from the experimentally measured fracture resistance curves. This allowed direct comparison of micromechanical properties to the macrofracture resistance of these fiber reinforced composites. Dissert. Abstr.

N94-31953 Ohio State Univ., Columbus.
THEORY OF THICK, LAMINATED COMPOSITE SHALLOW SHELLS Ph.D. Thesis
Jin-Der Paul Chang 1992 361 p
Avail: Univ. Microfilms Order No. DA9307734

This dissertation presents the derivation of a generalized shell theory with shear deformation and rotary inertia in curvilinear coordinates that yields a set of tenth order differential equations in terms of five independent displacement functions and five boundary conditions upon an edge of a shell. This theory includes two radii of curvature of the normal section cut along the coordinate lines and one radius of twist, which can also be used for a shell having two principal radii of curvature by setting the radius of twist to be infinite. The theory of general shells in curvilinear coordinates based on Love's second approximation can be reduced to a theory based on Love's first approximation. By using the assumptions for shallow shells having a planform projection, a theory of shallow shells with shear deformation and rotary inertia in cartesian coordinates is obtained. Further assumptions are made if a very shallow shell is used. The shallow shell theory is reduced to a simplified shallow shell theory, i.e., a generalized Donnell shell theory with shear deformation and rotary inertia. The present shallow shell theory and simplified shallow shell theory are formulated by employing a set of generalized constitutive equations of laminae. Further, the energy functionals, strain energy, kinetic energy, and loading potentials of these theories are presented. Closed-form solutions are obtained in free vibration and static deflections, due to different loading, for isotropic and cross-ply laminated shell panels with shear diaphragm boundaries. Comparisons are made among the results of the most accurate of the present theories and other various shear deformation theories and those from the three dimensional elasticity theory, available in recently published papers. It shows that the theory developed here gives very accurate results. Furthermore, by using the three present theories based on different assumptions and the thin shallow shell theory, extensive studies are made for isotropic and laminated composite shells in analyses of static deflections and free vibrations. The limits of accuracy for the simplified one of the present theories and the thin shallow shell theory are shown in comparison with the most accurate present theory. The important effects of shear deformation and rotary inertia are also demonstrated. Also, the analysis of characteristic behavior of shells is included by using various parameters. This clearly demonstrates the various parametric effects. Dissert. Abstr.

N94-31986 Northwestern Univ., Evanston, IL.
FRACTURE MECHANICS AND MICROMECHANISMS IN FIBER-REINFORCED COMPOSITES Ph.D. Thesis
Shuh-Huei Li 1993 225 p
Avail: Univ. Microfilms Order No. DA9327242

The resistance to fracture of monolithic-brittle matrix or quasi-brittle matrix materials increases significantly by use of fibers. The objective of this thesis is to investigate the mechanisms dominating enhanced toughness of matrix due to the presence of fibers. A micromechanical model is

developed to study the stability and growth of a bridged crack in a semi-infinite, brittle matrix composite reinforced with unidirectional, continuous fibers. This model considers microfracture mechanisms which primarily involve debonding associated with frictional sliding along fiber-matrix interfaces, and matrix cracking during tensile loading. The bridging stress of fiber and bridging factor which characterizes the crack opening are presented in closed form. Based on Eshelby's inclusion method, the energy approach is used to describe various stages of fracture processes (crack initiation interfacial debonding, width-through crack at bend-over point, and sequential multiple cracking). To verify the validity of the theoretical model, an experimental study was conducted with cement-based composites made with different volume fractions of steel fibers. The techniques of optical fluorescence microscopy (OFM) and epoxy impregnation were used to study the internal debonding phenomena of composites. The extent of the debonding cracks were observed prior to the bend-over point (BOP). A 'stable growth' of the debonding crack, where the debonding length increases with applied load, was also investigated in the study. Comparisons of model predictions of debonding behavior with experimental data appear to support the validity of the model. A theoretical model is also developed to analyze failure mechanisms of randomly aligned, discontinuous fiber-reinforced brittle matrix composites. The micromechanisms of debonding/sliding along intact fibers and pull-out of fibers are taken into account. The influence of spatial distribution of fibers, fiber aspect ratio, and fiber volume fraction on the cracking stress and tensile strength of a composite are examined. Critical conditions for multiple fracture associated with strain-hardening behavior are discussed as well. The model was applied to glass and steel fiber cement-based composites and compared with available experimental results. Dissert. Abstr.

N94-32012 Fairfax Materials Research, Inc., Alexandria, VA.
COMPUTER MODELLING OF CYCLIC DEFORMATION OF HIGH-TEMPERATURE MATERIALS Technical Progress Report, 1 Dec. 1993 - 28 Feb. 1994
M. S. Duesbery 28 Feb. 1993 14 p Limited Reproducibility: More than 20% of this document may be affected by microfiche quality
(Contract N00014-91-C-0067)
(AD-A277056) Avail: CASI HC A03

Current methods of lifetime assessment leave much to be desired. Typically, the expected life of a full-scale component exposed to a complex environment is based upon empirical interpretations of measurements performed on microscopic samples in controlled laboratory conditions. Extrapolation to the service component is accomplished by scaling laws, which, if used at all, are empirical; little or no attention is paid to synergistic interactions between the different components of the real environment. With the increasingly hostile conditions which must be faced in modern aerospace applications, improvement in lifetime estimation is mandated by both cost and safety considerations. This program aims at improving current methods of lifetime assessment by building in the characteristics of the micromechanisms known to be responsible for damage and failure. The broad approach entails the integration and, where necessary, augmentation of the micro-scale research results currently available in the literature into a macro-scale model with predictive capability. DTIC

N94-32023 Naval Postgraduate School, Monterey, CA.
SODIUM SULFATE CORROSION OF SILICON CARBIDE FIBER-REINFORCED LITHIUM ALUMINOSILICATE GLASS-CERAMIC MATRIX COMPOSITES M.S. Thesis
Leopoldo C. Maldia Dec. 1993 71 p Limited Reproducibility: More than 20% of this document may be affected by microfiche quality
(AD-A277224) Avail: CASI HC A04

Sodium sulfate hot corrosion of a SiC fiber-reinforced lithium aluminosilicate (LAS) glass-ceramic matrix composite was studied using Scanning Electron Microscope (SEM) and X-ray Diffraction (XRD). Changes in the microstructural chemical composition of the specimens were investigated. The samples provided by Naval Air Warfare Center (NAWC), Warminster, PA, were grouped as follows: (1) as-received, (2) Na2SO4 salt-coated and heat-treated in oxygen, (3) noncoated and heat-treated in oxygen, (4) Na2S4. Salt-coated and heat-treated in argon, and (5) noncoated and heat-treated in argon. Heat treatment was performed by NAWC for 100 hours at 900 C. Experimental data obtained indicated that the presence of Na2SO4 in an oxidative environment resulted in rapid corrosion of the matrix and SiC fibers and in the latter rings of SiO2 replaced what had previously been SiC. There was very limited degradation of the fibers and matrix exposed at the surface in the noncoated sample heat-treated in oxygen and in the salt-coated sample heat-treated in argon. A significant reduction in the amount of mullite in the matrices of all heat-treated samples was observed. Mullite dissolved into either the glassy phase or into the Beta-spodumene matrix. Lastly, the presence of distinct magnesium silicate crystalline phases in the salt-coated and heat-treated in oxygen sample implies that the MgO at the surface reacted with the SiO2 in the matrix. DTIC

N94-32024 Naval Postgraduate School, Monterey, CA.
FINITE ELEMENT ANALYSIS OF DAMAGE IN FIBROUS COMPOSITES USING A MICROMECHANICAL MODEL M.S. Thesis
Joseph M. Berner Dec. 1993 85 p Limited Reproducibility: More than 20% of this document may be affected by microfiche quality
(AD-A277226) Avail: CASI HC A05

The objective of this investigation is to study the damage mechanics of composite structures using a micromechanical approach for determining strength and stiffness degradation of the composite structures as damages, such as matrix cracking and fiber breakage, progress. The micromechanical cell method provides for analysis of stress at the fiber and matrix level while providing smeared composite properties for global structural analysis. As a result, the damage and failure criteria are expressed in terms of the fiber and matrix stress level of the composite structure. A correlation for stiffness reduction due to transverse cracking of a ceramic matrix composite under tensile loading is implemented in a three-dimensional finite element model. Next, thermal residual stresses from fabrication of the ceramic matrix composite are incorporated into the analysis. Finally, the finite element method is applied to a polymer matrix composite laminate with a center hole in order to study the progression of damage and final failure during tensile loading. The comparisons between the present predictions and the experimental results for the previous examples are very good. DTIC

N94-32070# Naval Energy and Environmental Support Activity, Port Hueneme, CA. Facilities Engineering Service Center.
BOND STRESS-SLIP CHARACTERISTICS OF FRP REBARS Interim Report, FY92 - FY93
L. J. Malvar Feb. 1994 51 p
(AD-A277191; NFESC-TR-2013-SHR) Avail: CASI HC A04/MF A01

The bond characteristics of four different types of glass fiber-reinforced plastic (GFRP) rebars with different surface deformations were analyzed experimentally. Local bond stress-slip data, as well as bond stress-radial deformation data, needed for constitutive modeling of the interface mechanics, were obtained for varying levels of confining pressure. In addition to bond stress and slip, radial stress and radial deformation were considered fundamental variables needed to provide for configuration-independent relationships. Each test specimen consisted of a 6 GFRP rebar embedded in a 3-inch-diameter, 4-inch-long cracked concrete cylinder subjected to a controlled, constant amount of confining axisymmetric radial pressure. Only 2.625 inches (the equivalent of five steel bar lugs) of contact were allowed between the bar and the concrete. For each rebar type, bond stress-slip and bond stress-radial deformation relationships were obtained for five levels of confining axisymmetric radial pressure. It was found that small surface indentations are sufficient to yield bond strengths comparable to that of steel bars. Effects of the deformations on tensile properties are discussed. It is also shown that radial pressure is an important parameter which can increase the bond strength threefold. DTIC

N94-32078 Drexel Univ., Philadelphia, PA.
MECHANICS OF THE SINGLE FIBER PULLOUT PROBLEM WITH SEVERAL INTERFACE CONDITIONS Ph.D. Thesis
Kishore Venkateswara Pochiraju 1993 162 p
Avail: Univ. Microfilms Order No. DA9319730

The fiber-matrix interface in fiber reinforced ceramic matrix composites plays a key role not only in the load transfer between matrix and fiber, but also in the micro-damage initiation and growth mechanisms. Consequently, the interface affects the overall strength of the composite and its toughness properties. In this regard, the response of the single fiber pull-out (or indentation) model to the application of a load at the end of the fiber is commonly used as a rational means by which the mechanics of the interface can be studied. This thesis presents a rigorous analysis of the single fiber pull-out (or push-in) problem. An analytical/computational method is

developed to determine the stress fields in the model subject to several fiber-matrix interface conditions, including perfect bonding, frictional sliding, and interfacial cracking. The analysis initially focuses on the singular stress fields near the fiber protrusion point and/or at the open/sliding interfacial crack fronts. A local analysis is carried out using the Muskhelishvili - Kolosov complex potential method from which separable power type radial stress singularities and the associated stress field characteristics are sought. Through singular stress analysis, accurate description of the local stress fields can be obtained within a scaling factor. In order to obtain the scaling factor in the local region and accurate stresses in the rest of the model, a refined finite element analysis is conducted with prescribed loading and boundary constraints. This global analysis provides the detailed stress fields throughout the model. A local-global stress matching is then conducted to determine the region in which a perfect match is observed between the spatial distributions of stresses obtained from the local analysis and the finite element analysis. This local-global matching procedure provides the scaling factor in the local field, thus completing the determination of the total stress field. Applying this local-global matching procedure, the characteristics of the stress fields are examined for several physical models. A simulation of frictional sliding problem of fiber is conducted based on Coulomb's law for frictional contact. Dissert. Abstr.

N94-32122# Aerospace Corp., El Segundo, CA.
HONEYCOMB SANDWICH STRUCTURES: VENTED VERSUS UNVENTED DESIGNS FOR SPACE SYSTEMS Final Report, Sep. 1992 - Oct. 1993
George Epstein and Susan Ruth Oct. 1993 24 p
(Contract F04701-88-C-0089)
(AD-A276713; TR-93(3904)-1; SMC-TR-94-02) Avail: CASI HC A03/MF A01

Several space systems programs have experienced significant anomalies associated with failures of unvented honeycomb sandwich structures. Based on documentation and personal experience, this report provides descriptions of the structures involved, the circumstances of the failures, and corrective actions. Of special note, it is concluded that failures occur due to internal pressure when the external environment is reduced in ambient pressure. Such failures are initiated at weak bond areas (presumed to result from a manufacturing defect - areas that were not previously identified/repaired). Once initiated, separation of the skin-to-core bond propagates very rapidly and has been described as explosive. It is recommended that honeycomb structures for space systems be adequately vented whenever possible. In situations where venting is not feasible, a series of recommendations is presented to minimize the likelihood of failure. Design and manufacturing parameters are listed for honeycomb sandwich panels that are not fully vented, in order to reduce the likelihood of failure. DTIC

N94-32265 Aeronautical Research Labs., Melbourne (Australia).
ASSESSMENT OF IMPACT DAMAGE IN COMPOSITE STRUCTURES
R. Jones, S. C. Galea, and J. J. Paul Dec. 1993 61 p Limited Reproducibility: More than 20% of this document may be affected by microfiche quality
(AD-A277063; ARL-TR-23; DODA-AR-008-409) Avail: Issuing Activity (Defense Technical Information Center (DTIC))

In order to provide through-life support for structural components fabricated from advanced composite materials, it is desirable to establish a damage tolerance methodology. There are many difficulties in meeting this objective, including the multiplicity of failure modes, the numerous types of potentially significant defects which may arise during manufacture or in service, and the sensitivity to moisture and temperature. This paper focuses on the problem of impact damage and reviews research undertaken at ARL in recent years related to the analysis and testing of impact damage composite laminates. It is shown that the residual strength of impact damaged laminates reduces to an asymptotic limit as the size of the damage increases and that uniaxial S-N curves for damaged laminates have a generic shape with a pronounced threshold (endurance) level. DTIC

N94-32342 Arizona State Univ., Tempe. Dept. of Mechanical and Aerospace Engineering.
MECHANICS OF FAILURE OF HIGH TEMPERATURE METAL MATRIX COMPOSITES Final Report, 15 Feb. 1990 - 30 Sep. 1993
Demitris A. Kouris 22 Dec. 1993 248 p Limited Reproducibility: More than 20% of this document may be affected by microfiche quality
(Grant AF-AFOSR-0235-90)
(AD-A277397; AFOSR-94-0072TR) Avail: CASI HC A11

Results of a three-year research effort aimed at developing an understanding of the factors controlling transverse strength and failure of intermetallic composites are presented. Experiments were conducted involving several aluminide matrix composites; two types of fibers were used in order to allow for large as well as small residual stresses. On the basis of the in situ observations and with the aid of high resolution strain mapping, the relevant damage mechanisms were identified. The experimental effort coupled with analytical models led to a number of conclusions that are important for the proper design of such composites. Among the important properties are the strength and sliding resistances of the interface, residual stresses, and fiber spacing. Therefore, optimum strength is achieved with either strongly bonded interfaces, or interfaces that debond easily but have large resistance to circumferential sliding. The latter condition could also be compatible with the requirement of debonding and relatively easy frictional sliding for maximum benefit from fiber reinforcement in longitudinal properties. The results suggest a potential benefit from having anisotropic interfacial properties, perhaps obtained through morphology, to allow easy sliding in the axial direction and more strongly resisted sliding in the circumferential direction. DTIC

N94-32496 Northwestern Univ., Evanston, IL.
EFFECTS OF INTERPHASES ON THE MECHANICAL, THERMAL AND HYGROMECHANICAL RESPONSE OF FIBER-REINFORCED COMPOSITES Ph.D. Thesis
Heung Soap Choi 1993 270 p
Avail: Univ. Microfilms Order No. DA9327174

The effects of fiber-matrix interphases on the micro- and macro-mechanical properties of unidirectionally fiber-reinforced composites have been studied for composites subjected to transverse uniaxial, biaxial and shear loadings, uniform temperature changes and uniform changes of moisture concentration. The interphases have been modeled by the spring-layer model which accounts for continuity of tractions, but allows radial and circumferential displacement jumps across the interphase that are linearly related to the normal and tangential tractions. Numerical calculations in basic cells have been carried out using the boundary element method. For the isothermal case the results display the effects of variation of interphase stiffness on the fields of stress and deformation and on the effective elastic constants for square array, 45 deg rotated square array and hexagonal array composites with and without interphase failure and radial matrix cracking. For a hexagonal array, under the assumption that the failure mechanisms follow the periodicity of the composite, the stress intensity factors at the tip of L-shaped and perpendicular-shaped matrix cracks and the reduction of the effective elastic moduli due to the matrix cracks and interphase damage have been calculated and the conditions for matrix crack propagation and extension of interphase damage have been analyzed. A fiber with a reduced interphase stiffness contained in a unidirectionally fiber reinforced composite gives rise to higher stresses at its interphase as well as at the interphases of neighboring fibers. For a hexagonal array composite, detailed numerical results are presented. Three cases have been investigated: (1) a perfect composite, (2) a perfect composite which contains a single fiber with a lower interphase stiffness, (3) a perfect composite which contains a single fiber with interphase cracks and a lower interphase stiffness. The effects of the interphases on the distribution of residual stresses induced by a uniform temperature change have also been investigated. The influence of thermally induced residual stresses on the micro- and macro-mechanical strength and stiffness properties of a hexagonal array composite subjected to monotonically increasing uniaxial transverse loading have been studied. Finally, the hygro-mechanical behavior for a uniform specific moisture concentration has been investigated by using the analogy between temperature and moisture effects. Dissert. Abstr.

N94-32501 California Univ., Santa Barbara.
MECHANICS OF CRACKING FOR COMPOSITE MATERIAL Ph.D. Thesis
Shrwai Ho 1992 145 p
Avail: Univ. Microfilms Order No. DA9317170

Cracking in the system is responsible for the reduction of strength for the vast majority of engineering materials. The object of this thesis is to introduce the Linear Elastic Fracture Mechanics to discuss the state of

knowledge on the cracking behavior of Composite Materials. This has implications for the science of the subject - basic understanding and modeling - and for practical considerations to aid high performance engine development. Several models were proposed in this study. Tunneling, a commonly observed cracking process, is inspected in this thesis: a new model for tunneling crack is introduced. Formula for steady-state energy release rate G(sub ss), which make it convenient for finite element analyses, is presented, and the relevance of G(sub ss) is studied. The concept is applied to micro cracking in brittle matrix composites caused by thermal expansion mismatch and tunneling cracks in a laminated 0/90 ceramic/matrix composite. Comparisons between experiment results and modeling are also included. Another more practical concern is trying to reconcile design practices for ductile alloys and monolithic ceramics, and thereby provide a theoretical link between design with and of ceramic-matrix composites. For a monolithic panel, even a small hole reduces the load-carrying capacity by a factor of 3: this is notch-sensitive. For a ductile alloy a small hole does not reduce much the load-carrying capacity: this is notch-insensitive. The main goal of that study is to determine the maximum load-carrying capacity of a ceramic-matrix composite panel with a hole. The basic model is large-scale bridging. Bridging laws shape, width, and periodic effects are all discussed in the thesis. An extended model, two-level-bridging model, is also included. Most engineering composite components exhibit failure behaviors that are governed by anisotropic and heterogeneous characteristics. In this thesis, a spatial rescaling was found to reduce plane elasticity problems for orthotropic materials. Guided by this technique and other analytic results, a systematic analysis is conducted for fracture specimens to investigate the role of material orthotropy in fracture behavior of unidirectional composites. All numerical calibrations are presented with fitting formulas in the relevant parameter regimes. The effect of material orthotropy on fracture behavior of unidirectional composites is thus quantified. Dissert. Abstr.

N94-32591 Berkeley Applied Science and Engineering, Inc., San Francisco, CA.

DEVELOPMENT OF AN ADVANCED CONTINUUM THEORY FOR COMPOSITE LAMINATES, VOLUME 1 Final Report, 1 Jan. 1991 - 31 Dec. 1993

M. Panahandeh, A. Masud, and G. R. Ghanimati 31 Dec. 1993 172 p Limited Reproducibility: More than 20% of this document may be affected by microfiche quality

(Contract F49620-91-C-0019)

(AD-A277275; AFOSR-94-0043TR-Vol-1) Avail: CASI HC A08

A continuum theory with a micro-macro structure was developed for composite laminates that satisfies the traction and displacement continuity requirements at interfaces. The interlaminar stresses were included in the model in a natural way and without any ad hoc assumptions. The built-in microstructure of the continuum model can account for the effects of curvature and geometric nonlinearity. A set of constitutive relations in terms of material properties of individual constituents was developed which is capable of modeling fiber orientation and stacking sequence. The theory was further expanded to include the effects of temperature where a set of coupled thermomechanical field equations with corresponding constitutive relations were derived. Development of the theory for cylindrical and spherical geometries was completed and wave motions in flat and curved geometries was studied. A layerwise shear-deformable multi-director C(sup 0) finite element formulation for the theory was developed which accounts for three dimensional effects, allows thickness variation, and permits the warping of the deformed normal, while satisfying all continuity requirements. Volume 1 includes the micro-macro continuum model of composite laminates as well as linear theory and wave motions in cylindrical and sperical laminates. DTIC

N94-32592# Berkeley Applied Science and Engineering, Inc., San Francisco, CA.

DEVELOPMENT OF AN ADVANCED CONTINUUM THEORY FOR COMPOSITE LAMINATES, VOLUME 2 Final Report, 1 Jan. 1991 - 31 Dec. 1993

M. Panahandeh, A. Masud, and G. R. Ghanimati 31 Dec. 1993 125 p

(Contract F49620-91-C-0019)

(AD-A277276; AFOSR-94-0043TR-Vol-2) Avail: CASI HC A06/MF A02

A continuum theory with a micro-macro structure was developed for composite laminates that satisfies the traction and displacement continuity requirements at interfaces. The interlaminar stresses were included in the model in a natural way and without any ad hoc assumptions. The built-in microstructure of the continuum model can account for the effects of curvature and geometric nonlinearity. A set of constitutive relations in terms of material properties of individual constituents was developed which is capable of modeling fiber orientation and stacking sequence. The theory was further expanded to include the effects of temperature where a set of coupled thermomechanical field equations with corresponding constitutive relations were derived. Development of the theory for cylindrical and spherical geometries was completed and wave motions in flat and curved geometries was studied. A layerwise shear-deformable multi-director C(sup 0) finite element formulation for the theory was developed which accounts for three dimensional effects, allows thickness variation, and permits the warping of the deformed normal, while satisfying all continuity requirements. Volume 2 includes the finite element method formulation of the layer-wise shear deformable composite shell theory as well as numerical simulations. DTIC

N94-32604# Army Research Lab., Aberdeen Proving Ground, MD.

A THERMAL VISCOELASTIC ANALYSIS FOR THICK-WALLED COMPOSITE CYLINDERS

Larry S. Chien and Jerome T. Tzeng 18 Mar. 1994 39 p

(AD-A274143; ARL-TR-310) Avail: CASI HC A03/MF A01

The linear quasistatic thermal viscoelastic behavior of a three dimensional thick laminated composite cylinder is investigated. The cylinder is loaded with a temperature change; however, thermomechanical coupling effects are neglected. The correspondence principle is employed to convert the thermoviscoelastic problem to its corresponding thermoelasticity problem in Laplace transform space. A closed-form formulation is then developed for each layer, assuming a state of generalized plane strain, to solve for a general solution of the corresponding thermoelastic problem. The Laplace transformed solution is completed by satisfying boundary conditions at the inner and outer surfaces of the cylinder and continuity conditions between adjacent layers. The solution process is expedited by replacing two undetermined coefficients in the assumed form of the thermoelastic solution with the normal stresses at the inner and outer of the cylinder and satisfying the continuity conditions between adjacent layers. Finally, direct Laplace transform inversion is used to yield the quasistatic thermoviscoelastic solution. DTIC

N94-32624 Phasex Corp., Lawrence, MA.

IMPROVED OXIDATION RESISTANCE OF 3-D CARBON/CARBON COMPOSITES Final Report, 1 Jul. 1992 - 28 Feb. 1993

Val Krukonis, Michael P. Coffey, and Scott D. Anderson 14 Jan. 1994 37 p Limited Reproducibility: More than 20% of this document may be affected by microfiche quality

(Contract F49620-92-C-0036)

(AD-A277349; AFOSR-94-0081TR) Avail: CASI HC A03

Carbon fiber reinforced silicon carbide matrix composites (C/SiC) were made by a process termed Supercritical Fluid Infiltration. A preceramic polymer, e.g., a polycarbosilane which can pyrolyze to form SiC, is dissolved in a supercritical fluid, the solution conveyed into a tightly woven preform of carbon fiber, and the preceramic polymer caused to deposit in the interstitial volume surrounding the fibers. Subsequent pyrolysis of the polymer forms the SiC matrix and fiber coating. Supercritical propane at conditions of 140 deg C, 4000 psi dissolves polycarbsilane to a concentration level of 30% (w/w), a level that results on substantial infiltration and deposition of the polymer. The yield of SiC from the parent polymer upon pyrolysis was determined to be about 50% (w/w); the polymer was fractionated using supercritical propane (in a process termed increasing pressure profiling), and it was found that some of the low molecular weight fractions gave extremely low yields of SiC (less than 25%) whereas some of the high molecular weight fractions yielded over 80% SiC. When the parent polymer was used for the infiltration studies the deposited material was modular in appearance suggesting that the liquid low molecular weight portion of the polymer was predominately and adversely influencing the uniformity. DTIC

N94-32642# Sandia National Labs., Albuquerque, NM.

MULTIPLE SIZE SCALE STRUCTURES IN SILICA/SILOXANE COMPOSITES STUDIED BY SMALL-ANGLE SCATTERING

G. Beaucage, D. W. Schaefer, T. Ulibarri, and E. Black 1993 6 p Presented at the 207th Spring National Meeting of the American Chemical

Society (ACS), San Diego, CA, 13-18 Mar. 1994
(Contract DE-AC04-94AL-85000)
(DE94-007300; SAND-93-2474C; CONF-940301-19) Avail: CASI HC A02/MF A01

The physical properties of in-situ produced composites, such as the TEOS-polysiloxane based systems, are directly related to the complex interaction of structural features from the nanoscopic to macroscopic scales. The nature of these structural interactions are a key element in understanding and controlling mechanical properties in these systems. We believe that the smallest scale structures, in the nanometer range, correlate with properties such as the modulus while large-scale structures on the micron scale effect failure in these materials. This paper discusses techniques for analysis of structural features and interrelation of structural features over these wide ranges of size using small-angle light, x-ray and neutron scattering. Combination of data from different instruments allows for characterization of the interaction between these different size scale features. DOE

N94-32665# Lawrence Livermore National Lab., CA.
INFLUENCE OF VOLUME FRACTION OF COMPONENT MATERIALS AND INTERLAYER BOND STRENGTH ON FRACTURE TOUGHNESS OF MULTI-LAYER Al 6090-25 VOLUME PERCENT SiCp AND Al 5182 LAMINATES
C. K. Syn, S. Stoner, D. R. Lesuer, and O. D. Sherby Nov. 1993 12 p Presented at the 94th Annual Meeting of the Minerals, Metals and Materials Society, San Francisco, CA, 27 Feb. - 3 Mar. 1994
(Contract W-7405-eng-48)
(DE94-007141; UCRL-JC-115698; CONF-940204-5) Avail: CASI HC A03/MF A01

Multilayer laminates of Al 6090/SiC/25p MMC and Al 5182 were prepared by hot pressing alternating layers of the component materials at 450 C in an argon gas atmosphere. Tensile properties, interlayer normal and shear bond strengths, and fracture toughness were measured in the T6-treated and untreated conditions. Fracture toughness was also measured as a function of the volume fraction of the MMC component. Yield and tensile strengths increased substantially by the T6 treatment while the total-elongation and interlayer bond strengths decreased even more substantially. Fracture toughness, on the other hand, did not change appreciably by the T6 treatment. The fracture toughness increased perceptibly with an increase in the volume percent of the MMC component. DOE

N94-32858*# National Aeronautics and Space Administration. Lewis Research Center, Cleveland, OH.
METCAN DEMONSTRATION MANUAL, VERSION 1.0 Final Report
H.-J. Lee and P. L. N. Murthy Apr. 1992 131 p
(RTOP 510-01-50)
(NASA-TM-105607; E-6944; NAS 1.15:105607) Avail: CASI HC A07/MF A02

The various features of the Metal Matrix Composite Analyzer (METCAN) computer program to simulate the high temperature nonlinear behavior of continuous fiber reinforced metal matrix composites are demonstrated. Different problems are used to demonstrate various capabilities of METCAN for both static and cyclic analyses. A complete description of the METCAN output file is also included to help interpret results. Author

N94-32860*# McDonnell Aircraft Co., Saint Louis, MO.
DEVELOPMENT OF THERMOPLASTIC COMPOSITE AIRCRAFT STRUCTURES Final Report, Apr. 1989 - Apr. 1991
Michael P. Renieri, Steven J. Burpo, Lance M. Roundy, Stephanie A. Todd, and H. J. Kim Mar. 1992 121 p Original contains color illustrations
(Contract NAS1-18862)
(NASA-CR-189593; NAS 1.26:189593) Avail: CASI HC A06/MF A02; 4 functional color pages

Efforts focused on the use of thermoplastic composite materials in the development of structural details associated with an advanced fighter fuselage section with applicability to transport design. In support of these designs, mechanics developments were conducted in two areas. First, a dissipative strain energy approach to material characterization and failure prediction, developed at the Naval Research Laboratory, was evaluated as a design/analysis tool. Second, a finite element formulation for thick composites was developed and incorporated into a lug analysis method which incorporates pin bending effects. Manufacturing concepts were developed for an upper fuel cell cover. A detailed trade study produced two promising concepts: fiber placement and single-step diaphragm forming. Based on the innovative design/manufacturing concepts for the fuselage section primary structure, elements were designed, fabricated, and structurally tested. These elements focused on key issues such as thick composite lugs and low cost forming of fastenerless, stiffener/moldine concepts. Manufacturing techniques included autoclave consolidation, single diaphragm consolidation (SDCC) and roll-forming. Author

N94-32863*# Boeing Co., Renton, WA.
APPLICATION OF A DESIGN-BUILD-TEAM APPROACH TO LOW COST AND WEIGHT COMPOSITE FUSELAGE STRUCTURE Report, 15 May 1989 - 31 Jul. 1990
L. B. Ilcewicz, T. H. Walker, K. S. Willden, G. D. Swanson, G. Truslove, S. L. Metschan, and C. L. Pfahl Dec. 1991 146 p
(Contract NAS1-18889; RTOP 510-02-13-01)
(NASA-CR-4418; NAS 1.26:4418) Avail: CASI HC A07/MF A02

Relationships between manufacturing costs and design details must be understood to promote the application of advanced composite technologies to transport fuselage structures. A team approach, integrating the disciplines responsible for aircraft structural design and manufacturing, was developed to perform cost and weight trade studies for a twenty-foot diameter aft fuselage section. Baseline composite design and manufacturing concepts were selected for large quadrant panels in crown, side, and keel areas of the fuselage section. The associated technical issues were also identified. Detailed evaluation of crown panels indicated the potential for large weight savings and costs competitive with aluminum technology in the 1995 timeframe. Different processes and material forms were selected for the various elements that comprise the fuselage structure. Additional cost and weight savings potential was estimated for future advancements. Author

N94-32877*# Sikorsky Aircraft, Stratford, CT.
INNOVATIVE FABRICATION PROCESSING OF ADVANCED COMPOSITE MATERIALS CONCEPTS FOR PRIMARY AIRCRAFT STRUCTURES Final Report
Christos Kassapoglou, Al J. DiNicola, and Jack C. Chou Feb. 1992 248 p
(Contract NAS1-18799; RTOP 510-02-11)
(NASA-CR-189558; NAS 1.26:189558) Avail: CASI HC A11/MF A03

The autoclave based THERM-X(sub R) process was evaluated by cocuring complex curved panels with frames and stiffeners. The process was shown to result in composite parts of high quality with good compaction at sharp radius regions and corners of intersecting parts. The structural properties of the postbuckled panels fabricated were found to be equivalent to those of conventionally tooled hand laid-up parts. Significant savings in bagging time over conventional tooling were documented. Structural details such as cocured shear ties and embedded stiffener flanges in the skin were found to suppress failure modes such as failure at corners of intersecting members and skin stiffeners separation. Author

N94-32904*# Texas A&M Univ., College Station. Dept. of Aerospace Engineering.
ANALYSIS OF NEW COMPOSITE ARCHITECTURES Final Interim Report, 1 Jul. 1992 - 30 Jun. 1993
John D. Whitcomb Apr. 1994 52 p
(Grant NAG3-1270; RTOP 505-62-10)
(NASA-CR-195303; E-8705; NAS 1.26:195303) Avail: CASI HC A04/MF A01

Global/local method in conjunction with a special macro finite element is used to gain computational efficiency in the simulation of textile composites behavior. Results are included to demonstrate the effectiveness of the method. Also, 2D finite elements are used to study boundary effects in plain weave composite specimens subjected to extension, shear, and flexure loads. Effective extension, shear, and flexural moduli were found to be quite sensitive to specimen size. For extension and flexure loads stress distributions were affected by a free surface, but the free surface boundary effect did not appear to propagate very far into the interior. For shear load, the boundary effect appeared to propagate much further into the interior. The report is in the form of two technical articles, the first describes

the global/local method while the second describes the use of the 2D finite elements. Author (revised)

N94-32939*# National Aeronautics and Space Administration. Langley Research Center, Hampton, VA.
COMPARISON OF THE COMPRESSIVE STRENGTHS FOR STITCHED AND TOUGHENED COMPOSITE SYSTEMS
James R. Reeder Apr. 1994 46 p
(RTOP 505-63-50-04)
(NASA-TM-109108; NAS 1.15:109108) Avail: CASI HC A03/MF A01

The compression strength of a stitched and a toughened matrix graphite/epoxy composite was determined and compared to a baseline unstitched untoughened composite. Two different layups with a variety of test lengths were tested under both ambient and hot/wet conditions. No significant difference in strength was seen for the different materials when the gage lengths of the specimens were long enough to lead to a buckling failure. For shorter specimens, a 30 percent reduction in strength from the baseline was seen due to stitching for both a 48-ply quasi-isotropic and a (0/45/0/-45/90/-45/0/45/0)s laminate. Analysis of the results suggested that the decrease in strength was due to increased fiber misalignment due to the stitches. An observed increasing strength with decreasing gage length, which was seen for all materials, was explained with a size effect model. The model assumed a random distribution of flaws (misaligned fibers). The toughened materials showed a small increase in strength over the baseline material for both laminates presumably due to the compensating effects of a more compliant matrix and straighter fibers in the toughened material. The hot/wet strength of the stitched and baseline material fell 30 percent below their ambient strengths for shorter, nonbuckling specimen, while the strength of the toughened matrix material only fell 20 percent. Video images of the failing specimen were recorded and showed local failures prior to global collapse of the specimen. These images support the theory of a random distribution of flaws controlling composite failure. Failed specimen appearance, however, seems to be a misleading indication of the cause of failure. Author (revised)

N94-33008# Southwest Research Inst., San Antonio, TX.
FRACTURE MICROMECHANICS OF CONTINUOUS FIBER AND TEXTILE REINFORCED METAL AND CERAMIC MATRIX COMPOSITES
D. L. Davidson Feb. 1994 52 p
(Contract N00014-93-C-0040)
(AD-A277434; SWRI-06-5555/1) Avail: CASI HC A04/MF A01

This report summarizes progress on fatigue crack growth through unidirectional SCS-6/titanium alloy composites and the fatigue and fracture of ceramic matrix composites reinforced with continuous fibers, both large and small, in unidirectional and woven forms. The fiber/matrix interaction is detailed for SCS-6/titanium alloy composites near stress concentrations, and it is shown how that is similar to measurements of fiber stress in the wake of fatigue cracks. The main theme of the work on ceramic matrix composites is the effect of fiber architecture on fatigue behavior. DTIC

N94-33018 Department of the Navy, Washington, DC.
SURFACE CONFORMING FLEXIBLE EDDY CURRENT PROBE FOR SCANNING VARYING SURFACE CONTOURS Patent
Susan N. Vernon, inventor (to Navy) and John M. Liu, inventor (to Navy) 11 Jan. 1994 19 p Filed 6 Nov. 1992
(AD-D016173; US-Patent-5,278,498; US-Patent-Appl-SN-972341; US-Patent-Class-324-234) Avail: US Patent and Trademark Office

A flexible core eddy current probe is disclosed for testing of curved or irregular surfaces. The core is comprised of a flexible binder loaded with a powdered magnetic material and then formed into a specific flexible core shape continuously adaptable to irregular or curved surfaces. The flexible core probe has specific application to carbon fiber reinforced composite components having contoured surfaces. DTIC

N94-33029# New Mexico Inst. of Mining and Technology, Socorro. Dept. of Metallurgical and Materials Engineering.
INTERFACE ENGINEERING IN OXIDE FIBER/OXIDE MATRIX COMPOSITES Annual Report, 1 Mar. 1993 - 28 Feb. 1994
K. K. Chawla 28 Feb. 1994 33 p
(Contract N00014-89-J-1459)
(AD-A277672) Avail: CASI HC A03/MF A01

We have shown in earlier work that significant improvements upon the mechanical properties of the alumina + 15 w/o zirconia (PRD-166) fiber/borosilicate glass matrix and mullite (Nextel 480 and 550) fiber/mullite matrix composites could be achieved using interface engineering approach. This approach involves a control of the microstructure, roughness of the interface, and the thermal expansion mismatch between the fiber and matrix in order to improve the strength and fracture toughness of the composite. We have made a qualitative comparison of the elemental distribution in the PRD-166/glass (N51A) composites, with and without an SnO2 coating, on fibers using secondary ion mass spectrometry (SIMS). The results confirmed that tin dioxide serves as an effective barrier between this fiber and the silica-based glass. The tensile strength and toughness of the interface between SnO2 and flat alumina substrate were obtained by a laser spallation technique. DTIC

N94-33121*# National Aeronautics and Space Administration. Langley Research Center, Hampton, VA.
SECOND NASA ADVANCED COMPOSITES TECHNOLOGY CONFERENCE
John G. Davis, Jr., comp. and Herman L. Bohon, comp. Jun. 1992 447 p Conference held in Lake Tahoe, NV, 4-7 Nov. 1991
(RTOP 510-02-13-01)
(NASA-CP-3154; L-17106; NAS 1.55:3154) Avail: CASI HC A19/MF A04

The conference papers are presented. The Advanced Composite Technology (ACT) Program is a major multi-year research initiative to achieve a national goal of technology readiness before the end of the decade. Conference papers recorded results of research in the ACT Program in the specific areas of automated fiber placement, resin transfer molding, textile preforms, and stitching as these processes influence design, performance, and cost of composites in aircraft structures. These papers will also be included in the Ninth Conference Proceedings to be published by the Federal Aviation Administration as a separate document. For individual titles, see N94-33122 through N94-33137.

N94-33122*# National Aeronautics and Space Administration. Langley Research Center, Hampton, VA.
DESIGNER'S UNIFIED COST MODEL
William T. Freeman, L. B. Ilcewicz, G. D. Swanson, and T. Gutowski *In its* Second NASA Advanced Composites Technology Conference Jun. 1992 p 27-46 (For primary document see N94-33121 09-24)
Avail: CASI HC A03/MF A04

A conceptual and preliminary designers' cost prediction model has been initiated. The model will provide a technically sound method for evaluating the relative cost of different composite structural designs, fabrication processes, and assembly methods that can be compared to equivalent metallic parts or assemblies. The feasibility of developing cost prediction software in a modular form for interfacing with state of the art preliminary design tools and computer aided design programs is being evaluated. The goal of this task is to establish theoretical cost functions that relate geometric design features to summed material cost and labor content in terms of process mechanics and physics. The output of the designers' present analytical tools will be input for the designers' cost prediction model to provide the designer with a data base and deterministic cost methodology that allows one to trade and synthesize designs with both cost and weight as objective functions for optimization. The approach, goals, plans, and progress is presented for development of COSTADE (Cost Optimization Software for Transport Aircraft Design Evaluation). Author

N94-33123*# Analytical Services and Materials, Inc., Hampton, VA.
COINS: A COMPOSITES INFORMATION DATABASE SYSTEM
Shahid Siddiqi, Louis F. Vosteen, Ralph Edlow, and Teck-Seng Kwa *In* NASA. Langley Research Center, Second NASA Advanced Composites Technology Conference Jun. 1992 p 47-55 (For primary document see N94-33121 09-24)
Avail: CASI HC A02/MF A04

An automated data abstraction form (ADAF) was developed to collect information on advanced fabrication processes and their related costs. The information will be collected for all components being fabricated as part of the Advanced Composite Technology (ACT) program and included in a COmposites INformation System (COINS) data base. The aim of the COINS development effort is to provide future airframe preliminary design and

fabrication teams with a tool through which production cost can become a deterministic variable in the design optimization process. The effort was initiated by NASA Langley to implement the recommendations of a working group comprised of representatives from the commercial airframe companies. The principal working group recommendation was to reinstitute collection of composite part fabrication data in a format similar to the DOD/NASA Structural Composites Fabrication Guide. The fabrication information collection form was automated with current user friendly computer technology. The new automated form and features that make the form easy to use by an aircraft structural design manufacturing team are described. Author

N94-33124*# National Aeronautics and Space Administration. Langley Research Center, Hampton, VA.

COMPOSITE FUSELAGE SHELL STRUCTURES RESEARCH AT NASA LANGLEY RESEARCH CENTER

James H. Starnes, Jr. and Mark J. Shuart *In its* Second NASA Advanced Composites Technology Conference Jun. 1992 p 57-83 (For primary document see N94-33121 09-24)

Avail: CASI HC A03/MF A04

Fuselage structures for transport aircraft represent a large portion of both the weight and cost of these aircraft primary structures. Composite materials offer the potential for reducing both the weight and cost of these structures, but only limited studies of the response and failure of composite fuselage structures have been conducted. The research is described which is being conducted and planned at NASA Langley to understand the critical behavior of composite fuselage structures and to validate the structural mechanics methodology being developed for stiffened composite fuselage shell structure subjected to combined internal pressure and mechanical loads. Stiffened shell and curved stiffened panel designs are currently being developed and analyzed, and these designs will be fabricated and then tested to study critical fuselage behavior and to validate structural analysis and design methodology. The research includes studies of the effects of combined internal pressure and mechanical loads on nonlinear stiffened panel and shell behavior, the effects of cutouts and other gradient producing discontinuities on composite shell response, and the effects of local damage on pressure containment and residual strength. Scaling laws are being developed that relate full scale and subscale behavior of composite fuselage shells. Author

N94-33125*# Lockheed Aeronautical Systems Co., Marietta, GA.

STRUCTURAL TESTING OF THE TECHNOLOGY INTEGRATION BOX BEAM

C. F. Griffin *In* NASA. Langley Research Center, Second NASA Advanced Composites Technology Conference Jun. 1992 p 85-97 (For primary document see N94-33121 09-24)

Avail: CASI HC A03/MF A04

A full scale section of a transport aircraft wing box was designed, analyzed, fabricated, and tested. The wing box section, which was called the technology integration box beam, contained blade stiffened covers and T-stiffened channel spars constructed using graphite-epoxy materials. Covers, spars, and the aluminum ribs were assembled using mechanical fasteners. The box beam was statically tested for several loading conditions to verify the stiffness and strength characteristics of the composite wing design. Failure of the box beam occurred at 125 pct. of design limit load during the combined unbending and torsion ultimate design load test. It appears that the failure initiated at a stiffener runout location in the upper cover which resulted in rupture of the upper cover and portions of both spars. Author

N94-33126*# National Aeronautics and Space Administration. Langley Research Center, Hampton, VA.

TECHNOLOGY INTEGRATION BOX BEAM FAILURE STUDY Status Report

Mark J. Shuart, D. R. Ambur, D. D. Davis, Jr., Randall C. Davis, G. L. Farley, C. G. Lotts, and J. T. Wang *In its* Second NASA Advanced Composites Technology Conference Jun. 1992 p 99-111 (For primary document see N94-33121 09-24)

Avail: CASI HC A03/MF A04

Composite structures have the potential to be cost effective, structurally efficient primary aircraft structures. As part of the Advanced Composite Technology (ACT) program to exploit this potential for heavily loaded aircraft structures, the design and fabrication of the technology integration box beam (TIBB) was completed. The TIBB is an advanced composite prototype structure for the center wing section of the Lockheed C-130 aircraft. The TIBB was tested for downbending, upbending, torsion, and combined upbending and torsion load conditions to verify the design. The TIBB failed at 83 percent of design ultimate load for the combined upbending and torsion load condition. Current analytical and experimental results are described for a study of the mechanisms that led to the failure of the TIBB. Experimental results include load, strain, and deflection data. An analytical study was conducted of the TIBB structural response. Analytical results include strain and deflection results from a global analysis of the TIBB. Derived from text

N94-33127*# National Aeronautics and Space Administration. Langley Research Center, Hampton, VA.

DEVELOPMENT OF STITCHED/RTM COMPOSITE PRIMARY STRUCTURES

Susan M. Kullerd (Lockheed Engineering and Sciences Co., Hampton, VA.) and Marvin B. Dow *In its* Second NASA Advanced Composites Technology Conference Jun. 1992 p 115-140 (For primary document see N94-33121 09-24)

Avail: CASI HC A03/MF A04

The goal of the NASA Advanced Composites Technology (ACT) Program is to provide the technology required to gain the full benefit of weight savings and performance offered by composite primary structures. Achieving the goal is dependent on developing composite materials and structures which are damage tolerant and economical to manufacture. Researchers at NASA Langley and Douglas Aircraft Co. are studying stitching reinforcement combined with resin transfer molding (RTM) to create structures meeting the ACT program goals. The research is aimed at materials, processes, and structural concepts for application in both transport wings and fuselages. Empirical guidelines are being established for stitching reinforcement in primary structures and test data are reported in another paper. New data are presented herein from evaluation tests of thick (96 ply) and thin (16 ply) stitched laminates and from selection tests of RTM composite resins. Tension strength, compression strength, and post impact compression strength data are reported. Elements of a NASA Langley program to expand the science base for stitched/RTM composites are discussed. Derived from text

N94-33128*# Douglas Aircraft Co., Inc., Long Beach, CA.

RESIN TRANSFER MOLDING FOR ADVANCED COMPOSITE PRIMARY WING AND FUSELAGE STRUCTURES

Alan Markus *In* NASA. Langley Research Center, Second NASA Advanced Composites Technology Conference Jun. 1992 p 141-167 (For primary document see N94-33121 09-24)

Avail: CASI HC A03/MF A04

The stitching and resin transfer molding (RTM) processes developed at Douglas Aircraft Co. are successfully demonstrating significant cost reductions with good damage tolerance properties. These attributes were identified as critical to application of advanced composite materials to commercial aircraft primary structures. The RTM/stitching developments, cost analyses, and test results are discussed of the NASA Advanced Composites Technology program. Derived from text

N94-33129*# National Aeronautics and Space Administration. Langley Research Center, Hampton, VA.

TEST AND ANALYSIS RESULTS FOR COMPOSITE TRANSPORT FUSELAGE AND WING STRUCTURES

Jerry W. Deaton, Susan M. Kullerd, Ram C. Madan, and Victor L. Chen *In its* Second NASA Advanced Composites Technology Conference Jun. 1992 p 169-193 (For primary document see N94-33121 09-24)

Avail: CASI HC A03/MF A04

Automated tow placement (ATP) and stitching of dry textile composite preforms followed by resin transfer molding (RTM) are being studied as cost effective manufacturing processes for obtaining damage tolerant fuselage and wing structures for transport aircraft. Data are presented to assess the damage tolerance of ATP and RTM fuselage elements with stitched-on stiffeners from compression tests of impacted three J-stiffened panels and from stiffener pull-off tests. Data are also presented to assess the damage tolerance of RTM wing elements which had stitched skin and

stiffeners from impacted single stiffener and three blade stiffened compression tests and stiffener pull-off tests. Derived from text

N94-33130*# National Aeronautics and Space Administration. Langley Research Center, Hampton, VA.
TENSION FRACTURE OF LAMINATES FOR TRANSPORT FUSELAGE. PART 1: MATERIAL SCREENING
T. H. Walker (Boeing Commercial Airplane Co., Seattle, WA.), W. B. Avery (Boeing Commercial Airplane Co., Seattle, WA.), L. B. Ilcewicz (Boeing Commercial Airplane Co., Seattle, WA.), C. C. Poe, Jr., and C. E. Harris *In its* Second NASA Advanced Composites Technology Conference Jun. 1992 p 197-238 (For primary document see N94-33121 09-24)
(Contract NAS1-18889)
Avail: CASI HC A03/MF A04

Transport fuselage structures are designed to contain pressure following a large penetrating damage event. Application of composites to fuselage structures requires a data base and supporting analysis on tension damage tolerance. Tests with 430 fracture specimens were used to accomplish the following: (1) identify critical material and laminate variables affecting notch sensitivity, (2) evaluate composite failure criteria, and (3) recommend a screening test method. Variables studied included fiber type, matrix toughness, lamination manufacturing process, and intraply hybridization. The laminates found to have the lowest notch sensitivity were manufactured using automated tow placement. This suggests a possible relationship between the stress distribution and repeatable levels of material inhomogeneity that are larger than found in traditional tape laminates. Laminates with the highest notch sensitivity consisted of toughened matrix materials that were resistant to a splitting phenomena that reduces stress concentrations in load bearing plies. Parameters for conventional fracture criteria were found to increase with the crack length of the smallest notch sizes studied. Most materials and laminate combinations followed less than a square root singularity for the largest crack sizes studied. Specimen geometry, notch type, and notch size were evaluated in developing a screening test procedure. Results indicate that a range of notch sizes must be tested to determine notch sensitivity. Author (revised)

N94-33131*# Iowa Univ., Iowa City. Dept. of Biomedical Engineering.
INDENTABILITY OF CONVENTIONAL AND NEGATIVE POISSON'S RATIO FOAMS **c27**
R. S. Lakes and K. Elms *In* NASA. Langley Research Center, Second NASA Advanced Composites Technology Conference Jun. 1992 p 239-242 (For primary document see N94-33121 09-24)
Avail: CASI HC A01/MF A04

The indentation resistance of foams, both of conventional structure and of reentrant structure giving rise to negative Poisson's ratio, is studied using holographic interferometry. In holographic indentation tests, reentrant foams had higher yield strength and lower stiffness than conventional foams of the same original relative density. Calculated energy absorption for dynamic impact is considerably higher for reentrant foam than conventional foam. Author

N94-33132*# Boeing Commercial Airplane Co., Seattle, WA.
LOCAL DESIGN OPTIMIZATION FOR COMPOSITE TRANSPORT FUSELAGE CROWN PANELS
G. D. Swanson, L. B. Ilcewicz, T. H. Walker, D. Graesser, M. Tuttle, and Z. Zabinsky *In* NASA. Langley Research Center, Second NASA Advanced Composites Technology Conference Jun. 1992 p 243-262 (For primary document see N94-33121 09-24)
(Contract NAS1-18889)
Avail: CASI HC A03/MF A04

Composite transport fuselage crown panel design and manufacturing plans were optimized to have projected cost and weight savings of 18 and 45 percent, respectively. These savings are close to those quoted as overall NASA Advanced Composite Technology (ACT) program goals. Three local optimization tasks were found to influence the cost and weight of fuselage crown panels. The effects are summarized of each task and the task associated with a design cost model is described in detail. Studies were performed to evaluate the relationship between manufacturing cost and design details. A design tool was developed to aid in these studies. The development of the design tool included combining cost and performance constraints with a random search optimization algorithm. The resulting software was used in a series of optimization studies that evaluated the sensitivity of design variables, guidelines, criteria, and material selection on cost. The effect of blending adjacent design points in a full scale panel subjected to changing load distributions and local variations was shown to be important. Technical issues and directions for future work were identified. Author (revised)

N94-33133*# Boeing Commercial Airplane Co., Seattle, WA.
COMPOSITE FUSELAGE CROWN PANEL MANUFACTURING TECHNOLOGY
Kurtis Willden, S. Metschan, C. Grant, and T. Brown *In* NASA. Langley Research Center, Second NASA Advanced Composites Technology Conference Jun. 1992 p 263-291 (For primary document see N94-33121 09-24)
(Contract NAS1-18889)
Avail: CASI HC A03/MF A04

Commercial fuselage structures contain significant challenges in attempting to save manufacturing costs with advanced composite technology. Assembly issues, materials costs, and fabrication of elements with complex geometry are each expected to drive the cost of composite fuselage structure. Key technologies, such as large crown panel fabrication, were pursued for low cost. An intricate bond panel design and manufacturing concept were selected based on the efforts of the Design Build Team. The manufacturing processes selected for the intricate bond design include multiple large panel fabrication with Advanced Tow Placement (ATP) process, innovative cure tooling concepts, resin transfer molding of long fuselage frames, and use of low cost materials forms. The process optimization for final design/manufacturing configuration included factory simulations and hardware demonstrations. These efforts and other optimization tasks were instrumental in reducing costs by 18 pct. and weight by 45 pct. relative to an aluminum baseline. The qualitative and quantitative results of the manufacturing demonstrations were used to assess manufacturing risks and technology readiness. Author (revised)

N94-33134*# National Aeronautics and Space Administration. Langley Research Center, Hampton, VA.
RECENT PROGRESS IN NASA LANGLEY RESEARCH CENTER TEXTILE REINFORCED COMPOSITES PROGRAM
H. Benson Dexter, Charles E. Harris, and Norman J. Johnston *In its* Second NASA Advanced Composites Technology Conference Jun. 1992 p 295-323 (For primary document see N94-33121 09-24)
Avail: CASI HC A03/MF A04

Research was conducted to explore the benefits of textile reinforced composites for transport aircraft primary structures. The objective is to develop and demonstrate the potential of affordable textile reinforced composite materials to meet design properties and damage tolerance requirements of advanced aircraft structural concepts. Some program elements include development of textile preforms, processing science, mechanics of materials, experimental characterization of materials, and development and evaluation of textile reinforced composite structural elements and subcomponents. Textile 3-D weaving, 3-D braiding, and knitting and/or stitching are being compared with conventional laminated tape processes for improved damage tolerance. Through-the-thickness reinforcements offer significant damage tolerance improvements. However, these gains must be weighted against potential loss in in-plane properties such as strength and stiffness. Analytical trade studies are underway to establish design guidelines for the application of textile material forms to meet specific loading requirements. Fabrication and testing of large structural parts are required to establish the potential of textile reinforced composite materials. Author

N94-33135*# Lockheed Aeronautical Systems Co., Marietta, GA.
ADVANCED TEXTILE APPLICATIONS FOR PRIMARY AIRCRAFT STRUCTURES
Anthony C. Jackson, Ronald E. Barrie, Bharat M. Shah, and Jay G. Shukla *In* NASA. Langley Research Center, Second NASA Advanced Composites Technology Conference Jun. 1992 p 325-352 (For primary document see N94-33121 09-24)
(Contract NAS1-18888)
Avail: CASI HC A03/MF A04

Advanced composite primary structural concepts were evaluated for low cost, damage tolerant structures. Development of advanced textile

preforms for fuselage structural applications with resin transfer molding and powder epoxy materials are now under development. Author

N94-33136*# Grumman Aerospace Corp., Bethpage, NY.
COMPARISON OF RESIN FILM INFUSION, RESIN TRANSFER MOLDING, AND CONSOLIDATION OF TEXTILE PREFORMS FOR PRIMARY AIRCRAFT STRUCTURE
J. Suarez and S. Dastin *In* NASA. Langley Research Center, Second NASA Advanced Composites Technology Conference Jun. 1992 p 353-386 (For primary document see N94-33121 09-24)
Avail: CASI HC A03/MF A04

Innovative design concepts and cost effective fabrication processes were developed for damage tolerant primary structures that can perform at a design ultimate strain level of 6000 micro inch/inch. Attention focused on the use of textile high performance fiber reinforcement concepts that provide improved damage tolerance and out-of-plane load capability, low cost resin film infusion (RFI) and resin transfer molding (RTM) processes, and thermoplastic forming concepts. The fabrication of wing 'Y' spars by four different materials and/or processes methods is described: fabricated using IM7 angle interlock 0 to 90 deg woven preforms with + or - 45 deg plies stitched with Toray high strength graphite thread and processed using RFI and 3501-6 epoxy; fabricated using G40-800 knitted/stitched preforms and processed using RFI and 3501-6 epoxy; fabricated using G40-800 knitted/stitched preforms using RTM and Tactix 123/H41 epoxy; and fabricated preforms using AS4(6K)/PEEK 150 g commingled angle interlock 0 to 90 deg woven preforms with + or - 45 deg commingled plies stitched using high strength graphite thread and processed by consolidation. Structural efficiency, processability, and acquisition cost are compared. Author

N94-33137*# Boeing Co., Seattle, WA. Defense and Space Group.
CHARACTERIZATION AND MANUFACTURE OF BRAIDED COMPOSITES FOR LARGE COMMERCIAL AIRCRAFT STRUCTURES
Mark J. Fedro and Kurtis Willden *In* NASA. Langley Research Center, Second NASA Advanced Composites Technology Conference Jun. 1992 p 387-428 (For primary document see N94-33121 09-24)
(Contract NAS1-18889)
Avail: CASI HC A03/MF A04

Braided composite materials has been recognized as a potential cost effective material form for fuselage structural elements. Consequently, there is a strong need for more knowledge in the design, manufacture, test, and analysis of textile structural composites. Advance braided composite technology is advanced towards applications to a large commercial transport fuselage. The mechanics are summarized of materials and manufacturing demonstration results which were obtained in order to acquire an understanding of how braided composites can be applied to a commercial fuselage. Textile composites consisting of 2-D, 2-D triaxial, and 3-D braid patterns with thermoplastic and two resin transfer molding resin systems were studied. The structural performance of braided composites was evaluated through an extensive mechanical test program. Analytical methods were also developed and applied to predict the following: internal fiber architecture; stiffness; fiber stresses; failure mechanisms; notch effects; and the history of failure of the braided composite specimens. The applicability of braided composites to a commercial transport fuselage was further assessed through a manufacturing demonstration. Author

N94-33165 CSA Engineering, Inc., Palo Alto, CA.
STRUCTURAL INTEGRITY OF INTELLIGENT MATERIALS AND STRUCTURES Report, 1 Jul. 1993 - 31 Jan. 1994
Warren C. Gibson and Bryce L. Fowler 25 Feb. 1994 44 p Limited Reproducibility: More than 20% of this document may be affected by microfiche quality
(Contract F49620-93-C-0026)
(AD-A278397; AFOSR-94-0166TR) Avail: Issuing Activity (Defense Technical Information Center (DTIC))

Intelligent materials open new avenues to improve performance, reliability, and longevity of future aerospace vehicle structures by allowing the materials themselves to become active elements for multiple system functions. However, the application of intelligent materials and structures has been inhibited because the effects of microstructural interactions between intelligent and host material elements have heretofore not been well characterized. This research implemented and applied three analytical approaches to the study of stress concentrations and cracking around embedded sensor/actuator elements. One was an analytical method based on high-order Ritz functions for accurate representation of steep strain gradients. The second was a conventional finite element approach using very fine meshes, and the third was a finite-element-based computation of energy release rates suitable for predicting crack growth. Among other interesting results, the analyses compared the effects of applied loads with the effects of actuation strains and found that the applied loads were more likely to cause cracking or delamination than actuation. DTIC

N94-33178 California Univ., Santa Barbara. Dept. of Materials.
ON THE MECHANICS OF MICROBALLOON-REINFORCED METAL MATRIX COMPOSITES
M. Y. He and F. W. Zok Apr. 1994 46 p Limited Reproducibility: More than 20% of this document may be affected by microfiche quality
(Contract N00014-93-I-0224)
(AD-A277928) Avail: CASI HC A03

The elastic/plastic response of ceramic microballoon reinforced metal matrix composites subject to uniaxial loading are examined using finite element analysis. The microballoons are assumed to be spherical and their morphology characterized by the ratio of wall thickness, t, to radius, R. The key parameters investigated are the relative wall thickness, t/R, the modulus ratio (matrix/ceramic) and the yield and hardening characteristics of the matrix. The emphasis of the study is on the overall stress-strain response of the composite, the development of matrix plasticity and the development of stress within the microballoon. Author (DTIC)

N94-33180 David Sarnoff Research Center, Princeton, NJ.
CERAMIC AND METAL COMPOSITE CIRCUIT-BOARD-LEVEL TECHNOLOGY FOR APPLICATION SPECIFIC ELECTRONIC MODULES (ASEM) Technical Report, 22 Dec. 1993 - 23 Mar. 1994
B. J. Thaler, A. H. Kumar, A. Sussman, and A. N. Prabhu 23 Mar. 1994 34 p Limited Reproducibility: More than 20% of this document may be affected by microfiche quality
(Contract DAAB07-94-C-C009; ARPA Order A840)
(AD-A277961) Avail: CASI HC A03

The quarterly progress for the Ceramic/Metal Composite Circuit-Board-Level Technology for Application Specific Electronic Modules is described in this report. Data is reported for the following tasks: Metal Core Fabrication, LTCC Ceramic Development, and Thin Film Interconnect Structure Integration. DTIC

N94-31033*# Toronto Univ., North York (Ontario). Inst. for Aerospace Studies.
THERMAL-VACUUM RESPONSE OF POLYMER MATRIX COMPOSITES IN SPACE
R. C. Tennyson and R. Matthews *In* NASA. Marshall Space Flight Center, LDEF Materials Results for Spacecraft Applications Dec. 1993 p 283-299 (For primary document see N94-31012 09-12)
Avail: CASI HC A03/MF A04

N94-31034*# Aerospace Corp., El Segundo, CA.
THE IMPACT OF LDEF RESULTS ON THE SPACE APPLICATION OF METAL MATRIX COMPOSITES
Gary L. Steckel and Tuyen D. Le *In* NASA. Marshall Space Flight Center, LDEF Materials Results for Spacecraft Applications Dec. 1993 p 301-318 (For primary document see N94-31012 09-12)
(Contract F04701-88-C-0089)
Avail: CASI HC A03/MF A04

N94-31035*# Auburn Univ., AL. Materials Engineering Program.
SPACE ENVIRONMENTAL EFFECTS ON POLYMER COMPOSITES: RESEARCH NEEDS AND OPPORTUNITIES
Bor Z. Jang, J. Bianchi, Y. M. Liu, and C. P. Chang *In* NASA. Marshall Space Flight Center, LDEF Materials Results for Spacecraft Applications Dec. 1993 p 319-333 (For primary document see N94-31012 09-12)
Avail: CASI HC A03/MF A04

N94-31036*# Boeing Defense and Space Group, Seattle, WA.
LOW-EARTH ORBIT EFFECTS ON ORGANIC COMPOSITE MATERIALS FLOWN ON LDEF
Pete E. George and Harry W. Dursch *In* NASA. Marshall Space Flight

Center, LDEF Materials Results for Spacecraft Applications Dec. 1993 p 335-354 (For primary document see N94-31012 09-12)
(Contracts NAS1-18224; NAS1-19247)
Avail: CASI HC A03/MF A04

N94-33301*# TRW Systems Group, Redondo Beach, CA.
LEVERAGING METAL MATRIX COMPOSITES TO REDUCE COSTS IN SPACE MECHANISMS
Ted Nye, Rex Claridge, and Jim Walker *In* NASA. Lewis Research Center, The 28th Aerospace Mechanisms Symposium May 1994 p 129-134 (For primary document see N94-33291 09-15)
(Contracts F33615-90-C-3200; F33733-89-C-1011)
Avail: CASI HC A02/MF A04

25 INORGANIC AND PHYSICAL CHEMISTRY

Includes chemical analysis, e.g., chromatography; combustion theory; electrochemistry; and photochemistry.

For related information see also *77 Thermodynamics and Statistical Physics.*.

N94-31153# Drexel Univ., Philadelphia, PA.
FUEL PROPERTY EFFECTS ON ENGINE COMBUSTION PROCESSES
N. P. Cernansky 10 Jan. 1994 2 p
(Contract DE-FG04-87AL-44658)
(DE94-005529; DOE/AL-44658/T2) Avail: CASI HC A01/MF A01

Our engine studies have concentrated on 2 areas of interest to autoignition and emissions from engines. In the first, we investigated the effect of nitric oxide (NO) on the reactivity and autoignition behavior of 87 PRF. In the second study, we continued work on the effects of blending ethers on the reactivity and autoignition of a primary reference fuel blend, 87 PRF, with emphasis placed on the chemical interactions between ethers and the baseline fuel. The effects of nitric oxide (NO) on the reactivity and autoignition behavior of 87 PRF were examined in our research engine under motored conditions at compression ratios of 5.2 and 8.2. The most significant conclusions of our study are: (1) nitric oxide does interact with the hydrocarbon oxidation at conditions typically experienced by the end gas in a fired engine; (2) the effect is complex and, depending on the reaction environment, the same concentration of NO can produce dramatically different results. These results are particularly important given the fact that residual fractions and recycled exhaust gases in spark ignited engines typically result in about 200-600 ppm of NO in the unburned charge. The octane enhancing ethers, MTBE, ETBE, TAME, and DIPE, were blended into 87 PRF at a constant 0 atom fraction of 1.94% in the fuel mixtures and the mixtures were tested under motored conditions at our new compression ratio of 8.2. This new compression ratio allows studies on autoignition behaviors of 87 PRF with and without ethers. The results showed that, when using 87 PRF/ether mixtures, reactivity was significantly reduced as indicated by the higher inlet temperature required to initiate reactivity, significantly lower maximum CO concentration and the significantly higher inlet temperature required for autoignition. DOE

N94-31154# Iowa State Univ. of Science and Technology, Ames.
AN AXIAL APPROACH TO DETECTION IN CAPILLARY ELECTROPHORESIS Ph.D. Thesis
J. A. Taylor May 1993 131 p
(Contract W-7405-eng-82)
(DE94-005556; IS-T-1656) Avail: CASI HC A07/MF A02

Our approach involves on-axis illumination of the compounds inside the capillary detection region and is applied to absorbance and fluorescence detection. Absorbance measurements were made by focussing an incident laser beam into one capillary end; by using signals collected over the entire length of analyte band, this enhances the analytical path length of conventional absorbance detection 60x. This instrument offers a 15x improvement in detection limits. Three fluorescence detection experiments are discussed, all of which involve insertion of an optical fiber into the capillary. The first uses a high refractive index liquid phase to obtain total internal reflectance along capillary axis, this reducing light scatter. The second uses a charge-coupled device camera for simultaneous imaging of a capillary array (this may be useful in genome sequencing, etc.). The third is a study of fluid motion inside the capillary under pressure-driven and electroosmotic flow. The thesis is divided into four parts. DOE

N94-31238 International Business Machines Corp., San Jose, CA.
INFRARED SPECTROELECTROCHEMICAL STUDY OF CYANIDE ADSORPTION AND REACTIONS AT PLATINUM ELECTRODES IN AQUEOUS PERCHLORATE ELECTROLYTE
Kevin Ashley, Daniel L. Feldheim, Diane B. Parry, Mahesh G. Samant, and Michael R. Philpott 18 Feb. 1994 36 p Limited Reproducibility: More than 20% of this document may be affected by microfiche quality
(Contract N00014-92-C-0173)
(AD-A276402; TR-07) Avail: CASI HC A03

In situ infrared (IR) spectroelectrochemistry is used to investigate the behavior of cyanide (CN) at polycrystalline platinum surfaces in aqueous perchlorate (CLO4(-)) electrolyte. IR spectroelectrochemical data reveal the existence of a number of surface, as well as solution, cyanide species in the interfacial region. Within the double-layer potential region, there is IR evidence for several forms of absorbed cyanide. When the potential is made sufficiently positive, cyanide is oxidized to form cyanate. Other solution cyanide species which may be formed at the platinum-cyanide solution interface include hydrogen cyanide and square planar platinum cyanide complex. Author (DTIC)

N94-31248# Naval Air Warfare Center, Warminster, PA. Air Vehicle and Crew Systems Technology Dept.
EMPIRICAL AND SEMI-EMPIRICAL RELATIONSHIPS OF LIQUID-VAPOR, SOLID-VAPOR, AND SOLID-LIQUID SURFACE ENERGIES Final Report
William E. Frazier 1 Sep. 1993 28 p
(AD-A276480; NAWCADWAR-93053-60) Avail: CASI HC A03/MF A01

Surface energy, frequently referred to as surface tension, plays a critical role in materials processing and the evolution of a material's microstructure and properties. Processes critically dependent upon surface energy include casting, rapid solidification processes, flotation separation, smelting, degassing of liquid metals and solidification processing to name a few. However, despite its technological importance, there is a dearth of credible surface energy data available for most alloys and a number of elements. This paper serves as a compilation of useful data and presents correlations that may be used to estimate surface energy. DTIC

N94-31282# Lehigh Univ., Bethlehem, PA. Center for Solid State Studies.
AN EXTENDED APPROACH TO OXIDATIONS AND NITRIDATIONS OF Si AND Ge(x)Si(1-x) MATERIALS Final Report, 1 Jun. 1992 - 31 Dec. 1993
Ralph J. Jaccodine and Donald R. Young 1 Jan. 1994 11 p
(Contract DAAL03-92-G-0224)
(AD-A276056; ARO-29282.1-MS) Avail: CASI HC A03/MF A01

The effect of germanium on the hot electron current of metal-oxide-semiconductor devices has been studied by avalanche electron injection from the silicon to silicon dioxide. Different doses of germanium ranging from 10(exp 12) to 10(exp 15) atoms/sq cm are implanted into Si-SiO2 interface. The lucky hot electron population is suppressed by germanium implantation. We have used the charge-voltage technique to measure the interface state density. The interface state density increase caused by Ge implantation is negligible if the dose is lower than 10(exp 14) Ge/sq cm. We have also used different implantation energies to locate the Ge peak at different locations in the Si. We found that when the peak is at Si-SiO2 interface, the hot electron population is the lowest. Our results show that Ge implantation is a promising method to solve the hot carrier problem that has become important in submicrometer devices. DTIC

N94-31286 Illinois Univ., Urbana-Champaign.
SHOCK TUBE IGNITION AND COMBUSTION OF ALUMINUM/MAGNESIUM ALLOY PARTICLES IN OXYGEN AT HIGH PRESSURE Ph.D. Thesis
Ted Anthony Roberts 1993 320 p
Avail: Univ. Microfilms Order No. DA9329149

The ignition and combustion of Al, Mg, and Al/Mg alloy particles in 99 percent O2/1 percent N2 mixtures is investigated at high temperatures and pressures for rocket engine applications. The 20 micron particles contain

0, 5, 10, 20, 40, 60, 80, and 100 weight percent Mg alloyed with Al, and are ignited in oxygen using the reflected shock in a shock tube near the endwall. Using this technique, the ignition delay and combustion times of the particles are measured at temperatures up to 3250 K as a function of Mg content for oxygen pressures of 8.5, 17, and 34 atm. An ignition model is developed which employs a simple lumped capacitance energy equation and temperature and pressure dependent particle and gas properties. Good agreement is achieved between the measured and predicted trends in the ignition delay times. For the particles investigated, the contribution of heterogeneous reaction to the heating of the particle is found to be significant at lower temperatures, but may be neglected at gas temperatures above 3000 K. As little as 10 percent Mg reduces the ignition delay time substantially at all pressures tested. The particle ignition delay times decrease with increasing Mg content, and this reduction becomes less pronounced as oxidizer temperature and pressure are increased.
Dissert. Abstr.

N94-31293# IBM Research Lab., San Jose, CA.
INTERACTION OF WATER WITH METAL SURFACES
Sheng-Bai Zhu and Michael R. Philpott 18 Feb. 1994 32 p
(Contract N00014-92-C-0173)
(AD-A276260; TR-08) Avail: CASI HC A03/MF A01

A new class of potential suitable for modeling the adsorption of water on different metal sites is described. The new potentials are simple in form and convenient for use in computer simulations. In their real space form they comprise three parts: a pair-wise sum of spatial anisotropic 12-6 potentials, a pair-wise-sum of isotopic short range potentials, and an image potential. Two modifications of the potential are developed. In the first, the anisotropic potential acts only on the oxygen atom and not on the protons. In the second, the potential acts on all the atoms of the water molecule. In practical calculations it is convenient to transform the potential to a reciprocal space form in the manner described by Steele. DTIC

N94-31305# Brookhaven National Lab., Upton, NY.
INFRARED AND NEAR INFRARED TRANSIENT ABSORPTION SPECTROSCOPY OF MOLECULAR FREE RADICALS
T. J. Sears, M. Wu, G. E. Hall, B. C. Chang, G. Hansford, J. C. Bloch, and R. W. Field 1993 8 p Presented at the OE/LASE 1993: International Society for Optical Engineering (SPIE) Conference, Los Angeles, CA, 13-23 Jan. 1993
(Contract DE-AC02-76CH-00016)
(DE94-005446; BNL-49888; CONF-930159-59) Avail: CASI HC A02/MF A01

The advantages of absorption spectroscopy at low absorbances include a linear relationship between signal size and number of absorbing molecules, line of sight measurement, and easily interpretable lineshape functions. The main disadvantage is due to the necessity of measuring a small change in light intensity, usually in the presence of a strong background, which limits the sensitivity. In this work, recent results obtained using absorption techniques with continuous wave lasers to measure vibrational and electronic spectra in the mid- and near-infrared of small free radicals are reported. The radical of interest was generated by excimer laser photolysis of a chemically stable precursor molecule and detected by measuring the transient decrease in power of a continuous wave probe laser that traversed the photolyzed volume before being imaged onto a detector. DOE

N94-31348 Princeton Univ., NJ. Dept. of Aerospace and Mechanical Sciences.
IGNITION STUDIES IN NONPREMIXED HYDROGEN/AIR COMBUSTION
Final Report
Chung K. Law and Thomas G. Kreutz 24 Jan. 1994 27 p Limited Reproducibility: More than 20% of this document may be affected by microfiche quality
(Contract DAAL03-90-G-0222)
(AD-A275954; ARO-27565.3-EG) Avail: CASI HC A03

Ignition in nonpremixed counterflowing jets of fuel against heated air has been investigated experimentally, computationally, and analytically. Using H2/air ignition as the primary test system, the dominant chemical kinetics of ignition has been identified as well as the role of temperature, pressure, aerodynamic straining, and fuel concentration on the ignition process. In addition, the coupling of mass transport and aerodynamic straining to the chemical kinetics in nonpremixed ignition has been clarified. The methodologies developed for investigating hydrogen/air ignition have been extended to ignition of more complex and realistic fuels such as methane, n-butane, and isobutane. DTIC

N94-31349# Lawrence Livermore National Lab., CA.
IMAGING AMS
S. P. H. T. Freeman (Oxford Univ., England.), C. B. Ramsey (Oxford Univ., England.), and R. E. M. Hedges (Oxford Univ., England.) Dec. 1993 13 p Presented at the 6th International Conference on Accelerator Mass Spectrometry, Canberra, Australia, 17 Sep. - 1 Oct. 1993
(Contract W-7405-eng-48)
(DE94-006662; UCRL-JC-115791; CONF-930960-9) Avail: CASI HC A03/MF A01

The benefits of simultaneous high effective mass resolution and large spectrometer acceptance that accelerator mass spectrometry has afforded the bulk analysis of material samples by secondary ion mass spectrometry may also be applied to imaging SIMS. The authors are exploring imaging AMS with the addition to the Oxford (sup 14)C-AMS system of a scanning secondary ion source. It employs a sub micron probe and a separate Cs flood to further increase the useful ion yield. The source has been accommodated on the system by directly injecting sputtered ions into the accelerator without mass analysis. They are detected with a range of devices including new high-bandwidth detectors. Qualitative mass spectra may be easily generated by varying only the post-accelerator analysis magnet. Selected ion signals may be used for imaging. In developing the instrument for bioscience research the authors are establishing its capability for measuring the lighter elements prevalent in biological tissue. Importantly, the machine can map the distributions of radiocarbon labeled compounds with an efficiency of about 1(per thousand). A background due to misidentification of non-(sup 14)C ions as a result of the reduced ion mass filtering is too small to hinder high magnification microscopy. DOE

N94-31352# Lawrence Livermore National Lab., CA.
AMS BEYOND 2000
J. C. Davis 28 Dec. 1993 15 p Presented at the 6th International Conference on Accelerator Mass Spectrometry, Canberra, Australia, 17 Sep. - 1 Oct. 1993
(Contract W-7405-eng-48)
(DE94-006666; UCRL-JC-114145; CONF-930960-8) Avail: CASI HC A03/MF A01

The occasion of this conference, the Sixth International Conference on Accelerator Mass Spectrometry, falls sixteen years after the remarkable triple simultaneous discovery of this powerful isotopic measurement. In the interval since the Fifth Conference in Paris in 1991, new facilities of both large and small size have become fully operational, achieving impressive gains in both measurement throughput and precision. The purpose of this short review is to extrapolate from recent gains and experience and to project the status of the field beyond the coming millennial date. AMS achieved instant application in archaeology and the geosciences and its early growth was stimulated by the excitement caused by the early results. The ability to obtain an accurate radiocarbon date with a sample one thousand times smaller than possible with scintillation or gas counting, the ability to trace (sup 14)CO2 in sea water with a similar thousand fold shrinkage in sample size, and the wide utility of (sup 10)Be, (sup 26)Al, (sup 36)Cl, and (sup 129)I as tracers and chronometers of erosion, hydrology and paleoclimate were sufficient to drive the partial conversion of existing accelerators and the construction of new dedicated ones. These applications remain the core of the present field and continue to justify its growth. The past few years, however, have seen developments in new fields. Biomedicine, chemical kinetics, materials science, forensic dosimetry, and arms control/counter proliferation have been explored. These applications have varying promise and will influence development of AMS programs in new ways in the future. DOE

N94-31459# Pennsylvania State Univ., University Park. Dept. of Chemistry.
A NEW MECHANISM FOR SURFACE DIFFUSION: MOTION OF A SUBSTRATE-ADSORBATE COMPLEX
S. J. Stranick, A. N. Parikh, D. L. Allara, and P. S. Weiss 8 Dec. 1993 17 p

(Contract N00014-91-J-1630)
(AD-A276072; TR-10) Avail: CASI HC A03/MF A01

We propose a new mechanism for diffusion of surface adsorbates in which motion of the substrate atoms to which the adsorbates are attached results in the motion of the substrate-adsorbate complex. We show an experimental example -- the motion of self-assembled monolayers (SAM's) of CH3O2C(CH2)15SH on gold which we have observed by recording time-lapse movies with scanning tunneling microscopy. DTIC

N94-31471 Toronto Univ. (Ontario).
TURBULENCE STRUCTURE OF A PREMIXED FLAME IN A COAXIAL FREE AIR JET IN THE PRESENCE OR ABSENCE OF A BASE FLOW Ph.D. Thesis
Roland Alan Cusworth 1992 316 p
(ISBN-0-315-78739-2) Avail: Univ. Microfilms Order No. DANN78739

The base region surrounding the nozzle exit plane of rockets has a strong influence on the structure of the hot turbulent exhaust plume. It has also been established that numerical simulations of such flows are strongly dependent on the turbulence model employed. The present experimental study is an attempt and to provide benchmark data on the turbulence structure of this type of flow, for turbulence model validation purposes and to shed some light into the base region effect. The real flow situation of interest is modelled in the laboratory by a premixed hydrogen/air flame in a co-flowing air in the presence or absence of a base region between the central and annular jets. The main experimental diagnostic tool used is an Argon-ion, two-dimensional (two-color) laser Doppler velocimeter, with a relevant data acquisition and processing system. Mean axial and radial velocities, as well as the three turbulence intensities and shear intensity were obtained along the centerline and nine cross-sections of the flow. A two control volume arrangement was used to measure direct correlations of the axial fluctuating velocities from which the axial turbulence macro-scale was derived. The macro-scale and the measured turbulence kinetic energy provide experimental data on the dissipation rate of the turbulence kinetic energy, an important constituent variable in all turbulence models, which has been neglected in almost all previous experimental investigations. The results obtained indicate that, in a fuel-rich exhaust plume, the temperature would increase due to promotion of secondary combustion by the base, and thus increase both infrared radiation emissions and microwave attenuation in the vicinity of the nozzle exit. In the case of a fuel-lean flame, downstream of the base flow region the temperature would be suppressed due to the strong influx of cold surrounding air, and thus reduce the production of infrared radiation and microwave attenuation. Due to the lack of a low velocity recirculation zone, secondary combustion in the nonbase fuel rich exhaust plume is less likely to occur; but, the nonbase exhaust may produce a longer detectable infrared signal, since the temperature in the thermal layer decreases more slowly than in the case of the base flame.

Dissert. Abstr.

N94-31493# University of Southern California, Los Angeles.
COMBUSTION-RELATED STUDIES USING WEAKLY-BONDED COMPLEXES
R. A. Beaudet Jun. 1993 26 p
(Contract DE-FG03-89ER-14053)
(DE94-006632; DOE/ER-14053/T5) Avail: CASI HC A03/MF A01

This work is concerned with microscopic-level phenomena of importance in combustion. Weakly bonded adducts formed in supersonic expansions are investigated spectroscopically and used to limit the angles and impact parameters of biomolecular encounters. Also examined are species in which a free radical such as oxygen is bonded to a stable molecule in a shallow well outside the reaction barrier. These species can be used for several studies such as those involving photoinitiated reactions. The main experimental approach uses tunable diode laser absorption spectroscopy to monitor and characterize in detail the complexes of interest, and laser photoinitiation and LIF/MPI detection to examine biomolecular processes in which the adducts are used as precursors. In the first phase of this research, geometries and other molecular properties are being determined from vibrational-rotational spectra. In the second phase, these complexes will be used as precursors to study photoinitiated reactions in precursor geometry limited environments. DOE

N94-31526# Massachusetts Inst. of Tech., Cambridge.
STRUCTURE AND DYNAMICS OF MICROEMULSIONS IN BULK, AT INTERFACES, AND IN CONFINED GEOMETRIES
1993 21 p
(Contract DE-FG02-90ER-45429)
(DE94-006043; DOE/ER-45429/T1) Avail: CASI HC A03/MF A01

The authors have been constructing a special purpose small angle neutron scattering spectrometer (SAND) in collaboration with IPNS of Argonne National Laboratory and Texaco Research Laboratories in Beacon, New York. The spectrometer, having a moderate neutron flux, will be uniquely suited for detailed studies of complex fluids in their various phases. This spectrometer will be fully available to general users of the small angle scattering community after a year of testing and upon installation of the auxiliary equipment. The general research objective of the MIT group is to continue studies of the microstructural relationship to phase-behavior in three-component microemulsion systems. Specifically, they shall study the (1) variation of bulk structures when a microemulsion undergoes a non-wetting to wetting transition, (2) correlating interfacial reflectivity measurements of these wetting transitions to the SANS results, (3) use the contrast variation technique they recently developed for measuring the mean and Gaussian curvatures of the surfactant sheet to study the structural inversion of water-in-oil to oil-in-water microemulsions and the transition of disordered bicontinuous microemulsion to ordered lamellar phases, (4) investigation of the effects of spatial confinement on the phase behavior and structure of bicontinuous microemulsions, and finally (5) they shall continue the study of the recently discovered non-exponential relaxation of droplet density fluctuations near the critical and percolation points in water-in-oil droplet microemulsions. DOE

N94-31574 Technische Univ., Berlin (Germany). Fachbereich Physik.
ELECTROCHEMICAL SURFACE MODIFICATION OF SILICON MONOCRYSTALS: A SURFACE ANALYTIC EXAMINATION Ph.D. Thesis [ELEKTROCHEMISCHE OBERFLAECHENMODIFIZIERUNG VON SILIZIUMEINKRISTALLEN: EINE OBERFLAECHEANALYTISCHE UNTERSUCHUNG]
Thomas Bitzer 1992 157 p In GERMAN Limited Reproducibility: More than 20% of this document may be affected by microfiche quality
(ETN-94-95733) Avail: Issuing Activity (European Space Agency (ESA))

After photoelectrochemical processing, the n-silicon monocrystals are characterized using X-ray and ultraviolet photoelectron spectroscopy, diffraction of low energy electrons and high resolution electron energy loss spectroscopy. A combined electrochemistry/ultrahigh vacuum system was specially developed. Electronic properties, stochiometry and morphology of differently oriented silicon electrodes during the electrochemical erosion of an electrolytic oxide film in aqueous ammonium fluoride solutions are examined ex situ with good time resolution. The correlation of the anodic dark current with the structure of the silicon/electrolyte interface was discussed. The influence of electrolyte chemical composition and pH value on hydrogen termination is investigated and a model of dynamic behavior of dark current was developed. The hydrogenation of (111) oriented silicon surfaces was optimized and a process for electrochemical preparation of atomic Si(111)-1 by 1:H surfaces is presented. The electronic structure of electrochemically synthesized surface was characterized by ultraviolet photoelectron spectroscopy and compared with band structure calculation results. ESA

N94-31591 Technische Univ., Eindhoven (Netherlands).
OXIDE PIGMENTS IN WATER: THE COLLOID-CHEMICAL POINT OF VIEW Ph.D. Thesis
S. G. J. Heijman 16 Jun. 1993 163 p Limited Reproducibility: More than 20% of this document may be affected by microfiche quality
(PB94-148616) Avail: Issuing Activity (National Technical Information Service (NTIS))

The effect of polyacrylic acid type dispersing agents on the stability against coagulation of titanium dioxide particles in water is investigated. Because polyacrylic acid is a charged polymer, two mechanisms are important: electrostatic stabilization and steric stabilization. At low salt concentrations the electrostatic stabilization is the most important mechanism. During the drying process of the paint film, the ionic strength is increasing and consequently the electrostatic stabilization is decreasing. Under these circumstances the additional steric stabilization is necessary to prevent coagulation. Two methods are evaluated in order to measure

the hydrodynamic layer thickness of the adsorbed polymer layer. Because the layer is relatively thin (3 nm), the methods normally used to measure the hydrodynamic layer thickness are not applicable. The hydrodynamic layer thickness is an indication for the steric stabilization properties of a dispersing agent. Electrostatic stabilization of the pigment dispersion can be quantified by measuring the zeta potential of the dispersion. A combination of both parameters gives an indication of the working mechanism of a dispersing agent. NTIS

N94-31679# Helsinki Univ. of Technology, Espoo (Finland). Lab. of Physical Chemistry and Electrochemistry.
PREPARATION OF CATALYST PARTICLES USING METHODS OF COLLOID CHEMISTRY. PART 1: PREPARATION OF SILICA PARTICLES FROM ALCOHOL SOLUTIONS
R. Lindberg 29 Sep. 1993 31 p
(PB94-135597; ISBN-951-22-1761-9) Avail: CASI HC A03/MF A01

Monodisperse silica particles ranging from 50 to 1500 nm in diameter with a standard deviation of 2 to 15 percent can be precipitated from tetraethyl orthosilicate (TEOS) in aqueous ethanol solutions containing ammonia. Three reactions are generally used to describe the hydrolysis and condensation of silicon alkoxides: hydrolysis, alcohol condensation, and water condensation. Final particle size is dependent on the silicon alkoxide and alcohol. Particles prepared in methanol solutions are the smallest and the particle size increases with increasing chain length of the alcohol. Influence of ammonia, water, and TEOS concentrations on the particle size, monodispersity, and aggregation of particles is presented. NTIS

N94-31795 Case Western Reserve Univ., Cleveland, OH.
A MODEL OF CONCURRENT FLOW FLAME SPREAD OVER A THIN SOLID FUEL Ph.D. Thesis
Paul Vincent Ferkul 1993 157 p
Avail: Univ. Microfilms Order No. DA9321871

A numerical model is developed to examine laminar flame spread and extinction over a thin solid fuel in low-speed concurrent flows. The model provides a more precise fluid-mechanical description of the flame by incorporating an elliptic treatment of the upstream flame stabilization zone near the fuel burnout point. Parabolic equations are used to treat the downstream flame, which has a higher flow Reynolds number. The parabolic and elliptic regions are coupled smoothly by an appropriate matching of boundary conditions. The solid phase consists of an energy equation with surface radiative loss and a surface pyrolysis relation. Steady spread with constant flame and pyrolysis lengths is found possible for thin fuels and this facilitates the adoption of a moving coordinate system attached to the flame with the flame spread rate being an eigenvalue. Calculations are performed in purely forced flow in a range of velocities which are lower than those induced in a normal gravity buoyant environment. Both quenching and blowoff extinction are observed. The results show that as flow velocity or oxygen percentage is reduced, the flame spread rate, the pyrolysis length, and the flame length all decrease, as expected. The flame standoff distance from the solid and the reaction zone thickness, however, first increase with decreasing flow velocity, but eventually decrease very near the quenching extinction limit. The short, diffuse flames observed at low flow velocities and oxygen levels are consistent with available experimental data. The maximum flame temperature decreases slowly at first as flow velocity is reduced, then falls more steeply close to the quenching extinction limit. Low velocity quenching occurs as a result of heat loss. At low velocities, surface radiative loss becomes a significant fraction of the total combustion heat release. In addition, the shorter flame length causes an increase in the fraction of conduction downstream compared to conduction to the fuel. These heat losses lead to lower flame temperatures, and ultimately, extinction. This extinction mechanism differs from that of blowoff, where the flame is unable to be stabilized due to the high flow velocity. Dissert. Abstr.

N94-31824 California Univ., Los Angeles.
A NUMERICAL METHOD FOR MIXING/CHEMICALLY REACTING COMPRESSIBLE FLOW WITH FINITE RATE CHEMISTRY Ph.D. Thesis
Vinh That Ton 1993 172 p
Avail: Univ. Microfilms Order No. DA9318724

An efficient and accurate numerical method is presented to solve conservation laws for time-dependent multicomponent flows of compressible reactive gaseous mixtures with and without finite rate chemical reactions. An essentially non-oscillatory (ENO) shock capturing scheme for solving hyperbolic equations is extended to solve this system of conservation laws in a fully coupled way. The thermodynamic properties of the mixture are modeled accurately in the extension. The stiff chemical kinetic terms are split from the fluid motion by the fractional step algorithm. A complex chemical kinetic system with finite rate chemistry is used in the calculation to study transient combustion processes. A new technique for proper treatment of the stiff source terms is utilized, so that a correct solution of stiff combustion waves can be obtained even for large time steps and grid sizes. Numerical difficulties associated with contact surfaces for multicomponent mixing flow and stiffness of detonation wave problems are eliminated. Several test problems of one and two space dimensions, inviscid and viscous, with and without chemical reactions, are presented. A numerical study of the mechanism for enhancement of mixing and combustion with potential applications to scramjet combustor design is presented. Dissert. Abstr.

N94-31883* National Aeronautics and Space Administration. Lewis Research Center, Cleveland, OH.
SOLID SURFACE (Videotape)
Dec. 1992 Videotape: 7 min. 5 sec. playing time, in color, with sound
(NASA-TM-109746; NONP-VT-94-9946) Avail: CASI VHS A01/BETA A22

This video tape describes the development of the Solid Surface Combustion Experiment (SSCE) by researchers at NASA LeRC. The experiment studies fire spreading over a small solid fuel sample subjected to microgravity conditions in Earth orbit. Buoyant convection, which determines the heat transfer in fires on Earth, disappears in microgravity; hence, this experiment will help researchers understand how fires act on Earth. CASI

N94-32033 Instituto Superior Tecnico, Lisbon (Portugal). Dept. of Mechanical Engineering.
NATO ADVANCED STUDY INSTITUTE ON UNSTEADY COMBUSTION. VOLUME 2: RESEARCH PAPERS, SEPTEMBER 6-17, 1993
F. E. Culick, M. V. Heitor, and J. H. Whitelaw 17 Sep. 1993 242 p
Limited Reproducibility: More than 20% of this document may be affected by microfiche quality
(Contract DAJA45-93-M-0151)
(AD-A276572) Avail: CASI HC A11

Partial contents include the following: Experimental Investigations on a Flat Pulse Combustor; Numerical Simulation of a Flat Pulse Combustor; Structural Analysis of Prime Soot Clusters Formed in Diffusion Flames; The Effect of Moisture on the Spontaneous Heating of Coal; Initiation of Detonation in Vacuum with Propellant Particles; Solid Propellant Unsteady Combustion Under High Pressure; Autosolitons Structure in Heterogeneous Media; Generation of Sound in Turbulent Flow with Coherent Structures at Closed Volumes; Combustion Chamber as a Whistle; An Experimental and Numerical Investigation of Premixed Combustion in a Vortex in a Laboratory Dump Combustor; The Influence of Fuel/Air Mixture Oscillations on the Formation of Self-Sustained Combustion Instabilities in Premixed Combustion Systems; and Oscillation in Ducted Kerosene Spray Flames. DTIC

N94-32110 Sandia National Labs., Albuquerque, NM.
DETERMINATION OF BPSG THIN-FILM PROPERTIES USING IR REFLECTION SPECTROSCOPY OF PRODUCT WAFERS
T. M. Niemczyk (New Mexico Univ., Albuquerque.), J. E. Franke (New Mexico Univ., Albuquerque.), Liz-Hong Zhang (New Mexico Univ., Albuquerque.), D. M. Haaland, and K. J. Radigan 1993 6 p Presented at the Fall Meeting of the Materials Research Society (MRS), Boston, MA, 29 Nov. - 3 Dec. 1993 Limited Reproducibility: More than 20% of this document may be affected by microfiche quality
(Contract DE-AC04-94AL-85000)
(DE94-006591; SAND-93-1635C; CONF-931108-77) Avail: Issuing Activity (Department of Energy (DOE))

Borophosphosilicate glass (BPSG) thin films are widely used in the microelectronics industry as passivation layers, planarization layers, low-fusion-temperature dielectrics, etc. Currently available analytical methods for determining boron and phosphorus content in BPSG films do not meet the demands of at-line or in-situ quality control process monitoring. Infrared (IR) spectroscopy satisfies many of the at-line or in-situ issues, but has

only recently been capable of providing quantitative results using undoped and unpatterned silicon substrates. Three BPSG calibration sets were analyzed using infrared external reflection-absorption spectroscopy: (1) 21 films deposited on undoped silicon coated with 0.1 micron of silicon dioxide, (2) 21 films deposited on undoped silicon, and (3) 9 films deposited on microelectronics product wafers. A multivariate partial least squares analysis of the spectral data for the first large data set showed that boron content, phosphorus content, and film thickness can be quantified with precisions of 0.10 wt%, 0.12 wt%, and 30 A, respectively. The second large data set yielded similar results. The precisions obtained for the nine product wafer samples were 0.13 wt%B, 0.09 wt%P, and for film thickness 103 A.
DOE

N94-32124# Army Research Lab., Aberdeen Proving Ground, MD.
CONDENSED-PHASE PROCESSES DURING SOLID PROPELLANT COMBUSTION. 3: PRELIMINARY DEPTH-PROFILING STUDIES ON XM39, JA2, M9, M30, AND HMX2 Final Report, Nov. 1990 - Oct. 1991
Michael A. Schroeder, Robert A. Fifer, Martin S. Miller, Rose A. Pesce-Rodriguez, and Claire J. Selawski Jan. 1994 30 p
(DA Proj. 1L1-61102-AH-43)
(AD-A276595; ARL-TR-346) Avail: CASI HC A03/MF A01

This report describes preliminary depth-profiling studies on the chemical changes in the burned layers of propellant samples that have been burned in air then quenched by dropping them into water. The changes described here are mainly those observable by infrared spectroscopy using an infrared microscope. Depth-profiling is obtained either by examining the cross section of a burned propellant sample or by abrasive blasting small amounts of material from the burned surface and examining the remaining surface in the infrared microscope. The propellants and compositions studied include XM39, JA2, M9, M30, and HMX2. For the nitramine-binder compositions XM39 and HMX2, the surface layers seem to consist of a layer of molten oxidizer (RDX or HMX) tens to hundreds of micrometers thick, overlaid by a 10- or 20-micrometer-thick layer of binder and/or its decomposition products. In the case of the nitrate ester compositions JA2 and M9, the chemical changes observable by infrared spectroscopy seem to be very near the surface, within approximately 10 micrometers. This is in agreement with our scanning electron microscope observations and with results in the literature.
DTIC

N94-32140# Princeton Univ., NJ. Dept. of Chemistry.
ANALYSIS OF FORWARD AND INVERSE PROBLEMS IN CHEMICAL DYNAMICS AND SPECTROSCOPY
H. Rabitz 1993 9 p
(Contract DE-FG02-86ER-13480)
(DE94-007607; DOE/ER-13480/4) Avail: CASI HC A02/MF A01

During the past year, progress was made in exploring the relation of between chemical mechanisms and resultant combustion behavior, and the relation between potential surface features and dynamical observables. The first category of study also included theory of lumping or simplification of complex kinetic mechanisms. A systematic approach is being developed understanding and practical execution of kinetic models, including with transport In the second area of research on potential surfaces, we are exploring forward analysis of how potential features influence laboratory observable cross sections and rate constants, as well as development of inverse analysis algorithms. In the latter category, considerable progress has been made on developing an algorithm which is stable and capable of reliably inverting high resolution laboratory spectroscopic data back to intramolecular potentials. A collaboration is under way in this case, with the laboratory program of Marsha Lester, and preliminary results indicate that high quality potential surfaces can be extracted in this fashion. DOE

N94-32216# Purdue Univ., West Lafayette, IN. Dept. of Chemistry.
SOME PERSPECTIVES ON SOLUTION-PHASE ELECTRON-TRANSFER PROCESSES
Joseph T. Hupp and Michael J. Weaver Feb. 1994 56 p
(Contract N00014-91-J-1409)
(AD-A276906; TR-145) Avail: CASI HC A04/MF A01

The kinetics of electron-transfer (ET) process is a subject graced by a remarkable diversity as well as importance in chemistry and biology. Of the manifold types of chemical ET reactions, those occurring in solution and at electrode-solution interfaces have been the subject of a notably concerted and fruitful research effort. This activity was in large part spawned, and subsequently spurred, by the development of the theoretical treatments by Rudy Marcus and others, now broadly know as 'Marcus theory.' The happy circumstances that enabled the formulation of such quantitative theoretical relationships for solution-phase ET kinetics having true predictive and interpreatative value have acted as a considerable impetus to the development of an increasingly diverse and impressive range of experimental activities.
DTIC

N94-32231 Texas Univ., Austin. Dept. of Chemical Engineering.
ELECTRICAL COMMUNICATION BETWEEN GLUCOSE OXIDASE AND ELECTRODES BASED ON POLY(VINYLIMIDAZOLE) COMPLEX OF Os(bpy)2Cl2 Technical Report, Oct. 1992 - Dec. 1993
Ravi Rajagopalan, Timothy J. Ohara, and Adam Heller 17 Feb. 1994 23 p Sponsored by ONR Limited Reproducibility: More than 20% of this document may be affected by microfiche quality
(AD-A276585) Avail: CASI HC A03

Glucose oxidase was electrically wired to glassy carbon electrodes by redox hydrogels based on poly(N-vinyl imidazole) (PVI) complexed with Os(bpy)2Cl2 (PVI-Os). The hydrogels were formed by crosslinking PVI-Os and glucose oxidase with poly(ethylene glycol) diglycidyl ether (PEGDGE). Glucose was electrooxidized on the PVI-Os based wired enzyme electrodes at 350 mV versus SCE. The dependence of the electrooxidation current on pH, ionic strength, film thickness, weight fraction of the enzyme in the redox hydrogel, and oxygen partial pressure for electrodes rotating at 1000 rpm is described.
DTIC

N94-32233# Aerospace Corp., El Segundo, CA. Technology Operations.
SOFT X RAY PHOTOELECTRON SPECTROSCOPY STUDY OF THE INTERACTION OF Cr WITH MoS2(0001)
Thomas D. Durbin, Jeffrey R. Lince, Stephen V. Didziulis, David K. Shuh, and Jory A . Yarmoff 14 Jan. 1994 42 p
(Contract F04701-88-C-0089)
(AD-A276916; TR-93(3935)-2; SMC-TR-94-06) Avail: CASI HC A03/MF A01

The solid lubricant MoS2 must exhibit good adhesion to high-Cr steels used in moving mechanical assemblies on spacecraft to provide an effective antiwear lifetime. The adhesion can be maximized by tailoring the interfacial reactivity between the Cr at the steel surface and MoS2. To this end, we studied the interaction of Cr with the MoS2(0001) surface with core-level and valence-band soft x ray photoelectron spectroscopy employing synchrotron radiation (hv=150 to 400 eV). Cr vapor-deposited at room temperature formed relatively flat films on MoS2(0001). The Cr underwent a limited chemical reaction with the MOS2 substrate to form a chromium sulfide and Mo metal. The Mo metal formed a thin layer between the Cr film and the MoS2 substrate. In contrast, reacted S was incorporated throughout the Cr film, with its concentration enhanced at the surface. Annealing the Cr-covered sample drove the reaction between Cr and MoS2, forming additional Mo metal that alloyed with Cr, and several adsorbed S species on the Cr film surface. Annealing also caused partial coalescence of the Cr-containing portion of the film, uncovering parts of the Cr-Mo alloy. The reactivity of Cr with respect to MoS2(0001) is greater than that of Fe and somewhat less than that of Mn. The results indicate that cleaning the surface of a steel device before MoS2 film deposition will expose bare Fe and Cr metal, which could increase the metal/lubricant adhesion.
DTIC

N94-32234# Naval Command, Control and Ocean Surveillance Center, San Diego, CA. Research, Development, Technology and Evaluation Div.
CONTROL EXPERIMENTS IN LIQUID METAL COMBUSTION
T. R. Ogden and L. A. Parnell Feb. 1994 11 p
(AD-A276918) Avail: CASI HC A03/MF A01

This paper describes control experiments in liquid metal combustion. Preliminary results are reported for the effectiveness of open-loop control techniques in improving closed-cycle liquid metal combustion. The effects of non-axisymmetric nozzle shapes and pulsed oxidant flow rate on the combustion process are tested by measuring the total fuel utilization at the point of end-of-run pressurization, which is characteristic of this type of combustor, and by observing the jet/bath dynamics using X-radiography. Nozzle geometry and oxidant flow rate are the parameters used to control the combustion process. The reacting jet stability and rate of end-of-run pressurization is affected somewhat by the nozzle geometry however, no significant effect is observed on the total fuel utilization achieved. Pulsed

oxidant injection produces an expected large effect in bath/jet dynamics as the oxidant flow rate is pulsed from 3 to 20 gr/sec, but no statistically significant change in total utilization is demonstrated. The causes of combustion chamber pressurization during the combustion process and at end-of-run are discussed. In an effort to explain significant pressurization of the combustion chamber developed during the combustion process, chamber pressure dependence on oxidant purity grade, oxidant flow rate and hydrogen content are reported. The presence of relatively small amounts of hydrocarbons introduced during combustor fabrication produces significant pressurization of the combustion chamber throughout the combustion period, while the chamber pressure has relatively little dependence on the oxidant mass flow rate or oxidant purity. No significant effect of pressurization caused by hydrocarbons on maximum fuel utilization is observed. DTIC

N94-32251# Oak Ridge National Lab., TN.
A COMPARISON BETWEEN TWO MONTE CARLO CODES ON DETERMINATION OF TRANSIENT CHEMICAL YIELDS
R. N. Hamm, J. E. Turner, and A. Chatterjee 1993 14 p Presented at the Department of Energy Monte Carlo Workshop, Irving, CA, 28-29 Apr. 1993
(Contract DE-AC05-84OR-21400)
(DE94-007224; CONF-9304148-2) Avail: CASI HC A03/MF A01

Monte Carlo computer codes have been independently developed at several laboratories for performing calculations of radiolysis of water. The different codes involve a wide variety of models and related assumptions in treating the many physical and chemical processes that occur. Because few detailed aspects of such computations can be directly checked by experiment, it is important to make comparisons of various predicted microscopic distributions. This paper compares results obtained with codes developed at Lawrence Berkeley Laboratory and at Oak Ridge National Laboratory. Both codes were used to calculate the spatial distributions of various radical species in spurs along the tracks of energetic electrons. Similarities and differences in the results of this preliminary study are shown. Additional work is planned. DOE

N94-32304 Utah Univ., Salt Lake City. Dept. of Chemistry.
CHEMICAL STRUCTURE AND KINETICS AT LIQUID/SOLID INTERFACES Report, 1 Jun. 1989 - 1 Mar. 1993
Joel M. Harris 1 Mar. 1993 7 p Limited Reproducibility: More than 20% of this document may be affected by microfiche quality
(Contract N00014-89-J-1412)
(AD-A277112) Avail: CASI HC A02

This program of research was to develop spectroscopic and kinetic methods for exploring chemical structure and molecular dynamics at interfaces between dielectric solids and liquids. The research was carried out using fluorescence and vibrational spectroscopy from probe molecules where spectral and temporal differences in emission, absorption, or scattering provide information about the surface onto which they are adsorbed or bound. Studies focused on the interfacial chemistry of insulating surfaces in contact with liquids. The spectral and temporal response of bound or adsorbed molecules were used to observe differences in the chemical environment at the liquid-solid interface. Time resolution was also valuable in sorting out heterogeneous surface environments from differences in emission rate constants, adsorption rates, and reaction kinetics. DTIC

N94-32352 Calgary Univ. (Alberta). Dept. of Chemistry.
INTRODUCTION TO ELECTROCHEMICAL IMPEDANCE
Petr Vanysek 24 Feb. 1994 78 p Limited Reproducibility: More than 20% of this document may be affected by microfiche quality
(AD-A277081) Avail: Issuing Activity (Defense Technical Information Center (DTIC))

An overview of principles of impedance in electrochemistry, some pitfalls, practical information on experimentation and data evaluation and other pertinent observations are given. DTIC

N94-32376# California Univ., Berkeley. Lawrence Berkeley Lab.
RECOVERY OF CARBOXYLIC ACIDS AT PH GREATER THAN PKa Ph.D. Thesis
L. A. Tung Aug. 1993 388 p
(Contract DE-AC03-76SF-00098)
(DE94-007030; LBL-34669) Avail: CASI HC A17/MF A04

The economics of producing carboxylic acids by fermentation is often dominated, not by the fermentation cost, but by the cost of recovering and purifying the acids from dilute aqueous solutions. Experiments were performed to measure uptakes of lactic and succinic acids as functions of pH by basic polymeric sorbents; sorbent regeneration was also tested. Performance at pH greater than pK(sub a) and regenerability depend on sorbent basicity; apparent pK(sub a) and monomer pK(sub a) can be used to predict sorbent performance. Two basic amine extractants, Alamine 336 and Amberlite LA-2, in were also studied; they are able to sustain capacity to higher pH in diluents that stabilize the acid-amine complex through H bonding. Secondary amines perform better than tert-amines in diluents that solvate the additional proton. Competitive sulfate and phosphate, an interference in fermentation, are taken up by sorbents more strongly than by extractants. The third step in the proposed fermentation process, the cracking of the trimethylammonium (TMA) carboxylate, was also examined. Because lactic acid is more soluble and tends to self-esterify, simple thermal cracking does not remove all TMA; a more promising approach is to esterify the TMA lactate by reaction with an alcohol. DOE

N94-32414# Tulsa Univ., OK. Dept. of Chemical Engineering.
VOLATILES COMBUSTION IN FLUIDIZED BEDS
R. P. Hesketh and R. A. Pendergrass 1993 40 p
(Contract DE-FG22-92PC-92539)
(DE94-008382; DOE/PC-92539/5) Avail: CASI HC A03/MF A01

The goal of this project is to investigate the conditions in which volatiles will burn within both the dense and freeboard regions of fluidized beds. Experiments using a fluidized bed operated at incipient fluidization will be performed to characterize the effect of particle surface area, initial fuel concentration, and particle type on the inhibition of volatiles within a fluidized bed. The work conducted during the period 4 September, 1993 through 3 December, 1993 is reported in this technical progress report. The experimental work during this time period consists primarily of reactor start-up and data collection. Results of stoichiometric combustion of propane in air at three temperatures and a residence time of approximately 3 s are reported. The results of a detailed chemical kinetic model of propane and methane are reported for the theoretical work for this quarter. These results give further evidence that the inhibition of propane and methane combustion is caused by the sand particles. DOE

N94-32594 Michigan Univ., Ann Arbor.
ENERGY TRANSFER PROPERTIES AND MECHANISMS
J. R. Barker 1993 16 p Limited Reproducibility: More than 20% of this document may be affected by microfiche quality
(Contract DE-FG02-85ER-13442)
(DE94-007403; DOE/ER-13442/8) Avail: CASI HC A03

Since no single experimental technique is the best method for energy transfer experiments, we have used both time-dependent infrared fluorescence (IRF) and time-dependent thermal lensing (TDTL) to study energy transfer in various systems. We are investigating pump-probe techniques employing resonance enhanced multiphoton ionization (REMPI). IRF was used to study benzene, azulene, and toluene. TDTL was used to study CS2 and SO2 (data not given for latter). Large molecule energy transfer mechanisms are discussed. DOE

N94-32616 Argonne National Lab., IL.
COMPUTATIONAL CHEMISTRY ON PARALLEL COMPUTERS
R. J. Harrison, R. Shepard, and A. F. Wagner 1994 5 p Limited Reproducibility: More than 20% of this document may be affected by microfiche quality
(Contract W-31-109-eng-38)
(DE94-008106; ANL/CHM/PP-73485) Avail: CASI HC A01

The recent successful adaptation of mainline computational chemistry codes to parallel computers introduces a new era of cost-effective, computer-intensive chemistry applications and paves the way for future applications on massively parallel centralized computers being developed under the High Performance Computer and Communications Initiative. Parallel computer architecture offers the promise of inexpensive supercomputing for the price of effort in algorithm adaptations to parallelism. In chemical sciences-supported work at Argonne, beginning efforts at algorithm changes in computational chemistry codes has resulted in program performances on the group's 12-processor Alliant computer superior to that on one-processor Cray X-MP or Y-MP computers. The effort so far has focused on sophisticated and highly accurate electronic structure

production codes for determining the forces between atoms and molecules responsible for chemical structure, spectra, and reactivity. Some effort has also been invested in trajectory simulations of molecular dynamics. The American-made Alliant computer (model FX/2812) is one of the latest generation of shared-memory group or division size computers that generally cost about an order of magnitude less than the laboratory or university size computers such as Crays. DOE

N94-32694*# Computational Fluid Dynamics Research Corp., Huntsville, AL.

ADVANCED CFD METHODOLOGY FOR FAST TRANSIENTS ENCOUNTERED IN NONLINEAR COMBUSTION INSTABILITY PROBLEMS. VOLUME 2: USER'S GUIDE Final Report

Z. J. Wang, H. Q. Yang, M. Z. Pindera, and A. J. Przekwas Jul. 1992 74 p Original contains color illustrations

(Contract NAS8-38489; SBIR-11.04-6576A(Vol-2))

(NASA-CR-191352; NAS 1.26:191352; CFDRC-4110/2-Vol-2) Avail: CASI HC A04/MF A01; 1 functional color page

Successful analysis of nonlinear combustion instability problems greatly depends on the accuracy of the numerical methods used to solve governing transient equations. The work undertaken during phase 1 and phase 2 of this research has focused on the development and assessment of popular state-of-the-art numerical methods for the treatment of compressible flows. As an end product of this project, a 3D Navier-Stokes solver, FASTRAN (FAst TRansient ANalysis) code was developed for fast transient compressible flows. Author (revised)

N94-32696*# Computational Fluid Dynamics Research Corp., Huntsville, AL.

ADVANCED CFD METHODOLOGY FOR FAST TRANSIENTS ENCOUNTERED IN NONLINEAR COMBUSTION INSTABILITY PROBLEMS. VOLUME 1: THEORY AND VALIDATION Final Report

H. Q. Yang, Z. J. Wang, M. Z. Pindera, and A. J. Przekwas Jul. 1992 169 p Original contains color illustrations

(Contract NAS8-38489; SBIR-11.04-6576A(Vol-1))

(NASA-CR-191351; NAS 1.26:191351; CFDRC-4110/2-Vol-1) Avail: CASI HC A08/MF A02; 1 functional color page

Successful analysis of nonlinear combustion instability problems greatly depends on the accuracy of the numerical methods used to solve the governing transient equations. The work undertaken during phase 1 and phase 2 of this research has focused on the development and assessment of popular state-of-the-art numerical methods for the treatment of compressible flows. As an end product of this project, a 3D Navier-Stokes solver, FASTRAN (FAst TRansient ANalysis) code was developed for fast transient compressible flows. Author (revised)

N94-32743# Los Alamos National Lab., NM. Chemical Sciences and Technology Div.

SURFACE PROBES OF POROUS TOLUENE/WATER ICES: ADSORPTION KINETICS AND ANNEALING SPECTRA MEASURED BY SECOND HARMONIC GENERATION

Bryan F. Henson and Jeanne M. Robinson 1994 11 p Presented at the International Symposium on Optoelectronic and Microwave Engineering, Los Angeles, CA, 22-28 Jan. 1994

(Contract W-7405-eng-36)

(DE94-007564; LA-UR-94-606; CONF-940114-3) Avail: CASI HC A03/MF A01

We have applied the technique of second harmonic generation to the study of the solid/vapor interface of porous toluene/water ice films at low temperature. The ice samples are condensed from the vapor onto a cold support at 90 K and are typically approximately 500 microns thick with an internal surface area of approximately 200 m(exp 2). The ices are transparent to both the 532 nm probe laser and to the 266 nm second harmonic signal. Second harmonic light is generated from surfaces throughout the bulk of the porous sample. Significant differences in the efficiency for second harmonic generation from water and toluene enable the species specific study of annealing and adsorption in this binary system. Measurements of the coverage dependent adsorption of toluene on water ice, and the observation of a coverage dependent liquid-solid phase transition in a few monolayers of toluene adsorbed on water ice at temperatures below the bulk toluene melting temperature are presented. DOE

N94-32767 Dow Corning Corp., Carrollton, KY.

METHYL CHLORIDE BY WAY OF OXYHYDROCHLORINATION OF METHANE

Nov. 1993 47 p Limited Reproducibility: More than 20% of this document may be affected by microfiche quality

(Contract DE-AC22-91PC-91030)

(DE94-009129; DOE/PC-91030/T7) Avail: Issuing Activity (Department of Energy (DOE))

The purpose of this contract is to develop a process for converting light alkane gases to methyl chloride via oxyhydrochlorination using highly selective, stable catalysts in fixed-bed reactors designed to remove the large amount of heat generated, so as to control the reaction temperature. Further, the objective is to obtain the engineering data base necessary for developing a commercially feasible process and to evaluate the economics of the process. This document reports significant progress this quarter toward the development of a stable heterogeneous packed bed catalyst for the oxyhydrochlorination of methane. This quarter's data shows a catalyst which gave an average 18% methane conversion and 78% MeCl selectivity for a 12 day period of time. The PDU (process development unit) design engineering effort made significant progress this quarter. A bid on a modular unit by Xytel Corporation was received and evaluated. The pre-engineering estimate showed that costs were considerably higher than the original project capital estimates. A rigorous effort was made to eliminate all nonessential equipment and scope of work. A reduced scope was agreed upon and in the second round both Xytel and the Dow Corning in-house facilities engineering team were allowed to bid on the package. DOE

N94-32801# Lawrence Livermore National Lab., CA.

ANALYTIC PROPERTIES OF THE OCP AND IONIC MIXTURES IN THE STRONGLY COUPLED FLUID STATE

H. E. DeWitt 2 Dec. 1993 11 p Presented at the 7th International Workshop on the Physics of Nonideal Plasmas, Rostock, Germany, 27 Sep. - 1 Oct. 1993

(Contract W-7405-eng-48)

(DE94-008216; UCRL-JC-115806; CONF-9309148-1) Avail: CASI HC A03/MF A01

Exact results for the Madelung constants and first order anharmonic energies are given for the inverse power potentials with the Coulomb potential as the softest example. Similar exact results are obtained using the analysis of Rosenfeld on the gamma yields infinity limit for the OCP internal energy, direct correlation function, screening function, and bridge functions. Knowing these exact limits for the fluid phase of the OCP allows one to determine the nature of the thermal corrections to the strongly coupled results. Solutions of the HNC equation modified with the hard sphere bridge function give an example. DOE

N94-32826# Utah Univ., Salt Lake City. Dept. of Chemistry.

TIME-RESOLVED ANALYTICAL METHODS FOR LIQUID/SOLID INTERFACES

J. M. Harris 15 Nov. 1993 8 p

(Contract DE-FG03-93ER-14333)

(DE94-008352; DOE/ER-14333/1) Avail: CASI HC A02/MF A01

Chemical phenomena occurring at boundaries between insulating solids and liquids (adsorption, partition, monolayer self-assembly, catalysis, and chemical reactions) are important to energy-related analytical chemistry. These phenomena are central to chromatography, solid-phase extraction, immobilized analytical reagents, and optical sensors. Chemical interactions in these processes cannot generally be identified solely by equilibrium surface concentrations, since the steady-state behavior does not reveal the mechanism or rates of surface reactions. Therefore, the goal is to develop surface-sensitive spectroscopies by which chemical kinetics at liquid/solid interfaces can be observed on time-scales from nanoseconds to seconds. In the first year, we have used Joule-discharge heating kinetics to study pore structure of silica gels; effects of pore diameter, particle size, and chemical modification on pore connectivity were investigated. Temperature-jump relaxation measurements of sorption/desorption kinetics at liquid/solid interfaces were also carried out using Joule heating; kinetic barriers to sorption of ions from solution were found for both C-18 and Cl surfaces. Through a collaboration with Fritz-Haber Institute in Berlin, we were able to acquire laser temperature-jump data on kinetics at liquid/solid interfaces using a colloidal sample. We also quantified the rate of migration of covalently attached ligands on silica surfaces; from the temperature

dependence, the large energy barrier to migration was estimated. A review of applications of electronic spectroscopy (absorption and fluorescence) to reversed-phase chromatographic interfaces was published. DOE

N94-32840# Lawrence Livermore National Lab., CA.
PRECONDITIONED TIME-DIFFERENCE METHODS FOR ADVECTION-DIFFUSION-REACTION EQUATIONS
C. Aro, G. Rodrigue, and D. Wolitzer Jan. 1994 4 p Presented at the Colorado Conference on Iterative Methods, Breckenridge, CO, 4-10 Apr. 1994
(Contract W-7405-eng-48)
(DE94-006472; UCRL-JC-115840; CONF-9404103-1) Avail: CASI HC A01/MF A01

Explicit time differencing methods for solving differential equations are advantageous in that they are easy to implement on a computer and are intrinsically very parallel. The disadvantage of explicit methods is the severe restrictions placed on step size due to stability. Stability bounds for explicit time differencing methods on advection - diffusion - reaction problems are generally quite severe and implicit methods are used instead. The linear systems arising from these implicit methods are large and sparse so that iterative methods must be used to solve them. In this paper we develop a methodology for increasing the stability bounds of standard explicit finite differencing methods by combining explicit methods, implicit methods, and iterative methods in a novel way to generate new time-difference schemes, called preconditioned time-difference methods. DOE

N94-32868*# Southwest Research Inst., San Antonio, TX. Engine, Fuel, and Vehicle Research Div.
IGNITION DELAYS, HEATS OF COMBUSTION, AND REACTION RATES OF ALUMINUM ALKYL DERIVATIVES USED AS IGNITION AND COMBUSTION ENHANCERS FOR SUPERSONIC COMBUSTION Final Report
Thomas W. Ryan, III, S. T. Schwab, and W. W. Harlowe Feb. 1992 20 p
(Contract NAS1-18191; SwRI Proj. 01-1302; RTOP 505-62-40-01)
(NASA-CR-189581; NAS 1.26:189581) Avail: CASI HC A03/MF A01

The subject of this paper is the design of supersonic combustors which will be required in order to achieve the needed reaction rates in a reasonable sized combustor. A fuel additive approach, which is the focus of this research, is the use of pyrophorics to shorten the ignition delay time and to increase the energy density of the fuel. Pyrophoric organometallic compounds may also provide an ignition source and flame stabilization mechanism within the combustor, thus permitting use of hydrocarbon fuels in supersonic combustion systems. Triethylaluminum (TEA) and trimethylaluminum (TMA) were suggested for this application due to their high energy density and reactivity. The objective here is to provide comparative data for the ignition quality, the energy content, and the reaction rates of several different adducts of both TEA and TMA. The results of the experiments indicate the aluminum alkyls and their more stable derivatives reduce the ignition delay and total reaction time to JP-10 jet fuel. Furthermore, the temperature dependence of ignition delay and total reaction time of the blends of the adducts are significantly lower than in neat JP-10. Author (revised)

N94-32886 UOP, Inc., Des Plaines, IL.
THE DEVELOPMENT OF PRECIPITATED IRON CATALYSTS WITH IMPROVED STABILITY
H. Abrevaya 27 Dec. 1993 278 p Limited Reproducibility: More than 20% of this document may be affected by microfiche quality
(Contract DE-AC22-87PC-79812)
(DE94-008711; DOE/PC-79812/T17) Avail: CASI HC A13

Precipitated iron catalysts are expected to be used in next generation slurry reactors for large-scale production of transportation fuels from synthesis gas. These reactors are expected to operate at higher temperatures and lower H2:CO ratios relative to the Sasol Arge reactor. The feasibility of using iron catalysts has been demonstrated under relatively mild Arge-type conditions but not under more severe slurry conditions. Possibly, an improvement in catalytic stability will be needed to make iron catalysts suitable for slurry operation. This program was aimed at identifying the chemical principles governing the deactivation of precipitated iron catalysts during Fischer-Tropsch synthesis and use of these chemical principles in the design of more stable catalysts. A new precipitated Fe catalyst was developed in this program for slurry reactor operation. The new Fe catalyst is predicted to perform slightly below the performance targets for slurry bubble column operation. Stability targets appear to be achievable. This catalyst did not noticeably deactivate during 1,740 hours on-stream. Compared to the selectivity target, an excess of 2 percent C1 + C2 was formed at 265 C. Based on the initial catalyst inventory in the autoclave, the catalyst seems to be short of the activity target by a factor of 1.8 at 265 C and 1.3 at 275 C. However, actual specific activities are likely to be closer to target because of catalyst inventory loss across the filter during the run and because catalytic activities were underestimated at low conversions. DOE

N94-32887# Utah Univ., Salt Lake City.
LIGAND INTERMEDIATES IN METAL-CATALYZED REACTIONS
J. A. Gladysz 10 Aug. 1993 12 p
(Contract DE-FG03-93ER-14321)
(DE94-008713; DOE/ER-14321/T2) Avail: CASI HC A03/MF A01

Achievements are reported for the following four areas: pi/sigma equilibria in aldehyde and ketone complexes; thermodynamic ligand binding affinities: alpha, beta unsaturated organic carbonyl compounds; a new form of coordinated carbon: an unsupported C3 chain that spans two different transition metals; and a new form of coordinated carbon: a C3 chain that is anchored by a metal on each end and spanned by a third. DOE

N94-32888# Altamira Instruments, Inc., Pittsburgh, PA.
DIRECT AROMATIZATION OF METHANE
Oct. 1993 7 p
(Contract DE-AC22-92PC-92109)
(DE94-008719; DOE/PC-92109/T3) Avail: CASI HC A02/MF A01

The pyrolysis of methane in the absence of a quench was studied at temperatures between 900 and 1050 C and methane flows of 80 to 200 Scc/minute. At 1050 C and a methane flow rate of 100 Scc/minute, methane conversion ranged between 15 and 19 percent with the major products being benzene, acetylene, and ethylene. The benzene molar selectivity was approximately 50 percent, corresponding to molar yield of approximately 7.5 to 10 percent. The reaction resulted in the formation of visible amounts of solid carbon, particularly at 1050 C. The resulting solid consisted partly of carbon and partly of a yellowish tar-like material which was soluble in toluene and contained various heavy hydrocarbons and polyring aromatics. DOE

N94-32889# Kentucky Univ., Lexington. Center for Applied Energy Research.
TECHNOLOGY DEVELOPMENT FOR IRON FISCHER-TROPSCH CATALYSTS
B. H. Davis 1993 36 p
(Contract DE-AC22-91PC-90056)
(DE94-008723; DOE/PC-90056/T13) Avail: CASI HC A03/MF A01

Slurry phase Fischer-Tropsch synthesis was conducted with an ultrafine iron oxide catalyst promoted with either K or Zr or both. Pretreatment in CO yielded higher conversions and a more stable catalyst than activation in hydrogen or synthesis gas. Hydrogen pretreatment of K promoted catalysts and synthesis gas activation in general were less effective. Mossbauer spectroscopy and XRD showed X-Fe5C2 and (epsilon)-Fe(2.2)C were formed during pretreatment in CO and did not depend on promoters present. Catalysts pretreated in H2 were reduced to metallic Fe and Fe3O4; promotion with K and Zr decreased the extent of reduction. Hydrogen pretreated catalysts with K lost surface area and carbided rapidly under synthesis conditions. Activation in synthesis gas reduced all catalysts to Fe3O4. Subsequent synthesis did not effect the phase present for the unpromoted and Zr promoted catalysts while those with K formed X-Fe5C2 and (epsilon)-Fe(2.2)C. It is concluded that pretreatment type is more important to the catalyst activity during the early period of synthesis than the impact of promotion with K and Zr. DOE

N94-32948*# National Aeronautics and Space Administration. Lewis Research Center, Cleveland, OH.
CET93 AND CETPC: AN INTERIM UPDATED VERSION OF THE NASA LEWIS COMPUTER PROGRAM FOR CALCULATING COMPLEX CHEMICAL EQUILIBRIA WITH APPLICATIONS
Bonnie J. McBride, Martin A. Reno, and Sanford Gordon Washington NASA, Washington Mar. 1994 34 p

(RTOP 505-62-52)
(NASA-TM-4557; E-8297; NAS 1.15:4557) Avail: CASI HC A03/MF A01

The NASA Lewis chemical equilibrium program with applications continues to be improved and updated. The latest version is CET93. This code, with smaller arrays, has been compiled for use on an IBM or IBM-compatible personal computer and is called CETPC. This report is intended to be primarily a users manual for CET93 and CETPC. It does not repeat the more complete documentation of earlier reports on the equilibrium program. Most of the discussion covers input and output files, two new options (ONLY and comments), example problems, and implementation of CETPC. Author

N94-32973 Department of the Navy, Washington, DC.
DIELECTRIC VISCOMETER INCLUDING FIXED AND VARIABLE CELLS Patent
John G. Williams, inventor (to Navy), Thomas M. Donnellan, inventor (to Navy), and Ronald E. Trabocco, inventor (to Navy) 18 Jan. 1994 7 p Filed 22 Jun. 1992
(AD-D016139; US-Patent-5,279,149; US-Patent-Appl-SN-902138; US-Patent-Class-73-54.01) Avail: US Patent and Trademark Office

A parallel plate dielectric viscometer is provided for measuring the viscosity of a substance having differing substance dielectric properties at differing substance viscosities. Two electrodes are disposed in opposition to each other forming a variable dielectric cell having a dielectric distance between the electrodes. The viscosity of the substance is varied and force is applied to the substance to vary the dielectric distance according to the varying viscosity. The rate of change of the dielectric distance with respect to time is used to determine the viscosity of the substance. The viscosity may be varied by heating the substance and force may be applied to the substance by way of one of the electrodes such that the dielectric distance between the electrodes decreases as the substance becomes more viscous. A fixed cell may also be provided in order to correct for the effects of chemical changes in the substance. DTIC

N94-33036*# Eloret Corp., Palo Alto, CA.
COMPUTED POTENTIAL ENERGY SURFACES FOR CHEMICAL REACTIONS Final Technical Report, 1 Jul. 1987 - 31 Jan. 1994
Stephen P. Walch 9 May 1994 11 p
(Contract NCC2-478)
(NASA-CR-195835; NAS 1.26:195835) Avail: CASI HC A03/MF A01

Quantum mechanical methods have been used to compute potential energy surfaces for chemical reactions. The reactions studied were among those believed to be important to the NASP and HSR programs and included the recombination of two H atoms with several different third bodies; the reactions in the thermal Zeldovich mechanism; the reactions of H atom with O2, N2, and NO; reactions involved in the thermal De-NO(x) process; and the reaction of CH(squared Pi) with N2 (leading to 'prompt NO'). These potential energy surfaces have been used to compute reaction rate constants and rates of unimolecular decomposition. An additional application was the calculation of transport properties of gases using a semiclassical approximation (and in the case of interactions involving hydrogen inclusion of quantum mechanical effects). Author (revised)

N94-33242 Stanford Univ., CA. Dept. of Mechanical Engineering.
TURBULENT REACTING FLOWS AND SUPERSONIC COMBUSTION Final Report, 15 Feb. 1990 - 14 Oct. 1993
C. T. Bowman, R. K. Hanson, M. G. Mungal, and W. C. Reynolds 15 Dec. 1993 32 p Limited Reproducibility: More than 20% of this document may be affected by microfiche quality
(Grant AF-AFOSR-0151-90)
(AD-A277462; AFOSR-94-0080TR) Avail: CASI HC A03

An experimental and computational investigation of supersonic combustion flows has been carried out. The principal objective of the research was to gain a more fundamental understanding of mixing and chemical reaction in supersonic flows. The research effort comprised three inter-related elements: (1) an experimental study of mixing and combustion in a supersonic plane mixing layer; (2) development of laser-induced fluorescence techniques for time-resolved multidimensional imaging of species concentration, temperature, velocity and pressure; and, (3) analyses and numerical simulations of compressible reacting flows. The specific objectives and results of the research of each of these program elements are summarized in this report. DTIC

N94-33260# Lawrence Livermore National Lab., CA.
ENHANCED THERMAL CAPACITY AEROGELS SUMMARY REPORT, FY 1993
L. W. Hrubesh, P. R. Coronado, and J. F. Poco Dec. 1993 13 p
(Contract W-7405-eng-48)
(DE94-008888; UCRL-CR-115799-Summ) Avail: CASI HC A03/MF A01

In a continuation of work done previously, the authors have fabricated a set of silica aerogels and then chemically modified their internal surfaces for the purpose of inhibiting the effects of sintering at high temperatures. They performed surface nitridation of silica aerogels, i.e., the replacement of surface oxygen atoms with nitrogen atoms, by reacting ammonia gas with the silica surfaces at elevated temperatures. After pre-oxidizing the aerogels, they exposed three sets of samples to anhydrous ammonia gas under different processing conditions. Each set contained silica aerogels of three different densities: 0.07 g/cc, 0.16 g/cc, and 0.29 g/cc. The treated samples, together with companion untreated reference samples, were sent to NASA Ames Research Laboratory for high temperature testing. They also fabricated two carbon aerogel cylinders: 7 cm diameter x 1.5 cm thick. These samples were also delivered to NASA Ames Research Laboratory for high temperature tests. DOE

N94-31025*# National Aeronautics and Space Administration. Marshall Space Flight Center, Huntsville, AL.
FLUORESCENCE OBSERVATIONS OF LDEF EXPOSED MATERIALS AS AN INDICATOR OF INDUCED MATERIAL REACTIONS
Roger C. Linton, Ann F. Whitaker, and Rachel R. Kamenetzky *In its* LDEF Materials Results for Spacecraft Applications Dec. 1993 p 159-178 (For primary document see N94-31012 09-12)
Avail: CASI HC A03/MF A04

N94-31040*# National Aeronautics and Space Administration. Lyndon B. Johnson Space Center, Houston, TX.
AN OVERVIEW OF THE EVALUATION OF OXYGEN INTERACTION WITH MATERIALS-THIRD PHASE (EOIM-3) EXPERIMENT: SPACE SHUTTLE MISSION 46
Lubert J. Leger, Steven L. Koontz, James T. Visentine, and Donald Hunton *In* NASA. Marshall Space Flight Center, LDEF Materials Results for Spacecraft Applications Dec. 1993 p 391-417 (For primary document see N94-31012 09-12)
Avail: CASI HC A03/MF A04

N94-31043*# Marquette Univ., Milwaukee, WI. Dept. of Mechanical and Industrial Engineering.
EFFECTS OF ORBITAL EXPOSURE ON RTV DURING THE LDEF MISSION
William E. Brower, Jr., S. V. Golub, and Robert A. Bauer *In* NASA. Marshall Space Flight Center, LDEF Materials Results for Spacecraft Applications Dec. 1993 p 455-463 (For primary document see N94-31012 09-12)
Avail: CASI HC A02/MF A04

N94-31050*# National Aeronautics and Space Administration. Marshall Space Flight Center, Huntsville, AL.
WHAT LDEF MEANS FOR DEVELOPMENT AND TESTING OF MATERIALS
Ann F. Whitaker, Wayne K. Stuckey, and Bland A. Stein *In its* LDEF Materials Results for Spacecraft Applications Dec. 1993 p 541-546 (For primary document see N94-31012 09-12)
Avail: CASI HC A02/MF A04

N94-31051*# Wales Univ., Swansea. Dept. of Physics.
ATOMIC OXYGEN DAMAGE CHARACTERIZATION BY PHOTOTHERMAL SCANNING
A. W. Williams, N. J. Wood, and A. B. Zakaria *In* NASA. Marshall Space Flight Center, LDEF Materials Results for Spacecraft Applications Dec. 1993 p 547-553 (For primary document see N94-31012 09-12)
Avail: CASI HC A02/MF A04

26 METALLIC MATERIALS

Includes physical, chemical, and mechanical properties of metals, e.g., corrosion; and metallurgy.

N94-31083 Stockholm Univ. (Sweden). Dept. of Physics.
A POLYNOMIAL REPRESENTATION OF THE VALENCE ORBITAL IONIZATION POTENTIALS
J. Blomquist and P. Kjaell Jul. 1993 15 p Limited Reproducibility: More than 20% of this document may be affected by microfiche quality
(USIP-93-06; ETN-94-95938) Avail: Issuing Activity (European Space Agency (ESA))

The ionization energy of the valence electrons (3d, 4s, 4p) for the elements from Ti to Ni was calculated for a large number of configurations with the X alpha model. The calculated ionization energies were fitted to second order polynomials of the population and the atomic number. A comparison with a widely used similar expression is made. ESA

N94-31258 Wisconsin Univ., Milwaukee. Dept. of Materials Engineering.
PROCESS PARAMETER-GROWTH ENVIRONMENT-FILM PROPERTY RELATIONSHIPS FOR REACTIVE SPUTTER DEPOSITED METAL (V, Nb, Zr, Y, Au) OXIDE, NITRIDE, AND OXYNITRIDE FILMS Final Report, 1 Jan. 1989 - 30 Jun. 1993
Carolyn R. Aita 30 Sep. 1993 102 p Limited Reproducibility: More than 20% of this document may be affected by microfiche quality
(Contract DAAL03-89-K-0022)
(AD-A276382; ARO-26427.12-MS) Avail: Issuing Activity (Defense Technical Information Center (DTIC))

The research developed process parameter-growth environment-film property relations (phase maps) for model sputter-deposited transition metal oxides, nitrides, and oxynitrides grown by reactive sputter deposition at low temperature. Optical emission spectrometry was used for plasma diagnostics. The results summarized here include the role of sputtered metal-oxygen molecular flux in oxide film growth; structural differences in highest valence oxides including conditions for amorphous growth; and using fundamental optical absorption edge features to probe short range structural disorder. Eight appendices containing sixteen journal articles are included. DTIC

N94-31314# Oak Ridge National Lab., TN.
ENHANCEMENT OF OXIDATION RESISTANCE OF SILICON CARBIDE BY HIGH-DOSE AND MULTI-ENERGY ALUMINUM IMPLANTATION
Z. Yang (Stevens Inst. of Tech., Hoboken, NJ.), H. Du (Stevens Inst. of Tech., Hoboken, NJ.), M. Libera (Stevens Inst. of Tech., Hoboken, NJ.), S. P. Withrow, L. M. Casas, and R. T. Lareau 1993 6 p Presented at the Fall Meeting of the Materials Research Society (MRS), Boston, MA, 29 Nov. - 3 Dec. 1993
(Contract DE-AC05-84OR-21400)
(DE94-006560; CONF-931108-70) Avail: CASI HC A02/MF A01

High-dose and multi-energy aluminum implantation of alpha-SiC (0001) was carried out to achieve a broad aluminum distribution extending from the sample surface to a depth of approximately 350 nm. Oxidation resistance of the implanted crystals was studied in 1 atm flowing oxygen at 1300C. Aluminum implantation resulted in a 45% improvement in the oxidation resistance of alpha-SiC as compared with unimplanted crystals due to the formation of structurally dense mullite (3Al(2)O(3).2SiO(2)) in the oxidation scale. DOE

N94-31325# Washington State Univ., Pullman. Dept. of Mechanical and Materials Engineering.
METAL INDUCED EMBRITTLEMENT
R. G. Hoagland Nov. 1993 11 p
(Contract DE-FG06-87ER-45287)
(DE94-007450; DOE/ER-45287/6) Avail: CASI HC A03/MF A01

This section summarizes the progress made in this program since the its renewal on June 1, 1992 to date. This program is seeking to characterize the cause of embrittlement that results when certain solid metals and their alloys are exposed to other metals, usually, but not necessarily, in liquid form. The research is examining a number of factors that influence the degree of embrittlement and is also attempting to develop the basis for understanding, the underlying cause of embrittlement. Accordingly, the program involves both theoretical and experimental approaches. DOE

N94-31345# Sandia National Labs., Albuquerque, NM.
HIGH TEMPERATURE DUCTILITY LOSS IN TITANIUM ALLOYS: A REVIEW
B. B. Rath, M. A. Imam, B. K. Damkroger, and G. R. Edwards 1994 16 p Presented at the 1994 TMS Annual Meeting on Actinides, San Francisco, CA, 27 Feb. - 3 Mar. 1994
(Contract DE-AC04-94AL-85000)
(DE94-006606; SAND-94-0283C; CONF-940221-3) Avail: CASI HC A03/MF A01

It is well known that two phase titanium alloy systems suffer from an abrupt drop in ductility at elevated temperatures in the range of 1,000 to 1,150 K. This loss of ductility is manifested by easy decohesion of polycrystalline aggregates along the grain boundaries of the high temperature beta phase. If the alloy is in a state of tensile stress at the aforementioned temperatures, cracks initiate at the grain boundaries and propagate readily through the alloy, leading to premature failure. This phenomenon is a cause of major concern in titanium alloy fabrication and welding. Several mechanisms have been proposed to explain high temperature crack nucleation and growth along the boundaries. A critical review of the phenomenon and possible mechanisms responsible for the observed behavior will be discussed. DOE

N94-31420# Office National d'Etudes et de Recherches Aerospatiales, Paris (France).
MICROSTRUCTURES AND MECHANICAL PROPERTIES OF Al3Ti-BASED ALLOYS: ANALYSIS IN SINGLE PHASE AND MULTIPHASE SYSTEMS Ph.D. Thesis - Paris 6 Univ. [STRUCTURES ET PROPRIETES MECANIQUES D'ALLIAGES DERIVES D'AL3TI: ETUDE EN SYSTEMES MONOPHASE ET POLYPHASE]
Laurence Potez 1993 272 p In FRENCH Original contains color illustrations
(ISSN 0078-3781)
(ONERA-NT-1993-6; ETN-94-96062) Avail: CASI HC A12/MF A03

Two routes of ductilization of the Al3Ti-DO22 compound are explored: the development of Ll2Al3Ti based alloys with ternary additions (Cr, Mn, Cu); and the use of the nonequilibrium melt spinning process, in order to produce a fine dispersion of an Al3Ti based phase in an Al matrix. The alloys are fully characterized using X-ray diffraction and both scanning and transmission electron microscopy. Differential scanning calorimetry and microhardness tests are used to assess the thermal stability of the structures. Ll2 single phase field is identified in the ternary systems Al-Ti-M (M = Cr, Mn, Cu) but its extent varies strongly with both temperature and composition. The existence of a two phase Ll2-Al2Ti field is demonstrated in the Al-Ti-Cu system. Moreover, several antiphase modulations are identified under high resolution microscopy. Melt spun ribbons exhibit locally a two phase Al-Ll2 structure in the Al-Ti-Cu and Al-Ti-Fe systems and a two phase Al-DO22 structure in the Al-Ti-Mo system. The production of alloy rods by hot extrusion is restricted to a volume fraction smaller than 50 percent of the intermetallic phase. Compression tests reveal that the two phase alloys are considerably more resistant than the single phase at room temperature. This behavior is attributed to a strong effect of modulus between the matrix and the intermetallic phase. Dynamic strain ageing and plastic instabilities are observed at 300 C in both the two phase and single phase alloys. ESA

N94-31456# Naval Surface Warfare Center, Bethesda, MD. Machinery Research and Development Directorate.
TRANSMISSIBILITY OF NICKEL-TITANIUM SHAPE MEMORY ALLOY SPRINGS Technical Report, Oct. 1992 - Apr. 1993
Edward J. Graesser Dec. 1993 26 p
(AD-A276055; CarderockDiv-MRD-93/25) Avail: CASI HC A03/MF A01

A research study was undertaken to measure the transmissibility of nickel-titanium (Ni-Ti) shape memory alloy (SMA) springs and compare the results to corresponding data on steel and Inconel springs. It was motivated by interest in an effective metal alternative to rubber-based machinery isolation mounts, with possible active control features. Ni-Ti was used due to its well known properties of shape memory and high intrinsic damping. Acceleration transmissibility was measured on a spring-mass system. Due to the distributed mass in the spring coils, standing waves occurred at high frequencies. However, due to the high intrinsic damping in Ni-Ti, the standing wave resonance peaks were as much as 20 db lower than corresponding peaks in steel and Inconel springs. Thus the capability of

Ni-Ti springs for high frequency vibration isolation is significantly better than that of steel or Inconel. Also, it is judged that the Ni-Ti material could be used in a variety of other isolation mount designs with a high likelihood for further improvement in passive isolation properties. In addition, it may be possible to use the shape memory effect in active control concepts. DTIC

N94-31486# Argonne National Lab., IL.
CREEP PROPERTIES OF VANADIUM-BASE ALLOYS
H. M. Chung, B. A. Loomis, and D. L. Smith Dec. 1993 10 p Presented at the 6th International Conference on Fusion Reactor Materials, Stresa, Italy, 27 Sep. - 1 Oct. 1993
(Contract W-31-109-eng-38)
(DE94-006541; ANL/ET/CP-81785; CONF-930928-27) Avail: CASI HC A02/MF A01

Vanadium-base alloys are promising candidate materials for application in fusion reactor structural components because of several important advantages. V-4Cr-4Ti has been identified as one of the most promising candidate alloys and was selected for comprehensive tests and examination. In the present investigation, thermal creep rates and stress-rupture life of V-4Cr-4Ti and V-10Cr-5Ti alloys were determined at 600 C. The impurity composition and microstructural characteristics of creep-tested specimens were analyzed and correlated with measured creep. Results show that V-4Cr-4Ti, which contains impurity compositions typical of a commercially fabricated vanadium-based alloy, exhibits creep strength substantially superior to that of V-20Ti, HT-9, or Type 316 stainless steel. The V-10Cr-5Ti alloy exhibits creep strength somewhat higher than that of V-4Cr-4Ti. DOE

N94-31519# Universiteit Twente, Enschede (Netherlands).
CHEMICAL VAPOUR DEPOSITION OF TUNGSTEN FOR THE APPLICATION IN INTEGRATED CIRCUITS Ph.D. Thesis
Albert Hasper 1992 148 p Sponsored by Dutch Innovative Research Program
(ISBN-9-09-005151-1; ETN-94-96026) Copyright Avail: CASI HC A07/MF A02

The results of research aimed at the implementation of tungsten in a BiCMOS (Bipolar and CMOS) process is described. The growth of tungsten by the reactions of WF6 with H2, SiH4, and Si was studied with emphasis on reactor technology and device aspects. The cold wall reactor used for tungsten deposition is a nonisothermal system, and thus, large temperature differences occur between wafer and the heating hot plate, especially at the typical low pressures for LPCVD (Low Pressure Chemical Vapor Deposition). The problem of wafer temperature behavior in cold wall systems is described. A model that predicts the wafer temperature in such systems as a function of total pressure, gas composition, and coatings of wafer susceptor, is formulated. Experimentally found growth rates are compared with the growth rates predicted by a mathematical reactor simulation model. The combination of the mathematical reactor model and a step coverage model is described, measurement and analysis of selectively filled tungsten contacts are addressed, and the application of W-LPCVD on a BiCMOS process is described. ESA

N94-31581# Lawrence Livermore National Lab., CA.
TENSILE PROPERTIES OF COMMERCIALLY PURE VANADIUM FROM ROOM TEMPERATURE TO 1200 C
G. A. Henshall and S. G. Torres Dec. 1993 34 p
(Contract W-7405-eng-48)
(DE94-006622; UCRL-ID-114591) Avail: CASI HC A03/MF A01

The tensile properties of vanadium are sensitive to interstitial impurity content and, to some extent, on grain size and strain rate. Thus, it is problematic to use published tensile data for materials potentially varying in these quantities. This investigation was undertaken to fully characterize the tensile properties of the commercially pure vanadium used at Lawrence Livermore. Both sheet and rod stock were tested in vacuum from ambient temperature to 1200 C at strain rates 6.67 x 10(exp -5) to 6.67 x 10(exp -2) s(exp -1). The results of these experiments show that vanadium behaves in a manner typical of many bcc metals containing interstitial impurities. Local peaks in yield stress and ultimate tensile stress versus temperature curves are observed at intermediate temperatures. Serrated yielding also is observed in some temperature ranges. Changes in strain rate within the quasistatic regime have a relatively small, predictable effect. The rod and sheet stock have similar properties, except that the lower yield stress of the rod is less than that of the sheet over most of the temperature range studied. No plateau in yield strength versus temperature curve was observed for the rod. In both forms, and for all temperatures, vanadium is ductile. The elongation to failure reaches a minimum of approximately 35 percent at a temperature of 500 C and a maximum of approximately 140 percent at 1200 C. DOE

N94-31626# Pacific Northwest Lab., Richland, WA.
THE INFLUENCE OF TRANSMUTATION, VOID SWELLING, AND FLUX/SPECTRA UNCERTAINTIES ON THE ELECTRICAL PROPERTIES OF COPPER AND COPPER ALLOYS
D. J. Edwards, F. A. Garner, and L. R. Greenwood Sep. 1993 18 p Presented at the 6th International Conference on Fusion Reactor Materials, Stresa, Italy, 27 Sep. - 1 Oct. 1993
(Contract DE-AC06-76RL-01830)
(DE94-006213; PNL-SA-22452; CONF-930928-25) Avail: CASI HC A03/MF A01

A comparison of the predicted and measured electrical conductivities of MARZ copper and two copper alloys irradiated in the Fast Flux Test Facility (FFTF) shows that the calculated transmutation rates agree within 15% with those required to produce the observed changes. It also appears that the contribution of transmutants and void swelling to conductivity changes are directly additive. Of the three models studied, Euken's model has been found to best describe the contribution of void swelling to conductivity loss. DOE

N94-31627# Pacific Northwest Lab., Richland, WA.
DEFECT-SOLUTE INTERACTIONS NEAR IRRADIATION GRAIN BOUNDARIES
E. P. Simonen, J. S. Vetrano, H. L. Heinisch, and S. M. Bruemmer Nov. 1993 8 p Presented at the Fall Meeting of the Materials Research Society (MRS), Boston, MA, 29 Nov. - 3 Dec. 1993
(Contract DE-AC06-76RL-01830)
(DE94-006215; PNL-SA-22766; CONF-931108-61) Avail: CASI HC A02/MF A01

Defect-solute interactions control radiation-induced segregation (RIS) to interfacial sinks, such as grain boundaries, in metallic materials. The best studied system in this regard has been austenitic stainless steels. Measurements of grain boundary composition indicate that RIS of major alloying elements are in reasonable agreement with inverse-Kirkendall predictions. The steep and narrow composition profiles are shown to result from limited back diffusion near the boundary. Subsequently, defect-solute interactions that affect the near boundary defect concentrations strongly affect RIS. The variability in measured RIS may in part be caused by grain boundary characteristics. DOE

N94-31638# California Univ., Berkeley. Lawrence Berkeley Lab.
AGING EFFECTS ON THE MICROSTRUCTURE, SURFACE CHARACTERISTICS AND WETTABILITY OF Cu PRETINNED WITH Sn-Pb SOLDERS Ph.D. Thesis
H. S. Linch Nov. 1993 73 p
(Contract DE-AC03-76SF-00098)
(DE94-007033; LBL-34991) Avail: CASI HC A04/MF A01

This study investigates effects of aging in air and argon at 170 C on Cu coupons which were pretinned with 75Sn-25Pb, 8Sn-92Pb, and 5Sn-95Pb solders. Coatings were applied using electroplating or hot dipping techniques. The coating thickness was controlled between 3 to 30 microns and the specimens were aged for 0 hours, 2 hours, 24 hours, and 2 weeks. Wetting balance tests were used to evaluate the wettability of the test specimens. Microstructural development was evaluated using x ray diffraction, energy dispersive x ray and Auger spectroscopy, and optical and scanning electron microscopy. The wetting behavior of the test specimens is interpreted with respect to observed microstructural changes and as a function of aging time, solder composition, and processing conditions. DOE

N94-31666# Argonne National Lab., IL.
EFFECT OF IRRADIATION DAMAGE AND HELIUM ON THE SWELLING AND STRUCTURE OF VANADIUM-BASE ALLOYS
H. M. Chung, B. A. Loomis, and D. L. Smith Dec. 1993 15 p Presented at the 6th International Conference on Fusion Reactor Materials, Stresa,

Italy, 27 Sep. - 1 Oct. 1993
(Contract W-31-109-eng-38)
(DE94-006540; ANL/ET/CP-81786; CONF-930928-26) Avail: CASI HC A03/MF A01

Swelling behavior and microstructural evolution of V-Ti, V-Cr-Ti, and V-Ti-Si alloys were investigated after irradiation at 420 to 600 C up to 114 dpa. The alloys exhibited swelling maxima between 30 and 80 dpa and swelling decreased on irradiation to higher dpa. This is in contrast to the monotonically increasing swelling of binary alloys that contain Fe, Ni, Cr, Mo, W, and Si. Precipitation of dense Ti5Si3 promotes good resistance to swelling of the Ti-containing alloys and it was concluded that Ti of greater than 3 wt. percent and 400 to 1000 wppm Si are necessary to effectively suppress swelling. Swelling was minimal in V-4Cr-4Ti, identified as the most promising alloy based on good mechanical properties and superior resistance to irradiation embrittlement. V-20Ti doped with B exhibited somewhat higher swelling because of He generation. Lithium atoms, generated from transmutation of B-10, formed gamma-LiV2O5 precipitates and did not seem to produce undesirable effects on mechanical properties. DOE

N94-31871 Royal Military Coll. of Canada, Kingston (Ontario).
ACOUSTIC EMISSION FROM CRACK GROWTH IN 7050 ALUMINUM AND 7075 ALUMINUM AS A FUNCTION OF TEMPERATURE AND HEAT TREATMENT
S. L. McBride and Y. Hong Feb. 1993 14 p
(DREP-CRS-93-15; DSIS-94-01128; CTN-94-61218) Avail: CASI HC A03/MF A01

The acoustic emission behavior of aluminum alloys 7050 and 7075 was investigated under various conditions of temperature and heat treatment. The two alloys are chemically and mechanically very similar apart from the presence of Mg2Si inclusions in the 7075 aluminum. During fatigue crack propagation, the amplitude of each acoustic emission signal was recorded for analysis along with the specimen load, number of load cycles, time, and crack length at which the signal occurred. It is shown that the crack propagation acoustic emission behavior is quite different for the two alloys. For similar heat treatment and temperature conditions, the number and amplitude of the acoustic emission events in 7050 and 7075 aluminum decreases with increasing temperature and with increasing overaging time. The measured amplitudes of the acoustic emission signals are linearly related to the source energy. For 7050 aluminum, the acoustic emission source energy is a fixed fraction of the strain energy release rate for fatigue crack advance. This fraction is a function of heat treatment and ambient crack growth temperature. For 7075 aluminum the acoustic emission source energy is independent of the strain energy release rate. This behavior may be due to the effect of Mg2Si inclusions within the process zone.
Author (CISTI)

N94-31918# Oak Ridge National Lab., TN.
CREEP-FATIGUE CRITERIA AND INELASTIC BEHAVIOR OF MODIFIED 9Cr-1Mo STEEL AT ELEVATED TEMPERATURES
M. B. Ruggles and T. Ogata Feb. 1994 60 p Prepared for Electric Power Research Inst., Palo Alto, CA
(Contract DE-AC05-84OR-21400)
(DE94-007915; ORNL/M-3198) Avail: CASI HC A04/MF A01

The ever increasing demand for safety requires that stringent and conservative methodology be developed for design and analysis of reactor components. At present modified 9Cr-1Mo steel is a candidate material for construction of steam generators in fast breeder reactors. Therefore high-temperature material properties and extensive insight into deformation behavior and creep-fatigue life are required to develop design guidelines for use of modified 9Cr-1Mo steel in actual plant components. However, existing information on creep-fatigue and deformation response of modified 9Cr-1Mo steel is insufficient, and further experimental and modeling efforts are needed. A joint effort between the Electric Power Research Institute (EPRI) in the United States and the Central Research Institute of Electric Power Industry (CRIEPI) in Japan was started in 1991 to investigate the inelastic behavior of and to develop creep-fatigue criteria for modified 9Cr-1Mo steel at elevated temperatures. The current program focuses on uniaxial and biaxial fatigue, creep, and creep-fatigue tests. Results of this effort are presented in this report. Section 2 introduces the test material and experimental arrangement. Uniaxial exploratory deformation tests and unified constitutive equations for inelastic analysis of modified 9Cr-1Mo steel are presented in Sections 3 and 4, respectively. Axial fatigue and creep-fatigue test results are discussed in Section 5. Section 6 is devoted to constant stress creep tests. Biaxial fatigue and creep-fatigue tests are described in Section 7. Progress in creep-fatigue life evaluation is reported in Section 8. DOE

N94-31995 Pennsylvania State Univ., University Park. Dept. of Materials Science and Engineering.
PREDICTION OF HYDROGEN ENTRY AND PERMEATION IN METALS AND ALLOYS Final Report, 1 Oct. 1990 - 30 Sep. 1993
H. W. Pickering 30 Sep. 1993 15 p Limited Reproducibility: More than 20% of this document may be affected by microfiche quality
(Contract N00014-91-J-1189)
(AD-A276637) Avail: CASI HC A03

This Grant focused on the investigation of the factors which affect hydrogen entry and permeation into metals/alloys that by themselves or in combination with other materials are used under conditions for which hydrogen embrittlement and cracking are a major concern. Factors that affect H entry include a broad range of metallurgical, environmental and interface properties such as adsorption, surface segregation, surface films and recesses in the surface. Research during this grant period focused on understanding how these parameters control hydrogen entry. The specific investigations included both aqueous and gas phase charging of hydrogen, utilizing primarily electrochemical techniques, in particular hydrogen permeation with the IPZ model, and microscopic methods in the case of aqueous phase charging, and ultra high resolution scanning tunneling microscopy (STM) in the case of gas phase charging. DTIC

N94-31997 Purdue Univ., West Lafayette, IN. Dept. of Chemistry.
THE ADSORPTION OF SULFATE ON GOLD(111) IN ACIDIC AQUEOUS MEDIA: ADLAYER STRUCTURAL INFERENCES FROM INFRARED SPECTROSCOPY AND SCANNING TUNNELING MICROSCOPY
Xiao-Ping Gao, Michael J. Weaver, and Gregory J. Edens Feb. 1994 22 p Limited Reproducibility: More than 20% of this document may be affected by microfiche quality
(Contract N00014-91-J-1409)
(AD-A276643; TR-148) Avail: CASI HC A03

The potential-dependent adsorption of sulfate on ordered Au(111) from acidic aqueous electrolytes has been examined in-situ by means of infrared reflection-absorption spectroscopy (IRAS) and by atomic-resolution scanning microscopy (STM) in order to explore further the nature of the adsorbate bonding and the structural changes attending the formation of the ordered adlayer at high potentials, as observed recently by using STM. Solution conditions that encompassed aqueous sulfuric acid, sulfuric acid/sulfate electrolytes of varying pH, and dilute sulfate in excess perchloric acid were selected in order to facilitate comparisons with recent adsorbate compositional data extracted from chronocoulometric and radiotracer measurements which utilized the last type of electrolyte. Essentially the same ordered adlayer structures were deduced by STM to form at suitably high potentials (greater than 0.8 V vs. SCE) in both sulfuric acid and the mixed sulfate/excess perchloric acid media. The adlayer, which exhibits a (sq. rt.3 x sq. rt.7) symmetry, involves a fractional sulfate coverage of 0.2, in accordance with chronocoulometic and radiotracer data. The possibility that the ordered sulfate adlayer incorporates coadsorbed hydronium cations is discussed; such coadsorption is suggested by the presence of additional tunneling maxima in the STM images. The IRAS data display a prominent S-O stretching band (nu(sub so)) at 1155-1220 cm(exp -1). The appearance of this nu(sub so) feature is also insensitive to the electrolyte conditions, including pH, consistent with its assignment to adsorbed sulfate, rather than to bisulfate. DTIC

N94-32004# Georgia Inst. of Tech., Atlanta.
PROCESSABLE, CHEMICAL ROUTES TO BINARY METAL SULFIDES Interim Technical Report No. 6, 1 Jul. 1992 - 1 Mar. 1994
William S. Rees, Jr. and Gertrud Kraeuter 8 Mar. 1994 16 p
(Contract N00014-92-J-1828)
(AD-A277006) Avail: CASI HC A03/MF A01

Metal thiolates of the general formula M(SR)2 (M = Pb, Zn, Cd) and Cl-Hg-SR (R = alkyl) have been prepared and characterized by spectroscopic techniques, TGA and, in selected cases, single crystal X-ray diffraction. The metal bis(thiolate) compounds can be converted into the related metal sulfides by thermolyses. The solid state materials have been

characterized by XRPD, SEM and, in selected cases, by particle size determination. The volatile pyrolytic co-products have been isolated and characterized by GC/MS. The decomposition pathways of mercury chlorothiolates are more complicated and depend on the nature of the organic group present in Cl-Hg-SR. DTIC

N94-32047# Pratt and Whitney Aircraft, West Palm Beach, FL. Government Engines and Space Propulsion.

FATIGUE IN SINGLE CRYSTAL NICKEL SUPERALLOYS

Charles Annis and Daniel P. Deluca 15 Feb. 1994 9 p

(AD-A276662; PW/GESP-FR21998-22) Avail: CASI HC A02/MF A01

This program investigates the seemingly unusual behavior of single crystal airfoil materials. The fatigue initiation processes in single crystal (SC) materials are significantly more complicated and involved than fatigue initiation and subsequent behavior of a (single) macrocrack in conventional, isotropic, materials. To understand these differences is the major goal of this project. DTIC

N94-32060# Purdue Univ., West Lafayette, IN. Dept. of Chemistry.

A NEW-TYPE OF LONG-RANGE RESTRUCTURING OF ORDERED METAL SURFACES INDUCED BY LATERAL ADSORBATE INTERACTIONS: IODIDE ON AU(110) ELECTRODES

Xiaoping Gao and Michael J. Weaver Feb. 1994 18 p

(Contract N00014-91-J-1409)

(AD-A276633; TR-150) Avail: CASI HC A03/MF A01

A new form of long-range surface restructuring of Au(110) is reported, specifically for Au(110) in aqueous iodide electrolyte at high electrode potentials where an ordered iodide adlayer is present. In-situ scanning tunneling microscopy reveals the formation of periodic terrace strips paralleling the direction with widths, ca 25-40 A, that diminish as the surface potential is increased. The (1 x 1) substrate unit cell, however, remains unaffected. The restructuring is postulated to be due to dipole-dipole repulsive interactions destabilizing terrace sites distant from steps, and hence limiting the size of the substrate-adlayer domains. DTIC

N94-32064 California Univ., Berkeley. Lawrence Berkeley Lab.

WORK HARDENING BEHAVIOR IN ALUMINUM ALLOY 2090 Ph.D. Thesis

C. Tseng Dec. 1993 64 p Limited Reproducibility: More than 20% of this document may be affected by microfiche quality

(Contract DE-AC03-76SF-00098)

(DE94-007036; LBL-35057) Avail: Issuing Activity (Department of Energy (DOE))

An investigation into the work hardening behavior of an aluminum alloy 2090-T81 Al-3.05Cu-2.16Li-0.12Zr at various test temperatures, heat treatment conditions and microstructures was conducted. One microstructure consisted of unrecrystallized, highly textured grains, and the other microstructure was composed of recrystallized grains. Microstructural effects on work hardening were divided into two levels of contribution: the grain structure level, which consisted of the grain size and shape, subgrains and texture, and the microconsistent level, which included the precipitates and solutes. Two heat treatments were studied: the as-received, peak-aged condition, and the solution heat treated condition where the as-received plate was re-solutionized. Observations of the deformed surface of both as-received grain structures at various prestrains indicated that there was no correlation between an increase in slip homogeneity and an increase in work hardening. The increase in out-of-plane grain rotation at lower temperatures was not primarily responsible for the increase in work hardening. In addition, the fully plastic deformation microstructure for the unrecrystallized microstructure appeared very inhomogeneous as the grains deformed in bands; there were also bands of grains that had very little to no deformation. From the work hardening plots it was found that an unrecrystallized, (110)/112/ textured grain structure with a homogeneous distribution of subgrains produced the highest rate of work hardening between 300 K and 77 K. When the microconstituents are added to both grain structures, both the work hardening rate in the elastic-plastic and fully plastic regimes and the level of work hardening at which the elastic-plastic to fully plastic transition occurred were affected. DOE

N94-32091# California Univ., Los Angeles. Dept. of Chemistry and Biochemistry.

METAL CLUSTERS: DYNAMICS AND STRUCTURE Final Report, 15 Dec. 1991 - 14 Dec. 1993

Emily A. Carter 14 Dec. 1993 14 p

(Contract N00014-89-J-1492)

(AD-A276842) Avail: CASI HC A03/MF A01

During the tenure of this grant, we have examined the dynamics and structure of metal clusters in the gas phase and on surfaces. We have extended the concept of cluster to also examine metallic interactions in two-dimensional islands and thin films. We have used both quantum mechanical approaches and classical Monte Carlo/Molecular Dynamics simulations. In addition, we have continued our development of a new first principles dynamics scheme specifically designed with atomic clusters in mind. The projects we have completed include: (1) the electronic structure and metal-metal bonding in low-lying states of Pt2 and Pt3; (2) structure and growth mechanisms of Pd two-dimensional clusters (islands) on bcc(110) substrates as a function of coverage; (3) structure, growth, and interdiffusion of Ni films on Ag(100); and (4) development of a systematic guide to choosing the size and shape of a simulation cell using periodic boundary conditions for use in studying interfaces between crystalline solids of different density and symmetry. DTIC

N94-32098# Argonne National Lab., IL.

THE NEW METALS AND ALLOYS INDEXES, SEARCH MANUAL: A PHASE DIAGRAM RESEARCH TOOL

M. H. Mueller, P. L. Wallace, T. C. Huang, and J. N. Dann 1993 12 p Presented at the Fall Meeting of the Minerals, Metals and Materials Society: Physical Metallurgy and Materials, Pittsburgh, PA, 17-21 Oct. 1993

(Contract W-31-109-eng-38)

(DE94-005371; ANL/FE/CP-81703; CONF-931009-19) Avail: CASI HC A03/MF A01

A new Metals and Alloys (M&A) Indexes to the powder diffraction file (PDF) has been developed. These indexes will be immediately useful to material scientists because the indexes share many features with references such as Hansen, Elliot, Shunk, Pearson, and Villars and Calvert. These indexes, as contained in the search manual, may be used independently or in conjunction with the powder diffraction file. The book contains four indexes: two contain data for all materials in the M&A PDF and two contain supporting data. The permuted-sort Alphabetical Formula Index brings together all entries containing a given element in alphabetical formula order. It has n entries for an n-component material and a straight-line format for the element being sorted to simplify reading the index. Thus, chemical knowledge can make identifications easier. Further, within binary and ternary phase diagrams, phases are listed in compositional order to facilitate direct use in phase diagram research. The Pearson Symbol Code Index has entries arranged in order of the Pearson symbol code, hence one can find all the materials with a given structure and, if desired, compare their atomic contents and lattice parameters. The latter are in the standard crystal data setting to aid in structural comparisons. The Common Names Index cross-references common metallurgical names, such as austenite or cementite, to the appropriate PDF data. The Strukturbericht Symbol Index cross-references Strukturbericht symbols and the equivalent Pearson symbols and structure prototypes. Examples of the uses of this index in phase diagram research are given. DOE

N94-32109 Argonne National Lab., IL.

IRRADIATION-ASSISTED STRESS CORROSION CRACKING OF MATERIALS FROM COMMERCIAL BWRs: ROLE OF GRAIN-BOUNDARY MICROCHEMISTRY

H. M. Chung, W. E. Ruther, J. E. Sanecki, A. G. Hins, and T. F. Kassner Dec. 1993 18 p Presented at the Water Reactor Safety Information Meeting, Bethesda, MD, 25-27 Oct. 1993 Limited Reproducibility: More than 20% of this document may be affected by microfiche quality

(Contract W-31-109-eng-38)

(DE94-006542; ANL/ET/CP-80141; CONF-931079-17) Avail: CASI HC A03

Constant-extension-rate tensile tests and grain-boundary analysis by Auger electron spectroscopy were conducted on high- and commercial-purity (HP and CP) Type 304 stainless steel (SS) specimens. The specimens were from irradiated boiling-water reactor (BWR) components. The tests were performed to determine susceptibility to irradiation-assisted stress

corrosion cracking (IASCC) and to identify the mechanisms of intergranular failure. The susceptibility of HP neutron absorber tubes to intergranular stress corrosion cracking (IGSCC) was higher than that of CP absorber tubes or CP control blade sheath. Contrary to previous beliefs, susceptibility to intergranular fracture could not be correlated with radiation-induced segregation of impurities such as Si, P, C, N, or S, but a correlation was obtained with grain-boundary Cr concentration. This indicated a role for Cr depletion that promotes IASCC. Detailed analysis of grain-boundary chemistry was conducted on neutron absorber tubes that were fabricated from two similar heats of HP Type 304 SS of virtually identical bulk chemical composition but exhibiting a significant difference in susceptibility to IGSCC for similar fluence. Grain-boundary concentrations of Cr, Ni, Si, P, S, and C in the crack-resistant and susceptible HP heats were virtually identical. However, grain boundaries of the cracking-resistant material contained less N and more B and Li (transmutation product from B) than those of the crack-susceptible material indicating beneficial effects of low N and high B contents. DOE

N94-32169# Purdue Univ., West Lafayette, IN. Dept. of Chemistry.
VIBRATIONAL SPECTROSCOPY AT METAL-SOLUTION INTERFACES: SOME PERSPECTIVES AND PROSPECTS FOR ELECTROCHEMICAL SURFACE SCIENCE
Michael J. Weaver, N. Kizhakevariam, X. Jiang, I. Villegas, and C. Stuhlmann Feb. 1994 13 p
(Contract N00014-91-J-1409)
(AD-A276781; TR-143) Avail: CASI HC A03/MF A01

Some recent applications of surface vibrational spectroscopies to electrochemical and related interfacial systems are illustrated by means of studies undertaken in the authors' laboratory. The utility of infrared reflection-absorption spectroscopy (IRAS) for linking the structural behavior of absorbates on ordered metal surfaces in electrochemical and vacuum environments is discussed with reference to a vacuum-based study of CO/D2O coadsorption on Pt(111). The use of atomic-resolution scanning tunneling microscopy in tandem with in-situ IRAS for electrochemical adlayer structural elucidation is noted. Some virtues of surface-enhanced Raman spectroscopy (SERS) for examining metal-adsorbate vibrations on transition metals in both electrochemical and high-pressure gas-phase systems are also briefly illustrated, specifically for rhodium surface oxidation.
Author (DTIC)

N94-32237# Galaxy Scientific Corp., Pleasantville, NJ.
FATIGUE TESTING OF 2024-T3 MATERIAL AFTER FOUR CYCLES OF PMB STRIPPING Final Report
Nov. 1993 58 p
(Contract DTFA03-89-C-00043)
(AD-A276926; DOT/FAA/CT-93/43) Avail: CASI HC A04/MF A01

The goal of this program was to determine the effect of plastic media blasting (PMB), an alternative to chemical paint removal, on the fatigue life of 2024-T3 aluminum. Two surface treatments, anodized and alclad, of three thicknesses: 0.032 inch, 0.040 inch, and 0.050 inch were considered. A number of alclad and anodized aluminum panels of the alloy and thicknesses specified were subjected to four cycles of PMB. The blast parameters were identical to those used in a previous FAA program. Almen strips tests were performed to quantify the blast intensity. A fatigue testing program was conducted on both the 'as received' and the PMB treated material. Reductions in mean fatigue life were observed for all materials tested after PMB treatment. These reductions were statistically significant for the 0.032 alclad and 0.040 anodized specimens. DTIC

N94-32240# Army Research Lab., Watertown, MA. Materials Directorate.
STUDY OF TYPE 2 AND 3 ANODIZED Al 5052-0 IN AQUEOUS DS2 SOLUTIONS
Chester V. Zabielski and Milton Levy Jan. 1994 10 p
(AD-A276960; ARL-TR-335) Avail: CASI HC A02/MF A01

Corrosion behavior studies using short-time electrochemical techniques and long-term immersion tests of types 2 and 3 anodized Al 5052-0 and uncoated Al 5052-0 were conducted in 30 volume percent DS2 aqueous decontaminating solution. Test data indicated that type 3 anodized Al 5052-0 provided significantly greater resistance to degradation than type 2 anodized Al 5052-0 or uncoated Al 5052-0. DTIC

N94-32371 Naval Postgraduate School, Monterey, CA.
CONTINUOUS MEASUREMENT OF AGING RESPONSE IN ALUMINUM ALLOYS BY EDDY CURRENT METHODS M.S. Thesis
Silvester G. Mata Dec. 1993 70 p Limited Reproducibility: More than 20% of this document may be affected by microfiche quality
(AD-A277233) Avail: CASI HC A04

The objective of this research was to further investigate the use of a sensor system to continuously monitor the aging response of heat treatable aluminum alloys. This concept of continuous monitoring is referred to as Intelligent Processing. The bridge consists of eddy current coils incorporated in an impedance bridge circuit, with modifications following earlier work by Esarey. The system continuously monitors a material property, resistivity, indicative of the aging process. The results of such continuous measurements, combined with mechanical test data, will allow one to gain active control of the aging process and hence the material properties of aluminum alloys. The ultimate results would be higher reliability of engineering structures. The increased precision in control of heat treatment processes would allow more narrow performance and greater service life of engineering structures. DTIC

N94-32374# Lawrence Livermore National Lab., CA.
RECENT ADVANCES AND DEVELOPMENTS IN REFRACTORY ALLOYS
T. G. Nieh and J. Wadsworth Nov. 1993 13 p Presented at the Fall Meeting of the Materials Research Society (MRS), Boston, MA, 29 Nov. - 3 Dec. 1993
(Contract W-7405-eng-48)
(DE94-007929; UCRL-JC-116117; CONF-931108-90) Avail: CASI HC A03/MF A01

Refractory metal alloys based on Mo, W, Re, Ta, and Nb (Cb) find applications in a wide range of aerospace applications because of their high melting points and high-temperature strength. This paper presents recent progress in the understanding and applications of these alloys. Recent studies to improve the oxidation and mechanical behavior of refractory metal alloys, and particularly Nb alloys, are also discussed. Some Re structures, for extremely high temperature applications (greater than 2000 C), made by CVD and P/M processes, are also illustrated. Interesting work on the development of new W alloys (W-HfC-X) and the characterization of some commercial refractory metals, e.g., K-doped W, TZM, and Nb-1%Zr, continues. Finally, recent developments in high temperature composites reinforced with refractory metal filaments, and refractory metal-based intermetallics, e.g., Nb3Al, Nb2Be17, and MoSi2, are briefly described.
DOE

N94-32416# Auburn Univ., AL.
HIGH TEMPERATURE MATERIALS TECHNOLOGY RESEARCH FOR ADVANCED THERMIONIC SYSTEMS
R. H. Zee and M. F. Rose 1993 10 p
(Contract DE-FG03-93SF-19645)
(DE94-008444; DOE/SF-19645/T4) Avail: CASI HC A02/MF A01

The effort was concentrated on two aspects of modeling of deformation in refractory alloy single crystals: deformation map in a tube with a (111) axial orientation and creep retardation due to solution strengthening (both effects are important in bcc single crystalline refractory alloys for high temperature emitters). Lattice misfit parameters are given between tungsten and 3 solutes (Re, Nb, Hf). DOE

N94-32498 Cornell Univ., Ithaca, NY.
A STATE VARIABLE MATERIAL MODEL FOR SUPERPLASTIC TITANIUM-6 PERCENT Al-4 PERCENT V Ph.D. Thesis
Daniel Abbott Mosher 1993 140 p
Avail: Univ. Microfilms Order No. DA9318816

A material model has been developed for the superplastic titanium alloy, Ti-6Al-4V, which describes the material's large strain viscoplastic behavior. To simulate superplastic forming, a model is required which captures the complexities of the material's mechanical response. The primary challenges to develop an accurate model are to determine which microstructural features are significant, the manner in which they influence the flow kinetics, and the rate at which these features evolve during thermomechanical processing. The two phase alpha-beta titanium alloy of this study has numerous aspects of the microstructure which could affect flow, as well as having multiple deformation mechanisms. In this work, the alpha phase grain size and shape have been used to represent the

microstructural state. Physical experiments have been performed to obtain data on the uniaxial kinetics of flow at fixed microstructural state and the evolution of state. The uniaxial kinetics have been determined over the following ranges of uniaxial deformation rate, d, temperature, T, and alpha grain size, bar-L(sub 3) (exp eff): 10(exp -5) s(exp -l) less than d less than 10(exp -3) s(exp -1), 875 degrees C less than T less than 950 degrees C, and 5.7 microns less than bar-L(exp eff) (sub 3) less than 17.1 microns. A hyperbolic sine functional form has been developed to capture the uniaxial behavior, which is based on the transition between two deformation mechanisms. An orthotropic flow rule has been derived based on alpha grain shape, which adds only one additional parameter that can be evaluated through uniaxial tests and microstructural examination. Grain size evolution experiments have been performed at 900 and 925 degrees C over the ranges of d and L(exp eff) (sub 3) given above. Grain growth has been divided into static and deformation enhanced components. Functional forms and material parameters have been determined which closely match the path dependent change of alpha grain size. The use of alpha grain size as an estimate of the microstructural state captures some of the transients observed in the stress response. Other trends such as strain softening cannot be predicted by the model, implying that additional aspects of the microstructure play a significant role in the kinetics of flow. Dissert. Abstr.

N94-32514# Argonne National Lab., IL.
STRUCTURAL ORDERING IN LIQUID K-Te ALLOYS
J. Fortner, M. L. Saboungi, and J. E. Enderby 1994 9 p
(Contract W-31-109-eng-38)
(DE94-008477; ANL/CMT/PP-75501) Avail: CASI HC A02/MF A01

Neutron diffraction from molten K(sub x)Te(sub 1-x) is reported for x = 0.12 and x = 0.50 semiconducting alloys. The measured radial distribution functions (rdf) demonstrate the persistence of covalently bonded tellurium in the liquid. The rdf of the liquid K(sub 0.12)Te(sub 0.88), which is dominated by the Te-Te contribution, is remarkably similar to that of pure liquid tellurium, the notable exception being that the nearest neighbor peak is largely resolved and found to have a coordination number slightly less than 2. The K(sub 0.50)Te(sub 0.50) rdf clearly indicates Te-Te pairing in the melt, and unexpected departure from the presumed similar Cu(sub 0.50)Te(sub 0.50). These paired tellurium are most likely of the form (Te(sub 2))(sup 2-) Zintl ions. DOE

N94-32522# Lawrence Livermore National Lab., CA.
LIQUID-ASSISTED DIFFUSION BONDING OF NiAl
M. J. Strum and G. A. Henshall 1994 15 p Presented at the 2nd Advanced Joining Technologies for New Materials, Cocoa Beach, FL, 2-4 Mar. 1994
(Contract W-7405-eng-48)
(DE94-008687; UCRL-JC-115737; CONF-940367-2) Avail: CASI HC A03/MF A01

A new isothermal joining method is investigated which could allow full utilization of the high temperature properties of advanced intermetallic alloys, such as NiAl, by producing joint compositions which match the parent material after bonding. In this method, interlayers of the parent material constituents are pre-placed in stoichiometric proportions on the surfaces to be joined. Bonding occurs without the application of pressure by raising the temperature above the liquidus of the lower melting constituent. The constituents then interdiffuse to produce the parent material phase and homogenize to the proper stoichiometry. This method differs from conventional liquid-assisted diffusion bonding in that no foreign melting-point depressants are added. Interrupted bonding treatments were used to characterize the kinetics of the isothermal solidification and homogenization processes in NiAl couples, and the compositional profiles of the bond region were characterized by electron probe microanalysis. Homogenization, as defined by the Ni and Al concentration maxima, follows a logarithmic time dependence once the bond region becomes single-phase NiAl. DOE

N94-32614 Pacific Northwest Lab., Richland, WA.
STAGE 1 BEHAVIOR IN A STRESS CORROSION STUDY OF TYPE 304 STAINLESS STEEL
A. L. Lund (Washington State Univ., Richland.) and R. H. Jones 1994 13 p Presented at the Corrosion 1994: National Association of Corrosion Engineers (NACE) International Annual Conference, Baltimore, MD, 28 Feb. - 4 Mar. 1994 Limited Reproducibility: More than 20% of this document may be affected by microfiche quality
(Contract DE-AC06-76RL-01830)
(DE94-008054; PNL-SA-23410; CONF-940222-13) Avail: CASI HC A03

In stress corrosion studies, crack velocity plotted with respect to stress intensity generally yields a characteristic curve with three distinct regions. Stage 1 exhibits a threshold (K(sub ISCC)) followed by a rapid increase in crack velocity (da/dt) for small changes in stress intensity. Stage 2 is characterized by an essentially constant crack velocity with increases in the stress intensity. Stage 3 exhibits a rapid increase in crack velocity for small increases in stress intensity leading to fracture. Stage 1 behavior has been poorly characterized in literature due to previous emphasis on determining the threshold K(sub ISCC) and difficulty and uncertainty in measuring of a large increase in crack velocity with only incremental changes in stress intensity. Tests were conducted in the stage 1 regime to measure crack velocity as a function of constant stress intensity. Constant K specimens were prepared according to the Mostovoy design, a tapered double cantilever beam. Specimens were prepared from Type 304 stainless steel containing 0.06 weight percent C solution annealed at 1100 C for 1 hour, water quenched, and annealed at 625 C for 24 hours to produce sensitization. A sodium thiosulfate solution at 50 C was chosen as the test environment. DOE

N94-32636 Lawrence Livermore National Lab., CA.
ON THE FORMATION OF MUON- AND ZETA-PHASES IN Ag-Al SYSTEM BY MECHANICAL ALLOYING
M. R. Paruchuri (Carnegie-Mellon Univ., Pittsburgh, PA.), D. L. Zhang (Carnegie-Mellon Univ., Pittsburgh, PA.), and T. B. Massalski (Carnegie-Mellon Univ., Pittsburgh, PA.) Sep. 1993 25 p Limited Reproducibility: More than 20% of this document may be affected by microfiche quality
(Contract W-7405-eng-48)
(DE94-007125; UCRL-CR-114777) Avail: CASI HC A03

Pure silver and aluminum powders have been mechanically alloyed in a Spex mill. Four selected nominal compositions Ag(1-x)Al(x) (x = 0.20, 0.23, 0.26 and 0.37) were investigated by X-ray diffraction and differential scanning calorimetry, after being subjected to different times of ball milling. In all four selected compositions, the close packed hexagonal intermediate lambda-phase and the fcc alpha-phase (Ag-based solid solution) formed together during the first hour of milling, but subsequently the lambda-phase disappeared during continued milling except in the two alloys corresponding to 26 at.%Al and 37 at.%Al where the lambda-phase is the equilibrium phase. With continued milling, the complex cubic mu-phase formed in the alloys of nominal composition 20, 23 and 26 at.%Al where it is expected in equilibrium alloys. No amorphous phases have been observed in the mechanically alloyed powders in this system. DOE

N94-32672 Sandia National Labs., Albuquerque, NM.
GETTERING OF METAL IMPURITIES BY CAVITIES IN SILICON
S. M. Myers, D. M. Follstaedt, D. M. Bishop, and J. W. Medernach 1993 12 p Presented at the 7th International Conference on Silicon Materials Science and Technology, San Francisco, CA, 22-27 May 1994 Limited Reproducibility: More than 20% of this document may be affected by microfiche quality
(Contract DE-AC04-94AL-85000)
(DE94-005248; SAND-93-2047C; CONF-940537-1) Avail: CASI HC A03

Ion implantation of He into Si followed by annealing approximately greater than 700 C produces nanometer-scale cavities from which the He has diffused. Experiments utilizing Rutherford backscattering spectrometry and transmission electron microscopy show that these cavities trap Cu impurities with a binding energy of 2.2 +/- 0.2 eV relative to solution, whereas the binding energy in precipitates of the equilibrium silicide phase Cu3Si is determined to be 1.7 eV. Preliminary results indicate that Ni impurities also are bound more strongly at internal surfaces than in silicide precipitates. These findings suggest that cavity traps may provide exceptionally effective gettering of transition-metal impurities. Additional properties relevant to gettering are discussed, including fundamental differences between trapping and precipitation dynamics, the replacement of Cu by H atoms at internal surface sites cavity-associated electronic levels in the band gap, and microstructural stability of the cavities. DOE

N94-32699# Brookhaven National Lab., Upton, NY.
CHARACTERIZATION OF THE CORROSION RESISTANCE OF DUPLEX STAINLESS STEELS USING LOCAL CURRENT DENSITY MAPPING TECHNIQUES
A. Aldykiewicz and H. S. Isaacs 10 Jan. 1994 23 p
(Contract DE-AC02-76CH-00016)
(DE94-007980; BNL-60099) Avail: CASI HC A03/MF A01

An in situ investigation of the dissolution behavior of duplex stainless steel has been carried out in acidic solutions containing 2.0 M HCl with 2.0 M H2SO4 to determine differences in dissolution rates of the austenitic and ferritic phases. The current density distribution over the dissolving steel surface was measured using a vibrating electrode. The study demonstrated that this technique could quantify the differences in dissolution rates of the austenitic and ferritic phases under the conditions tested. The dissolution rates for the two phases peak at different potentials resulting in multiple current maxima. In addition, transients in dissolution behavior of the two phases at different potentials were observed using optical microscopy. Electron microscopy of the dissolved surface showed very high levels of aluminum and silicon enrichment on the austenitic phase.
DOE

N94-32754 Lawrence Livermore National Lab., CA.
CALCULATIONS OF NONSPHERICALLY AVERAGED CHARGE DENSITIES FOR SUBSTITUTIONALLY DISORDERED ALLOYS
P. P. Singh and A. Gonis Feb. 1994 9 p Presented at the NATO Advanced Study Workshop on Metallic Alloys: Experimental and Theoretical Perspectives, Boca Raton, FL, 16-21 Jul. 1993 Limited Reproducibility: More than 20% of this document may be affected by microfiche quality
(Contract W-7405-eng-48)
(DE94-008293; UCRL-JC-116372; CONF-930759-7) Avail: Issuing Activity (Department of Energy (DOE))

Based on screening transformations of muffin-tin orbitals introduced by Andersen et al., we have developed a formalism for calculating the nonspherically averaged charge densities of substitutionally disordered alloys using the Korringa - Kohn - Rostoker coherent potential approximation (KKR CPA) method in the atomic-sphere approximation (ASA). We have validated our method by calculating charge densities for ordered structures, where we find that our approach yields charge densities that are essentially indistinguishable from the results of full-potential methods. For substitutionally disordered alloys, where full-potential methods have not been implemented so far, our approach can be used to calculate reliable nonspherically averaged charge densities from spherically symmetric one-electron potentials obtained from the KKR-ASA CPA. We report on our study of differences in charge denisty between ordered AlLi in L1(sub o) phase and substitutionally disordered Al(0.5)Li(0.5) on face-centered cubic lattice.
DOE

N94-32781# Westinghouse Savannah River Co., Aiken, SC.
DEUTERIUM ABSORPTION AND MATERIAL PHASE CHARACTERISTICS OF SAES St198 Zr-Fe ALLOY
A. Nobile, W. C. Mosley, J. S. Holder, and K. N. Brooks Jan. 1994 36 p Revised
(Contract DE-AC09-89SR-18035)
(DE94-008275; WSRC-TR-92-557-Rev-1) Avail: CASI HC A03/MF A01

This document reports deuterium absorption and material phase characteristics of SAES St 198 Zr-Fe Alloy (76.5% Zr). Scanning electron microscope images of polished surfaces, electron probe microanalysis, and x-ray powder diffractometry indicated the presence of a primary Zr2Fe phase with secondary phases of ZrFe2, Zr5FeSn, alpha-Zr, and Zr6Fe3O. A statistically designed experiment to determine the effects of temperature, time, and vacuum quality on activation of St 198 revealed that, when activated at low temperature (350 C), deuterium absorption rate was slower when the vacuum quality was poor (2.5 Pa vs. 3 x 10(exp -4) Pa). However, at higher activation temperature (500 C), deuterium absorption rate was fast and was independent of vacuum quality. Deuterium pressure-composition-temperature (P-C-T) data are reported for St 198 in the temperature range 200 to 500 C. The P-C-T data over the full range of deuterium loading and at temperatures of 350 C and below is described an expression. At higher temperatures, one or more secondary reactions in the solid phase occur that slowly consume D2 from the gas phase. X-ray diffraction and other data suggest these reactions to be: 2Zr2FeD(x) yields xZrD2 + x/3 ZrFe2 + (2 - 2/3x) Zr2Fe and Zr2FeD(x) + (2 - 1/2x) D2 yields 2ZrD2 + Fe, for 0 less than x less than 3. Reaction between gas-phase deuterium and Zr2Fe formed in the first reaction accounts for the observed consumption of deuterium from the gas phase by this reaction.
DOE

N94-32782# Lehigh Univ., Bethlehem, PA. Dept. of Physics.
MOLTEN METAL ANALYSIS BY LASER PRODUCED PLASMAS
Yong W. Kim Feb. 1994 42 p
(Contract DE-FC07-91ID-13103)
(DE94-007014; DOE/ID-13103/T1) Avail: CASI HC A03/MF A01

A new method of molten metal analysis, based on time- and space-resolved spectroscopy of a laser-produced plasma (LPP) plume of a molten metal surface, was implemented in the form of a prototype LPP sensor-probe, allowing in-situ analysis in less than 1 minute. The research at Lehigh University was structured in 3 phases: laboratory verification of concept, comparison of LPP method with conventional analysis of solid specimens and field trials of prototype sensor-probe in small-scale metal shops, and design/production/installation of two sensor-probes in metal production shops. The accomplishments of the first 2 phases are reported.
DOE

N94-32795# Stanford Linear Accelerator Center, CA.
ANISOTROPIC PHASE SEPARATION THROUGH THE METAL-INSULATOR TRANSITION IN AMORPHOUS Mo-Ge AND Fe-Ge ALLOYS Ph.D. Thesis
M. J. Regan Dec. 1993 152 p
(Contract DE-AC03-76SF-00515)
(DE94-007259; SU-SLAC-427; SU-SLAC/SSRL-0061) Avail: CASI HC A08/MF A02

Since an amorphous solid is often defined as that which lacks long-range order, the atomic structure is typically characterized in terms of the high-degree of short-range order. Most descriptions of vapor-deposited amorphous alloys focus on characterizing this order, while assuming that the material is chemically homogeneous beyond a few near neighbors. By coupling traditional small-angle x-ray scattering which probes spatial variations of the electron density with anomalous dispersion which creates a species-specific contrast, one can discern cracks and voids from chemical inhomogeneity. In particular, one finds that the chemical inhomogeneities which have been previously reported in amorphous Fe(x)Ge(1-x) and Mo(x)Ge(1-x) are quite anisotropic, depending significantly on the direction of film growth. With the addition of small amounts of metal atoms (x less than 0.2), no films appear isotropic nor homogeneous through the metal/insulator transition. The results indicate that fluctuations in the growth direction play a pivotal role in preventing simple growth models of a columnar structure or one that evolves systematically as it grows. The anomalous scattering measurements identify the metal atoms (Fe or Mo) as the source of the anisotropy, with the Ge atoms distributed homogeneously. The author has developed a method for using these measurements to determine the compositions of the phase-separating species. The results indicate phase separation into an amorphous Ge and an intermetallic phase of stoichiometry close to FeGe2 or MoGe3. Finally, by manipulating the deposited power flux and rates of growth, Fe(x)Ge(1-x) films which have the same Fe composition x can be grown to different states of phase separation. These results may help explain the difficulty workers have had in isolating the metal/insulator transition for these and other vapor-deposited amorphous alloys.
DOE

N94-32805# Pittsburgh Univ., PA.
STUDIES OF THE FUNDAMENTAL NATURE OF CATALYTIC ACIDITY, SITES AND INTERMEDIATES Final Progress Report
1993 4 p
(Contract DE-FG02-87ER-13774)
(DE94-006999; DOE/ER-13774/4) Avail: CASI HC A01/MF A01

This project was concerned with the fundamental nature of catalyst acidity in the H-zeolites and silica/alumina cracking catalysts. This report summarizes the progress on this project over the past five years. The titles of the twelve papers generated by this research are provided in the attached bibliography in chronological order.
DOE

N94-32825# Auburn Univ., AL.
HIGH TEMPERATURE MATERIALS TECHNOLOGY RESEARCH FOR ADVANCED THERMIONIC SYSTEMS

R. H. Zee and M. F. Rose 1993 21 p
(Contract DE-FG03-93SF-19645)
(DE94-008341; DOE/SF-19645/T3) Avail: CASI HC A03/MF A01

The objective was to understand the strengthening mechanisms in advanced refractory alloys for high-temperature thermionic applications. During the first 6 months, the role of substitutional solutes in refractory alloy single crystals was identified and modeled using a simple size misfit factor as the governing parameter. During the past period, effort was concentrated on the strengthening effects in various refractory structures and the growth of refractory alloy single crystals. DOE

N94-32851 Oak Ridge National Lab., TN.
POTENTIAL APPLICATIONS OF FUSION NEUTRAL BEAM FACILITIES FOR ADVANCED MATERIAL PROCESSING
J. M. Williams, C. C. Tsai, W. L. Stirling, and J. H. Whealton Jan. 1994 21 p Presented at the Workshop on Plasma-Based Ion Implantation, Madison, WI, 4-6 Aug. 1993 Limited Reproducibility: More than 20% of this document may be affected by microfiche quality
(Contract DE-AC05-84OR-21400)
(DE94-009167; CONF-9308156-3) Avail: CASI HC A03

Surface processing techniques involving high energy ion implantation have achieved commercial success for semiconductors and biomaterials. However, wider use has been limited in good part by economic factors, some of which are related to the line of sight nature of the beam implantation process. Plasma source ion implantation is intended to remove some of the limitations imposed by directionality of beam systems and also to help provide economies of scale. The present paper will outline relevant technologies and areas of expertise that exist at Oak Ridge National Laboratory in relation to possible future needs in materials processing. Experience in generation of plasmas, control of ionization states, pulsed extraction, and sheath physics exists. Contributions to future technology can be made either for the immersion mode or for the extracted beam mode. Existing facilities include the High Power Test Facility, which could conservatively operate at 1 A of continuous current at 100 kV delivered to areas of about 1 m(exp 2). Higher instantaneous voltages and currents are available with a reduced duty cycle. Another facility, the High Heat Flux Facility, can supply a maximum of 60 kV and currents of up to 60 A for 2 s on a 10 percent duty cycle. Plasmas may be generated by use of microwaves, radio frequency induction, or other methods and plasma properties may be tailored to suit specific needs. In addition to ion implantation of large steel components, foreseeable applications include ion implantation of polymers, ion implantation of Ti alloys, Al alloys, or other reactive surfaces. DOE

N94-32852 Oak Ridge National Lab., TN.
STRUCTURE, STABILITY, AND MECHANICAL PROPERTIES OF INTERMETALLIC PHASES
J. H. Schneibel and C. T. Liu 1993 13 p Presented at the Fall Meeting of the Minerals, Metals and Materials Society: Physical Metallurgy and Materials, Pittsburgh, PA, 17-21 Oct. 1993 Limited Reproducibility: More than 20% of this document may be affected by microfiche quality
(Contract DE-AC05-84OR-21400)
(DE94-009178; CONF-931009-22) Avail: Issuing Activity (Department of Energy (DOE))

The importance of the structural stability of intermetallics with regard to their mechanical properties is illustrated with two case studies. First, the importance of structural and thermal defects for the strength of (weakly ordered) FeAl and (strongly ordered) NiAl is shown. Several inconsistencies and unresolved issues in the present understanding of point defects in FeAl are addressed. Since point defects alone may not explain the mechanical differences between these two materials, the role of dislocations is considered as well. It is shown that the differences in the atomic bonding of FeAl and NiAl, which determine the active slip systems, are likely to influence the compositional dependence of the strength of these two intermetallics. Second, the class of the trialuminides is reviewed with emphasis on Al3Ti. In addition to stabilizing a cubic crystal structure, the ratio of K/G, where K is the bulk modulus and G the shear modulus, needs to be increased in order to achieve extensive plastic deformation at room temperature. It is not clear, at the present time, to what extent macroalloying of trialuminides can achieve this goal, although promising results have been reported for Al3Ti containing relatively high concentrations (14 at. %) of chromium. DOE

N94-32892# Lawrence Livermore National Lab., CA.
DEPENDENCE OF X RAY ABSORPTION MAGNETIC CIRCULAR DICHROISM ON LAYER PERIODICITY IN IRON-PLATINUM MULTILAYERS
A. F. Jankowski, G. D. Waddill, and J. G. Tobin Nov. 1993 14 p Presented at the 40th National Symposium of the American Vacuum Society, Orlando, FL, 15-19 Nov. 1993
(Contract W-7405-eng-48)
(DE94-008786; UCRL-JC-115359; CONF-9311104-20) Avail: CASI HC A03/MF A01

Magnetic circular dichroism in x-ray absorption is observed in Fe/Pt multilayers. The magnetization and helicity are both in the plane of the Fe/Pt multilayers which are prepared by planar magnetron sputter deposition. Lattice and layer pair spacings are measured using grazing incidence and high angle x-ray scattering. The film composition and lattice growth are confirmed using Auger depth profiling and cross-section transmission electron microscopy, respectively. The state of the film magnetization is found to be dependent on the layer pair spacing as well as the relative thickness of the Fe to Pt layer. The maximum magnetic moment is measured for a (Fe (9.5 A)/Pt (9.5) A)(sub 92) multilayer. DOE

N94-32931*# National Aeronautics and Space Administration. Lewis Research Center, Cleveland, OH.
FRICTIONAL BEHAVIOR AND ADHESION OF Ag AND Au FILMS APPLIED TO ALUMINUM OXIDE BY OXYGEN-ION ASSISTED SCREEN CAGE ION PLATING (SCIP)
Talivaldis Spalvins and Harold E. Sliney Apr. 1994 13 p Presented at the ICMCTF 1994, San Diego, CA, 25-29 Apr. 1994; sponsored by the American Vacuum Society
(RTOP 505-63-5A)
(NASA-TM-106522; E-8645; NAS 1.15:106522) Avail: CASI HC A03/MF A01

A modified dc-diode ion plating system, by utilizing a metallic screen cage as a cathode, is introduced for coating nonconductors such as ceramics. Screen cage ion plating (SCIP) is used to apply Ag and Au lubricating films on aluminum oxide surfaces. This process has excellent ability to coat around corners to produce three-dimensional coverage of the substrate. A dramatic increase in adhesion is achieved when plating is performed in a reactive 50 percent O2 - 50 percent Ar glow discharge compared to the adhesion when plating is performed in 100 percent Ar. The presence of oxygen ion assistance contributes to the excellent adhesion as measured in a pull-type adhesion tester. The Ag and Au film adhesion is significantly increased (less than 70MPa) and generally exceeds the cohesion of the substrate such that portions of the alumina are pulled out. Author

N94-32964# Argonne National Lab., IL.
EXPERIMENTAL STUDIES ON THE EFFECT OF COHERENCY STRAINS ON COARSENING KINETICS: CURRENT STATUS AND FUTURE OUTLOOK
G. Muralidharan, J. E. Epperson, and H. Chen 1994 12 p Presented at the International Conference on Advances in Physical Metallurgy, Bombay, India, 9-11 Mar. 1994
(Contracts W-31-109-eng-38; DE-FG02-91ER-45439)
(DE94-008480; ANL/IPNS/CP-82301; CONF-940383-1) Avail: CASI HC A03/MF A01

The effect of coherency strains on the coarsening rate constant in Ostwald ripening is an area that is not well understood. We briefly review the extant experimental data on the effect of coherency strains on coarsening rates and explain the need to account for variations in coarsening rates due to composition and diffusivity effects before drawing any conclusions on the dependence of coarsening rates on the misfit parameter. Using the preexisting theories for coarsening rates in multi-component systems, we suggest a simple method to account for the composition dependence of coarsening rates arising from factors unrelated to coherency strain effects. We then present some of the results from our on-going work in the Ni-Al-Si system and explain the relevance of this study to our understanding of coarsening in internally-stressed systems. We conclude the presentation with our views on the direction of future research in this aspect of coarsening. DOE

N94-32993# Argonne National Lab., IL.
IRRADIATION-INDUCED PHASE TRANSFORMATIONS IN ZIRCONIUM ALLOYS
L. M. Howe (Atomic Energy of Canada Ltd., Chalk River, Ontario.), D. Phillips (Atomic Energy of Canada Ltd., Chalk River, Ontario.), A. T. Motta (Pennsylvania State Univ., University Park.), and P. R. Okamoto Feb. 1994 24 p Presented at the 8th International Conference on Surface Modification of Metals By Ion Beams, Kanazawa, Japan, 13-17 Sep. 1993
(Contract W-31-109-eng-38)
(DE94-008484; ANL/MSD/CP-82244; CONF-9309251-2) Avail: CASI HC A03/MF A01

Ar-40 and Bi-209 ion irradiations of Zr3Fe were performed at 35-725 K using 15-1500 keV ions. Results are presented on the role of deposited-energy density on the nature of the damaged regions in individual cascades produced by ion bombardment of Zr3Fe. Comparison is also made between irradiation-induced amorphization of Zr3Fe during electron irradiation and under ion bombardments. Dependence of damage production on incident electron energy in Zr3Fe was also determined. Preliminary results are also discussed for amorphization of ZrFe2, Zr(Cr,Fe)2, and ZrCr2 by electron irradiation. Results of a recent investigation on amorphization of Zr(Cr,Fe)2 and Zr2(Ni,Fe) precipitates in Zircaloy-4 are discussed in the context of previous experimental results of neutron and electron irradiations and likely amorphization mechanisms are proposed. DOE

N94-33182 Cornell Univ., Ithaca, NY. Dept. of Chemistry.
INDUCED ADSORPTION OF CHLORIDE AND BROMIDE BY SUBMONOLAYER AMOUNTS OF COPPER UNDERPOTENTIALLY DEPOSITED ON Pt(111)
R. Gomez, J. M. Feliu, and H. D. Abruna 14 Mar. 1994 43 p Limited Reproducibility: More than 20% of this document may be affected by microfiche quality
(Contract N00014-84-K-0656)
(AD-A278023; TR-35) Avail: CASI HC A03

The underpotential deposition of submonolayer amounts of copper induces an enhanced adsorption of chloride and bromide on Pt(111) and is reflected in exceedingly sharp voltammetric peaks. The adsorbed anions are believed to be in contact with the platinum surface and in the vicinity of the electrodeposited copper. The electrosorption valency for chloride anions was estimated to be about one. This effect of induced adsorption was not observed on Pt(100) pointing to the sensitivity of the process to the surface structure. The advantages of working with low concentrations of metals in UPD studies is illustrated. DTIC

N94-33270 Lawrence Livermore National Lab., CA.
PHASE RELATIONSHIPS AND STABILITY OF THE (MU)- AND (ZETA)-PHASES IN THE Ag-Al-X (X=Zn, Ga, Ge) SYSTEMS
M. R. Paruchuri and T. B. Massalaski Sep. 1993 18 p Limited Reproducibility: More than 20% of this document may be affected by microfiche quality
(Contract W-7405-eng-48)
(DE94-009391; UCRL-CR-114778) Avail: CASI HC A03

Details of phase relationships in three ternary systems, Ag-Al-X (X=Zn, Ga, Ge) near the Ag-rich corner at 400 C are presented. Metallography, x-ray diffraction, scanning electron microscopy and x-ray spectroscopy have been used to establish the respective isothermal sections at 400 C. In each case, the mu-phase and the zeta-phase of the Ag-Al binary system extend into the ternary system and terminate at a three-phase region involving the Ag-rich primary solid solution (alpha(sub 1)-phase) in the Ag-Al-Zn and Ag-Al-Ga systems, and the Ge-rich primary solid solution (alpha(sub 2)-phase) in the Ag-Al-Ge ternary system. The stability ranges of the mu and zeta-phases follow approximately constant electron concentration lines. The solid solubilities of Zn, Ga and Ge in the mu-phase are relatively small, compared with those in the zeta-phase (up to 18 at. %). No ternary phase appears to exist in the Ag-rich portions studied in the three ternary systems. DOE

N94-33281# Army Armament Research, Development and Engineering Center, Watervliet, NY.
SIMPLER J(SUB Ic) TEST AND DATA ANALYSIS PROCEDURES FOR HIGH STRENGTH STEELS Final Report
J. H. Underwood, E. J. Troiano, and R. T. Abbott Jan. 1994 27 p
(AD-A277731; ARCCB-TR-94001) Avail: CASI HC A03/MF A01

Tests of five medium and high strength steels were used to investigate some prospective simplification in J(sub Ic) test and data analysis procedures. Three-point bend specimens with material strengths of 500 to 1500 MPa and nominal thickness of 10 mm were tested at room temperature. The investigation included J(sub Ic) tests using measured crack-mouth displacement to calculate load-line displacement based on an expression that relates the two displacements; a simple zero-point adjustment for J versus Delta-a curves, whereby certain intermediate Delta-a values are shifted to the blunting line to correct for errors at low values of Delta-a; and a comparison of Delta-a and J(sub Ic) results from the load-drop method, which gives a simple measure of crack growth after maximum load, with results from the usual unloading compliance method. The various results and comparisons are discussed in relation to their usefulness as general J(sub Ic) test procedure for a variety of materials, or a limited use test for certain materials. Two specific test and data procedures are proposed for general use in J(sub Ic) testing as follows. A new expression is described that calculates load-line displacement for the bend specimen from measured crack-mouth displacement, for a range of a/W values and strain hardening exponents. The expression makes possible a single-displacement unloading compliance J(sub Ic) test for the bend specimen using a single, standard, crack-mouth clip gage. A simple zero-shift procedure is proposed for general use with J(sub Ic) tests and for addition to ASTM Method E-813. The procedure adjusts the zero point of Delta-a so that on average the Delta-a values lie on the blunting line over the J-range of 20 to 60 percent of the provisional fracture toughness, J(sub Q). DTIC

N94-31017*# Boeing Defense and Space Group, Seattle, WA.
ANODIZED ALUMINUM ON LDEF
Johnny L. Golden *In* NASA. Marshall Space Flight Center, LDEF Materials Results for Spacecraft Applications Dec. 1993 p 61-71 (For primary document see N94-31012 09-12)
(Contracts NAS1-19247; NAS1-18224)
Avail: CASI HC A03/MF A04

27 NONMETALLIC MATERIALS

Includes physical, chemical, and mechanical properties of plastics, elastomers, lubricants, polymers, textiles, adhesives, and ceramic materials.

For composite materials see *24 Composite Materials.*

N94-31059# Office of Naval Research European Office, FPO New York, NY.
PIEZOELECTRIC MATERIALS RESEARCH IN EUROPE
John A. Sampsonions 28 May 1993 551 p
(AD-A276207; ONREUR-93-7-R) Avail: CASI HC A24/MF A04

The Office of Naval Research (ONR) and Office of Naval Research European Office (ONR Europe) recently sponsored an international workshop on advances in piezoelectric materials and current research thrusts in Europe. 'Perspectives on Piezoelectric Materials Research' was held at Elvetham Hall, near Basingstoke, England, 21-24 Feb. 1993. The 27 invited delegates were drawn from industry, academia, and government research organizations in nine countries: Denmark, France, the Federal Republic of Germany (FRG), Italy, Slovenia, Spain, Switzerland, the United Kingdom (U.K.), and the United States (U.S.). Abstracts and viewgraphs from the international meeting have been included in this report. DTIC

N94-31069 Helsinki Univ. of Technology, Espoo (Finland). Lab. of Polymer Technology.
REACTIONS OF ELECTROPHILIC MALEIC ANHYDRIDE AND EPOXY GROUPS WITH NUCLEOPHILIC FUNCTIONALITIES SUCH AS CARBOXYL, HYDROXYL, AND AMINE GROUPS. POLYMER TECHNOLOGY PUBLICATION SERIES NO. 16 Literature Review
P. Hietaoja and R. Holsti-Miettinen Aug. 1993 36 p Limited Reproducibility: More than 20% of this document may be affected by microfiche quality
(ISSN 0785-7144)
(PB94-135589; ISBN-951-22-1712-0) Avail: Issuing Activity (National Technical Information Service (NTIS))

The desired chemical reactions which may take place under twin screw extruder conditions have been reviewed. Effects of time, temperature, and catalysts have been summerized. Applications for polymer blending have been discussed. The study of chemical reactions between two polymers is often very complicated and therefore most of the work has been made with low molecular weight monomers or oligomers. NTIS

N94-31072 Selskapet for Industriell og Teknisk Forskning, Trondheim (Norway). Corrosion Center.
EVALUATION OF CORROSION PROTECTIVE ORGANIC COATINGS FOR STEEL STRUCTURES IN FRESH WATER Final Report
U. Steinsmo 9 Aug. 1993 40 p
(PB94-138484; STF34-A93158) Avail: Issuing Activity (National Technical Information Service (NTIS))

The report presents a summary of the final results from a 6 year program 'Evaluation of Corrosion Protective Organic Coatings for Steel Structures in Fresh Water'. 76 paint systems from 19 different main suppliers have been tested. The test program involved three different humidity cabinet tests, two water immersion tests, and long term exposure test in fresh water at three different fresh water sites and in cold humid air in two mountain tunnels. The importance of microbial activity has been investigated. In addition water uptake and water diffusivity have been determined and electrochemical studies performed. NTIS

N94-31198# Sandia National Labs., Livermore, CA.
A COMPATIBILITY STUDY OF FEFO WITH VARIOUS CONTAINMENT MATERIALS
T. J. Shepodd, S. H. Goods, and P. Foster 1994 6 p Presented at the International Symposium on Energetic Materials Technology and Exhibits, Orlando, FL, 21-24 Mar. 1994
(Contract DE-AC04-94AL-85000)
(DE94-005753; SAND-94-8508C; CONF-940348-2) Avail: CASI HC A02/MF A01

Compatibility between fluid bis-(2-fluoro- 2,2-dinitroethyl) formal (FEFO) and a number of organic and metallic materials was evaluated at 22 and 74 C for up to 8 months. The metals included common structural alloys and elemental metals that the extrudable explosive might contact in its service life. The organic materials included flexible materials for use as collapsible extrusion membranes or permeation barriers, rigid engineering resins (matrices for composite vessels), and polymer viscosity modifiers. DOE

N94-31199# Lawrence Livermore National Lab., CA.
SOL-GEL METAL OXIDE AND METAL OXIDE/POLYMER MULTILAYERS APPLIED BY MENISCUS COATING
J. A. Britten and I. M. Thomas Oct. 1993 9 p Presented at the 25th Boulder Damage Symposium: Annual Symposium on Optical Materials for High-Power Lasers, Boulder, CO, 27-29 Oct. 1993
(Contract W-7405-eng-48)
(DE94-005813; UCRL-JC-114730; CONF-931054-5) Avail: CASI HC A02/MF A01

We are developing a meniscus coating process for manufacturing large-aperture dielectric multilayer high reflectors (HR's) at ambient conditions from liquid suspensions. Using a lab-scale coater capable of coating 150 mm square substrates, we have produced several HR's which give 99% + reflection with 24 layers and with edge effects confined to about 10 mm. In calendar 1993, we are taking delivery of an automated meniscus coating machine capable of coating substrates up to 400 mm wide and 600 mm long. The laser-damage threshold and failure stress of sol-gel thin films can be substantially increased through the use of soluble polymers which act as binders for the metal oxide particles comprising the deposited film. Refractive index control of the film is also possible through varying the polymer/oxide ratio. Much of our present effort is in optimizing oxide particle/binder/solvent formulations for the high-index material. Films from colloidal zirconia strengthened with polyvinylpyrollidone (PVP) have given best results to date. An increase in the laser damage threshold (LDT) for single layers has been shown to significantly increase with increased polymer loading, but as yet the LDT for multilayer stacks remains low. DOE

N94-31201# Ohio State Univ., Columbus.
MOLECULAR/POLYMERIC MAGNETISM
1993 13 p
(Contract DE-FG02-86ER-45271)
(DE94-005888; DOE/ER-45271/T7) Avail: CASI HC A03/MF A01

Accomplishments during this past grant period span three areas of research. (1) Following models the authors and others have proposed, they have synthesized numerous new materials to test the generality of magnetism in molecular/polymeric systems. This activity is capped by their disclosure of the first room temperature molecular based magnet V(TCNE)x y(soivent). (2) They have extensively studied the magnetic transitions and related phenomena in decamethylferrocenium tetracyanoethanide, (FeCp*2)(TCNE), V(TCNE)x(center dot)y(solvent), and related materials, and developed an initial understanding of the key roles played by disorder, anisotropy, dimensionality, and spin magnitude. They have tested theirs and others' models for the origin of magnetic exchange between local sites, and models for control of (Tc), determining successes and shortcomings. They briefly summarize here the major breakthroughs, accomplishments, and discoveries that have occurred during this period. DOE

N94-31206 Illinois Univ., Urbana-Champaign.
AN INVESTIGATION OF THE SPIN-COATING PROCESS AND A MODEL FOR THREE-DIMENSIONAL REGULAR FOAMS Ph.D. Thesis
Weiqun Zhou 1993 153 p
Avail: Univ. Microfilms Order No. DA9329211

The thesis consists of two independent parts. The first part is entitled: An investigation of the spin-coating process; the second part is entitled: A model for three-dimensional regular foams. For spin-coating, a detailed numerical investigation of the spin-coating process has been performed. Our numerical approach takes advantage of the known asymptotic structure of the solution to the governing equations, and uses an adaptive scheme with multiple grids to achieve substantial improvements in accuracy and efficiency over previous approaches. As a result, the final coating thickness may be predicted, with good accuracy and efficiency, in terms of the spin speed and various material properties. For foam rheology, a model for the 3-D regular foam is developed. The 3-D model is considerably more realistic than the 2-D model used by previous researchers. The static shape of a foam cell is governed by the Young-Laplace equation, with one free boundary. The general problem was solved numerically, while asymptotic approximations were pursued for the limit of the gas volume fraction approaching unity. To study the rheology, we need to determine the geometry of the tessellating cells under deformation. To this end, a formalism is developed, which takes advantage of the affine movement of particular points of the tessellating cells (face centers, centroid of cell). Finally, as an example, the stretch of our 3-D model is examined in detail. Significant differences between the 3-D and 2-D models are observed. Most notably, the elastic modulus predicted by the 3-D model is lower and decreases faster with stretch than that predicted by the 2-D model, which suggests that the 3-D model might give closer agreement with experiments than the 2-D model. Dissert. Abstr.

N94-31276 Lehigh Univ., Bethlehem, PA. Materials Research Center.
PROCESSING OF NOVEL NANOPARTICLE DISPERSION STRENGTHENED CERAMICS FOR IMPROVED MECHANICAL PERFORMANCE Annual Report No. 2, 15 Dec. 1992 - 14 Dec. 1993
Helen M. Chan, Martin P. Harmer, M. Thompson, J. Fang, and I. Chou 14 Dec. 1993 65 p Limited Reproducibility: More than 20% of this document may be affected by microfiche quality
(Contract N00014-92-J-1635)
(AD-A275965) Avail: CASI HC A04

Results from a previous study carried out by the Lehigh group demonstrated Al2O3:SiC nanocomposites exhibited superior mechanical behavior relative to single phase alumina only when the samples had been annealed (2 h at 1300 C in argon) subsequent to industrial machining. These results were rationalized by postulating that on annealing of the machined specimens: (1) The extent of healing of grinding induced flaws is more significant in the nanocomposite than in alumina. (2) The machining induced residual stresses are relaxed to a lesser degree in the nanocomposite than in alumina. Further model studies have now been carried out which provide definitive evidence that both of the above assumptions are correct. Observation of indentation induced cracks both prior to, and after annealing, revealed that in the nanocomposite cracking

is predominantly transgranular, and crack healing takes place on annealing. For the case of single phase alumina, however, the crack morphology is predominantly intergranular, and annealing causes crack growth. DTIC

N94-31284# Clarkson Univ., Potsdam, NY.
RELIABILITY OF MULTILAYER COPPER/POLYIMIDE Final Report
S. V. Babu, D. H. Rasmussen, and D. W. Lawrence Nov. 1993 24 p
(Contract F30602-88-D-0028)
(AD-A276228; RL-TR-93-215) Avail: CASI HC A03/MF A01

The reliability of copper/polyimide (PI) multilayer structures was analyzed and found to depend on processing and environmental conditions. Copper films were deposited by thermal evaporation and patterned by contact lithography. Preimidized P12590-D polyimide films were spin coated over the copper with upper layers deposited as required. While the electrical characteristics of the multilayer structures generally behaved as expected, the softening of the underlying PI films led to observation of film buckling and dielectric breakdown in some samples. Consequently, alternate low temperature plasma and laser techniques for depositing copper on PI films, instead of PI films on copper, were explored to improve the reliability of the resulting Cu/PI multilayer structures. Copper films were deposited on PI substrates by radio frequency (13.56 MHz) plasma-induced reduction and excimer laser-induced ablation of copper formate. While the Cu/PI interface appears clean, the reduction of the formate was not complete with some residual carbon contamination in the copper film. Several methods for improving the purity of the Cu films were investigated. Diamondlike carbon (DLC) films are excellent barriers for the diffusion of Cu in Cu/Si structures. DLC films, due to their excellent compatibility with PI, may play a similar useful role in Cu/PI structures and improve their reliability. DTIC

N94-31297# Martin Marietta Labs., Baltimore, MD.
MOLECULAR INTERACTIONS AT METAL/POLYIMIDE INTERFACES: A CORRELATION WITH ADHESION AND BOND DURABILITY Annual Report, 1 Nov. 1992 - 31 Oct. 1993
G. D. Davis, B. J. Rees, P. L. Whisnant, K. M. Liechti, and A. Shirani 18 Feb. 1994 38 p
(Contract N00014-93-C-0004)
(AD-A276301; MML-TR-94-08) Avail: CASI HC A03/MF A01

Molecular interactions between a substrate and an overlayer control the intrinsic adhesion between the two materials and this intrinsic adhesion, in turn, is a critical component of the measured adhesion which also includes factors related to plastic deformation of the materials. Because virtually all measurements of adhesion include these other factors, accurate values for the intrinsic adhesion have not been available in the past. To develop a means to measure this parameter, nonlinear von Karman plate theory has been used for a consistent analysis of pressurized circular, island and peninsula blister specimens. The configurations considered ranged from linear plates to membranes. Interfacial energy release rates and fracture mode-mixes were extracted. For a given pressure and all possible materials and delamination length to thickness (aspect, a/h) ratios, the peninsula blister provided the highest energy release rate, followed by the island and circular blisters. The extent of yielding in delaminating copper films was greatest with the circular blister. The stress levels in the island blister were notably lower. While extensive yielding was still present in peninsula blister configurations with a/h = 100 and 500, there was none for a/h = 10. A scheme for extending the utility of blister specimens to higher aspect ratios was developed and analyzed. DTIC

N94-31354# Lawrence Livermore National Lab., CA.
COST-EFFECTIVE CERAMIC MACHINING: SUMMARY OF THREE-BODY WEAR EXPERIMENTS
L. V. Griffith Nov. 1993 55 p
(Contract W-7405-eng-48)
(DE94-007757; UCRL-ID-115678) Avail: CASI HC A04/MF A01

Loose-abrasive grinding experiments were conducted to compare relative grinding rates of BK7 glass, Si nitride, and alumina zirconia. Si nitride and alumina zirconia machined at about the same rate, while BK7 glass machined 6-8 times faster. Surface finish and subsurface were measured. Surface roughness of the ceramics is better than that of glass. Empirical equations for relating roughness and Preston coefficients were only qualitatively successful. Diamond and B4C yield about the same removal rate, but this is not basis enough for recommending the cheaper abrasive for the fixed-abrasive machining process. B4C is more friable than diamond, producing sharp cutting surfaces; however B4C may not be a good abrasive for precision grinding. SiC produced excellent surface finish but low removal rates. DOE

N94-31454 Utah Univ., Salt Lake City.
RELIABILITY ANALYSIS OF STRUCTURAL CERAMICS SUBJECTED TO BIAXIAL FLEXURE Ph.D. Thesis
Luen-Yuan Chao 1993 153 p
Avail: Univ. Microfilms Order No. DA9319428

Two weakest-link fracture statistics formulations for multiaxial loading, Batdorf's flaw density and orientation distribution approach and Evans' elemental strength approach, were compared for identical fracture criteria and flaw-size distribution function. Despite some fundamental differences in the methodology used in calculating fracture probabilities for multiaxial loading, the two approaches gave identical predictions. A recent contradictory conclusion reported in the literature is shown to be incorrect. Fracture stresses of a sintered alumina and silicon nitride were assessed in qualified uniaxial (three-point and four-point) and biaxial (uniform-pressure-on-disk) flexure tests in inert conditions (dry N2, 100 MPa/s stressing rate). The size and stress-state effects on the inert fracture stress of alumina were explained by a reliability analysis based on randomly oriented surface flaws and a mixed-mode fracture criterion. Fracture stresses of silicon nitride were in accord with a reliability analysis based on volume flaws with preferred orientation (crack plane normal to the maximum principal stress) and a normal stress fracture criterion. The preferred orientation of the flaws in silicon nitride resulted from stress-induced nucleation of cracks around pores. Alumina ceramic was also tested in deionized water at a low stressing rate (1 MPa/s). The decreased fracture stresses measured in both uniaxial and biaxial flexure tests in water as compared to the inert fracture stresses were consistent with subcritical crack growth behavior inferred from dynamic fatigue tests in water. The analysis of the size and stress-state effects on and time-dependent degradation of fracture stresses included consideration of the statistical uncertainties (90 percent confidence intervals) of the estimated Weibull (Weibull modulus, m, and characteristic strength, sigma(sub theta)) and slow-crack-growth (stress-intensity exponent, N, and critical crack growth rate, V(sub C)) parameters. Results suggested that subcritical crack growth and strength degradation were more severe in biaxial flexure than in uniaxial flexure, which implies an interaction between stress state and subcritical crack growth. Statistical analysis and correlation between pore-size distribution and fracture stress distribution using the theory of extreme-value statistics is presented for a sintered silicon nitride. The pore size distribution on a polished surface of this material was characterized using an automatic optical image analyzer. The distribution measured on the two dimensional plane surface was transformed to a population (volume) distribution using the Schwartz-Saltykov diameter method. The population pore-size distribution and the distribution of the pore size at fracture origins were correlated by extreme-value statistics. Fracture stress distribution was then predicted from the extreme-value pore size distribution using a linear elastic fracture mechanics model of annular crack around pore and the fracture toughness of the ceramic. The predicted strength distribution was in good agreement with strength measurements in bending. In particular, the extreme-value statistics analysis explained the nonlinear trend in the linearized Weibull plot of measured strengths without having to postulate a lower-bound strength. Dissert. Abstr.

N94-31509# Clark-Atlanta Univ., GA.
NOVEL ELECTROACTIVE POLYMERS AND BLOCK COPOLYMERS Final Report, 15 Aug. 1989 - 14 Aug. 1993
Ishrat M. Khan 12 Oct. 1993 12 p
(Contract DAAL03-89-G-0087)
(AD-A276119; ARO-27141.7-CH-SM) Avail: CASI HC A03/MF A01

Synthesis, characterization and properties of microphase separated mixed (ionic and electronic) conducting or MIEC block copolymers are reported. Polyomega-methoxyocta (oxyethylene)methacrylate-block-4-vinylpyridine, abbreviated as PMG8-4VP, and poly3-methylthiophene-block-omega-methoxyocta (oxyethylene)methacrylate, abbreviated as P(3MT-MG8), have been synthesized. Both block copolymer series may be appropriately doped to generate separate electronic and ionic conducting microdomains in the overall solid matrix. Also, highly ionic conductive solid polymer electrolytes have been prepared by blending poly(ethylene oxide), poly(2- or 4-vinylpyridine) and LiC1O4. All blends were prepared by the

solution blending process. Optimum blend compositions have been determined such that dimensionally stable elastomeric materials with ionic conductivities around 10(exp -5)S/cm at 25 C are obtained. DTIC

N94-31510# Pittsburgh Univ., PA.
BIOCATALYTIC PROCESSING POLYMERS IN SUPERCRITICAL FLUIDS Final Report, 15 Jun. 1990 - 14 Dec. 1993
Alan J. Russell Jan. 1994 15 p
(Contract DAAL03-90-G-0145)
(AD-A276120; ARO-28043.13-LS) Avail: CASI HC A03/MF A01

The performance and behavior of enzymes in non-aqueous environments has been explored under a variety of conditions, including high temperature and pressure. This work is both of fundamental interest, for providing information on enzyme behavior in non-aqueous environments, as well as of industrial importance, in that commercial processes which could benefit from the use of enzymes often operate in organic solvent, or at temperatures and pressures far from ambient. The work was directed at several topics within this general theme, including (1) biocatalysis in supercritical fluids--a study of the effect of smooth variations in solvent properties on enzyme activity; (2) biocatalysis in microemulsion systems--a study of the effect of microemulsion system variables on enzyme solubilization and activity; and (3) spectroscopic investigation of subtilisin in organic solvent--a study of the conformation of an enzyme in organic solvent as compared to its conformation in aqueous solution. DTIC

N94-31513 Technische Univ., Darmstadt (Germany). Fachbereich Physik.
COMPETITION BETWEEN CRYSTALLIZATION AND MIXING/DEMIXING IN POLYMER MIXTURE Ph.D. Thesis [KONKURRENZ ZWISCHEN KRISTALLISATION UND MISCHEN/ENTMISCHEN IN POLYMERMISCHUNGEN]
Yong Li 1991 143 p In GERMAN Limited Reproducibility: More than 20% of this document may be affected by microfiche quality
(ETN-94-95753) Avail: CASI HC A07

The competition between crystallization and mixing/demixing was systematically studied in polymer systems, as well as their mutual influence and the resulting morphologies and overmolecular structures, taking as example the model system poly-epsilon-caprolacton/polystyrol. The correlation between structure formation and the preparative parameters was determined. The characteristics of the structures resulting from the two opposite processes were analyzed. The resulting structure was especially characterized as a function of the temperature and the composition of the mixture, with a view to the multiphasic nature of the overmolecular structure. It is shown that the morphology of a polymer system can be adjusted by controlling the competition crystallization and mixing/demixing. ESA

N94-31557# Lawrence Livermore National Lab., CA.
ELECTROSTATIC REDUCTION OF PARTICULATES FOR LASER RESISTANT HAFNIA COATINGS
M. D. Miller, R. Chow, and G. E. Loomis Dec. 1993 8 p Presented at the 25th Boulder Damage Symposium: Annual Symposium on Optical Materials for High-Power Lasers, Boulder, CO, 27-29 Oct. 1993
(Contract W-7405-eng-48)
(DE94-005824; UCRL-JC-114845; CONF-931054-3) Avail: CASI HC A02/MF A01

The authors have reduced by 50% particulate defect density of hafnia coatings deposited onto silicon substrates through the use of electric fields, physical barriers and deposition rate. In an effort to reduce the number of hafnia (HfO2) particulates deposited onto silicon wafers, parallel plate electrodes were placed on either side of the evaporant plume. The particulate level was determined as the deposition rate was varied from 0.75 angstrom/sec to 12 angstrom/sec. Then, parallel plate electrodes were placed on either side of the plume as a way of electrostatically deflecting hafnia particulates away from the substrates. Later a single plate electrode was used in conjunction with a physical barrier placed over the hearth. The results of the study indicate that minimal defects occur when a parallel plate electric field is applied in conjunction with a fast deposition rate. Using a screen as a physical barrier, and/or a single electrode had little or no effect. This data may be useful in the manufacture of multilayer optical coatings with high laser damage thresholds. DOE

N94-31585 Technische Univ., Delft (Netherlands).
SMALL CYLINDRICAL ADHESIVE BONDS Ph.D. Thesis
H. Poulis May 1993 149 p Limited Reproducibility: More than 20% of this document may be affected by microfiche quality
(PB94-148210) Avail: Issuing Activity (National Technical Information Service (NTIS))

During the last few years, problems have arisen with regard to the adhesive bonding of very small cylindrical parts. The aim of this thesis is to design a practical and basic guidance for engineers in order to optimize the design and facilitate the production of small cylindrical adhesive bonds with a minimum number of production steps, but in such a way that the results are as reproducible as possible. The suggestions with regard to an optimal bond strength and performance are based on a large number of experimental values as well as on finite element analyses. NTIS

N94-31649# Sandia National Labs., Albuquerque, NM.
ADSORPTION OF WATER TO THE METAL/POLYMER INTERFACE STUDIED BY NEUTRON AND X RAY REFLECTIVITY
M. S. Kent, D. C. McIntyre, G. S. Smith, S. Baker, S. Wages, A. Nyitray, and J. Browning 1993 3 p Presented at the 17th Annual Adhesion Society Meeting, Orlando, FL, 20-24 Feb. 1994
(Contract DE-AC04-94AL-85000)
(DE94-005578; SAND-93-3863C; CONF-940244-1) Avail: CASI HC A01/MF A01

Neutron reflectivity is among the few techniques able to probe a buried interface. Through the use of isotopic labeling, complicated interface structures may be determined with a resolution on the order of 5 angstroms. However, for highly complex thin film and interface structures, it is often necessary to perform complementary experiments to reduce the number of unknown variables, and thus enable an unambiguous interpretation of the neutron reflectivity. To this end, the authors have combined x-ray and neutron reflectivity to study changes in a metal/polymer interface (molybdenum/polyurethane, hereafter Mo/PU) upon exposure to a humid environment. In particular, the authors have tracked the adsorption of moisture to the interface and variations in the density of the interphase. This information was obtained as a function of the concentration of a silane coupling agent added to the bulk of the PU. Adhesion of the Mo/PU interface is important to programs in the DOE complex. This paper reports the first results of this study. DOE

N94-31650# Sandia National Labs., Albuquerque, NM.
DEPOSITION OF DLC VIA INTENSE ION BEAM ABLATION
G. P. Johnston (New Mexico Univ., Albuquerque.), P. Tiwari (Los Alamos National Lab., NM.), D. J. Rej (Los Alamos National Lab., NM.), H. A. Davis (Los Alamos National Lab., NM.), W. J. Waganaar (Los Alamos National Lab., NM.), and R. E. Muenchausen (Los Alamos National Lab., NM.) 1993 6 p Presented at the Fall Meeting of the Materials Research Society (MRS), Boston, MA, 29 Nov. - 3 Dec. 1993
(Contract DE-AC04-94AL-85000)
(DE94-005583; SAND-93-1544C; CONF-931108-51) Avail: CASI HC A02/MF A01

Diamond-like carbon films were prepared by high intensity pulsed ion beam ablation of graphite targets. A 350 key, 35 kA, 400 ns pulse width beam, consisting primarily of carbon ions and protons, was focused onto a graphite target at a fluence of 15-45J/cm(sup 2). Films were deposited onto substrates positioned i.n q n angular array from normal to the target to 90 degrees off normal. Deposition rates up to 30 nm per pulse, corresponding to an instantaneous deposition rate greater than 1 mm/sec, have been observed. Electrical resistivities between 1 and 1000 ohm-cm were measured for these films. XRD scans showed that no crystalline structure developed in the films. SEM revealed that the bulk of the films contain material with feature sizes on the order of 100 nm, but micron size particles were deposited as well. Both Raman and electron energy loss spectroscopy indicated significant amounts of sp(sup 3) bonded carbon present in most of the films. DOE

N94-31672# Rensselaer Polytechnic Inst., Troy, NY.
CHEMICAL INTERACTIONS BETWEEN PROTEIN MOLECULES AND POLYMER MEMBRANE MATERIALS
G. Belfort, J. Koehler, and J. Wood 15 Jul. 1993 11 p
(Contract DE-FG02-90ER-14114)
(DE94-006987; DOE/ER-14114/3) Avail: CASI HC A03/MF A01

The surface force apparatus is now operable; data collection is automatic. Hen egg lysozyme was chosen as model protein. Protein-protein, protein-mica, protein-polymer, and protein-surfactant interactions were studied. Circular dichroism was used to study changes in protein structure during adsorption. DOE

N94-31692# Toronto Univ. (Ontario). Dept. of Aerospace Science and Engineering.
SPACE HYPERVELOCITY MICROPARTICLE IMPACT DAMAGE IN POLYMER MATRIX COMPOSITES M.S. Thesis
Gerald N. Manuelpillai 1993 129 p
(ISBN-0-315-87057-5; CTN-94-61246) Copyright Avail: Micromedia Ltd., Technical Information Centre, 240 Catherine Street, Suite 305, Ottawa, Ontario, K2P 2G8, Canada HC/MF

The current state of knowledge concerning micrometeoroid, orbital debris, and hypervelocity impacts in space environments is reviewed. A database of hypervelocity impact effects on advanced composite materials was compiled, using data from both space- and ground-based systems. Particular emphasis was placed on data from the Long Duration Exposure Facility (LDEF) satellite. Experiments were performed to obtain data on hypervelocity impacts on impact damaged protective coatings on polymer matrix composites. Current NASA models for predicting micrometeoroid and orbital debris fluxes in earth vicinity and an impact fluence nomogram, which was developed using LDEF data, are detailed. The nomogram enables the user to estimate total impact damage over time for a given spacecraft size and orbit. The experimentally obtained impact damage data were also modelled in a manner similar to the LDEF data. Both linear and quadratic fits were obtained. An attempt was made to integrate the simulation and flight databases. By modifying the data to reflect the difference in materials and in impact angles, the simulation data matched the flight database quite well. CISTI

N94-31722# Montreal Univ. (Quebec). Dept. de Genie Mecanique.
EMPIRICAL OPTIMIZATION OF THE CONSOLIDATION OF THERMOPLASTIC PREPREGS M.S. Thesis [OPTIMISATION EMPIRIQUE DE LA CONSOLIDATION DES PREIMPREGNES THERMOPLASTIQUES]
Tsevi M. G. Vovor Jun. 1993 158 p In FRENCH
(ISBN-0-315-86455-9; CTN-94-61198) Copyright Avail: Micromedia Ltd., Technical Information Centre, 240 Catherine Street, Suite 305, Ottawa, Ontario, K2P 2G8, Canada HC/MF

Response surface methodology, a statistical method of optimization, is used to relate the degree of consolidation of prepreg thermoplastic composites to their processing parameters. A global consolidation index is obtained from partial indices related to common mechanical properties such as shear strength, giving a quantitative formulation of the rather qualitative notion of consolidation, and provides an objective function for optimization. Fractional multifactorial designs were used in the experimental runs, involving various combinations of the processing parameters (temperature, pressure, residence time). Regression polynomial models were then built, using the least squares based response surface approach. Analysis of the polynomial coefficients showed the relative importance of the processing parameters and their respective interactions. For both amorphous polycarbonate glass and semicrystalline polypropylene glass prepregs, processing temperature was the most important parameter. For the amorphous system, the main interaction was temperature residence time. For the other, pressure residence time and pressure cooling rate interactions are among the important effects. The saddle nature of the fitted surfaces suggests nonexistence of a well defined optimal zone in the region investigated. Author (CISTI)

N94-31745 Texas A&M Univ., College Station.
VISCOELASTIC FRACTURE CHARACTERIZATION OF POLYMERIC SOLIDS Ph.D. Thesis
Jin Seong Choi 1993 202 p
Avail: Univ. Microfilms Order No. DA9328700

Almost all engineering materials exhibit creep and relaxation behavior. The observed magnitude depends on temperature, stress level, and loading duration. Some polymers are further influenced by moisture contents as well. Attempts to predict the crack initiation and propagation in fracture of polymeric solid materials are complicated by all such variables. In this study, hard viscoelastic polymeric solid materials were used to develop the viscoelastic fracture characterizing parameter. Fracture mechanism at the crack tip or in the neighborhood of crack tip is affected by those time-dependent material behaviors. A continuum aspect of time-dependent fracture mechanics approach was utilized. In the time-independent material, a fracture mechanics theory has been well established. However, viscoelastic polymeric solids are the time-dependent materials, and analysis methods are more complicated due to the time-dependency and therefore, analysis methods are rare. In this study, single specimen test method called 'calibration curve' method was used. A hyperbolic tangent function was introduced as a new calibration function to develop the whole crack growth resistance curve. The basic idea for the development of this calibration method came from the key curve method. Unlike the key curve method, the calibration curve method curve-fits for an assumed deformation path during the crack growth process using the normalization scheme of dimensional analysis. This calibration curve contains all the information needed to generate both the fracture toughness value at crack initiation and the crack growth resistance curve for a growing crack. Using those calibration curves at different displacement rate loadings, the time function was developed to relate the viscoelastic quantities in the physical viscoelastic domain to the reference quantities in the reference elastic domain. The reference hyperbolic tangent calibration function was determined in the reference elastic domain using the same time function. A viscoelastic fracture mechanics theory was introduced. Extensive research efforts on fracture characterization of high molecular weight polymers have led to the development of a unique time-independent, elastic-like fracture characterizing parameter, J(sup *)(sub V)-integral, useful in describing the fracture behavior of nonlinear viscoelastic materials like ABS copolymer and modified PVC. Dissert. Abstr.

N94-31764# Fermi National Accelerator Lab., Batavia, IL.
DESIGN OF NEW POLYMERS TO IMPROVE RADIATION STABILITY OF PLASTIC SCINTILLATORS
N. Barashkov (Karpov, V. Y. Physical Chemistry Inst., Moscow, USSR.), N. Korotkikh (Karpov, V. Y. Physical Chemistry Inst., Moscow, USSR.), T. Novikova (Karpov, V. Y. Physical Chemistry Inst., Moscow, USSR.), F. Markley, A. Pla-Dalmau, G. Foster, and M. Rivard Nov. 1993 12 p
(Contract DE-AC02-76CH-03000)
(DE94-008220; FNAL-TM-1868) Avail: CASI HC A03/MF A01

Diffusion enhancers have been used to increase the radiation stability of scintillators. There is a danger that such additions will also allow the scintillation dyes to diffuse out of the matrix. Covalent bonding of the dyes into the matrix would eliminate any luminophore migration. We have demonstrated that dyes with vinyl and divinyl groups can be successfully bonded into a styrene matrix. Both primary and secondary luminophores have been bonded into the matrix and in several cases they have been compared with similar luminophores without the vinyl groups in otherwise identical compositions. In general the bonding does not greatly affect either the radiation stability of the composition or its light output, but is, therefore, proven to be an acceptable method of preventing luminophore migration. Scintillators with a base of aromatic or alicyclic epoxy resins have also been made with bonded luminophores. In these compositions, the bonding is accomplished by using luminophores with one or two amine groups or epoxy groups. When using the amines, they are first prereacted with the epoxy resin and the modified epoxy is then cured with hexahydrophthalic anhydride or trimethoxyboroxine. The emission and absorption spectra of many of these reactive luminophores are given, along with the light outputs and radiation stability of the resulting scintillators. DOE

N94-31780# Oak Ridge National Lab., TN.
IN-SITU TEM CRYSTALLIZATION OF ANORTHITE-GLASS FILMS ON (ALPHA)-AI2O3
M. P. Mallamaci (Minnesota Univ., Minneapolis.), C. B. Carter (Minnesota Univ., Minneapolis.), and J. Bentley 1993 6 p Presented at the Fall Meeting of the Materials Research Society, Boston, MA, 29 Nov. - 3 Dec. 1993 Sponsored in part by Oak Ridge Associated Universities, Inc., TN, and Martin Marietta Energy Systems, Inc., Oak Ridge, TN
(Contracts DE-AC05-84OR-21400; DE-AC05-76OR-00033; DE-FG02-92ER-45465)
(DE94-006317; CONF-931108-60) Avail: CASI HC A02/MF A01

Anorthite-glass films were grown by pulsed-laser deposition on single-crystal (alpha)-Al2O3 substrates which were pre-thinned to electron transparency. The glass films were crystallized in the transmission electron microscope (TEM), which allowed direct observation and video-recording of

the crystallization process. Crystallization of these films in the TEM resulted in the formation of hexagonal and orthorhombic anorthite. The orthorhombic phase was the predominant product of glass films grown at elevated substrate temperatures and displayed strong epitaxy with the underlying substrate. In contrast, the hexagonal phase was the major constituent of films grown at ambient substrate temperature and displayed no clear epitaxy with the substrate. The difference in degree of epitaxy and phase structure may be evidence of ordering at the original glass/oxide interface. DOE

N94-31851*# Vanderbilt Univ., Nashville, TN. Dept. of Applied Science and Engineering.

ELASTIC MODULUS MEASUREMENTS OF LDEF GLASSES AND GLASS-CERAMICS USING A SPECKLE TECHNIQUE

D. E. Wiedlocher and D. L. Kinser 1992 7 p

(Contract NAS8-32695; NAG8-156; NASA Order L-17761-D)

(NASA-CR-195911; NAS 1.26:195911) Avail: CASI HC A02/MF A01

Elastic moduli of five glass types and the glass-ceramic Zerodur, exposed to a near-earth orbit environment on the Long Duration Exposure Facility (LDEF), were compared to that of unexposed samples. A double exposure speckle photography technique utilizing 633 nm laser light was used in the production of the speckle pattern. Subsequent illumination of a double exposed negative using the same wavelength radiation produces Young's fringes from which the in-plane displacements are measured. Stresses imposed by compressive loading produced measurable strains in the glasses and glass-ceramic. Author

N94-31917 Imagination Resources, Inc., Dublin, OH.

MEASUREMENT OF VISCOSITY, DENSITY, AND GAS SOLUBILITY OF REFRIGERANT BLENDS IN SELECTED SYNTHETIC LUBRICANTS

R. C. Cavestri Jan. 1994 76 p Limited Reproducibility: More than 20% of this document may be affected by microfiche quality

(Contract DE-FG02-91CE-23810)

(DE94-007723; DOE/CE-23810/33C) Avail: Issuing Activity (Department of Energy (DOE))

Liquid/liquid miscibilities of four different 32 ISO VG polyolesters and one alkylbenzene at three concentrations have been determined with five refrigerant blends, including HC-290. A vapor lubricant equilibrium (VLE) viscosity reduction of 32 ISO VG mineral oil with HCFC-22 has been completed. Composite viscosity reduction information by the fractionate components from R-502 in 32 ISO VG mineral oil has been obtained from -10 C to 125 C isotherms. Vapor lubricant equilibrium (VLE) viscosity reduction for 32 ISO VG mixed acid polyolester with HFC-134a and HFC-143a has also been completed. Data is also presented for the viscosity reduction of 32 ISO VG branched acid polyolester by these same refrigerants. DOE

N94-31935# Pennsylvania State Univ., University Park. Materials Research Lab.

PASSIVE VIBRATION DAMPING MATERIALS: PIEZOELECTRIC CERAMIC COMPOSITES FOR VIBRATION DAMPING APPLICATIONS Annual Report, 1 Feb. 1993 - 31 Jan. 1994

Shoko Yoshikawa Feb. 1994 35 p

(Contract N00014-92-J-1391)

(AD-A276550) Avail: CASI HC A03/MF A01

The study to produce ultra-fine (less than 50 micrometers in diameter) lead zirconate titanate (PZT) ceramic fibers for passive damping application has been carried out under several aspects. Sol-gel chemistry was undertaken to produce stable spinnable sol, as well as high quality PZT fibers. Due to the extreme geometry of such fibers, special characterization and poling methods were established. Single fiber dielectric properties, polarization hysteresis, and mechanical properties have been measured. Several methods for applying optimum resistive coatings were also explored. The analytical model of passively damped polymer composites using resistively shunted piezoelectric fiber was further developed to predict the behavior of such composites. DTIC

N94-31942 Cornell Univ., Ithaca, NY.

TOUGHENING MECHANISMS IN THE HIGH STRAIN RATE DEFORMATION OF RUBBER-MODIFIED POLYMER GLASSES Ph.D. Thesis

Donald Joseph Buckley, Jr. 1993 386 p

Avail: Univ. Microfilms Order No. DA9318838

The deformation mechanisms operating in rubber-modified polymer glasses have been studied using real time small angle x ray scattering (RTSAXS) and transmission electron microscopy (TEM). Three series each of high impact polystyrenes (HIPS) and acrylonitrile butadiene styrenes (ABS) were examined under tensile impact and tensile creep loading at strain rates in the regime 0.01 to 50 /s while RTSAXS, x ray mass thickness, and lateral strain measurements were made. The plastic strains due to crazing, shear deformation, and cavitation were obtained at time resolutions of 1.6 to 10 ms as functions of the weight-averaged matrix molecular weight (M(sub w)), rubber phase microstructure, and strain rate. The HIPS series examined the effect of rubber particle size, internal particle structure, and rubber phase volume fraction on the deformation processes. Particle size and structure produced marginal effects on the distribution of the total strain among the various mechanisms and the impact toughness, but the toughness increased with increasing rubber volume fraction and decreasing interparticle spacing. Coarsening of the craze microstructure at high rubber weight fractions and low strain rates was attributed to stress-activated sorption of low molecular weight polybutadiene (PB) from the particles. The effects of matrix molecular weight, rubber weight fraction, and rubber particle size were examined in the three ABS series. No systematic change in the deformation behavior was observed in the M(sub w) and particle size series, but the shear strain, cavitation strain, and toughness all scaled with increasing rubber weight fraction. As in the HIPS series the craze microstructure coarsened with increase rubber content. The increase in toughness with volume fraction in both HIPS and ABS was attributed to increased crazing, cavitation, and shear deformation (in the ABS materials) with decreasing width of the interparticle ligaments of the matrix. The kinetics of the deformation mechanisms, equality of the crazing and cavitation strains, and TEM studies support a model of planar deformation zones consisting of interconnected crazes and voids, separated by elastically deformed material. Dissert. Abstr.

N94-31945 Lehigh Univ., Bethlehem, PA.

HIGH-TEMPERATURE DEFORMATION AND FRACTURE TOUGHNESS OF DUPLEX CERAMIC MICROSTRUCTURES Ph.D. Thesis

Jonathan David French 1993 176 p

Avail: Univ. Microfilms Order No. DA9325939

High temperature deformation and fracture toughness behavior of duplex ceramic microstructures were examined in this study to achieve a general understanding of the flow and fracture of this type of material. Two model systems were studied: Al2O3: c-ZrO2(Y) and Al2O3:YAG. A dual experimental approach was employed to study the equivolumetric compositions in relation to their single-phase constituents. Creep and fracture toughness at high temperatures were studied using indentation and more traditional techniques. In addition, the indentation crack length method for determining fracture toughness of brittle materials was evaluated at high temperatures. In general, the duplex microstructure exhibits a 'rule-of-mixtures' behavior, i.e., properties in between those of the single-phase constituents, for properties that are governed by the continuum nature of the material, such as tensile creep properties. A 'non-rule-of-mixtures' type behavior occurs for properties that have significant contributions from the interphase boundaries, such as the high temperature fracture. The tensile creep rates of the duplex microstructures were lower than their single-phase constituents. This was attributed to Y(sup +3) segregation to alumina grain boundaries that hinders the interface reaction believed to control diffusional creep in alumina. Accounting for the dopant effect, the tensile creep behavior of the duplex microstructures could be modeled using simple composite theory, applied to flow of two-phase materials. Indentation creep of the duplex microstructures relative to the single-phase constituents was system and temperature specific; however, under certain conditions similar trends were observed. The duplex microstructure of both systems exhibited higher fracture toughness values than their single-phase constituents at high temperatures, likely due to lower interfacial energies relative to the grain boundary energies of the single-phases. The indentation method was shown to be applicable to the measurement of high temperature fracture toughness, with some limitations. The measurement of high temperature creep properties with the indentation technique tests a range of stress and strain rates inaccessible to bulk techniques. Therefore, since different mechanisms are operative in the two techniques, correlation is limited. However, useful information can be obtained from this method as to the deformation behavior under the extremes

of stress, strain rate, and temperature, which may be applicable to machining or geological processes. Dissert. Abstr.

N94-31956 Ohio State Univ., Columbus.
A FRACTURE MECHANICS METHODOLOGY FOR CHARACTERIZING THE PERFORMANCE OF FLAWED POLYMERIC DIELECTRIC MATERIALS Ph.D. Thesis
Scott Frederick Popelar 1993 113 p
Avail: Univ. Microfilms Order No. DA9325570

A fracture mechanics approach for quantifying slow crack growth in thin polyimide films and assessing their structural integrity and life expectancy is developed. The methodology and techniques presented in this document may also be applied to other polymeric materials. A test protocol for studying slow crack growth has been developed, along with an analysis model which deduces crack length histories from measured load-point displacements of single edge notched fracture specimens. From the crack length histories, the crack growth rate is correlated with the stress intensity factor. A series of room temperature tests were performed on the model materials 50HN, 100HN, 300H, and 500HN Kapton type polyimide film, and the corresponding crack growth rates were correlated with the stress intensity factor. A very strong dependence of the crack growth rate on the stress intensity factor is observed for all of the films. To a first approximation, the fracture process of these films can be taken to be governed by a critical value of the stress intensity factor. The fracture toughness of the films decreases with decreasing film thickness. A temperature-dependent shift factor was developed which consolidated creep compliance data at different temperatures into a single master curve at an arbitrary reference temperature. This same shift factor was used to shift crack growth rate and crack growth initiation time data gathered at elevated temperatures to a common reference temperature. Slow crack growth tests were performed on Kapton type 300H polyimide film at different combinations of temperature and relative humidity in order to investigate the influence of temperature and relative humidity on the fracture of Kapton film. The slow crack growth resistance was found to decrease with increasing temperature and humidity. The value of the initiation stress intensity factor decreased linearly with increasing humidity at the same temperature. It was found that temperature only influences the dry initiation stress intensity factor. Crack growth rate correlations were shifted to a reference temperature and relative humidity using a generalized form of the WLF equation. Dissert. Abstr.

N94-31976# Houston Univ., TX.
CHEMICAL VAPOR DEPOSITION OF METAL NITRIDES, PHOSPHIDES, AND ARSENIDES
D. M. Hoffman 1994 2 p Prepared for Los Alamos National Lab., NM
(Contract W-7405-eng-36)
(DE94-008096; LA-Sub-94-41) Avail: CASI HC A01/MF A01

The author recently reported that dialkylamido complexes are promising precursors to nitride thin films. On this basis it was reasoned that transition metal and main group disilazide complexes in which the silicon has dialkylamido substituents are potential precursors to ternary silicon nitride films. Bulky disilazide ligands are known to stabilize main group and transition metal complexes with low coordination numbers. Reaction of dimethylamine with Cl3SiN(H)SiMe3 in hexane solution at 25 C gave the bulky disilazane ((Me2N)(sub 3)Si)N(H)SiMe3 (1) in 73 percent yield. Reaction of (1) with n-butyl lithium in benzene at 0 C produced ((Me2N)(sub 3)Si)N(Li)SiMe3 in 82 percent yield. LiN(Si(NMe2)(sub 3))(sub 2) was chemically prepared in 92 percent yield and was converted to the amine with 83 percent yield. The author examined the use of amido precursors for main group oxide thin films. Sn(NMe2)(sub 4) and Si(NMe2)(sub 4) react with oxygen in an atmospheric pressure chemical vapor deposition reactor to give SnO2 and SiO2 films, respectively. The films were deposited on quartz, silicon, and glass at substrate temperatures of 250 to 400 C. The results of the characterizations of the films and compounds are presented in this report. DOE

N94-31978 Queens Univ., Kingston (Ontario). Dept. of Chemistry.
AZO POLYMERS FOR REVERSIBLE OPTICAL STORAGE. 4. COOPERATIVE MOTION OF RIGID GROUPS IN SEMICRYSTALLINE POLYMERS
A. Natansohn, P. Rochon, M. Pezolet, P. Audet, and D. Brown 1 Mar. 1994 27 p Limited Reproducibility: More than 20% of this document may be affected by microfiche quality
(Contract N00014-93-1-0615)
(AD-A277107; TR-13) Avail: Issuing Activity (Defense Technical Information Center (DTIC))

Polarized light induces a preferred orientation of azobenzene groups through photochemical trans-cis-trans processes. Stronger orientation tendencies exist if the azo-containing polymers are crystalline or liquid crystalline and the cooperative reorientation of nonactive mesogens of similar shape has been demonstrated. This paper shows that cooperative reorientation is a more general phenomenon and can take place even for a nonactive rigid group of a different shape which is bonded in the main chain while the azobenzene groups are in the side chains. Comparison is made between a disperse red containing amorphous azo polymer (pDR1A) and a disperse red 19 - containing semicrystalline azo polymer (pDR19T) with phenylene diacrylate (PD) groups within the main chain. Dichroic ratios are obtained from infrared and electronic spectra and are correlated with a writing / erasing / rewriting sequence performed with an argon laser. A maximum birefringence of 0.08 can be obtained on pDR1A, while on pDR19T the birefringence is 0.27 in similar conditions. This is the result of a combination of the semicrystallinity of pDR19T and of the cooperative orientation of PD groups along with the azobenzene groups. The drawback in terms of optical storage is the longer time required to write or erase. DTIC

N94-31979 Queens Univ., Kingston (Ontario). Dept. of Chemistry.
RECENT DEVELOPMENTS IN POLYMERIC CHARGE TRANSFER COMPLEXES
A. Natansohn 1 Mar. 1994 14 p Limited Reproducibility: More than 20% of this document may be affected by microfiche quality
(Contract N00014-93-1-0615)
(AD-A277108; TR-12) Avail: Issuing Activity (Defense Technical Information Center (DTIC))

The recent literature on polymeric charge transfer complexes is reviewed with emphasis on the author's own work. After a definition of the area and a survey of investigations on the spatial arrangement of donor and acceptor sites in the solid state, a variety of applications of these complexes is presented. Electrically conductive polymers are excluded. These applications are: compatibilization of polymer blends, liquid crystalline supramolecular organization, new developments in photoconductivity, electroluminescence, nonlinear optical properties, photorefractivity, and reversible optical storage. DTIC

N94-31980 Queens Univ., Kingston (Ontario). Dept. of Chemistry.
REVERSIBLE OPTICAL STORAGE IN AZO POLYMERS
A. Natansohn and P. Rochon 1 Mar. 1994 12 p Limited Reproducibility: More than 20% of this document may be affected by microfiche quality
(Contract N00014-93-1-0615)
(AD-A277109; TR-9) Avail: Issuing Activity (Defense Technical Information Center (DTIC))

Amorphous high-Tg azobenzene containing polymers can be used as reversible information storage materials in the form of films. The procedure takes advantage of the photochemically activated trans-cis-trans isomerization of the azobenzene groups. The written information is stable below the polymer glass transition temperature. Writing and erasing can be performed up to 105 times on the same spot of the polymer film. The reorientation mechanism depends on the type of substituents bound to the azobenzene group, on the type of the neighboring group on the polymer chain, and on the tendency of the polymer to self-organize. The efficiency of the process depends on the maximum absorbance of the azobenzene group and can be tailored to reach unity. This property of azobenzene containing polymers can be used in optical and holographic memory, waveguides and sensors, and photonic devices. DTIC

N94-31981 Bowling Green State Univ., OH. Center for Photochemical Sciences.
PHOTOPOLYMERIZATION OF CYCLOHEXENE OXIDE: A VISIBLE LIGHT INITIATING SYSTEM AND MECHANISTIC INVESTIGATIONS
Yubai Bi and D. C. Neckers Feb. 1994 10 p Limited Reproducibility: More than 20% of this document may be affected by microfiche quality
(Contract N00014-91-J-1921)
(AD-A277110; TR-6) Avail: Issuing Activity (Defense Technical Information Center (DTIC))

A visible light initiator system for the photoinduced cationic polymerization of epoxides is reported. It uses free radical promoted cationic polymerization, the radical being generated from a visible light absorber. The developed system consists of an iodinated xanthene dye, a coinitiator and a diaryliodonium salt. Aromatic amines having low basicity and containing alpha-hydrogens are the preferred coinitiators for the polymerization of cyclohexene oxide. The system can efficiently photoinitiate the polymerization of certain cyclic ethers and can function at any wavelength of the visible spectrum depending on the dye's absorption spectrum and its oxidation/reduction potentials. Studies on photochemical reactions between each two of the three components and characterization of the polymer formed from cyclohexene oxide indicate that both the oxidative bleaching of the dye by the diaryliodonium salt and the reductive bleaching of the dye by the aromatic amine contribute to alpha amino radical formation and oxidation of the alpha amino radicals by diaryliodonium salts produces alpha-aminocarbocations which initiate the ring opening polymerization. Dye molecules are incorporated into the polymer in chain terminating processes. DTIC

N94-31982 Bowling Green State Univ., OH. Center for Photochemical Sciences.

MECHANICAL PROPERTIES OF ACRYLATE NETWORKS FORMED BY VISIBLE LASER-INDUCED POLYMERIZATION. 2. CONTROL OF THE MECHANICAL PROPERTIES

Afranio Torres-Filho and D. C. Neckers Feb. 1994 17 p Limited Reproducibility: More than 20% of this document may be affected by microfiche quality

(Contract N00014-91-J-1921)

(AD-A277111; TR-5) Avail: Issuing Activity (Defense Technical Information Center (DTIC))

The mechanical properties of some acrylate networks formed by visible laser-induced polymerization were studied as a function of the initial molecular composition of the reacting mixture. The study included, besides some changes in the monomer composition, the influence of the acidity of the medium when ionizable dyes were used as photoinitiators. It was also shown that the mechanical strength of the network polymers can be significantly improved by the addition of inorganic fillers which have been surface treated with silane coupling agents containing polymerizable groups, or by adding to the multifunctional acrylate monomers a solution containing a stronger preformed polymer. The work also describes different attempts to obtain an elastomeric material by copolymerizing a flexible acrylated oligomer with the networking monomers. DTIC

N94-32005# Missouri Univ., Rolla. Dept. of Chemistry.

SOLVENT DIFFUSION COEFFICIENT CONCENTRATION DEPENDENCE IN POLYMER SOLUTIONS Technical Report, 1 Apr. 1993 - 15 Feb. 1994

R. A. Waggoner, Frank D. Blum, and J. M. MacElroy 15 Feb. 1994 36 p

(Contract N00014-91-J-1274)

(AD-A277023; UMR-FDB-33) Avail: CASI HC A03/MF A01

Self-diffusion coefficients of several different solvents in polystyrene as well as methyl methacrylate in poly(methyl methacrylate) have been determined at polymer concentrations from 0 to 50 wt% at 25 deg C. The solvents used for the polystyrene solutions were toluene, ethylbenzene, cumene, t-butyl acetate, chloroform, and methyl ethyl ketone. The diffusion data was used to evaluate several theories for the concentration dependence of the solvent diffusion coefficients, and in most cases the reduced diffusion coefficients, of solvents in polymer-solvent systems. In addition to the experimental data presented here, literature data for several systems were also used to test the models. The theories evaluated were based on widely different concepts including electrical conductivity, tortuosity, kinetic theory, and free-volume. The results indicate that the kinetic theory and free-volume approaches fit the data most consistently, with the kinetic theory approach preferred at lower polymer concentrations and the free-volume approach favored at higher polymer concentrations. DTIC

N94-32016# Katholieke Univ. te Leuven (Belgium).

THE SIXTH SYMPOSIUM ON UNCONVENTIONAL PHOTOACTIVE SOLIDS. ABSTRACTS

19 Aug. 1993 188 p Symposium held in Leuven, Belgium, 15-19 Aug. 1993

(Contract DAJA45-93-M-0440)

(AD-A277198; R/D-7211-CH-02) Avail: CASI HC A09/MF A02

This volume contains the abstracts, reproduced as submitted by the authors, of the scientific contributions that will be presented at the Symposium as plenary lecture, short invited lecture, oral presentations or as poster presentations. In an effort each of you to read or discuss as many posters of different subfields as possible, the abstracts were arranged in a nontopical order but placed in alphabetical order based on the name of the participant presenting the poster. DTIC

N94-32017 North Carolina Univ., Chapel Hill. Dept. of Chemistry.

ISOMERIC POLY(BENZOPHENONE)S: SYNTHESIS OF HIGHLY CRYSTALLINE POLY (4, 4 FOOT-BENZOPHENONE) AND AMORPHOUS POLY (2, 5-BENZOPHENONE), A SOLUBLE POLY (P-PHENYLENE) DERIVATIVE

R. W. Phillips, V. V. Sheares, E. T. Samulski, and J. M. DeSimone 15 Mar. 1994 14 p Limited Reproducibility: More than 20% of this document may be affected by microfiche quality

(Contract N00014-92-J-1374)

(AD-A277261; TR-14) Avail: CASI HC A03

Nickel-catalyzed polymerization which employs the coupling of isomeric dichlorobenzophenones is described. The polymerization utilizes inexpensive readily available monomers, 4,4'-dichlorobenzophenone (4,4'-DCBP), and 2,5-dichlorobenzophenone (2,5-DCBP). The poly(4,4'-benzophenone) can be derivatized to be soluble during the synthesis by the use of a ketimine precursor that is subsequently hydrolyzed to give the target material. The polymerization of 2,5-dichlorobenzophenone yields a soluble derivative of poly(p-phenylene). The resulting polymers were characterized to confirm the composition, molar mass, and thermal properties. The Ni(O) catalyzed route proves to be facile and economically feasible and opens the way to a large variety of heterocyclic and phenyl-based homo- and copolymers. DTIC

N94-32069 Bowling Green State Univ., OH. Center for Photochemical Sciences.

A VISIBLE LIGHT INITIATING SYSTEM FOR FREE RADICAL PROMOTED CATIONIC POLYMERIZATION

Yubai Bi and D. C. Neckers 2 Feb. 1994 53 p Limited Reproducibility: More than 20% of this document may be affected by microfiche quality

(Contract N00014-91-J-1921)

(AD-A277164; TR-3-ONR) Avail: CASI HC A04

A new visible light free radical promoted cation in chain polymerization is reported. The system is based on electron transfer photoreduction of xanthene dye triplets by aromatic amines possessing a hydrogen on the alpha carbon atom to the nitrogen. Subsequent deprotonation of the amine radical cation followed by onium salt oxidation leads to formation of an alpha-amino carbenium ion and the latter initiates polymerization. Critical to the success of the system are the basicity of the amine, the oxidation potential of the onium salt, and the presence or absence of nucleophilic centers in the monomer to be polymerized. The scope and details of the system are discussed in the publication. DTIC

N94-32102# Sandia National Labs., Albuquerque, NM.

TEMPERATURE DEPENDENCE OF THE EXCITON-EXCITON ANNIHILATION RATE CONSTANT IN POLY(DI-N-HEXYLSILANE)

R. G. Kepler and Z. G. Soos 1993 4 p Presented at the Fall Meeting of the Materials Research Society (MRS), Boston, MA, 29 Nov. - 3 Dec. 1993

(Contract DE-AC04-94AL-85000)

(DE94-005584; SAND-94-0056C; CONF-931108-55) Avail: CASI HC A01/MF A01

Fluorescence depolarization studies of polysilane chains in solution have shown that energy transfer along the polymer chains occurs for only a very short time relative to the excited state lifetime and only over short distances before the excited states become trapped in long, low-energy segments. However, in solid films the authors have shown in previous work that excitons are highly mobile throughout their 600 ps lifetime at room temperature, presumably because energy transfer among neighboring, parallel chain segments becomes possible. In this paper the authors report that the exciton-exciton annihilation rate constant decreases by only a

factor of five between room temperature and 12 K, showing that the excitons do not become trapped even at low temperatures. DOE

N94-32103# Los Alamos National Lab., NM.
ION-IRRADIATION-INDUCED DENSIFICATION OF ZIRCONIA SOL-GEL THIN FILMS
T. E. Levine (Cornell Univ., Ithaca, NY.), E. P. Giannelis (Cornell Univ., Ithaca, NY.), P. Kodali, J. Tesmer, M. Nastasi, and J. W. Mayer 1994 6 p Presented at the Fall Meeting of the Materials Research Society (MRS), Boston, MA, 29 Nov. - 3 Dec. 1993
(Contract W-7405-eng-36)
(DE94-006248; LA-UR-94-310; CONF-931108-87) Avail: CASI HC A02/MF A01

We have investigated the densification behavior of sol-gel zirconia films resulting from ion irradiation. Three sets of films were implanted with neon, krypton, or xenon. The ion energies were chosen to yield approximately constant energy loss through the film, and the doses were chosen to yield similar nuclear energy deposition. Ion irradiation of the sol-gel films resulted in carbon and hydrogen loss as indicated by Rutherford backscattering spectrometry and forward recoil energy spectroscopy. Although the densification was hypothesized to result from target atom displacement, the observed densification exhibits a stronger dependence on electronic energy deposition. DOE

N94-32116 Lawrence Livermore National Lab., CA.
SURFACE CHEMISTRY AND DURABILITY OF BOROSILICATE GLASS
S. A. Carroll, W. L. Bourcier, and B. L. Phillips Jan. 1994 10 p Presented at the Fall Meeting of the Materials Research Society (MRS), Boston, MA, 29 Nov. - 3 Dec. 1993 Limited Reproducibility: More than 20% of this document may be affected by microfiche quality
(Contract W-7405-eng-48)
(DE94-006734; UCRL-JC-116104; CONF-931108-80) Avail: CASI HC A02

Important glass-water interactions are poorly understood for borosilicate glass radioactive waste forms. Preliminary results show that glass durability is dependent on reactions occurring at the glass-solution interface. CSG glass (18.2 wt. % Na2O, 5.97 wt. % CaO, 11.68 wt. % Al2O3, 8.43 wt. % B2O3, and 55.73 wt. % SiO2 dissolution and net surface H(sup +) and OH(sup (minus)) adsorption are minimal at near neutral pH. In the acid and alkaline pH regions, CSG glass dissolution rates are proportional to H(+) (sub adsorbed)(sup 2) and OH(-)(sub adsorbed)(sup 0.8), respectively. In contrast, silica gel dissolution and net H(+) and OH(-) adsorption are minimal and independent of pH in acid to neutral solutions. In the alkaline pH region, silica gel dissolution is proportional to OH(-)(sub adsorbed)(sup 0.9)(sub adsorbed). Although Na adsorption is significant for CSG glass and silica gel in the alkaline pH regions, it is not clear if it enhances dissolution, or is an artifact of depolymerization of the framework bonds. DOE

N94-32184# Army Belvoir Research and Development Center, Fort Belvoir, VA.
STATUS OF DEVELOPING A MULTIFUNCTIONAL AVIATION GREASE Final Report
In-Sik Rhee Jan. 1994 29 p
(AD-A276755; BRDEC-2546) Avail: CASI HC A03/MF A01

A program has been initiated to develop a new multifunctional helicopter grease. The purpose for the development of this new grease is to provide a product having significantly improved performance, reduce the overall logistics and supply burdens, reduce procurement costs, and control the continuing increase in proliferation of proprietary non-standard products. The effort during FY-91 - FY-92 was devoted to determine the preliminary target requirements and to formulate the experimental grease. In these efforts, the preliminary target requirements were developed based on what is believed to be achievable with current technology versus projected system requirements. Based on these preliminary target requirements, the experimental greases were formulated using an advanced lithium complex technology as thickener and a mix polyalphaolefin (PAO) synthetic base oil, a small amount of high viscosity mineral oils, and various additives. On the basis of the work completed to date, the experimental greases were very close to meeting the preliminary target requirements and are promising as the candidate aviation greases. DTIC

N94-32221# Missouri Univ., Rolla. Dept. of Chemistry.
NMR STUDIES OF ORGANIC THIN FILMS Annual Report, 1 Jan. 1993 - 28 Feb. 1994
Frank D. Blum 28 Feb. 1994 73 p
(Contract N00014-91-J-1274)
(AD-A276953; UMR-FDB-34) Avail: CASI HC A04/MF A01

A review of the literature on NMR studies of thin organic films is given with 212 references. Special focus is given to the following: (1) polymers at interfaces including: solid-liquid, elastomer-solid, solid-gas, and solid-solid systems; and (2) surface active phases which were bonded and non-bonded. DTIC

N94-32239# California Univ., Los Angeles.
THE 14TH ANNUAL WEST COAST THEORETICAL CHEMISTRY/STATISTICAL MECHANICS CONFERENCE
19 Jun. 1993 136 p Conference held in Los Angeles, CA, 17-19 Jun. 1993
(AD-A276942) Avail: CASI HC A07/MF A02

The agenda and abstracts are presented for the 14th Annual West Coast Theoretical Chemistry/Statistical Mechanics Conference. Abstracts include, but are not limited to, the following: Molecular Dynamics form First Principles - Metals, Colloids, Ionic Melts; Potential Function for Polyfluorinated Ethers; Surface Tension and Atomic Interactions in Simple Liquids: Argon, Krypton and Xenon; Molecular Dynamics Computer Simulations of Water and Aqueous Solutions using a Polarizable Water Model; Ab-initio Studies of Water Clusters; Theoretical Studies of Boron Compounds; Parallelization of Correlation Function Quantum Monte Carlo; Collisional Energy Transfer in Bimolecular Ion-Molecule Dynamics; Resonances in the CH+N2 Reaction; Modeling and Analysis of Electric Double Layers; and Calculation of Scanning Tunneling Microscopy Image of an Adsorbate: Application to Adenine Adsorbed on a Graphite Surface. CASI

N94-32246# HCC Science and Technology Co., Summit, NJ.
MULTIFUNCTIONAL MACROMOLECULES Final Report, 1 Jul. 1991 - 31 Jul. 1993
A. J. East, M. J. Sansone, and T. Findakly Oct. 1993 174 p
(Contract F49620-91-C-0062)
(AD-A277347; AFOSR-94-0082TR) Avail: CASI HC A08/MF A02

While numerous photorefractive polymers were synthesized by the incorporation of NLO chromophores and photoconductive components as side chains on a backbone, the most significant photorefractive behavior demonstration under this project was made in an electrooptic aminonitrostilbene methacrylate copolymer (P2ANS/MMA) without the addition of photoconductive compounds. By four wave mixing, photorefractive gratings were written in P2ANS/MMA using s-polarized and p-polarized writing beams and probed using orthogonally polarized probe beams. With probe beam orthogonally polarized to the write beams, well behaved, field dependent, stable responses ascribed to the photorefractive effect were observed. Diffraction efficiencies of 10(exp -4) to 10(exp -5) were obtained in 8 micrometer thick films under an applied field of 50 V/micrometer with response times of 1.5 to 2 minutes. Increasing the sample thickness to 100 micrometers is projected to result in a diffraction efficiency of 1 to 3 percent. DTIC

N94-32253 Edgewood Arsenal, Aberdeen Proving Ground, MD. Research Development and Engineering Center.
INFLUENCE OF TRACE COMPONENTS ON THE VISCOELASTIC PROPERTIES OF A POLYMER SOLUTION Final Report, Oct. 1986 - Feb. 1989
Seok H. Hong and Wendel J. Shuely Aug. 1993 35 p Limited Reproducibility: More than 20% of this document may be affected by microfiche quality
(AD-A277171; ERDEC-TR-086) Avail: CASI HC A03

Research on characterization of viscoelastic properties of ultrahigh molecular weight polymer solutions led to the discovery of variations in rheological properties combined with variable dissolution behavior for certain polymer-liquid systems. The reference solutions exhibited extreme intra sample variations; therefore, the influence of processing and trace impurities on rheological property variance was studied. Measurements of first normal stress difference, apparent viscosity, and dynamic viscoelastic properties were performed as a function of controlled addition of components with

specific molecular interactions with polymers or solvents (e.g., various salts, surfactant, and chelating reagents). In addition, processing treatments such as filtration and centrifugation were applied and their influence on rheological properties of the polymer solution was determined. DTIC

N94-32358# Argonne National Lab., IL.
CHARACTERIZATION OF INTERFACE STRUCTURE IN MULTILAYERS USING SPECULAR X RAY REFLECTANCE
E. E. Fullerton Jan. 1994 5 p Presented at the 2nd Topical Meeting on Physics of X Ray Multilayer Structures, Jackson Hole, WY, 13-17 Mar. 1994
(Contract W-31-109-eng-38)
(DE94-007698; ANL/MSD/CP-82073; CONF-940379-1) Avail: CASI HC A01/MF A01

This paper discusses the quantitative analysis of specular reflectivity from a series of Nb/Si multilayers sputtered at various Ar pressures. Interfacial reactions and changes in cumulative roughness with Ar pressure can be quantitatively determined, in agreement with TEM. DOE

N94-32364# Missouri Univ., Rolla. Dept. of Chemistry.
DYNAMICS OF BLOCK POLY(STYRENE-CO-VINYLPYRIDINE) (SVP) IN SOLUTION AND ON SILICA
Frank D. Blum, M. Xie, B. R. Sinha, and F. C. Schwab 1 Mar. 1994 4 p
(Contract N00014-91-J-1274)
(AD-A277139; UMR-FDB-35) Avail: CASI HC A01/MF A01

Deuterium NMR relaxation measurements have been used to probe the dynamics of specifically labelled poly(styrene-co-vinyl pyridine) in solution and on silica. Of particular interest in this study was the comparison of the dynamics of the adsorbed polymers on silica with those of the block copolymer and homopolymer in solution. We found that in toluene, the styrene segments on the surface-bound polymer had enhanced mobility over that in toluene solution. This enhanced mobility does not extend to the other solvent systems tested (CCl4 and CCl4/CH3OH). For the latter systems, the styrene mobility on the surface bound-polymer was lower than those of the corresponding solutions, as expected. Thus, we conclude that this enhanced mobility probably occurs only in the presence of thermodynamically good solvents for styrene. A comparison of lower molecular weight (10 kg/mol) block copolymer and styrene homopolymer were also made in toluene. These results were interpreted through the use of the Hall-Helfand model for chain dynamics as indicating limited aggregation of the block copolymer in solution. DTIC

N94-32365# Queens Univ., Kingston (Ontario). Dept. of Chemistry.
COMPATIBILITY STUDIES OF SOME AZO POLYMER BLENDS
Shuang Xie, Almeria Natansohn, and Paul Rochon 1 Mar. 1994 6 p
(AD-A277141; TR-10) Avail: CASI HC A02/MF A01

Azo polymers have many special properties. In the search for new materials for optical applications, such as reversible optical storage and nonlinear optical devices, azo polymers have attracted much attention. Polymers with low azo concentrations are particularly useful. The writing and erasing efficiency depends on the energy input from the irradiation light during the process. In principle, lower energies would be required to induce local variations of optical properties in polymers with low azo concentrations. DTIC

N94-32367# Army Research Lab., Adelphi, MD.
PROCESSING AND CHARACTERIZATION OF FUNCTIONALLY GRADIENT CERAMIC MATERIALS Final Report
M. E. ODay, L. C. Sengupta, E. Ngo, S. Stowell, and R. Lancto Feb. 1994 19 p
(AD-A277154; ARL-TR-337) Avail: CASI HC A03/MF A01

Tape casting of ceramic materials offers the flexibility of gradually altering the electronic or structural properties of two dissimilar systems in order to improve their compatibility. This research outlines the processing and fabrication of two systems-of functionally gradient materials. The systems are both electronic ceramic composites consisting Ba(1-x)Sr(x)TiO3 (BSTO) and alumina or a second oxide additive. These composites would be used in phased array antenna systems, therefore, the electronic properties of the material have specific requirements in the microwave frequency regions. The composition of the tapes are varied to provide a graded dielectric constant, which gradually increases from that of air (dielectric constant = 1) to that of the ceramic (dielectric constant = 1500). This allows maximum penetration of incident microwave radiation as well as minimum energy dissipation and insertion loss into the entire phase shifting device. DTIC

N94-32377# Ames Lab., IA.
THE INTRAMOLECULAR CYCLIZATION OF BIS-2,5-DIMETHYLENE-2,5-DIHYDROFURANS AND BIS-2,5-DIMETHYLENE-2,5-DIHYDROTHIOPHENES: AN APPROACH TO MACROCYCLES Ph.D. Thesis
D. A. Klumpp 11 Jan. 1994 207 p
(Contract W-7405-eng-82)
(DE94-007060; IS-T-1627) Avail: CASI HC A10/MF A03

The first two papers of this dissertation present our work with the intramolecular cyclizations of a pair of p-quinodimethanes. The p-quinodimethanes were generated by flash vacuum pyrolysis (FVP) and were linked by a bridging chain. The third paper of this dissertation presents our work in the synthetic manipulation of the products formed from the intramolecular reactions of the p-quinodimethanes. DOE

N94-32381# Bowling Green State Univ., OH. Center for Photochemical Sciences.
INTRAMOLECULAR CHARGE TRANSFER COMPLEXES AS FLUORESCENCE PROBES FOR UV AND VISIBLE LIGHT INDUCED ACRYLATE POLYMERIZATION
Jiancheng Song, Afranio Torres-Filho, and D. C. Neckers Feb. 1994 8 p
(Contract N00014-91-J-1921)
(AD-A277129; TR-4) Avail: CASI HC A02/MF A01

Intramolecular charge transfer complexes (ICTC) of derivatives of DANSYL AMIDE such as 1,5-DASB and 2,5-DASB, were used as fluorescence probes for cure monitoring of photocurable polymer systems. This technique is based upon the difference in fluorescence intensity from the parallel and perpendicular conformations of the excited state of the complex and is based on the dependence of the relative population of each conformation on the microviscosity of the system. As the curing reaction proceeds, the steady state fluorescence emission spectra of the probes were all found to exhibit hypsochromic spectral shifts due to the increase in matrix microviscosity. A linear correlation between the fluorescence intensity ratios and the extent of polymerization, measured by transmission FTIR spectrometry, was obtained for different types of acrylated polymers, cured with UV or visible (VIS) initiators. DTIC

N94-32391# California Univ., Santa Barbara. Dept. of Materials.
EFFECT OF SURFACE FORCES ON THE RHEOLOGY OF PARTICLE-LIQUID SYSTEMS AND THE CONSOLIDATION OF CERAMIC POWDERS Annual Report, 1 Feb. 1993 - 31 Jan. 1994
Fred F. Lange 31 Jan. 1994 81 p
(Contract N00014-90-J-1441)
(AD-A277092; TR-8; TR-9; TR-10; TR-11; TR-12) Avail: CASI HC A05/MF A01

More reliable ceramics require improved processing reliability. Heterogeneities bought with powders and those inadvertently introduced during processing as well as non-uniform and undefined phase distributions contribute to unreliable processing. Colloidal powder treatments can eliminate many heterogeneities and ensure more uniform phase distributions. To ensure that new heterogeneities are not introduced, colloidally treated powders must be piped, as slurries, directly to a die cavity. Slurry consolidation methods based on particle partitioning, e.g., pressure filtration and centrifugation are emphasized in this review. Interparticle potentials play a dominant role in governing the slurry viscosity, maximum particle packing density, and the rheology of the consolidate body. These roles will be reviewed with the objective to understand how damage free bodies can be consolidate from slurries to increase the structural reliability of ceramics and their composites. DTIC

N94-32404 New Mexico Univ., Albuquerque.
PRESSURELESS SINTERING OF CERAMIC COMPOSITES Final Report
Martin W. Weiser 17 Jan. 1994 63 p Limited Reproducibility: More than 20% of this document may be affected by microfiche quality
(Grant AF-AFOSR-0265-90)
(AD-A277274; AFOSR-94-0056TR) Avail: CASI HC A04

This project examined the pressureless sintering and densification

behavior of model ceramic composites. The effect of inclusion aspect ratio on densification was studied using SiC whiskers and fibers in an Al2O3 matrix. Composites had maximum sintered density when made from fibers with aspect ratios around ten. This peak in the density is a result of the density of short aspect composites being inhibited by inclusion size considerations while long aspect composites are prevented from densifying by percolation related effects. How inhomogeneous inclusion distribution affects densification was studied using SiC(sub p)/Al2O3 composites. Three different types of inhomogeneity known as concentration, amplitude, and size were investigated. The sintered density was maximized at moderate levels of inclusion inhomogeneity. We also found that various salts were effective coagulating agents for slip casting Al2O3/ZrO2 composites. The drying of composites found that percolation limits the green density of particulate composites. The fracture toughness of Mn-Zn ferrites was increased from 0.9 to 2.8 MPa square root of m by addition of 25 volume percent partially stabilized ZrO2. Transient liquid phase sintering of composites is not an effective densification method. DTIC

N94-32408# Lehigh Univ., Bethlehem, PA. Energy Research Center.
ROBOTIC WELD OVERLAY COATINGS FOR EROSION CONTROL
B. F. Levin, J. N. DuPont, and A. R. Marder 20 Oct. 1993 57 p
(Contract DE-FG22-92PC-92542)
(DE94-008004; DOE/PC-92542/T4) Avail: CASI HC A04/MF A01

In the previous period of work, twelve overlay hardfacing alloys were selected for erosion testing based upon a literature review. All twelve coatings were deposited on 1018 steel substrates using the plasma arc welding process. Ten samples from each coating were prepared for erosion testing. The coating deposition and sample preparation procedures were described in the previous quarterly report. During the past quarter, all the coatings were erosion tested at 400 C. The erosion resistance of each coating was evaluated by determining the steady state erosion rate. In addition, the microstructure of each coating was characterized before and after the erosion tests. This progress report describes the erosion test results and coating microstructures. Also, a preliminary analysis on the relationships, between weld overlay coating hardness, microstructure, and erosion resistance will be discussed. DOE

N94-32490 Pittsburgh Univ., PA.
LUBRICATION WITH BINARY MIXTURES: LIQUID-LIQUID EMULSION IN ELASTOHYDRODYNAMICS AND METAL FORMING Ph.D. Thesis
Songhao Wang 1992 155 p
Avail: Univ. Microfilms Order No. DA9318009

In this work we first investigate the lubrication of an EHD conjunction with binary mixtures of mineral oil and water, for small droplet size of the dispersed phase. Our emulsified lubricant is a homogeneous isotropic continuum of two components, and we employ the extended Reynolds equations of Al-Sharif et al. We find that the film thickness varies linearly with the logarithm of the droplet radius and also with the inlet volume fraction. Interestingly, with inlet volume fraction as low as 10 percent, oil pooling can occur, which agrees qualitatively with experimental observations. Second, based on the present Plasto-Hydrodynamic model of cold rolling lubrication, we examine the characteristics of lubrication with emulsion in this condition. We are able to predict several experimentally observed phenomena, e.g. an increase in the yield stress of the workpiece leads to increased volume fraction, i.e., enhanced pooling ahead of the conjunction. The effect of varying the parameters of the problem on pressure, film thickness, and volume fraction distributions are also discussed. Finally, for metal rolling lubrication, the influence of the elastic deformation at inlet zone is considered. The elasto-plastohydrodynamic lubrication model leads to more reasonable result than the plasto-hydrodynamic model.
Dissert. Abstr.

N94-32517# EG and G Energy Measurements, Inc., Idaho Falls.
JOINING OF SILICON NITRIDES USING OXYNITRIDE GLASSES
M. H. OBrien Mar. 1993 40 p
(Contract DE-AC07-76ID-01570)
(DE94-008517; EGG-SCM-10713) Avail: CASI HC A03/MF A01

This report presents a study on commercial silicon nitrides that were successfully joined using oxynitride glasses. Sintered silicon nitride was joined by either closed or glass-filled joints. Glass-filled joints were successfully used on hot-pressed silicon nitrides and were comparable in fast fracture strength to unjoined silicon nitrides up to approximately 1000C. Above that temperature, strengths decreased rapidly and glass flow failure began. The study observed that time-dependent failure currently limits the service temperatures of glass-filled joints. Creep failure occurred in excess of 1000C. Between 900 and 1000C, slow crack growth failure was observed. Cavitation (or viscous deformation) was the rate-controlling mechanism of slow crack growth. DOE

N94-32518# Akron Univ., OH.
COMPATIBILITY OF REFRIGERANTS AND LUBRICANTS WITH ELASTOMERS
G. R. Hamed, R. H. Seiple, and Orawan Taikum Jan. 1994 529 p
(Contract DE-FG02-91CE-23810)
(DE94-008552; DOE/CE-23810/14) Avail: CASI HC A23/MF A04

The information contained in this report is designed to assist the air-conditioning and refrigeration industry in the selection of suitable elastomeric gasket and seal materials that will prove useful in various refrigerant and refrigeration lubricant environments. In part 1 of the program the swell behavior in the test fluids has been determined using weight and in situ diameter measurements for the refrigerants and weight, diameter and thickness measurements for the lubricants. Weight and diameter measurements are repeated after 2 and 24 hours for samples removed from the refrigerant test fluids and 24 hours after removal from the lubricants. Part 2 of the testing program includes the evaluation of tensile strength, hardness, weight, and dimensional changes after immersion aging in refrigerant/lubricant mixtures of selected elastomer formulations at elevated temperature and pressure. DOE

N94-32578 Massachusetts Univ., Lowell. Dept. of Chemistry.
NEW DEVELOPMENTS IN SECOND-ORDER NONLINEAR OPTICAL POLYMERIC MATERIALS Technical Report, 1 Jun. 1993 - 31 May 1994
S. K. Tripathy, W. K. Kim, B. Bihari, D. W. Cheong, and J. Kumar 17 Mar. 1994 12 p Limited Reproducibility: More than 20% of this document may be affected by microfiche quality
(Contract N00014-90-J-1148)
(AD-A277409; TR-94-11) Avail: CASI HC A03

Second harmonic generation (SHG) from the spin coated films of an asymmetrically substituted polydiacetylene, namely poly((8-butoxy cardonyl) methyl urethanyl) 1-(5-pyrimidyl)- octa-1,3- diyne (BPOD), is reported. The macromolecules assemble to produce the organization responsible for SHG without recourse to poling. d33 of the spin coated film (0.19 to 0.31 micrometers thickness) are between 0.78 to 0.88 pm/V without absorption correction and 3.32 to 5.57 pm/V after correction. Angular and polarization dependence study of the second harmonic response suggests that the film has in-plane isotropy as a whole and the net dipole is nearly perpendicular to the film surface. Spontaneous orientation of the polymer chains during the film formation seems to be responsible for the noncentrosymmetric alignment of the polymer. SHG from the Langmuir-Blodgett films are also reported. DTIC

N94-32579# Massachusetts Univ., Lowell. Dept. of Chemistry.
STABLE SECOND-ORDER NONLINEAR OPTICAL MATERIALS BASED ON INTERPENETRATING POLYMER NETWORKS Technical Report, 1 Jun. 1993 - 31 May 1994
S. Marturunkakul, J. I. Chen, L. Li, X. L. Jiang, and R. J. Jeng 17 Mar. 1994 7 p
(Contract N00014-90-J-1148)
(AD-A277410; TR-94-07) Avail: CASI HC A02/MF A01

Nonlinear optical (NLO) polymers have shown increased potential in practical applications, such as frequency doubling and electro-optic modulation, due to their large nonlinearity and ease of processing. A practical NLO polymer will need to possess large second-order nonlinearity, excellent temporal stability at elevated temperatures, and low optical loss. A number of NLO polymers have been developed to exhibit large second-order NLO coefficients comparable to those of the inorganic NLO materials which are currently in use in devices. However, the major drawback of NLO polymers is the decay of their electric field induced second-order optical nonlinearities. This decay is a result of the relaxation of the NLO chromophores from the induced noncentrosymmetric alignment to a random configuration. Numerous efforts have been made to minimize this decay through different approaches. Recently, we have reported on an approach to stable second-order NLO polymers using an interpenetrating polymer network (IPN) structure. This IPN system, with the hybrid properties of a high glass transition temperature

(T(sub g)), an extensively crosslinked network, and permanent entanglements, exhibited excellent temporal stability at elevated temperatures. In this report, a new IPN system, modified from the one reported earlier, with higher degree of crosslinking density and larger NLO chromophore density is investigated. DTIC

N94-32610 Massachusetts Univ., Lowell. Dept. of Chemistry.
NONLINEAR OPTICAL POLYMERS DERIVED FROM ORGANIC/INORGANIC COMPOSITES Technical Report, 1 Jun. 1993 - 31 May 1994
S. K. Tripathy, J. Kumar, J. I. Chen, S. Marturunkakul, and R. J. Jeng 18 Mar. 1994 12 p Limited Reproducibility: More than 20% of this document may be affected by microfiche quality
(Contract N00014-90-J-1148)
(AD-A277408; TR-94-10) Avail: CASI HC A03

A general approach to the development of multicomponent multifunctional stable NLO materials based on sol-gel reactions has been discussed. We have shown that these second order NLO organic/inorganic composites exhibit excellent room temperature stability of the second order optical nonlinearity. The final structure is an orientationally ordered organic/inorganic network. After an initial decay, excellent long term stability at elevated temperatures, ranging from 100 to 120 C, is observed for a number of different systems. The second order optical nonlinearities are reasonably large for practical device considerations. DTIC

N94-32617 Argonne National Lab., IL.
MECHANICAL PROPERTIES OF VACUUM-SINTERED YTTRIA CERAMICS
A. S. Wagh, D. Roberts, T. Suratwala, M. McMann, and R. B. Poeppel 1994 13 p Limited Reproducibility: More than 20% of this document may be affected by microfiche quality
(Contract W-31-109-eng-38)
(DE94-008138; ANL/MCT/PP-71579) Avail: CASI HC A03

Mechanical properties of vacuum sintered dense yttria ceramics have been studied. Values of flexural strength, fracture toughness, and thermal shock behavior, better than those reported in the literature, are reported. Microscopic investigations reveal elastic strain energy and cleavage step formation as the major contributors to the fracture energy. DOE

N94-32618# Carborundum Co., Niagara Falls, NY.
ENGINEERING SCALE DEVELOPMENT OF THE VAPOR-LIQUID-SOLID (VLS) PROCESS FOR THE PRODUCTION OF SILICON CARBIDE FIBRILS
W. E. Hollar, Jr. and W. H. Mills Sep. 1993 115 p Prepared for Oak Ridge National Lab., Oak Ridge, TN
(Contract DE-AC05-84OR-21400)
(DE94-007132; ORNL/Sub-86-SD861/01) Avail: CASI HC A06/MF A02

Vapor-liquid-solid (VLS) SiC fibrils are used as reinforcement in ceramic matrix composites (CMC). A program has been completed for determining process scaleup parameters and to produce material for evaluation in a CMC. The scaleup is necessary to lower production cost and increase material availability. Scaleup parameters were evaluated in a reactor with a vertical dimension twice that of the LANL reactor. Results indicate that the scaleup will be possible. Feasibility of recycling process gas was demonstrated and the impact of postprocessing on yields determined. DOE

N94-32632 Oak Ridge National Lab., TN.
CERAMIC TECHNOLOGY PROJECT DATABASE Summary Report, Sep. 1993
B. L. P. Keyes Jan. 1994 162 p Limited Reproducibility: More than 20% of this document may be affected by microfiche quality
(Contract DE-AC05-84OR-21400)
(DE94-008494; ORNL/M-3155) Avail: CASI HC A08

Data presented in this report represent an intense effort to improve processing methods, testing methods, and general mechanical properties of candidate ceramics for use in advanced heat engines. Materials discussed include GN-10, GS-44, GTE PY6, NT-154, NT-164, sintered reaction-bonded silicon nitrides, silicon nitride combined with rare-earth oxides, NT-230, Hexoloy SX-G1, Dow Corning's beta-Si3N4, and a few whisker-reinforced ceramic composites. Information in this report was taken from the project's semiannual and bimonthly progress reports and from final reports summarizing the results of individual studies. Test results are presented in tabular form and in graphs. The objective of this report is to make available the test results from these studies but not to draw conclusions from those data. DOE

N94-32640 Oak Ridge National Lab., TN.
COMPOSITIONS AND CHEMICAL BONDING IN CERAMICS BY QUANTITATIVE ELECTRON ENERGY-LOSS SPECTROMETRY
J. Bentley, L. L. Horton, C. J. McHargue, S. McKernan, and C. B. Carter 1993 6 p Presented at the Materials Research Society Meeting, Pittsburgh, PA, 29 Nov. - 3 Dec. 1993 Limited Reproducibility: More than 20% of this document may be affected by microfiche quality
(Contracts DE-AC05-84OR-21400; DE-AC05-76OR-00033)
(DE94-007208; CONF-9311153-2) Avail: CASI HC A02

Quantitative electron energy-loss spectrometry was applied to a range of ceramic materials at a spatial resolution of less than 5 nm. Analysis of Fe L(sub 23) white lines indicated a low-spin state with a charge transfer of approximately 1.5 electrons/atom onto the Fe atoms implanted into (amorphized) silicon carbide. Gradients of 2 to 5% in the Co:O stoichiometry were measured across 100-nm-thick Co3O4 layers in an oxidized directionally solidified CoO-ZrO2 eutectic, with the highest O levels near the ZrO2. The energy-loss near-edge structures were dramatically different for the two cobalt oxides; those for CO3O4 have been incorrectly ascribed to CoO in the published literature. Kinetically stabilized solid solubility occurred in an AlN-SiC film grown by low-temperature molecular beam epitaxy (MBE) on alpha(6H)-SiC, and no detectable interdiffusion occurred in couples of MBE-grown AlN on SiC following annealing at up to 1750C. In diffusion couples of polycrystalline AlN on SiC, interfacial 8H sialon (aluminum oxy-nitride) and pockets of Si3N4-rich beta(prime) sialon in the SiC were detected. DOE

N94-32655 Edgerton, Germeshausen and Grier, Inc., Idaho Falls, ID.
INORGANIC POLYMER ENGINEERING MATERIALS
M. L. Stone Jun. 1993 24 p Limited Reproducibility: More than 20% of this document may be affected by microfiche quality
(Contract DE-AC07-76ID-01570)
(DE94-008519; EGG-SCM-10804) Avail: CASI HC A03

Phosphazene-based, inorganic-polymer composites were produced and evaluated as potential engineering materials. The thermal, chemical, and mechanical properties of several different composites made from one polymer formulation were measured. The measured properties are very good, and the composites show excellent promise for structural applications in harsh environments. Chopped fiberglass, mineral, cellulose, and woodflour filled composites were tested. Chopped fiberglass filled composites showed the best overall properties. The phosphazene composites are very hard and rigid. They have low dielectric constants and typical linear thermal expansion coefficients for polymers. In most cases, the phosphazene materials performed as well or better than analogous, commercially available, filled phenolic composites. After 3 to 5 weeks of exposure, both the phosphazene and phenolics were degraded to aqueous bases and acids. The glass filled phosphazene samples were least affected. DOE

N94-32656 Northwestern Univ., Evanston, IL. Dept. of Physics and Astronomy.
ENERGETICS, BONDING MECHANISM, AND ELECTRONIC STRUCTURE OF CERAMIC/CERAMIC AND METAL/CERAMIC INTERFACES
A. J. Freeman 1994 19 p Limited Reproducibility: More than 20% of this document may be affected by microfiche quality
(Contract DE-FG02-88ER-45372)
(DE94-008551; DOE/ER-45372/6) Avail: CASI HC A03

The objectives of this project were to study the theory of the structure of the metal/ceramic interface (heterophase ceramic interfaces), ferroelectronic materials and their epitaxially grown oxide thin films (superlattice structure), perovskites, antiferroelectric, and electro-optic materials. DOE

N94-32657 Utah Univ., Salt Lake City.
FABRICATION, PHASE TRANSFORMATION STUDIES AND CHARACTERIZATION OF SiC-AlN-Al2OC CERAMICS
A. V. Virkar, Qiang Tian, and Jong Chen 1993 9 p Limited Reproducibility: More than 20% of this document may be affected by microfiche quality

(Contract DE-FG03-93ER-45482)
(DE94-008587; DOE/ER-45482/1) Avail: Issuing Activity (Department of Energy (DOE))

During the first year of the grant, research was conducted in three areas. Research underway on the effect of coherency strains on phase separation in the AlN-Al2OC was written into a manuscript. A study of interdiffusion in the SiC-AlN system was initiated. Work on theoretical analysis for determination of symmetry of morphology of phase separation in a hexagonal system was initiated. A brief description of the progress during the past six months is given, followed by a summary of work planned for next year. DOE

N94-32687 Lawrence Livermore National Lab., CA.
STRUCTURE-PROPERTY RELATIONSHIPS OF CARBON AEROGELS
R. W. Pekala, C. T. Alviso, and F. M. Kong Dec. 1993 4 p Presented at the 3rd Pacific Polymer Conference, Gold Coast, Australia Limited Reproducibility: More than 20% of this document may be affected by microfiche quality
(Contract W-7405-eng-48)
(DE94-007120; UCRL-JC-114787; CONF-931255-1) Avail: CASI HC A01

Of the organic reactions in sol-gel polymerizations, the most studied reaction is the aqueous polycondensation of resorcinol with formaldehyde; the resulting crosslinked gels are supercritically dried from CO2 to give resorcinol-formaldehyde (RF) aerogels. These aerogels can be pyrolyzed to form vitreous carbon monoliths with black color, high porosity, ultrafine cell/pore size, high surface area, and interconnected particles of the organic precursor. The structure and properties of the carbon aerogels depend on R/C (resorcinol/catalyst) ratio of starting solution, pyrolysis temperature, and chemical activation. Each variable is discussed. Carbon aerogels provide an almost ideal electrode material (in double-layer capacitors) owing to low electrical resistivity (less than 40 mohm-cm), controllable pore size distribution (5-500 angstrom), and high volumetric surface areas (app ximately 500 m(exp 2)/cm(exp 3)). DOE

N94-32698# Westinghouse Savannah River Co., Aiken, SC.
AN INVESTIGATION OF THE RADIOLYTIC STABILITY OF A RESORCINOL-FORMALDEHYDE ION EXCHANGE RESIN
C. L. Crawford, N. E. Bibler, and J. P. Bibler 1993 26 p Presented at the Waste Management 1994, Tucson, AZ, 27 Feb. - 3 Mar. 1994
(Contract DE-AC09-89SR-18035)
(DE94-007971; WSRC-MS-93-550; CONF-940225-67) Avail: CASI HC A03/MF A01

Radiolytic stability of a resorcinol-formaldehyde polycondensation type cation exchange resin was investigated for up to 1 x 10(exp 9) rads total dose. The resorcinol-formaldehyde resin is a resin that has potential cesium decontamination applications at Pacific Northwest and Savannah River. We have determined both radiation and storage effects on performance of the resin using 101-AW Hanford simulant and ASTM type 1 water. Distribution coefficient determinations, total carbon analysis, and physical observations lead us to conclude that radiation up to 1 x 10(exp 8) rads does not significantly affect the performance of the resin. The resin is more stable to radiation in water than in 101-AW Hanford simulant. Also radiation or storage does not affect the thermal stability of the resin. Gas production rates for several resin slurries increased in the order of resin/101-AW Hanford simulant, resin/ASTM water, and resin/0.5 M HNO3. H2 is produced from radiolysis of resin in 101-AW Hanford simulant with a G value of G(H2) of 0.11 +/- 0.02 molecules/100 eV and in 0.5 M HNO3 with a G value of G(H2) of 0.27 +/- 0.02 molecules/100 eV. DOE

N94-32722# Queens Univ., Kingston (Ontario). Dept. of Chemistry.
MICROSTRUCTURE OF COPOLYMERS CONTAINING DISPERSE RED 1 AND METHYL METHACRYLATE
Shuang Xie, Almeria Natansohn, and Paul Rochon 1 Mar. 1994 7 p
(AD-A277140; TR-11) Avail: CASI HC A02/MF A01

Two series of copolymers containing disperse red 1 and methyl methacrylate have been synthesized: poly(4'- (((2- (acryloyloxy)ethyl) ethyl) amino) -4 - nitroazobenzene - co-methylmethacrylate) (poly - (DRIA-co-MMA)) and poly(4'- (((2- (methacryloyloxy) ethyl) ethyl) amino) -4- nitroazobenzene -co-methyl methacrylate) (poly(DR1M -co-MMA)). The sequence distribution of the two series of copolymers is calculated on the basis of the estimated reactivity ratio values and analyzed by 13C-NMR spectroscopy. Methylmethacrylate centered triad MMD, DMD, and MMM and disperse red 1 centered triad DDD fractions are derived from the alpha-methyl carbon of MMA and carbonyl carbon in poly (DR1A-co-MMA). Good agreement is found between the spectral deconvolution results and the calculated results. Polymer tacticity is analyzed with the main chain quaternary carbon and carbonyl carbon in poly(DR1M-co-MMA). No spectral sequence distribution information is available for this series. DTIC

N94-32727# Sandia National Labs., Albuquerque, NM.
TEMPERATURE-HUMIDITY-BIAS AGING TECHNIQUE TO IDENTIFY DEFECTIVE SURFACE MOUNT CAPACITORS
R. Chanchani 1994 11 p Presented at the 14th Capacitor and Resistor Technology Symposium, Jupiter Beach, FL, 21-24 Mar. 1994
(Contract DE-AC04-94AL-85000)
(DE94-005354; SAND-94-0054C; CONF-940337-2) Avail: CASI HC A03/MF A01

Ceramic chip capacitors can potentially crack due to thermal stresses in a surface mount assembly process. The electrical performance of the cracked capacitors will degrade with time, and they will prematurely short. In high reliability applications, the cracked capacitors must be identified and eliminated. We have developed and demonstrated the temperature-humidity-bias (THB) aging technique to identify cracked capacitors. The initial phase of the study involved setting up automated test equipment to monitor 100 surface mounted capacitors at 85% relative humidity, 85 degrees C with 50 volts dc bias. The capacitors subjected to severe thermal shock were aged along with control samples. Failure mode analysis was done on the failed capacitors. The capacitors with surface cracks short-out within the first 8 hours of aging, whereas the capacitors that failed after a longer aging time (8 to 1000 hours) had a shorting path in an internal void. Internal voids are typical defects introduced during manufacturing of multilayer ceramic (MLC) capacitors. In the second phase of the study, we used the THB aging technique to study the effect of surface mount processes on capacitor cracking and, thus the reliability. The surface mount processes studied were vapor phase, infrared (IR) and convection belt reflow soldering. The results showed that 6.3% of vapor phase soldered capacitors, and 1.25% of the IR and convection belt soldered capacitors had cracks. In all capacitors, regardless of the solder process used, an additional 3 to 4% of the capacitors failed due to a shorting path in the internal void. The results of this study confirm that this technique can be used to screen cracked capacitors and compare different solder and manufacturing processes. DOE

N94-32729# Sandia National Labs., Albuquerque, NM.
CONJUGATED POLYMER FLUORESCENCE: INTERPLAY OF CORRELATIONS AND ALTERNATION
Z. G. Soos (Princeton Univ., NJ.), D. S. Galvao (Bell Communications Research, Inc., Red Bank, NJ.), S. Etemad (Bell Communications Research, Inc., Red Bank, NJ.), and R. G. Kepler 1993 6 p Presented at the Fall Meeting of the Materials Research Society, Boston, MA, 29 Nov. - 3 Dec. 1993
(Contract DE-AC04-94AL-85000)
(DE94-005587; SAND-93-1587C; CONF-931108-89) Avail: CASI HC A02/MF A01

Conjugated polymers can have high conductivity on doping, large nonlinear optical response in semiconducting state, and be used as LED's. These polymers include polyactylene, polydiacetylenes, polysilanes, polythiophene, poly-p- phenylenevinylene. Polymer fluorescence is related to the lowest singlet excited state S(sub 1). Polymer and oligomer data are shown for the excitation energy ratio of the two-photon and one-photon gaps. There is a ratio crossover with increasing e-e correlations in any centrosymmetri chain with an insulating ground state. The pi-conjugated polymers present various band gaps at constant correlations, and single-particle gaps can be related to the structure. The nature of the lowest singlet excited state depends sensitively on both correlations and alternation. DOE

N94-32739# Department of the Navy, Washington, DC.
MASS-LOADED COATING FOR REDUCING THE RESONANT FREQUENCY OF A CERAMIC DISC Patent Application
Patrick Monahan, inventor (to Navy) 27 Sep. 1993 10 p
(AD-D016095; US-Patent-Appl-SN-127178) Avail: CASI HC A02/MF A01

A mass-loaded coating includes a predetermined mass of powdered

lead which is mixed preferably in a ratio of 3:1 with a liquid polyurethane primer. When painted onto the surface of a disk or plate, the coating mass-loads the disc and lowers the resonant frequency of the disk without significantly increasing the physical dimensions of the disk. Thicker consistency adhesives, such as spreadable paste adhesives or thick putty-like adhesives may be substituted for mass-loading objects having irregular surface textures or complex shapes. DTIC

N94-32751 Lawrence Livermore National Lab., CA.
MICROANALYTICAL STUDY OF DEFECT FORMATION IN THIN BISMUTH STRONTIUM CALCIUM COPPER OXIDE FILMS
R. H. Howell, A. Chaiken, and R. G. Musket et al Jan. 1994 12 p Presented at the OE/LASE 1994: Conference on Optics, Electro-Optics, and Laser Applications in Science and Engineering, Los Angeles, CA, 22-29 Jan. 1994 Limited Reproducibility: More than 20% of this document may be affected by microfiche quality
(Contract W-7405-eng-48)
(DE94-008217; UCRL-JC-115842; CONF-940142-25) Avail: Issuing Activity (Department of Energy (DOE))

Thin bismuth strontium calcium copper oxide (BSCCO) films and BSCCO/insulator/BSCCO trilayers have been prepared on SiTiO3 and MgO substrates by evaporation from elemental sources in an ozone atmosphere. Accurate control of the stoichiometry is achieved through monitoring of the atomic fluxes by use of in situ atomic absorption spectroscopy as well as by reflection high energy electron diffraction (RHEED). Nevertheless, nanometer-scale, second phase precipitates are sometimes observed. These defects and the flat regions around them have been probed by a variety of microanalytical techniques, including Rutherford backscattering spectroscopy (RBS), particle-induced x ray emission (PIXE), atomic force microscopy (AFM), microscopic secondary ion mass spectroscopy, and transmission electron microscopy (TEM). DOE

N94-32788# Nebraska Univ., Lincoln. Dept. of Electrical Engineering.
CONDUCTIVE PAINTS Progress Report, 1 Dec. 1993 - 28 Feb. 1994
R. J. Soukup and N. J. Ianno 1994 4 p
(Contract DE-FG01-92CE-15974)
(DE94-008508; DOE/CE-15974/T7) Avail: CASI HC A01/MF A01

Paints were sprayed onto glass substrates and air dried or baked. Hardness was measured and found to be maximum at baking temperature of 300 C. No measurable adhesion to delrin, teflon, or nylon was obtained; however, adhesion to Plexiglas was obtained and measured. DOE

N94-32796# Sandia National Labs., Albuquerque, NM.
NUCLEATION AND GROWTH OF CUBIC BORON NITRIDE FILMS PRODUCED BY ION-ASSISTED PULSED LASER DEPOSITION
T. A. Friedmann, D. L. Medlin, P. B. Mirkarimi, K. F. McCarty, E. J. Klaus, D. R. Boehme, H. A. Johnsen, M. J. Mills, and D. K. Ottesen 1993 7 p Presented at the Fall Meeting of the Materials Research Society (MRS), Boston, MA, 29 Nov. - 3 Dec. 1993
(Contract DE-AC04-94AL-85000)
(DE94-007295; SAND-93-3872C; CONF-931108-85) Avail: CASI HC A02/MF A01

We are studying the boron nitride system using a pulsed excimer laser to ablate from hexagonal BN (cBN) targets to form cubic BN (cBN) films. We are depositing BN films on heated (25-800 C) Si (100) surfaces and are using a broad-beam ion source operated with Ar and N2 source gases to produce BN films with a high percentage of sp3-bonded cBN. In order to optimize growth and nucleation of cBN films, parametric studies of the growth parameters have been performed. The best films to date show greater than 85% sp3-bonded BN as determined from Fourier-transform infrared (FTIR) reflection spectroscopy. High resolution transmission electron microscopy (TEM) and selected area electron diffraction confirm the presence of cBN in these samples. The films are polycrystalline and show grain sizes up to 30--40 mn. We find from both the FTIR and TEM analyses that the cBN content in these films evolves with growth time. Initially, the films are deposited as hBN and the cBN nucleates on this hBN underlayer. Importantly, the position of the cBN IR phonon also changes with growth time. Initially this mode appears near 1130 cm(exp -1) and the position decreases with growth time to a constant value of 1085 cm(exp -1). Since in bulk cBN this IR mode appears at 1065 cm(exp -1), a large compressive stress induced by the ion bombardment is suggested. In addition, we report on the variation in cBN percentage with temperature. DOE

N94-32798# Argonne National Lab., IL.
EXTENDED-RANGE ORDER IN GLASSES
A. J. G. Ellison, D. L. Price, M. L. Saboungi, T. Egami, Rui-Zhong Hu, and W. S. Howells 1994 20 p
(Contract W-31-109-eng-38)
(DE94-008135; ANL/MSD/PP-77692) Avail: CASI HC A03/MF A01

A new type of order is identified in complex glasses, characterized by diffraction peaks at values of the wave vector below those typical of intermediate-range order. Combined neutron and anomalous x-ray diffraction studies of one glass exhibiting this behavior, vitreous rubidium germanate, indicate it to be associated with chemical ordering of the two cations with respect to each other. DOE

N94-32803# Sandia National Labs., Livermore, CA.
COMPILATION OF DIAMOND-LIKE CARBON PROPERTIES FOR BARRIERS AND HARD COATINGS
D. A. Outka, Wen L. Hsu, D. R. Boehme, N. Y. C. Yang, D. K. Ottesen, H. A. Johnsen, W. M. Clift, and T. J. Headley Feb. 1994 54 p
(Contract DE-AC04-76DR-00789)
(DE94-008231; SAND-94-8219) Avail: CASI HC A04/MF A01

Diamond-like carbon (DLC) is an amorphous form of carbon which resembles diamond in its hardness, lubricity, and interest for hardness, lubricity, and resistance to chemical attack. Such properties make DLC of use in barrier and hard coating technology. This report examines a variety of properties of DLC coatings which are relevant to its use as a protective coating. This includes examining substrates on which DLC coatings can be deposited; the resistance of DLC coatings to various chemical agents; adhesion of DLC coatings; and characterization of DLC coatings by electron microscopy, FTIR, sputter depth profiling, stress measurements, and nanoindentation. DOE

N94-32819# Sandia National Labs., Albuquerque, NM.
CHARACTERIZATION OF CROSSLINKED ELECTROOPTIC POLYIMIDES
M. B. Meinhardt, P. A. Cahill, C. H. Seager, A. J. Beuhler, D. A. Wargowski, K. D. Singer, T. C. Kowalczyk, and T. Z. Kosc 1993 7 p Presented at the OE/LASE 1994: Conference on Optics, Electro-Optics, and Laser Applications in Science and Engineering, Los Angeles, CA, 22-29 Jan. 1994
(Contract DE-AC04-94AL-85000)
(DE94-007934; SAND-93-1752C; CONF-940142-23) Avail: CASI HC A02/MF A01

The electrooptical properties of Ultradel(trademark) 9000D polyimides doped with dyes DCM and DADC, a bis(carbazole) analog of DCM with improved thermal stability, are reported. Cure temperatures were restricted to 240C or less to minimize potential thermal degradation of these dyes. Low poling fields of 30 V/(mu)m were used in these experiments and yielded r(sub 13) coefficients in the 0.1-0.8 pm/V range. Photothermal deflection measurements of dye-doped Ultradel 9000D samples showed low optical absorption losses in systems cured at 175C, but losses exceeded 20 dB/cm in samples cured at 300C. DOE

N94-32847# Texas Technological Univ., Lubbock.
METAL ION COMPLEXATION BY IONIZABLE CROWN ETHERS
R. A. Bartsch Jul. 1993 38 p
(Contract DE-FG05-88ER-13832)
(DE94-008301; DOE/ER-13832/36) Avail: CASI HC A03/MF A01

Cyclic and acyclic polyether compounds with pendent carboxylic acid, phosphonic acid monoethyl ester, sulfonic acid, phosphinic acid, and hydroxamic acid groups have been synthesized. The proton-ionizable polyethers can come with and without lipophilic groups. Two types of lipophilic di-ionizable lariat ethers have been prepared. Conformations of proton-ionizable lariat ethers have been probed. Competitive alkali metal cation transport by syn-(decyl)dibenzo- 16-crown-5-oxyacetic acid and lipophilic proton-ionizable dibenzo lariat ethers in polymer-supported liquid membranes was studied. Complexation of alkali metal cations with ionized lariat ethers was studied. Condensation polymerization of cyclic and acyclic dibenzo polyethers containing pendent mono-ionizable groups with formaldehyde produces novel ion exchange resins with both ion exchange sites for metal ion complexation and polyether binding sites for metal ion

recognition. Resins prepared from lariat ether dibenzo phosphonic acid monoethyl esters show strong sorption of divalent heavy metal cations with selectivity for Pb(2+). DOE

N94-32855# Lawrence Livermore National Lab., CA.
X RAY ABSORPTION STUDY OF PULSED LASER DEPOSITED BORON NITRIDE FILMS
A. Chaiken, L. J. Terminello, J. Wong, G. L. Doll, and T. Sato 2 Feb. 1994 8 p Presented at the Fall Meeting of the Materials Research Society (MRS), Boston, MA, 29 Nov. - 3 Dec. 1993
(Contract W-7405-eng-48)
(DE94-008295; UCRL-JC-114133; CONF-931108-91) Avail: CASI HC A02/MF A01

B and N K-edge x-ray absorption spectroscopy measurements have been performed on three BN thin films grown on Si substrates using ion-assisted pulsed laser deposition. Comparison of the films' spectra to those of several single-phase BN powder standards shows that the films consist primarily of sp2 bonds. Other features in the films's spectra suggest the presence of secondary phases, possibly cubic or rhombohedral BN. Films grown at higher deposition rates and higher ion-beam voltages are found to be more disordered, in agreement with previous work. DOE

N94-32891 Oak Ridge National Lab., TN.
EFFECT OF ELEVATED TEMPERATURE AND CYCLIC LOADING ON PROPERTIES AND DAMAGE MODES IN CERAMIC COMPOSITES
K. L. Reifsnider, W. W. Stinchcomb, L. Oleksuk, S. S. Lee, and D. P. Stinton Nov. 1993 30 p Prepared in cooperation with Virginia Polytechnic Inst. and State Univ., Blacksburg, VA Limited Reproducibility: More than 20% of this document may be affected by microfiche quality
(Contract DE-AC05-84OR-21400)
(DE94-008736; ORNL/Sub-87-SA946/03; CCMS-93-18) Avail: CASI HC A03

This report discusses the results of a ongoing program of research concerned with the investigation of the effects of elevated temperature on the properties and performance of ceramic composites. The present report is concerned with just two aspects of the general program, the changes in properties and damage modes due to the effects of exposure of two ceramic composite systems to high temperature air and multiaxial loading. Two material systems and specimen configurations are discussed. Tubular specimens fabricated at the Oak Ridge National Laboratory using a SiC/SiC combination were tested quasi-statically at elevated temperatures. Changes in stiffness as a function of time and temperature were observed, and an SEM study revealed substantial differences in the microstructure associated with that exposure. Flat Nicalon/CAS-2 coupons were fabricated by the Corning Glass Company, subjected to elevated temperature soaks for various periods of time and temperature, and then tested monotonically and under cyclic loading. Changes in damage and failure modes were observed in that system, and a new surface damage mode on the fiber was discovered, possibly due to frictional sliding. The present report discusses the observations, interpretations, and some micromechanical modeling associated with these activities and discusses the consequences of these temperature effects on future 'designs' of material systems. DOE

N94-32935 Oak Ridge National Lab., TN.
MATERIALS DEVELOPMENT PROGRAM: CERAMIC TECHNOLOGY PROJECT BIBLIOGRAPHY, 1984-1992
Mar. 1994 61 p Limited Reproducibility: More than 20% of this document may be affected by microfiche quality
(Contract DE-AC05-84OR-21400)
(DE94-009297; ORNL/M-3201) Avail: Issuing Activity (Department of Energy (DOE))

The Ceramic Technology for Advanced Heat Engines Project was begun in 1983 to meet the ceramic materials needs of the companion DOE automotive engine program, the Advanced Gas Turbine (AGT) project, and the Heavy Duty Transport (low-heat-rejection, heavy-duty diesel) project. The goal is to develop an industry technology base for reliable and cost effective ceramics for applications in advanced automotive gas turbine and diesel engines. Research areas were identified following extensive input from industry and academia. Majority of research is done by industry (60%); work is also done at colleges and universities, in-house, and at other national laboratories and government agencies. In the beginning, reliability of ceramic components was the key issue. The reliability issues have largely been met and, at the present time, cost is the driving issue, especially in light of the highly cost-sensitive automotive market. Emphasis of the program has now been shifted toward developing cost-effective ceramic components for high-performance engines in the near-term. This bibliography is a compilation of publications done in conjunction with the Ceramic Technology Project since its beginning. Citations were obtained from reports done by participants in the project. We have tried to limit citations to those published and easily located. The end date of 1992 was selected. DOE

N94-32945*# National Aeronautics and Space Administration. Lewis Research Center, Cleveland, OH.
CONVERSION OF POLYMERS OF METHYL- AND VINYLSILANE TO Si-C CERAMICS
Frances I. Hurwitz, Terrance A. Kacik, Xin-Ya Bu, John Masnovi, Paula J. Heimann, and Kassahun Beyene Apr. 1994 8 p Presented at the MRS Spring Meeting, San Francisco, CA, 4-8 Apr. 1994, sponsored by the Materials Research Society
(Contract NCC3-63; RTOP 505-63-51)
(NASA-TM-106554; E-8704; NAS 1.15:106554) Avail: CASI HC A02/MF A01

Poly(methylsilane) and poly(vinylsilane) were synthesized using a titanocene catalyst, and their pyrolytic conversion to ceramics was followed using a combination of thermal analysis and infrared spectroscopy. The two polymers have distinctly different backbone structures, as determined by Si NMR; methylsilane polymerizes to a polysilane, while vinylsilane polymers have predominately polycarbosilane backbone, with some polysilane structure as well. The pyrolysis path and char yield were dependent primarily on backbone structure, with little influence of polymer molecular weight. The majority of the weight loss on conversion occurs below 650 degrees C, although bond rearrangement continues to 1400 degrees C. Poly(vinylsilane) produced a C-rich Si-C ceramic in which the carbon was dispersed on a sufficiently fine level to show resistance to oxidation on heating in air to 1400 degrees C. Author

N94-32952# Materials Research Society, Pittsburg, PA.
SILICON-BASED OPTOELECTRONIC MATERIALS SYMPOSIUM AND MATERIALS RESEARCH SOCIETY PROCEEDINGS, VOLUME 298 Final Report, 15 Jun. - 14 Dec. 1993
John Ballance 14 Dec. 1993 476 p Proceedings held in San Francisco, CA, 12-14 Apr. 1993
(Contract F49620-93-1-0383)
(AD-A277518; AFOSR-94-0041TR) Avail: CASI HC A21/MF A04

Although silicon is at the heart of the microelectronics revolution, its low optical efficiency has limited its use in optoelectronic applications. The potential significance of combining communications and display technology with microelectronics technology has generated considerable activity directed at developing a silicon-compatible optoelectronic material. The last few years have seen some interesting and potentially important advances in this area. Symposium B was organized as a forum for the various groups studying the physics, materials science, processing, and applications of silicon-based optoelectronic materials to present their most recent results in this rapidly growing field. Talks were organized into five basic areas: Si(1-x)Ge(x), rare earth-doped silicon (this session was organized jointly with symposium, E, Rare Earth Doped Semiconductors), silicon nanoparticles, porous silicon, and applications. Many of the key research groups in each of these areas were represented at the meeting. DTIC

N94-32954# Minnesota Univ., Minneapolis. Dept. of Chemical Engineering and Materials Science.
PHASE BEHAVIOR, STRUCTURE, AND PROPERTIES OF MODEL BLOCK POLYMERS Final Report, 15 Apr. 1990 - 14 Oct. 1993
Frank S. Bates 14 Oct. 1993 15 p
(Grant AF-AFOSR-0207-90)
(AD-A277530; AFOSR-94-0094TR) Avail: CASI HC A03/MF A01

This project brought together three distinct experimental methods in an integrated investigation of the phase behavior, structure, and properties of block copolymers in the vicinity of the order-disorder transition. Anionic polymerization of polydiene diblock copolymers followed by catalytic hydrogenation was used to produce three classes of model saturated hydrocarbon materials. Dynamic mechanical spectroscopy and large amplitude dynamic shearing were employed to probe and manipulate,

respectively, the melt state microstructure. Small angle neutron scattering (SANS) experiments provided detailed information regarding the structure of the materials. A significant achievement during this work was the development of a dynamic shearing device that could be operated in situ with a SANS instrument. Together with the spectrum of materials produced, this combined scattering-rheology technique has led to a qualitative improvement in our understanding of block copolymer phase behavior and uncovered a rich polymorphism that is accompanied by dramatic variations in physical properties. Two new parameters have been shown to play a crucial role in determining block copolymer phase behavior. The degree of polymerization controls the extent of composition fluctuations which strongly affects the types of phases encountered near the order-disorder transition. Conformational asymmetry, which is controlled by the block volume and radius of gyration, leads to different phases on either side of the phase diagram. These effects have not been accounted for theoretically. DTIC

N94-32960 Department of the Navy, Washington, DC.
METHOD AND APPARATUS FOR INHIBITING THE DISBONDING OF A PAINT FROM METAL SURFACES Patent
Martin W. Kendig, inventor (to Navy) 30 Nov. 1993 6 p Filed 10 Jun. 1992
(AD-D016106; US-Patent-5,266,623; US-Patent-Appl-SN-896695;
US-Patent-Class-524-236) Avail: US Patent and Trademark Office

A method and the required materials for coating metal surfaces to prevent disbonding of the coating and metal surface is discussed. A polymer coating material has high molecular weight cations added thereto and can be used to paint steel or other metal surfaces subject to cathodic ionization. DTIC

N94-32975 Department of the Navy, Washington, DC.
INTERPENETRATING POLYMER NETWORK ACOUSTIC DAMPING MATERIAL Patent
Usman A. Sorathia, inventor (to Navy), William L. Yeager, inventor (to Navy), and Timothy L. Dapp, inventor (to Navy) 17 Aug. 1993 5 p Filed 28 Aug. 1991
(AD-D016141; US-Patent-5,237,018; US-Patent-Appl-SN-751352;
US-Patent-Class-525-454) Avail: US Patent and Trademark Office

Improved acoustic damping materials comprise interpenetrating polymer networks having a soft polymer component and a hard polymer component. The soft polymer component, constituting from 75 to 95, preferably 90, percent by weight of the material, is made by polymerizing an aromatic diisocyanate with a polyalkylene ether glycol, and the hard polymer component is a vinyl ester polymer made by polymerization of the acrylate or methacrylate ester of the diglycidyl ether of a polyphenol. The curing of the mixture is carried out at room temperature in presence of a peroxide and an aromatic amine. The mixture of ingredients, while liquid, may be injected into mechanical devices, such as shafts of rotating equipment whose noise is to be dampened, and allowed to cure therein. DTIC

N94-32985 Massachusetts Univ., Lowell. Dept. of Chemistry.
LOW LOSS SECOND-ORDER NONLINEAR OPTICAL POLYMERS BASED ON ALL ORGANIC SOL-GEL MATERIALS
R. J. Jeng, G. H. Hsiue, J. I. Chen, S. Marturunkakul, and L. Li 16 Mar. 1994 23 p Limited Reproducibility: More than 20% of this document may be affected by microfiche quality
(Contract N00014-90-J-1148)
(AD-A277482; TR-94-06-ONR; Rept-1148-94-06) Avail: Issuing Activity (Defense Technical Information Center (DTIC))

A new class of all organic sol-gel second-order nonlinear optical (NLO) materials based on hexa(methoxymethyl) melamine (HMM) has been developed. Two NLO active chromophores, 4-(4'nitrophenylazo) aniline (DO3) and 4-amino-4'-nitrobiphenyl (ANB), were incorporated into the melamine matrices. The samples exhibit second-order optical nonlinearity after poling and curing at 220 C for 30 min. DO3/HMM and ANB/HMM samples show a second harmonic coefficient, d33 of 10.7 and 1.8 pm/V at 1064 nm, respectively. The temporal stability of both systems has been studied at room temperature as well as at 100 C. Waveguide optical losses of samples at 633 and 830 nm are reported. DTIC

N94-33010# Materials Sciences Corp., Fort Washington, PA.
BRIEFING AND REVIEW MEETING IMPLEMENTATION OF THE MILITARY HANDBOOK 17 FOR POLYMER MATRIX AND METAL MATRIX COMPOSITES
Crystal H. Newton 14 Mar. 1994 6 p
(Contract DAAL01-93-C-4064)
(AD-A277446) Avail: CASI HC A02/MF A01

Support of the metal matrix composites effort, as the equivalent of a MIL-HDBK-17 working group, is included in the Secretariat contract. Preparation, of a document for publication was not included in the revised proposal since this was not mentioned in the RFP. The draft outline of the metal matrix handbook was revised. A volume with three parts is planned. Volunteers will draft some of the sections and additional sections will be written by the MMCIAC. The goal is a draft handbook by the New Orleans meeting, sufficient to be assigned a military handbook number. In addition to draft handbook sections, test matrix information is under development. Buchanan at McDonald Douglas has a MMC database he is willing to contribute to the handbook. DTIC

N94-33024*# National Aeronautics and Space Administration. Lewis Research Center, Cleveland, OH.
DEVELOPMENT AND PRELIMINARY EVALUATION OF ARYL ESTER BOUNDARY ADDITIVES FOR PERFLUOROPOLYETHERS
John R. Williams (Draper, Charles Stark Lab., Inc., Cambridge, MA.), Debra K. Feuchter (Calspan Corp., Fairview Park, OH.), and William R. Jones, Jr. May 1994 10 p Presented at the International Rolling Element Bearing Symposium, San Diego, CA, 12-14 Apr. 1994; sponsored by DOD
(Contract NAS3-25685; RTOP 233-02-0D)
(NASA-TM-106603; E-8878; NAS 1.15:106603) Avail: CASI HC A02/MF A01

A series of additives were developed for evaluation as boundary lubrication enhancers for perfluoropolyethers. They are composed of a hydrocarbon aryl component (for lubrication improvement) and a fluorinated side chain (for solubility enhancement). The two moieties are joined by an ester linkage. Five boundary additives were evaluated in a perfluoropolyether basestock (Fomblin Z25) using a specially designed four-ball apparatus. Additives were evaluated at a one wt percent concentration. Conditions included: an atmosphere of dry air at atmospheric pressure, a 200N load, a speed of 100 rpm, room temperature, and 440C stainless steel specimens. Two monoesters, 2,4,6-trimethyl E2 and H5PDFO yielded wear rate reductions of approximately 60 and 35 percent, respectively. One diester, H4(E2)(sub 2), had no activity, while two other diesters (a diester of bisphenol A and H4(E4)(sub 2)) were pro-wear. Author

N94-33054# Massachusetts Univ., Lowell. Dept. of Chemistry.
A RELAXATION STUDY OF POLED NONLINEAR OPTICAL POLYMERS BY INFRARED REFLECTION-ABSORPTION SPECTROSCOPY
Sutiyao Marturunkakul, Jeng I. Chen, Y. M. Chen, J. Kumar, and Sukany K. Tripathy 14 Mar. 1994 6 p
(Contract N00014-90-J-1148)
(AD-A277513; Rept-1148-94-05) Avail: CASI HC A02/MF A01

The relaxation of poled nonlinear optical (NLO) chromophores in polymer films was characterized by infrared reflection-absorption spectroscopy. Both a guest-host system and a photo-crosslinkable polymer system were investigated. Polymethylmethacrylate doped with either 2-methyl 4-nitroaniline or 4(4'-nitrophenylazo) aniline was studied. The photo-crosslinkable polymer system, polyvinylcinnamate doped with 3-cinnamoyloxy 4-(4-(N,N-diethylamino) 2-cinnamoyloxy phenyl azo)nitrobenzene, was also investigated. Doped NLO active molecules were aligned using the corona poling technique. Infrared spectra as a function of time were used to monitor the relaxation behavior of the oriented dyes after poling. Relaxation of NLO molecules was followed at various characteristic vibrational frequencies. The relaxation behavior of both systems were found to be consistent with those studied by the second harmonic generation technique. DTIC

N94-33058# Rutgers - The State Univ., Piscataway, NJ. Dept. of Mechanics and Materials Science.
THE FERROELECTRIC BEHAVIOR OF ODD-NUMBERED NYLONS
B. Z. Mei, J. I. Scheinbeim, and B. A. Newman Aug. 1993 24 p
(Contract N00014-91-J-1078)
(AD-A278126; TR-29-ONR) Avail: CASI HC A03/MF A01

The combined results of the present investigation of Nylon 5 and Nylon 9 and the previous investigation of Nylon 11 and Nylon 7 reveal that the odd-numbered nylons exhibit classic ferroelectric J-E and D-E hysteresis behavior at room temperature. In addition, the remanent polarization, P, of Nylon 5 and Nylon 9 are found to be 125 approximately 130 mC/sq meters and 65 approximately 70 mC/sq meters, respectively. The remanent polarization of the odd nylon series is observed to increase linearly with increasing dipole density as does the melting point. The coercive field also shows a linear increase with dipole density. The present study also shows that both uniaxially oriented and unoriented odd-numbered nylons exhibit ferroelectric hysteresis behavior, and that the ferroelectric response can be significantly enhanced by uniaxial orientation. DTIC

N94-33082# Massachusetts Univ., Lowell. Dept. of Chemistry.
NOVEL POLYDIACETYLENES AS MATERIALS FOR SECOND AND THIRD ORDER NONLINEAR OPTICS
W. H. Kim, B. Bihari, C. E. Masse, J. Kumar, and Sukany K. Tripathy 18 Mar. 1994 8 p
(Contract N00014-90-J-1148)
(AD-A277512; Rept-1148-94-09) Avail: CASI HC A02/MF A01

The objective of this investigation was to develop stable nonlinear optical (NLO) materials which possess both second and third order NLO properties. These materials were envisioned as having a polydiacetylene (PDA) backbone with a second order active NLO chromophoric substituent consisting of a donor group, a p-conjugated bridge, and an acceptor group. The choice of a PDA backbone in this investigation was twofold. In terms of third order NLO properties, the extensive p-conjugation of the PDA backbone leads to large ultrafast third order effects. In terms of second order NLO properties, the high thermal stability and rigidity of the PDA matrix in a perfect polymeric single crystal is expected to prevent the randomization of the NLO chromophores in the noncentrosymmetric environment. This paper focuses on the synthesis and NLO properties of the unsymmetrical diacetylene monomers, ((9-Butoxy carbonyl) methyl urethanyl) 1-(4-urethanyl 4'-urethanyl 4'-nitrobiphenyl)-nona 2,4-diyne, and ((9-Butoxy carbonyl)methyl urethanyl) 1-(4-urethanyl 4'-nitroazo-benzene)-nona 2,4-diyne. The high entropy flexible urethanyl side group was chosen to satisfy the monomer packing requirements for polymerization and enhance the solubility of the PDA's. DTIC

N94-33138# Rutgers - The State Univ., Piscataway, NJ.
ELECTRIC FIELD-INDUCED CHANGES IN ODD-NUMBERED NYLONS Technical Report, 1 Jun. 1993 - 31 May 1994
J. I. Scheinbeim and B. A. Newman Aug. 1993 29 p
(Contract N00014-91-J-1078)
(AD-A278003; TR-28) Avail: CASI HC A03/MF A01

Most studies of ferroelectricity and piezoelectricity in polymers have been directed towards poly(vinylidene fluoride) and its copolymers. A long series of investigations in our laboratory of the odd-numbered nylons has culminated in the discovery that these polymers are also ferroelectric and piezoelectric. These studies are important not only to test the generality of the phenomena discovered in poly(vinylidine fluoride), but to examine the effect of hydrogen bonding on ferroelectricity and piezoelectricity in polymers. One important result of this work was the discovery of a mechanism to stabilize the piezoelectric activity of these hydrogen bonded polymers to the melting point. DTIC

N94-33166 Naval Air Warfare Center, Warminster, PA. Vehicle and Crew Systems Technology Dept.
EVALUATION OF THE HUGHES CONVERSION COATING TOUCH-UP PEN Final Report, Jan. - Jun. 1993
John Deitzel (Jaylords, Inc., Philadelphia, PA.) and Stephen J. Spadafora 22 Jul. 1993 15 p Limited Reproducibility: More than 20% of this document may be affected by microfiche quality
(AD-A278398; NAWCADWAR-93050-60) Avail: Issuing Activity (Defense Technical Information Center (DTIC))

Chromate conversion coatings are common surface pretreatments for aluminum substrates on Navy aircraft, weapon platforms, and ground support equipment. While this chromated process performs satisfactorily, future restrictions require the elimination or minimization of chromium emissions from this process. One approach to minimize emissions is through the incorporation of new touch-up procedures. A chemical film touch-up pen developed by Hughes Ground Systems Group offers the potential to provide the required paint adhesion and corrosion protection for aluminum for repair applications. The Naval Air Warfare Center Aircraft Division at Warminster performed a study of this pen and the following is a description of the evaluation. DTIC

N94-33247# Rutgers - The State Univ., Piscataway, NJ. Dept. of Mechanics and Materials Science.
ELECTROSTRICTIVE RESPONSE OF ELASTOMERIC POLYMERS
Jerry I. Scheinbeim, Brian A. Newman, Z. Y. Ma, and J. W. Lee Aug. 1993 14 p
(Contract N00014-91-J-1078)
(AD-A277983; TR-30) Avail: CASI HC A03/MF A01

It is well known that the electrostrictive response of all materials is small at low applied electric fields. However, the electrostrictive strains (S) are related to the square of the applied field (E). It therefore appeared reasonable to assume that for a soft polymeric material, a large thickness response, d(sub T)(d(sub T) = partial derivative of S/partial derivative of E), might be obtained by application of sufficiently high D.C. bias fields (approx. 20MV /m) to a film while driving the film with an A.C. signal. Under such high electric fields, d(sub T) values greater than 3 A/V were obtained for a low crystallinity poly(vinylidene fluoride) (PVF2) film containing 65% by weight of a plasticizer tricresyl phosphate (TCP). Values of 6 A/V were obtained for certain classes of thermoplastic elastomers, i.e., polyurethanes. These values are considerably greater than those obtained from conventional piezoelectric ceramic materials and an order of magnitude greater than the 0.25 A/V obtained from polarized PVF2. In addition, large elastic strains (greater than 3%) were observed as a function of applied D.C. field. DTIC

N94-33348 Massachusetts Univ., Lowell. Dept. of Chemistry.
SECOND-ORDER NONLINEAR OPTICAL POLYMERS: FROM FUNDAMENTALS TO APPLICATIONS
Sutiyao Marturunkakul, Jeng I. Chen, Lian Li, Mario Cazeca, and Sandip Sengupya 17 Mar. 1994 11 p Limited Reproducibility: More than 20% of this document may be affected by microfiche quality
(Contract N00014-90-J-1148)
(AD-A277514; Rept-1148-94-08) Avail: CASI HC A03

Successful development of materials for photonic applications requires an understanding of the nonlinear optical process, chemistry and processing of materials, and technologies for device fabrications. We are able to successfully use different chemistries to develop several types of crosslinked and networked systems. Significant progress in improving material properties has been accomplished. Promising results have been observed in several materials developed. A prototype frequency doubling device has been prepared; second harmonic Cerenkov radiation emitting green and blue light have been observed. Relevant chemical modifications to fine-tune or enhance the desired properties will need to be iteratively performed to obtain optimized properties for practical applications. DTIC

N94-33350 Gumbs (R.) Associates, East Brunswick, NJ.
NOVEL SOL-GEL DEPOSITION FOR REPAIR OF CONDUCTING PATHS IN POLYCERAMIC SYSTEMS Final Report, 1 Jul. - 31 Dec. 1993
Guang-Way Jang 24 Feb. 1994 32 p Limited Reproducibility: More than 20% of this document may be affected by microfiche quality
(Contract F49620-93-C-0048)
(AD-A278381; AFOSR-94-0187TR) Avail: CASI HC A03

The present project involves research and development of conducting polymer sol-gel composites for repair of conducting paths in polyceramic systems. During Phase 1, we developed and carried out the synthesis of processible conducting polymers and organic/inorganic hybrid sol-gel materials. Sol-gel composite materials prepared during Phase 1, I have high electrical conductivity (ca. 30 S/cm) and adhere strongly on the surface of ceramic materials. The conductivity of ITO glass was the same as its original value after repairing a crack with these sol-gel composites. Conductive sol-gel composites can be prepared with a very small amount of processible conducting polymers, ca. 3%. Composites with high concentration of conducting polymers (70% - 90%), however, showed better stability. Sol-gel metal oxides and conducting polymers are also ideal electrode materials for the fabrication of multilayer capacitors and rechargeable batteries. Upon completion of the present work, it is evident that the feasibility of the technology proposed for repairing conducting paths in polyceramic systems was demonstrated. DTIC

N94-33352# United Technologies Research Center, East Hartford, CT.
NOVEL PRECURSOR APPROACHED FOR CMC DERIVED BY POLYMER PYROLYSIS Final Report, 15 Dec. 1990 - 14 Dec. 1993
Wayde R. Schmidt 15 Feb. 1994 56 p
(Contract F49620-91-C-0017)
(AD-A278383; R94-970051-3; AFOSR-94-0198TR) Avail: CASI HC A04/MF A01

A family of reactive endblocked poly(methylvinylsilane), PMVS, polymers was developed for fabricating fiber-reinforced silicon carbide ceramic matrix composites (CMC's). Control of reaction conditions was optimized to synthesize a baseline PMVS in multiple batches and sufficient quantity to examine modifications of the polymer chemistry during processing and pyrolysis. The conversion of PMVS to carbon-rich nanocrystalline silicon carbide ceramic was studied using a variety of analytical techniques, including thermal analysis, infrared and nuclear magnetic resonance spectroscopy, x-ray diffraction, and electron microscopy. The excess C in PMVS ceramic chars was effectively scavenged with an added Si source. Perhydropoly(silazane), PHPS, provided a polymer precursor source of Si3N4 and excess Si. Blends of PHPS and PMVS had higher char yields (70-85%) than either component polymer and generated novel nanocrystalline ceramics with heating to 1600 C. Crystal growth was inhibited in chars derived from these blends. Added elemental Si reacted with the excess C and enhanced crystal growth of SiC above the melting point of Si. Representative CMC's with good mechanical properties were fabricated using several PMVS-based matrix sources. The CMC's showed load vs. deflection curves typical of non-brittle failure and tensile specimens showed fibrous failure. DTIC

N94-31013*# National Aeronautics and Space Administration. Marshall Space Flight Center, Huntsville, AL.
THE PERFORMANCE OF THERMAL CONTROL COATINGS ON LDEF AND IMPLICATIONS TO FUTURE SPACECRAFT
Donald R. Wilkes (AZ Technology, Huntsville, AL.), Edgar R. Miller (AZ Technology, Huntsville, AL.), Richard J. Mell (AZ Technology, Huntsville, AL.), Paul S. LeMaster (AZ Technology, Huntsville, AL.), and James M. Zwiener *In its* LDEF Materials Results for Spacecraft Applications Dec. 1993 p 3-20 (For primary document see N94-31012 09-12)
Avail: CASI HC A03/MF A04

N94-31014*# Boeing Defense and Space Group, Seattle, WA.
PERFORMANCE OF SILVERED TEFLON (TRADEMARK) THERMAL CONTROL BLANKETS ON SPACECRAFT
Gary Pippin, Wayne Stuckey, and Carol Hemminger *In* NASA. Marshall Space Flight Center, LDEF Materials Results for Spacecraft Applications Dec. 1993 p 21-30 (For primary document see N94-31012 09-12)
Avail: CASI HC A02/MF A04

N94-31015*# National Aeronautics and Space Administration. Marshall Space Flight Center, Huntsville, AL.
SPACE ENVIRONMENT DURABILITY OF BETA CLOTH IN LDEF THERMAL BLANKETS
Roger C. Linton, Ann F. Whitaker, and Miria M. Finckenor *In its* LDEF Materials Results for Spacecraft Applications Dec. 1993 p 31-45 (For primary document see N94-31012 09-12)
Avail: CASI HC A03/MF A04

N94-31016*# McDonnell-Douglas Aerospace, Huntington Beach, CA.
SPACE STATION WP-2 APPLICATION OF LDEF MLI RESULTS
Charles A. Smith, Mark M. Hasegawa, and Cherie A. Jones *In* NASA. Marshall Space Flight Center, LDEF Materials Results for Spacecraft Applications Dec. 1993 p 47-60 (For primary document see N94-31012 09-12)
Avail: CASI HC A03/MF A04

N94-31018*# European Space Agency. European Space Research and Technology Center, ESTEC, Noordwijk (Netherlands).
FOLLOW-UP ON THE EFFECTS OF THE SPACE ENVIRONMENT ON UHCRE THERMAL BLANKETS
Francois Levadou and Marc vanEesbeek *In* NASA. Marshall Space Flight Center, LDEF Materials Results for Spacecraft Applications Dec. 1993 p 73-84 (For primary document see N94-31012 09-12)
Avail: CASI HC A03/MF A04

N94-31022*# National Aeronautics and Space Administration. Marshall Space Flight Center, Huntsville, AL.
ATOMIC OXYGEN EROSION CONSIDERATIONS FOR SPACECRAFT MATERIALS SELECTION
Ann F. Whitaker and Rachel R. Kamenetzky *In its* LDEF Materials Results for Spacecraft Applications Dec. 1993 p 117-123 (For primary document see N94-31012 09-12)
Avail: CASI HC A02/MF A04

N94-31023*# National Aeronautics and Space Administration. Langley Research Center, Hampton, VA.
PERFORMANCE OF SELECTED POLYMERIC MATERIALS ON LDEF
Philip R. Young, Wayne s. Slemp, and Bland A. Stein *In* NASA. Marshall Space Flight Center, LDEF Materials Results for Spacecraft Applications Dec. 1993 p 125-142 (For primary document see N94-31012 09-12)
Avail: CASI HC A03/MF A04

N94-31024*# National Aeronautics and Space Administration. Lewis Research Center, Cleveland, OH.
ATOMIC OXYGEN INTERACTION AT DEFECT SIGHTS IN PROTECTIVE COATINGS ON POLYMERS FLOWN ON LDEF
Bruce A. Banks, Kim K. deGroh, Bruce M. Auer, Linda Gebauer, and Cynthia LaMoreaux *In* NASA. Marshall Space Flight Center, LDEF Materials Results for Spacecraft Applications Dec. 1993 p 143-158 (For primary document see N94-31012 09-12)
Avail: CASI HC A03/MF A04

N94-31026*# Southwest Research Inst., San Antonio, TX.
LASER-INDUCED FLUORESCENCE OF SPACE-EXPOSED POLYURETHANE
Ralph H. Hill, Jr. *In* NASA. Marshall Space Flight Center, LDEF Materials Results for Spacecraft Applications Dec. 1993 p 179-192 (For primary document see N94-31012 09-12)
Avail: CASI HC A03/MF A04

N94-31030*# Vanderbilt Univ., Nashville, TN.
PHYSICAL PROPERTIES OF GLASSES EXPOSED TO EARTH-FACING AND TRAILING-SIDE ENVIRONMENTS ON LDEF
David E. Wiedlocher, Donald L. Kinser, Robert A. Weller, Robert A. Weeks, and Marcus H. Mendenhall *In* NASA. Marshall Space Flight Center, LDEF Materials Results for Spacecraft Applications Dec. 1993 p 227-243 (For primary document see N94-31012 09-12)
(Contracts NAG8-156; NAS8-32695; L-17761D)
Avail: CASI HC A03/MF A04

N94-31037*# National Aeronautics and Space Administration. Langley Research Center, Hampton, VA.
SUMMARY OF MATERIALS AND HARDWARE PERFORMANCE ON LDEF
Harry Dursch (Boeing Defense and Space Group, Seattle, WA.), Gary Pippin (Boeing Defense and Space Group, Seattle, WA.), and Lou Teichman *In* NASA. Marshall Space Flight Center, LDEF Materials Results for Spacecraft Applications Dec. 1993 p 355-369 (For primary document see N94-31012 09-12)
(Contracts NAS1-18224; NAS1-19247)
Avail: CASI HC A03/MF A04

N94-31039*# National Aeronautics and Space Administration. Lyndon B. Johnson Space Center, Houston, TX.
GROUND-BASED SIMULATION OF LEO ENVIRONMENT: INVESTIGATIONS OF A SELECT LDEF MATERIAL: FEP TEFLON (TRADEMARK)
Jon B. Cross (Los Alamos National Lab., NM.) and Steven L. Koontz *In* NASA. Marshall Space Flight Center, LDEF Materials Results for Spacecraft Applications Dec. 1993 p 379-389 (For primary document see N94-31012 09-12)
Avail: CASI HC A03/MF A04

N94-31041*# Rome Lab., Griffiss AFB, NY.
ANALYSIS OF LEADING EDGE AND TRAILING EDGE COVER GLASS SAMPLES BEFORE AND AFTER TREATMENT WITH ADVANCED SATELLITE CONTAMINATION REMOVAL TECHNIQUES

S. P. Hotaling *In* NASA. Marshall Space Flight Center, LDEF Materials Results for Spacecraft Applications Dec. 1993 p 419-436 (For primary document see N94-31012 09-12)
Avail: CASI HC A03/MF A04

N94-31042*# Alabama Univ., Huntsville. Surface Science Labs.
PRELIMINARY RESULTS FROM THE CONCAP-2-01 AND EIOM-3 EXPERIMENTS ON STS-46
John C. Gregory and Ganesh N. Raikar *In* NASA. Marshall Space Flight Center, LDEF Materials Results for Spacecraft Applications Dec. 1993 p 439-453 (For primary document see N94-31012 09-12)
Avail: CASI HC A03/MF A04

N94-31046*# National Aeronautics and Space Administration. Ames Research Center, Moffett Field, CA.
CHARACTERIZATION OF POLYMER DECOMPOSITION PRODUCTS BY LASER DESORPTION MASS SPECTROMETRY
Joan B. Pallix, Kenneth A. Lincoln, Charles J. Miglionico, Robert E. Roybal, Charles Stein, and Jon H. Shively *In* NASA. Marshall Space Flight Center, LDEF Materials Results for Spacecraft Applications Dec. 1993 p 499-509 (For primary document see N94-31012 09-12)
Avail: CASI HC A03/MF A04

N94-33131*# Iowa Univ., Iowa City. Dept. of Biomedical Engineering.
INDENTABILITY OF CONVENTIONAL AND NEGATIVE POISSON'S RATIO FOAMS
R. S. Lakes and K. Elms *In* NASA. Langley Research Center, Second NASA Advanced Composites Technology Conference Jun. 1992 p 239-242 (For primary document see N94-33121 09-24)
Avail: CASI HC A01/MF A04

N94-33311*# European Space Tribology Lab., Risley (England).
A COMPARISON OF THE PERFORMANCE OF SOLID AND LIQUID LUBRICANTS IN OSCILLATING SPACECRAFT BALL BEARINGS
S. Gill *In* NASA. Lewis Research Center, The 28th Aerospace Mechanisms Symposium May 1994 p 229-244 (For primary document see N94-33291 09-15)
Avail: CASI HC A03/MF A04

N94-33313*# National Aeronautics and Space Administration. Lewis Research Center, Cleveland, OH.
THE PRELIMINARY EVALUATION OF LIQUID LUBRICANTS FOR SPACE APPLICATIONS BY VACUUM TRIBOMETRY
W. R. Jones, Jr., S. V. Pepper, P. Herrera-Fierro, D. Feuchter, T. J. Toddy, D. T. Jayne, D. R. Wheeler, P. B. Abel, E. Kingsbury, and W. Morales et al *In its* The 28th Aerospace Mechanisms Symposium May 1994 p 265-277 (For primary document see N94-33291 09-15)
Avail: CASI HC A03/MF A04

28 PROPELLANTS AND FUELS

Includes rocket propellants, igniters, and oxidizers; their storage and handling procedures; and aircraft fuels.

For related information see also *07 Aircraft Propulsion and Power, 20 Spacecraft Propulsion and Power,* and *44 Energy Production and Conversion.*

N94-31579# Sandia National Labs., Albuquerque, NM.
LASER DIODE IGNITION (LDI)
W. J. Kass, L. A. Andrews, C. M. Boney, Weng W. Chow, J. W. Clements, J. A. Merson, F. J. Salas, R. J. Williams, and L. R. Hinkle 1994 7 p Presented at the 1994 NASA Pyrotechnic Systems Workshop, Albuquerque, NM, 8-9 Feb. 1994
(Contract DE-AC04-94AL-85000)
(DE94-006590; SAND-94-0259C; CONF-940245-2) Avail: CASI HC A02/MF A01 (US Sales Only)

This paper reviews the status of the laser diode ignition (LDI) program at Sandia National Labs. One-watt laser diodes have been characterized for use with a single explosive actuator. Extensive measurements of the effect of electrostatic discharge (ESD) pulses on the laser diode optical output have been made. Characterization of optical fiber and connectors over temperature has been done. Multiple laser diodes have been packaged to ignite multiple explosive devices and an eight element laser diode array has been recently tested by igniting eight explosive devices at predetermined 100 ms intervals. DOE

N94-31827# Sandia National Labs., Albuquerque, NM.
A LOW COST IGNITER UTILIZING AN SCB AND TITANIUM SUB-HYDRIDE POTASSIUM PERCHLORATE PYROTECHNIC
R. W. Bickes, Jr., M. C. Grubelich, J. K. Hartman, C. B. McCampbell, and J. K. Churchill 1993 4 p Presented at the 1994 National Aeronautics and Space Administration Pyrotechnic Systems Workshop, Albuquerque, NM, 8-9 Feb. 1994
(Contract DE-AC04-94AL-85000)
(DE94-006467; SAND-93-1734C; CONF-940245-1) Avail: CASI HC A01/MF A01

A conventional NSI (NASA standard initiator) normally employs a hot-wire ignition element to ignite ZPP (zirconium potassium perchlorate). With minor modifications to the interior of a header similar to an NSI device to accommodate an SCB (semiconductor bridge), a low cost initiator was obtained. In addition, the ZPP was replaced with THKP (titanium subhydride potassium perchlorate) to obtain increased overall gas production and reduced static-charge sensitivity. This paper reports on the all-fire and no-fire levels obtained and on a dual mix device that uses THKP as the igniter mix and a thermite as the output mix. DOE

N94-32114 Lawrence Livermore National Lab., CA.
SCENARIOS FOR MULTI-UNIT INERTIAL FUSION ENERGY PLANTS PRODUCING HYDROGEN FUEL
B. G. Logan Dec. 1993 6 p Presented at the 11th International Workshop on Laser Interaction and Related Plasma Phenomena, Monterey, CA, 25-29 Oct. 1993 Limited Reproducibility: More than 20% of this document may be affected by microfiche quality
(Contract W-7405-eng-48)
(DE94-006614; UCRL-JC-114495; CONF-931048-6) Avail: CASI HC A02

This work describes the following: (1) the motivation for considering fusion, in general, and Inertial Fusion Energy (IFE), in particular, to produce hydrogen fuel powering low-emission vehicles; (2) the general requirements for any fusion electric plant to produce hydrogen by water electrolysis at costs competitive with present consumer gasoline fuel costs per passenger mile, for advanced car architectures meeting President Clinton's 80 mpg advanced car goal; and (3) a comparative economic analysis for the potential cost of electricity (CoE) and corresponding cost of hydrogen (CoH) from a variety of multi-unit IFE plants with one to eight target chambers sharing a common driver and target fab facility. Cases with either heavy-ion or diode-pumped, solid-state laser drivers are considered, with 'conventional' indirect drive target gains versus 'advanced, e.g. Fast Ignitor' direct drive gain assumptions, and with conventional steam balance-of-plant (BoP) versus advanced MHD plus steam combined cycle BoP, to contrast the potential economics under 'conventional' and 'advanced' IFE assumptions, respectively. DOE

N94-32132# North Carolina State Univ., Raleigh. Dept. of Chemical Engineering.
NOVEL APPROACHES TO THE PRODUCTION OF HIGHER ALCOHOLS FROM SYNTHESIS GAS
22 Nov. 1993 25 p
(Contract DE-AC22-90PC-90043)
(DE94-006770; DOE/PC-90043/T12) Avail: CASI HC A03/MF A01

This document reports work during this quarter on the project to produce higher alcohols from synthesis gas. A set of four methanol synthesis runs was conducted. Significant catalyst deactivation was experienced, and essentially all of the oil was lost from the reactor over the course of two weeks of operation. Three screening runs of potential high temperature oil were also conducted. However, essentially no oil remained in the reactor after completion of each run. A 1%Rh/1.3%Re/Al2O3 catalyst was prepared from Re and Rh carbonyls with the objective of obtaining intimate contact between Rh and Re atoms. The catalytic activity of this catalyst was explored. Mo was deposited on the catalyst from both molybdenum hexacarbonyl (Mo(CO)6) and (NH4)6Mo7O24(center dot)4H2O.The catalytic activity of the molybdenum promoted catalysts was found to be the highest achieved to date under this contract. DOE

N94-32133# Lehigh Univ., Bethlehem, PA.
HIGH OCTANE ETHERS FROM SYNTHESIS GAS-DERIVED ALCOHOLS
K. Klier, R. G. Herman, O. C. Feeley, and M. A. Johansson Nov. 1993 20 p
(Contract DE-AC22-90PC-90044)
(DE94-006774; DOE/PC-90044/12) Avail: CASI HC A03/MF A01

The objective of the proposed research is to synthesize oxygenated fuel ethers, primarily methyl isobutyl ether (MIBE) and methyl tertiary butyl ether (MTBE), directly from coal-derived H2/CO/CO2 synthesis via alcohol mixtures that are rich in methanol and 2-methyl-1-proanol (isobutanol). The overall scheme involves gasification of coal, purification and shifting of the synthesis gas, higher alcohol synthesis, and direct synthesis of ethers. Both organic and inorganic catalysts will be investigated, and the better catalysts will be subjected to long term performance studies. The project is divided into the following three tasks: (1) synthesis of high octane ethers from alcohol mixtures containing predominantly methanol and 2-methyl-1-propanol over superacid resins, (2) inorganic catalysts for the synthesis of high octane ethers form alcohols, and (3) long term performance and reaction engineering for scale-up of the alcohols-to-ether process. A summary of technical progress is provided in this report. DOE

N94-32148# Lawrence Livermore National Lab., CA.
THE HYDROGEN HYBRID OPTION
J. R. Smith 15 Oct. 1993 12 p Presented at the Workshop on Advanced Components for Electric and Hybrid Electric Vehicles, Gaithersburg, MD, 27-28 Oct. 1993
(Contract W-7405-eng-48)
(DE94-006733; UCRL-JC-115425; CONF-9310282-1) Avail: CASI HC A03/MF A01

The energy efficiency of various piston engine options for series hybrid automobiles are compared with conventional, battery powered electric, and proton exchange membrane (PEM) fuel cell hybrid automobiles. Gasoline, compressed natural gas (CNG), and hydrogen are considered for these hybrids. The engine and fuel comparisons are done on a basis of equal vehicle weight, drag, and rolling resistance. The relative emissions of these various fueled vehicle options are also presented. It is concluded that a highly optimized, hydrogen fueled, piston engine, series electric hybrid automobile will have efficiency comparable to a similar fuel cell hybrid automobile and will have fewer total emissions than the battery powered vehicle, even without a catalyst. DOE

N94-32150# Pennsylvania State Univ., University Park.
ADVANCED THERMALLY STABLE JET FUELS
H. H. Schobert, S. Eser, C. Song, P. G. Hatcher, P. M. Walsh, and M. M. Coleman Jul. 1993 124 p
(Contract DE-FG22-92PC-92104)
(DE94-006760; DOE/PC-92104/T3) Avail: CASI HC A06/MF A02

This project was initiated on August 1, 1992. The starting date resulted in this project being one month out of synchronization with the normal quarterly calendar (i.e., January, April, July, and October). On advice of Mr. John Augustine, DOE/PETC, the present report is prepared to cover only two months work, so that future quarterly reports will be aligned with the conventional reporting schedule. A significant pressure dependence was observed for the pyrolysis of n-tetradecane at 450 C for 30 min. It appears that at least two processes are affected by the reactant pressure, but in opposite directions. The influence of inert gas pressure is dependent on both the initial sample volume and the pressure range. However, when the inert gas pressure is within a certain specific range, the changes in the sample volume have no impact on n-tetradecane conversion. Below or above this range, increasing inert gas pressure can either decrease or increase conversion, depending on the sample volume. DOE

N94-32583# Union Carbide Corp., South Charleston, WV.
HETEROGENEOUS CATALYTIC PROCESS FOR ALCOHOL FUELS FROM SYNGAS
Jul. 1993 23 p
(Contract DE-AC22-91PC-90046)
(DE94-008729; DOE/PC-90046/T8) Avail: CASI HC A03/MF A01

The principal objectives of this project are to discover and evaluate novel heterogeneous catalysis for conversion of syngas to oxygenates having use as fuel enhancers, to explore novel reactor and process concepts applicable in this process, and to develop the best total process for converting syngas to liquid fuels. This project is being pursued as two concurrent tasks. Task 1 involves catalyst research and development and is being largely conducted by catalyst chemists and analytical specialists. Task 2 is largely an engineering activity, and includes process conceptualization and economics and bench-scale process evaluation of systems developed in Task 1. The current targets for isobutanol-producing catalysts are to produce an equimolar mixture of methanol and isobutanol with a productivity for isobutanol of more than 50 g/Kg-hr. The present report describes technical progress in Task 1, Catalyst Studies, in catalyst preparation (potassium effects) and in determining the effects of process variables on catalyst performance. Task 1 conclusions are presented. Progress in Task 2, Engineering Studies, is reported in reaction engineering. Conclusions reached from the engineering studies are also presented. DOE

N94-33013# Waterloo Univ. (Ontario). Dept. of Chemistry.
LASER AND FOURIER TRANSFORM SPECTROSCOPY OF NOVEL PROPELLANT MOLECULES Final Report, 1 Apr. 1990 - 30 Sep. 1993
Peter F. Bernath Jan. 1994 20 p
(Contract F29601-91-C-0100)
(AD-A277506; AD-E201761; PL-TR-93-3088) Avail: CASI HC A03/MF A01

A wide variety of molecules were studied by the techniques of Fourier transform spectroscopy and visible laser spectroscopy. Molecules studied include CCN, CaBHsub4, CHsub3N, CN, IF, ICl, IBr, BC, CH, Csub2, Csub3, Csub60, LiF, AlF, AlCl, HF, HCl, BeFsub2, BiH, AlH, BaH, and GaH. These molecules were detected by infrared, visible and ultraviolet emission and absorption measurements. DTIC

29 MATERIALS PROCESSING

Includes space-based development of products and processes for commercial applications.

For biological materials see *55 Space Biology*.

N94-31884* National Aeronautics and Space Administration. Lewis Research Center, Cleveland, OH.
DEFYING GRAVITY (Videotape)
1993 Videotape: 7 min. playing time, in color, with sound
(NASA-TM-109747; NONP-VT-94-9947) Avail: CASI VHS A01/BETA A22

This video tape examines microgravity research that is ongoing at LeRC. The video details the development of the Multiple Axis Space Test and its use in training the Mercury 7 astronauts. The LeRC drop tower is discussed, and a comparison is made between research being done at LeRC and rides anyone can experience at the nearby Cedar Point Amusement Park. CASI

N94-31944 Toledo Univ., OH.
AN EXPERIMENTAL STUDY OF VOID FORMATION DURING ALUMINUM SOLIDIFICATION IN REDUCED GRAVITY Ph.D. Thesis
Francis Paul Chiaramonte, III 1993 133 p
Avail: Univ. Microfilms Order No. DA9326130

Void formation due to volumetric shrinkage and liquid/vapor reorientation during aluminum solidification was observed in real time using a radiographic viewing system in normal and reduced gravity. An end-chill directional solidification furnace with water quench was designed and constructed to solidify aluminum samples during the approximately 16 seconds of reduced gravity (+/- 0.02 g) achieved by flying an aircraft through a parabolic trajectory. In the first series of tests, the aluminum was contained in a vacuum sealed, pyrolytic boron nitride crucible. An ullage space was present during each test. Void formation was recorded for two cases: a nonwetting system and a wetting system where wetting occurs between the aluminum and the crucible lid. The void formation in the nonwetting case was similar in normal and reduced gravity, with a single vapor cavity forming at the top of the crucible. In the wetting case in reduced gravity, surface tension caused two voids to form in the top corners of the crucible, but in normal gravity only one large void forms across the top. In the second series of tests, the aluminum was contained in a pyrolytic boron nitride crucible which was placed in a stainless steel container and sealed in an Ar/4 percent H2 environment. An ullage space was present during each test.

Void formation was recorded for two cases: a nonwetting system and a wetting system where wetting occurs between the aluminum and one side wall and lid. The void formation in the nonwetting case was similar in normal and reduced gravity with a single vapor cavity forming at the top of the crucible; although the meniscus became more convex in reduced gravity. In the wetting case, the aluminum did not climb up the corners in one-g and one large symmetric void resulted at the top when solidified. In the wetting case during reduced gravity, the molten aluminum was drawn up the wetted wall and partially across the lid by a capillary underpressure; however, on the nonwetting wall the aluminum moved down. One void resulted along the nonwetting side of the container continuing to the top on the same side. Dissert. Abstr.

N94-32715 Colorado Univ., Boulder.
BOUNDARY ELEMENT ANALYSIS OF THREE-DIMENSIONAL NONLINEAR HYDRODYNAMICS IN A REDUCED GRAVITY ENVIRONMENT Ph.D. Thesis
Stephen Holbrook Sutherland 1992 172 p
Avail: Univ. Microfilms Order No. DA9318140

The development and implementation of a numerical technique for solving problems in two and three dimensional nonlinear hydrodynamics is described. The computational method, which employs both boundary element and finite element techniques, is an extension to three dimensions of recently developed two dimensional approaches supplemented with an explicit treatment of surface tension effects. Four, eight, and twelve node quadrilateral elements are implemented in the method. All element integrals that arise in the discretization process are evaluated numerically, which enables modeling of very general fluid domains. Test cases involving two and three dimensional nonlinear hydrodynamics including nonlinear solitary wave propagation and run-up, two dimensional nonlinear standing waves with and without surface tension effects, harmonic wave excitation in a cylindrical geometry, and axisymmetric free oscillation of an annular fluid body under low-gravity conditions are solved with the method to demonstrate its capability and accuracy. The test-case analysis predictions are compared with theoretical results and experimental data with good correlation obtained in each instance. Dissert. Abstr.

N94-33037*# Colorado Univ., Boulder. Center for Space Construction.
A LARGE MOTION ZERO-GRAVITY SUSPENSION SYSTEM FOR EXPERIMENTAL SIMULATION OF ORBITAL CONSTRUCTION AND DEPLOYMENT M.S. Thesis
Timothy Milton Straube Dec. 1993 62 p
(Grants NAGw-1388; NAG1-1490)
(NASA-CR-195881; NAS 1.26:195881; CSC-93-34) Avail: CASI HC A04/MF A01

The design and implementation of a vertical degree of freedom suspension system is described which provides a constant force off-load condition to counter gravity over large displacements. By accommodating motions up to one meter for structures weighing up to 100 pounds, the system is useful for experiments which simulate orbital construction events such as docking, multiple component assembly, or structural deployment. A unique aspect of this device is the combination of a large stroke passive off-load device augmented by electromotive torque actuated force feedback. The active force feedback has the effect of reducing break-away friction by a factor of twenty over the passive system alone. The thesis describes the development of the suspension hardware and the control algorithm. Experiments were performed to verify the suspensions system's effectiveness in providing a gravity off-load and simulating the motion of a structure in orbit. Additionally, a three dimensional system concept is presented as an extension of the one dimensional suspension system which was implemented. Author (revised)

31 ENGINEERING (GENERAL)

Includes vacuum technology; control engineering; display engineering; cryogenics; and fire prevention.

N94-31073 Selskapet for Industriell og Teknisk Forskning, Trondheim (Norway). Div. of Refrigeration Engineering.
APPLICATION OF NATURAL REFRIGERANTS: A RATIONAL SOLUTION TO A PRESSING PROBLEM
G. Lorentzen 25 Mar. 1993 13 p See also PB93-201382
(PB94-138781; STF11-A93032) Avail: Issuing Activity (National Technical Information Service (NTIS))

Experience has shown that release to the atmosphere of large quantities of chemicals which are foreign to nature often leads to unforeseen problems. A better strategy must be to use substances which are already present in the biosphere, and for which natural circulation systems already exist. Ammonia has been used for generations and can be applied successfully for a wide field. Propane has advantages for some special applications. Recent research has shown that carbon dioxide can be used as a near ideal refrigerant in many cases with new and energy efficient thermodynamic cycles. NTIS

N94-31364# Naval Surface Warfare Center, Dahlgren, VA.
NAVAL SURFACE WARFARE CENTER DAHLGREN DIVISION TECHNICAL DIGEST: ADVANCED MATERIALS TECHNOLOGY
Sep. 1993 153 p
(AD-A276448; NSWCDD/MP-93/200) Avail: CASI HC A08/MF A02

The Dahlgren Division conducts full-spectrum research, development, test and evaluation (RDT and E), and fleet support on advanced materials and materials processes for application to ordnance and weapon systems. We emphasize various core technologies such as advanced ceramics, warhead materials, electrochemistry, polymer science, acoustic materials, composites, magnetostrictive materials, semiconductor materials, thermal management materials, radiation sensor materials, energetic materials, biotechnology, surface science, and nondestructive evaluation. Spin-off technologies for dual use are also actively pursued. This issue of the Digest includes articles on engineered materials, energetic materials, and the characterization of materials. DTIC

N94-31604# American Foundreymens' Society, Des Plaines, IL.
EXPANDABLE PATTERN CASTING RESEARCH
1993 104 p Prepared in cooperation with Southern Research Inst., Birmingham, AL
(Contract DE-FC07-89ID-12869)
(DE94-004342; DOE/ID-12869/3) Avail: CASI HC A06/MF A02

The Expandable Pattern Casting (EPC) Process is a developing foundry technology that allows designers the opportunity to consolidate parts, reduce machining, and minimize assembly operations. An air gauging system was developed for measuring foam patterns; exact shrinkage depended on type and density of the foam. Compaction studies showed that maximum sand densities in cavities and under overhangs are achieved with vibrational amplitudes 0.001-0.004 in., and that sand moved most freely within a few inches of the top free surface. Key to complete mold filling while minimizing casting defects lies in removing the foam decomposition products. The most precise iron castings were made by EPC in four commercial EPC foundries, with attention paid to molding and compaction. EP cast 60-45-12 ductile iron had yield strengths, ultimate strengths, and elastic modulus similar to conventionally cast ductile iron cast from the same ladle. DOE

N94-31838 Selskapet for Industriell og Teknisk Forskning, Trondheim (Norway). Div. of Safety and Reliability.
SCIENTIFIC BASIS FOR SAFETY SCIENCE
J. Vatn and G. Aem 1 Jul. 1993 134 p See also NUREG/CR-1278-F, NUREG/CR-3518-V1, and NUREG/CR-3518-V2
(PB94-138534; STF75-A93038) Avail: Issuing Activity (National Technical Information Service (NTIS))

This report summarizes the results from a seminar about the scientific basis for safety science. The seminar was held 22-24 April, 1993. Papers presented at the seminar are included, along with comments. Scientific standards for safety science are presented. NTIS

N94-32412 Sandia National Labs., Albuquerque, NM.
SANDIA TECHNOLOGY ENGINEERING AND SCIENCE ACCOMPLISHMENTS
Feb. 1994 72 p Limited Reproducibility: More than 20% of this document may be affected by poor print
(Contract DE-AC04-94AL-85000)
(DE94-008312; SAND-93-2687) Avail: Issuing Activity (Department of Energy (DOE))

This report briefly discusses the following research being conducted at Sandia Laboratories: Advanced Manufacturing -- Sandia technology helps

keep US industry in the lead; Microelectronics -- Sandia's unique facilities transform research advances into manufacturable products; Energy -- Sandia's energy programs focus on strengthening industrial growth and political decisionmaking; Environment -- Sandia is a leader in environmentally conscious manufacturing and hazardous waste reduction; Health Care -- New biomedical technologies help reduce cost and improve quality of health care; Information & Computation -- Sandia aims to help make the information age a reality; Transportation -- This new initiative at the Labs will help improve transportation, safety, efficiency, and economy; Nonproliferation -- Dismantlement and arms control are major areas of emphasis at Sandia; and Awards and Patents -- Talented, dedicated employees are the backbone of Sandia's success. DOE

N94-32484* Creare, Inc., Hanover, NH. Engineering Research and Development Services.

THE 4 K STIRLING CRYOCOOLER DEMONSTRATION Final Report No. 8, 1 May 1990 - 30 Apr. 1992

W. Dodd Stacy 22 Sep. 1992 38 p

(Contract NAS7-1111; SBIR-08.12-3800)

(NASA-CR-191792; NAS 1.26:191792; TM-1563) Avail: CASI HC A03/MF A01

This report briefly summarizes the results and conclusions from an SBIR program intended to demonstrate an innovative Stirling cycle cryocooler concept for efficiently lifting heat from 4 K. Refrigeration at 4 K, a temperature useful for superconductors and sensitive instruments, is beyond the reach of conventional regenerative thermodynamic cycles due to the rapid loss of regenerator matrix heat capacity at temperatures below about 20 K. To overcome this fundamental limit, the cryocooler developed under this program integrated three unique features: recuperative regeneration between the displacement gas flow streams of two independent Stirling cycles operating at a 180 degree phase angle, tailored distortion of the two expander volume waveforms from sinusoidal to perfectly match the instantaneous regenerator heat flux from the two cycles and thereby unload the regenerator, and metal diaphragm working volumes to promote near isothermal expansion and compression processes. Use of diaphragms also provides unlimited operating life potential and eliminates bearings and high precision running seals. A phase 1 proof-of-principle experiment demonstrated that counterflow regenerator operation between 77 K and 4 K increases regenerator effectiveness by minimizing metal temperature transient cycling. In phase 2, a detailed design package for a breadboard cryocooler was completed. Fabrication techniques were successfully developed for manufacturing high precision miniature parallel plate recuperators, and samples were produced and inspected. Process development for fabricating suitably flat diaphragms proved more difficult and expensive than anticipated, and construction of the cryocooler was suspended at a completion level of approximately 75%. Subsequent development efforts on other projects have successfully overcome diaphragm fabrication difficulties, and alternate funding is currently being sought for completion and demonstration testing of the 4 K Stirling cryocooler.

Author

N94-32839# Lawrence Livermore National Lab., CA.

LLNL CASTING TECHNOLOGY

A. B. Shapiro, ed. and W. J. Comfort, III, ed. Jan. 1994 9 p

(Contract W-7405-eng-48)

(DE94-008282; UCRL-ID-116320) Avail: CASI HC A02/MF A01

Competition to produce cast parts of higher quality, lower rejection rate, and lower cost is a fundamental factor in the global economy. To gain an edge on foreign competitors, the US casting industry must cut manufacturing costs and reduce the time from design to market. Casting research and development (R&D) are the key to increasing US competiveness in the casting arena. Lawrence Livermore National Laboratory (LLNL) is the home of a wide range of R&D projects that push the boundaries of state-of-the art casting. LLNL casting expertise and technology include: casting modeling research and development, including numerical simulation of fluid flow, heat transfer, reaction/solidification kinetics, and part distortion with residual stresses; special facilities to cast toxic material; extensive experience casting metals and nonmetals; advanced measurement and instrumentation systems. Department of Energy (DOE) funding provides the leverage for LLNL to collaborate with industrial partners to share this advanced casting expertise and technology. At the same time, collaboration with industrial partners provides LLNL technologists with broader insights into casting industry issues, casting process data, and the collective experience of industry experts. Casting R&D is also an excellent example of dual-use technology; it is the cornerstone for increasing US industrial competitiveness and minimizing waste nuclear material in weapon component production. Annual funding for casting projects at LLNL is $10M, which represents 1% of the total LLNL budget. Metal casting accounts for about 80% of the funding. Funding is nearly equally divided between development directed toward US industrial competitiveness and weapon component casting. DOE

N94-32857*# Hydrogen Consultants, Inc., Littleton, CO.

METAL HYDRIDE HEAT PUMP ENGINEERING DEMONSTRATION AND EVALUATION MODEL Final Report

Franklin E. Lynch Oct. 1993 64 p

(Contract NAS9-17819)

(NASA-CR-188286; NAS 1.26:188286) Avail: CASI HC A04/MF A01

Future generations of portable life support systems (PLSS's) for space suites (extravehicular mobility units or EMU's) may require regenerable nonventing thermal sinks (RNTS's). For purposes of mobility, a PLSS must be as light and compact as possible. Previous venting PLSS's have employed water sublimators to reject metabolic and equipment heat from EMU's. It is desirable for long-duration future space missions to minimize the use of water and other consumables that need to be periodically resupplied. The emission of water vapor also interferes with some types of instrumentation that might be used in future space exploration. The test article is a type of RNTS based on a metal hydride heat pump (MHHP). The task of reservicing EMU's after use must be made less demanding in terms of time, procedures, and equipment. The capability for quick turnaround post-EVA servicing (30 minutes) is a challenging requirement for many of the RNTS options. The MHHP is a very simple option that can be regenerated in the airlock within the 30 minute limit by the application of a heating source and a cooling sink. In addition, advanced PLSS's must provide a greater degree of automatic control, relieving astronauts of the need to manually adjust temperatures in their liquid cooled ventilation garments (LCVG's). The MHHP includes automatic coolant controls with the ability to follow thermal load swings from minimum to maximum in seconds. The MHHP includes a coolant loop subsystem with pump and controls, regeneration equipment for post-EVA servicing, and a PC-based data acquisition and control system (DACS). Derived from text

N94-32861*# National Aeronautics and Space Administration. Lewis Research Center, Cleveland, OH.

CONTROLLING HAZARDOUS ENERGY SOURCES (LOCKOUT/TAGOUT)

Manuel B. Dominguez Oct. 1991 16 p

(NASA-TM-105290; E-6627; NAS 1.15:105290) Avail: CASI HC A03/MF A01

The minimum requirements as established by the Occupational Safety and Health Administration (OSHA) standard 29 CFR 1910.147 are discussed for preventing the unexpected operation of equipment or release of energy which could cause injury to personnel, damage to equipment, harm to the environment, or loss or compromise of test data. Safety requirements both for government and contractor personnel are explained for potentially hazardous energy sources during work operations at LeRC (Cleveland and Plum Brook Stations). Basic rules are presented to ensure protection against harmful exposures, and baseline implementation requirements are discussed from which detailed lockout/tagout procedures can be developed for individual equipment items. Examples of energy sources covered by this document include electrical, pneumatic, mechanical, chemical, cryogenic, thermal, spring tension/compression suspended or moving loads, and other potentially hazardous sources. Activities covered by this standard include, but are not limited to, construction, maintenance, installation, calibration, inspection, cleaning, or repair. Author (revised)

N94-32449*# Lawrence Livermore National Lab., CA.

FLEXIBLE MANUFACTURING FOR PHOTONICS DEVICE ASSEMBLY

Shin-yee Lu, Michael D. Pocha, Oliver T. Strand, and K. David Young *In* NASA, Washington, Technology 2003: The Fourth National Technology Transfer Conference and Exposition, Volume 2 Feb. 1994 p 246-251

(For primary document see N94-32420 09-99)

(Contract W-745-eng-48)

Avail: CASI HC A02/MF A04

32 COMMUNICATIONS AND RADAR

Includes radar; land and global communications; communications theory; and optical communications.

For related information see also *04 Aircraft Communications and Navigation* and *17 Space Communications, Spacecraft Communications, Command and Tracking.* For search and rescue see *03 Air Transportation and Safety,* and *16 Space Transportation.*

N94-31062# Defence Research Establishment, Ottawa (Ontario).
PEAK DETECTION OF SWERLING TYPE TARGETS. PART 1: DETECTION PROBABILITIES IN WHITE NOISE
Anastasios Drosopoulos and George Haslam Dec. 1993 49 p
(AD-A276217; DREO-1193-Pt-2) Avail: CASI HC A03/MF A01

Peak detection is an alternative to the commonly used threshold detection scheme in radar systems. The present report is the first part in an investigation of peak detection performance, for Swerling type targets, in an arbitrary noise/clutter background. In this report, peak detection is compared with classic fixed threshold detection in uncorrelated white noise. A methodology is also developed, capable of handling arbitrary stochastic signal and noise/clutter models. DTIC

N94-31063# Defence Research Establishment, Ottawa (Ontario).
EVALUATION OF HardSys/HardDraw, AN EXPERT SYSTEM FOR ELECTROMAGNETIC INTERACTIONS MODELLING
Marc Dion May 1993 60 p
(AD-A276218; DREO-1175; X5-XD) Avail: CASI HC A04/MF A01

The Department of National Defense and the National Research Council have sponsored the development of HardSys/HardDraw, an expert system for the modelling of electromagnetic interactions in complex systems. This report gives a description of HardSys/HardDraw and reviews the main concepts used in its design. Various aspects of its implementation, user interaction and modelling concepts are evaluated. Some deficiencies are identified and enhancements are proposed to overcome them. Concepts of uncertainty are reviewed and an approach using confidence factors and fuzzy arithmetic is developed. A new method relating both the frequency and time domains is presented and is applied for the calculation of failure index and shielding effectiveness. DTIC

N94-31093 Ecole Nationale Superieure des Telecommunications, Paris (France). Groupe Theorie des Communications.
CHANNEL EQUALIZATION FOR BLOCK TRANSMISSION SYSTEMS
Ghassan KawasKaleh Jan. 1993 35 p Limited Reproducibility: More than 20% of this document may be affected by microfiche quality
(ISSN 0751-1345)
(TELECOM-93-D-002; ETN-94-95885) Avail: CASI HC A03

For communication over channels subject to fast time variation, for example, the HF channel, the information symbols are arranged in the form of blocks separated by known symbols. Such a system is called a block transmission system. Its known convenient receiver is the Nonlinear Data Directed Estimator (NDDE). Appropriate equalization methods for this system are derived, using a nonstationary innovations representation based on Cholesky factorization in order to define a noise whitener and a maximum likelihood block detector. Zero forcing and minimum mean squared error block linear and block decision feedback equalizers are also derived. Their performances are evaluated and compared. They are shown to perform better than the conventional equalizers. As compared with the NDDE, the deduced block decision feedback equalizers have better performance and are much less complex. Whereas the NDDE uses the Levinson algorithm to solve M/2 Toeplitz systems of decreasing order (where M is the number of symbols per block), the deduced equalizers need to process only one Toeplitz system. The Schur algorithm, proposed for Cholesky factorization, allows the complexity to be further reduced. ESA

N94-31097 Ecole Nationale Superieure des Telecommunications, Paris (France). Groupe Image.
PHASE UNWRAPPING PROBLEMS IN ISAR IMAGES [PROBLEMES DE DEVELOPPEMENT DE PHASE DANS LES IMAGES ISAR]
Jean-Pierre Veran Dec. 1992 17 p In FRENCH Limited Reproducibility: More than 20% of this document may be affected by microfiche quality
(ISSN 0751-1345)
(TELECOM-93-D-008; ETN-94-95889) Avail: CASI HC A03

The problem of the phase unwrapping in the ISAR (Interoferometric Synthetic Aperture Radar) images is studied. This problem is tricky when the image is noisy and when the local gradient is high (like in mountainous areas). A theoretical approach is chosen and work in a continuous space is carried out. A formal analogy with a problem of magnetostatics is proposed, and, using simple physics tools, an expression of the unwrapped phase is obtained. Unfortunately this result is not fully transposable to a discrete space (real case). However, implementations which would improve the performance of the existing algorithms are discussed. ESA

N94-31171 Ecole Nationale Superieure des Telecommunications, Paris (France). Dept. Economie et Management.
ECONOMIC ANALYSIS OF THE HERTZIAN SPECTRUM Ph.D. Thesis [L'ANALYSE ECONOMIQUE DU SPECTRE HERTZIEN]
Eva Kalman 1993 365 p In FRENCH Sponsored by ARECOM, and France Telecom Limited Reproducibility: More than 20% of this document may be affected by microfiche quality
(ISSN 0751-1353)
(TELECOM-93-E-012; ETN-94-95901) Avail: CASI HC A16

Economic characteristics of the hertzian resource are outlined. The economic value of the spectrum is determined by the heteorogeneous quality of frequencies (relative rarity) and by their quantity, strictly limited at each moment in time (absolute rarity). Institutional characteristics of the hertzian spectrum, and allocation and evaluation methods are discussed. An attempt to quantify spectrum evaluation is given. ESA

N94-31174 Ecole Nationale Superieure des Telecommunications, Paris (France).
FAST AUTODIDACTIC ADAPTIVE EQUALIZATION ALGORITHMS Ph.D. Thesis [ALGORITHMES ACCELERES D'EGALISATION ADAPTATIVE AUTODIDACTE]
Katia Hilal 1993 203 p In ENGLISH and FRENCH Limited Reproducibility: More than 20% of this document may be affected by microfiche quality
(ISSN 0751-1353)
(TELECOM-93-E-018; ETN-94-95904) Avail: CASI HC A10

Autodidactic equalization by adaptive filtering is addressed in a mobile radio communication context. A general method, using an adaptive stochastic gradient Bussgang type algorithm, to deduce two low cost computation algorithms is given: one equivalent to the initial algorithm and the other having improved convergence properties thanks to a block criteria minimization. Two start algorithms are reworked: the Godard algorithm and the decision controlled algorithm. Using a normalization procedure, and block normalization, the performances are improved, and their common points are evaluated. These common points are used to propose an algorithm retaining the advantages of the two initial algorithms. This thus inherits the robustness of the Godard algorithm and the precision and phase correction of the decision control algorithm. The work is completed by a study of the stable states of Bussgang type algorithms and of the stability of the Godard algorithms, initial and normalized. The simulation of these algorithms, carried out in a mobile radio communications context, and under severe conditions on the propagation channel, gave a 75% reduction in the number of samples required for the processing in relation with the initial algorithms. The improvement of the residual error was of a much lower return. These performances are close to making possible the use of autodidactic equalization in the mobile radio system. ESA

N94-31182# European Space Agency. European Space Research and Technology Center, ESTEC, Noordwijk (Netherlands). Working Group on Satellite Communications Policy.
EUROPE AT THE CROSSROADS: THE FUTURE OF ITS SATELLITE COMMUNICATIONS INDUSTRY Final Report
Pierre Bartholome, ed. and B. Battrick, ed. Nov. 1993 59 p Original contains color illustrations
(ESA-SP-1166; ISBN-9-29-092101-3; ETN-94-95860) Copyright Avail: CASI HC A04/MF A01; ESA, EPD, ESTEC, Noordwijk, Netherlands, HC

Ways of adapting the European Space Agency's role to the new industrial environment of satellite communications, which is characterized by the disappearance of traditional monopolies and the introduction of competition, are presented. As far as ESA is concerned, it is found that a

general consensus exists to recommend that the agency should take a much wider view of its role as a research and development (R&D) organization. It should no longer restrict its field of activity to space technology only, but should take a more global approach. More emphasis should be placed on the development of complete communications systems and of commercial applications. European industry indeed feels very strongly that it is not getting from ESA the support it needs to match the performance of its foreign competitors on the world markets. It can only succeed commercially in the fierce competition with the U.S. and Japan if a substantial R&D program is defined and funded at European level, as required by the magnitude of the financial effort necessary. It is concluded that anything the agency untertakes in the future to redress the situation would produce much greater dividends if it were part of a coherent plan where all the European partners play their role in a cooperative spirit. It is recommended that the European Commission should, as a matter of urgency, take steps to institute a concertation mechanism involving all major players with a view to defining and developing a coherent strategy for Europe. ESA

N94-31190 Politecnico di Milano (Italy). Dipt. di Elettronica e Informazione.

FILTERING AND RECOGNITION OF MOVING BOATS IN RADAR IMAGES [FILTRAGGIO E RICONOSCIMENTO DI NATANTI IN MOVIMENTO IN IMMAGINI RADAR]

Cesare Alippi Jun. 1993 26 p In ITALIAN

(Rept-93-039; ETN-94-95808) Avail: Issuing Activity (Politecnico di Milano, Piazza Leonardo da Vinci 32, 20133 Milan, Italy)

The problems of filtering, recognition, and classification of objects in two dimensional images are addressed. In particular, a problem relating to the recognition of boats in harbors or canals in radar generated images is considered. The main objective is to determine the outlines of ships for subsequent identification of the direction of motion. The solution proposed must respect stringent requirements of real time development. The classical neural solution is considered. The solution is ultimately interpretable as a classical adaptive solution in which the convolution masking coefficients are determined as a function of learning. ESA

N94-31253 Defence Research Establishment, Ottawa (Ontario).

AN ADAPTIVE KALMAN FILTER EXCISOR FOR SUPPRESSING NARROWBAND INTERFERENCE

Brian W. Kozminchuk Nov. 1993 47 p Limited Reproducibility: More than 20% of this document may be affected by microfiche quality

(AD-A276286; DREO-TN-93-20) Avail: CASI HC A03

Several reports have been written by the author which characterize the performance of a Kalman filtering technique to suppress narrowband interference from direct sequence spread spectrum communications systems in a non-adaptive context, i.e., when the user has some a priori knowledge of the interference characteristics. This report expands on this technique by presenting an adaptive scheme which is useful for the situation when the interference characteristics are unknown. In this context, the Kalman filter must 'learn' to achieve optimal performance through the adjustment of one of its parameters. The criterion for optimality is the minimization of the mean-squared error at the output of the canceller, where this error consists of spread spectrum signal, noise and residual interference. The reasonable assumption is made that minimizing the mean of this squared error with respect to the appropriate Kalman filter parameter is equivalent to minimizing the mean squared value of the residual interference. Examples of the dynamic behavior of the adaptive interference suppressor are presented for narrowband Gaussian noise interference with bandwidths ranging from 1% to 5% of the chip rate. DTIC

N94-31254 Defence Research Establishment, Ottawa (Ontario).

SUBSPACE ESTIMATION WITHOUT EIGENVECTORS FOR ADAPTIVE BEAMFORMING

Mylene Toulgoat, Christoph Gierull, and Ross M. Turner Dec. 1993 32 p Limited Reproducibility: More than 20% of this document may be affected by microfiche quality

(AD-A276287; DREO-1194) Avail: CASI HC A03

This report describes a new fast projection technique for adaptive beamforming. It is based on a technique proposed by Yeh where Gram-Schmidt orthogonalization is applied to N rows of the covariance matrix to obtain the signal subspace. In Yeh's technique, N is equal to L the number of jammers. This technique, applied to bearing estimation, requires a priori knowledge of the number of sources. Even though it gives good results when the number of sources is much smaller than the number of array elements, the performance of Yeh's technique degrades severely as the number of jammers increases. We improve the technique by taking a larger number of rows in the orthogonalization: we add a thresholding procedure to the technique in order to optimize N. We compared this new technique, called Subspace Estimation Without Eigenvectors (SEWE), with other fast projection techniques. SEWE was shown to give superior performance in terms of the Signal-to-Noise-Plus-Jammer Ratio achievable with a given computational load, except when a very high SNJR is required. DTIC

N94-31260# Illinois Univ., Urbana.

SPREAD-SPECTRUM RADIO SYSTEMS AND NETWORKS Final Report, 21 May 1991 - 20 Jul. 1993

Michael B. Pursley and Dilip V. Sarwate 25 Oct. 1993 6 p

(Contract DAAL03-91-G-0154)

(AD-A276449; ARO-27994.10-EL) Avail: CASI HC A02/MF A01

As part of the research completed under the subject contract, we showed that the effectiveness of error-control coding in a frequency-hop radio system can be increased greatly by the use of side information developed in the radio receiver. For slow-frequency-hop transmission, the inclusion of test symbols in each dwell interval provides a simple method for the derivation of side information for that dwell interval. Requirements on the reliability of the side information are presented in two other publications, and their implications in determining the necessary number of test symbols per dwell interval are described. When applied to a frequency-hop radio, concatenated coding provides a method for simultaneously achieving a larger communication range and greater protection against partial-band interference than can be obtained by systems without error-control coding or even most systems with a single form of coding. DTIC

N94-31267# Sandia National Labs., Albuquerque, NM.

FEATURE DISCOVERY IN GRAY LEVEL IMAGERY FOR ONE-CLASS OBJECT RECOGNITION

M. W. Koch and M. M. Moya 1993 7 p Presented at the IEEE World Congress on Computational Intelligence, Orlando, FL, 26 Jun. - 2 Jul. 1993

(Contract DE-AC04-94AL-85000)

(DE94-005268; SAND-93-4040C; CONF-9306304-1) Avail: CASI HC A02/MF A01

Feature extraction transforms an object's image representation to an alternate reduced representation. In one-class object recognition, we would like this alternate representation to give improved discrimination between the object and all possible non-objects and improved generation between different object poses. Feature selection can be time-consuming and difficult to optimize so we have investigated unsupervised neural networks for feature discovery. We first discuss an inherent limitation in competitive type neural networks for discovering features in gray level images. We then show how Sanger's Generalized Hebbian Algorithm (GHA) removes this limitation and describe a novel GHA application for learning object features that discriminate the object from clutter. Using a specific example, we show how these features are better at distinguishing the target object from other nontarget object with Carpenter's ART 2-A as the pattern classifier. DOE

N94-31299# Naval Postgraduate School, Monterey, CA.

KALMAN FILTERING APPROACH TO BLIND EQUALIZATION M.S. Thesis

Mehmet Kutlu Dec. 1993 79 p

(AD-A276320) Avail: CASI HC A05/MF A01

Digital communication systems suffer from the channel distortion problem which introduces errors due to intersymbol interference. The solution to this problem is provided by equalizers which use a training sequence to adapt to the channel. However in many cases in which a training sequence is unfeasible, the channel must be adapted blindly. Most of the blind equalization algorithms known so far have problems of convergence to local minima. Our intention is to offer an alternative approach by using extended Kalman filtering and hidden Markov models. They seem to yield more efficient algorithms which take the statistics of the transmitted sequence into consideration. The theoretical development of these new algorithms is

discussed in this thesis. Also these algorithms have been simulated under different conditions. The results of simulations and comparisons with existing systems are provided. The models for simulations are presented as MATLAB codes. DTIC

N94-31300# Naval Postgraduate School, Monterey, CA.
PREDICTING ANTENNA PARAMETERS FROM ANTENNA PHYSICAL DIMENSIONS M.S. Thesis
Steven E. Lundholm Dec. 1993 209 p
(AD-A276442) Avail: CASI HC A10/MF A03

This report details the development and provides the documentation for custom computer software applications that evaluate antenna parameters. The applications are written in Mathcad 3.1 for the following antenna types: linear, planar, and circular arrays; folded dipole; caged dipole; and parabolic reflectors with helical and spiral feeds. Inputs to the applications are limited to the antenna's physical dimensions. In some cases, ground parameters are required. The chapters are structured to provide the user with the necessary information needed to use and interpret the software for each antenna type. The software applications are provided as appendices and give examples of each antenna type. Outputs of the applications provide various numerical and performance predictions, as well as far-field radiation patterns. The results computed are consistent with predictions provided in applicable publications, as well as those calculated by numerical antenna analysis programs such as ELNEC. DTIC

N94-31317# Argonne National Lab., Idaho Falls, ID.
OBSERVATION OF THE TRAVELING COMPONENT OF AN X RAY STANDING WAVE FIELD
B. Lai, W. B. Yun, J. Chrzas, and P. J. Viccaro 1994 16 p
(Contract W-31-109-eng-38)
(DE94-007671; ANL/APS/PP-73889) Avail: CASI HC A03/MF A01

We present the first systematic experimental study of the traveling component of a standing wave field, formed by interference of an incident beam with its specularly reflected part from a plane interface. The traveling component of the standing wave field propagates parallel to the interface and its existence manifests the dynamical aspect of the standing wave field. In our experiment, a multilayer structure was used to aid in the observation of the traveling wave component. The data measured are explained using a finite thickness diffraction grating model. DOE

N94-31334# Naval Command, Control and Ocean Surveillance Center, San Diego, CA. Research, Development, Technology and Evaluation.
THE HIGH-FREQUENCY BENCHMARK PROPAGATION PROGRAM Final Report
J. A. Ferguson and C. H. Shellman Oct. 1993 18 p
(AD-A276323; NCCOSC/RDT/E-TD-2608) Avail: CASI HC A03/MF A01

The High-Frequency Benchmark is a computer code being developed to employ a sophisticated ray tracing program coupled with a state-of-the-art ionospheric model chosen by the user. The merging of these two major components depends critically on the development of a spatial smoothing routine that accepts arbitrary ionospheric models as inputs. A significant improvement in the spatial interpolation has been made which enhances the flexibility of the model. The latest version of the Parameterized Ionospheric Model has been incorporated. This report describes these improvements and enhancements. DTIC

N94-31371# Rome Lab., Hanscom AFB, MA.
FORMULATION OF TIME-DOMAIN PLANAR NEAR-FIELD MEASUREMENTS WITHOUT PROBE CORRECTION Report, Sep. 1991 - Aug. 1993
Thorkild B. Hansen and Arthur D. Yaghjian Sep. 1993 106 p
(AF Proj. 2304)
(AD-A276380; RL-TR-93-210) Avail: CASI HC A06/MF A02

This report addresses the problem of formulating planar near-field antenna measurements in the time domain, so that a single set of time-domain near-field measurements yields the far-field pattern in the time domain or over a wide range of frequencies. The time-domain planar near-field techniques are developed for both acoustic and electromagnetic fields and the space outside the region occupied by the antenna is assumed to be isotropic and homogeneous. Probe correction is ignored, that is, it is assumed that the probe is ideal so that the exact values of the field on the measurement plane are known. Two fundamentally different approaches are used in deriving time-domain formulas which give the fields in the half space z greater than z sub 0, in terms of their values on the plane z = z sub 0. In the first approach the time-domain formulas are obtained by inverse Fourier transforming the corresponding frequency-domain formulas. Since this approach requires extensive use of the frequency domain near-field formulas, we start by giving a rigorous derivation and review of the frequency-domain formulation that addresses a number of subtleties that have not been dealt with adequately in the literature. As part of this review, planar near-field formulas for the static electric and magnetic fields are derived for the first time. In the second approach the time-domain near-field formulas are derived directly in the time domain. The equivalence of the resulting time-domain formulas obtained by the two different approaches demonstrates the validity of the formulas and the utility of both approaches. DTIC

N94-31384# State Univ. of New York, Stony Brook. Dept. of Electrical Engineering.
COMMUNICATIONS NETWORKS IN STRESSED ENVIRONMENTS Final Report, 1 Jan. 1991 - 31 Dec. 1993
Stephen S. Rappaport and T. G. Robertazzi 31 Dec. 1993 10 p
(Contract N00014-91-J-4063)
(AD-A275967) Avail: CASI HC A02/MF A01

Communications techniques and performance models are devised for communications networks in which mobile platforms, volatile traffic patterns, and interference are significant features. The main focus is on network organization and control configurations that support communications among semi-autonomous mobile platforms. Example platforms can support data gathering sensors and communications equipment aboard guided or maneuverable space vehicles satellites, aircraft, ships, or grounded vehicles or persons. Network configurations with limited and/or shared communications resources are considered. Analytical models are devised to characterize major performance issues. Matters of concern include maintaining network connectivity with mobile platforms that have active communications links, methods for allocating communications resources to gateways, dynamic assignment of resources, and access rights. Topics investigated have included: acquisition of spread spectrum signals, low-delay channel access protocols, call hand-off schemes, telecommunications traffic performance of mobile networks, computation vs. communication considerations, high speed packet switching, and aspects of self-organizing communications networks. DTIC

N94-31385# Air Force Inst. of Tech., Wright-Patterson AFB, OH.
A STUDY OF THEORETICAL MODELS FOR MANAGING TECHNOLOGY CHANGE AND A COMPARISON TO A RADIO FREQUENCY IDENTIFICATION IMPLEMENTATION M.S. Thesis
Mark S. Reboulet and Phillip L. Robinson Sep. 1993 137 p
(AD-A276012; AFIT/GLM/LA/93S-36) Avail: CASI HC A07/MF A02

This research developed an aggregate model for technological implementation in organizations. The aggregate model drew information from various theoretical models and aggregated those elements that were common to several of the models. Those elements included: information availability, anticipated profitability, probability of success, user attitudes, political attitudes, external pressure, teamwork, strategic planning, resource availability, and training. Individuals involved at various organizational levels of a radio frequency identification implementation were interviewed to see if the aggregate model could be useful to managers. The researchers found evidence that each of the elements of the aggregate model could be beneficial to managers considering implementing new technologies. Also, the researchers found that individuals at different organizational levels tended to view these elements differently. Additionally, the researchers recommended several elements that could be added to the model. DTIC

N94-31386# Naval Postgraduate School, Monterey, CA. Dept. of Electrical and Computer Engineering.
ANALYSIS USING BI-SPECTRAL RELATED TECHNIQUE Final Report, 1 Oct. 1992 - 30 Sep. 1993
Ralph Hippenstiel 17 Nov. 1993 60 p
(AD-A276017; NPS-EC-93-020) Avail: CASI HC A04/MF A01

This report investigates the use of bispectral related techniques to extract detection / classification clues from time frequency representations. Earlier results have indicated that 1.5-D spectral techniques (a degenerate

version of the bispectrum) has potential signal to noise ratio (SNR) gain over conventional techniques. This is partially due to the rejection of Gaussian like perturbations by the cumulant based techniques. The third order moment for Gaussian zero mean random processes is essentially zero. It is assumed that the independence of the instantaneous power spectrum (IPS) from analytic signal representations and the Gaussian character of the noise causes minimal distortion of the output variables, hence permit signal characterization at low to moderate SNRs. The performance is demonstrated on synthetic signals and on segments of the NOSC data set. DTIC

N94-31401# Naval Postgraduate School, Monterey, CA.
WAVEFORM GENERATION FOR ULTRA-WIDEBAND RADAR SYSTEM M.S. Thesis
Hsiao-Feng Chiang Dec. 1993 86 p
(AD-A276352) Avail: CASI HC A05/MF A01

In the current literature, ultra-wideband (UWB) waveforms are said to possess several potential advantages such as penetration of foliage, walls and ground, as well as target identification and detection of stealth targets. Due to the potential advantages of UWB waveforms, UWB power sources are currently being developed. This thesis investigates the Fourier synthesis method of waveform generation which is to be used with ultra-wideband radar. The major advantages of this method over traditional methods are that accurate control of pulse shapes and pulse repetition intervals (PRI) can be generated. In this thesis, the Fourier method is extended to generation of binary coded waveforms for UWB systems. The generation of such codes is important as it allows for the use of longer coded pulses. These coded pulses contain more energy and improve signal to noise ratio (SNR) while still retaining the range resolution and other benefits of smaller pulse widths. DTIC

N94-31418# Office National d'Etudes et de Recherches Aerospatiales, Paris (France).
ELECTROMAGNETIC SCATTERING THROUGH LOADED APERTURE PANELS WITH NONZERO CONTACT IMPEDANCE Ph.D. Thesis - Univ. des Sciences et Techniques de Lille [DIFFRACTION ELECTROMAGNETIQUE A TRAVERS DES OUVERTURES CHARGEES PAR DES PANNEAUX DOTES D'UNE IMPEDANCE DE CONTACT NON NULLE]
Marc Sternberg 1993 214 p In FRENCH Original contains color illustrations
(ISSN 0078-3781)
(ONERA-NT-1993-2; ETN-94-96060) Avail: CASI HC A10/MF A03

Electromagnetic scattering through loaded apertures made of materials of finite conductivity (such as composite materials), which can be characterized by a surface impedance, is analyzed. These apertures consist of panels bound to an infinite, perfectly conductive plane by an interface of nonzero contact impedance. The case of panels that do not overlap with the surrounding structure is first treated, and the consequences of an evenly distributed contact impedance around the aperture are examined. The numerical results generated by a code based on the method of moments are compared with theoretical and experimental results. The effect of electrical contact through a set of points is studied, both numerically and experimentally. The effect of overlapping is investigated. A method for characterizing the quality of the contact between the panel and the metallic support is proposed. ESA

N94-31419# Office National d'Etudes et de Recherches Aerospatiales, Paris (France).
RADAR IMAGE CLASSIFICATION BY TEXTURE MEASUREMENTS Ph.D. Thesis - Paris 6 Univ. [CLASSIFICATION D'IMAGES DE RADAR PAR MESURES DE TEXTURE]
Anne Beaupere 1993 182 p In FRENCH Original contains color illustrations
(ISSN 0078-3781)
(ONERA-NT-1993-3; ETN-94-96061) Avail: CASI HC A09/MF A02

Radar image classification by texture analysis, (the spatial distribution of gray levels) as opposed to radiometric analysis, is addressed. It was demonstrated that although the statistical distributions of texture and speckle are different, the bias is generally very small and depends to a large extent on the surface observed. The results are used to classify the image in four major categories: water, urban areas, forest, and farmland. The classification results are interpreted by radar texture simulation. Two models that use the surface roughness and the alternation of shadows and reflective surfaces to develop an automatic radar image interpretation tool taking into account a wide diversity of ground models and texture signatures are proposed. This technique offers broad perspectives for both military and civil applications by supplying information that is often not visible to the naked eye. ESA

N94-31446 Naval Research Lab., Washington, DC.
A MULTICHANNEL ARCHITECTURE FOR NAVAL TASK FORCE COMMUNICATION Final Report
William A. Thoet, Dennis J. Baker, and Dennis N. McGregor 30 Jan. 1994 31 p Limited Reproducibility: More than 20% of this document may be affected by microfiche quality
(AD-A276230; NRL/FR/5520-94-9703) Avail: CASI HC A03

This report describes a new architecture for mobile, narrowband, broadcast radio networks, which is called the Multichannel Architecture (MCA). We compare the performance limits of an MCA network to a single-channel architecture based on an ideal handoff assigned multiple access (IHAMA) protocol. Both architectures have been proposed for Naval intratask force communications with HF and line-of-sight UHF radio. Formulas for the network load capacity for each architecture are derived for several important cases, and simulation results are presented for those cases where analytical results are not available. Based on equivalent equipment, the load capacity of MCA is shown to exceed that of IHAMA. MCA also outperformed IHAMA in other performance areas such as delay, the ability to handle voice and virtual circuits, and jam resistance. DTIC

N94-31463# Naval Postgraduate School, Monterey, CA.
LOW SIDELOBE REFLECTOR ANTENNA DESIGN FOR COMMUNICATIONS M.S. Thesis
Nelson A. Aramas 23 Sep. 1993 75 p
(AD-A276079) Avail: CASI HC A04/MF A01

The current antenna used in the Marine Radio AN/MRC-142 is a focal point fed reflector with a first sidelobe of -10 dB. A new antenna design is required with a sidelobe reduction of another 10 dB, and a minimum impact on the system upgrade cost. An improved feed consisting of a fed dipole and disk in the vicinity of a parasitic ring was designed for use with the current reflector. The disk acts as a ground plane for the dipole, with the ring narrowing the beamwidth, resulting in a stronger edge taper on the reflector. An existing computer code based on the the method of moments was used to compute the gain and the radiation pattern. Circular parabolic reflectors of 36 inches and 48 inches were analyzed. The results show that the 36 inch reflector cannot satisfy the conditions over the entire frequency band (1350 to 1850 MHz) simultaneously. The 48 inch reflector came very close to satisfying all the conditions, although the sidelobe level is off by approximately 2 dB at wide angles in the H-plane. DTIC

N94-31464# Wright Lab., Wright-Patterson AFB, OH.
DIRECT-SEQUENCE SPREAD-SPECTRUM PERFORMANCE IN A MULTIPATH FADING ENVIRONMENT Final Report, 6 Jan. - 24 Aug. 1993
Terry D. Nebergall Sep. 1993 54 p
(AF Proj. 9994)
(AD-A276080; WL-TR-93-1135) Avail: CASI HC A04/MF A01

The performance of coherent direct-sequence spread-spectrum communication systems with specular multipath fading is analyzed in terms of average probability of error. Approximations to such are based on the characteristic-function method. The probability mass function of the correlation receiver output is also derived with this approach. Numerical results are presented for various multipath environments with deterministic gain coefficients and channel coding applications. DTIC

N94-31466# Boston Univ., MA. Dept. of Electrical Computer and Systems Engineering.
SEGMENT-BASED ACOUSTIC MODELS FOR CONTINUOUS SPEECH RECOGNITION Progress Report, 1 Oct. - 31 Dec. 1993
Mari Ostendorf and J. R. Rohlicek 11 Feb. 1994 12 p
(Contract N00014-92-J-1778)
(AD-A276109) Avail: CASI HC A03/MF A01

In work, we are interested in the problem of large vocabulary,

speaker-independent continuous speech recognition, and primarily in the acoustic modeling component of this problem. In developing acoustic models for speech recognition, we have conflicting goals. On one hand, the models should be robust to inter- and intra-speaker variability, to the use of a different vocabulary in recognition than in training, and to the effects of moderately noisy environments. In order to accomplish this, we need to model gross features and global trends. On the other hand, the models must be sensitive and detailed enough to detect fine acoustic differences between similar words in a large vocabulary task. To answer these opposing demands requires improvements in acoustic modeling at several levels: the frame level (e.g. signal processing), the phoneme level (e.g. modeling feature dynamics), and the utterance level (e.g. defining a structural context for representing the intra-utterance dependence across phonemes). This project address the problem of acoustic modeling specifically focusing on modeling at the segment level and above. DTIC

N94-31503*# National Aeronautics and Space Administration. Goddard Space Flight Center, Greenbelt, MD.

NASCOM SYSTEM DEVELOPMENT PLAN: SYSTEM DESCRIPTION, CAPABILITIES, AND PLANS, FY 94-2

Apr. 1994 179 p

(NASA-TM-109744; NAS 1.15:109744; Rept-540-030) Avail: CASI HC A09/MF A02

The Nascom System Development Plan (NSDP) for FY 94-2 contains 17 sections. It is a management document containing the approved plan for maintaining the Nascom Network System. Topics covered include an overview of Nascom systems and services, major ground communication support systems, low-speed data system, voice system, high-speed data system, Nascom support for NASA networks, Nascom planning for NASA missions, and network upgrade and advanced systems developments and plans. CASI

N94-31551# Vrije Univ., Amsterdam (Netherlands).

MULTIPLE SCATTERING OF POLARIZED RADIATION IN PLANETARY ATMOSPHERES Ph.D. Thesis

Willem Maria Frans Wauben 1992 187 p

(ETN-94-96018) Avail: CASI HC A09/MF A02

Multiple scattering of polarized radiation in planetary atmospheres is addressed in studies of calculation methods for observations of the reflected sunlight and the internal radiation field, which give information on the constituents and the vertical structure of planetary atmospheres. An adding/doubling method and other computational methods which give insight into the general behavior of the polarized radiation in planetary atmospheres are considered. The relationship between the single scattering characteristics and the polarized radiation in optically thin atmospheres is shown. The main characteristics of the radiation in optically thick atmospheres can be explained by using asymptotic expressions. The main differences between the polarized radiation in atmospheres of intermediate optical thickness, but containing different particles, are explained by using the first order radiation and asymptotic expressions. An approximative method shows the variation of the polarized radiation near the boundaries of the atmosphere. Observations of radiation scattered in the atmosphere of Venus are investigated. It is shown that the main features of the observed internal intensities and fluxes as functions of altitude are described by a cloud/gas atmospheric model of Venus. Pioneer Venus polarimetric data are analyzed by using a cloud/haze model. It is found that at a wavelength of 0.935 micrometers the observations can be explained in terms of this cloud/haze model, but that the agreement is less satisfactory at shorter wavelengths. Thus, the polarization observations at these shorter wavelengths may contain information that can be used for a further refinement of the atmospheric model. ESA

N94-31573 Technische Univ., Berlin (Germany). Fachbereich Elektrotechnik.

SPECTRAL ANALYSIS METHOD AND SAMPLE GENERATION FOR REAL TIME VISUALIZATION OF SPEECH Ph.D. Thesis [VERFAHREN DER SPEKTRALANALYSE UND MUSTERGENERIERUNG FUER DIE REALZEITVISUALISIERUNG GESPROCHENER SPRACHE]

Klaus Hobohm 1993 194 p In GERMAN Limited Reproducibility: More than 20% of this document may be affected by microfiche quality

(ETN-94-95732) Avail: CASI HC A09

A method for translating speech signals into optical models, characterized by high sound discrimination and learnability and designed to provide to deaf persons a feedback towards control of their way of speaking, is presented. Important properties of speech production and perception processes and organs involved in these mechanisms are recalled in order to define requirements for speech visualization. It is established that the spectral representation of time, frequency and amplitude resolution of hearing must be fair and continuous variations of acoustic parameters of speech signal must be depicted by a continuous variation of images. A color table was developed for dynamic illustration and sonograms were generated with five spectral analysis methods such as Fourier transformations and linear prediction coding. For evaluating sonogram quality, test persons had to recognize consonant/vocal/consonant words and an optimized analysis method was achieved with a fast Fourier transformation and a postprocessor. A hardware concept of a real time speech visualization system, based on multiprocessor technology in a personal computer, is presented. ESA

N94-31608 Technische Univ., Berlin (Germany). Fachbereich Physik.

STRUCTURE ESTIMATION OF PHASE OBJECTS FROM THE DIFFRACTION NEAR FIELD: MICROWAVE AND MODEL CALCULATIONS Ph.D. Thesis [STRUKTURBESTIMMUNG VON PHASENOBJEKTEN AUS DEM BEUGUNGSNAHFELD: MIKROWELLENMESSUNGEN UND MODELLRECHNUNGEN]

Marco Alexander Krumbuegel 1993 176 p In GERMAN Limited Reproducibility: More than 20% of this document may be affected by microfiche quality

(ETN-94-95737) Avail: Issuing Activity (European Space Agency (ESA))

The diffraction near field behind big, flat plate phase objects with wedge angles between 30 and 150 degrees are examined with a modified Mach Zehnder interferometer for 3 cm microwaves, in order to allow amplitude and phase to be accurately and continuously measured with dependence on wave polarization. The uniform asymptotic theory, developed for nontransparent objects, was adapted to phase objects using a canonic transformation. A strong polarization dependent overestimation between theory and experiment is found, particularly when the electric field vector is perpendicular to object axis. A modification of the Born approximation was developed in order to apply scattering theory to dielectric objects, which allows the multiple scattering inside the object to be taken into account, using a complex transmission factor. Threshold and extreme values criteria for reconstruction of object data were developed, based on calculations with the method of moments and the new approximation and measured field distributions. It is shown that the wedge angle can be estimated from highness and position of wedge extreme values in case of low refractivity objects; it is found that the best method is the estimation of minima in spatial frequency spectrum. ESA

N94-31615# Technische Univ., Darmstadt (Germany). Fachbereich Informatik.

STUDY OF STRUCTURES OF DIFFERENT COMPLEXITY FOR THE COMMUNICATION BETWEEN TWO PROCESSORS Ph.D. Thesis [STRUKTURUNTERSUCHUNGEN VERSCHIEDENER KOMPLEXITAETSMASSE FUER DIE KOMMUNIKATION ZWISCHEN ZWEI PROZESSOREN]

Bernd Halstenberg 1991 78 p In GERMAN

(ETN-94-95750) Avail: CASI HC A05/MF A01

The structure of the complexity of communication between two processors was investigated. For functions defined on the Cartesian product of two finite sets the communication complexity is defined as the number of bits that have to be exchanged when two processors want to compute the function value and the input to each of them consists only of one component of the input pair. This definition is extended to nondeterministic and probabilistic models. Based on this definition for functions with a finite domain, non uniform complexity classes are defined. It is shown that the relations between these classes correspond to the polynomial time complexity classes for various Turing machine models in many aspects. On the other hand, certain pairs of classes are shown not to be equal; until now the corresponding inequalities are conjectured but unproved to hold for the polynomial time classes. ESA

N94-31645# Technische Univ., Delft (Netherlands). Faculty of Technical Mathematics and Informatics.

VIRTUAL ANNOTATION: VERBAL COMMUNICATION IN VIRTUAL REALITY

Jouke C. Verlinden, Jay David Bolter, and Charles vanderMast 1993 10 p
(ISSN 0922-5641)
(Rept-93-67; ETN-94-96112) Copyright Avail: CASI HC A02/MF A01

A system that was developed to explore communication in virtual reality and which offers a simple and powerful method to embed verbal communication in simulations and visualizers by means of voice annotation is described. The prototype demonstrates that the addition of verbal communication opens up a range of new uses for virtual environments. A similar voice annotation facility is easily added to existing visualizers and simulations, and it enables reading, writing and communicating. ESA

N94-31683# National Inst. of Standards and Technology, Boulder, CO. Electromagnetic Fields Div.

APERTURE EXCITATION OF ELECTRICALLY LARGE, LOSSY CAVITIES

D. A. Hill, J. W. Adams, M. T. Ma, A. R. Ondrejka, and B. F. Riddle Sep. 1993 81 p
(PB94-145711; NIST/TN-1361) Avail: CASI HC A05/MF A01

The document presents a theory based on power balance for aperture excitation of electrically large, lossy cavities. The theory yields expressions for shielding effectiveness, cavity Q, and cavity time constant. In shielding effectiveness calculations, the incident field can be either a single plane wave or a uniformly random field to model reverberation chamber or random field illumination. The Q theory includes wall loss, absorption by lossy objects within the cavity, aperture leakage, and power received by antennas within the cavity. Extensive measurements of shielding effectiveness, cavity Q, and cavity time constant were made on a rectangular cavity, and good agreement with theory was obtained for frequencies from 1 to 18 GHz. NTIS

N94-31708# Manitoba Univ., Winnipeg. Dept. of Electrical and Computer Engineering.

THE DEVELOPMENT OF ACTIVE INTEGRATED ANTENNAS AND A DESIGN METHODOLOGY Ph.D. Thesis

David J. Roscoe Jun. 1993 189 p
(ISBN-0-315-86119-3; CTN-94-61184) Copyright Avail: Micromedia Ltd., Technical Information Centre, 240 Catherine Street, Suite 305, Ottawa, Ontario, K2P 2G8, Canada HC/MF

Active antennas permit the current distribution along the antenna structure to be altered in a controlled manner. A design methodology has been developed and verified as a useful engineering tool which allows for the analysis of an arbitrarily shaped active integrated travelling wave antenna. An electromagnetic based circuit simulator is used in conjunction with a post-processor to determine the current distribution and to calculate the radiation characteristics. In addition, a noise model has been developed and used to calculate the output temperature of active integrated traveling wave antennas. These tools have been verified experimentally, with good agreement between calculated and measured results. An active integrated antenna has been designed, modeled, fabricated, and verified experimentally. The structure is a series distribution of microstrip transmission line and amplifiers. This antenna possesses numerous characteristics unachievable by traditional passive elements, but some undesirable traits such as poor noise temperature performance have been identified. Some applications of this type of active antenna are presented, including active element phased arrays. Author (CISTI)

N94-31731# Concordia Univ., Loyola Campus, Montreal (Quebec). Dept. of Electrical and Computer Engineering.

LINEARLY SEPARABLE STACK-LIKE ARCHITECTURE FOR THE DESIGN OF WEIGHTED ORDER STATISTIC FILTERS WITH APPLICATION IN IMAGE PROCESSING M.S. Thesis

Christian Emanuel Savin Sep. 1993 100 p
(ISBN-0-315-87284-5; CTN-94-61238) Copyright Avail: Micromedia Ltd., Technical Information Centre, 240 Catherine Street, Suite 305, Ottawa, Ontario, K2P 2G8, Canada HC/MF

The problem of designing a weighted order statistic (WOS) filter for estimating a signal from its noise corrupted observation is considered. A new approach for WOS filter design is introduced by defining a more general type of filter configuration than the traditionally used linearly separable stack (LSS) filter design. The new type of filter architecture is characterized by a linearly separable Boolean function and is designated a linearly separable stacklike (LSSL) filter. It is shown that LSSL filters satisfy a new property called the generalized stacking property. Due to this property, the fundamentals of the optimality theory that have been developed for the class of stack filters remain valid in the framework of LSSL filters. It is shown that in the multilevel signal domain, a LSSL filter architecture performs the operation of WOS filtering. An adaptive algorithm for designing WOS filters in the domain of LSSL filter architecture is derived. An implementation of the proposed design algorithm is constructed using a binary level least mean squares algorithm. The proposed design and implementation is applied to the problem of restoring images corrupted with impulsive noise. Simulation results show that the WOS filters designed with the new method provide better results than those obtained using LSS filter architecture. Author (CISTI)

N94-31761# Lawrence Livermore National Lab., CA.

THE DEVELOPMENT AND TESTING OF A BACKSCATTER ABSORPTION GAS IMAGING (BAGI) SYSTEM DESIGNED TO IMAGE AT A RANGE OF 300 m

T. J. Kulp, R. Kennedy, M. Delong, D. Garvis, and J. Stahovec Apr. 1993 16 p Presented at the Society of Photo-Optical Instrumentation Engineers OE/Aerospace Science and Sensing Meeting, Orlando, FL, 11-16 Apr. 1993
(Contract W-7405-eng-48)
(DE94-006192; UCRL-JC-115032; CONF-930445-28) Avail: CASI HC A03/MF A01

The backscatter absorption gas imaging (BAGI) technique is a laser remote sensing method that fuses the chemical detection attributes of chemical lidar with the visualization capability of imaging laser radar (ladar) to allow real-time television images of invisible gas plumes to be made. The BAGI technique is carried out by actively imaging a scene with radiation having a wavelength absorbed by the gas to be visualized. Gas plumes present in the scene become visible in the image when they attenuate a portion of the backscattered radiation. Currently, all BAGI instruments that have been developed operate in the infrared (IR) and image gases via their fundamental vibrational transitions. The laser sources that have been used are the CO2 and the IR helium neon. The target range at which the current BAGI instruments are capable of operating varies between about 6 and 110 m. The imaging device used in those systems is an active raster-scanner that scans the beam of a continuous wave (C-W) laser and the instantaneous field-of-view (IFOV) of an infrared detector. In this paper, we summarize the design and preliminary performance evaluation of a new raster-scanning BAGI imager that is intended for long-range operation, at a target range of 300 m. A system capable of imaging at this range is desired to make airborne gas imaging from a low-flying airplane or helicopter possible. The system uses a 20 W CO2 laser and a redesigned scanner that employs telescopic transmission and receiving optics. Model predictions of the performance of the new system and some recent field testing results are presented. Issues relating to gas imaging at long ranges are also discussed. DOE

N94-31781# Lawrence Livermore National Lab., CA.

DISPERSION RELATIONS FOR A PLASMA-FILLED HELIX-LOADED-WAVEGUIDE

M. A. Makowski, E. B. Hooper, and B. W. Stallard Jan. 1994 23 p
(Contract W-7405-eng-48)
(DE94-006333; UCRL-ID-115969) Avail: CASI HC A03/MF A01

The propagation of waves on bounded, magnetized plasma columns arises in connection with a variety of applications. To this end, dispersion relations are developed for a variety of multi-region circularly symmetric configurations. These include the following: a sheath helix in free space; a plasma column in free space; a plasma filled conducting tube; a plasma filled sheath-helix in free space; a sheath helix within a conducting cylinder; a plasma filled sheath-helix within a conducting cylinder; and a plasma column within a sheath-helix contained within a conducting cylinder. The latter configuration is of the most interest for whistler wave excitation for plasma thruster applications, since it includes the effect of a vacuum region separating the plasma column from the helical excitation structure. DOE

N94-31784# Lawrence Livermore National Lab., CA.

PEM PUBLIC KEY CERTIFICATE CACHE SERVER

T. Cheung Dec. 1993 18 p
(Contract W-7405-eng-48)
(DE94-006404; UCRL-MA-115651) Avail: CASI HC A03/MF A01

Privacy Enhanced Mail (PEM) provides privacy enhancement services to users of Internet electronic mail. Confidentiality, authentication, message integrity, and non-repudiation of origin are provided by applying cryptographic measures to messages transferred between end systems by the Message Transfer System. PEM supports both symmetric and asymmetric key distribution. However, the prevalent implementation uses a public key certificate-based strategy, modeled after the X.509 directory authentication framework. This scheme provides an infrastructure compatible with X.509. According to RFC 1422, public key certificates can be stored in directory servers, transmitted via non-secure message exchanges, or distributed via other means. Directory services provide a specialized distributed database for OSI applications. The directory contains information about objects and then provides structured mechanisms for accessing that information. Since directory services are not widely available now, a good approach is to manage certificates in a centralized certificate server. This document describes the detailed design of a centralized certificate cache serve. This server manages a cache of certificates and a cache of Certificate Revocation Lists (CRL's) for PEM applications. PEMapplications contact the server to obtain/store certificates and CRL's. The server software is programmed in C and ELROS. To use this server, ISODE has to be configured and installed properly. The ISODE library 'libisode.a' has to be linked together with this library because ELROS uses the transport layer functions provided by 'libisode.a.' The X.500 DAP library that is included with the ELROS distribution has to be linked in also, since the server uses the DAP library functions to communicate with directory servers. DOE

N94-31796# Montreal Univ. (Quebec). Dept. de Mathematiques Appliquees.
FRACTAL AND SPECTRAL ANALYSIS M.S. Thesis [ANALYSE FRACTALE ET SPECTRALE]
Marko Lemieux Dec. 1992 140 p In FRENCH
(ISBN-0-315-86460-5; CTN-94-61199) Copyright Avail: Micromedia Ltd., Technical Information Centre, 240 Catherine Street, Suite 305, Ottawa, Ontario, K2P 2G8, Canada HC/MF

The fractal dimension of noise can be evaluated with the aid of classical methods borrowed from fractal analysis. Nevertheless, these methods are generally incompatible with spectral analysis processes. A study is presented of a method for calculating the dimension of a signal based on its amplitude spectrum. In effect, the slope determined by the principal coefficients of a discrete spectrum is a function of the fractal dimension of the corresponding signal. The maxima spectrum method combines low pass filtering, a large window of analysis, and linear regression. This technique requires a good mastery of the fast Fourier transform. As an application, comparative trials were performed on various signals with the above method and two other methods derived from fractal analysis. The results obtained are similar to those from classical methods of fractal analysis while the signal is pure or complex and if the frequency distribution is known. Nevertheless, the proposed technique fails if the distribution is unknown, as is the case with complex signals obtained from sums of pure noise originating from different families. CISTI

N94-31925 Research Inst. of National Defence, Linkoeping (Sweden). Huvudavdelning foer Informationsteknologi.
DIVISION OF MICROWAVE TECHNOLOGY Annual Report, FY 1992-1993 [INSTITUTIONEN FOER MIKROVAGSTEKNIK ARSRAPPORT 1992/1993]
J. Svedin Oct. 1993 36 p In SWEDISH See also PB91-240168 and N90-29537
(PB94-148079; FOA-C-30726-3.2) Avail: Issuing Activity (National Technical Information Service (NTIS))

This report gives a brief summary of the activities at the Division of Microwave Technology, Fiscal Year 1992/1993. NTIS

N94-31952 Cornell Univ., Ithaca, NY.
HIGH-RESOLUTION SYNTHETIC APERTURE RADAR OBSERVATIONS OF THE MOON Ph.D. Thesis
Nicholas John Sholto Stacy 1993 224 p
Avail: Univ. Microfilms Order No. DA9319369

Variations in radar backscatter from planetary surfaces are related to differences in the local slope and the electrical and structural properties of the top surface layer. The top few meters of the surface of the moon consist of fine-grained unconsolidated rock material containing exposed and buried rocks. Previous lunar radar measurements have shown a depolarized backscatter component related to the abundance of surface and subsurface rocks and a linearly polarized component associated with subsurface backscatter. High spatial resolution observations of the lunar surface were conducted using the Arecibo Observatory 12.6 cm wavelength radar in 1990 and 1992 with the aim of analyzing local variations in the surface backscatter properties. In the finest spatial resolution mode, a pulsed pseudo-random code with a 10 MHz bandwidth was transmitted and approximately 24 minutes of data was processed to achieve pixel resolutions smaller than 40 m in both dimensions. To obtain this fine resolution over a large area, a focused delay-Doppler algorithm was developed. This new data processing method applies range and frequency offsets to the raw data that permit processing with an algorithm similar to that used for strip mode synthetic aperture radar. A circularly polarized wave was transmitted and both senses of circular polarization were received. Stokes vector analysis was used to estimate the circularly and linearly polarized backscatter components. The comparison of these measurements to a model of quasi-specular and diffuse backscatter from surface and subsurface structures yielded estimates of the surface dielectric constant and showed that subsurface quasi-specular scattering is required for this model to explain the linearly polarized backscatter power. Images of the lunar poles show enhanced backscatter with a circular polarization ratio of approximately 0.9 from the radar facing inner walls and ejecta of several impact craters. This result is mainly attributed to diffuse backscatter from exposed and buried rocks. The orientation of the linearly polarized backscatter component was found to correlate with surface topography confirming that this component is, in general, the result of transmission through the surface. Results of an interferometric experiment show that interferometric phase fringes related to topography can be generated from data acquired several months apart. Dissert. Abstr.

N94-31998# Phillips Lab., Hanscom AFB, MA.
PERFORMANCE STATISTICS BULLETIN. HIGH LATITUDE METEOR SCATTER PROPAGATION OCTOBER, NOVEMBER, DECEMBER 1990, JANUARY 1991 Interim Report
A. D. Bailey, J. M. Quinn, P. M. Bench, and W. I. Klemetti 26 Jan. 1994 268 p
(AF Proj. 4643)
(AD-A276693; AD-E201781; PL-TR-94-2023; ERP-1142) Avail: CASI HC A12/MF A03

A representative sampling of meteor scatter propagation performance statistics is presented from the PL/GP High Latitude Meteor Scatter Test Bed. The data address questions of meteor scatter propagation under disturbed ionospheric conditions, as well as normal meteor scatter propagation in the polar region. The time and frequency variations of the propagation transfer function are characterized over the 35 to 147 MHz range, including the availability of useful meteor trails, the potential communication capacity associated with those trails, the occurrence and persistence of ionospheric scatter and sporadic E-layers, variations in the signal-to-noise ratios of each scatter return and the effects of auroral and polar cap absorption (PCA) events on meteor scatter propagation and communications. Statistics covering Arrival Rate, Duration, Duty Cycle, and Noise Temperature are presented. This bulletin is one of a series covering the test bed operation from February 1990 through September 1992. DTIC

N94-32049 Rome Lab., Hanscom AFB, MA.
PROCEEDINGS OF THE 1993 ANTENNA APPLICATIONS SYMPOSIUM, VOLUME 1
Paul Mayes Feb. 1994 283 p Limited Reproducibility: More than 20% of this document may be affected by microfiche quality
(AD-A277202; RL-TR-94-20-Vol-1) Avail: Issuing Activity (Defense Technical Information Center (DTIC))

The Proceedings of the 1993 Antenna Applications Symposium is a collection of state-of-the-art papers relating to phased array antennas, multibeam antennas, satellite antennas, microstrip antennas, reflector antennas, HF, VHF, UHF and various other antennas. DTIC

N94-32050 Rome Lab., Hanscom AFB, MA.
PROCEEDINGS OF THE 1993 ANTENNA APPLICATIONS SYMPOSIUM, VOLUME 2
Paul Mayes Feb. 1994 255 p Limited Reproducibility: More than 20% of this document may be affected by microfiche quality
(AD-A277203; RL-TR-94-20-Vol-2) Avail: Issuing Activity (Defense Technical Information Center (DTIC))

The Proceedings of the 1993 Antenna Applications Symposium is a collection of state-of-the-art papers relating to phased array antennas, multibeam antennas, satellite antennas, microstrip antennas, reflector antennas, HF, VHF, UHF and various other antennas. DTIC

N94-32067 Institut fuer Kosmosforschung, Berlin (Germany).
THE SECOND INTERNATIONAL WORKSHOP ON DISCRETE TIME DOMAIN MODELLING OF ELECTROMAGNETIC FIELDS AND NETWORKS. PROGRAM AND INFORMATION
Oct. 1993 23 p Workshop held in Berlin, Germany, 28-29 Oct. 1993 Limited Reproducibility: More than 20% of this document may be affected by microfiche quality
(AD-A277136; R/D-7121-EE-03) Avail: Issuing Activity (Defense Technical Information Center (DTIC))

Due to advances in different areas of microwave and millimeter-wave techniques, demand for efficient CAD tools has grown. This statement is today as true as it was at our last workshop held two years ago in Munich on this topic. The numerical analysis in time domain is attractive since it describes the evolution of physical quantities in a natural way. The two basic concepts, the modelling of fields and networks, are more closely related than it seems at first glance. In the TLM method, for example, the network model is the basis for modelling electromagnetic fields. Another example is the application of generalized S-matrix methods and diacoptics in field theory. The purpose of this conference is to stimulate synoptic considerations of field and network theory and to promote a lively exchange between researchers engaged in these fields. DTIC

N94-32073 Delaware Univ., Newark. Dept. of Mathematical Sciences.
PERFORMANCE METRICS FOR LOW PROBABILITY OF INTERCEPT-COMMUNICATION SYSTEM Final Report, 1 Oct. 1990 - 30 Sep. 1993
Glen Prescott Oct. 1993 94 p Limited Reproducibility: More than 20% of this document may be affected by microfiche quality
(Grant AF-AFOSR-0018-91)
(AD-A277346; AFOSR-94-0085TR) Avail: CASI HC A05

The research consisted of two distinct but interrelated problems. First, the researchers performed the research necessary to establish and describe a set of metrics and theorems for Low Probability of Intercept Waveforms. This led to the development of a design and analysis methodology and capability for Low Probability of Intercept signals and systems. This methodology and capability resulted in an algorithmic approach to LPI design and is composed of two primary elements - an analytical-based, computer-aided system to evaluate the detectability of LPI waveforms, and computer simulation models which allow the LPI communication link to be simulated and evaluated against the effects of Jawing and intercept receivers. Secondly, as these tools were being developed, the researchers conducted basic research into the design of the next generation LPI waveforms and possible strategies for detecting them. The two research tasks were complementary effects. This research effort had elements of both basic and applied research. The theorems and metrics led to the development of a tool to analyze waveform detectability which will serve two functions. It can be used as a design instrument for the engineer who must select the most effective LPI modulation technique for a given system: and furthermore it can also be used to facilitate basic research in the area of waveform detectability. DTIC

N94-32083# Phillips Lab., Hanscom AFB, MA.
PERFORMANCE STATISTICS BULLETIN. HIGH LATITUDE METOR SCATTER PROPAGATION, FEBRUARY, MARCH, APRIL, MAY 1992 Interim Report, Feb. - May 1992
Alan D. Bailey, John M. Quinn, Patricia M. Bench, and Wayne I. Klemetti 2 Feb. 1994 269 p
(AF Proj. 4643)
(AD-A276667; PL-TR-94-2027; ERP-1146) Avail: CASI HC A12/MF A03

A representative sampling of meteor scatter propagation performance statistics is presented from the PL/GP High Latitude Meteor Scatter Test Bed. The data address questions of meteor scatter propagation under disturbed ionospheric conditions, as well as normal meteor scatter propagation in the polar region. The time and frequency variations of the propagation transfer function are characterized over the 35 to 147 MHz range, including the availability of useful meteor trails, the potential communication capacity associated with those trails, the occurrence and persistence of ionospheric scatter and sporadic E-layers, variations in the signal to noise ratios of each scatter return, and the effects of auroral and polar cap absorption (PCA) events on meteor scatter propagation and communications. Statistics covering arrival rate, duration, duty cycle, and noise temperature are presented. This bulletin is one of a series covering the test bed operation from February 1990 through September 1992. DTIC

N94-32085 Center for Mathematics and Computer Science, Amsterdam (Netherlands). Dept. of Operations Research, Statistics, and System Theory.
THE USE OF SERVICE LIMITS FOR EFFICIENT OPERATION OF MULTI-STATION SINGLE-MEDIUM COMMUNICATION SYSTEMS
S. C. Borst, O. J. Boxma, and H. Levy Jun. 1993 27 p Sponsored by Netherlands Organization for Applied Scientific Research TMO Limited Reproducibility: More than 20% of this document may be affected by microfiche quality
(ISSN 0924-0659)
(CWI-BS-R9312; ETN-94-96221) Copyright Avail: Issuing Activity (European Space Agency (ESA))

Time limits and service limits are the major mechanisms used for controlling a large variety of multistation single medium computer communication systems like the Token Ring and FDDI (Fiber Distributed Data Interface). The proper use of these mechanisms is still not understood and rules for efficient system operation are not available. A study aimed at the derivation of such rules is presented. A cyclic polling model with different service limits (k-limited service) at the different queues is used. Interest is in determining these k-limit values so as to minimize the mean waiting cost of messages in the system. A simple approximative approach is proposed for two major problems: one in which a limit is set on the token rotation time and one in which no limits are imposed. The approach is tested for a variety of cases and is shown to be very effective. ESA

N94-32087# Institute for Defense Analyses, Alexandria, VA.
SYSTEM ANALYSIS OF ULTRA-WIDEBAND INSTRUMENTATION RADARS: IMPULSE VERSUS STEPPED-CHIRP APPROACHES Final Report, Jan. 1992 - Nov. 1993
James Ralston Nov. 1993 23 p
(Contract MDA903-89-C-0003)
(AD-A276624; AD-E501749; IDA-P-2831; IDA/HQ-93-43524) Avail: CASI HC A03/MF A01

As part of an ongoing effort to determine the utility of ultra-wideband (UWB) radar systems for military application, an experimental program was developed and executed to collect terrain clutter data using high resolution waveforms in the ultra high frequency (UHF) spectral region. Two approaches to the design of the radar instrumentation to be used to collect these data were considered: an impulse system with a nominal 1 ns pulse duration and a conventional stepped-chirp instrumentation radar covering the same frequency range. A novel feature of the program was the use of a scanned linear aperture to simulate the use of a large, ideally weighted real aperture antenna system. In this paper, the theoretical analysis done to predict and compare the performance expected from either system approach is presented in terms of the noise-equivalent reflectivity of the clutter measurement system, the time to collect data, and the impact of the linearly scanned aperture on sensitivity, angular resolution, and data collection time. DTIC

N94-32101# Ames Lab., IA.
PHOTONIC BAND GAP MATERIALS
C. M. Soukoulis (Iowa State Univ. of Science and Technology, Ames.) 1993 6 p Presented at the North Atlantic Treaty Organization (NATO) Advanced Study Meeting of Institute on Nanophas Materials, Corfu, Greece, 20 Jun. - 2 Jul. 1993

(Contract W-7405-eng-82)
(DE94-005566; IS-M-751; CONF-9306223-4) Avail: CASI HC A02/MF A01

An overview of the theoretical and experimental efforts in obtaining a photonic band gap, a frequency band in three dimensional dielectric structures in which electromagnetic waves are forbidden, is presented. DOE

N94-32113 Sandia National Labs., Albuquerque, NM.
ITS VERSION 3.0: POWERFUL, USER-FRIENDLY SOFTWARE FOR RADIATION MODELLING
R. P. Kensek, J. A. Halbleib, and G. D. Valdez 1993 24 p Presented at the International Ultraviolet and Electron Beam Curing Conference and Exhibition, Orlando, FL, 1-5 May 1994 Limited Reproducibility: More than 20% of this document may be affected by microfiche quality
(Contract DE-AC04-94AL-85000)
(DE94-006607; SAND-93-2077C; CONF-940566-1) Avail: CASI HC A03

The Integrated Tiger Series (ITS) is a powerful, but user-friendly, software package permitting state-of-the-art modelling of electron and/or photon radiation effects. The programs provide Monte Carlo solutions for linear time-independent coupled electron/photon radiation transport problems, with or without the presence of macroscopic electric and magnetic fields. The ITS system combines operational simplicity and physical accuracy in order to provide experimentalist and theorists alike with a method for the routine but rigorous solution of sophisticated radiation transport problems. DOE

N94-32121# Carnegie-Mellon Univ., Pittsburgh, PA. Dept. of Computer Science.
ELECTRONIC MAIL AND ORGANIZATIONAL KNOWLEDGE: MEDIA USE IN A GLOBAL CORPORATION
Robert E. Kraut and Paul Attewell Dec. 1993 20 p
(AD-A276707; CMU-CS-93-208) Avail: CASI HC A03/MF A01

Several attributes of communication media influence the costs of their use and utility, and these in turn have the potential to influence their patterns of use and organizational consequences. The goal of this paper is to examine some of these media attributes and their consequences in a large international firm. The data come from a survey of 973 employees of a multi-national corporation. They show that the distinguishing attributes of different media are not dominant: people whose jobs require substantial communication are likely to communicate heavily using all media available to them. The best predictor of which medium is used is the extent to which the medium can put people into contact with their important communication partners. When the job is the unit of analysis, the data from this survey do not support the media richness hypothesis - that use is determined by the fit between the richness of a medium and the degree to which people have complex, ambiguous, or social jobs. Yet when one takes a single conversation as a unit of analysis, the data show that media differing in interactivity and expressiveness are valuable for different tasks. Employees who use electronic mail extensively are better informed about their company and more committed to its management's goals. One reason for their superior knowledge about the organization seems to be that electronic mail promotes 'information spillover' from a focal recipient to others less directly interested in a message, without subjecting these marginal parties to the burdens of interruption and information overload. DTIC

N94-32158# Phillips Lab., Hanscom AFB, MA.
PERFORMANCE STATISTICS BULLETIN. HIGH LATITUDE METEOR SCATTER PROPAGATION FEBRUARY, MARCH, APRIL, MAY 1991 Interim Report
Alan D. Bailey, John M. Quinn, Patricia M. Bench, and Wayne I. Klemetti 1 Feb. 1994 266 p
(AD-A276723; AD-E201779; PL-TR-94-2021; ERP-1140) Avail: CASI HC A12/MF A03

A representative sampling of meteor scatter propagation performance statistics is presented from the PL/GP High Latitude Meteor Scatter Test Bed. The data address questions of meteor scatter propagation under disturbed ionospheric conditions, as well as normal meteor scatter propagation in the polar region. The time and frequency variations of the propagation transfer function are characterized over the 35 to 147 MHz range, including the availability of useful meteor trails, the potential communication capacity associated with those trails, the occurrence and persistence of ionospheric scatter and sporadic E-layers, variations in the signal-to-noise ratios of each scatter return and the effects of auroral and polar cap absorption (PCA) events on meteor scatter propagation and communications. Statistics covering Arrival Rate, Duration, Duty Cycle, and Noise Temperature are presented. This bulletin is one of a series covering the test bed operation from February 1990 through September 1992. DTIC

N94-32159 Phillips Lab., Hanscom AFB, MA.
PERFORMANCE STATISTICS BULLETIN. HIGH LATITUDE METEOR SCATTER PROPAGATION OCTOBER, NOVEMBER, DECEMBER 1991, JANUARY 1992 Interim Report
Alan D. Bailey, John M. Quinn, Patricia M. Bench, and Wayne I. Klemetti 1 Feb. 1994 269 p Limited Reproducibility: More than 20% of this document may be affected by microfiche quality
(AD-A276724; AD-E201778; PL-TR-94-2020; ERP-1139) Avail: Issuing Activity (Defense Technical Information Center (DTIC))

A representative sampling of meteor scatter propagation performance statistics is presented from the PL/GP High Latitude Meteor Scatter Test Bed. The data address questions of meteor scatter propagation under disturbed ionospheric conditions, as well as normal meteor scatter propagation in the polar region. The time and frequency variations of the propagation transfer function are characterized over the 35 to 147 MHz range, including the availability of useful meteor trails, the potential communication capacity associated with those trails, the occurrence and persistence of ionospheric scatter and sporadic E-layers, variations in the signal-to-noise ratios of each scatter return and the effects of auroral and polar cap absorption (PCA) events on meteor scatter propagation and communications. Statistics covering Arrival Rate, Duration, Duty Cycle, and Noise Temperature are presented. This bulletin is one of a series covering the test bed operation from February 1990 through September 1992. DTIC

N94-32161# ARCO Power Technologies, Inc., Washington, DC.
ELECTROMAGNETIC WAVE REFLECTION FROM IRREGULAR PLASMA LAYERS Final Report, 31 Aug. 1989 - 2 Sep. 1993
Dennis Papadopoulos, Ramy Shanny, and Robert D. Short 31 Aug. 1993 34 p
(Contract F19628-89-C-0174)
(AD-A276727; AD-E201774; PL-TR-93-2204) Avail: CASI HC A03/MF A01

The general theory describing reflection of electromagnetic waves from irregular reflectors was formulated by using path integral techniques (Dashen, 1979; Flatte, 1979). The general formulae reproduce the well known reflection coefficients for wave scattering from random rough surfaces derived by using Kirchhoff's theory or perturbation theory (Ogilvie, 1991). The theory was used to determine the degradation of an OTH radar signal scattered from irregular Artificial Ionospheric Mirrors (AIM). The cases of density irregularities induced by fluctuations in the ambient neutral density and by fluctuations in the heater power were separately examined. Scaling laws and bounds for minimal signal loss were derived. DTIC

N94-32179# Naval Postgraduate School, Monterey, CA.
DEVELOPMENT OF A FREQUENCY-DOMAIN ELECTROMAGNETIC SCATTERING MEASUREMENT SYSTEM M.S. Thesis
Kenneth K. Oh Dec. 1993 74 p
(AD-A276738) Avail: CASI HC A04/MF A01

This thesis describes the development of a system for measuring frequency-domain scattered fields in the Transient Electromagnetic Scattering Range at the Naval Postgraduate School. The new system employs a stepped-frequency CW waveform and utilizes an HP-8510B network analyzer as an RF front-end and a coherent receiver. A pair of AEL H1498 antennas was installed to cover a frequency range of 2 GHz to 18 GHz. An HP-82300C BASIC Language Processor was installed on a COMPAQ Deskpro-386 PC, and an HP-BASIC program was developed for remote control of the HP-8510B with data acquisition over the HPIB bus. A post-processing algorithm was created using MatLab for background subtraction, calibration, and deconvolution. A set of RCS measurements was made using various size spheres, and the postprocessing outputs were compared to computed values. Good agreement between these measurements and computed data indicates excellent accuracy of the measurement system and valid operations of the postprocessing algorithm. DTIC

N94-32183# Naval Postgraduate School, Monterey, CA.
APPLIED COMPUTATIONAL ELECTROMAGNETICS SOCIETY JOURNAL, VOLUME 9, NUMBER 1, MARCH 1994
Mar. 1994 107 p
(AD-A276753) Avail: CASI HC A06/MF A02

The partial contents of this document include the following: On the Use of Bivariate Spline Interpolation of Slot Data in the Design of Slotted Waveguide Arrays; A Technique for Determining Non-Integer Eigenvalues for Solutions of Ordinary Differential Equations; Antenna Modeling and Characterization of a VLF Airborne Dual Trailing Wire Antenna System; Electromagnetic Scattering from Two-Dimensional Composite Objects; and Use of a Stealth Boundary with Finite Difference Frequency Domain Simulations of Simple Antenna Problems. DTIC

N94-32185# SRI International Corp., Menlo Park, CA.
HIGH-PERFORMANCE SPEECH RECOGNITION USING CONSISTENCY MODELING Technical Report, 4 Aug. 1992 - 4 Aug. 1993
Vassilios Digilakis, Peter Monaco, Hy Murveit, and Mitchel Weintraub Mar. 1994 11 p
(AD-A276775) Avail: CASI HC A03/MF A01

The goal of this project conducted by SRI International (SRI) is to develop consistency modeling technology. Consistency modeling aims to reduce the number of improper independence assumptions used in traditional speech-recognition algorithms so that the resulting speech-recognition hypotheses are more self-consistent and, therefore, more accurate. Consistency is achieved by conditioning HMM output distributions on state and observations histories, P(x/s,H). The technical objective of the project is to find the proper form of the probability distribution, P; the proper history vector, H; the proper feature vector, x; and to develop the infrastructure (e.g. efficient estimation and search techniques) so that consistency modeling can be effectively used. During the first year of this effort, SRI focused on developing the appropriate base technologies for consistency modeling. We developed genonic hidden Markov model (HMM) technology, our choice for P above, and Progressive Search technology for HMM systems which allows us to develop and use complex HMM formulations in an efficient manner. Papers describing these two techniques are included in the appendix of this report and are briefly summarized below. This report also describes other accomplishments of Year 1 including the initial exploitation of discrete and continuous consistency modeling and the development of a scheme for efficiently computing Gaussian probabilities. DTIC

N94-32188# Lawrence Livermore National Lab., CA.
USING TSAR WITH THE POST-PROCESSING FAR-FIELD OPTION
S. T. Pennock Oct. 1993 5 p
(Contract W-7405-eng-48)
(DE94-006615; UCRL-MA-115257) Avail: CASI HC A01/MF A01

The TSAR EM code has contained far-field projection algorithms for some time. One drawback to previous versions of TSAR has been the necessity to run the field advancement routines each and every time to generate far-field data. A change has been made to TSAR to allow tangential fields on the projection surface to be saved to a file. These fields can then be used with a new postprocessor, POSTFAR, to produce far-field points at any desired location without rerunning the field advancement portion of TSAR. This will save large amounts of time in producing far-field calculations and allow calculation of other test point locations. If the tangential field data is saved to an 8 mm tape, these calculations may be made at a much later date. DOE

N94-32230# Massachusetts Univ., Amherst. Dept. of Electrical and Computer Engineering.
DISCRETE-EVENT-DYNAMIC-SYSTEM-BASED APPROACHES FOR SCHEDULING TRANSMISSIONS IN MULTIHOP PACKET RADIO NETWORKS Annual Report, Oct. 1991 - Sep. 1992
Christos G. Cassandras 1993 4 p
(Contract N00014-91-J-2025)
(AD-A276566) Avail: CASI HC A01/MF A01

In the classic transmission scheduling problem, the nodes of a packed radio network (PRN) broadcast fixed-length packets over a common resource (the channel). Packet transmissions are subject to interference constraints; for example, if a node is transmitting a packet, then all adjacent (neighboring) nodes must refrain from transmission. One then adopts a slotted time model where every slot is allocated to a set of nodes which can simultaneously transmit without conflict. Thus, a node generally belongs to one or more of these sets (called transmission sets). Our approach is based on viewing the transmission scheduling problem as a single server multiclass polling problem with simultaneous resource possession. Here, a class corresponds to a transmission set. The server corresponds to a channel operating with deterministic service times: a service time is equal to one time slot required for transmitting a packet. The scheduling problem is then equivalent to assigning the server (equivalently, each time slot) to a particular transmissions set. The simultaneous resource possession feature arises because the server is assigned to a transmission set, i.e. it can simultaneously provide service to packets from all nodes which belong to that set. The construction of the transmission set is dependent upon the topology and connectivity of the PRN and is equivalent to a graph partitioning problem. For our purposes, we assume M transmission sets have been specified. Finally, we allow for overlapping transmission sets, i.e. a node can belong to two or more difference transmission sets. DTIC

N94-32235 Advisory Group for Aerospace Research and Development, Neuilly-Sur-Seine (France).
ATMOSPHERIC PROPAGATION EFFECTS THROUGH NATURAL AND MAN-MADE OBSCURANTS FOR VISIBLE TO MM-WAVE RADIATION [LES EFFETS DES CONDITIONS DEFAVORABLES DE PROPAGATION SUR LES SYSTEMES OPTIQUES, IR ET A ONDES MILLIMETIQUES]
Nov. 1993 209 p In FRENCH Presented at the Electromagnetic Wave Propagation Panel Symposium, Palma de Mallorca, Spain, 17-20 May 1993 Limited Reproducibility: More than 20% of this document may be affected by microfiche quality
(AD-A276919; AGARD-CP-542; ISBN-92-835-0727-4) Avail: Issuing Activity (Defense Technical Information Center (DTIC))

Modern, precision-guided weapons require that guidance and target acquisition/recognition systems take into account the effects of the propagation environment. Successful performance must be obtained under adverse weather conditions such as haze, clouds, fog, rain, and snow and under adverse battlefield conditions such as dust, smoke, and man-made obscurants. Sensors operate at wavelengths ranging across the millimeter, IR, and the visible regions of the electromagnetic spectrum. Propagation effects vary drastically over this wavelength span and systems may employ a combination of sensors to mitigate adverse environmental conditions. The effectiveness of countermeasures such as multispectral obscurants and multispectral camouflage also depends on atmospheric properties. System performance is measured in terms of probability of detection, probability of recognition, and, ultimately, in terms of probability of a kill. A partial listing of the processes that affect theses probabilities and, in turn, are affected by the propagation environment includes extinction, angles and amplitude scintillation, target to background contrast, contrast transmission, and clutter characteristics. The symposium addresses the following topics: natural obscurants, multispectral camouflage, man-made obscurants and battlefield-induced phenomena, and target and background signatures. DTIC

N94-32282 Naval Postgraduate School, Monterey, CA. Dept. of Electrical and Computer Engineering.
LOW ALTITUDE NEAR-THE-HORIZON PROPAGATION: A COMPARISON BETWEEN RPO AND M-LAYER M.S. Thesis
Chi-Wei Wu Dec. 1993 140 p Limited Reproducibility: More than 20% of this document may be affected by microfiche quality
(AD-A277358; NPS-EC-93-022) Avail: CASI HC A07

Predictions of propagation loss made by the computer programs Radio Physical Optics (RPO) Computer Software Configuration Item (CSCI) and M-Layer are compared. The results of the high frequency parabolic equation approximation, as formulated in RPO, agree almost always with those derived from the low frequency modal computation as formulated in M-Layer. But at low altitudes in the neighborhood of the radar horizon, deviations between RPO and M-Layer become significant for some cases. RPO appears not to be able to properly account for the effects of a high altitude surface-based duct at a short range. Since the discrepancies fall in regions of importance to naval operations, a definitive resolution is an urgent task to be undertaken in the immediate future. DTIC

N94-32283# Naval Research Lab., Washington, DC.
DESIGN, DEVELOPMENT, AND TESTING OF A NETWORK FREQUENCY SELECTION SERVICE (NFSS) Final Report
Dennis J. Baker and Jastej Dhingra 14 Feb. 1994 195 p
(AD-A277362; NRL/MR/5520-94-7442) Avail: CASI HC A09/MF A03

This report focuses on the design, development, and testing of a prototype Network Frequency Selection Service (NFSS) that would automate the selection of a single, best frequency for operation of a single-channel network. After selecting the operating frequency, the NFSS proceeds to set the client network's transmitter and receiver to the chosen frequency. The NFSS is intended to be used as a scheduled service. During the periods when the NFSS is active, it normally tests a subset of the candidate frequencies, along with the previously chosen best frequency, and chooses the new best frequency from among this subset. Eventually, over several such active periods, all candidate frequencies are tested. The client network operates in its normal manner between activations of the NFSS. In the prototype NFSS, the 'best' frequency is the one that minimizes the frequency selection metric, which contains in order of importance: the number of relay nodes disconnected from the main body of the network, the number of relay nodes needed to form a backbone network, the number of links that the given topology falls short of being a fully connected network, and the index of the frequency in the sequential collection of candidate frequencies. DTIC

N94-32297# Phillips Lab., Hanscom AFB, MA.
PERFORMANCE STATISTICS BULLETIN. HIGH LATITUDE METEOR SCATTER PROPAGATION, NOVEMBER AND DECEMBER 1989, AND JANUARY 1990 Interim Report, Nov. - Dec. 1989, Jan. 1990
Alan D. Bailey, Jen C. Ostergaard, Regina M. Burton, Carlton H. Curtis, and Wayne I. Klemetti 22 Nov. 1993 216 p
(AD-A276688; AD-E201753; PL-TR-93-2234; ERP-1133) Avail: CASI HC A10/MF A03

A representative sampling of meteor scatter propagation performance statistics is presented from the PL/GP High Latitude Meteor Scatter Test Bed (HLMSTB). The data address questions of meteor scatter propagation under disturbed ionospheric conditions, as well as normal meteor scatter propagation in the polar region. The time and frequency variations of the propagation transfer function are characterized over the 35 to 147 MHz range, including the availability of useful meteor trails, the potential communication capacity associated with those trails, the occurrence and persistence of ionospheric scatter and sporadic E-layers, variations in the signal to noise ratios of each scatter return, and the effects of auroral and polar cap absorption (PCA) events on meteor scatter propagation and communications. Statistics covering arrival rate, duration, duty cycle, and noise temperature are presented. This bulletin is one of a series of polar meteor scatter data bulletins. DTIC

N94-32298# Phillips Lab., Hanscom AFB, MA.
PERFORMANCE STATISTICS BULLETIN. HIGH LATITUDE METEOR SCATTER PROPAGATION Interim Report, Feb. - May 1990
Alan D. Bailey, John M. Quinn, Patricia M. Bench, and Wayne I. Klemetti 26 Jan. 1994 268 p
(AF Proj. 4643)
(AD-A276694; AD-E201783; PL-TR-94-2025; ERP-1144) Avail: CASI HC A12/MF A03

A representative sampling of meteor scatter propagation performance statistics is presented from the PL/GP High Latitude Meteor Scatter Test Bed. The data address questions of meteor scatter propagation under disturbed ionospheric conditions, as well as normal meteor scatter propagation in the polar region. The time and frequency variations of the propagation transfer function are characterized over the 35 to 147 MHz range, including the availability of useful meteor trails, the potential communication capacity associated with those trails, the occurrence and persistence of ionospheric scatter and sporadic E-layers, variations in the signal-to-noise ratios of each scatter return and the effects of auroral and polar cap absorption (PCA) events on meteor scatter propagation and communications. Statistics covering Arrival Rate, Duration, Duty Cycle, and Noise Temperature are presented. This bulletin is one of a series covering the test bed operation from February 1990 through September 1992. DTIC

N94-32299# Phillips Lab., Hanscom AFB, MA.
PERFORMANCE STATISTICS BULLETIN. HIGH LATITUDE METEOR SCATTER PROPAGATION Interim Report, Jun. - Sep. 1990
Alan D. Bailey, John M. Quinn, Patricia M. Bench, and Wayne I. Klemetti 26 Jan. 1994 268 p
(AF Proj. 4643)
(AD-A276695; AD-E201782; PL-TR-94-2024; ERP-1143) Avail: CASI HC A12/MF A03

A representative sampling of meteor scatter propagation performance statistics is presented from the PL/GP High Latitude Meteor Scatter Test Bed. The data address questions of meteor scatter propagation under disturbed ionospheric conditions, as well as normal meteor scatter propagation in the polar region. The time and frequency variations of the propagation transfer function are characterized over the 35 to 147 MHz range, including the availability of useful meteor trails, the potential communication capacity associated with those trails, the occurrence and persistence of ionospheric scatter and sporadic E-layers, variations in the signal-to-noise ratios of each scatter return and the effects of auroral and polar cap absorption (PCA) events on meteor scatter propagation and communications. Statistics covering Arrival Rate, Duration, Duty Cycle, and Noise Temperature are presented. This bulletin is one of a series covering the test bed operation from February 1990 through September 1992. DTIC

N94-32300# Phillips Lab., Hanscom AFB, MA.
PERFORMANCE STATISTICS BULLETIN. HIGH LATITUDE METEOR SCATTER PROPAGATION Interim Report, Jun. - Sep. 1991
Alan D. Bailey, John M. Quinn, Patricia M. Bench, and Wayne I. Klemetti 1 Feb. 1994 268 p
(AF Proj. 4643)
(AD-A276696; AD-E201780; PL-TR-94-2022; ERP-1141) Avail: CASI HC A12/MF A03

A representative sampling of meteor scatter propagation performance statistics is presented from the PL/GP High Latitude Meteor Scatter Test Bed. The data address questions of meteor scatter propagation under disturbed ionospheric conditions, as well as normal meteor scatter propagation in the polar region. The time and frequency variations of the propagation transfer function are characterized over the 35 to 147 MHz range, including the availability of useful meteor trails, the potential communication capacity associated with those trails, the occurrence and persistence of ionospheric scatter and sporadic E-layers, variations in the signal-to-noise ratios of each scatter return and the effects of auroral and polar cap absorption (PCA) events on meteor scatter propagation and communications. Statistics covering Arrival Rate, Duration, Duty Cycle, and Noise Temperature are presented. This bulletin is one of a series covering the test bed operation from February 1990 through September 1992. DTIC

N94-32310 North Carolina State Univ., Raleigh.
COMMUNICATION NETWORKS FOR AUTONOMOUS MOBILE ROBOT COMPUTER ARCHITECTURES AND DISTRIBUTED REAL-TIME COMPUTING Ph.D. Thesis
Caglan Mehmet Aras 1993 137 p
Avail: Univ. Microfilms Order No. DA9316600

Communication networks play an increasingly important role in many areas of computing. This dissertation introduces an interprocessor communication network for mobile robot computer architectures and real-time communication networks for distributed real-time computing. In both cases, the objective of the research is to provide communication with very low delay. Mobile robot tasks such as collision avoidance and dynamic navigation change over time and exhibit a high degree of cooperation. The segmented bus is a reconfigurable interconnection network for intelligent mobile robot applications. The segmented bus employs a preemptive circuit-switched message transfer technique for low delay. For mobile robot applications, analysis suggests that message delays are lower on the segmented bus as compared to alternatives such as the multiple bus. Interactive real-time message streams are used in continuous media distributed sensing and command/control applications. These streams require low end-to-end delay bounds and zero-loss. This dissertation offers solutions to message-stream admission and low latency message transfers for interactive real-time message streams on communication networks. The proposed adaptive stream admission procedure is shown to admit more streams to a network

than previous approaches. The proposed preemphasis cut-through data transfer mechanism reduces the minimum achievable end-to-end delay bound of a packet-switched network to values approaching circuit-switched techniques. To obtain low latencies on integrated broadband networks, the asynchronous transfer mode (ATM) must support bound-delay, zero-loss data transfers. A message-level delay control mechanism based on preemptive cut-through is presented. Hardware and software to implement message-level delay control are described results show a significant reduction in computation requirements when message-level delay control is used on ATM switch processors. Dissert. Abstr.

N94-32332 Range Commanders Council, White Sands Missile Range, NM. Tele-Communications Group.
IRIG J ASYNCHRONOUS ASCII TIME CODE FORMATS
Mar. 1994 8 p Limited Reproducibility: More than 20% of this document may be affected by microfiche quality
(AD-A277244; RCC-212-94) Avail: CASI HC A02

This standard describes two American Standard Code for Information Interchange (ASCII) time formats to be used to transfer time over conventional asynchronous telecommunications circuits. DTIC

N94-32477*# Amerasia Technology, Inc., Westlake Village, CA.
ADVANCED SATELLITE COMMUNICATION SYSTEM Final Report
Edward J. Staples and Sen Lie May 1992 92 p
(Contract NAS3-25862; SBIR-14.05-9388)
(NASA-CR-194211; NAS 1.26:194211) Avail: CASI HC A05/MF A01

The objective of this research program was to develop an innovative advanced satellite receiver/demodulator utilizing surface acoustic wave (SAW) chirp transform processor and coherent BPSK demodulation. The algorithm of this SAW chirp Fourier transformer is of the Convolve - Multiply - Convolve (CMC) type, utilizing off-the-shelf reflective array compressor (RAC) chirp filters. This satellite receiver, if fully developed, was intended to be used as an on-board multichannel communications repeater. The Advanced Communications Receiver consists of four units: (1) CMC processor, (2) single sideband modulator, (3) demodulator, and (4) chirp waveform generator and individual channel processors. The input signal is composed of multiple user transmission frequencies operating independently from remotely located ground terminals. This signal is Fourier transformed by the CMC Processor into a unique time slot for each user frequency. The CMC processor is driven by a waveform generator through a single sideband (SSB) modulator. The output of the coherent demodulator is composed of positive and negative pulses, which are the envelopes of the chirp transform processor output. These pulses correspond to the data symbols. Following the demodulator, a logic circuit reconstructs the pulses into data, which are subsequently differentially decoded to form the transmitted data. The coherent demodulation and detection of BPSK signals derived from a CMC chirp transform processor were experimentally demonstrated and bit error rate (BER) testing was performed. To assess the feasibility of such advanced receiver, the results were compared with the theoretical analysis and plotted for an average BER as a function of signal-to-noise ratio. Another goal of this SBIR program was the development of a commercial product. The commercial product developed was an arbitrary waveform generator. The successful sales have begun with the delivery of the first arbitrary waveform generator. Derived from text

N94-32576# Johns Hopkins Univ., Laurel, MD. Applied Physics Lab.
HIGH PEAK POWER MICROWAVES: A HEALTH HAZARD Final Report, 1 Aug. - 31 Dec. 1992
Henry A. Kues 1 Dec. 1993 101 p Prepared in cooperation with Wilmer Ophthalmological Inst., Baltimore, MD
(Contract MIPR-92MM2600)
(AD-A277168) Avail: CASI HC A06/MF A02

Prior research has established the ability of microwave exposure to produce a variety of biological effects including ocular changes. Investigations in our laboratory have demonstrated corneal endothelial lesions, increased vascular permeability, electroretinographic changes, and structural damage. The present study was designed to verify previous results using high-peak-power pulsed microwave exposure (1.25 GHz, 1 MW peak power, 1 or 16 Hz, and pulse duration of 0.5 or 10 microns) and to determine the extent of ocular damage. For this study we employed the rhesus monkey (Macaca mulatta) whose ocular anatomy and physiology is very similar to the human eye. Each subject was given a battery of clinical diagnostic tests prior to exposure and again following completion of all exposures. Each restrained subject was exposed for 4 hours, on three consecutive days over a three week period. Although some tests such as routine slit lamp examination failed to show any changes, both ERG and histopathology documented significant microwave induced retinal alteration. These results document the ability of high-peak-power pulsed microwaves to result in clinically significant ocular changes. The effects observed in this study demonstrate that under certain exposure conditions microwaves could present a human health hazard. DTIC

N94-32625# Department of the Navy, Washington, DC.
SYSTEM FOR MONITORING AND ANALYZING FIELD ENERGY EXPOSURE Patent Application
John F. Scarzello, inventor (to Navy), Adam C. Feaga, inventor (to Navy), and Daniel S. Lenko, inventor (to Navy) 6 Dec. 1993 30 p
(AD-D016115; US-Patent-Appl-SN-186711; Navy-Case-75176) Avail: CASI HC A03/MF A01

A portable electromagnetic field exposure dosimeter includes a triaxial ferrite-loaded coil sensor, a group of amplifiers and bandpass filters, a data control board, and a computer. The triaxial sensor receives electromagnetic radiation along three orthogonal axes for measurement which is channeled through a group of amplifiers and then bandpass filtered into three frequency signal ranges. One frequency range corresponds to exposure at 60 Hz and two of its harmonics. The second frequency range corresponds to high frequency pulsed energy. The third frequency range reflects body motion of a tested individual. The data control board converts such filtered signals into digital code and controls the flow of the converted data to random access memory and to the computer. The computer performs a Fast Fourier Transform on the converted data from the 60 Hz frequency range and then stores or displays the analyzed data as a function of frequency and time. The computer also stores or displays the data from the other two frequency ranges. DTIC

N94-32661 Los Alamos National Lab., NM.
ANALYSIS OF DIETZ'S SINGLE, RECTANGULAR PULSE THEORY FOR THE GENERATION OF RADIATION VIA PHOTOELECTRONS
T. M. Dipp Dec. 1993 57 p Limited Reproducibility: More than 20% of this document may be affected by microfiche quality
(Contract W-7405-eng-36)
(DE94-006131; LA-12629-MS) Avail: Issuing Activity (Department of Energy (DOE))

The generation of radiation via photoelectrons induced off of a conducting surface has been analytically modeled and computationally simulated by several researchers. This paper analyzes and compares Dietz's theory predictions with my research to form a unified foundation of consistent, inter-supporting results that should provide confidence in the independently performed basic research and resulting scaling laws and predictions. In doing so, this paper concentrated on Dietz's small-spot, single, rectangular, 'weak' pulse theory and equations, which involve nonrelativistic, monoenergetic photoelectrons emitted normal to a conducting surface in vacuum. In this paper I: (1) analytically compare Dietz's theory equations with my theory equations, (2) compare Dietz's theoretical scaling laws with my Particle-In-Cell (PIC) code simulation results, and (3) make Dietz's equations easier to use in predicting and optimizing photoelectron-generated radiation. As a result, it is shown that Dietz's equations match my theory's equations in their predicted scaling laws, differing only slightly in their coefficients and unique model parameters. Also, Dietz's equations generally agree with the PIC code results. Finally, optimization analysis showed that theoretical conversion efficiencies for typical real metals can meet and exceed values of 10(exp -5) if optimal photon energies of 15 to 20 eV are used. Even better efficiencies should be possible if the small-spot constraint is violated as well. DOE

N94-32679# Los Alamos National Lab., NM.
ETHICS AND RATIONALITY IN INFORMATION-ENRICHED DECISIONS: A MODEL FOR TECHNICAL COMMUNICATION
S. B. Dressel, P. Carlson, and M. J. Killingsworth 1993 5 p Presented at the 41st Annual Conference of the Society for Technical Communication, Minneapolis, MN, May 1994
(Contract W-7405-eng-36)
(DE93-040251; LA-UR-93-2864; CONF-940534-2) Avail: CASI HC A01/MF A01

In a technological culture, information has a crucial impact upon decisions, but exactly how information plays into decisions is not always clear. Decisions that are effective, efficient, and ethical must be rational. That is, we must be able to determine and present good reasons for our actions. The topic in this paper is how information relates to good reasons and thereby affects the best decisions. A brief sketch of a model for decision-making, is presented which offers a synthesis of theoretical approaches to argument and to information analysis. Then the model is applied to a brief hypothetical case. The main purpose is to put the model before an interested audience in hopes of stimulating discussion and further research. DOE

N94-32745# Los Alamos National Lab., NM.
COVICS: A COVERT VIDEO COMMUNICATIONS SYSTEM
Roger Bracht and Tom Kuckertz 1994 11 p Presented at the Radio Frequency Expo West, San Jose, CA, 23 Mar. 1994
(Contract W-7405-eng-36)
(DE94-007568; LA-UR-94-597; CONF-940378-1) Avail: CASI HC A03/MF A01 (US Sales Only)

A covert video communications system compatible with narrow band satellite use has been developed. The system communications by modulating reflected energy. This means that no energy is actively generated at the passive end of the link. Only the antenna is impedance is modulated to return the information. The recovered signal is then coherently demodulated to recover the information. The system uses microstrip antennas, operates at 10 GHz, and has a range of about 5 km. The video is slow scan and is updated every 2 seconds, and can be sent over a 2400 baud line such as is required for some satellite communications systems. A combination of discrete cosine transform and video differencing was used to achieve a high degree of video compression. DOE

N94-32756# Lawrence Livermore National Lab., CA.
LONG DISTANCE TRANSMISSION OF 15 Gb/s DIGITAL USING SUBCARRIER MULTIPLEXING AND EXTERNAL MODULATION
K. Hugenberg, M. Lowry, D. Beckedahl, and J. Blair Mar. 1994 9 p Presented at the DOD Fiber Optics Conference 1994, McLean, VA, 22-24 Mar. 1994
(Contract W-7405-eng-48)
(DE94-008298; UCRL-JC-115711; CONF-940363-3) Avail: CASI HC A02/MF A01

This paper provides an overview of a high-speed link design using subcarrier multiplexing techniques with external modulators. Although we have few experimental results to data, we feel the techniques and technology described in this paper will enable the simultaneous transmission of multichannel analog video and up to 15 Gb/s of digital data on a single wavelength. Furthermore, we show preliminary modeling that would indicate that at least four channels of 2.5 Gb/s can be sent over distances exceeding 500 km using a new dispersion technique that takes advantage of subcarrier multiplexing. DOE

N94-32897*# DENMAR, Inc., Marietta, GA.
MOM3D METHOD OF MOMENTS CODE THEORY MANUAL Final Report
John F. Shaeffer Mar. 1992 165 p Prepared for Lockheed Advanced Development Co., Sunland, CA
(Contract NAS1-18603; RTOP 505-69-30-01)
(NASA-CR-189594; NAS 1.26:189594) Avail: CASI HC A08/MF A02

MOM3D is a FORTRAN algorithm that solves Maxwell's equations as expressed via the electric field integral equation for the electromagnetic response of open or closed three dimensional surfaces modeled with triangle patches. Two joined triangles (couples) form the vector current unknowns for the surface. Boundary conditions are for perfectly conducting or resistive surfaces. The impedance matrix represents the fundamental electromagnetic interaction of the body with itself. A variety of electromagnetic analysis options are possible once the impedance matrix is computed including backscatter radar cross section (RCS), bistatic RCS, antenna pattern prediction for user specified body voltage excitation ports, RCS image projection showing RCS scattering center locations, surface currents excited on the body as induced by specified plane wave excitation, and near field computation for the electric field on or near the body. Author

N94-32971# Naval Command, Control and Ocean Surveillance Center, San Diego, CA. RDT and E Div.
BROADBAND, HIGH-POWER, 2-30 MHz, TWIN-WHIP ANTENNA. COMPUTER AND 1/10-SCALE MODEL DESIGN STUDY Final Report
R. S. Abramo Jan. 1994 72 p
(DA Proj. S13-37)
(AD-A277619; NRAD-TD-2597) Avail: CASI HC A04/MF A01

This report presents the results of a study conducted to design a whip-type antenna that covers the entire 2-30 MHz frequency range, has improved efficiency over previous single-whip designs, and is capable of accepting 3-6 kilowatts of RF input power. The Numerical Electromagnetic Code Version 4 (NEC4) was used to design two versions of twin-whip antennas that incorporate resistive - inductive - capacitive (RLC) circuit elements to achieve the required performance. A 1/10-scale model antenna was built and tested to verify the numerical designs. DTIC

N94-32986# Naval Postgraduate School, Monterey, CA.
AN EXPLORATORY STUDY OF NEURO LINGUISTIC PROGRAMMING AND COMMUNICATION ANXIETY M.S. Thesis
Lois M. Brunner Dec. 1993 96 p
(AD-A277756) Avail: CASI HC A05/MF A01

This thesis is an exploratory study of Neuro-Linguistic Programming (NLP), and its capabilities to provide a technique or a composite technique that will reduce the anxiety associated with making an oral brief or presentation before a group, sometimes referred to as Communication Apprehension. The composite technique comes from NLP and Time Line Therapy, which is an extension to NLP. Student volunteers (17) from a Communications course given by the Administrative Sciences Department were taught this technique. For each volunteer, an informational oral presentation was made and videotaped before the training and another informational oral presentation made and videotaped following the training. The before and after training presentations for each individual volunteer were evaluated against criteria for communications anxiety and analyzed to determine if there was a noticeable reduction of anxiety after the training. Anxiety was reduced in all of the volunteers in this study. DTIC

N94-33001# Naval Underwater Ordnance Station, Newport, RI. Warfare Center Div.
HIGH FREQUENCE AND AUTOMATIC LINK ESTABLISHMENT (HF AND ALE) RADIO PROPAGATION TEST TO ANTARCTICA Final Report
P. E. Gilles, J. R. Katan, and B. L. Pease 1 Feb. 1994 194 p
(AD-A277730; NUWC-NPT-TR-10427) Avail: CASI HC A09/MF A03

Recent federal/military standards in the area of automatic link establishment (ALE) for HF radios have been developed that coordinate frequency selection between communicating terminals, allowing them to adapt to skywave conditions. This study focused on evaluating the utility of these state-of-the-art radios in the polar environment. A quick-look evaluation of this technology was demonstrated over a radio circuit between Christchurch, New Zealand, and McMurdo Station, Antarctica. This transauroral link, operated by the U.S. Navy for the National Science Foundation, is the primary link for all operational, logistical, and emergency communications for U.S. operations between the Antarctic and the outside world. Daily plots of the measured signal to noise ratio, probability of bit error, and channel quality are presented and analyzed. Because of the initial success of this technology demonstration, additional experiments were designed for deployment in FY 1993 to answer not only operational issues, but also to collect data for further scientific studies and engineering improvements. DTIC

N94-33025# Naval Postgraduate School, Monterey, CA.
MULTICAST COMMUNICATION WITH GUARANTEED QUALITY OF SERVICE M.S. Thesis
Eric B. Boyer 16 Dec. 1993 103 p
(AD-A277650) Avail: CASI HC A06/MF A02

In this thesis, we address the problem of constructing multicast data distribution trees with guaranteed quality of service (QoS) for supporting multiparty interactions. We present an approach that integrates reservation with tree construction to facilitate a guaranteed quality of service. The proposed approach is based on the use of information about participants registered before the interaction starts. We first identify the design goals for multicast tree construction with minimum QoS requirements. We then describe a protocol to locate a set of distribution centers for an interaction

that depends upon the current load distribution, locations of the participants, and their QoS requirements. The protocol sets up a suitable number of center-specific trees for the interaction transparently. We compare the quality of the resulting trees on large, hypothetical networks with that of sender-specific and Steiner trees. Our results show that center-specific trees, built around the centers located by our approach, reserve fewer resources than sender-specific trees even for a significant number of simultaneous senders while sacrificing minimally in the average delay faced by each receiver. DTIC

N94-33026# Naval Research Lab., Washington, DC.
NOISE CANCELLATION FOR CELP VOICE ENCODERS IN AN F/A-18 NOISE ENVIRONMENT Interim Report, Jan. 1991 - Jan. 1993
David A. Heide 18 Mar. 1994 23 p
(AD-A277652; NRL/FR/5530-94-9712) Avail: CASI HC A03/MF A01

Because of the severe noise environment in the Navy's F/A-18 jet aircraft, it has always been very difficult to achieve highly intelligible speech using low data rate voice encoders such as the 2.4 kbps LPC-10. As a result, all voice encoding has been done with a high data rate 16.0 kbps CVSD algorithm. The main focus of this research was to develop a technique that could retain the acceptable intelligibility of the high rate encoders while still significantly lowering the data rate required. To achieve these results, a noise cancellation preprocessor was developed to be used in tandem with the new 4.8 kbps CELP encoder that is being implemented in the STU-3. While many noise reduction techniques were investigated, the best results were accomplished by first reducing the noise through spectral subtraction and then enhancing the important resonant formants of the speech. The results indicated that when the noise cancellation preprocessor was added to the CELP encoder, the DRT intelligibility scores were improved by a significant 5.0 points, making the speech much more acceptable for possible use in the F/A-18. DTIC

N94-33081 Japan Broadcasting Corp., Tokyo. Recording and Mechanical Engineering Research Div.
AN EXPERIMENTAL COMPACT HI-VISION VCR USING METAL EVAPORATED TAPE
Koji Kamijo, Toshiyuki Matsui, and Kazutoshi Mutou Mar. 1994 17 p
(ISSN 0027-657X)
(NHK-Labs-Note-423) Copyright Avail: Issuing Activity (Japan Broadcasting Corp., Tokyo)

We studied VCR systems and made an experimental setup to design a Hi-Vision camera-VCR. We used a nonsegmented tape transport system, a TCI (time compressed integration) two-channel FM recording system, a lower shifting FM modulator, and a quadruple multiple FM demodulator with reduced Moire interference. The tape used a metal evaporated tape with superior recording ability in short wavelength areas. We realized high quality playback video signals from detailed analysis of the FM characteristics on a magnetic recording channel of the metal evaporated tape. The performances of this VCR are: the minimum recording wavelength of 0.37 micrometers, the baseband bandwidth of 20 MHz for luminance and 7 MHz for chrominance, and SNR of 41 dB for luminance and 45 dB for chrominance. Author (revised)

N94-33083*# Houston Univ., TX. Dept. of Electrical Engineering.
THE 20 GHz CIRCULARLY POLARIZED, HIGH TEMPERATURE SUPERCONDUCTING MICROSTRIP ANTENNA ARRAY Final Report
Jarrett D. Morrow, Jeffery T. Williams, Stuart A. Long, and John C. Wolfe 31 May 1994 71 p
(Grant NAG9-593)
(NASA-CR-195097; NAS 1.26:195097; TR-94-13) Avail: CASI HC A04/MF A01

The primary goal was to design and characterize a four-element, 20 GHz, circularly polarized microstrip patch antenna fabricated from YBa2Cu3O(x) superconductor. The purpose is to support a high temperature superconductivity flight communications experiment between the space shuttle orbiter and the ACTS satellite. This study is intended to provide information into the design, construction, and feasibility of a circularly polarized superconducting 20 GHz downlink or cross-link antenna. We have demonstrated that significant gain improvements can be realized by using superconducting materials for large corporate fed array antennas. In addition, we have shown that when constructed from superconducting materials, the efficiency, and therefore the gain, of microstrip patches increases if the substrate is not so thick that the dominant loss mechanism for the patch is radiation into the surface waves of the conductor-backed substrate. We have considered two design configurations for a superconducting 20 GHz four-element circularly polarized microstrip antenna array. The first is the Huang array that uses properly oriented and phased linearly polarized microstrip patch elements to realize a circularly polarized pattern. The second is a gap-coupled array of circularly polarized elements. In this study we determined that although the Huang array operates well on low dielectric constant substrates, its performance becomes extremely sensitive to mismatches, interelement coupling, and design imperfections for substrates with high dielectric constants. For the gap-coupled microstrip array, we were able to fabricate and test circularly polarized elements and four-element arrays on LaAlO3 using sputtered copper films. These antennas were found to perform well, with relatively good circular polarization. In addition, we realized a four-element YBa2Cu3O(x) array of the same design and measured its pattern and gain relative to a room temperature copper array. The patterns were essentially the same as that for the copper array. The measured gain of the YBCO antenna was greater than that for the room temperature copper design at temperatures below 82K, reaching a value of 3.4 dB at the lowest temperatures. Author (revised)

N94-33093# Rutgers - The State Univ., New Brunswick, NJ. Center for Mathematical Sciences.
DESIGN OF FREE SPACE INTERCONNECTED SIGNAL PROCESSOR Final Technical Report, Apr. 1991 - Feb. 1993
Miles Murdocca and Thomas Stone Dec. 1993 44 p
(Contract F30602-88-D-0028)
(AD-A278129; RL-TR-93-260) Avail: CASI HC A03/MF A01

Progress is described on a collaborative effort between the Photonics Center at Rome Laboratory (RL), Griffiss AFB and Rutgers University, through the RL Expert Science and Engineering (ES&E) program. The goal of the effort is to develop a prototype random access memory (RAM) that can be used in a signal processor for a computing model that consists of cascaded arrays of optical logic gates interconnected in free space with regular patterns. The effort involved the optical and architectural development of a cascadable optical logic system in which microlaser pumped S-SEED devices serve as logic gates. At the completion of the contract, two gate-level layouts of the module were completed which were created in collaboration with RL personnel. The basic layout of the optical system has been developed, and key components have been tested. The delayed delivery of microlaser arrays precluded completion of the processor during the contract period, but preliminary testing was made possible through the use of other microlaser devices. DTIC

N94-33159# Naval Postgraduate School, Monterey, CA.
COASTAL BOUNDARY LAYER AND REFRACTIVITY MEASUREMENTS USING THE GROUND-BASED HIGH RESOLUTION INTERFEROMETER SOUNDER (GB-HIS) M.S. Thesis
Roy R. Ledesma Dec. 1993 81 p
(AD-A277980) Avail: CASI HC A05/MF A01

Timesections of potential temperature, dewpoint temperature, modified radar refractivity (M), and the vertical derivative of the modified radar refractivity (dM/dZ) from radiosondes and the Ground-based High Resolution Interferometer Sounder (GB-HIS) during three experiments are studied to analyze refractive effects in the coastal boundary layer and evaluate GB-HIS performance. In May of 1991 and 1992, the GB-HIS instrument was deployed on the Research Vessel Point Sur during research cruises off the central California coast. In August and September of 1993, the GB-HIS was deployed during the Variation of Coastal Atmospheric Refractivity (VOCAR) experiment at the Naval Air Station in Point Mugu, California. Comparisons of radiosonde observations with the GB-HIS is capable of depicting large-scale air mass changes in the coastal boundary layer with high temporal resolution. As a result, the general location of some refractive layers in the coastal boundary layer can be determined with the GB-HIS data. Small scale features in the moisture timesections from the raob data were not resolved by the GB-HIS with significant skill. The inability of the GB-HIS to capture the vertical moisture gradients seriously limits its ability to monitor refractive conditions. DTIC

N94-33160# Naval Postgraduate School, Monterey, CA.
AN ANALYSIS OF CELLULAR TELEPHONE AND INMARSAT SYSTEMS FOR PROVIDING RADIO DATA LINK COMPUTER COMMUNICATIONS FOR US NAVY VESSELS M.S. Thesis
David L. Cooper, Jr. Dec. 1993 69 p
(AD-A278143) Avail: CASI HC A04/MF A01

This thesis examines radio frequency data link computer communications systems with emphasis on their potential application to ship/shore communications. Covered are two systems that experts believe hold the most promise for DOD application, International Maritime Satellite (INMARSAT) and cellular radiotelephones. An analysis of system capabilities, cost, and future potential is performed for each, and then the two systems are compared. In addition, a thorough discussion of the security issues for each system and final conclusions/recommendations are presented. The conclusions suggest that increased cellular radiotelephone usage vice INMARSAT by fleet units would optimize fleet readiness and improve supply system performance. Based on these conclusions, this author's recommendation is that all Navy ships be equipped with a cellular telephone system, while all aircraft carriers and amphibious aircraft carriers be equipped with both cellular and INMARSAT systems. DTIC

N94-33172 Northeast Radio Observatory Corp., Westford, Mass. Haystack Observatory.
MILLSTONE HILL RADAR STUDIES OF PLASMA WAVES AND TURBULENCE Annual Report, Nov. 1992 - Oct. 1993
John C. Foster 15 Mar. 1994 6 p Limited Reproducibility: More than 20% of this document may be affected by microfiche quality
(Contract F49620-93-1-0019)
(AD-A278409; AFOSR-94-0223TR) Avail: Issuing Activity (Defense Technical Information Center (DTIC))

The Millstone Hill UHF radar was used as a diagnostic tool for investigating plasma waves and turbulence. During the 15-month interval covered by the first year of this award, experiments were performed using an alternating-code technique in order to assess this capability for use as a plasma diagnostic. Experiments at fixed antenna position and with real-time interaction investigated phenomena near perpendicular flow angle when looking very close to perpendicular magnetic aspect angle conditions. Analysis of prior data showed that when flow angle is varied through perpendicular while holding 0 degree aspect angle, an abrupt change in sign of the line of sight phase velocity is observed. Preparations were continued for bistatic coherent backscatter experiments in FY 94 using the MIDAS-C data acquisition system developed at Millstone Hill for use as a bistatic receiver in Canada. DTIC

N94-33173 California Inst. of Tech., Pasadena. Dept. of Electrical Engineering.
RELIABLE COMMUNICATION IN THE PRESENCE OF SEVERE NOISE OR JAMMING Final Report, 1 Oct. 1990 - 30 Sep. 1993
Robert J. McEliece 30 Sep. 1993 4 p Limited Reproducibility: More than 20% of this document may be affected by microfiche quality
(Grant AF-AFOSR-0037-91)
(AD-A278410; AFOSR-94-0210TR) Avail: Issuing Activity (Defense Technical Information Center (DTIC))

It has been shown that the ultimate limits for some classes of multi-user communications systems can be computed by single linear programs. This theory can be applied to ordinary telephone networks and to TDMA communications networks. DTIC

N94-33186 Naval Command, Control and Ocean Surveillance Center, San Diego, CA. RDT and E Div.
AN APPROXIMATE MODEL FOR VERTICAL POLARIZATION AND SURFACE ROUGHNESS USING THE PARABOLIC EQUATION
Herbert V. Hitney Mar. 1994 3 p Limited Reproducibility: More than 20% of this document may be affected by microfiche quality
(DA Proj. MP9-2)
(AD-A278091) Avail: Issuing Activity (Defense Technical Information Center (DTIC))

This presentation gives an approximate method that allows vertical polarization and sea surface roughness effects to be included in parabolic equation (PE) radio wave propagation models. This method was implemented in the hybrid radio physical optics (RPO) propagation model, and several comparisons of RPO results to waveguide results are presented. DTIC

N94-33254# Naval Command, Control and Ocean Surveillance Center, San Diego, CA. RDT and E Div.
THE EFFECTS OF A MULTIPATH CHANNEL AND INTERFERENCE ON COHERENT M-PSK DIGITAL COMMUNICATION SYSTEMS Final Report, Oct. 1992 - Sep. 1993
R. C. North, R. A. Axford, and D. Bryan Nov. 1993 81 p
(ONR Proj. RC32W11)
(AD-A278158; NCCOSC/RDT/E-TR-1636) Avail: CASI HC A05/MF A01

This report derives expressions for the average probability of symbol error of coherent M-ary phase-shift-keyed (M-PSK) communication system operating under the following nonideal conditions: (1) time-invariant multipath channel consisting of a direct path and a single multipath, (2) intentional/unintentional interference consisting of either a continuous wave (CW) signal or a bandpass filtered white Gaussian noise signal (bandwidth is variable), and (3) additive white Gaussian noise. Exact solutions are derived for coherent binary phase shift-keyed (BPSK) while both exact and upper bound solutions (shown to be tighter than the Chernoff bound) are derived for coherent M-PSK. One particular example, line-of-sight ultrahigh frequency (LOS UHF) radio, is used extensively to exercise the derived expressions and illustrate typical system performance. These results pertain to receiver with no means of compensation for the nonideal channel conditions. Methods of compensation for multipath and interference, like adaptive equalization, beamforming, spatial diversity, and multichannel adaptive equalization, are presently under investigation by the authors. The results in this report will help determine the performance gain offered by these methods of compensation DTIC

N94-33261# Naval Postgraduate School, Monterey, CA.
GENERATION OF THE AMBIGUITY FUNCTION FOR ULTRA WIDEBAND RADAR WAVEFORMS M.S. Thesis
Efrain Leon Dec. 1993 84 p
(AD-A277913) Avail: CASI HC A05/MF A01

The Ambiguity Function is one of the tools used to study the suitability of waveforms for radar applications. An understanding of this function gives the radar engineer an insight into different radar waveforms and permits him to select the best design for a particular system application. This thesis investigates the Ambiguity Function for ultra wideband radar waveforms generated by the Fourier Synthesis Method, which provides the capability to produce very narrow pulses in a coherent and controllable form. Since, for ultra wideband radar waveforms, the transmitted signal is a baseband signal without sinusoidal carrier, the Ambiguity Function for this kind of waveform should be generated by Doppler processing in the time domain rather than in the frequency domain, as is done for conventional radar waveforms. In this thesis, the Ambiguity Function has been generated and analyzed for two different this wideband radar waveforms by means of computer simulation of a radar receiver which incorporates time-Doppler processing. DTIC

N94-33334 Air Force Inst. of Tech., Wright-Patterson AFB, OH. School of Engineering.
ASSESSING THE VULNERABILITY OF MULTI-COMMODITY NETWORKS WITH FAILING COMPONENTS M.S. Thesis
Alan R. Robinsoln Mar. 1994 170 p Limited Reproducibility: More than 20% of this document may be affected by microfiche quality
(AD-A278434; AFIT/GOR/ENS/94M-12) Avail: Issuing Activity (Defense Technical Information Center (DTIC))

This research proposes an analytical approach for assessing flow disturbance, or 'compromise,' based on limited sampling of arc flow information in multicommodity, or multiple origin-destination (O-D), networks with failing arcs. There were three objectives established for this research. The first objective was to bound the expected flow, given the arcs fail with certain probabilities, which was accomplished by reviewing current approaches for single-commodity networks and extending the results to the multicommodity case. The second objective was to determine the best placement of flow monitors to obtain the most accurate estimates of O-D pair volumes. This was accomplished using a multicriteria approach for defining and evaluating all possible monitor placement strategies satisfying monitor availability. The O-D pair volumes were estimated using the l(sub p)-norm metric for varied levels of p. The final objective was to define a compromise metric providing confident assessments on the occurrence of 'compromise.' This was accomplished using simple regression techniques

to generate confidence intervals around the expected flow for each O-D pair. The approach proposed in this research is provided as an initial look into 'compromise' assessment based on limited network information.
DTIC

N94-33347 Phillips Lab., Hanscom AFB, MA.
PERFORMANCE STATISTICS BULLETIN. HIGH LATITUDE METEOR SCATTER PROPAGATION, JUNE, JULY, AUGUST, SEPTEMBER 1992 Interim Report
Alan D. Bailey, John M. Quinn, Patricia M. Bench, and Wayne I. Klemetti 2 Feb. 1994 268 p Limited Reproducibility: More than 20% of this document may be affected by microfiche quality
(AF Proj. 4643)
(AD-A277508; AD-E201796; PL-TR-94-2026; ERP-1145) Avail: CASI HC A12

A representative sampling of meteor scatter propagation performance statistics is presented from the PL/GP High Latitude Meteor Scatter Test Bed. The data address questions of meteor scatter propagation under disturbed ionospheric conditions, as well as normal meteor scatter propagation in the polar region. The time and frequency variations of the propagation transfer function are characterized over the 35 to 147 MHz range, including the availability of useful meteor trails, the potential communication capacity associated with those trails, the occurrence and persistence of ionospheric scatter and sporadic E-layers, variations in the signal-to-noise ratios of each scatter return and the effects of auroral and polar cap absorption (PCA) events on meteor scatter propagation and communications. Statistics covering Arrival Rate, Duration, Duty Cycle, and Noise Temperature are presented. This bulletin is one of a series covering the test bed operation from February 1990 through September 1992.
DTIC

N94-33353# City Univ. of New York, NY. Graduate Center.
APPLIED HARMONIC ANALYSIS Final Report, 1 Jan. 1989 - 31 Aug. 1993
Louis Auslander 31 Aug. 1993 4 p
(Contract F49620-89-C-0020)
(AD-A278384; AFOSR-94-0140TR) Avail: CASI HC A01/MF A01

Recent work by the CUNY group under the direction of Professor Louis Auslander has continued to study application of the Weil transform to radar signal processing and, in a parallel effort, to multi-access spread spectrum communications. The main thrust of the work is the relationship between the Weil transform of a waveform and the ambiguity surface of the wave-form. The study of this relationship has led to a fundamental observation: the cancellation properties of a waveform necessary for the creation of a thumbtack-like ambiguity surface may be viewed as arising from the pattern of zeros and the non-trivial winding numbers of the Weil transform of the waveform. This point of view is exposited and used to reinterpret classical radar waveform design techniques, while also providing a new method for radar waveform design. Additionally, a new technique for modifying or shaping waveforms has been developed. This consists of changing a waveforms has been developed. This consists of changing a waveform by multiplying its Weil transform by doubly-periodic functions and taking the inverse Weil transform to produce a new signal. DTIC

N94-33354 City Univ. of New York, NY.
A NEW TOOL FOR SIGNAL PROCESSING Final Report, 1 Jul. 1992 - 31 Oct. 1993
Louis Auslander 31 Oct. 1993 4 p Limited Reproducibility: More than 20% of this document may be affected by microfiche quality
(Contract F49620-92-J-0412)
(AD-A278385; AFOSR-94-0139TR) Avail: CASI HC A01

Recent work has continued to study applications of the Weil transform to radar signal processing and, in a parallel effort, to multi-access spread spectrum communications. The main thrust of the work is the relationship between the Weil transform of a waveform and the ambiguity surface of the wave-form. The study of this relationship has led to a fundamental observation: the cancellation properties of a waveform necessary for the creation of a thumbtack-like ambiguity surface may be viewed as arising from the pattern of zeros and non-trivial winding numbers of the Weil transform of the waveform. This point of view is exposited and used to reinterpret classical radar waveform design techniques, while also providing a new method for radar waveform design. Additionally, a new technique for modifying or 'shaping' waveforms has been developed. This consists of changing a wave-form by multiplying its Weil transform by doubly-periodic functions and taking the inverse Weil transform to produce a new signal.
DTIC

N94-31002 Centre de Recherches en Physique de l'Environnement, Issy-les-Moulineaux (France).
RADAR MEASUREMENTS [MESURES RADAR]
Frank Roux *In* CNES, Subtropical Climates and Their Evolution: From Space-Based Observation to Modelling Oct. 1993 p 467-494 In FRENCH (For primary document see N94-30981 09-47)
Copyright Avail: Issuing Activity (CEPADUES-Editions, 111, rue Nicolas-Vauquelin, 31100 Toulouse, France)

N94-31428*# Jet Propulsion Lab., California Inst. of Tech., Pasadena.
CHANNEL AND TERMINAL DESCRIPTION OF THE ACTS MOBILE TERMINAL
B. S. Abbe, M. J. Agan, C. C. Girardey, and T. C. Jedrey *In* NASA. Marshall Space Flight Center, The Second Annual International Space University Alumni Conference Feb. 1994 p 26-33 (For primary document see N94-31425 09-12)
Avail: CASI HC A02/MF A02

N94-31433*# Telstra Corp. Ltd., Sydney (Australia).
HUBLESS SATELLITE COMMUNICATIONS NETWORKS
Peter Alan Robinson *In* NASA. Marshall Space Flight Center, The Second Annual International Space University Alumni Conference Feb. 1994 p 92-95 (For primary document see N94-31425 09-12)
Avail: CASI HC A01/MF A02

N94-31435*# Rutgers Univ., Piscataway, NJ. Center for Computer Aids for Industrial Productivity.
APPLICATION OF THE WAVELET TRANSFORM FOR SPEECH PROCESSING
Stephane Maes (Belgian National Foundation for Scientific Research, Brussels.) *In* NASA. Marshall Space Flight Center, The Second Annual International Space University Alumni Conference Feb. 1994 p 112-120 (For primary document see N94-31425 09-12)
Avail: CASI HC A02/MF A02

N94-31437*# Tsukuba Space Center (Japan).
MULTISATELLITE CONSTELLATION CONFIGURATION SELECTION FOR MULTIREGIONAL HIGHLY ELLIPTICAL ORBIT CONSTELLATIONS
Mark G. Matossian (Colorado Univ., Boulder.) *In* NASA. Marshall Space Flight Center, The Second Annual International Space University Alumni Conference Feb. 1994 p 126-136 Sponsored by NASDA; Science and Technology Agency; and NSF (For primary document see N94-31425 09-12)
Avail: CASI HC A03/MF A02

N94-32437*# Rome Lab., Griffiss AFB, NY.
AUTOMATIC TRANSLATION AMONG SPOKEN LANGUAGES
Sharon M. Walter and Kelly Costigan *In* NASA, Washington, Technology 2003: The Fourth National Technology Transfer Conference and Exposition, Volume 2 Feb. 1994 p 139-142 (For primary document see N94-32420 09-99)
Avail: CASI HC A01/MF A04

N94-32461*# National Aeronautics and Space Administration. Hugh L. Dryden Flight Research Facility, Edwards, CA.
THE CONSTANT CURRENT LOOP: A NEW PARADIGM FOR RESISTANCE SIGNAL CONDITIONING
Karl F. Anderson *In* NASA, Washington, Technology 2003: The Fourth National Technology Transfer Conference and Exposition, Volume 2 Feb. 1994 p 349-361 (For primary document see N94-32420 09-99)
Avail: CASI HC A03/MF A04

N94-32468*# Naval Command, Control and Ocean Surveillance Center, San Diego, CA.
VOICE AND VIDEO TRANSMISSION USING XTP AND FDDI
John Drummond, Edwin Cheng, and Will Gex *In* NASA, Washington, Technology 2003: The Fourth National Technology Transfer Conference

and Exposition, Volume 2 Feb. 1994 p 416-421 (For primary document see N94-32420 09-99)
Avail: CASI HC A02/MF A04

N94-33150 Defence Research Establishment, Ottawa (Ontario). Surface Radar Section.
THE APPLICATION OF A RADIAL BASIS FUNCTION NEURAL NETWORK FOR RADAR TRACKING OVER THE SEA
Henry Leung and Eloi Bosse *In* Defence Research Establishment Atlantic, CRAD Signal and Information Processing Working Group Workshop on Neural Networks, Volume 1 Feb. 1993 p 3-26 (For primary document see N94-33149 09-63)
Avail: Issuing Activity (Defence Research Establishment Atlantic, P.O. Box 1012, Dartmouth, NS B2Y 3Z7 Canada)

N94-33152 Speech Technology Research Ltd., Victoria (British Columbia).
NEURAL NETWORKS APPLIED TO THE PHONEMIC SEGMENTATION OF SPEECH
Roy C. Snell and B. C. Dickson *In* Defence Research Establishment Atlantic, CRAD Signal and Information Processing Working Group Workshop on Neural Networks, Volume 1 Feb. 1993 p 69-81 (For primary document see N94-33149 09-63)
Avail: Issuing Activity (Defence Research Establishment Atlantic, P.O. Box 1012, Dartmouth, NS B2Y 3Z7 Canada)

N94-33153 Defence Research Establishment, Ottawa (Ontario). Communications Electronic Warfare Section.
AUTOMATIC MODULATION RECOGNITION
Rene Lamontagne *In* Defence Research Establishment Atlantic, CRAD Signal and Information Processing Working Group Workshop on Neural Networks, Volume 1 Feb. 1993 p 83-103 (For primary document see N94-33149 09-63)
Avail: Issuing Activity (Defence Research Establishment Atlantic, P.O. Box 1012, Dartmouth, NS B2Y 3Z7 Canada)

N94-33155 Defence Research Establishment Suffield, Ralston (Alberta).
PERIODIC AND CHAOTIC SIGNAL GENERATION IN A RECURSIVE ARTIFICIAL NEURAL NETWORK
Simon A. Barton *In* Defence Research Establishment Atlantic, CRAD Signal and Information Processing Working Group Workshop on Neural Networks, Volume 1 Feb. 1993 p 145-170 (For primary document see N94-33149 09-63)
Avail: Issuing Activity (Defence Research Establishment Atlantic, P.O. Box 1012, Dartmouth, NS B2Y 3Z7 Canada)

N94-33310*# MATRA Marconi Space, Toulouse (France). Automatic Control Systems and Propulsion Div.
POINTING AND TRACKING SPACE MECHANISM FOR LASER COMMUNICATION
A. Brunschvig and M. deBoisanger *In* NASA. Lewis Research Center, The 28th Aerospace Mechanisms Symposium May 1994 p 211-228 (For primary document see N94-33291 09-15)
Avail: CASI HC A03/MF A04

N94-33319*# Jet Propulsion Lab., California Inst. of Tech., Pasadena.
THE GALILEO HIGH GAIN ANTENNA DEPLOYMENT ANOMALY
Michael R. Johnson *In* NASA. Lewis Research Center, The 28th Aerospace Mechanisms Symposium May 1994 p 359-377 (For primary document see N94-33291 09-15)
Avail: CASI HC A03/MF A04

N94-33346 Royal Military Coll. of Canada, Kingston (Ontario). Dept. of Electrical and Computer Engineering.
A HEURISTIC MULTIPLE TARGET TRACKER
J. C. F. Beaupre, M. Farooq, and J. M. J. Roy *In its* Proceedings of the Symposium/Workshop on Applications of Expert Systems in DND Apr. 1992 p 218-237 (For primary document see N94-33335 09-66)
Avail: Issuing Activity (Royal Military Coll. of Canada, Vimy Post Office, Kingston, ON K7K 5L0 Canada)

33 ELECTRONICS AND ELECTRICAL ENGINEERING

Includes test equipment and maintainability; components, e.g., tunnel diodes and transistors; microminiaturization; and integrated circuitry.

For related information see also *60 Computer Operations and Hardware* and *76 Solid-State Physics.*

N94-31057# Old Dominion Univ., Norfolk, VA. Dept. of Electrical and Computer Engineering.
ELECTRON-BEAM CONTROLLED SEMICONDUCTOR SWITCHES Final Report, 2 Jan. 1990 - 31 Aug. 1993
Karl Schoenbach 2 Nov. 1993 113 p
(Contract DAAL03-90-G-0018)
(AD-A276198; ARO-26821.8-PH) Avail: CASI HC A06/MF A02

The final report consists of an overview of the experimental and modeling studies on electron-beam controlled semiconductor switches and, for more details, reprints of the papers published under this contract. Also included in the final report are results of those studies which have not yet been published in the open literature. DTIC

N94-31066# Rome Lab., Griffiss AFB, NY.
FAULT COVERAGE MEASUREMENT FOR DIGITAL MICROCIRCUITS Report, Oct. 1988 - Sep. 1993
Kevin A. Kwiat, Warren H. Debany, Jr., Heather B. Dussault, Mark J. Gorniak, and Anthony R. Macera Dec. 1993 29 p
(AD-A276226; RL-TR-93-217) Avail: CASI HC A03/MF A01

Procedure 5012 governs the measurement and reporting of fault coverage for digital microcircuits. This report expands on the published version of Procedure 5012 and explains the rationale behind the requirements of the procedure. The complete text of 5012, with additional annotations, is included in this technical report. DTIC

N94-31079# Puerto Rico Univ., Rio Piedras.
EXPERIMENTAL AND THEORETICAL STUDIES OF HYDROGENATED AMORPHOUS SEMICONDUCTOR ALLOYS AND SUPERLATTICES Final Report, 15 Sep. 1989 - 14 Dec. 1993
Zvi S. Weisz and Manuel Gomez 4 Feb. 1994 132 p
(Contract DAAL03-89-G-0114)
(AD-A276159; ARO-25715.6-MS-SAH) Avail: CASI HC A07/MF A02

We developed the photocarrier grating technique for carrier mobility-lifetime products (micro-Tau) measurements. Applying this technique to hydrogenated amorphous silicon (a-Si:H), we obtained micro-Tau values ranging from 10(exp -8) to 10(exp -5) sq cm/V for the majority and 10(exp -10) to 10(exp -8) for the minority carrier. This served as a basis for quality evaluation of differnt methods of preparation. We established that the dominant recombination mechanism is the 'defect pool' mechanism. Using the semiconductor-electrolyte system, we studied the density of localized states in a-Si:H and compared it to crystalline silicon. We found in a-Si:H an overall density of localized states in 10(exp -18)/cu cm. In crystalline Si only surface states were found, of an overall density of 10(exp -12) sq/cm. The sq cm states are centered around 0.2 eV the conduction band edge. The transport properties of two other disordered systems that may be relevant to a-Si:H were studied theoretically. These systems consist of metal cermets and of small colloidal suspensions. DTIC

N94-31150# Los Alamos National Lab., NM.
HIGH-POWER MICROWAVE-TUBE TRANSMITTERS
W. North Jan. 1994 385 p
(Contract W-7405-eng-36)
(DE94-005340; LA-12687-MS) Avail: CASI HC A17/MF A04 (US Sales Only)

High-Power Microwave-Tube Transmitters describes in detail high-power microwave-tube transmitters and the various subsystems that comprise them. Relying on his long experience as a designer of radar systems and rf stations for particle accelerators, the author also imparts lessons he has learned from his work and opinions he has formed on the transmitter design. DOE

N94-31152# Pacific Northwest Lab., Richland, WA.
HIGH-TEMPERATURE SUPERCONDUCTING TRANSFORMER PERFORMANCE, COST, AND MARKET EVALUATION
J. A. Dirks, J. E. Dagle, J. G. DeSteese, H. D. Huber, S. A. Smith, J. W. Currie, S. B. Merrick, and T. A. Williams Sep. 1993 204 p
(Contract DE-AC06-76RL-01830)
(DE94-005494; PNL-7318) Avail: CASI HC A10/MF A03

Recent laboratory breakthroughs in high-temperature superconducting (HTS) materials have stimulated both the scientific community and general public with questions regarding how these materials can be used in practical applications. While there are obvious benefits from using HTS materials (most notably the potential for reduced energy losses in the conductors), a number of issues (such as overall system energy losses, cost, and reliability) may limit applications of HTS equipment, even if the well known materials problems are solved. This study examined the future application potential of HTS materials to power transformers. This study effort was part of a U.S. Department of Energy (DOE) Office of Energy Storage and Distribution (OESD) research program, Superconductivity Technology for Electric Power Systems (STEPS). The study took a systems perspective to gain insights to help guide DOE in managing research designed to realize the vision of HTS applications. Specific objectives of the study were as follows: to develop an understanding of the fundamental HTS transformer design issues that can provide guidance for developing practical devices of interest to the electric utility industry; to identify electric utility requirements for HTS transformers and to evaluate the potential for developing a commercial market; to evaluate the market potential and national benefits for HTS transformers that could be achieved by a successful HTS development program; to develop an integrated systems analysis framework, which can be used to support R&D planning by DOE, by identifying how various HTS materials characteristics impact the performance, cost, and national benefits of the HTS application. DOE

N94-31168 Ecole Nationale Superieure des Telecommunications, Paris (France).
A NEURON NETWORK FOR IMAGE CLASSIFICATION: FROM ALGORITHM TO IMPLANTATION Ph.D. Thesis [UN RESEAU DE NEURONES POUR LA CLASSIFICATION D'IMAGES: DE L'ALGORITHME A L'IMPLANTATION]
Anne Trotin 1993 170 p In FRENCH Limited Reproducibility: More than 20% of this document may be affected by microfiche quality
(ISSN 0751-1353)
(TELECOM-93-E-005; ETN-94-95898) Avail: CASI HC A08

The feasibility of implanting a neural network particular algorithm on a VLSI (Very Large Scale Integration) digital circuit is addressed. The target application is image recognition. The Neocognitron was used since it possesses particularly important tolerance capacities to image deformation in generalization phase, and a structure of local connections and shared weight which designates it as a good candidate for hardware integration. The general study of the model led to the carrying out of diverse transformations on the start algorithm in order to reduce the complexity of the operating phase processing. The learning was also modified, which allowed the size of different network layers to be automatically determined. The work was validated by simulations on a data base of postal code numerical manuscript extracts. The results obtained show that the simplifications carried out sometimes improve performances. The study of a digital integrated circuit allowed the complexity of the problem to be evaluated. It appears that the Neocognitron after modifications can be implanted. This nevertheless calls for the choice of a given application which allows an adapted structure to be defined. ESA

N94-31170 Ecole Nationale Superieure des Telecommunications, Paris (France). Dept. Electronique.
STUDY OF CONTINUOUS-TIME AND MIXED ANALOG-DIGITAL OPERATORS Ph.D. Thesis [ETUDES D'OPERATEURS ANALOGIQUES TEMPS-CONTINU ET MIXTES ANALOGIQUES-NUMERIQUES]
Fuji Yang 1993 156 p In FRENCH Limited Reproducibility: More than 20% of this document may be affected by microfiche quality
(ISSN 0751-1353)
(TELECOM-93-E-010; ETN-94-95900) Avail: CASI HC A08

The study of elementary analog operators is addressed. Different techniques for 'transconductor' realization were studied, and architectures giving good linearity and low consumption were proposed. The transconductor study was applied to continuous time high frequency filtering. The design of Gm-C filters was studied. Nonlinear operators studied are: a CMOS multiplier, a family of nonlinear operators for neural network implementation. Mixed analog-digital operators allow operations between an analog signal and a digital signal. Potential applications of mixed operators are presented. ESA

N94-31240# Naval Postgraduate School, Monterey, CA.
VLSI IMPLEMENTATION OF STRAY INSENSITIVE SWITCHED CAPACITOR COMPOSITE OPERATIONAL AMPLIFIERS M.S. Thesis
Gregory A. Silvernagel Dec. 1993 127 p
(AD-A276461) Avail: CASI HC A07/MF A02

In this research, analog active circuits are implemented in VLSI technology by combining the properties of switched capacitors and composite amplifiers. This combined design improves upon the single operational amplifier's finite design, limited bandwidth, lower slew rate, as well as enhancing the overall network passive and active sensitivities. The switched capacitor is implemented using both the toggle switched capacitor and the modified open floating resistor techniques. The composite operational amplifier is implemented using the C20A-1 and C20A-2 designs from the CNOA-i possibilities. These four designs are produced on a single microchip that includes the two phase nonoverlapping clock circuit and the switches. The microchip is tested in a finite gain circuit and the results are used to evaluate the performance of the design. Shortcomings in the circuit performance are identified and the analysis is used to improve network simulations as well as provide guidance for design improvements. The design improvements are incorporated in a second generation microchip that is fabricated in a low noise analog process. DTIC

N94-31281 Naval Air Warfare Center, China Lake, CA. Weapons Div.
THE 18TH ANNUAL ELECTRONICS MANUFACTURING SEMINAR
Feb. 1994 184 p Seminar held in Ridgecrest, CA, 23-24 Feb. 1994 Limited Reproducibility: More than 20% of this document may be affected by microfiche quality
(AD-A276038; NAWC-WPNS-TP-8183) Avail: CASI HC A09

Presented are the proceedings of the 18th Annual Electronics Manufacturing Seminar, held on 23-24 February 1994, in Ridgecrest, Calif. The proceedings include the papers presented at the Seminar and cover all aspects of soldering technology and electronics manufacturing. The proceedings are a compilation of information provided by both nongovernment and government sources. The proceedings are published in the interest of furthering communication and broadening awareness of current activities among soldering technology and electronics manufacturing specialists. DTIC

N94-31373 Technische Univ., Berlin (Germany). Fachbereich Elektrotechnik.
A SERIES RESONANT CONVERTER IN HALF BRIDGE CIRCUITS WITH COMBINED SERIAL AND PARALLEL CHARGE COUPLING AND SEVERAL OUTPUT CIRCUITS Ph.D. Thesis [EIN SERIENRESONANZUMRICHTER IN HALBBRUECKENSCHALTUNG MIT KOMBINIERTER SERIELLER UND PARALLELER LASTAUSKOPPLUNG UND MEHREREN AUSGANGSKREISEN]
Manfred Schlenk 1993 162 p In GERMAN Limited Reproducibility: More than 20% of this document may be affected by microfiche quality
(ETN-94-95739) Avail: CASI HC A08

A method for dimensioning series oscillating circuit converters is described. The properties of oscillating circuits, quasiresonant and multiresonant converters were reviewed. Parallel power coupling is shown to provide lossless circuits, even with secondary converter discharge, but the efficiency is lower than with serial coupling. A combination of both couplings was proposed for operating the converter in nominal charge and voltage area. The ratio of parallel to serial resonance capacitors is shown to be dependent on converter maximal efficiency and natural frequencies of both oscillating circuits. The properties of control process for resonant converters are presented. The dimensioning of elementary values of the resonance circuit for a converter with serial/parallel charge coupling and ohmic charge is described. A calculation process was developed for voltages and currents in the secondary circuit. It is shown that the dynamic behavior of converters with several output circuits is strongly influenced by the coupling of output spools. ESA

N94-31374 Technische Univ., Berlin (Germany). Fachbereich Verkehrswesen.
THEORETICAL PRINCIPLES FOR DESIGNING LONG STATOR/LINEAR MOTORS WITH IRON Ph.D. Thesis [THEORETISCHE GRUNDLAGEN ZUR AUSLEGUNG VON EISENBEHAFTETEN LANGSTATOR-LINEARMOTOREN]
Rolf Hellinger 1993 153 p In GERMAN Limited Reproducibility: More than 20% of this document may be affected by microfiche quality
(ETN-94-95741) Avail: CASI HC A08

Elements for dimensioning synchronous linear motors for rail transportation are presented. A calculation analytic method was developed, which is based on the introduction of the specific magnetic conductance function, which takes into account the influence of stator and excitation windings. Electromotive and inertia forces were estimated with the stator current function and the magnetic air gap flux density and the results were verified using the finite element method for solving Maxwell equations. The short circuit currents in the stator winding were evaluated by means of calculated inductivities. Some perturbations, such as sliding and oscillation forces were calculated. Some results were validated on the TRANSRAPID test vehicle. ESA

N94-31445# Minnesota Univ., Minneapolis. Dept. of Electrical Engineering.
CONCURRENT ARCHITECTURES FOR VLSI SIGNAL AND IMAGE PROCESSING Final Report, Mar. 1990 - Sep. 1993
Keshab K. Parhi 1 Nov. 1993 7 p
(Contract DAAL03-90-G-0063)
(AD-A276124; ARO-27076.39-EL) Avail: CASI HC A02/MF A01

This final report summarizes the research results obtained with support from ARO for the grant DAAL-90-G-0063 (27076-EL). In this project, we studied approaches for high speed and low power recursive and adaptive digital filtering and coding and design methodologies and synthesis for high performance digital signal processing (DSP) systems. DTIC

N94-31483# Sandia National Labs., Albuquerque, NM.
HIGH-PERFORMANCE GaAs/AlGaAs OPTICAL PHASE MODULATORS FOR MICROWAVE/PHOTONIC INTEGRATED CIRCUITS
V. M. Hietala, S. H. Kravitz, M. G. Armendariz, G. A. Vawter, R. F. Carson, and R. E. Leibenguth 1993 9 p Presented at the OE/LASE 1994 Conference on Optics, Electro-Optics, and Laser Applications in Science and Engineering, Los Angeles, CA, 22-29 Jan. 1994
(Contract DE-AC04-94AL-85000)
(DE94-006361; SAND-93-1590C; CONF-940142-7) Avail: CASI HC A02/MF A01

High speed, high performance optical phase modulators are being developed for use in a coherent photonic integrated circuit (PIC) technology. These phase modulators are the critical component of a PIC program at Sandia National Laboratories targeted for microwave/millimeter wave signal processing and control including phased-array antenna control. The primary design goals for these modulators are amenability for integration into PICs, high 'figure of merit' (FOM: phase shift per unit length-voltage), and large bandwidths allowing for operation at millimeter wave frequencies. Depletion edge translation optical phase modulators (GaAs/AlGaAs based) have been selected as the device technology of choice due to their high FOM (greater than 60 deg/V-mm at 1.3 micron). These modulators unfortunately suffer from a large terminal capacitance which greatly limits speed. To overcome this problem, a distributed electrode design based on the use of slow-wave coplanar strips has been developed. Device design and measurements are presented. DOE

N94-31494# Naval Research Lab., Washington, DC.
ANALYSIS OF KEY PERFORMANCE PARAMETERS OF PHASE SAMPLING DIGITAL RF MEMORIES Interim Report, 1 Jul. - 18 Nov. 1992
Mark D. Virden 21 Jan. 1994 15 p
(AD-A276019; NRL/FR/5742-94-9705) Avail: CASI HC A03/MF A01

This report explores several performance features of phase sampling digital RF memories (DRFM), starting with the phase sampling process itself. Spurious signal levels, bandwidth, and processing of simultaneous signals are analyzed using computer modeling of DRFM functions. The preferred phase sampling technique is to make phase comparisons between samples of the input signal and its 180 degree analog. The input amplifier and the noise immunity of the phase comparator determine the dynamic range. Theoretical spurious levels are tabulated for 2, 4, 8, and 16-state sampling. The data reveal no differences between two-state and four-state sampling. Other tables show output levels for simultaneous signals into eight-state and two-state DRFMS at different combinations of input amplitudes. The advantages of the phase DRFM are large bandwidth, large input signal dynamic range without automatic gain control, and the capability for direct output phase modulation. DTIC

N94-31517# Universiteit Twente, Enschede (Netherlands).
A SILICON CONDENSER MICROPHONE: MODELLING AND ELECTRONIC CIRCUITRY Ph.D. Thesis
Armand Gijsbertus H. vanderDonk 1992 198 p
(ISBN-9-09-005279-8; ETN-94-96024) Avail: CASI HC A09/MF A03

The operational mechanism of condenser microphones and some aspects concerning microphone terminology are described. A model of condenser microphones, concerning microphones with a highly tensioned diaphragm as well as microphones with a diaphragm without any initial stress, is presented. Expressions of the mechanical, the electrical, and the total sensitivity are derived. Some practical limitations concerning the influence of temperature changes during operation and the maximum allowable sound pressure are described. An optimization procedure with respect to the sensitivity, which takes into account the maximum allowable sound pressure, is presented. The noise contribution of the microphone preamplifier is considered. Amplifiers, consisting of a MOSFET and a bias resistor or bias diode, and amplifiers, consisting of a JFET and a bias resistor, are analyzed. The integration of a silicon condenser microphone with a PMOS source follower is addressed. Design criteria concerning the integration of the CMOS process and a specific microphone fabrication process are presented. The principle of electromechanical feedback is described. The electrical and mechanical problems and the limitations of feedback are discussed. The feedback was analyzed and tested for two types of actuator signals. The principle of operation of a DC voltage converter as a substitution of a low voltage electret is described. Experimental results of a converter realized in CMOS and the practical operation in combination with a silicon condenser microphone are presented. ESA

N94-31518# Universiteit Twente, Enschede (Netherlands).
A SILICON CONDENSER MICROPHONE: MATERIALS AND TECHNOLOGY Ph.D. Thesis
Patrick Richard Scheeper 1993 204 p Sponsored by Stichting voor Fundamenteel Onderzoek der Materie
(ISBN-9-09-005899-0; ETN-94-96025) Avail: CASI HC A10/MF A03

The development of a condenser microphone in silicon for application in hearing aids is described. The main design criteria are the size (area about 3 by 3 sq mm), the sensitivity (about 10 mV/Pa), and the frequency response (100 to 7 kHz +/-3 dB). A model for the condenser microphone, describing the quasi static as well as the dynamic behavior, is presented. This model is used as a tool to design and optimize microphones. The applicability of Chemical Vapor Deposited (CVD) silicon nitride as a diaphragm material is investigated. The sticking of the diaphragm to the backplate, which is a troublesome phenomenon during the fabrication of the microphones, is investigated. Two different condenser microphone designs are described. It is shown that with one of these designs it is possible to meet the requirements of a hearing aid microphone. A special type of diaphragm that is provided with corrugations, in order to control and improve the mechanical sensitivity of the diaphragm, is addressed. ESA

N94-31520# Universiteit Twente, Enschede (Netherlands).
MODULE GENERATION FOR SELF-TESTING INTEGRATED SYSTEMS Ph.D. Thesis, 21 Jan. 1992
Ronald Pieter vanRiessen 1991 218 p Sponsored by Dutch Program for Innovative Research
(ISBN-9-09-004570-8; ETN-94-96027) Copyright Avail: CASI HC A10/MF A03

Hardware used for self test in VLSI (Very Large Scale Integrated) systems is reviewed, and an architecture to control the test hardware in an integrated system is presented. Because of the increase of test times, the use of self test techniques has become practically and economically viable for VLSI systems. Beside the reduction in test times and costs, self test also provides testing at operational speeds. Therefore, a suitable

combination of scan path and macrospecific (self) tests is required to reduce test times and costs. An expert system that can be used in a silicon compilation environment is presented. The approach requires a minimum of testability knowledge from a system designer. A user friendly interface was described for specifying and modifying testability requirements by a testability expert. A reason directed backtracking mechanism is used to solve selection failures. Both the hierarchical testable architecture and the design for testability expert system are used in a self test compiler. The definition of a self test compiler was given. A self test compiler is a software tool that selects an appropriate test method for every macro in a design. The hardware to control a macro test will be included in the design automatically. As an example, the integration of the self-test compiler in a silicon compilation system PIRAMID was described. The design of a demonstrator circuit by self test compiler is described. This circuit consists of two self testable macros. Control of the self test hardware is carried out via the test access port of the boundary scan standard. ESA

N94-31535# Universiteit Twente, Enschede (Netherlands).
A HIERARCHICAL APPROACH TO TEST GENERATION FOR CMOS VLSI CIRCUITS Ph.D. Thesis
Edward Christiaan Weening 1992 151 p Sponsored by Dutch Program for Innovative Research
(ISBN-9-09-005449-9; ETN-94-96022) Copyright Avail: CASI HC A08/MF A02

A hierarchical approach to the automatic test pattern generation for large digital VLSI circuits, fabricated in CMOS technology, is developed and implemented. The use of information on the circuit's hierarchy, which is readily available from most modern CAD (Computer Aided Design) systems, speeds up the test generation process considerably and enhances the quality of the tests generated. The hierarchical test generation tool can also be integrated in future CAD systems making test generation and testability enhancement during circuit design feasible. The hierarchical approach is described at the switch, functional, and behavioral level. A test pattern generation algorithm at the switch level is presented. Test generation and fault simulation algorithms both using OBDD (Ordered Binary Decision Diagram) functional descriptions of the circuit modules are presented. A test plan generation method at the behavioral level is presented. Practical results show that the hierarchical approach to test generation is more efficient than a conventional, non-hierarchical approach, especially for switch level faults. The results also show that the use of Design For Testability (DFT) circuitry is supported at the behavioral level. ESA

N94-31536# Universiteit Twente, Enschede (Netherlands). Biomedical Engineering Div.
EMPLOYMENT OF A POROUS GOLD ACTUATOR IN ISFET-BASED COULOMETRIC SENSOR-ACTUATOR SYSTEMS WITH APPLICATION TO PROTEIN CHARACTERIZATION Ph.D. Thesis
Jiang Luo 1993 170 p Sponsored by Univ. Twente, and Stichting voor Fundamenteel Onderzoek der Materie
(ISBN-9-09-005887-7; ETN-94-96023) Copyright Avail: CASI HC A08/MF A02

Technological and theoretical aspects of the development and application of ISFET based coulometric sensor-actuator systems are described. An application of such a system to the characterization of proteins is suggested. Diffusion and migration processes at the coulometric sensor-actuator systems with a planar actuator in the application of acid base titration were studied. To minimize the delay time and to limit the diffusion of the species, a porous noble metal actuator is proposed, instead of a planar one, closely covering the gate of the ISFET. The adaptation of the conventional ISFET technology, by which a flat ISFET is proposed and fabricated, is described. An analytical model to describe the developed ISFET based coulometric sensor-actuator systems with gate-covering porous actuator is proposed. A way to operate the developed coulometric sensor-actuator system for a dynamical measurement of the buffer capacity of an analyte is introduced. The buffer capacity as a distinct parameter to characterize proteins was measured. The preliminary results obtained from the measurement of lysozyme and ribonuclease showed different buffer capacities at different pH values. More studies are necessary to further investigate the applicability of this method to characterize proteins. ESA

N94-31571 Technische Univ., Berlin (Germany). Fachbereich Elektrotechnik.
HIERARCHICAL FAULT CATALOG PROCESS FOR DIAGNOSIS OF ANALOG CIRCUITS Ph.D. Thesis [HIERARCHISCHES FEHLERKATALOGVERFAHREN ZUR DIAGNOSE ANALOGER SCHALTUNGEN]
Albert Hoefel 1993 126 p In GERMAN Limited Reproducibility: More than 20% of this document may be affected by microfiche quality
(ETN-94-95730) Avail: Issuing Activity (European Space Agency (ESA))

A practical approach for diagnosis of analog circuits with focus on implementation systems is presented. A fault catalog, which allows a transparent access to the knowledge base, was developed using hierarchical error simulations, assuming a modular structure of the system to be diagnosed. This hierarchical dictionary contains references between the fault cause, some defective circuit components and their interaction, a state at the circuit interface which differs from the nominal behavior and measurable variations of the node voltages inside the circuit. Each fault is classified in a hierarchical structure, regarding its effect on the circuit, the immediate effect at the interface of circuit components and the effect on circuit functionalities. An integration of external knowledge such as accident statistical data from production final controls was made possible. A learning algorithm was added for future correction and enhancement of fault catalog. Object oriented knowledge representation and programming were used for implementing the system. A special expert system shell was implemented for testing the concept, with comfortable system interfaces. Passive systems are shown to be successfully diagnosed, but stability problems appear to be reinforced by fault simulation, because their efficiency strongly depends on individual properties of isolated circuits. ESA

N94-31575 Technische Univ., Berlin (Germany). Fachbereich Verkehrswesen.
APPLICABLE DIMENSIONING AND MEASURE AND TECHNOLOGICAL EXAMINATION OF LONG STATOR-LINEAR MOTORS FOR MAGNETIC HIGH-SPEED RAILWAYS Ph.D. Thesis [ANWENDUNGSNAHE DIMENSIONIERUNG UND MESSTECHNISCHE UEBERPRUEFUNG VON LANGSTATOR-LINEARMOTOREN FUER MAGNETSCHNELLBAHNEN]
Ruediger Fuerst 1993 281 p In GERMAN Limited Reproducibility: More than 20% of this document may be affected by microfiche quality
(Grant BMFT-TV8202/8406)
(ETN-94-95734) Avail: CASI HC A13

Results of measurements aimed at verification of the characteristic magnitudes of long stator/linear motors are presented. Both TRANSRAPID 06 and 07 vehicles were used for tests and the maximal velocity reached 435 km/h. Stator current and voltage, effective power, efficiency, power factor and electromotive force were measured for all dynamic states of the vehicle: acceleration, inertial cruise and braking. The results were discussed in the case of perturbations and incidents of the linear motor, such as electrical short circuits in the long stator winding. Requirements for dimensioning the linear motor were identified and the influence of stator and excitation parameters on the curve electromotive force versus velocity was estimated. ESA

N94-31576 Technische Univ., Berlin (Germany). Fachbereich Elektrotechnik.
REAL TIME SIMULATION MODEL FOR DESIGNING CONVERTER REGULATION Ph.D. Thesis [ECHTZEIT-SIMULATIONSMODELL FUER DEN ENTWURF VON UMRICHTERSTEUERUNGEN]
Lahcene Benbaouche 1993 189 p In GERMAN Limited Reproducibility: More than 20% of this document may be affected by microfiche quality
(ETN-94-95735) Avail: Issuing Activity (European Space Agency (ESA))

A digital real time simulation model for examination of functionality of a network connected converter is achieved following the principle of hybrid computers. The converter and its components such as input filter, pulse inverter, and coupling impedance were simulated and the analog calculation elements and digital control electronics were designed as components. A microcomputer interface was added so that the values of the simulated passive components and the variables of the control system, which is based on pulse width modulation, could be modified. The discretization of the mathematical model and the solution of nonlinear differential equations were represented in state space. Symmetrical and shift controls were compared considering pulse inverter output signal distortion factor. Transfer

functions of the multivariable system and decoupling of active and passive powers were estimated. Object oriented programming of the system was achieved with TURBOPASCAL programming language. ESA

N94-31593 Sandia National Labs., Albuquerque, NM.
FRACTIONAL-FACTORIAL PROCESS DEVELOPMENT TECHNIQUES
J. D. McBrayer and J. S. Bowers 1993 7 p Presented at the 14th Capacitor and Resistor Technology Symposium, Jupiter Beach, FL, 21-24 Mar. 1994 Limited Reproducibility: More than 20% of this document may be affected by microfiche quality
(Contract DE-AC04-94AL-85000)
(DE94-005580; SAND-93-2128C; CONF-940337-1) Avail: CASI HC A02

The use of fractional-factorial main effects experimental design techniques have been used to transfer, develop and characterize many of the processes used in the fabrication of High-Energy-Density capacitors. This paper will present the approach and experimental methods used to evaluate several of these processes. The results include main-effects experimental data from an assembly experiment, an arc-spray/pull test experiment, and a plating/pre-tinning experiment. An analysis of the results and technique will be presented. This analysis will highlight the advantages and disadvantages to this approach. A list of the lessons learned will also be included, especially those things that should be avoided. DOE

N94-31594 Sandia National Labs., Albuquerque, NM.
EVIDENCE FOR A CORRECT SiO2 VOLTAGE ACCELERATION MODEL
W. M. Miller, N. F. Smith, C. Messick, and J. A. Shideler 1993 12 p Presented at the 1993 International Integrated Reliability Workshop, Lake Tahoe, CA, 24-27 Oct. 1993 Limited Reproducibility: More than 20% of this document may be affected by microfiche quality
(Contract DE-AC04-94AL-85000)
(DE94-006578; SAND-93-1830C; CONF-9310147-2) Avail: CASI HC A03

We present experimental evidence that SiO2 breakdown is best described by the E-model of Baglee and McPherson as opposed to the 1/E model of Lee, Chen and Hu. The experiment was performed on 1765 fully processed capacitors over a range of electric fields of 7.25 MV/cm to 11 MV/cm and temperatures of 25C to 200 C. In addition, we also present a curious data point at low electric fields that we ascribe to a change in breakdown mechanism. DOE

N94-31598# Little (Arthur D.), Inc., Cambridge, MA.
FEASIBILITY STUDY FOR THE RECYCLING OF NICKEL METAL HYDRIDE ELECTRIC VEHICLE BATTERIES
J. C. Sabatini, E. L. Field, I. C. Wu, M. R. Cox, B. M. Barnett, and J. T. Coleman Jan. 1994 99 p Prepared for Midwest Research Inst., Golden, CO
(Contract DE-AC02-83CH-10093)
(DE94-000268; NREL/TP-463-6153) Avail: CASI HC A05/MF A02

This feasibility study examined three possible recycling processes for two compositions (AB(sub 2) and AB(sub 5)) of nickel metal hydride electric vehicle batteries to determine possible routes for recovering battery materials. Analysts examined the processes, estimated the costs for capital equipment and operation, and estimated the value of the reclaimed material. They examined the following three processes: (1) a chemical process that leached battery powders using hydrochloric acid, (2) a pyrometallurical process, and (3) a physical separation/chemical process. The economic analysis revealed that the physical separation/chemical process generated the most revenue. DOE

N94-31609 Technische Univ., Berlin (Germany). Fachbereich Elektrotechnik.
EXAMINATION OF FAST SEMICONDUCTOR DIODES (RECOVERY) WITH RESPECT TO SWITCHING VALVES IN PWM AND RESONANCE DEVICES Ph.D. Thesis [UNTERSUCHUNG VON SCHNELLEN HALBLEITERDIODEN (RECOVERY) IN VERBINDUNG MIT ABSCHALTBAREN VENTILEN IN PWM- UND RESONANZSCHALTUNGEN]
Hagen Gebhardt 1993 152 p In GERMAN Sponsored by DFG Limited Reproducibility: More than 20% of this document may be affected by microfiche quality
(ETN-94-95740) Avail: CASI HC A08

The behavior of fast semiconductor power diodes for applications with high values of di/dt and du/dt is examined. The failure process of the diode was estimated as a function of current transformation velocity and blocking layer temperature with nominal intensity. A specification methodology was introduced from these measurements, which allows the rupture current profile of the examined diode to be predicted for a given application and voltage charge and losses to be evaluated. The conditions of implementation of highly reverse diodes in direct current converters were written and the diode behavior in inductive and capacitive circuits is investigated. The implementation of fast diodes in Pulse Width Modulation (PWM) circuits is examined. SPICE (Simulation Program with Integrated Circuit Emphasis), which provides models of active and passive components for analog circuits in power electronics, is presented. ESA

N94-31616# Universiteit Twente, Enschede (Netherlands).
ANALYSIS AND SYNTHESIS OF MOS TRANSLINEAR CIRCUITS Ph.D. Thesis
Remco John Wiegerink 1992 169 p
(ISBN-9-09-005495-2; ETN-94-96029) Copyright Avail: CASI HC A08/MF A02

Work to generalize and extend the translinear circuit principle to implementation by MOS transistors operating in strong inversion and saturation, is presented. The MOS Translinear (MTL) circuit principle was derived based on the ideal square law transistor characteristic. Both translinear loops containing a single type of transistor and loops containing both n and p type transistors were investigated. In the latter case not all transistor parameters can be dropped from the resulting equation. For loops containing only one type of transistor all transistor parameters cancel and the result is a temperature and process independent relation between the drain current of the transistors. The influence of device imperfections on the MTL principle was analyzed and a systematic analysis method for MTL networks was developed. Two MTL circuit design strategies are proposed: one to implement a desired transfer function by combining the basic functions; and one using the program MTLPLOT as an interactive design tool to approximate a desired transfer function by an MTL loop equation. The designs are illustrated by a four quadrant current multiplier and a nonlinear signal processing function. ESA

N94-31711# Royal Military Coll. of Canada, Kingston (Ontario). Dept. of Electrical and Computer Engineering.
AN INVESTIGATION OF A NOVEL MICROSTRIP MAGIC-T
M. W. Katsube Apr. 1992 143 p
(ISBN-0-315-86218-1; CTN-94-61187) Copyright Avail: Micromedia Ltd., Technical Information Centre, 240 Catherine Street, Suite 305, Ottawa, Ontario, K2P 2G8, Canada HC/MF

?he magic T device is commonly found in waveguide form and has unique power division and isolation characteristics which find wide application in the microwave field. The design of such a device in microstrip technology using aperture coupling is investigated. Aperture coupling is a recent method for coupling electromagnetic energy from one substrate layer to another. It has a number of advantages including the separate integration of top and bottom layer circuitry, whereby the ground plane provides the isolation between the respective layers. Results indicate that this working device in microstrip exhibits the required properties of a magic T. Theoretical analysis is pursued to produce ideal circuit models based on modal analysis. A first order approximation is made using the dominant mode, with Lorentz reciprocity and the Poynting theorem. Experimental findings show very good narrow band characteristics with possible broadband operation upon further optimization of the T-branch, which at this stage is the limiting factor. The slot coupling shows good characteristics from about 12 to 18 GHz. The aperture coupled microstrip magic T shows excellent potential in performance for future applications such as integration into microstrip antennas and multilayer processing systems. Author (CISTI)

N94-31726# Montreal Univ. (Quebec). Dept. de Genie Electrique.
SIMULATION OF NON-UNIFORM TRANSMISSION LINES FOR WEAKLY DISPERSIVE STRUCTURES M.S. Thesis [SIMULATION DE LIGNES DE TRANSMISSION NON-UNIFORMES POUR DES STRUCTURES PEU DISPERSIVES]
Ricardo Bricout May 1992 180 p In FRENCH
(ISBN-0-315-86525-3; CTN-94-61206) Copyright Avail: Micromedia Ltd., Technical Information Centre, 240 Catherine Street, Suite 305, Ottawa, Ontario, K2P 2G8, Canada HC/MF

A study was conducted to obtain the frequency response of microwave

passive circuits containing non-uniform (coupled) transmission lines. By analyzing a general structure in which propagation occurs in an inhomogeneous medium, the performance of common devices like couplers, filters, and matching networks could be improved. The number of discontinuities was kept to a minimum in order to avoid parasitic effects. Most of the work in the study is based on quasi-transverse electromagnetic mode transmission lines, and in order to obtain the desired parameters, it was assumed that a quasi-static analysis is sufficiently accurate. The analysis is based on the spectral domain approach coupled to the method of moments if required by the complexity of the structure. The simulation of the circuit response uses a Chebyshev polynomial decomposition to solve the propagation problem. The results presented include a miniature hybrid microwave integrated circuit interdigital capacitor model, with the measured and simulated response for some test samples. Results are also included for a semi-reentrant mode coupler, soft transitions, and their applications to millimeter wave filters. Double strip suspended substrate lines were used in some circuits. Comparisons were made with measured data if possible and with data obtained with a microwave circuit simulator.

Author (CISTI)

N94-31785# Pacific Northwest Lab., Richland, WA.
MODAL ANALYSIS OF MULTITERMINAL HIGH VOLTAGE DIRECT CURRENT TRANSMISSION
J. E. Dagle Dec. 1993 87 p
(Contract DE-AC06-76RL-01830)
(DE94-006426; PNL-9011) Avail: CASI HC A05/MF A01

This report describes a first phase of effort in providing the Bonneville Power Administration (BPA) with comprehensive tools for model-based analysis of interactions between the Pacific HVDC Intertie (PDCI) and the alternating current (ac) system containing it. The work builds upon the transient stability model coded by Control Technologies, Inc. (CTI) for use in the Electric Power Research Institute (EPRI) Extended Transient-Midterm Stability Package (ETMSP). The general thrust of the effort is that CM's model be interfaced to and tested against all tools provided by EPRI's Power System Analysis Package (PSAPAC) and that these tools be used to investigate options for PDCI use in testing and control of western system dynamics. This will require refinements to the tools, the model, and western system case data. The PSAPAC tool for eigenanalysis is the Small Signal Stability Package (SSSP), useful for performing modal analysis of the multiterminal HVDC (MTDC) system. Such analyses are necessary to design and test an expanded role of the PDCI for power system control. This study focused on testing the application of the MTDC with SSSP. Modifications were made to enable SSSP to read the MTDC model. The PSAPAC and SSSP tools and the MTDC model were evaluated for accuracy and consistency using several modal analysis techniques, including Prony analysis on ETMSP-generated data. Although SSSP appears to be useful in analyzing the PDCI modes, inconsistencies limit the overall usefulness of that approach. The modal frequencies and damping identified by SSSP are inconsistent, indicating SSSP has difficulty analyzing the MTDC representation of the dc systems. The differences between the new and existing models can be used to identify the particular modeling issues associated with SSSP which are presently resulting in inconsistent results.

DOE

N94-31848 Swedish Inst. for Materials Testing, Boras.
INFLUENCE OF CARBON DIOXIDE ON ELECTRONIC EQUIPMENT: FIRE EXTINGUISHING WITH LOW CONCENTRATION [KOLDIOXIDS (CO2) PAVERKAN PA ELEKTRONIK: SLAECKNING MEDLAGA KONCENTRATIONER]
M. Arvidson and H. Persson 1993 41 p In SWAHILI Limited Reproducibility: More than 20% of this document may be affected by microfiche quality
(PB94-148749; SP-RAPP-1993:20) Avail: CASI HC A03

Discharge tests and a literature survey have been conducted to investigate the risk for damage on electrical equipment due to low temperatures and electrostatic charges when carbon dioxide (CO2) fire protection systems are operated. The work concentrated on total flooding systems. No indication of adverse effects from CO2 on electrical equipment has been found. Fire tests in a 21.8 cu m room with a computer, electrical cables, or waste paper respectively was performed to investigate the needed CO2 concentration for extinction. At the lowest concentration tested, 26 to 28 volume percent, the fires in the computer and in the cables were extinguished satisfactorily. The fire in the paper reignited when the room was ventilated again.

NTIS

N94-31905 Colorado Univ., Boulder.
FINITE ELEMENT ANALYSIS OF TIME-INDEPENDENT SUPERCONDUCTIVITY Ph.D. Thesis
James Joseph Schuler 1993 262 p
Avail: Univ. Microfilms Order No. DA9320476

The focus of the thesis research is the development of electromagnetic (EM) finite elements based upon a generalized four-potential variational principle. The final goal of this research is to formulate, develop, and validate finite element models that can accurately capture electromagnetic, thermal, and material phase changes in a superconductor. The use of the four-potential variational principle allows for downstream coupling of electromagnetic fields with the thermal, mechanical, and quantum effects exhibited by superconducting materials. The use of variational methods to model an electromagnetic system allows for a greater range of applications than just the superconducting problem. In fact, the four-potential variational principle can be used to solve a broader range of EM problems than any of the currently available formulations. It also reduces the number of independent variables from six to four while easily dealing with conductor/insulator interfaces. This methodology has been applied to a range of EM field problems. Seven problems are presented here. These applications show the power of the four-potential variational method, when augmented by Lagrange multiplier weighted constraint equations, to solve diverse EM field problems. All of the finite element models predict EM quantities exceptionally well and match the expected physical behavior. The results obtained with these finite element models display in previously unseen detail the physics of the superconducting charge carriers within the boundary layer of a Ginzburg-Landau superconductor. These results are compared to the physics of a low viscosity fluid problem. From this analogy, a physical argument is advanced about superconductors. This argument is that the small resistance that exists within a superconductor is similar in origin to the viscous effects of fluids and can be attributed to collisions that occur between moving and static charge carriers.

Dissert. Abstr.

N94-31919# Brookhaven National Lab., Upton, NY.
THE ZINC ELECTRODE: REACTIONS AND MECHANISMS
J. McBreen 1993 11 p Presented at the Symposium on Science of Advanced Batteries, Cleveland, OH, 8-9 Nov. 1993
(Contracts DE-AC02-76CH-00016; DE-FG05-89ER-45384)
(DE94-007977; BNL-60038; CONF-9311115-2) Avail: CASI HC A03/MF A01

The zinc electrode in alkaline electrolyte is unusual in that supersaturated zincate solutions can form during discharge and spongy or mossy zinc deposits can form on charge at low overvoltages. This paper reports on in situ x-ray absorption (XAS) results on supersaturated zincate and on mossy deposits.

DOE

N94-31928# Raytheon Co., Lexington, MA. Research Div.
RF VACUUM MICROELECTRONICS Quarterly Progress Report No. 9, 1 Oct. - 31 Dec. 1993
D. K. Arch 15 Feb. 1994 12 p
(Contract MDA972-91-C-0030)
(AD-A276512) Avail: CASI HC A03/MF A01

We summarize our progress towards developing a thin film edge emitter vacuum transistor capable of 1 GHz modulation. The second fabrication run of vacuum transistors was carried out and is approximately 90% complete. Fabrication is anticipated to be completed in early January 1994.

DTIC

N94-32056# Texas Univ., Austin. Dept. of Chemical Engineering.
HYDROGEN PEROXIDE ELECTRODES BASED ON ELECTRICAL CONNECTION OF REDOX CENTERS OF VARIOUS PEROXIDASES TO ELECTRODES THROUGH A THREE-DIMENSIONAL ELECTRON RELAYING POLYMER NETWORK Technical Report, Oct. 1992 - Dec. 1993
Mark S. Vreeke and Adam Heller 16 Feb. 1994 25 p Sponsored by ONR
(AD-A276543; TR-009-1993) Avail: CASI HC A03/MF A01

Hydrogen Peroxide has been shown to be efficiently electro-reduced at an electrode modified with a hydrophilic, permeable film of horseradish peroxidase covalently bound to a 3-dimensional epoxy network having polyvinyl pyridine (PVP)-complexed Os(bpy)2C1+2/+3 redox centers. Four peroxide sensing cathodes based on peroxidases from Arthromyces ramosus, horseradish and bovine milk are compared. Their sensitivity at O.OV (SCE) ranges from 0.1 - 1.0 A sq cm/M, and their limiting currents relate to the enzyme's ability to complex with the redox epoxy network. DTIC

N94-32111# Sandia National Labs., Albuquerque, NM.
THE ADVENT OF FAILURE ANALYSIS SOFTWARE TECHNOLOGY
C. L. Henderson and R. D. Barnard 1994 10 p Presented at the International Reliability Physics Symposium, San Jose, CA, 11-14 Apr. 1994
(Contract DE-AC04-94AL-85000)
(DE94-006593; SAND-94-0402C; CONF-940453-2) Avail: CASI HC A02/MF A01

The increasing complexity of integrated circuits demands that software tools, in addition to hardware tools, be used for successful diagnosis of failure. A series of customizable software tools were developed that organize failure analysis information and provide expert level help to failure analysts to increase their productivity and success. DOE

N94-32112 Sandia National Labs., Albuquerque, NM.
NOVEL FAILURE ANALYSIS TECHNIQUES USING PHOTON PROBING WITH A SCANNING OPTICAL MICROSCOPE
E. I. Cole, Jr., J. M. Soden, J. L. Rife, D. L. Barton, and C. L. Henderson 1993 11 p Presented at the International Reliability Physics Symposium, San Jose, CA, 11-14 Apr. 1994 Limited Reproducibility: More than 20% of this document may be affected by microfiche quality
(Contract DE-AC04-94AL-85000)
(DE94-006594; SAND-93-2429C; CONF-940453-3) Avail: CASI HC A03

Three new failure analysis techniques for integrated circuits (IC's) were developed using localized photon probing with a scanning optical microscope (SOM). The first two are light-induced voltage alteration (LIVA) imaging techniques that do the following: (1) localize open-circuited and damaged junctions; and (2) image transistor logic states. The third technique uses the SOM to control logic states optically from the IC backside. LIVA images are produced by monitoring the voltage fluctuations of a constant current power supply as a laser beam is scanned over the IC. High selectivity for localizing defects was demonstrated using the LIVA approach. Logic state mapping results, similar to previous work using biased optical beam induced current (OBIC) and laser probing approaches were also produced using LIVA. Application of the two LIVA based techniques to backside failure analysis was demonstrated using an infrared laser source. Optical logic state control is based upon earlier work examining transistor response to photon injection. The physics of each method and their applications for failure analysis are described. DOE

N94-32136# Lawrence Livermore National Lab., CA.
PROMISING FUTURE ENERGY STORAGE SYSTEMS: NANOMATERIAL BASED SYSTEMS, Zn-AIR, AND ELECTROMECHANICAL BATTERIES
R. Koopman and J. Richardson Oct. 1993 8 p Presented at the Workshop on Advanced Components for Electric and Hybrid Electric Vehicles, Gaithersburg, MD, 27-28 Oct. 1993
(Contract W-7405-eng-48)
(DE94-007443; UCRL-JC-115382; CONF-9310282-2) Avail: CASI HC A02/MF A01

Future energy storage systems will require longer shelf life, higher duty cycles, higher efficiency, higher energy and power densities, and be fabricated in an environmentally conscious process. This paper describes several possible future systems which have the potential of providing stored energy for future electric and hybrid vehicles. Three of the systems have their origin in the control of material structure at the molecular level and the subsequent nanoengineering into useful device and components: aerocapacitors, nanostructure multilayer capacitors, and the lithium ion battery. The zinc-air battery is a high energy density battery which can provide vehicles with long range (400 km in autos) and be rapidly refueled with a slurry of zinc particles and electrolyte. The electromechanical battery is a battery-sized module containing a high-speed rotor integrated with an iron-less generator mounted on magnetic bearings and housed in an evacuated chamber. DOE

N94-32199 Naval Research Lab., Washington, DC.
DESIGN OF A HIGH POWER X-BAND MAGNICON AMPLIFIER
S. H. Gold, O. A. Nezhevenko, V. P. Yakovlev, and B. Hafizi 14 Feb. 1994 44 p Limited Reproducibility: More than 20% of this document may be affected by microfiche quality
(AD-A277001; NRL/MR/6790-94-7408) Avail: CASI HC A03

We present a design study for an X-band frequency-doubling magnicon amplifier driven by a 500 keV, 172 A beam from a field emission diode. This study makes use of steady state particle simulations employing the realistic fields of magnicon cavities connected by beam tunnels and includes the effects of finite electron beam diameter. The simulations propagate an electron beam through a sequence of deflection cavities at 5.7 GHz, followed by an output cavity that operates at 11.4 GHz. The deflection cavities and the output cavity contain synchronously rotating TM modes. The deflection cavities progressively spin up the beam transverse momentum, until alpha defined equal to v(sub perpendicular)/v(sub z) is greater than or equal to 1, where v(sub perpendicular) and v(sub z) are the velocity components perpendicular and parallel to the axial magnetic field. The output cavity uses this synchronously gyrating beam to generate microwave radiation at twice the drive frequency. Self consistency of the simulation is achieved by iteration until power balance exists in each cavity and until the optimum RF phase in each cavity is determined. The final magnicon circuit should produce 20 to 50 MW at 11.4 GHz, depending on initial beam diameter, with a drive power of 1kW at 5.7 GHz. DTIC

N94-32215# Applied Science and Technology, Inc., Woburn, MA.
MATERIALS PROCESSING AND MANUFACTURING TECHNOLOGIES FOR DIAMOND SUBSTRATES MULTICHIP MODULES
Evelio Sevillanon 12 Feb. 1994 4 p
(Contract N00014-93-C-2026)
(AD-A276904) Avail: CASI HC A01/MF A01

We have succeeded in transferring the high growth rate diamond process from our 8 kW prototype to our 75 kW reactor. Additionally, we generated the first free-standing diamond films of greater than 4 in. x 4 in. size. Our efforts have concentrated on the following: improving the growth rate and film quality of the diamond growth process, exploring the operating envelope of the 75 kW reactor, and designing improvements to fully realize the potential of the large scale high growth system. New program components have been initiated for developing release techniques on large substrates, improving film flatness, and improving uniformity of thickness and morphology. A thermal conductivity, test stand is in the planning stages for in-house testing of samples in the near future. DTIC

N94-32258# Office of Naval Research, Arlington, VA.
WORKSHOP ON COMMERCIALIZATION OF PULSED POWER SCIENCE AND TECHNOLOGY PROCEEDINGS
20 Aug. 1993 147 p Workshop held in San Francisco, CA, 18-20 Aug. 1993
(AD-A276987) Avail: CASI HC A07/MF A02

The new international environment has opened opportunities for pulsed power research that were not possible a few years ago. Pulsed power technology developed with Department of Defense support was primarily directed towards Department of Defense goals -- perhaps more so than other areas of critical technology. There are, however, many significant applications for pulsed power in the commercial sector. The ability to tailor power pulse shapes and sequences and efficiently deliver energy in a pulsed, rather than DC or traditional AC mode, opens new horizons for commercial applications of lasers and accelerators, in medicine and pollution control, advanced motor control, and many other areas. There will be many applications for efficient, long-lived, reliable pulsed power that can be matched to applications requiring specialized voltage and current. The 1993 Workshop on Commercialization of Pulsed Power Science and Technology brought together experts in the full range of problems facing technology transfer to discuss the issues facing commercialization and marketing. Those involved represented in addition to pulsed power expertise, experience in licensing, development, product engineering and marketing of new technology. The Workshop Proceedings provides a summary of discussion and expertise in all these areas. DTIC

N94-32259 Leeds Univ. (England).
PROCEEDINGS OF THE INTERNATIONAL WORKSHOP ON COMPUTATIONAL ELECTRONICS

Aug. 1993 338 p Workshop held in Leeds, England, 11-13 Aug. 1993 Limited Reproducibility: More than 20% of this document may be affected by microfiche quality
(Contract DAJA45-93-M-0162)
(AD-A277020; R/D-7071-EE-03) Avail: CASI HC A15

The 1993 International Workshop on Computational Electronics took place at Leeds in England. The aim of the workshop is to allow researchers to focus on the computational aspects of solid-state device modelling. This encompasses new device and carrier transport models, numerical and computational techniques, computational implementation of transport theory (including quantum), developments in modelling electronic structures, and new techniques in computer visualization of models. This year an underlying theme associated with compound semiconductor devices was adopted, but contributions on all aspects of solid-state modelling for all types of material were invited. DTIC

N94-32301 Ghent Univ. (Belgium).
NOVEL OPTOELECTRONIC DEVICES BASED ON COMBINING GaAs AND InP ON Si Final Report
P. Demeester 1993 9 p Limited Reproducibility: More than 20% of this document may be affected by microfiche quality
(Contract DAJA45-90-C-0003)
(AD-A277018; R/D-6291-EE-01) Avail: CASI HC A02

This work has concentrated on basic technologies for the fabrication of devices which can be used in optical interconnect and optical computing applications. One of the most important issues is the technology for integration of different devices on the same substrate. Three different possibilities were investigated: heteroepitaxial growth, epitaxial lift-off and patterned epitaxy. The heteroepitaxial technique and the epitaxial lift-off can be used to integrate optoelectronic and electronic devices on the same substrate (resulting in optoelectronic integrated circuits or OEIC's). In terms of device performance and material quality, very good results were obtained with the epitaxial lift-off. This was reflected in the realization of a number of interesting devices and optoelectronic integrated circuits. The heteroepitaxial growth still suffers from the large defect density and although clear improvements were obtained, no good device results could be obtained. As an alternative the bonding by atomic rearrangement was also successfully investigated. The patterned growth technique has a different application field and has important advantages in the fabrication of photonic integrated circuits (PIC) where two (or more) optoelectronic devices are integrated and coupled optically (e.g. laser and waveguide). DTIC

N94-32303 Army Research Lab., Fort Monmouth, NJ. Electronics and Power Sources Directorate.
PERFORMANCE OF THE SONY LITHIUM-ION RECHARGEABLE BATTERY Technical Report, Dec. 1991 - Dec. 1992
George Au and Martin Sulkes Dec. 1993 37 p Limited Reproducibility: More than 20% of this document may be affected by microfiche quality
(AD-A277076; ARL-TR-71) Avail: CASI HC A03

Sony lithium-ion cells type 20500 were tested and evaluated at different temperatures, discharge rates from C/2 to 3C, and with different charge voltage cutoffs. The capacity was typical 0.8 Ah at the C/2 rate at 25 C when charged to 4.1-volt cutoff. An energy density of 70 Wh/kg and 400 or more cycles was demonstrated. Charging to 4.25 volts and higher cutoffs was tested without a safety problem. The Sony charger provided a constant potential charge at 8.2 volts (4.1 volts/cell). It replaces 90% of capacity within one hour and it shut off the charging after 2-1/2 hours. DTIC

N94-32307# Parma Univ. (Italy).
WOCSDICE 1993
1993 132 p The 17th European Workshop on Compound Semiconductor Devices and Integrated Circuits was held in Parma, Italy, 31 May - 2 Jun. 1993
(Contract DAJA45-93-M-0211)
(AD-A276766; R/D-7096-EE-03) Avail: CASI HC A07/MF A02

Session 1 on materials and basic technologies included the following topics: AlGaAs Substrate Surface Cleaning by Hydrogen ECR Plasma; Alloying Behavior of AuGeNi-Type Ohmic Contacts for III-V Homo- and Heterostructures; The Thermal Stability of MBE-Grown Al Schottky Contacts; Dependence of Low Temperature Mobility on the Free Electron Density in Al(x)Ga(1-x)As Containing DX Centers; and Structural Characterization of MOVPE Grown GaAs/InP and InP/GaAs Heterostructures. Session 2 was on optoelectronic devices and circuits, including Current Status of InP-based Integrated Technology for Microwave and Optoelectronic Applications. Session 3 was on field-effect devices, including Optimizing the Pseudomorphic Channels in MODFET's. Session 4 was on noise. Sessions 5-9 were on topics related to sessions 1-4, except Session 6 on heterostructure bipolar transistors. Session 10 was on the same topic as 6, but Session 11 was on Power Applications. Derived from text

N94-32329 Yardney Technical Products, Inc., Pawcatuck, CT.
DEVELOPMENT OF SILVER-ZINC CELLS OF IMPROVED CYCLE LIFE AND ENERGY DENSITY Final Report, 16 Aug. 1991 - 15 Jan. 1992
Roberto Serenyi and Stanley D. James 3 Mar. 1994 12 p Limited Reproducibility: More than 20% of this document may be affected by microfiche quality
(Contract N60921-91-C-0205)
(AD-A277311; NSWCDD-TR-92/296) Avail: Issuing Activity (Defense Technical Information Center (DTIC))

Substantial increases in the cost effectiveness and range of naval underwater vehicles are possible by virtue of advances made, in this program, to silver-zinc, vehicle propulsion batteries. To improve battery cycle life and energy density, electropermeable membranes (EPM's) were used as additives and/or as coatings for the negative electrodes and as coatings for conventional separator materials. Also, bismuth oxide was tested as an additive to the negative electrodes and P2291-40/20, a radiation-grafted polyethylene film, as a separator used in conjunction with silver-treated cellophane. EPM's used as negative electrode additives and also as coatings for Celgard 2500 microporous polypropylene greatly improved cells. Cells with EPM's used as coatings for the negative electrodes failed rapidly because of an error in formulation. Cells with 10 percent bismuth oxide in the negative electrodes exhibited substantially lower capacity than the standard cells and were removed from the test. Cells with radiation-grafted polyethylene separators provided fewer cycles than the standard cells, with 5 percent higher capacity and 6 percent lower utilization of active materials by cycle 60. However, the slightly better capacity of these cells, realized due to the additional space available for active materials, does not compensate for their generally unimpressive performance. DTIC

N94-32336 Naval Postgraduate School, Monterey, CA.
OPTIMAL ADAPTIVE ESTIMATION ALGORITHM FOR HARMONIC CURRENT REDUCTION USING POWER LIMITED ACTIVE LINE CONDITIONERS M.S. Thesis
Joel E. Zupfer Dec. 1993 51 p Limited Reproducibility: More than 20% of this document may be affected by microfiche quality
(AD-A277354) Avail: CASI HC A04

The ability to measure and compensate for power line harmonics has become a growing area of interest because of today's commonly used electronic equipment. Since the number and relative magnitudes of the harmonics on the power line are a function of the load, estimation of an equivalent load can be accomplished. Because of variation in the load, the need for an adaptive algorithm is imperative. Thus far, few algorithms for determining harmonic contents have not dealt with the problem associated with the limited power of the line conditioner. This thesis deals with a previously known harmonic compensating algorithm and introduces a new algorithm which both compensates for harmonic noise and estimates the load as a transformation matrix depending on the associated transfer function of the active line conditioner in use. DTIC

N94-32386# Sandia National Labs., Albuquerque, NM.
FROM DISPLAY AND PWB TO MCMs: LARGE PANEL MANUFACTURING
D. W. Palmer and W. Worobey 1994 10 p Presented at the International Society for Hybrid Multichip Modules, Denver, CO, 13-15 Apr. 1994
(Contract DE-AC04-94AL-85000)
(DE94-007855; SAND-94-0009C; CONF-9404118-1) Avail: CASI HC A02/MF A01

Considerable manufacturing development is currently aimed at reducing high density Multichip Module (MCM) cost through the use of large panels (greater than 40 cm x 40 cm) to fabricate many interconnection substrates in parallel. This drive for low cost MCM manufacturing is aided by the growing base of similar panel technology for the Printed Wiring Board (PWB) and Flat Panel display industries. It is toward this experience that

the infant large panel MCM efforts are looking. In particular, the MCM Consortium formed by the Electronic Industry Association (EIA) and funded under the federal TRP effort is charged with developing a line of equipment optimized for large panel, fine line manufacture. PWB line definition research into large panels of glass and smooth non-woven laminate at 2-4 mil lines and spaces reveals that present equipment and processes are extendible well beyond commercial PWB product. In contrast, the ultra-cleanliness and spin coating of the silicon integrated circuit technology prove too expensive when scaled from 150mm diameter wafers to 560mm panels. Thus low waste photoresist (and other polymer dielectrics) application methods are needed for large panel manufacture. Similarly, PWB contact photomasking is nearing limits at 2-4 mil feature size, and projection or maskless direct write processes may be needed. Even small hand-held flat panel displays are manufactured from large panels to reduce the cost per display for conductive and dielectric layer deposition and patterning. In addition, as low cost flat displays become larger and improve in resolution, the line pitch and density approach that needed in high density MCM's. DOE

N94-32478*# Physical Sciences, Inc., Andover, MA.
ARCING IN SPACE STRUCTURES IN LOW EARTH ORBIT Final Report, 1 Jan. 1990 - 29 Dec. 1991
B. L. Upschulte, W. J. Marinelli, G. Weyl, and K. L. Carleton Jan. 1992 127 p
(Contract NAS3-25797; SBIR-10.01-9030)
(NASA-CR-194223; NAS 1.26:194223; PSI-2123/TR-1153) Avail: CASI HC A07/MF A02

This report describes results of an experimental and theoretical program to investigate arcing of structures containing dielectric and conducting materials when they are biased negatively with respect to a plasma. An argon ion source generated Ar(+) ions of directed energy 20 to 40 eV and density approximately 10(exp 7) cm(exp -3) that impinged upon samples containing a dielectric material on top of a negatively biased Kovar plate. Arcing events were studied for bias voltages between -300 and -1000V with respect to the ion beam. The samples were Dow Corning 93-500 adhesive on Kovar, fused silica cover slips bonded on Kovar, and silicon solar cells mounted on Kovar. Measurements of discharge current, Kovar plate voltage, and radiation from the arc versus time were carried out. Microsecond duration exposure images and optical spectra in the 0.24 to 0.40 micron band were also acquired during arcing events. Arcing events were found to be associated with exposed adhesive and means were found to eliminate arcing altogether. The charging of a silica cover plate and the fields around the plate were calculated using a particle-in-cell code. Models were developed to explain the ignition of the arc and the physical processes occurring during the discharge. Author

N94-32509 Naval Postgraduate School, Monterey, CA.
RADIATION TOLERANT, HIGH SPEED, LOW POWER, GALLIUM ARSENIDE LOGIC M.S. Thesis
Kurt A. Wolfe Dec. 1993 116 p Limited Reproducibility: More than 20% of this document may be affected by microfiche quality
(AD-A277293) Avail: Issuing Activity (Defense Technical Information Center (DTIC))

Gallium arsenide (GaAs) circuits are largely immune to slowly accumulated radiation doses and therefore do not need the shielding required by complementary metal oxide semiconductor (CMOS) devices. This attribute renders GaAs circuits particularly attractive for spacecraft and military applications. However, it has been shown that GaAs circuits with short gate length transistors are excessively susceptible to single event upsets (SEU) due to enhanced charge collection at the edges of the gate called 'edge effect.' This thesis studies the SEU problem in two parts. Extensive computer modeling and simulation of a charged particle passing through various transistors of a low power, two-phase dynamic MESFET logic (TDFL) test chip was conducted using HSPICE in the first part. In the second part, new GaAs logic topologies are developed, simulated, and layed out in integrated circuits which require less power than directly coupled MESFET logic (DCFL) and should be less susceptible to single event upsets than TDFL circuits. DTIC

N94-32521# EG and G Energy Measurements, Inc., Idaho Falls.
ENERGY STORAGE SPECIFICATION REQUIREMENTS FOR HYBRID-ELECTRIC VEHICLE
A. F. Burke Sep. 1993 36 p
(Contract DE-AC07-76ID-01570)
(DE94-008642; EGG-EP-10949) Avail: CASI HC A03/MF A01

A study has been made of energy storage unit requirements for hybrid-electric vehicles. The drivelines for these vehicles included both primary energy storage units and/or pulse power units. The primary energy storage units were sized to provide 'primary energy' ranges up to 60 km. The total power capability of the drivelines were such that the vehicles had 0 to 100 km/h acceleration times of 10 to 12 s. The power density requirements for primary energy storage devices to be used in hybrid vehicles are much higher than that for devices to be used in electric vehicles. The energy density and power density requirements for pulse-power devices for hybrid vehicles, are not much different than those in an electric vehicle. The cycle life requirements for primary energy-storage units for hybrid vehicles are about double that for electric vehicles, because of the reduced size of the storage units in the hybrid vehicles. The cycle life for pulse-power devices for hybrid vehicles is about the same as for electric vehicles having battery load leveling. Because of the need for additional components in the hybrid driveline, the cost of the energy storage units in hybrid vehicles should be much less (at least a factor of two) than those in electric vehicles. There are no presently available energy storage units that meet all the specifications for hybrid vehicle applications, but ultracapacitors and bipolar lead-acid batteries are under development that have the potential for meeting them. If flywheel systems having a mechanical system energy density of 40 to 50 W(center dot)h/kg and an electrical system power density of 2 to 3 kw/kg can be developed, they would have the potential of meeting specifications for primary storage and pulse power units. DOE

N94-32582# Allied-Signal Aerospace Co., Kansas City, MO.
NEW THICK FILM FEEDTHROUGH CONFIGURATIONS
C. T. Fritsche Mar. 1994 8 p
(Contract DE-AC04-76DP-00613)
(DE94-008706; KCP-613-5330) Avail: CASI HC A02/MF A01

An investigation determined that thick film feedthroughs could successfully be printed with 12-mil holes in 20-mil square pads, 10-mil holes in 15-mil square pads, 6 x 12-mil oval-shaped holes in 10 x 35-mil rectangular pads, and 6 x 9-mil oval-shaped holes in 10 x 25-mil rectangular pads. The results were verified by printing test vehicles containing the four feedthrough configurations, electrically testing the feedthroughs for continuity, and cross-sectioning each of the feedthroughs in two axes. DOE

N94-32593# Lawrence Livermore National Lab., CA.
CONDUCTIVITY MEASUREMENTS OF CERIA-BASED SOLID ELECTROLYTES USING AC IMPEDANCE
G. B. Balazs and R. S. Glass Feb. 1994 15 p Presented at the 185th Electrochemical Society Meeting, San Francisco, CA, 22-27 May 1994
(Contract W-7405-eng-48)
(DE94-007380; UCRL-JC-116378; CONF-940529-1) Avail: CASI HC A03/MF A01

The ionic conductivities of cerium oxide samples doped separately with oxides of the entire lanthanide series (except promethium) and yttrium were measured using AC impedance. A wide variation in conductivities was observed, from 1 x 10(exp -2) S/cm for Ce(0.8)Sm(0.2)O(1.9) to 2 x 10(exp -4) S/cm for undoped ceria at 600 C. Many of these ceria systems exhibited ionic conductivities higher than those of zirconia systems, making ceria a logical choice for certain low temperature applications. A correlation was found between the ionic radii of the dopant and the corresponding ionic conductivities, with ceria doped with Gd2O3, Sm2O3, and Y2O3 exhibiting the highest values. In addition, the relative contributions of the grain boundaries and grain interiors to the overall resistance was measured. The ceria/samaria and ceria/gadolinia systems showed a different response than the ceria/yttria system with regard to the effect of sintering time on the relative contributions. DOE

N94-32607 Argonne National Lab., IL.
PROCEEDINGS OF THE AD HOC WORKSHOP ON CERAMICS FOR LI/FeS2 BATTERIES
1993 240 p Workshop held in Oak Brook, IL, 29-30 Sep. 1993 Limited Reproducibility: More than 20% of this document may be affected by microfiche quality

(Contract W-31-109-eng-38)
(DE94-007460; ANL/CMT/Proc-81920; CONF-9309203) Avail: CASI HC A11

Representatives from industry, the U.S. Advanced Battery Consortium (USABC), DOE, national laboratories, and other government agencies met to develop recommendations and actions for accelerating the development of ceramic components critical to the successful introduction of the Li/FeS2 bipolar battery for electric vehicles. Most of the workshop is devoted to electrode materials, bipolar designs, separators, and bipolar plates. The bulk of this document is viewgraphs and is divided into: ceramics, USABC overview, SAFT's Li/FeS2 USABC program, bipolar Li/FeS2 component development, design requirements for bipolar plates, separator design requirements, compatibility of ceramic insulators with lithium, characterization of MgO for use in separators, resistivity measurements of separators, sintered AlN separators for LiMS batteries, etc. DOE

N94-32650# Sandia National Labs., Albuquerque, NM.
THIN-FILM DECOUPLING CAPACITORS FOR MULTI-CHIP MODULES
D. Dimos, S. J. Lockwood, R. W. Schwartz, and M. S. Rogers 1994 6 p Presented at the 44th Electronic Components and Technology Conference, Washington, DC, 1-4 May 1994
(Contract DE-AC04-94AL-85000)
(DE94-007743; SAND-94-0163C; CONF-940596-2) Avail: CASI HC A02/MF A01

Thin-film decoupling capacitors based on ferroelectric lead lanthanum zirconate titanate (PLZT) films are being developed for use in advanced packages, such as multi-chip modules. These thin-film decoupling capacitors are intended to replace multi-layer ceramic capacitors for certain applications, since they can be more fully integrated into the packaging architecture. The increased integration that can be achieved should lead to decreased package volume and improved high-speed performance, due to a decrease in interconnect inductance. PLZT films are fabricated by spin coating using metal carboxylate/alkoxide solutions. These films exhibit very high dielectric constants ((var epsilon) greater than or equal to 900), low dielectric losses (tan(delta) = 0.01), excellent insulation resistances (rho greater than 10(exp 13) (Omega)-cm at 125 C), and good breakdown field strengths (E(sub B) = 900 kV/cm). For integrated circuit applications, the PLZT dielectric is less than 1 micron thick, which results in a large capacitance/area (8-9 nF/sq mm). The thin-film geometry and processing conditions also make these capacitors suitable for direct incorporation onto integrated circuits and for packages that require embedded components. DOE

N94-32662 Los Alamos National Lab., NM.
PARTICLE-IN-CELL (PIC) CODE SIMULATION RESULTS AND COMPARISON WITH THEORY SCALING LAWS FOR PHOTOELECTRON-GENERATED RADIATION
T. M. Dipp Dec. 1993 80 p Limited Reproducibility: More than 20% of this document may be affected by microfiche quality
(Contract W-7405-eng-36)
(DE94-006132; LA-12628-MS) Avail: Issuing Activity (Department of Energy (DOE))

The generation of radiation via photoelectrons induced off of a conducting surface was explored using Particle-In-Cell (PIC) code computer simulations. Using the MAGIC PIC code, the simulations were performed in one dimension to handle the diverse scale lengths of the particles and fields in the problem. The simulations involved monoenergetic, nonrelativistic photoelectrons emitted normal to the illuminated conducting surface. A sinusoidal, 100% modulated, 6.3263 ns pulse train, as well as unmodulated emission, were used to explore the behavior of the particles, fields, and generated radiation. A special postprocessor was written to convert the PIC code simulated electron sheath into far-field radiation parameters by means of rigorous retarded time calculations. The results of the small-spot PIC simulations were used to generate various graphs showing resonance and nonresonance radiation quantities such as radiated lobe patterns, frequency, and power. A database of PIC simulation results was created and, using a nonlinear curve-fitting program, compared with theoretical scaling laws. Overall, the small-spot behavior predicted by the theoretical scaling laws was generally observed in the PIC simulation data, providing confidence in both the theoretical scaling laws and the PIC simulations. DOE

N94-32663# Sandia National Labs., Albuquerque, NM.
THE RELATIVE PERFORMANCE OF FeS2 AND CoS IN LONG-LIFE THERMAL-BATTERY APPLICATIONS
R. A. Guidotti and F. W. Reinhardt 1994 8 p Presented at the 185th Electrochemical Society Meeting, San Francisco, CA, 22-27 May 1994
(Contract DE-AC04-94AL-85000)
(DE94-006145; SAND-93-3865C; CONF-940529-2) Avail: CASI HC A02/MF A01

The relative performance of FeS2 and CoS2 was measured in single cells based on the LiBr-KBr-LiF 0 eutectic electrolyte over a temperature range of 400 to 550 C using both standard (dry) and flooded anodes. This electrolyte is designed to be used in long-life thermal-battery applications because it has a lower melting point (313 C) and a higher electrical conductivity than the standard LiCl-KCl eutectic (m.p.= 352 C). The cells were continuously pulsed for 1 ms every 10 ms from a background current density of 190 mA/sq cm to 1,130 mA/sq cm until end of life. DOE

N94-32680# United Solar Systems Corp., Troy, MI.
RESEARCH ON STABLE, HIGH-EFFICIENCY AMORPHOUS SILICON MULTIJUNCTION MODULES
S. Guha Mar. 1994 60 p
(Contract DE-AC02-83CH-10093)
(DE94-000298; NREL/TP-411-6396) Avail: CASI HC A04/MF A01

This report describes the progress made during the first half of Phase 3 of the R&D program to obtain high-efficiency amorphous silicon alloy multijunction modules. The highlight of the work includes (1) demonstration of the world's highest initial module efficiency (area of 0.09 m(exp 2)) of 11.4% as confirmed by NREL, and (2) demonstration of stable module efficiency of 9.5% after 1-sun light soaking for 1000 h at 50 C. In addition, fundamental studies were carried out to improve material properties of the component cells of the multijunction structure and to understand the optical losses associated with the back reflector. DOE

N94-32688 Lawrence Livermore National Lab., CA.
AUTOMATED FIBER PIGTAILING TECHNOLOGY
O. T. Strand, M. E. Lowry, S. Y. Lu, D. C. Nelson, D. J. Nikkel, M. D. Pocha, and K. D. Young Feb. 1994 6 p Presented at the 44th Electronic Components and Technology Conference, Washington, DC, 1-4 May 1994 Limited Reproducibility: More than 20% of this document may be affected by microfiche quality
(Contract W-7405-eng-48)
(DE94-007072; UCRL-JC-116148; CONF-940596-1) Avail: CASI HC A02

The high cost of optoelectronic (OE) devices is due mainly to the labor-intensive packaging process. Manually pigtailing such devices as single-mode laser diodes and modulators is very time consuming with poor quality control. The Photonics Program and the Engineering Research Division at LLNL are addressing several issues associated with automatically packaging OE devices. A furry automated system must include high-precision fiber alignment, fiber attachment techniques, in-situ quality control, and parts handling and feeding. This paper will present on-going work at LLNL in the areas of automated fiber alignment and fiber attachment. For the fiber alignment, we are building an automated fiber pigtailing machine (AFPM) which combines computer vision and object recognition algorithms with active feedback to perform sub-micron alignments of single-mode fibers to modulators and laser diodes. We expect to perform sub-micron alignments in less than five minutes with this technology. For fiber attachment, we are building various geometries of silicon microbenches which include on-board heaters to solder metal-coated fibers and other components in place; these designs are completely compatible with an automated process of OE packaging. We have manually attached a laser diode, a thermistor, and a thermo-electric heater to one of our microbenches in less than 15 minutes using the on-board heaters for solder reflow; an automated process could perform this same exercise in only a few minutes. Automated packaging techniques such as these will help lower the costs of OE devices. DOE

N94-32700# Sandia National Labs., Albuquerque, NM.
APPLICATION OF THE MODIFIED VOLTAGE-DIVIDING POTENTIOMETER TO OVERLAY METROLOGY IN A CMOS/BULK PROCESS
R. A. Allen (National Inst. of Standards and Technology, Gaithersburg, MD.), M. W. Cresswell (National Inst. of Standards and Technology, Gaithersburg, MD.), L. W. Linholm (National Inst. of Standards and

Technology, Gaithersburg, MD.), J. C. Owen, III (National Inst. of Standards and Technology, Gaithersburg, MD.), C. H. Ellenwood (National Inst. of Standards and Technology, Gaithersburg, MD.), T. A. Hill, J. D. Benecke, S. R. Volk, and H. D. Stewart 1 Feb. 1994 21 p Presented at the Institute of Electrical and Electronics Engineers (IEEE) International Conference on Microelectronic Test Structures, San Diego, CA, 22-24 Mar. 1994

(Contract DE-AC04-94AL-85000)

(DE94-007937; SAND-94-0405C; CONF-940369-2) Avail: CASI HC A03/MF A01

The measurement of layer-to-layer feature overlay will, in the foreseeable future, continue to be a critical metrological requirement for the semiconductor industry. Meeting the image placement metrology demands of accuracy, precision, and measurement speed favors the use of electrical test structures. In this paper, a two-dimensional, modified voltage-dividing potentiometer is applied to a short-loop VLSI process to measure image placement. The contributions of feature placement on the reticle and overlay on the wafer to the overall measurement are analyzed and separated. Additional sources of uncertainty are identified, and methods developed to monitor and reduce them are described. DOE

N94-32721# Department of the Navy, Washington, DC.

OXIDATION RESISTANT COPPER Patent Application

Alan S. Edelstein, inventor (to Navy), Forrest H. Kaatz, inventor (to Navy), and Vincent G. Harris, inventor (to Navy) 15 Nov. 1993 22 p

(AD-D016099; US-Patent-Appl-SN-151693) Avail: CASI HC A03/MF A01

Oxidation resistant particles composed of copper and at least one metal having a valence of +2 or +3 and having an intermediate lattice energy for the metal in its hydroxide form are presented. The metal is selected from nickel, cobalt, iron, manganese, cadmium, zinc, tin, magnesium, calcium and chromium. In one embodiment, the phases of copper and at least one metal in the particles are separate and the concentration of the metal is greater near the surface of the particles than inwardly thereof. Process for making the oxidation resistant copper particles includes the steps of dissolving a copper salt and a salt of at least one of the metals in a suitable solvent or diluent; forming primary particles of copper and at least one metal in basic form by mixing a base and the salt solution; separating, washing and drying the primary particles; reducing the primary particles to metallic form; and heat treating the particles in metallic form at an elevated temperature. DTIC

N94-32786# Sandia National Labs., Albuquerque, NM.

AN ELECTRICAL TEST SYSTEM FOR CONDUCTOR FORMATION PROCESS ANALYSIS

T. A. Estes and R. J. Rhodes 1994 7 p Presented at the Institute for Interconnecting and Packaging Electronic Printed Circuits Spring Expo, Boston, MA, 24-27 Apr. 1994

(Contract DE-AC04-94AL-85000)

(DE94-007291; SAND-94-0597C; CONF-9404112-1) Avail: CASI HC A02/MF A01

Sandia National Laboratories has designed and built an electrical test system which fulfills a requirement to quickly, accurately, and precisely measure the resistance of conductors formed on Printed Wiring Board (PWB) substrates. This requirement stems from the need to measure small variations in conductors and thus to determine the source of the variations. With this test technology, experiments can be conducted with new materials, equipment, and processes in a timely and scientific manner. Conductor formation processes can be optimized for both conductor yield and uniformity, and process equipment can be fine-tuned prior to processing product to ensure that conductor attributes fulfill requirements. Significant resources were spent by Sandia National Laboratories and Texas Instruments modifying commercially available two-probe testers. AT&T has built a two-probe tester and obtained a commercially available 'bed-of-nails' test system. The two-probe systems have limitations in speed and precision; the 'bed-of-nails' system has proved to be superior to the two-probe designs but is expensive and lacks test pattern flexibility and ease of use. Due to the need to establish a testing technology which meets the requirements of Sandia National Laboratories and the National Center for Manufacturing Sciences PWB Consortium Imaging Team (current Imaging Team members; AT&T, Texas Instruments, AlliedSignal, IBM, and Sandia National Laboratories), a prototype test system was designed and built by Sandia. This paper will discuss the design and performance of the test system and the results of a comparison to other test systems. DOE

N94-32806# Sandia National Labs., Albuquerque, NM.

OVERVIEW OF SANDIA'S ELECTRIC VEHICLE BATTERY PROGRAM

R. P. Clark 1993 3 p Presented at the 1993 Automotive Technology Development Contractors' Meeting, Dearborn, MI, 18-21 Oct. 1993

(Contract DE-AC04-94AL-85000)

(DE94-008944; SAND-94-0630C; CONF-9310169-2) Avail: CASI HC A01/MF A01

Sandia National Laboratories is actively involved in several projects which are part of an overall Electric Vehicle Battery Program. Part of this effort is funded by the United States Department of Energy/Office of Transportation Technologies (DOE/OTT) and the remainder is funded through the United States Advanced Battery Consortium (USABC). DOE/OTT supported activities include research and development of zinc/air and sodium/sulfur battery technologies as well as double layer capacitor (DLC) R&D. Projects in the USABC funded work include lithium/polymer electrolyte (LPE) R&D, sodium/sulfur activities and battery test and evaluation. DOE

N94-32809# Sandia National Labs., Albuquerque, NM.

HIGH-PERFORMANCE GaAs/AlGaAs OPTICAL PHASE MODULATORS FOR MICROWAVE PHOTONIC INTEGRATED CIRCUITS

V. M. Hietala, S. H. Kravitz, M. G. Armendariz, G. A. Vawter, and R. F. Carson 1994 4 p Presented at the 1994 Institute of Electrical and Electronics Engineers (IEEE) Microwave Theory Technique Symposium, San Diego, CA, 23-27 May 1994

(Contract DE-AC04-94AL-85000)

(DE94-007376; SAND-94-0477C; CONF-9405112-1) Avail: CASI HC A01/MF A01

A high-performance high-speed optical phase modulator for photonic integrated circuit (PIC) use is described. Integration of these optical phase modulators into a real system (compass) is also discussed. The optical phase modulators are based on depletion-edge translation and have experimentally provided optical phase shifts in excess of 60 degrees/V(center dot)mm with approximately 4 dB/cm loss while simultaneously demonstrating bandwidths in excess of 10 GHz. DOE

N94-32828# Edgerton, Germeshausen and Grier, Inc., Idaho Falls, ID.

EDD-7 ELECTRIC CHARGE POINT METER TEST RESULTS

C. R. Mersman Sep. 1993 71 p

(Contract DE-AC07-76ID-01570)

(DE94-008515; EGG-EP-10999) Avail: CASI HC A04/MF A01

The results of tests evaluating the electric switching portion of the EDD-7 Electric Charge Point Meter (ECPM) are presented. The ECPM is a modified parking meter that allows the purchase of 120 or 240 volt electric power. The ECPM is designed to make electricity available at any vehicle parking location. The test results indicate that the ECPM operated without failure through a series of over current and ground fault tests at three different test temperatures. The magnitude of current required to trip the over current protection circuitry varied with temperature while the performance of the ground fault interruption circuitry did not change significantly with the test temperature. DOE

N94-32905*# National Aeronautics and Space Administration. Lewis Research Center, Cleveland, OH.

THEORETICAL AND EXPERIMENTAL STUDY OF MICROSTRIP-TO-SLOT LINE UNIPLANAR TRANSITION

Jong-Gwan Yook (Michigan Univ., Ann Arbor.), Nihad I. Dib (Michigan Univ., Ann Arbor.), Linda P. B. Katehi (Michigan Univ., Ann Arbor.), Rainee N. Simons (NYMA, Inc., Brook Park, OH.), and Susan R. Taub May 1994 7 p Proposed for presentation at the 1994 IEEE AP-S International Symposium and URSI Radio Science Meeting, Seattle, WA, 19-24 Jun. 1994; sponsored by IEEE

(Contract NAS3-27186; RTOP 506-44-2C)

(NASA-TM-106566; E-8743; NAS 1.15:106566) Avail: CASI HC A02/MF A01

Recent advances in MMCI technology make it possible to construct transitions from CPW-to-microstrip with via hole, microstrip-to-slot line and microshield line-to-CPW all of which have potential applications in the feed network of antennas. In this study we investigate the characteristics of the

microstrip-to-slot line uniplanar transition using the finite element methods (FEM) and finite difference time domain (FDTD) techniques, and compared the theoretical results with the measurements. In both cases, the results agree with the measurements within a few percent. Author

N94-32917 Central Research Inst. of Electric Power Industry, Tokyo (Japan). Energy and Environment Lab.
DEVELOPMENT OF NICKEL AND METAL HYDRIDE SECONDARY BATTERY
T. Ikeya, K. Kumai, and T. Iwahori May 1993 23 p Limited Reproducibility: More than 20% of this document may be affected by microfiche quality
(DE94-757270; CRIE-T-92089) Avail: CASI HC A03

This paper describes contrivances on a nickel/metal hydride secondary battery using a hydrogen absorbing alloy modified by mechanical processing, and reports the battery characteristics. The test electrode (cathode) was made from a hydrogen absorbing alloy powder which has been mixed with cobalt powder at 20%, mechanically processed in a rotating ball mill, rolled into sheets, and sandwiched with nickel mesh sheets. The counter electrode is a sintered nickel electrode, the electrolyte uses potassium hydroxide aqueous solution, and the separators are made of polypropylene non-woven fabric. The result of battery characteristic tests using the test electrodes indicated that the battery has longer life than conventional batteries. A nickel electrode capacity regulated battery having the same configuration as practically used batteries exhibited no capacity decrease even after 1000 charge/discharge cycles. The main factor for this was thought that metals added by the mechanical processing are bonded locally on the alloy surface forming electrically conductive microstructure accompanying dissolving and depositing reactions to produce cobalt alloy that shows catalytic activity on the alloy surface. DOE

N94-32957# California Univ., Los Angeles.
VLSI FOR HIGH-SPEED DIGITAL SIGNAL PROCESSING Quarterly Progress Report, 1 Oct. - 31 Dec. 1993
Alan N. Willson, Jr. 21 Dec. 1993 5 p
(Contract N00014-91-J-1852)
(AD-A277617) Avail: CASI HC A01/MF A01

During the past quarter we have made considerable progress on the design and layout of the five-processor ring IC, although we missed the deadline for the Jan. 1994 MOSIS 0.8 micron CMOS fabrication run. The next available run has an Apr. 6 deadline, and we hope to have our chip on the run, or at the worst on the following one. We are trying to be as cautious as possible in our fabrication of this rather expensive chip in order to maximize our chances that only one fabrication run will be necessary. As we have mentioned previously, the chip will be a drop in replacement for our one-processor chip, which was found fully functional on its first fabrication, and which was described in our previous progress report. We have also made good progress on our IBM PC boards. DTIC

N94-32962 Department of the Navy, Washington, DC.
GROUNDING RING FOR GROUND ADAPTERS Patent
Nicholas F. Schade, inventor (to Navy) 11 Jan. 1994 5 p Filed 3 Jul. 1991
(AD-D016118; US-Patent-5,278,352; US-Patent-Appl-SN-725719; US-Patent-Class-174-65) Avail: US Patent and Trademark Office

The present invention relates to a grounding ring which may be used in ground adapters. The grounding ring has a structure resembling a miniature box girder with an irregular hexagonal cross section and is bent into a toroidal configuration. The grounding ring is characterized by increased wall areas for establishing electrical contact between a surface of a conductor and a surface of a stuffing tube, grounding conduit, or shield grounding fitting. The grounding ring provides improved EM performance and better capacitive coupling. DTIC

N94-32967 Department of the Navy, Washington, DC.
BUFFERED FEEDTHROUGH CROSSBAR SWITCH Patent
William J. Haber, inventor (to Navy) 11 Jan. 1994 9 p Filed 11 Apr. 1991
(AD-D016145; US-Patent-5,278,548; US-Patent-Appl-SN-685588; US-Patent-Class-340-825.79) Avail: US Patent and Trademark Office

An improved crossbar switch in which internal buffering is performed for all input signals across the chip and in which an extra input for each output channel of the crossbar switch element is provided. DTIC

N94-32976 Department of the Navy, Washington, DC.
DIGITAL BEAMFORMING AND FILTERING CIRCUIT Patent
Douglas L. Odell, inventor (to Navy) 7 Dec. 1993 8 p Filed 11 May 1992
(AD-D016142; US-Patent-5,268,877; US-Patent-Appl-SN-880824; US-Patent-Class-367-103) Avail: US Patent and Trademark Office

A beamformer system is disclosed which includes an array of sensors such as hydrophones which produce signals from which information relating to a target is to be determined. The beamformer system includes a channel for each sensor, the channel including a variable length shift register which provides bulk delay to received signals, a FIR interpolation filter which provides vernier delay and shading. The system also includes a summation tree which adds the received signals and a sign extension/bit reversal filter to avoid overflow. DTIC

N94-33034# Virginia Univ., Charlottesville. School of Engineering and Applied Science.
RESEARCH ON HIGH RELIABILITY REFRACTORY OHMIC CONTACTS FOR GaAs FETs AND MODFETs Final Report
W. T. Anderson Feb. 1994 40 p
(Contract N00014-91-P-2037)
(AD-A276848; UVA/525469/EE94/101) Avail: CASI HC A03/MF A01

The following topics are covered: high temperature characteristics of amorphous TiWSi(x) nonalloyed ohmic contacts to GaAs, all-refractory GaAs FET using amorphous TiWSi(x) source/drain metallization and graded In(x)Ga(1-x)As layers, high selectivity patterned substrate epitaxy of In(x)Ga(1-x)As/GaAs (0 less than or equal to x less than or equal to 1) by conventional low pressure organometallic vapor phase epitaxy (LPOMVPE), a simplified model describing enhanced growth rates during vapor phase selective epitaxy, and all-refractory GaAs FET for high temperature applications. CASI

N94-33044*# Arizona State Univ., Tempe.
ADVANCED HIGH FREQUENCY PARTIAL DISCHARGE MEASURING SYSTEM Final Report
George G. Karady May 1994 31 p
(Grant NAG3-1139)
(NASA-CR-195240; NAS 1.26:195240; ASU-DWA-0080) Avail: CASI HC A03/MF A01

This report explains the Advanced Partial Discharge Measuring System in ASU's High Voltage Laboratory and presents some of the results obtained using the setup. While in operation an insulation is subjected to wide ranging temperature and voltage stresses. Hence, it is necessary to study the effect of temperature on the behavior of partial discharges in an insulation. The setup described in this report can be used to test samples at temperatures ranging from -50 C to 200 C. The aim of conducting the tests described herein is to be able to predict the behavior of an insulation under different operating conditions in addition to being able to predict the possibility of failure. Derived from text

N94-33052*# National Aeronautics and Space Administration. Lewis Research Center, Cleveland, OH.
CHARACTERISTICS OF III-V SEMICONDUCTOR DEVICES AT HIGH TEMPERATURE
Rainee N. Simons (NYMA, Inc., Brook Park, OH.), Paul G. Young (Toledo Univ., OH.), Susan R. Taub, and Samuel A. Alterovitz Jun. 1994 6 p Presented at the Second International High Temperature Electronics Conference, Charlotte, NC, 5-10 Jun. 1994; sponsored by Sandia National, Phillips and Wright Laboratories
(Contract NAS3-25266; RTOP 506-44-2C)
(NASA-TM-106574; E-8801; NAS 1.15:106574) Avail: CASI HC A02/MF A01

This paper presents the development of III-V based pseudomorphic high electron mobility transistors (PHEMT's) designed to operate over the temperature range 77 to 473 K (-196 to 200 C). These devices have a pseudomorphic undoped InGaAs channel that is sandwiched between an AlGaAs spacer and a buffer layer; gate widths of 200, 400, 1600, and 3200 micrometers; and a gate length of 2 micrometers. Measurements were performed at both room temperature and 473 K (200 C) and show that the drain current decreases by 30 percent and the gate current increases to about 9 microns A (at a reverse bias of -1.5 V) at the higher

temperature. These devices have a maximum DC power dissipation of about 4.5 W and a breakdown voltage of about 16 V. Author (revised)

N94-33091 Westinghouse Science and Technology Center, Pittsburgh, PA.
ADVANCED SILICON TECHNOLOGY FOR MICROWAVE CIRCUITS Final Report
J. R. Szedon, T. J. Smith, M. H. Hanes, A. K. Agarwal, and M. M. Sopira 8 Mar. 1994 120 p Limited Reproducibility: More than 20% of this document may be affected by microfiche quality
(Contract N00014-91-C-2313)
(AD-A278039) Avail: CASI HC A06

MICROX is a silicon-on-insulator (SOI) technology using high resistivity (greater than 3,000 ohm-cm) silicon substrates to integrate RF and digital circuits. Channel length (down to 1/4 micrometers) and gate arrangement influences on frequency, power, and noise performance of FET's were characterized. Processing steps for MICROX MMIC's (Miniature Microwave Integrated Circuits) were identified and developed. The best MICROX power result was 250 mW per mm of gate periphery (8.45 dB of associated gain, 49% Power Added Efficiency (PAE)) at 2 GHz from a non-LDD device (gate length of 0.55 micrometers). At 10 GHz an LDD FET (gate length, 1/4 Am) delivered 60 mW/mm of power (PAE, 19%; gain, 4.6 dB). The best broadband noise figure (non-LDD FET; gate length, 0.48 micrometer) was 0.8 dB with 17.7 dB of associated gain at 2 GHz. These results are superior to those reported for alternative types of high frequency silicon FETS. Demonstration circuits (several L/S band amplifiers, a multi-bit attenuator, and a FET mixer) were selected, designed, simulated, and implemented in MICROX. MICROX provides higher frequency capability than alternative silicon approaches by eliminating parasitic capacitances associated with low resistivity bulk silicon. With silicon IC fabrication methods, MICROX offers a reduced risk route to high volume, low cost manufacturing of RF and high speed digital IC's, compared to GaAs. DTIC

N94-33116*# National Aeronautics and Space Administration. Lewis Research Center, Cleveland, OH.
ANALYSIS OF A SLOT COUPLED COPLANAR WAVEGUIDE FED PATCH ANTENNA
Jui-Ching Cheng (Michigan Univ., Ann Arbor.), Nihad I. Dib (Michigan Univ., Ann Arbor.), Linda P. B. Katehi (Michigan Univ., Ann Arbor.), Rainee N. Simons (NYMA, Inc., Brook Park, OH.), and Richard Q. Lee May 1994 7 p Proposed for presentation at the 1994 IEEE AP-S International Symposium and URSI Radio Science Meeting, Seattle, WA, 19-24 Jun. 1994; sponsored by IEEE
(Contract NAS3-27186; RTOP 506-44-2C)
(NASA-TM-106567; E-8749; NAS 1.15:106567) Avail: CASI HC A02/MF A01

A slot-coupled CPW fed patch antenna is analyzed using two different techniques: the Spectral Domain Method and the Finite Difference Time Domain Method. The results from both techniques are in good agreement with experimentally obtained data. Author

N94-33142# New Mexico Univ., Albuquerque. Dept. of Electrical Engineering and Computer Science.
REPETITIVELY PULSED BACKWARD-WAVE OSCILLATOR INVESTIGATIONS Final Report
Edl Schamiloglu 31 Mar. 1994 113 p
(Contract F49620-92-J-0157)
(AD-A278281; AFOSR-94-0232TR) Avail: CASI HC A06/MF A02

The Pulsed Power and Plasma Science Laboratory at the University of New Mexico (UNM) has completed its initial phase of research on repetitively pulsed high power backward-wave oscillators (BWO's). The aggressive program that we had established seeked to address three basic goals: (1) understand the physics of high efficiency vacuum BWO's using the Sinus-6 repetitively pulsed electron beam accelerator, (2) study vacuum and initiate plasma-filled long pulse BWO operations using the modified PI-110A accelerator, and (3) study the prospects of incorporating ferroelectric ceramic cathodes in high power electron beam-driven microwave sources to improve their operations in the long pulse regime. DTIC

N94-33163 United Technologies Research Center, East Hartford, CT.
ADVANCED MATERIAL PROCESSING FOR INTEGRATED-OPTIC FREQUENCY DOUBLING SYSTEMS Final Report, 1 Feb. 1991 - 30 Nov. 1993
R. A. Rubino and D. E. Cullen 30 Nov. 1993 27 p Limited Reproducibility: More than 20% of this document may be affected by microfiche quality
(Contract F49620-91-C-0022)
(AD-A278394; UTRC-R94-970053-1; AFOSR-94-0237TR) Avail: Issuing Activity (Defense Technical Information Center (DTIC))

This purpose of this two year program has been to investigate novel materials processing techniques for the purpose of producing highly efficient, nonlinear waveguide frequency doublers compatible with the integration of compact semiconductor sources. Practical, direct conversion, semiconductor sources of blue-light have still to be proven, thereby motivating the research of waveguide second-harmonic generation (SHG). DTIC

N94-33169 Universiteit Twente, Enschede (Netherlands). Dept. of Electrical Engineering.
ANALYSIS AND DESIGN OF A HIGH SPEED, WIDE RANGE STEPWISE TUNABLE OPTICAL FILTER/AMPLIFIER
J. H. Laarhuis and A. M. J. Koonen 1993 8 p
(ISSN 0924-3755)
(PB94-149572; Memo-INF-93-18; TIOS-93-10; ETN-93-94691) Copyright Avail: Issuing Activity (Universiteit Twente, Enschede, Netherlands)

A fast stepwise tunable filter with a large tuning range is presented. It comprises a cascade of two 3-4 based amplifying Fabry-Perot filters. The tandem filter fits within the STRIDIS interconnection strategy recently proposed and described. ESA

N94-33177 Aerospace Corp., El Segundo, CA. Technology Operations.
TEMPERATURE DEPENDENCE OF SINGLE-EVENT BURNOUT IN n-CHANNEL POWER MOSFET'S
G. H. Johnson, R. D. Schrimpf, K. F. Galloway, and R. Koga 15 Mar. 1994 13 p Limited Reproducibility: More than 20% of this document may be affected by microfiche quality
(Contract F04701-88-C-0089)
(AD-A277921; TR-92(2940)-16; SMC-TR-94-11) Avail: CASI HC A03

The temperature dependence of single-event burnout (SEB) in n-channel power metal-oxide-semiconductor field effect transistors (MOSFET's) is investigated experimentally and analytically. Experimental data are presented which indicate that the SEB susceptibility of the power MOSFET decreases with increasing temperature. A previously reported analytical model that describes the SEB mechanism is updated to include temperature variations. This model is shown to agree with the experimental trends. DTIC

N94-33181 Department of the Navy, Washington, DC.
LIGHTWEIGHT ZINC ELECTRODE Patent
William A. Ferrando, inventor (to Navy) 1 Feb. 1994 9 p Filed 27 Jul. 1993
(AD-D016181; US-Patent-5,283,138; US-Patent-Appl-SN-97181; US-Patent-Class-429-217) Avail: US Patent and Trademark Office

This document describes a light weight zinc electrode made of a sintered mat of copper metal coated graphite fibers, a composite material of zinc active material, and a hydrogel dispersed in a solid, impervious, inert polymer matrix. The composite material surrounds the individual copper metal coated graphite fibers of the sintered mat which support the composite material and provide paths of electrical conductivity throughout the composite material. DTIC

N94-33249# Howard Univ., Washington, DC.
OPTICALLY SWITCHED SUBMILLIMETER-WAVE OSCILLATOR Final Report, Apr. 1992 - Dec. 1993
Michael G. Spencer and Xiao Tang 8 Feb. 1994 29 p
(Contract DAAL03-92-G-0257)
(AD-A278014) Avail: CASI HC A03/MF A01

There exists a critical need for efficient local oscillators for heterodyne mixers operating in the 300 to 3000 GHz region. Applications include space-based submillimeter wave imaging arrays, airborne atmosphere spectroscopy, all-weather imaging radar, non-destructive testing, plasma diagnostics, weapon and contraband detection, and communications. In order to address these problems, we propose a novel low power semiconductor device which uses time delays from a common optical

pulse train to achieve a much higher frequency electrical pulse train, which contains a strong component and appreciable power of the desired submillimeter-wave harmonic for the output and which can be readily coupled electrically or radiatively to a receiver. In our effort, we developed a concept of linear array of ten optical switches. The microwave output from the switches can be in the 100 - 200 GHz frequency range. In order to implement this concept, a single photo-conductive switch of polycrystalline InGaAs was fabricated and tested. DTIC

N94-32460*# National Aeronautics and Space Administration. John F. Kennedy Space Center, Cocoa Beach, FL.
UNIVERSAL SIGNAL CONDITIONING AMPLIFIER
Pedro J. Medelius (I-NET, Inc., Cocoa Beach, FL.), Carl Hallberg (I-NET, Inc., Cocoa Beach, FL.), and Jim Cecil *In* NASA, Washington, Technology 2003: The Fourth National Technology Transfer Conference and Exposition, Volume 2 Feb. 1994 p 342-348 (For primary document see N94-32420 09-99)
Avail: CASI HC A02/MF A04

N94-33340 Royal Military Coll. of Canada, Kingston (Ontario). Dept. of Electrical and Computer Engineering.
A DIAGNOSTIC EXPERT SYSTEM FOR DIGITAL CIRCUITS
R. W. Backlund and J. D. Wilson *In its* Proceedings of the Symposium/Workshop on Applications of Expert Systems in DND Apr. 1992 p 102-112 (For primary document see N94-33335 09-66)
Avail: Issuing Activity (Royal Military Coll. of Canada, Vimy Post Office, Kingston, ON K7K 5L0 Canada)

34 FLUID MECHANICS AND HEAT TRANSFER

Includes boundary layers; hydrodynamics; fluidics; mass transfer; and ablation cooling.

For related information see also *02 Aerodynamics* and *77 Thermodynamics and Statistical Physics.*

N94-31184 University of Southern California, Los Angeles.
THE SMALL-SCALE TOPOLOGY OF A 2:1 ASPECT-RATIO ELLIPTIC JET Ph.D. Thesis
Thomas Robert Austin 1993
Avail: Issuing Activity (MIT Libraries, Rm. 14-0551, Cambridge, MA 02139-4307)

The topology of the large-scale vortices and associated small-scale structures that together constitute the free shear layer of a subsonic 2:1 aspect-ratio elliptic jet is investigated by phase-averaged analyses of turbulent velocity signals. The range of Reynolds numbers is extended in this investigation from 4 x 10(exp 4) to 1.7 x 10(exp 5) based on nozzle hydraulic diameter and corresponds to exit velocities from 20 to 85 m/s. Axisymmetric forcing at the preferred mode frequency at St = 0.42 is performed to induce a collective interaction among the initial vortices to form coherent structures at the preferred mode frequency near the nozzle. Successive vortex mergings are effectively suppressed such that the evolution of the turbulent flow from the nozzle to the end of the potential core is driven solely by azimuthally deforming, self-inducting vortices. The effects of vortex self-induction on the large-scale entrainment and the small-scale production processes, respectively, can be isolated from vortex merging effects. An initial azimuthally varying distribution of vorticity is created in the boundary layer at the jet exit. The degree of asymmetry of the initial boundary layer thickness is dictated by the nozzle geometry, Reynolds number, temperature and frequency content. The self-induction mechanism is primarily responsible for the downstream evolution of the azimuthally deforming elliptic vortices and it is also modified by the initial vorticity distribution. The jet temperature is elevated to study the effects of nonconstant density, or nonhomogeneity, on the large-scale entrainment process. The nonhomogeneous elliptic jet entrains 30 percent more mass than a homogeneous elliptic jet and up to three times more mass than a nonhomogeneous axisymmetric jet throughout the first eight exit diameters downstream. The preferred mode forced case entrains approximately as much mass as the natural case verifying that vortex self-induction is responsible for mass entrainment in small aspect-ratio asymmetric jets and that vortex merging is a second order effect. The Peak-Valley-Counting technique identifies an asymmetric distribution of small-scale structures primarily in the minor axis region of the natural elliptic jet with maxima occurring just downstream of the toroidal vortex cores. The preferred mode forced case induces a more symmetric distribution of small scales throughout the vortex cores and a 25 percent increase in the total small-scale population over the natural case. Small-scale distributions in the natural and forced elliptic jet correlate well to measured cones of combustion activity in chemically reacting shear flows. Therefore, the control of large- and small-scale mixing processes in a subsonic jet may be passively enhanced by asymmetric nozzle geometry and actively enhanced by preferred mode forcing. Dissert. Abstr.

N94-31185 Universiteit Twente, Enschede (Netherlands). Dept. of Applied Mathematics.
A PRIORI TESTS OF LARGE EDDY SIMULATION OF THE COMPRESSIBLE PLANE MIXING LAYER
A. W. Vreman, Bernard J. Geurts, and J. G. M. Kuerten 12 Aug. 1993 50 p Limited Reproducibility: More than 20% of this document may be affected by microfiche quality
(ISSN 0169-2690)
(MEMO-1152; ETN-94-95726) Avail: CASI HC A03

Three important aspects for the assessment of the possibilities of Large Eddy Simulation (LES) of compressible flow are investigated. In particular the magnitude of all subgrid terms, the role of the discretization errors, and the correlation of the turbulent stress tensor with several subgrid models are studied. The basis of the investigation is a Direct Numerical Simulation (DNS) of the two and three dimensional compressible mixing layers using a finite volume method on a sufficiently fine grid. With respect to the first aspect, the exact filtered Navier-Stokes equations are derived and all terms are classified according to their order of magnitude. It is found that the pressure dilatation subgrid term in the filtered energy equation, which is usually neglected in the modeling practice, is as large as the pressure velocity subgrid term, which in general is modeled. The second aspect yields the result that second and fourth order accurate spatial discretization methods give rise to discretization errors which are larger than the corresponding subgrid terms if the ratio between the filter width and the grid spacing is close to one. Even if an exact representation for the subgrid scale contributions is assumed, LES is accurate only if this ratio is sufficiently larger than one. The turbulent stress tensor is investigated in more detail. A priori tests of subgrid models for this tensor yield poor correlations for Smagorinsky's model, which is purely dissipative, while the non-eddy viscosity models considered correlate considerably better. ESA

N94-31209 California Univ., San Diego.
THE EFFECT OF AN AXIAL FLOW COMPONENT ON A CIRCULAR CYLINDER WAKE Ph.D. Thesis
Christine Gladding Lewis 1993 130 p
Avail: Univ. Microfilms Order No. DA9317509

A series of experiments were conducted to determine what effect a variation in the level of streamwise vorticity would have on the wake of a bluff body. These experiments investigate changes in wake dynamics caused by the introduction of a steady spanwise component of flow, which creates a steady influx of streamwise vorticity. To accomplish this, a cylinder in a uniform flow field is suddenly moved at constant velocity in the spanwise direction. The steady state flow condition is studied. The control cylinder technique is used to control the end conditions, to make the unperturbed flow parallel. Two primary modes of shedding are observed in the laminar cylinder wake, depending on the ratio of the axial cylinder velocity to the uniform flow velocity (V/U). For ratios of V/U less than four, oblique laminar shedding occurs. The direction and angle of the oblique shedding are controlled by the sign and magnitude of the ratio V/U. For larger ratios of V/U, shedding occurs in the form of trailing vortices. At a critical ratio of V/U, the vortex sheet appears to breakdown, and spectra are completely broadband. The steady-state motion can be compared, via Galilean transformation, to that of the yawed cylinder in a steady flow. Oblique shedding and trailing vortices have also been observed in yawed cylinder wakes. The relationship between shedding angle, frequency, wavelength, mean vorticity, and V/U is discussed. These results are compared to relationships found to occur in naturally occurring oblique shedding and to yawed cylinder results. Dissert. Abstr.

N94-31211 Michigan Univ., Ann Arbor.
RESPONSE OF WALL TURBULENCE TO HIGH FREQUENCY STREAMWISE AND SPANWISE OSCILLATIONS Ph.D. Thesis
Wen-Je Jung 1993 200 p
Avail: Univ. Microfilms Order No. DA9319555

In an attempt to gain a better understanding of the dynamics of nonequilibrium turbulent wall flows, the response of wall turbulence to two classes of perturbations, namely, streamwise oscillations and spanwise oscillations, has been investigated by direct numerical simulation. Nondimensional periods of oscillation, T(sub osc)(sup +) = T(sub osc) u(sub tau)(exp 2)/nu, ranging from 25 to 2000 and amplitudes of oscillation ranging from 30 to 80 percent have been studied. Significant suppression of turbulence is observed with spanwise oscillations at T(sub osc)(sup +) = 100, which is accompanied by reductions of 60 percent in the overall turbulence production and 40 percent in the turbulent drag. Analysis of the dynamics of near-wall turbulence structures reveals that these reductions are due to a continual shift of near wall streamwise vortices relative to the wall layer streaks. In the case of streamwise oscillations, no net reduction was observed at any of the frequencies investigated. The dynamics of the flow in the presence of both classes of oscillations has been classified in terms of the value of the nondimensional periods of oscillation T(sub osc)(sup +). Dissert. Abstr.

N94-31217 Iowa State Univ. of Science and Technology, Ames.
A SOLUTION ADAPTIVE STRUCTURED-UNSTRUCTURED GRID PROCEDURE FOR UNSTEADY FLOWS Ph.D. Thesis
Sanjay R. Mathur 1993 112 p
Avail: Univ. Microfilms Order No. DA9321195

A solution adaptive hybrid grid method for the computation of 2-D, unsteady flows is presented. The method is capable of handling multiple component, complex geometries in relative motion, such as those encountered in turbomachinery analysis. The numerical approach uses a hybrid structured-unstructured zonal grid topology along with modeling equations and solution techniques that are most appropriate in the individual domains, thus, combining the advantages of both structured and unstructured grid methods. The viscous flow region in the immediate vicinity of the airfoils is resolved using a third order accurate, implicit, upwind solution of the Navier-Stokes equations on structured, O-type grids. Explicit solutions of the Euler equations are obtained in the rest of the domain that consists of an unstructured mesh made up of triangular cells. The use of both central- and upwind-difference flux schemes is investigated for the unstructured domains. Methodologies for accurate, conservative transfer of information at the interface between the structured and unstructured domains as well as that between two unstructured grid regions. Both time-averaged and time-resolved results are presented for test cases and are compared with available experimental data. The quality of the results obtained by the present method is comparable with those obtained by methods based on fully structured grids. Calculations performed using the solution adaptation capabilities are also presented. Dissert. Abstr.

N94-31218 Michigan Univ., Ann Arbor.
ON THE STRUCTURE AND STABILITY OF SLENDER VISCOUS VORTICES Ph.D. Thesis
Ernst Wilhelm Mayer 1993 329 p
Avail: Univ. Microfilms Order No. DA9319584

The phenomenon of vortex breakdown, in which the flow near the axis of a rotating fluid suffers a sudden disruption, was first observed in the late 1950's. Despite having been the subject of intensive research since then, a fundamental understanding of the phenomenon has not yet been achieved. This thesis is an attempt at achieving such by way of a unified approach to each aspect which may be involved, the working hypothesis being that breakdown may best be understood as a nonlinear evolution problem. Treated in detail are the first two steps in such a program, which are first to understand the structure of the steady flows which may give rise to breakdown and then to investigate their stability. A family of similarity solutions to the Navier-Stokes equations, modeling the flows in leading-edge-type vortices, is presented. These solutions show a strong retardation of the axial flow in the core when the flow is subject to an adverse axial pressure gradient. The stability of several types of swirling base flows to 3-D disturbances is studied, revealing a rich variety of neutral and exponentially growing eigenmodes of both an inviscid and viscous character. The above axial retardation is also shown to be capable of inducing a linear instability of the flow, indicating the possibility of a secondary instability phenomenon. Implications of these results for the study of the full breakdown itself are discussed. Dissert. Abstr.

N94-31219 Massachusetts Inst. of Tech., Cambridge.
ON WAVE INTERACTIONS OF ROTATIONAL AND IRROTATIONAL FLOWS Ph.D. Thesis
Qingyuan Lu 1992
Avail: Issuing Activity (MIT Libraries, Rm. 14-0551, Cambridge, MA 02139-4307)

This thesis takes rotationality into account in the classical water wave problem and centers on the wave interactions of rotational and irrotational flows for an inviscid fluid. The rotational stability of irrotational waves is analyzed. The Cauchy solution of a mean perturbed vorticity equation is obtained for a basic flow consisting two plane waves, and it is shown that rotational perturbations experience algebraic growth. The stability characteristics of the basic flow consisting of a gravity wave and a weak parallel shear flow are also explored. A Rayleigh-like equation for the normal velocity perturbation is derived. It is shown that the eigenvalues of this equation are complex for a large class of basic flows indicating that the existing weak shear flow can destabilize the gravity waves. Furthermore, a resonant triad consisting of a pair of gravity waves with equal wave lengths and a third component of a steady rotational flow is studied. A system of coupled nonlinear equations for the surface wave amplitudes and the rotational flow field has been derived. Thereafter, the rotational medium is treated as passive. Here it is found that there are two distinct effects of a rotational medium on gravity waves. The first effect is the wave scattering mechanism by the normal vorticity of the rotational flow. The other is an instability mechanism caused by the normal velocity of the rotational flow. This instability indicates that the incident surface waves may lose coherence and therefore cannot survive in a rotational medium. This may offer a partial explanation of the observed attenuation of waves in distant ship wakes. The analysis has also been extended to the interfacial waves of a two layered flow in the presence of rotationality.
Author (revised)

N94-31221# Stockholm Univ. (Sweden). Dept. of Meteorology.
A FULLY TWO-DIMENSIONAL, NON-OSCILLATORY ADVECTION SCHEME FOR MOMENTUM AND SCALAR TRANSPORT EQUATIONS
Elias Valur Holm 17 Nov. 1993 63 p
(ISSN 0349-0467)
(DM-66; ETN-94-95880) Avail: CASI HC A04/MF A01

The advection scheme developed is a fully two dimensional and nonoscillatory extension of the one dimensional Crowley type mass conservative schemes. The fully two dimensional scheme includes new cell to cell fluxes directed along the local flow direction, and the distribution of the advected variable within each cell is approximated by a fully two dimensional polynomial. Compared to the standard timesplit approach, the fully two dimensional approach is an order of magnitude more computationally effective in our tests. Furthermore, it removes the instability associated with the use of the standard timesplit approach in deformational flow. It is also directly applicable to momentum advection in, for example, incompressible flows. A problem with the application of the present scheme to momentum advection is that kinetic energy and enstrophy are dissipated too quickly when the solution is underresolved. ESA

N94-31229*# National Aeronautics and Space Administration. Lewis Research Center, Cleveland, OH.
COMPUTATIONAL STUDY OF SINGLE-EXPANSION-RAMP NOZZLES WITH EXTERNAL BURNING
Shaye Yungster and Charles J. Trefny Apr. 1992 28 p Presented at the 32nd Aerospace Sciences Meeting, Reno, NV, 10-13 Jan. 1994
(Contract NCC3-233; RTOP 505-90-5R)
(NASA-TM-106550; ICOMP-94-5; E-8702; NAS 1.15:106550; AIAA Paper 94-0024) Copyright Avail: CASI HC A03/MF A01

A computational investigation of the effects of external burning on the performance of single expansion ramp nozzles (SERN) operating at transonic speeds is presented. The study focuses on the effects of external heat addition and introduces a simplified injection and mixing model based on a control volume analysis. This simplified model permits parametric and scaling studies that would have been impossible to conduct with a detailed CFD analysis. The CFD model is validated by comparing the computed pressure

distribution and thrust forces, for several nozzle configurations, with experimental data. Specific impulse calculations are also presented which indicate that external burning performance can be superior to other methods of thrust augmentation at transonic speeds. The effects of injection fuel pressure and nozzle pressure ratio on the performance of SERN nozzles with external burning are described. The results show trends similar to those reported in the experimental study, and provide additional information that complements the experimental data, improving our understanding of external burning flowfields. A study of the effect of scale is also presented. The results indicate that combustion kinetics do not make the flowfield sensitive to scale. Author

N94-31241# Naval Postgraduate School, Monterey, CA.
NUMERICAL ANALYSIS OF SINGLE-VORTEX/FREE-SURFACE INTERACTION M.S. Thesis
Craig F. Merrill Dec. 1993 87 p
(AD-A276462) Avail: CASI HC A05/MF A01

The interaction of a single Lamb vortex with a free surface is analyzed numerically through the use of a finite-difference technique. The individual effects of gravity, viscosity, and surface tension are investigated within the range of the applicability of the phenomenon and the code used. The vortex is allowed to build up to its full strength in a relatively small time and then the evolution of the free surface, streamlines, and other details of the flow are calculated. The results have shown that the smaller the proximity of the vortex to the free surface, the larger the scar produced on its down-wash side. The effect of the surface tension is to reduce the amplitude of the free surface elevation. The viscous effects appear to be relatively small even though the calculations are, out of necessity, confined to a limited range of the governing parameters, as in all finite difference calculations. DTIC

N94-31245# Wisconsin Univ., Madison. Center for Mathematical Sciences.
OSCILLATIONS IN PISTON-DRIVEN SHEAR FLOW OF A NON-NEWTONIAN FLUID Summary Report
David S. Malkus, John A. Nohel, and Bradley J. Plohr Feb. 1994 17 p
(Contracts DAAL03-91-C-0027; DAAL03-92-G-0185)
(AD-A276472; CMS-TSR-94-8) Avail: CASI HC A03/MF A01

In recent experiments on piston-driven shear flow of a highly elastic and very viscous non-Newtonian fluid, Lim and Schowalter observed nearly periodic oscillations in the particle velocity at the channel wall for particular values of the constant volumetric flow rate. Such periodicity has been characterized as a 'stick/slip' phenomenon caused by the failure of the fluid to adhere to the wall. We suggest an alternative explanation for these oscillations using a dynamic mathematical model based on the Johnson-Segalman-Oldroyd constitutive relation, the key feature of which is a non-monotonic relationship between steady shear stress and strain rate. The resulting three-dimensional equations of motion and stress are reduced to one space dimension, consistent with experimental results. In the inertialess approximation, the equations governing the flow can be viewed as a continuous family of quadratic ordinary differential equations coupled by the non-local constraint that fixes the volumetric flow rate. Varying the flow rate, the numerical simulation of solutions to this system exhibits transitions to and from a regime with persistent oscillations that compare favorably with the Lim-Schowalter observations. When the time-asymptotic behavior is cyclic, large shear strain rates are observed in a thin but macroscopic layer near the wall. The transitions are explained using spectral analysis of the linear (infinite dimensional) operator resulting from linearization of the quadratic system about a discontinuous steady state with a jump discontinuity in the stress components. The persistent oscillations arise as a Hopf bifurcation to periodic orbits as the volumetric flow rate is increased beyond a critical value. DTIC

N94-31268# Sandia National Labs., Albuquerque, NM.
ANALYSIS OF THE PHOTODIODE BOUNDARY LAYER TRANSITION INDICATOR
D. W. Kuntz, A. C. Wilken, and J. L. Payne 1994 15 p Presented at the 32nd Aerospace Sciences Meeting and Exhibit, Reno, NV, 11-14 Jan. 1994
(Contract DE-AC04-94AL-85000)
(DE94-005311; SAND-93-1274C; AIAA Paper 94-0454; CONF-940152-2)
Avail: CASI HC A03/MF A01

The photodiode transition indicator is a device which has been successfully used to determine the onset of boundary layer transition on numerous hypersonic flight vehicles. The exact source of the electromagnetic radiation detected by the photodiode at transition was not understood. In some cases early saturation of the device occurred, and the device failed to detect transition. Analyses have been performed to determine the source of the radiation producing the photodiode signal. The results of these analyses indicate that the most likely source of the radiation is blackbody emission from the heatshield material bordering the quartz window of the device. Good agreement between flight data and calculations based on this radiation source has been obtained. Analyses also indicate that the most probable source of the radiation causing early saturation is blackbody radiation from carbon particles which break away from the nosetip during the ablation process. DOE

N94-31341# Arizona State Univ., Tempe. Dept. of Mechanical Engineering.
LASER-INDUCED FLUORESCENCE/PARTICLE TRACKING SYSTEM FOR STRATIFIED FLOW RESEARCH Final Report, 1 Oct. 1992 - 30 Sep. 1993
H. J. Fernando 30 Sep. 1993 11 p
(Contract N00014-92-J-4101)
(AD-A275917; EFD-003) Avail: CASI HC A03/MF A01

The research conducted has two components. In the first part, a model that deals with turbulent mixing across sharp density interfaces subjected to homogeneous turbulence was developed. The analysis was essentially based on the rapid distortion theory approach of Hunt, which reckon on the empirical observation that the dissipation rate of turbulent kinetic energy above an interface is independent on the height z. The homogeneous turbulence was modeled using the classical von Karman spectra and the interfacial motions were assumed to be governed by the linear internal-wave equations. It was further assumed that the first mode of internal waves governs the interfacial motions, thus simplifying the interfacial boundary conditions; the latter have been a major difficulty in modeling fluid motions near sharp density interfaces. DTIC

N94-31422# Office National d'Etudes et de Recherches Aerospatiales, Paris (France).
ANALYSIS OF STRONG ACOUSTIC EXCITATION ON THE BREAKUP AND DISPERSION OF A LIQUID JET Ph.D. Thesis - Ecole Centrale de Paris [CONTRIBUTION A L'ETUDE DE L'INFLUENCE D'UNE EXCITATION ACOUSTIQUE INTENSE SUR LA RUPTURE ET LA DISPERSION D'UN JET LIQUIDE]
Bernard Labegorre 1993 280 p In FRENCH Original contains color illustrations
(ISSN 0078-3781)
(ONERA-NT-1993-9; ETN-94-96064) Avail: CASI HC A13/MF A03

The effect of strong acoustic waves on the breakup and dispersion of cylindrical liquid jets is considered with regard to combustion instabilities of liquid injection burners. An experimental study showed that a strong acoustic excitation modifies jet stability at low injection velocities (by reduction of the breakup length). This phenomenon, which exhibits saturation and threshold effects, is especially sensitive to excitation intensity. A linearized analysis of forced instabilities of a liquid jet shows that turbulence induced by acoustics, which appears for all breakup modes, can explain the observations with low speed injection. The literature shows that a strong acoustic excitation presents dispersive and agglomeration effects on a particle. Previous works include physical description and numerical methods, which might describe the turbulent dispersion of particles and turbulence induced by strong acoustic excitation. These points remain to be improved. Numerical simulations, made without consideration of turbulence, confirmed the experimentally observed dispersive effects of transverse waves applied on a cylindrical jet. This study can provide a basis for future investigations where quantitative experimental results will necessarily be obtained. ESA

N94-31460# Pennsylvania State Univ., University Park.
RESEARCH IN MARINE BOUNDARY LAYER INTERMITTENCY
John C. Wyngaard 20 Jan. 1994 3 p
(AD-A276076) Avail: CASI HC A01/MF A01

Wind-tunnel calibrations of turbulent-pressure sensors usually reveal deviations from ideal response. These deviations are typically reported in dimensional form (e.g., in microbars) or as a fraction of the dynamic

pressure. Neither presentation gives a direct indication of the reliability of pressure statistics measured in a turbulent flow. We derive a general response equation for a turbulent-pressure probe. The coefficients in the equation are obtainable from standard wind-tunnel calibration results. The form of the response equation makes it straightforward to relate the errors in measured pressure statistics of the turbulence. We demonstrate this by evaluating the reliability of measurements of some important pressure covariances, including the pressure-transport term in the turbulent kinetic energy (TKE) budget in the unstable surface layer. The preliminary finding is that the Nishiyama-Bedard sensor is capable of measuring pressure transport of TKE there to within 10-20%. DTIC

N94-31467# Naval Research Lab., Washington, DC.
ADDITIONAL CAPABILITIES OF THE UNIFIED WAVES MODEL Memorandum Report
J. M. Witting 29 Sep. 1993 34 p
(NR Proj. RR0-3204)
(AD-A276114; NRL-MR-5194) Avail: CASI HC A03/MF A01

The initial report on the 'unified waves model' describes a procedure to compute water wave propagation over long distances accurately at low cost, and for a wide variety of physical situations. This report outlines recent developments that extend its capabilities. These involve: (1) inclusion of a variable depth, (2) addition of a wavemaker, and (3) the ability to send steady nonuniform flows through the computational domain. Examples of calculations employing the new capabilities are given. DTIC

N94-31476# Virginia Polytechnic Inst. and State Univ., Blacksburg. Dept. of Aerospace and Oceanengineering.
THREE-DIMENSIONAL VELOCITY MEASUREMENTS ON A 6:1 PROLATE SPHEROID AT 10 DEG ANGLE OF ATTACK
Christopher J. Chesnakas, Roger L. Simpson, and Michael M. Madden 18 Jan. 1994 230 p Revised
(Contract N00014-91-J-1732)
(AD-A276485; VPI-AOE-202-Rev) Avail: CASI HC A11/MF A03

The flow in the cross flow separation region of a 6:1 prolate spheroid at 10 degrees angle of attack, Re(sub L) = 4.20 x 10(exp 6), was investigated using a novel three dimensional fiber optic laser doppler velocimeter (LDV). The probe was used to measure three simultaneous, orthogonal velocity components from within the model. The design and operation of this LDV probe is described and velocity, Reynolds stress, and velocity triple product measurements are presented from the inner boundary layer through the boundary layer edge. DTIC

N94-31477# Office National d'Etudes et de Recherches Aerospatiales, Paris (France).
MIXTURE MODEL SIMULATING REACTIVE TURBULENT FLOWS: TESTING OF EULERIAN-LAGRANGIAN PROBABILISTIC MODELS Ph.D. Thesis - Rouen Univ. [MODELISATION DU MELANGE POUR LA SIMULATION D'ECOULEMENTS REACTIFS TURBULENTS: ESSAIS DE MODELES PROBABILISTES EULERIENS LAGRANGIENS]
Fabienne Pit 1993 224 p In FRENCH Original contains color illustrations
(ISSN 0078-3781)
(ONERA-NT-1993-13; ETN-94-96065) Avail: CASI HC A10/MF A03

A model developed to simulate reactive turbulent flows with a noninfinitely fast chemistry using a joint Probability Density Function (PDF) is described. It is very complicated to solve the joint velocity and concentration PDF time variation equation analytically or numerically. But the problem can be simplified by integrating this equation in the velocity space. The result is a hybrid Eulerian-Lagrangian probabilistic approximation. The equation is then simulated by a Monte-Carlo method. In this equation, the small scale mixing phenomenon is represented by a model. The new model was compared with conventional mean exchange models in the case of a thermal mixing layer and a reactive mixing layer. The computation results were promising. It was demonstrated that the new model could be used for complex industrial two dimensional (2D) axisymmetric configurations (the bluff body) and 3D configuration (DEXTRE combustion chamber). ESA

N94-31559# Cranfield Inst. of Tech., Bedford (England). Dept. of Aerospace Studies.
VISCOUS LIMITER FUNCTIONS FOR MODEL CONVECTION-DIFFUSION EQUATIONS
E. F. Toro May 1993 23 p Revised
(Cranfield-Aero-9103; ISBN-1-871564-60-3; ETN-94-96068) Avail: CASI HC A03/MF A01; Cranfield Univ. of Technology, Coll. of Aeronautics, Cranfield, Bedford MK43 0AL, England, HC

Viscous Limiter Functions (VLF's), for use with Riemann problem based shock capturing methods as applied to viscous flows, are presented. In particular, viscous flux limiters are derived. The analysis pertains to a linear convection diffusion model equation. These VLF's combine the physical viscosity, the role of which is maximized, with numerical viscosity, whose role is minimized, to capture oscillation free solutions to convection diffusion equations. Assessment of the concepts presented is carried out through numerical experiments on linear and nonlinear model equations with exact solutions. ESA

N94-31563 California Univ., Irvine.
COMPUTATIONAL RADIATIVE HEAT TRANSFER IN HOMOGENEOUS AND NONHOMOGENEOUS NONSCATTERING MEDIA Ph.D. Thesis
Perry Lee Fuehrer 1993 208 p
Avail: Univ. Microfilms Order No. DA9315778

A computational methodology was developed for calculating radiative heat transfer in gaseous nonhomogeneous nonscattering media with complex emission and absorption spectra. The technique can be used in both equilibrium and nonequilibrium situations. Test cases applied to an Aeroassisted Orbital Transfer Vehicle (AOTV) were investigated, and results are presented herein. Nonequilibrium compositions and temperatures were taken from NASA-Langley three-dimensional hypersonic flowfield calculations that include real-gas effects and finite-rate chemical kinetics. This output was used as input to the NASA-Ames NEQAIR code to compute local values of spectral emission and absorption coefficients. For each spatial point considered, total (spectrally integrated) properties were computed, and these total properties were used to make the radiation calculations. Use of total properties was found to yield remarkably accurate values of total intensity when compared to exact results for the cases examined in the AOTV flowfield. Results are presented for three markedly different lines of sight along with heat flux calculations for six receiver locations. Also an examination of using the technique in a differential formulation for the calculation of the gradient of intensity at a point is conducted. A more accurate intensity and gradient of intensity calculation is made assuming linear spatial variations of spectral emission and absorption coefficients. The method is also compared to exact integration over the line structure of the 2143 cm(exp -1) band of CO for nonhomogeneous paths. These results are compared to calculations using the exponential wide-band model along with either the nonhomogeneous wide-band scaling or the transmission-path-adjustment algorithm. Finally, three nonhomogeneous lines of sight in water vapor were investigated using the exponential wide-band model. Water vapor was chosen due to its five bands which are spread throughout the spectrum. Comparison is made between wide-band scaling and the transmission path-adjustment method. Dissert. Abstr.

N94-31588 Technische Univ., Delft (Netherlands).
FLUID-STRUCTURE INTERACTION IN CASE OF WATER HAMMER WITH CAVITATION Ph.D. Thesis
A. S. Tijsseling 29 Jun. 1993 246 p Prepared in cooperation with Waterloopkundig Lab., Delft, Netherlands Limited Reproducibility: More than 20% of this document may be affected by microfiche quality
(PB94-148277) Avail: CASI HC A11

The transient behavior of liquid-filled pipe systems is studied. The time scale is acoustic. Pressure waves in the liquid, and axial, lateral, and torsional stress waves in the pipes are the dominant phenomena. The phenomena in the liquid (water hammer) and the phenomena in the pipe system (structural dynamic) influence each other if significant radial and axial pipe motions occur. When, in addition, the dynamic pressure drops to the vapor pressure, vapor bubbles will form in the liquid (cavitation). The major new element of the present work is in the simultaneous occurrence of fluid-structure interaction (FSI) and cavitation, which is investigated both theoretically and experimentally. An extensive review of literature on the subject is given. One dimensional basic equations are obtained by integration of general three dimensional equations for fluid dynamics and structural

linear elasticity. Three FSI-mechanisms (junction, Poisson, and friction-coupling) are taken into account. The governing equations, formulated as a hyperbolic set of fourteen first-order partial differential equations, are solved by the method of characteristics. Vapor cavitation is numerically simulated by the relatively simple concentrated cavity model. NTIS

N94-31660# Technische Univ., Delft (Netherlands). Faculty of Technical Mathematics and Informatics.
SOLUTION OF THE INCOMPRESSIBLE NAVIER-STOKES EQUATIONS IN GENERAL COORDINATES BY KRYLOV SUBSPACE AND MULTIGRID METHODS
S. Zeng, C. Vuik, and P. Wesseling 1993 22 p
(ISSN 0922-5641)
(Rept-93-64; ETN-94-96109) Copyright Avail: CASI HC A03/MF A01

Three iterative methods are studied: preconditioned GMRES (Generalized Minimal Residual) with ILU preconditioning, GMRESR with multigrid as inner loop and multigrid for the solution of the incompressible Navier-Stokes equations in general coordinates. Robustness and efficiency of the three methods are investigated and compared. Numerical results show that the second method is very promising. ESA

N94-31689# Groningen Rijksuniv. (Netherlands). Dept. of Mathematics.
CELL-VERTEX DISCRETISATION OF THE DRIVEN CAVITY FLOW WITHOUT ARTIFICIAL DIFFUSION
F. O. O. Wagener Jun. 1993 32 p
(W-9317; ETN-94-96178) Avail: CASI HC A03/MF A01

To solve the compressible Navier-Stokes equations in a driven cavity test case, traditional cell vertex discretization using the midpoint rule and artificial diffusion did not produce a steady state solution where it should. This is due to a loose treatment of the boundary. A more satisfactory and working alternative is proposed, which moreover has the virtue of making artificial diffusion superfluous. ESA

N94-31691# Groningen Rijksuniv. (Netherlands). Dept. of Mathematics.
SIMULATIONS OF THE CREATION AND MOTION OF VORTEX RINGS
R. S. Heeg Aug. 1993 61 p Sponsored by Groningen Rijksuniv.
(W-9319; ETN-94-96180) Avail: CASI HC A04/MF A01

Numerical solutions of the instationary axisymmetric incompressible Navier-Stokes equations concerning vortex rings are presented. They are compared with several experiments and discussed from a physical point of view. The influence of the boundary conditions on the convergence of the numerical scheme is also discussed. ESA

N94-31703# Technische Univ., Delft (Netherlands). Faculty of Technical Mathematics and Informatics.
FINITE VOLUME DISCRETIZATION OF THE k-EPSILON TURBULENCE MODEL IN GENERAL COORDINATES
M. Zijlema 1993 43 p
(ISSN 0922-5641)
(Rept-93-90; ETN-94-96135) Copyright Avail: CASI HC A03/MF A01

A formulation and finite volume discretizations of the k-epsilon turbulence model in general coordinates are discussed. Implementation of Dirichlet and Neumann boundary conditions are considered. The need for positive schemes in the implementation of the k-epsilon model is evaluated. Test problems were solved in order to assess the performance of the method. The method is demonstrated by applying it to the calculation of a turbulent flow across staggered tube banks. ESA

N94-31717# Montreal Univ. (Quebec). Dept. de Genie Mecanique.
FINITE ELEMENT NUMERICAL SIMULATION OF TURBULENT FLOWS M.S. Thesis [SIMULATION NUMERIQUE PAR ELEMENTS FINIS DES ECOULEMENTS TURBULENTS]
Abdelkader Baggag Apr. 1993 142 p In FRENCH
(ISBN-0-315-86416-8; CTN-94-61193) Copyright Avail: Micromedia Ltd., Technical Information Centre, 240 Catherine Street, Suite 305, Ottawa, Ontario, K2P 2G8, Canada HC/MF

Incompressible steady state turbulent flows are simulated numerically using a finite element method. Since the direct numerical simulation of turbulent behavior of fluids is beyond the capability of present day computers, the object of the study was to evaluate the suitability of algebraic turbulence models for computation of turbulent flows. An algebraic turbulence model using a two-layer concept was implemented into a generic incompressible Navier-Stokes solver. The spatial discretization of the flow field is realized by the finite element method of the averaged Navier-Stokes equations. To satisfy mass conservation, an augmented Lagrangian implementation of Uzawa's algorithm is used. It is known that algebraic and two-equation turbulence models require knowledge of the normal distance to the wall. A technique allowing the evaluation of this normal distance on an unstructured grid is evaluated and implemented. The algorithmic requirements and the appropriate strategy of resolution are determined for the considered model, and the methodology is applied in both two and three dimensional configurations. Simulation results are presented for turbulent flow around a NACA0012 airfoil and on a flat plane. Author (CISTI)

N94-31720# Montreal Univ. (Quebec). Dept. de Genie Civil.
NUMERICAL MODELLING OF TURBULENCE M.S. Thesis [MODELISATION NUMERIQUE DE LA TURBULENCE]
Patrick Beauchemin Nov. 1992 78 p In FRENCH
(ISBN-0-315-86439-7; CTN-94-61196) Copyright Avail: Micromedia Ltd., Technical Information Centre, 240 Catherine Street, Suite 305, Ottawa, Ontario, K2P 2G8, Canada HC/MF

A mathematical model that solves the pressure velocity form of the steady state Navier-Stokes equations is described. This finite element model uses the penalty function method to remove one degree of freedom at every computational node. In addition, a new approach is introduced which renders the matrix in the resulting set of algebraic equations symmetric and banded. This approach is named the linearized source term method. After a survey of different turbulence closure models, the mathematical model coupled with an algebraic closure model is applied to a practical case study. Since its domain of applicability is not restricted to the Navier-Stokes equation, the linearized source term method is then applied to the resolution of another nonlinear equation: a simplified form of a turbulence closure model. Author (CISTI)

N94-31730# Concordia Univ., Loyola Campus, Montreal (Quebec). Dept. of Mechanical Engineering.
FINITE ELEMENT VORTICITY-BASED METHODS FOR THE SOLUTION OF THE INCOMPRESSIBLE AND COMPRESSIBLE NAVIER-STOKES EQUATIONS Ph.D. Thesis
Grant Guevremont Aug. 1993 178 p
(ISBN-0-315-87265-9; CTN-94-61237) Copyright Avail: Micromedia Ltd., Technical Information Centre, 240 Catherine Street, Suite 305, Ottawa, Ontario, K2P 2G8, Canada HC/MF

Finite element vorticity-based methods are applied to the analysis of viscous flows. Analysis is carried out in terms of a stream function vorticity formulation for two dimensional (2D) flows and a velocity vorticity formulation for 2D and three dimensional (3D) flows. Second order equations are obtained for the variables and the discretization is based on the weak-Galerkin weighted residual method. The proposed stream function vorticity approach reverses the traditional imposition of wall boundary conditions. The finite element method is used to naturally impose the no-slip condition on the stream function equation accurate for complex geometries. This method is extended to 2D subsonic external lifting flow. The unknown stream function value on the airfoil for lifting flow is obtained by enforcing a continuous pressure distribution over the entire airfoil. This is imposed naturally through the finite element discretized vorticity transport equation. The finite element weak-Galerkin method used in the proposed velocity vorticity scheme is extended to 2D and 3D subsonic internal flow. A new accurate wall vorticity boundary condition is also proposed. The stream function and vorticity or the velocity and vorticity are solved simultaneously using a Newton method. No artificial viscosity was required to stabilize the iteration algorithm. Author (CISTI)

N94-31744 Princeton Univ., NJ.
MICROMECHANICS AND EFFECTIVE PROPERTIES OF PARTICULATE COMPOSITES AND FLUID SUSPENSIONS Ph.D. Thesis
Tsung-Muh Chen 1993 161 p
Avail: Univ. Microfilms Order No. DA9328076

It is well-known that the addition to a homogeneous continuum of a second particulate material having different physical properties can greatly alter the effective properties of the resulting two-phase system. In general, the effective properties of the medium will depend on the physical properties of both constituent phases, as well as the volume fraction, geometry, shape, and spatial distribution of the dispersed particles. The term 'effective

property' usually implies that a multi-phase system is being approximated as a macroscopically homogeneous continuum. This approximation is valid when a multi-phase system is viewed on a representative length scale, or more specifically the representative averaging domain, can only be defined on the basis of an assumption about the macroscopic homogeneity of a multi-phase system; that is, any volume-averaged property remains the same regardless of the spatial position of an averaging domain. In the first part of this study, attention is focused on the overall behavior of particulate composites. A general framework emanating from the eigenstrain concept introduced by Eshelby is presented for determining the effective elastic moduli of two-phase composites. Subsequently, a complete formulation of the many-particle interaction problem is given, and a new approach avoiding the problem of non-absolute convergence is also presented. Some existing models are then recovered from the far-field solution, in which the interaction between neighboring particles is neglected, due to mathematical analogy, the effective viscosity of fluid suspension is obtained from the results of particulate composites as the limiting case of an incompressible matrix containing either rigid spheres or spherical cavities. The present framework is further combined with phenomenological plastic analysis to investigate the overall elasto-(visco-)plastic behavior of particulate composites. Finally, an analogous framework for the determination of effective conductivities of random dispersions of rigid-spheres is presented. Dissert. Abstr.

N94-31774 Colorado Univ., Boulder.
SURFACE FLUXES OF TRACE GASES DERIVED FROM CONVECTIVE-LAYER PROFILES Ph.D. Thesis
Kenneth J. Davis 1992 291 p
Avail: Univ. Microfilms Order No. DA9318086

Nonlocal gradient and variance functions relating the surface and entrainment fluxes of a passive scalar to the mean mixing ratio and variance profiles in the cloud-free, convective boundary layer have been determined from large eddy simulations. These functions can be used to calculate the surface and entrainment fluxes of trace gases over a large area, given profile measurements within the convective boundary layer. This dissertation develops the convective layer gradient technique for estimating fluxes and demonstrates two potentially valuable applications. An attempt is made to verify the large eddy simulation gradient functions with aircraft observations from the First ISLSCP Field Experiment and the San Joaquin Valley Air Quality Study. Results show general agreement with the simulated gradient functions but precise comparison is made difficult by scatter in the aircraft derived functions. The gradient functions are used to estimate forest emissions of nonmethane hydrocarbons using tethered balloon profiles. Mean emission estimates from profiles collected during the Amazon Boundary Layer Experiment 2A and the Rural Oxidants in the Southern Environment 1 experiment show good agreement with estimates made from budget arguments. Daytime isoprene emissions from the dry season Amazon are estimated to be 3860 +/- 1380 microgram m(exp -2) hr(exp -1). Summer, daytime isoprene emissions from an Alabama pine-oak forest are estimated to be 4040 +/- 3200 microgram m(exp -2) hr(exp -1), alpha-pinene emissions 1750 +/- 1060 microgram m(exp -2) hr(exp -1), and beta-pinene emissions 770 +/- 560 microgram m(exp -2) hr(exp -1). Fluxes from individual profiles are very scattered and expected diurnal cycles in emission rates are not distinguishable. This technique provides a valuable means of measuring biogenic hydrocarbon emissions, a precursor to photochemical ozone production. The convective layer gradient technique holds the potential for remote estimation of surface fluxes over large areas using remote profiling technology, such as differential absorption lidar (DIAL). An attempt to estimate ozone deposition rates using an ozone DIAL system was unsuccessful. The minimum signal to noise ratio for successful ozone deposition estimates using this DIAL system and the convective layer gradient technique was derived and is less than the signal to noise level in the analyzed DIAL observations. Dissert. Abstr.

N94-31778 British Columbia Univ., Vancouver.
INCOMPRESSIBLE VISCOUS FLOW IN TUBES WITH OCCLUSIONS Ph.D. Thesis
Huaxiong Huang 1991 249 p
(ISBN-0-315-75467-2) Avail: Univ. Microfilms Order No. DANN75467

Viscous, incompressible flow in tubes with partial occlusion is investigated using numerical and experimental procedures. The study is related to the problem of atherosclerosis, one of the most common diseases of the circulatory system. One of the computational difficulties in solving the incompressible Navier-Stokes equations is the lack of pressure or vorticity boundary conditions. A finite difference approach, referred to as the interior constraint (IC) method, is proposed to resolve this difficulty. As a general numerical method, it is formulated for both the stream function-vorticity and primitive (physical) variable formulations. The procedure is explained using a one dimensional model with extensive numerical tests presented for two dimensional cases, including flow in a driven cavity and flow over a backward facing step. Results are obtained with second-order accuracy. Next, the IC method is applied to flow in a tube with an occlusion, which is used as the model for blood flow in stenosed arteries in the study of the pathology of atherosclerosis. Numerical results are obtained for both steady and pulsatile flows. Results are compared with those of SIMPLE, one of the commercially available numerical algorithms. The pulsatile flow study revealed several interesting new features. It suggested that the high shear stress is not likely to initiate atherosclerosis lesions. The recirculation region, which is a prominent feature of the unsteady flow, is more likely to cause the initiation and development of the disease. Experimental measurements for steady flow complement the numerical study and show qualitative agreement. Dissert. Abstr.

N94-31799# Montreal Univ. (Quebec). Dept. de Genie Mecanique.
AN ADAPTIVE METHOD FOR THE EXACT RESOLUTION OF SHOCK WAVES AND CONTACT DISCONTINUITIES M.S. Thesis [UNE METHODE ADAPTIVE POUR LA RESOLUTION EXACTE DES ONDES DE CHOC ET DES DISCONTINUITES DE CONTACT]
Marius Paraschivoiu Jul. 1993 146 p In FRENCH
(ISBN-0-315-86498-2; CTN-94-61202) Copyright Avail: Micromedia Ltd., Technical Information Centre, 240 Catherine Street, Suite 305, Ottawa, Ontario, K2P 2G8, Canada HC/MF

A methodology is presented which allows improved resolution of discontinuities that appear when solving the Euler equations. The basic principle is to take full advantage of Roe's upwind difference scheme, which is able to solve discontinuities with exact resolution when a grid line is oriented and located along the discontinuity. Based on this property, a technique is suggested that moves and adapts the grid to align and position an element interface on the discontinuities. For unsteady discontinuities, the exact solution is obtained when the cell interface moves at the same speed as the discontinuities. The shock waves and contact discontinuities are located using a wave model based on the properties of the acoustic waves, the entropy wave, and the shear wave. The neighboring mesh is then moved on the shocks or slip lines using the speed of those waves. An algorithm is implemented in a two-dimensional finite volume solver on unstructured triangular mesh. Mass, momentum, and energy fluxes at the interface are solved using an approximate Riemann solver based on Roe's scheme. The method is proven to find the exact solution for analytical test cases and to improve drastically the sharpness of the discontinuities for more complex geometries. For unsteady flows, the shock location is captured with great accuracy at any time position. Author (CISTI)

N94-31843 Stevens Inst. of Tech., Hoboken, NJ.
COMPUTATIONAL STUDY OF SIMULTANEOUS HEAT AND MASS TRANSFER IN TURBULENT SEPARATED FLOWS Ph.D. Thesis
Abdelghani Zigh 1993 196 p
Avail: Univ. Microfilms Order No. DA9328536

Many real problems of engineering interest contain regions of highly turbulent flow that exhibit separation and recirculation. An understanding of heat and mass transfer characteristics in these regions is of considerable importance in industrial practice. In this study, a finite volume numerical method is developed and utilized for the prediction and analysis of flow over a cascade of turbine blades involving simultaneous heat and mass transfer. The renormalization group (RNG) approach based nonlinear k-epsilon turbulence model is utilized to describe the flow field. The computational procedure involves the simultaneous solution of the time averaged equations of motion, heat, mass, and turbulent kinetic energy and its dissipation in generalized body-fitted coordinates. The first part of this study is aimed at the development of an algorithm and its validation through the analysis of a number of benchmark test cases. These include the turbulent flow with and without heat transfer downstream of an abrupt channel expansion, turbulent flows in the wake of a flat plate and isolated airfoils, and flow past airfoil cascades with and without trailing edge separation. The results are compared with the available experimental data and shown to be in excellent agreement. The second part involved parametric

study of the transpiration cooling of a turbine blade cascade. Flow past turbine blade cascades with simultaneous heat and mass transfer are analyzed for Reynolds numbers from 5 x 10(exp 5) to 2 x 10(exp 6) and flow angles from -30 deg to 55 deg. The effects of the separation were appreciable in the suction side and the Nusselt and Sherwood numbers in the separation zone reached a maximum at the reattachment point. It is found that the behavior of the separated shear layer plays an important part upon the heat transfer in the recirculation zone. Correlations between the average and the maximum Nusselt numbers and the Reynolds number as well as the average and the maximum Sherwood numbers and the Reynolds number suitable for application to turbine blades are developed. The last part of this study involved the prediction of stalled flow in axial compressor cascades. The performance of the algorithm is analyzed and the results from the present study are compared with the available experimental and computational results. Dissert. Abstr.

N94-31844 Colorado Univ., Boulder.
STEADY THERMAL CONVECTION IN MULTIPLE LIQUID LAYERS Ph.D. Thesis
Ajay Prakash 1993 376 p
Avail: Univ. Microfilms Order No. DA9320471

Convective flow in multiple liquid layers confined in a rectangular cavity is investigated using analytical, numerical, and experimental techniques. The cavity is subjected to differential heating, either parallel to or perpendicular to the interfaces between liquid layers. Thermal convection in the liquid layers results from buoyancy and from temperature induced changes in interfacial tension. Since the genesis of buoyancy is gravity, buoyancy effects are significantly reduced in a low-gravity environment. Definition of a space flight experiment aboard the upcoming IML-2 mission along with validation of fluid dynamical models with ground based experimentation are the objectives of this investigation. Flow in shallow cavities subjected to differential heating parallel to the interfaces is analytically investigated using the method of matched asymptotic expansions. Natural convection, without the influence of thermocapillary forces, is investigated in two and three layer systems. In low-gravity environments, thermocapillary convection with deformable interfaces is also studied. Ground based experiments to visualize the flow field are conducted. Particle streak line photography is used to visualize the flow. Particle displacement tracking is used to evaluate the velocity vector field, and holographic interferometry is used to visualize the temperature field. Numerical simulation is performed with the computer code FIDAP. Convection due to differential heating perpendicular to the interfaces is investigated using a linear stability analysis. Two and three layers of infinite horizontal extent are considered. Ground based experiments are conducted to visualize the temperature field in two and three layer systems confined in a box. Fluid dynamical models relying on mechanical coupling are experimentally validated for certain fluid combinations, while for other fluid combinations significant disparity is observed. An immobile interface is observed in the experiments, while the models predict a mobile interface. The discrepancy is attributed either to interfacial contamination in the form of molecular monolayers or to a very thin shear layer in the vicinity of the interface which could not be visualized. The existence of monolayers must be considered a real possibility for liquid combinations used in practical applications. A liquid combination exhibiting reasonable resistance to contaminant formation has been identified for the space flight experiment. Dissert. Abstr.

N94-31886* National Aeronautics and Space Administration. Lewis Research Center, Cleveland, OH.
THERMOCAPILLARY CONVECTION IN EVAPORATING SESSILE DROPS (Videotape)
1986 Videotape: 28 min. 30 sec. playing time, in color, with sound (NASA-TM-109758; NONP-VT-94-9958) Avail: CASI VHS A01/BETA A22

The purpose of this video is to understand the effects of surface tension on fluid convection. The fluid system chosen is the liquid sessile droplet to show the importance in single crystal growth, the spray drying and cooling of metal, and the advance droplet radiators of the space stations radiators. A cross sectional representation of a hemispherical liquid droplet under ideal conditions is used to show internal fluid motion. A direct simulation of buoyancy-dominant convection and surface tension-dominant convection is graphically displayed. The clear differences between two mechanisms of fluid transport, thermocapillary convection, and bouncy dominant convection is illustrated. CASI

N94-31941 Cornell Univ., Ithaca, NY.
MULTIGRID DIAGONAL IMPLICIT SOLUTIONS FOR COMPRESSIBLE TURBULENT FLOWS AND THEIR EVALUATION Ph.D. Thesis
Rama Rajaraja Varma 1993 144 p
Avail: Univ. Microfilms Order No. DA9325308

A numerical scheme to solve the two dimensional Navier-Stokes equations is developed and applied to several compressible turbulent flows over airfoils. A method for evaluating the quality of these solutions is then developed and illustrated with representative examples. The distinguishing features of the numerical scheme are its implicitness for improving stability, the diagonalization of the matrices in the implicit operator for computational efficiency, and the implementation within a multigrid procedure for convergence acceleration. A finite volume approximation is used for spatial discretization of the governing equations to handle complicated geometries. Artificial dissipation is added in the form of an adaptive blend of second and fourth differences of the solution to maintain robustness and stability. The viscous terms are treated explicitly to maintain the diagonal form. Results of simulations of viscous transonic flows past airfoils are presented. The computed flow field quantities are compared with those from other computations and experiments to confirm the accuracy of the method. Comparisons of convergence rates are made to demonstrate the efficiency of the method. In solutions to the Navier-Stokes equations it is important that the added numerical dissipation does not overwhelm the real viscous dissipation. In order to verify this, it is necessary to be able to estimate quantitatively the effect of numerical dissipation. A method for estimating the integrated effect of numerical dissipation on solutions to the Navier-Stokes equations is developed in this dissertation. The method is based on integration of the momentum equations and the computation of corrections due to numerical dissipation to the drag integral. These corrections can then be considered as estimates of the error due to dissipation. Solutions to the Navier-Stokes equations for laminar and turbulent flows over airfoils are used to illustrate the method. The errors due to numerical dissipation are compared with the total numerical errors in the solutions. The effects of different boundary conditions on the numerical dissipation are evaluated, providing means of judging the quality of the solutions. Dissert. Abstr.

N94-31988 Massachusetts Inst. of Tech., Cambridge.
OBSERVATIONS OF TURBULENCE, INTERNAL WAVES AND BACKGROUND FLOWS: AN INQUIRY INTO THE RELATIONSHIPS BETWEEN SCALES OF MOTION Ph.D. Thesis
Kurt Lewis Polzin 1992
Avail: Issuing Activity (MIT Libraries, Rm. 14-0551, Cambridge, MA 02139-4307)

Oceanic profiles of temperature, salinity, horizontal velocity, rate of dissipation of turbulent kinetic energy (epsilon) and rate of dissipation of thermal variance (chi) are used to examine the parameterization of turbulent mixing in the ocean due to internal waves. Observations from the far field of a seamount in a region of negligible large-scale flow were examined to address the issue of the buoyancy scaling of epsilon. These data exhibited large variations in background stratification with depth, but the internal wave characteristics were not substantially differentiable from the GM prescription. Data from an upper-ocean front, a warm core ring and a region of steep topography were analyzed in order to examine the parameter dependence of epsilon in internal wave fields which exhibited potentially nonstationary characteristics. Evidence was provided which implied the internal wave field in an upper ocean front was interacting with and modified by the background flow. Inhomogeneity and anisotropy of the internal wave field were noted in that data set. On the basis of a number of theoretical Richardson number probability distributions (Ri = N(sup 2)/S(sup 2), where S(sup 2) is the sum of the squared vertical derivatives of horizontal velocity), the nominal dissipation scaling of the Kunze et al. model was determined to be E(sup 2)N(sup 3). This scaling is altered to the observed epsilon similar to E(sup 2)N(sup 2) scaling by a statistical dependence between N(sup 2) and S(sup 2) which reduces the occurrence of supercritical Ri values. This statistical dependence is hypothesized to be an effect of the turbulent momentum and buoyancy fluxes on the internal wave shear and strain profiles caused by shear instability. The statistical dependence between N(sup 2) and S(sup 2) exhibited a buoyancy scaling which was interpreted

as resulting from the decreasing ratio between the time scale of the shear instability mechanism (T equivalent to 2(pi)/N) and the adiabatic time scale (T equivalent to 2(pi)/(Nf)(exp 1/2)) of the internal wave field (f is the Coriolis parameter). We argue that saturated spectral theories are valid only in the limit where a separation exists between the two time scales, i.e. for large N, low internal wave frequency content, and small f. These results have immediate implications for oceanic mixing driven by internal wave motions. Dissert. Abstr.

N94-32042# Naval Postgraduate School, Monterey, CA.
HOTWIRE MEASUREMENTS OF THE TURBULENT FLOW INTO A CASCADE OF CONTROLLED-DIFFUSION COMPRESSOR BLADES M.S. Thesis
Bryce E. Wakefield Dec. 1993 64 p
(AD-A277297) Avail: CASI HC A04/MF A01

Turbulence measurements near the leading edge of a compressor stator were made in a subsonic cascade wind tunnel with a hotwire system. Using a single hot-film probe, velocity and turbulence distortion data were obtained about the leading edge of the Controlled-Diffusion (CD) blades in order to verify Laser Doppler Velocimetry (LDV) data taken in earlier studies. Measurements were conducted at a Mach number of .25, a Reynolds number of 711,000, and an inlet flow angle of 48 deg. Turbulence profiles obtained in the pitch-wise direction were found to be in good agreement with previous LDV measurements. These data indicated a localized increase in turbulence around the leading edge due to the interaction of the free-shear layer with the inlet turbulence. This free-shear layer extends over the separation bubble, which forms on the suction side of the blades' leading edge. DTIC

N94-32045# Groningen Rijksuniv. (Netherlands). Dept. of Mathematics.
ON AN ADAPTATION METHOD FOR DENSE, 2D, C-TYPE GRIDS M.S. Thesis
M. A. Vis Jun. 1993 61 p Prepared in cooperation with National Aerospace Lab.
(W-9321; ETN-94-96182) Avail: CASI HC A04/MF A01

The study of the practical application of an adaptive grid method for high resolution (dense), 2D (two dimensional), C type grids around aerofoils is presented. For testing, the method was applied to the adaptation of a grid used for the simulation of a viscous flow around the RAE2822 aerofoil. The method may be suitable for adapting high resolution grids. ESA

N94-32076 North Carolina State Univ., Raleigh.
A NON-LOCAL MODEL FOR PREDICTION OF THE PROBABILITY DENSITY FUNCTION OF TURBULENT FLUCTUATIONS IN BOUNDARY-LAYER FLOWS Ph.D. Thesis
Michael John Brown 1993 151 p
Avail: Univ. Microfilms Order No. DA9320826

A mathematical model has been developed to predict the probability density function (pdf) and related statistical quantities of turbulent fluctuations in horizontally homogeneous boundary layer flows. The model is nonlocal, i.e., turbulent fluctuations are produced by vertical and longitudinal transport of fluid properties over finite distances from upstream positions. Fluid properties are assumed to be carried by fluid parcels. The likelihoods of parcel transport between two points and of property conservation during transport are determined using a point source dispersion model and a Lagrangian autocorrelation function, respectively. The model requires as input the mean vertical profile of the property being transported, as well as vertical profiles of the mean velocity, vertical mass eddy diffusivity, and Lagrangian time scale. Model assumptions have been tested by comparing model predictions with velocity measurements from a wind tunnel simulation of the neutral atmospheric boundary layer. The agreement between measured and model-predicted pdf's improved significantly when it was assumed that a parcel can take on a range of possible velocities, rather than the local mean value, when it mixes with the surrounding fluid. Model-predicted sigma(sub u) profiles were found to be sensitive to the form of the mean velocity, eddy diffusivity, and Lagrangian time scale profiles. With realistic input, however, model-predicted pdf and sigma(sub u) profiles were reasonably simulated. Model-predicted sigma(sub u) profiles collapsed onto one curve when scaled by u(sub *), decreased with height, and gave a surface value of sigma(sub u)/u(sub *) approximately 2.5. The model also predicted that sigma(sub u)/bar-U(z) should be an increasing function of z(sub 0), in agreement with field measurements. A method for predicting the Reynolds shear stress was proposed and preliminary results appear promising. Dissert. Abstr.

N94-32123 California Univ., San Diego, La Jolla.
EFFECTS OF BUOYANCY ON FLUID FLOWS AND TURBULENCE Final Report, 1 Oct. 1991 - 30 Sep. 1993
Charles W. VanAtta 18 Feb. 1994 3 p Limited Reproducibility: More than 20% of this document may be affected by microfiche quality
(Contract N00014-92-J-1121)
(AD-A276586) Avail: CASI HC A01

The main thrust of our studies has been focused on studying the effects of buoyancy on fluid flows and turbulence, having direct significance to geophysical flows, in particular keeping in mind the effects on the mixing of scalars, such as salinity and temperature. DTIC

N94-32149# City Coll. of the City Univ. of New York, NY.
STUDIES IN PHYSICO-CHEMICAL HYDRODYNAMICS OF EXTENDED SYSTEMS
G. I. Sivashinsky 1993 16 p
(Contract DE-FG02-88ER-13822)
(DE94-006752; DOE/ER-13822/7) Avail: CASI HC A03/MF A01

The object of the proposed research program is a unified theoretical approach to the description of a variety of physico-chemical hydrodynamic systems characterized by a significant disparity between the spatial scales involved. By appropriately performed averaging over short scales, one may considerably simplify the original problem, sometimes even lowering its effective dimensionality, and thereby making the latter quite tractable either analytically or numerically. Specifically, the author plans to study: (1) the hydrodynamic aspects of flameholding and flammability in premixed gas flames, (2) large-scale structures in Rayleigh-Benard-Marangoni convection in nonreactive and reactive liquid layers, (3) nonlinear dynamics of interfacial instabilities dominated by viscosity effects, and (4) negative viscosity effects and formation of large-scale structures in liquid layers driven at small scales. DOE

N94-32256# California Univ., Los Angeles. Dept. of Mechanical Aerospace and Nuclear Engineering.
SURFACE BOUNDARY CONDITIONS AND RELATED TECHNICAL ISSUES CONCERNING BURNETT EQUATIONS FOR 2-D HYPERSONIC FLOW Final Technical Report, 15 Nov. 1991 - 14 Nov. 1993
Xiao-Lin Zhong 14 Jan. 1994 21 p
(Contract F49620-92-J-0090)
(AD-A277322; AFOSR-94-0074TR) Avail: CASI HC A03/MF A01

Research on studying steady and transient rarefied hypersonic flow by using the Burnett equations and developing accurate and efficient numerical methods for both the Navier-Stokes and Burnett equations were conducted in three aspects: (1) A new method of formulating the additional boundary conditions for the Burnett equations was presented. The 2-D Burnett equations with first order slip conditions seem to be able to improve the Navier-Stokes equations in two dimensions in the continuum transition regime, though more validation work is needed for the Burnett equations. (2) The first Burnett solutions for axisymmetric flow have been obtained. (3) The high-order ENO schemes have been used to obtain time-accurate solutions of the Navier-Stokes equations to study the unsteady hypersonic shock-shock interference heating on a cylinder. The results show that the inherent unsteadiness has a strong effect on surface heating rates. The ENO schemes were found to work well for numerical simulations of transient hypersonic flow. DTIC

N94-32279# Iowa State Univ. of Science and Technology, Ames. Engineering Research Inst.
INCORPORATING RADIAL MIXING IN AXISYMMETRIC STREAMLINE CURVATURE THROUGH-FLOW ANALYSIS Final Technical Report, May 1992 - Sep. 1993
D. G. Grabowska and P. Kavanagh Sep. 1993 114 p
(Contract F49620-92-J-0226)
(AD-A277325; ISU-ERI-AMES-94-088; AFOSR-94-0079TR) Avail: CASI HC A06/MF A02

The development of governing equations for hub-to-tip streamline curvature solutions in turbomachinery passages and blade rows and incorporating viscous radial mixing is presented. Arbitrary passage geometries

and quasi-orthogonal description are accounted for. Fortran program coding is carried out for the special case of unbladed, axial-flow passages. Flow solutions are obtained by iteration based on fixed streamline patterns in the meridional plane followed by further iterations involving readjustment of the streamlines until overall convergence is obtained. Simple examples are presented to illustrate the solution technique. DTIC

N94-32361 Arnold Engineering Development Center, Arnold AFS, TN.
A CRITICAL EVALUATION OF METHODS FOR IMPOSING SOLID-WALL BOUNDARY CONDITIONS IN INVISCID FLOW Final Report, Aug. - Sep. 1993
S. L. Keeling (Calspan Corp., Arnold AFS, TN.) Mar. 1994 37 p
Limited Reproducibility: More than 20% of this document may be affected by microfiche quality
(AD-A276959; AEDC-TR-93-23) Avail: CASI HC A03

This report presents a critical evaluation of widely used methods for imposing discrete solid-wall boundary conditions for the numerical computation of inviscid flows. Specifically, it shows that some of these methods are only provisionally correct. Also, an explanation is given for the success of others. In particular, the report shows that a method involving contravariant velocity components can generate distortions in computed flows. Because complex CFD calculations can be difficult to interpret, the claims made here are demonstrated with explicit solutions to simple model problems. This work emphasizes that subtle and erroneous effects can result from the use of apparently natural numerical methods. It also emphasizes the importance of developing simple tests for these computational methods to elucidate the possible consequences of their use. DTIC

N94-32373# Sandia National Labs., Albuquerque, NM.
PARALLEL PARTICLE SIMULATIONS OF LOW-DENSITY FLUID FLOWS
S. Plimpton and T. Bartel 1993 4 p Presented at the High Performance Computing 1994: Grand Challenges in Computer Simulation, La Jolla, CA, 11-15 Apr. 1994
(Contract DE-AC04-94AL-85000)
(DE94-007858; SAND-93-2556C; CONF-940428-2) Avail: CASI HC A01/MF A01

Direct Simulation Monte Carlo (DSMC) is a simulation technique that uses particles to model fluids at low densities where continuum formulations break down. Monte Carlo rules are used to perform particle collisions and chemical reactions and a grid is used to locate nearby particles. We describe our implementation of a large-scale DSMC model on the thousand-processor nCUBE 2 and Intel Paragon machines. It includes body-fitted irregular grids and particle weighting to reduce the numbers of particles and grid cells that must be used. Our parallel methods for load-balancing and performing irregular communication on the distributed-memory machines are also discussed. The parallel machines have enabled us to run large simulations (10(exp 7) particles, 10(exp 4) grid cells, 10(exp 4) timesteps) at speeds up to 40 times faster (on our nCUBE 2) than on a Cray Y-MP processor. For illustration purposes, we include results from some of these large-scale simulations. DOE

N94-32410# Duke Univ., Durham, NC. Dept. of Mathematics.
HIGH-RESOLUTION NUMERICAL METHODS FOR COMPRESSIBLE MULTI-PHASE FLOW IN HIERARCHICAL POROUS MEDIA
J. A. Trangenstein 15 Mar. 1994 19 p
(Contract DE-FG05-92ER-25145)
(DE94-008261; DOE/ER-25145/T1) Avail: CASI HC A03/MF A01

This is the second year in the proposed three-year effort to develop high-resolution numerical methods for multi-phase flow in hierarchical porous media. The issues being addressed in this research are: Computational efficiency: field-scale simulation of enhanced oil recovery, whether for energy production or aquifer remediation, is typically highly under-resolved. This is because rock transport properties vary on many scales, and because current numerical methods have low resolution. Effective media properties: since porous media are formed through complex geologic processes, they involve significant uncertainty and scale-dependence. Given this uncertainty, knowledge of ensemble averages of flow in porous media can be preferable to knowledge of flow in specific realizations of the reservoir. However, current models of effective properties do not represent the observed behavior very well. Relative permeability models present a good example of this problem. In practice, these models seldom provide realistic representations of hysteresis, interfacial tension effects or three-phase flow; there are no models that represent well all three effects simultaneously. Wave propagation: since numerical methods must use the models for compoutations, oscillations could erroneously be attributed to numerical error rather than modeling difficulties. When wave propagation is well-understood by analysis, it can provide useful information about the expected behavior of the flows, and can assist in the development of high-resolution numerical methods. DOE

N94-32480*# Nektonics, Inc., Cambridge, MA.
CHEMICAL VAPOR DEPOSITION FLUID FLOW SIMULATION MODELLING TOOL
Edward T. Bullister Jun. 1992 136 p
(Contract NAS1-19102; SBIR-15.03-5777; RTOP 324-02-02)
(NASA-CR-189648; NAS 1.26:189648) Avail: CASI HC A07/MF A02

Accurate numerical simulation of chemical vapor deposition (CVD) processes requires a general purpose computational fluid dynamics package combined with specialized capabilities for high temperature chemistry. In this report, we describe the implementation of these specialized capabilities in the spectral element code NEKTON. The thermal expansion of the gases involved is shown to be accurately approximated by the low Mach number perturbation expansion of the incompressible Navier-Stokes equations. The radiative heat transfer between multiple interacting radiating surfaces is shown to be tractable using the method of Gebhart. The disparate rates of reaction and diffusion in CVD processes are calculated via a point-implicit time integration scheme. We demonstrate the use above capabilities on prototypical CVD applications. Author (revised)

N94-32485 Virginia Univ., Charlottesville.
COMPUTATIONAL MODELING OF CONVECTIVE HEAT TRANSFER TO LIQUID HYDROGEN COOLANT Ph.D. Thesis
Robert George Carlisle 1992 193 p
Avail: Univ. Microfilms Order No. DA9324896

A computational algorithm capable of modeling the flow down a coolant duct of a fluid whose thermophysical properties vary with temperature was created and applied. The algorithm is formulated separately in two and three dimensions. Both approaches use space marching of the parabolized Navier-Stokes equations combined with the iterative recalculation of the fluid properties and turbulent intensities. The two-dimensional algorithm also iteratively couples the temperature distribution in the fluid with the heat transfer distribution in the bounding material. The externally applied heat transfer modeled approximates anticipated conditions in the cowl lip of the National Aerospace Plane (NASP). The proposed cooling by liquid hydrogen of the large surface heat transfer caused by external shock/shock interaction was found to give temperatures in the leading edge material that were close to the thermal limits of prospective materials. It was found that the performance of the coolant (i.e. the ability to cool the structure below a specific temperature) was very sensitive to inlet conditions of the coolant fluid as well as to the mass flow rate. The spread of the heat transfer on passing through the bounding material was found to be considerable and significantly reduced the maximum temperature of the fluid. The results of the three dimensional modeling showed that the principal restraint on the ability of the duct flow to convect heat was the build up of heat in corner boundary layers. It was found that the addition of a vortex to the center of the cross-stream flow in the inlet was not effective in decreasing the maximum temperature of the heated fluid. Dirichlet boundary conditions (i.e. specified temperatures) calculated from the two-dimensional algorithm were applied to the three-dimensional algorithm and demonstrated similarity between the heat transfer coefficients calculated by both methods. Dissert. Abstr.

N94-32497 Waterloo Univ. (Ontario).
A CRITICAL EVALUATION OF THE REYNOLDS STRESS TURBULENCE CLOSURE FOR THE FLOW OF A TURBULENT FREE-STREAM OVER A TURBULENT BOUNDARY LAYER Ph.D. Thesis
John C. Mackinnon 1992 296 p
(ISBN-0-315-75792-2) Avail: Univ. Microfilms Order No. DANN75792

This thesis is concerned with the evaluation of a Reynolds stress turbulence closure (the Reynolds Stress Model) for the flow of a turbulent free-stream over the turbulent boundary layer on a flat plate. The interaction of turbulent flow with underlying boundary layer formed on a surface is a complex flow of interest in many practical engine problems. In order to

advance the ability of turbulence models to predict these flows, a clear understanding of the capability of existing models to account for important physical phenomena is necessary. The Reynolds Stress Model involves a set of partial differential equations representing conservation of turbulent stresses, where the stresses represent the transfer of momentum by turbulent fluctuations. In the present work, the thin shear layer form of the coupled governing equations were solved numerically using a finite volume method. Model predictions with the conventional Reynolds Stress Model (denoted CSM) have been compared to experimental data of local, mean and turbulent quantities gathered over a wide range of free-stream turbulence conditions. Based on comparison experimental data, it is found here that the CSM in general gives good predictions of local parameters, with the exception of the boundary layer thickness delta(sub 995). Experimentally observed effects of profile changes as a function of the free-stream turbulence intensity, I(sub infinity), and ratio of the free-stream length scale to boundary layer thickness, L(sub upsilon)(exp infinity) /delta, are also generally well predicted. It is identified that the CSM does not properly account for the effect of the wall on the external turbulence, resulting in the turbulent stress normal to the wall being attenuated at too great a distance. The conventionally applied gradient diffusion model of the third order correlations is also seen to under predict the experimental data when free-stream turbulence is present. New model formulations proposed to improve the treatment of these two aspects are developed and are shown to give better predictions. Dissert. Abstr.

N94-32511 Kentucky Univ., Lexington.
ADDITIVE TURBULENT DECOMPOSITION OF THE INCOMPRESSIBLE AND COMPRESSIBLE NAVIER-STOKES EQUATIONS Final Report, 1991- 1993
J. M. McDonough, Y. Yang, and X. Zhong 1993 27 p Limited Reproducibility: More than 20% of this document may be affected by microfiche quality
(Contract F49620-92-J-0113)
(AD-A277321; AFOSR-94-0076TR) Avail: CASI HC A03

Research results summarizing the past two years' efforts are presented. These include analysis of both the large and small-scale equations of additive turbulent decomposition (ATD) for the two dimensional incompressible Navier-Stokes equations. Both of these solution procedures are complete for Cartesian coordinates and check out is essentially finished for generalized coordinates. We discuss our method used to filter solutions to the large-scale equations, and the domain decomposition methods we are employing to recouple local small-scale solutions to produce global solutions on the small scale. We also present results obtained from our large-scale equations/chaotic map turbulence modeling approach for intermittent flow. DTIC

N94-32561# California Univ., Los Angeles. Dept. of Mathematics.
ANALYSIS AND COMPUTATION FOR VORTEX DYNAMICS AND RAREFIED GASES Final Technical Report, 1 Oct. 1989 - 30 Sep. 1993
Russel E. Caflisch 29 Nov. 1993 4 p
(Grant AF-AFOSR-0003-90)
(AD-A277415; AFOSR-94-0093TR) Avail: CASI HC A01/MF A01

Through support of this grant, a number of research projects on vortex dynamics and rarefied gas dynamics were completed. A few of the most outstanding results were the following: An analytic theory for singularity formation on the fluid interface in the Rayleigh-Taylor problem was developed and shown to agree with numerical results. Singular solutions were found by direct computation for Moore's approximation of the three dimensional Euler equations for axisymmetric flow with swirl. Generic form singularities for hyperbolic and elliptic equations were classified using catastrophe theory. The results were applied to shock waves, vortex sheets, and, in preliminary work, patterns in convective flows. DTIC

N94-32652 Lawrence Livermore National Lab., CA.
NOTES ON THE LANGEVIN MODEL FOR TURBULENT DIFFUSION OF MARKED PARTICLES
H. C. Rodean 26 Jan. 1994 122 p Limited Reproducibility: More than 20% of this document may be affected by microfiche quality
(Contract W-7405-eng-48)
(DE94-007847; UCRL-ID-115869) Avail: Issuing Activity (Department of Energy (DOE))

Three models for scalar diffusion in turbulent flow (eddy diffusivity, random displacement, and on the Langevin equation) are briefly described. The model's random velocity increment based Fokker-Planck equation is introduced, and then, they are examined in more detail in the reverse order. The Fokker-Planck equation is the Eulerian equivalent of the Lagrangian Langevin equation, and the derivation is outlined. The procedure for obtaining the deterministic and stochastic components of the Langevin equation from Kolmogorov's 1941 inertial range theory and the Fokker-Planck equation is described. It is noted that a unique form of the Langevin equation can be determined for diffusion in one dimension but not in two or three. The Langevin equation for vertical diffusion in the non-Gaussian convective boundary layer is presented and successively simplified for Gaussian inhomogeneous turbulence and Gaussian homogeneous turbulence in turn. The Langevin equation for Gaussian inhomogeneous turbulence is mathematically transformed into the random displacement model. It is shown how the Fokker-Planck equation for the random displacement model is identical in form to the partial differential equation for the eddy diffusivity model. It is noted that the Langevin model is applicable in two cases in which the other two are not valid: (1) close in time and distance to the point of scalar release; and (2) the non-Gaussian convective boundary layer. The two- and three-dimensional cases are considered in Part 3. DOE

N94-32709# Sandia National Labs., Albuquerque, NM.
THERM3D: A BOUNDARY ELEMENT COMPUTER PROGRAM FOR TRANSIENT HEAT CONDUCTION PROBLEMS
M. S. Ingber (New Mexico Univ., Albuquerque.) Feb. 1994 25 p
(Contract DE-AC04-94AL-85000)
(DE94-008112; SAND-93-7072) Avail: CASI HC A03/MF A01

The computer code THERM3D implements the direct boundary element method (BEM) to solve transient heat conduction problems in arbitrary three dimensional domains. This particular implementation of the BEM avoids performing time consuming domain integrations by approximating a 'generalized forcing function' in the interior of the domain with the use of radial basis functions. An approximate particular solution is then constructed, and the original problem is transformed into a sequence of Laplace problems. The code is capable of handling a large variety of boundary conditions including isothermal, specified flux, convection, radiation, and combined convection and radiation conditions. The computer code is benchmarked by comparisons with analytic and finite element results. DOE

N94-32849 Lawrence Livermore National Lab., CA.
A STUDY OF NEAR-SURFACE AND UNDERWATER EXPLOSIONS BY COMPUTER SIMULATIONS
M. Kamegai and J. W. White Feb. 1994 12 p Limited Reproducibility: More than 20% of this document may be affected by microfiche quality
(Contract W-7405-eng-48)
(DE94-009038; UCRL-ID-116360) Avail: CASI HC A03

Computer simulations were made for 13 near-surface and underwater explosions from generic 1-kt and 10-kt sources. The objective is to calculate energy coupling to the water and to understand conditions that drive signals into the ocean sound channel. The simulation used the CALE computer program which was previously validated using the WIGWAM test data. A 1-kt underwater explosion achieves its maximum coupling at about 20 m DOB, and the downward kinetic energy is less than 15% of the yield. As the source is lifted above the surface the coupling efficiency decreases dramatically. A comparison of underwater explosion simulations for the two different yields confirmed that hydrodynamic dimensions scale by the cube root of the yield. DOE

N94-32867*# Lockheed Aeronautical Systems Co., Marietta, GA.
SHEAR FLOW CONTROL OF COLD AND HEATED RECTANGULAR JETS BY MECHANICAL TABS. VOLUME 1: RESULTS AND DISCUSSION
W. H. Brown and K. K. Ahuja May 1989 357 p
(Contract NAS3-25409)
(NASA-CR-182296-Vol-1; NAS 1.26:182296-Vol-1; LG89ER0059-Vol-1)
Avail: CASI HC A16/MF A03

The effects of mechanical protrusions on the jet mixing characteristics of rectangular nozzles for heated and unheated subsonic and supersonic jet plumes were studied. The characteristics of a rectangular nozzle of aspect ratio 4 without the mechanical protrusions were first investigated. Intrusive probes were used to make the flow measurements. Possible

errors introduced by intrusive probes in making shear flow measurements were also examined. Several scaled sizes of mechanical tabs were then tested, configured around the perimeter of the rectangular jet. Both the number and the location of the tabs were varied. From this, the best configuration was selected. The conclusions derived were: (1) intrusive probes can produce significant errors in the measurements of the velocity of jets if they are large in diameter and penetrate beyond the jet center; (2) rectangular jets without tabs, compared to circular jets of the same exit area, provide faster jet mixing; and (3) further mixing enhancement is possible by using mechanical tabs. Author

N94-32869*# Lockheed Aeronautical Systems Co., Marietta, GA.
SHEAR FLOW CONTROL OF COLD AND HEATED RECTANGULAR JETS BY MECHANICAL TABS. VOLUME 2: TABULATED DATA
W. H. Brown and K. K. Ahuja May 1989 523 p
(Contract NAS3-25409; RTOP 505-62-00)
(NASA-CR-182296-Vol-2; NAS 1.26:182296-Vol-2; LG89ER0059-Vol-2)
Avail: CASI HC A22/MF A04

The effects of mechanical protrusions on the jet mixing characteristics of rectangular nozzles for heated and unheated subsonic and supersonic jet plumes were studied. The characteristics of a rectangular nozzle of aspect ratio 4 without the mechanical protrusions were first investigated. Intrusive probes were used to make the flow measurements. Possible errors introduced by intrusive probes in making shear flow measurements were also examined. Several scaled sizes of mechanical tabs were then tested, configured around the perimeter of the rectangular jet. Both the number and the location of the tabs were varied. From this, the best configuration was selected. This volume contains tabulated data for each of the data runs cited in Volume 1. Baseline characteristics, mixing modifications (subsonic and supersonic, heated and unheated) and miscellaneous charts are included. Author

N94-32871*# Vigyan Research Associates, Inc., Hampton, VA.
COMPUTATION OF THREE-DIMENSIONAL COMPRESSIBLE BOUNDARY LAYERS TO FOURTH-ORDER ACCURACY ON WINGS AND FUSELAGES Final Report
Venkit Iyer Jan. 1990 275 p
(Contract NAS1-18585; RTOP 505-60-31-05)
(NASA-CR-4269; NAS 1.26:4269) Avail: CASI HC A12/MF A03

A solution method, fourth-order accurate in the body-normal direction and second-order accurate in the stream surface directions, to solve the compressible 3-D boundary layer equations is presented. The transformation used, the discretization details, and the solution procedure are described. Ten validation cases of varying complexity are presented and results of calculation given. The results range from subsonic flow to supersonic flow and involve 2-D or 3-D geometries. Applications to laminar flow past wing and fuselage-type bodies are discussed. An interface procedure is used to solve the surface Euler equations with the inviscid flow pressure field as the input to assure accurate boundary conditions at the boundary layer edge. Complete details of the computer program used and information necessary to run each of the test cases are given in the Appendix.
Author

N94-32872*# Georgia Inst. of Tech., Atlanta.
ENHANCEMENT OF MIXING IN A RECTANGULAR JET BY MECHANICAL TABS
W. H. Brown and K. K. Ahuja Apr. 1990 86 p
(Grant NAG3-1062; RTOP 505-62-00)
(NASA-CR-185207; A-8402; NAS 1.26:185207) Avail: CASI HC A05/MF A01

This effort was conducted to obtain additional test data/configurations required to better understand the effects of tab length and width on jet mixing enhancement for a rectangular nozzle. The configurations tested were a six-tab configuration defined by NASA, a full-height tab configuration, and two-tab configurations with selected tab lengths and widths. Additional test data were also required for all candidate configurations to better interpret the data. Test data from this effect are presented. On the basis of these data, the following general observations were noted: The six-tab rectangular nozzle configuration provided a lower peak velocity than either the two-tab or four-tab configuration; and the rectangular nozzle with a full-height tab had about the same peak velocity as the two-tab configuration; however, the full-height tab configuration had a somewhat lower centerline velocity. Author

N94-32946*# National Aeronautics and Space Administration. Ames Research Center, Moffett Field, CA.
INCREMENTAL TRIANGULATION BY WAY OF EDGE SWAPPING AND LOCAL OPTIMIZATION
N. Lyn Wiltberger Jan. 1994 43 p
(RTOP 505-59-50)
(NASA-TM-103979; A-92196; NAS 1.15:103979) Avail: CASI HC A03/MF A01

This document is intended to serve as an installation, usage, and basic theory guide for the two dimensional triangulation software 'HARLEY' written for the Silicon Graphics IRIS workstation. This code consists of an incremental triangulation algorithm based on point insertion and local edge swapping. Using this basic strategy, several types of triangulations can be produced depending on user selected options. For example, local edge swapping criteria can be chosen which minimizes the maximum interior angle (a MinMax triangulation) or which maximizes the minimum interior angle (a MaxMin or Delaunay triangulation). It should be noted that the MinMax triangulation is generally only locally optical (not globally optimal) in this measure. The MaxMin triangulation, however, is both locally and globally optical. In addition, Steiner triangulations can be constructed by inserting new sites at triangle circumcenters followed by edge swapping based on the MaxMin criteria. Incremental insertion of sites also provides flexibility in choosing cell refinement criteria. A dynamic heap structure has been implemented in the code so that once a refinement measure is specified (i.e., maximum aspect ratio or some measure of a solution gradient for the solution adaptive grid generation) the cell with the largest value of this measure is continually removed from the top of the heap and refined. The heap refinement strategy allows the user to specify either the number of cells desired or refine the mesh until all cell refinement measures satisfy a user specified tolerance level. Since the dynamic heap structure is constantly updated, the algorithm always refines the particular cell in the mesh with the largest refinement criteria value. The code allows the user to: triangulate a cloud of prespecified points (sites), triangulate a set of prespecified interior points constrained by prespecified boundary curve(s), Steiner triangulate the interior/exterior of prespecified boundary curve(s), refine existing triangulations based on solution error measures, and partition meshes based on the Cuthill-McKee, spectral, and coordinate bisection strategies. Author (revised)

N94-32947*# National Aeronautics and Space Administration. Lewis Research Center, Cleveland, OH.
MODIFICATION OF THE MML TURBULENCE MODEL FOR ADVERSE PRESSURE GRADIENT FLOWS M.S. Thesis - Akron Univ., 1993
Julianne M. Conley Apr. 1994 96 p
(RTOP 505-62-52)
(NASA-TM-106544; E-8690; NAS 1.15:106544) Avail: CASI HC A05/MF A01

Computational fluid dynamics is being used increasingly to predict flows for aerospace propulsion applications, yet there is still a need for an easy to use, computationally inexpensive turbulence model capable of accurately predicting a wide range of turbulent flows. The Baldwin-Lomax model is the most widely used algebraic model, even though it has known difficulties calculating flows with strong adverse pressure gradients and large regions of separation. The modified mixing length model (MML) was developed specifically to handle the separation which occurs on airfoils and has given significantly better results than the Baldwin-Lomax model. The success of these calculations warrants further evaluation and development of MML. The objective of this work was to evaluate the performance of MML for zero and adverse pressure gradient flows, and modify it as needed. The Proteus Navier-Stokes code was used for this study and all results were compared with experimental data and with calculations made using the Baldwin-Lomax algebraic model, which is currently available in Proteus. The MML model was first evaluated for zero pressure gradient flow over a flat plate, then modified to produce the proper boundary layer growth. Additional modifications, based on experimental data for three adverse pressure gradient flows, were also implemented. The adapted model, called MMLPG (modified mixing length model for pressure gradient flows), was then evaluated for a typical propulsion flow problem, flow through a transonic diffuser. Three cases

were examined: flow with no shock, a weak shock and a strong shock. The results of these calculations indicate that the objectives of this study have been met. Overall, MMLPG is capable of accurately predicting the adverse pressure gradient flows examined in this study, giving generally better agreement with experimental data than the Baldwin-Lomax model. Author

N94-32958 Department of the Navy, Washington, DC.
MAGNETOHYDRODYNAMIC BOUNDARY LAYER CONTROL SYSTEM Patent
James C. Meng, inventor (to Navy) 28 Dec. 1993 6 p Filed 11 Feb. 1993
(AD-D016120; US-Patent-5,273,465; US-Patent-Appl-SN-016325; US-Patent-Class-440-6) Avail: US Patent and Trademark Office

An active boundary layer control system for marine vehicles is disclosed. The boundary layer control system comprises a plurality of magnets and seawater electrodes placed in circumferential rows around the beam of the hull. The magnets and electrodes are positioned so that a Lorentz force generated by the interacting magnetic and electric fields will drive the boundary layer flow in an axial direction toward the aft end of the bull. The boundary control system reduces turbulence and may relaminarize boundary layer flow, thereby reducing radiated noise. DTIC

N94-32969*# National Aeronautics and Space Administration. Lewis Research Center, Cleveland, OH.
INSTITUTE FOR COMPUTATIONAL MECHANICS IN PROPULSION (ICOMP) Annual Report No. 8, 1993
Charles E. Feiler, ed. Apr. 1994 91 p
(Contract NCC3-233; RTOP 505-90-5K)
(NASA-TM-106542; ICOMP-94-01; E-8686; NAS 1.15:106542) Avail: CASI HC A05/MF A01

The Institute for Computational Mechanics in Propulsion (ICOMP) is operated by the Ohio Aerospace Institute (OAI) and the NASA Lewis Research Center in Cleveland, Ohio. The purpose of ICOMP is to develop techniques to improve problem-solving capabilities in all aspects of computational mechanics related to propulsion. This report describes the accomplishments and activities at ICOMP during 1993. Author

N94-33009# Science Applications International Corp., McLean, VA.
FLUID DYNAMICS LAGRANGIAN SIMULATION MODEL Final Report
Ellis Hyman 8 Feb. 1994 137 p
(Contract N00014-89-C-2106)
(AD-A277438; SAIC-94/1017) Avail: CASI HC A07/MF A02

The work performed by Science Applications International Corporation (SAIC) on this contract, Fluid Dynamics Lagrangian Simulation Model, Contract Number N00014-89-C-2106, SAIC Project Number 01-0157-03-0768, focused on a number of research topics in fluid dynamics. The work was in support of the programs of NRL's Laboratory for Computational Physics and Fluid Dynamics and covered the period from 10 September 1989 to 9 December 1993. In the following sections, we describe each of the efforts and the results obtained. Much of the research work has resulted in journal publications. These are included in Appendices of this report for which the reader is referred for complete details. DTIC

N94-33020*# National Aeronautics and Space Administration. Langley Research Center, Hampton, VA.
IMPLEMENTATION OF A VIBRATIONALLY LINKED CHEMICAL REACTION MODEL FOR DSMC
A. B. Carlson and Graeme A. Bird Apr. 1994 11 p
(RTOP 232-01-04-04)
(NASA-TM-109109; NAS 1.15:109109) Avail: CASI HC A03/MF A01

A new procedure closely linking dissociation and exchange reactions in air to the vibrational levels of the diatomic molecules has been implemented in both one- and two-dimensional versions of Direct Simulation Monte Carlo (DSMC) programs. The previous modeling of chemical reactions with DSMC was based on the continuum reaction rates for the various possible reactions. The new method is more closely related to the actual physics of dissociation and is more appropriate to the particle nature of DSMC. Two cases are presented: the relaxation to equilibrium of undissociated air initially at 10,000 K, and the axisymmetric calculation of shuttle forebody heating during reentry at 92.35 km and 7500 m/s. Although reaction rates are not used in determining the dissociations or exchange reactions, the new method produces rates which agree astonishingly well with the published rates derived from experiment. The results for gas properties and surface properties also agree well with the results produced by earlier DSMC models, equilibrium air calculations, and experiment. Author

N94-33070*# National Aeronautics and Space Administration. Lewis Research Center, Cleveland, OH.
RENORMALIZATION GROUP THEORY OF BOLGIANO SCALING IN BOUSSINESQ TURBULENCE
Robert Rubinstein May 1994 19 p
(Contract NCC3-233; RTOP 505-90-5K)
(NASA-TM-106602; ICOMP-94-8; E-8877; NAS 1.15:106602; CMOTT-94-2) Avail: CASI HC A03/MF A01

Bolgiano scaling in Boussinesq turbulence is analyzed using the Yakhot-Orszag renormalization group. For this purpose, an isotropic model is introduced. Scaling exponents are calculated by forcing the temperature equation so that the temperature variance flux is constant in the inertial range. Universal amplitudes associated with the scaling laws are computed by expanding about a logarithmic theory. Connections between this formalism and the direct interaction approximation are discussed. It is suggested that the Yakhot-Orszag theory yields a lowest order approximate solution of a regularized direct interaction approximation which can be corrected by a simple iterative procedure. Author

N94-33162 Pennsylvania State Univ., University Park. Dept. of Mechanical Engineering.
THE STRUCTURE OF HIGH REYNOLDS NUMBER TURBULENT BOUNDARY LAYERS, PART A Final Technical Report, Dec. 1989 - Dec. 1993
James G. Brasseur 15 Feb. 1994 17 p Limited Reproducibility: More than 20% of this document may be affected by microfiche quality
(Grant AF-AFOSR-0113-90)
(AD-A278392; AFOSR-94-0207TR) Avail: CASI HC A03

We provide a summary of our accomplishments under a three-year 'mini URI' program in collaboration with researchers at Yale and Princeton universities. Whereas the central theme of the program is high Reynolds number wall-bounded turbulence, studies at Penn State included analysis of fundamental issues of scale interactions in high Reynolds number turbulence dynamics, the use of the wavelet decomposition and generalized filtering techniques in describing the relationship between the Fourier-spectral description of scale and the physical-space description of structure, direct numerical simulation of passive scalar sources in low Reynolds number turbulent boundary layers and analysis of scalar evolution in relationship to laboratory data, the relationship between homogeneous turbulent shear flow and the inertial sublayer in high Reynolds number turbulent boundary layers, and the development and application of sophisticated data analysis techniques which intimately combine graphical and quantitative analysis within a fully interactive 'analytical environment.' A brief summary of the accomplishments in each area of development is presented. DTIC

N94-33164 Michigan Univ., Ann Arbor. Gas Dynamics Labs.
SCALAR IMAGING VELOCIMETRY STUDIES OF TURBULENT FLOW STRUCTURE AND DYNAMICS Final Report, 1 Oct. 1991 - 30 Sep. 1993
Werner J. Dahm 31 Dec. 1993 76 p Limited Reproducibility: More than 20% of this document may be affected by microfiche quality
(Contract F49620-92-J-0025)
(AD-A278395; AFOSR-94-0164TR) Avail: CASI HC A05

The first fully-resolved, nonintrusive, experimental measurements of the spatio-temporal structure and dynamics of the full nine-component velocity gradient tensor field gradient-u(x,t) in a turbulent flow are here obtained by applying the scalar imaging velocimetry technique to laboratory turbulent flow scalar field data. A variational method implementing this concept is described in which weighted residuals of the conserved scalar transport equation, the continuity condition, and a derivative smoothness condition are minimized over the space of velocity fields. The technique is applied to direct numerical simulation (DNS) data for the limiting case of turbulent mixing of a Sc = 1 passive scalar field. The spatial velocity fields u(x,t) obtained correlate well with the exact DNS results, as do statistics of the velocity and velocity gradient fields. The method is then applied to fully resolved four dimensional Sc much greater than 1 scalar field imaging measurements from a laboratory turbulent flow. Results give the first fully resolved data for the time-varying (u, v, w) vector velocity

component fields simultaneously everywhere on a regular three dimensional spatial grid in a turbulent flow. Direct differentiation of these fields yields the spatial structure in the full velocity gradient tensor field components. From these, the vector vorticity field wi(x,t) and tensor strain rate field epsilon-ij(x,t) are extracted, as are the kinetic energy density field k(x;t), the kinetic energy dissipation rate field phi(x;t), and the enstrophy field W(x;t). Finally, extraction of the time evolution in these fields is demonstrated by applying this scalar imaging velocimetry method to perform the inversion for the velocity field at several sequential time steps. DTIC

N94-33290*# National Aeronautics and Space Administration. Ames Research Center, Moffett Field, CA.

BACKWARD-FACING STEP MEASUREMENTS AT LOW REYNOLDS NUMBER, Re(SUB h)=5000

Srba Jovic (Eloret Corp., Palo Alto, CA.) and David M. Driver Feb. 1994 26 p Original contains color illustrations

(RTOP 505-59-50)

(NASA-TM-108807; A-94043; NAS 1.15:108807) Avail: CASI HC A03/MF A01; 2 functional color pages

An experimental study of the flow over a backward-facing step at low Reynolds number was performed for the purpose of validating a direct numerical simulation (DNS) which was performed by the Stanford/NASA Center for Turbulence Research. Previous experimental data on back step flows were conducted at Reynolds numbers and/or expansion ratios which were significantly different from that of the DNS. The geometry of the experiment and the simulation were duplicated precisely, in an effort to perform a rigorous validation of the DNS. The Reynolds number used in the DNS was Re(sub h)=5100 based on step height, h. This was the maximum possible Reynolds number that could be economically simulated. The boundary layer thickness, d, was approximately 1.0 h in the simulation and the expansion ratio was 1.2. The Reynolds number based on the momentum thickness, Re(sub theta), upstream of the step was 610. All of these parameters were matched experimentally. Experimental results are presented in the form of tables, graphs and a floppy disk (for easy access to the data). An LDV instrument was used to measure mean velocity components and three Reynolds stresses components. In addition, surface pressure and skin friction coefficients were measured. LDV measurements were acquired in a measuring domain which included the recirculating flow region. Author

N94-32455*# National Aeronautics and Space Administration. Lyndon B. Johnson Space Center, Houston, TX.

ELECTROMAGNETIC PROBE TECHNIQUE FOR FLUID FLOW MEASUREMENTS

G. D. Arndt and J. R. Carl *In* NASA, Washington, Technology 2003: The Fourth National Technology Transfer Conference and Exposition, Volume 2 Feb. 1994 p 301-310 (For primary document see N94-32420 09-99)

Avail: CASI HC A02/MF A04

35 INSTRUMENTATION AND PHOTOGRAPHY

Includes remote sensors; measuring instruments and gages; detectors; cameras and photographic supplies; and holography.

For aerial photography see *43 Earth Resources and Remote Sensing*. For related information see also *06 Aircraft Instrumentation*, and *19 Spacecraft Instrumentation*.

N94-31085 Stockholm Univ. (Sweden). Dept. of Physics.

PARTICLE IDENTIFICATION IN A SEGMENTED CALORIMETER (NUMASS TEST DATA, SEPTEMBER 1991)

Q.-P. Zhang 15 Sep. 1993 25 p Limited Reproducibility: More than 20% of this document may be affected by microfiche quality

(USIP-93-08; ETN-94-95940) Avail: Issuing Activity (European Space Agency (ESA))

The ZEUS T60 uranium/scintillator calorimeter was the main detector in the NUMASS test run, which took place at the Super Proton Synchrotron (SPS) facility. Additional scintillators were embedded in the calorimeter for high precision measurement of the arrival time for hadronic particle. High energy pion beams were used to test the performance of the calorimeter and to measure the arrival time distribution for hadrons. The segmentation of the calorimeter makes it possible to measure different shower profiles in the detector which is then used to identify and discriminate against contamination in the pion beam of electrons and muons. The particle identification is described. ESA

N94-31096 Ecole Nationale Superieure des Telecommunications, Paris (France). Groupe Image.

TRACKING ROADS IN AN AERIAL IMAGE BY KALMAN FILTERING Progress Report, Jan. - Mar. 1993 [SUIVI DE ROUTES DANS UNE IMAGE AERIENNE PAR FILTRAGE DE KALMAN, JANVIER - MARS 1993]

Jean-Pierre Veran 1993 35 p In FRENCH Limited Reproducibility: More than 20% of this document may be affected by microfiche quality

(ISSN 0751-1345)

(TELECOM-93-D-007; ETN-94-95888) Avail: CASI HC A03

The possibility of tracking roads in aerial images in order to achieve an automatic extraction of the road network is studied. An analogy with the classical problem of moving targets tracking is proposed and an algorithm for roads tracking based on Kalman filtering is developed. For this, as observation space, both the image of the contours and the image of the gradient direction extracted from the original image with a classical Canny-Deriche detector are used. The modelization and the initialization of the parameters is possible because hypothesis on the roads characteristics was made. To improve this tracking tool, the radiometric information was used in a test a posteriori and two criteria to detect bad tracks were defined. It is shown how it is possible to take advantage of data extracted from a map of the region under study and previously registered. More precisely, information about crossroads (position, topology) is used so that the algorithm becomes robust when going through such areas. This also enables an automatic initialization of the tracking process and leads, with a recursive use of the program, to the possibility of recovering on the image the road network previously extracted from the map. ESA

N94-31283# Pennsylvania State Univ., University Park. Dept. of Chemistry.

ANALYTICAL APPLICATIONS OF SCANNING TUNNELING MICROSCOPY

P. S. Weiss 10 Oct. 1993 20 p

(Contract N00014-91-J-1630)

(AD-A276066; TR-9) Avail: CASI HC A03/MF A01

Recent progress and applications of scanning tunneling microscopy and scanning tunneling spectroscopy in molecular identification are presented. In particular, the difficulties in the direct interpretation of images are elaborated. The current limitations as well as the potential of this technique are discussed. DTIC

N94-31492*# Labsphere, Inc., North Sutton, NH.

CUSTOM UNIFORM SOURCE SYSTEM Final Report

John L. Balcom 15 Feb. 1994 25 p

(Contract NAS5-32349)

(NASA-CR-189332; NAS 1.26:189332; LAB-RP-10717-1; CSTM-USS-4000) Avail: CASI HC A03/MF A01

The purpose and scope of this final report is to provide information on the Custom Uniform Source System (CSTM-USS-4000). The report includes documentation and summaries of the results for the work performed under the contract. The Annex contain laboratory test findings, photographs, and drawings of the sphere system. Author

N94-31515# Technische Univ., Darmstadt (Germany). Fachbereich Physik.

CONCEPT, CONSTRUCTION AND TESTING OF A HIGH RESOLUTION QCLAM ELECTRON SPECTROMETER WITH LARGE SOLID ANGLE AND HIGH IMPULSE ACCEPTANCE FOR THE ELECTRON ACCELERATOR S-DALINAC Ph.D. Thesis [KONZEPTION, AUFBAU UND ERPROBUNG EINES HOCHAUFLOESENDEN QCLAM-ELEKTRONENSPEKTROMETERS MIT GROSSEM RAUMWINKEL UND HOHER IMPULSAKZEPTANZ AM ELEKTRONENBESCHLEUNIGER S-DALINAC]

Martin Knirsch 1991 91 p In GERMAN

(ETN-94-95755) Avail: CASI HC A05/MF A01

A magnetic QCLAM electron spectrometer was designed, constructed, and tested for the electron accelerator S-DALINAC. It consists of a

quadrupole magnet and a dipole magnet. The solid angle is 35 mst, and energies up to 200 MeV with an impulse acceptance of +/- 10% scattering angle can be detected. The fields of quadrupole and dipole magnets were measured with Hall probes and agree within 1% of the design valves. The imaging characteristics of the spectrometer were tested using elastically scattered electrons. A method to determine the electron trajectories in the target plane was developed. The scattered electrons are measured with a detector system with three multi wire drift chambers. A shielding system was constructed to suppress the background in the detector system due to gamma rays and neutrons. ESA

N94-31629# California Univ., Berkeley. Lawrence Berkeley Lab.
PHOTOELECTRON DIFFRACTION AND HOLOGRAPHY: PRESENT STATUS AND FUTURE PROSPECTS
C. S. Fadley, S. Thevuthasan, and A. P. Kaduwela Jul. 1993 29 p Presented at the 5th International Conference on Electron Spectroscopy, Kiev, Ukraine, 26 Jul. 1 Aug. 1993
(Contract DE-AC03-76SF-00098)
(DE94-006298; LBL-35054; CONF-930764-1) Avail: CASI HC A03/MF A01

Photoelectron diffraction and photoelectron holography, a newly developed variant, can provide a rich range of information concerning surface structure. These methods are sensitive to atomic type, chemical state, and spin state. The theoretical prediction of diffraction patterns is also well developed at both the single scattering and multiple scattering levels, and quantitative fits of experiment to theory can lead to structures with accuracies in the +/-0.03 A range. Direct structural information can also be derived from forward scattering in scanned-angle measurements at higher energies, path length differences contained in scanned-energy data at lower energies, and holographic inversions of data sets spanning some region in angle and energy space. Diffraction can also affect average photoelectron emission depths. Circular dichroism in core-level emission can be fruitfully interpreted in terms of photoelectron diffraction theory, as can measurements with spin-resolved core-spectra, and studies of surface magnetic structures and phase transitions should be possible with these methods. Synchrotron radiation is a key element of fully utilizing these techniques. DOE

N94-31783# Lawrence Livermore National Lab., CA.
STELLAR X RAY POLARIMETER POLARIZER DEVELOPMENT AND CALIBRATION AT LEA/LLNL
K. Ziock, E. Silver, and M. Raffanti 1993 12 p Presented at the Annual Meeting of the Society of Photo-Optical Instrumentation Engineers, San Diego, CA, 11-16 Jul. 1993
(Contract W-7405-eng-48)
(DE94-006400; UCRL-JC-115262; CONF-930722-58) Avail: CASI HC A03/MF A01

A large area, thin graphite crystal and a lithium scattering block are used as the polarization sensitive elements of the Stellar X-Ray Polarimeter (SXRP). The authors discuss the construction, selection and characterization of these two polarizing elements. In addition, they describe the plans for calibration of the completed instrument and the facility where it will be conducted. DOE

N94-31831 Pacific Northwest Lab., Richland, WA.
MILLIMETER WAVE, HIGH-RESOLUTION, HOLOGRAPHIC SURVEILLANCE SYSTEM
D. L. McMakin, D. M. Sheen, H. D. Collins, T. E. Hall, R. R. Smith, and J. G. Droppo, Jr. 1993 12 p Presented at the International Symposium on Substance Identification Technologies, Innsbruck, Austria, 4-8 Oct. 1993 Limited Reproducibility: More than 20% of this document may be affected by microfiche quality
(Contract DE-AC06-76RL-01830)
(DE94-004269; PNL-SA-22151; CONF-9310164-8) Avail: Issuing Activity (Department of Energy (DOE))

Millimeter wave holographic imaging systems capable of imaging through clothing to detect contraband, metal, plastic, or ceramic weapons may provided a practical solution to personnel inspection needs in mass transportation centers. Traditional inspection systems, such as metal detectors and x-ray imaging systems, have limitations for the detection of concealed weapons. Metal detectors are limited because they cannot detect plastic weapons and x-ray imaging systems are limited in use due to radiological health considerations. A prototype millimeter wave holographic surveillance system has been developed and demonstrated at the Pacific Northwest Laboratory (PNL). The prototype millimeter wave holographic surveillance system developed at PNL consists of a sequentially switched 2 (times) 64 element array coupled to a 35 GHz bi-static transceiver. The sequentially switched array of antennas can be used to obtain the holographic data at high speed by electronically sequencing the antennas along one dimension and performing a mechanical scan along the other dimension. A one-dimensional mechanical scan be be performed in about one second. The prototype system scans an aperture of 0.75 by 2.05. This system has been demonstrated and images have been obtained on volunteers at Sea-Tac International airport in Seattle, Washington. DOE

N94-31929# Carnegie-Mellon Univ., Pittsburgh, PA. Dept. of Computer Science.
A PARAPERSPECTIVE FACTORIZATION METHOD FOR SHAPE AND MOTION RECOVERY
Conrad J. Poelman and Takeo Kanade 11 Dec. 1993 36 p
(Contract F33615-90-C-1465; ARPA Order 7597)
(AD-A276513; CMU-CS-93-219) Avail: CASI HC A03/MF A01

The factorization method, first developed by Tomasi and Kanade, recovers both the shape of an object and its motion from a sequence of images, using many images and tracking many feature points to obtain highly redundant feature position information. The method robustly processes the feature trajectory information using singular value decomposition (SVD), taking advantage of the linear algebraic properties of orthographic projection. However, an orthographic formulation limits the range of motions the method can accommodate. Paraperspective projection, first introduced by Ohta, is a projection model that closely approximates perspective projection by modeling several effects not modeled under orthographic projection, while retaining linear algebraic properties. Our paraperspective factorization method can be applied to a much wider range of motion scenarios, such as image sequences containing significant translational motion toward the camera or across the image. The method also can accommodate missing or uncertain tracking data, which occurs when feature points are occluded or leave the field of view. We present the results of several experiments which illustrate the method's performance in a wide range of situations, including an aerial image sequence of terrain taken from a low-altitude air plane. DTIC

N94-32002# Naval Air Warfare Center, Orlando, FL. Training Systems Div.
NIGHT VISION CAMCORDER SYSTEM Interim Report, Oct. 1992 - Oct. 1993
John H. Allen and Richard C. Hebb Oct. 1993 36 p
(DA Proj. RM-3-3-T-24)
(AD-A277004; NAWCTSD-TR-93-021) Avail: CASI HC A03/MF A01

In order to obtain night vision device imagery, a portable lightweight night vision camcorder system has been designed. This system has the capability to record night vision imagery in confined quarters (e.g., cockpits) and other remote sites under various environmental conditions. The system is composed of a commercial third generation night vision monocular, a special optical coupler, and a consumer camcorder. Engineering drawings for the optical coupler are included as an appendix. Laboratory experiments were performed to determine the night vision camcorder system imaging characteristics. The results of these experiments indicate that the limiting resolution of recorded night vision video is about 30% to 40% of the limiting resolution of the third generation monocular, depending upon the type of video filming method used. DTIC

N94-32051# Naval Surface Warfare Center, Silver Spring, MD.
PVDF PRESSURE TRANSDUCERS FOR SHOCK WAVE AND EXPLOSIVES RESEARCH
Paul Gustavson, Douglas Tasker, and Jerry Forbes 16 Feb. 1994 59 p
(AD-A277319; NAVSWC-TR-91-506) Avail: CASI HC A04/MF A01

A polyvinylidene fluoride (PVDF) piezoelectric pressure transducer is described in this report. Techniques for its use and experimental applications are described in detail. DTIC

N94-32393# Naval Air Warfare Center, China Lake, CA. Weapons Div.
WAVELET TRANSFORM OF FIXED PATTERN NOISE IN FOCAL PLANE ARRAYS Final Report

Gary A. Hewer and Wei Kuo Feb. 1994 28 p
(AD-A276963; NAWC-WPNS-TP-8185) Avail: CASI HC A03/MF A01

This report summarizes research on the infrared fixed pattern noise on a microbolometer. The report demonstrates that Daubechies wavelets filter the noise in a predictable manner and present a new approximate model for the noise, power-law shot noise. DTIC

N94-32681 Pacific Northwest Lab., Richland, WA.
ULTRA WIDE BAND RADAR HOLOGRAPHIC IMAGING OF SUBSURFACE TARGETS

H. D. Collins and R. P. Gribble Aug. 1993 8 p Presented at the 20th Annual Review of Progress in Quantitative Nondestructive Evaluation (NDE), Brunswick, ME, 1-6 Aug. 1993 Limited Reproducibility: More than 20% of this document may be affected by microfiche quality
(Contract DE-AC06-76RL-01830)
(DE94-004271; PNL-SA-22301; CONF-9308167-6) Avail: CASI HC A02

This report discusses ultra wide band (i.e., 60 ps impulse) radar holography which is a unique technique for imaging subsurface targets with extremely high lateral and depth resolution. The large frequency bandwidth, typically 100%, provides excellent depth resolution and the synthetic aperture optimum lateral resolution of one-half wavelength at the center pulse frequency. Radar impulse holography can simply be described as a multi-frequency detection and imaging technique where the target's broadband time waveform signals are recorded over a defined aperture; decomposed into their discrete frequency components as single frequency holograms, and reconstructed into a composite image. Computer generated holograms are constructed for each frequency component in the 3-dB pulse bandwidth and plane wave angular spectra computed to provide unique detection analysis with respect to target identification, etc. The hologram at each frequency component in the pulse can be thought of as a diffraction lens for each reflecting point on the target. A complex target consists, of a multitude of points, and the recorded hologram becomes the superposition of these individual diffraction lens. It is a unique diffraction pattern capable of defining the target's image and scattering characteristics in the near- and far-field. DOE

N94-32706# New Mexico State Univ., Las Cruces.
THE LOS ALAMOS NATIONAL LABORATORY PRECISION DOUBLE CRYSTAL SPECTROMETER

D. V. Morgan, C. J. Stevens, and R. J. Liefield 1994 58 p Prepared for Los Alamos National Lab., NM
(Contract W-7405-eng-36)
(DE94-008075; LA-Sub-94-39) Avail: CASI HC A04/MF A01

This report discusses the following topics on the LANL precision double crystal x ray spectrometer: motivation for construction of the instrument, a brief history of the instrument, mechanical systems, motion control systems, computer control system, vacuum system, alignment program, scan programs, observations of the copper K alpha lines, and characteristics and specifications. DOE

N94-32728# EG and G Energy Measurements, Inc., Las Vegas, NV.
A 10 GHz BANDWIDTH, SINGLE TRANSIENT, DIGITIZED OSCILLOSCOPE WITH 20 GHz CAPABILITY

C. L. Hudson (EG and G Energy Measurements, Inc., Santa Barbara, CA.), S. M. Kocimski (EG and G Energy Measurements, Inc., Santa Barbara, CA.), J. Spector (EG and G Energy Measurements, Inc., Pleasanton, CA.), J Thomas (EG and G Energy Measurements, Inc., Woburn, MA.), and R. R. Woodstra (EG and G Energy Measurements, Inc., Albuquerque, NM.) 1993 11 p Presented at the 7th Photonics Workshop, Menlo Park, CA, 4-5 Oct. 1993
(Contract DE-AC08-93NV-11265)
(DE94-005400; EGG-11265-2021; CONF-9310225-2) Avail: CASI HC A03/MF A01

EG&G/EM has developed an oscilloscope with a -3 dB bandwidth greater than 10 GHz. Its rolloff characteristics are such that single-transient data greater than 20 GHz may be captured. A demountable CCD camera records the oscilloscope trace and is provided with PC-compatible capture and data processing software. The capabilities of the oscilloscope, camera, and its processing software are described and examples of the system's performance is shown. DOE

N94-32811# Pacific Northwest Lab., Richland, WA.
PERFORMANCE OF AN ION TRAP INDUCTIVELY COUPLED PLASMA MASS SPECTROMETER

D. W. Koppenaal, C. J. Barinaga, and M. R. Smith Jan. 1994 3 p Presented at the 1994 Winter Conference on Plasma Spectrochemistry, San Diego, CA, 10-15 Jan. 1994
(Contract DE-AC06-76RL-01830)
(DE94-007470; PNL-SA-22700; CONF-940167-1) Avail: CASI HC A01/MF A01

A prototype instrument comprising an inductively coupled plasma ion source and an ion trap mass spectrometer detector has been constructed, operated, and tested for improved elemental and isotopic analysis. The rationale for this work follows from recent achievements in the ion trap mass spectrometry (ITMS) field and the realization that coupling this mass spectrometer with the powerful ICP ion source may provide distinct analytical advantages. Potential benefits could include increased sensitivity (resulting from analyte ion isolation and subsequent detection against a dark background), atomic isobar resolution (extremely high ITMS resolution has been demonstrated), destruction of polyatomic interferences (via collisional dissociation or in-trap chemistry), and size reduction of instrumentation. Derived from text

N94-32821# Brookhaven National Lab., Upton, NY.
IONIZATION EM CALORIMETRY WITH ACCORDION ELECTRODES AND LIQUID KRYPTON OR ARGON

V. Radeka Nov. 1993 14 p Presented at the 4th International Conference on Calorimetry in High-Energy Physics, Elba, Italy, 19-25 Sep. 1993
(Contract DE-AC02-76CH-00016)
(DE94-009082; BNL-49806; CONF-9309166-4) Avail: CASI HC A03/MF A01

The results of a study and tests of a liquid krypton/argon electromagnetic calorimeter with accordion electrode structure are briefly summarized. This includes the calorimeter response to electrons and muons, energy, pointing and timing resolution, and a measurement by multiple sampling. The electrode layout with fine segmentation is illustrated. DOE

N94-32983*# National Aeronautics and Space Administration. Lewis Research Center, Cleveland, OH.
STABILIZED ALUMINA/ETHANOL COLLOIDAL DISPERSION FOR SEEDING HIGH TEMPERATURE AIR FLOWS

Judith H. Wernet and Mark P. Wernet May 1994 10 p Proposed for presentation at the Symposium on Laser Anemometry: Advances and Applications, Lake Tahoe, NV, 19-23 Jun. 1994; sponsored by ASME
(RTOP 505-62-50)
(NASA-TM-106591; E-8858; NAS 1.15:106591) Avail: CASI HC A02/MF A01

Seeding air flows with particles to enable measurements of gas velocities via laser anemometry and/or particle image velocimetry techniques can be quite exasperating. The seeding requirements are compounded when high temperature environments are encountered and special care must be used in selecting a refractory seed material. The pH stabilization techniques commonly employed in ceramic processing are used to obtain stable dispersions for generating aerosols of refractory seed material. By adding submicron alumina particles to a preadjusted pH solution of ethanol, a stable dispersion is obtained which when atomized produces a high quality aerosol. Commercial grade alumina powder is used with a moderate size distribution. The technique is not limited to alumina/ethanol and is also demonstrated with an alumina/H2O system. Other ceramic powders in various polar solvents could also be used once the point of zero charge (pH(sub pzc)) of the powder in the solvent has been determined. Author

N94-32459*# National Aeronautics and Space Administration. Goddard Space Flight Center, Greenbelt, MD.
A NEW HIGH-SPEED IR CAMERA SYSTEM

Jeffrey W. Travis, Peter K. Shu, Murzy D. Jhabvala, Michael S. Kasten, Samuel H. Moseley, Sean C. Casey, Lawrence K. McGovern, Philip J. Luers, Philip W. Dabney, and Ravi C. Kaipa et al *In* NASA, Washington, Technology 2003: The Fourth National Technology Transfer Conference and Exposition, Volume 2 Feb. 1994 p 332-341 (For primary document see N94-32420 09-99)
Avail: CASI HC A02/MF A04

N94-32470*# Jet Propulsion Lab., California Inst. of Tech., Pasadena.
THE TRUSTWORTHY DIGITAL CAMERA: RESTORING CREDIBILITY TO THE PHOTOGRAPHIC IMAGE
Gary L. Friedman *In* NASA, Washington, Technology 2003: The Fourth National Technology Transfer Conference and Exposition, Volume 2 Feb. 1994 p 430-435 (For primary document see N94-32420 09-99)
Avail: CASI HC A02/MF A04

36 LASERS AND MASERS

Includes parametric amplifiers.
For related information see also *76 Solid-State Physics.*

N94-31148# Sandia National Labs., Albuquerque, NM.
TRANSIENT RADIATION-INDUCED ABSORPTION IN THE MATERIALS FOR A GSGG LASER
P. J. Brannon Nov. 1993 25 p
(Contract DE-AC04-94AL-85000)
(DE94-005316; SAND-93-2417) Avail: CASI HC A03/MF A01

Materials used in the optical elements of a 1,061 m GSGG (gadolinium scandium gallium garnet) laser have been tested for transient radiation-induced absorption. The transient radiation-induced absorption in KK1, Schott S7005 and S7010, and M382 glasses have been determined for discrete wavelengths in the range 440-750 nm. Also, the transient radiation-induced absorption in 'pure' and MgO doped LiNbO3 has been measured at 1,061 nm. Mathematical expressions composed of exponentials are fitted to the data. DOE

N94-31200# Colorado Univ., Boulder.
NEAR RESONANT ABSORPTION BY ATOMS IN INTENSE FLUCTUATING LASER FIELDS
S. J. Smith Jan. 1994 26 p
(Contract DE-FG02-85ER-13421)
(DE94-005873; DOE/ER-13421/10) Avail: CASI HC A03/MF A01

The objective of this program was to make quantitative measurements of the effects of higher-order phase/frequency correlations in a laser beam on nonlinear optical absorption processes in atoms. The success of this program was due in large part to a unique experimental capability for modulating the extracavity beam of a stabilized (approximately less than 200 kHz) continuous-wave laser with statistically-well-characterized stochastic phase (or frequency) fluctuations, in order to synthesize laser bandwidths to approximately 20 MHz (depending on noise amplitude), with profiles variable between Gaussian and Lorentzian (depending on noise bandwidth). Laser driven processes investigated included the following: (1) the optical Autler-Towns effect in the 3S(sub 1/2) (F = 2, M(sub F) = 2) yields 3P(sub 3/2) (F = 3, M(sub F) = 3) two-level Na resonance, using a weak probe to the 4D(sub 5/2) level; (2) the variance and spectra of fluorescence intensity fluctuations in the two-level Na resonance; (3) the Hanle effect in the (sup 1)S(sub 0) - (sup 3)P(sub 1), transition at lambda = 555.6 nm in Yb-174; (4) absorption (and gain) of a weak probe, when the probe is a time-delayed replica of the resonant (with the two-level Na transition) pump laser; and (5) four-wave-mixing in a phase-conjugate geometry, in a sodium cell, and, finally, in a diffuse atomic sodium beam. The experimental results from these several studies have provided important confirmation of advanced theoretical methods. DOE

N94-31255 Defence Research Establishment, Ottawa (Ontario).
LASER SAFETY MANUAL FOR DREO
N. Brousseau Nov. 1993 17 p Limited Reproducibility: More than 20% of this document may be affected by microfiche quality
(AD-A276288; DREO-TN-93-36) Avail: CASI HC A03

This document contains the information and regulations needed to establish a safe working environment in research laboratories where laser radiation is used. It is based on the American National Standard for the Safe Use of Lasers (ANSI Z136.1-1986) and it contains additional provisions for medical surveillance to protect the Department of National Defence from damage claims. DTIC

N94-31269# Lawrence Livermore National Lab., CA.
THE ROLE OF DEFECTS IN LASER DAMAGE OF MULTILAYER COATINGS
M. R. Kozlowski and R. Chow 21 Dec. 1993 9 p Presented at the 25th Boulder Damage Symposium: Annual Symposium on Optical Materials for High-Power Lasers, Boulder, CO, 27-29 Oct. 1993
(Contract W-7405-eng-48)
(DE94-006731; UCRL-JC-113493; CONF-931054-7) Avail: CASI HC A02/MF A01

Laser induced damage to optical coatings is generally a localized phenomenon associated with coating defects. The most common of the defect types are the well-known nodule defect. This paper reviews the use of experiments and modeling to understand the formation of these defects and their interaction with laser light. Of particular interest are efforts to identify which defects are most susceptible to laser damage. Also discussed are possible methods for stabilizing these defects (laser conditioning) or preventing their initiation (source stabilization, spatter particle trapping). DOE

N94-31278# Stanford Univ., CA. Edward L Ginzton Lab. of Physics.
HIGH-POWER CW DIODE-LASER-ARRAY-PUMPED SOLID-STATE LASERS AND EFFICIENT NONLINEAR OPTICAL FREQUENCY CONVERSION Final Report, 20 Sep. 1990 - 30 Sep. 1993
Robert L. Byer 29 Dec. 1993 53 p
(Contract DAAL03-90-C-0026)
(AD-A276126; GL-5129; ARO-28348.4-PH-A) Avail: CASI HC A04/MF A01

During the past three years we have made substantial progress toward the goal of a fiber coupled, diode laser pumped 100W cw Nd:YAG minislab laser. We have diode pumped a 1W ring cavity laser and have operated it in a single frequency. We have diode pumped a testbed minislab Nd:YAG laser using fiber coupled diode laser bars and generated 5W of cw, TEMoo mode output power. We have designed and are implementing a 50W cw minislab Nd:YAG laser to be pumped by 25 diode laser bars coupled through optical fibers. We plan, in the second phase of this program, to achieve the 100W cw output power level in a minislab Nd:YAG laser approach proposed as the goal of this research program. In addition, we have demonstrated single frequency control of a high power Nd:YAG laser oscillator by injection locking; have frequency stabilized Nd:YAG oscillators by locking to high finesse Fabry Perot resonators; have absolutely stabilized Nd:YAG to one part in 10 to the -13th power by locking to iodine; have frequency converted Nd:YAG by second harmonic generation to 11.2W of cw TEMoo mode green output; have demonstrated the first cw 2 microns OPO in lithium niobate; and have demonstrated the first cw singly resonant OPO with 2W of output in a single frequency in KTP. DTIC

N94-31358# Stanford Univ., CA. Physics Lab.
NEW MATERIAL FOR HIGH AVERAGE POWER INFRARED GENERATION: QPM-DB GaAs Technical Report, 1 Sep. 1992 - 30 Nov. 1993
Robert L. Byer 13 Jan. 1994 32 p
(Contract DAAL03-92-G-0400)
(AD-A276389; SU-GL-5133; ARO-30708.2-PH) Avail: CASI HC A03/MF A01

We are investigating quasi-phase-matched diffusion-bonded (QPM-DB) GaAs for nonlinear infrared applications. We have fabricated diffusion-bonded stacks of up to nine layers, which we have used to demonstrate quasi-phase-matched second-harmonic generation pumped by 10.6-micrometers CO2 laser output. Preliminary optical damage tests of diffusion-bonded-stacked GaAs indicate a power handling capability in excess of other currently available nonlinear infrared materials. Numerical calculations modeling nonlinear frequency conversion and projectioned device performance are included in this report. DTIC

N94-31472 Alberta Univ., Edmonton.
AUTOMATIC RESONATOR ALIGNMENT AND POWER STABILIZATION OF HIGH POWER C02 LASERS Ph.D. Thesis
Dale Richard Akitt 1992 221 p
(ISBN-0-315-77217-4) Avail: Univ. Microfilms Order No. DANN77217

The high power carbon dioxide laser has become a very important tool in the area of industrial materials processing. This is due primarily to the enormous optical intensities which the device can attain. Unfortunately, it has proved increasingly difficult to construct machines capable of maintaining a consistently uniform output beam at elevated power levels, for extended periods. These difficulties are often attributed to thermal

distortion of the resonator optics. Because of this fact, researchers have invested considerable effort in the construction of water cooled, thermally stable optical benches, upon which to mount the resonator components. This approach is very expensive, and has provided only a partial solution to the problem. A different approach, and the subject of this thesis, is to construct a feedback control system which actively repositions the optical elements, so as to maintain optimum resonator alignment. Preliminary experiments demonstrated that this concept was indeed feasible. In this first study, a circular array of small thermistors was utilized as the feedback element. Indicators of mode uniformity in the vertical and horizontal directions were extracted from the array using electronic techniques. A relay type controller monitored these error measures and subsequently activated a pair of motor-micrometers fitted to one of the primary resonator mirrors. Although this thermistor-based system demonstrated the viability of the concept, the sensor array's slow response limited its performance. Subsequent experiments utilizing high speed pyroelectric detectors in place of the thermistors solved the problem. The next series of experiments was dedicated to finding a method of simultaneously aligning both primary resonator mirrors. This was accomplished by configuring the sensor array to monitor not only beam uniformity, but also beam position. A new controller was then developed which adjusted one mirror based on the position of the output beam, while the second mirror was employed to continuously maintain mode uniformity. This 'two mirror' control system has demonstrated the ability to consistently maintain optimum resonator alignment for indefinite periods, at arbitrary power levels up to 10 kW. Dissert. Abstr.

N94-31485# Sandia National Labs., Albuquerque, NM.
DOE REACTOR-PUMPED LASER PROGRAM
J. R. Felty (Department of Energy, Germantown, MD.), R. J. Lipinski, D. A. McArthur, and P. S. Pickard 1993 8 p Presented at the OE/LASE 1994 Conference on Optics, Electro-Optics, and Laser Applications in Science and Engineering, Los Angeles, CA, 22-29 Jan. 1994
(Contract DE-AC04-94AL-85000)
(DE94-006372; SAND-93-2719C; CONF-940142-11) Avail: CASI HC A02/MF A01

FALCON is a high power, steady state, nuclear reactor-pumped laser (RPL) concept that is being developed by the Department of Energy. The FALCON program has experimentally demonstrated reactor-pumped lasing in various mixtures of xenon, argon, neon, and helium at wavelengths of 585, 703, 725, 1271, 1733, 1792, 2032, 2630, 2650, and 3370 nm with intrinsic efficiency as high as 2.5 percent. The major strengths of a reactor-pumped laser are continuous high-power operation, modular construction, self-contained power, compact size, and a variety of wavelengths (from visible to infrared). These characteristics suggest numerous applications not easily accessible to other laser types. A ground-based RPL could beam its power to space for such activities as illuminating geosynchronous communication satellites in the earth's shadow to extend their lives, beaming power to orbital transfer vehicles, removing space debris, and providing power to a lunar base during the long lunar night. The compact size and self-contained power also makes an RPL very suitable for ship basing so that power-beaming activities could be situated around the globe. The continuous high power of an RPL opens many potential manufacturing applications such as deep-penetration welding and cutting of thick structures, wide-area hardening of metal surfaces by heat treatment or cladding application, wide-area vapor deposition of ceramics onto metal surfaces, production of submicron sized particles for manufacturing of ceramics, wide-area deposition of diamond-like coatings, and three dimensional ceramic lithography. DOE

N94-31532# Vrije Univ., Amsterdam (Netherlands).
TRANSVERSE MODE ANALYSIS OF HOLE-COUPLED FREE-ELECTRON LASERS Ph.D. Thesis
Bart Faatz 1992 122 p Sponsored by Netherlands Organization for Scientific Research, and Euratom
(ETN-94-96019) Avail: CASI HC A06/MF A02

The influence of the aperture on the Free Electron Laser (FEL) intracavity mode structure was investigated. Both the influence of the electron beam and of the resonator geometry are investigated, with emphasis on the latter. The basic equations describing the interaction between the electrons and the combined undulator and radiation fields are derived. A Three Dimensional Axisymmetric (TDA) code was extended to allow multiple passes of the light wave in a resonator geometry including apertures in one or both mirrors. To determine the influence of the aperture on the mode structure, simulations were performed in a resonator including the gain medium but without aperture. The same resonator generators were investigated including an aperture in the upstream mirror. The FELIX (FEL for Infrared eXperiments project) geometry and beam parameters are used to simulate the first experiments with FELIX. ESA

N94-31545# Vrije Univ., Amsterdam (Netherlands).
FREE ELECTRONS AS A VERSATILE SOURCE OF COHERENT RADIATION Ph.D. Thesis
Rene Johan Bakker 1993 119 p Sponsored by Netherlands Organization for Scientific Research Prepared in cooperation with FOM-Inst. voor Plasmafysica
(ETN-94-96011) Avail: CASI HC A06/MF A02

The construction of the Free Electron Laser (FEL) for Infrared experiments (FELIX) user facility is addressed. The objectives for this project were to construct an FEL, capable of producing high power short pulse radiation, continuously and rapidly tunable from 8 to 80 micrometers. Additionally, an optional phase locking scheme was designed in order to obtain narrow bandwidth radiation, that is, radiation with a bandwidth equal to a single longitudinal cavity mode. At present, FELIX covers the wavelength range from 6.5 to 110 micrometers. It is argued that the design objectives can be obtained with a high quality (for example, low energy spread) electron beam consisting of high current short pulse electron bunches. With FELIX, the electron beam consists of 5 ps long electron bunches (full width) with a current up to 60 A. The beam energy ranges from 15 to 45 MeV. The performance of the system producing this electron beam is discussed. It consists of a thermionic gun, a prebuncher, a buncher, and two standard commercial linac sections. The gun is modulated at 1 GHz in order to obtain bunches with a duration of 280 ps. After compression to 35 ps by the prebuncher, the bunches are accelerated to 3.8 MeV in the buncher and simultaneously compressed to 6 ps. Further compression is obtained in the first linac. The performance of the system is more than adequate, for example a root mean square energy spread of 0.3 behind the RF linac. The selection of narrow band radiation, which is useful for high resolution spectroscopy applications from the output of FELIX, is presented. ESA

N94-31561# Technische Univ., Darmstadt (Germany). Fachbereich Physik.
TIME EVOLUTION AND FILAMENTATION OF KrF(STAR) LASER GAS DISCHARGES Ph.D. Thesis [ZEITLICHE ENTWICKLUNG UND FILAMENTIERUNG VON KRF(STAR)-LASERGASENTLADUNGEN]
Thomas Mueller 1992 150 p In GERMAN Sponsored by BMFT
(ETN-94-95758) Avail: CASI HC A07/MF A02

Independent KrF(star) high pressure laser gas discharges were theoretically and experimentally investigated. An analytic discharge model was developed for the homogeneous phase of the discharge, starting from a Maxwellian velocity distribution of the electron component. The model was experimentally tested by measurements of the small signal amplification as well as the ignition and burn voltage on a short duration spark preionized excimer laser. Calculations and experiments show that the magnitude of perturbations and the time constant of their development strongly depend on the laser gas composition. The results are especially important for the extension of the laser pulse which is the first step towards an improvement of the beam quality. ESA

N94-31580# Lawrence Livermore National Lab., CA.
TWO-GIGAWATT BURST-MODE OPERATION OF THE INTENSE MICROWAVE PROTOTYPE (IMP) FREE-ELECTRON LASER (FEL) FOR THE MICROWAVE TOKAMAK EXPERIMENT (MTX)
B. Felker, S. Allen, H. Bell, J. Bowman, M. Delong, M. Fenstermacher, S. W. Ferguson, W. F. Fields, IV, D. Hathaway, and E. B. Hooper et al Oct. 1993 6 p Presented at the Symposium on Fusion Engineering, Hyannis, MA, 11-15 Oct. 1993
(Contract W-7405-eng-48)
(DE94-006613; UCRL-JC-114260; CONF-931018-83) Avail: CASI HC A02/MF A01

The MTX explored the plasma heating effects of 140 GHz microwaves from both gyrotrons and from the IMP FEL wiggler. The gyrotron was long pulse length (0.5 seconds maximum) and the FEL produced short pulse length, high peak power, single and burst modes of 140 GHz microwaves.

Full-power operations of the IMP FEL wiggler were commenced in April 1992 and continued into October 1992. The Experimental Test Accelerator 2 (ETA-2) provided a 50-nanosecond, 6-MeV, 2 to 3 k-Amp electron beam that was introduced colinear into the IMP FEL with a 140 GHz gyrotron master oscillator (MO). The FEL was able to amplify the MO signal from approximately 7 kW to peaks consistently in the range of 1 to 2 GW. This microwave pulse was transmitted into the MTX and allowed the exploration of the linear and nonlinear effects of short pulse, intense power in the MTX plasma. Single pulses were used to explore and gain operating experience in the parameter space of the IMP FEL, and finally evaluate transmission and absorption in the MTX. Single-pulse operations were repeatable. After the MTX was shut down burst-mode operations were successful at 2 kHz. This paper describes the IMP FEL, microwave transmission system to MTX, the diagnostics used for calorimetric measurements, and the operations of the entire microwave system. A discussion of correlated and uncorrelated errors that affect FEL performance is made. Linear and nonlinear absorption data of the microwaves in the MTX plasma is presented. DOE

N94-31599# Lawrence Livermore National Lab., CA.
USING LASER ABSORPTION SPECTROSCOPY TO MONITOR COMPOSITION AND PHYSICAL PROPERTIES OF METAL VAPORS
L. V. Berzins 3 Sep. 1993 14 p Presented at the Society of Photo-Optical Instrumentation Engineer's (SPIE) International Symposium on Optical Tools for Manufacturing and Advanced Automation, Boston, MA, 7-10 Sep. 1993
(Contract W-7405-eng-48)
(DE94-001530; UCRL-JC-112979; CONF-9309199-8) Avail: CASI HC A03/MF A01

The Atomic Vapor Laser Isotope Separation (AVLIS) program has been using laser absorption spectroscopy to monitor vapor densities for over 15 years. Laser absorption spectroscopy has proven itself to be an accurate and reliable method to monitor both density and composition. During this time the diagnostic has moved from a research tool toward a robust component of a process control system. The hardware used for this diagnostic is discussed elsewhere at this symposium. This paper describes how the laser absorption spectroscopy diagnostic is used as a component of a process control system as well as supplying detailed measurements on vapor densities, composition, flow velocity, internal and kinetic temperatures, and constituent distributions. Examples will be drawn from the uranium AVLIS program. In addition, potential applications such as composition control in the production of metal matrix composites or aircraft alloys will be discussed. DOE

N94-31622# Sandia National Labs., Albuquerque, NM.
SEMICONDUCTOR MICROCAVITY LASERS
P. L. Gourley, J. R. Wendt, G. A. Vawter, M. E. Warren, T. M. Brennan, and B. E. Hammons 1994 15 p Presented at the International Symposium on Optoelectronic and Microwave Engineering, Los Angeles, CA, 22-28 Jan. 1994
(Contract DE-AC04-94AL-85000)
(DE94-006143; SAND-94-0147C; CONF-940114-2) Avail: CASI HC A03/MF A01

New kinds of semiconductor microcavity lasers are being created by modern semiconductor technologies like molecular beam epitaxy and electron beam lithography. These new microcavities exploit 3-dimensional architectures possible with epitaxial layering and surface patterning. The physical properties of these microcavities are intimately related to the geometry imposed on the semiconductor materials. Among these microcavities are surface-emitting structures which have many useful properties for commercial purposes. This paper reviews the basic physics of these microstructured lasers. DOE

N94-31624# Los Alamos National Lab., NM.
DIAGNOSTICS OF HIGH-BRIGHTNESS SHORT-PULSE LASERS AND THE PLASMAS THEY GENERATE
G. A. Kyrala, R. D. Fulton, J. A. Cobble, G. T. Schappert, and A. J. Taylor 1994 13 p Presented at the OE/LASE 1994: Conference on Optics, Electro-Optics, and Laser Applications in Science and Engineering, Los Angeles, CA, 22-29 Jan. 1994
(Contract W-7405-eng-36)
(DE94-006165; LA-UR-94-271; CONF-940142-3) Avail: CASI HC A03/MF A01

The properties of a laser influence the interaction of the intense laser light with materials. The authors will describe some of the diagnostics that they have implemented at the Los Alamos Bright Source to correlate the changes in the x-ray spectrum and temporal history of a laser generated silicon plasmas with the changes of the incident XeCl laser light. One property is of special interest, the existence of a short prepulse. They find that the prepulse enhances the generation of the x-rays from a later pulse. DOE

N94-31636# Lawrence Livermore National Lab., CA.
LARGE-AREA CONDITIONING OF OPTICS FOR HIGH-POWER LASER SYSTEMS
L. M. Sheehan, M. R. Kozlowski, F. Rainer, and M. C. Staggs 21 Dec. 1993 10 p Presented at the 25th Boulder Damage Symposium: Annual Symposium on Optical Materials for High-Power Lasers, Boulder, CO, 27-29 Oct. 1993
(Contract W-7405-eng-48)
(DE94-007028; UCRL-JC-114998; CONF-931054-8) Avail: CASI HC A02/MF A01

In order to reach the high fluence goals of the Beamlet laser at Lawrence Livermore National Laboratory (LLNL), the polarizers in the system must be laser conditioned to increase their damage thresholds. Research has shown that by using a six-step raster conditioning program, the damage thresholds of the HfO2/SiO2 multilayer polarizer coatings can be increased to meet the Beamlet 3-ns design goal of 8 J/cm(exp 2). Because of the large size of the polarizers (73 cm by 37 cm by 9 cm), a large-area conditioning facility was constructed capable of rastering a one-meter optic, weighing as much as 400 pounds, at any specified use angle. A large translational stage moves the optic in a raster pattern through a stationary, 10-Hz rep-rated, 1064-nm beam with 10-ns pulses. A scatter measurement diagnostic allows on-the-fly evaluation of laser induced damage and logs the coordinates of the damage. Laser energy is measured pulse-to-pulse in order to ensure stability during a scan. A small amount of minor coating damage does occur during the process, but the damage does not grow upon further irradiation. This damage causes only a small increase in total scatter compared to that due to the preexisting defects, and would not influence the system performance. DOE

N94-31748# Laval Univ. (Quebec). Faculte des Sciences et de Genie Physique.
STUDY OF THE DYNAMICS OF A NONLINEAR COUPLED-CAVITY LASER SYSTEM M.S. Thesis [ETUDE DE LA DYNAMIQUE D'UN SYSTEME LASER A CAVITE COUPLEE NON LINEAIRE]
Francois Martin Jul. 1993 100 p In FRENCH
(ISBN-0-315-86717-5; CTN-94-61225) Copyright Avail: Micromedia Ltd., Technical Information Centre, 240 Catherine Street, Suite 305, Ottawa, Ontario, K2P 2G8, Canada HC/MF

A study was conducted with the objective of demonstrating the possibility of generating ultrashort pulses by coupling a nonlinear Fabry-Perot interferometer with a continuous Nd-YAG laser. It is shown that the response of a nonlinear Fabry-Perot interferometer can become complex if the incident intensity is sufficiently high. In effect, it is possible to observe bistable or chaotic behavior, phenomena which are not yet treated in the literature on cavity lasers coupled to a nonlinear interferometer. An analysis is then presented of the dynamics of coupling between a cavity laser and interferometer. The analysis takes into account such concepts as the time for establishing a synchronized mode regime and the nonlinearity level to be exceeded for operating the laser system in the synchronized mode regime or the commutation regime. Different experimental configurations are studied, and a proposal is finally developed for a final configuration which should generate a continuous train of short pulses. CISTI

N94-31797# Montreal Univ. (Quebec). Dept. de Genie Electronique et de Genie Informatique.
ALGORITHMS AND PARALLEL ARCHITECTURES FOR LASER ACOUSTIC IMAGING M.S. Thesis [ALGORITHMES ET ARCHITECTURES PARALLELES POUR IMAGERIE ACOUSTIQUE LASER]
Hakim Khali Mar. 1993 107 p In FRENCH

(ISBN-0-315-86466-4; CTN-94-61200) Copyright Avail: Micromedia Ltd., Technical Information Centre, 240 Catherine Street, Suite 305, Ottawa, Ontario, K2P 2G8, Canada HC/MF

In many signal processing applications, the required information is usually found in the frequency contents of the signals to be analyzed. In most cases, Fourier transforms are used for the analysis, but this kind of transform is unable to provide temporal information. This problem can be overcome by using time-frequency transforms. A study is presented of a particular time-frequency transform called the wavelet transform, which is used as a basic tool in the design of a monitor for nondestructive testing. The instrument must be able to detect defects in materials and determine their positions. The algorithms used in the study are described, and three approaches are developed and implemented: vector processing, parallel processing, and special purpose very large scale integration architectures. Models were built and simulated, and it is shown that this work can be integrated in a high-level synthesis tool for special purpose signal processing architectures. Author (CISTI)

N94-31840 Norges Tekniske Hoegskole, Trondheim.
LASER APPLICATIONS IN WOOD PROCESSING
B. M. Broenstad, N. Auman, and K. Toennessen 27 Aug. 1993 11 p Presented at the Fourth NOLAMP Conference, Soenderborg, Norway, Aug. 1993 Prepared in cooperation with Selskapet for Industriell og Teknisk Forskning, Trondheim, Norway
(PB94-138567; ISBN-82-595-7449-7) Avail: Issuing Activity (National Technical Information Service (NTIS))

Lasers have been used for special woodprocessing purposes for more than twenty years. Besides dieboard manufacturing, which was one of the earliest applications, CO2 lasers are also used for different cutting, marking and engraving operations. High quality slots in varying depths are produced in wood and different plywood materials at high cutting speeds and with excellent accuracy. Decorative marking operations are performed by means of masking techniques, or by moving a defocused beam over the workpiece. Formerly collected and stored data is directly used for laser cutting of card-board and 3D map modeling. Examples of products are shown, processing data given and limitations discussed. NTIS

N94-31936# Naval Research Lab., Washington, DC.
METHODS FOR SBS THRESHOLD REDUCTION Final Report
A. M. Scott (Defence Research Agency, Malvern, England.), W. T. Whitney, and M. T. Duignan 30 Jan. 1994 59 p
(AD-A276554; NRL/FR/5640-94-9704) Avail: CASI HC A04/MF A01

We have investigated methods for reducing the threshold for stimulated Brillouin scattering (SBS) using a frequency-narrowed Cr,Tm,Ho:YAG laser operating at 2.12 micrometers. The SBS medium was carbon disulfide. Single-focus SBS and threshold reduction by using two foci, a loop, and a ring have been demonstrated. Theories for the loop-SBS and the ring-SBS geometries have been developed and compared with experimental results. Backscatter power, energy, and conjugate fidelity data are presented. DTIC

N94-31996 Loughborough Univ. of Technology (England).
MECHANISMS OF LASER INDUCED REACTIONS IN OPAQUE HETEROGENEOUS ENVIRONMENTS Final Report
F. Wilkinson Nov. 1993 209 p Limited Reproducibility: More than 20% of this document may be affected by microfiche quality
(Contract DAJA45-90-C-0022)
(AD-A276642; R/D-6294-CH-01) Avail: CASI HC A10

The technique of laser flash photolysis has been applied to both heterogeneous and homogeneous samples in order to increase understanding of the mechanisms of laser induced reactions at surfaces. Nanosecond diffuse reflectance laser flash photolysis has been used to study triplet state absorption and fluorescence emission of monomers and dimers of acridine orange and other dyes which are shown to aggregate when adsorbed on microcrystalline cellulose and on other surfaces. The properties of excited states within dyed fabrics have been evaluated in several cases. The mechanism of the yellowing of thermomechanical paper pulp has also been investigated and transients studied on nanosecond timescales for the first time. Triplet-triplet energy transfer from benzophenone to oxazine dyes, from eosin to anthracene, and from anthracene to azomethine dyes has been studied on both cellulose and silica surfaces. This work demonstrates the occurrence of energy transfer by static and dynamic mechanisms depending on both the nature of the surface and the adsorbed species. The first picosecond studies exciting directly into the charge transfer absorption bands of aromatic hydrocarbon/oxygen complexes formed in the presence of high pressures of oxygen have been carried out to demonstrate the role of charge-transfer interactions in determining the singlet oxygen formation efficiencies during quenching of electronically excited states by molecular oxygen. Nanosecond laser excitation of a series of naphthalene and anthracene derivatives in the presence and absence of oxygen has clearly demonstrated for the first time the importance of charge transfer interactions in determining oxygen quenching constants and singlet oxygen formation efficiencies. DTIC

N94-32128# Lawrence Livermore National Lab., CA.
IMPACT OF OBSERVED HYPERFINE SPLITTING ON X-RAY LASER GAIN
J. Nilsen, J. A. Koch, J. H. Scofield, B. J. MacGowan, J. C. Moreno, and L. B. DaSilva Nov. 1993 6 p Presented at the 9th American Physical Society (APS) Topical Conference on Atomic Processes in Plasmas, San Antonio, TX, 15 Nov. 1993
(Contract W-7405-eng-48)
(DE94-005822; UCRL-JC-114568; CONF-9311168-1) Avail: CASI HC A02/MF A01

Line broadening mechanisms play an important role in determining the gain of X-ray laser transitions. Typically Doppler broadening is the primary mechanism which determines the linewidth of these transitions. However, the authors present cases where the hyperfine effect is the dominant line broadening mechanism. Studying laser lines, which tend to have gain narrowed linewidths, enables one to observe these dramatic hyperfine effects which would be difficult to observe in opacity or Stark broadened lines. In this work the authors report the observation of hyperfine splitting on an X-ray laser transition and discuss how hyperfine splitting has a major impact on the laser gain. In the experiments they measure the lineshape of the 3p to 3s, J = 0 to 1 transition in neon-like niobium and zirconium and observe a 28 m-angstrom splitting between the two largest hyperfine components in the niobium(Z=41) line at 145.9 angstroms, in good agreement with theory. In zirconium(Z=40), no splitting is observed since the hyperfine effect is proportional to the nuclear moment, and zirconium has zero nuclear moment, as is typical for even-Z elements. The hyperfine effect is shown to effect transitions which have a 2p(sub 1/2) vacancy in the closed neon-like core much more than those with a 2p(sub 3/2) vacancy. A comparison of the neon-like niobium laser spectrum with that of zirconium shows a dramatic reduction in the relative intensity of the niobium laser lines with the 2p(sub 1/2) vacancy. The authors also report the unusual behavior noticed recently in low-Z neon-like X-ray lasers in which ions with odd Z lase poorly, if at all, relative to ions with even Z. The hyperfine effect is shown to have a substantial impact on the gain of the low-Z and helps explain their poor performance. DOE

N94-32134# Sandia National Labs., Albuquerque, NM.
HIGH CONVERSION EFFICIENCY PUMPED-CAVITY SECOND HARMONIC GENERATION OF A DIODE LASER
D. M. Keicher Jan. 1994 114 p
(Contract DE-AC04-94AL-85000)
(DE94-006805; SAND-93-0909) Avail: CASI HC A06/MF A02

To investigate the feasibility of producing a compact, efficient blue laser source, pumped-cavity second harmonic generation of diode lasers was explored. It is desirable to have such lasers to increase optical disk storage density, for color displays and for under-the-sea green-blue optical signal transmission. Based on assumed cavity losses, a cavity was designed and numerical analysis predicted an overall conversion efficiency to the second harmonic wavelength of 76% from a 75 mW diode laser. The diode laser used in these experiments had a single longitudinal and a single transverse mode output at 860 nm. The best conversion efficiency obtained (26%) was less than optimum due to the 2.5% single-pass linear losses associated with the cavity. However, calculations based on these higher losses are in good agreement with the experimentally determined values. In addition, a factor of 1.65 increase in the second harmonic output power is anticipated by reducing the input mirror reflectivity to better impedance-match the cavity. With this relatively low second harmonic conversion, the power to light conversion is 7.8%. DOE

N94-32202# General Atomic Co., San Diego, CA. RF Physics and Technology Div.

FUSION APPLICATIONS OF HIGH POWER MILLIMETER WAVE SOURCES

R. L. Freeman and T. V. George Jan. 1994 2 p Presented at the International Conference on Millimeter and Submillimeter Waves, San Diego, CA, 10-14 Jan. 1994

(Contract DE-AC03-89ER-52153)

(DE94-007374; GA-A-21517; CONF-940132-1) Avail: CASI HC A01/MF A01

Heating by means of high power electron cyclotron (EC) waves in the mm wavelength range is considered to be one of the most attractive approaches for heating fusion plasmas to the temperatures required to achieve ignition. EC waves have also been used to drive plasma current by using directional launch and to stabilize MHD instabilities in tokamak plasmas through localized heating or current drive. Experiments are planned on both JET and TFTR to measure the alpha particle distribution by scattering EC waves. DOE

N94-32252# Lawrence Livermore National Lab., CA.

SOL-GEL COATINGS FOR HIGH POWER LASER OPTICS: PAST, PRESENT, AND FUTURE

I. M. Thomas 21 Dec. 1993 11 p Presented at the 25th Boulder Damage Symposium: Annual Symposium on Optical Materials for High-Power Lasers, Boulder, CO, 27-29 Oct. 1993

(Contract W-7405-eng-48)

(DE94-007240; UCRL-JC-115120; CONF-931054-9) Avail: CASI HC A03/MF A01

An investigation into the preparation of sol-gel coatings for high power lasers was started at LLNL in 1983 and AR coatings were successfully developed for use in the Nova laser in 1984. Several other large lasers now use these coatings. Subsequent work on HR coatings resulted in AlOOH/SiO2 and later ZrO2 or HfO2/SiO2 systems of good optical performance. The use of organic polymer binders gave increased damage threshold and enhanced optical performance. We are in the process of scaling up HR fabrication for substrates approximately 38 cm square. Concurrently we are developing sol-gel random phase plates for laser beam smoothing. These have a patterned surface design of silica which induces phase shifts in the beam by variation in the optical path length. Plates of this type on 80 cm diameter substrates have been used successfully on the Nova. DOE

N94-32270# Los Alamos National Lab., NM.

TI:SAPPHIRE BASED ULTRAFAST PUMP-PROBE LASER SOURCE IN THE VIOLET AND ULTRAVIOLET

G. Rodriguez, J. P. Roberts, and A. J. Taylor 1994 10 p Presented at the OE/LASE 1994: Conference on Optics, Electro-Optics, and Laser Applications in Science and Engineering, Los Angeles, CA, 22-29 Jan. 1994

(Contract W-7405-eng-36)

(DE94-007542; LA-UR-94-502; CONF-940142-26) Avail: CASI HC A02/MF A01

Frequency conversion of an ultrafast 810 nm Ti:sapphire laser has produced 15 mJ, 165-fs pulses at 405 nm with an energy conversion efficiency of 35%. Upon tripling the fundamental to 270 nm, an energy of 0.8 mJ is obtained. Unconverted to 405-nm light is used to generate an ultrafast supercontinuum in water that extends from 200 nm to 600 nm. The system operates at a 5 Hz repetition rate, and is useful for applications in deep ultraviolet pump-probe ultrafast spectroscopy. DOE

N94-32305 University Coll., Galway (Ireland).

BACKSCATTER AND TRANSMISSION OF AEROSOL AT UV THROUGH MIDDLE IR WAVELENGTHS Interim Report No. 3, Mar. - Jun. 1993

7 Dec. 1993 14 p Limited Reproducibility: More than 20% of this document may be affected by microfiche quality

(Contract DAJA45-92-C-0024)

(AD-A277127; R/D-6798-EN-01) Avail: CASI HC A03

Simultaneous measurements of backscatter and transmission coefficients, sigma(sub b) and sigma(sub e), for obscuring and biological aerosols using a Nd:YAG pulsed laser system at 1064, 532, and 266 nm wavelengths are being investigated in the laboratory. The experimental arrangement has been satisfactorily tested at 1064 and 532 nm for well-characterized water drops yielding sigma(sub e) = 14.4 +/- 0.4 sigma(sub b) and sigma(sub e) = (53.1 +/- 3.2) sigma(sub b) respectively. A catalogue of pollen and spore species measured at Mace Head using a seven-day recording volumetric spore trap is presented. Pollen number concentration for individual pollen species is presented for April 1993 whilst total number concentration is presented for April and May 1993 at Mace Head for both pollen and spore species. DTIC

N94-32366# MetroLaser, Irvine, CA.

PHOTOTHERMAL LASER DEFLECTION, AN INNOVATIVE TECHNIQUE TO MEASURE PARTICLES IN EXHAUSTS Final Report, Aug. 1989 - Feb. 1990

Cecil F. Hess Oct. 1993 48 p

(Contract F08635-89-C-0350)

(AD-A277151; AFESC/ESL-TR-90-16) Avail: CASI HC A03/MF A01

Photothermal Laser Deflection (PLD) is an analytical technique to measure in real-time the mass concentration of particles and gaseous exhaust pollutants in a variety of combustion devices (e.g., gas turbine engines and rockets). PLD uses a pump laser to locally heat the particle or gaseous species, thus changing the refractive index of the surrounding gas to form a thermal lens. A probe laser beam travelling through the thermal lens is temporarily deflected, and the amount of deflection is proportional to the species mass concentration. The experiments and analyses conducted during phase 1 demonstrated the feasibility of PLD in measuring the mass concentration of both soot particles and NO2 at a repetition rate of 25 HZ. PLD response was linear at soot concentrations from 0.3 to 10 mg/cubic meters at NO2 concentrations from approximately 6 to 208 ppm. Strategies to measure lower concentrations have been defined and include focusing the probe beam onto the face of the bi-cell detector. The large dynamic range, fast acquisition rate, and ability to measure particulate and gaseous pollutants makes PLD superior to other available methods. DTIC

N94-32406 Naval Research Lab., Washington, DC.

GYROTRONS AND FREE ELECTRON LASERS FOR ATMOSPHERIC SENSING Interim Report

Wallace M. Manheimer 28 Feb. 1994 69 p Limited Reproducibility: More than 20% of this document may be affected by microfiche quality

(AD-A277281; NRL/MR/6707-94-7444) Avail: Issuing Activity (Defense Technical Information Center (DTIC))

The development of gyrotrons and free electron lasers over the past decade and a half have naturally led to investigations of additional applications for them. This work looks into applications in the area of atmospheric sensing. Specific gyrotron applications include cloud radars, sensors for atmospheric turbulence, and measurement schemes for upper atmosphere trace impurities. To be useful as atmospheric sensors, free electron lasers must be made much more compact. Several development strategies for accomplishing this are possible. It appears that there are numerous potential applications for both gyrotrons and free electron lasers as atmospheric sensors. DTIC

N94-32413# Utah Univ., Salt Lake City.

LASER FLASH PHOTOLYSIS, EPR AND RAMAN STUDIES OF LIQUIDS AT ELEVATED PRESSURES

E. M. Eyring 19 Nov. 1993 6 p

(Contract DE-FG03-93ER-14340)

(DE94-008351; DOE/ER-14340/1) Avail: CASI HC A02/MF A01

A laser flash photolysis kinetic study of a W(CO)(sub 5) intermediate reacting with several different substituted 2,2(prime)-bipyridine ligands at pressures up to 150 MPa in liquid toluene has confirmed the considerable influence of steric hindrance on the mechanism of a thermal ring closure reaction. A similar laser flash photolysis kinetic study has been carried out with Mo(CO)(sub 6) and several bidentate ligands resembling 2,2(prime)-bipyridine dissolved in supercritical carbon dioxide. A much larger negative activation volume is found in supercritical carbon dioxide than observed previously with this solute system dissolved in liquid toluene. Rate of replacement of one polydentate ligand by another stronger chelating agent in the first coordination sphere of aqueous gadolinium(III) ion was measured over a range of pressures and other variables using a stopped-flow spectrophotometer. Two consecutive first order reaction steps are observed that show acid-catalysis. DOE

N94-32603# Sandia National Labs., Albuquerque, NM.
CHEMISORBED-MOLECULE POTENTIAL-ENERGY SURFACES AND ELECTRONICALLY-STIMULATED PROCESSES
D. R. Jennison, E. B. Stechel, A. R. Burns, and S. Y. Li 1994 15 p Presented at the OE/LASE 1994: Conference on Optics, Electro-Optics, and Laser Applications in Science and Engineering, Los Angeles, CA, 22-29 Jan. 1994
(Contract DE-AC04-94AL-85000)
(DE94-007932; SAND-94-0317C; CONF-940142-22) Avail: CASI HC A03/MF A01

Three topics illustrate some central physics of processes produced by UV-laser and low-energy electron stimulation. First, a multidimensional ground-state potential energy surface (PES) for NH3:Pd(111), computed using ab initio local-density functional theory, allows dramatically different dynamics depending on poorly-known excited-state forces. We use quantum-resolved experimental data to argue that stimulated desorption is dominated by a direct path off the surface, following placement of the wavepacket on a molecule-surface hard wall accessed by internal molecular motion. This illustrates the questionable relevance of one dimensional models for understanding molecule-surface dynamics. Second, we study the image-charge model of excited state forces experienced by ions produced, for example, by hot carrier attachment. Ab initio results show that this model totally fails at molecule-surface distances typical of chemisorption. Finally, we present a purely electronic adiabatic model of excited state PESs and use it to argue that, if significant covalent interactions occur between an adsorbate and a surface, hot carrier attachment does not simply produce singly-charged ions. Instead, attachment creates excitations of the molecule-surface bond occur and, in some cases, may result in multiply-charged ions. DOE

N94-32608 California Univ., Santa Barbara.
HIGH SPEED, STRAINED LAYER, MULTIQUANTUM WELL, GaInAsP AND GaAs LASERS AND HETEROSTRUCTURES Final Report
John Bowers, Larry Coldren, Gary Y. Robinson, and M. J. Hafich Dec. 1993 63 p Limited Reproducibility: More than 20% of this document may be affected by microfiche quality
(Contract F19628-89-K-0042; ARPA Order 7144)
(AD-A277287; RL-TR-93-241) Avail: Issuing Activity (Defense Technical Information Center (DTIC))

This report is divided into three sections, the first covering the work done in the area of high speed InGaAs/GaAs strained quantum well lasers, the second in the material growth and laser fabrication in the InGaAs/AlInGaAs system, and the third in the gas source molecular beam epitaxy (GSMBE) of In materials. This contract began at a time when quantum well laser bandwidths were severely limited for unknown reasons and the largest bandwidths were in bulk lasers. This has all changed now. Strained quantum well lasers were fabricated during the initial phase of this program resulting in anomalously large damping rates in quantum well lasers. Large damping rates result in small bandwidth because the lasers become critically damped at a low frequency. During the second portion of the contract, a theory describing the reasons for the resonance frequency, damping frequency, K factor, intensity noise, internal efficiency, injection efficiency, and wavelength chirping has been derived. Theoretical and experimental evidence in this program shows that carrier transport can lead to significant low frequency parasitic-like rolloff that reduces the modulation response by as much as a factor of six in quantum well lasers. DTIC

N94-32613# Los Alamos National Lab., NM.
A HISTORICAL PERSPECTIVE ON FIFTEEN YEARS OF LASER DAMAGE THRESHOLDS AT LLNL
F. Rainer, F. P. DeMarco, M. C. Staggs, M. R. Kozlowski, L. J. Atherton, and L. M. Sheehan 21 Dec. 1993 14 p Presented at the 25th Boulder Damage Symposium: Annual Symposium on Optical Materials for High-Power Lasers, Boulder, CO, 27-29 Oct. 1993
(Contract W-7405-eng-48)
(DE94-007930; UCRL-JC-114997; CONF-931054-10) Avail: CASI HC A03/MF A01

We have completed a fifteen year, referenced and documented compilation of more than 15,000 measurements of laser-induced damage thresholds (LIDT) conducted at the Lawrence Livermore National Laboratory (LLNL). These measurements cover the spectrum from 248 to 1064 nm with pulse durations ranging from less than 1 ns to 65 ns and at pulse-repetition frequencies (PRF) from single shots to 6.3 kHz. We emphasize the changes in LIDTs during the past two years since we last summarized our database. We relate these results to earlier data concentrating on improvements in processing methods, materials, and conditioning techniques. In particular, we highlight the current status of antireflective (AR) coatings, high reflectors (HR), polarizers, and frequency conversion crystals used primarily at 355 nm and 1064 nm. DOE

N94-32629# Lawrence Livermore National Lab., CA.
X RAY IMAGING AND X RAY SOURCE DEVELOPMENT AT LAWRENCE LIVERMORE NATIONAL LABORATORY
J. Trebes, R. Balhorn, and E. Anderson Dec. 1993 8 p Presented at the 4th International Conference on X Ray Microscopy, Chenogolovka, Russia, 20-24 Sep. 1993
(Contract W-7405-eng-48)
(DE94-007077; UCRL-JC-115163; CONF-9309290-2) Avail: CASI HC A02/MF A01

The Laser Program at Lawrence Livermore National Laboratory has a continuing effort to develop both x-ray sources and x-ray microscopy. This effort includes the ongoing development of: (1) a wide range of x-ray lasers at the Nova Laser Facility; (2) a zone plate lens--multilayer mirror based x-ray microscope; (3) three dimensional, high resolution x-ray microscopy; (4) short wavelength, normal incidence multilayer x-ray mirrors; (5) compact, high average power lasers for producing x-ray lasers and laser plasma x-ray sources. We have constructed and operated an x-ray laser based transmission x-ray microscope. The advantage offered by the x-ray laser source is the extreme high brightness allows high resolution images to be made on a timescale faster than that for x-ray damage effects to appear. The microscope, consists of the x-ray laser, a multilayer coated, near normal incidence spherical mirror used as a condenser, a silicon nitride specimen holder, an x-ray zone plate used as an objective lens, and a microchannel plate x-ray detector. The x-ray laser used is the Ni-like Ta x-ray laser operating with a wavelength of 4.48 nm, a pulselength of 200 spec, a divergence of 10 mrad, and an output energy of 10 microjoules. DOE

N94-32654# Texas Technological Univ., Lubbock. Pulsed Power Lab.
HIGH POWER SWITCH DESIGN FOR THE NOVA UPGRADE LASER (PROJECT HERCULES: HIGH ENERGY RESEARCH CONCERNING THE ULTIMATE LIFETIME OF EXPERIMENTAL SWITCHES) Final Report, 15 Aug. 1991 - 31 May 1993
Michael Giesselmann 1993 23 p Prepared for LANL, NM
(Contract W-7405-eng-48)
(DE94-007921; UCRL-CR-116290) Avail: CASI HC A03/MF A01

A test facility was constructed to test high power ignitrons using an electrolytic bank. The goal of this project, which was named Hercules (High Energy Research Concerning the Ultimate Lifetime of Experimental Switches), was to test the lifetime and switching characteristics of high power ignitrons for Lawrence Livermore's laser upgrade program. The main tubes of interest that have been tested were the NL-9000A from Richardson Electronics and the BK-1002 from English Electric Valve (EEV). Both tubes have stainless steel, cup style anodes. Both tubes were connected in series for the tests. Required test parameters were Ipeak = 300 kA and Qtransfer = 200 C. During the tests, the BK-1002 tube failed due to ignitor shorting. The average forward voltage drop across the EEV tube was almost twice than the drop across the NL-9000A. After the tube failure, the BK-1002 was replaced by a NL-1057 to continue testing of the NL-9000A. DOE

N94-32659# Lawrence Livermore National Lab., CA.
HIGH AVERAGE POWER PULSED PHASE CONJUGATE LASER WITH BIREFRINGENCE CORRECTION
M. W. Bowers, A. K. Hankla, and G. F. Jacobson Nov. 1993 8 p Presented at the CLEO 1994: Conference on Lasers and Electro-Optics, Anaheim, CA, 8-13 May 1994
(Contract W-7405-eng-48)
(DE94-006049; UCRL-JC-115687; CONF-940582-1) Avail: CASI HC A02/MF A01

We have developed a Nd:YAG laser that delivers 2.5 Joules per 10 ns pulse at a 10 Hz repetition rate. The output beam is a flat top with 1.5 times diffraction limited beam quality with 7% depolarization. DOE

N94-32684 Texas Univ., Austin. Inst. for Fusion Studies.
SUPERLUMINOUS LASER PULSE IN AN ACTIVE MEDIUM
D. L. Fisher and T. Tajima Dec. 1993 14 p Limited Reproducibility: More than 20% of this document may be affected by microfiche quality
(Contract DE-FG05-80ET-53088)
(DE94-007110; IFSR-635; DOE/ET-53088/635) Avail: CASI HC A03

Physical conditions are obtained to make the propagation velocity of a laser pulse and thus the phase velocity of the excited wake be at any desired value, including that equal to or greater than the speed of light. The provision of an active-plasma laser medium with an appropriately shaped pulse allows not only replenishment of laser energy loss to the wakefield but also acceleration of the group velocity of photons. A stationary solitary solution in the accelerated frame is obtained from the model equations and simulations thereof for the laser, plasma and atoms. This approach has applications in photonics and telecommunications as well as wakefield accelerators. DOE

N94-32704# Pacific Northwest Lab., Richland, WA.
A NONCRITICALLY PHASE MATCHED FEMTOSECOND OPTICAL PARAMETRIC OSCILLATOR NEAR 3 MICRONS
G. R. Holtom, R. A. Crowell, and X. S. Xie Feb. 1994 6 p Presented at the 9th Advanced Solid-State Lasers Meeting, Salt Lake City, UT, 7-10 Feb. 1994
(Contract DE-AC06-76RL-01830)
(DE94-008050; PNL-SA-23676; CONF-940226-5) Avail: CASI HC A02/MF A01

An optical parametric oscillator designed for the 3 micron spectral region is described. Pulses shorter than 100 fs are produced. Alignment is simple and conversion efficiency is good. DOE

N94-32707# Argonne National Lab., IL.
HIGH-ENERGY CHEMICAL PROCESSES: LASER IRRADIATION OF AROMATIC HYDROCARBONS
A. D. Trifunac, A. D. Liu, and D. M. Loffredo 1994 6 p
(Contract W-31-109-eng-38)
(DE94-008107; ANL/CHM/PP-74944) Avail: CASI HC A02/MF A01

Recent studies of the high-energy photochemical degradation of polycyclic aromatic hydrocarbons (PAH's) in solution have furthered our fundamental understanding of the way in which radiation interacts with matter. A new comprehensive mechanism that unifies many of the seemingly contradictory observations in radiation and photochemistry has been proposed on the basis of evidence gathered using specialized techniques such as transient optical spectroscopy and transient dc conductivity. The PAH molecules were activated by two-photon ionization, and behavior of the transient ions were monitored as a function of photon energy. It was found that a greater percentage of ions retain sufficient energy to decompose when higher energy light was used. When these cations decompose they leave a trail of products that establish a 'high-energy' decomposition pathway that involves proton transfer from the ion, a mechanism hitherto not considered in photoionization processes. DOE

N94-32753# Lawrence Livermore National Lab., CA.
PUMP-PROBE METHOD FOR INVESTIGATING LASER ABLATION AND OPTICAL DAMAGE THRESHOLD MECHANISMS IN OPTICAL MATERIALS
L. L. Chase Sep. 1993 14 p Presented at the Nuclear Instruments and Methods in Physics Research on Radiation Effects in Insulators, Nagoya, Japan, Sep. 1993
(Contract W-7405-eng-48)
(DE94-008291; UCRL-JC-114770; CONF-9309259-5) Avail: CASI HC A03/MF A01

The method developed for investigating laser-surface interactions by measuring the ratio of ablation threshold fluence for a pair of picosecond or subpicosecond laser pulses to the single-pulse ablation threshold was applied to ZnS (wurtzite) and to the borosilicate glass BK-7. Each sample was exposed to 1000 pulse pairs of 580-nm dye laser radiation. For ZnS, linear absorption was found to be the cause of the cumulative optical damage mechanism; the linear absorption is probably caused by defects states (such as color centers) near the surface. The nonlinear behavior of BK-7 suggests that avalanche ionization could be the damage mechanism. Results for both materials show that intrinsic multiphoton absorption mechanisms may not be significant indicators of optical damage mechanisms even when they lead to very high free-carrier densities and energy absorption. DOE

N94-32760# Los Alamos National Lab., NM.
SHORT-PULSE, HIGH-INTENSITY LASERS AT LOS ALAMOS
Antoinette J. Taylor, Jeffrey P. Roberts, George Rodriguez, Robert D. Fulton, George A. Kyrala, and Gottfried T. Schappert 1994 6 p Presented at the 11th International Workshop on Laser Interaction and Related Plasma Phenomena, Monterey, CA, 25-29 Oct. 1993
(Contract W-7405-eng-36)
(DE94-007545; LA-UR-94-528; CONF-931048-10) Avail: CASI HC A02/MF A01

Advances in ultrafast lasers and optical amplifiers have spurred the development of terawatt-class laser systems capable of delivering focal spot intensities approaching 10(exp 20) W/cm(exp 2). At these extremely high intensities, the optical field strength is more than twenty times larger than the Bohr electric field, permitting investigations of the optical properties of matter in a previously unexplored regime. The authors describe two laser systems for high intensity laser interaction experiments: the first is a terawatt system based on amplification of femtosecond pulses in XeCl which yields 250 mJ in 275 fs and routinely produces intensities on target in excess of 10(exp 18) W/cm(exp 2). The second system is based on chirped pulse amplification of 100-fs pulses in Ti:sapphire. DOE

N94-32761# Los Alamos National Lab., NM. Chemical Science and Technology Div.
REPETITIVELY PULSED Cr:LISAF LASER FOR LIDAR APPLCATIONS
Tsutomu Shimada, James W. Early, Charles S. Lester, and Nigel J. Cockroft 1994 6 p Presented at the 9th Advanced Solid-state Lasers Meeting, Salt Lake City, UT, 7-10 Feb. 1994
(Contract W-7405-eng-36)
(DE94-007546; LA-UR-94-526; CONF-940226-4) Avail: CASI HC A02/MF A01

A Cr:LiSAF laser has been successfully operated at time averaged powers up to 11 W and at pulse repetition rates to 12 Hz. During Q-switch operation, output energy as high as 450 mJ (32 ns FWHM) was obtained. Finally, line narrowed Q-switched pulses from the Cr:LiSAF laser were successfully used as a tunable light source for lidar to measure atmospheric water content. DOE

N94-32794# Lawrence Livermore National Lab., CA.
PROGRESS IN UNDERSTANDING AND IMPROVING X RAY LASERS
J. Nilsen, J. C. Moreno, J. A. Koch, J. H. Scofield, B. J. MacGowan, and L. B. DaSilva 11 Jan. 1994 7 p Presented at the LASERS 1993: International Conference on Lasers and Applications, Lake Tahoe, NV, 6-10 Dec. 1993
(Contract W-7405-eng-48)
(DE94-006048; UCRL-JC-116080; CONF-931237-6) Avail: CASI HC A02/MF A01

We discuss the use of a prepulse technique to achieve lasing in low-Z neon-like ions on the 3p yields 3s(J = 0 yields 1) transition. In neon-like titanium (Z=22), chromium (Z=24), iron (Z=26), nickel (Z=28), zinc (Z=30), and germanium (Z=32) this transition lases at 326, 285, 255, 231, 212 and 196 A, respectively. We present results using this technique on selenium (Z=34) and show how the J = 0 yields 1 transition at 182 A suddenly becomes a strong line. The observation that the low-Z ions with odd Z have not lased lead us to investigate the potential impact of hyperfine splitting on the laser gain. In our experiments we measure the lineshape of the 3p yields 3s(J = 0 yields 1) transition in neon-like niobium and zirconium and observe a 28 m(A) splitting between the two largest hyperfine components in the niobium (Z=41) line at 145.9 in good agreement with theory. In zirconium (Z=40), no splitting is observed since the hyperfine effect is proportional to the nuclear moment, and the principal isotopes of zirconium have zero nuclear moment, as is typical for even-Z elements. Finally, we discuss the use of low density foams for the laser target and present results which show lasing in zirconium aerogel with an initial density of 90 mg/cm(exp 3). DOE

N94-32845# Stanford Research Inst., Menlo Park, CA. Accelerator Center.
SELECTED APPLICATIONS OF PLANAR PERMANENT MAGNET MULTIPOLES IN FEL INSERTION DEVICE DESIGN
R. Tatchyn Aug. 1993 8 p Presented at the 15th International Free Electron Laser Conference, The Hague, Netherlands, 23-27 Aug. 1993
(Contract DE-AC03-76SF-00515)
(DE94-009014; SU-SLAC-PUB-6320; SLAC/SSRL-0049; CONF-930855-9)
Avail: CASI HC A02/MF A01

In recent work, a new class of magnetic multipoles based on planar configurations of permanent magnet (PM) materials was developed. These structures, in particular the quadrupole and sextupole, feature fully open horizontal apertures, and are comparable in effectiveness to conventional iron multipole structures. In this paper, results of recent measurements of planar PM quadrupoles and sextupoles are reported, and selected applications to FEL insertion device design are considered. DOE

N94-32848 Stanford Research Inst., Menlo Park, CA. Accelerator Center.
A RELIABLE LOW-MAINTENANCE FLASHLAMP-PUMPED Ti:SAPPHIRE LASER OPERATING AT 120 PPS
K. H. Witte Mar. 1994 2 p Presented at the LASERS 1993 International Conference on Lasers and Applications, Lake Tahoe, NV, 6-10 Dec. 1993 Limited Reproducibility: More than 20% of this document may be affected by microfiche quality
(Contract DE-AC03-76SF-00515)
(DE94-009030; SU-SLAC-PUB-6443; CONF-931237-9) Avail: CASI HC A01

Flashlamp-pumped Ti:sapphire lasers were reported to produce high-energy pulses with broad tunability. However, with the flashlamps operating at close to their explosion energy, and considering the thermal loading effects in the laser rod, these lasers were restricted to low repetition rates (typically around 10 PPS). Higher repetition rates at constant laser pulse energy reduce the flashlamp lifetime drastically. The author reports on a reliable flashlamp-pumped Ti:sapphire laser that was operating at 120 PPS for over 10(exp 9) shots with the only cavity or pump chamber maintenance being flashlamp changes less than every 2 x 10(exp 8) pulses--the lowest maintenance reported. A specular dual-lamp pump chamber was used to pump a 4 mm x 6 in., 0.1% doped Ti:sapphire rod. This resulted in a very low lasing threshold, which ensured a stable output at low pump levels. The criterion for pump power was to obtain a highly stable output at the edge of the selected tuning range, from 790 to 860 nm. The combination of flashlamp walls, flashlamp flow tubes, and rod solarization. DOE

N94-32968 Department of the Navy, Washington, DC.
MULTIFREQUENCY, RAPIDLY SEQUENCED OR SIMULTANEOUS TUNABLE LASER Patent
Richard Scheps, inventor (to Navy) 4 Jan. 1994 19 p Filed 26 Oct. 1992
(AD-D016169; US-Patent-5,276,695; US-Patent-Appl-SN-970328; US-Patent-Class-372-20) Avail: US Patent and Trademark Office

A tunable solid state laser produces a laser emission at one or more wavelengths simultaneously. The tunable solid state laser includes a laser resonator defined by an output coupler reflective element, two fold mirrors, and one or more high reflectivity end elements to form a reflective path in a laser resonator cavity there between with a laser crystal disposed in the laser resonator cavity. A means for optically exciting the laser crystal is appropriately disposed for end pumping the laser crystal to produce a laser emission in a predetermined range of wavelengths. A wavelength dispersing element such as a prism is disposed in the laser resonator cavity between one of the fold mirrors and the high reflectivity end elements for tuning the laser emission at one or more of the desired wavelengths in the predetermined range of wavelengths, the dispersing element being transparent to the laser emission over the predetermined range of wavelengths. DTIC

N94-33000# FOM-Inst. voor Plasmafysica, Rijnhuizen, Jutphaas (Netherlands).
INTERNATIONAL FREE ELECTRON LASER CONFERENCE
27 Aug. 1993 290 p Conference held in The Hague, Netherlands, 23-27 Aug. 1993
(Contract DAJA45-93-M-0434)
(AD-A277576; R/D-7110-CH-02) Avail: CASI HC A13/MF A03

Presented is a book of abstracts for the 15th International Free Electron Laser Conference. A partial listing of contents include: initial performance of Los Alamos advanced free electron laser, first observation of amplification of spontaneous emission achieved with the Darmstadt IR FEL, performance and tuning characteristics of the ENEA compact FEL, a millimeter-range FEL experiment using the coherent synchrotron radiation emitted from electron bunches, demonstration of ultraviolet lasing with a low energy beam, and experiments with grating-coupled free electron lasers. CASI

N94-33003 Army Research Lab., Adelphi, MD.
LARGE-DIAMETER InGaAs/AlGaAs VERTICAL-CAVITY SURFACE-EMITTING LASERS WITH LOW THRESHOLD CURRENT DENSITY FABRICATED USING A SIMPLE CHEMICAL ETCH PROCESS Final Report
Richard P. Leavitt, John L. Bradshaw, George J. Simonis, and John T. Pham Mar. 1994 15 p Limited Reproducibility: More than 20% of this document may be affected by microfiche quality
(AD-A277733; ARL-TN-32) Avail: CASI HC A03

We have demonstrated threshold current densities below 800 A/sq cm in large-diameter (75 microns less than d less than 150 microns) vertical-cavity surface emitting lasers fabricated from an epitaxial structure containing a single In(0.2)Ga(0.8)As quantum well in a one wavelength long Fabry-Perot resonant cavity. The fabrication process uses a circular Au/Cr/Au disk as both the p-type contact and the mask for chemically etching individual diodes. DTIC

N94-33012# California Univ., Berkeley. Dept. of Physics.
ULTRAFAST X RAY SOURCES Final Report, Aug. 1989 - Aug. 1993
Roger W. Falcone Aug. 1993 125 p
(Grant AF-AFOSR-0476-89)
(AD-A277455; AFOSR-94-0063TR) Avail: CASI HC A06/MF A02

During the contract period we made progress in six areas: development of ultrashort pulse x-ray sources; generation of subpicosecond, unicycle electromagnetic pulses; propagation of intense short pulse lasers in plasmas; new x-ray lasers; new high-intensity, short pulse lasers; diagnosis of multiphoton ionized plasmas. Our work resulted in thirty-one publications, which are listed in section 3 of this report. Publications not previously been sent to AFOSR are included in this report. Our work has resulted in forty-five conference presentations, which are listed in section 4 of this report. Four additional invited talks are currently scheduled. DTIC

N94-33102 Wright Lab., Wright-Patterson AFB, OH.
COMPARISON OF COHERENT TO INCOHERENT DETECTION AT 2.09 MICROMETERS USING A SOLID STATE LADAR SYSTEM Final Report, 27 Mar. 1991 - 21 Sep. 1993
Jay A. Overbeck Feb. 1994 128 p Limited Reproducibility: More than 20% of this document may be affected by microfiche quality
(AF Proj. 0100)
(AD-A277159; WL-TR-94-1038) Avail: CASI HC A07

A 2.09 LADAR system has been built to compare coherent to incoherent detection. The 2.09 micron wavelength is of interest for its high atmospheric transmission and because it is eye safe. The 2.09 micron system presented within is capable of either a coherent or incoherent operational mode, is tunable in a small region around 2.09 microns, and is being used to look at the statistical nature of the LADAR return pulses for typical glint and speckle targets. In order to compare coherent to incoherent detection the probability of detection will be investigated as the primary performance criterion of interest. The probability of detection is dependent on both the probability of false alarm and the probability density function representing the signal current output from the detector. These probability distributions are different for each detection technique and for each type of target. Furthermore, the probability of detection and the probability of false alarm are both functions of the dominating noise source(s) in the system. A description of the theoretical expectations of this system along with the setup of the LADAR system and how it is being used to collect data for both coherent and incoherent detection will be presented. DTIC

N94-33282# Phillips Lab., Kirtland AFB, NM.
PHASE-ONLY CORRECTION OF SCINTILLATED LASER BEAMS: DOWNRANGE EXPERIMENTAL RESULTS Final Report
L. McMackin, J. D. Gonglewski, B. Venet, M. P. Jelonek, and J. M. Spinherne Mar. 1994 12 p
(AF Proj. 9993)
(AD-A277778; AD-E201838; PL-TR-93-1058) Avail: CASI HC A03/MF A01

Results of Horizontal Propagation Experiment (HoPe) that was performed at the Phillips Laboratory Starfire Optical Range are presented. In this experiment, a laser beam was phase corrected using an adaptive optics system located at the transmitting site and focused toward a target located two miles away. Irradiance patterns of the corrected and uncorrected beam were recorded at the target site. Weather and atmospheric turbulence characteristics along the optical path were recorded at the same time. Strehl ratios calculated from the recorded images show that phase-only correction of a horizontally propagated laser beam can significantly improve the energy collected on-axis even under strongly scintillated conditions. Time-averaged Strehl ratios were improved by as much as a factor of five. Improvements in Strehl for varying turbulence conditions and the effect of hardware limitations on the results are discussed. DTIC

N94-32448*# Spire Corp., Bedford, MA. Optoelectronics Div.
HIGH POWER DIODE LASERS FOR SOLID-STATE LASER PUMPS
Kurt J. Linden and Patrick N. McDonnell *In* NASA, Washington, Technology 2003: The Fourth National Technology Transfer Conference and Exposition, Volume 2 Feb. 1994 p 233-245 (For primary document see N94-32420 09-99)
(Contracts NAS1-18660; NAS1-19301)
Avail: CASI HC A03/MF A04

37 MECHANICAL ENGINEERING

Includes auxiliary systems (nonpower); machine elements and processes; and mechanical equipment.

N94-31194 Chalmers Univ. of Technology, Goeteborg (Sweden). Dept. of Applied Physics.
VIBRATIONS OF A HEAVY TRUCK DIESEL ENGINE AND GEARBOX UNIT: EXAMINING STRUCTURE-BORNE SOUND TRANSMISSION WITH STATISTICAL ENERGY ANALYSIS M.S. Thesis
Bo Gaerdhagen and Bo-Goeran Emretsson Apr. 1993 96 p Limited Reproducibility: More than 20% of this document may be affected by microfiche quality
(ISSN 0283-8338)
(CTH-E-93-04; ETN-94-95952) Avail: Issuing Activity (European Space Agency (ESA))

Statistical Energy Analysis (SEA) is used for examining structure borne sound transmission in a heavy truck diesel engine and gearbox unit. SEA is considered to be applicable for frequencies above 1 kHz in the investigated case. The connection between the engine and the gearbox is not accurately described by the SEA model. This problem is circumvented by using two SEA models. The vibration transmission in the engine block is strongly influenced by in plane waves. The low modal count for the in plane waves reduces the prediction capability of the SEA model. Real noise sources in the engine and gearbox unit are complex. The examination was therefore limited to analysis using artificial excitation, simulating the sources. A rating of the relative strength of real noise sources in the engine and gearbox unit is presented. This rating is derived from measurements on a firing and externally driven engine. ESA

N94-31319# Argonne National Lab., IL.
REVIEW AND STATUS OF MAGLEV IN THE UNITED STATES
H. T. Coffey 1993 40 p Presented at the International Conference on Speed Technology for Railway and Maglev Vehicles, Yokohama, Japan, 22-25 Nov. 1993
(Contract W-31-109-eng-38)
(DE94-006832; ANL/ES/CP-82064; CONF-931102-3) Avail: CASI HC A03/MF A01

This report contains a slide show on the status and future of Maglev type transportation systems in the United States. DOE

N94-31333# Naval Postgraduate School, Monterey, CA.
ROTORDYNAMIC EFFECTS DRIVEN BY FLUID FORCES FROM A GEOMETRICALLY IMPERFECT LABYRINTH M.S. Thesis
William C. Williston, Jr. Dec. 1993 43 p
(AD-A276424) Avail: CASI HC A03/MF A01

The forces on a rotor due to asymmetric pressure distributions resulting from a single gland non-circular labyrinth seal in a circular outer casing are analyzed for the purpose of understanding the possible causes of synchronous vibration due to seal intolerance. A lumped parameter model is developed for flow in the azimuthal direction inside the seal gland. The sealing knife imperfections causing the non-circularity may be due to manufacturing defects or in service ware. The resulting continuity and momentum equations are solved using a regular linear perturbation technique. Results from this model indicate under what conditions seal imperfections can generate forces of the same order of magnitude as rotor mass unbalance. DTIC

N94-31379 Sheffield Univ. (England). Robotics Research Group.
A HIGH-PERFORMANCE MULTI-ARM ENVIRONMENT: THEORETICAL ASPECTS AND PRACTICAL IMPLEMENTATION
A. M. S. Zalzala, G. I. Dodds, and G. W. Irwin May 1993 24 p Sponsored by United Kingdom Science and Engineering Research Council Limited Reproducibility: More than 20% of this document may be affected by microfiche quality
(Grant ST79)
(RR-479; ETN-94-96056) Avail: CASI HC A03

The development of a multiarm robotic system, where the practical implementation of the system involves motion coordination of two multijoint RTX robots with six degrees of freedom, hosted by a SPARC IPC workstation, is reported. A planning scheme is introduced to provide accurate and coordinated collision free motion. In addition, taking into account the need for high productivity in industrial environments, minimum time movements are imposed by increasing the manipulators' performance to a maximum, thus providing a high performance workcell. A real time case study is included to show the validity and efficiency of the system. ESA

N94-31469 Virginia Polytechnic Inst. and State Univ., Blacksburg.
CONTROL OF A FLEXIBLE SPACE ROBOT TRACKING A MOVING TARGET Ph.D. Thesis
Yi-Feng Chen 1993 109 p
Avail: Univ. Microfilms Order No. DA9323764

This dissertation is concerned with a space robot consisting of a rigid platform, two articulated flexible arms and a rigid end-effector. The task is to ferry some payload and to dock smoothly with an orbiting target whose motion is either known or not known a priori. The dynamical equations for planar motion of the space robot are derived by means of Lagrange's equations. They are then separated into two sets of equations suitable for rigid-body maneuver control design and vibration suppression control design. A perturbation method is used when the target motion is known a priori and direct partitioning is used when the target motion is not known. Both approaches are under the assumption that maneuver motions are much larger than elastic motions. As far as the rigid-body maneuver control is concerned, optimal trajectory planning is carried out off-line by means of the global optimization method under the assumption that the target motion is known a priori. In contrast, when the target motion is not known a priori, online feedback tracking control is carried out by means of an algorithm based on Liapunov-like methodology and using on-line measurements of the target motion. As far as the vibration suppression control is concerned, the use of the piezoelectric sensor/actuator pairs dispersed along the flexible arms is proposed. Collocated sensors/actuators for vibration control exhibit good performance. The actuators are designed to compensate for the disturbances caused by the rigid-body maneuver and to realize the LQR feedback control. Assuming that the number of actuators along each flexible arm is equal to the number of modes used to model the beam, the LQR control design is based on a linear time-varying system without persistent disturbances. Problems related to the digital implementation of the control algorithms are also discussed. Some undesirable effects, such as the bursting phenomenon and even system instability, can occur if the control algorithms are realized in discrete-time. To prevent these problems, the modified discrete-time control schemes are developed. Numerical examples are used to demonstrate the control algorithms. Dissert. Abstr.

N94-31524# Westinghouse Savannah River Co., Aiken, SC.
SOLID-STATE RESISTANCE UPSET WELDING: A PROCESS WITH UNIQUE ADVANTAGES FOR ADVANCED MATERIALS
W. R. Kanne, Jr. 1993 18 p Presented at the 2nd Advanced Joining Technologies for New Materials, Cocoa Beach, FL, 2-4 Mar. 1994
(Contract DE-AC09-89SR-18035)
(DE94-005941; WSRC-MS-93-305; CONF-940367-1) Avail: CASI HC A03/MF A01

Solid-state resistance upset welding is suitable for joining many alloys that are difficult to weld using fusion processes. Since no melting takes place, the weld metal retains many of the characteristics of the base metal. Resulting welds have a hot worked structure, and thereby have higher strength than fusion welds in the same mate. Since the material being joined is not melted, compositional gradients are not introduced, second phase materials are minimally disrupted, and minor alloying elements do not affect weldability. Solid-state upset welding has been adapted for fabrication of structures considered very large compared to typical resistance welding applications. The process has been used for closure of capsules, small vessels, and large containers. Welding emphasis has been on 304L stainless steel, the material for current applications. Other materials have, however, received enough attention to have demonstrated capability for joining alloys that are not readily weldable using fusion welding methods. A variety of other stainless steels (including A-286), superalloys (including TD nickel), refractory metals (including tungsten), and aluminum alloys (including 2024) have been successfully upset welded. DOE

N94-31568 Maryland Univ., College Park.
KINEMATIC SYNTHESIS AND ANALYSIS OF A NOVEL CLASS OF SIX-DOF PARALLEL MINIMANIPULATORS Ph.D. Thesis
Farhad Tahmasebi 1993 221 p
Avail: Univ. Microfilms Order No. DA9327504

A new class of six degree of freedom (six-DOF) parallel minimanipulators is introduced. The minimanipulators are designed to provide high resolution and high stiffness in fine-manipulation operations. Two-DOF planar mechanisms (e.g., five-bar linkages, pantographs) and inextensible limbs are used to improve positional resolution and stiffness of the minimanipulators. The two-DOF mechanisms serve as drivers for the minimanipulators. The minimanipulators require only three inextensible limbs and, unlike most of the six-limbed parallel manipulators, their direct kinematics can be reduced to solving a polynomial in a single variable. All of the minimanipulator actuators are base-mounted. As a result, higher payload capacity, smaller actuator sizes, and lower power dissipation can be obtained. Inverse kinematics of the minimanipulators has been reduced to solving three decoupled quadratic equations, each of which contains only one unknown. Kinematic inversion is used to reduce the direct kinematics of the minimanipulator to an eighth-degree polynomial in the square of a single variable. Hence, the maximum number of assembly configurations for the minimanipulator is sixteen. It is proved that the sixteen solutions are eight pairs of reflected configurations with respect to the plane passing through the lower ends of the three limbs. The Jacobian and stiffness matrices of two types of minimanipulators are derived. It is shown that, at a central configuration, the stiffness matrix of the first type minimanipulator (driven by bidirectional linear stepper motors) can be decoupled, if proper design parameters are chosen. It is also shown that the stiffness of the minimanipulators is higher than that of the Stewart platform. Guidelines for obtaining large stiffness values and for designing the drivers of the second type minimanipulator (simplified five-bar linkages) are established. An algorithm is developed to determine the workspace of the minimanipulators. Given any orientation for the output link, three dimensional representation of the workspace is obtained. Guidelines for avoiding discontinuities inside of the workspace are established. Necessary and sufficient conditions for both inverse and direct kinematics singularities of the minimanipulators are obtained. Guidelines for avoiding direct kinematics singularities, which occur within the minimanipulator workspace, are established. Dissert. Abstr.

N94-31569 Iowa State Univ. of Science and Technology, Ames.
REMOTE ROBOT MANIPULATOR COUPLED WITH REMOTE-CONTROLLED GUIDE VEHICLE FOR SOIL SAMPLING IN HAZARDOUS WASTE SITES Ph.D. Thesis
Kiho Kim 1993 127 p
Avail: Univ. Microfilms Order No. DA9321180

The important initial step for remediation of hazardous waste is contaminant analysis since the cleanup operation can not begin until the contaminants in hazardous waste sites have been clearly identified. Ames Laboratory, one of the U.S. Department of Energy sites, has developed a robotic sampling system for automation of real-time contaminant analysis in situ which will provide the advantage of lowering the cost per sample, eliminating personnel exposure to hazardous environments, and allowing quicker results. Successful accomplishment of real-time contaminant analysis will require a remote manipulator to perform the sampling tasks in remote and unstructured surroundings, and a remote-controlled guide vehicle to move a remote manipulator into the desired sampling location. This thesis focuses on the design and construction of a remote-controlled guide vehicle to move the robotic sampling system into the contaminated field to obtain soil samples at the desired locations, the development of an integrated dynamic model of a remote manipulator, the identification of dynamic parameters in the integrated dynamic model, and the design of a mobile robotic sampling system. A four-wheeled vehicle prototype has been constructed and its performance tested manually in the field to verify the design requirements. To remotely control the vehicle, mechanical requirements to activate the brake, throttle, transmission, and steering linkages were determined based on experimental results. A teleoperated control utilizing hundred feet long umbilical cords was first employed to remotely control the vehicle. Next, the vehicle was modified to remotely operate in the field by radio control without the aid of long umbilical cords, satisfying all the design specifications. To reduce modeling error in the robotic system, the integrated dynamic system comprised of a remote manipulator (located on a trailer pulled by the remote-controlled guide vehicle) and its drive system has been modeled. The friction model as a function of velocity is included. The dynamic parameters such as velocity-dependent friction and gravity torque in the integrated dynamic model have been determined based on experimental results. Finally, a robotic arm, a sampling tool, and a soil recovery fixture for a mobile robotic sampling system to be mounted on the remote-controlled guide vehicle have been designed and analyzed. The integrated dynamic model for the robotic arm (mounted on the remote-controlled guide vehicle) and its drive system has also been developed. Dissert. Abstr.

N94-31621# EG and G Mound Applied Technologies, Miamisburg, OH.
Nd-YAG LASER WELDING OF THE FIBER OPTIC CONNECTOR TO THE HEADER SHELL ON THE 2SL ACTUATOR
J. T. Adams and J. J. Kwiatkowski 14 Jan. 1994 12 p
(Contract DE-AC04-88DP-43495)
(DE94-006104; MLM-3790) Avail: CASI HC A03/MF A01

An investigation was completed to determine the feasibility of laser welding a fiber optic connector at a right angle to the header shell of the 2SL actuator. The work was completed at the request of Los Alamos National Laboratory (LANL). These studies showed a minimal temperature rise at the fiber-to-connector shell seal area and essentially no loss in light transmission after welding. Both metallographic sections and tensile pull-test failure values were obtained. This study proves feasibility and with minimal change in parameters the penetration can be easily increased, which will yield higher tensile pull-test failure values. DOE

N94-31651# Sandia National Labs., Livermore, CA.
SOOT AND LIQUID-PHASE FUEL DISTRIBUTIONS IN A NEWLY DESIGNED OPTICALLY ACCESSIBLE DI DIESEL ENGINE
J. E. Dec and C. Espey Oct. 1993 18 p Presented at the 1993 Diesel Emission Reduction Workshop, La Jolla, CA, Jul. 1993
(Contract DE-AC04-76DR-00789)
(DE94-005648; SAND-93-8690C; CONF-9307164-1) Avail: CASI HC A03/MF A01

Two-dimensional (2-D) laser-sheet imaging has been used to examine the soot and liquid-phase fuel distributions in a newly designed, optically accessible, direct-injection diesel engine of the heavy-duty size class. The design of this engine preserves the intake port geometry and basic dimensions of a Cummins N-series production engine. It also includes several unique features to provide considerable optical access. Liquid-phase fuel and soot distribution studies were conducted at a medium speed (1,200 rpm) using a Cummins closed-nozzle fuel injector. The scattering was used to obtain planar images of the liquid-phase fuel distribution. These images show that the leading edge of the liquid-phase portion of the fuel jet reaches a maximum length of 24 mm, which is about half the

combustion bowl radius for this engine. Beyond this point virtually all the fuel has vaporized. Soot distribution measurements were made at a high load condition using three imaging diagnostics: natural flame luminosity, 2-D laser-induced incandescence, and 2-D elastic scattering. This investigation showed that the soot distribution in the combusting fuel jet develops through three stages. First, just after the onset of luminous combustion, soot particles are small and nearly uniformly distributed throughout the luminous region of the fuel jet. Second, after about 2 crank angle degrees a pattern develops of a higher soot concentration of larger sized particles in the head vortex region of the jet and a lower soot concentration of smaller sized particles upstream toward the injector. Third, after fuel injection ends, both the soot concentration and soot particle size increase rapidly in the upstream portion of the fuel jet. DOE

N94-31654# Technical Research Centre of Finland, Espoo. Metals Lab.
AN EXPERIMENTAL AND ANALYTICAL INVESTIGATION OF A THREADED FASTENER [TUKIRUUVIN VAESYMISTARKASTELU]
Sisko Sipilae Nov. 1993 54 p In FINNISH Sponsored by Technology Development Center, and Technical Research Centre of Finland
(ISSN 1235-0613)
(VTT-JULK-786; ISBN-9-51-384134-0; ETN-94-96036) Copyright Avail: CASI HC A04/MF A01

The fatigue strength of a connecting rod consisting of a threaded bar and an integral lug end was analyzed both experimentally and analytically. Different geometries and manufacturing methods were considered. These included cut and rolled threads, lugs which were welded to the threaded bar or machined with the threads from a single piece of material, and rods both with and without a reduced section between the threads and lug end. Fatigue tensile tests showed the reduced section between lug and threads and sometimes the lug itself to be the weakest point of the component. The rods with a welded lug and a reduced section between threads and lug were found to have the highest fatigue strengths. Rolled threads showed higher fatigue strength than did cut threads at the endurance limit. All analytically determined fatigue limits were conservative compared to test results. ESA

N94-31656# Technical Research Centre of Finland, Espoo. Production Engineering Lab.
JOINING OF ALUMINA BY VACUUM BRAZING [ALUMIINIOKSIDIN LIITTAEMINEN TYHJOEJUOTTAMALLA]
Liisa Heikinheimo, Mika Siren, and Pentti Kauppinen Aug. 1993 53 p In FINNISH Sponsored by Technology Development Center, and Technical Research Centre of Finland
(ISSN 1235-0605)
(VTT-TIED-1495; ISBN-9-51-384429-3; ETN-94-96039) Copyright Avail: CASI HC A04/MF A01

The active brazing method for diffusion bonding of ceramics to metals is addressed. This method is very flexible compared to the traditional Mo-manganese coating with subsequent brazing that includes four process steps: in active brazing the process is done in one step. The joint properties are favorable, the residual stress build up is limited if the braze is correctly selected and the thermal cycle is controlled, and the resulting strength and leak tightness are good. In experimental work the joinability of alumina to titanium and Ni superalloys was studied by wetting experiments, nondestructive test and shear strength measurements. The spreading of the braze is affected not only by the surface conditions of mating materials but also by the type of the brazing alloy. The Ag-Cu base alloys give better wetting, strength and leak tightness properties than the Ag base alloys. A shear test method was developed for the mechanical testing of metal-ceramic joints. However, the sample geometry affects the measured values, namely a smaller specimen size provides better results. The correlation between the C-SAM results, which describe the ratio between the true bonded area and unbonded area, and measured shear strength values is presented. The dependence between the measured strength and the area of the joint defects becomes obvious and should be studied in more detail. ESA

N94-31714# Toronto Univ. (Ontario). Dept. of Mechanical Engineering.
MOTION AND FORCE CONTROL OF COORDINATED ROBOTS Ph.D. Thesis
Yan-Ru Hu Jul. 1993 193 p
(ISBN-0-315-86323-4; CTN-94-61190) Copyright Avail: Micromedia Ltd., Technical Information Centre, 240 Catherine Street, Suite 305, Ottawa, Ontario, K2P 2G8, Canada HC/MF

Motion and force control methods are developed for coordinated robots assumed to grasp an object rigidly. The control problem is defined in a system theoretical framework where desired trajectories of motion and force are tracked asymptotically. Both joint redundant and nonredundant robots are considered. Four motion and force control problems are defined and solved. Motion and force control of coordinated robots in the presence of model uncertainty is developed based on an adaptive scheme used to estimate the unknown constant parameters of the robots, the object, and the environment. The problem of control of redundant robots in the presence of obstacles in the environment is addressed by defining the extended task space. The problem of optimal control of redundant robots focuses on minimizing torque loading at the joints; locally and globally optimal control laws are developed. Motion and force control of robots in the presence of joint flexibility is accomplished by developing a unified controller to regulate the motion, the contact and internal forces, and the joint elastic force, and to distribute the load between the robots. An experimental setup using two commercial robots has confirmed the results of the theoretical analysis. Author (CISTI)

N94-31721# Montreal Univ. (Quebec). Dept. de Genie Industriel.
A CONTRIBUTION TO THE REPRESENTATION AND IDENTIFICATION OF SEMI-FLEXIBLE ROBOTS M.S. Thesis [CONTRIBUTION A LA REPRESENTATION ET A L'IDENTIFICATION DES ROBOTS SEMI-SOUPLES]
Louise Cleroux Aug. 1992 105 p In FRENCH
(ISBN-0-315-86450-8; CTN-94-61197) Copyright Avail: Micromedia Ltd., Technical Information Centre, 240 Catherine Street, Suite 305, Ottawa, Ontario, K2P 2G8, Canada HC/MF

A representation model for a semi-flexible robot is developed from a combination of the usual Denavit Hartenberg (1955) model, a beam model for every link, and a spring model for every joint. Based on Castigliano's theorem, all the beam deflection modes are considered possible in addition to the springs. The model is able to represent three dimensional errors. Simulations of the model provide interesting results. Effects of arm postures and load categories on the flexible structure are easily visualized from the deformation surfaces obtained. Identification of nongeometric parameters is partially demonstrated using the minimization algorithms of Nelder-Mead (1964) and Powell (1964). The forces used in calculating the strain imposed are the ones felt at the robot base. With these, the three nongeometric parameters of a one degree of freedom planar robot are identified with two sets of data. The six nongeometric parameters of a two degrees of freedom planar robot have been identified with 97 percent success using only six sets of data. A subprogram was developed to calculate the forces at the robot base, based on the flexible structure and the tool tip forces. The nongeometric parameters for a one degree of freedom planar robot were then identified. Author (CISTI)

N94-31724 Maryland Univ., College Park.
ROBOT GRASPING: STABILITY AND OPTIMIZATION ISSUES Ph.D. Thesis
K. Venugopal Varma 1993 134 p
Avail: Univ. Microfilms Order No. DA9327512

In many robotic applications, robot end effectors are used to grasp and manipulate objects. To obtain stable grasps, force and moment balances must be satisfied. Geometric constraints that guarantee force and moment balances are presented. The constraints are used for determining whether a set of finger/object contact points result in a stable grasp. It is recognized that appropriate contact points and sufficient finger forces are required for generating a stable grasp. A stable grasp can be viewed as a static equilibrium state of the object that is maintained when the end effector replaces the object's support. Once an object is grasped, one has to assess the grasping quality. Grasping quality is defined as the capacity of the grasp to resist external forces and moments (disturbances). Grasping quality can be formulated as a mathematical optimization problem in which the finger forces that minimize an objective function and balance the external disturbances are sought. The value of the objective function and the finger forces represent the quality of the grasp for given external disturbances. Three grasping quality (objective) functions are examined and their values together with the resulting finger forces are evaluated. A precision

grasp of a pencil with four finger contacts as used in handwriting is analyzed. A model of the grasp is developed and finger contacts are determined. The optimal finger contacts are evaluated for two different objective functions. This problem formulation results in finger contacts that closely resemble the contacts employed by human beings. The pencil grasping model was used to predict the normal pressure on the writing surface for different stroke directions. These pressure variations are compared with human handwriting samples that correlated well with the model results. The constraints that result in a stable grasp and the grasping quality measure provide the necessary information for assessing the success rate of mechanical grippers in performing complex tasks. Dissert. Abstr.

N94-31754# Laval Univ. (Quebec). Dept. de Genie Mecanique.
APPLICATION OF CONTACT MECHANICS FOR THE VALIDATION OF ROBOTIZED OPERATIONS OF GRASPING OBJECTS SUBJECTED TO STATIC AND DYNAMIC FORCE FIELDS M.S. Thesis [APPLICATION DE LA MECHANIQUE DES CONTACTS POUR LA VALIDATION D'OPERATIONS ROBOTISEES DE PREHENSION D'OBJETS SOUMIS A DES CHAMPS DE FORCES STATIQUES ET DYNAMIQUES]
Traore Sibiri Mar. 1993 103 p In FRENCH
(ISBN-0-315-86831-7; CTN-94-61231) Copyright Avail: Micromedia Ltd., Technical Information Centre, 240 Catherine Street, Suite 305, Ottawa, Ontario, K2P 2G8, Canada HC/MF

Planning, implementation, and validation of applications of robotized grasping are done most of the time on the basis of experiments or by trial and error on the manipulator itself. To avoid the resulting losses in time and money, it would be desirable to be able to develop a more rigorous approach for treating and validating cases of grasping by employing a computer simulation of the pressure and shear force distributions resulting from static and dynamic loadings in the grasper/object contact zones. A simplified model of distribution of pressure and shear stress in the contact zones has been developed based on the method of Winkler (elastic contact) and as a function of contact geometry. The validity of the grasping was defined taking account of the gravitational and dynamic force fields as well as the grasping force transmitted to the points of contact. Experiments on the GMF-S300 robot allowed testing of certain aspects of the proposed approach at different stages of the project. CISTI

N94-31804* National Aeronautics and Space Administration. Lewis Research Center, Cleveland, OH.
HIGH TEMPERATURE NASP ENGINE SEAL DEVELOPMENT (Videotape)
1992 Videotape: 6 min. 25 sec. playing time, in color, with sound
(NASA-TM-109750; NONP-VT-94-9950) Avail: CASI VHS A01/BETA A22

This video details research being conducted at the Lewis Research Center on high temperature engine seal design for the National Aerospace Plane. To maximize the speed, the jets on the NASP extract oxygen from the air rather than carry large liquid fuel tanks; this creates temperatures within the jet of over 5000 F. To prevent these potentially explosive gases from escaping, researchers are developing new technologies for use in the engine seals. Two examples explained are the ceramic wafer seal and the braided ceramic rope seal. Computer simulations and laboratory footage are used to illustrate the workings of these seals. Benefits for other aerospace and industrial applications, as well as for the space shuttle, are explored. CASI

N94-31874# Toronto Univ. (Ontario). Dept. of Mechanical Engineering.
MODEL IDENTIFICATION OF A RECONFIGURABLE ROBOT MANIPULATOR M.S. Thesis
Shiyi Jia 1993 152 p
(ISBN-0-315-87109-1; CTN-94-61249) Copyright Avail: Micromedia Ltd., Technical Information Centre, 240 Catherine Street, Suite 305, Ottawa, Ontario, K2P 2G8, Canada HC/MF

The issue of model identification of an advanced modular and reconfigurable robot system, the IRIS Facility, is addressed. Theoretical insights into the methodology of parameter estimation are developed and the theory is applied experimentally to the IRIS Facility. In the theoretical study, the classical least squares (LS) algorithm is presented. It is found that LS estimates contain bias when measurement noise is present. To compensate the bias in LS estimates, two modified LS algorithms are proposed: the bias compensating LS algorithm and the instrumental variables method. The applicability of these two algorithms to robot parameter estimation is discussed and evaluated by simulation examples. Using the proposed algorithms, the dynamic parameters of the IRIS Facility are determined experimentally. The results confirm the theoretical analysis that the modified LS estimates are more accurate than the original LS estimates. The experimental work also provides a set of reliable parameters for the facility users and control system designers. Recommendations are given for improving the estimation process and related issues. Author (CISTI)

N94-31878# Toronto Univ. (Ontario). Dept. of Mechanical Engineering.
AUTOMATIC ANALYSIS OF FORCE DISTRIBUTION IN MULTI-FINGERED ARTICULATED HANDS M.S. Thesis
Mahyar Amani 1993 154 p
(ISBN-0-315-87205-5; CTN-94-61253) Copyright Avail: Micromedia Ltd., Technical Information Centre, 240 Catherine Street, Suite 305, Ottawa, Ontario, K2P 2G8, Canada HC/MF

A kinematic and force analysis of multifingered, multijointed dexterous hands is presented. The analysis involves calculation of the basis for null space of the grasp matrix. An algorithm is developed to perform all necessary analyses of dexterous hands. All equality and inequality constraints are automatically formulated in a constraint matrix. These include unisense constraints, frictional constraints, and joint torque limits. The reduction of the constraint matrix into a compact form is also presented. The algorithm is written in Fortran and is user-friendly and capable of handling all practical grasping problems. Different types of contact may be examined, including soft finger contact and point contact with and without friction. The software can easily determine the feasibility of a grasp for a given set of contact forces/torques, and may potentially be combined with either routines to compute the optimum value of contact wrench intensities and joint torque values. Author (CISTI)

N94-31973 Stanford Univ., CA.
CONTROL OF A FLEXIBLE-LINK ROBOTIC ARM MANIPULATING AN UNKNOWN DYNAMIC PAYLOAD Ph.D. Thesis
Lawrence John Alder 1993 180 p
Avail: Univ. Microfilms Order No. DA9317744

When light-weight space-based robots, such as the space shuttle's RMS (remote manipulator system), manipulate massive payloads such as satellites, significant structural bending is induced in the links of the robot. In addition, space-based robots will often manipulate payloads that are not rigid bodies: for example, satellites may contain fuel or have flexible appendages. This dissertation contributes new basic technology that will enable flexible-link manipulators to perform precise end-point control of payloads while simultaneously controlling the unknown internal dynamics of the payload. The approach taken here combines high-performance control with an innovative identification algorithm. In addition, to facilitate the development of controllers, a numerically efficient procedure to merge payload and arm dynamic models is presented. First, controllers incorporating end-point feedback with a known payload are made robust to high-frequency modelling errors, sensor noise, and sensor bias using frequency-weighted linear quadratic Gaussian design methods. Using end-point position measurements as the primary sensor, the robot is then capable of actively damping the internal payload dynamics an order of magnitude faster than the natural damping rate--if it knows the payload parameter. However, with this type of controller small parameter variations in the payload can lead to poor performance or instability. This research has therefore also developed an identification algorithm that updates the end-point controller parameters; this enables the system to achieve high performance when the payload dynamics are not known a priori. By using a nominal control law, the identification problem can be reduced to detecting and identifying eigenvalues of a closed system. To identify these eigenvalues, a generic algorithm capable of determining the eigenvalues of a system in real time has been developed: even the order of the system need not be known in advance. With this approach, moreover, the identification algorithm does not require that the system inject broad-band excitation in order to work accurately. An experimental robotic system was designed and built to test these emerging control strategies. All of the control strategies have been verified on the experimental robot. Experimental results demonstrate, for the first time, precision end-point control of a very flexible singlelink robot arm with unknown dynamic payloads. Dissert. Abstr.

N94-32166# Massachusetts Inst. of Tech., Cambridge. Artificial Intelligence Lab.

PARALLEL METHODS FOR SYNTHESIZING WHOLE-HAND GRASPS FROM GENERALIZED PROTOTYPES

Nancy S. Pollard Jan. 1994 283 p

(Contracts N00014-91-J-4038; N00014-92-J-1814)

(AD-A276798; AI-TR-1464) Avail: CASI HC A13/MF A03

This report addresses the problem of acquiring objects using articulated robotic hands. Standard grasps are used to make the problem tractable, and a technique is developed for generalizing these standard grasps to increase their flexibility to variations in the problem geometry. A generalized grasp description is applied to a new problem situation using a parallel search through hand configuration space, and the result of this operation is a global overview of the space of good solutions. The techniques presented in this report have been implemented, and the results are verified using the Salisbury three-finger robotic hand. DTIC

N94-32236# Naval Research Lab., Washington, DC.

PINCHED PROPAGATION OF HIGH-POWER, PULSED ELECTRON BEAMS FOR WELDING AND MATERIALS PROCESSING APPLICATIONS Interim Report

Richard F. Fernsler, Richard F. Hubbard, and Martin Lampe 3 Jan. 1994 59 p

(ARPA Order 7781)

(AD-A276925; NRL/MR/6790-93-7403) Avail: CASI HC A04/MF A01

Electron beams are used commercially as intense heating sources for welding and related materials processing applications. The beams used for welding operate continuously with energy up to 200 keV and current approximately 1 A. Because these beams are severely degraded by propagation in air over any substantial range, most present-day electron-beam welders require vacuum pumping and precision focusing, which has severely restricted utilization of the technology. Over the past few decades, a different class of electron-beam generators has been developed that produces pulsed beams with energies of several MeV, currents of 1 kA or more, radii as small as 1 mm, pulse lengths of tens of ns, and pulse repetition rates up to several kHz. We show here that beams of this type can propagate in ambient air, in a tightly pinched mode and with acceptable stability, over distances of a few tens of cm. We determine the constraints on the choice of beam parameters, due mainly to the effects of gas scattering and the resistive instability. We show that stability can be enhanced, and the acceptable parameter range extended considerably, by using a narrow conducting pipe filled with air or another gas to guide the beam to the workpiece. DTIC

N94-32261# Naval Postgraduate School, Monterey, CA.

CORRELATION OF FLUX COMPOSITION AND INCLUSION CHARACTERISTICS WITH SUBMERGED ARC WELD METAL PROPERTIES IN HY-100 STEEL M.S. Thesis

Kent W. Kettell Sep. 1993 107 p

(AD-A277040) Avail: CASI HC A06/MF A02

Submerged arc weldments of HY-100 steel prepared under standard conditions with five commercially available fluxes were analyzed to discern a basis for the variation in mechanical properties associated with different flux use. The variations in flux chemistry resulted in alloyed weldments with diverse weld metal mechanical properties as evident by Charpy impact, tensile, dynamic tear, and microhardness tests. The microstructures and macrostructures were examined using optical and electron microscopy in order to determine the basis for the variations in strength and toughness. Scanning electron microscope and energy dispersive x-ray experiments were performed to determine the size, type, distribution and volume fraction of the non-metallic inclusions in the weld metal. Inclusion characterization revealed that the role of the flux in alloying had a more significant effect on the strength and toughness than did the presence of specific inclusions. DTIC

N94-32272*# National Aeronautics and Space Administration. Lewis Research Center, Cleveland, OH.

DEVELOPMENT OF LIGHTWEIGHT RADIATORS FOR LUNAR BASED POWER SYSTEMS

Albert J. Juhasz and Harvey S. Bloomfield May 1994 12 p Proposed for presentation at the 5th European Symposium on Space and Environmental Control Systems and the 24th International Conference on Environmental Systems, Friedrichshafen, Germany, 20-23 Jun. 1994; sponsored by ESA, SAE, ASME, AIChE, and AIAA

(RTOP 233-02-0B)

(NASA-TM-106604; E-8880; NAS 1.15:106604) Avail: CASI HC A03/MF A01

This report discusses application of a new lightweight carbon-carbon (C-C) space radiator technology developed under the NASA Civil-Space Technology Initiative (CSTI) High Capacity Power Program to a 20 kWe lunar based power system. This system comprises a nuclear (SP-100 derivative) heat source, a Closed Brayton Cycle (CBC) power conversion unit with heat rejection by means of a plane radiator. The new radiator concept is based on a C-C composite heat pipe with integrally woven fins and a thin walled metallic liner for containment of the working fluid. Using measured areal specific mass values (1.5 kg/m2) for flat plate radiators, comparative CBC power system mass and performance calculations show significant advantages if conventional heat pipes for space radiators are replaced by the new C-C heat pipe technology. Author

N94-32320 Computational Mechanics Co., Austin, TX.

NEW MICRO- AND MACROSCOPIC MODELS OF CONTACT AND FRICTION Final Technical Report, 1 Nov. 1990 - 31 Oct. 1993

W. W. Tworzydlo, W. Cecot, J. T. Oden, and C. H. Yew 29 Nov. 1993 185 p Limited Reproducibility: More than 20% of this document may be affected by microfiche quality

(Contract F49620-91-C-0011)

(AD-A277240; TR-93-10; AFOSR-94-0045TR) Avail: CASI HC A09

This is the final report for the three year research project dedicated to the development of new asperity-based models of frictional interfaces. The main concept is to combine statistical homogenization methods with a realistic nonlinear finite element analysis of surface micro-asperities, and thus produce new asperity-based models of contact and friction. Research in the project started with the development of a complete theory and software for the statistical homogenization of random surface parameters. The next stage focused on the development of a finite element code for modeling surface asperities. This code is based on a proprietary h/p adaptive finite element kernel, which has been customized for the analysis of elastic and elasto-viscoplastic asperities with contact, molecular-range adhesion, and sliding resistance. To verify the new asperity-based interface models, special experiments were designed and performed for custom-shaped asperities and for rough engineering surfaces. The results of these experiments compare favorably with asperity-based theoretical and numerical predictions, and thus confirm the feasibility and practical value of the new models developed in this project. These models will be applicable in the analysis and control of a broad range of contact and friction phenomena, such as friction-induced squeaks and noises, tribology of bearings, electrical and thermal connectors, the mechanism of wear, and many others. DTIC

N94-32334 Naval Postgraduate School, Monterey, CA.

AN EXPERIMENTAL TESTBED FOR A FREE-FLOATING MANIPULATOR M.S. Thesis

Douglas L. Maddox Dec. 1993 44 p Limited Reproducibility: More than 20% of this document may be affected by microfiche quality

(AD-A277350) Avail: CASI HC A03

The attitude control of a multibody system in a gravity free environment has been an ongoing field of study for decades. Although most methods involve the use of thrusters, some algorithms exist that utilize internal motion of the system for reorientation. These algorithms reduce the expenditure of the limited amount of onboard fuel so as to extend the useful life span of the system. An experimental facility for testing existing algorithms and algorithms to be developed in the future for motion planning of multibody space systems are developed as part of this research. The multibody system developed is comprised of a two link space vehicle/manipulator system. The system is mounted on air bearings and floats freely on a flat glass table. The robotic system is controlled in real time using a VME based controller with support from a SPARC station. DTIC

N94-32370 Naval Postgraduate School, Monterey, CA.

DESIGN OF A TWO DIMENSIONAL PLANER PRESSURIZED AIR LABYRINTH SEAL TEST RIG M.S. Thesis

Joseph S. Konicki Dec. 1993 86 p Limited Reproducibility: More than

20% of this document may be affected by microfiche quality
(AD-A277232) Avail: CASI HC A05

A two-dimensional planer labyrinth seal test rig was designed to operate with air supplied at 45 psig and temperatures up to 150 F. The rig operates with a manually specified test section pressure up to 30 psig yielding Mach numbers to 0.9 and gap Reynolds numbers to 100,000. The air flow rate through the seal will be controlled by setting inlet pressure and adjusting an outlet control valve. The test section measurements are 18 inches wide by 1.5 inches depth by 6 inches in length and provides for 10:1 large scale geometry seals to be used to facilitate measurements. Design maximum seal gap size is 0.15 inches. The test section has a glass viewing port to allow flow field measurement by non-intrusive means such as Laser Doppler Velocimeter (LDV) with seals containing up to 5 sealing knives. Measurements of pressure, temperature and flow fields can also be simultaneously measured by probes inserted in the seal itself, or mounted on the removable/replaceable top plate. Inlet flow is conditioned through the use of a dump diffuser incorporating screens, honeycombs, expansion and contraction portions. The inlet flow to the test section can be modified from uniform to various non-uniform conditions by employing profile generators such as screens and winglets. A detailed mechanical design has been conducted including stress analysis and seal flow rate predictions. DTIC

N94-32479*# Nichols Research Corp., Huntsville, AL.
DEVELOPMENT OF AN AUTOMATED WIRE DELIVERY SYSTEM FOR ROBOTIC WELDING APPLICATIONS Final Report, 18 Apr. 1990 - 18 Jul. 1992
Timothy B. Morris 9 Jul. 1992 37 p
(Contract NAS8-38477; SBIR-05.05-2200)
(NASA-CR-194216; NAS 1.26:194216; NRC-TR-92-143) Avail: CASI HC A03/MF A01

Our Phase 1 study showed new techniques and procedures are required for maintaining the delivery of filler wire into the weld pool for robotic VPPA (variable polarity plasma arc) and GTA (gas tungsten arc) welding applications. Toward this end, the development and implementation of an autonomous wire delivery system appears very feasible utilizing existing proven technologies. In our Phase 1 research effort, we investigated the requirements necessary of a wire delivery system to assure a quality weldment. We also evaluated various sensing technologies for their ability to provide information related to delivery of the wire into the weld pool. Finally, we described the types of software necessary for the automatic wire delivery system. Several approaches for automating the wire delivery system have been suggested, and we recommend the building of a prototype system in our Phase 2 effort as a logical step in the application of this technology to robotic GTA and VPPA welding. Such a prototype would contain the necessary hardware components, sensors and control software for evaluating the performance of the system as applied to the berthing port, main engine and external fuel tank. This tool would be used to demonstrate the worth and plausibility of automating the wire delivery system for each of these applications. Author

N94-32682 Oak Ridge National Lab., TN.
A NEW SOLUTION METHOD FOR THE INVERSE KINEMATIC JOINT VELOCITY CALCULATIONS OF REDUNDANT MANIPULATORS
F. G. Pin, P. F. R. Belmans, J. C. Culioli, D. D. Carlson, and F. A. Tulloch 1994 8 p Presented at the Institute of Electrical and Electronics Engineers (IEEE) International Conference on Robotics, San Diego, CA, 8-13 May 1994 Limited Reproducibility: More than 20% of this document may be affected by microfiche quality
(Contracts DE-AC05-84OR-21400; DE-AC05-76OR-00033)
(DE94-004427; CONF-940550-10) Avail: CASI HC A02

A new analytical method to resolve underspecified systems of algebraic equations is presented. The method is referred to as the Full Space Parameterization (FSP) method and utilizes easily-calculated projected solution vectors to generate the entire space of solutions of the underspecified system. Analytic parameterizations for both the space of solutions and the null space of the system reduce the determination of a task-requirement-based single solution to a m - n dimensional problem, where m - n is the degree of underspecification, or degree of redundancy, of the system. An analytical solution is presented to directly calculate the least-norm solution from the parameterized space and the results are compared to solutions of the standard pseudo-inverse algorithm which embodies the (least-norm) Moore-Penrose generalized inverse. Application of the new solution method to a variety of systems and task requirements are discussed and sample results using four-link planar manipulators with one or two degrees of redundancy and a seven degree-of-freedom manipulator with one or four degrees of redundancy are presented to illustrate the efficiency of the new FSP method and algorithm. DOE

N94-32718# Department of the Navy, Washington, DC.
FLEXIBLE DRIVE SHAFT COUPLING Patent Application
Stanley Olson, inventor (to Navy) 12 Jul. 1993 21 p
(AD-D016096; US-Patent-Appl-SN-089915) Avail: CASI HC A03/MF A01

A flexible drive shaft coupling with two stage torsional flexibility is introduced. The flexible drive shaft coupling allows axial, radial, and bending misalignment of the input and output shafts while vibrationally isolating the shafts from one another. At low torque, power is transmitted from the input shaft through an elastomeric ring to the output shaft. At higher torque the elastomeric ring is deformed to allow contact between a less resilient snubber assembly and a drive plate mechanically connected to the output shaft. Power is transmitted through less resilient snubber assemblies which provide for greater power transmission. The axis of the coupling can be provided with a flexible spool assembly to allow transmission of exhaust mass from the input shaft to the output shaft. DTIC

N94-32741*# Case Western Reserve Univ., Cleveland, OH. Dept. of Electrical Engineering and Applied Physics.
CONTROL STRATEGIES FOR SYSTEMS WITH LIMITED ACTUATORS Final Report
Vincent R. Marcopoli and Stephen M. Phillips Apr. 1994 27 p
(Grant NAG3-1232; RTOP 505-62-50)
(NASA-CR-195307; E-8714; NAS 1.26:195307) Avail: CASI HC A03/MF A01

This work investigates the effects of actuator saturation in multi-input, multi-output (MIMO) control systems. The adverse system behavior introduced by the saturation nonlinearity is viewed here as resulting from two mechanisms: controller windup - a problem caused by the discrepancy between the limited actuator commands and the corresponding control signals, and directionality - the problem of how to use nonlimited actuators when a limited condition exists. The tracking mode and Hanus methods are two common strategies for dealing with the windup problem. It is seen that while these methods alleviate windup, performance problems remain due to plant directionality. Though high gain conventional antiwindup as well as more general linear methods have the potential to address both windup and directionality, no systematic design method for these schemes has emerged; most approaches used in practice are application driven. An alternative method of addressing the directionality problem is presented which involves the introduction of a control direction preserving nonlinearity to the Hanus antiwindup system. A nonlinearity is subsequently proposed which reduces the conservation inherent in the former direction-preserving approach, improving performance. The concept of multivariable sensitivity is seen to play a key role in the success of the new method.
Author (revised)

N94-32758# Department of Energy, New York, NY. Environmental Measurements Lab.
LOW POWER, CONSTANT-FLOW AIR PUMP SYSTEMS
Michael D. Polito and Brian Albert Jan. 1994 28 p
(DE94-007463; EML-558) Avail: CASI HC A03/MF A01

A rugged, yet small and lightweight constant-flow air pump system has been designed. Flow control is achieved using a novel approach which is three times more power efficient than previous designs. The resultant savings in battery size and weight makes these pumps ideal for sampling air on balloon platforms. The pump package includes meteorological sensors and an onboard computer that stores time and sensor data and turns the constant-flow pump circuit on/off. Some applications of these systems are also presented. DOE

N94-32778 Argonne National Lab., IL.
ON THE UNSTEADY-MOTION THEORY OF MAGNETIC FORCES FOR MAGLEV
S. S. Chen, S. Zhu, and Y. Cai Nov. 1993 69 p Limited Reproducibility:

More than 20% of this document may be affected by microfiche quality
(Contract W-31-109-eng-38)
(DE94-007765; AD-A277696; ANL-93/39) Avail: CASI HC A04

Motion-dependent magnetic forces are the key elements in the study of magnetically levitated vehicle (maglev) system dynamics. In the past, most maglev-system designs were based on a quasisteady-motion theory of magnetic forces. This report presents an experimental and analytical study that will enhance our understanding of the role of unsteady-motion-dependent magnetic forces and demonstrate an experimental technique that can be used to measure those unsteady magnetic forces directly. The experimental technique provides a useful tool to measure motion-dependent magnetic forces for the prediction and control of maglev systems. DOE

N94-32893*# National Aeronautics and Space Administration. Lewis Research Center, Cleveland, OH.
SIMULTANEOUS PRESSURE MEASUREMENT AND HIGH-SPEED PHOTOGRAPHY STUDY OF CAVITATION IN A DYNAMICALLY LOADED JOURNAL BEARING
D. C. Sun (State Univ. of New York, Binghamton.), David E. Brewe (Army Research Lab., Cleveland, OH.), and Philip B. Abel Feb. 1994 17 p Presented at the ASME/STLE Tribology Conference, San Diego, CA, 18-21 Oct. 1992; sponsored by ASME and the Society of Tribologists and Lubrication Engineers
(DA Proj. 1L1-61102-AH-45; RTOP 505-63-5A)
(NASA-TM-106456; E-6834; NAS 1.15:106456; ARL-TR-10) Avail: CASI HC A03/MF A01

Cavitation of the oil film in a dynamically loaded journal bearing was studied using high-speed photography and pressure measurement simultaneously. Comparison of the visual and pressure data provided considerable insight into the occurrence and nonoccurrence of cavitation. It was found that (1) for the submerged journal bearing, cavitation typically occurred in the form of one bubble with the pressure in the cavitation bubble close to the absolute zero; and (2) for cavitation-producing operating conditions, cavitation did not always occur; with the oil film then supporting a tensile stress. Author

N94-32900*# North Dakota Univ., Grand Forks.
MANUAL FOR AUTOMATIC GENERATION OF FINITE ELEMENT MODELS OF SPIRAL BEVEL GEARS IN MESH Final Report
G. D. Bibel, S. Reddy, and A. Kumar Apr. 1994 58 p
(Grant NAG3-1476; DA Proj. 1L1-62211-A-47-A; RTOP 505-62-36)
(NASA-CR-191009; E-8671; NAS 1.26:191009; ARL-CR-121) Avail: CASI HC A04/MF A01

The goal of this research is to develop computer programs that generate finite element models suitable for doing 3D contact analysis of faced milled spiral bevel gears in mesh. A pinion tooth and a gear tooth are created and put in mesh. There are two programs: Points.f and Pat.f to perform the analysis. Points.f is based on the equation of meshing for spiral bevel gears. It uses machine tool settings to solve for an N x M mesh of points on the four surfaces, pinion concave and convex, and gear concave and convex. Points.f creates the file POINTS.OUT, an ASCI file containing N x M points for each surface. (N is the number of node points along the length of the tooth, and M is nodes along the height.) Pat.f reads POINTS.OUT and creates the file tl.out. Tl.out is a series of PATRAN input commands. In addition to the mesh density on the tooth face, additional user specified variables are the number of finite elements through the thickness, and the number of finite elements along the tooth full fillet. A full fillet is assumed to exist for both the pinion and gear. Author

N94-32902*# National Aeronautics and Space Administration. Lewis Research Center, Cleveland, OH.
FEED-FORWARD CONTROL OF GEAR MESH VIBRATION USING PIEZOELECTRIC ACTUATORS
Gerald T. Montague (NYMA, Inc., Brook Park, OH.), Albert F. Kascak, Alan Palazzolo, Daniel Manchala, and Erwin Thomas May 1994 21 p
(DA Proj. 1L1-61102-AH-45; RTOP 505-62-06; RTOP 505-63-5B)
(NASA-TM-106366; E-8168; NAS 1.15:106366; ARL-TR-416) Avail: CASI HC A03/MF A01

This paper presents a novel means for suppressing gear mesh-related vibrations. The key components in this approach are piezoelectric actuators and a high-frequency, analog feed-forward controller. Test results are presented and show up to a 70-percent reduction in gear mesh acceleration and vibration control up to 4500 Hz. The principle of the approach is explained by an analysis of a harmonically excited, general linear vibratory system. Author

N94-32929*# Akron Univ., OH.
A PROCEDURE FOR 3-D CONTACT STRESS ANALYSIS OF SPIRAL BEVEL GEARS Final Report
A. Kumar and G. Bibel Mar. 1994 87 p
(Grant NAG3-1476; DA Proj. 1L1-62211-A-47-A; RTOP 505-62-10)
(NASA-CR-194472; E-8613; NAS 1.26:194472; ARL-CR-72) Avail: CASI HC A05/MF A01

Contact stress distribution of spiral bevel gears using nonlinear finite element static analysis is presented. Procedures have been developed to solve the nonlinear equations that identify the gear and pinion surface coordinates based on the kinematics of the cutting process and orientate the pinion and the gear in space to mesh with each other. Contact is simulated by connecting GAP elements along the intersection of a line from each pinion point (parallel to the normal at the contact point) with the gear surface. A three dimensional model with four gear teeth and three pinion teeth is used to determine the contact stresses at two different contact positions in a spiral bevel gearset. A summary of the elliptical contact stress distribution is given. This information will be helpful to helicopter and aircraft transmission designers who need to minimize weight of the transmission and maximize reliability. Author (revised)

N94-32979*# National Aeronautics and Space Administration. Lewis Research Center, Cleveland, OH.
SPUR, HELICAL, AND SPIRAL BEVEL TRANSMISSION LIFE MODELING
Michael Savage (Akron Univ., OH.), Kelly L. Rubadeux (Akron Univ., OH.), Harold H. Coe, and John J. Coy Apr. 1994 13 p Proposed for presentation at the 30th Joint Propulsion Conference, Indianapolis, IN, 27-29 Jun. 1994; sponsored by AIAA, SAE, ASME, and ASEE
(DA Proj. 1L1-62211-A-47-A; RTOP 505-62-10)
(NASA-TM-106552; E-8707; NAS 1.15:106552; ARL-TR-390; AIAA Paper 94-3079) Avail: CASI HC A03/MF A01

A computer program, TLIFE, which estimates the life, dynamic capacity, and reliability of aircraft transmissions, is presented. The program enables comparisons of transmission service life at the design stage for optimization. A variety of transmissions may be analyzed including: spur, helical, and spiral bevel reductions as well as series combinations of these reductions. The basic spur and helical reductions include: single mesh, compound, and parallel path plus revert star and planetary gear trains. A variety of straddle and overhung bearing configurations on the gear shafts are possible as is the use of a ring gear for the output. The spiral bevel reductions include single and dual input drives with arbitrary shaft angles. The program is written in FORTRAN 77 and has been executed both in the personal computer DOS environment and on UNIX workstations. The analysis may be performed in either the SI metric or the English inch system of units. The reliability and life analysis is based on the two-parameter Weibull distribution lives of the component gears and bearings. The program output file describes the overall transmission and each constituent transmission, its components, and their locations, capacities, and loads. Primary output is the dynamic capacity and 90-percent reliability and mean lives of the unit transmissions and the overall system which can be used to estimate service overhaul frequency requirements. Two examples are presented to illustrate the information available for single element and series transmissions. Author

N94-33061# Aerospace Corp., El Segundo, CA. Technology Operations.
TORQUE CHARACTERISTICS OF SOLID LUBRICATED PRECISION BEARINGS DURING OSCILLATORY MOTION
Reinhold Bauer and Paul D. Fleischauer 31 Jan. 1994 36 p
(Contract F04701-93-C-0094)
(AD-A278133; TR-93(3935)-11; SMC-TR-94-13) Avail: CASI HC A03/MF A01

MoS2 sputter-coated as well as uncoated (bare) angular-contact ball bearings were tested with various cage materials in a low-speed regime. Various self-lubricating polymers either neat or with additives and metallic cages were tested. The emphasis of this paper is to report on significant

torque increases torque bumps observed during non-ball overlap, oscillatory motion for some race/cage combinations. In some race/cage combinations torque bumps can be minimized by proper run-in. No attempt was made to run the bearings to failure, although certain race/cage combinations did in fact fail before the end of test. DTIC

N94-33251 Army Armament Research, Development and Engineering Center, Watervliet, NY.
A REVIEW OF WELDMENT FAILURE MODES AND WELDABILITY TESTING METHODS Final Report
George Young Jan. 1994 29 p Limited Reproducibility: More than 20% of this document may be affected by microfiche quality
(AD-A278096; ARCCB-TR-94003) Avail: CASI HC A03

An engineering study was conducted that reviewed typical weldment failure modes and the types of weldability test procedures currently used to predict behavioral response of a material that is to be welded. In comparing the design effectiveness of these tests, each has certain inherent technical advantage/disadvantages associated with it. The tests, if used appropriately, can save untold time and costs associated with poorly welded structures/components that fail in service prematurely. They are divided into two major categories, direct and indirect, related to the test methodology or procedure used to generate results. Specifically, direct tests make use of actual weldments, while indirect tests utilize basic metallurgical principles to predict weld behavior. From this study, it should be apparent that determining what the most appropriate weldability test procedure is for obtaining useful results for a given situation is critical to the success of that test. DTIC

N94-32450*# National Aeronautics and Space Administration. Lyndon B. Johnson Space Center, Houston, TX.
APPLICATION OF DEXTEROUS SPACE ROBOTICS TECHNOLOGY TO MYOELECTRIC PROSTHESES
Clifford Hess, Larry C. H. Li, Kristin A. Farry, and Ian D. Walker *In* NASA, Washington, Technology 2003: The Fourth National Technology Transfer Conference and Exposition, Volume 2 Feb. 1994 p 255-268 (For primary document see N94-32420 09-99)
Avail: CASI HC A03/MF A04

N94-32451*# Naval Surface Warfare Center, Panama City, FL.
NAVY OMNI-DIRECTIONAL VEHICLE (ODV) DEVELOPMENT PROGRAM
Hillery McGowen *In* NASA, Washington, Technology 2003: The Fourth National Technology Transfer Conference and Exposition, Volume 2 Feb. 1994 p 269-278 (For primary document see N94-32420 09-99)
Avail: CASI HC A02/MF A04

N94-32452*# Jet Propulsion Lab., California Inst. of Tech., Pasadena.
APPLYING ROBOTICS TO HAZMAT
Richard V. Welch and Gary O. Edmonds *In* NASA, Washington, Technology 2003: The Fourth National Technology Transfer Conference and Exposition, Volume 2 Feb. 1994 p 279-287 (For primary document see N94-32420 09-99)
Avail: CASI HC A02/MF A04

N94-33296*# National Aeronautics and Space Administration. Lewis Research Center, Cleveland, OH.
DESIGN, CHARACTERIZATION AND CONTROL OF THE UNIQUE MOBILITY CORPORATION ROBOT
Virgilio B. Velasco, Jr. (Case Western Reserve Univ., Cleveland, OH.), Wyatt S. Newman (Case Western Reserve Univ., Cleveland, OH.), Bruce Steinetz, Carlo Kopf, and John Malik *In its* The 28th Aerospace Mechanisms Symposium May 1994 p 63-78 (For primary document see N94-33291 09-15)
(Contract NAS3-26285)
Avail: CASI HC A03/MF A04

N94-33297*# Maryland Univ., College Park.
DEVELOPMENT OF AN INTERCHANGEABLE END EFFECTOR MECHANISM FOR THE RANGER TELEROBOTIC VEHICLE
Robert Cohen and David L. Akin *In* NASA. Lewis Research Center, The 28th Aerospace Mechanisms Symposium May 1994 p 79-89 (For primary document see N94-33291 09-15)
Avail: CASI HC A03/MF A04

N94-33299*# National Aeronautics and Space Administration. John F. Kennedy Space Center, Cocoa Beach, FL.
INNOVATIVE MECHANISM FOR MEASURING THE MASS PROPERTIES OF AN OBJECT
Kedron R. Wolcott (I-NET, Inc., Cocoa Beach, FL.), Todd A. Graham, and Keith L. Doty *In* NASA. Lewis Research Center, The 28th Aerospace Mechanisms Symposium May 1994 p 107-121 (For primary document see N94-33291 09-15)
Avail: CASI HC A03/MF A04

N94-33300*# Lockheed Missiles and Space Co., Sunnyvale, CA.
SPACE STATION FREEDOM SOLAR ARRAY TENSION MECHANISM DEVELOPMENT
Curtis Allmon and Bert Haugen *In* NASA. Lewis Research Center, The 28th Aerospace Mechanisms Symposium May 1994 p 123-128 (For primary document see N94-33291 09-15)
Avail: CASI HC A02/MF A04

N94-33305*# Lockheed Engineering and Sciences Co., Houston, TX.
PIP PIN RELIABILITY AND DESIGN
Lane P. Skyles *In* NASA. Lewis Research Center, The 28th Aerospace Mechanisms Symposium May 1994 p 153-158 (For primary document see N94-33291 09-15)
Avail: CASI HC A02/MF A04

N94-33308*# Space Systems/Loral, Palo Alto, CA.
TWO-AXIS ANTENNA POSITIONING MECHANISM
Michelle Herald and Leilani C. Wai *In* NASA. Lewis Research Center, The 28th Aerospace Mechanisms Symposium May 1994 p 183-197 (For primary document see N94-33291 09-15)
Avail: CASI HC A03/MF A04

N94-33312*# European Space Tribology Lab., Risley (England).
DEVELOPMENT OF LONG-LIFE, LOW-NOISE LINEAR BEARINGS FOR ATMOSPHERIC INTERFEROMETRY
E. W. Roberts, R. B. Watters, S. Gill, R. Birner, G. Lange, and W. Posselt *In* NASA. Lewis Research Center, The 28th Aerospace Mechanisms Symposium May 1994 p 245-264 (For primary document see N94-33291 09-15)
Avail: CASI HC A03/MF A04

N94-33314*# Draper (Charles Stark) Lab., Inc., Cambridge, MA.
DESIGN OF A HIGH-SPEED RELIABLE BALL BEARING
Herbert B. Singer and Erik Gelotte *In* NASA. Lewis Research Center, The 28th Aerospace Mechanisms Symposium May 1994 p 279-283 (For primary document see N94-33291 09-15)
Avail: CASI HC A01/MF A04

N94-33315*# Lockheed Missiles and Space Co., Sunnyvale, CA.
MSAT BOOM JOINT TESTING AND LOAD ABSORBER DESIGN
D. H. Klinker, K. Shuey, and D. R. St.Clair *In* NASA. Lewis Research Center, The 28th Aerospace Mechanisms Symposium May 1994 p 285-302 (For primary document see N94-33291 09-15)
Avail: CASI HC A03/MF A04

N94-33316*# Lockheed Missiles and Space Co., Sunnyvale, CA.
SPECIAL TEST EQUIPMENT AND FIXTURING FOR MSAT REFLECTOR ASSEMBLY ALIGNMENT
Jeffrey A. Young, Michael R. Zinn, and David R. McCarten *In* NASA. Lewis Research Center, The 28th Aerospace Mechanisms Symposium May 1994 p 303-322 (For primary document see N94-33291 09-15)
Avail: CASI HC A03/MF A04

N94-33317*# Astro Aerospace Corp., Carpinteria, CA.
DEPLOYABLE AND RETRACTABLE TELESCOPING TUBULAR STRUCTURE DEVELOPMENT
M. W. Thomson *In* NASA. Lewis Research Center, The 28th Aerospace Mechanisms Symposium May 1994 p 323-338 (For primary document see N94-33291 09-15)
Avail: CASI HC A03/MF A04

N94-33321*# G and H Technology, Inc., Camarillo, CA.
PAYLOAD HOLDDOWN AND RELEASE MECHANISM
Dale Chaput, Mark Visconti, Michael Edwards, and Tom Moran *In* NASA. Lewis Research Center, The 28th Aerospace Mechanisms Symposium May 1994 p 395-411 (For primary document see N94-33291 09-15)
Avail: CASI HC A03/MF A04

N94-33322*# Naval Research Lab., Washington, DC.
ADVANCED RELEASE TECHNOLOGIES PROGRAM
Bill Purdy *In* NASA. Lewis Research Center, The 28th Aerospace Mechanisms Symposium May 1994 p 413-427 (For primary document see N94-33291 09-15)
Avail: CASI HC A03/MF A04

38 QUALITY ASSURANCE AND RELIABILITY

Includes product sampling procedures and techniques; and quality control.

N94-31065# Naval Command, Control and Ocean Surveillance Center, San Diego, CA. Research, Development, Technology and Evaluation Div.
EVALUATION OF NONDESTRUCTIVE INSPECTION TECHNIQUES FOR QUALITY CONTROL OF ALUMINA-CERAMIC HOUSING COMPONENTS Final Report
R. R. Kurkchubasche, R. P. Johnson, and J. D. Stachiw Sep. 1993 75 p
(NR Proj. SO3-97)
(AD-A276220; NCCOSC/RDT/E-TR-1588) Avail: CASI HC A04/MF A01

Alumina-ceramic pressure housings have been shown to be feasible and cost-effective alternatives to housings made from more traditional materials such as steel, titanium, or aluminum. The high specific compressive strength, and high specific elastic modulus of alumina ceramic allow engineers to design pressure housings having weight-to-displacement ratios lower than 0.60 for a service depth of 20,000 feet while remaining neutrally buoyant. Titanium housings designed to the same requirements have weight-to-displacement ratios in excess of 0.85. Although the difference may, at first glance, seem negligible, it accounts for a tripling of the housing payload weight capacity when alumina ceramic is substituted for titanium. The transition of alumina-ceramic pressure housing components from the developmental stage to the operational environment brings on the requirement for the capability of nondestructively inspecting these components for gross fabrication flaws and for in-service damage which may have occurred. Various radiographic and ultrasonic inspection methods are evaluated and compared based on their ability to detect defects, determine defect location, and characterize defect size and shape in large alumina-ceramic components used for deep submergence pressure housing applications. Recommendations based on the findings of the study are made for the nondestructive inspection of alumina-ceramic components. DTIC

N94-31166 Ecole Nationale Superieure des Telecommunications, Paris (France).
A GENERIC MODEL FOR DATA ACQUISITION: CONNECTIONIST METHODS OF INFORMATION PROCESSING Ph.D. Thesis [UN MODELE GENERIQUE POUR L'ACQUISITION DE DONNEES: METHODES CONNEXIONNISTES DE TRAITEMENT DE L'INFORMATION]
Jacques Ehrlich 1993 285 p In FRENCH Limited Reproducibility: More than 20% of this document may be affected by microfiche quality
(ISSN 0751-1353)
(TELECOM-93-E-003; ETN-94-95896) Avail: CASI HC A13

EDDAKS (Event Driven Data Acquisition Kernel System), for the quality control of products created in industrial production processes, is proposed. It is capable of acquiring information about discrete event systems by synchronizing to them via the events. EDDAKS consists of EdObjects, forming a hierarchy, which react to EdEvents, and perform processing operations on messages. The hierarchy of EdObjects consists (from bottom up) of the Sensor, the Phase, the Extracter, the Dynamic Spreadsheet, and EDDAKS itself. The first three levels contribute to building the internal representation: a state vector characterizing a product in the course of production. The Dynamic Spreadsheet, is a processing structure that can be parameterized, used to perform calculations on a set of internal representations in order to deliver the external representation to the user. A system intended for quality control of the products delivered by a concrete production plant was generated by EDDAKS and used to validate. Processing methods using the multilayer perceptron model were considered. Two contributions aimed at improving the performance of this network are proposed. One consists of implanting a conjugate gradient method. The effectiveness of this method depends on the determination of an optimum gradient step that is efficiently calculated by a linear search using a secant algorithm. The other is intended to reduce the connectivity of the network by adapting it to the problem to be solved. It consists of identifying links having little or no activity and destroying them. This activity is determined by evaluating the covariance between each of the inputs of a cell and its output. An experiment in which nonlinear prediction is applied to a civil engineering problem is described. ESA

N94-31605# Pacific Northwest Lab., Richland, WA.
PROCESS MAPPING: A USER-FRIENDLY TOOL FOR PROCESS IMPROVEMENT
M. L. Carson and L. O. Levine Sep. 1993 4 p Presented at the 2nd International Symposium on Productive and Quality Improvement with a Focus on Government, Washington, DC, 8-10 Sep. 1993
(Contract DE-AC06-76RL-01830)
(DE94-004357; PNL-SA-22168; CONF-9309168-4) Avail: CASI HC A01/MF A01

Process maps aid administrative process improvement efforts by documenting processes in a rigorous yet understandable way. Icons, graphics, and text support process documentation, analysis, and improvement. DOE

N94-31872 Defence Research Establishment Pacific, Victoria (British Columbia).
ULTRASONIC CHARACTERIZATION OF DAMAGE IN A SIMULATED CF-18 COMPOSITE STRUCTURE
K. I. McRae, R. D. Finlayson, W. R. Sturrock, and D. S. Liesch Feb. 1993 32 p
(DREP-LN-93-26; DSIS-94-01061; CTN-94-61219) Avail: CASI HC A03/MF A01

A simulated CF-18 aircraft door component was constructed and subjected to treatment during manufacturing with the object of inducing damage in the composite material in a known and well-defined manner. The simulated component was then sent to participants in a nondestructive evaluation study. Results are reported for tests conducted with a scanning apparatus and data acquisition system which consisted of three components: ultrasonic transducer and scanner comprising a two-axis scanning frame to which a modified commercial transducer was attached; an acquisition system for ultrasonic data known as Signal Processing Ultrasonic Device (SPUD); and a data analysis and display system (DETECT/NDE) specifically designed to manipulate large three dimensional ultrasonic data sets. A series of five large-area scans was performed, each scan about 52 cm square. A total of eight regions of interest were identified for a more detailed analysis of the delamination damage, seven detailed scans covering a 13-cm square and one covering a 20.8-cm square. It was often possible to identify the probable source of the damage as that resulting from impact or caused by overloading of fasteners. Flaws of all significant dimensions were located and fully characterized using the ultrasonic procedure. Author (CISTI)

N94-32088# Nondestructive Testing Information Analysis Center, San Antonio, TX.
BENCHMARKING OF THE STATE-OF-THE-ART IN NONDESTRUCTIVE TESTING/EVALUATION FOR APPLICABILITY IN THE COMPOSITE ARMORED VEHICLE (CAV) ADVANCED TECHNOLOGY DEMONSTRATOR (ATD) PROGRAM, PHASE 1 Report, 5 Apr. - 15 Nov. 1993
Gary W. Carriveau Nov. 1993 70 p
(Contract DLA900-90-D-0123)
(AD-A276660; NTIAC-7304-103; TARDEC-TR-13604) Avail: CASI HC A04/MF A01

This technology assessment report is the result of compilation, review, and assessment of information and data concerning the development and use of NDE/T as applied to advanced composites that may be used in the CAV (Composite Armored Vehicle) ATD (Advanced Technology

Demonstrator) Program. This information has been gained from both published literature and as well as work in progress. It includes the results of a detailed bibliographic search using all the data bases held within the Defense Technical Information Center, supplemented wherever possible by other data bases. In addition, direct contacts and academic, industrial, and government research and development centers and applications laboratories were made. Discussions and recommendations contained in this report focus on the current state-of-the-art of composite NDE/T technologies and their capabilities and limitations for both the classical post process and real-time in-process inspection techniques. Furthermore, this effort includes an assessment of future developments and research trends including a projected time line. DTIC

N94-32387*# National Aeronautics and Space Administration, Washington, DC.
MANAGEMENT OF GOVERNMENT QUALITY ASSURANCE FUNCTIONS FOR NASA CONTRACTS
Apr. 1993 66 p
(NHB-5300.4(2B-2); NAS 1.18:5300.4(2B-2)) Avail: CASI HC A04/MF A01

This handbook sets forth requirements for NASA direction and management of government quality assurance functions performed for NASA contracts and is applicable to all NASA installations. These requirements will standardize management to provide the minimum oversight and effective use of resources. This handbook implements Federal Acquisition Regulation (FAR) Part 46, NASA FAR Supplement 18-46, Quality Assurance, and NMI 7410.1. Achievement of established quality and reliability goals at all levels is essential to the success of NASA programs. Active participation by NASA and other agency quality assurance personnel in all phases of contract operations, including precontract activity, will assist in the economic and timely achievement of program results. This involves broad participation in design, development, procurement, inspection, testing, and preventive and corrective actions. Consequently, government, as well as industry, must place strong emphasis on the accomplishment of all functions having a significant bearing on quality and reliability from program initiation through end-use of supplies and services produced. For purposes of implementing NASA and other agency agreements, and to provide for uniformity and consistency, the terminology and definitions prescribed herein and in a future handbook shall be utilized for all NASA quality assurance delegations and subsequent redelegations. Derived from text

N94-32481*# Bio-Imaging Research, Inc., Lincolnshire, IL.
DIFFERENTIAL PHASE ACOUSTIC MICROSCOPE FOR MICRO-NDE Final Report
David D. Waters, T. L. Pusateri, and S. R. Huang May 1992 108 p Revised
(Contract NAS1-19099; SBIR-04.09-6425A; RTOP 324-02-00)
(NASA-CR-189617; NAS 1.26:189617; BIR-2380) Avail: CASI HC A06/MF A02

A differential phase scanning acoustic microscope (DP-SAM) was developed, fabricated, and tested in this project. This includes the acoustic lens and transducers, driving and receiving electronics, scanning stage, scanning software, and display software. This DP-SAM can produce mechanically raster-scanned acoustic microscopic images of differential phase, differential amplitude, or amplitude of the time gated returned echoes of the samples. The differential phase and differential amplitude images provide better image contrast over the conventional amplitude images. A specially designed miniature dual beam lens was used to form two foci to obtain the differential phase and amplitude information of the echoes. High image resolution (1 micron) was achieved by applying high frequency (around 1 GHz) acoustic signals to the samples and placing two foci close to each other (1 micron). Tone burst was used in this system to obtain a good estimation of the phase differences between echoes from the two adjacent foci. The system can also be used to extract the V(z) acoustic signature. Since two acoustic beams and four receiving modes are available, there are 12 possible combinations to produce an image or a V(z) scan. This provides a unique feature of this system that none of the existing acoustic microscopic systems can provide for the micro-nondestructive evaluation applications. The entire system, including the lens, electronics, and scanning control software, has made a competitive industrial product for nondestructive material inspection and evaluation and has attracted interest from existing acoustic microscope manufacturers. Author (revised)

N94-32862*# Draper (Charles Stark) Lab., Inc., Cambridge, MA.
HIERARCHICAL MODELING FOR RELIABILITY ANALYSIS USING MARKOV MODELS B.S./M.S. Thesis - MIT
Arturo Fagundo May 1994 116 p
(Contract NAS9-18426)
(NASA-CR-188288; NAS 1.26:188288; CSDL-T-1220) Avail: CASI HC A06/MF A02

Markov models represent an extremely attractive tool for the reliability analysis of many systems. However, Markov model state space grows exponentially with the number of components in a given system. Thus, for very large systems Markov modeling techniques alone become intractable in both memory and CPU time. Often a particular subsystem can be found within some larger system where the dependence of the larger system on the subsystem is of a particularly simple form. This simple dependence can be used to decompose such a system into one or more subsystems. A hierarchical technique is presented which can be used to evaluate these subsystems in such a way that their reliabilities can be combined to obtain the reliability for the full system. This hierarchical approach is unique in that it allows the subsystem model to pass multiple aggregate state information to the higher level model, allowing more general systems to be evaluated. Guidelines are developed to assist in the system decomposition. An appropriate method for determining subsystem reliability is also developed. This method gives rise to some interesting numerical issues. Numerical error due to roundoff and integration are discussed at length. Once a decomposition is chosen, the remaining analysis is straightforward but tedious. However, an approach is developed for simplifying the recombination of subsystem reliabilities. Finally, a real world system is used to illustrate the use of this technique in a more practical context. Author

N94-32901*# NYMA, Inc., Brook Park, OH. Engineering Services Div.
EVALUATION OF PYROLYSIS AND ARC TRACKING ON CANDIDATE WIRE INSULATION DESIGNS FOR SPACE APPLICATIONS Final Report
Thomas J. Stueber, Ahmad Hammoud, Mark W. Stavnes, and Kenneth Hrovat May 1994 7 p
(Contract NAS3-27186; RTOP 323-57-4A)
(NASA-CR-195332; E-8849; NAS 1.26:195332) Avail: CASI HC A02/MF A01

Polyimide wire insulation has been found to be vulnerable to pyrolization and arc tracking due to momentary short circuit arcing events. This report compares arc tracking susceptibility of candidate insulation configurations for space wiring applications. The insulation types studied in this report were gauge 20 (0.81 mm dia.) hybrid wiring constructions using polyimide, tetrafluoroethylene (TFE), cross-linked ethylene tetrafluoroethylene (XL-ETFE) and/or polytetrafluoroethylene (PTFE) insulations. These constructions were manufactured according to military wiring standards for aerospace applications. Arc track testing was conducted under DC bias and vacuum (10(exp -6) torr). The tests were conducted to compare the various insulation constructions in terms of their resistance to arc tracking restrike. The results of the tests are presented. Author

N94-32953# State Univ. of New York, Stony Brook. Dept. of Applied Mathematics and Statistics.
STOCHASTIC MODELS IN RELIABILITY THEORY Final Report, 1 Dec. 1991 - 30 Nov. 1993
Laurence Baxter Dec. 1993 5 p
(Contract F49620-92-J-0101)
(AD-A277529; AFOSR-94-0087TR) Avail: CASI HC A01/MF A01

During the two years of research supported by this grant, the PI worked on several different problems in reliability theory, both statistical estimation and stochastic modeling, as well as topics in manufacturing. DTIC

N94-33032*# National Aeronautics and Space Administration. Lewis Research Center, Cleveland, OH.
IMPLEMENTING SOFTWARE SAFETY IN THE NASA ENVIRONMENT
Martha S. Wetherholt and Charles F. Radley May 1994 19 p Presented at the Safety Through Quality Conference, Old Windsor, England, 6-7 Jun. 1994; sponsored by the Real Time Associates, Ltd.
(Contract NAS3-26764; RTOP 323-88-03)
(NASA-TM-106597; E-8870; NAS 1.15:106597) Avail: CASI HC A03/MF A01

Until recently, NASA did not consider allowing computers total control

of flight systems. Human operators, via hardware, have constituted the ultimate safety control. In an attempt to reduce costs, NASA has come to rely more and more heavily on computers and software to control space missions. (For example, software is now planned to control most of the operational functions of the International Space Station.) Thus the need for systematic software safety programs has become crucial for mission success. Concurrent engineering principles dictate that safety should be designed into software up front, not tested into the software after the fact. 'Cost of Quality' studies have statistics and metrics to prove the value of building quality and safety into the development cycle. Unfortunately, most software engineers are not familiar with designing for safety, and most safety engineers are not software experts. Software written to specifications which have not been safety analyzed is a major source of computer related accidents. Safer software is achieved step by step throughout the system and software life cycle. It is a process that includes requirements definition, hazard analyses, formal software inspections, safety analyses, testing, and maintenance. The greatest emphasis is placed on clearly and completely defining system and software requirements, including safety and reliability requirements. Unfortunately, development and review of requirements are the weakest link in the process. While some of the more academic methods, e.g. mathematical models, may help bring about safer software, this paper proposes the use of currently approved software methodologies, and sound software and assurance practices to show how, to a large degree, safety can be designed into software from the start. NASA's approach today is to first conduct a preliminary system hazard analysis (PHA) during the concept and planning phase of a project. This determines the overall hazard potential of the system to be built. Shortly thereafter, as the system requirements are being defined, the second iteration of hazard analyses takes place, the systems hazard analysis (SHA). During the systems requirements phase, decisions are made as to what functions of the system will be the responsibility of software. This is the most critical time to affect the safety of the software. From this point, software safety analyses as well as software engineering practices are the main focus for assuring safe software. While many of the steps proposed in this paper seem like just sound engineering practices, they are the best technical and most cost effective means to assure safe software within a safe system. Author

N94-33038*# National Aeronautics and Space Administration. Lewis Research Center, Cleveland, OH.

PSIDD: A POST-SCAN INTERACTIVE DATA DISPLAY SYSTEM FOR ULTRASONIC SCANS

Don J. Roth and Steven A. Szatmary Washington Nov. 1993 24 p Original contains color illustrations

(RTOP 510-01-50)

(NASA-TM-4545; E-8167; NAS 1.15:4545) Avail: CASI HC A03/MF A01; 10 functional color pages

An ultrasonic data display system was developed at NASA Lewis Research Center that allows the user to interactively examine digitized waveforms and processed information associated with any specific scan location of an ultrasonic contact scan. This information is displayed on a video display monitor and includes acquired time-domain waveforms, frequency-domain magnitude and phase spectra, and ultrasonic properties (pulse velocity, phase velocity, reflection coefficient, attenuation coefficient, attenuation coefficient error) as a function of frequency for a material. This report describes the system features and illustrates the system's usefulness for nondestructive materials characterization. Author

N94-33088# Rome Lab., Griffiss AFB, NY.

ACCELERATED RELIABILITY TESTING UTILIZING DESIGN OF EXPERIMENTS Report, May - Sep. 1993

Barry T. McKinney Dec. 1993 146 p

(AF Proj. 2338)

(AD-A277989; RL-TR-93-249) Avail: CASI HC A07/MF A02

This report documents a system-level Accelerated Reliability testing methodology. The method requires no specific assumptions of a Time-to-Failure distribution nor a stress/performance model. The methodology results in a multi-stress environmental test based on Design of Experiments, specifically a one-third fractional factorial design. The test data are modeled by the method of orthogonal polynomials. Although the data are collected in a high-stress environment, an operational performance estimate can established without extrapolating beyond the test data limits. DTIC

N94-33101*# National Aeronautics and Space Administration. Goddard Space Flight Center, Greenbelt, MD.

SPACE FLIGHT PRINTED WIRING BOARD MEASLING INVESTIGATION

Walter B. Thomas, III May 1994 18 p

(RTOP 312-00-00)

(NASA-TM-104602; Rept-94B00071; NAS 1.15:104602) Avail: CASI HC A03/MF A01

A flight printed wiring board (PWB) for a satellite project was observed to have a high incidence of measling. Other PWB's produced for the program by the same manufacturer did not exhibit the degree of measling as did the 'measle-prone' board. Measling susceptibility during hand soldering and measling effects on PWB insulation resistance were investigated for three production PWB's. Measling resistance was significantly different between the three boards: the 'worst' exhibited five times the number of measles as the 'best' board. 'Severe' measling (that which is likely to affect board reliability) did not exist on the 'best' board, even under extreme soldering conditions (399 degrees C for 12-15 sec.), whereas the 'worst' board showed an average of one 'severe' measle for every two pads under more normal soldering conditions (288-343 degrees C for 2-5 sec.). Both soldering time and temperature affected measling, with time having a slightly greater influence (2 percent versus 12 percent). Measling effects on PWB insulation resistance were inconclusive. These were evaluated by in situ resistance measurements on the same three boards at elevated temperature and humidity. The measured resistance for all three boards decreased for exposures greater than 50 degrees C and 50 percent relative humidity. The 'measle-prone' board showed a resistance decrease at only 25 degrees C and 50 percent relative humidity. However, no definitive difference was detected between measled and not-measled (control) samples. The boards evaluated were production boards, so the effect of interlayer traces connecting the plated-through holes was not controlled. It is likely the resistance measurements were over different volumes of PWB laminate, which would account for the widely varying resistances measured. Thermomechanical measurements on board laminate materials did not reveal any differences attributed to measling. Differences in glass transition temperature were significantly different when measured by DTA, but not by SDT. Laminate thermal expansion differences were significant for the 35 degrees C evaluations, but not for any higher temperatures. Author

N94-32458*# National Aeronautics and Space Administration. Goddard Space Flight Center, Greenbelt, MD.

A VERSATILE NONDESTRUCTIVE EVALUATION IMAGING WORKSTATION

E. James Chern and David W. Butler *In* NASA, Washington, Technology 2003: The Fourth National Technology Transfer Conference and Exposition, Volume 2 Feb. 1994 p 326-331 (For primary document see N94-32420 09-99)

Avail: CASI HC A02/MF A04

39 STRUCTURAL MECHANICS

Includes structural element design and weight analysis; fatigue; and thermal stress.

For applications see *05 Aircraft Design, Testing and Performance* and *18 Spacecraft Design, Testing and Performance.*

N94-31091 Chalmers Univ. of Technology, Goeteborg (Sweden). Dept. of Applied Acoustics.

MODEL UPDATING OF VIBRATING SYSTEMS BASED ON MEASURED OR CALCULATED FREQUENCY RESPONSE FUNCTIONS Thesis

Carl-Ove Kolmodin and Martin Spaang Mar. 1993 40 p Sponsored by Volvo AB, Goeteberg Limited Reproducibility: More than 20% of this document may be affected by microfiche quality

(ISSN 0283-8338)

(CTH-E-93-03; ETN-94-95951) Avail: Issuing Activity (European Space Agency (ESA))

A method for updating analytical models using measured frequency response functions was investigated. The possibility of using measured data as input data is investigated using a vibrator isolator. A simple model

is used and the isolator properties are updated from dynamic measurements made on the isolator. The quality of the model and the need for an accurate theoretical model and high quality measurement data are discussed. The basic theory is presented and the completeness of measured coordinates are stressed. The use of this updating technique for the updating of finite element models are investigated. An exact theoretically derived with Euler-Bernoulli theory was used as input data for the updating. ESA

N94-31213 Virginia Polytechnic Inst. and State Univ., Blacksburg.
VIBRATION CONTROL AND DESIGN OF COMPOSITE CANTILEVERS TAKING INTO ACCOUNT STRUCTURAL UNCERTAINTIES AND DAMAGE Ph.D. Thesis
Donghoon Oh 1993 219 p
Avail: Univ. Microfilms Order No. DA9323788

Within this work a study of the vibrations of laminated composite cantilevers exhibiting structural uncertainties and damage is accomplished. The study is performed within both the Classical Lamination (CLT) and the First-order Transverse Shear Deformation Theories (FSDT). Upon comparing the natural frequencies and mode shapes obtained by both theories, the effects of transverse shear deformation will be emphasized. Other nonclassical effects, such as the bending-twist coupling and the warping restraint on the cantilevered structure, are also considered. Structural tailoring and optimization are implemented as passive techniques of vibration control. To deal with structural uncertainties, a probabilistic discretization technique for the governing system is developed. Statistical properties of natural frequencies are obtained by means of a second-moment method and a first-order perturbation technique. Structural tailoring is reconsidered to reduce the sensitivity of the dynamic behavior to parameter uncertainties. Next, the damage effect on the structure is considered in the design process. As a result, the problem of the robustness of structures in the presence of damage is addressed. This work also deals with the active feedback control of cantilevered structure systems. An efficient control technique for continuous structures, namely modal control, is adopted, and the control gain is obtained by an optimal control law. The comparison of controlled and uncontrolled dynamic responses is made between two models based on CLT and FSDT with emphasis on the influence played by transverse shear deformation and warping restraint. Dissert. Abstr.

N94-31288 Massachusetts Inst. of Tech., Cambridge.
DEFORMATION AND RUPTURE OF CYLINDRICAL SHELLS UNDER DYNAMIC LOADING Ph.D. Thesis
Michelle S. HooFatt 1992
Avail: Issuing Activity (MIT Libraries, Rm. 14-0551, Cambridge, MA 02139-4307)

The dynamic plastic response and failure of unstiffened and ring stiffened cylindrical shells subjected to dynamic loads were studied. The proposed solution methodology, based on a simple computational model of the shell and the concept of equivalence parameters, incorporated two main load-resisting mechanisms in the shell stretching in the longitudinal direction and bending in the circumferential direction. From this method, the complicated two-dimensional cylindrical shell problem was reduced to a one-dimensional problem of a string on-foundation. In particular, the magnitude of the transient and final shape of the transverse deflections of the shell undergoing impact and explosive-type loading were predicted. In order to predict shell failure, the solution for the transient deflection was coupled with a simple fracture criterion--the critical strain to rupture. Both exact and approximate solutions for the impact and impulsive loading of the unstiffened shell were compared and gave similar results for high velocity impact and impulsive loading. In the ring-stiffened shell, the overall deflection profile was shown to consist of both a global and local (between stiffeners) deflection field thereby revealing a complex interplay between the stiffener and the bay. Furthermore, a parametric study on the stiffened shell showed that string-on-foundation model for which ring-stiffeners are represented by lumped masses and springs is a promising method of analyzing the structure. Dissert. Abstr.

N94-31312# Oak Ridge National Lab., TN.
EFFECT OF VIBRATORY STRESS RELIEF DURING WELDING OF THICK STAINLESS STEEL PLATE
S. Spooner, S. A. David, X. L. Wang, C. R. Hubbard, T. M. Holden, and J. H. Root 1993 5 p Presented at the American Welding Society International Conference on Modeling and Control of Joining Processes, Orlando, FL, 8-10 Dec. 1993
(Contract DE-AC05-84OR-21400)
(DE94-006557; CONF-931234-6) Avail: CASI HC A01/MF A01

Residual strains were measured in two welded 25-mm thick plates of type 304 stainless steel by the neutron diffraction technique. The filler metal employed to weld these plates was type 308 stainless steel. One of the two welds was prepared without any vibratory stress relief treatment and the other was vibrated at a frequency below the resonant condition which gives a fraction the resonant amplitude during welding. In both plates the largest residual stress component found in the heat affected zone and in the base metal is along the fusion joint (longitudinal) and is found at the boundary between the weld zone and the heat affected zone. This longitudinal component is 300 +/- 50 MPa in tension. The associated normal stress was close to zero and the transverse stress was 80 +/- 50 MPa. Variations in residual stresses with thickness through the base metal plate were small. The treated plate and untreated plate showed nearly identical patterns of stress distribution. Differences in the measured stresses between the vibratory-stress-relief treated and the untreated plates fall within the error bars of the stress determination in these particular 25 mm thick 300-type stainless steel plates. DOE

N94-31316# Sandia National Labs., Albuquerque, NM.
TEARING RESISTANCE OF A THIN SHELL AGAINST PROJECTILE PENETRATION: MATERIAL PROPERTY EFFECTS
K. V. Trinh Jan. 1994 28 p
(Contract DE-AC04-76DR-00789)
(DE94-007466; SAND-93-8221) Avail: CASI HC A03/MF A01

This report presents results from a series of finite element analyses performed to study material effects on the tearing resistance of a thin shell subjected to projectile penetration. These analyses simulated a round, slender projectile impacting the top center of a metallic cylindrical shell at high speed. We varied eight selected shell material properties systematically using an L18 matrix (design of experiment technique). From the results, we determined effects of the eight properties on the minimum projectile velocity required to penetrate the shell. The material properties examined here included: yield strength, hardening and recovery characteristics, heat coefficient, initial porosity, and damage exponent (a void growth parameter). The DYNA2D finite element code along with the Sandia plasticity/damage model for ductile metals were used in the analyses. DOE

N94-31375# Technische Univ., Berlin (Germany). Sonderforschungsbereich 181 Hochfrequenter Rollkontakt der Fahrzeugraeder.
CONSIDERING TIES ELASTICITIES IN HIGH FREQUENCY RAIL DYNAMICS [DIE BERUECKSICHTIGUNG VON SCHWELLENELASTIZITAETEN IN DER HOCHFREQUENTEN GLEISDYNAMIK]
K. Knothe, N. Ilias, M. Goetz, and B. Ripke May 1993 22 p In GERMAN
(ILR-Mitt-281(1993); ETN-94-95743) Avail: CASI HC A03/MF A01

The eigenfrequencies of elastic railroad ties are experimentally and numerically determined. The eigenfrequencies were experimentally obtained for vertical and lateral eigenoscillations shapes. A finite element program, which contains interpolation hermitian polynomials, was used for calculating eigenfrequencies; bending and shear stiffnesses were taken into consideration and the coupling between flexion and torsion was neglected. The results were compared with data obtained for rigid ties. An approximation formula for eigenfrequency calculation of ties, based on the assumption of a beam with constant stiffness and subjected to shear deformation and torsional inertia, was given. A model which takes into account the elastic properties of ties was developed for calculating the compliance of rails in the frequency area. From the results it can be deduced that elastic calculations for ties are only necessary for frequencies lower than 200 Hz. ESA

N94-31376 Ecole Centrale de Lyon (France). Dept. de Mecanique des Solides.
CONTRIBUTIONS TO THE VALIDATION OF THE CJS MODEL FOR GRANULAR MATERIALS Ph.D. Thesis [CONTRIBUTIONS A LA VALIDATION DU MODELE CJS POUR LES MATERIAUX GRANULAIRES]
Khadija Elamrani 1992 167 p In FRENCH Limited Reproducibility:

More than 20% of this document may be affected by microfiche quality
(ECL-92-56; ETN-94-95908) Avail: CASI HC A08

Behavior model validation in the field of geotechnics is addressed, with the objective of showing the advantages and limits of the CJS (Cambou Jafari Sidoroff) behavior model for granular materials. Several levels are addressed: theoretical analysis of the CJS model to reveal consistence and first capacities; shaping (followed by validation by confrontation with other programs) of a computation code by finite elements (FINITEL) to integrate this model and prepare it for complex applications; validation of the code/model structure thus constituted by comparing its results to those of experiments in the case of nonhomogeneous (superficial foundations) problems. ESA

N94-31479 Northwestern Univ., Chicago, IL.
MODELING OF FRACTURE AND DAMAGE IN QUASIBRITTLE MATERIALS Ph.D. Thesis
Milan Jirasek 1993 254 p
Avail: Univ. Microfilms Order No. DA9327222

The dissertation presents several mathematical models useful for the simulation of fracture and damage propagation in quasi-brittle materials, which are characterized by the development of a large nonlinear process zone prior to failure. The simplest one is the R-curve model based on the replacement of the nonlinear fracture process zone by an equivalent linear elastic crack with a variable resistance against crack propagation. This approach is generalized by taking into account the effect of the loading rate. The emphasis is on the static loading rates rather than the dynamic ones, and creep in the bulk of the specimen is incorporated into the mathematical description. Another important class of models is based on the representation of a mechanical system by an assembly of interacting particles. A dynamic particle model is developed for the simulation of fracture of large sea ice floes during their impact on obstacles such as platforms or artificial islands. It is demonstrated that this model is capable of producing realistic results in terms of both the contact force history and the fracture pattern. Macroscopic fracture energy of random particle systems is studied as a function of the microscopic parameters using the size effect method. An effective numerical procedure for tracing a piecewise linear load-displacement curve is developed. The previously proposed continuum-based microplane model is carefully analyzed and shown to perform poorly in certain situations. The conditions under which the model gives unsatisfactory results are described and the reasons for the poor performance are explained. Modifications on the microscopic level do not remedy the situation and a macro-level modification is unavoidable. A promising concept of the revised version is advocated by presenting improvements of the behavior in several elementary situations. The dissertation is concluded by a localization analysis of a new concept of nonlocal averaging, strictly based on a micromechanically justified derivation. The analysis of the bifurcation at peak stress is followed by an incremental analysis of the post-peak behavior. It is shown that the new formulation preserves the essential properties of the original nonlocal approach and has some interesting added features. Dissert. Abstr.

N94-31544# Institut National des Sciences Appliquees, Lyon (France). Lab. de Mecanique des Solides.
CONTRIBUTION TO THE STUDY OF MULTIAXIAL FATIGUE UNDER PERIODIC OR RANDOM STRESSES Ph.D. Thesis [CONTRIBUTION A L'ETUDE DE LA FATIGUE MULTIAXIALE SOUS SOLLICITATIONS PERIODIQUES OU ALEATOIRES]
Jean-Louis Robert 1992 225 p In FRENCH
(ISAL-92-0004; ETN-94-95919) Avail: CASI HC A10/MF A03

A study aiming to give a random multiaxial fatigue life prediction method, by adapting to this problem long fatigue life criteria and Rainflow counting methods, is presented. Five 'classical' fatigue criteria for multiaxial and periodical stresses are analyzed. A criterion based upon the determination of the critical plane, experiencing the maximum damage evaluated with tangential and normal stresses on this plane, is proposed. The comparison between all criteria is made with 100 experimental tests collected in the literature. The criterion gives especially good predictions when principal stresses directions are fixed. Four rainflow counting methods are examined and a new one is proposed. Two ways of comparison are developed: rainflow cumulatives are modeled by a probability densities law and theoretical fatigue life predictions are calculated with either a linear or a nonlinear damage law. A method to calculate the constants of materials for these two approaches is described. It allows identical Woehler curves to be reproduced. Uniaxial loading histories measured on lorry components are used to compare these rainflow counting methods. A random multiaxial fatigue life prediction method is developed. Both counting variable and criterion proposed are based upon the tangential octahedric stress. The validation of the criterion is made by using experimental tests. The method is applied to loading histories and is satisfactory. ESA

N94-31562# Ecole Centrale de Lyon (France).
METHODOLOGY FOR DAMAGE STUDY OF A TUBE-GRILL CONTACT Ph.D. Thesis [METHODOLOGIE POUR L'ETUDE DE L'ENDOMMAGEMENT D'UN CONTACT TUBE-GRILLE]
Jean-Marc Voisin 1992 109 p In FRENCH
(ECL-92-49; ETN-94-95911) Avail: CASI HC A06/MF A02

Research for the 'ideal material' for the tube-grill contact of a steam generator is presented. A test bench (shock and sliding movements) was created to approach real operating conditions leading to matter loss of the stressed pieces. Study of bonding and cracking led to the development of a test procedure which characterizes the behavior of different materials in small fretting stressed contact. Experimental study gave the following conclusions. At vibratory test level, geometrical singularities of contact must be avoided. This is essentially a design problem. A bore of greater hardness than the tube is prejudicial for a good joint-holding with regard to wear. At the bonding simulation level, the test, being of a more general character, can show the catastrophic risks of cracking. The behavior of the materials put in contact must not lead to strong local stresses, otherwise the cracks can initiate and propagate to the periphery of the contact by a fatigue mechanism. The reliability of the installation requires that the stresses be weak since crack presence can not be allowed. ESA

N94-31707# Montreal Univ. (Quebec). Dept. de Genie Metallurgique.
THERMAL-MECHANICAL FATIGUE CRACK GROWTH IN AIRCRAFT ENGINE MATERIALS Ph.D. Thesis
Yi Dai May 1993 353 p
(ISBN-0-315-86543-1; CTN-94-61209) Copyright Avail: Micromedia Ltd., Technical Information Centre, 240 Catherine Street, Suite 305, Ottawa, Ontario, K2P 2G8, Canada HC/MF

A thermal mechanical fatigue (TMF) testing rig was built which is capable of studying the fatigue behaviors of gas turbine engine materials under simultaneous changes of temperatures and strains or stress. An advance alternating current potential drop (ACPD) measurement system was also developed which is capable of performing on-line monitoring of fatigue crack initiation and growth in specimen testing under isothermal and TMF conditions. Fatigue crack initiation and short crack growth data were obtained for titanium alloy specimens designed with notch features associated with bolt holes of compressor discs. TMF data were also obtained for two titanium alloys used in aircraft engine components. Those data explained the material fatigue behavior encountered in full-scale component testing. A complete fractographic analysis was performed on the tested specimens enhancing the understanding of the fatigue crack growth mechanisms and helping to formulate an analytical crack growth model. The ACPD fatigue crack monitoring technique was applied to the low cycle fatigue testing of Pratt & Whitney 1480 monocrystalline nickel alloy. A completely automated, computer controlled test procedure was developed which could obtain crack initiation and growth data with greater speed, precision, and reliability than previous methods. Author (CISTI)

N94-31737# Toronto Univ. (Ontario). Dept. of Aerospace.
POINT-CONTACT AND POINT-IMPACT DYNAMICS FOR MULTIBODY CHAINS M.S. Thesis
Ralph Rainer Jahn 1993 150 p
(ISBN-0-315-87056-7; CTN-94-61245) Copyright Avail: Micromedia Ltd., Technical Information Centre, 240 Catherine Street, Suite 305, Ottawa, Ontario, K2P 2G8, Canada HC/MF

Open multibody chains are used to model robotic manipulator arms. Point-contact and point-impact dynamics are simulated as they relate to multibody chains, with a view toward application to manipulator systems used in space. To make the simulation effort tractible, contact surfaces are modelled as points. This is of significance to many space applications where a large number of contact and impact situations deal with small contact areas such as contact with structures along edges and corners. A Newton-Euler approach is implemented in conjunction with the finite element

method to model the mass and flexibility properties of the robotic links. Rigid systems and flexible systems are considered separately. The necessary simulation dynamics for a multibody chain is given, followed by a description of the point-contact strategy for the respective system. Outlines of the point-impact solution algorithm for each respective system are also presented along with simulation results for various examples. Several important programming considerations are described along with the numerical procedures implemented in the simulators. CISTI

N94-31777 Virginia Polytechnic Inst. and State Univ., Blacksburg.
RANDOM VIBRATIONS OF COMPOSITE BEAMS AND PLATES Ph.D. Thesis
Ahmad Shehadeh Abdelnaser 1993 181 p
Avail: Univ. Microfilms Order No. DA9312867

In this study, a generalized modal approach is presented to solve more general vibration problems of composite beams and plates. The coupled systems of partial differential equations, representing the equations of motion, are uncoupled into modal equations by utilizing the eigenfunctions of the system and its adjoint. A method is presented to obtain these eigenfunctions for beams with arbitrary boundary conditions and for plates with Levy-type boundary conditions. The forced vibration solutions obtained by this method are then used to calculate the random response characteristics of beams and plates subjected to spatially and temporally correlated random loads. In the analysis of beams, both symmetric cross-ply and angle-ply configurations have been considered. In the symmetric cross-ply configuration with no torsional loads, of course, the warping effects are absent. The angle-ply case, however, includes torsion-warping effects and coupled bending-torsion motions. A simple displacement field is introduced to reflect warping in the third-order shear deformation theory. In the analysis of plates two configurations of the laminates have also been considered: symmetric cross-ply and antisymmetric angle-ply. At this time, these are the only two configurations which can be solved by the closed-form modal analysis approach for the Levy-type boundary conditions. In both cases of the beams and plates, the numerical results with and without shear deformations are obtained and compared. The result for no shear deformation theory are obtained with the classical lamination theory. The results have also been obtained for the first-order shear deformation theory with a somewhat simpler displacement field which has been commonly used in the past. The numerical results are obtained for the global response quantities such as frequencies, displacements, and crossing rates as well as for the local response quantities such as normal and shear stresses across a cross section. The numerical results obtained with various deformation theories for the frequencies as well as response quantities are compared to evaluate the effect of the shear deformations. For thicker and rigid beams and plates, one observes large differences in the frequencies and responses obtained with (the first and third-order shear deformation theories) and without consideration of shear deformations (classical theory). For the frequencies and global responses, both the first and third-order theories give about the same results. Dissert. Abstr.

N94-31819* National Aeronautics and Space Administration. Lewis Research Center, Cleveland, OH.
FUTUREPATH 3 (Videotape)
Oct. 1989 Videotape: 28 min. 55 sec. playing time, in color, with sound
(NASA-TM-109762; NONP-VT-94-9962) Avail: CASI VHS A01/BETA A22

The story of research and technology at NASA Lewis Research Center's Structures Division is presented. The job and designs of the Structures Division needed for flight propulsion is described including structural mechanics, structural dynamics, fatigue, and fracture. The video briefly explains why properties of metals used in structural mechanics need to be tested. Examples of tests and simulations used in structural dynamics (bodies in motion) are briefly described. Destructive and non-destructive fatigue/fracture analysis is also described. The arc sprayed monotape (a composite material) is explained, as are the programs in which monotape plays a roll. Finally, the National Aero-Space Plane (NASP or x-30) is introduced, including the material development and metal matrix as well as how NASP will reduce costs for NASA. CASI

N94-31841 Selskapet for Industriell og Teknisk Forskning, Trondheim (Norway). Div. of Production Engineering.
ACCEPTANCE CRITERIA FOR WELD DEFECTS IN ALUMINIUM WELDMENTS
M. Hval 4 Aug. 1993 56 p Sponsored by Nordisk Industrifond
(PB94-138575; STF20-A93124) Avail: Issuing Activity (National Technical Information Service (NTIS))

The report demonstrates the use of fracture mechanics to determine the significance of crack-like defects in aluminium weldments. In order to do so, fracture toughness data of 25 and 50 mm aluminum weld were determined. These results showed a large variation in the fracture toughness properties of the weldment, where the most critical zones were the fusion line and the hardness minimum of the HAZ. The fracture assessment was verified by comparing the results with four wide plate tests. The results of the defect assessment were dependent on the tensile input data for the weldments. For safe predictions it is proposed to use tensile input data for the average of the base material and the HAZ properties. On basis of the results simple defect acceptance criteria were determined for the weldments. NTIS

N94-31849 Ecole Polytechnique, Montreal (Quebec). Dept. of Mechanical Engineering.
FEASIBILITY STUDY OF COLD EXPANSION PROCESSES MODELLING Final Report
Marie Bernard, Bui-Quoc Thang, Denis Julien, and Sylvain Forgues Mar. 1993 258 p
(DSIS-94-01186; CTN-94-61216) Avail: CASI HC A12/MF A03

A comprehensive review is presented of the cold expansion techniques currently used for the improvement of fatigue strength of fastened joints. Two common practices of generating residual stress fields responsible for increasing fatigue life are cold working of the open hole before fastener installation and interference fit fastener systems. Most of the materials studied were aluminum, and experimental work has shown that the benefits of cold working on fatigue life enhancement were substantial in some cases, particularly in the high cycle fatigue region. The performance of cold working depends on several parameters, the most influential being the material characteristics, degree of cold working, and remote applied stress. Analytical work characterizing cold working in order to establish the residual stress distribution uses several simplified assumptions, and analytical results may sometimes be unrealistic compared to results from experiments or finite element methods. Life prediction methods for cold worked materials, relaxation of the compressive residual stress during cycling, and nondestructive examination methods applied to cold working problems are also summarized. Author (CISTI)

N94-31870 Ecole Centrale de Lyon (France). Dept. Materiaux-Mecanique Physique.
CRACKING INDUCED IN SMALL FRETTING: APPLICATION TO THE CASE OF AERONAUTICAL ALUMINUM ALLOYS Ph.D. Thesis [FISSURATION INDUITE EN PETITS DEBATTEMENTS: APPLICATION AU CAS D'ALLIAGES D'ALUMINIUM AERONAUTIQUES]
Zhong Rong Zhou 1992 164 p In FRENCH Limited Reproducibility: More than 20% of this document may be affected by microfiche quality
(ECL-92-50; ETN-94-95906) Avail: CASI HC A08

Work aimed at defining bases for justifying the resistance to fretting of aluminum alloys used in aeronautics is presented. The friction characteristics of woodchips obtained for various experimental configurations are presented. The very notion of fretting resistance is stripped of sense since intrinsic properties of susceptible materials do not exist to describe the very different experimental configurations. The use of fretting maps which can separate the local stress that the first bodies support in terms of 'overcharge' or 'overdeformation' and derive the various responses of the material is proposed. The dynamics of the phenomenon regarding cracking are considered. By this response mode, the various alloys can be better separated. The introduction of these maps, and in particular the separation of 'local stress' maps and 'material response,' appears susceptible to strongly modify the behavior of users confronted with fretting problems, identification of them, and choice of remedies. Expected developments are discussed. In a nonclassical fashion, the study results in the proposal of a characterization test called static fretting fatigue, of which first results give hope for better account to be taken of the combined effect of loads related to contact or unrelated to contact. ESA

N94-31904 Washington Univ., Seattle.
THE FINITE ELEMENT METHOD WITH ASYMPTOTIC SELF-SIMILAR SOLUTIONS Ph.D. Thesis
Marvin Luke 1993 161 p
Avail: Univ. Microfilms Order No. DA9326385

The application of self-similar solutions of the second kind as FEM special elements was examined. Self-similar solutions of the second kind are solutions to degenerate problems in physics where solution unknowns appear as exponents along with simple coefficients. They are of special interest because they represent the asymptotic solution for a wide class of non-degenerate initial conditions. In these problems the existence of an asymptotic solution is known, but the exact solution form is unknown. Self-similar solutions arise for two distinct classes of problems: (1) time-dependent point-source problems in which the solution is valid far away from the initial source, and (2) boundary layer type problems where the solution is valid in a small region where large changes occur. A finite element method is constructed that uses these asymptotic self-similar solutions. Two examples are solved. The first concerns a nonlinear time-dependent heat equation where the specific heat of the medium depends on whether it is heating or cooling. A self similar solution of the second kind is used as the solution representation for an infinite element. Unlike existing infinite element formulations the developed infinite element exhibits correct spatial and time asymptotic behavior. The interior region contains standard finite elements where the generalized trapezoidal method is used for time integration. An incomplete field method approximately enforces continuity of the solution both spatially and as a function of time at the element boundary interface. The results are compared with standard methods and found to be superior. The second example concerns an ordinary differential equation with a rapidly oscillating solution near a boundary. A special element is constructed to represent the solution in this region. This is coupled with hierarchical finite elements on the rest of the domain. Excellent results are achieved. Potential applications of self-similar solutions of the second kind in the finite element method are discussed. Dissert. Abstr.

N94-31912# Montreal Univ. (Quebec). Dept. de Metallurgie et Genie des Materiaux.
FATIGUE CRACK PROPAGATION AND FRACTOGRAPHY OF 3Y-TZP AND ZTA Ph.D. Thesis
Changzun Zhou Oct. 1992 297 p
(ISBN-0-315-86561-X; CTN-94-61213) Copyright Avail: Micromedia Ltd., Technical Information Centre, 240 Catherine Street, Suite 305, Ottawa, Ontario, K2P 2G8, Canada HC/MF

Cyclic tensile fatigue and compression fatigue were studied in 3-mole-percent yttria stabilized tetragonal zirconia polycrystals (3Y-TZP) and zirconia toughened alumina (ZTA) subjected to stress induced transformation. Clear striation-like dark bands separated by larger bright zones were observed in the tensile fatigue crack propagation of 3Y-TZP precracked specimens. The dark bands corresponded to matching depressions on the two opposite fractured surfaces and to regions of smaller amounts of transformation as confirmed by Raman spectroscopy. Hysteresis loops from a strain gauge placed at the fatigue crack tip of 3Y-TZP showed that fatigue crack propagation in a single cycle occurred in three stages: slow, very rapid, and slow propagation. The rapid propagation was always associated with presence of visible striations on the fatigue fracture surface and was triggered by a small amount of unloading in a load cycle. Fatigue resistance increased with increased stress intensity factor, a phenomenon believed to result from a transformation toughening effect. Fatigue crack propagation retardation was observed after a sustained load cycling, and fatigue crack propagation acceleration was observed during minor cycling. Explanations are suggested for both effects. Formation of four different zones on compression fatigue fracture surfaces is also explained.
Author (CISTI)

N94-31955 Iowa State Univ. of Science and Technology, Ames.
VIBRATIONAL AND ACOUSTIC RESPONSE OF RIBBED PLATES Ph.D. Thesis
Ten-Bin Juang 1993 231 p
Avail: Univ. Microfilms Order No. DA9321175

A self-consistent mathematical formulation, using the Fourier transform method and a direct Gaussian numerical integration scheme, is developed and verified for analysis of both vibrational and acoustic responses of infinite submerged ribbed plates. Further steps developed from standard theories make structural intensity, acoustic intensity, and acoustic power calculations possible in the nearfield and farfield and are demonstrated in this work. The direct numerical integration scheme adopted to obtain responses has proved to be straightforward and reliable. Although the double integration expression in some responses makes the technique infeasible, a practical way to overcome that difficulty is demonstrated using a standard branch-cut integration to eliminate one integration step analytically. The model and numerical scheme readily allow investigation of additional interesting topics, like the passband and stopband characteristic and the mode localization phenomenon that are observed in ribbed structures. Furthermore, an extension to comprehension of the mechanisms that generate the mode localization phenomenon on disordered structures has been realized. A secondary effort examines natural modes of vibration and acoustic radiation for finite stiffened multiple-span beams with the efficient transfer matrix method. This model shows that the mode localization phenomenon exists on disordered stiffened beams both under free-free and hinged-hinged end conditions. The sensitivity of the response to attachment disorder (perturbations in rib stiffness and location) has also been examined. An elaborate vibrational and acoustic experiment has been carried out on a baffled, stiffened, two-span, hinged beam to examine the existence of the localized modes and verify the predicted acoustic responses. Moreover, the radiation efficiency of finite beams has been investigated for comparison of the radiation behavior presented by the different stiffened beam arrangements. A thorough investigation of mode localization, frequency passbands and stopbands, structural and acoustic intensities, and radiated acoustic power is presented for analysis of submerged infinite ribbed plates with variable rib materials geometry and spacing (periodic and nonperiodic). A second investigation of localized natural modes is demonstrated for analysis and experiment of finite stiffened beams in air. Dissert. Abstr.

N94-31961 Stanford Univ., CA.
A SEPARATION TECHNIQUE FOR ASYMPTOTIC-NUMERIC SOLUTION FOR GENERAL SHELLS OF REVOLUTION Ph.D. Thesis
Khaliq ur-Rehman Shad 1993 135 p
Avail: Univ. Microfilms Order No. DA9326558

Response of axisymmetric shell structures can be expressed through the state vector formulation for each circumferential harmonic of deformation. Based on the state vector equation and asymptotic method, an efficient approach for the solution of shells of revolution is presented in this study. At a transition point, where an asymptotic solution does not remain accurate, a new subelement is introduced by dividing the shell element into three parts. Through the introduction of subelement and division of the solution into the slowly varying and the rapidly varying solutions, the transition point problem is so handled, that the number of each type of solution remains constant in a subelement. The asymptotic solution is used for the rapidly varying solutions and power series for the slowly varying solutions over a reduced system of equations. The order of reduced system is the same as the total number of slowly varying solutions present. The method is applied to isotropic and anisotropic shells, and static as well as dynamic loading effects are handled. The technique developed enjoys the advantage of capturing the rapid variation in the behavior of shells over a coarse mesh, whereas purely numerical methods require a very fine mesh and a fair amount of user judgement to capture such a variation in the response of the shell structures. This rapid variation of solutions which is restricted to the edge effects for the problems of statics is present throughout the shell meridian in case of the dynamic response and stability problems, and it further enhances the importance of the present approach. As the solution in most parts is based on an analytic approach, time is saved in both setting up data and solving the problem. The accuracy and effectiveness of the approach is demonstrated in the several examples presented. These include shells of various geometry under different boundary conditions, the working out of resonant frequency and mode shapes for various types of shells, the effect of the degree of orthotropy and the variation of stress through the thickness of the composite shells. Dissert. Abstr.

N94-31964 Michigan Univ., Ann Arbor.
VIBRATION LOCALIZATION IN DUAL-SPAN AXIALLY MOVING ELASTIC SYSTEMS Ph.D. Thesis
Abdulghaffar Azhari Aljawi 1993 188 p
Avail: Univ. Microfilms Order No. DA9319475

To date, vibration localization in the large class of systems modeled

by multispan axially moving materials has not been examined. These systems are common in many engineering applications, such as band saw blades, power transmission, belts and chains, and magnetic and paper tapes. An investigation of the vibration localization phenomenon in two-span, axially moving beams is presented. The effects of tension disorder, interspan coupling, and transport speed on the confinement of the natural modes of free vibration are studied. The equations governing the transverse vibration of the two-span, axially moving beam are derived through Hamilton's principle and solution methods are developed. Numerical results demonstrate that normal mode localization indeed occurs for both stationary and translating disordered two-span beams, especially for small interspan coupling. The occurrence of localization is characterized by a peak deflection much greater in one span than in the other. In the stationary disordered case, localization becomes more pronounced as interspan coupling decreases, i.e., as the span axial tension increases. For an axially translating beam with identical spans, the two loci in each pair of natural frequencies may exhibit a single or double crossing (depending on the value of tension) when plotted against the axial transport speed. These crossings become veerings when the beam is disordered, and localization is strongest at those speeds where the eigenvalue veerings occur. A perturbation approach, which provides additional insights into the sensitivity of the system to disorder, is also utilized. Analytical expressions are obtained in the limiting cases of weak and strong interspan coupling. Findings show that the sensitivity of the system to disorder primarily depends upon disorder and interspan coupling strengths. Finally, an investigation of the localization phenomenon is performed for a more complete model of a band/wheel system. The effects of tension disorder on the confinement of the natural modes of free vibration are investigated both theoretically and experimentally. It is shown that results obtained with the simple interspan coupling model are in qualitative agreement with those of the more complex model, thereby confirming the usefulness of the model featuring a simple coupling mechanism. Analytical predictions from the simple model are also very nicely validated by the experimental results. Dissert. Abstr.

N94-31965 Michigan Univ., Ann Arbor.
INFLUENCES OF PRESSURE-SENSITIVE YIELDING AND NON-SINGULAR STRESS ON PLANE-STRESS ELASTIC-PLASTIC CRACK-TIP FIELDS Ph.D. Thesis
Zine El Abidine BenAoun 1993 103 p
Avail: Univ. Microfilms Order No. DA9319489

In this study, we investigate the effects of elasticity and nonsingular stress terms on the asymptotic plane-stress mode 1 crack-tip fields for pressure-sensitive materials under small scale yielding. Perfectly plastic behavior is assumed and plastic dilatancy is introduced by the normality flow rule. A closed-form general asymptotic solution for singular centered fan sectors is given as a function of mu which is a pressure sensitivity parameter introduced in the yield condition. When elastic perfectly plastic behavior is considered, the results of finite element computations show the existence of elastic sectors bordering the stress-free crack faces. The near-tip stresses of the finite element results agree well with those of the corresponding asymptotic analysis. The angular spans of the elastic and plastic sectors vary with the value of mu. They also vary, for a specific pressure sensitivity parameter, with the value of the nonsingular stress term (T-stress) in the asymptotic expansion of the linear elastic crack-tip stresses, which is the normal stress in the direction of the crack line. In particular, the elastic sector span is in general shown to decrease with increasing T-stress. The parameter mu as well as the nonsingular stress term also have significant effects on the sizes and shapes of the plastic zones. The contribution of hydrostatic stress in the yield criterion for this class of pressure-sensitive materials extends the boundary of the plastic zone much farther in front of the crack-tip than that for incompressible Mises materials. Also, as the T-stress increases, the height of the plastic zone increases substantially for materials with a large pressure sensitivity. In zirconia ceramics, the dilatational phase transformation strain from tetragonal to monoclinic phase is limited to 4 percent. This condition is also considered in our study. Our computational results show that the phase transformation zones for strong transformation zirconia ceramics with large mu can be approximated by those for elastic perfectly plastic materials with no limit on plastic dilatation strain. The phase transformation zone height and the corresponding radial variation of the phase transformation strain can be used to estimate the effects of the T-stress on toughening. Dissert. Abstr.

N94-31974 California Inst. of Tech., Pasadena.
NONLINEAR EFFECTS IN INTERFACIAL FRACTURE Ph.D. Thesis
Philippe Hubert Geubelle 1993 245 p
Avail: Univ. Microfilms Order No. DA9316842

The issue of the non-coplanar quasistatic propagation of a crack in homogeneous and bimaterial sheets is investigated. Through a preliminary linear analysis, it is shown that the interface crack kinking problem is confronted, in most practical cases, with difficulties which do not arise in the homogeneous situation: the crack path as predicted by the maximum energy release rate criterion cannot be determined uniquely and an additional length parameter, absent in the homogeneous case, needs to be specified to assure uniqueness. Following that development, the assumption of small deformations is relinquished and it is shown how the size of the nonlinear zone imparts possibly the physical significance of the additional length parameter. The analysis is performed numerically in the homogeneous and bimaterial cases within the framework of the nonlinearly elastic theory of plane stress and using a 'boundary layer' approach. Material and geometrical nonlinearities are combined through the use of the Generalized Neo-Hookean (GNH) model. As the length of the crack extension becomes comparable to the size of the nonlinear zone, a transition is observed between the value of the energetically most favorable kink angle predicted by the linear theory and a unique a 'nonlinear' value which is found to be independent of the crack extension length and the far-field loading conditions. The results of the crack propagation analysis are related to those of a detailed asymptotic analysis of the structure of the near-tip stress and deformation fields for the GNH class of hyperelastic materials. The investigation addresses the symmetric (mode 1) and nonsymmetric (mixed-mode) homogeneous situations, the rigid substrate case, and the general bimaterial problem which allows for an arbitrary choice, on both sides of the interface, of the three material parameters characterizing the GNH model. The asymptotic analysis allows quantification of the effect of the 'hardening' characteristics on the blunting of the crack and the associated stress and strain singularities, and shows that the near-tip fields corresponding to a general nonsymmetric loading are, in the homogeneous situation, related to those of the symmetric (mode 1) case through a rotation which depends on the material characteristics and the far-field loading conditions. A somewhat similar property is obtained in the bimaterial problem, where the existence of a nonoscillatory and 'contact-free' solution is confirmed for all material combinations. Dissert. Abstr.

N94-32079 Utah State Univ., Logan.
NONLINEAR VIBRATION ANALYSIS OF LAMINATED PLATES ON LINEAR AND NONLINEAR ELASTIC FOUNDATIONS Ph.D. Thesis
Yan-Shin Shih 1992 188 p
Avail: Univ. Microfilms Order No. DA9316784

Solutions to free undamped large amplitude vibrations of arbitrarily laminated thin rectangular and quadrilateral plates on elastic foundations based on an assumed mode shape are determined. S-S-S-S and C-C-C-C boundary conditions with movable and immovable edges are considered in chapter 3. S-S-S-S, C-S-C-S, and C-C-C-C boundary conditions with stress-free edges of rectangular and quadrilateral plates are considered in chapters 4 and 5. The governing equations of motion of plates on linear Winkler, Pasternak foundations and a nonlinear Winkler foundation are provided using von Karman's theory. The Galerkin's method reduces the von Karman equation to a time-dependent ordinary differential equation and solutions are then obtained by using the Runge-Kutta method. The effects on the nonlinear frequency of several parameters such as amplitude, material lamination, aspect ratio, and boundary conditions as related to stress-free edges and the influence of elastic foundation constants are provided. Dissert. Abstr.

N94-32135 Sandia National Labs., Albuquerque, NM.
EXPERIMENTAL MEASUREMENT OF DYNAMIC FAILURE AND FRAGMENTATION PROPERTIES OF METALS
D. E. Grady and M. E. Kipp 1993 30 p Presented at the National Science Foundation (NSF) Symposium on Dynamic Failure Mechanics of Modern Materials, Pasadena, CA, 3-5 Feb. 1994 Limited Reproducibility: More than 20% of this document may be affected by microfiche quality

(Contract DE-AC04-94AL-85000)
(DE94-007377; SAND-93-2679C; CONF-940256-1) Avail: Issuing Activity (Department of Energy (DOE))

An experimental method for determining failure and fragmentation properties of metals in catastrophic breakup events has been pursued in this work. Spherical samples of the test metals were launched at high velocities with a two-stage light-gas gun facility and subjected to controlled impulsive loading by impact on a stationary non-metallic plate. Fragmentation and motion of the debris were diagnosed with multiple flash radiography. Methods for determining critical failure properties and the fragmentation toughness of the test metals were explored. DOE

N94-32273# Wisconsin Univ., Madison. Center for Mathematical Sciences.
ELASTIC AS LIMIT OF VISCOELASTIC RESPONSE, IN A CONTEXT OF SELF-SIMILAR VISCOUS LIMITS Summary Report
Anthanasios E. Tzavaras Mar. 1994 38 p
(Contract N00014-93-C-0015; NSF DMS-92-09049)
(AD-A277043) Avail: CASI HC A03/MF A01

We study the equations of one-dimensional isothermal elastic response as the small viscosity limit of the equations of viscoelasticity, in a context of self-similar viscous limits for Riemann data. THe limiting procedure is justified and a solution of the Riemann problem for the equations of elasticity is obtained. The emerging solution is composed of two wave fans, each consisting of rarefactions, shocks and contact discontinuities, separated by constant states. At shocks the self-similar viscous solution has the internal structure of traveling waves, and an admissibility criterion identified by Wendroff is fulfilled. DTIC

N94-32275 Virginia Univ., Charlottesville. School of Engineering and Applied Science.
CONTROL AND STABILIZATION OF DISTRIBUTED PARAMETER SYSTEMS; THEORETICAL AND COMPUTATIONAL ASPECTS Final Report
I. Lasiecka and R. Triggiani Feb. 1994 98 p Limited Reproducibility: More than 20% of this document may be affected by microfiche quality
(Grant AF-AFOSR-0511-89)
(AD-A277239; UVA/525714/AM94/101; AFOSR-94-0054TR) Avail: CASI HC A05

In this research, the issue of uniform stabilization has been investigated for large classes of conservative systems arising in elasticity. In the case of linear problems, two types of feedback have been considered: dissipative feedback operators acting only on the 'velocity' and generally nondissipative feedback based on Riccati operators and acting on the full pair of position and velocity. In nonlinear problems, feedback of the first type have been studied. Numerical implementation for both types of feedbacks have received special attention. DTIC

N94-32351 Imperial Coll. of Science and Technology, London (England). Dept. of Mechanical Engineering.
THE CYCLIC FATIGUE BEHAVIOUR OF ADHESIVE JOINTS Interim Report No. 3, Jul. - Dec. 1993
A. J. Kinloch, M. Fernando, and P. Lam 10 Dec. 1993 5 p Limited Reproducibility: More than 20% of this document may be affected by microfiche quality
(Contract DAJA45-93-C-0008)
(AD-A277080; R/D-6869-MS-01) Avail: Issuing Activity (Defense Technical Information Center (DTIC))

The work has progressed well and we have: (1) developed an automatic data acquisition method; (2) determined the compliance of the specimen, both experimentally and theoretically; (3) measured the static adhesive fracture energy, G sub c; and (4) measured the cyclic fatigue behavior at 25 deg C and 55% r.h. DTIC

N94-32486 Stanford Univ., CA.
DYNAMIC ERROR COMPENSATION IN ROBOTIC TRUSSES Ph.D. Thesis
Allen R. Boronkay 1993 385 p
Avail: Univ. Microfilms Order No. DA9326429

A robotic truss is an active structure comprised of links which inherently can be loaded only in tension or compression. Unlike passive truss structures, a robotic truss can execute large motions by adjusting the lengths of its links through the use of actuators. The importance of the truss structure for robotics has been neither fully recognized nor fully exploited in prior work. This property and its consequences for design are the focus of this thesis. Robotic trusses are shown to have advantages in metrology, modularity, stiffness-to-weight ratio, natural frequencies, modeling, and simplicity. The robotic truss's qualities make dual coarse/fine actuation interesting for some applications, such as machining. In dual actuation, each leg of the robotic truss has two actuators, one for large, relatively slow motions and one for small, high speed motions. A dynamic model for a simple robotic truss with dual actuation and control strategies for it, including the possibility for distributed control, are developed. The model is used to show that a dual actuated robotic truss can achieve a dynamic stiffness of over 200 N/micron (1.14 x 10(exp 6) lb/in.) which is sufficient for precision machining. The modeling, design, construction, and performance of an experimental differential solenoid fine actuator are examined. While this work uses machining as a focus, the robotic truss may find innumerable other applications. It is especially appropriate for cases in which high precision is needed. Electronics assembly, in particular, could benefit from the robotic truss's combination of metrological advantages and high natural frequencies. Dissert. Abstr.

N94-32637 Lawrence Livermore National Lab., CA.
AUTOMATIC CONTACT IN DYNA3D FOR VEHICLE CRASHWORTHINESS
R. G. Whirley and B. E. Engelmann 15 Jul. 1993 17 p Presented at the Annual Winter Meeting of the American Society of Mechanical Engineers, New Orleans, LA, 28 Nov. - 3 Dec. 1993 Limited Reproducibility: More than 20% of this document may be affected by microfiche quality
(Contract W-7405-eng-48)
(DE94-007143; UCRL-JC-114598; CONF-931121-38) Avail: CASI HC A03

This paper presents a new formulation for the automatic definition and treatment of mechanical contact in explicit nonlinear finite element analysis. Automatic contact offers the benefits of significantly reduced model construction time and fewer opportunities for user error, but faces significant challenges in reliability and computational costs. This paper discusses in detail a new four-step automatic contact algorithm. Key aspects of the proposed method include automatic identification of adjacent and opposite surfaces in the global search phase, and the use of a smoothly varying surface normal which allows a consistent treatment of shell intersection and corner contact conditions without ad-hoc rules. The paper concludes with three examples which illustrate the performance of the newly proposed algorithm in the public DYNA3D code. DOE

N94-32639 Westinghouse Savannah River Co., Aiken, SC.
MODELING OF RESIDUAL STRESS MITIGATION IN AUSTENITIC STAINLESS STEEL PIPE GIRTH WELDMENT
M. Li (Oregon Graduate Inst. of Science and Technology, Beaverton.), D. G. Atteridge (Oregon Graduate Inst. of Science and Technology, Beaverton.), W. E. Anderson (Oregon Graduate Inst. of Science and Technology, Beaverton.), and S. L. West 1994 10 p Presented at the American Welding Society International Conference on Modeling and Control of Joining Processes, Orlando, FL, 8-10 Dec. 1993 Limited Reproducibility: More than 20% of this document may be affected by microfiche quality
(Contract DE-AC09-89SR-18035)
(DE94-007184; WSRC-MS-94-080; CONF-931234-8) Avail: CASI HC A02

This study provides numerical procedures to model 40-cm-diameter, schedule 40, Type 304L stainless steel pipe girth welding and a newly proposed post-weld treatment. The treatment can be used to accomplish the goal of imparting compressive residual stresses at the inner surface of a pipe girth weldment to prevent/retard the intergranular stress corrosion cracking (IGSCC) of the piping system in nuclear reactors. This new post-weld treatment for mitigating residual stresses is cooling stress improvement (CSI). The concept of CSI is to establish and maintain a certain temperature gradient across the pipe wall thickness to change the final stress state. Thus, this process involves sub-zero low temperature cooling of the inner pipe surface of a completed girth weldment, while simultaneously keeping the outer pipe surface at a slightly elevated temperature with the help of a certain heating method. Analyses to obtain quantitative results on pipe girth welding and CSI by using a thermo-elastic-plastic finite element model are described in this paper. Results demonstrate the potential effectiveness

of CSI for introducing compressive residual stresses to prevent/retard IGSCC. Because of the symmetric nature of CSI, it shows great potential for industrial application. DOE

N94-32733# Department of the Navy, Washington, DC.
VIBRATION DAMPENER AND METHOD FOR MAKING SAME Patent Application
Wendell Maciejewski, inventor (to Navy) 22 Nov. 1993 14 p
(AD-D016094; US-Patent-Appl-SN-155606) Avail: CASI HC A03/MF A01

There is disclosed a vibration dampener comprising a body for disposition between two relatively movable members, the body being formed from a carrier of a gel material and particles having electrorheological properties embedded in the carrier with the particles electrically aligned and pseudo-bonded. Upon a displacement force being applied to the body, as by one of the members, the particles resist motion relative to other of the particles. There is further disclosed a method for making the aforesaid vibration dampener wherein the dampener has a current passed through it while the carrier cures into a gel material. DTIC

N94-32735*# National Aeronautics and Space Administration. Lewis Research Center, Cleveland, OH.
STRUCTURAL PROBABILITY CONCEPTS ADAPTED TO ELECTRICAL ENGINEERING
Eric P. Steinberg (Ohio Univ., Athens.) and Christos C. Chamis Mar. 1994 18 p Presented at the 35th AIAA Structures, Structural Dynamics and Materials Conference, Hilton Head, SC, 18-20 Apr. 1994; sponsored by AIAA
(RTOP 584-03-11)
(NASA-TM-106499; E-8493; NAS 1.15:106499; AIAA Paper 94-1383)
Avail: CASI HC A03/MF A01

Through the use of equivalent variable analogies, the authors demonstrate how an electrical subsystem can be modeled by an equivalent structural subsystem. This allows the electrical subsystem to be probabilistically analyzed by using available structural reliability computer codes such as NESSUS. With the ability to analyze the electrical subsystem probabilistically, we can evaluate the reliability of systems that include both structural and electrical subsystems. Common examples of such systems are a structural subsystem integrated with a health-monitoring subsystem, and smart structures. Since these systems have electrical subsystems that directly affect the operation of the overall system, probabilistically analyzing them could lead to improved reliability and reduced costs. The direct effect of the electrical subsystem on the structural subsystem is of secondary order and is not considered in the scope of this work. Author

N94-32771 Oak Ridge National Lab., TN.
REACTOR PRESSURE VESSEL STRUCTURAL INTEGRITY RESEARCH IN THE US NUCLEAR REGULATORY COMMISSION HSST AND HSSI PROGRAMS
W. E. Pennell and W. R. Corwin 1994 10 p Presented at the British Nuclear Energy Society International Conference on Thermal Reactor Safety Assessment, Manchester, England, 23-26 May 1994 Limited Reproducibility: More than 20% of this document may be affected by microfiche quality
(Contract DE-AC05-84OR-21400)
(DE94-006550; CONF-940594-1) Avail: CASI HC A02

This report discusses development on the technology used to assess the safety of irradiation-embrittled nuclear reactor pressure vessels containing flaws. Fracture mechanics tests on reactor pressure vessel steel have shown that local brittle zones do not significantly degrade the material fracture toughness, constraint relaxation at the crack tip of shallow surface flaws results in increased fracture toughness, and biaxial loading reduces but does not eliminate the shallow-flaw fracture toughness elevation. Experimental irradiation investigations have shown that the irradiation-induced shift in Charpy V-notch versus temperature behavior may not be adequate to conservatively assess fracture toughness shifts due to embrittlement and the wide global variations of initial chemistry and fracture properties of a nominally uniform material within a pressure vessel may confound accurate integrity assessments that require baseline properties. DOE

N94-32842 Sandia National Labs., Albuquerque, NM.
OVERVIEW OF SHOCK PHYSICS CODES FOR ARMOR ANALYSIS
M. McGlaun 1993 8 p Presented at the 5th Annual TACOM Combat Vehicle Survivability Symposium, Monterey, CA, 28 Feb. - 3 Mar 1994 Limited Reproducibility: More than 20% of this document may be affected by microfiche quality
(Contract DE-AC04-94AL-85000)
(DE94-008948; SAND-93-2552C; CONF-940255-1) Avail: Issuing Activity (Department of Energy (DOE))

Shock physics codes for armor analysis and the computers used to run the codes have improved dramatically over the last five years. Improved algorithms and material models allow accurate and efficient modeling of conventional armor. Desktop workstations routinely perform two-dimensional calculations, and massively parallel computers can perform three-dimensional calculations. New developments in codes and computers promise improved accuracy, increased capabilities, and faster simulation. This paper describes the current state of armor analysis codes and the computers used to run the codes. Armor analysis code features fall into one of five categories: mesh, solution algorithm, material model, heuristic, or computer. This paper discusses the current state of each of these categories and discusses the additional work needed. DOE

N94-32883*# National Aeronautics and Space Administration. Lewis Research Center, Cleveland, OH.
FLUTTER ANALYSIS OF A SUPERSONIC CASCADE IN TIME DOMAIN USING AN ADI EULER SOLVER
T. S. R. Reddy (Toledo Univ., OH.), M. A. Bakhle (Toledo Univ., OH.), and D. L. Huff Apr. 1992 25 p
(RTOP 535-03-01)
(NASA-TM-105625; E-6966; NAS 1.15:105625) Avail: CASI HC A03/MF A01

The aeroelastic stability of a two-dimensional cascade oscillating in supersonic axial flow is analyzed in the time domain. The aeroelastic model consists of a single degree of freedom typical section structural model for each blade of the cascade and an unsteady two-dimensional cascade aerodynamic model based on the Euler equations. The Euler equations are solved using a time accurate Alternating Direction Implicit (ADI) solution scheme. The aeroelastic equations are integrated in time. The effect of interblade phase angle is included in the aeroelastic analysis by an appropriate choice of initial and boundary conditions. Flutter predictions are obtained from the time response of a flat plate cascade in single degree of freedom pitching motion. The results correlate well with those obtained from a separate frequency domain flutter analysis for all values of interblade phase angles considered. Flutter results are then presented for cascades having airfoil sections representative of a supersonic throughflow fan. The validity of the time integration method for a cascade of airfoils at various interblade phase angles is demonstrated. Author

N94-32903*# National Aeronautics and Space Administration. Marshall Space Flight Center, Huntsville, AL.
A CASE STUDY OF ANALYSIS METHODS FOR LARGE DEFLECTIONS OF A CANTILEVER BEAM
L. D. Craig May 1994 34 p
(NASA-TM-108454; NAS 1.15:108454) Avail: CASI HC A03/MF A01

A load case study of geometric nonlinear large deflections of a cantilever beam is presented. The bending strain must remain elastic. Closed form solution and finite element methods of analysis are illustrated and compared for three common load cases. A nondimensional nomogram for each case is presented in the summary. Author

N94-32907*# Draper (Charles Stark) Lab., Inc., Cambridge, MA.
LIMITING VIBRATION IN SYSTEMS WITH CONSTANT AMPLITUDE ACTUATORS THROUGH COMMAND PRESHAPING M.S Thesis - MIT
Keith Eric Rogers May 1994 117 p
(Contract NAS9-18426)
(NASA-CR-188284; NAS 1.26:188284; CSDL-T-1214) Copyright Avail: CASI HC A06/MF A02

The basic concepts of command preshaping were taken and adapted to the framework of systems with constant amplitude (on-off) actuators. In this context, pulse sequences were developed which help to attenuate vibration in flexible systems with high robustness to errors in frequency identification. Sequences containing impulses of different magnitudes were approximated by sequences containing pulses of different durations. The effects of variation in pulse width on this approximation were examined. Sequences capable of minimizing loads induced in flexible systems during

execution of commands were also investigated. The usefulness of these techniques in real-world situations was verified by application to a high fidelity simulation of the space shuttle. Results showed that constant amplitude preshaping techniques offer a substantial improvement in vibration reduction over both the standard and upgraded shuttle control methods and may be mission enabling for use of the shuttle with extremely massive payloads. Author

N94-32932*# National Aeronautics and Space Administration. Lewis Research Center, Cleveland, OH.

COMPLIANCE MEASUREMENTS OF CHEVRON NOTCHED FOUR POINT BEND SPECIMEN

Anthony Calomino, Raymond Bubsey, and Louis J. Ghosn Apr. 1994 26 p

(RTOP 505-63-12)

(NASA-TM-106538; E-8679; NAS 1.15:106538) Avail: CASI HC A03/MF A01

The experimental stress intensity factors for various chevron notched four point bend specimens are presented. The experimental compliance is verified using the analytical solution for a straight through crack four point bend specimen and the boundary integral equation method for one chevron geometry. Excellent agreement is obtained between the experimental and analytical results. In this report, stress intensity factors, loading displacements and crack mouth opening displacements are reported for different crack lengths and different chevron geometries, under four point bend loading condition. Author

N94-32940*# Tennessee Technological Univ., Cookeville. Center for Manufacturing Research and Technology Utilization.

STRAIN SENSING USING OPTICAL FIBERS Final Report

Richard Houghton and Steven Hiles 6 May 1994 192 p

(Contract NCC8-8)

(NASA-CR-195807; NAS 1.26:195807; TR-MCTR-0594-07; TTU-124-894-83) Avail: CASI HC A09/MF A02

The main source of attenuation which will be studied is the optical fiber's sensitivity to bending at radii that are much larger than the radius of the fiber. This type of environmental attenuation causes losses that are a function of the severity of the bend. The average attenuation caused by bending varies exponentially with the bend radius. There are many different fibers, sources, and testing equipment available. This thesis describes tests that were performed to evaluate the variables that effect bending related attenuation and will discuss the consistency of the results. Descriptions and comparisons will be made between single mode and multimode fibers as well as instrumentation comparisons between detection equipment. Detailed analysis of the effects of the whispering gallery mode will be performed along with theorized methods for characterization of these modes. Derived from text

N94-32982 Southampton Univ. (England). Inst. of Sound and Vibration Research.

AN ANALYTICAL STUDY OF THE VIBRATION OF BEAMS FITTED WITH NEUTRALIZERS. PART 2: ASSESSMENT OF THE EFFECTS OF MOUNTING CONFIGURATIONS

P. Clark and R. G. White Jan. 1993 66 p

(ISVR-TR-225-Pt-2) Copyright Avail: Issuing Activity (Inst. of Sound and Vibration Research, Univ. of Southampton, Southampton SO9 5NH, England)

The control of vibration in beams or other one-dimensional structures is of considerable interest in practical engineering. With the majority of industrial machinery installations it is this type of structure, for example, pipe work and other mechanical linkages, which forms one of the main vibration paths which bypass isolator systems. It is well-known that the introduction of discontinuities into these types of structures significantly affects the vibration transmission properties of the complete system. One such discontinuity is the vibration neutralizer. In this report, the effects of mounting configuration upon the performance of the device as a vibration attenuator are presented using the concept of vibrational power transmission. Author

N94-33011# Virginia Univ., Charlottesville.

EFFECTIVE COMPUTATIONAL STRATEGY FOR PREDICTING THE RESPONSE OF COMPLEX SYSTEMS Final Report, 30 Sep. 1990 - 31 Aug. 1993

Ahmed K. Noor 8 Dec. 1993 25 p

(Grant AF-AFOSR-0369-90)

(AD-A277452; UVA/525733/CEAM94/101; AFOSR-94-0096TR) Avail: CASI HC A03/MF A01

An effective computational strategy is developed for generating the response of complex systems using (small or large) perturbations from the response of a simple structure (or a simpler mathematical/discrete model of the original structure). Two general approaches are developed for selecting the simpler model and establishing the relations between the original and simpler models. The two approaches are: decomposition or partitioning strategy, and hierarchical modeling strategy. Two effective partitioning strategies are used. The first is based on uncoupling of load-carrying mechanisms, and the second is based on symmetry transformations. The hierarchical modeling used is a predictor-corrector iterational process based on using a simple mathematical model in the predictor phase and correcting the response using a more accurate mathematical model. The strategies have been applied to several problems including: thermal buckling and postbuckling of multilayered composite plates; and nonlinear dynamic analysis of composite shells. DTIC

N94-33118*# National Aeronautics and Space Administration. Langley Research Center, Hampton, VA.

STRUCTURAL DAMPING STUDIES AT CRYOGENIC TEMPERATURES

Clarence P. Young, Jr. (North Carolina Univ., Raleigh.) and Ralph D. Buehrle May 1994 34 p

(RTOP 505-59-54-01)

(NASA-TM-109073; NAS 1.15:109073) Avail: CASI HC A03/MF A01

Results of an engineering study to measure changes in structural damping properties of two cryogenic wind tunnel model systems and two metallic test specimens at cryogenic temperatures are presented. Data are presented which indicate overall, a trend toward reduced structural damping at cryogenic temperatures (-250 degrees F) when compared with room temperature damping properties. The study was focused on structures and materials used for model systems tested in the National Transonic Facility (NTF). The study suggests that the significant reductions in damping at extremely cold temperatures are most likely associated with changes in mechanical joint compliance damping rather than changes in material (solid) damping. Author

N94-33143 Northwestern Univ., Evanston, IL. Technological Inst.

NONLOCAL THEORY FOR FRACTURING OF QUASIBRITTLE MATERIALS Final Report

Zdenek P. Bazant 1 Mar. 1994 220 p Limited Reproducibility: More than 20% of this document may be affected by microfiche quality

(Grant AF-AFOSR-0140-91)

(AD-A278283; Rept-0650-350-0457; AFOSR-94-0204TR) Avail: CASI HC A10

The failure of quasibrittle materials, which include concrete, rock, high-performance ceramics and fiber composites, cannot be treated according to the classical theories of plasticity or fracture mechanics because growth of zones of strain softening damage due to cracking must be considered. The mathematical treatment involves difficulties with spurious excessive localization. To remedy them, the nonlocal continuum concept was previously introduced, however, without theoretical foundation. The principal objective of the research has been to formulate the nonlocal damage concept on the basis of micromechanics of systems of growing and interacting cracks. This has led to a new model in which the nonlocal interactions are based on a smeared crack influence function, are tensorial and directional, and directional, and exhibit a power-type long-range decay. An iterative method for solving a Fredholm integral equation for the crack interactions in a finite element code has also been formulated. Advances have further been made in several related problems of micro-macro correlation. The applicability limits of the classical Weibull theory of random micro-strength have been identified and a nonlocal probabilistic generalization derived. The time dependence and rate effect in damage evolution have been described on the basis of the activation theory for bond ruptures. The problems of scaling and size effect associated with damage have

been analyzed, both theoretically and experimentally (with tests on concretes, fiber composites and rocks). DTIC

N94-33356# Illinois Univ., Chicago. Dept. of Civil Engineering Mechanics and Metallurgy.
FUNDAMENTAL STUDIES IN CRACK INITIATION Annual Report, 15 Sep. 1992 - 14 Sep. 1993
John Botsis Oct. 1993 38 p
(Contract F49620-92-J-0493)
(AD-A278387; AFOSR-94-0227TR) Avail: CASI HC A03/MF A01

Mechanistic investigations of damage evolution before crack initiation in an amorphous polymer show that damage consists of a core of highly dense crazing and a peripheral less dense zone of crazing. Damage characterization is carried out at consecutive configurations of the damage zone. Analysis of the kinematics of damage at different times involves comparisons of the inertia moments of damage distributions. The results indicate that damage evolution between consecutive configurations can be approximated by a linear transformaiion of the space variables. Thus, the process of damage growth can be described by translation and deformation of the damage zone. The growth rates of the damage zone movements decrease until crack initiation. In all cases, the average densities exhibit a damping type behavior with the number of cycles. The crack initiates within a core zone immediately ahead of the stress concentrator. The experimental results suggest that damage density within the core zone is independent of the loading conditions considered herein. This value is approximately equal to the damage density around the crack tip during slow crack propagation. The crack length at initiation is found to increase exponentially with the stress level. A simple decaying exponential relationship relates the crack initiation times and the applied stress level. This result is consistent with the fracture models based on absolute reaction theories. DTIC

N94-31031*# Auburn Univ., AL. Mechanical Engineering.
MORPHOLOGY CORRELATION OF CRATERS FORMED BY HYPERVELOCITY IMPACTS
Gary D. Crawford, M. Frank Rose, and Ralph H. Zee *In* NASA. Marshall Space Flight Center, LDEF Materials Results for Spacecraft Applications Dec. 1993 p 245-257 (For primary document see N94-31012 09-12)
Avail: CASI HC A03/MF A04

N94-31032*# National Aeronautics and Space Administration. Marshall Space Flight Center, Huntsville, AL.
MICROMETEOROID/SPACE DEBRIS EFFECTS ON MATERIALS
James M. Zwiener and Miria M. Finckenor *In its* LDEF Materials Results for Spacecraft Applications Dec. 1993 p 259-279 (For primary document see N94-31012 09-12)
Avail: CASI HC A03/MF A04

42 GEOSCIENCES (GENERAL)

N94-31606# Oak Ridge National Lab., TN.
PROCEEDINGS OF A JOINT US-JAPAN SEMINAR IN THE ENVIRONMENTAL SCIENCES
D. L. DeAngelis, ed. Nov. 1993 244 p Seminar held in Honolulu, HI, 24-30 Apr. 1988
(Contract DE-AC05-84OR-21400)
(DE94-004727; ORNL/TM-12392; ESDP-4124344; CONF-8804344) Avail: CASI HC A11/MF A03

The Joint US-Japan Seminar in the Environmental Sciences was based on the premises that questions remain concerning the factors that control many of the regularities observed in ecological communities and that increased collaboration between researchers in the United States and Japan can contribute to answering these questions. The papers included in this report resulted from the Seminar. These papers as well as workshop discussions summarized here outline the main issues that face theoretical ecology today. The papers cover four different areas of theoretical ecology: (1) individual species adaptations, (2) ecological community-food web interactions, (3) food web theory, and (4) concepts related to the ecosystem. Individual projects are processed separately for the databases. DOE

43 EARTH RESOURCES AND REMOTE SENSING

Includes remote sensing of earth resources by aircraft and spacecraft; photogrammetry; and aerial photography.
For instrumentation see *35 Instrumentation and Photography.*

N94-31068 Office of Technology Assessment, Washington, DC.
GLOBAL CHANGE RESEARCH AND NASA'S EARTH OBSERVING SYSTEM Background Paper
Nov. 1993 56 p See also PB93-231322, PB94-134640 and PB94-134657 Limited Reproducibility: More than 20% of this document may be affected by microfiche quality
(PB94-126992; OTA-BP-ISC-122) Avail: CASI HC A04

The United States is spending oillions of dollars in a multiyear Global Change Research Program (the USGCRP) to monitor, understand, and ultimately predict the nature of global changes and the mechanisms that cause them. The background report examines the direction and scope of USGCRP and its most expensive component, NASA's Earth Observing System (EOS) of satellites. In particular, it examines how well USGCRP and EOS are fulfilling their scientific objectives, whether some program elements are missing or need to be strengthened, and whether the program is meeting the needs of policymakers. The background paper describes the number of suggestions to improve the value of the USGCRP to both scientists and policymakers. The background paper also explicates the continuing debate over whether the sensors and satellites planned by USGCRP: (1) will be able to acquire data in sufficient detail to elucidate the mechanisms responsible for global change; and (2) are appropriate for long-term monitoring of key indices of global change. NTIS

N94-31074 Technische Univ., Delft (Netherlands). Faculteit der Geodesie.
FILTERING OF SATELLITE ALTIMETRY DATA WITH OPTIMAL SMOOTHING CUBIC SPLINES TO COMPUTE GEOID HEIGHTS, ALONG-TRACT GEOID AND GRAVITY GRADIENTS IN THE INDONESIAN WATERS AND ITS SURROUNDINGS
R. Rummel Sep. 1993 143 p See also PB87-213336 Limited Reproducibility: More than 20% of this document may be affected by microfiche quality
(PB94-147527) Avail: CASI HC A07

In the report, at first the basic principles of satellite altimetry and its oceanographic, geophysic and geodetic applications are discussed. Since the authors use the Geosat/ERM data, a review of the Geosat Satellite is briefly given. The theory behind the method to compute the geoid gradients and gravity gradients is described. The method takes advantage of the high precision and the data density in profile direction. For obtaining the vertical components a transformation from an oblique system into an orthogonal system is needed. Problems in the construction of geoid heights as a function of obtained distance, and the filtering of noise will be solved with optimal smoothing cubic splines using the GCV-criterion yielding the minimal value of the true mean square error. Next to the function, the error of the spline function will be estimated using the propagation law of covariances. NTIS

N94-31075 Technische Univ., Delft (Netherlands). Faculteit der Geodesie.
APPLICATION OF RADON TRANSFORMATION FOR IMPROVED ANALYSIS OF SPARSELY SAMPLED DATA: A FEASIBILITY STUDY
R. F. Hanssen Nov. 1993 151 p See also PB93-197283 Limited Reproducibility: More than 20% of this document may be affected by microfiche quality
(PB94-147535) Avail: CASI HC A08

The Radon transform depicts line-integrals in the space domain as pointvalues in the Radon domain. The set of all possible line-integrals yields a continuous coverage of the Radon domain. In this manner, lineations in the space domain become visible in the Radon domain, as they have a deviating Radon amplitude. The location of this amplitude represents the position parameters of the corresponding line. The Radon domain representation can also be found for a discrete homogeneously sampled set of data. The first impulse for this study originates from the field of satellite altimetry, and therefore the authors will throughout this thesis now and then refer to altimetry and altimetry data. Satellite altimetry has become an important technique for studying several properties of ocean areas, as

well for geodesists as for oceanographers, climatologists, geophysicist etc. A satellite altimeter measures the shape of the ocean surface which is simultaneously a good approximation of the marine geoid (i.e. the equipotential ocean surface). For geodetic or geophysical applications, it is desirable to compute the gravity anomaly or vertical deflection from the geoid height. NTIS

N94-31165 Ecole Nationale Superieure des Telecommunications, Paris (France).
AUTOMATIC EXTRACTION OF CARTOGRAPHIC OBJECTS BY FUSION OF DATA EXTRACTED FROM SATELLITE IMAGES Ph.D. Thesis [EXTRACTION AUTOMATIQUE D'OBJETS CARTOGRAPHIQUES PAR FUSION D'INFORMATIONS EXTRAITES D'IMAGES SATELLITES]
Stephane Houzelle 1993 177 p In FRENCH Limited Reproducibility: More than 20% of this document may be affected by microfiche quality
(ISSN 0751-1353)
(TELECOM-93-E-001; ETN-94-95895) Avail: CASI HC A09

An attempt to formalize aspects related to multisensor fusion is made. The characterization of the fact that a sensor may be redundant, or complementary in relation to another sensor, is addressed. For this, information theory provides a very important mathematical framework, allowing quantitative measurement of the redundancy or complementary levels existing between two sensors. A formalization of concepts encountered in multisensor fusion allowing better development of potential fusion strategies is proposed. A generic cell of data fusion is defined, attempting to characterize whichever data fusion process. The problem of integration can then, in this formalization, be regarded as the association of different fusion cells. Within the framework of this formalization, two types of strategies aiming at detecting bridges, and extracting build-up areas, are examined. An expert system for interpretation allowing simultaneous detection of several types of objects to be controlled is presented. This system is based on a modeling of manipulated objects (sensors, semantic objects, image primitives, etc.) satisfying description independence constraints. It lies on a blackboard type architecture, which seems particularly well suited to the management of several sensor usage. The study results show the indispensable character of multisensor fusion in scene analysis. ESA

N94-31496# Texas Univ., El Paso. Dept. of Electrical Engineering.
OPTICAL AND IMAGE TRANSMISSION THROUGH DESERT ATMOSPHERES Final Report
Carlos McDonald, Gerardo Carrillo, Luis Carrillo, Miguel Nunez, and Rick Gamboa 25 Jan. 1994 145 p
(Contract DAAL03-89-G-0108)
(AD-A276022; ARO-27259.2-GS-SAH) Avail: CASI HC A07/MF A02

Based on a unique experimental technique, measurement results are presented on the passive, remote sensing of the optical modulation transfer function of desert atmospheres (MTF(sub A)), including the DC, low, and high spatial cutoff frequency components which are attributed to contrast, aerosol, and turbulence, respectively. In particular, use of this technique has made it possible to directly measure the low spatial frequency cutoff of the aerosol component. This technique is based on utilizing digital image processing of remote video scenes which include two optically identical castellated targets which are located at different distances and are contrasted against the horizon sky. Ratios of apparent contrast and FFT calculations are used to determine the MTF(sub A) components, including the spatial cutoff frequencies of the aerosol and turbulence components, independent of the imaging system and actual properties of the targets. The experimental technique is described along with current MTF(sub A) component measurements. DTIC

N94-31504# Geological Survey, Reston, VA.
GAS HYDRATE DETECTION AND MAPPING ON THE US EAST COAST
T. S. Ahlbrandt and W. P. Dillon 1993 20 p Presented at the Fuels Technology Contractors' Review Meeting, Morgantown, WV, 16-18 Nov. 1993
(Contract DE-AI21-83MC-20422)
(DE94-005959; DOE/MC-20422/94/C0315; CONF-931156-15) Avail: CASI HC A03/MF A01

Project objectives are to identify and map gas hydrate accumulations on the U.S. eastern continental margin using remote sensing (seismic profiling) techniques and to relate these concentrations to the geological factors that control them. In order to test the remote sensing methods, gas hydrate-cemented sediments will be tested in the laboratory and an effort will be made to perform similar physical tests on natural hydrate-cemented sediments from the study area. Gas hydrate potentially may represent a future major resource of energy. Furthermore, it may influence climate change because it forms a large reservoir for methane, which is a very effective greenhouse gas; its breakdown probably is a controlling factor for sea-floor landslides; and its presence has significant effect on the acoustic velocity of sea-floor sediments. DOE

N94-31553 Maryland Univ., College Park.
DEVELOPMENT OF A STATISTICAL METHOD FOR ESTIMATING THE DOWNWARD LONGWAVE RADIATION AT THE SURFACE FROM SATELLITE OBSERVATIONS Ph.D. Thesis
Hai-Tien Lee 1993 166 p
Avail: Univ. Microfilms Order No. DA9327454

A new technique was developed statistically for estimating the DLR using the HIRS/2 clear-column radiances from NOAA polar orbiting satellites. Simulated radiation data were used in the model development and validation. Two categories of regression equations were studied. They are the linear models and the emissivity/transmissivity-approach models. It was found that the emissivity/transmissivity models are superior than the linear ones in the aspects of the RMS errors of the DLR estimates as well as in the residual spread patterns. For both clear and cloudy conditions, when instrument noise is included, the regression RMS errors of the emissivity and transmissivity models range from about 4 to 9 W/sq. m. Sensitivity studies show that DLR is the most sensitive to the error in the cloud amount on average. Overall, the combined DLR errors, excluding the contribution of the error in the surface pressure estimation, range from about 7 to 12 W/sq. m when there are +/- 10% uncertainties in cloud base heights. When the cloud amount uncertainties rise to 30%, the range of the combined DLR error ranges from about 10 to 25 W/sq. m. The standard deviations of DLR differences found in the validations are about 9 W/sq. m with mean differences at about +/-1 W/sq. m. For cloudy skies, cloud base height and the effective cloud amount are needed. The DLR estimated with different cloud data sources, however, has not been examined. Since the sensitivity study shows that the DLR error due to the uncertainty of the cloud amount usually dominates the other error components, it is believed that an accurate estimate of the cloud amount is more important for cloudy-sky DLR estimation. Despite these limitations noted above, our analysis indicates that the physical statistical method developed in this study should provide estimates of the DLR to within about 10 W/sq. m RMS directly from the HIRS observations if the cloud properties can be accurately estimated. Furthermore, it is expected that the errors will be considerably smaller for monthly average, except where persistent extreme conditions occur. Dissert. Abstr.

N94-31570 Kansas Univ., Lawrence.
SATELLITE RADAR ALTIMETRY OVER THE CONTINENTAL ICE SHEETS Ph.D. Thesis
Curt H. Davis 1992 192 p
Avail: Univ. Microfilms Order No. DA9313095

We conducted a review of the dielectric and physical properties of ice and snow to determine estimates for the depth of penetration in dry polar snow at altimeter frequencies. Minimum penetration estimates between 6 to 9 m were calculated for dry polar snow based upon the most recent reported dielectric data. In addition, an analysis of in situ radar data from East Antarctica showed that the penetration depth of dry polar snow varied with surface elevation and distance from the coast. By approximating the altimeter's antenna pattern and transmitted pulse shape with Gaussian functions, we derived a closed-form analytical solution for the return power volume scattered from beneath the ice sheet surface. The volume scattering model was then combined with the Brown surface scattering model. By applying the combined model to averaged altimeter waveforms, we showed that it accurately described variations in altimeter waveform shapes produced by differing contributions of surface and volume scattering to the received power. Next we developed an algorithm based upon the combined surface/volume scattering model that is capable of retracking individual (10/s) altimeter waveforms. Because the model is nonlinear, an iterative least-squares procedure was used to fit the combined model to altimeter return waveforms. The algorithm was used to retrack over 400,000 return waveforms from the Greenland and Antarctic ice sheets. By retracking individual altimeter waveforms we made quantitative estimates of the

geographical and seasonal variations in the near-surface properties of the ice sheet. The surface properties were correlated with elevation, latitude, and microwave brightness temperature data. Specifically, the estimated extinction coefficient of snow, k(sub e), varied from 0.48 to 0.13 m(exp -1) over the latitudes from 65 to 72 deg N on the central portion of the Greenland ice sheet and from 0.20 to 0.10 m(exp -1) over a section of Wilkes land in East Antarctica where the elevation increased from 2550 to 3150 m. Also, significant seasonal variations in the surface properties were observed in some areas of both the Greenland and Antarctic data sets. Finally we compared the surface elevations estimated from our retracking algorithm with the surface elevations produced from the NASA and ESA retracking algorithms. The NASA algorithm produced the most accurate elevation-change estimates when seasonal variations were present. Dissert. Abstr.

N94-31592 Technische Univ., Delft (Netherlands). Faculteit der Geodesie.

POSSIBLE IMPROVEMENTS OF SATELLITE EPHEMERIS PROGRAMS USED IN GEODESY

R. J. Valten Aug. 1993 106 p Limited Reproducibility: More than 20% of this document may be affected by microfiche quality
(PB94-148681) Avail: CASI HC A06

Possible improvements of ephemeris programs with respect to process speed are discussed. For some special cases fast algorithms are examined. These algorithms are tested in the program IRVORB. Satellite orbit dynamics (SOD) is discussed in chapter 2 to illustrate the origin of the formulae which are used in chapters 4, 5, and 6. Chapter 3 discusses some general considerations that must be made when programming computers. The first algorithm, which might improve process speed, is discussed in chapter 4. It concerns the iteration of the elliptic Kepler equation. Chapter 5 discusses the geopotential acceleration. Koop and Stelpstra introduced a fast recursion scheme for the calculation of Legendre functions and their derivatives. This method is implemented in IRVORB for the calculation of the geopotential acceleration. A third attempt to improve the process speed of orbital routines is discussed in chapter 6. Chapter 7 discusses the main results of this study. NTIS

N94-31603# Nevada Univ., Reno. Water Resources Center.

HYDROLOGIC DATABASE USER'S MANUAL

J. B. Champman, K. J. Gray, and C. B. Thompson Sep. 1993 102 p
(Contract DE-AC08-90NV-10845)
(DE94-003950; DOE/NV-10845/31) Avail: CASI HC A06/MF A02

The Hydrologic Database is an electronic filing cabinet containing water-related data for the Nevada Test Site (NTS). The purpose of the database is to enhance research on hydrologic issues at the NTS by providing efficient access to information gathered by a variety of scientists. Data are often generated for specific projects and are reported to DOE in the context of specific project goals. The originators of the database recognized that much of this information has a general value that transcends project-specific requirements. Allowing researchers access to information generated by a wide variety of projects can prevent needless duplication of data-gathering efforts and can augment new data collection and interpretation. In addition, collecting this information in the database ensures that the results are not lost at the end of discrete projects as long as the database is actively maintained. This document is a guide to using the database. DOE

N94-31658# Technical Research Centre of Finland, Espoo. Instrument Lab.

IMAGING DEVICES FOR SATELLITE REMOTE SENSING [SATELLIITIKAUKOKARTOITUKSEN KUVAUSLAITTEET]

Jari Tahvanainen Oct. 1993 33 p In FINNISH
(ISSN 1235-0605)
(VTT-TIED-1517; ISBN-9-51-384451-X; ETN-94-96041) Copyright Avail: CASI HC A03/MF A01

Data collection by detecting electromagnetic radiation reflected or emitted from objects on the Earth surface (remote sensing) is addressed. When detecting terrestrial materials with remote sensing systems (sensors and platforms) from satellite, the atmosphere affects electromagnetic energy levels and limits usable wavelength bands. Short wavelengths of electromagnetic radiation (gamma, X and UV portions of electromagnetic spectrum) are reflected almost totally from water vapor, which is always present in the atmosphere. Also atmospheric gas molecules and particles such as aerosols, dust, haze, smoke, etc. cause absorption and scattering of radiation energy on their own special spectral regions. The drawback of absorption and scattering can often be avoided by using more suitable, less affected wavelength bands. For example water vapor affects very little on microwave radiation and so imaging using this band is possible through clouds. Microwave detection can also be used at night time as the system itself supplies the detected radiation. Radar sensors are examples of active remote sensing instruments. Each terrestrial feature has its own reflectance and emittance characteristics, which often identify the imaged feature and its state. By using remote sensing images it is often possible get information also at features on which solar radiation can not reach directly. For example terrestrial plants often tell about the properties of soil under them. ESA

N94-31733# Toronto Univ. (Ontario). Dept. of Geography.

ESTIMATION OF VISIBLE AND NEAR-INFRARED REFLECTIVITY FOR PEYTO GLACIER BASIN USING SATELLITE DATA M.S. Thesis

Andrew Timothy Lowe 1993 142 p
(ISBN-0-315-87039-7; CTN-94-61241) Copyright Avail: Micromedia Ltd., Technical Information Centre, 240 Catherine Street, Suite 305, Ottawa, Ontario, K2P 2G8, Canada HC/MF

Performance of energy balance models in simulating glacier mass balance depends on the accurate representation of the spatial variation of surface reflectivity. A method is presented for estimating surface reflectivity from Landsat-5 imagery and digital terrain data. A two-stream solar radiation model is constructed to compute the incoming shortwave irradiance, path radiance, and vertical transmission for a homogeneous atmosphere. Topographic correction is made using digital terrain data. Landsat-5 band reflectances corrected for atmospheric effects are combined into a measure of surface reflectivity for the visible, near-infrared, and total portions of the solar spectrum using a simple weighting strategy. The procedure is applied to Peyto Glacier Basin, Alberta. The two-stream solar radiation model performs well. Estimated surface reflectivity measurements indicate considerable agreement with the field observations and literature. The study also demonstrates the sensitivity of snow and ice reflectivity to variations in slope angle and orientation. Author (CISTI)

N94-31853# European Space Agency. European Space Research and Technology Center, ESTEC, Noordwijk (Netherlands).

EUROPEAN IMAGING SPECTROSCOPY AIRCRAFT CAMPAIGN

T. D. Guyenne, comp. Noordwijk, Netherlands Dec. 1993 107 p Workshop held in Ispra, Italy, 15-17 Apr. 1991
(ESA-SP-360; ISBN-92-9092-282-6; ETN-94-95800) Copyright Avail: CASI HC A06/MF A02

Papers concerning the results of the European Imaging Spectroscopy Aircraft Campaign (EISAC) evaluation program, which officially ended in Dec. 1991, are presented. EISAC itself was flown in the period 15 May - 15 Jun. 1989. The evaluation program put its main emphasis on the following topics: radiometric correction of data; atmospheric correction of data; spectral signature modeling; definition and evaluation of relevant surface parameters to be received by future spaceborne instruments regarding especially the modeling of a combined vegetation and ocean badness (that is midband frequency, band width, number of bands) of the Medium Resolution Imaging Spectrometer (MERIS) on the first ESA Polar Platform Mission; data analysis in terms of applications in agriculture, forestry, soil science, and oceanography. For individual titles, see N94-31854 through N94-31868.

N94-31854# Ludwig-Maximilians-Univ., Munich (Germany). Arbeitsgruppe Fernerkundung.

THE EUROPEAN IMAGING SPECTROSCOPY AIRBORNE CAMPAIGN (EISAC). DATA TAKES AND EVALUATION PROGRAMME: AN OVERVIEW

J. Bodechtel and S. Sommer *In* ESA, European Imaging Spectroscopy Aircraft Campaign Dec. 1993 p 7-12 (For primary document see N94-31853 09-43)
Copyright Avail: CASI HC A02/MF A02

The activities of the European Imaging Spectroscopy Airborne Campaign (EISAC) initiated jointly by the European Space Agency (ESA) and the Joint Research Center (JRC) of the Commission of the European Communities, are summarized. In the framework of the campaign, flights

over 7 European test sites were performed in May/Jun. 1989. The EISAC data evaluation program comprised a wide range of applications in agriculture, forestry, geology/pedology and oceanography/marine biology. In a first phase, data evaluation was concentrated on quality assessment, radiometric and atmospheric correction of the airborne data. The second phase dealt with spectra signature modeling and with the definition and evaluation of relevant surface parameters, aiming towards optimized approaches for the exploitation of the data of future spaceborne imaging spectrometers with medium and high spatial resolution. ESA

N94-31855# Joint Research Centre of the European Communities, Ispra (Italy). Remote Sensing Applications Inst.

GROUND BASED RADIOMETRIC AND ATMOSPHERIC MEASUREMENTS

G. Maracci, G. Andreoli, and B. Hosgood *In* ESA, European Imaging Spectroscopy Aircraft Campaign Dec. 1993 p 13-16 (For primary document see N94-31853 09-43)

Copyright Avail: CASI HC A01/MF A02

An overview of the work performed during the coordination of the radiometric ground truth of the European Imaging Spectroscopy Airborne Campaign (EISCAT) is given. In this campaign, two different airborne imaging spectrometers were flown over several different test sites in Europe, both on land and at sea. The two scanners were the Programmable Multispectral Imager/Fluorescence Line Imager (PMI/FLI) and a multispectral band scanner. Some examples of how the data acquired in the field entered or might enter in the analysis of the airborne imaging spectrometry data are given. ESA

N94-31856# Nansen Environmental and Remote Sensing Center, Solheimsvik (Norway).

NORSMAP 1989: NORWEGIAN REMOTE SENSING SPECTROSCOPY FOR MAPPING AND MONITORING OR ALGAL BLOOMS AND POLLUTION

Lasse H. Pettersson, Ola M. Johannessen, and Oeyvind Frette *In* ESA, European Imaging Spectroscopy Aircraft Campaign Dec. 1993 p 17-25 Sponsored by Norwegian State Pollution Control Authority; Royal Norwegian Council for Scientific and Industrial Research; and Norwegian Space Center (For primary document see N94-31853 09-43)

Copyright Avail: CASI HC A02/MF A02

NORSMAP, a multi-institutional research program established to evaluate the potential of airborne imaging spectrometry for the monitoring of algal blooms in the North and Adriatic Seas, is reported. A Compact Airborne Spectrographic Imager (CASI) was operated from surveillance aircraft for a three week period in May 1989. The European Imaging Spectrometry Airborne Campaign (EISAC'89) also selected the NORSMAP region as one of the test sites to be flown over by the Fluorescence Line Imager (FLI) and the 64 channel Geophysical Environmental Research (GER) corporation Imaging Spectrometer (GERIS). The airborne activities were coordinated with field investigations carried out by research vessels. These measurements covered a wide range of physical, biological and optical ocean parameters. A spectrometer was installed on the research vessels to provide near surface waterleaving radiance spectra. In addition, a large number of other in situ biological, optical, and physical parameters were measured. Water masses covering a wide range of optical properties were analyzed and chlorophyll a concentrations in the range from 0.8 to 5 microg/l were observed. A good large scale match between the in situ and airborne data are found, although the point to point comparison are not too convincing. ESA

N94-31857# Joint Research Centre of the European Communities, Ispra (Italy). Environmental Mapping and Modelling Unit.

ANALYSIS OF GER IMAGING SPECTROMETRY DATA FOR THE IDENTIFICATION OF SOIL AND VEGETATION PARAMETERS IN LAND DEGRADATION STUDIES

Joachim Hill, Wolfgang Mehl, and Jacques Megier *In* ESA, European Imaging Spectroscopy Aircraft Campaign Dec. 1993 p 27-33 (For primary document see N94-31853 09-43)

Copyright Avail: CASI HC A02/MF A02

The potential use of remote sensing techniques, especially using the Geophysical Environment Research (GER) corporation imaging spectrometer, for ecological surveys in the Mediterranean area, at local and regional scales, are assessed. The aim was to identify and monitor degradational processes that may result from the instability of the biological communities, the accelerated erosion by water, and accidental or deliberate fires. In order to efficiently use remotely sensed data for monitoring the degradation of Mediterranean lands, it is necessary to extract physical parameters that can be used to describe cover and status of vegetation canopies, to identify important vegetation communities in terms of dominant species, and to discriminate areas already affected from erosion. An experiment which had the Ardeche region (France) as its test site is reported. Details of atmospheric corrections, geocoding of airborne spectrometry data, radiometric data quality, adaptive noise filtering and spectral unmixing are given. The results are presented. They suggest identification capabilities for vegetation and soil related environmental indicators. ESA

N94-31858# Deutsche Forschungsanstalt fuer Luft- und Raumfahrt, Oberpfaffenhofen (Germany). Optoelectronics Inst.

INFLIGHT CALIBRATION, PREPROCESSING, AND DATA EVALUATION OF GER 2 IMAGING SPECTROMETRY DATA

F. Lehmann, K. Lehmann, H. Rothfuss, and R. Richter *In* ESA, European Imaging Spectroscopy Aircraft Campaign Dec. 1993 p 35-42 (For primary document see N94-31853 09-43)

Copyright Avail: CASI HC A02/MF A02

The inflight calibration and preprocessing of the Geophysical Environment Research (GER) imaging spectrometer data is reported. This GER scanner, which covers a spectral range from 0.47 to 2.45 micrometer in 63 bands, was used during the European Imaging Spectrometry Airborne Campaign (EISAC'89). An application for environmental research is reported, in which the spectral response of vegetation cover on and near to unprotected waste deposits was examined for signatures which could be related to the influence of stress caused by the buried material. A further application for exploration and soil/vegetation studies is reported. In both studies, the GER airborne scanner proved to be a useful tool. ESA

N94-31859# Wageningen Agricultural Univ. (Netherlands). Dept. of Soil Science and Geology.

POSSIBILITIES OF GER DATA FOR SOIL SURFACE CHARACTERISTICS IN THE ALMADEN AREA

G. F. Epema *In* ESA, European Imaging Spectroscopy Aircraft Campaign Dec. 1993 p 43-48 (For primary document see N94-31853 09-43)

Copyright Avail: CASI HC A02/MF A02

Geophysical Environment Research (GER) imaging spectrometer data, from the European Imaging Spectroscopy Aircraft Campaign (EISAC'89), of the Almaden area (Spain) were examined for retrieving information on bare soils (with special emphasis on mineralogy). Different parameters describing absorption features are calculated for the image data. Differences in some parameters, like width and depth of absorption dip exist between bare soils. Noise of the GER data makes it difficult to evaluate exactly how much new information this parameter approach adds to traditional image processing techniques. ESA

N94-31860# Reading Univ. (England). Dept. of Geography.

THE EFFECTS OF VEGETATION ON THE ABILITY TO MAP SOILS USING GERIS DATA

R. J. Murphy and G. Wadge *In* ESA, European Imaging Spectroscopy Aircraft Campaign Dec. 1993 p 49-55 (For primary document see N94-31853 09-43)

(Contract NERC-F60/G6/12; NERC-GT4/88/GT/99)

Copyright Avail: CASI HC A02/MF A02

Geophysical Environment Research Imaging Spectrometer (GERIS) data from the Almaden (Spain) test site were used to explore the effects that varying proportions of live and dead vegetation cover had on the ability to perform thematic mapping of the geological substrate based on soil types. After calibration to reflectance a least squares unmixing analysis was performed using image endmembers and proportions maps of vegetation and soil/rock components generated. Despite a low signal to noise ratio, three soil/rock and four vegetation endmembers were successfully mapped and validated from field estimates. A quantitative assessment was made of the effects of live and dead vegetation on the ability of the unmixing analysis to distinguish between granite and slate soils. Granite soils were more easily misidentified as slate soils due to vegetation cover than vice versa. Dead vegetation was shown to have a greater impact on soil spectra

than live vegetation. The ability to distinguish between the soils was lost at 50 to 60% vegetation cover. ESA

N94-31861# Technische Univ., Munich (Germany). Remote Sensing Working Group.
INVESTIGATION ON CORRECTION MODELS FOR AIRBORNE IMAGING SPECTROMETRY DATA FROM THE EISAC-CAMPAIGN FOR GEOSCIENTIFIC PURPOSES
G. Loercher, J. Henkel, and F. Jaskolla *In* ESA, European Imaging Spectroscopy Aircraft Campaign Dec. 1993 p 57-60 (For primary document see N94-31853 09-43)
Copyright Avail: CASI HC A01/MF A02

On the base of the airborne spectrometry data from the European Imaging Spectroscopy Aircraft Campaign (EISAC), covering the test sites Almaden (Spain) and Upper Rhine Valley (Germany), investigations were focused on radiometric quality and radiometric correction. Besides an evaluation of the spectrometry data one of the main objectives was to develop different radiometric correction algorithms. The idea was to improve several correction methods for imaging spectrometry that are independent from additional data (for example atmospheric parameters). A further goal was to compare the accuracy of these algorithms and to estimate their applicability on imaging spectrometry data for geoscientific purposes. ESA

N94-31862# Consiglio Nazionale delle Ricerche, Bari (Italy). Ist. Elaborazione Segnali ed Immagini.
FEASIBILITY EVALUATION OF NEW DATA INTERPRETATION APPROACHES FOR VEGETATION ANALYSIS FROM AIRBORNE IMAGING SPECTROSCOPY
P. Blonda, C. Caroppo, R. Loizzo, and G. Pasquariello *In* ESA, European Imaging Spectroscopy Aircraft Campaign Dec. 1993 p 61-66 (For primary document see N94-31853 09-43)
Copyright Avail: CASI HC A02/MF A02

The activity performed in the framework of the European Imaging Spectroscopy Aircraft Campaign (EISAC) is described. Moniteq's Fluorescence Line Imager Programmable Multispectral Imager (FLI/PMI) data acquired on the Almaden (Spain) test site are analyzed. The aim is to define an experimental approach to provide a quantitative representation of the vegetation red edge reflectance curve. The results of the correlation with the ground truth information are presented. ESA

N94-31863# British National Space Centre, Huntingdon (England). Remote Sensing Applications Development Unit.
MONITORING FERTILIZER APPLICATION BY IMAGING SPECTROMETRY (SOMERSET LEVELS TEST SITE)
A. R. Jones, A. K. Wilson, and S. A. Briggs *In* ESA, European Imaging Spectroscopy Aircraft Campaign Dec. 1993 p 67-73 (For primary document see N94-31853 09-43)
Copyright Avail: CASI HC A02/MF A02

An experiment, undertaken within the framework of the European Imaging Spectroscopy Aircraft Campaign (EISAC), to evaluate the potential of airborne imaging spectrometry for detecting changes in the spectral response of grasslands associated with controlled applications of nitrogen fertilizer, is described. Different levels of fertilizer applications can be distinguished by the spectral response of the vegetation canopy detected from the airborne data. The use of a linear mixing model for characterizing the vegetation community suggests that changes in the spectral response due to different fertilizer levels are mostly influenced by changes in the physical structure of the canopy. An objective overview of the capabilities of the Moniteq Programmable Multispectral Imager (PMI) system for terrestrial applications is presented and the relevance of advancements in sensor technology for future campaigns is demonstrated. ESA

N94-31864# Wageningen Agricultural Univ. (Netherlands). Dept. of Landsurveying and Remote Sensing.
HIGH RESOLUTION SPECTROSCOPY IN AGRICULTURE: RESULTS OF THE EISAC 1989 CAMPAIGN
J. G. P. W. Clevers and C. Bueker *In* ESA, European Imaging Spectroscopy Aircraft Campaign Dec. 1993 p 75-79 (For primary document see N94-31853 09-43)
Copyright Avail: CASI HC A01/MF A02

A study, which uses the SAIL canopy reflectance model for evaluating the influence of varying crop parameters, such as Leaf Area Index (LAI) and leaf angle distribution, and external parameters, such as soil reflectance and irradiation conditions, on the theoretical position of the red edge, is reported. Results show that the position of the red edge is independent of soil background, but is largely influenced by LAI. This means that one may get an interaction between two effects of crop stress, namely a lower LAI and a lower chlorophyll content of the leaves. Results show that the solar zenith angle and the atmosphere have only a minor influence on the position of the red edge. During the European Imaging Spectroscopy Aircraft Campaign (EISAC'89), data of a nitrogen experiment at the Somerset test site (UK) were recorded with the Programmable Multispectral Imager (PMI). The analysis of the spectral data depicts a clear spectral shift of the red edge to shorter wavelengths according to decreased nitrogen nutrition of the grassland. Furthermore, different canopy parameters, such as fresh weight, dry matter weight or chlorophyll content were correlated more clearly to the red edge index than to radiance values in individual spectral bands or the normalized difference vegetation index. ESA

N94-31865# Technische Univ., Munich (Germany). Inst. for Geography.
EXTRACTION OF AGRICULTURAL PARAMETERS FROM IMAGING-SPECTROMETRY DATA AND SIMULATED MERIS DATA THROUGH RED EDGE ANALYSIS
Heike Bach and Wolfram Mauser *In* ESA, European Imaging Spectroscopy Aircraft Campaign Dec. 1993 p 81-91 (For primary document see N94-31853 09-43)
(Contract DFG-Ma-875/2-2)
Copyright Avail: CASI HC A03/MF A02

Airborne Imaging Spectrometry (IS) data of the GERIS (Geophysical Environmental Research (GER) IS) scanner and the Compact Airborne Spectrographic Imager (CASI) sensor were analyzed with regard to their information content concerning plant parameters. The data of the aircraft campaigns were combined with a set of agricultural ground truth and field spectrometry. The preprocessing of the IS data, above all, consists of a conversion of the radiance values into reflectance. The resulting reflectance values of the wavelength region, which contains the most characteristic spectral features of vegetation, the red edge, were parameterized. Two methods (inverted Gaussian fit, second derivative) were used and their advantages and limitations were determined. A strong correlation between the vegetation height of corn and the inflection wavelength of the red edge was found. This correlation was confirmed for different sensors, different methods for extracting the inflection wavelength, different times and different soil backgrounds. The possibility to use data of the future Medium Resolution Imaging Spectrometer (MERIS) sensor for red edge analysis was tested. Although MERIS does not seem very promising for vegetation studies, slight changes of the band setting could drastically improve its performance. ESA

N94-31866# Joanneum Research Centre, Graz (Austria). Image Processing and Computer Graphics Inst.
EVALUATION OF FLUORESCENCE LINE IMAGER (FLI) AIRBORNE IMAGING SPECTROMETER DATA FOR ROADSIDE TREE DAMAGE ASSESSMENT
C. Banninger *In* ESA, European Imaging Spectroscopy Aircraft Campaign Dec. 1993 p 93-99 (For primary document see N94-31853 09-43)
Copyright Avail: CASI HC A02/MF A02

Fluorescence Line Imager (FLI) data acquired along five major transit routes in Austria proved only partly successful in delineating exhaust emission related damage to tree stands bordering the roadways, as determined by changes in the position of the reflectance red edge in the 690 to 750 nm wavelength region defined by the slope-intercept method. The nature and extent of the tree damage present and the shortcomings of the spectral data sets acquired limited the usefulness of FLI data for damage detection in forests lying adjacent to roadways. ESA

N94-31867# Ghent Univ. (Belgium). Satellite Remote Sensing Research Programme.
EXTRACTION OF FORESTS STAND AGE PARAMETERS FROM AIRBORNE IMAGING SPECTROSCOPY DATA
Marc M. Leysen, Boudewijn P. DeRoover, Roland E. Goossens, and Robert R. DeWulf *In* ESA, European Imaging Spectroscopy Aircraft Campaign Dec. 1993 p 101-105 (For primary document see N94-31853 09-43)
Copyright Avail: CASI HC A01/MF A02

The information content of airborne imaging spectroscopy data on two different age parameters of oak stands, average stand age and development stage, is assessed. Mean radiance spectra are extracted from 3 by 3 pixel windows and from largest possible homogeneous zones in the stands, both sets of samples fully covering the range of stand ages. Selection of the optimal bands for prediction of stand age parameters is based upon analysis of variance of the spectral response to both stand age parameters. Regression analysis is used to model the relationship between average stand age and radiance in the selected bands. The bands covering the near infrared range are the most suited for both stand age parameters. Approximate SPOT band data are simulated through interpolation of original Geophysical Environment Research (GER) radiances. Simulated SPOT XS3 data yield comparable discriminative power for this purpose in comparison to individual GER channel data. ESA

N94-31868# Ludwig-Maximilians-Univ., Munich (Germany). Lehrstuhl fuer Landnutzungsplanung und Naturschutz.

EVALUATION OF GER- AND FLI-DATA WITH REFERENCE TO FOREST

B. Koch and B. Coenradie *In* ESA, European Imaging Spectroscopy Aircraft Campaign Dec. 1993 p 107-113 (For primary document see N94-31853 09-43)

Copyright Avail: CASI HC A02/MF A02

Geophysical Environment Research (GER) and Fluorescence Line Imager (FLI) data were investigated in order to classify different forest types. The investigations on the data proved that the radiometric performance of the sensors need to be improved for utilization in forestry. The results of the evaluation showed that a high spectral resolution as provided by the GER and FLI instrument gives a better chance to pick the most object conform spectral information. For the classification itself a relatively low number of well positioned bands provided the same separability as a high number. ESA

N94-31938# Army Topographic Engineering Center, Fort Belvoir, VA.

ALTERNATIVES TO HIERARCHICAL TECHNIQUES IN STEREO CORRELATION Scientific Paper

F. R. Norvelle Mar. 1994 10 p

(AD-A276570; TEC-R-217) Avail: CASI HC A02/MF A01

When digital stereo correlation methods are used to generate elevation data from stereo images of the terrain, the likelihood that the correlation process will be successful throughout the whole of the stereo model can be enhanced significantly by using hierarchical, multi-scale, pyramidal, coarse-to-fine, etc., techniques. One main advantage of these techniques is that the correlation data obtained at a lower resolution in the hierarchical procedure is used to guide and control the correlation process at the next higher resolution and, consequently, the user can be reasonably assured that the correlation process will not get 'lost'. Unfortunately, constraints imposed by results obtained at the lower resolution can also lead to generation of erroneous elevation data in some circumstances. For example, if the terrain is spotted with individual trees, buildings or other structures, the correlation process, when performed on the low resolution images, will include approximations to the heights of these features in the resulting elevation data. These are erroneous elevations compared to the 'bald earth' and their influence will be carried from one step to the next in the hierarchical procedure. The result will be a noisy digital elevation model (DEM) containing approximations to the elevations of trees and structures on the terrain and not just the terrain itself. Noisy elevation data can be minimized as necessary by using non-hierarchical techniques such as full-resolution correlation or the 'Iterative Orthophoto Refinements (IOR)' method. DTIC

N94-31999# Edgewood Arsenal, Aberdeen Proving Ground, MD. Research Development and Engineering Center.

REMOTE INFRARED VAPOR DETECTION OF VOLATILE ORGANIC COMPOUNDS Final Report, Oct. 1991 - Sep. 1993

R. T. Kroutil, R. J. Combs, R. B. Knapp, and G. W. Small Sep. 1993 36 p Prepared in cooperation with Ohio Univ., Athens, GA

(AD-A276982; ERDEC-TR-111) Avail: CASI HC A03/MF A01

In many open-air monitoring applications of Fourier transform spectrometry (FTS), the lack of a valid background reference spectrum limits the ability to perform quantitative measurements. Suppression of the broad band detector envelope overcomes this limitation. Interferogram processing provides a means of suppressing the broad band background, while maintaining the target spectral signatures of interest. A combination of interferogram segment selection, digital filtering, and pattern discrimination techniques achieve the background suppression of the variable broad band detector envelope. The spectral band position, width, and strength of the target vapor determine the parameters that are used for background suppression. Interferogram segment selection depends primarily on spectral band width. Digital filter design requires inputs of spectral band position and width. The pattern discrimination techniques compensate for variation in the spectral band contour with signal strength. The FTS in the laboratory and open-air trials demonstrate the utility of the background suppression approach in environmental monitoring of volatile organic compounds. DTIC

N94-32025 Naval Postgraduate School, Monterey, CA.

SHIPTRACK DATABASE ANALYSIS M.S. Thesis

Douglas E. Mays Dec. 1993 72 p Limited Reproducibility: More than 20% of this document may be affected by microfiche quality

(AD-A277228) Avail: CASI HC A04

The radiative characteristics of collected commercial and Navy ship tracks are described through an analysis of AVHRR (Advanced Very High Resolution Radiometer) satellite imagery. The analysis is conducted in a format to show the usefulness of a database approach to processing large amounts of ship track data. Twelve cases are analyzed: 9 commercial ship tracks and 3 Navy ship tracks. Satellite imagery for the above 12 cases was collected during the summer months of 1993 off the western coast of the United States. 306 Navy ship reports are associated with 55 satellite images. This data subset was subdivided and cross-referenced to provide statistical data on Navy track formation when a given report was under favorable track formation conditions. Reflectance signatures of the collected tracks show an increase through the first few hours of track formation. The emittance values of the tracks collected from night-time satellite imagery showed the expected decrease as droplet radius decreases. Nuclear powered vessels showed no evidence of track formation. The utility of database analysis for large datasets of observed ship tracks was demonstrated to be a viable method for future analysis of the 4000+ observed ship tracks in the collected imagery. DTIC

N94-32100# Brookhaven National Lab., Upton, NY.

EVALUATION OF SULFATE AEROSOL OPTICAL DEPTHS OVER THE NORTH ATLANTIC AND COMPARISON WITH SATELLITE OBSERVATIONS

C. M. Berkowitz (Pacific Northwest Lab., Richland, WA.), S. J. Ghan (Pacific Northwest Lab., Richland, WA.), C. M. Benkovitz, R. Wagener, S. Nemesure, and S. E. Schwartz Nov. 1993 8 p Presented at the 74th American Meteorological Society Annual Meeting, Nashville, TN, 23-28 Jan. 1994

(Contracts DE-AC02-76CH-00016; DE-AC06-76RL-01830)

(DE94-005457; BNL-49758; PNL-SA-22751; CONF-940115-22) Avail: CASI HC A02/MF A01

It has been postulated that scattering of sunlight by aerosols can significantly reduce the amount of solar energy absorbed by the climate system. Aerosol measurement programs alone cannot provide all the information needed to evaluate the radiative forcing due to anthropogenic aerosols. Thus, comprehensive global-scale aerosol models, properly validated against surface-based and satellite measurements, are a fundamental tool for evaluating the impacts of aerosols on the planetary radiation balance. Analyzed meteorological fields from the European Centre for Medium-Range Weather Forecasts are used to drive a modified version of the PNL Global Chemistry Model, applied to the atmospheric sulfur cycle. The resulting sulfate fields are used to calculate aerosol optical depths, which in turn are compared to estimates of aerosol optical depth based on satellite observations. DOE

N94-32119# Mission Research Corp., Santa Barbara, CA.

AUTOMATED DETECTION OF SHIP TRACKS IN MULTISPECTRAL SATELLITE DATA Progress Report No. 1, 1 Dec. 1993 - 31 Jan. 1994

Mark Fisk 31 Jan. 1994 23 p

(Contract N00014-93-C-0197)

(AD-A276697) Avail: CASI HC A03/MF A01

The objectives of this work are to develop robust ship track detection methods, demonstrate their utility using satellite imagery, and design the framework of an automated ship track detection system for operational use. The approach is to (1) use geographical and multispectral information

to reduce the data stream greatly based on contexts for which ship tracks are physically allowed; (2) optimally enhance satellite images using multispectral signals; (3) apply state-of-the-art edge-detection, dilation and erosion operators in order to find and enhance candidate ship tracks with weak signatures; (4) determine features or parameters that best characterize the higher reflectivity and curvilinearity of ship tracks; (5) apply rule-based and cluster analysis techniques to reduce the data stream to a limited number of subscenes with potential tracks; (6) apply state-of-the-art neural net and statistical discriminant analysis methods as final detection filters; (7) assess detection success and error rates; (8) develop a prototype design of the automated system. The algorithms used here are the kind that have exhibited success on this or similar problems. DTIC

N94-32160# Ohio State Univ., Columbus. Dept. of Geodetic Science and Surveying.

WORLD HEIGHT SYSTEM DEFINITION AND IMPLEMENTATION Final Report, 9 Sep. 1992 - 11 Dec. 1993

Richard H. Rapp and Nagarajan Balasubramania Dec. 1993 34 p

(Contract F19628-92-K-0026)

(AD-A276725; PL-TR-94-2001; AD-E201777) Avail: CASI HC A03/MF A01

Height systems of the world are inconsistent at the + or - 1 m level of accuracy. This report discusses two procedures that attempt to determine an ideal equipotential surface for heights and the connection of regional vertical datums. One method uses 18 stations whose precise geocentric coordinates are known along with the orthometric or mean sea level height with respect to a regional vertical datum. This information is combined with gravity data (for geoid undulation determination) in a general least squares adjustment. The results include the separation between a reference ellipsoid and the ideal (geoid) surface as well as the connection of the regional datums to the geoid. One finds, for example, the origin of the NAVD88 system (U.S.) is 40 + or - 4 cm below the geoid while the ODN (Newlyn) (England) is 26 + or - 23 cm below the geoid. A second procedure to examine the difference between vertical datums used Doppler positioned stations on various vertical drums. Using a degree 360 potential coefficient model, for geoid undulation determination, the separation between several datums was determined. For example, the NN datum used in Germany appears to be 91 cm higher than the reference surface of the ODN (Newlyn) datum used in England. The methods and results described in this report form a foundation for the development of a world height system. DTIC

N94-32203# Oak Ridge National Lab., TN.

A MODEL GEOPHYSICS PROGRAM

J. E. Nyquist 1994 8 p Presented at the Symposium on the Application of Geophysics to Environmental and Engineering Problems, Boston, MA, 27-31 Mar. 1994

(Contract DE-AC05-84OR-21400)

(DE94-007415; CONF-940353-3) Avail: CASI HC A02/MF A01

In 1993, I tested a radio-controlled airplane designed by Jim Walker of Brigham Young University for low-elevation aerial photography. Model-air photography retains most of the advantages of standard aerial photography - the photographs can be used to detect lineaments, to map roads and buildings, and to construct stereo pairs to measure topography - and it is far less expensive. Proven applications on the Oak Ridge Reservation include: updating older aerial records to document new construction, using repeated overflights of the same area to capture seasonal changes in vegetation and the effects of major storms, and detecting waste trench boundaries from the color and character of the overlying grass. Aerial photography is only one of many possible applications of radio-controlled aircraft. Currently, I am funded by the Department of Energy's Office of Technology Development to review the state of the art in microavionics, both military and civilian, to determine ways this emerging technology can be used for environmental site characterization. Being particularly interested in geophysical applications, I am also collaborating with electrical engineers at Oak Ridge National Laboratory to design a model plane that will carry a three-component flux-gate magnetometer and a global positioning system, which I hope to test in the spring of 1994. DOE

N94-32214 Colorado Univ., Boulder.

THE EFFECTS OF ALTIMETER SAMPLING CHARACTERISTICS: SOME GEOSAT EXAMPLES Final Report

Michael E. Parke and George Born 20 Jan. 1994 29 p Limited Reproducibility: More than 20% of this document may be affected by microfiche quality

(Contract N00014-92-J-6004)

(AD-A276899; NRL-CR/7320-93-0004) Avail: CASI HC A03

Altimetric satellites have characteristic sampling patterns in both space and time. This paper looks at the distortions of oceanographic and atmospheric signals as seen in geosat altimeter data. Because of the pattern of ground tracks lain down by Geosat, measurements of oceanographic and atmospheric phenomena can be distorted spatially as well as temporally. As a result, phenomena measured by altimetric measurements can appear as propagating waves with both wavelength and wavenumber different from the original phenomena. These changes, if not understood, can result in misinterpretation of results from altimeter data. Also, in some parts of the world, distorted signals satisfy the dispersion relation of other oceanographic waves, or two phenomena can both have the same distorted dispersion relations. A paper describing the results of this research is in preparation and will be submitted to the Journal of Geophysical Research Oceans. DTIC

N94-32249 Los Alamos National Lab., NM.

STATISTICS OF TIME AVERAGED ATMOSPHERIC SCINTILLATION

P. Stroud 1994 11 p Presented at the Society of Photo-Optical Instrumentation Engineers Conference on Intelligent Information Systems, Orlando, FL, 4-8 Apr. 1994 Limited Reproducibility: More than 20% of this document may be affected by microfiche quality

(Contract W-7405-eng-36)

(DE94-006998; LA-UR-94-691; CONF-940449-1) Avail: CASI HC A03

A formulation has been constructed to recover the statistics of the moving average of the scintillation Strehl from a discrete set of measurements. A program of airborne atmospheric propagation measurements was analyzed to find the correlation function of the relative intensity over displaced propagation paths. The variance in continuous moving averages of the relative intensity was then found in terms of the correlation functions. An empirical formulation of the variance of the continuous moving average of the scintillation Strehl has been constructed. The resulting characterization of the variance of the finite time averaged Strehl ratios is being used to assess the performance of an airborne laser system. DOE

N94-32492 Boston Univ., MA.

RESEARCH AND APPLICATIONS OF A CANOPY REFLECTANCE MODEL Ph.D. Thesis

Yecheng Wu 1993 151 p

Avail: Univ. Microfilms Order No. DA9317929

Remotely sensed data are commonly used to obtain quantitative information on biophysical characteristics of vegetation for large areas. These biophysical characteristics of vegetation and their spatial and temporal distribution are critical inputs to ecological models that describe the interaction between the land surface and climate, energy balance, and hydrologic and biogeochemical cycle. They can also be used for timber inventory and forest mapping of large areas. In this dissertation, the Li-Strahler canopy reflectance model and multispectral satellite data are used to estimate remotely the parameters of crown size, tree count density, cover, foliage biomass, and total standing biomass for nine coniferous forest stands on a transect of western and central Oregon. The spatial pattern of the test stands in the Oregon transect are statistically analyzed using computer simulated models and field measurements. A modified version of the model is also used to estimate regional forest type, crown size, and density on a stand-by-stand basis of portions of the Sierra Nevada Mountains in California using Landsat TM imagery. Dissert. Abstr.

N94-32523 Centre National d'Etudes Spatiales, Toulouse (France).

FROM OPTICS TO RADAR, SPOT AND ERS APPLICATIONS [DE L'OPTIQUE AU RADAR, LES APPLICATIONS DE SPOT ET ERS]

Dec. 1993 443 p In ENGLISH and FRENCH Colloquim held in Paris, France, 10-13 May 1993 Original contains color illustrations

(ISSN 0766-1002)

(ISBN-2-85428-345-7; ETN-94-95852) Copyright Avail: Issuing Activity (CEPADUES-Editions, 111 rue Nicolas-Vauquelin, 31100 Toulouse, France)

The applications of SPOT and ERS-1 to environmental monitoring, marine and ice mapping, and detecting nonrenewable resources (that is geological

surveys) and renewable resources (forests, crops, and land use) are addressed. In most cases specific case studies are presented and the advantages and disadvantages of SPOT and ERS are discussed. The advantage of the microwave remote sensors on ERS-1 synthetic aperture radar (SAR) is their independence of clouds and daylight, that is, measurement at a given time is always ensured. However, optical satellite data, such as that from SPOT, can not be replaced by SAR data, for example, because of the lower spatial resolution and speckle that characterizes SAR data. Applications of SAR interferometry with ERS-1 are also presented. Image processing techniques are addressed. For individual titles, see N94-32524 through N94-32575.

N94-32524 Joint Research Centre of the European Communities, Ispra (Italy). Remote Sensing Applications Inst.

THE COMPLEMENTARY NATURE OF THE SPOT AND ERS-1 SYSTEMS AND THEIR PLACE IN MAJOR INTERNATIONAL PROGRAMMES

R. Klersy *In* CNES, From Optics to Radar, SPOT, and ERS Applications Dec. 1993 p 37-42 (For primary document see N94-32523 09-43)

Copyright Avail: Issuing Activity (CEPADUES-Editions, 111 rue Nicolas-Vauquelin, 31100 Toulouse, France)

International programs concerned with the effects and extent of global climate and environmental change are considered. These programs require information at scales that can best be supplied, in many cases, by spaceborne earth observing sensors. The present situation is reviewed with a special emphasis on the complementary contributions of both SPOT and the synthetic aperture radar on board the European Space Agency's (ESA) ERS-1. The technical characteristics relevant to the international programs are reviewed and their respective contributions are evaluated. Two of the programs are examined in more detail in order that the full complementarity of the two systems can be demonstrated. For this purpose the Commission of the European Communities (CEC) monitoring agriculture with remote sensing (MARS) and tropical forest mapping and monitoring (TREES) (tropical ecosystem environment observations by satellite) programs were selected. ESA

N94-32525 Centre National d'Etudes Spatiales, Toulouse (France).

FROM OPTICS TO RADAR: ENVIRONMENTAL PROBLEMS AND THE SPOT/ERS SYSTEMS

Roy Gibson *In its* From Optics to Radar, SPOT, and ERS Applications Dec. 1993 p 45-51 (For primary document see N94-32523 09-43)

Copyright Avail: Issuing Activity (CEPADUES-Editions, 111 rue Nicolas-Vauquelin, 31100 Toulouse, France)

The great success of the SPOT and ERS-1 satellites is recognized and whether or not the environment community needs a continuation of these programs is discussed. The necessity for institutional environment authorities, who have the financial power to put systems like SPOT and ERS onto a truly operational basis, to define their needs and ensure future satellite systems will produce data that these agencies will be happy to buy, is discussed. It is suggested that environment agencies and departments are integrated into the decision making and financing process. ESA

N94-32526 Institute for Image Processing Computer Mapping, Graz (Austria).

FEASIBILITY IN THE USE OF SATELLITE REMOTE SENSING DATA AS A FAST REACTION TOOL FOR NATURAL DISASTER RELIEF

Klaus Granica and Ursula Schmitt *In* CNES, From Optics to Radar, SPOT, and ERS Applications Dec. 1993 p 53-58 (For primary document see N94-32523 09-43)

Copyright Avail: Issuing Activity (CEPADUES-Editions, 111 rue Nicolas-Vauquelin, 31100 Toulouse, France)

A study to obtain timely and pertinent information on a glacier lake outburst in the Himalayas (Nepal) by satellite remote sensing means is reported. Image processing methods were used for the analysis of the remote sensing data, especially for the location and quantification of the flood surge trace. The integration of the gained information in a geographic information system (GIS) environment delivered the required knowledge. A prerequisite for the realization of the needs for fast relief is the existence of reference data. These are maps or satellite data of prior date, and especially in high relief digital elevation models (DEM) must be available. Remote sensing data, especially SPOT data, are feasible for the mapping of the accumulation area and the destroyed settlements. For the mapping of trails and bridges higher spatial resolution is needed, which is fulfilled by SPOT panchromatic and in the near future through LANDSAT 6. Further investigations could also give information on risk areas and creation of hazard maps. ESA

N94-32527 Office de la Recherche Scientifique et Technique Outre-Mer, Montpellier (France).

CONTRIBUTION OF SAR ERS1 DATA TO STUDY THE FRENCH GUIANA TROPICAL COAST ENVIRONMENT [APPORT DES DONNEES SAR-ERS1 A L'ETUDE DE L'ENVIRONNEMENT COTIER TROPICAL GUYANAIS]

M. Lointier, J. P. Rudant, J. P. Deroin, M. T. Prost, C. Charron, B. Deffontaines, D. Raymond, and J. P. Cautru *In* CNES, From Optics to Radar, SPOT, and ERS Applications Dec. 1993 p 59-69 In FRENCH Sponsored by CNES; Ministere de l'Environnement et du Cadre de Vie; Ministere de l'Enseignement Superieur et de la Recherche; Bureau de Recherches Geologiques et Minieres; and Conseil Regional (For primary document see N94-32523 09-43)

(BRGM-93034) Copyright Avail: Issuing Activity (CEPADUES-Editions, 111 rue Nicolas-Vauquelin, 31100 Toulouse, France)

A study to show how ERS-1 synthetic aperture radar (SAR) data can be used in coastal studies and which discusses the issue of processing data of different spatial resolution is reported. In geological mapping, a lot of meanders are controlled by structural features, as well as basaltic veins; the morphological contrasts make a detailed lithological mapping possible. In coastal morphology, ERS-1 is able to detect the coast line and main structures such as sand bar like 'cheniers'. In the area of Malmanoury-Karouabo the synergetic use of optical and radar data to monitor coastal changes is discussed. In hydrology, most of the coastal watersheds have particular relations with the ocean, and during the rainy season, coastal swamps are supplied by floods. To understand these relations between all the flows, and where they go, multitemporal data from ERS-1 is analyzed to test which parameters could be detected. Applications of this work are in general mapping, irrigation, and rural planning; in this part of the country, like others in tropical regions, most of the population and human activities are concentrated on coastal zones. ESA

N94-32528 Copenhagen Univ. (Denmark). Inst. of Geography.

MONITORING LAND COVER AND CROP TYPES IN DENMARK USING ERS-1 SAR AND OPTICAL SATELLITE IMAGES

Bjarne Fog, Jan Nyholm Poulsen, Inge Sandholt, Henning Skriver, and Michael Stjernholm *In* CNES, From Optics to Radar, SPOT, and ERS Applications Dec. 1993 p 71-80 Sponsored by Danish Space Board Original contains color illustrations (For primary document see N94-32523 09-43)

Copyright Avail: Issuing Activity (CEPADUES-Editions, 111 rue Nicolas-Vauquelin, 31100 Toulouse, France)

A study indicating that the combined use of SPOT multispectral data and ERS-1 synthetic aperture radar (SAR) data can be beneficial for agricultural land use mapping is reported. The study area, the eastern part of the Jutland (Denmark), and available satellite data are described together with the procedure for the coregistration of satellite images and preprocessing. Methods and results of classification are described. It is found that the combination of a SPOT image from the early part of the growing season, where cloud free images are most easily obtained, with SAR images from the later part of the growing season is particularly promising. The implication of this could be the inclusion of the SAR data in, for example, the EEC control schemes for agricultural subsidies or other purposes requiring early delivery of classification results. The obvious benefit is that image acquisition for the middle part of the growing season could be planned and would be independent of the weather conditions. Another benefit is naturally the lower cost of data. It is however also clear that improvements can be added to the described procedures. The per pixel classification method used proved to be far better than anticipated, but it is also clear that a segment based classification method should be better suited for the nature of the SAR data. ESA

N94-32529 Institut Geographique National Espace, Toulose (France).

OPTICS AND RADAR: COHABITATION, RIVALITY OR HAPPY MARRIAGE. TOWARDS NEW PLANNING TOOLS [OPTIQUE ET RADAR: COHABITATION, RIVALITE OU MARIAGE HEUREUX. VERS DE NOUVEAUX OUTILS D'AMENAGEMENT]

Bertrand Galtier *In* CNES, From Optics to Radar, SPOT, and ERS

Applications Dec. 1993 p 83-90 In FRENCH (For primary document see N94-32523 09-43)

Copyright Avail: Issuing Activity (CEPADUES-Editions, 111 rue Nicolas-Vauquelin, 31100 Toulouse, France)

The history of SPOT and ERS-1 satellites and the use, in environmental management, and mapping are addressed. It is decided that the optimal utilization of ERS may not be found through a rivalry against SPOT or the other sources of geographic information. The history of SPOT has shown that the attempt to make classical maps from SPOT was a failure. SPOT's success was born from a completely new approach of the geographic information market. New products were conceived, taking into account the technical advantages and disadvantages of the satellite and its competitors, and after having clearly identified the fields where these products were clearly preferable. This was, for example, the field of emergency and project mapping, where the SPOT image map appears as one of the best available products. It is suggested that the same kind of approach must be adopted with ERS. It must not be attempted to force applications where ERS is clearly weaker. However, there are many fields where the future of ERS seems to be very bright, and a lot of progress has already been accomplished in the geometric modelization of images, or in application such as forestry. In the field of three dimensional application, radar images may even be a tool more efficient than any other one. The localization is a good example of a possible synergy between SPOT and ERS: ERS may serve as a geometric reference for SPOT space triangulation. In the tropical areas, ERS image maps, despite some unsolved problems concerning the visual aspect of the image, may fill the lack of good georeferenced geographic information. ESA

N94-32530 Centre d'Etudes Techniques de l'Equipment, Lyon (France).
THE CONTRIBUTION OF SATELLITE DATA IN COMMUNICATION INFRASTRUCTURE PROJECTS [L'APPORT DES DONNEES SATELLITES DANS LES PROJETS D'INFRASTRUCTURES DE COMMUNICATION]

Martine Chatain, Veronique Poujade, and Lionel Laurore *In* CNES, From Optics to Radar, SPOT, and ERS Applications Dec. 1993 p 91-96 In FRENCH Original contains color illustrations (For primary document see N94-32523 09-43)

Copyright Avail: Issuing Activity (CEPADUES-Editions, 111 rue Nicolas-Vauquelin, 31100 Toulouse, France)

A study carried out in the Amberieu-Grenoble region, France, which used a geographic information system (GIS) to plan the route to be taken by a motorway is reported. Information on the land use in the proposed region was supplied by SPOT. The image processing is described. Both multispectral and panchromatic images were acquired. The spatial perception supplied by the three dimensional images is a useful tool which needs to be complemented by processing of texture. The SPOT and GIS images were useful in evaluating the evolution of the environment and the economic factors surrounding new motorways. ESA

N94-32531 Institut Geographique National Espace, Toulose (France).
THE USE OF ERS IMAGES FOR MAPPING [UTILISATION CARTOGRAPHIQUE DES IMAGES ERS]

Patrick Gigord *In* CNES, From Optics to Radar, SPOT, and ERS Applications Dec. 1993 p 97-107 In FRENCH (For primary document see N94-32523 09-43)

Copyright Avail: Issuing Activity (CEPADUES-Editions, 111 rue Nicolas-Vauquelin, 31100 Toulouse, France)

The ERS data enabled complementation and diversification of the range of mapping products. The adaptation to the 'spacemap' production line of ERS imagery provided an interesting alternative to SPOT imagery in areas where the latter suffers from heavy cloud cover. The satisfactory internal balance of the ERS imagery enabled the validation of a reliable geometric correction model, avoiding in the process the frequent identification problems which arise when it comes to selecting ground control points, and also providing, at a similar cost, performance levels which are identical to SPOT's. The low incidence angle which was selected for ERS was the consequence of noticeably increasing the relief effect. The production of precisely located orthoimages requires the use of highly accurate digital terrain models. In mountain areas, the layover phenomenon frequently results in a loss of information, a dramatic problem in cartographic applications. Despite major efforts in terms of readability improvement, the planimetric use of ERS imagery proved disappointing versus that of SPOT. SPOT did not succeed in replacing aerial photography for the production of topographic maps, but it managed to open a new market: that of spacemaps. In a similar way, ERS does have its limitations, while cartographic requirements still must be met in world regions where optical sensors are inefficient. ESA

N94-32532 Technical Research Centre of Finland, Espoo.
SPOT IMAGERY FOR UPDATING LAND COVER INFORMATION OF 1:50,000 NUMERICAL TOPOGRAPHIC MAPS

E. Parmes *In* CNES, From Optics to Radar, SPOT, and ERS Applications Dec. 1993 p 109-115 (For primary document see N94-32523 09-43)

Copyright Avail: Issuing Activity (CEPADUES-Editions, 111 rue Nicolas-Vauquelin, 31100 Toulouse, France)

A method for updating the land cover information of 1:50,000 numerical topographic maps by the map supervised interpretation of SPOT imagery is described. It relies on the fact that more and more of the maps to be updated are in numerical form, and can be used in the numerical analysis of satellite imagery: both for the change detection and for the a priori estimation of correct assignment of changes. The change detection method uses the old numerical map's information to associate the satellite image's spectral classes, derived by an n dimensional histogram clustering method, to the corresponding map classes. The detectability of changes in land cover depend strongly on the features or satellite image channels used, the season of the satellite observations, and the land cover classes present in the area. The method uses the confusions between classpairs, derived from the intersection of the map and the satellite imagery, for the elimination of false change indications, which result from the spectral unseparability of classpairs. ESA

N94-32533 ISTAR, Valbonne (France).
EXAMPLE OF SPOT/ERS-1 COMPLEMENTARITY

F. Perlant *In* CNES, From Optics to Radar, SPOT, and ERS Applications Dec. 1993 p 117-127 (For primary document see N94-32523 09-43)

Copyright Avail: Issuing Activity (CEPADUES-Editions, 111 rue Nicolas-Vauquelin, 31100 Toulouse, France)

The main differences between SPOT and ERS-1 are described and a practical application, the SPOT/ERS image maps, is presented. Focus is on the technical aspects of the specific geocoded products generation process, in particular the radiometry and geometry. Limitations and constraints are discussed and results are presented. Complementary studies using digital elevation models (DEM) and special radar products containing phase informations are presented. ESA

N94-32534 Centre National de Teledetection, Tunis (Tunisia).
THE USE OF SPOT, AND THE CONTRIBUTION OF ERS-1, IN THE ASSESSMENT OF URBAN PRESSURE ON AGRICULTURE LAND IN GREATER TUNIS (TUNISIA) [ETUDE AVEC SPOT DE LA PRESSION URBAINE SUR LES TERRES AGRICOLES DANS LE GRAND TUNIS ET APPORT DE ERS-1]

L. Bouassida, L. Aouni, C. Gouinaud, L. Laurore, and M. Galaup *In* CNES, From Optics to Radar, SPOT, and ERS Applications Dec. 1993 p 129-139 In FRENCH Original contains color illustrations (For primary document see N94-32523 09-43)

Copyright Avail: Issuing Activity (CEPADUES-Editions, 111 rue Nicolas-Vauquelin, 31100 Toulouse, France)

A retrospective study of the evolution of Greater Tunis from 1975-1991 and its impact on agricultural areas was carried out using LANDSAT and SPOT images. This study allowed the establishment of images describing the dynamic change of urban areas. A land use map of Greater Tunis in 1990 was realized using SPOT images. This map is the basic source document for updating the urban surveying plan. ERS-1 data was tested mainly for urban classification. The outputs of this study were integrated in to geographic data base systems. ESA

N94-32535 Centre d'Etude Spatiale des Rayonnements, Toulouse (France).
RESTORATION OF INTERFEROMETRIC, POLARIMETRIC, RADIOMETRIC, AND TEXTURAL INFORMATION IN SAR IMAGES [RESTAURATION DES INFORMATIONS RADIOMETRIQUES POLARIMETRIQUES INTERFEROMETRIQUES ET TEXTURALES DANS LES IMAGES SAR]
A. Lopes *In* CNES, From Optics to Radar, SPOT, and ERS Applications Dec. 1993 p 143-152 In FRENCH (For primary document see N94-32523 09-43)
Copyright Avail: Issuing Activity (CEPADUES-Editions, 111 rue Nicolas-Vauquelin, 31100 Toulouse, France)

The basic properties of speckle in synthetic aperture radar (SAR) images and their influence on the various parameters are presented. Speckle reduction methods developed to handle these quantities are described. For radiometric channels, a reduction in filtering enables the use of classic algorithms for image processing. The formalisms used to handle variations in magnitude enables speckle reduction methods to be developed which combine the polarimetric, frequency, temporal, and textural aspects. ESA

N94-32536 GEC-Marconi Research Centre, Chelmsford (England).
ASSESSMENT OF REGION-BASED METHODS FOR AUTOMATED SAR/OPTICAL REGISTRATION, ATTRIBUTE EXTRACTION, AND CLASSIFICATION
A. J. Sephton, C. J. Oddy, and A. J. Rye *In* CNES, From Optics to Radar, SPOT, and ERS Applications Dec. 1993 p 153-164 Prepared in cooperation with MATRA Sep Imagerie et Informatique, Saint Quentinen Yvelines, France (For primary document see N94-32523 09-43)
Copyright Avail: Issuing Activity (CEPADUES-Editions, 111 rue Nicolas-Vauquelin, 31100 Toulouse, France)

A number of regional based methods for automated registration of SPOT multispectral and ERS-1 Synthetic Aperture Radar (SAR) images are evaluated and compared in the areas of co-image registration, attribute extraction, and classification. The images were recorded in the Kent area (England). The main scope of the work was directed towards the detection of areas of forestry. The three methods investigated which might be used in an operational system for automated co-image registration and attribute extraction were as follows: post segmentation, region matching method; edge map correlation method; and the 'jiggling' method. While all the techniques are shown to be effective when tested on the SPOT data alone, correlation with the ERS-1 data is found to be dependent on the particular features under observation. Some ideas on how the edge map correlation method may be extended are given. A comparison of the results of the region based, supervised, classification techniques found that the performance attained with the neural network method was more reliable than the statistical technique. Classification accuracies of approximately 90 percent were achieved from a combination of SPOT and ERS-1 data. This overall superiority in performance probably arises from the weaker assumptions made about the underlying nature of the input data for this method. For both the statistical and neural network techniques, a small (approximately 5 percent) improvement in results was found over using the SPOT data alone. By providing pattern data for the neural network based on region attributes rather than at the pixel level, problems of slow training rates were avoided, though of course this technique can only be used where a good segmentation can be produced for the particular scene. ESA

N94-32537 MATRA Sep Imagerie et Informatique, Saint Quentin en Yvelines (France). Lab. de Traitement des Images et du Signal.
ROBUST MULTISOURCE CLASSIFICATION METHOD USING THE MARKOV RANDOM FIELD METHODS [UNE METHODE ROBUSTE DE CLASSIFICATION MULTI-SOURCES UTILISANT DES PROCESSUS ALEATOIRES MARKOVIENS]
Laurent Peytavin, Frank Dansaert, and A. J. Sephton *In* CNES, From Optics to Radar, SPOT, and ERS Applications Dec. 1993 p 165-173 In FRENCH (For primary document see N94-32523 09-43)
Copyright Avail: Issuing Activity (CEPADUES-Editions, 111 rue Nicolas-Vauquelin, 31100 Toulouse, France)

Taking advantage of the complementarity between the optical sensors of SPOT and the Synthetic Aperture Radar (SAR) sensors of ERS-1, new techniques based on Markov random field image models and on neural network driven relaxation were developed and tested for some Earth resources monitoring applications such as forest canopy assessment and urban zone extent evaluation. These techniques make multisource pixel based classification more robust and potentially faster. The first results showed that the multisources regularization induced a nearly total recovery of the forest hidden by the clouds. Compared to a monosource classification on ERS data the classification precision is improved. Compared to a microwave classification on SPOT data the results are significantly improved as soon as the local cloud cover rate is above 5 percent. ESA

N94-32538 SCOT Conseil, Ramonville (France).
TECHNIQUE OF ERS-1 IMAGE PROCESSING IN ASSOCIATION WITH SPOT DATA [TECHNIQUE DE TRAITEMENT DES IMAGES ERS 1 EN ASSOCIATION AVEC DES DONNEES SPOT]
Maylis Galaup, Jochen Harms, and Jean-Guilhem Cailton *In* CNES, From Optics to Radar, SPOT, and ERS Applications Dec. 1993 p 175-177 In FRENCH Original contains color illustrations (For primary document see N94-32523 09-43)
Copyright Avail: Issuing Activity (CEPADUES-Editions, 111 rue Nicolas-Vauquelin, 31100 Toulouse, France)

Within the pilot project, 'Integration of ERS-1 data into the European project of agriculture statistics,' new techniques of image classification were tested. The automatic segmentation of optical data is used as a base for the field (classifies) applied to the ERS-1 data. An initial analysis of ERS-1 images by photointerpretation and application of classical optical image processing techniques lead to research into processing methods which are more adapted to radar images. Three of these methods were tested on the region of Seville (Spain). ESA

N94-32539 National Mapping and Resource Information Authority (Philippines).
AIRBORNE SAR AS A COMPLEMENT TO SPOT HRV IN LAND-COVER CLASSIFICATION: THE USE OF NORMALIZATION AND PRINCIPAL COMPONENTS ANALYSIS
Marvilyn P. Palaganas *In* CNES, From Optics to Radar, SPOT, and ERS Applications Dec. 1993 p 179-190 (For primary document see N94-32523 09-43)
Copyright Avail: Issuing Activity (CEPADUES-Editions, 111 rue Nicolas-Vauquelin, 31100 Toulouse, France)

A study which investigates the effect of the inclusion of Synthetic Aperture Radar (SAR) data to SPOT High Resolution Visible (HRV) data in the overall classification accuracy in delineating general land cover types is reported. The SPOT HRV sensor is a 'pushbroom' scanner. The SAR data was acquired on board the STAR aircraft in digital format and recorded on high density digital tape. Details of the image registration, filtering, texture transform, SAR and optical data integration, classification, and ground verification, are given. It was found that an increased overall accuracy was attained in the combination of the two data sets. However, a comparison of the classification accuracies of the specific land cover types varied with different methods used in the integration of the radar data to the optical data in the digital classification. ESA

N94-32540 MATRA Sep Imagerie et Informatique, Saint Quentin en Yvelines (France). Lab. de Traitement des Images et du Signal.
PRODUCTION OF TERRAIN DATA: OPTICAL RADAR COMPLEMENTARITY [PRODUCTION DE DONNEES TERRAIN: COMPLEMENTARITE OPTIQUE-RADAR]
H. Ancey, B. Carron, M. Mariton, and J. A. Sirat *In* CNES, From Optics to Radar, SPOT, and ERS Applications Dec. 1993 p 191-197 In FRENCH (For primary document see N94-32523 09-43)
Copyright Avail: Issuing Activity (CEPADUES-Editions, 111 rue Nicolas-Vauquelin, 31100 Toulouse, France)

Algorithmic breakthroughs which should improve the processing tools and the geometric quality of SPOT and ERS-1 images are focused upon. The complementarity of SPOT and ERS-1 Synthetic Aperture Radar (SAR) data is addressed, and specific studies which are needed in altimetry analyses are considered. ESA

N94-32541 Aerospatiale, Cannes (France).
FUSION OF MULTISPECTRAL (XS) AND PANCHROMATIC (P) SPOT IMAGES AND RADAR IMAGES [FUSION D'IMAGES SPOT MULTISPECTRALE (XS) ET PANCHROMATIQUE (P), ET D'IMAGES RADAR]

Marc Mangolini, Thierry Ranchin, and Lucien Wald *In* CNES, From Optics to Radar, SPOT, and ERS Applications Dec. 1993 p 199-209 In FRENCH (For primary document see N94-32523 09-43)
Copyright Avail: Issuing Activity (CEPADUES-Editions, 111 rue Nicolas-Vauquelin, 31100 Toulouse, France)

A way of increasing the spatial resolution of SPOT multispectral images (XS) using the corresponding panchromatic image (P) is presented, as well as the injection of information derived from ERS-1 into the former images. Existing methods for merging P and XS are analyzed before presenting a new method which aims at simulating 10 m resolution multispectral images that contain the same spectral information as the XS images. The following step consists of injecting detectable objects of the ERS-1 image into the SPOT images. These two fusion steps are both implemented using multiresolution analysis and the wavelet transform. Although the present method might be refined, it already provides very interesting results. ESA

N94-32542 Norwegian Defence Research Establishment, Kjeller.
SHIP TRAFFIC MONITORING AND OIL SPILL DETECTION USING THE ERS-1 SAR
Terje Wahl, Tom Anderssen, Knut Eldhuset, and Aage Skoeelv *In* CNES, From Optics to Radar, SPOT, and ERS Applications Dec. 1993 p 211-220 (For primary document see N94-32523 09-43)
Copyright Avail: Issuing Activity (CEPADUES-Editions, 111 rue Nicolas-Vauquelin, 31100 Toulouse, France)

A fast processing and distribution chain for ERS-1 Synthetic Aperture Radar (SAR) images was developed in Norway. Large quantities of ERS-1 images were analyzed to assess the capability of ERS-1 for ship detection, ship wake imaging, and oil slick detection. Automatic detection and analysis of ships and ship wakes using the 30 m resolution SAR Fast Delivery product was demonstrated. For oil spill detection use was made of 100 m resolution images of high radiometric quality. Ships above 120 m length are generally seen in ERS-1 images under most weather conditions. Ships smaller than 100 m may sometimes become practically invisible in the SAR images because of the strong backscatter from the sea surface at some wind speed (an effect due to the steep incidence angle of ERS-1). Ship wake signatures in ERS-1 images are very similar to those in SEASAT images. The most frequent wake feature is the dark turbulent wake. Several confirmed observations of oil slicks were reported. At low wind speed, natural surface slicks may in some cases be classified as oil slicks. Due to very strong winds, no oil slick signatures were seen in ERS-1 images from the wrecked oil tanker 'Braer'. ESA

N94-32543 MATRA Marconi Space (England).
SAR IMAGE FEATURE EXTRACTION SYSTEM: A PRE-OPERATIONAL APPLICATION OF ERS-1 SAR
I. J. Green, F. G. Sawyer, and S. B. Dunster *In* CNES, From Optics to Radar, SPOT, and ERS Applications Dec. 1993 p 221-230 Sponsored by British National Space Centre Original contains color illustrations (For primary document see N94-32523 09-43)
Copyright Avail: Issuing Activity (CEPADUES-Editions, 111 rue Nicolas-Vauquelin, 31100 Toulouse, France)

The Synthetic Aperture Radar (SAR) Image Feature Extraction System (SIFES), which was developed to demonstrate the capabilities of an end to end SAR system, is described. The first application to be demonstrated by the SIFES facility is ship traffic monitoring; for this, SIFES will be operated in a Ship Detection Workstation (SDWS) mode to extract information about shipping imaged by SAR. The workstation contains a processing chain which was assembled from algorithms developed during the project. These enable the automatic processing of input SAR image data to extract shipping information. The workstation has a powerful processing capability to rapidly execute these algorithms. Results are displayed as the data is processed allowing the operator to change algorithm parameters to optimize system performance. SAR data throughput is extremely large. The SDWS contains careful data management and storage which is required for efficient and rapid processing. The output product from the SDWS is a map of shipping in the coverage area. This can be sent electronically to end users of the information. An overview of the SDWS including a description of the hardware system, software, and algorithm chain, is presented. Results from the system are also presented and assessed. Recommendations for future operational SAR system applications are given. ESA

N94-32544 Mashinstroyeniye, Moscow (USSR).
ALMAZ MARINE APPLICATIONS [LES APPLICATIONS MARINES D'ALMAZ]
E. Xenofontov *In* CNES, From Optics to Radar, SPOT, and ERS Applications Dec. 1993 p 231-235 (For primary document see N94-32523 09-43)
Copyright Avail: Issuing Activity (CEPADUES-Editions, 111 rue Nicolas-Vauquelin, 31100 Toulouse, France)

Details of the Synthetic Aperture Radar (SAR) carried onboard Almaz-1 are given, and its advantages when compared to instruments of visible and infrared ranges are addressed. An assessment of experiments within the Ocean 1 program are assessed. It is noted that the possibility of recording the atmosphere and ocean surface processes is connected with the changes of sea surface scattering properties due to these processes. The main contribution into the sea surface radioscattering is made by short gravity capillary waves from 1 to 30 cm long, which exist practically everywhere on the ocean surface. To interpret radar images correctly it is necessary to understand the processes of obtaining images from SAR. These processes are addressed, and examples of interpreting ocean surface radar images are given. These examples concern the following: surface waves and swell; internal waves; currents, circulations, and whirl; fronts and frontal zones; underwater topography; oil pollutions; ship traces; and sea ice and icebergs. ESA

N94-32545 Ice Centre Environment Canada, Ottawa (Ontario).
THE USE OF ERS-1 WITHIN AN OPERATIONAL ICE MONITORING PROGRAM
Thomas Carrieres *In* CNES, From Optics to Radar, SPOT, and ERS Applications Dec. 1993 p 237-245 (For primary document see N94-32523 09-43)
Copyright Avail: Issuing Activity (CEPADUES-Editions, 111 rue Nicolas-Vauquelin, 31100 Toulouse, France)

ERS-1 Synthetic Aperture Radar (SAR) data was used to supplement regular sources of operational information at Ice Centre Environment Canada (ICEC). Experiences gained during the 1993 Canadian east coast Winter ice season with data acquisition and ordering are reviewed. Principles applied to aircraft-borne SAR image analysis are summarized and comparisons made with ERS-1 SAR. A validation experiment held in Feb. 1993 in the southern Gulf of St Lawrence is also addressed. During the experiment the aircraft SAR was used to image ice within four hours of an ERS-1 overpass. Ground measurements at selected points are discussed in relation to the coincident image samples. ESA

N94-32546 Geoscience Consultants, Paris (France).
THE USE OF SPOT AND ERS-1 IMAGES TO MAP THE ERUPTION OF NEVADO SABANCAYA (PROVINCE OF AREQUIPA, SOUTH PERU) AND EVALUATE ASSOCIATED RISKS [SUIVI DE L'ERUPTION DE NEVADO SABANCAYA (PROVINCE D'AREQUIPA, SUD PEROU) PAR IMAGES SPOT ET ERS1 ET CARTOGRAPHIE ET EVALUATION DES RISQUES ASSOCIES]
R. Guillande, D. Huaman, J. Chorowicz, J. C. Thouret, and F. LeGuern *In* CNES, From Optics to Radar, SPOT, and ERS Applications Dec. 1993 p 247-250 In FRENCH Original contains color illustrations (For primary document see N94-32523 09-43)
Copyright Avail: Issuing Activity (CEPADUES-Editions, 111 rue Nicolas-Vauquelin, 31100 Toulouse, France)

The eruption of the Nevado Sabancaya, which began a phreatomagnetic eruptive process on 28 May 1990 after 4 years of weak fumorallic and seismic activity, is addressed. The eruption had been foreseen by comparing images of Jul. 1986 and 1989 that showed differences in the ice cap within the crater. The eruption was monitored since Jun. 1990 by acquisition of six SPOT images. The images proved to be very helpful to analyze the impact on the regional environment, the evolution of the crater, and also the neighboring glaciers where lahars were generated. Other volcanological techniques and field observations were used to control satellite observation. Both field and satellite techniques complete each other. The lack of resources of the local geophysicists was partially compensated by remote analysis of SPOT images in France. ERS-1 images were acquired but are not available yet because of malfunctioning of the Cotopaxi reception station. Geometric simulation of Synthetic Aperture Radar (SAR) images were produced to determine whether or not deformation observed on the volcano will be visible on radar images and to help programming of the next

images in order to have the maximum information on the strategic area of the volcano. The delay of availability of SPOT as well as ERS images seems to be the major inconvenience in the use of satellite images for monitoring erupting volcanoes. This is less important in the case of monitoring of sleepy but potentially dangerous volcanoes. Satellite observation coupled with seismic monitoring transmitted by ARGOS beacons could be a minimal system for monitoring the hundreds of potentially dangerous volcanoes throughout the world. ESA

N94-32547 Groupement Scientifique de Teledetection de Strasbourg (France). Inst. de Geologie.

COMPARISON OF SPOT, ERS-1, SEASAT, LANDSAT TM, AND MERGED IMAGERY FOR GEOLOGICAL INVESTIGATIONS

H. Yesou (Service Regional de Traitement d'Image et de Teledetection, Strasbourg, France.), Y. Besnus, J. C. Pion, J. Pion, and P. DeFraipont *In* CNES, From Optics to Radar, SPOT, and ERS Applications Dec. 1993 p 251-262 Original contains color illustrations (For primary document see N94-32523 09-43)

Copyright Avail: Issuing Activity (CEPADUES-Editions, 111 rue Nicolas-Vauquelin, 31100 Toulouse, France)

An appraisal of the relative geological mapping performance of the most widely available remotely sensed data was carried out. A fracturing study at a local scale of a grinitic body is presented. A comparison of these results with those derived from a previous regional scale analysis, points out that the best data are not the same at the two scales. This is not linked to sensors resolution but to the nature of the geological objects that are pointed out at regional and local scales. The best results were obtained with merged SEASAT-SPOT imagery and with combined LANDSAT Thematic Mapper (TM)-SPOT panchromatic data, respectively. ESA

N94-32548 International Inst. for Aerospace Survey and Earth Sciences, Enschede (Netherlands).

OPTIMAL GEOLOGICAL DATA EXTRACTION FROM SPOT-RADAR SYNERGISM WITH SAMPLES FROM DJEBEL AMOUR (ALGERIA), RED SEA HILLS (SUDAN), SIRTE BASIN (LIBYA), AND MAGDALENA VALLEY (COLOMBIA)

B. N. Koopmans and E. Ricchetti *In* CNES, From Optics to Radar, SPOT, and ERS Applications Dec. 1993 p 263-274 Original contains color illustrations (For primary document see N94-32523 09-43)

Copyright Avail: Issuing Activity (CEPADUES-Editions, 111 rue Nicolas-Vauquelin, 31100 Toulouse, France)

An optimal synergism procedure was worked out combining SPOT information with radar information especially for geological applications. Combinations of data from four different sensors were examined: ERS-1 radar and SPOT multispectral (XS); SPOT and Shuttle Imaging Radar (SIR A); SPOT and SIR B; and LANDSAT multispectral scanner and airborne Synthetic Aperture Radar (SAR). The data was obtained from four different study areas, the details of which are given. An HIS transformation was performed on SPOT XS and LANDSAT data resulting in a color enhancement making rock differentiation in the areas possible. To obtain the full benefit of the spectral information from SPOT and the textural and pattern information from radar (ERS-1, SIR A, SIR B, and airborne radar), a synergistic image was produced using the hue and saturation information from SPOT/LANDSAT and the intensity values from radar data. On the basis of a comparison of single radar or single SPOT data with synergistic SPOT radar data an evaluation was made regarding mapping of geologic lithologic boundaries and recognition of structural features like faults and folding. Information from SPOT and the satellite radar are found to be complementary. ESA

N94-32549 Paris VI Univ. (France). Dept. Geotectonique.

RESPECTIVE CONTRIBUTIONS OF VIS-PIR, SAR-ERS 1, AND AIRBORNE RADAR DATA FOR MORPHOSTRUCTURAL AND MORPHONEOTECTONIC ANALYSIS: PRACTICAL EXAMPLES [APPORT RESPECTIF DES DONNEES VIS-PIR, SAR-ERS 1 ET RADAR AEROPORTE POUR L'ANALYSE MORPHOSTRUCTURALE ET MORPHONEOTECTONIQUE: EXEMPLES D'APPLICATIONS]

Daniel Raymond, Jean Chorowicz, Benoit Deffontaines, Pascal Luxey, Jean-Paul Rudant, and Tekin Yurur *In* CNES, From Optics to Radar, SPOT, and ERS Applications Dec. 1993 p 275-285 In FRENCH (For primary document see N94-32523 09-43)

Copyright Avail: Issuing Activity (CEPADUES-Editions, 111 rue Nicolas-Vauquelin, 31100 Toulouse, France)

A multiscale approach for morphostructural interpretation is addressed. The following methodology was assessed: compared analysis of all imagery available in the studied area at different scales and various wavelenghts including radar data, where the drainage pattern is extracted and anomalies underlined; these anomalies are also enhanced by the drainage patterns given by topographic maps permitting comparisons and validation. This methodology was applied to morphostructural studies at various scales in several test areas. In the small 1 by 10 km size area of Pezenas (southern France), SPOT and airborne ESAR German radar scenes were used to evidence new faults: some of them are potential structural guides for oil prospecting. From a LANDSAT Thematic Mapper scene combined with a Synthetic Aperture Radar (SAR) ERS-1 scene of Erzincan (Turkey) in a 100 by 100 km size mountainous area, the northeastern segment of the Ovacik fault was analyzed. Drainage pattern anomalies and offsets have given the amount of recent strike slip motion along the fault. In these examples, drainage pattern anomalies are closely related to the regional tectonic framework: according to its high sensibility to slope effects, the radar tool is convenient for drainage pattern analysis and morphostructural work. ESA

N94-32550* Jet Propulsion Lab., California Inst. of Tech., Pasadena.

USE OF SPOT AND ERS-1 SAR DATA TO STUDY THE TECTONIC AND CLIMATIC HISTORY OF ARID REGIONS [UTILISATION DE DONNEES SPOT ET SAR ERS-1 POUR L'ETUDE DE L'HISTOIRE TECTONIQUE ET CLIMATIQUE DES REGIONS ARIDES]

Tom G. Farr and Gilles F. Peltzer *In* CNES, From Optics to Radar, SPOT, and ERS Applications Dec. 1993 p 287-288 In ENGLISH and FRENCH Sponsored by NASA, Washington (For primary document see N94-32523 09-43)

Copyright Avail: Issuing Activity (CEPADUES-Editions, 111 rue Nicolas-Vauquelin, 31100 Toulouse, France)

In order to separate the effects of the different tectonic and climatic processes on the shapes of desert piedmonts, a modified conic equation was fitted to digital topographic data for individual alluvial fans in Death Valley (California, U.S.). The topographic data were obtained from a SPOT panchromatic stereo pair and from the airborne interferometric SAR (Synthetic Aperture Radar) (TOPSAR). The conic fit allows parameters for the epex position, slope, and radial curvature to be compared with unit age, uplift rate, and climatic conditions. Preliminary results indicate that slope flattens with age and radial curvature is concave up, but decreases with age. Work is continuing on correlation of fit residuals and apex position with fan unit age. This information will help in the determination of tectonic uplift rates and the climatic history of the western U.S. ERS-1 SAR images were used to study an area of western China where a large strike slip fault crosses a series of alluvial fans and stream valleys. Previous analysis of SPOT panchromatic images of the area shows that offsets fans and streams can be recognized. Measurement of the rate of motion of this fault will help in the overall model of deformation of the Asian tectonic plate in response to the collision of the Indian plate. ESA

N94-32551 Bureau de Recherches Geologiques et Minieres, Orleans (France).

STRUCTURAL STUDY IN AN ALTERITIC REGION: CONTRIBUTION OF ERS-1 SAR DATA OF THE MAUGES PLATEAU (LOIRE ATLANTIQUE, FRANCE) [ETUDE STRUCTURALE EN MILIEU ALTERITIQUE: APPORT DES DONNEES SAR ERS' DU PLATEAU DES MAUGES (LOIRE ATLANTIQUE, FRANCE)]

Jean-Yves Scanvic, J. M. Brosse, J. F. Desprats, Francois M. Girault, and M. Imbault *In* CNES, From Optics to Radar, SPOT, and ERS Applications Dec. 1993 p 289-299 In FRENCH (For primary document see N94-32523 09-43)

(BRGM-93032) Copyright Avail: Issuing Activity (CEPADUES-Editions, 111 rue Nicolas-Vauquelin, 31100 Toulouse, France)

An experimental survey, a part of a pilot project aiming to evaluate geological interest of ERS Synthetic Aperture Radar (SAR) data in specific conditions, 10 m alteritic formations masking the substratum, is reported. Two SAR images were processed and visually interpreted. These images were acquired under different conditions: ascending and descending mode, May and Sep., after a 10 day rainy period and 10 days without rain. The two interpretations are quite different. The May image reveals a quantity of

valuable structural informations outlining the different units mapped by drilling, scattered field observations, geochemistry, geophysics and optical remote sensing. Particularly, a buried granitic body, well mapped by gravimetry is enhanced on the surface through radar discontinuities. On the other hand, the information outlined by the Sep. second image is quite null as far as geology is concerned, which is important for hydrography network, roads, villages and forests. As a preliminary conclusion it appears radar imagery is quite a valuable tool for structural analysis in the plateau des Mauges conditions but acquisition characteristics have a great influence on the geological interpretation capacity. It appears absolutely necessary, more than in optical remote sensing, to optimize selection of appropriate data and all weather radar capacity make this possible. ESA

N94-32552 Bureau de Recherches Geologiques et Minieres, Orleans (France).

EVALUATION OF THE POTENTIAL OF SAR DATA FOR MAPPING OF LANDSLIDE RISKS [EVALUATION DU POTENTIEL DES DONNEES SAR POUR LA CARTOGRAPHIE DU RISQUE DE MOUVEMENTS DE TERRAIN]

Jean-Yves Scanvic, Claudie Carnec, Francois Girault, and Ollivier Rouzeau *In* CNES, From Optics to Radar, SPOT, and ERS Applications Dec. 1993 p 301-311 In FRENCH Sponsored by CNES (For primary document see N94-32523 09-43)

(BRGM-93033) Copyright Avail: Issuing Activity (CEPADUES-Editions, 111 rue Nicolas-Vauquelin, 31100 Toulouse, France)

The evolution of the mapping of natural risks is reported. An experiment to evaluate the Synthetic Aperture Radar (SAR) capacity for landslides mapping over the Chicamocha Valley (Columbia), which has been proposed and accepted for ERS-1 and the Japanese JERS, is addressed. A GIS (Geographic Information System) was prepared with SPOT and LANDSAT data, Digital Elevation Models (DEM) and derivated files, and a geological map. Some methodological aspects were studied such as simulation of stereopairs of airborne SAR over Taiwan, but realization of the Chicamocha Valley study is still pending, due to lack of data. For this reason a substitute test site was chosen in Boulc (France), where, till now geodesic space measurement have been realized with the DORIS (Doppler Orbitography and Radiopositioning Integrated by Satellite) system. ESA

N94-32553 Office de la Recherche Scientifique et Technique Outre-Mer, Paris (France).

STUDY OF SUBPOLAR GLACIERS OF SPITZBERGEN USING SPOT, ERS-1, AND HYPSOMETRIC DATA: RESULTS AND PERSPECTIVES [ETUDE DES GLACIERS SUB-POLAIRES DU SPITZBERG A L'AIDE DES DONNEES SPOT, ERS1 ET HYPSOMETRIQUES: RESULTATS ET PERSPECTIVES]

J.-F. Parrot (Paris VI Univ., France.), B. Lefauconnier (Norsk Polarinst., Oslo.), C. Mering (Paris VI Univ., France.), N. Lyberis (Paris VI Univ., France.), H. Taud (Paris VI Univ., France.), J.-P. Rudant (Paris VI Univ., France.), and J. Chorowicz (Paris VI Univ., France.) *In* CNES, From Optics to Radar, SPOT, and ERS Applications Dec. 1993 p 313-322 In FRENCH Sponsored in part by Commission of the European Communities (For primary document see N94-32523 09-43)

Copyright Avail: Issuing Activity (CEPADUES-Editions, 111 rue Nicolas-Vauquelin, 31100 Toulouse, France)

The surface state of subpolar glaciers were studied on the basis of combined SPOT and ERS-1 data. The approximately 64 sq km training zone of the Brogger and Loven glaciers is situated in the northwestern Spitsbergen, 79 deg. north. The SPOT data present extensive shaded zones arising from the combination of low Sun elevation (7 to 15 deg) and mountainous topography. The SPOT reflectance values were corrected using the slope orientation and dip parameters from the Digital Elevation Model (DEM) combined with the corresponding Sun elevation and azimuth. The reflectances of the shaded and illuminated zones were restored to a new image based on the XS1 versus XS3 bidimensional histogram. This new image provides a map of the different surface states of the glacier which is homogeneous in both the shaded and illuminated zones. The ERS-1 data are not influenced by the Sun's position but the incidence angle gives rise to geometric distortions. An attempt was made to reduce the speckle by using low pass filters and filters based on contrast and morphological criterion. A new reconstruction morphological filter, which reduces significantly the speckle while preserving the structure of the original image, was developed. Geometrical corrections were done using the DEM. The comparison of processed ERS-1 image with the DEM shows that the ERS-1 values of the glacier surfaces depend mainly on the dip angle of the ground surface and allows one to reconstruct partial DEM of glacier surfaces from ERS-1 data. ESA

N94-32554 SCOT Conseil, Ramonville (France).

INTEGRATION OF ERS-1 IMAGES INTO THE EUROPEAN AGRICULTURE STATISTICS PROJECT ACTION 4: THEMATIC ASPECT [INTEGRATION DES IMAGES ERS1 AU PROJET EUROPEEN DE STATISTIQUES AGRICOLES ACTION 4: ASPECT THEMATIQUE]

Maylis Galaup, Jochen Harms, and Hans Kohl *In* CNES, From Optics to Radar, SPOT, and ERS Applications Dec. 1993 p 325-328 In FRENCH Original contains color illustrations (For primary document see N94-32523 09-43)

Copyright Avail: Issuing Activity (CEPADUES-Editions, 111 rue Nicolas-Vauquelin, 31100 Toulouse, France)

Within the Action 4 of the Monitoring the Agriculture by Remote Sensing (MARS) project, the use and integration of ERS-1 data is tested for the field of agriculture. Two of the Action 4 test sites, Seville (Spain) and Great Driffield (UK), were chosen for this purpose. With support of optical data (SPOT, LANDSAT) ERS-1 data are visually interpreted. The results indicate the usefulness of ERS-1 data to complement optical data for agriculture applications. ESA

N94-32555 Centre d'Etude Spatiale des Rayonnements, Toulouse (France).

USE OF SPOT AND ERS-1 TO MAP TROPICAL VEGETATION AND MANGROVE DYNAMICS IN GUIANA [CARTOGRAPHIE DE LA VEGETATION TROPICALE ET SUIVI DE LA DYNAMIQUE DES MANGROVES DE GUYANE PAR SPOT ET ERS-1]

P. Hery, D. Ducrot-Gambart, A. Lopes, E. Mougin, G. Marty, F. Fromard, F. Blasco, J. P. Rudant, M. Lointier, and M. T. Prost *In* CNES, From Optics to Radar, SPOT, and ERS Applications Dec. 1993 p 329-341 In FRENCH Sponsored in part by Programme National de Teledetection Spatiale and ESA Original contains color illustrations (For primary document see N94-32523 09-43)

(Contract CNES/92/0393)

Copyright Avail: Issuing Activity (CEPADUES-Editions, 111 rue Nicolas-Vauquelin, 31100 Toulouse, France)

Assessment of combination and complementarity of SPOT and ERS-1 SAR (Synthetic Aperture Radar) data was performed in a study on tropical vegetation mapping and mangrove dynamic monitoring in French Guiana. Three channels SPOT and two ERS-1 images recorded at 23 and 35 deg of incidence angle were used jointly in a supervised classification. Results show that the main information comes from the SPOT data, nevertheless, in some cases, ERS-1 data appear very helpful for discriminating vegetation classes. On the other hand, ERS-1 data cannot be used alone with satisfactory results. The utilization of ERS-1 SAR data, in tropical vegetation studies, necessarily implies the combination of multitemporal data and multispectral data including available other SAR data (the Japanese JERS-1) and optical data (SPOT, LANDSAT). ESA

N94-32556 Joint Research Centre of the European Communities, Ispra (Italy).

A CASE STUDY COMPARING MULTI-TEMPORAL ERS-1 SAR DATA AND SPOT DATA FOR TROPICAL FOREST MAPPING

M. M. Leysen, J. A. Conway, and A. J. Sieber *In* CNES, From Optics to Radar, SPOT, and ERS Applications Dec. 1993 p 343-352 Original contains color illustrations (For primary document see N94-32523 09-43)

Copyright Avail: Issuing Activity (CEPADUES-Editions, 111 rue Nicolas-Vauquelin, 31100 Toulouse, France)

In the frame of the joint ESA Commission of the European Communities (CEC) TREES (Tropical Ecosystem Environment observation by Satellite) project, ERS-1 Synthetic Aperture Radar (SAR) data of West Africa are evaluated on their information content for mapping tropical ecosystems. A supervised classification methodology to exploit both the tonal and textural characteristics of ERS-1 SAR imagery is described. Supervised classifications are carried out on a multitemporal ERS-1 SAR data set and a monotemporal SPOT panchromatic data set. The resulting classifications are compared on the basis of their accuracy for the discrimination at the forest/nonforest level. It was found that the classification accuracies for the ERS-1 SAR

data (65 percent) are inferior to those obtained from the SPOT panchromatic data (95 percent). Factors limiting the results obtained are discussed for both sensors and possible analysis improvements suggested. ESA

N94-32557 SOTEMA, Ramonville Saint-Agne (France).
RAPID ESTIMATES OF CROP ACREAGE AND PRODUCTION AT EUROPEAN SCALE USING HIGH RESOLUTION IMAGERY
H. deBoissezon, G. Gonzales, B. Pous, and M. Sharman *In* CNES, From Optics to Radar, SPOT, and ERS Applications Dec. 1993 p 353-364 Original contains color illustrations (For primary document see N94-32523 09-43)
Copyright Avail: Issuing Activity (CEPADUES-Editions, 111 rue Nicolas-Vauquelin, 31100 Toulouse, France)

The methodology used to supply rapid estimations of the extent and growth of crops in Europe using SPOT and LANDSAT Thematic Mappers (TM) is described. The information obtained is transferred to the Agriculture Directorate at the European Community Statistical office so that precise updates of agriculture production is at hand. In order for this information to be exploitable, it must be delivered without delays. A maximum delay of 10 days from the acquisition of the images to the production of information has been enforced. The operational implications and constraints are addressed to show how the Action 4 system is, at present, completely operational. ESA

N94-32558 Institute of Geodesy and Cartography, Warsaw (Poland). Remote Sensing and Spatial Information Center.
APPLICATION OF ERS-1 SAR DATA FOR HYDROLOGICAL STUDIES
K. Dabrowska-Zielinska, M. Gruszczynska, M. Janowska, and A. Wielogorska *In* CNES, From Optics to Radar, SPOT, and ERS Applications Dec. 1993 p 365-369 (For primary document see N94-32523 09-43)
Copyright Avail: Issuing Activity (CEPADUES-Editions, 111 rue Nicolas-Vauquelin, 31100 Toulouse, France)

Synthetic Aperture Radar (SAR) data were used to assess soil moisture. The project was carried out for the Obra river valley (Poland) during the season of 1992. The study area was covered by grassland with the variety of soil types and soil water conditions. Simultaneously to ERS-1 overpass the soil moisture in the 20 ground points, for different soil layers and soil water potential representing the dielectric constant of soils, was measured. Three successive SAR images were taken to make the color composite on which the ground observations were located. The value of nine pixels were taken as the average for further investigations of correlation with ground measurements. The point of ground observation was located in the middle of each block of nine pixels. The first investigation shows that there is a relation between the microwave signal recorded by SAR and soil moisture in the depth of 0 to 10 cm. ESA

N94-32559 Centre de Recherches en Physique de l'Environnement, Velizy (France).
SYNERGY OF THERMAL INFRARED AND MICROWAVE REMOTE SENSING FOR EVAPORATION ESTIMATION
O. Taconet, A. Vidal, F. Rahman, L. Rakotoarivony, S. Laguette, and D. Vidal-Madjar *In* CNES, From Optics to Radar, SPOT, and ERS Applications Dec. 1993 p 373-383 (For primary document see N94-32523 09-43)
Copyright Avail: Issuing Activity (CEPADUES-Editions, 111 rue Nicolas-Vauquelin, 31100 Toulouse, France)

The principles of thermal infrared/microwave synergy for determination of surface evaporation are addressed. This synergy was studied during Mac Europe/Orgeval 91 experiment when simultaneous high resolution optical and microwave AIRSAR images were taken over wheat fields. Concommittance of acquisition is not sufficient to have images interpretable in the different bands. Optical images with minority of cumulus are adequate to obtain vegetation index but could not be used for thermal band due to complex feedbacks between vegetation mass transfers and variable solar sky condition. Use of thermal band needs stable clear or cloudy sky. Direct 1-layer models of evaporation are still satisfactory during the Orgeval experiment. The synergy for the estimation of vegetation structure (foliage density and aerodynamical displacement height) was studied. Optical vegetation index and vegetation water content from cloud models are used to derive Leaf Area Index (LAI) over wheat. Microwave derivations of LAI compared to the optical ones are too highly variable to be reliable to derive evaporation, especially for wheat canopies with low cover as encountered after the maturation. ESA

N94-32560 Wageningen Agricultural Univ. (Netherlands). Dept. of Soil Science and Geology.
MONITORING LANDSURFACE CHARACTERISTICS IN NIGER USING COMPLEMENTARY SPOT AND ERS-1 SAR DATA
Gerrit F. Epema and Peter J. vanOevelen *In* CNES, From Optics to Radar, SPOT, and ERS Applications Dec. 1993 p 385-396 Sponsored in part by Commission of the European Communities and Beleidscommissie Remote Sensing Original contains color illustrations (For primary document see N94-32523 09-43)
Copyright Avail: Issuing Activity (CEPADUES-Editions, 111 rue Nicolas-Vauquelin, 31100 Toulouse, France)

In the Sahelian zone of Niger, possibilities of SPOT and ERS-1 Synthetic Aperture Radar (SAR) for determining surface characteristics were examined. Preliminary results show that SPOT dry season data are good to discriminate bare surfaces with differences in iron content. Multitemporal SPOT data during the rainy season make it possible to discriminate a range of vegetation and crop types in this area and to follow their development. ERS-1 SAR information is very difficult to use separately in this area. A more integrated and synergetic approach in combination with optical sensors and some field check is necessary. Because the variation, both spatially and spectrally, within and between some classes is gradual for both SPOT and ERS-1 SAR, classification will remain difficult. ESA

N94-32561 Bureau de Recherches Geologiques et Minieres, Orleans (France). Remote Sensing Dept.
EUROPEAN MARS PROJECT: THE POTENTIAL INTEGRATION OF SPOT AND AIR- AND SATELLITE-BORNE RADAR DATA OVER TWO PILOT AREAS FOR AGRICULTURAL STATISTICS. PROSPER PROGRAMME AND ERS-1 PILOT PROJECT
C. King, J. F. Desprats, J. M. Terres, and J. C. Porchier *In* CNES, From Optics to Radar, SPOT, and ERS Applications Dec. 1993 p 397-411 In FRENCH Sponsored in part by Joint Research Centre of the European Communities and CNES Original contains color illustrations (For primary document see N94-32523 09-43)
(Contract BRGM-CB47-73)
(BRGM-93035) Copyright Avail: Issuing Activity (CEPADUES-Editions, 111 rue Nicolas-Vauquelin, 31100 Toulouse, France)

As part of the European Monitoring the Agriculture by Remote Sensing (MARS) project, whose objective is to provide regular information on crops in Europe, radar data from two complementary programs were evaluated to see how they may overcome some of the problems posed by seasonal cloudiness (which can upset the observation calendars and thus subsequent exploitation of the data). The radar data evaluated came from an airborne E-SAR radar operating in the X channel, and the ERS-1 ESA pilot project. The study areas were Great Driffield (U.K.) and La Beauce (France). An area survey provided reference data for 15 sites, in order to compare the classification performances for several data sets, including just SPOT data, a temporal series of ERS-1 data, and coupled SPOT/radar data using either the C channel from ERS-1 or the X channel of E-SAR. Two possibilities of using radar data for crop discrimination were evaluated: either a procedure mixing optical and radar data that aims at improving the optical data at the lowest possible cost by adding data from one or more radar images; or a procedure discarding the optical domain, using only a multitemporal series of radar images. The results show the interest and the limits of the two options. A mixed procedure would make it possible to refine surface estimates for certain groups of crops, for example Summer crops. The X channel, which was only tested in airborne mode, led to significant performance. The multitemporal ERS-1 data provided part of the required crop inventory objectives, but filtering techniques are being developed that might improve the performance of such data and it might confirm the potential of ERS-1 data to be substituted in case of cloudy conditions. ESA

N94-32562 Office de la Recherche Scientifique et Technique Outre-Mer, Yaounde (Cameroon).

COMPARING SPOT AND SIR A FOR MAPPING SUPERFICIAL FORMATIONS IN TROPICAL FOREST REGIONS: EXAMPLE OF THE YAOUNDY REGION (CAMEROON) [COMPARAISON DE SPOT ET SIR A POUR LA CARTOGRAPHIE DES FORMATIONS SUPERFICIELLES EN ZONE FORESTIERE TROPICALE: EXEMPLE DE LA REGION DE YAOUNDE (CAMEROUN)]

F. Seyler and J. Noel *In* CNES, From Optics to Radar, SPOT, and ERS Applications Dec. 1993 p 413-434 In FRENCH Original contains color illustrations (For primary document see N94-32523 09-43)

Copyright Avail: Issuing Activity (CEPADUES-Editions, 111 rue Nicolas-Vauquelin, 31100 Toulouse, France)

The relation between ground organization surface topography and forest cover was studied using remote sensing images to extrapolate ground knowledge. Two types of hill were studied in Yaoundy (Cameroon): an average inselberg hill with thin organic soil layer, and a low hill with a ferritic organization. The morphological characteristics of these two types of hill were extracted from Digital Terrain Models (DTM), and two SPOT images and a Spaceborne Imaging Radar (SIR A) image were analyzed to evaluate their capabilities of discriminating these characters and their spatial extension. It was found that a thematic map could be produced by analyzing the texture on the SIR A image and superimposing the information obtained from the SPOT image. To analyze relief on a local level, SIR A did not enable a better interpretation than SPOT. However, extrapolation of morphological characteristics for regional mapping is made possible by SIR A, in this case. It is thought that use of ERS-1 would confirm these conclusions. ESA

N94-32563 Geosys, Ramonville (France).

POSSIBLE COMPLEMENTARITY OF SPOT/ERS IN MAPPING LAND USE: STUDY ON AGRICULTURAL LAND IN BRITTANY (FRANCE) [CARTOGRAPHIE DE L'OCCUPATION DU SOL POSSIBLE COMPLEMENTARITE SPOT/ERS: UNE ETUDE SUR UN PAYSAGE AGRICOLE BRETON]

S. Louahala, M. Normand, C. Loumagne, A. Vidal, C. Cann, D. Vidal-Madjar, C. Ottle, P. Olivier, P. Merot, and A. Craves et al *In* CNES, From Optics to Radar, SPOT, and ERS Applications Dec. 1993 p 435-444 In FRENCH Original contains color illustrations (For primary document see N94-32523 09-43)

Copyright Avail: Issuing Activity (CEPADUES-Editions, 111 rue Nicolas-Vauquelin, 31100 Toulouse, France)

A hydrological space observatory was implemented on a small agricultural watershed in the center of Brittany. The main objective is to study the usefulness of the ERS-1 Synthetic Aperture Radar (SAR) images for water resources monitoring. During 1992, a great number of ERS-1 images were acquired together with extensive ground truth. It is shown, as one of preliminary results, that thanks to its all weather capacity to obtain time series of data, the SAR images can be used in conjunction with SPOT data to map the soil occupation. ESA

N94-32564 SCOT Conseil, Ramonville (France).

LAND COVER CHANGE DETECTION WITH ERS-1 DATA AND DATA FROM OTHER REMOTE SENSING SATELLITES. EXAMPLE: THE DELTA OF THE RIVER EBRO (SPAIN)

Jochen Harms *In* CNES, From Optics to Radar, SPOT, and ERS Applications Dec. 1993 p 445-446 Original contains color illustrations (For primary document see N94-32523 09-43)

Copyright Avail: Issuing Activity (CEPADUES-Editions, 111 rue Nicolas-Vauquelin, 31100 Toulouse, France)

Information was acquired with the help of 'traditional means' (SPOT, topo-maps, Corine Land Cover) and stored in a database. Different SPOT images were classified to receive information on the quantity and quality of land cover changes in the past years (1985-1992). Recent SPOT images are used together with ERS-1 images to understand the content of the radar signal. Therefore the ERS-1 images are rectified on a common base with the SPOT images. Different filtering procedures are used to reduce the speckle noise in the radar images. Following this, different techniques are used to classify the radar images: supervised and unsupervised classification of mono and multitemporal ERS-1 images; segmentation of mono and multitemporal ERS-1 images and classification on the base of this segmentation. Additionally, SPOT images are merged with ERS-1 images and classified with different techniques (for example principal components). ERS-1 images will be used to detect land cover changes. Images will be merged to identify the advantages and limitations of C band radar. First results of the project indicate the advantage of using radar data in combination with optical data. The technique of automatic classification by segmentation at field based classification was identified as the most promising technique for change detection measurements in coastal regions. ESA

N94-32565 Food and Agriculture Organization of the United Nations, Rome (Italy). Remote Sensing Centre.

ERS-1 SAR AND OPTICAL DATA FOR LAND USE/LAND COVER MAPPING: A CASE STUDY IN A SAVANNAH ZONE OF GUINEA

J. F. Dallemand, J. Lichtenegger, V. Kaufmann, B. Barry, N. Diaby, and P. Reichert *In* CNES, From Optics to Radar, SPOT, and ERS Applications Dec. 1993 p 447-456 (For primary document see N94-32523 09-43)

Copyright Avail: Issuing Activity (CEPADUES-Editions, 111 rue Nicolas-Vauquelin, 31100 Toulouse, France)

Results of an assessment of the use of ERS-1 Synthetic Aperture Radar (SAR) data for land use/land cover mapping in a savannah zone of West Africa are presented. Optical data (SPOT, LANDSAT Thematic Mapper (TM)) were compared with microwave data (Spaceborne Imaging Radar (SIR A), ERS-1). LANDSAT TM data were initially geocoded with a Digital Terrain Model (DTM) and then registered with ERS-1 data. Multispectral SPOT data were interpreted at 1:100,000 and 1:50,000 scale. Standard and adaptive SAR filters were compared. Two methods of optical/microwave data integration were tested: intensity hue saturation transformation and optical/radar color combination. It appeared that identification of land use classes was not satisfactory using ERS-1 data of a single date. Better results were obtained in the case of a multitemporal SAR approach and especially when combining dry season optical data with rainy season SAR data. In this latter case it becomes possible to define more detailed visual interpretation keys. The complementarity of SPOT multispectral (XS) and ERS-1 SAR data for flooded rice fields monitoring is very promising due to the strong backscatter variations during the crop cycle. ESA

N94-32566 European Space Agency. ESRIN, Frascati (Italy). Earth Observation Div.

SAR INTERFEROMETRY WITH ERS-1

S. N. Coulson, G. A. Solaas, F. Rocca, C. Prati, A. Monti-Guarnieri, P. Hartl, M. Reich, and C. Werner *In* CNES, From Optics to Radar, SPOT, and ERS Applications Dec. 1993 p 457-472 Original contains color illustrations (For primary document see N94-32523 09-43)

Copyright Avail: Issuing Activity (CEPADUES-Editions, 111 rue Nicolas-Vauquelin, 31100 Toulouse, France)

Activities and results to date within the framework of an ESA mission working group ERS-1 FRINGE, which exploits the techniques of Interferometric Synthetic Aperture Radar (INSAR) with ERS-1 for precise measurement of the Earth's surface topography and movement, are described. It was found that INSAR provides accurate values of surface height with spatial resolution and independent of cloud cover. Preliminary results indicate that terrain height errors of less than 10 m are achievable with ERS-1. The capability of ERS-1 to measure cm scale movement of surface features through differential INSAR was demonstrated. The technique of differential INSAR opens the door to many new potential SAR applications including crustal dynamics, fault slip detection and volcanology. ESA

N94-32567 Centre National d'Etudes Spatiales, Toulouse (France).

EVALUATION OF SURFACE PHASE CHANGE ON LARGE ZONES [EVALUATION DES CHANGEMENTS DE PHASE DE SURFACE SUR DE GRANDES ZONES]

D. Massonnet, B. Rogron, and C. Carmona *In its* From Optics to Radar, SPOT, and ERS Applications Dec. 1993 p 473-481 (For primary document see N94-32523 09-43)

Copyright Avail: Issuing Activity (CEPADUES-Editions, 111 rue Nicolas-Vauquelin, 31100 Toulouse, France)

Differential interferometry effects over agricultural surfaces were obtained using SEASAT data. These effects were attributed to soil swelling following irrigation. These effects were studied using ERS-1 data with the goal of assessing the usefulness of interferometric products for crop classification. By interferometric product, is understood not only 'non topographic' phase differences, but also additional information such as coherence. A site was

selected which allows opportunistic differential interferometry through a combination of close orbital tracks and a moderate topography. On this site of more than 300,000 sq km several hundreds of agricultural units were selected. The information gathered on each unit was the amplitudes of the images of the pair, the coherence of the pair and the difference of phase which cannot be explained by orbital or topographic effects. Several definitions of coherence were tested from the point of view of classification power, computational load and convergence speed. One of them seems more interesting than the standard one. A simple double target modelization, was studied to separate the uncoherent part of a pixel from the coherent one. The existence of targets able to change their amplitude while keeping a high degree of coherence is a critical point for the inversion of such a model. Although more focused studies are now envisioned on sites where ground truth is available, preliminary results show the high potential of differential interferometry for crop classification. ESA

N94-32568* Jet Propulsion Lab., California Inst. of Tech., Pasadena.
TECHNIQUES AND APPLICATIONS OF SAR INTERFEROMETRY FOR ERS-1
Charles L. Werner (Zurich Univ., Switzerland.), David L. Small (Zurich Univ., Switzerland.), Paul A. Rosen, Scott Hensley, and Howard A. Zebker *In* CNES, From Optics to Radar, SPOT, and ERS Applications Dec. 1993 p 483-490 Sponsored by NASA, Washington Original contains color illustrations (For primary document see N94-32523 09-43)
Copyright Avail: Issuing Activity (CEPADUES-Editions, 111 rue Nicolas-Vauquelin, 31100 Toulouse, France)

The ERS-1 Synthetic Aperture Radar (SAR) demonstrated that it is possible to measure high resolution topography over large areas using interferometry with repeat orbit data sets. Given that the ERS-1 orbit is known with high precision, an automatic system for generation of interferograms is presented. Least squares estimation using ground control points provides an accurate method for determining the precise interferometric baseline. The system parameters which affect the accuracy of the Digital Elevation Models (DEM's) are errors in the interferometric baseline, decorrelation caused by baseline separation, thermal noise, and surface change. An adaptive filter based on the local interferometric coherence was developed to improve phase unwrapping of the interferogram. Final accuracies of the DEM's generated for single scene pairs in Alaska (U.S.) and Bonn (Germany) are on the order of 5 to 10 m. ESA

N94-32569 Politecnico di Milano (Italy). Dipt. di Elettronica.
DEVELOPMENTS IN ERS-1 SAR INTERFEROMETRY: USE OF THE SPECTRAL SHIFT
F. Gatelli, A. Monti-Guarnieri, F. Parizzi, P. Pasquali, C. Prati, and F. Rocca *In* CNES, From Optics to Radar, SPOT, and ERS Applications Dec. 1993 p 491-500 (For primary document see N94-32523 09-43)
Copyright Avail: Issuing Activity (CEPADUES-Editions, 111 rue Nicolas-Vauquelin, 31100 Toulouse, France)

Synthetic Aperture Radar (SAR) surveys from separate passes shows relative shifts of the ground wavenumber spectra that depend on the local slope. The exploitation of the spectral shift for different applications is discussed: generation of 'low noise' interferograms benefiting phase unwrapping; generation of quick look interferograms; and decorrelation reduction by means of Tunable Interferometric SAR (TINSAR) systems. ESA

N94-32570 Centre National d'Etudes Spatiales, Toulouse (France).
DIFFERENTIAL INTERFEROMETRY STUDY OF AN EARTHQUAKE [ETUDE DU SITE D'UN TREMBLEMENT DE TERRE PAR INTERFEROMETRIE DIFFERENTIELLE]
D. Massonnet, M. Rossi, F. Adragna, and C. Carmona *In its* From Optics to Radar, SPOT, and ERS Applications Dec. 1993 p 501-509 Original contains color illustrations (For primary document see N94-32523 09-43)
Copyright Avail: Issuing Activity (CEPADUES-Editions, 111 rue Nicolas-Vauquelin, 31100 Toulouse, France)

ERS-1 satellite images of the Los Angeles (California, U.S.) region taken on four separate dates surrounding the Landers earthquake of 28 Jun. 1992, were analyzed to verify the feasibility of mapping crustal movements with differential interferometry. The results obtained prove that it is possible to obtain interferometric fringes despite the elapsed 105 days between the data takes of the most interesting pair of images. The combination of an image pair spanning the earthquake with a Digital Elevation Model (DEM) proves the possibility of determining the orbital positions of the satellite when taking the images without the help of any artificial ground target (image locking technique) and without working with exceptionally close orbits, despite the relatively rough topography of the site. The result is a map of the coseismic moves caused by the earthquake. This map matches closely the geophysical modelization obtained. ESA

N94-32571 Centre National d'Etudes Spatiales, Toulouse (France).
PRECISION AND LEVEL OF ARTEFACTS IN THE COMPUTATION OF DIGITAL TERRAIN MODELS BY INTERFEROMETRY [PRECISION ET NIVEAU D'ARTEFACTS DANS LES CALCULS DE MODELES NUMERIQUES DE TERRAIN PAR INTERFEROMETRIE]
D. Massonnet, F. Perlant, and T. Rabaute *In its* From Optics to Radar, SPOT, and ERS Applications Dec. 1993 p 511-523 Original contains color illustrations (For primary document see N94-32523 09-43)
Copyright Avail: Issuing Activity (CEPADUES-Editions, 111 rue Nicolas-Vauquelin, 31100 Toulouse, France)

The future of Digital Elevation Model (DEM) extraction by radar interferometry, is discussed. This depends critically on the amount of phase artefact due to terrain surface phase changes or atmospheric depth variations and also on the importance of decorrelation between scenes, due to target modifications or to intertrack distance. Some of these, such as the statistics of the intertrack distance, may be obtained through the features of the system, and be improved by multiple scene acquisition. Other artefacts, either linked to atmospheric conditions or specific target behavior, are much more difficult to characterize. A statistical approach for the latter is proposed and a large surface of interferometric data is processed in order to gather an experimental assessment of the amount of artefact occurring with varying conditions of observation related to intertrack distance, terrain nature, terrain shape and time elapsed between observations. According to their spatial signatures, artefacts may be spotted visually (for instance in the case of a loss of coherence over a water surface) or only after the DEM has been completed (in the case of low frequency atmospheric depth variations). In any case, the comparison of the interferometric DEM and of a DEM obtained by standard techniques is the ultimate tool. Several examples of such a comparison are shown. ESA

N94-32572 Stuttgart Univ. (Germany). Inst. fuer Navigation.
FIELDS OF EXPERIMENTS IN ERS-1 SAR INTERFEROMETRY IN BONN AND NAPLES
Philipp Hartl and Karl-Heinz Thiel *In* CNES, From Optics to Radar, SPOT, and ERS Applications Dec. 1993 p 525-534 Original contains color illustrations (For primary document see N94-32523 09-43)
Copyright Avail: Issuing Activity (CEPADUES-Editions, 111 rue Nicolas-Vauquelin, 31100 Toulouse, France)

An experiment to show that Interferometric Synthetic Aperture Radar (INSAR) plays an important role in generating Digital Terrain Models (DTM's) and in detecting small changes in the Earth's surface during two successive orbits is presented. The experiment was carried out in Bonn (Germany) in March 1992, with a three day repetition orbit. A description of the fieldwork, the deployment of corner reflectors, the measurements and the data analysis is given. Also some further investigations concerning the capability of the SAR for absolute height and spatial resolution were carried out. Another experiment in Naples (Italy) performed using the 35 day repetition orbit of ERS-1 is also addressed. Using ascending and descending orbits, the movements linked to the relaxation phase were measured. ESA

N94-32573 Mashinstroyeniye, Moscow (USSR).
THE PROCESSING TECHNOLOGY AND SOME APPLICATIONS OF ALMAZ-1 DATA
I. V. Elizavetin *In* CNES, From Optics to Radar, SPOT, and ERS Applications Dec. 1993 p 535-540 (For primary document see N94-32523 09-43)
Copyright Avail: Issuing Activity (CEPADUES-Editions, 111 rue Nicolas-Vauquelin, 31100 Toulouse, France)

The 'Almaz' space program, developed on the base of unique space platform for accommodation of a vast instrument set for the Earth remote sensing is addressed. The remote sensing capacity is used for exploration and practical monitoring of natural resources in various spectrum ranges of electromagnetic waves for the sake of ecology, agriculture, forestry, geology, cartography and other fields of a national economy. The main

observation system onboard Almaz spacecraft, represented by high resolution Synthetic Aperture Radar (SAR) for all weather, round the clock radar survey of land and ocean surface, is addressed. Almaz-1 spacecraft was launched into the Earth's orbit on Mar. 31 1991. The technology of image processing, and the application of Almaz-1 data for stereomapping and interferometric investigations are discussed. ESA

N94-32574 Centre National des Techniques Spatiales (Algeria).
QUANTITATIVE ANALYSIS OF WOODY VEGETATION IN SOUDANO-SAHALIAN REGION. TEXTURAL APPROACH (APPLICATION TO A BURKINA FASO REGION) [ESTIMATION QUANTITATIVE DE LA VEGETATION LIGNUEUSE EN REGION SOUDANO-SAHELIENNE. APPROCHE TEXTURALE (APPLICATION A UNE REGION DU BURKINA FASO)]
K. Djaroudib *In* CNES, From Optics to Radar, SPOT, and ERS Applications Dec. 1993 p 541-552 In FRENCH Prepared in cooperation with Louvain Univ, Belgium Original contains color illustrations (For primary document see N94-32523 09-43)
Copyright Avail: Issuing Activity (CEPADUES-Editions, 111 rue Nicolas-Vauquelin, 31100 Toulouse, France)

A study which showed the contribution of textural information in the quantitative analysis of woody biomass in remotely sensed data is presented. The idea was to establish correlations between measured radiations or their combinations, vegetation indexes for example, and parameters characterizing the vegetal cover such as overlapping amount relative to the soil or leaf area index. However, the influence of some covers to spectral indexes in precise seasons risk to give doubtful results. In Soudano-Sahalian region, during the rainy season, the spectral signature of herbaceous stratum in a savanna with trees, is predominant for vegetation index calculations. This makes the spectral approach doubtful at this vegetative stage. Another element which should characterize the state of a cover and will be complementary to its spectral information, is its spatial arrangement or its texture. High resolution spatial data reinforce this idea and permit to distinguish different textures of a cover: a black blob on panchromatic SPOT data represents a trees or a group of trees. Thus two different overlapping areas are presented according to two different textures and the hypothesis is that a relation exists between overlapping density of trees and their spatial arrangement. This arrangement was quantified thanks to the textural parameters calculation derived from cooccurrence matrices, and their correlations with other parameters characterizing the vegetal cover were tested. Results are presented. ESA

N94-32575 Centre de Cooperation Internationale en Recherche Agronomique pour le Developpement, Montpellier (France).
STATISTICAL ANALYSIS AND MAPPING OF COTTON AND FOOD CROP CULTIVATION SURFACES IN THE WEST OF BURKINA FASO: CONTRIBUTION OF COMBINED SPOT P AND XS DATA [EVALUATION STATISTIQUE ET CARTOGRAPHIQUE DES SURFACES CULTIVEES EN COTON ET EN VIVRIER DANS L'OUEST DU BURKINA FASO: APPPORT DE LA COMBINAISON DES DONNEES SPOT P ET XS]
G. Laine, M. Cances, S. Pare, and A. Tollet *In* CNES, From Optics to Radar, SPOT, and ERS Applications Dec. 1993 p 553-564 In FRENCH Original contains color illustrations (For primary document see N94-32523 09-43)
Copyright Avail: Issuing Activity (CEPADUES-Editions, 111 rue Nicolas-Vauquelin, 31100 Toulouse, France)

A study to assess the possibilities of using remote sensing techniques for agricultural statistics is presented. Computed aided photointerpretation of SPOT multispectral (XS) and panchromatic (P) data was used to identify the cultivated zone. The cotton/grain crop distribution is obtained every year by digital processing of SPOT XS data within the farmed area thus defined. ESA

N94-33019*# Purdue Univ., West Lafayette, IN. School of Electrical Engineering.
EARTH OBSERVATIONAL RESEARCH USING MULTISTAGE EOS-LIKE DATA Final Report, 1 Aug. 1986 - 31 May 1994
C. J. Johannsen and D. A. Landgrebe 31 May 1994 22 p
(Grant NAGw-925)
(NASA-CR-195833; NAS 1.26:195833) Avail: CASI HC A03/MF A01

This grant was funded as a part of a program in which both research and educational impact were intended. Research work under this grant is directed at the understanding and use of future hyperspectral data such as that from imaging spectrometers. Specifically, the objectives of the work were: to prepare suitable means for analyzing data from sensors which have large numbers of spectral bands, to advance the fundamental understanding of the manner in which soils and vegetative materials reflect high spectral resolution optical wavelength radiation, and to maximize the impact of the results on the educational community. Over the life of the grant, the work has thus involved basic earth science research and information system technique understanding and development in a mutually supportive way. However, during the later years it became necessary to focus the work primarily on the first and last areas, due to a steadily decreasing level of effort. Derived from text

N94-33269 Bristol Univ. (England).
SNOWMELT FORECASTING. FURTHER COLD REGIONS DEVELOPMENT OF OPERATIONAL HYDROLOGICAL FORECASTING, VOLUME 2
K. M. Sambles and M. G. Anderson Mar. 1994 94 p Limited Reproducibility: More than 20% of this document may be affected by microfiche quality
(Contract DAJA45-89-C-0028)
(AD-A278123; R/D-6194-EN-01-Vol-2) Avail: Issuing Activity (Defense Technical Information Center (DTIC))

This volume contains all the information that is required to operate the computer simulation model SNOMO. The input file required, the operational logic of SNOMO and the output produced by SNOMO are discussed in detail. A full listing of the SNOMO Fortran-77 code is included. DTIC

N94-30996 Centre National d'Etudes Spatiales, Toulouse (France). Lab. d'Etudes et de Recherches en Teledetection Spatiale.
RADIATION/REMOTE SENSING: REVIEW OF THE PRINCIPAL DEFINITIONS [RAYONNEMENT/TELEDETECTION: RAPPEL DES PRINCIPALES DEFINITIONS]
G. Dedieu (Centre National de la Recherche Scientifique, Toulouse, France.) *In its* Subtropical Climates and Their Evolution: From Space-Based Observation to Modelling Oct. 1993 p 315-32 In FRENCH (For primary document see N94-30981 09-47)
Copyright Avail: Issuing Activity (CEPADUES-Editions, 111, rue Nicolas-Vauquelin, 31100 Toulouse, France)

N94-31004 Ecole Normale Superieure, Paris (France). Lab. d'Ecologie.
BEHAVIOR AND DYNAMICS OF TROPICAL FORESTS AND SAVANNAS [FONCTIONNEMENT ET DYNAMIQUE DES FORESTS ET SAVANES TROPICALES]
J. C. Menaut *In* CNES, Subtropical Climates and Their Evolution: From Space-Based Observation to Modelling Oct. 1993 p 527-546 In FRENCH (For primary document see N94-30981 09-47)
Copyright Avail: Issuing Activity (CEPADUES-Editions, 111, rue Nicolas-Vauquelin, 31100 Toulouse, France)

N94-31006 Toulouse Univ. (France). Lab. d'Aerologie.
AIRBORNE INSTRUMENTS [INSTRUMENTS AEROPORTES]
A. Druilhet *In* CNES, Subtropical Climates and Their Evolution: From Space-Based Observation to Modelling Oct. 1993 p 559-585 In FRENCH (For primary document see N94-30981 09-47)
Copyright Avail: Issuing Activity (CEPADUES-Editions, 111, rue Nicolas-Vauquelin, 31100 Toulouse, France)

N94-32463*# National Aeronautics and Space Administration. John F. Kennedy Space Center, Cocoa Beach, FL.
MAPPING ANALYSIS AND PLANNING SYSTEM FOR THE JOHN F. KENNEDY SPACE CENTER
C. R. Hall (Bionetics Corp., Cocoa Beach, FL.), M. J. Barkaszi (Bionetics Corp., Cocoa Beach, FL.), M. J. Provancha (Bionetics Corp., Cocoa Beach, FL.), N. A. Reddick (Bionetics Corp., Cocoa Beach, FL.), C. R. Hinkle (Bionetics Corp., Cocoa Beach, FL.), B. A. Engel (Purdue Univ., West Lafayette, IN.), and B. R. Summerfield *In* NASA, Washington, Technology 2003: The Fourth National Technology Transfer Conference and Exposition, Volume 2 Feb. 1994 p 375-387 (For primary document see N94-32420 09-99)
Avail: CASI HC A03/MF A04

N94-32464*# National Aeronautics and Space Administration. John C. Stennis Space Center, Bay Saint Louis, MS.
REMOTE SENSING FOR HURRICANE ANDREW IMPACT ASSESSMENT Abstract Only
Bruce A. Davis and Nicholas Schmidt *In* NASA, Washington, Technology 2003: The Fourth National Technology Transfer Conference and Exposition, Volume 2 Feb. 1994 p 388 (For primary document see N94-32420 09-99)
Avail: CASI HC A01/MF A04

N94-32465*# National Aeronautics and Space Administration. John C. Stennis Space Center, Bay Saint Louis, MS.
REMOTE SENSING FOR URBAN PLANNING
Bruce A. Davis, Nicholas Schmidt, John R. Jensen, Dave J. Cowen, Joanne Halls, Sunil Narumalani, and Bryan Burgess *In* NASA, Washington, Technology 2003: The Fourth National Technology Transfer Conference and Exposition, Volume 2 Feb. 1994 p 389-393 (For primary document see N94-32420 09-99)
Avail: CASI HC A01/MF A04

N94-32466*# National Aeronautics and Space Administration. John C. Stennis Space Center, Bay Saint Louis, MS.
REMOTE SENSING AND THE MISSISSIPPI HIGH ACCURACY REFERENCE NETWORK
Mark Mick, Timothy M. Alexander, and Stan Woolley *In* NASA, Washington, Technology 2003: The Fourth National Technology Transfer Conference and Exposition, Volume 2 Feb. 1994 p 394-403 (For primary document see N94-32420 09-99)
Avail: CASI HC A02/MF A04

44 ENERGY PRODUCTION AND CONVERSION

Includes specific energy conversion systems, e.g., fuel cells; global sources of energy; geophysical conversion; and windpower.

For related information see also *07 Aircraft Propulsion and Power, 20 Spacecraft Propulsion and Power,* and *28 Propellants and Fuels.*

N94-31070 Swedish Inst. for Materials Testing, Boras.
DATABASES AND DEMANDS FOR SOLAR HEATING MATERIALS [DATABASER OCH KRAV FOER SOLFANGARMATERIAL]
H. Wennerholm 1993 45 p In SWEDISH
(PB94-137494; SP-RAPP-1993:16) Avail: Issuing Activity (National Technical Information Service (NTIS))

Numerous problems with materials in solar energy systems have demonstrated the need for data to assess their performance and durability. The report describes a database of solar materials that provides basic material data for designers, manufacturers and researchers in solar energy. Within the framework of selecting materials for a higher benefit in solar energy applications the database provides performance data, mechanical data, outdoor exposure data based on figures from manufacturers and researchers. NTIS

N94-31071 Swedish Inst. for Materials Testing, Boras.
SOLAR ENERGY IN CHINA
H. Wennerholm 1993 36 p Limited Reproducibility: More than 20% of this document may be affected by microfiche quality
(PB94-137502; SP-RAPP-1993:36) Avail: CASI HC A03

The report presents the progress, status and goals of the Chinese national solar energy programs since 1970's. It applies specially to solar water heating, solar drying, passive solar, solar cookers, and solar photovoltaics. In China, an expert team has been organized, a number of technology development centers for new and renewable sources of energy have been set up and some demonstration projects are under way. Shortage of energy in China can not be expected to be overcome in a short period of time. The only way out is to adopt various kinds of energy conservation measures and increase the utilization of NRSE, while expanding the production of conventional energy. NTIS

N94-31233*# National Aeronautics and Space Administration. Goddard Space Flight Center, Greenbelt, MD.
THE 1988 GODDARD SPACE FLIGHT CENTER BATTERY WORKSHOP
Thomas Y. Yi, ed. 1993 449 p Workshop held in Greenbelt, MD, 1-3 Nov. 1988
(NASA-CP-3237; NAS 1.55:3237) Avail: CASI HC A19/MF A04

This document contains the proceedings of the 21st annual Battery Workshop held at Goddard Space Flight Center, Greenbelt, Maryland on November 1-3, 1988. The Workshop attendees included manufacturers, users, and government representatives interested in the latest developments in battery technology as they relate to high reliability operations and aerospace use. The subjects covered included battery testing methodologies and criteria, life testing of nickel-cadmium cells, testing and operation of nickel-hydrogen batteries in low earth orbit, and nickel-hydrogen technology issues and concerns. Derived from text

N94-31234# Edgerton, Germeshausen and Grier, Inc., Idaho Falls, ID.
FEASIBILITY STUDY TO EVALUATE PLASMA QUENCH PROCESS FOR NATURAL GAS CONVERSION APPLICATIONS
C. P. Thomas, P. C. Kong, and B. A. Detering 1993 6 p Presented at the Fuels Technology Contractors' Review Meeting, Morgantown, WV, 16-18 Nov. 1993
(DE94-000086; CONF-931156-21) Avail: CASI HC A02/MF A01

The objective of this work was to conduct a feasibility study on a new process, called the plasma quench process, for the conversion of methane to acetylene. FY-1993 efforts were focused on determining the economic viability of this process using bench scale experimental data which was previously generated. This report presents the economic analysis and conclusions of the analysis. Future research directions are briefly described. DOE

N94-31235 Midwest Research Inst., Golden, CO.
PHOTOVOLTAICS: PROGRAM OVERVIEW, FISCAL YEAR 1993
Feb. 1994 39 p Limited Reproducibility: More than 20% of this document may be affected by poor print
(Contract DE-AC02-83CH-10093)
(DE94-000246; DOE/CH-10093/264) Avail: Issuing Activity (Department of Energy (DOE))

This overview is divided into sections titled: 1993 PV program accomplishments, PV systems for today's markets generate power and experience, systems development and testing prepares products for market, advances in manufacturing hasten availability of innovations, cooperative research improves PV technology, additional achievements in cooperative R&D, and summary of PV program services. DOE

N94-31236# Midwest Research Inst., Golden, CO.
ROLE OF POLYCRYSTALLINITY IN CdTe AND CuInSe2 PHOTOVOLTAIC CELLS
J. R. Sites (Colorado State Univ., Fort Collins.) Feb. 1994 32 p
(Contract DE-AC02-83CH-10093)
(DE94-000293; NREL/TP-451-6215) Avail: CASI HC A03/MF A01

This report describes work to conduct several investigations of thin-film polycrystalline solar cells. An analysis of high-efficiency solar cells fabricated at the University of South Florida showed significant reduction in forward recombination current, and the cells were stable over a 3-month test period. Transient voltage effects were documented in a large number of polycrystalline cells and were attributed to long-lived trapping states sensitive to voltage changes near one-half open-circuit voltage. Collection efficiency and its voltage dependence were carefully calculated. The typical effect on photocurrent at operating voltages is about 2% for CuInSe2, and less for other cells. DOE

N94-31264# Midwest Research Inst., Golden, CO.
SOLAR RESOURCE: UTILITY LOAD-MATCHING ASSESSMENT
R. Perez (State Univ. of New York, Albany.), R. Seals (State Univ. of New York, Albany.), and R. Stewart (State Univ. of New York, Albany.) Mar. 1994 48 p
(Contract DE-AC02-83CH-10093)
(DE94-000297; NREL/TP-411-6292) Avail: CASI HC A03/MF A01

This report describes work performed to estimate the load-matching capability of photovoltaics (PV) for a selected group of utilities in the continental United States. The report provides an initial quantitative estimate

of this capability for 20 utilities. This characteristic is important because it may indicate that the effective capacity, hence the value, of PV is higher than is traditionally assigned to such non-controllable, non-dispatchable resources. Load-matching capability is determined experimentally by analyzing the interaction between the load requirements of each utility and the output of locally sited PV systems. This type of investigation requires site- and time-specific insolation data that are not commonly available. Here, the needed data were inferred from geostationary satellite remote sensing of the Earth's cloud cover. A secondary objective of this study was to evaluate the suitability of this approach. The results of this investigation are presented in this report. DOE

N94-31266# Horizon Data Corp., Reston, VA. Power Information Center.

DRAFT MINUTES OF IAPG MECHANICAL WORKING GROUP MEETING

D. M. Skinner 15 Dec. 1993 22 p Presented at the Interagency Advanced Power Group (IAPG) Mechanical Meeting, Albuquerque, NM, 3-4 Nov. 1993

(Contract DE-AC01-90CE-90053)

(DE94-004954; CONF-9311149-Summ.) Avail: CASI HC A03/MF A01

This report provides the draft minutes of the Interagency Advanced Power Group meeting held November 3-4, 1993. Topics addressed are: materials for thermal management; photovoltaic programs in the Air Force; ground based radar advanced power system development program; battery research; generator prognostics & diagnostics equipment; a thermal flight experiment test program; power systems assessment; overview: Phillip's space thermal technologies branch; and development of actuator thermal management. DOE

N94-31272# AMAX Research and Development Center, Golden, CO.

DEVELOPMENT OF VANADIUM-PHOSPHATE CATALYSTS FOR METHANOL PRODUCTION BY SELECTIVE OXIDATION OF METHANE

R. L. McCormick, M. C. Jha, and R. D. Streuber Dec. 1993 17 p

(Contract DE-AC22-92PC-92110)

(DE94-006759; DOE/PC-92110/T4) Avail: CASI HC A03/MF A01

This document is the fourth quarterly technical progress report under Contract No. DE-AC22-92PC92110, 'Development of Vanadium-Phosphate Catalysts for Methanol Production by Selective Oxidation of Methane.' During this quarter, the authors focused primarily on catalyst activity testing in the microreactor. Additional blank runs using methane and methanol were performed. Initial attempts at preparing a silica supported catalyst are described. These results are discussed in detail and plans for the coming quarter are outlined. DOE

N94-31279# Midwest Research Inst., Golden, CO.

AUTOMATED SOLAR CELL ASSEMBLY TEAMED PROCESS RESEARCH

M. J. Nowlan (Spire Corp., Bedford, MA.), S. J. Hogan (Spire Corp., Bedford, MA.), G. Darkazalli (Spire Corp., Bedford, MA.), W. F. Breen (Spire Corp., Bedford, MA.), J. M. Murach (Spire Corp., Bedford, MA.), and S. F. Sutherland (Spire Corp., Bedford, MA.) Feb. 1994 34 p

(Contract DE-AC02-83CH-10093)

(DE94-000295; NREL/TP-411-6264) Avail: CASI HC A03/MF A01

This report describes work done under Phase 3A of the PVMaT project to address problems that are generic to the photovoltaics (PV) industry. Crystalline silicon solar cells were used in the majority of all terrestrial power modules shipped in 1992. Spire's analysis in Phase 1 of the PVMaT project indicated that the use of thin (less than or equal to 200 microns) silicon cells can substantially reduce module manufacturing costs, provided that processing yields remain as high as they are now for processing standard thickness cells. Because present solar cell tabbing and interconnecting processes have unacceptably high yield losses with such thin cells, the objective of this Phase 3A subcontract is to use Spire's light soldering technology and experience in designing and fabricating solar cell tabbing and interconnecting equipment to develop high yield throughput, fully automated processes for tabbing and interconnecting thin cells. DOE

N94-31487# Southern California Gas Co., Los Angeles.

ECONOMIC FEASIBILITY ANALYSIS OF DISTRIBUTED ELECTRIC POWER GENERATION BASED UPON THE NATURAL GAS FIRED FUEL CELL

Sep. 1993 5 p Prepared for Manes Associates, Inc., Huntington Beach, CA

(Contract DE-FC21-92MC-29227)

(DE94-005795; DOE/MC-29227/3588) Avail: CASI HC A01/MF A01

This report is an account of the work performed from May 1, 1993 to July 30, 1993 on the economic feasibility generating electrical power by natural gas-fired fuel cells. The study is comprised of a survey of energy users, the development of numeric models of an energy distribution system and a central plant utilities system that includes a fuel cell. A model of the capital cost of the hardware elements is combined with a series of ownership scenarios and an operations model that provide the necessary input for a model of the cost of ownership of a fuel cell-based power generation system. The primary model development tasks are complete. The remaining study emphasis is to perform an economic analysis of varied ownership scenarios using the model. This report outlines the progress to date. DOE

N94-31648# Ames Lab., IA.

PROCEEDINGS OF THE SEVENTEENTH DOE SOLAR PHOTOCHEMISTRY RESEARCH CONFERENCE

1993 212 p Conference held in Brainerd, MN, 6-10 Jun. 1993

(Contract W-7405-eng-82)

(DE94-005552; IS-5097; CONF-9306113) Avail: CASI HC A10/MF A03

The Seventeenth DOE Solar Photochemistry Research Conference sponsored by the Division of Chemical Sciences, Office of Basic Energy Sciences, is being held June 6-10, 1993, at Cragun's Lodge and Conference Center, Brainerd, Minnesota The meeting is hosted this year by the Ames Laboratory of Iowa State University. The purpose of the meeting is to foster cooperation, collaboration, and exchange of current research ideas among grantees and contractors of the DOE Division of Chemical Sciences engaged in fundamental research on solar photochemical energy conversion. This conference provides a special opportunity for interaction among investigators from diverse traditional chemistry disciplines who share the common good of providing the knowledge and concepts needed for production of low cost fuels and chemicals or electricity by photochemical conversion of solar energy. Our special guest plenary lecturer is Professor Graham Fleming, of the University of Chicago, who will speak on ultrafast spectroscopic studies of molecular dynamics in the condensed phase. The remaining presentations on Monday will feature further investigations of ultrafast phenomena in solvation, electron transfer, and charge separation at interfaces. These will lead into the topical sessions which follow on photosynthesis, molecular models, photoinduced charge transfer in homogeneous and heterogeneous solutions, inorganic photochemistry, and photoelectrochemistry. As an added feature, the photoelectrochemistry session will include six short introductory lectures for the benefit of nonspecialists on outstanding issues and problems in that field. In this volume may be found a copy of the program, the abstracts of 28 formal presentations and 59 posters, as well as an address listing of the 114 participants. DOE

N94-31655# Technical Research Centre of Finland, Espoo. Metals Lab.

METAL HYDRIDES IN HYDROGEN ENERGY SYSTEMS [METALLIHYDRIDIT VETYENERGIAJAERJESTELMISSAE]

Seppo Taehtinen Oct. 1992 42 p In FINNISH Sponsored by Technical Research Centre of Finland

(ISSN 1235-0605)

(VTT-TIED-1407; ISBN-9-51-384301-7; ETN-94-96037) Copyright Avail: CASI HC A03/MF A01

The viability of the hydride storage unit in solar hydrogen energy systems was assessed from testing results conducted in simulated solar hydrogen system environment. Hydride storage unit was shown to match technically well with the solar hydrogen energy system as a part of the hydrogen storage subsystem. Hydrogen could be stored using pressures from 5 bar to 30 bar at ambient temperature and subsequently liberated in different pressure ranges depending on the temperature of the hydride storage unit. The maximum flow rate of the hydrogen was over 10 Nl H2/min and the degree of the reversibility was better than 95%. ESA

N94-31762# Pacific Northwest Lab., Richland, WA.

DEVELOPMENT OF A CATALYTIC SYSTEM FOR GASIFICATION OF WET BIOMASS

D. C. Elliott, L. J. Sealock, M. R. Phelps, G. G. Neuenschwander, and T. R. Hart Aug. 1993 15 p Presented at the 1st Biomass Conference of

the Americas: Energy, Environment, Agriculture, and Industry, Burlington, VT, 30 Aug. - 2 Sep. 1993
(Contract DE-AC06-76RL-01830)
(DE94-006216; PNL-SA-22582; CONF-9308106-3) Avail: CASI HC A03/MF A01

A gasification system is under development at Pacific Northwest Laboratory that can be used with high-moisture biomass feedstocks. The system operates at 350 C and 205 atm using a liquid water phase as the processing medium. Since a pressurized system is used, the wet biomass can be fed as a slurry to the reactor without drying. Through the development of catalysts, a useful processing system has been produced. This paper includes assessment of processing test results of different catalysts. Reactor system results including batch, bench-scale continuous, and engineering-scale processing results are presented to demonstrate the applicability of this catalytic gasification system to biomass. The system has utility both for direct conversion of biomass to fuel gas or as a wastewater cleanup system for treatment of unconverted biomass from bioconversion processes. By the use of this system, high conversion of biomass to fuel gas can be achieved. Medium-Btu is the primary product. Potential exists for recovery/recycle of some of the unreacted inorganic components from the biomass in the aqueous byproduct stream. DOE

N94-31767# Kauppa-ja Teollisuusministerio, Helsinki (Finland). Energy Dept.
NEMO: ADVANCED ENERGY SYSTEMS AND TECHNOLOGIES
P. Lund (Helsinki Univ. of Technology, Otaniemi, Finland.) 1993 144 p In FINNISH
(DE94-721996; KTM/E-B-150) Avail: CASI HC A07/MF A02

In this report, the contents and major results of the national research program on advanced energy system and technologies (NEMO) are presented. The NEMO-program was one of the energy research programs of the Ministry of Trade and Industry during 1988-1992. Helsinki University of Technology had the responsibility of the overall coordination of the program. NEMO has been the largest resource allocation into advanced energy systems in Finland so far. The total budget was 70 million FIM. The focus of the program has been in solar energy, wind power, and energy storage. Hydrogen and fuel cells have been included in smaller amount. On all major fields of the NEMO-program, useful and high quality results have been obtained. Results of international significance include among others arctic wind energy, new approaches for the energy storage problem in solar energy applications, and the development of a completely new storage battery. International collaboration has been given high priority. The NEMO-program has also been active in informing the industries of the various business and utilization possibilities that advanced energy technologies offer. For example, major demonstration plants of each technology group have been realized. It is recommended that the further R and D should be still more focused on commercial applications. Through research efforts at universities, a good technology base should be maintained, whereas the industries should take a stronger position in commercializing new technology. Parallel to technology R and D, more public resources should be allocated for market introduction. DOE

N94-31811# Arkansas Univ., Fayetteville.
BIOLOGICAL CONVERSION OF SYNTHESIS GAS
R. Basu, K. T. Klasson, E. R. Johnson, M. Takriff, E. C. Clausen, and J. L. Gaddy Sep. 1993 246 p
(Contract DE-FG21-90MC-27225)
(DE94-000094; DOE/MC-27225/3625) Avail: CASI HC A11/MF A03

Based upon the results of this culture screening study, Rhodospirillum rubrum is recommended for biocatalysis of the water gas shift reaction and Chlorobium thiosulfatophilum is recommended for H2S conversion to elemental sulfur. Both bacteria require tungsten light for growth and can be co-cultured together if H2S conversion is not complete (required concentration of at least 1 ppM), thereby presenting H2 uptake by Chlorobium thiosulfatophilum. COS degradation may be accomplished by utilizing various CO-utilizing bacteria or by indirectly converting COS to elemental sulfur after the COS first undergoes reaction to H2 in water. The second alternative is probably preferred due to the low expected concentration of COS relative to H2S. Mass transfer and kinetic studies were carried out for the Rhodospirillum rubrum and Chlorobium thiosulfatophilum bacterial systems. Rhodospirillum rubrum is a photosynthetic anaerobic bacterium which catalyzes the biological water gas shift reaction: CO + H2O yields CO2 + H2. Chlorobium thiosulfatophilum is also a photosynthetic anaerobic bacteria, and converts H2S and COS to elemental sulfur. DOE

N94-31812 Pennsylvania State Univ., University Park.
IN-SITU CHARACTERIZATION OF GROWTH AND INTERFACES IN a-Si:H DEVICES
R. W. Collins, C. R. Wronski, I. An, Y. Lu, and H. V. Nguyen Feb. 1994 78 p Prepared for Midwest Research Inst., Golden, CO Limited Reproducibility: More than 20% of this document may be affected by microfiche quality
(Contract DE-AC02-83CH-10093)
(DE94-000291; NREL/TP-451-6135) Avail: CASI HC A05

This report describes work to reach two goals -- an individual goal and a wide-gap team goal. The individual goal was to investigate the 'top junction' for defects using the spectroscopic ellipsometry technique. This will include an evaluation if specific defects are associated with C, B, Sn (diffusing from the transparent conducting oxide TCO) or Na (diffusing from the glass). It may include an assessment of the function of a graded a-SiC:H buffer layer. As defects are identified and characterized, their influence on the transport properties will be assessed. This should lead to better parameters used as input to models for the electronic materials and device performance. The goal of the wide-gap team was to demonstrate, characterize, and understand improved doped and undoped 'wide gap' materials for use in achieving 15%-efficient stabilized photovoltaic modules ('wide gap' materials are defined by this team to have a band gap greater than or = 1.9 eV). The major conclusions of the research are discussed in the report. DOE

N94-32143# Astropower, Inc., Newark, DE.
SILICON-FILM(TM) PHOTOVOLTAIC MANUFACTURING TECHNOLOGY
W. R. Bottenberg, R. B. Hall, E. L. Jackson, S. Lampo, W. P. Mulligan, and A. M. Barnett Feb. 1994 41 p Prepared for Midwest Research Inst., Golden, CO
(Contract DE-AC02-83CH-10093)
(DE94-000202; NREL/TP-411-5815) Avail: CASI HC A03/MF A01

This report describes work under a subcontract to upgrade AstroPower, Inc.'s facility to produce 1.22 m(exp 2) Silicon-Film(trademark) PV modules with an output of 170 Wp. The focus for the first year of the PVMaT Phase 2A project is to establish the baseline process capability and optimize the performance of the present machine. This first year's activities accelerated the advance of Silicon-Film(trademark) manufacturing technology in several ways. First, the project led directly to plans to make an early introduction of a large solar cell product. The successful fabrication of 646 cm(exp 2) wafers and solar cells paved the way for dramatically increasing the power output per solar cell. Second was the establishment of a basis for the design and construction of a 2.4 MW/yr wafer machine. Another important contribution was the determination of the importance of H(+) implantation processes for polycrystalline silicon technologies. DOE

N94-32174# Lawrence Livermore National Lab., CA.
A SOLAR ARRAY MODULE FABRICATION PROCESS FOR HALE SOLAR ELECTRIC UAVs
P. G. Carey, R. C. Aceves, N. J. Colella, J. B. Thompson, and K. A. Williams Dec. 1993 5 p
(Contract W-7405-eng-48)
(DE94-006212; UCRL-ID-115268) Avail: CASI HC A01/MF A01

We describe a fabrication process to manufacture high power to weight ratio flexible solar array modules for use on high altitude long endurance (HALE) solar electric unmanned air vehicles (UAV's). A span-loaded flying wing vehicle, known as the RAPTOR Pathfinder, is being employed as a flying test bed to expand the envelope of solar powered flight to high altitudes. It requires multiple light weight, flexible solar array modules able to endure adverse environmental conditions. At high altitudes the solar UV flux is significantly enhanced relative to sea level and extreme thermal variations occur. Our process involves first electrically interconnecting solar cells into an array followed by laminating them between top and bottom laminated layers into a solar array module. After careful evaluation of candidate polymers, fluoropolymer materials have been selected as the array laminate layers because of their inherent abilities to withstand the hostile conditions imposed by the environment. DOE

N94-32383# Sandia National Labs., Albuquerque, NM.
RENEWABLE ENERGY TECHNOLOGY DEVELOPMENT AT SANDIA NATIONAL LABORATORIES
P. C. Klimas 1994 9 p Presented at the New Mexico Conference on the Environment, Albuquerque, NM, 24-26 Apr. 1994
(Contract DE-AC04-94AL-85000)
(DE94-007734; SAND-94-0497C; CONF-9404107-4) Avail: CASI HC A02/MF A01

The use of renewable energy technologies is typically thought of as an integral part of creating and sustaining an environment that maximizes the overall quality of life of the Earth's present inhabitants and does not leave an undue burden on future generations. Sandia National Laboratories has been a leader in developing many of these technologies over the last two decades. This paper describes innovative solar, wind and geothermal energy systems and components that Sandia is helping to bring to the marketplace. A common but special aspect of all of these activities is that they are conducted in partnership with non-federal government entities. A number of these partners are from New Mexico. DOE

N94-32648# Sandia National Labs., Albuquerque, NM. Renewable Energy Program Development Office.
SOLAR ACTIVITIES AT SANDIA NATIONAL LABORATORIES
Paul C. Klimas and David E. Hasti 1994 14 p Presented at the Globalcon: Congress and Exhibition for Energy and Environmental Technologies, Anaheim, CA, 6-7 Apr. 1994
(Contract DE-AC04-94AL-85000)
(DE94-007737; SAND-94-0552C; CONF-940443-1) Avail: CASI HC A03/MF A01

The use of renewable energy technologies is typically thought of as an integral part of creating and sustaining an environment that maximizes the overall quality of life of the Earth's present inhabitants and does not leave an undue burden on future generations. Sandia National Laboratories has been a leader in developing and deploying many of these technologies over the last two decades. A common but special aspect of all of these activities is that they are all conducted in cooperation with various types of partners. Some of these partners have an interest in seeing these systems grow in the marketplace, while others are primarily concerned with economic benefits that can come from immediate use of these renewable energy systems. This paper describes solar thermal and photovoltaic technology activities at Sandia that are intended to accelerate the commercialization of these solar systems. DOE

N94-32660 Los Alamos National Lab., NM.
A SIMPLE MODEL FOR DETERMINING PHOTOELECTRON-GENERATED RADIATION SCALING LAWS
T. M. Dipp Dec. 1993 76 p Limited Reproducibility: More than 20% of this document may be affected by microfiche quality
(Contract W-7405-eng-36)
(DE94-006130; LA-12674) Avail: Issuing Activity (Department of Energy (DOE))

The generation of radiation via photoelectrons induced off of a conducting surface was explored using a simple model to determine fundamental scaling laws. The model is one-dimensional (small-spot) and uses monoenergetic, nonrelativistic photoelectrons emitted normal to the illuminated conducting surface. Simple steady-state radiation, frequency, and maximum orbital distance equations were derived using small-spot radiation equations, a sin(exp 2) type modulation function, and simple photoelectron dynamics. The result is a system of equations for various scaling laws, which, along with model and user constraints, are simultaneously solved using techniques similar to linear programming. Typical conductors illuminated by low-power sources producing photons with energies less than 5.0 eV are readily modeled by this small-spot, steady-state analysis, which shows they generally produce low efficiency (eta(sub rsL) less than 10(exp -10.5)) pure photoelectron-induced radiation. However, the small-spot theory predicts that the total conversion efficiency for incident photon power to photoelectron-induced radiated power can go higher than 10(exp -5.5) for typical real conductors if photons having energies of 15 eV and higher are used, and should go even higher still if the small-spot limit of this theory is exceeded as well. Overall, the simple theory equations, model constraint equations, and solution techniques presented provide a foundation for understanding, predicting, and optimizing the generated radiation, and the simple theory equations provide scaling laws to compare with computational and laboratory experimental data. DOE

N94-32701# Horizon Data Corp., Reston, VA. Power Information Center.
INTERAGENCY ADVANCED POWER GROUP: STEERING GROUP MEETING MINUTES
18 Nov. 1993 69 p Meeting held in Fort Belvoir, VA, 18 Nov. 1993
(Contract DE-AC01-90CE-90053)
(DE94-007951; DOE/CE-90053/T62) Avail: CASI HC A04/MF A01

This document contains the draft meeting minutes of the Steering Group of the Interagency Advanced Power Group. Included are the discussions resulting from the presentation of working group reports and the results of a discussion of IAPG policies and procedures. In the appendix are the reports of the following working groups: Electrical, Mechanical, Solar, and Systems. DOE

N94-32705# Oak Ridge National Lab., TN.
FLYWHEEL ENERGY STORAGE TECHNOLOGY WORKSHOP
D. OKain, comp. and D. Howell, comp. 1993 453 p Workshop held in Oak Ridge, TN, 2-4 Nov. 1993
(Contract DE-AC05-84OR-21400)
(DE94-008064; CONF-9311155) Avail: CASI HC A20/MF A04

Advances in recent years of high strength/lightweight materials, high performance magnetic bearings, and power electronics technology has spurred a renewed interest by the transportation, utility, and manufacturing industries in flywheel energy storage (FES) technologies. FES offers several advantages over conventional electrochemical energy storage, such as high specific energy and specific power, fast charging time, long service life, high turnaround efficiency (energy out/energy in), and no hazardous/toxic materials or chemicals are involved. Potential applications of FES units include power supplies for hybrid and electric vehicles, electric vehicle charging stations, space systems, and pulsed power devices. Also, FES units can be used for utility load leveling, uninterruptable power supplies to protect electronic equipment and electrical machinery, and for intermittent wind or photovoltaic energy sources. The purpose of this workshop is to provide a forum to highlight technologies that offer a high potential to increase the performance of FES systems and to discuss potential solutions to overcome present FES application barriers. This document consists of viewgraphs from 27 presentations. DOE

N94-32725# Midwest Research Inst., Golden, CO. National Renewable Energy Lab.
BIOMASS POWER INDUSTRY: ASSESSMENT OF KEY PLAYERS AND APPROACHES FOR DOE AND INDUSTRY INTERACTION
Jan. 1994 35 p
(Contract DE-AC02-83CH-10093)
(DE94-000238; DOE/CH-10093/257) Avail: CASI HC A03/MF A01

A review team established by the Department of Energy conducted an assessment of the U.S. biomass power industry. The review team visited with more than 50 organizations representing all sectors of the biomass power industry including utilities, independent power producers, component manufacturers, engineering and construction contractors, agricultural organizations, industrial users, and regulatory organizations. DOE solicited industry input for the development of the Biomass Power Division's Five Year Plan. DOE believed there was a critical need to obtain industry's insight and working knowledge to develop the near- and long-term plans of the program. At the heart of this objective was the desire to identify near-term initiatives that the program could pursue to help accelerate the further development of biomass power projects. DOE

N94-32762# Los Alamos National Lab., NM. Electronics Research Group.
POLYMER ELECTROLYTE FUEL CELLS
S. Gottesfeld 1994 11 p Presented at the 11th International Seminar on Primary and Secondary Battery Technology and Application, Deerfield Beach, FL, 28 Feb. - 3 Mar. 1994
(Contract W-7405-eng-36)
(DE94-007558; LA-UR-94-659; CONF-940210-1) Avail: CASI HC A03/MF A01

The recent increase in attention to polymer electrolyte fuel cells (PEFC's) is the result of significant technical advances in this technology and the

initiation of some projects for the demonstration of complete PEFC-based power system in a bus or in a passenger car. A PEFC powered vehicle has the potential for zero emission, high energy conversion efficiency and extended range compared to present day battery powered EV's. This paper describes recent achievements in R&D on PEFC's. The major thrust areas have been: (1) demonstration of membrane/electrode assemblies with stable high performance in life tests lasting 4000 hours, employing ultra-low Pt loadings corresponding to only 1/2 oz of Pt for the complete power source of a passenger car; (2) effective remedies for the high sensitivity of the Pt electrocatalyst to impurities in the fuel feed stream; and (3) comprehensive evaluation of the physicochemical properties of membrane and electrodes in the PEFC, clarifying the water management issues and enabling effective codes and diagnostics for this fuel cell. DOE

N94-32763# Purdue Univ., West Lafayette, IN.
DEVELOPMENT OF A COMPUTER MODEL FOR POLYCRYSTALLINE THIN-FILM CuInSe2 AND CdTe SOLAR CELLS
J. L. Gray, R. J. Schwartz, and Y. J. Lee Mar. 1994 62 p Prepared for Midwest Research Inst., Golden, CO
(Contract DE-AC02-83CH-10093)
(DE94-006853; NREL/TP-451-6398) Avail: CASI HC A04/MF A01

Solar cells operate by converting the radiation power from sun light into electrical power through photon absorption by semiconductor materials. The elemental and compound material systems widely used in photovoltaic applications can be produced in a variety of crystalline and non-crystalline forms. Although the crystalline group of materials have exhibited high conversion efficiencies, their production cost are substantially high. Several candidates in the poly- and micro-crystalline family of materials have recently gained much attention due to their potential for low cost manufacturability, stability, reliability and good performance. Among those materials, CuInSe2 and CdTe are considered to be the best choices for production of thin film solar cells because of the good optical properties and almost ideal band gap energies. Considerable progress was made with respect to cell performance and low cost manufacturing processes. Recently conversion efficiencies of 14.1 and 14.6% have been reported for CuInSe2 and CdTe based solar cells respectively. Even though the efficiencies of these cells continue to improve, they are not fully understood materials and there lies an uncertainty in their electrical properties and possible attainable performances. The best way to understand the details of current transport mechanisms and recombinations is to model the solar cells numerically. By numerical modeling, the processes which limit the cell performance can be sought and therefore, the most desirable designs for solar cells utilizing these materials as absorbers can be predicted. The problems with numerically modeling CuInSe2 and CdTe solar cells are that reported values of the pertinent material parameters vary over a wide range, and some quantities such as carrier concentration are not explicitly controlled. DOE

N94-32765# Solarex Corp., Newtown, PA.
LARGE-AREA, TRIPLE-JUNCTION a-Si ALLOY PRODUCTION SCALE-UP
R. Oswald, J. ODowd, and W. Ashenfelter Mar. 1994 18 p Prepared for Midwest Research Inst., Golden, CO
(Contract DE-AC02-83CH-10093)
(DE94-006856; NREL/TP-411-6397) Avail: CASI HC A03/MF A01

This report describes work to improve the efficiency of large-area, multi-junction amorphous silicon (a-Si) alloy modules. Equipment capable of producing modules up to 0.74 m(exp 2) in area is on line and process development has begun. Preliminary cost analysis/reduction has begun to ensure that these development efforts will result in a commercialization of the large-area technology. The approach was to transfer the high-efficiency multi-junction technology from R&D into the manufacturing environment by using three different substrate sizes. Initial attempts to transfer the multijunction silicon process were made using a 0.1 m(exp 2) substrate (approximately 1 ft(exp 2)). These efforts resulted in a module with a measured aperture area efficiency of 10.32%. Simultaneous with the transfer of the silicon technology, the most complicated aspect of the technology transfer, Solarex began process development techniques on large-area modules by using the 0.37 m(exp 2) substrates. These efforts resulted in modules with a total area efficiency of 7%. Finally, initial runs on substrates 0.74 m(exp 2) were made to debug the large-area equipment in preparation of transferring the knowledge gained in the processing of the smaller substrates. DOE

N94-32823# Fuel Cell Engineering Corp., Danbury, CT.
DETAILED DESIGN OF THE 2MW DEMONSTRATION PLANT
16 Sep. 1993 26 p
(Contract DE-FC21-92MC-29237)
(DE94-000042; DOE/MC-29237/3512) Avail: CASI HC A03/MF A01

This document provides a summary of the design of the 2MW carbonate fuel cell power plant which will be built and tested under DOE cooperative agreement DE-FC2l-92MC29237. The report is divided into sections which describe the process and stack module design, and appendices which provide additional design detail. Section 2.0 provides an overview of the program, including the project objectives, site location, and schedule. A description of the overall process is presented in Section 3.0. The design of the fuel cell stack modules is described in section 5.0, which discusses the design of the fuel cell stacks, multi-stack enclosures, and stack modules. Additional detail is provided in a report appendix, the Final Design Criteria Summary. This is an abstract of the design criteria used in the design of the submodules and modules. DOE

N94-32918 Central Research Inst. of Electric Power Industry, Tokyo (Japan). Energy and Environment Lab.
FIELD OPERATION TEST OF UTILITY INTERACTIVE LOAD CONDITIONER WITH PHOTOVOLTAIC CELLS AT A DEMONSTRATION HOUSE
K. Ishihara, Y. Mita, T. Iwahori, and J. Iga May 1993 32 p Limited Reproducibility: More than 20% of this document may be affected by microfiche quality
(DE94-757271; CRIE-T-92090) Avail: CASI HC A03

This paper reports the result of a field operation test of a utility load conditioner in a demonstration house equipped with photovoltaic cells. The photovoltaic cells have an area of 42 m(exp 2) and a capacity of 8.6 kW at 250 V. The utility load conditioner is of single-phase, three-wire type, with a power converting capacity of 5 kW/6 kVA. The storage battery consists of two banks of sealed lead-acid batteries, each bank comprising 18 cells of 12 V - 65 Ah in series. As a result of the testing, the load conditioner was verified to cause only the excess power generated by the photovoltaic cells during daytime to flow into the storage battery banks under a reverse current flow operation mode. When the photovoltaic cell output is below power demand, the load conditioner draws as much power as is short from the storage battery banks. Under a storage battery absorbing operation mode, the conditioner makes the storage battery absorb the excess power while suppressing the reverse flow. Autonomous operation during a power failure, transfer to the storage battery absorbing operation mode, and return to the reverse current flow operation mode at power failure restoration have all operated smoothly without overcharging the storage batteries. A high energy storage efficiency of 70% in a pumped storage power plant has been achieved in a week-long operation. DOE

N94-32919 Central Research Inst. of Electric Power Industry, Tokyo (Japan).
OPTIMAL PLANNING OF RESIDENTIAL PHOTOVOLTAIC SYSTEMS UNDER VARIOUS RATE STRUCTURE
E. Imamura and H. Asano May 1993 24 p Limited Reproducibility: More than 20% of this document may be affected by microfiche quality
(DE94-757272; CRIE-Y-93001) Avail: CASI HC A03

With respect to residential electric power utilization and supply systems utilizing photovoltaic power generation, the installation inducible economic conditions were searched using a linear programming technique, and influences by charge systems were evaluated and discussed. A photovoltaic system model consists of a photovoltaic panel, a control panel incorporated inverter, and a storage battery set. For the amount of power generated by the photovoltaic system, mean values for total insolation in Tokyo each for winter, summer, and intermediate seasons were used, assuming the photovoltaic system efficiency at 10% and the battery charge/discharge efficiency at 70%. Residential power load patterns were hypothesized from 200 to 1000 kWh/month depending on the demand scale. As a result of the analysis, it was made clear that the condition the photovoltaic system is accepted by residential housing is such that the price for the photovoltaic system including the inverter becoming 1/5 of the present price, and the price for the battery including the charge/discharge control device becoming 1/3 make the cost break-even. In the case of time-band based charge system, it is shown that the case where the ratio of daytime charge to

nighttime charge is three makes the coordination of the battery and the photovoltaic system optimal. DOE

N94-32965 Sandia National Labs., Albuquerque, NM.
OPERATIONAL EXPERIENCE AND EVALUATION OF A DUAL-ELEMENT STRETCHED-MEMBRANE HELIOSTAT
J. W. Strachan and Geest VanDer, J. Jan. 1994 38 p Limited Reproducibility: More than 20% of this document may be affected by microfiche quality
(Contract DE-AC04-94AL-85000)
(DE94-008827; SAND-93-2453) Avail: CASI HC A03

A dual-element, stretched-membrane central receiver heliostat was designed and manufactured in 1989 by a private US company engaged in the development of commercial central receiver solar technology. The two-module collector, with a collection area of 97.5 sq m, extends stretched-membrane mirror technology on several fronts with face-down stow capability and a digital controller that integrates tracking and focusing control on a single programmable control board. The solar collector was installed at Sandia's National Solar Thermal Test Facility in Albuquerque, NM, and it was evaluated over a three-and-a-half year period which ended in Sep. 1993. The measured performance and the operational and maintenance characteristics of this commercial prototype are the subject of this report. The results of beam quality measurements, tracking repeatability tests, measurements of beam movement in elevated winds, performance tests of the focusing system, and all-day beam quality and tracking tests are presented, and the authors offer a detailed discussion of the knowledge gained through operation and maintenance and of the improvements made or suggested to the heliostat's design. DOE

N94-33015# Air Force Academy, CO. Research Lab.
ROOM TEMPERATURE MOLTEN SALTS FOR ADVANCED ENERGY CONVERSION AND STORAGE
John S. Wilkes 1994 12 p
(AD-A277777) Avail: CASI HC A03/MF A01

Very high energy density electrical power sources will be required by the Air Force for operations in space. New high performance electrolytes are being developed to enable a new generation of electrochemical power sources. DTIC

N94-31028*# National Aeronautics and Space Administration. Marshall Space Flight Center, Huntsville, AL.
IMPACT OF LDEF PHOTOVOLTAIC EXPERIMENT FINDINGS UPON SPACECRAFT SOLAR ARRAY DESIGN AND DEVELOPMENT REQUIREMENTS
Leighton E. Young *In its* LDEF Materials Results for Spacecraft Applications Dec. 1993 p 201-215 (For primary document see N94-31012 09-12)
Avail: CASI HC A03/MF A04

N94-31427*# National Aeronautics and Space Administration. Lewis Research Center, Cleveland, OH.
SOLAR LUNAR POWER
Sheila G. Bailey and Geoffrey A. Landis *In* NASA. Marshall Space Flight Center, The Second Annual International Space University Alumni Conference Feb. 1994 p 8-25 (For primary document see N94-31425 09-12)
Avail: CASI HC A03/MF A02

N94-33292*# Lockheed Missiles and Space Co., Sunnyvale, CA.
SPACE STATION FREEDOM SOLAR ARRAY CONTAINMENT BOX MECHANISMS
Mark E. Johnson, Bert Haugen, and Grant Anderson *In* NASA. Lewis Research Center, The 28th Aerospace Mechanisms Symposium May 1994 p 1-16 (For primary document see N94-33291 09-15)
Avail: CASI HC A03/MF A04

N94-33293*# ISRO Satellite Centre, Peenya, Bangalore (India). Spacecraft Mechanisms Group.
INSAT-2A AND 2B DEVELOPMENT MECHANISMS
M. N. Sathyanarayan, M. Nageswara Rao, B. S. Nataraju, N. Viswanatha, M. Laxmana Chary, K. S. Balan, V. Sridhara Murthy, Raju Aller, and H. N. Suresha Kumar *In* NASA. Lewis Research Center, The 28th Aerospace Mechanisms Symposium May 1994 p 17-34 (For primary document see N94-33291 09-15)
Avail: CASI HC A03/MF A04

45 ENVIRONMENT POLLUTION

Includes atmospheric, noise, thermal, and water pollution.

N94-31275# Army War Coll., Carlisle Barracks, PA. Strategic Studies Inst.
NATO CONTRIBUTIONS TO EUROPEAN ENVIRONMENTAL SECURITY Final Report
Kent H. Butts 30 Dec. 1993 61 p
(AD-A275918) Avail: CASI HC A04/MF A01

Environmental issues are promoting instability and conflict at an ever increasing rate. Forward-thinking international security strategists suggest that these catalytic issues be addressed before they lead to costly conflict. The U.S. Department of Defense has committed itself to using DOD assets to address these environmental problems. This study builds upon these visionary concepts to recommend that NATO develop an environmental assistance program to address issues that threaten stability in regions strategically important to European security. With NATO searching for a new mission to demonstrate its relevance in the post-cold war era, such a program has great potential benefit in helping to mitigate significant environment problems. It would also allow NATO to promote military-to-military contacts and enhance communication with former adversaries. DTIC

N94-31339# Aberdeen Proving Ground, MD. Edgewood Research Development and Engineering Center.
IN-BED MULTIPORT SAMPLING SYSTEM Final Report, Nov. 1991 - May 1993
L. C. Buettner, J. J. Mahle, and D. K. Friday Dec. 1993 17 p
(DA Proj. 101-62622-A-553)
(AD-A275908; ERDEC-TR-134) Avail: CASI HC A03/MF A01

Knowledge of the transient behavior in fixed-bed separation processes is required to design advanced air purification systems. Measuring transient behavior experimentally can be difficult because of rapid changes in pressure and temperature in the bed. An apparatus has been developed which simultaneously isolates multiple vapor phase concentration samples at selected axial positions within the bed for subsequent analysis. Results are presented for the calibration operation of this sampling apparatus using a laboratory pressure swing adsorption system. DTIC

N94-31347# Columbia Univ., Palisades, NY.
INVESTIGATION OF CARBON DIOXIDE IN THE CENTRAL SOUTH PACIFIC OCEAN (WOCE SECTIONS P-16C AND P-17C) DURING THE TUNES/2 EXPEDITION OF THE R/V THOMAS WASHINGTON, JULY-AUGUST, 1991
T. Takahashi, J. G. Goddard, S. Rubin, D. W. Chipman, and S. C. Sutherland Dec. 1993 163 p
(Contract DE-FG02-90ER-60983)
(DE94-006638; DOE/ER-60983/3) Avail: CASI HC A08/MF A02

This report summarizes the results of carbon dioxide and associated hydrographic measurements made during the oceanographic expedition, TUNES/2, aboard the R/V Thomas Washington in the central South Pacific Ocean. During the 40 day expedition, the total carbon dioxide concentration in 1000 seawater samples were determined using a coulometer system and the pCO2 in 940 seawater samples were determined using an equilibrator/gas chromatograph system. The alkalinity values in 900 water samples were computed using these measurements. In addition, 156 coulometric measurements were made for the Certified Reference Solutions (Batch No. 6) and yielded a mean value of 2303.2 +/- 1.5 (mu)mol/kg. The chemical characteristics for the major water masses have been determined. DOE

N94-31582# Pacific Northwest Lab., Richland, WA.
INFORMATION RESOURCES FOR US DEPARTMENT OF ENERGY POLLUTION PREVENTION PROGRAMS
K. L. Peterson, L. J. Snowden-Swan, and R. S. Butner Jan. 1994 62 p

(Contract DE-AC06-76RL-01830)
(DE94-006677; PNL-9002) Avail: CASI HC A04/MF A01

In support of the U.S. Department of Energy's (DOE's) pollution prevention efforts being conducted under the aegis of DOE's Office of Environmental Restoration and Waste Management (EM) program, Pacific Northwest Laboratory was tasked with evaluating pollution prevention information resources. The goal of this activity was to improve the effectiveness of DOE's pollution prevention activities through improved information flow, both within the complex and, more specifically, between DOE and other organizations that share similar pollution prevention challenges. This report presents findings with respect to the role of information collection and dissemination within the complex, opportunities for teaming from successes of the private sector, and specific information needs of the DOE pollution prevention community. These findings were derived from a series of interviews with pollution prevention coordinators from across the DOE complex, review of DOE site and facility pollution prevention plans, and workshops with DOE information users as well as an information resources workshop that brought together information specialists from private industry, nonprofit organizations, as well as state and regional pollution prevention assistance programs. DOE

N94-31596# Oak Ridge National Lab., TN.
THE GLOBAL CLIMATOLOGY NETWORK PRECIPITATION DATA
T. C. Peterson (National Climatic Data Center, Asheville, NC.), D. R. Easterling (National Climatic Data Center, Asheville, NC.), R. S. Vose, and J. K. Eischeid 1993 7 p Presented at the Symposium on Precipitation and Evaporation, Bratislava, Czechoslovakia, 20-24 Sep. 1993
(Contracts DE-AC05-84OR-21400; DE-AI05-90OR-21956; DE-AI05-90ER-60952)
(DE93-019199; CONF-9309223-1) Avail: CASI HC A02/MF A01

Several years ago, in response to growing concern about global climate change, the US National Climatic Data Center and the Carbon Dioxide Information Analysis Center undertook an effort to create a baseline global land surface climate data set called the Global Historical Climatology Network (GHCN, Vose et al., 1992). GHCN was created by merging several large existing climate data sets into one data base. Fifteen separate data sets went into the creation of the GHCN version 1.0. GHCN version 1.0 was released in 1992. It has 7,533 precipitation stations, but the number of stations varies with time. A slight majority (55%) have records in excess of 50 years, and a significant proportion (13%) have records in excess of 100 years. The longest period of record for any given station is 291 years (1697-1987 for Kew, United Kingdom). DOE

N94-31600 State Univ. of New York, Albany.
TREATMENT OF CLOUD RADIATIVE EFFECTS IN GENERAL CIRCULATION MODELS
W. C. Wang 1993 23 p Limited Reproducibility: More than 20% of this document may be affected by poor print
(Contract DE-FG02-90ER-61073)
(DE94-001864; DOE/ER-61073/3) Avail: Issuing Activity (Department of Energy (DOE))

This is a renewal proposal for an on-going project of the Department of Energy (DOE)/Atmospheric Radiation Measurement (ARM) Program. The objective of the ARM Program is to improve the treatment of radiation-cloud in GCMs so that reliable predictions of the timing and magnitude of greenhouse gas-induced global warming and regional responses can be made. The ARM Program supports two research areas: (1) The modeling and analysis of data related to the parameterization of clouds and radiation in general circulation models (GCMs); and (2) the development of advanced instrumentation for both mapping the three-dimensional structure of the atmosphere and high accuracy/precision radiometric observations. The present project conducts research in area (1) and focuses on GCM treatment of cloud life cycle, optical properties, and vertical overlapping. The project has two tasks: (1) Development and Refinement of GCM Radiation-Cloud Treatment Using ARM Data; and (2) Validation of GCM Radiation-Cloud Treatment. DOE

N94-31601# State Univ. of New York, Albany. Atmospheric Sciences Research Center.
TIME-DEPENDENT BEHAVIOR OF MOUNT PINATUBO AEROSOL
J. Michalsky and N. Larson 1993 5 p Presented at the Optical Society of America Meeting on Optical Remote Sensing of the Atmosphere, Salt Lake City, UT, 8-12 Mar. 1993
(Contracts DE-FG02-90ER-61072; DE-AC06-76RL-01830)
(DE94-001877; DOE/ER-61072/6; CONF-930346-4) Avail: CASI HC A01/MF A01

The 15-16 June 1991 eruption of Mount Pinatubo delivered approximately 20 million metric tons of SO2 to the stratosphere. The SO2 plume from Mount Pinatubo straddled the equator resulting in a more symmetrical global distribution of the H2SO4-H2O aerosol that results from the photochemical conversion of the SO2. This paper follows the aerosol optical depth change over three-northern mid-latitude sites for the first sixteen months following the eruption. The technique to derive volcanic aerosol optical depth from ground-based measurements (which are, by their nature, total column aerosol optical depth measurements) follows the technique developed in an earlier paper to examine El Chichon aerosol. The three sites' time-dependent behavior is discussed and compared. Comparison of El Chichon and Mount Pinatubo aerosol optical depth change with time is also discussed for the one site that operated before, through, and after both eruptions. DOE

N94-31602# State Univ. of New York, Albany. Atmospheric Sciences Research Center.
CONCENTRATION SYSTEM PERFORMANCE DEGRADATION IN THE AFTERMATH OF MOUNT PINATUBO
J. J. Michalsky, R. Perez, R. Seals, and P. Ineichen 1993 7 p Presented at the SOLAR 1993: American Society of Mechanical Engineers (ASME)/American Solar Energy Society (ASES) Joint Solar Energy Conference, Washington, DC, 25-28 Apr. 1993
(Contracts DE-FG02-90ER-61072; DE-AC04-76DP-00789; NSF INT-90-02363)
(DE94-001879; DOE/ER-61072/8; CONF-930435-10) Avail: CASI HC A02/MF A01

Major volcanic eruptions occur every few years, but most have little effect on solar radiation or climate. However, in the last ten years two volcanoes have decreased solar radiation and influenced weather at a level that might be expected at the frequency of about once a century. The Mexican volcano El Chichon and the Philippine volcano Mount Pinatubo put 6 and 20 million metric tons of SO2 in the stratosphere, respectively. SO2 is converted into H2SO4, which mixes with water to produce aerosol. Since there is no weather in the stratosphere and the aerosol is small, these aerosol particles remain suspended until coagulation and sedimentation bring them to the troposphere where they are removed by normal wet and dry deposition processes. The extinction in the direct solar irradiance from El Chichon was found to peak during the winter of 1983 at about 11% for northern, mid latitudes. Mount Pinatubo's peak extinction during 1992 was about 15%. Data from four northern, mid-latitude sites are examined to compare the direct consequences of the volcano's eruption on the performance of concentrating solar energy systems and the indirect effects that may be associated with Mount Pinatubo's perturbation of the weather. DOE

N94-31611 Technische Univ., Berlin (Germany). Inst. fuer Luft- und Raumfahrt.
THE CONTRIBUTION OF AERONAUTICS AND ASTRONAUTICS TO THE QUALITY OF LIFE ON EARTH [UEBER DEN BEITRAG DER LUFT- UND RAUMFAHRT ZUR LEBENSQUALITAET AUF DER ERDE]
Heinz-Hermann Koelle and Michael Mielke 1 Aug. 1993 70 p In GERMAN Limited Reproducibility: More than 20% of this document may be affected by microfiche quality
(ILR-Mitt-283(1993); ETN-94-95745) Avail: CASI HC A04

A century of aviation and four decades of space flight and their respective developments in the 20th century are considered. The contributions of aeronautics and astronautics with respect to improving the quality of life on Earth are projected for the 21st century by analyzing the potential of the respective technologies to the individual elements comprising a formal goal system defining the 'quality of life'. The individual fields of specific activities as well as individual projects, are evaluated with respect to their potential contributions during the next hundred years. The results obtained are compared with the potential contributions of maritime and surface transportation systems which are considered to form the transportation sector of society. Eight other sectors of society are evaluated in the same manner to allow a comparison of their contributions with the transportation

sector in general, and the contributions of the fields of aeronautics and astronautics in particular. ESA

N94-31625# Argonne National Lab., IL.
EMISSIONS OF GREENHOUSE GASES FROM THE USE OF TRANSPORTATION FUELS AND ELECTRICITY
M. A. DeLuchi Nov. 1993 523 p
(Contract W-31-109-eng-38)
(DE94-006166; ANL/ESD/TM-22-Vol-2) Avail: CASI HC A22/MF A04

This volume contains the appendices to the report on Emission of Greenhouse Gases from the Use of Transportation Fuels and Electricity. Emissions of methane, nitrous oxide, carbon monoxide, and other greenhouse gases are discussed. Sources of emission including vehicles, natural gas operations, oil production, coal mines, and power plants are covered. The various energy industries are examined in terms of greenhouse gas production and emissions. Those industries include electricity generation, transport of goods via trains, trucks, ships and pipelines, coal, natural gas and natural gas liquids, petroleum, nuclear energy, and biofuels. DOE

N94-31657# Technical Research Centre of Finland, Espoo. Heating and Ventilation Lab.
CONTROL AND MONITORING OF HEAVY METAL EMISSIONS [RASKASMETALLIPAEAESTOEJEN VALVONTA JA TARKKAILU]
Leena Aunela and Kari Larjava Sep. 1993 50 p In FINNISH Sponsored by the Ministry of Environment
(ISSN 1235-0605)
(VTT-TIED-1508; ISBN-9-51-384442-0; ETN-94-96040) Copyright Avail: CASI HC A03/MF A01

The control and monitoring of heavy metal emissions has not become an established practice in Finland. Control and monitoring regulations are issued to plants on a discretionary case by case basis. In Germany the air protection law as well as its subordinated decrees and technical instructions define the principles governing the control and monitoring of heavy metals released into the atmosphere within individual industries. The German practice and its applicability as a model for Finland are examined. The methods used to measure heavy metal concentrations are currently selected by the measurers themselves and the suitability of these methods is not subject to official control. Determining heavy metal concentrations in the flue gases of thermic processes is a demanding task since many different contributing factors are associated with its implementation. It is typical for heavy metals that they occur simultaneously in the vaporous and particulate phases. A sample of both phases must be taken simultaneously in order to determine the total concentration. The situation in Finland with regard to the collection of particulate heavy metals is quite good, because of the established particle measurement practice. Integrating the particle collection line into the vapor phase collection line makes it more difficult to satisfy the requirements of particle sampling (isokinetic sampling, the use of several measuring points). The processing and analysis of particulate samples must be further developed in order to obtain accurate and comparable results. ESA

N94-32144 Allied-Signal Aerospace Co., Kansas City, MO.
VALIDATION OF THE ENVIRONMENTALLY CONSCIOUS MANUFACTURING INTEGRATED DEMONSTRATION HARDWARE
R. D. Carter Nov. 1993 10 p Limited Reproducibility: More than 20% of this document may be affected by microfiche quality
(Contract DE-AC04-76DP-00613)
(DE94-003824; KCP-613-5307) Avail: CASI HC A02

This paper describes electrical and environmental testing that were performed on the Environmentally Conscious Manufacturing Integrated Demonstration (ECM ID) units. An analysis of the testing data comparing the ECM units with units processed using traditional processes showed that there was no statistical difference in functional performance or reliability. DOE

N94-32195# Industrial Coll. of the Armed Forces, Washington, DC.
STRATEGIES FOR SURVIVAL IN THE NEW ENVIRONMENTAL ERA Report, Aug. 1992 - Apr. 1993
Louisa H. McAllister Apr. 1993 37 p
(AD-A276827; NDU/ICAF-93-RS1) Avail: CASI HC A03/MF A01

Preservation of the environment has become an issue of primary importance worldwide; hence, American industry can expect a future in which public and private sector insistence on environmentally safe products--already high--will rise steadily and increasingly determine economic viability. This report focuses on the causes and effects of air pollution and the requirements of the Clean Air Act Amendments of 1990. To survive in today's environmentally sensitive atmosphere, companies must recognize and accept that the environment has become deeply entrenched as one of the central concerns of the American consumer. Moreover, to be successful, companies must be willing to make substantial organizational and operational changes. Several strategies for survival are suggested. Although the task will not be easy, the companies that succeed will find themselves among the most respected and profitable in the world. DTIC

N94-32354# Lawrence Livermore National Lab., CA.
CARBON CYCLE MODELING CALCULATIONS FOR THE IPCC
D. J. Wuebbles and A. K. Jain 12 Aug. 1993 19 p Presented at the International Panel on Climate Change Meeting, Carqueiranne, France, 18 Sep. 1993
(Contract W-7405-eng-48)
(DE94-004332; UCRL-JC-115337; CONF-9309300-1) Avail: CASI HC A03/MF A01

We carried out essentially all the carbon cycle modeling calculations that were required by the IPCC Working Group 1. Specifically, IPCC required two types of calculations, namely, 'inverse calculations' (input was CO2 concentrations and the output was CO2 emissions), and the 'forward calculations' (input was CO2 emissions and output was CO2 concentrations). In particular, we have derived carbon dioxide concentrations and/or emissions for several scenarios using our coupled climate-carbon cycle modelling system. DOE

N94-32590# Oulu Univ. (Finland). Dept. of Economics.
CARBON DIOXIDE ABATEMENT AS A DIFFERENTIAL GAME
O. Tahvonen 1993 31 p
(DE94-722023; OY/TTO-DP-4) Avail: CASI HC A03/MF A01

The report combines predictions on greenhouse warming, CO2 abatement costs and adaptation costs in a differential game framework. The specified model makes it possible to solve the payoffs of the subgame perfect solution of a two state variable nonautonomous problem with N unequal countries. Abatement cost parameters are calibrated with a global energy sector model and climate parameters are based on empirical time series. Simulation suggests that the backstop technology assumption in the abatement cost model may imply drastic cuts in optimal emission levels. Compared to the Nash noncooperative equilibrium a pareto optimal agreement is found to be beneficial for developing countries but more costly for the industrial world. Given the present damage estimates, the losses due to an emission stabilizing agreement may be 400 times higher than maximum potential gains from cooperation. DOE

N94-32600# Argonne National Lab., IL. Center for Transportation Research.
GREENHOUSE GAS EMISSION IMPACTS OF ELECTRIC VEHICLES UNDER VARYING DRIVING CYCLES IN VARIOUS COUNTRIES AND US CITIES
Michael Q. Wang and William W. Marr 10 Feb. 1994 23 p Presented at the 5th Global Warming Science and Policy International Conference and Expo, San Francisco, CA, 4-7 Apr. 1994
(Contract W-31-109-eng-38)
(DE94-007647; ANL/ES/CP-82079; CONF-940422-1) Avail: CASI HC A03/MF A01

Electric vehicles (EV's) can reduce greenhouse gas emissions, relative to emissions from gasoline-fueled vehicles. However, those studies have not considered all aspects that determine greenhouse gas emissions from both gasoline vehicles (GV's) and EV's. Aspects often overlooked include variations in vehicle trip characteristics, inclusion of all greenhouse gases, and vehicle total fuel cycle. In this paper, we estimate greenhouse gas emission reductions for EV's, including these important aspects. We select four US cities (Boston, Chicago, Los Angeles, and Washington, D.C.) and six countries (Australia, France, Japan, Norway, the United Kingdom, and the United States) and analyze greenhouse emission impacts of EV's in each city or country. We also select six driving cycles developed around the world (i.e., the US federal urban driving cycle, the Economic Community of Europe cycle 15, the Japanese 10-mode cycle, the Los Angeles 92 cycle, the New York City cycle, and the Sydney cycle). Note that we have

not analyzed EV's in high-speed driving (e.g., highway driving), where the results would be less favorable to EV's; here, EV's are regarded as urban vehicles only. We choose one specific driving cycle for a given city or country and estimate the energy consumption of four-passenger compact electric and gasoline cars in the given city or country. Finally, we estimate total fuel cycle greenhouse gas emissions of both GV's and EV's by accounting for emissions from primary energy recovery, transportation, and processing; energy product transportation; and powerplant and vehicle operations. DOE

N94-32690# Oak Ridge National Lab., TN.
HOMOGENEOUS GLOBAL MEAN TEMPERATURE TIME SERIES
T. C. Peterson (National Climatic Data Center, Asheville, NC.), D. R. Easterling (National Climatic Data Center, Asheville, NC.), R. S. Vose, and J. K. Eischeid 1993 3 p Presented at the 74th American Meteorological Society Annual Meeting, Nashville, TN, 23-28 Jan. 1994
(Contract DE-AC05-84OR-21400)
(DE94-002194; CONF-940115-10) Avail: CASI HC A01/MF A01

A multi-agency effort has been underway to create a homogeneous global baseline data set suitable for studying climate change. The joint release of the Global Historical Climatology Network (GHCN) version 1 in 1992 by the National Climatic Data Center/NOAA and the Carbon Dioxide Information Analysis Center/DOE gave the climate research community the largest monthly land surface global climate data set available to date with over 6,000 temperature stations, 39% of which have more than 50 years of data, and 10% have more than 100 years of data. Fifteen different global or regional data sets were merged to create GHCN version 1. Ten of these source data sets have temperature data, but only two have been tested and adjusted for inhomogeneities in the station time series. The majority of the station temperature time series in GHCN have not been systematically examined for discontinuities. DOE

N94-32691# Brookhaven National Lab., Upton, NY.
FINE RESOLUTION ATMOSPHERIC SULFATE MODEL DRIVEN BY OPERATIONAL METEOROLOGICAL DATA: COMPARISON WITH OBSERVATIONS
C. M. Benkovitz, S. E. Schwartz, C. M. Berkowitz, and R. C. Easter Sep. 1993 10 p Presented at the 74th American Meteorological Society Annual Meeting, Nashville, TN, 23-28 Jan. 1994
(Contracts DE-AC02-76CH-00016; DE-AC06-76RL-01830)
(DE94-002994; BNL-49536; CONF-940115-11) Avail: CASI HC A02/MF A01

The hypothesis that anthropogenic sulfur aerosol influences clear-sky and cloud albedo and can thus influence climate has been advanced by several investigators; current global-average climate forcing is estimated to be of comparable magnitude, but opposite sign, to longwave forcing by anthropogenic greenhouse gases. The high space and time variability of sulfate concentrations and column aerosol burdens were established by observational data; however, geographic and time coverage provided by data from surface monitoring networks is very limited. Consistent regional and global estimates of sulfate aerosol loading, and the contributions to this loading from different sources can be obtained only by modeling studies. Here we describe a sub-hemispheric to global-scale Eulerian transport and transformation model for atmospheric sulfate and its precursors, driven by operational meteorological data, and we reportthe results of calculations for Oct. 1986 for the North Atlantic and adjacent continental regions. The model, which is based on the Global Chemistry Model, uses meteorological data from the 6-hour forecast model of the European Center for Medium-Range Weather Forecast to calculate transport and transformation of sulfur emissions. Time- and location-dependent dry deposition velocities were estimated using the methodology of Wesely and colleagues. Chemical reactions include gaseous oxidation of SO2 and DMS by OH, and aqueous oxidation of SO2 by H2O2 and O3. Anthropogenic emissions were from the NAPAP and EMEP 1985 inventories and biogenic emissions based on Bates et al. Calculated sulfate concentrations and column burdens exhibit high variability on spatial scale of hundreds of km and temporal scale of days. Calculated daily average sulfate concentrations closely reproduce observed concentrations at locations widespread over the model domain. DOE

N94-32692# Brookhaven National Lab., Upton, NY.
FORMATION OF GAS-PHASE PEROXIDES IN A RURAL ATMOSPHERE: AN INTERPRETATION OF THE RECENT SOS/SERON FIELD RESULTS
J. H. Lee, I. N. Tang, and J. B. Weinstein-Lloyd Sep. 1993 7 p Presented at the 74th American Meteorological Society Annual Meeting, Nashville, TN, 23-28 Jan. 1994
(Contracts DE-AC02-76CH-00016; DE-FG02-91ER-61206)
(DE94-002995; BNL-49600; CONF-940115-12) Avail: CASI HC A02/MF A01

Hydrogen perioxide (H2O2) and certain organic peroxides such as hydroxymethyl-hydroperoxide (HMHP), are gas-phase oxidants present in the atmosphere at ppbv concentration levels. These oxidants play an important role in atmospheric chemistry. In addition, precipitation containing H2O2 is toxic to trees, and it has also been suggested that organic peroxides formed presumably by ozone reactions with biogenic alkenes are responsible for leaf disorders. Recently, we have developed a nonenzymatic method or aqueous-phase H2O2 measurement, using Fenton reagent and fluorescent hydroxy-benzoic acid. The new method, in conjunction with the well-known method of p-hydroxyphenylacetic acid and horseradish peroxidase for total peroxides, and together with an improved gas scrubber to mitigate sampling line problems, has been successfully deployed in recent SOS/SERON field measurements in rural Georgia. For the first time, continuously measured and speciated gas-phase peroxide data have become available, making it possible to examine some aspects of the ozone chemistry leading to the formation of these oxidants. It is observed that daily H2O2 maximum frequently occurs at a different time than does HMHP and that H2O2 concentration, but not HMHP, tends to correlate with solar fluxes measured at the same location. These findings seem to indicate that the formation mechanisms for H2O2 and organic peroxides are basically different. It is likely that H2O2 is formed from radical-radical recombination, while HMHP is formed by ozone-alkene reactions. Since the gas-phase ozone-alkene reactions are usually too slow to account for the diurnal concentration variations observed for HMHP, heterogeneous processes involving ozone and alkenes are also a possibility. DOE

N94-32693# California Univ., Davis.
PROCEEDINGS OF THE NINTH ANNUAL PACIFIC CLIMATE (PACLIM) WORKSHOP
K. T. Redmond, ed. and V. L. Tharp, ed. Mar. 1993 21 p Workshop held in Asilomar, CA, 21-24 Apr. 1992
(Contract DE-FC03-90ER-61010)
(DE94-003024; CONF-9204273-Summ) Avail: CASI HC A03/MF A01

We describe the climatology of the western United States as seen from two 1-month perspectives, Jan. and Jul. 1988, of the National Meteorological Center large-scale global analysis, the Colorado State University Regional Atmospheric Modeling System (RAMS), and various station observation sets. An advantage of the NMC analysis and the RAMS is that they provide a continuous field interpolation of the meteorological variables. It is more difficult to describe spatial meteorological fields from the available sparse station networks. We assess accuracy of the NMC analysis and RAMS by finding differences between the analysts, the model, and station values at the stations. From these comparisons, we find that RAMS has much more well-developed mesoscale circulation, especially in the surface wind field. However, RAMS climatological and transient fields do not appear to be substantially closer than the large-scale analysis to the station observations. The RAMS model does provide many other meteorological variables, such as precipitation, which are not readily available from the archives of the global analysis. Thus, RAMS could, at the least, be a tool to augment the NMC large-scale analyses. DOE

N94-32703# Illinois Dept. of Energy and Natural Resources, Springfield.
REMOVAL OF CO2 FROM FLUE GASES BY ALGAE
C. Akin (Institute of Gas Technology, Chicago, IL.), A. Maka (Institute of Gas Technology, Chicago, IL.), S. Patel (Institute of Gas Technology, Chicago, IL.), J. Conrad (Institute of Gas Technology, Chicago, IL.), and J. Benemann 1993 33 p
(Contract DE-FC22-92PC-92521)
(DE94-008039; DOE/PC-92521/T97) Avail: CASI HC A03/MF A01

The objective of this research program is to determine the feasibility of the alga Botryococcus braunii as a biocatalyst for the photosynthetic conversion of flue gas CO2 to hydrocarbons. Free and immobilized cells

of Botryococcus braunii were grown in aqueous medium supplemented with nitrogen, phosphorus, and mineral nutrients. Air and CO2 enriched air (10% to 15% (v/v) CO2) in the gas phase and 0.2% to 2% NaHCO3 in the liquid medium served as the carbon source. Growth and hydrocarbon formation characteristics of free and immobilized cultures of Botryococcus braunii were determined in bench-scale photobioreactors. Technical and economic feasibility of the conversion of flue gas CO2 to hydrocarbons by Botryococcus braunii culture systems was evaluated. In free cell systems, the hexane extractable oil productivity was about 15 to 37 grams of oil per 100 grams of cell dry weight. In immobilized cell systems, the oil production ranged between 5% and 47% at different immobilization systems and immobilized surface locations, with an average of 19% of cell biomass dry weight. The feasibility and economic evaluation estimated the cost of oil produced from flue gas CO2 by algae to range between $45 and $75 per barrel assuming that a hydrocarbon yield of about 50% of the biomass weight is achievable and a credit of $60 per ton of carbon removed is available. A future research program leading to development of a multistage process, consisting of closed systems for heavy inoculum buildup followed by lower cost open systems for oil production is recommended. DOE

N94-32711# Massachusetts Univ., Boston.
DIAGNOSTIC STUDIES OF CLIMATE VARIABILITY
R. S. Bradley and H. F. Diaz 1993 7 p
(Contract DE-FG02-89ER-69017)
(DE94-003629; DOE/ER-69017/5) Avail: CASI HC A02/MF A01

Research in 1992-93, the second year of the project, involved, inter alia, the following topics: continuation of studies of proxy climatic records to try to extend the record of large-scale climatic conditions back into previous centuries and to determine if there are reliable regional analogs for larger scale climatic fluctuations; examination of indices of long-term climatic variability to determine if climate has become more, or less, variable over time. This involves studies of both instrumental and proxy data sets for sites throughout the world; Continuation of studies of mid-winter polar boundary layer climate as a possible indicator of greenhouse gas-induced climate changes; documentation of the linkages between observed temperature and precipitation changes on regional space scales and changes in large-scale atmospheric circulation patterns; regridding of global temperature anomalies using an equidistant grid, optimal interpolation scheme, and stratification of data by extent of urbanization at each station, then recomputation of regional and hemispheric temperature trends. Significant progress was made in all of these areas. In the report, we summarize results of the work accomplished. DOE

N94-32712# Harvard Univ., Cambridge, MA. Dept. of Applied Science.
PHYSICAL BASIS FOR CLIMATE CHANGE MODELS
R. Goody and M. Gerstell 18 Oct. 1993 3 p
(Contract DE-FC03-90ER-61010)
(DE94-003827; DOE/ER-61010/T22) Avail: CASI HC A01/MF A01

The objectives for this research were two-fold: to identify means of using measurements of the outgoing radiation stream from earth to identify mechanisms of climate change; and to develop a flexible radiation code based upon the correlated-k method to enable rapid and accurate calculations of the outgoing radiation. The intended products are three papers and a radiation code. The three papers are to be on Entropy fluxes and the dissipation of the climate system, Radiation fingerprints of climate change, and A rapid correlated-k code. DOE

N94-32750# Pacific Northwest Lab., Richland, WA.
AN EVALUATION OF RAMS RADIATION SCHEMES BY FIELD MEASUREMENTS
S. Zhong and J. C. Doran Feb. 1994 5 p Presented at the RAMS Workshop, Ft. Collins, CO, 15-17 Feb. 1994
(Contract DE-AC06-76RL-01830)
(DE94-008053; PNL-SA-23581; CONF-940265-1) Avail: CASI HC A01/MF A01

At present, two radiation schemes are used in RAMS: the Mahrer and Pielke (M-P) scheme and the Chen and Cotton (C-C) scheme. The M-P scheme requires little computational expense, but does not include the radiative effects of liquid water or ice; the C-C scheme accounts for the radiative effects of liquid water and ice but is fairly expensive computationally. For simulations with clouds, the C-C scheme is obviously a better choice, but for clear sky conditions, RAMS users face a decision regarding which radiation scheme to use. It has been noted that the choice of radiation scheme may result in significantly different results for the same case. To examine the differences in the radiative fluxes and the boundary layer structure corresponding to the two radiation schemes in RAMS we have carried out a study where RAMS was used to simulate the same case with two different radiation schemes. The modeled radiative fluxes by the two schemes were then compared with the field measurements. A description of the observations and the case study, a comparison and discussion of the results, and a summary and conclusions follow. DOE

N94-32752# Argonne National Lab., IL.
IDENTIFICATION OF RESEARCH RELATING TO THE CRITICAL LOADS CONCEPT AND ITS POTENTIAL APPLICATION TO THE REGULATION OF ACIDIC DEPOSITION
N. Bhatti Dec. 1993 31 p
(Contract W-31-109-eng-38)
(DE94-008234; ANL/DIS/TM-4) Avail: CASI HC A03/MF A01

The overwhelming majority of strategies currently implemented to regulate acidic deposition have focused on source-based or emission-control techniques. In the past few years, however, the fact that such source-based strategies may not be sufficient to prevent adverse ecological effects and may therefore need to be supplemented with other control options, such as receptor-based strategies, has become apparent. Partly in response to this insufficiency of regulatory controls, the U.S. Congress has required the National Acid Precipitation Assessment Program to determine what deposition levels are needed to prevent such ecological damage, whether such safe deposition levels (i.e., critical loads) can realistically be identified, and what the costs and benefits of attaining such deposition levels are. This report reviews and culls the existing research on these alternative control strategies, emphasizing the critical loads concept, to determine the advantages and limitations and the cost-benefit relationships associated with receptor-based control options. The results of this study indicate that in spite of the significant limitations associated with the critical loads concept, this strategy dominates all discussions of nonsource-based control options and offers considerable advantages, including cost effectiveness, over the more traditional source-based control methods. Summaries of 10 of the most relevant studies dealing with alternative control strategies and the costs and benefits associated with them are also presented in this report. DOE

N94-32784# Oak Ridge National Lab., TN.
ENVIRONMENTAL ISSUES RELATED TO BIOMASS: AN OVERVIEW
M. Hughes (Department of Agriculture, Washington, DC.) and J. W. Ranney 1993 11 p Presented at the 1st Biomass Conference of the Americas: Energy, Environment, Agriculture, and Industry, Burlington, VT, 30 Aug. - 2 Sep. 1993
(Contract DE-AC05-84OR-21400)
(DE94-007226; CONF-9308106-4) Avail: CASI HC A03/MF A01

Now that public attention has grown increasingly focused on environmentalism and climate change, the commercial use of biomass could greatly accelerate. Renewable feedstocks like biomass can provide better environmentally balanced sources of energy and other nonfood products than fossil fuels. The future of biomass is uncertain, however, because public attention focuses on both its potential and its challenges. This paper is divided into five sections. Section 2 briefly addresses economic environmental issues. The extent to which externalities are accounted for in the market price of fuels plays a significant role in determining both the ultimate size of biofuel markets and the extent of the environmental benefits of feedstock cultivation and conversion processes. Sections 3 and 4 catalog the main hazards and benefits that are likely to arise in the large-scale commercialization of biomass fuel and note where the major uncertainties lay. Environmental issues arise with the cultivation of each feedstock and with each step in the process of its conversion to fuel. Feedstocks are discussed in Section 3 in terms of three main groups: wastes, energy crops, and traditional agricultural crops. In Section 4, conversion processes are also divided into three groups, on the basis of the end energy carrier: gas, liquid, and solid and electricity. Section 5 provides a conclusion and summary. DOE

N94-32789# Lawrence Livermore National Lab., CA.
CLIMATE EFFECTS OF ANTHROPOGENIC SULFATE: SIMULATIONS FROM A COUPLED CHEMISTRY/CLIMATE MODEL

C. C. Chuang, J. E. Penner, K. E. Taylor, and J. J. Walton Sep. 1993 7 p Presented at the 74th American Meteorological Society Annual Meeting, Nashville, TN, 23-28 Jan. 1994
(Contract W-7405-eng-48)
(DE94-004352; UCRL-JC-114078; CONF-940115-15) Avail: CASI HC A02/MF A01

In this paper, we use a more comprehensive approach by coupling a climate model with a 3-D global chemistry model to investigate the forcing by anthropogenic aerosol sulfate. The chemistry model treats the global-scale transport, transformation, and removal of SO2, DMS, and H2SO4 species in the atmosphere. The mass concentration of anthropogenic sulfate from fossil fuel combustion and biomass burning is calculated in the chemistry model and provided to the climate model where it affects the shortwave radiation. We also investigate the effect, with cloud nucleation parameterized in terms of local aerosol number, sulfate mass concentration, and updraft velocity. Our simulations indicate that anthropogenic sulfate may result in important increases in reflected solar radiation, which would mask locally the radiative forcing from increased greenhouse gases. Uncertainties in these results will be discussed. DOE

N94-32790# Argonne National Lab., IL.
NATIONAL US PUBLIC POLICY ON GLOBAL WARMING DERIVED FROM OPTIMIZATION OF ENERGY USE AND ENVIRONMENTAL IMPACT STUDIES
R. Reck 1993 7 p Presented at the International Symposium on Environmental Policy for ESSD Achievement, Seoul, Republic of Korea, 22-23 Oct. 1993
(Contract W-31-109-eng-38)
(DE94-004606; ANL/ER/CP-81397; CONF-9310249-1) Avail: CASI HC A02/MF A01

This paper will discuss possible United States policy responses to global warming. The components of a voluntary program for emissions control will be presented as well as regulatory options including a carbon tax and tradeable permits. The advantages and disadvantages of both options will be discussed as well as the need for a consistent overall policy response to climate change. DOE

N94-32812# Pacific Northwest Lab., Richland, WA.
FOOD SECURITY IN THE CONTEXT OF GLOBAL ENVIRONMENTAL CHANGE
N. J. Rosenberg Nov. 1993 18 p Presented at the Agriculture in the Context of Global Change Conference, Cincinnati, OH, 7-11 Nov. 1993
(Contract DE-AC06-76RL-01830)
(DE94-007481; PNL-SA-23709; CONF-9311191-1) Avail: CASI HC A03/MF A01

United Nations predictions and other sources indicate that world population could grow to 8.5 billion by 2025 (Keyfitz 1989) and 11 billion by the end of the coming century (UNFPA 1990). As new information becomes available on the effectiveness of population control programs, the rise of virulent diseases and other factors, these numbers change -- sometimes smaller, sometimes larger still. Whatever the numbers actually turn out to be, global agricultural production will have to increase several-fold from present levels to feed and clothe the growing population and to improve worldwide standards of nutrition. The capacity of global agriculture to ensure food security through increased and sustained agricultural production depends on our ability to manage, conserve and in some cases increase the resource base available to the industry of agriculture. The resources that underpin agriculture are land, water and genetic diversity. The first two of these are the subject of this paper. Genetic diversity is the subject of another paper in this volume. DOE

N94-32814 Los Alamos National Lab., NM.
MEXICO CITY OZONE CONCENTRATIONS AS A FUNCTION OF READILY-AVAILABLE METEOROLOGICAL PARAMETERS
M. J. Brown 1994 20 p Presented at the Institute of Mexican Petroleum (IMP) Conference, Mexico City, Mexico, Feb. 1994 Limited Reproducibility: More than 20% of this document may be affected by microfiche quality
(Contract W-7405-eng-36)
(DE94-007576; LA-UR-94-572; CONF-940266-1) Avail: CASI HC A03

Daily maximum ozone concentrations measured at four sites within the Mexico City basin during the winter months are plotted as functions of different meteorological parameters that are routinely measured at surface stations. We found that ozone concentrations are most strongly correlated to the increase in daytime temperature and the maximum daytime wind speed. We also discovered that high ozone values at the sites in the southern end of the basin occur when winds come out of the northeast. In contrast, wind direction was found to be uncorrelated with high ozone values at the northern sites. From straightforward combinations of the meteorological variables, we derived some simple rules for estimating lower and upper bounds on the ozone concentration. Scatter in the data was too long to give significance to best-fit equations and statistics. Additionally, a small rawinsonde data set was used to investigate ozone's dependence on boundary-layer height and near-surface temperature gradient. Results were inconclusive, however, due to the small size of the data set. DOE

N94-32817 Lawrence Livermore National Lab., CA.
QUANTIFIED ESTIMATES OF TOTAL GWPs FOR GREENHOUSE GASES TAKING INTO ACCOUNT TROPOSPHERIC CHEMISTRY
D. J. Wuebbles, J. S. Tamaresis, and K. O. Patten Nov. 1993 130 p Limited Reproducibility: More than 20% of this document may be affected by microfiche quality
(Contract W-7405-eng-48)
(DE94-007846; UCRL-ID-115850) Avail: CASI HC A07

The purpose of this report is to give an interim account of the progress being made at Lawrence Livermore National Laboratory (LLNL) in developing an improved capability for assessing the direct and indirect effects on Global Warming Potentials. Much of our current efforts are being devoted to improving the capability for modeling of global tropospheric processes in our state-of-the-art zonally-averaged chemical radiative-transport model of the troposphere and stratosphere. These efforts are in preparation for an improved evaluation and better quantification of the indirect GWP's resulting from effects on tropospheric ozone from ethane and other gases with significant human-related emissions. There are three major findings that should result from this project that should have significant impacts on EPA and its programs. First, the current and ongoing studies of the direct and indirect GWP's should have a significant influence on the continuing national and international assessments of climate change. Second, the improved capability for modeling of chemical and physical processes should lead to enhanced understanding of the controlling factors influencing ozone, hydroxyl and other key tropospheric constituents. Third, the enhanced modeling capability should be important to future studies of human-related influences on tropospheric and stratospheric chemical processes. DOE

N94-32882 Lawrence Livermore National Lab., CA.
STATISTICAL INTERCOMPARISON OF GLOBAL CLIMATE MODELS: A COMMON PRINCIPAL COMPONENT APPROACH
S. K. Sengupta and J. S. Boyle Nov. 1993 43 p Limited Reproducibility: More than 20% of this document may be affected by microfiche quality
(Contract W-7405-eng-48)
(DE94-008671; UCRL-ID-116155; PCMDI-13) Avail: CASI HC A03

Variables describing atmospheric circulation and other climate parameters derived from various GCM's and obtained from observations can be represented on a spatio-temporal grid (lattice) structure. The primary objective of this paper is to explore existing as well as new statistical methods to analyze such data structures for the purpose of model diagnostics and intercomparison from a statistical perspective. Among the several statistical methods considered here, a new method based on common principal components appears most promising for the purpose of intercomparison of spatio-temporal data structures arising in the task of model/model and model/data intercomparison. A strategy for such an intercomparison is outlined in two steps: First, the commonality of spatial structures in two (or more) fields is captured in the common principal vectors, and second, the corresponding principal components obtained as time series are then compared on the basis of similarities in their temporal evolution. DOE

N94-32894# Argonne National Lab., IL.
DRY DEPOSITION OF PAN TO GRASSLAND VEGETATION
P. V. Doskey, M. L. Wesely, D. R. Cook, and W. Gao 1994 6 p Presented at the 74th American Meteorological Society Annual Meeting, Nashville, TN, 23-28 Jan. 1994
(Contract W-31-109-eng-38)
(DE94-005111; ANL/ER/CP-80342; CONF-940115-17) Avail: CASI HC A02/MF A01

Peroxyacetyl nitrate or PAN (CH3C(O)OONO2) is formed in the lower troposphere via photochemical reactions involving nitrogen oxides (NO(x)) and non-methane hydrocarbons (NMHC's). PAN has a lifetime in the free troposphere of about three months and is removed by photolysis or reaction with OH. Dry deposition will decrease its lifetime, although the few measurements that were made indicate that this process is slow. Measurements of the uptake of PAN by alfalfa in growth chambers indicated that the dry deposition velocity (downward flux divided by concentration at a specified height) was 0.75 cm/s. Garland and Penkett measured a dry deposition velocity of 0.25 cm/s for PAN to grass and soil in a return-flow wind tunnel. Shepson et al. analyzed trends of PAN and O3 concentrations in the stable nocturnal boundary layer over mixed, deciduous/coniferous forests at night, when leaf stomata were closed, and concluded that the deposition velocity for PAN was at least 0.5 cm/s. We measured the dry deposition velocity of PAN to a grassland site in the midwestern United States with a modified Bowen ratio technique. Experiments were conducted on selected days during Sep., Oct., and Nov. of 1990. An energy balance Bowen ratio station was used to observe the differences in air temperature and water vapor content between heights of 3.0 and 0.92 m and to evaluate the surface energy balance. Air samples collected at the same two heights in Teflon (reg sign) bags were analyzed for PAN by a gas chromatographic technique. We present an example of the variations of PAN concentrations and gradients observed during the day and compare measurements of the dry deposition velocity to expectations based on the physicochemical properties of PAN. DOE

N94-32920 Institute of Energy Economics of Japan.
CURRENT POLICIES OF THE MAJOR COUNTRIES COPING WITH THE GLOBAL WARMING PROBLEM AND-THE ENERGY DEMAND AND SUPPLY
10 Nov. 1993 193 p Limited Reproducibility: More than 20% of this document may be affected by microfiche quality
(DE94-757291; IEE-SR-248) Avail: CASI HC A09

Investigation and analysis were made of attitude maintained by the US, EC, Germany and France to cope with the global warming and energy problems after the conclusion of the Framework Convention on Climate Change. Intending to take large scale and long term measures, the US framed the Energy Policy Act, ratified the Convention and announced the Action Program. For the environmental protection, the EC maintains a positive attitude however with rather weak measures taken. All EC's program to decrease CO2 emissions aims at the compensation of decrease in East Germany for the increase in South Europe. However, if the carbon energy tax can not be introduced, it is difficult to achieve the aim. Germany has the most drastic aim established to decrease CO2 emissions by 25 to 30%. Even after achieving the aim, Germany will be equal to the present EC in CO2 emissions per person. Therefore, German people are judged to be not considerably sacrificial. Having positively introduced the nuclear power since the oil crisis, France is a developed country where CO2 emissions are very small per person, aiming at stabilization of the emissions. DOE

N94-32966# Lawrence Livermore National Lab., CA.
EFFECTS OF LONG-TERM ELEVATED ATMOSPHERIC CO2 CONCENTRATIONS ON PINUS PONDEROSA
K. A. Surano, ed. and J. R. Kercher, ed. Oct. 1993 140 p
(Contract W-7405-eng-48)
(DE94-008832; UCRL-ID-115638) Avail: CASI HC A07/MF A02

This report details the results from an experiment of the effects of long-term elevated atmospheric CO2 concentrations on ponderosa pine (Pinus ponderosa) saplings and seedlings. The study began in 1983 as a pilot study designed to explore the feasibility of using open-top chambers for continuous multi-year exposures on sapling-sized trees and to examine possible CO2 responses so that future research could be adequately designed. However, following the first year of exposure, preliminary results from the study indicated that measurements of CO2 responses should be intensified. Open-top chambers proved suitable for use in multiyear exposures of mature trees. With respect to the preliminary examination of CO2 responses, many interesting observations were made. The nature of the preliminary results suggests that future long-term field CO2 exposures on perennial species may be critical to the understanding and preparation for future environments. Other research reported here attempted to adapt an existing western coniferous forest growth and succession model for use in elevated CO2 scenarios using differential species responses, and assessed the usefulness of the model in that regard. Seven papers were processed separately for inclusion in the appropriate data bases. DOE

N94-33105 Aberdeen Proving Ground, MD.
FOCUSED FEASIBILITY STUDY FINAL FIELD SAMPLING PLAN
Oct. 1993 61 p Limited Reproducibility: More than 20% of this document may be affected by microfiche quality
(AD-A277445) Avail: CASI HC A04

At the direction of APG-DSHE, the project has been separated into three work phases to allow for data evaluation and risk determination before a full focused feasibility study is conducted. Phase 1 of the project consists of an aerial photography investigation, surface/marine geophysical surveys, a flowmeter logging program, sampling surface and subsurface soils, an ecological risk assessment of the Beach Point Test Site, and analysis of chemical groundwater data generated through the separate Canal Creek Groundwater Monitoring Program. Tasks described for Phase 2 of the FFS will be performed upon evaluation of data needs identified subsequent to completion of the Phase 1 tasks. Phase 2 investigations include installation of additional groundwater monitoring wells, sampling of the new and previously existing monitoring wells, a flowmeter logging program, downhole geophysical logging of new monitoring wells (and one previously existing well), and possible soil gas surveys. Phase 3 tasks may be performed after phase 1, and at any point thereafter, if it is determined that contamination found in the Beach Point Test Site warrants treatment. DTIC

N94-33110 Israel Inst. for Biological Research, Ness-Ziona.
TRANSPORT AND DIFFUSION IN TURBULENT FIELDS MODELING AND MEASUREMENTS TECHNIQUES
Hadassah Kaplan, Nathan Dinar, Avi Lacser, and Yehudah Alexander
1993 458 p The 35th Oholo Conference held in Eilat, Israel, 28 Oct. - Nov. 1, 1991 Limited Reproducibility: More than 20% of this document may be affected by microfiche quality
(AD-A278114) Avail: Issuing Activity (Defense Technical Information Center (DTIC))

This volume contains the invited and contributed lectures that were presented at the 35th Oholo Conference, held in Eilat, Israel, during 28 Oct. - 1 Nov. 1991. This meeting, in common with the 28th Oholo Conference (1984) in Zichron Yaakov, was organized by the Environmental Sciences Division of the Israel Institute for Biological Research. The present conference dealt with theoretical, experimental, and practical aspects of 'Transport and Diffusion in Turbulent Fields'. The scientists attending the meeting came from over a dozen different countries and met to exchange ideas and share results of research in the following broad range of topics: (1) Basic studies and novel methods in modeling atmospheric processes--theory and experiments involving eddy flow; turbulent mixing, transport, and diffusion in various media, ranging from microscale to macroscale; (2) Analysis of concentration fluctuations--theoretical developments; observations in different atmospheric conditions; (3) Experimental techniques and methods of data acquisition--use of various sensors; laboratory experiments and observations in the atmosphere and in the ocean; and (4) Interactions and feedback between theoretical models and experimental results. DTIC

N94-33170*# Denver Univ., CO. Dept. of Engineering.
COUNTING PARTICLES EMITTED BY STRATOSPHERIC AIRCRAFT AND MEASURING SIZE OF PARTICLES EMITTED BY STRATOSPHERIC AIRCRAFT Final Technical Report, 1 May 1990 - 31 Dec. 1992
James Charles Wilson 19 Apr. 1994 28 p
(Contract NCC2-666)
(NASA-CR-195908; NAS 1.26:195908) Avail: CASI HC A03/MF A01

The ER-2 condensation nuclei counter (CNC) has been modified to reduce the diffusive losses of particles within the instrument. These changes have been successful in improving the counting efficiency of small particles at low pressures. Two techniques for measuring the size distributions of particles with diameters less than 0.17 micrometers have been evaluated. Both of these methods, the differential mobility analyzer (DMA) and the diffusion battery, have fundamental problems that limit their usefulness for stratospheric applications. We cannot recommend either for this application. Newly developed, alternative methods for measuring small particles include inertial separation with a low-loss critical orifice and thin-plate impactor

device. This technique is now used to collect particles in the multisample aerosol collector housed in the ER-2 CNC-2, and shows some promise for particle size measurements when coupled with a CNC as a counting device. The modified focused-cavity aerosol spectrometer (FCAS) can determine the size distribution of particles with ambient diameters as small as about 0.07 micrometers. Data from this instrument indicates the presence of a nuclei mode when CNC-2 indicates high concentrations of particles, but cannot resolve important parameters of the distribution. Derived from text

N94-31003 Universite des Sciences et Techniques de Lille (France). Lab. d'Optique Atmospherique.
DESERT AEROSOLS: SOURCES, TRANSPORTS, AND IMPACTS DETERMINED BY REMOTE SENSING [LES AEROSOLS DESERTIQUES: SOURCES, TRANSPORTS, IMPACTS DETERMINES PAR TELEDETECTION]
I. Jankowiak and D. Tanre *In* CNES, Subtropical Climates and Their Evolution: From Space-Based Observation to Modelling Oct. 1993 p 495-523 In FRENCH (For primary document see N94-30981 09-47)
Copyright Avail: Issuing Activity (CEPADUES-Editions, 111, rue Nicolas-Vauquelin, 31100 Toulouse, France)

N94-31007 Paris-Sud Univ., Orsay (France). Lab. d'Ecologie Vegetale.
CARBON BALANCE IN A FOREST ECOSYSTEM [BILAN CARBONE D'UN ECOSYSTEME FORESTIER]
Bernard Saugier *In* CNES, Subtropical Climates and Their Evolution: From Space-Based Observation to Modelling Oct. 1993 p 587-618 In FRENCH (For primary document see N94-30981 09-47)
Copyright Avail: Issuing Activity (CEPADUES-Editions, 111, rue Nicolas-Vauquelin, 31100 Toulouse, France)

N94-31008 Toulouse Univ. (France). Lab. d'Aerologie.
SOURCES AND WELLS OF MINOR ATMOSPHERIC CONSTITUENTS OF CLIMATIC IMPORTANCE [SOURCES ET PUITS DE CONSTITUANTS MINEUR ATMOSPHERIQUES D'INTERET CLIMATIQUE]
Robert Delmas *In* CNES, Subtropical Climates and Their Evolution: From Space-Based Observation to Modelling Oct. 1993 p 619-638 In FRENCH (For primary document see N94-30981 09-47)
Copyright Avail: Issuing Activity (CEPADUES-Editions, 111, rue Nicolas-Vauquelin, 31100 Toulouse, France)

N94-31010 Centre National de la Recherche Scientifique, Verrieres-Le Buisson (France). Service d'Aeronomie.
THE OZONE AND THE PHYSICO-CHEMICAL PROCESSES IN TROPICAL REGIONS [OZONE ET PROCESSUS PHYSICO-CHIMIQUES DANS LES REGIONS TROPICALES]
Gerard Megie (Paris VI Univ., France.) and Gerard Ancellet (Paris VI Univ., France.) *In* CNES, Subtropical Climates and Their Evolution: From Space-Based Observation to Modelling Oct. 1993 p 669-685 In FRENCH (For primary document see N94-30981 09-47)
Copyright Avail: Issuing Activity (CEPADUES-Editions, 111, rue Nicolas-Vauquelin, 31100 Toulouse, France)

N94-31011 Centre National d'Etudes Spatiales, Toulouse (France). Lab. d'Etudes et de Recherches en Teledetection Spatiale.
MODELING OF THE CONTINENTAL BIOSPHERE [MODELISATION DE LA BIOSPHERE CONTINENTALE]
Philippe Martin *In its* Subtropical Climates and Their Evolution: From Space-Based Observation to Modelling Oct. 1993 p 687-70 In FRENCH (For primary document see N94-30981 09-47)
Copyright Avail: Issuing Activity (CEPADUES-Editions, 111, rue Nicolas-Vauquelin, 31100 Toulouse, France)

46 GEOPHYSICS

Includes aeronomy; upper and lower atmosphere studies; ionospheric and magnetospheric physics; and geomagnetism.
For space radiation see *93 Space Radiation.*

N94-31104 Massachusetts Inst. of Tech., Cambridge.
MAGNETOHYDRODYNAMICS OF THE EARTH'S CORE. 1: STEADY, ROTATING MAGNETOCONVECTION. 2: MAGNETIC ROSSBY WAVES Ph.D. Thesis
Michael I. Bergman 1992
Avail: Issuing Activity (MIT Libraries, Rm. 14-0551, Cambridge, MA 02139-4307)

We review the evidence for core-mantle thermal coupling, which includes spatial correlation between the static magnetic field features, lateral thermal anomalies in the lower mantle, core-mantle boundary topography, and possibly virtual geomagnetic pole (VGP) path during magnetic dipole reversals. Maps of the main magnetic field at the Earth's surface suggest that anomalous electrical currents may be present in the equatorial zone, with a large azimuthal wavenumber m = 1 contribution. We invert the surface magnetic field for the magnitude of ideal magnetic dipoles distributed in various ways throughout the outer core. We find a better, smoother fit with equatorial dipoles than with polar dipoles. The equatorial anomalies in the surface main field correlate with regions of high surface magnetic secular variation, further suggesting persistent motions in the core. Although the convective equations are highly non-linear due to the high Rayleigh number of the Earth's core, so that time-dependent motions are certainly present, we are interested here in the possibility of steady motions that result from either free convection or forced convection and that might cause static features in the magnetic field. We provide destabilization in our model by uniformly fluxing buoyancy across the bottom boundary with a concominant buoyancy sink at the top boundary. The Rayleigh number Ra is a measure of the destabilization. We first apply our method to a non-rotating, electrically insulating spherical fluid shell in order to demonstrate the method's viability. We then look for solutions in a rapidly rotating spherical fluid shell (high Taylor number Ta). We next return to the rotating spherical shell, impose a poloidal magnetic field, and look for the magnetic analog of the polar models. When the Lorentz force is comparable to the Coriolis force (Elsasser number El = O(1)), the modes fill the shell and most efficiently transport buoyancy. Finally, we study axisymmetric flows forced by a high buoyancy flux across the upper boundary near the equator and a low flux near the poles. A second topic that we study in this thesis involves a possible consequence of compositional convection in the Earth's core: the formation of a stably stratified layer at the top of the outer core. Dissert. Abstr.

N94-31222# Stockholm Univ. (Sweden). Dept. of Meteorology.
ODIN AERONOMY SCIENCE: A PHASE-A REPORT BY THE AERONOMY SCIENCE WORKING GROUP FOR THE ODIN SATELLITE
D. P. Murtagh, G. Witt, R. Mewe, H. vanderWoerd, N. Kaempfer, P. Taalas, J. Askne, and A. Winnberg 21 Sep. 1993 32 p
(ISSN 0280-4441)
(AP-31; ETN-94-95881) Avail: CASI HC A03/MF A01

The phase A study of a satellite with the joint goals of studying the Earth's atmosphere and the interstellar medium using sub-mm techniques is reported. The satellite was given the name Odin. The main instrument is a four channel sub-mm receiver with bands at 425, 480, 551, and 515 GHz. The bands are tunable to at best +/- 1 and are served by two channel spectrometers with selectable resolutions of 0.1 and 1 MHz. In addition, an optical spectrometer covering the wavelength region 200 to 800 nm with a channel at 1.27 micrometers is included to obtain complementary measurements by the Differential Optical Absorption Spectroscopy (DOAS) technique. ESA

N94-31303# Naval Command, Control and Ocean Surveillance Center, San Diego, CA. Research, Development, Technology and Evaluation.
ATMOSPHERIC EFFECTS ASSESSMENT PROGRAM: IONOSPHERIC SOUNDING Final Report, period ending Oct. 1993
R. A. Sprague Feb. 1994 18 p
(NR Proj. R03-GE-81)
(AD-A276447; NCCOSC/RDT/E-TD-2609) Avail: CASI HC A03/MF A01

This document reports efforts on two main goals: to study the short-term ionospheric variability and to study the effects of this variability on high frequency (HF) skywave field strength. To achieve the first goal, ionospheric soundings are being done at 5-minute intervals at San Diego, CA, and at Logan, UT. This time interval was chosen to adequately resolve variations produced by locally generated gravity waves. To study the effects of short-term ionospheric variability on high frequency communications, a circuit is being established to measure the variability of the received HF signal strength. The chosen circuit will have the transmitter located in Forsyth, MT, and the receiver in Imperial Beach, CA (approximately 20 miles south of NRaD). DTIC

N94-31326# Tel-Aviv Univ. (Israel). Dept. of Geophysics and Planetary Sciences.

ANALYSIS OF IONOSPHERIC PARAMETERS IN EUROPE AND CREATION OF THE PREDICTION ALGORITHM Final Report

E. E. Tsedilina and A. Eviatar Feb. 1993 121 p

(Contract DAJA45-92-C-0006)

(AD-A276342) Avail: CASI HC A06/MF A02

Investigation of the correlation and gradient characteristics of the basic parameters of the ionospheric profile (foF2 and H'F) and Maximum usable frequency (MUF(3000)F2) were estimated with the aim of the creation of ionospheric model for HF radio predictions and communications. Ionospheric data on European sounding stations (Digisondes) spaced at the distances of 1000 to 1100 km from each other were used for the period in one year from September 1990 to October 1991. Various diurnal and seasonal dependencies for all characteristics considered were obtained. DTIC

N94-31351# Army Engineer Waterways Experiment Station, Vicksburg, MS. Environmental Lab.

MICROWAVE DIELECTRIC BEHAVIOR OF SOILS. REPORT 1: SUMMARY OF RELATED RESEARCH AND APPLICATIONS

John O. Curtis Dec. 1993 119 p

(AD-A275980; WES/TR/EL-93-25-Rept-1) Avail: CASI HC A06/MF A02

As a precursor to developing a well-documented database of complex electrical properties of soils as a function of signal frequency, sample moisture, sample temperature, and soil type, a comprehensive study of existing data collection methodology and analytical modeling was undertaken. Of particular utility are chronological tables of experimental and analytical milestones as well as an extensive reference list. Several appendices are included that are helpful in understanding soil/electromagnetic wave interactions and new concepts in modeling soil structure. DTIC

N94-31353# Army Engineer Waterways Experiment Station, Vicksburg, MS. Environmental Lab.

MICROWAVE DIELECTRIC BEHAVIOR OF SOILS. REPORT 2: A UNIQUE COAXIAL MEASUREMENT APPARATUS

John O. Curtis Dec. 1993 49 p

(AD-A275982; WES/TR/EL-93-25-Rept-2) Avail: CASI HC A03/MF A01

A reflection/transmission laboratory apparatus and data collection methodology are described that can be used to measure the complex dielectric response of moist soils over the 100 MHz to 18 GHz frequency range. The experimental setup includes a square cross-sectional coaxial sample holder, a vector network analyzer system for signal generation and detection, and an external bath for sample temperature control. Data collected on liquids whose dielectric response is well known verify that the electrical property calculation algorithm functions properly. DTIC

N94-31369# Colorado School of Mines, Golden.

PROCEEDINGS OF THE 4TH TUNNEL DETECTION SYMPOSIUM ON SUBSURFACE EXPLORATION TECHNOLOGY

R. M. Miller and R. F. Dennis 29 Apr. 1993 693 p Symposium held in Golden, CO, 26-29 Apr. 1993

(Contract DAAK70-92-C-0015)

(AD-A276372) Avail: CASI HC A99/MF A06

These Proceedings document the 47 technical papers delivered during the Fourth Tunnel Detection Symposium on Subsurface Exploration Technology held 26-29 April 1993 in Golden, Colorado. The objective of the Symposium was the exchange of technical information on the most recent advances in subsurface exploration technology. Previous series of symposia on this subject (1981, 1984 and 1988) were focused on the application of detecting and locating deep tunnels (to 300 meters) in hard rock geological environments. The scope of this symposium was expanded to include a wider variety of subsurface applications, viz., shallow tunnels (to 30 meters), natural cavities, historical, archaeological and other underground structures, buried utilities, environmental clean-up, etc. Subjects discussed included field methods and experimentation, instrumentation, methods for analysis of field data and interpretation, field problems, application of theories of subsurface exploration, mathematical and scale modeling, and related subjects. DTIC

N94-31457# Army Engineer Waterways Experiment Station, Vicksburg, MS. Environmental Lab.

MICROWAVE DIELECTRIC BEHAVIOR OF SOILS. REPORT 3: MEASUREMENT AND MODELING

John O. Curtis Dec. 1993 91 p

(AD-A276060; WES/TR/EL-93-25-Rept-3) Avail: CASI HC A05/MF A01

Making use of a coaxial reflection/transmission experimental procedure described in Report 2 of this series, a large number of complex dielectric property measurements were made of soil samples that ranged in texture from a poorly graded sand to a pure nonswelling clay mineral. Two methods of modeling the results are discussed. One is an equivalent circuit representation that accounts for both low-frequency conductivity and higher frequency dielectric relaxation losses in the soil/water mixture. The other model consists of a fractal description of soil structure combined with the concept of long-range electrical connectivity at less than 100 percent saturation. DTIC

N94-31525# Geological Survey, Denver, CO.

ANALYSIS OF DEEP SEISMIC REFLECTION AND OTHER DATA FROM THE SOUTHERN WASHINGTON CASCADES

W. D. Stanley and S. Y. Johnson 1993 8 p Presented at the Fuels Technology Contractors' Review Meeting, Morgantown, WV, 16-18 Nov. 1993

(Contract DE-AT21-92MC-29267)

(DE94-005958; DOE/MC-29267/94/C0314; CONF-931156-16) Avail: CASI HC A02/MF A01

Limited possibilities exist for new hydrocarbon exploration regimes in the Pacific Northwest. Extensive geophysical studies have been used to outline a proposed sedimentary basin hidden beneath volcanic rocks of the Cascades region of southwestern Washington (Stanley et. al, 1992, AAPG Bull. 76, 1569-1585). Electrical geophysical imaging using the magnetotelluric (MT) method first detected thick, electrically conductive sequences believed to represent late Cretaceous to Oligocene marine sedimentary rocks. The conductive section occurs at depths from about 1 km to 10 km in the area west of a line between Mt. Rainier and Mt. Adams, extending westward to a line between Mt. St. Helens and just west of Morton, WA. The conductive rocks reaches thicknesses as great as 10 km. The anomalous rocks appear to be very near the surface in the axis of anticanes that bring Eocene marine shales to shallow depths. Careful consideration of physical properties and the correspondence of the morphology of the units to known fold sets suggests that the high conductivities are related to lithologic/stratigraphic units rather than to variations in physical properties. Our preference for the lithology of the anomalous section, based upon a study of regional geology and structure, is one dominated by marine shales of Eocene and older age. Other possible lithologies that have been evaluated for the conductive section include nonmarine sedimentary units of Tertiary age, highly altered volcanic flows, and pre-Tertiary metasedimentary rocks with large percentages of graphite. We refer to this anomalously conductive region as the southern Washington Cascades conductor (SWCC). DOE

N94-31527 Brookhaven National Lab., Upton, NY.

CLOUD STUDIES SEEN FROM A PHYSICAL CHEMIST'S PERSPECTIVE

S. E. Schwartz Nov. 1993 10 p Presented at the 6th European Symposium on Physico-Chemical Behaviour of Atmospheric Pollutants, Varese, Italy, 18-22 Oct. 1993 Limited Reproducibility: More than 20% of this document may be affected by microfiche quality

(Contract DE-AC02-76CH-00016)

(DE94-006059; BNL-49744; CONF-9310268-1) Avail: CASI HC A02

Substantial advances have been made in recent years in describing the rates of chemical reactions in clouds. Inputs to these calculations are concentrations of reagent species, solubilities of reactive gases, rate expressions for interphase mass transport, rate expressions for

aqueous-phase reaction of the dissolved species, the liquid-water content of the cloud and its drop-size spectrum, and the composition of the cloudwater (especially pH) as it affects solubility and reaction rates. Armed with this information one can calculate the rates of reactions of interest. The question still remains as to the accuracy of such calculations. To answer this one needs field measurements, of cloud properties and the concentrations of reagents -- to permit evaluation of reaction rates -- and of differences in composition that may be attributed to chemical reaction. However, determination of rates and extents of in-cloud reactions presents a major challenge because of uncertainties associated with measurements of concentration changes. Even attribution of a measured composition change to a specific reaction is difficult. Another challenge to the field measurement community is determining the size dependence of cloudwater composition (especially pH) and the resultant difference between reaction rates based on bulk composition and actual reaction rates integrated over the cloud droplet spectrum. This paper reviews these issues and offers suggestions for field measurements to confirm model based-understanding of these processes. DOE

N94-31773 Stanford Univ., CA.
LIGHTNING-INDUCED COUPLING OF THE RADIATION BELTS TO GEOMAGNETICALLY CONJUGATE IONOSPHERIC REGIONS Ph.D. Thesis
William Cargill Burgess 1993 168 p
Avail: Univ. Microfilms Order No. DA9317753

Very low frequency (VLF) radio observations in Antarctica and North America provide the first evidence that bursts of energetic electrons from the earth's radiation belts commonly precipitate into geomagnetically conjugate ionospheric regions in response to lightning. The electrons, with energies ranging from tens of keV to over one MeV, appear to be scattered out of their otherwise stable trap in the earth's magnetic field by magnetospheric interactions with a regularly observed class of transient, lightning-generated VLF radio waves known as ducted whistlers. The precipitating electrons ionize atmospheric molecules at altitudes between 40 and 90 km, creating transient enhancements of ionization levels in conjugate locations. These ionospheric disturbances can be detected by their characteristic perturbations, sometimes called 'Trimpi events,' of the amplitude and phase of VLF transmitter signals propagating subionospherically within 200 to 250 km of the disturbed areas. The first detailed, one-to-one comparison of such signal perturbations, monitored in conjugate regions, with the multipath structure, arrival azimuths, and predicted electron scattering of simultaneously observed ducted whistlers suggests that every ducted whistler precipitates bursts of radiation belt electrons. If so, the estimated rate at which ducted whistlers contribute to radiation belt losses is comparable to that predicted for plasmaspheric hiss, a different class of magnetospheric wave that is often considered to control the structure of the belts. Lightning could therefore play a significant role in the maintenance of radiation belt equilibrium. Dissert. Abstr.

N94-31834# Toronto Univ. (Ontario). Dept. of Geography.
THE BASEMENT FRACTURE PATTERN OF SOUTHERN ONTARIO: A TECTONIC INTERPRETATION BASED ON LANDSAT TM IMAGERY, AIRPHOTOS AND FIELD DATA M.S. Thesis
Andrea Loy Rutty 1993 190 p
(ISBN-0-315-87086-9; CTN-94-61248) Copyright Avail: Micromedia Ltd., Technical Information Centre, 240 Catherine Street, Suite 305, Ottawa, Ontario, K2P 2G8, Canada HC/MF

The fracture pattern in the area overlying the Proterozoic central metasedimentary belt boundary zone (CMBBZ) and its north northeast trending extension below the flat-lying Paleozoic strata and Quaternary cover between Lake Ontario and Kashagawigamog Lake, southern Ontario, has been determined using Landsat satellite imagery, aerial photographs, and field studies. Image processing routines and photogeologic methods for delineating regional bedrock fracture patterns in highly glaciated and cultivated terrains are presented. Three principal sets of lineament orientations are found throughout the study area. These fractures are parallel to joints and faults within the Paleozoic strata, interpreted to be pre-Cenozoic in age. The approximately 023 deg trend parallels the underlying CMBBZ and may be related to its reactivation during late Cretaceous extension. Pop-up structures in the Balsam Lake area nucleated on joints parallel to the 106-108 deg lineament set and appear to be post-glacial in age.
Author (CISTI)

N94-31970 California Univ., Los Angeles.
TRANSPORT PHENOMENA IN THE EARTH'S PLASMA SHEET Ph.D. Thesis
Vassilis Angelopoulos 1993 196 p
Avail: Univ. Microfilms Order No. DA9317905

We present a series of studies that utilize observation and modeling in order to characterize transport in the earth's plasma sheet out to distances of 23 R(sub E). After a brief description of the dissertation's goals in Chapter 1, we analyze in Chapter 2 representative cases of high speed flows in the inner central plasma sheet along with the concurrent behavior of the plasma and magnetic field. We argue that such flows are organized in 10 min. time scale entities of convection enhancements that we term bursty bulk flow (BBF) events. BBF's have a substructure that is on a 1 min time scale, referred to as 'flow bursts'. BBF's represent intervals of enhanced, predominantly earthward transport of mass energy and magnetic flux. In Chapter 3, we use an algorithm to automatically detect BBF's and study their statistical properties. BBF's cause the plasma sheet to be in a more dipolarized, higher temperature state for a long time after their subsidence. Despite their short duration, BBF's can account for most of the measured earthward transport of particles, energy, and magnetic flux in the plasma sheet. The concept of BBF's as a particular state of transport in the plasma sheet is applied in Chapter 4 to the study of the non-BBF, quiet state of the inner plasma sheet. We construct the average ion velocity pattern in the quiet inner plasma sheet. We show that a semi-empirical magnetic field model of the magnetotail along with the inferred cross tail electric field and the measured average density reproduce the observed velocity averages assuming that the flow is the sum of corrotation, an E x B flow, and a model-derived diamagnetic drift Despite the qualitative agreement of the average flow pattern with our model calculations, the flow exhibits variability much larger than its average. The non-BBF flow is highly irregular and fundamentally unsteady, a reason why convection in the quiet state of the plasma sheet may be able to avoid a pressure balance inconsistency with the lobes. Chapter 5 explores whether a segregation of plasma sheet states similar to the one applied to the inner plasma sheet can also be extended to the outer plasma sheet.
Dissert. Abstr.

N94-31984 Cornell Univ., Ithaca, NY. Lab. of Plasma Studies.
THEORETICAL STUDIES ON IONOSPHERIC IRREGULARITIES AND ION DIODE PERFORMANCE Final Report, 1 Jan. 1989 - 31 Aug. 1993
R. N. Sudan 31 Aug. 1993 18 p Limited Reproducibility: More than 20% of this document may be affected by microfiche quality
(Contract N00014-89-J-1770)
(AD-A277115) Avail: Issuing Activity (Defense Technical Information Center (DTIC))

Work accomplished is divided into three parts: ionospheric physics; ion diodes, magnetic insulation, and plasma opening switches; and subgrid modeling in numerical computations and other research. Abstracts of published and conference papers are presented. CASI

N94-32007 Observatorio del Ebro, Roquetas (Spain).
EUROCAP PROGRAM-EBRE STATION Interim Report No. 1, Sep. - Nov. 1993
Luis F. Alberca Nov. 1993 3 p Limited Reproducibility: More than 20% of this document may be affected by microfiche quality
(Contract DAJA45-93-C-0041)
(AD-A277044; R/D-7131-EE-0041) Avail: CASI HC A01

Hourly vertical incidence ionograms have been obtained with the digisonde and copy of the ARTIST output in 5 1/4 inch floppy disks sent to Forth Monmouth regularly. The digisonde has been working with a good performance for this period. The refrigerating system of the shielding room of the digisonde has been improved to keep the temperature at the convenient level. A new set of receiving antennas is under construction. They will provide a better receiving signal and a better discrimination between ordinary and extraordinary rays. DTIC

N94-32077 Cornell Univ., Ithaca, NY.
RADAR SCATTERING FROM THE SUMMER POLAR MESOSPHERE: THEORY AND OBSERVATIONS Ph.D. Thesis
John Yungdo Nagamich Cho 1993 220 p
Avail: Univ. Microfilms Order No. DA9319373

The anomalously large radar reflectivities observed in the summer

polar mesosphere have eluded satisfactory explanation until now. We propose that the following chain of causality is responsible for the so-called polar mesosphere summer echoes (PMSE): The uniquely low temperatures in the summer mesopause produce ice aerosols. Because the aerosols exist in a plasma, they become electrically charged. The ambient electrons become coupled to the aerosols through electric fields and their effective diffusivity is retarded due to the large size of the aerosols. The reduction in diffusivity allows electron density inhomogeneities to be maintained at the radar Bragg scales. The radar waves are then scattered by the inhomogeneities. We support the above concept by developing a quantitative theory of ambipolar diffusion in the mesosphere. We then apply the results to isotropic turbulence and Fresnel radar scatter to show that the observed radar reflectivities can be explained by the theory. We show that the presence of realistic charged aerosols are sufficient to explain PMSE. We also show that dressed aerosol radar scatter, proposed by others as a generation mechanism for PMSE, can only apply to echoes detected by UHF radars. We present data taken with the Sondrestrom 1.29-GHz radar and attribute it to dressed aerosol scatter. In the summer of 1991, we used the Cornell University portable radar interferometer (CUPRI) to observe the mesosphere while rockets carrying in situ sensors were flown through two PMSE occurrences and a noctilucent cloud/PMSE event. We present a selection of first results from this campaign (NLC-91). The first simultaneous height comparison between noctilucent clouds and PMSE show that the radar scattering region was near or slightly above the visible cloud layer. We also infer from aspect sensitivity measurements and Doppler spectrograms that there were two distinct types of PMSE: enhanced turbulent scatter and partial (Fresnel) reflection from steep edges in the electron density. Both mechanisms require an anomalously low electron diffusion coefficient. Dissert. Abstr.

N94-32118 Phillips Lab., Hanscom AFB, MA.
ATMOSPHERIC STRUCTURE SIMULATION: AN AUTOREGRESSIVE MODEL FOR SMOOTH GEOPHYSICAL POWER SPECTRA WITH KNOWN AUTOCORRELATION FUNCTION Interim Report, 1 Oct. 1991 - 20 Jan. 1993
James H. Brown 5 Feb. 1993 59 p Limited Reproducibility: More than 20% of this document may be affected by microfiche quality
(AD-A276691; AD-E201762; PL-TR-93-2185; ERP-1128) Avail: CASI HC A04

Within a defined domain, geophysical phenomena often are characterized by smooth continuous power spectral densities having a negative power law slope. Frequently, Fourier transform analysis has been employed to generate synthetic scenes from pseudorandom arrays by passing the stochastic data through a Fourier filter having a desired correlation structure and power spectral dependency. This report examines the possibility of producing synthetic structure by invoking autoregression analysis as contrasted with the Fourier method. Since computations that apply multidimensional fast Fourier transforms to large data arrays consume enormous resources and time, the goal of this study is to seek an alternative method to reduce the computational burden. Future editions of the Phillips Laboratory Strategic High Altitude Atmospheric Radiance Code (SHARC) will feature an ability to calculate structured radiance. The methods explored herein provide a process that can complement or in some cases supplement methods presently being used. DTIC

N94-32154 Army Cold Regions Research and Engineering Lab., Hanover, NH.
A REASSESSMENT OF THE IN-SITU DIELECTRIC CONSTANT OF POLAR FIRN
Austin Kovacs, Anthony J. Gow, and Rexford M. Morey Dec. 1993 28 p Limited Reproducibility: More than 20% of this document may be affected by microfiche quality
(AD-A276999; CRREL-93-26) Avail: CASI HC A03

The success in using VHF and UHF frequency systems for sounding polar ice sheets has been tempered by an uncertainty in the in-situ dielectric constant epsilon' which controls the effective velocity V(sub e) of an electromagnetic wave propagating in an air-ice mixture. An empirical equation for determining epsilon' versus density (specific gravity, rho) was proposed in 1968 by Robin et al. where epsilon' = (1 + 0.851 rho)(exp 2). However, this expression has met with uncertainty because wide-angle radar refraction sounding techniques have produced values of epsilon' that are lower than Robin's equation predicts. This report discusses radar soundings made on the McMurdo Ice Shelf, Antarctica, and compares the resulting epsilon' values with Robin's equation, laboratory measurements on firn and ice, and other expressions given in the literature for determining epsilon' versus the specific gravity of dry firn and ice. Our findings indicate that the form of Robin's equation is valid. However, our analysis also indicates the expression could be slightly improved to read epsilon' = (1 + 0.845 rho)(exp 2). Reasons are suggested as to why previous wide-angle radar sounding studies did not reproduce Robin's findings. DTIC

N94-32335 Naval Postgraduate School, Monterey, CA.
AN ANALYSIS OF IONOSPHERIC DAYGLOW FROM OBSERVATIONS OF THE NAVAL POSTGRADUATE SCHOOL MIDDLE ULTRAVIOLET SPECTROGRAPH (MUSTANG) M.S. Thesis
Antony C. Marron Dec. 1993 70 p Limited Reproducibility: More than 20% of this document may be affected by microfiche quality
(AD-A277351) Avail: CASI HC A04

Middle ultraviolet spectra of the atmospheric airglow were obtained from a March 1992 rocket flight of the NPS MUSTANG instrument. These spectra are analyzed from 1900 to 3100 A, over an altitude range of 100 to 320 km. The data are modeled with computer generated synthetic spectra for the following emissions: N2 Vegard Kaplan (VK); N2 Lyman - Birge - Hopfield (LBH); and NO gamma, delta, and epsilon bands. A best fit procedure was developed. The resulting synthetic spectra agree well with obtained airglow data. Confirmation was made of the theoretical self absorption versus non-self absorption processes of the NO (0,0), (1,0), and (2,0) gamma resonance band emissions. NO self absorption is a necessary inclusion of any atmospheric nitric oxide analysis stratagem. Profiles of temperature versus altitude and NO column density versus altitude for the rocket flight are estimated. DTIC

N94-32337 Naval Postgraduate School, Monterey, CA.
THERMOSPHERIC MODELING ACCURACIES USING F10.7 AND Ap M.S. Thesis
John J. Adler Dec. 1993 72 p Limited Reproducibility: More than 20% of this document may be affected by microfiche quality
(AD-A277355) Avail: CASI HC A04

This thesis analyzes the accuracy of the 45 day forecasted F10.7 and Ap values given by the Air Force Space Forecast Center. These forecasts are generated daily to aid many agencies in their fields of endeavor. The U.S. Space Command uses the values in orbit prediction routines by way of atmospheric density models. This thesis shows that the F10.7 forecasts are accurate from one to seven days out, then deteriorate for the latter 38 days. Conversely, Ap forecasts are less accurate from one to five days out, then improve beyond the sixth day. The effects of forecasting errors upon satellite lifetimes are then shown using the Lifetime 4.1 orbital propagation model with a Jacchia 1971 atmosphere. Propagating a typical satellite for 45 days over various configurations of altitudes and eccentricities showed that only a narrow altitude band from 250 to 325 km is affected. Regions above or below this band are not significantly affected with errors in F10.7 or Ap. DTIC

N94-32338# Colorado Univ., Boulder.
TIME-RESOLVED IR SPECTROSCOPY, ENERGY TRANSFER, AND STATE-TO-STATE COLLISION DYNAMICS OF ATMOSPHERIC SPECIES Final Report, 1 Dec. 1990 - 30 Nov. 1993
David J. Nesbitt 28 Jan. 1994 18 p
(Grant AF-AFOSR-0055-90)
(AD-A277372; AFOSR-94-0057TR) Avail: CASI HC A03/MF A01

Achievements under the AFOSR grant have been in the following areas. We have developed a new method for state-to-state collisional energy transfer in crossed molecular beams, based on high sensitivity direct IR laser absorption, and allowing absolute cross sections to be obtained by measurement of absolute number densities of the scattering species (CH4, H2O, and HF with rare gases). Polarization methods have been developed to study alignment of J states, based on rapid modulation (75 kHz) of a single mode diode laser, and used to study collisional alignment of CO2 in supersonic jets. High resolution flash kinetic spectroscopy has been used to investigate reaction kinetics of OH radical with hydrocarbons, as well as to obtain absolute quantum yields for photofragmentation of HNO3 and H2O2 at 193 and 248 nm. Pressure broadening rates of OH radical relevant to IR 'airglow' detection and characterization have been measured. A new capability has been developed

for measuring state-resolved energy transfer in 'hot atom' collisions of open shell radicals. By absolute absorbance measurements and analysis of high resolution Doppler profiles, both integral and differential cross sections to a specific final J state are obtained for Cl + HCl scattering. DTIC

N94-32346 Dartmouth Coll., Hanover, NH. Dept. of Physics.
SELF-CONSISTENT EFFECTS OF MAGNETOSPHERIC HYDROMAGNETIC WAVES ON RING CURRENT IONS Annual Technical Report, 1 Jan. - 31 Dec. 1993
Mary Hudson 31 Dec. 1993 15 p Limited Reproducibility: More than 20% of this document may be affected by microfiche quality
(Contract F49620-93-1-0101)
(AD-A277406; AFOSR-94-0113TR) Avail: CASI HC A03

Major progress was made in obtaining an explanation for the rapid formation of new electron and proton radiation belts during the March 30, 1991 geomagnetic storm sudden commencement. Preliminary work on proton acceleration during the same event was reported at the Fall AGU meeting in December, an important feature of the simulation code that has been developed is the ability to post-process data runs after the trajectories of several hundred thousand ions or electrons have been followed through the inbound and outbound propagation time of the wave fields, which is about 100 seconds of real time. As a first step in the development of the three-dimensional MHD fluid-gyrokinetic particle hybrid code, a three-dimensional MHD version of the code in generalized orthogonal coordinates has been developed. DTIC

N94-32493 Colorado Univ., Boulder.
FORCED LIBRATION OF MERCURY AND GEODETIC DETERMINATION OF A POSSIBLE FLUID CORE Ph.D. Thesis
Xiaoping Wu 1993 181 p
Avail: Univ. Microfilms Order No. DA9320491

The possibility of determining the existence and size of a fluid core in Mercury by a combined orbiter-lander mission is investigated. Microwave Doppler and range measurements from earth to the orbiter would determine the spacecraft orbit accurately, and radio range measurements from the orbiter to the lander would determine the obliquity of Mercury and the amplitude of its 88-day forced libration in longitude. These measurements can be used to determine the fractional maximum moment of inertia of the anticipated fluid core. Consider covariance analyses are carried out to assess the performance of a simulated set of measurements consisting of 30 separate 8-hour arcs of data. Earth to orbiter ranging and Doppler tracking data with 3 cm and 1 x 10(exp -14) respective accuracies are assumed, plus orbiter to lander ranging with 1 m accuracy. The force model includes Mercury's gravity field, solar radiation pressure on the spacecraft body and on the antenna, thermal and albedo radiation from Mercury, and solid Mercury tides. The uncertainties for the estimated libration amplitude and the obliquity are shown to be 0.26 and 0.03 arcsec for the model employed. The resulting uncertainty for the fractional core moment of inertia is 0.45 percent. Moreover, the Love number k(sub 2) can be determined with an accuracy of 0.01. Based on a planet model with a rigid mantle, a homogeneous and incompressible fluid core, and a nonhydrostatic core-mantle boundary (CMB), the fluid motion and pressure fields are determined for both the free and forced motion problems. The perturbed eigenfrequencies and eigenfunctions are calculated for low degree and order inertial waves. The effect of CMB topography in the case of Mercury's forced libration is that the pressure torque on the mantle nearly equals the gravitational torque of the sun on the fluid core. Thus the mantle librates almost exactly as if it were driven by the torque of the sun on the entire planet including the core. This result means that it is still possible to detect the fluid core even with the presence of a nonhydrostatic CMB. Dissert. Abstr.

N94-32647# Los Alamos National Lab., NM.
VARIATIONAL ELLIPTIC SOLVER FOR ATMOSPHERIC APPLICATIONS
Piotr K. Smolarkiewicz (National Center for Atmospheric Research, Boulder, CO.) and Len G. Margolin Mar. 1994 39 p
(Contract W-7405-eng-36)
(DE94-007725; LA-12712-MS) Avail: CASI HC A03/MF A01

We discuss a conjugate gradient type method -- the conjugate residual -- suitable for solving linear elliptic equations that result from discretization of complex atmospheric dynamical problems. Rotation and irregular boundaries typically lead to nonself-adjoint elliptic operators whose matrix representation on the grid is definite but not symmetric. On the other hand, most established methods for solving large sparse matrix equations depend on the symmetry and definiteness of the matrix. Furthermore, the explicit construction of the matrix can be both difficult and computationally expensive. An attractive feature of conjugate gradient methods in general is that they do not require any knowledge of the matrix; and in particular, convergence of conjugate residual algorithms do not rely on symmetry for definite operators. We begin by reviewing some basic concepts of variational algorithms from the perspective of a physical analogy to the damped wave equation, which is a simple alternative to the traditional abstract framework of the Krylov subspace methods. We derive two conjugate residual schemes from variational principles, and prove that either definiteness or symmetry ensures their convergence. We discuss issues related to computational efficiency and illustrate our theoretical considerations with a test problem of the potential flow of a Boussinesq fluid flow past a steep, three-dimensional obstacle. DOE

N94-32736# Los Alamos National Lab., NM.
HIGH RESOLUTION PROPERTIES OF THE MARINE ATMOSPHERIC BOUNDARY LAYER
D. Cooper, W. Cottingame, W. Eichinger, P. Forman, C. Lebeda, D. Poling, and R. Thorton 1994 5 p Presented at the 21st Conference on Agricultural and Forest Meteorology, Boston, MA, Mar. 1994
(Contract W-7405-eng-36)
(DE94-006235; LA-UR-94-101; CONF-940368-1) Avail: CASI HC A01/MF A01

Los Alamos National Laboratory (LANL) participated in the Central Equatorial Pacific Experiment (CEPEX) by fielding a water-vapor Raman lidar on board the Research Vessel Vickers. The lidar measured water vapor concentration from the surface to lower tropospheric altitudes in order to support the CEPEX goal of evaluating a hypothesis regarding feedback mechanisms for global circulation models. This report describes some of the features observed within the marine Atmospheric Boundary Layer (ABL) and the lower troposphere. Data was collected continuously 24 hours per day over the equatorial Pacific from March 8th to March 21st of 1993 while in route between Guadalcanal and Christmas Island (the transect was at approximately 2 degrees south latitude). The lidar collected vertical transects of water vapor concentration up to 10 km during night operations and 4 km in the day. The vertical lidar profiles of water vapor were produced by summing the data over a period up to 600 seconds. The water-vapor Raman lidar measured the properties of the marine ABL as well as the lower and mid-troposphere. From the lidar water vapor profiles, 'images' of water vapor concentration versus altitude and date or sea surface temperature will be produced along with other products such as latent heat fluxes. The Raman water vapor lidar data will be used to better understand the role of transport and exchange at the ocean-atmosphere interface and throughout the marine atmosphere. DOE

N94-32772# Lawrence Livermore National Lab., CA.
A LONG-TERM SIMULATION OF SURFACE FLUXES AND SOIL MOISTURE
J. Kim, R. L. Lee, and M. Ek Sep. 1993 6 p Presented at the 74th American Meteorological Society Annual Meeting, Nashville, TN, 23-28 Jan. 1994
(Contract W-7405-eng-48)
(DE94-006661; UCRL-JC-114411; CONF-940115-24) Avail: CASI HC A02/MF A01

The heat fluxes over land surfaces play important roles in shaping atmospheric flows on various temporal and spatial scales. Fast and McCorcle showed that sea-breeze-like mesoscale circulations can develop over land surfaces of heterogeneous soil type and soil moisture. Evaporation from land surfaces is one of the major moisture sources for the summertime convective precipitation in extratropics. General circulation model studies also indicate that surface characteristics cause a significant impact on the simulated climate. DOE

N94-32816# Sandia National Labs., Albuquerque, NM.
NMR CHARACTERIZATION OF SHOCKED QUARTZ
M. B. Boslough, R. T. Cygan, R. A. Assink, and R. J. Kirkpatrick 1994 6 p Presented at the National Institute for Research in Inorganic Materials (NIRIM) Symposium on Advanced Materials, Tsukuba, Japan, 13-17 Mar.

1994
(Contract DE-AC04-94AL-85000)
(DE94-007733; SAND-94-0328C; CONF-940380-1) Avail: CASI HC A02/MF A01

We have characterized experimentally and naturally-shocked quartz (both synthetic and natural samples) by solid state nuclear magnetic resonance (NMR) spectroscopy. Relaxation analysis of experimentally-shocked samples provides a means for quantitative characterization of the amorphous/disordered silica component NMR spectra demonstrate that magnetization in both the amorphous and crystalline components follows power-law behavior as a function of recycle time. This observation is consistent with the relaxation of nuclear spins by paramagnetic impurities. A fractal dimension can be extracted from the power-law exponent associated with each phase, and relative abundances can be extracted from integrated intensities of deconvolved peaks. NMR spectroscopy of naturally-shocked sandstone from Meteor Crater, Arizona (USA) led to the discovery of a new amorphous hydroxylated silica phase. Solid state NMR spectra of both experimentally and naturally shocked quartz were unexpectedly rich in microstructural information, especially when combined with relaxation analysis and cross-polarization studies. We suggest solid state NMR as a potentially useful tool for examining shock-induced microstructural changes in other inorganic compounds, with possible implications for shock processing of structural ceramics. DOE

N94-32874 Argonne National Lab., IL.
PARAMETERIZING ATMOSPHERE-LAND SURFACE EXCHANGE FOR CLIMATE MODELS WITH SATELLITE DATA: A CASE STUDY FOR THE SOUTHERN GREAT PLAINS CART SITE
W. Gao 1994 7 p Presented at the 5th Annual Symposium on Global Change Studies, Nashville, TN, 24-28 Jan. 1994 Limited Reproducibility: More than 20% of this document may be affected by microfiche quality
(Contract W-31-109-eng-38)
(DE94-005109; ANL/ER/CP-80788; CONF-940131-2) Avail: Issuing Activity (Department of Energy (DOE))

High-resolution satellite data provide detailed, quantitative descriptions of land surface characteristics over large areas so that objective scale linkage becomes feasible. With the aid of satellite data, researchers examined the linearity of processes scaled up from 30 m to 15 km. If the phenomenon is scale invariant, then the aggregated value of a function or flux is equivalent to the function computed from aggregated values of controlling variables. The linear relation may be realistic for limited land areas having no large surface contrasts to cause significant horizontal exchange. However, for areas with sharp surface contrasts, horizontal exchange and different dynamics in the atmospheric boundary may induce nonlinear interactions, such as at interfaces of land-water, forest-farm land, and irrigated crops-desert steppe. The linear approach, however, represents the simplest scenario and is useful for developing an effective scheme for incorporating subgrid land surface processes into large-scale models. Our studies focus on coupling satellite data and ground measurements with a satellite-data-driven land surface model to parameterize surface fluxes for large-scale climate models. In this case study, we used surface spectral reflectance data from satellite remote sensing to characterize spatial and temporal changes in vegetation and associated surface parameters in an area of about 350 x 400 km covering the southern Great Plains (SGP) Cloud and Radiation Testbed (CART) site of the US Department of Energy's Atmospheric Radiation Measurement (ARM) Program. DOE

N94-32895# Lawrence Livermore National Lab., CA.
A CORRELATED k-DISTRIBUTION MODEL OF THE HEATING RATES FOR ATMOSPHERIC MIXTURES OF H2O, CO2, O3, CH4, AND N2O IN THE 0-2500 cm(EXP -1) WAVE NUMBER REGION AT ALTITUDES BETWEEN 0 AND 60 km
A. S. Grossman and K. E. Grant Sep. 1993 5 p Presented at the 74th American Meteorological Society Annual Meeting, Nashville, TN, 23-28 Jan. 1994
(Contract W-7405-eng-48)
(DE94-005136; UCRL-JC-115044; CONF-940115-18) Avail: CASI HC A01/MF A01

The main purposes of this paper are to first use the direct method of GGFP to calculate the transmission of the individual molecules H2O, CO2, O3, CH4, and N2O, plus the transmission of a mixture of all these molecules. Second, to use the G2 model for overlapping k-distributions to calculate the transmission for the CH4-N2O and H2O-CO2 systems in the spectral regions in which there are overlapping absorption features. For the wavenumber interval 0-2500 cm(exp -1) and altitude range of 0-60 km, a calculation of the atmospheric heating rates, upward fluxes, and downward fluxes will be made for each of the above cases and compared to line by line calculations. DOE

N94-32999 Keo Consultants, Brookline, MA.
HIGH FREQUENCY ACTIVE AURORAL RESEARCH PROGRAM (HAARP) IMAGER Final Report, 29 Aug. 1991 - 29 Aug. 1993
Cyril Lance and Robert Eather 30 Sep. 1993 322 p Limited Reproducibility: More than 20% of this document may be affected by microfiche quality
(Contract F19628-91-C-0141)
(AD-A277469; AD-E201833; PL-TR-93-2219) Avail: CASI HC A14

A low-light-level monochromatic imaging system was designed and fabricated which was optimized to detect and record optical emissions associated with high-power RF heating of the ionosphere. The instrument is capable of detecting very low intensities, of the order of 1 Rayleigh, from typical ionospheric atomic and molecular emissions. This is achieved through co-adding of ON images during heater pulses and subtraction of OFF (background) images between pulses. Images can be displayed and analyzed in real time and stored in optical disc for later analysis. Full image processing software is provided which was customized for this application and uses menu or mouse user interaction. DTIC

N94-33006# Columbia Univ., New York, NY. Lab. of Applied Geophysics.
FINITE-ELEMENT MODELING OF THE BLOCKAGE AND SCATTERING OF LG PROPAGATION Annual Report, 1 Dec. 1992 - 30 Nov. 1993
Yu-Chiung Teng 30 Nov. 1993 58 p
(Contract F49620-93-1-0073)
(AD-A277430; AFOSR-94-0099TR) Avail: CASI HC A04/MF A01

The problem of Lg wave blockage is being investigated using finite element models of island margin, basin, and basin with an uplifted Moho to simulate wave propagation across the Barents Sea basin. Results from the first year follow. The efficiency of the crust as a Lg wave guide strongly depends on the frequency content of an impulsive source. The effects of a basin on Lg propagation also depends on the basin width and the velocity contrast between the sedimentary basin and the surrounding granitic/basaltic crust. For a high velocity contrast, the Lg wave form is significantly lengthened. The presence of an uplifted Moho alone does not appear to have a major blockage effect on Lg wave propagation. The finite element codes with the fast execution algorithm prove to be well suited as tools for the modeling purposes intended in this research. DTIC

N94-33028# Naval Civil Engineering Lab., Port Hueneme, CA. Facilities Service Center.
PROCEDURES FOR COMPUTING SITE SEISMICITY Final Report, Oct. 1992 - Jan. 1994
John Ferritto Feb. 1994 180 p
(DA Proj. RM3-3-F-60)
(AD-A277666; NFESC-TR-2016-SHR) Avail: CASI HC A09/MF A02

This report was prepared as part of the Navy's Seismic Hazard Mitigation Program. The Navy has numerous bases located in seismically active regions throughout the world. Safe effective design of waterfront structures requires determining expected earthquake ground motion. The Navy's problem is further complicated by the presence of soft saturated marginal soils that can significantly amplify the levels of seismic shaking as evidenced in the 1989 Loma Prieta earthquake. The Naval Facilities Engineering Command's seismic design manual, NAVFAC P355.I, requires a probabilistic assessment of ground motion for design of essential structures. This report presents the basis for the Navy's Seismic Hazard Analysis procedure that was developed and is intended to be used with the Seismic Hazard Analysis computer program and user's manual. This report also presents data on geology and seismology to establish the background for the seismic hazard model developed. The procedure uses the historical epicenter data base and available geologic data, together with source models, recurrence models, and attenuation relationships to compute the probability distribution of site acceleration and an appropriate spectra. This report discusses the developed

stochastic model for seismic hazard evaluation and the associated research. DTIC

N94-33041# Naval Command, Control and Ocean Surveillance Center, San Diego, CA. RDT and E Div.
SPATIAL CORRELATION OF IONOSPHERIC VARIABILITY
R. A. Sprague Mar. 1994 3 p
(ONR Proj. ZW82)
(AD-A278105) Avail: CASI HC A01/MF A01

This presentation discusses a year long experimental campaign to determine the magnitude and spatial correlation of ionospheric variations. DTIC

N94-33111 Alberta Univ., Edmonton.
THE SPATIAL DEVELOPMENT OF THE MAGNETOSPHERIC LOW-LATITUDE BOUNDARY LAYER Ph.D. Thesis
John R. Manuel 1992 157 p
(ISBN-0-315-77418-5) Avail: Univ. Microfilms Order No. DANN77418

The low-latitude boundary layer (LLBL) comprises a large fraction of the magnetospheric boundary layer, making it a potentially important site for transport of mass, momentum, and energy from the high-speed magnetosheath plasma into the magnetosphere. I have examined, by computer simulation, the processes involved in the spatial development of a 6.4 R(sub E) (Earth radii) long section of the dayside LLBL from a thin and laminar boundary layer to a broad and turbulent one capable of significant transport. The computer simulation developed for this purpose is based on the full set of ideal magnetohydrodynamic (MHD) equations that govern the dynamics of most magnetospheric plasmas and uses a two dimensional nonperiodic simulation geometry to permit the realistic downstream development of the boundary layer. Simulations started from several realistic initial conditions all exhibit the formation of a LLBL that broadens with downstream distance, from an upstream thickness of 0.12 R(sub E) to as much as approximately 0.7 R(sub E) downstream, and reproduces many of the observed boundary layer characteristics. The broadening occurs through the action of Reynold and Maxwell stresses generated by the Kelvin-Helmholtz (KH) instability in the boundary layer which deposit momentum and energy into the LLBL. The KH instability also transports mass into the LLBL by mixing plasma across the boundary layer through continuous vortex roll ups and mergings and also appears capable of aiding diffusive transport processes by steepening density gradients at the magnetopause enough to trigger any of a number of possible diffusion processes. Simulations have also shown that the downstream development of the boundary layer may be slowed and possibly stopped in the presence of a flow-aligned component of the magnetosheath magnetic field. For example, for a magnetosheath magnetic field which is initialized to tilt 30 degrees away from perpendicular to the flow, the KH instability still develops, but fails to generate the large, merging vortices necessary to the success of the transport processes because the vortices lose kinetic energy to magnetic field distortions as they wind up the magnetic field. The magnetosheath magnetic field is thus capable of nonlinearly stabilizing the KH instability in the LLBL even though the LLBL is linearly unstable to the KH instability. Dissert. Abstr.

N94-33184 Institut Royal Meteorologique de Belgique, Dourbes. Ionospheric Station.
EUROCAP PROGRAM Interim Report No. 1, 1 Aug. - 31 Oct. 1993
J. C. Jodogne 11 Feb. 1994 4 p Limited Reproducibility: More than 20% of this document may be affected by microfiche quality
(Contract DAJA45-93-C-0042)
(AD-A278084; R/D-7150-EE-01) Avail: Issuing Activity (Defense Technical Information Center (DTIC))

Vertical soundings were recorded hourly with the Digisonde 256 and the Artist facility from Aug. - Oct. 1993. During these three months, the Digisonde 256 worked perfectly and only few hourly records are missing. Interruptions of the recording were mainly due to short mains failures. A software problem delayed the production of the output data due to the fact that we had to interact with University of Massachusetts, Lowell, group to solve it. DTIC

N94-33272# RADEX, Inc., Bedford, MA.
SIMULATION OF CO2 RELEASE AT 800 km ALTITUDE
A. Setayesh 31 Aug. 1993 22 p
(Contract F19628-90-C-0191)
(AD-A276692; RXR-93081; PL-TR-93-2177; SR-7) Avail: CASI HC A03/MF A01

The SOCRATES contamination-interaction code has been used to simulate the reactions of 0 + CO2 yields CO2(v) + O, O + CO2 - CO(v) + O2, and CO2 + H - CO + OH(v) at an altitude of 800 km in both ram and wake directions of the spacecraft. These simulations show that the radiation from these reactions can be measurable for the parameters which have been used in these calculations. The investigation carries out the simulations as much as 30 km from the spacecraft. The radiative intensity of CO(v) and OH(v) show the highest and lowest, respectively. DTIC

N94-33285# Naval Command, Control and Ocean Surveillance Center, San Diego, CA. RDT and E Div.
DIURNAL, SEASONAL AND SOLAR ACTIVITY VARIATIONS OF F-REGION PARAMETERS
A. K. Paul Mar. 1994 3 p
(ONR Proj. ZW82)
(AD-A278106) Avail: CASI HC A01/MF A01

This abstract describes a presentation at the Radio Science Meeting in Boulder, CO. The presentation was on diurnal, seasonal, and solar activity variations of F-region parameters. DTIC

N94-33351# North Carolina Central Univ., Durham.
HIGH RESOLUTION MOLECULAR SPECTROSCOPY OF ATMOSPHERIC SPECIES Final Report, 1 Jul. 1989 - 30 Sep. 1993
Jyotsna M. Dutta and Charles R. Jones 24 Feb. 1994 16 p
(Contract F49620-89-C-0080)
(AD-A278382; AFOSR-94-0184TR) Avail: CASI HC A03/MF A01

Laboratory-based pressure-broadening data has long provided information that is both of practical importance for technological applications and of fundamental interest for understanding molecular interactions and dynamics. During this project period the temperature dependence of the collision-broadened line widths of H2O and HDO were studied between 100 k and 600 K. Selected transitions were between 250 GHz and 500 GHz and the broadening gases were 02, N2, H2, and He. Low temperature measurements were made in a collisionally cooled cell to circumvent the limitations imposed by the low vapor pressure of the sample gas at temperatures far below their freezing points. The experimentally determined values were compared with earlier experimental and theoretical works. DTIC

N94-30998 Universite des Sciences et Techniques de Lille (France). Lab. d'Optique Atmospherique.
MATTER-RADIATION INTERACTIONS IN THE ATMOSPHERE [INTERACTIONS MATIERE-RAYONNEMENT DANS L'ATMOSPHERE]
Y. Fouquart *In* CNES, Subtropical Climates and Their Evolution: From Space-Based Observation to Modelling Oct. 1993 p 383-411 In FRENCH (For primary document see N94-30981 09-47)
Copyright Avail: Issuing Activity (CEPADUES-Editions, 111, rue Nicolas-Vauquelin, 31100 Toulouse, France)

N94-31106*# Massachusetts Inst. of Tech., Cambridge. Dept. of Earth, Atmospheric and Planetary Sciences.
PATTERNS OF DEFORMATION AND VOLCANIC FLOWS ASSOCIATED WITH LITHOSPHERIC LOADING BY LARGE VOLCANOES ON VENUS Abstract Only
Patrick J. McGovern and Sean C. Solomon *In its* Tectonic History of the Terrestrial Planets Mar. 1993 1 p (For primary document see N94-31105 09-91)
Avail: CASI HC A01/MF A03

47 METEOROLOGY AND CLIMATOLOGY

Includes weather forecasting and modification.

N94-30981 Centre National d'Etudes Spatiales, Toulouse (France).
SUBTROPICAL CLIMATES AND THEIR EVOLUTION: FROM SPACE-BASED OBSERVATION TO MODELLING [LES CLIMATS SUBTROPICAUX ET LEUR EVOLUTION: DE L'OBSERVATION SPATIALE A LA MODELISATION]

Oct. 1993 684 p In ENGLISH and FRENCH Presented at CNES 1992, International Summer School Session, Toulouse, France, Sep. 1992 (ISBN-2-85-428333-3; ETN-94-95799) Copyright Avail: Issuing Activity (CEPADUES-Editions, 111, rue Nicolas-Vauquelin, 31100 Toulouse, France)

The lectures and conferences given during the school on subtropical climate studies are presented. The main topics are: oceanic and energy general circulation, climate flow, sea-atmosphere interactions, West and North Africa climate, dynamics of tropical regions, tropical squall lines, the climate of the Mediterranean Sea, energy radiation, remote sensing, satellite data uses, radar data and measurements, aerosols from desert and arid zones, behavior of tropical forests and savannas, airborne equipment, ozone content, and chemical composition of the atmosphere land biosphere. For individual titles, see N94-30982 through N94-31011.

N94-30982 Centre National de la Recherche Scientifique, Gif-sur-Yvette (France). Centre des Faibles Radioactivites.

THE EARTH'S CLIMATE: PAST, PRESENT, AND FUTURE [LE CLIMAT DE LA TERRE: PASSE, PRESENT ET FUTUR]

J. C. Duplessy *In* CNES, Subtropical Climates and Their Evolution: From Space-Based Observation to Modelling Oct. 1993 p 13-3 In FRENCH (For primary document see N94-30981 09-47)

Copyright Avail: Issuing Activity (CEPADUES-Editions, 111, rue Nicolas-Vauquelin, 31100 Toulouse, France)

The Earth's climate evolution is reviewed. Climate variations have occurred for about 2.9 times 10 to the 9th power years, but air temperatures have varied only within a narrow range. Mountain building and continental drift are the main factors responsible for long term climatic changes. On the 10,000 to 100,000 year scale, seasonal insolation changes determined by orbital geometry trigger the global Earth's climate. Interactions between the various components of the climatic system (ocean atmosphere cryosphere) are responsible for variations which may be very abrupt. They constitute a nonlinear response of the climatic system to slowly varying forcing factors such as insolation or atmospheric greenhouse gas concentration. ESA

N94-30983 Centre National de la Recherche Scientifique, Paris (France). Lab. de Meteorologie Dynamique.

ENERGETIC AND GENERAL CIRCULATION [CIRCULATION GENERALE ET ENERGETIQUE] **c48**

Robert Sadourny *In* CNES, Subtropical Climates and Their Evolution: From Space-Based Observation to Modelling Oct. 1993 p 41-7 In FRENCH (For primary document see N94-30981 09-47)

Copyright Avail: Issuing Activity (CEPADUES-Editions, 111, rue Nicolas-Vauquelin, 31100 Toulouse, France)

The transfer of energy from equatorial to polar regions is performed either by the oceanic or atmospheric circulation. The behavior of the general atmospheric circulation in tropical regions is correlated to energy sources and wells. Satellite observations are of great help for studying the Earth's energy balance. The equations describing the radiative energy exchanges between the Earth and space are shown. The atmospheric energy wells and sources and the Hadley's-Walker energy model are explained. The kinetic description of the trade winds and of the Hadley's cell are given. The barocline instabilities and their influence over general atmospheric circulation are studied. ESA

N94-30984 Centre National de la Recherche Scientifique, Paris (France). Lab. d'Oceanographie Dynamique et de Climatologie.

GENERAL OCEAN CIRCULATION [CIRCULATION GENERALE OCEANIQUE] **c48**

P. Delecluse *In* CNES, Subtropical Climates and Their Evolution: From Space-Based Observation to Modelling Oct. 1993 p 81-9 In FRENCH Prepared in cooperation with Paris VI Univ., Fran ce and Office de la Recherche Scientifique et Technique Outre-Mer (For primary document see N94-30981 09-47)

Copyright Avail: Issuing Activity (CEPADUES-Editions, 111, rue Nicolas-Vauquelin, 31100 Toulouse, France)

Physical properties of the ocean and the atmosphere are compared. The energy exchanges between both fluids are reviewed. Forces acting in the ocean are presented and the set of governing equations is established. The study is carried out for cases when the ocean is forced by the wind. The general circulation is discussed with the thermocline structure under thermohaline stresses. The North Atlantic Deep Water belt is described to illustrate space and time scales. The study of particle trajectories of the North Atlantic Deep Water belt shows that numerical modeling is in agreement with Gordon's Scheme. The results show that global oceanic circulation can be well understood by numerical models, but difficulties arise from the lack of observational data. ESA

N94-30985 Centre National de Recherches Meteorologiques, Toulouse (France).

CLIMATOLOGIC FLUX IN TROPICAL OCEAN [FLUX CLIMATOLOGIQUES EN OCEAN TROPICAL] **c48**

S. Planton *In* CNES, Subtropical Climates and Their Evolution: From Space-Based Observation to Modelling Oct. 1993 p 99-120 In FRENCH (For primary document see N94-30981 09-47)

Copyright Avail: Issuing Activity (CEPADUES-Editions, 111, rue Nicolas-Vauquelin, 31100 Toulouse, France)

The air-sea flux climatologies are based on the application of empirical to atmospheric parameters and sea surface temperatures. The calculation of the meridional heat transport in the ocean inferred from the surface net heat flux reveals the discrepancies between different available estimates. These discrepancies are notable in the climatological estimates of the energy budget of the Warm Pool of the western tropical Pacific. They reflect uncertainties related to observation errors, errors in the used empirical formulae or sampling errors. The overall uncertainty of the annual mean net heat flux is about 40 W/sq m for the Tropical Pacific. New flux climatologies with expected lower uncertainties are based on the use of satellite data. Fluxes are retrieved either through statistical method or through a physical modeling. ESA

N94-30986 Centre National de la Recherche Scientifique, Paris (France). Lab. d'Oceanographie Dynamique et de Climatologie.

LOW FREQUENCE VARIABILITY OF THE OCEAN ATMOSPHERE COUPLED SYSTEM [VARIABILITE BASSE FREQUENCE DU SYSTEME COUPLE OCEAN-ATMOSPHERE] **c48**

P. Delecluse *In* CNES, Subtropical Climates and Their Evolution: From Space-Based Observation to Modelling Oct. 1993 p 121-140 In FRENCH Prepared in cooperation with Paris VI Univ., Fran ce and Office de la Recherche Scientifique et Technique Outre-Mer (For primary document see N94-30981 09-47)

Copyright Avail: Issuing Activity (CEPADUES-Editions, 111, rue Nicolas-Vauquelin, 31100 Toulouse, France)

The physical characteristics of equatorial regions are given and their dynamics are described. The equatorial waves theory is reviewed. In the oceanic equatorial zones, the thermocline is very pronounced and near to the surface, indicating that the barocline phase velocity is high. Dynamical space and scales and eigenmodes are calculated. The El Nino anomalous behavior is described: it is due to the phenomenon known as southern oscillations, it is responsible for the ocean-atmosphere variations and is named ENSO (El Nino Southern Oscillations). The 1982 to 1983 event is described and compared to previous ones. A model for describing ENSO is presented. ESA

N94-30987 Centre National de la Recherche Scientifique, Paris (France). Lab. de Meteorologie Dynamique.

INTERACTION PROCESSES BETWEEN THE OCEAN AND THE ATMOSPHERE [LES PROCESSUS D'INTERACTION ENTRE L'OCEAN ET L'ATMOSPHERE] **c48**

H. LeTreut *In* CNES, Subtropical Climates and Their Evolution: From Space-Based Observation to Modelling Oct. 1993 p 141-151 In FRENCH (For primary document see N94-30981 09-47)

Copyright Avail: Issuing Activity (CEPADUES-Editions, 111, rue Nicolas-Vauquelin, 31100 Toulouse, France)

The main physical processes which affect the ocean/atmosphere interactions are reviewed. In particular, the physical processes which maintain the atmospheric and oceanic boundary layers, as well as the atmospheric surface processes are described. Parameterizations used in large scale models are reviewed. Some additional elements of complexity, such as clouds in the atmosphere and phytoplankton in the ocean are included. Few investigations were carried out to study coupling between ocean and atmosphere boundary layers, which are known to be complex ones. ESA

N94-30988 Centre National de la Recherche Scientifique, Palaiseau (France). Lab. de Meteorologie Dynamique.

DYNAMIC CLIMATOLOGY OF WEST AFRICA [CLIMATOLOGIE DYNAMIQUE DE L'AFRIQUE DE L'OUEST]

P. deFelice (Ecole Polytechnique, Palaiseau, France.) *In* CNES, Subtropical Climates and Their Evolution: From Space-Based Observation to Modelling Oct. 1993 p 153-169 In FRENCH (For primary document see N94-30981 09-47)

Copyright Avail: Issuing Activity (CEPADUES-Editions, 111, rue Nicolas-Vauquelin, 31100 Toulouse, France)

Mean meteorological fields are displayed on several tropospheric levels for Summer and Winter. The following West Africa perturbation phenomena are described: Winter cold waves, Summer east waves and squall lines. The differences which distinguish tropical and equatorial zones meteorology are summarized. The velocity, temperature and geopotential mean fields are calculated from Meteosat data and analysis performed by the European center of mean term meteorological predictions. The cold advection phenomenon which occur during cold seasons is described. Three criteria describing the intertropical front are reviewed. Future developments in African climatology studies are considered. ESA

N94-30989 Office National de la Meteorologie, Algiers (Algeria).

SOME ASPECTS OF THE DROUGHT IN NORTH AFRICA AND IN THE MEDITERRANEAN BASIN [QUELQUES ASPECTS DE LA SECHERESSE EN AFRIQUE DU NORD ET DANS LE BASSIN MEDITERRANEEN]

Mohammed Kadi *In* CNES, Subtropical Climates and Their Evolution: From Space-Based Observation to Modelling Oct. 1993 p 171-198 In FRENCH (For primary document see N94-30981 09-47)

Copyright Avail: Issuing Activity (CEPADUES-Editions, 111, rue Nicolas-Vauquelin, 31100 Toulouse, France)

The results of studies concerning recent precipitation data from the Mediterranean basin are discussed. The data shows that meteorological drought is more apparent in the 1980's. However, chronic disruptive situations were observed. The North Atlantic oscillations, the sea surface temperature in the North Atlantic Ocean, the so called Mediterranean oscillations and the strength and position of some atmospheric circulation are potential indicators of the meteorological aspects of drought for this basin. In the context of climate change, more observations and research is needed on this phenomena because data on drought in this region remain rare. ESA

N94-30990 Centre National de la Recherche Scientifique, Palaiseau (France).

DYNAMICS IN THE TROPICS AND SYNOPTIC DISTURBANCES

Daniel L. Cadet *In* CNES, Subtropical Climates and Their Evolution: From Space-Based Observation to Modelling Oct. 1993 p 201-214 (For primary document see N94-30981 09-47)

Copyright Avail: Issuing Activity (CEPADUES-Editions, 111, rue Nicolas-Vauquelin, 31100 Toulouse, France)

The importance of tropical perturbations of synoptic scale is discussed within the framework of the general circulation of the tropics. It is based on the concept of energetics. The scale organization of convection in the tropical belt, which is occurring on a small scale and can give rise to the large scale east-west cells and the upper troposphere tropical jet, is explained. The tropical perturbations affecting different regions of the tropics are described. The major differences between them is discussed and the common features are emphasized. The perturbations affecting West Africa and the Indian subcontinent are described. ESA

N94-30991 Office de la Recherche Scientifique et Technique Outre-Mer, Paris (France). Lab. d'Oceanographie Dynamique et de Climatologie.

LOW FREQUENCY VARIABILITY OBSERVED IN THE TROPICAL ATLANTIC OCEAN [VARIABILITE BASSE FREQUENCE OBSERVEE DANS L'OCEAN ATLANTIQUE TROPICAL] **c48**

Alain Morliere (Paris VI Univ., France.) *In* CNES, Subtropical Climates and Their Evolution: From Space-Based Observation to Modelling Oct. 1993 p 215-231 In FRENCH (For primary document see N94-30981 09-47)

Copyright Avail: Issuing Activity (CEPADUES-Editions, 111, rue Nicolas-Vauquelin, 31100 Toulouse, France)

The yearly and seasonal variability of parameters describing the upper layers of the Atlantic tropical ocean are considered. These parameters play a role in the ocean-atmosphere interactions and the most important one is certainly the sea surface temperature. Equilibrium changes between the heat flow through the sea's surface, the horizontal or vertical advection and mixing layer phenomena induce temperature changes at the ocean's surface. The variability of the tropical Atlantic sea's surface can be easily correlated to wind variations and is controlled by seasonal signals. Yearly changes similar to those concerning El Nino and eigenvalue oscillations controlled by meridian signals are also observed in the Atlantic. ESA

N94-30992 Centre National de Recherches Meteorologiques, Toulouse (France).

TROPICAL SQUALL LINES [LES LIGNES DE GRAINS TROPICALES]

J.-L. Redelsperger (Centre National de la Recherche Scientifique, Toulouse, France.) *In* CNES, Subtropical Climates and Their Evolution: From Space-Based Observation to Modelling Oct. 1993 p 233-259 In FRENCH (For primary document see N94-30981 09-47)

Copyright Avail: Issuing Activity (CEPADUES-Editions, 111, rue Nicolas-Vauquelin, 31100 Toulouse, France)

The present knowledge on tropical squall lines is summarized. The atmospheric convection plays a major role in the general atmospheric circulation and, in particular, in tropical and intertropical regions. The rainfalls produced by convective atmospheric motions are essential for life and climate evolutions. The analysis of annual rainfall as a function of the latitude shows the effect of: cloud systems, tropical squall lines, tropical cyclones, convection during the day, and extratropical cyclones. Several international cooperation experiments were carried out to study tropical rainfall systems. Two of them are considered; The GATE (Global Atmospheric program's Atlantic Tropical Experiment) and the COPT81 (French acronym for deep tropical convection, 1981). ESA

N94-30993 Universidad Complutense, Madrid (Spain). Dept. Geofisica y Meteorologia.

THE CLIMATE OF THE MEDITERRANEAN BASIN: ITS SENSITIVITY TO GLOBAL CHANGE

Manuel deCastro *In* CNES, Subtropical Climates and Their Evolution: From Space-Based Observation to Modelling Oct. 1993 p 261-280 (For primary document see N94-30981 09-47)

Copyright Avail: Issuing Activity (CEPADUES-Editions, 111, rue Nicolas-Vauquelin, 31100 Toulouse, France)

The peculiarities of the climate in the Mediterranean basin, due to the geographic location and to the presence of a warm sea enclosed and surrounded by a complex orography, are discussed. The interaction of general circulation with Mediterranean basin climate is studied. The aim was to underline the fact that in this particular geographical area any attempt of climate forecasting requires both improvements to the general circulation models and better knowledge of the connection between local and regional meteorological processes and the nature of large scale circulation. In this respect, specific studies are required in the area. Studies considered to be of special importance are proposed. ESA

N94-30994 Centre National de la Recherche Scientifique, Toulouse (France).

EFFECTS OF THE DEEP TROPICAL CONVECTION IN THE LARGE SCALE ATMOSPHERIC FLOW [LES EFFETS DE LA CONVECTION PROFONDE TROPICALE SUR L'ECOULEMENT ATMOSPHERIQUE DE GRANDE ECHELLE]

P. Bougeault *In* CNES, Subtropical Climates and Their Evolution: From Space-Based Observation to Modelling Oct. 1993 p 281-299 In FRENCH (For primary document see N94-30981 09-47)

Copyright Avail: Issuing Activity (CEPADUES-Editions, 111, rue Nicolas-Vauquelin, 31100 Toulouse, France)

A global approach to study large tropical clouds is presented. It is called the convection parameterization method. A scale analysis of the tropical zone motions and the principles of cloud convection are discussed. The thermodynamic variables, the temperature and moisture profiles in convective clouds and a convective ascendence model are reviewed. It is shown how, by applying the global thermodynamic balance method, the effects can be experimentally assessed. The following approaches used in convection parameterization in climate models are summarized: the Kuo approach, the Arakawa Schubert calculation, the Bourgeault mass flow scheme. ESA

N94-30995 Paris VI Univ., Villefranche-sur-Mer (France). Lab. Physique et Chimies Marines.

THE OCEAN-ATMOSPHERE INTERACTIONS IN THE MEDITERRANEAN SEA [LES INTERACTIONS OCEAN-ATMOSPHERE EN MEDITERRANEE] **c48**

J. P. Bethoux *In* CNES, Subtropical Climates and Their Evolution: From Space-Based Observation to Modelling Oct. 1993 p 301-312 In FRENCH (For primary document see N94-30981 09-47)

Copyright Avail: Issuing Activity (CEPADUES-Editions, 111, rue Nicolas-Vauquelin, 31100 Toulouse, France)

The Mediterranean Sea is a plot area for air-sea interaction studies and can be considered as a small scale model for studying different phenomena of the terrestrial ocean. In particular, climate drives concentration basin dynamics and dense water formation. Marine data allows hypothesis and models for studying paleoclimate or recent climate changes. The Mediterranean Sea thermal balance shows that the water evaporation losses are superior to fresh water gains. The east and west Mediterranean sea zones are concentration basins and their water dynamics are the result of interactions with the atmospheric circulation. The dense water thermal changes in the west Mediterranean zone can be an indicator of the greenhouse effect increase. ESA

N94-30996 Centre National d'Etudes Spatiales, Toulouse (France). Lab. d'Etudes et de Recherches en Teledetection Spatiale.

RADIATION/REMOTE SENSING: REVIEW OF THE PRINCIPAL DEFINITIONS [RAYONNEMENT/TELEDETECTION: RAPPEL DES PRINCIPALES DEFINITIONS] **c43**

G. Dedieu (Centre National de la Recherche Scientifique, Toulouse, France.) *In its* Subtropical Climates and Their Evolution: From Space-Based Observation to Modelling Oct. 1993 p 315-32 In FRENCH (For primary document see N94-30981 09-47)

Copyright Avail: Issuing Activity (CEPADUES-Editions, 111, rue Nicolas-Vauquelin, 31100 Toulouse, France)

The following concepts which allow studying the electromagnetic radiation phenomena are discussed: the solid angle, the black body radiation, the natural body's thermal emissions. The differences between bulk and surface reflections is stressed. The equation of the spectral two dimensional reflectance and that of the albedo, the ratio between emitted and reflected radiation powers, are given. The basic principles for calculating the radiation energy balance are summarized. Radiometric measurements of an extended light source are carried out. Terrestrial luminosity at long and short wavelengths is studied. ESA

N94-30997 Centre National d'Etudes Spatiales, Toulouse (France).

SPACE EQUIPMENT FOR EARTH OBSERVATIONS [LES INSTRUMENTS SPATIAUX D'OBSERVATION DE LA TERRE] **c19**

Marc Leroy *In its* Subtropical Climates and Their Evolution: From Space-Based Observation to Modelling Oct. 1993 p 329-38 In FRENCH (For primary document see N94-30981 09-47)

Copyright Avail: Issuing Activity (CEPADUES-Editions, 111, rue Nicolas-Vauquelin, 31100 Toulouse, France)

The operation principles of space equipment are summarized. Earth observation from space has known an important development these last years and will probably grow even more rapidly in the short term. A wide variety of space instruments, active or passive, in the optical or microwave range can be found. The principles of measurement of these space instruments are reviewed. The notion of temporal resolution is made clear through the description of the orbits used in the field of Earth observation. The link between instrument measurement and input radiance is clarified. ESA

N94-30998 Universite des Sciences et Techniques de Lille (France). Lab. d'Optique Atmospherique.

MATTER-RADIATION INTERACTIONS IN THE ATMOSPHERE [INTERACTIONS MATIERE-RAYONNEMENT DANS L'ATMOSPHERE] **c46**

Y. Fouquart *In* CNES, Subtropical Climates and Their Evolution: From Space-Based Observation to Modelling Oct. 1993 p 383-411 In FRENCH (For primary document see N94-30981 09-47)

Copyright Avail: Issuing Activity (CEPADUES-Editions, 111, rue Nicolas-Vauquelin, 31100 Toulouse, France)

The following basic phenomena and equations describing interactions between matter and radiation are reviewed: light transfer equation; light absorption, diffusion and emission; Bouguer law, optical thickness, phase function, thermodynamic equilibrium; molecular coefficient and energy absorption, absorption spectra of atmospheric gases, Doppler effect, Voigt form, light transmission coefficient, bandwidth models. The main radiation variables, concepts, and units are defined. ESA

N94-30999 Joint Research Centre of the European Communities, Ispra (Italy). Remote Sensing Applications Inst.

MODELING THE INTERACTION BETWEEN SOLAR RADIATION AND TERRESTRIAL SURFACES

Michel M. Verstraete and Bernard Pinty *In* CNES, Subtropical Climates and Their Evolution: From Space-Based Observation to Modelling Oct. 1993 p 413-430 (For primary document see N94-30981 09-47)

Copyright Avail: Issuing Activity (CEPADUES-Editions, 111, rue Nicolas-Vauquelin, 31100 Toulouse, France)

The reasons for modeling the interaction between solar radiation and terrestrial surfaces, the required approximations, and the way they affect the level of representativity of the models, and the principles and rationale of model inversion against observed data, are reviewed. Significant progress was achieved towards the design of realistic models of bidirectional reflectance of natural surfaces, and this effort is a major element in the stragegy to retrieve quantitative information from satellite remote sensing data. Important limitations remain in model design, and the lack of comprehensive data sets of reflectances, coupled with exhaustive descriptions and measurements of the optical and structural properties of the observed surfaces, make it difficult to validate existing models. In the mean time, urgent environmental issues require immediate attention, and more empirical approaches may be necessary. ESA

N94-31000 Centre National de la Recherche Scientifique, Palaiseau (France). Lab. de Meteorologie Dynamique.

THE USE OF METEOROLOGICAL SATELLITE DATA FOR STUDYING TROPICAL ATMOSPHERIC PHENOMENA [L'UTILISATION DES DONNEES DE SATELLITES METEOROLOGIQUES POUR L'ETUDE DE PHENOMENES ATMOSPHERIQUES TROPICAUX]

Michel Desbois (Ecole Polytechnique, Palaiseau, France.) *In* CNES, Subtropical Climates and Their Evolution: From Space-Based Observation to Modelling Oct. 1993 p 431-445 In FRENCH (For primary document see N94-30981 09-47)

Copyright Avail: Issuing Activity (CEPADUES-Editions, 111, rue Nicolas-Vauquelin, 31100 Toulouse, France)

Meteorological satellites provide two kinds of atmospheric products in an operational way: cloud track winds and temperature and humidity profiles. These products have a limited accuracy but are useful in tropical areas. The content of the satellite information allows the study of parameters such as the elements of the radiative budget, the cloudiness characteristics, and precipitations. The useful methodologies are reviewed and illustrated with examples of applications to specific studies of tropical phenomena. The perspectives offered by new space sensors and necessary research developments are reviewed. ESA

N94-31001 Institut National de la Recherche Agronomique, Villenave d'Ornon (France). Station de Bioclimatologie.

THE SURFACE PARAMETERS: REMOTE SENSING OBSERVATIONS AND CLIMATOLOGY APPLICATIONS [LES PARAMETRES DE SURFACE: OBSERVATION PAR TELEDETECTION ET APPLICATIONS EN CLIMATOLOGIE]

Jean-Pierre Lagouarde *In* CNES, Subtropical Climates and Their Evolution: From Space-Based Observation to Modelling Oct. 1993 p 447-465 In FRENCH (For primary document see N94-30981 09-47)

Copyright Avail: Issuing Activity (CEPADUES-Editions, 111, rue Nicolas-Vauquelin, 31100 Toulouse, France)

The state of the earth surface determines the exchange process between the soil and the atmosphere, which have a certain influence over climate phenomena. Several parameters, which are suitable indicators of surface conditions, can be observed by satellites. Some examples of remote sensing potentialities for studying global vegetation and climate phenomena, in particular over tropical zones, are presented. Several methods were developed for applying teledetection data in climate studies. Some of these data can be used directly, such as those for albedo cartography in general circulation meteorology. Algorithms were developed for cases where data

has to be transformed, for instance, rain or evaporation mapping from surface temperature data. However, improvements of algorithms and of the accuracy of present satellite data are still needed. ESA

N94-31002 Centre de Recherches en Physique de l'Environnement, Issy-les-Moulineaux (France).
RADAR MEASUREMENTS [MESURES RADAR] **c32**
Frank Roux *In* CNES, Subtropical Climates and Their Evolution: From Space-Based Observation to Modelling Oct. 1993 p 467-494 In FRENCH (For primary document see N94-30981 09-47)
Copyright Avail: Issuing Activity (CEPADUES-Editions, 111, rue Nicolas-Vauquelin, 31100 Toulouse, France)

The radar operation principles, some applications, and data analysis techniques are summarized. Special attention is given to meteorological, Doppler, polarization diversity, and wind profiling radars. The design parameters and the radar equation and historical facts are summarized. Some of the latest developments on meteorological radars are related to onboard and space radars. One of the difficulties is the attenuation of satellite emissions by rain, which leads to the development of reliable data processing algorithms. The electronic radar components acquired suitable reliability and the data processing techniques allow in most cases accurate quantitative results. ESA

N94-31003 Universite des Sciences et Techniques de Lille (France). Lab. d'Optique Atmospherique.
DESERT AEROSOLS: SOURCES, TRANSPORTS, AND IMPACTS DETERMINED BY REMOTE SENSING [LES AEROSOLS DESERTIQUES: SOURCES, TRANSPORTS, IMPACTS DETERMINES PAR TELEDETECTION] **c45**
I. Jankowiak and D. Tanre *In* CNES, Subtropical Climates and Their Evolution: From Space-Based Observation to Modelling Oct. 1993 p 495-523 In FRENCH (For primary document see N94-30981 09-47)
Copyright Avail: Issuing Activity (CEPADUES-Editions, 111, rue Nicolas-Vauquelin, 31100 Toulouse, France)

Dust particles or desert aerosols come from arid and half arid zones, in particular from the Sahara, which is responsible for 25 percent of the total amount of aerosols. During desert storms, the dust can be carried by the wind and reach the Atlantic sea surface and the Caribbean. For accurately modeling dust transport phenomena, the dust plumes to be studied have to be localized and their evolution has to be daily and yearly described. Present satellite sensors do not allow continuous sensing of the motion of dust clouds. The use of satellite imagery for studying aerosol characteristics and dust transport phenomena is summarized. ESA

N94-31004 Ecole Normale Superieure, Paris (France). Lab. d'Ecologie.
BEHAVIOR AND DYNAMICS OF TROPICAL FORESTS AND SAVANNAS [FONCTIONNEMENT ET DYNAMIQUE DES FORESTS ET SAVANES TROPICALES] **c43**
J. C. Menaut *In* CNES, Subtropical Climates and Their Evolution: From Space-Based Observation to Modelling Oct. 1993 p 527-546 In FRENCH (For primary document see N94-30981 09-47)
Copyright Avail: Issuing Activity (CEPADUES-Editions, 111, rue Nicolas-Vauquelin, 31100 Toulouse, France)

The tropical zones cover approximately one third of the earth's land surface. The tropical forests and the savannas show similar characteristics. This particularity allows the tropical African forest to be used as a model for studying the world's tropical forests. The general characteristics and the behavior of the savanna's ecosystem are dicussed. The dynamics of the savanna's ecosystem mainly depends on grass/tree regulative exchanges and on the soil water content. The importance of applying a model for studying soil, vegetation, and atmospheric interactions is explained. The effects of the following phenomena are discussed: atmospheric carbon dioxide content, temperature increase, rainfall distribution, soil occupation/use, and the disturbances caused by natural or human activities. ESA

N94-31005 Paris VII Univ. (France). Unite de Physico-Chimie et Geochimie de l'Atmosphere.
ARID REGIONS AND WIND EROSION [ZONES ARIDES ET EROSION EOLIENNE]
G. Bergametti *In* CNES, Subtropical Climates and Their Evolution: From Space-Based Observation to Modelling Oct. 1993 p 547-557 In FRENCH (For primary document see N94-30981 09-47)
Copyright Avail: Issuing Activity (CEPADUES-Editions, 111, rue Nicolas-Vauquelin, 31100 Toulouse, France)

Soil dust particles are carried by the wind from desert zones to the atmosphere. The causes, the models, and some consequences of wind erosion phenomena are discussed. The problem of modeling wind soil erosion, due to the lack of knowledge in the field of viscous flow velocity limits and the particle's size, is considered. The relationship between the atmospheric boundary layer and wind erosion effects are reviewed. The physical mechanisms for saltating and suspending particles from the soil are summarized. Theoretical and experimental approaches for evaluating vertical particle flow are discussed. ESA

N94-31006 Toulouse Univ. (France). Lab. d'Aerologie.
AIRBORNE INSTRUMENTS [INSTRUMENTS AEROPORTES] **c43**
A. Druilhet *In* CNES, Subtropical Climates and Their Evolution: From Space-Based Observation to Modelling Oct. 1993 p 559-585 In FRENCH (For primary document see N94-30981 09-47)
Copyright Avail: Issuing Activity (CEPADUES-Editions, 111, rue Nicolas-Vauquelin, 31100 Toulouse, France)

Spaceborne remote sensing measurements allow the study of surface boundary conditions. In order to reach the objectives, the techniques, the equipment, and the data processing systems have to be developed and validated. The airborne measurement is the necessary intermediate step to link Earth surface phenomena to remote sensing data. The technique is illustrated by means of the FIFE (First ISLSCP Field Experiment) project. The usefulness of aeroplanes for studying trace components, turbulence phenomena, and atmosphere vertical fine structure is demonstrated. Some methods used in airborne remote sensing are summarized. ESA

N94-31007 Paris-Sud Univ., Orsay (France). Lab. d'Ecologie Vegetale.
CARBON BALANCE IN A FOREST ECOSYSTEM [BILAN CARBONE D'UN ECOSYSTEME FORESTIER] **c45**
Bernard Saugier *In* CNES, Subtropical Climates and Their Evolution: From Space-Based Observation to Modelling Oct. 1993 p 587-618 In FRENCH (For primary document see N94-30981 09-47)
Copyright Avail: Issuing Activity (CEPADUES-Editions, 111, rue Nicolas-Vauquelin, 31100 Toulouse, France)

The ecosystem characteristics, the main elements of carbon balance in forests, and data from well known regions are given. However, most results must be taken as an indication instead of as the absolute truth: up to now, there is no ecosystem where all the required parameters and variables are measured. In order to improve the understanding of the forest ecosystems and the effect of several phenomena, research programs are focalized into two directions: modeling present forest ecosystem; studying, modeling, and simulating the effect of global changes on the balance of carbon of forests. In order to understand the role of trees in CO2 formation it is necessary to pass from local to global scale, which requires the use of satellite remote sensing technology. ESA

N94-31008 Toulouse Univ. (France). Lab. d'Aerologie.
SOURCES AND WELLS OF MINOR ATMOSPHERIC CONSTITUENTS OF CLIMATIC IMPORTANCE [SOURCES ET PUITS DE CONSTITUANTS MINEUR ATMOSPHERIQUES D'INTERET CLIMATIQUE] **c45**
Robert Delmas *In* CNES, Subtropical Climates and Their Evolution: From Space-Based Observation to Modelling Oct. 1993 p 619-638 In FRENCH (For primary document see N94-30981 09-47)
Copyright Avail: Issuing Activity (CEPADUES-Editions, 111, rue Nicolas-Vauquelin, 31100 Toulouse, France)

An overview of sources and sinks of atmospheric minor constituents of climatic importance is given. The role in the atmosphere, and of sources and sinks in general of the greenhouse gases, carbon dioxide, methane, nitrous oxide, chlorofluorocarbons, tropospheric ozone, and precursors, is described. The attention is focalized on tropical regions, especially Africa, where the dominant source is biomass burning which induces important photochemical formation of ozone and contributes significantly to rainwater acidification. ESA

N94-31009 Centre National de la Recherche Scientifique, Montpellier (France).
CLIMATIC EVOLUTION AND DESERTIZATION [EVOLUTION CLIMATIQUE ET DESERTISATION]

H. N. LeHouerou *In* CNES, Subtropical Climates and Their Evolution: From Space-Based Observation to Modelling Oct. 1993 p 639-668 In FRENCH (For primary document see N94-30981 09-47)
Copyright Avail: Issuing Activity (CEPADUES-Editions, 111, rue Nicolas-Vauquelin, 31100 Toulouse, France)

The concept of desertization, or the irreversible growth of new desert areas onto arid zones, is discussed. The phenomenon is characterized by the gradual disappearance of vegetation, which becomes concentrated nearby water sources. Several scenarios for explaining the desertization phenomena which take into account the effects of CO2 pollution and the increase of about 3C of the Earth's temperature, are summarized. Up to now, these scenarios are not reliable concerning predictions of seasonal changes. It is shown that the albedo has no effect on the climate, at least for local effects. The human activities and the zones of high population densities are under continuous desertization danger. New technologies such as remote sensing are valuable tools for helping the environment management. ESA

N94-31010 Centre National de la Recherche Scientifique, Verrieres-Le Buisson (France). Service d'Aeronomie.
THE OZONE AND THE PHYSICO-CHEMICAL PROCESSES IN TROPICAL REGIONS [OZONE ET PROCESSUS PHYSICO-CHIMIQUES DANS LES REGIONS TROPICALES] **c45**
Gerard Megie (Paris VI Univ., France.) and Gerard Ancellet (Paris VI Univ., France.) *In* CNES, Subtropical Climates and Their Evolution: From Space-Based Observation to Modelling Oct. 1993 p 669-685 In FRENCH (For primary document see N94-30981 09-47)
Copyright Avail: Issuing Activity (CEPADUES-Editions, 111, rue Nicolas-Vauquelin, 31100 Toulouse, France)

Population growth, industrial production, and transportation induce changes in the chemical composition of the atmosphere, which disturb the Earth's environment. The tropospheric ozone content is correlated to climate changes. The processes controlling the distribution of ozone in the troposphere are discussed. The ozone percentage in tropical regions is highly dependent on the presence of ozone wells (by photolysis and the rupture of OH and HO2 radicals) and on the biomass burning processes. Experimental results demonstrate the corrrelation between the low troposphere's composition and the emission of burned savanna products. ESA

N94-31011 Centre National d'Etudes Spatiales, Toulouse (France). Lab. d'Etudes et de Recherches en Teledetection Spatiale.
MODELING OF THE CONTINENTAL BIOSPHERE [MODELISATION DE LA BIOSPHERE CONTINENTALE] **c45**
Philippe Martin *In its* Subtropical Climates and Their Evolution: From Space-Based Observation to Modelling Oct. 1993 p 687-70 In FRENCH (For primary document see N94-30981 09-47)
Copyright Avail: Issuing Activity (CEPADUES-Editions, 111, rue Nicolas-Vauquelin, 31100 Toulouse, France)

Modeling the dynamics of the terrestrial biosphere proceeds in four steps: a calculation of the area which can be colonized by vegetation; a parameterization of the exchanges of energy, water, momentum, carbon dioxide, or other physical and chemical quantities; a simulation of local ecological dynamics; and a description of migratory processes. Seven generic models of ecological dynamics, namely, probabilistic, inferential, threshold, statistical, response surface, ecophysiological, and mechanistic models, are described. Existing vegetation schemes are not suited to describe the continental biosphere in a general circulation model. Scaling issues accociated with the representation of migratory processes are also discussed. The CFL (Courant, Friedrichs, and Lewis) stability criterion insures that a model does not transfer atmospheric information more rapidly through space than time. Conversly, a vegetation model should give the landscape enough time for movements of vegetation across the landscape to be properly registered. The migration criterion guarantees that this is the case. A coupled climate/vegetation model respects the criterion when the ratio of its climatic and vegetation space is approximately five orders of magnitude smaller than the ratio of its time scales. ESA

N94-31239# Naval Postgraduate School, Monterey, CA. Dept. of Operations Research.
A COMPARISON OF PREDICTORS FOR FIRST-GUESS WIND SPEED ERRORS
Donald P. Gaver and Patricia A. Jacobs Dec. 1993 36 p
(AD-A276460; NPS-OR-93-020) Avail: CASI HC A03/MF A01

Numerical meteorological models are used to assist in the prediction of weather. Each run of a numerical model produces forecasts of meteorological variables which are used as preliminary predictions of the future values of these variables. These initial predictions are referred to as first-guess values. Estimation of the mean-square first-guess error is required in the optimal interpolation process in the numerical prediction of atmospheric variables. Several predictors for the mean-square error of the first-guess wind speeds are studied. The results suggest that prediction using observed covariates tend to be better than those using first-guess covariates. However, observed covariates are not always available. Predictions using first-guess covariates are better at the 250 mb level than the 850 or 500 mb levels. Of those first-guess covariates studied, first-guess wind speed appears to be the best. DTIC

N94-31322# Argonne National Lab., IL.
IMPLEMENTATION OF INSTRUMENTS AND FACILITIES AT THE SGP CART SITE
D. L. Sisterson and M. L. Wesely 1994 7 p Presented at the 3rd Atmospheric Radiation Measurement Science Team Meeting, Norman, OK, 1-5 Mar. 1994
(Contract W-31-109-eng-38)
(DE94-006839; ANL/ER/CP-80451; CONF-940373-1) Avail: CASI HC A02/MF A01

This report discusses the installation of instruments and trailers at the southern Great Plains Clouds and Radiation Testbed site. DOE

N94-31554 Pennsylvania State Univ., University Park.
REGIONAL SOURCES OF ERROR GROWTH IN THE NATIONAL METEOROLOGICAL CENTER'S MEDIUM-RANGE FORECAST MODEL Ph.D. Thesis
Carolyn A. Reynolds 1993 223 p
Avail: Univ. Microfilms Order No. DA9326932

The full spatial structure of systematic and random error growth in the National Meteorological Center's Medium-Range Forecast Model is investigated in an effort to identify the sources of error growth. The random error growth is partitioned into two types: external error growth, which is due to model deficiencies, and internal error growth, which is the unstable growth of errors in the initial conditions. Data from winter 1987, summer 1990, and winter 1992 are compared to assess seasonal variations in regional error growth, as well as to forecast model improvement. The tropical upper-tropospheric easterly bias in the forecast model is strongest in the regions of the upper-tropospheric westerlies. The structure of the evolution with forecast time of the U-field variance is consistent with the theory of stronger meridional propagation of extratropical disturbances where the U-field is westerly and energy accumulation where delta(U)/delta(x) is negative. The spatial structure of the external error growth in the extratropics reveals that the representation of orography in the model is inadequate. There is evidence of enhanced external error growth over the Rockies, Himalayas, and Antarctica. In the tropics, high external error at the 200 mb level is closely associcated with deep convection. There is evidence of significant model improvements in the tropics at the 850 mb level between 1987 and 1992. Internal error growth in the mid-latitudes is strongly associated with blocking phenomena, especially over the North Atlantic and Europe. In the tropics, there is some evidence of internal error accumulation in regions where delta(U)/delta(x) is negative. The results of this study are physically meaningful and in agreement with previous predictability studies, as well as current knowledge of forecast model deficiencies, while at the same time, providing new information about the full spatial and temporal distributions of forecast errors. Dissert. Abstr.

N94-31597# Wisconsin Univ., Madison. Dept. of Atmospheric and Oceanic Sciences.
BOUNDARY-LAYER CUMULUS OVER LAND: SOME OBSERVATIONS AND CONCEPTUAL MODELS
R. B. Stull 1993 16 p Presented at the ECMWF Workshop on Boundary-Layer Clouds, Reading, England, 8-11 Jun. 1993
(Contract DE-FG02-92ER-61361)
(DE93-040820; CONF-9306252-1) Avail: CASI HC A03/MF A01

Starting in 1980, the Boundary Layer Research Team at the University

of Wisconsin has been systematically studying the formation and evolution of nonprecipitating boundary-layer cumulus clouds (BLCu) in regions of fair weather (anticyclones) over land (Stull, 1980). Our approach is to quantify the average statistical characteristics of the surface, thermals, boundary layer, and clouds over horizontal regions of roughly 20 km in diameter. Within such a region over land, there is typically quite a variation in land use, and associated variations in surface albedo and moisture. DOE

N94-31743 Illinois Univ., Urbana-Champaign.
FIELD STUDIES OF RAINDROP OSCILLATIONS WITH APPLICATIONS TO RADAR METEOROLOGY Ph.D. Thesis
Ali Tokay 1993 181 p
Avail: Univ. Microfilms Order No. DA9329183

The characteristics and causes of raindrop oscillations were studied from two field experiments in Hawaiian and Illinois showers. The former experiment (HaRP) focused on the onset of raindrop oscillations as well as oscillations frequencies of small raindrops, whereas the latter experiment (ISWS) had a broader purpose to investigate the oscillation characteristics of moderate-to-large sized raindrops including amplitudes as well as frequencies, and oscillation causes. Raindrop oscillations were found to start at a diameter of d = 1.0 to 1.1 mm in both HaRP and ISWS experiments, consistent with 1991 laboratory observations of Beard, Kubesh, and Ochs and with the expected onset of eddy shedding. Most of the oscillation frequencies (greater than 95%) were near the fundamental harmonic (f2) with only a few observed near the first harmonic (f3) in both experiments. The oscillation frequencies around the fundamental harmonic showed a sized dependency that crossed the theoretical value for f2 at about d = 1.5 to 1.6 mm. The oscillation amplitude measurements determined from the vertical extent of the dash streaks showed good agreement with the 1988 data of Sterlyadkin, whereas the oscillation amplitudes estimated from the distortion indicated somewhat larger values of d greater than 2 mm. Eddy shedding was found to be the most likely cause of small raindrop oscillations because of the onset oscillations near 1.0 mm and weak forcing by drop collisions, turbulence, and wind shear. The influence of raindrop oscillations on dual-polarization radar parameters was investigated for the observed and theoretical size distributions using axis ratios based on different sets of calculations and measurements. Differential reflectivity (Z sub DR) decreased by as much as 0.74 dB from its value for non-oscillating raindrops. Similar change caused by raindrop oscillations were also found for the other dual-polarization parameters, such as the circular and linear depolarization ratios (CDR, LDR), differential phase shift, and differential specific attenuation. Dissert. Abstr.

N94-31775 Utah State Univ., Logan.
THE PROPERTIES OF SUNFLECKS IN A FLEXIBLE PLANT CANOPY, AND THEIR RELATIONSHIP TO TURBULENCE Ph.D. Thesis
Hongliang Tong 1992 175 p
Avail: Univ. Microfilms Order No. DA9316793

The properties of sunflecks within alfalfa canopies and their relationship to atmospheric turbulence above the canopies were quantified. Transient light environment in an alfalfa canopy was observed being highly dynamic, lasting from fractions of seconds to minutes in duration. Both probabilistic analysis and autocorrelation analysis indicate that the mean duration of sunflecks ranges from 0.1 to 1.6 seconds with most frequent sunflecks having durations of 0.2 to 0.8 seconds. Power spectral analysis suggests that winds have significant influences on the properties of sunflecks in the alfalfa canopies. Calculated power spectra of photosynthetically active radiation (PAR) time series within the canopies show clear linear relationships with the mean wind speeds and the spectra of vertical velocity measured 16 m above the canopies. This implies that the properties of sunflecks may be evaluated from the measured properties of turbulence. Results also show that the total variances of the PAR time series increase with increased wind, and the enhancement in variance is more apparent in lower canopy as wind increases. This suggests that the wind-induced movement of plants can reduce the vertical light gradient with canopy depth. Also, frequency distributions of sunfleck irradiance were found to disobey the normal distribution laws, but to be skewed. The skewness is affected by both canopy depth and wind. Smaller canopy depth and stronger winds can cause larger skewness. An attempt was made to use the beta distributions to simulate the PAR irradiance distributions, and the simulated results seem acceptable. The PAR spatial series were also characterized. Spatial power spectral analysis suggests that small-scale spatial heterogeneity is a predominant feature of light environment in alfalfa canopies, and lower solar elevation seems to decrease the spatial variability. In addition, similar analyses were conducted for an aspen canopy. The power spectra of the PAR time series measured within the aspen crown indicates that wind-induced leaf flutter can yield rapid sunflecks of 6 Hz in frequency. Dissert. Abstr.

N94-31791 North Carolina State Univ., Raleigh.
NUMERICAL SIMULATIONS OF MONSOON RAINFALL WITH THE NRL/NCSU REGIONAL NESTED GRID MODEL Ph.D. Thesis
Kirankumar Venkata Alapati 1993 209 p
Avail: Univ. Microfilms Order No. DA9316598

The short-range prediction of monsoon circulations and associated weather is a challenging problem. Two important physical processes which affect the dynamics as well the thermodynamics of the monsoon are the cumulus convection and the energy and the mass transfer in the atmospheric boundary layer. From the modeling point of view, horizontal and vertical resolutions, numerical techniques and data preparation are important components. A limited area numerical model with different boundary layer and cumulus parameterizations has been developed to simulate various physical processes and rainfall associated with the Asian summer monsoon. The model developed for this research is based on a version of the Naval Research Laboratory's nested grid model. Two different cumulus parameterization schemes, one developed by Kuo and the other by Betts-Miller, are used to simulate the monsoon rainfall during three different periods of the monsoon during which rainfall was moderate to heavy. Results indicate that the monsoon processes and associated rainfall are better predicted with the Kuo scheme. Uncertainties present in the adjustment parameter used in the Betts-Miller scheme lead to poor predictions. These results indicate necessity for further testing of the Betts-Miller scheme for the monsoon region. Model forecast showed considerable sensitivity to the sea surface temperature distribution. When observed sea surface temperatures are used, predicted rainfall is considerably higher than with the climatological values. Model results also indicated higher rainfall rates when a diabatic initialization scheme is used. With an increased vertical resolution in the boundary layer and better boundary layer physics, the sixteen layer model predicted significant diurnal variation of the height of the boundary layer over land and very little variation over the oceans. Also, forecast errors in the predicted fields are reduced particularly in the lower troposphere. Circulation patterns and the temporal and spatial distributions of rainfall are also better predicted with increased vertical resolution. Dissert. Abstr.

N94-31889 Kansas Univ., Lawrence.
RADAR RAINFALL MEASUREMENTS FROM SPACE Ph.D. Thesis
Duc Cong Kieu 1992 348 p
Avail: Univ. Microfilms Order No. DA9327538

Existing spaceborne rain-rate retrieval algorithms have unreasonable assumptions, and usually yield unrealistic and/or inaccurate rain-rate estimates. The relative errors in the rain-rate estimates of existing algorithms are typically larger than 50 percent. Practical constraints, and spatial and temporal variability of rain have made the potential rain rate estimation from a spaceborne platform very erroneous. The robust rain-rate retrieval (RRR) algorithm accurately extracts rain-rate profiles, using information from active and passive microwave sensors. Simulation results show that the total error in the RRR algorithm is within 20 percent. The RRR algorithm binds the rain-rate and rain-parameter estimators with guess intervals, utilizes radar properties of rain and concepts from existing rain-rate retrieval algorithms to further refine the rain-rate estimators, employs an adaptive weighted nonlinear least-squares technique, accounts for the presence of melting layers, and robustly produces unique and accurate rain-rate profiles. Measurement of rainfall from space will provide climatological data over regions where rain gauges are sparse, particularly over the oceans and developing countries. The planned Tropical Rainfall Measuring Mission (TRMM) radar will scan from side to side (i.e., the SSS mode). The proposed conical scanning (CS) mode offers many advantages over the side-to-side scanning (SSS) mode. For example, the high surface-clutter interference near vertical in the SSS mode is absent in the CS mode. The CS mode can be attained in three ways. They involve the use of a mechanically scanned parabolic-reflector antenna or fixed array, a single large fixed vertical electronically space-fed antenna, and two small tilted electronically

scanned space-fed antenna. The work here studied the feasibility of space-fed array (i.e., lens arrays and reflect arrays), active arrays, parabolic reflectors for the rain radar in the CS mode. Dissert. Abstr.

N94-31937# Kansas Univ. Center for Research, Inc., Lawrence. Radar Systems and Remote Sensing Lab.

SCATTEROMETER WIND-SPEED EXPONENTS: A REVIEW AND SAXON 35-GHz MEASUREMENTS

Xiao-Ping Wang Aug. 1993 45 p

(Contract N00014-89-J-3221)

(AD-A276568; CRINC/RSL-TR-8621-2) Avail: CASI HC A03/MF A01

Wind exponents Gamma are very important in the study of radar scattering cross-section under ocean-surface conditions. Most experiments apply the ordinary least-square regression (OLR). However, OLR accounts for error in only one variable in the regression, and therefore the results of OLR may not be statistically correct. In contrast, the orthogonal regression (OR) provides a good way to estimate two correlation variables (x,y) when both of them have errors. The best results are obtained if x and y have similar scales. Our study shows that OR has agreement with OLR when x is perfectly known without errors. Otherwise, OR and OLR have different results. For example, SAXON-FPN experiment (35 GHz) data demonstrates that orthogonal regression (OR) and ordinary linear regression (OLR) methods have similar wind exponent, Gamma, if the wave and the wind directions are same. If however, the directions are not the same, the estimates disagree. In this case, the estimate of Gamma from OR and OLR methods. Thus, it is seen that the wind exponent Gamma, has a highest value in both OR and OLR methods. Thus, it is seen that the wind exponent, Gamma, has a highest value when the wind direction and the wave direction are normal to the radar. DTIC

N94-31989 Massachusetts Inst. of Tech., Cambridge.

CUMULUS CONVECTION PARAMETERIZATION AND NUMERICAL MODELLING OF MOIST ATMOSPHERES Ph.D. Thesis

Nilton de Oliveira Renno 1992

Avail: Issuing Activity (MIT Libraries, Rm. 14-0551, Cambridge, MA 02139-4307)

A hydrological cycle is explicitly included in a one-dimensional radiative-convective equilibrium model which is coupled to a 'swamp' surface and tested with various cumulus convection schemes: the Moist Convective Adjustment scheme (Manabe et al, 1965), the Kuo (1974) scheme, the GISS (1974) Model scheme, the GISS (1983) Model II scheme, and the Emanuel (1991) scheme. Our results show that when the flux of incoming solar radiation is above a critical value -- dependent on the choice of the cumulus convection scheme -- equilibrium is not possible (a runaway greenhouse occurs). When the atmosphere's relative humidity is kept fixed at climatological values, the runaway greenhouse is inhibited. Furthermore, while the mass flux schemes (GISS (1974), GISS (1983), and Emanuel (1991)) produce an abrupt runaway greenhouse -- which occurs through a finite amplitude instability generated by the interaction of infrared radiation fluxes with detrained water vapor at the level of neutral buoyancy -- the other schemes produce a smooth transition to the runaway greenhouse. In addition, our results show that the Moist Convective Adjustment scheme breaks down when the runaway greenhouse is approached, and that the various cumulus schemes tested produce a decrease in the relative humidity of the middle-upper troposphere when the atmosphere's CO2 content is doubled. These schemes are not consistent with each other since they not only lead to different critical solar forcing for a runaway greenhouse to occur, but also produce very different water vapor profiles in the equilibrium atmosphere and have different lapse-rate feedbacks. Finally, using the scheme proposed by Emanuel (1991), we show that the atmospheric water vapor content and, therefore, the sensitivity of the equilibrium temperature to changes in the solar forcing, as well as the critical solar forcing in order for the runaway greenhouse to occur, depend crucially on the microphysics of cumulus convection. These results indicate that a physically-based cumulus convection scheme is of crucial importance in climate simulations, and that a poor cumulus convection scheme can produce artificial sensitivities in numerical simulations of moist atmospheres.

Dissert. Abstr.

N94-32019# Naval Postgraduate School, Monterey, CA.

SHORT TERM TELECONNECTIONS ASSOCIATED WITH AN INDIVIDUAL TROPICAL CYCLONE M.S. Thesis

Stephen C. Woll Dec. 1993 138 p

(AD-A277210) Avail: CASI HC A07/MF A02

The short term teleconnections associated with an individual western Pacific tropical cyclone were investigated using an atmospheric general circulation model. The general strategy was to use the GCM, in combination with several tropical cyclone bogusing procedures, to isolate the effects on the global circulation of the tropical cyclone. The bogusing procedures were used to alter the tropical cyclone in the initial conditions for the model. The primary modeling experiments involved using the tropical cyclone bogusing procedures to include or exclude the tropical cyclone from the initial conditions. The difference between model results that contained the tropical cyclone and those that did not were used to analyze the global response to the tropical cyclone. These results showed a strong and persistent teleconnection response in the extratropical Northern Hemisphere. This response was mainly evident in slowly propagating Rossby waves in the 200 mb height field. Examinations of the teleconnection mechanisms showed that the east Asian-north Pacific jet played a major role in the development of the teleconnection. In particular the following occurred: (1) the 200 mb height responses showed a consistent relationship with the jet; (2) the jet acted as a waveguide for the Rossby wave energy; and (3) the regions of potential barotropic instability which flank the jet were often colocated with areas of wave amplification. DTIC

N94-32021 Naval Postgraduate School, Monterey, CA.

THE EVOLUTION OF JET FEATURES DURING THE 1993 EAST COAST WHITE HURRICANE: A CASE STUDY USING THE GLOBAL SPECTRAL MODEL M.S. Thesis

Anton J. Kraft Dec. 1993 179 p Limited Reproducibility: More than 20% of this document may be affected by microfiche quality

(AD-A277217) Avail: CASI HC A09

During the period of 12-14 Mar. 1993 a major snow storm, later described as a White Hurricane, formed over the Gulf of Mexico, moved east-northeast across the Florida panhandle, and then headed northeast along the eastern seaboard. The extreme weather produced by this storm was responsible for 243 deaths and $1 billion in property damage. Because the storm was accompanied by unusually strong jet streaks, a diagnostic of the storm kinetic energy contents and generation of kinetic energy was undertaken. The vertically integrated kinetic energy (IKE) and vertically integrated generation of kinetic energy (IGK) are shown to be effective tools in determining how jet streaks influenced the development of this storm. Specifically, IKE can indicate geographically where jet streak maxima are located, whereas IGK can provide a measure of the effect of transverse circulations aloft. In addition, IGK combined with IKE can indicate if the jet streak is weakening or strengthening. The data used in this case study were primarily the National Weather Service's Global Spectral Model aviation forecast and analysis. These data were further interpolated for use in VISUAL, which is a meteorological diagnostic and display program developed primarily at the Naval Postgraduate School. DTIC

N94-32030 Colorado Univ., Boulder.

ESTIMATION AND ANALYSIS OF CLIMATE-SCALE RAINFALL OVER THE TROPICAL PACIFIC Ph.D. Thesis

Wesley Keith Berg 1993 216 p

Avail: Univ. Microfilms Order No. DA9320396

The relatively recent advent of spaceborne passive microwave technology, which has the ability to see beyond the cloud tops viewed by traditional visible and infrared sensors, has provided new prospects for global rainfall estimation. Using data from the Special Sensor Microwave/Imager (SSM/I) a database of monthly rainfall estimates has been produced over the global oceans for a three and one half year period from July 1987 through December 1990. Comparisons with in situ observations from a group of Pacific atoll rain gauge sites were used to calibrate the monthly estimates. These estimates were then compared to monthly rainfall estimates made from visible and infrared satellite observations. Based on this comparison, the SSM/I estimates were found to be as good or better than the other techniques, although the sampling provided by the SSM/I was determined to be the major limiting factor. A quantitative assessment of the errors revealed the uncertainty in the monthly SSM/I rainfall estimates averaged over 2.5 degrees latitude/longitude bins to be on the order of 20 to 25 percent of the monthly values. A subsequent analysis of the monthly SSM/I rainfall time series revealed both the major

features of the precipitation distributions and the seasonal fluctuations to agree with expected values. In addition, evidence of a strong interannual signal corresponding to the 1986-87 El Nino and the ensuing 1988-89 La Nina was found. Finally, an EOF analysis of the resulting monthly rainfall time series was performed which showed strong seasonal and interannual signals as well as evidence of variability over semiannual and intraseasonal time scales. Dissert. Abstr.

N94-32046# Army Topographic Engineering Center, Fort Belvoir, VA.
SELECTION OF CLIMATE STATION DATA USING CLUSTERING AND TRIANGULATED IRREGULAR NETWORK TECHNIQUES Technical Report, Mar. 1992 - Jan. 1993
Kevin R. Slocum Oct. 1993 32 p
(DA Proj. 4A1-62784-A-855)
(AD-A276658; TEC-0041) Avail: CASI HC A03/MF A01

This report presents a methodology of adding an elevation variable to the process of selecting climate station data for computer modeling. Various techniques are used in this method which include statistical correlation of climatic variables, clustering of climate station data, and development of a triangulated irregular network (TIN) internal graphic layer with nodes representing climate station locations. Improvements to the climate station data selection process are documented. DTIC

N94-32054 State Univ. of New York, Albany. Atmospheric Sciences Research Center.
USE OF AIR FORCE CLOUD COVER DATA TO EVALUATE AND IMPROVE CLOUD FORECASTS AND PARAMETERIZATIONS IN MESOCALE METEOROLOGICAL MODELS Annual Report, 1 Oct. 1992 - 30 Sep. 1993
Chris Walcek 28 Oct. 1993 17 p Limited Reproducibility: More than 20% of this document may be affected by microfiche quality
(Contract F49621-92-J-0018)
(AD-A277384; AFOSR-94-0112TR) Avail: CASI HC A03

This research utilizes satellite and surfaced derived cloud observations to improve our diagnostic capability of areal cloud coverage. In particular, a new relationship between relative humidity, vertical velocity, and cloud cover has been tested. Results of this research will be used to complement existing cloud cover parameterization in both regional scale and global scale models. Improved forecasts of fractional areal of cloud cover is the number one meteorological research priority of the U.S. Air Force. DTIC

N94-32057# Air Force Environmental Technical Applications Center, Scott AFB, IL.
STATION CLIMATIC SUMMARIES: CHINA, THE FORMER USSR, AND MONGOLIA
Feb. 1994 681 p
(AD-A276548; USAFETAC/DS-94/037) Avail: CASI HC A99/MF A06

This report contains a collection of summarized monthly and annual climatic data for specific locations in China, the former Union of Soviet Socialist Republics (USSR), and Mongolia. The last entry in this collection is February 1992. Summarized climatological elements are: percent frequency of occurrence of ceiling and visibility; means, extremes and number of days with specified values of temperature, precipitation, and snowfall; means of relative humidity, vapor pressure, dew point, pressure altitude, and cloud cover; prevailing wind direction, with mean and extreme speeds; and number of days with thunderstorms and fog. DTIC

N94-32094# Naval Postgraduate School, Monterey, CA.
THE INFLUENCE OF CUMULUS PARAMETERIZATION ON MODEL FORECASTS OF RAPID OCEANIC CYCLOGENESIS M.S. Thesis
James W. Allen Dec. 1993 242 p
(AD-A277207) Avail: CASI HC A11/MF A03

Numerous studies have left little doubt that latent heat release (LHR) can significantly influence many features of extratropical cyclone systems. Recent experiments with the NCAR/PSU mesoscale model indicated that not only did different moisture parameterizations significantly affect model forecasts, but that forecasts for different cyclonic systems responded very differently to the parameterizations. Model output from the NCAR/PSU model is examined for two cyclonic systems, with four different parameterization experiments used to produce four forecasts for each system. The output was then examined in three and four dimensions to qualitatively and quantitatively determine the direct and indirect effects of latent heat release on model output. The results clearly showed the difference in the general dynamics of the two cyclones. One demonstrated a very strong reliance on diabatic processes for its early development, becoming more adiabatic late in its history, while the other initially developed very adiabatically and became more diabatic after about the mid-point of the forecast period. The cyclonic system that started out diabatically was more sensitive to moisture parameterization. The models clearly showed the differences between precipitation fields generated by the different parameterizations. In particular, allowing evaporation of precipitation in non-saturated layers greatly decreased the areal extent of light precipitation, while having minimal effect in areas of heavy precipitation. DTIC

N94-32117# Phillips Lab., Hanscom AFB, MA.
SENSITIVITY ANALYSIS OF THE AVHRR INFRARED CIRRUS MODEL
Allan J. Bussey and Robert P. DEntremont 19 Jul. 1993 42 p
(AD-A276690; AD-E201756; PL-TR-93-2166; ERP-1126) Avail: CASI HC A03/MF A01

We have studied the sensitivity to errors of a cirrus cloud analysis technique using NOAA Advanced Very High Resolution Radiometer (AVHRR) multispectral imagery. The sensitivity analysis reveals possible errors in computing optical depths and altitudes for nighttime cirrus cloud data samples taken from the First ISCCP Regional Experiment (FIRE) Phase 1 intensive field observations. The Appendix contains plots of the computed errors found in the study. DTIC

N94-32162 Reading Univ. (England).
COORDINATION OF MESOSCALE METEOROLOGICAL RESEARCH BETWEEN ASL AND EUROPEAN GROUP Final Report, 1 Feb. 1990 - 31 Dec. 1993
R. P. Pearce 31 Dec. 1993 23 p Limited Reproducibility: More than 20% of this document may be affected by microfiche quality
(Contract DAJA45-90-C-0021)
(AD-A276730; R/D-6323-EN-01) Avail: CASI HC A03

This report summarizes the activities undertaken by the US Army Mesomet Panel during the contract period. For the period to 31st March, 1993, nine interim reports were submitted and these contain full details of these activities. For the final period, 1st April - 31st December 1993, a more detailed account is provided here and includes, as Annex 2, the report of the Panel's final meeting in Munster, Germany, 9th-10th September, 1993. Its executive summary contains five important recommendations, all directed towards the future modeling activities at ARL. These arise from the lessons learned from the Mesomet Model Comparison Project undertaken during the contract period and subsequent Mesomet Workshop held in El Paso in June, 1992. Section 3 sets out what the Panel feels have been its achievements during the contract period, one in which considerable changes in policy direction occurred, some of which will have been influenced by the Panel's advice. Attention is drawn to the role of the Panel in involving the wider mesomet modeling community in ASL's activities, particularly through the Mesomet Model Comparison Project and El Paso Workshop. A major publication arising from these activities is a Mesometeorology Modeling monograph to be published by the American Meteorological Society in 1994. This is described in section 4. DTIC

N94-32164# Florida State Univ., Tallahassee. Dept. of Meteorology.
RECURVATURE DYNAMICS OF A TYPHOON Progress Report, 1 Jan. - 31 Dec. 1993
T. N. Krishnamurti 31 Dec. 1993 3 p
(Contract N00014-91-1-0243)
(AD-A276792) Avail: CASI HC A01/MF A01

This paper deals with high resolution numerical weather prediction experiments for the recent Bangladesh Tropical Cyclone (Apr. 1991). This devastating storm resulted in well over 100,000 deaths. The results from global model experiments carried out at a horizontal resolution of 213 waves (triangular truncation) and from a regional model at a horizontal resolution of 46 km are presented. Recent improvements in the model's parameterization of cumulus convection, land surface parameterization (the specification of ground wetness), and enhanced evaporation over low wind speed regions were included in the sensitivity studies. DTIC

N94-32260 Naval Research Lab., Monterey, CA.
TYPHOON HAVENS HANDBOOK FOR THE WESTERN PACIFIC AND INDIAN OCEANS, CHANGE 3 Final Report

Dennis C. Perryman, Richard E. Gilmore, and Ronald E. Englebretson Dec. 1993 290 p Limited Reproducibility: More than 20% of this document may be affected by microfiche quality
(AD-A277030; NRL/PU/7541-93-0014) Avail: CASI HC A13

Thirty-one ports in the western Pacific and Indian Oceans are evaluated to describe their potentials as havens for ships threatened by typhoons. These evaluations are designed to serve as decision-making aids for force commanders, ship captains, and ship-routing personnel. A general introductory section describes tropical cyclones and discusses ship performance in storms, warning services, and calculation of danger zones. Mean storm tracks for four ocean areas are depicted in appendices.
DTIC

N94-32268# Pacific Northwest Lab., Richland, WA.
A PARAMETERIZATION OF CLOUD DROPLET NUCLEATION
S. J. Ghan, C. C. Chuang, and J. E. Penner Jan. 1994 7 p Presented at the 74th American Meteorological Society Annual Meeting, Nashville, TN, 23-28 Jan. 1994
(Contract DE-AC06-76RL-01830)
(DE94-007469; PNL-SA-23042; CONF-940115-31) Avail: CASI HC A02/MF A01

Droplet nucleation is a fundamental cloud process. The number of aerosols activated to form cloud droplets influences not only the number of aerosols scavenged by clouds but also the size of the cloud droplets. Cloud droplet size influences the cloud albedo and the conversion of cloud water to precipitation. Global aerosol models are presently being developed with the intention of coupling with global atmospheric circulation models to evaluate the influence of aerosols and aerosol-cloud interactions on climate. If these and other coupled models are to address issues of aerosol-interactions, the droplet nucleation process must be adequately represented. Ghan et al. have introduced a droplet nucleation parameterization for a single aerosol type that offers certain advantages over the popular Twomey parameterization. Here we describe the generalization of that parameterization to the case of multiple aerosol types, with estimation of aerosol mass as well as number activated. DOE

N94-32278 Naval Research Lab., Monterey, CA.
TROPICAL CYCLONE FORECASTERS REFERENCE GUIDE. 5: NUMERICAL TRACK FORECAST GUIDANCE Final Report
Richard A. Jeffries, Charles R. Sampson, Lester E. Carr, III, and Jan-Hwa Chu Dec. 1993 44 p Limited Reproducibility: More than 20% of this document may be affected by microfiche quality
(AD-A277318; NRL/PU/7515-93-0011) Avail: CASI HC A03

One of the keys to safe and successful naval operations in the tropics is a thorough understanding of tropical meteorology. The Tropical Cyclone Forecasters Reference Guide is designed primarily as a ready reference for midlatitude forecasters required to provide tropical meteorology support to staff commanders. This report provides a comprehensive overview of numerical forecast guidance used to assess tropical cyclone motion and is chapter 5 of the reference guide. Subjects discussed include global and regional numerical modeling, major warning center operations, tropical cyclone numerical forecast aids, numerical modeling terminology, and applications of numerical forecast guidance to tropical cyclone forecasting.
DTIC

N94-32716# Pennsylvania State Univ., University Park.
AN INTEGRATED CLOUD OBSERVATION AND MODELING INVESTIGATION IN SUPPORT OF THE ARM PROGRAM
28 Jul. 1993 11 p
(Contract DE-FG02-90ER-61071)
(DE94-003160; DOE/ER-61071/3) Avail: CASI HC A03/MF A01

This annual technical progress report, based on the same four divisions used in our original proposal, provides only a brief synopsis of the research carried out during the past three years. We have also included a brief description of algorithms and computer programs that were transferred to the ARM management. Such transfers of knowledge and technique are vital for the success of the ARM program. Various members of our research group participated in two major field programs: the First ISSCP Regional Experiment (FIRE) Cirrus 2 Experiment held in Nov. 1991, in Kansas; and the Atlantic Stratocumulus Transition Experiment (ASTEX) held in the Azores in Jun. 1992. Although our participation in these campaigns was funded primarily through other agencies, the data collected in these programs were essential for certain components of our research. The graphical user interface programs that were transferred to ARM were a direct outgrowth of these field activities as well. In addition, we collected a variety of data at Penn State using our 94 GHz radar, microwave radiometer, wind profilers, and other instruments. Again these data were acquired to meet the needs of our proposed research.
DOE

N94-32717# State Univ. of New York, Albany. Atmospheric Sciences Research Center.
USE OF CLOUD OBSERVATIONS AND MESOSCALE METEOROLOGY MODELS TO EVALUATE AND IMPROVE CLOUD PARAMETERIZATIONS
C. J. Walcek 30 Sep. 1993 5 p
(Contract DE-FG02-92ER-61364)
(DE94-003610; DOE/ER-61364/2) Avail: CASI HC A01/MF A01

This research program utilizes satellite and surface-derived cloud observations together with standard meteorological measurements to evaluate and improve our ability to accurately diagnose cloud coverage. Results of this research will be used to compliment existing or future parameterizations of cloud effects in general circulation models, since nearly all cloud parameterizations must specify a fractional area of cloud coverage when calculating radiative or dynamic cloud effects, and current parameterizations rely on rather crude cloud cover estimates. During the first phase of this research program, our goal is to evaluate and improve the methods for calculating cloud cover within a mesoscale meteorology model. To accomplish this, a mesoscale meteorology model will be quantitatively evaluated using available cloud cover databases including the U.S. Air Force 3DNEPH and RTNEPH satellite-derived cloud fields, as well as CART data as they become available. During the second phase of this research, the cloud cover data and improved parameterizations of cloud coverage developed during the first phase will be incorporated into a mesoscale meteorology model. Model forecasts which utilize the observed cloud coverage and depth should be improved relative to forecasts which crudely specify cloud properties.
DOE

N94-32726# Los Alamos National Lab., NM.
WIND-SPEED MEASUREMENTS WITH A SCANNING ELASTIC-BACKSCATTER LIDAR
W. T. Buttler and W. E. Eichinger 1994 5 p Presented at the 21st American Meteorological Society Conference on Agricultural and Forest Meteorology, San Diego, CA, 7-10 Mar. 1994
(Contract W-7405-eng-36)
(DE94-004974; LA-UR-93-4526; CONF-940362-1) Avail: CASI HC A01/MF A01

During the 1992 Summer Olympics, the Los Alamos National Laboratory (LANL) lidar team participated in the Barcelona Air Quality Initiative (BAQI). One of the main objectives of this experiment was the remote measurement of wind speeds around the city to verify wind speeds and directions predicted by the Nonhydrostatic Mesoscale Model (MEMO). Remote determination of wind velocities in the mixing layer is important for the verification and determination of critical input parameters of urban-pollution transport models. Most present elastic-backscatter lidar wind speed measurement methods rely on data acquired over time periods between 5 to 10 minutes and 30 minutes to 1 hour. Lidar can measure the spatial properties of the wind field over large volumes of space. This capability is an improvement over present methods, which rely on instruments attached to balloons that measure only those winds along the path the balloon travels. The material that follows describes the principles implicit in the measurement of winds with an elastic-backscatter lidar, as well as the maximum cross-correlation algorithm used to extract wind speeds from lidar data acquired during the Summer Olympics at Barcelona, Spain, in July 1992.
DOE

N94-32737*# National Aeronautics and Space Administration. Langley Research Center, Hampton, VA.
NOAA-9 EARTH RADIATION BUDGET EXPERIMENT (ERBE) SCANNER OFFSETS DETERMINATION
Lee M. Avis, Jack Paden, Robert B. Lee, III, Dhirendra K. Pandey, Joseph C. Stassi, Robert S. Wilson, Carol J. Tolson, and William C. Bolden May 1994 27 p
(RTOP 665-45-20-01)
(NASA-TM-109086; NAS 1.15:109086) Avail: CASI HC A03/MF A01

The Earth Radiation Budget Experiment (ERBE) instruments are designed

to measure the components of the radiative exchange between the Sun, Earth and space. ERBE is comprised of three spacecraft, each carrying a nearly identical set of radiometers: a three-channel narrow-field-of-view scanner, a two-channel wide-field-of-view (limb-to-limb) non-scanning radiometer, a two-channel medium field-of view (1000 km) non-scanning radiometer, and a solar monitor. Ground testing showed the scanners to be susceptible to self-generated and externally generated electromagnetic noise. This paper describes the pre-launch corrective measures taken and the post-launch corrections to the NOAA-9 scanner data. The NOAA-9 scanner has met the mission objectives in accuracy and precision, in part because of the pre-launch reductions of and post-launch data corrections for the electromagnetic noise. Author

N94-32759# Pacific Northwest Lab., Richland, WA.
WATER VAPOR FROM SUNRADIOMETRY IN COMPARISON WITH MICROWAVE AND BALLOON-SONDE MEASUREMENTS AT THE SOUTHERN GREAT PLAINS ARM SITE
J. J. Michalsky (State Univ. of New York, Albany.), L. C. Harrison (State Univ. of New York, Albany.), and J. C. Liljegren Jan. 1994 5 p Presented at the 5th Annual Symposium on Global Change Studies, Nashville, TN, 24-28 Jan. 1994
(Contract DE-AC06-76RL-01830)
(DE94-007479; PNL-SA-23229; CONF-940131-5) Avail: CASI HC A01/MF A01

Water vapor plays a fundamental role in weather and climate. It is the most important greenhouse gas and the most variable in space and time. The DOE Atmospheric Radiation Measurement program is devoting a large fraction of its resources for the accurate characterization of the column abundance and the distribution of water vapor with altitude. Balloon sondes, microwave radiometers, and Raman lidars are the major instruments either currently in use or under consideration for these tasks. Although the Multi-Filter Rotating Shadowband Radiometer (MFRSR) is primarily intended for use in accurate measurements of spectral short-wave radiation and in the measurement of spectral extinction by aerosol, it has the potential to measure total column water vapor as well. The authors report on a preliminary investigation of the MFRSR's capabilities with regard to accurate measurements of total column water vapor at times when there is a clear path to the sun, i.e., cloudless conditions. DOE

N94-32791# Lawrence Livermore National Lab., CA.
SIMULATION OF A PRECIPITATION EVENT IN THE WESTERN UNITED STATES
Jinwon Kim and S. T. Soong Sep. 1993 6 p Presented at the 74th American Meteorological Society Annual Meeting, Nashville, TN, 23-28 Jan. 1994
(Contract W-7405-eng-48)
(DE94-004835; UCRL-JC-114412; CONF-940115-23) Avail: CASI HC A02/MF A01

Wintertime precipitation is the major water resource in the western United States. Thus correct assessment of the wintertime precipitation is important in planning the summertime water supply and the development of future water resources. Precipitation forecast is also important for early warning of flooding. Regional precipitation depends chiefly on the large scale flow and local topography. Large scale moisture influx determines the amount of moisture available for the precipitation. Topography affects two major factors in the local precipitation: low-level vertical motion and local water vapor transport. Topography also affects partitioning the total precipitation into rain and snow since the snow line is usually lower than the peaks of major mountain ranges during wintertime. Modeling the features of regional precipitation has been intensely studied. Previous studies show that limited area models nested within large scale models or analysis can capture realistic features of storms. As limited area models usually have much finer spatial resolutions than large scale models, parameterized precipitation processes developed for large scale models may not be adequate for limited area models. We present a simulation of twelve-day precipitation over California from 11-23 Feb. 1986. We focus on features of precipitation such as the local distribution, total amount, and the occurrence of snowfall and rainfall. The simulation is carried out using a primitive-equation limited-area model. DOE

N94-32921# Pennsylvania State Univ., University Park. Dept. of Meteorology.
DEVELOPMENT AND TESTING OF IMPROVED TECHNIQUES FOR MODELING THE HYDROLOGIC CYCLE IN A MESOSCALE WEATHER PREDICTION SYSTEM Annual Report, 15 Dec. 1992 - 14 Dec. 1993
Thomas T. Warner 14 Dec. 1993 16 p
(Contract F49620-92-J-0118)
(AD-A277416; AFOSR-94-0130TR) Avail: CASI HC A03/MF A01

This research addresses the problem of moisture and temperature initializations in regional scale meteorological prediction models. Specifically, two approaches are used: one involving radar data and the second involving improved soil moisture content information. The model is initialized with rawinsonde data and then is forced to match convective signatures identified from WSR-57 radar data. Data from NOAA AVHRR radiometer data is used to initialize soil moisture information and generate large scale moisture fields. Methods of continuously updating soil moisture fields are under development. DTIC

N94-32937# Los Alamos National Lab., NM.
PERFORMANCE OF A NEW WIND UPDATING SYSTEM FOR A PROGNOSTIC METEOROLOGICAL MODEL IN THE ENVIRONS OF MEXICO CITY
M. D. Williams 1993 31 p Presented at the IMP Workshop, Mexico City, Mexico, Dec. 1993
(Contract W-7405-eng-36)
(DE94-006243; LA-UR-94-229; CONF-931251-1) Avail: CASI HC A03/MF A01

Los Alamos National Laboratory and Institute Mexicano del Petroleo are completely a joint study of options for improving air quality in Mexico City. The US Department of Energy supported the efforts of the Los Alamos investigators, while PEMEX supported the efforts of the Mexican researchers. One of the first steps in the process was to develop an understanding of the existing air quality situation. In this context we have modified a three-dimensional, prognostic, higher order turbulence model for atmospheric circulation (HOTMAC) to treat domains which include an urbanized area. This sophisticated meteorological model is required because of the complexity of the terrain and the relative paucity of meteorological data. Mexico City lies at an elevation of approximately 7500 feet above sea level in a 'U' shaped basin which opens to the north. The city occupies a major part of the southwest portion of the basin. Upper level winds are provided by rawinsondes at the airport, while low-level winds are measured at several sites within the city. Many of the sites have obstructed upwind fetches for a variety of directions. During the wintertime when the worst air quality episodes occur, the winds are frequently light, and out of the northeast at lower levels, while above 1000 meters above the surface they are usually from the southwest. This means the winds are light within the city, but significant slope winds develop which influence the behavior of the pollutants. Frequently, the winds in the basin change as a seabreeze penetrates the basin from the northeast. The seabreeze produces a much different wind regime after its arrival in the late afternoon or early evening. This makes it important to update the winds in a realistic fashion. DOE

N94-33004*# National Aeronautics and Space Administration. Marshall Space Flight Center, Huntsville, AL.
OPERATIONS SUMMARY FOR THE CONVECTION AND MOISTURE EXPERIMENT (CAMEX)
V. L. Griffin, A. R. Guillory, M. Susko, and J. E. Arnold Mar. 1994 188 p Original contains color illustrations
(NASA-TM-108445; NAS 1.15:108445) Avail: CASI HC A09/MF A02; 10 functional color pages

During the fall of 1993, NASA sponsored a field program called the Convection and Moisture Experiment (CAMEX) at Wallops Island, Virginia. CAMEX was a multidisciplinary experiment design to measure the three dimensional moisture fields over Wallops Island and to characterize the multifrequency radiometric signature of tropical convection over the Gulf Stream and southeastern Atlantic Ocean. This document summarizes the daily CAMEX activities, including ground and aircraft (NASA ER-2) operations, and includes 'quick-look' summaries of data acquisition along with data examples provided by the various CAMEX PI's. Author

N94-33065*# Vigyan Research Associates, Inc., Hampton, VA.
DROP SIZE DISTRIBUTIONS AND RELATED PROPERTIES OF FOG FOR FIVE LOCATIONS MEASURED FROM AIRCRAFT
J. Allen Zak Apr. 1994 131 p Sponsored in part by FAA, Atlantic City, NJ
(Contract NAS1-19341; RTOP 505-64-13-67)
(NASA-CR-4585; NAS 1.26:4585; DOT/FAA/CT-94/02) Avail: CASI HC A07/MF A02

Fog drop size distributions were collected from aircraft as part of the Synthetic Vision Technology Demonstration Program. Three west coast marine advection fogs, one frontal fog, and a radiation fog were sampled from the top of the cloud to the bottom as the aircraft descended on a 3-degree glideslope. Drop size versus altitude versus concentration are shown in three dimensional plots for each 10-meter altitude interval from 1-minute samples. Also shown are median volume radius and liquid water content. Advection fogs contained the largest drops with median volume radius of 5-8 micrometers, although the drop sizes in the radiation fog were also large just above the runway surface. Liquid water content increased with height, and the total number of drops generally increased with time. Multimodal variations in number density and particle size were noted in most samples where there was a peak concentration of small drops (2-5 micrometers) at low altitudes, midaltitude peak of drops 5-11 micrometers, and high-altitude peak of the larger drops (11-15 micrometers and above). These observations are compared with others and corroborate previous results in fog gross properties, although there is considerable variation with time and altitude even in the same type of fog. Author (revised)

N94-33089 Naval Research Lab., Monterey, CA.
FORECASTERS HANDBOOK FOR THE PHILIPPINE ISLANDS AND SURROUNDING WATERS Final Report
Forrest R. Williams, Glenn H. Jung, and Ronald E. Englebretson Dec. 1993 357 p Limited Reproducibility: More than 20% of this document may be affected by microfiche quality
(AD-A277993; NRL/PU/7541-92-0001) Avail: CASI HC A16

The analysis and forecasting of atmospheric and oceanic conditions important to air/ sea operations in the Philippine Islands area are described. The area covered includes the islands -- Luzon the Visayas (the central islands) and Mindanao -- from about 4.7 deg N to 21.5 N and 117 E to 127 E; and the Philippine Sea, Luzon Strait, South China Sea, and Sulu Sea. Seasonal climatologies of the southwest and northeast monsoons and tradewind regime, plus electromagnetic and ducting conditions, are presented. Appendices provide additional climatologies, a study of tropical cyclone characteristics, climatic normals for 60 Philippine stations, and percent frequencies of wave heights. Five case studies examine current accuracy of the Navy Operational Global Atmospheric Prediction System (NOGAPS) model analyses and prognoses. Tropical cyclone bulletins issued by the Joint Typhoon Warning Center, Guam, are identified and described; forecast philosophies are discussed. Interaction of Typhoon Yunya and the eruption of Mount Pinatubo volcano in June 1991 is described, and the dangers posed to aviation by volcanic ash are discussed. DTIC

N94-33288*# Wisconsin Univ., Madison. Space Science and Engineering Center.
TRMM-RELATED RESEARCH: TROPICAL RAINFALL AND ENERGY ANALYSIS EXPERIMENT Final Report
Verner E. Suomi, S. Ackerman, B. Hinton, and D. Martin May 1994 11 p Original contains color illustrations
(Grant NAG5-1586)
(NASA-CR-195834; NAS 1.26:195834) Avail: CASI HC A03/MF A01; 1 functional color page

The overall science objective of the participation in TRMM is the determination of daily rainfall and latent heating in the tropical atmosphere using TRMM and complementary spacecraft observations. The major focus these first three years has been to extend, in space and time, the TRMM satellite observations of rainfall. Observations from TRMM active and passive microwave radiometers will provide the fundamental observations for understanding the hydrological cycle of the tropics. Due to the orbit of the TRMM satellite and the extreme variability of convective rain systems, the TRMM observations provide rainfall estimates representative of a one month period. Monthly mean rainfall rates provide valuable information; however, this time scale limitation neglects the great value of the data towards a better understanding of the physics of tropical convection. Many tropical periodicities will not be characterized by these monthly averages, e.g. diurnal cycles, the 4-6 day easterly waves, and the 30 to 60 day cycle. In the spatial domain, due to its orbit, the TRMM satellite will over-fly many convective systems only once. Indeed, some precipitating systems will not be sampled at all. Observations from geostationary satellites can be used to extend the TRMM observations to smaller time and space scales. Although geostationary satellites cannot probe the interiors of precipitating systems, they do observe their life cycles. To acquire information on cloud water content and rain rate, it is proposed to combine geostationary and other satellite observations with the TRMM satellite measurements.
Derived from text

48 OCEANOGRAPHY

Includes biological, dynamic, and physical oceanography; and marine resources.

For related information see also *43 Earth Resources and Remote Sensing.*

N94-31053# Washington Univ., Seattle. Applied Physics Lab.
OCEAN ACOUSTIC PROPAGATION MEASUREMENTS AND WAVE PROPAGATION IN RANDOM MEDIA
Terry E. Ewart and Stephen A. Reynolds Apr. 1993 24 p
(Contract N00014-90-J-1260)
(AD-A276165) Avail: CASI HC A03/MF A01

Over the last two decades, observations of acoustic scintillations in the ocean have been useful in testing theories that predict the statistics for wave propagation in random media (WPRM). Ocean acoustic observations differ from scattering processes observed in other WPRM sub-fields in two important ways. First, the statistics of the refractive index can be determined accurately from oceanographic measurements. Hence, exacting tests of theories can be done when careful measurements of the medium and the wavefield are made synoptically. Second, the scattering of acoustic energy is predominantly influenced by the ocean internal wave field, which tends to exhibit statistical stationarity in many ocean regimes, and not by non-stationary turbulent processes, as observed in the atmosphere. We discuss space/time acoustic propagation experiments carried out in three scattering regimes: (1) weak, where the Rytov approximation is valid; (2) moderate, where multiple scattering theory is required; and (3) the case where multiple scattering in a single medium irregularity is encountered. A review is presented of the measurements and comparisons with theory. It is clear from field and numerical experiments that 2-point statistics cannot possibly explain the observations of intensity. Because two-point statistics are the norm when interpreting both medium and wavefield measurements, the possible failure of Gaussian statistics must be addressed. This has yet to be done. We will discuss remaining issues for which we believe further study is needed. DTIC

N94-31250# Army Engineer Waterways Experiment Station, Vicksburg, MS.
ADCIRC: AN ADVANCED THREE-DIMENSIONAL CIRCULATION MODEL FOR SHELVES, COASTS, AND ESTUARIES. USER'S MANUAL FOR ADCIRC-2DDI Technical Report No. 2
J. J. Westerink, R. A. Luettich, Jr., C. A. Blain, and Norman W. Scheffner Jan. 1994 168 p
(AD-A276150; WES/TR/DRP-92-6-2) Avail: CASI HC A08/MF A02

This report describes the use of model ADCIRC-2DDI, a two-dimensional, depth-integrated, finite-element-based hydrodynamic circulation code. ADCIRC-2DDI solves the shallow-water equations in their full nonlinear form and can be forced with elevation boundary conditions, zero normal boundary fluxes, variable spatial and temporal free surface stress and atmospheric pressure forcing functions in addition to Coriolis and tidal potential forcing terms. The algorithms that comprise ADCIRC-2DDI allow for extremely flexible spatial discretizations, which results in a highly effective minimization of the discrete size of any problem. Furthermore, these algorithms show good stability characteristics, generate no spurious artificial modes, have no inherent artificial damping, and are extremely efficient. The resulting model can be applied to computational domains ranging from the deep ocean to estuaries. Furthermore, the model is able to efficiently run months to years of simulation while providing detailed intra-tidal response characteristics. A complete description of all user aspects is

given in this document, including code setup and a description of all input and output files. Both model-specific and general modeling practices are discussed. Finally, two examples are presented. Sample input and output files for these examples are included in Appendices A and B. DTIC

N94-31448# Naval Postgraduate School, Monterey, CA.
THE EFFECT OF WESTERLY WIND BURSTS ON A TROPICAL OCEAN GENERAL CIRCULATION MODEL M.S. Thesis
Charles A. Weddle Dec. 1993 141 p
(AD-A276423) Avail: CASI HC A07/MF A02

A primitive equation general circulation model with imbedded mixed layer physics has been used to investigate the response of the equatorial Pacific ocean to daily varying winds and westerly wind bursts. The major issue addressed by this study is the impact of daily varying winds, including westerly wind bursts, in the modeling of the tropical Pacific ocean and El Nino. In the developmental phase, the sensitivity of the model to the integration time step and the domain size were investigated. The results of this work were used to determine the optimal time step and model domain size for the main experimental model runs. In the experimental phase, the model was spun-up using time averaged wind stresses. The model ocean was then exposed to two years of realistic daily varying wind stresses covering the period of 1991 and 1992. The model developed an El Nino like response that corresponded in several respects with observed features of the 1991-92 El Nino. The model also developed tropical instability waves in the eastern Pacific similar to those observed in situ and in satellite SST images. The model's responses to the tropical cyclones that occurred during 1991-92 were also consistent in several ways with observations. DTIC

N94-32000# Naval Research Lab., Bay Saint Louis, MS.
SURFACE FORWARD-SCATTERED ACOUSTIC MEASUREMENTS AND ANALYSIS Final Report
E. J. Yoerger, M. Wilson, and S. T. McDaniel Jun. 1993 5 p
(AD-A276998; NRL/PP/7174-93-0034) Avail: CASI HC A01/MF A01

A shallow water, high-frequency acoustic experiment was conducted off the coast of Panama City Florida during August 1991. Acoustic measurements of surface forward scattering, surface reverberation, and direct path intensities were made utilizing two large stationary towers resting on the seafloor. Each tower was equipped with horizontal and vertical receiving arrays, while the two sources were located on only one of the towers. The water bottom was 30 m deep and covered with a fine, rippled sand. The range of acoustic frequencies varied from 20 kHz to l8O kHz. Concurrent environmental measurements including wave heights, sound velocity profiles, and sample cores were made. This paper reports on the surface forward-scattered measurements made at 24 kHz. DTIC

N94-32066 Royal Australian Navy Hydrographic Service, Canberra.
HYDROGRAPHIC SERVICE ROYAL AUSTRALIAN NAVY Annual Report, 1992 - 1993
1993 48 p Limited Reproducibility: More than 20% of this document may be affected by microfiche quality
(AD-A277134; DODA-AR-008-886) Avail: Issuing Activity (Defense Technical Information Center (DTIC))

This Publication contains reports on the following: (1) Hydrographic survey; (2) Navigation services; (3) Oceanographic data acquisition; (4) Environmental services; and (5) Co-ordination and development. DTIC

N94-32072# Naval Postgraduate School, Monterey, CA.
AIR-SEA INTERACTION PATTERNS IN THE EQUATORIAL PACIFIC M.S. Thesis
John E. Kent Dec. 1993 194 p
(AD-A277305) Avail: CASI HC A09/MF A03

We have investigated air-sea interaction patterns in the equatorial Pacific during the 1991-1992 El Nino/Southern Oscillation (ENSO) event. Our study focused on the identification of spatial and temporal relationships between sea surface temperatures, subsurface temperatures, and winds. These relationships were examined using time series and statistical analyses of atmosphere and ocean data from the moored buoys of the Tropical Oceans-Global Atmosphere (TOGA) program. Our results strongly suggest that the heat content of the ocean mixed layer greatly affected air-sea interactions. In almost all regions, mixed layer warming was followed within one week by increased winds. In most cases, the mixed layer warming before wind events was accompanied by a thickening of the mixed layer, suggesting that internal waves were strongly influencing air-sea interactions. Increased winds tended to precede surface cooling and subsurface warming by a few days. There were strong correlations between warming (cooling) thermocline temperature and increased (decreased) zonal winds at the central and eastern equatorial Pacific buoys. In the central Pacific, thermocline warming (cooling) was associated with westerlies (easterlies). This suggested that equatorially trapped Kelvin waves warmed and thickened the mixed layer, resulting in increased zonal winds. In the central Pacific, these local zonal winds then reinforced the Kelvin waves through downwelling and upwelling. Ocean temperature inversions were found throughout the Pacific. DTIC

N94-32181# Naval Postgraduate School, Monterey, CA.
PREDICTION OF THE PLANE WAVE BEAMFORMED ACOUSTIC ARRIVAL STRUCTURE FOR THE 1992 BARENTS SEA COASTAL TOMOGRAPHY TEST
John L. Mykyta Dec. 1993 46 p
(AD-A276741) Avail: CASI HC A03/MF A01

In an effort to solve the forward propagation problem associated with the 1992 Barents Sea Polar Front Experiment Tomography Test, the transmission of a 224 Hz pulse signal from a near bottom sound source to a vertical hydrophone array was simulated based on three-dimensional ray theory. Through numerical raytracing, followed by eigenray searches and estimations of ray amplitudes, searches and estimations of ray amplitudes, phases and travel times, the arrival structure as a function of time and elevation angle was constructed. The simulation was performed for both a two-dimensional and three-dimensional modeled ocean environment in order to examine the significance of three-dimensional effects. The predicted arrival structures compare well with the observed data. Three-dimensional effects proved to be significant only for the latest arrivals. DTIC

N94-32220# Naval Postgraduate School, Monterey, CA.
THREE DIMENSIONAL VORTICITY FIELD IN THE CALIFORNIA CURRENT SYSTEM M.S. Thesis
Gonzalo Montenegro Mar. 1993 110 p
(AD-A276951) Avail: CASI HC A06/MF A02

Hydrographic data has traditionally been used only to determine dynamical features, specifically dynamic topography and geostrophic currents relative to an assumed level of no motion. However, the assumption of geostrophic balance has been questioned because of the neglect of ageostrophic effects. Measuring vorticity and vertical motion has always been technically demanding and costly. Due to the importance of these parameters new techniques have been developed, among them a diagnostic technique known as the C-vector Method, which uses the wind stress and the geostrophic balance as forcing functions to infer these quantities. Using this technique, the three dimensional vorticity field was computed for the California current system during the Coastal Transition Zone (CTZ) program. Hydrographic (CTD) and wind data sets were used assuming a quasi-geostrophic system. Also computed was vertical vorticity of the C-vector, known as the Psi function, which has a direct relationship with the vertical velocity, making it possible to infer upward or downward motion in coastal waters. A satisfying correlation was found between surface temperature fields, satellite imagery, and vertical motions inferred from the Psi function. The C-vector has therefore been shown to be a very reliable method of diagnosing vorticity and vertical circulation. DTIC

N94-32284# Environmental Research Inst. of Michigan, Ann Arbor.
VALIDATION SUPPORT OF THE ERIM OCEAN MODEL Technical Report, 4 Feb. 1993 - 3 Feb. 1994
M. A. True 28 Feb. 1994 36 p
(Contract N00014-93-C-2019)
(AD-A277364; ERIM-251600-4-F) Avail: CASI HC A03/MF A01

The ERIM Ocean Model (EOM) is a comprehensive program for the simulation of SAR images of the ocean surface. EOM was delivered to NRL and integrated into the NASE Modeling System in 1991. The purpose of the NASE-EOM module is to simulate ocean surface effects as seen by SAR sensors. The purpose of the validation phase of the NASE-EOM project was to determine which of EOM's physics are reliable and which physics need improvement. To that end, a series of validation tests were run using NASE-EOM. For the code-to-theory test, the action spectral

density equation was solved in EOM and compared with the linear solution. The results showed some numerical diffusion in EOM's solution which were reduced with finer spectral grid spacing. The code-to-code comparison consisted of a series of feature tables. The final validation test was the code-to-data comparison. The 11 test cases were run on the NASE Modeling System at NRL and the simulations were compared to experimental data. The simulated SAR signals were similar to each other and to the data for most test case, but the simulated clutter had different appearances in the SAR codes due to differences in the simulation of the propagation of the waves during the SAR imaging time, the averaging to reduce the speckle, and the angular dependence of the equilibrium wave height spectrum. DTIC

N94-32321 Scripps Institution of Oceanography, La Jolla, CA.
PROFILING ALACE INSTRUMENTS Final Report, 1 Apr. 1989 - 31 Mar. 1992
Jeff Sherman 20 Mar. 1993 28 p Limited Reproducibility: More than 20% of this document may be affected by microfiche quality
(Contract N00014-89-C-6014)
(AD-A277246; NRL-CR/7330-93-0001) Avail: Issuing Activity (Defense Technical Information Center (DTIC))

The autonomous Lagrangian circulation explorer (ALACE) is a free drifting oceanographic float which drifts at a level of neutral buoyancy and periodically rises to the surface where it transmits data to System Argos satellites and is located by them. The basic float was intended to observe ocean currents but recent developments, described in this report, have led to three new versions with expanded capabilities. One model reports temperature profiles from each ascent cycle. A second reports profiles of both temperature and conductivity from which sound speed profiles can be calculated. A third instrument observes microtemperature profiles on repeated vertical profiles and records them internally. At the end of its mission this float must be located from its Argos signals and recovered. All three floats have been field tested and their performances are discussed. The sound speed profiles obtained from the first conductivity and temperature measurements are accurate to 0.25 m/s after correcting for instrument drift using relatively stable climatological temperature versus salinity relations at depth. Subsequent sensor improvements are believed to have reduced drift. DTIC

N94-32325# Naval Postgraduate School, Monterey, CA. Dept. of Meteorology.
ESTIMATING SUBPYCNOCLINE DENSITY FLUCTUATIONS IN THE CALIFORNIA CURRENT REGION FROM UPPER OCEAN OBSERVATIONS
Robert L. Haney, Robert A. Hale, and Curtis A. Collins Feb. 1994 75 p
(AD-A277278; NPS-MR-94-001) Avail: CASI HC A04/MF A01

A method for extending upper ocean density observations to the deep ocean is tested using a large number of deep CTD stations in the California current. The specific problem considered is that of constructing the best estimate for the density profile below a certain depth, D, given an observed profile above that depth. For this purpose, the estimated disturbance profile is modeled as a weighted sum of empirical vertical modes (empirical orthogonal functions, EOF's). The EOF's were computed from the surface to 2000 m using 126 largely independent CTD stations off Pt. Sur, California. Separate computations were made for the summer half-year (mid-April to mid-October) and the winter half-year (mid-October to mid-April). For each observed density profile, the EOF weights that determine the estimated profile were obtained by performing a successive least squares fit of the disturbance density profile above D to the first N EOF's. In this study, N was taken to be 7, which is the number of EOF's considered necessary to account for the 'signal' in the profiles. The estimated profiles were then verified against the observed profiles to 2000 m, and the results are presented as a function of the depth D. DTIC

N94-32327 Naval Postgraduate School, Monterey, CA.
ENSO FORCED VARIATIONS OF THE SEA SURFACE TEMPERATURE AND ADJUSTED SEA LEVEL ALONG THE WEST COAST OF THE UNITED STATES M.S. Thesis
John B. Skillman Dec. 1993 98 p Limited Reproducibility: More than 20% of this document may be affected by microfiche quality
(AD-A277306) Avail: CASI HC A05

Daily coastal surface temperature and adjusted sea level data for the period 1955-1988 were used to characterize the surface temperature and adjusted sea level anomalies and the propagation of features along the west coast of the United States during El Nino-southern oscillation (ENSO). The strong ENSO years examined were 1957-58, 1972-73, and 1982-83. Moderate ENSO years used were 1966, 1976, and 1987. To look at regional differences in the signals, the time series of daily coastal surface temperature and adjusted sea level were divided into three distinct regions: the southern region (i.e., Southern California), the central upwelling region (i.e., Central California), and the northern region (i.e., Northern California, Oregon, and Washington). The anomaly series were compared with cross-spectral analysis. Phase speeds and wavenumbers were estimated from the difference in phase between La Jolla and the other stations as a function of frequency band. These were used to characterize the structure of waves associated with the propagation of the positive surface temperature and adjusted sea level anomalies. These wave characteristics were found to be consistent with coastally trapped internal Kelvin waves, due to their phase speed, wavelength, and nondispersive nature. Phase speeds for frequencies corresponding to 4-20 day periods were 60-100 km/day, based on temperature and sea level. A regression of wavenumber against frequency gives phase speeds of about 65-85 km/day that are consistent with Kelvin wave theory for typical west coast ocean structure and bathymetry. DTIC

N94-32400 Scripps Institution of Oceanography, La Jolla, CA. Marine Physical Lab.
MULTI-SCALE STUDIES OF SEAFLOOR TOPOGRAPHY Final Report, 1 Oct. 1990 - 30 Sep. 1993
Fred N. Spiess Jan. 1994 5 p Limited Reproducibility: More than 20% of this document may be affected by microfiche quality
(Contract N00014-91-J-1095)
(AD-A277008; MPL-U-2/94) Avail: CASI HC A01

An important aspect of this program is provision of surface ship hull mounted echo sounding data in the Pacific Natural Laboratory area for comparison with the deeply towed system output. The seagoing portion of this element was carried out in July, 1993, by Dr. Peter Lonsdale using the SeaBeam 2000 system installed in R/V Melville. Initial data reduction was carried out at sea and data are available for eventual statistical comparisons and analyses. DTIC

N94-32401 Scripps Institution of Oceanography, La Jolla, CA. Marine Physical Lab.
LONG TRANSECT SEAFLOOR SEISMIC ARRAY: A COMPONENT OF SAMSON (SOURCES OF AMBIENT MICRO SEISMIC OCEAN IC NOISE) Final Report, 1 Nov. 1989 - 30 Sep. 1993
Spahr C. Webb Jan. 1994 6 p Limited Reproducibility: More than 20% of this document may be affected by microfiche quality
(Contract N00014-89-J-1088)
(AD-A277009; MPL-U-10/94) Avail: CASI HC A02

During the SAMSON experiment, an array of at least twelve seafloor instruments was deployed to measure ambient seismo-acoustic noise. SAMSON is a large, coordinated experiment featuring several land and seafloor seismic arrays directed at studying the generation and propagation of very low frequency (1 mHz to 1 Hz) ambient noise. Surface waves were measured at the coast by the FRF array (established by NCEL), by a pressure array near the coast, and in deep water with wave buoys which are part of the ONR funded SWADE program. The seismic array extended from shallow into deep water from the North Carolina coast. Data from the array was incoherently processed and principally used to study the evolution of the seafloor noise field as a function of distance from the coast and with depth. The array also serves to tie together measurements made by the three coherent arrays: the first on land, the second in the shallow water very near the coast, and the third in deep water beyond the shelf. Some instruments of the incoherent array were elements of the two marine coherent arrays. DTIC

N94-32402 Scripps Institution of Oceanography, La Jolla, CA. Marine Physical Lab.
OCEAN OPTICS, OCEAN IMAGING AND OPTICAL TOMOGRAPHY Final Report, 1 Oct. 1988 - 30 Sep. 1993
Jules S. Jaffe Jan. 1994 6 p Limited Reproducibility: More than 20% of this document may be affected by microfiche quality
(Contract N00014-89-J-1419)
(AD-A277010; MPL-U-1/94) Avail: CASI HC A02

The broad goal of this research is to address the problem of understanding the propagation of light in the ocean and its ramifications for underwater imaging. In particular, we are interested in developing inversion algorithms for determining the total absorption and scattering coefficients and the small angle values of the volume scattering function from simple optical experiments such as the propagation of collimated light beams over distances of several total attenuation lengths. This is particularly important in understanding the limitations of current computer models which predict the propagation of light underwater. DTIC

N94-32881 Lawrence Livermore National Lab., CA.
OCEAN VARIABILITY AND ITS INFLUENCE ON THE DETECTABILITY OF GREENHOUSE WARMING SIGNALS
B. D. Santer, U. Mikolajewicz, W. Brueggemann, K. Hasselmann, H. Hoeck, E. Maier-Reimer, and U. Cubasch Jan. 1994 75 p Limited Reproducibility: More than 20% of this document may be affected by microfiche quality
(Contract W-7405-eng-48)
(DE94-008670; UCRL-ID-115329; PCMDI-14) Avail: CASI HC A04

Recent investigations have considered whether it is possible to achieve early detection of greenhouse-gas-induced climate change by observing changes in ocean variables. In this study, we use model data to assess some of the uncertainties involved in estimating when we could expect to detect ocean greenhouse warming signals. We distinguish between detection periods and detection times. As defined here, detection period is the length of a climate time series which must be available in order to detect a given linear trend in the presence of the natural climate variability. Detection period is defined in model years and is independent of reference time and the real time evolution of the signal. Detection time is computed for an actual time-evolving signal from a greenhouse warming experiment and depends on the experiment's start date. Two sources of uncertainty are considered - those associated with the level of natural variability or noise, and those associated with the time-evolving signals. We analyze the ocean signal and noise for spatially-averaged ocean circulation indices such as ice volume, heat and fresh water fluxes, rate of deep water formation, salinity, temperature, and transport of mass. The signals for these quantities are taken from recent time-dependent greenhouse warming experiments performed by the Hamburg group with a coupled ocean-atmosphere general circulation model. The natural variability noise is derived from a 300-year control run performed with the same coupled atmosphere-ocean model and from two long (greater than 3,000 year) stochastic forcing experiments in which an uncoupled ocean model was forced by white noise surface flux variations. In the first experiment the stochastic forcing was restricted to the fresh water fluxes, while in the second experiment the ocean model was additionally forced by variations in wind stress and heat fluxes. The mean states and ocean variability are very different in the three natural variability integrations. DOE

N94-32959 Department of the Navy, Washington, DC.
BIOLUMINESCENCE BATHYPHOTOMETER Patent
Kenneth M. Ferer, inventor (to Navy), James F. Case, inventor (to Navy), Edith A. Widder, inventor (to Navy), Steven A. Bernstein, inventor (to Navy), and Mark Lowenstine, inventor (to Navy) 23 Nov. 1993 17 p Filed 8 Jul. 1992
(AD-D016102; US-Patent-5,264,906; US-Patent-Appl-SN-910378; US-Patent-Class-356-28) Avail: US Patent and Trademark Office

A high intake, defined excitation, vertical Profiling survey, bioluminescence bathyphotometer system is discussed. The system was designed to measure, from a statistically significant sample with a calibrated hydromechanical stimulus, the following: (1) the bioluminescence of phytoplankton and zooplankton organisms in the oceanic water column to depths of 400 meters in absolute units of photons per second per volume (intensity) or photons per volume (total flux); (2) the concentration of bioluminescent population in flashes per volume; (3) the average light intensity per bioluminescent event; and (4) population flash dynamics. DTIC

N94-32981*# Woods Hole Oceanographic Inst., MA.
LIGHT IN THERMAL ENVIRONMENTS (LITE) WORKSHOP Final Technical Report, 1993
1993 59 p Workshop held in Woods Hole, MA, 10-12 Jan. 1993 Sponsored in part by NSF and RIDGE
(Grant NAGw-3452)
(NASA-CR-195851; NAS 1.26:195851) Avail: CASI HC A04/MF A01

Light emitted from high temperature black smokers (350 C) at mid-ocean ridge spreading centers has been documented, but the source of this light and its photochemical and biological consequences have yet to be investigated. Preliminary studies indicate that thermal radiation alone might account for the 'glow' and that a novel photoreceptor in shrimp colonizing black smoker chimneys may detect this 'glow.' A more controversial question is whether there may be sufficient photon flux of appropriate wavelengths to support geothermally-driven photosynthesis (GDP) by microorganisms. Although only a very low level of visible and near infrared light may be emitted from any single hydrothermal vent, several aspects of the light make it of more than enigmatic interest. First, the light is clearly linked to geophysical (and perhaps geochemical) processes; its attributes may serve as powerful index parameters for monitoring change in these processes. Second, while the glow at a vent orifice is a very local phenomenon, more expansive subsurface environments may be illuminated, thereby increasing the spatial scale at which biological consequences of this light might be considered. Third, in contrast to intermittent bioluminescent light sources in the deep sea, the light emitted at vents almost certainly glows or flickers continuously over the life of the individual black smokers (years to decades); collectively, light emitted from black smokers along the ocean's spreading centers superimposed on background Cerenkov radiation negates the concept of the deep sea as an environment devoid of abiotic light. Finally, the history of hydrothermal activity predates the origin of life; light in the deep sea has been a continuous phenomenon on a geological time scale and may have served either as a seed or refugium for the evolution of biological photochemical reactions or adaptations. Derived from text

N94-33045*# Columbia Univ., Palisades, NY.
EVOLUTION OF UPWELLING FRONTS OFF THE COAST OF PORTUGAL Final Technical Report
8 May 1994 44 p
(Grant NAGw-2058)
(NASA-CR-195692; NAS 1.26:195692) Avail: CASI HC A03/MF A01

We have analyzed the spatial and temporal variability of chlorophyll in the Atlantic Ocean off the Portugal coast using satellite imagery from 1979 to 1986 in conjunction with wind data. The spatial patterns in the imagery show the typical inshore-offshore and east-west gradients, while the temporal patterns show seasonal high winter values and low summer values. In the satellite imagery for the period 1979-1986, stable mesoscale and large scale patterns recurred despite interannual differences in absolute satellite-derived pigment concentrations. Author (revised)

N94-33057# Naval Postgraduate School, Monterey, CA.
EVOLUTION OF DIURNAL SURFACE WINDS AND SURFACE CURRENTS FOR MONTEREY BAY M.S. Thesis
Michael D. Foster Dec. 1993 97 p
(AD-A277649) Avail: CASI HC A05/MF A02

The diurnal-period fluctuations of winds and surface currents are analyzed for Sep. 1992 in and around Monterey Bay. Wind records are compared for three coastal stations and two mooring sites. Remotely-sensed surface current observations from two CODAR (HF radar) sites are used to explore the ocean's response to diurnal-period forcing. An average diurnal cycle is formed at each wind station and at all CODAR bins. The earliest sea breeze response is seen at the coastal wind stations where morning winds accelerate toward the coastal mountain ranges. A few hours later, the coastal winds accelerate to the southeast down the Salinas Valley. Offshore afternoon winds rotate from their normal alongshore orientation to also become aligned with the valley. The CODAR-derived surface currents respond in less than the two-hour sampling rate to the onset of the diurnal onshore winds. Currents accelerate in the direction of the Salinas Valley. As the day progresses, the more offshore currents rotate clockwise out from under the winds in a possible Ekman or inertial adjustment that continues throughout the night and spreads onshore. In the afternoon, a complicated eddy pattern develops near shore in a possible response to the coastal boundary. DTIC

N94-33062# Massachusetts Inst. of Tech., Cambridge. Dept. of Earth Atmospheric and Planetary Sciences.
QUANTITATIVE MODELING OF BOTTOM MORPHOLOGY AND SUBBOTTOM PROPERTIES Final Technical Report, Nov. 1989 - May 1993

Thomas H. Jordan May 1993 92 p
(Contract N00014-90-J-1584)
(AD-A278142) Avail: CASI HC A05/MF A01

The objectives of this research were threefold: (1) to provide the methodology needed to quantify the two-dimensional variations in bottom topography and three-dimensional variations in subbottom properties observed within the ARSRP Central Atlantic study area; (2) to apply this methodology to geological data sets collected in the study area; and (3) to use the resulting geological models to understand the bottom reverberations observed at long ranges across the study area and other parts of the deep ocean. DTIC

N94-33085# Coastal Engineering Research Center, Vicksburg, MS.
INDEX AND BULK PARAMETERS FOR FREQUENCY-DIRECTION SPECTRA MEASURED AT CERC FIELD RESEARCH FACILITY Final Report, Sep. 1989 - Aug. 1990
Charles E. Long and Wendy L. Smith Mar. 1994 86 p
(AD-A277759; CERC-94-2) Avail: CASI HC A05/MF A01

A multiyear series of wind wave frequency-direction spectral measurements has been undertaken at the Field Research Facility of the Coastal Engineering Research Center, U.S. Army Engineer Waterways Experiment Station. Cross-spectra of surface-corrected signals from a linear array of nine bottom-mounted pressure sensors have been used in conjunction with an iterative maximum likelihood algorithm to estimate frequency-direction spectra in about 8 m of water, approximately 900 M offshore. This report provides an index of and describes a means of access to 1,505 spectral observations obtained from September 1989 to August 1990. This period represents the fourth year of data collection. In addition to a list of data collection start times, a set of bulk parameters are provided to characterize the observations. Included are characteristic wave height, spectral peak frequency and corresponding peak period, peak wave direction, and directional spread. Time series graphs of these parameters, as well as local winds and currents, illustrate some of the salient climatology. DTIC

N94-33109# Woods Hole Oceanographic Inst., MA.
FINE AND MICROSTRUCTURE OBSERVATIONS AT FIEBERLIN G GUYOT R/V NEW HORIZON CRUISE REPORT
Ellyn T. Montgomery and John M. Toole Nov. 1993 33 p
(Contract N00014-89-J-1073)
(AD-A277917; WHOI-93-51) Avail: CASI HC A03/MF A01

This report describes fine structure and microstructure profile data taken on a cruise to Fieberling Guyot, a seamount in the northeast subtropical Pacific Ocean. The work performed at sea, instruments used, data return and processing procedures are summarized. This cruise took place between March 4 and March 28, 1991 on the R/V New Horizon, and was part of the interdisciplinary Accelerated Research Initiative (ARI) for Abrupt Topography sponsored by the Office of Naval Research. An overall goal of the ARI was to understand the physical, biological, and geological processes occurring near a seamount. The scientific objective of the Seamount Mixing Cruise was to collect data describing the oceanic fine-scale velocity and density fields, as well as the related turbulence and mixing in the vicinity of the seamount. The High Resolution Profiler (HRP) was deployed 95 times above and around the seamount. As well, two test dives were conducted on the way to the site, and eight deployments completed in deep basins off the southern California coast before returning to port. Three near-synoptic surveys of the seamount were completed with the deployment of 128 Expendable Current Profilers (XCP's). The temperature field of the upper 760 meters of water within a 50 kilometer radius of the seamount was mapped using 144 Expendable Bathythermographs (XBT's). DTIC

N94-33176# Woods Hole Oceanographic Inst., MA.
[DEEP WATER STUDIES OF CTD DATA] Report, 10 Oct. 1988 - 12 Dec. 1990
Bruce A. Warren 16 Dec. 1993 2 p
(Contract N00014-89-J-1076)
(AD-A277741) Avail: CASI HC A01/MF A01

The major accomplishments of this grant were as follows: (1) discovery and description of a broad but thin near-bottom boundary current on the Kenyan continental rise; (2) detection of a deep western-boundary current along the Carlsberg Ridge in the Arabian Basin; (3) some new ideas about the pattern of deep-water circulation in the Arabian Sea; and (4) quantification of property budgets and renewal time in the oxygen-minimum layer of the Arabian Sea. DTIC

N94-33185 Naval Command, Control and Ocean Surveillance Center, San Diego, CA. RDT and E Div.
A COMPARISON OF ROUGH SURFACE PARABOLIC EQUATION MODELS
A. E. Barrios Mar. 1994 3 p Limited Reproducibility: More than 20% of this document may be affected by microfiche quality
(DA Proj. MP9-2)
(AD-A278090) Avail: Issuing Activity (Defense Technical Information Center (DTIC))

Several parabolic equation models currently exist that model radio wave propagation over the ocean. Few of these models can accurately account for rough surface effects over an ocean environment. Several techniques to account for these effects, implemented within the split-step parabolic equation (PE) algorithm, are investigated. DTIC

N94-33243# Woods Hole Oceanographic Inst., MA.
FLUID MECHANICAL MEASUREMENTS WITHIN THE BOTTOM BOUNDARY LAYER OVER THE NORTHERN CALIFORNIA CONTINENTAL SHELF DURING STRESS
J. J. Fredericks, John H. Trowbridge, A. J. Williams, III, Steven J. Lintz, and Bradford Butman Sep. 1993 110 p
(Contracts N00014-89-J-1067; N00014-89-J-1058)
(AD-A277916; WHOI-93-32) Avail: CASI HC A06/MF A02

In studying the processes controlling particle distribution of fine sediments over the continental shelf, the height, structure and dynamics of the bottom boundary layer must be better understood. The Sediment Transport Events on Shelves and Slopes (STRESS) program provides a comprehensive set of data over the bottom half of the water column at the 90 m and the 130 m isobaths along the northern California continental shelf during the winters of 1988-89 and 1990-91. This report presents the STRESS salinity, temperature, velocity, wave characteristics and attenuation data. The report describes the processing, provides plots and tables of the data and corresponding statistics for evaluation of the data, and documents the data files. The combined set of moored and tripod mounted instrument measurements provides integrated, hourly-averaged profiles of the lower half of the water column at the four sites which can be used for analysis and modeling purposes. DTIC

N94-33244 Oregon State Univ., Corvallis. Coll. of Oceanic and Atmospheric Sciences.
SEASOAR AND CTD OBSERVATIONS DURING A COARE SURVEYS CRUISE, W9211C, 22 JANUARY - 22 FEBRUARY, 1993
A. Huyer, P. M. Kosro, R. OMalley, and J. Fleischbein Oct. 1993 328 p Limited Reproducibility: More than 20% of this document may be affected by microfiche quality
(AD-A277925) Avail: CASI HC A15

An international Coupled Ocean-Atmosphere Response Experiment (COARE) was conducted in the warm-pool region of the western equatorial Pacific Ocean over a four-month period from November 1992 through February 1993. Most of the oceanographic and meteorological observations were concentrated in the Intensive Flux Array (IFA) centered at 1 deg 45 min S, 156 deg 0 min E. As part of this experiment, the R/V Wecoma conducted three survey cruises on the R/V Wecoma; each cruise included measurements of the temperature, salinity and velocity distribution in the upper 300 m of the ocean, and continuous meteorological measurements of wind, air temperature, humidity, etc. Most of these measurements were along a butterfly pattern that was sampled repeatedly during the three COARE Surveys cruises, W9211A and W911B, and W9211C. This report summarizes the Seasoar and CTD observations from Wecoma's third COARE Surveys cruise, W9211C. It also provides a cruise narrative, and a brief description of the data processing procedures. Derived from text

N94-33245 Woods Hole Oceanographic Inst., MA.
CRUISE REPORT: OCEANUS 250 LEG 4 HIGH RESOLUTION PROFILER SURVEY FOR THE NORTH ATLANTIC TRACER RELEASE EXPERIMENT, 25 MARCH - 24 APRIL, 1992
Ellyn T. Montgomery and Raymond W. Schmitt, Jr. Aug. 1993 45 p Limited Reproducibility: More than 20% of this document may be affected

by microfiche quality
(Contract N00014-92-1323)
(AD-A277935; WHOI-93-39) Avail: CASI HC A03

This report describes fine structure and microstructure profile data taken on R/V Oceanus cruise 250 leg 4, between March 25 and April 24, 1992. During this cruise, an area of the Canary Basin near the Subduction Experiment's central mooring was surveyed with the High Resolution Profiler (HRP). The goals of the survey were to describe the hydrographic properties of the water adequately to recommend a location for the North Atlantic Tracer Release Experiment (NATRE) tracer injection, and to characterize the microstructure for comparison with the NATRE results. The work performed at sea, instrumentation, data return and processing procedures will be summarized in this report. DTIC

N94-30983 Centre National de la Recherche Scientifique, Paris (France). Lab. de Meteorologie Dynamique.
ENERGETIC AND GENERAL CIRCULATION [CIRCULATION GENERALE ET ENERGETIQUE]
Robert Sadourny *In* CNES, Subtropical Climates and Their Evolution: From Space-Based Observation to Modelling Oct. 1993 p 41-7 In FRENCH (For primary document see N94-30981 09-47)
Copyright Avail: Issuing Activity (CEPADUES-Editions, 111, rue Nicolas-Vauquelin, 31100 Toulouse, France)

N94-30984 Centre National de la Recherche Scientifique, Paris (France). Lab. d'Oceanographie Dynamique et de Climatologie.
GENERAL OCEAN CIRCULATION [CIRCULATION GENERALE OCEANIQUE]
P. Delecluse *In* CNES, Subtropical Climates and Their Evolution: From Space-Based Observation to Modelling Oct. 1993 p 81-9 In FRENCH Prepared in cooperation with Paris VI Univ., Fran ce and Office de la Recherche Scientifique et Technique Outre-Mer (For primary document see N94-30981 09-47)
Copyright Avail: Issuing Activity (CEPADUES-Editions, 111, rue Nicolas-Vauquelin, 31100 Toulouse, France)

N94-30985 Centre National de Recherches Meteorologiques, Toulouse (France).
CLIMATOLOGIC FLUX IN TROPICAL OCEAN [FLUX CLIMATOLOGIQUES EN OCEAN TROPICAL]
S. Planton *In* CNES, Subtropical Climates and Their Evolution: From Space-Based Observation to Modelling Oct. 1993 p 99-120 In FRENCH (For primary document see N94-30981 09-47)
Copyright Avail: Issuing Activity (CEPADUES-Editions, 111, rue Nicolas-Vauquelin, 31100 Toulouse, France)

N94-30986 Centre National de la Recherche Scientifique, Paris (France). Lab. d'Oceanographie Dynamique et de Climatologie.
LOW FREQUENCE VARIABILITY OF THE OCEAN ATMOSPHERE COUPLED SYSTEM [VARIABILITE BASSE FREQUENCE DU SYSTEME COUPLE OCEAN-ATMOSPHERE]
P. Delecluse *In* CNES, Subtropical Climates and Their Evolution: From Space-Based Observation to Modelling Oct. 1993 p 121-140 In FRENCH Prepared in cooperation with Paris VI Univ., Fran ce and Office de la Recherche Scientifique et Technique Outre-Mer (For primary document see N94-30981 09-47)
Copyright Avail: Issuing Activity (CEPADUES-Editions, 111, rue Nicolas-Vauquelin, 31100 Toulouse, France)

N94-30987 Centre National de la Recherche Scientifique, Paris (France). Lab. de Meteorologie Dynamique.
INTERACTION PROCESSES BETWEEN THE OCEAN AND THE ATMOSPHERE [LES PROCESSUS D'INTERACTION ENTRE L'OCEAN ET L'ATMOSPHERE]
H. LeTreut *In* CNES, Subtropical Climates and Their Evolution: From Space-Based Observation to Modelling Oct. 1993 p 141-151 In FRENCH (For primary document see N94-30981 09-47)
Copyright Avail: Issuing Activity (CEPADUES-Editions, 111, rue Nicolas-Vauquelin, 31100 Toulouse, France)

N94-30991 Office de la Recherche Scientifique et Technique Outre-Mer, Paris (France). Lab. d'Oceanographie Dynamique et de Climatologie.
LOW FREQUENCY VARIABILITY OBSERVED IN THE TROPICAL ATLANTIC OCEAN [VARIABILITE BASSE FREQUENCE OBSERVEE DANS L'OCEAN ATLANTIQUE TROPICAL]
Alain Morliere (Paris VI Univ., France.) *In* CNES, Subtropical Climates and Their Evolution: From Space-Based Observation to Modelling Oct. 1993 p 215-231 In FRENCH (For primary document see N94-30981 09-47)
Copyright Avail: Issuing Activity (CEPADUES-Editions, 111, rue Nicolas-Vauquelin, 31100 Toulouse, France)

N94-30995 Paris VI Univ., Villefranche-sur-Mer (France). Lab. Physique et Chimies Marines.
THE OCEAN-ATMOSPHERE INTERACTIONS IN THE MEDITERRANEAN SEA [LES INTERACTIONS OCEAN-ATMOSPHERE EN MEDITERRANEE]
J. P. Bethoux *In* CNES, Subtropical Climates and Their Evolution: From Space-Based Observation to Modelling Oct. 1993 p 301-312 In FRENCH (For primary document see N94-30981 09-47)
Copyright Avail: Issuing Activity (CEPADUES-Editions, 111, rue Nicolas-Vauquelin, 31100 Toulouse, France)

51 LIFE SCIENCES (GENERAL)

N94-31294# Florida Univ., Gainesville.
INTERNATIONAL JOURNAL OF QUANTUM CHEMISTRY. QUANTUM BIOLOGY SYMPOSIUM NUMBER 20. PROCEEDINGS OF THE INTERNATIONAL SYMPOSIUM ON THE APPLICATION OF FUNDAMENTAL THEORY TO PROBLEMS OF BIOLOGY AND PHARMACOLOGY Final Report, 28 Feb. 1993 - 27 Feb. 1994
Rodney J. Bartlett Feb. 1994 260 p Symposium held in St. Augustine, FL, 13-20 Mar. 1993
(Contract DAAH04-93-C-0072)
(AD-A276294; ARO-31084.1-PH-CF) Avail: CASI HC A12/MF A03

The format of the symposium adopted for the past few years was followed again this year with a compact eight-day schedule with an integrated program of biology, quantum chemistry, and condensed matter physics. The topics of the sessions covered by these proceedings include Modeling of Biomolecules and Intramembranal Systems, Protein-DNA Interactions, Electron Transport Mechanisms in Biological Systems, and Computational Approaches to Molecular Design. The articles have been subjected to the ordinary refereeing procedures of the International Journal of Quantum Chemistry. The articles presented in the sessions on quantum chemistry, condensed matter physics, and associated poster sessions are published in a separate volume of the International Journal of Quantum Chemistry. DTIC

N94-31533# Amsterdam Univ. (Netherlands).
SPECTRAL INHOMOGENEITY OF THE BACTERIAL LIGHT-HARVESTING ANTENNAE: CAUSES AND CONSEQUENCES Ph.D. Thesis
Frank vanMourik 1993 125 p Sponsored in part by Netherlands Organization for Scientific Research, and United Kingdom Science and Engineering Research Council
(Grant EEC-SC1-0004-C)
(ETN-94-96020) Avail: CASI HC A06/MF A02

A general introduction to bacterial photosynthesis, light harvesting, the importance of exciton interaction, exciton theory, the disordered dimer, and larger aggregates (LH-1), is presented. The following studies are then reported: exciton interactions in the light harvesting antenna of photosynthetic bacteria studied with triplet singlet spectroscopy and singlet triplet annihilation on the B820 subunit form of Rhodospirillum rubrum; spectroscopic characterization of the low light B800-850 light harvesting complex of Rhodopseudomonas palustris, strain 2.1.6; self assembly of the LH-1 light harvesting antenna of Rhodospirillum rubrum, a time-resolved study of the aggregation of the B820 subunit; excitation transfer dynamics and spectroscopic properties of the light harvesting BChl a complex of Prosthecochloris aestuarii; spectral inhomogeneity of the light harvesting antenna of Rhodospirillum rubrum probed by T-S spectroscopy and singlet

triplet annihilation at low temperatures; and energy transfer and aggregate size effects in the inhomogeneously broadened core light harvesting complex of Rhodobacter sphaeroides. ESA

N94-32226 Center for Mathematics and Computer Science, Amsterdam (Netherlands). Dept. of Analysis, Algebra and Geometry.
ON THE RECIPROCAL RELATIONSHIP BETWEEN LIFE HISTORIES AND POPULATION DYNAMICS
Odo Diekmann (Leiden Univ., Netherlands.) and J. A. J. Metz (Leiden Univ., Netherlands.) May 1993 16 p Submitted for publication Sponsored by Netherlands Organization for Applied Scientific Research TMO Limited Reproducibility: More than 20% of this document may be affected by microfiche quality
(ISSN 0924-2953)
(CWI-AM-R9302; ETN-94-96166) Copyright Avail: Issuing Activity (European Space Agency (ESA))

A possible mathematical framework for dealing with the following reciprocal questions is presented: how life history mechanisms shape the size and structure of populations; and how past population dynamics may have molded present day life histories. This framework is thought to be more general than comparable frameworks presented in the past; still sufficiently well specified to allow a directed search for both general theorems and tractable special cases; and still considerably less encompassing than one would wish. Within that framework, possible technical approaches to the questions above are discussed. Speculations about possible extensions to larger biological contexts are made in conclusion. ESA

N94-32228 Center for Mathematics and Computer Science, Amsterdam (Netherlands). Dept. of Analysis, Algebra and Geometry.
THE LEGACY OF KERMACK AND MCKENDRICK
O. Diekmann (Leiden Univ., Netherlands.), J. A. P. Heesterbeek (Cambridge Univ., England.), and J. A. J. Metz (Leiden Univ., Netherlands.) Jul. 1993 18 p Submitted for publication Sponsored by Netherlands Organization for Applied Scientific Research TMO Limited Reproducibility: More than 20% of this document may be affected by microfiche quality
(ISSN 0924-2953)
(CWI-AM-R9304; ETN-94-96168) Copyright Avail: Issuing Activity (European Space Agency (ESA))

Starting from the pioneering work by Kermack and McKendrick of 1927, issues of interest in deterministic epidemic modeling are reviewed. These include: classification of dynamics, the influence of heterogeneity, and submodels for the contact process. ESA

N94-32267# Washington State Univ., Pullman.
TOWARDS A DETAILED UNDERSTANDING OF THE STRUCTURAL VARIABILITY IN LIGNINS: A NEW APPROACH
N. G. Lewis and G. H. N. Towers 1993 16 p
(Contract DE-FG06-91ER-20022)
(DE94-007449; DOE/ER-20022/T1) Avail: CASI HC A03/MF A01

This reporting period witnessed a number of exciting and important breakthroughs in the study of lignin synthesis in plants and resulted in a significant deviation from the work plan originally proposed. Taken together, the authors' results reveal an emerging picture of a highly ordered assembly of the lignin polymer at the plasma membrane/cell-wall interface, in contrast to original considerations projecting a random series of coupling reactions. The Progress Report is divided into two sections: the first section reflects the interlocking research completed to date in the laboratories of N.G. Lewis and G.H.N. Towers. In the broadest sense, the Lewis group has focused mainly on woody plants, whereas the Towers laboratory examined similar processes in cereals/grasses. The second section compiles published work, a summary of manuscripts in preparation, and work currently underway for year three of the existing grant. DOE

N94-32269# Sandia National Labs., Livermore, CA.
A GENETIC ALGORITHM BASED METHOD FOR DOCKING FLEXIBLE MOLECULES
R. S. Judson, E. P. Jaeger, and A. M. Treasurywala Nov. 1993 38 p
(Contract DE-AC04-76DR-00789)
(DE94-007525; SAND-93-8688) Avail: CASI HC A03/MF A01

The authors describe a computational method for docking flexible molecules into protein binding sites. The method uses a genetic algorithm (GA) to search the combined conformation/orientation space of the molecule to find low energy conformation. Several techniques are described that increase the efficiency of the basic search method. These include the use of several interacting GA subpopulations or niches; the use of a growing algorithm that initially docks only a small part of the molecule; and the use of gradient minimization during the search. To illustrate the method, they dock Cbz-GlyP-Leu-Leu (ZGLL) into thermolysin. This system was chosen because a well refined crystal structure is available and because another docking method had previously been tested on this system. Their method is able to find conformations that lie physically close to and in some cases lower in energy than the crystal conformation in reasonable periods of time on readily available hardware. DOE

N94-32516# Princeton Univ., NJ.
DEVELOPMENT AND APPLICATION OF PHOTOSENSITIVE DEVICE SYSTEMS TO STUDIES OF BIOLOGICAL AND ORGANIC MATERIALS
S. M. Gruner and G. T. Reynolds 14 Sep. 1993 11 p
(Contract DE-FG02-87ER-60522)
(DE94-008503; DOE/ER-60522/7) Avail: CASI HC A03/MF A01

This progress report summarizes results, as of August 1993, for DOE grant DE-FG-02-76ER60522 during the fiscal period 1/1/93 to 12/31/93, which is the first year of a 3-year grant cycle. The overall goals of the grant are to develop advanced x-ray detector technologies, especially as applicable for biological and materials research at the national laboratories, and to train graduate and post-doctoral students on the use of these technologies via the performance of original biological and materials research. As summarized below, there has been good progress toward achieving the research goals of the original 3-year proposal; in consequence, the research plan and the total budget for the rest of 1993 and beyond is still well described by the original proposal. Accomplishments since the last progress report include: (1) A 1k x 1k fiber optically coupled CCD detector was assembled, tested at CHESS and is slated for extended user trials this Fall. A 2k x 2k CCD detector is being assembled for permanent installation at CHESS. (2) X-ray detector phosphors, calibration techniques, and system software have been developed. (3) The design of a Pixel Array Detector, a collaborative project with the Advanced Photon Source, has been initiated. (4) The properties of biomembrane lipids under extremes of pressure have been investigated. High pressure instrumentation and techniques have been developed. (5) The physics of mesophase formation in biomembrane lipid, surfactant, and polymeric systems have been studied. This includes study of the interaction of membrane proteins with elastically strained lipid bilayers. (6) Work has been initiated on the use of thermal diffuse scatter from proteins as a probe of protein dynamics. (7) Studies on luminescent phenomena have been reported. Since the last progress report (dated 15 May 1992), this work has resulted in 10 published papers, 7 abstracts, 1 Ph.D. thesis and 1 technical report. DOE

N94-32622 Illinois Univ., Urbana. Dept. of Cell and Structural Biology.
THE ORGANIZATION OF THE SUPRACHIASMATIC CIRCADIAN PACEMAKER OF THE RAT AND ITS REGULATION BY NEUROTRANSMITTERS AND MODULATORS Final Technical Report, 1 Apr. 1990 - 30 Sep. 1993
Martha U. Gillette, Dong Chen, Steven Demarco, Jian Ding, and Lia Faiman 2 Feb. 1994 62 p Limited Reproducibility: More than 20% of this document may be affected by microfiche quality
(Grant AF-AFOSR-0205-90)
(AD-A277324; AFOSR-94-0047TR) Avail: CASI HC A04

Our research addresses the cellular organization and regulation of a biological clock that controls daily (circadian) rhythms of behavior (e.g., performance), physiology and metabolism in mammals. This clock, located in the brain's suprachiasmatic nucleus (SCN), can be removed in a slice of hypothalamus, maintained in a life support system for up to 3 days and studied directly. Using this approach, progress in the 3 1/2 years of this award has been made in: (1) localizing time-keeping properties within the SCN of rat, (2) identifying electrophysiological properties of neurons in the major SCN subdivisions, (3) establishing regulatory roles for serotonin, a neuromodulatory input from the brain's arousal center in the raphe nuclei, as well as for neuropeptide Y, an input from the intergeniculate area, (4) determining the level of glutamic acid decarboxylase (GAD), the biosynthetic enzyme for the inhibitory neurotransmitter GABA, in SCN over the circadian cycle, and (5) examining the involvement of glutamate/nitric oxide signal transduction in mediating light entrainment of the SCN through retinal inputs.

This project involves both individual and interactive research projects at the University of Illinois and the USAF School of Aerospace Medicine.
DTIC

N94-32769 California Univ., Santa Cruz.
NINTH INTERNATIONAL WORKSHOP ON PLANT MEMBRANE BIOLOGY
1993 285 p Workshop held in Monterey, CA, 19-24 Jul. 1992 Limited Reproducibility: More than 20% of this document may be affected by microfiche quality
(Contract DE-FG03-92ER-20081)
(DE94-005690; CONF-9207229) Avail: CASI HC A13

This report is a compilation of abstracts from papers which were discussed at a workshop on plant membrane biology. Topics include: plasma membrane ATP-ases; plant-environment interactions, membrane receptors; signal transduction; ion channel physiology; biophysics and molecular biology; vaculor H+ pumps; sugar carriers; membrane transport; and cellular structure and function. DOE

N94-32890# Clemson Univ., SC. Dept. of Biological Sciences.
THE MAGNESIUM CHELATION STEP IN CHLOROPHYLL BIOSYNTHESIS
J. Weinstein Feb. 1994 19 p
(Contract DE-FG09-89ER-13989)
(DE94-008727; DOE/ER-13989/4) Avail: CASI HC A03/MF A01

Mg-chelatase catalysis is the first step unique to chlorophyll synthesis, namely the insertion of magnesium into protoporphyrin IX. When pea (Pisum sativum L., cv. Spring) chloroplasts are lyzed in a buffer lacking magnesium and the thylakoids removed by centrifugation, the remaining mixture of light membranes and soluble proteins (LM/S) has high Mg-chelatase activity. Several lines of evidence are presented to show that the magnesium insertion catalyzed by this preparation is a two-step reaction consisting of activation followed by magnesium chelation. An activated state of Mg-chelatase is achieved by preincubating LM/S with ATP. The activated state is observed as the elimination of the approximately 6 min lag in the rate of magnesium chelation upon addition of the prophyrin substrate. The activity of LM/S assayed at low protein concentrations can be greatly enhanced by preincubating at high protein concentrations (12 mg/ml is optimal). This activation effect requires the presence of both LM and S fractions, as well as ATP. Both steps require ATP, but at different concentrations; the first step is optimal at greater than 0.5 mM (EC(sub 50) = 0.3 mM) and the second step is optimal at 0.3 mM (EC(sub 50) less than 0.2 mM). ATP in the first step could be replaced by ATP(gamma)S; this analog could not sustain activity in the second step. This activated state was stable for at least 30 min at room temperature, but chilling of preincubated LM/S on ice for 30 min caused an almost complete loss of the activated state. DOE

N94-32896# Brookhaven National Lab., Upton, NY.
LIGHT UTILIZATION AND PHOTOINHIBITION OF PHOTOSYNTHESIS IN MARINE PHYTOPLANKTON
P. G. Falkowski, R. Greene, and Z. Kolber 1993 49 p Presented at the 41st Harden Conference on Photoinhibition of Photosynthesis, London, England, 5-10 Sep. 1993
(Contract DE-AC02-76CH-00016)
(DE94-005505; BNL-49821; CONF-9309312-1) Avail: CASI HC A03/MF A01

Based on the record of the oldest identifiable fossils, the first oxygenic photosynthetic organisms appeared about 2 x 10(exp 9) years ago in the form of marine single celled, planktonic procaryotes. In the intervening eons, phytoplankton have evolved and diversified; presently they represent at least 11 classes of procaryotic and euacaryotic photoautotrophs. While the carbon of these organisms cumulatively amounts to only 1 to 2% of the global plant biomass, they fix between 35 and 50 gigatonnes (x 10(exp 9) metric tons) of carbon annually, about 40% of the global total. On average, each gram of phytoplankton chlorophyll converts about 6% of the photosynthetically active radiation (440 to 700 nm) incident on the sea surface to photochemical energy. Despite a great deal of variability in ocean environments, this photosynthetic conversion efficiency is relatively constant for integrated water column production. Here we review the factors determining light utilization efficiency of phytoplankton in the oceans and the physiological acclimations which have evolved to optimize light utilization efficiency. DOE

N94-33098# Kentucky Univ., Lexington. Dept. of Pathology.
CHARACTERIZATION AND UTILIZATION OF OPIATE-LIKE HIBERNATION FACTORS Report, 15 Jul. 1992 - 15 Dec. 1993
Peter R. Oeltgen 8 Dec. 1993 69 p
(Contract DAMD17-92-C-2026; DA Proj. 3M1-62787-A-874)
(AD-A278136) Avail: CASI HC A04/MF A01

A hibernation induction trigger (HIT) molecule derived from the plasma of deeply hibernating woodchucks exerts profound effects mimicking a hibernation-like state when infused I.C.V. or I.V. in primates. The profound opiate-like behavioral and physiological depression occurring shortly after the infusion of the HIT-containing albumin fraction include hypothermia, bradycardia, long-term hypophagia and markedly depressed renal function. All of the aforementioned effects are reversed or retarded by the infusion of the opiate antagonists, naloxone and naltrexone. Such evidence enforces our hypothesis that the HIT molecule is not specific for hibernators, but that it may initiate its action through specific opioid receptor(s). We have shown that only DADLE, a delta class of opiate, could induce hibernation in summer-active ground squirrels (the traditional bioassay) in a fashion similar to those injected with HIT. Such evidence indicates that this delta opioid mimics the action of the HIT molecule and may be intimately involved in natural winter and summer-induced hibernation. Recently, we have developed a rapid in vitro bioassay utilizing the criteria of DNA and protein synthesis inhibition to monitor the metabolic inhibitory activity of hibernating plasma, and plasma fractions as well as the metabolic effects of the delta opioids DADLE and D-Pen 2.5-Enkephalin (DPDPE). DTIC

N94-33250 Technical Univ. of Denmark, Lyngby.
FUTURE DIRECTIONS OF NONLINEAR DYNAMICS IN PHYSICAL AND BIOLOGICAL SYSTEMS. (PHYSICA D NONLINEAR, VOLUME 68, NUMBER 1)
P. L. Christiansen, J. C. Eilbeck, and R. D. Parmentier 15 Sep. 1993 196 p Limited Reproducibility: More than 20% of this document may be affected by poor print and microfiche quality
(Contract DAJA45-92-M-0163)
(AD-A278085; R/D-6891-MA-02) Avail: Issuing Activity (Defense Technical Information Center (DTIC))

Early in 1990 a scientific committee was formed for the purpose of organizing a high-level scientific meeting on future directions of nonlinear dynamics in physical and biological systems, in honor of Alwyn Scott's 60th birthday (December 25, 1991). As preparations for the meeting proceeded, they were met with an unusually broad-scale and high level of enthusiasm on the part of the international nonlinear science community, resulting in a participation by 168 scientists from 23 different countries in the conference, which was held July 23 to August 1 1992. The contributions to this present volume have been grouped into the following chapters: solitons, superconducting devices, biomolecular dynamics, nonlinear optics, and classical and quantum mechanical lattice dynamics. DTIC

52 AEROSPACE MEDICINE

Includes physiological factors; biological effects of radiation; and effects of weightlessness on man and animals.

N94-31195# Ecole Nationale Superieure des Telecommunications, Paris (France).
INTERACTIVE RECONSTRUCTION OF ANATOMICAL STRUCTURES WITH FREE-FORM SURFACES Ph.D. Thesis [RECONSTRUCTION INTERACTIVE D'ELEMENTS ANATOMIQUES A L'AIDE DE SURFACES DE FORME LIBRE]
Rene Ebel 1993 318 p In FRENCH
(ISSN 0751-1353)
(TELECOM-93-E-002; ETN-94-95980) Avail: CASI HC A14/MF A03

An approach to the mathematical description of the surface of a three dimensional (3D) reconstruction of an anatomical structure from a set of 3D data point samples is described. The approach could be compared to CAGD (Computer Aided Geometric Design) insofar as it is based on interactivity and on the use of free form patches to describe the surfaces. The advantage of this approach lies in the quality of the surfaces obtained

(G(sup 1) continuity or tangent plane continuity is satisfied) and in the possibility of performing reconstructions from arbitrary sets of 3D points. It is assumed that the elements to be reconstructed are smooth and that they are simple enough to enable interactivity. Reconstruction of treelike structures such as blood vessels are addressed, distinguishing three constituent elements: tubular parts, 'caps,' and 'junctions'. For each one, a particular method of reconstruction is developed. The modeling of a tubular element begins with an interactive step of estimation of axial positions. The next steps consist of automatically fitting a right generalized cylinder on the data by an iterative optimization technique. The resulting surface is composed of B spline patches. Elements like 'caps' and 'junctions' are created automatically, by the prolongation of the tubular surface with Bezier-Gregory patches. The reconstruction method proposed for tubular surfaces is extended to organs with more general forms. This time, the user is requested to associate a predefined polyhedral structure with the data. After this interactive operation, the computer produces automatically a surfacic approximation of the data by means of triangular and rectangular Bezier-Gregory patches joined with G(sup 1) continuity. ESA

N94-31323# California Univ., Berkeley. Lawrence Berkeley Lab.
HYDROGENATED AMORPHOUS SILICON (a-Si:H) BASED GAMMA CAMERA: MONTE CARLO SIMULATIONS
H. Lee, J. S. Drewery, W. S. Hong, T. Jing, S. N. Kaplan, A. Mireshghi, and V. Perez-Mendez Jan. 1994 12 p Presented at the SPIE Medical Imaging Conference, Newport Beach, CA, 13-18 Feb. 1994
(Contract DE-AC03-76SF-00098)
(DE94-007042; LBL-35050; CONF-940254-1) Avail: CASI HC A03/MF A01

A new gamma camera using a-Si:H photodetectors has been designed for the imaging of heart and other small organs. In this new design, the photomultiplier tubes and the position sensing circuitry are replaced by 2-D array of a-Si:H p-i-n pixel photodetectors and readout circuitry which are built on a substrate. Without the photomultiplier tubes this camera is light weight, hence, it can be made portable. To predict the characteristics and the performance of this new gamma camera, we did Monte Carlo simulations. In the simulations, 128 x 128 imaging array of various pixel sizes were used. Tc-99m (140keV) and Tl-201) (70keV) were used as radiation sources. From the simulations, we could obtain the resolution of the camera and the overall system, and the blurring effects due to scattering in the phantom. Using the Wiener filter for image processing, restoration of the blurred image could be achieved. Simulation results of a-Si:H based gamma camera were compared with those of a conventional gamma camera. DOE

N94-31363# Clemson Apparel Research, Pengleton, SC.
MINIMIZATION OF CARPAL TUNNEL SYNDROME Final Report, 12 Dec. 1989 - 30 Jun. 1993
Ed Hill 13 Jan. 1994 26 p
(Contract DLA900-87-D-0017)
(AD-A276409) Avail: CASI HC A03/MF A01

The objectives of this report was to develop an attachment and method to reduce the risk of Carpal Tunnel Syndrome on a side seam operation called French Felling. In addition, the research assisted in identifying the cause of the high incidence of CTS in French Felling operators and a workstation device was designed to minimize its occurrence. DTIC

N94-31414* National Aeronautics and Space Administration, Washington, DC.
AEROSPACE MEDICINE AND BIOLOGY: A CONTINUING BIBLIOGRAPHY WITH INDEXES (SUPPLEMENT 388)
May 1994 59 p
(NASA-SP-7011(388); NAS 1.21:7011(388)) Avail: CASI HC A04

This bibliography lists 132 reports, articles and other documents introduced into the NASA Scientific and Technical Information Database. Subject coverage includes: aerospace medicine and physiology, life support systems and man/system technology, protective clothing, exobiology and extraterrestrial life, planetary biology, and flight crew behavior and performance. CASI

N94-31490# Acoustical Society of America, New York, NY.
MINUTES: ACCREDITED STANDARDS COMMITTEE ON BIOACOUSTICS, S3. US TAG FOR ISO/TC 43, ACOUSTICS, IEC/TC 29 ELECTROACOUSTICS, AND ISO/TC 108/SC4 HUMAN EXPOSURE TO MECHANICAL VIBRATION AND SHOCK
7 Oct. 1993 88 p Meeting held in Denver, CO, 7 Oct. 1993
(AD-A276201) Avail: CASI HC A05/MF A01

The following topics are presented: (1) approval of the minutes of the Ottawa, Canada meeting held 20 May 1993 (S1/384); (2) organization; (3) standards approved by ANSI in 1992/1993 and published (or being published) by ASA; (4) organizational matters and reports on working groups, including reports on letter ballots and international matters; (5) S3 liaison working groups; (6) international matters; (7) review of standards more than five years in existence; (8) new international standards available; (9) procedural ballots; (10) other business; (11) new business; (12) future meetings; and (13) adjournment. DTIC

N94-31652# Universiteit Twente, Enschede (Netherlands).
PERSPECTIVES OF GLUCOSE SENSING BASED ON A CHARGE-MODULATING COMPETITION REACTION Ph.D. Thesis
Jans Kruise 1993 164 p Sponsored by Ministry of Economic Affairs
(ISBN-9-09-005754-4; ETN-94-96030) Avail: CASI HC A08/MF A02

Diabetes mellitus is introduced, existing detection principles for glucose sensors are reviewed, and a method based on a charge modulating competition reaction for measurement of glucose dependent concentration of either oxygen, hydrogen peroxide or gluconic acid, as opposed to an enzyme based glucose sensor, is proposed. The detection principal, based on a competition reaction between glucose and a charged glucose derivative, is described. Both species can bind to receptor molecules present in a porous membrane. Due to the competition reaction, the concentration of bound charged glucose derivative depends on the glucose concentration in the sample solution. The aim is to find a method to detect this glucose dependent concentration of bound charged groups in the receptor membrane. The development of a Donnan potential across the membrane solution interface is modeled. Optimal system parameters, which lead to a maximum sensitivity of the Donnan potential towards changes in glucose concentration, are derived. The feasibility of static potentiometric detection of a Donnan potential with an ISFET based device is discussed. ISFET based membrane conductivity and miniature conductivity sensor are described. Measurement results of membranes in which the bound charge (of charged glucose derivatives) can be modulated by glucose are given. The membranes were characterized using the so called ion step method. This method was also used to prove the operation of the competition reaction between glucose and the charged glucose derivative. The effect of changes in glucose concentration on the membrane conductivity was investigated. ESA

N94-31738 Defence and Civil Inst. of Environmental Medicine, North York (Ontario).
PROCEEDINGS OF THE DCIEM DIVER THERMAL PROTECTION WORKSHOP
R. Y. Nishi, ed. Jan. 1992 218 p Workshop held in North York, Ontario, 31 Jan. - 2 Feb. 1989
(DCIEM-92-10; DSIS-92-03143; CTN-94-61181) Avail: Issuing Activity
(Defence and Civil Inst. of Environmental Medicine, 1133 Sheppard Ave. W., P.O. Box 2000, North York, ON M3M 3B9 Canada)

As a result of a renewed interest in diver thermal protection, a workshop was organized under the auspices of the America, Britain, Canada, and Australia Information Exchange Program on Naval Diving in order to bring together representatives from all the components associated with military diving. Papers were presented at the workshop on active and passive diver thermal protection, medical implications of diving in cold water, diving suit buoyancy characteristics, thermal insulation materials, diving suit undergarments, hot-water heating and electrical heating of diving suits, improvement of cold tolerance in humans, thermoregulation, diver monitoring systems, and test facilities. Separate abstracts have been prepared for four papers from this workshop. For individual titles, see N94-31739 through N94-31742.

N94-31739 Naval Coastal Systems Center, Panama City, FL. Materials Science Branch.
THERMOTROPIC LIQUID CRYSTALS: A VARIABLE Clo MATERIAL
c54
Rand R. Biggers *In* Defence and Civil Inst. of Environmental Medicine, Proceedings of the DCIEM Diver Thermal Protection Workshop Jan. 1992 p 33-39 (For primary document see N94-31738 09-52)
Avail: Issuing Activity (Defence and Civil Inst. of Environmental Medicine, 1133 Sheppard Ave. W., P.O. Box 2000, North York, ON M3M 3B9 Canada)

Thermotropic liquid crystals comprise a class of mesophase materials with variable heat transfer characteristics. Utilization of their unique thermal transport properties in a diving garment would add an additional dimension of flexibility to diver thermal protection. The response of the effective thermal conductivity of liquid crystals to applied fields is sufficiently strong that an excellent opportunity exists to exploit the heat transfer characteristics of these materials to produce variable-Clo garments. The effects of alternating current fields on the thermal transfer rate in N-(p-methoxy benzylidene)-p- butylaniline (MBBA) were studied. The results suggest that the best utilization of liquid crystals would be in a cooling mode. The minimum thermal conductivity of MBBA gives it a Clo value roughly one half that of an equivalent thickness of neoprene. It is expected that when more liquid crystals are accurately measured, they might approach the Clo values of thinsulate. Recent experiments have suggested that inclusion of liquid crystal cells in a thinsulate undergarment would provide a cooling ability while retaining about 95 percent of the garment's insulating ability. A composite thinsulate and liquid crystal undergarment could provide nine hours of protection against hypothermia, compared to three hours with the conventional garment. Author (CISTI)

N94-31740 Defence and Civil Inst. of Environmental Medicine, Toronto (Ontario). Environmental Physiology Section.
REVIEW OF PHARMACOLOGICAL APPROACH TO IMPROVE COLD TOLERANCE
A. L. Vallerand and I. Jacobs *In its* Proceedings of the DCIEM Diver Thermal Protection Workshop Jan. 1992 p 119-123 (For primary document see N94-31738 09-52)
Avail: Issuing Activity (Defence and Civil Inst. of Environmental Medicine, 1133 Sheppard Ave. W., P.O. Box 2000, North York, ON M3M 3B9 Canada)

It has been shown that beta-adrenergic drugs increase heat protection in humans exposed to comfortable ambient temperatures. The influence of a mixture of ephedrine and caffeine on cold tolerance was investigated in male subjects during 3-hour exposures to 10 C air. The drug ingestion reduced the total drop in core, mean skin, and mean body temperatures, thus producing significantly warmer final core, mean skin, and mean body temperatures compared to placebo ingestion. The drug ingestion increased the total 3-hour energy expenditure by 18.6 percent compared to that of the placebo ingestion in the cold. Using the non-protein respiratory exchange ratio to calculate the rates of substrate oxidation, it was found that the drug ingestion increased carbohydrate oxidation by 41.7 percent above that of the placebo, but did not alter lipid or protein metabolism. The results demonstrate that the ingestion of a mixture of ephedrine and caffeine improves cold tolerance in man by significantly increasing body temperatures in the cold. These improvements were caused by a greater energy expenditure, which appears to be dependent on an enhanced carbohydrate utilization. Author (CISTI)

N94-31741 Defence and Civil Inst. of Environmental Medicine, Toronto (Ontario). Environmental Physiology Section.
LIPID METABOLISM IN COLD-EXPOSED HUMANS
A. L. Vallerand and I. Jacobs *In its* Proceedings of the DCIEM Diver Thermal Protection Workshop Jan. 1992 p 139-142 (For primary document see N94-31738 09-52)
Avail: Issuing Activity (Defence and Civil Inst. of Environmental Medicine, 1133 Sheppard Ave. W., P.O. Box 2000, North York, ON M3M 3B9 Canada)

Changes in lipid utilization associated with cold exposure in humans was investigated along with the role of plasma triglyceride (TG) and lipolysis in lipid metabolism during cold exposure. Male subjects were subjected to an intravenous fat tolerance test (an index of plasma TG utilization) at thermal neutrality, in 10 C cold, and in the cold 24 hours after the first cold test. Rates of substrate oxidation were calculated from indirect calorimetry, and changes in plasma glycerol levels were measured as an index of lipolysis. Cold exposure reduced mean body temperature by 3.2 C and increased energy expenditure 2.6 times compared to warm values. Cold exposure also increased fat oxidation by 71 percent and plasma glycerol levels, but did not alter removal rates of the infused plasma TG. The second cold test was accompanied by a further increase in fat utilization and plasma glycerol levels, with unchanged fat tolerance. The results show that cold exposure in humans significantly increases the oxidation of lipid, and that plasma TG does not appear to be an important energy substrate in the cold. It is suggested that white adipose tissue and possibly intramuscular TG, not plasma TG, are the preferred sources of fatty acids for oxidation in cold-exposed humans. Author (CISTI)

N94-31742 Toronto Univ. (Ontario). Dept. of Physiology.
ERRORS ASSOCIATED WITH THE USE OF HEAT FLOW TRANSDUCERS
M. B. Ducharme and J. Frim *In* Defence and Civil Inst. of Environmental Medicine, Proceedings of the DCIEM Diver Thermal Protection Workshop Jan. 1992 p 213-221 (For primary document see N94-31738 09-52)
Avail: Issuing Activity (Defence and Civil Inst. of Environmental Medicine, 1133 Sheppard Ave. W., P.O. Box 2000, North York, ON M3M 3B9 Canada)

Direct assessment of heat flux from the body is a basic measurement in thermal physiology. Heat flux transducers (HFTs) are increasingly being used for that purpose, but questions have been raised about the accuracy of the manufacturer's constant of calibration and the effect of the thermal resistance of the HFT on the true thermal flux from the skin. Two different types of waterproofed HFTs were checked for their calibration using the Rapid-K heat flow meter conductivity instrument. The mean difference between the recalibrations and the manufacturer's constants was +20.2 = or - 7.1 percent for Thermonetics HFTs and -0.7 = or - 4.8 percent for Concept Engineering HFTs. The significant difference in the calibration error between the two manufacturers becomes an important criterion for selecting HFTs. A model capable of simulating a large range of insulation values was used to study the effect of the underlying tissue insulation on the relative error in thermal flux due to the HFT thermal resistance. The data show that the deviation from the true value increases with the reciprocal of the underlying tissue insulation. The underestimation of heat flux through the skin measured by an HFT is minimum when the HFT is used on vasoconstricted skin in cool subjects, but becomes important when used on warm vasodilated subjects. Author (CISTI)

N94-31746 Colorado Univ., Boulder.
MUSCLE DISUSE THROUGH TAIL-SUSPENSION: ETIOLOGY AND THERAPEUTICS Ph.D. Thesis
Ellis Calvin Gayles 1993 110 p
Avail: Univ. Microfilms Order No. DA9320424

Humans and animals experience a loss of muscle mass and size during exposure to the weightless environment of space. This effect is seen predominantly in the postural muscles of the leg. In order to more extensively study these effects, ground based models have been developed to mimic the effects of space flight on the mammalian musculoskeletal system. For rats or mice, the most common model involves suspending the animal by its tail such that the hind limbs are unloaded and the animal is tilted 30 degrees head down. The animal may only use its forelimbs for locomotion. In addition to unloading of the hind limbs, other physiological effects of suspension include anorexia, diuresis, and stress. The present research investigated the etiology of these suspension effects on mouse muscle mass and protein. Additionally, the sex and genotype dependence of these effects was also investigated. Two different therapeutic treatments were also developed to ameliorate the effects of suspension on the muscles. The results of the present studies estimate that unloading is responsible for approximately 50 percent of the suspension effect on muscle. Anorexia and stress are estimated to account for the other 50 percent. The effect of suspension on muscle mass was independent of sex or genotype; however the effect of suspension on muscle protein did demonstrate a genotype dependence. A resistance exercise regimen was developed to reduce the effects of suspension on the muscles. Suspended mice were required to walk on a grid with weight attached to their tails. This exercise regimen was performed daily during the suspension period. The daily exercise did not reduce the loss of muscle mass or muscle protein in the exercised

mice. Pulsed electromagnetic fields (PEMF's) were also investigated as a method of muscle stimulation to reduce the effects of suspension. These fields had a positive effect on muscle mass and protein content. Suspended mice exposed to the PEMF's maintained more muscle mass than normal suspended mice. Additionally, mice exposed to the PEMF's averaged more muscle protein than non-field mice. These results suggest that PEMF's may provide an efficacious method for the alleviation of suspension effects on muscle. Dissert. Abstr.

N94-31960 State Univ. of New York, Stony Brook.
ISOLATING STRAIN PARAMETERS CORRELATED TO SKELETAL ADAPTATION Ph.D. Thesis
Ted S. Gross 1993 176 p
Avail: Univ. Microfilms Order No. DA9328176

The close association between skeletal morphology and parameters such as strain magnitude, strain rate, and strain energy density suggest that the cellular populations of bone perceive and respond to mechanically induced deformations within the tissue. However, the specific stimulus responsible for the control and maintenance of skeletal tissue has yet to be defined. In this study, we develop an in vivo model of skeletal adaptation, assess whether physical stimuli are necessary to maintain bone mass in the adult skeleton, isolate mechanical parameters correlated to sites of adaptation induced by an exogenous loading regimen, and lastly validate these relationships by their ability to predict adaptation in the same model under alternate loading conditions. The right radii of three groups of five adult male turkeys were functionally isolated via parallel metaphyseal osteotomies. The left radius served as an intact, contra-lateral control. The first group of animals remained unloaded for a period of eight weeks. The remaining two groups were exposed to a four week exogenous loading regimen placing the bone primarily in bending. The groups were identical except for the orientation of the transcutaneous loading pins, which were rotated 90 degrees in the transverse plane in the last group of animals (group 'B'). Using multiple step-backward regression, adaptive responses were related to candidate mechanical parameters defined by orthotropic finite element models whose geometry was based upon each animal's intact control radius. Eight weeks of disuse induced a mean (+/- S.D.) 12.1 +/- 7.1 percent reduction of bone mass. The loss was achieved primarily via uniform endosteal expansion suggesting that the entire cortex is sensitive to mechanical stimuli. The exogenous loading regimen induced a 20.4 +/- 28.8 percent increase in bone area in group 'A', and a 35.2 +/- 32.8 percent increase in group 'B', primarily via periosteal expansion. In both groups, the location of greatest periosteal expansion corresponded with sites of minimum rather than maximum strain magnitudes. Of the many candidate correlates, only the surface epsilon(sub zz) gradient in the circumferential direction was validated by its ability to predict adaptation in the alternate loading group. The predictive power of this parameter is particularly intriguing when considering possible physiologic mechanisms of cellular signal transduction such as streaming potentials and cellular communication via gap junctions. Dissert. Abstr.

N94-32156# Naval Air Warfare Center, Warminster, PA. Aircraft Div.
VALIDATION AND SENSITIVITY ANALYSIS OF TEXAS HUMAN THERMAL MODEL PREDICTIONS DURING COLD WATER IMMERSION Final Report, Mar. - Sep. 1992
Barry S. Shender and Jonathan W. Kaufman 1 Feb. 1993 153 p
(AD-A275240; NAWCADWAR-93069-60) Avail: CASI HC A08/MF A02

The Texas Human Thermal Model has been used to simulate the effects of thermal stresses on individuals under a variety of conditions. AS part of a U.S. Navy effort to develop integrated protection garments, the Model has been modified to predict tolerance to cold water immersion with garments whose CLO values are less than 0.1. Other program modifications have been implemented leading to easier use, enhanced speed and versatility and accuracy of predictions. With these modifications, a validation of Model performance was done using human data obtained from Finnish cold water immersion suit assessments. Limitations in Model performance were found but predictions of rectal temperature (T(sub re)) were in reasonable agreement to actual results. A sensitivity analysis was also performed to determine which Model parameters were most effected by cold water immersions. The condition tested was head-out immersion in 40 deg F water by 160 lb man with a 10 mm mean skinfold thickness. Based on the thermal end points, the Model was sensitive to body segmental changes in CLO (ordered from most to least sensitive): chest and abdomen, leg, head, arm, foot, and hand. Mean skinfold thickness, basal metabolic rate, body weight and level of exercise metabolic rate up to 100 BTU/her were the most important physical parameters affecting Model performance. Lowering the water temperatures to 28 deg F caused a simple shift by in segment temperature predictions with respect to 40 deg F estimates. The overall shapes of the curves at 28 and 40 deg F were essentially the same, though the 28 deg F curves had steeper slopes leading to a faster fall to critical temperatures. DTIC

N94-32347* National Aeronautics and Space Administration, Washington, DC.
AEROSPACE MEDICINE AND BIOLOGY: A CONTINUING BIBLIOGRAPHY WITH INDEXES (SUPPLEMENT 389)
Jun. 1994 98 p
(NASA-SP-7011(389); NAS 1.21:7011(389)) Avail: CASI HC A05

This bibliography lists 234 reports, articles, and other documents recently introduced into the NASA Scientific and Technical Information System. Subject coverage includes: aerospace medicine and physiology, life support systems and man/system technology, protective clothing, exobiology and extraterrestrial life, planetary biology, and flight crew behavior and performance. Author

N94-32348* National Aeronautics and Space Administration, Washington, DC.
AEROSPACE MEDICINE AND BIOLOGY: A CONTINUING BIBLIOGRAPHY WITH INDEXES (SUPPLEMENT 385)
Feb. 1994 168 p
(NASA-SP-7011(385); NAS 1.21:7011(385)) Avail: CASI HC A08

This bibliography lists 536 reports, articles and other documents introduced into the NASA Scientific and Technical Information System Database. Subject coverage includes: aerospace medicine and physiology, life support systems and man/system technology, protective clothing, exobiology and extraterrestrial life, planetary biology, and flight crew behavior and performance. Author

N94-32623 David Sarnoff Research Center, Princeton, NJ.
MODELS OF THE NEURONAL MECHANISMS OF TARGET LOCALIZATION OF THE BARN OWL Final Report, 11 Sep. 1990 - 20 Sep. 1993
John Pearson Nov. 1993 24 p Limited Reproducibility: More than 20% of this document may be affected by microfiche quality
(Contract F49620-89-C-0131)
(AD-A277332; AFOSR-94-0061) Avail: CASI HC A03

Models of the computation of sound direction in the brainstem and midbrain of the barn owl (tyto alba) were developed. Nucleus laminaris is the first site of interaural time-delay (ITD) processing. It was shown that standard neuron models would have to have unrealistically fast time constants in order to match the 10 micro-second ITD resolution characteristic of laminaris neurons. Three physiological reasonable, qualitatively distinct alternatives, were developed. Nucleus ventralis lemnisci lateralis pars posterior (VLVp) and the lateral shell of the central nucleus of the inferior colliculus (ICL) are the first two stages of interaural level differences (ILD) processing. It was shown how a thermometer code of ILD could be formed in VLVp through competitive dynamics, and how the ILD-tuned responses of ICL neurons could derive from the VLVp through lateral inhibition. It was shown how this architecture could be modified to achieve near independence from the average binaural level. Experimentalists are now checking the predictions of these models of ILD and ITD processing. DTIC

N94-32732# Los Alamos National Lab., NM. Laser Sciences and Applications Group.
NONINVASIVE SPECTROSCOPIC DIAGNOSIS OF SUPERFICIAL OCULAR LESIONS AND CORNEAL INFECTIONS
J. R. Mourant, I. J. Bigio, T. Johnson, T. Shimada, D. C. Gritz, and K. Storey-Held 1994 10 p Presented at the OE/LASE 1994 Conference on Optics, Electro-Optics, and Laser Applications in Science and Engineering, Los Angeles, CA, 22-29 Jan. 1994
(Contract W-7405-eng-36)
(DE94-006231; LA-UR-94-16; CONF-940142-8) Avail: CASI HC A02/MF A01

The potential of a rapid noninvasive diagnostic system to detect tissue

abnormalities on the surface of the eye has been investigated. The optical scatter signal from lesions and normal areas on the conjunctival sclera of the human eye were measured in vivo. It is possible to distinguish nonpigmented pingueculas from other lesions. The ability of the system to detect malignancies could not be tested because none of the measured and biopsied lesions were malignant. Optical scatter and fluorescence spectra of bacterial and fungal suspensions, and corneal irritations were also collected. Both scattering and fluorescence show potential for diagnosing corneal infections. DOE

N94-33040# Army Research Inst. of Environmental Medicine, Natick, MA.
NUMERICAL MODEL OF THE THERMAL BEHAVIOR OF AN EXTREMITY IN A COLD ENVIRONMENT INCLUDING COUNTER-CURRENT HEAT EXCHANGE BETWEEN THE BLOOD VESSELS
Avraham Shitzer, Leander A. Stroschein, Paul Vital, Richard R. Gonzales, and Kent B. Pandolf Mar. 1994 122 p
(AD-A278099; USARIEM-T94-10) Avail: CASI HC A06/MF A02

A numerical model of the thermal behavior of an extremity, e.g., finger, is presented. The model includes the effects of: (1) heat conduction, (2) metabolic heat generation, (3) heat transport by blood perfusion, (4) heat exchange between the tissue and the large blood vessels, and (5) arterio-venous heat exchange. Heat exchange with the environment through a layer of thermal insulation, depicted by thermal handwear is also considered. The tissue is subdivided into four concentric layers. The layers described, from the center outward, as core, muscle, fat, and skin. Differential heat balance equations are formulated for the tissue and the major artery and the major vein. These coupled equations are solved numerically by the alternating direction method employing a Thomas algorithm. The numerical scheme was tested extensively for stability and convergence. Results of the convergence tests are presented and discussed and the dependence on the number of grid points is demonstrated. Plots of tissue and blood temperatures along selected nodes of the model are shown for different combinations of parameters. The effect of counter-current heat exchange between the artery and the vein on the thermal balance of the extremity is presented. This shows clearly the conservation of energy achieved due to this mechanism. The report is concluded by considering the effects of cold induced vasodilation on tissue temperature cycling. DTIC

N94-33069 Ecole Nationale Superieure des Telecommunications, Paris (France). Dept. Images.
FAST NONSUPERVISED 3D REGISTRATION OF PET AND MR IMAGES OF THE BRAIN
Jean-Francois Mangin (Commissariat a l'Energie Atomique, Orsay, France.), Vincent Frouin (Commissariat a l'Energie Atomique, Orsay, France.), Isabelle Bloch, Bernard Bendriem, and Jaime Lopez-Krahe 1993 46 p Submitted for publication Limited Reproducibility: More than 20% of this document may be affected by microfiche quality
(ISSN 0751-1337)
(TELECOM-93-C-006; ETN-94-95979) Avail: CASI HC A03

A fully nonsupervised methodology dedicated to the fast registration of PET (Positron Emission Tomography) and MR (Magnetic Resonance) images of the brain is proposed. Discrete representations of the surfaces of interest (head or brain surface) are automatically extracted form both images. A shape independent surface matching algorithm yields a rigid body transformation, which allows the transfer of information between both modalities. A 3D (three dimensional) extension of the chamfer matching principle makes up the core of this surface matching algorithm. The optimal transformation is inferred from the minimization of a quadrative generalized distance between discrete surfaces, taking into account between modalities differences in the localization of the segmented surfaces. The minimization process is efficiently performed via the precomputation of a 3D distance map. Validation studies using a dedicated brain shaped phantom showed that the maximum registration error was of the order of the PET pixel size (2 mm) for the wide variety of tested configurations. The software is routinely used in a clinical context by physicians (more than 50 registrations performed). The entire registration process requires about five minutes on a conventional workstation. ESA

N94-33092 Massachusetts General Hospital, Boston. Labs. of Photomedicine.
DEVELOPMENT OF A VIDEO FLUORESCENCE SYSTEM FOR ASSESSING BURN DEPTH Final Report, 26 May 1992 - 25 Dec. 1993
John A. Parrish, Norman S. Nishioka, Maya Jerath, Dominic Bua, and Geoffrey Silver 14 Jan. 1994 24 p Limited Reproducibility: More than 20% of this document may be affected by microfiche quality
(Contract DAMD17-92-J-2019; DA Proj. 3M2-63004-D-805)
(AD-A278127) Avail: CASI HC A03

The ultimate objective of our research is to develop an integrated laser-based system for treating burn injury. The first phase of this development effort was funded under the present contract. The objective was to design, construct and optimize a diagnostic system suitable for clinical use in humans that accurately determines burn depth. The diagnostic system utilizes an exogenously administered fluorescent dye to label skin vasculature that is detected by a fluorescence imaging system. During the past year the design criteria for such a system were formulated, the components acquired and the system constructed. A series of experiments have been carried out in animals to test and optimize the system. We have demonstrated that the ratio of fluorescence intensity detected by the system at a burn site to that detected from normal skin, can be used to accurately determine the extent of burn injury. The burn diagnostic system is now ready for clinical deployment to gather further data and refine the system. DTIC

N94-33268 Army Research Inst. of Environmental Medicine, Natick, MA.
MEDICAL PROBLEMS IN HIGH MOUNTAIN ENVIRONMENTS. A HANDBOOK FOR MEDICAL OFFICERS Final Report
Allen Cymerman and Paul B. Rock Feb. 1994 64 p Limited Reproducibility: More than 20% of this document may be affected by microfiche quality
(AD-A278095; USARIEM-TN94-2) Avail: Issuing Activity (Defense Technical Information Center (DTIC))

This Technical Note describes the physiological and medical basis for the prevention and treatment of altitude-related illnesses and a description of the reduced mental and physical performance incurred by troops in an operational high terrestrial altitude environment. Medical officers are provided with background information for the diagnosis, prevention, and management of the primary altitude-induced medical problems: acute mountain sickness (AMS), high altitude pulmonary edema (HAPE), and high altitude cerebral edema (HACE). Secondary medical problems are also reviewed as are precautionary and contributory sea-level medical conditions and general physiological and psychological factors affecting the performance of soldiers at altitude. DTIC

N94-32471*# National Aeronautics and Space Administration. Lyndon B. Johnson Space Center, Houston, TX.
VIRTUAL REALITY IN MEDICAL EDUCATION AND ASSESSMENT
Laurie A. Sprague (LinCom Corp., Houston, TX.), Brad Bell (LinCom Corp., Houston, TX.), Tim Sullivan (LinCom Corp., Houston, TX.), Mark Voss (LinCom Corp., Houston, TX.), Andrew F. Payer (Texas Univ., Galveston.), and Stewart Michael Goza *In* NASA, Washington, Technology 2003: The Fourth National Technology Transfer Conference and Exposition, Volume 2 Feb. 1994 p 439-443 (For primary document see N94-32420 09-99)
Avail: CASI HC A01/MF A04

53 BEHAVIORAL SCIENCES

Includes psychological factors; individual and group behavior; crew training and evaluation; and psychiatric research.

N94-31243# Southeastern Center for Electrical Engineering Education, Inc., Saint Cloud, FL.
SITUATIONAL AWARENESS: A FEASIBILITY INVESTIGATION OF NEAR-THRESHOLD SKILLS DEVELOPMENT Final Report, 27 Jul. 1987 - 31 May 1991
Grant E. Secrist and Bryce O. Hartman Jan. 1994 75 p
(Contract F33615-87-C-0614)
(AD-A276467; AL/AO-TR-1994-0002) Avail: CASI HC A04/MF A01

A decisive capability possessed by superior fighter-attack pilots is

keen situational awareness. In this report, we examine the trainability of near-threshold information acquisition and processing skills that appear to be vital to heightened situational awareness. The investigation served two purposes: (1) determine the effects or near-threshold training on target detection, recognition, and identification performance; and (2) assess the general transfer of this training to velocity discrimination and peripheral vision two-flash threshold performance. Ten flight-qualified AFROTC cadets served as trainees. Each trainee received 5,040 near-threshold training trials over five consecutive days. The findings indicate that near-threshold skills are trainable. Group and individual learning curves reflected consistent improvement in target detection, recognition, and identification accuracy at target durations down to 33 ms. Statistically significant differences were found between group baseline and post-training performance. DTIC

N94-31291# Naval Command, Control and Ocean Surveillance Center, San Diego, CA. Research, Development, Technology and Evaluation.
TOWARDS SIMPLICITY: NOISE AND COOPERATION IN THE PERFECT INTEGRATOR Professional Paper
A. R. Bulsara Feb. 1994 19 p
(AD-A276256) Avail: CASI HC A03/MF A01

Neuroscientists have known for decades that sensory information is encoded in the intervals between the action potentials or spikes characterizing neural firing events. Statistical analyses of experimentally obtained spike trains have shown the existence of a significant random component in the inter-spike intervals. There has been speculation, of late, that the noise may actually facilitate the transmission of sensory information; certainly there exists evidence that noise in networks of neurons can dynamically alter the properties of the membrane potential and the time constants. This paper describes the recent rekindling of interest in the Stochastic Resonance phenomenon leading to speculation that such nonlinear cooperative effects may occur naturally in living systems. DTIC

N94-31440# Maryland Univ., Baltimore. School of Medicine.
DEVELOPMENT AND ENHANCEMENT OF A MODEL OF PERFORMANCE AND DECISION MAKING UNDER STRESS IN A REAL LIFE SETTING Quarterly Report No. 11, 1 Nov. 1993 - 31 Jan. 1994
Colin F. Mackenzie 9 Feb. 1994 18 p
(Contract N00014-91-J-1540)
(AD-A276029) Avail: CASI HC A03/MF A01

A large portion of the quarter has been taken up with video-analysis and administrative requirements for reapproval of the protocol by the Institutional Review Board. A few additional cases have been videotaped in conjunction with Holter monitoring and blood pressure (BP) recording of the anesthesia care providers. DTIC

N94-31990 Massachusetts Inst. of Tech., Cambridge.
MODEL-BASED SCIENTIFIC DISCOVERY: A STUDY IN SPACE BIOENGINEERING Ph.D. Thesis
Nicolas Groleau 1992
Avail: Issuing Activity (MIT Libraries, Rm. 14-0551, Cambridge, MA 02139-4307)

This thesis describes a novel system that modifies the theory contained in a model of the normal human orientation system. This system, called MARIKA, demonstrates automated scientific discovery in an actual scientific domain through techniques adapted from diagnosis and design. MARIKA comprises a simulation module, a constraint propagation module and a model revision module. The module is captured in a simulation environment that produces time-varying signals. The model parameters are represented as constrained range variables and the input, output and intermediary signals are segmented in time and approximated by linear combinations of a set of four simple shape adequate for the vestibular domain. The model linear differential equations and boundary conditions are transformed into constraints on the curve fit parameters and the model parameters. Some extensions are also provided to cover simple non-linear cases and steady state conditions. Clinical data are abstracted using the shapes predicted by the model. These data are then compared to simulation predictions by propagating the constraints relating the model and the curve fit parameters. In case of contradiction, the model is modified by either extending the range of model parameters to pathological values or altering the structure of the model according to pre-indexed methods. MARIKA correctly models normal vestibular data and several end organ and nervous processing defects. MARIKA demonstrates the synergy of diagnosis and design techniques, qualitative and quantitative representation, and modeling, simulation, and artificial intelligence for a routine form of automated scientific discovery. MARIKA's set of shapes could readily be enhanced to be used to perform model-based theory refinement on a variety of linear domains. These encouraging results could lead to a useful clinical vestibular tool and to a space vestibular adaptation scientific discovery system.
Dissert. Abstr.

N94-32035 Aerospace Medical Research Labs., Brooks AFB, TX. Aerospace Medicine Directorate.
ANALYSIS OF PURSUIT TRACKING EYE MOVEMENTS IN PILOTS AND NONFLIERS Final Report, 1 Jan. 1993 - 1 Jan. 1994
Edward J. Engelken, Kennith W. Stevens, Ann F. Bell, and Jack D. Enderle 1 Jan. 1994 7 p Limited Reproducibility: More than 20% of this document may be affected by microfiche quality
(AF Proj. ILIR; AF Proj. 7755)
(AD-A276597; AL/AO-PC-1994-0003) Avail: CASI HC A02

Pursuit tracking eye movements were recorded and analyzed from a group of Air Force pilots and a group of nonflying Air Force Members. The tracking performance of the pilots was compared to the performance of the nonfliers. Subjects tracked a small spot of light moving sinusoidally in the horizontal plane at frequencies ranging from 0.2 to 1.0 Hz while their eye movements were recorded. An adaptive nonlinear digital filter was used to separate the total tracking response (TTR) into smooth pursuit (SP) and saccadic (SA) components. There were no significant differences in tracking performance between pilots and nonfliers. DTIC

N94-32096 Loyola Univ., Chicago, IL. Hearing Inst.
DETERMINATION OF MULTIPLE SOUND SOURCES Annual Report, 1 Sep. 1992 - 1 Sep. 1993
William A. Yost, Stanley Sheft, and Raymond Dye 1 Oct. 1993 16 p Limited Reproducibility: More than 20% of this document may be affected by microfiche quality
(Contract F49620-92-J-0489)
(AD-A277379; AFOSR-94-0127TR) Avail: CASI HC A03

We have completed the final construction of the sound-deaden listening room and the digital library of stored words, numbers, and letters, from nine English speaking males. We conducted pilot experiments on 20 subjects listening to one and two sound sources at a time. The results of the pilot experiments indicated that the sound room was well calibrated and allowed us to determine that a few of the words, letters, and numbers should be recorded. In addition the pilot experiment suggested a few modifications to our protocol. The new utterances have been recorded, the protocol modifications made, and a new set of 10 subjects were tested. The results from this additional set indicated that we had a good listening room, set of utterances, and procedure. From October until January of 1993 we will test the headphone listening protocol making adjustments where necessary. We plan to collect data in the full experiment starting late January 1994.
DTIC

N94-32187# Naval Aerospace Medical Research Lab., Pensacola, FL.
EFFECTS OF METHAMPHETAMINE AND FATIGUE ON LONG- AND SHORT-TERM MEMORY Interim Report, 1993
R. R. Stanny, A. H. McCardie, and D. F. Neri Nov. 1993 27 p
(AD-A276452; NAMRL-1387) Avail: CASI HC A03/MF A01

We examined the effects of a 10 mg/70 kg oral dose of d-methamphetamine HCl on fatigue-related deficits of short- and long-term memory. We used a recognition memory-search task with two memory loads. In one experimental condition, stimuli were committed to long-term memory (LTM) and performance was rendered automatic by extensive practice with consistently mapped stimuli and responses. In a second condition, the task was organized so that recognition depended on short-term memory (STM) despite equally extensive practice. After 7680 training trials, 13 subjects performed the task at 90-min intervals in a 13.5-h, sustained-performance session that began at 1930 and ended at 0900. At 0116, seven subjects were administered capsules containing 10 mg/70-kg body weight d-methamphetamine HCl, double-blind. The remaining subjects were administered a placebo. Memory-trace strengths and decision speeds declined during the early part of the night in all experimental conditions. The methamphetamine treatment reversed these effects within approximately 2 h of administration. The methamphetamine treatment also reversed an increasing trend in lapse probabilities. The stimulant did not merely produce

criterion shifts that led subjects to respond impulsively (more rapidly but less accurately). These results suggest that the methamphetamine treatment produced genuine increases in accuracy of recognition and that any criterion shifts that may have occurred were more than compensated for by increased accuracy. DTIC

N94-32276 York Univ. (Ontario).
SENSORY SENSITIVITIES AND DISCRIMINATIONS AND THEIR ROLES IN AVIATION Final Report, 1 Nov. 1990 - 31 Oct. 1993
David M. Regan 30 Nov. 1993 137 p Limited Reproducibility: More than 20% of this document may be affected by microfiche quality
(Grant AF-AFOSR-0080-91)
(AD-A277312; AFOSR-94-0078TR) Avail: CASI HC A07

Evidence that intersubject differences in the ability to process motion-defined (MD) shape are not predicted by the ability to process luminance-defined (LD) shape, that motion is processed by hierarchical manner, that discrimination and detection can be dissociated for MD form, and that spatial discrimination for MD and LD form are not entirely mediated by the same mechanism is as follows. Reducing presentation duration or dot lifetime from 1.0 to 0.1 sec progressively reduced the visibility of a MD bar, but did not reduce orientation discrimination for the bar when visibility was held constant. Detection and/or recognition of MD letters can be degraded by removal of brain tissue underlying prestriate cortex without affecting contrast sensitivity, Snellen acuity, low contrast acuity, or sensitivity to motion. Shape discrimination for an MD rectangle can be as low as 2 to 3 percent, as good as for an LD rectangle. Evidence is reported for a neural mechanism sensitive to shape independently of size. Evidence is reported for a neural mechanism directly sensitive to time to collision with an approaching object. A method is reported for measuring intersubject differences in discrimination of time to contact. A titration method for uncovering the color-defined form system is reported. The 40 Hz human brain response indexes magnocellular activity. By recording the magnetic field of the brain, an audio-visual integration area in the brain has been identified. Responses to texture-defined form and color-defined form have been unconfounded from responses to luminance-defined form. A technique for measuring intersubject differences in susceptibility to glare has been developed and is being used in a prospective study of flying safety. Also, the test quantifies visual status in cataract patients. DTIC

N94-32277 Carnegie-Mellon Univ., Pittsburgh, PA.
A DIFFERENTIAL THEORY OF LEARNING FOR EFFICIENT STATISTICAL PATTERN RECOGNITION Final Report, 30 Sep. 1989 - 29 Sep. 1993
John Hampshire and B. V. Kumar 15 Dec. 1993 445 p Limited Reproducibility: More than 20% of this document may be affected by microfiche quality
(Grant AF-AFOSR-0551-89)
(AD-A277313; AFOSR-94-0073TR) Avail: CASI HC A19

Probabilistic learning strategies currently use are inefficient, requiring high classifier complexity and large training samples. In this report, we introduce and analyze an asymptotically efficient differential learning strategy. It guarantees the best generalization allowed by the chosen classifier paradigm. Differential learning also requires the classifier with minimal complexity. The theory is demonstrated in several real-world machine learning/pattern recognition tasks. DTIC

N94-32344 North Carolina Univ., Chapel Hill. Dept. of Computer Science.
VISUAL ENCODING OF SPATIAL RELATIONS Annual Report, 1 Jan. - 31 Dec. 1993
Christina A. Burbeck 26 Jan. 1994 11 p Limited Reproducibility: More than 20% of this document may be affected by microfiche quality
(Contract F49620-92-J-0114)
(AD-A277400; AFOSR-94-0115TR) Avail: CASI HC A03

Psychophysical and theoretical research was conducted on the processes underlying the encoding of relative spatial locations of objects and edges of single objects. Work was done on developing a model of shape representation, called Object Representation by Cores, that is based on previous findings, sponsored by this grant, that the area over which position information is gathered scales with the distance being judged. Experimental work included measuring orientation discrimination thresholds for cone stimuli of various widths and measuring bisection thresholds for stimuli with sinusoidally modulated edges, where both edge modulation frequency and object width were manipulated. Results of both studies verified the key assumption of the model: the scale of the boundariness detector that contributes to perception of object shape covaries with object width. Studies continued on the perception of area. A new line of research was begun on the nature of information observers have about scenes containing multiple objects. DTIC

N94-32345# New York Univ., New York.
VISUAL NEURAL DEVELOPMENT AND CHROMATIC ABERRATION Annual Report, 15 Mar. 1992 - 14 Mar. 1993
Laurence T. Maloney 14 Mar. 1993 5 p
(Contract F49620-92-J-0187)
(AD-A277402; AFOSR-94-0109TR) Avail: CASI HC A01/MF A01

The purpose of the research is to (1) develop and test new methods to study the internal visual representation of the shape and surface properties of objects, and the mechanisms that calibrate it; (2) use the methods to investigate the representation of contour, shape and surface properties; (3) use the methods to study the representation of visual space; and (4) study visual (re-)calibration mechanisms. DTIC

N94-32419 Connecticut Univ., Storrs. Dept. of Communication Sciences.
AUDITORY PERCEPTION Annual Report, 1 Jan. - 31 Dec. 1993
Marion F. Cohen 23 May 1994 7 p Limited Reproducibility: More than 20% of this document may be affected by microfiche quality
(Contract F49620-93-1-0070)
(AD-A277414; AFOSR-94-0105TR) Avail: CASI HC A02

The experiments described in this report were designed to study the effects of certain acoustic cues on detectability of a delayed signal. The purpose was to gain insight into how the ear suppresses multiple hearings in a reverberant setting. Results of the experiments indicate that a signal, intended to simulate and echo, is more difficult to detect when it is following an identical masker, intended to simulate a primary sound, than when it is leading that masker. If, however, the signal is not acoustically similar to the masker, this asymmetry disappears, even if the masker is equally effective in the simultaneous condition. Further, if the signal and masker are not identical, but share an important acoustic attribute such as harmonicity, the asymmetry is observed. In summary, detectability of the delayed signal seems to be dependent on the strength of acoustic connection between the signal and masker, whereas detectability of the leading signal does not demonstrate that dependence. DTIC

N94-32495 Illinois Univ., Urbana-Champaign.
INFORMATION THEORY FOR ARM VISUO-MOTOR COORDINATION Ph.D. Thesis
Tarcisio Passos Ribe deCampos 1993 166 p
Avail: Univ. Microfilms Order No. DA9328987

The present work addresses the information processing of visuo-motor coordination. The aim of this research is to develop an adaptive model for coordinating mechanical action of an arm according to visual information. As a result, a large neural map has been generated which has been used to guide a pneumatically driven robot arm through a vision system consisting of image boards and two stereo cameras. This engineering approach has been employed to test the algorithm which might share close features with the way that biological beings solve the same sensory-motor task. Basically, arm postures are represented through their projections onto a set of image planes. Based on the link orientations and lengths as visual primitives extracted from these images, a topological state-space is characterized. Arm kinematics is defined as transformations of topological hypersurfaces, the intersections of which represent all possible postures which any redundant arm possesses in reaching an arbitrary target position. The self-organizing feature map has learned how the topological hypersurfaces transform in the state-space during arbitrary movements of the arm. The analyses of these transformations helped in idealizing a connectionistic model for kinematics. A model for the collision-free motion of a redundant arm manipulator moving in a workspace with obstacles is presented. A mapping of the arm surface onto a set of lattices, in which visual, motor information, and surface location are encoded, is adaptively developed through a learning procedure fed by trial movements. The map, which carries topographical features of the arm surface, is then used to guide the arm avoiding collisions with obstacles in unpredictable positions. The main achievements of this research are the topographical neural model for

obstacle-avoidance and the connectionist model for kinematics for redundant arms. Both models have been developed based on the analyses of a dynamic geometry, induced by the arm movements, embedded in a denoted visuo-motor space. The topographical neural model presents similar features with the motor cortex which might provide some insight for understanding biological visuo-motor control. Dissert. Abstr.

N94-32577# Florida Univ., Gainesville. Dept. of Psychology.
MECHANISMS OF TEMPORAL PATTERN DISCRIMINATION BY HUMAN OBSERVERS Final Technical Report, 1 Oct. 1990 - 31 Dec. 1993
Robert D. Sorkin 15 Feb. 1994 157 p
(Grant AF-AFOSR-0065-91)
(AD-A277407; AFOSR-94-0129TR) Avail: CASI HC A08/MF A02

The project's first component studied how human listeners discriminate two temporal patterns of tones. The stimuli were non-speech, non-musical tone sequences that conveyed arhythmic or partly rhythmic time patterns. The results indicated that the temporal pattern discrimination process depends on the timing of the sequences and whether they overlap in time. Listeners can perform the task very well when the patterns do not overlap and are presented to separate ears and/or at different tone frequencies. At long time separations, the listener's discrimination mechanism reduces the input information to two lists of intertone times, and the decision is based on the correlation between the lists (a temporal correlation process). At short time separations, the mechanism computes statistics based on the summed envelope of the two input waveforms (a single channel process). The project's second component consisted of analytical and computer modeling of multi-element detection systems. New results were obtained on the performance of statistically optimal detector arrays and on arrays that combine their binary outputs. The project's third component studied how observers process information in multi-element, visual signal detection. The results describe how performance depends on display element reliability, coding, and arrangement. DTIC

N94-32956# Northwestern Univ., Evanston, IL.
READING: INTERACTION WITH MEMORY Final Report, 1 Mar. 1990 - 31 Aug. 1993
Gail McKoon 15 Dec. 1993 170 p
(Grant AF-AFOSR-0246-90)
(AD-A277547; AFOSR-94-0097TR) Avail: CASI HC A08/MF A02

The topic of the supported research was reading and the ways information in memory can contribute to the inference processes that occur during reading. One source of information for inference processes is short-term memory for parts of a text that have already been read. Experiments investigated how this information is made available to allow, for example, inferences that decide the correct referent of a pronoun, or inferences that relate via causality two events described by the text. Experiments also examined the local representation constructed for a text, testing our proposal that locally available information is structured by the linguistic, semantic, and pragmatic means by which the information is expressed. A second line of research examined interactions between inference processes and well-known information from long-term memory, examining knowledge of the semantic structures of verbs, knowledge of what concepts are frequently associated with each other, and knowledge about how lexical items are used in various contexts. DTIC

N94-32997# Illinois Univ., Urbana. Dept. of Psychology.
REMINDING-BASED LEARNING Annual Technical Report, 21 Jan. 1993 - 20 Jan. 1994
Brian H. Ross 8 Feb. 1994 12 p
(Grant AF-AFOSR-0447-89)
(AD-A277424; AFOSR-94-0126TR) Avail: CASI HC A03/MF A01

When learning new cognitive skills involving problem solving, novices are often reminded of earlier problems. The use of earlier problems is a common means of problem solving and affects the learning of the skill. This project has three aims in understanding this learning. First, the representation of the resulting generalizations is being examined. Generalizations formed from remindings are likely to be conservative, in that they may be more tied to the examples than many current theories allow. A main aim of the project is to distinguish and test different forms of this conservatism. Second, the development of problem solving expertise is examined by focusing on differences in how typical and atypical problems are solved. Third, the effects of such reminding-based learning in everyday problem solving is examined to extend the findings and test some theoretical ideas that are difficult to investigate in more formal domains. This report provides an overview of this work and the progress on these objectives during the last year. DTIC

N94-32998# Smith-Kettlewell Inst. of Visual Sciences, San Francisco, CA. Eye Research.
VISUAL PROCESSING OF OBJECT VELOCITY AND ACCELERATION Annual Technical Report, 16 Jan. 1993 - 15 Jan. 1994
Suzanne McKee 4 Feb. 1994 3 p
(Contract F49620-92-J-0156)
(AD-A277425; AFOSR-94-0102TR) Avail: CASI HC A01/MF A01

Human observers can easily detect a signal dot moving, in apparent motion, on a trajectory embedded in a background of random-direction motion noise. A high detection rate is possible even though the spatial and temporal characteristics (step size and frame rate) of the signal are identical to the noise, making the signal indistinguishable from the noise on the basis of a single pair of frames. The success rate for detecting the signal dot was as high as 90% when the probability of mismatch from frame-to-frame, based on nearest neighbor matching was 0.3, control experiments showed that trajectory detection is not based on detecting a 'string' of collinear dots, i.e., a stationary position cue. Nor is a trajectory detected because produces stronger signals in independent 'local' motion detectors. For one thing, trajectory detection improves with increases in duration, up to 250-400 msec, a duration longer than the integration typically associated with a single motion detector. Moreover, the signal dot need not travel in a straight line to be detectable. The signal dot was as reliably detected when it changed its direction a small amount (less than 30 deg) each frame. Consistent with this, circular paths of sufficiently low curvature were as detectable as straight trajectories. DTIC

N94-33053 Draper (Charles Stark) Lab., Inc., Cambridge, MA.
INVESTIGATION OF DRIVE-REINFORCEMENT LEARNING AND APPLICATION OF LEARNING TO FLIGHT CONTROL Final Report, 1 Jan. 1989 - 1 Aug. 1993
Walter L. Baker, Stephen C. Atkins, Leemon C. Baird, III, Mark A. Koenig, and Peter J. Millington Aug. 1993 503 p Limited Reproducibility: More than 20% of this document may be affected by microfiche quality
(Contract F33615-88-C-1740)
(AD-A277442; CSDL-R-2575; WL-TR-93-1153) Avail: CASI HC A22

This report describes results obtained during a multiphase research program having the broad aim of investigating the application of learning systems to automatic control in general and to flight control in particular. The first phase analyzed the drive-reinforcement learning paradigm and examined its application to automatic control, with mixed results. The second phase compared a number of alternative strategies for learning augmented control and resulted in the conception of a new hybrid adaptive/learning control scheme. Subsequently, in the third phase, this hybrid control approach was more fully developed and applied to several nonlinear dynamical systems, including a cart-pole system, aeroelastic oscillator, and a three degree of freedom aircraft. The fourth phase revisited drive-reinforcement learning from the point of view of optimal control and successfully applied a version embedded in the associative control process architecture to regulate an aeroelastic oscillator. The fifth phase examined the problem of learning augmented estimation and resulted in the development of a preliminary estimation scheme consistent with the hybrid control approach. In the sixth and final phase, the hybrid control methodology was applied to a nonlinear, six degree of freedom flight control problem and then demonstrated via a challenging multiaxis maneuver. DTIC

N94-33068*# National Aeronautics and Space Administration. Ames Research Center, Moffett Field, CA.
AUTOGENIC-FEEDBACK TRAINING AS A TREATMENT FOR AIRSICKNESS IN HIGH-PERFORMANCE MILITARY AIRCRAFT: TWO CASE STUDIES
Patricia S. Cowings, William B. Toscano, Neal E. Miller, and Samuel Reynoso Mar. 1994 22 p
(RTOP 199-70-12-14)
(NASA-TM-108810; A-94048; NAS 1.15:108810) Avail: CASI HC A03/MF A01

The purpose of this paper is to present a detailed description of the physiological and performance responses of two military pilots undergoing

a treatment for motion sickness. The treatment used, Autogenic-Feedback Training (AFT), is an operant conditioning procedure where subjects are taught to control several of their autonomic responses and thereby suppress their motion sickness symptoms. Two male, active duty military pilots (U.S. Navy and U. S. Marine Corps), ages 30 and 35, were each given twelve 30-minute training sessions. The primary criterion for success of training was the subject's ability to tolerate rotating chair motion sickness tests for progressively longer periods of time and at higher rotational velocities. A standardized diagnostic scale was used during motion sickness to assess changes in the subject's perceived malaise. Physiological data were obtained from one pilot during tactical maneuvers in an F-18 aircraft after completion of his training. A significant increase in tolerance to laboratory-induced motion sickness tests and a reduction in autonomic nervous system (ANS) response variability was observed for both subjects after training. Both pilots were successful in applying AFT for controlling their airsickness during subsequent qualification tests on F-18 and T-38 aircraft and were returned to active duty flight status. Author

N94-33241 Hawaii Univ., Honolulu. Dept. of Psychology.
FROM ANIMALS TO ANIMATS Final Report, 30 Sep. 1992 - 29 Sep. 1993
Herbert L. Roitblat 29 Sep. 1993 9 p The Second International Conference on the Simulation of Adaptive Behavior was held in Hololulu, HI, 7-11 Dec. 1992 Limited Reproducibility: More than 20% of this document may be affected by microfiche quality
(Contract F49620-92-J-0530)
(AD-A277427; AFOSR-94-0071TR) Avail: CASI HC A02

This project provided partial support for an international conference on the simulation of adaptive behavior. The conference was held in Honolulu, HI on December 7-11, 1992. It was attended by more than 100 scientists from the US, Europe, and Asia. The main topic of the conference was how to use theories of animal behavior as a guide in the construction of robots and other autonomous agents. Contributors discussed how to develop behavior-based artificial intelligence, perception and motor control, action selection and the structuring of behavioral sequences, cognitive maps and internal world models, learning, evolution and adaptation, and collective behavior. DTIC

N94-33326 Minnesota Univ., Minneapolis. Dept. of Psychology.
WORKSHOP ON VISUAL PERCEPTION: COMPUTATION AND PSYCHOPHYSICS Final Report, 15 Jan. 1993 - 14 Jan. 1994
David C. Knill and Whitman Richards 1 Mar. 1994 15 p Workshop held in Chatham, MA, 14-17 Jan. 1993 Limited Reproducibility: More than 20% of this document may be affected by microfiche quality
(Contract F49620-93-1-0124)
(AD-A278412; AFOSR-94-0219TR) Avail: Issuing Activity (Defense Technical Information Center (DTIC))

The workshop brought together researchers in computational vision and psychophysics to discuss ways of conceptualizing and modeling problems in visual perception. Such a conceptualization requires common frameworks for formulating problems in perception. Workshop participants considered what formal tools and structures these frameworks should provide in order to be most useful for the study of human vision. Several recently proposed frameworks based on the formulation of Bayesian, probabilistic inference served as the focal point for evaluation and discussion. DTIC

N94-33327# Yale Univ., New Haven, CT. School of Medicine.
STRESS-INDUCED ENHANCEMENT OF THE STARTLE REFLEX Final Report, 1 Oct. 1990 - 30 Sep. 1993
Michael Davis 30 Sep. 1993 8 p
(Grant AF-AFOSR-0035-91)
(AD-A278414; AFOSR-94-0173TR) Avail: CASI HC A02/MF A01

A major goal of the work funded by the Air Force has been to evaluate the role of the amygdala in both conditioned and unconditioned fear and anxiety. This work showed that the central nucleus of the amygdala, and its direct projection to a particular part of the acoustic startle pathway, were critically involved in the performance or expression of fear-potentiated startle. DTIC

N94-33333 Wake Forest Univ., Winston-Salem, NC. Dept. of Physiology and Pharmacology.
NEOSTRIATAL NEURONAL ACTIVITY AND BEHAVIOR Final Report, 1 Jun. 1992 - 30 Sep. 1993
Donald J. Woodward 30 Sep. 1993 4 p Limited Reproducibility: More than 20% of this document may be affected by microfiche quality
(Contract F49620-92-J-0301)
(AD-A278429; AFOSR-94-0175TR) Avail: Issuing Activity (Defense Technical Information Center (DTIC))

The overall goal of the 'University Initiative' project 'Neostriatal Neuronal Activity and Behavior' was to establish a new technical approach for the study of ensembles of single neurons in CNS during tasks requiring sensory motor integration. An aim was to establish methodology for chronic implant of arrays of recording electrodes in rat neostriatum and other regions. Instrumentation was to be developed to allow amplification and spike sorting to be done for up to 64 concurrent spike trains. An acquisition system was to record the time events of spike trains, stimuli, and behavior events for up to four days continuously. An analysis capability was to provide a wide range of standard analysis procedures including histograms and rasters. A new approach for neuron ensemble analysis was to be developed to deal with statistical fluctuations of ensemble patterned activity across trials. Experimental studies were to study neuronal population activity during a series of tasks including tone and treadmill locomoting and a delayed matching-to-sample task with a spatial memory requirement. Computational simulation was to be done to explore short-term memory properties of the local circuitry between medium spiny neurons in neostriatum. Development of the experimental approach was the primary goal. Extended experimental analysis was secondary for this type of developmental project. DTIC

N94-32472*# National Aeronautics and Space Administration. Goddard Space Flight Center, Greenbelt, MD.
TECHNOLOGY TRANSFER OF OPERATOR-IN-THE-LOOP SIMULATION
K. H. Yae (Iowa Univ., Iowa City.), H. C. Lin (Iowa Univ., Iowa City.), T. C. Lin (Iowa Univ., Iowa City.), and H. P. Frisch *In* NASA, Washington, Technology 2003: The Fourth National Technology Transfer Conference and Exposition, Volume 2 Feb. 1994 p 444-455 (For primary document see N94-32420 09-99)
Avail: CASI HC A03/MF A04

54 MAN/SYSTEM TECHNOLOGY AND LIFE SUPPORT

Includes human engineering; biotechnology; and space suits and protective clothing.

For related information see also *16 Space Transportation.*

N94-31224# European Space Agency. European Space Research and Technology Center, ESTEC, Noordwijk (Netherlands). Thermal Control and Life Support Div.
ATMOSPHERE QUALITY STANDARDS IN MANNED SPACE VEHICLES
Jun. 1992 238 p
(ISSN 0379-4059)
(ESA-PSS-03-401-Issue-1; ETN-94-95872) Copyright Avail: CASI HC A11/MF A03

The various parameters which define the physical, chemical, and biological status of the atmospheres of space vehicles are described. Each of these atmospherical parameters is given standard values as required for the different situations encountered in space missions. Data on the following are given: respiration physiology; decompression physiology; atmospheric parameters; atmospheric contamination; environmental control and safety aspects. ESA

N94-31302# Naval Health Research Center, San Diego, CA.
A REVIEW OF MICROCLIMATE COOLING SYSTEMS IN THE CHEMICAL, BIOLOGICAL, RADIOLOGICAL ENVIRONMENT
T. Derion and R. S. Pozos 22 Sep. 1993 29 p
(NR Proj. M33-P-30)
(AD-A276446; NHRC-93-23) Avail: CASI HC A03/MF A01

Soldiers may work in hot environments and under conditions posing a biological, chemical, or nuclear threat. Chemical protective overgarments

are worn to prevent contact with toxins; however, they prevent dissipation of body heat. This review addresses the effectiveness of microclimate cooling systems in alleviating thermal strain in personnel encapsulated in protective overgarments during exertion in the heat. Air, liquid, and passive ice cooling systems are primarily reviewed, but other methodologies are also discussed. Air cooling can increase tolerance time fourfold, but high ambient temperature air cooling may be dangerous. Liquid cooling is effective in reducing heat strain at light to moderate work loads and is beneficial when applied to the thighs during lower-body exercise. Overcooling and discomfort can occur with a liquid-cooled system due to cutaneous vasoconstriction. Liquid-cooled systems are heavy and require excessive maintenance, and tube compression can result in interrupted coolant flow. Air cooling is inefficient compared to liquid cooling because of air's lower specific heat. Ice cooling may only be suitable for short-term work and is generally less effective than either air or liquid cooling although the wearer can move about untethered. The best cooling system design approach may be indicated by consideration of the unique cooling needs of personnel performing specific tasks in various environments. DTIC

N94-31380*# National Aeronautics and Space Administration. Marshall Space Flight Center, Huntsville, AL.

TECHNICAL ASSESSMENT OF MIR-1 LIFE SUPPORT HARDWARE FOR THE INTERNATIONAL SPACE STATION

K. L. Mitchell, R. M. Bagdigian, R. L. Carrasquillo, D. L. Carter, G. D. Franks, D. W. Holder, Jr., C. F. Hutchens, K. Y. Ogle, J. L. Perry, and C. D. Ray Mar. 1994 183 p Original contains color illustrations

(NASA-TM-108441; NAS 1.15:108441) Avail: CASI HC A09/MF A02; 7 functional color pages

NASA has been progressively learning the design and performance of the Russian life support systems utilized in their Mir space station. In 1992, a plan was implemented to assess the benefits of the Mir-1 life support systems to the Freedom program. Three primary tasks focused on: evaluating the operational Mir-1 support technologies and understanding if specific Russian systems could be directly utilized on the American space station and if Russian technology design information could prove useful in improving the current design of the planned American life support equipment; evaluating the ongoing Russian life support technology development activities to determine areas of potential long-term application to the U.S. space station; and utilizing the expertise of their space station life support systems to evaluate the benefits to the current U.S. space station program which included the integration of the Russian Mir-1 designs with the U.S. designs to support a crew of six. Author (revised)

N94-31447* Carnegie-Mellon Univ., Pittsburgh, PA. Dept. of Computer Science.

DIGIT-EYES: VISION-BASED HUMAN HAND TRACKING

James M. Rehg and Takeo Kanade 31 Dec. 1993 26 p Limited Reproducibility: More than 20% of this document may be affected by microfiche quality

(Grant NGT-50559)

(NASA-CR-195913; NAS 1.26:195913; AD-A276417; CMU-CS-93-220) Avail: CASI HC A03

Passive sensing of human hand and limb motion is important for a wide range of applications from human-computer interaction to athletic performance measurement. High degree of freedom articulated mechanisms like the human hand are difficult to track because of their large state space and complex image appearance. This article describes a model-based hand tracking system, called Digit-Eyes, that can recover the state of a 27 degree of freedom hand model from gray scale images at speeds of up to 10 Hz. We employ kinematic and geometric hand models, along with a high temporal sampling rate, to decompose global image patterns into incremental, local motions of simple shapes. Hand pose and joint angles are estimated from line and point features extracted from images of unmarked, unadorned hands, taken from one or more viewpoints. We present some preliminary. results on a three dimensional mouse interface based on the Digit-Eyes sensor. DTIC

N94-31839 Selskapet for Industriell og Teknisk Forskning, Trondheim (Norway). Div. of Safety and Reliability.

SYSTEMS FOR THE MONITORING OF WORKING CONDITIONS RELATING TO HEALTH AND SAFETY: EXTENSIVE DESCRIPTION. NORWAY

S. Sklet 2 Sep. 1993 76 p

(PB94-138542; STF75-A93042) Avail: Issuing Activity (National Technical Information Service (NTIS))

Different Norwegian systems for the monitoring of working conditions relating to health and safety are described in this report. The descriptions will be part of the European Health and Safety Database. The European Health and Safety Database is a product of the European Foundation for the Improvement of Living and Working Conditions (European Foundation) and contains descriptions of information systems useful for monitoring working conditions related to health and safety in the European Community Countries and other European countries. The project has been sponsored by the Nordic Council of Ministers, Working Environment Committee. NTIS

N94-31852 Technische Univ., Berlin (Germany). Inst. fuer Luft- und Raumfahrt.

DESIGN OF A LOGISTICS MODEL FOR BUILDING AND SUPPORTING A LUNAR STATION [ENTWURF EINES LOGISTIK-MODELLS FUER DEN BAU UND DEN BETRIEB EINER MONDSTATION]

Richard Huhn 1 May 1993 85 p In GERMAN Limited Reproducibility: More than 20% of this document may be affected by microfiche quality

(ILR-Mitt-282(1993); ETN-94-95744) Avail: CASI HC A05

A simulation model that allows five transportation systems for logistic support of a lunar base to be compared on the basis of their cost effectiveness is presented. Over a life cycle of 50 years, four different growth rates of the lunar base were considered. The annual average size of the scientific staff and the annual lunar output were given as input data of this model. Taking into account the increasing annual lunar output and the required propellants per year for the transportation system, the annual volume of imports, the annual number of launches, the average costs per year, and the cost effectiveness were calculated. This simulation model consists of about 65 equations. To check the plausibility of the calculated trends, the results of a standard run are presented. ESA

N94-31954 Michigan Univ., Ann Arbor.

TRIPPING OVER OBSTACLES: BIOMECHANICAL ANALYSES OF HOW YOUNG AND OLD TRY TO AVOID IT Ph.D. Thesis

Hsieh-Ching Chen 1993 135 p

Avail: Univ. Microfilms Order No. DA9319500

The objective of this research was to determine the biomechanical factors that significantly affect gait patterns, planning, motor control, and fall avoidance strategies required to successfully negotiate obstacles. The results of this research are presented as a series of three experimental studies and a biomechanical model simulation study. In the first study, the gait patterns of healthy young and old adults were examined as they approached and stepped over fixed obstacles of different heights. The results suggest that the old adults adopt a more conservative strategy for crossing obstacles than young adults. The second study examined the effectiveness of avoidance strategies used by young and old healthy adults as they walked and stepped over a virtual obstacle that appeared from 200 to approximately 1000 ms before reaching it. The results suggested that delays as small as 50 or 100 ms in noticing or reacting to obstacles may significantly lower subjects' rates of success in avoiding them. Age group differences were found, but they were not pronounced. The third study examined the effect of divided attention in young and old healthy adults as they walked and stepped over an obstacle under time-critical conditions. The results showed attention distraction significantly decreased subjects' ability to avoid obstacles under time critical conditions. The old had a significantly higher risk of obstacle contact than the young under these conditions. In the final study, two different biomechanical models were used to simulate the response to a trip. A phase 1 model predicted body kinematics and dynamics from swing foot toe-off until 100 ms after contact of the swing foot with the obstacle. The phase 2 model predicted the recovery response from 100 ms after obstacle contact until the swing foot was extended forward and recontacted the ground or for 200 ms if recontact had not occurred by that time. The results showed the maximum available rate of torque development in the swing hip flexor and the stance leg ankle plantaflexor muscles may largely determine the ability to recover from a trip. Dissert. Abstr.

N94-32034 Software Options, Inc., Cambridge, MA.

BEYOND THE READ-EVAL LOOP: THE ARTIFACTS SYSTEM

Mike Karr 14 Feb. 1994 19 p Limited Reproducibility: More than 20% of this document may be affected by microfiche quality
(Contracts N00014-85-C-0710; N00014-90-C-0024)
(AD-A276589) Avail: CASI HC A03

The purpose of the Artifacts System is to structure complex, evolving data, to assist users in their cooperative effort to develop such data, and to integrate the tools that operate on and produce this data. A key element in the design is to eliminate what is the usual interaction with a computer-based system: run a tool to achieve a desired effect. Rather, users of the Artifacts System set up structures that indicate desired results and browse these structures in hypertext-like fashion; tool invocation is usually implicit. Version and configuration management is an integral part of the system, not a facility on the side. DTIC

N94-32171# Army Aeromedical Research Lab., Fort Rucker, AL.
EVALUATION OF INTENSITY DISTRIBUTION PROFILES FOR US. ARMY ROTORCRAFT POSITION LIGHTING ADAPTED FOR IMAGE INTENSIFIER OPERATIONS Final Report
Ellen H. Snook, Clarence E. Rash, and Malcolm N. Colbert Sep. 1993 175 p
(DA Proj. 3M1-62787-A-879)
(AD-A276459; USAARL-93-36) Avail: CASI HC A08/MF A02

Compatibility problems with image intensifier (I2) devices and cockpit/interior lighting have been investigated and well documented. However, I2 compatibility with position/exterior lighting is only in the early stages of development. In the Army aviation community, attempts have been made to reduce the detrimental effects of position light intensity on I2 devices by operating lights in dim mode or by masking lights. In these modified lighting configurations, requirements in Federal Aviation Administration (FAA) regulations are not always satisfied. In this investigation, the intensity distribution profiles for currently employed lighting strategies were evaluated. Further subjective evaluation of the entire position light system, as a whole, is strongly recommended in order to determine all factors that may have impact on the modification of exterior lighting and/or requirements. Exterior lighting must be acceptable in both the civilian/military aviation environments. DTIC

N94-32302 Logicon Technical Services, Inc., Dayton, OH.
METHODS FOR MEASURING CHARACTERISTICS OF NIGHT VISION GOGGLES Final Report, Mar. 1989 - Nov. 1991
Harry L. Task, Richard T. Hartman, Peter L. Marasco, and Annette R. Zobel Oct. 1993 55 p Limited Reproducibility: More than 20% of this document may be affected by microfiche quality
(AF Proj. 7184)
(AD-A277046; AL/CF-TR-1993-0177) Avail: CASI HC A04

There are many parameters that are used to describe and specify night vision goggles (NVG's) such as resolution, field of view, brightness gain, distortion, etc. However, standardized test procedures for determining the value of these parameters have not been established. Informal comparison studies have shown that measurements of some of these parameters may vary considerably (as much as a factor of two) depending on the method, equipment, and procedures used to make the measurements. The purpose of this technical report is to document specific procedures for measuring most of the major parameters used to specify NVG's to help standardize methodology and improve accuracy and comparability between measuring organizations. DTIC

N94-32379# Army Aeromedical Research Lab., Fort Rucker, AL.
UNIT SPECIFIC CREW REST STRATEGIES: PHASE 1 EVALUATION OF THE 1/212TH AVIATION BATTALION DURING SHIFTWORK TRANSITIONS Final Report
Carlos A. Comperatore, James A. Chiaramonte, Kathy L. Lawhorn, and Lawrence W. Allan Jan. 1994 51 p
(DA Proj. 3M1-62787-A-879)
(AD-A277122; USAARL-94-3) Avail: CASI HC A04/MF A01

Army aviation commanders are deeply concerned with the implementation of crew rest strategies which are both practical and effective. Maintaining peak performance of individuals rotating from one work shift to another is of paramount concern. General guidelines often provide appropriate information, but they do not provide strategies or specific schedules of crew rest tailored to the unit's specific mission demands, environmental conditions, and strength. A complement to general recommendations and guidelines is the use of unit-specific crew rest strategies. This concept involves a two-phase process. In phase one, the unit's existing response to a characteristic mission or training exercise is evaluated by determining the amount of rest obtained by a representative sample of crew members. The results of the phase 1 evaluations provide descriptive quantitative information of daily rest periods, and the impact of mission driven work schedules and environmental conditions on crew rest quality. Phase 2 provides rhythms, sleep/wake cycles, shiftwork schedules, and methods for regulating the body's biological clock to prevent sleep loss during characteristic mission. This report contains a summation of the results of a phase 1 evaluation of shiftwork schedules used by the 1/212th Army Aviation Training Battalion at Fort Rucker, Alabama. Shiftwork schedules used by 1/212th aviators and aircrew included shifts from daytime to early morning, to nighttime, and to afternoon duty hours. DTIC

N94-32580 Taylor (S. R.) and Associates, Bartlesville, OK.
NOVEL ULTRASONIC METHOD FOR FOOD HYDRATION Final Report, Mar. - Oct. 1993
S. R. Taylor and J. C. Hansen Mar. 1994 33 p Limited Reproducibility: More than 20% of this document may be affected by microfiche quality
(Contract DAAK60-93-C-0020)
(AD-A277411; Natick-TR-94/014) Avail: CASI HC A03

This report summarizes the work accomplished in the successful completion of phase 1 of this SBIR project. The overall conclusion is that the ultrasonic activation during aerosol dehydration results in significant increases in evaporation/dehydration rates. These improvements in dehydration rates allow for much more rapid and energy-efficient processing, thus reducing dehydration costs. DTIC

N94-32596 Pacific Northwest Lab., Richland, WA.
THE ROLE OF GUIDELINE-BASED DESIGN TOOLS
J. A. Fox Oct. 1993 6 p Presented at the Human Factors and Ergonomics Society Meeting, Seattle, WA, 11-15 Oct. 1993 Limited Reproducibility: More than 20% of this document may be affected by microfiche quality
(Contract DE-AC06-76RL-01830)
(DE94-007482; PNL-SA-21969; CONF-9310100-8) Avail: CASI HC A02

User System Interface (USI) design guidelines are one of the more popular tools that have been developed to aid designers in creating effective interfaces. When used properly, guidelines can provide the basis for a structured design methodology throughout the system life cycle. A survey published by Mosier and Smith (1986) provides an in-depth account of guideline usage. That 1986 survey showed that guidelines were used in varying degrees by virtually all types of people involved in the design and evaluation of USIs. Design guidelines are one of the older USI design tools, and the continued popularity of guidelines can be seen by the continued updating and expansion of guideline compendiums to keep up with new advances in the field. DOE

N94-32609 Aerospace Medical Research Labs., Brooks AFB, TX.
AIRCREW EYE/RESPIRATORY PROTECTION (AERP): 16-HOUR EXTENDED WEAR EVALUATION OF CHEMICAL PROTECTIVE EQUIPMENT Final Report, 9 Feb. - 31 Dec. 1993
Sarah A. Nunneley and Roberta L. Russell Feb. 1994 14 p Limited Reproducibility: More than 20% of this document may be affected by microfiche quality
(AD-A277288; AL-TP-1993-0014) Avail: Issuing Activity (Defense Technical Information Center (DTIC))

Sixteen-hour wear tests were conducted for the aircrew eye/respiratory protection (AERP) and associated clothing and equipment. Two subjects each carried out simulated tanker/transport and fighter/attack scenarios. No major problems were encountered. DTIC

N94-32697*# Umpqua Research Co., Myrtle Creek, OR. Aerospace Div.
CATALYTIC METHODS USING MOLECULAR OXYGEN FOR TREATMENT OF PMMS AND ECLSS WASTE STREAMS, VOLUME 2 Final Report, Apr. 1990 - Apr. 1992
James R. Akse 12 May 1992 217 p
(Contract NAS8-38490; SBIR-12.02-5201(Vol-2))
(NASA-CR-190299; NAS 1.26:190299) Avail: CASI HC A10/MF A03

Catalytic oxidation has proven to be an effective addition to the baseline sorption, ion exchange water reclamation technology which will be used

on Space Station Freedom (SSF). Low molecular weight, polar organics such as alcohols, aldehydes, ketones, amides, and thiocarbamides which are poorly removed by the baseline multifiltration (MF) technology can be oxidized to carbon dioxide at low temperature (121 C). The catalytic oxidation process by itself can reduce the Total Organic Carbon (TOC) to below 500 ppb for solutions designed to model these waste waters. Individual challenges by selected contaminants have shown only moderate selectivity towards particular organic species. The combined technology is applicable to the more complex waste water generated in the Process Materials Management System (PMMS) and Environmental Control and Life Support System (ECLSS) aboard SSF. During the phase 3 Core Module Integrated Facility (CMIF) water recovery tests at NASA MSFC, real hygiene waste water and humidity condensate were processed to meet potable specifications by the combined technology. A kinetic study of catalytic oxidation demonstrates that the Langmuir-Hinshelwood rate equation for heterogeneous catalysts accurately represent the kinetic behavior. From this relationship, activation energy and rate constants for acetone were determined. Author (revised)

N94-32936*# National Aeronautics and Space Administration. Ames Research Center, Moffett Field, CA.
AN INVESTIGATION OF ACOUSTIC NOISE REQUIREMENTS FOR THE SPACE STATION CENTRIFUGE FACILITY
Timothy Castellano Feb. 1994 28 p
(RTOP 960-60-90)
(NASA-TM-108811; A-94050; NAS 1.15:108811) Avail: CASI HC A03/MF A01

Acoustic noise emissions from the Space Station Freedom (SSF) centrifuge facility hardware represent a potential technical and programmatic risk to the project. The SSF program requires that no payload exceed a Noise Criterion 40 (NC-40) noise contour in any octave band between 63 Hz and 8 kHz as measured 2 feet from the equipment item. Past experience with life science experiment hardware indicates that this requirement will be difficult to meet. The crew has found noise levels on Spacelab flights to be unacceptably high. Many past Ames Spacelab life science payloads have required waivers because of excessive noise. The objectives of this study were (1) to develop an understanding of acoustic measurement theory, instruments, and technique, and (2) to characterize the noise emission of analogous Facility components and previously flown flight hardware. Test results from existing hardware were reviewed and analyzed. Measurements of the spectral and intensity characteristics of fans and other rotating machinery were performed. The literature was reviewed and contacts were made with NASA and industry organizations concerned with or performing research on noise control. Author

N94-33050*# National Aeronautics and Space Administration. Lyndon B. Johnson Space Center, Houston, TX.
USE OF A PITCH ADJUSTABLE FOOT RESTRAINT SYSTEM: OPERATOR STRENGTH CAPABILITY AND LOAD REQUIREMENTS
Robert P. Wilmington (Lockheed Engineering and Sciences Co., Houston, TX.), Jeffrey Poliner (Lockheed Engineering and Sciences Co., Houston, TX.), and Glenn K. Klute May 1994 33 p
(Contract NAS9-18800)
(NASA-TP-3477; S-764; NAS 1.60:3477) Avail: CASI HC A03/MF A01

The zero-gravity environment creates a need for a proper human body restraint system to maintain a comfortable posture with less fatigue and to maximize productivity. In addition, restraint systems must be able to meet the loading demands of maintenance and assembly tasks performed on orbit. The shuttle's primary intravehicular astronaut restraint system is currently a foot loop design that attaches to flat surfaces on the shuttle, allowing for varying mounting locations and easy egress and ingress. However, this design does not allow for elevation, pitch, or foot loop length adjustment. Several prototype foot restraint systems are being evaluated for use aboard the space station and the space shuttle. The JSC Anthropometry and Biomechanics Laboratory initiated this study to quantify the maximum axial forces and moments that would be induced on a foot loop type of restraint while operators performed a torque wrench task, also allowing for angling the restraint pitch angle to study yet another effect. Results indicate that the greatest forces into the torque wrench and into the foot restraint system occur while the operator performs an upward effort. This study did not see any significant difference in the operators' force due to pitch orientation. Thus, in a work environment in which hand holds are available, no significant influence of the pitch angle on forces imparted to the restraint system existed. Author (revised)

N94-33084 State Univ. of New York, Buffalo. Dept. of Physiology.
EFFECTS OF COMBINED BREATHING IMPEDIMENTS ON DIVER'S RESPIRATORY PERFORMANCE Annual Progress Report, 1 Feb. 1993 - 31 Jan. 1994
Claes Lundgren 31 Jan. 1994 9 p Limited Reproducibility: More than 20% of this document may be affected by microfiche quality
(Contract N00014-93-1-0509)
(AD-A277437) Avail: CASI HC A02

Combinations of flow resistance (R), elastance (E) and static lung loading are present to varying degrees in all breathing gear for divers. We have, in earlier studies, determined the maximal acceptable levels for two of these loads, when acting alone, to be: E: 7 cm H20/L, R: such that the external work of breathing equals 1.5 to 2.0 J/L. Fractions of the acceptable levels of R and E (when acting alone) were combined such that the total fraction was 1. The subjects were exposed to five of these combinations (%R/%E): 100/0, 75/25, 50/50, 25/75, 0/100. No static lung load was imposed. Results are from 3, in an ongoing series of 12, submerged, air-breathing divers exposed in a hyperbaric chamber to 1.45 and 6.8 ATA; exercise was performed in the prone position at 60% of VO(2). The mean end-tidal CO2 values were 46.7 mm Hg at the shallow depth and 52.4 mm Hg at the great depth but were unaffected by the R/E combination. V(E) was not affected differently by the R/E combinations, but the tidal volumes were reduced 8-20% by increased E. The ERV was reduced by about 20% with the higher E. Similarly, the VC was reduced by about 15%. The T(sub i)/T(sub tot) was not affected by the R/E combinations but it increased from 0.45 to 0.47 with depth. The dyspnea scores were not different for the different loads. This leads to the conclusion that R and E are additive in their effects on divers' respiratory performance. DTIC

N94-33171 Federal Aviation Administration, Cambridge, MA.
COCKPIT ELECTRONIC DISPLAY WORKSHOP: PROCEEDINGS (COMPUTER DISKETTE)
Dec. 1993 2 p Workshop was held
(AD-M000330; DOT-VNTSC-FAA-93-21-CD; DOT/FAA/RD-93/42-CD; NONP-DTIC-DK-94-11178) Avail: Issuing Activity (Defense Technical Information Center (DTIC))

Thirty-six government, academic, and industry human factors professionals participated in a workshop convened at the Volpe National Transportation Systems Center to identify human factors issues associated with depicting terminal area operations information on electronic cockpit displays. Two working groups, formed from the meeting attendees, identified a variety of research issues associated with the identification, distribution, and electronic presentation of terminal area information to flight crews. These two disks contain the original workshop proceedings formatted in Microsoft Word 5.1 for Macintosh. DTIC

N94-33349 Wright Lab., Wright-Patterson AFB, OH.
AN EXPERIMENTAL STUDY OF PILOT/VEHICLE DYNAMICS USING A TILT ROTOR FLYING MACHINE Final Report, May 1992 - Jun. 1993
David B. Doman Jun. 1993 291 p Limited Reproducibility: More than 20% of this document may be affected by microfiche quality
(AD-A277516; WL-TR-93-3063) Avail: CASI HC A13

A laboratory Tilt Rotor Flying Machine (TROFM) is designed and built for the purpose of conducting an experimental study of the effects of command systems on human pilot behavior. The aircraft is mounted on a two-axis pivot stand which gives the fuselage 2 degrees of freedom; pitch and yaw. Analytical models are derived using Lagrangian and Newtonian techniques. Identification of the aircraft characteristics is based on a nonparametric Discrete Fourier Transform technique and a maximum likelihood parameter estimation scheme. Attitude command, rate command and unaugmented systems are designed and implemented in real time using a digital computer. An investigation of the effects of command systems, displays and tasks on human pilot behavior is conducted. Pilot and pilot-vehicle describing functions are obtained from time histories of dynamic tracking tasks where the pilot attempts to track a random appearing input. Correlations between Cooper-Harper ratings and quantitative descriptions of pilot behavior are made. The experimental results compare favorably to

the classical theory of man-machine system dynamics which is based on the cross-over model. The results of this study indicate that desirable controlled elements in man-machine systems have the characteristics of a simple tracker. DTIC

N94-31429*# University of Southern California, Los Angeles. Inst. of Aerospace Systems Architecture and Technology.
THE NOMAD EXPLORER ASSEMBLY ASSIST VEHICLE: AN ARCHITECTURE FOR RAPID GLOBAL EXTRATERRESTRIAL BASE INFRASTRUCTURE ESTABLISHMENT
Madhu Thangavelu (Rockwell International Corp., Downey, CA.) *In* NASA. Marshall Space Flight Center, The Second Annual International Space University Alumni Conference Feb. 1994 p 34-56 (For primary document see N94-31425 09-12)
Avail: CASI HC A03/MF A02

N94-31739 Naval Coastal Systems Center, Panama City, FL. Materials Science Branch.
THERMOTROPIC LIQUID CRYSTALS: A VARIABLE Clo MATERIAL
Rand R. Biggers *In* Defence and Civil Inst. of Environmental Medicine, Proceedings of the DCIEM Diver Thermal Protection Workshop Jan. 1992 p 33-39 (For primary document see N94-31738 09-52)
Avail: Issuing Activity (Defence and Civil Inst. of Environmental Medicine, 1133 Sheppard Ave. W., P.O. Box 2000, North York, ON M3M 3B9 Canada)

N94-32435*# Ergonomic-Interface Keyboard Systems, Inc., La Jolla, CA.
THE VERTICAL
Stephen L. Albert and Jeffrey B. Spencer *In* NASA, Washington, Technology 2003: The Fourth National Technology Transfer Conference and Exposition, Volume 2 Feb. 1994 p 124-129 (For primary document see N94-32420 09-99)
Avail: CASI HC A02/MF A04

N94-32453*# Jet Propulsion Lab., California Inst. of Tech., Pasadena.
ADVANCED TELEOPERATION: TECHNOLOGY INNOVATIONS AND APPLICATIONS
Paul S. Schenker, Antal K. Bejczy, and Won S. Kim *In* NASA, Washington, Technology 2003: The Fourth National Technology Transfer Conference and Exposition, Volume 2 Feb. 1994 p 288-292 (For primary document see N94-32420 09-99)
Avail: CASI HC A01/MF A04

55 SPACE BIOLOGY

Includes exobiology; planetary biology; and extraterrestrial life.

N94-32389* National Aeronautics and Space Administration. Ames Research Center, Moffett Field, CA.
THE QUEST FOR CONTACT (Videotape)
1 Feb. 1992 Videotape: 32 min. playing time, in color, with sound
(NASA-TM-109778; NONP-VT-94-9978) Avail: CASI VHS A01/BETA A22

This video details the history and current efforts of NASA's Search for Extraterrestrial Intelligence program. The video explains the use of radiotelescopes to monitor electromagnetic frequencies reaching the Earth, and the analysis of this data for patterns or signals that have no natural origin. The video presents an overview of Frank Drake's 1960 'Ozma' experiment, the current META experiment, and planned efforts incorporating an international Deep Space Network of radiotelescopes that will be trained on over 800 stars. CASI

59 MATHEMATICAL AND COMPUTER SCIENCES (GENERAL)

N94-33286*# Institute for Computer Applications in Science and Engineering, Hampton, VA.
CUMULATIVE REPORTS AND PUBLICATIONS THROUGH DECEMBER 31, 1993 Final Report
Mar. 1994 100 p
(Contract NAS1-19480; RTOP 505-90-52-01)
(NASA-CR-194889; NAS 1.26:194889) Avail: CASI HC A05/MF A02

This document contains a complete list of ICASE reports. Since ICASE reports are intended to be preprints of articles that will appear in journals or conference proceedings, the published reference is included when it is available. Author

60 COMPUTER OPERATIONS AND HARDWARE

Includes hardware for computer graphics, firmware, and data processing.

For components see *33 Electronics and Electrical Engineering.*

N94-31587 Technische Univ., Delft (Netherlands).
DELFT ISING COMPUTING ENGINE Ph.D. Thesis
Y. Fonk Jun. 1993 136 p Limited Reproducibility: More than 20% of this document may be affected by microfiche quality
(PB94-148251) Avail: CASI HC A07

The thesis describes a novel, extremely fast and cost effective special-purpose computer for performing simulations of Ising and Ising-like models: the Delft Ising Computing Engine (DICE). DICE lifts the ceiling of the computational power available to a physicist for the type of simulations for which it has been designed. DICE is a parallel and fully pipelined computer that consists of a linear array of tightly-coupled identifical processors driven by a single controller. It serves as a coprocessor to a Silicon Graphics UNIX host. Except for the host interface, the machine operates synchronously at a clock speed of 20 MHz. DICE is extendible by means of auxiliary processors for particularly nasty measurements. The hardware peculiarities of DICE are hidden from its users. They see a high-level programmable virtual machine created by software running on the host. This virtual machine uses a database in which all the parameters relevant to a simulation are stored, and automatically generates the information required by DICE. NTIS

N94-31816* National Aeronautics and Space Administration. Lewis Research Center, Cleveland, OH.
THE VISION MACHINES (Videotape)
Apr. 1993 Videotape: 22 min. playing time, in color with sound
(NASA-TM-109757; NONP-VT-94-9957) Avail: CASI VHS A01/BETA A22

The thoughts of computer scientists at LeRC on the direction that computer development is taking and future implications are explored. Experts discuss the coming information superhighway and technologies such as fiber optics and neural networks. The impact of future computers on education, laboratory research, telecommunications, and science visualization. CASI

N94-31934# Carnegie-Mellon Univ., Pittsburgh, PA. Dept. of Computer Science.
AN ANALYSIS OF INSTRUCTION-CACHED SIMD COMPUTER ARCHITECTURE Ph.D. Thesis
Todd E. Rockoff Dec. 1993 247 p
(Contract F33615-90-C-1465; ARPA Order 7597)
(AD-A276519; CMU-CS-93-218) Avail: CASI HC A11/MF A03

In a single instruction-stream/multiple data-stream (SIMD) computer, calculations are performed by simple processing elements (PE's) that are not independently capable of program-control operations. In lock-step, the PE's execute one program that is sequenced by a single system controller. Large numbers of these simple PE's are obtained through replication of a PE chip containing many identical PE's. A state-of-the-art SIMD computer is regulated by a single system clock that is distributed throughout the

computer. On each system clock cycle, the system controller broadcasts the next instruction to be executed by the PE's. The system clock interval allows time to distribute a PE instruction throughout the computer, an action that typically requires more time than the minimum interval of a clock regulating the PE's themselves within the PE chips. The disparity between the highest rate of PE operation and the rate of global instruction broadcast gives rise to a heretofore uncompensated clock-rate limitation. To overcome this limitation, instruction-cached SIMD computer architecture provides for a small instruction buffer to be placed within the replicated PE chip. This buffer stores repeated instruction sequences for subsequent retrieval at the relatively high rate attainable within the PE chip. The instruction buffer and its control mechanism comprise a SIMD instruction cache, or 1-cache. DTIC

N94-31972 George Mason Univ., Fairfax, VA.
DOME: DYNAMIC OPTIMIZATION ON MULTIPROCESSOR ENGINES, A STATISTICAL APPROACH Ph.D. Thesis
Fotios N. Barlos 1993 192 p
Avail: Univ. Microfilms Order No. DA9316548

To efficiently handle a continuous increase in the volume of information, elaborate multicomputer database machines and sophisticated software tools are employed. Maximum exploitation of parallelism dictates an even partitioning of the computation across the processing sites. To achieve a uniform load is difficult when the data are highly skewed since characterizing the expected workload can introduce significant overhead. We develop a query optimization approach, named Dynamic Optimization on Multiprocessor Engines (DOME), that uses a dynamic sampling methodology to determine the frequency distribution along each level of the query tree. DOME covers the three main multiprocessor query optimization areas of Workload Partitioning, Site Selection, and Operation Ordering. The DOME optimizer samples the input relations of a query tree and subsequently performs the computation of the query on the samples to generate the intermediate results of the tree. Contrary to previous static optimizers that use analytical formulas to estimate the frequency distribution of the relations at higher levels of the query tree DOME derives the required frequency distribution by analyzing the characteristics of the developed sampled relations. We prove that the application of the same relational operation on relations and their samples produces relations with the same statistical characteristics. We implemented DOME on an Intel i860 hypercube system with 32 nodes and test its behavior through extensive experimentation. DOME provides uniform workload distribution across all the tests. The Workload Partitioning algorithms yields an order of magnitude factor improvement over prior approaches for highly skewed data during Project-Join execution sequences. The Site Selection algorithms provide approximately a six fold factor improvement over a static allocation approach for Join operation. The Operation Ordering approach provides approximately a 20 percent improvement over a random resolver for Three-Way Join operations with a sample size of 10 percent of the input relation. Overall, DOME provides savings across the whole domain of the input datasets, and the savings become significant as the skewness of the input relations grows.
Dissert. Abstr.

N94-32147# Lawrence Livermore National Lab., CA.
MICA, A FACILITY TO ACHIEVE PORTABILITY FOR MESSAGE-PASSING AND DYNAMIC MEMORY MANAGEMENT IN FORTRAN
J. C. Brown and A. A. Mirin Jan. 1994 14 p
(Contract W-7405-eng-48)
(DE94-006692; UCRL-ID-115975) Avail: CASI HC A03/MF A01

MICA, which stands for Macro Interface for Communication and Allocation, is a macro facility for message passing and dynamic memory management for Fortran programs on Unix platforms. A combination of CPP and M4 preprocessing is used to provide the macro interface. CPP is used for conditional compilation according to machine architecture and selected memory management and message passing options. M4 is used for translating the macro calls into the appropriate Fortran code sequences. Several supporting Fortran subprograms are included. DOE

N94-32163 Naval Postgraduate School, Monterey, CA.
AN ANALOG PREPROCESSING ARCHITECTURE FOR HIGH-SPEED ANALOG-TO-DIGITAL CONVERSION M.S. Thesis
Jorge A. Esparza Dec. 1993 168 p Limited Reproducibility: More than 20% of this document may be affected by microfiche quality
(AD-A276737) Avail: CASI HC A08

This thesis investigates the feasibility of implementing an analog-to-digital converter (ADC) based on a new symmetrical number system (SNS). This preprocessing architecture decomposes the analog amplitude analyzing function of an ADC into a number of sub-operations (moduli). Each sub-operation folds the analog signal with a folding period proportional to the value of the modulus. Through the use of the SNS encoding and recombining the results of the sub-operations, a definitive performance enhancement is achieved. The number of comparators required is reduced considerably, allowing more bandwidth to be used in the folding circuits. The overall design effort demonstrates a 9-bit design with a total of 23 comparators. SPICE simulations are developed and the performance demonstrated. Also identified are the areas in which further research is required. DTIC

N94-32766# Sandia National Labs., Albuquerque, NM.
MULTIMEDIA AS A DESKTOP AND CLASSROOM TOOL
S. Nelson Feb. 1994 11 p
(Contract DE-AC04-94AL-85000)
(DE94-009118; SAND-94-0249) Avail: CASI HC A03/MF A01

The major thrust of the study leading to this report was a quick but in-depth understanding of the process for using multimedia computer equipment for information exchange within our engineering office and within the school environment. That is, how feasible is it to augment the typical office memo or school instruction sheet with pictures, video, and sounds? What specialized skills, hardware, and software are needed by those of us who want to use the technology? The brief study period allowed for an examination of available hardware and software, observation of current approaches to multimedia within our particular environment, and the development of applications, all within the context of several project areas: the Sandia Science Advisors program; a Sandia scientific project associated with the National Information Infrastructure Testbed; the curriculum of Monte Vista Elementary School of Albuquerque public schools; and the University of New Mexico Medical School health scene project. DOE

N94-32783# Oak Ridge National Lab., TN.
A MINIATURIZED ASIC-BASED MULTICHANNEL SCALER INSTRUMENT
M. N. Ericson, G. W. Turner, D. E. McMillan, B. S. Hoffheins, R. A. Todd, and J. M. Hiller 1993 5 p Presented at the 1993 IEEE Nuclear Science Symposium and Medical Imaging Conference, San Francisco, CA, 2-5 Nov. 1993
(Contract DE-AC05-84OR-21400)
(DE94-007222; CONF-931107-34) Avail: CASI HC A01/MF A01

A miniaturized multichannel scaler instrument was developed to address size and operational constraints for data acquisition in a portable laser-induced luminescence system. The multichannel scaling (MCS) function is implemented as a programmable application specific integrated circuit (ASIC) with standard interfaces for control and data acquisition. The instrument is microcontroller-based with sufficient computing power for data manipulation and algorithmic processing. The unit includes electronics for laser control and amplification and pulse height discrimination of PMT pulses. Modification of the instrument should allow use in nuclear, chemical, and spectroscopy related applications including Mossbauer experiments. Interfaces are incorporated allowing both computer-controlled and stand alone operation. Implementation of the MCS function as an ASIC and comparison with conventional implementations are discussed. Full characterization of the MCS is presented including differential non-linearity (DNL), bin dead time, and bandwidth measurements. DOE

N94-32978 Department of the Navy, Washington, DC.
TOROIDAL COMPUTER MEMORY FOR SERIAL AND PARALLEL PROCESSORS Patent
Allen D. Parks, inventor (to Navy) and James C. Perry, inventor (to Navy)
11 Jan. 1994 8 p Filed 29 Jun. 1990
(AD-D016144; US-Patent-5,278,966; US-Patent-Appl-SN-546595;
US-Patent-Class-395-425) Avail: US Patent and Trademark Office

The toroidal computer memory system utilizes toroidal memory paths in its architecture to enable memory locations along those paths to be obtained in a single access, as compared to multiple accesses typically required by

conventional linear computer memory. The storage/retrievable media is designed to replicate paths on the surface of a torus. By defining certain parameters and the mathematical properties of these memory paths in the electronics of a controller, points on the memory paths can be accessed from the storage/retrieval media more efficiently than conventional computer memory. DTIC

N94-33252# Aerospace Corp., El Segundo, CA. Technology Operations.
THE IMPACT OF ASIC DEVICES ON THE SEU VULNERABILITY OF SPACE-BORNE COMPUTERS
R. Koga, W. R. Crain, K. B. Crawford, S. J. Hansel, and S. D. Pinkerton 30 Jan. 1994 14 p
(Contract F04701-93-C-0094)
(AD-A278134; TR-0091(6940-05)-6; SMC-TR-94-17) Avail: CASI HC A03/MF A01

Application specific integrated circuits (ASIC's) offer a number of advantages over traditional multi-component microcircuits including reductions in both size and power dissipation, and are therefore prime candidates to replace such microcircuits in space-borne electronics systems. The results of recent tests of the susceptibilities of various ASIC devices to cosmic ray and trapped proton induced single event upset (SEU) and latchup are reported here and are compared to the susceptibilities of the devices that they would replace. This comparison leads to a discussion of the impact of ASIC devices on the SEU susceptibility of space-borne computers. DTIC

N94-32433*# Jet Propulsion Lab., California Inst. of Tech., Pasadena.
SPACECRAFT ON-BOARD INFORMATION EXTRACTION COMPUTER (SOBIEC)
David Eisenman, Robert E. DeCaro, and David W. Jurasek *In* NASA, Washington, Technology 2003: The Fourth National Technology Transfer Conference and Exposition, Volume 2 Feb. 1994 p 107-116 (For primary document see N94-32420 09-99)
Avail: CASI HC A02/MF A04

N94-32434*# Analex Space Systems, Inc., Cocoa Beach, FL.
PEN-BASED COMPUTERS: COMPUTERS WITHOUT KEYS
Cheryl L. Conklin *In* NASA, Washington, Technology 2003: The Fourth National Technology Transfer Conference and Exposition, Volume 2 Feb. 1994 p 117-123 (For primary document see N94-32420 09-99)
(Contract NAS10-11675)
Avail: CASI HC A02/MF A04

61 COMPUTER PROGRAMMING AND SOFTWARE

Includes computer programs, routines, alogorithms, and specific applications, e.g., CAD/CAM.

N94-31087 Stockholm Univ. (Sweden). Dept. of Physics.
SUMMARY OF SOME DATA PROCESSING ROUTINES IN THE MOLECULAR PHYSICS GROUP OF STOCKHOLM UNIVERSITY
Olli Launila and Jonas Jonsson Sep. 1993 116 p Limited Reproducibility: More than 20% of this document may be affected by microfiche quality
(USIP-93-05; ETN-94-95942) Avail: Issuing Activity (European Space Agency (ESA))

The development of computer based routines for analysis of molecular spectra is addressed. The goal in their development was to facilitate much of the 'trivial' work, like measuring plates, typing down data, constructing explicit models for different multiplicities, assessing raw data, etc. Different programs developed during the past years, as well as updates of older programs, are presented together with an outline of general organization of data transport and processing strategies. A rational data handling strategy is vital and should consist of simple data formats and programs capable of using these, preferably without ever having to specify to the program the data format in question. Therefore, the programs should be carefully constructed and 'intelligent', and the formats should be economic and easily readable. Also, the program source codes should be available to anyone who might want to modify and recompile them. It is hoped that this set of programs will facilitate much of the spectroscopy work. ESA

N94-31094 Ecole Nationale Superieure des Telecommunications, Paris (France). Groupe Modelisation.
THE GENERALIZED MULTI DELAY ADAPTIVE FILTER: STRUCTURE AND CONVERGENCE ANALYSIS
E. Moulines, O. AitAmrane, and Y. Grenier 15 Mar. 1993 38 p Revised Sponsored by Centre National d'Etudes des Telecommunications Limited Reproducibility: More than 20% of this document may be affected by microfiche quality
(ISSN 0751-1345)
(TELECOM-93-D-004; ETN-94-95886) Avail: CASI HC A03

A view of frequency domain LMS algorithms as particular implementations of a more general scheme, the Generalized Multi Delay Filter (GMDF), is presented. Frequency domain adaptive filters have long been recognized as an attractive alternative to time domain algorithms when dealing with systems with large impulse response and/or correlated input. Frequency domain LMS adaptive schemes essentially retain the attractive features of frequency domain implementations, while requiring a processing delay considerably smaller than the length of the impulse response. Within this general class of algorithms, implementations based on the weighted overlap and add reconstruction algorithms are focused on; these variants provide an independent control of the overall processing delay and of the rate of update of the filter coefficients, allowing a tradeoff between the computational complexity and the rate of convergence. An analysis of the performance of this new scheme is presented and insight into the influence of impulse response segmentation on the behavior of the adaptive algorithm is provided. Exact analytical expressions for the steady state mean square error are derived. Necessary and sufficient conditions for the convergence of the algorithm to the optimal solution within finite variance are obtained, and translate into bounds for the stepsize parameter. Simulations are presented to support the analysis and to demonstrate the practical usefulness of the GMDF algorithm in applications where large impulse response have to be processed. ESA

N94-31163# Loughborough Univ. of Technology (England). Dept. of Mathematical Sciences.
A NEW METHODOLOGY OF SYSTEM PARAMETER ESTIMATION
J. T. Ma and Q. H. Wu Jan. 1994 16 p
(Maths-Rept-A-208; ETN-94-95868) Avail: CASI HC A03/MF A01

A new methodology of system parameter estimation based on the evolutionary programming (EP) to estimate the generator parameters is presented. The EP is very powerful for searching the real values of the parameters with measurements of generator outputs which are highly contaminated by noises, in contrast to the extended Kalman filter which is currently used for parameter estimation. Comparison between the two different methodologies is given to show the potential of applications of the EP to parameter estimation and system modeling. ESA

N94-31164# Loughborough Univ. of Technology (England). Dept. of Mathematical Sciences.
OPTIMAL REACTIVE POWER DISPATCH OF POWER SYSTEMS USING NONLINEAR PROGRAMMING
J. T. Ma and Q. H. Wu Jan. 1994 15 p
(Maths-Rept-A-209; ETN-94-95869) Avail: CASI HC A03/MF A01

The economical operation and planning of power systems using a nonlinear programming method is reported. The optimal reactive power dispatch of power systems with a number of constraints is solved by the BFGS (Broyden, Fletcher, Goldfarb, and Shanno) method to reduce transmission network power loss and improve voltage control of the transmission network. The simulation study is carried out based on the IEEE 30 bus system. The simulation results show that the BFGS method can be used with modifications to enhance the economical operation of power systems. ESA

N94-31178 Politecnico di Milano (Italy). Dipt. di Elettronica e Informazione.
DESIGN PATTERNS MIXING GENERICITY AND INHERITANCE IN THE DEVELOPMENT OF REUSABLE COMPONENTS
Piero Fraternali Jun. 1993 22 p

(Rept-93-021; ETN-94-95803) Avail: Issuing Activity (Politecnico di Milano, Piazza Leonardo da Vinci 32, 20133 Milan, Italy)

Genericity and inheritance are both considered helpful means in the design of well organized collections of software components, particularly as they foster the factorization of commonalities among modules and thus the production of more compact, yet extensible code. However, the availability of both primitives in a single programming language gives application designers more than one way to organize a system into a collection of modules. It is not always clear which solution is preferable under which respect. Genericity and inheritance have been contrasted, and some design guidelines are proposed, mainly in the context of software production in-the-small. Investigations on the role of inheritance and genericity in the design, maintenance, and reuse of collections of software components are reported. Results of a broad review of existing libraries are presented. From this, a set of 'canonical' design patterns, patterns displaying different mixtures of inheritance and genericity, is extracted. These patterns are contrasted with respect to qualitative dimensions concerning both the developers and the users of the library, namely: factorization, extendibility, shrinkability, time and space efficiency, ease of reuse, cost localization, and sideward compatibility. ESA

N94-31188 Politecnico di Milano (Italy). Dipt. di Elettronica e Informazione.

TECHNIQUES FOR INCREASING THE ROBUSTNESS OF ITERATIVE ALGORITHMS FOR MULTI-RESOURCES LOCATION PROBLEMS [TECNICHE PER AUMENTARE LA ROBUSTEZZA DEGLI ALGORITMI ITERATIVI PER PROBLEMI DI LOCALIZZAZIONE MULTI-RISORSE]

Giovanni Righini May 1993 49 p In ITALIAN Sponsored in part by Ministry of University and Scientific and Technological Research

(Rept-93-037; ETN-94-95806) Avail: Issuing Activity (Politecnico di Milano, Piazza Leonardo da Vinci 32, 20133 Milan, Italy)

Multi-resource location problems can be seen as combinations of single resource allocation and location problems; therefore, many of the algorithms proposed in the literature have an iterative structure in which the two phases of allocation and location alternate until convergence to a local optimum solution. Some procedures inspired by the principal of local search are proposed. The procedures are in a position to perturb the local optimum configuration for possibly converging to a better solution. Problems in the euclidean plane and on graphs are considered in static and dynamic versions in which the input data varies with time. The validity of the technique is illustrated with results relating to an experimental proof carried out. ESA

N94-31189 Politecnico di Milano (Italy). Dipt. di Elettronica e Informazione.

EXACT SOLUTION OF THE SINGLE MACHINE SCHEDULING PROBLEM WITH EARLINESS AND FLOW TIME PENALTIES

Mauro DellAmico, Silvano Martello, and Daniele Vigo 1993 21 p

(Rept-93-038; ETN-94-95807) Avail: Issuing Activity (Politecnico di Milano, Piazza Leonardo da Vinci 32, 20133 Milan, Italy)

Given a set of tasks with associated processing times, deadlines, flow time penalties, and earliness penalties, the problem of determining a task schedule, on one machine, to minimize the total cost incurred by the penalties is considered. The problem is NP hard in the strong sense. A lower bound based on a preemptive relaxation, an approximation algorithm, and two exact approaches, one based on branch and bound and one on dynamic programming, is presented. An overall exact algorithm is obtained by combining these two approaches. Extensive computational experiments show the effectiveness of the proposed algorithms. ESA

N94-31192 Politecnico di Milano (Italy). Dipt. di Elettronica e Informazione.

A WORST-CASE ANALYSIS OF AN APPROXIMATE ALGORITHM FOR FINDING THE MINIMUM HAMILTONIAN CYCLE ON PATHS

Giovanni Righini and Marco Trubian Jun. 1993 10 p Sponsored in part by Ministry of University and Scientific and Technological Research

(Rept-93-042; ETN-94-95811) Avail: Issuing Activity (Politecnico di Milano, Piazza Leonardo da Vinci 32, 20133 Milan, Italy)

An algorithm for the problem of constructing the minimum length hamiltonian cycle, passing through some given paths, is presented. The value of the solution given by the algorithm is guaranteed to be not worse than 2 times the optimal value. ESA

N94-31212 Politecnico di Milano (Italy). Dipt. di Elettronica e Informazione.

A FINITE STATE MACHINE MODEL FOR OBJECT ORIENTED SYSTEMS

Stefano Paraboschi Jun. 1993 19 p

(Rept-93-040; ETN-94-95809) Avail: Issuing Activity (Politecnico di Milano, Piazza Leonardo da Vinci 32, 20133 Milan, Italy)

A Finite State Machine (FSM) model of an object system is proposed. Attributes, inheritance, and subtyping relations are characterized in the model, and a classification of composition mechanisms and a metric to compare subtypes is provided. FSM's provide a good model for objects since they represent in a natural way the concept of state which is not adequately represented in classical formalization models. This representation of states and dynamics introduces a new and more general definition of behavior compatibility. ESA

N94-31223# European Space Agency, Paris (France). ESA Board for Software Standardisation and Control.

GUIDE TO SOFTWARE QUALITY ASSURANCE

Jul. 1993 52 p

(ISSN 0379-4059)

(ESA-PSS-05-11-Issue-1; ETN-94-95883) Copyright Avail: CASI HC A04/MF A01

Software quality assurance is defined and explained, guidelines on how to do it are presented, and the contents of a Software Quality Assurance Plan (SQAP) are detailed. A general discussion of the principles of SQA is presented. This expands upon ESA Procedures, Specifications, and Standards PSS-05-0, which describes the software enigineering standards that apply to all deliverable software implemented for the ESA, either in house or by industry. All the mandatory practices in ESA PSS-05-0 that apply to software quality assurance are repeated. ESA

N94-31251 Minnesota Univ., Minneapolis. Dept. of Computer Science.

DESIGN AND ANALYSIS OF SCALABLE PARALLEL ALGORITHMS Final Report, 27 Aug. 1990 - 26 Aug. 1993

Vipin Kumar 15 Nov. 1993 13 p Limited Reproducibility: More than 20% of this document may be affected by microfiche quality

(Contract DAAL03-90-G-0201)

(AD-A276255; ARO-28408.1-MA-SDI) Avail: CASI HC A03

The objective of this research is to develop efficient parallel algorithms for a variety of problems and to analyze the scalability of new and existing parallel algorithms. Scalability analysis is an important tool used for predicting the performance of an algorithm-architecture combination when one or more of the hardware related parameters (interconnection network, speed of processors, speed of communication channels, number of processors) are changed. The problems studied as a part of this project come from diverse domains such as solution of differential equations, discrete optimization, neural network based learning, sorting and graph algorithms. In particular, we have studied parallel algorithms for solving linear systems using the preconditioned conjugate gradient method, partitioning of finite element meshes, balancing load in unstructured tree search arising in discrete optimization, the backpropagation neural network learning algorithm, dynamic programming, fast Fourier transform, sorting, shortest-path computation for graphs, robot motion planning, and matrix multiplication. DTIC

N94-31263# SRI International Corp., Menlo Park, CA.

PROOF OF CONCEPT FOR THE REWRITE RULE MACHINE: INTERENSEMBLE STUDIES Final Report

Jose Meseguer 23 Feb. 1994 83 p

(Contract N00014-90-C-0210)

(AD-A276506) Avail: CASI HC A05/MF A01

The main goal was to learn through simulation about the functionality and performance on realistic applications of an RRM system consisting of a collection of RRM ensemble chips (each such chip being a SIMD processor) connected on a network, and to design mechanisms to support the simultaneous parallel computation of applications across many such ensemble chips. To achieve these goals we first built a high-level interensemble simulator and ran a collection of benchmarks on it under varying assumptions about several architectural parameters to obtain a first estimate of the communication requirements for the RRM and to determine the feasibility of those requirements in view of existing network

technology. Using a second, very detailed register-transfer level simulator of a single ensemble and the performance results of a collection of applications run on it, together with modeling above the ensemble level, we also estimated interensemble performance; in this way we were able to obtain more detailed and accurate interensemble performance estimates. Mechanisms supporting parallel computations across many ensembles were also studied and designed. DTIC

N94-31277# Colorado Univ., Boulder.
ALGORITHMS AND STRUCTURES FOR REAL-TIME SIGNAL PROCESSING Final Report, 1 Jun. 1988 - 31 May 1992
Clifford T. Mullis 4 Feb. 1994 4 p Revised
(Contract DAAL03-88-K-0058)
(AD-A276101; CU-153-6951; ARO-25470.9-EL) Avail: CASI HC A01/MF A01

The study of digital signal processing is to a large extent the study of algorithms, but there is a natural classification into algorithms for design and algorithms for actual processing. Our research has been mainly concerned with the latter classification and has addressed structural constraints which arise because of resource limits and/or a desire for efficiency. This has led in a number of problems to some algebraic decomposition of algorithms with the intent of achieving parallelism and quality, as measured by the degree of approximation (bias) and roundoff noise and similar errors (variance). More recently, we have been studying problems which involve both classes of algorithms; for example, what is a good design (filter function or window) which must conform to structural constraints dictated by processing considerations. This has proven to be a rich area of application. DTIC

N94-31328# Software Options, Inc., Cambridge, MA.
EXTENDER'S GUIDE FOR ARTIFACTS AND DRAFTS
Michael Karr, Glenn Holloway, and Steve Rosen 8 Feb. 1994 86 p
(AD-A276344) Avail: CASI HC A05/MF A01

To extend artifact and/or draft functionality in E-L, you must first have a working knowledge of how E-L is used. E-L is extended from within, by using the system to develop new functionality and then to augment the plexes that describe the structure of the artifacts system. This guide assumes you are familiar with the E-L Users' Manual. To add a tool to the system, you will also need to know how to develop C or Common Lisp programs using E-L, so you should also have read either the C and Unix Artifacts Manual or the Common Lisp Artifacts Manual. DTIC

N94-31335# Rome Lab., Griffiss AFB, NY.
DEVELOPING THE MULTIMEDIA USER INTERFACE COMPONENT (MUSIC) FOR THE ICARUS PRESENTATION SYSTEM (IPS) Report, Jun. - Aug. 1993
Ingrid Bartnik Dec. 1993 21 p
(AF Proj. 4594)
(AD-A276341; RL-TM-93-6) Avail: CASI HC A03/MF A01

Rome Lab's Intelligence Technology branch provides modeling and simulation support to a variety of intelligence consumers and analysts, across a wide spectrum of application areas. Much of the research, development and capabilities demonstrations take place in the ICARUS Prototype Development and Demonstration Facility, named after the character from Greek Mythology who built the first prototype to solve a problem. In order to provide a cohesive development and demonstration architecture, as well as to advance the state-of-the-art in user interfaces and presentation techniques, the ICARUS Presentation System was envisioned, being comprised of two components: the Interactive VuGraph (InterVu) System and the Multimedia User Interface Component (MUSIC). This report documents the initial research, design and implementation of a prototype of the MUSIC system. DTIC

N94-31343# Carnegie-Mellon Univ., Pittsburgh, PA. Management Sciences Research Group.
A PARALLEL IMPLEMENTATION OF THE COLUMN SUBTRACTION ALGORITHM
T. H. Smith 22 Dec. 1993 23 p
(Contract N00014-85-K-0198)
(AD-A275922; MSRR-596) Avail: CASI HC A03/MF A01

We have implemented Harche and Thompson's column subtraction algorithm for the set partitioning problem on the CN-200 Connection Machine. The implementation involved partitioning the large array of processors in the CM-2 into segments and letting each segment explore a different part of the search tree generated by the column subtraction algorithm. Our reported computational results indicate that the segments are highly utilized and that good speed-ups are obtained as the number of segments is increased. DTIC

N94-31357# Institute for Defense Analyses, Alexandria, VA.
A COMPARISON OF PRODUCT REALIZATION FRAMEWORKS Final Report
Brian S. Cohen, Earl Ecklund, Michael Frame, Michael W. Marean, and Stephen Yencho Oct. 1993 68 p
(Contract MDA903-89-C-0003)
(AD-A275992; IDA-D-1439; IDA/HQ-93-44605; AD-E501747) Avail: CASI HC A04/MF A01

In 1991, DoD established seven key science and technology thrust areas to assist in planning for investment in defense technology. The goals of thrust 7 are to develop new industrial capabilities that will lower product unit costs and life-cycle costs, shorten the lead time in design and manufacture of products, and increase product quality. This document reviews a set of software products, applications, and standards which are potential components of a DoD thrust 7 product realization infrastructure to support design and manufacturing activities for the advanced technology demonstrations (ATDs). This study is a quick sampling of software products and frameworks and is not intended to be either complete or comprehensive. The reviewed frameworks were each designed to meet the needs of a specific engineering discipline. No final recommendations or judgments about particular frameworks were made since a rigorous and detailed analysis of requirements has not been performed. None of the reviewed frameworks met all of the perceived needs for a thrust 7 and ATD framework, such as the need to design and analyze ATD products both within and across engineering disciplines. The best option for obtaining a product realization framework to accommodate thrust 7 needs appears to be the federation of multiple existing framework technologies to achieve the needed capabilities. Future work should include the extension of this study to cover all relevant frameworks and associated technology. The thrust 7 ATD requirements should be analyzed in order to properly recommend a framework that meets those requirements. DTIC

N94-31370# Software Options, Inc., Cambridge, MA.
E-L USER'S MANUAL
Judy G. Townley 17 Feb. 1994 50 p
(Contract N00014-85-C-0710)
(AD-A276378) Avail: CASI HC A03/MF A01

E-L is a software development environment that reflects a fresh look at how the design of a programming system and the design of the languages it supports can reinforce each other in ways that increase software productivity. The benefits of this coordinated environment-and-language design are reflected most directly in E-L's tools for manipulating programs. In E-L, one sets up a structure that indicates a desired result. E-L uses a strategy called opportunistic scheduling to minimize manual tool invocation and to mediate the objectives of maximizing the use of tools and maximizing responsiveness. Most tool invocations are automatic, typically in response to editing or to actions taken by other tools, which are themselves automatically invoked. Because tools are scheduled, not run immediately, the system can optimize the use of resources. For example, the system may locate idle machines on the network and use them for invocations. The system will usually not run more than one scheduled tool on any one machine at a time (to minimize swapping and thrashing). DTIC

N94-31383# Air Force Inst. of Tech., Wright-Patterson AFB, OH.
THE DEVELOPMENT AND USE OF AN EVALUATION MECHANISM FOR THE ASSESSMENT OF SOFTWARE CONFIGURATION MANAGEMENT TOOLS M.S. Thesis
Wayne M. Descheneau and Neil W. Robinson Dec. 1993 122 p
(AD-A275961; AFIT/GSS/LAS/93D-3) Avail: CASI HC A06/MF A02

This study investigated the development of a mechanism for use in the evaluation of Software Configuration Management (SCM) tool's. An examination of applicable DoD standards identified the SCM requirements that could be levied on a development contractor, and a literature search revealed the functionality common to various automated tools. These two sets of information were organized into a matrix, and for each requirement

that was met, the intersection on the matrix of the requirement and each functionality used to meet that requirement was checked. In addition to the matrix, the mechanism consisted of general information about a given tool and an area to substantiate each requirement identified as being met by the tool. The evaluation mechanism was then used to assess two commercially available SCM tools: Aide-De-Camp and the Product Configuration Management System. The evaluation mechanism prescribes a method for evaluating complex SCM tools and forces the evaluator to gain intimate knowledge of a tool to effectively assess the tool's merits for a given effort. DTIC

N94-31443# Rice Univ., Houston, TX.
PARALLEL STRUCTURED OPTIMIZATION ALGORITHMS FOR INVERSE PROBLEMS Final Report, 15 Apr. 1990 - 14 Aug. 1993
John E. Dennis, Jr. and Richard A. Tapia 25 Oct. 1993 11 p
(Contract DAAL03-90-G-0093)
(AD-A276053; ARO-26932.28-MA-SDI) Avail: CASI HC A03/MF A01

The final report contains results for interior point methods, optimization with simulation constraints, large scale nonlinear methods, and parallel direct search methods. DTIC

N94-31449# Naval Postgraduate School, Monterey, CA.
A MODEL AND ALGORITHMS FOR A SOFTWARE EVOLUTION CONTROL SYSTEM M.S. Thesis
Salah E. Badr Dec. 1993 463 p
(AD-A276431) Avail: CASI HC A20/MF A04

This dissertation introduces an evolution control system (ECS) for the Computer Aided Prototyping System (CAPS). The purpose of the ECS is to automate the scheduling and the assignment of tasks to the software designers based on management policies and the dependencies in a model of the software configuration. The ECS controls the software evolution process in an incrementally evolving software system where the steps to be scheduled are only partially known. Time required, the set of subtasks for each step, and the input/output constraints between steps are all uncertain, and are all subject to change as evolution steps are carried out. The ECS provides computer assistance for managing such changes and partially automates the control of the design team and the project data. The ECS manages both the development/prototyping data and the design team through scheduling the software tasks and assigning them to members of the design team. The main goals of this system are: managing the evolution steps from the moment they are proposed until their completion; reaching a feasible schedule that meets the deadline requirements or minimizes the largest amount that a deadline is missed if all deadlines cannot be met and provides for the earliest possible completion for those steps that either do not have deadlines or have under-estimated deadlines; maximizing the efforts of software designers by maximizing concurrent assignments; supporting incremental replanning as additional information becomes available; and minimizing wasted design effort due to schedule reorganization as well as workers forced to wait for completion of subtasks. DTIC

N94-31461# Naval Research Lab., Washington, DC.
CONSISTENCY CHECKS FOR SCR-STYLE REQUIREMENTS SPECIFICATIONS Final Report
Constance L. Heitmeyer and Bruce G. Labaw 31 Dec. 1993 15 p
(AD-A276077; NRL/FR/5540-93-9586) Avail: CASI HC A03/MF A01

This report describes a class of software tools that check formal requirements specifications for consistency with a requirements model. The model, which describes properties of requirements specifications based on the SCR (Software Cost Reduction) approach to requirements, is summarized. Two experiments are described in which condition tables and mode transition tables in an updated version of the A-7 requirements document were checked for selected properties using tools we developed. The significant number of errors found by the tools is summarized. Tool-based techniques and manual techniques for performing consistency checks are compared, and several additional consistency checks, derived from the formal model, are identified. Our work is compared with related work by Parnas and SRI concerning the automated checking of tabular specifications. Conclusions are presented concerning the utility, cost, and scalability of tool-based consistency checking. DTIC

N94-31465# IBM Federal Systems Div., Gaithersburg, MD.
SOFTWARE REUSE CASE STUDY: TRILLIUM Final Report
David Dikel, Jonathan Rosoff, Paul Kengor, Jonathan Lichtenstein, and George DeMarco 13 Sep. 1993 58 p Prepared in cooperation with Applied Expertise, Inc., Arlington, VA
(Contract F19628-93-C-0129)
(AD-A276108; IBM-05021-002) Avail: CASI HC A04/MF A01

DoD has identified software reuse as a central strategy for improving the quality, timelines and cost efficiency of its weapons, command and control and other automated information systems. However, to reap full benefits from software reuse technology, DoD must change the way it does business. The question is how. This study provides a commercial example in which software reuse is specifically gauged and encouraged as a means to improve quality, timeliness and life-cycle cost. TRILLIUM's recommended software reuse practices are based upon over ten years of successful experience. Reuse is not isolated, but viewed as one of several activities, all of which are needed to ensure software capability. Further, evidence suggests that TRILLIUM has been widely adopted by managers and practitioners throughout Bell's supplier organizations (who have chosen to market TRILLIUM to their customers). As such, this example appears to provide the right goals, long-term experience base and successful approach for getting effective software reuse into practice. While there are clear differences between DoD and Bell, we believe that the experiences and lessons learned by Bell and its suppliers can provide perspective and insights to those who develop and implement DoD policy. DTIC

N94-31475# Stanford Univ., CA. Dept. of Aeronautics and Astronautics.
ControlShell: A REAL-TIME SOFTWARE FRAMEWORK Quarterly Progress Report, Apr. - Jun. 1993
J. C. Latombe, R. H. Cannon, and S. A. Schneider Jun. 1993 45 p
(Contract N00014-92-J-1809)
(AD-A276481) Avail: CASI HC A03/MF A01

We are creating a new paradigm for building and maintaining complex real-time software systems for the control of moving mechanical systems. This objective is being met through the simultaneous development of both a powerful software environment and cogent motion planning and control capabilities. Our research concentrates on three key areas: building an innovative, powerful, real-time software framework; implementing new distributed control architectures for intelligent mechanical systems; and developing distribution architectures and new algorithms for the computationally hard motion planning and direction problem. DTIC

N94-31484# Sandia National Labs., Albuquerque, NM.
AN APPLICATION REFERENCE MODEL FOR LAYERED MANUFACTURING
P. R. Kennicott 1994 23 p Presented at the International Conference on Rapid Product Development, Stuttgart, Germany, 31 Jan. 1994
(Contract DE-AC04-94AL-85000)
(DE94-006368; SAND-94-0123C; CONF-940154-1) Avail: CASI HC A03/MF A01

The Intelligent Manufacturing Systems (IMS) test case 6 project (rapid product development) was set up to demonstrate rapid product development and three dimensional measurement techniques where the agencies performing the work were distributed over different countries. Test case 6 provided a unique opportunity to examine the process by which an application protocol (AP) of the Standard for Exchange of Product Data (STEP) is prepared. The test case had a well defined scope, the production of simple parts by means of layered manufacturing techniques. The information concerned with this manufacture was similarly well defined, due to the requirement that the information be transmitted among the organizations participating in the test case. STEP is an international standard specifying the data content and format for storage and exchange of product data throughout the product's life cycle. STEP has been under development since 1984 and is just now emerging as an international standard. STEP is specified as a series of information models using the EXPRESS computer language. For purposes of data exchange, a mapping to a physical file format is specified. Informally, product data can be defined as all the data about a product which one might wish to save. This definition implies some variation in the amount of data to be saved in any one instance. In the case of test case 6, one would certainly wish to save the IGES files describing the part. One may or may not wish to save the manufacturing parameters. While there are many parts of STEP with different purposes,

the important series of parts for the purposes of standardizing product data are those dealing with application protocols. An application protocol specifies the details of product data within the context of a single application (in this case, layered manufacturing). Other AP's deal with such subjects as configuration-managed solid parts and associated drafting. DOE

N94-31522# Technische Univ., Delft (Netherlands). Faculty of Technical Mathematics and Informatics.

LORE AND REASON MAINTENANCE

Bob Goedhart 1993 55 p

(ISSN 0922-5641)

(Rept-93-88; ETN-94-96133) Copyright Avail: CASI HC A04/MF A01

The knowledge representation language LORE was developed within the Delfi project aiming at a general purpose language for the development of knowledge based systems. The language combines several techniques developed in the field of AI (Artificial Intelligence) and can be used without posing restrictions to the application area it is used in. The knowledge engineering environment Delfi3 consists of several system components, such as a compiler, a linker, and an interpreter, for this language. The interpreter is the most important component, since it performs the actual execution of the knowledge base. The formal specification of this execution process is modeled in the execution model. The execution model of the language LORE is studied and extended with techniques from the field of reason maintenance. The use of these techniques will enable the interpreter to record and inspect its results, and to use these results in future inferences. This will result in a more efficient execution and, on top of that, in a database of reasons (the reason base) that can be used for other purposes as well. The results of the implementation of this execution model are compared with results from literature. ESA

N94-31542# Institut National Polytechnique, Grenoble (France). Lab. d'Informatique Fondamentale et d'Intelligence Artificielle.

POLYHEDRIC OBJECT RECOGNITION BY INDEXING IN A MODEL BASE Ph.D. Thesis [RECONNAISSANCE D'OBJETS POLYEDRIQUES PAR INDEXATION DANS UNE BASE DE MODELES]

Humberto Sossa 1992 133 p In FRENCH Sponsored by CONACYT, Mexico

(ETN-94-95913) Avail: CASI HC A07/MF A02

The problem of object recognition in presence of a large model base is addressed. The indexing of models can be described as follows: given a group of image indexes, quickly extract from the model base the models containing the index group. Since the combinatorial of the classic paradigm is prohibitive in this case, an indexing method by graph hashing is proposed. The principles are described: coding of image and models under a graph form, management of a model base by hash-coded tables, comparison of graphs on the basis of their polynomial characterization, and access to the model base. The system implemented according to these principles is described and experimental results are presented. ESA

N94-31543# Institut National Polytechnique, Grenoble (France). Lab. de Genie Informatique.

EXTENSION OF THE LUSTRE LANGUAGE AND APPLICATION TO CIRCUIT DESIGN: THE LUSTRE V4 LANGUAGE AND THE POLLUX SYSTEM Ph.D. Thesis [EXTENSION DU LANGAGE LUSTRE ET APPLICATION A LA CONCEPTION DE CIRCUITS: LE LANGAGE LUSTRE-V4 ET LE SYSTEME POLLUX]

Frederic Rocheteau 1992 205 p In FRENCH

(ETN-94-95918) Avail: CASI HC A10/MF A03

The study of possible applications of the synchronous declarative language LUSTRE to the description of hardware circuits, and more particularly, given these characteristics, its data stream aspect notably, to data paths, is addressed. In relation to real time systems, of which the programming and verification constitute the preferred application domain of this language, synchronous circuits are generally much more regular and of a more important size. In order to allow an easy description of these applications, an extension of LUSTRE was developed. It adds to the language, while conserving its rigorous semantics: structured data and manipulation operators, a concept of generic subprograms, and limited recursion. The POLLUX system was then developed around this language. It decomposes into the following: a precompiler for semantic analysis of a program, to assure consistence; and various postprocessors of which the principal one is a synchronous circuit generator implanted afterwards on PAM, a machine based on prediffused programmable circuits--the other principal postprocessors are a classical sequential code generator, a graphical interface to pass from a text program to a scheme block and vice versa. ESA

N94-31577 Technische Univ., Berlin (Germany). Fachbereich Informatik.

COMPOSITIONALITY OF APPLICATION ORIENTED STRUCTURING MECHANISMS FOR ALGEBRAIC SPECIFICATION LANGUAGES WITH INITIAL SEMANTICS Ph.D. Thesis

Ingo Classen 1993 94 p Limited Reproducibility: More than 20% of this document may be affected by microfiche quality

(ETN-94-95736) Avail: CASI HC A05

Specification concepts and structuring operations, which take into account structural relationships between components of a complex system and reduce the gap between the language level and the level of mathematical constructions are presented. The theoretical study was aimed to support structuring on syntactical and semantical levels, in order to facilitate a systematic development of structured systems. The theory was formulated with respect to the abstract notion of specification frames, and was based on structural properties of such frames like compositionality, which can be expressed in terms of category theory. Two aspects of structural relationships were discussed from a syntactical point of view: sharing was considered with respect to parametrized specifications and parameter passing, assuming two kinds of sorting strategies (quick sort and mergesort); structural equivalence was regarded with respect to parametrized specifications. Amalgamation constructions, based on the level of elementary specifications, were proposed to support structuring operations on the semantical level. It is concluded that the theory can be applied to the design of software systems. ESA

N94-31646# Technische Univ., Delft (Netherlands). Faculty of Technical Mathematics and Informatics.

AUTOMATIC GENERATION OF CONTEXT-SENSITIVE TEXTUAL HELP

Johannes J. deGraaff, Piyawadee Noi Sukaviriya, and Charles A. P. G. vanderMast 1993 10 p Sponsored by Sun Microsystems Inc., and Siemans A. G.

(ISSN 0922-5641)

(Rept-93-68; ETN-94-96113) Copyright Avail: CASI HC A02/MF A01

The automatic generation of help is addressed. Graphical user interfaces tend to get more and more complex, and consequently, the user needs help to work with these interfaces. Development of good help systems is very time consuming, if only because the help system needs to change whenever the specifications do. The context of the research is the User Interface Design Environment (UIDE) which uses high level application and interface representations to generate interfaces and help. Based on descriptions of an interface, help can be generated to answer two questions: why is an object not usable (grayed out); and how can it be made usable. Pre and post conditions, part of the semantics and sequencing control representations in UIDE, are used to answer these questions. The help system uses unsatisfied preconditions to explain why an object in the interface is disabled. A standard set of templates is used to translate often occurring predicates into text. A planner is used to derive how to enable the object in question. The help system looks at those predicates that must become true to enable the object, and searches for objects with corresponding post conditions. ESA

N94-31659# Universiteit Twente, Enschede (Netherlands). Tele-Informatics and Open Systems Group.

PERFORMABILITY MODELLING USING DyQNtool+

Boudewijn R. Haverkort and Anne-Marie Maass 13 Oct. 1993 16 p Presented at the 5th International Workshop on Petri Nets and Performance Models, Toulouse, France, 22-24 Oct. 1993

(ISSN 0924-3755)

(Memo-INF-93-45; TIOS-93-27; ETN-94-96107) Copyright Avail: CASI HC A03/MF A01

DyQNtool+, a tool for performability modeling based on the Dynamic Queueing Network concept, an approach in which stochastic Petri nets and queueing networks are combined, is described. In particular, DyNQNtool+ makes use of the tools SPNP (Stochastic Petri Net Package) and SHARPE (a tool for learning about stochastic models) for the computation of complex performability measures. With DyNQtool+, dynamic queueing network models can be easily constructed. The tool takes care

of the automatic translation of these models to a Markov reward model which is subsequently analyzed by performability analysis techniques. ESA

N94-31682 Rutherford Appleton Lab., Chilton (England). Central Computing Dept.

ARNOLDI CODE FOR COMPUTING SELECTED EIGENVALUES OF SPARSE REAL UNSYMMETRIC MATRICES

J. A. Scott Dec. 1993 45 p See also PB93-179588

(PB94-145182; RAL-93-097) Avail: Issuing Activity (Nationai Technical Information Service (NTIS))

Arnoldi methods can be more effective than subspace iteration methods for computing the dominant eigenvalues of a large sparse real unsymmetric matrix. In this paper we consider variants of the method of Arnoldi and discuss the design and development of a code to implement these methods. The new code, which is called EB13, offers the user the choice of a basic Arnoldi algorithm, an Arnoldi algorithm with Chebychev acceleration, and a Chebychev preconditioned Arnoldi algorithm. Each method is available in blocked and unblocked form. The performance of each option in the EB13 package is compared with that of subspace iteration on a range of test problems and, on the basis of the results, advice is offered to the user on the appropriate choice of method. NTIS

N94-31685 Rutherford Appleton Lab., Chilton (England).

GKS-9X: AN EXPERIMENTAL APPLICATION

L. B. Damnjanovic and D. A. Duce Nov. 1993 45 p See also PB93-232270

(PB94-147048; RAL-93-088) Avail: Issuing Activity (National Technical Information Service (NTIS))

The Graphical Kernel System-9x (GKS-9x) refers to the current state (Draft International Standard) of the revision of GKS which was published as an International Standards Organization (ISO) standard for computer graphics programming in August 1985. A part of the GKS-9x standard was implemented at Rutherford Appleton Laboratory to explore the feasibility of the new concepts as well as the behavior of GKS-9x. This paper explores the effects of the number of primitives manipulated in an application on the experimental GKS-9x implementation performance. It also identifies the major factors which increase the GKS-9x function execution times. Finally, the improvement in speed obtained when optimization was included in the traversal process is analyzed and discussed. The application was made based on the seating plan of a theater consisting of 1,154 seats. NTIS

N94-31686 Gesellschaft fuer Mathematik und Datenverarbeitung, Bonn (Germany).

REPORT ON IMPLEMENTING PART RELATIONSHIPS USING VML METACLASSES

M. Halper, J. Geller, and Y. Perl 1993 88 p Prepared in cooperation with New Jersey Inst. of Tech., Newark Limited Reproducibility: More than 20% of this document may be affected by microfiche quality

(PB94-147485; GMD-224) Copyright Avail: Issuing Activity (National Technical Information Service (NTIS))

This report describes the result of a joint project of the New Jersey Institute of Technology, NJ, and GMD-IPSI, Darmstadt, Germany, on the development of a metaclass library of part-of semantic relationships. The metaclass library has been implemented for the open object-oriented VODAK database management system developed at GMD-IPSI and is available with the VODAK software release. NTIS

N94-31687 Gesellschaft fuer Mathematik und Datenverarbeitung, Saint Augustin (Germany).

DESIGN METHODS BASED ON NETS: DEMON Final Report

E. Best 1993 427 p See also PB92-116110 Limited Reproducibility: More than 20% of this document may be affected by microfiche quality

(PB94-147493; GMD-217) Copyright Avail: CASI HC A19

This report describes the results of the ESPRIT Basic Research Action Number 3148 DEMON (design methods based on nets). Its main body consists of chapters 1 to 6 which survey and present the results of the six working groups of DEMON. This main text is surrounded by an initial chapter which summarizes and evaluates the results in the light of the initial statement of DEMON, and a final chapter 7 which contains the list of publications of DEMON. NTIS

N94-31694# Technische Univ., Delft (Netherlands). Faculty of Technical Mathematics and Informatics.

A GAUSS-SEIDEL TYPE SOLVER FOR SPECIAL CONVEX PROGRAMS, WITH APPLICATION TO FRICTIONAL CONTACT MECHANICS

E. A. H. Vollebregt 1993 26 p

(ISSN 0922-5641)

(Rept-93-77; ETN-94-96122) Copyright Avail: CASI HC A03/MF A01

A method that solves the constrained minimization of a convex function, when the constraints g(sub j)(x(sub 1),...,x(sub n)) less than or equal to 0 are function of only a few variables and can be partitioned in some way, is described. A proof of convergence is given which is based on the fact that the function values that are generated decrease. The relation to the nonlinear equation solver TanGS is shown, together with results for TanGS. The solver is applied to the solution of tangential traction in contact mechanics. ESA

N94-31695# Technische Univ., Delft (Netherlands). Faculty of Technical Mathematics and Informatics.

USING ATOMIC ACTIONS IN REPLICA GROUPS TO SIMPLIFY THE REPLICATION IMPLEMENTATION

L. H. A. Bouwmeester, P. G. Kluit, and F. Ververs 1993 23 p

(ISSN 0922-5641)

(Rept-93-78; ETN-94-96123) Copyright Avail: CASI HC A03/MF A01

Active replica groups require complex protocols implementing ordering and delivery guarantees to ensure state consistency. These protocols have an impact on the performance of the replica groups. A demonstration that using atomic actions in the replication infrastructure allows the use of a simpler protocol is given. Execution failures of this protocol to ensure the ordering and delivery guarantees can now be managed within atomic actions by relying on their serialization property. The atomic actions are integrated in the replication infrastructure in such a way that interacting groups are not aware of each other's group membership changes. ESA

N94-31704# Technische Univ., Delft (Netherlands). Faculty of Technical Mathematics and Informatics.

DESIGNING IN VIRTUAL REALITY: MODELLING OBJECTS IN A VIRTUAL ENVIRONMENT (MOVE)

P. A. J. Brijs, T. S. Hoek, C. A. P. G. vanderMast, and G. J. F. Smets 1993 16 p

(ISSN 0922-5641)

(Rept-93-91; ETN-94-96136) Copyright Avail: CASI HC A03/MF A01

A CAD (Computer Aided Design) system developed to provide designers with modeling tools that can be used in a virtual environment is described. The design of the environment and the way in which the user is assisted to perform his task in the virtual environment are discussed. The MOVE system allows the user to operate in an intuitive and everyday style of work. This is done by offering tools that can be grabbed and handled. Each tool enables a designer to directly manipulate and transform the virtual models in a specific way, providing appropriate visual, auditory and tactile feedback during the operation. With these tools designers can recapture the three dimensional aspect of building and shaping models, which is lost when working behind computer screens. CAD systems for use in a virtual environment offer designers the possibility to not only see their products in an early stage of design, but to also simulate and explore using them, without having to manufacture a physical model. Parts of the functionality of the MOVE system and the way the four level approach by Foley was used to develop the program are described. ESA

N94-31713# Toronto Univ. (Ontario). Dept. of Mechanical Engineering.

CAD-BASED OFF-LINE PLANNING FOR AN ACTIVE-VISION SYSTEM Ph.D. Thesis

Xiaoyu He Jun. 1993 184 p

(ISBN-0-315-86317-X; CTN-94-61189) Copyright Avail: Micromedia Ltd., Technical Information Centre, 240 Catherine Street, Suite 305, Ottawa, Ontario, K2P 2G8, Canada HC/MF

Development of an active vision system for three dimensional object recognition by robots was based on an approach combining object pre-marking and active sensing. A set of problems within the framework of the proposed active vision system was investigated. The optimal object pre-marking problem is defined as determining the minimum number of markers and their best locations on a given set of objects. A dynamic programming based method is developed to solve this problem. The problem

of optimal placement of a mobile camera is addressed in terms of guaranteeing the detection of markers on a viewed object. This problem is divided into two sub-problems: determining the camera's initial location(s) for detecting an initial marker, and determining the camera's secondary locations for detecting an additional marker when the first acquired image is insufficient for recognizing the object. The former is solved based on probability theory and computational geometry; the second is solved by a similar method as well as utilizing a-priori knowledge of marker locations. The problems of object pre-marking and camera placement are also integrated into a single problem. The I-DEAS computer-aided design package is used to facilitate the solution methods. A prototype of the proposed active vision system was implemented for the experimental verification of the methods developed. Author (CISTI)

N94-31715# Toronto Univ. (Ontario). Dept. of Electrical and Computer Engineering.

MORPHOLOGICAL DIRECTIONAL CODING OF IMAGES Ph.D. Thesis

Samuel Ziheng Zhou Oct. 1993 182 p

(ISBN-0-315-86336-6; CTN-94-61191) Copyright Avail: Micromedia Ltd., Technical Information Centre, 240 Catherine Street, Suite 305, Ottawa, Ontario, K2P 2G8, Canada HC/MF

Image feature extraction is used in image coding for exploiting the properties of the human visual system in order to achieve good perceptual quality at a low bit rate. A new image coding scheme, morphological directional coding (MDC), is introduced. In MDC, feature extraction is accomplished through various types of nonlinear morphological filters. Each image is decomposed into a hierarchy of image features which are subsequently encoded by appropriate coding methods based on the perceptual significance of the features. Sequential filters are used to generate a multiresolution representation in which line features of different width resolutions are separated. A morphological directional filter bank is developed to group the extracted line features according to their orientations so that the features can be represented efficiently by subsampling and modeling. A hierarchical vector quantization scheme is developed to encode information regarding edges, textures, and smooth regions. A hybrid vector structuring element decomposition algorithm is also developed for fast implementation of morphological filters. Using this algorithm can significantly reduce the computational complexity of a morphological filter using the structural element. Author (CISTI)

N94-31718# Montreal Univ. (Quebec). Dept. de Genie Electrique et Informatique.

STEREOSCOPIC CORRESPONDENCE BASED ON THE STRUCTURE OF SHADING M.S. Thesis [CORRESPONDANCE STEREOSCOPIQUE BASEE SUR LA STRUCTURE DE L'OMBRAGE]

Michel Albert Audette Aug. 1992 189 p In FRENCH

(ISBN-0-315-86418-4; CTN-94-61194) Copyright Avail: Micromedia Ltd., Technical Information Centre, 240 Catherine Street, Suite 305, Ottawa, Ontario, K2P 2G8, Canada HC/MF

A region-based two-view matching algorithm is proposed for solving the correspondence problem in stereoscopic vision. In the algorithm, regions are computed from the Gaussian (K) and mean (H) curvature information of the image intensity surface. A region, defined as a connected area of constant K/H sign combination, constitutes the footprint of a local section of the intensity surface. Neighborhood information is made explicit by means of an adjacency graph representation of the region map. The adjacency graph is the dual of the modified Voronoi diagram of the region map, which is computed by isotropically growing each region. Matching is attempted between nodes of identical shape types in the two region maps by comparing their intra-regional characteristics along with the topological configuration of their immediate neighborhoods. The disparity map is established through a coarse-to-fine strategy. The interpolation technique is a two-stage algorithm: a least median of squares approximation and a weighted bicubic spline interpolation. The final product, computed from disparity vectors produced at the finest resolution level, is a dense disparity function which can be used to obtain the structure and motion of the elements of the scene. Author (CISTI)

N94-31728# Laval Univ. (Quebec). Dept. de Genie Electrique.

VOLUMETRIC MODELLING OF THREE DIMENSIONAL SCENES BY OCTREE DECOMPOSITION OF GEOMETRIC MODELS M.S. Thesis [MODELISATION VOLUMETRIQUE DES SCENES TRI-DIMENSIONNELLES PAR DECOMPOSITION OCTAIRE DE MODELES GEOMETRIQUES]

Pierre Vachon Nov. 1993 101 p In FRENCH

(ISBN-0-315-86866-X; CTN-94-61235) Copyright Avail: Micromedia Ltd., Technical Information Centre, 240 Catherine Street, Suite 305, Ottawa, Ontario, K2P 2G8, Canada HC/MF

Certain applications of three dimensional vision profit from volumetric representation offered by octrees. Since these structures are typically difficult to obtain starting from a simple geometric description, a method of conversion has been developed with a view to allow creation of volumetric models. This conversion permits passage from a simple geometric format to an octree format through a recursive partitioning of space. The algorithm to carry out the conversion is implemented in software called Octavue which allows the user to enter geometric scenes, adjust partitioning parameters, and visualize the resulting octree structures. Further improvements to the algorithm and software are proposed. A user guide to Octavue is appended. CISTI

N94-31752# Laval Univ. (Quebec). Dept. de Genie Electrique.

METHODS OF IMPLEMENTING THE VITERBI ALGORITHM ON A MASSIVELY PARALLEL COMPUTER OF THE SIMD (SINGLE INSTRUCTION MULTIPLE DATA) TYPE M.S. Thesis [METHODES DE REALISATION DE L'ALGORITHME DE VITERBI SUR ORDINATEUR MASSIVEMENT PARALLELE DE TYPE SIMD]

Sebastien Roy Apr. 1993 99 p In FRENCH

(ISBN-0-315-86783-3; CTN-94-61229) Copyright Avail: Micromedia Ltd., Technical Information Centre, 240 Catherine Street, Suite 305, Ottawa, Ontario, K2P 2G8, Canada HC/MF

Methods for parallelization of the Viterbi algorithm are proposed with a view to their implementation on a massively parallel computer. The computer in question, the MasPar MP1, is characterized by a single instruction multiple data architecture, which implies certain constraints on the level of efficiency of the algorithms proposed. The fixed objective is to obtain the optimum efficiency and the maximum speed possible on the MasPar, taking account of the constraints of the parallel architecture and the Viterbi algorithm itself. In addition to the ordinary Viterbi algorithm, a decoder for trellis coded modulation codes is also realized on the MasPar. Finally, a new suboptimal decoding algorithm is tested with the goal of improving the exploitation of the architecture and the internal topology of the MasPar. The decoder software thus obtained allow rapid carrying out of simulations of experimental communication systems. The study of the proposed parallel algorithms and their performance can also be useful in the design of future decoders for very large scale integration. CISTI

N94-31810# Software Productivity Consortium, Herndon, VA.

OVERVIEW OF MEGAPROGRAMMING COURSE: LECTURES AND EXERCISES

Feb. 1994 130 p See also AD-M000313, AD-M000314, AD-M000315, and AD-M000316 Prepared for Virginia Center of Excellance for Software Reuse and Technology Transfer, Herndon

(Contract MDA972-92-J-1018)

(AD-A276169; SPC-93028-CMC) Avail: CASI HC A07/MF A02

The traditional approach to software development has a lot of limitations and problems associated with it. There's a technique that is different from the traditional software development process. It's called megaprogramming. Megaprogramming is in the research stage, although individual ideas within megaprogramming have been in use within industry for years. Because megaprogramming is in its infancy, some of the terms and some of the specific details may change. The underlying concepts and principles behind megaprogramming are unlikely to change. Today, this manual explains traditional software development concepts and introduces mega-programming. DTIC

N94-31932# Massachusetts Inst. of Tech., Cambridge. Artificial Intelligence Lab.

HIERARCHICAL MIXTURES OF EXPERTS AND THE EM ALGORITHM Memorandum Report

Michael I. Jordan and Robert A. Jacobs 6 Aug. 1993 31 p

(Contract N00014-90-J-1942; NSF ASC-92-17041; NSF IRI-90-13991; NSF ECS-92-16531)
(AD-A276516; AIM-1440; CBCL-Memo-83) Avail: CASI HC A03/MF A01

We present a tree-structured architecture for supervised learning. The statistical model underlying the architecture is a hierarchical mixture model in which both the mixture coefficients and the mixture components are generalized linear models (GLIM's). Learning is treated as a maximum likelihood problem; in particular, we present an Expectation-Maximization (EM) algorithm for adjusting the parameters of the architecture. We also develop an on-line learning algorithm in which the parameters are updated incrementally. Comparative simulation results are presented in the robot dynamics domain. DTIC

N94-31933# Massachusetts Inst. of Tech., Cambridge. Artificial Intelligence Lab.

ON THE CONVERGENCE OF STOCHASTIC ITERATIVE DYNAMIC PROGRAMMING Memorandum Report

Tommi Jaakkola, Michael I. Jordan, and Satinder P. Singh Aug. 1993 15 p

(Contract N00014-90-J-1942; NSF ASC-92-17041; NSF ECS-92-16531; NSF IRI-90-13991)
(AD-A276517; AIM-1441; CBCL-Memo-84) Avail: CASI HC A03/MF A01

Recent developments in the area of reinforcement learning have yielded a number of new algorithms for the prediction and control of Markovian environments. These algorithms, including the TD(lambda) algorithm of Sutton (1988) and the Q-learning algorithm of Watkins (1989), can be motivated heuristically as approximations to dynamic programming (DP). We provide a rigorous proof of convergence of these DP-based learning algorithms by relating them to the powerful techniques of stochastic approximation theory via a new convergence theorem. The theorem establishes a general class of convergent algorithms to which both TD(lambda) and Q-learning belong. DTIC

N94-31940 Carnegie-Mellon Univ., Pittsburgh, PA. Dept. of Computer Science.

A REDUNDANT DISK ARRAY ARCHITECTURE FOR EFFICIENT SMALL WRITES

Daniel Stodolsky, Mark Holland, William V. Courtright, II, and Garth A. Gibson 20 Oct. 1993 67 p Limited Reproducibility: More than 20% of this document may be affected by microfiche quality

(Contract MDA972-90-C-0035; NSF ECD-89-07068; ARPA Order 7330)
(AD-A276645; CMU-CS-93-200) Avail: CASI HC A04

Parity encoded redundant disk arrays provide highly reliable, cost effective secondary storage with high performance for reads and large writes. Their performance on small writes, however, is much worse than mirrored disks--the traditional, highly reliable, but expensive organization for secondary storage. Unfortunately, small writes are a substantial portion of the I/O workload of many important, demanding applications such as on-line transaction processing. This paper presents parity logging, a novel solution to the small write problem for redundant disk arrays. Parity logging applies journalling techniques to substantially reduce the cost of small writes. We provide a detailed analysis of parity logging and competing schemes--mirroring, floating storage, and RAID level 5--and verify these models by simulation. Parity logging provides performance competitive with mirroring, the best of the alternative single failure tolerating disk array organizations. However, its overhead is close to the minimum offered by RAID level 5. Finally, parity logging can exploit data caching much more effectively than all three alternative approaches. DTIC

N94-31966 Carnegie-Mellon Univ., Pittsburgh, PA.

LARGE-SCALE SHAPE OPTIMIZATION: NUMERICAL METHODS, PARALLEL ALGORITHMS, AND APPLICATIONS TO AERODYNAMIC DESIGN Ph.D. Thesis

Carlos Eduardo Orozco 1993 150 p
Avail: Univ. Microfilms Order No. DA9322751

Motivated by flight vehicle design problems, this work focuses on large-scale optimization problems in which the design variables are parameters describing shape. It deals with several Sequential Quadratic Programming methods that can be used to advantage for the solution of shape optimization problems that involve systems governed by nonlinear partial differential equations. Its main contribution is the development of a family of Coordinate Basis Infeasible Path (CBIP) optimization methods and its implementation in highly parallel architectures. The methods avoid the solution of the discretized form of the state equations at each design iteration by embedding them as equality constraints in the optimization problem. CBIP methods make use of a decomposition into nonorthogonal subspaces that exploits Jacobian and Hessian sparsity in an optimal fashion. In the absence of a line search, the resulting algorithms require the solution of just two or three linear systems per optimization iteration. They are therefore more efficient than traditional path-following methods which typically require many stiffness matrix solves to fully converge the nonlinear state equations at each optimization iteration. In the massively parallel implementation, the construction and solution of the algebraic systems is performed in parallel, as are sensitivity computations associated with the state variables. Parallelism is thus extended to computation of the gradient of the objective function with respect to the state variables, the Lagrange multipliers, the gradient of the state equations with respect to the design variables, and the projected gradient. The parallel optimization algorithms require no additional communication routines nor parallel data structures beyond those needed for the parallel solution of the state equations. The algorithms are applied to a two dimensional aerodynamic design problem, that of determining the shape of an airfoil which produces a desired pressure distribution in the presence of compressible potential flow. Shape optimization problems of up to 90 shape variables, 8,316 state variables, and 16,264 finite elements are solved. The parallel efficiency of the algorithms, i.e., the portion of time spent on parallel tasks relative to the overall time, is high, and they scale well, for a practical number of design variables. Dissert. Abstr.

N94-31994 Carnegie-Mellon Univ., Pittsburgh, PA. Dept. of Computer Science.

A THEORY OF DISTRIBUTED TIME

Sean W. Smith Dec. 1993 138 p Limited Reproducibility: More than 20% of this document may be affected by microfiche quality

(Contract F33615-93-1-1330; NSF CCR-88-58087)
(AD-A276631; CMU-CS-93-231) Avail: CASI HC A07

Natural intuition organizes experience into a linear sequence of discrete events, but this approach is inappropriate for asynchronous distributed systems, where information is distributed and perception is delayed. Distributed environments require a distributed notion of time, to abstract away not only irrelevant physical detail but also irrelevant temporal and computations detail. By expressing distributed systems concepts that are difficult to talk about in terms of real time and by distinguishing what really 'happens' from what physically occurred, a theory of distributed time would provide a natural framework for solving problems in distributed environments. This paper lays the groundwork for that claim by formally building such a theory. This research improves on previous work on time in distributed systems by supporting temporal relations more general than partial orders, by supporting abstraction through multiple levels of temporal relations, by separating the family of temporal relations an application consults from the particular clock implementations that track them, and by providing a single arena to consider these issues for a wide range of applications. DTIC

N94-32080# Carnegie-Mellon Univ., Pittsburgh, PA. Dept. of Computer Science.

INCREMENTAL RECOMPILATION FOR STANDARD ML OF NEW JERSEY

Robert Harper, Frank Pfenning, Peter Lee, and Eugene Rollins Feb. 1994 12 p

(Contract F19628-91-C-0168; ARPA Order 8313)
(AD-A276522; CMU-CS-94-116) Avail: CASI HC A03/MF A01

The design and implementation of an incremental recompilation manager (IRM) for Standard ML of New Jersy (SML/NJ) is described. Truly separate compilation is difficult to implement correctly and efficiently for SML because one compilation unit may depend not only on the interface of another, but also on its implementation. In this paper we present an integrated compilation system base on the 'visible compiler' primitives provided by SML/NJ that supports 'smart recompilation' to minimize system build time in most situations. Large systems are presented as hierarchical source groups. An automatic dependency analyzer determines constraints on the order in which sources must be considered. By abstracting away from the specifics

of the SML/NJ compiler, the IRM readily generalizes to arbitrary 'compilation tools' such as parser generators and embedded languages. DTIC

N94-32081# Carnegie-Mellon Univ., Pittsburgh, PA. Dept. of Computer Science.
AN MS-DOS FILE SYSTEM FOR UNIX
Alessandro Forin and Gerald R. Malan Sep. 1993 24 p
(Contract DABT63-93-C-0054)
(AD-A276523; CMU-CS-93-196) Avail: CASI HC A03/MF A01

We have written DosFs, a new file system for UNIX that uses MS-DOS data structures for permanent storage. DosFs can be used anywhere a traditional UNIX file system can be used, and it can mount disks written by MS-DOS as regular UNIX partitions. DosFs can be used as the root partition and exported by an NFS server. Our motivation for this work was efficient disk space utilization; DosFs provides from 10 to 13 percent better disk utilization than the 4.3 BSD Fast File System (FFS). In addition, we found that the disk block allocation algorithm used by DosFs lets us exploit large contiguous disk operations, providing a five-fold improvement over FFS for uncached operations. To the best of our knowledge, this is the first file system implementation that allows the user to specify the logical block size at mount time. A user can mount the same file system with a larger block size when file accesses tend to be sequential and a smaller one when they tend to be scattered. The MS-DOS structures were designed for a single-user system and do not support access control. We solved this problem with simple extensions that are backward-compatible with MS-DOS. DTIC

N94-32086*# Carnegie-Mellon Univ., Pittsburgh, PA. Dept. of Computer Science.
UTILITY-BASED PLANNING
Sven Koenig and Reid G. Simmons Nov. 1993 43 p
(Grant NAGw-1175)
(NASA-CR-195878; NAS 1.26:195878; AD-A276521; CMU-CS-93-222)
Avail: CASI HC A03/MF A01

The design and implementation of an incremental recompilation manager (IRM) for Standard ML of New Jersey (SML/NJ) is described. Truly separate compilation is difficult to implement correctly and efficiently for SML because one compilation unit may depend not only on the interface of another, but also on its implementation. In this paper we present an integrated compilation system based on the visible compiler primitives provided by SML/NJ that supports 'smart recompilation' to minimize system build time in most situations. Large systems are presented as hierarchical source groups. An automatic dependency analyzer determines constraints on the order in which sources must be considered. By abstracting away from the specifics of the SML/NJ compiler, the IRM readily generalizes to arbitrary 'compilation tools' such as parser generators and embedded languages. DTIC

N94-32093 Dayton Univ., OH. Research Inst.
VISUAL EVALUATION OF COMPUTER-GENERATED TEXTURES Final Report, Oct. 1990 - Mar. 1993
George A. Geri, Don R. Lyon, and Yehoshua Y. Zeevi Jan. 1994 42 p
Limited Reproducibility: More than 20% of this document may be affected by microfiche quality
(Contract F33615-90-C-0005)
(AD-A277201; AL/HR-TR-1993-0189) Avail: Issuing Activity (Defense Technical Information Center (DTIC))

Textures generated by superimposing sinusoidal luminance distributions can be used to simulate the natural terrain textures often used in flight simulator imagery. Since the visual system is spatially inhomogeneous with the periphery being generally less sensitive than the center of the visual field, simpler, more easily generated textures can potentially be used to simulate terrain that is farther from the operator's point of regard. The minimal number of component sinusoids required to generate textures that are visually acceptable in the visual periphery was estimated for the discrimination of complex suprathreshold textures. Specifically, similarity ratings were obtained to determine the effects of component orientation and component phase-bandwidth on the cortical magnification factor (CMF) associated with that discrimination. The textures were designed to be both specifically by a relatively small number of localized spectral components and sufficiently complex to approximate natural images. The number of component orientations was found to be a particularly important determinant of texture discrimination in that its effect on rated similarity was largely independent of the total number of components making up the texture. When the number of components was varied, a CMF of 2 was sufficient to equate the similarity ratings obtained at 0.75 deg and 20 deg. Under the same conditions, a CMF of 4 clearly overcorrected the data. The estimated CMF for texture discrimination is much smaller than that found for the discrimination of simple 2-D spatial frequency and suggests that either quantitatively different cortical mechanisms or different cortical areas are responsible for the two types of discrimination. DTIC

N94-32130# Adaptive Solutions, Inc., Beaverton, OR.
HIGH PERFORMANCE HARDWARE AND SOFTWARE FOR PATTERN RECOGNITION AND IMAGE PROCESSING Status Report, 8 Nov. 1993 - 31 Jan. 1994
Wendell A. Henry 15 Feb. 1994 5 p
(Contract N00014-93-C-0234)
(AD-A276405) Avail: CASI HC A01/MF A01

The contract was given tentative funding approval on November 8, 1993. At that time work on Phase 1 of the contract started. The contract was formally approved December 30, 1993. During the first three months of the contract efforts have centered on planning and scheduling the Phase 1 projects and beginning work on the defined tasks. Progress was made in the definition and design of the CNAPS/PC hardware board (image processing accelerator board that plugs into a PC) that will be developed during Phase 1. Likewise, progress was made in the initial design and prototyping of the software to be developed in this phase of the project. DTIC

N94-32131# Trusted Information Systems, Inc., Los Angeles, CA.
INTEGRATED TRUSTED SYSTEM DEVELOPMENT ENVIRONMENT PROCESS Final Report, Apr. 1991 - Dec. 1992
Terry C. Benzel, Douglas W. Rothnie, and Stephen D. Crocker Oct. 1993 145 p
(Contract F30602-91-C-0049)
(AD-A276414; RL-TR-93-193) Avail: CASI HC A07/MF A02

The Integrated Trusted System Development Environment (ITSDE) Process project has further extended and refined the Integrated Development Process (IDP) defined previously by the authors. The result is a set of integrated Data Item Descriptions (DID's) for use with the process and tailoring directions for producing the DID's. The IDP describes a software development process for developing trusted systems under DoD-STD-2167A. The process is based on an approach which integrates the Trusted Compute System Criteria (TCSEC) requirements contained in DOD-5200-28-STD into the software development process required by DoD-STD-2167A. The IDP focuses on development of 2167A DID's which have been tailored to include TCSEC deliverables. The IDP describes how these items can be produced in a manner which minimizes the impact on cost and budget, while increasing assurance in the product's trustworthiness. The majority of the work reported here was performed during the period 1 Apr 91. DTIC

N94-32145# Pacific Northwest Lab., Richland, WA.
CMS PREPROCESSING SUBSYSTEM USER'S GUIDE: SOFTWARE VERSION 2.0
B. T. Didier, J. D. Gash, F. L. Greitzer, S. L. Havre, J. V. Ramsdell, and C. R. Turney Dec. 1993 75 p
(Contract DE-AC06-76RL-01830)
(DE94-005327; PNL-8995) Avail: CASI HC A04/MF A01

The Common Mapping Standard (CMS) Data Production System (CDPS) produces and distributes CMS data in compliance with the Common Mapping Standard Interface Control Document. CDPS is composed of two subsystems, the CMS Preprocessing Subsystem (CPS) and the CMS Distribution Subsystem (CDS). This guide describes the operation of CPS. CPS is responsible for the management of source data and the production of CMS data from source data. The CPS system was developed for use on a workstation running Ultrix 4.2, the X Window System Version X11R4, and motif Version 1.1. This subsystem is organized into four major functional groups and supports production of CMS data from source chart, indose, and elevation data products. DOE

N94-32146# Pacific Northwest Lab., Richland, WA.
CMS DISTRIBUTION SUBSYSTEM USER'S GUIDE
J. D. Gash, F. L. Greitzer, L. D. Hatfield, M. H. Portwood, and C. R.

Turney Dec. 1993 112 p
(Contract DE-AC06-76RL-01830)
(DE94-005328; PNL-8994) Avail: CASI HC A06/MF A02

The Common Mapping Standard (CMS) Data Production System (CDPS) produces and distributes CMS data in compliance with the Common Mapping Standard Interface Control Document. CDPS is composed of two subsystems the CMS Distribution Subsystem (CDS) and the CMS Preprocessing Subsystem (CPS). This guide describes the operation of CDS. CDS is responsible for the management of archived CMS data, the management of production orders, and the generation of theater databases. This subsystem was developed for use on a workstation running Ultrix 4.2, the X Window System Version X11R4, and motif Version 1.1. CDS is organized into seven major functional groups and supports archiving and distributing CMS data for selected products. DOE

N94-32212 Massachusetts Inst. of Tech., Cambridge. Artificial Intelligence Lab.
METHODS FOR PARALLELIZING SEARCH PATHS IN PHRASING
Carl DeMarcken Aug. 1993 115 p Limited Reproducibility: More than 20% of this document may be affected by microfiche quality
(Contract N00014-91-J-4038; NSF ASC-92-17041)
(AD-A276876; AI-TR-1453) Avail: CASI HC A06

Many search problems are commonly solved with combinatoric algorithms that unnecessarily duplicate and serialize work at considerable computational expense. There are techniques available that can eliminate redundant computations and perform remaining operations concurrently, effectively reducing the branching factors of these algorithms. This thesis applies these techniques to the problem of parsing natural language. The result is an efficient programming language that can reduce some of the expense associated with principle-based parsing and other search problems. The language is used to implement various natural language parsers, and the improvements are compared to those that result from implementing more deterministic theories of language processing. DTIC

N94-32213 Massachusetts Inst. of Tech., Cambridge. Artificial Intelligence Lab.
TRANSLUCENT PROCEDURES, ABSTRACTION WITHOUT OPACITY
Guillermo J. Rozas Oct. 1993 180 p Limited Reproducibility: More than 20% of this document may be affected by microfiche quality
(Contract N00014-92-J-4097; NSF MIP-90-01651)
(AD-A276877; AI-TR-1427) Avail: CASI HC A09

This report introduces translucent procedures as a new mechanism for implementing behavioral abstractions. Like an ordinary procedure, a translucent procedure can be invoked, and this provides an obvious way to capture a behavior. Translucent procedures, like ordinary procedures, can be manipulated as first-class objects and combined using functional composition. But unlike ordinary procedures, translucent procedures have structure that can be examined in well-specified non-destructive ways, without invoking the procedure. DTIC

N94-32219 Virginia Center of Excellance for Software Reuse and Technology Transfer, Herndon.
MULTIGRAPH: AN ARCHITECTURE FOR MODEL-BASED PROGRAMMING. MODEL-BASED PROGRAM SYNTHESIS FOR PARALLEL COMPUTING. PREMOS: PROGRAMMING ENVIRONMENT FOR MODEL-BASED PROGRAM SYNTHESIS, VERSION 01.00.00
Janos Sztipanovits, Ben Abbott, and Hubertus Franke Mar. 1994 59 p Limited Reproducibility: More than 20% of this document may be affected by microfiche quality
(Contract MDA972-92-J-1018)
(AD-A276949; SPC-93154-CMC) Avail: CASI HC A04/MF A01

This presentation consists of three presentations related to model-based software synthesis. The first presentation provides an overview of the MULTIGRAPH Architecture (MGA), which is used as a generic framework for model-based programming. Evolution of the architecture has been driven by the requirements of specific applications. Characteristics of these application domains and their impact on the basic design of MGA are discussed. The second presentation discusses Model-Based Program Synthesis for Parallel Computing. Automatic program synthesis is one of the prime disciplines that can contribute to the advancement of the software engineering of reactive systems. A large, high-performance parallel instrumentation system used for analysis of turbine engine strain gauge signals produced during altitude testing is presented as an illustration. The system is called the Computer Assisted Dynamic Data Analysis and Monitoring System (CADDMAS). The third presentation discusses a Programming Environment for Model-Based Program Synthesis. The development of model-based programming environments is driven by two opposite forces: specialization and Standardization. The presentation addresses the design and implementation of tools which satisfy both above-mentioned forces. In order to overcome this dilemma, the MULTIGRAPH Architecture uses meta-tools. This presentation focuses on the design and implementation of meta-tools and their coordination to form a harmonic environment. DTIC

N94-32257 Yale Univ., New Haven, CT. Dept. of Computer Science.
AN ALGORITHM FOR PROBABILISTIC, TOTALLY-ORDERED TEMPORAL PROJECTION
Drew McDermott Mar. 1994 57 p Limited Reproducibility: More than 20% of this document may be affected by microfiche quality
(Contract N00014-91-J-1577)
(AD-A277341; YaleU/DCS/RR-1014) Avail: Issuing Activity (Defense Technical Information Center (DTIC))

Temporal projection, defined as the prediction of what might happen when a plan is executed, is an important component of many planning algorithms. To achieve efficiency, it is desirable for a projection to be a totally ordered event sequence. To cope with uncertainty, the events must be generated using probabilistic rules. We require a rule language that allows us to specify what can happen when an event occurs, as well as what events can occur when certain propositions are true. The language has a formal semantics, which allows us to prove that a set of rules has a unique model (if it is consistent). This language supports a Monte Carlo style of projection, in which event sequences are sampled randomly using the probabilities in the rules. The output of the projector is a timeline that allows a planning algorithm to test the truth of propositions at arbitrary points. The algorithms for building and retrieving from the timeline can be shown to be correct. Experiments show that for a typical theory, the time to build a timeline is a quadratic function of the number of events in the timeline. DTIC

N94-32287 Nijmegen Univ. (Netherlands). Dept. of Informatics.
INFORMAL INTRODUCTION TO THE EXTENDED AFFIX GRAMMAR FORMALISM AND ITS COMPILER
M. Seutter 13 Sep. 1993 56 p Limited Reproducibility: More than 20% of this document may be affected by microfiche quality
(Grant SION-612-317-404)
(TR-93-19; ETN-94-96213) Avail: Issuing Activity (European Space Agency (ESA))

The Extended Affix Grammar (EAG) formalism, a formalism for describing both the context free and the context sensitive syntax of languages, and its compiler are introduced. EAG is a member of the family of two level grammars. They are very closely related to two level van Wijngaarden grammars. To a description in EAG the EAG compiler may be applied, generating either a recognizer or a transducer or a translator or a syntax directed editor for the language described. Attention is paid to the ideas behind the language and the language concepts are elucidated by examples. The use of the compiler and the options that may be used to steer the generation process are discussed. ESA

N94-32294 Stanford Univ., CA.
APPLICATIONS OF DATA COMPRESSION TO 3-D SCALAR FIELD VISUALIZATION Ph.D. Thesis
Paul Ning 1993 133 p
Avail: Univ. Microfilms Order No. DA9326533

Scientific visualization is the use of computer graphics techniques for analyzing and displaying experimental or simulated data, and has been promoted as an efficient tool for understanding large, multidimensional datasets that arise in many applications. The use of visualization does not eliminate, however, the problem of data management; rather, data management issues must be addressed by the visualization tools themselves. Thus, it is only natural to apply data compression techniques in order to improve the performance of visualization systems. In this dissertation, we demonstrate how compression can be beneficial to both isosurface generation and volume rendering, two common techniques for displaying volumetric (three dimensional) scalar fields. Isosurface generation involves

the construction of a polygonal model which approximates a contour surface in the volume. The number of polygons generated can be quite large, however, which increases rendering time and storage costs. We develop a variable-resolution isosurface generation algorithm which constructs accurate surface models over a wide range of compressed polygon counts. This algorithm imposes an octree hierarchy on the volume data, and applies tree pruning techniques to find good surface models at lower resolutions. Instead of extracting and displaying a single surface, volume rendering treats the entire three dimensional scalar field as a collection of sources and attenuators, and integrates these contributions along the viewing direction to form a projected image of the translucent volume. A volume renderer requires access to all of the scalar field samples, as well as to several derived quantities. For large datasets, the storage used by these methods can be very high, and rendering speed is generally slow. We introduce a compressed volume format based on vector quantization that provides storage savings and that may also be exploited for faster rendering. Dissert. Abstr.

N94-32330# Wright Research Development Center, Wright-Patterson AFB, OH. Flight Dynamics Lab.

QUAD4 SEMINAR Report, Jan. - Mar. 1989

Vipperla B. Venkayya and Victoria A. Tischler Apr. 1993 258 p Revised

(AD-A277366; WRDC-TR-89-3046) Avail: CASI HC A12/MF A03

NASTRAN (NASA Structural Analysis Program) is the most widely used general purpose structural analysis program in the world. This program was originally developed in the mid-sixties, and the first version was released in 1968. This development in the form of enhancements and maintenance was continued until 1972 as a single government version under the sponsorship of NASA. Since then the government version is being developed as COSMIC-NASTRAN, while a commercial version is being marketed by McNeal and Swendler Corporation (MSC) as MSC-NASTRAN. Even through the basic structure of these two versions remains the same, there are significant differences in capabilities and efficiencies. Around 1980 the MSC introduced a new plate bending element called the QUAD4 to its element library. It is one of the most versatile plate bending elements, even though its theoretical basis is somewhat controversial. DTIC

N94-32353# Sandia National Labs., Albuquerque, NM.

INTERACTIVE GRAPHICAL MODEL BUILDING USING TELEPRESENCE AND VIRTUAL REALITY

C. Cooke (Massachusetts Inst. of Tech., Cambridge.) and S. Stansfield 1993 5 p Presented at the IEEE International Conference on Robotics, San Diego, CA, 8-13 May 1994

(Contract DE-AC04-94AL-85000)

(DE94-001421; SAND-93-1977C; CONF-940550-2) Avail: CASI HC A01/MF A01

This paper presents a prototype system developed at Sandia National Laboratories to create and verify computer-generated graphical models of remote physical environments. The goal of the system is to create an interface between an operator and a computer vision system so that graphical models can be created interactively. Virtual reality and telepresence are used to allow interaction between the operator, computer, and remote environment. A stereo view of the remote environment is produced by two CCD cameras. The cameras are mounted on a three degree-of-freedom platform which is slaved to a mechanically-tracked, stereoscopic viewing device. This gives the operator a sense of immersion in the physical environment. The stereo video is enhanced by overlaying the graphical model onto it. Overlay of the graphical model onto the stereo video allows visual verification of graphical models. Creation of a graphical model is accomplished by allowing the operator to assist the computer in modeling. The operator controls a 3-D cursor to mark objects to be modeled. The computer then automatically extracts positional and geometric information about the object and creates the graphical model. DOE

N94-32390 Materials Research Labs., Ascot Vale (Australia).

GRAFTED - GRAphical FAULT TREE EDitor: A FAULT TREE DESCRIPTION PROGRAM FOR TARGET VULNERABILITY/SURVIVABILITY ANALYSIS. USER MANUAL

Michael E. Buckland, Mark Webster, and Frank J. Tkalcevic Dec. 1993 28 p Limited Reproducibility: More than 20% of this document may be affected by microfiche quality

(AD-A277067; MRL-GD-0057; DODA-AR-008-614) Avail: Issuing Activity (Defense Technical Information Center (DTIC))

A computer program, the GRAphical Fault Tree EDitor (GRAFTED), was written to simplify data entry and modification of component fault tree descriptions (FTD) used in military platform vulnerability/survivability analysis. GRAFTED uses a unique, graphical, screen based data entry procedure to define and display both individual system component parameters, and their hierarchical relationship in the overall system FTD. The generated component and system FTD output is in a format that is directly readable by the MRL version of the General Vulnerability Assessment Model, (GVAM), suite of computer programs. Although GRAFTED was specifically designed to generate FTD's for GVAM, it could be easily modified to accommodate data input formats and FTD output for other assessment procedures that require user friendly data entry and graphical fault tree editing and visualisation. This version of GRAFTED was written specifically for Tektronix UNIX workstations, and only runs on these machines. DTIC

N94-32504# Massachusetts Inst. of Tech., Cambridge. Artificial Intelligence Lab.

Emacs LISP IN EDWIN SCHEME

Matthew Birkholz Sep. 1993 121 p

(Contract N00014-92-J-4097; NSF MIP-90-01651)

(AD-A276721; AI-TR-1451) Avail: CASI HC A06/MF A02

The MIT-Scheme program development environment includes a general-purpose text editor, Edwin, that has an extension language, Edwin Scheme. Edwin is very similiar to another general-purpose text editor, GNU Emacs, which also has an extension language, Emacs Lisp. The popularity of GNU Emacs has lead to a large library of tools written in Emacs Lisp. The goal of this thesis is to implement a useful subset of Emacs Lisp in Edwin Scheme. This subset was chosen to be sufficient for simple operation of the GNUS news reading program. DTIC

N94-32508 Carnegie-Mellon Univ., Pittsburgh, PA. Software Engineering Inst.

CASE STUDIES OF SOFTWARE PROCESS IMPROVEMENT METHODS Final Report

Daniel J. Paulish Dec. 1993 63 p Limited Reproducibility: More than 20% of this document may be affected by microfiche quality

(Contract F19628-90-C-0003)

(AD-A277289; CMU/SEI-93-TR-26; ESC-TR-93-200) Avail: CASI HC A04

This report describes the case studies approach applied at a number of Siemens software development organizations to observe the impact of software process improvement methods. In addition, the report provides guidance to software development organizations that want to improve their processes. A set of organization performance measures are defined to help an organization observe its software process improvement over time. An approach is given for selecting software process improvement methods. The report concludes with a description of common implementation problems and recommendations for organizations to improve their software processes. DTIC

N94-32584# Sandia National Labs., Livermore, CA.

OPT++: AN OBJECT-ORIENTED CLASS LIBRARY FOR NONLINEAR OPTIMIZATION

J. C. Meza Mar. 1994 21 p

(Contract DE-AC04-76DR-00789)

(DE94-008890; SAND-94-8225) Avail: CASI HC A03/MF A01

Object-oriented programming is becoming a popular way of developing new software. The promise of this new programming paradigm is that software developed through these concepts will be more reliable and easier to re-use, thereby decreasing the time and cost of the software development cycle. This report describes the development of a C++ class library for nonlinear optimization. Using object-oriented techniques, this new library was designed so that the interface is easy to use while being general enough so that new optimization algorithms can be added easily to the existing framework. DOE

N94-32585# Lawrence Livermore National Lab., CA.

ON THE IMPLEMENTATION OF ERROR HANDLING IN DYNAMIC INTERFACES TO SCIENTIFIC CODES Ph.D. Thesis

C. J. Solomon Nov. 1993 51 p
(Contract W-7405-eng-48)
(DE94-008970; UCRL-LR-116004) Avail: CASI HC A04/MF A01

With the advent of powerful workstations with windowing systems, the scientific community has become interested in user friendly interfaces as a means of promoting the distribution of scientific codes to colleagues. Distributing scientific codes to a wider audience can, however, be problematic because scientists, who are familiar with the problem being addressed but not aware of necessary operational details, are encouraged to use the codes. A more friendly environment that not only guides user inputs, but also helps catch errors is needed. This thesis presents a dynamic graphical user interface (GUI) creation system with user controlled support for error detection and handling. The system checks a series of constraints defining a valid input set whenever the state of the system changes and notifies the user when an error has occurred. A naive checking scheme was implemented that checks every constraint every time the system changes. However, this method examines many constraints whose values have not changed. Therefore, a minimum evaluation scheme that only checks those constraints that may have been violated was implemented. This system was implemented in a prototype and user testing was used to determine if it was a success. Users examined both the GUI creation system and the end-user environment. The users found both to be easy to use and efficient enough for practical use. Moreover, they concluded that the system would promote distribution. DOE

N94-32599# Argonne National Lab., Idaho Falls, ID.
DESIGN OF GRAPHIC SCREENS USING NEURO LINGUISTIC PROGRAMMING
S. Alenka Brown-VanHoozer 1994 6 p Presented at the 1994 Society for Computer Simulation Multiconference, San Diego, CA, 11-15 Apr. 1994
(Contract W-31-109-eng-38)
(DE94-007634; ANL/IFR/CP-80791; CONF-940456-11) Avail: CASI HC A02/MF A01

Neuro linguistic programming (NLP) is an explicit and powerful model of human experience and communication which can be instrumental in designing pragmatic visual displays. It is a new approach to interacting with humans, based on modeling and outcomes. The original creators of NLP studied people who were successful in outcomes with their patients and modeled what these people did. Over sixteen years, the technique has crossed over into law, politics, business, and education. The intended use that is described in this paper is focused on the human factor aspect and visual display designs. DOE

N94-32641 Oak Ridge National Lab., TN.
IMPLEMENTATION AND DISPLAY OF COMPUTER AIDED DESIGN (CAD) MODELS IN MONTE CARLO RADIATION TRANSPORT AND SHIELDING APPLICATIONS
T. J. Burns 1994 10 p Presented at the 8th International Conference on Radiation Shielding, Arlington, TX, 24-27 Apr. 1994 Limited Reproducibility: More than 20% of this document may be affected by microfiche quality
(Contract DE-AC05-84OR-21400)
(DE94-007221; CONF-940424-22) Avail: CASI HC A02

An X-window application capable of importing geometric information directly from two Computer Aided Design (CAD) based formats for use in radiation transport and shielding analyses is being developed at ORNL. The application permits the user to graphically view the geometric models imported from the two formats for verification and debugging. Previous models, specifically formatted for the radiation transport and shielding codes can also be imported. Required extensions to the existing combinatorial geometry analysis routines are discussed. Examples illustrating the various options and features which will be implemented in the application are presented. The use of the application as a visualization tool for the output of the radiation transport codes is also discussed. DOE

N94-32651 Sandia National Labs., Albuquerque, NM.
VARYING EXECUTION DISCIPLINE TO INCREASE PERFORMANCE
P. L. Campbell and A. B. Maccabe 22 Dec. 1993 44 p Limited Reproducibility: More than 20% of this document may be affected by microfiche quality
(Contract DE-AC04-94AL-85000)
(DE94-007844; SAND-93-4088) Avail: CASI HC A03

This research investigates the relationship between execution discipline and performance. The hypothesis has two parts: (1) different execution disciplines exhibit different performance for different computations; and (2) these differences can be effectively predicted by heuristics. A machine model is developed that can vary its execution discipline. That is, the model can execute a given program using either the control-driven, data-driven, or demand-driven execution discipline. This model is referred to as a 'variable-execution-discipline' machine. The instruction set for the model is the Program Dependence Web (PDW). The first part of the hypothesis will be tested by simulating the execution of the machine model on a suite of computations, based on the Livermore Fortran Kernel (LFK) Test (a.k.a. the Livermore Loops), using all three execution disciplines. Heuristics are developed to predict relative performance. These heuristics predict the execution time under each discipline for one iteration of each loop and the number of iterations taken by that loop; then the heuristics use those predictions to develop a prediction for the execution of the entire loop. Similar calculations are performed for branch statements. The second part of the hypothesis will be tested by comparing the results of the simulated execution with the predictions produced by the heuristics. If the hypothesis is supported, then the door is open for the development of machines that can vary execution discipline to increase performance. DOE

N94-32668 California Univ., Berkeley. Lawrence Berkeley Lab.
THE LIMITS OF INTELLIGENCE IN DESIGN
K. Papamichael and J. P. Protzen May 1993 10 p Presented at the 4th International Symposium on System Research, Informatics and Cybernetics, Baden-Baden, Germany, 3-4 Aug. 1993 Limited Reproducibility: More than 20% of this document may be affected by microfiche quality
(Contract DE-AC03-76SF-00098)
(DE94-004668; LBL-31742; CONF-9308203-1) Avail: Issuing Activity (Department of Energy (DOE))

A new, comprehensive design theory is presented, applicable to all design domains such as engineering and industrial design, architecture, city and regional planning, and, in general, any goal-oriented activity that involves decision making. The design process is analyzed into fundamental activities that are characterized with respect to the nature of knowledge requirements and the degree to which they can be specified and delegated to others, in general, and to computers in particular. The characterization of design problems as 'wicked', or 'ill-defined', design has been understood as a rational activity, that is 'thinking before acting'. The new theory presented in this paper suggests that design is 'thinking and feeling while acting', supporting the position that design is only partially rational. Intelligence, 'natural' or 'artificial', is only one of two requirements for design, the other being emotions. Design decisions are only partially inferred, that is, they are not entirely the product of reasoning. Rather, design decisions are based on judgment that requires the notion of 'good' and 'bad', which is attributed to feelings, rather than thoughts. The presentation of the design theory extends to the implications associated with the limits of intelligence in design, which, in turn, become constraints on the potential role of computers in design. Many of the current development efforts in computer-aided design violate these constraints, especially in the implementation of expert systems and multi-criterion evaluation models. These violations are identified and discussed in detail. Finally, specific areas for further research and development in computer-aided design are presented and discussed. DOE

N94-32749# Westinghouse Hanford Co., Richland, WA.
DEVELOPING A PERSONAL-COMPUTER-BASED RECORDS RETENTION SYSTEM USING PARADOX(TM)
B. Sprouse and S. Wray Oct. 1993 9 p Presented at the 38th Association of Records Managers and Administrators (ARMA) Annual Meeting, Seattle, WA, 17-20 Oct. 1993
(Contract DE-AC06-87RL-10930)
(DE94-007984; WHC-SA-1705; CONF-9310300-1) Avail: CASI HC A02/MF A01

Many records managers are confronted with large caches of records stored in corners, attics, or warehouses that seem to be 'out of sight, out of mind.' Much of this information becomes 'lost' because it is not properly identified and cataloged. Perhaps the records have always been stored in

these places because the lack of an alternative. In these situations, the records manager must organize and catalog the records and provide solutions to the records management and storage problems. A simple personal computer-based records management system can be developed that will provide organization, accountability, and retrievability of the records. By developing a basic database structure and implementing some basic records management principles, a records manager can gain control of even the most extreme displays of records mismanagement. This paper will discuss practical ways of establishing a records system that provides for database tracking using off-the-shelf database software packages. Database examples using Paradox software will be used to explain the basic concepts for developing records systems. The paper will also discuss developing and performing a records assessment, researching applicable requirements, writing a records management plan, implementing the records system, and testing and modifying the system. DOE

N94-32773*# National Aeronautics and Space Administration. Lewis Research Center, Cleveland, OH.

ON THE USE OF COMPUTERS FOR TEACHING FLUID MECHANICS

Thomas J. Benson Jun. 1994 18 p Proposed for presentation at the ASME Fluids Engineering Division Summer Meeting, Lake Tahoe, NV, 19-23 Jun. 1994; sponsored by ASME

(RTOP 505-62-52)

(NASA-TM-106587; E-8851; NAS 1.15:106587) Avail: CASI HC A03/MF A01

Several approaches for improving the teaching of basic fluid mechanics using computers are presented. There are two objectives to these approaches: to increase the involvement of the student in the learning process and to present information to the student in a variety of forms. Items discussed include: the preparation of educational videos using the results of computational fluid dynamics (CFD) calculations, the analysis of CFD flow solutions using workstation based post-processing graphics packages, and the development of workstation or personal computer based simulators which behave like desk top wind tunnels. Examples of these approaches are presented along with observations from working with undergraduate co-ops. Possible problems in the implementation of these approaches as well as solutions to these problems are also discussed. Author (revised)

N94-32775*# Boeing Co., Seattle, WA.

INTERPRETER COMPOSITION ISSUES IN THE FORMAL VERIFICATION OF A PROCESSOR-MEMORY MODULE Final Report

David A. Fura and Gerald C. Cohen Hampton, VA NASA May 1994 69 p

(Contract NAS1-18586; RTOP 505-64-50-04)

(NASA-CR-4594; NAS 1.26:4594) Avail: CASI HC A04/MF A01

This report describes interpreter composition techniques suitable for the formal specification and verification of a processor-memory module using the HOL theorem proving system. The processor-memory module is a multichip subsystem within a fault-tolerant embedded system under development within the Boeing Defense and Space Group. Modeling and verification methods were developed that permit provably secure composition at the transaction-level of specification, significantly reducing the complexity of the hierarchical verification of the system. Author (revised)

N94-32776*# SRI International Corp., Menlo Park, CA.

MODEL-BASED RECONFIGURATION: DIAGNOSIS AND RECOVERY Final Report

Judy Crow and John Rushby Hampton, VA NASA May 1994 66 p

(Contract NAS1-18226; RTOP 505-64-50-04)

(NASA-CR-4596; NAS 1.26:4596) Avail: CASI HC A04/MF A01

We extend Reiter's general theory of model-based diagnosis to a theory of fault detection, identification, and reconfiguration (FDIR). The generality of Reiter's theory readily supports an extension in which the problem of reconfiguration is viewed as a close analog of the problem of diagnosis. Using a reconfiguration predicate 'rcfg' analogous to the abnormality predicate 'ab,' we derive a strategy for reconfiguration by transforming the corresponding strategy for diagnosis. There are two obvious benefits of this approach: algorithms for diagnosis can be exploited as algorithms for reconfiguration and we have a theoretical framework for an integrated approach to FDIR. As a first step toward realizing these benefits we show that a class of diagnosis engines can be used for reconfiguration and we discuss algorithms for integrated FDIR. We argue that integrating recovery and diagnosis is an essential next step if this technology is to be useful for practical applications. Author (revised)

N94-32899*# National Aeronautics and Space Administration. Lyndon B. Johnson Space Center, Houston, TX.

BUCKY INSTRUCTION MANUAL, VERSION 3.3

James P. Smith May 1994 61 p

(NASA-TM-104793; S-766; NAS 1.15:104793) Avail: CASI HC A04/MF A01

The computer program BUCKY is a p-version finite element package for the solution of structural problems. The current version of BUCKY solves the 2-D plane stress, 3-D plane stress plasticity, 3-D axisymmetric, Mindlin and Kirchoff plate bending, and buckling problems. The p-version of the finite element method is a highly accurate version of the traditional finite element method. Example cases are presented to show the accuracy and application of BUCKY. Author

N94-32906*# National Aeronautics and Space Administration. Ames Research Center, Moffett Field, CA.

TRANSLATING AN AI APPLICATION FROM LISP TO ADA: A CASE STUDY

Gloria J. Davis Nov. 1991 7 p

(RTOP 549-03-61)

(NASA-TM-103845; A-91094; NAS 1.15:103845) Avail: CASI HC A02/MF A01

A set of benchmarks was developed to test the performance of a newly designed computer executing both Lisp and Ada. Among these was AutoClassII -- a large Artificial Intelligence (AI) application written in Common Lisp. The extraction of a representative subset of this complex application was aided by a Lisp Code Analyzer (LCA). The LCA enabled rapid analysis of the code, putting it in a concise and functionally readable form. An equivalent benchmark was created in Ada through manual translation of the Lisp version. A comparison of the execution results of both programs across a variety of compiler-machine combinations indicate that line-by-line translation coupled with analysis of the initial code can produce relatively efficient and reusable target code. Author

N94-32928*# Institute for Computer Applications in Science and Engineering, Hampton, VA.

A SOFTWARE ARCHITECTURE FOR MULTIDISCIPLINARY APPLICATIONS: INTEGRATING TASK AND DATA PARALLELISM Final Report

Barbara Chapman (Wien Univ., Austria.), Piyush Mehrotra, John VanRosendale, and Hans Zima Mar. 1994 26 p Submitted for publication

(Contract NAS1-19480; FWF-P8989-PHY; BMWF-GZ-308.9281-IV/3/93; RTOP 505-90-52-01)

(NASA-CR-194896; NAS 1.26:194896; ICASE-94-18) Avail: CASI HC A03/MF A01

Data parallel languages such as Vienna Fortran and HPF can be successfully applied to a wide range of numerical applications. However, many advanced scientific and engineering applications are of a multidisciplinary and heterogeneous nature and thus do not fit well into the data parallel paradigm. In this paper we present new Fortran 90 language extensions to fill this gap. Tasks can be spawned as asynchronous activities in a homogeneous or heterogeneous computing environment; they interact by sharing access to Shared Data Abstractions (SDA's). SDA's are an extension of Fortran 90 modules, representing a pool of common data, together with a set of Methods for controlled access to these data and a mechanism for providing persistent storage. Our language supports the integration of data and task parallelism as well as nested task parallelism and thus can be used to express multidisciplinary applications in a natural and efficient way. Author

N94-32972# Washington Univ., Seattle. Dept. of Computer Science and Engineering.

MESH OPTIMIZATION

Hughes Hoppe, Tony DeRose, Tom Duchamp, John McDonald, and Werner Stuetzle 1994 35 p

(Contract DE-FG06-85ER-25006; NSF CCR-89-57323)

(AD-A277644; TR-93-01-01) Avail: CASI HC A03/MF A01

We present a method for solving the following problem: Given a set of data points scattered in three dimensions and an initial triangular mesh M(sub O), produce a mesh M, of the same topological type as M(sub O), that fits the data well and has a small number of vertices. Our approach is to minimize an energy function that explicitly models the competing desires of conciseness of representation and fidelity to the data. We show that mesh optimization can be effectively used in at least two applications: surface reconstruction from unorganized points and mesh simplification (the reduction of the number of vertices in an initially dense mesh of triangles). DTIC

N94-33027# New York Univ., New York. Inst. of Mathematical Sciences.

MACHINE ASSISTED IMPLEMENTATION OF COMPLEX ALGORITHMS AND LABOR INTENSIVE SOFTWARE, CLOSING REPORT

Robert A. Paige 22 Feb. 1994 5 p

(Contract N00014-90-J-1890)

(AD-A277662) Avail: CASI HC A01/MF A01

Our project stated the following broad goals: (1) to design a practical tool capable of automating major aspects of programming--essentially, a generalization of YACC and MACSYMA to facilitate implementation of a wide class of complex nonnumerical algorithms (in addition to parsing); (2) to design and implement complexity based specification languages; (3) to integrate problem specification, program design, verification, and analysis within a single unified framework; (4) to design and efficiently implement pattern directed rule systems for semantic analysis; and (5) to make it easier to teach and understand algorithms and software engineering. DTIC

N94-33030# Carnegie-Mellon Univ., Pittsburgh, PA. Dept. of Computer Science.

SynRGen: AN EXTENSIBLE FILE REFERENCE GENERATOR

Maria R. Ebling and M. Satyanarayanan Feb. 1994 16 p

(Contracts F33615-90-C-1465; F19628-93-C-0193)

(AD-A277678; CMU-CS-94-119) Avail: CASI HC A03/MF A01

SynRGen, a synthetic file reference generator operating at the system call level, is capable of modeling a wide variety of usage environments. It achieves realism through trace-inspired micromodels and flexibility by combining these micromodels stochastically. A micromodel is a parameterized piece of code that captures the distinctive signature of an application. We have used SynRGen extensively for stress testing the Coda File System. We have also performed a controlled experiment that demonstrates SynRGen's ability to closely emulate real users-within 20% of many key system variables. In this paper we present the rationale, detailed design, and evaluation of SynRGen and mention its applicability to broader uses such as performance evaluation. DTIC

N94-33031# Army Engineer Waterways Experiment Station, Vicksburg, MS. Information Technology Lab.

THEORY AND APPLICATION OF IMAGE ENHANCEMENT Final Report

Michael G. Ellis, Sr. and Roy L. Campbell, Jr. Feb. 1994 467 p

(AD-A277896; WES/TR/ITL-94-1) Avail: CASI HC A20/MF A04

The conventional methods for image enhancement cannot be satisfactorily applied to the restoration of many types of images. This report explores standard image enhancement algorithms with emphasis on possible extensions to allow for real-time applications. The artifacts introduced by compression algorithms can often be compensated for by proper restoration techniques. A desktop conferencing system is prototyped in this report as a test-bed application to evaluate both real-time compression and real-time enhancement algorithms. DTIC

N94-33049*# Mississippi State Univ., Mississippi State. NSF Engineering Research Center for Computational Field Simulation.

TRANSFORMATION OF TWO AND THREE-DIMENSIONAL REGIONS BY ELLIPTIC SYSTEMS Final Report

C. Wayne Mastin 4 May 1994 30 p

(Grant NsG-1577)

(NASA-CR-195849; NAS 1.26:195849) Avail: CASI HC A03/MF A01

Several reports are attached to this document which contain the results of our research at the end of this contract period. Three of the reports deal with our work on generating surface grids. One is a preprint of a paper which will appear in the journal Applied Mathematics and Computation. Another is the abstract from a dissertation which has been prepared by Ahmed Khamayseh, a graduate student who has been supported by this grant for the last two years. The last report on surface grids is the extended abstract of a paper to be presented at the 14th IMACS World Congress in July. This report contains results on conformal mappings of surfaces, which are closely related to elliptic methods for surface grid generation. A preliminary report is included on new methods for dealing with block interfaces in multiblock grid systems. The development work is complete and the methods will eventually be incorporated into the National Grid Project (NGP) grid generation code. Thus, the attached report contains only a simple grid system which was used to test the algorithms to prove that the concepts are sound. These developments will greatly aid grid control when using elliptic systems and prevent unwanted grid movement. The last report is a brief summary of some timings that were obtained when the multiblock grid generation code was run on the Intel IPSC/860 hypercube. Since most of the data in a grid code is local to a particular block, only a small fraction of the total data must be passed between processors. The data is also distributed among the processors so that the total size of the grid can be increase along with the number of processors. This work is only in a preliminary stage. However, one of the ERC graduate students has taken an interest in the project and is presently extending these results as a part of his master's thesis. Author (revised)

N94-33051# Office National d'Etudes et de Recherches Aerospatiales, Paris (France).

USE AND ADMINISTRATION OF UNIX (TM) SYSTEMS [UTILISATION ET ADMINISTRATION DES SYSTEMES UNIX]

Christian Pelissier 1992 278 p In FRENCH

(ISSN 0078-3781)

Avail: CASI HC A13/MF A03

The first part of this paper presents the Unix system from a user stand point. It concerns beginners, developers, and system administrators. Most of the commands are discussed and illustrated with examples. Others, because of their importance, are explained in detail. These are Shell and C-shell interpreters, the Make and SCCS utilities, the vi text editor and the mail utility. The second part describes system administration. It discusses the various aspects of this specialty beginning with the most elementary operations such as how to declare users and devices. The network is not forgotten since it covers TCP/IP, NFS, NIS, electronic mail, UUCP, and X-Window. System security is developed in the last chapter. The Unix versions covered in this paper are AT&T System 5 R2 and R3 as well as BSD 4.2 and 4.3 through the particular implementation of computer manufacturers. Author (revised)

N94-33075*# Institute for Computer Applications in Science and Engineering, Hampton, VA.

ON THE MINIMUM OF INDEPENDENT GEOMETRICALLY DISTRIBUTED RANDOM VARIABLES Final Report

Gianfranco Ciardo (College of William and Mary, Williamsburg, VA.), Lawrence M. Leemis (College of William and Mary, Williamsburg, VA.), and David Nicol (College of William and Mary, Williamsburg, VA.) Mar. 1994 18 p Submitted for publication

(Contract NAS1-19480; RTOP 505-90-52-01)

(NASA-CR-194883; NAS 1.26:194883; ICASE-94-12) Avail: CASI HC A03/MF A01

The expectations E(X(sub 1)), E(Z(sub 1)), and E(Y(sub 1)) of the minimum of n independent geometric, modifies geometric, or exponential random variables with matching expectations differ. We show how this is accounted for by stochastic variability and how E(X(sub 1))/E(Y(sub 1)) equals the expected number of ties at the minimum for the geometric random variables. We then introduce the 'shifted geometric distribution' and show that there is a unique value of the shift for which the individual shifted geometric and exponential random variables match expectations both individually and in the minimums. Author (revised)

N94-33090 Naval Postgraduate School, Monterey, CA.

MULTIPLE-VALUED PROGRAMMABLE LOGIC ARRAY MINIMIZATION BY SOLUTION SPACE SEARCH M.S. Thesis

Charles G. Wendt Dec. 1993 60 p Limited Reproducibility: More than 20% of this document may be affected by microfiche quality

(AD-A278033) Avail: CASI HC A04

A minimal realization of a multiple-valued programmable logic array

can only be achieved by exhaustive search. However, an exhaustive search is unrealistic even with the high speed CPU's in use today. Heuristic algorithms have been developed that provide near-minimal solutions using significantly less CPU time. This thesis investigates a new type of heuristic that uses implicant operations (combine, reshape, and cut) to move through the solution space. The choice of move is dynamically controlled by feedback from a queue of previous moves, called a TABU queue. This new heuristic performs better than existing heuristics in certain situations, but it requires more CPU time than direct cover methods. in addition, this heuristic provides a unique capability to fix the move acceptance probabilities associated with the basic implicant operations. Fixing move acceptance probabilities allows a study of the solution space of multiple-valued logic functions under controlled conditions. For example, tile results of a preliminary study into the solution space of a four-valued, three variable special function (SF) are presented. This suggests that the search space is not homogeneous; rather it suggests that the space is segmented with restrictive access between segments. The results of such studies will be a basis for improving the performance of current and future minimization heuristics. DTIC

N94-33097# Center for Mathematics and Computer Science, Amsterdam (Netherlands). Dept. of Computer Science.
MADE: A MULTIPLE APPLICATION DEVELOPMENT ENVIRONMENT
Ivan Herman, Graham J. Reynolds, and Jacques Davy Sep. 1993 22 p (ISSN 0169-118X)
(CWI-CS-R9360; ETN-94-96154) Copyright Avail: CASI HC A03/MF A01

An overview of MADE, an ESPRIT (European Strategic Program for Research and development in Information Technology) project aiming at the development of a programming environment for multimedia applications is presented. The resulting software library is based on C++, and it is planned to operate on UNIX workstations as well as on PC (Personal Computer) based platforms. Possible application scenarios where the MADE environment can be of a great help for multimedia programming are described. ESA

N94-33114*# Research Inst. for Computing and Information Systems, Houston, TX.
SELECTION CRITERIA AND FACILITATION TRAINING FOR THE STUDY OF GROUPWARE Final Technical Report
Barry P. Robichaux (Houston Univ., TX.) Nov. 1993 45 p
(Contract NCC9-16; RICIS Proj. IR-01b)
(NASA-CR-195906; NAS 1.26:195906) Avail: CASI HC A03/MF A01

Computer support for planning and decision making groups is a growing trend in the 90s. Groupware is a name often applied to group software and has been defined as 'computer-based systems that support groups engaged in a common task (or goal) and that provide an interface to a shared environment'. Unlike most single-user software, groupware assists user groups in their collaboration, coordination, and communication efforts. This paper focuses on groupware to support the meeting process. These systems are often called group decision support systems (GDSS), electronic meeting systems (EMS), or group support systems (GSS). The term 'meeting support groupware' is used here to include any computer-based system to support meetings. In order to understand this technology, one must first understand groups, what they do and the problems they face, and groupware, a wide range of technology to support group work. Guidelines for selecting groups for study as part of an overall research plan are provided in this document. These were taken from the literature and from persons for whom the information in this paper was targeted. Also, guidelines for facilitation training are discussed. Familiarity with known and accepted techniques are the principle duties of the facilitator and any form of training must include practice in using these techniques. Derived from text

N94-33179 Naval Postgraduate School, Monterey, CA.
INCREASING THE PRACTICAL IMPACT OF FORMAL METHODS FOR COMPUTER-AIDED SOFTWARE DEVELOPMENT: SOFTWARE SLICING, MERGING AND INTEGRATION
Valdis Berzins 15 Oct. 1993 79 p Limited Reproducibility: More than 20% of this document may be affected by microfiche quality
(AD-A277929) Avail: CASI HC A05

The goals of this workshop were to: (1) identify the key technical problems in computer aided software evolution; (2) clarify the relations to other parts of computer science; (3) examine plausible technical approaches and assess advantages and disadvantages; and (4) identify directions for future work that can have a practical impact. The papers for the workshop fall into these main areas: software maintenance and evolution; software specification methods; software merging, slicing, and restructuring; and software verification, testing, and synthesis. Derived from text

N94-33183 Carnegie-Mellon Univ., Pittsburgh, PA. Graduate School of Industrial Administration.
MIXED 0-1 PROGRAMMING BY LIFT-AND-PROJECT IN A BRANCH-AND-CUT FRAMEWORK
Egon Balas, Sebastian Ceria, and Gerard Cornuejols 25 Feb. 1994 38 p Limited Reproducibility: More than 20% of this document may be affected by microfiche quality
(Contract N00014-89-J-1063; NSF DDM-92-01340)
(AD-A278045; MSRR-603) Avail: CASI HC A03

We investigate the computational issues that need to be addressed when incorporating general cutting planes for mixed 0-1 programs into a branch-and-cut framework. The cuts we use are of the lift-and-project variety. Some of the issues addressed have a theoretical answer but others are of an experimental nature and are settled by comparing alternatives on a set of test problems. The resulting code is a robust solver for mixed 0-1 programs. We compare it with several existing codes. DTIC

N94-33188 California Univ., San Diego, La Jolla. Dept. of Electrical and Computer Engineering.
FAULTLESS SOFTWARE PROJECT Final Report, 1 Feb. 1989 - 31 Mar. 1993
William Howden Jun. 1993 10 p Limited Reproducibility: More than 20% of this document may be affected by microfiche quality
(Contract N00014-89-J-1751)
(AD-A278161) Avail: CASI HC A02

Research has focused in three areas. The first is the development of a general platform paradigm for informal program verification and understanding. The second is the development of practical methods for the reconstruction of functional specifications from code. The third is the development of formal, statistical models for the evaluation of testing methods. DTIC

N94-33279# Carnegie-Mellon Univ., Pittsburgh, PA. Dept. of Computer Science.
STRUCTURING Z SPECIFICATIONS WITH VIEWS
Daniel Jackson Mar. 1994 27 p
(Contract F33615-93-1-1330; NSF CCR-93-08726)
(AD-A277618; CMU-CS-94-126) Avail: CASI HC A03/MF A01

A view is a partial specification of a program, consisting of a state space and a set of operations. A full specification is obtained by composing several views and linking them through their states (by asserting invariants across views) and through their operations (by defining external operations as combinations of operations from different views). By encouraging multiple representations of the program's state, view structuring lends clarity and terseness to the specification of operations. And by separating different aspects of functionality, it brings modularity at the grossest level of organization, so that specifications can accommodate change more gracefully. View structuring in Z is demonstrated with a few small examples. The features of Z that make it especially well suited to composing views are discussed, along with some hints for adapting other languages to the purpose. DTIC

N94-33284 Scranton Univ., PA. Dept. of Computing Sciences.
Ada SUPPORT FOR THE MATHEMATICAL FOUNDATIONS OF SOFTWARE ENGINEERING Final Report
John Beidler 16 Nov. 1993 40 p Limited Reproducibility: More than 20% of this document may be affected by microfiche quality
(Contract DAAL03-92-G-0410)
(AD-A278031) Avail: CASI HC A03

Three topics were selected as targets for this project: program correctness, finite state devices, and program complexity (timing). A variety of artifacts were developed to support course material, programming assignments, and laboratory assignments in the mathematics of software engineering. The program correctness artifact centers on an artifact, called Assert. Assert is an Ada package that assists users in testing program

assertions. The finite state device target is supported by several artifacts. One artifact in a course module, with laboratory and programming assignments, centers on the use of finite state device concepts in programming and the classical representations of finite state devices in Ada. The second finite state device artifact is a Turing Machine simulator that simulates a Turing machine with from one to three tapes. The timing target centered on generalizations of the classical Towers of Hanoi problem. The traditional Towers of Hanoi problem appears in many computing texts as a recursion example. Our study of the Towers of Hanoi problem led to the observation that there is no formal proof for the Towers of Hanoi problem when more than three spindles are used. This problem lends itself to substantial experimentation among the students as they compete to develop the program with the best timing results. All software developed through this grant has been forwarded for inclusion in the Public Ada Library (PAL) DTIC

N94-33287*# National Aeronautics and Space Administration. Goddard Space Flight Center, Greenbelt, MD.
MODIS. VOLUME 1: MODIS LEVEL 1A SOFTWARE BASELINE REQUIREMENTS
Edward Masuoka, Albert Fleig, Philip Ardanuy, Thomas Goff, Lloyd Carpenter, Carl Solomon, and James Storey Apr. 1994 78 p
(Contract NAS5-31331; RTOP 920-00-00)
(NASA-TM-104594-Vol-1; Rept-94B00058-Vol-1; NAS 1.15:104594-Vol-1)
Avail: CASI HC A05/MF A01

This document describes the level 1A software requirements for the moderate resolution imaging spectroradiometer (MODIS) instrument. This includes internal and external requirements. Internal requirements include functional, operational, and data processing as well as performance, quality, safety, and security engineering requirements. External requirements include those imposed by data archive and distribution systems (DADS); scheduling, control, monitoring, and accounting (SCMA); product management (PM) system; MODIS log; and product generation system (PGS). Implementation constraints and requirements for adapting the software to the physical environment are also included. Author (revised)

N94-31120*# Louisiana State Univ., Baton Rouge. Dept. of Physics and Astronomy.
AN EFFICIENT THREE-DIMENSIONAL POISSON SOLVER FOR SIMD HIGH-PERFORMANCE-COMPUTING ARCHITECTURES Abstract Only
H. Cohl *In* Lunar and Planetary Inst., Workshop on Physics of Accretion Disks Around Compact and Young Stars 1994 p 1 (For primary document see N94-31116 09-90)
(Grants NAGw-2447; NSF AST-90-08166)
Avail: CASI HC A01/MF A01

N94-32429*# Wright Lab., Wright-Patterson AFB, OH. Avionics Directorate.
COMMON MODELING SYSTEM FOR DIGITAL SIMULATION
Rick Painter *In* NASA, Washington, Technology 2003: The Fourth National Technology Transfer Conference and Exposition, Volume 2 Feb. 1994 p 65-79 (For primary document see N94-32420 09-99)
Avail: CASI HC A03/MF A04

N94-32430*# PDA Engineering, Santa Ana, CA.
ANALYTICAL DESIGN PACKAGE (ADP2): A COMPUTER AIDED ENGINEERING TOOL FOR AIRCRAFT TRANSPARENCY DESIGN
J. E. Wuerer, M. Gran, and T. W. Held *In* NASA, Washington, Technology 2003: The Fourth National Technology Transfer Conference and Exposition, Volume 2 Feb. 1994 p 80-92 (For primary document see N94-32420 09-99)
Avail: CASI HC A03/MF A04

N94-32431*# Allied-Signal Corp., Kansas City, MO.
ASSEMBLY FLOW SIMULATION OF A RADAR
W. C. Rutherford and P. M. Biggs *In* NASA, Washington, Technology 2003: The Fourth National Technology Transfer Conference and Exposition, Volume 2 Feb. 1994 p 93-96 (For primary document see N94-32420 09-99)
(Contract DE-AC04-76DP-00613)
Avail: CASI HC A01/MF A04

N94-32432*# National Aeronautics and Space Administration. Lyndon B. Johnson Space Center, Houston, TX.
CONFIG: INTEGRATED ENGINEERING OF SYSTEMS AND THEIR OPERATION
Jane T. Malin, Dan Ryan, and Land Fleming *In* NASA, Washington, Technology 2003: The Fourth National Technology Transfer Conference and Exposition, Volume 2 Feb. 1994 p 97-104 (For primary document see N94-32420 09-99)
Avail: CASI HC A02/MF A04

N94-32436*# Ensco, Inc., Melbourne, FL.
A SYSTEMS APPROACH TO COMPUTER-BASED TRAINING
Gaylen W. Drape *In* NASA, Washington, Technology 2003: The Fourth National Technology Transfer Conference and Exposition, Volume 2 Feb. 1994 p 130-136 (For primary document see N94-32420 09-99)
Avail: CASI HC A02/MF A04

N94-32438*# Idaho National Engineering Lab., Idaho Falls.
A PC PROGRAM TO OPTIMIZE SYSTEM CONFIGURATION FOR DESIRED RELIABILITY AT MINIMUM COST
Steven W. Hills and Ali S. Siahpush *In* NASA, Washington, Technology 2003: The Fourth National Technology Transfer Conference and Exposition, Volume 2 Feb. 1994 p 143-150 (For primary document see N94-32420 09-99)
Avail: CASI HC A02/MF A04

N94-32439*# Defense Mapping Agency Systems Center, Fairfax, VA.
EVOLVING SOFTWARE REENGINEERING TECHNOLOGY FOR THE EMERGING INNOVATIVE-COMPETITIVE ERA
Phillip Q. Hwang, Evan Lock, and Noah Prywes *In* NASA, Washington, Technology 2003: The Fourth National Technology Transfer Conference and Exposition, Volume 2 Feb. 1994 p 151-160 (For primary document see N94-32420 09-99)
Avail: CASI HC A02/MF A04

62 COMPUTER SYSTEMS

Includes computer networks and special application computer systems.

N94-31099 Ecole Nationale Superieure des Telecommunications, Paris (France). Dept. Signal.
IMPLANTING ALGORITHMS ON PARALLEL MACHINES [IMPLANTATION D'ALGORITHMES SUR MACHINES PARALLELES]
Jesus Sanchez Oct. 1993 84 p In FRENCH Limited Reproducibility: More than 20% of this document may be affected by microfiche quality
(ISSN 1242-1345)
(TELECOM-93-D-017; ETN-94-95891) Avail: CASI HC A05

The implanting of algorithms on parallel machines necessitates knowledge of the algorithm and, more markedly than for sequential machines, of the target architecture. The adequation between the algorithm and the architecture is fundamental for obtaining performant implantations. A greedy approach consisting of using the most resources possible (processors, communication links, buses, etc.) of the parallel machines, that is, to 'parallelize' the algorithm to the maximum, can bring an important improvement in the calculation time caused by problems due to the communication, synchronization between processors, etc. The hardware and software on which implantation is to take place must therefore be well understood. The characteristics of the different hardware topologies normally used by parallel machine builders are described, and criteria to use to compare them are addressed. The software part of implantations is addressed, describing the principal programming languages used in parallel machines and the different existing interprocessor mechanisms. ESA

N94-31149# Sandia National Labs., Albuquerque, NM.
SANDIA'S RESEARCH NETWORK FOR SUPERCOMPUTING 1993: A DEMONSTRATION OF ADVANCED TECHNOLOGIES FOR BUILDING HIGH-PERFORMANCE NETWORKS
S. A. Gossage and M. O. Vahle Dec. 1993 18 p
(Contract DE-AC04-94AL-85000)
(DE94-005319; SAND-93-3807) Avail: CASI HC A03/MF A01

Supercomputing '93, a high-performance computing and communications conference, was held November 15th through 19th, 1993 in Portland, Oregon. For the past two years, Sandia National Laboratories has used this conference to showcase and focus its communications and networking endeavors. At the 1993 conference, the results of Sandia's efforts in exploring and utilizing Asynchronous Transfer Mode (ATM) and Synchronous Optical Network (SONET) technologies were vividly demonstrated by building and operating three distinct networks. The networks encompassed a Switched Multimegabit Data Service (SMDS) network running at 44.736 megabits per second, an ATM network running on a SONET circuit at the Optical Carrier (OC) rate of 155.52 megabits per second, and a High Performance Parallel Interface (HIPPI) network running over a 622.08 megabits per second SONET circuit. The SMDS and ATM networks extended from Albuquerque, New Mexico to the showroom floor, while the HIPPI/SONET network extended from Beaverton, Oregon to the showroom floor. This paper documents and describes these networks. DOE

N94-31177 Politecnico di Milano (Italy). Dipt. di Elettronica e Informazione.

THE ANT SYSTEM: AN AUTOCATALYTIC OPTIMIZING PROCESS

Marco Dorigo, Vittorio Maniezzo, and Alberto Colorni Sep. 1993 37 p (Rept-91-016-Rev; ETN-94-95802) Avail: Issuing Activity (Politecnico di Milano, Piazza Leonardo da Vinci 32, 20133 Milan, Italy)

An analogy with the way ant colonies function suggested the definition of a new computational paradigm, called the 'ant system'. It is proposed as a viable approach to stochastic combinatorial optimization. The main characteristics of this model are positive feedback and distributed computation, together with the use of a constructive greedy heuristic. Positive feedback accounts for rapid discovery of good solutions, distributed computation avoids premature convergence, and the greedy heuristic helps the procedure to find acceptable solutions in the early stages of the search process. The proposed methodology is applied to the classical traveling salesman problem, and simulation results are reported. The working of the algorithm is discussed, and it is compared with tabu search and simulated annealing in the case of the traveling salesman problem. It is shown how the ant system can be applied to other optimization problems like the asymmetric traveling salesman, the quadratic assignment, and job shop scheduling. ESA

N94-31183 Ecole Nationale Superieure des Telecommunications, Paris (France). Dept. Informatique.

A PROBABILISTIC VIEW OF DATALOG PARALLELIZATION

Sergio Lifschitz and Victor Vianu 1993 20 p Limited Reproducibility: More than 20% of this document may be affected by microfiche quality

(Grants CAPES/MEC-1245/90-13; NSF IRI-92-21268) (ISSN 0751-1353) (TELECOM-93-D-021; ETN-94-95894) Avail: Issuing Activity (European Space Agency (ESA))

A pure parallelization strategy applicable to all Datalog programs is proposed. Since completeness is not guaranteed, a complementary single processor evaluation step has to be foreseen, which can be very costly in some cases. However, it is shown that in most cases, the global performance of the algorithm (including complementary step) is excellent. This is justified by a probabilistic analysis of the behavior of the algorithm and by results of implantations on randomly generated data. It is considered that any information on the data base is available and therefore, that every instance holds. In practice this is not always true. In this case for more structured data, the strategy no longer presents a good behavior. With more information on the data, adaptations must be foreseen so that good performances can be attained. ESA

N94-31249# Naval Postgraduate School, Monterey, CA. Dept. of Computer Science.

SCHEDULING TECHNIQUES FOR MULTIPLE PROCESSOR SYSTEMS IN REAL-TIME ENVIRONMENTS M.S. Thesis

John H. Quigg Sep. 1993 76 p

(AD-A276149) Avail: CASI HC A05/MF A01

Directed Acyclic Graph Scheduling is a technique used to implement the real-time execution of Digital Signal Processing applications on multiple-processor data-flow machines that support variable-grained parallelism. The approach used in the Navy's AN/UYS-2 Digital Signal Processor statically schedules an application graph at run-time using a First-Come-First-Served (FCFS) policy. Research by Shukla and Zaky Shukla 91 developed a new algorithm, the Revolving Cylinder (RC), to ameliorate the inherently non-deterministic output flow of the FCFS scheduling approach currently used in the system. Although the RC technique solved the problem of output-flow determinism there was no broad coverage of other current research in the very specialized field of real-time data-flow machines. This thesis reviews Revolving Cylinder analysis and then surveys, compares, and evaluates research in the field using the review as a baseline for comparison. The RC approach is best at improving the throughput and output flow determinism of a narrow range of applications on a particular architecture. Each of the other approaches offer improvements over RC scheduling in either performance as measured by throughput or through flexibility in applications handled. For each of these improvements, however, significant trade-offs are made and so improvements become relative when they affect system robustness and an ability to handle repeated execution of application graphs. The AN/UYS-2 can implement RC scheduling with a minimum of cost and no hardware reconfiguration and this makes it the best approach for short-term system. DTIC

N94-31259 Carnegie-Mellon Univ., Pittsburgh, PA. Dept. of Computer Science.

LIST RANKING AND LIST SCAN ON THE CRAY C-90

Margaret Reid-Miller and Guy E. Blelloch 16 Feb. 1994 37 p Limited Reproducibility: More than 20% of this document may be affected by microfiche quality

(Contract F33615-93-1-1330; NSF CCR-92-58525)

(AD-A276411; CMU-CS-94-101) Avail: CASI HC A03

List ranking and list scan are two primitive operations used in many parallel algorithms that use list, trees, and graph data structures. But vectorizing and parallelizing list ranking is a challenge because it is highly communication intensive and dynamic. In addition, the serial algorithm is very simple and has very small constants. In order to compete a parallel algorithm must also be simple and have small constants. A parallel algorithm due to Wyllie is such an algorithm, but it is not work efficient -- its performance degrades for longer and longer linked lists. In contrast, work efficient PRAM algorithms developed to date have very large constants. We introduce a new fully vectorized and parallelized algorithm that is both work efficient and has small constants. However, it does not achieve O(log n) running time. But we contend that work efficiency and small constants is more important, given that vector and multiprocessor machines are used for problems that are much larger than the number of processors and, therefore, the O(log n) time is never achieved in practice. In particular, to the best of our knowledge our implementation of list ranking and list scan on the CRAY C-90 is the fastest implementation to date. In addition, it is the first implementation of which we are aware that outperforms fast workstations. DTIC

N94-31641# Technische Univ., Delft (Netherlands). Faculty of Technical Mathematics and Informatics.

SOME CALCULATIONS ON SUPERSYMMETRIC GRAPHS AS COMMUNICATION NETWORKS

P. G. Kluit 1993 18 p

(ISSN 0922-5641)

(Rept-93-72; ETN-94-96117) Copyright Avail: CASI HC A03/MF A01

A mathematical comment on Peper's study on efficient network topologies for extensible massively parallel computers is presented. Peper studied the application of supersymmetric planar graphs as communication networks in massively parallel computers. Essential in such a network is the presence of some simple routing function. A routing function in a network gives for every pair of nodes P and Q a signpost that indicates which way to start for a shortest path from P to Q. Unfortunately, such a routing function is absent in Peper's exposition. By embedding the graph in a hyperbolic plane and applying some simple differential geometry, a routing function is supplied. The same embedding allows for a very concise proof of the theorem that supersymmetric graphs are smooth (that is, contain no extreme nodes). Peper proves this theorem in a combinatorial nonuniform way, considering several cases and subcases. Another detailed combinatorial analysis is found in Peper's derivation of the uniform exponentiality of supersymmetric graphs. The simplification of this derivation by using some hyperbolic geometry is questioned. It turns out that it can be simplified without using hyperbolic geometry. ESA

N94-31662# Technische Univ., Delft (Netherlands). Faculty of Technical Mathematics and Informatics.
INVARIANCE OF THE GENERALIZED STEADY-STATE FOR 1-D DISTRIBUTED PARAMETER SYSTEMS
L. Dekker 15 Aug. 1993 19 p
(ISSN 0922-5641)
(Rept-93-66; ETN-94-96111) Copyright Avail: CASI HC A03/MF A01

Invariance is proven for some linear 1-D (one dimensional) distributed parameter systems. Discussions are based upon the use of a mathematical formulation of the generalized steady state as an infinite series expansion of the time derivatives of the two corner input signals. This formulation, together with the property of decomposition invariance, offers easy to exploit massive parallelism. Spatial decomposition invariance is considered for 1-D diffusion systems. The boundary conditions of the diffusion system are conceived to be corner input signals forcing a uniquely defined 2-corner generalized steady state onto the diffusion system. It is proven that this 2-corner generalized steady state has the property to be invariant under spatial system decomposition. Spatial decomposition invariance of the generalized steady state is further considered for two other 1-D distributed parameter systems of second order in space: a diffusion system with uniformly distributed damping and a convection diffusion system. It is pointed out for the convection diffusion system that the proof used for the diffusion system (without damping) remains valid, because of the structure of this proof, for other 1-D distributed parameter systems. It is also shown, through transformation of a convection diffusion system successively into a diffusion system with damping and then into a diffusion system, that the generalized steady state is invariant under transformation of the state variable. ESA

N94-31663# Argonne National Lab., IL.
A COMPARISON OF DISTRIBUTED MEMORY AND VIRTUAL SHARED MEMORY PARALLEL PROGRAMMING MODELS
J. A. Keane (Manchester Univ., England.), A. J. Grant (Manchester Univ., England.), and M.-Q. Xu Apr. 1993 16 p Presented at the 4th Meiko User Society Conference, Southampton, England, Apr. 1993
(Contract W-31-109-eng-38)
(DE94-005473; ANL/MCS/CP-81645; CONF-9304227-1) Avail: CASI HC A03/MF A01

The virtues of the different parallel programming models, shared memory and distributed memory, have been much debated. Conventionally the debate could be reduced to programming convenience on the one hand, and high scalability factors on the other. More recently the debate has become somewhat blurred with the provision of virtual shared memory models built on machines with physically distributed memory. The intention of such models/machines is to provide scalable shared memory, i.e. to provide both programmer convenience and high scalability. In this paper, the different models are considered from experiences gained with a number of systems ranging from applications in both commerce and science to languages and operating systems. Case studies are introduced as appropriate. DOE

N94-31700# Technische Univ., Delft (Netherlands). Faculty of Technical Mathematics and Informatics.
GENERALIZED STEADY-STATE METHOD FOR SOLVING 2-D DIFFUSION SYSTEMS
L. Dekker 1993 20 p
(ISSN 0922-5641)
(Rept-93-83; ETN-94-96128) Copyright Avail: CASI HC A03/MF A01

Massively parallel modeling of distributed parameter systems through the generalized steady state method is described. This method is explained for one and two dimensional diffusion systems. The arising models are shown to contain explicit parallelism proportional to the physical size of the system. This together with the invariance property under spatial system decomposition makes these models promising for simulation of distributed parameter systems through massively parallel processing. ESA

N94-31920# Lawrence Livermore National Lab., CA.
THE FELICIA BULLETIN BOARD SYSTEM AND THE IRBIS ANONYMOUS FTP SERVER: COMPUTER SECURITY INFORMATION SOURCES FOR THE DOE COMMUNITY
W. J. Orvis 3 Nov. 1993 22 p
(Contract W-7405-eng-48)
(DE94-008219; UCRL-MA-115837) Avail: CASI HC A03/MF A01

The Computer Incident Advisory Capability (CIAC) operates two information servers for the DOE community, FELICIA (formerly FELIX) and IRBIS. FELICIA is a computer Bulletin Board System (BBS) that can be accessed by telephone with a modem. IRBIS is an anonymous ftp server that can be accessed on the Internet. Both of these servers contain all of the publicly available CIAC, CERT, NIST, and DDN bulletins, virus descriptions, the VIRUS-L moderated virus bulletin board, copies of public domain and shareware virus-detection/protection software, and copies of useful public domain and shareware utility programs. This guide describes how to connect these systems and obtain files from them. DOE

N94-32032# Columbia Univ., New York, NY. Dept. of Chemistry.
COMBINATORIAL ION SENSORS Annual Report, 15 Feb. 1993 - 14 Feb. 1994
W. C. Still 14 Feb. 1994 2 p
(Contract N00014-93-1-0288)
(AD-A276567) Avail: CASI HC A01/MF A01

The objective is to develop a massively parallel combinatorial method for preparing and screening ionophores which selectively bind group IIB and divalent transition metals. The accomplishments were: During the past year, we have prepared for and begun preparation of an encoded combinatorial library of cyclen-based receptors and also validated a color-based assay for detecting certain metal-binding ligands. The latter study was designed as a positive control to show that good metal-binding polymer-supported ligands could be detected visually from a library of relatively poor ionophoric ligands. DTIC

N94-32052 Massachusetts Univ., Amherst.
PROBLEMS IN SURVIVABLE MULTI-MEDIA NETWORKS Final Report
C. G. Cassandras, J. F. Kurose, and D. Towsley 1994 5 p Limited Reproducibility: More than 20% of this document may be affected by microfiche quality
(Contract N00014-90-J-1293)
(AD-A277370) Avail: CASI HC A01

Our research funded under ONR contact N00014-90-J-1293 can be broadly divided into three areas: (1) call admission in high speed networks; (2) optimal routing in the presence of state information; and (3) the effects of model uncertainties on routing in networks. DTIC

N94-32165# Massachusetts Inst. of Tech., Cambridge. Artificial Intelligence Lab.
THE NAMED-STATE REGISTER FILE
Peter R. Nuth Aug. 1993 129 p
(Contract N00014-88-K-0738)
(AD-A276796; AI-TR-1459) Avail: CASI HC A07/MF A02

This thesis introduces the Named-State Register File (NSF), a fine-grain, fully-associative register file. The NSF allows fast context switching between concurrent threads as well as efficient sequential program performance. The NSF holds more live data than conventional register files, and it requires less spill and reload traffic to switch between contexts. This thesis demonstrates an implementation of the Named-State Register File and estimates the access time and chip area required for different organizations. Architectural simulations of large sequential and parallel applications show that the NSF can reduce execution time by 9% to 17% compared to alternative register files. DTIC

N94-32196 Nijmegen Univ. (Netherlands). Dept. of Informatics.
TRANSFORMATIONAL DERIVATION OF (PARALLEL) PROGRAMS USING SKELETONS
Eerke A. Boiten (Technische Univ., Eindhoven, Netherlands.), A. Max Geerling, and Helmut A. Partsch Sep. 1993 18 p Limited Reproducibility: More than 20% of this document may be affected by microfiche quality
(Grant NF-63/62-518)
(TR-93-20; ETN-94-96214) Avail: Issuing Activity (European Space Agency (ESA))

A framework for the derivation of programs for arbitrary (in particular, parallel) architectures, motivated by a generalization of the derivation process for sequential algorithms is described. The central concept in this approach is that of a skeleton: on the one hand, a higher order function for targeting transformational derivations, and, on the other hand, representing an elementary computation on the intended architecture. Skeletons thus form a basis for intermediate languages, that can be implemented once and for all, as a process separate from individual program developments. The

available knowledge on the derivation of (higher order) functional programs can be used for deriving parallel ones. The method is reviewed and illustrated with an example (trapezoidal rule on SIMD processor array). ESA

N94-32243 Massachusetts Inst. of Tech., Cambridge.
PARALLEL AND DISTRIBUTED COMPUTING COMBINATORIAL ALGORITHMS Final Report, 1 Feb. 1992 - 31 Oct. 1993
Tom Leighton 1 Oct. 1993 25 p Limited Reproducibility: More than 20% of this document may be affected by microfiche quality
(Contract F49620-92-J-0125)
(AD-A277333; AFOSR-94-0051TR) Avail: CASI HC A03

The first methods for tolerating more than a small number of worst-case faults in commonly used networks such as the butterfly, the mesh of trees, and other hypercubic networks are presented. Previously, work on the fault tolerance properties of these networks was limited to showing how to overcome a single fault by adding an extra stage of hardware to the networks. DTIC

N94-32248# Argonne National Lab., IL.
MOVING BASISplus AND TECHLIBplus FROM VAX/VMS TO UNIX
R. Dominiak 1993 20 p Presented at the 1993 Annual Information Dimensions Exchange Association Meeting, San Diego, CA, 15-19 Nov. 1993
(Contract W-31-109-eng-38)
(DE94-004696; ANL/IPD/CP-81274; CONF-9311152-1) Avail: CASI HC A03/MF A01

BASISplus is used at the Laboratory by the Technical Information Services (TIS) Department which is part of the Information and Publishing Division at ARGONNE. TIS operates the Argonne Information Management System (AIM). The AIM System consists of the ANL Libraries On-Line Database (a TECHLIBplus database), the Current Journals Database (IDI's current contents search), the ANL Publications Tracking Database (a TECHLIBplus database), the Powder Diffraction File Database, and several CD-ROM databases available through a Novell network. The AIM System is available from the desktop of ANL staff through modem and network connections, as well as from the 10 science libraries at ARGONNE. TIS has been a BASISplus and TECHLIBplus site from the start, and never migrated from BASIS K. The decision was made to migrate from the VAX/VMS platform to a UNIX platform. Migrating a product from one platform to another involves many decisions and considerations. These justifications, decisions, and considerations are explored in this report. DOE

N94-32274 Electronics Research Lab., Adelaide (Australia).
PARALLEL PROCESSING FOR DIFFERENCING AND HISTOGRAMMING
Vaughan Clarkson and Pinaki S. Ray Oct. 1993 32 p Limited Reproducibility: More than 20% of this document may be affected by microfiche quality
(AD-A277060; ERL-0692-RR; DODA-AR-008-135) Avail: Issuing Activity (Defense Technical Information Center (DTIC))

Algorithms which take advantage of massively parallel and vector architectures are formulated for the calculation of the differences of times-of-arrival derived from a sequence of time samples. The application which generated the work is the classification of pulse trains which are detected by an electronic support measures receiver. Four algorithms are proposed, of which three have been implemented and tested on several machines. The results obtained through testing are compared with each other and with results for more conventional architectures. It is found that one of the machines, the massively parallel MASPAR MP-1 computer, is able to perform histogramming fastest through exploitation of its data-parallel architecture. Several suggestions are made which could significantly improve performance on all architectures. DTIC

N94-32291 Nijmegen Univ. (Netherlands). Dept. of Mathematics and Computer Science.
AN EPISTEMIC PROOF SYSTEM FOR PARALLEL PROCESSES
M. vanHulst and J.-J. C. Meyer 16 Aug. 1993 21 p Limited Reproducibility: More than 20% of this document may be affected by microfiche quality
(TR-93-17; ETN-94-96211) Avail: Issuing Activity (European Space Agency (ESA))

A study aiming to employ epistemic logic to reason about parallel programs is presented. A proof system for the correctness of parallel programs using knowledge in distributed systems is presented and proven sound and relatively complete with respect to a formal Kripke style semantics that supports truly concurrent computations. ESA

N94-32323# Naval Undersea Warfare Center, Newport, RI.
MASSIVELY PARALLEL SYSTEMS DESIGN FOR REAL-TIME EMBEDDED APPLICATIONS
Thomas C. Choinski and Chin-Hwa Lee 14 Feb. 1994 16 p Presented at the Systems Reengineering Technology Workshop, Monterey, CA, 8-10 Feb. 1994
(AD-A277256; NUWC-NPT-10591) Avail: CASI HC A03/MF A01

This paper describes a generic approach to mitigate risk when reengineering for high throughput massively parallel systems. The approach entails baselining the existing system, capturing the functional requirements, estimating initial processing requirements through a high level analysis, benchmarking a subset of the functionality on a low throughput computer, and modeling the high throughput application to determine the detailed processing requirements for scaling. DTIC

N94-32356# Los Alamos National Lab., NM.
THE OPERATOR SHELL: A MEANS OF PRIVILEGE DISTRIBUTION UNDER UNIX
M. Neuman and G. Christoph 1994 10 p Presented at the 3rd FedUNIX Annual Conference on System Administration, Networking, and Security, Washington, DC, 4-9 Apr. 1994
(Contract W-7405-eng-36)
(DE94-007566; LA-UR-94-604; CONF-9404110-1) Avail: CASI HC A02/MF A01

The Operator Shell (Osh) is a setuid root, security enhanced, restricted shell for providing fine-grain distribution of system privileges for a wide range of usages and requirements. Osh offers a marked improvement over other Unix privilege distribution systems in its ability to specify access to both commands and files, auditing features, and familiar interface. This paper describes the design, features, security considerations, internals, and applications of the Operator Shell. DOE

N94-32357# Argonne National Lab., IL.
PARALLEL MONTE CARLO REACTOR NEUTRONICS
R. N. Blomquist and F. B. Brown 1994 7 p Presented at the 1994 Society for Computer Simulation Multiconference, San Diego, CA, 11-15 Apr. 1994
(Contract W-31-109-eng-38)
(DE94-007642; ANL/RA/CP-81815; CONF-940456-12) Avail: CASI HC A02/MF A01

The issues affecting implementation of parallel algorithms for large-scale engineering Monte Carlo neutron transport simulations are discussed. For nuclear reactor calculations, these include load balancing, recoding effort, reproducibility, domain decomposition techniques, I/O minimization, and strategies for different parallel architectures. Two codes were parallelized and tested for performance. The architectures employed include SIMD, MIMD-distributed memory, and workstation network with uneven interactive load. Speedups linear with the number of nodes were achieved. DOE

N94-32482*# Electronic Associates, Inc., Long Branch, NJ.
CONSTRUCTION OF A PARALLEL PROCESSOR FOR SIMULATING MANIPULATORS AND OTHER MECHANICAL SYSTEMS Final Report, Apr. 1990 - Aug. 1991
George Hannauer 20 Aug. 1991 58 p
(Contract NAS5-30905; SBIR-05.03-1100)
(NASA-CR-191327; NAS 1.26:191327) Avail: CASI HC A04/MF A01

This report summarizes the results of NASA Contract NAS5-30905, awarded under phase 2 of the SBIR Program, for a demonstration of the feasibility of a new high-speed parallel simulation processor, called the Real-Time Accelerator (RTA). The principal goals were met, and EAI is now proceeding with phase 3: development of a commercial product. This product is scheduled for commercial introduction in the second quarter of 1992. Author (revised)

N94-32483*# Integrated Parallel Technology, Pleasanton, CA.
VME ROLLBACK HARDWARE FOR TIME WARP MULTIPROCESSOR SYSTEMS Final Report

Michael J. Robb and Calvin A. Buzzell 25 Sep. 1992 51 p
(Contract NAS7-1102; SBIR-06.08-4448)
(NASA-CR-191796; NAS 1.26:191796) Avail: CASI HC A04/MF A01

The purpose of the research effort is to develop and demonstrate innovative hardware to implement specific rollback and timing functions required for efficient queue management and precision timekeeping in multiprocessor discrete event simulations. The previously completed phase 1 effort demonstrated the technical feasibility of building hardware modules which eliminate the state saving overhead of the Time Warp paradigm used in distributed simulations on multiprocessor systems. The current phase 2 effort will build multiple pre-production rollback hardware modules integrated with a network of Sun workstations, and the integrated system will be tested by executing a Time Warp simulation. The rollback hardware will be designed to interface with the greatest number of multiprocessor systems possible. The authors believe that the rollback hardware will provide for significant speedup of large scale discrete event simulation problems and allow multiprocessors using Time Warp to dramatically increase performance. Derived from text

N94-32646# Argonne National Lab., IL.
GIGABITS TO THE DESKTOP: INSTALLING TOMORROW'S NETWORKS TODAY
Timothy C. Kuhfuss and Paul T. Phillips 1994 20 p Presented at the International Conference on Advanced Science and Technology, Naperville, IL, 1 Mar. 1994
(Contract W-31-109-eng-38)
(DE94-007701; ANL/ECT/CP-82125; CONF-940377-1) Avail: CASI HC A03/MF A01

Argonne is one of the US Department of Energy's world class research institutions. Leading edge computing tools and networks allow Argonne to maintain and enhance this reputation. One current effort to deploy leading edge tools is the Argonne 'Gigabits to the Desktop' project. While the delivering and using gigabits to the desktop is little more than a hope at this time, this paper discusses the hurdles to achieving it and how to tear down as many hurdles as possible. Under this project, four distinct areas are being investigated and enhanced. This paper discusses briefly the applications and tools that we see driving the requirement for gigabits to the desktop. It will touch on a functional description of our ideal workstations, architectures and the candidates for the next generation network capable of delivering gigabits. Lastly, it provides an in-depth analysis of physical layer options and attempt to prove that this area, while the least risky, must be done properly, with the proper media. This paper assumes one important point. It assumes that bandwidth is essentially free. We discuss network architectures and physical installation recommendations which have a fixed cost. However, on a campus, there is no marginal cost for additional packets on these networks once the network infrastructure is installed. This point is important when extrapolating our conclusions to the wide area. The marginal cost of a packet sent to a commercial network is usually nonzero. This fact may prove to be a great hindrance in migrating the applications mentioned beyond the organizational boundaries. DOE

N94-32683 Ames Lab., IA.
DEVELOPMENT OF A LOW-LATENCY SCALAR COMMUNICATION ROUTINE ON MESSAGE-PASSING ARCHITECTURES Ph.D. Thesis
R. Pai 11 Jan. 1994 68 p Limited Reproducibility: More than 20% of this document may be affected by microfiche quality
(Contract W-7405-eng-82)
(DE94-007061; IS-T-1704) Avail: Issuing Activity (Department of Energy (DOE))

One of the most significant advances in computer systems over the past decade is parallel processing. To be scalable to a large number of processing nodes and to be able to support multiple levels and forms of parallelism and its flexible use, new parallel machines have to be multicomputer architectures that have general networking support and extremely low internode communication latencies. The performance of a program when ported to a parallel machine is limited mainly by the internode communication latencies of the machine. Therefore, the best parallel applications are those that seldom require communications which must be routed through the nodes. Thus the ratio of computation time to that of communication time is what determines, to a large extent, the performance metrics of an algorithm. The cost of synchronization and load imbalance appear secondary to that of the time required for internode communication and I/O, for communication intensive applications. This thesis is organized in chapters. The first chapter deals with the communication strategies in various message-passing computers. A taxonomy of inter-node communication strategies is presented in the second chapter and a comparison of the strategies in some existing machines is done. The implementation of communication in nCUBE Vertex O.S is explained in the third chapter. The fourth chapter deals with the communication routines in the Vertex O.S, and the last chapter explains the development and implementation of the scalar communication call. Finally some conclusions are presented. DOE

N94-32734*# Odyssey Research Associates, Inc., Ithaca, NY.
FORMAL SEMANTICS FOR A SUBSET OF VHDL AND ITS USE IN ANALYSIS OF THE FTPP SCOREBOARD CIRCUIT Report, Jan. - Dec. 1992
Mark Bickford 5 Apr. 1994 67 p
(Contract NAS1-18972; RTOP 505-64-10-13)
(NASA-CR-191577; NAS 1.26:191577; TM-92-0045) Avail: CASI HC A04/MF A01

In the first part of the report, we give a detailed description of an operational semantics for a large subset of VHDL, the VHSIC Hardware Description Language. The semantics is written in the functional language Caliban, similar to Haskell, used by the theorem prover Clio. We also describe a translator from VHDL into Caliban semantics and give some examples of its use. In the second part of the report, we describe our experience in using the VHDL semantics to try to verify a large VHDL design. We were not able to complete the verification due to certain complexities of VHDL which we discuss. We propose a VHDL verification method that addresses the problems we encountered but which builds on the operational semantics described in the first part of the report. Author

N94-32995# Washington Univ., Seattle. Dept. of Computer Science and Engineering.
PRINCIPLES OF ULTRADEPENDABILITY IN CHAOTIC ROUTING Final Report, 1 Oct. 1990 - 30 Sep. 1993
Lawrence Snyder 30 Sep. 1993 9 p
(Contract N00014-91-J-1007)
(AD-A277422) Avail: CASI HC A02/MF A01

Generally, the routers that are used in state-of-the-art parallel computers are a form of oblivious router known as demonstration order routers. Examples include the iPSC/2, nCUBE, DELTA, Paragon, Dash, J-Machine, etc. In networks based on these routers, all packets between source S and destination D take a single path, oblivious to network congestion and faults. This can lead to the following: poor performance under high loads when congestion can be significant; and system failure in large or unmaintainable systems where faults are likely. For these two reasons--performance and dependability--adaptive routing techniques have long been advocated. Adaptive routers can be divided into two broad classes, minimal adaptive, in which packets always take a shortest path to their destinations, and nonminimal adaptive, in which packet routes are not restricted to shortest paths. Though there have been many proposals for both types, it is generally true that nonminimal adaptive routers are superior minimal adaptive routers. This is consistent with one's intuition. Although a minimal adaptive router can bypass congestion by sending packets along alternate paths, they discover the congestion too late. That is, when there are no alternate forward paths to choose from, the packet's forward progress is stalled and is now contributing to the congestion. This affect motivates nonminimal adaptive routing in which a packet can back up or deroute, and go around congestion when there are no forward paths. DTIC

N94-33002 Center for Mathematics and Computer Science, Amsterdam (Netherlands). Dept. of Computer Science.
FINDING ALL PERIODS AND INITIAL PALINDROMES OF A STRING IN PARALLEL
Dany Breslauer and Zvi Galil Nov. 1992 13 p Limited Reproducibility: More than 20% of this document may be affected by microfiche quality
(Grant NSF CCR-90-14605) (ISSN 0169-118X)
(AD-B175069; CWI-CS-R9248; ETN-94-94728) Copyright Avail: CASI HC A03

An optimal O(log log n) time CRCW-PRAM algorithm for computing all period lengths of a string is presented. Previous parallel algorithms compute the period only if it is shorter than half of the length of the string. The

algorithm can be used to find all initial palindromes of a string in the same time and processor bounds. Both algorithms are the fastest possible over a general alphabet. A lower bound is derived for finding initial palindromes by modifying a known lower bound for finding the period length of a string. When p processors are available the bounds become Theta((n/p) + log log(sub (1 + p)/n) 2p). ESA

N94-32440*# Dakota Scientific Software, Inc., Rapid City, SD. Dept. of Computer Science.
A HIGH-SPEED LINEAR ALGEBRA LIBRARY WITH AUTOMATIC PARALLELISM
Michael L. Boucher *In* NASA, Washignton, Technology 2003: The Fourth National Technology Transfer Conference and Exposition, Volume 2 Feb. 1994 p 161-168 (For primary document see N94-32420 09-99)
Avail: CASI HC A02/MF A04

63 CYBERNETICS

Includes feedback and control theory, artificial intelligence, robotics and expert systems.

For related information see also *54 Man/System Technology and Life Support.*

N94-31061# Thinkalong Software, Inc., Brownsville, CA.
DISCOVERY SYSTEMS FOR MANUFACTURING Final Report, 1 Dec. 1991 - 1 Dec. 1993
Dan Woods and Jack Parks Jan. 1994 108 p
(Contract F33615-92-C-5802)
(AD-A276216; WL-TR-94-4008) Avail: CASI HC A06/MF A02

This has been a three-part project: (1) enhancing generalized discovery tools on our existing computer platform, (2) building specialized discovery tools, and (3) applying generalized and specialized discovery tools to specific materials related projects including protein studies and crystallography. During the work, we have had the opportunity to incorporate some of our other activities, including studies we have done in biomedical fields using our discovery system. We have also folded in some of our external work in design. Portions of this other work are included in this report because it serves to illustrate key points we wish to make. This report includes portions of contributions made by our consultants, W. B. Dress and A. G. Jackson. We begin our report with a review of the philosophical aspects of what we call computational theory formation. We then present the computer tool that has been extended as part of this work, the goal of which is to address the issues brought up in the first section. Finally, the three different applications mentioned above are introduced. DTIC

N94-31064# Naval Postgraduate School, Monterey, CA. Dept. of Mechanical Engineering.
MACHINERY MONITORING AND DIAGNOSTICS USING PSEUDO WIGNER-VILLE DISTRIBUTION AND BACKPROPAGATION NEURAL NETWORK M.S. Thesis
Lloyd H. Jones Sep. 1993 54 p
(AD-A276219) Avail: CASI HC A04/MF A01

Artificial Neural Networks provide a data based approach to problem solving, patterned after neurological systems, which has proven successful on unique and noisy data. The pseudo Wigner-Ville distribution provides an excellent characterization of a stationary or non-stationary input signal by transforming a time signal into a joint time-frequency domain. This characterization provides an energy level associated with any processed characteristic frequency, which when used as an input to an artificial neural network will aide in the detection of location and severity of machinery faults. Research is presented where the union of an artificial neural network, utilizing the highly successful backpropagation paradigm, and the pseudo Wigner-Ville distribution are demonstrated and shown to provide remarkable success as a tool for machinery monitoring. DTIC

N94-31100 Ecole Nationale Superieure des Telecommunications, Paris (France). Dept. Images.
REPORT OF THE 'MATHEMATICAL MODELS FOR NEURAL NETWORKS' COURSE [RAPPORT DU STAGE 'MODELES MATHEMATIQUES POUR RESEAUX DE NEURONES']
Mireille Lefevre (Electricite de France, Chatou.) 1993 28 p In FRENCH Limited Reproducibility: More than 20% of this document may be affected by microfiche quality
(ISSN 1242-1345)
(TELECOM-93-D-019; ETN-94-95892) Avail: CASI HC A03

The training course 'mathematical models for neural networks' aimed to define a mathematical frame for the study of multilayer neural networks, considered as adaptive systems controlled by synaptic matrices. The developments presented are based on mathematical tools such as tensor products, convex analysis, and viability and control theory. The main points emphasized are the definition of an incremental learning algorithm named heavy algorithm, the elaboration of learning algorithms deduced from either gradient, subgradient or Newton methods and the building of special algorithms applied to control process. ESA

N94-31157# Loughborough Univ. of Technology (England). Dept. of Mathematical Sciences.
A GREEN'S FUNCTION APPROACH TO ANALYSING THE EFFECTS OF RANDOM SYNAPTIC BACKGROUND ACTIVITY IN A MODEL NEURAL NETWORK
Paul C. Bressloff Nov. 1993 31 p
(Maths-Rept-A-202; ETN-94-95862) Avail: CASI HC A03/MF A01

The effect of randomly distributed synaptic background activity on the states of self sustained firing in a model neural network with shunting is investigated. Using mean field theory, the steady state of the network is expressed in terms of an ensemble averaged single neuron Green's function. This Green's function is shown to satisfy a matrix equation identical in form to that found in the tight binding alloy model of excitations on a one dimensional disordered lattice. The ensemble averaging is then performed using a coherent potential approximation, thus allowing the steady state firing rate of the network to be determined. The firing rate is found to decrease as the mean level of background activity across the network is increased; a uniform background (zero variance) leads to a greater reduction than a randomly distributed one (nonzero variance). ESA

N94-31158# Loughborough Univ. of Technology (England). Dept. of Mathematical Sciences.
FEASIBILITY AND STABILITY RESULTS FOR CONSTRAINED STABLE GENERALIZED PREDICTIVE CONTROL
J. A. Rossiter, B. Kouvaritakis, and J. R. Gossner Nov. 1993 24 p
(Maths-Rept-A-203; ETN-94-95863) Avail: CASI HC A03/MF A01

Predictive control strategies which handle input and output constraints are considered. The difficulty with these approaches is that, in an attempt to optimize output tracking over a finite horizon, they tend to drive the controls to the constraint limits; this can lead to infeasibility which, in the case of systems with poles and/or zeros outside the unit circle, leads to instability. The necessary and sufficient conditions for feasibility and stability are developed and an algorithm which overcomes finite horizon infeasibility and gives stability and asymptotic tracking is presented. ESA

N94-31161# Loughborough Univ. of Technology (England). Dept. of Mathematical Sciences.
A DIRECT DIGITAL DESIGN FOR A MULTICHANNEL STRUCTURAL TEST SYSTEM USING THE CHARACTERISTIC LOCUS METHOD
J. A. Rossiter, R. W. Pratt, and K. J. Smith Dec. 1993 8 p Sponsored in cooperation with British Aerospace (Military Aircraft) Ltd.
(Grant SERC-GR/G59990)
(Maths-Rept-A-206; ETN-94-95866) Avail: CASI HC A02/MF A01

A direct digital design for multichannel structural test systems, which are used in aerospace and automotive industries to investigate fatigue and vibration properties of structures, is addressed. The direct digital design considered uses the charateristic locus method. The design process for a two input, two output system is described and compared to an earlier analog design which is shown to be unstable when implemented digitally. It was shown that an earlier design carried out in continuous time did not anticipate the effects of discretization and hence an apparently good design in continuous time led to a poor design in discrete time. However, if the design is carried out in discrete time such problems will not arise. It was also shown that design using an approximately exact commutative controller is much easier than a design using a more traditional CL design technique. ESA

N94-31176 Politecnico di Milano (Italy). Dipt. di Elettronica e Informazione.
ON THE USE OF GENETIC ALGORITHMS TO SOLVE THE TIME-TABLE PROBLEM
Alberto Colorni (Consiglio Nazionale delle Ricerche, Milan, Italy.), Marco Dorigo, and Vittorio Maniezzo Apr. 1992 26 p Revised
(Rept-90-060-Rev; ETN-94-95801) Avail: Issuing Activity (Politecnico di Milano, Piazza Leonardo da Vinci 32, 20133 Milan, Italy)

The results of an investigation of the possibilities offered by Genetic Algorithms (GA's) to solve the timetable problem are presented. This problem was chosen since it is representative of the class of multiconstrained, NP hard, combinatorial optimization problems with real world application. The model is presented, including the definition of a hierarchical structure for the objective function and the generalized genetic operators which can be applied to matrices representing timetables. The outcomes of the utilization of the implemented system to the specific case of the generation of a school timetable is reported. Two versions of the GA, with and without local search, are compared both to a handmade timetable and to two other approaches based on simulated annealing and tabu search. Results show that GA with local search and tabu search with relaxation both outperform simulated annealing and handmade timetables. ESA

N94-31186 Politecnico di Milano (Italy). Artificial Intelligence and Robotics Project.
CONCEPTS AND ENVIRONMENT [CONCETTI E AMBIENTE]
Anio O. Arigoni (Bologna Univ., Italy.), Vittorio Maniezzo, and Anna Navarra Apr. 1993 29 p In ITALIAN
(Rept-93-032; ETN-94-95804) Avail: Issuing Activity (Politecnico di Milano, Piazza Leonardo da Vinci 32, 20133 Milan, Italy)

A review of the principal psychological models proposed to explain the processes of concept formation consequent to interaction with the environment is presented. Only those models which are sufficiently advanced to allow an implementation on computer are reviewed. The objective is to identify fundamental aspects of the theory confronting the development of the cognitive structure in specific systems at the sensorimotor level. Consideration is given to which systems have the best results, in particular for defining new inductive classification and adaptive control algorithms for autonomous robots. ESA

N94-31193 Ecole Nationale Superieure des Telecommunications, Paris (France). Dept. Images.
ART: ADAPTIVE RESONANCE THEORY [LA FAMILLE ART]
Mireille Lefevre (Electricite de France, Chatou.) 1993 35 p In FRENCH Limited Reproducibility: More than 20% of this document may be affected by microfiche quality
(ISSN 1242-1345)
(TELECOM-93-D-020; ETN-94-95893) Avail: Issuing Activity (European Space Agency (ESA))

The ART theory developed by Carpenter and Grossberg is addressed. This theory yields to neuronal models which are capable of classifying a set of data in an unsupervised way and with an a priori unknown number of clusters emerging from the self organization. It is also possible to introduce a supervision by cooperation between several ART modules. ESA

N94-31207 Notre Dame Univ., IN.
CAMERA-SPACE MANIPULATION WITH NATURAL VISUAL INFORMATION Ph.D. Thesis
Umesh Arvind Korde 1993 159 p
Avail: Univ. Microfilms Order No. DA9328896

Camera-space manipulation is a precise and robust approach to robot hand/eye coordination in practical, three-dimensional situations. The acquisition of visual information necessary for camera-space manipulation has so far been simplified by placing easily detectable visual 'cues' on the objects involved in the task. This work concerns the development of an approach to speedy and precise extraction of visual information from 'natural' features on the objects. This approach invokes asymbiosis between the estimation procedure of camera-space manipulation and image analysis, in which each procedure builds on progressively improving information 'learned' by the other, both during a particular cycle of a repetitive task, and from one task-cycle to the next. The idea was implemented in a three-dimensional automobile wheel-loading task, in which the natural features were circular. The relative locations of video cameras were such that error-propagation from the estimation procedure to object positioning would be near a minimum. The image-analysis procedure developed in this work could respond to the availability of better information. Its speed and precision improved continually with improving accuracy of the estimation procedure. This procedure can be expected to be more suitable for camera-space manipulation than methods based on the Hough transform. Finally, a method to generalize the approach to tasks involving a class of features was proposed and tested. Dissert. Abstr.

N94-31301# Physical Optics Corp., Torrance, CA.
SMART ENVIRONMENTAL MONITOR BASED ON NEURAL NETWORKS AND MULTI-SPECTRAL PATTERN RECOGNITION Final Report, Mar. - Sep. 1993
Tai-Wei Lu Sep. 1993 19 p
(Contract DACA76-93-C-0004)
(AD-A276445; TEC-0048) Avail: CASI HC A03/MF A01

In phase 1 of this project, Physical Optics Corporation (POC) accomplished the goal of the original proposal which was to develop and optimize a unique neural network (NN) algorithm that performs rapid spectral signal processing and identification. POC's NN algorithm was tested with extremely noisy Raman spectra from Lawrence Livermore National Laboratory and experimentally showed at least ten times better sensitivity and reliability than conventional spectral signal processing methods. POC built a portable demonstration system with POC's NN and successfully demonstrated real-time spectral signature identification operations. POC proposed, for phase 2 implementation, a holographic optical neural network (HONN) system that is capable of rapid hyperspectral imaging through an acoustic-optic tunable filter (AOTF), real-time spectral feature identification, and mapping. The success of the phase 2 project will make automatic and rapid hyperspectral image analysis and feature location possible. DTIC

N94-31315# Argonne National Lab., IL.
OTTER 3.0 REFERENCE MANUAL AND GUIDE
W. W. McCune Jan. 1994 58 p
(Contract W-31-109-eng-38)
(DE94-007457; ANL-94/6) Avail: CASI HC A04/MF A01

OTTER (Organized Techniques for Theorem-proving and Effective Research) is a resolution-style theorem-proving program for first-order logic with equality. OTTER includes the inference rules binary resolution, hyperresolution, UR-resolution, and binary paramodulation. Some of its other abilities and features are conversion from first-order formulas to clauses, forward and back subsumption, factoring, weighting, answer literals, term ordering, forward and back demodulation, evaluable functions and predicates, and Knuth-Bendix completion. OTTER is coded in C, is free, and is portable to many different kinds of computers. DOE

N94-31372# Technische Univ., Berlin (Germany). Fachbereich Informatik.
AN ACTIVE COMPUTER SUPPORTED MEDIUM FOR DISTRIBUTED PLANNING IN ENTERPRISES Ph.D. Thesis [EIN AKTIVES COMPUTERGESTUETZTES MEDIUM ZUR VERTEILTEN PLANUNG IM UNTERNEHMEN]
Olaf F. Mehlmann 1993 187 p In GERMAN
(ETN-94-95738) Avail: CASI HC A09/MF A02

A computer aided system for supporting cooperative planning processes and active decision making is presented. The computer was regarded as an active medium and communication and coordination processes were used as a theoretical basis of the study in the framework of collaborative work. Intelligence was regarded as a property of a social group, which is developed through interactions of individuals. The enterprise to be planned was regarded as an accommodating, virtual product. The system was designed for automatically identifying unaccommodativeness in quantitative plannings and consequent communication needs. The system was based on the method of quantitative reasoning, which allows fuzzy, probabilistically interpreted interval numbers to be processed and soft interdependencies to be represented. The system was implemented on a personal computer with an object oriented, user friendly interface. ESA

N94-31482 Stanford Univ., CA.
CONTINGENCY-TOLERANT ROBOT MOTION PLANNING AND CONTROL Ph.D. Thesis
Wonyun Choi 1993 144 p
Avail: Univ. Microfilms Order No. DA9326443

This dissertation describes a new approach and enables techniques to build the navigation system of a mobile robot operating in a partially known environment. The main layout of this environment is known in advance, but the locations and shapes of some smaller objects may not be known. Environments of this type include shop-floors, offices, etc. The problem is to automatically determine how the robot should move from one position to another without colliding with objects in the environment. In order to be both efficient and robust, the navigation system should interweave a planning component and reaction component. The planning component should take advantage of available prior knowledge to produce globally efficient plans. However, it should be aware that knowledge may be incomplete and generate lesser-committed plans that leave some freedom of choice at execution time to deal with contingencies. The reaction component should organize the robot's behavior according to both the ongoing plan and the sensory inputs. The main idea underlying the approach proposed in this dissertation is to let the reaction component share some global knowledge of the robot's environment with the planning component. Based on this idea, we have developed a new type of navigation system where the planning component generates a lesser-committed motion plan, called a channel, represented by a sequence of parallelepipedic cells, and the reaction component uses artificial potential fields to pull the robot toward its goal within the channel, while repelling it away from unexpected obstacles. Various arrangements of unexpected obstacles may be encountered during navigation. The treatment of these arrangements by the reaction component is organized in three layers: channel navigation, local replanning, and global replanning. The most common and simpler cases are processed by the first layer using less complex techniques, while less frequent but more complex cases are handled by the other layers using more complex techniques. This navigation system applies to mobile robots with holonomic or nonholonomic constraints. Three versions of the system have been implemented. They have been experimented with simulated robots and a real mobile robot. Experimental results are discussed in this report. Dissert. Abstr.

N94-31500 Sheffield Univ. (England). Robotics Research Group.
A NEURAL NETWORK METHODOLOGY FOR ENGINEERING APPLICATIONS: THE LEARNING CONTROL OF ROBOTIC SYSTEMS
Ali M. S. Zalzala May 1993 9 p Limited Reproducibility: More than 20% of this document may be affected by microfiche quality
(RR-480; ETN-94-96057) Avail: CASI HC A02

A methodology for the application of artificial neural networks in engineering applications is presented. In this approach, the conventional control model is used to provide knowledge to the designed network; hence, this gives a further insight into the solution of the specific task. The presented method is implemented for different modules of robot control with outstanding success. ESA

N94-31514# Technische Univ., Darmstadt (Germany). Fachbereich Informatik.
ADAPTIVE OPERATING SYSTEMS CONCEPTS Ph.D. Thesis [ADAPTIVE BETRIEBSSYSTEMKONZEPTE]
Andreas Heck 1991 225 p In GERMAN
(ETN-94-95754) Avail: CASI HC A10/MF A03

A model for an adaptive computer operating system which adapts to the respective requirements in a flexible and simple way is presented. The concept of adaptivity is explained, and the status of the research into adaptive operating systems models is described. The support of adaptivity in the structure of an operating system using the developed model is explained. Several adaptive procedures were described within this model. Examples demonstrate the improvements brought about by adaptive systems as compared to static procedures. The model was extended for applications in distributed operating systems. The great flexibility of the concept with respect to adaptations within the operating system is demonstrated. ESA

N94-31546# Vrije Univ., Amsterdam (Netherlands).
AN EXPERT SYSTEM ARCHITECTURE FOR HETEROGENEOUS DOMAINS: A CASE-STUDY IN THE LEGAL FIELD Ph.D. Thesis
Robert Frederik Walker 1992 399 p Sponsored by Netherlands Organization for Scientific Research
(ETN-94-96012) Copyright Avail: CASI HC A17/MF A04

EXPANDER (expert system architecture allowing nonhomogeneous distributed knowledge representation), intended to operate in heterogeneous domains where several structurally different sources of knowledge must be combined in order to successfully solve a complex task, is described. It supports a distributed knowledge base in which the knowledge is kept in separate and autonomous modules. The resulting modularity offers considerable flexibility in choosing a range of knowledge representation formalisms and reasoning methods to accommodate domain intricacies. The philosophy behind EXPANDER is to provide extended flexibility: the possibility to tailor an expert system to a particular domain even if this entails the use of many different knowledge representation formalisms and reasoning mechanisms. A global overview of the legal domain is given and the PROLEXS expert system is introduced. The design of a generic expert system architecture is described, and the system is tailored to the legal domain, with emphasis on generic aspects with respect to heterogeneous domains. Implementation aspects are considered. ESA

N94-31623# Los Alamos National Lab., NM.
THE FUTURE OF OPEN ARCHITECTURE PROCESS CONTROL SYSTEMS
R. A. Gore 1994 18 p Presented at the 13th Energy-sources Technology Conference and Exhibition (ETCE) on Wind Energy, New Orleans, LA, 23-26 Jan. 1994
(Contract W-7405-eng-36)
(DE94-006163; LA-UR-94-0274; CONF-940113-7) Avail: CASI HC A03/MF A01

The author relates some of his experience in the acquisition and use of flexible controllers, and summarizes what he has learned and what a few other people are doing. What the author calls a 'flexible' system could also be called open architecture system. Where one defines OA as the use of well defined and documented software and hardware with interfaces that will permit the system to be modified by the user. Such systems could be based on either accepted or defacto standards for hardware and software. In addition to just sharing the author's experiences, this presentation is appropriate because of the relatively new encouragement that the Laboratory is receiving to work with American industry in the manufacturing area. DOE

N94-31647# Technische Univ., Delft (Netherlands). Faculty of Technical Mathematics and Informatics.
DIGITAL STATE-FEEDBACK H(INFINITY) CONTROL OF PRITCHARD-SALAMON SYSTEMS: A POPOV FUNCTION APPROACH
Florin Dan Barb, Vlad Ionescu, and Willem deKoning 1993 35 p
(ISSN 0922-5641)
(Rept-93-69; ETN-94-96114) Copyright Avail: CASI HC A03/MF A01

The digital state feedback H(infinity) control problem for Pritchard-Salamon infinite dimensional systems with unbounded input and output operators is addressed. A discrete Popov function based solution is given in terms of the solvability of a discrete time Riccati equation associated to the equivalent discrete time, time invariant system obtained by lifting the T periodically continuous time system. ESA

N94-31735# Toronto Univ. (Ontario). Dept. of Aerospace Science and Engineering.
REAL-TIME CONTROL OF THE TRUSSARM VARIABLE-GEOMETRY-TRUSS MANIPULATOR UTILIZING MACHINE VISION M.S. Thesis
David Allan Fenske 1993 66 p
(ISBN-0-315-87054-0; CTN-94-61243) Copyright Avail: Micromedia Ltd., Technical Information Centre, 240 Catherine Street, Suite 305, Ottawa, Ontario, K2P 2G8, Canada HC/MF

Trussarm is a variable geometry truss manipulator concept consisting of double octahedral truss modules. Trussarm changes shape by having hinged joints and three active members or actuators at its midplane. To prove the Trussarm concept, a prototype module was built. In an attempt to improve the control system for the Trussarm, machine vision was chosen to provide it with a method of sensing its workspace. The PAMI-Virtek Vision System from the University of Waterloo, which can track the six free-space coordinates of their special target in real time, was acquired

and adapted to the prototype Trussarm module. A control system for Trussarm was then devised to take advantage of the vision system. This control system was simulated using FORTRAN to prove the concept and then successfully implemented in the laboratory, allowing real-time visual control of the Trussarm for the first time. Author (CISTI)

N94-31750# Laval Univ. (Quebec). Dept. de Genie Electrique.
A NEURAL NETWORK MODEL FOR THE VISUAL PERCEPTION OF THE DEPTH OF A SCENE FROM STEREOSCOPY AND SHADING Ph.D. Thesis [UN MODELE DE RESEAU NEURONIQUE POUR LA PERCEPTION VISUELLE DE LA PROFONDEUR D'UNE SCENE A PARTIR DE LA STEREOSCOPIE ET DE L'OMBRAGE]
Richard Lepage Aug. 1993 289 p In FRENCH
(ISBN-0-315-86753-1; CTN-94-61227) Copyright Avail: Micromedia Ltd., Technical Information Centre, 240 Catherine Street, Suite 305, Ottawa, Ontario, K2P 2G8, Canada HC/MF

An artificial neural network was developed to carry out the fusion of stereoscopic vision and shading analysis to reconstruct the depth of an observed scene, starting from two illuminated images which may originate from two cameras. The reconstruction of depth from two dimensional images is an essential step before high level treatments which consist of the recognition and the memorization of the elements in the three dimensional scene observed. The edges contained in each of the two images are first detected. The identical edges in each of the images are then paired by the stereoscopy algorithm and the disparities measured indicate the depth of the scene observed at different edge positions. A shading analysis of one of the images produces an estimate of the relative depth for the slight variations of the exterior surface. A relaxation network combines the two analyses and allows for the obtaining of a dense mesh of depth measurements. CISTI

N94-31757# Laval Univ. (Quebec). Dept. de Genie Electrique.
STRATEGY FOR TRACKING AND GRABBING A MOVING OBJECT WITH THE AID OF A DECOUPLABLE MANIPULATOR WITH SIX DEGREES OF FREEDOM GENERAL ARCHITECTURE, GUIDED BY A VISION SYSTEM Ph.D. Thesis [STRATEGIE POUR LE SUIVI ET LA SAISIE D'UN OBJET MOBILE A L'AIDE D'UN MANIPULATEUR DECOUPLABLE A 6DDL D'ARCHITECTURE GENERALE GUIDE PAR UN SYSTEME DEVISION]
Jean Cote Sep. 1993 91 p In FRENCH
(ISBN-0-315-86864-3; CTN-94-61234) Copyright Avail: Micromedia Ltd., Technical Information Centre, 240 Catherine Street, Suite 305, Ottawa, Ontario, K2P 2G8, Canada HC/MF

In the studied problem of tracking and grabbing a moving object with a manipulator guided by a vision system, the motion of the object is unknown and it is not necessarily constrained to the manipulator's attainable workspace. The concept of generalized inverse kinematic functions for prescribed points situated outside of the manipulator workspace is presented. Using this new approach, it is possible to make a real vector of the linkage coordinates correspond to any Cartesian vector of three dimensional space while minimizing the Euclidian distance between the point whose position is given by this vector and the end effector of the manipulator. To control the manipulator, a trajectory planning algorithm is developed. The algorithm is based on a polynomial interpolation preserving continuity of position, velocity, and acceleration along the trajectory of each linkage. A graphic simulator, developed mainly to validate the tracking and trajectory planning algorithms, is also presented. The simulator allows study of any manipulator configuration described with the aid of Hartenberg Denavit parameters. CISTI

N94-31794 Clarkson Univ., Potsdam, NY.
TRAJECTORY LEARNING WITH A DIRECT DRIVE ROBOTIC MANIPULATOR Ph.D. Thesis
Nabeel H. Salem 1993 240 p
Avail: Univ. Microfilms Order No. DA9320008

It is common knowledge that human performance of most tasks improves with practice. There is no reason why the same should not be true for robotic manipulators. If an accurate evaluation of task performance can be made, then the performance error can be used to infer command error. The command can then be updated the next time the task is performed in order to obtain an improvement in robot trajectory tracking performance. The key to getting an iterative learning algorithm to converge is the availability of an accurate mathematical model of the robot arm dynamics. Unfortunately, commercial robots, with rare exceptions, are very difficult to model. This is due to the effects of high friction and backlash which are introduced by massive links driven only indirectly through highly-geared motors. In this study, the problems associated with advanced manipulator control due to the lack of suitable experimental manipulators have been mitigated through the use of a high performance custom built arm based on direct drive technology (high torque motors designed to eliminate the need for gears by coupling directly to the robot joint axes). This experimental direct drive manipulator (DDMan) has been used to evaluate our particular learning control ideas. Three iterative learning algorithms have been tested on the DDMan. The first algorithm is based on subtracting the estimate of the command error from the robot command control law in an iterative manner. The other two learning algorithms use optimization techniques to modify the robot model and torque command for the next robot trajectory movement. The experimental results indicates that the robot trajectory tracking accuracy has improved significantly. Numerical simulations are used to examine the learning sensitivity to model parameter errors. Dissert. Abstr.

N94-31798# Montreal Univ. (Quebec). Dept. de Genie Electrique.
ADAPTIVE CONTROL OF A ROBOT IN CARTESIAN COORDINATES: ANALYSIS AND IMPLEMENTATION M.S. Thesis [COMMANDE ADAPTIVE DE ROBOT EN COORDONNEES CARTESIENNES: ANALYSE ET REALISATION]
Sylvain Robert Jul. 1993 100 p In FRENCH
(ISBN-0-315-86493-1; CTN-94-61201) Copyright Avail: Micromedia Ltd., Technical Information Centre, 240 Catherine Street, Suite 305, Ottawa, Ontario, K2P 2G8, Canada HC/MF

An analysis is presented of an adaptive controller for trajectory tracking and its real-time implementation on a two degree of freedom SCARA robot. The control law consists of a proportional derivative regulator plus feedforward compensation of the estimated dynamics. The stability of this control scheme can be demonstrated by the Liapunov method, which allows deduction of a law of adaptation of the control parameters. This controller directly utilizes an assigned trajectory expressed in Cartesian coordinates. A conversion to the coordinates of articulation is thereby avoided, which improves the precision and reduces the number of calculations required. The practical implementation of the controller is based on the Motorola DSP96002 microprocessor and a library of programmed floating point matrix functions. Experimental results are reported which validate the theoretical developments and demonstrate the controller performance. Results obtained with a simple proportional derivative controller are also shown for comparison. CISTI

N94-31800# Montreal Univ. (Quebec). Dept. de Genie Electrique et de Genie Informatique.
STUDY OF A PATH PLANNING AND TRACKING SYSTEM FOR AN ARTICULATED MOBILE ROBOT M.S. Thesis [ETUDE D'UN SYSTEME DE PLANIFICATION ET DE SUIVI DE CHEMIN POUR UN ROBOT MOBILE ARTICULE]
Isabelle Girard Jun. 1993 141 p In FRENCH
(ISBN-0-315-86502-4; CTN-94-61203) Copyright Avail: Micromedia Ltd., Technical Information Centre, 240 Catherine Street, Suite 305, Ottawa, Ontario, K2P 2G8, Canada HC/MF

Three methods based on the control approach are studied for possible application to path planning and tracking for an articulated mobile robot. The path planning problem is formulated as a control problem, and system entries are sought which will steer the system from an initial to a final configuration. The three methods considered (Murray and Sastry (1990), Tilbury and Sastry (1992), and Fernandez, Li and Gurvits), all use sinusoids as control inputs. The first two are rejected, while the third gives a good motion planner. Its principal limitation is a relatively long computation time. For path tracking, the lateral and orientation offsets of the robot are defined with respect to the point on the path which is closest to the actual position of the robot. To develop the motion controllers that will correct these offsets, the dynamic model of the system is linearized to obtain two decoupled systems that characterize the translational and the rotational motion. The controller of each of these systems comprises a feedforward component and a feedback component. The behavior of the control system is analyzed using simulations. These show the robustness of the control strategy under the influence of different initial conditions and constant perturbations. Author (CISTI)

N94-31801# Montreal Univ. (Quebec). Dept. de Genie Electrique.
DEVELOPMENT OF A FEEDFORWARD CONTROLLER FOR A FLEXIBLE MANIPULATOR M.S. Thesis [MISE AU POINT D'UN CONTROLEUR ANTICIPATIF POUR UN MANIPULATEUR FLEXIBLE]
Koorush Ziarati Jan. 1993 139 p In FRENCH
(ISBN-0-315-86515-6; CTN-94-61205) Copyright Avail: Micromedia Ltd., Technical Information Centre, 240 Catherine Street, Suite 305, Ottawa, Ontario, K2P 2G8, Canada HC/MF

A test bench comprising a motor, elastic joint, and rigid or flexible arm was built and used to test a feedforward controller based on the knowledge of the dynamic model of the rigid system to which a quasi-static correction has been added. This control was computed off-line and applied in real time to the system. To reduce the disturbance effects and ensure system stability at the end of the trajectory, a feedback signal computed through measurement of motor angle was applied first. A second feedback signal computed from evaluating the flexible arm curvature was added to the above scheme. The deformation of the flexible link was measured with strain gauges. A model of the system was formulated by taking into account both the joint elasticity and the arm flexibility effects. The model parameters were measured experimentally and validated by comparing simulation and test results. A software package was developed for simulation and real-time implementation. The control strategy was also tested by experiment and simulation. The multistage controller allows control of flexible robots. Tracking error is low for slow and averaged velocity tracking trajectories. The simplicity of calculation indicates a potential for control implementation in real time for flexible robots with several degrees of freedom. Author (CISTI)

N94-31808 National Oceanic and Atmospheric Administration, Boulder, CO. Space Environment Lab.
PROCEEDINGS OF THE INTERNATIONAL WORKSHOP ON ARTIFICIAL INTELLIGENCE APPLICATIONS IN SOLAR-TERRESTRIAL PHYSICS
J. Joselyn, H. Lundstedt, and J. Trolinger Dec. 1993 224 p Conference held in Lund, Sweden, 22-24 Sep. 1993 Limited Reproducibility: More than 20% of this document may be affected by microfiche quality
(PB94-142064) Avail: CASI HC A10

The first workshop on Artificial Intelligence (AI) Applications in Solar-Terrestrial Physics was held at the University in Lund, Sweden. The Workshop's three-day schedule included sessions on theory, applications, and data bases, demonstrations, and ample time for discussion. The sessions consisted of invited reviews, short contributions, computer presentations, and posters. The value of data access via Internet was shown when Yohkoh images, Stanford magnetograms, and NOAA's solar and geophysical images were displayed and discussed on the final day of the Workshop. NTIS

N94-31821# Groningen Rijksuniv. (Netherlands). Dept. of Mathematics.
UNIVERSAL APPROXIMATION IN p-MEAN BY NEURAL NETWORKS
Robert M. Burton (Corvallis Environmental Research Lab., OR.) and Herold G. Dehling 1993 10 p
(W-9320; ETN-94-96181) Avail: CASI HC A02/MF A01

The representation capabiiities of single hidden layer feedforward neural nets are studied. The aim is to show that a neural network with a single hidden layer and a non polynomial transfer function can approximate any function f: R(sup d) onto R arbitrarily well in a local L(sup p) norm. ESA

N94-31826# Universiteit Twente, Enschede (Netherlands). Dept. of Applied Mathematics.
LIGHT-TRAFFIC ANALYSIS FOR QUEUES WITH SPATIALLY DISTRIBUTED ARRIVALS
Dirk P. Kroese and Volker Schmidt 26 Jul. 1993 29 p
(ISSN 0169-2690)
(MEMO-1150; ETN-94-95724) Avail: CASI HC A03/MF A01

The following continuous polling system is considered: customers arrive according to a homogeneous Poisson process (or a more general stationary point process) and wait on a circle in order to be served by a single server. The server is 'greedy', in the sense that he always moves (with constant speed) towards the nearest customer. The customers are served according to an arbitrary service time distribution, in the order in which they are encountered by the server. First order and second order Taylor expansions are found for the expected configuration of customers, for the mean queue length, and for expectation and distribution function of the workload. It is shown that under light traffic conditions the greedy server works more efficiently than the cyclically polling server. ESA

N94-31833# Toronto Univ. (Ontario).
A REAL-TIME COMPUTER CONTROL AND TRAJECTORY GENERATION ENVIRONMENT FOR TRUSSARM M.S. Thesis
Joseph P. Sallmen 1993 228 p
(ISBN-0-315-87060-5; CTN-94-61247) Copyright Avail: Micromedia Ltd., Technical Information Centre, 240 Catherine Street, Suite 305, Ottawa, Ontario, K2P 2G8, Canada HC/MF

A variable geometry truss shows promise as a next-generation design for a manipulator for space applications. A proof of concept one-bay version of octohedral geometry (Trussarm Mark I) has been constructed. It is outfitted with an industrial motion controller capable of independent closed-loop proportional integral derivative control on each actuator. The objective is to provide a user/machine interface for the control and evaluation of Trussarm. The overall system (hardware and software) is examined, focusing on the computer programming and operator interface. The theoretical preliminaries of the electro mechanical control, the kinematics of Trussarm, and trajectory design are described, followed by an in-depth discussion of the Trussarm Trajectory Generator and Trussarm Control Environment, two computer programs which allow testing and demonstration of the Trussarm facility. The software requirements are listed, followed by a detailed design and implementation. Plots of trajectory data from Trussarm are presented. References are made throughout to how the current system may accommodate a four-bay Trussarm, the next design. Author (CISTI)

N94-31842 Maryland Univ., College Park.
SAFE NAVIGATION AND ACTIVE VISION FOR AUTONOMOUS VEHICLES: A PURPOSIVE AND DIRECT SOLUTION Ph.D. Thesis
Gin-Shu Young 1993 191 p
Avail: Univ. Microfilms Order No. DA9327522

Two capabilities strongly desired in the operation of autonomous vehicles are safe navigation and active vision. It is a challenge to develop autonomous vehicles capable of operating in complicated, unpredictable, and hazardous environments. To navigate autonomous vehicles safely, obstacles such as protrusions, depressions, and steep terrains must be discriminated from terrain before any path planning and obstacle avoidance activity is undertaken. In the first part of the dissertation, a purposive and direct approach to obstacle detection for safe navigation has been developed. The method finds obstacles in a two dimensional image-based space, as opposed to three dimensional reconstructed space, using optical flow. The theory derives from new visual linear invariants based on optical flow. Employing the linear invariance property, obstacles can be directly detected by using a reference flow line obtained from measured optical flow. The main features of this approach are that two dimensional visual information (i.e., optical flow) is directly used to detect obstacles and no range, three dimensional motion, or three dimensional scene geometry is recovered; the method of finding protrusions and depressions is valid for the vehicle (or camera) undergoing general six degree of freedom motion; and the error sources involved are reduced to a minimum, since the only information required is one component of optical flow. A number of experiments from both synthetic and real image data suggest that the approach is effective and robust. The method is demonstrated on both ground and air vehicles. To enhance the capability of active vision, the computer controlled camera system must be calibrated. In the second part of this dissertation, a purposive and direct method for the calibration of the camera system is developed. The method calibrates all the joint poses and link frames of the manipulator and the camera poses related to the same world frame. The solution for the manipulator, camera-to-manipulator, and base-to-world calibration is developed in closed form. The main features of this technique are that only the form of one equation solving one parameter is used and the camera-to-manipulator and base-to-world calibration are the by-products of the manipulator calibration procedure. Dissert. Abstr.

N94-31873# Quebec Univ., Chicoutimi.
ANALYSIS AND DESIGN OF A FORMAL NEURAL NETWORK FOR FILTERING A DYNAMIC SIGNAL M.S. Thesis [ANALYSE ET CONCEPTION D'UN RESEAU DE NEURONES FORMELS POUR LE FILTRAGE D'UN SIGNAL DYNAMIQUE]
M. Abderrahim Ennaji Sep. 1992 220 p In FRENCH

(ISBN-0-315-86932-1; CTN-94-61220) Copyright Avail: Micromedia Ltd., Technical Information Centre, 240 Catherine Street, Suite 305, Ottawa, Ontario, K2P 2G8, Canada HC/HC

A detailed analysis is made of the capacity of a feedforward neural network for filtering signals. This network is trained to memorize and generalize a dynamic signal. A number of neural network architectures are studied to bring out the specific qualities related to filtering of dynamic signals. A proposed model demonstrates the capacity of a feedforward network to memorize a dynamic signal, to generalize it at the amplitude and frequency level, to reconstruct an already learned signal, to reproduce any signal with added noise in the form of high and low frequency components, and to filter a signal in the manner of a high-pass, low-pass, bandstop, or bandpass filter. The study focuses on the possibility of reducing the size of training data to eventually decrease the convergence time without affecting model performance. The number of nodes in the network is optimized and a relation is established between the signal to be learned and the number of nodes in the input and cache layers. CISTI

N94-31875# Toronto Univ. (Ontario). Dept. of Mechanical Engineering.
PHOTOPYROELECTRIC SPECTROSCOPY AS A NON-INTRUSIVE TECHNIQUE FOR THE DETERMINATION OF THE OPTICAL ABSORPTION SPECTRA OF MULTIPLE QUANTUM WELL SAMPLES M.S. Thesis
Christine Alison daSilva 1993 160 p
(ISBN-0-315-87164-4; CTN-94-61250) Copyright Avail: Micromedia Ltd., Technical Information Centre, 240 Catherine Street, Suite 305, Ottawa, Ontario, K2P 2G8, Canada HC/MF

Photopyroelectric (PPE) spectroscopy is a new and nonintrusive technique for the measurement of optical absorption spectra in bulk and thin-film materials. The technique is used for the first time to measure the optical absorption spectra of AlGaAs/GaAs multiple quantum wells (MQW) on a semi-insulating (SI) GaAs substrate. First, the motivation for and the current state of characterizing MQWs is discussed. The features of PPE spectroscopy and some other methods of characterizing are then detailed. An improved model of a three-layer specimen, the pyroelectric detector, and the signal generation system is presented. This model is then adapted to a computer program which offers several options, among which is the calculation of the optical absorption spectra. These calculations are made in conjunction with experimentally obtained PPE spectra of the MQW and substrate materials. Semiquantitative spectra for the optical absorption coefficients of an AlGaAs/GaAs MQW in the 900 to 1080 nm wavelength range were calculated. The computer adaptation of the theoretical model was found to simulate all the correct trends in PPE spectra. An accurate prediction of the PPE spectrum of a SI GaAs sample at 16 kHz modulation frequency was made. Author (CISTI)

N94-31876# Toronto Univ. (Ontario). Dept. of Mechanical Engineering.
REAL-TIME CONTROL AND APPLICATION TO ROBOTICS: HARDWARE AND SOFTWARE ARCHITECTURES M.S. Thesis
Chin Zhou 1993 171 p
(ISBN-0-315-87192-X; CTN-94-61251) Copyright Avail: Micromedia Ltd., Technical Information Centre, 240 Catherine Street, Suite 305, Ottawa, Ontario, K2P 2G8, Canada HC/MF

Systems were designed and real-time control architectures implemented for three experimental facilities developed as test beds for verification and experimental studies of new robotic control schemes. These setups use complex real-time control systems and are characterized by modular and open hardware and software architectures that can be easily reconfigured and control levels that can be directly assessed. Computer hardware suitable for real-time control applications is studied systematically to achieve well-designed system architectures and full utilization of hardware resources. Two hardware architectures were designed and implemented, one a VERSA-module Eurocards bus based architecture implemented for a telerobot system, the other a two-level distributed parallel multiprocessor architecture implemented in a multi-arm facility and a coordinated dual-arm system. A versatile real-time software environment for the three setups was designed based on a multiprocessor resource limited hardware configuration. The software consists of the following hierarchical levels: an extended computer module level, a real-time operating system (RTOS), an abstract robot control level, and a user integration level. At the last level, the software is independent of hardware and the RTOS and is easily reconfigurable. Author (CISTI)

N94-31962 Wisconsin Univ., Milwaukee.
HIGH-SPEED PATH CONSTRAINED MANIPULATOR OPERATION USING OPTIMAL-FEEDBACK COMBINED CONTROLLER Ph.D. Thesis
Akihiko Kumagai 1993 152 p
Avail: Univ. Microfilms Order No. DA9328005

Feedback control schemes for manipulators for high-speed/high-accuracy trajectory execution are studied. Also separately from this issue, kinematic singularity problems and a model based feedback control method for parallel manipulators are studied. For the first part, a near-minimum time feedback controller is developed using the non-uniform time scaling technique. Using this controller, the speed of a manipulator is automatically adjusted reacting to the experienced parameter errors and external disturbances. The controller moves the manipulator to follow a given path within a near-minimum time using the available actuator torque capacities in the most efficient manner and maintaining the stability of the controller. A scheme to maintain the stability of feedback controllers for saturated input torque conditions is introduced by locally applying the non-uniform time scaling technique. A variable gain control scheme is combined with the non-uniform time scaling technique to develop a near-minimum time class controller to provide satisfactory accurate trajectory control under extremely uncertain dynamic environment. The uniform time scaling technique is used to strengthen the stability effect of feedback controllers. For the second part, a general theory is developed for obtaining global properties, such as unstable configurations, of parallel manipulators using direct kinematic polynomial discriminants and Jacobians. The unstable configurations of the platform of a parallel manipulator occur when two branches of the direct kinematics coalesce into one, and the discriminant of the direct kinematic polynomial vanishes. The Jacobian of the direct kinematics, which relates the passive joint velocities and the active joint velocities, is also singular at the unstable configurations. The workspace and accessibility regions of the platform of parallel manipulators are obtained by analyses of the direct and inverse kinematic polynomials and the topological maps between the joint space and task space. The dynamic equations of parallel manipulators are derived using two different approaches, the Newton-Euler formulation and the Lagrangian formulation with the Lagrange multipliers. Then a model based feedback controller is developed using these dynamic equations. Dissert. Abstr.

N94-31991 Massachusetts Inst. of Tech., Cambridge.
ROBOT MOTION VISION BY FIXATION Ph.D. Thesis
M. Ali Taalebinezhaad 1992
Avail: Issuing Activity (MIT Libraries, Rm. 14-0551, Cambridge, MA 02139-4307)

In numerous current and future applications ranging from autonomous navigation of mobile robots to collision avoidance systems for cars, an imaging system (installed on a moving vehicle) takes 2D images of an environment with the aim of finding the motion of the vehicle (translational and rotational velocities) as well as the structure of the environment (shape). In machine vision, this problem is referred to as the general motion vision problem. This thesis introduces a direct method called fixation for solving this general motion vision problem, arbitrary motion relative to an arbitrary environment. Avoiding feature correspondence and optical flow has been the motivation behind this direct method which uses the spatio-temporal brightness gradients of the images directly. The fixation method results in a linear constraint equation (Fixation Constraint Equation) which explicitly expresses the rotational velocity in terms of the translational velocity. The combination of this constraint equation with the Brightness-Change Constraint Equation (a fundamental equation which relates the motion to the brightness gradients at any image point) solves the general motion vision problem. In contrast to previous direct methods, the fixation method does not impose any severe restrictions on the motion or the environment. Moreover, the fixation method neither requires tracked images as its input or uses tracking for obtaining fixated images. Instead, it introduces a novel technique called the pixel shifting process to construct fixated images for any arbitrary fixation point. This is done entirely in software without any need to move the imaging system for tracking. This fixation method has been successfully tested in the real world environment for the recovery of the motion and shape in the general case. The experimental results are presented and the implementation issues and techniques are discussed. Dissert. Abstr.

N94-32036 Naval Undersea Warfare Center, Newport, RI.
ADAPTIVE CONTROL OF TELEROBOTIC SYSTEMS WORN BY HUMANS Final Report
J. B. Bagley, Jr. 27 Sep. 1993 94 p Limited Reproducibility: More than 20% of this document may be affected by microfiche quality
(AD-A276608; NUWC-NPT-TD-10212) Avail: CASI HC A05

A distinguishing feature of man is his ability to invent mechanical devices to augment his physical capabilities. Traditionally, these machines have been master-slave devices with man controlling the activities of the machine. Recent work has been done to develop a control architecture for the coupled man-machine systems; however, these systems rely on a complete and detailed description of the device and its operating environment. The necessity of an environmental model places limitations on the machine's ability to perform different tasks. This report discusses how environmental dependence can be overcome through the use of a parameter estimator, which operates on data contained in the system. This report first verifies the performance of the control architecture. A linear estimation technique is then used to allow the system to adapt to an unknown time-invariant environment. Also discussed is how the results of the adaptations can be extended to the problem of an unknown time-varying environment. DTIC

N94-32053 Yale Univ., New Haven, CT. School of Medicine.
NEURAL NETWORKS FOR MODEL-BASED RECOGNITION Final Report, 1 May 1990 - 30 Sep. 1993
Gene Gindi 30 Sep. 1993 5 p Limited Reproducibility: More than 20% of this document may be affected by microfiche quality
(Grant AF-AFOSR-0224-90)
(AD-A277375; AFOSR-94-0048TR) Avail: CASI HC A01

During this grant period, the investigators explored issues involving the use of neural nets for object recognition. The PI, Gene Gindi moved from Yale to Stony Brook late in the grant period, and continued the brunt of the work at Stony Brook under a subcontractual arrangement with Yale. A colleague, Eric Mjolsness, became the titular PI during this period, and a postdoc involved in this work, Anand Rangarajan, stayed at Yale but had his salary partially paid during the SUNY subcontractual period. This final progress report is authored by Gene Gindi. DTIC

N94-32061# Industrial Coll. of the Armed Forces, Washington, DC.
APPLICATION OF ARTIFICIAL INTELLIGENCE TO THE DOD CORPORATE INFORMATION MANAGEMENT (CIM) PROGRAM
Howard E. Bylund, Jr. Apr. 1993 33 p
(AD-A276656; NDU-ICAF-93-F40) Avail: CASI HC A03/MF A01

This paper analyzes the DoD Corporate Information Management (CIM) Program and the level of Artificial Intelligence being inserted into the program. This analysis is done by using commercial business activities as a baseline. It addresses the introduction of Artificial Intelligence (AI) through the benchmark process of the DoD CIM. It was found that this benchmark process of the CIM, similar to the DoD Total Quality Management (TQM) process, is determining the level of technology insertion into the CIM. It is recommended that this process continue and that, as with other technologies, AI be incorporated as demonstrated beneficial through the benchmark process. DTIC

N94-32095 University of Southern California, Los Angeles. Dept. of Electrical Engineering.
MODELING AND CONTROL OF NONLINEAR SYSTEMS Final Report, 1 May 1991 - 31 Aug. 1993
John E. Hauser 10 Jan. 1994 5 p Limited Reproducibility: More than 20% of this document may be affected by microfiche quality
(Grant AF-AFOSR-0255-91)
(AD-A277377; AFOSR-94-0052TR) Avail: CASI HC A01

We have conducted research on the modeling and control of nonlinear systems. Our efforts have been directed toward understanding the control of truly nonlinear behavior as well as the synthesis of control laws for systems that can be nearly transformed into linear systems (via approximate feedback linearization). We have introduced a new framework for understanding and analyzing the stability and control of nonlinear maneuvering systems. This approach is based on the concept of transverse dynamics. We have demonstrated the usefulness of this approach in the control of the swinging energy of the pendulum for an experimental cart and pendulum system. On the theoretical side, we have provided a new method for the construction of converse Lyapunov functions for exponentially stable periodic orbits. New techniques for the approximate feedback linearization of nonlinear systems have been developed. In order to construct a feedback linearizing coordinate transformation, a class of optimization problems has been formulated for finding approximate solutions to an appropriate system of partial differential equations. In contrast to previous results, this approach does not require differentiation of the data describing the system and is therefore applicable to systems with, for example, tabular data. DTIC

N94-32127# Lawrence Livermore National Lab., CA.
EXPLORING PHASE SPACE CONCEPTS IN THE FORECASTING OF TIME SERIES WITH ARTIFICIAL NEURAL NETWORKS
R. D. Rogers and V. Vemuri 13 Sep. 1993 8 p Presented at the American Nuclear Society (ANS) Winter Meeting, San Francisco, CA, 14-18 Nov. 1993
(Contract W-7405-eng-48)
(DE94-005810; UCRL-JC-115072; CONF-931160-40) Avail: CASI HC A02/MF A01

The authors study the performance of feedforward artificial neural networks in forecasting future values of several different time series. They explore both short- and long-term prediction of several periodic time series. They find that a significant source of error in long-term prediction of time series is introduced by a phase shift between the network output and the time series. They explore the origin of this phase shift and suggest strategies for minimizing its effect. They find that the phase diagrams of the time series and the neural network forecast contain useful diagnostic information. DOE

N94-32152# Massachusetts Inst. of Tech., Cambridge. Artificial Intelligence Lab.
GEOMETRIC STRUCTURE OF THE ADAPTIVE CONTROLLER OF THE HUMAN ARM
Reza Shadmehr and Ferdinando Mussa-Ivaldi 21 Jul. 1993 35 p
(Contract N00014-90-J-1946; NSF ASC-92-17041)
(AD-A276797; AI-1437) Avail: CASI HC A03/MF A01

The objects with which the hand interacts with may significantly change the dynamics of the arm. How does the brain adapt control of arm movements to this new dynamics? We show that adaptation is via composition of a model of the task's dynamics. By exploring generalization capabilities of this adaptation we infer some of the properties of the computational elements with which the brain formed this model; the elements have broad receptive fields and encode the learned dynamics as a map structured in an intrinsic coordinate system closely related to the geometry of the skeletomusculature. The low-level nature of these elements suggests that they may represent a set of primitives with which a movement is represented in the CNS. DTIC

N94-32175# Los Alamos National Lab., NM.
NEURAL NETWORK DEFINITIONS OF HIGHLY PREDICTABLE PROTEIN SECONDARY STRUCTURE CLASSES
A. Lapedes, E. Steeg, and R. Farber 1994 9 p Presented at the Neural Information Processing Systems (NIPS) Conference, Denver, CO, 30 Nov. - 2 Dec. 1993
(Contract W-7405-eng-36)
(DE94-006234; LA-UR-94-110; CONF-9311171-2) Avail: CASI HC A02/MF A01

We use two co-evolving neural networks to determine new classes of protein secondary structure which are significantly more predictable from local amino sequence than the conventional secondary structure classification. Accurate prediction of the conventional secondary structure classes - alpha helix, beta strand, and coil - from primary sequence has long been an important problem in computational molecular biology. Neural networks have been a popular method to attempt to predict these conventional secondary structure classes. Accuracy has been disappointingly low. The algorithm presented here uses neural networks to simultaneously examine both sequence and structure data and to evolve new classes of secondary structure that can be predicted from sequence with significantly higher accuracy than the conventional classes. These new classes have both similarities to and differences with the conventional alpha helix, beta strand, and coil. DOE

N94-32193 Center for Mathematics and Computer Science, Amsterdam (Netherlands). Dept. of Operations Research, Statistics, and System Theory.

A POLLING SYSTEM WITH A DORMANT SERVER

S. C. Borst Jun. 1993 39 p Sponsored by Netherlands Organization for Applied Scientific Research TMO Limited Reproducibility: More than 20% of this document may be affected by microfiche quality

(ISSN 0924-0659)

(CWI-BS-R9313; ETN-94-96222) Copyright Avail: Issuing Activity (European Space Agency (ESA))

A polling system with a dormant server, that is, a polling system in which the server may be allowed to make a halt at a queue when there are no customers present in the system, is studied. A pseudo conservation law for a general model is derived and used to compare the dormant and the non dormant server case. The question at which queues the server should make a halt to minimize the mean total amount of work in the system is addressed. Subsequently attention is directed in particular to a globally gated polling system in which the server makes a halt at its home base when there are no customers present in the system. For that system, explicit expressions for the LST of the cycle time distribution, for the LST of the waiting time distribution at each of the queues, and for the pgf of the joint queue length distribution at polling epochs, are derived. The waiting time at each of the queues is shown to be smaller (in the increasing convex ordering sense) than in the non dormant server case. ESA

N94-32198 Center for Mathematics and Computer Science, Amsterdam (Netherlands). Dept. of Operations Research, Statistics, and System Theory.

MULTISERVER QUEUES WITH IMPATIENT CUSTOMERS

O. J. Boxma and P. R. deWaal Nov. 1993 23 p Sponsored in part by Koninklijke/Shell-Lab.; and Netherlands Organization for Applied Scientific Research TMO Limited Reproducibility: More than 20% of this document may be affected by microfiche quality

(ISSN 0924-0659)

(CWI-BS-R9319; ETN-94-96228) Copyright Avail: Issuing Activity (European Space Agency (ESA))

Multiserver queues in which customers leave when their service is not started before the expiration of a stochastic deadline are studied. Insensitive bounds and sharp approximations for the overflow probability are derived. Assigning costs to servers and to the loss of impatient customers, the problem of determining the number of servers that minimizes a certain cost function are also considered. ESA

N94-32281# Massachusetts Inst. of Tech., Cambridge. Artificial Intelligence Lab.

UNDERGRADUATE ROBOTICS PROJECTS IN SUPPORT OF RESEARCH ON NEURAL NETWORKS Final Report, 15 Jan. - 15 Jul. 1993

Christopher Atkeson 15 Jul. 1993 3 p

(Contract F49620-93-1-0104)

(AD-A277331; AFOSR-94-0088TR) Avail: CASI HC A01/MF A01

This grant was successful both in developing sensor systems and in educating undergraduate students. There were several reasons to ask students to develop these systems. First and foremost is the educational value of having a student build a complete system. This challenge is much greater than a typical course laboratory experiment. The student must propose, refine, and choose among different variants of any particular approach. The system must be designed, built, debugged, documented, and, most importantly, evaluated. Any particular version of the system may suggest future revisions or new approaches. In some cases there are commercially available systems the researchers could use, but in many cases they had trouble finding off the shelf systems that are light and inexpensive enough to suit their purposes. DTIC

N94-32340# Boston Univ., MA. Center for Adaptive Systems.

NEURAL MODELS OF SPATIAL ORIENTATION IN NOVEL ENVIRONMENTS Annual Report, 1 Sep 1992 - 31 Aug. 1993

Stephen Grossberg Jan. 1994 23 p

(Contract F49620-92-J-0499)

(AD-A277383; AFOSR-94-0116TR) Avail: CASI HC A03/MF A01

Completed work on this grant analyzes problems of three dimensional vision, visual search, spatial mapping, planning, and action, all of which utilize spatial representations to control adaptive behaviors in real time. Highlights include significant contributions towards solving the classical figure-ground problem for biological vision, the motor equivalence problem for flexible arm movement control including tool use, the problem of self-organizing body-centered spatial representations for movement planning and spatial orientation, and the problem of carrying out fast visual search for targets among multiple distractors. New research directions include projects which have been developed to frontally attack core problems concerning how a rapidly moving agent can self-organize spatial representations, use these representations for real-time movement planning, and transform spatial movement plans into appropriate motor commands for movement control and real-time navigation. Specific projects include retinal image processing, formation of egocentric maps of object positions from optic flow, detection of moving objects from optic flow, integration of eqocentric and allocentric representations for autonomous navigation investigation of spatial reference frames, and transformations between frames for real-time flexible speech articulator control. DTIC

N94-32359*# Draper (Charles Stark) Lab., Inc., Cambridge, MA.

FUZZY LOGIC APPLICATION FOR MODELING MAN-IN-THE-LOOP SPACE SHUTTLE PROXIMITY OPERATIONS M.S. Thesis - MIT

Robert B. Brown May 1994 146 p

(Contract NAS9-18426)

(NASA-CR-188283; NAS 1.26:188283; CSDL-T-1205) Copyright Avail: CASI HC A07/MF A02

A software pilot model for Space Shuttle proximity operations is developed, utilizing fuzzy logic. The model is designed to emulate a human pilot during the terminal phase of a Space Shuttle approach to the Space Station. The model uses the same sensory information available to a human pilot and is based upon existing piloting rules and techniques determined from analysis of human pilot performance. Such a model is needed to generate numerous rendezvous simulations to various Space Station assembly stages for analysis of current NASA procedures and plume impingement loads on the Space Station. The advantages of a fuzzy logic pilot model are demonstrated by comparing its performance with NASA's man-in-the-loop simulations and with a similar model based upon traditional Boolean logic. The fuzzy model is shown to respond well from a number of initial conditions, with results typical of an average human. In addition, the ability to model different individual piloting techniques and new piloting rules is demonstrated. Author (revised)

N94-32787# Sandia National Labs., Albuquerque, NM.

A MULTITASKING BEHAVIORAL CONTROL SYSTEM FOR THE ROBOTIC ALL TERRAIN LUNAR EXPLORATION ROVER (RATLER)

P. Klarer 1994 7 p Presented at the CIRFFSS 1994:AIAA/National Aerospace and Space Administration Conference on Intelligent Robots in Field, Factory, Service and Space, Houston, TX, 21-24 Mar. 1994

(Contract DE-AC04-94AL-85000)

(DE94-007293; SAND-94-0408C; CONF-940365-3) Avail: CASI HC A02/MF A01

The design of a multitasking behavioral control system for the Robotic All Terrain Lunar Exploration Rover (RATLER) is described. The control system design attempts to ameliorate some of the problems noted by some researchers when implementing subsumption or behavioral control systems, particularly with regard to multiple processor systems and real-time operations. The architecture is designed to allow both synchronous and asynchronous operations between various behavior modules by taking advantage of intertask communications channels and by implementing each behavior module and each interconnection node as a stand-alone task. The potential advantages of this approach over those previously described in the field are discussed. An implementation of the architecture is planned for a prototype Robotic All Terrain Lunar Exploration Rover (RATLER) currently under development and is briefly described. DOE

N94-32943*# Houston Univ., TX. Dept. of Electrical Engineering.

STATE-SPACE SELF-TUNER FOR ON-LINE ADAPTIVE CONTROL Final Report, 1 Jun. 1989 - 31 May 1994

L. S. Shieh 1994 9 p

(Grant NAG9-380)

(NASA-CR-195836; NAS 1.26:195836) Avail: CASI HC A02/MF A01

Dynamic systems, such as flight vehicles, satellites and space stations, operating in real environments, constantly face parameter and/or structural

variations owing to nonlinear behavior of actuators, failure of sensors, changes in operating conditions, disturbances acting on the system, etc. In the past three decades, adaptive control has been shown to be effective in dealing with dynamic systems in the presence of parameter uncertainties, structural perturbations, random disturbances and environmental variations. Among the existing adaptive control methodologies, the state-space self-tuning control methods, initially proposed by us, are shown to be effective in designing advanced adaptive controllers for multivariable systems. In our approaches, we have embedded the standard Kalman state-estimation algorithm into an online parameter estimation algorithm. Thus, the advanced state-feedback controllers can be easily established for digital adaptive control of continuous-time stochastic multivariable systems. A state-space self-tuner for a general multivariable stochastic system has been developed and successfully applied to the space station for on-line adaptive control. Also, a technique for multistage design of an optimal momentum management controller for the space station has been developed and reported in. Moreover, we have successfully developed various digital redesign techniques which can convert a continuous-time controller to an equivalent digital controller. As a result, the expensive and unreliable continuous-time controller can be implemented using low-cost and high performance microprocessors. Recently, we have developed a new hybrid state-space self tuner using a new dual-rate sampling scheme for on-line adaptive control of continuous-time uncertain systems. Derived from text

N94-32980*# Tennessee State Univ., Nashville. Center of Excellence in Information Systems.

PARAMETRIC ROBUST CONTROL AND SYSTEM IDENTIFICATION: UNIFIED APPROACH Semiannual Status Report, 1 Nov. 1993 - 30 Apr. 1994

Leehyun Keel 10 May 1994 8 p

(Grant NAG5-2109)

(NASA-CR-195826; NAS 1.26:195826) Avail: CASI HC A02/MF A01

Despite significant advancement in the area of robust parametric control, the problem of synthesizing such a controller is still a wide open problem. Thus, we attempt to give a solution to this important problem. Our approach captures the parametric uncertainty as an H(sub infinity) unstructured uncertainty so that H(sub infinity) synthesis techniques are applicable. Although the techniques cannot cope with the exact parametric uncertainty, they give a reasonable guideline to model the unstructured uncertainty that contains the parametric uncertainty. An additional loop shaping technique is also introduced to relax its conservatism. Derived from text

N94-32992# Texas Univ., Austin. Center for Numerical Analysis.

PARALLEL SUPERCOMPUTING: ADVANCED METHODS, ALGORITHMS, AND SOFTWARE FOR LARGE-SCALE LINEAR AND NONLINEAR PROBLEMS

G. F. Carey and D. M. Young 1993 45 p

(Contract DE-FG05-87ER-25048)

(DE94-008446; DOE/ER-25048/T8) Avail: CASI HC A03/MF A01

The program outlined here is directed to research on methods, algorithms, and software for distributed parallel supercomputers. Of particular interest are finite element methods and finite difference methods together with sparse iterative solution schemes for scientific and engineering computations of very large-scale systems. Both linear and nonlinear problems will be investigated. In the nonlinear case, applications with bifurcation to multiple solutions will be considered using continuation strategies. The parallelizable numerical methods of particular interest are a family of partitioning schemes embracing domain decomposition, element-by-element strategies, and multi-level techniques. The methods will be further developed incorporating parallel iterative solution algorithms with associated preconditioners in parallel computer software. The schemes will be implemented on distributed memory parallel architectures such as the CRAY MPP, Intel Paragon, the NCUBE3, and the Connection Machine. We will also consider other new architectures such as the Kendall-Square (KSQ) and proposed machines such as the TERA. The applications will focus on large-scale three-dimensional nonlinear flow and reservoir problems with strong convective transport contributions. These are legitimate grand challenge class computational fluid dynamics (CFD) problems of significant practical interest to DOE. The methods developed and algorithms will, however, be of wider interest. DOE

N94-32996# Texas Univ., Houston. Dept. of Neurobiology and Anatomy.

ANALYSIS AND SYNTHESIS OF ADAPTIVE NEURAL ELEMENTS AND ASSEMBLES Final Technical Report, 1 Oct. 1990 - 30 Sep. 1993

John H. Byrne 30 Sep. 1993 13 p

(Grant AF-AFOSR-0027-91)

(AD-A277423; AFOSR-94-0095TR) Avail: CASI HC A03/MF A01

The overall objectives of this research were to investigate mechanisms underlying neural plasticity, learning, and memory. Between 1 Oct. 1990 and 30 Sep. 1993, progress was made in eight areas: (1) Voltage-clamp experiments analyzed membrane currents in a neuron that is modified during learning. (2) These data were incorporated into a single-cell model of associative learning. (3) The single-cell model was incorporated into a small neural network and simulations examined the functions of interneurons and the consequences of plasticity at multiple sites. (4) Additional simulations with the single-cell model examined potential cellular mechanisms for operant conditioning. (5) As a first step toward identifying additional loci for learning-induced modifications, the synaptic interactions were characterized among neurons that function as a central pattern generator (CPG). (6) Experiments also characterized how transmitters modulated the properties of the neurons and synaptic connections in the CPG and altered the electrical activity in the CPG. (7) These data were used to develop a model of the CPG, and simulations examined the mechanisms underlying the generation of rhythmic neural activity. (8) A realistic model of a bursting neuron was used to examine mechanisms underlying the generation and modulation of endogenous rhythmic neuronal activity. In addition, a computer program that is a general-purpose simulator for neural networks and action potentials was developed and has been made available to others. These results have provided general insights into information processing and storage in the nervous system. DTIC

N94-33014# Brown Univ., Providence, RI. Inst. for Brain and Neural Systems.

PROCEEDINGS OF THE NIPS 1993 POSTCONFERENCE WORKSHOP ON PULLING IT ALL TOGETHER: METHODS FOR COMBINING NEURAL NETWORKS

Michael P. Perrone 15 Mar. 1994 95 p

(Contract N00014-91-J-1316)

(AD-A277507) Avail: CASI HC A05/MF A01

This report is the proceedings workshop. The goal of the workshop was to examine theoretical aspects and heuristic methods for combining existing neural network algorithms to generate systems which have improved performance properties. This report includes an outline and summary of the workshop as well as the slides used in each participant's presentation. DTIC

N94-33043# Dayton Univ., OH. Research Inst.

CORRELATION FILTER SYNTHESIS USING NEURAL NETWORKS Final Technical Report, Jun. 1991 - Apr. 1993

Steven C. Gustafson and David L. Flannery Dec. 1993 173 p

(Contract F19628-91-K-0014)

(AD-A278124; RL-TR-93-239) Avail: CASI HC A08/MF A02

Excellent results were obtained using neural networks to synthesize filters for optical correlators, including filters for both cluttered backgrounds and target rotation angles not used in training. The most significant results employed new stretch and hammer neural networks which constitute an important and enduring advance because they train with guaranteed upper bounds on computational effort and generalize with guaranteed lower bounds on smoothness and stability. These results indicate good prospects for training neural networks to synthesize filters for a wide range of target distortions, and this approach has clear advantages compared to searching stored filters. DTIC

N94-33149 Defence Research Establishment Atlantic, Dartmouth (Nova Scotia).

CRAD SIGNAL AND INFORMATION PROCESSING WORKING GROUP WORKSHOP ON NEURAL NETWORKS, VOLUME 1

B. A. McArthur, ed. Feb. 1993 243 p Workshop held in Dartmouth, Nova Scotia, 6-7 May 1992

(DREA-TC-93-305-Vol-1; DSIS-93-02664-Vol-1; CTN-94-61183) Avail: Issuing Activity (Defence Research Establishment Atlantic, P.O. Box 1012, Dartmouth, NS B2Y 3Z7 Canada)

A workshop was held to provide the Canadian defense research

establishments and military colleges with a forum for the exchange of information related to the theory, design, and application of neural networks. Nine papers described defense related applications of neural networks, including radar, sonar, speech, pattern recognition, target acquisition and tracking, modulation recognition, and multisensor data fusion. Four papers were devoted to neural network theory and design. Separate abstracts have been prepared for nine papers from this workshop. For individual titles, see N94-33150 through N94-33158.

N94-33150 Defence Research Establishment, Ottawa (Ontario). Surface Radar Section.

THE APPLICATION OF A RADIAL BASIS FUNCTION NEURAL NETWORK FOR RADAR TRACKING OVER THE SEA **c32**

Henry Leung and Eloi Bosse *In* Defence Research Establishment Atlantic, CRAD Signal and Information Processing Working Group Workshop on Neural Networks, Volume 1 Feb. 1993 p 3-26 (For primary document see N94-33149 09-63)

Avail: Issuing Activity (Defence Research Establishment Atlantic, P.O. Box 1012, Dartmouth, NS B2Y 3Z7 Canada)

A new technique based on a radial basis function (RBR) neural network has been developed as a solution to the low-angle tracking problem. Computer simulations were carried out to evaluate the performance of the tracking algorithm. It was shown, using simulated data, that the new technique is able to track both stationary and moving targets under low signal to noise ratio environments with high accuracy. It was also demonstrated using real-life multipath data that the new technique is robust in the sense that it is insensitive to array errors and the nature of the background noise. The RBF network could track low flying targets under high sea-state conditions with very high performance in terms of resolution accuracy; in the two experiments conducted, the largest deviation was less than one meter. The algorithm is superior to the MUSIC algorithm in terms of robustness, resolvability, and estimation accuracy. Author (CISTI)

N94-33151 Defence Research Establishment Atlantic, Dartmouth (Nova Scotia).

SOME NEURAL COMPUTING APPROACHES TO TARGET TRACKING

Joseph N. Maksym *In its* CRAD Signal and Information Processing Working Group Workshop on Neural Networks, Volume 1 Feb. 1993 p 27-50 (For primary document see N94-33149 09-63)

Avail: Issuing Activity (Defence Research Establishment Atlantic, P.O. Box 1012, Dartmouth, NS B2Y 3Z7 Canada)

Multiple targets, false detections, and maneuvers present difficulties in the application of tracking and data association algorithms. Potential applications of neural networks in target tracking and data association problems are examined. While neural computing has proven useful for many pattern recognition and control applications, it is not yet clear how and where neural networks should be used in systems for tracking targets. Preliminary work on the application of neural networks as adjuncts to more conventional Kalman filter tracking systems is discussed. The possible use of neural networks is applied to model selection in a multiple-model approach to tracking maneuvering targets as well as to measurement to track data association. The focus is on Hopfield and probabilistic networks. A character recognition example illustrates the implementation of a combined Hopfield and probabilistic network approach. Author (CISTI)

N94-33152 Speech Technology Research Ltd., Victoria (British Columbia).

NEURAL NETWORKS APPLIED TO THE PHONEMIC SEGMENTATION OF SPEECH **c32**

Roy C. Snell and B. C. Dickson *In* Defence Research Establishment Atlantic, CRAD Signal and Information Processing Working Group Workshop on Neural Networks, Volume 1 Feb. 1993 p 69-81 (For primary document see N94-33149 09-63)

Avail: Issuing Activity (Defence Research Establishment Atlantic, P.O. Box 1012, Dartmouth, NS B2Y 3Z7 Canada)

A technique frequently used to develop software for identifying and classifying patterns is the construction of an expert system. Such a technique can be difficult and time-consuming to apply. Recent advances in neural networks have provided an alternative approach to the pattern classification problem. Using a corpus of already classified data, it is possible to design a neural network and train it to reproduce the classification results indicated on the training data. This approach completely removes the requirement for specifying the rules to be used and also greatly simplifies the final system implementation. The classification results obtained using an expert system are compared to those using a neural network for the problem of identifying nasalized segments of human speech. The waveform analysis used involves tenth order fixed frame linear prediction. Preliminary experiments on a limited data set indicate that the neural network approach will prove to be an effective tool for classifying nasal murmurs in human speech. The use of three output nodes corresponding to nasal, non-nasal, and mixed frames appears to improve the classification efficiency significantly. Since separate networks can be trained to recognize the nasal characteristics of individuals or groups, the process can be easily adapted to any application. Author (CISTI)

N94-33153 Defence Research Establishment, Ottawa (Ontario). Communications Electronic Warfare Section.

AUTOMATIC MODULATION RECOGNITION **c32**

Rene Lamontagne *In* Defence Research Establishment Atlantic, CRAD Signal and Information Processing Working Group Workshop on Neural Networks, Volume 1 Feb. 1993 p 83-103 (For primary document see N94-33149 09-63)

Avail: Issuing Activity (Defence Research Establishment Atlantic, P.O. Box 1012, Dartmouth, NS B2Y 3Z7 Canada)

To automate the problem of surveillance of the radio spectrum in electronic warfare (EW) applications, an intercept and analysis testbed is being built by Defence Research Establishment Ottawa's Communications EW section. As part of the testbed's narrowband digital signal processing subsystem, automatic modulation recognition (AMR) algorithms are being developed to identify the signal modulation type among several known to be in use in a given environment. Time and frequency domain features of the AMR system are reviewed and preliminary test results are presented in which the features are used in combination with an artificial neural network (ANN). It was proposed to increase the robustness of the system by improving the set of features and by using a classifier able to map complex decision regions. The results showed that both ways contributed to improve the system accuracy. Using the classic probabilistic classifier on the new set of features provided impressive results on the order of 94 percent for signal to noise ratios as low as 5 dB. The performance was further improved up to 99.8 percent using an ANN. Author (CISTI)

N94-33154 Defence Research Establishment Atlantic, Dartmouth (Nova Scotia).

MULTI-SENSOR DATA FUSION FOR TARGET ACQUISITION

Rony Philippe *In its* CRAD Signal and Information Processing Working Group Workshop on Neural Networks, Volume 1 Feb. 1993 p 129-143 (For primary document see N94-33149 09-63)

Avail: Issuing Activity (Defence Research Establishment Atlantic, P.O. Box 1012, Dartmouth, NS B2Y 3Z7 Canada)

The Canadian Department of National Defense has undertaken the study and development of intelligent systems for acquiring and identifying noncooperative vehicles using a number of sensors such as geophones, microphones, and electromagnetic sensors. By integrating the data from multiple sensors, the goal is to provide as fine a level of discrimination as possible. As a first step, it is necessary to determine the signal features which will serve to discriminate between the vehicles. Once an appropriate set of features has been selected, use of neural nets is proposed for classifying and/or identifying the various signatures and for coming to a decision on the identity of the unknown vehicle. The neural network should prove well suited for the expected variability of the signatures of vehicles due to the noise and uncertainties of a combat environment. In parallel with the search for appropriate signal features, work is beginning in the simulation of neural nets used for character recognition and for controlling phased-array antennas which are made to adaptively produce a peak and null in the radiation pattern in specific directions. Author (CISTI)

N94-33155 Defence Research Establishment Suffield, Ralston (Alberta).

PERIODIC AND CHAOTIC SIGNAL GENERATION IN A RECURSIVE ARTIFICIAL NEURAL NETWORK **c32**

Simon A. Barton *In* Defence Research Establishment Atlantic, CRAD Signal and Information Processing Working Group Workshop on Neural Networks, Volume 1 Feb. 1993 p 145-170 (For primary document see N94-33149 09-63)

Avail: Issuing Activity (Defence Research Establishment Atlantic, P.O. Box 1012, Dartmouth, NS B2Y 3Z7 Canada)

The behavior of artificial neural networks of recursive nonlinear processing elements can be rapidly moved from stability, through complex periodicity, to chaotic activity and back again, by only slight and subtle changes in a parameter that controls the steepness of the nonlinear node response functions. It is shown that a simple recursive network of only three sigmoidal nodes can exhibit cyclical behavior whose periodicity depends on the magnitude of a node response parameter, s. High values of s produce chaotic signals. From the numerically estimated values of s for which each period doubling occurs, a value of 4.669 is obtained for Feigenbaum's (1980) universal constant delta (4.669201...), thus confirming that this is a chaotic system. Chaotic and complex cyclical patterns can also arise in networks containing many nodes. The practical implications for artificial neural network applications and the possible biological significance of this effect are discussed. Author (CISTI)

N94-33156 Communications Research Centre, Ottawa (Ontario).
MODULAR NEURAL NETWORK ARCHITECTURES
William C. Treurniet *In* Defence Research Establishment Atlantic, CRAD Signal and Information Processing Working Group Workshop on Neural Networks, Volume 1 Feb. 1993 p 171-207 (For primary document see N94-33149 09-63)
Avail: Issuing Activity (Defence Research Establishment Atlantic, P.O. Box 1012, Dartmouth, NS B2Y 3Z7 Canada)

A number of proposed neural network architectures may be applied to the problem of phoneme classification in speech recognition. Experiments were conducted exploring the utility of some of these architectures including Hampshire and Waibel's Meta-Pi network, Nowlan and Hinton's system of experts, and Smieja's Minos architecture. In general, these modular structures did not perform better than single networks trained with the same data. Some explanations for this lack of improvement are suggested. Two new modular architectures were also designed and tested. The first employed 14 time delay neural network (TDNN) modules to map the complete input space to a different representation of reduced dimensionality. The second consisted of 49 TDNNs, each with one output unit, trained to discriminate one phoneme class from all the others. The first was able to identify 52.4 percent of the test cases correctly but the second only achieved 39.1 percent correct generalization. The same data used to train the latter modular systems were used to train single multilayer networks and TDNN's. For 38 and 49 classes the multilayer networks achieved 43 percent and 45.5 percent correct generalization respectively, while the TDNN's corresponding performances were 46.1 percent and 45.7 percent correct. The results suggest that modular architectures do not produce improved generalization performance compared to single networks. Author (CISTI)

N94-33157 Defence Research Establishment Pacific, Victoria (British Columbia).
NEAREST-NEIGHBOUR SEARCH IN CONSTANT TIME: AN ALTERNATIVE TO NEURAL NETWORKS FOR PATTERN MATCHING APPLICATIONS
Pierre Zakarauskas and John M. Ozard *In* Defence Research Establishment Atlantic, CRAD Signal and Information Processing Working Group Workshop on Neural Networks, Volume 1 Feb. 1993 p 209-229 (For primary document see N94-33149 09-63)
Avail: Issuing Activity (Defence Research Establishment Atlantic, P.O. Box 1012, Dartmouth, NS B2Y 3Z7 Canada)

Neural networks divide decision space with hyperplanes whose positions are adjusted during training, and the decision regions thus obtained are not necessarily optimal for noisy data. Neural networks also have the disadvantage of a rapid increase in training time for very large problems. To obtain robust pattern matching for problems where the number of patterns becomes very large, an alternate algorithm is proposed. This algorithm finds the training pattern closest to a test pattern, in a time which is asymptotically constant with the total number of patterns. The algorithm first partitions the search space and finds which partition each of the training patterns falls into. When a test pattern is supplied, it is compared to all patterns within the partitions which are within a given distance R to the test pattern. If the distance d between the closest pattern found during the first pass and the test pattern is less than R, the search stops; if not, a second pass is done using d as a search parameter to select partitions. This algorithm guarantees that the nearest neighbor is found. The mean number of operations done to find the nearest neighbor is presented as a function of the density of patterns per partition and the dimensionality of the search space. A global minimum mean number of operations is shown to exist at slightly less than one pattern per partition. Author (CISTI)

N94-33158 Defence Research Establishment Atlantic, Dartmouth (Nova Scotia).
NUMERICAL OPTIMIZATION TECHNIQUES IN NEURAL NETWORK TRAINING
Roy C. Snell *In* Defence Research Establishment Atlantic, CRAD Signal and Information Processing Working Group Workshop on Neural Networks, Volume 1 Feb. 1993 p 231-242 (For primary document see N94-33149 09-63)
Avail: Issuing Activity (Defence Research Establishment Atlantic, P.O. Box 1012, Dartmouth, NS B2Y 3Z7 Canada)

Numerical optimization methods are presented as an alternative to the standard backpropagation (BP) algorithm used in the training of multilayer perceptrons. This type of neural network is frequently the one chosen as a method of solving problems in the areas of pattern classification and nonlinear prediction. Aside from network topology considerations, the most significant problem encountered in the use of neural nets is the training process. The formulas used in the standard BP training technique for multilayer perceptrons are first derived. The training algorithm is then examined in the context of the unconstrained minimization of a multivariate function. A review of the standard methods used in numerical optimization points out the inefficiencies of BP, such as the fixed step size which produces divergence and oscillations in the worst cases and slower convergence in others. Alternative methods to improve training are suggested, focusing on the Fletcher Reeves Polak Ribiere minimization algorithm. A number of numerical examples are used to illustrate the increased efficiency of the proposed methods. Author (CISTI)

N94-33168# Aerospace Corp., El Segundo, CA. Technology Operations.
DATA PROCESSING ALGORITHMS FOR ON-BOARD SATELLITE EVENT ANALYSIS
R. Koga, S. D. Pinkerton, and N. Katz 30 Jan. 1994 13 p
(Contract F04701-93-C-0094)
(AD-A278406; TR-0091(6940-05)-8; SMC-TR-94-16) Avail: CASI HC A03/MF A01

Event rates encountered by satellite-borne sensors typically exceed the available telemetry bandwidth, necessitating on-board data analysis. One method of reducing output telemetry requirements, employed by data processing units (DPU's) on several recent and forthcoming satellites (VIKING, CRRES, CAMMICE), is to partition the underlying event parameter spaces into disjoint classes and to downlink statistics based on these classes rather than individual events. The DPU's utilize a hardware implemented binary search algorithm to classify each valid event into one of several mass and mass per charge-state (M/Q) groups, using look-up tables written under software control. Mass and M/Q group boundaries are defined via polynomial curves in the underlying parameter spaces. The boundary curves were obtained using a combination of global and local least-squares approximation algorithms applied to preflight sensor calibration data. DTIC

N94-33174 North Carolina Univ., Charlotte. Dept. of Mathematics.
CONFERENCE ON OPERATOR, WAVELET AND CONTROL THEORY
Final Report, 1 Apr. - 30 Sep. 1993
Xingde Dai 30 Sep. 1993 19 p Limited Reproducibility: More than 20% of this document may be affected by microfiche quality
(Contract F49620-93-1-0180)
(AD-A277429; AFOSR-94-0089TR) Avail: CASI HC A03

The conference on Interaction Between Operator Theory, Wavelet Theory and Control Theory, was held May 1-2, 1993 in Charlotte NC. The event was organized and hosted by the University of North Carolina at Charlotte. The main purpose of the conference was to bring researchers together, in so doing, to encourage an interchange of information and stimulation of cooperative efforts. DTIC

N94-33325 Texas Univ., Austin. Dept. of Electrical and Computer Engineering.
ADAPTIVE CONTROL OF NONLINEAR AND STOCHASTIC SYSTEMS Final Report, 1 Jan. 1992 - 31 Dec. 1993
Gunzburger and Aristotle Arapostathis 28 Feb. 1994 10 p Limited Reproducibility: More than 20% of this document may be affected by microfiche quality
(Contract F49620-92-J-0083)
(AD-A278411; AFOSR-94-0218TR) Avail: Issuing Activity (Defense Technical Information Center (DTIC))

Significant progress was made in a number of aspects of nonlinear and stochastic systems. Important contributions in the adaptive control of finite state Markov chains under partial observations were solved, and significant progress was made along more general directions. A project in surveying the literature on the ergodic control problem for discrete-time controlled Markov processes was completed. This work presented a comprehensive account of the considerable research on this problem over the past three decades. Further extending this effort, we embarked on writing a research monograph entitled 'Ergodic Control of Markov Chains and Stochastic Games' intended for publication as a volume in the series of 'Applications of Mathematics' by Springer-Verglag. A controlled switching diffusion model was developed to study the hierarchical control of flexible manufacturing systems. This study led to significant results in optimal control of stochastic hybrid system in both the discounted and average cost cases. In the area of deterministic nonlinear systems, numerical aspects of approximation linearization were investigated. DTIC

N94-33330 Texas Univ., El Paso. Dept. of Electrical Engineering.
INVESTIGATION OF MODULARLY CONFIGURED ATTACHED PROCESSORS WITH INTELLIGENT MEMORIES Report, 1 Oct. 1993 - 31 Mar. 1994
Glenn Gibson, Vijay Singh, Sanjay Singh, Yu-Cheng Liu, and Yi-Chieh Chang 31 Mar. 1994 56 p Limited Reproducibility: More than 20% of this document may be affected by microfiche quality
(Contract N00014-93-1-1343)
(AD-A278418) Avail: Issuing Activity (Defense Technical Information Center (DTIC))

A new architecture for high performance parallel attached processors is described. Based on this architecture, an attached processor can be implemented as multiple memory-to-memory pipelines, each being constructed with a class of fundamental components. The unique features are that the attached processor can be configured to match a set of algorithms and its memory controllers can be programmed to fit the access patterns required by the algorithms. As a result, high utilization of the processing logic for given sets of algorithms can be obtained. An example based on matrix multiplication is used for illustration. Finally, design issues related to the implementation of the attached processor based on an MCM technology are discussed. DTIC

N94-32421*# National Aeronautics and Space Administration. Ames Research Center, Moffett Field, CA.
REFINING FUZZY LOGIC CONTROLLERS WITH MACHINE LEARNING
Hamid R. Berenji *In* NASA, Washington, Technology 2003: The Fourth National Technology Transfer Conference and Exposition, Volume 2 Feb. 1994 p 3-6 (For primary document see N94-32420 09-99)
Avail: CASI HC A01/MF A04

N94-32422*# Bureau of Mines, Tuscaloosa, AL.
A FUZZY CLASSIFIER SYSTEM FOR PROCESS CONTROL
C. L. Karr and J. C. Phillips *In* NASA, Washington, Technology 2003: The Fourth National Technology Transfer Conference and Exposition, Volume 2 Feb. 1994 p 7-16 (For primary document see N94-32420 09-99)
Avail: CASI HC A02/MF A04

N94-32423*# Naval Air Warfare Center, Lakehurst, NJ. Aircraft Div.
FUZZY-NEURAL CONTROL OF AN AIRCRAFT TRACKING CAMERA PLATFORM
Dennis McGrath *In* NASA, Washington, Technology 2003: The Fourth National Technology Transfer Conference and Exposition, Volume 2 Feb. 1994 p 17-23 (For primary document see N94-32420 09-99)
Avail: CASI HC A02/MF A04

N94-32424*# American Welding Inst., Louisville, TN.
EMPIRICAL MODELING FOR INTELLIGENT, REAL-TIME MANUFACTURE CONTROL
Xiaoshu Xu *In* NASA, Washington, Technology 2003: The Fourth National Technology Transfer Conference and Exposition, Volume 2 Feb. 1994 p 24-33 (For primary document see N94-32420 09-99)
Avail: CASI HC A02/MF A04

N94-32425*# Naval Surface Warfare Center, Silver Spring, MD.
NEURAL NETWORK WAVELET TECHNOLOGY: A FRONTIER OF AUTOMATION
Harold Szu *In* NASA, Washington, Technology 2003: The Fourth National Technology Transfer Conference and Exposition, Volume 2 Feb. 1994 p 34-39 (For primary document see N94-32420 09-99)
Avail: CASI HC A02/MF A04

N94-33306*# National Aeronautics and Space Administration. Lewis Research Center, Cleveland, OH.
INTELLIGENT CONTROL OF A MULTI-DEGREE-OF FREEDOM REACTION COMPENSATING PLATFORM SYSTEM USING FUZZY LOGIC
Benjamin B. Choi, Charles Lawrence, and Yueh-Jaw Lin *In its* The 28th Aerospace Mechanisms Symposium May 1994 p 159-165 (For primary document see N94-33291 09-15)
Avail: CASI HC A02/MF A04

64 NUMERICAL ANALYSIS

Includes iteration, difference equations, and numerical approximation.

N94-31082 Grenoble-1 Univ. (France). Lab. Artemis.
FORMAL VERIFICATION OF SYSTOLIC MULTIPLIERS WITH THE BOYER-MOORE THEOREM PROVER
Laurence Pierre (Provence Univ., Marseille, France.) Jul. 1992 31 p Limited Reproducibility: More than 20% of this document may be affected by microfiche quality
(RR-897-M; ETN-94-95937) *Avail: Issuing Activity (European Space Agency (ESA))

A recursive functional modeling and an associated inductive proof methodology, specialized for the formal verification of systolic multipliers, is presented; these techniques are implemented in the Boyer-Moore logic. The software for the automatic translation between circuit descriptions written in VHSIC Hardware Design Language (VHDL) and the Boyer-Moore formalism is being realized, in order to include the automatic formal proof of systolic multipliers in the PREVAIL environment. The two significant examples given in this report demonstrate the feasibility and the efficiency of the method. ESA

N94-31092 Ecole Nationale Superieure des Telecommunications, Paris (France). Groupe Image.
TRIANGULAR NORMS AND CONORMS: A GENERAL TOOL FOR GENERATING FUZZY MATHEMATICAL MORPHOLOGIES [NORMES ET CONORMES TRIANGULAIRES: UN OUTIL GENERAL POUR LA GENERATION DE MORPHOLOGIES MATHEMATIQUES FLOUES]
Isabelle Bloch Jan. 1993 59 p In FRENCH Limited Reproducibility: More than 20% of this document may be affected by microfiche quality
(ISSN 0751-1345)
(TELECOM-93-D-001; ETN-94-95884) Avail: CASI HC A04

Several definitions for mathematical morphology operations working on fuzzy sets are proposed in the literature. Most of them are based on the same construction principle: translating set relationships into functional ones. A study which shows that triangular norms and conorms, which can be interpreted as fuzzy intersection and union, constitute a general tool for generating a large class of fuzzy morphologies and unify the previous approaches, is presented. The derived morphological operations preserve almost all properties satisfied by classical mathematical morphology. They inherit directly notions related to data fusion and decision theory derived from the interpretation of T-norms and T-conorms in terms of combination of uncertain, imprecise, partial information. ESA

N94-31095 Ecole Nationale Superieure des Telecommunications, Paris (France). Groupe Image.

COMPUTING THE PRECISION OF LOCALIZATION IN A PLANE USING PROJECTIVE INVARIANTS

Patrick Horain (Universidad Autonoma de Barcelona, Bellaterra, Spain.) 4 Dec. 1992 12 p Limited Reproducibility: More than 20% of this document may be affected by microfiche quality

(ISSN 0751-1345)

(TELECOM-93-D-005; ETN-94-95887) Avail: CASI HC A03

The use of projective invariants to localize objects in a plane from a single perspective image is addressed. Special attention is paid to the precision of the result. A method is proposed to estimate the final uncertainty, and to minimize it. This method may be adapted to volumic invariants, and may be useful when using invariants for object recognition. ESA

N94-31156# Loughborough Univ. of Technology (England). Dept. of Mathematical Sciences.

STRUCTURAL PROPERTIES OF INVERSE LINEAR SYSTEMS

A. C. Pugh, N. P. Karampetakis, A. I. G. Vardulakis, and G. E. Hayton Nov. 1993 12 p

(Maths-Rept-A-200; ETN-94-95861) Avail: CASI HC A03/MF A01

It was shown that some of the finite and infinite properties of a square inverse system are related to the corresponding properties of the original system. Equivalent invertible systems are seen to give rise to inverses which are similarly equivalent. An extension to the case of inverses of generalized transfer function matrices is also considered. ESA

N94-31159# Loughborough Univ. of Technology (England). Dept. of Mathematical Sciences.

SYMPLECTIC RUNGE-KUTTA SCHEMES 3: CANONICAL ELEMENTARY DIFFERENTIALS

M. Sofroniou and W. Oevel Nov. 1993 11 p

(Maths-Rept-A-204; ETN-94-95864) Avail: CASI HC A03/MF A01

Results demonstrating that the symplecticity condition for Runge-Kutta schemes may be eliminated by suitable parameterization of the order conditions are used to reexamine the relationship between order conditions for canonical Runge-Kutta methods and canonical elementary differentials. It is shown that the canonical elementary differential can be specified in terms of one rooted candidate per tree. ESA

N94-31160# Loughborough Univ. of Technology (England). Dept. of Mathematical Sciences.

SYMBOLIC DERIVATION OF RUNGE-KUTTA METHODS

M. Sofroniou Nov. 1993 24 p

(Maths-Rept-A-205; ETN-94-95865) Avail: CASI HC A03/MF A01

A symbolic computer package, Butcher.m, which may be used to explore and derive Runge-Kutta methods is presented. The package makes use of the graph theoretical formalism attributed to John Butcher. Runge-Kutta methods and the representation used for the free parameters are introduced. The concept of rooted trees and their correspondence with the elementary differentials appearing in a Taylor series expansion of the solution is also introduced. The derivation and implementation of the order conditions is symbolically demonstrated. Solving the resulting nonlinear equations is a very difficult proposition. The Groebner bases algorithm, implemented as part of Mathematica's 'solve' command, which may be used to obtain solutions, is outlined. Butcher's simplifying assumptions and their implementation are explained. These play a crucial role in the derivation of high order schemes. The use of the package is illustrated with several examples. ESA

N94-31162# Loughborough Univ. of Technology (England). Dept. of Mathematical Sciences.

OBSERVATIONS OF THE NOTION OF MINIMALITY IN THE GENERALIZED STATE SPACE

A. C. Pugh, N. P. Karampetakis, A. I. Vardulakis, and G. E. Hayton Jan. 1994 24 p Sponsored in part by Greek National Foundation

(Maths-Rept-A-207; ETN-94-95867) Avail: CASI HC A03/MF A01

The notion of minimality in the conventional state space is explored in the generalized state space context. In the regular case two disctinct notions are seen to accrue to the term, one which has a true dynamic meaning and one which does not. Some implications for generalized state space systems possessing either of these properties are revealed by a number of results and examples. ESA

N94-31169 Ecole Nationale Superieure des Telecommunications, Paris (France).

MODULATION AND CODING FOR THE GAUSSIAN CHANNEL, POSSIBLY AFFECTED BY FLUCTUATIONS Ph.D. Thesis [MODULATION ET CODAGE POUR LE CANAL GAUSSIEN, EVENTUELLEMENT AFFECTE DE FLUCTUATIONS]

Weidong Zhang 1993 152 p In FRENCH Limited Reproducibility: More than 20% of this document may be affected by microfiche quality

(ISSN 0751-1353)

(TELECOM-93-E-009; ETN-94-95899) Avail: Issuing Activity (European Space Agency (ESA))

As a technique for obtaining good codes without loss of spectral efficiency, coded modulation relies on a joint design of coding and modulation. For the same purpose but using different means, a system which combines a Maximum Distance Separable (MDS) code, particularly a q-ary (n, k) Reed-Solomon one, and a q-ary Phase Shift Keying (PSK) modulation, is studied. This scheme is clearly different from that of Ungerboeck since it does not involve constellation partitioning, but it results in a Euclidean distance distribution close to that of random coding, which was used by Shannon for proving the channel capacity theorem, provided that q, n and k are large enough. Thus it is possible to obtain by deterministic means the same performance as by random coding, and the criterion for searching good codes, instead of the minimum distance one, may be a measure of similarity of the normalized distance distribution with respect to random coding. Good performance can be achieved only if decoding the MDS code actually works in the Euclidean space. In other words, soft decoding is mandatory. The Battail-Fang algorithm with some modification is used. In a system using PSK, quantification is often performed only on the phase of the received signal. An attempt to perform it on both the phase and the amplitude was made. A performance improvement results since better use is made of the information provided by the channel. The results of both theoretical analysis and computer simulation reported supply evidence of favor of designing codes by means closer to those of the origin, that is, information theory. ESA

N94-31187 Politecnico di Milano (Italy). Dipt. di Elettronica e Informazione.

A WORST-CASE ANALYSIS OF TWO APPROXIMATE ALGORITHMS FOR THE SYMMETRIC TRAVELLING SALESMAN PROBLEM

Giovanni Righini and Marco Trubian May 1993 10 p Sponsored in part by Ministry of University and Scientific and Technological Research

(Rept-93-036; ETN-94-95805) Avail: Issuing Activty (Politecnico di Milano, Piazza Leonardo da Vinci 32, 20133 Milan, Italy)

Two algorithms for the asymmetric traveling salesman problem are presented. The worst case performance of both algorithms is bounded by quantities which are independent of the size of the problem (number of vertices) but depend on the weights associated to the arcs. The second algorithm improves a bound previously found under an identical hypothesis. ESA

N94-31231# Office National d'Etudes et de Recherches Aerospatiales, Paris (France).

DOUBLY ASYMPTOTIC APPROXIMATIONS: THEORETICAL AND NUMERICAL ANALYSES Ph.D. Thesis - Paris 6 Univ. [ETUDE THEORIQUE ET NUMERIQUE DES METHODES DE DOUBLES APPROXIMATIONS ASYMPTOTIQUES]

Sophie Ortola 1993 117 p In FRENCH

(ISSN 0078-3781)

(ONERA-NT-1993-7; ETN-94-95875) Avail: CASI HC A06/MF A02

The solution of fluid structure interaction problems for internal harmonic excitation of a structure is addressed. Doubly Asymptotic Approximations (DAA's) are approximate relations for solving the exterior acoustic problem. For a geometrically simple problem, the responses given by the DAA approach are analyzed for the interaction and for the acoustic problems. For the acoustic problem, when DAA relations are applied on the spherical edge of the fluid domain, the frequency domains of validity of these methods can be determined for a given excitation harmonic. For the associated unidimensional axisymmetric problems, iterative methods were developed, based on the characteristics of the DAA operators, to calculate the exact

exterior acoustic solutions over the whole frequency range. The iterative process expected to be the most efficient, numerically, is applied for the three dimensional case. In the upper frequency range, the iterative solutions are then extended by a new approximate solution obtained by translation of a DAA relation. A variety of numerical methods, using DAA and iterative methods, are proposed for solving the fluid structure interaction problem. ESA

N94-31252 Defence Research Establishment, Ottawa (Ontario).
DESCRIPTION OF A PACKAGE FOR THE ANALYSIS AND DISPLAY OF THE RESULTS OF NUMERICAL SIMULATIONS
Marc Dion Dec. 1993 47 p Limited Reproducibility: More than 20% of this document may be affected by microfiche quality
(AD-A276285; DREO-TN-93-21) Avail: CASI HC A03

An interactive and versatile program was written for a VAX/VMS system to plot and manipulate the results of some simulation programs. It was first developed to display results from SPICE (a circuit simulation program) but has been modified to accept almost any data in ASCII files. Another version of the program was written for the plotting and manipulation of results during the simulations. This document provides a detailed description of the programs and their commands. DTIC

N94-31274# Argonne National Lab., IL.
A SURVEY OF NUMERICAL CUBATURE OVER TRIANGLES
J. N. Lyness and R. Cools 1993 25 p Presented at the Joint Meeting of the Canadian Mathematical Society, the American Mathematical Society, and the Mathematical Association of America on Computation 1943-1993, Vancouver, Ontario, 15-19 Aug. 1993
(Contract W-31-109-eng-38)
(DE94-006810; ANL/MCS/CP-81883; CONF-9308116-1) Avail: CASI HC A03/MF A01

This survey collects together theoretical results in the area of numerical cubature over triangles and is a vehicle for a current bibliography. We treat first the theory relating to regular integrands and then the corresponding theory for singular integrands with emphasis on the 'full corner singularity.' Within these two sections we treat successively approaches based on transforming the triangle into a square, formulas based on polynomial moment fitting, and extrapolation techniques. Within each category we quote key theoretical results without proof, and relate other results and references to these. Nearly all the references we have found may be readily placed in one of these categories. This survey is theoretical in character and does not include recent work in adaptive and automatic integration. DOE

N94-31309# Argonne National Lab., IL.
FIRST THEORY INSTITUTE ON COMPUTATIONAL DIFFERENTIATION
C. H. Bischof, ed., A. Griewank, ed., and P. M. Khademi, ed. 1993 35 p Presented at the 1st Theory Institute on Computational Differentiation Workshop, Argonne, IL, 24-26 May 1993
(Contract W-31-109-eng-38)
(DE94-006491; ANL/MCS-TM-183; CONF-9305285) Avail: CASI HC A03/MF A01

Computational differentiation (CD) is concerned with tools, techniques, and mathematics for generating, with little human effort, efficient and accurate derivative codes from programs written in such computer languages as C and FORTRAN. The primary purposes of the meeting were to explore the deep complexity issues that lie at the heart of the computation of derivatives from computer programs and to provide a forum for brainstorming on future research directions, including the applications of automatic differentiation (AD) in scientific computing and the development of AD tools. DOE

N94-31311# Argonne National Lab., IL.
NONLINEARITY AS AN ORIGIN OF NONUNIQUENESS IN SOLUTION OF HARTREE'S EQUATION
M. Ya. Amusia and A. F. Ioffe 1993 4 p Presented at the 1993 International Symposium on Nonlinear Theory and Its Applications, Honolulu, HI, 5-10 Dec. 1993
(Contract W-31-109-eng-38)
(DE94-006538; ANL/PHY/CP-81870; CONF-931252-1) Avail: CASI HC A01/MF A01

There is almost no doubt that the surrounding macroscopical world, its chemistry and biology is described by the Schredinger equation, which includes all particles and their interaction. In a very large scale of distances the interaction is of electromagnetic nature and can be presented as a sum of potential energies of all pairs of particles. The solution of the Schredinger equation gives the wave function of any considered system and via it all observable characteristics can be calculated, in principle. The Schredinger equation is linear so it has unique solutions. However containing coordinates and momenta of all particles of the system, it is almost unsolvable for really macroscopical objects and must be simplified. One of the most important steps in this direction was made by Hartree in the twenties, leading to nonlinear equations which bear his name. The wave function of a multielectron system is approximated in Hartree's method by the product of one-particle wave functions, which are selected in a definite fashion. We consider a system of N identical Fermi-particles moving in the Coulomb attractive field of a nucleus of charge Z and interacting one with another via the pair potential V(r1,r2) where r1 and r2 are the radius vectors of the particles. Derived from text

N94-31359# Naval Command, Control and Ocean Surveillance Center, San Diego, CA. Research, Development, Technology and Evaluation Div.
TEXTURE GENERATION ON IRREGULAR REGIONS
J. F. Richardson Jan. 1994 8 p
(AD-A275999) Avail: CASI HC A02/MF A01

This paper describes a technique for the solution of systems of symmetric parabolic partial differential equations that are associated with the generation of biologic texture generating equations on the highly irregular regions associated with complex image geometries. This technique, when used with an automatic grid generation program, allows for the direct and efficient generation of textures on complex surfaces. Since there is a one to one correspondence between the generated texture in the transformed domain and the original surface, there is no need to map the generated texture pattern back to the surface of interest. This technique can be applied to large systems of reaction-diffusion equations, thus expanding the set of patterns that can be produced using models based upon reaction-diffusion equations. In addition, textures based upon variable diffusion constants can be generated including a wide range of anisotropic textures. DTIC

N94-31360# Army Research Lab., Aberdeen Proving Ground, MD.
REMARKS ON A RESULT OF LAV CARVALHO Final Report, Oct. 1992 - May 1993
N. P. Bhatia and W. O. Egerland Feb. 1994 13 p
(AD-A276404; ARL-TR-351) Avail: CASI HC A03/MF A01

The report comments on two papers in the Journal of Mathematical Analysis and Applications and contains two new propositions that supplement results that were previously published by the authors. The note was submitted for publication in the Journal of Mathematical Analysis and Applications and is presently under review. DTIC

N94-31388 Amsterdam Univ. (Netherlands). Inst. for Logic, Language and Computation.
LAMBEK CALCULUS IS L-COMPLETE
Mati Pentus (Moscow State Univ., Russia.) Nov. 1993 40 p Limited Reproducibility: More than 20% of this document may be affected by microfiche quality
(ISSN 0928-3307)
(LP-93-14; ETN-94-96005) Avail: CASI HC A03/MF A01

A proof that the Lambek calculus is complete with respect to L models, that is, free semi group models, is given. The completeness with respect to relational models over the natural linear order of integers is also proved. ESA

N94-31391 Amsterdam Univ. (Netherlands). Dept. of Mathematics and Computer Science.
AN ALGEBRAIC VIEW ON ROSETTA
Theo M. V. Janssen Sep. 1993 21 p Submitted for publication Limited Reproducibility: More than 20% of this document may be affected by microfiche quality
(ISSN 0923-3292)
(CL-93-02; ETN-94-96008) Avail: CASI HC A03

A mathematical model of compositional translation is developed using basic universal algebra. The Rosetta system, which has as its main principle the principle of compositionality of translation, is considered in the

perspective of the developed model, and other instances of the model are mentioned. Aspects related to the formal power of the method are discussed. ESA

N94-31393 Amsterdam Univ. (Netherlands). Dept. of Mathematics and Computer Science.
PROVING THEOREMS OF THE LAMBEK CALCULUS OF ORDER 2 IN POLYNOMIAL TIME
Erik Aarts (OTS, Utrecht, Netherlands.) May 1993 16 p Limited Reproducibility: More than 20% of this document may be affected by microfiche quality
(Contract NF-102/62-356) (ISSN 0928-3323)
(CT-93-05; ETN-94-96010) Avail: CASI HC A03

In the Lambek calculus of order 2, only sequents are allowed in which the depth of nesting of implications is limited to 2. A proof that the decision problem of provability in the calculus can be solved in time polynomial in the length of the sequent is given. A normal form for proofs of second order sequents is defined. It is shown that for every proof there is a normal form proof with the same reading. With this normal form, two algorithms that decide about probability of sequents in polynomial time can be given. ESA

N94-31394 Sheffield Univ. (England). Dept. of Automatic Control and Systems Engineering.
NONLINEAR MODEL VALIDATION USING CORRELATION TESTS
S. A. Billings and Q. M. Zhu Jul. 1993 18 p Limited Reproducibility: More than 20% of this document may be affected by microfiche quality
(Grant SERC-GR/H3528.6)
(RR-463; ETN-94-96055) Avail: CASI HC A03

Higher order correlation tests which use model residuals combined with system inputs and outputs are presented to check the validity of a general class of nonlinear models. The method is illustrated by testing both simple and complex nonlinear system models. It is thought that these tests should be applicable to a wide class of nonlinear models including neural nets. ESA

N94-31399# Westinghouse Savannah River Co., Aiken, SC.
A REVIEW OF SENSITIVITY ANALYSIS TECHNIQUES
D. M. Hamby 1993 36 p
(Contract DE-AC09-89SR-18035)
(DE94-007192; WSRC-MS-93-576) Avail: CASI HC A03/MF A01

Mathematical models are utilized to approximate various highly complex engineering, physical, environmental, social, and economic phenomena. Model parameters exerting the most influence on model results are identified through a 'sensitivity analysis.' A comprehensive review is presented of more than a dozen sensitivity analysis methods. The most fundamental of sensitivity techniques utilizes partial differentiation whereas the simplest approach requires varying parameter values one-at-a-time. Correlation analysis is used to determine relationships between independent and dependent variables. Regression analysis provides the most comprehensive sensitivity measure and is commonly utilized to build response surfaces that approximate complex models. DOE

N94-31409 Amsterdam Univ. (Netherlands). Dept. of Mathematics and Computer Science.
COMPARING MODELS OF THE NON-EXTENSIONAL TYPED LAMBDA-CALCULUS
Raymond Hoofman Oct. 1993 21 p Limited Reproducibility: More than 20% of this document may be affected by microfiche quality
(ISSN 0928-3315)
(ML-93-19; ETN-94-95995) Avail: CASI HC A03

'Powerset models' of the nonextensional typed lambda calculus are compared. It is shown that the choice of a certain minimal interpretation, with respect to a certain class of interpretations, of the type constructor 'double arrow pointing to the right' yields models with a maximal theory (in that class). ESA

N94-31412 Sheffield Univ. (England). Dept. of Automatic Control and Systems Engineering.
ON WAVELET REPRESENTATIONS OF DIFFERENTIAL EQUATIONS
S. P. Banks and A. Moser Jul. 1993 15 p Limited Reproducibility: More than 20% of this document may be affected by microfiche quality
(RR-482; ETN-94-96058) Avail: CASI HC A03

The wavelet expansion of the solutions of nonlinear differential equations is considered. It is shown that, using Lie series, an infinite dimensional linear system is obtained and an existence result for periodic orbits is proved. The numerical computation of solutions is generalized from Euler's method to general wavelet expansions. ESA

N94-31413 Sheffield Univ. (England). Dept. of Automatic Control and Systems Engineering.
IDENTIFICATION OF POLYNOMIAL AND RATIONAL NARMAX MODELS
Q. M. Zhu and S. A. Billings Aug. 1993 13 p Limited Reproducibility: More than 20% of this document may be affected by microfiche quality
(Grant SERC-GR/H3528.6)
(RR-483; ETN-94-96059) Avail: Issuing Activity (European Space Agency (ESA))

The identification of polynomial and rational NARMAX models is studied, and a unified least squares algorithm is introduced. The NARMAX model can be used to describe the stochastic behaviors of both linear and nonlinear systems. The identification of two fluid loading systems and a wave flume system in unidirectional and directional sea states are included to illustrate the results. ESA

N94-31441# Wisconsin Univ., Madison. Center for Mathematical Sciences.
MULTIVARIATE SPLINE APPROXIMATION Final Report, 27 Sep. 1990 - 26 Sep. 1993
Carl R. DeBoor and Amos Ron 22 Dec. 1993 6 p
(Contract DAAL03-90-G-0090)
(AD-A276034; ARO-27690.22-MA) Avail: CASI HC A02/MF A01

We started out with the goal of understanding approximation order in a multivariate context, including the approximation of surfaces. In addition, we wanted to understand better the use and analysis of our approach to multivariate polynomial interpolation. We ended up concentrating on approximation from shift-invariant spaces of functions on R(exp d) real space. Here, S is shift-invariant if f is an element of S implies that also f(. - alpha) is an element of S for any integer vector alpha. The simple, yet widely applicable, model we considered concerns the behavior, as H approaches 0, of the distance between f and S of a suitably smooth f from the scaled space S(sub h)(sup h) := (f(./h) : f is an element of S(sub h)), with each S(sub h) a shift-invariant space. Examples of such spaces are provided by finite elements on a regular grid, in particular box spline spaces, also the spaces which make up the multiresolution analysis generated by wavelets. DTIC

N94-31451 Amsterdam Univ. (Netherlands). Inst. for Logic, Language and Computation.
ON THE EQUIVALENCE OF LAMBEK CATEGORIAL GRAMMARS AND BASIC CATEGORIAL GRAMMARS
Wojcieh Buszkowski (Adam Mickiewicz Univ., Poznan, Poland.) Jul. 1993 22 p Sponsored by EEC Limited Reproducibility: More than 20% of this document may be affected by microfiche quality
(ISSN 0928-3307)
(LP-93-07; ETN-94-95999) Avail: CASI HC A03

It is known that Lambek categorial grammars (LCG's) are weakly equivalent to context free grammars (CFG's), hence also to BCGs (basic CG's), by Gaifman's theorem. It is shown that for any product free LCG G, there is an equivalent BCG G' which results from expanding the initial type assignment of G by means of some Lambek derivable formulae, as expected by many authors and erroneously proven by some. The construction uses a modification of Pentus' argument and the interpretation of Gaifman's theorem on the basis of the Lambek calculus. The latter is presented more carefully and, as a result, a proof of Gaifman's theorem is obtained in which the Lambek calculus is essentially involved. ESA

N94-31453 Amsterdam Univ. (Netherlands). Inst. for Logic, Language and Computation.
COMPLETENESS AND DECIDABILITY OF THE MIXED STYLE OF INFERENCE WITH COMPOSITION
Makoto Kanazawa (Stanford Univ., CA.) Oct. 1993 19 p Limited Reproducibility: More than 20% of this document may be affected by

microfiche quality
(ISSN 0928-3307)
(LP-93-09; ETN-94-96001) Avail: CASI HC A03

A complete calculus for mixed inference with composition is presented and it is proved that it has the finite model property and is therefore decidable. A variant of the calculus complete with respect to functional models is presented and completeness and decidability of other styles of inference involving composition, including dynamic inference, are mentioned. A trend in one corner of logic is to regard the meaning of a sentence as a relation on information states. This 'dynamic' perspective gives rise to a number of new conceptions of inference, allowing different answers to the question of what it means for conclusion C to follow from premises P(sub 1), ..., P(sub n). One such dynamic notion of inference is what van Benthem calls mixed inference, which is of particular interest for its connection to Veltman's update semantics. Mixed inference is investigated with respect to such standard logical questions as axiomatizability and decidability. Other dynamic styles of inference are discussed. ESA

N94-31474# Wisconsin Univ., Madison. Center for Mathematical Sciences.

FRAMES AND STABLE BASES FOR SHIFT-INVARIANT SUBSPACES OF L(SUB 2)(IR(SUP d)) Summary Report

Amos Ron and Zuowei Shen Feb. 1994 44 p
(Contract DAAL03-90-G-0090; NSF DMS-92-24748; NSF DMS-90-00053; NSF DMS-91-02857)
(AD-A276470; CMS-TSR-94-7) Avail: CASI HC A03/MF A01

We study in this paper certain types of bases for shift-invariant subspaces. Our primary objective is to connect among three important families of basis sets: shift-invariant sets. Weyl-Heisenberg sets, and affine (wavelet) sets. The present paper is the first in a series of three, and is concerned with the basic theory of shift-invariant bases for the shift-invariant spaces. DTIC

N94-31529# National Academy of Sciences - National Research Council, Washington, DC. Board on Mathematical Sciences.

A CROSS-DISCIPLINARY REPORT ON THE MATHEMATICAL SCIENCES APPLIED TO MATERIALS SCIENCE, PART 1 Final Report, 1 Feb. 1992 - 31 Oct. 1993

John R. Tucker 26 Oct. 1993 10 p
(Contract DAAL03-92-G-0013)
(AD-A276116; ARO-29397.1-MA-Pt-1) Avail: CASI HC A02/MF A01

This project produced a National Research Council report from the Board on Mathematical Sciences, Mathematical Research in Materials Science. Opportunities and Perspectives, that documents and presents technical details of fruitful collaborations between the mathematical sciences and materials science, and indicates areas of mathematical sciences research holding the most promise for advancing materials science. Written primarily for mathematical and materials science researchers with an interest in advancing research at this interface, as well as for federal and state agency representatives interested in encouraging such collaborations, it focuses on directions for potentially promising collaboration between materials scientists and mathematical scientists, and encourages both communities to increase such collaborations. It emphasizes that both the mathematical sciences and materials science communities have much to win from an increase in cross-disciplinary collaborations, and presents recommendations for facilitating mathematical sciences research that bears on important issues in materials science, including recommendations on how to attract students and young researchers to this area. It seeks to encourage research directions in the mathematical sciences that complement vital materials science research, and raise awareness of the value of quantitative methods in materials science. DTIC

N94-31539# Cranfield Inst. of Tech., Bedford (England). Dept. of Aerospace Science.

FULLY DISCRETE ARBITRARY-ORDER SCHEMES FOR A MODEL HYPERBOLIC CONSERVATION LAW

J. Shi and E. F. Toro Jun. 1993 24 p
(Cranfield-Aero-9307; ISBN-1-871564-63-8; ETN-94-96070) Avail: CASI HC A03/MF A01; Cranfield Univ. of Technology, Coll. of Aeronautics, Cranfield, Bedford MK43 0AL, England, HC

An approach for constructing two level explicit fully discrete arbitrary order conservative numerical methods for one dimensional scalar hyperbolic equation is presented. To illustrate the technique fully discrete second, third, and fourth order conservative numerical schemes are given. Numerical experiments indicate that the second order methods are not accurate for problems requiring long time evolution, and a dramatic improvement of the numerical solution is seen when the accuracy changes from second to fourth order. The foundations for developing high order methods that are applicable to nonlinear systems of hyperbolic conservation laws are presented. There are two major problems to be addressed. One is the problem of monotonicity of the schemes near high gradients (for example shocks) and the other is the extension of the approach to nonlinear systems. These issues are the subjects of current research. ESA

N94-31540# Cranfield Inst. of Tech., Bedford (England). Dept. of Aerospace Science.

A SIMPLIFIED VON NEUMANN METHOD FOR LINEAR STABILITY ANALYSIS

Jian Shi Jun. 1993 20 p
(Cranfield-Aero-9310; ISBN-1-871564-62-X; ETN-94-96071) Avail: CASI HC A03/MF A01; Cranfield Univ. of Technology, Coll. of Aeronautics, Cranfield, Bedford MK43 0AL, England, HC

The issue of linear stability analysis for two and three level explicit and implicit one dimensional finite different numerical schemes is investigated. An approach which simplifies the Von Neumann method is presented. It was proved that the new technique is efficient and effective for linear stability study. This is especially true for high order and complicated numerical schemes. ESA

N94-31541# Cranfield Inst. of Tech., Bedford (England). Dept. of Aerospace Science.

MULTIDIMENSIONAL WAF-TYPE SCHEMES FOR MODEL CONSERVATION LAWS

E. F. Toro and S. J. Billett Sep. 1993 51 p
(Cranfield-Aero-9312; ISBN-1-871564-65-4; ETN-94-96072) Avail: CASI HC A03/MF A01; Cranfield Univ. of Technology, Coll. of Aeronautics, Cranfield, Bedford MK43 0AL, England, HC

The use of the Weighted Average Flux (WAF) approach to generate first and second order accurate finite volume schemes in one, two, and three space dimensions is explored. The derived schemes have multidimensional upwinding aspects and good stability properties. Oscillation free methods that are second order accurate in smooth flow by making use of one dimensional limiter functions are constructed. Some numerical results are presented. ESA

N94-31552# Technische Univ., Delft (Netherlands). Faculty of Technical Mathematics and Informatics.

TWO MODELS SOLVING THE INCREASING ENERGY PROBLEM OF THE CONTINUOUS HOPFIELD NETWORK MODEL

M. A. Odijk 1993 20 p
(ISSN 0922-5641)
(Rept-93-87; ETN-94-96132) Copyright Avail: CASI HC A03/MF A01

The integral term of the energy function of a continuous Hopfield network is often neglected in order to use the model for optimization purposes. Unfortunately, this diminishes the computational power of the model. What is more, omitting the integral term may cause the energy to increase, thus, disturbing the computations. One solution to overcome these problems is to omit the decay term in the motion equation. Then, the integral term can be deleted in a natural manner. Another solution is to increase the gain exponentially during the state evolution. It can be shown that when applying one of those solutions the Hopfield energy function without the integral term is a Liapunov function for the motion equation. The idea of omitting the decay term or increasing the gain is not new. However, it is claimed that the theoretical support is presented. In particular, it can be shown that both solutions yield models that have equal computational power. There also exists an interesting physical relation between the two solutions. ESA

N94-31642# Technische Univ., Delft (Netherlands). Faculty of Technical Mathematics and Informatics.

STIRLING'S FORMULA AND APPROXIMATIONS FOR n(FACTORIAL) AND THE MIDDLE RATIO

J. G. Besjes and W. J. vanHorssen 1993 25 p

(ISSN 0922-5641)
(Rept-93-73; ETN-94-96118) Copyright Avail: CASI HC A03/MF A01

It is shown elementary that n(factorial)e(exp n)n(exp -n-(1/2)) tends to a limit 'a' greater than 0 for n approaches infinity. Sharp bounds for 'a' are given. Semiconvergent series for n(factorial) and the middle ratio are found, giving rise to inequalities. In principle many more terms of the series can be obtained giving more intricate inequalities. ESA

N94-31643# Technische Univ., Delft (Netherlands). Faculty of Technical Mathematics and Informatics.

GENERALIZATION OF A THEOREM OF KUSMIN

Karma Dajani and Cor Kraaikamp 1993 19 p Sponsored in part by Netherlands Organization for Scientific Research
(ISSN 0922-5641)
(Rept-93-74; ETN-94-96119) Copyright Avail: CASI HC A03/MF A01

A Gauss-Kusmin theorem for the natural extension of the regular continued fraction expansion is given. A generalization of a theorem by D.E. Knuth is obtained by similar techniques. ESA

N94-31644# Technische Univ., Delft (Netherlands). Faculty of Technical Mathematics and Informatics.

QUALITATIVE PROPERTIES OF TWO-DIMENSIONAL PREDATOR-PREY SYSTEMS

R. E. Kooij and Z. Zegeling 1993 34 p
(ISSN 0922-5641)
(Rept-93-75; ETN-94-96120) Copyright Avail: CASI HC A03/MF A01

The number of limit cycles appearing in two dimensional predator-prey systems is investigated. Uniqueness of limit cycles is proved for systems with a functional response more general than the standard Holling types 2 and 3. The transformation to Lienard systems is discussed. Examples of systems with at least two limit cycles are given. The aim is to indicate in which cases no, one, or at least two limit cycles appear. ESA

N94-31665 Argonne National Lab., IL.

FINITE-PART INTEGRALS AND THE EULER-MACLAURIN EXPANSION

J. N. Lyness 1993 10 p Presented at the International Symposium on Special Functions, Approximation, Numericqal Quadrature, and Orthogonal Polynomials, West Lafayette, IN, 2-4 Dec. 1993 Limited Reproducibility: More than 20% of this document may be affected by microfiche quality
(Contract W-31-109-eng-38)
(DE94-006539; ANL/MCS/CP-81897; CONF-931249-1) Avail: CASI HC A02

The context of this note is the discretization error made by the m-panel trapezoidal rule when the integrand has an algebraic singularity at one end, say x = 0, of the finite integration interval. In the absence of a singularity, this error in described by the classical Euler-Maclaurin summation formula, which is an asymptotic expansion in inverse integer powers of m. When an integrable singularity (x(sup alpha) with alpha greater than -1) is present, Navot's generalization is valid. This introduces negative fractional powers of m into the expansion. Ninham has generalized this result to noninteger alpha satisfying alpha less than -1. In this note, we extend these results to all alpha by providing the nontrivial extension to negative integer alpha. This expansion differs from the previous expansions by the introduction of a term log m. DOE

N94-31673# Technische Univ., Delft (Netherlands). Faculty of Technical Mathematics and Informatics.

TRACTABLE DEDUCTION IN SOME FRAGMENTS OF AUTO-EPISTEMIC LOGIC

G. J. Akkerman 1993 18 p Sponsored by Netherlands Organization for Scientific Research
(ISSN 0922-5641)
(Rept-93-89; ETN-94-96134) Copyright Avail: CASI HC A03/MF A01

The three fragments of default logic that have been shown to have tractable decision problems by Kautz and Selman, are considered and it is shown that the corresponding decision problems for auto-epistemic logic have similar complexities. This serves to demonstrate that stratified theories (for which, due to its allowing only one extension, all decision problems collapse in to one) form not the only reasonable tractable fragment of auto-epistemic logic. ESA

N94-31676# Groningen Rijksuniv. (Netherlands). Dept. of Mathematics.

THE CAMERON-MARTIN THEOREM

Erik G. F. Thomas 8 Jun. 1993 15 p Presented at the Seminar for Stochastic Analysis, Groningen, Netherlands
(W-9315; ETN-94-96177) Avail: CASI HC A03/MF A01

In a previous study the abstract version of the Cameron Martin theorem for Gaussian measures on a general locally convex space was stated and proved following methods introduced by Schwartz. A study showing how the classical result of Cameron and Martin may be recovered from the abstract result is presented, and further examples are given. ESA

N94-31684# Utrecht State Univ. (Netherlands). Dept. of Computer Science.

ABSTRACTS OF THE WORKSHOP ON COMPUTATIONAL GEOMETRY (CG 1992) Abstracts Only

1992 92 p Conference held in Utrecht, Netherlands, 12-13 Mar. 1992 See also AD-A155399
(PB94-147022; RUU-CS-92-10) Avail: CASI HC A05/MF A01

This document contains abstracts of the papers that were presented at the 8th European Workshop on Computational Geometry (CG '92), held in Utrecht, The Netherlands, 12-13 March 1992, and supported by EURICS, The Eindhoven-Utrecht Research Institute in Computing Science. The final program contains 27 presentations, leading to a diverse and interesting program. NTIS

N94-31690# Groningen Rijksuniv. (Netherlands). Dept. of Mathematics.

HETEROCLINIC ATTRACTORS: TIME AVERAGES AND MODULI OF TOPOLOGICAL CONJUGACY

Floris Takens 1993 15 p
(W-9318; ETN-94-96179) Avail: CASI HC A03/MF A01

Heteroclinic 'attractors,' which differ from usual attractors in the sense that they are only attracting from one side, are considered, as in an example by Bowen of a smooth (at least C cubed) vector field in the plane with two saddle points and two saddle connections. The eigenvalues of the linearized vector fields at the saddle points are supposed to be so that the cycle, consisting of the two saddle connections, is attracting from the inside. The special property of the example is that for no orbit, converging to this cycle, there is a corresponding 'physical measure.' ESA

N94-31693# Technische Univ., Delft (Netherlands). Faculty of Technical Mathematics and Informatics.

A HYLAND-BERNSTEIN APPROACH TO THE DIGITAL CONTROL OF PRITCHARD-SALAMON SYSTEMS

Florin Dan Barb and Willem deKoning 1993 17 p
(ISSN 0922-5641)
(Rept-93-76; ETN-94-96121) Copyright Avail: CASI HC A03/MF A01

The fixed, finite order digital linear quadratic Gaussian (LQG) control of Pritchard-Salamon infinite dimensional systems with unbounded input and output operators is considered. A set of necessary conditions is given in terms of the solvability of a discrete time Hyland-Bernstein system of equations: two modified Riccati equations and two modified Lyapunov equations coupled by a projection operator. ESA

N94-31696# Technische Univ., Delft (Netherlands). Faculty of Technical Mathematics and Informatics.

A PREDATOR-PREY MODEL WITH IVLEV'S FUNCTIONAL RESPONSE

R. E. Kooij and A. Zegeling 1993 20 p
(ISSN 0922-5641)
(Rept-93-79; ETN-94-96124) Copyright Avail: CASI HC A03/MF A01

The uniqueness of limit cycles is proved for a two dimensional predator-prey system with a functional response of Ivlev's type. The system of planar autonomous ordinary differential equations is transformed to a Lienard system to which a modified theorem of Zhang Zhifen is applied. ESA

N94-31701# Technische Univ., Delft (Netherlands). Faculty of Technical Mathematics and Informatics.

PAIRWISE-COMPARISON USING THE LOGARITHMIC LEAST SQUARES METHOD AND THE GENERALIZED PSEUDOINVERSE

M. Kwiesielewicz 1993 17 p Sponsored by Tech. Univ.
(ISSN 0922-5641)
(Rept-93-84; ETN-94-96129) Copyright Avail: CASI HC A03/MF A01

The logarithmic least square method is one of the methods used to rank a finite number of stimuli based on their pairwise comparison. In the case of one decision maker the problem can be solved using the geometric mean method. It is then assumed that the solution is geometrically normalized. In the case of multiple decision makers a set of linear equations is obtained and if there is a different number of judgements for each pair of the compared objects the geometric normalization assumption can not be used directly. It is shown that by applying the generalized pseudoinverse, the solution that is geometrically normalized and consistent with the case of one decision maker is obtained. To define the pseudoinverse the spectral decomposition is used. The structure of the general solution is presented and the existence of the general solution is discussed. ESA

N94-31702# Technische Univ., Delft (Netherlands). Faculty of Technical Mathematics and Informatics.

SIMPLE PATCH: A NEW HEURISTIC FOR THE PRODUCT TRAVELING SALESMAN PROBLEM

Gregor A. vanAcken, Jan Bertus Molenkamp, and Rene vanDal 1993 16 p Sponsored by Japan International Science and Technology Exchange Center

(ISSN 0922-5641)

(Rept-93-85; ETN-94-96130) Copyright Avail: CASI HC A03/MF A01

A heuristic Simple Patch is described and compared to other heuristics for the product Traveling Salesman Problem (TSP). Besides the heuristics for the Euclidean TSP and the heuristic uniflow, these heuristics include an algorithm of Gilmore and Gomory. This algorithm gives an optimal solution to the TSP for a special class of matrices; in case of a product matrix it only generates an upper bound. Terminology and basic concepts used are introduced and solvable cases of the product TSP are considered. An interesting research subject is to find classes of matrices for which a given heuristic always generates an optimal solution. A proof of the fact that the improvement algorithm 2-Opt (starting with an arbitrary tour) yields an optimal solution for the symmetric product TSP in polynomial time is given. Heuristics for the product TSP based on the idea of subtour patching are described. Worst case analyses of the three subtour patching heuristics and a complexity analysis of the heuristic Simple Patch are given. The results of a computational experiment are presented. ESA

N94-31755# Laval Univ. (Quebec). Faculte des Sciences de l'Education.

MULTIPLE REGRESSION AND MEASUREMENT ERRORS: RELATIVE EFFICIENCY OF TWO MODELS, THE STANDARD MODEL AND FULLER'S MODEL, FOR ESTIMATING STRUCTURAL RELATIONSHIPS Ph.D. Thesis [LA REGRESSION MULTIPLE ET LES ERREURS DE MESURE: EFFICACITE RELATIVE DE DEUX MODELES, LE MODELE STANDARD ET LE MODELE DE FULLER, A ESTIMER DES RELATIONS STRUCTURELLES]

Denis Savard Nov. 1993 390 p In FRENCH

(ISBN-0-315-86834-1; CTN-94-61232) Copyright Avail: Micromedia Ltd., Technical Information Centre, 240 Catherine Street, Suite 305, Ottawa, Ontario, K2P 2G8, Canada HC/MF

Research was conducted with the object of supplying certain indications which would allow researchers to utilize multiple regression more effectively when it is applied to variables affected by measurement error. Using a Monte Carlo method, a comparison was made of the relative efficiency of two regression models for estimating the structural relationships of the kind that are encountered in the educational field. The main hypothesis of the research stipulates that on the whole, Fuller's model, conceived specifically for taking measurement errors into account, would have an advantage over the standard model for the situations investigated. Six specific hypotheses complete this hypothesis, one for each of the independent variables, still presuming an advantage for Fuller's method. Simulations were carried out using 3,000 structural relationships which gave place to 9,000 regression analyses. Fuller's model had the advantage in three of the six criteria studied, while the standard model is more advantageous in the other three. It appears probable that Fuller's model gives better results in the presence of larger samples than those used in this research, i.e. samples sizes of 30 and 100. CISTI

N94-31763# Los Alamos National Lab., NM.

A BRIEF INTRODUCTION TO SYMPLECTIC INTEGRATORS AND RECENT RESULTS

P. J. Channell 1994 17 p Presented at the Symplectic Integrators Workshop, Waterloo, Ontario, 14-20 Oct. 1993

(Contract W-7405-eng-36)

(DE94-006225; LA-UR-94-0063; CONF-9310269-1) Avail: CASI HC A03/MF A01

The author begins with a brief synopsis about Hamiltonian systems and symplectic maps. A symplectic integrator is a symplectic map phi(q,p;t) that systematically approximates the time t flow of a Hamiltonian system. Systematic means: (1) in time step, t, i.e. the error should vanish as some power of the time step, and (2) in order of approximation, i.e. one would like a hierarchy of such (phi) that have errors that vanish as successively higher powers of the time step. Currently, the authors known two general types of symplectic integrators: (1) implicit integrators that are derived from a generating function or from algebraic conditions on Runge-Kutta schemes, and (2) explicit integrators that are derived from integrable Hamiltonians or from algebraic conditions on Runge-Kutta schemes. DOE

N94-31939# Carnegie-Mellon Univ., Pittsburgh, PA. Dept. of Computer Science.

PRINCIPAL COMPONENT ANALYSIS WITH MISSING DATA AND ITS APPLICATION TO OBJECT MODELING

Heung-Yeung Shum, Katsushi Ikeuchi, and Raj Reddy Dec. 1993 44 p

(Contracts F33615-90-C-1465; DAAH04-94-G-0006; NSF IRI-92-24521)

(AD-A276644; CMU-CS-93-213) Avail: CASI HC A03/MF A01

Observation-based object modeling often requires integration of shape descriptions from different views. In current conventional methods, to sequentially merge multiple views, accurate description of each surface patch has to be precisely known in each view, and transformation between any adjacent views needs to be accurately recovered. When noisy data and mismatches are present, recovered transformation becomes erroneous. In addition, the transformation error accumulates and propagates along the sequence, which results in an inaccurate object model. To overcome these problems, we have developed a weighted least square (WLS) approach which simultaneously recovers object shape and transformation among different views without recovering inter-frame motion as an intermediate step. We show that object modeling from a sequence of range images is a problem of principal component analysis with missing data (PCAMD), which can be generalized as a WLS minimization problem. An efficient algorithm is devised to solve the problem of PCAMD. After we have segmented surface regions in each view and tracked over all the sequence, we construct a 3F x P normal measurement matrix of surface normals, and an F x P distance measurement matrix of normal distances to the origin for all visible P regions appeared over the whole sequence of F views, respectively. These two measurement matrices, which have many missing elements due to noise, occlusion, and mismatching, enable us to formulate multiple view merging as a combination of two WLS problems. A two-step algorithm, which employs the quaternion representation of the rotation matrix, is presented to compute surface descriptions and transformations among different views simultaneously. DTIC

N94-32018 Stanford Univ., CA. Dept. of Electrical Engineering.

RECURSIVE ANALYSIS OF MATRIX SCATTERING FUNCTIONS Final Report, 1 Nov. 1990 - 31 Oct. 1993

Roman Sobolewski 31 Dec. 1993 13 p Limited Reproducibility: More than 20% of this document may be affected by microfiche quality

(Grant AF-AFOSR-0060-91)

(AD-A277264; AFOSR-94-0055TR) Avail: CASI HC A03

The researchers conducted investigations in the following areas: Structured Matrix Factorization, Application to Root Location and Stability Problems, Interpolation Theory, Time-Variant, and Displacement Theory. Certain survey papers were written for special occasions, and a set of notes for a special short course in Brazil was published by the University of Sao Paulo. DTIC

N94-32022# Alabama Univ., University.

PENETRABLE WEDGE ANALYSIS

Robert W. Scarstein 3 Feb. 1994 11 p

(Contract N00014-93-1-6014)

(AD-A277219; NRL-CR-7181-94-0004) Avail: CASI HC A03/MF A01

The required inner products in the Galerkin solution of the integral equation, using a basis of exponential-weighted Laguerre polynomials, are expressed as a series of algebraic forms. We are presently evaluating

these series to get a feel for the invertibility of the integral equation (transformed to a system of linear equations), prior to any inclusion of the anticipated asymptotic behavior from the Sommerfeld half-space problem. If this unmodified system of the first kind inverts nicely, then its inverse can be used to express the boundary value problem as a system of the second kind; resulting in a whole new set of opportunities for iterative or perturbation series approaches. DTIC

N94-32048# Army Research Lab., Watertown, MA. Materials Directorate.

MINIMIZATION OF COMPUTATIONAL REQUIREMENTS IN THE HYBRID STRESS FINITE ELEMENT METHOD Final Report

Erik Saether Feb. 1994 42 p

(AD-A277120; ARL-TR-336) Avail: CASI HC A03/MF A01

The hybrid stress method has demonstrated many improvements over conventional displacement-based elements. A main detraction from the method, however, has been the higher computational cost in forming element stiffness coefficients due to matrix inversions and manipulations as required by the technique. By utilizing special transformations of initially assumed stress fields, a spanning set of orthonormalized stress modes can be generated which simplify the matrix equations and allow explicit expressions for element stiffness coefficients to be derived. The developed methodology is demonstrated using several selected 2-D quadrilateral and 3-D hexahedral elements. DTIC

N94-32084 Center for Mathematics and Computer Science, Amsterdam (Netherlands). Dept. of Operations Research, Statistics, and System Theory.

LINE TRANSECTS, COVARIANCE FUNCTIONS AND SET APPROXIMATION

A. J. Cabo and A. J. Baddeley May 1993 32 p Sponsored by Netherlands Organization for Applied Scientific Research TMO Limited Reproducibility: More than 20% of this document may be affected by microfiche quality

(ISSN 0924-0659)

(CWI-BS-R9311; ETN-94-96220) Copyright Avail: Issuing Activity (European Space Agency (ESA))

A geometric transform of sets, based upon intersections of the set with lines, is introduced. Many basic integral geometric formulae used in stereology can be expressed as identities concerning this transform. It is also closely related to the glance function used by Waksman to construct a metric for subsets of the plane. That construction is modified to obtain a new metric eta for 'regular' sets S contained in R(sup d). The metric eta is shown to be topologically equivalent to the Hausdorff metric on convex sets. The covariance function is proved to be a continuous functional with respect to this new metric on classes of uniformly bounded regular sets. ESA

N94-32106 Center for Mathematics and Computer Science, Amsterdam (Netherlands). Dept. of Analysis, Algebra and Geometry.

MULTIPARAMETER QUANTUM GROUPS AND MULTIPARAMETER R-MATRICES

Michiel Hazewinkel Sep. 1993 38 p Sponsored by Netherlands Organization for Applied Scientific Research TMO Limited Reproducibility: More than 20% of this document may be affected by microfiche quality

(ISSN 0924-2953)

(CWI-AM-R9307; ETN-94-96217) Copyright Avail: Issuing Activity (European Space Agency (ESA))

There exists an vertical matrix (n 2) + 1 parameter quantum group deformation of GL(sub n). An explicit R matrix for this multiparameter family is given. This gives additional information on the nature of this family and facilitates some calculations. This explicit R matrix satisfies the Yang-Baxter Equation (YBE). All solutions of the YBE under the restriction r(sup ab)(sub cd) 0 unless (a, b) = (c, d) are described. One kind of the most general constituents of these solutions precisely corresponds to the vertical matrix (n 2) + 1 parameter quantum group mentioned above. A description of which solutions extend to an enhanced Yang-Baxter operator is given and link invariants are defined. Preliminary results on these link invariants are presented. ESA

N94-32107 Center for Mathematics and Computer Science, Amsterdam (Netherlands). Dept. of Operations Research, Statistics, and System Theory.

KAPLAN-MEIER ESTIMATORS OF INTERPOINT DISTANCE DISTRIBUTIONS FOR SPATIAL POINT PROCESSES

Adrian J. Baddeley (Leiden Univ., Netherlands.) and Richard D. Gill (Utrecht State Univ., Netherlands.) Jul. 1993 33 p Sponsored by Netherlands Organization for Applied Scientific Research TMO Limited Reproducibility: More than 20% of this document may be affected by microfiche quality

(ISSN 0924-0659)

(CWI-BS-R9315; ETN-94-96224) Copyright Avail: Issuing Activity (European Space Agency (ESA))

When a spatial point process is observed through a bounded window, edge effects hamper the estimation of characteristics such as the empty space function F, the nearest neighbor distance distribution G, and the reduced second order moment function K. A proposal and a study of product limit type estimators of F, G, and K based on the analogy with censored survival data, where the distance from a fixed point to the nearest point of the process is right censored by its distance to the boundary of the window, is presented. The resulting estimators have a ratio unbiasedness property that is standard in spatial statistics. The empty space function F of any stationary point process is shown to be absolutely continuous and so is the product limit estimator of F. The estimators are strongly consistent when there are independent replications or when the sampling window becomes large. A central limit theorem for independent replications within a fixed observation window, and asymptotic theory for independent replications of sparse Poisson processes, is outlined. In simulations the new estimators are generally much more efficient than the 'border method' estimator but (for estimators of K) somewhat less efficient than sophisticated edge corrections. ESA

N94-32108 Center for Mathematics and Computer Science, Amsterdam (Netherlands). Dept. of Operations Research, Statistics, and System Theory.

CONTROL OF A RANDOM WALK WITH NOISY DELAYED INFORMATION

Eithan Altman (Institut National de Recherche d'Informatique et d'Automatique, Valbonne, France.) and Ger Koole Aug. 1993 16 p Sponsored by Netherlands Organization for Applied Scientific Research TMO Limited Reproducibility: More than 20% of this document may be affected by microfiche quality

(ISSN 0924-0659)

(CWI-BS-R9316; ETN-94-96225) Copyright Avail: Issuing Activity (European Space Agency (ESA))

The control of a random walk on the set of nonnegative integers is considered. The controller has two actions. It makes decisions based on a noisy information on the current state but on full information on previous states and actions. The optimality of a threshold policy, where the threshold depends on the last known action, and the noisy information on the current state, is established. The result is applied to a problem of control of service and a problem of a control of flow in the presence of uncontrolled flows. ESA

N94-32167# Massachusetts Inst. of Tech., Cambridge. Artificial Intelligence Lab.

ALGEBRAIC FUNCTIONS FOR RECOGNITION

Amnon Shashua Jan. 1994 12 p

(Contracts N00014-91-J-1270; N00014-92-J-1879)

(AD-A276803; AIM-1452; CBCL-MEMO-90) Avail: CASI HC A03/MF A01

In the general case, a trilinear relationship between three perspective views is shown to exist. The trilinearity result is shown to be of much practical use in visual recognition by alignment. This yields a direct method that cuts through the computations of camera transformation, scene structure, and epipolar geometry. The proof of the central result may be of further interest as it demonstrates certain regularities across homographies of the plane and introduces new view invariants. Experiments on simulated and real image data were conducted including a comparative analysis with epipolar intersection and the linear combination methods, with results indicating a greater degree of robustness in practice and a higher level of performance in re-projection tasks. DTIC

N94-32191 Center for Mathematics and Computer Science, Amsterdam (Netherlands). Dept. of Analysis, Algebra and Geometry.
NUMERICAL DETECTION AND CONTINUATION OF CODIMENSION-TWO HOMOCLINIC BIFURCATIONS
A. R. Champneys (Bath Univ., England.) and Y. A. Kuznetsov (Academy of Sciences, USSR, Pushchino.) Sep. 1993 50 p Sponsored by Science Research Council Limited Reproducibility: More than 20% of this document may be affected by microfiche quality
(Grant NWO-B-80-61) (ISSN 0924-2953)
(CWI-AM-R9308; ETN-94-96218) Copyright Avail: Issuing Activity (European Space Agency (ESA))

A numerical procedure for the automatic accurate location of certain codimension two homoclinic singularities along curves of codimension one homoclinic bifurcations to hyperbolic equilibria in autonomous systems of ordinary differential equations is presented. The procedure also allows for the continuation of multiple codimension homoclinic orbits in the relevant number of free parameters. All known codimension two bifurcations that involve a unique homoclinic orbit are considered. In each case the known theoretical results are reviewed and a regular test function is derived. In particular, the test functions for global degeneracies involving the orientation of a homoclinic loop are presented. The incorporation of such a procedure into an existing boundary value method for homoclinic continuation is shown and implemented using the continuation code AUTO. Several examples are studied, including Chua's electronic circuit and the FitzHugh Nagumo equations. In each case, the method is shown to reproduce codim 2 bifurcation points previously found using ad hoc methods, and, in some cases, to obtain new results. ESA

N94-32194 Center for Mathematics and Computer Science, Amsterdam (Netherlands). Dept. of Operations Research, Statistics, and System Theory.
ON INTERPOLATING RANDOM FIELDS USING A FINITE NUMBER OF OBSERVATIONS
Kacha O. Dzhaparidze (Technische Univ., Delft, Netherlands.) and Rene H. P. Janssen (Technische Univ., Delft, Netherlands.) Jul. 1993 16 p Sponsored by Netherlands Organization for Applied Scientific Research TMO Limited Reproducibility: More than 20% of this document may be affected by microfiche quality
(ISSN 0924-0659)
(CWI-BS-R9314; ETN-94-96223) Copyright Avail: Issuing Activity (European Space Agency (ESA))

The best in the mean square sense linear interpolator for a zero mean weakly stationary random field is expressed in terms of orthonormal polynomials associated with the spectral distribution function of this field. Results are applied to a zero mean real Gaussian field. ESA

N94-32197 Center for Mathematics and Computer Science, Amsterdam (Netherlands). Dept. of Operations Research, Statistics, and System Theory.
AREA-INTERACTION POINT PROCESSES
A. J. Baddeley (Leiden Univ., Netherlands.) and M. N. M. VanLieshout (Vrije Univ., Amsterdam, Netherlands.) Nov. 1993 18 p Sponsored by Netherlands Organization for Applied Scientific Research TMO Limited Reproducibility: More than 20% of this document may be affected by microfiche quality
(ISSN 0924-0659)
(CWI-BS-R9318; ETN-94-96227) Copyright Avail: Issuing Activity (European Space Agency (ESA))

A Markov point process that exhibits a range of clustered, random, and ordered patterns according to the value of an interaction parameter, is introduced. In contrast to pairwise interaction processes, this model has interaction terms of all orders. The likelihood is closely related to the empty space function F, paralleling the relation between the Strauss process and Ripley's K-function. It is shown that in complete analogy with pairwise interaction processes, the pseudolikelihood equations for this model are a special case of the Takacs Fiksel method, and the model is the limit of a sequence of auto-logistic lattice processes. ESA

N94-32200 Leiden Univ. (Netherlands). Dept. of Mathematics and Computer Science.
A STABILITY ESTIMATE BASED ON NUMERICAL RANGES WITH APPLICATION TO A SPECTRAL DISCRETIZATION OF A CONVECTION-DIFFUSION EQUATION
J. L. M. vanDorsselaer and W. Hundsdorfer Oct. 1993 12 p Submitted for publication Sponsored by Netherlands Organization for Applied Scientific Research TMO Limited Reproducibility: More than 20% of this document may be affected by microfiche quality
(TW-93-12; ETN-94-96201) Avail: Issuing Activity (European Space Agency (ESA))

The stability of numerical processes for solving initial value problems is addressed. A stability result which is related to a theorem by Von Neumann, where the requirements to be satisfied are less severe and easier to verify, is presented. As an illustration, a simple convection-diffusion equation is considered. For the spatial discretization, a spectral collocation method based on so called Legendre - Gauss - Lobatto points is used and the temporal discretization is based on a one step method. The fully discrete numerical process is shown stable, provided that the temporal step size is bounded by a constant depending only on the convection-diffusion equation, the number of collocation points, and the one step method under consideration. ESA

N94-32204 Center for Mathematics and Computer Science, Amsterdam (Netherlands). Dept. of Analysis, Algebra and Geometry.
SOME PROBLEMS OF APPLIED ALGEBRA
Michiel Hazewinkel Aug. 1993 28 p Sponsored by Netherlands Organization for Applied Scientific Research TMO Limited Reproducibility: More than 20% of this document may be affected by microfiche quality
(ISSN 0924-2953)
(CWI-AM-R9306; ETN-94-96170) Copyright Avail: Issuing Activity (European Space Agency (ESA))

In contrast to 'classical' applied mathematics a number of applications of algebra and combinatorics are discussed. These are detection arrays, chip wiring diagrams, packing problems, and voting systems. Particular attention is paid to the times of symmetry, ability to calculate symbolically, and notation. ESA

N94-32206 Leiden Univ. (Netherlands). Dept. of Mathematics and Computer Science.
ON THE ERROR COMMITTED BY STOPPING THE NEWTON ITERATION IN RUNGE-KUTTA METHODS AND LINEAR MULTISTEP METHODS
J. Groeneweg Nov. 1993 61 p Limited Reproducibility: More than 20% of this document may be affected by microfiche quality
(TW-93-13; ETN-94-96202) Avail: CASI HC A04/MF A01

The numerical solution of stiff initial value problems, for nonlinear ordinary differential equations, by Runge-Kutta methods and linear multistep methods that are implicit is addressed. For stiff problems it is common practice to use Newton iteration, or a variant thereof, for solving the system of algebraic equations occurring in each time step of such step by step methods. The error committed by stopping the Newton type iteration was previously studied mainly theoretically. Theoretical upper bounds for this error are confirmed by numerical experiments. In some of the experiments even smaller errors appear to be present than is to be expected according to the theory. ESA

N94-32207 Leiden Univ. (Netherlands). Dept. of Mathematics and Computer Science.
STABILITY ESTIMATES FOR FAMILIES OF MATRICES OF NONUNIFORMLY BOUNDED ORDER
M. N. Spijker and F. A. J. Straetemans Nov. 1993 23 p Submitted for publication Limited Reproducibility: More than 20% of this document may be affected by microfiche quality
(TW-93-14; ETN-94-96203) Avail: Issuing Activity (European Space Agency (ESA))

The problem of establishing upper bounds for the norm of the n-th power of square matrices is addressed. The focus is on upper bounds that are valid for families of matrices of finite, but nonuniformly bounded, order. Such upper bounds are relevant to the stability analysis of numerical methods for solving differential equations. In the famous Kreiss matrix theorem a condition, on the resolvent of matrices, occurs which implies

that the norm of the n-th power does not grow faster than linearly with n. A slightly stronger version of this resolvent condition is studied, which is often satisfied in cases of practical interest. This version is proved to imply a growth at a rate that is essentially lower than in the case of the classical Kreiss resolvent condition. A condition, on the iterated resolvent of matrices, which is related to one of the assumptions occurring in the Hille-Yosida theorem, is considered. This condition is known to imply a growth at a rate O(n(exp 1/2)). It is proved that, when a slightly stronger version of the iterated resolvent condition is in force, there is growth at a rate that is at most O(n(exp p)), with p greater than or equal to 0 and less than 1/2. ESA

N94-32227 Center for Mathematics and Computer Science, Amsterdam (Netherlands). Dept. of Analysis, Algebra and Geometry.

STEEPEST DESCENT PATHS FOR INTEGRALS DEFINING THE MODIFIED BESSEL FUNCTIONS OF IMAGINARY ORDER

N. M. Temme Jun. 1993 15 p Sponsored by Netherlands Organization for Applied Scientific Research TMO Limited Reproducibility: More than 20% of this document may be affected by microfiche quality

(ISSN 0924-2953)

(CWI-AM-R9303; ETN-94-96167) Copyright Avail: Issuing Activity (European Space Agency (ESA))

The followng modified Bessel function of third kind of purely imaginary order is considered for real values of the parameters nu, x, x greater than 0: K(sub i(nu))(x) = integral zero to infinity (e exp (-xcosht))(cos (nu)t dt). This function plays an important role in certain problems of mathematical physics. It is the kernel of the Kontorovich Lebedev transform. The paths of steepest descent (the saddle point contours) of this integral are described, giving non oscillatory integrals. The resulting integral representations are important for obtaining asymptotic expansions and for constructing numerical algorithms. Non oscillating integrals representing I(sub i(nu))(x), the modified Bessel function of first kind of purely imaginary order, are also considered. Similar results for the ordinary Bessel functions are summarized. ESA

N94-32244 University of Southern California, Los Angeles. Dept. of Mathematics.

APPROXIMATION THEORY AND COMPUTATIONAL METHODS FOR THE IDENTIFICATION AND CONTROL OF DISTRIBUTED PARAMETER SYSTEMS Final Report, 1 Nov. 1990 - 31 Oct. 1993

I. G. Rosen 16 Dec. 1993 14 p Limited Reproducibility: More than 20% of this document may be affected by microfiche quality

(Grant AF-AFOSR-0076-91)

(AD-A277335; AFOSR-94-0053TR) Avail: CASI HC A03

A brief overview and summary of the research carried out in the area of approximation theory and computational methods for the identification and control of distributed parameter systems is provided. In particular, this final report details our efforts during the period 1 Nov. 1990 - 31 Oct. 1993 on projects involving the adaptive control and estimation and on-line identification of distributed parameter systems (including a collaborative experimental-effort with Air Force personnel at Phillips Laboratory at Edwards Air Force Base), the identification and control of degenerate distributed parameter systems, multigrid methods for the solution of optimal LQR control problems for infinite dimensional systems, wavelet based approximation in the optimal LQ control of distributed parameter systems, the identification of nonlinear Volterra equations with application to materials with memory, the LQ control of linear and nonlinear distributed parameter systems with infinite spatial domain, and optimal control and estimation of thermoelastic systems with applications to thermo-acoustic refrigeration. DTIC

N94-32245# Maryland Univ., College Park. Inst. for Physical Science and Technology.

POLYNOMIAL INTERPOLATION AND APPROXIMATION OF REAL FUNCTIONS. 2: SYMMETRICAL INTERPOLATION FOR THE TRIANGLE Final Report

Qi Chen and Ivo Babuska Nov. 1993 27 p

(Contract N00014-93-I-0131)

(AD-A277345; BN-1158) Avail: CASI HC A03/MF A01

This is the second paper in a series to discuss the approximation efficacy of polynomial interpolation of functions. In particular, the approximation accuracy depends sensitively on the locations of the interpolation nodes. We address the problem of finding the optimal symmetrical polynomial interpolation schemes for the triangle. The table for the symmetrical mean minimal interpolation sets for the triangle is given in this paper. An adaptive scheme for determining the interpolation order is also presented. DTIC

N94-32286 Carnegie-Mellon Univ., Pittsburgh, PA. Graduate School of Industrial Administration.

PERFECT 0, +/- MATRICES

Michele Conforti, Gerard Cornuejols, and Carla De Francesco Oct. 1993 13 p Limited Reproducibility: More than 20% of this document may be affected by microfiche quality

(Contract N00014-89-J-1063)

(AD-A277387) Avail: CASI HC A03

Perfect graphs and perfect 0,1 matrices are well studied in the literature. Here we introduce perfect 0 +/- 1 matrices. Our main result is a characterization of these matrices in terms of a family of perfect 0,1 matrices. DTIC

N94-32292 Nijmegen Univ. (Netherlands). Dept. of Informatics.

MULTIPLE INHERITANCE VIA INTERSECTION TYPES

Adriana B. Compagnoni and Benjamin C. Pierce 30 Aug. 1993 27 p Sponsored in part by United Kingdom Science and Engineering Research Council; ESPRIT Basic Research Actions TYPES and CONFER; and Netherlands Organization for Applied Scientific Research TMO Limited Reproducibility: More than 20% of this document may be affected by microfiche quality

(TR-93-18; ECS-LFCS-93-275; ETN-94-96212) Avail: CASI HC A03

Combining intersection types with higher order subtyping yields a typed model of object oriented programming with multiple inheritance. Objects, message passing, subtyping, and inheritance appear as programming idioms in a typed lambda calculus, a modeling technique that facilitates experimentation and helps in distinguishing between essential aspects of the object oriented style (encapsulation and subtype polymorphism, which are directly reflected in the low level type system) and useful but inessential programming idioms such as inheritance. The target calculus, a natural generalization of system F(sup omega) with intersection types, is of independent interest. Basic structural properties are established and a proof of type soundness using a simple semantics based on partial equivalence relations is given. ESA

N94-32331 Maryland Univ., College Park. Inst. for Physical Science and Technology.

ETA PERCENT-SUPERCONVERGENCE IN THE INTERIOR OF LOCALLY REFINED MESHES OF QUADRILATERALS: SUPERCONVERGENCE OF THE GRADIENT IN FINITE ELEMENT SOLUTIONS OF LAPLACE'S AND POISSON'S EQUATIONS

I. Babuska, T. Strouboulis, S. K. Gangaraj, and C. S. Upadhyay Jan. 1994 178 p Sponsored by ARO and Texas Advanced Research Program Limited Reproducibility: More than 20% of this document may be affected by microfiche quality

(Contract N00014-90-J-1030; NSF CCR-88-20279; NSF MSS-90-25110)

(AD-A277242; BN-1161; CMC-93-09) Avail: CASI HC A09

This paper is the third in a series in which we study the superconvergence of finite element solutions by a computer-based approach. We studied classical superconvergence and we introduced the new concept of eta percent superconvergence and showed that it can be employed to determine regions of least error for the derivatives of the finite element solution in the interior of any grid of triangular elements. Here we use the same ideas to study the superconvergence of the derivatives of the finite element solution in the interior of complex grids of quadrilaterals of the type used in practical computations. DTIC

N94-32341# Maryland Univ., College Park. Inst. for Physical Science and Technology.

FINITE ELEMENT SOLUTION TO THE HELMHOLTZ EQUATION WITH HIGH WAVE NUMBER. PART 1: THE h-VERSION OF THE FEM Final Report

Frank Ihlenburg and Ivo Babuska Nov. 1993 45 p

(Contract N00014-93-I-0131)

(AD-A277396; BN-1159-Pt-1) Avail: CASI HC A03/MF A01

The h-version of the finite element method with piecewise linear approximation has been applied to solve a one-dimensional model problem

for the Helmholtz equation. The main practical purpose of the investigation is to lay theoretical ground for safe rules of the thumb how to choose the mesh width of the FE-model depending on the wavenumber. In this context, we present new results for stability and error estimation of the FE-solution. Following the analysis, numerical results are discussed. DTIC

N94-32349 Center for Mathematics and Computer Science, Amsterdam (Netherlands). Dept. of Computer Science.
COMBINATORY REDUCTION SYSTEMS: INTRODUCTION AND SURVEY
Jan Willem Klop, Vincent vanOostrom, and Femke vanRaamsdonk Sep. 1993 29 p Sponsored by Commission of the Europen Communities and Netherlands Organization for Applied Scientific Research TNO Limited Reproducibility: More than 20% of this document may be affected by microfiche quality
(ISSN 0169-118X)
(CWI-CS-R9362; ETN-94-96156) Copyright Avail: CASI HC A03

A class of orthogonal CRS's (combinatory reduction systems) is introduced and illustrated with many examples, its expressive power is discussed, and an outline of a short proof of confluence is given. This proof is a direct generalization of Aczel's original proof, which is close to the well known confluence proof for lambda calculus by Tait and Martin-Loef. There is a well known connection between the parallel reduction featuring in the latter proof and the concept of 'developments,' and a classical lemma in the theory of lambda calculus is that of 'finite developments,' a strong normalization result. It turns out that the notion of 'parallel reduction' used in Aczel's proof gives rise to a generalized form of developments, called 'superdevelopments.' The results of a comparison of CRS's with the strongly related format of higher order rewriting, Nipkow's HRS's (higher order rewrite systems), are mentioned. ESA

N94-32507 Center for Mathematics and Computer Science, Amsterdam (Netherlands). Dept. of Operations Research, Statistics, and System Theory.
THE p-q-r-MEDIAL AXIS ALGORITHM REQUIRES ONLY LOCAL OPERATIONS
Peter F. M. Nacken Nov. 1993 10 p Sponsored by Netherlands Organization for Applied Scientific Research TNO Limited Reproducibility: More than 20% of this document may be affected by microfiche quality
(ISSN 0924-0659)
(CWI-BS-R9317; ETN-94-96226) Copyright Avail: Issuing Activity (European Space Agency (ESA))

The proof of a conjecture that the detection of the medial axis defined by a p-q-r-metric requires only local operations (restricted to a 16 point neighborhood) on the distance transformed image is presented. This is related to the relative positions the centers of spheres defined by the p-q-r-metric can have, if one sphere is included in the other. The conjecture is proved by considering the extension of chamfer metrics to R squared, and a general algorithm is described. ESA

N94-32653# Sandia National Labs., Albuquerque, NM.
BOUNDS ON LEAST-SQUARES FOUR-PARAMETER SINE-FIT ERRORS DUE TO HARMONIC DISTORTION AND NOISE
J. P. Deyst (National Inst. of Standards and Technology, Gaithersburg, MD.), T. M. Souders (National Inst. of Standards and Technology, Gaithersburg, MD.), and O. M. Solomon 1994 16 p Presented at the Instrumentation and Measurement Technology Conference, Hammamatsu, Japan, 10-12 May 1994
(Contract DE-AC04-94AL-85000)
(DE94-007859; SAND-94-0254C; CONF-940557-1) Avail: CASI HC A03/MF A01

Least-squares sine-fit algorithms are used extensively in signal processing applications. The parameter estimates produced by such algorithms are subject to both random and systematic errors when the record of input samples consists of a fundamental sine wave corrupted by harmonic distortion or noise. The errors occur because, in general, such sine-fits will incorporate a portion of the harmonic distortion or noise into their estimate of the fundamental. Bounds are developed for these errors for least-squares four-parameter (amplitude, frequency, phase, and offset) sine-fit algorithms. The errors are functions of the number of periods in the record, the number of samples in the record, the harmonic order, and fundamental and harmonic amplitudes and phases. The bounds do not apply to cases in which harmonic components become aliased. DOE

N94-32670 Lawrence Livermore National Lab., CA.
THE 2D DETERMINISTIC RADIATION TRANSPORT WITH THE DISCONTINUOUS FINITE ELEMENT METHOD
D. Kershaw and J. Harte 11 Nov. 1993 27 p Limited Reproducibility: More than 20% of this document may be affected by microfiche quality
(Contract W-7405-eng-48)
(DE94-004687; UCRL-ID-115525) Avail: CASI HC A03

This report provides a complete description of the analytic and discretized equations for 2D deterministic radiation transport. This computational model has been checked against a wide variety of analytic test problems and found to give excellent results. We make extensive use of the discontinuous finite element method. DOE

N94-32675# Sandia National Labs., Albuquerque, NM.
NOTE ON THE VARIANCE OF AUTOSPECTRAL DENSITY PROCESSED USING WELCH'S METHOD
D. O. Smallwood 1993 9 p Presented at the Annual Technical Meeting and Exposition of the Institute of Environmental Sciences, Rosemont, IL, 1-6 May 1994
(Contract DE-AC04-94AL-85000)
(DE94-005352; SAND-93-4104C; CONF-940510-1) Avail: CASI HC A02/MF A01

The variance of an estimate of an autospectral density (power spectral density) obtained using Welch's method is examined. This error is examined in terms of a normalized error measure. Particular attention is given to the temporal windows and overlap processing. DOE

N94-33033*# Institute for Computer Applications in Science and Engineering, Hampton, VA.
AN APPROXIMATE RIEMANN SOLVER FOR MAGNETOHYDRODYNAMICS (THAT WORKS IN MORE THAN ONE DIMENSION) Final Report
Kenneth G. Powell (Michigan Univ., Ann Arbor.) Apr. 1994 16 p Submitted for publication
(Contract NAS1-19480; RTOP 505-90-52-01)
(NASA-CR-194902; NAS 1.26:194902; ICASE-94-24) Avail: CASI HC A03/MF A01

An approximate Riemann solver is developed for the governing equations of ideal magnetohydrodynamics (MHD). The Riemann solver has an eight-wave structure, where seven of the waves are those used in previous work on upwind schemes for MHD, and the eighth wave is related to the divergence of the magnetic field. The structure of the eighth wave is not immediately obvious from the governing equations as they are usually written, but arises from a modification of the equations that is presented in this paper. The addition of the eighth wave allows multidimensional MHD problems to be solved without the use of staggered grids or a projection scheme, one or the other of which was necessary in previous work on upwind schemes for MHD. A test problem made up of a shock tube with rotated initial conditions is solved to show that the two-dimensional code yields answers consistent with the one-dimensional methods developed previously. Author

N94-33060 Pittsburgh Univ., PA. Dept. of Mathematics and Statistics.
ON THE COMPUTATION OF SIMPLICAL APPROXIMATIONS OF IMPLICITLY DEFINED TWO-DIMENSIONAL MANIFOLDS
Monica L. Brodzik and Werner C. Rheinboldt Apr. 1994 17 p Limited Reproducibility: More than 20% of this document may be affected by poor print
(Contract N00014-90-J-1025; NSF CCR-92-03488)
(AD-A278132; ICMA-94-187) Avail: Issuing Activity (Defense Technical Information Center (DTIC))

A method is presented for the computation of a simplicial approximation covering a specified subset M sub o of a two-dimensional manifold M in Rn defined implicitly as the solution set of a nonlinear system F(x) = 0 of n-2 equations in n unknowns. The given subset M sub o is a subset of M is the intersection of M with some polyhedral domain in Rn and is assumed to be bounded and non-empty. The method represents an extension of a local simplicial approximation process developed earlier by the second author. DTIC

N94-33120*# National Aeronautics and Space Administration. Lewis Research Center, Cleveland, OH.
DIRECT REPLACEMENT OF ARBITRARY GRID-OVERLAPPING BY NON-STRUCTURED GRID
Kai-Hsiung Kao and Meng-Sing Liou May 1994 17 p
(Contract NCC3-233; RTOP 505-90-5K)
(NASA-TM-106601; ICOMP-94-7; E-8875; NAS 1.15:106601) Avail: CASI HC A03/MF A01

A new approach that uses nonstructured mesh to replace the arbitrarily overlapped structured regions of embedded grids is presented. The present methodology uses the Chimera composite overlapping mesh system so that the physical domain of the flowfield is subdivided into regions which can accommodate easily-generated grid for complex configuration. In addition, a Delaunay triangulation technique generates nonstructured triangular mesh which wraps over the interconnecting region of embedded grids. It is designed that the present approach, termed DRAGON grid, has three important advantages: eliminating some difficulties of the Chimera scheme, such as the orphan points and/or bad quality of interpolation stencils; making grid communication in a fully conservative way; and implementation into three dimensions is straightforward. A computer code based on a time accurate, finite volume, high resolution scheme for solving the compressible Navier-Stokes equations has been further developed to include both the Chimera overset grid and the nonstructured mesh schemes. For steady state problems, the local time stepping accelerates convergence based on a Courant - Friedrichs - Leury (CFL) number near the local stability limit. Numerical tests on representative steady and unsteady supersonic inviscid flows with strong shock waves are demonstrated.
Author (revised)

N94-33175 Ohio State Univ., Columbus. Dept. of Mathematics.
A STUDY OF WEAK SOLUTIONS AND THEIR REGULARIZATIONS BY NUMERICAL METHODS Final Report, 1 Jul. 1992 - 30 Jun. 1993
George Majda 30 Jun. 1993 16 p Limited Reproducibility: More than 20% of this document may be affected by microfiche quality
(Grant AF-AFOSR-0309-91)
(AD-A277453; AFOSR-94-0065TR) Avail: CASI HC A03

Consider the incompressible Euler equations with vortex sheet initial data. For this initial value problem, there are a number of outstanding conjectures: This initial value problem does not have a unique weak or measure-valued solution, a selection principle is required to pick out a unique solution. The limit of vanishing viscosity (in the Navier Stokes equations) provides the correct selection principle, and different regularizations, such as adding viscosity or smoothing the initial vortex sheet, may converge to different limits as the regularization tends to zero.
DTIC

N94-33255# Naval Command, Control and Ocean Surveillance Center, San Diego, CA. RDT and E Div.
A THEORY OF CONDITIONAL INFORMATION WITH APPLICATIONS
P. G. Calabrese Mar. 1994 12 p
(AD-A278164) Avail: CASI HC A03/MF A01

The development of conditional propositions, deduction between conditionals, and boolean-like operations on conditionals, and their associated probabilities are here unified in terms of boolean relations of the form B = 0 defined on an initially relation-free algebra of boolean polynomials that transcend an initial domain of discourse. The conditional proposition (a/b) is assigned the conditional probability P(a/b), which is different from the probability that (a/b) is a tautology. The resulting algebraic techniques and demonstrated in several examples such as by simplifying a circular rule-based expert system and removing its circularity and by deriving logical and probability formulas for keeping communication lines open.
DTIC

N94-33265# Naval Postgraduate School, Monterey, CA.
LEAST SQUARES APPROXIMATION BY G1 PIECEWISE PARAMETRIC CUBES M.S. Thesis
Marion R. Holmes Dec. 1993 70 p
(AD-A277978) Avail: CASI HC A04/MF A01

Parametric piecewise cubic polynomials are used throughout the computer graphics industry to represent geometric curved shapes. The exploration of the use of parametric curves and surfaces can be viewed as the birth of Computer Aided Geometric Design (CAGD). In this thesis, least squares approximation is used for fitting a geometrically continuous (G1) piecewise parametric cubic polynomial to a sequence of ordered points in the plane. Cubic Bezier curves are used as a basis. The parameterization, the control points, the number of knots, and their locations are determined as part of the approximation process. A development of the algorithm is given, along with some results for a variety of sets of ordered data.
DTIC

N94-32467*# National Aeronautics and Space Administration. Ames Research Center, Moffett Field, CA.
A VISUAL DETECTION MODEL FOR DCT COEFFICIENT QUANTIZATION
Albert J. Ahumada, Jr. and Andrew B. Watson *In* NASA, Washington, Technology 2003: The Fourth National Technology Transfer Conference and Exposition, Volume 2 Feb. 1994 p 404-415 (For primary document see N94-32420 09-99)
Avail: CASI HC A03/MF A04

65 STATISTICS AND PROBABILITY

Includes data sampling and smoothing; Monte Carlo method; and stochastic processes.

N94-31191 Politecnico di Milano (Italy). Dipt. di Elettronica e Informazione.
REPRESENTATION, PREDICTION AND IDENTIFICATION OF CYCLOSTATIONARY PROCESSES: A STATE-SPACE APPROACH
Sergio Bittanti, Paolo Bolzern, Giuseppe deNicolao, and Luigi Piroddi 1993 32 p Sponsored in part by Ministry of University and Scientific and Technological Research, and CNR
(Rept-93-041; ETN-94-95810) Avail: Issuing Activity (Politecnico di Milano, Piazza Leonardo da Vinci 32, 20133 Milan, Italy)

A view of state-space Gaussian CycloStationary (CS) processes in discrete time is presented. The connections among three alternative descriptions are investigated: jointly periodic autocovariance functions, state-space stochastic models (Markovian representations), and Auto Regressive Moving Average models with periodic coefficients (PARMA). Background regarding deterministic periodic systems is given and the properties of state-space representations are investigated. A classification of the various types of state-space representations is provided. PARMA models are investigated from a state-space point of view. The equivalence between input-output and state-space representations, the linear prediction problem, the canonical factorization of PARMA models, and its role in identification, are addressed. The following remarks are made in conclusion: the assumption of Gaussianity was made so that first and second order moments suffice to completely characterize a CS process; most results straightforwardly extend anyway to the case of non-Gaussian (wide sense) CS processes; a point to be noted is that in the non-Gaussian case the Kalman predictor is no more optimal but is just the optimal predictor within the class of linear prediction rules.
ESA

N94-31462# Naval Research Lab., Washington, DC.
DETECTION OF A CHI-SQUARE FLUCTUATING TARGET IN GAUSSIAN NOISE Final Report
David M. Drumheller 7 Feb. 1994 13 p
(NR Proj. R03-5-B-03)
(AD-A276078; NRL/FR/7140-94-9700) Avail: CASI HC A03/MF A01

Detection of a target is often performed by applying a binary hypothesis test on the output of a matched-filter receiver. This report presents a derivation of the probability density function and cumulative probability function of the matched-filter output for a chi-square fluctuating target in Gaussian noise. The cumulative probability function is used to determine the probability of target detection for a given false alarm probability.
DTIC

N94-31590 Institut des Hautes Etudes Scientifiques, Bures-sur-Yvette (France).
DYNAMICAL ENTROPY OF GENERALIZED QUANTUM MARKOV CHAINS
Y. M. Park Nov. 1993 19 p Limited Reproducibility: More than 20% of this document may be affected by microfiche quality
(PB94-148483; IHES/P/93/60) Avail: Issuing Activity (National Technical Information Service (NTIS))

We compute the dynamical entropy in the sense of Connes, Narnhofer, and Thirring of shift automorphism of generalized quantum Markov chains as defined by Accardi and Frigerio. For any generalized quantum Markov chain defined via a finite set of conditional density amplitudes, we show that the dynamical entropy is equal to the mean entropy. NTIS

N94-31661# Technische Univ., Delft (Netherlands). Faculty of Technical Mathematics and Informatics.

A NOTE ON COCYCLES IN A SEMIDIRECT PRODUCT

Karma Dajani 1993 15 p Sponsored by Netherlands Organization for Scientific Research

(ISSN 0922-5641)

(Rept-93-65; ETN-94-96110) Copyright Avail: CASI HC A03/MF A01

Cocycles of a nonsingular ergodic action taking values in a semidirect product were previously studied. By examining their essential range, it was proved that in the topology of convergence in measure, recurrence is a generic property. A continuation of the study of such cocycles is presented. The essential range is shown to be an extension of certain subgroups in the essential range of each coordinate cocycle; this allows the essential range to be viewed as a generalized semidirect product. When the range of the cocycle is contained in R(sup +) (alpha sign) R, sufficient conditions for the projection in the second coordinate to be trivial are given. ESA

N94-31697# Technische Univ., Delft (Netherlands). Faculty of Technical Mathematics and Informatics.

DIAGONAL BAND PROBABILITY DISTRIBUTIONS

Adrianus M. H. Meeuwissen 22 Sep. 1993 31 p

(ISSN 0922-5641)

(Rept-93-80; ETN-94-96125) Copyright Avail: CASI HC A03/MF A01

A class of bivariate diagonal band probability distributions is studied. From a computational point of view, these distributions are very attractive for the simulation of dependent random variables. A characterization of the class of all mixtures of diagonal band distributions is given. Conditions are given for the continuity and for the continuous differentiability of the mixtures. The mixture with the least relative information with respect to the uniform density given a correlation is also calculated and a practical approximation for this probability density is given. The regression of Y on X, E(Y/X = x), is studied. ESA

N94-31698# Technische Univ., Delft (Netherlands). Faculty of Technical Mathematics and Informatics.

PROBABILITY DISTRIBUTIONS WITH GIVEN MARGINALS AND GIVEN CORRELATION THAT HAVE MAXIMAL ENTROPY

Adrianus M. H. Meeuwissen and Tim Bedford 20 Sep. 1993 33 p

(ISSN 0922-5641)

(Rept-93-81; ETN-94-96126) Copyright Avail: CASI HC A03/MF A01

A joint probability distribution that can be used to model a partially unknown distribution is investigated. For two random variables, the joint distribution with maximal entropy, given the marginal distributions and the rank correlation between the random variables, is studied. This distribution is given by the solution of a nonlinear system of equations. A recurrence relation for the coefficients of the Taylor series expansion of this solution is derived. An algorithm to solve the nonlinear system of equations numerically for the computation of a discretized version of the distribution is given. ESA

N94-31699# Technische Univ., Delft (Netherlands). Faculty of Technical Mathematics and Informatics.

THE LAPLACE FUNCTIONAL AND PALM MEASURE OF A QUASI-COX PROCESS WHICH IS DRIVEN BY A MARKOV CHAIN

John G. M. Schoenmakers 1993 15 p

(ISSN 0922-5641)

(Rept-93-82; ETN-94-96127) Copyright Avail: CASI HC A03/MF A01

A quasi-Cox point process in a polish phase space half open interval (0, infinity), open at the right, times U is studied. Let W be a continuous time Markov chain on a finite space A. Consider a realization (f(t)), t greater than or equal to 0, of the chain W. The instant where f makes his k-th jump from a to b, a and b both are a member of A, will be denoted by tau(sub ab; k; f). On U there will be given a set of sigma finite measures the set of (nu(sub a); a is a member of A). Then given a realization f of the Markov chain, the constructed process is the convolution of a Poisson point process with intensity nu(sub f(t))(du)dt and countable many one point processes on the lines the set (tau(sub ab; k; f)) times U, denoted by P(sub ab; k; f). It is shown that the Laplace functional of this process satisfies a specific functional equation and can be represented as a product integral. The Palm and intensity measures of the quasi-Cox process are also derived. Quasi-Cox processes arise in many applications of point processes. For example, the point process of excursions of a Markov process from a finite set of recurrent states is studied. ESA

N94-32142# Massachusetts Inst. of Tech., Cambridge. Artificial Intelligence Lab.

ON THE RELATIONSHIP BETWEEN GENERALIZATION ERROR, HYPOTHESIS COMPLEXITY, AND SAMPLE COMPLEXITY FOR RADIAL BASIS FUNCTIONS

Partha Niyogi and Federico Girosi Jan. 1994 26 p

(Contracts N00014-93-1-0385; N00014-92-J-1879)

(AD-A276802; AIM-1467; CBCL-MEMO-88) Avail: CASI HC A03/MF A01

In this paper, we bound the generalization error of a class of Radial Basis Function networks for certain well defined function learning tasks in terms of the number of parameters and number of examples. We show that the total generalization error is partly due to the insufficient representational capacity of the network (because of its finite size) and partly due to insufficient information about the target function (because of finite number of samples). We make several observations about generalization error which are valid irrespective of the approximation scheme. Our result also sheds light on ways to choose an appropriate network architecture for a particular problem. DTIC

N94-32205 Leiden Univ. (Netherlands). Dept. of Mathematics and Computer Science.

UNDISCOUNTED MARKOV DECISION CHAINS WITH PARTIAL INFORMATION; AN ALGORITHM FOR COMPUTING A LOCALLY OPTIMAL PERIODIC POLICY

A. Hordijk and J. A. Loeve 1993 18 p Sponsored by Netherlands Organization for Applied Scientific Research TMO Limited Reproducibility: More than 20% of this document may be affected by microfiche quality

(TW-93-10; ETN-94-96200) Avail: Issuing Activity (European Space Agency (ESA))

An algorithm of successive approximation type that computes a locally optimal periodic policy for a Markov decision chain with partial state information is constructed. Convergence properties are shown. Under certain conditions the policy found by the algorithm is shown to be locally optimal (or a saddle point) in the class of all admissible Markov policies. The case where the limiting policy is stationary is studied, and the previously mentioned conditions are automatically fulfilled. The algorithm is applied to a queueing network with server control. ESA

N94-32225 Center for Mathematics and Computer Science, Amsterdam (Netherlands). Dept. of Operations Research, Statistics, and System Theory.

ON CONSTRUCTING MULTI-VARIATE ORTHONORMAL POLYNOMIALS ASSOCIATED WITH SPECTRAL DISTRIBUTION FUNCTIONS

Kacha O. Dzhaparidze (Technische Univ., Delft, Netherlands.) and Rene H. P. Janssen (Technische Univ., Delft, Netherlands.) Apr. 1993 38 p Sponsored by Netherlands Organization for Applied Scientific Research TMO Limited Reproducibility: More than 20% of this document may be affected by microfiche quality

(ISSN 0924-0659)

(CWI-BS-R9310; ETN-94-96165) Copyright Avail: Issuing Activity (European Space Agency (ESA))

With a spectral distribution function of a random field are associated orthonormal polynomials in several variables. Recurrence relations between these polynomials which yield an algorithm for construction are presented. In the special case of polynomials in a single variable, these relations were already known, as opposed to the multi dimensional case treated. ESA

N94-32229 Center for Mathematics and Computer Science, Amsterdam (Netherlands). Dept. of Analysis, Algebra and Geometry.

A CELL-CYCLE MODEL REVISITED

Odo Diekmann (Leiden Univ., Netherlands.), Mats Gyllenberg (Lulea Univ., Sweden.), Horst Thieme (Arizona State Univ., Tempe.), and Sjoerd M.

Verduyn Lunel (Vrije Univ., Amsterdam, Netherlands.) Jul. 1993 21 p Presented at Conference Internationale Sur Les Equations Differentielles, Marrakech, Morocco, 11-14 Sep. 1992 Sponsored in part by Netherlands Organization for Applied Scientific Research TMO: Bank of Sweden Tercentary Foundation; Swedish Council for Forestry and Agricultural Research; Carl Trygger Foundation; and Swedish Cancer Foundation Limited Reproducibility: More than 20% of this document may be affected by microfiche quality
(Grant NSF DMS-91-01979) (ISSN 0924-2953)
(CWI-AM-R9305; ETN-94-96169) Copyright Avail: Issuing Activity (European Space Agency (ESA))

A perturbation theory for strongly continuous semigroups of operators and their adjoints is explained in the context of a cell division model involving size structure. The theory is based on renewal equations describing the cumulative effect of divisions, rather than on infinitesimal generators. ESA

N94-32339# Florida State Univ., Tallahassee. Dept. of Statistics.
STATISTICAL INFERENCE FOR COHERENT SYSTEMS FROM PARTIAL INFORMATION AND IN RESAMPLING TECHNIQUES IN SURVIVAL ANALYSIS Final Report, 1 Sep. 1990 - 31 Aug. 1993
Hani Doss 30 Sep. 1993 5 p
(Grant AF-AFOSR-0202-90)
(AD-A277382; AFOSR-94-0092TR) Avail: CASI HC A01/MF A01

Research supported in the period of the grant produced significant results of use in the areas of reliability assessment, design of systems for dependabilities, Markov chain analysis, goodness of fit tests, and censored and truncated data analysis. The PI effectively disseminated his results through invited talks at significant national meetings and through published journals. DTIC

N94-32350 Center for Mathematics and Computer Science, Amsterdam (Netherlands). Dept. of Operations Research, Statistics, and System Theory.
STOCHASTIC REALIZATION OF A GAUSSIAN STOCHASTIC CONTROL SYSTEM
J. H. VanSchuppen Nov. 1993 22 p Submitted for publication Sponsored in part by Netherlands Organization for Applied Scientific Research TMO Limited Reproducibility: More than 20% of this document may be affected by microfiche quality
(Contract SC1-CT92-0779) (ISSN 0924-0659)
(CWI-BS-R9320; ETN-94-96229) Copyright Avail: Issuing Activity (European Space Agency (ESA))

The stochastic realization problem of representing a stationary Gaussian process as the observation process of a Gaussian stochastic control system is considered. The problem formulation includes that the last m components of the observation process form the Gaussian white noise input process to the system. Identifiability of this class of systems motivates the problem. The results include a necessary and sufficient condition for the existence of a stochastic realization. A subclass of Gaussian stochastic control systems is defined that is almost a canonical form for this stochastic realization problem. For a structured Gaussian stochastic control system an equivalent condition for identifiability of the parametrization is stated. ESA

N94-32673# Sandia National Labs., Albuquerque, NM.
ARITHMETIC AVERAGING: A VERSATILE TECHNIQUE FOR SMOOTHING AND TREND REMOVAL
E. L. Clark 1993 18 p Presented at the 40th International Instrumentation Symposium, Baltimore, MD, 1-5 May 1994
(Contract DE-AC04-94AL-85000)
(DE94-005274; SAND-93-3979C; CONF-940581-1) Avail: CASI HC A03/MF A01

Arithmetic averaging is simple, stable, and can be very effective in attenuating the undesirable components in a complex signal, thereby providing smoothing or trend removal. An arithmetic average is easy to calculate. However, the resulting modifications to the data, in both the time and frequency domains, are not well understood by many experimentalists. This paper discusses the following aspects of averaging: (1) types of averages -- simple, cumulative, and moving; and (2) time and frequency domain effects of the averaging process. DOE

N94-32744# Los Alamos National Lab., NM. Statistics Group.
ASPECTS OF MODELING UNCERTAINTY AND PREDICTION
Michael D. McKay 1993 14 p Presented at the International Workshop on Model Uncertainty: Its Characterization and Quantification, Annapolis, MD, 20-22 Oct. 1993
(Contract W-7405-eng-36)
(DE94-007565; LA-UR-94-605; CONF-9310294-1) Avail: CASI HC A03/MF A01

Probabilistic assessment of variability in model prediction considers input uncertainty and structural uncertainty. For input uncertainty, understanding of practical origins of probabilistic treatments as well as restrictions and limitations of methodology is much more developed than for structural uncertainty. There is a simple basis for structural uncertainty that parallels that for input uncertainty. Although methodologies for assessing structural uncertainty for models in general are very limited, more options are available for submodels. DOE

N94-33276# Massachusetts Inst. of Tech., Cambridge. Artificial Intelligence Lab.
CONVERGENCE RESULTS FOR THE EM APPROACH TO MIXTURES OF EXPERTS ARCHITECTURES
Michael I. Jordan and Lei Xu Nov. 1993 35 p
(Contract N00014-90-J-1942; NSF ASC-92-17041)
(AD-A276801; AIM-1458; CBCL-MEMO-87) Avail: CASI HC A03/MF A01

The Expectation-Maximization (EM) algorithm is an iterative approach to maximum likelihood parameter estimation. Jordan and Jacobs recently proposed an EM algorithm for the mixture of experts architecture and the hierarchical mixture of experts architecture. They showed empirically that the EM algorithm for these architectures yields significantly faster convergence than gradient ascent. In the current paper we provide a theoretical analysis of this algorithm. We show that the algorithm can be regarded as a variable metric algorithm with its searching direction having a positive projection on the gradient of the log likelihood. We also analyze the convergence of the algorithm and provide an explicit expression for the convergence rate. In addition, we describe an acceleration technique that yields a significant speedup in simulation experiments. DTIC

66 SYSTEMS ANALYSIS

Includes mathematical modeling; network analysis; and operations research.

N94-31296# National Academy of Sciences - National Research Council, Washington, DC.
MATHEMATICAL RESEARCH IN MATERIALS SCIENCE OPPORTUNITIES AND PERSPECTIVES, PART 2 Final Report
1993 142 p
(Contract DAAL03-92-G-0013)
(AD-A276298; ARO-29397.2-MA-Pt-2) Avail: CASI HC A07/MF A02

This National Research Council report from the Board on Mathematical Sciences documents and presents technical details of fruitful collaborations between the mathematical sciences and materials science, and indicates areas of mathematical sciences research holding the most promise for advancing materials science. Written primarily for mathematical and materials science researchers with an interest in advancing research at this interface, as well as for federal and state agency representatives interested in encouraging such collaborations, it focuses on directions for potentially promising collaboration between materials scientists and mathematical scientists, and encourages both communities to increase such collaborations. It emphasizes that both the mathematical sciences and materials science communities have much to gain from an increase in cross-disciplinary collaborations, and presents recommendations for facilitating mathematical sciences research that bears on important issues in materials science, including recommendations on how to attract students and young researchers to this area. It seeks to encourage research directions in the mathematical sciences that complement vital materials science research, and raise awareness of the value of quantitative methods in materials science. It is available through National Academy Press. DTIC

N94-33335 Royal Military Coll. of Canada, Kingston (Ontario).
PROCEEDINGS OF THE SYMPOSIUM/WORKSHOP ON APPLICATIONS OF EXPERT SYSTEMS IN DND
Georges Akhras, ed. and Pierre Roberge, ed. Apr. 1992 241 p Symposium/Workshop held in Kingston, Ontario, 23-24 Apr. 1992
(DSIS-93-00343; CTN-94-61182) Avail: Issuing Activity (Royal Military Coll. of Canada, Vimy Post Office, Kingston, ON K7K 5L0 Canada)

A symposium was organized with the intent of creating a vehicle, within the Canadian Department of National Defence, to promote, stimulate, and demystify the development of expert systems and their applications to engineering. Papers were presented on expert systems for applications such as electronic warfare, mission scheduling, threat evaluation, aircraft and avionics maintenance, digital circuit diagnostics, particle accelerator control, air traffic control, search and rescue tracking, and building inspection. More general topics such as knowledge acquisition and expert system development were also included. Separate abstracts have been prepared for 11 papers from this symposium. For individual titles, see N94-33336 through N94-33346.

N94-33336 National Defence Headquarters, Ottawa (Ontario). Director Signals Engineering and Maintenance.
A DECISION SUPPORT SYSTEM FOR ELECTRONIC WARFARE ANALYSTS
J. G. L. Dumouche and A. L. Jenkins *In* Royal Military Coll. of Canada, Proceedings of the Symposium/Workshop on Applications of Expert Systems in DND Apr. 1992 p 15-34 (For primary document see N94-33335 09-66)
Avail: Issuing Activity (Royal Military Coll. of Canada, Vimy Post Office, Kingston, ON K7K 5L0 Canada)

A main goal of electronic warfare (EW) is to identify enemy units and determine their intentions. This is accomplished through the analysis of data obtained by EW support measures (ESM). One of the techniques employed by EW analysts is to use deployment templates as defined in doctrinal publications to predict the deployment and intentions of the enemy forces being faced. A prototype decision support system (DSS) has been written in the Smalltalk programming language to make use of doctrinal templates to assist EW analysts in estimating enemy locations, identities, and intentions. The DSS consists of a window-based user interface plus interfaces with the following: a database of doctrinal templates, a tactical database, an inference calculator, and a database of inferred templates to search the tactical database for a possible match to a selected template or an element of it. The DSS also has the ability to compute a certainty factor for each match. A template database browser is provided to allow entering of different doctrinal templates in a database. The use of the DSS is reviewed, with illustrations of the database browser displays and search results. Initial reactions to the DSS suggest that it is a tool that will greatly enhance the working environment of EW analysts. Author (CISTI)

N94-33337 Royal Military Coll. of Saint-Jean, Richelain (Quebec).
SCHEDULING FIGHTER MISSIONS USING AN EXPERT SYSTEM WITH AN OPERATIONS RESEARCH MODULE
J. Genest, L. Lefebvre, G. Savard, and M. Vachon *In* Royal Military Coll. of Canada, Proceedings of the Symposium/Workshop on Applications of Expert Systems in DND Apr. 1992 p 35-48 (For primary document see N94-33335 09-66)
Avail: Issuing Activity (Royal Military Coll. of Canada, Vimy Post Office, Kingston, ON K7K 5L0 Canada)

Aircraft serviceability is the ratio between the number of aircraft ready for flight and the total number available. One of the main goals in scheduling missions is to maintain a high serviceability rate while meeting operational and training requirements. This is a complex problem for aircraft maintainers since aircraft may break down unexpectedly after missions, making it difficult to follow a preset schedule. A three-step approach is proposed which combines an expert system, an optimization module, and a critique module to assist aircraft maintainers and operators in the production of a mission schedule. The approach first prepares an initial schedule using an optimization model. The expert system then reviews the schedule to enforce domain specific heuristics based on the experience of maintainers and operators. The schedule is then evaluated by maintainers in conjunction with a critique module which, using machine learning techniques, will refine the heuristics used by the expert system. This approach is currently being developed for a F-18 squadron using an expert system shell called ART-IM and an operations research system running on a personal computer. Favorable results were obtained from each module and they are now being integrated in an application running in the Microsoft Windows environment. Author (CISTI)

N94-33338 Alberta Research Council, Edmonton. Dept. of Advanced Computing Engineering.
THE CF-18 DIAGNOSTIC AND MAINTENANCE EXPERT SYSTEM PROJECT **c01**
J. B. Tubman, M. D. Brinsmead, C. C. Lumb, M. M. Mendoza, and I. S. L. Tan *In* Royal Military Coll. of Canada, Proceedings of the Symposium/Workshop on Applications of Expert Systems in DND Apr. 1992 p 74-92 (For primary document see N94-33335 09-66)
Avail: Issuing Activity (Royal Military Coll. of Canada, Vimy Post Office, Kingston, ON K7K 5L0 Canada)

A feasibility study is being conducted to investigate the appropriateness and practicality of applying expert system technologies to the maintenance of CF-18 aircraft. The target application is two radar test sets, designated AN/USM-469, for testing and fault isolating replaceable subassemblies of the CF-18 AN/APG-65 radar. There are 72 different subassemblies that can be connected to the test sets, and the study concentrated on the radar transmitter as the unit under test. The test program for the radar transmitter contains a sequence of at least 160 test procedures partitioned into 14 groups, the first eight of which must be performed in a given sequence and the last six may be reordered according to the procedure most likely to find a reported fault. The purpose of the expert system would be to assist technicians in making this sequencing decision. The approach taken to accomplish this task is described with reference to the general and special resequencing problems, design and implementation of the test system database, and field testing. It was concluded that the expert system approach is not likely to yield a significant speedup in maintenance time for radar transmitters. The approach was impeded by the need to rerun unneeded safety tests many times if a lot of resequencing takes place. Author (CISTI)

N94-33339 Canadian Forces Base Trenton, Astra (Ontario).
AN EXPERT SYSTEM APPLICATION FOR TROUBLESHOOTING THE CF18 F404 ENGINE **c07**
W. D. E. Allan and R. C. Best *In* Royal Military Coll. of Canada, Proceedings of the Symposium/Workshop on Applications of Expert Systems in DND Apr. 1992 p 93-101 (For primary document see N94-33335 09-66)
Avail: Issuing Activity (Royal Military Coll. of Canada, Vimy Post Office, Kingston, ON K7K 5L0 Canada)

Troubleshooting the CF-18 F404 engine often involves referring to data recorded by the Inflight Engine Condition Monitoring System (IECMS), which routinely records engine and aircraft parameters during flight. A software suite has been developed for graphically presenting these data. Troubleshooting procedures have been amended to include the analysis of the plots, focusing on features unique to known faults. An expert system application is proposed to provide assistance to technicians in utilizing this information in the troubleshooting process. The ability of the system to recognize the fault signatures and to be readily updated with new patterns will be central to the success of the proposed application. The role of the system in supporting second and third line maintenance activities is also discussed. An overriding consideration in the application of expert system technology to the maintenance of the F404 engine is the necessity to maintain the level of expertise of the technicians. The system will provide recommendations for solutions, but final maintenance decisions must always rest with the technician. Author (CISTI)

N94-33340 Royal Military Coll. of Canada, Kingston (Ontario). Dept. of Electrical and Computer Engineering.
A DIAGNOSTIC EXPERT SYSTEM FOR DIGITAL CIRCUITS **c33**
R. W. Backlund and J. D. Wilson *In its* Proceedings of the Symposium/Workshop on Applications of Expert Systems in DND Apr. 1992 p 102-112 (For primary document see N94-33335 09-66)
Avail: Issuing Activity (Royal Military Coll. of Canada, Vimy Post Office, Kingston, ON K7K 5L0 Canada)

A scheme is presented for a diagnostic expert system which is capable of troubleshooting a faulty digital circuit or producing a reduced test vector set for a non-faulty digital circuit. It is based on practical fault-finding logic

and utilizes artificial intelligence techniques. The program uses expert knowledge comprised of two components: that which is contained within the program in the form of rules and heuristics, and that which is derived from the circuit under test in the form of specific device information. Using both forward and backward tracking algorithms, signal paths comprised of device and gate interconnections are identified from each output pin to the primary input pins which have effect on them. Beginning at the output, the program proceeds to validate each device in each signal path by forward propagating test values through the device to the output, and backward propagating the same values to the primary inputs. All devices in the circuit are monitored for each test applied and their performance is recorded. Device or gate validation occurs when the recorded history shows that a device has been toggled successfully through all necessary states. When run on a circuit which does not contain a fault, the program determines a reduced test vector set for that circuit. Author (CISTI)

N94-33341 Royal Military Coll. of Canada, Kingston (Ontario). Dept. of Mathematics and Computer Science.

MANAGEMENT OF UNCERTAINTY IN KNOWLEDGE-BASED SYSTEMS: A MILITARY PERSPECTIVE **c82**

M. C. McKean, J. Fugere, and L. Niem *In its* Proceedings of the Symposium/Workshop on Applications of Expert Systems in DND Apr. 1992 p 113-132 (For primary document see N94-33335 09-66)

Avail: Issuing Activity (Royal Military Coll. of Canada, Vimy Post Office, Kingston, ON K7K 5L0 Canada)

An overview is provided of the uncertainty management problem. Uncertainty management approaches using knowledge based systems must process both qualitative and quantitative information. Implemented systems capable of solving or assisting in the solution of practical problems can be classified as first-, second-, and next-generation systems. These systems range in their approach to uncertainty management from rigid add-on techniques for the case of rule-based first generation systems to multiple approaches for next generation systems. Evidence is presented to show that knowledge based systems, where wisely applied, can lead to a more efficient and effective military. A case study is described which uses the Bayesian reasoning tool (BaRT) in identifying whether an aircraft is friend or foe. The BaRT approach is based on the contention that hypotheses and relations in a given domain can be represented in a network of low-order probabilistic relationships between clusters of semantically related hypotheses. BaRT has been successfully applied to a number of military classification problems. Author (CISTI)

N94-33342 McMaster Univ., Hamilton (Ontario). Dept. of Electrical and Computer Engineering.

KNOWLEDGE ENGINEERING FOR PACES, THE PARTICLE ACCELERATOR CONTROL EXPERT SYSTEM **c73**

P. C. Lind, W. F. S. Poehlman, J. W. Stark, and T. Cousins *In* Royal Military Coll. of Canada, Proceedings of the Symposium/Workshop on Applications of Expert Systems in DND Apr. 1992 p 133-152 (For primary document see N94-33335 09-66)

Avail: Issuing Activity (Royal Military Coll. of Canada, Vimy Post Office, Kingston, ON K7K 5L0 Canada)

The KN-3000 used at Defense Research Establishment Ottawa is a Van de Graaff particle accelerator employed primarily to produce monoenergetic neutrons for calibrating radiation detectors. To provide training and assistance for new operators, it was decided to develop an expert system for accelerator operation. Knowledge engineering aspects of the expert system are reviewed. Two important issues are involved: the need to encapsulate expert knowledge into the system in a form that facilitates automatic accelerator operation and to partition the system so that time-consuming inferencing is minimized in favor of faster, more algorithmic control. It is seen that accelerator control will require fast, narrowminded decision making for rapid fine tuning, but slower and broader reasoning for machine startup, shutdown, fault diagnosis, and correction. It is also important to render the knowledge base in a form conducive to operator training. A promising form of the expert system involves a hybrid system in which high level reasoning is performed on the host machine that interacts with the user, while an embedded controller employs neural networks for fast but limited adjustment of accelerator performance. This partitioning of duty facilitates a hierarchical chain of command yielding an effective mixture of speed and reasoning ability. Author (CISTI)

N94-33343 Royal Military Coll. of Canada, Kingston (Ontario). Dept. of Chemistry and Chemical Engineering.

THE HYPERMEDIA TECHNOLOGY AS FRONT END TO KNOWLEDGE PROCESSING SYSTEMS **c82**

P. R. Roberge *In its* Proceedings of the Symposium/Workshop on Applications of Expert Systems in DND Apr. 1992 p 153-168 (For primary document see N94-33335 09-66)

Avail: Issuing Activity (Royal Military Coll. of Canada, Vimy Post Office, Kingston, ON K7K 5L0 Canada)

A major challenge to the development of expert systems is the development of high-grade user interfaces. Hypertext technology is ideally suited to facilitate the design of intuitive user interfaces for decision support systems. Some of the inefficiencies of expert systems can be overcome by integrating the features of hypertext and some of the weaknesses in hypertext systems can be overcome by using expert systems. This complementarity is illustrated with examples from systems recently developed to either the prototype level or simply as proof of concept for teaching or training applications. Two commercial hypertext products, Ntergaid's HyperWriter and OWL International's Guide were selected to create a hypertext interface to some expertise management systems. Four projects are reviewed: a flexible knowledge based system for management of chemical power source systems aboard aircraft; a failure analyst to support personnel involved with stress corrosion cracking problems; and expert systems on corrosion prevention coatings and information processing for materials performance. Author (CISTI)

N94-33344 Royal Military Coll. of Canada, Kingston (Ontario). Dept. of Engineering Management.

A PROBLEM-SOLVING APPROACH TO KNOWLEDGE ACQUISITION **c82**

J. G. Dumais and A. L. Jenkins *In its* Proceedings of the Symposium/Workshop on Applications of Expert Systems in DND Apr. 1992 p 169-188 (For primary document see N94-33335 09-66)

Avail: Issuing Activity (Royal Military Coll. of Canada, Vimy Post Office, Kingston, ON K7K 5L0 Canada)

Current approaches to knowledge acquisition (KA) are primarily prototyping and modelling. Many expert system (ES) projects developed under both approaches never result in a working system because of deficiencies in the ES development process. A KA methodology is defined which should solve some of these problems and consequently make ES's more affordable. A phased development process is proposed. The methodology uses the characteristics of the task to determine first the problem solving model which best resembles the strategy used by the expert in solving problems. Furthermore, this problem solving model suggests the relevant knowledge types as well as the general structure in which they must be represented to be useful in solving problems. Based on this information, the methodology suggests appropriate techniques to further assist the knowledge engineer in the iterative elicitation of the relevant knowledge types. Finally, the elicited knowledge is validated.

Author (CISTI)

N94-33345 Air Transport Group Headquarters, Astra (Ontario).

A NEURAL NETWORK APPLICATION TO SEARCH AND RESCUE SATELLITE AIDED TRACKING (SARSAT) **c18**

Ivan W. Taylor and Michel O. Vigneault *In* Royal Military Coll. of Canada, Proceedings of the Symposium/Workshop on Applications of Expert Systems in DND Apr. 1992 p 189-201 (For primary document see N94-33335 09-66)

Avail: Issuing Activity (Royal Military Coll. of Canada, Vimy Post Office, Kingston, ON K7K 5L0 Canada)

The Search and Rescue Satellite Aided Tracking (SARSAT) system uses polar orbiting satellites to monitor the earth's surface for emergency locator transmitters (ELT's). A detected ELT signal is retransmitted to ground facilities for processing. The ELT location is determined by fitting a Doppler curve to the signal, and this location estimate is then sent for transmission to a rescue unit for action. The heuristic based approach to predict the location accuracy category of SARSAT hits based on the parameters of the Doppler curve fit work reasonably well but are far from ideal. They consistently have difficulty identifying very good solutions when they occur and very poor solutions when they occur. Normal data fitting techniques based on multiple linear regression do not work well because SARSAT data are inherently nonlinear. Neural networks were thus applied

to SARSAT data as a nonlinear data fitting technique. A neural network program was trained on a sample of 173 observations and tested on a sample of 172 observations. Results are compared to the current method. Although the results so far have been promising, they are still far from ideal. Other artificial intelligence technologies such as fuzzy logic, expert systems, and inductive learning are being investigated to enhance the neural network approach. Author (CISTI)

N94-33346 Royal Military Coll. of Canada, Kingston (Ontario). Dept. of Electrical and Computer Engineering.
A HEURISTIC MULTIPLE TARGET TRACKER **c32**
J. C. F. Beaupre, M. Farooq, and J. M. J. Roy *In its* Proceedings of the Symposium/Workshop on Applications of Expert Systems in DND Apr. 1992 p 218-237 (For primary document see N94-33335 09-66)
Avail: Issuing Activity (Royal Military Coll. of Canada, Vimy Post Office, Kingston, ON K7K 5L0 Canada)

The potential of applying recent developments in expert systems to multiple target tracking (MTT) is investigated. Standard MTT algorithms can generate relatively unreliable target state estimates. The multiple hypotheses tracker (MHT) is a very powerful algorithm, and demanding in computer resources, which can handle difficult situations by differing the formulation of hard decisions and which forms hypothetical tracks with associated probability values. It is proposed that heuristics can be formulated to improve MHT performance. These rules act on the tracks, hypotheses, and corresponding probability values to decide which hypotheses are most representative of reality. In effect, the MHT algorithm is modified to accept and process knowledge of the context or environment in which it operates and on its own strengths and weaknesses. To evaluate the performance of this concept, a prototype has been built which simulates the environment of a small military flight training school as viewed through the returns of a modified area surveillance radar. In a scenario involving nine targets behaving within regulated directives, the tracking prototype successfully displays timely, accurate, and dependable information. Author (CISTI)

N94-31432*# Hong Kong Univ. Dept. of Civil and Structural Engineering.
EVALUATING SUCCESS LEVELS OF MEGA-PROJECTS
Mohan M. Kumaraswamy *In* NASA. Marshall Space Flight Center, The Second Annual International Space University Alumni Conference Feb. 1994 p 76-91 (For primary document see N94-31425 09-12)
Avail: CASI HC A03/MF A02

67 THEORETICAL MATHEMATICS

Includes topology and number theory.

N94-31244# Wisconsin Univ., Madison. Center for Mathematical Sciences.
STRICTLY POSITIVE DEFINITE FUNCTIONS ON SPHERES Summary Report
Amos Ron and Xingping Sun Feb. 1994 23 p
(Contract NSF DMS-92-24748; DAAL03-90-G-0090)
(AD-A276471; CMS-TSR-94-6) Avail: CASI HC A03/MF A01

In this paper we study strictly positive definite functions on the unit sphere of the m-dimensional Euclidean space. Such functions can be used for solving a scattered data interpolation problem on spheres. Since positive definite functions on the sphere were already characterized by Schoenberg some fifty years ago, the issue here is to determine what kind of positive definite functions are actually strictly positive definite. The study of this problem was initiated recently by Xu and Cheney, where certain sufficient conditions were derived. A new approach, which is based on a critical connection between this problem and that of multivariate polynomial interpolation on spheres, is presented here. The relevant interpolation problem is subsequently analyzed by three different complementary methods. The first is based on the de Boor Ron general least solution for the multivariate polynomial interpolation problem. The second, which is suitable only for $m = 2$, is based on the connection between bivariate harmonic polynomials and univariate analytic polynomials, and reduces the problem to the structure of the integer zeros of bounded univariate exponentials. Finally, the last method invokes the realization of harmonic polynomials as the polynomial kernel of the laplacian, thereby exploiting some basic relations between homogeneous ideals and their polynomial kernels. DTIC

N94-31389 Amsterdam Univ. (Netherlands). Dept. of Philosophy.
WHAT COMES FIRST IN DYNAMIC SEMANTICS: A COMPOSITIONAL, NON-REPRESENTATIONAL ACCOUNT OF NATURAL LANGUAGE PRESUPPOSITION Ph.D. Thesis - Edinburgh Univ.
David Ian Beaver Nov. 1993 93 p Limited Reproducibility: More than 20% of this document may be affected by microfiche quality
(ISSN 0928-3307)
(LP-93-15; ETN-94-96006) Avail: CASI HC A05

The Context Change Potential (CCP) model of presupposition is formally elaborated and modified within a propositionally dynamic logic, a first order dynamic logic, and within a three sorted type theory. A non structural formal model of global accommodation is defined. ESA

N94-31390 Amsterdam Univ. (Netherlands). Dept. of Computational Linguistics.
THE INTERPRETATION OF FREE FOCUS
Noor vanLeusen and Laszlo Kalman Jul. 1993 41 p Limited Reproducibility: More than 20% of this document may be affected by microfiche quality
(ISSN 0928-3293)
(CL-93-01; ETN-94-96007) Avail: CASI HC A03

An analysis of the interpretation focus, that is, focus which is not 'bound' by a focusing adverb, is presented. Utterances containing free focus act as answers to questions or as replies; thus, their use is contextually more restricted than that of bound focus. Utterances containing free focus can only occur felicitously in certain licensing contexts so, in a sense, free focus is 'bound' by the context. A claim that these licensing contexts can be characterized in terms of an exhaustivity requirement on the antecedent of the focused constituent is made. Free focus is defined, starting from the concept of focus as the most prominent constituent of an utterance. A distinction is made between free focus and three other types of prominent elements: contrastive topic, comment, and bound focus. The semantics of free focus are outlined, with special regard to the contextual prerequisites of using it. Generally recognized conditions are explained, which turn out to be necessary but not sufficient conditions. An additional condition, called the exhaustivity condition, is introduced. The proposal is justified by examining the various constructions in which free focus is involved. A distinction between various functions that focusing can have is made, and the various linguistic expression types that can be focused are reviewed. Certain requirements on the features that a formal semantic theory should have in order to account for the facts related to free focus are formulated. ESA

N94-31403 Amsterdam Univ. (Netherlands). Inst. for Logic, Language and Computation.
RESUMPTIVE QUANTIFIERS IN EXCEPTION SENTENCES
Friederike Moltmann (California Univ., Los Angeles.) Oct. 1993 29 p Limited Reproducibility: More than 20% of this document may be affected by microfiche quality
(ISSN 0928-3307)
(LP-93-11; ETN-94-96003) Avail: CASI HC A03

A study of what appears to be a clear instance of polyadic quantification in natural language, namely, polyadic quantification in exception sentences, is presented. In connection with this, a semantic analysis of exception constructions in general is also presented. Various results concerning exception sentences with polyadic quantifiers are presented. In particular, it is shown that even though the polyadic quantifiers which exception phrases may apply to are iterations of monadic quantifiers and hence reducible polyadic quantifiers in Keenan's sense, the resulting quantifiers are not generally reducible, that is, they are not generally expressible as iterations of monadic quantifiers. ESA

N94-31404 Amsterdam Univ. (Netherlands). Dept. of Mathematics and Computer Science.
BINARY QUANTIFIERS AND RELATIONAL SEMANTICS
Natasha Alechina 8 Nov. 1993 37 p Limited Reproducibility: More than 20% of this document may be affected by microfiche quality
(ISSN 0928-3307)
(LP-93-13; ETN-94-96004) Avail: Issuing Activity (European Space Agency (ESA))

An attempt to extend the treatment of unary generalized quantifiers proposed by van Lambalgen and van Benthem and Alechina to the binary case is presented. A binary quantifier IIx(phi, psi) can be understood as 'typically, phi's are psi's'. After investigating some formal properties of these quantifiers, an embedding of predicate conditional logic into a logic with binary quantifiers is defined and possible applications of binary quantifiers in formalizing defeasible reasoning are discussed. ESA

N94-31407 Amsterdam Univ. (Netherlands). Inst. for Logic, Language and Computation.

ON THE INDEPENDENT AXIOMATIZABILITY OF MODAL AND INTERMEDIATE LOGICS

Alexander Chagrov (Tver State Univ., Russia.) and Michael Zakharyaschev (Academy of Sciences, USSR, Moscow.) Sep. 1993 16 p Sponsored in part by Netherlands Organization for Scientific Research Limited Reproducibility: More than 20% of this document may be affected by microfiche quality

(ISSN 0928-3315)

(ML-93-17; ETN-94-95993) Avail: CASI HC A03

Questions concerning independent axiomatizations of logics are addressed. A solution to the following problem, connected with efforts to describe the lattices of all normal modal and intermediate logics, is given: whether or not every normal or intermediate logic has an independent set of axioms. ESA

N94-31408 Amsterdam Univ. (Netherlands). Dept. of Mathematics and Computer Science.

EXTENSIONAL REALIZABILITY

Jaap vanOosten 30 Sep. 1993 30 p Limited Reproducibility: More than 20% of this document may be affected by microfiche quality

(ML-93-18; ETN-94-95994) Avail: CASI HC A03

Extensional realizability, a modification of Kleene's original definition, where a notion of 'x and y are equivalent as realizers of A' is built in, and where it is then required that realizers of A to B code operations which send equivalent realizers of A to equivalent realizers of B, is addressed. Inductive definitions for two approaches to do this are presented. It is shown that r(sub e) and e realizability are not equivalent as interpretations of intuitionistic Heyting arithmetic HA. A characterization of e realizability over a conservative extension HA(sup infinity) of HA + Markov's principle is obtained. More precisely, HA(sup infinity) has variables alpha of a new sort, and the notion 'alpha realizes A' for formulas A in the extended language is defined. Toposes generalizing notions of extensional realizability in the same way as Hyland's 'effective topos' generalizes Kleene's realizability are addressed. ESA

N94-31410 Amsterdam Univ. (Netherlands). Dept. of Mathematics and Computer Sciences.

THE DECIDABILITY OF DEPENDENCY IN INTUITIONISTIC PROPOSITIONAL LOGIC

L. A. Chagrova (Tver State Univ., Russia.) and Dick DeJongh Nov. 1993 13 p Limited Reproducibility: More than 20% of this document may be affected by microfiche quality

(ISSN 0928-3315)

(ML-93-20; ETN-94-95996) Avail: CASI HC A03

A definition is given for formulae A(sub 1), ..., A(sub n) in some theory T which is formalized in a propositional calculus S to be independent with respect to S. It is shown that, for intuitionistic propositional logic IPC, dependency (with respect to IPC itself) is decidable. This is an almost immediate consequence of Pitts' uniform interpolation theorem for IPC. A reasonably simple infinite sequence of IPC formulae F(sub n)(p, q) is given such that IPC formulae A and B are dependent if and only if at least one of the F(sub n)(A, B) is provable. ESA

N94-31411 Amsterdam Univ. (Netherlands). Dept. of Philosophy.

SUMS AND QUANTIFIERS

Jaap vanderDoes May 1993 41 p Submitted for publication Sponsored by EEC Limited Reproducibility: More than 20% of this document may be affected by microfiche quality

(ISSN 0928-3307)

(LP-93-05; ETN-94-95997) Avail: CASI HC A03

The semantics of plural noun phrases is addressed in a study on systematic ways to combine the standard theory of quantification with the sum theory of collections. The research is carried out within an extensional type theory. In such a framework the theories can be connected by giving ways to transform determiners in type ((et)((et)t)), that is, relations between sets, to ones in type ((et)(((et)t)t)), that is, relations between sets and sets of sets. It is assumed for simplicity that common nouns only hold of individuals (denote sets) and that only verb phrases are collective (denote sets of sets). Given that collections viewed as sums may be identified with sets, such 'lifted' determiner denotations are suitable to be used in a collective setting. ESA

N94-31416 Amsterdam Univ. (Netherlands). Dept. of Mathematics and Computer Science.

EFFECTIVE TRUTH

G. K. Dzhaparidze 21 Sep. 1993 29 p Sponsored by Netherlands Organization for Scientific Research Limited Reproducibility: More than 20% of this document may be affected by microfiche quality

(ISSN 0928-3315)

(ML-93-15; ETN-94-95991) Avail: CASI HC A03

The notion of effective truth defined in terms of game (dialogue) semantics and very much resembling recursive realizability is introduced. This notion seems to be a natural alternative for the classical notion of truth which satisfies the 'constructivistic' demands. At the same time it serves as a natural justification of 'resource conscious' effects reflected in substructural logics, the logic corresponding to effective truth is a version of linear logic. ESA

N94-31417 Amsterdam Univ. (Netherlands). Dept. of Mathematics and Computer Science.

CORRESPONDENCE THEORY FOR EXTENDED MODAL LOGICS, VERSION 3.0

Maarten deRijke Oct. 1993 33 p Sponsored by Netherlands Foundation for Philosophical Research Limited Reproducibility: More than 20% of this document may be affected by microfiche quality

(ISSN 0928-3315)

(ML-93-16; ETN-94-95992) Avail: CASI HC A03

Issues of reducibility of modal conditions to first order formulas are addressed. The Sahlqvist van Benthem and Gabbay Ohlbach Simmons algorithms are studied and extended. The central notion, correspondence and reducibility is defined; roughly speaking, a formula is reducible for certain variables if it is equivalent to a formula in which those variables do not occur. For most practical purposes actual reductions are obtained by making appropriate substitutions for the forbidden variables. An analysis of what makes the Sahlqvist van Benthem and Gabbay Ohlbach Simmons algorithms work is made; the analysis involves both a semantic description of the substitution mechanisms, and a syntactic characterization of the formulas allowing such substitutions. A less algorithmic perspective is adopted, and reducibility results are obtained by imposing restrictions on languages and their interpretations. A frequent complaint about the actual use of the Sahlqvist van Benthem algorithm has been its alleged obscurity, so special attention is given to using the algorithms. ESA

N94-31450 Amsterdam Univ. (Netherlands). Dept. of Philosophy.

UPDATES IN DYNAMIC SEMANTICS

Paul Dekker 28 May 1993 46 p Sponsored by EEC Limited Reproducibility: More than 20% of this document may be affected by microfiche quality

(ISSN 0928-3307)

(LP-93-06; ETN-94-95998) Avail: CASI HC A03

A reformulation of Groenendijk and Stokhof's system of dynamic predicate logic (DPL) as an update semantics is given. The basic semantic notion is that of update of information about the values of variables. It is shown that the dynamics of interpretation involved, and the validity of certain classical logical equivalences, can be more precisely characterized in the update formulation of DPL. The system is shown to be extended with a perspicuous and uniform account of adnominal and adverbial quantification (symmetric as well as asymmetric). ESA

N94-31468 Amsterdam Univ. (Netherlands). Inst. for Logic, Language and Computation.

WEAKS VS. STRONG READINGS OF DONKEY SENTENCES AND MONOTONICITY INFERENCE IN A DYNAMIC SETTING

Makoto Kanazawa (Stanford Univ., CA.) Oct. 1993 49 p Submitted

for publication Limited Reproducibility: More than 20% of this document may be affected by microfiche quality
(ISSN 0928-3307)
(LP-93-10; ETN-94-96002) Avail: CASI HC A03

A study showing that the availability of what some authors have called the weak reading and the strong reading of donkey sentences with relative clauses is systematically related to monotonicity properties of the determiner is presented. The correlation is different from what has been observed in the literature in that it concerns not only right monotonicity, but also left monotonicity (persistence/antipersistence). A claim that the reading selected by a donkey sentence with a double monotone determiner is in fact the one that validates inference based on the left monotonicity of the determiner is made. This accounts for the lack of strong reading in donkey sentences with MON determiners, which have been neglected in the literature. The relevance of other natural forms of inference is considered and it is suggested how monotonicity inference might play a central role in the actual process of interpretation. The formal theory is couched in dynamic predicate logic with generalized quantifiers. ESA

N94-31589 Institut des Hautes Etudes Scientifiques, Bures-sur-Yvette (France).
SU(2) WZNW MODEL AT HIGHER GENERA FROM GAUGE FIELD FUNCTIONAL INTEGRAL
K. Gawedzki Dec. 1993 15 p Limited Reproducibility: More than 20% of this document may be affected by microfiche quality
(PB94-148467; IHES/P/93/66) Avail: CASI HC A03

We compute the gauge field functional integral giving the scalar product of the SU(2) Chern-Simons theory states on a Riemann surface of genus greater than 1. The result allows the expression of the higher genera partition functions of the SU(2) WZNW conformal field theory by explicit finite dimensional integrals. Our calculation may also shed new light on the functional integral of the Liouville theory. NTIS

N94-31639# California Univ., Berkeley. Lawrence Berkeley Lab.
MODERN INTEGRAL EQUATION TECHNIQUES FOR QUANTUM REACTIVE SCATTERING THEORY Ph.D. Thesis
S. M. Auerbach Nov. 1993 200 p
(Contract DE-AC03-76SF-00098)
(DE94-007039; LBL-34923) Avail: CASI HC A09/MF A03

Rigorous calculations of cross sections and rate constants for elementary gas phase chemical reactions are performed for comparison with experiment, to ensure that our picture of the chemical reaction is complete. We focus on the H/D + H2 yields H2/DH + H reaction, and use the time independent integral equation technique in quantum reactive scattering theory. We examine the sensitivity of H + H2 state resolved integral cross sections sigma(sub v-prime j-prime, vj)(E) for the transitions (v = 0, j = 0) to (v-prime = 1, j-prime = 1, 3), to the difference between the Liu - Siegbahn - Truhlar - Horowitz (LSTH) and double many body expansion (DMBE) ab initio potential energy surfaces (PES). This sensitivity analysis is performed to determine the origin of a large discrepancy between experimental cross sections with sharply peaked energy dependence and theoretical ones with smooth energy dependence. We find that the LSTH and DMBE PESs give virtually identical cross sections, which lends credence to the theoretical energy dependence. DOE

N94-31770 Institut des Hautes Etudes Scientifiques, Bures-sur-Yvette (France).
CONFORMAL FIELD THEORY AND GEOMETRY OF STRINGS
J. Froehlich (Eidgenoessische Technische Hochschule, Zurich, Switzerland.) and K. Gawedzki (Centre National de la Recherche Scientifique, Gif-sur-Yvette, France.) Nov. 1993 47 p See also PB92-125038 and PB93-215499 Limited Reproducibility: More than 20% of this document may be affected by microfiche quality
(PB94-148442; IHES/P/93/59) Avail: CASI HC A03

What is quantum geometry. This question is becoming a popular leitmotiv in theoretical physics and in mathematics. Conformal field theory may catch a glimpse of the right answer. We review global aspects of the geometry of conformal fields, such as duality and mirror symmetry, and interpret them within Connes' non-commutative geometry. NTIS

N94-31825 State Univ. of New York, Stony Brook.
LATTICE GEOMETRODYNAMICS Ph.D. Thesis
Mark Corrado Galassi 1992 132 p
Avail: Univ. Microfilms Order No. DA9317284

I present the results of my work aimed at making Regge Calculus a practical tool for numerical relativity. The principal results are a formalism for solving the Regge equations in the general case, a working software package r(3)+1 which implements these methods, and a collection of numerical results produced by this software. The formalism for solving the Regge equations consists of a set of algorithms for constructing and analyzing arbitrary simplicial lattices, calculating deficit angles, and (for the first time) calculating the Jacobian of the Regge equations. I also present a definition of lapse and shift in Regge Calculus. At this time, the software package consists of approximately ten thousand lines of C++ code which offer a user interface, lattice analysis routines, and routines to calculate and solve the Regge equations with arbitrary choice lapse and shift. The Regge equations are solved using Newton's method and conjugate gradient methods. The numerical runs presented here (1) confirm the validity of the methods used; (2) examine the structure of diffeomorphism freedom in Regge Calculus, giving the first verification that one can choose lapse and shift freely; (5) examine the Bianchi identities and quantify the extent to which time evolution in Regge Calculus preserves constraints, finding that the constraints are proportional to the third power of the lattice spacing.
Dissert. Abstr.

N94-32192 Center for Mathematics and Computer Science, Amsterdam (Netherlands). Dept. of Analysis, Algebra and Geometry.
QUANTUM HOMOGENEOUS SPACES, DUALITY, AND QUANTUM 2-SPHERES
Marhijs S. Dijkhuizen and Tom H. Koornwinder Sep. 1993 25 p Sponsored by Netherlands Organization for Applied Scientific Research TMO Limited Reproducibility: More than 20% of this document may be affected by microfiche quality
(ISSN 0924-2953)
(CWI-AM-R9309; ETN-94-96219) Copyright Avail: Issuing Activity (European Space Agency (ESA))

For a quantum group, G, the notion of quantum homogeneous G-space is defined. Two methods to construct such spaces are discussed. The first one makes use of quantum subgroups, the second more general one is based upon the notion of infinitesimal invariance with respect to certain two sided coideals in the Hopf algebra dual to the Hopf algebra of G. These methods are applied to the quantum group SU(2). As two sided coideals, the subspaces spanned by twisted primitive elements in the sl(2) quantized universal enveloping algebra are taken. A one parameter series of mutually nonisomorphic quantum 2-spheres is obtained, together with the spectral decomposition of the corresponding right regular representation of quantum SU(2). The link with the quantum spheres defined by Podles is established. ESA

N94-32589# Los Alamos National Lab., NM.
NUMERICAL TRANSPORT THEORY
Edward W. Larsen (Michigan Univ., Ann Arbor.) 1994 12 p
(Contract W-7405-eng-36)
(DE94-009064; LA-SUB-94-3) Avail: CASI HC A03/MF A01

The basic problem addressed in the project was that of accelerating the iterative convergence of Discrete Ordinates (S(sub N)) problems. Important previous work on this problem, much of which was done at LANL, has shown that the Diffusion Synthetic Acceleration (DSA) method can be a very effective acceleration procedure. However, in two-dimensional geometries, only the diamond differenced S(sub N) equations have been efficiently solved using DSA. This is because, for the 2-D diamond-differenced S(sub N) equations, the standard DSA procedure leads to a relatively simple discretized low-order diffusion equation that for many problems can be efficiently solved by a multigrid method. For other discretized versions of the S(sub N) equations, the standard DSA procedure leads to much more complicated discretizations of the low-order diffusion equation that have not been efficiently solved by multigrid (or other) methods. In this project, we have developed a new procedure to obtain discretized diffusion equations for DSA-accelerating the convergence of the S(sub N) equations using certain lumped discontinuous finite element spatial differencing methods. The idea is to use an asymptotic analysis for the derivation of the discretized diffusion equation. This is based on the fact that diffusion theory is an asymptotic limit of transport theory. The asymptotic analysis

also shows that the schemes considered in this project are highly accurate for diffusive problems with spatial meshes that are optically thick. Specifically, we apply this DSA procedure to a lumped Linear Discontinuous (LD) scheme for slab geometry and a lumped Bilinear Discontinuous (BLD) scheme for x,y-geometry. Our theoretical and numerical results indicate that these schemes are very accurate and can be solved efficiently using the new method. We describe the concept that underlies the DSA method. We describe the basic asymptotic relationship between transport and diffusion theory. DOE

70 PHYSICS (GENERAL)

For precision time and time interval (PTTI) see *35 Instrumentation and Photography;* for geophysics, astrophysics or solar physics see *46 Geophysics, 90 Astrophysics,* or *92 Solar Physics.*

N94-31084 Stockholm Univ. (Sweden). Dept. of Physics.
INSTRUMENTATION FOR EXELFS MEASUREMENTS USING CONVERGENT BEAM DIFFRACTION COUPLING TO THE ELECTRON ENERGY LOSS SPECTROMETER
Zou Wei Yuan, Stefan Csillag, and Mohammed A. Tafreshi Aug. 1993 17 p Limited Reproducibility: More than 20% of this document may be affected by microfiche quality
(USIP-93-07; ETN-94-95939) Avail: Issuing Activity (European Space Agency (ESA))

Convergent beam diffraction coupling between a JEOL-100C scanning transmission microscope and an electron energy loss spectrometer is realized for the purpose of Extended Energy Loss Fine Structure (EXELFS) measurements. The working principle, the instrumentation for this coupling mode and some specific details, such as condenser system, shadow image, focusing conditions and measurements of convergent angles are described and discussed. The combination of a quadrupole and cylindrical lens for magnifying the image and increasing the dispersion of spectrum, together with a new type of compensation circuit for stray magnetic fields and the arrangement of the parallel recording system are also reported. ESA

N94-31167 Ecole Nationale Superieure des Telecommunications, Paris (France).
REGULAR WAVELETS: APPLICATION TO FIXED IMAGE COMPRESSION Ph.D. Thesis [ONDELETTES REGULIERES: APPLICATION A LA COMPRESSION D'IMAGES FIXES]
Olivier Rioul 1993 254 p In ENGLISH and FRENCH Limited Reproducibility: More than 20% of this document may be affected by microfiche quality
(ISSN 0751-1353)
(TELECOM-93-E-004; ETN-94-95897) Avail: Issuing Activity (European Space Agency (ESA))

The study of the effect of new mathematical properties brought by wavelet theory on subband coding, for still image compression problems, is addressed. Using a theoretical analysis of discrete time multiresolution decomposition, it is shown that, within the framework, the practical novelty of wavelets reduces to the 'regularity' property of octave band filter banks used in subband coding schemes. Tools which make a systematic study of regularity possible, for applications such as image compression, are derived. A mathematical study of the regularity property is investigated, in which optimal regularity estimation algorithms are derived. Several filter bank design algorithms are proposed, which can balance regularity against other filter properties (orthogonality, linear phase response, frequency selectivity, etc.) which are generally believed to be relevant for image coding. Fast algorithms are derived, for which substantial reduction of computational load required by octave band filter banks is possible. An experimental study of filter properties is carried out, for a simple still image compression scheme, in which the wavelet transform is separable. In this restricted framework, the potential interest of regularity is emphasized, in competition with other criteria such as frequency selectivity and linear phase. ESA

N94-31397# Lawrence Livermore National Lab., CA.
ELEMENT-SPECIFIC MAGNETIC HYSTERESIS MEASUREMENTS, A NEW APPLICATION OF CIRCULARLY POLARIZED SOFT X-RAYS
H.-J. Lin (Bell Telephone Labs., Inc., Murray Hill, NJ.), C. T. Chen (Bell Telephone Labs., Inc., Murray Hill, NJ.), G. Meigs (Bell Telephone Labs., Inc., Murray Hill, NJ.), Y. U. Idzerda (Naval Research Lab., Washington, DC.), A. Chaiken (Naval Research Lab., Washington, DC.), G. A. Prinz (Naval Research Lab., Washington, DC.), and G. H. Ho (Pennsylvania Univ., Philadelphia.) Sep. 1993 7 p Presented at the Annual Meeting of the Society of Photo-Optical Instrumentation Engineers, San Diego, CA, 11-16 Jul. 1993
(Contract W-7405-eng-48)
(DE94-007122; UCRL-JC-114794; CONF-930722-59) Avail: CASI HC A02/MF A01

Element-specific magnetic hysteresis measurements on heteromagnetic materials have been achieved by using circularly polarized soft x-rays. Dramatically different Fe and Co hysteresis curves of Fe/Cu/Co trilayers were obtained by recording the magnetic circular dichroism (MCD) at their respective L(sub 3) white lines as a function of applied magnetic field. The data resolve the complicated hysteresis curves, observed by conventional magnetometry, and determine the individual magnetic moments for the Fe and Co layers. Fine hysteresis features, imperceptible in the conventional curves, were also observed, demonstrating a new application of circularly polarized soft x-rays in the investigation of magnetic systems. DOE

N94-31560# Technische Univ., Darmstadt (Germany).
DEVELOPMENT AND IMPLEMENTATION OF A FULL-POTENTIAL ASW METHOD Ph.D. Thesis [ENTWICKLUNG UND IMPLEMENTATION EINES FULL-POTENTIAL-ASW-VERFAHRENS]
Volker Eyert 1991 192 p In GERMAN
(ETN-94-95757) Avail: CASI HC A09/MF A02

A full potential method based on the standard ASW (Augmented Spherical Waves) procedure was developed with a view to the calculation of the electronic characteristics of solid bodies. The standard ASW procedure is presented. Its detailed knowledge is a prerequisite for the understanding of the full potential method. The electronic and magnetic characteristics of the high temperature superconductors K2NiF4 and K2CuF4, analyzed in the framework of the ASW procedure, are discussed. The development and implementation of the full potential method are outlined. As applications of this method, calculations concerning the electronic characteristics of copper and beryllium as well as electric field gradients were performed. ESA

N94-31725 Michigan Univ., Ann Arbor.
PENETRATION DISTANCES AND THEIR APPLICATIONS TO PATH PLANNING Ph.D. Thesis
Chong Jin Ong 1993 183 p
Avail: Univ. Microfilms Order No. DA9319601

The proximal relationship of two objects is of interest for many reasons, e.g., the interference detection problem in robot motion planning. When the mathematical representations of two objects are separated the natural measure of the proximal relationship is the shortest Euclidean distance. However, much less is known when the representations intersect. In this dissertation, one of the main foci is the characterization and computation of measures of the proximal relationship between two intersecting objects. We call these measures penetration distances. A formal exposition of penetration distances and their mathematical properties is given. A penetration distance is defined by the least 'movement' needed to separate the two objects. In general, 'movement' involves both rotation and translation. Several ways of measuring the degree of rotation and translation are introduced and each yields a different definition of penetration distance. In the special case of convex objects, it is shown that the various penetration distances are the same and are determined from translational motion alone. The above-mentioned penetration distances are difficult to compute. An important contribution of this thesis is the development of a new penetration distance based on ideas of 'growing' the mathematical representations of objects. It is called the growth distance and can be computed easily for a pair of convex objects. The mathematical properties and computational aspects of the growth distance are developed at length. For instance, its relationship to the other penetration distances is determined. When two objects are separated, the growth distance is also a measure of separation. An important application of the growth distance is to path finding for robotic systems in the presence of obstacles. Our approach is to convert the path finding problem into an optimization problem. The objective is to minimize the 'amount' of collision along the path. This novel approach

involves searching among collision paths. Problems unique to this formulation are discussed. Our approach has several advantages over existing approaches and has performed well in several examples. Dissert. Abstr.

N94-31906 Kentucky Univ., Lexington.
NONLINEAR ANALYSIS OF SPRINGS USING HELICAL FINITE ELEMENTS Ph.D. Thesis
David Allen Bruner 1993 92 p
Avail: Univ. Microfilms Order No. DA9321508

The coil spring is one of the most commonly used components in mechanical systems. Its versatility as an energy storage device stems from its unique geometry. A spring has greatly different characteristics if all of its useful energy storage modes, such as compression, extension, torsion, and lateral bending, are considered. The analysis of these modes encompassing all of the deformations present in the wire, including shear deformation and axial deformation along the wire centerline, is difficult to obtain analytically. The phenomenon of large geometric deformation can frequently occur with a loaded spring and further complicate the analysis. In this work, the geometry of a generalized helix is the basis for a finite element. This finite element exactly matches the shape of springs with variable radius and pitch. This generality in shape combined with inclusion of shear and axial deformation modes gives a complete tool for the accurate modeling of springs. A nonlinear large deflection technique previously developed for two dimensional large deflection studies is extended to three dimensions for use with the helical finite element. An iterative technique, based on fictitious forces which correct geometric nonlinearities, enables analysis of spring loading cases which cause large nonlinear deformations. The helical finite element is verified by means of linear and nonlinear numerical test cases. Experimental tests are designed and conducted to evaluate the effectiveness of the model. The results of these numerical and experimental tests are presented and demonstrate the accuracy of the developed model. Dissert. Abstr.

N94-33161# North Carolina Agricultural and Technical State Univ., Greensboro.
COMPUTATIONAL METHODS IN CONTINUUM MECHANICS Final Report
Bolindra N. Borah, Robert E. White, A. Kyrillidis, S. Shankarlingham, and Y. Ji 30 Nov. 1993 17 p
(Contract DAAL03-90-G-0216)
(AD-A278144) Avail: CASI HC A03/MF A01

The primary objectives of this research are the development of algorithms which are applicable to non-linear continuum mechanic problems, especially to Stefan's Problems and Fluid Flows in Porous Media (Richard's Equation). We have studied 2-D and 3-D related problems. The codes are written in Cray Fortran and vectorization is done on the Cray Y-MP. The results obtained by Compact ADI, Finite Difference SOR and ADI are compared. It is seen that Compact ADI is superior. Six scientific research papers have been presented/published in various conferences and journals in the last two years. All of the papers are attached in the appendix as attachments. Author

71 ACOUSTICS

Includes sound generation, transmission and attenuation.
For noise pollution see *45 Environmental Pollution.*

N94-31060# Georgetown Univ., Washington, DC. Dept. of Physics.
NONINVASIVE SPECTRAL ANALYSIS AND BEAM MAPPING OF FOCUSED ULTRASOUND, PART 1 Final Report, 1 Apr. 1989 - 30 Sep. 1993
Walter Mayer, Thomas Neighbors, Herbert Ruf, John Wolf, and Qicao Zhu Jan. 1994 135 p
(Contract N00014-89-J-1795)
(AD-A276211) Avail: CASI HC A07/MF A02

This is a report on the noninvasive analysis of ultrasonic fields where nonlinear distort initially sinusoidal sound fields, with the main emphasis being placed on the acousto-optic (schlieren) investigation of line-focused ultrasound propagating in water. Computational models and experimental results are presented as well as some results of phenomena related to reflection and transmission at boundaries of pulsed sound fields. DTIC

N94-31076 Chalmers Univ. of Technology, Goeteborg (Sweden). Dept. of Applied Acoustics.
MODELLING THE LATE PART OF ROOM IMPULSE RESPONSES USING ADAPTIVE FILTERING: ON THE RECREATION OF REALITY
Sven Landstroem and Jan Skoglund 1993 45 p Limited Reproducibility: More than 20% of this document may be affected by microfiche quality
(ISSN 0283-8338)
(CTH-E-93-01; ETN-94-95949) Avail: Issuing Activity (European Space Agency (ESA))

The late part of a monaural Room Impulse Response (RIR) was modeled using statistical methods in order to explore possible redundancies. This type of modeling can, for example, be used to simplify synthetization of RIR's or to decrease the storage needs. By regarding the impulse response as time series and applying system identification theory, an ARMA filter can be used to reproduce the late part Finite Impulse Response (FIR) coefficients from a Gaussian white noise sequence. To investigate the audible differences between the original and a modeled RIR, listening tests were performed. Three anechoic source signals convolved with the RIR's were presented to 9 listeners (all musicians). The tests indicated that differences were not audible to the average listener, even though one listener consistently detected all differences. ESA

N94-31077 Chalmers Univ. of Technology, Goeteborg (Sweden). Dept. of Applied Acoustics.
QUALITY OF SOUND IN LARGE ROOMS: ALTERATION OF ROOM IMPULSE RESPONSES
Per Linusson Feb. 1993 77 p Limited Reproducibility: More than 20% of this document may be affected by microfiche quality
(ISSN 0283-8338)
(CTH-E-93-02; ETN-94-95950) Avail: Issuing Activity (European Space Agency (ESA))

Psychoacoustic testing of Room Impulse Responses (RIR), using editing techniques and listening tests with help of auralization is considered. Using these techniques the question of when the reverberation tail is subjectively diffuse was studied. This question is of great interest, for example for auralization techniques. Binaural Room Impulse Responses (BRIR's) were measured in two positions in a concert hall. Their respective reverberation tails were substituted by editing. Listening tests indicated that even with a connection time of 400 ms, some test persons could consistently detect differences with speech as source signal. With music (piano) as source signal the 'limit' of the diffuse part was somewhere between 200 to 400 ms. In the second listening test an individual reflection was substituted with a diffuse one by editing. Three types of diffuse reflections were used. The results indicated that it is possible to improve the subjective quality with a diffuse reflection. Furthermore the character of the diffuse reflection is significant. ESA

N94-31090 Chalmers Univ. of Technology, Goeteborg (Sweden). Dept. of Applied Acoustics.
A PILOT STUDY OF COMFORT CRITERIA AND SOUND QUALITY METRICS FOR SOUND INSIDE CABINS OF PROPELLER-DRIVEN AIRCRAFT
Mendel Kleiner Mar. 1993 49 p Limited Reproducibility: More than 20% of this document may be affected by microfiche quality
(Contract NUTEK-92-05162P) (ISSN 0283-832X)
(CTH-F-93-03; ETN-94-95948) Avail: Issuing Activity (European Space Agency (ESA))

A pilot study on comfort criteria and sound quality metrics for aircraft interior cabin sound due to propeller and aerodynamic noise is presented. Literature searches on these subjects were made using various international data bases. Several suggested metrics are reviewed. Some results using aircraft sound data are reported. Using a personal computer based system with a signal acquisition/replay board and commercial software it was possible to successfully change the sound quality of recorded propeller aircraft noise signals in several ways. An audio demonstration tape of some of these test signals is available in R-DAT format. A strategy for work in the fields of metrics, sound comfort and sound quality for aircraft interior cabin sound is outlined. Currently available software and hardware for sound quality work are reviewed and short summaries of a number of related articles and papers are featured. ESA

N94-31226# Office National d'Etudes et de Recherches Aerospatiales, Paris (France).
SCATTERING OF A RANDOM ACOUSTIC FIELD BY AN INFINITE CYLINDER: APPLICATION TO THE MODELIZATION OF THE ACOUSTIC ENVIRONMENT OF THE 'ARIANE 5' LAUNCHER SCALE-MODEL USING EXPERIMENTAL DATA Ph.D. Thesis - Conservatoire National des Arts et Metiers de Paris [DIFFRACTION D'UN CHAMP ACOUSTIQUE A CARACTERE ALEATOIRE PAR UN CYLINDRE INFINI: APPLICATION A LA MODELISATION DE L'ENVIRONNEMENT ACOUSTIQUE DE LA MAQUETTE 'ARIANE 5' A PARTIR DES DONNEES EXPERIMENTALES]
Jean Varnier 1993 131 p In FRENCH Original contains color illustrations
(ISSN 0078-3781)
(ONERA-NT-1993-11; ETN-94-95877) Avail: CASI HC A07/MF A02

The prediction of the acoustic environment of a launcher at takeoff is made possible by the following simplifications: the launcher is represented by a portion of an infinite cylinder and the incident acoustic field is compared to a superposition of plane waves. The analytical formulation for the scattered field induced by a plane wave is reviewed and the random case is investigated under two aspects: acoustic pressure generated on the cylinder wall, and space correlation functions of the resulting field. The above theoretical concepts allow, using measurements carried out during the firing test of captive Ariane 5 scale model, the proposal of a separation method of the assumed components (lateral and vertical) of the incident acoustic field, modelized by uncorrelated plane waves. This approach is based on some hypotheses which may be partly specified by the simulation of the experimental cross correlation functions. It seems possible to reconstruct, using a definite number of plane waves, the entire experimental data (at least in the flow frequency range), and to characterize the acoustic field for a given test condition. ESA

N94-31242# Naval Postgraduate School, Monterey, CA.
A PRELIMINARY INVESTIGATION OF HIGH AMPLITUDE STANDING WAVES WITH LASER DOPPLER ANEMOMETRY M.S. Thesis
Timothy J. Corrigan 16 Nov. 1993 53 p
(AD-A276463) Avail: CASI HC A04/MF A01

A previous study of thermoacoustic heat transport phenomena reported measurements of the acoustically induced temperature difference (Delta)T generated across short, poorly thermally conducting plates situated in high amplitude acoustic standing waves. That study focused on the dependence of (Delta)T on the position of the plates in the standing wave, the mean gas pressure and acoustic pressure amplitude. For a given mean gas pressure, there was a threshold acoustic pressure amplitude above which irregularities appeared in the plots of (Delta)T vs kx. There was evidence that some velocity-dependent effect might be the cause of the discrepancies. An investigation of the acoustic velocity field in high amplitude standing waves has been initiated to determine whether there are measurable irregularities in the velocity field that can account for the observed behavior. The use of Laser Doppler Anemometry (LDA) provided accurate measurements of the velocity behavior of a gas in an empty resonator, as well as in a resonator with a crude thermoacoustic stack. Preliminary results are reported. The major conclusions are that LDA measurements of acoustic velocity fields provide reliable results and there are no significant velocity perturbations evident in our measurements. A videotape of acoustically induced flow in the resonator with a stack indicate that significant velocity perturbations do exist on time scales other than acoustic. DTIC

N94-31257 Naval Postgraduate School, Monterey, CA.
COMPUTER IMPLEMENTATION OF ARNOTT'S FORMULATION OF THERMOACOUSTICS USING MATLAB M.S. Thesis
Argirios L. Gamaletsos 18 Nov. 1993 72 p Limited Reproducibility: More than 20% of this document may be affected by microfiche quality
(AD-A276356) Avail: Issuing Activity (Defense Technical Information Center (DTIC))

This thesis describes a Matlab computer program that implements Arnott's formulation of thermoacoustics. The program calculates the resonance frequency and quality factor of a thermoacoustic prime mover below onset of self-oscillation. The results of this analysis are compared to measured values for both a closed end and an open end prime mover and to predictions of a standing wave analysis of prime movers. DTIC

N94-31336*# National Aeronautics and Space Administration. Ames Research Center, Moffett Field, CA.
INVESTIGATION OF SONIC BOOM FOR THE SPACE SHUTTLE: HIGH CROSS-RANGE ORBITER
Raymond M. Hicks, Joel P. Mendoza, and Lionel L. Levy, Jr. [1993] 12 p
(NASA-TM-108238; NAS 1.15:108238) Avail: CASI HC A03/MF A01

Recent studies of a proposed low cross-range straight-wing space shuttle orbiter have shown that the sonic boom created during reentry may be objectionable, particularly at low supersonic Mach number. Because of this, additional tests have been conducted to determine the sonic-boom overpressure for a blended wing-body shape proposed for use as a high cross-range shuttle orbiter. Two mission profiles, in which a constant angle of attack was held during the supersonic portion of the flight, were studied. In one case the angle of attack was 60 degrees; in the other 25 degrees. The sonic-boom pressure signatures were measured in a wind tunnel and used to estimate overpressures for both missions. A technique for alleviating the boom is indicated. Author (revised)

N94-31337*# National Aeronautics and Space Administration. Ames Research Center, Moffett Field, CA.
INVESTIGATION OF SONIC BOOM FOR THE SPACE SHUTTLE: LOW CROSS-RANGE ORBITER
Lionel L. Levy, Jr., Raymond M. Hicks, and Joel P. Mendoza [1993] 10 p
(NASA-TM-108237; NAS 1.15:108237) Avail: CASI HC A02/MF A01

It is desired that the Space Shuttle Orbiter be capable of landing at airports equipped to handle present-day jet transports. Since the majority of such airports are located near heavily populated areas, an investigation has been undertaken to determine whether or not the sonic boom generated during reentry of Space Shuttle Orbiters is potentially a serious problem. The investigation was concerned with the low cross-range orbiter and reentry concept proposed by Faget of the Manned Spacecraft Center (MSC). This report describes the approach used and presents the results obtained to date. Author (revised)

N94-31653# Technische Univ., Eindhoven (Netherlands).
AEROACOUSTIC SOURCES IN INTERNAL FLOWS Ph.D. Thesis
Marinus Carolus Adri Peters 1993 252 p Sponsored by Netherlands Foundation for Technical Sciences, and N.V. Nederlandse Gasunie
(Grant ETN-71.1403)
(ISBN-9-03-86-0282-0; ETN-94-96031) Copyright Avail: CASI HC A12/MF A03

The basic equations describing the production of aeroacoustic sound are derived, and approximations to the basic equations are presented leading to inhomogeneous convected wave equations. Different models to describe the generation and convection of vorticity at high Reynolds numbers are described, with special attention to the so called Kutta condition, which in potential flow models accounts for the action of viscous forces at sharp edges. Results of the various potential flow methods are compared for starting flows such as the starting flow past a wedge, out of a two dimensional channel exit and in a T junction. The periodic vortex formation process in several configurations is addressed. Results of an experimental investigation into the propagation and reflection of acoustic waves in a long open ended pipe are described. Accurate experimental data on the influence of a low Mach number (turbulent) mean flow on the reflection coefficient and damping coefficient were obtained using a multimicrophone method. As an application of the computational methods, flow induced resonances in a system with two side branches, that is, in a tandem T junction and in a cross junction, are addressed. ESA

N94-31846 Notre Dame Univ., IN.
EXPERIMENTAL AND COMPUTATIONAL STUDIES ON PROPELLER NOISE DUE TO INFLOW DISTORTION Ph.D. Thesis
Srinivasan Subramanian 1993 298 p
Avail: Univ. Microfilms Order No. DA9320189

Large-scale non-uniformities in the approach flow to a propeller result in periodic unsteady blade forces that radiate tonal noise at the blade passing frequencies and its higher harmonics. The current research focuses on a combined theoretical and experimental approach to study this propeller aeroacoustic problem. The theoretical study employs the classical acoustic analogy in conjunction with two-dimensional unsteady aerodynamic theory.

The experimental side of this research is conducted in an anechoic flow facility and employs a four-bladed marine propeller. Both isolated and cyclical distortions are investigated. The radiative properties due to isolated distortions is first studied by operating the propeller behind the wake of a rod. Qualitative comparisons of the measured directivities match well with the analyses from theory. Next, the analysis is extended to cyclical distortions in the incoming flow. The theoretical analysis accounts for the effect of mean blade loading on the unsteady blade forces and provides an upper and lower bound for the resulting far field noise radiation. The experimental study employs non-uniform flow generators that provide a three-cycle and four-cycle azimuthal variation in the approach flow. An extensive comparison of the measured noise levels with the theoretical predictions shows an excellent agreement both in magnitude and directivity. Dissert. Abstr.

N94-31899 Catholic Univ. of America, Washington, DC.
BOUNDARY CONTROL OF SCATTERING Ph.D. Thesis
Terence John Bazow 1993 226 p
Avail: Univ. Microfilms Order No. DA9318375

The essence of the acoustic scattering problem is to determine the acoustic fields that result from the presence of a body (scatterer) in a known ensonification field. The scattering problem is formulated as a constrained optimization problem solving for that surface admittance which minimizes radiated energy in a restricted subset of farfield directions. The imposed constraints are that the total field must satisfy the admittance boundary condition at the scatterer's surface, and the scattered field must satisfy both the Helmholtz equation and the radiation condition in the region exterior to the scatterer. For a specified surface admittance distribution, approximate solutions for the scattering problem are obtained by applying the discrete form of the axisymmetric Helmholtz integral representation coupled with a piecewise constant collocation scheme. Nonlinear minimization techniques are then used to find the admittance distribution that minimizes the scattered energy in a selected farfield angular sector. For this investigation, the scattering bodies are rotational ellipsoids and the surface admittance is both complex and axisymmetric. The ensonification field is a packet of plane waves containing a few sinusoidal waves with different frequencies or with a few directions of incidence. Three factors are found to directly affect optimization calculations for the acoustic fields that result from the scatterer's presence. First is the farfield sector over which minimization is desired. Second is the constraint imposed on the admittance distribution. The third factor is the convergence domain for the solutions to the direct scattering problem. The numerical simulations demonstrate that the Helmholtz integral representation coupled with nonlinear minimization techniques yield useful solutions. Further, the approach and numerical techniques provide credible estimates of optimal admittance distributions and the scattered fields over a range of spatial and geometric arrangements. Dissert. Abstr.

N94-32059# Georgetown Univ., Washington, DC. Dept. of Physics.
NONINVASIVE SPECTRAL ANALYSIS AND BEAM MAPPING OF FOCUSED ULTRASOUND, PART 2 Final Report
Walter Mayer, Thomas Neighbors, Herbert Ruf, John Wolf, and Qicao Zhu Jan. 1994 74 p
(Contract N00014-89-J-1795)
(AD-A276629) Avail: CASI HC A04/MF A01

Appendix A outlines the steps necessary for using the line focus software, LFOCUS.EXE, developed to support ONR research on optical probing of ultrasonic fields. Section A.2 outlines the hardware requirements for program execution. Since the software is menu driven rather than batch processed, Section A.3 provides a short user's guide for the menu driven interface. Section A.4 describes the output file structure used for data post processing. DTIC

N94-32089# Woods Hole Oceanographic Inst., MA.
SOUND SCATTERING BY CYLINDERS OF NONCIRCULAR CROSS SECTION Ph.D. Thesis
Daniel T. DiPerna Feb. 1994 91 p
(Contract N00014-89-J-1729)
(AD-A276663; WHOI-93-47) Avail: CASI HC A05/MF A01

This thesis investigates a new method for predicting the farfield scattered pressure of a plane wave due to an infinite cylinder of noncircular cross section. Both impenetrable and penetrable fluid boundary conditions will be treated for several types of cross sections and for a large frequency range. This new method requires the conformal mapping of both the exterior and interior of a closed surface to a semi-infinite strip. Numerically efficient algorithms will be presented for both of these cases. A new method for satisfying the boundary conditions will be developed, as well as an efficient algorithm for generating the required modal functions on the boundary. Numerical results are presented for cross sections in the shape of an ellipse, square, and three leaf clover. In all cases, the results compare extremely well with exact or high frequency asymptotic results. DTIC

N94-32125# Naval Undersea Warfare Center, Newport, RI.
WAVEVECTOR-FREQUENCY ANALYSIS WITH APPLICATIONS TO ACOUSTICS
Wayne A. Strawderman 1994 574 p
(AD-A276618) Avail: CASI HC A24/MF A04

This monograph presents an approach to the description and analysis of acoustic fields and systems that parallels and extends one developed by electrical engineers to describe and analyze electrical signals and systems. This approach, called wavevector-frequency analysis, complements traditional methods of acoustics. Wavevector-frequency analysis is simply the description and interpretation of a space-time field or system in terms of the Fourier conjugates of the independent spatial and temporal variables of the field or system. The Fourier conjugate of the spatial vector variable is called the wavevector, and the Fourier conjugate of the time variable is the frequency. The formalism of this approach to acoustics evolved over the course of an extended research effort to understand and characterize certain acoustic fields associated with turbulent flow. A brief description of this research effort will put the evolution of this approach in perspective. DTIC

N94-32262# Naval Postgraduate School, Monterey, CA.
PULSE-SPLITTING AND AM-FM CONVERSION IN A NONLINEAR DISPERSIVE MEDIUM M.S. Thesis
William F. Coleman Dec. 1993 74 p
(AD-A277041) Avail: CASI HC A04/MF A01

Experimental and theoretical results are presented for nonlinear dispersive waveguide modes in an acoustic duct. We report observations of a localized envelope which splits into two disturbances moving with two different velocities of propagation. As a consequence, we predict that if a signal is amplitude modulated at the source, spatial beating between the two disturbances will occur, and at periodic positions in space the signal will become frequency modulated. These results can have applications in an all-optical AM-FM conversion and in high data rate fiber optic communications. DTIC

N94-32418# Federal Aviation Administration, Cambridge, MA.
HELIPORT NOISE MODEL (HNM) VERSION 2.2 (USER'S GUIDE) Final Report, Oct. 1989 - Feb. 1994
Gregg G. Fleming and Edward J. Rickley 23 May 1994 91 p
(AD-A277072; DOT-VNTSC-FAA-94-3; DOT/FAA/EE-94-01) Avail: CASI HC A05/MF A01

The John A. Volpe National Transportation Systems Center (Volpe Center), in support of the Federal Aviation Administration, Office of Environment and Energy, has developed Version 2.2 of the Heliport Noise Model (HNM). The HNM is a computer program used for determining the impact of helicopter noise in the vicinity of terminal operations. This document, prepared by the Volpe Center's Acoustics Facility, is a User's Guide for HNM Version 2.2. It presents: (1) computer system requirements and installation procedures; (2) an overview of HNM capabilities and the user's implementation of these capabilities; (3) the elements of a heliport case study; (4) a step-by-step tutorial for preparing and running a case study; and (5) the interpretation of HNM Version 2.2 output. Also presented, in the Appendices of this document, are the following: (1) a discussion of the technical revisions made to several internal algorithms - primarily revisions which are transparent to HNM users; (2) a discussion of the helicopter noise Data Base used by the HNM; and (3) a summary of error messages in the HNM. DTIC

N94-32930*# National Aeronautics and Space Administration. Langley Research Center, Hampton, VA.
A MATHEMATICAL MODEL FOR SIMULATING NOISE SUPPRESSION OF LINED EJECTORS
Willie R. Watson Apr. 1994 30 p

(RTOP 505-59-52-02)
(NASA-TP-3425; L-17283; NAS 1.60:3425) Avail: CASI HC A03/MF A01

A mathematical model containing the essential features embodied in the noise suppression of lined ejectors is presented. Although some simplification of the physics is necessary to render the model mathematically tractable, the current model is the most versatile and technologically advanced at the current time. A system of linearized equations and the boundary conditions governing the sound field are derived starting from the equations of fluid dynamics. A nonreflecting boundary condition is developed. In view of the complex nature of the equations, a parametric study requires the use of numerical techniques and modern computers. A finite element algorithm that solves the differential equations coupled with the boundary condition is then introduced. The numerical method results in a matrix equation with several hundred thousand degrees of freedom that is solved efficiently on a supercomputer. The model is validated by comparing results either with exact solutions or with approximate solutions from other works. In each case, excellent correlations are obtained. The usefulness of the model as an optimization tool and the importance of variable impedance liners as a mechanism for achieving broadband suppression within a lined ejector are demonstrated. Author

N94-33017 Department of the Navy, Washington, DC.
ACOUSTIC WINDOW Patent
David M. Bullat, inventor (to Navy), Philip C. Bradshaw, inventor (to Navy), and Jay C. Brown, inventor (to Navy) 4 Jan. 1994 7 p Filed 19 Nov. 1992
(AD-D016171; US-Patent-5,276,658; US-Patent-Appl-SN-987497; US-Patent-Class-367-174) Avail: US Patent and Trademark Office

A cost-effective, producible improved apparatus for and method of fabricating a transducer acoustic window for a marine environment has acceptable acoustic energy transmitting properties and appropriate mechanical properties to withstand the rigors associated with varying velocities of flowing water, fluctuating temperatures, changing ambient pressures, the abuse attendant operations, etc., that are routinely encountered during a prolonged deployment. The acoustic window has a cast CONAP 1556 polyurethane window portion that extends over a hull opening and on a bearing surface rim about the opening. A number of equidistantly, circumferentially spaced stainless steel inserts are molded in the cast polyurethane window portion. DTIC

N94-33023*# BBN Systems and Technologies Corp., Cambridge, MA.
RECIPROCITY-BASED EXPERIMENTAL DETERMINATION OF DYNAMIC FORCES AND MOMENTS: A FEASIBILITY STUDY Final Report
Istvan L. Ver and Michael S. Howe May 1994 72 p Prepared for Georgia Inst. of Tech., Atlanta, GA
(Contract NAS1-19061; BBN Proj. 621697; RTOP 538-03-14-01)
(NASA-CR-194905; NAS 1.26:194905; BBN-7967) Avail: CASI HC A04/MF A01

BBN Systems and Technologies has been tasked by the Georgia Tech Research Center to carry Task Assignment No. 7 for the NASA Langley Research Center to explore the feasibility of 'In-Situ Experimental Evaluation of the Source Strength of Complex Vibration Sources Utilizing Reciprocity.' The task was carried out under NASA Contract No. NAS1-19061. In flight it is not feasible to connect the vibration sources to their mounting points on the fuselage through force gauges to measure dynamic forces and moments directly. However, it is possible to measure the interior sound field or vibration response caused by these structureborne sound sources at many locations and invoke principle of reciprocity to predict the dynamic forces and moments. The work carried out in the framework of Task 7 was directed to explore the feasibility of reciprocity-based measurements of vibration forces and moments. Author

N94-33096# Pennsylvania State Univ., University Park. Applied Research Lab.
STATISTICAL CHARACTERISTICS OF BISTATIC SURFACE SCATTER AND MEAN BISTATIC SURFACE SCATTERING STRENGTHS
P. D. Neumann and R. L. Culver Mar. 1994 136 p
(Contract N00039-92-C-0100)
(AD-A278155; ARL-TR-94-07) Avail: CASI HC A07/MF A02

The characterization of reverberation, from the surface, the bottom, and/or the volume, is important in advancing the understanding of the mechanisms involved in underwater sound scattering. Numerous experiments and much theoretical work have been done in the area of monostatic reverberation, but the area of bistatic reverberation has been much less researched. This certainly is a result of the much more complex geometries involved in bistatic reverberation. This dissertation studied the statistics of bistatic surface reverberation data from the FLIP experiment conducted in January of 1992. The data were verified as homogeneous and normally distributed using the Kolmogorov-Smirnov two-sample test with a confidence interval equal to 0.1, using a technique by which ensembles from different times were combined. Meaningful deviations from a normal distribution were observed at the highest wind speed of 7.2 m/s. DTIC

N94-33146 Florida Univ., Gainesville. Dept. of Psychology.
COMPLEX AUDITORY SIGNALS Annual Technical Report, 1 Jan. 1993 - 31 Jan. 1994
David M. Green 28 Feb. 1994 12 p Limited Reproducibility: More than 20% of this document may be affected by microfiche quality
(Contract F49620-92-J-0139)
(AD-A278391; AFOSR-94-0213TR) Avail: CASI HC A03

This progress report covers the period from Jan. 1993 - Jan. 1994. First, we list the papers published during the period. Next, we list the papers submitted for publication and the papers presented at scientific meetings. The personnel are then listed, and, finally we conclude with a brief discussion of the problem areas in which future research efforts will be concentrated. We feel that more research should be devoted to this topic. Not only is this research needed to understand the basic stimulus variables in more detail, but it is needed in order to apply this research to real-world situations. In most realistic situations, the change in the auditory spectrum occurs at different times and with different degrees of synchrony among the components of the complex. DTIC

N94-32456*# Army Armament Munitions and Chemical Command, Watervliet, NY. Benet Labs.
COMPUTERIZED ULTRASONIC TESTING SYSTEM (CUTS) FOR IN-PROCESS THICKNESS DETERMINATION
J. Frankel, M. Doxbeck, S. C. Schroeder, and A. Abbate *In* NASA, Washington, Technology 2003: The Fourth National Technology Transfer Conference and Exposition, Volume 2 Feb. 1994 p 311-317 (For primary document see N94-32420 09-99)
Avail: CASI HC A02/MF A04

72 ATOMIC AND MOLECULAR PHYSICS

Includes atomic structure, electron properties, and molecular spectra.

N94-31146# Iowa State Univ. of Science and Technology, Ames. Ames Lab.
THEORETICAL STUDIES OF ZIRCONIUM AND CARBON CLUSTERS WITH MOLECULAR DYNAMICS SIMULATIONS Ph.D. Thesis
B. Zhang Aug. 1993 131 p
(Contract W-7405-eng-82)
(DE94-005276; IS-T-1662) Avail: CASI HC A07/MF A02

In this dissertation, we will present a systematic study of structures of fullerenes ranging from C(20) to C(100) by introducing a novel scheme. Using our new scheme, we not only reproduce all known fullerene structures but also successfully predicted several other fullerene structures which were confirmed by experiments. By utilizing the tight-binding molecular-dynamic (TBMD) simulation, we also studied the dynamical behavior of fullerenes: Vibrations, thermal disintegration of individual clusters as well as collisions between fullerenes. If the beauty of carbon fullerene is not enough, people found that carbon can also form tubules and even speculated that they can form three-dimensional graphite-like networks. By extending our fullerene structure searching scheme, we performed a search for the ground-state structure of three dimensional carbon network. We found the most stable structure people ever proposed for simple cubic based networks. From the difference of this new form of carbon and graphite in the electronic and vibrational properties, we propose an experimental probe to identify these novel three-dimensional carbon networks. DOE

N94-31147# Fermi National Accelerator Lab., Batavia, IL.
STATE OF HADRON COLLIDER PHYSICS
P. D. Grannis Dec. 1993 28 p Presented at the 9th Workshop on Proton-Antiproton Collider Physics, Tsukuba, Japan, 18-22 Oct. 1993
(Contract DE-AC02-76CH-03000)
(DE94-005279; FNAL/C-93/384; CONF-9310247-4) Avail: CASI HC A03/MF A01

The 9th Topical Workshop on Proton-Antiproton Collider Physics in Tsukuba Japan demonstrated clearly the enormous breadth of physics accessible in hadron colliders. Although no significant chinks were reported in the armor of the Standard Model, new results presented in this meeting have expanded our knowledge of the electroweak and strong interactions and have extended the searches for non-standard phenomena significantly. Much of the new data reported came from the CDF and D0 experiments at the Fermilab collider. Superb operation of the Tevatron during the 1992-1993 run and significant advances on the detector fronts -- in particular, the emergence of the new D0 detector as a productive physics instrument in its first outing and the addition of the CDF silicon vertex detector -- enabled much of this advance. It is noteworthy, however, that physics from the CERN collider experiments UA1 and UA4 continued to make a large impact at this meeting. In addition, very interesting summary talks were given on new results from HERA, cosmic ray experiments, on super-hadron collider physics, and on e(+)e(-) experiments at LEP and TRISTAN. These summaries are reported elsewhere. DOE

N94-31151# Argonne National Lab., IL.
ANALYSIS OF BEAM-ON-TARGET INTERACTION IN A NEUTRON-SOURCE TEST FACILITY
A. Hassanein and D. Smith Oct. 1993 19 p Presented at the 6th International Conference on Fusion Reactor Materials, Stresa, Italy, 27 Sep. - 1 Oct. 1993
(Contract W-31-109-eng-38)
(DE94-005392; ANL/EP/CP-79740-Rev.; CONF-930928-3-Rev.) Avail: CASI HC A03/MF A01

The need is urgent for a high-flux, high-energy neutron test facility to evaluate the performance of fusion reactor materials. An accelerator-based deuterium-lithium source is generally considered the most reasonable approach to a high-flux neutron source in the near future. The idea is to bombard a high-energy (20-40 MeV) deuteron beam into a lithium jet target to produce high-energy neutrons in order to simulate a fusion reactor environment via the Li (d, n) nuclear stripping reaction. Deposition of the high-energy deuteron beam and the subsequent response of the lithium jet are modeled and evaluated in detail. To assess the feasibility of this concept, the analysis is done parametrically for various deuteron beam energies, beam currents, and jet velocities. A main requirement for a successful operation is to keep the free jet surface at a minimum temperature to reduce surface evaporation of lithium into the vacuum system. The effects of neutron-generated heating and irradiation on the jet-supporting back plate are also evaluated. The back plate must maintain a reasonable lifetime during system operation. DOE

N94-31202# Argonne National Lab., IL.
TIME-RESOLVED INFRARED ABSORPTION STUDIES APPLIED TO THE STUDY OF RADICAL PLUS MOLECULE REACTIONS
G. A. Bethardy, R. G. Macdonald, and F. J. Northrup 1994 8 p Presented at the OE/LASE 1994: Conference on Optics, Electro-Optics, and Laser Applications in Science and Engineering, Los Angeles, CA, 22-29 Jan. 1994
(Contract W-31-109-eng-38)
(DE94-005921; ANL/CHM/CP-81658; CONF-940142-10) Avail: CASI HC A02/MF A01

Reaction of the cyano radical (CN) with ethane (C2H6) was studied using time resolved infrared absorption to monitor the product hydrogen cyanide (HCN) in individual ro-vibrational states. Pulse laser photolysis was used to provide an initial excess of the CN radical and the time dependence of individual ro-vibrational states of the high frequency anti-symmetric stretching mode of HCN (0,0,v3) was followed. These experiments reveal that the initial product state distribution of HCN is not highly excited in the HCN(0,0,v3) vibrational manifold. DOE

N94-31227# Office National d'Etudes et de Recherches Aerospatiales, Paris (France).
DEVELOPMENT OF A 3D NUMERICAL CODE TO CALCULATE THE TRAJECTORIES OF THE BLOW OFF ELECTRONS EMITTED BY A VACUUM SURFACE DISCHARGE: APPLICATION TO THE STUDY OF THE ELECTROMAGNETIC INTERFERENCE INDUCED ON A SPACECRAFT Ph.D. Thesis - Paris VI Univ. [DEVELOPPEMENT D'UN CODE NUMERIQUE 3D SIMULANT LES TRAJECTOIRES DES ELECTRONS EMIS PAR UNE DECHARGE DE SURFACE SOUS VIDE: APPLICATION A L'ETUDE DES PERTURBATIONS ELECTROMAGNETIQUES SUR SATELLITE]
Etienne Froger 1993 292 p In FRENCH Original contains color illustrations
(ISSN 0078-3781)
(ONERA-NT-1993-12; ETN-94-95878) Avail: CASI HC A13/MF A03

A description of the electromagnetic behavior of a satellite subjected to an electric discharge is given using a specially developed numerical code. One of the particularities of vacuum discharges, obtained by irradiation of polymers, is the intense emission of electrons into the spacecraft environment. Electromagnetic radiation, associated with the trajectories of the particles around the spacecraft, is considered as the main source of the interference observed. In the absence of accurate orbital data and realistic ground tests, the assessment of these effects requires numerical simulation of the interaction between this electron source and the spacecraft. This is done by the GEODE particle code which is applied to characteristic configurations in order to estimate the spacecraft response to a discharge, which is simulated from a vacuum discharge model designed in laboratory. The spacecraft response to a current injection is simulated by the ALICE numerical three dimensional code. The comparison between discharge and injection effects, from the results given by the two codes, illustrates the representativity of electromagnetic susceptibility tests and the main parameters for their definition. ESA

N94-31237 International Business Machines Corp., San Jose, CA.
MOLECULAR DYNAMICS COMPUTER SIMULATIONS OF CHARGED METAL ELECTRODE-AQUEOUS ELECTROLYTE INTERFACES
Michael R. Philpott and James N. Glosli 18 Feb. 1994 29 p Limited Reproducibility: More than 20% of this document may be affected by microfiche quality
(Contract N00014-92-C-0173)
(AD-A276401; TR-09) Avail: CASI HC A03

When two different substances are joined, material flows across the interface (sometimes imperceptibly almost) until the chemical potentials of the component species are equalized. When the substances are solid or liquid and some of the chemical species are charged, then the interface develops a net electrical polarization due to the formation of an electric double layer. The main goal of this program of study is to give a molecular basis for understanding the structure and dynamics of electrical double layers at charged metal-aqueous electrolyte interface. The aim is to unify current separate descriptions of surface adsorption and solution behavior and, ultimately, to include a detailed treatment of the surface crystallography and electronic properties of the metal. DTIC

N94-31270# Lawrence Livermore National Lab., CA.
EMISSION FROM FERROELECTRIC CATHODES
S. E. Sampayan, G. J. Caporaso, C. L. Holmes, E. J. Lauer, D. Prosnitz, D. O. Trimble, and G. A. Westenskow May 1993 50 p Presented at the Workshop on High Intensity Electron Sources, Legnaro, Italy, 24-28 May 1993
(Contract W-7405-eng-48)
(DE94-006732; UCRL-JC-112646-Rev-1; CONF-9305155-3-Rev-1) Avail: CASI HC A03/MF A01

The authors have recently initiated an investigation of electron emission from ferroelectric cathodes. The experimental apparatus consisted of an electron diode and a 250 kV, 12 ohm, 70 ns pulsed high voltage power source. A planar triode modulator driven by a synthesized waveform generator initiates the polarization inversion and allows inversion pulse tailoring. The pulsed high voltage power source is capable of delivering two high voltage pulses within 50 (mu)s of each other and is capable of operating at a sustained repetition rate of 5 Hz. The initial measurements indicate that emission current densities above the Child-Langmuir Space Charge Limit, J(sub CL), are possible. They explain this effect to be based

on a non-zero initial energy of the emitted electrons. They also determined that this effect is strongly coupled to relative timing between the inversion pulse and application of the main anode-cathode pulse. They also have initiated brightness measurements of the emitted beam and estimate a preliminary lower bound to be on the order of 10(exp 9) A/sq m-rad(exp 2) for currents close to J(sub CL) and factor of two less at currents over 4J(sub CL). As in previous measurements at this laboratory, they performed the measurement using a pepper pot technique. Beamlet profiles are recorded with a fast phosphor and gated cameras. They describe their apparatus and preliminary measurements. DOE

N94-31310# Argonne National Lab., IL.
ANALYSIS OF THE HIGH ENERGY BEHAVIOR OF THE FORWARD SCATTERING PARAMETERS - SIGMA(tot), RHO AND B
M. M. Block (Northwestern Univ., Evanston, IL), F. Halzen (Wisconsin Univ., Madison.), B. Margolis (McGill Univ., Montreal, Quebec.), and A. R. White 1993 28 p Presented at the 23rd International Symposium on Multiparticle Dynamics, Aspen, CO, 13-17 Sep. 1993
(Contracts W-31-109-eng-38; DE-AC02-76ER-02289; DE-AC02-76ER-00881)
(DE94-006537; ANL-HEP-CP-94-9; CONF-9309297-4) Avail: CASI HC A03/MF A01

Recent experimental results, namely, the remeasurement of the rho value by UA4/2 at (radical)s = 546 GeV, together with a new analysis by the E710 group of sigma(sub tot), rho and B at (radical)s = 1800 GeV, as well as their measurement of sigma(sub tot) and B at (radical)s = 1020 GeV, have provided important anchor points for the high energy behavior of (anti p)p scattering. The authors analyze high energy (anti p)p and pp data, using two distinct (and dissimilar) analysis techniques: (1) asymptotic amplitude analysis, under the assumption that they have reached 'asymptopia', and (2) an eikonal model whose amplitudes are designed to mimic real QCD amplitudes. The former gives strong evidence for a log (s/s(sub 0)) dependence at current energies and not log(sup 2)(s/s(sub 0)), and demonstrates that odderons are not necessary to explain the experimental data. The latter gives a unitary model for extrapolation into true 'asymptopia' from current energies, allowing them to predict the values of the total cross section at future supercolliders. Using their QCD-model, the authors obtain sigma(sub tot)(16 TeV)= 106 (+/-) 4 mb and sigma(sub tot)(40 TeV) = 120 (+/-) 5 mb. DOE

N94-31320# Argonne National Lab., IL.
ELIMINATION OF TWO ATOMIC ELECTRONS BY A SINGLE HIGH ENERGY PHOTON
M. Y. Amusia and A. F. Ioffe 1993 18 p Presented at the Eliminations of Two Atomic Electrons by Single High Energy Photon, Argonne, IL, 4-5 Oct. 1993
(Contract W-31-109-eng-38)
(DE94-006834; ANL/PHY/CP-81852; CONF-9310281-1) Avail: CASI HC A03/MF A01

This report discusses the following topics: mechanism of two-electron photoionization; multiple photoionization near inner shell thresholds; double ionization accompanying Compton-effect; and the investigation of secondary photon emission in coincidence with double charged ion production. DOE

N94-31321# Argonne National Lab., IL.
HIGH-TEMPERATURE STUDY OF O+H2CO YIELDS OH+HCO
J. P. Hessler, Hong Du, and P. J. Ogren 1994 6 p Presented at the 207th Spring National Meeting of the American Chemical Society, San Diego, CA, 13-18 Mar. 1994
(Contract W-31-109-eng-38)
(DE94-006837; ANL/CHM/CP-81226; CONF-940301-9) Avail: CASI HC A02/MF A01

In our previous studies of the reactions of the methyl radical with molecular oxygen, we noticed that after the methyl radical has been consumed the reactions which control the concentration of hydroxyl are hydroxyl-hydroxyl recombination, the titled reaction, and the reaction between hydroxyl and formaldehyde. From the long-time temporal behavior of hydroxyl we have been able to extract the rate coefficient for the titled reaction over the temperature range 1580 to 2250 K. When we combine our data with the low temperature data of Klemm et al, we obtain the rate expression k(T) = 2.59 x 10(exp -16) T(exp 1.67) exp(-891/T(K)) cu cm/s(exp -1). This result is consistent with the earlier recommendation of Herron which is based on a Bond-Energy-Band-Order calculation adjusted to agree with the experimental results at 700 K. DOE

N94-31398# Brookhaven National Lab., Upton, NY.
BNL POSSIBILITIES
P. H. Pile 1993 10 p Presented at the U.S./Japan Seminar on Hyperon-Nucleon Interactions, Maui, HI, 24-28 Oct. 1993
(Contract DE-AC02-76CH-00016)
(DE94-007179; BNL-49921; CONF-9310259-2) Avail: CASI HC A02/MF A01

The Brookhaven National Laboratory AGS facility provides the intense kaon and pion beams necessary for detailed studies of the hyperon-nucleon interaction. A description of available beams is provided along with a summary of the current and future physics program. DOE

N94-31402# Aspen Center for Physics, CO.
SUMMARY OF THE 1993 WINTER ACP WORKSHOP ON COLLECTIVE DYNAMICS IN DISORDERED SYSTEM Final Report, 1 Jan. - 31 Dec. 1993
M. Turner 20 Feb. 1994 6 p Workshop held in Aspen, CO, 3-9 Jan. 1993
(Contract N00014-93-1-0271)
(AD-A276355) Avail: CASI HC A02/MF A01

This document is comprised of a list of presentation titles and conference participants. DTIC

N94-31405# California Univ., Berkeley. Lawrence Berkeley Lab.
TRANSPORT PROPERTIES OF QUARK AND GLUON PLASMAS
H. Heiselberg 1 Dec. 1993 13 p Presented at the Pre-equilibrium Parton Dynamics, Berkeley, CA, 23 Aug. - 3 Sep. 1993
(Contract DE-AC03-76SF-00098)
(DE94-007043; LBL-34911; CONF-9308181-2) Avail: CASI HC A03/MF A01

The kinetic properties of relativistic quark-gluon and electron-photon plasmas are described in the weak coupling limit. The troublesome Rutherford divergence at small scattering angles is screened by Debye screening for the longitudinal or electric part of the interactions. The transverse or magnetic part of the interactions is effectively screened by Landau damping of the virtual photons and gluons transferred in the QED and QCD interactions respectively. Including screening a number of transport coefficients for QCD and QED plasmas can be calculated to leading order in the interaction strength, including rates of momentum and thermal relaxation, electrical conductivity, viscosities, flavor and spin diffusion of both high temperature and degenerate plasmas. Damping of quarks and gluons as well as color diffusion in quark-gluon plasmas is, however, shown not to be sufficiently screened and the rates depends on an infrared cut-off of order the 'magnetic mass,' m(sub mag) approximately g(sup 2)T. DOE

N94-31507# Fermi National Accelerator Lab., Batavia, IL.
HYPERON POLARIZATION AND MAGNETIC MOMENTS
J. Lach Dec. 1993 24 p Presented at the 3rd Workshop on Relativistic Aspects of Nuclear Physics, Rio de Janeiro, Brazil, 25-27 Aug. 1993
(Contract DE-AC02-76CH-03000)
(DE94-006041; FNAL/C-93/381; CONF-9308210-1) Avail: CASI HC A03/MF A01

Inclusively produced hyperons with significant polarization were first observed at Fermilab about seventeen years ago. This and subsequent experiments showed that Lambda(degree) were produced polarized while bar-Lambda(degree) had no polarization in the same kinematical region. This set the stage for many experiments which showed that most hyperons are produced polarized. Recent Fermilab experiments have showed that this phenomena is even more complex and theoretical understanding is still lacking. Nevertheless polarized hyperon beams have been an extremely useful experimental tool in measuring hyperon magnetic moments. Recently, magnetic moment precession of channeled particles in bent crystals has been observed. This opens the possibility of measuring the magnetic moments of charmed baryons. DOE

N94-31508# Lawrence Livermore National Lab., CA.
SPECTROSCOPY AND ATOMIC PHYSICS IN EBIT AND SUPEREBIT

P. Beiersdorfer, M. Chen, V. Decaux, S. Elliott, D. Knapp, R. Marrs, A. Osterheld, K. Widmann, and M. Bitter 16 Dec. 1993 20 p Presented at the 9th Biennial Topical Conference on Atomic Processes in Plasmas, San Antonio, TX, 19-23 Sep. 1993
(Contract W-7405-eng-48)
(DE94-006050; UCRL-JC-114373; CONF-9309119-3) Avail: CASI HC A03/MF A01

An overview is given of x-ray measurements in progress on the Livermore electron beam ion trap facilities. The measurements include detailed investigations oi the satellite spectrum of heliumlike krypton Kr(sup 34+) for diagnostic applications in future tokamak fusion reactors, precise measurements of the 2-2 transition energies in neonlike U(sup 82+) through lithiumlike U(sup 89+) to test the predictions of QED theory, and investigations of line formation by innershell ionization and non-resonant electron capture for the development of line diagnostics applicable to non-equilibrium plasmas. DOE

N94-31511# Technische Univ., Darmstadt (Germany). Fachbereich Physik.
EXPERIMENTAL INVESTIGATION OF PHONON EIGENVECTORS USING X RAY INTERFERENCE FIELDS Ph.D. Thesis [EXPERIMENTELLE UNTERSUCHUNG VON PHONONEIGENVEKTOREN MIT ROENTGENINTERFERENZFELDERN]
Alexis N. Zounek 1991 122 p In GERMAN Sponsored by BMFT
(ETN-94-95751) Avail: CASI HC A06/MF A02

The Thermally Diffuse Scattering (TDS) of x-ray interference fields in GaAs was measured, and the data were analyzed together with those of existing measurements on Si, with a view to the investigation of phonon eigenvectors. The contribution of multiphonon processes was taken into account using a specially developed lattice dynamics model. A method was established to separate the contributions of TDS and Compton scattering. For GaAs as well as for Si, eigenvectors were directly determined by adapting the single-phonon scattering. ESA

N94-31516# Technische Univ., Darmstadt (Germany). Fachbereich Physik.
ENERGY AND ANGULAR DISTRIBUTIONS OF SECONDARY IONS DURING ELECTRONIC SPUTTERING OF NONCONDUCTING SURFACES Ph.D. Thesis [ENERGIE- UND WINKELVERTEILUNGEN VON SEKUNDAERIONEN BEIM ELEKTRONISCHEN SPUTTERN VON NICHTLEITER-OBERFLAECHEN]
Robert Moshammer 1991 87 p In GERMAN
(ETN-94-95756) Avail: CASI HC A05/MF A01

Energy and angular distributions of desorbed particles were measured during irradiation of nonconducting solid substances with heavy ions to get additional information about sputtering in the range of electronic energy loss. The developed system allows a significantly more accurate measurement of the secondary ion energy distribution than previously as well as for the first time an angular distribution. The projectile incidence angle is shown to be an important parameter for the angular distribution of organic molecular ions. No directed emission is found for secondary ions from inorganic substances, even for those with large mass. Positive ions are emitted with higher energy than negative ions with comparable mass. Comparison of the experimental results with models shows that fragile organic molecular ions are removed from the surface by the shock wave. The emission of lighter fragment ions is compatible with the approach of an outflowing gas. ESA

N94-31534# Amsterdam Univ. (Netherlands).
THE MEASUREMENT OF THE HADRONIC ENERGY FLOW AND JET PRODUCTION WITH THE ZEUS CALORIMETER IN DEEP INELASTIC SCATTERING EVENTS AT HERA Ph.D. Thesis
Paulus Johannes deJong 1993 204 p Sponsored by Stichting voor Fundamenteel Onderzoek der Materie
(ETN-94-96021) Avail: CASI HC A10/MF A03

A study which shows that the hadronic energy flow (resulting from the struck proton) in deep inelastic scattering events can be measured with a high resolution calorimeter, used to distinguish between a number of these models, test the predictions of various structure function parametrizations in the new kinematical region, and find evidence for the occurrence of higher order processes involving gluons in deep inelastic scattering, is presented. The kinematics and physics at the HERA collider and the ZEUS detector are described. The emphasis is on the role of calorimetry. Hardware and offline software for measurements are described. Monte Carlo generator programs, and the fragmentation and quantum chromodynamics model they implement, are described. Application to ZEUS data is described. Various distributions of the reconstructed kinematics and the hadronic energy flow are presented and compared to Monte Carlo data. A cone jet finding algorithm is applied to the data. ESA

N94-31537# Vrije Univ., Amsterdam (Netherlands).
INFLUENCE OF LONG-RANGE CORRELATIONS ON THE SPECTRAL FUNCTIONS AND RESPONSE OF 48Ca AND 90Zr Ph.D. Thesis
Guestl Adonis Rijsdijk 1993 109 p
(ETN-94-96017) Avail: CASI HC A06/MF A02

The calculation of single particle strength distributions or spectral functions is addressed. An additional aim is the study of the influence of single particle strength fragmentation on the nuclear response. Proton-hole spectral functions are calculated by solving the Dyson equation for the one-body Green function. The calculations are performed for the nuclei Ca-48 and Zr-90 using a parameterized form of the G-matrix of the Bonn meson exchange potential as an effective interaction. Response functions are calculated taking into account the fragmentation of the single particle strength explicitly. ESA

N94-31548# Vrije Univ., Amsterdam (Netherlands).
COLLECTIVE AND QUASIPARTICLE EXCITATIONS IN LIGHT Pb ISOTOPES Ph.D. Thesis
Adrianus Johannes Ma Plompen 1993 124 p
(ETN-94-96014) Avail: CASI HC A06/MF A02

The structure at high spin of the light Pb isotopes Pb-192 and Pb-196 was investigated by studying the gamma decay of these nuclei. The aim was to establish the rotational bands that were expected to be based on the known intruder configurations. However, in a brief study of the nucleus Pb-196, the previous indications for such a band based on the O(+) intruder state appeared to be elusive, and the structure based on the 11(-) intruder state turned out to be quite different from what was expected. It was realized only after the full fledged study of Pb-192 that the excitation energy pattern of the levels that decay via the 11(-) intruder state is probably a rather general feature. In particular, neutron intruder excitations in addition to the proton excitations are needed to achieve stable rotating configurations, which therefore occur at higher excitation energy and spin. ESA

N94-31549# Vrije Univ., Amsterdam (Netherlands).
DIAMAGNETISM IN HELIUM RYDBERG ATOMS Ph.D. Thesis
Tonny vanderVeldt 1993 122 p
(ETN-94-96015) Avail: CASI HC A06/MF A02

Experiments on highly excited helium Rydberg atoms in magnetic fields are addressed. Theories of the hydrogen and helium Rydberg atom in a magnetic and an electric field are summarized. For experiments in magnetic fields, a magnet, an excitation chamber to screen the interaction region for stray electric fields, and an enhancement cavity to increase the intensity of UV laserlight for the excitation process, were built. The following investigations are reported: the helium atom in a pure magnetic field in the low field regime, where well resolved angular momentum manifolds are recorded; the helium Rydberg atom in parallel electric and magnetic fields; and the quasi-Landau structure of helium Rydberg states using scaled energy spectroscopy. ESA

N94-31607# Brookhaven National Lab., Upton, NY.
IONIZING RADIATION EFFECTS ON SILICON TEST STRUCTURES
H. W. Kraner, R. Beuttenmuller, W. Chen, J. A. Kierstead, Z. Li, Y. Zhang, L. Dou, E. Fretwurst, and G. Lindstroem Dec. 1993 18 p Presented at the 1st International Conference on Large Scale Applications and Radiation Hardness of Semiconductor Detectors, Florence, Italy, 7-9 Jul. 1993
(Contract DE-AC02-76CH-00016)
(DE94-006060; BNL-49823; CONF-9307163-1) Avail: CASI HC A03/MF A01

The effects of Co-60 gamma irradiation on MOSCAPS and special junction diode detectors have been studied. The capacitors were used to elicit the charge accumulation and anneal in two types of thermally grown oxides representative of those used in routine detector processing. Ion

implanted, oxide passivated junction detectors having 0.25 and 1 cm(exp 2) areas and perimeter to area ratios of 1 (a square), 2 and 5 were designed and constructed to amplify the ionizing effects expected to largely affect junction edges through changes in fixed oxide charges. Detectors were exposed to over 4 Mrad and showed clear increases in leakage current in proportion to the junction edge length. Annealing schedules were determined to provide a continuous response to incremental irradiations and subsequent room temperature anneals of leakage current. Besides an increase in gate threshold, little effect on the C(V) response was found. PISCES simulation of the edge fields using different fixed oxide charge revealed regions of very high lateral fields near the junction edges for fixed charges in the 2 x 10(exp 12)/cm(exp 2) range expected from the capacitor studies which could be responsible for the observed leakage currents. DOE

N94-31613# Technische Univ., Darmstadt (Germany). Fachbereich Physik.

OPTIMAL DETECTOR STRATEGIES FOR THE PHASE CONTRAST IMAGING FOR SCANNING TRANSMISSION ELECTRON MICROSCOPES Ph.D. Thesis [OPTIMALE DETEKTORSTRATEGIEN FUER DIE PHASENKONTRASTABBILDUNG IM RASTER-TRANSMISSIONS-ELEKTRONENMIKROSKOP]

Michael Hammel 1992 130 p In GERMAN Sponsored by DFG
(ETN-94-95747) Avail: CASI HC A07/MF A02

The applicability of the principle of multiple signal imaging for the Scanning Transmission Electron Microscope (STEM) is addressed. The study was limited to the bright field imaging of objects whose structure can be modeled in a simple way. Imaging theory, and the concept of transfer function and its relation to the signal to noise ratio are explained. Experimental investigations demonstrate that a phase contrast procedure can be quantified for the conventional method of signal acquisition using a nonsegmented circular detector. The different detector strategies are outlined. Statements about the optimal detector configuration are given, nearly independently of the object. ESA

N94-31614# Technische Univ., Darmstadt (Germany). Fachbereich Physik.

CONTROL HEAVY ION COLLISIONS IN THE SYSTEMS Ar-40 + Ca-40 AND Si-28 + Si-28, AND THE NATURE OF PARTICLE EMISSION IN FUSION-EVAPORATION REACTIONS Ph.D. Thesis [ZENTRALE SCHWERIONENSTOESSE IN DEN SYSTEMEN 40AR + 40CA UND 28SI + 28SI UND DIE NATUR DER TEILCHENEMISSION IN FUSION-VERDAMPFUNGS-REAKTIONEN]

Andreas Oberstedt 1991 111 p In GERMAN
(Contract BMFT-06-DA-184-I)
(ETN-94-95749) Avail: CASI HC A06/MF A02

The system Ar-40 + Ca-40 was investigated at 15 MeV/h in the heavy ion accelerator UNILAL to study the influence of the incident energy on pre-equilibrium effects. Neutrons were detected in coincidence with evaporation rest nuclei, whose mass distribution was measured by a special time of flight spectrometer and explained by the emission of light particles using a statistical model. The isotropic equilibrium contribution was separated from the angle dependent pre-equilibrium contribution using the energy spectra and the angular distribution of the neutrons. The dependence of the particle emission in central collisions of the system Si-28 + Si-28 was investigated in the accelerator VICKSI. Mass and charge numbers of the evaporation test nuclei were determined. A statistical model shows that emission is due to light particles. The results provide information pertaining to the equation of state of the nuclear matter. ESA

N94-31620# Texas Univ. at Dallas, Richardson. Dept. of Physics.

ELEMENTARY PARTICLE PHYSICS

J. M. Izen Jan. 1994 11 p
(Contract DE-FG05-92ER-40736)
(DE94-006071; DOE/ER-40736/1) Avail: CASI HC A03/MF A01

Much of the work was connected with experimental measurements made at the Beijing Spectrometer operating at sq. root of s = 4.03 GeV. The effort has now moved to investigating the physics derived from the sq. root of s = 4.03 GeV data, including D(sub s) production, absolute D(sub s) branching fractions (hadronic, leptonic, and inclusive semileptonic), D°D and D°D° production, absolute D hadronic branching fractions, D° branching fractions, and an upper limit on the nu(sub tau) mass. DOE

N94-31637# California Univ., Berkeley. Lawrence Berkeley Lab.

DOUBLE ROTATION NMR STUDIES OF ZEOLITES AND ALUMINOPHOSPHATE MOLECULAR SIEVES Ph.D. Thesis

R. Jelinek Jul. 1993 202 p
(Contract DE-AC03-76SF-00098)
(DE94-007032; LBL-34881) Avail: CASI HC A10/MF A03

The goal is to study the organization and structures of guest atoms and molecules and their reactions on internal surfaces within pores of zeolites and aluminophosphate molecular sieves. Al-27 and Na-23 double rotation NMR (DOR) is used since it removes the anisotropic broadening in NMR spectra of quadrupolar nuclei, thus increasing resolution. This work concentrates on probing aluminum framework atoms in aluminophosphate molecular sieves and sodium extraframework cations in porous aluminosilicates. In aluminophosphates, ordering and electronic environments of the framework Al-27 nuclei are modified upon adsorption of water molecules within the channels; a relation is sought between the sieve channel topology and the organization of adsorbed water, as well as the interaction between the Al nuclei and the water molecules. Extraframework Na(sup +) cations are directly involved in adsorption processes and reactions in zeolite cavities. DOE

N94-31668# Argonne National Lab., IL.

DOUBLE PHOTOIONIZATION OF HELIUM WITH SYNCHROTRON X RAYS: PROCEEDINGS

Jan. 1994 114 p Presented at the Double Photoionization of Helium (He) with Synchrotron X Rays Workshop, Argonne, IL, 4 Oct. 1993
(Contract W-31-109-eng-38)
(DE94-006737; ANL/PHY-94/1; CONF-9310190) Avail: CASI HC A06/MF A02

This report contains papers on the following topics: overview and comparison of photoionization with charged particle impact; the ratio of double to single ionization of helium: the relationship of photon and bare charged particle impact ionization; double photoionization of helium at high energies; Compton scattering of photons from electrons bound in light elements; electron ionization and the Compton effect in double ionization of helium; elimination of two atomic electrons by a single energy photon; double photoionization of helium at intermediate energies; double photoionization: gauge dependence, Coulomb explosion; single and double ionization by high energy photon impact; The effect of Compton scattering on the double to single ionization ratio in helium; and double ionization of He by photoionization and Compton scattering. DOE

N94-31669# Fermi National Accelerator Lab., Batavia, IL.

B LIFETIMES AT CDF

J. E. Skarha (Johns Hopkins Univ., Baltimore, MD.) Jan. 1994 11 p Presented at the 9th Workshop on Proton-Antiproton Collider Physics, Tsukuba, Japan, 18-22 Oct. 1993
(Contract DE-AC02-76CH-03000)
(DE94-006850; FNAL/C-93/402-E; CONF-9310247-11) Avail: CASI HC A03/MF A01

Measurements of the average b-hadron lifetime using inclusive B yields J/psi X events, the individual B(sub u) and B(sub d) lifetimes and their ratio using exclusive B yields psi K events, and the B(sub s) lifetime using semileptonic B(sub s) yields l nu D(sub s) X events are presented. The results were obtained from a 21.3 pb(exp -1) sample of square root of s = 1.8 TeV (bar p)p collisions collected in 1992-93 at the Fermilab Tevatron collider and required the precise position measurements of the recently installed CDF silicon vertex detector. DOE

N94-31670# Fermi National Accelerator Lab., Batavia, IL.

STUDY OF ASSOCIATED GAUGE BOSON PRODUCTION AT D0: W GAMMA PRODUCTION

A. L. Spadafora (Superconducting Super Collider Lab., Dallas, TX.) Jan. 1994 12 p Presented at the 9th Workshop on Proton-Antiproton Collider Physics, Tsukuba, Japan, 18-22 Oct. 1993
(Contract DE-AC02-76CH-03000)
(DE94-006951; FNAL/C-94/016-E; CONF-9310247-14) Avail: CASI HC A03/MF A01

Preliminary results are presented from a study of (bar p)p yields W gamma + X at square root of s = 1800 GeV at D0 using data from its recently completed first run at the Fermilab Tevatron Collider. The analysis is performed in both the electron and muon channels. In each channel 10

events are observed, which, after subtracting backgrounds, agrees with the standard model expectation. Study of this process is a direct test of the couplings of the WW gamma vertex. Using a Monte Carlo calculation of the dependence of the number of expected events on these couplings, we set preliminary limits (at the 95 percent confidence level) on the anomalous couplings of -2.5 less than or equal to Delta kappa less than or equal to 2.7 (lambda = 0) and -1.2 less than or equal to lambda less than or equal to 1.1 (Delta kappa = 0). DOE

N94-31671# Fermi National Accelerator Lab., Batavia, IL.
THE D0 UPGRADE
S. Gruenendahl (Rochester Univ., NY.) Jan. 1994 12 p Presented at the 9th Workshop on Proton-Antiproton Collider Physics, Tsukuba, Japan, 18-22 Oct. 1993
(Contract DE-AC02-76CH-03000)
(DE94-006953; FNAL/C-94/023-E; CONF-9310247-16) Avail: CASI HC A03/MF A01

In order to maximize the physics potential of the Fermilab Tevatron proton antiproton collider complex, both the accelerator system and the two large collider detectors are undergoing major upgrades during the remainder of this decade. For the D0 detector, the upgrade focuses on implementation of an integrated magnetic tracker in the central region of the detector, accompanied by those modifications to other parts of the apparatus necessary to cope with the increase in interaction rate provided by the collider. DOE

N94-31681 Rutherford Appleton Lab., Chilton (England).
PRACTICAL NEUTRON TRAINING COURSE: COURSE NOTES
S. M. Bennington, A. C. Hannon, and J. B. Forsyth Dec. 1993 39 p See also DE85-702837 and PB92-200187
(PB94-145158; RAL-93-083) Avail: Issuing Activity (National Technical Information Service (NTIS))

The aim of this course is to provide students who are just starting work in neutron scattering with practical experience of running neutron scattering experiments. The course is constructed so as to provide an introduction to the practicalities of running neutron scattering experiments, especially those performed on a pulsed neutron source. It is intended to be similar in structure to a university undergraduate course, and it is divided into a series of experiments which explore various aspects of neutron scattering. The course is not meant to be a complete self-contained introduction to neutron scattering as this would take considerably longer than one week, but it attempts to provide foundations and to introduce ideas that will be built upon in subsequent practical work. Chapter headings include the following: detector set up, transmission-related properties of materials, diffraction, single crystal neutron diffraction, beryllium filter spectrometer, and the crystal analyzer spectrometer. Appendices include: GENIE basics, useful conversion factors, description of the test beamline, checklist on how to perform a run, d-spacings and selection rules for simple crystal systems, and crystal structures of some metallic elements. NTIS

N94-31749# Laval Univ. (Quebec). Dept. de Physique.
MECHANISMS OF FORMATION AND OF DE-EXCITATION IN THE REACTION Mg-24 + C-12 YIELDS 9 ALPHA AT 35MeV PER NUCLEON M.S. Thesis [MECANISMES DE FORMATION ET DE DESEXCITATION DANS LA REACTION MG-24 + C-12 YIELDS 9 ALPHA A 35 MEV PAR NUCLEON]
Yves Larochelle Jul. 1993 131 p In FRENCH
(ISBN-0-315-86746-9; CTN-94-61226) Copyright Avail: Micromedia Ltd., Technical Information Centre, 240 Catherine Street, Suite 305, Ottawa, Ontario, K2P 2G8, Canada HC/MF

Experiments were conducted at the Chalk River Laboratories on the mechanisms of formation of highly excited nuclei and their de-excitation following a collision between heavy ions at intermediate energies. Investigation of the reactions utilized a matrix of 80 detectors mounted in five concentric rings. The detectors in the three inner rings are of the phoswich type and the 32 detectors in the other two rings are the CsI(Tl) type. Implementation of the technique of secondary beams originating from a superconducting cyclotron beam enabled establishment of a new parametrization of the response of CsI as a function of the energy, charge, and mass of the particles. Results are presented related to the complete breakup of the system into nine alpha particles. This output path presents the advantage of containing the total charge of the system and also of eliminating the ambiguity of isotopic identification. In particular, the angular distributions and the correlation functions obtained are compared to different theoretical models. CISTI

N94-31753# Laval Univ. (Quebec). Dept. de Physique.
SPECTROSCOPIC STUDY OF THE MOLECULAR COLLISIONS (HYDROGEN-NITROGEN AND HYDROGEN-OXYGEN) AT ENERGIES OF SEVERAL MeV M.S. Thesis [ETUDE SPECTROSCOPIQUE DES COLLISIONS MOLECULAIRES (HYDROGENE-AZOTE ET HYDROGENE-OXYGENE) A DES ENERGIES DE QUELQUES MEV]
Jacinthe Plante Jan. 1993 153 p In FRENCH
(ISBN-0-315-86794-9; CTN-94-61230) Copyright Avail: Micromedia Ltd., Technical Information Centre, 240 Catherine Street, Suite 305, Ottawa, Ontario, K2P 2G8, Canada HC/MF

Results are presented from a systematic study concerning the constant velocity collisions between hydrogen projectiles (H(+), H2(+), and H3(+) at 1 MeV/nucleon) and two gases (O2 and N2). These collisions are of interest for atmospheric studies, in particular for protonic auroras. Emission spectra in the ultraviolet and visible (1200 to 6000 Angstroms) were recorded as a function of type of projectile in order to study the role of accompanying electrons in the various collisional processes, and as a function of the target gas pressure in order to determine the relative importance of single and multiple collisions in this process. The observations confirm the formation of the neutral nitrogen atom, resolving a question which was posed in recent work. These observations suggest the absence of most of the atomic and molecular hydrogen lines. It is the same for the first vibrational levels of the C 2-Sigma(sub u(+)) - X 2-Sigma(sub g (+)) bands of N2(+), even if the latter have already been excited by electron impact to energies comparable to those of the electrons which accompany the H2(+) and H3(+) projectiles in the study. CISTI

N94-31779# Oak Ridge National Lab., TN.
PERTURBATIVE AND NONPERTURBATIVE EM LEPTON PAIR PRODUCTION IN RELATIVISTIC HEAVY-ION COLLISIONS
V. E. Oberacker, J. C. Wells, A. S. Umar, and M. R. Strayer 1993 11 p Presented at the NATO Advanced Study Institute on Hot and Dense Nuclear Matter, Bodrum, Turkey, 26 Sep. - 9 Oct. 1993
(Contract DE-AC05-84OR-21400)
(DE94-006315; CONF-930999-6) Avail: CASI HC A03/MF A01

In this talk, the authors focus on electromagnetic dilepton production from the QED-vacuum in relativistic heavy-ion collisions. Heavy ions in relativistic motion generate strong time-dependent EM fields with large Fourier components which give rise to sizable pair production. There are several motivations for this study: Lepton pair production by hadronic (Drell-Yan) processes has been widely discussed as a possible signature of the quark-gluon plasma formation. The dominant background will come from electromagnetic sources and could even mask the signals from the plasma phase. Electromagnetically produced lepton pairs also impose severe constraints on the design of relativistic heavy-ion colliders such as RHIC and LHC. In addition to the free pair production discussed above, pair-production with capture of the negatively charged lepton into a bound state is also possible. This change of the charge state of the ions is the leading mechanism for beam loss of relativistic colliders. Accurate predictions of the cross section for this process are important because the cross section increases with energy. DOE

N94-31832# Concordia Univ., Montreal (Quebec). Dept. of Physics.
PRODUCTION OF CHARGINOS AND NEUTRALINOS FOR THE REACTION POSITRON ELECTRON YIELDS Z' BOSON YIELDS CHARGINO(+) (SUB I) CHARGINO(-) (SUB J) OR NEUTRALINO (SUB I) NEUTRALINO (SUB J) IN SU(2) (SUB L) X SU(2) (SUB R) X U(1) (SUB B-L) M.S. Thesis
Scott Walter Eby-Frederick Aug. 1993 108 p
(ISBN-0-315-87316-7; CTN-94-61239) Copyright Avail: Micromedia Ltd., Technical Information Centre, 240 Catherine Street, Suite 305, Ottawa, Ontario, K2P 2G8, Canada

All left-right supersymmetry models contain a second Z(0) boson, Z'. If the Z' is massive enough it will decay into charginos and neutralinos. The particular model considered is an extension of the supersymmetric standard model which has been modified to include both left and right symmetry groups. The cross sections have been calculated for the production of

charginos and neutralinos in the reaction in which a positron electron pair decays into a Z' boson which then yields pairs of charginos or neutralinos. The Z'-reaction was evaluated at the center of mass energy up to 2 TeV for different sets of parameters. Since the chargino and neutralino masses were chosen in the range above 50 GeV, their widths are expected to be on the order of a fraction of a GeV. Unless the charginos or neutralinos in question turn out to be stable, the decay of these particles should occur well within a detector. Within such widths, experiments should be able to observe not the charginos and neutralinos themselves, but their decay products. The expected decay products are listed. Author (CISTI)

N94-31915# Windsor Univ. (Ontario). Dept. of Physics.
PRODUCTION AND DETECTION OF METASTABLE ATOMIC OXYGEN Ph.D. Thesis
Lance Richard Leclair Jun. 1993 172 p
(ISBN-0-315-87364-7; CTN-94-61223) Copyright Avail: Micromedia Ltd., Technical Information Centre, 240 Catherine Street, Suite 305, Ottawa, Ontario, K2P 2G8, Canada HC/MF

The metastable species O(1S) has been observed following the dissociation of O2, N2O, and CO2 molecules by pulsed electron impact. A crossed beam apparatus was used to obtain time-of-flight spectra of the fragments. A novel detector consisting of a layer of freshly deposited Xe was employed. O(1S) atoms impinging on the surface quickly form XeO excimers which rapidly decay, producing easily detected photons. In the case of O2 and N2O, present results indicate that this method is sensitive solely to O(1S) with high quantum efficiency. In the case of CO2, the Xe layer is sensitive to O(1S) and the metastable CO(a3Pi). Low resolution optical spectra of the emissions which follow the arrival of O(1S) at the Xe layer reveal bands at 375, 550, and 725 nm, while CO(a3Pi) fragments impinging on the layer produce emissions below 350 nm. Time-of-flight and released kinetic energy spectra for all target gases are presented along with excitation functions from threshold to 1,000 eV. These were made using a Bethe-Born calibration technique. Maximum cross sections for O(1S) production were also determined. Author (CISTI)

N94-31921 Rutherford Appleton Lab., Chilton (England).
BARYOGENESIS FROM A PRIMORDIAL LEPTON ASYMMETRY
S. A. Abel and K. E. C. Benson 21 Dec. 1993 29 p Prepared in cooperation with Oxford Univ., Englan d
(PB94-145166; RAL-93-103) Avail: Issuing Activity (National Technical Information Service (NTIS))

We examine the generation of baryon asymmetry at the weak scale from a primordial lepton asymmetry. If the electroweak phase transition is first order, partial reflection of tau leptons off the bubble walls and the resulting hypercharge transport into the symmetric phase, gives rise to a baryon number consistent with observation. NTIS

N94-31922 Rutherford Appleton Lab., Chilton (England).
PROBING LEPTON NUMBER VIOLATION VIA MAJORANA NEUTRINOS AT HADRON SUPERCOLLIDERS
A. Datta, M. Guchait, and A. Pilaftsis Nov. 1993 32 p Prepared in cooperation with Jadavpur Univ., Calcutta, India
(PB94-147055; RAL-93-074) Avail: Issuing Activity (National Technical Information Service (NTIS))

The possibility of discovering heavy Majorana neutrinos and lepton number violation via the like sign dilepton signal at hadron supercolliders is investigated. The cross-sections for the production of these neutrinos singly as well as in pairs are computed both in three and four generation scenarios within the framework of the gauge group SU(2)(sub L) X(circled) U(1)(sub Y) and the dominant processes are identified. The suppression of the Standard model background by suitable kinematical cuts is also discussed. NTIS

N94-31923 Rutherford Appleton Lab., Chilton (England).
F0-975, A0-980 AS EYE-WITNESSES OF CONFINEMENT
F. E. Close, Y. L. Dokshitzer, V. N. Gribov, V. A. Khoze, and M. G. Ryskin Nov. 1993 19 p Prepared in cooperation with Lund Univ., Sweden; Kozponti Fizikai Kutato Intezet, Budapest, Hungary; Durham Univ., England; and Academy of Sciences (USSR), Saint Petersburg
(PB94-147105; RAL-93-049) Avail: Issuing Activity (National Technical Information Service (NTIS))

We investigate some phenomenological consequences of an idea that the f(sub 0)(975) and a(sub 0)(980) play a special role in the dynamics of quark confinement. NTIS

N94-31993 Massachusetts Inst. of Tech., Cambridge.
A MODEL OF THE ION CHEMISTRY OF ELECTRIFIED CONVECTION Ph.D. Thesis
Robert A. Boldi 1992
Avail: Issuing Activity (MIT Libraries, Rm. 14-0551, Cambridge, MA 02139-4307)

To examine the chemical effects of the reactions induced by the ions, electrons, and photons produced in and around a lightning channel, a two-dimensional, axisymmetric dynamical/chemical model of electrified convection has been developed. This model considers approximately 800 thermal and photochemical reactions among 165 neutrals, ions, water clusters, and electrons; effects of pressure, temperature, and electric fields upon the reaction coefficients are explicitly considered. Because the aim of this thesis to focus on ion production and their subsequent gas-phase reactions, aqueous-phase chemistry has not been considered (although heterogeneous loss is represented) and the dynamics and microphysics are specified in a relatively simple manner. The ion and UV-photon generation mechanisms dominate the overall production of many neutrals such as atomic O, N, and H, and are responsible for elevated mixing ratios of the sparingly soluble or short lived chemical families that derive from these species (i.e. NO(x), O(x)). In general, the ion and UV-induced reactions contribute equally to the production of both O((sup 3)P) and O ((sup1)D) and consequently are equally important in the overall chemistry of O3 and OH and other derivative chemical species. The Electrified model represents a net-loss process for some chemical species, primarily due to enhanced in-cloud OH levels. On a global basis this model accounts for the annual destruction of 1.8 Tg of CO, 0.45 Tg of CH4, and 2 x 10(exp -4) Tg of OCS. Once again, these are small fractions of the currently estimated annual source strengths of these species (1600 Tg CO, 525 Tg CH4, and 0.4 Tg OCS). This model is now being refined to include (1) a better representation of heterogeneous loss to the ice phase and (2) feedback between space charge (ions) and the electric field and it is being expanded to include the full range of aqueous-phase chemistry. Additionally (1) a better understanding of the electric-field-strength dependent reactions of e(sup -) and O2 with water would be valuable in quantifying the production of the HO(sub y) family and (2) modeling the production of corona from water would improve the simulation of aqueous-phase ion chemistry. Dissert. Abstr.

N94-32008 Rutherford Appleton Lab., Chilton (England).
RESULTS FROM THE H1 EXPERIMENT AT HERA
J. Dainton Jan. 1994 29 p See also DE93-766345
(PB94-145174; RAL-94-012) Avail: Issuing Activity (National Technical Information Service (NTIS))

First results from the H1 experiment at the high energy electron-proton (ep) collider HERA are presented. Based on an integrated ep luminosity of about 25 nb(sup -1) accumulated during the first data taking period in 1992, first measurements of soft and hard photoproduction and of deep inelastic ep scattering (DIS) have been made. The total photoproduction cross section is measured to be 156 +/- 2 +/- 18 (sys) (mu)b at less than W(sub (gamma)p) greater or equal to 197 GeV. Hard partonic dynamics in photoproduction are observed, and resolved photon contributions inferred in which first hints of interactions involving gluonic components of real photon structure are seen. A measurement of the proton structure function F(sub 2)(x,Q(sub 2)) in the new kinematic region of Bjorken x (x(sub Bj)) between about 10(sup -4) and about 10(sup -2) is presented showing a substantial rise as (x(sub Bj)) decreases. Measurements of the characteristics of hadronic energy flow in such low x DIS events are presented, and a class of events with a large pseudorapidity interval devoid of hadronic energy close to the proton beam direction is reported. NTIS

N94-32044# Naval Postgraduate School, Monterey, CA.
X RAY PULSE CONSIDERATIONS AND ELECTRON FLOW IN HIGH VOLTAGE DIODES M.S. Thesis
Michael O. Callahan Dec. 1993 78 p
(AD-A277301) Avail: CASI HC A05/MF A01

Electrical breakdown in high voltage diodes has been studied since the 1920's, yet it is still not well understood. This study characterizes the

electron flow during breakdown in a high voltage vacuum diode. This was accomplished by measuring the x rays produced when electrons strike the anode of the diode. Current measurements taken during the experiment include both the displacement and conduction electron current, so the x-ray signal is the best measure of the conduction current. Knowledge of the electron flow is important in determining the mechanism of breakdown. The currently accepted explosive electron emission (EEE) model for electrical breakdown can not properly account for the energy required to form cathode spots. Schwirzke proposed a new model that involves an ionization process and a subsequent unipolar arc that accounts for the energy to form the spots. Electron flow for the two models is very different. The EEE model requires a large current density for several nanoseconds before plasma formation, whereas the new model predicts a large current density that develops simultaneously with the plasma formation. The results of this experiment support the predictions of the new model. DTIC

N94-32082# California Univ., San Diego, La Jolla. Dept. of Physics.
POSITRON-MOLECULE INTERACTIONS Final Technical Report, 1 Oct. 1989 - 31 Dec. 1993
Clifford M. Surko 14 Feb. 1994 9 p
(Contract N00014-89-J-1769)
(AD-A276542; TR-3-ONR) Avail: CASI HC A02/MF A01

The objective of this research was to study the interaction of positrons with molecules at energies below the threshold for positronium atom formation. While there is evidence that positrons bind or form long-lived resonances with large atoms and molecules, this phenomenon is not understood. This phenomenon has a number of potentially important scientific and technological applications, including aspects of atomic and molecular physics, the formation of positive ions for mass spectrometry, and gamma ray astronomy. Many facets of the interaction of low energy positrons with molecules were illuminated, including the scaling of positron annihilation rate with molecular ionization potential and the identification of other trends as a function of chemical structure. Spectra of the gamma ray radiation resulting when a positron annihilates on a molecule were also measured. The measurements indicate that the site of positron binding is on the C-H bond in hydrocarbon molecules and on the fluorine atoms in fluorine compounds. The measured annihilation rates on large aromatics indicate that these molecules are likely to be an important source of the annihilation radiation observed from the interstellar medium. DTIC

N94-32097# Joint Inst. for Nuclear Research, Dubna (USSR). Lab. of Neutron Physics.
NN-INTERACTION IN (1)S0-STATE: VIRTUAL LEVEL OR DIBARYON RESONANCE? [NN-VZAIMODEJSTVIE V (1)S0-SOSTOYANIL: VIRTUAL'NYL UROVEN' ILI DIBARIONNYL REZONANS?]
S. B. Borzakov 1993 4 p In RUSSIAN
(DE94-606492; JINR-R-15-93-29) Avail: CASI HC A01/MF A01 (US Sales Only)

The experimental and theoretical evidence for the existence of a quasi-stationary state ofthe neutron and the proton, with J(sup (pi))=0(sup +), is discussed. The experimental methods for conducting such a state observation are proposed. DOE

N94-32139# Los Alamos National Lab., NM.
THE NIJMEGEN HYPERON-NUCLEON POTENTIALS
R. Timmerm.ans 17 Feb. 1994 9 p Presented at the US/Japan Seminar on Hyperon-Nucleon Interactions, Maui, HI, 24-28 Oct. 1993
(Contract W-7405-eng-36)
(DE94-007557; LA-UR-94-676; CONF-9310259-3) Avail: CASI HC A02/MF A01

The Nijmegen YN potential models are reviewed. Differences with the models constructed by the Juelich group are highlighted. A mini-review is given of the status of the scalar mesons and their relevance for the NN and YN interactions. Finally, the reactions (bar N)N yields (bar Y)Y are discussed. DOE

N94-32141# Argonne National Lab., IL.
A GENERAL STOCHASTIC LIOUVILLE THEORY FOR SEQUENTIAL AND SUPEREXCHANGE ELECTRON-TRANSFER REACTIONS INVOLVING THREE MARCUS POTENTIAL SURFACES
J. Tang 1994 26 p
(Contract W-31-109-eng-38)
(DE94-007695; ANL/CHM/PP-80246) Avail: CASI HC A03/MF A01

A general theory for nonadiabatic electron-transfer reactions at high temperature involving Marcus parabolic potential surfaces is presented. The theory can be applied to a three-component system with a donor, a bridging intermediate and an acceptor as well as to a system with charge separation from a photo-excited state followed by charge recombination to a third or ground state. Using the nonperturbative stochastic Liouville approach, analytical expressions are derived for the superexchange and the sequential electron-transfer rate constants covering all three conditions: the 'nondegenerate,' the 'degenerate' and the 'quasi-degenerate' regimes. DOE

N94-32170# Purdue Univ., West Lafayette, IN. Dept. of Chemistry.
CHARGE-DEPENDENT ATOMIC-SCALE STRUCTURES OF HIGH-INDEX AND (110) GOLD ELECTRODE SURFACES AS REVEALED BY SCANNING TUNNELING MICROSCOPY
Xiaoping Gao, Gregory J. Edens, Antoinette Hamelin, and Michael J. Weaver Feb. 1994 48 p
(Contract N00014-91-J-1409)
(AD-A276782; TR-149) Avail: CASI HC A03/MF A01

The atomic and nanoscale structures of high-index gold surfaces in aqueous perchloric acid electrolyte as revealed by in-situ scanning tunneling microscopy (STM) under electrode potential control are reported with the objective of ascertaining systematically the terrace-step morphology and superstructures as a function of the crystallographic orientation. Six faces, Au(221), (331), (533), (311), (210), and (410), two each lying in the three fcc crystallographic zones, were selected to investigate the role of the step orientation and terrace width for non-vicinal faces. Data for the low-index surface Au(110) are also included for comparison with Au(331) and (221), since all three feature formally a n(111)-(111) terrace-step structure. Measurements of the double-layer capacitance as a function of the electrode potential, E, in dilute (10 mM) perchloric acid were also undertaken in order to evaluate the potential of zero charge (E sub pzc) for each surface and to check the potential-dependent surface stability. The two surfaces in the (111)-(100) zone, Au(533) and (311), both display essentially (1 x 1) (i.e bulk-termination) atomic structures at positive electrode charges (i.e. for E greater than E sub pzc), yet exhibit significant surface relaxation at negative charges involving edge-atom depression and row buckling. For the surfaces in the (111)-(110) zone, Au(221) and (331), however, such surface relaxation is seen even at positive electrode charges. This behavioral difference can be understood on the basis of the differing step structures present in the two zones. Moreover, Au(331) undergoes a reversible (1 x 2) reconstruction at negative charges, involving row pairing. DTIC

N94-32173# Texas Univ., Austin. Dept. of Physics.
MEDIUM ENERGY MEASUREMENTS OF N-N PARAMETERS
D. Ambrose, M. Bachman, P. Coffey, G. Glass, B. Jobst, K. H. McNaughton, C. Nguyen, and P. J. Riley 1 Oct. 1993 84 p
(Contract DE-FG05-88ER-40446)
(DE94-006067; DOE/ER-40446/6) Avail: CASI HC A05/MF A01

The authors report here progress made during the three year period January 1, 1990, to December 31, 1993, for the Department of Energy three-year grant number DE-FG05-88ER40446, third year. A major part of the work has been associated with nucleon-nucleon (N-N) research carried out at the Nucleon Physics Laboratory (NPL) at the Los Alamos Meson Physics Facility (LAMPF). During this period they also completed data acquisition and analyses of a TRIUMF experiment, but they have no further plans for experimental work at TRIUMF. Other research has been and will be continued to be carried out at BNL, and involves two rare kaon decay experiments, BNL E791, now completed, and a second generation rare kaon decay experiment, E871, which has just this summer completed an engineering test run. The authors are now also members of a proposed experiment, STAR, (solenoidal tracker at RHIC) to be carried out at the Relativistic Heavy Ion Collider Facility, RHIC, at BNL. The past three years have been a time of rapid change in the focus of the experimental program. A LAMPF experiment, E1097, in which they spent a large amount of effort during the past three years, was terminated due to funding shortages after they had fabricated the detector, but before data acquisition, and consequently they increased their participation in the rare kaon experiment at BNL, E871. It now appears that there will be no LAMPF N-N program after 1993, so that the research efforts will concentrate on the BNL rare

kaon decay measurement, E871, and on STAR. The authors expect that STAR, which requires the fabrication of a large colliding beam detector facility, will use an increasing amount of their research efforts during the next few years. In what follows they describe recent progress on the LAMPF and TRIUMF N-N measurements, on the BNL rare kaon decay work, and on the initial work with the STAR group. DOE

N94-32177# Oak Ridge National Lab., TN.
ATOMIC AND MOLECULAR DATA NEEDS FOR FUSION
D. R. Schultz 1993 12 p Presented at the 9th Biennial Topical Conference on Atomic Processes in Plasmas, San Antonio, TX, 19-23 Sep. 1993
(Contract DE-AC05-84OR-21400)
(DE94-006555; CONF-9309119-5) Avail: CASI HC A03/MF A01

Atomic and molecular processes in plasmas play a crucial role in the development of net energy producing magnetic fusion devices. In light of this fact, presented here is a survey of the broad needs of fusion energy research and a review of the status of the existing database. Emphasis is placed on the relatively new needs for data as novel materials are evaluated for use in the next devices and as components such as the divertor take on more significance for demonstration and practical reactors. Also, examples are given of recent or ongoing data evaluation efforts, the role of national and international data centers is discussed, and some summarizing comments are given. DOE

N94-32178# New Orleans Univ., LA.
ELECTRONIC AND NUCLEAR FACTORS IN INTRAMOLECULAR CHARGE AND EXCITATION TRANSFER PROCESSES
P. Piotrowiak 1993 4 p Presented at the 17th Solar Photochemistry Research Conference, Brainerd, MN, 6-10 Jun. 1993
(Contract DE-FG05-92ER-14310)
(DE94-006598; CONF-9306113-2) Avail: CASI HC A01/MF A01

A qualitative discussion is given of initial work on the following topics: intramolecular triplet excitation transfer bands, donor - bridge - acceptor systems with a tethered ion, and depolarization of transient microwave conductivity. A number of special compounds were synthesized, such as spiranes; 2,6-diamino- dihydro anthracene precursor; and para- amino- nitro- biphenyl and -terphenyl. DOE

N94-32250# California Univ., Berkeley. Lawrence Berkeley Lab.
ADVANCES AND APPLICATIONS OF DYNAMIC-ANGLE SPINNING NUCLEAR MAGNETIC RESONANCE Ph.D. Thesis
J. H. Baltisberger Jun. 1993 219 p
(Contract DE-AC03-76SF-00098)
(DE94-007031; LBL-34883) Avail: CASI HC A10/MF A03

This dissertation describes nuclear magnetic resonance experiments and theory which have been developed to study quadrupolar nuclei (those nuclei with spin greater than one-half) in the solid state. Primarily, the technique of dynamic-angle spinning (DAS) is extensively reviewed and expanded upon in this thesis. Specifically, the improvement in both the resolution (two-dimensional pure-absorptive phase methods and DAS angle choice) and sensitivity (pulse-sequence development), along with effective spinning speed enhancement (again through choice of DAS conditions or alternative multiple pulse schemes) of dynamic-angle spinning experiment was realized with both theory and experimental examples. The application of DAS to new types of nuclei (specifically the Rb-87 and Rb-85 nuclear spins) and materials (specifically amorphous solids) has also greatly expanded the possibilities of the use of DAS to study a larger range of materials. This dissertation is meant to demonstrate both recent advances and applications of the DAS technique, and by no means represents a comprehensive study of any particular chemical problem. DOE

N94-32271# Los Alamos National Lab., NM.
ANTIPROTON PRODUCTION IN HEAVY ION COLLISIONS
B. V. Jacak 1993 13 p Presented at the NATO Advanced Study Institute on Hot and Dense Nuclear Matter, Bodrum, Turkey, 5 Oct. 1993
(Contract W-7405-eng-36)
(DE94-007552; LA-UR-94-713; CONF-9310293-1) Avail: CASI HC A03/MF A01

In high energy p-p and alpha-alpha collisions, baryons are observed predominantly at rapidities near those of target and projectile; the mean rapidity shift of projectile and target nucleons is approximately one unit. In the central rapidity region, the number of baryons is quite small. In fact, the number of baryons and antibaryons is rather similar, indicating that most of these baryons are CREATED particles rather than projectile and target fragments. Antibaryon production is of interest in heavy ion collisions as enhanced antiquark production has been predicted as a potential signature of quark-gluon plasma formation. Antibaryons also provide a sensitive probe of the hadronic environment, via annihilation and/or mean field effects upon their final distributions. However, the collision dynamics also affect the baryon and antibaryon distributions. Baryons are more shifted toward midrapidity in nucleus-nucleus and p-p nucleus collisions than in p-p collisions, increasing the probability of annihilating the antibaryons. The interpretation of antibaryon yields is further complicated by collective processes which may take place in the dense hadronic medium formed in nucleus-nucleus collisions. Jahns and coworkers have shown that multistep processes can increase antibaryon production near threshold. Antiproton production is clearly very interesting, but is sensitive to a combination of processes taking place in the collision. The final number of observed antiprotons depends on the balance between mechanisms for extra antiproton production beyond those from the individual nucleon-nucleon collisions and annihilation with surrounding baryons. We can hope to sort out these things by systematic studies, varying the system size and beam energy. I will review what is known about antiproton production at both the AGS and SPS, and look at trends going from p-p to p-nucleus to nucleus-nucleus collisions. DOE

N94-32355 Brookhaven National Lab., Upton, NY.
ANALYTICAL SOLUTIONS OF MINIMUM IONIZATION PARTICLE INDUCED CURRENT SHAPES OF SILICON DETECTORS AND SIMULATION OF CHARGE COLLECTION PROPERTIES
V. Eremin (Academy of Sciences, USSR, Saint Petersburg.), W. Chen, and Z. Li Nov. 1993 8 p Presented at the 1993 IEEE Nuclear Science Symposium and Medical Imaging Conference, San Francisco, CA, 2-5 Nov. 1993 Limited Reproducibility: More than 20% of this document may be affected by microfiche quality
(Contract DE-AC02-76CH-00016)
(DE94-007523; BNL-49816; CONF-931107-35) Avail: CASI HC A02

A new analytical, one dimensional method to obtain the induced current shapes and simulation of charge shapes for p(sup +) -n-n(sup +) silicon detectors in the case of minimum ionization particle has been developed here. Exact solutions have been found for both electron and hole current shapes. Simulations of induced charge shapes of detectors have also been given. The results of this work are consistent with the earlier work where a semi-analytical method had been used. DOE

N94-32360 State Univ. of New York, Stony Brook. Dept. of Physics.
COOLING AND TRAPPING OF NEUTRAL ATOMS Technical Report, 1992 - 1993
Harold Metcalf 1993 7 p Limited Reproducibility: More than 20% of this document may be affected by microfiche quality
(Contract N00014-90-J-1012)
(AD-A276957) Avail: CASI HC A02

The subject of this research is the quantization of atomic motion. Atoms can easily be cooled to kinetic energies below 0.2 MHz, which is below the light shifts in a weak standing wave. At low excitation rates, an optical standing wave may be viewed as producing a sinusoidal potential. Atoms are then confined in the lambda space between the planes of the standing wave, but have a deBroglie wavelength of approximately equal to lambda/10 or more. Thus their motion is quantized by the light field. We have evidence of this quantization of motion from direct RF spectroscopy of the vibrational states in the wells. The position of the rf peaks do not correspond to the calculated energy intervals and do not shift with laser parameters as expected. DTIC

N94-32368# Calspan Corp., Buffalo, NY. Research Center.
MONOENERGETIC NEUTRAL PARTICLE TRANSPORT IN SEMI-INFINITE MEDIA Final Report, May 1991 - Dec. 1992
Barry D. Ganapol Sep. 1993 46 p
(Contract F30602-88-D-0026)
(AD-A277155; RL-TR-93-176) Avail: CASI HC A03/MF A01

A large class of half-space transport problems for neutral particles is considered including single and adjacent half-space geometries. Localized and distributed sources emitting particles either in a particular direction,

isotropically or with a given angular distribution are considered. All solutions are based on the solution to the well-known albedo problem. A numerical Laplace transform inversion is used to generate highly accurate benchmark solutions which can be used to assess the error incurred by numerical transport algorithms. DTIC

N94-32375# Columbia Univ., New York, NY. Dept. of Chemistry.
THEORETICAL STUDIES OF ELECTRON TRANSFER AND OPTICAL SPECTROSCOPY
R. A. Friesner 1993 19 p
(Contract DE-FG02-90ER-14162)
(DE94-006985; DOE/ER-14162/3) Avail: CASI HC A03/MF A01

Progress was made in three areas. First, we have made major strides in developing our PSGVB electronic structure code including high level electron correlation methods needed to treat complex structures like semiconductor clusters. Secondly, we have developed a one-electron pseudopotential model for semiconductor clusters which reproduces the experimental bandgap as a function of cluster size without adjustable parameters. We are currently using the model to calculate absorption spectra as opposed to just the bandgap via a dispersed polaron formalism. Finally, we have developed two novel quantum dynamical methods, one involving surface hopping and the second utilizing Redfield theory. These methods will be applied to calculation of the relaxation of an excited electron in a semiconductor cluster and also to electron transfer through DNA. DOE

N94-32512# Texas Univ., Austin. Center for Particle Physics.
RESEARCH PROGRAM IN PARTICLE PHYSICS
E. C. G. Sudarshan, D. A. Dicus, J. L. Ritchie, and K. Lang May 1993 55 p
(Contracts DE-FG03-93ER-40757; DE-FG05-85ER-40200)
(DE94-008449; DOE/ER-40757/322) Avail: CASI HC A04/MF A01

This report is the progress report for DOE funded support of particle physics work at the University of Texas, Austin. Support was divided between theoretical and experimental programs, and each is reviewed separately in the report. Theoretical effort was divided between three general areas: quantum gravity and mathematical physics; phenomenology; and quantum mechanics and quantum field theory. Experimental effort was primarily directed toward AGS experiments at Brookhaven, to look for rare kaon decays. AGS experiments 791 and 871 are described, along with BNL experiment 888. DOE

N94-32515# Argonne National Lab., IL.
FORMATION MECHANISM AND YIELD OF MOLECULES EJECTED FROM ZnS, CdS, AND FeS2 DURING ION BOMBARDMENT
S. Nikzad, W. F. Calaway, M. J. Pellin, C. E. Young, D. M. Gruen, and T. A. Tombrello 1994 29 p
(Contract W-31-109-eng-38)
(DE94-008487; ANL/CHM/PP-76357) Avail: CASI HC A03/MF A01

Neutral species ejected from single crystals of ZnS, CdS, and FeS2 during ion bombardment by 3 keV Ar(sup +) were detected by laser post-ionization followed by time-of-flight mass spectrometry. While metal atoms (Fe, Zn, Cd) and S2 were the dominant species observed, substantial amounts of S, FeS, Zn2, ZnS, Cd2, and CdS were also detected. The experimental results demonstrate that molecules represent a larger fraction of the sputtered yield than was previously believed from secondary ion mass spectrometry experiments. In addition, the data suggest that the molecules are not necessarily formed from adjacent atoms in the solid and that a modified form of the recombination model could provide a mechanism for their formation. DOE

N94-32587# Fermi National Accelerator Lab., Batavia, IL.
JET PHYSICS AND QCD TESTS AT THE TEVATRON COLLIDER
R. Plunkett Feb. 1994 28 p Presented at the Conference on Physics in Collision, Heidelberg, Germany, 16-18 Jun. 1993
(Contract DE-AC02-76CH-03000)
(DE94-008987; FNAL/C-94/045-E; CONF-9306251-3) Avail: CASI HC A03/MF A01

Results are presented detailing the status of tests of perturbative QCD in hard parton-parton collisions generated by high energy collisions of protons and antiprotons at the Fermilab Collider. Recent data from the CDF and DO experiments are compared to Next-to-Leading Order QCD calculations in hadronic jet production, prompt photon production, jet production in events with W bosons, and b-quark production. DOE

N94-32598 Argonne National Lab., IL.
WAVE PACKET STUDIES OF THE VIBRATIONAL PREDISSOCIATION OF THREE AND FOUR-ATOM VAN DER WAALS COMPLEXES
S. K. Gray 1994 25 p Presented at the Royal Society of Chemistry Conference, Durham, England, 2-8 Apr. 1994 Limited Reproducibility: More than 20% of this document may be affected by microfiche quality
(Contract W-31-109-eng-38)
(DE94-007623; ANL/CHM/CP-81637; CONF-9404106-1) Avail: CASI HC A03

Vibrational predissociation of XI2 and X2I2 van der Waals complexes, with X = He and Ne, is studied with wave packets. Three dimensional calculations are carried out on the three-atom systems. Suitable X..I potential interactions are determined, and product distributions are predicted. Reduced dimension models of X2I2(v prime) yields 2X + I2(v less than v prime) are investigated. Comparison is made with available experimental results. Mechanistic issues, including the role of intramolecular vibrational relaxation resonances, are addressed. DOE

N94-32605 Pacific Northwest Lab., Richland, WA.
MOLECULAR SCIENCE RESEARCH CENTER Annual Report, 1992
M. L. Knotek Jan. 1994 192 p Limited Reproducibility: More than 20% of this document may be affected by microfiche quality
(Contract DE-AC06-76RL-01830)
(DE94-007464; PNL-8999) Avail: CASI HC A09

The Molecular Science Research Center is a designated national user facility, available to scientists from universities, industry, and other national laboratories. After an opening section, which includes conferences hosted, appointments, and projects, this document presents progress in the following fields: chemical structure and dynamics; environmental dynamics and simulation; macromolecular structure and dynamics; materials and interfaces; theory, modeling, and simulation; and computing and information sciences. Appendices are included: MSRC staff and associates, 1992 publications and presentations, activities, and acronyms and abbreviations. DOE

N94-32615 Argonne National Lab., IL.
RATE COEFFICIENT FOR THE REACTION H + O2 YIELDS OH + O: RESULTS FROM 2000 TO 5300 K
J. P. Hessler and Hong Du 1994 9 p Limited Reproducibility: More than 20% of this document may be affected by microfiche quality
(Contract W-31-109-eng-38)
(DE94-008105; ANL/CHM/PP-75156) Avail: CASI HC A02

Tunable-laser flash absorption has recently provided an unprecedented extension of the temperature range over which the rate of the reaction H + O2 yields OH + O has been measured, resolving an 18-year-old controversy over the high-temperature behavior of the rate of the most important reaction in combustion. Studies have shown that the rate of the above reaction follows a simple Arrhenius expression, k(T) = 1.62 x 10(exp -10) exp(-7474/T(K)) cm(exp 3)/s, from 960 to 5300 K. Previously, measurements by one group extended only up to 3300 K. At 2600 K, the highest temperature studied by three other groups, the measured rates differed by 220 percent. To obtain the new results, a shock wave was used to quickly heat a sample and the rate of production of OH directly behind the shock wave was measured by tuning the wavelength of a pulsed dye laser to a region of strong absorption by the OH molecule. The strength of this absorption was measured as a function of distance behind the shock wave by directing the light from the laser beam onto a linear-array detector. This technique is capable of measuring the rates of very fast reactions, and is ideal for precise studies at very high temperatures where the rates of chemical reactions are the fastest. DOE

N94-32621 Northwestern Univ., Evanston, IL.
EXPERIMENTAL INVESTIGATIONS AND MOLECULAR DYNAMICS SIMULATIONS OF RADIATION INDUCED SURFACE DAMAGE Final Report, 15 Aug. 1991 - 14 Aug. 1993
P. C. Stair, L. D. Marks, D. Seidman, and E. Weitz Jan. 1994 24 p Limited Reproducibility: More than 20% of this document may be affected by microfiche quality
(Grant AF-AFOSR-0303-91)
(AD-A277323; AFOSR-94-0083TR) Avail: CASI HC A03

The research is part of a several year study of the electron stimulated desorption (ESD) behavior of transition metal oxides. The original objective of this research was the development and implementation of an ESD O atom source to be used in Low Earth Orbital (LEO) simulations of materials damage. Though the desorption of neutral particles has been widely postulated, most of the ESD results found in the literature are measurements of ejected ions. The principal reason for this is the ease of ion detection and the inherently low sensitivity of detectors to neutral particles. Most information pertaining to the relative abundance of neutral versus ion desorption is the result of indirect measurements. Despite extensive experimentation including the application of resonant enhanced multiphoton ionization for the selective detection of atomic oxygen the production of atomic oxygen via ESD was never detected. From careful calibration experiments the upper limit to the neutral to ion yield, O/O(+), by ESD was calculated to be 10. From electron microscopy studies of both the reconstructed Ir(001) and Si(001) surfaces, the controversy between the existing models in literature (+/- 0.016 nm for the Ir(001)-5x1 models and +/-0.005 nm for the Si(001)-2x1 models) could be resolved for the first time using a combination of UHV-TED and UHV-HREM techniques. DTIC

N94-32627 Fermi National Accelerator Lab., Batavia, IL.
A SEARCH FOR RAPIDITY GAPS IN JET EVENTS AND A STUDY OF COLOR COHERENCE IN MULTIJET EVENTS AT D0
F. Borcherding 1993 10 p Presented at the 9th Workshop on Proton-Antiproton Collider Physics, Tsukuba, Japan, 18-22 Oct. 1993 Limited Reproducibility: More than 20% of this document may be affected by microfiche quality
(Contract DE-AC02-76CH-03000)
(DE94-006849; FNAL/C-93/388-E; CONF-9310247-12) Avail: CASI HC A02

The authors present studies of Rapidity Gaps and Color Coherence in jet events at the DO Detector for data taken during the recent Tevatron collider run at (radical)s = 1.8 TeV. An upper limit of f((Delta)(eta)(sub c) greater than 3) less than 1.2 x 10(exp -2) at 95% C.L. on the true rapidity gap fraction is given. The color coherence results indicate the angle ordering approximation as modeled in the Herwig Monte Carlo represents the collider as well. DOE

N94-32628# Sandia National Labs., Albuquerque, NM.
COMPLETE MODEL DESCRIPTION OF AN ELECTRON BEAM USING ACCEPT MONTE CARLO SIMULATION CODE
D. E. Weiss (Minnesota Mining and Mfg. Co., Saint Paul.) and R. P. Kensek 1993 25 p Presented at the International Ultraviolet and Electron Beam Curing Conference and Exhibition, Orlando, FL, 1-5 May 1994
(Contract DE-AC04-94AL-85000)
(DE94-007063; SAND-93-2084C; CONF-940566-2) Avail: CASI HC A03/MF A01

A 3D model of a low voltage electron beam has been constructed using the ITS/ACCEPT Monte Carlo code in order to validate the code for this application and improve upon 1D slab geometry simulations. A line source description update to the code allows complete simulation of a low voltage electron beam with any filament length. Faithful reproduction of the geometric elements involved, especially the window support structure, can account for 90-95% of the dose received by routine dosimetry. With a 3D model, dose distributions in non-web articles can be determined and the effects of equipment modifications can be anticipated in advance. DOE

N94-32630# Stanford Linear Accelerator Center, CA.
THE FORM FACTORS OF THE NUCLEONS
G. G. Petratos Dec. 1993 7 p Presented at the Workshop on Electron Nucleus Scattering, Elba, Italy, 5-10 Jul. 1993
(Contract DE-AC03-76SF-00515)
(DE94-007096; SU-SLAC-PUB-6328; CONF-9307145-3) Avail: CASI HC A02/MF A01

The study of the electromagnetic form factors of the nucleons are of fundamental importance in understanding nucleon structure. The form factors contain all the information about the deviation from pointlike structure of the charge and magnetization current distributions of the nucleons. The hope is that measurements at sufficiently large momentum transfers can provide a microscopic understanding of the nucleon wave functions in terms of their constituent quark amplitudes. Recent measurements of the electric G(sub E)(Q(sup 2)) and magnetic G(sub M)(Q(sup 2)) form factors of the nucleons are reviewed and compared to theoretical calculations based on non-perturbative QCD sum rules, diquark, relativistic constituent quark, and vector meson dominance (VMD) models. A short summary of ongoing and future measurements is also presented. DOE

N94-32643 State Univ. of New York, Stony Brook.
IONIZATION PROBES OF MOLECULAR STRUCTURE AND CHEMISTRY
P. M. Johnson Jan. 1994 6 p Limited Reproducibility: More than 20% of this document may be affected by microfiche quality
(Contract DE-FG02-86ER-13590)
(DE94-007605; DOE/ER-13590/13) Avail: CASI HC A02

The development of new techniques for the study of chemical systems is vital for progress in understanding commercially and environmentally important chemical reactions such as combustion, atmospheric ozone depletion, chemical etching in semiconductor manufacture, etc. The very high light flux obtainable from current tunable lasers enables the user to obtain a diagnostic response from molecules present in extremely small concentrations. It is the goal of this research to understand the photophysics of molecule-laser interactions and to devise new spectroscopic analysis techniques which tell us more about the molecules and enable their detection in difficult environments. With high powered pulsed lasers, an almost inevitable end product of the molecule-laser interaction is ionization of the molecule via the absorption of one or several photons. This provides an opportunity for detection because it is easy to collect and count ions. The challenge is to extract information from the ionization event, which typically does not convey the spectral signatures which allow detailed characterization. The author is presently exploiting the very high Rydberg states present just below the energy of each ionic state as referenced to the neutral ground state. By creating and field ionizing these Rydberg states, he is able to extract the states of the molecular ion from the continuum absorption. When he detects the resulting ion in a mass spectrometer, he calls the technique Mass Analyzed Threshold Ionization (MATI) spectroscopy. The information obtained from the experiment is equivalent to having an infrared spectrum of the ion responsible for each parent mass peak in a mass spectrometer sampling a mixture. The identity and structure of each species can be determined. The bulk of the effort in the last year has been involved with understanding the detailed mechanism of this technique and extending it to allow different light sources. DOE

N94-32644 Princeton Univ., NJ. Dept. of Chemical Engineering.
MOLECULAR INTERACTIONS IN DILUTE SUPERCRITICAL MIXTURES: MOLECULAR DYNAMICS INVESTIGATION
P. G. Debenedetti 1993 10 p Limited Reproducibility: More than 20% of this document may be affected by microfiche quality
(Contract DE-FG02-87ER-13714)
(DE94-007610; DOE/ER-13714/T2) Avail: CASI HC A02

Research was done in the following areas: computational and theoretical studies of molecular interactions in supercritical mixtures; supercooled liquids, network fluids, and glasses; and fast algorithms for simulating large systems on a vector processor. DOE

N94-32666# Oak Ridge National Lab., TN.
ADJACENT-CELL PRECONDITIONERS FOR SOLVING OPTICALLY THICK NEUTRON TRANSPORT PROBLEMS
Y. Y. Azmy 1994 9 p Presented at the 8th International Conference on Radiation Shielding, Arlington, TX, 24-27 Apr. 1994
(Contract DE-AC05-84OR-21400)
(DE94-007219; CONF-940424-20) Avail: CASI HC A02/MF A01

We develop, analyze, and test a new acceleration scheme for neutron transport methods, the Adjacent-cell Preconditioner (AP) that is particularly suited for solving optically thick problems. Our method goes beyond Diffusion Synthetic Acceleration (DSA) methods in that it's spectral radius vanishes with increasing cell thickness. In particular, for the ID case the AP method converges immediately, i.e. in one iteration, to 10(exp -4) pointwise relative criterion in problems with dominant cell size of 10 mfp or thicker. Also, the AP has a simple formalism and is cell-centered hence, multidimensional and high order extensions are easier to develop, and more efficient to implement. DOE

N94-32689 Stanford Linear Accelerator Center, CA.
MINIMAX: MULTIPARTICLE PHYSICS AT THE TEVATRON COLLIDER
J. D. Bjorken Jan. 1994 6 p Presented at the 23rd International Symposium on Multiparticle Dynamics, Aspen, CO, 13-17 Sep. 1993 Limited Reproducibility: More than 20% of this document may be affected by microfiche quality
(Contract DE-AC03-76SF-00515)
(DE94-007095; SU-SLAC-PUB-6430; CONF-9309297-5) Avail: CASI HC A02

The author and two dozen others are engaged in a small test/experiment in the Fermilab Tevatron collider. It is called Minimax, and its purpose is to explore large-cross-section physics in the forward direction. The primary goal of Minimax is search for events containing the residue of disoriented chiral condensate (dcc) produced in the primary collision. The theoretical ideas are very speculative. But if they are right, they could provide an interpretation of the Centauro/anti-Centauro anomalies claimed to have been seen in cosmic-ray events. In this paper, the history and status of Minimax is described. DOE

N94-32708# Argonne National Lab., IL.
SEMILEPTONIC DECAYS OF MESONS IN THE SO(4) MODEL
F. Iachello (Yale Univ., New Haven, CT.) and T. S. H. Lee 1994 13 p
(Contracts W-31-109-eng-38; DE-FG02-91ER-40608)
(DE94-008108; ANL/PHY/PP-73096) Avail: CASI HC A03/MF A01

We present results of a calculation of semileptonic decays of mesons in the string-like U(4) SU(sub f)(n) SU(sub s) (2) SU(sub c)(3) model with U(4) implies SO(4) dynamic symmetry. The calculation describes the available data as accurately as the semirelativistic quark model. We make predictions for several exclusive decays which can be tested by future experiments. DOE

N94-32710# Argonne National Lab., IL.
CHIRAL SYMMETRY AND THE THRESHOLD GAMMA(p) YIELDS PI(SUP 0)p REACTION
T. S. H. Lee and B. C. Pearce 1994 15 p
(Contract W-31-109-eng-38)
(DE94-008117; ANL/PHY/PP-71811) Avail: CASI HC A03/MF A01

The threshold gamma p yields pi(sup 0)p reaction is investigated by using a chiral invariant pi N model in a unitary, gauge invariant, dynamical calculation based on a chiral Lagrangian. It is shown that the chiral invariant pi N final state interaction significantly suppresses the E(sub 0+) amplitude from the value -2.4 x 10(exp -3) m(sub pi)(exp -1) predicted by the low energy theorem to -0.66 x 10(exp -3) m(sub pi)(exp -1). We discuss questions concerning the implications of the present results in interpreting the recent Mainz data and their multipole analysis. The experimental accuracy needed for investigating chiral symmetry breaking is illustrated. DOE

N94-32755# Lawrence Livermore National Lab., CA.
OCCUPIED AND UNOCCUPIED ORBITALS OF C60 AND C70
J. A. Carlisle, L. J. Terminello, and E. S. Hudson et al Mar. 1994 8 p Presented at the 2nd International Topical Conference on Optical Probes of Conjugated Polymers and Fullerenes, Salt Lake City, UT, 16-19 Feb. 1994
(Contract W-7405-eng-48)
(DE94-008294; UCRL-JC-116395; CONF-940262-2) Avail: CASI HC A02/MF A01

The full spectrum of occupied and unoccupied sigma and pi orbitals is presented for solid C60, C70, and graphite, using C1s emission and absorption spectroscopy. There are significant differences between C60 and C70, and even larger changes relative to their infinite analog graphite C(sub infinity). A comparison is made with photoemission and inverse photoemission results, along with first principles quasiparticle calculations. DOE

N94-32757# Argonne National Lab., IL.
RADIATION AND PHOTOCHEMISTRY SECTION Annual Report, Oct. 1992 - Nov. 1993
Nov. 1993 39 p
(Contract W-31-109-eng-38)
(DE94-008880; ANL/RPG-94/1) Avail: CASI HC A03/MF A01

The research described in this survey is a study of transient intermediates and chemistry induced by energetic radiation in the condensed phase. The survey is presented in two major parts: the first one studies ions, excited states, and other transients in the condensed phase; the second one studies the role of solvents in chemical reactivity. Some highlights of the past year were observations of ion-molecule reactions of excited aromatic cations via flash photolysis and transient dc conductivity; anion solvation study revealing role of solvent molecular structure; zeolite matrix study of C7H8 radical cation chemistry; and H atom reaction with O2, I(-), and comparison of diffusion of H, D, and muonium in ice. DOE

N94-32768# California Univ., Berkeley. Lawrence Berkeley Lab.
A GUIDE TO EXPERIMENTAL ELEMENTARY PARTICLE PHYSICS LITERATURE, 1988-1992
S. I. Alekhin (Gosudarstvennyi Komitet po Ispolzovaniyu Atomnoi Energii, Moscow, USSR.), V. V. Ezhela (Gosudarstvennyi Komitet po Ispolzovaniyu Atomnoi Energii, Moscow, USSR.), and B. B. Filimonov (Gosudarstvennyi Komitet po Ispolzovaniyu Atomnoi Energii, Moscow, USSR.) Sep. 1993 468 p Revised
(Contract DE-AC03-76SF-00098)
(DE94-007445; LBL-90-Rev) Avail: CASI HC A20/MF A04

We present an indexed guide to the literature in experimental particle physics for the years 1988-1992. About 4,000 papers are indexed by Beam/Target/Momentum, Reaction Momentum (including the final state), Final State Particle, and Accelerator/Detector/Experiment. All indices are cross-referenced to the paper's title and reference in the ID/Reference/Title Index. The information in this guide is also publicly available from a regularly updated computer database. DOE

N94-32780# Fermi National Accelerator Lab., Batavia, IL.
STUDIES OF JET PRODUCTION WITH THE D0 DETECTOR
H. Weerts (Michigan State Univ., East Lansing.) Jan. 1994 21 p Presented at the 9th Workshop on Proton-Antiproton Collider Physics, Tsukuba, Japan, 18-22 Oct. 1993
(Contract DE-AC02-76CH-03000)
(DE94-008271; FNAL/C-94/035-E; CONF-9310247-21) Avail: CASI HC A03/MF A01

During the first collider run at the Tevatron, the DO experiment has accumulated a large sample of events with jet final states, covering a jet E(sub T) range from about 30 to 400 GeV and pseudorapidities up to eta = 3.2. First results about the transverse energy flow as a function of the jet cone size R are obtained and presented. The study of the two leading E(sub T) jets in events results in a measurement of the dijet angular distribution 1/(sigma)d(sigma)/d(chi) as well as the triple differential cross section d(sup 3)(sigma)/dE(sub T)d(eta)(sub 1)d(eta)(sub 2) over a rapidity region not explored before. The correlation between E(sub T) of two jets and their distance in pseudorapidity is outlined as a test of resummation techniques and compared to a recent theoretical prediction. Finally, distributions are presented characterizing the topology of 3 jet events and they are compared to parton shower Monte Carlo's and to an O(alpha(sub s)(sup 3)) prediction at the tree level. DOE

N94-32797# Argonne National Lab., IL.
METAL CLUSTER-RARE GAS VAN DER WAALS COMPLEXES: MICROSCOPIC MODELS OF PHYSISORPTION
W. J. C. Menezes and M. B. Knickelbein 1994 5 p
(Contract W-31-109-eng-38)
(DE94-008134; ANL/CHM/PP-75637) Avail: CASI HC A01/MF A01

The first examples of metal cluster-rare gas van der Waals complexes have been produced using a molecular beam technique, providing novel microscopic models of rare gas physisorption phenomena that occur at low temperatures on extended metal surfaces. These studies show that the formation efficiency of these complexes vary dramatically with the number of metal atoms in the cluster. An interesting example is provided by iron clusters, in which the 13-atom iron cluster is relatively inert toward complexation with krypton atoms, whereas the neighboring 12- and 14-atom clusters form krypton adducts readily. Such results provide valuable insights into the surface topology (i.e., 'smoothness' or 'roughness') of metal clusters, which may in turn aid in developing a detailed microscopic understanding of related systems of technological interest, ranging from heterogeneous catalysts to cluster-assembled materials. DOE

N94-32804# Los Alamos National Lab., NM.
PROCEEDINGS OF THE INTERNATIONAL WORKSHOP ON LOW ENERGY MUON SCIENCE: LEMS 1993
M. Leon, ed. Jan. 1994 552 p Workshop held in Santa Fe, NM, 4-8 Apr. 1993
(Contract W-7405-eng-36)
(DE94-006495; LA-12698-C; CONF-9304145) Avail: CASI HC A24/MF A04

This report contains papers on research with low energy muons. The topics covered included the following: fundamental electroweak physics; muonic atoms and molecules, and muon catalyzed fusion; muon spin research; and muon facilities. These papers were indexed and cataloged separately. DOE

N94-32807# Lawrence Livermore National Lab., CA.
ELECTRON: CLUSTER INTERACTIONS
A. A. Scheidemann (Washington Univ., Seattle.), V. V. Kresin, and W. D. Knight Feb. 1994 19 p Presented at the Workshop on Positron Interactions With Atoms, Molecules and Clusters, Bielefeld, Germany, 14-17 Jul. 1993
(Contract W-7405-eng-48)
(DE94-009089; UCRL-JC-116383; CONF-930715-2) Avail: CASI HC A03/MF A01

Beam depletion spectroscopy was used to measure absolute total inelastic electron-sodium cluster collision cross sections in the energy range from E approximately 0.1 to E approximately 6 eV. The investigation focused on the closed shell clusters Na8, Na20, and Na40. The measured cross sections show an increase for the lowest collision energies where electron attachment is the primary scattering channel. The electron attachment cross section can be understood in terms of Langevin scattering connecting this measurement with the polarizability of the cluster. For energies above the dissociation energy, the measured electron-cluster cross section is energy independent, thus defining an electron-cluster interaction range. This interaction range increases with the cluster size. DOE

N94-32841# Stanford Research Inst., Menlo Park, CA. Accelerator Center.
CP VIOLATION AND THE TOP QUARK
D. Atwood Feb. 1994 3 p Presented at the 2nd International Workshop on Physics and Experiments at Linear E(sup +)e(sup -) Colliders; European Workshop at DESY, Waikoloa, HI, 26 Apr. - 3 May 1993
(Contract DE-AC03-76SF-00515)
(DE94-008930; SU-SLAC-PUB-6434; CONF-9304229-1) Avail: CASI HC A01/MF A01

We consider signals of CP violation in semi-leptonic decay of the top quark. We show that the transverse polarization asymmetries of the (tau)-lepton in the decay t yields brv is extremely sensitive to CP violation. As an illustration, we consider CP phases arising from the charged Higgs exchange in the Weinberg three Higgs doublet model. Qualitatively, the polarization asymmetries are enhanced over rate or energy asymmetries by a factor of O(m(sub t)/m(sub r)) is approximately equal to 100 with a corresponding increase in sensitivity to CP violating parameters. We also examine (tau) polarization in b decays via b yields cvr and find that may also be very effective in constraining CP violating effects such as those that arise from an extended Higgs sector. DOE

N94-32850# Oak Ridge National Lab., TN. Physics Div.
STRING-PARTON MODEL DESCRIPTION OF RELATIVISTIC HEAVY-ION COLLISIONS
A. S. Umar, D. J. Dean, and Strayer 1993 10 p Presented at the NATO Advanced Study Institute on Hot and Dense Nuclear Matter, Bodrum, Turkey, 26 Sept. - 9 Oct. 1993
(Contracts DE-AC05-84OR-21400; DE-FG05-87ER-40376)
(DE94-009164; CONF-930999-9) Avail: CASI HC A02/MF A01

Various models have been developed to address the ordinary hadronic physics that occurs in relativistic heavy-ion collisions. These include string-based fragmentation models such as the LUND model and its extensions in FRITIOF, which assume that excited hadrons behave as a chain of color dipoles that move like one dimensional relativistic strings. Interactions are introduced via multiple small momentum exchanges between the color dipoles of two overlapping strings. Other nondynamical models are the dual-parton model, in which the strings are formed by soft gluon exchange between the valence partons of the colliding hadrons. The quark-gluon string model, also based on the dual parton model, has been developed to study soft parton collisions and includes rescattering. The strings in the above models are in fact one dimensional constructions in momentum space, and string evolution is carried out in this space. We have developed a real-time dynamical model for studying the inclusive properties of hadronic collisions in three dimensions. The model is based on the Nambu-Goto string description of hadrons supplemented by extensions to incorporate the basic features of the parton model, together with a hadronization mechanism. The advantage of having a fully dynamical model is the possibility to explore the detailed time evolution of the hadronic matter. Furthermore, since the model is fully three dimensional, all of the transverse degrees of freedom are available to the evolving system. The model has been successfully applied to the study of high-energy e(+)e(-), pp, mu p, and mu A collisions. These calculations have been used to fix all of the parameters present in the model. For all of the calculations presented here, the model parameters have been held fixed at their predetermined values. DOE

N94-32876# Argonne National Lab., IL. Chemistry Div.
STRUCTURAL STUDIES OF PHOTOINDUCED INTRAMOLECULAR ELECTRON TRANSFER IN CYCLOPENTADIENYLNICKELNITROSYL
L. X. Chen, M. K. Bowman, Zhi-Yu Wang, J. R. Norris, and P. A. Montano 1994 52 p
(Contract W-31-109-eng-38)
(DE94-008467; ANL/CHM/PP-80920) Avail: CASI HC A04/MF A01

A structural study based on EXAFS, FTIR, and optical absorption spectroscopies was conducted on a photogenerated, metastable state of cyclopentadienylnickelnitrosyl (CpNiNO) produced by a reversible photochemical reaction. The photogenerated, metastable state with distinctively different EXAFS, IR, and optical absorption spectra from those of the ground state molecules was created by irradiating the sample with the 365 nm line of a mercury lamp at 20K . At the same temperature, the reverse reaction was induced by irradiation with the 313 nm line from the mercury lamp. Based on the analysis of the EXAFS data, the photogenerated, metastable state of CpNiNO has undergone considerable nuclear rearrangements compared to its ground state. The nuclear movement is characterized by a 0.12 a elongation of Ni-N bond and by a bending of Ni-N-O. A shift of the N-O stretching frequency from 1824 to 1387 cm(exp -1) was observed in the photoinduced reaction with 365 nm light, implying that a NO(-) like species results from intramolecular electron transfer from Ni to NO. The changes in the absorption spectra for the same reaction showed reduced absorption of the 385 nm band and a newly generated broad band near IR region. Temperature dependence of the Debye-Waller factor of CpNiNO was in good agreement with the diatomic harmonic oscillator for the Ni-N bond, but deviated for the Ni-O and the Ni-C bonds. Based on the structures obtained from EXAFS, ZINDO calculations for both the ground state and the photogenerated, metastable state of CpNiNO reproduced the general features of the observed absorption spectra and qualitatively explained the wavelength dependence of the reaction. The calculated partial charges on each atom in the ground state and the photogenerated, metastable state of CpNiNO are consistent with intramolecular electron transfer upon photoexcitation by 365 nm light. DOE

N94-33144 Maryland Univ., College Park. Inst. for Physical Science and Technology.
COHERENT PROCESSES IN ATOM IN STRONG RADIATION FIELDS Final Report, 1 Feb. 1991 - 30 Sep. 1993
C. W. Clark and T. J. McIlrath 30 Sep. 1993 5 p Limited Reproducibility: More than 20% of this document may be affected by microfiche quality
(Grant AF-AFOSR-0109-91)
(AD-A278388; AFOSR-94-0215TR) Avail: CASI HC A01

During this grant period work proceeded to study alternative methods of integrating the higher dimensional time-dependent partial differential equations that arise in the study of atoms interacting with intense laser radiation. Present methods use, for example, Taylor series propagators applied to finite difference and basis set models. We have more recently developed modified propagators based on polynomial extrapolation and rational polynomial extrapolation (Buelisch-Stoer) and have prepared versions that can be effectively vectorized on Cray YMP computers, and in the case of polynomial extrapolation, parallelized on massively parallel

computers. In addition, the stability and accuracy of the finite difference models have been compared to those based on interpolatory splines. The main effort in this grant was directed toward developing numerical integrators for the Schroedinger equation describing the interaction on atoms with circularly polarized light. DTIC

N94-33189# Stanford Research Inst., Menlo Park, CA. Linear Accelerator Center.
SPIN-STRUCTURE FUNCTION OF THE NEUTRON He-3: SLAC RESULTS
Z. E. Meziani Nov. 1993 5 p Presented at the 14th European Conference on Few-Body Problems in Physics, Amsterdam, Netherlands, 22-27 Aug. 1993
(Contracts DE-AC03-76SF-00515; DE-FG03-88ER-40439)
(DE94-008927; SLAC-PUB-6393; CONF-9308164-8) Avail: CASI HC A01/MF A01

A first measurement of the longitudinal asymmetry of deep-inelastic scattering of polarized electrons from a polarized He-3 target at energies ranging from 19 to 26 GeV has been performed at SLAC. The spin-structure function of the neutron g(sub 1)(sup n) was extracted from the measured asymmetries allowing for a test of the Ellis-Jaffe and Bjorken sum rules. The Quark Parton Model (QPM) interpretation of the nucleon spin-structure function is examined in light of the new results. DOE

N94-33277 Purdue Univ., West Lafayette, IN. Dept. of Chemistry.
A TANDEM MICROSCOPIC-ELECTROCHEMICAL EXAMINATION OF A CHARGE-INDUCED SURFACE PHASE SEQUENCE: ORDERED Au(110) IN AQUEOUS IODIDE ELECTROLYTES AS PROBED BY POTENTIODYNAMIC SCANNING TUNNELING MICROSCOPY
Xiaoping Gao, Gregory J. Edens, and Michael J. Weaver Feb. 1994 49 p Limited Reproducibility: More than 20% of this document may be affected by microfiche quality
(Contract N00014-91-J-1409)
(AD-A276905; TR-152) Avail: CASI HC A03

Atomic-level structural and dynamical aspects of the electrode potential-induced sequence of surface phases on ordered Au(110) in dilute aqueous alkali iodide electrolytes have been explored by scanning tunneling microscopy (STM) coupled with cyclic voltammetry. This system exhibits a potentially rich series of electro-induced phase transitions triggered primarily by increasing iodide adsorption towards more positive potentials, together with alkali cation coadsorption. Exploration of the real-space phase-transition dynamics, in particular, is facilitated by means of 'potentiodynamic' STM image sequences obtained during potential steps or especially voltammetric sweeps, thereby providing a direct link to conventional (macroscopic) electrochemical phenomena. At the most negative potentials, beyond ca -0.7 V vs SCE, Au(110) forms a largely uniform (1 x 3) phase. The microscopic steps associated with the formation and iodide adsorbate-induced removal of this reconstruction were examined by potentiodynamic STM. In cesium iodide electrolyte, 'one-missing-row' (1 x 3) and (1 x 2) regions are seen to be formed by periodic row displacement en route to the final 'three-missing-row' (1 x 3) phase. DTIC

N94-33278 Stanford Research Inst., Menlo Park, CA. Accelerator Center.
POLARIZED LEPTON-NUCLEON SCATTERING
E. Hughes Feb. 1994 56 p Presented at the 21st Annual SLAC Summer Institute on Particle Physics: Spin Structure in High-Energy Processes, Stanford, CA, 26 Jul. - 6 Aug. 1993 Limited Reproducibility: More than 20% of this document may be affected by microfiche quality
(Contract DE-AC03-76SF-00515)
(DE94-009027; SU-SLAC-PUB-6439; CONF-930767-2) Avail: CASI HC A04

Deep inelastic polarized lepton-nucleon scattering is reviewed in three lectures. The first lecture covers the polarized deep inelastic scattering formalism and foundational theoretical work. The second lecture describes the nucleon spin structure function experiments that were performed up through 1993. The third lecture discusses the implications of the results and future experiments aimed at high-precision measurements of the nucleon spin structure functions. DOE

N94-32447*# National Aeronautics and Space Administration. Marshall Space Flight Center, Huntsville, AL.
NEUTRAL ION SOURCES IN PRECISION MANUFACTURING
Steven C. Fawcett and Thomas W. Drueding *In* NASA, Washington, Technology 2003: The Fourth National Technology Transfer Conference and Exposition, Volume 2 Feb. 1994 p 223-232 (For primary document see N94-32420 09-99)
Avail: CASI HC A02/MF A04

73 NUCLEAR AND HIGH-ENERGY PHYSICS

Includes elementary and nuclear particles; and reactor theory. For space radiation see *93 Space Radiation.*

N94-31247# Massachusetts Inst. of Tech., Cambridge. Research Lab of Electronics.
PROCEEDINGS OF THE 37TH INTERNATIONAL SYMPOSIUM ON ELECTRON, ION, AND PHOTON BEAMS Final Report, 15 Apr. 1993 - 14 Apr. 1994
Henry I. Smith 11 Feb. 1994 876 p Symposium held in San Diego, CA, 1-4 Jun. 1993
(Contract N00014-93-1-0474)
(AD-A276478) Avail: CASI HC A99/MF A10

Topics covered include: lithographic patterning of self-assembled films; alignment signal failure detection and recovery in real time; marks for alignment and registration in projection electron lithography; improvement of heterodyne alignment technique for x-ray steppers; confocal filtering of the instantaneous image in scanned darkfield alignment; novel on-axis interferometric alignment method with sub-10 nm precision; focused-ion beam induced deposition of copper; focused ion beam XeF2 etching of materials for phase-shift masks; selective electroless plating on electron beam seeded nanostructures; modification of polymer surfaces and the fabrication of submicron-scale functionalized structures by deep-ultraviolet and electron-beam lithography; characteristics of ion beam assisted etching of GaAs: surface stoichiometry; and resolution limits in electron-beam induced tungsten deposition. DTIC

N94-31480 Brookhaven National Lab., Upton, NY.
THE DEVELOPMENT OF CVR COATINGS FOR PBR FUELS
R. E. Barletta, P. E. Vanier, M. B. Dowell, and J. A. Lennartz 1993 6 p Presented at the Fall Meeting of the Materials Research Society (MRS), Boston, MA, 29 Nov. - 3 Dec. 1993 Limited Reproducibility: More than 20% of this document may be affected by microfiche quality
(Contract DE-AC02-76CH-00016)
(DE94-004233; BNL-49703; CONF-931108-17) Avail: CASI HC A02

Particle bed reactors (PBR's) are being developed for both space power and propulsion applications. These reactors operate with exhaust gas temperatures of 2500 to 3000 K and fuel temperatures hundreds of degrees higher. One fuel design for these reactors consists of uranium carbide encapsulated in either carbon or graphite. This fuel kernel must be protected from the coolant gas, usually H2, both to prevent attack of the kernel and to limit fission product release. Refractory carbide coatings have been proposed for this purpose. The typical coating process used for this is a chemical vapor deposition. Testing of other components have indicated the superiority of refractory carbide coatings applied using a chemical vapor reaction (CVR) process, however technology to apply these coatings to large numbers of fuel particles with diameters on the order of 500 pm were not readily available. A process to deposit these CVR coatings on surrogate fuel consisting of graphite particles is described. Several types of coatings have been applied to the graphite substrate: NbC in various thicknesses and a bilayer coating consisting of NbC and TaC with a intermediate layer of pyrolytic graphite. These coated particles have been characterized prior to test; results are presented. DOE

N94-31488# Alabama Univ., University. Dept. of Physics and Astronomy.
HIGH ENERGY PHYSICS PROGRAM AT THE UNIVERSITY OF ALABAMA Annual Report
L. Baksay and J. K. Busenitz Oct. 1993 50 p
(Contract DE-FG05-84ER-40141)
(DE94-006544; DOE/ER-40141/T1) Avail: CASI HC A03/MF A01

The High Energy Physics group at the University of Alabama is a member of the L3 collaboration studying e(sup +)e(sup -) collisions near the Z degree pole at the LEP accelerator at CERN. About 2 million Z degree events have been accumulated and the experiment has been prolific in publishing results on the Z resonance parameters, the Z couplings to all leptons and quarks with mass less than half the Z mass, searches for new particles and interactions, and studies of strong interactions and/or weak charged current decays of quarks and leptons abundantly produced in Z decays. They are contributing to data analysis as well as to detector hardware. In particular, they are involved in a major hardware upgrade for the experiment, namely the design, construction, and commissioning of a silicon microvertex detector (SMD) which has successfully been installed for operation during the present grant period. A report is presented on their recent L3 activities and their plans for the next grant period of twelve months (1 Apr. 1994 - 31 Mar. 1995). Their main interests in data analysis are in the study of single photon final states and the physics made more accessible by the SMD, such as heavy flavor physics. Their hardware efforts continue to be concentrated on the high precision capacitive and optical alignment monitoring systems for the SMD and also includes gas monitoring for the muon system. They are also planning to participate in the coming upgrade of the L3 detector. DOE

N94-31505# Ohio State Univ., Columbus.
HIGH ENERGY PHYSICS STUDIES
1993 25 p
(Contract DE-FG02-91ER-40690)
(DE94-005970; DOE/ER-40690/2) Avail: CASI HC A03/MF A01

Research progress is reported in the following areas: lattice gauge theory, heavy meson decay and CP violation, light cone QCD, technicolor, supersymmetry, and other models beyond the standard model. DOE

N94-32099# Brookhaven National Lab., Upton, NY.
RHIC SPIN PHYSICS
G. Bunce 1993 6 p Presented at the 5th International Workshop on High Energy Spin Physics, Protvino, Russia, 20-24 Sep. 1993
(Contract DE-AC02-76CH-00016)
(DE94-005452; BNL-49719; CONF-9309323-1) Avail: CASI HC A02/MF A01

The physics potential of colliding beams of protons, polarized either longitudinally or transversely, at RHIC is remarkable. A luminosity of L = 2 x 10(exp 32) cm(exp -2) sec(exp -1) with 70 percent polarized beams will be available with up to 250 GeV energy in each beam. The proposal to collide polarized protons in RHIC was submitted in August 1992 and approved in October 1993, just after this workshop. The collaboration has been encouraged to complete research and development on Siberian Snakes, so that RHIC will be able to accelerate polarized protons early in its program. The expected date of the first heavy ion collisions is 1999. The spin physics program includes measurement of gluon and sea quark polarization in the longitudinally polarized proton, measurement and then application of parity violation in W and Z production, measurement of hard scattering parton-parton asymmetries, and quark polarization or transversity in transversely polarized protons. Single spin asymmetries allow sensitive searches for parity violation (longitudinal polarization) and correlations between quark spin and gluons (transverse). Probes include direct photons (to p(sub T) = 20 GeV/c), jets (to p(sub T) greater than 50 GeV/c), Drell-Yan pairs (to m(sub ll) = 9 GeV), W(sup +/-), and Z. Here, the collaboration emphasizes the new information included in the update, given to the Brookhaven PAC this September. DOE

N94-32407# San Francisco State Univ., CA. Dept. of Physics and Astronomy.
RESEARCH IN THEORETICAL HIGH-ENERGY PHYSICS Progress Report, Sep. 1992 - Sep. 1993
J. P. Greensite 1993 10 p
(Contract DE-FG03-92ER-40711)
(DE94-008388; DOE/ER-40711/T1) Avail: CASI HC A02/MF A01

Progress on problems in quantum gravity and QCD, made during the period Sep. 92 - Sep. 93, and proposed research for the coming year are summarized. Over the last year the author has proposed a dynamic mechanism underlying the observed Lorentzian signature of spacetime and a new quantization scheme for gravity, based on a transfer matrix approach. This transfer matrix formulation is not only a possible solution for the well-known 'problem of time' in quantum gravity, but also predicts that Newton's constant is not really a constant: it should be subject to quantum fluctuations. In addition, together with two European collaborators, the author has done some further work on the abelian projection model of quark confinement. This work in quantum gravity and QCD has been reported in various publications, and the author briefly describes each of these investigations. DOE

N94-32586# Fermi National Accelerator Lab., Batavia, IL.
THE FUTURE OF HIGH ENERGY PHYSICS IN THE US STATEMENT FOR THE SCIENCE SUBCOMMITTEE OF THE HOUSE SCIENCE, SPACE AND TECHNOLOGY COMMITTEE
J. Peoples, Jr. Jan. 1994 6 p
(Contract DE-AC02-76CH-03000)
(DE94-008986; FNAL-TM-1876) Avail: CASI HC A02/MF A01

This report discusses the procedures the United States is taking to stay among the world leaders in research of high energy physics. DOE

N94-32588# Fermi National Accelerator Lab., Batavia, IL.
THE FUTURE OF HIGH-ENERGY PHYSICS IN THE US: STATEMENT FOR THE 1994 HEPAP SUBPANEL
J. Peoples, Jr. Feb. 1994 11 p
(Contract DE-AC02-76CH-03000)
(DE94-008994; FNAL-TM-1877) Avail: CASI HC A03/MF A01

The United States has a superb capability for forefront research in elementary particle physics for the next decade -- but it can be realized only if there is sufficient funding to make efficient use of our existing world-class facilities. Throughout most of the past half century, the US has led the world in making contributions to our growing understanding of elementary particle physics. We are no longer the dominant force in the field, but we are still one of the leaders. The termination of the SSC is an enormous blow, but it need not end our participation in the field. We must first take advantage of what we have -- and that is considerable -- and then use it as the basis for a successful strategy for the first few decades in the next century. The US can make many important contributions to our field for the rest of this decade and for part of the next. But, after that, we will not long remain among the world's leaders unless we have the foresight to preserve and strengthen our capability to construct and operate world-class facilities. DOE

N94-32685 Texas Univ., Austin. Inst. for Fusion Studies.
PARTICLE DIFFUSION FROM THE BEAM-BEAM INTERACTION IN SYNCHROTRON COLLIDERS
J. K. Koga and T. Tajima Jan. 1994 13 p Limited Reproducibility: More than 20% of this document may be affected by microfiche quality
(Contract DE-FG05-80ET-53088)
(DE94-007111; IFSR-636; DOE/ET-53088/636) Avail: CASI HC A03

The authors investigate the beam-beam interaction in a synchrotron collider, specifically studying slow particle diffusion in phase space away from tune resonances. Using the tune and tune shift of contemporary large hadron colliders as reference parameters, the computation shows all particles diffusive after 10(exp 5) rotations in contrast to previous single particle tracking results. The diffusion coefficients are several orders of magnitude higher than the tracking code and increase exponentially with the action, caused by the collision induced variation of the second moment of the beams (x(exp 2)). DOE

N94-32731# Syracuse Univ., NY. Dept. of Physics.
FUSION WITH HIGHLY SPIN POLARIZED HD AND D2
A. Honig, S. Letzring, and S. Skupsky 17 Dec. 1993 23 p
(Contract DE-FG03-91SF-18862)
(DE94-006209; DOE/SF-18862/T2) Avail: CASI HC A03/MF A01

The experimental efforts over the past 5 years have been aimed at carrying out inertial confinement fusion (ICF) shots with spin-polarized D fuel. The authors successfully prepared polarized D in HD, and solved the problems of loading target shells with their carefully prepared isotopic mixtures, polarizing them so that the D polarization remains metastably frozen-in for about half a day, and carrying out the various cold transfer requirements at Syracuse, where the target is prepared, and at Rochester, where the cold target is inserted into the OMEGA fusion chamber. A principal concern during this past year was overcoming difficulties encountered in maintaining the integrity of the fragile cold target during

the multitude of cold-transfers required for the experiment. These difficulties arose from insufficient rigidity of the cold transfer systems, which were constrained to be of small diameter by the narrow central access bore of the dilution refrigerator, and were exacerbated by the multitude of required target shell manipulations between different environments, each with different coupling geometry, including target shell permeation, polarization, storage, transport, retrieval and insertion into OMEGA. The authors did solve all of these problems, and were able to position a cold, high density but unpolarized target with required precision in OMEGA. Upon shooting the accurately positioned unpolarized high density cold target, no neutron yield was observed. Inspection inside the OMEGA tank after the shot indicated the absence of neutron yield was due to mal-timing or insufficient retraction rate of OMEGA's fast shroud mechanism, resulting in interception of at least 20 of the 24 laser beams by the faulty shroud. In spite of this, all elements of the complex experiment the authors originally undertook have been successfully demonstrated, and the cold retrieval concepts and methods they developed are being utilized on the ICF upgrades at Rochester and at Livermore. DOE

N94-32748 Fermi National Accelerator Lab., Batavia, IL.
PROCEEDINGS OF THE WORKSHOP ON B PHYSICS AT HADRON ACCELERATORS
P. McBride, ed. (Superconducting Super Collider Lab., Dallas, TX.) and C. S. Mishra, ed. 1993 765 p Workshop held in Snowmass, CO, 21 Jun. - 2 Jul. 1993 Limited Reproducibility: More than 20% of this document may be affected by microfiche quality
(Contract DE-AC02-76CH-03000)
(DE94-007961; SSCL-SR-1225; CONF-9306258) Avail: Issuing Activity (Department of Energy (DOE))

This report contains papers on the following topics: measurement of angle (alpha); measurement of angle (beta); measurement of angle (gamma); other B physics; theory of heavy flavors; charged particle tracking and vertexing; e and gamma detection; muon detection; hadron ID; electronics, DAQ, and computing; and machine detector interface. DOE

N94-32802# Fermi National Accelerator Lab., Batavia, IL.
HYPERON POLARIZATION, CRYSTAL CHANNELING, AND E781 AT FERMILAB
J. Lach Jan. 1994 19 p Presented at the US/Japan Seminar on Hyperon-Nucleon Interactions, Maui, HI, 24-28 Oct. 1993
(Contract DE-AC02-76CH-03000)
(DE94-008224; FNAL/C-94/031; CONF-9310259-4) Avail: CASI HC A03/MF A01

Early experiments at Fermilab observed significant polarization of inclusively produced hyperons. These and subsequent experiments showed that lambda0 were produced polarized while lambdabar0 had no polarization in the same kinematical region. Other hyperons and antihyperons were also seen to be polarized. Recent Fermilab experiments have showed this to be a rich and complex phenomena. Theoretical understanding is still lacking. Fermilab E761 has shown that bent single crystals can be used to process the polarization of hyperons and from the precession angle measure the hyperon's magnetic moment. This opens the possibility of measuring the magnetic moments of charmed baryons. Finally, I will briefly discuss Fermilab E781, an experiment designed to study charmed particle production by sigma(-) hyperons. DOE

N94-32844# Texas Univ., Austin. Inst. for Fusion Studies.
THE 1994 INTERNATIONAL SHERWOOD FUSION THEORY CONFERENCE
1994 254 p Conference held in Dallas, TX, 14-16 Mar. 1994
(Contract DE-FG05-88ER-53266)
(DE94-008961; CONF-940328) Avail: CASI HC A12/MF A03

This report contains the abstracts of the paper presented at the 1994 International Sherwood Fusion Theory Conference. DOE

N94-32879# Department of Energy, Washington, DC. Assistant Secretary for Nuclear Energy.
INDEPENDENT SAFETY ASSESSMENT OF THE TOPAZ-2 SPACE NUCLEAR REACTOR POWER SYSTEM
Sep. 1993 31 p Revised
(DE94-008653; DOE/NE-0001P) Avail: CASI HC A03/MF A01

The independent safety assessment described in this study report was performed to assess the safety of the design and launch plans anticipated by the U.S. Department of Defense (DOD) in 1993 for a Russian-built, U.S.-modified TOPAZ-2 space nuclear reactor power system. Its conclusions, and the bases for them, were intended to provide guidance for the U.S. Department of Energy (DOE) management in the event that the DOD requested authorization under section 91b. of the Atomic Energy Act of 1954, as amended, for possession and use (including ground testing and launch) of a nuclear-fueled, modified TOPAZ-2. The scientists and engineers who were engaged to perform this assessment are nationally-known nuclear safety experts in various disciplines. They met with participants in the TOPAZ-2 program during the spring and summer of 1993 and produced a report based on their analysis of the proposed TOPAZ-2 mission. Their conclusions were confined to the potential impact on public safety and did not include budgetary, reliability, or risk-benefit analyses. DOE

N94-33342 McMaster Univ., Hamilton (Ontario). Dept. of Electrical and Computer Engineering.
KNOWLEDGE ENGINEERING FOR PACES, THE PARTICLE ACCELERATOR CONTROL EXPERT SYSTEM
P. C. Lind, W. F. S. Poehlman, J. W. Stark, and T. Cousins *In* Royal Military Coll. of Canada, Proceedings of the Symposium/Workshop on Applications of Expert Systems in DND Apr. 1992 p 133-152 (For primary document see N94-33335 09-66)
Avail: Issuing Activity (Royal Military Coll. of Canada, Vimy Post Office, Kingston, ON K7K 5L0 Canada)

74 OPTICS

Includes light phenomena; and optical devices.
For lasers see *36 Lasers and Masers.*

N94-31173 Ecole Nationale Superieure des Telecommunications, Paris (France).
THE CONOSCOPIC MICROSCOPE Ph.D. Thesis [LE MICROSCOPE CONOSCOPIQUE]
Eric LeFahler 1993 121 p In FRENCH Limited Reproducibility: More than 20% of this document may be affected by microfiche quality
(ISSN 0751-1353)
(TELECOM-93-E-017; ETN-94-95903) Avail: CASI HC A06

The understanding, study and development of the conoscopic microscope is addressed. A conoscopic holography approach based on physical optics (wave method) was developed. The three dimensional (3D) optical transfer function computation of a conoscopic system was developed. The 3D optical transfer function concept was extended to an optoinformatic system. This 3D optical transfer function will serve as a general tool for modeling conoscopic systems. A conoscopic microscope was physically realized. This necessitated a dimensioning study and test and implementation of optical electronic and computer components. The required software package for using the microscope was built. The influence of different physical and technological parameters (light quantity, measurement stability, precision, repeatibility, etc.) on this system were quantified. The microscope was tested on different hardware types (glass, silicon platelet, InP platelet) and satisfactory surface measurements were obtained. ESA

N94-31256 Pennsylvania State Univ., University Park. Dept. of Chemistry.
STUDYING TRANSIENT MOBILITY AND ENERGY LOSS USING SCANNING TUNNELING MICROSCOPY
M. J. Abrams and P. S. Weiss 31 Dec. 1993 23 p Limited Reproducibility: More than 20% of this document may be affected by microfiche quality
(Contract N00014-91-J-1630)
(AD-A276292; TR-11) Avail: CASI HC A03

We show how scanning tunneling microscopy can be used to determine aspects of transient mobility in the adsorption process, in chemical reactions, and energy transfer processes at surfaces. For adsorption from the gas phase both the mean accommodation length and the promptness of energy loss can be elucidated using real space imaging. DTIC

N94-31262# Northwestern Univ., Evanston, IL. Dept. of Materials Science and Engineering.
NEW AND EMERGING TECHNIQUES FOR IMAGING SURFACES Final Report
Ellen D. Williams (Maryland Univ., College Park.) and L. D. Marks Jan. 1994 45 p
(Contract N00014-93-1-0363)
(AD-A276497) Avail: CASI HC A03/MF A01

The development of techniques for real-time in-situ imaging of surfaces and for spatially resolved spectroscopic imaging of surfaces is reviewed. The capabilities of Field-Ion Microscopy, In-Situ Transmission Electron Microscopy, Low-Energy Electron Microscopy, Point Projection Microscopy, In-Situ Scanning Electron Microscopy, Near Field Scanning Optical Microscopy, Photo-emission Electron Microscopy, Plane-View Transmission Electron Microscopy, Reflection Electron Microscopy, Scanning Electron Microscopy with Polarization Analysis, Scanning Micro-cathodoluminescence, and Scanning Tunneling Microscopy are summarized. DTIC

N94-31271# Fermi National Accelerator Lab., Batavia, IL.
FINAL RESULTS FROM THE SDC DOPANT SEARCH FOR NEW GREEN WAVELENGTH SHIFTING (WLS) FIBERS, VOLUME 1
A. Pla-Dalmau, G. W. Foster, and G. Zhang Dec. 1993 99 p
(Contract DE-AC02-76CH-03000)
(DE94-006744; FNAL-TM-1873-Vol-1) Avail: CASI HC A05/MF A02

A scintillating tile/fiber design had been selected for the SDC calorimeter. It consisted of scintillator plates embedded with a wavelength shifting (WLS) fiber which was spliced to a clear fiber. Based on the results from previous radiation damage studies on different scintillating materials, SCSN38 had been chosen for the scintillating tile and BCF91 or Y7 for the WLS fiber. SCSN38 is a blue-emitting scintillator and both WLS fibers use K-27, a green-emitting compound, as dopant. K-27 has a decay time of approximately 12 ns which is long in comparison to that of most blue-emitting materials. Of all the factors that affect the speed of the scintillator tile/fiber calorimeter, the lifetime of the green-emitting dopant is the dominant component. To increase the speed of the calorimeter, it would be desirable that the green WLS fibers utilized had lifetimes between 3 and 5 ns. However, currently available green WLS fibers exhibit decay times between 7 and 12 ns. Development of new green-emitting WLS fibers with short decay times must be investigated. The goal of this project was to search for commercially available fluorescent compounds with lambda(sub abs) = 400-450 nm, lambda(sub em) = 450-550 nm, tau = 3-7 ns, and quantum efficiency of minimum 0.7 (current K-27 baseline). Large Stokes shift and low self-absorption were not important requirements since the optical pathlength for the shifted light was small. Characterization of the spectroscopic properties of these compounds after styrene polymerization is important since this is an essential part of the manufacturing of WLS fibers. This summary presents the transmittance and fluorescence data for each dopant tested. However, many fluorescence measurements using different excitation wavelengths and orientations were recorded. Volume 1 presents a plot for each dopant combining transmittance and the most representative fluorescence measurement. DOE

N94-31330# Stanford Univ., CA. Dept. of Electrical Engineering.
ADVANCED OPTICAL FIBER COMMUNICATION SYSTEMS Status Report, 1 Aug. 1993 - 1 Mar. 1994
Leonid G. Kazovsky 1 Mar. 1994 36 p
(Contract N00014-91-J-1857)
(AD-A276416) Avail: CASI HC A03/MF A01

Our research is focused on three major aspects of advanced optical fiber communication systems: dynamic wavelength division multiplexing (WDM) networks, fiber nonlinearities, and high dynamic range coherent analog optical links. In the area of WDM networks, we have designed and implemented two high-speed interface boards and measured their throughput and latency. Furthermore, we designed and constructed an experimental PSK/ASK transceiver that simultaneously transmits packet-switched ASK data and circuit-switched PSK data on the same optical carrier. In the area of fiber nonlinearities, we investigated the theoretical impact of modulation frequency on cross-phase modulation (XPM) in dispersive fibers. In the area of high dynamic range coherent analog optical links, we developed theoretical expressions for the RF power transfer ratio (or RF power gain) and the noise figure (NF) of angle-modulated links. We then compared the RF power gains and noise figures of these links to that of an intensity modulated direct detection (DD) link. DTIC

N94-31340# Aberdeen Proving Ground, MD. Edgewood Research Development and Engineering Center.
CHAMBER OPTICS FOR TESTING PASSIVE REMOTE SENSING VAPOR DETECTORS Final Report, Jan. - Jun. 1993
Dennis F. Flanigan Nov. 1993 59 p
(DA Proj. 104-63806-D-601)
(AD-A275909; ERDEC-TR-127) Avail: CASI HC A04/MF A01

There is a need to test the response of multiple remote sensing FTS to known concentrations of vapors with a carefully controlled temperature difference, delta T, between a background source, T(sub bg), and the gas, T(sub g). We have analyzed the various factors inherent in delivering a beam of specified radiance to the sensor including: the geometrical factors needed to assure that the background source fills the field of view, methods of multisensor viewing, and the effects of the transmittance of the additional optical elements. Several optical configurations will deliver a suitable beam. The telescopically based system delivers a spatially similar beam to what the sensor would see in the field. The two-lens system delivers an image at the entrance aperture that is functionally equivalent to a collimated beam at least for single detector spectroradiometers. The radiance analysis showed that the position of the optical elements is important. These results suggest that there is very little penalty to a one window cell, which might be substantially easier to design and build than a windowless cell. DTIC

N94-31550# Vrije Univ., Amsterdam (Netherlands).
SINGLE SCATTERING OF LIGHT BY ENSEMBLES OF PARTICLES WITH VARIOUS SHAPES Ph.D. Thesis
Foeke Kuik 1992 145 p
(ETN-94-96016) Avail: CASI HC A07/MF A02

Single scattering properties of ensembles of randomly oriented small particles are addressed. Results for computed, as well as measured, scattering matrices as functions of scattering angle are presented. Computational results, mainly pertaining to spheroids and finite cylinders, are discussed. Experimental work pertaining to ensembles of water droplets, randomly oriented SiO2 particles, and H2O ice crystals, is discussed. ESA

N94-31584 National Defence Research Establishment, Linkoeping (Sweden). Huvudavdeining foer Informationsteknologi.
FIBEROPTISK MAGNETFALTSENSOR (FIBER OPTIC MAGNETOMETER)
G. Mannerskog, S. Zyra, and J. P. Bengtsson Sep. 1993 42 p In SWAHILI See also PB87-19833 Limited Reproducibility: More than 20% of this document may be affected by microfiche quality
(PB94-148061; FOA-C-30730-3.1) Avail: CASI HC A03

A sensor element for measurement of low frequency magnetic fields has been developed. The element is based on the amorphous magnetostrictive material Vitrovac 4040. An optical fiber was glued to a thin strip of this material and strain originating from a magnetic field was measured. The strain was detected with a Mach-Zehnder interferometer. The output signal was fed back to the sensor element using a small solenoid. The measurement signal then became highly linear. Experiments show high directionality for the sensor. The minimum detectable flux density was 3nT/(square root of Hz) using an effective fiber length of 40 cm and a carrier at 1 mT. Considerably higher sensitivity is expected with a better sensor element and better signal processing. Polarization drift in the interferometer was also a limiting factor. The report contains a theoretical review of relevant magnetic field theory and interferometry. The experimental arrangement and the results obtained are described. Finally, results and possible improvements to the system are discussed. NTIS

N94-31736# Toronto Univ. (Ontario). Dept. of Aerospace Engineering.
FIBER OPTIC SENSORS FOR THE DETECTION OF SURFACE ACOUSTIC WAVES ON METALS M.S. Thesis
Derek John Glennie 1993 109 p
(ISBN-0-315-87055-9; CTN-94-61244) Copyright Avail: Micromedia Ltd., Technical Information Centre, 240 Catherine Street, Suite 305, Ottawa, Ontario, K2P 2G8, Canada HC/MF

The theory of fiber optic strain sensors for surface acoustic waves is explained along with the theory of laser generated ultrasound and modifications to the acoustic source generated when a laser pulse illuminates

a metal surface. Experiments were conducted to determine if surface acoustic waves could be generated on metal surfaces by a Nd-YAG laser pulse and whether a fiber optic Michelson interferometer could detect the waves in various configurations. Surface waves could indeed be generated and detected as hypothesized, and further experiments examined the decay of the surface acoustic waves with distance, the effects of varying the length of one arm of the acoustic wave sensor, and the acoustic wave amplitude versus laser pulse energy. To increase the amplitude of the surface acoustic waves without damaging the sample surface, a circular lens, a cylindrical lens, and a mask were used to modify the laser pulse before it illuminated the sample. Two experiments were conducted to determine if the interferometer could be used to investigate corrosion on the sample surface. On the basis of three corrosion simulations performed, the applicability of using that sensor for corrosion detection is in doubt. CISTI

N94-31751# Laval Univ. (Quebec). Dept. de Physique.
OPTIMIZATION OF Y JUNCTIONS IN INTEGRATED OPTICS M.S. Thesis [OPTIMISATION DE JONCTIONS Y EN OPTIQUE INTEGREE]
Louis Roy Nov. 1993 79 p In FRENCH
(ISBN-0-315-86782-5; CTN-94-61228) Copyright Avail: Micromedia Ltd., Technical Information Centre, 240 Catherine Street, Suite 305, Ottawa, Ontario, K2P 2G8, Canada HC/MF

Optical Y-junctions are one of the biggest limitations to the integration of optical circuits. A new approach is presented for increasing the angle of separation of the branches while limiting the radiation losses in the junction. Starting from the phenomenon of diffraction in three slots, a recreation of which is attempted in an optical waveguide, a study is presented of the behavior of the field in a structure which locally accelerates the phase front of the incident wave. Structures are proposed which prepare the field to change direction before being injected into branches. In spite of the difficulty of recreating the three-slot diffraction phenomenon, the final structure of the junction is nevertheless an improvement due to the phenomenon of local acceleration of the phase front which helps the separation of the incident wave. CISTI

N94-31756# Laval Univ. (Quebec). Dept. de Genie Electrique.
SYNCHRONIZED LASER SCANNING THREE DIMENSIONAL ACQUISITION SYSTEM M.S. Thesis [SYSTEME D'ACQUISITION 3-D A BALAYAGE LASER SYNCHRONISE]
Jean-Francois Tremblay Feb. 1993 81 p In FRENCH
(ISBN-0-315-86848-1; CTN-94-61233) Copyright Avail: Micromedia Ltd., Technical Information Centre, 240 Catherine Street, Suite 305, Ottawa, Ontario, K2P 2G8, Canada HC/MF

A three dimensional vision system is presented which is capable of providing the distance of objects on a 256 by 256 mesh coordinated in azimuth and in elevation. A scanner module added to an existing Jupiter camera of Servo-Robot Inc. allows directing the laser beam to a desired location. The camera, originally with one axis of rotation, was modified to have two axes of rotation. The supplementary axis works in strict relationship with the original scanning mechanism of the camera. The calibration method is modified to take into account this additional mechanism. The new module is carefully integrated with the camera which remains compact and lightweight so that it can easily be used by small robots. The characteristics of the Jupiter camera and the modified final product are described. The design of the second axis of rotation is reviewed with respect to the mechanical design and to the modifications of the controller electronics and software. Finally, the methods used for calibrating the second axis of rotation are summarized along with the results of representative experiments which illustrate some of the images captured by the new three dimensional camera. CISTI

N94-31850 Toronto Univ. (Ontario). Acousto-Optic Research Lab.
MANUFACTURE OF LIGHT-DAMAGE RESISTANT, PLANAR, SINGLE MODE WAVEGUIDE ON LITHIUM NIOBATE Interim Progress Report Phase 1, 1 Jul. 1988 - 31 Mar. 1989
Velimir M. Ristic Mar. 1989 60 p
(DSIS-94-01503; CTN-94-61257) Avail: CASI HC A04/MF A01

The photorefractive effect in LiNbO3 waveguides is described with reference to the origin of internal fields, the effects of impurities and atomic radii, and the energy level model for grating formation in a photorefractive material. It is evident that contamination of the crystal contributes to the photorefractive effect, and processing procedures are detailed which can be used to fabricate LiNbO3 devices while minimizing contamination. The photorefractive effect, also called optical damage, has both photovoltaic and photoconductive components and is mainly due to the photoionization of Fe(2) to the Fe(3) state and the generation of a free electron. Photorefractive effects in LiNbO3 channel waveguides were modelled theoretically and the models were experimentally verified. The electro-optically induced refractive index changes were measured by interferometric techniques. A thermal fixing technique to reduce photorefractive susceptibility was also modelled and tested. This technique relies on the mobility of H(+) ions at elevated temperatures. CISTI

N94-31877# Toronto Univ. (Ontario). Dept. of Medical Biophysics.
INVESTIGATION OF SCINTILLATOR AND FIBRE LIGHT IN PLASTIC SCINTILLATION DOSIMETRY M.S. Thesis
Steven Francis DeBoer 1993 129 p
(ISBN-0-315-87190-3; CTN-94-61252) Copyright Avail: Micromedia Ltd., Technical Information Centre, 240 Catherine Street, Suite 305, Ottawa, Ontario, K2P 2G8, Canada HC/MF

Plastic scintillation dosimetry is a new and promising method of measuring dose in a radiation therapy beam. In this dosimetry system, the light signal produced in a miniature scintillator is transmitted to a photomultiplier tube via fiber optic cables. This system offers many advantages over conventional dosimetry methods, but an undesired radiation induced light signal is produced in the optical fibers. In an investigation of this new dosimetry system, work focused on methods to increase the scintillator to fiber light ratio. Examination of the Cerenkov light produced in the fiber light has led to the development of equations that describe the collection of this light as a function of the fiber orientation within the electron beam for different fibers and different electron beam angular distributions. The results indicated that an increase in the scintillator to fiber light ratio by a factor of 2:1 is achievable by scintillator light shifting and optical filtering of the fiber light signal. An additional factor of 7:1 is expected from a theoretical analysis of the addition of coatings to the scintillator surface. Author (CISTI)

N94-32006# SRI International Corp., Menlo Park, CA.
IR MATERIALS PRODUCIBILITY Quarterly Report No. 6, Nov. 1993 - 31 Jan. 1994
A. Sher, M. A. Berding, A. T. Paxton, and M. W. Muller Feb. 1994 48 p
(Contract MDA972-92-C-0053; ARPA Order 8557)
(AD-A277028) Avail: CASI HC A03/MF A01

In this quarter we have completed an extensive paper on native point defects in Hg(0.8)Cd(0.2)Te, and submitted it to Physical Review B. We calculated the binding energy of a mercury vacancy tellurium anti-site defect complex in Hg(0.8)CdTe and estimated the complex density and its consequences on materials processing. The defect formation energies in CdTe and ZnSe, including gradient corrections to the local density approximation, were calculated, and estimates of the neutral defect concentrations in ZnSe were made. We have continued to develop a method to calculate the defect ionization energies in CdTe, ZnSe, and LiNbO3. Preliminary prediction of the defect densities in x=0.17 LWIR Hg(1-x)Zn(x)Te were made and compared to results in HgCdTe. We continued to develop a method to calculate the temperature dependence of the semiconductor bandgaps. Modifications of our thermodynamical codes for the LiNbO3 problem were made so that the stoichiometry and temperature may be specified and the defect densities determined. DTIC

N94-32013 Surveillance Research Lab., Salisbury (Australia).
ADVANCED INFRARED PHOTODETECTORS: MATERIALS REVIEW
Philip J. Picone Dec. 1993 35 p Limited Reproducibility: More than 20% of this document may be affected by microfiche quality
(AD-A277058; SRL-0117-RR; DODA-AR-008-157) Avail: Issuing Activity (Defense Technical Information Center (DTIC))

The present status of advanced infrared semiconductor detector materials and their application to infrared sensor array systems is reviewed. Techniques to increase device operating temperature are considered for various materials. Focal plane processing requirements are also considered. DTIC

N94-32037 University Coll. of North Wales, Bangor.
FAST ACTING OPTICAL DEFLECTION Final Report, Dec. 1989 - Feb. 1993

D. K. Das-Gupta 18 Jun. 1993 49 p Limited Reproducibility: More than 20% of this document may be affected by microfiche quality
(Contract DAJA45-90-C-0005; DA Proj. 1L1-61102-BH-57)
(AD-A276630; R/D-6310-MS-01) Avail: Issuing Activity (Defense Technical Information Center (DTIC))

The transmission spectra in the wavelength range of 400 nm to 1000nm have been studied with sinusoidal phase transmission gratings formed on photo-resist materials on glass substrates and dielectric mirrors (filters) formed by depositing multiple and alternate layers of 'High' and 'Low' inorganic dielectric materials on glass and polycarbonate substrates. With the sinusoidal crossed two groove profiles transmission gratings of groove depth approx. 896 on a single substrate a transmission was of less than 1% at 500-680nm and the transmittance did not exceed l2% over the entire range of 400-1000nm. The transmission over the visible part of the wavelength was poor although the gratings satisfied the required specification. The multiple layer all dielectric mirror, produced on one surface of a polycarbonate substrate (50mmx50mmx3mm) satisfied the following specification: less than 0.5% transmission at 532nm, less than 1.0% transmission from 694nm, 50% transmission from 400nm to 500nm and from 560 nm to 600 nm. The performance mentioned above satisfied adequately the required specification. DTIC

N94-32068 Physical Optics Corp., Torrance, CA. Research and Development Div.
OPTICAL PROCESSING OF MMW FOR AGILE BEAMSTEERING AND BEAMFORMING Final Report, 2 Jul. 1993 - 2 Jan. 1994
Lev Sadovnik 1 Feb. 1994 35 p Limited Reproducibility: More than 20% of this document may be affected by microfiche quality
(Contract N00014-93-C-0136)
(AD-A277161) Avail: CASI HC A03

There is little doubt than an electronically steered, stationary scanning antenna offers significant advantages over any gimbaled installation, especially for tactical missile seekers. A scanning phased array antenna reduces the demands on space and power and makes better use of the space available. It is widely believed that the millimeter wave (MMW) band (W-band) is the region of the RF spectrum which provides the best angular resolution. In fact, MMW sensor and seeker technologies have made significant advances in recent years, demonstrating their suitability for autonomous adverse weather, battlefield, and smart munition applications. Moreover, only the use of the W-band can produce an active seeker with imaging capability for on-board target identification. DTIC

N94-32138 California Univ., Berkeley. Lawrence Berkeley Lab.
DESIGN AND CHARACTERIZATION OF A PULSED X RAY SOURCE FOR FLUORESCENT LIFETIME MEASUREMENTS
S. C. Blankespoor (California Univ., Berkeley.) Dec. 1993 32 p Limited Reproducibility: More than 20% of this document may be affected by microfiche quality
(Contract DE-AC03-76SF-00098)
(DE94-007495; LBL-35092) Avail: Issuing Activity (Department of Energy (DOE))

To search for new, fast, inorganic scintillators, the author and his colleagues have developed a bench-top pulsed x-ray source for determining fluorescent lifetimes and wavelengths of compounds in crystal or powdered form. This source uses a light-excited x-ray tube which produces x-rays when light from a laser diode strikes its photocathode. The x-ray tube has a tungsten anode, a beryllium exit window, a 30 kV maximum tube bias, and a 50 HA maximum average cathode current. The laser produces 3 x 10(exp 7) photons at 650 nm per approximately 100 ps pulse, with up to 10(exp 7) pulses/sec. The time spread for the laser diode, x-ray tube, and a microchannel plate photomultiplier tube is less than 120 ps fwhm. The mean x-ray photon energy, at tube biases of 20, 25, and 30 kV, is 9.4, 10.3, and 11.1 keV, respectively. They measured 140, 230, and 330 x-ray photons per laser diode pulse per steradian at tube biases of 20, 25, and 30 kV, respectively. Background x-rays due to dark current occur at a rate of 1 x 10(exp 6) and 3 x 10(exp 6) photons/sec/steradian at tube biases of 25 and 30 kV, respectively. Data characterizing the x-ray output with an aluminum filter in the x-ray beam are also presented. DOE

N94-32151# Florida Inst. of Tech., Melbourne.
DEVELOPMENT OF PHASE-ONLY FILTERS FOR SENSOR IMAGERY Final Report, Mar. - Nov. 1993
Samuel P. Kozaitis Dec. 1993 33 p
(Contract F30602-93-C-0024)
(AD-A276722; RL-TR-93-248) Avail: CASI HC A03/MF A01

We used the statistical technique of factor analysis to design binary and ternary optical correlation filters to identify objects in the presence of unknown or non-repeatable distortions. We considered values of spatial frequencies of training set imagery as features and used those spatial frequencies in our filter depending on their variation across a training set. In addition, we provided general expressions for performance measures as a function of training set imagery. The potential of our approach was evaluated with infrared sensor imagery that varied in an unknown way. Our statistically designed filters were easily calculated and performed well in the presence of noise. Furthermore, the performance of our filters were varied by allowing for trade-offs in performance measures. Our filters reduced the sensitivity of binary and ternary phase-only filters to changes in an object's appearance when the input imagery varied in an unknown manner. DTIC

N94-32155 California Univ., Berkeley. Lawrence Berkeley Lab.
X RAY OPTICS FOR SCIENCE AND TECHNOLOGY Final Report, 1 Feb. 1990 - 21 Oct. 1993
David T. Attwood 22 Dec. 1993 21 p Limited Reproducibility: More than 20% of this document may be affected by microfiche quality
(Grant AF-AFOSR-0129-90)
(AD-A277369; AFOSR-94-0077TR) Avail: CASI HC A03

The University of California has conducted research on soft x-ray physics, optics and applications thereof to the physical and life sciences. With support from the Air Force Office of Scientific Research, the University was able to develop a student research and training program. In combination with support from the DOE and, more recently, DOD's Advanced Research Projects Agency (ARPA), a world leadership research group has been established, the Center for X-ray Optics (CXRO), which holds the world's record for highest resolution soft x-ray microscopy (300 A); maintains leadership in biomicroscopy and spatially resolved materials studies; produces reflective optics in the soft x-ray and extreme ultraviolet (EUV), which are among the best in the world; participates in an EUV lithography program which will permit the future industrial evolution from visible and ultraviolet microchip patterning to EUV nanochip production; and offers one of the nation's strongest programs for student training in the emerging fields of nanostructures fabrication for materials science, quantum electronics, and biomicroscopy. A recent review article from 'Physics Today' (August 1992), which highlights some of these activities, is attached, along with the most recent annual report submitted to AFOSR, as well as other materials relevant to the AFOSR program. Derived from text

N94-32180# Naval Postgraduate School, Monterey, CA.
A TECHNIQUE FOR MULTIPLEXING 3X3-COUPLER TERMINATED INTERFEROMETRIC FIBER-OPTIC SENSORS M.S. Thesis
Gregory J. Reid Dec. 1993 108 p
(AD-A276739) Avail: CASI HC A06/MF A02

This thesis investigates the multiplexing of Mach-Zehnder type 3x3 terminated fiber-optic sensors demodulated by either 'quadrature' or 'symmetric' methods using intensity modulation of the source. 3x3-couplers produce signals that permit unmodulated passive demodulation of interferometric signals. The theory is described and the results of a 2x1 element array optical demonstration are presented. Possible architectures using this demultiplexing technique are presented for several applications with different return line requirements. The technique was successfully demonstrated and warrants further investigation to increase the number of sensors and reduce the number of return lines for specific applications. The multiplexing technique presents the opportunity for possible cost savings over other phase generated carrier techniques, which require wavelength modulation of the source and significant optical path differences in the interferometers, and are therefore constrained to presently very expensive sources. The technique presented uses compatible low coherent laser sources such as Compact Disc quality (830 nm) devices. DTIC

N94-32186# Massachusetts Inst. of Tech., Cambridge. Artificial Intelligence Lab.
OPTICAL FLOW FROM 1D CORRELATION: APPLICATION TO A SIMPLE TIME-TO-CRASH DETECTOR
Tomaso Poggio and Nicola Ancona Oct. 1993 19 p

(Contracts N00014-91-J-1270; N00014-92-J-1879)
(AD-A276777; AIM-1375; CBCL-MEMO-74) Avail: CASI HC A03/MF A01

A new technique exploiting 1D correlation of 2D or even 1D patches between successive frames may be sufficient to compute an estimation of optical flow field. Sparse measurements are used to compute qualitative properties of the flow for different visual tasks. We can combine our technique with a scheme for detecting expansion or rotation in an algorithm which suggests interesting biological implications. The algorithm provides a rough estimate of time-to-crash. It is well-suited for VLSI implementations. It was tested on real image sequences. We show its performance and compare the results to previous approaches. DTIC

N94-32280# North Carolina Univ., Chapel Hill. Dept. of Chemistry.
POST-CALIBRATION CORRECTION FOR ROTATING-ANALYZER ELLIPSOMETER WITH OPTICAL FIBER BUNDLE DETECTION SYSTEM
S. Y. Kim, L. Spanos, and E. A. Irene 15 Mar. 1994 26 p
(Contract N00014-89-J-1178)
(AD-A277329; TR-64) Avail: CASI HC A03/MF A01

Spectroscopic ellipsometry with a rotating analyzer operated without a dark room is examined. The effect of the residual linear polarization at the output of an optical fiber bundle upon the ellipsometric constants is critically analyzed. The fraction of the linear polarization and the rotation angle of the polarization axis inside the optical fiber are the two key elements of the post-calibration correction. The spectral dependence of the calibration constants is corrected. DTIC

N94-32285 Massachusetts Inst. of Tech., Lexington. Lincoln Lab.
CONTROL AND RELIABILITY OF OPTICAL NETWORKS IN MULTIPROCESSORS
James J. Olsen 22 Dec. 1993 137 p Limited Reproducibility: More than 20% of this document may be affected by microfiche quality
(Contract F19628-90-C-0002)
(AD-A277385; TR-985; ESC-TR-93-237) Avail: Issuing Activity (Defense Technical Information Center (DTIC))

Optical communication links have great potential to improve the performance of interconnection networks within large parallel multiprocessors, but semiconductor laser drive control and reliability problems inhibit their wide use. This report describes a number of system-level solutions to these problems. The solutions are simple and inexpensive enough to be practical for implementation in the thousands of optical links that might be used in a multiprocessor. Semiconductor laser reliability problems are divided into two classes: transient errors and hard failures. It is found that for transient errors, the computer system might require a very low bit error rate (BER), such as 10(exp -23), without error control. Optical links cannot achieve such rates directly, but a much higher link-level BER (such as 10(exp -7)) would be acceptable with simple error detection coding. A feedback system is proposed that will enable lasers to achieve these error levels even when laser threshold current varies. Instead of conventional techniques using laser output monitors, a software-based feedback system can use BER levels for laser drive control. Experiments demonstrate that this method is feasible and has other benefits such as laser wearout tracking and optical loss compensation. For hard failures, one can provide redundant spare optical links to replace failed ones. Unfortunately, this involves the inclusion of many extra, otherwise unneeded optical links. A new approach, called 'bandwidth fallback,' is presented that allows continued use of partially failed channels while still accepting full-width data inputs, providing high reliability without any spare links. DTIC

N94-32324# North Carolina Univ., Chapel Hill. Dept. of Chemistry.
SI/SIO2 INTERFACE STUDIES BY IMMERSION ELLIPSOMETRY Technical Report No. 60
Q. Liu and E. A. Irene 15 Mar. 1994 8 p
(Contract N00014-89-J-1178)
(AD-A277277) Avail: CASI HC A02/MF A01

The mechanisms associated with Si/SiO2 interface annealing and thermal oxidation conditions were studied by spectroscopic immersion ellipsometry. Essentially, this surface sensitive ellipsometry technique uses liquids that match the refractive index of the films thereby optically removing the films. With the use of an optical model, it is shown that at high annealing temperatures viscous relaxation dominates, while at low annealing temperatures the suboxide reduction is apparent. It is also shown that with the thickening SiO2 overlayer, the thickness of the suboxide layer at the interface increases and the average radius of the crystalline silicon protrusions decreases for the three different orientation studied. These results are consistent with the commonly accepted Si oxidation model. DTIC

N94-32380# Alabama Univ., Huntsville. Environmental and Energy Center.
FIBER OPTIC CHEMICAL SENSORS Final Report, 23 May 1989 - 31 Mar. 1991
W. F. Arendale, R. Hatcher, Y. Garlington, J. Harwell, and T. Everett Oct. 1993 164 p
(Contract F08635-89-C-0288)
(AD-A277128; JRC-RR-91-08; AFESC/ESL-TR-91-08) Avail: CASI HC A08/MF A02

This final report describes a database that supports the development, engineering, and manufacturing of dependable chemical sensors which include fiber-optics in the design and which are suitable for use in the field by technicians. Inexperienced investigators using the database can start with the state of the art rather than starting over each time a requirement for a new chemical sensor is established. The expectations are shorter development times and reduced development and engineering costs. DTIC

N94-32385# Sandia National Labs., Albuquerque, NM.
RECONFIGURABLE OPTICAL SWITCHES WITH MONOLITHIC ELECTRICAL-TO-OPTICAL INTERFACES
J. Cheng, P. Zhou, J. C. Zolper, K. L. Lear, G. A. Vawter, R. E. Leibenguth, and A. C. Adams 1994 8 p Presented at the OE/LASE 1994: Conference on Optics, Electro-Optics, and Laser Applications in Science and Engineering, Los Angeles, CA, 22-29 Jan. 1994
(Contract DE-AC04-94AL-85000)
(DE94-007745; SAND-94-0524C; CONF-940142-27) Avail: CASI HC A02/MF A01

Vertical cavity surface-emitting lasers (VCSEL's) can be integrated with heterojunction phototransistors (HPT's) and heterojunction bipolar transistors (HBT's) on the same wafer to form high speed optical and optoelectronic switches, respectively, that can be optically or electrically addressed. This permits the direct communication and transmission of data between distributed electronic processors through an optical switching network. The experimental demonstration of an integrated optoelectronic HBT/VCSEL switch combining a GaAs/AlGaAs heterojunction bipolar transistor (HBT) with a VCSEL is described below, using the same epilayer structure upon which binary HPT/VCSEL optical switches are also built. The monolithic HBT/VCSEL switch has high current gain, low power dissipation, and a high optical to electrical conversion efficiency. Its modulation has been measured and modeled. DOE

N94-32392# Colorado Univ., Boulder. Optoelectronic Computing Systems Center.
STUDIES OF AN OPTICAL MULTI-PROCESSOR INTERCONNECT Final Report
Jon R. Sauer 1994 179 p
(Contract DASG60-91-C-1043)
(AD-A277093) Avail: CASI HC A09/MF A02

Optical fiber provides a very high capacity medium for point to point transmission of data. It is not a straightforward proposition to achieve the same level of success in networked fiber communication systems. A carefully designed system can approach terabyte-per-second capability. The purpose of this study was to investigate the performance of a generic optical distributed interconnect architecture for parallel processing. In particular, the target was the general purpose, easily programmable, tightly coupled, multiple-instruction stream, multiple data stream (MIMD) systems. We have proposed a fiber-optic interconnect system that is aimed at exploiting the advantages provided by both optics and electronics to provide a low latency, high throughput communication between processors and memory modules in a shared memory system. Decisions taken during any new design are to be based on the basic requirements placed on the system, the strengths and weakness of the implementation domain, and the identification of the problems that exist in past designs. DTIC

N94-32417*# Applied Research Corp., Landover, MD.
A LOW-COST, CCD SOLID STATE STAR TRACKER Final Report, 1 Dec. 1990 - 30 Nov. 1992
M. Chmielowski and D. Wynne 23 Dec. 1992 529 p
(Contract NAS5-31169; SBIR-09.12-8442)
(NASA-CR-192722; NAS 1.26:192722; R92-204) Avail: CASI HC A23

Applied Research Corporation (ARC) has developed an engineering model of a multi-star CCD-based tracker for space applications requiring radiation hardness, high reliability and low power consumption. The engineering unit compared favorably in functional performance tests to the standard NASA single-star tracker. Characteristics of the ARC star tracker are: field of view = 10 deg x 7.5 deg, sensitivity range of -1 to +5 star magnitude, NEA = 3 in x 3 in, linearity = 5 in x 5 in, and power consumption of 1-3 W (operating mode dependent). The software is upgradable through a remote link. The hardware-limited acquisition rate is 1-5 Hz for stars of +2 to +5 magnitude and 10-30 Hz for -1 to +2 magnitude stars. Mechanical and electrical interfaces are identical to the standard NASA star tracker. Author

N94-32510 Princeton Univ., NJ. Dept. of Mathematics.
MATHEMATICAL NONLINEAR OPTICS Final Technical Report, 1 Apr. 1990 - 1940 Sep. 1993
David W. McLaughlin 3 Jan. 1994 14 p Limited Reproducibility: More than 20% of this document may be affected by microfiche quality
(Grant AF-AFOSR-0161-90)
(AD-A277320; AFOSR-94-0062TR) Avail: CASI HC A03

The principal investigator, together with two post-doctoral fellows, several graduate students, and colleagues, has applied the modern mathematical theory of nonlinear waves to problems in nonlinear optics. Projects included the interaction of laser light with nematic liquid crystals, propagation through random nonlinear media, cross polarization instabilities and optical shocks for propagation along nonlinear optical fibers, and the dynamics of bistable optical switches coupled through both diffusion and diffraction. In the first project the extremely strong nonlinear response of a CW laser beam in a nematic liquid crystal medium produced striking undulation and filamentation of the CW beam which was observed experimentally and explained theoretically. In the second project the interaction of randomness with nonlinearity was investigated, as well as an effective randomness due to the simultaneous presence of many nonlinear instabilities. In the polarization problems theoretical hyperbolic structure (instabilities and homoclinic orbits) in the coupled nonlinear Schroedinger (NLS) equations was identified and used to explain cross polarization instabilities in both the focusing and defocusing cases, as well as to describe optical shocking phenomena. For the coupled bistable optical switches, a numerical code was carefully developed in two spatial and one temporal dimensions. The code was used to study the decay of temporal transients to 'on-off' steady states in a geometry which includes forward and backward longitudinal propagation, together with one dimensional transverse coupling of both electromagnetic diffraction and carrier diffusion. DTIC

N94-32626 Department of the Navy, Washington, DC.
PASSIVE, MULTI-CHANNEL FIBER OPTIC ROTARY JOINT ASSEMBLY Patent Application
Gregory Ames, inventor (to Navy) and Roger L. Morency, inventor (to Navy) 8 Nov. 1993 30 p Limited Reproducibility: More than 20% of this document may be affected by microfiche quality
(AD-D016116; US-Patent-Appl-SN-151396; Navy-Case-70935) Avail: CASI HC A03

A passive multi-channel optical fiber rotary joint couples optical fiber communication channels via axially bilaterally symmetrically disposed lens housings, or array pieces, for receiving miniature collimation lenses to one and the other sides of an image-derotation prism-and-prism rotational-drive subassembly including an image derotation prism which rotates at a predetermined ratio of the relative rotation of the array pieces. This establishes transverse pseudo-planar rotary interfaces respectively between the one and another array piece and the confronting sides of the prism-and-prism drive subassembly. Each channel at the axially outward side of each of one and the other array pieces includes a fiber and lens junction in which the fiber is attached to the axially outward side of the collimation lens at (1) a predetermined axially bilaterally symmetrical position chosen for maximum coupling of signal power through the joint, and (2) individual lateral positions relative to the lens chosen to provide coupling with a path of beam propagation perpendicular to the rotary interface at the other side of the collimation lens. DTIC

N94-32649# Sandia National Labs., Albuquerque, NM.
METAL-ION SPIN-ON GLASSES: NOVEL MATERIALS FOR ACTIVE WAVEGUIDES
Carol I. H. Ashby, Charles T. Sullivan, G. Allen Vawter, John P. Hohimer, G. Ronald Hadley, and Daniel R. Neal 1993 9 p Presented at the OE/LASE 1994: Conference on Optics, Electro-optics, and Laser Applications in Science and Engineering, Los Angeles, CA, 22-29 Jan. 1994
(Contract DE-AC04-94AL-85000)
(DE94-007738; SAND-93-1785C; CONF-940142-24) Avail: CASI HC A02/MF A01

Monolithic integration of a rare-earth-ion-based active waveguide on the same wafer as its diode pump laser would permit compact packaging of the technology demonstrated in fiber lasers and amplifiers. This new monolithic technology would offer the potential for developing compact infrared and visible (up-conversion) lasers, amplifiers, and other photonic integrated circuit components. One approach that we are investigating for such monolithic integration uses a high concentration of one or more rare-earth ions incorporated into polysiloxane spin-on glasses that are solvent-cast onto 3-5 semiconductor wafers. This 'fiber on a chip' technology substitute a relatively high-ion-concentration, short-length metal-ion spin-on glass (MISOG) waveguide for the low-ion-concentration, long-length fiber. Progress to data on developing MISOG waveguide materials and technology is discussed. DOE

N94-32674 Sandia National Labs., Albuquerque, NM.
CHARACTERIZATION OF THERMALLY STABLE DYE-DOPED POLYIMIDE BASED ELECTROOPTIC MATERIALS
M. B. Meinhardt, P. A. Cahill, C. H. Seager, A. J. Beuhler, and D. A. Wargowski 1993 9 p Presented at the Fall Meeting of the Materials Research Society (MRS), Boston, MA, 29 Nov. - 3 Dec. 1993 Limited Reproducibility: More than 20% of this document may be affected by microfiche quality
(Contract DE-AC04-94AL-85000)
(DE94-005309; SAND-93-1545C; CONF-931108-78) Avail: Issuing Activity (Department of Energy (DOE))

Polymeric electrooptic materials have the potential to replace electronic switches in applications which require minimization of heat dissipation while maintaining high switching speeds. Polyimide matrices incorporating electrooptic dyes are promising materials for such applications due to their low cost and compatibility with existing processing environments. Preparation and characterization of novel dye-doped polyimide films for electrooptics is described. Thermal stabilities of donor-acceptor 2,5-diaryl oxazoles were evaluated by differential scanning calorimetry. Absorptive losses in thin films of Ultradel 9000D(reg sign) doped with donor-acceptor oxazoles were measured by photothermal deflection spectroscopy. Absorptive losses at high doping levels may be explainable by dye-dye aggregation or dye degradation during the curing process. Lower doping levels, however, show losses of less than or = 3.0 dB/cm at 830 nm and less than or = 2.4 dB/cm at 1,320 nm. DOE

N94-32702*# Maxdem, Inc., San Dimas, CA.
NONLINEAR OPTICAL PROPERTIES OF RIGID-ROD POLYMERS Final Report, 9 Apr. 1990 - 9 Apr. 1992
Mark S. Trimmer and Ying Wang 6 May 1992 46 p
(Contract NAS7-1104; SBIR-04.08-5224)
(NASA-CR-191349; NAS 1.26:191349) Avail: CASI HC A03/MF A01

The purpose of this research project was to integrate enhanced third order nonlinear optical (NLO) properties, especially high x(exp (3)) (greater than 10(exp -8) esu), into Maxdem's novel conjugated rigid-rod polymers while retaining their desirable processing, mechanical, and thermal properties. This work primarily involved synthetic approaches to optimized materials. Author (revised)

N94-32719# Department of the Navy, Washington, DC.
TORQUE-BALANCED EXTENDABLE FIBER OPTIC CABLE Patent Application
Louis E. Sansone, inventor (to Navy) and Gregory Simonds, inventor (to

Navy) 6 Oct. 1993 12 p
(AD-D016097; US-Patent-Appl-SN-134192) Avail: CASI HC A03/MF A01

An extendable fiber optic cable includes an inner tubular core, a viscous gel received in the tubular core, a plurality of optical fibers suspended in the gel, reinforcing fibers which are braided around the inner core, and an elastomeric outer cover which is received over the reinforcing fibers. The cable is first formed in a straight configuration and then formed into a plurality of coiled segments wherein adjacent coiled segments are wound in alternating directions, i.e. clockwise, counterclockwise, clockwise, etc. Straight segments of wire are provided between the coiled segments wherein the cable is stretchable up to 50% of its relaxed length. The alternating coil segments prevent the cable from twisting and transmitting torque forces to the optical fibers. DTIC

N94-32720# Department of the Navy, Washington, DC.
FIBER OPTIC CONTINUOUS TRUE TIME-DELAY MODULATOR Patent Application
Ronald D. Esman, inventor (to Navy) 6 Aug. 1993 21 p
(AD-D016098; US-Patent-Appl-SN-102924) Avail: CASI HC A03/MF A01

The fiber optic true time-delay modulator generates a continuously variable true time-delay (i.e., phase shift) by utilizing the dispersion characteristic of single mode optical fibers. The signal to be variably delayed modulates a continuous wave optical signal from a tunable laser source which is applied to a dispersive optical fiber wherein the phase shift occurs. The optical intensity output of the dispersive optical fiber is converted back into electrical energy by a photodetector for use in radio frequency, microwave and millimeter wave electronic devices. The invention can be used to generate multiple synchronized output signals by using a multiple wavelength laser or by combining outputs from several independently tuned lasers. Also, frequency and phase shifting is inherently provided by modulating the time delay. DTIC

N94-32738# Department of the Navy, Washington, DC.
MULTI-LINE PASSIVE FIBER OPTIC SLIPRING Patent Application
Darrell T. Abney, inventor (to Navy) 30 Sep. 1993 13 p
(AD-D016092; US-Patent-Appl-SN-129725) Avail: CASI HC A03/MF A01

A multi-line, passive fiber optic slipring is provided. A plurality of transmitting optical fibers are terminated in a plurality of focusing lenses. The fibers and focusing lens are free to rotate about an axis rotation. A plurality of ellipsoidal mirrors are stacked on top of one another beneath the focusing lenses such that the axis of rotation passes through a first focal point of each of the plurality of ellipsoidal mirrors. Each of the focusing lenses focuses optical signals through the first focal point of a corresponding one of the ellipsoidal mirrors. The optical signals reflect from each corresponding mirror to a second focal point of the corresponding mirror. Each mirror is further provided with an optical aperture along the axis of rotation to allow the optical signals not focused on the first focal point of the corresponding mirror to pass through. Each of a plurality of receiving optical fibers is fixed at a corresponding one of the second focal points. DTIC

N94-32777*# National Aeronautics and Space Administration. Lewis Research Center, Cleveland, OH.
RADIOMETRY SPOT MEASUREMENT SYSTEM
Harry H. Chen and Stephen J. Lawn Apr. 1994 12 p
(RTOP 963-10-0F)
(NASA-TM-106561; E-8727; NAS 1.15:106561) Avail: CASI HC A03/MF A01

The radiometry spot measurement system (RSMS) has been designed for use in the Diffusive And Radiative Transport in Fires (DARTFire) experiment, currently under development at the NASA Lewis Research Center. The RSMS can measure the radiation emitted from a spot of specific size located on the surface of a distant radiation source within a controlled wavelength range. If the spot is located on a blackbody source, its radiation and temperature can be measured directly or indirectly by the RSMS. This report presents computer simulation results used to verify RSMS performance. Author (revised)

N94-32818 Sandia National Labs., Albuquerque, NM.
LIGHT SCATTERING STUDIES OF A MODEL ELECTRORHEOLOGICAL FLUID
T. C. Halsey (Chicago Univ., IL.) and J. E. Martin 1993 14 p Presented at the 4th International Conference on Electrorhelogical Fluids, Feldkirch, Austria, 20-23 Jul. 1993 Limited Reproducibility: More than 20% of this document may be affected by microfiche quality
(Contract DE-AC04-94AL-85000)
(DE94-007860; SAND-94-0393C; CONF-9307174-1) Avail: CASI HC A03

Electrorheological suspensions typically contain particles of approximately one (mu)m in diameter. Thus light-scattering offers a natural method of probing the microstructure of these suspensions. We report the development of an index matched single-scattering fluid, as well a slight-scattering studies of this fluid in both a quiescent and sheared regime. In the first case, the results are in agreement with a phenomenological theory of coarsening based on thermal fluctuations. In the second case, they agree with an 'independent droplet' model of the suspensions structure under shear. DOE

N94-32878 Sandia National Labs., Albuquerque, NM.
SANDIA'S PHOTONIC PROGRAM AND ITS CHANGING NATIONAL ROLE
R. F. Carson and W. J. Meyer 1994 11 p Presented at the OE/LASE 1994: Conference on Optics, Electro-Optics, and Laser Applications in Science and Engineering, Los Angeles, CA, 22-29 Jan. 1994 Limited Reproducibility: More than 20% of this document may be affected by microfiche quality
(Contract DE-AC04-94AL-85000)
(DE94-008616; SAND-94-0277C; CONF-940142-29) Avail: CASI HC A03

Photonics activities at Sandia National Laboratories are founded on an extensive materials research program. In 1988, the Compound Semiconductor Research Laboratory (CSRL) was established at Sandia to bring together device and materials research and development, in support of Sandia's role in weapons technologies. Recently, industrial competitiveness has been added as a major mission for the national laboratories. As a result, present photonics programs are not only directed towards internal applications-driven projects, but are increasingly tied to the Department Of Energy's (DOE's) Technology Transfer Initiatives (TTI's), Cooperative Research and Development Agreements (CRADA's), and participation in partnerships and consortia. This evolution yields a full range of photonics programs, ranging from materials synthesis and device fabrication to packaging, test, and subsystem development. This paper presents an overview of Sandia's photonics-program directions, using three applications as examples. DOE

N94-32994# Brookhaven National Lab., Upton, NY.
RHIC CHROMATIC CORRECTION SYSTEM
D. Trbojevic, J. Wei, S. Tepikian, S. Peggs, F. Dell, and T. Satogata 1993 5 p Presented at the Orbit Analysis Workshop, Upton, NY, 1-3 Dec. 1993
(Contract DE-AC02-76CH-00016)
(DE94-008532; BNL-49656; CONF-931254-4) Avail: CASI HC A01/MF A01

The chromaticity correction system, including the nonlinear correction, for the Relativistic Heavy Ion Collider (RHIC) is presented. Expected multipoles in the superconducting magnets have shown that the octupole and decapole might be large enough to reduce the momentum aperture and introduce undesirable nonlinear chromatic behavior of the machine. Simulations of these conditions have been performed with the accelerator physics tracking code TEAPOT. The chromatic dependence curves were obtained by the least square fitting. A correction to the first and the second order terms were applied by using two sextupole and two octupole circuits. The decapole correction system was applied to correct for the third order dependence on momentum. The long term tracking studies at injection did not include the decapole correction. The studies showed that the octupole correction system significantly improves the dynamical aperture at the injection. The decapole system would not be necessary at commissioning of the machine but the correction magnets will be available. At the top energy, as to be expected, the low beta quadrupoles are the dominant source of the nonlinear momentum dependence. DOE

N94-33073*# Physical Optics Corp., Torrance, CA. Research and Development Div.
RECONFIGURABLE ARRAY OF RADIATING ELEMENTS (RARE) CONTROLLED BY LIGHT Interim Technical Progress Report, 14 Jan. - 14 Apr. 1994
Lev Sadovnik Apr. 1994 13 p Original contains color illustrations
(Contract NAS5-38039)
(NASA-CR-195828; NAS 1.26:195828; Rept-3256) Avail: CASI HC A03/MF A01; 1 functional color page

The parameters of a silicon - dielectric - metal microstrip line were compared with those of a metal - dielectric - metal microstrip line from an actual FLAPS antenna. The proposed structure has higher losses; this is caused by the electrical conductivity of the illuminated silicon electrode being lower than is the case with a line using a copper top electrode. However, the value of these conductive losses is on the same order as the radiative losses in the microstrip line used in FLAPS antenna. These results point to the feasibility of using the proposed type of a microstrip line in a light-controlled reconfigurable MMW antenna with reasonable energy losses and with a reasonable light flux. Author

N94-33087# Physical Optics Corp., Torrance, CA. Research and Development Div.
A NOVEL OPTOELECTRONIC SYSTEM FOR DISTORTION-INVARIANT ATR Final Report, 2 Jul. 1993 - 2 Jan. 1994
Lev Sadovnik 1 Feb. 1994 32 p
(Contract N00014-93-C-0135)
(AD-A277985; POC-3225) Avail: CASI HC A03/MF A01

The proposed idea is to enhance existing optical correlation based automatic target recognition (ATR) by introducing scale, translation, and rotation invariance (STRI). Previously, STRI was achieved by utilizing a library of matched filters corresponding to various positions of rotation and scale variation. We find that simple preprocessing can eliminate the need for the library since any STR changes in the input image can be nullified by bringing an input image to what we call its archetype. Physical Optics Corporation's (POC's) new approach includes a segmentation preprocessor (required to select any potential object of interest in an image of a realistic scene), POC's invariant preprocessor, and a standard optical correlator. This combination will greatly increase recognition speed and will simplify the recognition training procedure since only one in-plane position of the target will be needed to provide STRI recognition. The Phase 1 research described in this report opened a new approach to invariant ATR in which in-phase object position will no longer be of concern and, therefore, the best matched filter can be exploited to attain maximum confidence of identification. This should result in the development of hardware capable of operating in a real-time mode. DTIC

N94-33140# Arizona Univ., Tucson. Optical Sciences Center.
RESEARCH IN THE OPTICAL SCIENCES Final Technical Report
Robert C. Powell Feb. 1994 59 p
(Contract F49620-91-C-0009)
(AD-A278271; AFOSR-94-0238TR) Avail: CASI HC A04/MF A01

This report discusses research progress in the optical sciences, including the areas of: Monte Carlo simulation of multiple quantum well infrared detectors, field of view micro-optics, optical elements for X-UV wavelengths, fundamental physics of MBE heterostructures, MBE growth of novel semiconductor heterostructures, optical nonlinearities in low-dimensional semiconductor structures, carrier relaxation studies in semiconductor lasers and in novel GaAs quantum well structures, spectral hole burning and instabilities in semiconductor lasers, surface characterization of semiconductor structures, propagation of short optical pulses in passive and active nonlinear all-optical switches, and atom optics. DTIC

N94-33141# Ohio State Univ., Columbus. Research Foundation.
VISUAL PERCEPTION OF 3-DIMENSIONAL STRUCTURE FROM DIFFERENT TYPES OF OPTICAL DEFORMATION Annual Technical Report, 15 Feb. 1993 - 15 Feb. 1994
James T. Todd 9 Feb. 1994 3 p
(Contract F49620-93-1-0116)
(AD-A278272; AFOSR-94-0222TR) Avail: CASI HC A01/MF A01

The research performed by James Todd during the past year of AFOSR support has examined the abilities of human observers to determine an object's 3-dimensional form from various types of optical information such as shading, texture, motion or binocular disparity, both individually and in combination. The results of this research have provided strong evidence that 3-dimensional structure may be perceptually represented in a manner that is similar to the Klein hierarchy of geometries, such that observers are most sensitive to those aspects of an object's structure that remain invariant over the largest number of possible transformations. The evidence to support this hypothesis has been obtained using a wide variety of converging operations, including judgments of euclidean 3D length, judgments of conformal properties such as 3D angles, and judgments of affine properties such as planarity. We have also examined how these judgments are influenced by combining different types of optical information using both computer simulations and direct viewing of natural scenes. DTIC

N94-33145# University of Southern California, Los Angeles.
STUDIES OF OPTICAL BEAM PHASE CONJUGATION AND ELECTROMAGNETIC SCATTERING PROCESS Final Technical Report, 1 Dec. 1990 - 30 Nov. 1993
Robert W. Hellwarth 30 Mar. 1994 28 p
(Contract F49620-91-C-0018)
(AD-A278389; AFOSR-94-0234TR) Avail: CASI HC A03/MF A01

In this project we have performed both experimental and theoretical studies of optical beam phase-conjugation and of electromagnetic scattering and propagation with intense optical fields. During the reporting period we have: demonstrated that atomic vapors require fewer photons to perform optical wave mixing than any other medium examined to date; showed theoretically that a one-joule broadband optical pulse, whose carrier wavelength is one micron, can impart nearly one GeV energy to a charged particle; established the stringent experimental upper limits on the hyperpolarizabilities of C60 and C70 molecules in solution; made the first direct time-of-flight measurements of the drift velocity of photoexcited carrier in any photorefractive insulator (n-type Bi12SiO20); determined the difference between the complex polarizabilities of different trap levels in insulators; made quantitative predictions and measurements of spatial harmonic content of photorefractive gratings; developed and applied moving-grating diagnostic techniques to photoexcited carriers; and demonstrated an exception to the law of exponential attenuation of weak monochromatic optical beams in a homogeneous medium. DTIC

N94-33187 International Society for Optical Engineering, Bellingham, WA.
PROCEEDINGS SPIE: CONFERENCE DIGEST, VOLUME 2104
James R. Birch, ed. and Terence J. Parker, ed. 10 Sep. 1993 714 p
The Eighteenth International Conference on Infrared and Millimeter Waves was held in Colchester, England, 6-10 Sep. 1993 Limited Reproducibility: More than 20% of this document may be affected by microfiche quality
(AD-A278107; R/D-7051-EE-02-Vol-2104) Avail: CASI HC A99/MF A06

The Eighteenth International Conference on Infrared and Millimeter Waves was held from 6-10 Sep. 1993, at the University of Essex in Colchester, UK. The scope of the Conference covers progress in all areas of infrared and millimeter wave science and technology, and the large number of contributions (more than 300) received from more than 25 countries demonstrates the importance of the field and the need for the Conference. DTIC

N94-33267 Manchester Univ. (England).
OPTICAL PROPERTIES OF DOPED SOL-GEL SILICA GLASSES Final Technical Report, 6 Jul. - 31 Dec. 1993
Terence A. King 4 Jan. 1994 56 p Limited Reproducibility: More than 20% of this document may be affected by microfiche quality
(Contract DAJA45-92-C-0005)
(AD-A278094; R/D-6709-EE-01) Avail: Issuing Activity (Defense Technical Information Center (DTIC))

Sol-gel optical composites were developed and characterized for potential applications in optics, lasers, nonlinear optics, and optoelectronics. Post-doped xerogels were index matched by in-situ polymerization of monomers to form inorganic-organic composites of low scatter and high optical quality. Characterization of the microstructure was made by visible and IR absorption and Raman Spectroscopy and optical quality by attenuation and scatter measurement. Doping techniques were optimized using hypercritical drying and vacuum impregnation and doping distribution monitored by laser-induced fluorescence. One-tenth wavelength surfaces were formed by novel optical polishing. Organic molecular dopants were

tested in laser and nonlinear systems. Initial third harmonic generation and Z-scan measurements have shown the potential for saturable absorption and optical limiting. DTIC

N94-33331 University of Central Florida, Orlando.
SIMPLIFIED ULTRA-HIGH RESOLUTION OPTIC FOR SOFT X RAY IMAGING Final Report, 1 Jul. 1992 - 31 Dec. 1993
W. T. Silfvast 31 Dec. 1993 10 p Limited Reproducibility: More than 20% of this document may be affected by microfiche quality
(Contract F49620-92-J-0405)
(AD-A278424; AFOSR-94-0192TR) Avail: Issuing Activity (Defense Technical Information Center (DTIC))

In this report, we outline the design considerations and construction of an EUV reflection imaging microscope. The parameters of the microscope and the debris measurements of the source are presented. The reasons for selecting a laser-produced plasma (LPP) source and a Schwarzschild objective are described. While most research efforts for the development of soft x ray sources such as soft x ray lasers pursue the generation of shorter and shorter wavelengths down to the 'water window,' the EUV and soft x ray spectral regions are also ideal wavelengths for applications in chemistry and biology due to the photon energy being close to the molecular bond energy. DTIC

N94-31029*# Georgia Tech Research Inst., Atlanta.
DEGRADATION OF OPTICAL COMPONENTS IN SPACE
M. D. Blue *In* NASA. Marshall Space Flight Center, LDEF Materials Results for Spacecraft Applications Dec. 1993 p 217-226 (For primary document see N94-31012 09-12)
Avail: CASI HC A02/MF A04

N94-32445*# Midwest Research Inst., Golden, CO.
OPTICAL PROCESSING FOR SEMICONDUCTOR DEVICE FABRICATION
Bhushan L. Sopori *In* NASA, Washington, Technology 2003: The Fourth National Technology Transfer Conference and Exposition, Volume 2 Feb. 1994 p 207-215 (For primary document see N94-32420 09-99)
Avail: CASI HC A02/MF A04

N94-32446*# Midwest Research Inst., Golden, CO.
A SCANNING DEFECT MAPPING SYSTEM FOR SEMICONDUCTOR CHARACTERIZATION
Bushnan L. Sopori *In* NASA, Washington, Technology 2003: The Fourth National Technology Transfer Conference and Exposition, Volume 2 Feb. 1994 p 216-222 (For primary document see N94-32420 09-99)
Avail: CASI HC A02/MF A04

N94-33298*# National Aeronautics and Space Administration. Marshall Space Flight Center, Huntsville, AL.
DIAMOND TURNING IN THE PRODUCTION OF X RAY OPTICS
Steven C. Fawcett *In* NASA. Lewis Research Center, The 28th Aerospace Mechanisms Symposium May 1994 p 91-105 (For primary document see N94-33291 09-15)
Avail: CASI HC A03/MF A04

N94-33307*# Dornier System G.m.b.H., Friedrichshafen (Germany).
HIGH PRECISION MOVING MAGNET CHOPPER FOR VARIABLE OPERATION CONDITIONS
Winfried Aicher and Manfred Schmid *In* NASA. Lewis Research Center, The 28th Aerospace Mechanisms Symposium May 1994 p 167-181 (For primary document see N94-33291 09-15)
Avail: CASI HC A03/MF A04

75 PLASMA PHYSICS

Includes magnetohydrodynamics and plasma fusion.

For ionospheric plasmas see *46 Geophysics*. For space plasmas see *90 Astrophysics*.

N94-31088 Royal Inst. of Tech., Stockholm (Sweden). Alfven Lab.
LABORATORY AND SPACE EXPERIMENTS AS A KEY TO THE PLASMA UNIVERSE
Carl-Gunne Faelthammar Aug. 1993 21 p Presented at the Symposium on Plasma-93, Allahabad, India, 11-14 Oct. 1993 Limited Reproducibility: More than 20% of this document may be affected by microfiche quality
(ISSN 1103-6613)
(TRITA-ALP-1993-01; ISRN-KTH/ALP/R-93/01-SE; ETN-94-95943) Avail: CASI HC A03

Almost all of the known matter in our universe is in the state of plasma. Because of the complexity of the plasma state, a reliable understanding has to be built on empirical knowledge, since theoretical models easily become misleading unless guided by experiment or observation. Thus, experiments in the laboratory and in situ measurements in space represent an essential, but often overlooked, key to the understanding of our universe. Information learned about the following is addressed: Earth's magnetosphere; classification of cosmic plasmas; electric currents in cosmic plasmas; magnetic field aligned electric fields; anomalous resistivity; magnetic mirror effect; electric double layers; acceleration of charged particles; coupling between magnetic fields and motion of matter; rapid release of magnetically stored energy; filamentary structures; cellular structures; and chemical separation. ESA

N94-31089 Royal Inst. of Tech., Stockholm (Sweden). Alfven Lab.
THE DOUBLE PROBE ELECTRIC FIELD EXPERIMENT ON FREJA: DESCRIPTION AND FIRST RESULTS
G. T. Marklund, L. G. Blomberg, P.-A. Lindqvist, C.-G. Faelthammar, G. Haerendel, F. S. Mozer, A. Pedersen, and P. Tanskanen Oct. 1993 25 p Limited Reproducibility: More than 20% of this document may be affected by microfiche quality
(ISSN 1103-6613)
(TRITA-ALP-1993-02; ISRN-KTH/ALP/R-93/02-SE; ETN-94-95944) Avail: Issuing Activity (European Space Agency (ESA))

A sophisticated double probe electric field instrument for high resolution measurements of the auroral fine structure was developed for the Freja mission. The instrument is equipped with a 4 Mbyte burst memory for high rate data sampling (6144 samples/s) and for temporary storage of data. It can be run in a number of different operational modes and provides information not only on the vector electric field but also on the satellite potential with a time resolution orders of magnitude better than on previous satellite missions. The plasma environment explored by Freja, that is, the plasma transition region between the upper ionosphere and the innermost magnetosphere, is a highly dynamic region characterized by a considerable degree of spatial and temporal structure on various scales, and is associated with various phenomena such as intense, irregular electric fields, weak double layers, transient electric fields, and low frequency electric field fluctuations. The preliminary results from the first six months of operation clearly demonstrate that the Freja electric field instrument with its burst memory capability and possibility of simultaneous vector electric field and interferometric density measurements is ideally suited for detailed studies of these phenomena. Moreover, the measurements may contribute significantly to the understanding of different aspects of the auroral electrodynamics such as the formation, energy transfer, and current closure mechanisms of different auroral arc structures, and, more generally, of the relationships between auroral electric fields, currents, particles, and optical emissions. ESA

N94-31205 Ohio Univ., Athens.
RADIATION FROM AN APERTURE INTO AN ANISOTROPIC PLASMA HALF-SPACE Ph.D. Thesis
Suthum Srikasem 1993 132 p
Avail: Univ. Microfilms Order No. DA9322370

The present studies are concerned with the radiation from a given source distribution immersed in an anisotropic plasma. These studies are separated into two parts: radiation in an unbounded plasma and radiation in plasma half-space over a conducting plane. In the first part, the problem is formulated by means of linear analysis, Bessel, and Fourier transform techniques. The integrals of the dyadic Green's function for an anisotropic plasma are evaluated with respect to an orthogonal coordinate system a-caret, b-caret, c-caret. The final solution is expressed in a closed form. This dyadic Green's function can be directly reduced to the case of an uniaxial or an isotropic medium. The rectangular aperture and dipole fields are determined for some specific orientation of the static magnetic field. Conventional image theory is applicable for the cases of isotropic, uniaxial, and anisotropic plasmas. However, in an anisotropic plasma, this theory is only applicable when the static magnetic field is perpendicular to the

conducting plane. In the second part, the image theory is reformulated by using the dyadic Green's function obtained in the first part, the boundary condition on the conducting plane, and the uniqueness theorem. This reformulation technique can be applied to an arbitrary orientation of the static magnetic field. In both parts, the field patterns of the rectangular aperture and dipole in isotropic, uniaxial, and anisotropic plasma are plotted to compare the difference. In an unbounded anisotropic plasma, both extraordinary and ordinary fields will always exist. The value of epsilon(sub 3) (compared to epsilon(sub 1) and epsilon(sub 2)) had the most significant effect on the field patterns. In the second part, for rectangular aperture, the orientation of the static magnetic field had the most significant effect on the extraordinary field pattern. In this case, when the static magnetic field is perpendicular to the conducting plane, then the amplitude of the field patterns are twice as in the case of an unbounded medium.

Dissert. Abstr.

N94-31273# TRW, Inc., Redondo Beach, CA. Applied Technology Div.
MHD SEED RECOVERY/REGENERATION, PHASE 2
1993 13 p
(Contract DE-AC22-87PC-79672)
(DE94-006772; DOE/PC-79672/T8) Avail: CASI HC A03/MF A01

Progress is reported on the following tasks: (Task 1) design, refurbish, and operate potassium formate 'backend' system, (Task 2) design, construct, and operate the calcium formate production proof-of-concept 'frontend' unit, (Task 5) project management and control, and (Task 6) Western seed studies. An outline for the final report is provided at the end of this document.

DOE

N94-31304# General Atomic Co., San Diego, CA.
OPERATION OF D3-D WITH ALL-GRAPHITE WALLS
K. L. Holtrop, G. L. Jackson, A. G. Kellman, R. L. Lee, and M. Hollerbach Oct. 1993 19 p Presented at the 40th National Symposium of the American Vacuum Society (AVS), Orlando, FL, 15-19 Nov. 1993
(Contract DE-AC03-89ER-51114)
(DE94-004858; GA-A-21487; CONF-9311104-15) Avail: CASI HC A03/MF A01

Recently, additional graphite coverage has been installed in the DIII-D tokamak, increasing the graphite tile coverage from 45% to approximately 90%. Due to a problem with copper impurity bursts during tokamak discharges, copper foam sheets between the graphite tiles and the Inconel wall have been replaced with GRAFOIL gaskets, which further increases the surface area of the graphite inside the DIII-D torus. Although additional graphite has the potential for improving DIII-D performance, if not properly conditioned it can also degrade tokamak discharges by contributing to increased low Z impurity influx and higher particle fueling. To address these concerns, improvements were implemented both in tile preparation and wall conditioning techniques. All previously installed tiles were grit-blasted with boron-carbide grit to remove co-deposited metal impurities and all tiles were outgassed to 1000 C prior to installation. The glow discharge system used for wall conditioning was modified to include a large area electrode. The only conditioning techniques used were baking and helium conditioning to avoid producing loosely bound carbon. Previously, H2 or D2 Taylor discharge cleaning was used extensively during the vent recovery phase. Recovery from the recent 7-month machine opening was extremely rapid with improved modes of energy confinement (H-mode) transitions observed on the 14th plasma discharge. In addition, very high confinement (VH-mode) discharges were obtained without boronization, which is further indication of the rapid vent recovery. Lower recycling/lower fueling efficiency was also observed during operation with all-graphite walls. We will also discuss the use of Ne and Ar glow, and qualification of the new graphite including outgassing tests of the GRAFOIL material.

DOE

N94-31324# General Atomic Co., San Diego, CA.
NONINDUCTIVE CURRENT DRIVE EXPERIMENTS ON D3-D, AND FUTURE PLANS
R. Prater, M. E. Austin, F. W. Baity, R. W. Callis, S. C. Chiu, J. S. deGrassie, R. L. Freeman, C. B. Forest, R. H. Goulding, and R. W. Harvey et al Feb. 1994 19 p Presented at the 5th International Toki Conference on Plasma Physics and Controlled Nuclear Fusion: Physics and Technology of Plasma Heating and Current Drive, Toki, Japan, 16-19 Nov. 1993
(Contracts DE-AC03-89ER-51114; DE-AC05-84OR-21400; W-7405-eng-48)
(DE94-007373; GA-A-21525; CONF-931178-1) Avail: CASI HC A03/MF A01

Experiments on D3-D (and other tokamaks) have shown that improved performance can follow from optimization of the current density profile. Increased confinement of energy and a higher limit on beta have both been found in discharges in which the current density profile is modified through transient means, such as ramping of current or elongation. Peaking of the current distribution to obtain discharges with high internal inductance has been found to be beneficial. Alternatively, discharges with broader profiles, as in the VH-mode or with high beta poloidal, have shown improved performance. Noninductive current drive is a means to access these modes of improved confinement on a steady state basis. Accordingly, experiments on noninductive current drive are underway on the D3-D tokamak using fast waves, electron cyclotron waves. Recent experiments on fast wave current drive have demonstrated the ability to drive up to 180 kA of noninductive current using 1.5 MW of power at 60 MHz, including the contribution from 1 MW of ECCD and the bootstrap current. Higher power rf current drive systems are needed to strongly affect the current profile on D3-D. An upgrade to the FWCD system is underway to increase the total power to 6 MW, using two additional antennas and two new 30 to 120 MHz transmitters. Additionally, a 1 MW prototype ECH system at 110 GHz is being developed (with eventual upgrade to 10 MW). With these systems, noninductive current drive at the 1 MA level will be available for experiments on profile control in D3-D.

DOE

N94-31366# Texas Univ., Austin. Inst. for Fusion Studies.
TRANSPORT SUPPRESSION BY SHEAR FLOW GENERATION IN MULTIHELICITY RESISTIVE-g TURBULENCE
H. Sugama (National Inst. for Fusion Science, Nagoya, Japan.) and W. Horton Nov. 1993 38 p
(Contract DE-FG05-80ET-53088)
(DE94-007108; DOE/ET-53088/631; IFSR-631) Avail: CASI HC A03/MF A01

Turbulent momentum transport given by the Reynolds stress is considered as one of the candidates explaining the production and sustainment of the mean shear flow in the H-mode plasmas. Here we describe the nature of the shear flow generation and transport reduction in the 3D multihelicity system. The profiles of the Reynolds stress, shear flow and thermal flux in the 3D case are compared with those in the 2D case. The Beklemishev-Horton theory for the anomalous transport which multiplies the 2D transport by the density of distinct mode rational surfaces is found to overestimate the observed flux due to the disappearance of a subset of modes on certain rational surfaces. The mixing-length theory, in which the anomalous transport is independent of the density of mode rational surfaces, underestimates the thermal flux.

DOE

N94-31378 Ecole Centrale de Lyon (France). Lab. de Mecanique des Fluides.
DEVELOPMENT AND APPLICATION OF A MULTIMESH AUTO-ADAPTIVE FINITE ELEMENT METHOD FOR THE CALCULATION OF AN ELECTRIC ARC PLASMA Ph.D. Thesis [DEVELOPPEMENT ET APPLICATION D'UNE METHODE D'ELEMENTS FINIS AUTO-ADAPTATIFS MULTIMAILLAGES POUR LE CALCUL D'UN PLASMA D'ARC ELECTRIQUE]
Jean Noel 1989 121 p In FRENCH Limited Reproducibility: More than 20% of this document may be affected by microfiche quality
(ECL-89-03; ETN-94-95910) Avail: CASI HC A06

The feasibility of a two dimensional computation code for electric arc plasma is addressed. The nonstationary physics of a plasma arc can intervene at high gradients on all the variables, a high convection, as well as the considerable pressure variations (in space and time). Here the spatial finesse needed for the treatment of high gradient zones, is obtained by the use of a finite element method, improved by a mesh auto-adaptivity. The chosen time integration method is of the Runge-Kutta type with time step adjustment. This is presented, with the numerical methodology principles (multimesh, regularization, time step control). Results obtained in the study of classical partial differential equation systems, simplified versions of the Navier-Stokes equations (Burger equation, Dwyer-Sanders flame model), are presented. The numerical treatment of a confined arc plasma required the preliminary definition of a representative system of equations. This system is presented, with the thermal and dynamic modelings carried out.

Different aspects of the models introduced are illustrated, and results obtained for an unstationary one dimensional arc plasma in industrial conditions are presented. Comparisons between these results and available experimental data are encouraging, but suggest that a better dynamic modeling is indispensable. ESA

N94-31396# Texas Univ., Austin. Inst. for Fusion Studies.
L-H CONFINEMENT MODE DYNAMICS IN THREE-DIMENSIONAL STATE SPACE
H. Sugama (National Inst. for Fusion Science, Nagoya, Japan.) and W. Horton Jan. 1994 40 p
(Contract DE-FG05-80ET-53088)
(DE94-007113; DOE/ET-53088/639; IFSR-639) Avail: CASI HC A03/MF A01

The dynamical model for the L-H confinement mode transitions consisting of three ordinary differential equations (3-ODE model) for the essential state variables is proposed. The model is derived from the energy balance equations for the resistive pressure-gradient-driven turbulence and describes temporal evolutions of three characteristic variables (u.k.f) the potential energy contained in the pressure gradient, the turbulent kinetic energy and the shear flow energy. The energy input to the peripheral plasma region is included as an external control parameter in the model. The model equations have stationary solutions corresponding to the L and H modes. The authors obtain the L to H and H to L transition with the energy input parameter changed. The type of the L-H transition, whether a first-order or second-order transition, is shown to be determined by the shear flow damping coefficient. They also find the parameter region in which the H mode stationary solution becomes unstable and bifurcates to the limit cycle which shows periodic oscillations characteristic of the ELM confinement state. DOE

N94-31400# Lawrence Livermore National Lab., CA.
INERTIAL FUSION WITH ULTRA-POWERFUL LASERS
M. Tabak, J. Hammer, M. Glinsky, W. Kruer, S. Wilks, J. Woodworth, E. M. Campbell, M. D. Perry, and R. Mason Oct. 1993 31 p Presented at the Fall Meeting of the Plasma Physics Division of the American Physical Society, St. Louis, MO, 1-5 Nov. 1993
(Contract W-7405-eng-48)
(DE94-007242; UCRL-JC-115500; CONF-931132-2) Avail: CASI HC A03/MF A01

Ultra-high intensity lasers can be used to ignite ICF capsules with a few tens of kilojoules of light and can lead to high gain with as little as 100 kilojoules of incident laser light. We propose a scheme with three phases. First, a capsule is imploded as in the conventional approach to inertial fusion to assemble a high density fuel configuration. Second, a hole is bored through capsule corona composed of ablated material, pushing critical density close to the high density core of the capsule, by employing the ponderomotive force associated with high intensity laser light. Finally, the fuel is ignited by suprathermal electrons, produced in the high intensity laser plasma interactions, which propagate from critical density to this high density core. This paper reviews two models of energy gain in ICF capsules and explains why ultra-high intensity lasers allow access to the model producing the higher gains. This new scheme also drastically reduces the difficulty of the implosion and thereby allows lower quality fabrication and less stringent beam quality and symmetry requirements from the implosion driver. The difficulty of the fusion scheme is transferred to the technological difficulty of producing the ultra-high-intensity laser and of transporting this energy to the fuel. DOE

N94-31406# Lawrence Livermore National Lab., CA.
STRUCTURAL DESIGN OF THE SUPERCONDUCTING POLOIDAL FIELD COILS FOR THE TOKAMAK PHYSICS EXPERIMENT
T. G. OConnor and J. P. Zbasnik Oct. 1993 6 p Presented at the Symposium on Fusion Engineering, Hyannis, MA, 11-15 Oct. 1993
(Contracts W-7405-eng-48; DE-AC02-76CH-03073)
(DE94-007078; UCRL-JC-114266; CONF-931018-84) Avail: CASI HC A02/MF A01

The Tokamak Physics Experiment concept design uses superconducting coils made from cable-in-conduit conductor to accomplish both magnetic confinement and plasma initiation. The Poloidal Field (PF) magnet system is divided into two subsystems, the central solenoid and the outer ring coils, the latter is focus of this paper. The eddy current heating from the pulsed operation is excessive for a case type construction; therefore, a 'no case' design has been chosen. This 'no case' design uses the conductor conduit as the primary structure and the electrical insulation (fiberglass/epoxy wrap) as a structural adhesive. The model integrates electromagnetic analysis and structural analysis into the finite element code ANSYS to solve the problem. PF coil design is assessed by considering a variety of coil current wave forms, corresponding to various operating modes and conditions. The structural analysis shows that the outer ring coils are within the requirements of the fatigue life and fatigue crack growth requirements. The forces produced by the Toroidal Field coils on the PF coils have little effect on the maximum stresses in the PF coils. In addition in an effort to reduce the cost of the coils new elongated PF coils design was proposed which changes the aspect ratio of the outer ring coils to reduce the number of turns in the coils. The compressive stress in the outer ring coils is increased while the tensile stress is decreased. DOE

N94-31512 Technische Univ., Darmstadt (Germany). Fachbereich Mathematik.
NUMERICAL METHOD FOR THE INVESTIGATION OF THE MAGNETOHYDRODYNAMIC STABILITY OF THREE DIMENSIONAL PLASMA EQUILIBRIA Ph.D. Thesis [NUMERISCHE VERFAHREN ZUR UNTERSUCHUNG DER MAGNETOHYDRODYNAMISCHEN STABILITAET DREIDIMENSIONALER PLASMAGLEICHGEWICHTE]
Carolin Schwab 1991 168 p In GERMAN Limited Reproducibility: More than 20% of this document may be affected by microfiche quality
(ETN-94-95752) Avail: CASI HC A08

A numerical method was developed to treat Magnetohydrodynamic (MHD) stability problems in three dimensional, toroidal plasma configurations. The fundamentals of MHD are presented. The ideal MHD stability problem is formulated as a time independent variational problem. A stability code was developed, and its fundamentals are outlined. The use of the Fourier formalism leads to the concept of mode families. The phase factor transformation was incorporated in the variational problem. The algebraic eigenvalue problem was solved using inverse vector iteration. ESA

N94-31530# Hampton Univ., VA.
STUDIES OF THE PLASMA TRIGGERING MECHANISM OF INVERSE PINCH SWITCH Final Report, 15 Sep. 1989 - 14 Sep. 1993
Kwang S. Han 10 Nov. 1993 26 p
(Contract DAAL03-89-G-0113)
(AD-A276117; ARO-26499.3-PH-SAH) Avail: CASI HC A03/MF A01

The plasma-puff triggering mechanism based on a hypocycloidal pinch geometry was investigated to determine the optimal operating conditions for the azimuthally uniform surface flashover which initiates plasma-puff under wide ranges of fill gas pressure of Ar, He and N2. The optimal fill gas pressure for the azimuthally uniform plasma-puff was about 120 mTorr less than P sub opt less than 450 Torr for He and N2. For Argon 120 mTorr less than P sub opt less than 5 Torr. The inverse pinch switch was triggered with the plasma-puff and the switching capability under various electrical parameters and working gas pressures of Ar. He and N2 was determined. It was also shown that the azimuthally uniform switching discharges were dependent on the type of fill gas and its fill pressure. A new concept of plasma-focus driven plasma-puff was also discussed in comparison with the hypocycloidal pinch plasma-puff triggering. The main discharge of inverse pinch switch with plasma-focus driven plasma-puff trigger is found to be more azimuthally uniform than that with hypocycloidal pinch plasma-puff trigger in a gas pressure region between 80 mTorr and 1 Torr. A comparative study of the INPIStron and a spark gap also reveals that the INPIStron with a low impedance Z = 9 ohms can transfer a high voltage pulse with a superior pulse-shape fidelity over that with a spark of Z = 100 ohms. DTIC

N94-31558# Colorado Univ., Boulder.
TOROIDAL PINCH EXPERIMENTS
S. Robertson 24 Jan. 1994 28 p
(Contract DE-FG02-87ER-53244)
(DE94-005876; DOE/ER-53244/20) Avail: CASI HC A03/MF A01

The effect of boundary conditions on plasma confinement in the reversed field pinch (RFP) was studied. Early theoretical studies of the magnetohydrodynamic stability of the reversed field pinch had shown that the pinch was unstable unless it was surrounded by a conducting shell which prevented the penetration of the magnetic field during the lifetime of the pinch. The presence of the sheer, however, complicated construction

and prevented control of the plasma equilibrium by feedback systems. This research project was undertaken to determine the effect on confinement of varying the magnetic penetration time of the shell. A reversed field pinch, the Reversatron, was constructed so that shells of varying thickness could be installed. Shells were made with magnetic penetration times both longer and shorter than the duration of the plasma discharge. These shells allowed the performance to be determined as a function of the magnetic penetration time of the shell. This research showed that a shell with a short penetration time degraded the discharges. Diagnostic measurements showed reductions in plasma current, discharge duration, and the Doppler temperature of impurity ions and showed increases in the plasma resistivity and loop voltage. The greater power input and lower temperature implied a reduced energy confinement time. Magnetic diagnostics showed that two classes of MHD instabilities with poloidal mode number m = 1 were responsible for the degraded confinement. These were the dynamo modes resonant on the magentic axis (with toroidal mode numbers -9, -10, -11, -12) and the external kink modes (with toroidal mode numbers 3, 4, 5, and 6). DOE

N94-31572 Technische Univ., Berlin (Germany). Fachbereich Physik.
STARK BROADENING OF THE 2S STATE OF HYDROGEN AND DEUTERIUM IN ARC PLASMAS OF LOW DENSITY Ph.D. Thesis [STARKVERBREITERUNG DES 2S-ZUSTANDS VON WASSERSTOFF UND DEUTERIUM IN BOGENPLASMEN NIEDRIGER DICHTE]
Andreas Steiger 1993 87 p In GERMAN Limited Reproducibility: More than 20% of this document may be affected by microfiche quality
(ETN-94-95731) Avail: Issuing Activity (European Space Agency (ESA))

The study is focused on the proof of the Stark broadening theory for the first excited state of electrons. The Stark broadening of 2S state of hydrogen and deuterium was measured by two-photons excitation from the fundamental state, for electrons whose number density varies from 3 times 10 to the 21st power to 1.1 times 10 to the 22nd power per cu m, with temperatures in the 7500 to 9000K range. A pulse laser was built for the excitation of the (1S - 2S) transition and a stabilized cascade arc was developed as plasma source, whose parameters were estimated by conventional emission and absorption spectroscopy of Balmer lines. Two-photons excitation was ascertained with nonlinear polarization spectroscopy and a cross polarization extinction power of 100 million was reached during the experiment, so that absorption degrees until 0.0001 could be measured with good reliability. A simple measuring process was obtained with analysis of nonlinear properties of polarization spectroscopy, which suppresses perturbating influences of small error polarizations on the line profile to be measured. An asymmetry of the 1S - 2S Stark profile is detected, which is explained by the fine structure splitting in low density plasmas. ESA

N94-31619# Texas Univ., Austin. Fusion Research Center.
PLASMA CONFINEMENT THEORY AND TRANSPORT SIMULATION
D. W. Ross Oct. 1993 27 p
(Contract DE-FG05-88ER-53266)
(DE94-006065; DOE/ER-53266/46; FRCR-440) Avail: CASI HC A03/MF A01

The objectives of the Fusion Research Center Theory Program continue to be: (1) to advance the transport studies of tokamaks, including development and maintenance of the Magnetic Fusion Energy Database; and (2) to provide theoretical interpretation, modeling, and equilibrium and stability studies for the TEXT-Upgrade tokamak. Publications and reports and conference presentations for the grant period are listed. Work is described in five basic categories: Magnetic Fusion Energy Database; Computational Support and Numerical Modeling; Support for TEXT-Upgrade and Diagnostics; Transport Studies; and Alfven Waves. DOE

N94-31664# Columbia Univ., New York, NY. Dept. of Applied Physics.
HIGH BETA TOKAMAK RESEARCH
G. A. Navratil, M. E. Mauel, T. H. Ivers, M. K. V. Sankar, E. Eisner, D. Gates, A. Garofalo, R. Kombargi, D. Maurer, and D. Nadle et al 1993 25 p
(Contract DE-FG02-86ER-53222)
(DE94-006513; DOE/ER-53222/T3) Avail: CASI HC A03/MF A01

During the past 6 months, experiments have been conducted with the HBT-EP tokamak in order to test and evaluate diagnostic systems, establish basic machine operation, document MHD behavior as a function of global discharge parameters, investigate conditions leading to passive stabilization of MHD instabilities, and quantify the external saddle coil current required for DC mode locking. In addition, the development and installation of new hardware systems has occurred. A prototype saddle coil was installed and tested. A five-position (n,m) = (1,2) external helical saddle coil was attached for mode-locking experiments. And, fabrication of the 32-channel UV tomography and the multipass Thomson scattering diagnostics have begun in preparation for installation later this year. DOE

N94-31667# Lawrence Livermore National Lab., CA.
QUENCH DETECTION AND INSTRUMENTATION FOR THE TOKAMAK PHYSICS EXPERIMENT MAGNETS
M. R. Chaplin, W. V. Hassenzahl, and J. H. Schultz Oct. 1993 6 p Presented at the Symposium on Fusion Engineering, Hyannis, MA, 11-15 Oct. 1993
(Contracts W-7405-eng-48; DE-AC02-76CH-03073)
(DE94-006656; UCRL-JC-114261; CONF-931018-79) Avail: CASI HC A02/MF A01

The design of the local instrumentation and control (I&C) system for the Tokamak Physics Experiment (TPX) superconducting poloidal-field (PF) and toroidal-field (TF) magnets is presented. The local I&C system monitors the status of the magnet systems and initiates the proper control sequences to protect the magnets from any foreseeable fault. Local I&C also stores magnet-system data for analysis and archiving. Quench detection for the TPX magnets must use a minimum of two independent sensing methods and is allowed a detection time of one second. Proposed detection methods include the measurement of normal-zone resistive voltage, cooling-path helium flow, local temperature in the winding pack, and local pressure in the winding pack. Fiber optic based isolation systems are used to remove high common-mode magnet voltages and eliminate ground loops. The data acquisition and fault detection systems are computer based. The design of the local I&C system incorporates redundant, fault tolerant, and/or fail-safe features at all component levels. As part of a quench detection research and development plan, a quench detection model coil has been proposed to test all detection methods. Initial cost estimates and schedule for the local I&C system are presented. DOE

N94-31727# Montreal Univ. (Quebec). Dept. de Genie Electrique.
TIME DOMAIN SPECTROSCOPY FOR STUDYING A MONOPOLE ANTENNA IMMERSED IN A PLASMA M.S. Thesis [SPECTROSCOPIE TEMPORELLE POUR L'ETUDE D'UNE ANTENNE MONOPOLE PLONGEE DANS UN PLASMA]
Pierre-Richard Renaud Mar. 1993 325 p In FRENCH
(ISBN-0-315-86526-1; CTN-94-61207) Copyright Avail: Micromedia Ltd., Technical Information Centre, 240 Catherine Street, Suite 305, Ottawa, Ontario, K2P 2G8, Canada HC/MF

Time domain spectroscopy (TDS) was applied to study the characteristics of antennas in plasmas. A time domain spectrometer was designed and its operation was tested by analyzing the response of several linear components. The spectrometer measures the complex reflection coefficient as well as the impedance of these loads over the 6-2500 MHz range. TDS results were compared with those found by frequency domain reflectometry (FDR) using a network analyzer. The TDS was then applied to investigating the response of a monopole cylindrical antenna immersed in a cold anisotropic plasma. TDS and FDR yielded results in excellent agreement over the 10-1000 MHz band. Beyond 1000 MHz the precision was negatively affected by the less than ideal short circuit used for calibraiion. The existence of sheath wave resonances below 1000 MHz was confirmed. It was also shown that in the presence of constant magnetic field, the resonances exhibited a shift towards higher frequencies. The effect of the plasma density (discharge current) and of the sheath thickness (controlled by a direct current polarization applied to the antenna) was also studied. The results obtained are in agreement with theory as well as with previously published data. Author (CISTI)

N94-31765# Lawrence Livermore National Lab., CA.
FIRST-WALL HEAT-FLUX MEASUREMENTS DURING ELMing H-MODE PLASMA
C. J. Lasnier, S. L. Allen, D. N. Hill, A. W. Leonard, and T. W. Petrie 28 Jan. 1994 22 p
(Contracts W-7405-eng-48; DE-AC03-84ER-51044)
(DE94-008310; UCRL-ID-116271) Avail: CASI HC A03/MF A01

We present measurements of the diverter heat flux in DIII-D for ELMing H-mode and radiative diverter conditions. In previous work, we have examined heat flux profiles in lower single-null diverted plasmas and measured the scaling of the peak heat flux with plasma current and beam power. One problem with those results was our lack of good power accounting. This situation has been improved to better than 80-90% accountability with the installation of new bolometer arrays, and the operation of the entire complement of 5 Infrared (IR) TV cameras using the DAPS (Digitizing Automated Processing System) video processing system for rapid inter-shot data analysis. We also have expanded the scope of our measurements to include a wider variety of plasma shapes (e.g., double-null diverters (DND), long and short single-null diverters (SND), and inside-limited plasmas), as well as more diverse discharge conditions. Double-null discharges are of particular interest because that shape has proven to yield the highest confinement (VH-mode) and beta of all DIII-D plasmas, so any future diverter modifications for DIII-D will have to support DND operation. In addition, the proposed TPX tokamak is being designed for double-null operation, and information on the magnitude and distribution of diverter heat flux is needed to support the engineering effort on that project. So far, we have measured the DND power sharing at the target plates and made preliminary tests of heat flux reduction by gas injection. DOE

N94-31766# Stanford Univ., CA. Dept. of Chemistry.
DEGENERATE FOUR-WAVE MIXING AS A DIAGNOSTIC OF PLASMA CHEMISTRY
R. N. Zare Mar. 1993 3 p
(Contract DE-FG03-92ER-14304)
(DE94-008588; DOE/ER-14304/1) Avail: CASI HC A01/MF A01

Degenerate four-wave mixing (DFWM) has been found suitable for in situ monitoring during plasma-enhanced chemical vapor deposition. DFWM has been used to monitor CH and C2 during synthesis of diamond thin films. Analysis of CH rotational and vibrational spectra confirmed the temperature trend predicted by the 1-D model. For substrate temperature 1200 K and free-stream temperatures of 3500 and 4300 K, the 1-D simulations predicted boundary layer thicknesses consistent with observations. The species concentration change across the boundary layer is dramatic; at 2 mm from the surface, both CH and C2 reach maximum concentration. It has been demonstrated that, using a conventional laser system, operating at visible wavelengths (low energies), DFWM is nonintrusive and can generate signals that are easily monitored. DOE

N94-31772 Institut des Hautes Etudes Scientifiques, Bures-sur-Yvette (France).
STABILITY AND INSTABILITY CRITERIA FOR MAGNETOHYDRODYNAMICS
S. Friedlander (Illinois Univ., Chicago.) and M. M. Vishik (Texas Univ., Austin.) Aug. 1993 20 p Limited Reproducibility: More than 20% of this document may be affected by microfiche quality
(Grant NSF DMS-91-23946)
(PB94-148475; IHES/P/93/41) Avail: Issuing Activity (National Technical Information Service (NTIS))

The motion of an electrically conducting ideal fluid is governed by the equations of magnetohydrodynamics (MHD) which reduce to the Euler equations in the absence of a magnetic field. Arnold's treatment for the stability of the Euler equations has been extended to the augmented system for ideal MHD by Holm et al (1985) and Friedlander and Vishik (1990). In contrast with the purely hydrodynamic problem, it is possible for MHD to obtain 3-dimensional examples in which the second variation of the energy is in fact definite. We note, however, that it is still a difficult task to check the remaining conditions associated with nonlinear stability concerning convexity and regularity. In this paper, we examine restrictions on the class of examples of MHD equilibria for which the second variation of the energy is definite. We follow the approach of Sadun and Vishik (1993) and consider the Arnold functional corresponding to localized high frequency disturbances. NTIS

N94-31776 California Inst. of Tech., Pasadena.
PULSED EXPANSION OF PLASMA IN A MAGNETIC THRUSTER Ph.D. Thesis
Fujio Iinoya 1993 397 p
Avail: Univ. Microfilms Order No. DA9316848

The inertial confinement fusion (ICF) pulse rocket is capable of both extremely high specific impulses and high thrust-to-weight ratios by virtue of intermittent nuclear fusion energy production isolated from the vehicle structure. The thruster of the rocket, which converts an initially isotropically expanding ICF debris plasma into a directed pulse jet exhaust, is to be fabricated out of magnetic field created by current coils attached to the vehicle. Thrust is obtained through the property that good conductors exclude magnetic fields. Because of the highly dynamic behavior of the flow, which is bounded by an interface whose motion is unknown a priori, the first problem which must be investigated is that of the bulk flow. Numerical simulations of the bulk flow process were conducted under both the thin-shell and the classical hydrodynamic approximations. In the former approach, all of the plasma is assumed to be collected into an azimuthally symmetric perfectly conducting thin shell at the interface due to interfacial pressure application. These calculations showed that, under idealized conditions, promising propulsive efficiencies could be obtained for a range of field-to-plasma energy ratios and thruster geometries. In the latter approach, the plasma is approximated as an unmagnetized perfectly conducting fluid obeying the laws of classical hydrodynamics. The hydrodynamic codes (both one and two dimensional) employed an advanced classical particle in cell (PIC) scheme, and were successful at capturing interface motions self-consistently. The shock arising from the interface deceleration was also captured correctly. One dimensional planar-geometry simulations gave results which matched well with analytical calculations for such processes as free expansion into a vacuum and shock tube problems. The formation of a shell-like structure originating from the interfacial regions was observed in simulations of large expansion ratio flows carried out in two dimensions, although these 'shells' did not necessarily stay at the interface. The idealized bulk flow analyses in this work are hoped to serve as a basis for more detailed studies of how the flow will behave with a real plasma and to help assess the feasibility and design issues of the device. Dissert. Abstr.

N94-31787# Colorado Univ., Boulder. Dept. of Astrophysical, Planetary, and Atmospheric Science.
COLLISIONAL AND CHAOTIC TRANSPORT OF ENERGETIC PARTICLES IN TOROIDAL PLASMA
J. R. Cary and S. G. Shasharina Mar. 1993 182 p
(Contract DE-FG02-85ER-53207)
(DE94-006504; DOE/ER-53207/10) Avail: CASI HC A09/MF A02

Progress is reported in three general areas of confinement plasma physics. First, an accurate theory was developed for the trapping/detrapping process in tokamaks with ripple and stellarators. Second, the alpha particle distribution was determined for the situation where both collisions and collisionless chaotic (ripple) transport are present. Finally, transport of the toroidally trapped particles in rippled tokamaks with up-down asymmetry was studied. DOE

N94-31809# Los Alamos National Lab., NM.
INSTABILITY HEATING OF SOLID-FIBER Z PINCHES Ph.D. Thesis
R. A. Riley, Jr. Feb. 1994 192 p
(Contract W-7405-eng-36)
(DE94-007055; LA-12722-T) Avail: CASI HC A09/MF A02

The Los Alamos High Density Z Pinch-II (HDZP-II) facility is used to study the dynamics of z-pinch plasmas generated from solid fibers of deuterated polyethylene CD(sub 2) with a range in radii of 3-60 microns. HDZP-II is a pulsed-power generator that delivers a current that rises to 700 kA in 100 ns through an inductive load. A multiframe circular schlieren records the evolution of the shape and size of the plasma on seven images taken at 10-ns intervals. These circular-schlieren images show very strong m=0 instability at the onset of current and a rapid radial expansion of the plasma. No higher-order instabilities are observed. An interferometer is used to infer the electron density and electron line density, giving a measure of the fraction of plasma contained within the outline of the circular-schlieren image at one time during the multiframe sequence. A three-channel x-ray crystal-reflection spectrometer provides the time-resolved, spatially-averaged electron temperature. The magnitude of the x-ray emission at these energies also gives qualitative information about the electron temperature and density at late times. A lower bound on the ion temperature is inferred from the particle pressure needed to balance the magnetic field pressure. The ion temperature rose above that of the electrons, strongly suggesting an additional heating term that puts energy directly into the ions. An ion heating term is proposed to explain

the observed rapid radial expansion and elevated ion temperatures. This heating term is based on the assumption that the observed m=0 instabilities reconnect, enclosing magnetic flux which degenerates into turbulence in the plasma. A 0-D simulation is developed to investigate the relevance of different physical models to the data presented. DOE

N94-31927 California Univ., Los Angeles.
COMPUTER MODELING OF ACTIVE EXPERIMENTS IN SPACE PLASMAS Ph.D. Thesis
Ross John Bollens 1993 176 p
Avail: Univ. Microfilms Order No. DA9319803

Our understanding of space plasmas is expanding rapidly. This is, in large part, due to the ambitious efforts of scientists from around the world who are performing large scale active experiments in the space plasma surrounding the earth. One such effort was designated the Active Magnetospheric Particle Tracer Explorers (AMPTE) and consisted of a series of plasma releases that were completed during 1984 and 1985. What makes the AMPTE experiments particularly interesting was the occurrence of a dramatic anomaly that was completely unpredicted. During the AMPTE experiment, three satellites traced the solar wind flow into the earth's magnetosphere. One satellite, built by West Germany, released a series of barium and lithium canisters that were detonated and subsequently photoionized via solar radiation, thereby creating an artificial comet. Another satellite, built by Great Britain and in the vicinity during detonation, carried, as did the first satellite, a comprehensive set of magnetic field, particle, and wave instruments. Upon detonation, what was observed by the satellites, as well as by aircraft and ground-based observers, was quite unexpected. The initial deflection of the ion clouds was not in the ambient solar wind's flow direction (V) but rather in the direction transverse to the solar wind and the background magnetic field (V x B). This result was not predicted by any existing theories or simulation models; it is the main subject discussed in this dissertation. A large three dimensional computer simulation was produced to demonstrate that this transverse motion can be explained in terms of a rocket effect. Due to the extreme computer resources utilized in producing this work, the computer methods used to complete the calculation and the visualization techniques used to view the results are also discussed. Dissert. Abstr.

N94-32031 European Office of Aerospace Research and Development, FPO New York, NY.
WORKSHOP ON MODELS FOR PLASMA SPECTROSCOPY
30 Sep. 1993 97 p Workshop held in Oxford, England, 27-30 Sep. 1993 Sponsored in part by LLNL Limited Reproducibility: More than 20% of this document may be affected by microfiche quality
(AD-A276565) Avail: CASI HC A05

A meeting was held at St. Johns College, Oxford from Monday 27th to Thursday 30th of September 1993 to bring together a group of physicists working on computational modelling of plasma spectroscopy. The group came from the UK, France, Israel and the USA. The meeting was organized by myself, Dr. Steven Rose of RAL and Dr. R.W. Lee of LLNL. It was funded by the U.S. European Office of Aerospace Research and Development and by LLNL. The meeting grew out of a wish by a group of core participants to make available to practicing plasma physicists (particularly those engaged in the design and analysis of experiments) sophisticated numerical models of plasma physics. Additional plasma physicists attended the meeting in Oxford by invitation. These were experimentalists and users of plasma physics simulation codes whose input to the meeting was to advise the core group as to what was really needed. DTIC

N94-32201# General Atomic Co., San Diego, CA.
FWCD AND ECCD EXPERIMENTS ON D3-D
R. Prater, M. E. Austin, F. W. Baity, R. W. Callis, S. C. Chiu, J. S. DeGrassie, R. L. Freeman, C. B. Forest, R. H. Goulding, and R. W. Harvey et al Feb. 1994 9 p Presented at the IAEA Meeting on Radio-Frequency Launchers for Plasma Heating and Current Drive, Naka, Japan, 10-12 Nov. 1993 Submitted for publication
(Contracts DE-AC03-89ER-51114; DE-AC05-84OR-21400; W-7405-eng-48)
(DE94-007371; GA-A-21518; CONF-9311140-2) Avail: CASI HC A02/MF A01

Fast wave current drive and electron cyclotron current drive experiments have been performed on the D3-D tokamak as part of the advanced tokamak program. The goal of this program is to develop techniques for controlling the profile of the current density in order to access regimes of improved confinement and stability. The experiments on fast wave current drive used a four strap antenna with 900 phasing between straps. A decoupler was used to help maintain the phasing, and feedback control of the plasma position was used to keep the resistive loading constant. RF pickup loops demonstrate that the directivity of the antenna is as expected. Plasma currents up to 0.18 MA were driven by 1.5 MW of fast wave power. Electron cyclotron current drive experiments at 60 GHz have shown 0.1 MA of plasma current driven by 1 MW of power. New fast wave and electron cyclotron heating systems are in development for D3-D, so that the goals of the advanced tokamak program can be carried out. DOE

N94-32415# Syracuse Univ., NY. Dept. of Physics.
NEW POLYMER TARGET-SHELL PROPERTIES AND CHARACTERIZATIONS
A. Honig, X. Wei, Q. Fan, N. Alexander, and N. Palmer 1993 6 p Presented at the 9th Target Fabrication Specialists Meeting, Monterey, CA, 6-8 Jul. 1993
(Contract DE-FG03-91SF-18862)
(DE94-008420; DOE/SF-18862/T2-App-A; CONF-9307127-1-App-A) Avail: CASI HC A02/MF A01

A method for characterizing ICF target shells is presented, based on measurement of the gas released from a single shell into a small volume. It utilizes cryogenic permeation systems developed in connection with our work on ICF targets containing nuclear spin-polarized deuterium. Permeation rates for polystyrene and parylene-coated-polystyrene shells are measured at temperatures from 350K down to 180K. Burst or implosion pressure can be determined over a full temperature range down to 20K. Shell temperature is calculated from its gas leakage rate, calibrated by permeation measurements over the temperature range. Lag of shell temperature compared with sample-chamber temperature during warming of the latter is attributed to the weakness of the thermal link provided by both radiative heat transfer and free molecular conduction with small accommodation coefficients for helium and deuterium gas at the structure to which the shell is conductively linked, or at the surface of a conductively isolated shell. Quantification of this lag can provide a measure of atomic scale roughness of the shell outer surface. Also presented are reversible pre-rupture leakage phenomena for polystyrene and parylene-coated-polystyrene shells. DOE

N94-32519# General Atomic Co., San Diego, CA.
AN EDGE DENSITY FLUCTUATION DIAGNOSTIC FOR D3-D USING LITHIUM BEAMS
D. M. Thomas Jan. 1994 41 p
(Contract DE-FG03-90ER-54081)
(DE94-008554; GA-A-21584) Avail: CASI HC A03/MF A01

The pivotal role played by edge physics in tokamak transport and performance is widely appreciated but not completely understood at this time. The evident bifurcation in transport behavior during the L-to-H transition and the modification of the edge region by edge localized modes (ELM's) are just two examples of this relationship. There is a clear need to understand the role that turbulence plays in the plasma transport problem. Various workers have seen a suppression of both the magnetic and plasma density fluctuations during the transition. It is clear that the turbulence and transport behavior are linked and we are coming to an understanding of the transition evolution, based on a model of shear suppression of the turbulence and the creation of a transport barrier. In the case of the H-mode, this barrier is known to form a short distance radially inside the location of the last closed flux surface. The VH-mode may be thought of as a natural extension of this situation where the transport barrier moves deeper into the core of the discharge. As summarized in the May 1989 report of the DOE Transport Task Force, one of the key issues to be addressed in making progress on the transport question was to characterize the nature of local fluctuations. The objective of our research was to develop and demonstrate the feasibility of one particular measurement technique to determine density fluctuations in the region of interest on the DIII-D tokamak. DOE

N94-32520# Lodestar Research Corp., Boulder, CO.
ICRF HEATING AND CURRENT DRIVE IN TFTR SUPERSHOT PLASMAS: DATA ANALYSIS AND INTERPRETATION OF ICRF/EDGE INTERACTIONS

R. E. Aamodt, D. A. Dippolito, and J. R. Myra 22 Sep. 1993 6 p
(Contract DE-FG03-93ER-54212)
(DE94-008586; DOE/ER-54212/1; LRC-93-43) Avail: CASI HC A02/MF A01

The relevance of RF-sheath-plasma interactions to ICRF (ion cyclotron range of frequencies) operation in TFTR (tokamak fusion test reactor) has been studied. Screen-screen and screen-limiter RF sheaths have been identified and analyzed for the old and new Bay M geometries on TFTR, including sheath voltages driven by both feeders and the central antenna conductor. Calculations have been carried out to determine the effects of ICRF on edge transport (profile flattening by E x B convection), impurity influx (delta Z(sub eff)) and edge electron heating (FS glow phenomena) as a function of edge plasma parameters, rf power and antenna phasing. It was found that many of the experimentally observed ICRF-edge plasma interactions on TFIR are consistent with the predictions of RF sheath theory. DOE

N94-32595# General Atomic Co., San Diego, CA.
EXPERIMENTAL SURVEY OF THE L-H TRANSITION CONDITIONS IN THE D3-D TOKAMAK
T. N. Carlstrom, P. Gohil, and J. C. Watkins Jan. 1994 7 p Presented at the IAEA Meeting on H-Mode Physics, Naka, Japan, 15-17 Nov. 1993
(Contracts DE-AC03-89ER-51114; DE-FG03-89ER-51121; DE-AC02-78ET-51013; DE-AC04-76DP-00789)
(DE94-007428; GA-A-21541; CONF-9311147-6) Avail: CASI HC A02/MF A01

We present the global analysis of a recent survey of the H-mode power threshold in D3-D using D(sup o) yields D(sup +) NBI after boronization of the vacuum vessel. Single parameter scans of B(sub T), I(sub p), density, and plasma shape have been carried out on the D3-D tokamak for neutral beam heated single-null and double-null diverted plasmas. In single-null discharges, the power threshold is found to increase approximately linearly with B(sub T) and n(sub e) but remains independent of I(sub p). In double-null discharges, the power threshold is found to be approximately independent of both B(sub T) and n(sub e). Various shape parameters such as plasma-wall gaps had only a weak effect on the power threshold. Imbalancing the double null configuration resulted in a large increase in the threshold power. DOE

N94-32611# General Atomics Technologies Corp., San Diego, CA.
RECENT VH-MODE RESULTS ON D3-D
T. H. Osborne, K. H. Burrell, and T. N. Carlstrom Jan. 1994 6 p Presented at the IAEA Meeting on H-Mode Physics, Naka, Japan, 15-17 Nov. 1993 Prepared in cooperation with California Univ., Los Angeles
(Contracts DE-AC03-89ER-51114; DE-FG03-86ER-53225; W-7405-eng-48; DE-AC05-84OR-21400)
(DE94-007429; GA-A-21554; CONF-9311147-5) Avail: CASI HC A02/MF A01

A regime of improved H-mode energy confinement, VH-mode, is obtained in the D3-D tokamak with adequate vessel conditioning. The improved confinement in VH-mode is consistent with the extension of the region of high E x B velocity shear turbulence suppression zone further in from the plasma boundary. The energy confinement enhancement in VH-mode can be limited by ELM's, localized momentum transfer events, or operation at high heating power or low q. Energy confinement enhancement improves with increasing triangularity of the plasma cross section and is independent of elongation. The termination of VH-mode is associated with an edge localized kink mode which is destabilized by both the large edge pressure gradient and edge current density. DOE

N94-32612# General Atomic Co., San Diego, CA.
OVERVIEW OF H-MODE STUDIES IN D3-D
R. J. Groebner, D. R Baker,, and S. L. Allen Jan. 1994 10 p Presented at the IAEA Meeting on H-Mode Physics, Naka, Japan, 15-17 Nov. 1993
(Contracts DE-AC03-89ER-51114; DE-FG03-89ER-51121; DE-FG03-86ER-53225; DE-AC05-84OR-21400; DE-AC03-76DP-00789)
(DE94-007430; GA-A-21520; CONF-9311147-4) Avail: CASI HC A02/MF A01

A major portion of the D3-D program includes studies of the L-H transition, of the VH-mode, of particle transport and control and of the power-handling capability of a diverter. Significant progress has been made in all of these areas and the purpose of this paper is to summarize the major results obtained during the last two years. An increased understanding of the origin of improved confinement in H-mode and in VH-mode discharges has been obtained; good impurity control has been achieved in several operating scenarios; studies of helium transport provide encouraging results from the point of view of reactor design; an actively pumped diverter chamber has controlled the density in H-mode discharges; and a radiative diverter is a promising technique for controlling the heat flux from the main plasma. DOE

N94-32619# Oak Ridge National Lab., TN.
CHARACTERIZATION OF ATOMIC AND MOLECULAR IMPURITY SOURCES AND TRANSPORT AT THE TOKAMAK EDGE
C. C. Klepper, J. T. Hogan, W. R. Hess, and D. Guilhem 1993 13 p Presented at the 9th Biennial Topical Conference on Atomic Processes in Plasmas, San Antonio, TX, 19-23 Sep. 1993
(Contract DE-AC05-84OR-21400)
(DE94-007212; CONF-9309119-4) Avail: CASI HC A03/MF A01

The characterization of impurity sources in the tokamak edge is challenging because of the highly localized nature of impurity generation. Detailed, spatially resolved, diagnostic information is needed, and three-dimensional (3-D) modeling is required for interpretation. There is also a need for a more extensive atomic and molecular data base for the conditions encountered in this region. The availability of new measurements of photon efficiencies for some relevant hydrocarbon molecules for plasma conditions typical for the tokamak edge and the development of a 3-D Monte Carlo impurities code have enabled the successful modeling of spatially resolved measurements in the vicinity of the pump limiter neutralizer plate and near the inner wall of Tore Supra. DOE

N94-32631# Texas Univ., Austin. Inst. for Fusion Studies.
ANOMALOUS THERMALIZATION OF FAST IONS IN MAGNETIZED PLASMA
K. R. Chen Nov. 1993 17 p
(Contract DE-FG05-80ET-53088)
(DE94-007109; DOE/ET-53088/634; IFSR-634) Avail: CASI HC A03/MF A01

A novel anomalous process causing the perpendicular energy of fast ions to be thermalized and lost on average to bulk ion heating, instead of classical slowing down and bulk electron heating, is investigated with PIC simulations. More than half of the fast ions are slowed down to the thermal ion level, although some are heated to twice their birth energy. The fast ion density perturbation is large. This process is excited by a new two-gyro-stream instability and may continually occur in a burning plasma. The implications for fusion ignition and fast ion confinement are assessed. DOE

N94-32664# Texas Univ., Austin. Inst. for Fusion Studies.
BASIC PRINCIPLES APPROACH FOR STUDYING NONLINEAR ALFVEN WAVE-ALPHA PARTICLE DYNAMICS
H. L. Berk, B. N. Breizman, and M. Pekker Jan. 1994 18 p Presented at the Meeting on Physics of High-Energy Particles in Toroidal Systems, Irvine, CA, 30 Aug. - 1 Sep. 1993
(Contract DE-FG05-80ET-53088)
(DE94-007112; DOE/ET-53088/637; IFSR-637; CONF-930888-1) Avail: CASI HC A03/MF A01

An analytical model and a numerical procedure are presented which give a kinetic nonlinear description of the Alfven-wave instabilities driven by the source of energetic particles in a plasma. The steady-state and bursting nonlinear scenarios predicted by the analytical theory are verified in the test numerical simulation of the bump-on-tail instability. A mathematical similarity between the bump-on-tail problem for plasma waves and the Alfven wave problem gives a guideline for the interpretation of the bursts in the wave energy and fast particle losses observed in the tokamak experiments with neutral beam injection. DOE

N94-32686 Texas Univ., Austin. Inst. for Fusion Studies.
MAGNETLESS MAGNETIC FUSION
A. D. Beklemishev and T. Tajima Feb. 1994 16 p Limited Reproducibility: More than 20% of this document may be affected by microfiche quality
(Contract DE-FG05-80ET-53088)
(DE94-007114; IFSR-646; DOE/ET-53088/646) Avail: CASI HC A03

The authors propose a concept of thermonuclear fusion reactor in

which the plasma pressure is balanced by direct gas-wall interaction in a high-pressure vessel. The energy confinement is achieved by means of the self-contained toroidal magnetic configuration sustained by an external current drive or charged fusion products. This field structure causes the plasma pressure to decrease toward the inside of the discharge and thus it should be magnetohydrodynamically stable. The maximum size, temperature and density profiles of the reactor are estimated. An important feature of confinement physics is the thin layer of cold gas at the wall and the adjacent transitional region of dense arc-like plasma. The burning condition is determined by the balance between these nonmagnetized layers and the current-carrying plasma. They suggest several questions for future investigation, such as the thermal stability of the transition layer and the possibility of an effective heating and current drive behind the dense edge plasma. The main advantage of this scheme is the absence of strong external magnets and, consequently, potentially cheaper design and lower energy consumption. DOE

N94-32730# Los Alamos National Lab., NM.
MEASUREMENT OF ICF FUEL ION TEMPERATURE ON NOVA
D. B. Harris and R. E. Chrien 1994 7 p Presented at the 11th International Workshop on Laser Interaction and Related Plasma Phenomena, Monterey, CA, 25-29 Oct. 1993
(Contract W-7405-eng-36)
(DE94-006150; LA-UR-94-345; CONF-931048-11) Avail: CASI HC A02/MF A01

A new diagnostic for measuring the average fuel ion temperature in inertial confinement fusion (ICF) targets at the time of peak burn has been constructed by Los Alamos and installed on the Nova Laser System at Lawrence Livermore National Laboratory. This ion-temperature diagnostic measures the time-of-flight of fusion neutrons and determines the thermonuclear-reaction-weighted ion temperature through the time-of-arrival distribution. Preliminary experiments have been designed and performed to test the diagnostic. These tests measured the ion temperature of targets designed to have varying temperatures and yields. Additionally, an experiment has been designed to examine the cause of the increase in yield degradation (compared to clean 1-D calculations) as the capsule convergence is increased. Understanding the cause of yield degradation in high convergence implosions is necessary to increase the confidence of the target performance for the next generation National Ignition Facility planned by the US ICF Program. DOE

N94-32800# Washington Univ., Seattle. Aerospace and Energetics Research Program.
COAXIAL SLOW SOURCE
R. D. Brooks and T. R. Jarboe 1993 10 p
(Contract DE-FG06-87ER-53243)
(DE94-008191; DOE/ER-53243/5; UWAERP-42) Avail: CASI HC A02/MF A01

This report describes work performed by the University of Washington Aerospace and Energetics Research Program involving the Field Reversed Configuration (FRC) approach to magnetic confinement fusion. The group's effort involved continued research on the Coaxial Slow Source annular FRC experimental device located on campus, as well as support for the Large s Experiment (LSX) operated by Spectra Technology Incorporated, Bellevue, Washington. DOE

N94-32810# General Atomic Co., San Diego, CA.
DIVERTOR PUMPING AND OTHER REACTOR APPLICATION ISSUES FOR H-MODE
R. D. Stambaugh, N. H. Brooks, and S. L. Allen Jan. 1994 8 p Presented at the IAEA Meeting on H-mode Physics, Naka, Japan, 15-17 Nov. 1993
(Contracts DE-AC03-89ER-51114; W-7405-eng-48; DE-AC05-84OR-21400; DE-AC04-76DP-00789; DE-FG03-89ER-51121)
(DE94-007431; GA-A-21542; CONF-9311147-3) Avail: CASI HC A02/MF A01

We summarize results from DIII-D in regard to issues for reactor application of H-mode. Recently, DIII-D has begun to operate a cryopump (D(sub 2) pumping speed = 31,000 ell/s at a pressure of 2 mTorr). Initial results are very favorable for density control in H-mode. The plasma density could be reduced by 50%. Energy confinement is unchanged so the temperature rises in proportion to the density drop. Ability to access these less collisional plasmas in H-mode is favorable to current drive application. With the all-graphite wall, impurity accumulation has been eliminated. The exceedingly good confinement of VH-mode offers the possibility of retaining good confinement while radiating copious power from the plasma edge using injected noble gas impurities. DOE

N94-32820# California Univ., Berkeley.
COOPERATIVE PROGRAM ON D3-D (FY 1993)
T. K. Fowler 1994 10 p
(Contract DE-FG03-89ER-51116)
(DE94-008343; DOE/ER-51116/T4) Avail: CASI HC A02/MF A01

This is a proposal to continue support of the authors' cooperative research program on DIII-D, under Department of Energy contract DE-FG03-89ER51116. The proposal describes work carried out recently in support of DIII-D data analysis and modeling, with a focus on divertors, edge physics and transport phenomena linking edge and core physics. Proposed work will continue to focus on edge physics, instabilities, the further development of codes to model the plasma, and data analysis in support of related experimental work. DOE

N94-32838# Lawrence Livermore National Lab., CA.
THE NUMERICAL TOKAMAK PROJECT (NTP) SIMULATION OF TURBULENT TRANSPORT IN THE CORE PLASMA: A GRAND CHALLENGE IN PLASMA PHYSICS
Dec. 1993 37 p
(Contract W-7405-eng-48)
(DE94-008279; UCRL-ID-115962) Avail: CASI HC A03/MF A01

The long-range goal of the Numerical Tokamak Project (NTP) is the reliable prediction of tokamak performance using physics-based numerical tools describing tokamak physics. The NTP is accomplishing the development of the most advanced particle and extended fluid model's on massively parallel processing (MPP) environments as part of a multi-institutional, multi-disciplinary numerical study of tokamak core fluctuations. The NTP is a continuing focus of the Office of Fusion Energy's theory and computation program. Near-term HPCC work concentrates on developing a predictive numerical description of the core plasma transport in tokamaks driven by low-frequency collective fluctuations. This work addresses one of the greatest intellectual challenges to our understanding of the physics of tokamak performance and needs the most advanced computational resources to progress. We are conducting detailed comparisons of kinetic and fluid numerical models of tokamak turbulence. These comparisons are stimulating the improvement of each and the development of hybrid models which embody aspects of both. The combination of emerging massively parallel processing hardware and algorithmic improvements will result in an estimated 10**2--10**6 performance increase. Development of information processing and visualization tools is accelerating our comparison of computational models to one another, to experimental data, and to analytical theory, providing a bootstrap effect in our understanding of the target physics. The measure of success is the degree to which the experimentally observed scaling of fluctuation-driven transport may be predicted numerically. The NTP is advancing the HPCC Initiative through its state-of-the-art computational work. We are pushing the capability of high performance computing through our efforts which are strongly leveraged by OFE support. DOE

N94-32911# Wisconsin Univ., Madison.
STABILITY OF TEARING MODES IN TOKAMAK PLASMAS
C. C. Hegna and J. D. Callen Feb. 1994 35 p
(Contract DE-FG02-86ER-53218)
(DE94-009205; UW-CPTC-94-1) Avail: CASI HC A03/MF A01

The stability properties of m greater than or = 2 tearing instabilities in tokamak plasmas are analyzed. A boundary layer theory is used to find asymptotic solutions to the ideal external kink equation which are used to obtain a simple analytic expression for the tearing instability parameter Delta(prime). This calculation generalizes previous work on this topic by considering more general toroidal equilibria (however, toroidal coupling effects are ignored). Constructions of Delta(prime) are obtained for plasmas with finite beta and for islands that have nonzero width. A simple heuristic estimate is given for the value of the saturated island width when the instability criterion is violated. A connection is made between the calculation of the asymptotic matching parameter in the finite beta and island width case to the nonlinear analog of the Glasser effect. DOE

N94-32912# Wisconsin Univ., Madison.
STABILITY OF BOOTSTRAP CURRENT DRIVEN MAGNETIC ISLANDS IN STELLARATORS
C. C. Hegna and J. D. Callen Mar. 1994 11 p
(Contract DE-FG02-86ER-53218)
(DE94-009207; UW-CPTC-94-3) Avail: CASI HC A03/MF A01

The stability of magnetic island producing perturbations due to fluctuations in the bootstrap current in stellarator configuration is examined. The stability criterion depends on the sign of the derivative of the rotational transform, the pressure gradient and the direction of the equilibrium bootstrap current which is determined by the structure of (parallel)B(parallel). It is found that quasi-helically symmetric stellarator configurations with p'/tau' less than 0 are unstable to the formation of bootstrap current driven magnetic islands. The stability of conventional stellarator configurations depends upon the field structure. DOE

N94-32915# Lawrence Livermore National Lab., CA.
ANALYTIC FORMULATION FOR THE AC ELECTRICAL CONDUCTIVITY IN TWO-TEMPERATURE, STRONGLY COUPLED, OVERDENSE PLASMA: FORTRAN SUBROUTINE
R. Cauble and W. Rozmus 21 Oct. 1993 20 p
(Contract W-7405-eng-48)
(DE94-009466; UCRL-ID-115325) Avail: CASI HC A03/MF A01

A FORTRAN subroutine for the calculation of the ac electrical conductivity in two-temperature, strongly coupled, overdense plasma is presented. The routine is the result of a model calculation based on classical transport theory with application to plasmas created by the interaction of short pulse lasers and solids. The formulation is analytic and the routine is self-contained. DOE

N94-32916# Central Research Inst. of Electric Power Industry, Tokyo (Japan).
STABILIZATION METHOD OF A.C. ARC PLASMA
M. Iwata, S. Yasui, and M. Shibuya May 1993 26 p
(DE94-757268; CRIE-W-92016) Avail: CASI HC A03/MF A01

A pulse adding method has been discussed in order to stabilize AC plasma. As a first step of discussing the effectiveness of the method, the relation between current gradient at the current zero point and current zero duration was investigated experimentally. The experiment used a plasma torch to generate AC plasma with a current of 200 A and added the pulses of 0 to 30 A to the current zero point. As a result, it was found that, if the current gradient in the pulse added to currents is raised to about 15 A/microsecond against the current zero duration for 10 to 100 microsecond without pulses, the current zero duration is largely reduced to about 0.2 microseconds and the plasma stability is enhanced. A transient analysis calculation revealed a result that, if the current gradient is raised at the current zero point by adding pulses, the current zero duration can be shortened because of rise in the transient recovery voltage. It was also discovered that a polarity change in tungsten electrodes can vary the current zero duration. DOE

N94-32922 Wisconsin Univ., Madison. Center for Plasma Theory and Computation.
ANOMALOUS TRANSPORT EQUATIONS IN TOROIDAL PLASMAS
A. I. Smolyakov (Saskatchewan Univ., Saskatoon.), A. Hirose (Saskatchewan Univ., Saskatoon.), and J. D. Callen Mar. 1994 12 p Limited Reproducibility: More than 20% of this document may be affected by microfiche quality
(Contract DE-FG02-86ER-53218)
(DE94-009206; UW-CPTC-94-2) Avail: Issuing Activity (Department of Energy (DOE))

Reduced transport equations for a toroidal plasma with fluctuations are derived. These equations include the effects of both anomalous and standard neoclassical transport, and allow clarification of the structure of convective fluxes caused by electrostatic and magnetic fluctuations. Special attention is paid to the combined effects of fluctuations and toroidicity on the transport. The formulation retains the effects of a magnetic field inhomogeneity on the anomalous transport. It is shown that phase space diffusion caused by the gradient in the equilibrium magnetic field appears as a pinch flux in the real space. DOE

N94-32977 Department of the Navy, Washington, DC.
ELECTRON ACCELERATION SYSTEM Patent
Han S. Uhm, inventor (to Navy) 1 Feb. 1994 6 p Filed 12 Sep. 1991
(AD-D016143; US-Patent-5,283,530; US-Patent-Appl-SN-758978; US-Patent-Class-328-233) Avail: US Patent and Trademark Office

A bore formed within a body of material storing a magnetic field at a saturation level, establishes a linear path along which an electron beam is focussed after the bore is ionized to form a plasma channel therein. The driving current of the beam is sharply decreased to cause simultaneous decay of the stored magnetic field from a saturation level inducing an electric field concentrated in the plasma channel to accelerate travel of trailing electrons in the beam with a high accelerating gradient.
Author (DTIC)

N94-33007# North Carolina Univ., Chapel Hill. Dept. of Chemistry.
ELECTRON CYCLOTRON RESONANCE PLASMA OXIDATION STUDIES OF InP
Y. Z. Hu, J. Joseph, and E. A. Irene 15 Mar. 1994 29 p
(Contract N00014-89-J-1178)
(AD-A277431; TR-61) Avail: CASI HC A03/MF A01

Electron cyclotron resonance plasma oxidation of InP was studied using both spectroscopic and single wavelength ellipsometry employed during the oxidation process. A two layer oxide was observed with the outer layer being In rich and the inner layer P rich as-confirmed from x-ray photoelectron spectroscopy and etch rate studies. Optical models and oxidation kinetics are analyzed. From positive substrate bias effects on oxidation rates, negative ion oxidant species were identified as dominant and oxide etching was observed at negative bias. DTIC

N94-33042# Naval Command, Control and Ocean Surveillance Center, San Diego, CA. RDT and E Div.
SIMULTANEOUS EXCITATION OF PARAMETRIC DECAY CASCADES AND THE OTSI IN 1D NUMERICAL SIMULATIONS BASED ON AAKAROV'S EQUATIONS
R. A. Sprague and J. A. Fejer Mar. 1994 3 p
(AD-A278108) Avail: CASI HC A01/MF A01

This presentation describes results from numerical simulations based on Zakarov's equations. These results show, that for relatively low pump pressures, the OTSI is stabilized by the presence of the cascade and thus, can coexist with the cascade. DTIC

N94-33048*# Alabama Univ., Huntsville. Dept. of Electrical and Computer Engineering.
IONOSPHERIC PLASMA OUTFLOW IN RESPONSE TO TRANSVERSE ION HEATING: SELF-CONSISTENT MACROSCOPIC TREATMENT Annual Progress Report No. 3, 1993 - 1994
N. Singh May 1994 37 p
(Grant NAGw-2903)
(NASA-CR-195820; NAS 1.26:195820; UAH-94-429) Avail: CASI HC A03/MF A01

We examined the various likely processes for creating the cavities and found that the mirror force acting on the transversely heated ions is the most likely mechanism. The pondermotive force causing the wave collapse was found to be a much weaker force than the mirror force on the transversely heated ions observed inside the cavities along with the lower hybrid waves. Using a hydrodynamic model for the polar wind we modeled the cavity formation and found that for the heating rate obtained from the observed waves, the mirror force does create cavities with depletions as observed. Some initial results from this study were published in a recent Geophysical Research Letters and were reported in the Fall AGU meeting in San Francisco. We have continued this investigation using a large-scale semikinetic model. Derived from text

N94-33074*# Lockheed Missiles and Space Co., Palo Alto, CA. Research and Development Div.
ANALYSIS OF DATA FROM THE PLASMA COMPOSITION EXPERIMENT ON THE INTERNATIONAL SUN-EARTH EXPLORER (ISEE 1) Final Report, 1 Jan. 1990 - 31 May 1994
O. W. Lennartsson 10 May 1994 183 p
(Contract NAS5-33047)
(NASA-CR-195880; NAS 1.26:195880; F-254279) Copyright Avail: CASI HC A09/MF A02

The Lockheed plasma composition experiment on the ISEE 1 spacecraft has provided one of the largest and most varied sets of data on earth's energetic plasma environment, covering both the solar wind, well beyond the bow shock, and the near equatorial magnetosphere to a distance of almost 23 earth radii. This report is an overview of the last four years of data analysis and archiving. The archiving for NSSDC includes most data obtained during the initial 28-months of instrument operation, from early November 1977 through the end of February 1980. The data products are a combination of spectra (mass and energy angle) and velocity moments. A copy of the data user's guide and examples of the data products are attached as appendix A. The data analysis covers three major areas: solar wind ions upstream and downstream of the day side bowshock, especially He(++) ions; terrestrial ions flowing upward from the auroral regions, especially H(+), O(+), and He(+) ions; and ions of both solar and terrestrial origins in the tail plasma sheet and lobe regions. Copies of publications are attached. Author (revised)

N94-33106 Aerospace Corp., El Segundo, CA. Technology Operations.
CHARACTERISTICS OF ION FLOW IN THE QUIET STATE OF THE INNER PLASMA SHEET
V. Angelopoulos, C. F. Kennel, F. V. Coroniti, R. Pellat, and M. G. Kivelson 15 Mar. 1994 9 p Limited Reproducibility: More than 20% of this document may be affected by microfiche quality
(Contract F04701-88-C-0089)
(AD-A277451; TR-93(3940)-7; SMC-TR-94-04) Avail: CASI HC A02

We use AMPTE/IRM and ISEE 2 data to study the properties of the high beta (beta(sub iota) greater than 0.5) plasma sheet, the inner plasma sheet (IPS). Bursty bulk flows (BBF's) are excised from the two databases, and the average flow pattern in the non-BBF (quiet) IPS is constructed. At local midnight this ensemble-average flow is predominantly duskward; closer to the flanks it is mostly earthward. The flow pattern agrees qualitatively with calculations based on the Tsyganenko model (T87), where the earthward flow is due to the ensemble-average cross tail electric field and the duskward flow is the diamagnetic drift due to an inward pressure gradient. The IPS is on the average in pressure equilibrium with the lobes. Because of its large variance the average flow does not represent the instantaneous flow field. Case studies also show that the non-BBF flow is highly irregular and inherently unsteady, a reason why earthward convection can avoid a pressure balance inconsistency with the lobes. The ensemble distribution of velocities is a fundamental observable of the quiet plasma sheet flow field. DTIC

N94-33113*# Smithsonian Astrophysical Observatory, Cambridge, MA.
PARTICIPATION IN THE SCIENTIFIC ACTIVITIES OF THE WAVES IN SPACE PLASMA (WISP) PROJECT Final Report, 15 Mar. 1992 - 14 Mar. 1994
Yakov L. Alpert and Mario D. Grossi Apr. 1994 54 p
(Grant NAG5-1925)
(NASA-CR-195903; NAS 1.26:195903) Avail: CASI HC A04/MF A01

This is the Final Report for Contract NAG5-1925, that consisted of experiment design, for possible use by the space science mission called WISP (Waves in Space Plasma). This mission is under study by the Canadian Space Agency and by NASA. Two WISP configurations are contemplated, under the name of BICEPS: one is called BOLAS, and the other WISPRS. Both these configurations are meant to perform bistatic sounding of the ionosphere, at a height close to F(sub 2) H(sub max) (about 350 Km), with a pair of satellites, either tethered or in free flight. Investigation A (with Y.L. Alpert as P.I.) addresses the subject of parametric decay effects, expected to arise in a magnetoplasma under the influence of high-intensity HF fields. Criteria were formulated that could be used in searching for parametric instabilities and of electric fields in the ionosphere and magnetosphere, by in-situ satellites, such as the BICEPS Pair. Investigation B (with M.D.Grossi as P.I.) addressed the bistatic measurement, by the BICEPS pair,of ionospheric features, such as large-scale and small-scale disturbances, travelling ionospheric disturbances, electron density irregularities, spread-F phenomena, etc. These measurements by BICEPS could be correlated with the waveform distortion and degradation experienced by microwave links from geosynchronous height to ground, such as the ACTS satellite, expected to radiate pulses as short as 1 nanosecond in the band 20 to 30 GHz. These links are transionospheric and propagate e.m. waves in the volume of the ionosphere where BICEPS operates. It will be possible, therefore, to correlate the two classes of measurements, and learn the causative mechanisms that are responsible for the time-spread and frequency-spread nature of communications waveforms at microwave, in geosynchronous height to ground paths. Derived from text

N94-33264# Naval Postgraduate School, Monterey, CA.
TIME RESOLVED MEASUREMENTS OF LIGHT PRODUCED BY ONSET OF PLASMA FORMATION ON ELECTRODES OF FAST PULSED HIGH VOLTAGE DIODES M.S. Thesis
Charles M. Wright 10 Dec. 1993 105 p
(AD-A277974) Avail: CASI HC A06/MF A02

Despite years of research on electrical breakdown of fast pulsed high vacuum diodes, the mechanisms of the process are far from being fully discovered. It is well known that electrical breakdown with plasma formation on the electrode surfaces, but there is disagreement on how this occurs. The most widely accepted model, the Explosive Electron Emission model predicts plasma formation on the cathode by means of ohmic heating caused by a field emitted current. Anode plasma formation under this model is explained as due to energy deposition by fast electrons. A new model proposes that adsorbed neutral molecules on the electrode surfaces play a key role in developing the conditions where unipolar arcs cause plasma formation on both electrodes. In this work, simultaneous measurements of the light produced at the electrodes shows that plasma is produced on the anode in less than 2 nanoseconds after it is produced at the cathode. These findings support the new model. DTIC

76 SOLID-STATE PHYSICS

Includes superconductivity.

For related information, see also *33 Electronics and Electrical Engineering* and *36 Lasers and Masers.*

N94-31055# North Carolina Univ., Chapel Hill. Dept. of Physics and Astronomy.
INDIUM-VACANCY COMPLEXES IN MERCURY CADMIUM TELLURIDE Final Report, 14 Mar. 1991 - 30 Sep. 1993
M. L. Swanson, William C. Huges, and J. C. Austin 30 Sep. 1993 10 p
(Contract DAAL03-91-G-0080)
(AD-A276177; ARO-27846.8-MS) Avail: CASI HC A02/MF A01

The goals of this research were to study specific defect configurations in Hg(0.79)Cd(0.21)Te (MCT), using perturbed angular correlation (PAC) measurements, with emphasis on the defect consisting of vacancies trapped at the donor impurity indium. The secondary goal was to study antisite defects and small indium precipitates. The first of these objectives was met with the identification and structural characterization of the In-V (Hg) complexes. It was determined that this defect does occur under appropriate conditions (reported in several publications), and that it consists of an indium impurity on a cation site, joined to a single vacancy at the (110) next site. The mysterious (111) orientation of the electric field gradient (EFG) observed for donor-vacancy complexes in MCT and other II-VI semiconductors was shown to result from the polarization of Te atoms surrounding the indium donor. The thermodynamics of the mercury-vacancy and indium-vacancy complexes were extensively characterized, resulting in good estimates of the migration energy for Hg vacancies and binding energies for vacancy-indium pairs. In-V (Hg) complexes were seen to interact with H impurities. No evidence of either antisite defects or small metal clusters was seen at doping levels up to 10(exp 17)In/cu cm. DTIC

N94-31056# Hawaii Univ., Honolulu.
PASSIVATION OF III-V COMPOUND SEMICONDUCTOR BASED DEVICES Final Report, 1 Oct. 1990 - 30 Sep. 1993
V. Malhotra 29 Nov. 1993 14 p
(Contract DAAL03-90-G-0209)
(AD-A276178; ARO-28214.10-EL-SAH) Avail: CASI HC A03/MF A01

Our results indicate that excellent passivation of SiN(x)/GaAs and SiN(x)/InP interfaces can be achieved using both liquid and gaseous sulfur treatments of the surface. It is important to note that the S-treated surfaces are stable in the presence of a 'soft' ECR plasma and are amenable to the environment of SiN(x) growth. Annealing appears to be a crucial step in achieving lower defect densities at the SiN(x)/III-V interfaces. A significant reduction in the interfacial defect density leads to unpinning of the Fermi-level at the interfaces. This permits fabrication of superior metal-semiconductor

(both Schottky and ohmic) junctions and metal-insulator-semiconductor FET's. Furthermore, reduction of defects at the interface also reduces the surface recombination velocity, thus improving the performance of minority carrier based devices. We have demonstrated that such is indeed the case by passivating AlGaAs/GaAs based heterojunction bipolar transistors and surface-emitting lasers. DTIC

N94-31067# Ames Lab., IA.
SYNTHESIS, CHARACTERIZATION, PHASE DIAGRAMS AND SUPERCONDUCTING, AND NORMAL STATE MAGNETIC PROPERTIES OF La(2-x)Sr(x)CuO4 (0 IS LESS THAN OR EQUAL TO x WHICH IS LESS THAN OR EQUAL TO 0.08) AND ELECTROCHEMICALLY OXIDIZED La(2-x)Sr(x)CuO(4 + DELTA) (0 IS LESS THAN OR EQUAL TO x WHICH IS LESS THAN OR EQUAL TO 0.33, 0 IS LESS THAN OR EQUAL TO DELTA WHICH IS LESS THAN OR EQUAL TO 0.12) Ph.D. Thesis
F. Chou Aug. 1993 157 p
(Contract W-7405-eng-82)
(DE94-005260; IS-T-1661) Avail: CASI HC A08/MF A02

La(2-x)Sr(x)CuO4 (0 less than or equal to x less than or equal to 0.15) can all be intercalated with oxygen by a novel electrochemical oxidation method. Bulk superconductivity is found with an onset (T(sub c)) approximately 40 K for the whole range 0.01 less than or equal to x less than or equal to 0.15; for x = 0.25 and 0.33, the electrochemical oxidation did not improve the superconducting properties. The magnetic susceptibility (chi)(T = 50-320 K) data for La2CuO(4.11) and La(1.92)Sr(0.08)CuO(4.07) are nearly identical with those of conventionally prepared La(1.85)Sr(0.15)CuO4, indicating that the hole doping level (p) in the CuO2 planes of the three compounds is nearly the same. Combined thermogravimetric analysis and iodometric titration experiments indicate that part of the intercalated oxygen has a formal valence close to -1. The maximum doped-hole concentration in the CuO2 planes that can be achieved from combined Sr-doping and electrochemical oxygen doping for 0 less than or equal to x less than or equal to 0.15 is p approximately 0.16 holes/formula unit. Oxygen can also intercalate into single crystal La2CuO4 through a slow electrochemical oxidation process. The required low current and long time for the charging process reflects that the oxygen intercalation for a single crystal is limited by its small specific surface area and long diffusion distance. The anisotropic superconducting, magnetic and transport properties are summarized and compared with those of polycrystalline La2CuO(4+(delta)) as well as of YBa2Cu3O(7-delta) and La(2-x)Sr(x)CuO4 single crystals. The single crystal La2CuO(4+(delta)) has a maximum (T(sub c)) approximately 40 K, which is lower than that (T(sub c)) approximately 42-45 of the corresponding polycrystalline samples. The magnetic phase diagram of La(2-x)Sr(x)CuO4 in the antiferromagnetic (AF) regime (0 less than or equal to x less than or equal to 0.02) has been derived from La-139 NQR studies from 4 to 250 K. DOE

N94-31081# Pennsylvania State Univ., University Park.
MODIFICATION OF SEMICONDUCTOR SURFACE PROPERTIES WITH CHEMICALLY BOUND MOLECULAR FILMS Final Report, 15 Jun. 1990 - 15 Dec. 1993
David L. Allara and S. Ashok Feb. 1994 12 p
(Contract DAAL03-92-G-0150)
(AD-A276162; ARO-27770.1-CH) Avail: CASI HC A03/MF A01

In line with the objectives, three parallel and connected thrusts were pursued: (1) investigation of the use of Langmuir-Blodgett (LB) films in MIS Schottky structures to modify the barrier properties of junctions made from SiO2/Si and GaAs(100); (2) the treatment of Si and GaAs(100) surfaces with inorganic P and S compounds in order to favorably modify the electrical behavior, primarily via passivation of surface traps; and (3) the development of self-assembled monolayers of organothiols, in particular, alkanethiolates on GaAs(100) as a means to modify the electrical properties of the surface and more recently as a new class of ultrahigh resolution lithographic resists for nanofabrication. In support of each of these thrusts, extensive work was carried out in two areas: characterization of the structure and composition of the surface films, primarily by infrared spectroscopy (IRS), x-ray photoelectron spectroscopy (XPS) and ellipsometry and characterization of the electrical behavior of the film and its interface with the semiconductor, primarily by fabrication of MIS Schottky diode structures and measurement of I-V and C-V response, but also including limited photoluminescence and photoreflectance measurements. All the work was directed ultimately for the chemically bonded molecular film samples. The LB films represented molecules adsorbed with no chemical bonding, the inorganic treatments represented chemically modified surfaces with molecular groups and the chemically bound inorganic films contained both the previous aspects. DTIC

N94-31307# Pacific Northwest Lab., Richland, WA.
ION-BEAM-DRIVEN AMORPHIZATION OF Ca2La8(Si4)6O2 SINGLE CRYSTALS
W. J. Weber, N. J. Hess, and L. M. Wang Nov. 1993 7 p Presented at the Fall Meeting of the Materials Research Society (MRS), Boston, MA, 29 Nov. - 3 Dec. 1993
(Contract DE-AC06-76RL-01830)
(DE94-006219; PNL-SA-22718; CONF-931108-67) Avail: CASI HC A02/MF A01

Single crystals of Ca2La8(SiO4)(sub 6)O2, with 1% Nd substituted for La, were irradiated with 0.8 MeV Ne(+) and 1.5 MeV Kr(+) ions from 15 to 773 K. The irradiations were carried out using the HVEM-Tandem Facility at Argonne National Laboratory. The structural changes and the ion fluence for complete amorphization were determined by in situ transmission electron microscopy. The ion fluence for complete amorphization increased with temperature in two stages associated with defect annealing processes. The critical temperature for amorphization increased from approximately 360 K for 0.8 MeV Ne(+) to approximately 710 K for 1.5 MeV Kr(+). During in situ annealing studies, irradiation-enhanced recrystallization was observed at 923 K. Spatially-resolved fluorescence spectra of the Nd ion excited with 488.0 mn laser excitation showed marked line-broadening toward the center of the amorphous regions. Initial measurements indicate the subtle shifts of the (sup 9)I(sub 9/2) groundstate energy levels can be measured by pumping directly into the excited state (sup 4)F(sub 3/2) manifold suggesting that the line broadening observed originates from a distribution of geometrically distorted Nd sites. DOE

N94-31327# State Univ. Coll. of New York, Buffalo. Dept. of Chemistry.
SILICONE GREASE AS A PRECURSOR TO A PSEUDO CROWN-ETHER LIGAND: CRYSTAL STRUCTURE OF (K(+)K(Me2SiO)7(+)) (HIn(CH2CMe3)3(-))4)
Melvyn R. Churchill, Charles H. Lake, Sun-Hua L. Chao, and O. T. Beachly, Jr. 25 Feb. 1994 14 p
(Contract N00014-90-J-1530)
(AD-A276343; SUNYBUF/DC/TR-38) Avail: CASI HC A03/MF A01

The crystallization of K((HIn(CH2CMe3)3)) from heptane in the presence of silicone grease led to the formation of the title compound, in which one potassium cation is surrounded by a planar cyclo-(Me2SiO)7 ligand; K+...O distances range from 2.86(3) to 2.99(4)A. DTIC

N94-31329# Aeronautical Radio, Inc., Annapolis, MD.
ACTIVE MATRIX LIQUID CRYSTAL DISPLAY. INDUSTRY SURVEY RESULTS Final Report, 1 Jul. - 1 Dec. 1993
K. Harris Dec. 1993 93 p
(Contract F33615-93-D-3800)
(AD-A276415; WL-TR-93-1176) Avail: CASI HC A05/MF A01

A survey exploring such aspects of AMLDC as resolution fixed configuration, viewing angle, contrast, luminance, grey shades, chromaticity, etc. was distributed to potential domestic producers and component manufacturers of AMLCD's. This report summarizes the responses received from the polled companies. The purpose of the survey was to determine current and near-future state-of-the-art AMLCD technology in the United States. DTIC

N94-31350 Picotronix, Inc., Ann Arbor, MI.
A 1-PICOSECOND InGaAs PHOTODETECTOR FOR OPERATION AT 1300-1600 nm Progress Report No. 2, 15 Sep. - 15 Nov. 1993
15 Nov. 1993 13 p Limited Reproducibility: More than 20% of this document may be affected by microfiche quality
(Contract N00014-93-C-0139)
(AD-A275959) Avail: CASI HC A03

During the past two months, we have grown a number of new InGaAs structures and characterized them for sensitivity, speed, resistivity, and optical absorption. We have concentrated on two new approaches that promise to shorten carrier lifetime while maintaining high sensitivity and resistivity. The first approach involves growing a superlattice of

low-temperature molecular beam epitaxy (MBE) InGaAs/InAlAs with post annealing, i.e. InGaAs:As/InAlAs:As. In this structure, the InGaAs:As serves as an absorbing layer while the InAlAs:As serves as a trapping layer. The second approach uses lattice-matched bulk (i.e., no superlattice) InGaAs:As. DTIC

N94-31395 Joint Inst. for Nuclear Research, Dubna (USSR). Lab. of Nuclear Problems.

LOW DISPERSION OF THE MUON PRECESSION FREQUENCY IN HTSC SAMPLES YBa2Cu3O(x) AND EuBa2Cu3O(x)

V. G. Grebinnik, V. N. Duginov, and V. A. Zhukov et al 1992 7 p Limited Reproducibility: More than 20% of this document may be affected by microfiche quality

(DE94-608388; JINR-R-14-92-345) Avail: CASI HC A02 (US Sales Only)

Measurements of the muon spin relaxation rate (mu SR) have been performed on monocrystalline unoriented grains YBa2Cu3O(sub 6.89) and ceramics EuBa2Cu3O(sub 6.84) in order to determine the magnetic field penetration depth lambda. Measurements were conducted on field-cooled samples with magnetic field 2.5 kG at temperatures 10 less than T less than 100 K. Experimental value of the muon precession frequency variance (Delta(omega)(sup 2))(sup 1/2)(T yields 0) was approximately equal to 2.5 mu/s, which corresponds to the magnetic field penetration depth perpendicular to CuO2 planes lambda(sub ab)(0) approximately equal to 1600 A. The result calls in question the traditional idea about the penetration depth measured with (mu)SR-experiment lambda(sub (mu)SR) as the lower limit of lambda(lambda greater than or equal to lambda(sub (mu)SR)) in strongly anisotropic high-T(sub c) superconductors. DOE

N94-31439# Texas A&M Univ., College Station. Center for Electronic Materials.

ELECTROOPTIC CRYSTAL GROWTH AND PROPERTIES Final Report

4 Feb. 1994 8 p

(Contract N00014-93-1-0920)

(AD-A276023) Avail: CASI HC A02/MF A01

A new member in the tungsten-bronze family of ferroelectric lead potassium niobate (PKN), with general formula Pb(1-x)K(2x)Nb2O6, has been grown as bulk single crystal. Growth of PKN with charge composition x = 0.23 has been achieved using the Czochralski technique of crystal pulling. Large diameter boules were grown in platinum crucibles at temperatures between 1280 and 1300 C. Crystallographic studies were conducted using x ray diffraction techniques. The samples were characterized for ferroelectric properties between 25 and 600 C and for optical absorption. This paper presents the crystal synthesis and the results of ferroelectric and optical characterization. Bulk single crystals of potassium tantalate niobate, KTa(1-x)Nb(x)O3, ferroelectric with different values of Ta/Nb ratios have been grown by temperature gradient transport technique (TGTT). A second attached paper presents the results of the crystal growth experiments, ferroelectric characterization techniques, and properties of potassium tantalate niobate crystals. Derived from text

N94-31455# North Carolina Univ., Raleigh. Dept. of Electrical and Computer Engineering.

GROWTH AND CHARACTERIZATION OF III-V SEMICONDUCTORS WITH RARE EARTH IMPURITIES FOR OPTOELECTRONIC DEVICES Report, 1 Oct. 1992 - 30 Sep. 1993

Robert M. Kolbas 30 Sep. 1993 2 p

(Contract N00014-93-1-0665)

(AD-A276021) Avail: CASI HC A01/MF A01

We have focused on evaluating the old samples by SIMS and implantation and have been able to obtain GaN:Er doped samples. Publications and presentations include: 'Molecular Beam Epitaxial Growth and Optical Characterization of Erbium Doped GaAs/AlGaAs Heterostructures' and 'Photoluminescence Study of Energy Transfer Processes in Erbium Doped Al(x)Ga(1-x)As Grown by MBE.' Derived from text

N94-31473# Illinois Univ., Urbana. Physics Lab.

[THE RELATIONSHIP OF THE ELECTRONIC STRUCTURES OF SEMICONDUCTOR SURFACES AND HETEROSTRUCTURES TO CRYSTAL GROWTH] Annual Report, 1 Oct. 1992 - 30 Sep. 1993

Yia-Chung Chang, S.-F. Ren, and Z.-Q. Gu 14 Feb. 1994 4 p

(Contract N00014-90-J-1267)

(AD-A276465) Avail: CASI HC A01/MF A01

The objective is to understand the electronic structures of semiconductor surfaces and heterostructures in relation to crystal growth. The approach is to perform first-principle theoretical calculations to determine the structures of surface and interface and to identify the main spectral features of the reflectance-difference spectra of (001) GaAs with transitions involving Ga-Ga dimers and As-As dimers. DTIC

N94-31489# Oak Ridge National Lab., TN.

INCOHERENT IMAGING BY Z-CONTRAST STEM: TOWARDS 1 ANGSTROM RESOLUTION

S. J. Pennycook, D. E. Jesson, and A. J. McGibbon Dec. 1993 9 p Presented at the Fall Meeting of the Materials Research Society, Boston, MA, 29 Nov. - 3 Dec. 1993

(Contract DE-AC05-84OR-21400)

(DE94-006551; CONF-931108-62) Avail: CASI HC A02/MF A01

By averaging phase correlations between scattered electrons, a high angle detector in the scanning transmission electron microscope (STEM) can provide an incoherent, Z-contrast image at atomic resolution. Phase coherence is effectively destroyed through a combination of detector geometry (transverse incoherence) and phonon scattering (longitudinal incoherence). Besides having a higher intrinsic resolution, incoherent imaging offers the possibility of robust reconstruction to higher resolutions, provided that some lower frequency information is present in the image. This should have value for complex materials and regions of complex atomic arrangements such as grain boundaries. Direct resolution of the GaAs sublattice with a 300 kV STEM is demonstrated. DOE

N94-31499# Lawrence Livermore National Lab., CA.

THE THRESHOLD ENERGY FOR DEFECT PRODUCTION IN SiC: A MOLECULAR DYNAMIC STUDY

J. Wong, T. DiazdelaRubia, M. W. Guinan, M. Tobin, J. M. Perlado, A. S. Perez, and J. Sanz 1 Oct. 1993 13 p Presented at the 6th International Conference on Fusion Reactor Materials, Stresa, Italy, 27 Sep. - 1 Oct. 1993

(Contract W-7405-eng-48)

(DE94-007123; UCRL-JC-114789; CONF-930928-28) Avail: CASI HC A03/MF A01

We discuss the results of molecular dynamics computer simulation studies of the threshold energy for defect production in beta-SiC. The simulations are performed with the Tersoff potential for SiC which provides accurate values of many of its defect properties. In addition, we show that it properly describes the melting behavior of SiC. Simulations were carried out for Si and C recoils in 3 dimensional cubic computational cells with periodic boundary conditions and up to 4096 atoms. The results show anisotropy in the threshold for Si and C recoils as well as for the recoil direction. The lowest threshold is 25 eV for C recoils along (111) and the highest is 85 eV for Si recoils along (110). Details of the defect configurations obtained will be discussed. DOE

N94-31501# Oak Ridge National Lab., TN.

ION BEAM SYNTHESIS OF IrSi3 BY 1-MeV Ir ION IMPLANTATION INTO Si(111)

T. P. Sjoreen and H.-J. Hinneberg Nov. 1993 6 p Presented at the Fall Meeting of the Materials Research Society, Boston, MA, 29 Nov. - 3 Dec. 1993

(Contract DE-AC05-84OR-21400)

(DE94-006556; CONF-931108-76) Avail: CASI HC A02/MF A01

The formation of a Si/IrSi3/Si heterostructure by 1-MeV Ir ion implantation and subsequent annealing has been studied for different doses (0.1 to 2.25 x 10(exp 17) Ir/sq cm), substrate temperatures (450 to 600 C), and annealing temperatures (1000 to 1200 C) using Rutherford backscattering spectrometry, ion channeling, and cross-sectional transmission electron microscopy. The heterostructure formation is observed to depend strongly on the processing conditions. The best structure, nearly continuous and precipitate-free, is obtained by implanting 1.8 to 2.0 x 10(exp 17) Ir/sq cm at a substrate temperature of 550 C and annealing at 1100 C for 5 hours. A stoichiometric IrSi3 layer can also be produced by furnace annealing at 1150 C for 1 hour or by rapid thermal annealing at 1200 C for 3 minutes. Other substrate temperatures generally lead to a structure with a discontinuous IrSi3 layer frequently interrupted by large surface precipitates or islands. Origin of these islands, as well as dependence of heterostructure on processing parameters, is discussed. DOE

N94-31502# Sandia National Labs., Albuquerque, NM.
III-V COMPOUND SEMICONDUCTOR STRIP-LOADED WAVEGUIDE DEVICES FOR PICs: DESIGN FOR MINIMUM CROSSTALK AND HIGH DENSITY
G. A. Vawter and G. R. Hadley 1993 7 p Presented at the OE/LASE 1994 Conference on Optics, Electro-Optics, and Laser Applications in Science and Engineering, Los Angeles, CA, 22-29 Jan. 1994
(Contract DE-AC04-94AL-85000)
(DE94-006588; SAND-93-1816C; CONF-940142-18) Avail: CASI HC A02/MF A01

Compact, low-cost photonic integrated circuits (PIC's) have long been a desire of systems engineers. Unfortunately, the majority of PIC's in use today use regrown buried heterostructure waveguides to achieve low crosstalk at reasonable packing density. These regrown structures are very expensive and limit PIC applications to high performance niches. The alternative low-cost approach is to use etched-rib, or strip-loaded, waveguides. Strip-loaded waveguides are simple to manufacture but may have guided slab-modes carrying unwanted light between devices within the PIC. These slab modes can result in very high crosstalk or low device density. This paper addresses techniques for control of stray light in strip-loaded PIC's. Methods include mesa isolation of waveguides and ion implantation outside the waveguide rib. In addition, some devices such as Mach-Zehnder interferometers and waveguide power combiners generate radiation and slab modes as a fundamental means of operation. Improved designs for both of these structures with proper removal of both radiated and slab-mode light and high contrast-ratio operation will be covered. DOE

N94-31506# Fermi National Accelerator Lab., Batavia, IL.
STUDY OF B(0) - BAR-B(0) MIXING IN D0
S. Igarashi Dec. 1993 10 p Presented at the 9th Workshop on Proton-Antiproton Collider Physics, Tsukuba, Japan, 18-22 Oct. 1993
(Contract DE-AC02-76CH-03000)
(DE94-006000; FNAL/C-93/386-E; CONF-9310247-10) Avail: CASI HC A02/MF A01

The probability of B(sup 0)-(bar B)(sup 0) mixing has been measured using the D0 detector. Non-isolated dimuon events are used to determine the ratio of like to unlike-sign pairs. The measured ratio is 0.48 +/- 0.04(stat.) +/- 0.03(syst.), compared with the expected value of 0.23 +/- 0.07 in the absence of B(sup 0)-(bar B)(sup 0) mixing. The combined mixing probability is measured to be 0.13 +/- 0.02(stat.) +/- 0.05(syst.) in good agreement with other experimental measurements. DOE

N94-31521# Universiteit Twente, Enschede (Netherlands).
ENGINEERING OF DAMAGE IN ION IMPLANTED SILICON Ph.D. Thesis
Jan Reinder Liefting 1992 92 p Sponsored by Netherlands Organization for Scientific Research, and Varian Ion Implant Systems
(ISBN-9-09-005097-3; ETN-94-96028) Copyright Avail: CASI HC A05/MF A01

A study on how secondary defect formation can be influenced by altering implant or anneal conditions and how this affects device performance is presented. Results of engineering the primary damage for low and high mass implants by performing the implants at elevated temperatures are presented. Implanting in this way enhances annealing during the implant and consequently reduces the amount of primary damage. It is investigated if engineering the primary damage in this way influences dislocation formation. TEM (Transmission Electron Microscopy) analysis of implants to doses which generate a total damage much higher than the critical amount is discussed. These implants generate roughly the same total amount of damage, but still dislocation formation should be different and this is studied. It is known that small interstitial clusters, formed during the implant, become stable dislocation loops by absorbing Si interstitials. Thus, dislocation formation could be engineered if alternative sinks for the interstitials could be introduced. It is thought that carbon can act as such a sink. For damage engineering, it is important to know how effective C is as a sink, and this is investigated. Dislocations can severely degrade the yield and quality of microelectronic devices. Several ways to avoid dislocation formation are introduced in a bipolar transistor fabrication process to investigate if device performance may be improved. Defects are considered to have only a negative influence on the quality of Si. This is correct if the defects trap metallic impurities and are positioned in the active regions of a device. A way of engineering the position of dislocations so that the metallic impurities can be placed in regions where they do not influence device performance is achieved. ESA

N94-31528# APA Optics, Inc., Blaine, MN.
GaAs/GaN STRAINED LAYER SUPERLATTICE MATERIALS FOR HIGH TEMPERATURE TRANSISTORS, PHASE 1 Final Report, 1 Jul. - Dec. 1992
Jonathan N. Kuznia 10 Jan. 1994 9 p
(Contract DAAL03-92-C-0036)
(AD-A276115; ARO-30481.1-EL-SBI-Phase-1) Avail: CASI HC A02/MF A01

During this program, we were successful in depositing single crystal layers of GaAs on GaAs on GaN epilayers and single crystal GaN on GaAs substrates. These two developments represent an impcrtant advance in the technology base required to grow GaN/GaAs short period superlattices. Due to the large difference in bandgap energy between GaAs and GaN (1.4-3.6 eV), superlattices based on these two materials can potentially provide electronic devices which operate at elevated temperatures over a wide range of wavelengths (365-860 nm). For the first time, tertiary butyl arsine (TBA) was used to grow GaAs on GaN substrates. From an industry safety perspective, this is extremely important since TBA is less toxic and deadly as compared to pure arsine. During this program, the growth of ternary GaAsN was also attempted. Unfortunately, poor results were obtained and further growths were curtailed. During the growth of the ternary GaAsN, an important growth aspect was determined. When attempting to grow GaAsN at low temperatures, arsenic incorporation far exceeded nitrogen leaving the film GaAs. At elevated temperatures, nitrogen was preferentially incorporated leaving a GaN film. Such growth knowledge will prove important for future GaAs/GaN superlattice work. During this program, we were successful in depositing single crystal GaN-GaAs, GaN/GaAs superlattices. DTIC

N94-31531# David Sarnoff Research Center, Princeton, NJ.
HIGH PERFORMANCE YBCO FILMS Report, 1 Dec. 1993 - 25 Feb. 1994
Edgar J. Denlinger, Aly Fathy, and David Kalokitis 25 Feb. 1994 9 p
(Contract N00014-91-C-0216; ARPA Order 8100)
(AD-A276493) Avail: CASI HC A02/MF A01

A program plan for Phase 3 of the contract was submitted and approved. It incorporates a silver capping layer and a glass/metal handle for support of a thin YBCO/magnesium fluoride microstrip structure. The basic technology can be applied to MCM's as well as millimeter wave circuit needs. A silver capping layer of thickness 5 microns was found to be compatible with glass and able to withstand processing temperatures of 550 C used for firing and annealing of the glass. However, after subjecting the silver/glass combination to 700 C (to simulate the effect of depositing a subsequent YBCO signal layer in the complete MCM structure), there was some degradation in the silver's conductivity as measured using the dielectric resonator technique. A thicker silver layer is apparently needed to adjust for the interfacial reaction between the silver and the glass. Silver was deposited on both STO and YBCO-covered samples with excellent adhesion. After heating the samples to 750 C in flowing nitrogen, the adhesion of the silver remained excellent when tested with scotch tape. DTIC

N94-31547# Vrije Univ., Amsterdam (Netherlands).
HIGH PRESSURE EXPERIMENTS ON THE Y-Ba-Cu-O SUPERCONDUCTORS: A MAJOR ROLE FOR HOLES Ph.D. Thesis
Engelina Nieske vanEenige 1992 143 p Sponsored by Netherlands Organization for Scientific Research
(ETN-94-96013) Avail: CASI HC A07/MF A02

The critical temperature (Tc) of members of the Y-Ba-Cu-O system was investigated as a function of pressure, by means of resistivity measurements. The apparatus used to generate high pressures is a diamond anvil cell. Resistivity measurements were carried out at up to 50 GPa. Y1BaCuO8, a high pressure dependence member, was investigated at up to 17 GPa; the Tc could be increased with 28K, primarily due to the increase of charge carriers in the planes. The Tc as a function of pressure of three '124' samples with a small part of either the Ba or Y atoms replaced by a different kind of atoms was investigated; replacing atoms near the planes with atoms of a different valency is found to decrease the

maximum Tc. High pressure experiments show that Y2Ba4Cu7O15.32, consisting of very thin alternating layers of YBa2Cu3O7 and YBa2Cu4O8, behaves as a multilayer of proximity coupled planes. Measurements of the upper critical field of CaLaBaCu3O7, a tetragonal version of YBa2Cu3O7, showed that the increase of the number of holes with pressure is exceptionally small, and hence the low dTc/dp. Experiments on Bi based conductors showed pressure dependence to fit the general picture. ESA

N94-31610 Technische Univ., Berlin (Germany). Fachbereich Physik.
HYDROGEN INCORPORATION AND RADIATION INDUCED DYNAMICS IN METAL-OXIDE-SILICON STRUCTURES: A STUDY USING NUCLEAR REACTION ANALYSIS Ph.D. Thesis
M. A. Briere 1993 138 p Limited Reproducibility: More than 20% of this document may be affected by microfiche quality
(ETN-94-95742) Avail: CASI HC A07

Resonant Nuclear Reaction Analysis (NRA), using the H-1/N-15, alpha gamma/c-12 reaction at 6.4 MeV, is successfully applied to the investigation of hydrogen incorporation and radiation induced migration in metal oxide silicon structures. The influence of processing parameters on the H content of thermal oxides, with and without gate material present, is studied. Hydrogen accumulation at the Si-SiO2 interface is reproducibly demonstrated for as-oxidized samples, as well as for oxides exposed to H2 containing atmospheres during subsequent thermal processing. The migration of hydrogen, from the bulk oxide to the silicon oxide interface during NRA, is investigated. It is found that the cross section for this migration, per incident N-15 ion, depends on the sample processing history. It is argued that the release is due to electron capture at Si-OH sites and that the migration is driven by reductions in the interfacial free energy associated with the incorporation of hydrogen within the strained oxide region. A similar migration of hydrogen during irradiation with 2.5 MeV electrons is presented, which suggests that the migration occurs preferentially under applied fields which are directed to the silicon interface. It is argued that this bias effect is due to holes, which modify the interfacial region so as to increase hydrogen solubility, that is explained by the diffusivity of the hydrogen species during N-15 irradiation, which suggest identification as neutral atomic hydrogen. The spatial distribution of hydrogen at the Si-SiO2 interface is shown to be confined to within ca. 2 nm of the metallurgical boundary, in agreement with measurements of the location of oxide charge states, paramagnetic centers, as well as the width of the strained transition region in the neighborhood of this interface. A direct correlation between the hydrogen content of the bulk oxide and the radiation generated oxide charges and interface states is presented. These data provide strong support for the important role of hydrogen in determining the radiation sensitivity of electronic devices. ESA

N94-31612 Technische Univ., Darmstadt (Germany). Fachbereich Physik.
ELECTRON SPIN RESONANCE MEASUREMENTS OF Er(3+) AND Mn(2+) IN THE HIGH TEMPERATURE SUPERCONDUCTOR COMPOUNDS La(2-x)Sr(x)CuO(4-DELTA) Ph.D. Thesis
[ELEKTRONENSPINRESONANZ-MESSUNGEN AN ER(3+) UND MN(2+) IN DEN HOCHTEMPERATUR-SUPRALEITER-VERBINDUNGEN LA(2-X)SR(X)CUO(4-DELTA)]
Lei Kan 1992 91 p In GERMAN Limited Reproducibility: More than 20% of this document may be affected by microfiche quality
(ETN-94-95746) Avail: Issuing Activity (European Space Agency (ESA))

The Electron Spin Resonance (ESR) of the magnetic doping impurities of Er(3+) and Mn(2+) in the high temperature superconductor compound La(2-x)Sr(x)CuO(4-delta) was investigated for a large variation of x and the Mn concentration. Besides ESR, the magnetic susceptibility and the electrical resistance were also measured to determine spin dynamics, and magnetic and electrical properties of the lanthanum compounds. The spin dynamics was described by a theoretical model. The ESR studies provides very interesting information about the spin dynamics of the Cu and Mn ions in the lanthanum compounds. The strong coupling between the magnetic moments of these ions (bottleneck domain) strongly reduces the broadening of the Mn(2+) ESR linewidth. The ESR measurements allow the study of the relaxation rates of the Cu spin system and other degrees of freedom. The Mn(2+) ESR signal could not be observed in the superconducting state since the transition temperature of the compounds is strongly reduced by the doping with Mn ions. ESA

N94-31628# Los Alamos National Lab., NM.
IMPURITIES AND CONDUCTIVITY IN A D-WAVE SUPERCONDUCTOR
A. V. Balatsky 1994 7 p Presented at the Strongly Correlated Electron Materials, Los Alamos, NM, 15-18 Dec. 1993
(Contract W-7405-eng-36)
(DE94-006222; LA-UR-94-96; CONF-931247-3) Avail: CASI HC A02/MF A01

Impurity scattering in the unitary limit produces low energy quasiparticles with anisotropic spectrum in a two-dimensional d-wave superconductor. The authors describe a new quasi-one-dimensional limit of the quasiparticle scattering, which might occur in a superconductor with short coherence length and with finite impurity potential range. The DC conductivity in a d-wave superconductor is predicted to be proportional to the normal state scattering rate and is impurity-dependent. They show that quasi-one-dimensional regime might occur in high-(Tc) superconductors with Zn impurities at low temperatures T approximately less than 10 K. DOE

N94-31630# Oak Ridge National Lab., TN.
CHARACTERIZATION OF THE RARE EARTH ORTHOPHOSPHATES AND Ce-DOPED LaPO4 BY X RAY ABSORPTION SPECTROSCOPY
D. K. Shuh (California Univ., Berkeley. Lawrence Berkeley Lab.), D. Perry (California Univ., Berkeley. Lawrence Berkeley Lab.), L. J. Terminello (Lawrence Livermore National Lab., CA.), L. A. Boatner, and M. M. Abraham 1993 6 p Presented at the Fall Meeting of the Materials Research Society, Boston, MA, 29 Nov. - 3 Dec. 1993
(Contracts DE-AC05-84OR-21400; DE-AC03-76SF-00098; W-7405-eng-48)
(DE94-006313; CONF-931108-73) Avail: CASI HC A02/MF A01

X-ray Absorption Spectroscopy (XAS) of the Rare Earth (RE) 3d levels yields sharp peaks near the edges as a result of strong, quasi-atomic 3d(sup 10)4f (yields) 3d(sup 9)4f(sup n+1) (M(sub 4,5)) transitions that contain a wealth of spectroscopic features. XAS is a useful technique for the characterization of 4f-occupancy, 4f-hybridization, and valence in RE-containing materials. The XAS measurements of the single crystal RE-orthophosphates, as well as a range of Ce doped (approximately 1-30%) LaPO4 hosts were performed at the 3d edge in the total electron yield mode at beamline 8-2 at the Stanford Synchrotron Radiation Laboratory (SSRL). The XAS spectra of the RE ions in the orthophosphate matrix generally resemble that of the corresponding RE metal and emphasize the major contribution of the trivalent state to the electronic transitions occurring at the 3d edge. There is no energy shift of the La and Ce absorption peaks with Ce doping and furthermore, no additional transitions are observed in either spectral region. However, accompanying the Ce doping there is a significant narrowing of the La absorption peak full width half maximum that contrasts to the Ce features that exhibit no contraction. The La and Ce spectra indicate that the Ce-doping of LaPO4 is purely substitutional. DOE

N94-31631# Los Alamos National Lab., NM.
THE 4f HEAVY FERMION PHOTOELECTRON SPECTRA DO NOT EXHIBIT THE KONDO SCALE
A. J. Arko, J. J. Joyce, A. B. Andrews, R. I. R. Blyth, R. J. Bartlett, Z. Fisk, P. C. Canfield, C. G. Olson, P. J. Benning, and D. M. Poirier et al 1994 8 p Presented at the Strongly Correlated Electron Materials, Los Alamos, NM, 15-18 Dec. 1993
(Contract W-7405-eng-36)
(DE94-006252; LA-UR-94-217; CONF-931247-1) Avail: CASI HC A02/MF A01

It has been the authors contention for some time that neither the Single Impurity Anderson Model (SIAM), as extended by Gunnarsson and Schonhammer (GS), or the non-crossing approximation (NCA) correctly describes the 4f photoelectron spectra of heavy fermions. Recently, they have concentrated on Yb heavy fermions since in these materials the Kondo resonance (KR) is fully occupied and thus accessible via photoemission. In particular, they have repeatedly pointed out that the width, position, spectral weight, lineshape, and temperature dependence of the features assumed to be the KR and its sidebands, are nearly independent of the Kondo temperature, T(sub K), while at the same time bearing a striking resemblance to the simple 4f core level spectra of pure Yb metal, or of Lu in isostructural Lu compounds. It is important to resolve these issues in view of the fundamental nature of the problem. Here, the authors chose to test the bulk vs. surface hypothesis by performing measurements on YbCu2Si2 and YbAl3 single crystals at hv approximately 120 eV (UPS)

and hv approximately 1,500 eV(XPS) to see if the n(sub f), hole occupancy, values increase markedly at XPS energies as the electron escape depth increases by about a factor of 3-5. Measurements were performed at both 300K and 20K using single crystals cleaved in-situ, with photoelectrons collected in normal emission for maximum bulk sensitivity. UPS measurements were performed at NSLS and the University of Wisconsin SRC, while XPS measurements were done at the University of Minnesota. The UPS, ultraviolet photoelectron spectra, and the L(sub 3) edge x-ray absorption and photoemission measurements are in fundamental disagreement. DOE

N94-31633# Los Alamos National Lab., NM.
EXPERIMENTAL EVIDENCE FOR LATTICE EFFECTS IN HIGH TEMPERATURE SUPERCONDUCTORS
S. J. L. Billinge, G. H. Kwei, and J. D. Thompson 18 Jan. 1994 51 p Presented at the Strongly Correlated Electron Materials, Los Alamos, NM, 15-18 Dec. 1993
(Contract W-7405-eng-36)
(DE94-006250; LA-UR-94-0277; CONF-931247-4) Avail: CASI HC A04/MF A01

We present an overview of the experimental evidence for the role of the lattice in the mechanism of high temperature superconductivity. It appears unlikely that a solely conventional electron-phonon interaction produces the pairing. However, there is ample evidence of strong electron and spin to lattice coupling and observations of a response of the lattice to the electronic state. We draw attention to the importance of the local structure in discussions of lattice effects in high-T(sub c) superconductivity. DOE

N94-31634# California Univ., Berkeley. Lawrence Berkeley Lab.
THE EFFECTS OF AMORPHOUS LAYER REGROWTH ON CARBON ACTIVATION IN GaAs AND InP
A. J. Moll (California Univ., Berkeley.), E. E. Haller (California Univ., Berkeley.), J. W. Ager, III, K. M. Yu, and W. Walukiewicz Nov. 1993 6 p Presented at the Fall Meeting of the Materials Research Society (MRS), Boston, MA, 29 Nov. - 3 Dec. 1993
(Contract DE-AC03-76SF-00098)
(DE94-006290; LBL-34289; CONF-931108-59) Avail: CASI HC A02/MF A01

The effect of the Ga dose on the activation of implanted carbon in GaAs is determined. The free hole concentration is found to depend on the amorphous layer created by the Ga co-implant. Initial results on C implantation in InP indicate the behavior of C is very different in InP when compared to GaAs. The role of precipitation in reducing the activation of C in both GaAs and InP is discussed. DOE

N94-31729# Laval Univ. (Quebec). Dept. de Physique.
PHOTONIC BANDGAPS IN PERIODIC DIELECTRIC STRUCTURES Ph.D. Thesis
Pierre R. Villeneuve Dec. 1993 124 p
(ISBN-0-315-86902-X; CTN-94-61236) Copyright Avail: Micromedia Ltd., Technical Information Centre, 240 Catherine Street, Suite 305, Ottawa, Ontario, K2P 2G8, Canada HC/MF

Photonic bandgaps are defined as frequency intervals for which electromagnetic wave propagation is forbidden in all 4 pi steradians within a dielectric structure with a periodic index of refraction. Since photonic bandgap materials can essentially suppress all states, the radiative dynamics within the materials can be strongly modified. By changing the atom-field radiative coupling, photonic bandgap materials could lead to the inhibition of spontaneous emission; if a local defect is introduced within the structure, it will behave like a high Q microcavity. The existence of bandgaps can be predicted from a strictly classical treatment of the vector wave equation. The numerical results depend on the formulation of the problem. Use of the plane-wave expansion can lead to accurate results but introduces two problems related to the dielectric discontinuities and the plane-wave cutoff. The rate of convergence is compared as a function of the number of expansion terms and an alternative is presented to the discontinuous step function representation of the dielectric structure. These functions will allow overcoming of the Gibbs phenomenon and eliminate spatial fluctuations of the dielectric function. Guidelines are given for generation of photonic bandgaps. Experiments at microwave frequencies demonstrate many of the properties of photonic bandgaps. Author (CISTI)

N94-31813 Xerox Palo Alto Research Center, CA.
RESEARCH ON THE STABILITY, ELECTRONIC PROPERTIES, AND STRUCTURE OF a-Si:H AND ITS ALLOYS
W. B. Jackson, N. Johnson, and N. Nickel Feb. 1994 53 p Prepared for Midwest Research Inst., Golden, CO Limited Reproducibility: More than 20% of this document may be affected by microfiche quality
(Contract DE-AC02-83CH-10093)
(DE94-000292; NREL/TP-451-6192) Avail: Issuing Activity (Department of Energy (DOE))

This report describes work focusing on the defect and transport properties of a-Si:H with particular emphasis on defect metastability. Light-induced defects remain the major impediment to higher stabilized solar cell efficiencies. The many years of research have shown that this is a difficult problem to solve, and we take the view that a solution can be found only with a deep understanding of the mechanism; this has been our main goal. The metastability is closely related to the intrinsic defect properties, so these studies have also led to a greatly improved model of all the electronic properties of a-Si:H. Section A of the report discusses a theoretical analysis of the defect pool model for the equilibrium dark defect density, with particular reference to whether there are significant charged defects. Section B discusses the use of an electronic transport model to analyze forward and reverse currents and extends it to the calculation of field dependences of bulk and contact currents, which give more precision to the analysis of defects from reverse bias thermal generation currents. Electronic transport is discussed in Section C. Work done on H transport and bonding is described in Section D. DOE

N94-31847# Sandia National Labs., Albuquerque, NM.
INORGANIC MATERIALS FOR ANOMALOUS-DISPERSION PHASE-MATCHED SECOND HARMONIC GENERATION: RUBIDIUM TITANYL ARSENATE ISOMORPHS, Rb(Ti(1-2x)Ln(x)Nb(x) OAsO4
M. T. Anderson, M. L. F. Phillips, and G. D. Stucky 1993 26 p Presented at the 1st Meeting of the Pacific Rim Ceramic Societies, Honolulu, HI, 7-10 Nov. 1993
(Contract DE-AC04-94AL-85000)
(DE94-006141; SAND-93-2743C; CONF-931142-6) Avail: CASI HC A03/MF A01

We report the synthesis and optical properties of Rb(Ti(1-2x)-Ln(x)Nb(x))OAsO4. The solid solubility of lanthanide ions in the materials decreases exponentially as the size of the lanthanide ion increases. The materials exhibit absorption spectra characteristic of the particular lanthanide ion in the structure. The spectral regions between absorption peaks are transparent and will allow the transmission of fundamental and second-harmonic radiation. The charge transfer band is red-shifted 0 to 27 nm relative to RbTiOAsO4 (midpoint 331 nm). Second-harmonic intensities measured at 532 nm decrease exponentially as lanthanide ion concentration increases. DOE

N94-31916# Los Alamos National Lab., NM.
FERMI SURFACE INSTABILITY AT 0.4 K IN A HEAVY-FERMION YbBiPt: SDW?
R. Movshovich, A. Lacerda, P. C. Canfield, J. D. Thompson, and Z. Fisk 1994 7 p Presented at the Strongly Correlated Electron Materials, Los Alamos, NM, 15-18 Dec. 1993
(Contract W-7405-eng-36)
(DE94-006224; LA-UR-94-73; CONF-931247-2) Avail: CASI HC A02/MF A01

The authors report results of resistivity measurements of heavy-fermion compound YbBiPt at ambient and hydrostatic pressures of up to approximately 6 kbars and in magnetic field up to 1 Tesla. They interpret the rise of resistivity below 0.4 K as partial gaping of the Fermi surface. From the temperature dependence of resistivity they obtain the value of the weak coupling energy gap of delta(sub 0)/k(sub B)T(sub c) = 1.65 (+-) 0.15. Magnetic field -- transition temperature phase diagram follows the weak coupling BCS expression remarkably well from T(sub c) to T(sub c)/4. These results support identification of 0.4 K transition as a Spin Density Wave formation. DOE

N94-31983 University of North Texas, Denton. Dept. of Physics.
[DEVELOPMENT OF SAMPLE CHARGE COMPENSATION FOR CHARACTERIZATION OF IMPURITIES IN SEMICONDUCTOR MATERIALS]

Floyd D. McDaniel 2 Feb. 1994 14 p Limited Reproducibility: More than 20% of this document may be affected by microfiche quality
(Contract N00014-90-J-1691)
(AD-A277113) Avail: Issuing Activity (Defense Technical Information Center (DTIC))

Because of the high sensitivities and small sample size capabilities, an accelerator mass spectrometry (AMS) system has been constructed at the Ion Beam Modification and Analysis Laboratory (IBMAL) at the University of North Texas. The AMS system, which has been developed through a collaboration with Texas Instruments Inc., the National Science Foundation, and the Office of Naval Research, has been applied to trace element analysis of stable isotopes in electronic materials. The terminal charge stripping inherent with tandem accelerator operation allows molecular interferences to be removed. The interferences of molecules that have approximately the same mass as the element of interest (e.g. (Si-28)2 and Fe-56) are one of the primary limits to high sensitivities for SIMS. Because AMS has increased sensitivities over SIMS for some elements by factors of 100 to 1000 due to the removal of molecular interferences, AMS is sometimes called 'Super-SIMS.' The unique capabilities of AMS allow new and more sensitive methods for the characterization of trace impurities in electronic materials. DTIC

N94-31985 University of Southern California, Los Angeles. Dept. of Electrical Engineering.
EPITAXIAL LIFTOFF TECHNOLOGY ONTO PROCESSED SILICON FOUNDRY WAFERS Annual Report, FY-1993
Eli Yablonovitch 1993 2 p Limited Reproducibility: More than 20% of this document may be affected by microfiche quality
(Contract N00014-93-1-0311)
(AD-A277116) Avail: Issuing Activity (Defense Technical Information Center (DTIC))

Technical objectives are to research the application of liftoff transfer of epitaxial material to foreign substrates including: surface chemistry and electrical, mechanical, thermal, and optical properties of Van der Waals bonded materials; III-V devices bonded to silicon circuitry and to other substrates with enhanced optical, electrical, or thermal properties; and integrated optical devices incorporating lifted-off material and/or devices with LiNbO3 glass or other substrates. This effort addresses the need for new technologies which can fully utilize the performance advantages of III-V (GaAs, InGaAs, InGaAsP, and InP) materials for electronic and optoelectronic applications. Specifically, the program is directed at demonstrating the potential of epitaxial liftoff as a technology to enable the realization of 'monolithic' optoelectronic devices with the characteristics of epitaxial material, that is, by transfer of epitaxial material to foreign substrates in a form that permits material processing and device fabrication to proceed as though the epitaxial material were grown directly on the substrate. DTIC

N94-32001# Georgia Inst. of Tech., Atlanta.
TETRAALKYLDIARSINES AS POTENTIAL PRECURSORS FOR ELECTRONIC MATERIALS: SYNTHESIS AND CHARACTERIZATION OF VARIOUS ISO-PROPYL ARSENIC COMPOUNDS Interim Technical Report No. 4, 1 Jul. 1992 - 1 Mar. 1994
Lawrence F. Brough, Liu Gang, Matthew A. Lipkovich, and Thomas J. Colacot 8 Mar. 1994 9 p
(Contract N00014-92-J-1828)
(AD-A277003) Avail: CASI HC A02/MF A01

Tetrakis (iso-propyl) diarsine was synthesized by the reaction of (i-Pr)AsLi with (i-Pr)2AsI. The lithium salt of the secondary arsine was produced following deprotonation of (i-Pr)2AsH, obtained by reduction of (i-Pr)2AsI, which was prepared by the thermolysis of (i-Pr)3AsI2. The X-ray crystal structure of (I-Pr)3AsII has been determined on the product of the reaction of (i-Pr)3As and I2. Compounds of the general form E= As(i-Pr), (E = O, S, Se) have been prepared. DTIC

N94-32003# Georgia Inst. of Tech., Atlanta.
NEW MOLECULAR-BASED ROUTES TO BINARY MAIN GROUP METAL SULFIDES Interim Technical Report No. 1, 1 Jul. 1992 - 1 Mar. 1994
William S. Rees, Jr. and Gertrud Kraeuter 8 Mar. 1994 14 p
(Contract N00014-92-J-1828)
(AD-A277005) Avail: CASI HC A03/MF A01

Metal thiolates of the general formula M(SR)2 (M = Pb, Zn, Cd) and Cl-Hg-SR (R = alkyl) have been prepared and characterized by IR and NMR spectroscopic techniques, TGA and, in selected cases, single crystal X-ray diffraction. The metal bis(thiolate) compounds can be converted into the related metal sulfides by thermolyses. The solid state materials have been characterized by XRPD, SEM and, in selected cases, by particle size determination. The volatile pyrolytic co-products have been isolated and characterized by GC/MS. The decomposition pathways of mercury chlorothiolates are more complicated and depend on the nature of the organic group present in Cl-Hg-SR. DTIC

N94-32011 Georgia Inst. of Tech., Atlanta.
GROUP 12 THIOLATES: SYNTHESES, CHARACTERIZATION AND DECOMPOSITION PATHWAYS Interim Report, 1 Jul. 1992 - 1 Mar. 1994
Gertrud Krauter, Virgil L. Goedken, Bernhard Neumuller, and William S. Rees, Jr. 8 Mar. 1994 10 p Limited Reproducibility: More than 20% of this document may be affected by microfiche quality
(Contract N00014-92-J-1828)
(AD-A277055; TR-5) Avail: CASI HC A02

Zinc and cadmium bis(alkylthiolate) compounds have been prepared and converted into the appropriate binary metal sulfides by thermal treatment. Several mercury chlorothiolates have been synthesized and characterized by single crystal x-ray diffraction. Their decomposition pathways are discussed. The prepared binary metal sulfides have been studied by XRPD and in selected cases - by particle size determination. The volatile co-products have been isolated and characterized by GC/MS. DTIC

N94-32040 Rochester Univ., NY. Dept. of Electrical Engineering.
THE CHARGING EFFECT IN HIGH-Tc SUPERCONDUCTING THIN FILMS Final Report, 1 Nov. 1991 - 31 Dec. 1993
Roman Sobolewski Jan. 1994 12 p Limited Reproducibility: More than 20% of this document may be affected by microfiche quality
(Contract F49620-92-J-0075)
(AD-A277265; AFOSR-94-0058TR) Avail: CASI HC A03

Experimental research has been conducted to elucidate the basic physics and possible applications of the charging effect in partially oxygen-depleted YBa2Cu3O(6+x) (YBCO) thin films. A novel laser-writing technique, suitable for patterning and fabrication of monolithic YBCO electronic devices has been developed. The technique allows us to define superconducting and insulating regions in the same sample and is based on local laser beam heating of the epitaxial YBCO film in either the presence or the absence of an oxygen atmosphere. Several test structures for our charging-effect experiments were fabricated using laser writing. The structures are fully monolithic with a partially oxygen-depleted channel and oxygen-rich source and drain electrodes. The devices were tested and showed a substantial charging effect, which we associate with the charge-transfer effects related to electric-field-enhanced changes of the crystalline order in oxygen-deficient YBCO. We have also fabricated and successfully tested laser-written YBCO microwave transmission structures and resonators. The developed devices represent a new approach for the high-temperature superconducting electronics, which consists of exploiting contrasting properties of the oxygen-poor and oxygen-rich YBCO phases to design novel devices. DTIC

N94-32041 Syracuse Univ., NY. Dept. of Physics.
PROCESSING BORON AND BORON CARBIDE THIN FILMS FOR PROTECTIVE COATINGS AND DEVICE FABRICATION Final Report, 15 Sep. 1992 - 14 Sep. 1993
Peter Dowben 14 Sep. 1993 10 p Limited Reproducibility: More than 20% of this document may be affected by microfiche quality
(Contract F49620-92-J-0503)
(AD-A277266; AFOSR-94-0059TR) Avail: CASI HC A02

The fabrication of boron and boron carbide heterojunction devices is based upon the success, thus far, of fabricating boron-carbide heterojunctions in the laboratory of Professor Dowben. We have pioneered the use of heavy boranes, carboranes, and phosphaboranes to make doped layers and semiconductors. DTIC

N94-32065# Stanford Linear Accelerator Center, CA.
ANOMALOUS SMALL ANGLE X RAY SCATTERING STUDIES OF AMORPHOUS METAL-GERMANIUM ALLOYS Ph.D. Thesis
M. Rice Dec. 1993 197 p

(Contract DE-AC03-76SF-00515)
(DE94-007258; SU-SLAC-434; SU-SLAC/SSRL-0065) Avail: CASI HC A09/MF A03

This dissertation addresses the issue of composition modulation in sputtered amorphous metal-germanium thin films with the aim of understanding the intermediate range structure of these films as a function of composition. The investigative tool used in this work is anomalous small-angle x-ray scattering (ASAXS). The primary focus of this investigation is the amorphous iron-germanium (a-Fe(x)Ge(100-x)) system with particular emphasis on the semiconductor-rich regime. Brief excursions are made into the amorphous tungsten-germanium (a-W(x)Ge(100-x)) and the amorphous molybdenum-germanium (a-Mo(x)Ge(100-x)) systems. All three systems exhibit an amorphous structure over a broad composition range extending from pure amorphous germanium to approximately 70 atomic percent metal when prepared as sputtered films. Across this composition range the structures change from the open, covalently bonded, tetrahedral network of pure a-Ge to densely packed metals. The structural changes are accompanied by a semiconductor-metal transition in all three systems as well as a ferromagnetic transition in the a-Fe(x)Ge(100-x) system and a superconducting transition in the a-Mo(x)Ge(100-x) system. A long standing question, particularly in the a-Fe(x)Ge(100-x) and the a-Mo(x)Ge(100-x) systems, has been whether the structural changes (and therefore the accompanying electrical and magnetic transitions) are accomplished by homogeneous alloy formation or phase separation. The application of ASAXS to this problem proves unambiguously that fine scale composition modulations, as distinct from the simple density fluctuations that arise from cracks and voids, are present in the a-Fe(x)Ge(100-x), a-W(x)Ge(100-x), and a-Mo(x)Ge(100-x) systems in the semiconductor-metal transition region. Furthermore, ASAXS shows that germanium is distributed uniformly throughout each sample in the x less than 25 regime of all three systems. DOE

N94-32092 Arizona State Univ., Tempe. Dept. of Physics.
CORRELATIONS BETWEEN MICROMAGNETIC, MICROSTRUCTURAL AND MICROCHEMICAL PROPERTIES IN ULTRATHIN EPITAXIAL MAGNETIC STRUCTURES Annual Report No. 1, 1 Jan. - 31 Dec. 1993
M. R. Scheinfein, J. S. Drucker, and G. G. Hembree 31 Dec. 1993 132 p Limited Reproducibility: More than 20% of this document may be affected by microfiche quality
(Contract N00014-93-1-0099)
(AD-A277200) Avail: Issuing Activity (Defense Technical Information Center (DTIC))

The proposed goal of this project is to obtain quantitative measurements of the microstructural, microchemical and micromagnetic properties of surfaces and interfaces of ultrathin films composed of magnetic materials deposited on non-magnetic, antiferromagnetic (metal) and insulating substrates. Surface microanalytic methods based on unique ultrahigh-vacuum scanning transmission electron microscope/scanning electron microscope (UHV-STEM/SEM) equipped with in-situ thin film preparation and characterization tools are being used. Magnetic characterization is performed in-situ using the surface magneto-optical Kerr effect (SMOKE). Additional magnetic microstructure measurements are being conducted in a novel STEM based electron holography system where absolutely calibrated nanometer resolution magnetometry is possible. Of the proposed systems for study outlined in the original proposal, work has begun on FE/Ag, Fe/Cu, Fe/CaF2 and Fe/CaF2/Si (half of the proposed systems). DTIC

N94-32104# Sandia National Labs., Albuquerque, NM.
ADVANCES IN MOVPE COMPOUND SEMICONDUCTOR EPITAXY MANUFACTURING TECHNOLOGY: FROM HIGH THROUGHPUT LARGE AREA REACTORS TO CLUSTER TOOLS
G. S. Tompa (Emcore Corp., Somerset, NJ.), P. A. Zawadzki (Emcore Corp., Somerset, NJ.), and K. Moy (Emcore Corp., Somerset, NJ.) 1993 4 p Presented at the 1994 Conference on GaAs Manufacturing, Las Vegas, NV, 2-5 May 1994
(Contract DE-AC04-94AL-85000)
(DE94-006367; SAND-93-2702C; CONF-940588-1) Avail: CASI HC A01/MF A01

Molecular Beam Epitaxy (MBE) and Metal Organic Vapor Phase Epitaxy (MOVPE) are the two leading production deposition technologies. In recent years, MOVPE has become the more versatile and more economical production technology. We have embarked on a next generation MOVPE systems development path which meets the large scale, high throughput needs of this growing high technology market, both today and tomorrow. The systems development task is discussed. DOE

N94-32115 Lawrence Livermore National Lab., CA.
AMORPHOUS/CRYSTALLINE STRUCTURE AND PHASE TRANSFORMATIONS IN METASTABLE SEMICONDUCTING Ge(1-x)Sn(x)
S. M. Lee (Lawrence Univ., Appleton, WI.) and K. Barmak (Lehigh Univ., Bethlehem, PA.) Dec. 1993 8 p Presented at the Fall Meeting of the Materials Research Society (MRS), Boston, MA, 29 Nov. - 3 Dec. 1993 Limited Reproducibility: More than 20% of this document may be affected by microfiche quality
(Contract W-7405-eng-48)
(DE94-006659; UCRL-JC-113900; CONF-931108-79) Avail: CASI HC A02

The semiconducting crystalline alloys, Ge(1-x)Sn(x), are of interest due to theoretical predictions about their electronic band structures which make them useful in infrared photodetectors. However the composition region where these alloys have the desired properties is greater than the equilibrium solid solubility limit of Sn in Ge (x less than or equal to 0.01). The authors have circumvented the solubility limits and produced thin (2,000 A) and thick (4-8 micron) films of Ge(1-x)Sn(x) (x less than or equal to 0.31) by RF sputtering. Differential scanning calorimetry (DSC) measurements were performed to study grain growth and crystallization processes in these highly metastable semiconductors. X-ray and electron diffraction measurements indicated the materials were amorphous, but the fact that some of the films were fine grained polycrystalline samples only became apparent in their DSC spectra. The authors present models that describe quantitatively the transformation behavior in both sets of films. DOE

N94-32153# Army Research Inst. of Environmental Medicine, Natick, MA.
RECOMMENDATIONS FOR METEOROLOGICAL DATA COLLECTION DURING PHYSIOLOGICAL FIELD STUDIES
W. R. Santee and R. W. Hoyt Mar. 1994 50 p
(AD-A276834; USARIEM-T94-9) Avail: CASI HC A03/MF A01

Adequate meteorological data are primary environmental requirements that should be collected during physiological field studies. This report describes the minimum and recommended levels of meteorological data collection during winter field studies. Cold weather models and indices are briefly discussed. Meteorological data collected by an automated weather station during a January 1988 field study at the Marine Corps Mountain Warfare Training Center, Bridgeport, CA are presented. DTIC

N94-32172# Oak Ridge National Lab., TN.
ORIENTED Si AND Ge NANOCRYSTALS FORMED IN Al2O3 BY ION IMPLANTATION AND ANNEALING
C. W. White, J. D. Budai, S. P. Withrow, S. J. Pennycook, D. S. Zhou, T. Vo-Dinh, D. M. Hembree, and R. H. Magruder Nov. 1993 10 p Presented at the Fall Meeting of the Materials Research Society (MRS), Boston, MA, 29 Nov. - 3 Dec. 1993
(Contract DE-AC05-84OR-21400)
(DE94-005593; CONF-931108-52) Avail: CASI HC A02/MF A01

Ion implantation followed by thermal annealing in a reducing atmosphere has been used to create a high density of oriented Si and Ge nanocrystals in (0001) Al2O3. Both types of nanocrystals are three dimensionally aligned with respect to the Al2O3 matrix, but the orientational relationships are different, and the two types of nanocrystals have different shapes in Al2O3. Implantation of Si and Ge in fused silica also produces nanocrystals, but in this case the nanocrystals are randomly oriented relative to each other. DOE

N94-32176# EG and G Energy Measurements, Inc., Goleta, CA.
ON THE NATURE OF STRIAE IN STRONTIUM BARIUM NIOBATE
R. R. Monchamp, G. B. Mihalik, and L. A. Franks 1993 16 p
(Contract DE-AC08-93NV-11265)
(DE94-006486; EGG-11265-2040) Avail: CASI HC A03/MF A01

Strontium barium niobate crystals were grown by the Czochralski technique. These crystals were 15 to 20 mm in diameter and 25 to 75 mm long. Two types of striae, designated as coarse and fine, were characterized. The coarse striae are optically dense and are spaced by

100 to 500 micron apart; the fine striae are optically less dense and spaced 5 to 50 micron apart. The origins of the striae are attributed to thermal fluctuations in the melt related to the control system and to rotation of the growing crystal in non-isothermal radial gradients. Analysis of the crystals would indicated that the coarse striae may contain increased concentrations of sodium. DOE

N94-32209 Rome Univ. (Italy).
THE 10TH INTERNATIONAL CONFERENCE ON INTERNAL FRICTION AND ULTRASONIC ATTENUATION IN SOLIDS (ICIFUAS)
9 Sep. 1993 227 p Conference held in Rome, Italy, 6-9 Sep. 1993 Limited Reproducibility: More than 20% of this document may be affected by microfiche quality
(Contract DAHA45-93-M-0293)
(AD-A276849) Avail: CASI HC A11

The purpose of this conference is as follows: to provide an International Forum for researchers in the field of elastic energy dissipation in solids by ultrasonic attenuation, internal friction, after effect, and vibration damping. The following top ics were discussed: Point defects, Dislocations, and their interaction with lattice imperfections; Phase transformations--displacive transitions and order-disorder transitions and precipitation; Hydrogen in metals and semiconductors; Oxide superconductors and fullerenes; Amorphous materials and superionic conductors; Ferroelectric and ceramic materials; Composites and polymers; Thin films; Electron and phonon relaxation; Grain boundaries, domain walls, and interfaces; General aspects of anelasticity and mechanical properties; Magneto-elastic interactions; and Experimental techniques, non-destructive testing, and industrial applications. DTIC

N94-32216# Georgia Inst. of Tech., Atlanta. Dept. of Chemistry.
NEW ZINC-BIS(DIALKYLAMIDES) POTENTIALLY USABLE AS SITE-SELECTIVE DOPANTS FOR p-TYPE ZnSe Interim Report, 1 Jul. 1992 - 1 Mar. 1994
William S. Rees, Jr. and Oliver Just 8 Mar. 1994 10 p
(Contract N00014-92-J-1820)
(AD-A276947; TR-3) Avail: CASI HC A02/MF A01

In earlier work, the effective utilization of Zn(NSi(CH3)32)2 as a site-selective dopant for the production of p-type ZnSe by OMVPE was demonstrated. Several new zinc-bis(dialkylamides) of the general form (R)(R')NZnN(R)(R') have been prepared. They have been characterized by 1H- and 13C-NMR, GC/MS, and elemental analysis. Vapor pressures and gas phase decomposition profiles have been examined. Correlations of vapor pressure and structure are discussed for this series of compounds. A mechanism for the site-selectivity observed in the incorporation of nitrogen is proposed. DTIC

N94-32247 Gosudarstvennyi Komitet po Ispolzovaniyu Atomnoi Energii, Serpukhov (USSR).
N(EXP n(n-1)/2)-STATE R-MATRIX RELATED WITH U(SUB q)(sl(n)) ALGEBRA AT q(EXP 2N) = 1
R. M. Kashaev and V. V. Mangazeev 1992 12 p Submitted for publication Limited Reproducibility: More than 20% of this document may be affected by microfiche quality
(DE94-608140; IHEP-TD-92-32) Avail: CASI HC A03 (US Sales Only)

The N(exp n(n-1)/2)-state R-matrix related with U(sub q)(sl(n)) algebra at q(exp 2N) = 1 is presented. Its matrix elements are interpreted as Boltzmann weights of an elementary box of some 2d lattice statistical model and given in terms of W-bar weights of the 'minimal' sl(n) chiral Potts model. The corresponding family of transfer matrices depends on n rapidity variables living on high genus algebraic curves, the latter being defined by n moduli. DOE

N94-32255# California Univ., Santa Barbara. Coll. of Engineering.
NOVEL GROWTH TECHNOLOGIES FOR IN SITU FORMATION OF SEMICONDUCTOR QUANTUM WIRE STRUCTURES Final Report
S. P. DenBaars 1994 14 p
(Contract N00014-92-J-1694)
(AD-A277188) Avail: CASI HC A03/MF A01

Novel growth technologies were developed for low dimensional quantum materials and devices. Non-hydride MOCVD and use of strain to produce InP quantum dots have been achieved. This ONR contract was key to our development of the less hazardous novel non-hydride sources, tertiary butyl arsine (TBA) and tertiary butyl phosphine (TBP) for the growth on InP based electronic devices. Indium Phosphide channel JFET were fabricated by MOCVD using tertiary butyl phosphine (TBP) as the alternative source for phosphine for the first time. We have developed the Stranski-Krastanow (SK) growth mode for the in-situ formation of InP quantum dots. It has been observed that many strained systems exhibit Stranski-Krastanow growth, where the epitaxy initiates in two dimensions but transforms to three dimensions with the formation of dislocations in response to the energetics and kinetics of the layer. DTIC

N94-32296# Sandia National Labs., Albuquerque, NM.
STABILITY AND PRECIPITATION KINETICS IN Si(1-y)C(y)/Si AND Si(1-x-y)Ge(x)C(y)/Si HETEROSTRUCTURES PREPARED BY SOLID PHASE EPITAXY
J. W. Strane (Cornell Univ., Ithaca, NY.), S. T. Picraux, H. J. Stein, S. R. Lee, J. Candelaria, D. Theodore, and J. W. Mayer 1993 6 p Presented at the Fall Meeting of the Materials Research Society, Boston, MA, 29 Nov. - 3 Dec. 1993
(Contract DE-AC04-94AL-85000)
(DE94-006589; SAND-93-1473C; CONF-931108-63) Avail: CASI HC A02/MF A01

This study investigates the stability of metastable Si(1-y)C(y)/Si heterostructures during rapid thermal annealing (RTA) over a temperature range of 1,000-1,150 C. Heterostructures of Si(1-y)C(y)/Si and Si(1-x-y)Ge(x)C(y)/Si (where x =0.77 and y is less than or equal to 0.0014) were formed by solid phase epitaxy from C implanted, preamorphized substrates using a 30 minute 700 C anneal in N2. The occupancy of C in substitution lattice sites was monitored by Fourier Transform Infrared Absorption spectroscopy. The layer strain was monitored by rocking curve X-ray diffraction and the structural changes in the layers were determined using plan-view and X-sectional transmission electron microscopy (TEM). For anneals of 1,150 C or above, all the substitutional C was lost from the Si lattice after 30 seconds. TEM verified that the strain relaxation was the result of C precipitating into highly aligned (beta)SiC particles rather than by the formation of extended defects. No nucleation barrier was observed for the loss of substitutional C. Preliminary results will also be discussed for Si(1-x-y)Ge(x)C(y)/Si heterostructures where there is the additional factor of the competition between strain energy and the chemical driving forces. DOE

N94-32306# Research Triangle Inst., Research Triangle Park, NC.
HETEROEPITAXIAL DIAMOND GROWTH Final Report, 1 Jan. - 31 Dec. 1993
R. J. Markunas, R. A. Rudder, J. B. Posthill, R. E. Thomas, and G. Hudson Feb. 1994 102 p
(Contract N00014-92-C-0081)
(AD-A277178; RTI/5294/94-Quarterly; RTI-83U-5294) Avail: CASI HC A06/MF A02

Technical highlights from 1993 include the following: Growth Chemistries: A clear correlation was observed between ionization potential of feedstock gasses and critical power necessary for inductive coupling of the plasma and consequent diamond growth. Substrate preparation and epitaxial film quality: Ion-implantation of C and O has been coupled with either electrochemical etching or acid cleaning for surface preparation prior to homoepitaxial growth. Reactor modifications: Key improvements were made to the RF reactor to allow for long growths to consolidate substrates. Liquid mass flow controllers were added to precisely meter both the water and selected alcohol. Ion-implantation and lift off: Lift off of diamond platelets has been achieved with two processes. Ion-implantation of either C or O followed by annealing and implantation of either C or O followed by water based electrolysis. Diamond characterization: Development of novel detect characterization techniques: (1) Etch delineation of defects by exposure to propane torch flame. (2) Hydrogen plasma exposure to enhance secondary electron emission and provide non-topographical defect contrast. Acetylene will react at room temperature with sites created by partial desorption of oxygen from the (100) diamond surface. Thermal desorption measurements give an apparent activation energy for CO desorption from diamond (100) of 45 kcal/mol. Quantum chemical calculations indicate an activation energy of 38 kcal/mol for CO desorption. Ab initio calculations on (100) surfaces indicates that oxygen adsorbed at one dimer site has an effect on the dimerization of an adjacent site. DTIC

N94-32322 Wales Univ. Inst. of Science and Technology, Cardiff. Dept. of Physics and Astronomy.
LOWERING THE SCHOTTKY BARRIER AT METAL OR SILICIDE/SI INTERFACES TO EXTEND THE RANGE OF INFRARED DETECTORS
Final Report, Sep. 1992 - Aug. 1993
C. L. Griffiths Nov. 1993 26 p Limited Reproducibility: More than 20% of this document may be affected by microfiche quality
(Grant AF-AFOSR-0342-90)
(AD-A277253; EOARD-TR-94-03) Avail: Issuing Activity (Defense Technical Information Center (DTIC))

Si and group IV based Schottky barriers (SB) below about 0.2 eV are of considerable technological importance since detectors based upon them will be able to probe deep into the infrared while maintaining well established processing techniques. Investigations relating to this problem have been carried out using ultrahigh vacuum techniques and x ray photoelectron spectroscopy. Two approaches have been pursued, one by tailoring the interface geometric and hence electronic structure and the other by using a reduced band gap material. The systems studied were Sn on Si(111) and Pt on Ge(111). Sn invokes several surface reconstructions on Si(111), one of which, the 2 times the square root of 3 structure, has an associated electronic structure with the Fermi level situated 0.14 +/- 0.10 eV above the valence band maximum (VBM). This means that the corresponding p-type SB is also 0.14 +/- 0.10 eV, well below the value of 0.22 eV found at the PtSi/Si(100) interface. Similarly, when Pt was deposited onto Ge(100), the Fermi level was positioned 0.12 +/- 0.04 eV above the VBM, again resulting in a p-type SB significantly lower than that at the PtSi/Si(100) interface. Chemical interactions at the Pt/Ge interface are discussed. DTIC

N94-32372# Argonne National Lab., IL.
DEFECT CASCADES PRODUCED BY NEUTRON IRRADIATION IN YBa2Cu3O(7-DELTA) SUPERCONDUCTORS
M. C. Frischherz, M. A. Kirk, and J. Farmer Feb. 1994 7 p Presented at the 7th IWCC International Workshop on Critical Currents in Superconductors, Alpbach, Austria, 24-27 Jan. 1994
(Contract W-31-109-eng-38)
(DE94-007700; ANL/MSD/CP-82067; CONF-940122-3) Avail: CASI HC A02/MF A01

The defect cascades produced by fast neutron irradiation of YBa2Cu3O(7-delta) single crystals were studied by transmission electron microscopy. The visible defects were found to have sizes between 1 and 5 nm. Defect densities were obtained as a function of neutron fluence between 2 and 8 x 10(exp 21) m(exp -2) (E greater than 0.1 MeV). The measured defect density scales linearly with fluence and amounts to 1 x 10(exp 22) m(exp -3) at a neutron fluence of 2 x 10(exp 2l) m(exp -2). The defect stability was studied at room temperature and through annealing to 400 C. DOE

N94-32384# Sandia National Labs., Albuquerque, NM.
INTRA-CASCADE SURFACE RECOMBINATION OF POINT DEFECTS DURING ION BOMBARDMENT OF Ge(001)
J. A. Floro, B. K. Kellerman, E. Chason, S. T. Picraux, D. K. Brice, and K. M. Horn 1993 6 p Presented at the Materials Research Society Meeting, Pittsburgh, PA, 29 Nov. - 3 Dec. 1993
(Contract DE-AC04-94AL-85000)
(DE94-007740; SAND-94-0357C; CONF-9311153-3) Avail: CASI HC A02/MF A01

Low energy Ar and Xe ion bombardment of Ge(001) produces large numbers of point defects on the Ge surface and in the near-surface regions. Defect concentrations on the surface are detected and quantified in real time during bombardment using in situ Reflection High Energy Electron Diffraction (RHEED). We report the energy dependence of the defect yield for 70-500 eV Ar and Xe ion bombardment, and the temperature dependence of the defect yield (defects/ion) during 200 eV ion bombardment. The defect yield drops rapidly as the substrate temperature during bombardment is varied from 175 to 400 K. We attribute the yield reduction to surface recombination of adatoms and vacancies produced in the same collision cascade. DOE

N94-32409# Sandia National Labs., Albuquerque, NM.
DEVELOPMENT, CHARACTERIZATION, AND APPLICATIONS OF HIGH TEMPERATURE SUPERCONDUCTOR NANOBRIDGE JOSEPHSON JUNCTIONS
J. R. Wendt, C. P. Tigges, V. M. Hietala, T. A. Plut, J. S. Martens, K. Char, and M. E. Johansson Mar. 1994 25 p
(Contract DE-AC04-94AL-85000)
(DE94-008113; SAND-94-0158) Avail: CASI HC A03/MF A01

A well-controlled, high-yield Josephson junction process in high temperature superconductors (HTS) is necessary for the demonstration of ultra-high-speed devices and circuits which exceed the capabilities of conventional electronics. The authors developed nanobridge Josephson junctions in high quality thin-film YBaCuO with dimensions below 100 nm fabricated using electron-beam nanolithography. They characterized this Josephson junction technology for process yield, junction parameter uniformity, and overall applicability for use in high-performance circuits. To facilitate the determination of junction parameters, they developed a measurement technique based on spectral analysis in the range of 90-160 GHz of phase-locked, oscillating arrays of up to 2,450 Josephson junctions. Because of the excellent yield and uniformity of the nanobridge junctions, they successfully applied the junction technology to a wide variety of circuits. These circuits included transmission-line pulse formers and 32 and 64-bit shift registers. The 32-bit shift register was shown to operate at clock speeds near 100 GHz and is believed to be one of the faster and more complex digital circuit demonstrated to date using high temperature superconductor technology. DOE

N94-32411# Lawrence Livermore National Lab., CA.
POINT DEFECT PRODUCTION, GEOMETRY, AND STABILITY IN SILICON: A MOLECULAR DYNAMICS SIMULATION STUDY
M. J. Caturla, T. D. delaRubia, and G. H. Gilmer Feb. 1994 8 p Presented at the Fall Meeting of the Materials Research Society (MRS), Boston, MA, 29 Nov. - 3 Dec. 1993
(Contract W-7405-eng-48)
(DE94-008292; UCRL-JC-116364; CONF-931108-92) Avail: CASI HC A02/MF A01

We present results of molecular dynamics computer simulation studies of the threshold energy for point defect production in silicon. We employ computational cells with 8000 atoms at ambient temperature of 10 K that interact via the Stillinger-Weber potential. Our simulations address the orientation dependence of the defect production threshold as well as the structure and stability of the resulting vacancy-interstitial pairs. Near the (111) directions, a vacancy tetrahedral-interstitial pair is produced for 25 eV recoils. However, at 30 eV recoil energy, the resulting interstitial is found to be the (110) split dumbbell configuration. This Frenkel pair configuration is lower in energy than the former by 1.2 eV. Moreover, upon warming of the sample from 10 K the tetrahedral interstitial converts to a (110) split before finally recombining with the vacancy. Along (100) directions, a vacancy-(110) split interstitial configuration is found at the threshold energy of 22 eV. Near (110) directions, a wide variety of closed replacement chains are found to occur for recoil energies up to 45 eV. At 45 eV, the low energy vacancy-(110) split configuration is found. At 300 K, the results are similar. We provide details on the atomic structure and relaxations near these defects as well as on their mobilities. DOE

N94-32597 Los Alamos National Lab., NM.
ATTEMPTS TO MODEL THE GENERATION OF NEW GRAIN BOUNDARIES DURING THE DEFORMATION OF POLYCRYSTALS
U. F. Kocks, J. D. Cotton, S. R. Chen, S. I. Wright, A. D. Rollett, J. D. Embury, and A. J. Beaudoin 1993 11 p Presented at the Fall Meeting of the Minerals, Metals and Materials Society: Physical Metallurgy and Materials, Pittsburgh, PA, 17-21 Oct. 1993 Limited Reproducibility: More than 20% of this document may be affected by microfiche quality
(Contract W-7405-eng-36)
(DE94-007527; LA-UR-93-4520; CONF-931009-21) Avail: CASI HC A03

We explore ways by which new orientations (nuclei) can arise during essentially homogeneous defo rmation in polycrystals. All of these can be categorized as generating new large-angle boundaries: one is due to excessive storage of dislocations of one sign parallel to existing grain boundaries; another is due to reactions of cell walls with grain edges; and in the last, new boundaries are created surrounding a domain of different slip system distribution. DOE

N94-32601# Argonne National Lab., IL. Materials Science Div.
EFFECT OF TWIN BOUNDARY DENSITY ON THE VORTEX MELTING TRANSITION IN YBa2Cu3O(7-DELTA) SINGLE CRYSTALS
W. K. Kwok, J. Fendrich, S. Fleshler, U. Welp, and G. W. Crabtree Jan. 1994 7 p Presented at the 7th IWCC International Workshop on Critical Currents in Superconductors, Alpbach, Austria, 24-27 Jan. 1994
(Contract W-31-109-eng-38)
(DE94-007684; ANL/MSD/CP-82175; CONF-940122-2) Avail: CASI HC A02/MF A01

The authors present magnetotransport rho(H,T) measurements in clean untwinned and twinned crystals of YBa2Cu3O(7-delta) in magnetic fields up to 8 Tesla for H parallel to c. In untwinned crystals, they show strong support for a vortex solid to liquid first order melting transition at a temperature T(sub m), much below the mean field transition temperature T(sub c)(H), characterized by an extremely sharp drop in resistivity rho(T(sub m)) and the appearance of hysteretic behavior at rho(H(sub m)). In densely twinned crystals, the sharp transition is replaced with a continuous transition at a higher temperature T(sub BG) greater than T(sub m). Furthermore, the cusp in T(sub BG)(theta) predicted by the Bose glass theory at fixed field is observed. In dilutely twinned crystals they demonstrate the competing effect of pinning and freezing at the phase transition. The vortex solid state at low fields is characterized by the appearance of a 'peak effect' just below the melting temperature. DOE

N94-32602# Argonne National Lab., IL. Science and Technology Center for Superconductivity.
HIGH T(SUB c) SUPERCONDUCTOR TUNNEL JUNCTIONS FOR PHOTON DETECTORS
John Zasadzinski (Illinois Inst. of Tech., Chicago.), Jun Chen, K. E. Gray, and D. G. Hinks Feb. 1994 9 p Presented at the International Conference on Millimeter and Submillimeter Waves, San Diego, CA, 10-14 Jan. 1994
(Contract W-31-109-eng-38)
(DE94-007686; ANL/MSD/CP-82165; CONF-940132-2) Avail: CASI HC A02/MF A01

Superconducting - insulator - superconducting (SIS) and normal metal counterelectrode (SIN) quasiparticle tunnel junctions on high T(sub c) superconductors (HTS) offer the possibility of low-noise, heterodyne, photon detection in the THz regime. We report progress on the development of such junctions using mechanical point contacts. In general, these contacts display the optimum characteristics that can be obtained from HTS native-surface tunnel barriers. The bismuthate, Ba(1-x)K(x)BiO3, (T(sub c) = 25 K), displays ideal, BCS, quasiparticle characteristics at T = 4.2 K; however, at temperatures T approximately T(sub c)/2 there is evidence of strong quasiparticle damping which may inhibit device performance. The cuprates typically display nonideal quasiparticle characteristics including large sub-gap conductances. Recent data for the new Hg-based cuprates (T(sub c) = 96 K) are promising in that they exhibit very low and flat sub-gap conductances as expected from a BCS density of states. Proximity effect tunnel junctions on Bi2Sr2CaCu2O8/Au bilayers have been studied using an In tip. An induced energy gap has been consistently observed in the Au layer and the data can be understood using the McMillan model. A few junctions show much improved sub-gap characteristics compared to ones made directly on the BSCCO surface and indicate that this approach may be suitable for mixer development. DOE

N94-32606# Lawrence Livermore National Lab., CA.
BORON AND HYDROGEN IN Ni3Al. PART 2: MECHANICAL TESTING OF BICRYSTALS
P. E. Johnson, W. Gourdin, A. Gonis, N. Kioussis, and M. Vaudin Jan. 1994 6 p Presented at the Fall Meeting of the Materials Research Society (MRS), Boston, MA, 29 Nov. - 3 Dec. 1993
(Contract W-7405-eng-48)
(DE94-007441; UCRL-JC-114159-Pt-2; CONF-931108-84-Pt-2) Avail: CASI HC A02/MF A01

To provide a sensitive measurement of the effect of boron segregation on the strength and ductility of Ni3Al grain boundaries, bicrystal tensile tests were performed on small specimens of boron doped Ni76Al24 cut from extremely large-grained boules. Five specimens with the same 'random' or low-symmetry grain boundary (disorientations measured by means of backscattered Kikuchi patterns) and two specimens with a second random grain boundary were tested in quenched and slow-cooled conditions. Duplicate tests performed in a low (7 ppM) water-vapor environment showed that the fracture mode and the stress and strain at fracture are altered by environmental embrittlement at individual, partially strengthened grain boundaries. DOE

N94-32634# Lawrence Livermore National Lab., CA.
FEMTOSECOND PROBE-PROBE TRANSMISSION STUDIES OF LT-GROWN GaAs NEAR THE BAND EDGE
H. B. Radousky, A. F. Bello, D. J. Erskine, L. N. Dinh, M. J. Bennahmias, M. D. Perry, T. R. Ditmire, and R. P. Mariella, Jr. Dec. 1993 8 p Presented at the Spring Meeting of the Materials Research Society, San Francisco, CA, 4-8 Apr. 1994
(Contract W-7405-eng-48)
(DE94-006660; UCRL-JC-115625; CONF-940411-1) Avail: CASI HC A02/MF A01

We have studied the near-edge optical response of a LT-grown GaAs sample which was deposited at 300 C on a Si substrate, and then annealed at 600 C. The Si was etched away to leave a 1 micron free standing GaAs film. Femtosecond transmission measurements were made using an equal pulse technique at four wavelengths between 825 and 870 nm. For each wavelength, we observe both a multipicosecond relaxation time, as well as a shorter relaxation time which is less than 100 femtoseconds. DOE

N94-32645# Argonne National Lab., IL. Materials Science Div.
SHORT COHERENCE LENGTH SUPERCONDUCTORS: INTERMEDIATE REGIME BETWEEN BCS AND BOSONS
Jan R. Engelbrecht (Los Alamos National Lab., NM.), Mohit Randeria, and Carlos A. R. SadeMelo Feb. 1994 5 p Presented at the Strongly Correlated Electron Materials, Los Alamos, NM, 15-18 Dec. 1993
(Contract W-31-109-eng-38)
(DE94-007694; ANL/MSD/CP-82054; CONF-931247-7) Avail: CASI HC A01/MF A01

In order to understand the high (Tc) materials, conventional superconductors and their metallic normal states are examined to see how generalizations of BCS pairing may lead to unconventional properties. The persistence of gap-like features in the normal state up to temperatures several times (Tc) is shown. The short coherence length and normal state pseudo-gaps are suggestive of preformed pairs which Bose condense at the superconducting transitions; the normal state is a degenerate Fermi system in which correlations lead to pseudo-gaps. It is argued that these deviations from Fermi liquid behavior are characteristic of the normal state of short coherence length superconductors. DOE

N94-32724# Oak Ridge National Lab., TN.
AB INITIO STUDY OF THE EPITAXIAL GROWTH OF Ge ON Si(100) SURFACE
V. Milman, S. J. Pennycook, D. E. Jesson, M. C. Payne, and I. Stich Nov. 1993 7 p Presented at the Fall Meeting of the Materials Research Society (MRS), Boston, MA, 29 Nov. - 3 Dec. 1993
(Contract DE-AC05-84OR-21400)
(DE94-007245; CONF-931108-83) Avail: CASI HC A02/MF A01

We identify the binding sites for adsorption of a single Ge atom on the Si(100) surface using ab initio total energy calculations. The calculated diffusion barriers are in excellent agreement with experimental estimates. Using a large supercell we resolve the controversy regarding the binding geometry and migration path for the adatom, and investigate the influence of the adatom on the buckling of Si dimers. The adatom induces a buckling defect that is frequently observed using scanning tunneling microscopy (STM); therefore, the study of single adatoms may be experimentally accessible. DOE

N94-32746# Los Alamos National Lab., NM. Center for Nonlinear Studies.
STRONGLY ANISOTROPIC s-WAVE VERSUS d-WAVE GAP IN CUPRATE SUPERCONDUCTORS: EVIDENCE AND THEORY
Baird Brandow 1994 5 p Presented at the Strongly Correlated Electron Materials, Los Alamos, NM, 15-18 Dec. 1993
(Contract W-7405-eng-36)
(DE94-007579; LA-UR-94-563; CONF-931247-8) Avail: CASI HC A01/MF A01

As is well known, the d-wave gap scenario for cuprate superconductors

has strong support from several lines of evidence: (1) evidence for strong gap anisotropy, e.g. the Stanford photoemission data; (2) evidence for gap nodes, e.g. the UBC studies of penetration depth lambda(sub L)(T) at low T(much less than T(sub c)); (3) a pairing interaction based on the strong quasiparticle repulsion at q = (pi,pi), the latter being clearly established from inelastic neutron scattering and NMR data; and, (4) the phenomenological theory also provides a source for the strong (and linear) resistivity. The d-wave gap scenario and theory are, therefore, very plausible. The authors now point out that there is a viable alternative scenario -- a highly anisotropic s-like gap form -- which is also consistent with the evidence just mentioned. This form is supported by additional experimental evidence, and by a qualitative dynamical argument, and also by detailed and nearly ab initio calculations based on a systematic theory. This theory is based on the assumption of strong electronic correlations of the type found in valence-fluctuation and heavy-fermion materials. DOE

N94-32747# Los Alamos National Lab., NM.
QUANTUM FLUCTUATIONS OF VORTICES IN JOSEPHSON-COUPLED SUPERCONDUCTORS
L. N. Bulaevskii and M. P. Maley 1994 19 p Presented at the Superconducting Superlattices and Multilayers and Oxide Superconductory Physics and Nanoengineering, Los Angeles, CA, 23-28 Jan. 1994
(Contract W-7405-eng-36)
(DE94-007609; LA-UR-94-538; CONF-940121-3) Avail: CASI HC A03/MF A01

The effect of quantum fluctuations of vortices on the low temperature specific heat and reversible magnetization in the mixed state in highly anisotropic layered superconductors is discussed. For reversible magnetization, M, the change of slope in the dependence of M vs ln B, observed in Bi(2:2:1:2), is explained. In the mean field approach, this slope should be almost B independent. The specific heat due to the vortex fluctuation contribution is predicted to be linear in T at low T. DOE

N94-32764# Mobil Tyco Solar Energy Corp., Billerica, MA.
THIN EFG OCTAGONS
J. P. Kalejs Mar. 1994 23 p Prepared for Midwest Research Inst., Golden, CO
(Contract DE-AC02-83CH-10093)
(DE94-006855; NREL/TP-411-6399) Avail: CASI HC A03/MF A01

This report describes work to advance the manufacturing line capabilities in crystal growth and laser cutting of Mobil Solar's unique edge-defined film-fed growth (EFG) octagon technology and to reduce the manufacturing costs of 10 cm x 10 cm polycrystalline silicon EFG wafers. The report summarizes the significant technical improvements in EFG technology achieved in the first 6 months of the PVMaT Phase 2 and the success in meeting program milestones. Technical results are reported for each of the three main pregrain areas: Task 5 -- Thin octagon growth (crystal growth) to reduce the thickness of the octagon to 200 microns; Task 6 -- Laser cutting-to improve the laser cutting process so as to produce wafers with decreased laser cutting damage at increased wafer throughput rates; and Task 7 -- Process control and product specification to implement advanced strategies in crystal growth process control and productivity designed to increase wafer yields. DOE

N94-32770 State Univ. of New York, Buffalo.
SUNY BEAMLINE FACILITIES AT THE NATIONAL SYNCHROTRON LIGHT SOURCE
P. Coppens 1993 55 p Limited Reproducibility: More than 20% of this document may be affected by microfiche quality
(Contract DE-FG02-86ER-45231)
(DE94-006343; DOE/ER-45231/8) Avail: Issuing Activity (Department of Energy (DOE))

This document presents information concerning: crystallography (single crystal studies); crystallography (powder diffraction); crystallography (surface structure); exafs and interface studies; and small angle scattering. DOE

N94-32779# Argonne National Lab., IL.
ISOTHERMAL SINTERING, MICROSTRUCTURE, AND SUPERCONDUCTING PROPERTIES OF Y1Ba2Cu3O(7-x) COMPOUND
R. N. Viswanath (Madras Univ., India.), S. Ramasmay (Madras Univ., India.), W. Schaper (Goettingen Univ., Germany.), K. Gehrke (Goettingen Univ., Germany.), and U. Balachandran 1994 42 p
(Contract W-31-109-eng-38)
(DE94-008132; ANL/MCT/PP-72124) Avail: CASI HC A03/MF A01

Polycrystalline YBa2CuO(7-x) was prepared by the solid state reaction method and characterized by x-ray powder diffraction method, Meissner effect, resistivity by the four probe method, and iodometric titrations. The material was processed at 930 C, and isothermal sintering behavior up to 96 was studied using positron lifetime, x-ray powder diffraction (SEM), four probe method for resistivity, and critical current vs magnetic field and differential thermal analysis (DTA). Two types of grain morphology are observed by SEM one below 36 and one above 36 sintering. DTA shows a peak around 954 C. Positron lifetime results reveal that the lifetime values and (tau)(sub 1) and (tau)(sub 2) arise from positron trapping in strained/deformed regions and microvoids formed in the triple defect junctions (TDJ), respectively. The size of the defect responsible for the pinning centers is estimated from positron lifetime data. Reasons for the lesser value of transport J(sub c) (24.72 A/sq cm), obtained in the compound sintered at 930 C are explained. The nature of defects related to the resistivity component in the compound is also discussed. DOE

N94-32785# Oak Ridge National Lab., TN.
PROPERTIES OF DOPED AND UNDOPED (Ca,Sr)CuO2 THIN FILMS
D. P. Norton, B. C. Chakoumakos, J. D. Budai, E. C. Jones, D. K. Christen, and D. H. Lowndes Dec. 1993 22 p Presented at the Electro Technical Laboratory Workshop on High Temperature Superconductors, Tokyo, Japan, 6-10 Dec. 1993
(Contract DE-AC05-84OR-21400)
(DE94-007230; CONF-931257-1) Avail: CASI HC A03/MF A01

The authors have studied the transport and structural properties of (Ca,Sr)CuO2, Sr(1-y)Nd(y)CuO2, and Sr(1-x)CuO(2-(delta)) thin films grown by pulsed-laser deposition. Stoichiometric 'infinite layer' (Ca,Sr)CuO2 thin films grown over a large range of growth conditions are insulators, while superconductivity is observed in Sr(1-y)Nd(y)CuO2 films with (Tc)(onset) (approximately) 28 K for y = 0.10. A Nd solubility limit of y = 0.10 is observed with the appearance of a new phase with c approximately 0.37 nm for y greater than 0.10. In addition, the transport and structural properties of Sr(1-x)CuO(2-(delta)) thin films grown by pulsed-laser deposition support the contention that the tetragonal phase is capable of accommodating a significant density of alkaline-earth deficiencies up to x less than or equal to 0.3. Resistivity measurements indicate a significant change in the carrier density of the CuO2 planes as Sr vacancies are introduced. In addition, an enigmatic anomaly in resistivity at 185 K is observed for Sr(0.85)CuO(2-(delta)) thin films. Magnetic measurements on these samples indicate that, although a significant drop in resistivity at 185 K is observed, it is not due to a superconducting transition. Hall measurements, as well as changes in resistivity with film growth conditions, suggest that the majority carriers in these Sr(1-x)CuO(2-(delta)) thin films are electrons even with the Sr-vacancies present. DOE

N94-32799# Washington Univ., Seattle.
NEAR EDGE X RAY SPECTROSCOPY THEORY
1994 9 p
(Contract DE-FG06-90ER-45415)
(DE94-008179; DOE/ER-45415/T1) Avail: CASI HC A02/MF A01

We propose to develop a quantitative theory of x-ray spectroscopies in the near edge region, within about 100 eV of threshold. These spectroscopies include XAFS (x-ray absorption fine structure), photoelectron diffraction (PD), and diffraction anomalous fine structure (DAFS), all of which are important tools for structural studies using synchrotron radiation x-ray sources. Of primary importance in these studies are many-body effects, such as the photoelectron self-energy, and inelastic losses. A better understanding of these quantities is needed to obtain theories without adjustable parameters. We propose both analytical and numerical calculations, the latter based on our x-ray spectroscopy codes FEFF. DOE

N94-32815# Argonne National Lab., IL.
NEW ADVANCES IN THE MODELING OF HIGH-TEMPERATURE SUPERCONDUCTORS
L. Freitag, P. Plassmann, and M. Jones 1994 7 p Presented at the 1994 Society for Computer Simulation Multiconference, San Diego, CA, 11-15 Apr. 1994

(Contract W-31-109-eng-38)
(DE94-007649; ANL/MCS/CP-82091; CONF-940456-13) Avail: CASI HC A02/MF A01

In this paper, we present a new discrete formulation that maintains discrete invariance and is suitable for use on nonorthogonal meshes. This formulation, unlike its predecessors, allows us to easily use adaptive mesh refinement to concentrate grid points where error contributions are large (near vortex centers). In this way we reduce the total number of grid points required to accurately capture vortex configurations and allow the possibility of solving problems previously considered intractable. To solve these large problems, we require the memory capabilities and computational power of state-of-the-art parallel computers. To use these machines, we have developed scalable libraries for adaptive mesh refinement and partitioning on two-dimensional triangular grids. This general-purpose software uses bisection of the longest side to refine triangles in which error contributions are large. These adaptive meshes are both unstructured and dynamic, and we present a new geometric partitioning, algorithm that strives to minimize communication cost by ensuring good partition aspect ratios. We present computational results showing the efficiency of these adaptive techniques for a superconductivity application. DOE

N94-32822# Brookhaven National Lab., Upton, NY.
RESISTIVITY MEASUREMENTS ON THE NEUTRON IRRADIATED DETECTOR GRADE SILICON MATERIALS
Zheng Li Nov. 1993 14 p Presented at the 1st International Conference on Large Scale Applications and Radiation Hardness of Semiconductor Detectors, Florence, Italy, 7-9 Jul. 1993
(Contract DE-AC02-76CH-00016)
(DE94-009083; BNL-49822; CONF-9307163-2) Avail: CASI HC A03/MF A01

Resistivity measurements under the condition of no or low electrical field (electrical neutral bulk (ENB) condition) were made on various device configurations on detector grade silicon materials after neutron irradiation. Results of the measurements have shown that the ENB resistivity increases with neutron fluence ((Phi)(sub n)) at low (phi)(sub n) (less than 10(exp 13) n/sq cm) and saturates at a value between 300 and 400 k(Omega)-cm at (phi)(sub n) approximately 10(exp 13) n/sq cm. Meanwhile, the effective doping concentration N(sub eff) in the space charge region (SCR) obtained from the C-V measurements of fully depleted p(sup +)/n silicon junction detectors was found to increase nearly linearly with (phi)(sub n) at high fluences ((phi)(sub n) greater than 10(exp 13) n/sq cm). The experimental results are explained by the deep levels crossing the Fermi level in the SCR and near perfect compensation in the ENB by all deep levels, resulting in N(sub eff) (SCR) nearly equal n or p (free carrier concentrations in the ENB). DOE

N94-32843# Argonne National Lab., IL.
ULTRAHIGH-CURRENT-DENSITY METAL-ION IMPLANTATION AND DIAMONDLIKE-HYDROCARBON FILMS FOR TRIBOLOGICAL APPLICATIONS
P. J. Wilbur (Colorado State Univ., Fort Collins.) Sep. 1993 56 p
(Contract W-31-109-eng-38)
(DE94-008958; ANL/OTM/CR-4) Avail: CASI HC A04/MF A01

The metal-ion-implantation system used to implant metals into substrates are described. The metal vapor required for operation is supplied by drawing sufficient electron current from the plasma discharge to an anode-potential crucible so a solid, pure metal placed in the crucible will be heated to the point of vaporization. The ion-producing, plasma discharge is initiated within a graphite-ion-source body, which operates at high temperature, by using an argon flow that is turned off once the metal vapor is present. Extraction of ion beams several cm in diameter at current densities ranging to several hundred micro-A/sq cm on a target 50 cm downstream of the ion source were demonstrated using Mg, Ag, Cr, Cu, Si, Ti, V, B, and Zr. These metals were implanted into over 100 substrates (discs, pins, flats, wires). A model describing thermal stresses induced in materials (e.g. ceramic plates) during high-current-density implantation is presented. Tribological and microstructural characteristics of iron and 304-stainless-steel samples implanted with Ti or B are examined. Diamondlike-hydrocarbon coatings were applied to steel surfaces and found to exhibit good tribological performance. DOE

N94-32875 Argonne National Lab., IL.
ELECTRON ENERGY DEPENDENCE OF AMORPHIZATION IN Zr3Fe
A. T. Motta (Pennsylvania State Univ., University Park.), L. M. Howe (Atomic Energy of Canada Ltd., Chalk River, Ontario.), and P. R. Okamoto Feb. 1994 7 p Presented at the Fall Meeting of the Materials Research Society (MRS), Boston, MA, 29 Nov. - 3 Dec. 1993 Limited Reproducibility: More than 20% of this document may be affected by microfiche quality
(Contract W-31-109-eng-38)
(DE94-008459; ANL/MSD/CP-82234; CONF-931108-93) Avail: CASI HC A02

This paper reports the results from a study conducted to determine the effect of electron energy on the dose-to-amorphization of Zr3Fe at 23-30 K. Zr3Fe samples were irradiated in the HVEM at Argonne National Laboratory, at 200 to 900 keV. Amorphization occurred at electron energies from 900 keV down to 250 keV. Three distinct regions were observed: between 900 and 700 key amorphization occurred at a constant low dose of approximately 4 x 10(exp 21) e cm(exp -2); a higher plateau at 10(exp 22) was observed between 600 and 400 keV, and finally there was a sharp increase in the dose-to-amorphization below 400 key, so that at 250 key the necessary dose was an order of magnitude higher than that at 900 keV. In the region below 400 keV there was evidence of a dependence of the dose-to-amorphization on the orientation of the sample with respect to the electron beam. The results can be analyzed in terms of a composite displacement cross section dominated at high energies by displacements of Zr and Fe atoms, by displacements of Fe atoms at intermediate energies and of secondary displacements of lattice atoms by recoil impurities at low energies. DOE

N94-32884 Lawrence Livermore National Lab., CA.
INTERFACE CONTROLLED AMORPHIZATION OF CRYSTALLINE Ni/Ti MULTILAYERS
A. F. Jankowski, J. P. Hayes, and P. B. Ramsey Dec. 1993 6 p Presented at the Fall Meeting of the Materials Research Society (MRS), Boston, MA, 29 Nov. - 3 Dec. 1993 Limited Reproducibility: More than 20% of this document may be affected by microfiche quality
(Contract W-7405-eng-48)
(DE94-008685; UCRL-JC-114168; CONF-931108-95) Avail: CASI HC A02

Solid-state amorphization (SSA) of crystalline interfaces is observed in the Ni/Ti multilayer system. The amorphization reaction nucleates at location(s) of crystallographic disorder, i.e. the multilayer interfaces. Microstructural analyses reveal the sputter-deposited growth structure to be epitaxial with semicoherent interfaces. Strain energy originating from interface lattice distortions varies as a function of the multilayer repeat spacing. Therefore, the interfacial energy effects the onset conditions for SSA. Differential thermal analysis is used to measure the critical temperature T(sub c) to the nucleation of the SSA, which is found to vary with the Ni/Ti multilayer pair spacing. DOE

N94-32908 Technische Univ., Munich (Germany).
THE 6TH INTERNATIONAL CONFERENCE ON MODULATED SEMICONDUCTOR STRUCTURES
27 Aug. 1993 570 p Conference held in Garmisch-Partenkirchen, Germany, 23-27 Aug. 1993 Limited Reproducibility: More than 20% of this document may be affected by microfiche quality
(Contract DAJA45-93-M-0294)
(AD-A276815; R/D-7125-EE-02) Avail: CASI HC A24

This workbook contains unreferred manuscripts of papers which will be presented at conference. The topics covered include the following: growth of wires and dots; transport properties in low dimensional systems; growth characterization transport; growth characterization and phonons; quantum wells -- electrical properties; vertical transport -- resonant tunneling; quantum wells, superlattices -- optical properties; metal/semiconductors and type 2 interfaces; atomic scale characterization; electronic excitation -- superlattices; and optical properties. DTIC

N94-32913# Los Alamos National Lab., NM.
PROCEEDINGS, STRONGLY CORRELATED ELECTRONIC MATERIALS: THE 1993 LOS ALAMOS SYMPOSIUM
K. S. Bedell 1994 662 p Proceedings held in Los Alamos, NM, 15-18 Dec. 1993

(Contract W-7405-eng-36)
(DE94-009293; LA-UR-94-1148; CONF-931247) Avail: CASI HC A99/MF A06

The subject included such topics as high temperature superconductors, heavy-fermion insulators and superconductors, the metal-insulator transition, the superconductor-insulator transition and unusual (non-Fermi liquid) normal metallic states. The symposium was structured around 13 invited review talks; with each talk, there were several (about 30) related short presentations and discussion sections (90 pages). The review talks and short papers were processed separately for the data base. DOE

N94-32933# California Univ., San Diego, La Jolla.
INVESTIGATION OF SUPERCONDUCTIVITY AND MAGNETISM IN d AND f-ELECTRON MATERIALS
1993 17 p
(Contract DE-FG03-86ER-45230)
(DE94-008535; DOE/ER-45230/T2) Avail: CASI HC A03/MF A01

Emphasis has been on high (Tc) cuprate superconductors, along with some experiments on heavy fermion materials. Approach involved the preparation of novel materials, including high (Tc) oxide and rare earth and uranium intermetallic compounds in polycrystals and single crystals, and the investigation of transport, thermal, and magnetic properties of these materials down to 50 mK, in magnetic fields up to 10 tesla, and pressures up to 160 kbar. Other measurements, such as neutron scattering, micro-SR, and photoemission, are carried out at national facilities. DOE

N94-32934 Lawrence Livermore National Lab., CA.
IMAGING OF SURFACE STRUCTURE WITH ENERGY-DEPENDENT PHOTOELECTRON DIFFRACTION
J. G. Tobin, G. D. Waddill, Hua Li, and S. Y. Tong Aug. 1993 10 p Presented at the 4th International Conference on the Structure of Surfaces, Shanghai, China, 16-19 Aug. 1993 Limited Reproducibility: More than 20% of this document may be affected by microfiche quality
(Contract W-7405-eng-48)
(DE94-009096; UCRL-JC-112889; CONF-9308154-4) Avail: Issuing Activity (Department of Energy (DOE))

Energy-dependent photoelectron diffraction (EDPD) has been used to determine the surface structure of a surface alloy. Direct imaging has been achieved by Fourier transformation of experimental energy-dependent photoelectron diffraction data. This holographic method, based upon the intersection of contour arcs associated with each measurement direction, can provide vectorial atomic positions with atomic resolution. Experimental analysis is supported by Fourier transformation of simulations from multiple scattering calculations. The surface geometry of c(2x2) Au/Cu(001) has been imaged in an elementally-specific manner, with clear, non-model-dependent discrimination of the surface alloy over the overlayer structure. DOE

N94-32944# Los Alamos National Lab., NM.
EVIDENCE FOR SYMMETRY BREAKING LOCAL DISTORTIONS IN THALLIUM BARIUM COPPER OXIDE
Janis H. Nickel, Patrick G. Allen, Guonguang Li, Jose MustredeLeon, Ian D. Raistrick, and Steven D. Conradson 1994 5 p Presented at the Strongly Correlated Electron Materials, Los Alamos, NM, 15-18 Dec. 1993
(Contract W-7405-eng-36)
(DE94-006149; LA-UR-94-343; CONF-931247-9) Avail: CASI HC A01/MF A01

Extended x-ray absorption fine structure (EXAFS) show local structural anomalies in Tl2Ba2CuO6, which reduce the crystal symmetry; this symmetry lowering is interpreted as an indication of the existence of localized states. A local structural model consistent with the EXAFS results consists of a fraction of the O(1) sites displaced from the midpoint of the Cu-Cu bond, and dimpling of the CuO2 planes when the O(1) site is not displaced from this midpoint. DOE

N94-32963 Sandia National Labs., Albuquerque, NM.
OPTICAL PROPERTIES OF LANTHANIDE-DOPED RbTiOAsO4 AND TRANSITION METAL-DOPED KTiOPO4
M. L. F. Phillips, M. T. Anderson, and M. B. Sinclair 1993 24 p Presented at the LASERS 1993: International Conference on Lasers and Applications, Lake Tahoe, NV, 6-10 Dec. 1993 Limited Reproducibility: More than 20% of this document may be affected by microfiche quality
(Contract DE-AC04-94AL-85000)
(DE94-008433; SAND-93-2112C; CONF-931237-7) Avail: CASI HC A03

We have synthesized derivatives of potassium titanyl phosphate (KTP) and rubidium titanyl (RTA) where Ti was replaced by transition metal or lanthanide ions, and K, Ti, P, or O was replaced by aliovalent counterions. Up to 5 mol % lanthanide ion can be substituted onto the Ti, and 100 mol % substitution of other transition metals onto the Ti sites in KTP can be made. The visible spectra of these doped KTP phases are characteristic of the dopant ions, with sharp, narrow transitions resulting from lanthanide substitution and broader absorptions from transition-metal dopants. Powder second harmonic generation (SHG) intensities diminish with increased dopant concentration. Decreases in SHG intensities parallel those seen in previously studied systems. The choice of counterion substantially impacts some dopant solubilities, but generally affects SHG intensity and visible spectrum to a lesser degree. Single crystals doped with Er(3+), Fe(3+), and Co(2+) have linear absorption coefficients in the range of 1 to 5 cm(exp -1). Changes in noncritical phase matching wavelength due to anomalous dispersion are calculated to be less than 1 nm at the dopant levels tested. DOE

N94-32988# Stanford Univ., CA. Dept. of Electrical Engineering.
SUPERCONDUCTING AND SEMICONDUCTING HYBRIDS AND ADVANCE MEMORY CONCEPTS FOR SUPERCONDUCTING ELECTRONICS Annual Report, 1 May 1993 - 30 Apr. 1994
M. R. Beasley and M. Horowitz 29 Mar. 1994 5 p
(Contract N00014-92-J-1886)
(AD-A277766) Avail: CASI HC A01/MF A01

The goal of this program is to explore advance alternatives to the standard approaches to memory in Josephson junction digital electronics. The work includes the systems, circuits, and materials aspects of the problem. DTIC

N94-32989# Argonne National Lab., IL.
MICROREFLECTANCE INFRARED STUDY OF ELECTRON-MOLECULAR VIBRATIONAL COUPLING AND LATTICE SOFTNESS IN BEDT-TTF SALTS
J. R. Ferraro (North Carolina State Univ., Raleigh.), Myung-Hwan Whangbo (North Carolina State Univ., Raleigh.), H. H. Wang, and P. Stout 1994 25 p
(Contracts W-31-109-eng-38; DE-FG05-86ER-45259)
(DE94-008490; ANL/CHM/PP-74824) Avail: CASI HC A03/MF A01

Microreflectance infrared (MR-IR) spectra were obtained for several (beta)- and (kappa)-phase salts of bis- (ethylenedithio) tetrathiafulvalene (BEDT-TTF or ET) and its deuterium analog d(sub 8)-ET by employing polarized and unpolarized light. The vibronic region of these MR-IR spectra provides information about the electron-molecular vibration (EMV) coupling, and the highest-frequency C-C-H bending vibration observed for an ET salt reflects the extent of its lattice softness. Under polarized light, the EMV coupling for an ET salt depends strongly upon how the light polarization vector is aligned with respect to the sample crystallographic axes. The lowest vibron frequency is indicative of increased EMV coupling. DOE

N94-32990 Argonne National Lab., IL.
CHARACTERIZATION OF NANOPARTICLES AND NANOPHASE MATERIALS
R. W. Siegel Feb. 1994 15 p Presented at the European Science Foundation (ESF) Explorative Workshop: Aerosol Methods and Advanced Techniques for Nanoparticle Science and Nanopowder Technology, Duisburg, Germany, 4-9 Oct. 1993 Limited Reproducibility: More than 20% of this document may be affected by microfiche quality
(Contract W-31-109-eng-38)
(DE94-008348; ANL/MSD/CP-80658; CONF-9310287-1) Avail: Issuing Activity (Department of Energy (DOE))

Structures of nanoparticles and nanophase materials, both metals and ceramics, have been investigated over the past several years by a wide range of experimental methods. These studies included observations by the following: x-ray and neutron scattering; transmission and scanning electron microscopy; Moessbauer, Raman, and positron annihilation spectroscopies; and most recently scanning tunneling microscopy and nuclear magnetic resonance. These experiments yielded considerable information about the structures of nanoparticles and nanophase materials

on a variety of length scales, but much about the local atomic arrangements in these new materials remains to be elucidated. Present status of our knowledge of these structures is reviewed and some future needs are considered. DOE

N94-32991# Stanford Univ., CA.
A QUEST FOR A NEW SUPERCONDUCTING STATE
J. P. Collman and W. A. Little 1993 9 p
(Contract DE-FG03-86ER-45245)
(DE94-008439; DOE/ER-45245/T2) Avail: CASI HC A02/MF A01

The authors report on their progress during the past twelve months and the work that is planned for the coming year. They have been working on a theory to describe the long range proximity effect discovered experimentally on Bi-Ag-Tl(2223) sandwiches during the period of the previous grant. This has led to the prediction of a novel effect which they refer to as a 'pair echo' which occurs in these sandwiches and is analogous to the familiar 'spin echo' seen in certain NMR experiments. Experimentally, they have extended the measurements of the proximity effect to lower temperatures and to other superconductors. They have completed high resolution studies of the thermal difference optical reflectance of the high (T(sub c)) superconductor Tl(2223), for temperatures both above and below the transition temperature, over a photon energy range from 0.3 eV to 5.3 eV. A striking anomaly in this thermal difference spectrum was found near 1.6 eV, which appears below (T(sub c)) and scales in magnitude with temperature like (Delta)(T)(sup 2) where (Delta)(T) is a BCS gap. This is precisely the kind of effect which they had hoped to find, based on a Holstein-like mechanism in these materials, and which they had predicted in a paper on 'Gap Modulation'. The proper interpretation of the effect observed should reveal the mechanism responsible for the superconductivity of the cuprates. They have completed a search for the so-called Zhang-modes in the above high (T(sub c)) superconductor Tl(2223) over the same energy range, 0.3 eV to 5.3 eV. These modes are predicted to exist if the proper description of the ground state of the system is that of a Hubbard model. DOE

N94-33005# Conductus, Inc., Sunnyvale, CA.
YBCO JOSEPHSON JUNCTION ARRAYS Final Report, 15 Jul. 1992 - 14 Jul. 1993
Randy Simon 14 Jul. 1993 29 p
(Contract F49620-92-C-0048)
(AD-A277426; AFOSR-94-0075TR) Avail: CASI HC A03/MF A01

Josephson junction arrays have long been suggested as efficient, tunable sources for upper microwave and mm-wave frequencies. Based on the fundamental properties of the junction and the ability to combine the power output of many junctions using an array, the circuit concept is quite promising. The challenge is to phase lock the junctions so that power adds coherently and a number of demonstrations with Nb junction arrays have been performed doing this. This program was intended to begin using YBCO junction arrays to demonstrate source potential at 77 K. Edge junctions have been used in arrays with up to 60000 junctions and the ability to couple power off-chip has been demonstrated directly for frequencies of at least 70-160 GHz. Power outputs have approached 1 micro W (in relatively narrow bands) and tunability has exceeded 20 GHz. Some novel array architectures have been built, including one with improved linewidth per unit junction, and new techniques developed for extracting junction statistics from array spectra. These techniques are used as feedback for process optimizations now in progress. DTIC

N94-33039# Wisconsin Univ., Madison. Dept. of Physics.
LOW ENERGY ION BEAM ASSISTED GROWTH OF HOMOEPITAXIAL SILICON FILMS AT LOW TEMPERATURE Final Report, 1 Mar. 1993 - 28 Feb. 1994
Kim W. Pierson 28 Feb. 1994 4 p
(Contract N00014-93-1-0195)
(AD-A278092) Avail: CASI HC A01/MF A01

The goal of this project was to lower the substrate temperature required to promote device quality epitaxial silicon growth below the 300 C mark set by a Japanese group led by T. Ohmi. Normally high substrate temperatures are required to achieve thin film epitaxial growth. A new thin film deposition technique called ion beam assisted deposition offers the possibility to grow epitaxial layers at low substrate temperatures. In this technique, while the atoms are condensing into the epilayer, they are bombarded by low energy noble gas ions. The kinetic energy of the incident ions supplants the thermal energy lost by lowering the substrate temperature and provides enough surface mobility so that the correct crystal structure can grow. Lower temperatures will reduce impurity and interlayer diffusion problems caused by high temperature growth processing steps. DTIC

N94-33055# Materials Research Society, Pittsburg, PA.
RARE EARTH DOPED SEMICONDUCTORS AND MATERIALS RESEARCH SOCIETY SYMPOSIUM PROCEEDINGS, VOLUME 301 Final Report, 5 Feb. 1993 - 4 Feb. 1994
John Ballance 4 Feb. 1994 432 p Proceedings held in San Francisco, CA, 13-15 Apr. 1993
(Contract F49620-93-1-0156)
(AD-A277517; AFOSR-94-0042TR) Avail: CASI HC A19/MF A04

The properties of rare earth ions in solids were studied in detail for decades, but until recently this work was restricted to dominantly ionic hosts such as fluorides and oxides, and to a lesser extent to more covalently bonded hosts, such as tetrahedral 2-6 semiconductors. The idea of rare earth elements incorporated into covalent semiconductors such as GaAs and Si may be traced to a short communication in 1963 by R.L. Bell (J. Appl. Phys. 34, 1563 (1963)) proposing a dc-pumped rare earth laser. At about the same time, three unpublished technical reports appeared as a result of U.S. Department of Defense sponsored research in rare earth doped Si, GaAs, and InP to fabricate LED's. Attempts by other researchers to identify sharp 4f specific emissions in these hosts essentially failed. DTIC

N94-33246 Conductus, Inc., Sunnyvale, CA.
HIGH TEMPERATURE SUPERCONDUCTING JOSEPHSON JUNCTION ARRAY SYSTEMS, PHASE 1 Final Report, 1 Jul. - 31 Dec. 1993
J. Martens, A. Pance, K. Char, M. Johansson, and S. Whiteley 25 Jan. 1994 29 p Limited Reproducibility: More than 20% of this document may be affected by microfiche quality
(Contract F49620-93-C-0041)
(AD-A277937; Rept-94001-SBIR-1-F; AFOSR-94-0132TR) Avail: CASI HC A03

High temperature superconducting Josephson arrays were investigated as possible millimeter wave sources. A junction technology was selected and improved to the point where radiation, near 1 microwatt off-chip, was measured from a variety of 2-dimensional arrays in the 70-160 GHz range. The arrays were tunable and were successfully coupled to a number of antennas for broadband, tunable transmission. Antennas for a variety of specific applications were selected on the basis of bandwidth requirements, impedance levels, polarization, and the possibility of sufficient monolithic integration. The final part of the program was a study of potential subsystems that would utilize these arrays. Interchip communications transceivers were studied and interchip coupling was demonstrated using two antenna-coupled arrays. The most promising application may be a monolithic clock source, near 100 GHz, for communications and signal processing systems. DTIC

N94-33248# Rockwell International Corp., Thousand Oaks, CA. Science Center.
QUANTUM WELL INFRARED PHOTODETECTOR FPA Final Report, 1 Sep. 1991 - 28 Feb. 1993
L. Kozlowski Mar. 1994 76 p
(Contract N00014-91-C-0163)
(AD-A278010; SC71061.FR) Avail: CASI HC A05/MF A01

The AT&T/Rockwell team met all the objectives of this collaborative program; AT&T supplied the QWIP detector arrays and Rockwell subsequently fabricated hybrid focal plane arrays using available high performance CMOS multiplexers, tested the hybrids, performed breadboard imaging demonstrations and delivered several hybrid FPA's. Eighteen hybrids were fabricated and evaluated. The collaboration yielded significant improvements in QWIP FPA performance and reliability and many milestones including: first BLIP LWIR FPA sensitivity demonstration at low photon backgrounds (less than 1 x 10(exp 12) photons/sq cm-sec) with the GaAs-based quantum well infrared photodetector (QWIP) technology, high LWIR FPA pixel operability; NE Delta T's as low as 5 mK at LWIR imaging backgrounds at f/1.4 and temperatures consistent with mechanical coolers (approx. 65K), increased coupling efficiency by over an order of magnitude; achieved effective quantum efficiency of approx. 10% with low crosstalk; effective quantum efficiencies of up to 30% under flood illumination, though

with high crosstalk; mean D* of 1 x10(exp 14) cm-Hz(exp 1/2)/W at 3.0 x 10(exp 9) photons/sq cm-sec background at 32.5K operating temperature with greater than 98% operability; maximum temperature for 9.5 microns m FPA BLIP sensitivity as high as 62K; excellent hybrid reliability by mechanically thinning the QWIP; and responsivity nonuniformity less than 3% rms, thus enabling greater than 83 dB dynamic range. DTIC

N94-33271# Oak Ridge National Lab., TN.
THE PATH FOR LONG RANGE CONDUCTION IN HIGH J(SUB c) TlBa2Ca2Cu3O(8+x) SPRAY-PYROLYZED DEPOSITS
D. M. Kroeger, A. Goyal, E. D. Specht, Z. L. Wang, J. E. Tkaczyk, J. A. Sutliff, and J. A. DeLuca 1993 9 p Presented at the Fall Meeting of the Minerals, Metals and Materials Society: Physical Metallurgy and Materials, Pittsburgh, PA, 17-21 Oct. 1993
(Contract DE-AC05-84OR-21400)
(DE94-007211; CONF-931009-20) Avail: CASI HC A02/MF A01

Grain boundary misorientations and local texture in polycrystalline TlBa2Ca2Cu3O(8+x) deposits prepared by thallination of spray-pyrolyzed precursor deposits on yttria-stabilized zirconia have been determined from transmission electron microscopy, electron backscatter diffraction patterns, and x ray diffraction. The deposits were polycrystalline, had small grains, and excellent c-axis alignment. The deposits contained colonies of grains with similar but not identical a-axis orientations. Most grain boundaries within a colony have small misorientation angles and should not be weak links. It is proposed that long range current flow occurs through a percolative network of small angle grain boundaries at colony intersections. DOE

N94-33273 Purdue Univ., West Lafayette, IN. Dept. of Chemistry.
SENSITIVITY OF ELECTROCHEMICAL ADLAYER STRUCTURE TO THE METAL CRYSTALLOGRAPHIC ORIENTATION: POTENTIAL-INDEPENDENT IODIDE ADSORPTION ON Au(100) IN COMPARISON WITH OTHER LOW-INDEX SURFACES
Xiaoping Gao, Gregory J. Edens, Fan-Chen Liu, and Michael J. Weaver Feb. 1994 43 p Limited Reproducibility: More than 20% of this document may be affected by microfiche quality
(Contract N00014-91-J-1409)
(AD-A276714; TR-153) Avail: CASI HC A03

The potential-dependent ordered atomic structures formed for iodide adsorption on Au(100) from dilute aqueous alkali iodide electrolytes as discerned by means of in-situ scanning tunneling microscopy (STM) are reported and compared to the corresponding behavior of the other two low-index faces, Au(111) and (110). As in related studies, emphasis is placed on linking the microscopic structural information to the voltammetric and other macroscopic electrochemical response including the use of 'potentiodynamic' STM tactics where real-space images are acquired during appropriate electrode potential steps or sweeps. While relatively low iodide coverages, theta(sub I) approximately equal to 0.1, are sufficient to lift the hexagonal Au(100) reconstruction, yielding large ordered (1 x 1) domains by ca-0.6 V vs SCE, ordered iodide adlayers are formed only above -0.2 V. A compressible incommensurate (2 sq rt 2 x p sq rt 2) phase (theta(sub I) approximately equal to 0.46 - 0.49) is observed between ca -0.2 and 0 V, which reverts to a distinct (2 sq rt of 2 x sq rt of 2)R45 deg structure (theta(sub I) approximately equal to 0.5) featuring uniform binding in twofold bridging sites. Interestingly, while the latter structure is retained locally at higher potentials, it is interspersed with narrow (3-4 atom wide) strips having a rotated hexagonal pattern. The latter becomes increasingly dense, and eventually dominant, towards higher potentials. This microscopically nonuniform (or spatially modulated) phase is noteworthy as well as unusual; the corresponding iodine phases on Au(111) and (110) display, as is common, structural uniformity at a given potential. DTIC

N94-33274# Purdue Univ., West Lafayette, IN. Dept. of Chemistry.
SCANNING TUNNELING MICROSCOPY AND INFRARED SPECTROSCOPY AS COMBINED IN-SITU PROBES OF ELECTROCHEMICAL ADLAYER STRUCTURE: CYANIDE ON Pt(111)
Christopher Stuhlmann, Ignacio Villegas, and Michael J. Weaver Feb. 1994 17 p
(Contract N00014-91-J-1409)
(AD-A276715; TR-147) Avail: CASI HC A03/MF A01

The spatial structure of irreversibly adsorbed cyanide adlayers on a Pt(111) electrode is deduced by means of in-situ scanning tunneling microscopy (STM) combined with infrared reflection-absorption spectroscopy (IRAS). The latter data suggests atop-like Pt-CN coordination. The STM images display a (2 sq rt of 3 x 2 sq rt of 3)R30 degree-7CN structure, with cyanides bound in symmetric atop sites surrounded by hexagonal clusters of CN, likely bound in near-atop sites. This arrangement, stable over the applied potential range -0.5 to 0 V vs SCE, gives way to a (2 x 2) structure and disordered adlayers at lower potentials. These findings are compared with previous structural information deduced from ex-situ electron diffraction. DTIC

N94-33275# Purdue Univ., West Lafayette, IN. Dept. of Chemistry.
NANOSCALE STRUCTURAL CHANGES UPON ELECTROOXIDATION OF Au(111) AS PROBED BY POTENTIODYNAMIC SCANNING TUNNELING MICROSCOPY
Xiaoping Gao and Michael J. Weaver Feb. 1994 15 p
(Contract N00014-91-J-1409)
(AD-A276780; TR-146) Avail: CASI HC A03/MF A01

Understanding the surface structural changes associated with, and resulting from, the electrochemical formation and removal of oxide films is of broadbased practical as well as fundamental importance. These reports chiefly involve STM imaging at a series of fixed potentials, either before and after voltammetric formation and removal of oxide layers, or additionally at suitable high electrode potentials so that surface oxide is present. Evident are several characteristic oxide-induced changes in surface morphology, including the formation of monolayer pits and related metal corrosion, disordering, and roughening. Of the unanswered questions, a central issue concerns the links between surface structural changes and the much discussed voltammetric features for the initial oxidation of ordered gold electrodes. DTIC

N94-33324# Crystal Systems, Inc., Salem, MA.
DEVELOPMENT OF MATERIALS FOR SPECTRAL HOLE BURNING APPLICATIONS Final Report, 16 Jun. 1993 - 15 Feb. 1994
Chandra P. Khattak, John A. Lesiczka, and Frederick Schmid 28 Feb. 1994 27 p
(Contract F49620-93-C-0035)
(AD-A278408; AFOSR-94-0242TR) Avail: CASI HC A03/MF A01

It was intended to evaluate growth of europium-doped yttrium aluminum oxide (Eu:Y3Al5O12, Eu:YAG) and europium-doped yttrium silicate (Eu:Y2SiO5, Eu:YSO) crystals to characterize these crystals for spectral hole burning application. After technical discussions at a topical workshop and agreement of the Technical Monitor, the scope of the program was enlarged to include growth of rare-earth doped mixed-oxide crystals and growth of Eu:YSO was de-emphasized as these crystals were available for characterization. The experimental effort involved producing YAG, YSO, and YAlO3 (YALO) host crystals and the dopants Eu, Tm, Tb, and Ce. High optical quality crystals of Eu:YAG, Tm:YAG, Tb:YAG, and Ce:YAG were fabricated from 6 cm diameter boules grown using the heat exchanger method (HEM). The samples were characterized for absorption as a function of wavelength at SRI International, Menlo Park, CA. Previously grown Ce:Gd3Sc2Al3O12 (Ce:GSAG) crystal was also characterized. The available data is insufficient for choosing a crystal for spectral hole burning application. It is necessary to explore other rare-earth doped mixed oxide crystals and carry out more characterization. DTIC

N94-33328# Stanford Univ., CA. Dept. of Electrical Engineering.
ELECTRICAL CHARACTERISTICS OF GaAs MESFET FABRICATION BY ION IMPLANTATION OF SI OR Se Final Report, 5 Jul. 1989 - 4 Oct. 1993
T. W. Sigmon 4 Oct. 1993 102 p
(Contract F49620-89-C-0094; ARPA Order 6860)
(AD-A278416; AFOSR-94-0228TR) Avail: CASI HC A06/MF A02

Since its synthesis in the 1920s by Goldschmidt, gallium arsenide has received much attention in the last few decades. In the mid-1980s, GaAs technology finally matured into the age of production. We saw a boom of companies dedicated to the growth of GaAs materials and the fabrication of GaAs devices and integrated circuits. Although GaAs is no longer being considered a general purpose material like silicon, it is now well established in several niche markets, such as direct broadcast satellite, microwave monolithic integrated circuits, and optoelectronics. DTIC

N94-33332 Pennsylvania State Univ., University Park. Dept. of Materials Science and Engineering.
MICROSTRUCTURES AND EPITAXY IN OXIDE SUPERCONDUCTOR THIN FILMS AND DEVICES Final Report, 1 Feb. 1992 - 31 Jan. 1994
Altaf H. Carim 1 Mar. 1994 17 p Limited Reproducibility: More than 20% of this document may be affected by microfiche quality
(Contract F49620-92-J-0159)
(AD-A278427; AFOSR-94-0191TR) Avail: Issuing Activity (Defense Technical Information Center (DTIC))

This report summarizes the work performed at the Pennsylvania State University (PSU) and the Westinghouse Science and Technology Center (WSTC) under the project entitled 'Microstructure and Epitaxy in Oxide Superconductor Thin Films and Devices,' AFOSR Grant F49620-92-J-0159. The total period of the project was 1 Feb. 1992 - 31 Jan. 1994. Results over the first year of the award, 1 Feb. 1992 - 31 Jan. 1993, were summarized in the annual (interim) report submitted earlier. The present document will therefore focus on the more recent activities during the second year of the project. DTIC

N94-33355 Johns Hopkins Univ., Baltimore, MD. Dept. of Electrical and Computer Engineering.
MATERIAL ENGINEERING OF THE NOVEL SEMICONDUCTOR STRUCTURES Final Report, 15 Feb. 1991 - 14 Feb. 1994
Jacob Khurgin 14 Feb. 1994 8 p Limited Reproducibility: More than 20% of this document may be affected by microfiche quality
(Grant AF-AFOSR-0183-91)
(AD-A278386; AFOSR-94-0230TR) Avail: CASI HC A02

Using photoluminescence (PL) excitation spectroscopy we measured trapping times and recombination times in stepped QW's and coupled QW's and related the results to the wavefunction/interface overlaps. Continuous wave PL excitation spectra of multiple narrow-stepped QW's at room temperature have been measured for the first time. It has been observed that PL intensity increases stronger than as a square of the excitation intensity, and we have attributed this phenomenon to the intricate blend of the radiative recombination between free carriers with the nonradiative recombination on the saturable interface traps. Using the CW PL data only, we have managed to measure both the trapping efficiency and ratio between electron and hole radiative and nonradiative decay times. The result of this research were published in the two separate articles in the Applied Physics Letters 2,4,8 and presented at international conferences 11-13. DTIC

77 THERMODYNAMICS AND STATISTICAL PHYSICS

Includes quantum mechanics; theoretical physics; and Bose and Fermi statistics.

For related information see also *25 Inorganic and Physical Chemistry* and *34 Fluid Mechanics and Heat Transfer.*

N94-31052 International Centre for Theoretical Physics, Trieste (Italy).
TOPOLOGICAL CONFORMAL ALGEBRA IN 2D GRAVITY COUPLED TO MINIMAL MATTER
S. Panda (Mehta Research Inst. of Mathematics and Mathematical Physics, Allahabad, India.) and S. Roy Sep. 1993 7 p Limited Reproducibility: More than 20% of this document may be affected by microfiche quality
(DE94-608122; IC-93/307) Avail: CASI HC A02 (US Sales Only)

An infinite number of topological conformal algebras with varying central charges are explicitly shown to be present in 2d gravity (treated both in the conformal gauge and in the light-cone gauge) coupled to minimal matter. The central charges of the underlying N = 2 theory in two different gauge choices are generically found to be different. The physical states in these theories are briefly discussed in the light of the N = 2 superconformal symmetry. DOE

N94-31054# Wisconsin Univ., Madison. Dept. of Materials Science and Engineering.
SOLIDIFICATION STRUCTURE SYNTHESIS IN UNDERCOOLED LIQUIDS Final Report, 11 Dec. 1989 - 30 Jun. 1993
J. H. Perepezko 18 Oct. 1993 95 p
(Contract DAAL03-90-G-0042)
(AD-A276166; ARO-27472.6-MS) Avail: CASI HC A05/MF A01

The undercooling of liquid metals is a fairly common observation, but the amount of undercooling is usually limited by the action of heterogeneous catalysts. When a liquid is subdivided into a fine droplet dispersion in order to isolate nucleation catalysis, substantial undercooling may be observed before the onset of solidification, as demonstrated by the increased undercooling limits established in the current work. At high undercooling, the solidification of alloys can result in the suppression of the usual crystallization reactions and in the formation of nonequilibrium phases with distinct and novel microstructures. A number of processing variables have been established to control undercooling including: droplet size, melt superheat, cooling rate, and droplet surface chemistry. The application of thermal analysis together with x-ray diffraction and microstructural examination methods has allowed for an evaluation of the kinetic competition during phase selection, for the determination of the decomposition and melting temperatures of metastable phases, and for the assessment of metastable phase diagrams. New advances have also been made in the understanding and control of heterogeneous nucleation and in probing the thermal history of rapidly solidifying samples by upquenching studies as well as in the development of new experimental capacity to study composites. The understanding developed from droplet undercooling studies has a direct application to Rapid Solidification Processing (RSP) and allows for an assessment of RSP treatment in terms of the influence of undercooling and metastable phase equilibria on phase selection and novel solidification microstructure development. The basic information that droplet studies yield also has a broad application to many aspects of solidification processing. DTIC

N94-31098 Ecole Nationale Superieure des Telecommunications, Paris (France). Groupe Image.
ENTROPY, INFORMATION (AND IMAGE), PART 1 [ENTROPIE, INFORMATION (ET IMAGE), PARTIE 1]
Henri Maitre 1993 10 p In FRENCH Limited Reproducibility: More than 20% of this document may be affected by microfiche quality
(ISSN 0751-1337)
(TELECOM-93-D-009; ETN-94-95890) Avail: CASI HC A02

The notion of entropy is introduced from its historical origins in physics: thermodynamics, statistical physics, quantum physics. Information theoretic versions of this concept are presented, along with mathematical attempts to build entropy on solid bases. This allows a convenient framework for the control of digital picture processing algorithm (to be presented in part 2) to be introduced. ESA

N94-31289 Massachusetts Inst. of Tech., Cambridge.
TAMING CHAOTIC CIRCUITS Ph.D. Thesis
Elizabeth Bradley 1992
Avail: Issuing Activity (MIT Libraries, Rm. 14-0551, Cambridge, MA 02139-4307)

The program 'Perfect Moment' is built around a collection of techniques. Given a differential equation, a control parameter, and two state-space points, the program explores the system's behavior, automatically choosing interesting and useful parameter values and constructing state-space portraits at each one. It then chooses a set of trajectory segments from those portraits, uses them to construct a composite path between the objectives, and finally causes the system to follow that path by switching the parameter value at the segment junctions. Rules embodying theorems and definitions from nonlinear dynamics are used to limit computational complexity by identifying areas of interest and directing and focusing the mapping and search on these areas. Reference trajectories found by this design tool exhibit a variety of interesting and useful properties. 'Perfect Moment' balances an inverted pendulum by 'pumping' the device up, over half a dozen cycles, using roughly one-sixth the torque that a traditional linear controller would exert in this task. In another example, the program uses a detour through a chaotic zone to stabilize a system about 300 times faster than would happen by waiting long enough for the system to reach a regime where traditional control methods obtain. Chaotic zones can also be used to steer trajectories across boundaries of basins of attraction, effectively altering the geometry and the convergence properties of the system's stability regions. An externally-induced chaotic attractor that overlaps the phase-locked loop's original lock range is demonstrated here;

the controller designed by the program uses this feature to extend the capture range out to the original lock range limits, allowing the circuit to acquire lock over a wider range of input frequencies than would otherwise be possible. Dissert. Abstr.

N94-31498 Colorado Univ., Boulder.
COMPRESSIBLE CONVECTION WITH IONIZATION Ph.D. Thesis
Mark Peter Rast 1992 321 p
Avail: Univ. Microfilms Order No. DA9318125

The influence of non-ideal effects associated with ionization upon the dynamics and thermodynamics of compressible convection is studied. Ionization causes changes in the particle number density, internal energy, specific heat and opacity of a fluid. The effects of the first three of these are studied with a simplified model involving pure hydrogen fluid. Linear and finite-amplitude analyses and fully nonlinear two-dimensional simulations are undertaken, with the numerical simulations performed on the massively parallel Connection Machine CM-2. Opacity effects are examined by analyzing solutions obtained from more realistic three-dimensional simulations of solar granulation carried out by Nordlund and Stein. Ionization effects are expected to influence the dynamics of granulation and acoustic mode excitation in the Sun and other stars, and likewise the coupling of convection with pulsations that occurs in stars such as white dwarfs and Cepheid variables. Both the global transport properties and the local dynamical properties of convective flows are affected by ionization. In regions of partial ionization, the enthalpy flux is dominated by latent heat transport. Strong temperature fluctuations and corresponding buoyancy forces develop wherever rapid changes in ionization state occur. These can result in narrow regions of intense vertical flow. The flow asymmetries reported in compressible ideal gas convection can either be enhanced or diminished depending on the vertical positioning of the partially ionized region within the domain. Ionization-induced variations in the radiative properties of a convecting fluid can result in thermal boundary layer instability and plume formation. The interval between plume formation events depends on the growth rate of the instability, the scale of the underlying convective motions and the phase speed of the perturbation. As plumes formed in the upper boundary layer descend, buoyancy forces remain significant as long as heat exchange and compressional heating result primarily in ionization of the fluid rather than in temperature equilibration. This can lead to supersonic vertical flows in an otherwise subsonic flow field, and can serve to excite acoustic oscillations, the phase of which can be abruptly altered by subsequent plume events. In the three-dimensional simulations, significant entrainment of surrounding fluid with depth gradually weakens the sheets and plumes of fast downflow. Dissert. Abstr.

N94-31712# Toronto Univ. (Ontario). Dept. of Physics.
PERTURBATIVE ASPECTS OF LOWER-DIMENSIONAL GAUGE THEORIES Ph.D. Thesis
Brian John Hand Jul. 1993 115 p
(ISBN-0-315-86269-6; CTN-94-61188) Copyright Avail: Micromedia Ltd., Technical Information Centre, 240 Catherine Street, Suite 305, Ottawa, Ontario, K2P 2G8, Canada HC/MF

The appearance of a chiral anomaly in the nonlocal regularization scheme is illustrated in the analysis of the two-dimensional chiral Schwinger model. The nonexistence of a measure factor necessary to preserve gauge invariance of the regularized theory is explicitly demonstrated. The one-loop vacuum polarization tensor in three dimensional quantum electrodynamics (QED3) is evaluated using analytic and nonlocal regularization. Both techniques are shown to yield gauge invariant results. The results are compared to those obtained using other regularization methods. A similar analysis is then performed on non-Abelian Chern-Simons theory, and it is found that there is no renormalization of the Chern-Simons parameter. The mass-shell behavior of the fermion propagator in massless QED3, a confining theory, is examined. A technique developed for ordinary four dimensional quantum electrodynamics is applied in which the charged asymptotic states in the theory are dressed with soft vector bosons in order to improve the representation of the infrared dynamics in perturbation theory. The resulting modification to the mass-shell behavior of the fermion propagator is determined with the result that the propagator no longer possesses a mass-shell singularity. Author (CISTI)

N94-31760# Los Alamos National Lab., NM.
NON-EQUILIBRIUM ELECTRODYNAMICS IN THE LARGE N EXPANSION
E. Mottola 1994 18 p Presented at the Third Thermal Field Theories Workshop, Alberta, Ontario, 15-28 Aug. 1993
(Contract W-7405-eng-36)
(DE94-006156; LA-UR-94-381; CONF-9308211-1) Avail: CASI HC A03/MF A01

An effective action technique for the time evolution of a closed system consisting of a mean field interacting with charged fluctuations is presented, and applied specifically to Quantum Electrodynamics. The effective action of QED is first developed in a systematic expansion in 1/N where N is the number of distinct fermion species. Then by making use of the Schwinger-Keldysh closed time path (CTP) formulation of field theory, causality of the resulting equations of motion is ensured. In QED, this technique may be used to study the quantum non-equilibrium effects of pair creation in strong electric fields and the scattering and transport processes of a relativistic e(+)e(-) plasma. Numerical results for these processes in lowest order are presented. The renormalization procedure, connection to quantum transport theory and extension to QCD and other applications of the method are also discussed. DOE

N94-31823# Stanford Linear Accelerator Center, CA.
NEW QCD RESULTS FROM STRING THEORY
Z. Bern (California Univ., Los Angeles.), L. Dixon, and D. A. Kosower Nov. 1993 8 p Presented at the 1993 International Conference on Strings, Berkeley, CA, 24-29 May 1993
(Contracts DE-AC03-76SF-00515; DE-FG03-91ER-40662)
(DE94-005226; SU-SLAC-PUB-6388; CONF-9305317-1) Avail: CASI HC A02/MF A01

We discuss new results in QCD obtained with string-based methods. These methods were originally derived from superstring theory and are significantly more efficient than conventional Feynman rules. This technology was a key ingredient in the first calculation of the one-loop five-gluon amplitude. We also present a conjecture for a particular one-loop helicity amplitude with an arbitrary number of external gluons. DOE

N94-31893 Politecnico di Milano (Italy). Dipt. di Elettronica e Informazione.
BIFURCATION AND DETERMINISTIC CHAOS IN DYNAMIC SYSTEMS [BIFORCAZIONI E CAOS DETERMINISTICO NEI SISTEMI DINAMICI]
Carlo Piccardi and Sergio Rinaldi Jul. 1993 86 p Presented at Convegno-Scuola su biosystemi e Complessita, Bressanone, Italy, 27-30 Sep. 1993
(Rept-93-047; ETN-94-95814) Avail: Issuing Activity (Politecnico di Milano, Piazza Leonardo da Vinci 32, 20133 Milan, Italy)

Papers on the following are presented: the asymptotic behavior of dynamic systems; structural stability and deterministic chaos; and the problems of chaotics induced by seasons in population dynamics. For individual titles, see N94-31894 through N94-31897.

N94-31894 Politecnico di Milano (Italy). Dipt. di Elettronica e Informazione.
ASYMPTOTIC BEHAVIOR OF DYNAMIC SYSTEMS [COMPORTAMENTO ASINTOTICO DEI SISTEMI DINAMICI]
Sergio Rinaldi *In its* Bifurcation and Deterministic Chaos in Dynamic Systems Jul. 1993 15 p Sponsored in part by Ministry of University and Scientific and Technological Research (For primary document see N94-31893 09-77)
Avail: Issuing Activity (Politecnico di Milano, Piazza Leonardo da Vinci 32, 20133 Milan, Italy)

Notions and results on the asymptotic behavior of nonlinear dynamic systems are presented. The principle characteristics of the four attraction categories, equilibria, cycles, tori, and strange attractors are demonstrated. ESA

N94-31895 Politecnico di Milano (Italy). Dipt. di Elettronica e Informazione.
STRUCTURAL STABILITY AND BIFURCATIONS [STABILITA STRUTTURALE E BIFORCAZIONI]
Sergio Rinaldi *In its* Bifurcation and Deterministic Chaos in Dynamic Systems Jul. 1993 24 p Sponsored in part by Ministry of University

and Scientific and Technological Research (For primary document see N94-31893 09-77)
Avail: Issuing Activity (Politecnico di Milano, Piazza Leonardo da Vinci 32, 20133 Milan, Italy)

The structural stability of nonlinear dynamic systems is addressed. Bifurcations with collisions, local bifurcations (Hopf, tangent and flip, and Nairmark-Sacker), and global bifurcations are studied. Phenomena cited are those of catastrophic transition, hysteresis, subharmonics, frequency coupling, and deterministic chaos. ESA

N94-31896 Politecnico di Milano (Italy). Dipt. di Elettronica e Informazione.
DETERMINISTIC CHAOS [IL CAOS DETERMINISTICO]
Sergio Rinaldi *In its* Bifurcation and Deterministic Chaos in Dynamic Systems Jul. 1993 21 p Sponsored in part by Ministry of University and Scientific and Technological Research (For primary document see N94-31893 09-77)
Avail: Issuing Activity (Politecnico di Milano, Piazza Leonardo da Vinci 32, 20133 Milan, Italy)

The problem of deterministic chaos, which is due to the existence of strange attractors, that is to the possibility that a dynamic system may have a decisive aperiodic behavior but confined in a limited region of the state space, is addressed. The appearance of chaos is described. Sensitivity to the initial conditions, fractal geometry of strange attractors, bifurcation in chaos, and reconstruction of time series attractors are studied. ESA

N94-31897 Politecnico di Milano (Italy). Dipt. di Elettronica e Informazione.
SEASONS AND CHAOS IN POPULATION DYNAMICS [STAGIONI E CAOS NELLA DINAMICA DELLE POPOLAZIONI]
Carlo Piccardi and Sergio Rinaldi *In its* Bifurcation and Deterministic Chaos in Dynamic Systems Jul. 1993 20 p Sponsored in part by Fondazione E.N.I. Enrico Mattei, and Politecnico di Milano (For primary document see N94-31893 09-77)
Avail: Issuing Activity (Politecnico di Milano, Piazza Leonardo da Vinci 32, 20133 Milan, Italy)

Examples in which the role of the season is determinant in generating a chaotic type of dynamics of some populations are presented. This emerges in an experimental approach, in which a series of data is numerically analyzed, and in a theoretical approach, in which the bifurcation of the mathematical model describing the phenomenology of the process is analyzed. ESA

N94-31911# Montreal Univ. (Quebec). Dept. de Mathematiques Appliquees.
THE KALUZA-KLEIN APPROACH AND GAUGE SUPERSYMMETRY Ph.D. Thesis [APPROCHE KALUZA-KLEIN ET SUPERSYMETRIE DE JAUGE]
Jean-Pierre Pare Dec. 1992 120 p In FRENCH
(ISBN-0-315-86553-9; CTN-94-61212) Copyright Avail: Micromedia Ltd., Technical Information Centre, 240 Catherine Street, Suite 305, Ottawa, Ontario, K2P 2G8, Canada HC/MF

A non-Abelian gauge supersymmetric Kaluza-Klein approach is presented for charged spinning particles and strings in a background of gravitational and Yang-Mills fields. The classical Kaluza-Klein approach is first generalized for a spinning particle. The spin is described by Grassmannian variables added to the principal bundle. This super symmetrization gives rise to a fermionic non-Abelian charge in addition to the bosonic one. This leads to a search for a supergroup action on the superprincipal bundle which leaves invariant the action of the spinning particle. The invariance of this action would lead to the conservation of a non-Abelian supercharge, generalizing the conservation law obtained for particles without spin. Lagrangian and Hamiltonian formulations are presented and the equations of motion are derived and discussed. The invariance of these formulations under a supergroup action leads to a conservation law of a non-Abelian supercharge. The bosonic part of this supercharge corresponds to the non-Abelian (bosonic) charge obtained for a particle without spin. The fermionic part is a non-physical charge. In the supersymmetric case, this decouples from all other dynamical variables and does not influence trajectories of spinning particles. These formulations are then extended for spinning strings.
Author (CISTI)

N94-31924 Rutherford Appleton Lab., Chilton (England).
TENSOR GAUGE POTENTIALS IN LOOP SPACE FORMULATION OF YANG-MILLS FIELDS
C. Hong-Mo, J. Faridani, and T. S. Tsun Nov. 1993 15 p Prepared in cooperation with Oxford Univ., Englan d
(PB94-147147; RAL-93-080) Avail: Issuing Activity (National Technical Information Service (NTIS))

It is shown that an antisymmetric rank-two tensor gauge potential of the type first found in string and supersymmetry theories occurs also in ordinary Yang-Mills theory when formulated in loop space, where it appears as a Lagrange multiplier for a zero curvature constraint necessary and sufficient for removing the inherent redundancy of loop variables. It is then further shown that the tensor potential acts there as the parallel 'phase' transport for monopoles. NTIS

N94-32043# Naval Postgraduate School, Monterey, CA.
HEAT TRANSFER STUDIES ON A RECTANGULAR CHANNEL WITH OFFSET PLATE FINS M.S. Thesis
Jeffrey M. Masterson Dec. 1993 49 p
(AD-A277300) Avail: CASI HC A03/MF A01

Convective heat transfer characteristics of a liquid cooled rectangular channel, containing offset plate fins, were investigated experimentally. The selected geometry was a 10x model of the fluid circulation passages in the commercially available SEM-E type electronic cooling modules. The test surface containing fins was made of aluminum and was heated at its base by a thermofoil heater. The Reynolds numbers were varied between 100-800, with water as the cooling fluid. Surface temperature measurements on the heated surface were used to determine the Colburn j factor. The effects of natural convection were also investigated. DTIC

N94-32513# California Univ., Santa Barbara. Dept. of Physics.
NUMERICAL SIMULATION OF QUANTUM MANY-BODY SYSTEMS
D. J. Scalapino and R. L. Sugar 1993 7 p
(Contract DE-FG03-85ER-45197)
(DE94-008451; DOE/ER-45197/8) Avail: CASI HC A02/MF A01

Understanding the physical properties of strongly interacting many-electron systems remains one of the central goals of condensed matter physics. In this project, the authors have developed and implemented numerical techniques, such as quantum Monte Carlo simulations, to study basic models of interacting electrons: the one-band Hubbard model for positive and negative U, the three-band CuO2 Hubbard model, the Holstein electron-phonon model, the periodic Anderson model, and the Kondo lattice. Such models exhibit a rich variety of physical properties. For example, the half-filled Holstein model undergoes a Peierls-charge-density wave transition. While away from half-filling there is competition between superconductivity and the Peierls-charge-density wave phase. The ground state of the half-filled 2D Hubbard model has long-range antiferromagnetic order. Away from half-filling, it has been found to have an attractive interaction in the singlet d(sub x(exp 2)-y(exp 2)) pairing channel, and it provides a model for the high-temperature cuprate superconductors. Similarly, it is believed that the periodic Anderson model and the Kondo lattice model provide a framework for understanding the heavy fermion materials which can exhibit antiferromagnetic and superconducting phases. Because of the strong coupling and the interplay between the different correlations, it is possible to tip these delicately balanced systems in favor of a given correlated state by the approximations one makes. Thus it is important to develop systematic, controlled calculations for these models. Numerical calculations provide an important approach for determining the properties of such models. A review of the work on these problems is presented. DOE

N94-32774*# Eloret Corp., Palo Alto, CA.
ARC-HEATER PERFORMANCE RESEARCH Final Technical Report, 1 Apr. 1990 - 31 Jan. 1994
Charles E. Shepard and Prabha Durgapal 29 Apr. 1994 9 p
(Contract NCC2-688)
(NASA-CR-195821; NAS 1.26:195821) Avail: CASI HC A02/MF A01

The tasks performed can be divided into the following categories: an analysis of the electric arc phenomena, especially near the electrodes; a parametric study of arcjet performance by means of a computer code (ARCFLO) and verification with experimental data where possible; the development of a data acquisition system to collect the above experimental

data using Ames arc-jets; and a study of the critical components (electrodes and constrictor disks) and suggestions of how to improve their performance. Author (revised)

N94-32824# Texas Univ., Austin. Dept. of Physics.
QUANTUM DYNAMICS IN DUAL SPACES
E. C.G. Sudarshan 1993 57 p
(Contract DE-FG03-93ER-40757)
(DE94-008303; DOE/ER-40757/020) Avail: CASI HC A04/MF A01

Quantum mechanics gives us information about spectra of dynamical variables and transition rates including scattering cross sections. They can be exhibited as spectral information in analytically continued spaces and their duals. Quantum mechanics formulated in these generalized spaces is used to study scattering and time evolution. It is shown that the usual asymptotic condition is inadequate to deal with scattering of composite or unstable particles. Scattering theory needs amendment when the interacting system is not isospectral with the free Hamiltonian, and the amendment is formulated. Perturbation theory in generalized spaces is developed and used to study the deletion and augmentation of the spectrum of the Hamiltonian. A complete set of algebraically independent constants for an interacting system is obtained. The question of the breaking of time symmetry is discussed. DOE

N94-32846 Oak Ridge K-25 Site, TN.
SOLGAS REFINED: A COMPUTERIZED THERMODYNAMIC EQUILIBRIUM CALCULATION TOOL
L. D. Trowbridge and J. M. Leitnaker Nov. 1993 80 p Limited Reproducibility: More than 20% of this document may be affected by microfiche quality
(Contract USECHQ-93-C-0001)
(DE94-009021; K/ETO-140) Avail: Issuing Activity (Department of Energy (DOE))

SOLGAS, an early computer program for calculating equilibrium in a chemical system, was made more user-friendly, and several 'bells and whistles' were added. The necessity to include elemental species was eliminated. The input of large numbers of starting conditions was automated. A revised format for entering data simplifies and reduces chances for error. Calculated errors by SOLGAS are flagged, and several programming errors are corrected. Auxiliary programs are available to assemble and partially automate plotting of large amounts of data. Thermodynamic input data can be changed 'on line. The program can be operated with or without a co-processor. Copies of the program, suitable for the IBM-PC or compatible with at least 384 bytes of low RAM, are available from the authors. DOE

N94-33148*# Wisconsin Univ., Milwaukee. Dept. of Mechanical Engineering.
PHYSICS OF HEAT PIPE REWETTING Final Technical Report, 1 Apr. 1991 - 31 Jan. 1994
S. H. Chan 1994 16 p
(Grant NAG9-525)
(NASA-CR-195902; NAS 1.26:195902) Avail: CASI HC A03/MF A01

This is the final report which summarizes the research accomplishments under the project entitled 'Physics of Heat Pipe Rewetting' under NASA Grant No. NAG 9-525, Basic, during the period of April 1, 1991 to January 31, 1994. The objective of the research project was to investigate both analytically and experimentally the rewetting characteristics of the heated, grooved plate. The grooved plate is to simulate the inner surface of the vapor channel in monogroove heat pipes for space station design. In such designs, the inner surface of the vapor channel is threaded with monogrooves. When the heat pipe is thermally overloaded, dryout of the monogroove surface occurs. Such a dryout surface should be promptly rewetted to prevent the failure of the heat pipe operation in the thermal radiator of the space station. Author

80 SOCIAL SCIENCES (GENERAL)

Includes educational matters.

N94-31806* National Aeronautics and Space Administration. Lewis Research Center, Cleveland, OH.
MARSVILLE: THE COSMIC VILLAGE (Videotape)
May 1993 Videotape: 7 min. 30 sec. playing time, in color, with sound
(NASA-TM-109752; NONP-VT-94-9952) Avail: CASI VHS A01/BETA A22

This video describes an educational student activity sponsored by the Challenger Center for Space Science Education and the Educational Information and Resource Center, which was held at the Lewis Research Center. Marsville was held in May 1992, involving students from schools in three counties around Cleveland. In commemoration of the International Space Year, students worked together to plan a simulated colony on Mars, which culminated in the erection of a balloon tent 'city' at the Lewis Research Center. CASI

N94-31807* National Aeronautics and Space Administration. Lewis Research Center, Cleveland, OH.
SPACE ACCELERATION MEASUREMENT SYSTEM (Videotape)
May 1993 Videotape: 23 min. playing time, in color, with sound
(NASA-TM-109754; NONP-VT-94-9954) Avail: CASI VHS A01/BETA A22

This training video, presented by the Lewis Research Center's Space Experiments Division, gives a background and detailed instructions for preparing the space acceleration measurement system (SAMS) for use. The SAMS measures, conditions, and records forces of low gravity accelerations, and is used to determine the effect of these forces on various experiments performed in microgravity. Inertial sensors are used to measure positive and negative acceleration over a specified frequency range. The video documents the SAMS' uses in different configurations during shuttle missions. CASI

N94-31815* National Aeronautics and Space Administration. Lewis Research Center, Cleveland, OH.
WELCOME TO THE OHIO AEROSPACE INSTITUTE (Videotape)
Nov. 1992 Videotape: 10 min. 22 sec. playing time, in color with souind
(NASA-TM-109756; NONP-VT-94-9956) Avail: CASI VHS A01/BETA A22

The mission and various programs administered by the Ohio Aerospace Institute, a consortium made up of 9 Ohio Universities, LeRC, and members of the Aerospace Industry are described. The video highlights the following: programs to bring aerospace research to K-12 classrooms; programs to allow graduate students access to laboratory equipment at LeRC; the creation of a statewide television network to link researchers in industry and academia; and focus groups to encourage collaboration between companies in aerospace research. CASI

N94-31817* National Aeronautics and Space Administration. Lewis Research Center, Cleveland, OH.
NASA REPORT TO EDUCATION, VOLUME 9 (Videotape)
Mar. 1991 Videotape: 26 min. 44 sec. playing time, in color, with sound
(NASA-TM-109760; NONP-VT-94-9960) Avail: CASI VHS A01/BETA A22

This is an edition of 'NASA Report to Education' covering NASA's Educational Workshop, Lewis Research Center's T-34 and the Space Exploration Initiative. The first segment shows NASA Education Workshop program (NEWEST - NASA Educational Workshops for Elementary School Teachers). Highlights of the 14 days of intense training, lectures, fieldtrips and simple projects that the educators went through to teach the program are included. Participants are shown working on various projects such as the electromagnetic spectrum, living in Space Station Freedom, experience in T-34, tour of tower at the Federal Aviation Administrative Facilities, conducting an egg survival system and an interactive video conference with astronaut Stori Musgrave. Participants share impressions of the workshop. The second segment tells how Lewis Research Center's T-34 aircraft is used to promote aerospace education in several Cleveland schools and excite students. CASI

N94-31887* National Aeronautics and Space Administration. Lewis Research Center, Cleveland, OH.
THE SKY IS YOUR CLASSROOM (Videotape)
1982 Videotape: 28 min. 30 sec. playing time, in color, with sound
(NASA-TM-109759; NONP-VT-94-9959) Avail: CASI VHS A01/BETA A22

An overview of NASA's 11th annual Aerospace Education Workshop Program is presented. A portion of activities that are performed during the workshop sessions, which are used to familiarize teachers with up-to-date information are shown. An overview of aerospace concepts and terms is provided. Activities shown include: how model rockets are used to teach about the principles of rocketry; how eggs are packaged to represent an astronaut landing on another planet; a trip to the Cleveland Museum of Natural History was used to introduce a telescope and planetarium; and a visit to LeRC. How lectures and discussion material are presented on such topics as the history of aircraft and the space shuttle is demonstrated. CASI

N94-32677# Lawrence Livermore National Lab., CA.
A FACILITATED MENTORING PROCESS FOR ENGINEERS
L. Donald and M. Clark Nov. 1993 12 p Presented at the 8th IEEE-USA Careers Conference, Dallas, TX, 14-15 Apr. 1994
(Contract W-7405-eng-48)
(DE94-005823; UCRL-JC-115706; CONF-940467-2) Avail: CASI HC A03/MF A01

Mentoring has been occurring in organizations for many, many years through a natural pairing process of people wanting to help one another. The numerous benefits of mentoring to both the protege and the mentor are widely known. We describe a Facilitated Mentoring Pilot Program for engineers, successfully completed in June, 1993. This career development tool can help make every engineer a leader. DOE

N94-32910# Pacific Northwest Lab., Richland, WA.
OPTIONS FOR SYSTEMIC CHANGE IN MATHEMATICS, SCIENCE, AND TECHNOLOGY EDUCATION: SCIENTIST/TEACHER PARTNERSHIPS
C. S. Glantz and L. Fayette Jan. 1994 4 p Presented at the 74th American Meteorological Society Annual Meeting, Nashville, TN, 23-28 Jan. 1994
(Contract DE-AC06-76RL-01830)
(DE94-007472; PNL-SA-23576; CONF-940115-30) Avail: CASI HC A01/MF A01

Options is a US Department of Energy/Pacific Northwest Laboratory (DOE/PNL) project whose goal is to assist Washington and Oregon middle schools having high percentages of students historically underrepresented in mathematics, science, and technology. The goal is to ensure that all students receive high-quality mathematics, science, and technology education throughout their middle school years. Teams of scientists work with teams of teachers from participating OPTIONS schools to initiate significant change in the manner in which science, mathematics, and technology are taught. As part of this effort, PNL scientists team up with teachers to develop curricula. DOE

N94-33066*# National Aeronautics and Space Administration, Washington, DC.
OPINION POLLS AND THE US CIVIL SPACE PROGRAM
Sylvia Doughty Fries Apr. 1992 11 p Presented at the Meeting of the American Inst. for Aeronautics and Astronautics, 29 Apr. 1992
(NASA-TM-109700; NAS 1.15:109700) Avail: CASI HC A03/MF A01

An analysis of two public opinion poles that sought to determine NASA's level of support among the American people is presented. One pole models public participation in policy-making as a pyramid. The model provides for three levels of public participation: the attentive public, the interested public, and the non-attentive public. The three groups are discussed in the context of how to best promulgate NASA's mission throughout the American public. CASI

N94-31436*# International Space Univ., Inc., Toronto (Ontario).
AN INNOVATIVE APPROACH TO SPACE EDUCATION
Christine Marton, Alain B. Berinstain, and John Criswick *In* NASA. Marshall Space Flight Center, The Second Annual International Space University Alumni Conference Feb. 1994 p 121-125 (For primary document see N94-31425 09-12)
Avail: CASI HC A01/MF A02

81 ADMINISTRATION AND MANAGEMENT

Includes management planning and research.

N94-31181# European Space Agency, Paris (France).
EUROPEAN BUSINESS CONFRONTED WITH THE 21ST CENTURY: MEN, THE ESSENTIAL RISK [LE SENTERPRISES EUROPEENNES FACE AU XXIE SIECLE: LES HOMMES, L'ENJEU ESSENTIEL]
T. D. Guyenne, ed. Nov. 1993 180 p In FRENCH Presented at the International Forum, Paris, France, 17-18 Nov. 1992 Original contains color illustrations
(ESA-SP-1167; ISBN-9-29-092105-6; ETN-94-95859) Copyright Avail: CASI HC A09/MF A02

Round table discussions concerning the following topics are presented: management of jobs and competencies at the heart of business strategies (predicting and managing the jobs which business need and will need and the integration of human resources, competencies, and know-how into business strategies); strategic analysis and prevision of competencies and jobs in European businesses (strategic scenarios and results of a study on competencies in the aerospace industries in the years to come); new training technologies; cooperation between the state, businesses, and education with regard to training; and men, culture, and ethics of business in the 21st century. ESA

N94-31197# Advisory Group for Aerospace Research and Development, Neuilly-Sur-Seine (France).
AGARD MEMBERSHIP, 1994 [LES MEMBRES DE L'AGARD, 1994]
Mar. 1994 70 p
(AGARD-Memb-94) Copyright Avail: CASI HC A04/MF A01

This publication contains lists of the National Delegates Board of AGARD, the Steering Committee, AGARD national coordinators, technical panels, the Technical Information Committee, and the Aerospace Applications Studies Committee, as of 1 March 1994. It also contains a list of the staff at AGARD Headquarters. Each list is separated by participating country and contains address, phone number, and fax number with each name. Derived from text

N94-31538# Cranfield Inst. of Tech., Bedford (England). Applied Psychology Unit.
DRUG-RELATED PROBLEMS IN THE WORKPLACE
A. Guppy Jun. 1993 20 p
(Cranfield-Aero-9306; ISBN-1-871564-61-1; ETN-94-96069) Avail: CASI HC A03/MF A01; Cranfield Univ. of Technology, Coll. of Aeronautics, Cranfield, Bedford MK43 0AL, England, HC

The introduction of workplace policies and procedures to minimize the existence of problems associated with substance use, which has become widespread among certain western nations over the last two decades, is considered. There is general agreement that the primary goal of such activities should be to minimize the effects on measures such as absenteeism, lost productivity, safety and health care costs that are seen as associated with substance misuse by employees. The evidence that significant associations exist between certain patterns of drug use and workplace problems within the safety and productivity domains is reviewed. An outline of relevant countermeasure alternatives is provided as well as some information concerning current trends in intervention within British based organizations. One of the aspects of workplace intervention that has received considerable attention in recent years concerns drug testing. There would appear to be much debate about the legal and ethical implications of certain drug testing programs, particularly where countries are perceiving pressure to require testing following the use of such procedures in the U.S. (Ontario Law Reform, 1992). For this reason a very brief review of drug testing programs is provided. ESA

N94-32074# Montreal Univ. (Quebec). Dept. de Mathematiques Appliquees.
PLANNING OF AIR CREW SCHEDULES M.S. Thesis [PLANIFICATION D'HORAIRES D'EQUIPAGES AERIENS]
Raphael Tcheune Sep. 1992 125 p In FRENCH

(ISBN-0-315-86506-7; CTN-94-61204) Copyright Avail: Micromedia Ltd., Technical Information Centre, 240 Catherine Street, Suite 305, Ottawa, Ontario, K2P 2G8, Canada HC/MF

Air crew schedule planning is important for reducing the operating costs of an airline. Planning these schedules must take into account such constraints as flight schedules, type of aircraft, location of flight departure and arrival, length of flight, crew fatigue, and regulations and agreements on crew working conditions. A scheduling optimization program has been developed for planning crew rotations for Air France which performs the scheduling in accordance with the company's present collective agreement. A study was conducted of a system for planning air crew schedules for Air France, following the regulations negotiated for the European market. The scheduling problem is formulated mathematically and relevant literature is reviewed. The method chosen for solving the scheduling problem uses the column generation principle and GENCOL software, which is for solving shortest path problems with constraints on an adequately constructed network. Two network models are developed in which the tasks to be done are disposed on arcs, each arc having resources which characterize the task and which must be consumed when the task is accomplished. The two models are tested on four data sets having 109, 218, 588, and 739 flight segments. The results obtained are satisfactory from the point of view of calculation time and quality of crew rotations. CISTI

N94-32222*# National Aeronautics and Space Administration, Washington, DC.

NASA STRATEGIC PLAN

May 1994 27 p
(NASA-TM-109780; NAS 1.15:109780) Avail: CASI HC A03/MF A01

The NASA Strategic Plan is a living document. It provides far-reaching goals and objectives to create stability for NASA's efforts. The Plan presents NASA's top-level strategy: it articulates what NASA does and for whom; it differentiates between ends and means; it states where NASA is going and what NASA intends to do to get there. This Plan is not a budget document, nor does it present priorities for current or future programs. Rather, it establishes a framework for shaping NASA's activities and developing a balanced set of priorities across the Agency. Such priorities will then be reflected in the NASA budget. The document includes vision, mission, and goals; external environment; conceptual framework; strategic enterprises (Mission to Planet Earth, aeronautics, human exploration and development of space, scientific research, space technology, and synergy); strategic functions (transportation to space, space communications, human resources, and physical resources); values and operating principles; implementing strategy; and senior management team concurrence.
Derived from text

N94-32678# Westinghouse Hanford Co., Richland, WA.

AGILE TOTAL QUALITY GUIDELINES FOR ENHANCING TEAMWORK AND SUCCESS

D. D. Brayton and R. R. Harris Aug. 1993 17 p Presented at the 48th Annual Quality Congress, Las Vegas, NV, 24-26 May 1994
(Contract DE-AC06-87RL-10930)
(DE93-019972; WHC-SA-2050; CONF-940538-1) Avail: CASI HC A03/MF A01

Companies implement total quality Programs to enable them to obtain performance leadership in meeting their business objectives. The successful corporations reach energy level of the corporate structure and change the overall culture of their operations. Limited success occurs when companies advocate total quality programs (e.g., high-powered training classes, tools and gimmicks), but are only partially effective in changing the culture of the work force. The ability to reach the 'grassroots' level employees with a total quality program effort is vital in changing the overall culture. First-line management, i.e., both project and supervisory leaders, must direct the total quality program effort. First-line management needs well defined guidelines (beyond the general company guidelines) for implementing a total quality program. Guidelines that allow the establishment of an agile total quality Program, which support upper management total quality program directives, yet are modifiable for their specific needs. The guidelines presented in this paper empower employees and improve the culture of the work environment through defined goals and teamwork to achieve success. DOE

N94-32723# Department of Energy, Washington, DC.

TOTAL QUALITY MANAGEMENT IMPLEMENTATION GUIDELINES

Dec. 1993 73 p
(DE94-007232; DOE/HR-0066) Avail: CASI HC A04/MF A01

These guidelines were designed by the Energy Quality Council to help managers and supervisors in the Department of Energy Complex bring Total Quality Management to their organizations. Because the Department is composed of a rich mixture of diverse organizations, each with its own distinctive culture and quality history, these guidelines are intended to be adapted by users to meet the particular needs of their organizations. For example, for organizations that are well along on their quality journeys and may already have achieved quality results, these guidelines will provide a consistent methodology and terminology reference to foster their alignment with the overall energy quality initiative. For organizations that are just beginning their quality journeys, these guidelines will serve as a startup manual on quality principles applied in the energy context. DOE

N94-32426*# Naval Command, Control and Ocean Surveillance Center, San Diego, CA. RDT&E Div.

NEW APPROACHES FOR REAL TIME DECISION SUPPORT SYSTEMS

D. Charles Hair and Kent Pickslay *In* NASA, Washington, Technology 2003: The Fourth National Technology Transfer Conference and Exposition, Volume 2 Feb. 1994 p 40-45 (For primary document see N94-32420 09-99)
Avail: CASI HC A02/MF A04

N94-32427*# Carnegie Group, Inc., Pittsburgh, PA.

KNOWLEDGE-BASED COMMODITY DISTRIBUTION PLANNING

Victor Saks and Ivan Johnson *In* NASA, Washington, Technology 2003: The Fourth National Technology Transfer Conference and Exposition, Volume 2 Feb. 1994 p 46-54 (For primary document see N94-32420 09-99)
Avail: CASI HC A02/MF A04

82 DOCUMENTATION AND INFORMATION SCIENCE

Includes information management; information storage and retrieval technology; technical writing; graphic arts; and micrography.

For computer documentation see *61 Computer Programming and Software.*

N94-31155# Oak Ridge National Lab., TN.

ACQUISITION INFORMATION MANAGEMENT SYSTEM TELECOMMUNICATION SITE SURVEY RESULTS

K. A. Hake and B. G. Key Sep. 1993 39 p
(Contract DE-AC05-84OR-21400)
(DE94-005688; ORNL/TM-12112) Avail: CASI HC A03/MF A01

The Army acquisition community currently uses a dedicated, point-to-point secure computer network for the Army Material Plan Modernization (AMPMOD). It must transition to the DOD supplied Defense Secure Network 1 (DSNET1). This is one of the first networks of this size to begin the transition. The type and amount of computing resources available at individual sites may or may not meet the new network requirements. This task surveys these existing telecommunications resources available in the Army acquisition community. It documents existing communication equipment, computer hardware, associated software, and recommends appropriate changes. DOE

N94-31172 Ecole Nationale Superieure des Telecommunications, Paris (France). Dept. Economie et Management.

STANDARDIZATION AND INTELLECTUAL PROPERTY CONTROL: A REFLECTION ON THE INFORMATICS CASE Ph.D. Thesis [CONTROLE DE LA STANDARDISATION ET PROPRIETE INTELLECTUELLE: UNE REFLEXION SUR LE CAS DE L'INFORMATIQUE]

Moises Lachman 1993 335 p In FRENCH Sponsored by Conselho Nacional de Pesquisas Limited Reproducibility: More than 20% of this document may be affected by microfiche quality
(ISSN 0751-1353)
(TELECOM-93-E-016; ETN-94-95902) Avail: CASI HC A15

The informatics industry is studied, as an industry whose dynamics are

based on the complementary relations holding between the hardware and the software. The development of this industry is reviewed, underlining theoretically and empirically the role played by the hardware and the software, the standards linking them, and the judicial framework ruling them. ESA

N94-31175 Nijmegen Univ. (Netherlands). Dept. of Informatics.
TRANSFORMATION OF DATABASE POPULATIONS AND OPERATIONS FROM THE CONCEPTUAL TO THE INTERNAL LEVEL
P. vanBommel, G. Kovacs, and A. Micsik 9 Nov. 1992 20 p Sponsored in part by Trans-European Mobility Scheme for European Communities Limited Reproducibility: More than 20% of this document may be affected by microfiche quality
(TR-92-27; ETN-94-95615) Avail: CASI HC A03

A framework for the automatic transformation of databases from the conceptual to the internal level is described. The approach fits in with the ANSI/SPARC three level architecture for database management systems. The framework consists of three components: structures (database schemata), populations (database contents) and operations (database manipulations). These components are described for modeling techniques, such as ER, NIAM and the Binary Relationship Model. On the internal level focus is on (nested) relational models. For each component on the conceptual level a separate transformation is provided to the internal level. The components are integrated by a central notion: the predicator. Further integration is obtained by means of basic population rules. ESA

N94-31228# National Inst. of Standards and Technology, Gaithersburg, MD. Office of Director.
PUTTING THE INFORMATION INFRASTRUCTURE TO WORK: REPORT OF THE INFORMATION INFRASTRUCTURE TASK FORCE COMMITTEE ON APPLICATIONS AND TECHNOLOGY
May 1994 116 p
(NIST/SP-857; ISBN-0-16-043188-3) Avail: CASI HC A06/MF A02; SOD

The Committee on Applications and Technology of the Information Infrastructure Task Force is charged with coordinating efforts to develop, demonstrate, and promote applications of information technology in several diverse areas and to develop and recommend technology strategies and policy to accelerate the implementation of the National Information Infrastructure (NII). The goal of this document is to focus the public debate on the uses of the NII and the benefits of advanced computing and communications technologies. Seven applications papers are presented which address manufacturing, electronic commerce, health care, education and lifelong learning, environmental monitoring, libraries, and government service delivery. In each of these papers a description of the application arena is given along with a summary of the current information technology uses, short and long term goals, and issues related to how these goals could be achieved. CASI

N94-31331# Naval Coastal Systems Center, Panama City, FL.
COVERT CHANNEL ANALYSIS OF TRUSTED SYSTEMS. A GUIDE TO UNDERSTANDING Final Report
Virgil Gligor Nov. 1993 124 p
(AD-A276418; NCSC-TG-030) Avail: CASI HC A06/MF A02

This document provides a set of good practices related to covert channel analysis of systems employed for processing classified and other sensitive information. It's written to help vendors and evaluators understand covert channel analysis requirements. It contains suggestions and recommendations derived from Trusted Computer System Evaluation Criteria (TCSEC) objectives which aren't required by the TCSEC. DTIC

N94-31338 FutureVision, Buchanan, GA.
SPACE INDUSTRIALIZATION: A GUIDE TO GOVERNMENT INFORMATION
Robert T. Weaver, Jr. May 1994 66 p
(Release-1.2) Avail: Issuing Activity (FutureVision, PO Box 580, Buchanan, GA 30110-0580)

This bibliography is an exhaustive listing of 336 non-technical reports issued by the federal government since 1980. Coverage includes launch vehicles and services, remote sensing, space nuclear power, the national aerospace plane, NASA, Space Station Freedom/Alpha and the activities/hardware of foreign space programs. Author

N94-31344# Air Force Inst. of Tech., Wright-Patterson AFB, OH. School of Logistics and Acquisition Management.
AN ANALYSIS OF THE RECORDS MANAGEMENT PROCESS TO DETERMINE THE IMPACT OF AUTOMATION ON PRODUCTIVITY M.S. Thesis
David A. Gaines and Trevor J. Nelson Dec. 1993 107 p
(AD-A275923; AFIT/GSS/LAR/93D-4) Avail: CASI HC A06/MF A02

This research was performed to study the effects of automation on Air Force records management productivity prior to widespread implementation of Document Librarian. Document Librarian is a software tool developed for Headquarters Air Force Materiel Command (HQ AFMC) to manage records in accordance with Air Force, Federal, and National Archives and Records Administration (NARA) regulations, and is currently undergoing developmental testing. One organization was used as a case study to determine the effects of Document Librarian on the organization's records management productivity. A records management process model was constructed and used to define the relevant tasks and outputs of their records management process. Administrative productivity indicators (API's), a productivity measuring technique, was then used to determine a measure of productivity for the tasks defined by the model. The results showed approximately a 30 to 31 percent increase in the records technician's productivity when records were managed with Document Librarian. DTIC

N94-31355# Defense Information Systems Agency, Arlington, VA. Center for Information Management.
DOD INFORMATION SYSTEMS CAPACITY MANAGEMENT FUNCTION Final Report
Charles A. Archer, Sr. 16 Nov. 1993 190 p
(AD-A275987) Avail: CASI HC A09/MF A02

This report provides the foundation and structure for development of policy for a Department of Defense (DoD) information systems capacity management (CM) function. The objective in this workshop was to provide a DoD-wide standard framework for conducting performance measurement and capacity planning activities across all defense information infrastructure (DII), information systems (IS), and configurations (i.e., mainframe/host computers, communication systems, and networks). In many ways, the activities described in this document are similar to collective CM processes used in the DoD today, primarily for mainframe environments. However, the processes modeled in this report were constructed as the 'best practices' of all approaches to capacity management, and have been extended to include all DoD communication and network systems. DTIC

N94-31365# Utrecht State Univ. (Netherlands). Dept. of Computer Science.
DETECTING THE EROSION OF HIERARCHIC INFORMATION STRUCTURES
P. D. Bruza (Nijmegen Univ., Netherlands.), T. W. C. Huibers, J. vanderLinden, and T. vanOpstal Mar. 1993 17 p
(ISSN 0924-3275)
(RUU-CS-93-10; ETN-94-95647) Avail: CASI HC A03/MF A01

The problem of detecting erosion in hierarchical information structures is studied. This problem manifests itself particularly in environments where there is little or no possibility to guarantee structures in accordance with a specification and furthermore where there is a high frequency of mutation of structures. The notion of information structure is formalized in terms of so called structural expressions. The erosion of information structures is paralleled by increased optionality in the associated structural expressions. In order to detect erosion the 'choice normal form' for structural expressions is introduced. In this normal form all implicit optionality is made explicit. It is shown how arbitrary structural expressions can be brought into the normal form via transformations which are semantic preserving. A graphical formalism is presented whereby analysis of erosion is made more convenient. ESA

N94-31392 Amsterdam Univ. (Netherlands). Dept. of Philosophy.
THE MEANING OF DUPLICATES IN THE RELATIONAL DATABASE MODEL
Karen L. Kwast and Sieger vanDenneheuvel May 1993 53 p Limited Reproducibility: More than 20% of this document may be affected by microfiche quality
(ISSN 0928-3323)
(CT-93-04; ETN-94-96009) Avail: CASI HC A04

The relational database model is defined in terms of sets, whereas SQL needs the distinct option of explicit duplicate removal. The underlying concept of duplicate tuples is defined, the operators of the relational algebra are generalized, and the connection with logic is studied. It is shown that 'baggy' operators are neither classical nor linear. The generalized system is applied in a formal interpretation of SQL. ESA

N94-31415# Universiteit Twente, Enschede (Netherlands). Centre for Telematics and Information Technology.

ON A FORMAL APPROACH TO THE METHODOLOGY OF INFORMATION PLANNING

Sjaak N. Brinkkemper, Marianne Geurts, Ilse vandeKamp, Jaap Acohen, and Rolf Engmann Aug. 1993 15 p

(ISSN 0924-3755)

(Memo-INF-93-42; ETN-94-95716) Copyright Avail: CASI HC A03/MF A01

Research of methodological aspects of information planning is mostly not performed in a rigorous formal way. The application of meta-modeling techniques to be able to formulate methodological statements about information planning on a more formal basis is proposed. This is demonstrated by a comparison of three information planning methods, an investigation of the practical application of these methods, and the composition of an improved method. ESA

N94-31452 Amsterdam Univ. (Netherlands). Center for Computer Science in Organization and Management.

INFORMATION ACQUISITION FROM MULTI-AGENT RESOURCES; ABSTRACT

Zhisheng Huang and Peter vanEmdeBoas 26 Aug. 1993 15 p Limited Reproducibility: More than 20% of this document may be affected by microfiche quality

(ISSN 0928-3307)

(LP-93-08; ETN-94-96000) Avail: CASI HC A03

The possibilities and impossibilities of strategies for dealing with the 'Judge puzzle' problem are investigated. Those situations where information can be combined without risking the undesirable situation that a derivable proposition contradicts the beliefs of all agents involved are characterized: the relevant notion is called absolute safety. It turns out that in that case only trivial solutions exist. It follows that any nontrivial strategy must use information about the epistemic states of the agents involved. Less restrictive notions of safety are investigated. The more interesting of these notions are those which involve not only propositions about the world but also epistemic information relating the knowledge of the various agents involved. For this purpose, the logic of belief dependence is used. The results characterizing the generalized safety notions generalize for this extended logic. A notion of almost safety within this framework which describes the safety of combining information under the hypothesis that agents eventually might have exchanged their information among themselves is presented. For this notion of almost safety an explicit solution to the Judge puzzle is given. ESA

N94-31583 Technische Univ., Eindhoven (Netherlands).

MANAGING CUSTOMER ORDER DRIVEN ENGINEERING. AN INTERDISCIPLINARY AND DESIGN ORIENTED APPROACH

D. R. Muntslag 1993 255 p Limited Reproducibility: More than 20% of this document may be affected by microfiche quality

(PB94-145083; ISBN-90-386-0251-0) Copyright Avail: CASI HC A12

This thesis addresses a specific subset of production situations, namely, the engineer-to-order plants which produce industrial equipment. This type of production plant is concerned with the engineering and production of complex industrial equipment to fill specific customer orders. These plants operate in a market which can be characterized as being extremely dynamic and erratic. The research described deals with the control of a nonphysical process, the customer order driven engineering which precedes the physical production of a product. Important decisions are made during this nonphysical phase which have a significant effect upon the performance of the whole company. NTIS

N94-31586 Technische Univ., Delft (Netherlands).

EFFECTIVE INFORMATION MODELLING SUPPORT Ph.D. Thesis

T. F. Verhoef 28 Jun. 1993 291 p Limited Reproducibility: More than 20% of this document may be affected by microfiche quality

(PB94-148236; ISBN-90-9006176-2) Avail: Issuing Activity (National Technical Information Service (NTIS))

To get a detailed insight, both in prescribed and applied modeling knowledge, especially in similarities and differences between prescribed and applied modeling knowledge, the authors perform an extensive investigation. In chapter 2, the authors present the approach they use to acquire and represent both prescribed and applied modeling knowledge. The results of applying their approach are presented in the three subsequent chapters. Chapter 3 deals with prescribed modeling knowledge, while chapters 4 and 5 are involved with representing applied modeling knowledge. Chapter 6 discusses conclusions, both on similarities and differences between prescribed and applied modeling knowledge. Based on these conclusions, they propose a model for effective information modeling support in chapter 7. The chapter also shows some applications. In chapter 8, the findings are evaluated. NTIS

N94-31640# Technische Univ., Delft (Netherlands). Faculty of Technical Mathematics and Informatics.

ON THE VALIDITY OF THE BLP MODEL

Edo Roos Lindgreen 1993 25 p

(Contract TGP92037) (ISSN 0922-5641)

(Rept-93-70; ETN-94-96115) Copyright Avail: CASI HC A03/MF A01

The Bell-LaPadula (BLP) model, a model for multilevel secure computer systems, plays a pivotal role in the trusted computer systems evaluation criteria (TCSEC). A limited though systematical attempt to investigate the validity of the BLP model, taking the model's original and current context into account, is presented. While the original model appears to be based on indefinite and sometimes questionable assumptions, it is argued that the current model must be considered invalid for its application in practice. ESA

N94-31768# Netherlands Bibliographical and Documentary Committee, Amsterdam.

CURRENT RESEARCH INFORMATION IN EUROPE: CONFERENCE PROCEEDINGS

M. J. deGoede 1993 130 p Conference held in Amsterdam, Netherlands, 2-4 Dec. 1993 Sponsored by Commission of the European Communities

(PB94-127933) Copyright Avail: CASI HC A07/MF A02

Contents: Current Research Information in the Information World; Current Research Information in the USA; Integrating Research Information Services--A Challenge to Meet Users' Needs; Q2--A Study to the Harmonization and Utilization of European 'R&D Project' Databases; Industrial Users of Current Research Information; German Current Research Databases; French Current Research Database; CRIB Current Research in Britain; Usages and Users of Social Sciences Research Information--The Database FORIS of the Social Sciences Information Center in Germany; NOD--Marketing the Dutch Current Research Database; Towards the Improvement of the Conditions for Electronic Publishing; The Future of Current Research Information Systems; Campus Wide Information Systems; International Databases on Current Research; DERPI--Central European Initiative for Data Exchange on Research Activities; BEST Europe--Present and Future; European Working Group on Research Databases. NTIS

N94-31829# Computer Graphics Systems Development Corp., Mountain View, CA.

TEXTURE LIBRARY FOR 3-DIMENSIONAL VISUALIZATION SYSTEMS Final Report

Roy Latham, Dave Marsh, P. Y. Cheng, and Stuart Wells 29 Dec. 1993 58 p Revised

(Contract DACA76-93-C-0010)

(AD-A276125) Avail: CASI HC A04/MF A01

A texture library is sought to serve DoD visual simulation training needs as well as civilian commercial applications. The design effort of the present study encompasses determination of pattern requirements, identification of methods for pattern generation, establishment of image generator requirements, identification of methods for categorizing patterns, and establishment of methods for compressing and distributing patterns. DTIC

N94-31888*# National Aeronautics and Space Administration, Washington, DC.

INDEX TO NASA NEWS RELEASES AND SPEECHES, 1993
Apr. 1994 86 p
(NASA-TM-109722; NAS 1.15:109722) Avail: CASI HC A05/MF A01

This issue of the Index to NASA News Releases and Speeches contains a listing of news releases distributed by the Office of Public Affairs, NASA Headquarters, and a selected listing of speeches presented by members of the Headquarters staff during 1993. The index is arranged in six sections: subject index, personal names index, news release number index, accession number index, speeches, and news releases. Author

N94-31930# Carnegie-Mellon Univ., Pittsburgh, PA. Dept. of Computer Science.
COMPILER TECHNIQUES FOR MANAGING DATA MOTION Ph.D. Thesis
John S. Pieper Dec. 1993 162 p
(Contract MDA972-90-C-0035; ARPA Order 7330)
(AD-A276514; CMU-CS-93-217) Avail: CASI HC A08/MF A02

Software caching, automatic algorithm blocking, and data overlays are different names for the same problem: compiler management of data movement throughout the memory hierarchy. Modern high-performance architectures often omit hardware support for moving data between levels of the memory hierarchy: iWarp does not include a data cache, and Cray supercomputers do not have virtual memory. These systems have effectively traded a more complicated programming model for performance by replacing a hardware-controlled memory hierarchy with a simple fast memory. The simpler memories have less logic in the critical path, so the cycle time of the memories is improved. For programs which fit in the resulting memory, the extra performance is great. Unfortunately, the driving force behind supercomputing today is a class of very large scientific problems, both in terms of computation time and in terms of the amount of data used. Many of these programs do not fit in the memory of the machines available. When architects trade hardware support for data migration to gain performance, control of the memory hierarchy is left to the programmer. Either the program size must be cut down to fit into the machine, or every loop which accesses more data than will fit into memory must be restructured by hand. This thesis describes how a compiler can relieve the programmer of this burden and automate data motion throughout the memory hierarchy without direct hardware support. DTIC

N94-32090# Industrial Coll. of the Armed Forces, Washington, DC.
LIFTING THE FOG OF CORPORATE INFORMATION MANAGEMENT Research Report, Aug. 1992 - Apr. 1993
Charles D. Miller Apr. 1993 49 p
(AD-A276680; NDU-ICAF-93-F22A) Avail: CASI HC A03/MF A01

Corporate information management (CIM) is a very complex, multifaceted program which is being implemented in the Department of Defense. It is so broad and all encompassing that it appears more as a vision than a program. The intent is to operate DOD like a business enterprise, by streamlining how we do business and then implementing state-of-the-art information technology. CIM will impact every facet of DOD, from administrative support to the 'warfighter' in combat. This paper takes a broad look at CIM from a layman's perspective and provides a simplified explanation of the program. DTIC

N94-32105 Nijmegen Univ. (Netherlands). Dept. of Information Systems.
EXPERIENCES WITH EDO: AN EVOLUTIONARY DATABASE OPTIMIZER
Patrick VanBommel 14 Jul. 1993 19 p Limited Reproducibility: More than 20% of this document may be affected by microfiche quality
(TR-93-23; ETN-94-96216) Avail: Issuing Activity (European Space Agency (ESA))

The database design tool EDO (Evolutionary Database Optimizer) is introduced. The term 'evolutionary' refers to a basic feature of the tool. After generating an initial pool of preliminary internal representations for a given conceptual data model, EDO allows a database designer to activate evolution strategies, modifying the preliminary internal representations into more desirable ones. The quality of the internal representations found as yet is used to perform a guided walk through the solution space of alternative internal representations for the conceptual model under consideration. This quality (called fitness) takes into account the expected storage space and the expected average response time of a candidate internal representation. ESA

N94-32210# Industrial Coll. of the Armed Forces, Washington, DC.
UNTYING THE GORDIAN DATA KNOT. A PAPER ON INFORMATION ENGINEERING (IE) AND CORPORATE INFORMATION MANAGEMENT (CIM) Report, Aug. 1992 - Apr. 1993
William F. Reyers Apr. 1993 37 p
(AD-A276862; NDU-ICAF-93-F22) Avail: CASI HC A03/MF A01

DOD must find the best way to transition the data in its legacy and migration systems which today are integrated into a gigantic gordian knot. The Defense Information Systems Agency (DISA) provided the above assessment in September 1992 as part of the DOD status report on the CIM initiative. This assessment succinctly identified the major challenge for CIM. The current data in DOD systems must transition to the future DOD systems. DOD has selected the Information Engineering approach to accomplish this data transition. As such, Information Engineering and its associated data standardization processes become the pacing factors for the successful implementation of CIM. With the success of CIM totally dependent on data standardization, it is important that we understand this effort, the progress to date, and the probability for ultimate success. This paper explores CIM and Information Engineering and discusses several impediments that can hinder CIM if left unaddressed. The paper also contains an alternative to the current data standardization process underway. DTIC

N94-32289 Nijmegen Univ. (Netherlands). Dept. of Information Systems.
AN INFORMATION SYSTEM ORGANIZED AS STRATIFIED HYPERMEDIA
C. A. J. Burgers, H. A. Proper, and T. P. vanderWeide 5 Jul. 1993 21 p Limited Reproducibility: More than 20% of this document may be affected by microfiche quality
(TR-93-12; ETN-94-96209) Avail: Issuing Activity (European Space Agency (ESA))

The integration between stratified hypermedia architecture and information systems is addressed. A relation between modern hypertext approaches and conventional data modeling techniques, such as PSM (Predicator Set Modeling), is investigated. This relation provides the mechanism of query by navigation, in order to facilitate the query formulation problem. ESA

N94-32290 Nijmegen Univ. (Netherlands). Dept. of Information Systems.
EVORM: A CONCEPTUAL MODELLING TECHNIQUE FOR EVOLVING APPLICATION DOMAINS
H. A. Proper and T. P. vanderWeide Jul. 1993 29 p Limited Reproducibility: More than 20% of this document may be affected by microfiche quality
(TR-93-16; ETN-94-96210) Avail: Issuing Activity (European Space Agency (ESA))

EVORM, a modeling technique for evolving application domains is presented. A delimitation of the concept of evolution is provided, based on an earlier developed general theory for such evolutions. This theory makes a distinction between the underlying information structure and its evolution on the one hand, and the description and semantics of operations on the information structure and its population on the other hand. Main issues within this theory are object typing, type relatedness and identification of objects. EVORM is the result of applying this general theory to the object role modeling technique PSM (Predicator Set Modeling), a generalization of ER, EER, FORM and NIAM (Natural language Information Analysis Method). ESA

N94-32293 Selskapet for Industriell og Teknisk Forskning, Trondheim (Norway). Norges Branntekniske Lab.
DESCRIPTION OF DCS (DATA CONVERTING SYSTEM) AND CT (CONE TOOL). A REPRINT OF A NOTE PUBLISHED IN FIRE AND MATERIALS TITLED FIRE TEST DATA AVAILABLE FOR YOUR PURPOSE
K. Opstad and L. E. Loenvik 25 Jun. 1993 9 p Repr. from Fire and Materials, Chichester, England See also PB93-182038
(PB94-138559; STF25-A93026) Avail: Issuing Activity (National Technical Information Service (NTIS))

The EUREFIC (European Reaction to Fire Classification) has produced a lot of fire test data, which are made available through a Data Converting System (DCS). DCS is a simple PC based program which transfers data logger files into a standard fire test data format, given by FDMS (A Fire Data Management System). DCS can also transfer standard data files into

data formats of common spread sheets. The EUREFIC program has made two models for assessing large scale performance of test materials. These models are integrated into a PC program named CT (Cone Tools). NTIS

N94-32382# Science Applications International Corp., San Diego, CA.
THE INTELLIGENT MONITORING SYSTEM: GENERIC DATABASE INTERFACE (GDI). REVISED USER MANUAL Technical Report, 27 Nov. 1991 - 25 Feb. 1994
Jean Anderson, Mari Mortell, Bonnie MacRitchie, and Howard Turner 3 Jan. 1994 140 p
(Contract MDA972-92-C-0026; ARPA Order 6266)
(AD-A277131; SAIC-93/1001) Avail: CASI HC A07/MF A02

The Generic Database Interface (GDI) is a common application programmable to multiple databases, providing two key capabilities: Database access and data management. Database access routines allow an application to connect to and query a database with the same GDI call whether the target database is ORACLE, POSTGRES, or SYBASE. Data to and from the database are managed in the native format of the application, making it possible to provide a seamless integration of application and database. DTIC

N94-32487 Memphis State Univ., TN.
THE RELATIONSHIP BETWEEN INTEGRATIVE TASK DESIGN FOR INFORMATION SYSTEMS PROFESSIONALS AND PERCEIVED INFORMATION SYSTEMS EFFECTIVENESS Ph.D. Thesis
Stanley E. Gambill 1992 128 p
Avail: Univ. Microfilms Order No. DA9311442

This dissertation examines the problem of task design for information systems (IS) professionals and investigates the relationship between integrative task design and perceived information systems effectiveness. A conceptual model was developed that integrated important job design factors from expectancy theory, goal setting theory, equity theory, and job characteristics theory. The model proposed that these important job design factors were positively related to perceived information systems effectiveness. One key issue which should be noted is that this study was concerned with perceived effectiveness of the total IS function, not just individual employees or systems. This is a departure from most prior studies dealing with task design. The level of analysis is usually the individual employee and the focus is on the relationship between task design and individual work motivation and performance. A field study was conducted where data was gathered via questionnaires from thirty organizations. Job design factors identified as important by participating organizations included feedback from the job, feedback on goals, goal specificity, employee voice, skill variety, and participation in goal setting. Results of the study also indicate that employee voice, feedback on goals, autonomy, task identity, goal specificity, and participation in goal setting are positively related to perceived information systems effectiveness as measured by hourly users of information systems services. Limitations of the research and practical implications for both IS practitioners and academics are discussed. Several avenues for future research are presented as well. Dissert. Abstr.

N94-32488 Rutgers - The State Univ., New Brunswick, NJ.
RELATIONSHIPS BETWEEN ACCESS AND USE IN INFORMATION SYSTEMS: REMOTE ACCESS TO AND BROWSING OF ONLINE CATALOGS Ph.D. Thesis
Pamela Snelson 1993 118 p
Avail: Univ. Microfilms Order No. DA9320536

Ownership of personal computers, automation of information resources, and installation of campus networks allow increased access to academic information systems. An interesting research question arises: How is accessibility related to the use of information systems? This study examined two groups of online catalog users segregated by their method of access to the online system: access via terminals located in the library or remote workstations connected to the campus network. An online survey collected demographic data, perceptions on source and terminal accessibility, and information on usage, task variety, and search satisfaction. Transaction logs furnished data on browsing behavior, while interviews of both groups of users provided additional information about remote use. Results indicate that remote use of online information systems is comparable to traditional in-library use. There are no statistically significant differences in information source accessibility, browsing, task variety, or satisfaction. However, overall perceptions of accessibility are high for both groups and contribute to subjective satisfaction. Task variety may be a function of accessibility and is also a contributing factor to satisfaction. Since these results do not support the original model, a revised model consonant with the data is proposed. The trends noted above are not limited to libraries and other information centers. Online catalogs are but one application of interactive computer systems. Automated teller machines and shopping via CompuServe are two examples of business transactions that are now conducted from remote sites. When considered in this broader context, online catalog searching is an example of human interaction with computers. Research conducted within the framework of online catalogs will be useful in the larger category of human adaptation to technological innovations. Dissert. Abstr.

N94-32499 George Mason Univ., Fairfax, VA.
A SIMULATION OF UNCERTAIN REASONING ON PARAMETRIC DATABASES USING DATA-DEPENDENCY DERIVED INFERENCE NETS Ph.D. Thesis
Robert E. Eek 1993 183 p
Avail: Univ. Microfilms Order No. DA9320193

Users of parametric databases must achieve high recall and precision (retrieval effectiveness) on pre-existing collections of uncertain data. Such databases, common in the military intelligence community, are used to identify and evaluate such things as radar systems whose characteristics are inherently imprecise and usually only partially known. Existing Boolean queries against such databases cannot reliably retrieve information when, as often occurs, newly observed data fall outside the parameter range limits of a database's records. This research first develops and then simulates a database query methodology that demonstrates high retrieval effectiveness on uncertain parametric data. The query methodology developed in this research addresses two issues necessary to the reliable, effective retrieval of uncertain and incomplete data. First, it provides a method for deriving verifiable argument structure in the form of inference nets using the data dependencies in a database scheme. That method can be used for inductive reasoning on parametric databases. Second, it proposes evidence evaluation methodologies that operate efficiently and reliably in a shared database environment. Two set-theoretic methods, fuzzy sets, and Baconian rough sets are discussed. The simulation applies data dependency derived inference nets and the two evidence evaluation models to parametric databases used by electronics intelligence (ELINT) analysts. The evaluation methods are implemented in a manner appropriate to parametric data ranges that represent statistical compilations of previously observed data values. The simulation compares the retrieval effectiveness of data dependency derived inference nets, one using fuzzy set and the other Baconian evaluation, to that of conventional database queries using Boolean evaluation methods. The data collections and associated observations used by the simulation include data variance where observations exceed recorded range limits. The results of this research demonstrate that database management systems designed for general business applications can support reasoning on uncertain information. The formal inference structuring method of data dependency derived inference nets is applicable to many areas where uncertain information must be processed. Dissert. Abstr.

N94-32506 Nijmegen Univ. (Netherlands). Dept. of Information Systems.
INFORMATION DISCLOSURE IN EVOLVING INFORMATION SYSTEMS: TAKING A SHOT AT A MOVING TARGET
H. A. Proper and T. P. vanderWeide 17 Sep. 1993 22 p Limited Reproducibility: More than 20% of this document may be affected by microfiche quality
(TR-93-22; ETN-94-96215) Avail: CASI HC A03

A manipulation language for evolving information systems is introduced. Evolving information systems go beyond the capacity of conventional database systems, not only as they incorporate a time dimension, but also since they allow all aspects of the system to evolve. The introduced language is related to the philosophy underlying NIAM (Natural language Information Analysis Method). This method investigates the grammar of the communication in the universe of discourse. Usually this grammar is depicted as an information structure diagram (NIAM or ER schema). The language Elisa-D, which is based on this grammar, is described. Queries in this language have a direct meaning in the universe of discourse, while natural language expressions are easily formalized in this language. ESA

N94-32633 Naval Postgraduate School, Monterey, CA.
MULTIDIMENSIONAL SCALING OF USER INFORMATION SATISFACTION M.S. Thesis
Synthia S. Jones Dec. 1993 120 p Limited Reproducibility: More than 20% of this document may be affected by microfiche quality
(AD-A277230) Avail: Issuing Activity (Defense Technical Information Center (DTIC))

The objective of this study was to determine if multidimensional scaling reveals more about user perception of satisfaction with information systems than did factor analysis. Multidimensional scaling shed a different light on information satisfaction data, making them easier to visualize and interpret. While the differences were not substantial between multidimensional scaling and factor analysis, we concluded that the possibility of remarkably new insights gained through multidimensional scaling were well worth the small marginal cost of undertaking the analysis. Multidimensional scaling (MDS) provides an information technology (IT) manager with possible new perspectives in the analysis of user's satisfaction with information and with information systems. The technique probes for meanings locked in user satisfaction data that are not accessible by other analytic procedures. IT managers should be, in all cases, skeptical of contrived hypothesis testing factor analyses that deal with satisfaction data only at its face value. MDS gives managers a tool by which they can identify meanings beyond the obvious. Coupled with the careful and effective use of the semantic differential question format, MDS is a powerful means to escape the fatal flaw in data gathered by survey questionnaires: socially desirable responses. DTIC

N94-32635# Westinghouse Savannah River Co., Aiken, SC.
MANAGING PERFORMANCE OF DB2 AD HOC REPORTS
A. Chow 1994 9 p Presented at the 4th Annual Conference of the International DB2 Users Group, San Diego, CA, 8-12 May 1994
(Contract DE-AC09-89SR-18035)
(DE94-006669; WSRC-MS-94-029; CONF-940595-1) Avail: CASI HC A02/MF A01

The DB2 financial reporting systems at Westinghouse Savannah River Company consists of 212 standardized reports that over 1034 users have accessed in 1993 to generate their reports. Each report has a range of selection criteria that the users can specify. Depending on the selection criteria, a report can access from a few rows to millions of rows of data. When this new DB2 system went into production in 1992, the CPU was at 100% utilization. From the beginning, ad hoc reports had a backlog of 4-5 days. Since DB2 was a new DBMS, most people blamed the poor report turn around times on DB2 as an inefficient DBMS and on a shortage of CPU cycles. Since we are unable to purchase a more powerful CPU, the only option left to us was to improve report turn around was system and application performance tuning. This document presents our efforts in these areas. Education of users in report submission was a starting point. And as to index tuning techniques that were applied, we created more friendly indexes, used clustering indexes, and used a reorganizing mechanism. A more efficient SQL was written which saved a lot of money. DOE

N94-32676# Oak Ridge National Lab., TN.
USING THE NATIONAL INFORMATION INFRASTRUCTURE FOR SOCIAL SCIENCE, EDUCATION, AND INFORMED DECISION MAKING
B. E. Tonn Jan. 1994 27 p
(Contract DE-AC05-84OR-21400)
(DE94-005442; ORNL/TM-12651) Avail: CASI HC A03/MF A01

The United States has aggressively embarked on the challenging task of building a National Information Infrastructure (NII). This infrastructure will have many levels, extending from the building block capital stock that composes the telecommunications system to the multitude of higher tier applications hardware and software tied to this system. This 'White Paper' presents a vision for a second and third tier national information infrastructure that focuses exclusively on the needs of social science, education, and decision making (NII-SSEDM). NII-SSEDM will provide the necessary data, information, and automated decision support and educational tools needed to help this nation solve its most pressing social problems. The proposed system has five components: data collection systems; databases; statistical analysis and modeling tools; policy analysis and decision support tools; and materials and software specially designed for education. This paper contains: a vision statement for each component; comments on progress made on each component as of the early 1990s; and specific recommendations on how to achieve the goals described in the vision statements. The white paper also discusses how the NII-SSEDM could be used to address four major social concerns: ensuring economic prosperity; health care; reducing crime and violence; and K-12 education. Examples of near-term and mid-term goals (e.g., pre-and post Year 2000) are presented for consideration. Although the development of NII-SSEDM will require a concerted effort by government, the private sector, schools, and numerous other organizations, the success of NH-SSEDM is predicated upon the identification of an institutional 'champion' to acquire and husband key resources and provide strong leadership and guidance. DOE

N94-32808# Sandia National Labs., Albuquerque, NM.
INFORMATION SYSTEMS TO ENHANCE TECHNOLOGY EXCHANGE
Tom Hunter, Mark Harrington, Charlene Harlan, and Eugene Drozhko 1994 4 p Presented at the Waste Management 1994, Tucson, AZ, 27 Feb. - 3 Mar. 1994
(Contract DE-AC04-94AL-85000)
(DE94-007744; SAND-93-3967C; CONF-940225-52) Avail: CASI HC A01/MF A01

A fundamental part of international technology exchange is the compilation and dissemination of information. Worldwide environmental problems and technology development activities form the basis for important opportunities across the world and especially for those in the former Soviet Union. Recently, important agreements have been reached among Russian institutes engaged in environmental work and the US Department of Energy (DOE) and its national laboratories. These agreements will allow a systematic compilation of information on environmental contamination problems in Russia that can be included in DOE's environmental information systems. A computer hardware and software system has been loaned to Russian scientists by the DOE for the sharing of environmental software and data, while establishing standards for future information networks. DOE

N94-32827# Edgerton, Germeshausen and Grier, Inc., Idaho Falls, ID.
PRELIMINARY EVALUATION OF THE UNIVERSITY OF SOUTH FLORIDA MOBILE DATA ACQUISITION SYSTEM, THE IDAHO NATIONAL ENGINEERING LABORATORY VERSATILE DATA ACQUISITION SYSTEM, AND THE AUTOLOGGER VEHICLE USER SURVEY SYSTEM PRODUCED BY INSTRUMENTAL SOLUTIONS OF OTTAWA, CANADA FOR THE SITE OPERATOR PROGRAM FIELD DATA COLLECTION
D. M. Kiser and R. A. Richardson Sep. 1993 39 p
(Contract DE-AC07-76ID-01570)
(DE94-008514; EGG-EP-10948) Avail: CASI HC A03/MF A01

The Electric Vehicle (EV) Site Operator Program is currently composed of thirteen Site Operators. In addition to operating electric vehicles for demonstration of the technology, the Site Operators also perform operational field testing. Data collected by the programs are input to the Site Operator Database at each site and transmitted, periodically, to the database at the INEL. As the program has expanded, some Site Operators have begun operating vehicles at sites remote from their offices. With the advent of these expanded test programs, it is necessary to consider in-vehicle, automated data acquisition systems. Three of these in-vehicle, data acquisition systems have been designed and constructed. The Mobile Data Acquisition System (MDAS) was designed and constructed by Sigma TecSystems, Inc. located in Tampa, Florida. The Versatile Data Acquisition System (VDAS) was designed and constructed at the INEL under the guidance of the Electric and Hybrid Vehicle (EHV) Program. The AUTOLOGGER Vehicle User Survey System produced by Instrumental Solutions of Ottawa, ON. Because the USF MDAS is a new system proposed for use by the Site Operator Program, the purpose of this report is to provide a preliminary evaluation of the MDAS by comparing the system to the proven VDAS. Data used to perform the comparison was acquired by a review of the MDAS literature provided by the USF, and by a demonstration of the MDAS and its performance, provided by the USF to INEL personnel. A brief discussion of the AUTOLOGGER is also included, for comparison, because it is being used by Southern California Edison (SCE), one of the Site Operator Program participants who recommends the unit as a good system. DOE

N94-32829*# National Aeronautics and Space Administration. Langley Research Center, Hampton, VA.

NASA/DOD AEROSPACE KNOWLEDGE DIFFUSION RESEARCH PROJECT. PAPER 5: AEROSPACE LIBRARIANS AND TECHNICAL INFORMATION SPECIALISTS AS INFORMATION INTERMEDIARIES: A REPORT OF PHASE 2 ACTIVITIES OF THE NASA/DOD AEROSPACE KNOWLEDGE DIFFUSION RESEARCH PROJECT

Thomas E. Pinelli and John M. Kennedy 1990 15 p Presented at the 81st Annual Conference of the Special Libraries Association Aerospace Division, Pittsburgh, PA, 13 Jun. 1990 See also A91-19804

(NASA-TM-109777; NAS 1.15:109777; AD-B175123L) Avail: CASI HC A03/MF A01

The objective of the NASA/DOD Aerospace Knowledge Diffusion Research Project is to provide descriptive and analytical data regarding the flow of scientific and technical information (STI) at the individual, organizational, national, and international levels, placing emphasis on the systems used to diffuse the results of federally funded aerospace STI. An overview of project assumptions, objectives, and design is presented and preliminary results of the phase 2 aerospace library survey are summarized. Phase 2 addressed aerospace knowledge transfer and use within the larger social system and focused on the flow of aerospace STI in government and industry and the role of the information intermediary in knowledge transfer. CASI

N94-32830*# National Aeronautics and Space Administration. Langley Research Center, Hampton, VA.

NASA/DOD AEROSPACE KNOWLEDGE DIFFUSION RESEARCH PROJECT. PAPER 6: AEROSPACE KNOWLEDGE DIFFUSION IN THE ACADEMIC COMMUNITY: A REPORT OF PHASE 3 ACTIVITIES OF THE NASA/DOD AEROSPACE KNOWLEDGE DIFFUSION RESEARCH PROJECT

Thomas E. Pinelli and John M. Kennedy 1990 19 p Presented at the 1990 Annual Conference of the American Society for Engineering Education Engineering Libraries Division, Toronto, Ontario, 27 Jun. 1990 See also A91-19803

(NASA-TM-109771; NAS 1.15:109771; AD-A252563) Avail: CASI HC A03/MF A01

The objective of the NASA/DOD Aerospace Knowledge Diffusion Research Project is to provide descriptive and analytical data regarding the flow of scientific and technical information (STI) at the individual, organizational, national, and international levels, placing emphasis on the systems used to diffuse the results of federally funded aerospace STI. An overview of project assumptions, objectives, and design is presented and preliminary results of the phase 3 survey of faculty and students are summarized. Phase 3 addressed the information-seeking habits, practices and attitudes of U.S. aerospace engineering and science students and faculty. In addition, it sought to determine the kind and extent of training/education which faculty and students receive in the use of information sources. CASI

N94-32831*# National Aeronautics and Space Administration. Langley Research Center, Hampton, VA.

NASA/DOD AEROSPACE KNOWLEDGE DIFFUSION RESEARCH PROJECT. PAPER 10: THE NASA/DOD AEROSPACE KNOWLEDGE DIFFUSION RESEARCH PROJECT

Thomas E. Pinelli, John M. Kennedy, and Rebecca O. Barclay 1991 16 p Repr. from Government Information Quarterly, v. 8, no. 2, 1991 p 219-233 See also A91-35445

(ISSN 0740-624X)

(NASA-TM-109769; NAS 1.15:109769; AD-A252152) Avail: CASI HC A03/MF A01

The goal of the NASA/DOD Aerospace Knowledge Diffusion Research Project is to further understanding of the dissemination of aerospace information and technology into the research and development process. The project covers practices of aerospace engineers and scientists in obtaining scientific and technical information (STI) as well as the transfer of STI between government and industry, between individuals and organizations in the academic community, and between non-U.S. groups. The benefits of STI diffusion for maximizing research and development productivity and the industrial competitiveness of the aerospace industry are discussed. CASI

N94-32832*# National Aeronautics and Space Administration. Langley Research Center, Hampton, VA.

NASA/DOD AEROSPACE KNOWLEDGE DIFFUSION RESEARCH PROJECT. PAPER 12: THE DIFFUSION OF FEDERALLY FUNDED AEROSPACE RESEARCH AND DEVELOPMENT (R/D) AND THE INFORMATION SEEKING BEHAVIOR OF US AEROSPACE ENGINEERS AND SCIENTISTS

Thomas E. Pinelli, John M. Kennedy, and Rebecca O. Barclay 1991 17 p Presented at the 82d Annual Conference of the Special Libraries Association, San Antonio, TX, 11 Jun. 1991 See also A92-29652

(NASA-TM-109404; NAS 1.15:109404) Avail: CASI HC A03/MF A01

In this paper, the diffusion of federally funded aerospace R&D is explored from the perspective of the information-seeking behavior of U.S. aerospace engineers and scientists. The following three assumptions frame this exploration: (1) knowledge production, transfer, and utilization are equally important components of the aerospace R&D process; (2) the diffusion of knowledge resulting from federally funded aerospace R&D is indispensable for the U.S. to remain a world leader in aerospace; and (3) U.S. government technical reports, produced by NASA and DOD, play an important, but as yet undefined, role in the diffusion of federally funded aerospace R&D. A conceptual model for federally funded aerospace knowledge diffusion, one that emphasizes U.S. goverment technical reports, is presented. Data regarding three research questions concerning the information-seeking behavior of U.S. aerospace engineers and scientists are also presented. Author (revised)

N94-32833*# National Aeronautics and Space Administration. Langley Research Center, Hampton, VA.

NASA/DOD AEROSPACE KNOWLEDGE DIFFUSION RESEARCH PROJECT. PAPER 18: SCIENTIFIC AND TECHNICAL INFORMATION (STI) POLICY AND THE COMPETITIVE POSITION OF THE US AEROSPACE INDUSTRY

Peter Hernon (Simmons Coll., Boston, MA.) and Thomas E. Pinelli Jan. 1992 11 p Presented at the 30th Aerospace Sciences Meeting of the American Institute of Aeronautics and Astronautics, Reno, NV, 9 Jan. 1992 See also A92-28233

(NASA-TM-109782; NAS 1.15:109782; AIAA Paper 92-0796; AD-B175124L) Avail: CASI HC A03/MF A01

With its contribution to trade, its coupling with national security, and its symbolism of U.S. technological strength, the U.S. aerospace industry holds a unique position in the Nation's industrial structure. Federal science and technology policy and Federal scientific and technical information (STI) policy loom important as strategic contributions to the U.S. aerospace industry's leading competitive position. However, three fundamental policy problems exist. First, the United States lacks a coherent STI policy and a unified approach to the development of such a policy. Second, policymakers fail to understand the relationship of STI to science and technology policy. Third, STI is treated as a part of general information policy, without any recognition of its uniqueness. This paper provides an overview of the Federal information policy structure as it relates to STI and frames the policy issues that require resolution. Author (revised)

N94-32834*# National Aeronautics and Space Administration. Langley Research Center, Hampton, VA.

NASA/DOD AEROSPACE KNOWLEDGE DIFFUSION RESEARCH PROJECT. PAPER 11: THE VOICE OF THE USER: HOW US AEROSPACE ENGINEERS AND SCIENTISTS VIEW DOD TECHNICAL REPORTS

Thomas E. Pinelli and John M. Kennedy 1991 64 p Presented at the 1991 Defense Technical Information Center's Managers Planning Conference, Solomon's Island, MD, 1 May 1991 See also A91-41123

(NASA-TM-109348; NAS 1.15:109348; AD-A252566) Avail: CASI HC A04/MF A01

The project serves to understand how the NASA/DOD research results are transferred into the aerospace R&D process, while providing a basis for understanding the aerospace information dissemination process itself and the implications of the process at the individual, organizational, national, and international levels. The project objectives include understanding the aerospace knowledge diffusion process at its various levels, with particular emphasis on the dissemination of government funded aerospace scientific and technical information (STI); understanding the international aerospace knowledge diffusion process at the individual and organizational levels,

emphasizing the policies and systems used to disseminate the results of government funded aerospace STI; understanding how government technical reports and aerospace librarians assist in the transfer and utilization of knowledge derived from federally funded aerospace R&D; gaining recognition and acceptance in the aerospace community that STI is a valuable resource for innovation, problem solving, and productivity; and assisting in optimizing the effectiveness and efficiency of the STI aerospace transfer system and exchange mechanism. These objectives will be achieved by providing descriptive and analytical data regarding the flow of STI. CASI

N94-32835*# National Aeronautics and Space Administration. Langley Research Center, Hampton, VA.
NASA/DOD AEROSPACE KNOWLEDGE DIFFUSION RESEARCH PROJECT. PAPER 1: THE VALUE OF SCIENTIFIC AND TECHNICAL INFORMATION (STI), ITS RELATIONSHIP TO RESEARCH AND DEVELOPMENT (R/D), AND ITS USE BY US AEROSPACE ENGINEERS AND SCIENTISTS
Thomas E. Pinelli, Rebecca O. Barclay, Myron Glassman, and Walter E. Oliu 1990 21 p Presented at the European Forum on External Information: A Decision Tool, Strasbourg, France, 19 Jan. 1990 See also A90-21931
(NASA-TM-109774; NAS 1.15:109774; AD-A252565) Avail: CASI HC A03/MF A01

This paper is based on the premise that scientific and technical information (STI), its use by aerospace engineers and scientists, and the aerospace research and development (R&D) process are related. We intend to support this premise with data gathered from numerous studies concerned with STI, the relationship of STI to the performance and management of R&D activities, and the information use and seeking behavior of engineers in general and aerospace engineers and scientists in particular. We intend to develop and present a synthesized appreciation of how aerospace R&D managers can improve the efficacy of the R&D process by understanding the role and value of STI in this process. Derived from text

N94-32836*# National Aeronautics and Space Administration. Langley Research Center, Hampton, VA.
NASA/DOD AEROSPACE KNOWLEDGE DIFFUSION RESEARCH PROJECT. REPORT 25: THE TECHNICAL COMMUNICATIONS PRACTICES OF BRITISH AEROSPACE ENGINEERS AND SCIENTISTS: RESULTS OF THE PHASE 4 RAeS MAIL SURVEY
Thomas E. Pinelli, Rebecca O. Barclay, and John M. Kennedy May 1994 46 p
(RTOP 505-90-00)
(NASA-TM-109098; NAS 1.15:109098) Avail: CASI HC A03/MF A01

The U.S. government technical report is a primary means by which the results of federally funded research and development (R&D) are transferred to the U.S. aerospace industry. However, little is known about this information product in terms of its actual use, importance, and value in the transfer of federally funded R&D. To help establish a body of knowledge, the U.S. government technical report is being investigated as part of the NASA/DOD Aerospace Knowledge Diffusion Research Project. In this report, we summarize the literature on technical reports and provide a model that depicts the transfer of federally funded aerospace R&D via the U.S. government technical report. We present results from our investigation of aerospace knowledge diffusion vis-a-vis the U.S. government technical report, and present the results of research that investigated aerospace knowledge diffusion vis-a-vis the technical communications practices of British aerospace engineers and scientists. Author

N94-32837*# National Aeronautics and Space Administration. Langley Research Center, Hampton, VA.
NASA/DOD AEROSPACE KNOWLEDGE DIFFUSION RESEARCH PROJECT. REPORT 24: THE TECHNICAL COMMUNICATIONS PRACTICES OF US AEROSPACE ENGINEERS AND SCIENTISTS: RESULTS OF THE PHASE 1 SAE MAIL SURVEY
Thomas E. Pinelli, Rebecca O. Barclay, and John M. Kennedy May 1994 53 p
(RTOP 505-90-00)
(NASA-TM-109088; NAS 1.15:109088) Avail: CASI HC A04/MF A01

The U.S. government technical report is a primary means by which the results of federally funded research and development (R&D) are transferred to the U.S. aerospace industry. However, little is known about this information product in terms of its actual use, importance, and value in the transfer of federally funded R&D. To help establish a body of knowledge, the U.S. government technical report is being investigated as part of the NASA/DOD Aerospace Knowledge Diffusion Research Project. In this report, we summarize the literature on technical reports and provide a model that depicts the transfer of federally funded aerospace R&D via the U.S. government technical report. We present results from our investigation of aerospace knowledge diffusion vis-a-vis the U.S. government technical report, and present the results of research that investigated aerospace knowledge diffusion vis-a-vis the technical communications practices of U.S. aerospace engineers and scientists affiliated with the Society of Automotive Engineers (SAE). Author

N94-32856# Stockholm Univ. (Sweden). Inst. of Physics.
A FLEXIBLE IBM-PC BASED DATA ACQUISITION SYSTEM FOR NUCLEAR PHYSICS EXPERIMENTS
B. Hovander, A. Johansson, G. Appelquist, A. Ekholm, K. Fransson, and C. Bohm Sep. 1992 8 p
(USIP-92-02; ETN-93-94845) Avail: CASI HC A02/MF A01

A SCSI-bus data acquisition module, which serves up to 15 12-bit NIM-standard spectroscopy ADC's, is described. When operating in cascade mode, 8 modules may serve up to 112 ADC's. The module was primarily developed for use in nuclear physics experiments. A typical system configuration consists of a data acquisition module, a SCSI-bus mass storage device (Video-8 or DAT), and a personal computer system controller. The latter also serves as a monitor allowing on-line evaluation of the quality of the incoming experimental data. The module has a micro-controller, a SCSI-bus controller, and a field programmable gate array as main components. The gate array implements most of the ADC arbitration and read-out logic. The module was designed to allow a high degree of flexibility. This was accomplished by allowing the control programs and gate array configurations to be down-loaded from the system controller. The design thus permits rather extensive functional modifications without changing the hardware. It also allows thorough testing by down-loading test programs and test configurations. ESA

N94-32987# Naval Research Lab., Bay Saint Louis, MS.
MDFF HELP LIBRARY, VERSION 2: ON-LINE DOCUMENTATION FOR THE MAP DATA FORMATTING FACILITY Final Report
S. A. Myrick, P. W. Wischow, M. C. Lohrenz, M. E. Trenchard, and M. L. Gendron 7 Mar. 1994 211 p
(AD-A277763; NRL/MR/7441-93-7071) Avail: CASI HC A10/MF A03

The purpose of this report is to describe on-line documentation for the Naval Research Laboratory's Map Data Formatting Facility (MDFF). The MDFF utilizes Digital Equipment Corporation (DEC) computers to process several types of data including Compressed Aeronautical Chart, Compressed Nautical Chart, and Digital Landmass System. Using DEC software utilities, online documentation has been developed that provides information pertaining to the processing and compression of these data types and to other topics that are specific to the MDFF. DTIC

N94-33256 Defense Technical Information Center, Alexandria, VA.
DTIC THESAURUS ON DISKETTE WITH dBASE 4.1 RUNTIME (COMPUTER DISKETTE)
1993 9 p See also AD-A268855, AD-M000310, AD-M000311, AD-M000309, and AD-M000312
(AD-M000306; NONP-DTIC-DK-94-2360) Avail: Issuing Activity (Defense Technical Information Center (DTIC))

The DTIC Thesaurus provides a basic multidisciplinary subject term vocabulary used by DTIC to index and retrieve scientific and technical information from its various databases and to aid DTIC's users in their information storage and retrieval operations. System capabilities of the diskette version include: posting term, user reference, and hierarchy search and display; posting term search by any word within the full term (KWOC listing); posting term and use reference search by truncated entry of the beginning characters of the first word(s) of the term; two drill-down expansions within thesaurus displays; and meaningful 'not found' messages displayed and retained on search screens. DTIC

N94-33257 Defense Technical Information Center, Alexandria, VA.
DTIC THESAURUS ON DISKETTE (ASC2) (COMPUTER DISKETTE)
1993 1 p See also AD-M000310, AD-M000311, AD-M000312,

AD-M000306, and AD-A268855
(AD-M000309; NONP-DTIC-DK-94-2362) Avail: Issuing Activity (Defense Technical Information Center (DTIC))

The DTIC Thesaurus provides a basic multidisciplinary subject term vocabulary used by DTIC to index and retrieve scientific and technical information from its various databases and to aid DTIC's users in their information storage and retrieval operations. System capabilities of the diskette version include: posting term, user reference, and hierarchy search and display; posting term search by any work within the full term (KWOC listing); posting term and use reference search by truncated entry of the beginning characters of the first word(s) of the term; two drill-down expansions within thesaurus displays; and meaningful 'not found' messages displayed and retained on search screens. DTIC

N94-33258 Defense Technical Information Center, Alexandria, VA.
DTIC THESAURUS ON DISKETTE WITHOUT RUNTIME (COMPUTER DISKETTE)
1993 1 p See also AD-M000311, AD-M000309, AD-M000312, AD-M000306 and AD-A268855
(AD-M000310) Avail: Issuing Activity (Defense Technical Information Center (DTIC))

The DTIC Thesaurus provides a basic multidisciplinary subject term vocabulary used by DTIC to index and retrieve scientific and technical information from its various databases and to aid DTIC's users in their information storage and retrieval operations. System capabilities of the diskette version include: posting terms, user reference, and hierarchy search and display; posting term search by any word within the full term (KWOC listing); posting term and use reference search by truncated entry of the beginning characters of the first word(s) of the term; two drill-down expansions with thesaurus displays; and meaningful 'not found' messages displayed and retained on search screens. DTIC

N94-33259 Defense Technical Information Center, Alexandria, VA.
DTIC THESAURUS ON DISKETTE WITHOUT RUNTIME (COMPUTER DISKETTE)
1993 See also AD-M000311, AD-M000309, AD-M000310, AD-M000306, and AD-A268855
(AD-M000312; NONP-DTIC-DK-94-2365) Avail: Issuing Activity (Defense Technical Information Center (DTIC))

The DTIC Thesaurus provides a basic multidisciplinary subject term vocabulary used by DTIC to index and retrieve scientific and technical information from its various databases and to aid DTIC's user in their information storage and retrieval operations. System capabilities of the diskette version include: posting term, user reference, and hierarchy search and display; posting term search by any word within the full term (KWOC listing); posting term and use reference search by truncated entry of the beginning characters of the first word(s) of the term; two drill-down expansions within thesaurus displays; and meaningful 'not found' messages displayed and retained on search screens. DTIC

N94-31038*# National Aeronautics and Space Administration. Marshall Space Flight Center, Huntsville, AL.
LDEF MATERIALS SPECIAL INVESTIGATION GROUP'S DATA BASES
John W. Strickland (BAMSI, Inc., Huntsville, AL.), Joan G. Funk (National Aeronautics and Space Administration. Langley Research Center, Hampton, VA.), and John M. Davis *In its* LDEF Materials Results for Spacecraft Applications Dec. 1993 p 371-376 (For primary document see N94-31012 09-12)
Avail: CASI HC A02/MF A04

N94-32428*# National Aeronautics and Space Administration. Ames Research Center, Moffett Field, CA.
A HYPERTEXT SYSTEM THAT LEARNS FROM USER FEEDBACK
Nathalie Mathe *In* NASA, Washington, Technology 2003: The Fourth National Technology Transfer Conference and Exposition, Volume 2 Feb. 1994 p 55-61 (For primary document see N94-32420 09-99)
Avail: CASI HC A02/MF A04

N94-32441*# University of Central Florida, Orlando. Dept. of Computer Science.
HIGH-SPEED DATA SEARCH
James N. Driscoll *In* NASA, Washington, Technology 2003: The Fourth National Technology Transfer Conference and Exposition, Volume 2 Feb. 1994 p 171-180 (For primary document see N94-32420 09-99)
Avail: CASI HC A02/MF A04

N94-32442*# Office of Naval Research, Arlington, VA.
DATABASE TOMOGRAPHY FOR COMMERCIAL APPLICATION
Ronald N. Kostoff and Henry J. Eberhart *In* NASA, Washington, Technology 2003: The Fourth National Technology Transfer Conference and Exposition, Volume 2 Feb. 1994 p 181-189 (For primary document see N94-32420 09-99)
Avail: CASI HC A02/MF A04

N94-32443*# Analex Space Systems, Inc., Cocoa Beach, FL.
AUTOMATED MAINFRAME DATA COLLECTION IN A NETWORK ENVIRONMENT
David L. Gross *In* NASA, Washington, Technology 2003: The Fourth National Technology Transfer Conference and Exposition, Volume 2 Feb. 1994 p 190-197 (For primary document see N94-32420 09-99)
Avail: CASI HC A02/MF A04

N94-32444*# National Aeronautics and Space Administration. Marshall Space Flight Center, Huntsville, AL.
BEGINNING THE 21ST CENTURY WITH ADVANCED AUTOMATIC PARTS IDENTIFICATION (API)
Fred Schramm and Don Roxby *In* NASA, Washington, Technology 2003: The Fourth National Technology Transfer Conference and Exposition, Volume 2 Feb. 1994 p 198-204 (For primary document see N94-32420 09-99)
Avail: CASI HC A02/MF A04

N94-32469*# University of Central Florida, Orlando.
AN INTELLIGENT INTERACTIVE VISUAL DATABASE MANAGEMENT SYSTEM FOR SPACE SHUTTLE CLOSEOUT IMAGE MANAGEMENT
James M. Ragusa, Gary Orwig, Michael Gilliam, David Blacklock, and Ali Shaykhian *In* NASA, Washington, Technology 2003: The Fourth National Technology Transfer Conference and Exposition, Volume 2 Feb. 1994 p 422-429 (For primary document see N94-32420 09-99)
(Grant NAG10-0058)
Avail: CASI HC A02/MF A04

N94-33341 Royal Military Coll. of Canada, Kingston (Ontario). Dept. of Mathematics and Computer Science.
MANAGEMENT OF UNCERTAINTY IN KNOWLEDGE-BASED SYSTEMS: A MILITARY PERSPECTIVE
M. C. McKean, J. Fugere, and L. Niem *In its* Proceedings of the Symposium/Workshop on Applications of Expert Systems in DND Apr. 1992 p 113-132 (For primary document see N94-33335 09-66)
Avail: Issuing Activity (Royal Military Coll. of Canada, Vimy Post Office, Kingston, ON K7K 5L0 Canada)

N94-33343 Royal Military Coll. of Canada, Kingston (Ontario). Dept. of Chemistry and Chemical Engineering.
THE HYPERMEDIA TECHNOLOGY AS FRONT END TO KNOWLEDGE PROCESSING SYSTEMS
P. R. Roberge *In its* Proceedings of the Symposium/Workshop on Applications of Expert Systems in DND Apr. 1992 p 153-168 (For primary document see N94-33335 09-66)
Avail: Issuing Activity (Royal Military Coll. of Canada, Vimy Post Office, Kingston, ON K7K 5L0 Canada)

N94-33344 Royal Military Coll. of Canada, Kingston (Ontario). Dept. of Engineering Management.
A PROBLEM-SOLVING APPROACH TO KNOWLEDGE ACQUISITION
J. G. Dumais and A. L. Jenkins *In its* Proceedings of the Symposium/Workshop on Applications of Expert Systems in DND Apr. 1992 p 169-188 (For primary document see N94-33335 09-66)
Avail: Issuing Activity (Royal Military Coll. of Canada, Vimy Post Office, Kingston, ON K7K 5L0 Canada)

83 ECONOMICS AND COST ANALYSIS

Includes cost effectiveness studies.

N94-31361# Massachusetts Inst. of Tech., Cambridge. Artificial Intelligence Lab.
A RADIAL BASIS FUNCTION APPROACH TO FINANCIAL TIME SERIES ANALYSIS Ph.D. Thesis
James M. Hutchinson Dec. 1993 151 p
(Contracts N00014-92-J-1879; N00014-93-1-0385; N00014-91-J-4038)
(AD-A276408; AI-TR-1457) Avail: CASI HC A08/MF A02

Nonlinear multivariate statistical techniques on fast computers offer the potential to capture more of the dynamics of the high dimensional, noisy systems underlying financial markets than traditional models, while making fewer restrictive assumptions. This thesis presents a collection of practical techniques to address important estimation and confidence issues for Radial Basis Function networks arising from such a data driven approach, including efficient methods for parameter estimation and pruning, a pointwise prediction error estimator, and a methodology for controlling the 'data mining' problem. Novel applications in the finance area are described, including customized, adaptive option pricing and stock price prediction. DTIC

N94-31617# Technische Univ., Delft (Netherlands). Faculty of Technical Mathematics and Informatics.
BUDGET ALLOCATION AND MONOPOLISTIC PRICING IN A MULTIPRODUCT FIRM
Hans vanMaaren and Jan Bertus Molenkamp 1993 16 p
(ISSN 0922-5641)
(Rept-93-86; ETN-94-96131) Copyright Avail: CASI HC A03/MF A01

The budget of a multiproduct dominant firm has to be allocated to the several production centers within the firm. The objective is to maximize the firm's profit given price demand functions and production functions of the individual products. A solution method based on Lagrange decomposition is presented. This results in a product ranking having a clear economic interpretation and an analysis of the allocation policy. ESA

84 LAW, POLITICAL SCIENCE AND SPACE POLICY

Includes NASA appropriation hearings; aviation law; space law and policy; international law; international cooperation; and patent policy.

N94-31732# Concordia Univ., Loyola Campus, Montreal (Quebec). Dept. of Geography, Public Policy and Pubic Administration Program.
COMMON PROPERTY RESOURCES AND LOW-LEVEL FLYING IN LABRADOR: FLIGHT, FIGHT OR FANCY? M.A. Thesis
Sherri Labour Sep. 1993 112 p
(ISBN-0-315-87318-3; CTN-94-61240) Copyright Avail: Micromedia Ltd., Technical Information Centre, 240 Catherine Street, Suite 305, Ottawa, Ontario, K2P 2G8, Canada HC/MF

Modern, low-level training flights have been conducted out of the air base at Goose Bay, Labrador since the early 1980s. The flying season is restricted to seven months a year (April to November) over two flight training areas totalling 99,000 square km. The flights usually last 60-90 minutes, often consist of two planes flying in formation, and may come as close as 30 m to the ground. Aboriginal groups have protested against these flights because of their possible effect on the environment and on native life styles based on a hunting and fishing economy. A study is presented which illustrates how the fundamentally different attitudes and values that Euro-Canadians and aboriginals attach to land are at the core of the conflict over low-level flying in Labrador. It is shown how common property resource management strategies can mediate the contrasting attitudes and values of the aboriginals and the Canadian Defence Department with respect to land and nature. Emphasis is placed on understanding the human side of the problem and the personal and political concerns of the people involved in the conflict. Author (CISTI)

N94-33067*# National Aeronautics and Space Administration, Washington, DC.
SPACE HISTORY, SPACE POLICY, AND EXECUTIVE LEADERSHIP
Sylvia K. Kraemer 1993 7 p Presented at the International Space History Symposium, Washington, DC, 14 Oct. 1993
(NASA-TM-109787; NAS 1.15:109787) Avail: CASI HC A02/MF A01

A lecture that attempts to establish the role of space historians in formulating space policy is presented. The discussion focusses on two adages and their relevance to space policy. The adages are as follows: 'write about what you know;' and 'good managers do things right; good executives do the right things.' CASI

N94-31431*# Instituto Tecnologico de Aeronautica, Sao Paulo (Brazil).
LEGAL REGIME OF HUMAN ACTIVITIES IN OUTER SPACE LAW
Carlo Golda *In* NASA. Marshall Space Flight Center, The Second Annual International Space University Alumni Conference Feb. 1994 p 66-75 (For primary document see N94-31425 09-12)
Avail: CASI HC A02/MF A02

85 URBAN TECHNOLOGY AND TRANSPORTATION

Includes applications of space technology to urban problems; technology transfer; technology assessment; and surface and mass transportation.

For related information see also *03 Air Transportation and Safety, 16 Space Transportation,* and *44 Energy Production and Conversion.*

N94-32462*# National Aeronautics and Space Administration. Lyndon B. Johnson Space Center, Houston, TX.
LITERACITY: A MULTIMEDIA ADULT LITERACY PACKAGE COMBINING NASA TECHNOLOGY, RECURSIVE ID THEORY, AND AUTHENTIC INSTRUCTION THEORY
Jerry Willis (Houston Univ., TX.), Dee Anna Willis (Houston Univ., TX.), Clare Walsh (Houston Univ., TX.), Elizabeth Stephens (Houston Univ., TX.), Timothy Murphy (Houston Univ., TX.), Jerry Price (Houston Univ., TX.), William Stevens (Lockheed Engineering and Sciences Co., Houston, TX.), Kevin Jackson (Department of Justice, Washington, DC.), James A. Villareal, and Bob Way *In* NASA, Washington, Technology 2003: The Fourth National Technology Transfer Conference and Exposition, Volume 2 Feb. 1994 p 365-374 (For primary document see N94-32420 09-99)
Avail: CASI HC A02/MF A04

88 SPACE SCIENCES (GENERAL)

No abstracts in this category.

89 ASTRONOMY

Includes radio, gamma-ray, and infrared astronomy, and astrometry.

N94-31210 Colorado Univ., Boulder.
EXTREME ULTRAVIOLET OPACITY SOURCES IN THE DA WHITE DWARF G191-B2B Ph.D. Thesis
Erik Wilkinson 1993 139 p
Avail: Univ. Microfilms Order No. DA9320489

The goal of this work is to evaluate the cause(s) of the short wavelength deficit apparent in existing extreme ultraviolet observations of the DA white dwarf G191-B2B. G191-B2B is a hot (T(sub eff) approximately equal to 55,000 K) white dwarf located 45 parsecs from earth in the constellation of Aurigae. Observations of G191-B2B with the Al/P and LX3000 photometers onboard the European X ray Observatory (EXOSAT) show the count rate of the Al/P photometer (170 A less than or equal to lambda less than or equal to 300 A) is almost ten times higher than the LX3000 (44 A less than or equal to lambda less than or equal to 300 A)

count rate. Pure hydrogen white dwarf model atmospheres predict the photometer count rates should be similar. This discrepancy suggests a short wavelength opacity source(s) is present in the photosphere of G191-B2B. A unique sounding rocket borne instrument with sufficient spectral resolution and sensitivity to investigate the implied opacity source(s) was designed, built, calibrated, and flown. The instrument made observations of G191-B2B between 200 A and 330 A with Delta-lamda = 2 A. The design, calibration, and flight performance of the instrument are discussed. Several absorption features in the spectrum are identified, their statistical significance is evaluated, and potential sources of the features are investigated. Dissert. Abstr.

N94-31786# Stanford Research Inst., Menlo Park, CA.
GAMMA LARGE AREA SILICON TELESCOPE (GLAST)
G. L. Godfrey Nov. 1993 16 p Presented at the 2nd Towards a Major Atmospheric Cerenkov Detector Workshop, Calgary, Ontario, 17-18 Jul. 1993
(Contract DE-AC03-76SF-00515)
(DE94-006439; SU-SLAC-PUB-6390; CONF-9307166-1) Avail: CASI HC A03/MF A01

The recent discoveries and excitement generated by EGRET have prompted an investigation into modern technologies ultimately leading to the next generation space-based gamma ray telescope. The goal is to design a detector that will increase the data acquisition rate by almost two orders of magnitude beyond EGRET, while at the same time improving on the angular resolution, the energy measurement of reconstructed gamma rays, and the triggering capability of the instrument. The GLAST proposal is based on the assertion that silicon particle detectors are the technology of choice for space application: no consumables, no gas volume, robust (versus fragile), long lived, and self triggering. The GLAST detector is roughly modeled after EGRET in that a tracking module precedes a calorimeter. The GLAST Tracker has planes of thin radiatior interspersed with planes of crossed-strip (x,y) 300 micron-pitch silicon detectors to measure the coordinates of converted electron-positron pairs. The gap between the layers (approximately 5 cm) provides a lever arm in track fitting resulting in an angular resolution of 0.1 deg at high energy (the low energy angular resolution at 100 MeV would be about 2 deg, limited by multiple scattering). A possible GLAST calorimeter is made of a mosaic of CsI crystals of order 10 r.l. in depth, with silicon photodiodes readout. The increased depth of the GLAST calorimeter over EGRET's extends the energy range to about 300 GeV. DOE

N94-31790 Massachusetts Univ., Amherst.
CO OBSERVATIONS IN EXTERNAL GALAXIES AND GAS MASS DETERMINATION Ph.D. Thesis
Shuding Xie 1993 250 p
Avail: Univ. Microfilms Order No. DA9316728

We investigate three aspects in the determinations of molecular gas masses from (sup 12)CO, (sup 13)CO, and dust emission. Using the (sup 12)CO, (sup 13)CO J = 2 - 1 and 1 - O as well as CS J = 2 - 1 data obtained with the 14 m FCRAO telescope, in conjunction with radiative transfer calculations, we estimate the average temperature and density of the molecular gas at the centers of two actively star-forming galaxies, NGC 2146 and IC 342. The physical conditions of the gas in the nuclei of these two galaxies differ from those in the disk of our own Galaxy. However, the CO luminosity to molecular gas mass ratios are found to be similar in these two galaxies. The ratios are within a factor of 2 of the value in the Milky Way if the Galactic CO abundance is assumed. We present a simple model to estimate the dust temperature distributions in galaxies based on the FIR/sub mm observations. The uncertainties in the dust mass owing to inexact modeling of the temperature distribution, uncertainty in the emissivity law, imprecision in the observed data, and the presence of a correlation between grain size and temperature are examined. The dust masses are estimated from the derived dust temperature distributions in 12 galaxies making use of the available data at 60, 100, 345, and 761 microns. The comparison between the dust masses obtained from our model calculations and the gas masses deduced from (sup 12)CO J = 1 - O observation yields an average H2-to-dust mass ratio of 181+/-(sup 119, sub 91). In the determination of H2 column density from (sup 13)CO emission the clumpiness of material in molecular clouds has not been considered in the evaluation of the uncertainties. We take this effect into account to examine the uncertainties owing to the use of the LTE approximation. The clumpy cloud model proposed by Kwan and Sanders (1986) is used over a wide range of parameters. Our calculations indicate that the largest uncertainty arises from the assumption that all levels possess a common excitation temperature in estimating the partition function. The partition function can be either over estimated, owing to subthermal excitations in high J levels, or underestimated, probably owing to an underestimate of the mean excitation temperature when the volumn filling factor is so small that the surface coverage factor of antenna beam is less than one. The uncertainties in N(H2) can be reduced by using an alternative formula to estimate the partition function. Dissert. Abstr.

N94-31898 Cornell Univ., Ithaca, NY.
NEAR INFRARED SURVEYS OF HIGH MASS STAR FORMING REGIONS Ph.D. Thesis
Samuel Thomas Megeath 1993 135 p
Avail: Univ. Microfilms Order No. DA9319366

We present near infrared surveys of the DR22, S184, and W3 high mass star forming regions. Each survey region shows evidence of recent massive star formation, either a maser or compact H II region. We have detected dense clusters in each region. The peak densities for the listed magnitude range of the DR22, S184, and W3 clusters are 83 (m(sub k) is less than 17), 56 (m(sub k) is less than 17), and 216 (m(sub K) is less than 16) stars per square arcminute. Deep J (1.25 micron), H (1.65 micron), and K (2.2 micron) images were obtained at the peak density positions for all three clusters. Color-magnitude diagrams show that 68 percent, 98 percent, and 73 percent of the stars in the DR22, S184, and W3 clusters have masses less than 3.6 solar mass. More than 87 percent of the stars in each cluster are consistent with the K versus H-K values of reddened T-Tauri stars. Color-color diagrams reveal that 23 to 72 percent of the sources in S184 show K-band excesses. These excesses are thought to arise in circumstellar disks and are of magnitudes typical for classical T-Tauri stars. In contrast, less than 27 percent of the stars in DR22 show excesses; the majority of the stars have colors consistent with reddened naked T-Tauri stars. H-K colors show that the S184 and W3 clusters have several magnitudes of internal extinction, while the DR22 cluster shows little internal extinction (less than 1 mag). We examine the K-band luminosity function, the number of stars detected per K-band magnitude interval, for each cluster. We find a peak at 15th magnitude for the DR22 cluster. A comparison of the peak with existing models results in an age for the DR22 cluster between 3 x 10(exp 5) years and 1 x 10(exp 6) years. We do not find similar peaks in the S184 and W3 cluster; however, peaks may be hidden by the high internal extinction observed in both clusters. Finally, we propose that the DR22 cluster is a young cluster which has been unveiled by an advancing H II region front. We suggest that the paucity of excesses in the DR22 cluster is the result of disk disruption by the advancing H II region. Dissert. Abstr.

N94-31914# Montreal Univ. (Quebec). Dept. de Sociologie.
CONSTRUCTION OF VISUAL REPRESENTATIONS AND TIME-SPACE ORGANIZATION OF RESOURCES IN ASTRONOMY Ph.D. Thesis [CONSTRUCTION DE REPRESENTATIONS VISUELLES ET ORGANISATION SPATIO-TEMPORELLE DES RESSOURCES EN ASTRONOMIE]
Luc Gauthier Sep. 1991 867 p In ENGLISH and FRENCH
(ISBN-0-315-86694-2; CTN-94-61222) Copyright Avail: Micromedia Ltd., Technical Information Centre, 240 Catherine Street, Suite 305, Ottawa, Ontario, K2P 2G8, Canada HC/MF

The components of the perceptual behavior of a group of astronomers was studied along with some examples of the organization of resources in space and time in astronomy. It is apparent that the work of constructing visual representations at the beginning of astronomical practice happens through the utilization of categories which are not explicitly defined but which nonetheless are no less effective in their incorporation into a perceptual behavior developed by astronomers during their training and their confrontation with their objective. The origin and nature of these categories is reviewed. The processes covered by the concept of laboratory work, as recently used in the sociology of the sciences are brought up to date. To do this, characteristics of astronomical practice with respect to the structure of utilization of resources in time and space were identified and contrasted through definition of the mechanisms allowing this structuring. These mechanisms should be considered to supplant the laboratory notion. CISTI

N94-31951 Washington Univ., Seattle.
A CHEMICAL ANALYSIS OF SOLAR NEIGHBORHOOD DWARFS Ph.D. Thesis
William John Spiesman 1993 154 p
Avail: Univ. Microfilms Order No. DA9326400

In this study we perform a chemical analysis of the most abundant stars of our galaxy, the low mass dwarfs. Little of the chemistry and physics that operate in low mass stars has been measured directly, and most of what we do know about them is based on theory or inferred from higher mass stars. Here we take a first close look at these unwieldy stars using high dispersion spectroscopy, modern stellar atmospheres, and synthetic spectrum techniques. Low mass dwarfs are particularly difficult to study. They are intrinsically faint, so even with modern detectors and large telescopes, we can study only those dwarfs that are very near the sun. Their cool atmospheres are incredibly complex with many molecules contributing to the opacity, and with deep, highly efficient convection. Their spectra are line rich, and since the surface gravities are so high, molecular and atomic lines are almost hopelessly broadened and blended. Despite the difficulties with analyzing these stars, the fact that the evolutionary status of all low mass dwarfs places them unambiguously on the main sequence (or the pre-main sequence) makes knowledge of their chemical content indispensable. Since their convective masses are large, results based on analyses of low mass stars are less susceptible to contamination by impurities which might be added to stellar atmospheres through accretion after star formation. We demonstrate that the temperature scale for the cool dwarfs must be shifted upwards towards warmer temperatures. We present abundance results for a sample of metal-poor and metal-rich K dwarfs showing that the trends of abundance ratios with metallicity seen in giants and in the warmer dwarfs also apply to the lower main sequence. We determine (O/Fe) for the first time from the TiO molecule, with results which are similar to those from atomic lines. Our abundance results for oxygen show that (O/Fe) does not rise above +0.5 for metal poor stars, even at low metallicities. We find that the correlation of sodium abundance with nitrogen that is seen in globular cluster giants also appears in Halo dwarfs. The abundance results for these unevolved stars are interpreted as consequences of the prestellar material from which these stars formed.
Dissert. Abstr.

N94-31968 Cornell Univ., Ithaca, NY.
MEASURING THE HUBBLE CONSTANT AND OUR VIRGO-INFALL VELOCITY INDEPENDENTLY Ph.D. Thesis
Nanyao Lu 1993 180 p
Avail: Univ. Microfilms Order No. DA9318864

We consider two volumes in the local space: AV and BV, in an approximately antipodal geometry relative to the Virgo Cluster (AV: 22(sup h) less than alpha less than 2(sup h), 0(sup o) less than delta less than 20(sup o) and 0 less than upsilon(sub h) less than 3,000 km s(exp -1); BV: 10(sup h)30(sup m) less than alpha less than 13(sup h)30(sup m), 0(sup o) less than delta less than 20(sup o) and 2,500 less than upsilon(sub h) less than 4,500 km s(exp -1). Comparing the galaxies in these two volumes via an I-band Tully-Fisher (TF) relation allows us to independently derive (1) A Hubble ratio, H(sub AB), between the two volumes; and (2) a model independent estimate of Delta(upsilon)(sub double bars), our peculiar velocity in the direction of the Virgo Cluster with respect to the uniformly expanding reference frame of the sample galaxies. High-quality HI 21cm data and I-band CCD photometry were obtained and are presented for the galaxies in the following two samples in the target volumes: (1) a main galaxy sample, called the CfA sample and consisting of 123 disk galaxies, is complete to B(sub T) = 14.5 and was used to derive H(sub AB) and Delta(upsilon)(sub double bar); and (2) a supplementary sample, called the faint sample and consisting of 73 galaxies with B(sub T) less than 14.5, was used to control the Malmquist bias. To reduce both the TF scatter and Malmquist bias, only CfA galaxies with a corrected HI width W(sub R) greater than W(sub R, sup min) were used in our TF analysis, where W(sub R, sup min) approximately equals 181 km s(exp -1) for the AV and approximately 234 for the BV sample. We then corrected the residual Malmquist bias and properly estimated the TF scatter by introducing two 'counterfeit' galaxies. Using the faint sample, we show that the TF dispersion has a dominant and well defined Gaussian peak with an intrinsic rms dispersion sigma(sub TF, sup 0) equivalent to 0.3 mag for W(sub R) greater than or approx. equal to 180 km s(exp -1). We finally found Delta(upsilon)(sub double bar) approximately equal to 410+/- 85 km/s and H(sub AB) approximately equal to 88 +/- 4 km/s Mpc(exp -1). We tested various local velocity models, using the above value of Delta(upsilon)(sub double bar) as a constraint, to explore the variation of H(sub AB)/H(sub O) (where H(sub O) is the postulated Hubble constant for each model). We found: (1) Pure Virgo-infall models in general give a consistent Delta(upsilon)(sub double bar). (2) A bi-infall model involving either a nearby Great Attractor (GA) or a distant GA gives a Delta(upsilon)(sub double bar) which is systematically lower. (3) H(sub AB)/H(sub O) has a mean of 0.95 and a variance less than approximately 6% among all the models. The small variation, attributed to the fact that only a tidal velocity field has effects on H(sub AB), makes the local measurements of H(sub O) meaningful. (4) Our best estimate for the Hubble constant is H(sub O) approximately equals (92 +/- 4)(1 + epsilon)km s(exp -1) Mpc(exp -1), where (1 + epsilon) accounts for the (unknown) possible systematic error in the distances of the local calibrators, which are few in number.
Dissert. Abstr.

N94-31969 Wollongong Univ. (Australia).
NEAR AND FAR INFRARED OBSERVATIONS OF PROTOSTARS AND DARK CLOUDS Ph.D. Thesis
Mark Gerard Suters 1992
Avail: Issuing Activity (MIT Libraries, Rm. 14-0551, Cambridge, MA 02139-4307)

Far infrared point source and extended emission data from the Infrared Astronomical Satellite (IRAS) survey are used to investigate the properties of star formation in the regions of high galactic latitude dark cloud complexes. The properties of individual sources are examined using near infrared spectroscopy and broad band spectral energy distributions. The IRAS signature of star formation is derived by comparing the far infrared colors of a sample of protostars with those of other common far infrared objects. The quality of the IRAS data is ignored for the purposes of this investigation. The criteria developed for identifying protostars from the IRAS Point Source Catalog discriminates against most non-protostellar objects, with the exception of galaxies and HII regions. Objects identified as protostellar according to other criteria are also likely to be identified by the criteria developed. Extended emission data in the far infrared is used to estimate the column density and temperature of several dark cloud complexes, and the optical extinction in the same regions is estimated with the Guide Star Catalog. Temperature and column density share an inverse relationship cloud cores are characterized by column densities above 10(exp 24) hydrogen atoms m(exp -2) and temperatures around 20 K, while the inter cloud medium has column densities below 10(exp 23) atoms m(exp -2) and temperatures above 50 K. The column density, as measured by IRAS, and the optical extinction appear to be related up to values of around 10(exp 25) atoms m(exp -2) and 5 magnitudes respectively but the IRAS detectors appear insensitive to material at higher densities than these. Near infrared spectra of a variety of objects chosen for their youth, including IRAS sources which satisfy the protostar criteria, are investigated. These spectra are categorized into three distinct groups of increasing youth: (1) T Tauri-like spectra, with flat H and K band continua, lacking both Br-gamma emission and CO absorption; (2) FU Orilike spectra, with Br-gamma emission, CO absorption, and 1.9 micron water absorption, and (3) embedded protostar spectra, with red continuum, Br-gamma emission, but lacking CO absorption. The spectral energy distributions (SED's) of the sources are also investigated, wing data at wavelengths from 0.3 micron to 100 microns. All of the objects studied in the near infrared have SED's characteristic of either T Tauri stars or of embedded protostars. There seems little correlation between the evolutionary status assigned to an object on the basis of its SED and that assigned from near infrared spectral features perhaps because the shape of the SED is independent of the evolution of the central object, and depends on geometric considerations such as the orientation of the circumstellar disk in relation to the line of sight from the Earth.
Dissert. Abstr.

N94-32189# Lawrence Livermore National Lab., CA.
DESIGN AND EARLY RESULTS OF THE SODIUM-LAYER LASER GUIDE STAR ADAPTIVE OPTICS EXPERIMENT AT THE LAWRENCE LIVERMORE NATIONAL LABORATORY
D. T. Gavel, C. E. Max, K. Avicola, H. D. Bissinger, J. M. Brase, J. Duff, H. W. Friedman, J. R. Morris, S. S. Olivier, and D. A. Rapp et al 30 Jul. 1993 8 p Presented at the ICO-16 Satellite Conference on Active and

Adaptive Optics, Garching, Germany, 2-5 Aug. 1993
(Contract W-7405-eng-48)
(DE94-006653; UCRL-JC-114837; CONF-9308215-1) Avail: CASI HC A02/MF A01

Adaptive optic systems promise to give diffraction limited performance to ground based telescopes operating at visible and near infrared wavelengths. However, because of the short spatial scale of atmospheric turbulence, the corrected field of view is limited to only a few arc seconds in the visible and to perhaps 10 arc seconds at L band (3.5 mu). A bright point source must be in this field of view as a wavefront reference, but the number density of natural stars is too small for full sky coverage at imaging wavelengths less than 3 mu. A sufficiently bright point source can be artificially generated by a laser, however, and investigations into the use of laser beacons has been proceeding for some time now. Our experiments at Livermore have concentrated on the formation of guide stars in the sodium mesospheric layer at 90 km altitude. We have also designed and built adaptive optics systems that use both artificial and natural guide stars. Experimental results to date have shown great promise for the practicality of this technique in astronomy. DOE

N94-32308 California Univ., Santa Cruz.
A CRITICAL EXAMINATION OF STELLAR ATMOSPHERE THEORY FOR METAL-POOR K-GIANT STARS Ph.D. Thesis
Cristina Morea DalleOre 1993 188 p
Avail: Univ. Microfilms Order No. DA9317939

State of the art model atmospheres are closely examined for a sample of nine bright K-giant stars. For one star, HD 122563, considered a standard for its wealth of data in the literature, the best available spectroscopic data and input parameters were used. We find a serious inconsistency in the atmosphere theory: in three, maybe four, of the stars in the sample, the temperature obtained from excitation and ionization equilibria differs by up to 300 K from the temperature obtained from accurate photometric sources. This error shows up as a slope in the derived Fe abundances versus excitation potential when the photometric temperatures are used. No clear correlation is found between the temperature discrepancy and star characteristics. Several possible causes of error are examined for HD 122563, the standard star. The analysis is carried out with different codes making use of various sets of atomic parameters; all yield comparable slopes. Assumptions made in the atmosphere code are tested; none of them affect the slope in a significant way. Non-LTE corrections are estimated, and a nonhomogeneous atmosphere model is computed yielding no effect on the slope. An analysis similar to the one performed in HD 122563 yields no significant slope in the solar Fe I abundances, ruling out the possibility of systematic errors in the values. A more comprehensive survey of solar Fe abundances is also performed, yielding greater understanding of previously discrepant solar (Fe/H) values in the literature. While these avenues do not lead to an explanation of the slope problem, they show that the slope is not an artifact of the data or of the analysis. Assuming that all elements behave like iron, we estimate possible errors of approximately plus or minus 0.2 dex for HD 122563 in the abundances of elements other than Fe, depending on the excitation potential of the lines adopted in the analysis. Ratios of element abundances calculated on lines with comparable excitation potential should not be affected. The magnitude of these errors does not affect the basic trends in abundance ratios versus metallicity; they are comparable to the observed and as yet unexplained scatter that plagues the same trends. Dissert. Abstr.

N94-32695*# Laser Power Research, San Diego, CA.
DIGITAL IMAGE PROFILERS FOR DETECTING FAINT SOURCES WHICH HAVE BRIGHT COMPANIONS Final Report
Elena Morris, Graham Flint, and Robert Slavey 27 May 1992 214 p
(Contract NAS7-1103; SBIR-08.18-0700)
(NASA-CR-191348; NAS 1.26:191348) Avail: CASI HC A10/MF A03

For this program, an image profiling system was developed which offers the potential for detecting extremely faint optical sources that are located in close proximity to bright companions. The approach employed is novel in three respects. First, it does not require an optical system wherein extraordinary measures must be taken to minimize diffraction and scatter. Second, it does not require detectors possessing either extreme uniformity in sensitivity or extreme temporal stability. Finally, the system can readily be calibrated, or nulled, in space by testing against an unresolved singular stellar source. Author (revised)

N94-32942*# Alabama Univ., Huntsville. Dept. of Physics.
BATSE DATA ANALYSIS Final Report, 4 Feb. - 4 Dec. 1993
William S. Paciesas 1 Feb. 1994 38 p
(Contract NAS8-38609)
(NASA-CR-195818; NAS 1.26:195818) Avail: CASI HC A03/MF A01

The Burst and Transient Source Experiment (BATSE) is one of four instruments on the Compton Observatory which was launched by the space shuttle Atlantis on 5 Apr. 1991. As of the end of Nov. 1993, BATSE detected more than 830 cosmic gamma ray bursts and more than 690 solar flares. Pulsed gamma rays have been detected from at least 16 sources and emission from at least 28 sources (including most of the pulsed sources) has been detected by the earth occultation technique. The daily BATSE operations tasks represent a substantial level of effort and involve a large team which includes MSFC personnel as well as contractors such as UAH. The effort is naturally divided into several areas: data operations, burst operations, occultation operations, and pulsar operations. UAH personnel have been involved to some extent in all of these as well as contributing to various areas of scientific data analysis. Derived from text

N94-31426*# National Aeronautics and Space Administration. Marshall Space Flight Center, Huntsville, AL.
MITIGATION OF ADVERSE ENVIRONMENTAL EFFECTS ON LUNAR-BASED ASTRONOMICAL INSTRUMENTS
Les Johnson, Kurtis L. Dietz, T. W. Armstrong, and B. L. Colborn *In its* The Second Annual International Space University Alumni Conference Feb. 1994 p 1-7 (For primary document see N94-31425 09-12)
Avail: CASI HC A02/MF A02

N94-31430*# Max-Planck-Inst. fuer Extraterrestrische Physik, Garching (Germany).
MULTIWAVELENGTH SEARCH FOR PROTOPLANETARY DISKS
Ralph Neuhaeuser and Theodor Schmidt-Kaler *In* NASA. Marshall Space Flight Center, The Second Annual International Space University Alumni Conference Feb. 1994 p 57-65 Sponsored by Hanns-Seidel-Stiftung and BMFT (For primary document see N94-31425 09-12)
Avail: CASI HC A02/MF A02

90 ASTROPHYSICS

Includes cosmology; celestial mechanics; space plasmas; and interstellar and interplanetary gases and dust.

For related information see also *75 Plasma Physics*.

N94-31086 Stockholm Univ. (Sweden). Dept. of Physics.
FIREWORKS IN VELOCITY AND CONFIGURATION SPACE APPLIED TO COSMOLOGY
Lennard Widlund Oct. 1993 17 p Revised Limited Reproducibility: More than 20% of this document may be affected by microfiche quality
(USIP-93-90; ETN-94-95941) Avail: CASI HC A03

A metagalactic model for the universe, in which the expansion is caused by a series of hierarchical explosions, is developed. The evolution of the distribution of matter is described by a Botzmann equation, for which solutions are found in the nonrelativistic case. By studying the evolution of the peculiar velocities in the metagalaxy, the model can be applied to metagalactic cosmology. An upper limit for the radius of the metagalaxy is obtained. This turns out to be too small to be compatible with the highest redshifts observed. Two modifications of the model are studied, but the difficulties still remain. ESA

N94-31116*# Lunar and Planetary Inst., Houston, TX. Publications Services Dept.
WORKSHOP ON PHYSICS OF ACCRETION DISKS AROUND COMPACT AND YOUNG STARS Abstracts Only
Edison P. Liang, ed. (Rice Univ., Houston, TX.) and Tomasz F. Stepinski, ed. 1994 18 p Workshop held in Houston, TX, 8-10 Apr. 1994
(Contract NASw-4574)
(NASA-CR-195756; NAS 1.26:195756; LPI-TR-94-03-Pt-1) Avail: CASI HC A03/MF A01

The papers that were presented at the Workshop on Physics of Accretion

Disks Around Compact and Young Stars are contained in this volume. The workshop was held on 8-10 Apr. 1994 in Houston, Texas. For individual titles, see N94-31117 through N94-31144.

N94-31117*# Gothenburg Univ. (Sweden).
ACCRETION DISKS AROUND BLACK HOLES Abstract Only
M. A. Abramowicz *In* Lunar and Planetary Inst., Workshop on Physics of Accretion Disks Around Compact and Young Stars 1994 p 1 (For primary document see N94-31116 09-90)
Avail: CASI HC A01/MF A01

The physics of accretion flow very close to a black hole is dominated by several general relativistic effects. It cannot be described by the standard Shakura Sunyaev model or by its relativistic version developed by Novikov and Thorne. The most important of these effects is a dynamical mass loss from the inner edge of the disk (Roche lobe overflow). The relativistic Roche lobe overflow induces a strong advective cooling, which is sufficient to stabilize local, axially symmetric thermal and viscous modes. It also stabilizes the non-axially-symmetric global modes discovered by Papaloizou and Pringle. The Roche lobe overflow, however, destabilizes sufficiently self-gravitating accretion disks with respect to a catastrophic runaway of mass due to minute changes of the gravitational field induced by the changes in the mass and angular momentum of the central black hole. One of the two acoustic modes may become trapped near the inner edge of the disk. All these effects, absent in the standard model, have dramatic implications for time-dependent behavior of the accretion disks around black holes. Author

N94-31118*# Louisiana State Univ., Baton Rouge. Dept. of Physics and Astronomy.
A TWISTED DISK EQUATION THAT DESCRIBES WARPED GALAXY DISKS Abstract Only
K. Barker *In* Lunar and Planetary Inst., Workshop on Physics of Accretion Disks Around Compact and Young Stars 1994 p 1 (For primary document see N94-31116 09-90)
(Grants NAGw-2447; NSF AST-90-08166)
Avail: CASI HC A01/MF A01

Warped H1 gas layers in the outer regions of spiral galaxies usually display a noticeably twisted structure. This structure is thought to arise primarily as a result of differential precession in the H1 disk as it settles toward a 'preferred orientation' in an underlying dark halo potential well that is not spherically symmetric. In an attempt to better understand the structure and evolution of these twisted, warped disk structures, we have utilized the 'twist-equation' formalism. Specifically, we have generalized the twist equation to allow the treatment of non-Keplerian disks and from it have derived the steady-state structure of twisted disks that develop from free precession in a nonspherical, logarithmic halo potential. This generalized equation can also be used to examine the time-evolutionary behavior of warped galaxy disks. Author (revised)

N94-31119*# Louisiana State Univ., Baton Rouge. Dept. of Physics and Astronomy.
A HETEROGENEOUS COMPUTING ENVIRONMENT FOR SIMULATING ASTROPHYSICAL FLUID FLOWS Abstract Only
J. Cazes *In* Lunar and Planetary Inst., Workshop on Physics of Accretion Disks Around Compact and Young Stars 1994 p 1 (For primary document see N94-31116 09-90)
(Grants NAGw-2447; NSF AST-90-08166)
Avail: CASI HC A01/MF A01

In the Concurrent Computing Laboratory in the Department of Physics and Astronomy at Louisiana State University we have constructed a heterogeneous computing environment that permits us to routinely simulate complicated three-dimensional fluid flows and to readily visualize the results of each simulation via three-dimensional animation sequences. An 8192-node MasPar MP-1 computer with 0.5 GBytes of RAM provides 250 MFlops of execution speed for our fluid flow simulations. Utilizing the parallel virtual machine (PVM) language, at periodic intervals data is automatically transferred from the MP-1 to a cluster of workstations where individual three-dimensional images are rendered for inclusion in a single animation sequence. Work is underway to replace executions on the MP-1 with simulations performed on the 512-node CM-5 at NCSA and to simultaneously gain access to more potent volume rendering workstations. Author

N94-31120*# Louisiana State Univ., Baton Rouge. Dept. of Physics and Astronomy.
AN EFFICIENT THREE-DIMENSIONAL POISSON SOLVER FOR SIMD HIGH-PERFORMANCE-COMPUTING ARCHITECTURES Abstract Only **c61**
H. Cohl *In* Lunar and Planetary Inst., Workshop on Physics of Accretion Disks Around Compact and Young Stars 1994 p 1 (For primary document see N94-31116 09-90)
(Grants NAGw-2447; NSF AST-90-08166)
Avail: CASI HC A01/MF A01

We present an algorithm that solves the three-dimensional Poisson equation on a cylindrical grid. The technique uses a finite-difference scheme with operator splitting. This splitting maps the banded structure of the operator matrix into a two-dimensional set of tridiagonal matrices, which are then solved in parallel. Our algorithm couples FFT techniques with the well-known ADI (Alternating Direction Implicit) method for solving Elliptic PDE's, and the implementation is extremely well suited for a massively parallel environment like the SIMD architecture of the MasPar MP-1. Due to the highly recursive nature of our problem, we believe that our method is highly efficient, as it avoids excessive interprocessor communication. Author (revised)

N94-31121*# Louisiana State Univ., Baton Rouge. Dept. of Physics and Astronomy.
THE DYNAMICAL SETTLING OF WARPED DISKS AND ANGULAR MOMENTUM TRANSPORT IN GALAXIES Abstract Only
P. Fisher *In* Lunar and Planetary Inst., Workshop on Physics of Accretion Disks Around Compact and Young Stars 1994 p 1 (For primary document see N94-31116 09-90)
(Grants NAGw-2447; NSF AST-90-08166)
Avail: CASI HC A01/MF A01

We present results of three-dimensional, hydrodynamic models of gaseous disks settling in a nonspherical potential. As the gas settles, differential precession creates a warped disk similar to the warps seen in spiral galaxies. A logarithmic potential, indicative of a massive halo, seems to induce warps more extreme than those produced by a l/r potential with a quadrupole distortion. Author

N94-31122*# Massachusetts Univ., Amherst.
OBSERVATIONS OF ACCRETION AND ANGULAR MOMENTUM REGULATION IN YOUNG CIRCUMSTELLAR DISKS AND THE IMPLICATIONS FOR PLANETARY FORMATION Abstract Only
P. Hartigan *In* Lunar and Planetary Inst., Workshop on Physics of Accretion Disks Around Compact and Young Stars 1994 p 2 (For primary document see N94-31116 09-90)
Avail: CASI HC A01/MF A01

Accretion disks around young stars produce excess infrared continuum associated with the disk and excess optical and ultraviolet continua associated with the boundary layer or 'hot spot' as material falls from the disk onto the stellar photosphere. When we subtract the excess continuum and photospheric contributions to the total spectrum, we can obtain high-quality emission line profiles of the Balmer lines as well as permitted lines from other elements. These emission lines often exhibit redshifted absorption, indicative of infalling material. Remarkably, objects with large accretion rates tend to rotate slower than their counterparts that lack accretion disks. Hence, there must be some process, probably involving magnetic fields, that allows the star to accrete large amounts of material from the disk without increasing its rotational velocity. Young stars typically do not have optically thick inner disks that do not accrete. Hence, either planets form within accretion disks, or the timescale for planetary formation is considerably shorter than approx. 3 x 10(exp 6) yr, the duration of the classical T Tauri star phase of young stellar evolution. Author (revised)

N94-31123*# Texas Univ., Austin. Dept. of Astronomy.
DISK INSTABILITY AND THE SPECTRAL EVOLUTION OF THE 1992 OUTBURST OF THE INTERMEDIATE POLAR GK PERSEI Abstract Only
S.-W. Kim, J. C. Wheeler, F. C. Bruhweiler, M. Fitzurka, K. Beuermann, K. Reinsch, and S. Mineshige *In* Lunar and Planetary Inst., Workshop on Physics of Accretion Disks Around Compact and Young Stars 1994 p 2 (For primary document see N94-31116 09-90)
Avail: CASI HC A01/MF A01

The disk instability model can explain the previous history of

dwarf-nova-like outbursts in the intermediate polar GK Per, which occur about once every three years. Disk models that reproduce the recurrence time and outburst light curves suggest that GK Per has a large effective inner disk radius (approx. 30-40 white dwarf radii) truncated by a strong magnetic field (10(exp 7) G). In this context, the effective radius is that of the portion of the disk that participates in the disk thermal instability. The radius derived is larger than the corotation radius, which must be an upper limit on the true dynamical inner radius of the disk. Disk instability models with this large effective inner radius predict that the ultraviolet continuum should be rather flat. Here we compare the predictions of the disk instability model to IUE observations of the 1981 outburst and to IUE and ROSAT observations of the recent 1992 outburst of GK Per. The model disk continuum spectral evolution is consistent with the observed UV and optical spectra, especially at maximum and in the early decay phase of the outburst. The consistency of the model with the observed UV spectra suggests that the effective inner radius of the disk is almost constant, independent of mass accretion rate, and that whatever structure lies between the effective inner radius and the corotation radius neither participates in the disk instability nor radiates substantially in the UV. The related physics of the inner disk region will be briefly discussed. Author (revised)

N94-31124*# Texas Univ., Austin. Dept. of Astronomy.

DISK IRRADIATION AND LIGHT CURVES OF X RAY NOVAE Abstract Only

S.-W. Kim, J. C. Wheeler, and S. Mineshige *In* Lunar and Planetary Inst., Workshop on Physics of Accretion Disks Around Compact and Young Stars 1994 p 2 (For primary document see N94-31116 09-90)

Avail: CASI HC A01/MF A01

We study the disk instability and the effect of irradiation on outbursts in the black hole X-ray nova system. In both the optical and soft X-rays, the light curves of several X-ray novae, A0620-00, GH 2000+25, Nova Muscae 1991 (GS 1124-68), and GRO J0422+32, show a main peak, a phase of exponential decline, a secondary maximum or reflare, and a final bump in the late decay followed by a rapid decline. Basic disk thermal limit cycle instabilities can account for the rapid rise and overall decline, but not the reflare and final bump. The rise time of the reflare, about 10 days, is too short to represent a viscous time, so this event is unlikely to be due to increased mass flow from the companion star. We explore the possibility that irradiation by X-rays produced in the inner disk can produce these secondary effects by enhancing the mass flow rate within the disk. Two plausible mechanisms of irradiation of the disk are considered: direct irradiation from the inner hot disk and reflected radiation from a corona or other structure above the disk. Both of these processes will be time dependent in the context of the disk instability model and result in more complex time-dependent behavior of the disk structure. We test both disk instability and mass transfer burst models for the secondary flares in the presence of irradiation. Author (revised)

N94-31125*# Rice Univ., Houston, TX. Dept. of Space Physics and Astronomy.

TIME-DEPENDENT BEHAVIOR OF ACTIVE GALACTIC NUCLEI WITH PAIR PRODUCTION Abstract Only

H. Li and C. D. Dermer *In* Lunar and Planetary Inst., Workshop on Physics of Accretion Disks Around Compact and Young Stars 1994 p 2 (For primary document see N94-31116 09-90)

Avail: CASI HC A01/MF A01

We study the properties of coupled partial differential equations describing the time-dependent behavior of the photon and electron occupation numbers for conditions likely to be found near active galactic nuclei (AGN). The processes governing electron acceleration are modeled by a stochastic accelerator, and we include acceleration by Alfvenic and whistler turbulence. The acceleration of electrons is limited by Compton and synchrotron losses, and the number density of electrons depends on pair production and annihilation processes. We also treat particle escape from the system. We examine the steady, (possibly) oscillatory, and unstable solutions that arise for various choices of parameters. We examine instabilities related to pair production and trapping and consider the formation of pair jets.

Author (revised)

N94-31126*# Rice Univ., Houston, TX. Dept. of Space Physics and Astronomy.

OBSERVATIONAL CONSTRAINTS ON BLACK HOLE ACCRETION DISKS Abstract Only

Edison P. Liang *In* Lunar and Planetary Inst., Workshop on Physics of Accretion Disks Around Compact and Young Stars 1994 p 2-3 (For primary document see N94-31116 09-90)

Avail: CASI HC A01/MF A01

We review the empirical constraints on accretion disk models of stellar-mass black holes based on recent multiwavelength observational results. In addition to time-averaged emission spectra, the time evolutions of the intensity and spectrum provide critical information about the structure, stability, and dynamics of the disk. Using the basic thermal Keplerian disk paradigm, we consider in particular generalizations of the standard optically thin disk models needed to accommodate the extremely rich variety of dynamical phenomena exhibited by black hole candidates ranging from flares of electron-positron annihilations and quasiperiodic oscillations in the X-ray intensity to X-ray novae activity. These in turn provide probes of the disk structure and global geometry. The goal is to construct a single unified framework to interpret a large variety of black hole phenomena. This paper will concentrate on the interface between basic theory and observational data modeling. Author (revised)

N94-31127*# Rice Univ., Houston, TX. Dept. of Space Physics and Astronomy.

NONLINEAR CALCULATIONS OF THE TIME EVOLUTION OF BLACK HOLE ACCRETION DISKS Abstract Only

C. Luo *In* Lunar and Planetary Inst., Workshop on Physics of Accretion Disks Around Compact and Young Stars 1994 p 3 (For primary document see N94-31116 09-90)

Avail: CASI HC A01/MF A01

Based on previous works on black hole accretion disks, I continue to explore the disk dynamics using the finite difference method to solve the highly nonlinear problem of time-dependent alpha disk equations. Here a radially zoned model is used to develop a computational scheme in order to accommodate functional dependence of the viscosity parameter alpha on the disk scale height and/or surface density. This work is based on the author's previous work on the steady disk structure and the linear analysis of disk dynamics to try to apply to x-ray emissions from black candidates (i.e., multiple-state spectra, instabilities, QPO's, etc.).

Author (revised)

N94-31128*# Louisiana State Univ., Baton Rouge. Dept. of Physics and Astronomy.

EVOLUTION OF VAPORIZING PULSARS Abstract Only

P. McCormick *In* Lunar and Planetary Inst., Workshop on Physics of Accretion Disks Around Compact and Young Stars 1994 p 3 (For primary document see N94-31116 09-90)

(Grants NAGw-2447; NSF AST-90-20855)

Avail: CASI HC A01/MF A01

We construct evolutional scenarios for LMXB's using a simplified stellar model. We discuss the origin and evolution of short-period, low mass binary pulsars with evaporating companions. We suggest that these systems descend from low-mass X-ray binaries and that angular momentum loss mainly due to evaporative wind drives their evolution. We derive limits on the energy and angular momentum carried away by the wind based on the observed low eccentricity. In our model the companion remains near contact, and its quasiadiabatic expansion causes the binary to expand. Short-term oscillations of the orbital period may occur if the Roche-lobe overflow forms an evaporating disk. Author (revised)

N94-31129*# Rice Univ., Houston, TX. Dept. of Space Physics and Astronomy.

CAN A VARIABLE ALPHA INDUCE LIMIT CYCLE BEHAVIOR AND EXPONENTIAL LUMINOSITY DECAY IN TRANSIENT SOFT X RAY SOURCES? Abstract Only **c93**

C. MeirellesFilho and Edison P. Liang *In* Lunar and Planetary Inst., Workshop on Physics of Accretion Disks Around Compact and Young Stars 1994 p 3-4 (For primary document see N94-31116 09-90)

Avail: CASI HC A01/MF A01

There has been, recently, a revival of the stability problem of accretion disks. Much of this renewed interest is due to recent observational data

on transient soft X-ray novae, which are low-mass X-ray binaries. It is widely believed that nonsteady mass transfer from the secondary onto the compact primary, through an accretion disk, is the reason for the observed spectacular events in the form of often repetitive outbursts, with recurrence times ranging from 1 to 60 yr and duration time on the scale of months. Though not having reached yet a consensus about the nature of the mechanism that regulates the mass transfer, the disk thermal instability model seems to be favored by the fact that the rise in the hard X-ray luminosity is prior to the rise in the soft X-ray luminosity, while the mass transfer instability model seems to be hindered by the fact that the luminosity during quiescence is unable to trigger the thermal instability. However, it should be stressed that, remarkably, the X-ray light curves of these X-ray novae all show overall exponential decays, a feature quite difficult to reproduce in the framework of the viscous disk model, which yields powerlike luminosity decay. Taking into account this observational constraint, we have studied the temporal evolution of perturbations in the accretion rate, under the assumption that alpha is radial and parameter dependent. The chosen dependence is such that the model can reproduce limit cycle behavior (the system is locally unstable but globally stable). However, the kind of dependence we are looking for in alpha does not allow us to use the usual Shakura and Sunyaev procedure in the sense that we no longer can obtain a linearized continuity equation without explicit dependence on the accretion rate. This is so because now we cannot eliminate the accretion rate by using the angular momentum conservation equation.

Author (revised)

N94-31130*# Rice Univ., Houston, TX. Dept. of Space Physics and Astronomy.

CONVECTIVE SOLAR NEBULA Abstract Only **c92**

C. MeirellesFilho and M. Reyes-Ruiz *In* Lunar and Planetary Inst., Workshop on Physics of Accretion Disks Around Compact and Young Stars 1994 p 4 (For primary document see N94-31116 09-90)

Avail: CASI HC A01/MF A01

Analyzing turbulent flows with rotation, Dubrulle and Valdettaro have concluded that some new effects come into play and may modify the standard picture we have concerning turbulence. In that respect the value of the Rossby number is of crucial importance since it will determine the transition between regimes where rotation is or is not important. With rotation there will be a tendency to constrain the motion to the plane perpendicular to the rotation axis and as a consequence the horizontal scale will increase as compared to the longitudinal one, which means that the turnover time in this direction will increase. The net effect is that the energy cascade down process is hindered by rotation. As a matter of fact, when rotation is present one observes two cascades: an enstrophy (vorticity) cascade from large scales to small scales; and an inverse energy cascade from small scales to large scales. Since the first process is not efficient on transporting energy to the dissipation range, what we see is energy storage in the large structures at the expense of the small structures. This kind of behavior has been confirmed experimentally. For a very large gamma we obtain, in the inertial range, a spectrum of k(exp -3) instead of the usual Kilmogorov's k(exp -5/3) spectrum. In reality, when rotation is dominant, energy gets stored in inertial waves that propagate it essentially in the longitudinal direction. In that case, we can no longer assign just one viscosity to the fluid and, what is most important, the concept of viscosity loses its meaning since we no longer have local transport of energy. Such results, however, were derived considering a hot disk, in which opacity is mainly given by electron scattering. In the present work we have applied the formulation developed in the previous work for the description of the viscous-stage solar nebula. Author (revised)

N94-31131*# Rice Univ., Houston, TX. Dept. of Space Physics and Astronomy.

ROTATIONAL EFFECTS IN TURBULENCE DRIVEN BY CONVECTION Abstract Only

C. MeirellesFilho, M. Reyes-Ruiz, and C. Luo *In* Lunar and Planetary Inst., Workshop on Physics of Accretion Disks Around Compact and Young Stars 1994 p 4-5 (For primary document see N94-31116 09-90)

Avail: CASI HC A01/MF A01

We have treated turbulence with rotation in a thin Keplerian disk. Highlighting implicit assumptions already existent in the alpha model together with a geometrical but physically reasonable deduction of the degrees of freedom of the largest eddies, which is of paramount importance in our formulation, we were able to obtain relations satisfied by parameters of the turbulence, such as turnover time and alpha. The effects of rotation in the turbulence we have taken implictly through an anisotropy factor (x) which is simply related to the Rossby number. Convection is the process assumed to generate turbulence, and we have used Canuto and Goldman's treatment of convective instability, whose characteristic growth time we have assumed equal to the turnover time. We have also used their procedure to obtain the turbulent viscosity. Author (revised)

N94-31132*# Texas Univ., Austin. Dept. of Astronomy.

A CONSTRAINT ON THE PAIR-DENSITY RATIO (Z+) IN AN ELECTRON-POSITRON PAIR WIND Abstract Only

M. D. Moscoso and J. C. Wheeler *In* Lunar and Planetary Inst., Workshop on Physics of Accretion Disks Around Compact and Young Stars 1994 p 5 (For primary document see N94-31116 09-90)

Avail: CASI HC A01/MF A01

We derive a constraint on the pair density ratio, z(sub +) = n(sub +)/n(sub p), in an electron-positron pair wind flowing away from the central region of an accretion disk around a compact object under the assumption of a coupling between electrons, positrons, and protons. The minimum rate at which positrons are injected into the annihilation volume is given by the observed annihilation flux per unit volume. This rate is then used to determine a minimum mass loss rate per unit area, M(dot)(sub *) for a given pair density ratio at the base of the streamline. The requirement that M(dot)(sub *) less than M(dot)(sub *)(sub Edd) (the mean Eddington mass loss rate per unit area) then places a lower limit on the pair density ratio, z(sub +,)(sub min). A positron annihilation line was observed in Nova Muscae 1991 by GRANAT/SIGMA. The narrow width and redshift of the line suggest that the pair production and annihilation regions are physically distinct. We hypothesize that an electron-positron pair wind transports the pairs from the production to the annihilation region and calculate z(sub +),(sub min). We then determine constraints on the physical parameters on the pair production region by comparing z(sub +),(sub min) with previous studies of two-temperature and one-temperature accretion disks with electron-positron pairs. Author (revised)

N94-31133*# Rice Univ., Houston, TX. Dept. of Space Physics and Astronomy.

CIRCUMSTELLAR MATERIAL AROUND YOUNG STARS IN ORION Abstract Only

C. R. ODell *In* Lunar and Planetary Inst., Workshop on Physics of Accretion Disks Around Compact and Young Stars 1994 p 5-6 (For primary document see N94-31116 09-90)

Avail: CASI HC A01/MF A01

The star cluster associated with the Orion nebula is one of the richest known. Lying at the nearside of the Orion Molecular cloud and at a distance of about 500 pc from us, it contains many premain-sequence stars with ages of about 300,000 yr. The nebula itself is a blister type, representing a wall of material ionized by the hottest star in the Trapezium group (member C). Although this is not the closest star formation region, it is probably the easiest place to detect circumstellar, possibly proto-planetary, material around these solar mass stars. This is because the same process of photoionization that creates the nebula also photoionizes these circumstellar clouds, thus rendering them easily visible. Moreover, their dust component is made visible by extinction of light from the background nebula. Young stars with circumstellar material were found in Orion on the second set of HST images and were called proplyds, indicating their special nature as circumstellar clouds caused to be luminous by being in or near a gaseous nebula. The brightest objects in the field had previously been seen in the optical and radio, and although their true nature had been hypothesized it was the HST images that made it clear what they are. The forms vary from cometlike when near the Trapezium to elliptical when further away, with the largest being 1000 AU and the bright portions of the smallest, which are found closest to the Trapezium, being about 100 AU in diameter. We now have a second set of HST observations made immediately after the refurbishment mission that provides even greater detail and reveals even more of these objects. About half of all the low-luminosity stars are propiyds. The poster paper describes quantitative tests about their fundamental structure and addresses the question of whether the circumstellar material is a disk or shell. One object (HST 16) is seen only in silhouette against the nebula and is easily resolved into an

elliptical form of optical depth monotonically increasing toward the central star. Author (revised)

N94-31134*# Louisiana State Univ., Baton Rouge. Dept. of Physics and Astronomy.

A STUDY OF ANGULAR MOMENTUM LOSS IN BINARIES USING THE FREE LAGRANGE METHOD Abstract Only

A. M. Rajasekhar *In* Lunar and Planetary Inst., Workshop on Physics of Accretion Disks Around Compact and Young Stars 1994 p 6 (For primary document see N94-31116 09-90)

(Grants NAGw-2447; NSF AST-90-20855)

Avail: CASI HC A01/MF A01

The evolution of a binary star system depends greatly on the angular momentum losses in the system brought about by gravitational radiation and mass outflow (e.g., evaporating winds and magnetic braking) from the secondary component of the binary. Using a three-dimensional hydrodynamic fluid code based on the free Lagrange method, we study the loss of specific angular momentum from a binary system due to an evaporative wind from the companion of a millisecond pulsar. We consider binaries of different mass ratios and winds of different initial velocities and in particular attempt to model the system PSR 1957+20. We are in the process of incorporating the effect of the radiation force from the pulsar and the magnetic field of the companion on the mass outflow. The latter effect would also enable us to study magnetic braking in cataclysmic variables and low-mass X-ray binaries. Author

N94-31135*# Rice Univ., Houston, TX. Dept. of Space Physics and Astronomy.

EVOLUTION OF PROTOPLANETARY DISKS WITH DYNAMO MAGNETIC FIELDS Abstract Only

M. Reyes-Ruiz and Tomasz F. Stepinski *In* Lunar and Planetary Inst., Workshop on Physics of Accretion Disks Around Compact and Young Stars 1994 p 6-7 (For primary document see N94-31116 09-90)

Avail: CASI HC A01/MF A01

The notion that planetary systems are formed within dusty disks is certainly not a new one; the modern planet formation paradigm is based on suggestions made by Laplace more than 200 years ago. More recently, the foundations of accretion disk theory where initially developed with this problem in mind, and in the last decade astronomical observations have indicated that many young stars have disks around them. Such observations support the generally accepted model of a viscous Keplerian accretion disk for the early stages of planetary system formation. However, one of the major uncertainties remaining in understanding the dynamical evolution of protoplanetary disks is the mechanism responsible for the transport of angular momentum and subsequent mass accretion through the disk. This is a fundamental piece of the planetary system genesis problem since such mechanisms will determine the environment in which planets are formed. Among the mechanisms suggested for this effect is the Maxwell stress associated with a magnetic field treading the disk. Due to the low internal temperatures through most of the disk, even the question of the existence of a magnetic field must be seriously studied before including magnetic effects in the disk dynamics. On the other hand, from meteoritic evidence it is believed that magnetic fields of significant magnitude existed in the earliest, PP-disk-like, stage of our own solar system's evolution. Hence, the hypothesis that PP disks are magnetized is not made solely on the basis of theory. Previous studies have addressed the problem of the existence of a magnetic field in a steady-state disk and have found that the low conductivity results in a fast diffusion of the magnetic field on timescales much shorter than the evolutionary timescale. Hence the only way for a magnetic field to exist in PP disks for a considerable portion of their lifetimes is for it to be continuously regenerated. In the present work, we present results on the self-consistent evolution of a turbulent PP disk including the effects of a dynamo-generated magnetic field.

Author (revised)

N94-31136*# California Univ., Irvine. Dept. of Physics.

THEORY OF PROTOSTELLAR ACCRETION DISKS Abstract Only

S. Ruden *In* Lunar and Planetary Inst., Workshop on Physics of Accretion Disks Around Compact and Young Stars 1994 p 8 (For primary document see N94-31116 09-90)

Avail: CASI HC A01/MF A01

I will present an overview of the current paradigm for the theory of gaseous accretion disks around young stars. Protostellar disks form from the collapse of rotating molecular cloud cores. The disks evolve via outward angular momentum transport provided by several mechanisms: gravitational instabilities, thermal convective turbulence, and magnetic stresses. I will review the conditions under which these mechanisms are efficient and consistent with the observed disk evolutionary timescales of several million years. Time permitting, I will discuss outbursts in protostellar disks (FU Orionis variables), the effect of planet formation on disk structure, and the dispersal of remnant gas. Author

N94-31137*# Texas Univ., Austin. Dept. of Astronomy.

THERMAL CONTINUA OF AGN ACCRETION DISKS Abstract Only

G. A. Shields and H. H. Coleman *In* Lunar and Planetary Inst., Workshop on Physics of Accretion Disks Around Compact and Young Stars 1994 p 8 (For primary document see N94-31116 09-90)

Avail: CASI HC A01/MF A01

We have computed the thermal continuum energy distribution of thermal radiation from the atmospheres of supermassive accretion disks around supermassive black holes. Non-LTE radiative transfer is combined with a model of the vertical structure at each radius appropriate to the low effective gravities of these disks. Locally, the Lyman edge of H can be in emission or absorption. When the emission is summed over the disk with Doppler and gravitational redshifts taken into account, the observed continuum typically shows little sign of a discontinuity near the Lyman edge. For relatively cool disks, the Lyman edge is in absorption, but it appears as a slope change extending over several hundred angstroms, rather than an abrupt discontinuity. Disks around Kerr black holes can explain the observed range of soft X-ray luminosities of AGN, but disks around Schwarzschild holes are much too faint in soft X-rays. Author (revised)

N94-31138*# Lunar and Planetary Inst., Houston, TX.

EVOLUTION OF DYNAMO-GENERATED MAGNETIC FIELDS IN ACCRETION DISKS AROUND COMPACT AND YOUNG STARS Abstract Only

Tomasz F. Stepinski *In its* Workshop on Physics of Accretion Disks Around Compact and Young Stars 1994 p 8-9 (For primary document see N94-31116 09-90)

Avail: CASI HC A01/MF A01

Geometrically thin, optically thick, turbulent accretion disks are believed to surround many stars. Some of them are the compact components of close binaries, while the others are throught to be T Tauri stars. These accretion disks must be magnetized objects because the accreted matter, whether it comes from the companion star (binaries) or from a collapsing molecular cloud core (single young stars), carries an embedded magnetic field. In addition, most accretion disks are hot and turbulent, thus meeting the condition for the MHD turbulent dynamo to maintain and amplify any seed field magnetic field. In fact, for a disk's magnetic field to persist long enough in comparison with the disk viscous time it must be contemporaneously regenerated because the characteristic diffusion time of a magnetic field is typically much shorter than a disk's viscous time. This is true for most thin accretion disks. Consequently, studying magentic fields in thin disks is usually synonymous with studying magnetic dynamos, a fact that is not commonly recognized in the literature. Progress in studying the structure of many accretion disks was achieved mainly because most disks can be regarded as two-dimensional flows in which vertical and radial structures are largely decoupled. By analogy, in a thin disk, one may expect that vertical and radial structures of the magnetic field are decoupled because the magnetic field diffuses more rapidly to the vertical boundary of the disk than along the radius. Thus, an asymptotic method, called an adiabatic approximation, can be applied to accretion disk dynamo. We can represent the solution to the dynamo equation in the form $B = Q(r)b(r,z)$, where Q(r) describes the field distribution along the radius, while the field distribution across the disk is included in the vector function b, which parametrically depends on r and is normalized by the condition $\max(b(z)) = 1$. The field distribution across the disk is established rapidly, while the radial distribution Q(r) evolves on a considerably longer timescale. It is this evolution that is the subject of this paper. Author (revised)

N94-31139*# Princeton Univ., NJ.

NONTHERMAL ACCRETION DISK MODELS AROUND NEUTRON STARS Abstract Only

M. Tavani and Edison P. Liang *In* Lunar and Planetary Inst., Workshop

on Physics of Accretion Disks Around Compact and Young Stars 1994 p 9 (For primary document see N94-31116 09-90)
Avail: CASI HC A01/MF A01

We consider the structure and emission spectra of nonthermal accretion disks around both strongly and weakly magnetized neutron stars. Such disks may be dissipating their gravitational binding energy and transferring their angular momentum via semicontinuous magnetic reconnections. We consider specifically the structure of the disk-stellar magnetospheric boundary where magnetic pressure balances the disk pressure. We consider energy dissipation via reconnection of the stellar field and small-scale disk turbulent fields of opposite polarity. Constraints on the disk emission spectrum are discussed. Author

N94-31140*# Louisiana State Univ., Baton Rouge. Dept. of Physics and Astronomy.
GRAVITATIONAL INSTABILITIES IN PROTOSTELLAR DISKS Abstract Only
J. E. Tohline *In* Lunar and Planetary Inst., Workshop on Physics of Accretion Disks Around Compact and Young Stars 1994 p 9-10 (For primary document see N94-31116 09-90)
(Grants NAGw-2447; NSF AST-90-08166)
Avail: CASI HC A01/MF A01

The nonaxisymmetric stability of self-gravitating, geometrically thick accretion disks has been studied for protostellar systems having a wide range of disk-to-central object mass ratios. Global eigenmodes with four distinctly different characters were identified using numerical, nonlinear hydrodynamic techniques. The mode that appears most likely to arise in normal star formation settings, however, resembles the 'eccentric instability' that was identified earlier in thin, nearly Keplerian disks: It presents an open, one-armed spiral pattern that sweeps continuously in a trailing direction through more than 2-pi radians, smoothly connecting the inner and outer edges of the disk, and requires cooperative motion of the point mass for effective amplification. This particular instability promotes the development of a single, self-gravitating clump of material in orbit about the point mass, so its routine appearance in our simulations supports the conjecture that the eccentric instability provides a primary route to the formation of short-period binaries in protostellar systems. Author (revised)

N94-31141*# Louisiana State Univ., Baton Rouge. Dept. of Physics and Astronomy.
THREE-DIMENSIONAL RADIATIVE TRANSFER CALCULATIONS ON AN SIMD MACHINE APPLIED TO ACCRETION DISKS Abstract Only
H. Vath *In* Lunar and Planetary Inst., Workshop on Physics of Accretion Disks Around Compact and Young Stars 1994 p 10 (For primary document see N94-31116 09-90)
(Grant NAGw-2447)
Avail: CASI HC A01/MF A01

We have developed a tool to solve the radiative transfer equation for a three-dimensional astrophysical object on the SIMD computer MasPar MP-1. With this tool we can rapidly calculate the image of such an object as seen from an arbitrary direction and at an arbitrary wavelength. Such images and spectra can then be used to directly compare observations with the model. This tool can be applied to many different areas in astrophysics, e.g., HI disks of galaxies and polarized radiative transfer of accretion columns onto white dwarfs. Here we use this tool to calculate the image and spectrum of a simple model of an accretion disk. Author

N94-31142*# Texas Univ., Austin. Dept. of Astronomy.
DYNAMICS OF FLUX TUBES IN ACCRETION DISKS Abstract Only
E. T. Vishniac and R. C. Duncan *In* Lunar and Planetary Inst., Workshop on Physics of Accretion Disks Around Compact and Young Stars 1994 p 10-11 (For primary document see N94-31116 09-90)
Avail: CASI HC A01/MF A01

The study of magnetized plasmas in astrophysics is complicated by a number of factors, not the least of which is that in considering magnetic fields in stars or accretion disks, we are considering plasmas with densities well above those we can study in the laboratory. In particular, whereas laboratory plasmas are dominated by the confining magnetic field pressure, stars, and probably accretion disks, have magnetic fields whose beta (ratio of gas pressure to magnetic field pressure) is much greater than 1. Observations of the Sun suggest that under such circumstances the magnetic field breaks apart into discrete flux tubes with a small filling factor. On the other hand, theoretical treatments of MHD turbulence in high-beta plasmas tend to assume that the field is more or less homogeneously distributed throughout the plasma. Here we consider a simple model for the distribution of magnetic flux tubes in a turbulent medium. We discuss the mechanism by which small inhomogeneities evolve into discrete flux tubes and the size and distribution of such flux tubes. We then apply the model to accretion disks. We find that the fibrilation of the magnetic field does not enhance magnetic buoyancy. We also note that the evolution of an initially diffuse field in a turbulent medium, e.g., any uniform field in a shearing flow, will initially show exponential growth as the flux tubes form. This growth saturates when the flux tube formation is complete and cannot be used as the basis for a self-sustaining dynamo effect. Since the typical state of the magnetic field is a collection of intense flux tubes, this effect is of limited interest. However, it may be important early in the evolution of the galactic magnetic field, and it will play a large role in numerical simulations. Finally, we note that the formation of flux tubes is an essential ingredient in any successful dynamo model for stars or accretion disks.
Author (revised)

N94-31143*# Texas Univ., Austin. Dept. of Astronomy.
THE PHYSICS OF BLACK HOLE X RAY NOVAE Abstract Only
J. C. Wheeler, S.-W. Kim, M. D. Moscoso, and S. Mineshige *In* Lunar and Planetary Inst., Workshop on Physics of Accretion Disks Around Compact and Young Stars 1994 p 11-12 (For primary document see N94-31116 09-90)
Avail: CASI HC A01/MF A01

X-ray transients that are established or plausible black hole candidates have been discovered at a rate of about one per year in the galaxy for the last five years. There are now well over a dozen black hole candidates, most being in the category of X-ray novae with low-mass companions. There may be hundreds of such transient systems in the galaxy yet to be discovered. Classic black hole candidates like Cygnus X-1 with massive companions are in the minority, and their census in the galaxy and magellanic clouds is likely to be complete. The black hole X-ray novae (BHXN) do not represent only the most common environment in which to discover black holes. Their time dependence gives a major new probe with which to study the physics of accretion into black holes. The BHXN show both a soft X-ray flux from an optically thick disk and a hard power law tail that is reminiscent of AGN spectra. The result may be new insight into the classical systems like Cyg X-1 and LMC X-1 that show similar power law tails, but also to accretion into supermassive black holes and AGN.
Author (revised)

N94-31144*# Louisiana State Univ., Baton Rouge. Dept. of Physics and Astronomy.
GAS DYNAMICS FOR ACCRETION DISK SIMULATIONS Abstract Only
R. Whitehurst *In* Lunar and Planetary Inst., Workshop on Physics of Accretion Disks Around Compact and Young Stars 1994 p 12 (For primary document see N94-31116 09-90)
Avail: CASI HC A01/MF A01

The behavior of accretion disks can largely be understood in terms of the basic physical processes of mass, energy, and momentum conservation. Despite this, detailed modeling of these systems using modern computational techniques is challenging and controversial. Disturbing differences exist between methods used widely in astrophysics, namely Eulerian finite-difference techniques and particle codes such as SPH. Therefore neither technique is fully satisfactory for accretion disk simulations. This paper describes a new fully Lagrangian method designed to resolve these difficulties. Author

N94-31280 Societe Francaise de Chimie-Physique, Paris.
PHYSICAL CHEMISTRY OF MOLECULES AND GRAINS IN SPACE
10 Sep. 1993 126 p Presented at the 50th International Meeting of th e Societe Francais de Physique, Mont Saint-Odile, France 6-10 Sep. 1993 Limited Reproducibility: More than 20% of this document may be affected by microfiche quality
(AD-A276037) Avail: CASI HC A07

Abstracts are presented for the 50th international meeting of Physical Chemistry of Molecules and Grains in Space. Topics include: Recent Developments in Astrochemistry; Photofragmentation of PAH ions; A Laser Vaporization Source for Spectroscopic Characterization of Refractory Compounds; The Effects of Varying Cosmic Ray Ionization Rates on the

Chemistry of Interstellar Clouds; Vibrational Excitation of Hydrogen Desorbed from a Carbon Surface; Photodesorption from CO Ices; Excitation Mechanisms of the C2 Swan Bands in Comet Halley's Spectrum; Grain Mantle Processing and IR Emission; Reactions of C+ Ions with Molecules at Low Temperatures; and On the Large Organic Molecules in the Interstellar Gas. CASI

N94-31495 Massachusetts Univ., Amherst.
THE STELLAR AND GASEOUS CONTENT OF MASSIVE LOW SURFACE BRIGHTNESS DISK GALAXIES Ph.D. Thesis
Patricia Marie Knezek 1993 321 p
Avail: Univ. Microfilms Order No. DA9316682

This dissertation presents a multi-wavelength study of a subset of an extreme type of galaxy, those which have low surface brightnesses, large disks, and large amounts of atomic gas, yet which have total dynamical masses similar to those of giant spiral galaxies. These systems may represent a significant, but largely unexplored, fraction of galaxies in the universe, and determining their star formation histories and evolution is critical to our attempts to understand the different modes of formation and evolution of all galaxies. Surface photometry at B and R, in conjunction with H(sub I), (sup 12)CO and far-infrared data, is used to try to determine if these galaxies had an early epoch of star formation that has since faded, have ongoing star formation with an unusual IMF, or are perhaps galaxies which have never efficiently formed stars due to a lack of molecular clouds. Results of our observations confirm earlier findings that these systems in general have very blue disks relative to higher surface brightness, gas-rich disk systems. This result makes it very difficult to explain these galaxies as 'faded disks.' Although they have prodigious amounts of H(sub I), there is little evidence of abundant (sup 12)CO or dust. Despite their physical similarities, they show an amazing variety of optical morphologies. Many have steep radial color gradients, perhaps due to changing metallicities. These systems tend to be in fairly isolated regions of the universe. The lack of nearby neighbors may have allowed them to form and evolve in a very different manner from typical high surface brightness galaxies. Some systems may, in fact, have undergone very little star formation over time. If this is true, this population could represent a valuable window into the early epochs of star formation in disk galaxies. Dissert. Abstr.

N94-31497 Wisconsin Univ., Madison.
DOUBLE-LINED PRE-MAIN-SEQUENCE BINARIES: A TEST OF PRE-MAIN-SEQUENCE EVOLUTIONARY THEORY Ph.D. Thesis
Chi-Wai Lee 1992 105 p
Avail: Univ. Microfilms Order No. DA9304164

This thesis is to test the calibrations of theoretical pre-main-sequence (PMS) evolutionary models. We compare the theoretical masses and ages of the components of five double-lined pre-main-sequence binaries with the dynamical mass ratios and the assumption of coeval formation of binary components. The spectral types and luminosity ratios of the components are derived from comparisons of selected lines in the observed spectra with synthetic binary spectra created from spectral standards. These are based on echelle observations obtained during 1989-1990. Theoretical masses and ages of the components are obtained by comparing with the theoretical evolutionary models of Mazzitelli and VandenBerg. All five binaries have components with theoretical masses and ages consistent with the dynamical mass ratios and the assumption of coeval formation. We find no substantial problems with the relative mass calibrations of the theoretical tracks, nor the assumption of coeval formation of binary components. These hold for binaries with ages ranging from approximately 10(exp 6) yr to few times 10(exp 6) yr. Assuming coeval formation of binary components, we compare the ranges of both the theoretical mass ratios and the dynamical mass ratios with the detectable range of dynamical mass ratios. The results show that the ranges of theoretical mass ratios and the dynamical mass ratio are small subsets of the detectable range of dynamical mass ratios. This finding indicates that this analysis is a significant test of the relative mass calibrations of the PMS tracks of Mazzitelli and VandenBerg. The binary P1540 with age of approximately 10(exp 5) yr is the youngest in our sample. The maximum age difference for the solutions that have theoretical mass ratios consistent with the dynamical mass ratio is only a few times 10(exp 5) yr. This is small compared to the ages of few times 10(exp 6) yr of the other binaries in the sample. This indicates it is possible that processes such as disk accretions have little effects on the evolution of the binaries after approximately 10(exp 5) yr. Dissert. Abstr.

N94-31556 Washington Univ., Seattle.
THE ORIGIN OF NEON-E: NEON-E IN SINGLE INTERSTELLAR SILICON CARBIDE AND GRAPHITE GRAINS Ph.D. Thesis
Robert Hill Nichols, Jr. 1992 158 p
Avail: Univ. Microfilms Order No. DA9317398

Anomalous noble gas components, such as Ne-E, measured in bulk SiC and graphite fractions separated from meteorites have previously supported the presolar origin of these mineral grains. These prior measurements, however, were performed on samples containing many thousands of grains; any result derived from such bulk measurements is only an average of the many, perhaps dissimilar, constituents. This work reports the first measurements of (sup 22)Ne-E and (sup 4)He in a suite of single micron-sized presolar SiC and graphite grains separated from the Murchison (CM) meteorite. The analyses were performed using a laser gas extraction technique and a high-sensitivity noble gas mass spectrometer. C- and N-isotopic compositions were determined via ion microprobe analyses on a subset of the suite of grains to further constrain their origin. This work confirms that SiC and graphite are the carriers of Ne-E(H) and Ne-E(L), respectively. Only 4 percent of the SiC grains and 30 percent of the graphite grains carry the anomalous gas above the spectrometer detection limits, implying that several inferences based on bulk noble gas measurements about the lifetimes of presolar grains and the abundances of these grains in meteorites should be reconsidered. That He-4 is found only in the Ne-E(H)-rich SiC grains provides strong evidence against a Na-22 origin of Ne-E(H). The He-4 and Ne-22 in the gas-rich SiC grains were probably produced either in the He-burning shell of low mass asymptotic giant branch (AGB) stars or in Wolf-Rayet stars during the WN-WC transition. Although the C-isotopic compositions of the gas-rich SiC grains argue against grain formation from pure He-shell material, AGB stars still appear to be the most plausible site for the formation of Ne-E(H). The graphite grains, which carry only (sup 22)Ne-E(L) without any He-4, probably formed from Wolf-Rayet stars near the WN-WC transition, with the Ne-E(L) being produced directly by the implantation of Ne. One gas-rich graphite grain, however, does not conform to a Wolf-Rayet origin. Although this grain could plausibly have formed from a nova with the Ne-E(L) being produced from the in situ decay of Na-22, the C-isotopic composition of this grain is inconsistent with such a scenario. The results of this work argue strongly against the popular belief that Ne-E(H) and Ne-E(L) are derived solely from the in situ decay of novae-produced Na-22. Dissert. Abstr.

N94-31566 Alabama Univ., Huntsville.
NUMERICAL SIMULATION OF INTERPLANETARY DYNAMICS Ph.D. Thesis
Chin-Chun Wu 1993 187 p
Avail: Univ. Microfilms Order No. DA9324492

This dissertation discusses investigations into the physics of the propagation of solar generated disturbances in the interplanetary medium. The motivation to initiate this study was two-fold: (1) understanding the fundamental physics of the nonlinear interactions of solar generated MHD shocks and non-homogeneous interplanetary medium, and (2) understanding the physics of solar generated disturbance effects on the Earth's environment, (i.e. the solar connection to the geomagnetic storm). In order to achieve these goals, the authors employed two numerical models to encompass these studies. In the first part, a one-dimensional MHD code with adaptive grids is used to study the evolution of interplanetary slow shocks (ISS), the interaction of a forward slow shock with a reverse slow shock, and the interaction of a fast shock with a slow shock. Results show that the slow shocks can be generated by a decreasing density, velocity or temperature perturbation or by a pressure pulse by following a forward fast shock and that slow shocks can propagate over 1 AU; results also show that the ISS never evolves into fast shocks. Interestingly, it is also found that an ISS could be 'eaten up' by an interplanetary fast shock (IFS) catching up from behind. This could be a reason that the slow shock has been difficult to observe near 1 AU. In addition, a forward slow shock could be dissipated by following a strong forward fast shock (Mach number greater than 1.7). In the second part, a fully three-dimensional (3D), time-dependent, MHD interplanetary global model (3D IGM) is used to study the relationship between different forms of solar activity and transient variations of the north-south component, B(sub x), of the interplanetary magnetic field, IMF, at 1 AU. One form of solar activity, the flare, is simulated by using a pressure pulse at different locations near the

solar surface and observing the simulated IMF evolution of B(sub theta) (= -B(sub x)) at 1 AU. Results show that, for a given pressure pulse, the orientation of the corresponding transient variation of B(sub x) has a strong relationship to the location of the pressure pulse and the initial conditions of the IMF. Dissert. Abstr.

N94-31567 California Univ., Santa Cruz.
REACTIVE FLOWS IN COMPACT OBJECTS Ph.D. Thesis
Francis Xavier Timmes 1993 204 p
Avail: Univ. Microfilms Order No. DA9328224

This thesis examines aspects of subsonic reactive flows in stars. Highlighted are fluid flows in which the velocity of the fluid is much less than the local sound speed of the fluid, and where the thermodynamic conditions of the fluid are conducive to nuclear reactions. Reactive flows of this nature are capable of generating self-sustained flame fronts, also known as deflagration waves. An introductory chapter on the astrophysics of reacting flows commences this thesis, followed by four chapters which apply this physics to the interiors of compact objects. The bifurcation between accretion-induced collapse of a white dwarf to a neutron star, and the explosion of the white dwarf in a Type 1a supernovae event is the subject of the second chapter. The fate of the accreting white dwarf is critically dependent upon the propagation speed of the laminar flame front that is ignited near or at the center of the star. The physical properties (speed, width, and density recovery time) of subsonic flame fronts are calculated from first principles, and the resulting implications discussed. Chapter three extends the body of literature on the thermal conductivity due to collisions between relativistic degenerate electrons, and provides convenient expressions for evaluation of the electron-electron contribution to the total thermal conductivity. Merging white dwarfs offer another bifurcation point towards accretion-induced collapse and is the subject of chapter four. Here carbon burning is ignited at the surface of the accreting white dwarf, and propagates inwards toward the center of the dwarf. Collapse of the dwarf to a neutron star probably ensues if the flame propagates to the center. One finds that for each value of the gravitational potential, there is a minimum density (hence a minimum mass) below which the flame becomes quenched before it reaches the center of the white dwarf. Closure of this thesis is attained on a possibly exciting, and certainly speculative note. The development and initial testing of implicit smooth particle hydrocode, which may turn out to be useful for subsonic reactive flows in multiple dimensions, is presented. Dissert. Abstr.

N94-31758 California Univ., Santa Cruz.
EVOLUTION OF STARS AND WINDS IN THE STARBURST GALAXY M82 Ph.D. Thesis
Jay Scott Doane 1993 95 p
Avail: Univ. Microfilms Order No. DA9328208

Standard time-dependent equations for the conversion of gas into stars are used to generate model starbursts. Included are provisions for recycling of gas and heavy elements from evolved stars and the loss of matter in a wind driven by supernova explosions. Free parameters include the initial mass function (IMF), star formation rate (SFR), amount of initial star-forming gas, and the amount of gas ejected from each supernova. These are constrained by data from the well-observed starburst galaxy M82 such as the current supernova rate, current amount of dynamical mass in the burst region, bolometric and ionizing photon luminosity of the burst region, amount of gas ejected since the onset of starburst, x ray luminosity in the galactic halo, and pressure of the optical clouds in the halo. The last three constraints require that the outflowing gas from the burst region be modeled as it moves into the galactic halo. We treat the wind as a one dimensional steady state flow issuing from the starburst core, subject to radiative losses in the outer galaxy. Our core starburst model succeeds in easily matching most of the observations when we employ a truncated IMF such that no stars form with a mass less than three solar mass. We find we can also fit the relevant observational parameters with a normal Salpeter IMF, but the range of times that the models fit is narrow, and the initial parameters have to be fine tuned for the agreement. Also of interest is that our SFR must be much higher than is common in the local solar neighborhood. We are unable, within reasonable parametric limitations, to generate with our central-source model what has been formerly interpreted as an extended thermal x ray flux, in agreement with recent observations. It is possible that a two-episode outflow can explain a majority of the observations in the outer galaxy. A primary, relatively cool wind consisting of thermally unstable regions may be responsible for the optical line emission and x rays, while a later, similarly unstable yet hotter wind could be responsible for the reacceleration of the extended radio synchrotron electrons. Dissert. Abstr.

N94-31782# Lawrence Livermore National Lab., CA.
STRONGLY COUPLED IONIC MIXTURES AND THE H/He EOS
H. E. DeWitt 2 Dec. 1993 19 p Presented at the Equation of State in Astrophysics Workshop, Saint-Malo, France, 14-18 Jun. 1993
(Contract W-7405-eng-48)
(DE94-006391; UCRL-JC-115805; CONF-9306287-2) Avail: CASI HC A03/MF A01

This paper summarizes recent work on the strongly coupled OCP and Binary Ionic Mixture equation of state and other thermodynamic quantities in white dwarf interior conditions for both fluid and solid phases with the assumption of a uniform background. Conditions for phase separation of different elements in fluid or solid phases is strongly dependent on deviations from the linear mixing rule which gives the equation of state as an additive function of the OCP equation of state. These deviations turn out to be small (a few parts in 10(exp 5)) and always positive including the case where the fraction of the higher Z component approaches 0. Also the equation of state of strongly coupled light elements (H and He particularly) obtained from simulations with a linear response description of the electrons is given for conditions appropriate to brown dwarf star interiors. Recent Livermore work on a band structure calculation of the enthalpy of H and He mixtures under jovian conditions is discussed. This work leads to a prediction of a high temperature (15,000 K) for miscibility of He in ionized H at 10 Mb. DOE

N94-31788 California Univ., Santa Cruz.
LINE-STRENGTH GRADIENTS AND KINEMATIC PROFILES IN ELLIPTICAL GALAXIES Ph.D. Thesis
Jose deJesusGonzalez-Gonzalez 1993 211 p
Avail: Univ. Microfilms Order No. DA9328211

The strength of several spectral features together with velocity dispersion and rotation were measured along the principal photometric axes of a sample of 40 elliptical galaxies. These line-strength and kinematic profiles were used to study the stellar population in these systems. The line-strength indices were measured with the Lick IDS system to compare the galaxy indices to model predictions for co-eval generations of stars as a function of age and metallicity. The IDS calibration yields the most comprehensive and up-to-date collection of models available. The Mg and Fe line-strengths indicate a high (Mg/Fe) abundance ratio in strong-lined galaxies relative to the calibrating stars. The Mg and Fe indices taken alone are not enough to separate the age and metallicity of composite stellar populations. The age-metallicity degeneracy has been broken in this study by including the H(sub beta) strength (a very age-sensitive index). The H(sub beta) index varies considerably among the galaxies while the more metallicity-sensitive indices do not vary as much. The well defined light-strength patterns in the galaxies reflect into remarkable age-metallicity trends when compared to the models. Taking the models as a reference, two specific conclusions are reached. First, although the mean stellar metallicity does not seem to vary significantly among strong and weak-lined galaxies (Delta bar-Z approximately less than 50 percent), these two types of galaxies are separated by a considerable age spread. The mean stellar age of weak-lined galaxies can be as small as approximately 4 to 6 Gyr, in contrast to ages of approximately 12 to 15 Gyr in strong-lined galaxies. And secondly, the typical H(sub beta) gradient is flat. The typical metallicity gradient reads to be Delta bar-Z/Delta log r approximately equal to -0.3, compared to a typical age gradient of Delta bar-age/Delta log r approximately equal to 3 Gyr per dex in radius (or approximately 40 percent at bar-age = 8 Gyr). If a population of old but blue stars contributes significantly to the optical light in weak-lined galaxies, their strong H(sub beta) absorption would not be an indication of a young age. Further observations in this direction are encouraged. Dissert. Abstr.

N94-31789 British Columbia Univ., Vancouver.
GRAVITATIONAL EFFECTS OF COSMIC STRINGS Ph.D. Thesis
Daniel Vollick 1992 161 p
(ISBN-0-315-75484-2) Avail: Univ. Microfilms Order No. DANN75484

Cosmic strings are line-like distributions of energy which may have formed in the early universe. Recent simulations of the evolution of cosmic

string networks show that strings have a significant amount of small scale structure (i.e. wiggles). In this thesis we will examine some of the gravitational effects produced by wiggly cosmic strings. One intriguing possibility is that cosmic strings produced the density perturbations which triggered the formation of galaxies and large-scale structure. Calculations by others which neglect the wiggles suggest that this scenario is ruled out. Using the Zel'dovich approximation and taking the wiggles into account I found that the wakes produced by the strings in cold dark matter can account for the observed large scale structure of the universe. Using the Gilbert equation I found that the size of the structure produced in hot dark matter is smaller but comparable to the size of the observed large scale structure. I also found that the wiggles can fragment the wakes into pieces which have the mass of a galaxy. One of the interesting observational effects of cosmic strings is the production of double images through gravitational lensing. The gravitational field of a wiggly string differs from the field of a straight string in that the curvature tensor outside a straight string is zero, whereas the curvature tensor diverges as one approaches a wiggly string. Could this make a significant observational difference? To examine this I calculated the effect of a wave pulse on the images of objects located behind the string and found that differences exist, but are small. Dissert. Abstr.

N94-31869 Massachusetts Univ., Amherst.
COMETARY MOLECULES Ph.D. Thesis
Weiguo Ge 1993 130 p
Avail: Univ. Microfilms Order No. DA9316652

A comprehensive model of the excitation and kinematics of cometary molecules has been developed and used to analyze data obtained on comet Levy (1990c). This work builds on previous studies to develop modes of the excitation and distribution of HCN and H2CO in the coma and to apply these modes to comet Levy in order to determine the physical parameters of the cometary coma and test models of the possible origin of H2CO in comets. The collision cross sections as a function of delta J have been considered in the excitation models for both molecules, based on quantum mechanical calculations. The vectorial model has been adopted for consideration of possible daughter species and a Monte Carlo calculation technique has been applied to develop both parent and daughter molecule models for H2CO so that we can calculate its production rate and discuss its original source. With the high quality of spectra for both HCN and H2CO molecules in comet Levy, we are able to use our models to constrain their abundance and some physical parameters of the coma. These new observational results confirm that microwave spectroscopy is an efficient tool to study cometary parent molecules, and help us understand the formation of our solar system. Dissert. Abstr.

N94-31913# Montreal Univ. (Quebec). Dept. de Physique.
STUDY OF STELLAR ASSOCIATIONS LOCATED IN THE REGION CONTAINED BETWEEN THE MAGELLANIC CLOUDS Ph.D. Thesis [ETUDE D'ASSOCIATIONS STELLAIRES SITUEES DANS LA REGION COMPRISE ENTRE LES NUAGES MAGELLAN]
Luc Grondin Dec. 1991 178 p In ENGLISH and FRENCH
(ISBN-0-315-86692-6; CTN-94-61221) Copyright Avail: Micromedia Ltd., Technical Information Centre, 240 Catherine Street, Suite 305, Ottawa, Ontario, K2P 2G8, Canada HC/MF

Fundamental characteristics that are required to understand the nature of the bridge linking the Magellanic Clouds were investigated. Photometry in the B, V, and I bands was applied to five stellar associations in the bridge allowing construction of a precise color-magnitude diagram for each association. The distance and age of these associations was determined along with the radial velocity of some of the stars. It was found that the five associations studied are found at distances on the order of 60 kiloparsecs (kpc), confirming that they belong to the Magellanic System. The age of the associations appears less than 16 million years, much younger than the time since the last hypothetical encounter between the Small and Large Magellanic Clouds. The stars were thus formed near their present position in a relatively tenuous medium. The initial mass function (IMF) has a less pronounced slope than that evaluated by Scalo for the system surrounding the Sun and by Mateo for a sample of Magellanic clusters. Nevertheless, it is comparable with the IMF obtained by Sagar and Richtler for five clusters in the Large Magellanic Cloud and that characterizing the open clusters of the Galaxy. A universal IMF hypothesis is thus favored. CISTI

N94-31926 State Univ. of New York, Stony Brook.
PLANETESIMAL DYNAMICS IN THE VICINITY OF A GROWING PROTOPLANET Ph.D. Thesis
David Michael Kary 1993 305 p
Avail: Univ. Microfilms Order No. DA9328200

This thesis describes calculations of the systematic component of spin angular momentum accretion. It also covers work on the impact probability for planetesimals evolving towards a planet due to gas drag. The rotation studies assume that a spherical planet on a circular orbit accretes from a uniform density two dimensional disk of planetesimals. For a nongravitating planet, these calculations give prograde rotation of less than one rotation/year. When planetary gravity is included and the planetesimal eccentricity is low, the rotation is strongly retrograde. As eccentricity grows, the rotation becomes prograde, reaching a strong peak, and then dropping toward the nongravitating limit. The peak is comparable to observed rotation rates, but when planetesimal eccentricities have a Rayleigh distribution little prograde rotation is produced. However, the observed spin rates may result from nonuniformities in the planetesimal disk, specifically, a gap in planetesimal semimajor axes around the planet. This gives extra impactors from the extremities of the accretion cone which produce strongly prograde rotation. In the gas drag studies planetesimals approaching a protoplanet on a circular orbit are studied using three-body numerical integrations. Planetesimals originate on circular orbits external to the planet's orbit and usually coplanar with it. Particles larger than a given size become trapped at resonances with the planet. The stability of resonance locks depends on the proximity of other resonances and often on a period-doubling transition to chaos. For modern planet densities, only a small fraction of the material not trapped in resonances hits the planet. Planets with extended atmospheres dense enough to trap planetesimals accrete much more efficiently. At large decay rates, impact probabilities vary inversely with the drag parameter. Particles whose vertical motions are large compared to the planet's radius have impact probabilities which vary inversely with their orbital inclination. The rotation induced by particles which hit the planet depends on the drag rate. Low drag rates produce prograde rotation since planetesimals are accreted from the extremities of the accretion zone, while large drag rates produce retrograde rotation, since the planetesimals are accreted from anywhere in the accretion zone, and their eccentricities are low. Dissert. Abstr.

N94-31946 Virginia Univ., Charlottesville.
STRUCTURE AND STABILITY OF SPHERICAL ACCRETION FLOWS ONTO COMPACT OBJECTS Ph.D. Thesis
John Charles Houck 1991 101 p
Avail: Univ. Microfilms Order No. DA9223411

We examine the structure of hypercritical accretion flows onto neutron stars, considering steady state, spherically symmetric flows with accretion rates in the range 10(exp -4) approximately less than M less than or equal to 10(exp 4) solar mass/yr. In this regime, the gravitational accretion energy is carried away by neutrinos. Our models include pair production, radiation diffusion, and general relativistic effects. At the lower accretion rates, free-fall toward the neutron star surface ceases and an extended, quasistatic radiation pressure supported envelope is present. This radiation pressure supported envelope is likely to be dynamically unstable. Applying these results to the case of SN1987A, we find that the luminosity at infinity from accretion onto a central neutron star should reach 50 percent of the Eddington luminosity within about six months of the explosion, approaching the Eddington luminosity within a year. We then examine the general structure and stability of spherical accretion flows onto compact objects. For simplicity, we assume that the cooling function has the form L varies as rho(exp beta - alpha) p(exp alpha). The dependence of the flow structure and stability on the accretion rate M, the form of the cooling function, and the ratio of specific heats (gamma) of the accreting material is discussed. We then discuss the application to post-supernova neutron star accretion flows and to observations of quasiperiodic variations in the x ray and optical emission from accreting white dwarfs in AM Her binaries. Post-supernova neutron star accretion flows are marginally unstable against radial shock oscillations. The nonlinear evolution of these oscillations may be an important aspect of the emergence of the neutron star from this accretion envelope. The parameter space over which white dwarf accretion shocks are unstable may be further extended by the existence of unstable nonradial oscillation modes. Because these modes can have oscillation periods ranging from

approximately 1 to 10 s, they are of interest in connection with both optical and x ray quasiperiodic oscillations observed in AM Her systems.
Dissert. Abstr.

N94-31947 Washington Univ., Seattle.
COMPOSITION AND PROPERTIES OF DUST FROM COMET HALLEY Ph.D. Thesis
Mark E. Lawler 1993 219 p
Avail: Univ. Microfilms Order No. DA9326371

A study of the elemental and morphological properties of cometary dust is made using elemental composition data from the PUMA and PIA impact mass spectrometers that analyzed Comet Halley's dust on flyby missions in 1986. The study is unique in its special rigorous selection procedures and its resulting high quality data sets, the largest of which contains mass spectra from 279 dust particles. The results include findings that anhydrous mafic silicates, many rich in Mg composition, are a predominant and ubiquitous constituent of cometary dust. Iron sulfides are probably also a common constituent. Both silicates and sulfides occur as mineral grains smaller than the typical particle size, and they are mixed intimately with abundant organic 'CHON' material. Sulfates and carbonates that would be produced by aqueous alteration seem to be very rare or nonexistent. Compositional dispersions of the major rock-forming elements in the cometary dust are quite unlike those seen in carbonaceous chondrites and serpentine-dominated hydrous interplanetary particles. The Halley data show evidence for olivines and low-Fe silicates that are absent from the hydrous smectite layer-silicate class of interplanetary particles, and this type of IDP also appears unlikely to be cometary material. The overall compositional dispersions in Halley's dust appear most similar to the anhydrous, porous chondritic class of interplanetary dust particles, lending additional support to the belief that this class of interplanetary particle has a cometary origin. Several lines of evidence indicate that extensive sublimation of volatile organic material in the dust occurs up to approximately 40,000 km from the comet nucleus, resulting in declining organic fractions in dust populations more distant from the nucleus. Sublimation may lead to fragmentation of the dust and elimination of the larger particles beyond this radius. Limited evidence has been found that published estimates of PUMA and PIA dust particle masses are too high by at least two orders of magnitude. The data appear consistent with a Greenberg-type model of organic CHON mantles on constituent silicate grains if sublimation of volatiles operates and produces the observed high variability in CHON-to-silicate composition. Dissert. Abstr.

N94-31948 Johns Hopkins Univ., Baltimore, MD.
IONIZED GAS IN THE HALOS OF EDGE-ON INFRARED-BRIGHT GALAXIES: EVIDENCE FOR STARBURST-DRIVEN SUPERWINDS Ph.D. Thesis
Matthew David Lehnert 1993 326 p
Avail: Univ. Microfilms Order No. DA9327629

Large scale, starburst driven outflows from galaxies ('superwinds') have a rich legacy in theoretical astrophysics and have been invoked to explain many aspects of galactic formation and evolution. Such winds should arise when the supernova rate is high enough to create a cavity of very hot shock-heated gas within a galaxy. This gas can then expand outward as a high speed wind that can accelerate and heat ambient interstellar or circum-galactic gas causing it to emit optical line radiation and/or thermal x rays. Theory suggests that such winds should be common in starburst galaxies and the nature of the winds should depend on the star formation rate and distribution. In order to systematize our observational understanding of superwinds (determine their incidence rate and the dependence of their properties on the star formation that drives them) and to make quantitative comparisons with the theory of superwinds, we have analyzed data from an optical spectroscopic and narrow-band imaging survey of an infrared flux-limited sample of about 50 IR-warm, starburst galaxies whose stellar disks are viewed nearly edge-on. This sample contains galaxies with infrared luminosities from approximately equal to 10(exp 10 to 12) solar luminosity and allows us to determine the properties of superwinds over a wide range of star formation rates. We have found that extra-planar emission-line gas is a very common feature of these edge-on, IR-bright galaxies and the properties of the extended emission-line gas are quantitatively consistent with the superwind theory. These properties are: radial pressure profiles that fall as approximately r(exp -2), pressures in the nuclei of these galaxies that are three orders of magnitude higher than the ambient pressure in the ISM of our galaxy, line ratios becoming more shock-like as one proceeds out along the galaxy minor axis, extra-planar filamentary and shell-like emission-line morphologies on scales of 100 s of pc to 10 s of Kpc, and the kinematic signatures of an outflow whose velocity is related to the star formation rate. Dissert. Abstr.

N94-31949 California Inst. of Tech., Pasadena.
HYDRODYNAMICS OF NEUTRON STAR INTERIORS AND LABORATORY SUPERFLUIDS Ph.D. Thesis
Tassilo Andreas Reisenegger 1993 124 p
Avail: Univ. Microfilms Order No. DA9325384

This thesis contains the following papers: (1) A new class of g-modes in neutron stars. In the fluid core of a neutron star, the ratio of the number densities of charged particles (protons and electrons) to neutrons is an increasing function of the mass density. This composition gradient stably stratifies the matter, giving rise to g-modes with periods ranging upward from a few milliseconds. Some of these modes are computed and their damping mechanisms are discussed. (2) Magnetic field decay in isolated neutron stars: We investigate mechanisms that promote the loss of magnetic flux from an isolated neutron star. Ambipolar diffusion involves a drift of the magnetic field and charged particles relative to the neutrons, opposed by frictional drag. Variants of it include both the buoyant rise and the dragging by superfluid neutron vortices of magnetic flux tubes. The charged particle flux decomposes into a solenoidal and an irrotational component. The irrotational component perturbs the chemical equilibrium, generating pressure gradients that effectively choke it. The solenoidal component can transport magnetic flux from the outer core to the crust on a short timescale. Flux that threads the inner core is permanently trapped unless particle interactions can rapidly smooth departures from chemical equilibrium. We speculate that Hall drift may lead to a turbulent cascade of the magnetic field in the solid crust, terminated by ohmic dissipation at small scales. (3) The spin-up problem in helium 2: The laminar spin-up of helium 2 is studied by solving the linearized two-fluid equations in a simple case. No direct interactions between vortex lines and container walls are included. Two mechanisms are identified for the transfer of angular momentum from the container to the interior fluid. Both involve a poloidal secondary flow. An analytic expression for the spin-up time is found. Dissert. Abstr.

N94-31950 Johns Hopkins Univ., Baltimore, MD.
THE CHEMICAL AND DYNAMICAL EVOLUTION OF THE GALAXY Ph.D. Thesis
Tammy Ann Smecker-Hane 1993 305 p
Avail: Univ. Microfilms Order No. DA9327664

I develop theoretical models of the chemical and dynamical evolution of galaxies and present a galactic structure survey-invaluable tools for uncovering the history of the formation of our galaxy. Important advances in my theoretical models are noninstantaneous recycling of newly synthesized elements such as iron from Type Ia supernovae (mergers of white dwarf binaries). I incorporate Type Ia supernovae in models of baryonic dark matter as stellar remnants. If dark halos consist mainly of white dwarfs, as has been proposed, then an excessive supernovae rate is predicted unless the binary fraction was virtually zero. The observed chemical abundance ratios of halo stars signify enrichment from only Type II supernovae. I explore the timescale for the onset of Type Ia supernovae as an upper-limit to the timescale of halo formation. The apparent inconsistency between differences in ages of halo stars (2 to 3 Gyr) and timescale inferred from Type Ia supernovae (approximately less than 0.1 Gyr) suggests galaxies formed from hierarchical substructure. I calculate chemical and dynamical evolution models of viscous disks with noninstantaneous recycling. Patterns of element ratios and scatter in the age-metallicity relationship are predicted throughout the disk. Characterized by radial flows of gas, these models are ideal for exploring new ideas on creating the galactic bulge from disk inflow. The high metallicity of bulge stars may not require an ad hoc variation of the stellar initial mass function if inflow alters the apparent yields in the bulge and solar neighborhood. I present an unbiased, magnitude-limited spectroscopic survey of F-G stars. Radial velocities accurate to approximately less than 10 km/s are derived and compared with predictions of galactic structure models. Distances are derived by photometric parallax, and three dimensional velocities are calculated using published proper motions. Calibration of spectral line strengths against metallicity is presented for standard stars. Evaluation of metallicities of program stars is forthcoming. These data will be useful for constraining

the existence of a metallicity gradient in the galactic halo, and determining correlations between kinematics and chemistry in the disk/halo transition.
Dissert. Abstr.

N94-31963 Catholic Univ. of America, Washington, DC.
A STUDY OF PHYSICAL CONDITIONS, RADIATIVE TRANSFER AND SHOCKS IN THE INTERSTELLAR MEDIUM Ph.D. Thesis
Cheng-Hsuan Lyu 1993 157 p
Avail: Univ. Microfilms Order No. DA9318378

Two basic physical problems due to radiative transfer and time-dependent shocks are explored. In the first problem, a detailed statistical equilibrium model dealing with the radiative transfer in the interstellar molecular clouds is developed. An improved treatment of the radiation field, including the 2.73 K background radiation field, is incorporated. This model is applied in an analysis of ultraviolet high dispersion (R approx. 8.6 x 10(exp 4)) echelle observations of molecular CO obtained with the Goddard High Resolution Spectrograph aboard the Hubble Space Telescope. Specifically, for the xi Per clouds, synthetic spectra were computed and fitted to the observed CO (2-0) and (3-0) bands in the A (sup 1)II - X (sup 1)sigma(+) system. Derived populations of the C I ground-state fine-structure levels and the Co ground-state rotational levels were used to derive densities of two of the three, and possibly four, detected cloud components. The velocity component displaying the strongest C I absorption reveals extraordinarily high pressure (P/k greater than 4.0 x 10(exp 4) cm(exp -3) K). For the xi Oph clouds, the computed relative populations of the 6 lowest rotational levels of CO, based upon the statistical equilibrium model, together with multiple Voigt profile fits were determined to reproduce successfully the observations of the rotational structure of the (5-0) and (6-0) bands in (12)C(16)O and (13)C(16)O. The abundance of Co is found to be (1.88 +/- 0.25) x 10(exp 15) cm(exp -2), and the isotope ratio of (12)C(16)O/(13)C(16)O is approximately 79 +/- 22. In the second interstellar shock problem, we find that the photoionization by the EUV/UV (including soft X-ray) flux from both the central Of star and the surrounding hot gas plasma is a significant mechanism in determining the dynamical processes in the interstellar bubble, where the He II emission should be observable. Shock ionization and photoionization by X-rays originating from the central hot O star are responsible for producing this emission. Furthermore, from an expanding supershell model, we find that the local cloud (less than or equal to 10 pc) at the periphery of Loop I is affected by a recent (less than or equal to 10(exp 5) years) supernova, and the shock velocity (the expansion velocity) is approximately 15 km s(exp -1). This cloud is substantially ionized where the ionization fraction of hydrogen is approximately 66 percent and that of helium is 36 percent. Dissert. Abstr.

N94-31987 Massachusetts Inst. of Tech., Cambridge.
A MULTI-FREQUENCY STUDY OF AN X RAY SELECTED SAMPLE OF ACTIVE GALACTIC NUCLEI Ph.D. Thesis
Bruce Alan Grossan 1992
Avail: Issuing Activity (MIT Libraries, Rm. 14-0551, Cambridge, MA 02139-4307)

The LASS (Large Area Sky Survey) experiment, which flew aboard the HEAO-1 spacecraft, carried out a 2-20 keV survey of the sky during 1977-1978. The X-ray sources from this survey make up the LASS catalog (Wood et al. 1979). Optical counterparts have been identified for greater than 86 percent of the LASS sources above a flux of approx. 0.95 microns (mu)Jy Q 5 keV (Remillard 1992b). The LASS error boxes, along with the more precise positions from the Modulation Collimator (MC) X-ray experiment (also aboard HEAO-1), subsequent X-ray imaging, and optical search techniques were all used to identify the LASS sources. From these identifications, a high-latitude (absolute value of b greater than 20 deg.), flux limited (greater than or equal to 0.95 (mu)Jy) sample of 96 emission line Active Galactic Nuclei (AGN) have been selected for study. The sample is referred to as the LMA (for the LASS/MC identified sample of AGN). The objective of this work is to produce multi-frequency spectra of this sample of objects, in order to determine and interpret the statistical properties of the sample over nearly the full range of observable wavelengths. Data were obtained for as much of the radio through hard X-ray (less than 20 keV) spectrum as possible for each object in the LMA. Radio, near infrared, and other measurements were taken from the literature, far IR fluxes were extracted from co-added observations from IRAS, UV spectra were obtained from the IUE archives, and original observations were performed (with the help of collaborators) in the radio, near IR, optical, UV, and X-ray to fulfill this goal. Correlation studies of the continuum bands found poor correlations of X-ray and radio flux, good correlations for 12 and 26 micron flux with X-ray flux, excellent correlations for optical and near IR fluxes with X-rays, and poor correlations of UV and X-ray fluxes. Correlation studies of the line and X-ray continuum flux yield a good correlation between the flux of (OIII), the strongest narrow emission line, and X-ray flux. The hard X-ray Luminosity Function (LF) of the LMA can be roughly described by a power law of slope -2.49 plus or minus 0.02 from 10(exp 42)-10(exp 48) erg s(exp -1), but the function steepens with increasing luminosity.
Dissert. Abstr.

N94-32028 California Univ., Los Angeles.
THE MANIFESTATIONS OF ENERGETIC ACTIVITY IN THE GALACTIC CENTER Ph.D. Thesis
Keven Isao Uchida 1993 281 p
Avail: Univ. Microfilms Order No. DA9319823

The Galactic center region exhibits anomalous gas motions that may either indicate the radial ejection of gas due to a energetic central outburst or, alternatively, orbital motion in a non axisymmetric central potential, such as that of a bar. The purpose of this dissertation has been to explore these alternatives by examining new evidence of energetic activity in the Galactic center region. Particular emphasis has been placed on the unusual infrared hotspot AFGL 5376 and the radio continuum shell G359.1-0.5. What these objects have in common, and what has drawn attention to them, is their association with prominent molecular gas features extending well out of the Galactic plane. The nonthermal shell G359.1-0.5 is completely ringed by one such massive protrusion. AFGL 5376 is associated with another -- a well-defined, 90-pc spur of gas. This dissertation also reports on a new set of far-infrared continuum structures (the IR Spurs) which, like the molecular features, extend away from the Galactic plane. The data which have been acquired and analyzed for this investigation include (1) millimeter-wave molecular line ((12)CO J = 2-1 and 1-0) observations of AFGL 5376 and G359.1-0.5, (2) lambda 21 cm neutral hydrogen line and continuum observations toward G359.1-0.5, and (3) 12, 25, 60 and 100 microns IRAS images of the 'IR Spurs'. In addition, a kinematic code was developed to model the expansion of, and the effects of Galactic shear on the localized molecular ring associated with and surrounding G359.1-0.5. The energy output from a star cluster composed of nearly 200 O-type stars is apparently needed to account for the expansion of the ring. AFGL 5376 provides strong evidence of a recent major release of energy from the Galactic center; it is the locus of a large-scale vertical shock which bisects the entire length of its associated molecular spur. It is most readily understood in terms of explosion-induced expansion motions from the nucleus. A central energy release is the favored hypothesis for the observed anomalous gas motions, although the response of the gas to a bar remains a viable alternative. Dissert. Abstr.

N94-32029 Harvard Univ., Boston, MA.
THE KINEMATICS OF DENSE CLUSTERS OF GALAXIES Ph.D. Thesis
Ann I. Zabludoff 1993 180 p
Avail: Univ. Microfilms Order No. DA9318699

To obtain the distribution of cluster velocity dispersions (sigma), we have measured redshifts in the fields of the 31 R greater than or equal to 1 Abell clusters with 0.02 less than or equal to z less than or equal to 0.05. At least 10 fields are contaminated by superimposed velocity peaks. We extract 25 dense clusters with sigma greater than or equal to 300 km s(exp -1) and with surface number densities one deviation above the mean for the Great Wall. From the CfA Redshift Survey, we obtain a volume-limited catalog of 31 groups with sigma greater than or equal to 100 km s(exp -1) and with the same surface density limit as for the clusters. By combining the two distributions, we obtain a well-defined sample over a wide range of dispersions. The groups compensate for incompleteness in the Abell catalog at low sigma. The Abell clusters populate the high-sigma tail. At sigma approximately equal to 700 km s(exp -l), the group and cluster distributions are consistent. The combined distribution is consistent with x-ray temperature distribution functions. We compare the distribution of sigma with those predicted by theoretical models of large-scale structure. The models include Gaussian and non-Gaussian initial conditions, different power spectra, flat and open cosmologies, and unbiased and biased galaxy formation. Open and biased Gaussian models predict a distribution with too steep a slope the normalizations of unbiased models tend to be too high. Skew-positive and broad models are most successful at reproducing

the data, skew-negative models are the worst. To examine the individual kinematics of well-sampled clusters, we develop a method for detecting departures from a Gaussian velocity distribution in systems with approximately 100-200 measured redshifts. We decompose the velocity distributions of eight clusters into sums of the orthogonal Gauss-Hermite functions. This method quantifies the asymmetric 3rd-order and symmetric 4th-order terms of each distribution while minimizing the effect of interlopers in the tails. Dissert. Abstr.

N94-32137# Lawrence Livermore National Lab., CA.
WINDS FROM DISKS IN COMPACT BINARIES
C. W. Mauche 27 Oct. 1993 13 p Presented at the 105th Annual Meeting of the Astronomical Society of the Pacific, San Diego, CA, 10-15 Jul. 1993
(Contract W-7405-eng-48)
(DE94-007452; UCRL-JC-115464; CONF-9307167-1) Avail: CASI HC A03/MF A01

We herein present an observational and theoretical review of the winds of compact binaries. After a brief consideration of the accretion disk coronae and winds of X-ray binaries, the review concentrates on the winds of cataclysmic variables (CV's). Specifically, we consider the related problems of the geometry and mass-loss rate of the winds of CV's, their ionization state and variability, and the results from studies of eclipsing CV's. Finally, the properties of bona fide accretion disk wind models are reviewed. DOE

N94-32309 Wisconsin Univ., Madison.
A STUDY OF THE NEUTRAL HYDROGEN DISTRIBUTION OF THE MILKY WAY THROUGH 21 cm EMISSION AND LYMAN ALPHA ABSORPTION Ph.D. Thesis
Athanassios Diplas 1992 171 p
Avail: Univ. Microfilms Order No. DA9304149

The focus of the thesis is the distribution of neutral hydrogen in the galactic disk and halo. The thesis consists of two projects. The first project is the study of the warp of the outer galaxy, via 21 cm emission. The second project deals with the H I distribution as derived from Ly alpha studies of stars hotter than B2 with the IUE. In the first part, we have used the Bell Laboratories Northern Hemisphere H I survey data of Stark and coworkers. These measurements are well suited for investigations of faint galactic H I emission because the sidelobe contamination of the data is low. We present a series of contour maps of n(sub H). The measurements permit us to probe with reliability the nature of the galactic warp and the extension of the gas to large z in the outer galaxy. For moderate R, the z distribution of the H I is complicated and reveals the existence of a confined component and an extended component. When viewed from the position of the sun, the warped and flaring outer galaxy extends to galactic latitudes as large as +25 degrees. In the second part of the thesis we studied the galactic interstellar H I distribution by analyzing existing absorption line data towards the complete sample of 554 B2 and hotter stars observed at high resolution with the IUE. This study more than doubles the number of lines of sight previously observed. We corrected the measured values of N(H I) for stellar contamination, and discarded approximately 40 percent of the B stars. The final working sample includes 388 stars. We present statistical averages for a number of quantities derived for the sample and study the changes in the H I to dust ratios with distance absolute value of z and with n(sub (H I)). The distribution of the gas away from the galactic plane is complex. Dissert. Abstr.

N94-32489 Arizona State Univ., Tempe.
ORGANIC ANALYSES OF THE MURCHISON METEORITE Ph.D. Thesis
George Cooper 1993 98 p
Avail: Univ. Microfilms Order No. DA9320585

Many compounds yielding clues to the organic chemistry and molecular composition of the early solar system have been identified in the Murchison meteorite. Among these are amino acid precursors: carboxy lactams, lactams, N-acetyl amino acids, and amino acid hydantoins (5-substituted hydantoins). Also found were precursors of acids: dicarboxylic acid mono amides, carboxylic acid amides, and cyclic imides. Precursors of hydroxy acids, hydroxy amides, are also numerous. Organic phosphorus compounds are reported. The corresponding organic sulfur compounds, sulfite, and water soluble and insoluble phosphate are also present. Laboratory experiments have indicated that unusual cyanate chemistry was possibly responsible for the formation of at least some of the amino and carboxylic acid precursors. A plausible mode of formation of the organic phosphorus and sulfur compounds, alkyl phosphonic and alkyl sulfonic acids, respectively, suggests a direct link between identified interstellar molecules and aqueous chemistry on the meteorite parent body. The compounds were extracted under gentle conditions to avoid, as much as possible, decomposition during extraction. The procedure included extraction of a powdered sample with room temperature water, cation and anion exchange chromatography, derivatization with the reagent N-methyl- N-(tert-butyl dimethyl silyl) trifluoro acetamide (MTBSTFA), and analysis by gas chromatography-mass spectrometry (GCMS) and high performance liquid chromatography (HPLC). Dissert. Abstr.

N94-32503# Stanford Research Inst., Menlo Park, CA. Linear Accelerator Center.
THE EVOLUTIONARY STATUS OF PSR 1259-63
L. Cominsky Dec. 1993 4 p Presented at the 4th Maryland Conference on Astrophysics, College Park, MD, 11-13 Oct. 1993
(Contract DE-AC03-76SF-00515)
(DE94-007094; SU-SLAC-PUB-6405; CONF-9310283-1) Avail: CASI HC A01/MF A01

The PSR 1259-63 system is unique in that it is the first radio pulsar found to be in a binary system with a massive main sequence companion. As such, it may be the evolutionary missing link connecting the radio pulsars to the X-ray emitting Be binaries. In this paper, we consider the conditions under which PSR 1259-63 may be the progenitor of the less eccentric, more slowly rotating X-ray Be binaries such as 4U0115+63, A0535+26, and A0538-66. Scenarios invoking the interaction of the pulsar with the stellar wind of the companion are proposed to account for the rapid spin-down phase that must occur in this system if it is evolutionarily linked to accreting X-ray binaries. The unexpected X-ray emission observed from PSR 1259-63 may indicate that the interaction between the pulsar and the Be star occurs at greater distances and produces a greater spin-down efficiency than was previously calculated. DOE

N94-32638 Brookhaven National Lab., Upton, NY.
TRANSVERSE ENERGY PRODUCTION WITH Si AND Au BEAMS AT AGS ENERGY: TOWARDS HOT AND DENSE HADRONIC MATTER
J. Barrette (McGill Univ., Montreal, Quebec.) 1993 5 p Presented at the 10th International Conference on Ultra-Relativistic Nucleus-nucleus Collisions, Borlaenge, Sweden, 20-24 Jun. 1993 Limited Reproducibility: More than 20% of this document may be affected by microfiche quality
(Contract DE-AC02-76CH-00016)
(DE94-007178; BNL-49968; CONF-930636-12) Avail: CASI HC A01

One of the main goals of the present heavy-ion reaction studies at the AGS and CERN is the understanding of the space-time evolution of the particle and energy density produced in such collisions. These are necessary ingredients if one wants to understand quantitatively the properties of matter at high temperature and density. In that respect, the study of inclusive global variables such as the transverse energy distribution gives valuable information on the reaction dynamics and, albeit indirectly, on the energy and baryon density reached in nucleus-nucleus collisions. In the spring of 1992, the AGS produced the first beam of very heavy ions, more specifically a beam of 11.4 GeV/c per nucleon Au-197. This is an important step for the field since it gives a first glimpse as to how the reaction dynamics evolves as the mass and volume of colliding systems reach the largest value that will be available in the future. The authors have used part of the E814 experimental set-up to study the transverse energy distribution produced in Au induced collisions. These data can be compared to similar data obtained with lighter beams and thus provide for the first time information on how the E(sub T) distribution evolves with the mass of the system as one reaches very large systems. DOE

N94-32914# Lawrence Livermore National Lab., CA.
CONVECTION IN TYPE 2 SUPERNOVAE Ph.D. Thesis
D. S. Miller 15 Oct. 1993 129 p
(Contract W-7405-eng-48)
(DE94-009373; UCRL-LR-115467) Avail: CASI HC A07/MF A02

Results are presented here from several two dimensional numerical calculations of events in Type 2 supernovae. A new 2-D hydrodynamics and neutrino transport code has been used to compute the effect on the supernova explosion mechanism of convection between the neutrinosphere

and the shock. This convection is referred to as exterior convection to distinguish it from convection beneath the neutrinosphere. The model equations and initial and boundary conditions are presented along with the simulation results. The 2-D code was used to compute an exterior convective velocity to compare with the convective model of the Mayle and Wilson 1-D code. Results are presented from several runs with varying sizes of initial perturbation, as well as a case with no initial perturbation but including the effects of rotation. The M&W code does not produce an explosion using the 2-D convective velocity. Exterior convection enhances the outward propagation of the shock, but not enough to ensure a successful explosion. Analytic estimates of the growth rate of the neutron finger instability are presented. It is shown that this instability can occur beneath the neutrinosphere of the proto-neutron star in a supernova explosion with a growth time of approximately 3 microseconds. The behavior of the high entropy bubble that forms between the shock and the neutrinosphere in one dimensional calculations of supernova is investigated. It has been speculated that this bubble is a site for gamma-process generation of heavy elements. Two dimensional calculations are presented of the time evolution of the hot bubble and the surrounding stellar material. Unlike one dimensional calculations, the 2D code fails to achieve high entropies in the bubble. When run in a spherically symmetric mode the 2-D code reaches entropies of approximately 200. When convection is allowed, the bubble reaches approximately 60 then the bubble begins to move upward into the cooler, denser material above it. DOE

N94-33112 Queens Univ., Kingston (Ontario).
THE ROLE OF GALAXY TYPE AND ENVIRONMENT IN DETERMINING THE PROPERTIES OF GLOBULAR CLUSTER SYSTEMS Ph.D. Thesis
Terry James Bridges 1992 221 p
(ISBN-0-315-76447-3) Avail: Univ. Microfilms Order No. DANN76447

We have investigated the dependence of globular cluster system (GCS) properties on parent galaxy type and environment. We have acquired deep B and V CCD photometry of the GCS's of NGC 1399, the Fornax cluster cD, and NGC 4594, a large-bulged spiral. We find that the clusters in NGC 1399 and NGC 4594 are bluer (more metal-poor) than the halo light, and we show that there is a radial color gradient in the NGC 1399 GCS. We confirm that NGC 1399 has a superabundant GCS, whereas NGC 4594 has a cluster specific frequency similar to other Sa/Sb galaxies. We also find a central deficit of clusters in NGC 4594, but it is not clear whether this was built in or was due to subsequent dynamical evolution. We have also obtained deep V CCD photometry of two poor cluster cDs, NGC 4073 (MKW 4) and NGC 5629 (AWN 3). NGC 4073 has a detectable GCS, but it is unlikely to be as cluster-rich as some rich cluster cD/gE galaxies (e.g. M87, NGC 1399). No GCS has been detected around NGC 5629. Some GCS properties, namely the mean cluster color (metallicity) and the degree of central concentration, depend on parent galaxy luminosity, whereas the cluster specific frequency depends on galaxy environment and to a lesser extent on galaxy type. On the other hand, the existence of cluster central deficits and color gradients does not seem to depend on galaxy attributes or environment. The finding of color gradients in some GCSs and not in others implies that cluster formation is dissipative in some cases and more prolonged and chaotic in others. It is argued that the available data are most consistent with globular clusters forming during protogalactic collapse, but slightly before the halo field populations.
Dissert. Abstr.

N94-33147 Chicago Univ., IL. Dept. of Astronomy and Astrophysics.
NUCLEAR PHYSICS AND ASTROPHYSICS
D. N. Schramm and A. V. Olinto Jun. 1993 11 p Limited Reproducibility: More than 20% of this document may be affected by microfiche quality
(Contract DE-FG02-91ER-40606)
(DE94-007168; DOE/ER-40606/3) Avail: Issuing Activity (Department of Energy (DOE))

The authors report on recent progress of research at the interface of nuclear physics and astrophysics. During the past year, the authors continued to work on Big Bang and stellar nucleosynthesis, the solar neutrino problem, the equation of state for dense matter, the quark-hadron phase transition, and the origin of gamma-ray bursts; and began studying the consequences of nuclear reaction rates in the presence of strong magnetic fields. They have shown that the primordial production of B and Be cannot explain recent detections of these elements in halo stars and have looked at spallation as the likely source of these elements. By looking at nucleosynthesis with inhomogeneous initial conditions, they concluded that the Universe must have been very smooth before nucleosynthesis. They have also constrained neutrino oscillations and primordial magnetic fields by Big Bang nucleosynthesis. On the solar neutrino problem, they have analyzed the implications of the SAGE and GALLEX experiments. They also showed that the presence of dibaryons in neutron stars depends weakly on uncertainties of nuclear equations of state. They have started to investigate the consequences of strong magnetic fields on nuclear reactions and implications for neutron star cooling and supernova nucleosynthesis. DOE

N94-31021*# Boeing Defense and Space Group, Seattle, WA.
MODEL OF SPACECRAFT ATOMIC OXYGEN AND SOLAR EXPOSURE MICROENVIRONMENTS
R. J. Bourassa and H. G. Pippin *In* NASA. Marshall Space Flight Center, LDEF Materials Results for Spacecraft Applications Dec. 1993 p 105-114 (For primary document see N94-31012 09-12)
(Contract NAS1-19247)
Avail: CASI HC A02/MF A04

91 LUNAR AND PLANETARY EXPLORATION

Includes planetology; and manned and unmanned flights.
For spacecraft design or space stations see *18 Spacecraft Design, Testing and Performance.*

N94-31105*# Massachusetts Inst. of Tech., Cambridge. Dept. of Earth, Atmospheric, and Planetary Sciences.
TECTONIC HISTORY OF THE TERRESTRIAL PLANETS Final Report, Oct. 1989 - Mar. 1993
Sean C. Solomon Mar. 1993 216 p
(Grant NAGw-1937)
(NASA-CR-195696; NAS 1.26:195696) Avail: CASI HC A10/MF A03

The topics covered include the following: patterns of deformation and volcanic flows associated with lithospheric loading by large volcanoes on Venus; aspects of modeling the tectonics of large volcanoes on the terrestrial planets; state of stress, faulting, and eruption characteristics of large volcanoes on Mars; origin and thermal evolution of Mars; geoid-to-topography ratios on Venus; a tectonic resurfacing model for Venus; the resurfacing controversy for Venus; and the deformation belts of Lavinia Planitia. For individual titles, see N94-31106 through N94-31115.

N94-31106*# Massachusetts Inst. of Tech., Cambridge. Dept. of Earth, Atmospheric and Planetary Sciences.
PATTERNS OF DEFORMATION AND VOLCANIC FLOWS ASSOCIATED WITH LITHOSPHERIC LOADING BY LARGE VOLCANOES ON VENUS Abstract Only **c46**
Patrick J. McGovern and Sean C. Solomon *In its* Tectonic History of the Terrestrial Planets Mar. 1993 1 p (For primary document see N94-31105 09-91)
Avail: CASI HC A01/MF A03

Magellan radar imaging and topography data are now available for a number of volcanoes on Venus greater than 100 km in radius. These data can be examined to reveal evidence of the flexural response of the lithosphere to the volcanic load. On Venus, erosion and sediment deposition are negligible, so tectonic evidence of deformation around large volcanoes should be evident except where buried by very young flows. Radar images reveal that most tectonic features and flow units on the flanks of these volcanoes have predominantly radial orientations. However, both Tepev Mons in Bell Regio and Sapas Mons in Atla Regio exhibit circumferential graben on their flanks. In addition, images reveal several flow units with an annular character around the north and west flanks of Tepev Mons. This pattern most likely results from ponding of flows in an annular flexural moat. Maat Mons in Atla Regio and Sif Mons in Eistla Regio are examples of volcanoes that lack circumferential graben and annular flows; discernible flow units and fractures on these constructs appear to be predominantly radial. Altimetry data can also provide evidence of flexural response. Tepev Mons is partially encircled by depressions that may be sections of a flexural moat that has not been completely filled. The locations of these depressions generally coincide with the annular flows described above. There is weaker evidence for such depressions around Maat Mons as

well. The lack of circumferential tectonic features around most volcanoes on Venus might be explained by gradual moat filling and coverage by radial flows. The depressions around Tepev (and possible Maat) may indicate that this process is currently continuing. We use analytic models of plate flexure in an axisymmetric geometry to constrain the elastic plate thickness supporting Tepev Mons. If we consider the outer radius of the ponded flows to be the edge of a moat, we find that models with elastic plate thickness of 10-20 km fit best. Finite element models of a volcanic load detached from the underlying lithosphere predict overthrusting and radial normal faulting at the volcano's edge. Such a mechanism for the formation of radial rift zones on Venus volcanoes would make such features analogous to structures on the flanks of volcanoes on Earth. Author (revised)

N94-31107*# Massachusetts Inst. of Tech., Cambridge. Dept. of Earth, Atmospheric, and Planetary Sciences.

ASPECTS OF MODELLING THE TECTONICS OF LARGE VOLCANOES ON THE TERRESTRIAL PLANETS

Patrick J. McGovern and Sean C. Solomon *In its* Tectonic History of the Terrestrial Planets Mar. 1993 2 p (For primary document see N94-31105 09-91)

Avail: CASI HC A01/MF A03

Analytic solutions for the response of planetary lithospheres to volcanic loads have been used to model faulting and infer elastic plate thicknesses. Predictions of the distribution of faulting around volcanic loads, based on the application of Anderson's criteria for faulting to the results of the models, do not agree well with observations. Such models do not give the stress state and stress history within the edifice. The effects of episodic load growth can also be treated. When these effects are included, models give much better agreement with observations. Derived from text

N94-31108*# Massachusetts Inst. of Tech., Cambridge. Dept. of Earth, Atmospheric, and Planetary Sciences.

STATE OF STRESS, FAULTING, AND ERUPTION CHARACTERISTICS OF LARGE VOLCANOES ON MARS

Patrick J. McGovern and Sean C. Solomon *In its* Tectonic History of the Terrestrial Planets Mar. 1993 89 p Submitted for publication (For primary document see N94-31105 09-91)

Avail: CASI HC A05/MF A03

The formation of a large volcano loads the underlying lithospheric plate and can lead to lithospheric flexure and faulting. In turn, lithospheric stresses affect the stress field beneath and within the volcanic edifice and can influence magma transport. Modeling the interaction of these processes is crucial to an understanding of the history of eruption characteristics and tectonic deformation of large volcanoes. We develop models of time-dependent stress and deformation of the Tharsis volcanoes on Mars. A finite element code is used that simulates viscoelastic flow in the mantle and elastic plate flexural behavior. We calculate stresses and displacements due to a volcano-shaped load emplaced on an elastic plate. Models variously incorporate growth of the volcanic load with time and a detachment between volcano and lithosphere. The models illustrate the manner in which time-dependent stresses induced by lithospheric plate flexure beneath the volcanic load may affect eruption histories, and the derived stress fields can be related to tectonic features on and surrounding martian volcanoes. Author (revised)

N94-31109*# California Univ., Los Angeles.

ORIGIN AND THERMAL EVOLUTION OF MARS

G. Schubert, Sean C. Solomon, D. L. Turcotte, M. J. Drake, and N. H. Sleep *In* MIT, Tectonic History of the Terrestrial Planets Mar. 1993 19 p (For primary document see N94-31105 09-91)

Avail: CASI HC A03/MF A03

The thermal evolution of Mars is governed by subsolidus mantle convection beneath a thick lithosphere. Models of the interior evolution are developed by parameterizing mantle convective heat transport in terms of mantle viscosity, the superadiabatic temperature rise across the mantle and mantle heat production. Geological, geophysical, and geochemical observations of the composition and structure of the interior and of the timing of major events in Martian evolution, such as global differentiation, atmospheric outgassing and the formation of the hemispherical dichotomy and Tharsis, are used to constrain the model computations. Isotope systematics of SNC meteorites suggest core formation essentially contemporaneously with the completion of accretion. Other aspects of this investigation are discussed. Author (revised)

N94-31110*# Massachusetts Inst. of Tech., Cambridge. Dept. of Earth, Atmospheric, and Planetary Sciences.

GEOID-TO-TOPOGRAPHY RATIOS ON VENUS: A GLOBAL PERSPECTIVE Abstract Only

Mark Simons and Sean C. Solomon *In its* Tectonic History of the Terrestrial Planets Mar. 1993 1 p (For primary document see N94-31105 09-91)

Avail: CASI HC A01/MF A03

Recently available spherical harmonic solutions for the geoid and topography of Venus are sufficiently high resolution that they can be used to address questions concerning the relationship between geoid and topography on a regional scale. We have approached this question by mapping the geoid-to-topography ratio (GTR) on a systematic global basis. For a given point on the surface, we consider the geoid and elevation values at all points on a gridded representation of those fields located within a specified distance of the reference point. From the set of paired values, we determine the correlation coefficient and the best-fitting straight line. The latter is the GTR at that position, and the former is a measure of the significance of the derived ratio. This procedure is then repeated for all points on the global grid, yielding maps of the GTR and the correlation coefficient. Unlike previous studies of the GRT on Venus, this apprach permits us to make an objective and systematic search for regions with anomalous GTR's as well as areas that do not demonstrate any strong correlation between geoid and topography. These maps can be updated regularly as new harmonic models of the Venus geoid are produced from new Magellan tracking data. This procedure permits the development of a global perspective on the relationship between GTR and venusian surface tectonics. Author (revised)

N94-31111*# Carnegie Institution of Washington, DC.

THE TECTONIC AND VOLCANIC EVOLUTION OF VENUS: CATASTROPHIC OR GRADUAL? Abstract Only

Sean C. Solomon *In* MIT, Tectonic History of the Terrestrial Planets Mar. 1993 1 p (For primary document see N94-31105 09-91)

Avail: CASI HC A01/MF A03

Radar imaging and altimetry data from the Magellan mission have yielded important new constraints on the tectonic and volcanic history of Venus and on its internal dynamics. The planet lacks global plate tectonics, but a number of chasm systems and corona moat structures have arcuate planforms, asymmetric topogrpahic profiles, and relief analogous to deep-sea trenches on Earth and may be products of limited lithospheric underthrusting or subduction. Several lines of evidence point to a crust and upper mantle stronger than would be predicted by simple extrapolation from Earth and the 450 K greater surface temperature; these include the unrelaxed depths of impact craters, apparently large values of elastic lithosphere thickness, and large ratios of gravity to topography. The density of impact craters indicates an averate crater retention age of about 500 My, but not more than 5% of the recognized craters have been volcanically embayed. This last observation has led to the proposal that Venus has been subjected to one or more global resurfacing events, the latest about 500 My ago, and that the volcanic flux during intervals between such events has been low. That more recent tectonic activity has been widespread, however, is indicated by the high relief and slopes of mountains, chasm walls, and plateau margins; the significant fraction (0.3) of impact craters deformed by younger faults; and the postformational vertical deformation of long channels. Interior dynamical scenarios advanced to account for episodic volcanic resurfacing include catastrophic overturn of a global lithosphere thickened by cooling or compositional buoyancy and strongly time-dependent mantle convective heat flux. Outgassing considerations and analogy with Earth and other terrestrial planets, however, suggests that such catastrophic models are unlikely. If the mantle of Venus cooled more efficiently than that of Earth because of, say, different boundary conditions, a different flow law, or a different degree of layering, then the planet may in the last 500 My have attained lesser mantle temperatures, lower mantle heat flux, and a significantly lesser rate of magma production than Earth yet still display evidence for ongoing convection and active tectonics. Such a 'cold Venus' scenario would be broadly consistent with observations yet be characterized by a gradual volcanic and tectonic evolution. Author (revised)

N94-31112*# Carnegie Institution of Washington, DC. Dept. of Terrestrial Magnetism.

KEEPING THAT YOUTHFUL LOOK

Sean C. Solomon *In* MIT, Tectonic History of the Terrestrial Planets Mar. 1993 2 p Repr. from Nature, v. 361, 14 Jan. 1993 (For primary document see N94-31105 09-91)

Avail: CASI HC A01/MF A03

The record of impact cratering on Venus, recently revealed from high-resolution radar imaging by the Magellan spacecraft, has been interpreted as indicating that the planet underwent catastrophic global resurfacing about 500 million years ago. Although other interpretations of the crater characteristics have been suggested, the possibility of geologically rapid global resurfacing on the planet that most resembles our own in terms of mass, density, and bulk composition has generated widespread interest. The mechanisms that could cause such a catastrophe are discussed. Derived from text

N94-31113*# Carnegie Institution of Washington, DC. Dept. of Terrestrial Magnetism.

A TECTONIC RESURFACING MODEL FOR VENUS

Sean C. Solomon *In* MIT, Tectonic History of the Terrestrial Planets Mar. 1993 2 p (For primary document see N94-31105 09-91)

Avail: CASI HC A01/MF A03

Two remarkable aspects of the population of impact craters on Venus are that craters at all sizes are indistinguishable from a random population and that the vast majority of craters have not been significantly modified by tectonic strain or by volcanic flows external to the crater rim, despite evidence from Magellan images that volcanic and tectonic features are widespread on Venus. One interpretation of these observations is that most of the surface dates from the end of a catastrophic global resurfacing event that ceased about 500 My ago, and that the small fraction of craters volcanically embayed or modified by deformation indicates that volcanic and tectonic activity subsequent to that time has been at much lower levels. An alternative model, in which resurfacing occurs episodically in patches a few hundred kilometers in extent and there is a wider spectrum of surface ages, also appears to be consistent with the characteristics of impact craters on Venus. A number of potential mechanisms for catastrophic resurfacing of Venus have been proposed, ranging from geologically sudden convective destabilization of the global lithosphere to strongly time-dependent heat flux and melt generation in the underlying mantle. In most of these geophysical models, resurfacing occurs implicitly or explicitly by volcanism. We explore the hypothesis that, at least in the geologically recent history of Venus, the primary resurfacing mechanism has been tectonic deformation rather than volcanism. We show how such a hypothesis provides at least as good an explanation of a wide range of observations as do volcanic resurfacing models. Finally, we explore the implications of tectonic resurfacing hypothesis for the controversy over the recent resurfacing history of the planet. Derived from text

N94-31114*# Carnegie Institution of Washington, DC. Dept. of Terrestrial Magnetism.

THE RESURFACING CONTROVERSY FOR VENUS: AN OVERVIEW AND A MECHANISTIC PERSPECTIVE Abstract Only

Sean C. Solomon *In* MIT,. Tectonic History of the Terrestrial Planets Mar. 1993 1 p (For primary document see N94-31105 09-91)

Avail: CASI HC A01/MF A03

Two remarkable aspects of the population of impact craters on Venus are that craters at all sizes are indistinguishable from a random population and that most craters have not been significantly modified by tectonic strain or by volcanic flows external to the crater rim, despite evidence from Magellan images that volcanic and tectonic features are widespread on Venus. One interpretation of these observations is that most of the surface dates from the end of a catastrophic global resurfacing event that ceased about 500 My ago, and that a small fraction of craters volcanicly embayed or modified by deformation indicate that volcanic and tectonic activity subsequent to that time has been at much lower levels. A competing scenario, in which resurfacing occurs episodically in patches a few hundred kilometers in extent and there is a wider spectrum of surface ages, also appears to be consistent with the characteristics of impact craters on Venus. While geological and statistical studies of the crater population on Venus offer some promise for distinguishing between these two hypotheses, consideration of the possible mechanisms of catastrophic episodic resurfacing provides an independent perspective. Potential mechanisms for catastrophic resurfacing of Venus range from geologically sudden convective destabilization of the global lithosphere to strongly time-dependent heat flux and melt generation in the underlying mantle. For most of these mechanisms, resurfacing occurs implicitly or explicitly by volcanism. An alternative hypothesis is that, at least in the geologically recent history of Venus, the primary resurfacing mechanism has been tectonic deformation rather than volcanism. Because the rate of surface strain should be controlled by the temperature-dependent strength of the lower crust, a geologically rapid transition in surface strain rates should be the natural result of planetary cooling. This transition would occur at comparable times for areas of similar crustal thickness and heat flow, but would be delayed for regions of thicker or hotter crust. The end of the era of high rates of tectonic resurfacing could thus appear as a 'catastrophe' over the 80% of the planet with an elevation within 1 Km of the mean, while continued deformation would give rise to 'episodic' resurfacing to much younger times in the highlands, a result consistent with lower crater densities seen in highland regions. Author (revised)

N94-31115*# Cornell Univ., Ithaca, NY. Center for Radiophysics and Space Research.

PLAINS TECTONISM ON VENUS: THE DEFORMATION BELTS OF LAVINIA PLANITIA

Steven W. Squyres, David G. Jankowski, Mark Simons, Sean C. Solomon, Bradford H. Hager, and George E. McGill *In* MIT, Tectonic History of the Terrestrial Planets Mar. 1993 21 p Repr. from Journal of Geophysical Research, v. 97, no. E8, 25 Aug. 1992 p 13, 579-13, 599 See also A92-52671 (For primary document see N94-31105 09-91)

Avail: CASI HC A03/MF A03

High-resolution radar images from the Magellan spacecraft have revealed the first details of the morphology of the Lavinia Planitia region of Venus. A number of geologic units can be distinguished, including volcanic plains units with a range of ages. Transecting these plains over much of the Lavinia region are two types of generally orthogonal features that we interpret to be compressional wrinkle ridges and extensional grooves. The dominant tectonic features of Lavinia are broad elevated belts of intense deformation that transect the plains with complex geometry. They are many tens to a few hundred kilometers wide, as much as 1000 km long, and elevated hundreds of meters above the surrounding plains. Two classes of deformation belts are seen in the Lavinia region. 'Ridge belts' are composed of parallel ridges, each a few hundred meters in elevation, that we interpret to be folds. Typical fold spacings are 5-10 km. 'Fracture belts' are dominated instead by intense faulting, with faults in some instances paired to form narrow grabens. There is also some evidence for modest amounts of horizontal shear distributed across both ridge and fracture belts. Crosscutting relationships among the belts show there to be a range in belt ages. In western Lavinia, in particular, many ridge and fracture belts appear to bear a relationship to the much smaller wrinkle ridges and grooves on the surrounding plains: ridge morphology tends to dominate belts that lie more nearly parallel to local plains wrinkle ridges, and fracture morphology tends to dominate belts that lie more nearly parallel to local plains grooves. We use simple models to explore the formation of ridge and fracture belts. We show that convective motions in the mantle can couple to the crust to cause horizontal stresses of a magnitude sufficient to induce the formation of deformation belts like those observed in Lavinia. We also use the small-scale wavelengths of deformation observed within individual ridge belts to place an approximate lower limit on the venusian thermal gradient in the Lavinia region at the time of deformation.

Author (revised)

N94-31145# Sandia National Labs., Albuquerque, NM.

FIBER OPTIC CHEMICAL SENSORS ON MARS

M. A. Butler, A. J. Ricco, F. J. Grunthaner, and A. L. Lane 1993 10 p Presented at the Space 1994 International Conference and Exposition on Engineering, Construction, and Operations in Space, Albuquerque, NM, 26 Feb. - 3 Mar. 1994

(Contract DE-AC04-94AL-85000)

(DE94-005251; SAND-93-1601C; CONF-940214-6) Avail: CASI HC A02/MF A01

A fiber optic chemical sensing instrument is described that will measure the reactivity of the martian soil and atmosphere. The self-contained instrument monitors reflectivity changes in reactive thin films caused by

chemical reactions with the martian soil or atmosphere. Data from over 200 separate thin-film-coated optical fibers are recorded simultaneously. This fiber optic sensing technology has many advantages for planetary exploration and monitoring applications on manned spacecraft, in addition to many practical terrestrial uses. DOE

N94-31805* National Aeronautics and Space Administration. Lewis Research Center, Cleveland, OH.
MARS: FIVE VIEWS ON WHAT IS KNOWN (Videotape)
Feb. 1993 Videotape: 29 min. playing time, in color, with sound
(NASA-TM-109751; NONP-VT-94-9951) Avail: CASI VHS A01/BETA A22

This video gives a historical survey of philosophy and scientific study of the nature of the surface of Mars and discussion of whether life existed or exists on Mars. Several Lewis researchers recount early telescope observations of Mars including the identification of 'channels' or possible ancient waterways on the surface. An overview of the accomplishments of the Mariner spacecraft in mapping the surface of Mars as well as a detailed description of the Viking missions to Mars are presented. The results of the Viking Biology Experiment, conducted by the Viking Lander, are highlighted. There is also a discussion of the possible presence of monuments and a huge 'face' on the Martian surface. The video includes several computer simulations of flight over the Martian surface. CASI

N94-31975 California Inst. of Tech., Pasadena.
ONE: MICROPHYSICS OF FROST METAMORPHISM: APPLICATIONS TO TRITON AND MARS. TWO: A GLOBAL ANALYSIS OF THE OZONE DEFICIT IN THE UPPER STRATOSPHERE AND LOWER MESOSPHERE. THREE: THE DIABATIC CIRCULATION IN THE STRATOSPHERE AS DIAGNOSED FROM MICROWAVE LIMB SOUNDER DATA Ph.D. Thesis
Janusz Bronistaw Eluszkiewicz 1993 130 p
Avail: Univ. Microfilms Order No. DA9316839

The present thesis is devoted to two broad subjects, planetary frost metamorphism and the terrestrial middle atmosphere, and consists of three papers. Paper 1 considers frost metamorphism on the surfaces of Triton and Mars. Based on an analysis of the microphysical processes involved in the pressureless sintering, it is concluded that fine-grained nitrogen and carbon dioxide frosts can undergo seasonal metamorphism into semitransparent layers on the surface of Triton and in the Martian seasonal polar caps, respectively. The presence of such layers explains a host of facts about Triton's surface and about the Martian seasonal caps. Paper 2 is devoted to elucidating a long-standing issue in the terrestrial middle atmosphere chemistry, the so-called 'ozone deficit problem.' Based on an analysis of data acquired by the Limb Infrared Monitor of the Stratosphere (LIMS) instrument between October 1978 and May 1979, it is concluded that current photochemical models systematically underestimate observed ozone abundances in the upper stratosphere and lower mesosphere. Three modifications to the accepted photochemical scheme, capable of providing a global solution to this problem, are proposed and discussed. Paper 3 differs from the other two in that it reports on results from an ongoing research effort. It considers the diabatic circulation in the stratosphere and lower mesosphere, using ozone and temperature measurements acquired by the Microwave Limb Sounder (MLS) instrument onboard the Upper Atmosphere Research Satellite (UARS). The present study extends past analyses of the diabatic circulation by considering a full annual cycle, November 1991-November 1992, and by taking advantage of the high vertical resolution of MLS data. In the tropical upper stratosphere and lower mesosphere, a semiannual oscillation (SAO) is observed in the computed circulation, with the region of downwelling reaching maximum spatial extent approximately 1 month before the equinox. The projected lifetime of UARS should enable the present analysis to be extended to several SAO cycles. Dissert. Abstr.

N94-31992 Massachusetts Inst. of Tech., Cambridge.
A STUDY OF AREAS OF LOW RADIO-THERMAL EMISSIVITY ON VENUS Ph.D. Thesis
Robert Joseph Wilt 1992
Avail: Issuing Activity (MIT Libraries, Rm. 14-0551, Cambridge, MA 02139-4307)

Observations performed by the Magellan radiometer experiment have confirmed previous findings that a few regions on Venus, primarily at higher elevations, possess unexpectedly low values of radiothermal emissivity, occasionally reaching as low as 0.3. Values of emissivity below 0.7 occur over about 1.5 percent of the surface, and are associated with several types of features, including highlands, volcanoes, tectonically uplifted terrain, and impact craters. There is a strong correlation of low emissivity and high elevation, but rather than decreasing gradually with elevation, the emissivity drops rapidly in a small altitude range above a certain 'critical radius'. The altitude at which the change in emissive properties occurs varies from feature to feature; on average, it lies at a planetary radius of about 6054 km. Notable exceptions to the association of low emissivity and high elevation exist; for example, Lakshmi Planum, Maat Mons, and the summits of many volcanoes display high emissivities at high elevations, while in some impact craters and plains areas we find low emissivities at low elevations. Two possible explanations for low emissivities have been advanced: (1) emission from a highly reflective single interface between the atmosphere and a surface material having a bulk dielectric constant of order 80 ('high-dielectric' model); and (2) emission from the surface of a low-loss soil having a more usual permittivity (of order 2) which contains subsurface scatterers composed of ordinary rock materials ('volume scattering' model). Theoretical results and Monte Carlo simulations are used to show that the previously proposed volume scattering model cannot account for the observed emissivities; however, scattering from a material with very low loss (loss factor of order 10(exp -3) or less) containing subsurface voids could produce the observed results. Consideration of the two models in light of the Magellan observations leads us to believe that the low emissivities on Venus result from the creation of a high-dielectic material by surface-atmosphere interaction, probably a loaded dielectric containing a conductive mineral. Dissert. Abstr.

N94-32326 California Univ., Los Angeles.
PLANETARY MAGNETOTAILS: MAGNETIC CONFIGURATION AND NONTHERMAL PLASMA Ph.D. Thesis
Carl Max Hammond, Jr. 1993 235 p
Avail: Univ. Microfilms Order No. DA9321918

This dissertation examines three aspects of planetary magnetotails: time averaged structure, interplanetary magnetic field (IMF) induced changes in structure, and relationship of the magnetic structure to the nonthermal plasma component. In chapter 2, we present images of the time averaged shape terrestrial magnetotail. Using these images, we model the neutral sheet and magnetopause and apply these models to the uranian magnetotail. Having presented models of the time averaged shape of planetary magnetotails in chapter 2, we use the same imaging technique, in chapter 5, to examine the effect of the IMF on the structure of the tail. During periods of southward IMF, we find changes in the tail consistent with substorm growth phase. We find the neutral sheet rotates in response to the B(sub y) component of the IMF. We then examine the tail plasma. We show an anomalous encounter with the uranian plasma sheet observed by the Voyager 2 spacecraft is consistent with an expanded plasma sheet resulting from an injection of plasma below 28 keV. We then utilize the results from large scale kinetic simulations to show that the amount of tail 'stretch' can affect the high energy particle distribution. Finally, we examine the stability of the kappa distribution to non-resonant interactions using a Monte Carlo algorithm. Dissert. Abstr.

N94-32740*# Geo Eco Arc Research, La Canada, CA.
BIOSPHERIC EFFECTS OF A LARGE EXTRATERRESTRIAL IMPACT: CASE STUDY OF THE CRETACEOUS/TERTIARY BOUNDARY CRATER Progress Report, FY 1993
Kevin O. Pope 10 May 1994 21 p
(Contract NASw-4812)
(NASA-CR-195827; NAS 1.26:195827) Avail: CASI HC A03/MF A01

The Chicxulub Crater in Yucatan, Mexico, is the primary candidate for the impact that caused mass extinctions at the Cretaceous/Tertiary boundary. The target rocks at Chicxulub contain 750 to 1500 m of anhydrite (CaSO4), which was vaporized upon impact, creating a large sulfuric acid aerosol cloud. In this study we apply a hydrocode model of asteroid impact to calculate the amount of sulfuric acid produced. We then apply a radiative transfer model to determine the atmospheric effects. Results include 6 to 9 month period of darkness followed by 12 to 26 years of cooling.
Author (revised)

N94-32923*# National Aeronautics and Space Administration. Lyndon B. Johnson Space Center, Houston, TX.

THE LUNAR SCOUT PROGRAM: AN INTERNATIONAL PROGRAM TO SURVEY THE MOON FROM ORBIT FOR GEOCHEMISTRY, MINERALOGY, IMAGERY, GEODESY, AND GRAVITY Report, 1991 - 1993

Donald A. Morrison, ed. Apr. 1994 147 p

(NASA-TM-104791; S-762; NAS 1.15:104791) Avail: CASI HC A07/MF A02

The Lunar Scout Program was one of a series of attempts by NASA to develop and fly an orbiting mission to the moon to collect geochemical, geological, and gravity data. Predecessors included the Lunar Observer, the Lunar Geochemical Orbiter, and the Lunar Polar Orbiter - missions studied under the auspices of the Office of Space Science. The Lunar Scout Program, however, was an initiative of the Office of Exploration. It was begun in late 1991 and was transferred to the Office of Space Science after the Office of Exploration was disbanded in 1993. Most of the work was done by a small group of civil servants at the Johnson Space Center; other groups also responsible for mission planning included personnel from the Charles Stark Draper Laboratories, the Lawrence Livermore National Laboratory, Boeing, and Martin Marietta. The Lunar Scout Program failed to achieve new start funding in FY 93 and FY 94 as a result of budget downturns, the de-emphasis of the Space Exploration Initiative, and the fact that lunar science did not rate as high a priority as other planned planetary missions, and was cancelled. The work done on the Lunar Scout Program and other lunar orbiter studies, however, represents assets that will be useful in developing new approaches to lunar orbit science. Derived from text

N94-33103*# Southwest Research Inst., San Antonio, TX. Instrumentation and Space Research Div.

PLASMA AND RADIO WAVES FROM NEPTUNE: SOURCE MECHANISMS AND PROPAGATION Final Report, 1 Jan. 1991 - 31 Mar. 1994

H. K. Wong 1994 34 p

(Grant NAGw-2412; SwRI Proj. 15-4167)

(NASA-CR-195877; NAS 1.26:195877) Copyright Avail: CASI HC A03/MF A01

This report summarizes results obtained through the support of NASA Grant NAGW-2412. The objective of this project is to conduct a comprehensive investigation of the radio wave emission observed by the planetary radio astronomy (PRA) instrument on board Voyager 2 as if flew by Neptune. This study has included data analysis, theoretical and numerical calculations, ray tracing, and modeling to determine the possible source mechanism(s) and locations of the Neptune radio emissions. We have completed four papers, which are included in the appendix. The paper 'Modeling of Whistler Ray Paths in the Magnetosphere of Neptune' investigated the propagation and dispersion of lighting-generated whistler in the magnetosphere of Neptune by using three dimensional ray tracing. The two papers 'Numerical Simulations of Bursty Radio Emissions from Planetary Magnetospheres' and 'Numerical Simulations of Bursty Planetary Radio Emissions' employed numerical simulations to investigate an alternate source mechanism of bursty radio emissions in addition to the cyclotron maser instability. We have also studied the possible generation of Z and whistler mode waves by the temperature anisotropic beam instability and the result was published in 'Electron Cyclotron Wave Generation by Relativistic Electrons.' Besides the aforementioned studies, we have also collaborated with members of the PRA team to investigate various aspects of the radio wave data. Two papers have been submitted for publication and the abstracts of these papers are also listed in the appendix. Derived from text

N94-33104*# Southwest Research Inst., San Antonio, TX. Instrumentation and Space Research Div.

DISTRIBUTION AND NATURE OF UV ABSORBERS ON TRITON'S SURFACE Annual Report

S. Alan Stern 1 Mar. 1994 47 p

(Grant NAGw-3402; SwRI Proj. 15-5653)

(NASA-CR-195886; NAS 1.26:195886) Avail: CASI HC A03/MF A01

Substantial evidence suggests that a UV Spectrally Absorbing Material (UV-SAM) exists on Triton's surface. This evidence is found in the positive slope in Triton's spectrum from the UV to the near-IR, and the increasing contrast in Triton's light curve in the blue and UV. Although it is now widely-thought that UV-SAM's exist on Triton, little is known about their distribution and spectral properties. The goal of this NDAP Project is to determine the spatial distribution and geological context of the UV-SAM material. We hope to determine if UV-SAM's on Triton are correlated with geologic wind streaks, craters, calderas, geomorphic/topographic units, regions containing (or lacking) volatile frosts, or some other process (e.g., magnetospheric interactions). Once the location and distribution of UV-SAM's has been determined, further constraints on their composition can be made by analyzing the spectrographic data set. To accomplish these goals, various data sets will be used, including Voyager 2 UV and visible images of Triton's surface, IUE and HST spectra of Triton, and a geologic map of the surface based on Voyager 2 and spectrophotometric data. The results of this research will be published in the planetary science literature. Derived from text

N94-33190*# Lunar and Planetary Inst., Houston, TX. Mars Surface and Atmosphere Through Time Study Group.

MARS: PAST, PRESENT, AND FUTURE. RESULTS FROM THE MSATT PROGRAM, PART 1 Abstracts Only

R. M. Haberle, ed. (National Aeronautics and Space Administration. Ames Research Center, Moffett Field, CA.) 1993 66 p Workshop held in Houston, TX, 15-17 Nov. 1993

(Contract NASw-4574)

(NASA-CR-194279; NAS 1.26:194279; LPI-TR-93-06-Pt-1) Avail: CASI HC A04/MF A01

This volume contains papers that were accepted for presentation at the workshop on Mars: Past, Present, and Future -- Results from the MSATT Program. Topics include, but are not limited to: Martian impact craters; thermal emission measurements of Hawaiian palagonitic soils with implications for Mars; thermal studies of the Martian surface; Martian atmospheric composition studies; temporal and spatial mapping of Mars' atmospheric dust opacity and surface albedo; studies of atmospheric dust from Viking IR thermal mapper data; the distribution of Martian ground ice at other epochs; numerical simulation of thermally induced near-surface flows over Martian terrain; the pH of Mars; the mineralogic evolution of the Martian surface through time; geologic controls of erosion and sedimentation on Mars; and dielectric properties of Mars' surface: proposed measurement on a Mars Lander. For individual titles, see N94-33191 through N94-33240.

N94-33191*# Lunar and Planetary Inst., Houston, TX.

DEPTH-DIAMETER RATIOS FOR MARTIAN IMPACT CRATERS: IMPLICATIONS FOR TARGET PROPERTIES AND EPISODES OF DEGRADATION Abstract Only

N. G. Barlow *In its* Mars: Past, Present, and Future. Results from the MSATT Program, Part 1 1993 p 1 (For primary document see N94-33190 09-91)

Avail: CASI HC A01/MF A01

This study determines crater depth through use of photoclinometric profiles. Random checks of the photoclinometric results are performed using shadow estimation techniques. The images are Viking Orbiter digital format frames; in cases where the digital image is unusable for photoclinometric analysis, shadow estimation is used to determine crater depths. The two techniques provide depth results within 2 percent of each other. Crater diameters are obtained from the photoclinometric profiles and checked against the diameters measured from the hard-copy images using a digitizer. All images used in this analysis are of approximately 40 m/pixel resolution. The sites that have been analyzed to date include areas within Arabia, Maja Valles, Memnonia, Acidalia, and Elysium. Only results for simple craters (craters less than 5 km in diameter) are discussed here because of the low numbers of complex craters presently measured in the analysis. General results indicate that impact craters are deeper than average. A single d/D relationship for fresh impact craters on Mars does not exist due to changes in target properties across the planet's surface. Within regions where target properties are approximately constant, however, d/D ratios for fresh craters can be determined. In these regions, the d/D ratios of nonpristine craters can be compared with the fresh crater d/D relationship to obtain information on relative degrees of crater degradation. This technique reveals that regional episodes of enhanced degradation have occurred. However, the lack of statistically reliable size-frequency distribution data prevents comparison of the relative ages of these events

between different regions, and thus determination of a large-scale episode (or perhaps several episodes) cannot be made at this time.

Derived from text

N94-33192*# National Aeronautics and Space Administration. Ames Research Center, Moffett Field, CA.

STATIONARY EDDIES IN THE MARS GENERAL CIRCULATION AS SIMULATED BY THE NASA-AMES GCM Abstract Only

J. R. Barnes (Oregon State Univ., Corvallis.), J. B. Pollack, and Robert M. Haberle *In* Lunar and Planetary Inst., Mars: Past, Present, and Future. Results from the MSATT Program, Part 1 1993 p 2 (For primary document see N94-33190 09-91)

Avail: CASI HC A01/MF A01

Quasistationary eddies are prominent in a large set of simulations of the Mars general circulation performed with the NASA-Ames GCM. Various spacecraft observations have at least hinted at the existence of such eddies in the Mars atmosphere. The GCM stationary eddies appear to be forced primarily by the large Mars topography, and (to a much lesser degree) by spatial variations in the surface albedo and thermal inertia. The stationary eddy circulations exhibit largest amplitudes at high altitudes (above 30-40 km) in the winter extratropical regions. In these regions they are of planetary scale, characterized largely by zonal wavenumbers 1 and 2. Southern Hemisphere winter appears to be dominated by a very strong wave 1 pattern, with both waves 1 and 2 being prominent in the Northern Hemisphere winter regime. This difference seems to be basically understandable in terms of differences in the topography in the two hemispheres. The stationary eddies in the northern winter extratropics are found to increase in amplitude with dust loading. This behavior appears to be at least partly associated with changes in the structure of the zonal-mean flow that favor a greater response to wave 1 topographic forcing. There are also strong stationary eddy circulations in the tropics and in the summer hemisphere. The eddies in the summer subtropics and extratropics are substantially stronger in southern summer than in northern summer. The summer hemisphere stationary circulations are relatively shallow and are characterized by smaller zonal scales than those in the winter extratropics.

Author

N94-33193*# National Aeronautics and Space Administration. Ames Research Center, Moffett Field, CA.

THERMAL EMISSION MEASUREMENTS (5-25 MICRONS) OF HAWAIIAN PALAGONITIC SOILS WITH IMPLICATIONS FOR MARS Abstract Only

J. F. Bell, III and T. L. Roush *In* Lunar and Planetary Inst., Mars: Past, Present, and Future. Results from the MSATT Program, Part 1 1993 p 2-3 (For primary document see N94-33190 09-91)

Avail: CASI HC A01/MF A01

The research presented here represents the initial phase of a broader project that is intended to provide data in the mid- and far-IR spectral region for both well-characterized iron oxides/oxyhydroxides and poorly crystalline or amorphous materials (e.g., palagonites). Such information can be used in the interpretation of data to be returned by the Mars Observer Thermal Emission Spectrometer (TES). Additionally, this same information will prove useful for assessing the information content of existing Kuiper Airborne Observatory, Mariner 7, and Mariner 9 spectra. which also cover the thermal IR wavelength region.

Derived from text

N94-33194*# California Inst. of Tech., Pasadena.

THERMAL STUDIES OF MARTIAN CHANNELS AND VALLEYS USING TERMOSKAN DATA: NEW RESULTS Abstract Only

B. H. Betts and B. C. Murray *In* Lunar and Planetary Inst., Mars: Past, Present, and Future. Results from the MSATT Program, Part 1 1993 p 3-4 (For primary document see N94-33190 09-91)

Avail: CASI HC A01/MF A01

The Termoskan instrument onboard the Phobos '88 spacecraft acquired the highest-spatial-resolution thermal data ever obtained for Mars. Included in the thermal images are 2 km/pixel midday observations of several major channel and valley systems, including significant portions of Shalbatana Vallis, Ravi Vallis, Al-Qahira Vallis, Ma'adim Vallis, the channel connecting Valles Marineris with Hydraotes Chaos, and channel material in Eos Chasma. Termoskan also observed small portions of the southern beginnings of Simud, Tiu, and Ares Valles and some channel material in Gangis Chasma. Simultaneous broad band visible data were obtained for all but Ma'adim Vallis. We find that most of the channels and valleys have higher inertias than their surroundings, consistent with Viking IRTM-based thermal studies of Martian channels. We see for the first time that thermal inertia boundaries closely match all flat channel floor boundaries. Combining Termoskan thermal data, relative observations from Termoskan visible channel data, Viking absolute bolometric albedos, and a thermal model of the Mars surface, we have derived lower bounds on channel thermal inertias. Lower bounds on typical channel thermal inertias range from 8.4 to 12.5 (10(exp -3) cal cm(exp -2) s(exp -1/2)K(exp -1)) (352 to 523 in SI units). Lower bounds on inertia differences with the surrounding heavily cratered plains range from 1.1 to 3.5 (46 to 147 in SI units). Atmospheric and geometric effects are not sufficient to cause the inertia enhancements. We agree with previous researchers that localized, dark, high inertia areas within channels are likely eolian in nature. However, the Temloskan data show that eolian deposits do not fill the channels, nor are they responsible for the overall thermal inertia enhancement. Thermal homogeneity and strong correlation of thermal boundaries with the channel floor boundaries lead us to favor noneolian overall explanations.

Derived from text

N94-33195*# Brown Univ., Providence, RI.

THE IMPORTANCE OF ENVIRONMENTAL CONDITIONS IN REFLECTANCE SPECTROSCOPY OF LABORATORY ANALOGS FOR MARS SURFACE MATERIALS Abstract Only

J. Bishop, S. Murchie, S. Pratt, J. Mustard, and C. Pieters *In* Lunar and Planetary Inst., Mars: Past, Present, and Future. Results from the MSATT Program, Part 1 1993 p 4-6 Sponsored by Keck Foundation (For primary document see N94-33190 09-91)

(Grants NAGw-28; NAGw-748)

Avail: CASI HC A01/MF A01

Reflectance spectra are presented here for a variety of particulate, ferric-containing analogs to Martian soil (Fe(3+)-doped smectites and palagonites) to facilitate interpretation of remotely acquired spectra. The analog spectra were measured under differing environmental conditions to evaluate the influence of exposure history on water content and absorption features due to H2O in these samples. Each of these materials contains structural OH bonded to metal cations, adsorbed H2O, and bound H2O (either in a glass, structural site, or bound to a cation). Previous experiments involving a variety of Mars analogs have shown that the 3 micron H2O band in spectra of palagonites is more resistant to drying than the 3 micron H2O band in spectra of montmorillonites. Other experiments have shown that spectra of ferrihydrite and montmorillonites doped with ferric sulfate also contain sufficient bound H2O to retain a strong 3 micron band under dry conditions. Once the effects of the environment on bound water in clays, oxides, and salts are better understood, the hydration bands measured via reflectance spectroscopy can be used to gain information about the chemical composition and moisture content of real soil systems. Such information would be especially useful in interpreting observations of Mars where subtle spatial variations in the strengths of metal-OH and H2O absorptions have been observed in telescopic and ISM spectra. We measured bidirectional reflectance spectra of several Mars soil analogs under controlled environmental conditions to assess the effects of moisture content on the metal-OH and H2O absorptions. The samples analyzed include chemically altered montmorillonites, ferrihydrite. and palagonites from Hawaii and Iceland. Procedures for preparation of the cation-exchanged montmorillonites, ferric-salt doped montmorillonites, and ferric oxyhydroxides are described in detail elsewhere.

Derived from text

N94-33196*# Brown Univ., Providence, RI.

FERRIC SULFATE MONTMORILLONITES AS MARS SOIL ANALOGS Abstract Only

J. L. Bishop, C. M. Pieters, and R. G. Burns *In* Lunar and Planetary Inst., Mars: Past, Present, and Future. Results from the MSATT Program, Part 1 1993 p 6-8 Sponsored by Keck Foundation (For primary document see N94-33190 09-91)

(Grants NAGw-28; NAGw-2220; NAGw-748)

Avail: CASI HC A01/MF A01

Spectroscopic analyses have shown that Fe(3+)-doped smectites prepared in the laboratory exhibit important similarities to the soils on Mars. Ferrihydrite in these smectites has features in the visible to near-infrared region that resemble the energies and band-strengths of features in reflectance spectra observed for several bright regions on Mars. Ferric - sulfate - montmorillonite samples have been prepared more recently because they are a good compositional match with the surface material

on Mars as measured by Viking. Reflectance spectra of montmorillonite doped with ferric sulfate in the interlayer regions include a strong 3 micron band that persists under dry conditions. This is in contrast to spectra of similarly prepared ferric-doped montmorillonites, which exhibit a relatively weaker 3 micron band under comparable dry environmental conditions. Presented here are reflectance spectra of a suite of ferric-sulfate exchanged montmorillonites prepared with variable ferric sulfate concentrations and variable pH conditions. Derived from text

N94-33197*# Research Support Instruments, Inc., Alexandria, VA.
CONSTRAINTS ON THE MARTIAN CRATERING RATE IMPOSED BY THE SNC METEORITES AND VALLIS MARINERIS LAYERED DEPOSITS Abstract Only
J. E. Brandenburg *In* Lunar and Planetary Inst., Mars: Past, Present, and Future. Results from the MSATT Program, Part 1 1993 p 8-10 (For primary document see N94-33190 09-91)
Avail: CASI HC A01/MF A01

Following two independent lines of evidence -- estimates of the age and formation time of a portion of the Martian geologic column exposed in the layered deposits and the crystallization and ejection ages of the SNC meteorites -- it appears that the Martian cratering rate must be double the lunar rate or even higher. This means models such as NHII or NHIII (Neukum and Hiller models II and III), which estimate the Martian cratering rate as being several times lunar are probably far closer to reality on Mars than lunar rates. The effect of such a shift is profound: Mars is transformed from a rather Moon-like place into a planet with vigorous dynamics, multiple large impacts, erosion, floods, and volcanism throughout its history. A strong shift upward in cratering rates on Mars apparently solves some glaring problems; however, it creates others. The period of time during which Earth-like atmospheric conditions existed, the liquid water era on Mars, persists in NHIII up to only 0.5 b.y. ago. Scenarios of extended Earth-like conditions on Mars have been discounted in the past because they would have removed many of the craters from the early bombardment era found in the south. It does appear that some process of crater removal was quite vigorous in the north during Mars' past. Evidence exists that the northern plains may have been the home of long-lived seas or perhaps even a paleo-ocean, so models exist for highly localized destruction of craters in the north. However, the question of how the ancient crater population could be preserved in the south under a long liquid-water era found in any high-cratering-rate models is a serious question that must be addressed. It does appear to be a higher-order problem because it involves low-energy dynamics acting in localized areas, i.e., erosion of craters in the south of Mars, whereas the two problems with the low-cratering-rate models involve high-energy events acting over large areas: the formation of the Vallis Marineris, the SNC ejecting impacts, and the global atmospheric pressure and temperature conditions that allow liquid water to exist as a robust entity anywhere on the Martian surface. In any case, it appears Mars is a more complex and dynamic planet than previously supposed. It has canyons dating from the middle to late period of its history that contain apparent lake sediments bedded deeper than most sediments on Earth. Recent multiple, violent impacts on Mars have apparently provided us with multiple random samples of its surface that all crystallized less than 1.5 b.y. ago. These things cannot be accommodated in our present cratering chronologies of Mars, based on 1x lunar cratering rates, without great difficulties. These difficulties suggest that a new chronology, probably based on NHII or even NHIII, should be adopted; this new chronology will provide us with a new view of Mars as a dynamic planet of rich history. Derived from text

N94-33198*# Massachusetts Inst. of Tech., Cambridge. Dept. of Earth, Atmospheric and Planetary Sciences.
DEPOSITION RATES OF OXIDIZED IRON ON MARS Abstract Only
R. G. Burns *In* Lunar and Planetary Inst., Mars: Past, Present, and Future. Results from the MSATT Program, Part 1 1993 p 10-12 (For primary document see N94-33190 09-91)
(Grant NAGw-2220)
Avail: CASI HC A01/MF A01

The reddened oxidized surface of Mars is indicative of temporal interactions between the Martian atmosphere and its surface. During the evolution of the Martian regolith, primary ferromagnesian silicate and sulfide minerals in basaltic rocks apparently have been oxidized to secondary ferric-bearing assemblages. To evaluate how and when such oxidized deposits were formed on Mars, information about the mechanisms and rates of chemical weathering of Fe(2+)-bearing minerals has been determined. In this paper, mechanisms and rates of deposition of ferric oxide phases on the Martian surface are discussed. Author

N94-33199*# European Space Agency. European Space Research and Technology Center, ESTEC, Noordwijk (Netherlands). Space Science Dept.
MARSNET: A EUROPEAN NETWORK OF STATIONS ON THE SURFACE OF MARS Abstract Only
A. F. Chicarro *In* Lunar and Planetary Inst., Mars: Past, Present, and Future. Results from the MSATT Program, Part 1 1993 p 12-14 (For primary document see N94-33190 09-91)
Avail: CASI HC A01/MF A01

Following an ESA preliminary study on the possible areas of European participation in the future international exploration of Mars and an ESA call for ideas of new missions, MARSNET, a network of small surface stations, was selected for further in-depth scientific and technical assessment studies as a potential European contribution to such exploration. Subsequently, the MARSNET phase A studies started in the autumn of 1991. The industrial kickoff took place in early January 1992, following the tender evaluation and the decision to select the Aerospatiale-led consortium including Dornier, Alcatel, Laben, and Etca to perform the industrial studies. The phase A studies ended in early 1993. However, critical items such as an instrument deployment device continue to be studied in the framework of ESA's Technology Research Program. The MARSNET mission consists of a network of three semihard landers to be placed on the Martian surface, several thousand kilometers apart, thus defining a regional/global seismological and meteorological network in the Tharsis region. The small stations would be targeted for landing at scientifically interesting sites in this region of Mars, which is the most likely area to still show tectonic activity; this would allow the seismometers to acquire data for the determination of the internal structure of the planet. Landing site geology and geochemistry will also be studied. Derived from text

N94-33200*# Colorado Univ., Boulder. Lab. for Atmospheric and Space Physics.
MARS ATMOSPHERIC DUST PROPERTIES: A SYNTHESIS OF MARINER 9, VIKING, AND PHOBOS OBSERVATIONS Abstract Only
R. T. Clancy, S. W. Lee, and G. R. Gladstone *In* Lunar and Planetary Inst., Mars: Past, Present, and Future. Results from the MSATT Program, Part 1 1993 p 14-15 (For primary document see N94-33190 09-91)
Avail: CASI HC A01/MF A01

We have modified a doubling-and-adding code to reanalyze the Mariner 9 IRIS spectra of Mars atmospheric dust as well as Viking IRTM EPF sequences in the 7, 9, and 20 micron channels. The code is capable of accurate emission/ absorption/scattering radiative transfer calculations over the 5-30 micron wavelength region for variable dust composition and particle size inputs, and incorporates both the Viking IRTM channel weightings and the Mariner 9 IRIS wavelength resolution for direct comparisons to these datasets. We adopt atmospheric temperature profiles according to the algorithm of Martin (1986) in the case of the Viking IRTM comparisons, and obtained Mariner 9 IRIS temperature retrievals from the 15 micron CO2 band for the case of the IRIS comparisons. We consider palagonite as the primary alternative to the montmorillonite composition of Mars atmospheric dust, based on several considerations. Palagonite absorbs in the ultraviolet and visible wavelength region due to its Fe content. Palagonite is also, in principal, consistent with the observed lack of clays on the Mars surface. Furthermore, palagonite does not display strong, structured absorption near 20 microns as does montmorillonite (in conflict with the IRIS observations). We propose that a palagonite composition with particle sizes roughly one-half that of the Toon et al. (1977) determination provide a much improved model to Mars atmospheric dust. Since palagonite is a common weathering product of terrrestrial basalts, it would not be unreasonable for palagonite to be a major surface component for Mars. The lack of even a minor component of Al-rich clays on the surface of Mars could be consistent with a palagonite composition for Mars dust if the conditions for basalt weathering on Mars were sufficiently anhydrous. Variations in palagonite composition could also lead to the inability of the modeled palagonite to fit the details of the 9 micron absorbtion indicated by the IRIS observations. Derived from text

N94-33201*# Martin Marietta Corp., Denver, CO. Planetary Sciences Lab.

MAGMATIC VOLATILES AND THE WEATHERING OF MARS Abstract Only

B. C. Clark *In* Lunar and Planetary Inst., Mars: Past, Present, and Future. Results from the MSATT Program, Part 1 1993 p 15-16 (For primary document see N94-33190 09-91)

Avail: CASI HC A01/MF A01

The sources for volatiles on Mars have been the subject of many hypotheses for exogenous influences including late accretion of volatile-enriched material, impact devolatilization to create massive early atmospheres, and even major bombardment by comets. However, the inventory of chemically active volatiles observable at the contemporary surface of Mars is consistent with domination by endogenous, subsequent planetary processes, viz., persistent magmatic outgassing. Volcanism on Mars has been widespread in both space and time. Notwithstanding important specific differences between the mantles of Earth and Mars, the geochemical similarities are such that the suite of gases emitted from Martian volcanic activity should include H2O, CO2, S-containing gases (e.g. H2S and/or SO2), and Cl-containing gases (e.g., Cl2 and/or HCl). H2O and CO2 exist in the atmosphere of Mars. Both are also present as surface condensates. However, spectroscopic observations of the Martian atmosphere clearly show that the S- and Cl-containing gases are severely depleted, with upper limits of less than or equal to 10(exp -7) the abundance of CO2. Likewise, there is no evidence of polar condensates of compounds of these elements as there is for CO2 and H2O. Within the soil, on the other hand, there has been direct measurement of incorporated H2O and abundant compounds containing S and Cl. Barring some as yet implausible geochemical sequestering process, the S/Cl ratio of about 6:1 in Martian soils implies a limit of 5% on the contribution of matter of solarlike composition (e.g., carbonaceous chondrite or cometary material) to these volatiles. Hence, exogenous sources are minor or not yet observed. From analysis of elemental trends in Martian soils, it has been recently shown that a simple two-component model can satisfy the Viking in situ measurements. Component A includes Si and most or all the Al, Ca, Ti, and Fe. Component B, taken as 16 +/- 3% by weight of the total, contains S and most or all the Cl and Mg. These results constrain several models of Martian soil mineralogy but are consistent with a mixture of silicates (such as Fe-rich clays and accessory minerals and soluble salts). The overall element profile is notably like shergottites, with significant incorporation of chemically reactive atmospheric gases from magmatic degassing. Derived from text

N94-33202*# Lunar and Planetary Inst., Houston, TX.

THERMAL AND HYDRAULIC CONSIDERATIONS REGARDING THE FATE OF WATER DISCHARGED BY THE OUTFLOW CHANNELS TO THE MARTIAN NORTHERN PLAINS Abstract Only

S. M. Clifford *In its* Mars: Past, Present, and Future. Results from the MSATT Program, Part 1 1993 p 16-17 (For primary document see N94-33190 09-91)

Avail: CASI HC A01/MF A01

The identification of possible shorelines in the Martian northern plains suggests that the water discharged by the circum-Chryse outflow channels may have led to the formation of transient seas, or possibly even an ocean, covering as much as one-third of the planet. Speculations regarding the possible fate of this water have included local ponding and reinfiltration into the crust; freezing, sublimation, and eventual cold-trapping at higher latitudes; or the in situ survival of this now frozen water to the present day -- perhaps aided by burial beneath a protective cover of eolian sediment or lavas. Although neither cold-trapping at higher latitudes nor the subsequent freezing and burial of flood waters can be ruled out, thermal and hydraulic considerations effectively eliminate the possibility that any significant reassimilation of this water by local infiltration has occurred given climatic conditions resembling those of today. The arguments against the local infiltration of flood water into the northern plains are two-fold. First, given the climatic and geothermal conditions that are thought to have prevailed on Mars during the Late Hesperian (the period of peak outflow channel activity in the northern plains), the thickness of the cryosphere in Chryse Planitia is likely to have exceeded 1 km. A necessary precondition for the widespread occurrence of groundwater is that the thermodynamic sink represented by the cryosphere must already be saturated with ice. For this reason, the ice-saturated cryosphere acts as an impermeable barrier that effectively precludes the local resupply of subpermafrost groundwater by the infiltration of water discharged to the surface by catastraphic floods. Note that the problem of local infiltration is not significantly improved even if the cryosphere were initially dry, for as water attempts to infiltrate the cold, dry crust, it will quickly freeze, creating a seal that prevents any further infiltration from the ponded water above. The second argument against the local infiltration of flood water in the northern plains is based on hydraulic considerations. Repeated impacts have likely brecciated the Martian crust down to a depth of roughly 10 km. Given a value of permeability no greater than that inferred for the top 10 km of the Earth's crust (approximately 10(exp -2) darcies), a timescale as much as a billion years or more for the Martian groundwater system to achieve hydrostatic equilibrium, and the approximately 2-4 km elevation difference between the outflow channel source regions and the northern plains, the water confined beneath the frozen crust of the northern plains should have been under a significant hydraulic head. Thus, the existence of a hydraulic pathway between the ponded flood waters above the northern plains and the confined aquifer lying beneath it would not have led to the infiltration of flood water back into the crust, but rather the additional expulsion of groundwater onto the surface. Derived from text

N94-33203*# Arizona State Univ., Tempe. Dept. of Geology.

REGIONAL SEDIMENTOLOGICAL VARIATIONS AMONG DARK CRATER FLOOR FEATURES: TOWARD A MODEL FOR MODERN EOLIAN SAND DISTRIBUTION ON MARS Abstract Only

K. S. Edgett and P. R. Christensen *In* Lunar and Planetary Inst., Mars: Past, Present, and Future. Results from the MSATT Program, Part 1 1993 p 17-18 (For primary document see N94-33190 09-91)

Avail: CASI HC A01/MF A01

It has been known since 1972 that many Martian craters have dark features on their floors, and that when seen at higher image resolution, some of the dark units are dune fields. Interpretations of thermal inertia derived from Viking Infrared Thermal Mapper (IRTM) data have been used to suggest that many dark intracrater features, including those where dunes are not observed in images, contain some amount of sand or particles in the range 0.1-10 mm. However, it has never been known if all these dark features consist of dunes. We assembled a set of 108 carefully constrained Viking IRTM observations for dark crater-floor units. The data and selection criteria are described in detail elsewhere. Studied in conjunction with Mariner 9 and Viking orbiter images of each crater, these data indicate that the dark crater-floor units in some regions have different thermal properties than those in other regions. Thermal inertias were computed using the Viking thermal model of H. H. Kieffer and corrected for atmospheric CO2 effects using the relationship for a dust-free atmosphere shown by Haberle and Jakosky. Derived from text

N94-33204*# Viale Univ., Rome (Italy).

AEROSOLS SCATTERING AND NEAR-INFRARED OBSERVATIONS OF THE MARTIAN SURFACE Abstract Only

S. Erard *In* Lunar and Planetary Inst., Mars: Past, Present, and Future. Results from the MSATT Program, Part 1 1993 p 18-19 (For primary document see N94-33190 09-91)

Avail: CASI HC A01/MF A01

The presence of a scattered contribution in the atmosphere of Mars is a major problem for spectroscopic observations of the surface in the infrared since the main mineralogical absorptions have a typical depth of 1% and could be easily masked or subdued by atmospheric scattering. An estimate of the aerosol contribution between 0.77 and 2.6 microns was previously derived above Tharsis from ISM imaging spectroscopic data acquired from the Phobos 2 spacecraft in 1989. It is used here to investigate the effect of the scattering on the criteria that allow the mineralogical characterization of the surface. Derived from text

N94-33205*# National Aeronautics and Space Administration. Ames Research Center, Moffett Field, CA.

A MODEL FOR THE EVOLUTION OF CO2 ON MARS Abstract Only

Robert M. Haberle, D. Tyler, C. P. McKay, and W. L. Davis *In* Lunar and Planetary Inst., Mars: Past, Present, and Future. Results from the MSATT Program, Part 1 1993 p 19-20 (For primary document see N94-33190 09-91)

Avail: CASI HC A01/MF A01

Our MSATT work has focused on the evolution of CO2 on Mars. We have constructed a model that predicts the evolution of CO2 on Mars from a specified initial amount at the end of the heavy bombardment to the present. The model draws on published estimates of the main process believed to affect the fate of CO2 during this period: chemical weathering, regolith uptake, polar cap formation, and atmospheric escape. Except for escape, the rate at which these processes act is controlled by surface temperatures that we calculate using a modified version of the Gierasch and Toon energy balance model. Various aspects of this work are covered. Derived from text

N94-33206*# Planetary Science Inst., Tucson, AZ.
POSSIBLE TEST OF ANCIENT DENSE MARTIAN ATMOSPHERE Abstract Only
W. K. Hartmann and S. Engel *In* Lunar and Planetary Inst., Mars: Past, Present, and Future. Results from the MSATT Program, Part 1 1993 p 20 (For primary document see N94-33190 09-91)
Avail: CASI HC A01/MF A01

We have completed preliminary calculations of the minimum sizes of bolides that would penetrate various hypothetical Martian atmospheres with surface pressures ranging from 6 to 1000 mbar for projectiles of various strengths. The calculations are based on a computer program. These numbers are used to estimate the diameter corresponding to the turndown in the crater diameter distribution due to the loss of these bodies, analogous to the dramatic turndown at larger sized already discovered on Venus due to this effect. We conclude that for an atmosphere greater than a few hundred millibars, a unique downward displacement in the diameter distribution would develop in the crater diameter distribution at D approximately = 0.5-4 km, due to loss of all but Fe bolides. Careful search for this displacement globally, as outlined here, would allow us to place upper limits on the pressure of the atmosphere contemporaneous with the oldest surfaces, and possibly to get direct confirmation of dense ancient atmospheres. Derived from text

N94-33207*# Jet Propulsion Lab., California Inst. of Tech., Pasadena.
GROUNDBASED MONITORING OF MARTIAN ATMOSPHERIC OPACITY Abstract Only
K. E. Herkenhoff and L. J. Martin *In* Lunar and Planetary Inst., Mars: Past, Present, and Future. Results from the MSATT Program, Part 1 1993 p 20-21 (For primary document see N94-33190 09-91)
Avail: CASI HC A01/MF A01

The amount of dust in the Martian atmosphere is variable in both space and time. The presence of aerosols in the Mars atmosphere complicates quantitative analysis of Martian surface properties. We have developed a model for Mars surface and atmospheric scattering based on equations in Hillier et al (1991). This formulation was chosen for its speed of computation and because it accounts for the spherical geometry of atmospheric scattering at high mission angles, i.e., near the planetary limb. Derived from text

N94-33208*# Colorado Univ., Boulder. Lab. for Atmospherics and Space Physics.
MARS ATMOSPHERIC LOSS AND ISOTOPIC FRACTIONATION BY SOLAR-WIND-INDUCED SPUTTERING AND PHOTOCHEMICAL ESCAPE Abstract Only
B. M. Jakosky, R. O. Pepin, R. E. Johnson, and J. L. Fox *In* Lunar and Planetary Inst., Mars: Past, Present, and Future. Results from the MSATT Program, Part 1 1993 p 21 (For primary document see N94-33190 09-91)
Avail: CASI HC A01/MF A01

We examine the effects of loss of Mars atmospheric constituents by solar-wind-induced sputtering and by photochemical escape during the last 3.8 b.y. Sputtering is capable of efficiently removing all species from the upper atmosphere including the light noble gases; N is removed by photochemical processes as well. Due to diffusive separation (by mass) above the homopause, removal from the top of the atmosphere will fractionate the isotopes of each species with the lighter mass being preferentially lost. For C and O, this allows us to determine the size of nonatmospheric reservoirs that mix with the atmosphere; these reservoirs can be CO2 adsorbed in the regolith or H2O in the polar ice caps. We have constructed both simple analytical models and time-dependent models of the loss from and supply of volatiles to the Martian atmosphere. Derived from text

N94-33209*# National Aeronautics and Space Administration. Lyndon B. Johnson Space Center, Houston, TX.
SNC METEORITES AND THEIR IMPLICATIONS FOR RESERVOIRS OF MARTIAN VOLATILES Abstract Only
J. H. Jones *In* Lunar and Planetary Inst., Mars: Past, Present, and Future. Results from the MSATT Program, Part 1 1993 p 21-23 (For primary document see N94-33190 09-91)
Avail: CASI HC A01/MF A01

The SNC meteorites and the measurements of the Viking landers provide our only direct information about the abundance and isotopic composition of Martian volatiles. Indirect measurements include spectroscopic determinations of the D/H ratio of the Martian atmosphere. A personal view of volatile element reservoirs on Mars is presented, largely as inferred from the meteoritic evidence. This view is that the Martian mantle has had several opportunities for dehydration and is most likely dry, although not completely degassed. Consequently, the water contained in SNC meteorites was most likely incorporated during ascent through the crust. Thus, it is possible that water can be decoupled from other volatile/incompatible elements, making the SNC meteorites suspect as indicators of water inventories on Mars. Derived from text

N94-33210*# Geological Survey, Flagstaff, AZ.
THE NORTHERN PLAINS MSATT MEETING, AND A CALL FOR A FIELD-ORIENTED SUCCESSOR TO MSATT Abstract Only
J. S. Kargel *In* Lunar and Planetary Inst., Mars: Past, Present, and Future. Results from the MSATT Program, Part 1 1993 p 23-24 (For primary document see N94-33190 09-91)
Avail: CASI HC A01/MF A01

The workshop was devoted to a review of our knowledge of the Martian northern plains and presentation of recent ideas pertaining to the geologic and climatic evolution of this interesting region. The meeting was held in Fairbanks to allow easy access to Mars-like terrains in central and northern Alaska. There is no place on Earth that is a close analog of the Martian northern plains, but parts of Alaska come reasonably close in some respects, so we may expect that some of the processes occurring there are similar to processes that have occurred on Mars. Derived from text

N94-33211*# Colorado Univ., Boulder. Lab. for Atmospheric and Space Physics.
TEMPORAL AND SPATIAL MAPPING OF ATMOSPHERIC DUST OPACITY AND SURFACE ALBEDO ON MARS Abstract Only
S. W. Lee, R. T. Clancy, G. R. Gladstone, and T. Z. Martin *In* Lunar and Planetary Inst., Mars: Past, Present, and Future. Results from the MSATT Program, Part 1 1993 p 24 (For primary document see N94-33190 09-91)
Avail: CASI HC A01/MF A01

The Mariner 9 and Viking missions provided abundant evidence that eolian processes are active over much of the surface of Mars. Past studies have demonstrated that variations in regional albedo and wind streak patterns are indicative of sediment transport through a region, while thermal inertia data (derived from the Viking Infrared Thermal Mapper (IRTM) datasets) are indicative of the degree of surface mantling by dust deposits. We are making use of the method developed by T. Z. Martin to determine dust opacity from IRTM thermal observations. We have developed a radiative transfer model that allows corrections for the effects of atmospheric dust loading on observations of surface albedo to be made. This approach to determining 'dust-corrected surface albedo' incorporates the atmospheric dust opacity, the single-scattering albedo and particle phase function of atmospheric dust, the bidirectional reflectance of the surface, and accounts for variable lighting and viewing geometry. Derived from text

N94-33212*# Atmospheric and Environmental Research, Inc., Cambridge, MA.
HOW WELL WAS TOTAL OZONE ABUNDANCE INFERRED WITH MARINER 9 Abstract Only
B. L. Lindner *In* Lunar and Planetary Inst., Mars: Past, Present, and Future. Results from the MSATT Program, Part 1 1993 p 25-26 (For primary document see N94-33190 09-91)
Avail: CASI HC A01/MF A01

Ozone is a key to understanding atmospheric chemistry on Mars. Over 20 photochemical models of the Martian atmosphere have been published, and O3 is often used as a benchmark for these models. O3 abundance has been inferred from instrumentation on several spacecraft, with the most complete coverage provided by Mariner 9. A radiative transfer computer model is used to re-examine the Mariner 9 UV spectra. Derived from text

N94-33213*# Atmospheric and Environmental Research, Inc., Cambridge, MA.

THE EFFECT OF POLAR CAPS ON OBLIQUITY Abstract Only

B. L. Lindner *In* Lunar and Planetary Inst., Mars: Past, Present, and Future. Results from the MSATT Program, Part 1 1993 p 26-27 (For primary document see N94-33190 09-91)

(Contract NASw-4614)

Avail: CASI HC A01/MF A01

Rubincam has shown that the Martian obliquity is dependent on the seasonal polar caps. In particular, Rubincam analytically derived this dependence and showed that the change in obliquity is directly proportional to the seasonal polar cap mass. Rubincam concludes that seasonal friction does not appear to have changed Mars' climate significantly. Using a computer model for the evolution of the Martian atmosphere, Haberle et al. have made a convincing case for the possibility of huge polar caps, about 10 times the mass of the current polar caps, that exist for a significant fraction of the planet's history. Since Rubincam showed that the effect of seasonal friction on obliquity is directly proportional to polar cap mass, a scenario with a ten-fold increase in polar cap mass over a significant fraction of the planet's history would result in a secular increase in Mars' obliquity of perhaps 10 degrees. Hence, the Rubincam conclusion of an insignificant contribution to Mars' climate by seasonal friction may be incorrect. Furthermore, if seasonal friction is an important consideration in the obliquity of Mars, this would significantly alter the predictions of past obliquity. Derived from text

N94-33214*# California Univ., Los Angeles. Inst. of Geophysics and Planetary Physics.

ESCAPE OF MARS ATMOSPHERIC CARBON THROUGH TIME BY PHOTOCHEMICAL MEANS Abstract Only

J. G. Luhmann, J. Kim, and A. F. Nagy *In* Lunar and Planetary Inst., Mars: Past, Present, and Future. Results from the MSATT Program, Part 1 1993 p 27 (For primary document see N94-33190 09-91)

Avail: CASI HC A01/MF A01

Luhmann et al. recently suggested that sputtering of the Martian atmosphere by re-entering O(+) pickup ions could have provided a significant route of escape for CO2 and its products throughout Mars' history. They estimated that the equivalent of C in an approximately 140-mbar CO2 atmosphere should have been lost this way if the Sun and solar wind evolved according to available models. Another source of escaping C (and O) that is potentially important is the dissociative recombination of ionospheric CO(+) near the exobase. We have evaluated the loss rates due to this process for 'ancient' solar EUV radiation fluxes of 1, 3, and 6 times the present flux in order to calculate the possible cumulative loss over the last 3.5 Gyr. Derived from text

N94-33215*# Lowell Observatory, Flagstaff, AZ.

MIGHT IT BE POSSIBLE TO PREDICT THE ONSET OF MAJOR MARTIAN DUST STORMS? Abstract Only

L. J. Martin, P. B. James, and R. W. Zurek *In* Lunar and Planetary Inst., Mars: Past, Present, and Future. Results from the MSATT Program, Part 1 1993 p 27-28 Sponsored in part by Space Telescope Science Inst. (For primary document see N94-33190 09-91)

(Grants NAGw-2257; NAGw-3311)

Avail: CASI HC A01/MF A01

The possible indicators of impending Martian dust storms are discussed. Topics covered include the following: seasonal effects, perihelion, recession of the north polar hood; and Hellas Basin. CASI

N94-33216*# Jet Propulsion Lab., California Inst. of Tech., Pasadena.

STUDIES OF ATMOSPHERIC DUST FROM VIKING IR THERMAL MAPPER DATA Abstract Only

T. Z. Martin *In* Lunar and Planetary Inst., Mars: Past, Present, and Future. Results from the MSATT Program, Part 1 1993 p 28 (For primary document see N94-33190 09-91)

Avail: CASI HC A01/MF A01

Following earlier work to map the dust opacity of the Mars atmosphere, a number of separate studies have been performed employing the radiometric measurements of the Viking IR Thermal Mappers. These efforts have resulted in a new perspective on the atmospheric dust distribution during the Viking Mission, as well as quantitative measures useful in the modeling of likely behavior at other times, and improved boundary conditions for circulation models of Mars. The significant findings from these studies are presented. Derived from text

N94-33217*# Geological Survey, Flagstaff, AZ.

GLOBAL COLOR VIEWS OF MARS Abstract Only

A. S. McEwen, L. A. Soderblom, T. L. Becker, E. M. Lee, and R. M. Batson *In* Lunar and Planetary Inst., Mars: Past, Present, and Future. Results from the MSATT Program, Part 1 1993 p 29 (For primary document see N94-33190 09-91)

Avail: CASI HC A01/MF A01

About 1000 Viking Orbiter red and violet filter images have been processed to provide global color coverage of Mars at a scale of 1 km/pixel. Individual image frames acquired during a single spacecraft revolution ('rev') were first processed through radiometric calibration, cosmetic cleanup, geometric control, reprojection, and mosaicking. A total of 57 'single-rev' mosaics have been produced. Phase angles range from 13 to 85 degrees. All the mosaics are geometrically tied to the Mars digital image mosaic (MDIM), a black-and-white base map with a scale of 231 m/pixel. Derived from text

N94-33218*# Colorado Univ., Boulder. Lab. for Atmospheric and Space Physics.

THE DISTRIBUTION OF MARTIAN GROUND ICE AT OTHER EPOCHS Abstract Only

M. T. Mellon and B. M. Jakosky *In* Lunar and Planetary Inst., Mars: Past, Present, and Future. Results from the MSATT Program, Part 1 1993 p 29-30 (For primary document see N94-33190 09-91)

Avail: CASI HC A01/MF A01

The past orbital evolution of Mars is examined in relation to changes in ice stability as well as the condensation, sublimation, and diffusion of atmospheric water in an exchange with the regolith. The Martian obliquity has undergone significant oscillations in its recent past. During periods of high obliquity, the solar energy would have been distributed such that the equatorial and midlatitude regions would have been colder that at present and the polar regions would have been warmer. Warmer polar regions would result in the sublimation of more polar cap water into the atmosphere and thus higher atmospheric water abundances. This combination of effects would have resulted in ground ice being stable globally. During periods of low obliquity the opposite would have occurred. Modeling results of the regolith thermal behavior and the molecular diffusion of water vapor within the regolith and in exchange with the atmosphere have shown significant quantities of ground ice can form at all latitudes within the top 50 cm to 1 m of the regolith during periods of high obliquity. The amount of ice that forms can be as much as the regolith pores can hold. During low obliquity most or all of this ice sublimes and diffuses away. Below this depth a longer-term stability is observed at some latitudes where ice steadily increases in concentration regardless of orbital oscillations that occur. Derived from text

N94-33219*# National Aeronautics and Space Administration. Lyndon B. Johnson Space Center, Houston, TX.

MINERALOGICAL DIVERSITY (SPECTRAL REFLECTANCE AND MOESSBAUER DATA) IN COMPOSITIONALLY SIMILAR IMPACT MELT ROCKS FROM MANICOUAGAN CRATER, CANADA Abstract Only

R. V. Morris, J. F. Bell, III, D. C. Golden, and H. V. Lauer, Jr. *In* Lunar and Planetary Inst., Mars: Past, Present, and Future. Results from the MSATT Program, Part 1 1993 p 30-32 (For primary document see N94-33190 09-91)

Avail: CASI HC A01/MF A01

Meteoritic impacts under oxidizing surface conditions occur on both earth and Mars. Oxidative alteration of impact melt sheets is reported at several terrestrial impact structures including Manicouagan, West Clearwater Lake, and the Ries Basin. A number of studies have advocated that a significant fraction of Martian soil may consist of erosional products of

oxidatively altered impact melt sheets. If so, the signature of the Fe-bearing mineralogies formed by the process may be present in visible and near infrared reflectivity data for the Martian surface. Of concern is what mineral assemblages form in impact melt sheets produced under oxidizing conditions and what their spectral signatures are. Spectral and Moessbauer data for 19 powder samples of impact melt rock from Manicouagan Crater are reported. Results show for naturally occurring materials that composite hematite-pyroxene bands have minima in the 910-nm region. Thus many of the anomalous Phobos-2 spectra, characterized by a shallow band minimum in the near-IR whose position varies between approximately 850 and 1000 nm, can be explained by assemblages whose endmembers (hematite and pyroxene) are accepted to be present on Mars. Furthermore, results show that a mineralogically diverse suite of rocks can be generated at essentially constant composition, which implies that variations in Martian surface mineralogy do not necessarily imply variations in chemical composition. CASI

N94-33220*# Lunar and Planetary Inst., Houston, TX.
MARTIAN SPECTRAL UNITS DERIVED FROM ISM IMAGING SPECTROMETER DATA Abstract Only
S. Murchie, J. Mustard, and R. Saylor *In its* Mars: Past, Present, and Future. Results from the MSATT Program, Part 1 1993 p 32-34 (For primary document see N94-33190 09-91)
Avail: CASI HC A01/MF A01

Based on results of the Viking mission, the soil layer of Mars has been thought to be fairly homogeneous and to consist of a mixture of as few as two components, a 'dark gray' basaltic material and a 'bright red' altered material. However, near-infrared reflectance spectra measured recently both telescopically and from spacecraft indicate compositional heterogeneity beyond what can be explained by just two components. In particular, data from the ISM imaging spectrometer, which observed much of the equatorial region at a spatial resolution of approximately 22 km, indicate spatial differences in the presence and abundance of Fe-containing phases, hydroxylated silicates, and H2O. The ISM data was used to define, characterize, and map soil 'units' based on their spectral properties. The spatial distribution of these 'units' were compared to morphologic, visible color, and thermal inertia features recognized in Viking data.
Derived from text

N94-33221*# National Aeronautics and Space Administration. Ames Research Center, Moffett Field, CA.
EDDY TRANSPORT OF WATER VAPOR IN THE MARTIAN ATMOSPHERE Abstract Only
J. R. Murphy (San Jose State Univ., CA.) and Robert M. Haberle *In* Lunar and Planetary Inst., Mars: Past, Present, and Future. Results from the MSATT Program, Part 1 1993 p 34 (For primary document see N94-33190 09-91)
Avail: CASI HC A01/MF A01

Viking orbiter measurements of the Martian atmosphere suggest that the residual north polar water-ice cap is the primary source of atmospheric water vapor, which appears at successively lower northern latitudes as the summer season progresses. Zonally symmetric studies of water vapor transport indicate that the zonal mean meridional circulation is incapable of transporting from north polar regions to low latitudes the quantity of water vapor observed. This result has been interpreted as implying the presence of nonpolar sources of water. Another possibility is the ability of atmospheric wave motions, which are not accounted for in a zonally symmetric framework, to efficiently accomplish the transport from a north polar source to the entirety of the Northern Hemisphere. The ability or inability of the full range of atmospheric motions to accomplish this transport has important implications regarding the questions of water sources and sinks on Mars: if the full spectrum of atmospheric motions proves to be incapable of accomplishing the transport, it strengthens arguments in favor of additional water sources. Preliminary results from a three dimensional atmospheric dynamical/water vapor transport numerical model are presented. The model accounts for the physics of a subliming water-ice cap, but does not yet incorporate recondensation of this sublimed water. Transport of vapor away from this water-ice cap in this three dimensional framework is compared with previously obtained zonally symmetric (two dimensional) results to quantify effects of water vapor transport by atmospheric eddies.
Author (revised)

N94-33222*# California Univ., Los Angeles. Dept. of Earth and Space Sciences.
IRTM BRIGHTNESS TEMPERATURE MAPS OF THE MARTIAN SOUTH POLAR REGION DURING THE POLAR NIGHT: THE COLD SPOTS DON'T MOVE Abstract Only
D. A. Paige, D. Crisp, M. L. Santee, and M. I. Richardson *In* Lunar and Planetary Inst., Mars: Past, Present, and Future. Results from the MSATT Program, Part 1 1993 p 34-35 (For primary document see N94-33190 09-91)
Avail: CASI HC A01/MF A01

A series of infrared thermal mapper (IRTM) south polar brightness temperature maps obtained by Viking Orbiter 2 during a 35-day period during the southern fall season in 1978 was examined. The maps show a number of phenomena that have been identified in previous studies, including day to day brightness temperature variations in individual low temperature regions and the tendency for IRTM 11-micron channel brightness temperatures to also decrease in regions where low 20-micron channel brightness temperatures are observed. The maps also show new phenomena, the most striking of which is a clear tendency for the low brightness temperature regions to occur at fixed geographic regions. During this season, the coldest low brightness temperatures appear to be concentrated in distinct regions, with spatial scales ranging from 50 to 300 km. There are approximately a dozen of these concentrations, with the largest centered near the location of the south residual polar cap. Other concentrations are located at Cavi Angusti and close to the craters Main, South, Lau, and Dana. Broader, less intense regions appear to be well correlated with the boundaries of the south polar layered deposits and the Mountains of Mitchell. No evidence for horizontal motion of any of these regions has been detected. Author (revised)

N94-33223*# Wyoming Univ., Laramie. Dept. of Atmospheric Science.
NUMERICAL SIMULATION OF THERMALLY INDUCED NEAR-SURFACE FLOWS OVER MARTIAN TERRAIN Abstract Only
T. R. Parish and A. D. Howard *In* Lunar and Planetary Inst., Mars: Past, Present, and Future. Results from the MSATT Program, Part 1 1993 p 35-39 (For primary document see N94-33190 09-91)
Avail: CASI HC A01/MF A01

Numerical simulations of the Martian near-surface wind regime using a mesoscale atmospheric model have shown that the thermally induced near-surface winds are analogous to terrestrial circulations. In particular, katabatic wind displays a striking similarity to flow observed over Antarctica. Introduction of solar radiation strongly perturbs the slope flows; anabatic conditions develop in middle to high latitudes during the daytime hours due to the solar heating of the sloping terrain. There appears to be a rapid transition from the katabatic to the anabatic flow regimes, emphasizing the primary importance of radiative exchanges at the surface in specifying the horizontal pressure gradient force. Author

N94-33224*# University of Southern California, Los Angeles. Dept. of Geological Sciences.
APRON HEIGHTS AROUND STEPPED MASSIFS IN THE CYDONIA MENSAE REGION: DO THEY RECORD THE LOCAL PALEOBATHYMETRY OF OCEANUS BOREALIS? Abstract Only
T. J. Parker and D. S. Gorsline *In* Lunar and Planetary Inst., Mars: Past, Present, and Future. Results from the MSATT Program, Part 1 1993 p 39-40 (For primary document see N94-33190 09-91)
Avail: CASI HC A01/MF A01

The use of photoclinometry and shadow measurements to determine the basin volume without linking the measurements to a global datum is described. Since the boundary, or shoreline, of the basin cannot be tied to the datum and typically has no useful local relative height to measure, what is needed is a number of measurements of the height of the paleoshorelines distributed across the basin. Photoclinometric profiles are being compiled from Viking Orbiter images of the Cydonia Mensae region, which includes images with high sun elevations, necessary to avoid shadows, and images with low sun elevations, to enable the use of shadow measurements as an independent check, at high resolution (40 to 100 m/pixel). Both asymmetric and symmetric photoclinometric profile models are being used, and the results cross checked with one another to minimize errors. An apron-height map, potentially a paleobathymetric map of part of the margin of Oceanus Borealis, can be compiled from this data to determine

whether variations in apron height are consistent with a lacustrine interpretation. Derived from text

N94-33225*# Worcester Polytechnic Inst., MA.
THE pH OF MARS Abstract Only
R. C. Plumb (Brown Univ., Providence, RI.), J. L. Bishop (Brown Univ., Providence, RI.), and J. O. Edwards (Brown Univ., Providence, RI.) *In* Lunar and Planetary Inst., Mars: Past, Present, and Future. Results from the MSATT Program, Part 1 1993 p 40-41 (For primary document see N94-33190 09-91)
Avail: CASI HC A01/MF A01

The Viking labeled release (LR) experiments provided data that can be used to determine the acid-base characteristics of the regolith. Constraints on the acid-base properties and redox potentials of the Martian surface material would provide additional information for determining what reactions are possible and defining formation conditions for the regolith. Calculations devised to determine the pH of Mars must include the amount of soluble acid species or base species present in the LR regolith sample and the solubility product of the carbonate with the limiting solubility. This analysis shows that CaCO3, either as calcite or aragonite, has the correct K(sub sp) to have produced the Viking LR successive injection reabsorption effects. Thus CaCO3 or another MeCO3 with very similar solubility characteristics must have been present on Mars. A small amount of soluble acid, but no more than 4 micro-mol per sample, could also have been present. It is concluded that the pH of the regolith is 7.2 +/- 0.1. Derived from text

N94-33226*# Geological Survey, Denver, CO.
THE MINERALOGIC EVOLUTION OF THE MARTIAN SURFACE THROUGH TIME: IMPLICATIONS FROM CHEMICAL REACTION PATH MODELING STUDIES Abstract Only
G. S. Plumlee, W. I. Ridley, J. D. DeBraal, and M. H. Reed *In* Lunar and Planetary Inst., Mars: Past, Present, and Future. Results from the MSATT Program, Part 1 1993 p 41-43 (For primary document see N94-33190 09-91)
Avail: CASI HC A01/MF A01

Chemical reaction path calculations were used to model the minerals that might have formed at or near the Martian surface as a result of volcano or meteorite impact driven hydrothermal systems; weathering at the Martian surface during an early warm, wet climate; and near-zero or sub-zero C brine-regolith reactions in the current cold climate. Although the chemical reaction path calculations carried out do not define the exact mineralogical evolution of the Martian surface over time, they do place valuable geochemical constraints on the types of minerals that formed from an aqueous phase under various surficial and geochemically complex conditions. Derived from text

N94-33227*# National Aeronautics and Space Administration. Ames Research Center, Moffett Field, CA.
CONTROLS ON THE CO2 SEASONAL CYCLE Abstract Only
J. B. Pollack, F. Forget, Robert M. Haberle, J. Schaeffer, and H. Lee *In* Lunar and Planetary Inst., Mars: Past, Present, and Future. Results from the MSATT Program, Part 1 1993 p 43 (For primary document see N94-33190 09-91)
Avail: CASI HC A01/MF A01

Surface pressure measurement performed by the Viking landers show substantial variations in pressure on seasonal timescales that are characterized by two local minima and two local maxima. These variations have widely been attributed to the seasonal condensation and sublimation of CO2 in the two polar regions. It has been somewhat of a surprise that the amplitude of the minimum and maximum that is dominated by the CO2 cycle in the north was much weaker than the corresponding amplitude of the south-dominated extrema. Another surprise was that the seasonal pressure cycle during years 2 and 3 of the Viking mission was so similar to that for year 1, despite the occurrence of two global dust storms during year 1 and none during years 2 and 3. An energy balance model that incorporates dynamical factors from general circulation model (GCM) runs in which the atmospheric dust opacity and seasonal date were systematically varied was used to model the observed seasonal pressure variations. The energy balance takes account of the following processes in determining the rates of CO2 condensation and sublimation at each longitudinal and latitudinal grid point: solar radiation, infrared radiation from the atmosphere and surface, subsurface heat conduction, and atmospheric heat advection. Condensation rates are calculated both at the surface and in the atmosphere. In addition, the energy balance model also incorporates information from the GCM runs on seasonal redistribution of surface pressure across the globe. Estimates of surface temperature of the seasonal CO2 caps were used to define the infrared radiative losses from the seasonal polar caps. The seasonal pressure variations measured at the Viking lander sites were closely reproduced. Author (revised)

N94-33228*# National Aeronautics and Space Administration. Ames Research Center, Moffett Field, CA.
THE WAVELENGTH DEPENDENCE OF MARTIAN ATMOSPHERIC DUST RADIATIVE PROPERTIES Abstract Only
J. B. Pollack, M. E. Ockert-Bell, R. Arvidson, and M. Shepard *In* Lunar and Planetary Inst., Mars: Past, Present, and Future. Results from the MSATT Program, Part 1 1993 p 44 (For primary document see N94-33190 09-91)
Avail: CASI HC A01/MF A01

One of the key radiative agents in the atmosphere of Mars is the suspended dust particles. A new analysis of two data sets of the Martian atmosphere is being carried out in order to better evaluate the radiative properties of the atmospheric dust particles. The properties of interest are the size distribution, optical constants, and other radiative properties, such as the single-scattering albedo and phase function. Of prime importance is the wavelength dependence of these radiative properties throughout the visible and near-infrared wavelengths. Understanding the wavelength dependence of absorption and scattering characteristics will provide a good definition of the influence that the atmospheric dust has on heating of the atmosphere. Derived from text

N94-33229*# Arizona State Univ., Tempe. Dept. of Geology.
EVIDENCE FOR ULTRAMAFIC LAVAS ON SYRTIS MAJOR Abstract Only
D. P. Reyes and P. R. Christensen *In* Lunar and Planetary Inst., Mars: Past, Present, and Future. Results from the MSATT Program, Part 1 1993 p 44-45 (For primary document see N94-33190 09-91)
Avail: CASI HC A01/MF A01

Pyroxene compositions from ISM data compared with pyroxene compositions of Apollo 12 pigeonite basalt, Shergotite meteorite, and pyroxenitic komatiite show that the Syrtis Major volcanic materials are consistent with pyroxenitic komatiite. Pyroxenitic komatiite is significant for the earth because it contains a large amount of MgO, implying generation under unique circumstances compared to typical basaltic compositions. Derived from text

N94-33230*# Arizona State Univ., Tempe. Dept. of Geography.
MARTIAN DELTAS: MORPHOLOGY AND DISTRIBUTION Abstract Only
J. W. Rice, Jr. and D. H. Scott *In* Lunar and Planetary Inst., Mars: Past, Present, and Future. Results from the MSATT Program, Part 1 1993 p 45-46 (For primary document see N94-33190 09-91)
Avail: CASI HC A01/MF A01

Recent detailed mapping has revealed numerous examples of Martian deltas. The location and morphology of these deltas are described. Factors that contribute to delta morphology are river regime, coastal processes, structural stability, and climate. The largest delta systems on Mars are located near the mouths of Maja, Maumee, Vedra, Ma'adim, Kasei, and Brazos Valles. There are also several smaller-scale deltas emplaced near channel mouths situated in Ismenius Lacus, Memnonia, and Arabia. Delta morphology was used to reconstruct type, quantity, and sediment load size transported by the debouching channel systems. Methods initially developed for terrestrial systems were used to gain information on the relationships between Martian delta morphology, river regime, and coastal processes. Author (revised)

N94-33231*# California Inst. of Tech., Pasadena. Div. of Geological and Planetary Sciences.
CARBONATE FORMATION ON MARS: LATEST EXPERIMENTS Abstract Only
S. K. Stephens, D. J. Stevenson, G. R. Rossman, and L. F. Keyser *In* Lunar and Planetary Inst., Mars: Past, Present, and Future. Results from the MSATT Program, Part 1 1993 p 46-48 (For primary document see N94-33190 09-91)
Avail: CASI HC A01/MF A01

Laboratory simulations of Martian CO2 storage address whether carbonate formation could have reduced CO2 pressure from a hypothetical greater than 1 bar to the present 7 mbar in less than or equal to 3 to 4 billion years. This problem is addressed with experiments and analysis designed to verify and improve previous kinetic measurements, reaction mechanisms, and product characterizations, with the goal of improving existing models of Martian CO2 history. A sensitive manometer monitored the pressure drop of CO2 due to uptake by powdered silicate for periods of 3 to 100+ days. Pressure drops for diopside 1 and basalt show rapid short-term (approximately one day) CO2 uptake and considerably slower long-term pressure drops. Curves for diopside 2, olivine 1, and olivine 2 are qualitatively similar to those for diopside 1, whereas quartz and plagioclase show near-zero short-term pressure drops and very slow long-term signals, indistinguishable from a leak (less than 10(exp 11) mol/sq m/s). Derived from text

N94-33232*# Geological Survey, Flagstaff, AZ.
GEOLOGIC CONTROLS OF EROSION AND SEDIMENTATION ON MARS Abstract Only
K. L. Tanaka, J. M. Dohm, and M. H. Carr *In* Lunar and Planetary Inst., Mars: Past, Present, and Future. Results from the MSATT Program, Part 1 1993 p 48-49 (For primary document see N94-33190 09-91)
Avail: CASI HC A01/MF A01

Because Mars has had a history of diverse erosional and depositional styles, a variety of erosional landforms and sedimentary deposits can be seen on Viking orbiter images. Here we review how geologic processes involving rock, water, and structure have controlled erosion and sedimentation on Mars. Additionally, we review how further studies will help refine our understanding of these processes. Author

N94-33233*# Cornell Univ., Ithaca, NY. Center for Radiophysics and Space Research.
POLAR SEDIMENT ACCUMULATION: ROLE OF SURFACE WINDS AT THE TWO POLES Abstract Only
P. C. Thomas and P. J. Gierasch *In* Lunar and Planetary Inst., Mars: Past, Present, and Future. Results from the MSATT Program, Part 1 1993 p 49 (For primary document see N94-33190 09-91)
Avail: CASI HC A01/MF A01

The accumulation of the large deposits of volatile and nonvolatile sediments at both Martian poles has occurred through periods of likely climate change. Most data on wind directions near the Martian poles and seasonal activity relate to a very short period of time, at one point in climate cycles. It is still uncertain what the net budgets to the poles are and how this budget (if known) would fit into longer climate/sediment cycles. Pending further data we examined the full suite of Viking high-resolution, high-latitude images for wind markers of all sizes and types. These probably represent timescales of formation from days to several tens of thousands of years. The goal is to estimate the effectiveness, and possible drivers, of wind systems that bring materials near the surface to the regions of polar sediments and that also remove materials from the polar areas. Author

N94-33234*# Lockheed Engineering and Sciences Co., Houston, TX.
THE MARTIAN SOURCES OF THE SNC METEORITES (TWO, NOT ONE), AND WHAT CAN AND CAN'T BE LEARNED FROM THE SNC METEORITES Abstract Only
A. H. Treiman *In* Lunar and Planetary Inst., Mars: Past, Present, and Future. Results from the MSATT Program, Part 1 1993 p 49-51 (For primary document see N94-33190 09-91)
Avail: CASI HC A01/MF A01

The SNC meteorites, which almost certainly originate in the Martian crust, have been inferred to come from a single impact crater site, but no known crater fits all criteria. Formation at two separate sites (S from one, NC from the other) is more consistent with the sum of petrologic, geochronologic, and cosmochronologic data. If the source craters for the SNC meteorites can be located, Mars science will advance considerably. However, many significant questions cannot be answered by the SNC meteorites. These questions await a returned sample. Author

N94-33235*# British Columbia Univ., Vancouver.
TEMPORAL CHANGES IN THE GEOGRAPHIC DISTRIBUTION, ELEVATION, AND POTENTIAL ORIGIN OF THE MARTIAN OUTFLOW CHANNELS Abstract Only
S. Tribe and S. M. Clifford *In* Lunar and Planetary Inst., Mars: Past, Present, and Future. Results from the MSATT Program, Part 1 1993 p 51-52 (For primary document see N94-33190 09-91)
Avail: CASI HC A01/MF A01

Observational evidence of outflow channel activity on Mars suggests that water was abundant in the planet's early crust. However, with the decline in the planet's internal heat flow, a freezing front developed within the regolith that propagated downward with time and acted as a thermodynamic sink for crustal H2O. One result of this thermal evolution is that, if the initial inventory of water on Mars was small, the cryosphere may have grown to the point where all the available water was taken up as ground ice. Alternatively, if the inventory of H2O exceeds the current pore volume of the cryosphere, then Mars has always possessed extensive bodies of subpermafrost groundwater. We have investigated the relative age, geographic distribution, elevation, and geologic setting of the outflow channels in an effort to accomplish the following: (1) identify possible modes of origin and evolutionary trends in their formation; (2) gain evidence regarding the duration and spatial distribution of groundwater in the crust; and (3) better constraint estimates of the planetary inventory of H2O. Author

N94-33236*# National Aeronautics and Space Administration. Ames Research Center, Moffett Field, CA.
OBLIQUITY VARIATION IN A MARS CLIMATE EVOLUTION MODEL Abstract Only
D. Tyler (San Jose State Univ., CA.) and Robert M. Haberle *In* Lunar and Planetary Inst., Mars: Past, Present, and Future. Results from the MSATT Program, Part 1 1993 p 52-53 (For primary document see N94-33190 09-91)
Avail: CASI HC A01/MF A01

The existence of layered terrain in both polar regions of Mars is strong evidence supporting a cyclic variation in climate. It has been suggested that periods of net deposition have alternated with periods of net erosion in creating the layered structure that is seen today. The cause for this cyclic climatic behavior is variation in the annually averaged latitudinal distribution of solar insolation in response to obliquity cycles. For Mars, obliquity variation leads to major climatological excursion due to the condensation and sublimation of the major atmospheric constituent, CO2. The atmosphere will collapse into the polar caps, or existing caps will rapidly sublimate into the atmosphere, dependent upon the polar surface heat balance and the direction of the change in obliquity. It has been argued that variations in the obliquity of Mars cause substantial departures from the current climatological values of the surface pressure and the amount of CO2 stored in both the planetary regolith and polar caps. In this new work we have modified the Haberle et al. model to incorporate variable obliquity by allowing the polar and equatorial insolation to become functions of obliquity, which we assume to vary sinusoidally in time. As obliquity varies in the model, there can be discontinuities in the time evolution of the model equilibrium values for surface pressure, regolith, and polar cap storage. The time constant, tau r, for the regolith to find equilibrium with the climate is estimated--depending on the depth, thermal conductivity, and porosity of the regolith--between 10(exp 4) and 10(exp 6) yr. Thus, using 2000-yr timesteps to move smoothly through the 0.1250 m.y. obliquity cycles, we have an atmosphere/regolith system that cannot be assumed in equilibrium. We have dealt with this problem by limiting the rate at which CO2, can move between the atmosphere and regolith, mimicking the diffusive nature and effects of the temperature and pressure waves, by setting the time rate of change of regolith storage proportional to the difference between equilibrium storage and current storage. Author

N94-33237*# European Space Agency. European Space Research and Technology Center, ESTEC, Noordwijk (Netherlands). Space Science Dept.
DIELECTRIC PROPERTIES OF MARS' SURFACE: PROPOSED MEASUREMENT ON A MARS LANDER Abstract Only
S. Ulamec and R. Grard *In* Lunar and Planetary Inst., Mars: Past, Present, and Future. Results from the MSATT Program, Part 1 1993

p 53-54 (For primary document see N94-33190 09-91)
Avail: CASI HC A01/MF A01

Recent studies of missions to Mars (MESUR by NASA and Marsnet by ESA) have suggested the development of semihard landers. One type was to be extremely basic, consisting mainly of a meteorological package, but with the possibility of other small, low-mass, low-power instruments. In particular, this type of lander was also considered for the exploration of the polar regions. Two methods to investigate the surface material at the landing site are discussed. Both measure the dielectric constant epsilon of the ground material. This information can then be used to elucidate the surface composition and structure. The determination of the permittivity would be of high scientific value, especially in the case of a landing on the polar ice. Author

N94-33238*# California Univ., Los Angeles.
THE INFLUENCE OF THERMAL INERTIA ON MARS' SEASONAL PRESSURE VARIATION AND THE EFFECT OF THE WEATHER COMPONENT Abstract Only
S. E. Wood and D. A. Paige *In* Lunar and Planetary Inst., Mars: Past, Present, and Future. Results from the MSATT Program, Part 1 1993 p 54-56 (For primary document see N94-33190 09-91)
Avail: CASI HC A01/MF A01

Using a Leighton-Murray type diurnal and seasonal Mars thermal model, we found that it is possible to reproduce the seasonal variation in daily-averaged pressures (approximately 680-890 Pa) measured by Viking Lander 1 (VL1), during years without global dust storms, with a standard deviation of less than 5 Pa. In this simple model, surface CO2, frost condensation, and sublimation rates at each latitude are determined by the net effects of radiation, latent heat, and heat conduction in subsurface soil layers. An inherent assumption of our model is that the seasonal pressure variation is due entirely to the exchange of mass between the atmosphere and polar caps. However, the results of recent Mars GCM modeling have made it clear that there is a significant dynamical contribution to the seasonal pressure variation. This 'weather' component is primarily due to large-scale changes in atmospheric circulation, and its magnitude depends somewhat on the dust content of the atmosphere. The overall form of the theoretical weather component at the location of VL1, as calculated by the AMES GCM, remains the same over the typical range of Mars dust opacities. Author (revised)

N94-33239*# Open Univ., Milton (England). Dept. of Earth Sciences.
CARBONATES, SURFATES, PHOSPHATES, NITRATES, AND ORGANIC MATERIALS: THEIR ASSOCIATION IN A MARTIAN METEORITE Abstract Only
I. P. Wright, M. M. Grady, and C. T. Pillinger *In* Lunar and Planetary Inst., Mars: Past, Present, and Future. Results from the MSATT Program, Part 1 1993 p 56-57 (For primary document see N94-33190 09-91)
Avail: CASI HC A01/MF A01

The debate concerning the evolution of CO2 on Mars continues. It would appear that in order to explain the valley networks and other relict fluvial landforms it is necessary to accept that liquid water was once present at the surface of Mars. This in turn requires, at some point in the planet's history, a higher surface temperature than exists today, proposition explained traditionally by an early dense CO2, atmosphere. However, there are a number of problems with this notion: for instance, CO2 alone is not an efficient greenhouse gas because of its tendency to form clouds. Moreover, if there was an early dense CO2 atmosphere, it is necessary to explain where the elemental constituents now reside. There are two possibilities for the latter, namely loss to outer space of atmospheric CO2 or the formation of vast carbonate deposits. While some models of atmospheric loss predict that up to 0.4 bar of CO2 could be removed from the Martian surface, this is still not enough to account for the original atmospheric inventory, usually considered to have been in the range of 1-5 bar. Thus, most models of the evolution of the Martian surface require removal of CO2 from the atmosphere and into carbonate deposits. However, as yet, the evidence for the existence of carbonates on Mars is fairly scant. This is an issue that would have been resolved by results obtained from Mars Observer. Author (revised)

N94-33240*# National Aeronautics and Space Administration. Ames Research Center, Moffett Field, CA. Search for Extraterrestrial Intelligence Inst.
SIMULTANEOUS LABORATORY MEASUREMENTS OF CO2 AND H2O ADSORPTION ON PALAGONITE: IMPLICATIONS FOR THE MARTIAN CLIMATE AND VOLATILE RESERVOIR Abstract Only
A. P. Zent and R. Quinn *In* Lunar and Planetary Inst., Mars: Past, Present, and Future. Results from the MSATT Program, Part 1 1993 p 57-58 (For primary document see N94-33190 09-91)
Avail: CASI HC A01/MF A01

We are measuring the simultaneous adsorption of H2O and CO2 on palagonite materials in order to improve the formulation of climate models for Mars. We report on the initial co-adsorption data. Models of the Martian climate and volatile inventory indicate that the regolith serves as one of the primary reservoirs of outgassed volatiles and that it exchanges H2O and CO2 with the atmosphere in response to changes in insolation associated with astronomical cycles. Physical adsorbate must exist on the surfaces of the cold particulates that constitute the regolith, and the size of that reservoir can be assessed through laboratory measurements of adsorption on terrestrial analogs. Many studies of the independent adsorption of H2O and CO2 on Mars analog were made and appear in the literature. Empirical expressions that relate the adsorptive coverage of each gas to the temperature of the soil and partial pressure have been derived based on the laboratory data. Numerical models incorporate these adsorption isotherms into climatic models, which predict how the adsorptive coverage of the regolith and hence, the pressure of each gas in the atmosphere will vary as the planet moves through its orbit. These models suggest that the regolith holds several tens to hundreds of millibars of CO2 and that during periods of high obliquity warming of the high-latitude regolith will result in desorption of the CO2, and a consequent increase in atmospheric pressure. At lower obliquities, the caps cool and the equator warms forcing the desorption of several tens of millibars of CO2, which is trapped into quasipermanent CO2 caps. Author (revised)

92 SOLAR PHYSICS

Includes solar activity, solar flares, solar radiation and sunspots. For related information see *93 Space Radiation.*

N94-31214 Arizona Univ., Tucson.
EVIDENCE OF SOLAR OSCILLATIONS IN RAYLEIGH-SCATTERED LIGHT Ph.D. Thesis
Marvin Edward Germain 1993 119 p
Avail: Univ. Microfilms Order No. DA9328609

A new instrument has been developed for making unimaged whole-disk observations of low-degree solar normal-mode oscillations. The apparatus, referred to as the sky monitor, does not track the solar disk, but instead measures the radiant flux scattered by the earth's atmosphere at 1.6 and 0.5 mu. The expected diurnal flux variation was obtained from a detailed radiative transfer calculation. Data were acquired for 15.5 months during 1991-92. Seventy-two days of data were analyzed for evidence of solar p modes in the frequency range 1800 to 4776 micro-Hz. Noise generated by the earth's atmosphere was reduced by scaling the Fourier amplitude computed from the infrared signal and subtracting it from the Fourier amplitude computed from the visible signal. A superimposed frequency analysis was then performed which revealed approximately 2 sigma peaks within 0.3 micro-Hz of symmetry-allowed locations, while no excess power was detected at the symmetry-forbidden frequencies. The probability of obtaining by chance the observed excess power density at symmetry-allowed frequencies and deficit of power density at symmetry-forbidden frequencies was computed to be 6.9 x 10(exp -3). Correcting the frequencies for solar-cycle variations, the probability was reduced to 2.9 x 10(exp -4). These results indicate that it is quite unlikely that the observed symmetry properties have occurred by chance, and support the hypothesis that solar normal-mode signals are manifested in the data. The amplitudes l prime/l(sub 0) averaged over radial order n of the $l = 0$ and $l = 2$, $m = 0$ modes were found to be (7.54 +/- 0.54) x 10(exp -7) and (7.68 +/- 0.56) x 10(exp -7), respectively. These results are about a factor of two smaller than the amplitude of total irradiance oscillations measured from space. While the rotational splitting of the $l = 2$ multiplet appears to be consistent

with that reported by Hill, results for l = 1 and l = 3 are inconclusive.
Dissert. Abstr.

N94-31491# Midwest Research Inst., Golden, CO. National Renewable Energy Lab.
USERS MANUAL FOR SERI QC SOFTWARE ASSESSING THE QUALITY OF SOLAR RADIATION DATA
Dec. 1993 201 p
(Contract DE-AC02-83CH-10093)
(DE93-018210; NREL/TP-463-5608) Avail: CASI HC A10/MF A03

This manual describes the procedures and software for assessing the quality of solar radiation data. This does not constitute quality control because quality control must take place during the preparations for data collection (selection, calibration, and installation of instruments), during the measurement process, and during the transmission (if any) and recording of the numerical values. Once the data are recorded, only quality assessment can be performed. If quality assessment is performed in real time or soon after the measurement process is completed, it can provide input to control the quality of future measurements. Furthermore, quality assessment can be used for quality control if data judged to be bad are deleted and/or modified. We do not subscribe to these actions because the deletion or modification of data destroys information that might be useful to the user. For example, if an instrument has gone through a gradual failure and all of the data that fail quality assessment criteria are deleted or modified, the user of the data may not be able to detect what was happening and will not question the accuracy of other data collected before the instrument completely failed. Therefore, the SERI QC procedures and software do not delete or modify data. Instead, flags are set to inform the user of any departure of the data from expected values. These flags indicate the magnitude and direction of such departures. For the flags to communicate as much information as possible, this manual attempts to identify and explain the probable causes of various flags. However, we cannot overemphasize the following: Flags only indicate that data do or do not fall within expected ranges. This does not mean that the data are or are not valid. DOE

N94-31595 National Oceanic and Atmospheric Administration, Boulder, CO. Space Environment Lab.
SOLAR PHYSICS AND TERRESTRIAL EFFECTS. A CURRICULUM GUIDE FOR TEACHERS, GRADE 7-12
Roger P. Briggs (Boulder Valley Public Schools, CO.), Robert J. Carlisle (Boulder Valley Public Schools, CO.), and Barbara B. Poppe Dec. 1993 100 p Limited Reproducibility: More than 20% of this document may be affected by microfiche quality
(PB94-142247) Avail: Issuing Activity (National Technical Information Service (NTIS))

The guide consists of three main parts: a short textbook, a hands-on activity guide, and resource listings. The textbook should provide the necessary background in solar physics for teachers. It could also be used by students, but is written largely at an adult level and therefore may not be easily understood by younger students. Problems for more advanced students are included at the end of each of the four sections and answers to the problems are given at the end of the section. The activity section offers ideas for hands-on experiences that can be done in the classroom, using materials that are cheap and easily available. Background information is available in the text for the activities. The resources and references section contains a wealth of further possibilities for exploring solar-terrestrial physics, including software, telecommunications, books, and supplies.
NTIS

N94-31632# California Univ., Berkeley. Lawrence Berkeley Lab.
COLLECTIVE ACCELERATION IN SOLAR FLARES
W. Barletta, A. M. Sessler, M. Xie, S. S. Gershtein, V. Krishan, and M. Reiser Nov. 1993 7 p Presented at the International Workshop on Acceleration and Radiation Generation in Space and Laboratory Plasmas, Kardmall, Greece, 10 Aug. - 4 Sep. 1993
(Contract DE-AC03-76SF-00098)
(DE94-006288; LBL-34842; CONF-9308206-2) Avail: CASI HC A02/MF A01

Solar flare data are examined with an eye to seeing if they suggest collective acceleration of ions. That, in fact, seems to be the case. The collective acceleration mechanism of Gershtein is reviewed, and the possibilities of the mechanism are discussed. DOE

N94-31792 Cornell Univ., Ithaca, NY.
THEORETICAL STUDIES OF MAGNETOHYDRODYNAMIC EQUILIBRIA AND DYNAMICS OF A SOLAR CORONAL LOOP Ph.D. Thesis
Dana Warfield Longcope 1993 355 p
Avail: Univ. Microfilms Order No. DA9318794

This work is concerned with the time evolution, both quasistatic and dynamical, of the magnetic fields in the solar corona, and its implications for the problem of solar coronal heating. A theoretical study is made of a collection of closed magnetic flux tubes whose footpoints are subject to slow, complicated photospheric displacements. A simple model is developed in which the effects of gravitation and curvature are ignored and the flux tubes are assumed to be long and thin. The governing equations for this model are those of nonideal reduced magnetohydrodynamics. A formalism is developed for isolating the purely quasistatic component of the system's evolution. Analytic calculations are carried out using this formalism to investigate the development of small-scale magnetic structure resulting from the footpoint motions, called a magnetic cascade. Furthermore the formalism admits a scenario whereby quasistatic evolution is interrupted by spontaneous dynamical behavior. This occurs when the present equilibrium is neutrally stable to a current driven MHD instability. The nonideal equations are solved under conditions of slow, continuous, random driving using a time dependent three dimensional computer code. The system is found to achieve a statistical steady state in which the electromechanical work done by the driving is balanced by ohmic and viscous dissipation. The most evident spatial features of these solutions are three dimensional current sheets which develop spontaneously in the interior. These are analyzed using Sweet-Parker reconnection theory. The global properties of the statistical steady state can be explained in terms of these current sheets. It is proposed that the observed current sheets develop when the present MHD equilibrium becomes unstable to current driven instabilities. At such a point the system would relax abruptly to a new equilibrium with lower magnetic energy, thereby liberating its excess energy as heat. A picture of this process is presented in terms of a greatly simplified low-dimensional analog of the reduced MHD system. This low-dimensional system is evolved numerically for long times and found to exhibit relaxations of varying amplitudes at random intervals. The statistical distribution of these events is compared to similar distributions observed in the solar corona. Dissert. Abstr.

N94-32343 Hawaii Univ., Honolulu. Inst. for Astronomy.
STEPS TOWARD UNDERSTANDING THE SOLAR DYNAMO Annual Report, 1 Feb. 1992 - 31 Jul. 1993
Barry LaBonte 31 Jul. 1993 18 p Limited Reproducibility: More than 20% of this document may be affected by microfiche quality
(Grant AF-AFOSR-0116-90)
(AD-A277398; AFOSR-94-0098TR) Avail: CASI HC A03

Progress has been made toward solving the problem of the solar dynamo. The flux tube dynamo has been defined as a promising model for future investigation. Surface solar magnetic fields have been observed to determine whether electric currents carried by the fields can yield information about the dynamo region. Observational tools have been developed to probe the internal solar magnetic fields. DTIC

N94-33047*# Iowa Univ., Iowa City. Dept. of Physics and Astronomy.
A COMPREHENSIVE ANALYSIS OF ELECTRON CONICAL DISTRIBUTIONS FROM MULTI-SATELLITE DATABASES Final Report
J. Douglas Menietti 1993 27 p
(Grant NAG5-2102; U-of-I Proj. 14251600)
(NASA-CR-195848; NAS 1.26:195848) Avail: CASI HC A03/MF A01

This report consists of a copy of a paper that has been submitted to the 'Journal of Geophysical Research', entitled 'DE 1 and Viking Observations Associated With Electron Conical Distributions,' and an abstract of another paper (included as an appendix to the report) that is about to be submitted to the same journal entitled 'Perpendicular Electron Heating by Absorption of Auroral Kilometric Radiation.' A bibliography of other papers that have been published as a result of this project follows. The purpose of this project was to use the DE 1 and Viking particle and wave data to better understand the source mechanism of electron conical distributions. We have shown that electron conics are often associated with upper hybrid

waves in the nightside auroral region. We have also shown that electron conics are observed near auroral kilometric radiation (AKR) source regions and may be the result of perpendicular heating due to waves. We have completed a statistical study of electron conics observed by DE-I and Viking. The study shows the occurrence frequency and location of electron conical distributions; there are some differences between the results of DE and Viking perhaps due to different regions sampled. Derived from text

N94-33080# Instituto de Pesquisas Espaciais, Sao Jose dos Campos (Brazil).
HIGH SENSITIVITY AND RESOLUTION DECIMETRIC SPECTROSCOPE: PRELIMINARY ANALYSIS OF SOLAR BURSTS M.S. Thesis
Francisco Carlos Roc Fernandes Jun. 1992 146 p In PORTUGESE (INPE-5537-TDI/525) Avail: CASI HC A07/MF A02

High sensitivity radio spectroscope in conjunction with a 9 meter diameter polar mounted antenna has been put into regular operation since December 1990. Spectroscope operates over band of 1600 +/- 100 MHz with high time (20-100 ms) and frequency (0.3-3 MHz) resolution. The data is recorded on 35 mm black and white film and is digitized. Characteristics of the antenna at various elevations and that of spectroscope are described in detail. Limitations of the existing spectroscope and near future plans are also presented. Up to January 1992, about 162 groups of solar bursts have been recorded by this spectroscope. They have been classified in two major categories: microwave and decimetric bursts, generated due to gyrosynchrotron and beam plasma interactions, respectively. Preliminary characteristics of 44 groups of the decimetric bursts, such as of the observed flux, total duration, and excitation and decay time, have suggested that they are likely to be decimetric type 3 bursts and are generated at the second harmonic by beam plasma interaction. Estimated beam density is of the order of 10(exp 4) cm(exp -3). Author (revised)

N94-31130*# Rice Univ., Houston, TX. Dept. of Space Physics and Astronomy.
CONVECTIVE SOLAR NEBULA Abstract Only
C. MeirellesFilho and M. Reyes-Ruiz *In* Lunar and Planetary Inst., Workshop on Physics of Accretion Disks Around Compact and Young Stars 1994 p 4 (For primary document see N94-31116 09-90)
Avail: CASI HC A01/MF A01

93 SPACE RADIATION

Includes cosmic radiation; and inner and outer earth's radiation belts.

For biological effects of radiation see *52 Aerospace Medicine*. For theory see *73 Nuclear and High-Energy Physics*.

N94-31101*# Alaska Univ., Fairbanks. Geophysical Inst.
THEORY, IMAGE SIMULATION, AND DATA ANALYSIS OF CHEMICAL RELEASE EXPERIMENTS Final Report, 1 Feb. 1990 - 31 Jan. 1994
Eugene M. Wescott 26 Apr. 1994 70 p Original contains color illustrations
(Grant NAG6-1)
(NASA-CR-194865; NAS 1.26:194865) Avail: CASI HC A04/MF A01; 2 functional color pages

The final phase of Grant NAG6-1 involved analysis of physics of chemical releases in the upper atmosphere and analysis of data obtained on previous NASA sponsored chemical release rocket experiments. Several lines of investigation of past chemical release experiments and computer simulations have been proceeding in parallel. This report summarizes the work performed and the resulting publications. The following topics are addressed: analysis of the 1987 Greenland rocket experiments; calculation of emission rates for barium, strontium, and calcium; the CRIT 1 and 2 experiments (Collisional Ionization Cross Section experiments); image calibration using background stars; rapid ray motions in ionospheric plasma clouds; and the NOONCUSP rocket experiments. For individual titles, see N94-31102 through N94-31102.

N94-31102*# Rice Univ., Houston, TX. Dept. of Space Physics and Astronomy.
CONVECTION AND ELECTRODYNAMIC SIGNATURES IN THE VICINITY OF A SUN-ALIGNED ARC: RESULTS FROM THE POLAR ACCELERATION REGIONS AND CONVECTION STUDY (POLAR ARCS)
L. A. Weiss, E. J. Weber, P. H. Reiff, J. R. Sharber, J. D. Winningham, F. Primdahl, I. S. Mikkelsen, C. Seifring, and Eugene M. Wescott *In* Alaska Univ., Theory, Image Simulation, and Data Analysis of Chemical Release Experiments 26 Apr. 1994 12 p Repr. from Auroral Plasma Dynamics Geophysical Monograph 80 (American Geophysical Union), 1993 p 69-80 (For primary document see N94-31101 09-93)
(Grants NAGw-1655; AF-AFOSR-0203-87; NSF ATM-91-03440)
Copyright Avail: CASI HC A03/MF A01; 2 functional color pages

An experimental campaign designed to study high-latitude auroral arcs was conducted in Sondre Stromfjord, Greenland, on February 26, 1987. The Polar Acceleration Regions and Convection Study (Polar ARCS) consisted of a coordinated set of ground-based, airborne, and sounding rocket measurements of a weak, sun-aligned arc system within the duskside polar cap. A rocket-borne barium release experiment, two DMSP satellite overflights, all-sky photography, and incoherent scatter radar measurements provided information on the large-scale plasma convection over the polar cap region while a second rocket instrumented with a DC magnetometer, Langmuir and electric field probes, and an electron spectrometer provided measurements of small-scale electrodynamics. The large-scale data indicate that small, sun-aligned precipitation events formed within a region of antisunward convection between the duskside auroral oval and a large sun-aligned arc further poleward. This convection signature, used to assess the relationship of the sun-aligned arc to the large-scale magnetospheric configuration, is found to be consistent with either a model in which the arc formed on open field lines on the dusk side of a bifurcated polar cap or on closed field lines threading an expanded low-latitude boundary layer, but not a model in which the polar cap arc field lines map to an expanded plasma sheet. The antisunward convection signature may also be explained by a model in which the polar cap arc formed on long field lines recently reconnected through a highly skewed plasma sheet. The small-scale measurements indicate the rocket passed through three narrow (less than 20 km) regions of low-energy (less than 100 eV) electron precipitation in which the electric and magnetic field perturbations were well correlated. These precipitation events are shown to be associated with regions of downward Poynting flux and small-scale upward and downward field-aligned currents of 1-2 micro-A/sq m. The paired field-aligned currents are associated with velocity shears (higher and lower speed streams) embedded in the region of antisunward flow. Author

N94-31103 Massachusetts Inst. of Tech., Cambridge.
THEORETICAL STUDIES OF X RAY EMISSION FROM CLUSTERS OF GALAXIES Ph.D. Thesis
John C. Tsai 1992
Avail: Issuing Activity (MIT Libraries, Rm. 14-0551, Cambridge, MA 02139-4307)

We have studied X-ray emission from clusters of galaxies by adopting two complementary approaches. The first consists of a detailed analysis of the available data on a single cluster. For this we have chosen to study the gas around M87 because it is the best observed cluster X-ray source and because all of the data have hitherto not been considered simultaneously. The second approach consists of studying the X-ray emission from a simulated cluster of galaxies. For this, we have used the cluster simulation of Katz & White. We have tested the CDM theory of structure formation by analyzing the nature of the cluster gas and by comparing the simulated cluster to real clusters. The cluster has also been used to test the accuracy of the standard deprojection technique used by observers to extract the cluster mass profile. We have reached the following conclusions concerning the intracluster gas around M87. First, the available data cannot be adequately modeled with density and temperature profiles that are single valued functions of radius (a single phase model). Because of this, we have investigated two multi-phase medium models. The first is the local timescale model of White & Sarazin and the second is an ad hoc power law model where the rate at which mass drops out of the ambient (single phase) medium is simply a power law in radius. We find that the models of White & Sarazin provide an improved fit to the data, whereas the power law model does not. This implies both that the data require

mass to be dropping out of the ambient medium and that the dropout rate is well parameterized by the local timescale model. The inferred mass accretion rates are consistent with previous determinations. The putative identification of absorption above the Galactic value from SSS data is not confirmed by our analysis. Moreover, we find that data from the SSS are inconsistent with those of the Einstein Observatory HRI and FPCS. Finally we study a self-consistent model where the gas that drops out of the flow in the local timescale model becomes X-ray absorbing gas.
Dissert. Abstr.

N94-31635 California Univ., Berkeley. Lawrence Berkeley Lab.
VARIOUS MAGNET OPTIONS FOR DELTA LAUNCHED VERSION OF ASTROMAG
M. A. Green Jul. 1993 7 p Presented at the International Cryogenic Engineering Conference and International Cryogenic Materials Conference, Albuquerque, NM, 12-16 Jul. 1993 Limited Reproducibility: More than 20% of this document may be affected by microfiche quality
(Contract DE-AC03-76SF-00098)
(DE94-006292; LBL-35003; CONF-930703-43) Avail: CASI HC A02

This report compares various superconducting magnet options for use in a particle astrophysics experiment to be launched with a Delta rocket into a sun synchronous orbit and an earth trailing solar orbit. The goals of the experiment are to study the incidence of anti particles coming from deep space and to study populations of light nuclei (up to atomic number 8) and gamma rays from deep space. The proposed superconducting coils, which would be made with an aluminum stabilized niobium titanium superconductor, would be cooled using stored superfluid helium. Both a sun synchronous orbit and an earth trailing solar orbit permit one to shield the magnetic and cryogen vessel behind the solar panels. This permits one to reduce the temperature of the cryostat outer vessel which results in an increased cryogen lifetime for the experiment. A number of superconducting coil and cryostat options were looked at in terms of total magnetic and cryostat mass, cryogen life time, complexity, and overall particle astrophysics capability for the attached detectors. DOE

N94-31709# Royal Military Coll. of Canada, Kingston (Ontario).
NEUTRON MEASUREMENTS AT THE COMMERCIAL AIRCRAFT ALTITUDES M.S. Thesis
Richard Kosierb Apr. 1993 207 p
(ISBN-0-315-86201-7; CTN-94-61185) Copyright Avail: Micromedia Ltd., Technical Information Centre, 240 Catherine Street, Suite 305, Ottawa, Ontario, K2P 2G8, Canada HC/MF

To provide more complete information of the neutron component of the galactic cosmic ray field at aircraft altitudes, an investigation was conducted in which a group of Air Canada and Air France pilots routinely carried neutron bubble detectors on their normal flight duties for a period of about one year. Each pilot carried one dosimeter, activating it on takeoff and resetting it on landing. A data base of over 600 flights was obtained. This work yielded measurements of the fast neutron flux of 1.436 to 2.259 neutrons per square cm per second (ncms) for the Air Canada and 2.033 to 2.909 ncms for the Air France flights. In addition, the pilots typically experienced an annual total dose equivalent (including neutrons and gamma rays) of 3.1 to 3.9 millisieverts per year. These results are found to be in agreement with other experimental and theoretical work. Consequently, the total dose equivalent experienced by the air crew is clearly above the new recommended dose limit of one millisievert per year for the general public, which would classify the flight crews in the same category as an atomic radiation worker. Author (CISTI)

N94-31890 Colorado Univ., Boulder.
RADIO EMISSION FROM PRE-MAIN-SEQUENCE STARS Ph.D. Thesis
Stephen Lee Skinner 1992 258 p
Avail: Univ. Microfilms Order No. DA9318135

This study focuses on the properties and physical origin of radio continuum emission from pre-main-sequence (PMS) stars. These are young stars, typically less than a few million years old, and are still in a phase of gravitational contraction that will ultimately be halted by the onset of hydrogen burning in their cores. First, I address the question of the origin of centimeter continuum emission in intermediate mass (approx. equal to 3-20 solar mass) PMS stars, the so-called 'Herbig Ae/Be stars'. A high-sensitivity radio survey of 57 such stars was undertaken using the Very Large Array and Australia Telescope, resulting in the detection of twelve stars. These observations provide a homogenous data base consisting of information on source sizes, radio luminosities, variability timescales, circular polarization, and spectral energy distributions in the wavelength range 2-20 cm. Using these data along with previously published spectroscopy, I conclude that centimeter radio emission from Herbig Ae/Be stars is predominantly thermal and in many cases wind-related. An unexpected result of the above program was the serendipitous detection of circularly polarized radio emission in the low mass (approx. equal to 1 solar mass) PMS star Hubble 4, a member of the class of 'weak-lined T Tauri stars' (WTTS). This provides some of the most convincing evidence to date for the existence of ordered magnetic fields in WTTS. In a second observing program, I have searched for evidence of cold (less than or equal to 50 K) circumstellar dust around WTTS, which might exist in the form of remnant disks. Of the sixteen WTTS that were observed in the wavelength range 450-1100 microns using the James Clerk Maxwell Telescope, only V836 Tau was detected. Its spectral energy distribution longward of 10 microns is consistent with that expected for a flat, axisymmetric circumstellar disk of mass approx. equal to 0.04 solar mass (= 42 Jupiter masses). This star may be a rare example of an object in which disk dispersal is underway, but not yet complete. Dissert. Abstr.

N94-31900 California Univ., Irvine.
A SEARCH FOR 100 TeV GAMMA RAY EMISSION FROM THE X RAY BINARY PULSAR 4U 0115+63 USING THE CYGNUS EXTENSIVE AIR-SHOWER ARRAY Ph.D. Thesis
Dimitris E. Alexandreas 1992 84 p
Avail: Univ. Microfilms Order No. DA9317861

A search has been performed for unpulsed and pulsed ultra high energy gamma ray emission from the x ray transient binary pulsar 4U 0115+63 over timescales ranging from one source-day to the entire data set. The motivation has been the detection at TeV energies of 4U 0115+63 by the Cerenkov telescope at Dugway, operated by the University Durham. The search has been performed in the database of the CYGNUS 1 extensive air-shower array that extends from April 1986 to March 1992 and contains 17,000 hours of data from the source direction. In the search for unpulsed emission, the background is estimated by creating random events from the actually detected data set, and the Li and Ma statistic is used to evaluate the statistical significance of a background fluctuation. The Rayleigh test and its power are employed in the search for pulsed emissions. No statistically significant evidence for emission can be found. No correlation with its 24-day orbital period can be seen. A 90 percent confidence level upper limit on the unpulsed continuous flux from 4U 0115+63 above 130 TeV is 7.0 x 10(exp -15) cm(exp -2) s(exp -1). This value agrees with that of the Whipple collaboration but is at least one order of magnitude lower than other upper limits or claimed detections. Dissert. Abstr.

N94-32129# Lawrence Livermore National Lab., CA.
GAMMA-RAY OPTICAL COUNTERPART SEARCH EXPERIMENT (GROCSE)
C. Akerlof (Michigan Univ., Ann Arbor.), M. Fatuzzo (Michigan Univ., Ann Arbor.), B. Lee (Michigan Univ., Ann Arbor.), R. Bionta, A. Ledebuhr, H. S. Park, S. Barthelmy, T. Cline, and N. Gehrels 15 Dec. 1993 7 p Presented at the BATSE Gamma-Ray Burst Workshop, Huntsville, AL, 21-23 Oct. 1993
(Contract W-7405-eng-48)
(DE94-007124; UCRL-JC-114984; CONF-9310252-5) Avail: CASI HC A02/MF A01

The requirements of a gamma-ray burst optical counterpart detector are reviewed. By taking advantage of real-time notification of bursts, new instruments can make sensitive searches while the gamma-ray transient is still in progress. A wide field of view camera at Livermore National Laboratories has recently been adapted for detecting GRB optical counterparts to a limiting magnitude of 8. A more sensitive camera, capable of reaching m(sub upsilon) = 14, is under development. DOE

N94-31129*# Rice Univ., Houston, TX. Dept. of Space Physics and Astronomy.
CAN A VARIABLE ALPHA INDUCE LIMIT CYCLE BEHAVIOR AND EXPONENTIAL LUMINOSITY DECAY IN TRANSIENT SOFT X RAY SOURCES? Abstract Only
C. MeirellesFilho and Edison P. Liang *In* Lunar and Planetary Inst.,

Workshop on Physics of Accretion Disks Around Compact and Young Stars 1994 p 3-4 (For primary document see N94-31116 09-90)
Avail: CASI HC A01/MF A01

99 GENERAL

N94-31196# Advisory Group for Aerospace Research and Development, Neuilly-Sur-Seine (France).
AGARD HIGHLIGHTS 94/1, APRIL 1994
Apr. 1994 55 p
(AGARD-Highlights-94/1) Copyright Avail: CASI HC A04/MF A01

Highlights of the activities and accomplishments of the Advisory Group for Aerospace Research and Development (AGARD) during the first quarter of 1994 are discussed. Topics covered include the new AGARD chairman and the new director; the von Karman Medal for 1993; guidance and control in aerospace operations and systems; CASHE (Computer-Aided Systems Human Engineering); and aerospace research and development in Italy. Changes since the last issue of Highlights are covered in the note from the director, including the change of AGARD's concentration to strictly aerospace technology. CASI

N94-31308# Los Alamos National Lab., NM.
WORKSHOP ON ADVANCES IN SMOOTH PARTICLE HYDRODYNAMICS
C. A. Wingate and W. A. Miller 1993 418 p Presented at the Workshop on Advances in Smooth Particle Hydrodynamics, Los Alamos, NM, 21-23 Sep. 1993
(Contract W-7405-eng-36)
(DE94-006221; LA-UR-93-4375; CONF-9309337-1) Avail: CASI HC A18/MF A04

These proceedings contain viewgraphs presented at the 1993 workshop held at Los Alamos National Laboratory. Discussed topics include: negative stress, reactive flow calculations, interface problems, boundaries and interfaces, energy conservation in viscous flows, linked penetration calculations, stability and consistency of the SPH method, instabilities, wall heating and conservative smoothing, tensors, tidal disruption of stars, breaking the 10,000,000 particle limit, modelling relativistic collapse, SPH without H, relativistic KSPH avoidance of velocity based kernels, tidal compression and disruption of stars near a supermassive rotation black hole, and finally relativistic SPH viscosity and energy. DOE

N94-31523# Brookhaven National Lab., Upton, NY.
LABORATORY DIRECTED RESEARCH & DEVELOPMENT PROGRAM
G. J. Ogeka and A. J. Romano Dec. 1993 98 p
(Contract DE-AC02-76CH-00016)
(DE94-005928; BNL-52351-Rev-12/93) Avail: CASI HC A05/MF A02

At Brookhaven National Laboratory the Laboratory Directed Research and Development (LDRD) Program is a discretionary research and development tool critical in maintaining the scientific excellence and vitality of the laboratory. It is also a means to stimulate the scientific community, fostering new science and technology ideas, which is the major factor in achieving and maintaining staff excellence, and a means to address national needs, within the overall mission of the Department of Energy and Brookhaven National Laboratory. This report summarizes research which was funded by this program during fiscal year 1993. The research fell in a number of broad technical and scientific categories: new directions for energy technologies; global change; radiation therapies and imaging; genetic studies; new directions for the development and utilization of BNL facilities; miscellaneous projects. Two million dollars in funding supported 28 projects which were spread throughout all BNL scientific departments. DOE

N94-31885* National Aeronautics and Space Administration. Lewis Research Center, Cleveland, OH.
NASA SELECT YEARENDER REVIEW (Videotape)
Dec. 1992 Videotape: 3 min. 15 sec. playing time, in color, with sound
(NASA-TM-109748; NONP-VT-94-9948) Avail: CASI VHS A01/BETA A22

This video presents an overview of the accomplishments of various divisions at LeRC in 1992. The following LeRC educational outreach and LeRC research programs are summarized: the Marsville Link-Up conducted with the Cleveland Public School district; the Advanced Ducted Propeller; the world's first Large Scale Slush Hydrogen Generator; seven experiments at the Microgravity Laboratory; and the completion of the Advanced Communication Technology Satellite. CASI

N94-32420*# National Aeronautics and Space Administration, Washington, DC.
TECHNOLOGY 2003: THE FOURTH NATIONAL TECHNOLOGY TRANSFER CONFERENCE AND EXPOSITION, VOLUME 2
Michael Hackett, comp. Feb. 1994 466 p Conference held in Anaheim, CA, 7-9 Dec. 1993
(NASA-CP-3249; NAS 1.55:3249) Avail: CASI HC A20/MF A04

Proceedings from symposia of the Technology 2003 Conference and Exposition, Dec. 7-9, 1993, Anaheim, CA, are presented. Volume 2 features papers on artificial intelligence, CAD&E, computer hardware, computer software, information management, photonics, robotics, test and measurement, video and imaging, and virtual reality/simulation. For individual titles, see N94-32421 through N94-32474.

N94-32421*# National Aeronautics and Space Administration. Ames Research Center, Moffett Field, CA.
REFINING FUZZY LOGIC CONTROLLERS WITH MACHINE LEARNING **c63**
Hamid R. Berenji *In* NASA, Washington, Technology 2003: The Fourth National Technology Transfer Conference and Exposition, Volume 2 Feb. 1994 p 3-6 (For primary document see N94-32420 09-99)
Avail: CASI HC A01/MF A04

In this paper, we describe the GARIC (Generalized Approximate Reasoning-Based Intelligent Control) architecture, which learns from its past performance and modifies the labels in the fuzzy rules to improve performance. It uses fuzzy reinforcement learning which is a hybrid method of fuzzy logic and reinforcement learning. This technology can simplify and automate the application of fuzzy logic control to a variety of systems. GARIC has been applied in simulation studies of the Space Shuttle rendezvous and docking experiments. It has the potential of being applied in other aerospace systems as well as in consumer products such as appliances, cameras, and cars. Author

N94-32422*# Bureau of Mines, Tuscaloosa, AL.
A FUZZY CLASSIFIER SYSTEM FOR PROCESS CONTROL **c63**
C. L. Karr and J. C. Phillips *In* NASA, Washington, Technology 2003: The Fourth National Technology Transfer Conference and Exposition, Volume 2 Feb. 1994 p 7-16 (For primary document see N94-32420 09-99)
Avail: CASI HC A02/MF A04

A fuzzy classifier system that discovers rules for controlling a mathematical model of a pH titration system was developed by researchers at the U.S. Bureau of Mines (USBM). Fuzzy classifier systems successfully combine the strengths of learning classifier systems and fuzzy logic controllers. Learning classifier systems resemble familiar production rule-based systems, but they represent their IF-THEN rules by strings of characters rather than in the traditional linguistic terms. Fuzzy logic is a tool that allows for the incorporation of abstract concepts into rule based-systems, thereby allowing the rules to resemble the familiar 'rules-of-thumb' commonly used by humans when solving difficult process control and reasoning problems. Like learning classifier systems, fuzzy classifier systems employ a genetic algorithm to explore and sample new rules for manipulating the problem environment. Like fuzzy logic controllers, fuzzy classifier systems encapsulate knowledge in the form of production rules. The results presented in this paper demonstrate the ability of fuzzy classifier systems to generate a fuzzy logic-based process control system. Author (revised)

N94-32423*# Naval Air Warfare Center, Lakehurst, NJ. Aircraft Div.
FUZZY-NEURAL CONTROL OF AN AIRCRAFT TRACKING CAMERA PLATFORM **c63**
Dennis McGrath *In* NASA, Washington, Technology 2003: The Fourth National Technology Transfer Conference and Exposition, Volume 2 Feb. 1994 p 17-23 (For primary document see N94-32420 09-99)
Avail: CASI HC A02/MF A04

A fuzzy-neural control system simulation was developed for the control of a camera platform used to observe aircraft on final approach to an

aircraft carrier. The fuzzy-neural approach to control combines the structure of a fuzzy knowledge base with a supervised neural network's ability to adapt and improve. The performance characteristics of this hybrid system were compared to those of a fuzzy system and a neural network system developed independently to determine if the fusion of these two technologies offers any advantage over the use of one or the other. The results of this study indicate that the fuzzy-neural approach to control offers some advantages over either fuzzy or neural control alone. Author

N94-32424*# American Welding Inst., Louisville, TN.
EMPIRICAL MODELING FOR INTELLIGENT, REAL-TIME MANUFACTURE CONTROL **c63**
Xiaoshu Xu *In* NASA, Washington, Technology 2003: The Fourth National Technology Transfer Conference and Exposition, Volume 2 Feb. 1994 p 24-33 (For primary document see N94-32420 09-99)
Avail: CASI HC A02/MF A04

Artificial neural systems (ANS), also known as neural networks, are an attempt to develop computer systems that emulate the neural reasoning behavior of biological neural systems (e.g. the human brain). As such, they are loosely based on biological neural networks. The ANS consists of a series of nodes (neurons) and weighted connections (axons) that, when presented with a specific input pattern, can associate specific output patterns. It is essentially a highly complex, nonlinear, mathematical relationship or transform. These constructs have two significant properties that have proven useful to the authors in signal processing and process modeling: noise tolerance and complex pattern recognition. Specifically, the authors have developed a new network learning algorithm that has resulted in the successful application of ANS's to high speed signal processing and to developing models of highly complex processes. Two of the applications, the Weld Bead Geometry Control System and the Welding Penetration Monitoring System, are discussed in the body of this paper.
Author (revised)

N94-32425*# Naval Surface Warfare Center, Silver Spring, MD.
NEURAL NETWORK WAVELET TECHNOLOGY: A FRONTIER OF AUTOMATION **c63**
Harold Szu *In* NASA, Washington, Technology 2003: The Fourth National Technology Transfer Conference and Exposition, Volume 2 Feb. 1994 p 34-39 (For primary document see N94-32420 09-99)
Avail: CASI HC A02/MF A04

Neural networks are an outgrowth of interdisciplinary studies concerning the brain. These studies are guiding the field of Artificial Intelligence towards the, so-called, 6th Generation Computer. Enormous amounts of resources have been poured into R/D. Wavelet Transforms (WT) have replaced Fourier Transforms (FT) in Wideband Transient (WT) cases since the discovery of WT in 1985. The list of successful applications includes the following: earthquake prediction; radar identification; speech recognition; stock market forecasting; FBI finger print image compression; and telecommunication ISDN-data compression. Author

N94-32426*# Naval Command, Control and Ocean Surveillance Center, San Diego, CA. RDT&E Div.
NEW APPROACHES FOR REAL TIME DECISION SUPPORT SYSTEMS **c81**
D. Charles Hair and Kent Pickslay *In* NASA, Washington, Technology 2003: The Fourth National Technology Transfer Conference and Exposition, Volume 2 Feb. 1994 p 40-45 (For primary document see N94-32420 09-99)
Avail: CASI HC A02/MF A04

NCCOSC RDT&E Division (NRaD) is conducting research into ways of improving decision support systems (DSS) that are used in tactical Navy decision making situations. The research has focused on the incorporation of findings about naturalistic decision-making processes into the design of the DSS. As part of that research, two computer tools were developed that model the two primary naturalistic decision-making strategies used by Navy experts in tactical settings. Current work is exploring how best to incorporate the information produced by those tools into an existing simulation of current Navy decision support systems. This work has implications for any applications involving the need to make decisions under time constraints, based on incomplete or ambiguous data. Author

N94-32427*# Carnegie Group, Inc., Pittsburgh, PA.
KNOWLEDGE-BASED COMMODITY DISTRIBUTION PLANNING **c81**
Victor Saks and Ivan Johnson *In* NASA, Washington, Technology 2003: The Fourth National Technology Transfer Conference and Exposition, Volume 2 Feb. 1994 p 46-54 (For primary document see N94-32420 09-99)
Avail: CASI HC A02/MF A04

This paper presents an overview of a Decision Support System (DSS) that incorporates Knowledge-Based (KB) and commercial off the shelf (COTS) technology components. The Knowledge-Based Logistics Planning Shell (KBLPS) is a state-of-the-art DSS with an interactive map-oriented graphics user interface and powerful underlying planning algorithms. KBLPS was designed and implemented to support skilled Army logisticians to prepare and evaluate logistics plans rapidly, in order to support corps-level battle scenarios. KBLPS represents a substantial advance in graphical interactive planning tools, with the inclusion of intelligent planning algorithms that provide a powerful adjunct to the planning skills of commodity distribution planners. Author (revised)

N94-32428*# National Aeronautics and Space Administration. Ames Research Center, Moffett Field, CA.
A HYPERTEXT SYSTEM THAT LEARNS FROM USER FEEDBACK **c82**
Nathalie Mathe *In* NASA, Washington, Technology 2003: The Fourth National Technology Transfer Conference and Exposition, Volume 2 Feb. 1994 p 55-61 (For primary document see N94-32420 09-99)
Avail: CASI HC A02/MF A04

Retrieving specific information from large amounts of documentation is not an easy task. It could be facilitated if information relevant in the current problem solving context could be automatically supplied to the user. As a first step towards this goal, we have developed an intelligent hypertext system called CID (Computer Integrated Documentation). Besides providing an hypertext interface for browsing large documents, the CID system automatically acquires and reuses the context in which previous searches were appropriate. This mechanism utilizes on-line user information requirements and relevance feedback either to reinforce current indexing in case of success or to generate new knowledge in case of failure. Thus, the user continually augments and refines the intelligence of the retrieval system. This allows the CID system to provide helpful responses, based on previous usage of the documentation, and to improve its performance over time. We successfully tested the CID system with users of the Space Station Freedom requirements documents. We are currently extending CID to other application domains (Space Shuttle operations documents, airplane maintenance manuals, and on-line training). We are also exploring the potential commercialization of this technique. Author (revised)

N94-32429*# Wright Lab., Wright-Patterson AFB, OH. Avionics Directorate.
COMMON MODELING SYSTEM FOR DIGITAL SIMULATION **c61**
Rick Painter *In* NASA, Washington, Technology 2003: The Fourth National Technology Transfer Conference and Exposition, Volume 2 Feb. 1994 p 65-79 (For primary document see N94-32420 09-99)
Avail: CASI HC A03/MF A04

The Joint Modeling and Simulation System is a tri-service investigation into a common modeling framework for the development digital models. The basis for the success of this framework is an X-window-based, open systems architecture, object-based/oriented methodology, standard interface approach to digital model construction, configuration, execution, and post processing. For years Department of Defense (DOD) agencies have produced various weapon systems/technologies and typically digital representations of the systems/technologies. These digital representations (models) have also been developed for other reasons such as studies and analysis, Cost Effectiveness Analysis (COEA) tradeoffs, etc. Unfortunately, there have been no Modeling and Simulation (M&S) standards, guidelines, or efforts towards commonality in DOD M&S. The typical scenario is an organization hires a contractor to build hardware and in doing so an digital model may be constructed. Until recently, this model was not even obtained by the organization. Even if it was procured, it was on a unique platform, in a unique language, with unique interfaces, and, with the result being UNIQUE maintenance required. Additionally, the constructors of the model expended more effort in writing the 'infrastructure' of the model/simulation (e.g., user interface, database/database management system, data journalizing/archiving, graphical presentations, environment characteristics, other components in the simulation, etc.) than in producing the model of

the desired system. Other side effects include: duplication of efforts; varying assumptions; lack of credibility/validation; and decentralization in policy and execution. J-MASS provides the infrastructure, standards, toolset, and architecture to permit M&S developers and analysts to concentrate on the their area of interest. Author (revised)

N94-32430*# PDA Engineering, Santa Ana, CA.
ANALYTICAL DESIGN PACKAGE (ADP2): A COMPUTER AIDED ENGINEERING TOOL FOR AIRCRAFT TRANSPARENCY DESIGN **c61**
J. E. Wuerer, M. Gran, and T. W. Held *In* NASA, Washington, Technology 2003: The Fourth National Technology Transfer Conference and Exposition, Volume 2 Feb. 1994 p 80-92 (For primary document see N94-32420 09-99)
Avail: CASI HC A03/MF A04

The Analytical Design Package (ADP2) is being developed as a part of the Air Force Frameless Transparency Program (FTP). ADP2 is an integrated design tool consisting of existing analysis codes and Computer Aided Engineering (CAE) software. The objective of the ADP2 is to develop and confirm an integrated design methodology for frameless transparencies, related aircraft interfaces, and their corresponding tooling. The application of this methodology will generate high confidence for achieving a qualified part prior to mold fabrication. ADP2 is a customized integration of analysis codes, CAE software, and material databases. The primary CAE integration tool for the ADP2 is P3/PATRAN, a commercial-off-the-shelf (COTS) software tool. The open architecture of P3/PATRAN allows customized installations with different applications modules for specific site requirements. Integration of material databases allows the engineer to select a material, and those material properties are automatically called into the relevant analysis code. The ADP2 materials database will be composed of four independent schemas: CAE Design, Processing, Testing, and Logistics Support. The design of ADP2 places major emphasis on the seamless integration of CAE and analysis modules with a single intuitive graphical interface. This tool is being designed to serve and be used by an entire project team, i.e., analysts, designers, materials experts, and managers. The final version of the software will be delivered to the Air Force in Jan. 1994. The Analytical Design Package (ADP2) will then be ready for transfer to industry. The package will be capable of a wide range of design and manufacturing applications. Author (revised)

N94-32431*# Allied-Signal Corp., Kansas City, MO.
ASSEMBLY FLOW SIMULATION OF A RADAR **c61**
W. C. Rutherford and P. M. Biggs *In* NASA, Washington, Technology 2003: The Fourth National Technology Transfer Conference and Exposition, Volume 2 Feb. 1994 p 93-96 (For primary document see N94-32420 09-99)
(Contract DE-AC04-76DP-00613)
Avail: CASI HC A01/MF A04

A discrete event simulation model has been developed to predict the assembly flow time of a new radar product. The simulation was the key tool employed to identify flow constraints. The radar, production facility, and equipment complement were designed, arranged, and selected to provide the most manufacturable assembly possible. A goal was to reduce the assembly and testing cycle time from twenty-six weeks. A computer software simulation package (SLAM 2) was utilized as the foundation for simulating the assembly flow time. FORTRAN subroutines were incorporated into the software to deal with unique flow circumstances that were not accommodated by the software. Detailed information relating to the assembly operations was provided by a team selected from the engineering, manufacturing management, inspection, and production assembly staff. The simulation verified that it would be possible to achieve the cycle time goal of six weeks. Equipment and manpower constraints were identified during the simulation process and adjusted as required to achieve the flow with a given monthly production requirement. The simulation is being maintained as a planning tool to be used to identify constraints in the event that monthly output is increased. 'What-if' studies have been conducted to identify the cost of reducing constraints caused by increases in output requirement. Author

N94-32432*# National Aeronautics and Space Administration. Lyndon B. Johnson Space Center, Houston, TX.
CONFIG: INTEGRATED ENGINEERING OF SYSTEMS AND THEIR OPERATION **c61**
Jane T. Malin, Dan Ryan, and Land Fleming *In* NASA, Washington, Technology 2003: The Fourth National Technology Transfer Conference and Exposition, Volume 2 Feb. 1994 p 97-104 (For primary document see N94-32420 09-99)
Avail: CASI HC A02/MF A04

This article discusses CONFIG 3, a prototype software tool that supports integrated conceptual design evaluation from early in the product life cycle, by supporting isolated or integrated modeling, simulation, and analysis of the function, structure, behavior, failures and operations of system designs. Integration and reuse of models is supported in an object-oriented environment providing capabilities for graph analysis and discrete event simulation. CONFIG supports integration among diverse modeling approaches (component view, configuration or flow path view, and procedure view) and diverse simulation and analysis approaches. CONFIG is designed to support integrated engineering in diverse design domains, including mechanical and electro-mechanical systems, distributed computer systems, and chemical processing and transport systems. Author

N94-32433*# Jet Propulsion Lab., California Inst. of Tech., Pasadena.
SPACECRAFT ON-BOARD INFORMATION EXTRACTION COMPUTER (SOBIEC) **c60**
David Eisenman, Robert E. DeCaro, and David W. Jurasek *In* NASA, Washington, Technology 2003: The Fourth National Technology Transfer Conference and Exposition, Volume 2 Feb. 1994 p 107-116 (For primary document see N94-32420 09-99)
Avail: CASI HC A02/MF A04

The Jet Propulsion Laboratory is the Technical Monitor on an SBIR Program issued for Irvine Sensors Corporation to develop a highly compact, dual use massively parallel processing node known as SOBIEC. SOBIEC couples 3D memory stacking technology provided by nCUBE. The node contains sufficient network Input/Output to implement up to an order-13 binary hypercube. The benefit of this network, is that it scales linearly as more processors are added, and it is a superset of other commonly used interconnect topologies such as: meshes, rings, toroids, and trees. In this manner, a distributed processing network can be easily devised and supported. The SOBIEC node has sufficient memory for most multi-computer applications, and also supports external memory expansion and DMA interfaces. The SOBIEC node is supported by a mature set of software development tools from nCUBE. The nCUBE operating system (OS) provides configuration and operational support for up to 8000 SOBIEC processors in an order-13 binary hypercube or any subset or partition(s) thereof. The OS is UNIX (USL SVR4) compatible, with C, C++, and FORTRAN compilers readily available. A stand-alone development system is also available to support SOBIEC test and integration. Author

N94-32434*# Analex Space Systems, Inc., Cocoa Beach, FL.
PEN-BASED COMPUTERS: COMPUTERS WITHOUT KEYS **c60**
Cheryl L. Conklin *In* NASA, Washington, Technology 2003: The Fourth National Technology Transfer Conference and Exposition, Volume 2 Feb. 1994 p 117-123 (For primary document see N94-32420 09-99)
(Contract NAS10-11675)
Avail: CASI HC A02/MF A04

The National Space Transportation System (NSTS) is comprised of many diverse and highly complex systems incorporating the latest technologies. Data collection associated with ground processing of the various Space Shuttle system elements is extremely challenging due to the many separate processing locations where data is generated. This presents a significant problem when the timely collection, transfer, collation, and storage of data is required. This paper describes how new technology, referred to as Pen-Based computers, is being used to transform the data collection process at Kennedy Space Center (KSC). Pen-Based computers have streamlined procedures, increased data accuracy, and now provide more complete information than previous methods. The end results is the elimination of Shuttle processing delays associated with data deficiencies. Author

N94-32435*# Ergonomic-Interface Keyboard Systems, Inc., La Jolla, CA.
THE VERTICAL **c54**
Stephen L. Albert and Jeffrey B. Spencer *In* NASA, Washington, Technology 2003: The Fourth National Technology Transfer Conference and Exposition, Volume 2 Feb. 1994 p 124-129 (For primary document

see N94-32420 09-99)
Avail: CASI HC A02/MF A04

'THE VERTICAL' computer keyboard is designed to address critical factors which contribute to Repetitive Motion Injuries (RMI) (including Carpal Tunnel Syndrome) in association with computer keyboard usage. This keyboard splits the standard QWERTY design into two halves and positions each half 90 degrees from the desk. In order to access a computer correctly. 'THE VERTICAL' requires users to position their bodies in optimal alignment with the keyboard. The orthopaedically neutral forearm position (with hands palms-in and thumbs-up) reduces nerve compression in the forearm. The vertically arranged keypad halves ameliorate onset occurrence of keyboard-associated RMI. By utilizing visually-reference mirrored mylar surfaces adjustable to the user's eye, the user is able to readily reference any key indicia (reversed) just as they would on a conventional keyboard. Transverse adjustability substantially reduces cumulative musculoskeletal discomfort in the shoulders. 'THE VERTICAL' eliminates the need for an exterior mouse by offering a convenient finger-accessible curser control while the hands remain in the vertically neutral position. The potential commercial application for 'THE VERTICAL' is enormous since the product can effect every person who uses a computer anywhere in the world. Employers and their insurance carriers are spending hundreds of millions of dollars per year as a result of RMI. This keyboard will reduce the risk.
Author

N94-32436*# Ensco, Inc., Melbourne, FL.
A SYSTEMS APPROACH TO COMPUTER-BASED TRAINING **c61**
Gaylen W. Drape *In* NASA, Washington, Technology 2003: The Fourth National Technology Transfer Conference and Exposition, Volume 2 Feb. 1994 p 130-136 (For primary document see N94-32420 09-99)
Avail: CASI HC A02/MF A04

This paper describes the hardware and software systems approach used in the Automated Recertification Training System (ARTS), a Phase 2 Small Business Innovation Research (SBIR) project for NASA Kennedy Space Center (KSC). The goal of this project is to optimize recertification training of technicians who process the Space Shuttle before launch by providing computer-based training courseware. The objectives of ARTS are to implement more effective CBT applications identified through a need assessment process and to provide an enhanced courseware production system. The system's capabilities are demonstrated by using five different pilot applications to convert existing classroom courses into interactive courseware. When the system is fully implemented at NASA/KSC, trainee job performance will improve and the cost of courseware development will be lower. Commercialization of the technology developed as part of this SBIR project is planned for Phase 3. Anticipated spin-off products include custom courseware for technical skills training and courseware production software for use by corporate training organizations of aerospace and other industrial companies.
Author

N94-32437*# Rome Lab., Griffiss AFB, NY.
AUTOMATIC TRANSLATION AMONG SPOKEN LANGUAGES **c32**
Sharon M. Walter and Kelly Costigan *In* NASA, Washington, Technology 2003: The Fourth National Technology Transfer Conference and Exposition, Volume 2 Feb. 1994 p 139-142 (For primary document see N94-32420 09-99)
Avail: CASI HC A01/MF A04

The Machine Aided Voice Translation (MAVT) system was developed in response to the shortage of experienced military field interrogators with both foreign language proficiency and interrogation skills. Combining speech recognition, machine translation, and speech generation technologies, the MAVT accepts an interrogator's spoken English question and translates it into spoken Spanish. The spoken Spanish response of the potential informant can then be translated into spoken English. Potential military and civilian applications for automatic spoken language translation technology are discussed in this paper.
Author

N94-32438*# Idaho National Engineering Lab., Idaho Falls.
A PC PROGRAM TO OPTIMIZE SYSTEM CONFIGURATION FOR DESIRED RELIABILITY AT MINIMUM COST **c61**
Steven W. Hills and Ali S. Siahpush *In* NASA, Washington, Technology 2003: The Fourth National Technology Transfer Conference and Exposition, Volume 2 Feb. 1994 p 143-150 (For primary document see N94-32420 09-99)
Avail: CASI HC A02/MF A04

High reliability is desired in all engineered systems. One way to improve system reliability is to use redundant components. When redundant components are used, the problem becomes one of allocating them to achieve the best reliability without exceeding other design constraints such as cost, weight, or volume. Systems with few components can be optimized by simply examining every possible combination but the number of combinations for most systems is prohibitive. A computerized iteration of the process is possible but anything short of a super computer requires too much time to be practical. Many researchers have derived mathematical formulations for calculating the optimum configuration directly. However, most of the derivations are based on continuous functions whereas the real system is composed of discrete entities. Therefore, these techniques are approximations of the true optimum solution. This paper describes a computer program that will determine the optimum configuration of a system of multiple redundancy of both standard and optional components. The algorithm is a pair-wise comparative progression technique which can derive the true optimum by calculating only a small fraction of the total number of combinations. A designer can quickly analyze a system with this program on a personal computer.
Author

N94-32439*# Defense Mapping Agency Systems Center, Fairfax, VA.
EVOLVING SOFTWARE REENGINEERING TECHNOLOGY FOR THE EMERGING INNOVATIVE-COMPETITIVE ERA **c61**
Phillip Q. Hwang, Evan Lock, and Noah Prywes *In* NASA, Washington, Technology 2003: The Fourth National Technology Transfer Conference and Exposition, Volume 2 Feb. 1994 p 151-160 (For primary document see N94-32420 09-99)
Avail: CASI HC A02/MF A04

This paper reports on a multi-tool commercial/military environment combining software Domain Analysis techniques with Reusable Software and Reengineering of Legacy Software. It is based on the development of a military version for the Department of Defense (DOD). The integrated tools in the military version are: Software Specification Assistant (SSA) and Software Reengineering Environment (SRE), developed by Computer Command and Control Company (CCCC) for Naval Surface Warfare Center (NSWC) and Joint Logistics Commanders (JLC), and the Advanced Research Project Agency (ARPA) STARS Software Engineering Environment (SEE) developed by Boeing for NAVAIR PMA 205. The paper describes transitioning these integrated tools to commercial use. There is a critical need for the transition for the following reasons: First, to date, 70 percent of programmers' time is applied to software maintenance. The work of these users has not been facilitated by existing tools. The addition of Software Reengineering will also facilitate software maintenance and upgrading. In fact, the integrated tools will support the entire software life cycle. Second, the integrated tools are essential to Business Process Reengineering, which seeks radical process innovations to achieve breakthrough results. Done well, process reengineering delivers extraordinary gains in process speed, productivity and profitability. Most importantly, it discovers new opportunities for products and services in collaboration with other organizations. Legacy computer software must be changed rapidly to support innovative business processes. The integrated tools will provide commercial organizations important competitive advantages. This, in turn, will increase employment by creating new business opportunities. Third, the integrated system will produce much higher quality software than use of the tools separately. The reason for this is that producing or upgrading software requires keen understanding of extremely complex applications which is facilitated by the integrated tools. The radical savings in the time and cost associated with software, due to use of CASE tools that support combined Reuse of Software and Reengineering of Legacy Code, will add an important impetus to improving the automation of enterprises. This will be reflected in continuing operations, as well as in innovating new business processes. The proposed multi-tool software development is based on state of the art technology, which will be further advanced through the use of open systems for adding new tools and experience in their use.
Author

N94-32440*# Dakota Scientific Software, Inc., Rapid City, SD. Dept. of Computer Science.
A HIGH-SPEED LINEAR ALGEBRA LIBRARY WITH AUTOMATIC PARALLELISM **c62**
Michael L. Boucher *In* NASA, Washignton, Technology 2003: The Fourth

National Technology Transfer Conference and Exposition, Volume 2 Feb. 1994 p 161-168 (For primary document see N94-32420 09-99)
Avail: CASI HC A02/MF A04

Parallel or distributed processing is key to getting highest performance workstations. However, designing and implementing efficient parallel algorithms is difficult and error-prone. It is even more difficult to write code that is both portable to and efficient on many different computers. Finally, it is harder still to satisfy the above requirements and include the reliability and ease of use required of commercial software intended for use in a production environment. As a result, the application of parallel processing technology to commercial software has been extremely small even though there are numerous computationally demanding programs that would significantly benefit from application of parallel processing. This paper describes DSSLIB, which is a library of subroutines that perform many of the time-consuming computations in engineering and scientific software. DSSLIB combines the high efficiency and speed of parallel computation with a serial programming model that eliminates many undesirable side-effects of typical parallel code. The result is a simple way to incorporate the power of parallel processing into commercial software without compromising maintainability, reliability, or ease of use. This gives significant advantages over less powerful non-parallel entries in the market. Author

N94-32441*# University of Central Florida, Orlando. Dept. of Computer Science.
HIGH-SPEED DATA SEARCH c82
James N. Driscoll *In* NASA, Washington, Technology 2003: The Fourth National Technology Transfer Conference and Exposition, Volume 2 Feb. 1994 p 171-180 (For primary document see N94-32420 09-99)
Avail: CASI HC A02/MF A04

The high-speed data search system developed for KSC incorporates existing and emerging information retrieval technology to help a user intelligently and rapidly locate information found in large textual databases. This technology includes: natural language input; statistical ranking of retrieved information; an artificial intelligence concept called semantics, where 'surface level' knowledge found in text is used to improve the ranking of retrieved information; and relevance feedback, where user judgements about viewed information are used to automatically modify the search for further information. Semantics and relevance feedback are features of the system which are not available commercially. The system further demonstrates focus on paragraphs of information to decide relevance; and it can be used (without modification) to intelligently search all kinds of document collections, such as collections of legal documents medical documents, news stories, patents, and so forth. The purpose of this paper is to demonstrate the usefulness of statistical ranking, our semantic improvement, and relevance feedback. Author

N94-32442*# Office of Naval Research, Arlington, VA.
DATABASE TOMOGRAPHY FOR COMMERCIAL APPLICATION c82
Ronald N. Kostoff and Henry J. Eberhart *In* NASA, Washington, Technology 2003: The Fourth National Technology Transfer Conference and Exposition, Volume 2 Feb. 1994 p 181-189 (For primary document see N94-32420 09-99)
Avail: CASI HC A02/MF A04

Database tomography is a method for extracting themes and their relationships from text. The algorithms, employed begin with word frequency and word proximity analysis and build upon these results. When the word 'database' is used, think of medical or police records, patents, journals, or papers, etc. (any text information that can be computer stored). Database tomography features a full text, user interactive technique enabling the user to identify areas of interest, establish relationships, and map trends for a deeper understanding of an area of interest. Database tomography concepts and applications have been reported in journals and presented at conferences. One important feature of the database tomography algorithm is that it can be used on a database of any size, and will facilitate the users ability to understand the volume of content therein. While employing the process to identify research opportunities it became obvious that this promising technology has potential applications for business, science, engineering, law, and academe. Examples include evaluating marketing trends, strategies, relationships and associations. Also, the database tomography process would be a powerful component in the area of competitive intelligence, national security intelligence and patent analysis. User interests and involvement cannot be overemphasized.
Author (revised)

N94-32443*# Analex Space Systems, Inc., Cocoa Beach, FL.
AUTOMATED MAINFRAME DATA COLLECTION IN A NETWORK ENVIRONMENT c82
David L. Gross *In* NASA, Washington, Technology 2003: The Fourth National Technology Transfer Conference and Exposition, Volume 2 Feb. 1994 p 190-197 (For primary document see N94-32420 09-99)
Avail: CASI HC A02/MF A04

The progress and direction of the computer industry have resulted in widespread use of dissimilar and incompatible mainframe data systems. Data collection from these multiple systems is a labor intensive task. In the past, data collection had been restricted to the efforts of personnel specially trained on each system. Information is one of the most important resources an organizations has. Any improvement in an organization's ability to access and manage that information provides a competitive advantage. This problem of data collection is compounded at NASA sites by multi-center and contractor operations. The Centralized Automated Data Retrieval System (CADRS) is designed to provide a common interface that would permit data access, query, and retrieval from multiple contractor and NASA systems. The methods developed for CADRS have a strong commercial potential in that they would be applicable for any industry that needs inter-department, inter-company, or inter-agency data communications. The widespread use of multi-system data networks, that combine older legacy systems with newer decentralized networks, has made data retrieval a critical problem for information dependent industries. Implementing the technology discussed in this paper would reduce operational expense and improve data collection on these composite data systems. Author

N94-32444*# National Aeronautics and Space Administration. Marshall Space Flight Center, Huntsville, AL.
BEGINNING THE 21ST CENTURY WITH ADVANCED AUTOMATIC PARTS IDENTIFICATION (API) c82
Fred Schramm and Don Roxby *In* NASA, Washington, Technology 2003: The Fourth National Technology Transfer Conference and Exposition, Volume 2 Feb. 1994 p 198-204 (For primary document see N94-32420 09-99)
Avail: CASI HC A02/MF A04

Under the direction of the NASA George C. Marshall Space Flight Center, Huntsville, Alabama, the development and commercialization of an advanced Automated Parts Indentification (API) system is being undertaken by Rockwell International Corporation. The new API system is based on a variable sized, machine-readable, two-dimensioanl matrix symbol that can be applied directly onto most metallic and nonmetallic materials using safe, permanent marking methods. Its checkerboard-like structure is the most space efficient of all symbologies. This high data-density symbology can be applied to products of different material sizes and geometries using application-dependent, computer-driven marking devices. The high fidelity markings produced by these devices can then be captured using a specially designed camera linked to any IBM-compatible computer. Applications of compressed symbology technology will reduce costs and improve quality, productivity, and processes in a wide variety of federal and commercial applications. Author

N94-32445*# Midwest Research Inst., Golden, CO.
OPTICAL PROCESSING FOR SEMICONDUCTOR DEVICE FABRICATION c74
Bhushan L. Sopori *In* NASA, Washington, Technology 2003: The Fourth National Technology Transfer Conference and Exposition, Volume 2 Feb. 1994 p 207-215 (For primary document see N94-32420 09-99)
Avail: CASI HC A02/MF A04

A new technique for semiconductor device processing is described that uses optical energy to produce local heating/melting in the vicinity of a preselected interface of the device. This process, called optical processing, invokes assistance of photons to enhance interface reactions such as diffusion and melting, as compared to the use of thermal heating alone. Optical processing is performed in a 'cold wall' furnace, and requires considerably lower energies than furnace or rapid thermal annealing. This technique can produce some device structures with unique properties that cannot be produced by conventional thermal processing. Some applications

of optical processing involving semiconductor-metal interfaces are described. Author

N94-32446*# Midwest Research Inst., Golden, CO.
A SCANNING DEFECT MAPPING SYSTEM FOR SEMICONDUCTOR CHARACTERIZATION c74
Bushnan L. Sopori *In* NASA, Washington, Technology 2003: The Fourth National Technology Transfer Conference and Exposition, Volume 2 Feb. 1994 p 216-222 (For primary document see N94-32420 09-99)
Avail: CASI HC A02/MF A04

We have developed an optical scanning system that generates maps of the spatial distributions of defects in single and polycrystalline silicon wafers. This instrument, called Scanning Defect Mapping System, utilizes differences in the scattering characteristics of dislocation etch pits and grain boundaries from a defect-etched sample to identify and count them. This system simultaneously operates in the dislocation mode and the grain boundary (GB) mode. In the 'dislocation mode,' the optical scattering from the etch pits is used to statistically count dislocations, while ignoring the GB's. Likewise, in the 'grain boundary mode' the system only recognizes the local scattering from the GB's to generate grain boundary distributions. The information generated by this instrument is valuable for material quality control, identifying mechanisms of defect generation and the nature of thermal stresses during the crystal growth, and the solar cell process design. Author

N94-32447*# National Aeronautics and Space Administration. Marshall Space Flight Center, Huntsville, AL.
NEUTRAL ION SOURCES IN PRECISION MANUFACTURING c72
Steven C. Fawcett and Thomas W. Drueding *In* NASA, Washington, Technology 2003: The Fourth National Technology Transfer Conference and Exposition, Volume 2 Feb. 1994 p 223-232 (For primary document see N94-32420 09-99)
Avail: CASI HC A02/MF A04

Ion figuring of optical components is a relatively new technology that can alleviate some of the problems associated with traditional contact polishing. Because the technique is non contacting, edge distortions and rib structure print through do not occur. This initial investigation was aimed at determining the effect of ion figuring on surface roughness of previously polished or ductile ground ceramic optical samples. This is the first step in research directed toward the combination of a pre-finishing process (ductile grinding or polishing) with ion figuring to produce finished ceramic mirrors. The second phase of the project is focusing on the development of mathematical algorithms that will deconvolve the ion beam profile from the surface figure errors so that these errors can be successfully removed from the optical components. In the initial phase of the project, multiple, chemical vapor deposited silicon carbide (CVD SiC) samples were polished or ductile ground to specular or near-specular roughness. These samples were then characterized to determine topographic surface information. The surface evaluation consisted of stylus profilometry, interferometry, and optical and scanning electron microscopy. The surfaces, were ion machined to depths from 0-5 microns. The finished surfaces were characterized to evaluate the effects of the ion machining process with respect to the previous processing methods and the pre-existing subsurface damage. The development of the control algorithms for figuring optical components has been completed. These algorithms have been validated with simulations and future experiments have been planned to verify the methods. This paper will present the results of the initial surface finish experiments and the control algorithms simulations. Author

N94-32448*# Spire Corp., Bedford, MA. Optoelectronics Div.
HIGH POWER DIODE LASERS FOR SOLID-STATE LASER PUMPS c36
Kurt J. Linden and Patrick N. McDonnell *In* NASA, Washington, Technology 2003: The Fourth National Technology Transfer Conference and Exposition, Volume 2 Feb. 1994 p 233-245 (For primary document see N94-32420 09-99)
(Contracts NAS1-18660; NAS1-19301)
Avail: CASI HC A03/MF A04

The development and commercial application of high power diode laser arrays for use as solid-state laser pumps is described. Such solid-state laser pumps are significantly more efficient and reliable than conventional flash-lamps. This paper describes the design and fabrication of diode lasers emitting in the 780 - 900 nm spectral region, and discusses their performance and reliability. Typical measured performance parameters include electrical-to-optical power conversion efficiencies of 50 percent, narrow-band spectral emission of 2 to 3 nm FWHM, pulsed output power levels of 50 watts/bar with reliability values of over 2 billion shots to date (tests to be terminated after 10 billion shots), and reliable operation to pulse lengths of 1 ms. Pulse lengths up to 5 ms have been demonstrated at derated power levels, and CW performance at various power levels has been evaluated in a 'bar-in-groove' laser package. These high-power 1-cm stacked-bar arrays are now being manufactured for OEM use. Individual diode laser bars, ready for package-mounting by OEM customers, are being sold as commodity items. Commercial and medical applications of these laser arrays include solid-state laser pumping for metal-working, cutting, industrial measurement and control, ranging, wind-shear/atmospheric turbulence detection, X-ray generation, materials surface cleaning, microsurgery, ophthalmology, dermatology, and dental procedures. Author

N94-32449*# Lawrence Livermore National Lab., CA.
FLEXIBLE MANUFACTURING FOR PHOTONICS DEVICE ASSEMBLY c31
Shin-yee Lu, Michael D. Pocha, Oliver T. Strand, and K. David Young *In* NASA, Washington, Technology 2003: The Fourth National Technology Transfer Conference and Exposition, Volume 2 Feb. 1994 p 246-251 (For primary document see N94-32420 09-99)
(Contract W-745-eng-48)
Avail: CASI HC A02/MF A04

The assembly of photonics devices such as laser diodes, optical modulators, and opto-electronics multi-chip modules (OEMCM), usually requires the placement of micron size devices such as laser diodes, and sub-micron precision attachment between optical fibers and diodes or waveguide modulators (usually referred to as pigtailing). This is a very labor intensive process. Studies done by the opto-electronics (OE) industry have shown that 95 percent of the cost of a pigtailed photonic device is due to the use of manual alignment and bonding techniques, which is the current practice in industry. At Lawrence Livermore National Laboratory, we are working to reduce the cost of packaging OE devices through the use of automation. Our efforts are concentrated on several areas that are directly related to an automated process. This paper will focus on our progress in two of those areas, in particular, an automated fiber pigtailing machine and silicon micro-technology compatible with an automated process. Author

N94-32450*# National Aeronautics and Space Administration. Lyndon B. Johnson Space Center, Houston, TX.
APPLICATION OF DEXTEROUS SPACE ROBOTICS TECHNOLOGY TO MYOELECTRIC PROSTHESES c37
Clifford Hess, Larry C. H. Li, Kristin A. Farry, and Ian D. Walker *In* NASA, Washington, Technology 2003: The Fourth National Technology Transfer Conference and Exposition, Volume 2 Feb. 1994 p 255-268 (For primary document see N94-32420 09-99)
Avail: CASI HC A03/MF A04

Future space missions will require robots equipped with highly dexterous robotic hands to perform a variety of tasks. A major technical challenge in making this possible is an improvement in the way these dexterous robotic hands are remotely controlled or teleoperated. NASA is currently investigating the feasibility of using myoelectric signals to teleoperate a dexterous robotic hand. In theory, myoelectric control of robotic hands will require little or no mechanical parts and will greatly reduce the bulk and weight usually found in dexterous robotic hand control devices. An improvement in myoelectric control of multifinger hands will also benefit prosthetics users. Therefore, as an effort to transfer dexterous space robotics technology to prosthetics applications and to benefit from existing myoelectric technology, NASA is collaborating with the Limbs of Love Foundation, the Institute for Rehabilitation and Research, and Rice University in developing improved myoelectric control multifinger hands and prostheses. In this paper, we will address the objectives and approaches of this collaborative effort and discuss the technical issues associated with myoelectric control of multifinger hands. We will also report our current progress and discuss plans for future work. Author

N94-32451*# Naval Surface Warfare Center, Panama City, FL.
NAVY OMNI-DIRECTIONAL VEHICLE (ODV) DEVELOPMENT PROGRAM c37

Hillery McGowen *In* NASA, Washington, Technology 2003: The Fourth National Technology Transfer Conference and Exposition, Volume 2 Feb. 1994 p 269-278 (For primary document see N94-32420 09-99)
Avail: CASI HC A02/MF A04

The Omni-Directional Vehicle (ODV) development program sponsored by the Office of Naval Research at the Coastal Systems Station has investigated the application of ODV technology for use in the Navy shipboard environment. ODV technology as originally received by the Navy in the form of the Cadillac-Gage Side Mover Vehicle was applicable to the shipboard environment with the potential to overcome conditions of reduced traction, ship motion, decks heeled at high angles, obstacles, and confined spaces. Under the Navy program, ODV technology was investigated and a series of experimental vehicles were built and successfully tested under extremely demanding conditions. The ODV drive system has been found to be applicable to autonomous, remotely, or manually operated vehicles. Potential commercial applications include multi-directional forklift trucks, automatic guided vehicles employed in manufacturing environments, and remotely controlled platforms used in nuclear facilities or for hazardous waste clean up tasks. Author

N94-32452*# Jet Propulsion Lab., California Inst. of Tech., Pasadena.
APPLYING ROBOTICS TO HAZMAT **c37**
Richard V. Welch and Gary O. Edmonds *In* NASA, Washington, Technology 2003: The Fourth National Technology Transfer Conference and Exposition, Volume 2 Feb. 1994 p 279-287 (For primary document see N94-32420 09-99)
Avail: CASI HC A02/MF A04

The use of robotics in situations involving hazardous materials can significantly reduce the risk of human injuries. The Emergency Response Robotics Project, which began in October 1990 at the Jet Propulsion Laboratory, is developing a teleoperated mobile robot allowing HAZMAT (hazardous materials) teams to remotely respond to incidents involving hazardous materials. The current robot, called HAZBOT III, can assist in locating characterizing, identifying, and mitigating hazardous material incidents without risking entry team personnel. The active involvement of the JPL Fire Department HAZMAT team has been vital in developing a robotic system which enables them to perform remote reconnaissance of a HAZMAT incident site. This paper provides a brief review of the history of the project, discusses the current system in detail, and presents other areas in which robotics can be applied removing people from hazardous environments/operations. Author

N94-32453*# Jet Propulsion Lab., California Inst. of Tech., Pasadena.
ADVANCED TELEOPERATION: TECHNOLOGY INNOVATIONS AND APPLICATIONS **c54**
Paul S. Schenker, Antal K. Bejczy, and Won S. Kim *In* NASA, Washington, Technology 2003: The Fourth National Technology Transfer Conference and Exposition, Volume 2 Feb. 1994 p 288-292 (For primary document see N94-32420 09-99)
Avail: CASI HC A01/MF A04

The capability to remotely, robotically perform space assembly, inspection, servicing, and science functions would rapidly expand our presence in space, and the cost efficiency of being there. There is considerable interest in developing 'telerobotic' technologies, which also have comparably important terrestrial applications to health care, underwater salvage, nuclear waste remediation and other. Such tasks, both space and terrestrial, require both a robot and operator interface that is highly flexible and adaptive, i.e., capable of efficiently working in changing and often casually structured environments. One systems approach to this requirement is to augment traditional teleoperation with computer assists -- advanced teleoperation. We have spent a number of years pursuing this approach, and highlight some key technology developments and their potential commercial impact. This paper is an illustrative summary rather than self-contained presentation; for completeness, we include representative technical references to our work which will allow the reader to follow up items of particular interest. Author

N94-32454*# Axiomatics Corp., Woburn, MA.
CONTINUOUS MEASUREMENT OF AIRCRAFT WING ICING **c03**
Stephen S. C. Yao *In* NASA, Washington, Technology 2003: The Fourth National Technology Transfer Conference and Exposition, Volume 2 Feb. 1994 p 295-300 (For primary document see N94-32420 09-99)
Avail: CASI HC A02/MF A04

Ice formation on the wings of aircraft is a problem that has plagued air travel since its inception. Several recent incidents have been attributed to ice formation on the lifting surfaces of wings. This paper describes a SBIR Phase 1 research effort on the use of small flat dielectric sensors in detecting a layer of ice above the sensor. The sensors are very small, lightweight, and inexpensive. The electronics package that controls the sensor is also small, and could be even smaller using commonly available miniaturization technologies. Thus, several sensors could be placed on a surface such that a representative ice thickness profile could be measured. The benefits offered by developing this technology go beyond the safety improvements realized by monitoring ice formation on the wings of an aircraft. Continuous monitoring of anti-icing fluid concentrations on the ground would warn the pilot of impending fluid failure as well as allowing the stations to use less de-icing solution per aircraft. This in turn would increase the safety of takeoffs and reduce the overall discharge of de-icing solution into the environment, thus reducing the biohazard of the de-icing procedure. Author

N94-32455*# National Aeronautics and Space Administration. Lyndon B. Johnson Space Center, Houston, TX.
ELECTROMAGNETIC PROBE TECHNIQUE FOR FLUID FLOW MEASUREMENTS **c34**
G. D. Arndt and J. R. Carl *In* NASA, Washington, Technology 2003: The Fourth National Technology Transfer Conference and Exposition, Volume 2 Feb. 1994 p 301-310 (For primary document see N94-32420 09-99)
Avail: CASI HC A02/MF A04

The probes described herein, in various configurations, permit the measurement of the volume fraction of two or more fluids flowing through a pipe. Each probe measures the instantaneous relative dielectric constant of the fluid in immediate proximity. As long as separation of the relative dielectric constant of the fluid is possible, several or even many fluids can be measured in the same flow stream. By using multiple probes, the velocity of each fluid can generally be determined as well as the distribution of each constituent in the pipe. The values are determined by statistical computation. There are many potential applications for probes of this type in industry and government. Possible NASA applications include measurements of helium/hydrazine flow during rocket tests at White Sands, liquid/gas flow in hydrogen or oxygen lines in Orbiter engines, and liquid/gaseous Freon flow in zero gravity tests with the KS135 aircraft at JSC. Much interest has been shown recently by the oil industry. In this a good method is needed to measure the fractions of oil, water, and natural gas flowing in a pipeline and the velocity of each. This particular problem involves an extension of what has been developed to date and our plans to solve this problem will be discussed herein. Author

N94-32456*# Army Armament Munitions and Chemical Command, Watervliet, NY. Benet Labs.
COMPUTERIZED ULTRASONIC TESTING SYSTEM (CUTS) FOR IN-PROCESS THICKNESS DETERMINATION **c71**
J. Frankel, M. Doxbeck, S. C. Schroeder, and A. Abbate *In* NASA, Washington, Technology 2003: The Fourth National Technology Transfer Conference and Exposition, Volume 2 Feb. 1994 p 311-317 (For primary document see N94-32420 09-99)
Avail: CASI HC A02/MF A04

A Computerized Ultrasonic Testing System (CUTS) was developed to measure, in real-time, the rate of deposition and thickness of chromium plated on the inside of thick steel tubes. The measurements are made from the outside of the tubes with the ultrasonic pulse-echo technique. The resolution of the system is 2.5 micron. (0.0001 in.) and the accuracy is better than 10 micron (0.0004 in.). The thickness is measured using six transducers mounted at different locations on the tube. In addition, two transducers are mounted on two reference standards, thereby allowing the system to be continuously calibrated. The tube temperature varies during the process, thus the input from eight thermocouples, located at the measurement sites, is used to calculate and compensate for the change in return time of the ultrasonic echo due to the temperature dependence of the sound velocity. CUTS is applicable to any commercial process where real-time change of thickness of a sample has to be known, with

the advantage of facilitating increased efficiency and of improving process control. Author

N94-32457*# National Aeronautics and Space Administration. Lyndon B. Johnson Space Center, Houston, TX.

MICROWAVE SENSOR FOR ICE DETECTION c06

G. D. Arndt, A. Chu, L. G. Stolarczyk, and G. L. Stolarczyk *In* NASA, Washington, Technology 2003: The Fourth National Technology Transfer Conference and Exposition, Volume 2 Feb. 1994 p 318-325 (For primary document see N94-32420 09-99)

Avail: CASI HC A02/MF A04

A microwave technique has been developed for detecting ice build-up on the wing surfaces of commercial airliners and highway bridges. A microstrip patch antenna serves as the sensor, with changes in the resonant frequency and impedance being dependent upon the overlying layers of ice, water and glycol mixtures. The antenna sensor is conformably mounted on the wing. The depth and dielectric constants of the layers are measured by comparing the complex resonant admittance with a calibrated standard. An initial breadboard unit has been built and tested. Additional development is now underway. Another commercial application is in the robotics field of remote sensing of coal seam thickness. Author

N94-32458*# National Aeronautics and Space Administration. Goddard Space Flight Center, Greenbelt, MD.

A VERSATILE NONDESTRUCTIVE EVALUATION IMAGING WORKSTATION c38

E. James Chern and David W. Butler *In* NASA, Washington, Technology 2003: The Fourth National Technology Transfer Conference and Exposition, Volume 2 Feb. 1994 p 326-331 (For primary document see N94-32420 09-99)

Avail: CASI HC A02/MF A04

Ultrasonic C-scan and eddy current imaging systems are of the pointwise type evaluation systems that rely on a mechanical scanner to physically maneuver a probe relative to the specimen point by point in order to acquire data and generate images. Since the ultrasonic C-scan and eddy current imaging systems are based on the same mechanical scanning mechanisms, the two systems can be combined using the same PC platform with a common mechanical manipulation subsystem and integrated data acquisition software. Based on this concept, we have developed an IBM PC-based combined ultrasonic C-scan and eddy current imaging system. The system is modularized and provides capacity for future hardware and software expansions. Advantages associated with the combined system are: (1) eliminated duplication of the computer and mechanical hardware, (2) unified data acquisition, processing and storage software, (3) reduced setup time for repetitious ultrasonic and eddy current scans, and (4) improved system efficiency. The concept can be adapted to many engineering systems by integrating related PC-based instruments into one multipurpose workstation such as dispensing, machining, packaging, sorting, and other industrial applications. Author

N94-32459*# National Aeronautics and Space Administration. Goddard Space Flight Center, Greenbelt, MD.

A NEW HIGH-SPEED IR CAMERA SYSTEM c35

Jeffrey W. Travis, Peter K. Shu, Murzy D. Jhabvala, Michael S. Kasten, Samuel H. Moseley, Sean C. Casey, Lawrence K. McGovern, Philip J. Luers, Philip W. Dabney, and Ravi C. Kaipa et al *In* NASA, Washington, Technology 2003: The Fourth National Technology Transfer Conference and Exposition, Volume 2 Feb. 1994 p 332-341 (For primary document see N94-32420 09-99)

Avail: CASI HC A02/MF A04

A multi-organizational team at the Goddard Space Flight Center is developing a new far infrared (FIR) camera system which furthers the state of the art for this type of instrument by the incorporating recent advances in several technological disciplines. All aspects of the camera system are optimized for operation at the high data rates required for astronomical observations in the far infrared. The instrument is built around a Blocked Impurity Band (BIB) detector array which exhibits responsivity over a broad wavelength band and which is capable of operating at 1000 frames/sec, and consists of a focal plane dewar, a compact camera head electronics package, and a Digital Signal Processor (DSP)-based data system residing in a standard 486 personal computer. In this paper we discuss the overall system architecture, the focal plane dewar, and advanced features and design considerations for the electronics. This system, or one derived from it, may prove useful for many commercial and/or industrial infrared imaging or spectroscopic applications, including thermal machine vision for robotic manufacturing, photographic observation of short-duration thermal events such as combustion or chemical reactions, and high-resolution surveillance imaging. Author

N94-32460*# National Aeronautics and Space Administration. John F. Kennedy Space Center, Cocoa Beach, FL.

UNIVERSAL SIGNAL CONDITIONING AMPLIFIER c33

Pedro J. Medelius (I-NET, Inc., Cocoa Beach, FL.), Carl Hallberg (I-NET, Inc., Cocoa Beach, FL.), and Jim Cecil *In* NASA, Washington, Technology 2003: The Fourth National Technology Transfer Conference and Exposition, Volume 2 Feb. 1994 p 342-348 (For primary document see N94-32420 09-99)

Avail: CASI HC A02/MF A04

A state-of-the-art instrumentation amplifier capable of being used with most types of transducers has been developed at the Kennedy Space Center. This Universal Signal Conditioning Amplifier (USCA) can eliminate costly measurement setup item and troubleshooting, improve system reliability and provide more accurate data than conventional amplifiers. The USCA can configure itself for maximum resolution and accuracy based on information read from a RAM chip attached to each transducer. Excitation voltages or current are also automatically configured. The amplifier uses both analog and digital state-of-the-art technology with analog-to-digital conversion performed in the early stages in order to minimize errors introduced by offset and gain drifts in the analog components. A dynamic temperature compensation scheme has been designed to achieve and maintain 12-bit accuracy of the amplifier from 0 to 70 C. The digital signal processing section allows the implementation of digital filters up to 511th order. The amplifier can also perform real-time linearizations up to fourth order while processing data at a rate of 23.438 kS/s. Both digital and analog outputs are available from the amplifier. Author

N94-32461*# National Aeronautics and Space Administration. Hugh L. Dryden Flight Research Facility, Edwards, CA.

THE CONSTANT CURRENT LOOP: A NEW PARADIGM FOR RESISTANCE SIGNAL CONDITIONING c32

Karl F. Anderson *In* NASA, Washington, Technology 2003: The Fourth National Technology Transfer Conference and Exposition, Volume 2 Feb. 1994 p 349-361 (For primary document see N94-32420 09-99)

Avail: CASI HC A03/MF A04

A practical single constant current loop circuit for the signal conditioning of variable-resistance transducers has been synthesized, analyzed, and demonstrated. The strain gage and the resistance temperature detector are examples of variable-resistance sensors. Lead wires connect variable-resistance sensors to remotely located signal-conditioning hardware. The presence of lead wires in the conventional Wheatstone bridge signal-conditioning circuit introduces undesired effects that reduce the quality of the data from the remote sensors. A practical approach is presented for suppressing essentially all lead wire resistance effects while indicating only the change in resistance value. Theoretical predictions supported by laboratory testing confirm the following features of the approach: (1) dc response; (2) the electrical output is unaffected by extremely large variation in the resistance of any or all lead wires; (3) the electrical output remains zero for no change in gage resistance; (4) the electrical output is inherently linear with respect to gage resistance change; (5) the sensitivity is double that of a Wheatstone bridge circuit; and (6) the same excitation wires can serve multiple independent gages. An adaptation of current loop circuit is presented that simultaneously provides an output signal voltage directly proportional to transducer resistance change and provides temperature information that is unaffected by transducer and lead wire resistance variations. These innovations are the subject of NASA patent applications. Author

N94-32462*# National Aeronautics and Space Administration. Lyndon B. Johnson Space Center, Houston, TX.

LITERACITY: A MULTIMEDIA ADULT LITERACY PACKAGE COMBINING NASA TECHNOLOGY, RECURSIVE ID THEORY, AND AUTHENTIC INSTRUCTION THEORY c85

Jerry Willis (Houston Univ., TX.), Dee Anna Willis (Houston Univ., TX.), Clare Walsh (Houston Univ., TX.), Elizabeth Stephens (Houston Univ., TX.),

Timothy Murphy (Houston Univ., TX.), Jerry Price (Houston Univ., TX.), William Stevens (Lockheed Engineering and Sciences Co., Houston, TX.), Kevin Jackson (Department of Justice, Washington, DC.), James A. Villareal, and Bob Way *In* NASA, Washington, Technology 2003: The Fourth National Technology Transfer Conference and Exposition, Volume 2 Feb. 1994 p 365-374 (For primary document see N94-32420 09-99)
Avail: CASI HC A02/MF A04

An important part of NASA's mission involves the secondary application of its technologies in the public and private sectors. One current application under development is LiteraCity, a simulation-based instructional package for adults who do not have functional reading skills. Using fuzzy logic routines and other technologies developed by NASA's Information Systems Directorate and hypermedia sound, graphics, and animation technologies the project attempts to overcome the limited impact of adult literacy assessment and instruction by involving the adult in an interactive simulation of real-life literacy activities. The project uses a recursive instructional development model and authentic instruction theory. This paper describes one component of a project to design, develop, and produce a series of computer-based, multimedia instructional packages. The packages are being developed for use in adult literacy programs, particularly in correctional education centers. They use the concepts of authentic instruction and authentic assessment to guide development. All the packages to be developed are instructional simulations. The first is a simulation of 'finding a friend a job.' Author

N94-32463*# National Aeronautics and Space Administration. John F. Kennedy Space Center, Cocoa Beach, FL.
MAPPING ANALYSIS AND PLANNING SYSTEM FOR THE JOHN F. KENNEDY SPACE CENTER c43
C. R. Hall (Bionetics Corp., Cocoa Beach, FL.), M. J. Barkaszi (Bionetics Corp., Cocoa Beach, FL.), M. J. Provancha (Bionetics Corp., Cocoa Beach, FL.), N. A. Reddick (Bionetics Corp., Cocoa Beach, FL.), C. R. Hinkle (Bionetics Corp., Cocoa Beach, FL.), B. A. Engel (Purdue Univ., West Lafayette, IN.), and B. R. Summerfield *In* NASA, Washington, Technology 2003: The Fourth National Technology Transfer Conference and Exposition, Volume 2 Feb. 1994 p 375-387 (For primary document see N94-32420 09-99)
Avail: CASI HC A03/MF A04

Environmental management, impact assessment, research and monitoring are multidisciplinary activities which are ideally suited to incorporate a multi-media approach to environmental problem solving. Geographic information systems (GIS), simulation models, neural networks and expert-system software are some of the advancing technologies being used for data management, query, analysis and display. At the 140,000 acre John F. Kennedy Space Center, the Advanced Software Technology group has been supporting development and implementation of a program that integrates these and other rapidly evolving hardware and software capabilities into a comprehensive Mapping, Analysis and Planning System (MAPS) based in a workstation/local are network environment. An expert-system shell is being developed to link the various databases to guide users through the numerous stages of a facility siting and environmental assessment. The expert-system shell approach is appealing for its ease of data access by management-level decision makers while maintaining the involvement of the data specialists. This, as well as increased efficiency and accuracy in data analysis and report preparation, can benefit any organization involved in natural resources management. Author

N94-32464*# National Aeronautics and Space Administration. John C. Stennis Space Center, Bay Saint Louis, MS.
REMOTE SENSING FOR HURRICANE ANDREW IMPACT ASSESSMENT Abstract Only c43
Bruce A. Davis and Nicholas Schmidt *In* NASA, Washington, Technology 2003: The Fourth National Technology Transfer Conference and Exposition, Volume 2 Feb. 1994 p 388 (For primary document see N94-32420 09-99)
Avail: CASI HC A01/MF A04

Stennis Space Center personnel flew a Learjet equipped with instrumentation designed to acquire imagery in many spectral bands into areas most damaged by Hurricane Andrew. The calibrated airborne multispectral scanner (CAMS), a NASA-developed sensor, and a Zeiss camera acquired images of these areas. The information derived from the imagery was used to assist Florida officials in assessing the devastation caused by the hurricane. The imagery provided the relief teams with an assessment of the debris covering roads and highways so cleanup plans could be prioritized. The imagery also mapped the level of damage in residential and commercial areas of southern Florida and provided maps of beaches and land cover for determination of beach loss and vegetation damage, particularly the mangrove population. Stennis Space Center personnel demonstrated the ability to respond quickly and the value of such response in an emergency situation. The digital imagery from the CAMS can be processed, analyzed, and developed into products for field crews faster than conventional photography. The resulting information is versatile and allows for rapid updating and editing. Stennis Space Center and state officials worked diligently to compile information to complete analyses of the hurricane's impact. Author (revised)

N94-32465*# National Aeronautics and Space Administration. John C. Stennis Space Center, Bay Saint Louis, MS.
REMOTE SENSING FOR URBAN PLANNING c43
Bruce A. Davis, Nicholas Schmidt, John R. Jensen, Dave J. Cowen, Joanne Halls, Sunil Narumalani, and Bryan Burgess *In* NASA, Washington, Technology 2003: The Fourth National Technology Transfer Conference and Exposition, Volume 2 Feb. 1994 p 389-393 (For primary document see N94-32420 09-99)
Avail: CASI HC A01/MF A04

Utility companies are challenged to provide services to a highly dynamic customer base. With factory closures and shifts in employment becoming a routine occurrence, the utility industry must develop new techniques to maintain records and plan for expected growth. BellSouth Telecommunications, the largest of the Bell telephone companies, currently serves over 13 million residences and 2 million commercial customers. Tracking the movement of customers and scheduling the delivery of service are major tasks for BellSouth that require intensive manpower and sophisticated information management techniques. Through NASA's Commercial Remote Sensing Program Office, BellSouth is investigating the utility of remote sensing and geographic information system techniques to forecast residential development. This paper highlights the initial results of this project, which indicate a high correlation between the U.S. Bureau of Census block group statistics and statistics derived from remote sensing data. Author

N94-32466*# National Aeronautics and Space Administration. John C. Stennis Space Center, Bay Saint Louis, MS.
REMOTE SENSING AND THE MISSISSIPPI HIGH ACCURACY REFERENCE NETWORK c43
Mark Mick, Timothy M. Alexander, and Stan Woolley *In* NASA, Washington, Technology 2003: The Fourth National Technology Transfer Conference and Exposition, Volume 2 Feb. 1994 p 394-403 (For primary document see N94-32420 09-99)
Avail: CASI HC A02/MF A04

Since 1986, NASA's Commercial Remote Sensing Program (CRSP) at Stennis Space Center has supported commercial remote sensing partnerships with industry. CRSP's mission is to maximize U.S. market exploitation of remote sensing and related space-based technologies and to develop advanced technical solutions for spatial information requirements. Observation, geolocation, and communications technologies are converging and their integration is critical to realize the economic potential for spatial informational needs. Global positioning system (GPS) technology enables a virtual revolution in geopositionally accurate remote sensing of the earth. A majority of states are creating GPS-based reference networks, or high accuracy reference networks (HARN). A HARN can be defined for a variety of local applications and tied to aerial or satellite observations to provide an important contribution to geographic information systems (GIS). This paper details CRSP's experience in the design and implementation of a HARN in Mississippi and the design and support of future applications of integrated earth observations, geolocation, and communications technology. Author (revised)

N94-32467*# National Aeronautics and Space Administration. Ames Research Center, Moffett Field, CA.
A VISUAL DETECTION MODEL FOR DCT COEFFICIENT QUANTIZATION c64
Albert J. Ahumada, Jr. and Andrew B. Watson *In* NASA, Washington, Technology 2003: The Fourth National Technology Transfer Conference

and Exposition, Volume 2 Feb. 1994 p 404-415 (For primary document see N94-32420 09-99)
Avail: CASI HC A03/MF A04

The discrete cosine transform (DCT) is widely used in image compression and is part of the JPEG and MPEG compression standards. The degree of compression and the amount of distortion in the decompressed image are controlled by the quantization of the transform coefficients. The standards do not specify how the DCT coefficients should be quantized. One approach is to set the quantization level for each coefficient so that the quantization error is near the threshold of visibility. Results from previous work are combined to form the current best detection model for DCT coefficient quantization noise. This model predicts sensitivity as a function of display parameters, enabling quantization matrices to be designed for display situations varying in luminance, veiling light, and spatial frequency related conditions (pixel size, viewing distance, and aspect ratio). It also allows arbitrary color space directions for the representation of color. A model-based method of optimizing the quantization matrix for an individual image was developed. The model described above provides visual thresholds for each DCT frequency. These thresholds are adjusted within each block for visual light adaptation and contrast masking. For given quantization matrix, the DCT quantization errors are scaled by the adjusted thresholds to yield perceptual errors. These errors are pooled nonlinearly over the image to yield total perceptual error. With this model one may estimate the quantization matrix for a particular image that yields minimum bit rate for a given total perceptual error, or minimum perceptual error for a given bit rate. Custom matrices for a number of images show clear improvement over image-independent matrices. Custom matrices are compatible with the JPEG standard, which requires transmission of the quantization matrix. Author

N94-32468*# Naval Command, Control and Ocean Surveillance Center, San Diego, CA.
VOICE AND VIDEO TRANSMISSION USING XTP AND FDDI **c32**
John Drummond, Edwin Cheng, and Will Gex *In* NASA, Washington, Technology 2003: The Fourth National Technology Transfer Conference and Exposition, Volume 2 Feb. 1994 p 416-421 (For primary document see N94-32420 09-99)
Avail: CASI HC A02/MF A04

The use of Xpress Transfer Protocol (XTP) and Fiber Distributed Data Interface (FDDI) provides a high speed and high performance network solution to multimedia transmission that requires high bandwidth. FDDI is an ANSI and ISO standard for a MAC and physical layer protocol that provides a signaling rate of 100 Mbits/sec and fault tolerance. XTP is a transport and network layer protocol designed for high performance and efficiency and is the heart of the SAFENET Lightweight Suite for systems that require performance or realtime communications. The testbed consists of several commercially available Intel based i486 PC's containing off-the-shelf FDDI cards, audio analog-digital converter cards, video interface cards, and XTP software. Unicast, multicast, and duplex audio transmission experiments have been performed using XTP software. Unicast and multicast video transmission is in progress. Several potential commercial applications are described. Author (revised)

N94-32469*# University of Central Florida, Orlando.
AN INTELLIGENT INTERACTIVE VISUAL DATABASE MANAGEMENT SYSTEM FOR SPACE SHUTTLE CLOSEOUT IMAGE MANAGEMENT **c82**
James M. Ragusa, Gary Orwig, Michael Gilliam, David Blacklock, and Ali Shaykhian *In* NASA, Washington, Technology 2003: The Fourth National Technology Transfer Conference and Exposition, Volume 2 Feb. 1994 p 422-429 (For primary document see N94-32420 09-99)
(Grant NAG10-0058)
Avail: CASI HC A02/MF A04

Status is given of an applications investigation on the potential for using an expert system shell for classification and retrieval of high resolution, digital, color space shuttle closeout photography. This NASA funded activity has focused on the use of integrated information technologies to intelligently classify and retrieve still imagery from a large, electronically stored collection. A space shuttle processing problem is identified, a working prototype system is described, and commercial applications are identified. A conclusion reached is that the developed system has distinct advantages over the present manual system and cost efficiencies will result as the system is implemented. Further, commercial potential exists for this integrated technology. Author (revised)

N94-32470*# Jet Propulsion Lab., California Inst. of Tech., Pasadena.
THE TRUSTWORTHY DIGITAL CAMERA: RESTORING CREDIBILITY TO THE PHOTOGRAPHIC IMAGE **c35**
Gary L. Friedman *In* NASA, Washington, Technology 2003: The Fourth National Technology Transfer Conference and Exposition, Volume 2 Feb. 1994 p 430-435 (For primary document see N94-32420 09-99)
Avail: CASI HC A02/MF A04

The increasing sophistication of computers has made digital manipulation of photographic images, as well as other digitally-recorded artifacts such as audio and video, incredibly easy to perform and increasingly difficult to detect. Today, every picture appearing in newspapers and magazines has been digitally altered to some degree, with the severity varying from the trivial (cleaning up 'noise' and removing distracting backgrounds) to the point of deception (articles of clothing removed, heads attached to other people's bodies, and the complete rearrangement of city skylines). As the power, flexibility, and ubiquity of image-altering computers continues to increase, the well-known adage that 'the photography doesn't lie' will continue to become an anachronism. A solution to this problem comes from a concept called digital signatures, which incorporates modern cryptographic techniques to authenticate electronic mail messages. 'Authenticate' in this case means one can be sure that the message has not been altered, and that the sender's identity has not been forged. The technique can serve not only to authenticate images, but also to help the photographer retain and enforce copyright protection when the concept of 'electronic original' is no longer meaningful. Author (revised)

N94-32471*# National Aeronautics and Space Administration. Lyndon B. Johnson Space Center, Houston, TX.
VIRTUAL REALITY IN MEDICAL EDUCATION AND ASSESSMENT **c52**
Laurie A. Sprague (LinCom Corp., Houston, TX.), Brad Bell (LinCom Corp., Houston, TX.), Tim Sullivan (LinCom Corp., Houston, TX.), Mark Voss (LinCom Corp., Houston, TX.), Andrew F. Payer (Texas Univ., Galveston.), and Stewart Michael Goza *In* NASA, Washington, Technology 2003: The Fourth National Technology Transfer Conference and Exposition, Volume 2 Feb. 1994 p 439-443 (For primary document see N94-32420 09-99)
Avail: CASI HC A01/MF A04

The NASA Johnson Space Center (JSC)/LinCom Corporation, the University of Texas Medical Branch at Galveston (UTMB), and the Galveston Independent School District (GISD) have teamed up to develop a virtual visual environment display (VIVED) that provides a unique educational experience using virtual reality (VR) technologies. The VIVED end product will be a self-contained educational experience allowing students a new method of learning as they interact with the subject matter through VR. This type of interface is intuitive and utilizes spatial and psychomotor abilities which are now constrained or reduced by the current two dimensional terminals and keyboards. The perpetual challenge to educators remains the identification and development of methodologies which conform the learners abilities and preferences. The unique aspects of VR provide an opportunity to explore a new educational experience. Endowing medical students with an understanding of the human body poses some difficulty challenges. One of the most difficult is to convey the three dimensional nature of anatomical structures. The ideal environment for addressing this problem would be one that allows students to become small enough to enter the body and travel through it - much like a person walks through a building. By using VR technology, this effect can be achieved; when VR is combined with multimedia technologies, the effect can be spectacular.
Author (revised)

N94-32472*# National Aeronautics and Space Administration. Goddard Space Flight Center, Greenbelt, MD.
TECHNOLOGY TRANSFER OF OPERATOR-IN-THE-LOOP SIMULATION **c53**
K. H. Yae (Iowa Univ., Iowa City.), H. C. Lin (Iowa Univ., Iowa City.), T. C. Lin (Iowa Univ., Iowa City.), and H. P. Frisch *In* NASA, Washington, Technology 2003: The Fourth National Technology Transfer Conference and Exposition, Volume 2 Feb. 1994 p 444-455 (For primary document see N94-32420 09-99)
Avail: CASI HC A03/MF A04

The technology developed for operator-in-the-loop simulation in space teleoperation has been applied to Caterpillar's backhoe, wheel loader, and off-highway truck. On an SGI workstation, the simulation integrates computer modeling of kinematics and dynamics, real-time computational and visualization, and an interface with the operator through the operator's console. The console is interfaced with the workstation through an IBM-PC in which the operator's commands were digitized and sent through an RS-232 serial port. The simulation gave visual feedback adequate for the operator in the loop, with the camera's field of vision projected on a large screen in multiple view windows. The view control can emulate either stationary or moving cameras. This simulator created an innovative engineering design environment by integrating computer software and hardware with the human operator's interactions. The backhoe simulation has been adopted by Caterpillar in building a virtual reality tool for backhoe design. Author

N94-32473*# National Aeronautics and Space Administration. Langley Research Center, Hampton, VA.

HIGH PERFORMANCE REAL-TIME FLIGHT SIMULATION AT NASA LANGLEY **c09**

Jeff I. Cleveland, II *In* NASA, Washington, Technology 2003: The Fourth National Technology Transfer Conference and Exposition, Volume 2 Feb. 1994 p 456-462 (For primary document see N94-32420 09-99)

Avail: CASI HC A02/MF A04

In order to meet the stringent time-critical requirements for real-time man-in-the-loop flight simulation, computer processing operations must be deterministic and be completed in as short a time as possible. This includes simulation mathematical model computational and data input/output to the simulators. In 1986, in response to increased demands for flight simulation performance, personnel at NASA's Langley Research Center (LaRC), working with the contractor, developed extensions to a standard input/output system to provide for high bandwidth, low latency data acquisition and distribution. The Computer Automated Measurement and Control technology (IEEE standard 595) was extended to meet the performance requirements for real-time simulation. This technology extension increased the effective bandwidth by a factor of ten and increased the performance of modules necessary for simulator communications. This technology is being used by more than 80 leading technological developers in the United States, Canada, and Europe. Included among the commercial applications of this technology are nuclear process control, power grid analysis, process monitoring, real-time simulation, and radar data acquisition. Personnel at LaRC have completed the development of the use of supercomputers for simulation mathematical model computational to support real-time flight simulation. This includes the development of a real-time operating system and the development of specialized software and hardware for the CAMAC simulator network. This work, coupled with the use of an open systems software architecture, has advanced the state of the art in real time flight simulation. The data acquisition technology innovation and experience with recent developments in this technology are described. Author (revised)

N94-32474*# ECC International Corp., Orlando, FL.

THE EFFECTS OF ABOVE REAL-TIME TRAINING (ARTT) IN AN F-16 SIMULATOR **c09**

Dutch Guckenberger, Kay Stanney, and Norman E. Lane *In* NASA, Washington, Technology 2003: The Fourth National Technology Transfer Conference and Exposition, Volume 2 Feb. 1994 p 463-470 (For primary document see N94-32420 09-99)

Avail: CASI HC A02/MF A04

In this application of above real-time training (ARTT), 24 mission-capable F-16 pilots performed three tasks on a part-task F-16A flight simulator under varying levels of time compression (i.e., 1.0x, 1.5x, 2.0x, and random). All subjects were then tested in a real-time (1.0x) environment. The three tasks under study were an emergency procedure (EP) task, a one versus two air combat maneuvering (ACM) task, and a stern conversion or air intercept task. All ARTT pilots performed the EP task with 28 percent greater accuracy and were better at dealing with a simultaneous MIG threat, reflected by a six-fold increase in the number of MIG kills compared to a real-time control group. In the stern conversion task, there were no statistical differences between groups. In the ACM task, those pilots trained in the mixed time accelerations were faster to acquire lock and were faster to kill both MIG threats than the other groups. These findings are generally consistent with previous findings that show positive effects of task variations (including time variations) during training. Also discussed are related research findings that support the benefits of ARTT and ARTT's impact on emergency procedure training. Further, a synthesis of multidiscipline research outlining the underlying theoretical basis for ARTT is presented. A proposed model of ARTT based on an analogy to Einstein's theory of special relativity is suggested. Conclusions and an outline of future research directions are presented. Successful current commercialization efforts are related as well as future efforts. Author (revised)

N94-32854# Executive Office of the President, Washington, DC.

AERONAUTICS AND SPACE REPORT OF THE PRESIDENT: FISCAL YEAR 1993 ACTIVITIES

1994 136 p Original contains color illustrations

Avail: CASI HC A07/MF A02

The annual Aeronautics and Space Report includes a comprehensive description of the programmed activities and the accomplishments of all agencies of the United States in the field of aeronautics and space activities during the preceding calendar year. This year's report was prepared on a fiscal year basis, which is consistent with the budgetary period now used in programs of the Federal Government. The following areas are covered: space launch activities; space science; space flight and space technology; space communications; aeronautical activities; studies of the planet earth; and other aeronautical and space activities. Derived from text

N94-32885*# National Aeronautics and Space Administration, Washington, DC.

RESEARCH AND TECHNOLOGY OBJECTIVES AND PLANS SUMMARY (RTOPS) Research and Technology Program, FY 1992

Feb. 1992 252 p

(NASA-TM-105441; NAS 1.15:105441) Avail: CASI HC A12/MF A03

This publication represents the NASA research and technology program for FY92. It is a compilation of the Summary portions of each of the RTOP's (Research and Technology Objectives and Plans) used for management review and control of research currently in progress throughout NASA. The RTOP Summary is designed to facilitate communication and coordination among concerned technical personnel in government, in industry, and in universities. The first section containing citations and abstracts of the RTOP's is followed by four indexes: Subject, Technical Monitor, Responsible NASA Organization, and RTOP Number. Author

N94-32949# Aerospace Corp., El Segundo, CA.

AEROSPACE SPONSORED RESEARCH Summary Report, 1 Oct. 1992 - 30 Sep. 1993

1 Apr. 1994 175 p

(ATR-93(8498)-1) Avail: CASI HC A08/MF A02

Broad guidelines for the direction and emphasis of the overall research and development activities at Aerospace Corporation are periodically developed to assess in detail the trends in relevant technologies and their application to military space systems. Research and development activities are conducted in these technical categories: spacecraft and launch vehicles, electronic device technology, communications and navigation technology, information sciences, environmental technology, surveillance technology, plans and analysis, modeling and simulation, and systems engineering. This ASR summary report for FY 1993 contains brief reports of 33 selected projects carried out under the ASR program. They are a representative sample of the wide range of Aerospace internal research interests, from basic science to operational space systems engineering. This volume also includes abstracts of all 103 projects undertaken in FY 1993, and a comprehensive listing of all professional publications and technical reports produced using ASR funds during FY 1991-1993. Derived from text

N94-33072*# National Aeronautics and Space Administration. John F. Kennedy Space Center, Cocoa Beach, FL.

CHRONOLOGY OF KSC AND KSC RELATED EVENTS FOR 1993

Ken Nail, Jr. Mar. 1994 289 p Prepared in cooperation with Sherikon Space Systems, Inc., Kennedy Space Center, FL
(NASA-TM-109196; NAS 1.15:109196; KSC-KHR-18) Avail: CASI HC A13/MF A03

This document is intended to serve as a record of KSC events and as a reference source for historians and other researchers. Arrangement is by day and month and individual articles are attributed to published sources. This edition has an index on p. 272. Author (revised)

Typical Subject Index Listing

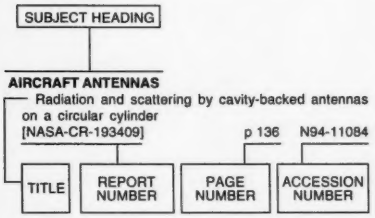

The subject heading is a key to the subject content of the document. Titles, report numbers, and accession numbers of pertinent documents are provided under each subject heading. When the title is insufficiently descriptive of the document content, a title extension is added, separated from the title by three hyphens. The report number helps to indicate the type of document cited (e.g., NASA report, NASA translation, NASA contractor report). The accession number is the number by which the document abstracts are arranged in this journal and by which the document is sold or requested. The page number helps you locate the citation in the abstract section. The titles, with title extensions if present, are arranged under each subject heading in ascending accession number order. The subject headings have been selected from the latest revision of the *NASA Thesaurus*.

A

ABERRATION
Visual neural development and chromatic aberration [AD-A277402] p 3800 N94-32345

ABLATION
Deposition of DLC via intense ion beam ablation [DE94-005583] p 3651 N94-31650
Development of lightweight ceramic ablators and arc-jet test results [NASA-TM-108798] p 3617 N94-33117

ABLATIVE MATERIALS
Development of lightweight ceramic ablators and arc-jet test results [NASA-TM-108798] p 3617 N94-33117

ABORT APPARATUS
Design, performance, and test standards for flight termination receivers/decoders. Volume 1: Design and performance requirements [AD-A277245] p 3602 N94-32333

ABSORBENTS
Double rotation NMR studies of zeolites and aluminophosphate molecular sieves [DE94-007032] p 3866 N94-31637

ABSORBERS (MATERIALS)
Interpenetrating polymer network acoustic damping material [AD-D016141] p 3663 N94-32975
Distribution and nature of UV absorbers on Triton's surface [NASA-CR-195886] p 3943 N94-33104

ABSORPTANCE
Anodized aluminum on LDEF p 3592 N94-31017

ABSORPTION
Deuterium absorption and material phase characteristics of SAES St198 Zr-Fe alloy [DE94-008275] p 3646 N94-32781

ABSORPTION SPECTRA
Near resonant absorption by atoms in intense fluctuating laser fields [DE94-005873] p 3714 N94-31200
Extreme ultraviolet opacity sources in the DA white dwarf G191-B2B p 3924 N94-31210
Infrared and near infrared transient absorption spectroscopy of molecular free radicals [DE94-005446] p 3632 N94-31305
Combustion-related studies using weakly-bonded complexes [DE94-006632] p 3633 N94-31493
Computational radiative heat transfer in homogeneous and nonhomogeneous nonscattering media p 3702 N94-31563
Characterization of the rare earth orthophosphates and Ce-doped LaPO4 by x ray absorption spectroscopy [DE94-006313] p 3898 N94-31630
Photopyroelectric spectroscopy as a non-intrusive technique for the determination of the optical absorption spectra of multiple quantum well samples [ISBN-0-315-87164-4] p 3833 N94-31875
Structural studies of photoinduced intramolecular electron transfer in cyclopentadienylnickelnitrosyl [DE94-008467] p 3874 N94-32876

ABSORPTION SPECTROSCOPY
Time-resolved infrared absorption studies applied to the study of radical plus molecule reactions [DE94-005921] p 3863 N94-31202
Infrared and near infrared transient absorption spectroscopy of molecular free radicals [DE94-005446] p 3632 N94-31305
Combustion-related studies using weakly-bonded complexes [DE94-006632] p 3633 N94-31493
Using laser absorption spectroscopy to monitor composition and physical properties of metal vapors [DE94-001530] p 3716 N94-31599
Fiber optic chemical sensors [AD-A277128] p 3881 N94-32380
X ray absorption study of pulsed laser deposited boron nitride films [DE94-008295] p 3662 N94-32855
Structural studies of photoinduced intramolecular electron transfer in cyclopentadienylnickelnitrosyl [DE94-008467] p 3874 N94-32876
Scanning tunneling microscopy and infrared spectroscopy as combined in-situ probes of electrochemical adlayer structure: Cyanide on Pt(111) [AD-A276715] p 3909 N94-33274

ABSTRACTS
Piezoelectric materials research in Europe [AD-A276207] p 3648 N94-31059
Workshop on Physics of Accretion Disks Around Compact and Young Stars [NASA-CR-195756] p 3927 N94-31116
The 1994 International Sherwood Fusion Theory Conference [DE94-008961] p 3877 N94-32844
International Free Electron Laser Conference [AD-A277576] p 3721 N94-33000

ACCELERATED LIFE TESTS
Accelerated reliability testing utilizing design of experiments [AD-A277989] p 3732 N94-33088
The preliminary evaluation of liquid lubricants for space applications by vacuum tribometry p 3606 N94-33313
Design of a high-speed reliable ball bearing p 3606 N94-33314

ACCELERATION (PHYSICS)
Space acceleration measurement system [NASA-TM-109754] p 3913 N94-31807

ACCELEROMETERS
Space acceleration measurement system [NASA-TM-109754] p 3913 N94-31807
OARE flight maneuvers and calibration measurements on STS-58 [NASA-TM-109093] p 3613 N94-32924

ACCEPTOR MATERIALS
Recent developments in polymeric charge transfer complexes [AD-A277108] p 3654 N94-31979
Novel polydiacetylenes as materials for second and third order nonlinear optics [AD-A277512] p 3664 N94-33082

ACCESS CONTROL
On the validity of the BLP model [REPT-93-70] p 3917 N94-31640

ACCESS TIME
The named-state register file [AD-A276796] p 3825 N94-32165

ACCIDENT PREVENTION
Controlling hazardous energy sources (lockout/tagout) [NASA-TM-105290] p 3669 N94-32861

ACCRETION DISKS
Workshop on Physics of Accretion Disks Around Compact and Young Stars [NASA-CR-195756] p 3927 N94-31116
Accretion disks around black holes p 3928 N94-31117
A twisted disk equation that describes warped galaxy disks p 3928 N94-31118
Observations of accretion and angular momentum regulation in young circumstellar disks and the implications for planetary formation p 3928 N94-31122
Disk irradiation and light curves of x ray novae p 3929 N94-31124
Observational constraints on black hole accretion disks p 3929 N94-31126
Nonlinear calculations of the time evolution of black hole accretion disks p 3929 N94-31127
Can a variable alpha induce limit cycle behavior and exponential luminosity decay in transient soft x ray sources? p 3929 N94-31129
Rotational effects in turbulence driven by convection p 3930 N94-31131
A constraint on the pair-density ratio (Z+) in an electron-positron pair wind p 3930 N94-31132
Evolution of protoplanetary disks with dynamo magnetic fields p 3931 N94-31135
Theory of protostellar accretion disks p 3931 N94-31136
Thermal continua of AGN accretion disks p 3931 N94-31137
Evolution of dynamo-generated magnetic fields in accretion disks around compact and young stars p 3931 N94-31138
Nonthermal accretion disk models around neutron stars p 3931 N94-31139
Gravitational instabilities in protostellar disks p 3932 N94-31140
Three-dimensional radiative transfer calculations on an SIMD machine applied to accretion disks p 3932 N94-31141
Dynamics of flux tubes in accretion disks p 3932 N94-31142
The physics of black hole x ray novae p 3932 N94-31143
Gas dynamics for accretion disk simulations p 3932 N94-31144
Planetesimal dynamics in the vicinity of a growing protoplanet p 3935 N94-31926
Structure and stability of spherical accretion flows onto compact objects p 3935 N94-31946
Winds from disks in compact binaries [DE94-007452] p 3938 N94-32137

ACCUMULATIONS
Studies of jet production with the D0 detector [DE94-008271] p 3873 N94-32780

ACCUMULATORS
Operational experience and evaluation of a dual-element stretched-membrane heliostat [DE94-008827] p 3763 N94-32965

ACCURACY
An investigation of airborne GPS/INS for high accuracy position and velocity determination [DE94-006139] p 3576 N94-31306
Airborne SAR as a complement to SPOT HRV in land-cover classification: The use of normalization and principal components analysis p 3750 N94-32539

ACETYLENE
Feasibility study to evaluate plasma quench process for natural gas conversion applications [DE94-000086] p 3758 N94-31234

Direct aromatization of methane
[DE94-008719] p 3638 N94-32888
Novel polydiacetylenes as materials for second and third order nonlinear optics
[AD-A277512] p 3664 N94-33082

ACID RAIN
Identification of research relating to the critical loads concept and its potential application to the regulation of acidic deposition
[DE94-008234] p 3767 N94-32752

ACIDITY
The adsorption of sulfate on gold(111) in acidic aqueous media: Adlayer structural inferences from infrared spectroscopy and scanning tunneling microscopy
[AD-A276643] p 3642 N94-31997
Studies of the fundamental nature of catalytic acidity, sites and intermediates
[DE94-006999] p 3646 N94-32805

ACOUSTIC ATTENUATION
Ocean acoustic propagation measurements and wave propagation in random media
[AD-A276165] p 3787 N94-31053
Determination of multiple sound sources
[AD-A277379] p 3799 N94-32096
Mass-loaded coating for reducing the resonant frequency of a ceramic disc
[AD-D016095] p 3660 N94-32739
A mathematical model for simulating noise suppression of lined ejectors
[NASA-TP-3425] p 3861 N94-32930
Interpenetrating polymer network acoustic damping material
[AD-D016141] p 3663 N94-32975
Digital beamforming and filtering circuit
[AD-D016142] p 3697 N94-32976

ACOUSTIC EMISSION
Ocean acoustic propagation measurements and wave propagation in random media
[AD-A276165] p 3787 N94-31053
Acoustic emission from crack growth in 7050 aluminum and 7075 aluminum as a function of temperature and heat treatment
[DREP-CRS-93-15] p 3642 N94-31871
Acoustic window
[AD-D016171] p 3862 N94-33017

ACOUSTIC EXCITATION
Analysis of strong acoustic excitation on the breakup and dispersion of a liquid jet
[ONERA-NT-1993-9] p 3701 N94-31422

ACOUSTIC FREQUENCIES
Surface forward-scattered acoustic measurements and analysis
[AD-A276998] p 3788 N94-32000

ACOUSTIC MEASUREMENT
Surface forward-scattered acoustic measurements and analysis
[AD-A276998] p 3788 N94-32000
An investigation of acoustic noise requirements for the Space Station centrifuge facility
[NASA-TM-108811] p 3805 N94-32936

ACOUSTIC MICROSCOPES
Differential phase acoustic microscope for micro-NDE
[NASA-CR-189617] p 3731 N94-32481

ACOUSTIC PROPAGATION
Ocean acoustic propagation measurements and wave propagation in random media
[AD-A276165] p 3787 N94-31053

ACOUSTIC PROPERTIES
Segment-based acoustic models for continuous speech recognition
[AD-A276109] p 3673 N94-31466
Prediction of the plane wave beamformed acoustic arrival structure for the 1992 Barents Sea coastal tomography test
[AD-A276741] p 3788 N94-32181

ACOUSTIC SCATTERING
Ocean acoustic propagation measurements and wave propagation in random media
[AD-A276165] p 3787 N94-31053
Scattering of a random acoustic field by an infinite cylinder: Application to the modelization of the acoustic environment of the 'Ariane 5' launcher scale-model using experimental data
[ONERA-NT-1993-11] p 3860 N94-31226
Boundary control of scattering p 3861 N94-31899
Surface forward-scattered acoustic measurements and analysis
[AD-A276998] p 3788 N94-32000
Penetrable wedge analysis
[AD-A277219] p 3845 N94-32022
Sound scattering by cylinders of noncircular cross section
[AD-A276663] p 3861 N94-32089
Statistical characteristics of bistatic surface scatter and mean bistatic surface scattering strengths
[AD-A278155] p 3862 N94-33096

ACOUSTIC VELOCITY
A preliminary investigation of high amplitude standing waves with laser Doppler anemometry
[AD-A276463] p 3860 N94-31242
Reactive flows in compact objects
p 3934 N94-31567
Profiling ALACE instruments
[AD-A277246] p 3789 N94-32321
Computerized Ultrasonic Testing System (CUTS) for in-process thickness determination
p 3862 N94-32456

ACOUSTICS
Quality of sound in large rooms: Alteration of room impulse responses
[CTH-E-93-02] p 3859 N94-31077
A pilot study of comfort criteria and sound quality metrics for sound inside cabins of propeller-driven aircraft
[CTH-F-93-03] p 3859 N94-31090
Computer implementation of Arnott's formulation of thermoacoustics using MATLAB
[AD-A276356] p 3860 N94-31257
Boundary control of scattering p 3861 N94-31899
Wavevector-frequency analysis with applications to acoustics
[AD-A276618] p 3861 N94-32125
Pulse-splitting and AM-FM conversion in a nonlinear dispersive medium
[AD-A277041] p 3861 N94-32262
Interpenetrating polymer network acoustic damping material
[AD-D016141] p 3663 N94-32975

ACOUSTO-OPTICS
Noninvasive spectral analysis and beam mapping of focused ultrasound, part 1
[AD-A276211] p 3859 N94-31060

ACRYLATES
Mechanical properties of acrylate networks formed by visible laser-induced polymerization. 2. Control of the mechanical properties
[AD-A277111] p 3655 N94-31982
Solvent diffusion coefficient concentration dependence in polymer solutions
[AD-A277023] p 3655 N94-32005
Intramolecular charge transfer complexes as fluorescence probes for UV and visible light induced acrylate polymerization
[AD-A277129] p 3657 N94-32381
Microstructure of copolymers containing disperse red 1 and methyl methacrylate
[AD-A277140] p 3660 N94-32722

ACRYLIC RESINS
Oxide pigments in water: The colloid-chemical point of view
[PB94-148616] p 3633 N94-31591

ACTIVE CONTROL
The development of active integrated antennas and a design methodology
[ISBN-0-315-86119-3] p 3675 N94-31708
Active control for fin buffet alleviation
[AD-A276844] p 3586 N94-32224
Dynamic error compensation in robotic trusses
p 3738 N94-32486
Study of dynamic stall phenomenon and its control using vorticity, stream function and circulation form of the unsteady Navier-Stokes equations p 3572 N94-32714
Magnetohydrodynamic boundary layer control system
[AD-D016120] p 3710 N94-32958
Active vortex control for a high performance wing
[AD-D016140] p 3573 N94-32974

ACTIVE GALACTIC NUCLEI
Workshop on Physics of Accretion Disks Around Compact and Young Stars
[NASA-CR-195756] p 3927 N94-31116
Time-dependent behavior of active galactic nuclei with pair production p 3929 N94-31125
A multi-frequency study of an x ray selected sample of active galactic nuclei p 3937 N94-31987

ACTS
Channel and terminal description of the ACTS mobile terminal p 3599 N94-31428

ACTUATORS
Draft minutes of IAPG Mechanical Working Group meeting
[DE94-004954] p 3759 N94-31266
Employment of a porous gold actuator in ISFET-based coulometric sensor-actuator systems with application to protein characterization
[ISBN-9-09-005887-7] p 3689 N94-31536
Nd-YAG laser welding of the fiber optic connector to the header shell on the 2SL actuator
[DE94-006104] p 3723 N94-31621
Dynamic error compensation in robotic trusses
p 3738 N94-32486
Control strategies for systems with limited actuators
[NASA-CR-195307] p 3727 N94-32741
Feed-forward control of gear mesh vibration using piezoelectric actuators
[NASA-TM-106366] p 3728 N94-32902
Limiting vibration in systems with constant amplitude actuators through command preshaping
[NASA-CR-188284] p 3739 N94-32907
Design, characterization and control of the Unique Mobility Corporation robot p 3603 N94-33296
Design, development, and testing of a lightweight optical sensor cover system p 3604 N94-33302
Pip pin reliability and design p 3605 N94-33305
High precision moving magnet chopper for variable operation conditions p 3605 N94-33307
Implementation of heaters on thermally actuated spacecraft mechanisms p 3607 N94-33320
Payload holddown and release mechanism
p 3607 N94-33321

ADA (PROGRAMMING LANGUAGE)
Translating an AI application from Lisp to Ada: A case study
[NASA-TM-103845] p 3820 N94-32906
Ada support for the mathematical foundations of software engineering
[AD-A278031] p 3822 N94-33284

ADAPTATION
Isolating strain parameters correlated to skeletal adaptation p 3797 N94-31960
Analysis and synthesis of adaptive neural elements and assemblies
[AD-A277423] p 3836 N94-32996

ADAPTERS
Grounding ring for ground adapters
[AD-D016118] p 3697 N94-32962

ADAPTIVE CONTROL
Fast autodidactic adaptive equalization algorithms
[TELECOM-93-E-018] p 3670 N94-31174
On the use of genetic algorithms to solve the time-table problem
[REPT-90-060-REV] p 3829 N94-31176
The ant system: An autocatalytic optimizing process
[REPT-91-016-REV] p 3824 N94-31177
Concepts and environment
[REPT-93-032] p 3829 N94-31186
Filtering and recognition of moving boats in radar images
[REPT-93-039] p 3671 N94-31190
ART: Adaptive Resonance Theory
[TELECOM-93-D-020] p 3829 N94-31193
A neural network methodology for engineering applications: The learning control of robotic systems
[RR-480] p 3830 N94-31500
Adaptive operating systems concepts
[ETN-94-95754] p 3830 N94-31514
Adaptive nonlinear control of spacecraft
p 3609 N94-31564
Motion and force control of coordinated robots
[ISBN-0-315-86323-4] p 3724 N94-31714
Adaptive control of a robot in Cartesian coordinates: Analysis and implementation
[ISBN-0-315-86493-1] p 3831 N94-31798
On-line physical parameter identification and adaptive control of a launch vehicle p 3602 N94-31891
Adaptive control of telerobotic systems worn by humans
[AD-A276608] p 3834 N94-32036
Geometric structure of the adaptive controller of the human arm
[AD-A276797] p 3834 N94-32152
Optimal adaptive estimation algorithm for harmonic current reduction using power limited active line conditioners
[AD-A277354] p 3693 N94-32336
A fuzzy classifier system for process control
p 3839 N94-32422
State-space self-tuner for on-line adaptive control
[NASA-CR-195836] p 3835 N94-32943
Adaptive control of nonlinear and stochastic systems
[AD-A278411] p 3839 N94-33325

ADAPTIVE FILTERS
Modelling the late part of room impulse responses using adaptive filtering: On the recreation of reality
[CTH-E-93-01] p 3859 N94-31076
The generalized multi delay adaptive filter: Structure and convergence analysis
[TELECOM-93-D-004] p 3808 N94-31094
Fast autodidactic adaptive equalization algorithms
[TELECOM-93-E-018] p 3670 N94-31174
An adaptive Kalman filter excisor for suppressing narrowband interference
[AD-A276286] p 3671 N94-31253
Concurrent architectures for VLSI signal and image processing
[AD-A276124] p 3688 N94-31445
Recursive analysis of matrix scattering functions
[AD-A277264] p 3845 N94-32018

ADAPTIVE OPTICS
Design and early results of the sodium-layer laser guide star adaptive optics experiment at the Lawrence Livermore National Laboratory
[DE94-006653] p 3926 N94-32189
Phase-only correction of scintillated laser beams: Downrange experimental results
[AD-A277778] p 3722 N94-33282
ADDITIVES
Fuel property effects on engine combustion processes
[DE94-005529] p 3631 N94-31153
Influence of trace components on the viscoelastic properties of a polymer solution
[AD-A277171] p 3656 N94-32253
Processing and characterization of functionally gradient ceramic materials
[AD-A277154] p 3657 N94-32367
Development and preliminary evaluation of aryl ester boundary additives for perfluoropolyethers
[NASA-TM-106603] p 3663 N94-33024
Torque characteristics of solid lubricated precision bearings during oscillatory motion
[AD-A278133] p 3728 N94-33061
Optical properties of doped sol-gel silica glasses
[AD-A278094] p 3884 N94-33267
ADDUCTS
Combustion-related studies using weakly-bonded complexes
[DE94-006632] p 3633 N94-31493
ADHESION
Molecular interactions at metal/polyimide interfaces: A correlation with adhesion and bond durability
[AD-A276301] p 3650 N94-31297
High performance YBCO films
[AD-A276493] p 3897 N94-31531
Soft x ray photoelectron spectroscopy study of the interaction of Cr with MoS2(0001)
[AD-A276916] p 3635 N94-32233
New micro- and macroscopic models of contact and friction
[AD-A277240] p 3726 N94-32320
Conductive paints
[DE94-008508] p 3661 N94-32788
Compilation of diamond-like carbon properties for barriers and hard coatings
[DE94-008231] p 3661 N94-32803
Frictional behavior and adhesion of Ag and Au films applied to aluminum oxide by oxygen-ion assisted Screen Cage Ion Plating (SCIP)
[NASA-TM-106522] p 3647 N94-32931
ADHESION TESTS
Small cylindrical adhesive bonds
[PB94-148210] p 3651 N94-31585
Nd-YAG laser welding of the fiber optic connector to the header shell on the 2SL actuator
[DE94-006104] p 3723 N94-31621
ADHESIVE BONDING
Molecular interactions at metal/polyimide interfaces: A correlation with adhesion and bond durability
[AD-A276301] p 3650 N94-31297
Small cylindrical adhesive bonds
[PB94-148210] p 3651 N94-31585
Shearographic inspection of a DeHavilland DHC-7
[AD-A276716] p 3566 N94-32157
The cyclic fatigue behaviour of adhesive joints
[AD-A277080] p 3738 N94-32351
ADHESIVES
Small cylindrical adhesive bonds
[PB94-148210] p 3651 N94-31585
The cyclic fatigue behaviour of adhesive joints
[AD-A277080] p 3738 N94-32351
ADJOINTS
A cell-cycle model revisited
[CWI-AM-R9305] p 3851 N94-32229
ADRENERGICS
Review of pharmacological approach to improve cold tolerance p 3796 N94-31740
ADSORPTION
Modification of semiconductor surface properties with chemically bound molecular films
[AD-A276162] p 3895 N94-31081
Infrared spectroelectrochemical study of cyanide adsorption and reactions at platinum electrodes in aqueous perchlorate electrolyte
[AD-A276402] p 3631 N94-31238
Interaction of water with metal surfaces
[AD-A276260] p 3632 N94-31293
A new mechanism for surface diffusion: Motion of a substrate-adsorbate complex
[AD-A276072] p 3632 N94-31459
Double rotation NMR studies of zeolites and aluminophosphate molecular sieves
[DE94-007032] p 3866 N94-31637
Adsorption of water to the metal/polymer interface studied by neutron and x ray reflectivity
[DE94-005578] p 3851 N94-31649
Chemical interactions between protein molecules and polymer membrane materials
[DE94-006987] p 3651 N94-31672
The adsorption of sulfate on gold(111) in acidic aqueous media: Adlayer structural inferences from infrared spectroscopy and scanning tunneling microscopy
[AD-A276643] p 3642 N94-31997
A new-type of long-range restructuring of ordered metal surfaces induced by lateral adsorbate interactions: Iodide on AU(110) electrodes
[AD-A276633] p 3643 N94-32060
Surface chemistry and durability of borosilicate glass
[DE94-006734] p 3656 N94-32116
Vibrational spectroscopy at metal-solution interfaces: Some perspectives and prospects for electrochemical surface science
[AD-A276781] p 3644 N94-32169
Ab initio study of the epitaxial growth of Ge on Si(100) surface
[DE94-007245] p 3904 N94-32724
Surface probes of porous toluene/water ices: Adsorption kinetics and annealing spectra measured by second harmonic generation
[DE94-007564] p 3637 N94-32743
Metal cluster-rare gas van der Waals complexes: Microscopic models of physisorption
[DE94-008134] p 3873 N94-32797
Time-resolved analytical methods for liquid/solid interfaces
[DE94-008352] p 3637 N94-32826
Induced adsorption of chloride and bromide by submonolayer amounts of copper underpotentially deposited on Pt(111)
[AD-A278023] p 3648 N94-33182
Mars atmospheric loss and isotopic fractionation by solar-wind-induced sputtering and photochemical escape p 3947 N94-33208
Simultaneous laboratory measurements of CO2 and H2O adsorption on palagonite: Implications for the Martian climate and volatile reservoir p 3952 N94-33240
Sensitivity of electrochemical adlayer structure to the metal crystallographic orientation: Potential-independent iodide adsorption on Au(100) in comparison with other low-index surfaces
[AD-A276714] p 3909 N94-33273
ADVANCED VERY HIGH RESOLUTION RADIOMETER
Shiptrack database analysis
[AD-A277228] p 3746 N94-32025
Sensitivity analysis of the AVHRR infrared cirrus model
[AD-A276690] p 3784 N94-32117
ADVECTION
A fully two-dimensional, non-oscillatory advection scheme for momentum and scalar transport equations
[DM-66] p 3700 N94-31221
AERIAL PHOTOGRAPHY
A paraperspective factorization method for shape and motion recovery
[AD-A276513] p 3712 N94-31929
A model geophysics program
[DE94-007415] p 3747 N94-32203
Remote sensing for hurricane Andrew impact assessment p 3758 N94-32464
AERIAL RECONNAISSANCE
Army scout/reconnaissance helicopters versus unmanned aerial vehicles
[AD-A276902] p 3579 N94-32232
Remote sensing for hurricane Andrew impact assessment p 3758 N94-32464
AEROACOUSTICS
Investigation of sonic boom for the Space Shuttle: High cross-range orbiter
[NASA-TM-108238] p 3860 N94-31336
Investigation of sonic boom for the Space Shuttle: Low cross-range orbiter
[NASA-TM-108237] p 3860 N94-31337
Aeroacoustic sources in internal flows
[ISBN-9-03-86-0282-0] p 3860 N94-31653
Experimental and computational studies on propeller noise due to inflow distortion p 3860 N94-31846
AERODYNAMIC CHARACTERISTICS
Modeling of aircraft unsteady aerodynamic characteristics. Part 1: Postulated models
[NASA-TM-109120] p 3586 N94-32951
AERODYNAMIC COEFFICIENTS
Design and initial testing of a facility to measure unsteady pressures on an oscillating cascade with supersonic leading edge locus p 3569 N94-31880
A critical assessment of UH-60 main rotor blade airfoil data
[NASA-TM-103985] p 3571 N94-32063
AERODYNAMIC CONFIGURATIONS
Prediction of transonic potential flow with slipstreams around configurations
[FFA-TN-1992-15] p 3568 N94-31220
Large-scale shape optimization: Numerical methods, parallel algorithms, and applications to aerodynamic design p 3815 N94-31966
A new method for calculating wing along aerodynamics to angle of attack 180 deg
[AD-A277965] p 3574 N94-33263
AERODYNAMIC DRAG
CFD-based drag prediction: State-of-the-art, theory, prospects
[AD-B179297] p 3567 N94-31180
Response of wall turbulence to high frequency streamwise and spanwise oscillations p 3700 N94-31211
Control of hypersonic aerodynamic forces with surface blowing p 3567 N94-31216
Shock-dependent, optimum thrust wings in supersonic flow p 3570 N94-32027
Aerodynamic drag of droplets in turbulent flow fields
[ISBN-0-315-75827-9] p 3571 N94-32491
AERODYNAMIC FORCES
Control of hypersonic aerodynamic forces with surface blowing p 3567 N94-31216
AERODYNAMIC HEAT TRANSFER
Computational study of simultaneous heat and mass transfer in turbulent separated flows p 3704 N94-31843
AERODYNAMIC HEATING
A novel CFD/structural analysis of a cross parachute
[DE94-005271] p 3568 N94-31578
Implementation of a vibrationally linked chemical reaction model for DSMC
[NASA-TM-109109] p 3710 N94-33020
AERODYNAMIC INTERFERENCE
Active control for fin buffet alleviation
[AD-A276844] p 3586 N94-32224
AERODYNAMIC LOADS
A novel CFD/structural analysis of a cross parachute
[DE94-005271] p 3568 N94-31578
Local design optimization for composite transport fuselage crown panels p 3629 N94-33132
AERODYNAMIC NOISE
A pilot study of comfort criteria and sound quality metrics for sound inside cabins of propeller-driven aircraft
[CTH-F-93-03] p 3859 N94-31090
A mathematical model for simulating noise suppression of lined ejectors
[NASA-TP-3425] p 3861 N94-32930
AERODYNAMIC STABILITY
Flutter analysis of a supersonic cascade in time domain using an ADI Euler solver
[NASA-TM-105625] p 3739 N94-32883
AERODYNAMIC STALLING
Computational prediction of stall flutter in spanwise-finite blade cascades p 3584 N94-31967
Study of dynamic stall phenomenon and its control using vorticity, stream function and circulation form of the unsteady Navier-Stokes equations p 3572 N94-32714
AERODYNAMICS
The effect of an axial flow component on a circular cylinder wake p 3699 N94-31209
Aeronautical engineering: A continuing bibliography with indexes (supplement 302)
[NASA-SP-7037(302)] p 3565 N94-31342
Aeronautical engineering: A continuing bibliography with indexes (supplement 303)
[NASA-SP-7037(303)] p 3565 N94-31361
Modular Simulator System (MSS). System/segment specification for the generic modular simulator system-flight dynamics module, volume 4
[AD-A276971] p 3590 N94-32396
Aeronautical engineering: A continuing bibliography with indexes (supplement 304)
[NASA-SP-7037(304)] p 3566 N94-32853
A new method for calculating wing along aerodynamics to angle of attack 180 deg
[AD-A277965] p 3574 N94-33263
Cumulative reports and publications through December 31, 1993
[NASA-CR-194889] p 3806 N94-33286
AEROELASTICITY
Aeroelastic vibrations of lifting surfaces
[ECL-91-01] p 3585 N94-31677
Computational prediction of stall flutter in spanwise-finite blade cascades p 3584 N94-31967
A finite-difference approximate-factorization algorithm for solution of the unsteady transonic small-disturbance equation
[NASA-TP-3129] p 3572 N94-32865
Flutter analysis of a supersonic cascade in time domain using an ADI Euler solver
[NASA-TM-105625] p 3739 N94-32883
AEROGELS
Structure-property relationships of carbon aerogels
[DE94-007120] p 3860 N94-32687

Enhanced thermal capacity aerogels summary report, FY 1993
[DE94-008888] p 3639 N94-33260

AERONAUTICAL ENGINEERING

Aeronautical engineering: A continuing bibliography with indexes (supplement 302)
[NASA-SP-7037(302)] p 3565 N94-31342
Aeronautical engineering: A continuing bibliography with indexes (supplement 303)
[NASA-SP-7037(303)] p 3565 N94-31381
Aircraft weight prediction capability. Volume 1: Weight study and results
[AD-A277206] p 3579 N94-32062
Aeronautical engineering: A continuing bibliography with indexes (supplement 304)
[NASA-SP-7037(304)] p 3566 N94-32853
Aeronautics and space report of the President: Fiscal year 1993 activities p 3966 N94-32854
Aviation human factors research in US universities: Potential contributions to national needs
[NASA-TM-108814] p 3575 N94-32927
Research and technology, 1993
[NASA-TM-106376] p 3567 N94-33046

AERONAUTICS

Research and Technology Objectives and Plans Summary (RTOPS)
[NASA-TM-105441] p 3966 N94-32885

AERONOMY

Odin aeronomy science: A phase-A report by the Aeronomy Science Working Group for the Odin satellite
[AP-31] p 3770 N94-31222

AEROSERVOELASTICITY

Aeroelastic vibrations of lifting surfaces
[ECL-91-01] p 3585 N94-31677

AEROSOLS

Desert aerosols: Sources, transports, and impacts determined by remote sensing p 3770 N94-31003
Optical and image transmission through desert atmospheres
[AD-A276022] p 3742 N94-31496
Time-dependent behavior of Mount Pinatubo aerosol
[DE94-001877] p 3764 N94-31601
Concentration system performance degradation in the aftermath of Mount Pinatubo
[DE94-001879] p 3764 N94-31602
Radar scattering from the summer polar mesosphere: Theory and observations p 3772 N94-32077
Evaluation of sulfate aerosol optical depths over the North Atlantic and comparison with satellite observations
[DE94-005457] p 3746 N94-32100
A parameterization of cloud droplet nucleation
[DE94-007469] p 3785 N94-32268
Backscatter and transmission of aerosol at UV through middle IR wavelengths
[AD-A277127] p 3718 N94-32305
Fine resolution atmospheric sulfate model driven by operational meteorological data: Comparison with observations
[DE94-002994] p 3766 N94-32691
Climate effects of anthropogenic sulfate: Simulations from a coupled chemistry/climate model
[DE94-004352] p 3767 N94-32789
Stabilized alumina/ethanol colloidal dispersion for seeding high temperature air flows
[NASA-TM-106591] p 3713 N94-32983
Counting particles emitted by stratospheric aircraft and measuring size of particles emitted by stratospheric aircraft
[NASA-CR-195908] p 3769 N94-33170
Aerosols scattering and near-infrared observations of the Martian surface p 3946 N94-33204
Groundbased monitoring of Martian atmospheric opacity p 3947 N94-33207

AEROSPACE ENGINEERING

AGARD highlights 94/1, April 1994
[AGARD-HIGHLIGHTS-94/1] p 3956 N94-31196
AGARD membership, 1994
[AGARD-MEMB-94] p 3914 N94-31197
An innovative approach to space education
p 3600 N94-31436
Aerospace test facilities at NASA LERC Plumbrook
[NASA-TM-109755] p 3602 N94-31814
Welcome to the Ohio Aerospace Institute
[NASA-TM-109756] p 3913 N94-31815
NASA strategic plan
[NASA-TM-109780] p 3915 N94-32222
NASA/DOD Aerospace Knowledge Diffusion Research Project. Paper 5: Aerospace librarians and technical information specialists as information intermediaries: A report of phase 2 activities of the NASA/DOD Aerospace Knowledge Diffusion Research Project
[NASA-TM-109777] p 3921 N94-32829
NASA/DOD Aerospace Knowledge Diffusion Research Project. Paper 6: Aerospace knowledge diffusion in the academic community: A report of phase 3 activities of the NASA/DOD Aerospace Knowledge Diffusion Research Project
[NASA-TM-109771] p 3921 N94-32830
NASA/DOD Aerospace Knowledge Diffusion Research Project. Paper 10: The NASA/DOD Aerospace Knowledge Diffusion Research Project
[NASA-TM-109769] p 3921 N94-32831
NASA/DOD Aerospace Knowledge Diffusion Research Project. Paper 12: The diffusion of federally funded aerospace research and development (R/D) and the information seeking behavior of US aerospace engineers and scientists
[NASA-TM-109404] p 3921 N94-32832
NASA/DOD Aerospace Knowledge Diffusion Research Project. Paper 18: Scientific and Technical Information (STI) policy and the competitive position of the US aerospace industry
[NASA-TM-109782] p 3921 N94-32833
NASA/DOD Aerospace Knowledge Diffusion Research Project. Paper 11: The voice of the user: How US aerospace engineers and scientists view DOD technical reports
[NASA-TM-109348] p 3921 N94-32834
NASA/DOD Aerospace Knowledge Diffusion Research Project. Paper 1: The value of scientific and technical information (STI), its relationship to Research and Development (R/D), and its use by US aerospace engineers and scientists
[NASA-TM-109774] p 3922 N94-32835
NASA/DOD Aerospace Knowledge Diffusion Research Project. Report 25: The technical communications practices of British aerospace engineers and scientists: Results of the phase 4 RAeS mail survey
[NASA-TM-109096] p 3922 N94-32836
NASA/DOD Aerospace Knowledge Diffusion Research Project. Report 24: The technical communications practices of US aerospace engineers and scientists: Results of the phase 1 SAE mail survey
[NASA-TM-109088] p 3922 N94-32837
Aeronautics and space report of the President: Fiscal year 1993 activities p 3966 N94-32854
Research and Technology Objectives and Plans Summary (RTOPS)
[NASA-TM-105441] p 3966 N94-32885

AEROSPACE ENVIRONMENTS

LDEF Materials Results for Spacecraft Applications
[NASA-CP-3257] p 3591 N94-31012
Space environment durability of beta cloth in LDEF thermal blankets p 3591 N94-31015
Impact of LDEF photovoltaic experiment findings upon spacecraft solar array design and development requirements p 3594 N94-31028
Physical properties of glasses exposed to Earth-facing and trailing-side environments on LDEF
p 3594 N94-31030
Space environmental effects on polymer composites: Research needs and opportunities p 3595 N94-31035
Physical chemistry of molecules and grains in space
[AD-A276037] p 3932 N94-31280
Modular Simulator System (MSS). System/segment specification for the generic modular simulator system-environment module, volume 13
[AD-A276980] p 3589 N94-32319
Vibration Isolation Technology (VIT) ATD project
[NASA-TM-106496] p 3567 N94-33064
Spacecraft environmental anomalies expert system
[AD-A277962] p 3612 N94-33262

AEROSPACE INDUSTRY

Welcome to the Ohio Aerospace Institute
[NASA-TM-109756] p 3913 N94-31815
NASA/DOD Aerospace Knowledge Diffusion Research Project. Paper 18: Scientific and Technical Information (STI) policy and the competitive position of the US aerospace industry
[NASA-TM-109782] p 3921 N94-32833

AEROSPACE MEDICINE

Aerospace medicine and biology: A continuing bibliography with indexes (supplement 388)
[NASA-SP-7011(388)] p 3795 N94-31414
Aerospace medicine and biology: A continuing bibliography with indexes (supplement 389)
[NASA-SP-7011(389)] p 3797 N94-32347
Aerospace medicine and biology: A continuing bibliography with indexes (supplement 385)
[NASA-SP-7011(385)] p 3797 N94-32348

AEROSPACE PLANES

Hypervelocity Tunnel 9 Mach 10/14 Calibration
[AD-A275960] p 3587 N94-31318
High temperature NASP engine seal development
[NASA-TM-109750] p 3725 N94-31804
Futurepath 3
[NASA-TM-109762] p 3735 N94-31819

AEROSPACE SCIENCES

An innovative approach to space education
p 3600 N94-31436
ISU in an era of partial reconvergence — International Space University p 3600 N94-31438
The sky is your classroom
[NASA-TM-109759] p 3914 N94-31887
Research and Technology Objectives and Plans Summary (RTOPS)
[NASA-TM-105441] p 3966 N94-32885

AEROSPACE SYSTEMS

Aerospace software engineering for advanced systems architectures
[AD-A277101] p 3581 N94-31977
Computer modelling of cyclic deformation of high-temperature materials
[AD-A277056] p 3623 N94-32012
Honeycomb sandwich structures: Vented versus unvented designs for space systems
[AD-A276713] p 3624 N94-32122
Deployable and retractable telescoping tubular structure development p 3607 N94-33317
Lessons learned from selecting and testing spaceflight potentiometers p 3607 N94-33318

AEROSPACE TECHNOLOGY TRANSFER

AGARD highlights 94/1, April 1994
[AGARD-HIGHLIGHTS-94/1] p 3956 N94-31196
Application of dexterous space robotics technology to myoelectric prostheses p 3729 N94-32450
NASA/DOD Aerospace Knowledge Diffusion Research Project. Paper 10: The NASA/DOD Aerospace Knowledge Diffusion Research Project
[NASA-TM-109769] p 3921 N94-32831

AEROTHERMODYNAMICS

The prediction of convective transfer on the thermal insulation of a solid-propellant rocket motor
[ONERA-NT-1993-15] p 3614 N94-31423

AFRICA

Dynamic climatology of West Africa
p 3778 N94-30988
Some aspects of the drought in North Africa and in the Mediterranean basin p 3778 N94-30989

AGE FACTOR

Tripping over obstacles: Biomechanical analyses of how young and old try to avoid it p 3803 N94-31954

AGING (MATERIALS)

Aging effects on the microstructure, surface characteristics and wettability of Cu pretinned with Sn-Pb solders
[DE94-007033] p 3641 N94-31638

AGING (METALLURGY)

Continuous measurement of aging response in aluminum alloys by eddy current methods
[AD-A277233] p 3644 N94-32371

AGRICULTURE

High resolution spectroscopy in agriculture: Results of the EISAC 1989 campaign p 3745 N94-31864
Extraction of agricultural parameters from imaging-spectrometry data and simulated MERIS data through red edge analysis p 3745 N94-31865
The use of SPOT, and the contribution of ERS-1, in the assessment of urban pressure on agriculture land in Greater Tunis (Tunisia) p 3749 N94-32534
Integration of ERS-1 images into the European Agriculture Statistics project Action 4: Thematic aspect
p 3753 N94-32554
Rapid estimates of crop acreage and production at European scale using high resolution imagery
p 3754 N94-32557
Food security in the context of global environmental change
[DE94-007481] p 3768 N94-32812

AIR COOLING

A review of microclimate cooling systems in the chemical, biological, radiological environment
[AD-A276446] p 3802 N94-31302

AIR FLOW

Design of a two dimensional planer pressurized air labyrinth seal test rig
[AD-A277232] p 3726 N94-32370
Low power, constant-flow air pump systems
[DE94-007463] p 3727 N94-32758
Stabilized alumina/ethanol colloidal dispersion for seeding high temperature air flows
[NASA-TM-106591] p 3713 N94-32983

AIR JETS

Turbulence structure of a premixed flame in a coaxial free air jet in the presence or absence of a base flow
[ISBN-0-315-78739-2] p 3633 N94-31471

AIR LAND INTERACTIONS

The surface parameters: Remote sensing observations and climatology applications p 3779 N94-31001
Surface fluxes of trace gases derived from convective-layer profiles p 3704 N94-31774

An evaluation of RAMS radiation schemes by field measurements
[DE94-008053] p 3767 N94-32750
Numerical simulation of thermally induced near-surface flows over Martian terrain p 3949 N94-33223
Carbonate formation on Mars: Latest experiments p 3950 N94-33231

AIR MASSES
Coastal boundary layer and refractivity measurements using the ground-based high resolution interferometer sounder (GB-HIS)
[AD-A277980] p 3683 N94-33159

AIR NAVIGATION
The contribution of aeronautics and astronautics to the quality of life on Earth
[ILR-MITT-283(1993)] p 3764 N94-31611
Flight technical error for category B non-precision approaches and missed approaches using non-differential GPS for course guidance
[PB94-142734] p 3576 N94-31680
Aircraft communication and navigation systems and communication and navigation systems
[AD-A277309] p 3582 N94-32328
Modular Simulator System (MSS). System/segment specification for the generic modular simulator system-navigation/communication module, volume 6
[AD-A276973] p 3590 N94-32398
An evaluation framework for designing a night vision, computer-based trainer
[AD-A278005] p 3590 N94-33139

AIR POLLUTION
Emissions of greenhouse gases from the use of transportation fuels and electricity
[DE94-006166] p 3765 N94-31625
Control and monitoring of heavy metal emissions
[VTT-TIED-1508] p 3765 N94-31657
Evaluation of sulfate aerosol optical depths over the North Atlantic and comparison with satellite observations
[DE94-005457] p 3746 N94-32100
Photothermal laser deflection, an innovative technique to measure particles in exhausts
[AD-A277151] p 3718 N94-32366
Carbon dioxide abatement as a differential game
[DE94-722023] p 3765 N94-32590
Fine resolution atmospheric sulfate model driven by operational meteorological data: Comparison with observations
[DE94-002994] p 3766 N94-32691
Identification of research relating to the critical loads concept and its potential application to the regulation of acidic deposition
[DE94-008234] p 3767 N94-32752
Mexico City ozone concentrations as a function of readily-available meteorological parameters
[DE94-007576] p 3768 N94-32814
Transport and diffusion in turbulent fields modeling and measurements techniques
[AD-A278114] p 3769 N94-33110

AIR PURIFICATION
In-bed multiport sampling system
[AD-A275908] p 3763 N94-31339
Removal of CO2 from flue gases by algae
[DE94-008039] p 3766 N94-32703

AIR QUALITY
Strategies for survival in the new environmental era
[AD-A276827] p 3765 N94-32195
Wind-speed measurements with a scanning elastic-backscatter lidar
[DE94-004974] p 3785 N94-32726
Performance of a new wind updating system for a prognostic meteorological model in the environs of Mexico City
[DE94-006243] p 3786 N94-32937
Transport and diffusion in turbulent fields modeling and measurements techniques
[AD-A278114] p 3769 N94-33110

AIR SAMPLING
In-bed multiport sampling system
[AD-A275908] p 3763 N94-31339
Low power, constant-flow air pump systems
[DE94-007463] p 3727 N94-32758
Counting particles emitted by stratospheric aircraft and measuring size of particles emitted by stratospheric aircraft
[NASA-CR-195908] p 3769 N94-33170

AIR TRAFFIC
The 1993 aviation system capacity plan
[AD-A276958] p 3575 N94-32620
Civil tiltrotor market penetration: Effects on Northeast corridor airport delay
[AD-A277534] p 3576 N94-32955
FAA aviation forecasts, fiscal years 1994-2005
[AD-A277808] p 3566 N94-33016

AIR TRAFFIC CONTROL
Evaluation for the development of taxiway lighting intensity standards
[AD-A276706] p 3588 N94-32120
Plan recognition for an air traffic control simulation
[DSIS-94-01221] p 3577 N94-32505
Three dimensional audio versus head down TCAS displays
[NASA-CR-177636] p 3576 N94-33063
Cockpit Electronic Display Workshop: A synopsis
[AD-A277728] p 3583 N94-33280
A heuristic multiple target tracker p 3686 N94-33346

AIR TRANSPORTATION
The contribution of aeronautics and astronautics to the quality of life on Earth
[ILR-MITT-283(1993)] p 3764 N94-31611
The 1993 aviation system capacity plan
[AD-A276958] p 3575 N94-32620
Airborne Trailblazer: Two decades with NASA Langley's 737 flying laboratory
[NASA-SP-4216] p 3566 N94-32793
Annual review of aircraft accident data: US air carrier operations, calendar year 1991
[PB94-158847] p 3575 N94-32925
Civil tiltrotor market penetration: Effects on Northeast corridor airport delay
[AD-A277534] p 3576 N94-32955
FAA aviation forecasts, fiscal years 1994-2005
[AD-A277808] p 3566 N94-33016

AIR WATER INTERACTIONS
Subtropical Climates and Their Evolution: From Space-Based Observation to Modelling
[ISBN-2-85-428333-3] p 3776 N94-30981
Climatologic flux in tropical ocean p 3777 N94-30985
Low frequence variability of the ocean atmosphere coupled system p 3777 N94-30986
Interaction processes between the ocean and the atmosphere p 3777 N94-30987
The ocean-atmosphere interactions in the Mediterranean Sea p 3779 N94-30995
Investigation of carbon dioxide in the central South Pacific Ocean (WOCE Sections P-16C and P-17C) during the TUNES/2 expedition of the R/V Thomas Washington, July-August, 1991
[DE94-006638] p 3763 N94-31347
The effect of westerly wind bursts on a tropical ocean general circulation model
[AD-A276423] p 3788 N94-31448
Research in marine boundary layer intermittency
[AD-A276076] p 3701 N94-31460
Air-sea interaction patterns in the equatorial Pacific
[AD-A277305] p 3788 N94-32072
ENSO forced variations of the sea surface temperature and adjusted sea level along the west coast of the United States
[AD-A277306] p 3789 N94-32327
High resolution properties of the marine atmospheric boundary layer
[DE94-006235] p 3774 N94-32736
Ocean variability and its influence on the detectability of greenhouse warming signals
[DE94-008670] p 3790 N94-32881
Index and bulk parameters for frequency-direction spectra measured at CERC Field Research Facility
[AD-A277759] p 3791 N94-33085
SEASOAR and CTD observations during a COARE surveys cruise, W9211C, 22 January - 22 February, 1993
[AD-A277925] p 3791 N94-33244

AIRBORNE EQUIPMENT
Airborne instruments p 3757 N94-31006
European Imaging Spectroscopy Aircraft Campaign
[ESA-SP-360] p 3743 N94-31853
The European Imaging Spectroscopy Airborne Campaign (EISAC). Data takes and evaluation programme: An overview p 3743 N94-31854
NORSMAP 1989: Norwegian remote sensing spectroscopy for mapping and monitoring or algal blooms and pollution p 3744 N94-31856
Analysis of GER imaging spectrometry data for the identification of soil and vegetation parameters in land degradation studies p 3744 N94-31857
Inflight calibration, preprocessing, and data evaluation of GER 2 imaging spectrometry data p 3744 N94-31858
Investigation on correction models for airborne imaging spectrometry data from the EISAC-campaign for geoscientific purposes p 3745 N94-31861
SATCOM feasibility study for search and rescue aircraft
[DSIS-94-01083] p 3575 N94-31902
Airborne Trailblazer: Two decades with NASA Langley's 737 flying laboratory
[NASA-SP-4216] p 3566 N94-32793

AIRBORNE LASERS
Statistics of time averaged atmospheric scintillation
[DE94-006998] p 3747 N94-32249

AIRBORNE RADAR
Airborne SAR as a complement to SPOT HRV in land-cover classification: The use of normalization and principal components analysis p 3750 N94-32539
The use of ERS-1 within an operational ice monitoring program p 3751 N94-32545
Optimal geological data extraction from SPOT-radar synergism with samples from Djebel Amour (Algeria), Red Sea Hills (Sudan), Sirte Basin (Libya), and Magdalena Valley (Colombia) p 3752 N94-32548
Respective contributions of VIS-PIR, SAR-ERS 1, and airborne radar data for morphostructural and morphoneotectonic analysis: Practical examples p 3752 N94-32549

AIRBORNE/SPACEBORNE COMPUTERS
An investigation of airborne GPS/INS for high accuracy position and velocity determination
[DE94-006139] p 3576 N94-31306
The maintenance of operational flight program
[AD-A276363] p 3565 N94-31367
Technologies for avionics embedded computer systems
[AD-A276364] p 3581 N94-31368
Testing Operational Flight Programs (OFP's)
[AD-A276361] p 3578 N94-31387
Low power, constant-flow air pump systems
[DE94-007463] p 3727 N94-32758
Data processing algorithms for on-board satellite event analysis
[AD-A278406] p 3838 N94-33168

AIRCRAFT ACCIDENT INVESTIGATION
Annual review of aircraft accident data: US air carrier operations, calendar year 1991
[PB94-158847] p 3575 N94-32925
Aircraft incident report: In-flight turbulence encounter and loss of portions of the elevators, China Airlines Flight CI-012, McDonnell Douglas MD-11-P, Taiwan Registration B-150 about 20 miles east of Japan, 7 December 1992
[PB94-910403] p 3576 N94-32938

AIRCRAFT ACCIDENTS
Rotorcraft ditchings and water-related impacts that occurred from 1982 - 1989, phase 2
[AD-A276473] p 3574 N94-31246
Estimating the impact of crashworthiness standards on mortality and morbidity events in the US Army rotary-wing aircraft mishaps
[AD-A277121] p 3575 N94-32363
Annual review of aircraft accident data: US air carrier operations, calendar year 1991
[PB94-158847] p 3575 N94-32925
Aircraft incident report: In-flight turbulence encounter and loss of portions of the elevators, China Airlines Flight CI-012, McDonnell Douglas MD-11-P, Taiwan Registration B-150 about 20 miles east of Japan, 7 December 1992
[PB94-910403] p 3576 N94-32938

AIRCRAFT ANTENNAS
Applied Computational Electromagnetics Society Journal, volume 9, number 1, March 1994
[AD-A276753] p 3679 N94-32183

AIRCRAFT COMMUNICATION
Communications networks in stressed environments
[AD-A275967] p 3672 N94-31384
SATCOM feasibility study for search and rescue aircraft
[DSIS-94-01083] p 3575 N94-31902
Aircraft communication and navigation systems and communication and navigation systems
[AD-A277309] p 3582 N94-32328
Modular Simulator System (MSS). System/segment specification for the generic modular simulator system-navigation/communication module, volume 6
[AD-A276973] p 3590 N94-32398

AIRCRAFT COMPARTMENTS
A pilot study of comfort criteria and sound quality metrics for sound inside cabins of propeller-driven aircraft
[CTH-F-93-03] p 3859 N94-31090

AIRCRAFT CONFIGURATIONS
A finite-difference approximate-factorization algorithm for solution of the unsteady transonic small-disturbance equation
[NASA-TP-3129] p 3572 N94-32865
Modeling of aircraft unsteady aerodynamic characteristics. Part 1: Postulated models
[NASA-TM-109120] p 3586 N94-32951

AIRCRAFT CONSTRUCTION MATERIALS
Damage tolerance aspects of a full composite airplane fuselage: Requirements, modelling, predictions, experiments
[LR-728] p 3578 N94-31674
Cracking induced in small fretting: Application to the case of aeronautical aluminum alloys
[ECL-92-50] p 3735 N94-31870

Location of impact damage sites in composite aircraft structures, task 3.4.1
[DSIS-94-01590] p 3621 N94-31892
Effects of frequency and amplitude variations of superimposed minor loading sequences on the corrosion fatigue behavior of aircraft structural aluminum alloys
p 3578 N94-31957
Innovative fabrication processing of advanced composite materials concepts for primary aircraft structures
[NASA-CR-189558] p 3626 N94-32877
Second NASA Advanced Composites Technology Conference
[NASA-CP-3154] p 3627 N94-33121
COINS: A composites information database system
p 3627 N94-33123
Composite fuselage shell structures research at NASA Langley Research Center p 3628 N94-33124
Structural testing of the technology integration box beam p 3628 N94-33125
Technology integration box beam failure study
p 3628 N94-33126
Development of stitched/RTM composite primary structures p 3628 N94-33127
Resin transfer molding for advanced composite primary wing and fuselage structures p 3628 N94-33128
Test and analysis results for composite transport fuselage and wing structures p 3628 N94-33129
Recent progress in NASA Langley Research Center textile reinforced composites program
p 3629 N94-33134
Advanced textile applications for primary aircraft structures p 3629 N94-33135
Comparison of resin film infusion, resin transfer molding, and consolidation of textile preforms for primary aircraft structure p 3630 N94-33136
Structural integrity of intelligent materials and structures
[AD-A278397] p 3630 N94-33165

AIRCRAFT CONTROL
Antiwindup analysis and design approaches for MIMO systems
[NASA-CR-195304] p 3584 N94-32075

AIRCRAFT DESIGN
Unmanned Air Vehicle/Remotely Piloted Vehicle analysis for lethal UAV/RPV
[AD-A276052] p 3578 N94-31442
Multidisciplinary optimization of high-speed civil transport configurations using variable-complexity modeling p 3578 N94-31881
A comparison of military and commercial aircraft development
[AD-A276830] p 3575 N94-32168
Analytical Design Package (ADP2): A computer aided engineering tool for aircraft transparency design
p 3823 N94-32430
Application of a design-build-team approach to low cost and weight composite fuselage structure
[NASA-CR-4418] p 3626 N94-32863
Second NASA Advanced Composites Technology Conference
[NASA-CP-3154] p 3627 N94-33121
Designer's unified cost model p 3627 N94-33122
COINS: A composites information database system
p 3627 N94-33123
Structural testing of the technology integration box beam p 3628 N94-33125
Local design optimization for composite transport fuselage crown panels p 3629 N94-33132
Recent progress in NASA Langley Research Center textile reinforced composites program
p 3629 N94-33134
The National Aerospace Plane (NASP): Development issues for the follow-on vehicle
[AD-A278417] p 3581 N94-33329

AIRCRAFT DETECTION
Fault detection and isolation for the Bluebird test bed aircraft
[AD-A277979] p 3586 N94-33086

AIRCRAFT ENGINES
An analysis of non-integerizing the aircraft engines Cost Effectiveness Analysis Spreadsheet Model (CEAMOD version 2.0)
[AD-A276251] p 3583 N94-31290
Thermal-mechanical fatigue crack growth in aircraft engine materials
[ISBN-0-315-86543-1] p 3734 N94-31707
Development of a cascade simulation of fan-passage flow
[AD-A277234] p 3584 N94-32026
Analysis of Navy aircraft engine and engine component warranties
[AD-A276936] p 3584 N94-32238
A user's manual for the cost effectiveness analysis spreadsheet model for aircraft engines (CEAMOD version 2.0)
[AD-A278042] p 3585 N94-33266
Analysis of intermediate level maintenance following F404-GE-400 engine component life reductions
[AD-A277918] p 3585 N94-33283
An expert system application for troubleshooting the CF18 F404 engine p 3585 N94-33339

AIRCRAFT EQUIPMENT
Modular Simulator System (MSS). System/segment specification for the generic modular simulator system-radar module, volume 8
[AD-A276975] p 3589 N94-32314

AIRCRAFT FUELS
Improved resealing procedures for the second deseal/reseal program in RAAF F111 aircraft fuel tanks
[AD-A277069] p 3580 N94-32378

AIRCRAFT HAZARDS
Aircraft icing handbook (update)
[AD-A276499] p 3574 N94-31678
WHIPICE — computer program for analysis of aircraft deicing
[NASA-TM-109749] p 3574 N94-31803

AIRCRAFT ICING
Aircraft icing handbook (update)
[AD-A276499] p 3574 N94-31678
WHIPICE — computer program for analysis of aircraft deicing
[NASA-TM-109749] p 3574 N94-31803
Continuous measurement of aircraft wing icing
p 3576 N94-32454
An experimental study of the flowfield on a semispan rectangular wing with a simulated glaze ice accretion
[NASA-CR-195301] p 3571 N94-32475

AIRCRAFT INDUSTRY
Prospects for the French fighter industry in a post-cold war environment: Is the future more than a mirage?
p 3565 N94-31959

AIRCRAFT INSTRUMENTS
Study of virtual prototyping of aircraft instruments
[CMC-0687-1090] p 3581 N94-31903

AIRCRAFT LANDING
Fuzzy-neural control of an aircraft tracking camera platform p 3839 N94-32423

AIRCRAFT LIGHTS
Evaluation of intensity distribution profiles for US. Army rotorcraft position lighting adapted for image intensifier operations
[AD-A276459] p 3804 N94-32171

AIRCRAFT MAINTENANCE
A laboratory study of multiple site damage in fuselage lap splices
[AD-A276151] p 3578 N94-31078
An analysis of the maintenance performance measurement system for LAMPS MK 3 helicopter squadrons
[AD-A276421] p 3565 N94-31332
An evaluation of aircraft maintenance performance factors in the objective wing
[AD-A276010] p 3565 N94-31362
Initial estimates of Integrated Maintenance Information System (IMIS) costs and benefits, volume 1
[AD-A276144] p 3565 N94-31830
Shearographic inspection of a DeHavilland DHC-7
[AD-A276716] p 3566 N94-32157
Human Computer Interface Specifications (HCIS) for the Integrated Maintenance Information System (IMIS)
[AD-A277184] p 3566 N94-32254
Fault detection and isolation for the Bluebird test bed aircraft
[AD-A277979] p 3586 N94-33086
A user's manual for the cost effectiveness analysis spreadsheet model for aircraft engines (CEAMOD version 2.0)
[AD-A278042] p 3585 N94-33266
Analysis of intermediate level maintenance following F404-GE-400 engine component life reductions
[AD-A277918] p 3585 N94-33283
Scheduling fighter missions using an expert system with an operations research module p 3853 N94-33337
The CF-18 diagnostic and maintenance expert system project p 3567 N94-33338
An expert system application for troubleshooting the CF18 F404 engine p 3585 N94-33339

AIRCRAFT MODELS
Controls design with crossfeeds for hovering rotorcraft using quantitative feedback theory
[NASA-CR-195765] p 3585 N94-31203
Numerical simulation of combined external/internal transonic flow on the forebody/inlet of the AV-8B Harrier 2 p 3569 N94-31759
Six degree of freedom flight dynamic model of a Mk-82 store
[AD-A277065] p 3580 N94-32362
Fault detection and isolation for the Bluebird test bed aircraft
[AD-A277979] p 3586 N94-33086

AIRCRAFT NOISE
Investigation of sonic boom for the Space Shuttle: High cross-range orbiter
[NASA-TM-108238] p 3860 N94-31336
Investigation of sonic boom for the Space Shuttle: Low cross-range orbiter
[NASA-TM-108237] p 3860 N94-31337
Common property resources and low-level flying in Labrador: Flight, fight or fancy?
[ISBN-0-315-87318-3] p 3924 N94-31732
Heliport Noise Model (HNM) version 2.2 (user's guide)
[AD-A277072] p 3861 N94-32418
Reciprocity-based experimental determination of dynamic forces and moments: A feasibility study
[NASA-CR-194905] p 3862 N94-33023

AIRCRAFT PERFORMANCE
Unmanned Air Vehicle/Remotely Piloted Vehicle analysis for lethal UAV/RPV
[AD-A276052] p 3578 N94-31442
Multidisciplinary optimization of high-speed civil transport configurations using variable-complexity modeling p 3578 N94-31881

AIRCRAFT PILOTS
Unit specific crew rest strategies: Phase 1 evaluation of the 1/212th Aviation Battalion during shiftwork transitions
[AD-A277122] p 3804 N94-32379

AIRCRAFT PRODUCTION COSTS
Designer's unified cost model p 3627 N94-33122
COINS: A composites information database system
p 3627 N94-33123
Composite fuselage crown panel manufacturing technology p 3629 N94-33133

AIRCRAFT RELIABILITY
An evaluation of aircraft maintenance performance factors in the objective wing
[AD-A276010] p 3565 N94-31362

AIRCRAFT SAFETY
Aircraft incident report: In-flight turbulence encounter and loss of portions of the elevators, China Airlines Flight CI-012, McDonnell Douglas MD-11-P, Taiwan Registration B-150 about 20 miles east of Japan, 7 December 1992
[PB94-910403] p 3576 N94-32938

AIRCRAFT STRUCTURES
Multiple-site damage in aircraft fuselage structures
[LR-729] p 3578 N94-31675
Location of impact damage sites in composite aircraft structures, task 3.4.1
[DSIS-94-01590] p 3621 N94-31892
Effects of frequency and amplitude variations of superimposed minor loading sequences on the corrosion fatigue behavior of aircraft structural aluminum alloys
p 3578 N94-31957
Finite element analysis of MB326H Macchi wing lower spar cap fatigue cracks
[AD-A277062] p 3580 N94-32264
Development of thermoplastic composite aircraft structures
[NASA-CR-189593] p 3626 N94-32860
Innovative fabrication processing of advanced composite materials concepts for primary aircraft structures
[NASA-CR-189558] p 3626 N94-32877
Second NASA Advanced Composites Technology Conference
[NASA-CP-3154] p 3627 N94-33121
Composite fuselage shell structures research at NASA Langley Research Center p 3628 N94-33124
Technology integration box beam failure study
p 3628 N94-33126
Resin transfer molding for advanced composite primary wing and fuselage structures p 3628 N94-33128
Recent progress in NASA Langley Research Center textile reinforced composites program
p 3629 N94-33134
Advanced textile applications for primary aircraft structures p 3629 N94-33135
Comparison of resin film infusion, resin transfer molding, and consolidation of textile preforms for primary aircraft structure p 3630 N94-33136
Characterization and manufacture of braided composites for large commercial aircraft structures
p 3630 N94-33137
Structural integrity of intelligent materials and structures
[AD-A278397] p 3630 N94-33165

AIRCRAFT TIRES
Computational methods for frictional contact with applications to the Space Shuttle orbiter nose-gear tire
p 3608 N94-32295

AIRCRAFT WAKES
A study of the development and attenuation of wing-generated, vortical wakes p 3570 N94-31971

AIRFOIL OSCILLATIONS
Design and initial testing of a facility to measure unsteady pressures on an oscillating cascade with supersonic leading edge locus p 3569 N94-31880
Flutter analysis of a supersonic cascade in time domain using an ADI Euler solver
[NASA-TM-105625] p 3739 N94-32883
AIRFOIL PROFILES
Shock-dependent, optimum thrust wings in supersonic flow p 3570 N94-32027
AIRFOILS
On an adaptation method for 2-dimensional C-type grids
[W-9322] p 3569 N94-31822
On an adaptation method for dense, 2D, C-type grids
[W-9321] p 3706 N94-32045
Fatigue in single crystal nickel superalloys
[AD-A276662] p 3843 N94-32047
The analysis of wake-induced unsteady aerodynamics related to higher harmonic control
[AD-A277914] p 3573 N94-33108
AIRFRAMES
Dual-band infrared imaging to detect corrosion damage within airframes and concrete structures
[DE94-006047] p 3580 N94-32658
AIRGLOW
Time-resolved IR spectroscopy, energy transfer, and state-to-state collision dynamics of atmospheric species
[AD-A277372] p 3773 N94-32338
AIRLINE OPERATIONS
Planning of air crew schedules
[ISBN-0-315-86506-7] p 3914 N94-32074
FAA aviation forecasts, fiscal years 1994-2005
[AD-A277808] p 3566 N94-33016
AIRPORTS
Determining the bearing capacity of flexible airfield pavements using a heavy weight deflectometer
[ISBN-0-315-86210-6] p 3587 N94-31710
The 1993 aviation system capacity plan
[AD-A276958] p 3575 N94-32620
ALASKA
The Northern Plains MSATT Meeting, and a call for a field-oriented successor to MSATT
p 3947 N94-33210
ALBEDO
Monoenergetic neutral particle transport in semi-infinite media
[AD-A277155] p 3870 N94-32368
Fine resolution atmospheric sulfate model driven by operational meteorological data: Comparison with observations
[DE94-002994] p 3766 N94-32691
Temporal and spatial mapping of atmospheric dust opacity and surface albedo on Mars
p 3947 N94-33211
ALBUMINS
Characterization and utilization of opiate-like hibernation factors
[AD-A278136] p 3794 N94-33098
ALCOHOLS
Heterogeneous catalytic process for alcohol fuels from syngas
[DE94-008729] p 3667 N94-32583
ALDEHYDES
Ligand intermediates in metal-catalyzed reactions
[DE94-008713] p 3638 N94-32887
ALFALFA
The properties of sunflecks in a flexible plant canopy, and their relationship to turbulence
p 3782 N94-31775
Dry deposition of PAN to grassland vegetation
[DE94-005111] p 3768 N94-32894
ALGAE
NORSMAP 1989: Norwegian remote sensing spectroscopy for mapping and monitoring or algal blooms and pollution p 3744 N94-31856
Removal of CO2 from flue gases by algae
[DE94-008039] p 3766 N94-32703
ALGEBRA
An algebraic view on Rosetta
[CL-93-02] p 3841 N94-31391
Multiparameter quantum groups and multiparameter R-matrices
[CWI-AM-R9307] p 3846 N94-32106
Algebraic functions for recognition
[AD-A276803] p 3846 N94-32167
Quantum homogeneous spaces, duality, and quantum 2-spheres
[CWI-AM-R9309] p 3857 N94-32192
Some problems of applied algebra
[CWI-AM-R9306] p 3847 N94-32204
N(exp n(n-1)/2)-state R-matrix related with U(sub q)(sl(n)) algebra at q(exp 2N) = 1
[DE94-608140] p 3902 N94-32247
A high-speed linear algebra library with automatic parallelism p 3828 N94-32440
ALGORITHMS
Implanting algorithms on parallel machines
[TELECOM-93-D-017] p 3823 N94-31099
Feasibility and stability results for constrained stable generalized predictive control
[MATHS-REPT-A-203] p 3828 N94-31158
Fast autodidactic adaptive equalization algorithms
[TELECOM-93-E-018] p 3670 N94-31174
On the use of genetic algorithms to solve the time-table problem
[REPT-90-060-REV] p 3829 N94-31176
The ant system: An autocatalytic optimizing process
[REPT-91-016-REV] p 3824 N94-31177
Concepts and environment
[REPT-93-032] p 3829 N94-31186
A worst-case analysis of two approximate algorithms for the symmetric travelling salesman problem
[REPT-93-036] p 3840 N94-31187
Techniques for increasing the robustness of iterative algorithms for multi-resources location problems
[REPT-93-037] p 3809 N94-31188
Exact solution of the single machine scheduling problem with earliness and flow time penalties
[REPT-93-038] p 3809 N94-31189
A worst-case analysis of an approximate algorithm for finding the minimum hamiltonian cycle on paths
[REPT-93-042] p 3809 N94-31192
Design and analysis of scalable parallel algorithms
[AD-A276255] p 3809 N94-31251
Feature discovery in gray level imagery for one-class object recognition
[DE94-005268] p 3671 N94-31267
Algorithms and structures for real-time signal processing
[AD-A276101] p 3810 N94-31277
Analysis of ionospheric parameters in Europe and creation of the prediction algorithm
[AD-A276342] p 3771 N94-31326
A parallel implementation of the column subtraction algorithm
[AD-A275922] p 3810 N94-31343
Proving theorems of the Lambek calculus of order 2 in polynomial time
[CT-93-05] p 3842 N94-31393
Identification of polynomial and rational NARMAX models
[RR-483] p 3842 N94-31413
Parallel structured optimization algorithms for inverse problems
[AD-A276053] p 3811 N94-31443
A hierarchical approach to test generation for CMOS VLSI circuits
[ISBN-9-09-005449-9] p 3689 N94-31535
Solution of the incompressible Navier-Stokes equations in general coordinates by Krylov subspace and multigrid methods
[REPT-93-64] p 3703 N94-31660
Algorithms and parallel architectures for laser acoustic imaging
[ISBN-0-315-86466-4] p 3716 N94-31797
Lattice geometrodynamics p 3857 N94-31825
Compiler techniques for managing data motion
[AD-A276514] p 3918 N94-31930
Hierarchical mixtures of experts and the EM algorithm
[AD-A276516] p 3814 N94-31932
On the convergence of stochastic iterative dynamic programming
[AD-A276517] p 3815 N94-31933
Principal component analysis with missing data and its application to object modeling
[AD-A276644] p 3845 N94-31939
Large-scale shape optimization: Numerical methods, parallel algorithms, and applications to aerodynamic design p 3815 N94-31966
Recursive analysis of matrix scattering functions
[AD-A277264] p 3845 N94-32018
On an adaptation method for dense, 2D, C-type grids
[W-9321] p 3706 N94-32045
Automated detection of ship tracks in multispectral satellite data
[AD-A276697] p 3746 N94-32119
High-performance speech recognition using consistency modeling
[AD-A276775] p 3679 N94-32185
Undiscounted Markov decision chains with partial information; an algorithm for computing a locally optimal periodic policy
[TW-93-10] p 3851 N94-32205
An algorithm for probabilistic, totally-ordered temporal projection
[AD-A277341] p 3817 N94-32257
Stochastic realization of a Gaussian stochastic control system
[CWI-BS-R9320] p 3852 N94-32350
The p-q-r-medial axis algorithm requires only local operations
[CWI-BS-R9317] p 3849 N94-32507
Production of terrain data: Optical radar complementarity p 3750 N94-32540
Bounds on least-squares four-parameter sine-fit errors due to harmonic distortion and noise
[DE94-007859] p 3849 N94-32653
Overview of shock physics codes for armor analysis
[DE94-008948] p 3739 N94-32842
Parallel supercomputing: Advanced methods, algorithms, and software for large-scale linear and nonlinear problems
[DE94-008446] p 3836 N94-32992
Finding all periods and initial palindromes of a string in parallel
[AD-B175089] p 3827 N94-33002
Noise cancellation for CELP voice encoders in an F/A-18 noise environment
[AD-A277652] p 3683 N94-33026
Machine assisted implementation of complex algorithms and labor intensive software, closing report
[AD-A277662] p 3821 N94-33027
Theory and application of image enhancement
[AD-A277896] p 3821 N94-33031
Fast nonsupervised 3D registration of PET and MR images of the brain
[TELECOM-93-C-006] p 3798 N94-33069
Multiple-valued programmable logic array minimization by solution space search
[AD-A278033] p 3821 N94-33090
Mixed 0-1 programming by lift-and-project in a branch-and-cut framework
[AD-A278045] p 3822 N94-33183
Convergence results for the EM approach to mixtures of experts architectures
[AD-A276801] p 3852 N94-33276
ALIGNMENT
Automatic resonator alignment and power stabilization of high power C02 lasers
[ISBN-0-315-77217-4] p 3714 N94-31472
Special test equipment and fixturing for MSAT reflector assembly alignment p 3606 N94-33316
ALKALI METALS
Metal ion complexation by ionizable crown ethers
[DE94-008301] p 3661 N94-32847
ALKALINE EARTH METALS
Properties of doped and undoped (Ca,Sr)CuO2 thin films
[DE94-007230] p 3905 N94-32785
ALKYL COMPOUNDS
New molecular-based routes to binary main group metal sulfides
[AD-A277005] p 3900 N94-32003
Processable, chemical routes to binary metal sulfides
[AD-A277006] p 3642 N94-32004
Group 12 thiolates: Syntheses, characterization and decomposition pathways
[AD-A277055] p 3900 N94-32011
Ignition delays, heats of combustion, and reaction rates of aluminum alkyl derivatives used as ignition and combustion enhancers for supersonic combustion
[NASA-CR-189581] p 3638 N94-32868
ALKYNES
New developments in second-order nonlinear optical polymeric materials
[AD-A277409] p 3658 N94-32578
ALLOYING
Defect-solute interactions near irradiation grain boundaries
[DE94-006215] p 3641 N94-31627
On the formation of muon- and zeta-phases in Ag-Al system by mechanical alloying
[DE94-007125] p 3645 N94-32636
ALLOYS
Metal induced embrittlement
[DE94-007450] p 3640 N94-31325
The new Metals and Alloys Indexes, search manual: A phase diagram research tool
[DE94-005371] p 3643 N94-32098
ALPHA PARTICLES
Mechanisms of formation and of de-excitation in the reaction Mg-24 + C-12 yields 9 alpha at 35MeV per nucleon
[ISBN-0-315-86746-9] p 3867 N94-31749
Collisional and chaotic transport of energetic particles in toroidal plasma
[DE94-006504] p 3889 N94-31787
Basic principles approach for studying nonlinear Alfven wave-alpha particle dynamics
[DE94-007112] p 3891 N94-32664
ALTERNATING CURRENT
Modal analysis of multiterminal high voltage direct current transmission
[DE94-006426] p 3691 N94-31785

Analytic formulation for the ac electrical conductivity in two-temperature, strongly coupled, overdense plasma: FORTRAN subroutine
[DE94-009466] p 3893 N94-32915
Stabilization method of A.C. arc plasma
[DE94-757268] p 3893 N94-32916

ALTERNATING DIRECTION IMPLICIT METHODS
An efficient three-dimensional Poisson solver for SIMD high-performance-computing architectures p 3823 N94-31120
Flutter analysis of a supersonic cascade in time domain using an ADI Euler solver
[NASA-TM-105625] p 3739 N94-32883

ALTIMETERS
The effects of altimeter sampling characteristics: Some Geosat examples
[AD-A276899] p 3747 N94-32214

ALTITUDE
Drop size distributions and related properties of fog for five locations measured from aircraft
[NASA-CR-4585] p 3787 N94-33065

ALUMINIDES
Structure, stability, and mechanical properties of intermetallic phases
[DE94-009178] p 3647 N94-32852

ALUMINUM
Anodized aluminum on LDEF p 3592 N94-31017
Interfacial behaviour: Wettability in SiC(sub p) metal matrix composites
[ISBN-0-315-87206-3] p 3621 N94-31835
An experimental study of void formation during aluminum solidification in reduced gravity p 3667 N94-31944
Compositions and chemical bonding in ceramics by quantitative electron energy-loss spectrometry
[DE94-007208] p 3659 N94-32640
Influence of volume fraction of component materials and interlayer bond strength on fracture toughness of multi-layer Al 6090-25 volume percent SiCp and Al 5182 laminates
[DE94-007141] p 3626 N94-32665
Evaluation of the Hughes conversion coating touch-up pen
[AD-A278398] p 3664 N94-33166

ALUMINUM ALLOYS
Shock tube ignition and combustion of aluminum/magnesium alloy particles in oxygen at high pressure p 3631 N94-31286
Microstructures and mechanical properties of Al3Ti-based alloys: Analysis in single phase and multiphase systems
[ONERA-NT-1993-6] p 3640 N94-31420
Powder metallurgical processing of fibre reinforced aluminium composites
[PB94-148285] p 3620 N94-31688
Acceptance criteria for weld defects in aluminium weldments
[PB94-138575] p 3735 N94-31841
Cracking induced in small fretting: Application to the case of aeronautical aluminum alloys
[ECL-92-50] p 3735 N94-31870
Acoustic emission from crack growth in 7050 aluminum and 7075 aluminum as a function of temperature and heat treatment
[DREP-CRS-93-15] p 3642 N94-31871
Effects of frequency and amplitude variations of superimposed minor loading sequences on the corrosion fatigue behavior of aircraft structural aluminum alloys p 3578 N94-31957
Work hardening behavior in aluminum alloy 2090
[DE94-007036] p 3643 N94-32064
Fatigue testing of 2024-T3 material after four cycles of PMB stripping
[AD-A276926] p 3644 N94-32237
Study of type 2 and 3 anodized Al 5052-0 in aqueous DS2 solutions
[AD-A276960] p 3644 N94-32240
Continuous measurement of aging response in aluminum alloys by eddy current methods
[AD-A277233] p 3644 N94-32371
A state variable material model for superplastic titanium-6 percent Al-4 percent V p 3644 N94-32498
Liquid-assisted diffusion bonding of NiAl
[DE94-008687] p 3645 N94-32522
Boron and hydrogen in Ni3Al. Part 2: Mechanical testing of bicrystals
[DE94-007441] p 3904 N94-32606
On the formation of muon- and zeta-phases in Ag-Al system by mechanical alloying
[DE94-007125] p 3645 N94-32636
Calculations of nonspherically averaged charge densities for substitutionally disordered alloys
[DE94-008293] p 3646 N94-32754
Phase relationships and stability of the (mu)- and (zeta)-phases in the Ag-Al-X (X=Zn, Ga, Ge) systems
[DE94-009391] p 3648 N94-33270

ALUMINUM ARSENIDES
A 1-picosecond InGaAs photodetector for operation at 1300-1600 nm
[AD-A275959] p 3895 N94-31350
High speed, strained layer, multiquantum well, GaInAsP and GaAs lasers and heterostructures
[AD-A277287] p 3719 N94-32608

ALUMINUM GALLIUM ARSENIDES
High-performance GaAs/AlGaAs optical phase modulators for microwave/photonic integrated circuits
[DE94-006361] p 3688 N94-31483
Epitaxial liftoff technology onto processed silicon foundry wafers
[AD-A277116] p 3900 N94-31985
Large-diameter InGaAs/AlGaAs vertical-cavity surface-emitting lasers with low threshold current density fabricated using a simple chemical etch process
[AD-A277733] p 3721 N94-33003
Characteristics of III-V semiconductor devices at high temperature
[NASA-TM-106574] p 3697 N94-33052

ALUMINUM GRAPHITE COMPOSITES
The impact of LDEF results on the space application of metal matrix composites p 3595 N94-31034

ALUMINUM OXIDES
Evaluation of nondestructive inspection techniques for quality control of alumina-ceramic housing components
[AD-A276220] p 3730 N94-31065
Processing of novel nanoparticle dispersion strengthened ceramics for improved mechanical performance
[AD-A275965] p 3649 N94-31276
Cost-effective ceramic machining: Summary of three-body wear experiments
[DE94-007757] p 3650 N94-31354
Reliability analysis of structural ceramics subjected to biaxial flexure p 3650 N94-31454
Joining of alumina by vacuum brazing
[VTT-TIED-1495] p 3724 N94-31656
Fatigue crack propagation and fractography of 3Y-TZP and ZTA
[ISBN-0-315-86561-X] p 3736 N94-31912
High-temperature deformation and fracture toughness of duplex ceramic microstructures p 3653 N94-31945
Oriented Si and Ge nanocrystals formed in Al2O3 by ion implantation and annealing
[DE94-005593] p 3901 N94-32172
Processing and characterization of functionally gradient ceramic materials
[AD-A277154] p 3657 N94-32367
Frictional behavior and adhesion of Ag and Au films applied to aluminum oxide by oxygen-ion assisted Screen Cage Ion Plating (SCIP)
[NASA-TM-106522] p 3647 N94-32931
Stabilized alumina/ethanol colloidal dispersion for seeding high temperature air flows
[NASA-TM-106591] p 3713 N94-32983
Perfluoropolyalkylether decomposition on catalytic aluminas
[NASA-TM-106547] p 3617 N94-33021
Interface engineering in oxide fiber/oxide matrix composites
[AD-A277672] p 3627 N94-33029
Development of materials for spectral hole burning applications
[AD-A278408] p 3909 N94-33324

AMBIGUITY
Generation of the ambiguity function for ultra wideband radar waveforms
[AD-A277913] p 3684 N94-33261

AMBIPOLAR DIFFUSION
Radar scattering from the summer polar mesosphere: Theory and observations p 3772 N94-32077

AMIDES
Intramolecular charge transfer complexes as fluorescence probes for UV and visible light induced acrylate polymerization
[AD-A277129] p 3657 N94-32381

AMINES
Reactions of electrophilic maleic anhydride and epoxy groups with nucleophilic functionalities such as carboxyl, hydroxyl, and amine groups. Polymer Technology Publication series no. 16
[PB94-135589] p 3648 N94-31069
Design of new polymers to improve radiation stability of plastic scintillators
[DE94-008220] p 3652 N94-31764
Microstructure of copolymers containing disperse red 1 and methyl methacrylate
[AD-A277140] p 3660 N94-32722

AMMONIA
Chemisorbed-molecule potential-energy surfaces and electronically-stimulated processes
[DE94-007932] p 3719 N94-32603
Enhanced thermal capacity aerogels summary report, FY 1993
[DE94-008888] p 3639 N94-33260

AMORPHOUS MATERIALS
Ion-beam-driven amorphization of Ca2La8(Si4)6O2 single crystals
[DE94-006219] p 3895 N94-31307
The effects of amorphous layer regrowth on carbon activation in GaAs and InP
[DE94-006290] p 3899 N94-31634
Deposition of DLC via intense ion beam ablation
[DE94-005583] p 3651 N94-31650
Reversible optical storage in azo polymers
[AD-A277109] p 3654 N94-31980
Isomeric poly(benzophenone)s: Synthesis of highly crystalline poly (4, 4 foot-benzophenone) and amorphous poly (2, 5-benzophenone), a soluble poly (p-phenylene) derivative
[AD-A277261] p 3655 N94-32017
Anomalous small angle x ray scattering studies of amorphous metal-germanium alloys
[DE94-007258] p 3900 N94-32065
On the formation of muon- and zeta-phases in Ag-Al system by mechanical alloying
[DE94-007125] p 3645 N94-32636
Anisotropic phase separation through the metal-insulator transition in amorphous Mo-Ge and Fe-Ge alloys
[DE94-007259] p 3646 N94-32795
Compilation of diamond-like carbon properties for barriers and hard coatings
[DE94-008231] p 3661 N94-32803
Electron energy dependence of amorphization in Zr3Fe
[DE94-008459] p 3906 N94-32875
Interface controlled amorphization of crystalline Ni/Ti multilayers
[DE94-008685] p 3906 N94-32884
Irradiation-induced phase transformations in zirconium alloys
[DE94-008484] p 3648 N94-32993
Fundamental studies in crack initiation
[AD-A278387] p 3741 N94-33356

AMORPHOUS SILICON
Experimental and theoretical studies of hydrogenated amorphous semiconductor alloys and superlattices
[AD-A276159] p 3686 N94-31079
Hydrogenated amorphous silicon (a-Si:H) based gamma camera: Monte Carlo simulations
[DE94-007042] p 3795 N94-31323
In-situ characterization of growth and interfaces in a-Si:H devices
[DE94-000291] p 3760 N94-31812
Research on the stability, electronic properties, and structure of a-Si:H and its alloys
[DE94-000292] p 3899 N94-31813
Research on stable, high-efficiency amorphous silicon multijunction modules
[DE94-000298] p 3695 N94-32680
Large-area, triple-junction a-Si alloy production scale-up
[DE94-006856] p 3762 N94-32765

AMPLIFICATION
Short-pulse, high-intensity lasers at Los Alamos
[DE94-007545] p 3720 N94-32760

AMPLIFIERS
Universal signal conditioning amplifier p 3699 N94-32460
Analysis and design of a high speed, wide range stepwise tunable optical filter/amplifier
[PB94-149572] p 3698 N94-33169

AMPLITUDE MODULATION
Pulse-splitting and AM-FM conversion in a nonlinear dispersive medium
[AD-A277041] p 3861 N94-32262

AMPTE (SATELLITES)
Computer modeling of active experiments in space plasmas p 3890 N94-31927

ANALOG CIRCUITS
Study of continuous-time and mixed analog-digital operators
[TELECOM-93-E-010] p 3687 N94-31170
VLSI implementation of stray insensitive switched capacitor composite operational amplifiers
[AD-A276461] p 3687 N94-31240
Hierarchical fault catalog process for diagnosis of analog circuits
[ETN-94-95730] p 3689 N94-31571

ANALOG DATA
An analog preprocessing architecture for high-speed analog-to-digital conversion
[AD-A276737] p 3807 N94-32163

ANALOG TO DIGITAL CONVERTERS
An analog preprocessing architecture for high-speed analog-to-digital conversion
[AD-A276737] p 3807 N94-32163

A flexible IBM-PC based data acquisition system for nuclear physics experiments
[USIP-92-02] p 3922 N94-32856

ANALOGS
The Northern Plains MSATT Meeting, and a call for a field-oriented successor to MSATT
p 3947 N94-33210

ANALYTICAL CHEMISTRY
Fiber optic chemical sensors
[AD-A277128] p 3881 N94-32380
Time-resolved analytical methods for liquid/solid interfaces
[DE94-008352] p 3637 N94-32826

ANALYZERS
Post-calibration correction for rotating-analyzer ellipsometer with optical fiber bundle detection system
[AD-A277329] p 3881 N94-32280

ANATOMY
Interactive reconstruction of anatomical structures with free-form surfaces
[TELECOM-93-E-002] p 3794 N94-31195

ANCHORS (FASTENERS)
Use of a pitch adjustable foot restraint system: Operator strength capability and load requirements
[NASA-TP-3477] p 3805 N94-33050

ANESTHESIA
Development and enhancement of a model of performance and decision making under stress in a real life setting
[AD-A276029] p 3799 N94-31440

ANGLE OF ATTACK
Tip effects on the vortex wake of an axisymmetric body at angle of attack p 3570 N94-31907
Active control for fin buffet alleviation
[AD-A276844] p 3586 N94-32224
An experimental study of the flowfield on a semispan rectangular wing with a simulated glaze ice accretion
[NASA-CR-195301] p 3571 N94-32475
Control of low-speed turbulent separated flow over a backward-facing ramp
[NASA-TM-109740] p 3573 N94-33071
Installed F/A-18 inlet flow calculations at 30 degrees angle-of-attack: A comparative study
[NASA-CR-195297] p 3573 N94-33119
A new method for calculating wing along aerodynamics to angle of attack 180 deg
[AD-A277965] p 3574 N94-33263

ANGULAR DISTRIBUTION
Energy and angular distributions of secondary ions during electronic sputtering of nonconducting surfaces
[ETN-94-95756] p 3865 N94-31516
Monoenergetic neutral particle transport in semi-infinite media
[AD-A277155] p 3870 N94-32368

ANGULAR MOMENTUM
Accretion disks around black holes
p 3928 N94-31117
The dynamical settling of warped disks and angular momentum transport in galaxies p 3928 N94-31121
Observations of accretion and angular momentum regulation in young circumstellar disks and the implications for planetary formation p 3928 N94-31122
Evolution of vaporizing pulsars p 3929 N94-31128
A study of angular momentum loss in binaries using the free Lagrange method p 3931 N94-31134
Evolution of protoplanetary disks with dynamo magnetic fields p 3931 N94-31135
Theory of protostellar accretion disks
p 3931 N94-31136
Trajectory planning for space manipulators
[AD-A277229] p 3611 N94-32369

ANGULAR RESOLUTION
The Los Alamos National Laboratory precision double crystal spectrometer
[DE94-008075] p 3713 N94-32706

ANHYDRIDES
Reactions of electrophilic maleic anhydride and epoxy groups with nucleophilic functionalities such as carboxyl, hydroxyl, and amine groups. Polymer Technology Publication series no. 16
[PB94-135589] p 3648 N94-31069

ANIMALS
From animals to animats
[AD-A277427] p 3802 N94-33241

ANISOTROPIC MEDIA
Ultrasonic tomography in fiber-reinforced composite materials p 3620 N94-31565

ANISOTROPIC SHELLS
A separation technique for asymptotic-numeric solution for general shells of revolution p 3736 N94-31961

ANISOTROPY
Radiation from an aperture into an anisotropic plasma half-space p 3885 N94-31205
Strongly anisotropic s-wave versus d-wave gap in cuprate superconductors: Evidence and theory
[DE94-007579] p 3904 N94-32746
Anisotropic phase separation through the metal-insulator transition in amorphous Mo-Ge and Fe-Ge alloys
[DE94-007259] p 3646 N94-32795

ANNEALING
Ionizing radiation effects on silicon test structures
[DE94-006060] p 3865 N94-31607
Oriented Si and Ge nanocrystals formed in Al2O3 by ion implantation and annealing
[DE94-005593] p 3901 N94-32172
Stability and precipitation kinetics in Si(1-y)C(y)/Si and Si(1-x-y)Ge(x)C(y)/Si heterostructures prepared by solid phase epitaxy
[DE94-006589] p 3902 N94-32296
Femtosecond probe-probe transmission studies of LT-grown GaAs near the band edge
[DE94-006660] p 3904 N94-32634
Compositions and chemical bonding in ceramics by quantitative electron energy-loss spectrometry
[DE94-007208] p 3659 N94-32640
Gettering of metal impurities by cavities in silicon
[DE94-005248] p 3645 N94-32672
Surface probes of porous toluene/water ices: Adsorption kinetics and annealing spectra measured by second harmonic generation
[DE94-007564] p 3637 N94-32743

ANNIHILATION REACTIONS
Time-dependent behavior of active galactic nuclei with pair production p 3929 N94-31125
B lifetimes at CDF
[DE94-006650] p 3866 N94-31669
Study of associated gauge boson production at D0: W gamma production
[DE94-006951] p 3866 N94-31670
Temperature dependence of the exciton-exciton annihilation rate constant in poly(di-n-hexylsilane)
[DE94-005584] p 3655 N94-32102

ANNUAL VARIATIONS
Regional sources of error growth in the National Meteorological Center's medium-range forecast model
p 3781 N94-31554
Seasons and chaos in population dynamics
p 3912 N94-31897
Forecasters handbook for the Philippine Islands and surrounding waters
[AD-A277993] p 3787 N94-33089
Controls on the CO2 seasonal cycle
p 3950 N94-33227
The influence of thermal inertia on Mars' seasonal pressure variation and the effect of the weather component p 3952 N94-33238
Diurnal, seasonal and solar activity variations of F-region parameters
[AD-A278106] p 3776 N94-33285

ANODES
X ray pulse considerations and electron flow in high voltage diodes
[AD-A277301] p 3868 N94-32044
High power switch design for the Nova upgrade laser (Project HERCULES: High Energy Research Concerning the Ultimate Lifetime of Experimental Switches)
[DE94-007921] p 3719 N94-32654

ANODIC COATINGS
Study of type 2 and 3 anodized Al 5052-0 in aqueous DS2 solutions
[AD-A276960] p 3644 N94-32240

ANODIZING
Anodized aluminum on LDEF p 3592 N94-31017

ANOMALIES
Spacecraft environmental anomalies expert system
[AD-A277962] p 3612 N94-33262
The Galileo high gain antenna deployment anomaly
p 3607 N94-33319

ANTARCTIC REGIONS
High frequence and automatic link establishment (HF and ALE) radio propagation test to Antarctica
[AD-A277730] p 3682 N94-33001

ANTENNA ARRAYS
Predicting antenna parameters from antenna physical dimensions
[AD-A276442] p 3672 N94-31300
Radar rainfall measurements from space
p 3782 N94-31889
Proceedings of the 1993 Antenna Applications Symposium, volume 1
[AD-A277202] p 3676 N94-32049
Proceedings of the 1993 Antenna Applications Symposium, volume 2
[AD-A277203] p 3677 N94-32050
Optical processing of MMW for agile beamsteering and beamforming
[AD-A277161] p 3880 N94-32068
Processing and characterization of functionally gradient ceramic materials
[AD-A277154] p 3657 N94-32367
The 20 GHz circularly polarized, high temperature superconducting microstrip antenna array
[NASA-CR-195097] p 3683 N94-33083
INSAT-2A and 2B development mechanisms
p 3803 N94-33293

ANTENNA DESIGN
Low sidelobe reflector antenna design for communications
[AD-A276079] p 3673 N94-31463
The development of active integrated antennas and a design methodology
[ISBN-0-315-86119-3] p 3675 N94-31708
Applied Computational Electromagnetics Society Journal, volume 9, number 1, March 1994
[AD-A276753] p 3679 N94-32183
Processing and characterization of functionally gradient ceramic materials
[AD-A277154] p 3657 N94-32367
Broadband, high-power, 2-30 MHz, twin-whip antenna. Computer and 1/10-scale model design study
[AD-A277619] p 3682 N94-32971
Reconfigurable Array of Radiating Elements (RARE) controlled by light
[NASA-CR-195828] p 3684 N94-33073
The 20 GHz circularly polarized, high temperature superconducting microstrip antenna array
[NASA-CR-195097] p 3683 N94-33083

ANTENNA FEEDS
Theoretical and experimental study of microstrip-to-slot line uniplanar transition
[NASA-TM-106566] p 3696 N94-32905

ANTENNA RADIATION PATTERNS
Predicting antenna parameters from antenna physical dimensions
[AD-A276442] p 3672 N94-31300
Formulation of time-domain planar near-field measurements without probe correction
[AD-A276380] p 3672 N94-31371
Proceedings of the 1993 Antenna Applications Symposium, volume 1
[AD-A277202] p 3676 N94-32049
Proceedings of the 1993 Antenna Applications Symposium, volume 2
[AD-A277203] p 3677 N94-32050
Using TSAR with the post-processing far-field option
[DE94-006615] p 3679 N94-32188
Particle-In-Cell (PIC) code simulation results and comparison with theory scaling laws for photoelectron-generated radiation
[DE94-006132] p 3695 N94-32662

ANTICOAGULANTS
Oxide pigments in water: The colloid-chemical point of view
[PB94-148616] p 3633 N94-31591

ANTIFERROMAGNETISM
Synthesis, characterization, phase diagrams and superconducting, and normal state magnetic properties of La(2-x)Sr(x)CuO4 (0 is less than or equal to x which is less than or equal to 0.08) and electrochemically oxidized La(2-x)Sr(x)CuO(4 + delta) (0 is less than or equal to x which is less than or equal to 0.33, 0 is less than or equal to delta which is less than or equal to 0.12)
[DE94-005260] p 3895 N94-31087

ANTIKNOCK ADDITIVES
Fuel property effects on engine combustion processes
[DE94-005529] p 3631 N94-31153

ANTIMISSILE DEFENSE
Basic and applied studies of the ram accelerator as a hypervelocity projectile launcher
[AD-A277392] p 3602 N94-32286
Vulnerability assessment of a space based weapon platform electronic system exposed to a thermonuclear weapon detonation
[DE94-007229] p 3611 N94-32667

ANTIPROTONS
F0-975, A0-980 as eye-witnesses of confinement
[PB94-147105] p 3868 N94-31923
Antiproton production in heavy ion collisions
[DE94-007552] p 3870 N94-32271
Studies of jet production with the D0 detector
[DE94-008271] p 3873 N94-32780

ANTIREFLECTION COATINGS
The role of defects in laser damage of multilayer coatings
[DE94-006731] p 3714 N94-31269
Sol-gel coatings for high power laser optics: Past, present, and future
[DE94-007240] p 3718 N94-32252

ANXIETY
An exploratory study of neuro linguistic programming and communication anxiety
[AD-A277756] p 3682 N94-32986
Stress-induced enhancement of the startle reflex
[AD-A278414] p 3802 N94-33327

APERTURES
Radiation from an aperture into an anisotropic plasma half-space p 3885 N94-31205
Transverse mode analysis of hole-coupled free-electron lasers
[ETN-94-96019] p 3715 N94-31532
Aperture excitation of electrically large, lossy cavities
[PB94-145711] p 3675 N94-31683

APOLLO 11 FLIGHT
Apollo 11 highlights
[NASA-TM-109763] p 3800 N94-31820

APPLICATION SPECIFIC INTEGRATED CIRCUITS
A miniaturized ASIC-based multichannel scaler instrument
[DE94-007222] p 3807 N94-32783
Ceramic and metal composite circuit-board-level technology for application specific electronic modules (ASEM)
[AD-A277961] p 3630 N94-33180
The impact of ASIC devices on the SEU vulnerability of space-borne computers
[AD-A278134] p 3808 N94-33252

APPLICATIONS OF MATHEMATICS
Cumulative reports and publications through December 31, 1993
[NASA-CR-194889] p 3806 N94-33286

APPLICATIONS PROGRAMS (COMPUTERS)
Symbolic derivation of Runge-Kutta methods
[MATHS-REPT-A-205] p 3840 N94-31160
Air Force Space Command satellite orbit predictor using parallel virtual machines
[AD-A276316] p 3601 N94-31298
Adaptive control of a robot in Cartesian coordinates: Analysis and implementation
[ISBN-0-315-86493-1] p 3831 N94-31798
WHIPICE — computer program for analysis of aircraft deicing
[NASA-TM-109749] p 3574 N94-31803
Lattice geometrodynamics p 3857 N94-31825
ITS version 3.0: Powerful, user-friendly software for radiation modelling
[DE94-006607] p 3678 N94-32113
MICA, a facility to achieve portability for message-passing and dynamic memory management in FORTRAN
[DE94-006692] p 3807 N94-32147
Low altitude near-the-horizon propagation: A comparison between RPO and M-layer
[AD-A277358] p 3679 N94-32282
Assembly flow simulation of a radar p 3823 N94-32431
A systems approach to computer-based training p 3823 N94-32436
Advanced CFD methodology for fast transients encountered in nonlinear combustion instability problems. Volume 2: User's guide
[NASA-CR-191352] p 3637 N94-32694
SOLGAS refined: A computerized thermodynamic equilibrium calculation tool
[DE94-009021] p 3913 N94-32846
METCAN demonstration manual, version 1.0
[NASA-TM-105607] p 3626 N94-32858
A software architecture for multidisciplinary applications: Integrating task and data parallelism
[NASA-CR-194896] p 3820 N94-32928
Snowmelt forecasting. Further cold regions development of operational hydrological forecasting, volume 2
[AD-A278123] p 3757 N94-33269
Structuring Z specifications with views
[AD-A277618] p 3822 N94-33279

APPROACH CONTROL
Flight technical error for category B non-precision approaches and missed approaches using non-differential GPS for course guidance
[PB94-142734] p 3576 N94-31680

APPROXIMATION
Multivariate spline approximation
[AD-A276034] p 3842 N94-31441
Universal approximation in p-mean by neural networks
[W-9320] p 3832 N94-31821
Solution of the average-passage equations for the incompressible flow through multiple-blade-row turbomachinery
[AD-A276515] p 3583 N94-31931
On the relationship between generalization error, hypothesis complexity, and sample complexity for radial basis functions
[AD-A276802] p 3851 N94-32142
Multiserver queues with impatient customers
[CWI-BS-R9319] p 3835 N94-32198
Approximation theory and computational methods for the identification and control of distributed parameter systems
[AD-A277335] p 3848 N94-32244
Polynomial interpolation and approximation of real functions. 2: Symmetrical interpolation for the triangle
[AD-A277345] p 3848 N94-32245
Numerical optimization techniques in neural network training p 3838 N94-33158

AQUEOUS SOLUTIONS
Biocatalytic processing polymers in supercritical fluids
[AD-A276120] p 3651 N94-31510
Oxide pigments in water: The colloid-chemical point of view
[PB94-148616] p 3633 N94-31591
Preparation of catalyst particles using methods of colloid chemistry. Part 1: Preparation of silica particles from alcohol solutions
[PB94-135597] p 3634 N94-31679
Study of type 2 and 3 anodized Al 5052-0 in aqueous DS2 solutions
[AD-A276960] p 3644 N94-32240
Recovery of carboxylic acids at pH greater than pKa
[DE94-007030] p 3636 N94-32376

ARABIAN SEA
Deep water studies of CTD data
[AD-A277741] p 3791 N94-33176

ARAGONITE
The pH of Mars p 3950 N94-33225

ARC DISCHARGES
Arcing in space structures in low Earth orbit
[NASA-CR-194223] p 3694 N94-32478
Arc-heater performance research
[NASA-CR-195821] p 3912 N94-32774

ARC HEATING
Arc-heater performance research
[NASA-CR-195821] p 3912 N94-32774
Development of lightweight ceramic ablators and arc-jet test results
[NASA-TM-108798] p 3617 N94-33117

ARC WELDING
Correlation of flux composition and inclusion characteristics with submerged arc weld metal properties in HY-100 steel
[AD-A277040] p 3726 N94-32261

ARCHITECTURE
Compiler techniques for managing data motion
[AD-A276514] p 3918 N94-31930

ARCHITECTURE (COMPUTERS)
An expert system architecture for heterogeneous domains: A case-study in the legal field
[ETN-94-96012] p 3830 N94-31546
Delft Ising computing engine
[PB94-148251] p 3806 N94-31587
The future of open architecture process control systems
[DE94-006163] p 3830 N94-31623
Algorithms and parallel architectures for laser acoustic imaging
[ISBN-0-315-86486-4] p 3716 N94-31797
Real-time control and application to robotics: Hardware and software architectures
[ISBN-0-315-87192-X] p 3833 N94-31876
An analysis of instruction-cached SIMD computer architecture
[AD-A276519] p 3806 N94-31934
An analog preprocessing architecture for high-speed analog-to-digital conversion
[AD-A276737] p 3807 N94-32163
MULTIGRAPH: An architecture for model-based programming. Model-based program synthesis for parallel computing. PREMOS: Programming environment for model-based program synthesis, version 01.00.00
[AD-A276949] p 3817 N94-32219
Parallel processing for differencing and histogramming
[AD-A277080] p 3826 N94-32274
An information system organized as stratified hypermedia
[TR-93-12] p 3918 N94-32289
Massively parallel systems design for real-time embedded applications
[AD-A277256] p 3826 N94-32323
The Operator Shell: A means of privilege distribution under Unix
[DE94-007566] p 3826 N94-32356
Studies of an optical multi-processor interconnect
[AD-A277093] p 3881 N94-32392
Common modeling system for digital simulation p 3823 N94-32429
Construction of a parallel processor for simulating manipulators and other mechanical systems
[NASA-CR-191327] p 3826 N94-32482
Gigabits to the Desktop: Installing tomorrow's networks today
[DE94-007701] p 3827 N94-32646
Development of a low-latency scalar communication routine on message-passing architectures
[DE94-007061] p 3827 N94-32683
Toroidal computer memory for serial and parallel processors
[AD-D016144] p 3807 N94-32978
Modular neural network architectures p 3838 N94-33156
Investigation of modularly configured attached processors with intelligent memories
[AD-A278418] p 3839 N94-33330

ARIANE LAUNCH VEHICLE
Scattering of a random acoustic field by an infinite cylinder: Application to the modelization of the acoustic environment of the 'Ariane 5' launcher scale-model using experimental data
[ONERA-NT-1993-11] p 3860 N94-31226

ARID LANDS
Arid regions and wind erosion p 3780 N94-31005
Climatic evolution and desertization p 3780 N94-31009
Use of SPOT and ERS-1 SAR data to study the tectonic and climatic history of arid regions p 3752 N94-32550

ARITHMETIC
Extensional realizability
[ML-93-18] p 3856 N94-31408

ARM (ANATOMY)
Geometric structure of the adaptive controller of the human arm
[AD-A276797] p 3834 N94-32152

ARMED FORCES (UNITED STATES)
Interagency Advanced Power Group: Steering Group meeting minutes
[DE94-007951] p 3761 N94-32701
Medical problems in high mountain environments. A handbook for medical officers
[AD-A278095] p 3798 N94-33268

ARMENIA
Station climatic summaries: China, the former USSR, and Mongolia
[AD-A276548] p 3784 N94-32057

ARMOR
Overview of shock physics codes for armor analysis
[DE94-008948] p 3739 N94-32842

ARSENATES
Inorganic materials for anomalous-dispersion phase-matched second harmonic generation: Rubidium titanyl arsenate isomorphs, Rb(Ti(1-2x)Ln(x)Nb(x))OAsO4
[DE94-006141] p 3899 N94-31847

ARSENIC COMPOUNDS
Tetraalkyldiarsines as potential precursors for electronic materials: Synthesis and characterization of various iso-propyl arsenic compounds
[AD-A277003] p 3900 N94-32001

ARTERIOSCLEROSIS
Incompressible viscous flow in tubes with occlusions
[ISBN-0-315-75467-2] p 3704 N94-31778

ARTIFICIAL INTELLIGENCE
OTTER 3.0 reference manual and guide
[DE94-007457] p 3829 N94-31315
Developing the Multimedia User Interface Component (MUSIC) for the Icarus Presentation System (IPS)
[AD-A276341] p 3810 N94-31335
An active computer supported medium for distributed planning in enterprises
[ETN-94-95738] p 3829 N94-31372
Proceedings of the International Workshop on Artificial Intelligence Applications in Solar-Terrestrial Physics
[PB94-142064] p 3832 N94-31808
Hierarchical mixtures of experts and the EM algorithm
[AD-A276516] p 3814 N94-31932
Application of Artificial Intelligence to the DoD Corporate Information Management (CIM) program
[AD-A276656] p 3834 N94-32061
Translucent procedures, abstraction without opacity
[AD-A276877] p 3817 N94-32213
High-speed data search p 3923 N94-32441
The limits of intelligence in design
[DE94-004668] p 3819 N94-32668
Model-based reconfiguration: Diagnosis and recovery
[NASA-CR-4596] p 3820 N94-32776
Translating an AI application from Lisp to Ada: A case study
[NASA-TM-103845] p 3820 N94-32906
From animals to animats
[AD-A277427] p 3802 N94-33241

ARTIFICIAL SATELLITES
Air Force Space Command satellite orbit predictor using parallel virtual machines
[AD-A276316] p 3601 N94-31298
General-relativistic celestial mechanics. 4: Theory of satellite motion
[PB94-147782] p 3601 N94-31769
Testing for preferred-frame effects in gravity with artificial Earth satellites
[PB94-148459] p 3610 N94-31771

Design, characterization, and control of the NASA three degree of freedom reaction compensation platform
p 3605 N94-33304

ASPECT RATIO
The small-scale topology of a 2:1 aspect-ratio elliptic jet
p 3699 N94-31184
Response of a cantilevered plate in supersonic flow
[AD-A277487] p 3580 N94-33107

ASSEMBLIES
Assembly flow simulation of a radar
p 3823 N94-32431
Special test equipment and fixturing for MSAT reflector assembly alignment
p 3606 N94-33316

ASSEMBLY
Fractional-factorial process development techniques
[DE94-005580] p 3690 N94-31593

ASSESSMENTS
GRAFTED - GRAphical fault tree EDitor: A fault tree description program for target vulnerability/survivability analysis. User manual
[AD-A277067] p 3818 N94-32390

ASTEROIDS
Keeping that youthful look --- impact cratering of Venus
p 3941 N94-31112

ASTRODYNAMICS
Planetesimal dynamics in the vicinity of a growing protoplanet
p 3935 N94-31926
The chemical and dynamical evolution of the galaxy
p 3936 N94-31950

ASTROMETRY
General-relativistic celestial mechanics. 4: Theory of satellite motion
[PB94-147782] p 3601 N94-31769

ASTRONAUTS
Legal regime of human activities in outer space law
p 3599 N94-31431
Defying gravity
[NASA-TM-109747] p 3667 N94-31884

ASTRONOMICAL MODELS
Fireworks in velocity and configuration space applied to cosmology
[USIP-93-90] p 3927 N94-31086
Nonthermal accretion disk models around neutron stars
p 3931 N94-31139
Gas dynamics for accretion disk simulations
p 3932 N94-31144
Evolution of stars and winds in the starburst galaxy M82
p 3934 N94-31758
The chemical and dynamical evolution of the galaxy
p 3936 N94-31950

ASTRONOMICAL PHOTOGRAPHY
A new high-speed IR camera system
p 3713 N94-32459

ASTRONOMICAL SPECTROSCOPY
Cometary molecules
p 3935 N94-31869
High sensitivity and resolution decimetric spectroscope: Preliminary analysis of solar bursts
[INPE-5537-TDI/525] p 3954 N94-33080
SNC meteorites and their implications for reservoirs of Martian volatiles
p 3947 N94-33209

ASTRONOMY
Construction of visual representations and time-space organization of resources in astronomy
[ISBN-0-315-86694-2] p 3925 N94-31914

ASTROPHYSICS
Physical chemistry of molecules and grains in space
[AD-A276037] p 3932 N94-31280
Various magnet options for Delta launched version of ASTROMAG
[DE94-006292] p 3955 N94-31635
Nuclear physics and astrophysics
[DE94-007168] p 3939 N94-33147

ASYMMETRY
A worst-case analysis of two approximate algorithms for the symmetric travelling salesman problem
[REPT-93-036] p 3840 N94-31187
Baryogenesis from a primordial lepton asymmetry
[PB94-145166] p 3868 N94-31921

ASYMPTOTES
Kaplan-Meier estimators of interpoint distance distributions for spatial point processes
[CWI-BS-R9315] p 3846 N94-32107

ASYMPTOTIC METHODS
Doubly asymptotic approximations: Theoretical and numerical analyses
[ONERA-NT-1993-7] p 3840 N94-31231
The finite element method with asymptotic self-similar solutions
p 3736 N94-31904
A separation technique for asymptotic-numeric solution for general shells of revolution
p 3736 N94-31961

ASYMPTOTIC PROPERTIES
Heteroclinic attractors: Time averages and moduli of topological conjugacy
[W-9318] p 3844 N94-31690
Bifurcation and deterministic chaos in dynamic systems
[REPT-93-047] p 3911 N94-31893
Asymptotic behavior of dynamic systems
p 3911 N94-31894
Penetrable wedge analysis
[AD-A277219] p 3845 N94-32022
Kaplan-Meier estimators of interpoint distance distributions for spatial point processes
[CWI-BS-R9315] p 3846 N94-32107

ASYMPTOTIC SERIES
Stirling's formula and approximations for n(factorial) and the middle ratio
[REPT-93-73] p 3843 N94-31642
Finite-part integrals and the Euler-Maclaurin expansion
[DE94-006539] p 3844 N94-31665
Stability of tearing modes in tokamak plasmas
[DE94-009205] p 3892 N94-32911

ATLANTIC OCEAN
Low frequency variability observed in the tropical Atlantic Ocean
p 3778 N94-30991
Operations summary for the convection and moisture experiment (CAMEX)
[NASA-TM-108445] p 3786 N94-33004
Evolution of upwelling fronts off the coast of Portugal
[NASA-CR-195692] p 3790 N94-33045
Quantitative modeling of bottom morphology and subbottom properties
[AD-A278142] p 3790 N94-33062
Cruise report: Oceanus 250 leg 4 high resolution profiler survey for the North Atlantic Tracer Release Experiment, 25 March - 24 April, 1992
[AD-A277935] p 3791 N94-33245

ATMOSPHERIC ATTENUATION
Optical and image transmission through desert atmospheres
[AD-A276022] p 3742 N94-31496
Field studies of raindrop oscillations with applications to radar meteorology
p 3782 N94-31743
Atmospheric propagation effects through natural and man-made obscurants for visible to MM-wave radiation
[AD-A276919] p 3679 N94-32235
Low altitude near-the-horizon propagation: A comparison between RPO and M-layer
[AD-A277358] p 3679 N94-32282

ATMOSPHERIC BOUNDARY LAYER
Research in marine boundary layer intermittency
[AD-A276076] p 3701 N94-31460
Boundary-layer cumulus over land: Some observations and conceptual models
[DE93-040820] p 3781 N94-31597
Surface fluxes of trace gases derived from convective-layer profiles
p 3704 N94-31774
A non-local model for prediction of the probability density function of turbulent fluctuations in boundary-layer flows
p 3706 N94-32076
High resolution properties of the marine atmospheric boundary layer
[DE94-006235] p 3774 N94-32736
An evaluation of RAMS radiation schemes by field measurements
[DE94-008053] p 3767 N94-32750
Coastal boundary layer and refractivity measurements using the ground-based high resolution interferometer sounder (GB-HIS)
[AD-A277980] p 3683 N94-33159

ATMOSPHERIC CHEMISTRY
Sources and wells of minor atmospheric constituents of climatic importance
p 3770 N94-31008
Cloud studies seen from a physical chemist's perspective
[DE94-008059] p 3771 N94-31527
Evaluation of sulfate aerosol optical depths over the North Atlantic and comparison with satellite observations
[DE94-005457] p 3746 N94-32100
Formation of gas-phase peroxides in a rural atmosphere: An interpretation of the recent SOS/SERON field results
[DE94-002995] p 3766 N94-32692
Biospheric effects of a large extraterrestrial impact: Case study of the Cretaceous/Tertiary boundary crater
[NASA-CR-195827] p 3942 N94-32740
Surface probes of porous toluene/water ices: Adsorption kinetics and annealing spectra measured by second harmonic generation
[DE94-007564] p 3637 N94-32743
Quantified estimates of total GWPs for greenhouse gases taking into account tropospheric chemistry
[DE94-007846] p 3768 N94-32817
Dry deposition of PAN to grassland vegetation
[DE94-005111] p 3768 N94-32894
A correlated k-distribution model of the heating rates for atmospheric mixtures of H2O, CO2, O3, CH4, and N2O in the 0-2500 cm(exp -1) wave number region at altitudes between 0 and 60 km
[DE94-005136] p 3775 N94-32895
A model for the evolution of CO2 on Mars
p 3946 N94-33205
Mars atmospheric loss and isotopic fractionation by solar-wind-induced sputtering and photochemical escape
p 3947 N94-33208
How well was total ozone abundance inferred with Mariner 9
p 3947 N94-33212
Escape of Mars atmospheric carbon through time by photochemical means
p 3948 N94-33214

ATMOSPHERIC CIRCULATION
Subtropical Climates and Their Evolution: From Space-Based Observation to Modelling
[ISBN-2-85-428333-3] p 3776 N94-30981
Energetic and general circulation
p 3777 N94-30983
Tropical squall lines
p 3778 N94-30992
Effects of the deep tropical convection in the large scale atmospheric flow
p 3778 N94-30994
Desert aerosols: Sources, transports, and impacts determined by remote sensing
p 3770 N94-31003
Regional sources of error growth in the National Meteorological Center's medium-range forecast model
p 3781 N94-31554
Numerical simulations of monsoon rainfall with the NRL/NCSU regional nested grid model
p 3782 N94-31791
The evolution of jet features during the 1993 east coast white hurricane: A case study using the global spectral model
[AD-A277217] p 3783 N94-32021
Coordination of mesoscale meteorological research between ASL and European group
[AD-A276730] p 3784 N94-32162
Variational elliptic solver for atmospheric applications
[DE94-007725] p 3774 N94-32647
Diagnostic studies of climate variability
[DE94-003629] p 3767 N94-32711
Wind-speed measurements with a scanning elastic-backscatter lidar
[DE94-004974] p 3785 N94-32726
High resolution properties of the marine atmospheric boundary layer
[DE94-006235] p 3774 N94-32736
A long-term simulation of surface fluxes and soil moisture
[DE94-006661] p 3774 N94-32772
Statistical intercomparison of global climate models: A common principal component approach
[DE94-008671] p 3768 N94-32882
Performance of a new wind updating system for a prognostic meteorological model in the environs of Mexico City
[DE94-006243] p 3786 N94-32937
Stationary eddies in the Mars general circulation as simulated by the NASA-Ames GCM
p 3944 N94-33192
Eddy transport of water vapor in the Martian atmosphere
p 3949 N94-33221

ATMOSPHERIC COMPOSITION
Carbon balance in a forest ecosystem
p 3770 N94-31007
Sources and wells of minor atmospheric constituents of climatic importance
p 3770 N94-31008
Climatic evolution and desertization
p 3780 N94-31009
The ozone and the physico-chemical processes in tropical regions
p 3770 N94-31010
Cloud studies seen from a physical chemist's perspective
[DE94-006059] p 3771 N94-31527
Time-dependent behavior of Mount Pinatubo aerosol
[DE94-001877] p 3764 N94-31601
Surface fluxes of trace gases derived from convective-layer profiles
p 3704 N94-31774
One: Microphysics of frost metamorphism: Applications to Triton and Mars. Two: A global analysis of the ozone deficit in the upper stratosphere and lower mesosphere. Three: The diabatic circulation in the stratosphere as diagnosed from Microwave Limb Sounder data
p 3942 N94-31975
Ionization probes of molecular structure and chemistry
[DE94-007605] p 3872 N94-32643
A correlated k-distribution model of the heating rates for atmospheric mixtures of H2O, CO2, O3, CH4, and N2O in the 0-2500 cm(exp -1) wave number region at altitudes between 0 and 60 km
[DE94-005136] p 3775 N94-32895
Effects of long-term elevated atmospheric CO2 concentrations on Pinus ponderosa
[DE94-008832] p 3769 N94-32966
Mars: Past, Present, and Future. Results from the MSATT Program, part 1
[NASA-CR-194279] p 3943 N94-33190
Mars atmospheric dust properties: A synthesis of Mariner 9, Viking, and Phobos observations
p 3945 N94-33200

Magmatic volatiles and the weathering of Mars
p 3946 N94-33201
Regional sedimentological variations among dark crater floor features: Toward a model for modern eolian sand distribution on Mars p 3946 N94-33203
A model for the evolution of CO2 on Mars
p 3946 N94-33205
Mars atmospheric loss and isotopic fractionation by solar-wind-induced sputtering and photochemical escape
p 3947 N94-33208
SNC meteorites and their implications for reservoirs of Martian volatiles p 3947 N94-33209
Studies of atmospheric dust from Viking IR thermal mapper data p 3948 N94-33216
Carbonate formation on Mars: Latest experiments
p 3950 N94-33231
Obliquity variation in a Mars climate evolution model
p 3951 N94-33236
Carbonates, surfates, phosphates, nitrates, and organic materials: Their association in a Martian meteorite
p 3952 N94-33239
High resolution molecular spectroscopy of atmospheric species
[AD-A278382] p 3776 N94-33351

ATMOSPHERIC CORRECTION
European Imaging Spectroscopy Aircraft Campaign
[ESA-SP-360] p 3743 N94-31853
The European Imaging Spectroscopy Airborne Campaign (EISAC). Data takes and evaluation programme: An overview p 3743 N94-31854
Ground based radiometric and atmospheric measurements p 3744 N94-31855

ATMOSPHERIC DENSITY
Thermospheric modeling accuracies using F10.7 and Ap
[AD-A277355] p 3773 N94-32337
Possible test of ancient dense Martian atmosphere
p 3947 N94-33206

ATMOSPHERIC EFFECTS
Atmospheric effects assessment program: Ionospheric sounding
[AD-A276447] p 3770 N94-31303
Statistics of time averaged atmospheric scintillation
[DE94-006998] p 3747 N94-32249
Biospheric effects of a large extraterrestrial impact: Case study of the Cretaceous/Tertiary boundary crater
[NASA-CR-195827] p 3942 N94-32740

ATMOSPHERIC GENERAL CIRCULATION MODELS
Energetic and general circulation
p 3777 N94-30983
The climate of the Mediterranean basin: Its sensitivity to global change p 3778 N94-30993
Modeling of the continental biosphere
p 3770 N94-31011
Treatment of cloud radiative effects in general circulation models
[DE94-001864] p 3764 N94-31600
Short term teleconnections associated with an individual tropical cyclone
[AD-A277210] p 3783 N94-32019
Physical basis for climate change models
[DE94-003827] p 3767 N94-32712
Use of cloud observations and mesoscale meteorology models to evaluate and improve cloud parameterizations
[DE94-003610] p 3785 N94-32717
A long-term simulation of surface fluxes and soil moisture
[DE94-006661] p 3774 N94-32772
Statistical intercomparison of global climate models: A common principal component approach
[DE94-006871] p 3768 N94-32882

ATMOSPHERIC HEAT BUDGET
Energetic and general circulation
p 3777 N94-30983

ATMOSPHERIC HEATING
Carbon dioxide abatement as a differential game
[DE94-722023] p 3765 N94-32590
A correlated k-distribution model of the heating rates for atmospheric mixtures of H2O, CO2, O3, CH4, and N2O in the 0-2500 cm(exp -1) wave number region at altitudes between 0 and 60 km
[DE94-005136] p 3775 N94-32895
A model for the evolution of CO2 on Mars
p 3946 N94-33205
The wavelength dependence of Martian atmospheric dust radiative properties p 3950 N94-33228
TRMM-related research: Tropical rainfall and energy analysis experiment
[NASA-CR-195834] p 3787 N94-33286

ATMOSPHERIC IONIZATION
Lightning-induced coupling of the radiation belts to geomagnetically conjugate ionospheric regions
p 3772 N94-31773

ATMOSPHERIC MODELS
Subtropical Climates and Their Evolution: From Space-Based Observation to Modelling
[ISBN-2-85-428333-3] p 3776 N94-30981
Climatologic flux in tropical ocean
p 3777 N94-30985
Carbon balance in a forest ecosystem
p 3770 N94-31007
Analysis of ionospheric parameters in Europe and creation of the prediction algorithm
[AD-A276342] p 3771 N94-31326
The High-Frequency Benchmark propagation program
[AD-A276323] p 3672 N94-31334
Regional sources of error growth in the National Meteorological Center's medium-range forecast model
p 3781 N94-31554
Cumulus convection parameterization and numerical modelling of moist atmospheres p 3783 N94-31989
Use of Air Force cloud cover data to evaluate and improve cloud forecasts and parameterizations in mesocale meteorological models
[AD-A277384] p 3784 N94-32054
Evaluation of sulfate aerosol optical depths over the North Atlantic and comparison with satellite observations
[DE94-005457] p 3746 N94-32100
Atmospheric structure simulation: An autoregressive model for smooth geophysical power spectra with known autocorrelation function
[AD-A276691] p 3773 N94-32118
Recommendations for meteorological data collection during physiological field studies
[AD-A276834] p 3901 N94-32153
Tropical cyclone forecasters reference guide. 5: Numerical track forecast guidance
[AD-A277318] p 3785 N94-32278
A critical examination of stellar atmosphere theory for metal-poor K-giant stars p 3927 N94-32308
Thermospheric modeling accuracies using F10.7 and Ap
[AD-A277355] p 3773 N94-32337
Proceedings of the Ninth Annual Pacific Climate (PACLIM) Workshop
[DE94-003024] p 3766 N94-32693
Physical basis for climate change models
[DE94-003827] p 3767 N94-32712
An evaluation of RAMS radiation schemes by field measurements
[DE94-008053] p 3767 N94-32750
Climate effects of anthropogenic sulfate: Simulations from a coupled chemistry/climate model
[DE94-004352] p 3767 N94-32789
Parameterizing atmosphere-land surface exchange for climate models with satellite data: A case study for the Southern Great Plains CART site
[DE94-005109] p 3775 N94-32874
Performance of a new wind updating system for a prognostic meteorological model in the environs of Mexico City
[DE94-006243] p 3786 N94-32937
Forecasters handbook for the Philippine Islands and surrounding waters
[AD-A277993] p 3787 N94-33089
Transport and diffusion in turbulent fields modeling and measurements techniques
[AD-A278114] p 3769 N94-33110
A model for the evolution of CO2 on Mars
p 3946 N94-33205
Possible test of ancient dense Martian atmosphere
p 3947 N94-33206
Groundbased monitoring of Martian atmospheric opacity p 3947 N94-33207
Mars atmospheric loss and isotopic fractionation by solar-wind-induced sputtering and photochemical escape
p 3947 N94-33208
Studies of atmospheric dust from Viking IR thermal mapper data p 3948 N94-33216
Eddy transport of water vapor in the Martian atmosphere p 3949 N94-33221
Numerical simulation of thermally induced near-surface flows over Martian terrain p 3949 N94-33223
Obliquity variation in a Mars climate evolution model
p 3951 N94-33236
Simultaneous laboratory measurements of CO2 and H2O adsorption on palagonite: Implications for the Martian climate and volatile reservoir p 3952 N94-33240

ATMOSPHERIC MOISTURE
Cloud studies seen from a physical chemist's perspective
[DE94-006059] p 3771 N94-31527
Cumulus convection parameterization and numerical modelling of moist atmospheres p 3783 N94-31989
Operations summary for the convection and moisture experiment (CAMEX)
[NASA-TM-108445] p 3786 N94-33004

ATMOSPHERIC OPTICS
Matter-radiation interactions in the atmosphere
p 3776 N94-30998
Design and early results of the sodium-layer laser guide star adaptive optics experiment at the Lawrence Livermore National Laboratory
[DE94-006653] p 3926 N94-32189
Groundbased monitoring of Martian atmospheric opacity p 3947 N94-33207
Temporal and spatial mapping of atmospheric dust opacity and surface albedo on Mars
p 3947 N94-33211

ATMOSPHERIC PHYSICS
Airborne instruments p 3757 N94-31006
Modeling of the continental biosphere
p 3770 N94-31011
Spectroscopic study of the molecular collisions (hydrogen-nitrogen and hydrogen-oxygen) at energies of several MeV
[ISBN-0-315-86794-9] p 3867 N94-31753
One: Microphysics of frost metamorphism: Applications to Triton and Mars. Two: A global analysis of the ozone deficit in the upper stratosphere and lower mesosphere. Three: The diabatic circulation in the stratosphere as diagnosed from Microwave Limb Sounder data
p 3942 N94-31975
Theoretical studies on ionospheric irregularities and ion diode performance
[AD-A277115] p 3772 N94-31984
Atmospheric structure simulation: An autoregressive model for smooth geophysical power spectra with known autocorrelation function
[AD-A276691] p 3773 N94-32118
Time-resolved IR spectroscopy, energy transfer, and state-to-state collision dynamics of atmospheric species
[AD-A277372] p 3773 N94-32338
Spatial correlation of ionospheric variability
[AD-A278105] p 3776 N94-33041

ATMOSPHERIC PRESSURE
Possible test of ancient dense Martian atmosphere
p 3947 N94-33206
Controls on the CO2 seasonal cycle
p 3950 N94-33227
Simultaneous laboratory measurements of CO2 and H2O adsorption on palagonite: Implications for the Martian climate and volatile reservoir p 3952 N94-33240

ATMOSPHERIC RADIATION
Treatment of cloud radiative effects in general circulation models
[DE94-001864] p 3764 N94-31600
Water vapor from sunradiometry in comparison with microwave and balloon-sonde measurements at the Southern Great Plains ARM Site
[DE94-007479] p 3786 N94-32759

ATMOSPHERIC REFRACTION
Coastal boundary layer and refractivity measurements using the ground-based high resolution interferometer sounder (GB-HIS)
[AD-A277980] p 3683 N94-33159

ATMOSPHERIC SCATTERING
Multiple scattering of polarized radiation in planetary atmospheres
[ETN-94-96018] p 3674 N94-31551
Performance statistics bulletin. High latitude meteor scatter propagation October, November, December 1990, January 1991
[AD-A276693] p 3676 N94-31998
Radar scattering from the summer polar mesosphere: Theory and observations p 3772 N94-32077
Performance statistics bulletin. High latitude metor scatter propagation, February, March, April, May 1992
[AD-A276667] p 3677 N94-32083
Performance statistics bulletin. High latitude meteor scatter propagation February, March, April, May 1991
[AD-A276723] p 3678 N94-32158
Performance statistics bulletin. High latitude meteor scatter propagation October, November, December 1991, January 1992
[AD-A276724] p 3678 N94-32159
Performance statistics bulletin. High latitude meteor scatter propagation, November and December 1989, and January 1990
[AD-A276688] p 3680 N94-32297
Performance statistics bulletin. High latitude meteor scatter propagation
[AD-A276694] p 3680 N94-32298
Performance statistics bulletin. High latitude meteor scatter propagation
[AD-A276695] p 3680 N94-32299
Performance statistics bulletin. High latitude meteor scatter propagation
[AD-A276696] p 3680 N94-32300
Aerosols scattering and near-infrared observations of the Martian surface p 3946 N94-33204
Groundbased monitoring of Martian atmospheric opacity p 3947 N94-33207

ATMOSPHERIC SOUNDING
Eurocap program-ebre station
[AD-A277044] p 3772 N94-32007
Gyrotrons and free electron lasers for atmospheric sensing
[AD-A277281] p 3718 N94-32406
Water vapor from sunradiometry in comparison with microwave and balloon-sonde measurements at the Southern Great Plains ARM Site
[DE94-007479] p 3786 N94-32759
Operations summary for the convection and moisture experiment (CAMEX)
[NASA-TM-108445] p 3786 N94-33004
Participation in the scientific activities of the Waves in Space Plasma (WISP) project
[NASA-CR-195903] p 3894 N94-33113
EUROCAP program
[AD-A278084] p 3776 N94-33184
An evaluation of three GPS receivers for use in the GPS sounder
[AD-A278157] p 3577 N94-33253

ATMOSPHERIC TEMPERATURE
Diagnostic studies of climate variability
[DE94-003629] p 3767 N94-32711
Mars atmospheric dust properties: A synthesis of Mariner 9, Viking, and Phobos observations
p 3945 N94-33200

ATMOSPHERIC TURBULENCE
Optical and image transmission through desert atmospheres
[AD-A276022] p 3742 N94-31496
The properties of sunflecks in a flexible plant canopy, and their relationship to turbulence
p 3782 N94-31775
Aircraft incident report: In-flight turbulence encounter and loss of portions of the elevators, China Airlines Flight CI-012, McDonnell Douglas MD-11-P, Taiwan Registration B-150 about 20 miles east of Japan, 7 December 1992
[PB94-910403] p 3576 N94-32938
Phase-only correction of scintillated laser beams: Downrange experimental results
[AD-A277778] p 3722 N94-33282

ATOMIC CLUSTERS
Metal clusters: Dynamics and structure
[AD-A276842] p 3643 N94-32091
Metal cluster-rare gas van der Waals complexes: Microscopic models of physisorption
[DE94-008134] p 3873 N94-32797

ATOMIC COLLISIONS
Results from the H1 experiment at HERA
[PB94-145174] p 3868 N94-32008
Analysis of forward and inverse problems in chemical dynamics and spectroscopy
[DE94-007607] p 3635 N94-32140

ATOMIC ENERGY LEVELS
Electronic and nuclear factors in intramolecular charge and excitation transfer processes
[DE94-006598] p 3870 N94-32178

ATOMIC EXCITATIONS
Mechanisms of formation and of de-excitation in the reaction Mg-24 + C-12 yields 9 alpha at 35MeV per nucleon
[ISBN-0-315-86746-9] p 3867 N94-31749
Production and detection of metastable atomic oxygen
[ISBN-0-315-87364-7] p 3868 N94-31915
Cooling and trapping of neutral atoms
[AD-A276957] p 3870 N94-32360

ATOMIC INTERACTIONS
High-temperature study of O+H2CO yields OH+HCO
[DE94-006837] p 3864 N94-31321

ATOMIC PHYSICS
Spectroscopy and atomic physics in EBIT and SuperEBIT
[DE94-006050] p 3864 N94-31508
Atomic and molecular data needs for fusion
[DE94-006555] p 3870 N94-32177

ATOMIC SPECTRA
Diamagnetism in helium Rydberg atoms
[ETN-94-96015] p 3865 N94-31549

ATOMIC STRUCTURE
The relationship of the electronic structures of semiconductor surfaces and heterostructures to crystal growth
[AD-A276465] p 3896 N94-31473
Collective and quasiparticle excitations in light Pb isotopes
[ETN-94-96014] p 3865 N94-31548
Various magnet options for Delta launched version of ASTROMAG
[DE94-006292] p 3955 N94-31635
Double rotation NMR studies of zeolites and aluminophosphate molecular sieves
[DE94-007032] p 3866 N94-31637
The adsorption of sulfate on gold(111) in acidic aqueous media: Adlayer structural inferences from infrared spectroscopy and scanning tunneling microscopy
[AD-A276643] p 3642 N94-31997
A new-type of long-range restructuring of ordered metal surfaces induced by lateral adsorbate interactions: Iodide on AU(110) electrodes
[AD-A276633] p 3643 N94-32060
Amorphous/crystalline structure and phase transformations in metastable semiconducting Ge(1-x)Sn(x)
[DE94-006659] p 3901 N94-32115
Charge-dependent atomic-scale structures of high-index and (110) gold electrode surfaces as revealed by scanning tunneling microscopy
[AD-A276782] p 3869 N94-32170
Lowering the Schottky barrier at metal or silicide/Si interfaces to extend the range of infrared detectors
[AD-A277253] p 3903 N94-32322
Theoretical studies of electron transfer and optical spectroscopy
[DE94-006985] p 3871 N94-32375
Numerical simulation of quantum many-body systems
[DE94-008451] p 3912 N94-32513
Computational chemistry on parallel computers
[DE94-008106] p 3636 N94-32616
Energetics, bonding mechanism, and electronic structure of ceramic/ceramic and metal/ceramic interfaces
[DE94-008551] p 3659 N94-32656
Calculations of nonspherically averaged charge densities for substitutionally disordered alloys
[DE94-008293] p 3646 N94-32754
Occupied and unoccupied orbitals of C60 and C70
[DE94-008294] p 3873 N94-32755
Near edge x ray spectroscopy theory
[DE94-008179] p 3905 N94-32799
Characterization of nanoparticles and nanophase materials
[DE94-008348] p 3907 N94-32990
Sensitivity of electrochemical adlayer structure to the metal crystallographic orientation: Potential-independent iodide adsorption on Au(100) in comparison with other low-index surfaces
[AD-A276714] p 3909 N94-33273
Nanoscale structural changes upon electrooxidation of Au(111) as probed by potentiodynamic scanning tunneling microscopy
[AD-A276780] p 3909 N94-33275
A tandem microscopic-electrochemical examination of a charge-induced surface phase sequence: Ordered Au(110) in aqueous iodide electrolytes as probed by potentiodynamic scanning tunneling microscopy
[AD-A276905] p 3875 N94-33277

ATOMS
Cooling and trapping of neutral atoms
[AD-A276957] p 3870 N94-32360
Coherent processes in atom in strong radiation fields
[AD-A278388] p 3874 N94-33144

ATTENUATION
Arithmetic averaging: A versatile technique for smoothing and trend removal
[DE94-005274] p 3852 N94-32673

ATTITUDE (INCLINATION)
Attitude dynamics of spinning rockets in space with internal mass motion p 3601 N94-31802

ATTITUDE CONTROL
Adaptive nonlinear control of spacecraft
p 3609 N94-31564
An experimental testbed for a free-floating manipulator
[AD-A277350] p 3726 N94-32334
The ALEXIS mission recovery
[DE94-007549] p 3611 N94-32813

ATTITUDE GYROS
Chaotic attitude motion of satellites in the central gravitational field
[ISBN-0-315-78768-6] p 3610 N94-31723
Performance analysis of an integrated GPS/inertial attitude determination system
[NASA-CR-188289] p 3577 N94-32864

ATTITUDE STABILITY
Chaotic attitude motion of satellites in the central gravitational field
[ISBN-0-315-78768-6] p 3610 N94-31723

AUDIO FREQUENCIES
Acoustic window
[AD-D016171] p 3862 N94-33017

AUDIO SIGNALS
Auditory perception
[AD-A277414] p 3800 N94-32419

AUDIO VISUAL MATERIAL
Multimedia as a desktop and classroom tool
[DE94-009118] p 3807 N94-32766

AUDITORY PERCEPTION
Spectral analysis method and sample generation for real time visualization of speech
[ETN-94-95732] p 3674 N94-31573
Determination of multiple sound sources
[AD-A277379] p 3799 N94-32096
Auditory perception
[AD-A277414] p 3800 N94-32419
Mechanisms of temporal pattern discrimination by human observers
[AD-A277407] p 3801 N94-32577
Models of the neuronal mechanisms of target localization of the barn owl
[AD-A277332] p 3797 N94-32623
Three dimensional audio versus head down TCAS displays
[NASA-CR-177636] p 3576 N94-33063
Complex auditory signals
[AD-A278391] p 3862 N94-33146

AUDITORY SIGNALS
Three dimensional audio versus head down TCAS displays
[NASA-CR-177636] p 3576 N94-33063
Complex auditory signals
[AD-A278391] p 3862 N94-33146

AURORAL ABSORPTION
Performance statistics bulletin. High latitude meter scatter propagation, February, March, April, May 1992
[AD-A276667] p 3677 N94-32083
Performance statistics bulletin. High latitude meteor scatter propagation February, March, April, May 1991
[AD-A276723] p 3678 N94-32158
Performance statistics bulletin. High latitude meteor scatter propagation October, November, December 1991, January 1992
[AD-A276724] p 3678 N94-32159
Performance statistics bulletin. High latitude meteor scatter propagation, November and December 1989, and January 1990
[AD-A276688] p 3680 N94-32297
Performance statistics bulletin. High latitude meteor scatter propagation
[AD-A276694] p 3680 N94-32298
Performance statistics bulletin. High latitude meteor scatter propagation
[AD-A276695] p 3680 N94-32299
Performance statistics bulletin. High latitude meteor scatter propagation
[AD-A276696] p 3680 N94-32300
Performance statistics bulletin. High latitude meteor scatter propagation, June, July, August, September 1992
[AD-A277508] p 3685 N94-33347

AURORAL ARCS
Convection and electrodynamic signatures in the vicinity of a Sun-aligned arc: Results from the Polar Acceleration Regions and Convection Study (Polar ARCS)
p 3954 N94-31102

AURORAL SPECTROSCOPY
Spectroscopic study of the molecular collisions (hydrogen-nitrogen and hydrogen-oxygen) at energies of several MeV
[ISBN-0-315-86794-9] p 3867 N94-31753

AURORAS
The double probe electric field experiment on Freja: Description and first results
[TRITA-ALP-1993-02] p 3885 N94-31089
High frequency active auroral research program (HAARP) imager
[AD-A277469] p 3775 N94-32999
A comprehensive analysis of electron conical distributions from multi-satellite databases
[NASA-CR-195848] p 3953 N94-33047

AUSTENITE
Modeling of residual stress mitigation in austenitic stainless steel pipe girth weldment
[DE94-007184] p 3738 N94-32639

AUSTENITIC STAINLESS STEELS
Defect-solute interactions near irradiation grain boundaries
[DE94-006215] p 3641 N94-31627
Characterization of the corrosion resistance of duplex stainless steels using local current density mapping techniques
[DE94-007980] p 3646 N94-32699

AUTOCORRELATION
Atmospheric structure simulation: An autoregressive model for smooth geophysical power spectra with known autocorrelation function
[AD-A276691] p 3773 N94-32118

AUTOMATIC CONTROL
Compiler techniques for managing data motion
[AD-A276514] p 3918 N94-31930
Automated fiber pigtailing technology
[DE94-007072] p 3695 N94-32688

A novel optoelectronic system for distortion-invariant ATR
[AD-A277985] p 3884 N94-33087
Knowledge engineering for PACES, the particle accelerator control expert system p 3854 N94-33342

AUTOMATION
Automated detection of ship tracks in multispectral satellite data
[AD-A276697] p 3746 N94-32119
Automatic translation among spoken languages p 3685 N94-32437

AUTOMOBILE ENGINES
Materials development program: Ceramic technology project bibliography, 1984-1992
[DE94-009297] p 3662 N94-32935

AUTOMOBILE FUELS
Fuel property effects on engine combustion processes
[DE94-005529] p 3631 N94-31153
Scenarios for multi-unit inertial fusion energy plants producing hydrogen fuel
[DE94-006614] p 3666 N94-32114
The hydrogen hybrid option
[DE94-006733] p 3667 N94-32148

AUTOMOBILES
The hydrogen hybrid option
[DE94-006733] p 3667 N94-32148

AUTOMORPHISMS
Dynamical entropy of generalized quantum Markov chains
[PB94-148483] p 3850 N94-31590

AUTONOMOUS NAVIGATION
Contingency-tolerant robot motion planning and control p 3830 N94-31482
Safe navigation and active vision for autonomous vehicles: A purposive and direct solution p 3832 N94-31842
Robot motion vision by fixation p 3833 N94-31991
Neural models of spatial orientation in novel environments
[AD-A277383] p 3835 N94-32340
A multitasking behavioral control system for the Robotic All Terrain Lunar Exploration Rover (RATLER)
[DE94-007293] p 3835 N94-32787

AUTONOMY
From animals to animats
[AD-A277427] p 3802 N94-33241

AUTOREGRESSIVE PROCESSES
Representation, prediction and identification of cyclostationary processes: A state-space approach
[REPT-93-041] p 3850 N94-31191
Atmospheric structure simulation: An autoregressive model for smooth geophysical power spectra with known autocorrelation function
[AD-A276691] p 3773 N94-32118

AVERAGE
Heteroclinic attractors: Time averages and moduli of topological conjugacy
[W-9318] p 3844 N94-31690
Arithmetic averaging: A versatile technique for smoothing and trend removal
[DE94-005274] p 3852 N94-32673

AVIATION METEOROLOGY
Drop size distributions and related properties of fog for five locations measured from aircraft
[NASA-CR-4585] p 3787 N94-33065

AVIONICS
The maintenance of operational flight program
[AD-A276363] p 3565 N94-31367
Technologies for avionics embedded computer systems
[AD-A276364] p 3581 N94-31368
Testing Operational Flight Programs (OFP's)
[AD-A276361] p 3578 N94-31387
SATCOM feasibility study for search and rescue aircraft
[DSIS-94-01083] p 3575 N94-31902
Aerospace software engineering for advanced systems architectures
[AD-A277101] p 3581 N94-31977
Getting a handle on designing for avionics software supportability and maintainability
[AD-A276362] p 3581 N94-32055
Modular Simulator System (MSS). System/segment specification for the generic modular simulator system-navigation/communication module, volume 6
[AD-A276973] p 3590 N94-32398
A framework for developing and managing reusable avionics software
[AD-A276846] p 3582 N94-32909

AXIAL FLOW
The effect of an axial flow component on a circular cylinder wake p 3699 N94-31209
On the structure and stability of slender viscous vortices p 3700 N94-31218
Solution of the average-passage equations for the incompressible flow through multiple-blade-row turbomachinery
[AD-A276515] p 3583 N94-31931
Incorporating radial mixing in axisymmetric streamline curvature through-flow analysis
[AD-A277325] p 3706 N94-32279
Flutter analysis of a supersonic cascade in time domain using an ADI Euler solver
[NASA-TM-105625] p 3739 N94-32883

AXIAL LOADS
Reliability analysis of structural ceramics subjected to biaxial flexure p 3650 N94-31454
Contribution to the study of multiaxial fatigue under periodic or random stresses
[ISAL-92-0004] p 3734 N94-31544

AXIAL STRESS
Contribution to the study of multiaxial fatigue under periodic or random stresses
[ISAL-92-0004] p 3734 N94-31544

AXIOMS
On the independent axiomatizability of modal and intermediate logics
[ML-93-17] p 3856 N94-31407

AXISYMMETRIC BODIES
Tip effects on the vortex wake of an axisymmetric body at angle of attack p 3570 N94-31907
A separation technique for asymptotic-numeric solution for general shells of revolution p 3736 N94-31961

AXISYMMETRIC FLOW
Accretion disks around black holes p 3928 N94-31117
Simulations of the creation and motion of vortex rings
[W-9319] p 3703 N94-31691
Incorporating radial mixing in axisymmetric streamline curvature through-flow analysis
[AD-A277325] p 3706 N94-32279

AXONS
Empirical modeling for intelligent, real-time manufacture control p 3839 N94-32424

AZERBAIJAN
Station climatic summaries: China, the former USSR, and Mongolia
[AD-A276548] p 3784 N94-32057

AZO COMPOUNDS
Azo polymers for reversible optical storage. 4. Cooperative motion of rigid groups in semicrystalline polymers
[AD-A277107] p 3654 N94-31978
Reversible optical storage in azo polymers
[AD-A277109] p 3654 N94-31980
Compatibility studies of some azo polymer blends
[AD-A277141] p 3657 N94-32365
Microstructure of copolymers containing disperse red 1 and methyl methacrylate
[AD-A277140] p 3660 N94-32722

AZULENE
Energy transfer properties and mechanisms
[DE94-007403] p 3636 N94-32594

B

B STARS
Evolution of dynamo-generated magnetic fields in accretion disks around compact and young stars p 3931 N94-31138
The evolutionary status of PSR 1259-63
[DE94-007094] p 3938 N94-32503

BACILLUS
Biocatalytic processing polymers in supercritical fluids
[AD-A276120] p 3651 N94-31510

BACKGROUND NOISE
Peak detection of Swerling type targets. Part 1: Detection probabilities in white noise
[AD-A276217] p 3670 N94-31062
A Green's function approach to analysing the effects of random synaptic background activity in a model neural network
[MATHS-REPT-A-202] p 3828 N94-31157
Long transect seafloor seismic array: A component of SAMSON (Sources of Ambient Micro Seismic Ocean ic Noise)
[AD-A277009] p 3789 N94-32401
Visual processing of object velocity and acceleration
[AD-A277425] p 3801 N94-32998
The application of a radial basis function neural network for radar tracking over the sea p 3686 N94-33150

BACKSCATTERING
The development and testing of a backscatter absorption gas imaging (BAGI) system designed to image at a range of 300 m
[DE94-006192] p 3675 N94-31761
Methods for SBS threshold reduction
[AD-A276554] p 3717 N94-31936
High-resolution synthetic aperture radar observations of the Moon p 3676 N94-31952
ITS version 3.0: Powerful, user-friendly software for radiation modelling
[DE94-006607] p 3678 N94-32113
Backscatter and transmission of aerosol at UV through middle IR wavelengths
[AD-A277127] p 3718 N94-32305
MOM3D method of moments code theory manual
[NASA-CR-189594] p 3682 N94-32897
Millstone Hill radar studies of plasma waves and turbulence
[AD-A278409] p 3684 N94-33172

BACKWARD DIFFERENCING
On the error committed by stopping the Newton iteration in Runge-Kutta methods and linear multistep methods
[TW-93-13] p 3847 N94-32206

BACKWARD FACING STEPS
Backward-facing step measurements at low Reynolds number, Re(sub h)=5000
[NASA-TM-108807] p 3711 N94-33290

BACKWARD WAVES
Repetitively pulsed backward-wave oscillator investigations
[AD-A278281] p 3698 N94-33142

BACTERIA
Spectral inhomogeneity of the bacterial light-harvesting antennae: Causes and consequences
[ETN-94-96020] p 3792 N94-31533

BAKING
Conductive paints
[DE94-008508] p 3661 N94-32788

BALL BEARINGS
Torque characteristics of solid lubricated precision bearings during oscillatory motion
[AD-A278133] p 3728 N94-33061
A comparison of the performance of solid and liquid lubricants in oscillating spacecraft ball bearings p 3606 N94-33311
Development of long-life, low-noise linear bearings for atmospheric interferometry p 3606 N94-33312
Design of a high-speed reliable ball bearing p 3606 N94-33314

BALLISTIC MISSILES
Vulnerability assessment of a space based weapon platform electronic system exposed to a thermonuclear weapon detonation
[DE94-007229] p 3611 N94-32667
Integrated safety program for the Nuclear Electric Propulsion Space Test Program
[DE94-004670] p 3615 N94-32669

BALLOON-BORNE INSTRUMENTS
Low power, constant-flow air pump systems
[DE94-007463] p 3727 N94-32758
Water vapor from sunradiometry in comparison with microwave and balloon-sonde measurements at the Southern Great Plains ARM Site
[DE94-007479] p 3786 N94-32759

BANGLADESH
Recurvature dynamics of a typhoon
[AD-A276792] p 3784 N94-32164

BARENTS SEA
Prediction of the plane wave beamformed acoustic arrival structure for the 1992 Barents Sea coastal tomography test
[AD-A276741] p 3788 N94-32181
Finite-element modeling of the blockage and scattering of LG propagation
[AD-A277430] p 3775 N94-33006

BARIUM OXIDES
On the nature of striae in strontium barium niobate
[DE94-006486] p 3901 N94-32176
Processing and characterization of functionally gradient ceramic materials
[AD-A277154] p 3657 N94-32367
High T(sub c) superconductor tunnel junctions for photon detectors
[DE94-007686] p 3904 N94-32602
The path for long range conduction in high J(sub c) TlBa2Ca2Cu3O(8+x) spray-pyrolyzed deposits
[DE94-007211] p 3909 N94-33271

BARYON RESONANCE
NN-interaction in (1)S0-state: Virtual level or dibaryon resonance?
[DE94-606492] p 3869 N94-32097

BARYONS
Baryogenesis from a primordial lepton asymmetry
[PB94-145166] p 3868 N94-31921
Antiproton production in heavy ion collisions
[DE94-007552] p 3870 N94-32271
Transverse energy production with Si and Au beams at AGS energy: Towards hot and dense hadronic matter
[DE94-007178] p 3938 N94-32638
Hyperon polarization, crystal channeling, and E781 at Fermilab
[DE94-008224] p 3877 N94-32802

BASE FLOW
On the structure and stability of slender viscous vortices p 3700 N94-31218
Turbulence structure of a premixed flame in a coaxial free air jet in the presence or absence of a base flow
[ISBN-0-315-78739-2] p 3633 N94-31471
BATTERY CHARGERS
EDD-7 Electric Charge Point Meter test results
[DE94-008515] p 3696 N94-32828
BAYES THEOREM
Fault detection and isolation for the Bluebird test bed aircraft
[AD-A277979] p 3586 N94-33086
Real-time sensor data validation
[NASA-CR-195295] p 3616 N94-33099
Management of uncertainty in knowledge-based systems: A military perspective p 3854 N94-33341
BCS THEORY
A quest for a new superconducting state
[DE94-008439] p 3908 N94-32991
BEADS
Empirical modeling for intelligent, real-time manufacture control p 3839 N94-32424
BEAM INJECTION
Experimental survey of the L-H transition conditions in the D3-D tokamak
[DE94-007428] p 3891 N94-32595
BEAM INTERACTIONS
RHIC spin physics
[DE94-005452] p 3876 N94-32099
Particle diffusion from the beam-beam interaction in synchrotron colliders
[DE94-007111] p 3876 N94-32685
BEAMFORMING
Subspace estimation without eigenvectors for adaptive beamforming
[AD-A276287] p 3671 N94-31254
Optical processing of MMW for agile beamsteering and beamforming
[AD-A277161] p 3880 N94-32068
Prediction of the plane wave beamformed acoustic arrival structure for the 1992 Barents Sea coastal tomography test
[AD-A276741] p 3788 N94-32181
Digital beamforming and filtering circuit
[AD-D016142] p 3697 N94-32976
BEAMS (RADIATION)
Optical processing of MMW for agile beamsteering and beamforming
[AD-A277161] p 3880 N94-32068
BEAMS (SUPPORTS)
Random vibrations of composite beams and plates p 3735 N94-31777
Vibrational and acoustic response of ribbed plates p 3736 N94-31955
An analytical study of the vibration of beams fitted with neutralizers. Part 2: Assessment of the effects of mounting configurations
[ISVR-TR-225-PT-2] p 3740 N94-32982
BEARING (DIRECTION)
Relative motion pinwheel
[AD-D016107] p 3577 N94-32961
BEARINGS
International Space Station Alpha's bearing, motor, and roll ring module developmental testing and results p 3603 N94-33295
BEHAVIOR
From animals to animats
[AD-A277427] p 3802 N94-33241
BELARUS
Station climatic summaries: China, the former USSR, and Mongolia
[AD-A276548] p 3784 N94-32057
BEND TESTS
Strain sensing using optical fibers
[NASA-CR-195807] p 3740 N94-32940
Technology integration box beam failure study p 3628 N94-33126
Simpler J(sub Ic) test and data analysis procedures for high strength steels
[AD-A277731] p 3648 N94-33281
BENDING
Control of a flexible-link robotic arm manipulating an unknown dynamic payload p 3725 N94-31973
QUAD4 seminar
[AD-A277366] p 3818 N94-32330
Compliance measurements of chevron notched four point bend specimen
[NASA-TM-106538] p 3740 N94-32932
BENDING FATIGUE
Fatigue behavior of unidirectional pultruded composite materials
[ISBN-0-315-86425-7] p 3621 N94-31719
BENDING MOMENTS
An approximate solution for interlaminar stresses in laminated composites p 3621 N94-31901
Technology integration box beam failure study p 3628 N94-33126
BENDING VIBRATION
Microreflectance infrared study of electron-molecular vibrational coupling and lattice softness in BEDT-TTF salts
[DE94-008490] p 3907 N94-32989
BENZENE
Energy transfer properties and mechanisms
[DE94-007403] p 3636 N94-32594
Microstructure of copolymers containing disperse red 1 and methyl methacrylate
[AD-A277140] p 3660 N94-32722
Direct aromatization of methane
[DE94-008719] p 3638 N94-32888
BESSEL FUNCTIONS
Steepest descent paths for integrals defining the modified Bessel functions of imaginary order
[CWI-AM-R9303] p 3848 N94-32227
BIBLIOGRAPHIES
Space industrialization: A guide to government information
[RELEASE-1.2] p 3916 N94-31338
Aeronautical engineering: A continuing bibliography with indexes (supplement 302)
[NASA-SP-7037(302)] p 3565 N94-31342
Aeronautical engineering: A continuing bibliography with indexes (supplement 303)
[NASA-SP-7037(303)] p 3565 N94-31381
Aerospace medicine and biology: A continuing bibliography with indexes (supplement 388)
[NASA-SP-7011(388)] p 3795 N94-31414
A guide to experimental elementary particle physics literature, 1988-1992
[DE94-007445] p 3873 N94-32768
Aeronautical engineering: A continuing bibliography with indexes (supplement 304)
[NASA-SP-7037(304)] p 3566 N94-32853
Materials development program: Ceramic technology project bibliography, 1984-1992
[DE94-009297] p 3662 N94-32935
Cumulative reports and publications through December 31, 1993
[NASA-CR-194889] p 3806 N94-33286
BICRYSTALS
Boron and hydrogen in Ni3Al. Part 2: Mechanical testing of bicrystals
[DE94-007441] p 3904 N94-32606
BIDIRECTIONAL REFLECTANCE
Modeling the interaction between solar radiation and terrestrial surfaces p 3779 N94-30999
Temporal and spatial mapping of atmospheric dust opacity and surface albedo on Mars p 3947 N94-33211
BIG BANG COSMOLOGY
Fireworks in velocity and configuration space applied to cosmology
[USIP-93-90] p 3927 N94-31086
Nuclear physics and astrophysics
[DE94-007168] p 3939 N94-33147
BINARY DATA
Binary quantifiers and relational semantics
[LP-93-13] p 3855 N94-31404
Spacecraft On-Board Information Extraction Computer (SOBIEC) p 3808 N94-32433
BINARY MIXTURES
Strongly coupled ionic mixtures and the H/He EOS
[DE94-006391] p 3934 N94-31782
Measurement of viscosity, density, and gas solubility of refrigerant blends in selected synthetic lubricants
[DE94-007723] p 3653 N94-31917
Processable, chemical routes to binary metal sulfides
[AD-A277006] p 3642 N94-32004
Lubrication with binary mixtures: Liquid-liquid emulsion in elastohydrodynamics and metal forming p 3658 N94-32490
Extended-range order in glasses
[DE94-008135] p 3661 N94-32798
Analytic properties of the OCP and ionic mixtures in the strongly coupled fluid state
[DE94-008216] p 3637 N94-32801
BINARY PHASE SHIFT KEYING
Advanced satellite communication system
[NASA-CR-194211] p 3681 N94-32477
The effects of a multipath channel and interference on coherent M-PSK digital communication systems
[AD-A278158] p 3684 N94-33254
BINARY STARS
Double-lined pre-main-sequence binaries: A test of pre-main-sequence evolutionary theory p 3933 N94-31497
Winds from disks in compact binaries
[DE94-007452] p 3938 N94-32137
The evolutionary status of PSR 1259-63
[DE94-007094] p 3938 N94-32503
BINARY SYSTEMS (MATERIALS)
High temperature ductility loss in titanium alloys: A review
[DE94-006606] p 3640 N94-31345
Micromechanics and effective properties of particulate composites and fluid suspensions p 3703 N94-31744
Nonlinear effects in interfacial fracture p 3737 N94-31974
New molecular-based routes to binary main group metal sulfides
[AD-A277005] p 3900 N94-32003
Group 12 thiolates: Syntheses, characterization and decomposition pathways
[AD-A277055] p 3900 N94-32011
BINAURAL HEARING
Mechanisms of temporal pattern discrimination by human observers
[AD-A277407] p 3801 N94-32577
Models of the neuronal mechanisms of target localization of the barn owl
[AD-A277332] p 3797 N94-32623
BIOACOUSTICS
Minutes: Accredited Standards Committee on Bioacoustics, S3. US TAG for ISO/TC 43, acoustics, IEC/TC 29 electroacoustics, and ISO/TC 108/SC4 human exposure to mechanical vibration and shock
[AD-A276201] p 3795 N94-31490
BIOASSAY
Characterization and utilization of opiate-like hibernation factors
[AD-A278136] p 3794 N94-33098
BIOASTRONAUTICS
Aerospace medicine and biology: A continuing bibliography with indexes (supplement 388)
[NASA-SP-7011(388)] p 3795 N94-31414
Muscle disuse through tail-suspension: Etiology and therapeutics p 3796 N94-31746
BIOCHEMISTRY
International Journal of Quantum Chemistry, Quantum Biology Symposium number 20. Proceedings of the International Symposium on the Application of Fundamental Theory to Problems of Biology and Pharmacology
[AD-A276294] p 3792 N94-31294
Biocatalytic processing polymers in supercritical fluids
[AD-A276120] p 3651 N94-31510
Development and application of photosensitive device systems to studies of biological and organic materials
[DE94-008503] p 3793 N94-32516
Ninth International Workshop on Plant Membrane Biology
[DE94-005690] p 3794 N94-32769
BIOCONVERSION
Spectral inhomogeneity of the bacterial light-harvesting antennae: Causes and consequences
[ETN-94-96020] p 3792 N94-31533
Development of a catalytic system for gasification of wet biomass
[DE94-006216] p 3759 N94-31762
Biological conversion of synthesis gas
[DE94-000094] p 3760 N94-31811
Removal of CO2 from flue gases by algae
[DE94-008039] p 3766 N94-32703
BIODYNAMICS
Tripping over obstacles: Biomechanical analyses of how young and old try to avoid it p 3800 N94-31954
Use of a pitch adjustable foot restraint system: Operator strength capability and load requirements
[NASA-TP-3477] p 3805 N94-33050
BIOENGINEERING
Model-based scientific discovery: A study in space bioengineering p 3799 N94-31990
BIOINSTRUMENTATION
Perspectives of glucose sensing based on a charge-modulating competition reaction
[ISBN-9-09-005754-4] p 3795 N94-31652
BIOLOGICAL EFFECTS
Aerospace medicine and biology: A continuing bibliography with indexes (supplement 389)
[NASA-SP-7011(389)] p 3797 N94-32347
Aerospace medicine and biology: A continuing bibliography with indexes (supplement 385)
[NASA-SP-7011(385)] p 3797 N94-32348
High peak power microwaves: A health hazard
[AD-A277168] p 3681 N94-32576
Effects of long-term elevated atmospheric CO2 concentrations on Pinus ponderosa
[DE94-008832] p 3769 N94-32966
BIOLOGICAL EVOLUTION
Qualitative properties of two-dimensional predator-prey systems
[REPT-93-75] p 3844 N94-31644
BIOLOGICAL MODELS (MATHEMATICS)
Two models solving the increasing energy problem of the continuous Hopfield network model
[REPT-93-87] p 3843 N94-31552

Qualitative properties of two-dimensional predator-prey systems
[REPT-93-75] p 3844 N94-31644
A predator-prey model with Ivlev's functional response
[REPT-93-79] p 3844 N94-31696
Tripping over obstacles: Biomechanical analyses of how young and old try to avoid it p 3803 N94-31954
Model-based scientific discovery: A study in space bioengineering p 3799 N94-31990
On the reciprocal relationship between life histories and population dynamics
[CWI-AM-R9302] p 3793 N94-32226
The legacy of Kermack and McKendrick
[CWI-AM-R9304] p 3793 N94-32228
A cell-cycle model revisited
[CWI-AM-R9305] p 3851 N94-32229
Research and applications of a canopy reflectance model p 3747 N94-32492
Numerical model of the thermal behavior of an extremity in a cold environment including counter-current heat exchange between the blood vessels
[AD-A278099] p 3798 N94-33040
Workshop on Visual Perception: Computation and Psychophysics
[AD-A278412] p 3802 N94-33326

BIOLUMINESCENCE
Bioluminescence bathyphotometer
[AD-D016102] p 3790 N94-32959

BIOMASS
Development of a catalytic system for gasification of wet biomass
[DE94-006216] p 3759 N94-31762
Biomass power industry: Assessment of key players and approaches for DOE and industry interaction
[DE94-000238] p 3761 N94-32725
Environmental issues related to biomass: An overview
[DE94-007226] p 3767 N94-32784
Climate effects of anthropogenic sulfate: Simulations from a coupled chemistry/climate model
[DE94-004352] p 3767 N94-32789
Light utilization and photoinhibition of photosynthesis in marine phytoplankton
[DE94-005505] p 3794 N94-32896

BIOMASS ENERGY PRODUCTION
Biomass power industry: Assessment of key players and approaches for DOE and industry interaction
[DE94-000238] p 3761 N94-32725

BIOMEDICAL DATA
Interactive reconstruction of anatomical structures with free-form surfaces
[TELECOM-93-E-002] p 3794 N94-31195

BIOPHYSICS
Spectral inhomogeneity of the bacterial light-harvesting antennae: Causes and consequences
[ETN-94-96020] p 3792 N94-31533
Future directions of nonlinear dynamics in physical and biological systems. (Physica D nonlinear, volume 68, number 1)
[AD-A278085] p 3794 N94-33250

BIOPROCESSING
Biocatalytic processing polymers in supercritical fluids
[AD-A276120] p 3651 N94-31510

BIOREACTORS
Biological conversion of synthesis gas
[DE94-000094] p 3760 N94-31811

BIOSPHERE
Subtropical Climates and Their Evolution: From Space-Based Observation to Modelling
[ISBN-2-85-428333-3] p 3776 N94-30981
Modeling of the continental biosphere p 3770 N94-31011

BIOSYNTHESIS
Towards a detailed understanding of the structural variability in lignins: A new approach
[DE94-007449] p 3793 N94-32267
The magnesium chelation step in chlorophyll biosynthesis
[DE94-008727] p 3794 N94-32890

BIPOLAR TRANSISTORS
Passivation of III-V compound semiconductor based devices
[AD-A276178] p 3894 N94-31056
Reconfigurable optical switches with monolithic electrical-to-optical interfaces
[DE94-007745] p 3861 N94-32385

BIPOLARITY
Chemical vapour deposition of tungsten for the application in integrated circuits
[ISBN-9-09-005151-1] p 3641 N94-31519

BIREFRINGENCE
Azo polymers for reversible optical storage. 4. Cooperative motion of rigid groups in semicrystalline polymers
[AD-A277107] p 3654 N94-31978
High average power pulsed phase conjugate laser with birefringence correction
[DE94-006049] p 3719 N94-32659

BISMALEIMIDE
Evolution of the interface properties with temperature in the T800H/ bismaleimide composites
[ONERA-NT-1993-14] p 3619 N94-31478

BISMUTH ALLOYS
Fermi surface instability at 0.4 K in a heavy-fermion YbBiPt: SDW?
[DE94-006224] p 3899 N94-31916

BISMUTH OXIDES
High T(sub c) superconductor tunnel junctions for photon detectors
[DE94-007686] p 3904 N94-32602

BIT ERROR RATE
Control and reliability of optical networks in multiprocessors
[AD-A277385] p 3881 N94-32285

BIVARIATE ANALYSIS
Diagonal band probability distributions
[REPT-93-80] p 3851 N94-31697

BLACK HOLES (ASTRONOMY)
Accretion disks around black holes p 3928 N94-31117
Disk irradiation and light curves of x ray novae p 3929 N94-31124
Observational constraints on black hole accretion disks p 3929 N94-31126
Nonlinear calculations of the time evolution of black hole accretion disks p 3929 N94-31127
The physics of black hole x ray novae p 3932 N94-31143

BLOCK COPOLYMERS
Novel electroactive polymers and block copolymers
[AD-A276119] p 3650 N94-31509
Dynamics of block poly(styrene-co-vinylpyridine) (SVP) in solution and on silica
[AD-A277139] p 3657 N94-32364
Phase behavior, structure, and properties of model block polymers
[AD-A277530] p 3662 N94-32954

BLOCKING
Compiler techniques for managing data motion
[AD-A276514] p 3918 N94-31930
Finite-element modeling of the blockage and scattering of LG propagation
[AD-A277430] p 3775 N94-33006

BLOOD
Numerical model of the thermal behavior of an extremity in a cold environment including counter-current heat exchange between the blood vessels
[AD-A278099] p 3798 N94-33040

BLOOD CIRCULATION
Incompressible viscous flow in tubes with occlusions
[ISBN-0-315-75467-2] p 3704 N94-31778

BLOOD FLOW
Incompressible viscous flow in tubes with occlusions
[ISBN-0-315-75467-2] p 3704 N94-31778

BLOOD PLASMA
Characterization and utilization of opiate-like hibernation factors
[AD-A278136] p 3794 N94-33098

BLOOD VESSELS
Numerical model of the thermal behavior of an extremity in a cold environment including counter-current heat exchange between the blood vessels
[AD-A278099] p 3798 N94-33040

BLOWING
Control of hypersonic aerodynamic forces with surface blowing p 3567 N94-31216

BLUFF BODIES
The effect of an axial flow component on a circular cylinder wake p 3699 N94-31209

BODY CENTERED CUBIC LATTICES
Metal clusters: Dynamics and structure
[AD-A276842] p 3643 N94-32091

BODY-WING CONFIGURATIONS
Multidisciplinary optimization of high-speed civil transport configurations using variable-complexity modeling p 3578 N94-31881

BOEING 737 AIRCRAFT
Airborne Trailblazer: Two decades with NASA Langley's 737 flying laboratory
[NASA-SP-4216] p 3566 N94-32793

BOEING 767 AIRCRAFT
A comparison of military and commercial aircraft development
[AD-A276830] p 3575 N94-32168

BOILERS
Methodology for damage study of a tube-grill contact
[ECL-92-49] p 3734 N94-31562
Creep-fatigue criteria and inelastic behavior of modified 9Cr-1Mo steel at elevated temperatures
[DE94-007915] p 3642 N94-31918

BOLIDES
Possible test of ancient dense Martian atmosphere p 3947 N94-33206

BOLOMETERS
Wavelet transform of fixed pattern noise in focal plane arrays
[AD-A276963] p 3712 N94-32393

BOLTZMANN DISTRIBUTION
Fireworks in velocity and configuration space applied to cosmology
[USIP-93-90] p 3927 N94-31086

BOLTZMANN TRANSPORT EQUATION
Monoenergetic neutral particle transport in semi-infinite media
[AD-A277155] p 3870 N94-32368

BONDED JOINTS
Small cylindrical adhesive bonds
[PB94-148210] p 3651 N94-31585
Joining of alumina by vacuum brazing
[VTT-TIED-1495] p 3724 N94-31656
Bond stress-slip characteristics of FRP rebars
[AD-A277191] p 3623 N94-32070
The cyclic fatigue behaviour of adhesive joints
[AD-A277080] p 3738 N94-32351

BONDING
Interfacial behaviour: Wettability in SiC(sub p) metal matrix composites
[ISBN-0-315-87206-3] p 3621 N94-31835
Energetics, bonding mechanism, and electronic structure of ceramic/ceramic and metal/ceramic interfaces
[DE94-008551] p 3659 N94-32656

BONES
Isolating strain parameters correlated to skeletal adaptation p 3797 N94-31960

BOOLEAN ALGEBRA
A theory of conditional information with applications
[AD-A278164] p 3850 N94-33255

BOOMS (EQUIPMENT)
MSAT boom joint testing and load absorber design p 3606 N94-33315
Deployable and retractable telescoping tubular structure development p 3607 N94-33317

BOOSTER ROCKET ENGINES
Possible effect of the chlorine oxide dimer on transient ozone loss in rocket plumes
[AD-A278135] p 3616 N94-33094

BORANES
Processing boron and boron carbide thin films for protective coatings and device fabrication
[AD-A277266] p 3900 N94-32041

BORN APPROXIMATION
Structure estimation of phase objects from the diffraction near field: Microwave and model calculations
[ETN-94-95737] p 3674 N94-31608

BORON
Determination of BPSG thin-film properties using IR reflection spectroscopy of product wafers
[DE94-006591] p 3634 N94-32110
Boron and hydrogen in Ni3Al. Part 2: Mechanical testing of bicrystals
[DE94-007441] p 3904 N94-32606

BORON CARBIDES
Processing boron and boron carbide thin films for protective coatings and device fabrication
[AD-A277266] p 3900 N94-32041

BORON NITRIDES
Nucleation and growth of cubic boron nitride films produced by ion-assisted pulsed laser deposition
[DE94-007295] p 3661 N94-32796
X ray absorption study of pulsed laser deposited boron nitride films
[DE94-008295] p 3662 N94-32855

BOROSILICATE GLASS
Surface chemistry and durability of borosilicate glass
[DE94-006734] p 3656 N94-32116
Pump-probe method for investigating laser ablation and optical damage threshold mechanisms in optical materials
[DE94-008291] p 3720 N94-32753

BOSONS
Study of associated gauge boson production at D0: W gamma production
[DE94-006951] p 3866 N94-31670
Production of charginos and neutralinos for the reaction positron electron yields Z' boson yields chargino(+) (sub i) chargino(-) (sub j) or neutralino (sub i) neutralino (sub j) in SU(2) (sub L) x SU(2) (sub R) x U(1) (sub B-L)
[ISBN-0-315-87316-7] p 3867 N94-31832
F0-975, A0-980 as eye-witnesses of confinement
[PB94-147105] p 3868 N94-31923
Short coherence length superconductors: Intermediate regime between BCS and bosons
[DE94-007694] p 3904 N94-32645

BOULES
Boron and hydrogen in Ni3Al. Part 2: Mechanical testing of bicrystals
[DE94-007441] p 3904 N94-32606
BOUNDARIES
Deep water studies of CTD data
[AD-A277741] p 3791 N94-33176
BOUNDARY CONDITIONS
Boundary control of scattering p 3861 N94-31899
Solution of the average-passage equations for the incompressible flow through multiple-blade-row turbomachinery
[AD-A276515] p 3583 N94-31931
Sound scattering by cylinders of noncircular cross section
[AD-A276663] p 3861 N94-32089
Surface boundary conditions and related technical issues concerning Burnett equations for 2-D hypersonic flow
[AD-A277322] p 3706 N94-32256
A critical evaluation of methods for imposing solid-wall boundary conditions in inviscid flow
[AD-A276959] p 3707 N94-32361
The 2D deterministic radiation transport with the discontinuous finite element method
[DE94-004687] p 3849 N94-32670
A finite-difference approximate-factorization algorithm for solution of the unsteady transonic small-disturbance equation
[NASA-TP-3129] p 3572 N94-32865
BOUNDARY ELEMENT METHOD
THERM3D: A boundary element computer program for transient heat conduction problems
[DE94-008112] p 3708 N94-32709
Boundary element analysis of three-dimensional nonlinear hydrodynamics in a reduced gravity environment p 3668 N94-32715
BOUNDARY LAYER CONTROL
Study of dynamic stall phenomenon and its control using vorticity, stream function and circulation form of the unsteady Navier-Stokes equations p 3572 N94-32714
Results for the hybrid laminar flow control experiment conducted in the NASA Langley 8-foot transonic pressure tunnel on a 7-foot chord model
[NASA-TM-107582] p 3601 N94-32870
Magnetohydrodynamic boundary layer control system
[AD-D016120] p 3710 N94-32958
BOUNDARY LAYER EQUATIONS
Computation of three-dimensional compressible boundary layers to fourth-order accuracy on wings and fuselages
[NASA-CR-4269] p 3709 N94-32871
BOUNDARY LAYER FLOW
Interaction processes between the ocean and the atmosphere p 3777 N94-30987
Boundary layer study on nozzle wall at hypersonic velocities p 3569 N94-31882
A non-local model for prediction of the probability density function of turbulent fluctuations in boundary-layer flows p 3706 N94-32076
A critical evaluation of methods for imposing solid-wall boundary conditions in inviscid flow
[AD-A276959] p 3707 N94-32361
Shear flow control of cold and heated rectangular jets by mechanical tabs. Volume 1: Results and discussion
[NASA-CR-182296-VOL-1] p 3708 N94-32867
Shear flow control of cold and heated rectangular jets by mechanical tabs. Volume 2: Tabulated data
[NASA-CR-182296-VOL-2] p 3709 N94-32869
Magnetohydrodynamic boundary layer control system
[AD-D016120] p 3710 N94-32958
Transport and diffusion in turbulent fields modeling and measurements techniques
[AD-A278114] p 3769 N94-33110
The structure of high Reynolds number turbulent boundary layers, part A
[AD-A278392] p 3710 N94-33162
BOUNDARY LAYER SEPARATION
Three-dimensional velocity measurements on a 6:1 prolate spheroid at 10 deg angle of attack
[AD-A276485] p 3702 N94-31476
An experimental study of the flowfield on a semispan rectangular wing with a simulated glaze ice accretion
[NASA-CR-195301] p 3571 N94-32475
Numerical analysis of transonic wing buffet p 3586 N94-32713
Study of dynamic stall phenomenon and its control using vorticity, stream function and circulation form of the unsteady Navier-Stokes equations p 3572 N94-32714
Control of low-speed turbulent separated flow over a backward-facing ramp
[NASA-TM-109740] p 3573 N94-33071
BOUNDARY LAYER STABILITY
Compressible convection with ionization p 3911 N94-31498
BOUNDARY LAYER TRANSITION
Analysis of the photodiode boundary layer transition indicator
[DE94-005311] p 3701 N94-31268
BOUNDARY LAYERS
Development of a cascade simulation of fan-passage flow
[AD-A277234] p 3584 N94-32026
Diagnostic studies of climate variability
[DE94-003629] p 3767 N94-32711
Stability of tearing modes in tokamak plasmas
[DE94-009205] p 3892 N94-32911
Fluid mechanical measurements within the bottom boundary layer over the Northern California continental shelf during stress
[AD-A277916] p 3791 N94-33243
BOUNDARY LUBRICATION
Development and preliminary evaluation of aryl ester boundary additives for perfluoropolyethers
[NASA-TM-106603] p 3663 N94-33024
BOUNDARY VALUE PROBLEMS
Fully discrete arbitrary-order schemes for a model hyperbolic conservation law
[CRANFIELD-AERO-9307] p 3843 N94-31539
A simplified Von Neumann method for linear stability analysis
[CRANFIELD-AERO-9310] p 3843 N94-31540
Penetrable wedge analysis
[AD-A277219] p 3845 N94-32022
A stability estimate based on numerical ranges with application to a spectral discretization of a convection-diffusion equation
[TW-93-12] p 3847 N94-32200
On the error committed by stopping the Newton iteration in Runge-Kutta methods and linear multistep methods
[TW-93-13] p 3847 N94-32206
Finite element solution to the Helmholtz equation with high wave number. Part 1: The h-version of the FEM
[AD-A277396] p 3848 N94-32341
Fourth-order 2N-storage Runge-Kutta schemes
[NASA-TM-109112] p 3573 N94-32950
Computational methods in continuum mechanics
[AD-A278144] p 3859 N94-33161
A study of weak solutions and their regularizations by numerical methods
[AD-A277453] p 3850 N94-33175
BOUSSINESQ APPROXIMATION
Renormalization group theory of Bolgiano scaling in Boussinesq turbulence
[NASA-TM-106602] p 3710 N94-33070
BOW WAVES
Analysis of data from the plasma composition experiment on the International Sun-Earth Explorer (ISEE 1)
[NASA-CR-195880] p 3893 N94-33074
BOX BEAMS
Structural testing of the technology integration box beam p 3628 N94-33125
Technology integration box beam failure study p 3628 N94-33126
BRAIDED COMPOSITES
Characterization and manufacture of braided composites for large commercial aircraft structures p 3630 N94-33137
BRAIN
Geometric structure of the adaptive controller of the human arm
[AD-A276797] p 3834 N94-32152
Sensory sensitivities and discriminations and their roles in aviation
[AD-A277312] p 3800 N94-32276
Neural network wavelet technology: A frontier of automation p 3839 N94-32425
The organization of the suprachiasmatic circadian pacemaker of the rat and its regulation by neurotransmitters and modulators
[AD-A277324] p 3793 N94-32622
Fast nonsupervised 3D registration of PET and MR images of the brain
[TELECOM-93-C-006] p 3798 N94-33069
BRANCHING (MATHEMATICS)
Bifurcation and deterministic chaos in dynamic systems
[REPT-93-047] p 3911 N94-31893
Structural stability and bifurcations p 3911 N94-31895
Numerical detection and continuation of codimension-two homoclinic bifurcations
[CWI-AM-R9308] p 3847 N94-32191
On the computation of simplical approximations of implicitly defined two-dimensional manifolds
[AD-A278132] p 3849 N94-33060
BRAYTON CYCLE
Development of lightweight radiators for lunar based power systems
[NASA-TM-106604] p 3726 N94-32272
BRAZING
Joining of alumina by vacuum brazing
[VTT-TIED-1495] p 3724 N94-31656
BRIGHTNESS
The stellar and gaseous content of massive low surface brightness disk galaxies p 3933 N94-31495
BRIGHTNESS TEMPERATURE
IRTM brightness temperature maps of the Martian south polar region during the polar night: The cold spots don't move p 3949 N94-33222
BRILLOUIN EFFECT
Methods for SBS threshold reduction
[AD-A276554] p 3717 N94-31936
BRILLOUIN ZONES
Strongly anisotropic s-wave versus d-wave gap in cuprate superconductors: Evidence and theory
[DE94-007579] p 3904 N94-32746
BRITTLE MATERIALS
Modeling of fracture and damage in quasibrittle materials p 3734 N94-31479
BRITTLENESS
Nonlocal theory for fracturing of quasibrittle materials
[AD-A278283] p 3740 N94-33143
BROADBAND
Waveform generation for ultra-wideband radar system
[AD-A276352] p 3673 N94-31401
Ultra wide band radar holographic imaging of subsurface targets
[DE94-004271] p 3713 N94-32681
Broadband, high-power, 2-30 MHz, twin-whip antenna. Computer and 1/10-scale model design study
[AD-A277619] p 3682 N94-32971
Generation of the ambiguity function for ultra wideband radar waveforms
[AD-A277913] p 3684 N94-33261
BROKEN SYMMETRY
Chiral symmetry and the threshold gamma(p) yields pi(sup 0)p reaction
[DE94-008117] p 3873 N94-32710
Quantum dynamics in dual spaces
[DE94-008303] p 3913 N94-32824
CP violation and the top quark
[DE94-008930] p 3874 N94-32841
Evidence for symmetry breaking local distortions in thallium barium copper oxide
[DE94-006149] p 3907 N94-32944
BROMIDES
Induced adsorption of chloride and bromide by submonolayer amounts of copper underpotentially deposited on Pt(111)
[AD-A278023] p 3648 N94-33182
BROWN DWARF STARS
Strongly coupled ionic mixtures and the H/He EOS
[DE94-006391] p 3934 N94-31782
BROWNIAN MOVEMENTS
The Laplace functional and Palm measure of a quasi-Cox process which is driven by a Markov chain
[REPT-93-82] p 3851 N94-31699
BSCCO SUPERCONDUCTORS
High T(sub c) superconductor tunnel junctions for photon detectors
[DE94-007686] p 3904 N94-32602
Microanalytical study of defect formation in thin bismuth strontium calcium copper oxide films
[DE94-008217] p 3661 N94-32751
BUCKLING
Ab initio study of the epitaxial growth of Ge on Si(100) surface
[DE94-007245] p 3904 N94-32724
BUDGETING
Budget allocation and monopolistic pricing in a multiproduct firm
[REPT-93-86] p 3924 N94-31617
BUFFETING
Active control for fin buffet alleviation
[AD-A276844] p 3586 N94-32224
Numerical analysis of transonic wing buffet p 3586 N94-32713
BUOYANCY
Effects of buoyancy on fluid flows and turbulence
[AD-A276586] p 3706 N94-32123
BUOYS
Profiling ALACE instruments
[AD-A277246] p 3789 N94-32321
BURNS (INJURIES)
Development of a video fluorescence system for assessing burn depth
[AD-A278127] p 3798 N94-33092
BURSTS
Development of high-pressure diaphragms for the AEDC impulse tunnel
[AD-A277053] p 3588 N94-32009

C

C-130 AIRCRAFT
Assessment of interior modifications in C-130 and C-141 aircraft for night vision goggle operations
[AD-A276843] p 3582 N94-32223
C-141 AIRCRAFT
Assessment of interior modifications in C-130 and C-141 aircraft for night vision goggle operations
[AD-A276843] p 3582 N94-32223
CADMIUM COMPOUNDS
Group 12 thiolates: Syntheses, characterization and decomposition pathways
[AD-A277055] p 3900 N94-32011
CADMIUM SELENIDES
The relationship of the electronic structures of semiconductor surfaces and heterostructures to crystal growth
[AD-A276465] p 3896 N94-31473
CADMIUM SULFIDES
Formation mechanism and yield of molecules ejected from ZnS, CdS, and FeS2 during ion bombardment
[DE94-008487] p 3871 N94-32515
CADMIUM TELLURIDES
Role of polycrystallinity in CdTe and CuInSe2 photovoltaic cells
[DE94-000293] p 3758 N94-31236
Development of a computer model for polycrystalline thin-film CuInSe2 and CdTe solar cells
[DE94-006853] p 3762 N94-32763
CAFFEINE
Review of pharmacological approach to improve cold tolerance p 3796 N94-31740
CALCITE
The pH of Mars p 3950 N94-33225
CALCIUM ISOTOPES
Influence of long-range correlations on the spectral functions and response of 48Ca and 90Zr
[ETN-94-96017] p 3865 N94-31537
CALCIUM OXIDES
The path for long range conduction in high J(sub c) TlBa2Ca2Cu3O(8+x) spray-pyrolyzed deposits
[DE94-007211] p 3909 N94-33271
CALCIUM SILICATES
Ion-beam-driven amorphization of Ca2La8(Si4)6O2 single crystals
[DE94-006219] p 3895 N94-31307
CALCULUS
Lambek calculus is L-complete
[LP-93-14] p 3841 N94-31388
Proving theorems of the Lambek calculus of order 2 in polynomial time
[CT-93-05] p 3842 N94-31393
Comparing models of the non-extensional typed lambda-calculus
[ML-93-19] p 3842 N94-31409
The decidability of dependency in intuitionistic propositional logic
[ML-93-20] p 3856 N94-31410
Completeness and decidability of the mixed style of inference with composition
[LP-93-09] p 3842 N94-31453
Lattice geometrodynamics p 3857 N94-31825
Combinatory reduction systems: Introduction and survey
[CWI-CS-R9362] p 3849 N94-32349
CALIBRATING
Viscoelastic fracture characterization of polymeric solids p 3652 N94-31745
Ground based radiometric and atmospheric measurements p 3744 N94-31855
Inflight calibration, preprocessing, and data evaluation of GER 2 imaging spectrometry data p 3744 N94-31858
OARE flight maneuvers and calibration measurements on STS-58
[NASA-TM-109093] p 3613 N94-32924
MODIS. Volume 2: MODIS level 1 geolocation, characterization and calibration algorithm theoretical basis document, version 1
[NASA-TM-104594-VOL-2] p 3613 N94-33289
CALIFORNIA
Differential interferometry study of an earthquake p 3756 N94-32570
Fluid mechanical measurements within the bottom boundary layer over the Northern California continental shelf during stress
[AD-A277916] p 3791 N94-33243
CALORIMETERS
Particle identification in a segmented calorimeter (NUMASS test data, September 1991)
[USIP-93-08] p 3711 N94-31085
The measurement of the hadronic energy flow and jet production with the ZEUS calorimeter in deep inelastic scattering events at HERA
[ETN-94-96021] p 3865 N94-31534
Gamma Large Area Silicon Telescope (GLAST)
[DE94-006439] p 3925 N94-31786
Ionization EM calorimetry with accordion electrodes and liquid krypton or argon
[DE94-009082] p 3713 N94-32821
CAMERAS
Hydrogenated amorphous silicon (a-Si:H) based gamma camera: Monte Carlo simulations
[DE94-007042] p 3795 N94-31323
CAD-based off-line planning for an active-vision system
[ISBN-0-315-86317-X] p 3813 N94-31713
Synchronized laser scanning three dimensional acquisition system
[ISBN-0-315-86848-1] p 3879 N94-31756
Gamma-ray optical counterpart search experiment (GROCSE)
[DE94-007124] p 3955 N94-32129
Fuzzy-neural control of an aircraft tracking camera platform p 3839 N94-32423
The trustworthy digital camera: Restoring credibility to the photographic image p 3714 N94-32470
CAMOUFLAGE
Atmospheric propagation effects through natural and man-made obscurants for visible to MM-wave radiation
[AD-A276919] p 3679 N94-32235
CANONICAL FORMS
Symplectic Runge-Kutta schemes 3: Canonical elementary differentials
[MATHS-REPT-A-204] p 3840 N94-31159
CANOPIES (VEGETATION)
The properties of sunflecks in a flexible plant canopy, and their relationship to turbulence p 3782 N94-31775
Research and applications of a canopy reflectance model p 3747 N94-32492
CANTILEVER BEAMS
A case study of analysis methods for large deflections of a cantilever beam
[NASA-TM-108454] p 3739 N94-32903
CAPACITANCE
Grounding ring for ground adapters
[AD-D016118] p 3697 N94-32962
CAPACITANCE SWITCHES
VLSI implementation of stray insensitive switched capacitor composite operational amplifiers
[AD-A276461] p 3687 N94-31240
CAPACITORS
VLSI implementation of stray insensitive switched capacitor composite operational amplifiers
[AD-A276461] p 3687 N94-31240
A series resonant converter in half bridge circuits with combined serial and parallel charge coupling and several output circuits
[ETN-94-95739] p 3687 N94-31373
Fractional-factorial process development techniques
[DE94-005580] p 3690 N94-31593
Evidence for a correct SiO2 voltage acceleration model
[DE94-006578] p 3690 N94-31594
Thin-film decoupling capacitors for multi-chip modules
[DE94-007743] p 3695 N94-32650
Temperature-humidity-bias aging technique to identify defective surface mount capacitors
[DE94-005354] p 3660 N94-32727
Overview of Sandia's electric vehicle battery program
[DE94-008944] p 3696 N94-32806
CAPE KENNEDY LAUNCH COMPLEX
Pen-based computers: Computers without keys p 3808 N94-32434
A systems approach to computer-based training p 3823 N94-32436
Chronology of KSC and KSC related events for 1993
[NASA-TM-109196] p 3966 N94-33072
CAPILLARY FLOW
Thermocapillary convection in evaporating sessile drops
[NASA-TM-109758] p 3705 N94-31886
CARBON
Theoretical studies of zirconium and carbon clusters with molecular dynamics simulations
[DE94-005276] p 3862 N94-31146
The effects of amorphous layer regrowth on carbon activation in GaAs and InP
[DE94-006290] p 3899 N94-31634
Deposition of DLC via intense ion beam ablation
[DE94-005583] p 3851 N94-31650
Structure-property relationships of carbon aerogels
[DE94-007120] p 3660 N94-32687
Compilation of diamond-like carbon properties for barriers and hard coatings
[DE94-008231] p 3661 N94-32803
Light utilization and photoinhibition of photosynthesis in marine phytoplankton
[DE94-005505] p 3794 N94-32896
Escape of Mars atmospheric carbon through time by photochemical means p 3948 N94-33214
CARBON CYCLE
Carbon cycle modeling calculations for the IPCC
[DE94-004332] p 3765 N94-32354
CARBON DIOXIDE
Application of natural refrigerants: A rational solution to a pressing problem
[PB94-138781] p 3668 N94-31073
Investigation of carbon dioxide in the central South Pacific Ocean (WOCE Sections P-16C and P-17C) during the TUNES/2 expedition of the R/V Thomas Washington, July-August, 1991
[DE94-006638] p 3763 N94-31347
Influence of carbon dioxide on electronic equipment: Fire extinguishing with low concentration
[PB94-148749] p 3691 N94-31848
Carbon cycle modeling calculations for the IPCC
[DE94-004332] p 3765 N94-32354
Carbon dioxide abatement as a differential game
[DE94-722023] p 3765 N94-32590
Removal of CO2 from flue gases by algae
[DE94-008039] p 3766 N94-32703
National US public policy on global warming derived from optimization of energy use and environmental impact studies
[DE94-004606] p 3768 N94-32790
A correlated k-distribution model of the heating rates for atmospheric mixtures of H2O, CO2, O3, CH4, and N2O in the 0-2500 cm(exp -1) wave number region at altitudes between 0 and 60 km
[DE94-005136] p 3775 N94-32895
A model for the evolution of CO2 on Mars p 3946 N94-33205
Mars atmospheric loss and isotopic fractionation by solar-wind-induced sputtering and photochemical escape p 3947 N94-33208
Escape of Mars atmospheric carbon through time by photochemical means p 3948 N94-33214
Controls on the CO2 seasonal cycle p 3950 N94-33227
Carbonate formation on Mars: Latest experiments p 3950 N94-33231
The influence of thermal inertia on Mars' seasonal pressure variation and the effect of the weather component p 3952 N94-33238
Simultaneous laboratory measurements of CO2 and H2O adsorption on palagonite: Implications for the Martian climate and volatile reservoir p 3952 N94-33240
Simulation of CO2 release at 800 km altitude
[AD-A276692] p 3776 N94-33272
CARBON DIOXIDE CONCENTRATION
Carbon balance in a forest ecosystem p 3770 N94-31007
Investigation of carbon dioxide in the central South Pacific Ocean (WOCE Sections P-16C and P-17C) during the TUNES/2 expedition of the R/V Thomas Washington, July-August, 1991
[DE94-006638] p 3763 N94-31347
Influence of carbon dioxide on electronic equipment: Fire extinguishing with low concentration
[PB94-148749] p 3691 N94-31848
Carbon cycle modeling calculations for the IPCC
[DE94-004332] p 3765 N94-32354
A correlated k-distribution model of the heating rates for atmospheric mixtures of H2O, CO2, O3, CH4, and N2O in the 0-2500 cm(exp -1) wave number region at altitudes between 0 and 60 km
[DE94-005136] p 3775 N94-32895
Effects of long-term elevated atmospheric CO2 concentrations on Pinus ponderosa
[DE94-008832] p 3769 N94-32966
Regional sedimentological variations among dark crater floor features: Toward a model for modern eolian sand distribution on Mars p 3946 N94-33203
Carbonate formation on Mars: Latest experiments p 3950 N94-33231
Obliquity variation in a Mars climate evolution model p 3951 N94-33236
Carbonates, surfates, phosphates, nitrates, and organic materials: Their association in a Martian meteorite p 3952 N94-33239
CARBON DIOXIDE LASERS
New material for high average power infrared generation: QPM-DB GaAs
[AD-A276389] p 3714 N94-31358
Automatic resonator alignment and power stabilization of high power C02 lasers
[ISBN-0-315-77217-4] p 3714 N94-31472
The development and testing of a backscatter absorption gas imaging (BAGI) system designed to image at a range of 300 m
[DE94-006192] p 3675 N94-31761

CARBON DIOXIDE REMOVAL
Removal of CO2 from flue gases by algae
[DE94-008039] p 3766 N94-32703
CARBON DISULFIDE
Methods for SBS threshold reduction
[AD-A276554] p 3717 N94-31936
Energy transfer properties and mechanisms
[DE94-007403] p 3636 N94-32594
CARBON FIBER REINFORCED PLASTICS
Unidirectional composites compressive behaviour: Test methods and micromechanical approach
[ONERA-NT-1993-10] p 3618 N94-31232
Evolution of the interface properties with temperature in the T800H/ bismaleimide composites
[ONERA-NT-1993-14] p 3619 N94-31478
Optimization of the forming parameters of PEEK/carbon fiber composite
[ISBN-0-315-86410-9] p 3620 N94-31716
Low velocity impact damage in carbon fiber/PEEK composite laminates
[ISBN-0-315-86546-6] p 3622 N94-31909
CARBON FIBERS
Optimization of the forming parameters of PEEK/carbon fiber composite
[ISBN-0-315-86410-9] p 3620 N94-31716
Surface conforming flexible eddy current probe for scanning varying surface contours
[AD-D016173] p 3627 N94-33018
Lightweight zinc electrode
[AD-D016181] p 3698 N94-33181
CARBON MONOXIDE
CO observations in external galaxies and gas mass determination p 3925 N94-31790
Vibrational energy transfer of diatomic gases in hypersonic expanding flows p 3570 N94-31958
A study of physical conditions, radiative transfer and shocks in the interstellar medium p 3937 N94-31963
Simulation of CO2 release at 800 km altitude
[AD-A276692] p 3776 N94-33272
CARBON 12
Mechanisms of formation and of de-excitation in the reaction Mg-24 + C-12 yields 9 alpha at 35MeV per nucleon
[ISBN-0-315-86746-9] p 3867 N94-31749
CARBON-CARBON COMPOSITES
Development of lightweight radiators for lunar based power systems
[NASA-TM-106604] p 3726 N94-32272
Improved oxidation resistance of 3-D carbon/carbon composites
[AD-A277349] p 3625 N94-32624
CARBONATES
Carbonate formation on Mars: Latest experiments p 3950 N94-33231
Carbonates, surfates, phosphates, nitrates, and organic materials: Their association in a Martian meteorite p 3952 N94-33239
CARBONYL COMPOUNDS
Novel approaches to the production of higher alcohols from synthesis gas
[DE94-006770] p 3666 N94-32132
Laser flash photolysis, EPR and Raman studies of liquids at elevated pressures
[DE94-008351] p 3718 N94-32413
Ligand intermediates in metal-catalyzed reactions
[DE94-008713] p 3638 N94-32887
CARBORANE
Processing boron and boron carbide thin films for protective coatings and device fabrication
[AD-A277266] p 3900 N94-32041
CARBOXYL GROUP
Reactions of electrophilic maleic anhydride and epoxy groups with nucleophilic functionalities such as carboxyl, hydroxyl, and amine groups. Polymer Technology Publication series no. 16
[PB94-135589] p 3648 N94-31069
CARBOXYLIC ACIDS
Recovery of carboxylic acids at pH greater than pKa
[DE94-007030] p 3636 N94-32376
Metal ion complexation by ionizable crown ethers
[DE94-008301] p 3661 N94-32847
CARGO AIRCRAFT
A comparison of military and commercial aircraft development
[AD-A276830] p 3575 N94-32168
CARRIER MOBILITY
Experimental and theoretical studies of hydrogenated amorphous semiconductor alloys and superlattices
[AD-A276159] p 3686 N94-31079
CASCADE FLOW
Computational study of simultaneous heat and mass transfer in turbulent separated flows p 3704 N94-31843
Design and initial testing of a facility to measure unsteady pressures on an oscillating cascade with supersonic leading edge locus p 3569 N94-31880
Development of a cascade simulation of fan-passage flow
[AD-A277234] p 3584 N94-32026
Hotwire measurements of the turbulent flow into a cascade of controlled-diffusion compressor blades
[AD-A277297] p 3706 N94-32042
Flutter analysis of a supersonic cascade in time domain using an ADI Euler solver
[NASA-TM-105625] p 3739 N94-32883
CASCADE RANGE (CA-OR-WA)
Analysis of deep seismic reflection and other data from the southern Washington Cascades
[DE94-005958] p 3771 N94-31525
CASCADE WIND TUNNELS
Hotwire measurements of the turbulent flow into a cascade of controlled-diffusion compressor blades
[AD-A277297] p 3706 N94-32042
CAST ALLOYS
Expandable pattern casting research
[DE94-004342] p 3668 N94-31604
CASTING
Expandable pattern casting research
[DE94-004342] p 3668 N94-31604
Processing and characterization of functionally gradient ceramic materials
[AD-A277154] p 3657 N94-32367
LLNL casting technology
[DE94-008282] p 3669 N94-32839
Leveraging metal matrix composites to reduce costs in space mechanisms p 3604 N94-33301
CASTINGS
Expandable pattern casting research
[DE94-004342] p 3668 N94-31604
CATACLYSMIC VARIABLES
Disk instability and the spectral evolution of the 1992 outburst of the intermediate polar GK Persei p 3928 N94-31123
A study of angular momentum loss in binaries using the free Lagrange method p 3931 N94-31134
Winds from disks in compact binaries
[DE94-007452] p 3938 N94-32137
CATALYSIS
Solidification structure synthesis in undercooled liquids
[AD-A276166] p 3910 N94-31054
Isomeric poly(benzophenone)s: Synthesis of highly crystalline poly (4, 4 foot-benzophenone) and amorphous poly (2, 5-benzophenone), a soluble poly (p-phenylene) derivative
[AD-A277261] p 3655 N94-32017
Heterogeneous catalytic process for alcohol fuels from syngas
[DE94-008729] p 3667 N94-32583
Catalytic methods using molecular oxygen for treatment of PMMS and ECLSS waste streams, volume 2
[NASA-CR-190299] p 3804 N94-32697
Methyl chloride by way of oxyhydrochlorination of methane
[DE94-009129] p 3637 N94-32767
The development of precipitated iron catalysts with improved stability
[DE94-008711] p 3638 N94-32886
Ligand intermediates in metal-catalyzed reactions
[DE94-008713] p 3638 N94-32887
The magnesium chelation step in chlorophyll biosynthesis
[DE94-008727] p 3794 N94-32890
CATALYSTS
Development of vanadium-phosphate catalysts for methanol production by selective oxidation of methane
[DE94-006759] p 3759 N94-31272
Development of a catalytic system for gasification of wet biomass
[DE94-006216] p 3759 N94-31762
Novel approaches to the production of higher alcohols from synthesis gas
[DE94-006770] p 3666 N94-32132
High octane ethers from synthesis gas-derived alcohols
[DE94-006774] p 3667 N94-32133
Heterogeneous catalytic process for alcohol fuels from syngas
[DE94-008729] p 3667 N94-32583
Methyl chloride by way of oxyhydrochlorination of methane
[DE94-009129] p 3637 N94-32767
Studies of the fundamental nature of catalytic acidity, sites and intermediates
[DE94-006999] p 3646 N94-32805
The development of precipitated iron catalysts with improved stability
[DE94-008711] p 3638 N94-32886
Technology development for iron Fischer-Tropsch catalysts
[DE94-008723] p 3638 N94-32889
Perfluoropolyalkylether decomposition on catalytic aluminas
[NASA-TM-106547] p 3617 N94-33021
CATALYTIC ACTIVITY
Development of vanadium-phosphate catalysts for methanol production by selective oxidation of methane
[DE94-006759] p 3759 N94-31272
Novel approaches to the production of higher alcohols from synthesis gas
[DE94-006770] p 3666 N94-32132
High octane ethers from synthesis gas-derived alcohols
[DE94-006774] p 3667 N94-32133
CATHODES
Emission from ferroelectric cathodes
[DE94-006732] p 3863 N94-31270
Hydrogen peroxide electrodes based on electrical connection of redox centers of various peroxidases to electrodes through a three-dimensional electron relaying polymer network
[AD-A276543] p 3691 N94-32056
CATHODIC COATINGS
Development of silver-zinc cells of improved cycle life and energy density
[AD-A277311] p 3693 N94-32329
CATIONS
Indium-vacancy complexes in mercury cadmium telluride
[AD-A276177] p 3894 N94-31055
Silicone grease as a precursor to a pseudo crown-ether ligand: Crystal structure of (K(+)K(Me2SiO)7(+))(HIn(CH2CMe3)3(-))4)
[AD-A276343] p 3895 N94-31327
A visible light initiating system for free radical promoted cationic polymerization
[AD-A277164] p 3655 N94-32069
High-energy chemical processes: Laser irradiation of aromatic hydrocarbons
[DE94-008107] p 3720 N94-32707
Method and apparatus for inhibiting the disbonding of a paint from metal surfaces
[AD-D016106] p 3663 N94-32960
CAUCHY PROBLEM
Viscous limiter functions for model convection-diffusion equations
[CRANFIELD-AERO-9103] p 3702 N94-31559
Elastic as limit of viscoelastic response, in a context of self-similar viscous limits
[AD-A277043] p 3738 N94-32273
CAVES
Proceedings of the 4th Tunnel Detection Symposium on Subsurface Exploration Technology
[AD-A276372] p 3771 N94-31369
CAVITATION FLOW
Fluid-structure interaction in case of water hammer with cavitation
[PB94-148277] p 3702 N94-31588
Simultaneous pressure measurement and high-speed photography study of cavitation in a dynamically loaded journal bearing
[NASA-TM-106456] p 3728 N94-32893
CAVITIES
Atomic oxygen interaction at defect sights in protective coatings on polymers flown on LDEF p 3593 N94-31024
Aperture excitation of electrically large, lossy cavities
[PB94-145711] p 3675 N94-31683
Gettering of metal impurities by cavities in silicon
[DE94-005248] p 3645 N94-32672
CAVITY FLOW
Steady thermal convection in multiple liquid layers p 3705 N94-31844
CCD STAR TRACKER
A low-cost, CCD solid state star tracker
[NASA-CR-192722] p 3882 N94-32417
CELESTIAL BODIES
Physical chemistry of molecules and grains in space
[AD-A276037] p 3932 N94-31280
CELESTIAL MECHANICS
General-relativistic celestial mechanics. 4: Theory of satellite motion
[PB94-147782] p 3601 N94-31769
CELL DIVISION
A cell-cycle model revisited
[CWI-AM-R9305] p 3851 N94-32229
CELL MEMBRANES (BIOLOGY)
Ninth International Workshop on Plant Membrane Biology
[DE94-005690] p 3794 N94-32769
CELLS (BIOLOGY)
Ninth International Workshop on Plant Membrane Biology
[DE94-005690] p 3794 N94-32769
CELLULOSE
Inorganic polymer engineering materials
[DE94-008519] p 3659 N94-32655

CENTER OF GRAVITY
General-relativistic celestial mechanics. 4: Theory of satellite motion
[PB94-147782] p 3601 N94-31769
CENTRAL NERVOUS SYSTEM
Neostriatal neuronal activity and behavior
[AD-A276429] p 3802 N94-33333
CENTRAL PROCESSING UNITS
Study of structures of different complexity for the communication between two processors
[ETN-94-95750] p 3674 N94-31615
Multiple-valued programmable logic array minimization by solution space search
[AD-A278033] p 3821 N94-33090
CENTRIFUGAL CASTING
Effect of surface forces on the rheology of particle-liquid systems and the consolidation of ceramic powders
[AD-A277092] p 3657 N94-32391
CENTRIFUGES
An investigation of acoustic noise requirements for the Space Station centrifuge facility
[NASA-TM-108811] p 3805 N94-32936
CERAMIC COATINGS
The development of CVR coatings for PBR fuels
[DE94-004233] p 3875 N94-31480
Mass-loaded coating for reducing the resonant frequency of a ceramic disc
[AD-D016095] p 3660 N94-32739
CERAMIC FIBERS
Passive vibration damping materials: Piezoelectric ceramic composites for vibration damping applications
[AD-A276550] p 3653 N94-31935
Pressureless sintering of ceramic composites
[AD-A277274] p 3657 N94-32404
CERAMIC MATRIX COMPOSITES
Processing of novel nanoparticle dispersion strengthened ceramics for improved mechanical performance
[AD-A275965] p 3649 N94-31276
Passive vibration damping materials: Piezoelectric ceramic composites for vibration damping applications
[AD-A276550] p 3653 N94-31935
Toughening mechanisms in fiber-reinforced ceramic-matrix composites p 3622 N94-31943
Finite element analysis of damage in fibrous composites using a micromechanical model
[AD-A277226] p 3623 N94-32024
Mechanics of the single fiber pullout problem with several interface conditions p 3623 N94-32078
Processing and characterization of functionally gradient ceramic materials
[AD-A277154] p 3657 N94-32367
Pressureless sintering of ceramic composites
[AD-A277274] p 3657 N94-32404
Mechanics of cracking for composite material p 3624 N94-32501
Ceramic Technology Project database
[DE94-008494] p 3659 N94-32632
Effect of elevated temperature and cyclic loading on properties and damage modes in ceramic composites
[DE94-008736] p 3662 N94-32891
Conversion of polymers of methyl- and vinylsilane to Si-C ceramics
[NASA-TM-106554] p 3662 N94-32945
Fracture micromechanics of continuous fiber and textile reinforced metal and ceramic matrix composites
[AD-A277434] p 3627 N94-33008
On the mechanics of microballoon-reinforced metal matrix composites
[AD-A277928] p 3630 N94-33178
Novel precursor approached for CMC derived by polymer pyrolysis
[AD-A278383] p 3665 N94-33352
CERAMICS
Physical properties of glasses exposed to Earth-facing and trailing-side environments on LDEF p 3594 N94-31030
Piezoelectric materials research in Europe
[AD-A276207] p 3648 N94-31059
Evaluation of nondestructive inspection techniques for quality control of alumina-ceramic housing components
[AD-A276220] p 3730 N94-31065
Processing of novel nanoparticle dispersion strengthened ceramics for improved mechanical performance
[AD-A275965] p 3649 N94-31276
Cost-effective ceramic machining: Summary of three-body wear experiments
[DE94-007757] p 3650 N94-31354
Naval Surface Warfare Center Dahlgren Division Technical Digest: Advanced materials technology
[AD-A276448] p 3668 N94-31364
Development and characterization of intermediary layers allowing the bond between a metal alloy and a plasma sprayed ceramic
[ECL-91-39] p 3619 N94-31377
Reliability analysis of structural ceramics subjected to biaxial flexure p 3650 N94-31454
Joining of alumina by vacuum brazing
[VTT-TIED-1495] p 3724 N94-31656
Characterization and growth mechanisms of the MgAl2O4 phase in Al2O3-reinforced Al-Mg composites
[ISBN-0-315-86531-8] p 3620 N94-31706
High temperature NASP engine seal development
[NASA-TM-109750] p 3725 N94-31804
Elastic modulus measurements of LDEF glasses and glass-ceramics using a speckle technique
[NASA-CR-195911] p 3653 N94-31851
High-temperature deformation and fracture toughness of duplex ceramic microstructures p 3653 N94-31945
Processing and characterization of functionally gradient ceramic materials
[AD-A277154] p 3657 N94-32367
Effect of surface forces on the rheology of particle-liquid systems and the consolidation of ceramic powders
[AD-A277092] p 3657 N94-32391
Proceedings of the Ad Hoc Workshop on Ceramics for Li/FeS2 batteries
[DE94-007460] p 3694 N94-32607
Mechanical properties of vacuum-sintered yttria ceramics
[DE94-008138] p 3659 N94-32617
Ceramic Technology Project database
[DE94-008494] p 3659 N94-32632
Compositions and chemical bonding in ceramics by quantitative electron energy-loss spectrometry
[DE94-007208] p 3659 N94-32640
Thin-film decoupling capacitors for multi-chip modules
[DE94-007743] p 3695 N94-32650
Energetics, bonding mechanism, and electronic structure of ceramic/ceramic and metal/ceramic interfaces
[DE94-008551] p 3659 N94-32656
Fabrication, phase transformation studies and characterization of SiC-AlN-Al2OC ceramics
[DE94-008587] p 3659 N94-32657
Temperature-humidity-bias aging technique to identify defective surface mount capacitors
[DE94-005354] p 3660 N94-32727
Effect of elevated temperature and cyclic loading on properties and damage modes in ceramic composites
[DE94-008736] p 3662 N94-32891
Materials development program: Ceramic technology project bibliography, 1984-1992
[DE94-009297] p 3662 N94-32935
Characterization of nanoparticles and nanophase materials
[DE94-008348] p 3907 N94-32990
Development of lightweight ceramic ablators and arc-jet test results
[NASA-TM-108798] p 3617 N94-33117
Nonlocal theory for fracturing of quasibrittle materials
[AD-A278283] p 3740 N94-33143
On the mechanics of microballoon-reinforced metal matrix composites
[AD-A277928] p 3630 N94-33178
Ceramic and metal composite circuit-board-level technology for application specific electronic modules (ASEM)
[AD-A277961] p 3630 N94-33180
Novel sol-gel deposition for repair of conducting paths in polyceramic systems
[AD-A278381] p 3664 N94-33350
Novel precursor approached for CMC derived by polymer pyrolysis
[AD-A278383] p 3665 N94-33352
CERENKOV RADIATION
Second-order nonlinear optical polymers: From fundamentals to applications
[AD-A277514] p 3664 N94-33348
CERIUM OXIDES
Conductivity measurements of ceria-based solid electrolytes using AC impedance
[DE94-007380] p 3694 N94-32593
CESIUM
An investigation of the radiolytic stability of a resorcinol-formaldehyde ion exchange resin
[DE94-007971] p 3660 N94-32698
CESIUM IODIDES
Mechanisms of formation and of de-excitation in the reaction Mg-24 + C-12 yields 9 alpha at 35MeV per nucleon
[ISBN-0-315-86746-9] p 3867 N94-31749
CHANGE DETECTION
SPOT imagery for updating land cover information of 1:50,000 numerical topographic maps p 3749 N94-32532
Land cover change detection with ERS-1 data and data from other remote sensing satellites. Example: The delta of the River Ebro (Spain) p 3755 N94-32564
Evaluation of surface phase change on large zones p 3755 N94-32567
CHANNELS (DATA TRANSMISSION)
Channel equalization for block transmission systems
[TELECOM-93-D-002] p 3670 N94-31093
Covert channel analysis of trusted systems. A guide to understanding
[AD-A276418] p 3916 N94-31331
CHAOS
Taming chaotic circuits p 3910 N94-31289
Chaotic attitude motion of satellites in the central gravitational field
[ISBN-0-315-78768-6] p 3610 N94-31723
Bifurcation and deterministic chaos in dynamic systems
[REPT-93-047] p 3911 N94-31893
Deterministic chaos p 3912 N94-31896
Seasons and chaos in population dynamics p 3912 N94-31897
CHARACTER RECOGNITION
Real time character recognition for F-111C video tape records
[AD-A277061] p 3580 N94-32263
CHARACTERIZATION
Synthesis, characterization, phase diagrams and superconducting, and normal state magnetic properties of La(2-x)Sr(x)CuO4 (0 is less than or equal to x which is less than or equal to 0.08) and electrochemically oxidized La(2-x)Sr(x)CuO(4 + delta) (0 is less than or equal to x which is less than or equal to 0.33, 0 is less than or equal to delta which is less than or equal to 0.12)
[DE94-005260] p 3895 N94-31067
Employment of a porous gold actuator in ISFET-based coulometric sensor-actuator systems with application to protein characterization
[ISBN-9-09-005887-7] p 3689 N94-31536
Stellar x ray polarimeter polarizer development and calibration at LEA/LLNL
[DE94-006400] p 3712 N94-31783
MODIS. Volume 2: MODIS level 1 geolocation, characterization and calibration algorithm theoretical basis document, version 1
[NASA-TM-104594-VOL-2] p 3613 N94-33289
CHARGE COUPLED DEVICES
Degradation of optical components in space p 3594 N94-31029
Development and application of photosensitive device systems to studies of biological and organic materials
[DE94-008503] p 3793 N94-32516
A 10 GHz bandwidth, single transient, digitized oscilloscope with 20 GHz capability
[DE94-005400] p 3713 N94-32728
High frequency active auroral research program (HAARP) imager
[AD-A277469] p 3775 N94-32999
CHARGE EXCHANGE
Influence of long-range correlations on the spectral functions and response of 48Ca and 90Zr
[ETN-94-96017] p 3865 N94-31537
CHARGE TRANSFER
Recent developments in polymeric charge transfer complexes
[AD-A277108] p 3654 N94-31979
The charging effect in high-Tc superconducting thin films
[AD-A277265] p 3900 N94-32040
Electronic and nuclear factors in intramolecular charge and excitation transfer processes
[DE94-006598] p 3870 N94-32178
Intramolecular charge transfer complexes as fluorescence probes for UV and visible light induced acrylate polymerization
[AD-A277129] p 3657 N94-32381
Compositions and chemical bonding in ceramics by quantitative electron energy-loss spectrometry
[DE94-007208] p 3659 N94-32640
CHARGE TRANSFER DEVICES
Deep water studies of CTD data
[AD-A277741] p 3791 N94-33176
CHARGED PARTICLES
Molecular dynamics computer simulations of charged metal electrode-aqueous electrolyte interfaces
[AD-A276401] p 3863 N94-31237
The Kaluza-Klein approach and gauge supersymmetry
[ISBN-0-315-86553-9] p 3912 N94-31911
Hydrodynamics of neutron star interiors and laboratory superfluids p 3936 N94-31949
Characterization of atomic and molecular impurity sources and transport at the tokamak edge
[DE94-007212] p 3891 N94-32619
CHARPY IMPACT TEST
Reactor pressure vessel structural integrity research in the US Nuclear Regulatory Commission HSST and HSSI Programs
[DE94-006550] p 3739 N94-32771
CHASSIGNITES
SNC meteorites and their implications for reservoirs of Martian volatiles p 3947 N94-33209

The Martian sources of the SNC meteorites (two, not one), and what can and can't be learned from the SNC meteorites p 3951 N94-33234

CHELATION

The magnesium chelation step in chlorophyll biosynthesis
[DE94-008727] p 3794 N94-32890

CHEMICAL ANALYSIS

Fiber optic chemical sensors on Mars
[DE94-005251] p 3941 N94-31145

An axial approach to detection in capillary electrophoresis
[DE94-005556] p 3631 N94-31154

Double rotation NMR studies of zeolites and aluminophosphate molecular sieves
[DE94-007032] p 3866 N94-31637

Composition and properties of dust from Comet Halley p 3936 N94-31947

A chemical analysis of solar neighborhood dwarfs p 3926 N94-31951

New zinc-bis(dialkylamides) potentially usable as site-selective dopants for p-type ZnSe
[AD-A276947] p 3902 N94-32218

Molecular Science Research Center
[DE94-007464] p 3871 N94-32605

Multiple size scale structures in silica/siloxane composites studied by small-angle scattering
[DE94-007300] p 3625 N94-32642

Molten metal analysis by laser produced plasmas
[DE94-007014] p 3646 N94-32782

Characterization of nanoparticles and nanophase materials
[DE94-008348] p 3907 N94-32990

CHEMICAL ATTACK

Characterization of the corrosion resistance of duplex stainless steels using local current density mapping techniques
[DE94-007980] p 3646 N94-32699

Compilation of diamond-like carbon properties for barriers and hard coatings
[DE94-008231] p 3661 N94-32803

CHEMICAL BONDS

Modification of semiconductor surface properties with chemically bound molecular films
[AD-A276162] p 3895 N94-31081

Design of new polymers to improve radiation stability of plastic scintillators
[DE94-008220] p 3652 N94-31764

A genetic algorithm based method for docking flexible molecules
[DE94-007525] p 3793 N94-32269

Compositions and chemical bonding in ceramics by quantitative electron energy-loss spectrometry
[DE94-007208] p 3659 N94-32640

Ab initio study of the epitaxial growth of Ge on Si(100) surface
[DE94-007245] p 3904 N94-32724

Metal ion complexation by ionizable crown ethers
[DE94-008301] p 3661 N94-32847

X ray absorption study of pulsed laser deposited boron nitride films
[DE94-008295] p 3662 N94-32855

CHEMICAL CLOUDS

Theory, Image Simulation, and Data Analysis of Chemical Release Experiments
[NASA-CR-194865] p 3954 N94-31101

CHEMICAL COMPOSITION

Cloud studies seen from a physical chemist's perspective
[DE94-006059] p 3771 N94-31527

Composition and properties of dust from Comet Halley p 3936 N94-31947

The chemical and dynamical evolution of the galaxy p 3936 N94-31950

A chemical analysis of solar neighborhood dwarfs p 3926 N94-31951

Group 12 thiolates: Syntheses, characterization and decomposition pathways
[AD-A277055] p 3900 N94-32011

Sodium sulfate corrosion of silicon carbide fiber-reinforced lithium aluminosilicate glass-ceramic matrix composites
[AD-A277224] p 3623 N94-32023

Organic analyses of the Murchison meteorite p 3938 N94-32489

Molecular Science Research Center
[DE94-007464] p 3871 N94-32605

On the formation of muon- and zeta-phases in Ag-Al system by mechanical alloying
[DE94-007125] p 3645 N94-32636

Ionization probes of molecular structure and chemistry
[DE94-007605] p 3872 N94-32643

SOLGAS refined: A computerized thermodynamic equilibrium calculation tool
[DE94-009021] p 3913 N94-32846

Evidence for ultramafic lavas on Syrtis Major p 3950 N94-33229

CHEMICAL DEFENSE

Aircrew Eye/Respiratory Protection (AERP): 16-hour extended wear evaluation of chemical protective equipment
[AD-A277288] p 3804 N94-32609

CHEMICAL EFFECTS

A model of the ion chemistry of electrified convection p 3868 N94-31993

CHEMICAL ELEMENTS

New zinc-bis(dialkylamides) potentially usable as site-selective dopants for p-type ZnSe
[AD-A276947] p 3902 N94-32218

CHEMICAL ENGINEERING

Performance of selected polymeric materials on LDEF p 3593 N94-31023

CHEMICAL EQUILIBRIUM

CET93 and CETPC: An interim updated version of the NASA Lewis computer program for calculating complex chemical equilibria with applications
[NASA-TM-4557] p 3638 N94-32948

CHEMICAL EXPLOSIONS

A compatibility study of FEFO with various containment materials
[DE94-005753] p 3649 N94-31198

CHEMICAL REACTIONS

Reactions of electrophilic maleic anhydride and epoxy groups with nucleophilic functionalities such as carboxyl, hydroxyl, and amine groups. Polymer Technology Publication series no. 16
[PB94-135589] p 3648 N94-31069

High-temperature study of O+H2CO yields OH+HCO
[DE94-006837] p 3864 N94-31321

Cloud studies seen from a physical chemist's perspective
[DE94-006059] p 3771 N94-31527

Modern integral equation techniques for quantum reactive scattering theory
[DE94-007039] p 3857 N94-31639

A numerical method for mixing/chemically reacting compressible flow with finite rate chemistry p 3634 N94-31824

A comparison between two Monte Carlo codes on determination of transient chemical yields
[DE94-007224] p 3636 N94-32251

Ionization probes of molecular structure and chemistry
[DE94-007605] p 3872 N94-32643

Time-resolved analytical methods for liquid/solid interfaces
[DE94-008352] p 3637 N94-32826

Computed potential energy surfaces for chemical reactions
[NASA-CR-195835] p 3639 N94-33036

The mineralogic evolution of the Martian surface through time: Implications from chemical reaction path modeling studies p 3950 N94-33226

CHEMICAL REACTORS

Direct aromatization of methane
[DE94-008719] p 3638 N94-32888

CHEMISORPTION

Chemisorbed-molecule potential-energy surfaces and electronically-stimulated processes
[DE94-007932] p 3719 N94-32603

CHINA

Solar energy in China
[PB94-137502] p 3758 N94-31071

Station climatic summaries: China, the former USSR, and Mongolia
[AD-A276548] p 3784 N94-32057

CHIPS (ELECTRONICS)

Universal signal conditioning amplifier p 3699 N94-32460

Thin-film decoupling capacitors for multi-chip modules
[DE94-007743] p 3695 N94-32650

VLSI for high-speed digital signal processing
[AD-A277617] p 3697 N94-32957

Buffered feedthrough crossbar switch
[AD-D016145] p 3697 N94-32967

CHIRAL DYNAMICS

Chiral symmetry and the threshold gamma(p) yields pi(sup 0)p reaction
[DE94-008117] p 3873 N94-32710

CHIRP

Advanced satellite communication system
[NASA-CR-194211] p 3681 N94-32477

CHIRP SIGNALS

System analysis of ultra-wideband instrumentation radars: Impulse versus stepped-chirp approaches
[AD-A276624] p 3677 N94-32087

CHLORIDES

Induced adsorption of chloride and bromide by submonolayer amounts of copper underpotentially deposited on Pt(111)
[AD-A278023] p 3648 N94-33182

CHLORINATION

Methyl chloride by way of oxyhydrochlorination of methane
[DE94-009129] p 3637 N94-32767

CHLORINE OXIDES

Possible effect of the chlorine oxide dimer on transient ozone loss in rocket plumes
[AD-A278135] p 3616 N94-33094

CHLOROPHYLLS

The magnesium chelation step in chlorophyll biosynthesis
[DE94-008727] p 3794 N94-32890

Evolution of upwelling fronts off the coast of Portugal
[NASA-CR-195692] p 3790 N94-33045

CHLOROPLASTS

The magnesium chelation step in chlorophyll biosynthesis
[DE94-008727] p 3794 N94-32890

CHOLESKY FACTORIZATION

Channel equalization for block transmission systems
[TELECOM-93-D-002] p 3670 N94-31093

CHROMATOGRAPHY

Organic analyses of the Murchison meteorite p 3938 N94-32489

Time-resolved analytical methods for liquid/solid interfaces
[DE94-008352] p 3637 N94-32826

CHROMIC ACID

Anodized aluminum on LDEF p 3592 N94-31017

CHROMIUM

Soft x ray photoelectron spectroscopy study of the interaction of Cr with MoS2(0001)
[AD-A276916] p 3635 N94-32233

CHROMIUM ALLOYS

Creep properties of vanadium-base alloys
[DE94-008541] p 3641 N94-31486

CHROMIUM STEELS

Creep-fatigue criteria and inelastic behavior of modified 9Cr-1Mo steel at elevated temperatures
[DE94-007915] p 3642 N94-31918

CHRONOLOGY

Extraction of forests stand age parameters from airborne imaging spectroscopy data p 3745 N94-31867

Chronology of KSC and KSC related events for 1993
[NASA-TM-109196] p 3966 N94-33072

CIRCADIAN RHYTHMS

Unit specific crew rest strategies: Phase 1 evaluation of the 1/212th Aviation Battalion during shiftwork transitions
[AD-A277122] p 3804 N94-32379

The organization of the suprachiasmatic circadian pacemaker of the rat and its regulation by neurotransmitters and modulators
[AD-A277324] p 3793 N94-32622

CIRCUIT BOARDS

From display and PWB to MCMs: Large panel manufacturing
[DE94-007855] p 3693 N94-32386

VLSI for high-speed digital signal processing
[AD-A277617] p 3697 N94-32957

Space flight printed wiring board measling investigation
[NASA-TM-104602] p 3732 N94-33101

Ceramic and metal composite circuit-board-level technology for application specific electronic modules (ASEM)
[AD-A277961] p 3630 N94-33180

CIRCUIT DIAGRAMS

Some problems of applied algebra
[CWI-AM-R9306] p 3647 N94-32204

CIRCUIT RELIABILITY

Interpreter composition issues in the formal verification of a processor-memory module
[NASA-CR-4594] p 3820 N94-32775

CIRCUITS

Taming chaotic circuits p 3910 N94-31289

Extension of the LUSTRE language and application to circuit design: The LUSTRE V4 language and the POLLUX system
[ETN-94-95918] p 3812 N94-31543

Validation of the Environmentally Conscious Manufacturing Integrated Demonstration hardware
[DE94-003824] p 3765 N94-32144

Digital beamforming and filtering circuit
[AD-D016142] p 3697 N94-32976

CIRCULAR CYLINDERS

The effect of an axial flow component on a circular cylinder wake p 3699 N94-31209

Single scattering of light by ensembles of particles with various shapes
[ETN-94-96016] p 3878 N94-31550

CIRCULAR POLARIZATION

Element-specific magnetic hysteresis measurements, a new application of circularly polarized soft x-rays
[DE94-007122] p 3858 N94-31397

High-resolution synthetic aperture radar observations of the Moon p 3676 N94-31952
The 20 GHz circularly polarized, high temperature superconducting microstrip antenna array [NASA-CR-195097] p 3683 N94-33083
Coherent processes in atom in strong radiation fields [AD-A276388] p 3874 N94-33144

CIRCULATORY SYSTEM
Incompressible viscous flow in tubes with occlusions [ISBN-0-315-75467-2] p 3704 N94-31778

CIRRUS CLOUDS
Sensitivity analysis of the AVHRR infrared cirrus model [AD-A276690] p 3784 N94-32117

CIVIL AVIATION
A comparison of military and commercial aircraft development [AD-A276830] p 3575 N94-32168
The 1993 aviation system capacity plan [AD-A276958] p 3575 N94-32620

CLASSIFICATIONS
Neural network definitions of highly predictable protein secondary structure classes [DE94-006234] p 3834 N94-32175

CLASSIFIERS
A fuzzy classifier system for process control p 3839 N94-32422

CLEANING
Fatigue testing of 2024-T3 material after four cycles of PMB stripping [AD-A276926] p 3644 N94-32237

CLEANLINESS
Design, development, and testing of a lightweight optical sensor cover system p 3604 N94-33302

CLIMATE
The Earth's climate: Past, present, and future p 3777 N94-30982
Energetic and general circulation p 3777 N94-30983
The Global Climatology Network precipitation data [DE93-019199] p 3764 N94-31596
Selection of climate station data using clustering and triangulated irregular network techniques [AD-A276658] p 3784 N94-32046
Station climatic summaries: China, the former USSR, and Mongolia [AD-A276548] p 3784 N94-32057
Homogeneous global mean temperature time series [DE94-002194] p 3766 N94-32690
Fine resolution atmospheric sulfate model driven by operational meteorological data: Comparison with observations [DE94-002994] p 3766 N94-32691
Proceedings of the Ninth Annual Pacific Climate (PACLIM) Workshop [DE94-003024] p 3766 N94-32693
Diagnostic studies of climate variability [DE94-003629] p 3767 N94-32711
Physical basis for climate change models [DE94-003827] p 3767 N94-32712
Climate effects of anthropogenic sulfate: Simulations from a coupled chemistry/climate model [DE94-004352] p 3767 N94-32789
Parameterizing atmosphere-land surface exchange for climate models with satellite data: A case study for the Southern Great Plains CART site [DE94-005109] p 3775 N94-32874
The effect of polar caps on obliquity p 3948 N94-33213
Obliquity variation in a Mars climate evolution model p 3951 N94-33236

CLIMATE CHANGE
The Earth's climate: Past, present, and future p 3777 N94-30982
Interaction processes between the ocean and the atmosphere p 3777 N94-30987
The climate of the Mediterranean basin: Its sensitivity to global change p 3778 N94-30993
Sources and wells of minor atmospheric constituents of climatic importance p 3770 N94-31008
Climatic evolution and desertization p 3780 N94-31009
Global change research and NASA's Earth Observing System [PB94-126992] p 3741 N94-31068
The complementary nature of the SPOT and ERS-1 systems and their place in major international programmes p 3748 N94-32524
Homogeneous global mean temperature time series [DE94-002194] p 3766 N94-32690
Proceedings of the Ninth Annual Pacific Climate (PACLIM) Workshop [DE94-003024] p 3766 N94-32693
Diagnostic studies of climate variability [DE94-003629] p 3767 N94-32711
Physical basis for climate change models [DE94-003827] p 3767 N94-32712
Biospheric effects of a large extraterrestrial impact: Case study of the Cretaceous/Tertiary boundary crater [NASA-CR-195827] p 3942 N94-32740
Environmental issues related to biomass: An overview [DE94-007226] p 3767 N94-32784
National US public policy on global warming derived from optimization of energy use and environmental impact studies [DE94-004606] p 3768 N94-32790
Quantified estimates of total GWPs for greenhouse gases taking into account tropospheric chemistry [DE94-007846] p 3768 N94-32817
Ocean variability and its influence on the detectability of greenhouse warming signals [DE94-008670] p 3790 N94-32881
Current policies of the major countries coping with the global warming problem and-the energy demand and supply [DE94-757291] p 3769 N94-32920
Polar sediment accumulation: Role of surface winds at the two poles p 3951 N94-33233

CLIMATOLOGY
Subtropical Climates and Their Evolution: From Space-Based Observation to Modelling [ISBN-2-85-428333-3] p 3776 N94-30981
Climatologic flux in tropical ocean p 3777 N94-30985
Dynamic climatology of West Africa p 3778 N94-30988
Dynamics in the tropics and synoptic disturbances p 3778 N94-30990
Effects of the deep tropical convection in the large scale atmospheric flow p 3778 N94-30994
The surface parameters: Remote sensing observations and climatology applications p 3779 N94-31001
Sources and wells of minor atmospheric constituents of climatic importance p 3770 N94-31008
Climatic evolution and desertization p 3780 N94-31009
Modeling of the continental biosphere p 3770 N94-31011
Cumulus convection parameterization and numerical modelling of moist atmospheres p 3783 N94-31989
Selection of climate station data using clustering and triangulated irregular network techniques [AD-A276658] p 3784 N94-32046
Station climatic summaries: China, the former USSR, and Mongolia [AD-A276548] p 3784 N94-32057
Sensitivity analysis of the AVHRR infrared cirrus model [AD-A276690] p 3784 N94-32117
Use of SPOT and ERS-1 SAR data to study the tectonic and climatic history of arid regions p 3752 N94-32550
Homogeneous global mean temperature time series [DE94-002194] p 3766 N94-32690
Proceedings of the Ninth Annual Pacific Climate (PACLIM) Workshop [DE94-003024] p 3766 N94-32693
Diagnostic studies of climate variability [DE94-003629] p 3767 N94-32711
Statistical intercomparison of global climate models: A common principal component approach [DE94-008671] p 3768 N94-32882
Forecasters handbook for the Philippine Islands and surrounding waters [AD-A277993] p 3787 N94-33089
The Northern Plains MSATT Meeting, and a call for a field-oriented successor to MSATT p 3947 N94-33210
The effect of polar caps on obliquity p 3948 N94-33213
Obliquity variation in a Mars climate evolution model p 3951 N94-33236
Simultaneous laboratory measurements of CO2 and H2O adsorption on palagonite: Implications for the Martian climate and volatile reservoir p 3952 N94-33240

CLINICAL MEDICINE
Development of a video fluorescence system for assessing burn depth [AD-A278127] p 3798 N94-33092
Characterization and utilization of opiate-like hibernation factors [AD-A278136] p 3794 N94-33098

CLOSED CYCLES
Control experiments in liquid metal combustion [AD-A276918] p 3635 N94-32234

CLOUD COVER
Use of Air Force cloud cover data to evaluate and improve cloud forecasts and parameterizations in mesocale meteorological models [AD-A277384] p 3784 N94-32054

CLOUD HEIGHT INDICATORS
Development of a statistical method for estimating the downward longwave radiation at the surface from satellite observations p 3742 N94-31553

CLOUD PHYSICS
Cloud studies seen from a physical chemist's perspective [DE94-006059] p 3771 N94-31527
Development of a statistical method for estimating the downward longwave radiation at the surface from satellite observations p 3742 N94-31553
Boundary-layer cumulus over land: Some observations and conceptual models [DE93-040820] p 3781 N94-31597
Radar scattering from the summer polar mesosphere: Theory and observations p 3772 N94-32077
A parameterization of cloud droplet nucleation [DE94-007469] p 3785 N94-32268

CLOUDS (METEOROLOGY)
Interaction processes between the ocean and the atmosphere p 3777 N94-30987
Effects of the deep tropical convection in the large scale atmospheric flow p 3778 N94-30994
Treatment of cloud radiative effects in general circulation models [DE94-001864] p 3764 N94-31600
Use of Air Force cloud cover data to evaluate and improve cloud forecasts and parameterizations in mesocale meteorological models [AD-A277384] p 3784 N94-32054
A parameterization of cloud droplet nucleation [DE94-007469] p 3785 N94-32268
An integrated cloud observation and modeling investigation in support of the ARM program [DE94-003160] p 3785 N94-32716
Use of cloud observations and mesoscale meteorology models to evaluate and improve cloud parameterizations [DE94-003610] p 3785 N94-32717
TRMM-related research: Tropical rainfall and energy analysis experiment [NASA-CR-195834] p 3787 N94-33288

CLUSTER ANALYSIS
Automated detection of ship tracks in multispectral satellite data [AD-A276697] p 3746 N94-32119
Database tomography for commercial application p 3923 N94-32442

CLUTTER
System analysis of ultra-wideband instrumentation radars: Impulse versus stepped-chirp approaches [AD-A276624] p 3677 N94-32087
Validation support of the ERIM ocean model [AD-A277364] p 3788 N94-32284

CMOS
A silicon condenser microphone: Modelling and electronic circuitry [ISBN-9-09-005279-8] p 3688 N94-31517
Chemical vapour deposition of tungsten for the application in integrated circuits [ISBN-9-09-005151-1] p 3641 N94-31519
A hierarchical approach to test generation for CMOS VLSI circuits [ISBN-9-09-005449-9] p 3689 N94-31535

COAL DERIVED GASES
High octane ethers from synthesis gas-derived alcohols [DE94-006774] p 3667 N94-32133

COASTAL CURRENTS
ADCIRC: An advanced three-dimensional circulation model for shelves, coasts, and estuaries. User's manual for ADCIRC-2DDI [AD-A276150] p 3787 N94-31250

COASTAL WATER
Surface forward-scattered acoustic measurements and analysis [AD-A276998] p 3788 N94-32000
Three dimensional vorticity field in the California current system [AD-A276951] p 3788 N94-32220
Evolution of upwelling fronts off the coast of Portugal [NASA-CR-195692] p 3790 N94-33045
Index and bulk parameters for frequency-direction spectra measured at CERC Field Research Facility [AD-A277759] p 3791 N94-33085

COASTS
The evolution of jet features during the 1993 east coast white hurricane: A case study using the global spectral model [AD-A277217] p 3783 N94-32021
ENSO forced variations of the sea surface temperature and adjusted sea level along the west coast of the United States [AD-A277306] p 3789 N94-32327
Contribution of SAR ERS1 data to study the French Guiana tropical coast environment [BRGM-93034] p 3748 N94-32527

Evolution of diurnal surface winds and surface currents for Monterey Bay
[AD-A277649] p 3790 N94-33057
Coastal boundary layer and refractivity measurements using the ground-based high resolution interferometer sounder (GB-HIS)
[AD-A277980] p 3683 N94-33159

COATING
Sol-gel metal oxide and metal oxide/polymer multilayers applied by meniscus coating
[DE94-005813] p 3649 N94-31199
An investigation of the spin-coating process and a model for three-dimensional regular foams
p 3649 N94-31206
Evaluation of the Hughes conversion coating touch-up pen
[AD-A278398] p 3664 N94-33166

COATINGS
Anodized aluminum on LDEF p 3592 N94-31017
Large-area conditioning of optics for high-power laser systems
[DE94-007028] p 3716 N94-31636
Sol-gel coatings for high power laser optics: Past, present, and future
[DE94-007240] p 3718 N94-32252

COBALT ALLOYS
Development of nickel and metal hydride secondary battery
[DE94-757270] p 3697 N94-32917

COBALT COMPOUNDS
Molecular/polymeric magnetism
[DE94-005888] p 3649 N94-31201
The relative performance of FeS2 and CoS in long-life thermal-battery applications
[DE94-006145] p 3695 N94-32663

COBALT OXIDES
Compositions and chemical bonding in ceramics by quantitative electron energy-loss spectrometry
[DE94-007208] p 3659 N94-32640

COCKPITS
Development of a reconfigurable helicopter flight control system
[ISBN-0-315-87218-7] p 3585 N94-31837
Study of virtual prototyping of aircraft instruments
[CMC-0687-1090] p 3581 N94-31903
Cockpit Electronic Display Workshop: Proceedings (computer diskette)
[AD-M000330] p 3805 N94-33171
Cockpit Electronic Display Workshop: A synopsis
[AD-A277728] p 3583 N94-33280

CODERS
Noise cancellation for CELP voice encoders in an F/A-18 noise environment
[AD-A277652] p 3683 N94-33026

CODING
Modulation and coding for the Gaussian channel, possibly affected by fluctuations
[TELECOM-93-E-009] p 3840 N94-31169
Waveform generation for ultra-wideband radar system
[AD-A276352] p 3673 N94-31401
Morphological directional coding of images
[ISBN-0-315-86336-6] p 3814 N94-31715
Beginning the 21st century with advanced Automatic Parts Identification (API) p 3923 N94-32444
The trustworthy digital camera: Restoring credibility to the photographic image p 3714 N94-32470
MOM3D method of moments code theory manual
[NASA-CR-189594] p 3682 N94-32897
Noise cancellation for CELP voice encoders in an F/A-18 noise environment
[AD-A277652] p 3683 N94-33026

COERCIVITY
The ferroelectric behavior of odd-numbered nylons
[AD-A278126] p 3663 N94-33058

COGNITION
Concepts and environment
[REPT-93-032] p 3829 N94-31186
Reminding-based learning
[AD-A277424] p 3801 N94-32997

COGNITIVE PSYCHOLOGY
Concepts and environment
[REPT-93-032] p 3829 N94-31186
Reading: Interaction with memory
[AD-A277547] p 3801 N94-32956

COHERENT RADAR
Comparison of coherent to incoherent detection at 2.09 micrometers using a solid state LADAR system
[AD-A277159] p 3721 N94-33102

COLD FLOW TESTS
Design of a cold-flow test facility for the high pressure fuel turbopump turbine of the Space Shuttle main engine
[AD-A276743] p 3615 N94-32182

COLD NEUTRONS
Fusion with highly spin polarized HD and D2
[DE94-006209] p 3876 N94-32731

COLD PLASMAS
Time domain spectroscopy for studying a monopole antenna immersed in a plasma
[ISBN-0-315-86526-1] p 3888 N94-31727

COLD ROLLING
Lubrication with binary mixtures: Liquid-liquid emulsion in elastohydrodynamics and metal forming
p 3658 N94-32490

COLD TOLERANCE
Review of pharmacological approach to improve cold tolerance p 3796 N94-31740
Lipid metabolism in cold-exposed humans
p 3796 N94-31741
Validation and sensitivity analysis of Texas human thermal model predictions during cold water immersion
[AD-A275240] p 3797 N94-32156
Numerical model of the thermal behavior of an extremity in a cold environment including counter-current heat exchange between the blood vessels
[AD-A278099] p 3798 N94-33040

COLD WATER
Validation and sensitivity analysis of Texas human thermal model predictions during cold water immersion
[AD-A275240] p 3797 N94-32156

COLD WORKING
Feasibility study of cold expansion processes modelling
[DSIS-94-01186] p 3735 N94-31849

COLLIMATION
Passive, multi-channel fiber optic rotary joint assembly
[AD-D016116] p 3882 N94-32626

COLLISION AVOIDANCE
Contingency-tolerant robot motion planning and control p 3830 N94-31482
Penetration distances and their applications to path planning p 3858 N94-31725
Three dimensional audio versus head down TCAS displays
[NASA-CR-177636] p 3576 N94-33063

COLLISION RATES
Constraints on the Martian cratering rate imposed by the SNC meteorites and Vallis Marineris layered deposits p 3945 N94-33197

COLLOIDS
Preparation of catalyst particles using methods of colloid chemistry. Part 1: Preparation of silica particles from alcohol solutions
[PB94-135597] p 3634 N94-31679
The sol-gel-xerogel transition
[AD-A276647] p 3616 N94-32038

COLOR
A search for rapidity gaps in jet events and a study of color coherence in multijet events at D0
[DE94-006849] p 3872 N94-32627
Global color views of Mars p 3948 N94-33217

COLOR CODING
A visual detection model for DCT coefficient quantization p 3850 N94-32467

COLOR VISION
Visual neural development and chromatic aberration
[AD-A277402] p 3800 N94-32345

COLOR-MAGNITUDE DIAGRAM
Study of stellar associations located in the region contained between the Magellanic Clouds
[ISBN-0-315-86692-6] p 3935 N94-31913

COLUMBUS SPACE STATION
Development concept for Dutch user support
[PB94-125523] p 3598 N94-31208

COMBINATORIAL ANALYSIS
On the use of genetic algorithms to solve the time-table problem
[REPT-90-060-REV] p 3829 N94-31176
The ant system: An autocatalytic optimizing process
[REPT-91-016-REV] p 3824 N94-31177
Combinatorial ion sensors
[AD-A276567] p 3825 N94-32032
Some problems of applied algebra
[CWI-AM-R9306] p 3847 N94-32204
Combinatory reduction systems: Introduction and survey
[CWI-CS-R9362] p 3849 N94-32349
Implementation and display of Computer Aided Design (CAD) models in Monte Carlo radiation transport and shielding applications
[DE94-007221] p 3819 N94-32641
On the computation of simplical approximations of implicitly defined two-dimensional manifolds
[AD-A278132] p 3849 N94-33060

COMBUSTIBLE FLOW
A numerical method for mixing/chemically reacting compressible flow with finite rate chemistry
p 3634 N94-31824
Advanced CFD methodology for fast transients encountered in nonlinear combustion instability problems. Volume 1: Theory and validation
[NASA-CR-191351] p 3637 N94-32696

COMBUSTION
NATO Advanced Study Institute on Unsteady Combustion. Volume 2: Research papers, September 6-17, 1993
[AD-A276572] p 3634 N94-32033
Studies in physico-chemical hydrodynamics of extended systems
[DE94-006752] p 3706 N94-32149
Volatiles combustion in fluidized beds
[DE94-008382] p 3636 N94-32414
Rate coefficient for the reaction H + O2 yields OH + O: Results from 2000 to 5300 K
[DE94-008105] p 3871 N94-32615
Ionization probes of molecular structure and chemistry
[DE94-007605] p 3872 N94-32643

COMBUSTION CHAMBERS
Combustor and nozzle effects on particulate behavior in solid rocket motors
[AD-A277304] p 3614 N94-32071

COMBUSTION CHEMISTRY
Fuel property effects on engine combustion processes
[DE94-005529] p 3631 N94-31153
Ignition studies in nonpremixed hydrogen/air combustion
[AD-A275954] p 3632 N94-31348
Combustion-related studies using weakly-bonded complexes
[DE94-006632] p 3633 N94-31493
Analysis of forward and inverse problems in chemical dynamics and spectroscopy
[DE94-007607] p 3635 N94-32140
Rate coefficient for the reaction H + O2 yields OH + O: Results from 2000 to 5300 K
[DE94-008105] p 3871 N94-32615

COMBUSTION CONTROL
Volatiles combustion in fluidized beds
[DE94-008382] p 3636 N94-32414

COMBUSTION PHYSICS
Computational study of single-expansion-ramp nozzles with external burning
[NASA-TM-106550] p 3700 N94-31229
Ignition studies in nonpremixed hydrogen/air combustion
[AD-A275954] p 3632 N94-31348
Analysis of strong acoustic excitation on the breakup and dispersion of a liquid jet
[ONERA-NT-1993-9] p 3701 N94-31422
A numerical method for mixing/chemically reacting compressible flow with finite rate chemistry
p 3634 N94-31824
Solid surface
[NASA-TM-109746] p 3634 N94-31883
Volatiles combustion in fluidized beds
[DE94-008382] p 3636 N94-32414

COMBUSTION PRODUCTS
Emissions of greenhouse gases from the use of transportation fuels and electricity
[DE94-006166] p 3765 N94-31625
Photothermal laser deflection, an innovative technique to measure particles in exhausts
[AD-A277151] p 3718 N94-32366
CET93 and CETPC: An interim updated version of the NASA Lewis computer program for calculating complex chemical equilibria with applications
[NASA-TM-4557] p 3636 N94-32948
Exposure assessment of JAVELIN missile combustion products
[AD-A278128] p 3616 N94-33059

COMBUSTION STABILITY
Analysis of strong acoustic excitation on the breakup and dispersion of a liquid jet
[ONERA-NT-1993-9] p 3701 N94-31422
Advanced CFD methodology for fast transients encountered in nonlinear combustion instability problems. Volume 2: User's guide
[NASA-CR-191352] p 3637 N94-32694
Advanced CFD methodology for fast transients encountered in nonlinear combustion instability problems. Volume 1: Theory and validation
[NASA-CR-191351] p 3637 N94-32696

COMETARY ATMOSPHERES
Cometary molecules p 3935 N94-31869
Composition and properties of dust from Comet Halley
p 3936 N94-31947

COMETS
Cometary molecules p 3935 N94-31869

COMFORT
A pilot study of comfort criteria and sound quality metrics for sound inside cabins of propeller-driven aircraft
[CTH-F-93-03] p 3859 N94-31090
THE VERTICAL p 3806 N94-32435

COMMAND AND CONTROL
Evolving software reengineering technology for the emerging innovative-competitive era
p 3823 N94-32439

COMMAND GUIDANCE
An experimental study of pilot/vehicle dynamics using a tilt rotor flying machine
[AD-A277516] p 3805 N94-33349
COMMERCIAL AIRCRAFT
A laboratory study of multiple site damage in fuselage lap splices
[AD-A276151] p 3578 N94-31078
Fracture and fatigue strength evaluation of multiple site damaged aircraft fuselages - curved panel testing and analysis
[AD-A277100] p 3579 N94-32015
A comparison of military and commercial aircraft development
[AD-A276830] p 3575 N94-32168
COMMODITIES
Knowledge-based commodity distribution planning
p 3915 N94-32427
COMMUNICATION EQUIPMENT
Communications networks in stressed environments
[AD-A275967] p 3672 N94-31384
Electronic mail and organizational knowledge: Media use in a global corporation
[AD-A276707] p 3678 N94-32121
COMMUNICATION NETWORKS
Acquisition information management system telecommunication site survey results
[DE94-005688] p 3915 N94-31155
Putting the information infrastructure to work: Report of the Information Infrastructure Task Force Committee on Applications and Technology
[NIST/SP-857] p 3916 N94-31228
Spread-spectrum radio systems and networks
[AD-A276449] p 3671 N94-31260
Advanced optical fiber communication systems
[AD-A276416] p 3878 N94-31330
Communications networks in stressed environments
[AD-A275967] p 3672 N94-31384
A multichannel architecture for Naval Task Force Communication
[AD-A276230] p 3673 N94-31446
Analysis of the effect of routing strategies for parallel implementations of a selected avionics application
[AD-A276069] p 3581 N94-31458
Study of structures of different complexity for the communication between two processors
[ETN-94-95750] p 3674 N94-31615
Welcome to the Ohio Aerospace Institute
[NASA-TM-109756] p 3913 N94-31815
The vision machines
[NASA-TM-109757] p 3806 N94-31816
Problems in survivable multi-media networks
[AD-A277370] p 3825 N94-32052
Performance metrics for low probability of intercept-communication system
[AD-A277346] p 3677 N94-32073
Discrete-event-dynamic-system-based approaches for scheduling transmissions in multihop packet radio networks
[AD-A276566] p 3679 N94-32230
Design, development, and testing of a Network Frequency Selection Service (NFSS)
[AD-A277362] p 3680 N94-32283
Control and reliability of optical networks in multiprocessors
[AD-A277385] p 3881 N94-32285
Communication networks for autonomous mobile robot computer architectures and distributed real-time computing p 3680 N94-32310
Voice and video transmission using XTP and FDDI
p 3685 N94-32468
Using the National Information Infrastructure for social science, education, and informed decision making
[DE94-005442] p 3920 N94-32676
Information systems to enhance technology exchange
[DE94-007744] p 3920 N94-32808
Multicast communication with guaranteed quality of service
[AD-A277650] p 3682 N94-33025
Reliable communication in the presence of severe noise or jamming
[AD-A278410] p 3684 N94-33173
MARSNET: A European network of stations on the surface of Mars p 3945 N94-33199
Assessing the vulnerability of multi-commodity networks with failing components
[AD-A278434] p 3684 N94-33334
COMMUNICATION SATELLITES
Multisatellite constellation configuration selection for multiregional highly elliptical orbit constellations
p 3600 N94-31437
Satellite communications industry
[AD-A276685] p 3610 N94-32039
An analysis of cellular telephone and INMARSAT systems for providing radio data link computer communications for US Navy vessels
[AD-A278143] p 3684 N94-33160
COMMUNICATION THEORY
Updates in dynamic semantics
[LP-93-06] p 3856 N94-31450
Assessing the vulnerability of multi-commodity networks with failing components
[AD-A278434] p 3684 N94-33334
COMPANION STARS
Evolution of dynamo-generated magnetic fields in accretion disks around compact and young stars
p 3931 N94-31138
Digital image profilers for detecting faint sources which have bright companions
[NASA-CR-191348] p 3927 N94-32695
COMPARATORS
An analog preprocessing architecture for high-speed analog-to-digital conversion
[AD-A276737] p 3807 N94-32163
COMPARISON
Finding all periods and initial palindromes of a string in parallel
[AD-B175069] p 3827 N94-33002
COMPASSES
Relative motion pinwheel
[AD-D016107] p 3577 N94-32961
COMPATIBILITY
Design patterns mixing genericity and inheritance in the development of reusable components
[REPT-93-021] p 3808 N94-31178
A compatibility study of FEFO with various containment materials
[DE94-005753] p 3649 N94-31198
Compatibility studies of some azo polymer blends
[AD-A277141] p 3657 N94-32365
Characterization of thermally stable dye-doped polyimide based electrooptic materials
[DE94-005309] p 3882 N94-32674
COMPILERS
Compiler techniques for managing data motion
[AD-A276514] p 3918 N94-31930
Incremental recompilation for Standard ML of New Jersey
[AD-A276522] p 3815 N94-32080
Utility-based planning
[NASA-CR-195878] p 3816 N94-32086
Informal introduction to the extended affix grammar formalism and its compiler
[TR-93-19] p 3817 N94-32287
Construction of a parallel processor for simulating manipulators and other mechanical systems
[NASA-CR-191327] p 3826 N94-32482
COMPLETENESS
Lambek calculus is L-complete
[LP-93-14] p 3841 N94-31388
COMPLEX COMPOUNDS
Recent developments in polymeric charge transfer complexes
[AD-A277108] p 3654 N94-31979
Wave packet studies of the vibrational predissociation of three and four-atom van der Waals complexes
[DE94-007623] p 3871 N94-32598
Ligand intermediates in metal-catalyzed reactions
[DE94-008713] p 3638 N94-32887
COMPLEX SYSTEMS
Effective computational strategy for predicting the response of complex systems
[AD-A277452] p 3740 N94-33011
Design and Monte Carlo analysis of an unmanned aerial vehicle
[AD-A277648] p 3580 N94-33056
COMPLEX VARIABLES
On the computation of simplical approximations of implicitly defined two-dimensional manifolds
[AD-A276132] p 3849 N94-33060
COMPONENT RELIABILITY
Stochastic models in reliability theory
[AD-A277529] p 3731 N94-32953
Assessing the vulnerability of multi-commodity networks with failing components
[AD-A278434] p 3684 N94-33334
COMPOSITE MATERIALS
Low-Earth orbit effects on organic composite materials flown on LDEF p 3595 N94-31036
Performance predictions for composite materials
[AD-A276451] p 3618 N94-31261
Electromagnetic scattering through loaded aperture panels with nonzero contact impedance
[ONERA-NT-1993-2] p 3673 N94-31418
Damage tolerance aspects of a full composite airplane fuselage: Requirements, modelling, predictions, experiments
[LR-728] p 3578 N94-31674
Micromechanics and effective properties of particulate composites and fluid suspensions p 3703 N94-31744
Optimization of composite material failure loads
[ISBN-0-315-87214-4] p 3621 N94-31836
Location of impact damage sites in composite aircraft structures, task 3.4.1
[DSIS-94-01590] p 3621 N94-31892
Benchmarking of the state-of-the-art in nondestructive testing/evaluation for applicability in the Composite Armored Vehicle (CAV) Advanced Technology Demonstrator (ATD) program, phase 1
[AD-A276660] p 3730 N94-32088
Nonlinear optical polymers derived from organic/inorganic composites
[AD-A277408] p 3659 N94-32610
Development of thermoplastic composite aircraft structures
[NASA-CR-189593] p 3626 N94-32860
Innovative fabrication processing of advanced composite materials concepts for primary aircraft structures
[NASA-CR-189558] p 3626 N94-32877
Second NASA Advanced Composites Technology Conference
[NASA-CP-3154] p 3627 N94-33121
COINS: A composites information database system
p 3627 N94-33123
Resin transfer molding for advanced composite primary wing and fuselage structures p 3628 N94-33128
Tension fracture of laminates for transport fuselage. Part 1: Material screening p 3629 N94-33130
Recent progress in NASA Langley Research Center textile reinforced composites program
p 3629 N94-33134
Ceramic and metal composite circuit-board-level technology for application specific electronic modules (ASEM)
[AD-A277961] p 3630 N94-33180
Lightweight zinc electrode
[AD-D016181] p 3698 N94-33181
Novel sol-gel deposition for repair of conducting paths in polyceramic systems
[AD-A278381] p 3664 N94-33350
COMPOSITE STRUCTURES
Ultrasonic characterization of damage in a simulated CF-18 composite structure
[DREP-LN-93-26] p 3730 N94-31872
Finite element analysis of damage in fibrous composites using a micromechanical model
[AD-A277226] p 3623 N94-32024
Benchmarking of the state-of-the-art in nondestructive testing/evaluation for applicability in the Composite Armored Vehicle (CAV) Advanced Technology Demonstrator (ATD) program, phase 1
[AD-A276660] p 3730 N94-32088
Assessment of impact damage in composite structures
[AD-A277063] p 3624 N94-32265
Development of thermoplastic composite aircraft structures
[NASA-CR-189593] p 3626 N94-32860
Application of a design-build-team approach to low cost and weight composite fuselage structure
[NASA-CR-4418] p 3626 N94-32863
Analysis of new composite architectures
[NASA-CR-195303] p 3626 N94-32904
Effective computational strategy for predicting the response of complex systems
[AD-A277452] p 3740 N94-33011
Second NASA Advanced Composites Technology Conference
[NASA-CP-3154] p 3627 N94-33121
Composite fuselage shell structures research at NASA Langley Research Center p 3628 N94-33124
Structural testing of the technology integration box beam p 3628 N94-33125
Technology integration box beam failure study
p 3628 N94-33126
Resin transfer molding for advanced composite primary wing and fuselage structures p 3628 N94-33128
Test and analysis results for composite transport fuselage and wing structures p 3628 N94-33129
Local design optimization for composite transport fuselage crown panels p 3629 N94-33132
Composite fuselage crown panel manufacturing technology p 3629 N94-33133
Advanced textile applications for primary aircraft structures p 3629 N94-33135
Characterization and manufacture of braided composites for large commercial aircraft structures
p 3630 N94-33137
Leveraging metal matrix composites to reduce costs in space mechanisms p 3604 N94-33301
COMPOSITION (PROPERTY)
Dielectric properties of Mars' surface: Proposed measurement on a Mars lander p 3951 N94-33237

COMPRESSIBLE BOUNDARY LAYER
Computation of three-dimensional compressible boundary layers to fourth-order accuracy on wings and fuselages
[NASA-CR-4269] p 3709 N94-32871
COMPRESSIBLE FLOW
A priori tests of large eddy simulation of the compressible plane mixing layer
[MEMO-1152] p 3699 N94-31185
An adaptive finite element method for unsteady compressible rotor airfoil aerodynamics
p 3567 N94-31204
Compressible convection with ionization
p 3911 N94-31498
Cell-vertex discretisation of the driven cavity flow without artificial diffusion
[W-9317] p 3703 N94-31689
Finite element vorticity-based methods for the solution of the incompressible and compressible Navier-Stokes equations
[ISBN-0-315-87265-9] p 3703 N94-31730
A numerical method for mixing/chemically reacting compressible flow with finite rate chemistry
p 3634 N94-31824
Solution of the average-passage equations for the incompressible flow through multiple-blade-row turbomachinery
[AD-A276515] p 3583 N94-31931
Multigrid diagonal implicit solutions for compressible turbulent flows and their evaluation
p 3705 N94-31941
High-resolution numerical methods for compressible multi-phase flow in hierarchical porous media
[DE94-008261] p 3707 N94-32410
Direct replacement of arbitrary grid-overlapping by non-structured grid
[NASA-TM-106601] p 3850 N94-33120
COMPRESSION LOADS
Elastic modulus measurements of LDEF glasses and glass-ceramics using a speckle technique
[NASA-CR-195911] p 3653 N94-31851
COMPRESSION TESTS
Unidirectional composites compressive behaviour: Test methods and micromechanical approach
[ONERA-NT-1993-10] p 3618 N94-31232
Comparison of the compressive strengths for stitched and toughened composite systems
[NASA-TM-109108] p 3627 N94-32939
Test and analysis results for composite transport fuselage and wing structures p 3628 N94-33129
COMPRESSIVE STRENGTH
Evaluation of nondestructive inspection techniques for quality control of alumina-ceramic housing components
[AD-A276220] p 3730 N94-31065
Comparison of the compressive strengths for stitched and toughened composite systems
[NASA-TM-109108] p 3627 N94-32939
Development of stitched/RTM composite primary structures p 3628 N94-33127
COMPRESSOR BLADES
Hotwire measurements of the turbulent flow into a cascade of controlled-diffusion compressor blades
[AD-A277297] p 3706 N94-32042
COMPTON EFFECT
Elimination of two atomic electrons by a single high energy photon
[DE94-006834] p 3864 N94-31320
COMPUTATION
Design and analysis of scalable parallel algorithms
[AD-A276255] p 3809 N94-31251
List ranking and list scan on the CRAY C-90
[AD-A276411] p 3824 N94-31259
Mixed 0-1 programming by lift-and-project in a branch-and-cut framework
[AD-A278045] p 3822 N94-33183
COMPUTATIONAL ASTROPHYSICS
A heterogeneous computing environment for simulating astrophysical fluid flows p 3928 N94-31119
COMPUTATIONAL CHEMISTRY
A genetic algorithm based method for docking flexible molecules
[DE94-007525] p 3793 N94-32269
Computational chemistry on parallel computers
[DE94-008106] p 3636 N94-32616
Molecular interactions in dilute supercritical mixtures: Molecular dynamics investigation
[DE94-007610] p 3872 N94-32644
Computed potential energy surfaces for chemical reactions
[NASA-CR-195835] p 3639 N94-33036
COMPUTATIONAL FLUID DYNAMICS
CFD-based drag prediction: State-of-the-art, theory, prospects
[AD-B179297] p 3567 N94-31180
A solution adaptive structured-unstructured grid procedure for unsteady flows p 3700 N94-31217
Prediction of transonic potential flow with slipstreams around configurations
[FFA-TN-1992-15] p 3568 N94-31220
Numerical analysis of single-vortex/free-surface interaction
[AD-A276462] p 3701 N94-31241
Grid sensitivity for aerodynamic optimization and flow analysis p 3568 N94-31287
Experimental and numerical simulation of helicopter rotor fuselage interaction
[ONERA-NT-1993-8] p 3568 N94-31421
Additional capabilities of the unified waves model
[AD-A276114] p 3702 N94-31467
Fluid-structure interaction in case of water hammer with cavitation
[PB94-148277] p 3702 N94-31588
Aeroacoustic sources in internal flows
[ISBN-9-03-86-0282-0] p 3860 N94-31653
Solution of the incompressible Navier-Stokes equations in general coordinates by Krylov subspace and multigrid methods
[REPT-93-64] p 3703 N94-31660
Cell-vertex discretisation of the driven cavity flow without artificial diffusion
[W-9317] p 3703 N94-31689
Simulations of the creation and motion of vortex rings
[W-9319] p 3703 N94-31691
Finite element vorticity-based methods for the solution of the incompressible and compressible Navier-Stokes equations
[ISBN-0-315-87265-9] p 3703 N94-31730
Numerical simulation of combined external/internal transonic flow on the forebody/inlet of the AV-8B Harrier 2 p 3569 N94-31759
Pulsed expansion of plasma in a magnetic thruster
p 3889 N94-31776
Incompressible viscous flow in tubes with occlusions
[ISBN-0-315-75467-2] p 3704 N94-31778
On an adaptation method for 2-dimensional C-type grids
[W-9322] p 3569 N94-31822
A new inverse method for generating high-speed aerodynamic flows with application to waverider design
p 3569 N94-31828
Computational study of simultaneous heat and mass transfer in turbulent separated flows
p 3704 N94-31843
Boundary layer study on nozzle wall at hypersonic velocities p 3569 N94-31882
Solution of the average-passage equations for the incompressible flow through multiple-blade-row turbomachinery
[AD-A276515] p 3583 N94-31931
Multigrid diagonal implicit solutions for compressible turbulent flows and their evaluation
p 3705 N94-31941
Large-scale shape optimization: Numerical methods, parallel algorithms, and applications to aerodynamic design p 3815 N94-31966
A study of the development and attenuation of wing-generated, vortical wakes p 3570 N94-31971
Incorporating radial mixing in axisymmetric streamline curvature through-flow analysis
[AD-A277325] p 3706 N94-32279
A critical evaluation of methods for imposing solid-wall boundary conditions in inviscid flow
[AD-A276959] p 3707 N94-32361
A novel potential/viscous flow coupling technique for computing helicopter flow fields
[NASA-CR-193272] p 3571 N94-32476
Additive turbulent decomposition of the incompressible and compressible Navier-Stokes equations
[AD-A277321] p 3708 N94-32511
Analysis and computation for vortex dynamics and rarefied gases
[AD-A277415] p 3708 N94-32581
Advanced CFD methodology for fast transients encountered in nonlinear combustion instability problems. Volume 1: Theory and validation
[NASA-CR-191351] p 3637 N94-32696
Numerical analysis of transonic wing buffet
p 3586 N94-32713
Boundary element analysis of three-dimensional nonlinear hydrodynamics in a reduced gravity environment p 3868 N94-32715
Computation of three-dimensional compressible boundary layers to fourth-order accuracy on wings and fuselages
[NASA-CR-4269] p 3709 N94-32871
A mathematical model for simulating noise suppression of lined ejectors
[NASA-TP-3425] p 3861 N94-32930
Modification of the MML turbulence model for adverse pressure gradient flows
[NASA-TM-106544] p 3709 N94-32947
Fourth-order 2N-storage Runge-Kutta schemes
[NASA-TM-109112] p 3573 N94-32950
Institute for Computational Mechanics in Propulsion (ICOMP)
[NASA-TM-106542] p 3710 N94-32969
Parallel supercomputing: Advanced methods, algorithms, and software for large-scale linear and nonlinear problems
[DE94-008446] p 3836 N94-32992
Direct replacement of arbitrary grid-overlapping by non-structured grid
[NASA-TM-106601] p 3850 N94-33120
Computational methods in continuum mechanics
[AD-A278144] p 3859 N94-33161
A study of weak solutions and their regularizations by numerical methods
[AD-A277453] p 3850 N94-33175
Cumulative reports and publications through December 31, 1993
[NASA-CR-194889] p 3806 N94-33286
COMPUTATIONAL GEOMETRY
Abstracts of the Workshop on Computational Geometry (CG 1992)
[PB94-147022] p 3844 N94-31684
Mesh optimization
[AD-A277644] p 3820 N94-32972
On the computation of simplical approximations of implicitly defined two-dimensional manifolds
[AD-A278132] p 3849 N94-33060
Least squares approximation by G1 piecewise parametric cubes
[AD-A277978] p 3850 N94-33265
COMPUTATIONAL GRIDS
A priori tests of large eddy simulation of the compressible plane mixing layer
[MEMO-1152] p 3699 N94-31185
A solution adaptive structured-unstructured grid procedure for unsteady flows p 3700 N94-31217
Grid sensitivity for aerodynamic optimization and flow analysis p 3568 N94-31287
Abstracts of the Workshop on Computational Geometry (CG 1992)
[PB94-147022] p 3844 N94-31684
Cell-vertex discretisation of the driven cavity flow without artificial diffusion
[W-9317] p 3703 N94-31689
On an adaptation method for 2-dimensional C-type grids
[W-9322] p 3569 N94-31822
On an adaptation method for dense, 2D, C-type grids
[W-9321] p 3706 N94-32045
Polynomial interpolation and approximation of real functions. 2: Symmetrical interpolation for the triangle
[AD-A277345] p 3848 N94-32245
Eta percent-superconvergence in the interior of locally refined meshes of quadrilaterals: Superconvergence of the gradient in finite element solutions of Laplace's and Poisson's equations
[AD-A277242] p 3848 N94-32331
New advances in the modeling of high-temperature superconductors
[DE94-007649] p 3905 N94-32815
Statistical intercomparison of global climate models: A common principal component approach
[DE94-008671] p 3768 N94-32882
Incremental triangulation by way of edge swapping and local optimization
[NASA-TM-103979] p 3709 N94-32948
Mesh optimization
[AD-A277644] p 3820 N94-32972
Parallel supercomputing: Advanced methods, algorithms, and software for large-scale linear and nonlinear problems
[DE94-008446] p 3836 N94-32992
Transformation of two and three-dimensional regions by elliptic systems
[NASA-CR-195849] p 3821 N94-33049
Direct replacement of arbitrary grid-overlapping by non-structured grid
[NASA-TM-106601] p 3850 N94-33120
COMPUTER AIDED DESIGN
Interactive reconstruction of anatomical structures with free-form surfaces
[TELECOM-93-E-002] p 3794 N94-31195
AGARD highlights 94/1, April 1994
[AGARD-HIGHLIGHTS-94/1] p 3956 N94-31196
Grid sensitivity for aerodynamic optimization and flow analysis p 3568 N94-31287
A comparison of product realization frameworks
[AD-A275992] p 3810 N94-31357
A model and algorithms for a software evolution control system
[AD-A276431] p 3811 N94-31449
Module generation for self-testing integrated systems
[ISBN-9-09-004570-8] p 3688 N94-31520

Extension of the LUSTRE language and application to circuit design: The LUSTRE V4 language and the POLLUX system
[ETN-94-95918] p 3812 N94-31543
GKS-9X: An experimental application
[PB94-147048] p 3813 N94-31685
Designing in virtual reality: Modelling Objects in a Virtual Environment (MOVE)
[REPT-93-91] p 3813 N94-31704
CAD-based off-line planning for an active-vision system
[ISBN-0-315-86317-X] p 3813 N94-31713
A new inverse method for generating high-speed aerodynamic flows with application to waverider design p 3569 N94-31828
Multidisciplinary optimization of high-speed civil transport configurations using variable-complexity modeling p 3578 N94-31881
Study of virtual prototyping of aircraft instruments
[CMC-0687-1090] p 3581 N94-31903
The Second International Workshop on Discrete Time Domain Modelling of Electromagnetic Fields and Networks. Program and information
[AD-A277136] p 3677 N94-32067
An analog preprocessing architecture for high-speed analog-to-digital conversion
[AD-A276737] p 3807 N94-32163
Interactive graphical model building using telepresence and virtual reality
[DE94-001421] p 3818 N94-32353
Analytical Design Package (ADP2): A computer aided engineering tool for aircraft transparency design p 3823 N94-32430
CONFIG: Integrated engineering of systems and their operation p 3823 N94-32432
Evolving software reengineering technology for the emerging innovative-competitive era p 3823 N94-32439
The role of guideline-based design tools
[DE94-007482] p 3804 N94-32596
Implementation and display of Computer Aided Design (CAD) models in Monte Carlo radiation transport and shielding applications
[DE94-007221] p 3819 N94-32641
The limits of intelligence in design
[DE94-004668] p 3819 N94-32668
On the computation of simplical approximations of implicitly defined two-dimensional manifolds
[AD-A278132] p 3849 N94-33060
Designer's unified cost model p 3627 N94-33122
COINS: A composites information database system p 3627 N94-33123
Least squares approximation by G1 piecewise parametric cubes
[AD-A277978] p 3850 N94-33265

COMPUTER AIDED MANUFACTURING

A comparison of product realization frameworks
[AD-A275992] p 3810 N94-31357
An application reference model for layered manufacturing
[DE94-006368] p 3811 N94-31484

COMPUTER AIDED MAPPING

SPOT imagery for updating land cover information of 1:50,000 numerical topographic maps p 3749 N94-32532

COMPUTER AIDED TOMOGRAPHY

Fast nonsupervised 3D registration of PET and MR images of the brain
[TELECOM-93-C-006] p 3798 N94-33069

COMPUTER ASSISTED INSTRUCTION

A systems approach to computer-based training p 3823 N94-32436
Literacy: A multimedia adult literacy package combining NASA technology, recursive ID theory, and authentic instruction theory p 3924 N94-32462
Virtual reality in medical education and assessment p 3798 N94-32471
On the use of computers for teaching fluid mechanics
[NASA-TM-106587] p 3820 N94-32773
An evaluation framework for designing a night vision, computer-based trainer
[AD-A278005] p 3590 N94-33139

COMPUTER COMPONENTS

VLSI for high-speed digital signal processing
[AD-A277617] p 3697 N94-32957

COMPUTER DESIGN

Delft Ising computing engine
[PB94-148251] p 3806 N94-31587
Control and reliability of optical networks in multiprocessors
[AD-A277385] p 3881 N94-32285
Formal semantics for a subset of VHDL and its use in analysis of the FTPP scoreboard circuit
[NASA-CR-191577] p 3827 N94-32734
Investigation of modularly configured attached processors with intelligent memories
[AD-A278418] p 3839 N94-33330

COMPUTER GRAPHICS

Interactive reconstruction of anatomical structures with free-form surfaces
[TELECOM-93-E-002] p 3794 N94-31195
Description of a package for the analysis and display of the results of numerical simulations
[AD-A276285] p 3841 N94-31252
Texture generation on irregular regions
[AD-A275999] p 3841 N94-31359
GKS-9X: An experimental application
[PB94-147048] p 3813 N94-31685
Texture library for 3-dimensional visualization systems
[AD-A276125] p 3917 N94-31829
Visual evaluation of computor-generated textures
[AD-A277201] p 3816 N94-32093
Applications of data compression to 3-D scalar field visualization p 3817 N94-32294
Interactive graphical model building using telepresence and virtual reality
[DE94-001421] p 3818 N94-32353
Design of graphic screens using Neuro Linguistic Programming
[DE94-007634] p 3819 N94-32599
Mesh optimization
[AD-A277644] p 3820 N94-32972
Least squares approximation by G1 piecewise parametric cubes
[AD-A277978] p 3850 N94-33265

COMPUTER INFORMATION SECURITY

Acquisition information management system telecommunication site survey results
[DE94-005688] p 3915 N94-31155
Covert channel analysis of trusted systems. A guide to understanding
[AD-A276418] p 3916 N94-31331
On the validity of the BLP model
[REPT-93-70] p 3917 N94-31640
PEM public key certificate cache server
[DE94-006404] p 3675 N94-31784
The FELICIA bulletin board system and the IRBIS anonymous FTP server: Computer security information sources for the DOE community
[DE94-008219] p 3825 N94-31920
Integrated Trusted System Development Environment Process
[AD-A276414] p 3816 N94-32131
The Operator Shell: A means of privilege distribution under Unix
[DE94-007566] p 3826 N94-32356

COMPUTER NETWORKS

Sandia's research network for Supercomputing 1993: A demonstration of advanced technologies for building high-performance networks
[DE94-005319] p 3823 N94-31149
Acquisition information management system telecommunication site survey results
[DE94-005688] p 3915 N94-31155
Putting the information infrastructure to work: Report of the Information Infrastructure Task Force Committee on Applications and Technology
[NIST/SP-857] p 3916 N94-31228
Performability modelling using DyQNtool+
[MEMO-INF-93-45] p 3812 N94-31659
Using atomic actions in replica groups to simplify the replication implementation
[REPT-93-78] p 3813 N94-31695
The vision machines
[NASA-TM-109757] p 3806 N94-31816
Selection of climate station data using clustering and triangulated irregular network techniques
[AD-A276658] p 3784 N94-32046
Problems in survivable multi-media networks
[AD-A277370] p 3825 N94-32052
The use of service limits for efficient operation of multi-station single-medium communication systems
[CWI-BS-R9312] p 3677 N94-32085
Undiscounted Markov decision chains with partial information; an algorithm for computing a locally optimal periodic policy
[TW-93-10] p 3851 N94-32205
Parallel and distributed computing combinatorial algorithms
[AD-A277333] p 3826 N94-32243
IRIG J asynchronous ASCII time code formats
[AD-A277244] p 3681 N94-32332
Automated mainframe data collection in a network environment p 3923 N94-32443
High performance real-time flight simulation at NASA Langley p 3591 N94-32473
Gigabits to the Desktop: Installing tomorrow's networks today
[DE94-007701] p 3827 N94-32646
Use and administration of UNIX (tm) systems p 3821 N94-33051

COMPUTER PROGRAMMING

Discovery systems for manufacturing
[AD-A276216] p 3828 N94-31061
Developing the Multimedia User Interface Component (MUSIC) for the Icarus Presentation System (IPS)
[AD-A276341] p 3810 N94-31335
E-L user's manual
[AD-A276378] p 3810 N94-31370
The development and use of an evaluation mechanism for the assessment of software configuration management tools
[AD-A275961] p 3810 N94-31383
Segment-based acoustic models for continuous speech recognition
[AD-A276109] p 3673 N94-31466
GKS-9X: An experimental application
[PB94-147048] p 3813 N94-31685
Design Methods based On Nets: DEMON
[PB94-147493] p 3813 N94-31687
Overview of megaprogramming course: Lectures and exercises
[AD-A276169] p 3814 N94-31810
On the convergence of stochastic iterative dynamic programming
[AD-A276517] p 3815 N94-31933
Incremental recompilation for Standard ML of New Jersey
[AD-A276522] p 3815 N94-32080
Integrated Trusted System Development Environment Process
[AD-A276414] p 3816 N94-32131
MULTIGRAPH: An architecture for model-based programming. Model-based program synthesis for parallel computing. PREMOS: Programming environment for model-based program synthesis, version 01.00.00
[AD-A276949] p 3817 N94-32219
EVORM: A conceptual modelling technique for evolving application domains
[TR-93-16] p 3918 N94-32290
A hypertext system that learns from user feedback p 3923 N94-32428
Spacecraft On-Board Information Extraction Computer (SOBIEC) p 3808 N94-32433
Evolving software reengineering technology for the emerging innovative-competitive era p 3823 N94-32439
Emacs Lisp in Edwin scheme
[AD-A276721] p 3818 N94-32504
MADE: A Multiple Application Development Environment
[CWI-CS-R9360] p 3822 N94-33097
Increasing the practical impact of formal methods for computer-aided software development: Software slicing, merging and integration
[AD-A277929] p 3822 N94-33179
Structuring Z specifications with views
[AD-A277618] p 3822 N94-33279

COMPUTER PROGRAMS

Summary of some data processing routines in the molecular physics group of Stockholm University
[USIP-93-05] p 3808 N94-31087
Model updating of vibrating systems based on measured or calculated frequency response functions
[CTH-E-93-03] p 3732 N94-31091
Standardization and intellectual property control: A reflection on the informatics case
[TELECOM-93-E-016] p 3915 N94-31172
Guide to software quality assurance
[ESA-PSS-05-11-ISSUE-1] p 3809 N94-31223
Computer implementation of Arnott's formulation of thermoacoustics using MATLAB
[AD-A276356] p 3860 N94-31257
Taming chaotic circuits p 3910 N94-31289
An analysis of non-integerizing the aircraft engines Cost Effectiveness Analysis Spreadsheet Model (CEAMOD version 2.0)
[AD-A276251] p 3583 N94-31290
First theory institute on computational differentiation
[DE94-006491] p 3841 N94-31309
OTTER 3.0 reference manual and guide
[DE94-007457] p 3829 N94-31315
Extender's guide for artifacts and drafts
[AD-A276344] p 3810 N94-31328
The High-Frequency Benchmark propagation program
[AD-A276323] p 3672 N94-31334
The maintenance of operational flight program
[AD-A276363] p 3565 N94-31367
Testing Operational Flight Programs (OFP's)
[AD-A276361] p 3578 N94-31387
Direct-sequence spread-spectrum performance in a multipath fading environment
[AD-A276080] p 3673 N94-31464

The future of open architecture process control systems
[DE94-006163] p 3830 N94-31623
Performability modelling using DyQNtool+
[MEMO-INF-93-45] p 3812 N94-31659
Damage tolerance aspects of a full composite airplane fuselage: Requirements, modelling, predictions, experiments
[LR-728] p 3578 N94-31674
Aeroelastic vibrations of lifting surfaces
[ECL-91-01] p 3585 N94-31677
The influence of the deorbit-burn manoeuvre on the footprint of a re-entry capsule
[LR-727] p 3609 N94-31705
Workshop on Models for Plasma Spectroscopy
[AD-A276565] p 3890 N94-32031
Noninvasive spectral analysis and beam mapping of focused ultrasound, part 2
[AD-A276629] p 3861 N94-32059
GRAFTED - GRAphical fault tree EDitor: A fault tree description program for target vulnerability/survivability analysis. User manual
[AD-A277067] p 3818 N94-32390
Heliport Noise Model (HNM) version 2.2 (user's guide)
[AD-A277072] p 3861 N94-32418
A PC program to optimize system configuration for desired reliability at minimum cost p 3823 N94-32438
Evolving software reengineering technology for the emerging innovative-competitive era
p 3823 N94-32439
User's guide for a flat wake rotor inflow/wake velocity prediction code, DOWN
[NASA-TM-104139] p 3572 N94-32873
BUCKY instruction manual, version 3.3
[NASA-TM-104793] p 3820 N94-32899
Manual for automatic generation of finite element models of spiral bevel gears in mesh
[NASA-CR-191009] p 3728 N94-32900
CET93 and CETPC: An interim updated version of the NASA Lewis computer program for calculating complex chemical equilibria with applications
[NASA-TM-4557] p 3638 N94-32948
Theory and application of image enhancement
[AD-A277896] p 3821 N94-33031
Implementing software safety in the NASA environment
[NASA-TM-106597] p 3731 N94-33032
Designer's unified cost model p 3627 N94-33122
Increasing the practical impact of formal methods for computer-aided software development: Software slicing, merging and integration
[AD-A277929] p 3822 N94-33179
Faultless software project
[AD-A278161] p 3822 N94-33188
A user's manual for the cost effectiveness analysis spreadsheet model for aircraft engines (CEAMOD version 2.0)
[AD-A278042] p 3585 N94-33266

COMPUTER STORAGE DEVICES

Extender's guide for artifacts and drafts
[AD-A276344] p 3810 N94-31328
The named-state register file
[AD-A276796] p 3825 N94-32165
Superconducting and semiconducting hybrids and advance memory concepts for superconducting electronics
[AD-A277766] p 3907 N94-32988
SynRGen: An extensible file reference generator
[AD-A277678] p 3821 N94-33030

COMPUTER SYSTEMS DESIGN

Implanting algorithms on parallel machines
[TELECOM-93-D-017] p 3823 N94-31099
LORE and reason maintenance
[REPT-93-88] p 3812 N94-31522
An expert system architecture for heterogeneous domains: A case-study in the legal field
[ETN-94-96012] p 3830 N94-31546
Compositionality of application oriented structuring mechanisms for algebraic specification languages with initial semantics
[ETN-94-95736] p 3812 N94-31577
On the validity of the BLP model
[REPT-93-70] p 3917 N94-31640
Design Methods based On Nets: DEMON
[PB94-147493] p 3813 N94-31687
Designing in virtual reality: Modelling Objects in a Virtual Environment (MOVE)
[REPT-93-91] p 3813 N94-31704
Experiences with EDO: An Evolutionary Database Optimizer
[TR-93-23] p 3918 N94-32105
Parallel and distributed computing combinatorial algorithms
[AD-A277333] p 3826 N94-32243
Communication networks for autonomous mobile robot computer architectures and distributed real-time computing p 3680 N94-32310
Massively parallel systems design for real-time embedded applications
[AD-A277256] p 3826 N94-32323
Modular Simulator System (MSS). Engineering design guide
[AD-A276967] p 3589 N94-32394
Modular Simulator System (MSS): Interface design document for the generic MSS
[AD-A277270] p 3590 N94-32403
High performance real-time flight simulation at NASA Langley p 3591 N94-32473
Developing a personal-computer-based records retention system using Paradox(tm)
[DE94-007984] p 3819 N94-32749
Selection criteria and facilitation training for the study of groupware
[NASA-CR-195906] p 3822 N94-33114

COMPUTER SYSTEMS PERFORMANCE

Sandia's research network for Supercomputing 1993: A demonstration of advanced technologies for building high-performance networks
[DE94-005319] p 3823 N94-31149
Performability modelling using DyQNtool+
[MEMO-INF-93-45] p 3812 N94-31659
Using atomic actions in replica groups to simplify the replication implementation
[REPT-93-78] p 3813 N94-31695
Compiler techniques for managing data motion
[AD-A276514] p 3918 N94-31930
The use of service limits for efficient operation of multi-station single-medium communication systems
[CWI-BS-R9312] p 3677 N94-32085

COMPUTER SYSTEMS PROGRAMS

The development and use of an evaluation mechanism for the assessment of software configuration management tools
[AD-A275961] p 3810 N94-31383

COMPUTER SYSTEMS SIMULATION

Proof of concept for the rewrite rule machine: Interensemble studies
[AD-A276506] p 3809 N94-31263

COMPUTER TECHNIQUES

Discovery systems for manufacturing
[AD-A276216] p 3828 N94-31061
Symbolic derivation of Runge-Kutta methods
[MATHS-REPT-A-205] p 3840 N94-31160
An analysis of the records management process to determine the impact of automation on productivity
[AD-A275923] p 3916 N94-31344
An active computer supported medium for distributed planning in enterprises
[ETN-94-95738] p 3829 N94-31372
Possible improvements of satellite ephemeris programs used in geodesy
[PB94-148681] p 3743 N94-31592
Designing in virtual reality: Modelling Objects in a Virtual Environment (MOVE)
[REPT-93-91] p 3813 N94-31704
On-line physical parameter identification and adaptive control of a launch vehicle p 3602 N94-31891
Beyond the read-eval loop: The artifacts system
[AD-A276589] p 3803 N94-32034
Performance metrics for low probability of intercept-communication system
[AD-A277346] p 3677 N94-32073
Transformational derivation of (parallel) programs using skeletons
[TR-93-20] p 3825 N94-32196
MULTIGRAPH: An architecture for model-based programming. Model-based program synthesis for parallel computing. PREMOS: Programming environment for model-based program synthesis, version 01.00.00
[AD-A276949] p 3817 N94-32219
Multiple inheritance via intersection types
[TR-93-18] p 3848 N94-32292
New approaches for real time decision support systems p 3915 N94-32426
Institute for Computational Mechanics in Propulsion (ICOMP)
[NASA-TM-106542] p 3710 N94-32969
An evaluation framework for designing a night vision, computer-based trainer
[AD-A278005] p 3590 N94-33139
Cumulative reports and publications through December 31, 1993
[NASA-CR-194889] p 3806 N94-33286

COMPUTER VIRUSES

The FELICIA bulletin board system and the IRBIS anonymous FTP server: Computer security information sources for the DOE community
[DE94-008219] p 3825 N94-31920

COMPUTER VISION

Computing the precision of localization in a plane using projective invariants
[TELECOM-93-D-005] p 3840 N94-31095
Camera-space manipulation with natural visual information p 3829 N94-31207
Digit-Eyes: Vision-based human hand tracking
[NASA-CR-195913] p 3803 N94-31447
Polyhedric object recognition by indexing in a model base
[ETN-94-95913] p 3812 N94-31542
CAD-based off-line planning for an active-vision system
[ISBN-0-315-86317-X] p 3813 N94-31713
Volumetric modelling of three dimensional scenes by octree decomposition of geometric models
[ISBN-0-315-86866-X] p 3814 N94-31728
Real-time control of the Trussarm variable-geometry-truss manipulator utilizing machine vision
[ISBN-0-315-87054-0] p 3830 N94-31735
A neural network model for the visual perception of the depth of a scene from stereoscopy and shading
[ISBN-0-315-86753-1] p 3831 N94-31750
Synchronized laser scanning three dimensional acquisition system
[ISBN-0-315-86848-1] p 3879 N94-31756
Strategy for tracking and grabbing a moving object with the aid of a decouplable manipulator with six degrees of freedom general architecture, guided by a vision system
[ISBN-0-315-86864-3] p 3831 N94-31757
Safe navigation and active vision for autonomous vehicles: A purposive and direct solution
p 3832 N94-31842
Robot motion vision by fixation p 3833 N94-31991
Visual evaluation of computer-generated textures
[AD-A277201] p 3816 N94-32093
Neural models of spatial orientation in novel environments
[AD-A277383] p 3835 N94-32340

COMPUTERIZED SIMULATION

Model of spacecraft atomic oxygen and solar exposure microenvironments p 3593 N94-31021
Evaluation of HardSys/HardDraw, an expert system for electromagnetic interactions modelling
[AD-A276218] p 3670 N94-31063
Modelling the late part of room impulse responses using adaptive filtering: On the recreation of reality
[CTH-E-93-01] p 3859 N94-31076
Scattering of a random acoustic field by an infinite cylinder: Application to the modelization of the acoustic environment of the 'Ariane 5' launcher scale-model using experimental data
[ONERA-NT-1993-11] p 3860 N94-31226
Molecular dynamics computer simulations of charged metal electrode-aqueous electrolyte interfaces
[AD-A276401] p 3863 N94-31237
ADCIRC: An advanced three-dimensional circulation model for shelves, coasts, and estuaries. User's manual for ADCIRC-2DDI
[AD-A276150] p 3787 N94-31250
Description of a package for the analysis and display of the results of numerical simulations
[AD-A276285] p 3841 N94-31252
Hydrogenated amorphous silicon (a-Si:H) based gamma camera: Monte Carlo simulations
[DE94-007042] p 3795 N94-31323
Developing the Multimedia User Interface Component (MUSIC) for the Icarus Presentation System (IPS)
[AD-A276341] p 3810 N94-31335
Using Monte Carlo techniques and parallel processing for debris hazard analysis of rocket systems
[DE94-007250] p 3609 N94-31382
The threshold energy for defect production in SiC: A molecular dynamic study
[DE94-007123] p 3896 N94-31499
Delft Ising computing engine
[PB94-148251] p 3806 N94-31567
Virtual annotation: Verbal communication in virtual reality
[REPT-93-67] p 3674 N94-31645
The influence of the deorbit-burn manoeuvre on the footprint of a re-entry capsule
[LR-727] p 3609 N94-31705
Model-based scientific discovery: A study in space bioengineering p 3799 N94-31990
Computer modelling of cyclic deformation of high-temperature materials
[AD-A277056] p 3623 N94-32012
On an adaptation method for dense, 2D, C-type grids
[W-9321] p 3706 N94-32045
Selection of climate station data using clustering and triangulated irregular network techniques
[AD-A276658] p 3784 N94-32046

The Second International Workshop on Discrete Time Domain Modelling of Electromagnetic Fields and Networks. Program and information
[AD-A277136] p 3677 N94-32067
Atmospheric structure simulation: An autoregressive model for smooth geophysical power spectra with known autocorrelation function
[AD-A276691] p 3773 N94-32118
Using TSAR with the post-processing far-field option
[DE94-006615] p 3679 N94-32188
Proceedings of the International Workshop on Computational Electronics
[AD-A277020] p 3692 N94-32259
Validation support of the ERIM ocean model
[AD-A277364] p 3788 N94-32284
Parallel Monte Carlo reactor neutronics
[DE94-007642] p 3826 N94-32357
Parallel particle simulations of low-density fluid flows
[DE94-007858] p 3707 N94-32373
High-resolution numerical methods for compressible multi-phase flow in hierarchical porous media
[DE94-008261] p 3707 N94-32410
Assembly flow simulation of a radar
p 3823 N94-32431
Literacity: A multimedia adult literacy package combining NASA technology, recursive ID theory, and authentic instruction theory p 3924 N94-32462
Technology transfer of operator-in-the-loop simulation
p 3802 N94-32472
High performance real-time flight simulation at NASA Langley p 3591 N94-32473
Construction of a parallel processor for simulating manipulators and other mechanical systems
[NASA-CR-191327] p 3826 N94-32482
VME rollback hardware for time warp multiprocessor systems
[NASA-CR-191796] p 3826 N94-32483
Molecular Science Research Center
[DE94-007464] p 3871 N94-32605
Complete model description of an electron beam using ACCEPT Monte Carlo simulation code
[DE94-007063] p 3872 N94-32628
Automatic contact in DYNA3D for vehicle crashworthiness
[DE94-007143] p 3738 N94-32637
Molecular interactions in dilute supercritical mixtures: Molecular dynamics investigation
[DE94-007610] p 3872 N94-32644
Particle-in-Cell (PIC) code simulation results and comparison with theory scaling laws for photoelectron-generated radiation
[DE94-006132] p 3695 N94-32662
Development of a computer model for polycrystalline thin-film CuInSe2 and CdTe solar cells
[DE94-006853] p 3762 N94-32763
The Numerical Tokamak Project (NTP) simulation of turbulent transport in the core plasma: A grand challenge in plasma physics
[DE94-008279] p 3892 N94-32838
Fluid Dynamics Lagrangian Simulation Model
[AD-A277438] p 3710 N94-33009
Implementation of a vibrationally linked chemical reaction model for DSMC
[NASA-TM-109109] p 3710 N94-33020
Simultaneous excitation of parametric decay cascades and the OTSI in 1D numerical simulations based on Aakarov's equations
[AD-A278108] p 3893 N94-33042
Design and Monte Carlo analysis of an unmanned aerial vehicle
[AD-A277648] p 3560 N94-33056
Visual perception of 3-dimensional structure from different types of optical deformation
[AD-A278272] p 3884 N94-33141
Computational methods in continuum mechanics
[AD-A278144] p 3859 N94-33161
How well was total ozone abundance inferred with Mariner 9 p 3947 N94-33212
Snowmelt forecasting. Further cold regions development of operational hydrological forecasting, volume 2
[AD-A278123] p 3757 N94-33269
Simulation of CO2 release at 800 km altitude
[AD-A276692] p 3776 N94-33272

COMPUTERS
Standardization and intellectual property control: A reflection on the informatics case
[TELECOM-93-E-016] p 3915 N94-31172
Pen-based computers: Computers without keys
p 3808 N94-32434

CONCATENATED CODES
Spread-spectrum radio systems and networks
[AD-A276449] p 3671 N94-31260

CONCRETE STRUCTURES
Dual-band infrared imaging to detect corrosion damage within airframes and concrete structures
[DE94-006047] p 3580 N94-32658

CONCRETES
Nonlocal theory for fracturing of quasibrittle materials
[AD-A278283] p 3740 N94-33143

CONCURRENT PROCESSING
Proof of concept for the rewrite rule machine: Interensemble studies
[AD-A276506] p 3809 N94-31263
Design Methods based On Nets: DEMON
[PB94-147493] p 3813 N94-31687

CONDENSATES
Minimax: Multiparticle physics at the Tevatron collider
[DE94-007095] p 3873 N94-32689

CONDENSATION NUCLEI
Counting particles emitted by stratospheric aircraft and measuring size of particles emitted by stratospheric aircraft
[NASA-CR-195908] p 3769 N94-33170

CONDENSED MATTER PHYSICS
International Journal of Quantum Chemistry. Quantum Biology Symposium number 20. Proceedings of the International Symposium on the Application of Fundamental Theory to Problems of Biology and Pharmacology
[AD-A276294] p 3792 N94-31294
Summary of the 1993 Winter ACP Workshop on Collective Dynamics in Disordered System
[AD-A276355] p 3864 N94-31402

CONDITIONED REFLEXES
Stress-induced enhancement of the startle reflex
[AD-A278414] p 3802 N94-33327

CONDITIONING (LEARNING)
Stress-induced enhancement of the startle reflex
[AD-A278414] p 3802 N94-33327

CONDUCTING FLUIDS
Stability and instability criteria for magnetohydrodynamics
[PB94-148475] p 3889 N94-31772

CONDUCTING POLYMERS
The Sixth Symposium on Unconventional Photoactive Solids. Abstracts
[AD-A277198] p 3655 N94-32016
Polymer electrolyte fuel cells
[DE94-007558] p 3761 N94-32762
Novel sol-gel deposition for repair of conducting paths in polyceramic systems
[AD-A278381] p 3864 N94-33350

CONDUCTION BANDS
Experimental and theoretical studies of hydrogenated amorphous semiconductor alloys and superlattices
[AD-A276159] p 3686 N94-31079

CONDUCTION ELECTRONS
X ray pulse considerations and electron flow in high voltage diodes
[AD-A277301] p 3868 N94-32044

CONDUCTIVE HEAT TRANSFER
Space Station WP-2 application of LDEF MLI results
p 3592 N94-31016
THERM3D: A boundary element computer program for transient heat conduction problems
[DE94-008112] p 3708 N94-32709
Numerical model of the thermal behavior of an extremity in a cold environment including counter-current heat exchange between the blood vessels
[AD-A278099] p 3798 N94-33040
Computational methods in continuum mechanics
[AD-A278144] p 3859 N94-33161

CONDUCTIVITY
Novel electroactive polymers and block copolymers
[AD-A276119] p 3650 N94-31509

CONDUCTIVITY METERS
Perspectives of glucose sensing based on a charge-modulating competition reaction
[ISBN-9-09-005754-4] p 3795 N94-31652

CONDUCTORS
A simple model for determining photoelectron-generated radiation scaling laws
[DE94-006130] p 3761 N94-32660
An electrical test system for conductor formation process analysis
[DE94-007291] p 3696 N94-32786
Grounding ring for ground adapters
[AD-D016118] p 3697 N94-32962

CONFERENCES
LDEF Materials Results for Spacecraft Applications
[NASA-CP-3257] p 3591 N94-31012
Workshop on Physics of Accretion Disks Around Compact and Young Stars
[NASA-CR-195756] p 3927 N94-31116
The 1988 Goddard Space Flight Center Battery Workshop
[NASA-CP-3237] p 3758 N94-31233
Proceedings of the 37th international symposium on electron, ion, and photon beams
[AD-A276478] p 3875 N94-31247
Physical chemistry of molecules and grains in space
[AD-A276037] p 3932 N94-31280
The 18th annual electronics manufacturing seminar
[AD-A276038] p 3687 N94-31281
International Journal of Quantum Chemistry. Quantum Biology Symposium number 20. Proceedings of the International Symposium on the Application of Fundamental Theory to Problems of Biology and Pharmacology
[AD-A276294] p 3792 N94-31294
Workshop on advances in smooth particle hydrodynamics
[DE94-006221] p 3956 N94-31308
First theory institute on computational differentiation
[DE94-006491] p 3841 N94-31309
Proceedings of the 4th Tunnel Detection Symposium on Subsurface Exploration Technology
[AD-A276372] p 3771 N94-31369
The Second Annual International Space University Alumni Conference
[NASA-CP-3253] p 3598 N94-31425
Minutes: Accredited Standards Committee on Bioacoustics, S3. US TAG for ISO/TC 43, acoustics, IEC/TC 29 electroacoustics, and ISO/TC 108/SC4 human exposure to mechanical vibration and shock
[AD-A276201] p 3795 N94-31490
Proceedings of a Joint US-Japan Seminar in the Environmental Sciences
[DE94-004727] p 3741 N94-31606
Proceedings of the Seventeenth DOE Solar Photochemistry Research Conference
[DE94-005552] p 3759 N94-31648
Double photoionization of helium with synchrotron x rays: Proceedings
[DE94-006737] p 3866 N94-31668
Proceedings of the DCIEM Diver Thermal Protection Workshop
[DCIEM-92-10] p 3795 N94-31738
Current Research Information in Europe: Conference proceedings
[PB94-127933] p 3917 N94-31768
Proceedings of the International Workshop on Artificial Intelligence Applications in Solar-Terrestrial Physics
[PB94-142064] p 3832 N94-31808
Aerospace software engineering for advanced systems architectures
[AD-A277101] p 3581 N94-31977
The Sixth Symposium on Unconventional Photoactive Solids. Abstracts
[AD-A277198] p 3655 N94-32016
Proceedings of the 1993 Antenna Applications Symposium, volume 1
[AD-A277202] p 3676 N94-32049
Proceedings of the 1993 Antenna Applications Symposium, volume 2
[AD-A277203] p 3677 N94-32050
The Second International Workshop on Discrete Time Domain Modelling of Electromagnetic Fields and Networks. Program and information
[AD-A277136] p 3677 N94-32067
The 10th International Conference on Internal Friction and Ultrasonic Attenuation in Solids (ICIFUAS)
[AD-A276849] p 3902 N94-32209
The 14th Annual West Coast Theoretical Chemistry/Statistical Mechanics Conference
[AD-A276942] p 3656 N94-32239
Workshop on Commercialization of Pulsed Power Science and Technology Proceedings
[AD-A276987] p 3692 N94-32258
Proceedings of the International Workshop on Computational Electronics
[AD-A277020] p 3692 N94-32259
WOCSDICE 1993 --- 17th European Workshop on Compound Semiconductor Devices and Integrated Circuits
[AD-A276766] p 3693 N94-32307
Technology 2003: The Fourth National Technology Transfer Conference and Exposition, volume 2
[NASA-CP-3249] p 3956 N94-32420
Proceedings of the Ad Hoc Workshop on Ceramics for Li/FeS2 batteries
[DE94-007460] p 3694 N94-32607
Proceedings of the Ninth Annual Pacific Climate (PACLIM) Workshop
[DE94-003024] p 3766 N94-32693
Interagency Advanced Power Group: Steering Group meeting minutes
[DE94-007951] p 3761 N94-32701
Flywheel Energy Storage Technology Workshop
[DE94-008064] p 3761 N94-32705
Proceedings of the Workshop on B Physics at Hadron Accelerators
[DE94-007961] p 3877 N94-32748
Proceedings of the International Workshop on Low Energy Muon Science: LEMS 1993
[DE94-006495] p 3874 N94-32804

The 1994 International Sherwood Fusion Theory Conference
[DE94-008961] p 3877 N94-32844
The 6th International Conference on Modulated Semiconductor Structures
[AD-A276815] p 3906 N94-32908
Proceedings, Strongly Correlated Electronic Materials: The 1993 Los Alamos Symposium
[DE94-009293] p 3906 N94-32913
Silicon-Based Optoelectronic Materials Symposium and Materials Research Society Proceedings, volume 298
[AD-A277518] p 3662 N94-32952
International Free Electron Laser Conference
[AD-A277576] p 3721 N94-33000
Proceedings of the NIPS 1993 Postconference Workshop on Pulling It All Together: Methods for Combining Neural Networks
[AD-A277507] p 3836 N94-33014
CRAD Signal and Information Processing Working Group Workshop on Neural networks, volume 1
[DREA-TC-93-305-VOL-1] p 3836 N94-33149
Cockpit Electronic Display Workshop: Proceedings (computer diskette)
[AD-M000330] p 3805 N94-33171
Conference on operator, wavelet and control theory
[AD-A277429] p 3838 N94-33174
The Northern Plains MSATT Meeting, and a call for a field-oriented successor to MSATT
p 3947 N94-33210
From animals to animats
[AD-A277427] p 3802 N94-33241
Cockpit Electronic Display Workshop: A synopsis
[AD-A277728] p 3583 N94-33280
The 28th Aerospace Mechanisms Symposium
[NASA-CP-3260] p 3603 N94-33291
Proceedings of the Symposium/Workshop on Applications of Expert Systems in DND
[DSIS-93-00343] p 3853 N94-33335

CONFIGURATION MANAGEMENT
The development and use of an evaluation mechanism for the assessment of software configuration management tools
[AD-A275961] p 3810 N94-31383
A model and algorithms for a software evolution control system
[AD-A276431] p 3811 N94-31449
Beyond the read-eval loop: The artifacts system
[AD-A276589] p 3803 N94-32034

CONFINEMENT
Toroidal pinch experiments
[DE94-005876] p 3887 N94-31558
Cooling and trapping of neutral atoms
[AD-A276957] p 3870 N94-32360
New polymer target-shell properties and characterizations
[DE94-008420] p 3890 N94-32415
Divertor pumping and other reactor application issues for H-mode
[DE94-007431] p 3892 N94-32810

CONFORMAL MAPPING
Sound scattering by cylinders of noncircular cross section
[AD-A276663] p 3861 N94-32089

CONGRESSIONAL REPORTS
Global change research and NASA's Earth Observing System
[PB94-126992] p 3741 N94-31068

CONICAL SCANNING
Radar rainfall measurements from space
p 3782 N94-31889

CONIFERS
Research and applications of a canopy reflectance model p 3747 N94-32492
Effects of long-term elevated atmospheric CO2 concentrations on Pinus ponderosa
[DE94-008832] p 3769 N94-32966

CONJUGATE GRADIENT METHOD
Design and analysis of scalable parallel algorithms
[AD-A276255] p 3809 N94-31251
Lattice geometrodynamics p 3857 N94-31825
Variational elliptic solver for atmospheric applications
[DE94-007725] p 3774 N94-32647

CONJUGATION
Conjugated polymer fluorescence: Interplay of correlations and alternation
[DE94-005587] p 3660 N94-32729

CONNECTORS
Nd-YAG laser welding of the fiber optic connector to the header shell on the 2SL actuator
[DE94-006104] p 3723 N94-31621
New thick film feedthrough configurations
[DE94-008706] p 3694 N94-32582

CONSERVATION EQUATIONS
Can a variable alpha induce limit cycle behavior and exponential luminosity decay in transient soft x ray sources? p 3929 N94-31129

CONSERVATION LAWS
Fully discrete arbitrary-order schemes for a model hyperbolic conservation law
[CRANFIELD-AERO-9307] p 3843 N94-31539
Multidimensional WAF-type schemes for model conservation laws
[CRANFIELD-AERO-9312] p 3843 N94-31541
A numerical method for mixing/chemically reacting compressible flow with finite rate chemistry
p 3634 N94-31824
A polling system with a dormant server
[CWI-BS-R9313] p 3835 N94-32193

CONSISTENCY
High-performance speech recognition using consistency modeling
[AD-A276775] p 3679 N94-32185

CONSOLIDATION
Empirical optimization of the consolidation of thermoplastic prepregs
[ISBN-0-315-86455-9] p 3652 N94-31722
Effect of surface forces on the rheology of particle-liquid systems and the consolidation of ceramic powders
[AD-A277092] p 3657 N94-32391

CONSTANTS
Experimental studies on the effect of coherency strains on coarsening kinetics: Current status and future outlook
[DE94-008480] p 3647 N94-32964

CONSTRAINTS
A Gauss-Seidel type solver for special convex programs, with application to frictional contact mechanics
[REPT-93-77] p 3813 N94-31694
Space Station Freedom solar array containment box mechanisms p 3603 N94-33292

CONSUMERS
Strategies for survival in the new environmental era
[AD-A276827] p 3785 N94-32195

CONTACT LOADS
Point-contact and point-impact dynamics for multibody chains
[ISBN-0-315-87056-7] p 3734 N94-31737
Development of a robotic simulator for studying interference and contact problems
[ISBN-0-315-86705-1] p 3588 N94-31747
Application of contact mechanics for the validation of robotized operations of grasping objects subjected to static and dynamic force fields
[ISBN-0-315-86831-7] p 3725 N94-31754
Automatic analysis of force distribution in multi-fingered articulated hands
[ISBN-0-315-87205-5] p 3725 N94-31878
Computational methods for frictional contact with applications to the Space Shuttle orbiter nose-gear tire
p 3608 N94-32295
New micro- and macroscopic models of contact and friction
[AD-A277240] p 3726 N94-32320
A procedure for 3-D contact stress analysis of spiral bevel gears
[NASA-CR-194472] p 3728 N94-32929

CONTACT RESISTANCE
Electromagnetic scattering through loaded aperture panels with nonzero contact impedance
[ONERA-NT-1993-2] p 3673 N94-31418

CONTAINERS
A compatibility study of FEFO with various containment materials
[DE94-005753] p 3649 N94-31198

CONTAMINANTS
An overview of the on-orbit contamination of the Long Duration Exposure Facility (LDEF) p 3598 N94-31049
Photothermal laser deflection, an innovative technique to measure particles in exhausts
[AD-A277151] p 3718 N94-32366

CONTAMINATION
Anodized aluminum on LDEF p 3592 N94-31017
Modeling of LDEF contamination environment
p 3592 N94-31019
Degradation of optical components in space
p 3594 N94-31029
Atmosphere quality standards in manned space vehicles
[ESA-PSS-03-401-ISSUE-1] p 3802 N94-31224
Information systems to enhance technology exchange
[DE94-007744] p 3920 N94-32808
Focused feasibility study final field sampling plan
[AD-A277445] p 3769 N94-33105

CONTEXT
The interpretation of free focus
[CL-93-01] p 3855 N94-31390

CONTEXT FREE LANGUAGES
Informal introduction to the extended affix grammar formalism and its compiler
[TR-93-19] p 3817 N94-32287

CONTINENTAL SHELVES
Gas hydrate detection and mapping on the US east coast
[DE94-005959] p 3742 N94-31504
Deep water studies of CTD data
[AD-A277741] p 3791 N94-33176
Fluid mechanical measurements within the bottom boundary layer over the Northern California continental shelf during stress
[AD-A277916] p 3791 N94-33243

CONTINUOUS RADIATION
Development of a frequency-domain electromagnetic scattering measurement system
[AD-A276738] p 3678 N94-32179

CONTINUOUS WAVE LASERS
Near resonant absorption by atoms in intense fluctuating laser fields
[DE94-005873] p 3714 N94-31200
High-power CW diode-laser-array-pumped solid-state lasers and efficient nonlinear optical frequency conversion
[AD-A276126] p 3714 N94-31278
The development and testing of a backscatter absorption gas imaging (BAGI) system designed to image at a range of 300 m
[DE94-006192] p 3675 N94-31761

CONTINUUM MECHANICS
Computational methods in continuum mechanics
[AD-A278144] p 3859 N94-33161

CONTINUUM MODELING
Development of an advanced continuum theory for composite laminates, volume 1
[AD-A277275] p 3625 N94-32591
Development of an advanced continuum theory for composite laminates, volume 2
[AD-A277276] p 3625 N94-32592

CONTINUUMS
Observations of accretion and angular momentum regulation in young circumstellar disks and the implications for planetary formation p 3928 N94-31122
Thermal continua of AGN accretion disks
p 3931 N94-31137

CONTOURS
Steepest descent paths for integrals defining the modified Bessel functions of imaginary order
[CWI-AM-R9303] p 3848 N94-32227
Surface conforming flexible eddy current probe for scanning varying surface contours
[AD-D016173] p 3627 N94-33018

CONTRACT MANAGEMENT
Management of government quality assurance functions for NASA contracts
[NHB-5300.4(2B-2)] p 3731 N94-32387

CONTRACTORS
Common modeling system for digital simulation
p 3823 N94-32429

CONTROL BOARDS
Optimal planning of residential photovoltaic systems under various rate structure
[DE94-757272] p 3762 N94-32919

CONTROL EQUIPMENT
International Space Station Alpha's bearing, motor, and roll ring module developmental testing and results
p 3603 N94-33295

CONTROL MOMENT GYROSCOPES
Adaptive nonlinear control of spacecraft
p 3609 N94-31564

CONTROL SIMULATION
Modular Simulator System (MSS). System/segment specification for the generic modular simulator system-flight controls module, volume 3
[AD-A276970] p 3590 N94-32395
Plan recognition for an air traffic control simulation
[DSIS-94-01221] p 3577 N94-32505

CONTROL STABILITY
Feasibility and stability results for constrained stable generalized predictive control
[MATHS-REPT-A-203] p 3828 N94-31158
Robot grasping: Stability and optimization issues
p 3724 N94-31724
Automatic analysis of force distribution in multi-fingered articulated hands
[ISBN-0-315-87205-5] p 3725 N94-31878
Antiwindup analysis and design approaches for MIMO systems
[NASA-CR-195304] p 3584 N94-32075
Control strategies for systems with limited actuators
[NASA-CR-195307] p 3727 N94-32741

CONTROL SURFACES
Active control for fin buffet alleviation
[AD-A276844] p 3586 N94-32224
Combined contamination and space environmental effects on solar cells and thermal control surfaces
[NASA-TM-106592] p 3617 N94-33022

CONTROL SYSTEMS DESIGN
A direct digital design for a multichannel structural test system using the characteristic locus method
[MATHS-REPT-A-206] p 3828 N94-31161
AGARD highlights 94/1, April 1994
[AGARD-HIGHLIGHTS-94/1] p 3956 N94-31196
Control of hypersonic aerodynamic forces with surface blowing p 3567 N94-31216
Control of a flexible space robot tracking a moving target p 3722 N94-31469
ControlShell: A real-time software framework
[AD-A276481] p 3811 N94-31475
A neural network methodology for engineering applications: The learning control of robotic systems
[RR-480] p 3830 N94-31500
Real time simulation model for designing converter regulation
[ETN-94-95735] p 3689 N94-31576
Digital state-feedback H(infinity) control of Pritchard-Salamon systems: A Popov function approach
[REPT-93-69] p 3830 N94-31647
A Hyland-Bernstein approach to the digital control of Pritchard-Salamon systems
[REPT-93-76] p 3844 N94-31693
Development of a feedforward controller for a flexible manipulator
[ISBN-0-315-86515-6] p 3832 N94-31801
A real-time computer control and trajectory generation environment for Trussarm
[ISBN-0-315-87060-5] p 3832 N94-31833
Development of a reconfigurable helicopter flight control system
[ISBN-0-315-87218-7] p 3585 N94-31837
Real-time control and application to robotics: Hardware and software architectures
[ISBN-0-315-87192-X] p 3833 N94-31876
On-line physical parameter identification and adaptive control of a launch vehicle p 3602 N94-31891
High-speed path constrained manipulator operation using optimal-feedback combined controller p 3833 N94-31962
Control of a flexible-link robotic arm manipulating an unknown dynamic payload p 3725 N94-31973
Adaptive control of telerobotic systems worn by humans
[AD-A276608] p 3834 N94-32036
Antiwindup analysis and design approaches for MIMO systems
[NASA-CR-195304] p 3584 N94-32075
Novel failure analysis techniques using photon probing with a scanning optical microscope
[DE94-006594] p 3692 N94-32112
Approximation theory and computational methods for the identification and control of distributed parameter systems
[AD-A277335] p 3848 N94-32244
Control strategies for systems with limited actuators
[NASA-CR-195307] p 3727 N94-32741
Active vortex control for a high performance wing
[AD-D016140] p 3573 N94-32974
Parametric robust control and system identification: Unified approach
[NASA-CR-195826] p 3836 N94-32980
Implementing software safety in the NASA environment
[NASA-TM-106597] p 3731 N94-33032
Investigation of drive-reinforcement learning and application of learning to flight control
[AD-A277442] p 3801 N94-33053
Pointing and tracking space mechanism for laser communication p 3606 N94-33310

CONTROL THEORY
Feasibility and stability results for constrained stable generalized predictive control
[MATHS-REPT-A-203] p 3828 N94-31158
Observations of the notion of minimality in the generalized state space
[MATHS-REPT-A-207] p 3840 N94-31162
Vibration control and design of composite cantilevers taking into account structural uncertainties and damage p 3733 N94-31213
A neural network methodology for engineering applications: The learning control of robotic systems
[RR-480] p 3830 N94-31500
Adaptive nonlinear control of spacecraft p 3609 N94-31564
A Hyland-Bernstein approach to the digital control of Pritchard-Salamon systems
[REPT-93-76] p 3844 N94-31693
On the convergence of stochastic iterative dynamic programming
[AD-A276517] p 3815 N94-31933
Modeling and control of nonlinear systems
[AD-A277377] p 3834 N94-32095
Control of a random walk with noisy delayed information
[CWI-BS-R9316] p 3846 N94-32108
Control experiments in liquid metal combustion
[AD-A276918] p 3635 N94-32234
Approximation theory and computational methods for the identification and control of distributed parameter systems
[AD-A277335] p 3848 N94-32244
Stochastic realization of a Gaussian stochastic control system
[CWI-BS-R9320] p 3852 N94-32350
Study of dynamic stall phenomenon and its control using vorticity, stream function and circulation form of the unsteady Navier-Stokes equations p 3572 N94-32714
Control strategies for systems with limited actuators
[NASA-CR-195307] p 3727 N94-32741
Parametric robust control and system identification: Unified approach
[NASA-CR-195826] p 3836 N94-32980
Investigation of drive-reinforcement learning and application of learning to flight control
[AD-A277442] p 3801 N94-33053
Conference on operator, wavelet and control theory
[AD-A277429] p 3838 N94-33174
Adaptive control of nonlinear and stochastic systems
[AD-A278411] p 3839 N94-33325

CONTROL VALVES
Design of a two dimensional planer pressurized air labyrinth seal test rig
[AD-A277232] p 3726 N94-32370

CONTROLLED ATMOSPHERES
Atmosphere quality standards in manned space vehicles
[ESA-PSS-03-401-ISSUE-1] p 3802 N94-31224

CONTROLLED FUSION
Anomalous thermalization of fast ions in magnetized plasma
[DE94-007109] p 3891 N94-32631
The 1994 International Sherwood Fusion Theory Conference
[DE94-008961] p 3877 N94-32844

CONTROLLERS
Taming chaotic circuits p 3910 N94-31289
An analysis of instruction-cached SIMD computer architecture
[AD-A276519] p 3806 N94-31934
High-speed path constrained manipulator operation using optimal-feedback combined controller p 3833 N94-31962
Control of a flexible-link robotic arm manipulating an unknown dynamic payload p 3725 N94-31973
Antiwindup analysis and design approaches for MIMO systems
[NASA-CR-195304] p 3584 N94-32075
Geometric structure of the adaptive controller of the human arm
[AD-A276797] p 3834 N94-32152
Refining fuzzy logic controllers with machine learning p 3839 N94-32421
A fuzzy classifier system for process control p 3839 N94-32422
Fuzzy-neural control of an aircraft tracking camera platform p 3839 N94-32423
Feed-forward control of gear mesh vibration using piezoelectric actuators
[NASA-TM-106366] p 3728 N94-32902
State-space self-tuner for on-line adaptive control
[NASA-CR-195836] p 3835 N94-32943
Operational experience and evaluation of a dual-element stretched-membrane heliostat
[DE94-008827] p 3763 N94-32965
Intelligent control of a multi-degree-of freedom reaction compensating platform system using fuzzy logic p 3605 N94-33306

CONVECTION
Convection and electrodynamic signatures in the vicinity of a Sun-aligned arc: Results from the Polar Acceleration Regions and Convection Study (Polar ARCS) p 3954 N94-31102
Convective solar nebula p 3930 N94-31130
Rotational effects in turbulence driven by convection p 3930 N94-31131
Compressible convection with ionization p 3911 N94-31498
Regional sources of error growth in the National Meteorological Center's medium-range forecast model p 3781 N94-31554
Surface fluxes of trace gases derived from convective-layer profiles p 3704 N94-31774
Thermocapillary convection in evaporating sessile drops
[NASA-TM-109758] p 3705 N94-31886
Cumulus convection parameterization and numerical modelling of moist atmospheres p 3783 N94-31989
A model of the ion chemistry of electrified convection p 3868 N94-31993
Convection in Type 2 supernovae
[DE94-009373] p 3938 N94-32914
Operations summary for the convection and moisture experiment (CAMEX)
[NASA-TM-108445] p 3786 N94-33004
Characteristics of ion flow in the quiet state of the inner plasma sheet
[AD-A277451] p 3894 N94-33106

CONVECTION CURRENTS
Tropical squall lines p 3778 N94-30992

CONVECTION-DIFFUSION EQUATION
Viscous limiter functions for model convection-diffusion equations
[CRANFIELD-AERO-9103] p 3702 N94-31559
A stability estimate based on numerical ranges with application to a spectral discretization of a convection-diffusion equation
[TW-93-12] p 3847 N94-32200

CONVECTIVE FLOW
Effects of the deep tropical convection in the large scale atmospheric flow p 3778 N94-30994
Compressible convection with ionization p 3911 N94-31498
Steady thermal convection in multiple liquid layers p 3705 N94-31844

CONVECTIVE HEAT TRANSFER
Origin and thermal evolution of Mars p 3940 N94-31109
A tectonic resurfacing model for Venus p 3941 N94-31113
The resurfacing controversy for Venus: An overview and a mechanistic perspective p 3941 N94-31114
Plains tectonism on Venus: The deformation belts of Lavinia Planitia p 3941 N94-31115
Development of a three-dimensional icing model for predicting ice accretion on aircraft
[ONERA-NT-1993-5] p 3574 N94-31230
Thermocapillary convection in evaporating sessile drops
[NASA-TM-109758] p 3705 N94-31886
Heat transfer studies on a rectangular channel with offset plate fins
[AD-A277300] p 3912 N94-32043
Computational modeling of convective heat transfer to liquid hydrogen coolant p 3707 N94-32485

CONVENTIONS
Current policies of the major countries coping with the global warming problem and-the energy demand and supply
[DE94-757291] p 3769 N94-32920

CONVERGENCE
The generalized multi delay adaptive filter: Structure and convergence analysis
[TELECOM-93-D-004] p 3808 N94-31094
Stirling's formula and approximations for n(factorial) and the middle ratio
[REPT-93-73] p 3843 N94-31642
Solution of the average-passage equations for the incompressible flow through multiple-blade-row turbomachinery
[AD-A276515] p 3583 N94-31931
On the convergence of stochastic iterative dynamic programming
[AD-A276517] p 3815 N94-31933
On the relationship between generalization error, hypothesis complexity, and sample complexity for radial basis functions
[AD-A276802] p 3851 N94-32142
Numerical transport theory
[DE94-009064] p 3857 N94-32589
Measurement of ICF fuel ion temperature on Nova
[DE94-006150] p 3892 N94-32730
Convergence results for the EM approach to mixtures of experts architectures
[AD-A276801] p 3852 N94-33276

CONVERGENT-DIVERGENT NOZZLES
Simulation of low-density nozzle plumes in non-zero ambient pressures
[NASA-TM-106501] p 3615 N94-32742

CONVEXITY
A Gauss-Seidel type solver for special convex programs, with application to frictional contact mechanics
[REPT-93-77] p 3813 N94-31694

COOLANTS
Computational modeling of convective heat transfer to liquid hydrogen coolant p 3707 N94-32485

COOLERS
The 4 K Stirling cryocooler demonstration
[NASA-CR-191792] p 3669 N94-32484

COOLING
Heat transfer studies on a rectangular channel with offset plate fins
[AD-A277300] p 3912 N94-32043

Cooling and trapping of neutral atoms
[AD-A276957] p 3870 N94-32360
Characterization of thermally stable dye-doped polyimide based electrooptic materials
[DE94-005309] p 3882 N94-32674

COOLING FLOWS (ASTROPHYSICS)
Accretion disks around black holes
p 3928 N94-31117
Structure and stability of spherical accretion flows onto compact objects p 3935 N94-31946

COOLING SYSTEMS
A review of microclimate cooling systems in the chemical, biological, radiological environment
[AD-A276446] p 3802 N94-31302
Thermocapillary convection in evaporating sessile drops
[NASA-TM-109758] p 3705 N94-31886
The 4 K Stirling cryocooler demonstration
[NASA-CR-191792] p 3669 N94-32484

COORDINATES
Geometric structure of the adaptive controller of the human arm
[AD-A276797] p 3834 N94-32152

COORDINATION
Coordination of mesoscale meteorological research between ASL and European group
[AD-A276730] p 3784 N94-32162

COPOLYMERIZATION
Reactions of electrophilic maleic anhydride and epoxy groups with nucleophilic functionalities such as carboxyl, hydroxyl, and amine groups. Polymer Technology Publication series no. 16
[PB94-135589] p 3648 N94-31069

COPOLYMERS
Viscoelastic fracture characterization of polymeric solids p 3652 N94-31745
Isomeric poly(benzophenone)s: Synthesis of highly crystalline poly (4, 4 foot-benzophenone) and amorphous poly (2, 5-benzophenone), a soluble poly (p-phenylene) derivative
[AD-A277261] p 3655 N94-32017
Microstructure of copolymers containing disperse red 1 and methyl methacrylate
[AD-A277140] p 3660 N94-32722

COPPER
Reliability of multilayer copper/polyimide
[AD-A276228] p 3650 N94-31284
The influence of transmutation, void swelling, and flux/spectra uncertainties on the electrical properties of copper and copper alloys
[DE94-006213] p 3641 N94-31626
Aging effects on the microstructure, surface characteristics and wettability of Cu pretinned with Sn-Pb solders
[DE94-007033] p 3641 N94-31638
Oxidation resistant copper
[AD-D016099] p 3696 N94-32721
Induced adsorption of chloride and bromide by submonolayer amounts of copper underpotentially deposited on Pt(111)
[AD-A278023] p 3648 N94-33182

COPPER ALLOYS
The influence of transmutation, void swelling, and flux/spectra uncertainties on the electrical properties of copper and copper alloys
[DE94-006213] p 3641 N94-31626

COPPER COMPOUNDS
Gettering of metal impurities by cavities in silicon
[DE94-005248] p 3645 N94-32672
Strongly anisotropic s-wave versus d-wave gap in cuprate superconductors: Evidence and theory
[DE94-007579] p 3904 N94-32746
Indentability of conventional and negative Poisson's ratio foams p 3629 N94-33131

COPPER OXIDES
High T(sub c) superconductor tunnel junctions for photon detectors
[DE94-007686] p 3904 N94-32602
Investigation of superconductivity and magnetism in d and f-electron materials
[DE94-008535] p 3907 N94-32933
The path for long range conduction in high J(sub c) TlBa2Ca2Cu3O(8+x) spray-pyrolyzed deposits
[DE94-007211] p 3909 N94-33271

COPPER SELENIDES
Role of polycrystallinity in CdTe and CuInSe2 photovoltaic cells
[DE94-000293] p 3758 N94-31236
Development of a computer model for polycrystalline thin-film CuInSe2 and CdTe solar cells
[DE94-006853] p 3762 N94-32763

CORNEA
High peak power microwaves: A health hazard
[AD-A277168] p 3681 N94-32576
Noninvasive spectroscopic diagnosis of superficial ocular lesions and corneal infections
[DE94-006231] p 3797 N94-32732

CORNERS
Shock impingement near mild hypersonic expansion corners p 3569 N94-31879

CORONAL LOOPS
Theoretical studies of magnetohydrodynamic equilibria and dynamics of a solar coronal loop
p 3953 N94-31792

COROTATION
Disk instability and the spectral evolution of the 1992 outburst of the intermediate polar GK Persei
p 3928 N94-31123

CORRECTION
NOAA-9 Earth Radiation Budget Experiment (ERBE) scanner offsets determination
[NASA-TM-109086] p 3785 N94-32737

CORRELATION
Near resonant absorption by atoms in intense fluctuating laser fields
[DE94-005873] p 3714 N94-31200
Influence of long-range correlations on the spectral functions and response of 48Ca and 90Zr
[ETN-94-96017] p 3865 N94-31537
Correlations between micromagnetic, microstructural and microchemical properties in ultrathin epitaxial magnetic structures
[AD-A277200] p 3901 N94-32092
Conjugated polymer fluorescence: Interplay of correlations and alternation
[DE94-005587] p 3660 N94-32729
Spatial correlation of ionospheric variability
[AD-A278105] p 3776 N94-33041

CORRELATION COEFFICIENTS
Nonlinear model validation using correlation tests
[RR-463] p 3842 N94-31394

CORROSION
Development and characterization of intermediary layers allowing the bond between a metal alloy and a plasma sprayed ceramic
[ECL-91-39] p 3619 N94-31377
Dual-band infrared imaging to detect corrosion damage within airframes and concrete structures
[DE94-006047] p 3580 N94-32658
Characterization of the corrosion resistance of duplex stainless steels using local current density mapping techniques
[DE94-007980] p 3646 N94-32699
Nanoscale structural changes upon electrooxidation of Au(111) as probed by potentiodynamic scanning tunneling microscopy
[AD-A276780] p 3909 N94-33275

CORROSION PREVENTION
Evaluation of corrosion protective organic coatings for steel structures in fresh water
[PB94-138484] p 3649 N94-31072
Method and apparatus for inhibiting the disbonding of a paint from metal surfaces
[AD-D016106] p 3663 N94-32960
Evaluation of the Hughes conversion coating touch-up pen
[AD-A278398] p 3664 N94-33166

CORROSION RESISTANCE
Evaluation of corrosion protective organic coatings for steel structures in fresh water
[PB94-138484] p 3649 N94-31072
Study of type 2 and 3 anodized Al 5052-0 in aqueous DS2 solutions
[AD-A276960] p 3644 N94-32240
Robotic weld overlay coatings for erosion control
[DE94-008004] p 3658 N94-32408
Characterization of the corrosion resistance of duplex stainless steels using local current density mapping techniques
[DE94-007980] p 3646 N94-32699

CORROSION TESTS
Evaluation of corrosion protective organic coatings for steel structures in fresh water
[PB94-138484] p 3649 N94-31072
Study of type 2 and 3 anodized Al 5052-0 in aqueous DS2 solutions
[AD-A276960] p 3644 N94-32240
Characterization of the corrosion resistance of duplex stainless steels using local current density mapping techniques
[DE94-007980] p 3646 N94-32699

CORRUGATED PLATES
Vibrational and acoustic response of ribbed plates
p 3736 N94-31955

COSMIC DUST
Circumstellar material around young stars in Orion
p 3930 N94-31133
CO observations in external galaxies and gas mass determination p 3925 N94-31790

COSMIC GASES
CO observations in external galaxies and gas mass determination p 3925 N94-31790

COSMIC PLASMA
Laboratory and space experiments as a key to the plasma universe
[TRITA-ALP-1993-01] p 3885 N94-31088

COSMIC RAYS
Mitigation of adverse environmental effects on lunar-based astronomical instruments
p 3598 N94-31426
Nuclear physics and astrophysics
[DE94-007168] p 3939 N94-33147

COSMIC X RAYS
Stellar x ray polarimeter polarizer development and calibration at LEA/LLNL
[DE94-006400] p 3712 N94-31783

COSMOLOGY
Gravitational effects of cosmic strings
[ISBN-0-315-75484-2] p 3934 N94-31789

COST ANALYSIS
An analysis of non-integerizing the aircraft engines Cost Effectiveness Analysis Spreadsheet Model (CEAMOD version 2.0)
[AD-A276251] p 3583 N94-31290
Economic feasibility analysis of distributed electric power generation based upon the natural gas fired fuel cell
[DE94-005795] p 3759 N94-31487
Budget allocation and monopolistic pricing in a multiproduct firm
[REPT-93-86] p 3924 N94-31617
Design of a logistics model for building and supporting a lunar station
[ILR-MITT-282(1993)] p 3803 N94-31852
Prospects for the French fighter industry in a post-cold war environment: Is the future more than a mirage?
p 3565 N94-31959
Identification of research relating to the critical loads concept and its potential application to the regulation of acidic deposition
[DE94-008234] p 3767 N94-32752

COST EFFECTIVENESS
Initial estimates of Integrated Maintenance Information System (IMIS) costs and benefits, volume 1
[AD-A276144] p 3565 N94-31830
Design of a logistics model for building and supporting a lunar station
[ILR-MITT-282(1993)] p 3803 N94-31852
A PC program to optimize system configuration for desired reliability at minimum cost p 3823 N94-32438
A user's manual for the cost effectiveness analysis spreadsheet model for aircraft engines (CEAMOD version 2.0)
[AD-A278042] p 3585 N94-33266

COST ESTIMATES
Feasibility study for the recycling of nickel metal hydride electric vehicle batteries
[DE94-000268] p 3690 N94-31598

COST REDUCTION
Status of developing a multifunctional aviation grease
[AD-A276755] p 3656 N94-32184
Thin EFG octagons
[DE94-006855] p 3905 N94-32764
LLNL casting technology
[DE94-008282] p 3669 N94-32839
Innovative fabrication processing of advanced composite materials concepts for primary aircraft structures
[NASA-CR-189558] p 3626 N94-32877
Composite fuselage crown panel manufacturing technology p 3629 N94-33133
Leveraging metal matrix composites to reduce costs in space mechanisms p 3604 N94-33301

COSTS
Design, development, and testing of a lightweight optical sensor cover system p 3604 N94-33302

COULOMB POTENTIAL
Analytic properties of the OCP and ionic mixtures in the strongly coupled fluid state
[DE94-006216] p 3637 N94-32801

COULOMETRY
Employment of a porous gold actuator in ISFET-based coulometric sensor-actuator systems with application to protein characterization
[ISBN-9-09-005887-7] p 3689 N94-31536

COUNTERFLOW
Ignition studies in nonpremixed hydrogen/air combustion
[AD-A275954] p 3632 N94-31348

COUNTERS
Counting particles emitted by stratospheric aircraft and measuring size of particles emitted by stratospheric aircraft
[NASA-CR-195908] p 3769 N94-33170

COUPLING
Instrumentation for EXELFS measurements using convergent beam diffraction coupling to the electron energy loss spectrometer
[USIP-93-07] p 3858 N94-31084
COUPLINGS
Flexible drive shaft coupling
[AD-D016096] p 3727 N94-32718
COVALENCE
Rare Earth Doped Semiconductors and Materials Research Society Symposium Proceedings, Volume 301
[AD-A277517] p 3908 N94-33055
COVALENT BONDS
Rare Earth Doped Semiconductors and Materials Research Society Symposium Proceedings, Volume 301
[AD-A277517] p 3908 N94-33055
COVARIANCE
Line transects, covariance functions and set approximation
[CWI-BS-R9311] p 3846 N94-32084
Note on the variance of autospectral density processed using Welch's method
[DE94-005352] p 3849 N94-32675
Statistical intercomparison of global climate models: A common principal component approach
[DE94-008671] p 3768 N94-32882
COVERINGS
Design and performance of the telescope and detector covers on the Extreme Ultraviolet Explorer satellite
p 3605 N94-33309
CRACK GEOMETRY
Nonlinear effects in interfacial fracture
p 3737 N94-31974
CRACK INITIATION
Thermal-mechanical fatigue crack growth in aircraft engine materials
[ISBN-0-315-86543-1] p 3734 N94-31707
Viscoelastic fracture characterization of polymeric solids p 3652 N94-31745
Cracking induced in small fretting: Application to the case of aeronautical aluminum alloys
[ECL-92-50] p 3735 N94-31870
Fundamental studies in crack initiation
[AD-A278387] p 3741 N94-33356
CRACK OPENING DISPLACEMENT
Stage 1 behavior in a stress corrosion study of Type 304 stainless steel
[DE94-008054] p 3645 N94-32614
Compliance measurements of chevron notched four point bend specimen
[NASA-TM-106538] p 3740 N94-32932
Simpler J(sub Ic) test and data analysis procedures for high strength steels
[AD-A277731] p 3648 N94-33281
CRACK PROPAGATION
High temperature ductility loss in titanium alloys: A review
[DE94-006606] p 3640 N94-31345
Reliability analysis of structural ceramics subjected to biaxial flexure p 3650 N94-31454
Modeling of fracture and damage in quasibrittle materials p 3734 N94-31479
Multiple-site damage in aircraft fuselage structures
[LR-729] p 3578 N94-31675
Thermal-mechanical fatigue crack growth in aircraft engine materials
[ISBN-0-315-86543-1] p 3734 N94-31707
Viscoelastic fracture characterization of polymeric solids p 3652 N94-31745
Acoustic emission from crack growth in 7050 aluminum and 7075 aluminum as a function of temperature and heat treatment
[DREP-CRS-93-15] p 3642 N94-31871
Low velocity impact damage in carbon fiber/PEEK composite laminates
[ISBN-0-315-86546-6] p 3622 N94-31909
Fatigue crack propagation and fractography of 3Y-TZP and ZTA
[ISBN-0-315-86561-X] p 3736 N94-31912
A fracture mechanics methodology for characterizing the performance of flawed polymeric dielectric materials
p 3654 N94-31956
Effects of frequency and amplitude variations of superimposed minor loading sequences on the corrosion fatigue behavior of aircraft structural aluminum alloys
p 3578 N94-31957
Nonlinear effects in interfacial fracture
p 3737 N94-31974
Fracture mechanics and micromechanisms in fiber-reinforced composites p 3622 N94-31986
Fracture and fatigue strength evaluation of multiple site damaged aircraft fuselages - curved panel testing and analysis
[AD-A277100] p 3579 N94-32015
Effects of interphases on the mechanical, thermal and hygromechanical response of fiber-reinforced composites p 3624 N94-32496
The effect of ductile phase (Nb) reinforcement morphology on the mechanical behavior of an intermetallic matrix (MoSi2) p 3615 N94-32500
Mechanics of cracking for composite material
p 3624 N94-32501
Joining of silicon nitrides using oxynitride glasses
[DE94-008517] p 3658 N94-32517
Stage 1 behavior in a stress corrosion study of Type 304 stainless steel
[DE94-008054] p 3645 N94-32614
Fracture micromechanics of continuous fiber and textile reinforced metal and ceramic matrix composites
[AD-A277434] p 3627 N94-33008
Simpler J(sub Ic) test and data analysis procedures for high strength steels
[AD-A277731] p 3648 N94-33281
Fundamental studies in crack initiation
[AD-A278387] p 3741 N94-33356
CRACK TIPS
Viscoelastic fracture characterization of polymeric solids p 3652 N94-31745
Influences of pressure-sensitive yielding and non-singular stress on plane-stress elastic-plastic crack-tip fields p 3737 N94-31965
CRACKING (CHEMICAL ENGINEERING)
Studies of the fundamental nature of catalytic acidity, sites and intermediates
[DE94-006999] p 3646 N94-32805
CRACKING (FRACTURING)
The impact of LDEF results on the space application of metal matrix composites p 3595 N94-31034
Reliability analysis of structural ceramics subjected to biaxial flexure p 3650 N94-31454
Acceptance criteria for weld defects in aluminium weldments
[PB94-138575] p 3735 N94-31841
Toughening mechanisms in fiber-reinforced ceramic-matrix composites p 3622 N94-31943
Nonlinear effects in interfacial fracture
p 3737 N94-31974
Fracture mechanics and micromechanisms in fiber-reinforced composites p 3622 N94-31986
Prediction of hydrogen entry and permeation in metals and alloys
[AD-A276637] p 3642 N94-31995
Fatigue in single crystal nickel superalloys
[AD-A276662] p 3643 N94-32047
Finite element analysis of MB326H Macchi wing lower spar cap fatigue cracks
[AD-A277062] p 3580 N94-32264
The effect of ductile phase (Nb) reinforcement morphology on the mechanical behavior of an intermetallic matrix (MoSi2) p 3615 N94-32500
Mechanics of cracking for composite material
p 3624 N94-32501
Nonlocal theory for fracturing of quasibrittle materials
[AD-A278283] p 3740 N94-33143
Structural integrity of intelligent materials and structures
[AD-A278397] p 3630 N94-33165
A review of weldment failure modes and weldability testing methods
[AD-A278096] p 3729 N94-33251
CRACKS
Processing of novel nanoparticle dispersion strengthened ceramics for improved mechanical performance
[AD-A275965] p 3649 N94-31276
Multiple-site damage in aircraft fuselage structures
[LR-729] p 3578 N94-31675
Finite element analysis of MB326H Macchi wing lower spar cap fatigue cracks
[AD-A277062] p 3580 N94-32264
Compliance measurements of chevron notched four point bend specimen
[NASA-TM-106538] p 3740 N94-32932
CRASHES
Estimating the impact of crashworthiness standards on mortality and morbidity events in the US Army rotary-wing aircraft mishaps
[AD-A277121] p 3575 N94-32363
CRASHWORTHINESS
Estimating the impact of crashworthiness standards on mortality and morbidity events in the US Army rotary-wing aircraft mishaps
[AD-A277121] p 3575 N94-32363
Automatic contact in DYNA3D for vehicle crashworthiness
[DE94-007143] p 3738 N94-32637
CRATERING
Constraints on the Martian cratering rate imposed by the SNC meteorites and Vallis Marineris layered deposits p 3945 N94-33197
CRATERS
Morphology correlation of craters formed by hypervelocity impacts p 3594 N94-31031
Micrometeoroid/space debris effects on materials
p 3595 N94-31032
CRAY COMPUTERS
List ranking and list scan on the CRAY C-90
[AD-A276411] p 3824 N94-31259
Compiler techniques for managing data motion
[AD-A276514] p 3918 N94-31930
CREEP PROPERTIES
Effects of oxidation and creep damage mechanisms on creep behavior in HIPed silicon nitrides
[DE94-006559] p 3618 N94-31313
Viscoelastic fracture characterization of polymeric solids p 3652 N94-31745
Creep-fatigue criteria and inelastic behavior of modified 9Cr-1Mo steel at elevated temperatures
[DE94-007915] p 3642 N94-31918
High temperature materials technology research for advanced thermionic systems
[DE94-008444] p 3644 N94-32416
Joining of silicon nitrides using oxynitride glasses
[DE94-008517] p 3658 N94-32517
CREEP STRENGTH
Effects of oxidation and creep damage mechanisms on creep behavior in HIPed silicon nitrides
[DE94-006559] p 3618 N94-31313
Creep properties of vanadium-base alloys
[DE94-006541] p 3641 N94-31486
CREEP TESTS
Creep properties of vanadium-base alloys
[DE94-006541] p 3641 N94-31486
Creep-fatigue criteria and inelastic behavior of modified 9Cr-1Mo steel at elevated temperatures
[DE94-007915] p 3642 N94-31918
CRETACEOUS-TERTIARY BOUNDARY
Biospheric effects of a large extraterrestrial impact: Case study of the Cretaceous/Tertiary boundary crater
[NASA-CR-195827] p 3942 N94-32740
CRITICAL FREQUENCIES
Analysis of ionospheric parameters in Europe and creation of the prediction algorithm
[AD-A276342] p 3771 N94-31326
CRITICAL TEMPERATURE
High pressure experiments on the Y-Ba-Cu-O superconductors: A major role for holes
[ETN-94-96013] p 3897 N94-31547
CROP GROWTH
Rapid estimates of crop acreage and production at European scale using high resolution imagery
p 3754 N94-32557
Statistical analysis and mapping of cotton and food crop cultivation surfaces in the west of Burkina Faso: Contribution of combined SPOT P and XS data
p 3757 N94-32575
CROP IDENTIFICATION
Monitoring land cover and crop types in Denmark using ERS-1 SAR and optical satellite images
p 3748 N94-32528
Rapid estimates of crop acreage and production at European scale using high resolution imagery
p 3754 N94-32557
European MARS project: The potential integration of SPOT and air- and satellite-borne radar data over two pilot areas for agricultural statistics. PROSPER programme and ERS-1 pilot project
[BRGM-93035] p 3754 N94-32561
Evaluation of surface phase change on large zones
p 3755 N94-32567
CROP INVENTORIES
European MARS project: The potential integration of SPOT and air- and satellite-borne radar data over two pilot areas for agricultural statistics. PROSPER programme and ERS-1 pilot project
[BRGM-93035] p 3754 N94-32561
CROSS FLOW
The effect of an axial flow component on a circular cylinder wake p 3699 N94-31209
CROSS POLARIZATION
Mathematical nonlinear optics
[AD-A277320] p 3882 N94-32510
CROSSLINKING
Electrical communication between glucose oxidase and electrodes based on poly(vinylimidazole) complex of Os(bpy)2Cl2
[AD-A276585] p 3635 N94-32231
Stable second-order nonlinear optical materials based on interpenetrating polymer networks
[AD-A277410] p 3658 N94-32579
Characterization of crosslinked electrooptic polyimides
[DE94-007934] p 3661 N94-32819
A relaxation study of poled nonlinear optical polymers by infrared reflection-absorption spectroscopy
[AD-A277513] p 3663 N94-33054

Second-order nonlinear optical polymers: From fundamentals to applications
[AD-A277514] p 3664 N94-33348
CROSSTALK
III-V compound semiconductor strip-loaded waveguide devices for PICs: Design for minimum crosstalk and high density
[DE94-006588] p 3897 N94-31502
CRUCIBLES
Ultrahigh-current-density metal-ion implantation and diamondlike-hydrocarbon films for tribological applications
[DE94-008958] p 3906 N94-32843
CRUDE OIL
Emissions of greenhouse gases from the use of transportation fuels and electricity
[DE94-006166] p 3765 N94-31625
CRUSTAL FRACTURES
The basement fracture pattern of southern Ontario: A tectonic interpretation based on Landsat TM imagery, airphotos and field data
[ISBN-0-315-87086-9] p 3772 N94-31834
CRYOGENIC COOLING
The 4 K Stirling cryocooler demonstration
[NASA-CR-191792] p 3669 N94-32484
CRYOGENIC EQUIPMENT
Various magnet options for Delta launched version of ASTROMAG
[DE94-006292] p 3955 N94-31635
CRYOGENIC FLUID STORAGE
Aerospace test facilities at NASA LERC Plumbrook
[NASA-TM-109755] p 3602 N94-31814
CRYOGENIC TEMPERATURE
Structural damping studies at cryogenic temperatures
[NASA-TM-109073] p 3740 N94-33118
CRYOGENIC WIND TUNNELS
Structural damping studies at cryogenic temperatures
[NASA-TM-109073] p 3740 N94-33118
CRYOGENICS
Various magnet options for Delta launched version of ASTROMAG
[DE94-006292] p 3955 N94-31635
Controlling hazardous energy sources (lockout/tagout)
[NASA-TM-105290] p 3669 N94-32861
CRYOPUMPING
Divertor pumping and other reactor application issues for H-mode
[DE94-007431] p 3892 N94-32810
CRYOSTATS
Various magnet options for Delta launched version of ASTROMAG
[DE94-006292] p 3955 N94-31635
CRYPTOGRAPHY
PEM public key certificate cache server
[DE94-006404] p 3675 N94-31784
The trustworthy digital camera: Restoring credibility to the photographic image p 3714 N94-32470
CRYSTAL DEFECTS
The 10th International Conference on Internal Friction and Ultrasonic Attenuation in Solids (ICIFUAS)
[AD-A276849] p 3902 N94-32209
Defect cascades produced by neutron irradiation in YBa2Cu3O(7-delta) superconductors
[DE94-007700] p 3903 N94-32372
A scanning defect mapping system for semiconductor characterization p 3885 N94-32446
Microanalytical study of defect formation in thin bismuth strontium calcium copper oxide films
[DE94-008217] p 3661 N94-32751
The path for long range conduction in high J(sub c) TlBa2Ca2Cu3O(8+x) spray-pyrolyzed deposits
[DE94-007211] p 3909 N94-33271
CRYSTAL DISLOCATIONS
Attempts to model the generation of new grain boundaries during the deformation of polycrystals
[DE94-007527] p 3903 N94-32597
Structure, stability, and mechanical properties of intermetallic phases
[DE94-009178] p 3647 N94-32852
CRYSTAL GROWTH
Electrooptic crystal growth and properties
[AD-A276023] p 3896 N94-31439
Characterization and growth mechanisms of the MgAl2O4 phase in Al2O3-reinforced Al-Mg composites
[ISBN-0-315-86531-8] p 3620 N94-31706
In-situ characterization of growth and interfaces in a-Si:H devices
[DE94-000291] p 3760 N94-31812
Thermocapillary convection in evaporating sessile drops
[NASA-TM-109758] p 3705 N94-31886
Chemical vapor deposition of metal nitrides, phosphides, and arsenides
[DE94-008096] p 3654 N94-31976
Oriented Si and Ge nanocrystals formed in Al2O3 by ion implantation and annealing
[DE94-005593] p 3901 N94-32172
Materials processing and manufacturing technologies for diamond substrates multichip modules
[AD-A276904] p 3692 N94-32215
Femtosecond probe-probe transmission studies of LT-grown GaAs near the band edge
[DE94-006660] p 3904 N94-32634
Thin EFG octagons
[DE94-008855] p 3905 N94-32764
Nucleation and growth of cubic boron nitride films produced by ion-assisted pulsed laser deposition
[DE94-007295] p 3661 N94-32796
Development of materials for spectral hole burning applications
[AD-A278408] p 3909 N94-33324
Novel precursor approached for CMC derived by polymer pyrolysis
[AD-A278383] p 3665 N94-33352
CRYSTAL LATTICES
Experimental evidence for lattice effects in high temperature superconductors
[DE94-006250] p 3899 N94-31633
CRYSTAL OPTICS
A noncritically phase matched femtosecond optical parametric oscillator near 3 microns
[DE94-008050] p 3720 N94-32704
CRYSTAL STRUCTURE
Experimental and theoretical studies of hydrogenated amorphous semiconductor alloys and superlattices
[AD-A276159] p 3686 N94-31079
Silicone grease as a precursor to a pseudo crown-ether ligand: Crystal structure of (K(+)K(Me2SiO)7(+)) (Hln(CH2CMe3)3(-))4)
[AD-A276343] p 3895 N94-31327
Incoherent imaging by Z-contrast stem: Towards 1 Angstrom resolution
[DE94-006551] p 3896 N94-31489
Experimental evidence for lattice effects in high temperature superconductors
[DE94-006250] p 3899 N94-31633
The effects of amorphous layer regrowth on carbon activation in GaAs and InP
[DE94-006290] p 3899 N94-31634
Practical neutron training course: Course notes
[PB94-145158] p 3867 N94-31681
Optimization of the forming parameters of PEEK/carbon fiber composite
[ISBN-0-315-86410-9] p 3620 N94-31716
Anomalous small angle x ray scattering studies of amorphous metal-germanium alloys
[DE94-007258] p 3900 N94-32065
The new Metals and Alloys Indexes, search manual: A phase diagram research tool
[DE94-005371] p 3643 N94-32098
SUNY beamline facilities at the National Synchrotron Light Source
[DE94-006343] p 3905 N94-32770
Properties of doped and undoped (Ca,Sr)CuO2 thin films
[DE94-007230] p 3905 N94-32785
Evidence for symmetry breaking local distortions in thallium barium copper oxide
[DE94-006149] p 3907 N94-32944
Low energy ion beam assisted growth of homoepitaxial silicon films at low temperature
[AD-A278092] p 3908 N94-33039
CRYSTAL SURFACES
Characterization and growth mechanisms of the MgAl2O4 phase in Al2O3-reinforced Al-Mg composites
[ISBN-0-315-86531-8] p 3620 N94-31706
CRYSTALLINITY
Experimental and theoretical studies of hydrogenated amorphous semiconductor alloys and superlattices
[AD-A276159] p 3686 N94-31079
Azo polymers for reversible optical storage. 4. Cooperative motion of rigid groups in semicrystalline polymers
[AD-A277107] p 3654 N94-31978
Isomeric poly(benzophenone)s: Synthesis of highly crystalline poly (4, 4 foot-benzophenone) and amorphous poly (2, 5-benzophenone), a soluble poly (p-phenylene) derivative
[AD-A277261] p 3655 N94-32017
The charging effect in high-Tc superconducting thin films
[AD-A277265] p 3900 N94-32040
Amorphous/crystalline structure and phase transformations in metastable semiconducting Ge(1-x)Sn(x)
[DE94-006659] p 3901 N94-32115
CRYSTALLIZATION
Solidification structure synthesis in undercooled liquids
[AD-A276166] p 3910 N94-31054
Silicone grease as a precursor to a pseudo crown-ether ligand: Crystal structure of (K(+)K(Me2SiO)7(+)) (Hln(CH2CMe3)3(-))4)
[AD-A276343] p 3895 N94-31327
Competition between crystallization and mixing/demixing in polymer mixture
[ETN-94-95753] p 3651 N94-31513
Optimization of the forming parameters of PEEK/carbon fiber composite
[ISBN-0-315-86410-9] p 3620 N94-31716
In-situ TEM crystallization of anorthite-glass films on (alpha)-Al2O3
[DE94-006317] p 3652 N94-31780
Strongly coupled ionic mixtures and the H/He EOS
[DE94-006391] p 3934 N94-31782
Amorphous/crystalline structure and phase transformations in metastable semiconducting Ge(1-x)Sn(x)
[DE94-006659] p 3901 N94-32115
CRYSTALLOGRAPHY
Charge-dependent atomic-scale structures of high-index and (110) gold electrode surfaces as revealed by scanning tunneling microscopy
[AD-A276782] p 3869 N94-32170
SUNY beamline facilities at the National Synchrotron Light Source
[DE94-006343] p 3905 N94-32770
Microreflectance infrared study of electron-molecular vibrational coupling and lattice softness in BEDT-TTF salts
[DE94-008490] p 3907 N94-32989
Sensitivity of electrochemical adlayer structure to the metal crystallographic orientation: Potential-independent iodide adsorption on Au(100) in comparison with other low-index surfaces
[AD-A276714] p 3909 N94-33273
CRYSTALS
Stellar x ray polarimeter polarizer development and calibration at LEA/LLNL
[DE94-006400] p 3712 N94-31783
Metal clusters: Dynamics and structure
[AD-A276842] p 3643 N94-32091
On the nature of striae in strontium barium niobate
[DE94-006486] p 3901 N94-32176
The Los Alamos National Laboratory precision double crystal spectrometer
[DE94-008075] p 3713 N94-32706
CUBES (MATHEMATICS)
Least squares approximation by G1 piecewise parametric cubes
[AD-A277978] p 3850 N94-33265
CUES
Modular Simulator System (MSS). System/segment specification for the generic modular simulator system-physical cues module, volume 10
[AD-A276977] p 3589 N94-32316
CUMULUS CLOUDS
Boundary-layer cumulus over land: Some observations and conceptual models
[DE93-040820] p 3781 N94-31597
Numerical simulations of monsoon rainfall with the NRL/NCSU regional nestsd grid model p 3782 N94-31791
Cumulus convection parameterization and numerical modelling of moist atmospheres p 3783 N94-31989
CURIE TEMPERATURE
Piezoelectric materials research in Europe
[AD-A276207] p 3648 N94-31059
CURING
Intramolecular charge transfer complexes as fluorescence probes for UV and visible light induced acrylate polymerization
[AD-A277129] p 3657 N94-32381
CURRENT DENSITY
Noninductive current drive experiments on D3-D, and future plans
[DE94-007373] p 3886 N94-31324
CURRENT DISTRIBUTION
Noninductive current drive experiments on D3-D, and future plans
[DE94-007373] p 3886 N94-31324
The form factors of the nucleons
[DE94-007096] p 3872 N94-32630
Multicast communication with guaranteed quality of service
[AD-A277650] p 3682 N94-33025
CURVED PANELS
Fracture and fatigue strength evaluation of multiple site damaged aircraft fuselages - curved panel testing and analysis
[AD-A277100] p 3579 N94-32015
Innovative fabrication processing of advanced composite materials concepts for primary aircraft structures
[NASA-CR-189558] p 3626 N94-32877

CURVES (GEOMETRY)
Least squares approximation by G1 piecewise parametric cubes
[AD-A277978] p 3850 N94-33265
CYANIDES
Time-resolved infrared absorption studies applied to the study of radical plus molecule reactions
[DE94-005921] p 3863 N94-31202
Infrared spectroelectrochemical study of cyanide adsorption and reactions at platinum electrodes in aqueous perchlorate electrolyte
[AD-A276402] p 3631 N94-31238
Scanning tunneling microscopy and infrared spectroscopy as combined in-situ probes of electrochemical adlayer structure: Cyanide on Pt(111)
[AD-A276715] p 3909 N94-33274
CYANO COMPOUNDS
Time-resolved infrared absorption studies applied to the study of radical plus molecule reactions
[DE94-005921] p 3863 N94-31202
CYCLIC COMPOUNDS
Metal ion complexation by ionizable crown ethers
[DE94-008301] p 3661 N94-32847
CYCLIC HYDROCARBONS
Electronic and nuclear factors in intramolecular charge and excitation transfer processes
[DE94-006598] p 3870 N94-32178
High-energy chemical processes: Laser irradiation of aromatic hydrocarbons
[DE94-008107] p 3720 N94-32707
CYCLIC LOADS
Effects of frequency and amplitude variations of superimposed minor loading sequences on the corrosion fatigue behavior of aircraft structural aluminum alloys
p 3578 N94-31957
The cyclic fatigue behaviour of adhesive joints
[AD-A277080] p 3738 N94-32351
Effect of elevated temperature and cyclic loading on properties and damage modes in ceramic composites
[DE94-008736] p 3662 N94-32891
CYCLOGENESIS
The influence of cumulus parameterization on model forecasts of rapid oceanic cyclogenesis
[AD-A277207] p 3784 N94-32094
CYCLOHEXANE
Photopolymerization of cyclohexene oxide: A visible light initiating system and mechanistic investigations
[AD-A277110] p 3654 N94-31981
CYCLONES
Short term teleconnections associated with an individual tropical cyclone
[AD-A277210] p 3783 N94-32019
Recurvature dynamics of a typhoon
[AD-A276792] p 3784 N94-32164
Tropical cyclone forecasters reference guide. 5: Numerical track forecast guidance
[AD-A277318] p 3785 N94-32278
Forecasters handbook for the Philippine Islands and surrounding waters
[AD-A277993] p 3787 N94-33089
CYCLOTRON RADIATION
Noninductive current drive experiments on D3-D, and future plans
[DE94-007373] p 3886 N94-31324
Electron cyclotron resonance plasma oxidation studies of InP
[AD-A277431] p 3893 N94-33007
CYCLOTRON RESONANCE
Electron cyclotron resonance plasma oxidation studies of InP
[AD-A277431] p 3893 N94-33007
CYCLOTRON RESONANCE DEVICES
Fusion applications of high power millimeter wave sources
[DE94-007374] p 3718 N94-32202
Gyrotrons and free electron lasers for atmospheric sensing
[AD-A277281] p 3718 N94-32406
CYLINDRICAL BODIES
An efficient three-dimensional Poisson solver for SIMD high-performance-computing architectures
p 3823 N94-31120
Scattering of a random acoustic field by an infinite cylinder: Application to the modelization of the acoustic environment of the 'Ariane 5' launcher scale-model using experimental data
[ONERA-NT-1993-11] p 3860 N94-31226
Small cylindrical adhesive bonds
[PB94-148210] p 3651 N94-31585
A thermal viscoelastic analysis for thick-walled composite cylinders
[AD-A274143] p 3625 N94-32604
CYLINDRICAL SHELLS
Deformation and rupture of cylindrical shells under dynamic loading p 3733 N94-31288
Tearing resistance of a thin shell against projectile penetration: Material property effects
[DE94-007466] p 3733 N94-31316
CZOCHRALSKI METHOD
On the nature of striae in strontium barium niobate
[DE94-006486] p 3901 N94-32176

D

DAMAGE
A laboratory study of multiple site damage in fuselage lap splices
[AD-A276151] p 3578 N94-31078
Vibration control and design of composite cantilevers taking into account structural uncertainties and damage
p 3733 N94-31213
Modeling of fracture and damage in quasibrittle materials p 3734 N94-31479
Engineering of damage in ion implanted silicon
[ISBN-9-09-005097-3] p 3897 N94-31521
Methodology for damage study of a tube-grill contact
[ECL-92-49] p 3734 N94-31562
Damage tolerance aspects of a full composite airplane fuselage: Requirements, modelling, predictions, experiments
[LR-728] p 3578 N94-31674
Multiple-site damage in aircraft fuselage structures
[LR-729] p 3578 N94-31675
Finite element analysis of damage in fibrous composites using a micromechanical model
[AD-A277226] p 3623 N94-32024
Dual-band infrared imaging to detect corrosion damage within airframes and concrete structures
[DE94-006047] p 3580 N94-32658
Effect of elevated temperature and cyclic loading on properties and damage modes in ceramic composites
[DE94-008736] p 3662 N94-32891
Comparison of resin film infusion, resin transfer molding, and consolidation of textile preforms for primary aircraft structure p 3630 N94-33136
DAMAGE ASSESSMENT
Low-Earth orbit effects on organic composite materials flown on LDEF p 3595 N94-31036
Summary of materials and hardware performance on LDEF p 3595 N94-31037
Methodology for damage study of a tube-grill contact
[ECL-92-49] p 3734 N94-31562
Evaluation of Fluorescence Line Imager (FLI) airborne imaging spectrometer data for roadside tree damage assessment p 3745 N94-31866
Ultrasonic characterization of damage in a simulated CF-18 composite structure
[DREP-LN-93-26] p 3730 N94-31872
Computer modelling of cyclic deformation of high-temperature materials
[AD-A277056] p 3623 N94-32012
Assessment of impact damage in composite structures
[AD-A277063] p 3624 N94-32265
Remote sensing for hurricane Andrew impact assessment p 3758 N94-32464
Feasibility in the use of satellite remote sensing data as a fast reaction tool for natural disaster relief
p 3748 N94-32526
Automatic contact in DYNA3D for vehicle crashworthiness
[DE94-007143] p 3738 N94-32637
Fundamental studies in crack initiation
[AD-A278387] p 3741 N94-33356
DAMPING
Chaotic attitude motion of satellites in the central gravitational field
[ISBN-0-315-78768-6] p 3610 N94-31723
Attitude dynamics of spinning rockets in space with internal mass motion p 3601 N94-31802
Mass-loaded coating for reducing the resonant frequency of a ceramic disc
[AD-D016095] p 3660 N94-32739
Interpenetrating polymer network acoustic damping material
[AD-D016141] p 3663 N94-32975
Deployable and retractable telescoping tubular structure development p 3607 N94-33317
DASSAULT AIRCRAFT
Prospects for the French fighter industry in a post-cold war environment: Is the future more than a mirage?
p 3565 N94-31959
DATA ACQUISITION
A generic model for data acquisition: Connectionist methods of information processing
[TELECOM-93-E-003] p 3730 N94-31166
Ground based radiometric and atmospheric measurements p 3744 N94-31855
Recommendations for meteorological data collection during physiological field studies
[AD-A276834] p 3901 N94-32153
Spacecraft On-Board Information Extraction Computer (SOBIEC) p 3808 N94-32433
Pen-based computers: Computers without keys
p 3808 N94-32434
Using the National Information Infrastructure for social science, education, and informed decision making
[DE94-005442] p 3920 N94-32676
A miniaturized ASIC-based multichannel scaler instrument
[DE94-007222] p 3807 N94-32783
Preliminary evaluation of the University of South Florida Mobile Data Acquisition System, the Idaho National Engineering Laboratory Versatile Data Acquisition System, and the Autologger Vehicle User Survey System produced by Instrumental Solutions of Ottawa, Canada for the Site Operator Program Field Data Collection
[DE94-008514] p 3920 N94-32827
A flexible IBM-PC based data acquisition system for nuclear physics experiments
[USIP-92-02] p 3922 N94-32856
Accelerated reliability testing utilizing design of experiments
[AD-A277989] p 3732 N94-33088
Statistical characteristics of bistatic surface scatter and mean bistatic surface scattering strengths
[AD-A278155] p 3862 N94-33096
Performance statistics bulletin. High latitude meteor scatter propagation, June, July, August, September 1992
[AD-A277508] p 3685 N94-33347
DATA BASE MANAGEMENT SYSTEMS
LDEF materials special investigation group's data bases p 3596 N94-31038
Transformation of database populations and operations from the conceptual to the internal level
[TR-92-27] p 3916 N94-31175
Report on implementing part relationships using VML metaclasses
[PB94-147485] p 3813 N94-31686
The advent of failure analysis software technology
[DE94-006593] p 3692 N94-32111
CMS Distribution Subsystem user's guide
[DE94-005328] p 3816 N94-32146
Atomic and molecular data needs for fusion
[DE94-006555] p 3870 N94-32177
Moving BASISplus and TECHLIBplus from VAX/VMS to UNIX
[DE94-004696] p 3826 N94-32248
The intelligent monitoring system: Generic Database Interface (GDI). Revised user manual
[AD-A277131] p 3919 N94-32382
An intelligent interactive visual database management system for Space Shuttle closeout image management
p 3923 N94-32469
A simulation of uncertain reasoning on parametric databases using data-dependency derived inference nets p 3919 N94-32499
Managing performance of DB2 Ad Hoc Reports
[DE94-006669] p 3920 N94-32635
Developing a personal-computer-based records retention system using Paradox(tm)
[DE94-007984] p 3819 N94-32749
The hypermedia technology as front end to knowledge processing systems p 3854 N94-33343
DATA BASES
LDEF materials special investigation group's data bases p 3596 N94-31038
Databases and demands for solar heating materials
[PB94-137494] p 3758 N94-31070
Transformation of database populations and operations from the conceptual to the internal level
[TR-92-27] p 3916 N94-31175
A probabilistic view of Datalog parallelization
[TELECOM-93-D-021] p 3824 N94-31183
The meaning of duplicates in the relational database model
[CT-93-04] p 3916 N94-31392
The Global Climatology Network precipitation data
[DE93-019199] p 3764 N94-31596
Hydrologic Database user's manual
[DE94-003950] p 3743 N94-31603
Current Research Information in Europe: Conference proceedings
[PB94-127933] p 3917 N94-31768
Texture library for 3-dimensional visualization systems
[AD-A276125] p 3917 N94-31829
Systems for the monitoring of working conditions relating to health and safety: Extensive description. Norway
[PB94-138542] p 3803 N94-31839
Shiptrack database analysis
[AD-A277226] p 3746 N94-32025
Experiences with EDO: An Evolutionary Database Optimizer
[TR-93-23] p 3918 N94-32105

Coordination of mesoscale meteorological research between ASL and European group
[AD-A276730] p 3784 N94-32162
EVORM: A conceptual modelling technique for evolving application domains
[TR-93-16] p 3918 N94-32290
Fiber optic chemical sensors
[AD-A277128] p 3881 N94-32380
The intelligent monitoring system: Generic Database Interface (GDI). Revised user manual
[AD-A277131] p 3919 N94-32382
Analytical Design Package (ADP2): A computer aided engineering tool for aircraft transparency design
p 3823 N94-32430
High-speed data search p 3923 N94-32441
Database tomography for commercial application
p 3923 N94-32442
Mapping analysis and planning system for the John F. Kennedy Space Center p 3757 N94-32463
Space flight risk data collection and analysis project: Risk and reliability database
[NASA-CR-195879] p 3603 N94-32494
Using the National Information Infrastructure for social science, education, and informed decision making
[DE94-005442] p 3920 N94-32676
Preliminary evaluation of the University of South Florida Mobile Data Acquisition System, the Idaho National Engineering Laboratory Versatile Data Acquisition System, and the Autologger Vehicle User Survey System produced by Instrumental Solutions of Ottawa, Canada for the Site Operator Program Field Data Collection
[DE94-008514] p 3920 N94-32827
MDFF HELP library, version 2: On-line documentation for the map data formatting facility
[AD-A277763] p 3922 N94-32987
Briefing and review meeting implementation of the military handbook 17 for polymer matrix and metal matrix composites
[AD-A277446] p 3663 N94-33010
COINS: A composites information database system
p 3627 N94-33123
DTIC Thesaurus on diskette with dBase 4.1 runtime (computer diskette)
[AD-M000306] p 3922 N94-33256
DTIC Thesaurus on diskette without runtime (computer diskette)
[AD-M000310] p 3923 N94-33258
DTIC Thesaurus on diskette without runtime (computer diskette)
[AD-M000312] p 3923 N94-33259
A new method for calculating wing along aerodynamics to angle of attack 180 deg
[AD-A277965] p 3574 N94-33263
Performance statistics bulletin. High latitude meteor scatter propagation, June, July, August, September 1992
[AD-A277508] p 3685 N94-33347

DATA COMPRESSION

Regular wavelets: Application to fixed image compression
[TELECOM-93-E-004] p 3858 N94-31167
Texture library for 3-dimensional visualization systems
[AD-A276125] p 3917 N94-31829
Applications of data compression to 3-D scalar field visualization p 3817 N94-32294
Neural network wavelet technology: A frontier of automation p 3839 N94-32425
MDFF HELP library, version 2: On-line documentation for the map data formatting facility
[AD-A277763] p 3922 N94-32987
Data processing algorithms for on-board satellite event analysis
[AD-A278406] p 3838 N94-33168

DATA CONVERSION ROUTINES

System for monitoring and analyzing field energy exposure
[AD-D016115] p 3681 N94-32625

DATA CORRELATION

Alternatives to hierarchical techniques in stereo correlation
[AD-A276570] p 3746 N94-31938

DATA FLOW ANALYSIS

An analysis of instruction-cached SIMD computer architecture
[AD-A276519] p 3806 N94-31934
Automated detection of ship tracks in multispectral satellite data
[AD-A276697] p 3746 N94-32119
Assessing the vulnerability of multi-commodity networks with failing components
[AD-A278434] p 3684 N94-33334

DATA INTEGRATION

Information acquisition from multi-agent resources; abstract
[LP-93-08] p 3917 N94-31452
Fusion of multispectral (XS) and Panchromatic (P) SPOT images and radar images p 3750 N94-32541

DATA LINKS

Study of structures of different complexity for the communication between two processors
[ETN-94-95750] p 3674 N94-31615
High frequence and automatic link establishment (HF and ALE) radio propagation test to Antarctica
[AD-A277730] p 3682 N94-33001
An analysis of cellular telephone and INMARSAT systems for providing radio data link computer communications for US Navy vessels
[AD-A278143] p 3684 N94-33160

DATA MANAGEMENT

Model borne data management system for wind tunnel testing, phase 2
[AD-A276296] p 3587 N94-31295
CMS Preprocessing Subsystem user's guide: Software version 2.0
[DE94-005327] p 3816 N94-32145
Atomic and molecular data needs for fusion
[DE94-006555] p 3870 N94-32177
Untying the gordian data knot. A paper on Information Engineering (IE) and Corporate Information Management (CIM)
[AD-A276862] p 3918 N94-32210
An algorithm for probabilistic, totally-ordered temporal projection
[AD-A277341] p 3817 N94-32257
Description of DCS (Data Converting System) and CT (Cone Tool). A reprint of a note published in Fire and Materials titled Fire Test Data Available for Your Purpose
[PB94-138559] p 3918 N94-32293
The intelligent monitoring system: Generic Database Interface (GDI). Revised user manual
[AD-A277131] p 3919 N94-32382
Automated mainframe data collection in a network environment p 3923 N94-32443

DATA PROCESSING

Radar measurements p 3685 N94-31002
Filtering of satellite altimetry data with optimal smoothing cubic splines to compute geoid heights, along-tract geoid and gravity gradients in the Indonesian waters and its surroundings
[PB94-147527] p 3741 N94-31074
Summary of some data processing routines in the molecular physics group of Stockholm University
[USIP-93-05] p 3808 N94-31087
Entropy, information (and image), part 1
[TELECOM-93-D-009] p 3910 N94-31098
First-wall heat-flux measurements during ELMing H-mode plasma
[DE94-008310] p 3888 N94-31765
The European Imaging Spectroscopy Airborne Campaign (EISAC). Data takes and evaluation programme: An overview p 3743 N94-31854
Noninvasive spectral analysis and beam mapping of focused ultrasound, part 2
[AD-A276629] p 3861 N94-32059
CMS Preprocessing Subsystem user's guide: Software version 2.0
[DE94-005327] p 3816 N94-32145
MULTIGRAPH: An architecture for model-based programming. Model-based program synthesis for parallel computing. PREMOS: Programming environment for model-based program synthesis, version 01.00.00
[AD-A276949] p 3817 N94-32219
Self-consistent effects of magnetospheric hydromagnetic waves on ring current ions
[AD-A277406] p 3774 N94-32346
Spacecraft On-Board Information Extraction Computer (SOBIEC) p 3808 N94-32433
Note on the variance of autospectral density processed using Welch's method
[DE94-005352] p 3849 N94-32675
MDFF HELP library, version 2: On-line documentation for the map data formatting facility
[AD-A277763] p 3922 N94-32987
Earth observational research using multistage EOS-like data
[NASA-CR-195833] p 3757 N94-33019
Fine and microstructure observations at Fieberlin g Guyot R/V new horizon cruise report
[AD-A277917] p 3791 N94-33109
Cruise report: Oceanus 250 leg 4 high resolution profiler survey for the North Atlantic Tracer Release Experiment, 25 March - 24 April, 1992
[AD-A277935] p 3791 N94-33245

DATA PROCESSING EQUIPMENT

A flexible IBM-PC based data acquisition system for nuclear physics experiments
[USIP-92-02] p 3922 N94-32856

DATA RECORDING

Model borne data management system for wind tunnel testing, phase 2
[AD-A276296] p 3587 N94-31295

DATA REDUCTION

Multiple regression and measurement errors: Relative efficiency of two models, the standard model and Fuller's model, for estimating structural relationships
[ISBN-0-315-86834-1] p 3845 N94-31755
A critical assessment of UH-60 main rotor blade airfoil data
[NASA-TM-103985] p 3571 N94-32063
Automated detection of ship tracks in multispectral satellite data
[AD-A276697] p 3746 N94-32119
BATSE data analysis
[NASA-CR-195818] p 3927 N94-32942
Analysis of data from the plasma composition experiment on the International Sun-Earth Explorer (ISEE 1)
[NASA-CR-195880] p 3893 N94-33074
Data processing algorithms for on-board satellite event analysis
[AD-A278406] p 3838 N94-33168

DATA RETRIEVAL

Automated mainframe data collection in a network environment p 3923 N94-32443

DATA SAMPLING

Application of radon transformation for improved analysis of sparsely sampled data: A feasibility study
[PB94-147535] p 3741 N94-31075

DATA STORAGE

Compiler techniques for managing data motion
[AD-A276514] p 3918 N94-31930
A redundant disk array architecture for efficient small writes
[AD-A276645] p 3815 N94-31940
An MS-DOS file system for UNIX
[AD-A276523] p 3816 N94-32081
Using TSAR with the post-processing far-field option
[DE94-006615] p 3679 N94-32188
Toroidal computer memory for serial and parallel processors
[AD-D016144] p 3807 N94-32978
DTIC Thesaurus on diskette (ASC2) (computer diskette)
[AD-M000309] p 3922 N94-33257

DATA STRUCTURES

Transformation of database populations and operations from the conceptual to the internal level
[TR-92-27] p 3916 N94-31175
Detecting the erosion of hierarchic information structures
[RUU-CS-93-10] p 3916 N94-31365
The meaning of duplicates in the relational database model
[CT-93-04] p 3916 N94-31392
Extension of the LUSTRE language and application to circuit design: The LUSTRE V4 language and the POLLUX system
[ETN-94-95918] p 3812 N94-31543
Report on implementing part relationships using VML metaclasses
[PB94-147485] p 3813 N94-31688
An MS-DOS file system for UNIX
[AD-A276523] p 3816 N94-32081

DATA SYSTEMS

CMS Preprocessing Subsystem user's guide: Software version 2.0
[DE94-005327] p 3816 N94-32145
CMS Distribution Subsystem user's guide
[DE94-005328] p 3816 N94-32146
Untying the gordian data knot. A paper on Information Engineering (IE) and Corporate Information Management (CIM)
[AD-A276862] p 3918 N94-32210
High-speed data search p 3923 N94-32441

DATA TRANSFER (COMPUTERS)

Sandia's research network for Supercomputing 1993: A demonstration of advanced technologies for building high-performance networks
[DE94-005319] p 3823 N94-31149
The FELICIA bulletin board system and the IRBIS anonymous FTP server: Computer security information sources for the DOE community
[DE94-008219] p 3825 N94-31920
Compiler techniques for managing data motion
[AD-A276514] p 3918 N94-31930
An MS-DOS file system for UNIX
[AD-A276523] p 3816 N94-32081
Description of DCS (Data Converting System) and CT (Cone Tool). A reprint of a note published in Fire and Materials titled Fire Test Data Available for Your Purpose
[PB94-138559] p 3918 N94-32293
Communication networks for autonomous mobile robot computer architectures and distributed real-time computing p 3680 N94-32310
IRIG J asynchronous ASCII time code formats
[AD-A277244] p 3681 N94-32332

Automated mainframe data collection in a network environment p 3923 N94-32443

DATA TRANSMISSION

Channel equalization for block transmission systems [TELECOM-93-D-002] p 3670 N94-31093

Towards simplicity: Noise and cooperation in the perfect integrator [AD-A276256] p 3799 N94-31291

Communications networks in stressed environments [AD-A275967] p 3672 N94-31384

Development of a low-latency scalar communication routine on message-passing architectures [DE94-007061] p 3827 N94-32683

COVICS: A covert video communications system [DE94-007568] p 3682 N94-32745

Long distance transmission of 15 Gb/s digital using subcarrier multiplexing and external modulation [DE94-008298] p 3682 N94-32756

DAYGLOW

An analysis of ionospheric dayglow from observations of the Naval Postgraduate School Middle Ultraviolet Spectrograph (MUSTANG) [AD-A277351] p 3773 N94-32335

DE HAVILLAND AIRCRAFT

Shearographic inspection of a DeHavilland DHC-7 [AD-A276716] p 3566 N94-32157

DEACTIVATION

The development of precipitated iron catalysts with improved stability [DE94-008711] p 3638 N94-32886

DEBONDING (MATERIALS)

Fracture mechanics and micromechanisms in fiber-reinforced composites p 3622 N94-31986

Mechanics of failure of high temperature metal matrix composites [AD-A277397] p 3624 N94-32342

DEBRIS

Using Monte Carlo techniques and parallel processing for debris hazard analysis of rocket systems [DE94-007250] p 3609 N94-31382

DECISION MAKING

An analysis of non-integerizing the aircraft engines Cost Effectiveness Analysis Spreadsheet Model (CEAMOD version 2.0) [AD-A276251] p 3583 N94-31290

An active computer supported medium for distributed planning in enterprises [ETN-94-95738] p 3829 N94-31372

Pairwise-comparison using the logarithmic least squares method and the generalized pseudoinverse [REPT-93-84] p 3844 N94-31701

Control of a random walk with noisy delayed information [CWI-BS-R9316] p 3846 N94-32108

New approaches for real time decision support systems p 3915 N94-32426

Knowledge-based commodity distribution planning p 3915 N94-32427

The limits of intelligence in design [DE94-004668] p 3819 N94-32668

Using the National Information Infrastructure for social science, education, and informed decision making [DE94-005442] p 3920 N94-32676

Ethics and rationality in information-enriched decisions: A model for technical communication [DE93-040251] p 3681 N94-32679

Selection criteria and facilitation training for the study of groupware [NASA-CR-195906] p 3822 N94-33114

A decision support system for electronic warfare analysts p 3853 N94-33336

DECISION THEORY

Tractable deduction in some fragments of auto-epistemic logic [REPT-93-89] p 3844 N94-31673

Hierarchical mixtures of experts and the EM algorithm [AD-A276516] p 3814 N94-31932

DECODERS

Design, performance, and test standards for flight termination receivers/decoders. Volume 1: Design and performance requirements [AD-A277245] p 3602 N94-32333

DECODING

Methods of implementing the Viterbi algorithm on a massively parallel computer of the SIMD (single instruction multiple data) type [ISBN-0-315-86783-3] p 3814 N94-31752

DECOMPOSITION

Characterization of polymer decomposition products by laser desorption mass spectrometry p 3597 N94-31046

Evidence for a correct SiO2 voltage acceleration model [DE94-006578] p 3690 N94-31594

Group 12 thiolates: Syntheses, characterization and decomposition pathways [AD-A277055] p 3900 N94-32011

Parallel supercomputing: Advanced methods, algorithms, and software for large-scale linear and nonlinear problems [DE94-008446] p 3836 N94-32992

Effective computational strategy for predicting the response of complex systems [AD-A277452] p 3740 N94-33011

Perfluoropolyalkylether decomposition on catalytic aluminas [NASA-TM-106547] p 3617 N94-33021

DECONTAMINATION

Study of type 2 and 3 anodized Al 5052-0 in aqueous DS2 solutions [AD-A276960] p 3644 N94-32240

An investigation of the radiolytic stability of a resorcinol-formaldehyde ion exchange resin [DE94-007971] p 3660 N94-32698

DECOUPLING

Thin-film decoupling capacitors for multi-chip modules [DE94-007743] p 3695 N94-32650

DEDUCTION

Tractable deduction in some fragments of auto-epistemic logic [REPT-93-89] p 3844 N94-31673

DEEP SPACE NETWORK

The quest for contact [NASA-TM-109778] p 3806 N94-32389

DEEP WATER

Estimating subpycnocline density fluctuations in the California current region from upper ocean observations [AD-A277278] p 3789 N94-32325

Deep water studies of CTD data [AD-A277741] p 3791 N94-33176

DEFECTS

Atomic oxygen interaction at defect sights in protective coatings on polymers flown on LDEF p 3593 N94-31024

Passivation of III-V compound semiconductor based devices [AD-A276178] p 3894 N94-31056

Experimental and theoretical studies of hydrogenated amorphous semiconductor alloys and superlattices [AD-A276159] p 3686 N94-31079

The role of defects in laser damage of multilayer coatings [DE94-006731] p 3714 N94-31269

Rotordynamic effects driven by fluid forces from a geometrically imperfect labyrinth [AD-A276424] p 3722 N94-31333

The threshold energy for defect production in SiC: A molecular dynamic study [DE94-007123] p 3896 N94-31499

Engineering of damage in ion implanted silicon [ISBN-9-09-005097-3] p 3897 N94-31521

Defect-solute interactions near irradiation grain boundaries [DE94-006215] p 3641 N94-31627

In-situ characterization of growth and interfaces in a-Si:H devices [DE94-000291] p 3760 N94-31812

Research on the stability, electronic properties, and structure of a-Si:H and its alloys [DE94-000292] p 3899 N94-31813

Acceptance criteria for weld defects in aluminium weldments [PB94-136575] p 3735 N94-31841

Fracture and fatigue strength evaluation of multiple site damaged aircraft fuselages - curved panel testing and analysis [AD-A277100] p 3579 N94-32015

Shearographic inspection of a DeHavilland DHC-7 [AD-A276716] p 3566 N94-32157

Temperature-humidity-bias aging technique to identify defective surface mount capacitors [DE94-005354] p 3660 N94-32727

Space flight printed wiring board measling investigation [NASA-TM-104602] p 3732 N94-33101

DEFENSE PROGRAM

NATO contributions to European environmental security [AD-A275918] p 3763 N94-31275

DoD information systems capacity management function [AD-A275987] p 3916 N94-31355

V-22: Dual-use technology or red herring? [AD-A276577] p 3579 N94-32058

Application of Artificial Intelligence to the DoD Corporate Information Management (CIM) program [AD-A276656] p 3834 N94-32061

Lifting the fog of corporate information management [AD-A276680] p 3918 N94-32090

A comparison of military and commercial aircraft development [AD-A276830] p 3575 N94-32168

Common modeling system for digital simulation p 3823 N94-32429

DTIC Thesaurus on diskette with dBase 4.1 runtime (computer diskette) [AD-M000306] p 3922 N94-33256

DTIC Thesaurus on diskette without runtime (computer diskette) [AD-M000310] p 3923 N94-33258

DTIC Thesaurus on diskette without runtime (computer diskette) [AD-M000312] p 3923 N94-33259

DEFINITION

Legal regime of human activities in outer space law p 3599 N94-31431

DEFLAGRATION

Reactive flows in compact objects p 3934 N94-31567

DEFLECTION

Deformation and rupture of cylindrical shells under dynamic loading p 3733 N94-31288

Fast acting optical deflection [AD-A276630] p 3879 N94-32037

Photothermal laser deflection, an innovative technique to measure particles in exhausts [AD-A277151] p 3718 N94-32366

A case study of analysis methods for large deflections of a cantilever beam [NASA-TM-108454] p 3739 N94-32903

DEFORMATION

Patterns of deformation and volcanic flows associated with lithospheric loading by large volcanoes on Venus p 3776 N94-31106

Vibration control and design of composite cantilevers taking into account structural uncertainties and damage p 3733 N94-31213

Computer modelling of cyclic deformation of high-temperature materials [AD-A277056] p 3623 N94-32012

High temperature materials technology research for advanced thermionic systems [DE94-008444] p 3644 N94-32416

DEGENERATION

Degenerate four-wave mixing as a diagnostic of plasma chemistry [DE94-008588] p 3889 N94-31766

DEGRADATION

Space environment durability of beta cloth in LDEF thermal blankets p 3591 N94-31015

Degradation of optical components in space p 3594 N94-31029

Physical properties of glasses exposed to Earth-facing and trailing-side environments on LDEF p 3594 N94-31030

Analysis of GER imaging spectrometry data for the identification of soil and vegetation parameters in land degradation studies p 3744 N94-31857

Combined contamination and space environmental effects on solar cells and thermal control surfaces [NASA-TM-106592] p 3617 N94-33022

Depth-diameter ratios for Martian impact craters: Implications for target properties and episodes of degradation p 3943 N94-33191

DEGREES OF FREEDOM

Six degree of freedom flight dynamic model of a Mk-82 store [AD-A277065] p 3580 N94-32362

Design and Monte Carlo analysis of an unmanned aerial vehicle [AD-A277648] p 3580 N94-33056

Design, characterization, and control of the NASA three degree of freedom reaction compensation platform p 3605 N94-33304

DEHYDRATED FOOD

Novel ultrasonic method for food hydration [AD-A277411] p 3804 N94-32580

DEHYDRATION

Novel ultrasonic method for food hydration [AD-A277411] p 3804 N94-32580

DEICING

Aircraft icing handbook (update) [AD-A276499] p 3574 N94-31678

WHIPICE --- computer program for analysis of aircraft deicing [NASA-TM-109749] p 3574 N94-31803

Continuous measurement of aircraft wing icing p 3576 N94-32454

DELAMINATING

Ultrasonic characterization of damage in a simulated CF-18 composite structure [DREP-LN-93-26] p 3730 N94-31872

Low velocity impact damage in carbon fiber/PEEK composite laminates [ISBN-0-315-86546-6] p 3622 N94-31909

Structural integrity of intelligent materials and structures
[AD-A278397] p 3630 N94-33165

DELAY
The generalized multi delay adaptive filter: Structure and convergence analysis
[TELECOM-93-D-004] p 3808 N94-31094
Civil tiltrotor market penetration: Effects on Northeast corridor airport delay
[AD-A277534] p 3576 N94-32955

DELTA WINGS
Shock-dependent, optimum thrust wings in supersonic flow p 3570 N94-32027

DELTAS
Martian deltas: Morphology and distribution p 3950 N94-33230

DEMODULATION
Phase-lock roll control of inertially pointing spacecraft p 3609 N94-31470
A technique for multiplexing 3x3-coupler terminated interferometric fiber-optic sensors
[AD-A276739] p 3880 N94-32180

DEMULTIPLEXING
A technique for multiplexing 3x3-coupler terminated interferometric fiber-optic sensors
[AD-A276739] p 3880 N94-32180

DENMARK
Monitoring land cover and crop types in Denmark using ERS-1 SAR and optical satellite images p 3748 N94-32528

DENSIFICATION
Ion-irradiation-induced densification of zirconia sol-gel thin films
[DE94-006248] p 3656 N94-32103
Pressureless sintering of ceramic composites
[AD-A277274] p 3657 N94-32404

DENSITY (MASS/VOLUME)
Effect of irradiation damage and helium on the swelling and structure of vanadium-base alloys
[DE94-006540] p 3641 N94-31666

DENSITY DISTRIBUTION
Estimating subpycnocline density fluctuations in the California current region from upper ocean observations
[AD-A277278] p 3789 N94-32325

DENSITY MEASUREMENT
An overview of the Evaluation of Oxygen Interaction with Materials-third phase (EOIM-3) experiment: Space Shuttle Mission 46 p 3596 N94-31040
Using laser absorption spectroscopy to monitor composition and physical properties of metal vapors
[DE94-001530] p 3716 N94-31599
Measurement of viscosity, density, and gas solubility of refrigerant blends in selected synthetic lubricants
[DE94-007723] p 3653 N94-31917
Estimating subpycnocline density fluctuations in the California current region from upper ocean observations
[AD-A277278] p 3789 N94-32325

DEPENDENCE
The decidability of dependency in intuitionistic propositional logic
[ML-93-20] p 3856 N94-31410

DEPLETION
Electron: Cluster interactions
[DE94-009089] p 3874 N94-32807

DEPLOYMENT
Deployable and retractable telescoping tubular structure development p 3607 N94-33317
The Galileo high gain antenna deployment anomaly p 3807 N94-33319

DEPOSITION
Electrostatic reduction of particulates for laser resistant hafnia coatings
[DE94-005824] p 3651 N94-31557
Deposition of DLC via intense ion beam ablation
[DE94-005583] p 3651 N94-31650
Low energy ion beam assisted growth of homoepitaxial silicon films at low temperature
[AD-A278092] p 3908 N94-33039
Induced adsorption of chloride and bromide by submonolayer amounts of copper underpotentially deposited on Pt(111)
[AD-A278023] p 3648 N94-33182
Deposition rates of oxidized iron on Mars p 3945 N94-33198
Obliquity variation in a Mars climate evolution model p 3951 N94-33236
Novel sol-gel deposition for repair of conducting paths in polyceramic systems
[AD-A278381] p 3664 N94-33350

DEPOSITS
The zinc electrode: Reactions and mechanisms
[DE94-007977] p 3691 N94-31919
Geologic controls of erosion and sedimentation on Mars p 3951 N94-33232
Polar sediment accumulation: Role of surface winds at the two poles p 3951 N94-33233
Carbonates, surfates, phosphates, nitrates, and organic materials: Their association in a Martian meteorite p 3952 N94-33239

DERIVATION
First theory institute on computational differentiation
[DE94-006491] p 3841 N94-31309

DESERTIFICATION
Climatic evolution and desertization p 3780 N94-31009

DESERTS
Arid regions and wind erosion p 3780 N94-31005
Optical and image transmission through desert atmospheres
[AD-A276022] p 3742 N94-31496

DESIGN ANALYSIS
Chamber optics for testing passive remote sensing vapor detectors
[AD-A275909] p 3878 N94-31340
Analysis and synthesis of MOS translinear circuits
[ISBN-9-09-005495-2] p 3690 N94-31616
Design Methods based On Nets: DEMON
[PB94-147493] p 3813 N94-31687
Modular Simulator System (MSS) management guide
[AD-A277098] p 3588 N94-32014
A low-cost, CCD solid state star tracker
[NASA-CR-192722] p 3882 N94-32417
A PC program to optimize system configuration for desired reliability at minimum cost p 3823 N94-32438
The relationship between integrative task design for information systems professionals and perceived information systems effectiveness p 3919 N94-32487
Design and evaluation of coils for a 50 mm diameter induction coilgun launcher
[DE94-005244] p 3603 N94-32671
Detailed design of the 2MW Demonstration Plant
[DE94-000042] p 3762 N94-32823
Application of a design-build-team approach to low cost and weight composite fuselage structure
[NASA-CR-4418] p 3626 N94-32863
Analysis and design of a high speed, wide range stepwise tunable optical filter/amplifier
[PB94-149572] p 3698 N94-33169

DESORPTION
Experimental investigations and molecular dynamics simulations of radiation induced surface damage
[AD-A277323] p 3871 N94-32621

DESTABILIZATION
On wave interactions of rotational and irrotational flows p 3700 N94-31219

DESTRUCTION
Using Monte Carlo techniques and parallel processing for debris hazard analysis of rocket systems
[DE94-007250] p 3609 N94-31382

DETECTION
Proceedings of the 4th Tunnel Detection Symposium on Subsurface Exploration Technology
[AD-A276372] p 3771 N94-31369
Detection of a chi-square fluctuating target in Gaussian noise
[AD-A276078] p 3850 N94-31462
Perspectives of glucose sensing based on a charge-modulating competition reaction
[ISBN-9-09-005754-4] p 3795 N94-31652
Microwave sensor for ice detection p 3583 N94-32457
Visual processing of object velocity and acceleration
[AD-A277425] p 3801 N94-32998
Real-time sensor data validation
[NASA-CR-195295] p 3616 N94-33099

DETERIORATION
Evidence for a correct SiO2 voltage acceleration model
[DE94-006578] p 3690 N94-31594

DETONATION
Using Monte Carlo techniques and parallel processing for debris hazard analysis of rocket systems
[DE94-007250] p 3609 N94-31382

DETONATION WAVES
A study of near-surface and underwater explosions by computer simulations
[DE94-009038] p 3708 N94-32849

DETONATORS
Laser Diode Ignition (LDI)
[DE94-006590] p 3666 N94-31579

DEUTERIUM
Stark broadening of the 2S state of hydrogen and deuterium in arc plasmas of low density
[ETN-94-95731] p 3888 N94-31572
Modern integral equation techniques for quantum reactive scattering theory
[DE94-007039] p 3857 N94-31639
Dynamics of block poly(styrene-co-vinylpyridine) (SVP) in solution and on silica
[AD-A277139] p 3657 N94-32364
New polymer target-shell properties and characterizations
[DE94-008420] p 3890 N94-32415
Experimental survey of the L-H transition conditions in the D3-D tokamak
[DE94-007428] p 3891 N94-32595
Fusion with highly spin polarized HD and D2
[DE94-006209] p 3876 N94-32731
Deuterium absorption and material phase characteristics of SAES St198 Zr-Fe alloy
[DE94-006275] p 3646 N94-32781

DEW POINT
Coastal boundary layer and refractivity measurements using the ground-based high resolution interferometer sounder (GB-HIS)
[AD-A277980] p 3683 N94-33159

DIABETES MELLITUS
Perspectives of glucose sensing based on a charge-modulating competition reaction
[ISBN-9-09-005754-4] p 3795 N94-31652

DIAGNOSIS
Hierarchical fault catalog process for diagnosis of analog circuits
[ETN-94-95730] p 3689 N94-31571
Development of a video fluorescence system for assessing burn depth
[AD-A278127] p 3798 N94-33092

DIAMAGNETISM
Diamagnetism in helium Rydberg atoms
[ETN-94-96015] p 3865 N94-31549
Transport phenomena in the Earth's plasma sheet p 3772 N94-31970
Isothermal sintering, microstructure, and superconducting properties of Y1Ba2Cu3O(7-x) compound
[DE94-008132] p 3905 N94-32779

DIAMOND FILMS
Degenerate four-wave mixing as a diagnostic of plasma chemistry
[DE94-008588] p 3889 N94-31766
Materials processing and manufacturing technologies for diamond substrates multichip modules
[AD-A276904] p 3692 N94-32215
Ultrahigh-current-density metal-ion implantation and diamondlike-hydrocarbon films for tribological applications
[DE94-006958] p 3906 N94-32843

DIAMONDS
Deposition of DLC via intense ion beam ablation
[DE94-005583] p 3651 N94-31650
Materials processing and manufacturing technologies for diamond substrates multichip modules
[AD-A276904] p 3692 N94-32215
Heteroepitaxial diamond growth
[AD-A277178] p 3902 N94-32306
Compilation of diamond-like carbon properties for barriers and hard coatings
[DE94-008231] p 3661 N94-32803
Diamond turning in the production of x ray optics p 3604 N94-33298

DIAPHRAGMS (MECHANICS)
A silicon condenser microphone: Materials and technology
[ISBN-9-09-005899-0] p 3688 N94-31518
Development of high-pressure diaphragms for the AEDC impulse tunnel
[AD-A277053] p 3588 N94-32009

DIATOMIC GASES
Vibrational energy transfer of diatomic gases in hypersonic expanding flows p 3570 N94-31958

DIATOMIC MOLECULES
Implementation of a vibrationally linked chemical reaction model for DSMC
[NASA-TM-109109] p 3710 N94-33020

DICHROISM
Element-specific magnetic hysteresis measurements, a new application of circularly polarized soft x-rays
[DE94-007122] p 3858 N94-31397
Azo polymers for reversible optical storage. 4. Cooperative motion of rigid groups in semicrystalline polymers
[AD-A277107] p 3654 N94-31978
Dependence of x ray absorption magnetic circular dichroism on layer periodicity in iron-platinum multilayers
[DE94-008786] p 3647 N94-32892

DIELECTRIC POLARIZATION
Electrical properties of double layer dielectric structures for space technology
[ISBN-0-315-86547-4] p 3610 N94-31910

DIELECTRIC PROPERTIES
Microwave dielectric behavior of soils. Report 3: Measurement and modeling
[AD-A276060] p 3771 N94-31457
Satellite radar altimetry over the continental ice sheets p 3742 N94-31570

Passive vibration damping materials: Piezoelectric ceramic composites for vibration damping applications
[AD-A276550] p 3653 N94-31935
Electromagnetic probe technique for fluid flow measurements p 3711 N94-32455
Microwave sensor for ice detection
p 3583 N94-32457
Dielectric viscometer including fixed and variable cells
[AD-D016139] p 3639 N94-32973
Dielectric properties of Mars' surface: Proposed measurement on a Mars lander p 3951 N94-33237

DIELECTRICS
Sol-gel metal oxide and metal oxide/polymer multilayers applied by meniscus coating
[DE94-005813] p 3649 N94-31199
Structure estimation of phase objects from the diffraction near field: Microwave and model calculations
[ETN-94-95737] p 3674 N94-31608
Photonic bandgaps in periodic dielectric structures
[ISBN-0-315-86902-X] p 3899 N94-31729
A fracture mechanics methodology for characterizing the performance of flawed polymeric dielectric materials
p 3654 N94-31956
Photonic band gap materials
[DE94-005566] p 3677 N94-32101
Determination of BPSG thin-film properties using IR reflection spectroscopy of product wafers
[DE94-006591] p 3634 N94-32110
Chemical structure and kinetics at liquid/solid interfaces
[AD-A277112] p 3636 N94-32304

DIENES
Phase behavior, structure, and properties of model block polymers
[AD-A277530] p 3662 N94-32954

DIESEL ENGINES
Soot and liquid-phase fuel distributions in a newly designed optically accessible DI diesel engine
[DE94-005648] p 3723 N94-31651
Materials development program: Ceramic technology project bibliography, 1984-1992
[DE94-009297] p 3662 N94-32935

DIFFERENTIAL ABSORPTION LIDAR
Gyrotrons and free electron lasers for atmospheric sensing
[AD-A277281] p 3718 N94-32406

DIFFERENTIAL CALCULUS
First theory institute on computational differentiation
[DE94-006491] p 3841 N94-31309

DIFFERENTIAL EQUATIONS
Symplectic Runge-Kutta schemes 3: Canonical elementary differentials
[MATHS-REPT-A-204] p 3840 N94-31159
Symbolic derivation of Runge-Kutta methods
[MATHS-REPT-A-205] p 3840 N94-31160
Taming chaotic circuits p 3910 N94-31289
On wavelet representations of differential equations
[RR-482] p 3842 N94-31412
Numerical detection and continuation of codimension-two homoclinic bifurcations
[CWI-AM-R9308] p 3847 N94-32191
A stability estimate based on numerical ranges with application to a spectral discretization of a convection-diffusion equation
[TW-93-12] p 3847 N94-32200
On the error committed by stopping the Newton iteration in Runge-Kutta methods and linear multistep methods
[TW-93-13] p 3847 N94-32206
Preconditioned time-difference methods for advection-diffusion-reaction equations
[DE94-006472] p 3838 N94-32840
A study of weak solutions and their regularizations by numerical methods
[AD-A277453] p 3850 N94-33175

DIFFERENTIAL GEOMETRY
Some calculations on supersymmetric graphs as communication networks
[REPT-93-72] p 3824 N94-31641

DIFFERENTIAL INTERFEROMETRY
Evaluation of surface phase change on large zones
p 3755 N94-32567
Developments in ERS-1 SAR interferometry: Use of the spectral shift p 3756 N94-32569
Differential interferometry study of an earthquake
p 3756 N94-32570
Performance analysis of an integrated GPS/inertial attitude determination system
[NASA-CR-188289] p 3577 N94-32864

DIFFRACTION
Photoelectron diffraction and holography: Present status and future prospects
[DE94-006298] p 3712 N94-31629

DIFFRACTION PATTERNS
Photoelectron diffraction and holography: Present status and future prospects
[DE94-006298] p 3712 N94-31629
Ultra wide band radar holographic imaging of subsurface targets
[DE94-004271] p 3713 N94-32681

DIFFUSION
Defect-solute interactions near irradiation grain boundaries
[DE94-006215] p 3641 N94-31627
Generalized steady-state method for solving 2-D diffusion systems
[REPT-93-83] p 3825 N94-31700
Design of new polymers to improve radiation stability of plastic scintillators
[DE94-008220] p 3652 N94-31764
Numerical transport theory
[DE94-009064] p 3857 N94-32589
Fabrication, phase transformation studies and characterization of SiC-AlN-Al2OC ceramics
[DE94-008587] p 3659 N94-32657
Adjacent-cell Preconditioners for solving optically thick neutron transport problems
[DE94-007219] p 3872 N94-32666
Ab initio study of the epitaxial growth of Ge on Si(100) surface
[DE94-007245] p 3904 N94-32724
Anomalous transport equations in toroidal plasmas
[DE94-009206] p 3893 N94-32922
Numerical model of the thermal behavior of an extremity in a cold environment including counter-current heat exchange between the blood vessels
[AD-A276099] p 3798 N94-33040

DIFFUSION COEFFICIENT
Solvent diffusion coefficient concentration dependence in polymer solutions
[AD-A277023] p 3655 N94-32005
Particle diffusion from the beam-beam interaction in synchrotron colliders
[DE94-007111] p 3876 N94-32685

DIFFUSION FLAMES
NATO Advanced Study Institute on Unsteady Combustion. Volume 2: Research papers, September 6-17, 1993
[AD-A276572] p 3634 N94-32033

DIFFUSION THEORY
Numerical transport theory
[DE94-009064] p 3857 N94-32589

DIFFUSION WELDING
Joining of alumina by vacuum brazing
[VTT-TIED-1495] p 3724 N94-31656
Liquid-assisted diffusion bonding of NiAl
[DE94-008687] p 3645 N94-32522

DIFFUSIVITY
Notes on the Langevin model for turbulent diffusion of marked particles
[DE94-007847] p 3708 N94-32652
Experimental studies on the effect of coherency strains on coarsening kinetics: Current status and future outlook
[DE94-008480] p 3647 N94-32964

DIGITAL COMPUTERS
MDFF HELP library, version 2: On-line documentation for the map data formatting facility
[AD-A277763] p 3922 N94-32987
An experimental study of pilot/vehicle dynamics using a tilt rotor flying machine
[AD-A277516] p 3805 N94-33349

DIGITAL DATA
Entropy, information (and image), part 1
[TELECOM-93-D-009] p 3910 N94-31098
An intelligent interactive visual database management system for Space Shuttle closeout image management
p 3923 N94-32469
MDFF HELP library, version 2: On-line documentation for the map data formatting facility
[AD-A277763] p 3922 N94-32987

DIGITAL ELECTRONICS
Study of continuous-time and mixed analog-digital operators
[TELECOM-93-E-010] p 3687 N94-31170
VLSI for high-speed digital signal processing
[AD-A277617] p 3697 N94-32957
Superconducting and semiconducting hybrids and advance memory concepts for superconducting electronics
[AD-A277766] p 3907 N94-32988
A diagnostic expert system for digital circuits
p 3699 N94-33340

DIGITAL FILTERS
The generalized multi delay adaptive filter: Structure and convergence analysis
[TELECOM-93-D-004] p 3808 N94-31094
Concurrent architectures for VLSI signal and image processing
[AD-A276124] p 3688 N94-31445
Remote infrared vapor detection of volatile organic compounds
[AD-A276982] p 3746 N94-31999
Digital beamforming and filtering circuit
[AD-D016142] p 3697 N94-32976

DIGITAL RADAR SYSTEMS
Analysis of key performance parameters of phase sampling digital RF memories
[AD-A276019] p 3688 N94-31494

DIGITAL SIMULATION
Numerical method for the investigation of the magnetohydrodynamic stability of three dimensional plasma equilibria
[ETN-94-95752] p 3887 N94-31512
Real time simulation model for designing converter regulation
[ETN-94-95735] p 3689 N94-31576
Methods of implementing the Viterbi algorithm on a massively parallel computer of the SIMD (single instruction multiple data) type
[ISBN-0-315-86783-3] p 3814 N94-31752
An analog preprocessing architecture for high-speed analog-to-digital conversion
[AD-A276737] p 3807 N94-32163
Common modeling system for digital simulation
p 3823 N94-32429

DIGITAL SYSTEMS
Fault coverage measurement for digital microcircuits
[AD-A276226] p 3686 N94-31066
A generic model for data acquisition: Connectionist methods of information processing
[TELECOM-93-E-003] p 3730 N94-31166
Concurrent architectures for VLSI signal and image processing
[AD-A276124] p 3688 N94-31445
The trustworthy digital camera: Restoring credibility to the photographic image p 3714 N94-32470
Digital image profilers for detecting faint sources which have bright companions
[NASA-CR-191348] p 3927 N94-32695
MDFF HELP library, version 2: On-line documentation for the map data formatting facility
[AD-A277763] p 3922 N94-32987
Advanced silicon technology for microwave circuits
[AD-A278039] p 3698 N94-33091

DIGITAL TECHNIQUES
A direct digital design for a multichannel structural test system using the characteristic locus method
[MATHS-REPT-A-206] p 3828 N94-31161
A Hyland-Bernstein approach to the digital control of Pritchard-Salamon systems
[REPT-93-76] p 3844 N94-31693
Alternatives to hierarchical techniques in stereo correlation
[AD-A276570] p 3746 N94-31938
Example of SPOT/ERS-1 complementarity
p 3749 N94-32533
Study of subpolar glaciers of Spitzbergen using SPOT, ERS-1, and hypsometric data: Results and perspectives
p 3753 N94-32553
Comparing SPOT and SIR A for mapping superficial formations in tropical forest regions: Example of the Yaoundy Region (Cameroon) p 3755 N94-32562
Precision and level of artefacts in the computation of digital terrain models by interferometry
p 3756 N94-32571
Fields of experiments in ERS-1 SAR interferometry in Bonn and Naples p 3756 N94-32572

DIMENSIONAL MEASUREMENT
Apron heights around stepped massifs in the Cydonia Mensae region: Do they record the local paleobathymetry of Oceanus Borealis? p 3949 N94-33224

DIMERS
Ab initio study of the epitaxial growth of Ge on Si(100) surface
[DE94-007245] p 3904 N94-32724
Possible effect of the chlorine oxide dimer on transient ozone loss in rocket plumes
[AD-A278135] p 3616 N94-33094

DIODES
Theoretical studies on ionospheric irregularities and ion diode performance
[AD-A277115] p 3772 N94-31984
X ray pulse considerations and electron flow in high voltage diodes
[AD-A277301] p 3868 N94-32044
Time resolved measurements of light produced by onset of plasma formation on electrodes of fast pulsed high voltage diodes
[AD-A277974] p 3894 N94-33264

DIPOLE ANTENNAS
Predicting antenna parameters from antenna physical dimensions
[AD-A276442] p 3672 N94-31300

DIRECT CURRENT
Modal analysis of multiterminal high voltage direct current transmission
[DE94-006426] p 3691 N94-31785

DIRECTIONAL ANTENNAS
Low sidelobe reflector antenna design for communications
[AD-A276079] p 3673 N94-31463
DIRECTIONAL SOLIDIFICATION (CRYSTALS)
An experimental study of void formation during aluminum solidification in reduced gravity p 3667 N94-31944
DIRECTIONAL STABILITY
Controls design with crossfeeds for hovering rotorcraft using quantitative feedback theory
[NASA-CR-195765] p 3585 N94-31203
DIRECTIVITY
Experimental and computational studies on propeller noise due to inflow distortion p 3860 N94-31846
DIRICHLET PROBLEM
Finite volume discretization of the k-epsilon turbulence model in general coordinates
[REPT-93-90] p 3703 N94-31703
DISASTERS
Feasibility in the use of satellite remote sensing data as a fast reaction tool for natural disaster relief p 3748 N94-32526
DISCONNECT DEVICES
Design and performance of the telescope and detector covers on the Extreme Ultraviolet Explorer satellite p 3605 N94-33309
Payload holddown and release mechanism p 3607 N94-33321
Advanced release technologies program p 3607 N94-33322
DISCRETE COSINE TRANSFORM
A visual detection model for DCT coefficient quantization p 3850 N94-32467
COVICS: A covert video communications system
[DE94-007568] p 3682 N94-32745
DISCRIMINANT ANALYSIS (STATISTICS)
A differential theory of learning for efficient statistical pattern recognition
[AD-A277313] p 3800 N94-32277
DISEASES
Muscle disuse through tail-suspension: Etiology and therapeutics p 3796 N94-31746
DISK GALAXIES
Three-dimensional radiative transfer calculations on an SIMD machine applied to accretion disks p 3932 N94-31141
The stellar and gaseous content of massive low surface brightness disk galaxies p 3933 N94-31495
DISK OPERATING SYSTEM (DOS)
An MS-DOS file system for UNIX
[AD-A276523] p 3816 N94-32081
DISLOCATIONS (MATERIALS)
Engineering of damage in ion implanted silicon
[ISBN-9-09-005097-3] p 3897 N94-31521
DISPERSING
Analysis of strong acoustic excitation on the breakup and dispersion of a liquid jet
[ONERA-NT-1993-9] p 3701 N94-31422
DISPERSION STRENGTHENING
Processing of novel nanoparticle dispersion strengthened ceramics for improved mechanical performance
[AD-A275965] p 3649 N94-31276
DISPLACEMENT
An efficient higher order theory for laminated composite plates and a finite element implementation p 3617 N94-31215
Electron energy dependence of amorphization in Zr3Fe
[DE94-008459] p 3906 N94-32875
DISPLAY DEVICES
Active matrix liquid crystal display. Industry survey results
[AD-A276415] p 3895 N94-31329
Theoretical basis for state vector comparison, relative position display, and relative position/rendezvous prediction
[AD-A277216] p 3608 N94-32020
PSIDD: A Post-Scan Interactive Data Display system for ultrasonic scans
[NASA-TM-4545] p 3732 N94-33038
Three dimensional audio versus head down TCAS displays
[NASA-CR-177636] p 3576 N94-33063
Cockpit Electronic Display Workshop: Proceedings (computer diskette)
[AD-M000330] p 3805 N94-33171
Cockpit Electronic Display Workshop: A synopsis
[AD-A277728] p 3583 N94-33280
An experimental study of pilot/vehicle dynamics using a tilt rotor flying machine
[AD-A277516] p 3805 N94-33349
DISSOLVING
Characterization of the corrosion resistance of duplex stainless steels using local current density mapping techniques
[DE94-007980] p 3646 N94-32699
DISTANCE
Measuring the Hubble constant and our Virgo-infall velocity independently p 3926 N94-31968
DISTORTION
Bounds on least-squares four-parameter sine-fit errors due to harmonic distortion and noise
[DE94-007859] p 3849 N94-32653
DISTRIBUTED PARAMETER SYSTEMS
Invariance of the generalized steady-state for 1-D distributed parameter systems
[REPT-93-66] p 3825 N94-31662
Generalized steady-state method for solving 2-D diffusion systems
[REPT-93-83] p 3825 N94-31700
Approximation theory and computational methods for the identification and control of distributed parameter systems
[AD-A277335] p 3848 N94-32244
Control and stabilization of distributed parameter systems; theoretical and computational aspects
[AD-A277239] p 3738 N94-32275
DISTRIBUTED PROCESSING
Using atomic actions in replica groups to simplify the replication implementation
[REPT-93-78] p 3813 N94-31695
A theory of distributed time
[AD-A276631] p 3815 N94-31994
CMS Distribution Subsystem user's guide
[DE94-005328] p 3816 N94-32146
Parallel and distributed computing combinatorial algorithms
[AD-A277333] p 3826 N94-32243
Communication networks for autonomous mobile robot computer architectures and distributed real-time computing p 3680 N94-32310
Modular Simulator System (MSS). Engineering design guide
[AD-A276967] p 3589 N94-32394
Modular Simulator System (MSS): Interface design document for the generic MSS
[AD-A277270] p 3590 N94-32403
Spacecraft On-Board Information Extraction Computer (SOBIEC) p 3808 N94-32433
A high-speed linear algebra library with automatic parallelism p 3828 N94-32440
High performance real-time flight simulation at NASA Langley p 3591 N94-32473
A software architecture for multidisciplinary applications: Integrating task and data parallelism
[NASA-CR-194896] p 3820 N94-32928
DISTRIBUTION FUNCTIONS
The kinematics of dense clusters of galaxies p 3937 N94-32029
On constructing multi-variate orthonormal polynomials associated with spectral distribution functions
[CWI-BS-R9310] p 3851 N94-32225
On the minimum of independent geometrically distributed random variables
[NASA-CR-194883] p 3821 N94-33075
DISULFIDES
Proceedings of the Ad Hoc Workshop on Ceramics for Li/FeS2 batteries
[DE94-007460] p 3694 N94-32607
The relative performance of FeS2 and CoS in long-life thermal-battery applications
[DE94-006145] p 3695 N94-32663
DITCHING (LANDING)
Rotorcraft ditchings and water-related impacts that occurred from 1982 - 1989, phase 2
[AD-A276473] p 3574 N94-31246
DIURNAL VARIATIONS
Evolution of diurnal surface winds and surface currents for Monterey Bay
[AD-A277649] p 3790 N94-33057
The influence of thermal inertia on Mars' seasonal pressure variation and the effect of the weather component p 3952 N94-33238
Diurnal, seasonal and solar activity variations of F-region parameters
[AD-A278106] p 3776 N94-33285
DIVERTERS
First-wall heat-flux measurements during ELMing H-mode plasma
[DE94-008310] p 3888 N94-31765
Overview of H-mode studies in D3-D
[DE94-007430] p 3891 N94-32612
Divertor pumping and other reactor application issues for H-mode
[DE94-007431] p 3892 N94-32810
Cooperative program on D3-D (FY 1993)
[DE94-008343] p 3892 N94-32820
DIVING (UNDERWATER)
Proceedings of the DCIEM Diver Thermal Protection Workshop
[DCIEM-92-10] p 3795 N94-31738
Effects of combined breathing impediments on diver's respiratory performance
[AD-A277437] p 3805 N94-33084
DOCUMENTATION
A hypertext system that learns from user feedback p 3923 N94-32428
DONOR MATERIALS
Recent developments in polymeric charge transfer complexes
[AD-A277108] p 3654 N94-31979
DOPED CRYSTALS
Growth and characterization of III-V semiconductors with rare earth impurities for optoelectronic devices
[AD-A276021] p 3896 N94-31455
Novel electroactive polymers and block copolymers
[AD-A276119] p 3650 N94-31509
Processing boron and boron carbide thin films for protective coatings and device fabrication
[AD-A277266] p 3900 N94-32041
Oriented Si and Ge nanocrystals formed in Al2O3 by ion implantation and annealing
[DE94-005593] p 3901 N94-32172
Conductivity measurements of ceria-based solid electrolytes using AC impedance
[DE94-007380] p 3694 N94-32593
Boron and hydrogen in Ni3Al. Part 2: Mechanical testing of bicrystals
[DE94-007441] p 3904 N94-32606
Characterization of thermally stable dye-doped polyimide based electrooptic materials
[DE94-005309] p 3882 N94-32674
Properties of doped and undoped (Ca,Sr)CuO2 thin films
[DE94-007230] p 3905 N94-32785
Characterization of crosslinked electrooptic polyimides
[DE94-007934] p 3661 N94-32819
Investigation of superconductivity and magnetism in d and f-electron materials
[DE94-008535] p 3907 N94-32933
Optical properties of lanthanide-doped RbTiOAsO4 and transition metal-doped KTiOPO4
[DE94-008433] p 3907 N94-32963
A relaxation study of poled nonlinear optical polymers by infrared reflection-absorption spectroscopy
[AD-A277513] p 3663 N94-33054
Rare Earth Doped Semiconductors and Materials Research Society Symposium Proceedings, Volume 301
[AD-A277517] p 3908 N94-33055
Development of materials for spectral hole burning applications
[AD-A278408] p 3909 N94-33324
DOPPLER RADAR
Radar measurements p 3685 N94-31002
DOSIMETERS
Investigation of scintillator and fibre light in plastic scintillation dosimetry
[ISBN-0-315-87190-3] p 3879 N94-31877
System for monitoring and analyzing field energy exposure
[AD-D016115] p 3681 N94-32625
Complete model description of an electron beam using ACCEPT Monte Carlo simulation code
[DE94-007063] p 3872 N94-32628
DOWNLINKING
Data processing algorithms for on-board satellite event analysis
[AD-A278406] p 3838 N94-33168
DOWNRANGE
Phase-only correction of scintillated laser beams: Downrange experimental results
[AD-A277778] p 3722 N94-33282
DRAG COEFFICIENTS
A critical assessment of UH-60 main rotor blade airfoil data
[NASA-TM-103985] p 3571 N94-32063
DRAG MEASUREMENT
Aerodynamic drag of droplets in turbulent flow fields
[ISBN-0-315-75827-9] p 3571 N94-32491
DRAG REDUCTION
Computational study of single-expansion-ramp nozzles with external burning
[NASA-TM-106550] p 3700 N94-31229
Shock-dependent, optimum thrust wings in supersonic flow p 3570 N94-32027
DRAINAGE PATTERNS
Respective contributions of VIS-PIR, SAR-ERS 1, and airborne radar data for morphostructural and morphoneotectonic analysis: Practical examples p 3752 N94-32549

DREDGING
Results of real-time testing and demonstration of the US Army Corps of Engineers real-time on-the-fly positioning system
[AD-A276160] p 3576 N94-31080
DROP SIZE
Solidification structure synthesis in undercooled liquids
[AD-A276166] p 3910 N94-31054
Cloud studies seen from a physical chemist's perspective
[DE94-006059] p 3771 N94-31527
Drop size distributions and related properties of fog for five locations measured from aircraft
[NASA-CR-4585] p 3787 N94-33065
DROPS (LIQUIDS)
Solidification structure synthesis in undercooled liquids
[AD-A276166] p 3910 N94-31054
Single scattering of light by ensembles of particles with various shapes
[ETN-94-96016] p 3878 N94-31550
Thermocapillary convection in evaporating sessile drops
[NASA-TM-109758] p 3705 N94-31886
A parameterization of cloud droplet nucleation
[DE94-007469] p 3785 N94-32268
Aerodynamic drag of droplets in turbulent flow fields
[ISBN-0-315-75827-9] p 3571 N94-32491
DROUGHT
Some aspects of the drought in North Africa and in the Mediterranean basin p 3778 N94-30989
DRUGS
Drug-related problems in the workplace
[CRANFIELD-AERO-9306] p 3914 N94-31538
DRY FRICTION
A Gauss-Seidel type solver for special convex programs, with application to frictional contact mechanics
[REPT-93-77] p 3813 N94-31694
DRYING
Thermocapillary convection in evaporating sessile drops
[NASA-TM-109758] p 3705 N94-31886
Conductive paints
[DE94-008508] p 3661 N94-32788
Dry deposition of PAN to grassland vegetation
[DE94-005111] p 3768 N94-32894
Physics of heat pipe rewetting
[NASA-CR-195902] p 3913 N94-33148
DRYING APPARATUS
Novel ultrasonic method for food hydration
[AD-A277411] p 3804 N94-32580
DUCTILITY
High temperature ductility loss in titanium alloys: A review
[DE94-006606] p 3640 N94-31345
DURABILITY
Space environment durability of beta cloth in LDEF thermal blankets p 3591 N94-31015
Molecular interactions at metal/polyimide interfaces: A correlation with adhesion and bond durability
[AD-A276301] p 3650 N94-31297
Surface chemistry and durability of borosilicate glass
[DE94-006734] p 3656 N94-32116
Development of stitched/RTM composite primary structures p 3628 N94-33127
Resin transfer molding for advanced composite primary wing and fuselage structures p 3628 N94-33128
DUST
Mars atmospheric dust properties: A synthesis of Mariner 9, Viking, and Phobos observations p 3945 N94-33200
Groundbased monitoring of Martian atmospheric opacity p 3947 N94-33207
Temporal and spatial mapping of atmospheric dust opacity and surface albedo on Mars p 3947 N94-33211
Studies of atmospheric dust from Viking IR thermal mapper data p 3948 N94-33216
The wavelength dependence of Martian atmospheric dust radiative properties p 3950 N94-33228
DUST STORMS
Desert aerosols: Sources, transports, and impacts determined by remote sensing p 3770 N94-31003
Arid regions and wind erosion p 3780 N94-31005
Might it be possible to predict the onset of major Martian dust storms? p 3948 N94-33215
DWARF STARS
Reactive flows in compact objects p 3934 N94-31567
A chemical analysis of solar neighborhood dwarfs p 3926 N94-31951
DYES
Mechanisms of laser induced reactions in opaque heterogeneous environments
[AD-A276642] p 3717 N94-31996
Characterization of thermally stable dye-doped polyimide based electrooptic materials
[DE94-005309] p 3882 N94-32674
Characterization of crosslinked electrooptic polyimides
[DE94-007934] p 3661 N94-32819
A relaxation study of poled nonlinear optical poimers by infrared reflection-absorption spectroscopy
[AD-A277513] p 3663 N94-33054
Development of a video fluorescence system for assessing burn depth
[AD-A278127] p 3798 N94-33092
DYNAMIC CHARACTERISTICS
Model updating of vibrating systems based on measured or calculated frequency response functions
[CTH-E-93-03] p 3732 N94-31091
Vibration control and design of composite cantilevers taking into account structural uncertainties and damage p 3733 N94-31213
Asymptotic behavior of dynamic systems p 3911 N94-31894
Structural stability and bifurcations p 3911 N94-31895
Seasons and chaos in population dynamics p 3912 N94-31897
Dynamics of block poly(styrene-co-vinylpyridine) (SVP) in solution and on silica
[AD-A277139] p 3657 N94-32364
Quantum dynamics in dual spaces
[DE94-008303] p 3913 N94-32824
DYNAMIC CONTROL
Real-time control of the Trussarm variable-geometry-truss manipulator utilizing machine vision
[ISBN-0-315-87054-0] p 3830 N94-31735
Study of a path planning and tracking system for an articulated mobile robot
[ISBN-0-315-86502-4] p 3831 N94-31800
A real-time computer control and trajectory generation environment for Trussarm
[ISBN-0-315-87060-5] p 3832 N94-31833
Real-time control and application to robotics: Hardware and software architectures
[ISBN-0-315-87192-X] p 3833 N94-31876
Control of a flexible-link robotic arm manipulating an unknown dynamic payload p 3725 N94-31973
Dynamics and control of orbiting flexible systems: A formulation with applications
[ISBN-0-315-75390-0] p 3611 N94-32502
Design, characterization and control of the Unique Mobility Corporation robot p 3603 N94-33296
DYNAMIC LOADS
Deformation and rupture of cylindrical shells under dynamic loading p 3733 N94-31288
Limiting vibration in systems with constant amplitude actuators through command preshaping
[NASA-CR-188284] p 3739 N94-32907
Intelligent control of a multi-degree-of freedom reaction compensating platform system using fuzzy logic p 3605 N94-33306
DYNAMIC MODELS
Application of contact mechanics for the validation of robotized operations of grasping objects subjected to static and dynamic force fields
[ISBN-0-315-86831-7] p 3725 N94-31754
On the reciprocal relationship between life histories and population dynamics
[CWI-AM-R9302] p 3793 N94-32226
Six degree of freedom flight dynamic model of a Mk-82 store
[AD-A277065] p 3580 N94-32362
String-parton model description of relativistic heavy-ion collisions
[DE94-009164] p 3874 N94-32850
DYNAMIC PRESSURE
Research in marine boundary layer intermittency
[AD-A276076] p 3701 N94-31460
DYNAMIC PROGRAMMING
Exact solution of the single machine scheduling problem with earliness and flow time penalties
[REPT-93-038] p 3809 N94-31189
What comes first in dynamic semantics: A compositional, non-representational account of natural language presupposition
[LP-93-15] p 3855 N94-31389
Performability modelling using DyQNtool+
[MEMO-INF-93-45] p 3812 N94-31659
CAD-based off-line planning for an active-vision system
[ISBN-0-315-86317-X] p 3813 N94-31713
On the convergence of stochastic iterative dynamic programming
[AD-A276517] p 3815 N94-31933
DOME: Dynamic optimization on multiprocessor engines, a statistical approach p 3807 N94-31972
DYNAMIC RANGE
Advanced optical fiber communication systems
[AD-A276416] p 3878 N94-31330
DYNAMIC RESPONSE
Model updating of vibrating systems based on measured or calculated frequency response functions
[CTH-E-93-03] p 3732 N94-31091
Controls design with crossfeeds for hovering rotorcraft using quantitative feedback theory
[NASA-CR-195765] p 3585 N94-31203
Deformation and rupture of cylindrical shells under dynamic loading p 3733 N94-31288
A study of the Space Station Freedom response to the disturbance environment p 3600 N94-31434
Chaotic attitude motion of satellites in the central gravitational field
[ISBN-0-315-78768-6] p 3610 N94-31723
Heave dynamics of an air cushion vehicle bag and finger skirt
[ISBN-0-315-87053-2] p 3568 N94-31734
Vibrational and acoustic response of ribbed plates p 3736 N94-31955
A separation technique for asymptotic-numeric solution for general shells of revolution p 3736 N94-31961
Reciprocity-based experimental determination of dynamic forces and moments: A feasibility study
[NASA-CR-194905] p 3862 N94-33023
Response of a cantilevered plate in supersonic flow
[AD-A277487] p 3580 N94-33107
DYNAMIC STABILITY
Structural stability and bifurcations p 3911 N94-31895
DYNAMIC STRUCTURAL ANALYSIS
A study of the Space Station Freedom response to the disturbance environment p 3600 N94-31434
Study of wave propagation and dynamic response of laminated composite structures
[AD-A276123] p 3619 N94-31444
Fluid-structure interaction in case of water hammer with cavitation
[PB94-148277] p 3702 N94-31588
Random vibrations of composite beams and plates p 3735 N94-31777
Futurepath 3
[NASA-TM-109762] p 3735 N94-31819
Vibrational and acoustic response of ribbed plates p 3736 N94-31955
Vibration localization in dual-span axially moving elastic systems p 3736 N94-31964
Nonlinear vibration analysis of laminated plates on linear and nonlinear elastic foundations p 3737 N94-32079
Control and stabilization of distributed parameter systems; theoretical and computational aspects
[AD-A277239] p 3738 N94-32275
Multiple size scale structures in silica/siloxane composites studied by small-angle scattering
[DE94-007300] p 3625 N94-32642
Structural damping studies at cryogenic temperatures
[NASA-TM-109073] p 3740 N94-33118
DYNAMICAL SYSTEMS
On wavelet representations of differential equations
[RR-482] p 3842 N94-31412
Bifurcation and deterministic chaos in dynamic systems
[REPT-93-047] p 3911 N94-31893
Asymptotic behavior of dynamic systems p 3911 N94-31894
Structural stability and bifurcations p 3911 N94-31895
Deterministic chaos p 3912 N94-31896
DYNAMO THEORY
Evolution of dynamo-generated magnetic fields in accretion disks around compact and young stars p 3931 N94-31138
Steps toward understanding the solar dynamo
[AD-A277398] p 3953 N94-32343

E

E REGION
Performance statistics bulletin. High latitude meteor scatter propagation February, March, April, May 1991
[AD-A276723] p 3678 N94-32158
Performance statistics bulletin. High latitude meteor scatter propagation October, November, December 1991, January 1992
[AD-A276724] p 3678 N94-32159
Performance statistics bulletin. High latitude meteor scatter propagation
[AD-A276694] p 3680 N94-32298
Performance statistics bulletin. High latitude meteor scatter propagation
[AD-A276695] p 3680 N94-32299

Performance statistics bulletin. High latitude meteor scatter propagation
[AD-A276696] p 3680 N94-32300
Performance statistics bulletin. High latitude meteor scatter propagation, June, July, August, September 1992
[AD-A277508] p 3685 N94-33347

EARLY WARNING SYSTEMS
Vulnerability assessment of a space based weapon platform electronic system exposed to a thermonuclear weapon detonation
[DE94-007229] p 3611 N94-32667

EARTH ALBEDO
The surface parameters: Remote sensing observations and climatology applications p 3779 N94-31001

EARTH ATMOSPHERE
Wind-speed measurements with a scanning elastic-backscatter lidar
[DE94-004974] p 3785 N94-32726

EARTH CORE
Magnetohydrodynamics of the Earth's core. 1: Steady, rotating magnetoconvection. 2: Magnetic Rossby waves p 3770 N94-31104

EARTH IONOSPHERE
Theory, Image Simulation, and Data Analysis of Chemical Release Experiments
[NASA-CR-194865] p 3954 N94-31101
Analysis of ionospheric parameters in Europe and creation of the prediction algorithm
[AD-A276342] p 3771 N94-31326
The High-Frequency Benchmark propagation program
[AD-A276323] p 3672 N94-31334
Theoretical studies on ionospheric irregularities and ion diode performance
[AD-A277115] p 3772 N94-31984
An analysis of ionospheric dayglow from observations of the Naval Postgraduate School Middle Ultraviolet Spectrograph (MUSTANG)
[AD-A277351] p 3773 N94-32335
Spatial correlation of ionospheric variability
[AD-A278105] p 3776 N94-33041
Ionospheric plasma outflow in response to transverse ion heating: Self-consistent macroscopic treatment
[NASA-CR-195820] p 3893 N94-33048
Participation in the scientific activities of the Waves in Space Plasma (WISP) project
[NASA-CR-195903] p 3894 N94-33113
Millstone Hill radar studies of plasma waves and turbulence
[AD-A278409] p 3684 N94-33172
EUROCAP program
[AD-A278084] p 3776 N94-33184

EARTH MAGNETOSPHERE
Theory, Image Simulation, and Data Analysis of Chemical Release Experiments
[NASA-CR-194865] p 3954 N94-31101
Computer modeling of active experiments in space plasmas p 3890 N94-31927
Analysis of data from the plasma composition experiment on the International Sun-Earth Explorer (ISEE 1)
[NASA-CR-195880] p 3893 N94-33074
Characteristics of ion flow in the quiet state of the inner plasma sheet
[AD-A277451] p 3894 N94-33106
Participation in the scientific activities of the Waves in Space Plasma (WISP) project
[NASA-CR-195903] p 3894 N94-33113

EARTH MANTLE
Magnetohydrodynamics of the Earth's core. 1: Steady, rotating magnetoconvection. 2: Magnetic Rossby waves p 3770 N94-31104

EARTH MOVEMENTS
SAR interferometry with ERS-1 p 3755 N94-32566
Differential interferometry study of an earthquake p 3756 N94-32570
Procedures for computing site seismicity
[AD-A277666] p 3775 N94-33028

EARTH OBSERVATIONS (FROM SPACE)
The processing technology and some applications of Almaz-1 data p 3756 N94-32573
Earth observational research using multistage EOS-like data
[NASA-CR-195833] p 3757 N94-33019

EARTH OBSERVING SYSTEM (EOS)
Global change research and NASA's Earth Observing System
[PB94-126992] p 3741 N94-31068
MODIS. Volume 1: MODIS level 1A software baseline requirements
[NASA-TM-104594-VOL-1] p 3823 N94-33287
MODIS. Volume 2: MODIS level 1 geolocation, characterization and calibration algorithm theoretical basis document, version 1
[NASA-TM-104594-VOL-2] p 3613 N94-33289

EARTH ORBITAL ENVIRONMENTS
The performance of thermal control coatings on LDEF and implications to future spacecraft p 3591 N94-31013
Performance of silvered Teflon (trademark) thermal control blankets on spacecraft p 3591 N94-31014
Space Station WP-2 application of LDEF MLI results p 3592 N94-31016
Anodized aluminum on LDEF p 3592 N94-31017
Follow-up on the effects of the space environment on UHCRE thermal blankets p 3592 N94-31018
Modeling of LDEF contamination environment p 3592 N94-31019
Model of spacecraft atomic oxygen and solar exposure microenvironments p 3593 N94-31021
Atomic oxygen erosion considerations for spacecraft materials selection p 3593 N94-31022
Performance of selected polymeric materials on LDEF p 3593 N94-31023
Atomic oxygen interaction at defect sights in protective coatings on polymers flown on LDEF p 3593 N94-31024
Fluorescence observations of LDEF exposed materials as an indicator of induced material reactions p 3593 N94-31025
Laser-induced fluorescence of space-exposed polyurethane p 3593 N94-31026
On the linearity of fast atomic oxygen effects p 3594 N94-31027
Low-Earth orbit effects on organic composite materials flown on LDEF p 3595 N94-31036
Summary of materials and hardware performance on LDEF p 3595 N94-31037
Ground-based simulation of LEO environment: Investigations of a select LDEF material: FEP Teflon (trademark) p 3596 N94-31039
An overview of the Evaluation of Oxygen Interaction with Materials-third phase (EOIM-3) experiment: Space Shuttle Mission 46 p 3596 N94-31040
Preliminary results from the CONCAP-2-01 and EIOM-3 experiments on STS-46 p 3596 N94-31042
Effects of orbital exposure on RTV during the LDEF mission p 3597 N94-31043
Spacecraft materials: Comparison between flight results obtained on LDEF and MIR p 3597 N94-31045
Design application and development of spacecraft in LEO utilizing LDEF results p 3597 N94-31047
An overview of the on-orbit contamination of the Long Duration Exposure Facility (LDEF) p 3598 N94-31049
What LDEF means for development and testing of materials p 3598 N94-31050
Space hypervelocity microparticle impact damage in polymer matrix composites
[ISBN-0-315-87057-5] p 3652 N94-31692
Combined contamination and space environmental effects on solar cells and thermal control surfaces
[NASA-TM-106592] p 3617 N94-33022

EARTH ORBITS
Semianalytic Satellite Theory (SST): Mathematical algorithms
[AD-A276836] p 3610 N94-32208
Combined contamination and space environmental effects on solar cells and thermal control surfaces
[NASA-TM-106592] p 3617 N94-33022

EARTH RADIATION BUDGET EXPERIMENT
NOAA-9 Earth Radiation Budget Experiment (ERBE) scanner offsets determination
[NASA-TM-109086] p 3785 N94-32737

EARTH RESOURCES
European Imaging Spectroscopy Aircraft Campaign
[ESA-SP-360] p 3743 N94-31853
The European Imaging Spectroscopy Airborne Campaign (EISAC). Data takes and evaluation programme: An overview p 3743 N94-31854

EARTH SURFACE
The surface parameters: Remote sensing observations and climatology applications p 3779 N94-31001
Homogeneous global mean temperature time series
[DE94-002194] p 3766 N94-32690
Parameterizing atmosphere-land surface exchange for climate models with satellite data: A case study for the Southern Great Plains CART site
[DE94-005109] p 3775 N94-32874

EARTH TERMINALS
Satellite communications industry
[AD-A276685] p 3610 N94-32039

EARTHQUAKES
Differential interferometry study of an earthquake p 3756 N94-32570
Procedures for computing site seismicity
[AD-A277666] p 3775 N94-33028

ECCENTRICITY
Testing for preferred-frame effects in gravity with artificial Earth satellites
[PB94-148459] p 3610 N94-31771

ECHO SOUNDING
Multi-scale studies of seafloor topography
[AD-A277008] p 3789 N94-32400

ECOLOGY
Behavior and dynamics of tropical forests and savannas p 3757 N94-31004
Proceedings of a Joint US-Japan Seminar in the Environmental Sciences
[DE94-004727] p 3741 N94-31606

ECONOMIC ANALYSIS
Economic analysis of the hertzian spectrum
[TELECOM-93-E-012] p 3670 N94-31171
Economic feasibility analysis of distributed electric power generation based upon the natural gas fired fuel cell
[DE94-005795] p 3759 N94-31487
Feasibility study for the recycling of nickel metal hydride electric vehicle batteries
[DE94-000268] p 3690 N94-31598
Scenarios for multi-unit inertial fusion energy plants producing hydrogen fuel
[DE94-006614] p 3666 N94-32114
Estimating the impact of crashworthiness standards on mortality and morbidity events in the US Army rotary-wing aircraft mishaps
[AD-A277121] p 3575 N94-32363
Recovery of carboxylic acids at pH greater than pKa
[DE94-007030] p 3636 N94-32376

ECONOMIC FACTORS
Using the National Information Infrastructure for social science, education, and informed decision making
[DE94-005442] p 3920 N94-32676
Optimal planning of residential photovoltaic systems under various rate structure
[DE94-757272] p 3762 N94-32919
FAA aviation forecasts, fiscal years 1994-2005
[AD-A277808] p 3566 N94-33016

ECONOMICS
The contribution of aeronautics and astronautics to the quality of life on Earth
[ILR-MITT-283(1993)] p 3764 N94-31611
Strategies for survival in the new environmental era
[AD-A276827] p 3765 N94-32195
Solar activities at Sandia National Laboratories
[DE94-007737] p 3761 N94-32648
Environmental issues related to biomass: An overview
[DE94-007226] p 3767 N94-32784

ECOSYSTEMS
Behavior and dynamics of tropical forests and savannas p 3757 N94-31004
Proceedings of a Joint US-Japan Seminar in the Environmental Sciences
[DE94-004727] p 3741 N94-31606

EDDY CURRENTS
Continuous measurement of aging response in aluminum alloys by eddy current methods
[AD-A277233] p 3644 N94-32371
A versatile nondestructive evaluation imaging workstation p 3732 N94-32458
Surface conforming flexible eddy current probe for scanning varying surface contours
[AD-D016173] p 3627 N94-33018

EDGE DETECTION
Automated detection of ship tracks in multispectral satellite data
[AD-A276697] p 3746 N94-32119

EDITING ROUTINES (COMPUTERS)
Emacs Lisp in Edwin scheme
[AD-A276721] p 3818 N94-32504

EDUCATION
European business confronted with the 21st century: Men, the essential risk
[ESA-SP-1167] p 3914 N94-31181
Satellite direct readout: Opportunities for science education
[AD-A276257] p 3609 N94-31292
An innovative approach to space education p 3600 N94-31436
ISU in an era of partial reconvergence — International Space University p 3600 N94-31438
Solar physics and terrestrial effects. A curriculum guide for teachers, grade 7-12
[PB94-142247] p 3953 N94-31595
Practical neutron training course: Course notes
[PB94-145158] p 3867 N94-31681
Marsville: The cosmic village
[NASA-TM-109752] p 3913 N94-31806
NASA report to education, volume 9
[NASA-TM-109760] p 3913 N94-31817
Defying gravity
[NASA-TM-109747] p 3667 N94-31884
The sky is your classroom
[NASA-TM-109759] p 3914 N94-31887
Recommendations for meteorological data collection during physiological field studies
[AD-A276834] p 3901 N94-32153

X ray optics for science and technology
[AD-A277369] p 3880 N94-32155
A systems approach to computer-based training
p 3823 N94-32436
Literacity: A multimedia adult literacy package combining NASA technology, recursive ID theory, and authentic instruction theory p 3924 N94-32462
Virtual reality in medical education and assessment
p 3798 N94-32471
Using the National Information Infrastructure for social science, education, and informed decision making
[DE94-005442] p 3920 N94-32676
A facilitated mentoring process for engineers
[DE94-005823] p 3914 N94-32677
Multimedia as a desktop and classroom tool
[DE94-009116] p 3807 N94-32766
On the use of computers for teaching fluid mechanics
[NASA-TM-106587] p 3820 N94-32773
OPTIONS for systemic change in mathematics, science, and technology education: Scientist/teacher partnerships
[DE94-007472] p 3914 N94-32910
An exploratory study of neuro linguistic programming and communication anxiety
[AD-A277756] p 3682 N94-32986
Ada support for the mathematical foundations of software engineering
[AD-A278031] p 3822 N94-33284

EFFICIENCY
Design patterns mixing genericity and inheritance in the development of reusable components
[REPT-93-021] p 3808 N94-31178

EFFLUENTS
Time-dependent behavior of Mount Pinatubo aerosol
[DE94-001877] p 3764 N94-31601
Concentration system performance degradation in the aftermath of Mount Pinatubo
[DE94-001879] p 3764 N94-31602

EIGENVALUES
Arnoldi code for computing selected eigenvalues of sparse real unsymmetric matrices
[PB94-145182] p 3813 N94-31682
Stability and instability criteria for magnetohydrodynamics
[PB94-148475] p 3889 N94-31772
Applied Computational Electromagnetics Society Journal, volume 9, number 1, March 1994
[AD-A276753] p 3679 N94-32183

EIGENVECTORS
Experimental investigation of phonon eigenvectors using x ray interference fields
[ETN-94-95751] p 3865 N94-31511

EJECTORS
A mathematical model for simulating noise suppression of lined ejectors
[NASA-TP-3425] p 3861 N94-32930

EL NINO
Low frequence variability of the ocean atmosphere coupled system p 3777 N94-30986
The effect of westerly wind bursts on a tropical ocean general circulation model
[AD-A276423] p 3788 N94-31448
Air-sea interaction patterns in the equatorial Pacific
[AD-A277305] p 3788 N94-32072
ENSO forced variations of the sea surface temperature and adjusted sea level along the west coast of the United States
[AD-A277306] p 3789 N94-32327

ELASTIC BENDING
A case study of analysis methods for large deflections of a cantilever beam
[NASA-TM-108454] p 3739 N94-32903

ELASTIC BODIES
Vibration localization in dual-span axially moving elastic systems p 3736 N94-31964

ELASTIC DEFORMATION
Deformation and rupture of cylindrical shells under dynamic loading p 3733 N94-31288

ELASTIC PLATES
State of stress, faulting, and eruption characteristics of large volcanoes on Mars p 3940 N94-31108

ELASTIC PROPERTIES
Considering ties elasticities in high frequency rail dynamics
[ILR-MITT-281(1993)] p 3733 N94-31375
Evaluating in-plane elastic constants of damaged carbon-epoxy laminates using a quantitative ultrasonic technique p 3621 N94-31793
Creep-fatigue criteria and inelastic behavior of modified 9Cr-1Mo steel at elevated temperatures
[DE94-007915] p 3642 N94-31918
Nonlinear effects in interfacial fracture
p 3737 N94-31974
Elastic as limit of viscoelastic response, in a context of self-similar viscous limits
[AD-A277043] p 3738 N94-32273
On the mechanics of microballoon-reinforced metal matrix composites
[AD-A277928] p 3630 N94-33178

ELASTOHYDRODYNAMICS
Lubrication with binary mixtures: Liquid-liquid emulsion in elastohydrodynamics and metal forming
p 3658 N94-32490

ELASTOMERS
Novel electroactive polymers and block copolymers
[AD-A276119] p 3650 N94-31509
NMR studies of organic thin films
[AD-A276953] p 3656 N94-32221
Compatibility of refrigerants and lubricants with elastomers
[DE94-008552] p 3658 N94-32518
Electrostrictive response of elastomeric polymers
[AD-A277983] p 3664 N94-33247

ELASTOPLASTICITY
Contributions to the validation of the CJS model for granular materials
[ECL-92-56] p 3733 N94-31376
Micromechanics and effective properties of particulate composites and fluid suspensions p 3703 N94-31744
Influences of pressure-sensitive yielding and non-singular stress on plane-stress elastic-plastic crack-tip fields p 3737 N94-31965

ELECTRETS
A silicon condenser microphone: Modelling and electronic circuitry
[ISBN-9-09-005279-8] p 3688 N94-31517

ELECTRIC ARCS
Development and application of a multimesh auto-adaptive finite element method for the calculation of an electric arc plasma
[ECL-89-03] p 3886 N94-31378
Arcing in space structures in low Earth orbit
[NASA-CR-194223] p 3694 N94-32478
Arc-heater performance research
[NASA-CR-195821] p 3912 N94-32774
Evaluation of pyrolysis and arc tracking on candidate wire insulation designs for space applications
[NASA-CR-195332] p 3731 N94-32901

ELECTRIC AUTOMOBILES
Greenhouse gas emission impacts of electric vehicles under varying driving cycles in various countries and US cities
[DE94-007647] p 3765 N94-32600

ELECTRIC BATTERIES
Draft minutes of IAPG Mechanical Working Group meeting
[DE94-004954] p 3759 N94-31266
Feasibility study for the recycling of nickel metal hydride electric vehicle batteries
[DE94-000268] p 3690 N94-31598
The zinc electrode: Reactions and mechanisms
[DE94-007977] p 3691 N94-31919
Promising future energy storage systems: Nanomaterial based systems, Zn-air, and electromechanical batteries
[DE94-007443] p 3692 N94-32136
The hydrogen hybrid option
[DE94-006733] p 3667 N94-32148
Performance of the Sony lithium-ion rechargeable battery
[AD-A277076] p 3693 N94-32303
Proceedings of the Ad Hoc Workshop on Ceramics for Li/FeS2 batteries
[DE94-007460] p 3694 N94-32607
Low power, constant-flow air pump systems
[DE94-007463] p 3727 N94-32758
Polymer electrolyte fuel cells
[DE94-007558] p 3761 N94-32762
EDD-7 Electric Charge Point Meter test results
[DE94-008515] p 3696 N94-32828
Optimal planning of residential photovoltaic systems under various rate structure
[DE94-757272] p 3762 N94-32919

ELECTRIC BRIDGES
A series resonant converter in half bridge circuits with combined serial and parallel charge coupling and several output circuits
[ETN-94-95739] p 3687 N94-31373

ELECTRIC CHARGE
EDD-7 Electric Charge Point Meter test results
[DE94-008515] p 3696 N94-32828

ELECTRIC CONDUCTORS
Analysis of Dietz's single, rectangular pulse theory for the generation of radiation via photoelectrons
[DE94-006131] p 3681 N94-32661

ELECTRIC CONNECTORS
Hydrogen peroxide electrodes based on electrical connection of redox centers of various peroxidases to electrodes through a three-dimensional electron relaying polymer network
[AD-A276543] p 3691 N94-32056

ELECTRIC CONTACTS
Research on high reliability refractory ohmic contacts for GaAs FETs and MODFETs
[AD-A276848] p 3697 N94-33034

ELECTRIC CURRENT
Laboratory and space experiments as a key to the plasma universe
[TRITA-ALP-1993-01] p 3885 N94-31088
Introduction to electrochemical impedance
[AD-A277081] p 3636 N94-32352

ELECTRIC DISCHARGES
Development of a 3D numerical code to calculate the trajectories of the blow off electrons emitted by a vacuum surface discharge: Application to the study of the electromagnetic interference induced on a spacecraft
[ONERA-NT-1993-12] p 3863 N94-31227
Advanced high frequency partial discharge measuring system
[NASA-CR-195240] p 3697 N94-33044

ELECTRIC ENERGY STORAGE
Promising future energy storage systems: Nanomaterial based systems, Zn-air, and electromechanical batteries
[DE94-007443] p 3692 N94-32136

ELECTRIC EQUIPMENT
Payload holddown and release mechanism
p 3607 N94-33321

ELECTRIC EQUIPMENT TESTS
Influence of carbon dioxide on electronic equipment: Fire extinguishing with low concentration
[PB94-148749] p 3691 N94-31848
Structural probability concepts adapted to electrical engineering
[NASA-TM-106499] p 3739 N94-32735

ELECTRIC FIELDS
The double probe electric field experiment on Freja: Description and first results
[TRITA-ALP-1993-02] p 3885 N94-31089
Electrostatic reduction of particulates for laser resistant hafnia coatings
[DE94-005824] p 3651 N94-31557
Evidence for a correct SiO2 voltage acceleration model
[DE94-006578] p 3690 N94-31594
Transport phenomena in the Earth's plasma sheet
p 3772 N94-31970
A model of the ion chemistry of electrified convection
p 3868 N94-31993
MOM3D method of moments code theory manual
[NASA-CR-189594] p 3682 N94-32897
Electric field-induced changes in odd-numbered nylons
[AD-A278003] p 3664 N94-33138
Electrostrictive response of elastomeric polymers
[AD-A277983] p 3664 N94-33247

ELECTRIC GENERATORS
Draft minutes of IAPG Mechanical Working Group meeting
[DE94-004954] p 3759 N94-31266
Workshop on Commercialization of Pulsed Power Science and Technology Proceedings
[AD-A276987] p 3692 N94-32258

ELECTRIC MOTOR VEHICLES
Energy storage specification requirements for hybrid-electric vehicle
[DE94-008642] p 3694 N94-32521
Proceedings of the Ad Hoc Workshop on Ceramics for Li/FeS2 batteries
[DE94-007460] p 3694 N94-32607
Overview of Sandia's electric vehicle battery program
[DE94-008944] p 3696 N94-32806
Preliminary evaluation of the University of South Florida Mobile Data Acquisition System, the Idaho National Engineering Laboratory Versatile Data Acquisition System, and the Autologger Vehicle User Survey System produced by Instrumental Solutions of Ottawa, Canada for the Site Operator Program Field Data Collection
[DE94-008514] p 3920 N94-32827
EDD-7 Electric Charge Point Meter test results
[DE94-008515] p 3696 N94-32828

ELECTRIC NETWORKS
The Second International Workshop on Discrete Time Domain Modelling of Electromagnetic Fields and Networks. Program and information
[AD-A277136] p 3677 N94-32067

ELECTRIC POTENTIAL
Role of polycrystallinity in CdTe and CuInSe2 photovoltaic cells
[DE94-000293] p 3758 N94-31236
NN-interaction in (1)S0-state: Virtual level or dibaryon resonance?
[DE94-606492] p 3869 N94-32097
Novel failure analysis techniques using photon probing with a scanning optical microscope
[DE94-006594] p 3692 N94-32112

High power switch design for the Nova upgrade laser (Project HERCULES: High Energy Research Concerning the Ultimate Lifetime of Experimental Switches)
[DE94-007921] p 3719 N94-32654
X ray absorption study of pulsed laser deposited boron nitride films
[DE94-008295] p 3662 N94-32855
Stabilization method of A.C. arc plasma
[DE94-757268] p 3893 N94-32916
Advanced high frequency partial discharge measuring system
[NASA-CR-195240] p 3697 N94-33044

ELECTRIC POWER PLANTS
Emissions of greenhouse gases from the use of transportation fuels and electricity
[DE94-006166] p 3765 N94-31625

ELECTRIC POWER SUPPLIES
The 1988 Goddard Space Flight Center Battery Workshop
[NASA-CP-3237] p 3758 N94-31233
Development of silver-zinc cells of improved cycle life and energy density
[AD-A277311] p 3693 N94-32329
Flywheel Energy Storage Technology Workshop
[DE94-008064] p 3761 N94-32705

ELECTRIC POWER TRANSMISSION
Optimal reactive power dispatch of power systems using nonlinear programming
[MATHS-REPT-A-209] p 3808 N94-31164

ELECTRIC WIRE
Evaluation of pyrolysis and arc tracking on candidate wire insulation designs for space applications
[NASA-CR-195332] p 3731 N94-32901

ELECTRICAL ENGINEERING
A silicon condenser microphone: Modelling and electronic circuitry
[ISBN-9-09-005279-8] p 3688 N94-31517
Structural probability concepts adapted to electrical engineering
[NASA-TM-106499] p 3739 N94-32735

ELECTRICAL FAULTS
A hierarchical approach to test generation for CMOS VLSI circuits
[ISBN-9-09-005449-9] p 3689 N94-31535
Hierarchical fault catalog process for diagnosis of analog circuits
[ETN-94-95730] p 3689 N94-31571
X ray pulse considerations and electron flow in high voltage diodes
[AD-A277301] p 3868 N94-32044
Time resolved measurements of light produced by onset of plasma formation on electrodes of fast pulsed high voltage diodes
[AD-A277974] p 3894 N94-33264

ELECTRICAL GROUNDING
Grounding ring for ground adapters
[AD-D016118] p 3697 N94-32962

ELECTRICAL IMPEDANCE
Electromagnetic scattering through loaded aperture panels with nonzero contact impedance
[ONERA-NT-1993-2] p 3673 N94-31418
Introduction to electrochemical impedance
[AD-A277081] p 3636 N94-32352

ELECTRICAL INSULATION
Chemical structure and kinetics at liquid/solid interfaces
[AD-A277112] p 3636 N94-32304
Evaluation of pyrolysis and arc tracking on candidate wire insulation designs for space applications
[NASA-CR-195332] p 3731 N94-32901

ELECTRICAL MEASUREMENT
Advanced high frequency partial discharge measuring system
[NASA-CR-195240] p 3697 N94-33044

ELECTRICAL PROPERTIES
Role of polycrystallinity in CdTe and CuInSe2 photovoltaic cells
[DE94-000293] p 3758 N94-31236
The influence of transmutation, void swelling, and flux/spectra uncertainties on the electrical properties of copper and copper alloys
[DE94-006213] p 3641 N94-31626
Research on the stability, electronic properties, and structure of a-Si:H and its alloys
[DE94-000292] p 3899 N94-31813
Hydrogen peroxide electrodes based on electrical connection of redox centers of various peroxidases to electrodes through a three-dimensional electron relaying polymer network
[AD-A276543] p 3691 N94-32056
The relative performance of FeS2 and CoS in long-life thermal-battery applications
[DE94-006145] p 3695 N94-32663
Research on stable, high-efficiency amorphous silicon multijunction modules
[DE94-000298] p 3695 N94-32680
The ferroelectric behavior of odd-numbered nylons
[AD-A278126] p 3663 N94-33058
Electrical characteristics of GaAs MESFET fabrication by ion implantation of Si or Se
[AD-A278416] p 3909 N94-33328

ELECTRICAL RESISTANCE
The constant current loop: A new paradigm for resistance signal conditioning p 3685 N94-32461
Space flight printed wiring board measling investigation
[NASA-TM-104602] p 3732 N94-33101

ELECTRICAL RESISTIVITY
Analysis of deep seismic reflection and other data from the southern Washington Cascades
[DE94-005958] p 3771 N94-31525
The influence of transmutation, void swelling, and flux/spectra uncertainties on the electrical properties of copper and copper alloys
[DE94-006213] p 3641 N94-31626
Fermi surface instability at 0.4 K in a heavy-fermion YbBiPt: SDW?
[DE94-006224] p 3899 N94-31916
Oxidation resistant copper
[AD-D016099] p 3696 N94-32721
Strongly anisotropic s-wave versus d-wave gap in cuprate superconductors: Evidence and theory
[DE94-007579] p 3904 N94-32746
Isothermal sintering, microstructure, and superconducting properties of Y1Ba2Cu3O(7-x) compound
[DE94-008132] p 3905 N94-32779
Properties of doped and undoped (Ca,Sr)CuO2 thin films
[DE94-007230] p 3905 N94-32785
An electrical test system for conductor formation process analysis
[DE94-007291] p 3696 N94-32786
Resistivity measurements on the neutron irradiated detector grade silicon materials
[DE94-009083] p 3906 N94-32822
Analytic formulation for the ac electrical conductivity in two-temperature, strongly coupled, overdense plasma: FORTRAN subroutine
[DE94-009466] p 3893 N94-32915
Lightweight zinc electrode
[AD-D016181] p 3698 N94-33181

ELECTRICITY
Solar activities at Sandia National Laboratories
[DE94-007737] p 3761 N94-32648

ELECTRO-OPTICAL EFFECT
Manufacture of light-damage resistant, planar, single mode waveguide on lithium niobate
[DSIS-94-01503] p 3879 N94-31850
Reconfigurable optical switches with monolithic electrical-to-optical interfaces
[DE94-007745] p 3881 N94-32385
Energetics, bonding mechanism, and electronic structure of ceramic/ceramic and metal/ceramic interfaces
[DE94-008551] p 3659 N94-32656
Characterization of crosslinked electrooptic polyimides
[DE94-007934] p 3661 N94-32819

ELECTRO-OPTICS
The conoscopic microscope
[TELECOM-93-E-017] p 3877 N94-31173
Electrooptic crystal growth and properties
[AD-A276023] p 3896 N94-31439
Manufacture of light-damage resistant, planar, single mode waveguide on lithium niobate
[DSIS-94-01503] p 3879 N94-31850
Recent developments in polymeric charge transfer complexes
[AD-A277108] p 3654 N94-31979
The sol-gel-xerogel transition
[AD-A276647] p 3616 N94-32038
Multifunctional macromolecules
[AD-A277347] p 3656 N94-32246
Stable second-order nonlinear optical materials based on interpenetrating polymer networks
[AD-A277410] p 3658 N94-32579
Energetics, bonding mechanism, and electronic structure of ceramic/ceramic and metal/ceramic interfaces
[DE94-008551] p 3659 N94-32656
Characterization of thermally stable dye-doped polyimide based electrooptic materials
[DE94-005309] p 3882 N94-32674
Reconfigurable Array of Radiating Elements (RARE) controlled by light
[NASA-CR-195828] p 3884 N94-33073

ELECTROACOUSTICS
Minutes: Accredited Standards Committee on Bioacoustics, S3. US TAG for ISO/TC 43, acoustics, IEC/TC 29 electroacoustics, and ISO/TC 108/SC4 human exposure to mechanical vibration and shock
[AD-A276201] p 3795 N94-31490

ELECTROCATALYSTS
Polymer electrolyte fuel cells
[DE94-007558] p 3761 N94-32762

ELECTROCHEMICAL CELLS
Dielectric viscometer including fixed and variable cells
[AD-D016139] p 3639 N94-32973
Room temperature molten salts for advanced energy conversion and storage
[AD-A277777] p 3763 N94-33015

ELECTROCHEMICAL OXIDATION
Synthesis, characterization, phase diagrams and superconducting, and normal state magnetic properties of La(2-x)Sr(x)CuO4 (0 is less than or equal to x which is less than or equal to 0.08) and electrochemically oxidized La(2-x)Sr(x)CuO(4 + delta) (0 is less than or equal to x which is less than or equal to 0.33, 0 is less than or equal to delta which is less than or equal to 0.12)
[DE94-005260] p 3895 N94-31067
Electrochemical surface modification of silicon monocrystals: A surface analytic examination
[ETN-94-95733] p 3633 N94-31574
Electrical communication between glucose oxidase and electrodes based on poly(vinylimidazole) complex of Os(bpy)2Cl2
[AD-A276585] p 3635 N94-32231

ELECTROCHEMISTRY
Infrared spectroelectrochemical study of cyanide adsorption and reactions at platinum electrodes in aqueous perchlorate electrolyte
[AD-A276402] p 3631 N94-31238
The zinc electrode: Reactions and mechanisms
[DE94-007977] p 3691 N94-31919
Hydrogen peroxide electrodes based on electrical connection of redox centers of various peroxidases to electrodes through a three-dimensional electron relaying polymer network
[AD-A276543] p 3691 N94-32056
Electrical communication between glucose oxidase and electrodes based on poly(vinylimidazole) complex of Os(bpy)2Cl2
[AD-A276585] p 3635 N94-32231
Introduction to electrochemical impedance
[AD-A277081] p 3636 N94-32352
Scanning tunneling microscopy and infrared spectroscopy as combined in-situ probes of electrochemical adlayer structure: Cyanide on Pt(111)
[AD-A276715] p 3909 N94-33274
Nanoscale structural changes upon electrooxidation of Au(111) as probed by potentiodynamic scanning tunneling microscopy
[AD-A276780] p 3909 N94-33275

ELECTRODE MATERIALS
Hydrogen peroxide electrodes based on electrical connection of redox centers of various peroxidases to electrodes through a three-dimensional electron relaying polymer network
[AD-A276543] p 3691 N94-32056
A new-type of long-range restructuring of ordered metal surfaces induced by lateral adsorbate interactions: Iodide on AU(110) electrodes
[AD-A276633] p 3643 N94-32060
Proceedings of the Ad Hoc Workshop on Ceramics for Li/FeS2 batteries
[DE94-007460] p 3694 N94-32607

ELECTRODEPOSITION
Computerized Ultrasonic Testing System (CUTS) for in-process thickness determination
p 3862 N94-32456

ELECTRODES
Molecular dynamics computer simulations of charged metal electrode-aqueous electrolyte interfaces
[AD-A276401] p 3863 N94-31237
Infrared spectroelectrochemical study of cyanide adsorption and reactions at platinum electrodes in aqueous perchlorate electrolyte
[AD-A276402] p 3631 N94-31238
The zinc electrode: Reactions and mechanisms
[DE94-007977] p 3691 N94-31919
The charging effect in high-Tc superconducting thin films
[AD-A277265] p 3900 N94-32040
Hydrogen peroxide electrodes based on electrical connection of redox centers of various peroxidases to electrodes through a three-dimensional electron relaying polymer network
[AD-A276543] p 3691 N94-32056
A new-type of long-range restructuring of ordered metal surfaces induced by lateral adsorbate interactions: Iodide on AU(110) electrodes
[AD-A276633] p 3643 N94-32060
Charge-dependent atomic-scale structures of high-index and (110) gold electrode surfaces as revealed by scanning tunneling microscopy
[AD-A276782] p 3869 N94-32170

Electrical communication between glucose oxidase and electrodes based on poly(vinylimidazole) complex of Os(bpy)2Cl2
[AD-A276585] p 3635 N94-32231
Structure-property relationships of carbon aerogels
[DE94-007120] p 3660 N94-32687
Arc-heater performance research
[NASA-CR-195821] p 3912 N94-32774
Ionization EM calorimetry with accordion electrodes and liquid krypton or argon
[DE94-009082] p 3713 N94-32821
Magnetohydrodynamic boundary layer control system
[AD-D016120] p 3710 N94-32958
Dielectric viscometer including fixed and variable cells
[AD-D016139] p 3639 N94-32973
Lightweight zinc electrode
[AD-D016181] p 3698 N94-33181
Time resolved measurements of light produced by onset of plasma formation on electrodes of fast pulsed high voltage diodes
[AD-A277974] p 3894 N94-33264

ELECTROLYTES
Molecular dynamics computer simulations of charged metal electrode-aqueous electrolyte interfaces
[AD-A276401] p 3863 N94-31237
Infrared spectroelectrochemical study of cyanide adsorption and reactions at platinum electrodes in aqueous perchlorate electrolyte
[AD-A276402] p 3631 N94-31238
Electrochemical surface modification of silicon monocrystals: A surface analytic examination
[ETN-94-95733] p 3633 N94-31574
The zinc electrode: Reactions and mechanisms
[DE94-007977] p 3691 N94-31919
A new-type of long-range restructuring of ordered metal surfaces induced by lateral adsorbate interactions: Iodide on AU(110) electrodes
[AD-A276633] p 3643 N94-32060
Charge-dependent atomic-scale structures of high-index and (110) gold electrode surfaces as revealed by scanning tunneling microscopy
[AD-A276782] p 3869 N94-32170
The relative performance of FeS2 and CoS in long-life thermal-battery applications
[DE94-006145] p 3695 N94-32663
Sensitivity of electrochemical adlayer structure to the metal crystallographic orientation: Potential-independent iodide adsorption on Au(100) in comparison with other low-index surfaces
[AD-A276714] p 3909 N94-33273
A tandem microscopic-electrochemical examination of a charge-induced surface phase sequence: Ordered Au(110) in aqueous iodide electrolytes as probed by potentiodynamic scanning tunneling microscopy
[AD-A276905] p 3875 N94-33277

ELECTROLYTIC CELLS
Polymer electrolyte fuel cells
[DE94-007558] p 3761 N94-32762

ELECTROMAGNETIC ABSORPTION
Matter-radiation interactions in the atmosphere
p 3776 N94-30998
Near resonant absorption by atoms in intense fluctuating laser fields
[DE94-005873] p 3714 N94-31200
Structural studies of photoinduced intramolecular electron transfer in cyclopentadienylnickelnitrosyl
[DE94-008467] p 3874 N94-32876

ELECTROMAGNETIC COUPLING
Lightning-induced coupling of the radiation belts to geomagnetically conjugate ionospheric regions
p 3772 N94-31773

ELECTROMAGNETIC FIELDS
Development of a 3D numerical code to calculate the trajectories of the blow off electrons emitted by a vacuum surface discharge: Application to the study of the electromagnetic interference induced on a spacecraft
[ONERA-NT-1993-12] p 3863 N94-31227
Formulation of time-domain planar near-field measurements without probe correction
[AD-A276380] p 3672 N94-31371
Finite element analysis of time-independent superconductivity p 3691 N94-31905
The Second International Workshop on Discrete Time Domain Modelling of Electromagnetic Fields and Networks. Program and information
[AD-A277136] p 3677 N94-32067
System for monitoring and analyzing field energy exposure
[AD-D016115] p 3681 N94-32625

ELECTROMAGNETIC INTERACTIONS
Evaluation of HardSys/HardDraw, an expert system for electromagnetic interactions modelling
[AD-A276218] p 3670 N94-31063
Microwave dielectric behavior of soils. Report 1: Summary of related research and applications
[AD-A275980] p 3771 N94-31351
Diagnostics of high-brightness short-pulse lasers and the plasmas they generate
[DE94-006165] p 3716 N94-31624
Baryogenesis from a primordial lepton asymmetry
[PB94-145166] p 3868 N94-31921
Short-pulse, high-intensity lasers at Los Alamos
[DE94-007545] p 3720 N94-32760
Proceedings of the International Workshop on Low Energy Muon Science: LEMS 1993
[DE94-006495] p 3874 N94-32804
MOM3D method of moments code theory manual
[NASA-CR-189594] p 3682 N94-32897

ELECTROMAGNETIC INTERFERENCE
An adaptive Kalman filter excisor for suppressing narrowband interference
[AD-A276286] p 3671 N94-31253

ELECTROMAGNETIC NOISE
Fractal and spectral analysis
[ISBN-0-315-86460-5] p 3676 N94-31796
Optimal adaptive estimation algorithm for harmonic current reduction using power limited active line conditioners
[AD-A277354] p 3693 N94-32336
Restoration of interferometric, polarimetric, radiometric, and textural information in SAR images
p 3750 N94-32535
NOAA-9 Earth Radiation Budget Experiment (ERBE) scanner offsets determination
[NASA-TM-109086] p 3785 N94-32737
Reliable communication in the presence of severe noise or jamming
[AD-A276410] p 3684 N94-33173

ELECTROMAGNETIC PROPERTIES
Evaluation of HardSys/HardDraw, an expert system for electromagnetic interactions modelling
[AD-A276218] p 3670 N94-31063

ELECTROMAGNETIC PULSES
Diagnostics of high-brightness short-pulse lasers and the plasmas they generate
[DE94-006165] p 3716 N94-31624
High peak power microwaves: A health hazard
[AD-A277168] p 3681 N94-32576
Superluminous laser pulse in an active medium
[DE94-007110] p 3720 N94-32684
Pump-probe method for investigating laser ablation and optical damage threshold mechanisms in optical materials
[DE94-008291] p 3720 N94-32753
Short-pulse, high-intensity lasers at Los Alamos
[DE94-007545] p 3720 N94-32760
Ultrafast x ray sources
[AD-A277455] p 3721 N94-33012

ELECTROMAGNETIC RADIATION
Radiation/remote sensing: Review of the principal definitions p 3757 N94-30996
Analysis of the photodiode boundary layer transition indicator
[DE94-005311] p 3701 N94-31268
Photonic band gap materials
[DE94-005566] p 3677 N94-32101
Electromagnetic wave reflection from irregular plasma layers
[AD-A276727] p 3678 N94-32161
System for monitoring and analyzing field energy exposure
[AD-D016115] p 3681 N94-32625
Analysis of Dietz's single, rectangular pulse theory for the generation of radiation via photoelectrons
[DE94-006131] p 3681 N94-32661

ELECTROMAGNETIC SCATTERING
Electromagnetic scattering through loaded aperture panels with nonzero contact impedance
[ONERA-NT-1993-2] p 3673 N94-31418
Multiple scattering of polarized radiation in planetary atmospheres
[ETN-94-96018] p 3674 N94-31551
Development of a frequency-domain electromagnetic scattering measurement system
[AD-A276738] p 3678 N94-32179
Applied Computational Electromagnetics Society Journal, volume 9, number 1, March 1994
[AD-A276753] p 3679 N94-32183
Studies of optical beam phase conjugation and electromagnetic scattering process
[AD-A278389] p 3884 N94-33145

ELECTROMAGNETIC SPECTRA
Economic analysis of the hertzian spectrum
[TELECOM-93-E-012] p 3670 N94-31171

ELECTROMAGNETIC WAVE FILTERS
Study of continuous-time and mixed analog-digital operators
[TELECOM-93-E-010] p 3687 N94-31170
Analysis and design of a formal neural network for filtering a dynamic signal
[ISBN-0-315-86932-1] p 3832 N94-31873
Advanced satellite communication system
[NASA-CR-194211] p 3681 N94-32477

ELECTROMAGNETIC WAVE TRANSMISSION
The High-Frequency Benchmark propagation program
[AD-A276323] p 3672 N94-31334
Photonic band gap materials
[DE94-005566] p 3677 N94-32101
Atmospheric propagation effects through natural and man-made obscurants for visible to MM-wave radiation
[AD-A276919] p 3679 N94-32235

ELECTROMAGNETISM
Applied Computational Electromagnetics Society Journal, volume 9, number 1, March 1994
[AD-A276753] p 3679 N94-32183

ELECTROMECHANICAL DEVICES
Promising future energy storage systems: Nanomaterial based systems, Zn-air, and electromechanical batteries
[DE94-007443] p 3692 N94-32136

ELECTROMOTIVE FORCES
Theoretical principles for designing long stator/linear motors with iron
[ETN-94-95741] p 3688 N94-31374
Applicable dimensioning and measure and technological examination of long stator-linear motors for magnetic high-speed railways
[ETN-94-95734] p 3689 N94-31575

ELECTRON ACCELERATION
Time-dependent behavior of active galactic nuclei with pair production p 3929 N94-31125
Electron acceleration system
[AD-D016143] p 3893 N94-32977

ELECTRON ACCELERATORS
Concept, construction and testing of a high resolution QCLAM electron spectrometer with large solid angle and high impulse acceptance for the electron accelerator S-DALINAC
[ETN-94-95755] p 3711 N94-31515
Repetitively pulsed backward-wave oscillator investigations
[AD-A278281] p 3698 N94-33142

ELECTRON ATTACHMENT
Electron: Cluster interactions
[DE94-009089] p 3874 N94-32807

ELECTRON BEAMS
Electron-beam controlled semiconductor switches
[AD-A276198] p 3686 N94-31057
Instrumentation for EXELFS measurements using convergent beam diffraction coupling to the electron energy loss spectrometer
[USIP-93-07] p 3358 N94-31084
Proceedings of the 37th international symposium on electron, ion, and photon beams
[AD-A276478] p 3875 N94-31247
Emission from ferroelectric cathodes
[DE94-006732] p 3863 N94-31270
Spectroscopy and atomic physics in EBIT and SuperEBIT
[DE94-006050] p 3864 N94-31508
Two-gigawatt burst-mode operation of the Intense Microwave Prototype (IMP) Free-Electron Laser (FEL) for the Microwave Tokamak Experiment (MTX)
[DE94-006613] p 3715 N94-31580
First-wall heat-flux measurements during ELMing H-mode plasma
[DE94-008310] p 3888 N94-31765
ITS version 3.0: Powerful, user-friendly software for radiation modelling
[DE94-006607] p 3678 N94-32113
Complete model description of an electron beam using ACCEPT Monte Carlo simulation code
[DE94-007063] p 3872 N94-32628
Electron energy dependence of amorphization in Zr3Fe
[DE94-008459] p 3906 N94-32875
Electron acceleration system
[AD-D016143] p 3893 N94-32977
Repetitively pulsed backward-wave oscillator investigations
[AD-A278281] p 3698 N94-33142

ELECTRON BUNCHING
Free electrons as a versatile source of coherent radiation
[ETN-94-96011] p 3715 N94-31545

ELECTRON CAPTURE
Spectroscopy and atomic physics in EBIT and SuperEBIT
[DE94-006050] p 3864 N94-31508

ELECTRON CYCLOTRON HEATING
Noninductive current drive experiments on D3-D, and future plans
[DE94-007373] p 3886 N94-31324
Two-gigawatt burst-mode operation of the Intense Microwave Prototype (IMP) Free-Electron Laser (FEL) for the Microwave Tokamak Experiment (MTX)
[DE94-006613] p 3715 N94-31580

FWCD and ECCD experiments on D3-D
[DE94-007371] p 3890 N94-32201
Fusion applications of high power millimeter wave sources
[DE94-007374] p 3718 N94-32202

ELECTRON DENSITY (CONCENTRATION)
Radar scattering from the summer polar mesosphere: Theory and observations p 3772 N94-32077
Electromagnetic wave reflection from irregular plasma layers
[AD-A276727] p 3678 N94-32161
Calculations of nonspherically averaged charge densities for substitutionally disordered alloys
[DE94-008293] p 3646 N94-32754
Anisotropic phase separation through the metal-insulator transition in amorphous Mo-Ge and Fe-Ge alloys
[DE94-007259] p 3646 N94-32795
A study of weak solutions and their regularizations by numerical methods
[AD-A277453] p 3850 N94-33175
Phase relationships and stability of the (mu)- and (zeta)-phases in the Ag-Al-X (X=Zn, Ga, Ge) systems
[DE94-009391] p 3648 N94-33270

ELECTRON DENSITY PROFILES
An analysis of ionospheric dayglow from observations of the Naval Postgraduate School Middle Ultraviolet Spectrograph (MUSTANG)
[AD-A277351] p 3773 N94-32335
EUROCAP program
[AD-A278084] p 3776 N94-33184

ELECTRON DIFFRACTION
Instrumentation for EXELFS measurements using convergent beam diffraction coupling to the electron energy loss spectrometer
[USIP-93-07] p 3858 N94-31084
Nucleation and growth of cubic boron nitride films produced by ion-assisted pulsed laser deposition
[DE94-007295] p 3661 N94-32796
Imaging of surface structure with energy-dependent photoelectron diffraction
[DE94-009096] p 3907 N94-32934

ELECTRON DIFFUSION
Radar scattering from the summer polar mesosphere: Theory and observations p 3772 N94-32077

ELECTRON DISTRIBUTION
A comprehensive analysis of electron conical distributions from multi-satellite databases
[NASA-CR-195848] p 3953 N94-33047

ELECTRON EMISSION
Emission from ferroelectric cathodes
[DE94-006732] p 3863 N94-31270
X ray pulse considerations and electron flow in high voltage diodes
[AD-A277301] p 3868 N94-32044
Time resolved measurements of light produced by onset of plasma formation on electrodes of fast pulsed high voltage diodes
[AD-A277974] p 3894 N94-33264

ELECTRON ENERGY
Free electrons as a versatile source of coherent radiation
[ETN-94-96011] p 3715 N94-31545
X ray pulse considerations and electron flow in high voltage diodes
[AD-A277301] p 3868 N94-32044
Electron energy dependence of amorphization in Zr3Fe
[DE94-008459] p 3906 N94-32875
Irradiation-induced phase transformations in zirconium alloys
[DE94-008484] p 3648 N94-32993

ELECTRON IMPACT
Production and detection of metastable atomic oxygen
[ISBN-0-315-87364-7] p 3868 N94-31915

ELECTRON IRRADIATION
Irradiation-induced phase transformations in zirconium alloys
[DE94-008484] p 3648 N94-32993

ELECTRON MICROSCOPES
In-situ TEM crystallization of anorthite-glass films on (alpha)-Al2O3
[DE94-008317] p 3652 N94-31780

ELECTRON MICROSCOPY
Microstructures and mechanical properties of Al3Ti-based alloys: Analysis in single phase and multiphase systems
[ONERA-NT-1993-6] p 3640 N94-31420

ELECTRON ORBITALS
Occupied and unoccupied orbitals of C60 and C70
[DE94-008294] p 3873 N94-32755
Investigation of superconductivity and magnetism in d and f-electron materials
[DE94-006535] p 3907 N94-32933

ELECTRON PARAMAGNETIC RESONANCE
Electron spin resonance measurements of Er(3+) and Mn(2+) in the high temperature superconductor compounds La(2-x)Sr(x)CuO(4-delta)
[ETN-94-95746] p 3898 N94-31612

ELECTRON PHONON INTERACTIONS
Experimental evidence for lattice effects in high temperature superconductors
[DE94-006250] p 3899 N94-31633

ELECTRON PLASMA
Transport properties of quark and gluon plasmas
[DE94-007043] p 3864 N94-31405

ELECTRON PRECIPITATION
Convection and electrodynamic signatures in the vicinity of a Sun-aligned arc: Results from the Polar Acceleration Regions and Convection Study (Polar ARCS)
p 3954 N94-31102

ELECTRON PROBES
Deuterium absorption and material phase characteristics of SAES St198 Zr-Fe alloy
[DE94-008275] p 3648 N94-32781

ELECTRON RADIATION
ITS version 3.0: Powerful, user-friendly software for radiation modelling
[DE94-006607] p 3678 N94-32113
Self-consistent effects of magnetospheric hydromagnetic waves on ring current ions
[AD-A277406] p 3774 N94-32346

ELECTRON SCATTERING
Convective solar nebula p 3930 N94-31130
Results from the H1 experiment at HERA
[PB94-145174] p 3868 N94-32008
Electron: Cluster interactions
[DE94-009089] p 3874 N94-32807

ELECTRON SPECTROSCOPY
Analytical applications of scanning tunneling microscopy
[AD-A276066] p 3711 N94-31283
Concept, construction and testing of a high resolution QCLAM electron spectrometer with large solid angle and high impulse acceptance for the electron accelerator S-DALINAC
[ETN-94-95755] p 3711 N94-31515

ELECTRON SPIN
Experimental evidence for lattice effects in high temperature superconductors
[DE94-006250] p 3899 N94-31633

ELECTRON TRAJECTORIES
Development of a 3D numerical code to calculate the trajectories of the blow off electrons emitted by a vacuum surface discharge: Application to the study of the electromagnetic interference induced on a spacecraft
[ONERA-NT-1993-12] p 3863 N94-31227

ELECTRON TRANSFER
A visible light initiating system for free radical promoted cationic polymerization
[AD-A277164] p 3655 N94-32069
A general stochastic Liouville theory for sequential and superexchange electron-transfer reactions involving three Marcus potential surfaces
[DE94-007695] p 3869 N94-32141
Some perspectives on solution-phase electron-transfer processes
[AD-A276906] p 3635 N94-32216
Theoretical studies of electron transfer and optical spectroscopy
[DE94-006985] p 3871 N94-32375
Structural studies of photoinduced intramolecular electron transfer in cyclopentadienylnickelnitrosyl
[DE94-008467] p 3874 N94-32876
A study of weak solutions and their regularizations by numerical methods
[AD-A277453] p 3850 N94-33175

ELECTRON TRANSITIONS
Stark broadening of the 2S state of hydrogen and deuterium in arc plasmas of low density
[ETN-94-95731] p 3888 N94-31572
Progress in understanding and improving x ray lasers
[DE94-006048] p 3720 N94-32794

ELECTRON-POSITRON PAIRS
A constraint on the pair-density ratio (Z+) in an electron-positron pair wind p 3930 N94-31132
Gamma Large Area Silicon Telescope (GLAST)
[DE94-006439] p 3925 N94-31786
F0-975, A0-980 as eye-witnesses of confinement
[PB94-147105] p 3868 N94-31923

ELECTRONIC BULLETIN BOARDS
The FELICIA bulletin board system and the IRBIS anonymous FTP server: Computer security information sources for the DOE community
[DE94-008219] p 3825 N94-31920

ELECTRONIC CONTROL
Custom uniform source system
[NASA-CR-189332] p 3711 N94-31492
International Space Station Alpha's bearing, motor, and roll ring module developmental testing and results
p 3803 N94-33295

ELECTRONIC COUNTERMEASURES
Analysis of key performance parameters of phase sampling digital RF memories
[AD-A276019] p 3688 N94-31494
Atmospheric propagation effects through natural and man-made obscurants for visible to MM-wave radiation
[AD-A276919] p 3679 N94-32235

ELECTRONIC EQUIPMENT
The 18th annual electronics manufacturing seminar
[AD-A276038] p 3687 N94-31281
Proceedings of the International Workshop on Computational Electronics
[AD-A277020] p 3692 N94-32259
Vulnerability assessment of a space based weapon platform electronic system exposed to a thermonuclear weapon detonation
[DE94-007229] p 3611 N94-32667

ELECTRONIC EQUIPMENT TESTS
Module generation for self-testing integrated systems
[ISBN-9-09-004570-8] p 3688 N94-31520
Validation of the Environmentally Conscious Manufacturing Integrated Demonstration hardware
[DE94-003824] p 3765 N94-32144
The CF-18 diagnostic and maintenance expert system project p 3567 N94-33338
A diagnostic expert system for digital circuits
p 3699 N94-33340

ELECTRONIC MAIL
PEM public key certificate cache server
[DE94-006404] p 3675 N94-31784
Electronic mail and organizational knowledge: Media use in a global corporation
[AD-A276707] p 3678 N94-32121

ELECTRONIC MODULES
Heat transfer studies on a rectangular channel with offset plate fins
[AD-A277300] p 3912 N94-32043
Detailed design of the 2MW Demonstration Plant
[DE94-000042] p 3762 N94-32823
Ceramic and metal composite circuit-board-level technology for application specific electronic modules (ASEM)
[AD-A277961] p 3630 N94-33180

ELECTRONIC PACKAGING
Flexible manufacturing for photonics device assembly
p 3669 N94-32449
Metal-ion spin-on glasses: Novel materials for active waveguides
[DE94-007738] p 3882 N94-32649
Automated fiber pigtailing technology
[DE94-007072] p 3695 N94-32688

ELECTRONIC WARFARE
Modular Simulator System (MSS). System/segment specification for the generic modular simulator system-electronic warfare module, volume 9
[AD-A276976] p 3589 N94-32315
Automatic modulation recognition
p 3686 N94-33153
A decision support system for electronic warfare analysts p 3853 N94-33336

ELECTRONS
Time-dependent behavior of active galactic nuclei with pair production p 3929 N94-31125
Elimination of two atomic electrons by a single high energy photon
[DE94-006834] p 3864 N94-31320
X ray pulse considerations and electron flow in high voltage diodes
[AD-A277301] p 3868 N94-32044
ITS version 3.0: Powerful, user-friendly software for radiation modelling
[DE94-006607] p 3678 N94-32113
Self-consistent effects of magnetospheric hydromagnetic waves on ring current ions
[AD-A277406] p 3774 N94-32346
Ionization EM calorimetry with accordion electrodes and liquid krypton or argon
[DE94-009082] p 3713 N94-32821

ELECTROPHORESIS
An axial approach to detection in capillary electrophoresis
[DE94-005556] p 3631 N94-31154

ELECTROPHYSIOLOGY
The organization of the suprachiasmatic circadian pacemaker of the rat and its regulation by neurotransmitters and modulators
[AD-A277324] p 3793 N94-32622

ELECTRORHEOLOGICAL FLUIDS
Vibration dampener and method for making same
[AD-D016094] p 3739 N94-32733
Light scattering studies of a model electrorheological fluid
[DE94-007860] p 3883 N94-32818

ELECTROSTATIC CHARGE
Influence of carbon dioxide on electronic equipment: Fire extinguishing with low concentration
[PB94-148749] p 3691 N94-31848
ELECTROSTATICS
Electrostatic reduction of particulates for laser resistant hafnia coatings
[DE94-005824] p 3651 N94-31557
ELECTROSTRICTION
Electrostrictive response of elastomeric polymers
[AD-A277983] p 3664 N94-33247
ELECTROWEAK MODEL
Proceedings of the International Workshop on Low Energy Muon Science: LEMS 1993
[DE94-006495] p 3874 N94-32804
ELEMENTARY EXCITATIONS
Collective and quasiparticle excitations in light Pb isotopes
[ETN-94-96014] p 3865 N94-31548
Impurities and conductivity in a D-wave superconductor
[DE94-006222] p 3898 N94-31628
Strongly anisotropic s-wave versus d-wave gap in cuprate superconductors: Evidence and theory
[DE94-007579] p 3904 N94-32746
ELEMENTARY PARTICLE INTERACTIONS
State of hadron collider physics
[DE94-005279] p 3863 N94-31147
BNL possibilities
[DE94-007179] p 3864 N94-31398
F0-975, A0-980 as eye-witnesses of confinement
[PB94-147105] p 3868 N94-31923
Positron-molecule interactions
[AD-A276542] p 3869 N94-32082
The Nijmegen hyperon-nucleon potentials
[DE94-007557] p 3869 N94-32139
Numerical simulation of quantum many-body systems
[DE94-008451] p 3912 N94-32513
A guide to experimental elementary particle physics literature, 1988-1992
[DE94-007445] p 3873 N94-32768
Studies of jet production with the D0 detector
[DE94-008271] p 3873 N94-32780
ELEMENTARY PARTICLES
Elementary particle physics
[DE94-006071] p 3866 N94-31620
A guide to experimental elementary particle physics literature, 1988-1992
[DE94-007445] p 3873 N94-32768
ELEVATION
Geoid-to-topography ratios on Venus: A global perspective p 3940 N94-31110
World height system definition and implementation
[AD-A276725] p 3747 N94-32160
Study of subpolar glaciers of Spitzbergen using SPOT, ERS-1, and hypsometric data: Results and perspectives p 3753 N94-32553
ELEVATION ANGLE
Prediction of the plane wave beamformed acoustic arrival structure for the 1992 Barents Sea coastal tomography test
[AD-A276741] p 3788 N94-32181
ELLIPSOMETERS
Post-calibration correction for rotating-analyzer ellipsometer with optical fiber bundle detection system
[AD-A277329] p 3881 N94-32280
ELLIPSOMETRY
Post-calibration correction for rotating-analyzer ellipsometer with optical fiber bundle detection system
[AD-A277329] p 3881 N94-32280
Si/SiO2 interface studies by immersion ellipsometry
[AD-A277277] p 3881 N94-32324
Electron cyclotron resonance plasma oxidation studies of InP
[AD-A277431] p 3893 N94-33007
ELLIPTIC DIFFERENTIAL EQUATIONS
Variational elliptic solver for atmospheric applications
[DE94-007725] p 3774 N94-32647
ELLIPTIC FUNCTIONS
Transformation of two and three-dimensional regions by elliptic systems
[NASA-CR-195849] p 3821 N94-33049
ELLIPTICAL GALAXIES
Line-strength gradients and kinematic profiles in elliptical galaxies p 3934 N94-31788
ELLIPTICAL ORBITS
Multisatellite constellation configuration selection for multiregional highly elliptical orbit constellations p 3600 N94-31437
Testing for preferred-frame effects in gravity with artificial Earth satellites
[PB94-148459] p 3610 N94-31771
EMBEDDED COMPUTER SYSTEMS
The maintenance of operational flight program
[AD-A276363] p 3565 N94-31367
Technologies for avionics embedded computer systems
[AD-A276364] p 3581 N94-31368
Testing Operational Flight Programs (OFP's)
[AD-A276361] p 3578 N94-31387
Interpreter composition issues in the formal verification of a processor-memory module
[NASA-CR-4594] p 3820 N94-32775
EMBRITTLEMENT
Metal induced embrittlement
[DE94-007450] p 3640 N94-31325
Boron and hydrogen in Ni3Al. Part 2: Mechanical testing of bicrystals
[DE94-007441] p 3904 N94-32606
Reactor pressure vessel structural integrity research in the US Nuclear Regulatory Commission HSST and HSSI Programs
[DE94-006550] p 3739 N94-32771
EMERGENCIES
Technical evaluation of the UH-60Q: Aircraft in typical aeromedical evacuation missions
[AD-A276944] p 3586 N94-32217
EMERGENCY BREATHING TECHNIQUES
Development and enhancement of a model of performance and decision making under stress in a real life setting
[AD-A276029] p 3799 N94-31440
EMISSION
Theoretical studies of x ray emission from clusters of galaxies p 3954 N94-31103
EMISSION SPECTRA
Observational constraints on black hole accretion disks p 3929 N94-31126
Spectroscopic study of the molecular collisions (hydrogen-nitrogen and hydrogen-oxygen) at energies of several MeV
[ISBN-0-315-86794-9] p 3867 N94-31753
An analysis of ionospheric dayglow from observations of the Naval Postgraduate School Middle Ultraviolet Spectrograph (MUSTANG)
[AD-A277351] p 3773 N94-32335
Thermal emission measurements (5-25 microns) of Hawaiian palagonitic soils with implications for Mars p 3944 N94-33193
EMISSIVITY
Development of a statistical method for estimating the downward longwave radiation at the surface from satellite observations p 3742 N94-31553
A study of areas of low radio-thermal emissivity on Venus p 3942 N94-31992
Dual-band infrared imaging to detect corrosion damage within airframes and concrete structures
[DE94-006047] p 3580 N94-32658
EMITTANCE
Performance of silvered Teflon (trademark) thermal control blankets on spacecraft p 3591 N94-31014
Vulnerability assessment of a space based weapon platform electronic system exposed to a thermonuclear weapon detonation
[DE94-007229] p 3611 N94-32667
EMITTERS
RF vacuum microelectronics
[AD-A276512] p 3691 N94-31928
EMPLOYMENT
European business confronted with the 21st century: Men, the essential risk
[ESA-SP-1167] p 3914 N94-31181
EMULSIONS
Structure and dynamics of microemulsions in bulk, at interfaces, and in confined geometries
[DE94-006043] p 3633 N94-31526
Lubrication with binary mixtures: Liquid-liquid emulsion in elastohydrodynamics and metal forming p 3658 N94-32490
END EFFECTORS
Control of a flexible space robot tracking a moving target p 3722 N94-31469
Robot grasping: Stability and optimization issues p 3724 N94-31724
Development of a robotic simulator for studying interference and contact problems
[ISBN-0-315-86705-1] p 3588 N94-31747
Application of contact mechanics for the validation of robotized operations of grasping objects subjected to static and dynamic force fields
[ISBN-0-315-86831-7] p 3725 N94-31754
Automatic analysis of force distribution in multi-fingered articulated hands
[ISBN-0-315-87205-5] p 3725 N94-31878
Parallel methods for synthesizing whole-hand grasps from generalized prototypes
[AD-A276798] p 3726 N94-32166
Application of dexterous space robotics technology to myoelectric prostheses p 3729 N94-32450
Development of an interchangeable end effector mechanism for the Ranger telerobotic vehicle p 3604 N94-33297
ENERGETIC PARTICLES
Collisional and chaotic transport of energetic particles in toroidal plasma
[DE94-006504] p 3889 N94-31787
Basic principles approach for studying nonlinear Alfven wave-alpha particle dynamics
[DE94-007112] p 3891 N94-32664
ENERGY ABSORPTION
Transient radiation-induced absorption in the materials for a GSGG laser
[DE94-005316] p 3714 N94-31148
Rotorcraft ditchings and water-related impacts that occurred from 1982 - 1989, phase 2
[AD-A276473] p 3574 N94-31246
MSAT boom joint testing and load absorber design p 3606 N94-33315
Load-limiting landing gear footpad energy absorption system p 3607 N94-33323
ENERGY BUDGETS
Controls on the CO2 seasonal cycle p 3950 N94-33227
ENERGY CONSERVATION
Gas dynamics for accretion disk simulations p 3932 N94-31144
The hydrogen hybrid option
[DE94-006733] p 3667 N94-32148
Renewable energy technology development at Sandia National Laboratories
[DE94-007734] p 3761 N94-32383
ENERGY CONSUMPTION
Greenhouse gas emission impacts of electric vehicles under varying driving cycles in various countries and US cities
[DE94-007647] p 3765 N94-32600
ENERGY CONVERSION
Room temperature molten salts for advanced energy conversion and storage
[AD-A277777] p 3763 N94-33015
ENERGY CONVERSION EFFICIENCY
High conversion efficiency pumped-cavity second harmonic generation of a diode laser
[DE94-006805] p 3717 N94-32134
A simple model for determining photoelectron-generated radiation scaling laws
[DE94-006130] p 3761 N94-32660
Polymer electrolyte fuel cells
[DE94-007558] p 3761 N94-32762
ENERGY DISSIPATION
Instrumentation for EXELFS measurements using convergent beam diffraction coupling to the electron energy loss spectrometer
[USIP-93-07] p 3858 N94-31084
Studying transient mobility and energy loss using scanning tunneling microscopy
[AD-A276292] p 3877 N94-31256
Observations of turbulence, internal waves and background flows: An inquiry into the relationships between scales of motion p 3705 N94-31988
Ion-irradiation-induced densification of zirconia sol-gel thin films
[DE94-006248] p 3656 N94-32103
The 10th International Conference on Internal Friction and Ultrasonic Attenuation in Solids (ICIFUAS)
[AD-A276849] p 3902 N94-32209
ENERGY DISTRIBUTION
Energy and angular distributions of secondary ions during electronic sputtering of nonconducting surfaces
[ETN-94-95756] p 3865 N94-31516
ENERGY GAPS (SOLID STATE)
GaAs/GaN strained layer superlattice materials for high temperature transistors, phase 1
[AD-A276115] p 3897 N94-31528
Photonic band gap materials
[DE94-005566] p 3677 N94-32101
Lowering the Schottky barrier at metal or silicide/Si interfaces to extend the range of infrared detectors
[AD-A277253] p 3903 N94-32322
Theoretical studies of electron transfer and optical spectroscopy
[DE94-006985] p 3871 N94-32375
ENERGY LEVELS
Near resonant absorption by atoms in intense fluctuating laser fields
[DE94-005873] p 3714 N94-31200
Spectroscopy and atomic physics in EBIT and SuperEBIT
[DE94-006050] p 3864 N94-31508
ENERGY METHODS
An approximate solution for interlaminar stresses in laminated composites p 3621 N94-31901

ENERGY POLICY
Current policies of the major countries coping with the global warming problem and-the energy demand and supply
[DE94-757291] p 3769 N94-32920
ENERGY SOURCES
Biomass power industry: Assessment of key players and approaches for DOE and industry interaction
[DE94-000238] p 3761 N94-32725
ENERGY SPECTRA
Design and characterization of a pulsed x ray source for fluorescent lifetime measurements
[DE94-007495] p 3880 N94-32138
ENERGY STORAGE
Solar lunar power p 3599 N94-31427
Metal hydrides in hydrogen energy systems
[VTT-TIED-1407] p 3759 N94-31655
NEMO: Advanced energy systems and technologies
[DE94-721996] p 3760 N94-31767
Nonlinear analysis of springs using helical finite elements p 3859 N94-31906
Development of silver-zinc cells of improved cycle life and energy density
[AD-A277311] p 3693 N94-32329
Energy storage specification requirements for hybrid-electric vehicle
[DE94-008642] p 3694 N94-32521
Flywheel Energy Storage Technology Workshop
[DE94-008064] p 3761 N94-32705
Room temperature molten salts for advanced energy conversion and storage
[AD-A277777] p 3763 N94-33015
ENERGY TECHNOLOGY
Solar resource: Utility load-matching assessment
[DE94-000297] p 3758 N94-31264
Laboratory Directed Research & Development Program
[DE94-005928] p 3956 N94-31523
NEMO: Advanced energy systems and technologies
[DE94-721996] p 3760 N94-31767
Renewable energy technology development at Sandia National Laboratories
[DE94-007734] p 3761 N94-32383
Sandia technology engineering and science accomplishments
[DE94-008312] p 3668 N94-32412
Solar activities at Sandia National Laboratories
[DE94-007737] p 3761 N94-32648
Flywheel Energy Storage Technology Workshop
[DE94-008064] p 3761 N94-32705
Biomass power industry: Assessment of key players and approaches for DOE and industry interaction
[DE94-000238] p 3761 N94-32725
ENERGY TRANSFER
Convective solar nebula p 3930 N94-31130
Vibrations of a heavy truck diesel engine and gearbox unit: Examining structure-borne sound transmission with statistical energy analysis
[CTH-E-93-04] p 3722 N94-31194
A fully two-dimensional, non-oscillatory advection scheme for momentum and scalar transport equations
[DM-66] p 3700 N94-31221
Numerical simulations of monsoon rainfall with the NRL/NCSU regional nested grid model
p 3782 N94-31791
Vibrational energy transfer of diatomic gases in hypersonic expanding flows p 3570 N94-31958
Transport phenomena in the Earth's plasma sheet
p 3772 N94-31970
Mechanisms of laser induced reactions in opaque heterogeneous environments
[AD-A276642] p 3717 N94-31996
Ion-irradiation-induced densification of zirconia sol-gel thin films
[DE94-006248] p 3656 N94-32103
Time-resolved IR spectroscopy, energy transfer, and state-to-state collision dynamics of atmospheric species
[AD-A277372] p 3773 N94-32338
Energy transfer properties and mechanisms
[DE94-007403] p 3636 N94-32594
ENGINE DESIGN
A numerical method for mixing/chemically reacting compressible flow with finite rate chemistry
p 3634 N94-31824
Mechanics of cracking for composite material
p 3624 N94-32501
Oscillating-flow loss test results in rectangular heat exchanger passages
[NASA-CR-185297] p 3615 N94-32792
A 1050 K Stirling space engine design
[NASA-CR-182149] p 3616 N94-32866
ENGINE FAILURE
Real-time sensor data validation
[NASA-CR-195295] p 3616 N94-33099
ENGINE INLETS
Inlet distortion in engines on VSTOL aircraft
[NASA-CR-195841] p 3584 N94-33035
Response of a cantilevered plate in supersonic flow
[AD-A277487] p 3580 N94-33107
ENGINE PARTS
Thermal-mechanical fatigue crack growth in aircraft engine materials
[ISBN-0-315-86543-1] p 3734 N94-31707
High temperature NASP engine seal development
[NASA-TM-109750] p 3725 N94-31804
Analysis of Navy aircraft engine and engine component warranties
[AD-A276936] p 3584 N94-32238
A user's manual for the cost effectiveness analysis spreadsheet model for aircraft engines (CEAMOD version 2.0)
[AD-A278042] p 3585 N94-33266
Analysis of intermediate level maintenance following F404-GE-400 engine component life reductions
[AD-A277918] p 3585 N94-33283
ENGINEERING
A facilitated mentoring process for engineers
[DE94-005823] p 3914 N94-32677
ENGINEERING MANAGEMENT
Managing customer order driven engineering. An interdisciplinary and design oriented approach
[PB94-145083] p 3917 N94-31583
ENGINEERS
A facilitated mentoring process for engineers
[DE94-005823] p 3914 N94-32677
NASA/DOD Aerospace Knowledge Diffusion Research Project. Paper 12: The diffusion of federally funded aerospace research and development (R/D) and the information seeking behavior of US aerospace engineers and scientists
[NASA-TM-109404] p 3921 N94-32832
NASA/DOD Aerospace Knowledge Diffusion Research Project. Paper 11: The voice of the user: How US aerospace engineers and scientists view DOD technical reports
[NASA-TM-109348] p 3921 N94-32834
NASA/DOD Aerospace Knowledge Diffusion Research Project. Paper 1: The value of scientific and technical information (STI), its relationship to Research and Development (R/D), and its use by US aerospace engineers and scientists
[NASA-TM-109774] p 3922 N94-32835
NASA/DOD Aerospace Knowledge Diffusion Research Project. Report 25: The technical communications practices of British aerospace engineers and scientists: Results of the phase 4 RAeS mail survey
[NASA-TM-109098] p 3922 N94-32836
NASA/DOD Aerospace Knowledge Diffusion Research Project. Report 24: The technical communications practices of US aerospace engineers and scientists: Results of the phase 1 SAE mail survey
[NASA-TM-109088] p 3922 N94-32837
ENGRAVING
Laser applications in wood processing
[PB94-138567] p 3717 N94-31840
ENTHALPY
Strongly coupled ionic mixtures and the H/He EOS
[DE94-006391] p 3934 N94-31782
ENTROPY
Entropy, information (and image), part 1
[TELECOM-93-D-009] p 3910 N94-31098
Physical basis for climate change models
[DE94-003827] p 3767 N94-32712
ENTROPY (STATISTICS)
Dynamical entropy of generalized quantum Markov chains
[PB94-148483] p 3850 N94-31590
Probability distributions with given marginals and given correlation that have maximal entropy
[REPT-93-81] p 3851 N94-31698
ENVIRONMENT EFFECTS
LDEF Materials Results for Spacecraft Applications
[NASA-CP-3257] p 3591 N94-31012
Space Station WP-2 application of LDEF MLI results
p 3592 N94-31016
Modeling of LDEF contamination environment
p 3592 N94-31019
Concentration system performance degradation in the aftermath of Mount Pinatubo
[DE94-001879] p 3764 N94-31602
Evaluation of Fluorescence Line Imager (FLI) airborne imaging spectrometer data for roadside tree damage assessment p 3745 N94-31866
Greenhouse gas emission impacts of electric vehicles under varying driving cycles in various countries and US cities
[DE94-007647] p 3765 N94-32600
Fine resolution atmospheric sulfate model driven by operational meteorological data: Comparison with observations
[DE94-002994] p 3766 N94-32691
Identification of research relating to the critical loads concept and its potential application to the regulation of acidic deposition
[DE94-008234] p 3767 N94-32752
ENVIRONMENT MANAGEMENT
Information resources for US Department of Energy pollution prevention programs
[DE94-006677] p 3763 N94-31582
Mapping analysis and planning system for the John F. Kennedy Space Center p 3757 N94-32463
ENVIRONMENT MODELS
Modeling of the continental biosphere
p 3770 N94-31011
Model of spacecraft atomic oxygen and solar exposure microenvironments p 3593 N94-31021
Possible test of ancient dense Martian atmosphere
p 3947 N94-33206
ENVIRONMENT POLLUTION
NATO contributions to European environmental security
[AD-A275918] p 3763 N94-31275
Information systems to enhance technology exchange
[DE94-007744] p 3920 N94-32808
ENVIRONMENT PROTECTION
NATO contributions to European environmental security
[AD-A275918] p 3763 N94-31275
Evaluating success levels of mega-projects
p 3599 N94-31432
Strategies for survival in the new environmental era
[AD-A276827] p 3765 N94-32195
Environmental issues related to biomass: An overview
[DE94-007226] p 3767 N94-32784
Current policies of the major countries coping with the global warming problem and-the energy demand and supply
[DE94-757291] p 3769 N94-32920
ENVIRONMENTAL CHEMISTRY
The mineralogic evolution of the Martian surface through time: Implications from chemical reaction path modeling studies p 3950 N94-33226
Controls on the CO2 seasonal cycle
p 3950 N94-33227
ENVIRONMENTAL CONTROL
Atmosphere quality standards in manned space vehicles
[ESA-PSS-03-401-ISSUE-1] p 3802 N94-31224
Technical assessment of Mir-1 life support hardware for the international space station
[NASA-TM-108441] p 3803 N94-31380
ENVIRONMENTAL ENGINEERING
Atomic oxygen erosion considerations for spacecraft materials selection p 3593 N94-31022
Technical assessment of Mir-1 life support hardware for the international space station
[NASA-TM-108441] p 3803 N94-31380
ENVIRONMENTAL MONITORING
Global change research and NASA's Earth Observing System
[PB94-126992] p 3741 N94-31068
Analysis of GER imaging spectrometry data for the identification of soil and vegetation parameters in land degradation studies p 3744 N94-31857
Monitoring fertilizer application by imaging spectrometry (Somerset Levels test site) p 3745 N94-31863
A model geophysics program
[DE94-007415] p 3747 N94-32203
Mapping analysis and planning system for the John F. Kennedy Space Center p 3757 N94-32463
Research and applications of a canopy reflectance model p 3747 N94-32492
From Optics to Radar, SPOT and ERS Applications
[ISBN-2-85428-345-7] p 3747 N94-32523
The complementary nature of the SPOT and ERS-1 systems and their place in major international programmes p 3748 N94-32524
From optics to radar: Environmental problems and the SPOT/ERS systems p 3748 N94-32525
Feasibility in the use of satellite remote sensing data as a fast reaction tool for natural disaster relief
p 3748 N94-32526
Contribution of SAR ERS1 data to study the French Guiana tropical coast environment
[BRGM-93034] p 3748 N94-32527
A case study comparing multi-temporal ERS-1 SAR data and SPOT data for tropical forest mapping
p 3753 N94-32556
Ocean variability and its influence on the detectability of greenhouse warming signals
[DE94-008670] p 3790 N94-32881

ENVIRONMENTAL SURVEYS
National US public policy on global warming derived from optimization of energy use and environmental impact studies
[DE94-004606] p 3768 N94-32790
Real-time centimeter positioning with GPS: A system developed by the US Army Corps of Engineers
[AD-A278152] p 3577 N94-33095
Cruise report: Oceanus 250 leg 4 high resolution profiler survey for the North Atlantic Tracer Release Experiment, 25 March - 24 April, 1992
[AD-A277935] p 3791 N94-33245
ENVIRONMENTAL TESTS
Atomic oxygen erosion considerations for spacecraft materials selection p 3593 N94-31022
Performance of selected polymeric materials on LDEF p 3593 N94-31023
Fluorescence observations of LDEF exposed materials as an indicator of induced material reactions p 3593 N94-31025
Laser-induced fluorescence of space-exposed polyurethane p 3593 N94-31026
On the linearity of fast atomic oxygen effects p 3594 N94-31027
Effects of orbital exposure on RTV during the LDEF mission p 3597 N94-31043
What LDEF means for development and testing of materials p 3598 N94-31050
Aerospace test facilities at NASA LERC Plumbrook
[NASA-TM-109755] p 3602 N94-31814
Validation of the Environmentally Conscious Manufacturing Integrated Demonstration hardware
[DE94-003824] p 3765 N94-32144
Accelerated reliability testing utilizing design of experiments
[AD-A277989] p 3732 N94-33088
ENZYME ACTIVITY
Biocatalytic processing polymers in supercritical fluids
[AD-A276120] p 3651 N94-31510
The sol-gel-xerogel transition
[AD-A276647] p 3616 N94-32038
Ninth International Workshop on Plant Membrane Biology
[DE94-005690] p 3794 N94-32769
ENZYMES
Biocatalytic processing polymers in supercritical fluids
[AD-A276120] p 3651 N94-31510
EPHEMERIDES
Possible improvements of satellite ephemeris programs used in geodesy
[PB94-148681] p 3743 N94-31592
EPIDEMIOLOGY
The legacy of Kermack and McKendrick
[CWI-AM-R9304] p 3793 N94-32228
EPITAXY
GaAs/GaN strained layer superlattice materials for high temperature transistors, phase 1
[AD-A276115] p 3897 N94-31528
Semiconductor microcavity lasers
[DE94-006143] p 3716 N94-31622
In-situ TEM crystallization of anorthite-glass films on (alpha)-Al2O3
[DE94-006317] p 3652 N94-31780
Epitaxial liftoff technology onto processed silicon foundry wafers
[AD-A277116] p 3900 N94-31985
The charging effect in high-Tc superconducting thin films
[AD-A277265] p 3900 N94-32040
Correlations between micromagnetic, microstructural and microchemical properties in ultrathin epitaxial magnetic structures
[AD-A277200] p 3901 N94-32092
Stability and precipitation kinetics in Si(1-y)C(y)/Si and Si(1-x-y)Ge(x)C(y)/Si heterostructures prepared by solid phase epitaxy
[DE94-006589] p 3902 N94-32296
Heteroepitaxial diamond growth
[AD-A277178] p 3902 N94-32306
Energetics, bonding mechanism, and electronic structure of ceramic/ceramic and metal/ceramic interfaces
[DE94-008551] p 3659 N94-32656
Ab initio study of the epitaxial growth of Ge on Si(100) surface
[DE94-007245] p 3904 N94-32724
Microanalytical study of defect formation in thin bismuth strontium calcium copper oxide films
[DE94-008217] p 3661 N94-32751
The 6th International Conference on Modulated Semiconductor Structures
[AD-A276815] p 3906 N94-32908
Low energy ion beam assisted growth of homoepitaxial silicon films at low temperature
[AD-A278092] p 3908 N94-33039
Microstructures and epitaxy in oxide superconductor thin films and devices
[AD-A278427] p 3910 N94-33332
EPOXY COMPOUNDS
Reactions of electrophilic maleic anhydride and epoxy groups with nucleophilic functionalities such as carboxyl, hydroxyl, and amine groups. Polymer Technology Publication series no. 16
[PB94-135589] p 3648 N94-31069
Photopolymerization of cyclohexene oxide: A visible light initiating system and mechanistic investigations
[AD-A277110] p 3654 N94-31981
EPOXY MATRIX COMPOSITES
Performance of selected polymeric materials on LDEF p 3593 N94-31023
Micromechanical analysis of the interface and basic damage modes in glass fiber/epoxy resin model composites
[ONERA-NT-1993-4] p 3618 N94-31225
Fatigue behavior of unidirectional pultruded composite materials
[ISBN-0-315-86425-7] p 3621 N94-31719
Evaluating in-plane elastic constants of damaged carbon-epoxy laminates using a quantitative ultrasonic technique p 3621 N94-31793
EPOXY RESINS
Design of new polymers to improve radiation stability of plastic scintillators
[DE94-008220] p 3652 N94-31764
Hydrogen peroxide electrodes based on electrical connection of redox centers of various peroxidases to electrodes through a three-dimensional electron relaying polymer network
[AD-A276543] p 3691 N94-32056
EQUALIZERS (CIRCUITS)
Kalman filtering approach to blind equalization
[AD-A276320] p 3671 N94-31299
EQUATIONS OF MOTION
General-relativistic celestial mechanics. 4: Theory of satellite motion
[PB94-147782] p 3601 N94-31769
Design and Monte Carlo analysis of an unmanned aerial vehicle
[AD-A277648] p 3580 N94-33056
Identification and control of structures in space
[NASA-CR-195910] p 3612 N94-33115
EQUATIONS OF STATE
Strongly coupled ionic mixtures and the H/He EOS
[DE94-006391] p 3934 N94-31782
Analytic properties of the OCP and ionic mixtures in the strongly coupled fluid state
[DE94-008216] p 3637 N94-32801
EQUATORIAL ELECTROJET
Theoretical studies on ionospheric irregularities and ion diode performance
[AD-A277115] p 3772 N94-31984
EQUATORIAL ORBITS
Testing for preferred-frame effects in gravity with artificial Earth satellites
[PB94-148459] p 3610 N94-31771
EQUATORIAL REGIONS
Low frequence variability of the ocean atmosphere coupled system p 3777 N94-30986
EQUILIBRIUM FLOW
The effect of an axial flow component on a circular cylinder wake p 3699 N94-31209
EQUIPMENT SPECIFICATIONS
An application reference model for layered manufacturing
[DE94-006368] p 3811 N94-31484
Design, performance, and test standards for flight termination receivers/decoders. Volume 1: Design and performance requirements
[AD-A277245] p 3602 N94-32333
The Los Alamos National Laboratory precision double crystal spectrometer
[DE94-008075] p 3713 N94-32706
EQUIPOTENTIALS
World height system definition and implementation
[AD-A276725] p 3747 N94-32160
EQUIVALENCE
On the equivalence of Lambek categorial grammars and basic categorial grammars
[LP-93-07] p 3842 N94-31451
ERBIUM
Electron spin resonance measurements of Er(3+) and Mn(2+) in the high temperature superconductor compounds La(2-x)Sr(x)CuO(4-delta)
[ETN-94-95746] p 3898 N94-31612
ERGODIC PROCESS
A note on cocycles in a semidirect product
[REPT-93-65] p 3851 N94-31661
Adaptive control of nonlinear and stochastic systems
[AD-A278411] p 3839 N94-33325
EROSION
Space Station WP-2 application of LDEF MLI results p 3592 N94-31016
Follow-up on the effects of the space environment on UHCRE thermal blankets p 3592 N94-31018
Atomic oxygen erosion considerations for spacecraft materials selection p 3593 N94-31022
On the linearity of fast atomic oxygen effects p 3594 N94-31027
Impact of LDEF photovoltaic experiment findings upon spacecraft solar array design and development requirements p 3594 N94-31028
Robotic weld overlay coatings for erosion control
[DE94-008004] p 3658 N94-32408
Geologic controls of erosion and sedimentation on Mars p 3951 N94-33232
Obliquity variation in a Mars climate evolution model p 3951 N94-33236
ERROR ANALYSIS
The generalized multi delay adaptive filter: Structure and convergence analysis
[TELECOM-93-D-004] p 3808 N94-31094
A comparison of predictors for first-guess wind speed errors
[AD-A276460] p 3781 N94-31239
A review of sensitivity analysis techniques
[DE94-007192] p 3842 N94-31399
Direct-sequence spread-spectrum performance in a multipath fading environment
[AD-A276080] p 3673 N94-31464
Regional sources of error growth in the National Meteorological Center's medium-range forecast model p 3781 N94-31554
Error analysis of real-time and post-processed orbit determination for the Geosat Follow-On altimetric satellite using GPS tracking p 3576 N94-31845
On the error committed by stopping the Newton iteration in Runge-Kutta methods and linear multistep methods
[TW-93-13] p 3847 N94-32206
Eta percent-superconvergence in the interior of locally refined meshes of quadrilaterals: Superconvergence of the gradient in finite element solutions of Laplace's and Poisson's equations
[AD-A277242] p 3848 N94-32331
Thermospheric modeling accuracies using F10.7 and Ap
[AD-A277355] p 3773 N94-32337
Finite element solution to the Helmholtz equation with high wave number. Part 1: The h-version of the FEM
[AD-A277396] p 3848 N94-32341
Note on the variance of autospectral density processed using Welch's method
[DE94-005352] p 3849 N94-32675
Aspects of modeling uncertainty and prediction
[DE94-007565] p 3852 N94-32744
ERROR CORRECTING CODES
Model-based reconfiguration: Diagnosis and recovery
[NASA-CR-4596] p 3820 N94-32776
ERROR DETECTION CODES
Consistency checks for SCR-style requirements specifications
[AD-A276077] p 3811 N94-31461
On the implementation of error handling in dynamic interfaces to scientific codes
[DE94-008970] p 3818 N94-32585
Model-based reconfiguration: Diagnosis and recovery
[NASA-CR-4596] p 3820 N94-32776
ERRORS
Multiple regression and measurement errors: Relative efficiency of two models, the standard model and Fuller's model, for estimating structural relationships
[ISBN-0-315-86834-1] p 3845 N94-31755
Principal component analysis with missing data and its application to object modeling
[AD-A276644] p 3845 N94-31939
On the relationship between generalization error, hypothesis complexity, and sample complexity for radial basis functions
[AD-A276802] p 3851 N94-32142
Bounds on least-squares four-parameter sine-fit errors due to harmonic distortion and noise
[DE94-007859] p 3849 N94-32653
ERS-1 (ESA SATELLITE)
From Optics to Radar, SPOT and ERS Applications
[ISBN-2-85428-345-7] p 3747 N94-32523
The complementary nature of the SPOT and ERS-1 systems and their place in major international programmes p 3748 N94-32524
From optics to radar: Environmental problems and the SPOT/ERS systems p 3748 N94-32525
Contribution of SAR ERS1 data to study the French Guiana tropical coast environment
[BRGM-93034] p 3748 N94-32527
Optics and radar: Cohabitation, rivality or happy marriage. Towards new planning tools p 3748 N94-32529

The use of ERS images for mapping
p 3749 N94-32531
Assessment of region-based methods for automated SAR/optical registration, attribute extraction, and classification p 3750 N94-32536
Robust multisource classification method using the Markov random field methods p 3750 N94-32537
Technique of ERS-1 image processing in association with SPOT data p 3750 N94-32538
Production of terrain data: Optical radar complementarity p 3750 N94-32540
Fusion of multispectral (XS) and Panchromatic (P) SPOT images and radar images p 3750 N94-32541
Ship traffic monitoring and oil spill detection using the ERS-1 SAR p 3751 N94-32542
SAR image feature extraction system: A pre-operational application of ERS-1 SAR p 3751 N94-32543
The use of ERS-1 within an operational ice monitoring program p 3751 N94-32545
The use of SPOT and ERS-1 images to map the eruption of Nevado Sabancaya (Province of Arequipa, South Peru) and evaluate associated risks p 3751 N94-32546
Comparison of SPOT, ERS-1, SEASAT, LANDSAT TM, and merged imagery for geological investigations
p 3752 N94-32547
Optimal geological data extraction from SPOT-radar synergism with samples from Djebel Amour (Algeria), Red Sea Hills (Sudan), Sirte Basin (Libya), and Magdalena Valley (Colombia) p 3752 N94-32548
Respective contributions of VIS-PIR, SAR-ERS 1, and airborne radar data for morphostructural and morphoneotectonic analysis: Practical examples
p 3752 N94-32549
Use of SPOT and ERS-1 SAR data to study the tectonic and climatic history of arid regions p 3752 N94-32550
Structural study in an alteritic region: Contribution of ERS-1 SAR data of the Mauges Plateau (Loire Atlantique, France)
[BRGM-93032] p 3752 N94-32551
Study of subpolar glaciers of Spitzbergen using SPOT, ERS-1, and hypsometric data: Results and perspectives
p 3753 N94-32553
Integration of ERS-1 images into the European Agriculture Statistics project Action 4: Thematic aspect
p 3753 N94-32554
Use of SPOT and ERS-1 to map tropical vegetation and mangrove dynamics in Guiana p 3753 N94-32555
A case study comparing multi-temporal ERS-1 SAR data and SPOT data for tropical forest mapping
p 3753 N94-32556
Application of ERS-1 SAR data for hydrological studies p 3754 N94-32558
Monitoring landsurface characteristics in Niger using complementary SPOT and ERS-1 SAR data
p 3754 N94-32560
European MARS project: The potential integration of SPOT and air- and satellite-borne radar data over two pilot areas for agricultural statistics. PROSPER programme and ERS-1 pilot project
[BRGM-93035] p 3754 N94-32561
Possible complementarity of SPOT/ERS in mapping land use: Study on agricultural land in Brittany (France)
p 3755 N94-32563
Land cover change detection with ERS-1 data and data from other remote sensing satellites. Example: The delta of the River Ebro (Spain) p 3755 N94-32564
ERS-1 SAR and optical data for land use/land cover mapping: A case study in a savannah zone of Guinea
p 3755 N94-32565
SAR interferometry with ERS-1 p 3755 N94-32566
Techniques and applications of SAR interferometry for ERS-1 p 3756 N94-32568
Developments in ERS-1 SAR interferometry: Use of the spectral shift p 3756 N94-32569
Differential interferometry study of an earthquake
p 3756 N94-32570
Precision and level of artefacts in the computation of digital terrain models by interferometry
p 3756 N94-32571
Fields of experiments in ERS-1 SAR interferometry in Bonn and Naples p 3756 N94-32572

ESSENTIALLY NON-OSCILLATORY SCHEMES
A numerical method for mixing/chemically reacting compressible flow with finite rate chemistry
p 3634 N94-31824

ESTERS
Metal ion complexation by ionizable crown ethers
[DE94-008301] p 3661 N94-32847
Interpenetrating polymer network acoustic damping material
[AD-D016141] p 3663 N94-32975
Development and preliminary evaluation of aryl ester boundary additives for perfluoropolyethers
[NASA-TM-106603] p 3663 N94-33024

ESTIMATES
Initial estimates of Integrated Maintenance Information System (IMIS) costs and benefits, volume 1
[AD-A276144] p 3565 N94-31830
Kaplan-Meier estimators of interpoint distance distributions for spatial point processes
[CWI-BS-R9315] p 3846 N94-32107

ESTIMATING
Estimating the impact of crashworthiness standards on mortality and morbidity events in the US Army rotary-wing aircraft mishaps
[AD-A277121] p 3575 N94-32363

ESTUARIES
ADCIRC: An advanced three-dimensional circulation model for shelves, coasts, and estuaries. User's manual for ADCIRC-2DDI
[AD-A276150] p 3787 N94-31250

ETCHING
Ionization probes of molecular structure and chemistry
[DE94-007605] p 3872 N94-32643

ETHANE
Time-resolved infrared absorption studies applied to the study of radical plus molecule reactions
[DE94-005921] p 3863 N94-31202

ETHERS
Fuel property effects on engine combustion processes
[DE94-005529] p 3631 N94-31153
Silicone grease as a precursor to a pseudo crown-ether ligand: Crystal structure of (K(+)K(Me2SiO)7(+))(HIn(CH2CMe3)3(-))4)
[AD-A276343] p 3895 N94-31327
High octane ethers from synthesis gas-derived alcohols
[DE94-006774] p 3667 N94-32133
The intramolecular cyclization of bis-2,5-dimethylene-2,5-dihydrofurans and bis-2,5-dimethylene-2,5-dihydrothiophenes: An approach to macrocycles
[DE94-007060] p 3657 N94-32377
Metal ion complexation by ionizable crown ethers
[DE94-008301] p 3661 N94-32847

ETHICS
Ethics and rationality in information-enriched decisions: A model for technical communication
[DE93-040251] p 3681 N94-32679

ETHYL ALCOHOL
Preparation of catalyst particles using methods of colloid chemistry. Part 1: Preparation of silica particles from alcohol solutions
[PB94-135597] p 3634 N94-31679
Stabilized alumina/ethanol colloidal dispersion for seeding high temperature air flows
[NASA-TM-106591] p 3713 N94-32983

ETHYL COMPOUNDS
Microstructure of copolymers containing disperse red 1 and methyl methacrylate
[AD-A277140] p 3660 N94-32722

ETHYLENE
Direct aromatization of methane
[DE94-008719] p 3638 N94-32888
Evaluation of pyrolysis and arc tracking on candidate wire insulation designs for space applications
[NASA-CR-195332] p 3731 N94-32901

ETIOLOGY
Muscle disuse through tail-suspension: Etiology and therapeutics p 3796 N94-31746

EUCLIDEAN GEOMETRY
Strictly positive definite functions on spheres
[AD-A276471] p 3855 N94-31244

EULER EQUATIONS OF MOTION
An adaptive method for the exact resolution of shock waves and contact discontinuities
[ISBN-0-315-86498-2] p 3704 N94-31799
A new inverse method for generating high-speed aerodynamic flows with application to waverider design
p 3569 N94-31828

EUROPE
European business confronted with the 21st century: Men, the essential risk
[ESA-SP-1167] p 3914 N94-31181
Europe at the crossroads: The future of its satellite communications industry
[ESA-SP-1166] p 3670 N94-31182
Analysis of ionospheric parameters in Europe and creation of the prediction algorithm
[AD-A276342] p 3771 N94-31326
Current Research Information in Europe: Conference proceedings
[PB94-127933] p 3917 N94-31768
The European Imaging Spectroscopy Airborne Campaign (EISAC). Data takes and evaluation programme: An overview p 3743 N94-31854
Integration of ERS-1 images into the European Agriculture Statistics project Action 4: Thematic aspect
p 3753 N94-32554
Rapid estimates of crop acreage and production at European scale using high resolution imagery
p 3754 N94-32557

EUROPEAN SPACE AGENCY
Guide to software quality assurance
[ESA-PSS-05-11-ISSUE-1] p 3809 N94-31223

EUROPEAN SPACE PROGRAMS
From optics to radar: Environmental problems and the SPOT/ERS systems p 3748 N94-32525

EUROPIUM COMPOUNDS
Low dispersion of the muon precession frequency in HTSC samples YBa2Cu3O(x) and EuBa2Cu3O(x)
[DE94-608388] p 3896 N94-31395

EUTECTICS
Compositions and chemical bonding in ceramics by quantitative electron energy-loss spectrometry
[DE94-007208] p 3659 N94-32640
The relative performance of FeS2 and CoS in long-life thermal-battery applications
[DE94-006145] p 3695 N94-32663

EVACUATING (TRANSPORTATION)
Technical evaluation of the UH-60Q: Aircraft in typical aeromedical evacuation missions
[AD-A276944] p 3586 N94-32217

EVALUATION
Evaluating success levels of mega-projects
p 3599 N94-31432
The European Imaging Spectroscopy Airborne Campaign (EISAC). Data takes and evaluation programme: An overview p 3743 N94-31854

EVAPORATION
The ocean-atmosphere interactions in the Mediterranean Sea p 3779 N94-30995
Thermocapillary convection in evaporating sessile drops
[NASA-TM-109758] p 3705 N94-31886
Recurvature dynamics of a typhoon
[AD-A276792] p 3784 N94-32164
Synergy of thermal infrared and microwave remote sensing for evaporation estimation p 3754 N94-32559

EVOKED RESPONSE (PSYCHOPHYSIOLOGY)
Stress-induced enhancement of the startle reflex
[AD-A278414] p 3802 N94-33327

EVOLUTION (DEVELOPMENT)
Experiences with EDO: An Evolutionary Database Optimizer
[TR-93-23] p 3918 N94-32105
Information disclosure in evolving information systems: Taking a shot at a moving target
[TR-93-22] p 3919 N94-32506

EXCIMER LASERS
Diagnostics of high-brightness short-pulse lasers and the plasmas they generate
[DE94-006165] p 3716 N94-31624
Short-pulse, high-intensity lasers at Los Alamos
[DE94-007545] p 3720 N94-32760
Nucleation and growth of cubic boron nitride films produced by ion-assisted pulsed laser deposition
[DE94-007295] p 3661 N94-32796

EXCIMERS
Production and detection of metastable atomic oxygen
[ISBN-0-315-87364-7] p 3868 N94-31915

EXCITATION
Intramolecular charge transfer complexes as fluorescence probes for UV and visible light induced acrylate polymerization
[AD-A277129] p 3657 N94-32381
Conjugated polymer fluorescence: Interplay of correlations and alternation
[DE94-005587] p 3660 N94-32729
Bioluminescence bathyphotometer
[AD-D016102] p 3790 N94-32959
Simultaneous excitation of parametric decay cascades and the OTSI in 1D numerical simulations based on Aakarov's equations
[AD-A278108] p 3893 N94-33042

EXCITONS
Temperature dependence of the exciton-exciton annihilation rate constant in poly(di-n-hexylsilane)
[DE94-005584] p 3655 N94-32102

EXHAUST EMISSION
Control and monitoring of heavy metal emissions
[VTT-TIED-1508] p 3765 N94-31657
Evaluation of Fluorescence Line Imager (FLI) airborne imaging spectrometer data for roadside tree damage assessment p 3745 N94-31866
Greenhouse gas emission impacts of electric vehicles under varying driving cycles in various countries and US cities
[DE94-007647] p 3765 N94-32600

EXHAUST GASES
Greenhouse gas emission impacts of electric vehicles under varying driving cycles in various countries and US cities
[DE94-007647] p 3765 N94-32600

Possible effect of the chlorine oxide dimer on transient ozone loss in rocket plumes
[AD-A278135] p 3616 N94-33094

EXHAUST NOZZLES
Computational study of single-expansion-ramp nozzles with external burning
[NASA-TM-106550] p 3700 N94-31229
Combustor and nozzle effects on particulate behavior in solid rocket motors
[AD-A277304] p 3614 N94-32071

EXOBIOLOGY
Aerospace medicine and biology: A continuing bibliography with indexes (supplement 388)
[NASA-SP-7011(388)] p 3795 N94-31414
Aerospace medicine and biology: A continuing bibliography with indexes (supplement 389)
[NASA-SP-7011(389)] p 3797 N94-32347
Aerospace medicine and biology: A continuing bibliography with indexes (supplement 385)
[NASA-SP-7011(385)] p 3797 N94-32348

EXOSPHERE
Escape of Mars atmospheric carbon through time by photochemical means p 3948 N94-33214

EXPERIMENT DESIGN
Tearing resistance of a thin shell against projectile penetration: Material property effects
[DE94-007466] p 3733 N94-31316
Accelerated reliability testing utilizing design of experiments
[AD-A277989] p 3732 N94-33088

EXPERT SYSTEMS
Evaluation of HardSys/HardDraw, an expert system for electromagnetic interactions modelling
[AD-A276218] p 3670 N94-31063
Information acquisition from multi-agent resources; abstract
[LP-93-08] p 3917 N94-31452
Module generation for self-testing integrated systems
[ISBN-9-09-004570-8] p 3688 N94-31520
LORE and reason maintenance
[REPT-93-88] p 3812 N94-31522
An expert system architecture for heterogeneous domains: A case-study in the legal field
[ETN-94-96012] p 3830 N94-31546
Hierarchical mixtures of experts and the EM algorithm
[AD-A276516] p 3814 N94-31932
Mapping analysis and planning system for the John F. Kennedy Space Center p 3757 N94-32463
An intelligent interactive visual database management system for Space Shuttle closeout image management p 3923 N94-32469
The limits of intelligence in design
[DE94-004668] p 3819 N94-32668
Spacecraft environmental anomalies expert system
[AD-A277962] p 3612 N94-33262
Proceedings of the Symposium/Workshop on Applications of Expert Systems in DND
[DSIS-93-00343] p 3853 N94-33335
Scheduling fighter missions using an expert system with an operations research module p 3853 N94-33337
The CF-18 diagnostic and maintenance expert system project p 3567 N94-33338
An expert system application for troubleshooting the CF18 F404 engine p 3585 N94-33339
A diagnostic expert system for digital circuits p 3699 N94-33340
Management of uncertainty in knowledge-based systems: A military perspective p 3854 N94-33341
Knowledge engineering for PACES, the particle accelerator control expert system p 3854 N94-33342
The hypermedia technology as front end to knowledge processing systems p 3854 N94-33343
A problem-solving approach to knowledge acquisition p 3854 N94-33344
A heuristic multiple target tracker p 3686 N94-33346

EXPLOSIONS
Fireworks in velocity and configuration space applied to cosmology
[USIP-93-90] p 3927 N94-31086
Using Monte Carlo techniques and parallel processing for debris hazard analysis of rocket systems
[DE94-007250] p 3609 N94-31382
Analysis of forward and inverse problems in chemical dynamics and spectroscopy
[DE94-007607] p 3635 N94-32140

EXPLOSIVES
PVDF pressure transducers for shock wave and explosives research
[AD-A277319] p 3712 N94-32051

EXPONENTIAL FUNCTIONS
Stirling's formula and approximations for n(factorial) and the middle ratio
[REPT-93-73] p 3843 N94-31642

EXPONENTS
Comparing models of the non-extensional typed lambda-calculus
[ML-93-19] p 3842 N94-31409

EXPOSURE
Performance of silvered Teflon (trademark) thermal control blankets on spacecraft p 3591 N94-31014
Physical properties of glasses exposed to Earth-facing and trailing-side environments on LDEF p 3594 N94-31030
Summary of materials and hardware performance on LDEF p 3595 N94-31037
Characterization of polymer decomposition products by laser desorption mass spectrometry p 3597 N94-31046
Controlling hazardous energy sources (lockout/tagout)
[NASA-TM-105290] p 3669 N94-32861
Effect of elevated temperature and cyclic loading on properties and damage modes in ceramic composites
[DE94-008736] p 3662 N94-32891
Exposure assessment of JAVELIN missile combustion products
[AD-A278128] p 3616 N94-33059

EXTERNAL STORE SEPARATION
Six degree of freedom flight dynamic model of a Mk-82 store
[AD-A277065] p 3580 N94-32362

EXTERNAL STORES
Six degree of freedom flight dynamic model of a Mk-82 store
[AD-A277065] p 3580 N94-32362

EXTINCTION
A model of concurrent flow flame spread over a thin solid fuel p 3634 N94-31795

EXTINGUISHING
Influence of carbon dioxide on electronic equipment: Fire extinguishing with low concentration
[PB94-148749] p 3691 N94-31848

EXTRACTION
High-temperature study of O+H2CO yields OH+HCO
[DE94-006837] p 3864 N94-31321
Time-resolved analytical methods for liquid/solid interfaces
[DE94-008352] p 3637 N94-32826

EXTRAPOLATION
Evaluating success levels of mega-projects p 3599 N94-31432
Computer modelling of cyclic deformation of high-temperature materials
[AD-A277056] p 3623 N94-32012
A new method for calculating wing along aerodynamics to angle of attack 180 deg
[AD-A277965] p 3574 N94-33263

EXTRATERRESTRIAL INTELLIGENCE
The quest for contact
[NASA-TM-109778] p 3806 N94-32389

EXTRATERRESTRIAL LIFE
Mars: Five views on what is known
[NASA-TM-109751] p 3942 N94-31805

EXTRATERRESTRIAL RADIO WAVES
Plasma and radio waves from Neptune: Source mechanisms and propagation
[NASA-CR-195877] p 3943 N94-33103

EXTRAVEHICULAR ACTIVITY
The Nomad Explorer assembly assist vehicle: An architecture for rapid global extraterrestrial base infrastructure establishment p 3599 N94-31429
Energy absorber for the CETA p 3604 N94-33303

EXTRAVEHICULAR MOBILITY UNITS
Metal hydride heat pump engineering demonstration and evaluation model
[NASA-CR-188286] p 3669 N94-32857

EXTREME ULTRAVIOLET EXPLORER SATELLITE
Design and performance of the telescope and detector covers on the Extreme Ultraviolet Explorer satellite p 3605 N94-33309

EXTREME ULTRAVIOLET RADIATION
Extreme ultraviolet opacity sources in the DA white dwarf G191-B2B p 3924 N94-31210
Simplified ultra-high resolution optic for soft x ray imaging
[AD-A278424] p 3885 N94-33331

EYE MOVEMENTS
Analysis of pursuit tracking eye movements in pilots and nonfliers
[AD-A276597] p 3799 N94-32035

F

F REGION
Diurnal, seasonal and solar activity variations of F-region parameters
[AD-A278106] p 3776 N94-33285

F 2 REGION
Analysis of ionospheric parameters in Europe and creation of the prediction algorithm
[AD-A276342] p 3771 N94-31326

F-111 AIRCRAFT
Real time character recognition for F-111C video tape records
[AD-A277061] p 3580 N94-32263

F-16 AIRCRAFT
Initial estimates of Integrated Maintenance Information System (IMIS) costs and benefits, volume 1
[AD-A276144] p 3585 N94-31830

F-18 AIRCRAFT
Noise cancellation for CELP voice encoders in an F/A-18 noise environment
[AD-A277652] p 3683 N94-33026
Installed F/A-18 inlet flow calculations at 30 degrees angle-of-attack: A comparative study
[NASA-CR-195297] p 3573 N94-33119
Scheduling fighter missions using an expert system with an operations research module p 3853 N94-33337
An expert system application for troubleshooting the CF18 F404 engine p 3585 N94-33339

FABRICATION
Automated solar cell assembly teamed process research
[DE94-000295] p 3759 N94-31279
Fractional-factorial process development techniques
[DE94-005580] p 3690 N94-31593
The charging effect in high-Tc superconducting thin films
[AD-A277265] p 3900 N94-32040
Silicon-Film(tm) photovoltaic manufacturing technology
[DE94-000202] p 3760 N94-32143
A solar array module fabrication process for HALE solar electric UAVs
[DE94-006212] p 3760 N94-32174
Analytical Design Package (ADP2): A computer aided engineering tool for aircraft transparency design p 3823 N94-32430
Optical processing for semiconductor device fabrication p 3885 N94-32445
Flexible manufacturing for photonics device assembly p 3669 N94-32449
Fabrication, phase transformation studies and characterization of SiC-AlN-Al2OC ceramics
[DE94-008587] p 3659 N94-32657
Innovative fabrication processing of advanced composite materials concepts for primary aircraft structures
[NASA-CR-189558] p 3626 N94-32877
Effect of elevated temperature and cyclic loading on properties and damage modes in ceramic composites
[DE94-008736] p 3662 N94-32891
Enhanced thermal capacity aerogels summary report, FY 1993
[DE94-008888] p 3639 N94-33260

FABRICS
Space environment durability of beta cloth in LDEF thermal blankets p 3591 N94-31015
Space Station WP-2 application of LDEF MLI results p 3592 N94-31016

FABRY-PEROT INTERFEROMETERS
Study of the dynamics of a nonlinear coupled-cavity laser system
[ISBN-0-315-86717-5] p 3716 N94-31748

FACTOR ANALYSIS
Development of phase-only filters for sensor imagery
[AD-A276722] p 3880 N94-32151
Multidimensional scaling of user information satisfaction
[AD-A277230] p 3920 N94-32633
Torque characteristics of solid lubricated precision bearings during oscillatory motion
[AD-A278133] p 3728 N94-33061

FACTORIAL DESIGN
Fractional-factorial process development techniques
[DE94-005580] p 3690 N94-31593
Accelerated reliability testing utilizing design of experiments
[AD-A277989] p 3732 N94-33088

FACTORIALS
Stirling's formula and approximations for n(factorial) and the middle ratio
[REPT-93-73] p 3843 N94-31642

FACTORIZATION
A paraperspective factorization method for shape and motion recovery
[AD-A276513] p 3712 N94-31929
Recursive analysis of matrix scattering functions
[AD-A277264] p 3845 N94-32018

FAIL-SAFE SYSTEMS
Quench detection and instrumentation for the Tokamak Physics Experiment magnets
[DE94-006656] p 3888 N94-31667

Deployable and retractable telescoping tubular structure development p 3607 N94-33317

FAILURE

Experimental measurement of dynamic failure and fragmentation properties of metals [DE94-007377] p 3737 N94-32135

Nonlocal theory for fracturing of quasibrittle materials [AD-A278283] p 3740 N94-33143

Pip pin reliability and design p 3605 N94-33305

FAILURE ANALYSIS

Performance predictions for composite materials [AD-A276451] p 3618 N94-31261

Optimization of composite material failure loads [ISBN-0-315-87214-4] p 3621 N94-31836

Computer modelling of cyclic deformation of high-temperature materials [AD-A277056] p 3623 N94-32012

Benchmarking of the state-of-the-art in nondestructive testing/evaluation for applicability in the Composite Armored Vehicle (CAV) Advanced Technology Demonstrator (ATD) program, phase 1 [AD-A276660] p 3730 N94-32088

The advent of failure analysis software technology [DE94-006593] p 3692 N94-32111

Novel failure analysis techniques using photon probing with a scanning optical microscope [DE94-006594] p 3692 N94-32112

Honeycomb sandwich structures: Vented versus unvented designs for space systems [AD-A276713] p 3624 N94-32122

Mechanics of failure of high temperature metal matrix composites [AD-A277397] p 3624 N94-32342

Torque characteristics of solid lubricated precision bearings during oscillatory motion [AD-A278133] p 3728 N94-33061

Technology integration box beam failure study p 3628 N94-33126

FAILURE MODES

Unidirectional composites compressive behaviour: Test methods and micromechanical approach [ONERA-NT-1993-10] p 3618 N94-31232

The advent of failure analysis software technology [DE94-006593] p 3692 N94-32111

A review of weldment failure modes and weldability testing methods [AD-A278096] p 3729 N94-33251

FAINT OBJECTS

Digital image profilers for detecting faint sources which have bright companions [NASA-CR-191348] p 3927 N94-32695

FAR FIELDS

Micromechanics and effective properties of particulate composites and fluid suspensions p 3703 N94-31744

Experimental and computational studies on propeller noise due to inflow distortion p 3860 N94-31846

Using TSAR with the post-processing far-field option [DE94-006615] p 3679 N94-32188

Particle-In-Cell (PIC) code simulation results and comparison with theory scaling laws for photoelectron-generated radiation [DE94-006132] p 3695 N94-32662

FAR INFRARED RADIATION

High precision moving magnet chopper for variable operation conditions p 3605 N94-33307

FAR ULTRAVIOLET RADIATION

Ground-based simulation of LEO environment: Investigations of a select LDEF material: FEP Teflon (trademark) p 3596 N94-31039

FARM CROPS

High resolution spectroscopy in agriculture: Results of the EISAC 1989 campaign p 3745 N94-31864

Extraction of agricultural parameters from imaging-spectrometry data and simulated MERIS data through red edge analysis p 3745 N94-31865

FAST FOURIER TRANSFORMATIONS

An efficient three-dimensional Poisson solver for SIMD high-performance-computing architectures p 3823 N94-31120

Atmospheric structure simulation: An autoregressive model for smooth geophysical power spectra with known autocorrelation function [AD-A276691] p 3773 N94-32118

FAST NEUTRONS

Defect cascades produced by neutron irradiation in YBa2Cu3O(7-delta) superconductors [DE94-007700] p 3903 N94-32372

FASTENERS

An experimental and analytical investigation of a threaded fastener [VTT-JULK-786] p 3724 N94-31654

Feasibility study of cold expansion processes modelling [DSIS-94-01186] p 3735 N94-31849

FATIGUE (BIOLOGY)

Effects of methamphetamine and fatigue on long- and short-term memory [AD-A276452] p 3799 N94-32187

FATIGUE (MATERIALS)

Fatigue crack propagation and fractography of 3Y-TZP and ZTA [ISBN-0-315-86561-X] p 3736 N94-31912

Effects of frequency and amplitude variations of superimposed minor loading sequences on the corrosion fatigue behavior of aircraft structural aluminum alloys p 3578 N94-31957

The cyclic fatigue behaviour of adhesive joints [AD-A277080] p 3738 N94-32351

Fracture micromechanics of continuous fiber and textile reinforced metal and ceramic matrix composites [AD-A277434] p 3627 N94-33008

FATIGUE LIFE

A laboratory study of multiple site damage in fuselage lap splices [AD-A276151] p 3578 N94-31078

Contribution to the study of multiaxial fatigue under periodic or random stresses [ISAL-92-0004] p 3734 N94-31544

Fatigue behavior of unidirectional pultruded composite materials [ISBN-0-315-86425-7] p 3621 N94-31719

Feasibility study of cold expansion processes modelling [DSIS-94-01186] p 3735 N94-31849

Active control for fin buffet alleviation [AD-A276844] p 3586 N94-32224

Fatigue testing of 2024-T3 material after four cycles of PMB stripping [AD-A276926] p 3644 N94-32237

FATIGUE TESTS

An experimental and analytical investigation of a threaded fastener [VTT-JULK-786] p 3724 N94-31654

Fatigue crack propagation and fractography of 3Y-TZP and ZTA [ISBN-0-315-86561-X] p 3736 N94-31912

Creep-fatigue criteria and inelastic behavior of modified 9Cr-1Mo steel at elevated temperatures [DE94-007915] p 3642 N94-31918

Effects of frequency and amplitude variations of superimposed minor loading sequences on the corrosion fatigue behavior of aircraft structural aluminum alloys p 3578 N94-31957

FAULT DETECTION

Quench detection and instrumentation for the Tokamak Physics Experiment magnets [DE94-006656] p 3888 N94-31667

Model-based reconfiguration: Diagnosis and recovery [NASA-CR-4596] p 3820 N94-32776

Fault detection and isolation for the Bluebird test bed aircraft [AD-A277979] p 3586 N94-33086

Assessing the vulnerability of multi-commodity networks with failing components [AD-A278434] p 3684 N94-33334

FAULT TOLERANCE

Fault coverage measurement for digital microcircuits [AD-A276226] p 3686 N94-31066

Quench detection and instrumentation for the Tokamak Physics Experiment magnets [DE94-006656] p 3888 N94-31667

Using atomic actions in replica groups to simplify the replication implementation [REPT-93-78] p 3813 N94-31695

Parallel and distributed computing combinatorial algorithms [AD-A277333] p 3826 N94-32243

Interpreter composition issues in the formal verification of a processor-memory module [NASA-CR-4594] p 3820 N94-32775

Model-based reconfiguration: Diagnosis and recovery [NASA-CR-4596] p 3820 N94-32776

Fault detection and isolation for the Bluebird test bed aircraft [AD-A277979] p 3586 N94-33086

FAULT TREES

GRAFTED - GRAphical fault tree EDitor: A fault tree description program for target vulnerability/survivability analysis. User manual [AD-A277067] p 3818 N94-32390

FEAR

Stress-induced enhancement of the startle reflex [AD-A278414] p 3802 N94-33327

FEASIBILITY

Feasibility study to evaluate plasma quench process for natural gas conversion applications [DE94-000086] p 3758 N94-31234

FEASIBILITY ANALYSIS

Proof of concept for the rewrite rule machine: Interensemble studies [AD-A276506] p 3809 N94-31263

Economic feasibility analysis of distributed electric power generation based upon the natural gas fired fuel cell [DE94-005795] p 3759 N94-31487

Feasibility study for the recycling of nickel metal hydride electric vehicle batteries [DE94-000268] p 3690 N94-31598

Feasibility in the use of satellite remote sensing data as a fast reaction tool for natural disastar relief p 3748 N94-32526

Removal of CO2 from flue gases by algae [DE94-008039] p 3766 N94-32703

Focused feasibility study final field sampling plan [AD-A277445] p 3769 N94-33105

FEED SYSTEMS

Development of an automated wire delivery system for robotic welding applications [NASA-CR-194216] p 3727 N94-32479

Buffered feedthrough crossbar switch [AD-D016145] p 3697 N94-32967

FEEDBACK

Controls design with crossfeeds for hovering rotorcraft using quantitative feedback theory [NASA-CR-195765] p 3585 N94-31203

A hypertext system that learns from user feedback p 3923 N94-32428

FEEDBACK CONTROL

Control of a flexible space robot tracking a moving target p 3722 N94-31469

Automatic resonator alignment and power stabilization of high power C02 lasers [ISBN-0-315-77217-4] p 3714 N94-31472

Adaptive nonlinear control of spacecraft p 3609 N94-31564

Digital state-feedback H(infinity) control of Pritchard-Salamon systems: A Popov function approach [REPT-93-69] p 3830 N94-31647

Development of a reconfigurable helicopter flight control system [ISBN-0-315-87218-7] p 3585 N94-31837

High-speed path constrained manipulator operation using optimal-feedback combined controller p 3833 N94-31962

A novel potential/viscous flow coupling technique for computing helicopter flow fields [NASA-CR-193272] p 3571 N94-32476

Control strategies for systems with limited actuators [NASA-CR-195307] p 3727 N94-32741

FEEDFORWARD CONTROL

Development of a feedforward controller for a flexible manipulator [ISBN-0-315-86515-6] p 3832 N94-31801

FEEDING (SUPPLYING)

Feed-forward control of gear mesh vibration using piezoelectric actuators [NASA-TM-106366] p 3728 N94-32902

FELDSPARS

In-situ TEM crystallization of anorthite-glass films on (alpha)-Al2O3 [DE94-006317] p 3652 N94-31780

FERMENTATION

Recovery of carboxylic acids at pH greater than pKa [DE94-007030] p 3636 N94-32376

FERMI LIQUIDS

Short coherence length superconductors: Intermediate regime between BCS and bosons [DE94-007694] p 3904 N94-32645

FERMI SURFACES

Fermi surface instability at 0.4 K in a heavy-fermion YbBiPt: SDW? [DE94-006224] p 3899 N94-31916

FERMIONS

The 4f heavy fermion photoelectron spectra do not exhibit the Kondo scale [DE94-006252] p 3898 N94-31631

Fermi surface instability at 0.4 K in a heavy-fermion YbBiPt: SDW? [DE94-006224] p 3899 N94-31916

Investigation of superconductivity and magnetism in d and f-electron materials [DE94-008535] p 3907 N94-32933

FERRIC IONS

The importance of environmental conditions in reflectance spectroscopy of laboratory analogs for Mars surface materials p 3944 N94-33195

FERROELECTRICITY

Emission from ferroelectric cathodes [DE94-006732] p 3863 N94-31270

Electrooptic crystal growth and properties [AD-A276023] p 3896 N94-31439

Thin-film decoupling capacitors for multi-chip modules [DE94-007743] p 3695 N94-32650

Energetics, bonding mechanism, and electronic structure of ceramic/ceramic and metal/ceramic interfaces
[DE94-008551] p 3659 N94-32656
The ferroelectric behavior of odd-numbered nylons
[AD-A278126] p 3663 N94-33058
Electric field-induced changes in odd-numbered nylons
[AD-A278003] p 3664 N94-33138

FERTILIZERS
Monitoring fertilizer application by imaging spectrometry (Somerset Levels test site) p 3745 N94-31863

FIBER COMPOSITES
Performance of selected polymeric materials on LDEF p 3593 N94-31023
On the mechanics of stress analysis of fiber-reinforced composites p 3619 N94-31481
On the constitutive response of transversely loaded fiber composites with compliant interphases p 3619 N94-31555
Ultrasonic tomography in fiber-reinforced composite materials p 3620 N94-31565
Powder metallurgical processing of fibre reinforced aluminium composites
[PB94-148285] p 3620 N94-31686
Optimization of the forming parameters of PEEK/carbon fiber composite
[ISBN-0-315-86410-9] p 3620 N94-31716
Fracture mechanics and micromechanisms in fiber-reinforced composites p 3622 N94-31986
Sodium sulfate corrosion of silicon carbide fiber-reinforced lithium aluminosilicate glass-ceramic matrix composites
[AD-A277224] p 3623 N94-32023
Finite element analysis of damage in fibrous composites using a micromechanical model
[AD-A277226] p 3623 N94-32024
Mechanics of the single fiber pullout problem with several interface conditions p 3623 N94-32078
Pressureless sintering of ceramic composites
[AD-A277274] p 3657 N94-32404
Effects of interphases on the mechanical, thermal and hygromechanical response of fiber-reinforced composites p 3624 N94-32496
The effect of ductile phase (Nb) reinforcement morphology on the mechanical behavior of an intermetallic matrix (MoSi2) p 3615 N94-32500
Improved oxidation resistance of 3-D carbon/carbon composites
[AD-A277349] p 3625 N94-32624
METCAN demonstration manual, version 1.0
[NASA-TM-105607] p 3626 N94-32858
Analysis of new composite architectures
[NASA-CR-195303] p 3626 N94-32904
Fracture micromechanics of continuous fiber and textile reinforced metal and ceramic matrix composites
[AD-A277434] p 3627 N94-33008
Surface conforming flexible eddy current probe for scanning varying surface contours
[AD-D016173] p 3627 N94-33018
Nonlocal theory for fracturing of quasibrittle materials
[AD-A278283] p 3740 N94-33143
Novel precursor approached for CMC derived by polymer pyrolysis
[AD-A278383] p 3665 N94-33352

FIBER OPTICS
Fiber optic chemical sensors on Mars
[DE94-005251] p 3941 N94-31145
Advanced optical fiber communication systems
[AD-A276416] p 3878 N94-31330
Fiberoptisk magnetfaltsensor (fiber optic magnetometer)
[PB94-148061] p 3878 N94-31584
Nd-YAG laser welding of the fiber optic connector to the header shell on the 2SL actuator
[DE94-006104] p 3723 N94-31621
Fiber optic sensors for the detection of surface acoustic waves on metals
[ISBN-0-315-87055-9] p 3878 N94-31736
The vision machines
[NASA-TM-109757] p 3606 N94-31816
A technique for multiplexing 3x3-coupler terminated interferometric fiber-optic sensors
[AD-A276739] p 3880 N94-32180
Fiber optic chemical sensors
[AD-A277128] p 3881 N94-32380
Studies of an optical multi-processor interconnect
[AD-A277093] p 3681 N94-32392
Mathematical nonlinear optics
[AD-A277320] p 3882 N94-32510
Passive, multi-channel fiber optic rotary joint assembly
[AD-D016116] p 3882 N94-32626
Gigabits to the Desktop: Installing tomorrow's networks today
[DE94-007701] p 3827 N94-32646
Automated fiber pigtailing technology
[DE94-007072] p 3695 N94-32688
Torque-balanced extendable fiber optic cable
[AD-D016097] p 3882 N94-32719
Fiber optic continuous true time-delay modulator
[AD-D016098] p 3883 N94-32720
Multi-line passive fiber optic slipring
[AD-D016092] p 3883 N94-32738
Long distance transmission of 15 Gb/s digital using subcarrier multiplexing and external modulation
[DE94-008298] p 3682 N94-32756
Strain sensing using optical fibers
[NASA-CR-195807] p 3740 N94-32940

FIBER ORIENTATION
Comparison of the compressive strengths for stitched and toughened composite systems
[NASA-TM-109108] p 3627 N94-32939

FIELD ALIGNED CURRENTS
Convection and electrodynamic signatures in the vicinity of a Sun-aligned arc: Results from the Polar Acceleration Regions and Convection Study (Polar ARCS) p 3954 N94-31102

FIELD COILS
Structural design of the superconducting Poloidal Field coils for the Tokamak Physics Experiment
[DE94-007078] p 3887 N94-31406

FIELD EFFECT TRANSISTORS
A silicon condenser microphone: Modelling and electronic circuitry
[ISBN-9-09-005279-8] p 3688 N94-31517
Employment of a porous gold actuator in ISFET-based coulometric sensor-actuator systems with application to protein characterization
[ISBN-9-09-005887-7] p 3689 N94-31536
Perspectives of glucose sensing based on a charge-modulating competition reaction
[ISBN-9-09-005754-4] p 3795 N94-31652
Radiation tolerant, high speed, low power, gallium arsenide logic
[AD-A277293] p 3694 N94-32509
Research on high reliability refractory ohmic contacts for GaAs FETs and MODFETs
[AD-A276848] p 3697 N94-33034
Characteristics of III-V semiconductor devices at high temperature
[NASA-TM-106574] p 3697 N94-33052
Advanced silicon technology for microwave circuits
[AD-A278039] p 3698 N94-33091
Temperature dependence of single-event burnout in n-channel power MOSFET's
[AD-A277921] p 3698 N94-33177
Electrical characteristics of GaAs MESFET fabrication by ion implantation of Si or Se
[AD-A278416] p 3909 N94-33328

FIELD THEORY (ALGEBRA)
Topological conformal algebra in 2D gravity coupled to minimal matter
[DE94-008122] p 3910 N94-31052
N(exp n(n-1)/2)-state R-matrix related with U(sub q)(si(n)) algebra at q(exp 2N) = 1
[DE94-008140] p 3902 N94-32247

FIELD THEORY (PHYSICS)
Experimental investigation of phonon eigenvectors using x ray interference fields
[ETN-94-95751] p 3865 N94-31511
Conformal field theory and geometry of strings
[PB94-148442] p 3857 N94-31770
New QCD results from string theory
[DE94-005226] p 3911 N94-31823
Wavevector-frequency analysis with applications to acoustics
[AD-A276618] p 3861 N94-32125
The future of high-energy physics in the US: Statement for the 1994 HEPAP Subpanel
[DE94-008994] p 3876 N94-32588

FIGHTER AIRCRAFT
Aircraft simulation and pilot proficiency: From surrogate flying towards effective training
[AD-B179300] p 3587 N94-31179
Prospects for the French fighter industry in a post-cold war environment: is the future more than a mirage? p 3565 N94-31959
Active control for fin buffet alleviation
[AD-A276844] p 3586 N94-32224

FINANCIAL MANAGEMENT
Managing performance of DB2 Ad Hoc Reports
[DE94-006669] p 3920 N94-32635

FINE STRUCTURE
Instrumentation for EXELFS measurements using convergent beam diffraction coupling to the electron energy loss spectrometer
[USIP-93-07] p 3858 N94-31084
The double probe electric field experiment on Freja: Description and first results
[TRITA-ALP-1993-02] p 3885 N94-31089
Near edge x ray spectroscopy theory
[DE94-008179] p 3905 N94-32799
Fine and microstructure observations at Fieberlin g Guyot R/V new horizon cruise report
[AD-A277917] p 3791 N94-33109
Cruise report: Oceanus 250 leg 4 high resolution profiler survey for the North Atlantic Tracer Release Experiment, 25 March - 24 April, 1992
[AD-A277935] p 3791 N94-33245

FINGERS
Numerical model of the thermal behavior of an extremity in a cold environment including counter-current heat exchange between the blood vessels
[AD-A276099] p 3798 N94-33040

FINITE DIFFERENCE THEORY
An efficient three-dimensional Poisson solver for SIMD high-performance-computing architectures p 3823 N94-31120
Nonlinear calculations of the time evolution of black hole accretion disks p 3929 N94-31127
Gas dynamics for accretion disk simulations p 3932 N94-31144
Numerical analysis of single-vortex/free-surface interaction
[AD-A276462] p 3701 N94-31241
A simplified Von Neumann method for linear stability analysis
[CRANFIELD-AERO-9310] p 3843 N94-31540
Applied Computational Electromagnetics Society Journal, volume 9, number 1, March 1994
[AD-A276753] p 3679 N94-32183
COVICS: A covert video communications system
[DE94-007568] p 3682 N94-32745
Preconditioned time-difference methods for advection-diffusion-reaction equations
[DE94-006472] p 3638 N94-32840
A finite-difference approximate-factorization algorithm for solution of the unsteady transonic small-disturbance equation
[NASA-TP-3129] p 3572 N94-32865
Theoretical and experimental study of microstrip-to-slot line uniplanar transition
[NASA-TM-106566] p 3696 N94-32905
Parallel supercomputing: Advanced methods, algorithms, and software for large-scale linear and nonlinear problems
[DE94-008446] p 3836 N94-32992
Analysis of a slot coupled coplanar waveguide fed patch antenna
[NASA-TM-106567] p 3698 N94-33116
Computational methods in continuum mechanics
[AD-A278144] p 3859 N94-33161

FINITE ELEMENT METHOD
Patterns of deformation and volcanic flows associated with lithospheric loading by large volcanoes on Venus p 3776 N94-31106
State of stress, faulting, and eruption characteristics of large volcanoes on Mars p 3940 N94-31108
An adaptive finite element method for unsteady compressible rotor airfoil aerodynamics p 3567 N94-31204
An efficient higher order theory for laminated composite plates and a finite element implementation p 3617 N94-31215
Design and analysis of scalable parallel algorithms
[AD-A276255] p 3809 N94-31251
Tearing resistance of a thin shell against projectile penetration: Material property effects
[DE94-007466] p 3733 N94-31316
Contributions to the validation of the CJS model for granular materials
[ECL-92-56] p 3733 N94-31376
Development and application of a multimesh auto-adaptive finite element method for the calculation of an electric arc plasma
[ECL-89-03] p 3886 N94-31378
Finite element numerical simulation of turbulent flows
[ISBN-0-315-86418-8] p 3703 N94-31717
Finite element vorticity-based methods for the solution of the incompressible and compressible Navier-Stokes equations
[ISBN-0-315-87265-9] p 3703 N94-31730
The finite element method with asymptotic self-similar solutions p 3736 N94-31904
Finite element analysis of time-independent superconductivity p 3691 N94-31905
Nonlinear analysis of springs using helical finite elements p 3859 N94-31906
Finite element analysis of damage in fibrous composites using a micromechanical model
[AD-A277226] p 3623 N94-32024
Minimization of computational requirements in the hybrid stress finite element method
[AD-A277120] p 3846 N94-32048
Finite element analysis of MB326H Macchi wing lower spar cap fatigue cracks
[AD-A277062] p 3580 N94-32264

Control and stabilization of distributed parameter systems; theoretical and computational aspects
[AD-A277239] p 3738 N94-32275
QUAD4 seminar
[AD-A277366] p 3818 N94-32330
Eta percent-superconvergence in the interior of locally refined meshes of quadrilaterals: Superconvergence of the gradient in finite element solutions of Laplace's and Poisson's equations
[AD-A277242] p 3848 N94-32331
Finite element solution to the Helmholtz equation with high wave number. Part 1: The h-version of the FEM
[AD-A277396] p 3848 N94-32341
Development of an advanced continuum theory for composite laminates, volume 2
[AD-A277276] p 3625 N94-32592
Automatic contact in DYNA3D for vehicle crashworthiness
[DE94-007143] p 3738 N94-32637
The 2D deterministic radiation transport with the discontinuous finite element method
[DE94-004687] p 3849 N94-32670
BUCKY instruction manual, version 3.3
[NASA-TM-104793] p 3820 N94-32899
Manual for automatic generation of finite element models of spiral bevel gears in mesh
[NASA-CR-191009] p 3728 N94-32900
A case study of analysis methods for large deflections of a cantilever beam
[NASA-TM-108454] p 3739 N94-32903
Analysis of new composite architectures
[NASA-CR-195303] p 3626 N94-32904
Theoretical and experimental study of microstrip-to-slot line uniplanar transition
[NASA-TM-106566] p 3696 N94-32905
A procedure for 3-D contact stress analysis of spiral bevel gears
[NASA-CR-194472] p 3728 N94-32929
Parallel supercomputing: Advanced methods, algorithms, and software for large-scale linear and nonlinear problems
[DE94-008446] p 3836 N94-32992
Finite-element modeling of the blockage and scattering of LG propagation
[AD-A277430] p 3775 N94-33006
On the mechanics of microballoon-reinforced metal matrix composites
[AD-A277928] p 3830 N94-33178

FINITE VOLUME METHOD
Multidimensional WAF-type schemes for model conservation laws
[CRANFIELD-AERO-9312] p 3843 N94-31541
Finite volume discretization of the k-epsilon turbulence model in general coordinates
[REPT-93-90] p 3703 N94-31703

FINS
Heat transfer studies on a rectangular channel with offset plate fins
[AD-A277300] p 3912 N94-32043
Active control for fin buffet alleviation
[AD-A276844] p 3586 N94-32224

FIR FILTERS
VLSI for high-speed digital signal processing
[AD-A277617] p 3697 N94-32957

FIRE EXTINGUISHERS
Influence of carbon dioxide on electronic equipment: Fire extinguishing with low concentration
[PB94-148749] p 3691 N94-31848

FIRE FIGHTING
Influence of carbon dioxide on electronic equipment: Fire extinguishing with low concentration
[PB94-148749] p 3691 N94-31848
Description of DCS (Data Converting System) and CT (Cone Tool). A reprint of a note published in Fire and Materials titled Fire Test Data Available for Your Purpose
[PB94-138559] p 3918 N94-32293
Glutinous water: Protecting vertical and overhead surfaces from fire spread
[AD-A277280] p 3575 N94-32405

FIRES
Solid surface
[NASA-TM-109746] p 3634 N94-31883
Description of DCS (Data Converting System) and CT (Cone Tool). A reprint of a note published in Fire and Materials titled Fire Test Data Available for Your Purpose
[PB94-138559] p 3918 N94-32293
Glutinous water: Protecting vertical and overhead surfaces from fire spread
[AD-A277280] p 3575 N94-32405

FISCHER-TROPSCH PROCESS
The development of precipitated iron catalysts with improved stability
[DE94-008711] p 3638 N94-32886
Technology development for iron Fischer-Tropsch catalysts
[DE94-008723] p 3638 N94-32889

FLAME PROPAGATION
Reactive flows in compact objects
p 3934 N94-31567
A model of concurrent flow flame spread over a thin solid fuel p 3634 N94-31795
A numerical method for mixing/chemically reacting compressible flow with finite rate chemistry
p 3634 N94-31824
Solid surface
[NASA-TM-109746] p 3634 N94-31883

FLAME RETARDANTS
Glutinous water: Protecting vertical and overhead surfaces from fire spread
[AD-A277280] p 3575 N94-32405

FLAME STABILITY
A model of concurrent flow flame spread over a thin solid fuel p 3634 N94-31795

FLAMES
A model of concurrent flow flame spread over a thin solid fuel p 3634 N94-31795

FLAMMABILITY
Glutinous water: Protecting vertical and overhead surfaces from fire spread
[AD-A277280] p 3575 N94-32405

FLASH LAMPS
A reliable low-maintenance flashlamp-pumped Ti:sapphire laser operating at 120 PPS
[DE94-009030] p 3721 N94-32848

FLASHOVER
Studies of the plasma triggering mechanism of inverse pinch switch
[AD-A276117] p 3887 N94-31530

FLATNESS
Space Station Freedom Solar Array tension mechanism development p 3604 N94-33300

FLAVOR (PARTICLE PHYSICS)
Proceedings of the Workshop on B Physics at Hadron Accelerators
[DE94-007961] p 3877 N94-32748

FLEXIBILITY
Adaptive operating systems concepts
[ETN-94-95754] p 3830 N94-31514
Flexible drive shaft coupling
[AD-D016096] p 3727 N94-32718

FLEXIBLE BODIES
Point-contact and point-impact dynamics for multibody chains
[ISBN-0-315-87056-7] p 3734 N94-31737
Control and stabilization of distributed parameter systems; theoretical and computational aspects
[AD-A277239] p 3738 N94-32275
Identification and control of structures in space
[NASA-CR-195910] p 3612 N94-33115
Space Station Freedom Solar Array tension mechanism development p 3604 N94-33300

FLEXIBLE SPACECRAFT
A study of the Space Station Freedom response to the disturbance environment p 3600 N94-31434
Dynamics and control of orbiting flexible systems: A formulation with applications
[ISBN-0-315-75390-0] p 3611 N94-32502

FLEXING
Reliability analysis of structural ceramics subjected to biaxial flexure p 3650 N94-31454

FLIGHT ALTITUDE
Neutron measurements at the commercial aircraft altitudes
[ISBN-0-315-86201-7] p 3955 N94-31709

FLIGHT CHARACTERISTICS
Modular Simulator System (MSS). System/segment specification for the generic modular simulator system-flight dynamics module, volume 4
[AD-A276971] p 3590 N94-32396

FLIGHT CLOTHING
Aircrew Eye/Respiratory Protection (AERP): 16-hour extended wear evaluation of chemical protective equipment
[AD-A277288] p 3804 N94-32609

FLIGHT CONTROL
Controls design with crossfeeds for hovering rotorcraft using quantitative feedback theory
[NASA-CR-195765] p 3585 N94-31203
Development of a reconfigurable helicopter flight control system
[ISBN-0-315-87218-7] p 3585 N94-31837
Antiwindup analysis and design approaches for MIMO systems
[NASA-CR-195304] p 3584 N94-32075
Active control for fin buffet alleviation
[AD-A276844] p 3586 N94-32224
Modular Simulator System (MSS). System/segment specification for the generic modular simulator system-flight controls module, volume 3
[AD-A276970] p 3590 N94-32395
Aircraft incident report: In-flight turbulence encounter and loss of portions of the elevators, China Airlines Flight CI-012, McDonnell Douglas MD-11-P, Taiwan Registration B-150 about 20 miles east of Japan, 7 December 1992
[PB94-910403] p 3576 N94-32938
Investigation of drive-reinforcement learning and application of learning to flight control
[AD-A277442] p 3801 N94-33053
Fault detection and isolation for the Bluebird test bed aircraft
[AD-A277979] p 3586 N94-33086
The analysis of wake-induced unsteady aerodynamics related to higher harmonic control
[AD-A277914] p 3573 N94-33108

FLIGHT CREWS
Situational awareness: A feasibility investigation of near-threshold skills development
[AD-A276467] p 3798 N94-31243
Neutron measurements at the commercial aircraft altitudes
[ISBN-0-315-86201-7] p 3955 N94-31709
Planning of air crew schedules
[ISBN-0-315-86506-7] p 3914 N94-32074
Assessment of interior modifications in C-130 and C-141 aircraft for night vision goggle operations
[AD-A276843] p 3582 N94-32223
Unit specific crew rest strategies: Phase 1 evaluation of the 1/212th Aviation Battalion during shiftwork transitions
[AD-A277122] p 3804 N94-32379
Cockpit Electronic Display Workshop: A synopsis
[AD-A277728] p 3583 N94-33280

FLIGHT HAZARDS
Rotorcraft ditchings and water-related impacts that occurred from 1982 - 1989, phase 2
[AD-A276473] p 3574 N94-31246

FLIGHT MECHANICS
Modeling of aircraft unsteady aerodynamic characteristics. Part 1: Postulated models
[NASA-TM-109120] p 3586 N94-32951

FLIGHT OPERATIONS
Common property resources and low-level flying in Labrador: Flight, fight or fancy?
[ISBN-0-315-87318-3] p 3924 N94-31732
Operations summary for the convection and moisture experiment (CAMEX)
[NASA-TM-108445] p 3786 N94-33004

FLIGHT PATHS
Flight technical error for category B non-precision approaches and missed approaches using non-differential GPS for course guidance
[PB94-142734] p 3576 N94-31680

FLIGHT PLANS
Plan recognition for an air traffic control simulation
[DSIS-94-01221] p 3577 N94-32505

FLIGHT SAFETY
Evaluation for the development of taxiway lighting intensity standards
[AD-A276706] p 3588 N94-32120
Aircraft incident report: In-flight turbulence encounter and loss of portions of the elevators, China Airlines Flight CI-012, McDonnell Douglas MD-11-P, Taiwan Registration B-150 about 20 miles east of Japan, 7 December 1992
[PB94-910403] p 3576 N94-32938
Three dimensional audio versus head down TCAS displays
[NASA-CR-177636] p 3576 N94-33063

FLIGHT SIMULATION
Variable-resolution imagery for flight simulation
[AD-A276199] p 3586 N94-31058
Controls design with crossfeeds for hovering rotorcraft using quantitative feedback theory
[NASA-CR-195765] p 3585 N94-31203
High performance real-time flight simulation at NASA Langley p 3591 N94-32473

FLIGHT SIMULATORS
Aircraft simulation and pilot proficiency: From surrogate flying towards effective training
[AD-B179300] p 3587 N94-31179
Modular Simulator System (MSS) management guide
[AD-A277098] p 3588 N94-32014
Visual evaluation of computer-generated textures
[AD-A277201] p 3816 N94-32093
Modular Simulator System (MSS). Executive report
[AD-A276966] p 3588 N94-32241
Modular Simulator System (MSS). Interface requirements specification for the generic MSS
[AD-A276965] p 3588 N94-32311
Modular Simulator System (MSS). System/segment specification for the generic MSS-system integration, volume 1
[AD-A276968] p 3588 N94-32312

Modular Simulator System (MSS). System/segment specification for the generic modular simulator system-flight station module, volume 2
[AD-A276969] p 3588 N94-32313
Modular Simulator System (MSS). System/segment specification for the generic modular simulator system-radar module, volume 8
[AD-A276975] p 3589 N94-32314
Modular Simulator System (MSS). System/segment specification for the generic modular simulator system-electronic warfare module, volume 9
[AD-A276976] p 3589 N94-32315
Modular Simulator System (MSS). System/segment specification for the generic modular simulator system-physical cues module, volume 10
[AD-A276977] p 3589 N94-32316
Modular Simulator System (MSS). System/segment specification for the generic modular simulator system-visual module, volume 11
[AD-A276978] p 3589 N94-32317
Modular Simulator System (MSS). System/segment specification for the generic modular simulator system-instructor/operator station module, volume 12
[AD-A276979] p 3589 N94-32318
Modular Simulator System (MSS). System/segment specification for the generic modular simulator system-environment module, volume 13
[AD-A276980] p 3589 N94-32319
Modular Simulator System (MSS). Engineering design guide
[AD-A276967] p 3589 N94-32394
Modular Simulator System (MSS). System/segment specification for the generic modular simulator system-flight controls module, volume 3
[AD-A276970] p 3590 N94-32395
Modular Simulator System (MSS). System/segment specification for the generic modular simulator system-flight dynamics module, volume 4
[AD-A276971] p 3590 N94-32396
Modular Simulator System (MSS). System/segment specification for the generic modular simulator system-propulsion module propulsion module, volume 5
[AD-A276972] p 3590 N94-32397
Modular Simulator System (MSS). System/segment specification for the generic modular simulator system-navigation/communication module, volume 6
[AD-A276973] p 3590 N94-32398
Modular Simulator System (MSS). System/segment specification for the generic modular simulator system-weapons module, volume 7
[AD-A276974] p 3590 N94-32399
Modular Simulator System (MSS): Interface design document for the generic MSS
[AD-A277270] p 3590 N94-32403
High performance real-time flight simulation at NASA Langley p 3591 N94-32473
An evaluation framework for designing a night vision, computer-based trainer
[AD-A278005] p 3590 N94-33139

FLIGHT TESTS

Utilizing a Russian space nuclear reactor for a United States space mission: Flight qualification issues
[DE94-004674] p 3613 N94-31265
Flight technical error for category B non-precision approaches and missed approaches using non-differential GPS for course guidance
[PB94-142734] p 3576 N94-31680
In flight measurement of steady and unsteady blade surface pressure of a single rotation large scale advanced prop-fan installed on the PTA aircraft
[NASA-CR-187096] p 3584 N94-32859
Flight test results of riblets at supersonic speeds
[NASA-TM-4387] p 3572 N94-32880
Synthetic vision technology demonstration. Volume 1: Executive summary
[DOT/FAA/RD-93/40-VOL-1] p 3582 N94-33076
Synthetic vision technology demonstration. Volume 2: Sensor tower testing
[DOT/FAA/RD-93/40-VOL-2] p 3582 N94-33077
Synthetic vision technology demonstration. Volume 3: Flight tests
[DOT/FAA/RD-93/40-VOL-3] p 3582 N94-33078
Synthetic vision technology demonstration. Volume 4: Appendices
[DOT/FAA/RD-93/40-VOL-4] p 3583 N94-33079
The analysis of wake-induced unsteady aerodynamics related to higher harmonic control
[AD-A277914] p 3573 N94-33108
Advanced release technologies program p 3607 N94-33322

FLIGHT TRAINING

Aircraft simulation and pilot proficiency: From surrogate flying towards effective training
[AD-B179300] p 3587 N94-31179
Modular Simulator System (MSS) management guide
[AD-A277098] p 3588 N94-32014
Modular Simulator System (MSS). Executive report
[AD-A276966] p 3588 N94-32241
Modular Simulator System (MSS). Interface requirements specification for the generic MSS
[AD-A276965] p 3588 N94-32311
Modular Simulator System (MSS). System/segment specification for the generic MSS-system integration, volume 1
[AD-A276968] p 3588 N94-32312
Modular Simulator System (MSS). System/segment specification for the generic modular simulator system-flight station module, volume 2
[AD-A276969] p 3588 N94-32313
Modular Simulator System (MSS). System/segment specification for the generic modular simulator system-radar module, volume 8
[AD-A276975] p 3589 N94-32314
Modular Simulator System (MSS). System/segment specification for the generic modular simulator system-electronic warfare module, volume 9
[AD-A276976] p 3589 N94-32315
Modular Simulator System (MSS). System/segment specification for the generic modular simulator system-physical cues module, volume 10
[AD-A276977] p 3589 N94-32316
Modular Simulator System (MSS). System/segment specification for the generic modular simulator system-visual module, volume 11
[AD-A276978] p 3589 N94-32317
Modular Simulator System (MSS). System/segment specification for the generic modular simulator system-instructor/operator station module, volume 12
[AD-A276979] p 3589 N94-32318
Modular Simulator System (MSS). System/segment specification for the generic modular simulator system-environment module, volume 13
[AD-A276980] p 3589 N94-32319
The effects of Above Real-Time Training (ARTT) in an F-16 simulator p 3591 N94-32474

FLOATING

VLSI implementation of stray insensitive switched capacitor composite operational amplifiers
[AD-A276461] p 3687 N94-31240

FLOATS

Profiling ALACE instruments
[AD-A277246] p 3789 N94-32321

FLOODS

Feasibility in the use of satellite remote sensing data as a fast reaction tool for natural disaster relief p 3748 N94-32526
Simulation of a precipitation event in the western United States
[DE94-004835] p 3786 N94-32791

FLOW CHARACTERISTICS

Oscillating-flow loss test results in rectangular heat exchanger passages
[NASA-CR-185297] p 3615 N94-32792
Control of low-speed turbulent separated flow over a backward-facing ramp
[NASA-TM-109740] p 3573 N94-33071

FLOW DISTORTION

Inlet distortion in engines on VSTOL aircraft
[NASA-CR-195841] p 3584 N94-33035

FLOW DISTRIBUTION

Computational study of single-expansion-ramp nozzles with external burning
[NASA-TM-106550] p 3700 N94-31229
Hypervelocity Tunnel 9 Mach 10/14 Calibration
[AD-A275960] p 3587 N94-31318
A novel CFD/structural analysis of a cross parachute
[DE94-005271] p 3568 N94-31578
On an adaptation method for dense, 2D, C-type grids
[W-9321] p 3706 N94-32045
Optical flow from 1D correlation: Application to a simple time-to-crash detector
[AD-A276777] p 3880 N94-32186
Design of a two dimensional planer pressurized air labyrinth seal test rig
[AD-A277232] p 3726 N94-32370
An experimental study of the flowfield on a semispan rectangular wing with a simulated glaze ice accretion
[NASA-CR-195301] p 3571 N94-32475
A novel potential/viscous flow coupling technique for computing helicopter flow fields
[NASA-CR-193272] p 3571 N94-32476
Results for the hybrid laminar flow control experiment conducted in the NASA Langley 8-foot transonic pressure tunnel on a 7-foot chord model
[NASA-TM-107582] p 3601 N94-32870
Computation of three-dimensional compressible boundary layers to fourth-order accuracy on wings and fuselages
[NASA-CR-4269] p 3709 N94-32871
Use of Navier-Stokes methods for the calculation of high-speed nozzle flow fields
[NASA-TM-106551] p 3573 N94-32984
Characteristics of ion flow in the quiet state of the inner plasma sheet
[AD-A277451] p 3894 N94-33106
Direct replacement of arbitrary grid-overlapping by non-structured grid
[NASA-TM-106601] p 3850 N94-33120

FLOW EQUATIONS

Prediction of transonic potential flow with slipstreams around configurations
[FFA-TN-1992-15] p 3568 N94-31220
Surface boundary conditions and related technical issues concerning Burnett equations for 2-D hypersonic flow
[AD-A277322] p 3706 N94-32256

FLOW MEASUREMENT

Hotwire measurements of the turbulent flow into a cascade of controlled-diffusion compressor blades
[AD-A277297] p 3706 N94-32042
Electromagnetic probe technique for fluid flow measurements p 3711 N94-32455
Shear flow control of cold and heated rectangular jets by mechanical tabs. Volume 1: Results and discussion
[NASA-CR-182296-VOL-1] p 3708 N94-32867
Shear flow control of cold and heated rectangular jets by mechanical tabs. Volume 2: Tabulated data
[NASA-CR-182296-VOL-2] p 3709 N94-32869
Scalar imaging velocimetry studies of turbulent flow structure and dynamics
[AD-A278395] p 3710 N94-33164
Calibration and validation studies in the LENS facility
[AD-A278403] p 3591 N94-33167
Backward-facing step measurements at low Reynolds number, Re(sub h)=5000
[NASA-TM-108807] p 3711 N94-33290

FLOW RESISTANCE

Effects of combined breathing impediments on diver's respiratory performance
[AD-A277437] p 3805 N94-33084

FLOW STABILITY

On the structure and stability of slender viscous vortices p 3700 N94-31218
Workshop on advances in smooth particle hydrodynamics
[DE94-006221] p 3956 N94-31308
Structure and stability of spherical accretion flows onto compact objects p 3935 N94-31946

FLOW VELOCITY

Oscillations in piston-driven shear flow of a non-Newtonian fluid
[AD-A276472] p 3701 N94-31245
Backward-facing step measurements at low Reynolds number, Re(sub h)=5000
[NASA-TM-108807] p 3711 N94-33290

FLOW VISUALIZATION

Parallel particle simulations of low-density fluid flows
[DE94-007858] p 3707 N94-32373

FLUE GASES

Removal of CO2 from flue gases by algae
[DE94-008039] p 3766 N94-32703

FLUENCE

Defect cascades produced by neutron irradiation in YBa2Cu3O(7-delta) superconductors
[DE94-007700] p 3903 N94-32372
Vulnerability assessment of a space based weapon platform electronic system exposed to a thermonuclear weapon detonation
[DE94-007229] p 3611 N94-32667
Resistivity measurements on the neutron irradiated detector grade silicon materials
[DE94-009083] p 3906 N94-32822

FLUID BOUNDARIES

Laser-induced fluorescence/particle tracking system for stratified flow research
[AD-A275917] p 3701 N94-31341
Sound scattering by cylinders of noncircular cross section
[AD-A276663] p 3861 N94-32089

FLUID DYNAMICS

A cross-disciplinary report on the mathematical sciences applied to materials science, part 1
[AD-A276116] p 3843 N94-31529
Steady thermal convection in multiple liquid layers p 3705 N94-31844
Effects of buoyancy on fluid flows and turbulence
[AD-A276586] p 3706 N94-32123
Chemical vapor deposition fluid flow simulation modelling tool
[NASA-CR-189648] p 3707 N94-32480
Fluid Dynamics Lagranglan Simulation Model
[AD-A277438] p 3710 N94-33009
Renormalization group theory of Bolgiano scaling in Boussinesq turbulence
[NASA-TM-106602] p 3710 N94-33070
The structure of high Reynolds number turbulent boundary layers, part A
[AD-A278392] p 3710 N94-33162

Scalar imaging velocimetry studies of turbulent flow structure and dynamics
[AD-A278395] p 3710 N94-33164

FLUID FILMS
Simultaneous pressure measurement and high-speed photography study of cavitation in a dynamically loaded journal bearing
[NASA-TM-106456] p 3728 N94-32893

FLUID FLOW
A heterogeneous computing environment for simulating astrophysical fluid flows p 3928 N94-31119
Reactive flows in compact objects p 3934 N94-31567
Parallel particle simulations of low-density fluid flows
[DE94-007858] p 3707 N94-32373
Electromagnetic probe technique for fluid flow measurements p 3711 N94-32455
Computational modeling of convective heat transfer to liquid hydrogen coolant p 3707 N94-32485

FLUID JETS
Analysis of strong acoustic excitation on the breakup and dispersion of a liquid jet
[ONERA-NT-1993-9] p 3701 N94-31422
Enhancement of mixing in a rectangular jet by mechanical tabs
[NASA-CR-185207] p 3709 N94-32872

FLUID MECHANICS
Mathematical research in materials science opportunities and perspectives, part 2
[AD-A276298] p 3852 N94-31296
Chemical vapor deposition fluid flow simulation modelling tool
[NASA-CR-189648] p 3707 N94-32480
On the use of computers for teaching fluid mechanics
[NASA-TM-106587] p 3820 N94-32773
Fluid mechanical measurements within the bottom boundary layer over the Northern California continental shelf during stress
[AD-A277916] p 3791 N94-33243

FLUID-SOLID INTERACTIONS
Doubly asymptotic approximations: Theoretical and numerical analyses
[ONERA-NT-1993-7] p 3840 N94-31231
Fluid-structure interaction in case of water hammer with cavitation
[PB94-148277] p 3702 N94-31588

FLUORESCENCE
Fluorescence observations of LDEF exposed materials as an indicator of induced material reactions p 3593 N94-31025
An axial approach to detection in capillary electrophoresis
[DE94-005556] p 3631 N94-31154
Final results from the SDC dopant search for new green wavelength shifting (WLS) fibers, volume 1
[DE94-006744] p 3878 N94-31271
Evaluation of Fluorescence Line Imager (FLI) airborne imaging spectrometer data for roadside tree damage assessment p 3745 N94-31866
Evaluation of GER- and FLI-data with reference to forest p 3746 N94-31868
Temperature dependence of the exciton-exciton annihilation rate constant in poly(di-n-hexylsilane)
[DE94-005584] p 3655 N94-32102
Design and characterization of a pulsed x ray source for fluorescent lifetime measurements
[DE94-007495] p 3880 N94-32138
Intramolecular charge transfer complexes as fluorescence probes for UV and visible light induced acrylate polymerization
[AD-A277129] p 3657 N94-32381
Conjugated polymer fluorescence: Interplay of correlations and alternation
[DE94-005587] p 3660 N94-32729
Noninvasive spectroscopic diagnosis of superficial ocular lesions and corneal infections
[DE94-006231] p 3797 N94-32732
Development of a video fluorescence system for assessing burn depth
[AD-A278127] p 3798 N94-33092

FLUORIDES
PVDF pressure transducers for shock wave and explosives research
[AD-A277319] p 3712 N94-32051

FLUTTER
Aeroelastic vibrations of lifting surfaces
[ECL-91-01] p 3585 N94-31677
Flutter analysis of a supersonic cascade in time domain using an ADI Euler solver
[NASA-TM-105625] p 3739 N94-32883

FLUTTER ANALYSIS
Computational prediction of stall flutter in spanwise-finite blade cascades p 3584 N94-31967
Flutter analysis of a supersonic cascade in time domain using an ADI Euler solver
[NASA-TM-105625] p 3739 N94-32883

FLUX DENSITY
Transport phenomena in the Earth's plasma sheet p 3772 N94-31970
Development of silver-zinc cells of improved cycle life and energy density
[AD-A277311] p 3693 N94-32329
Transverse energy production with Si and Au beams at AGS energy: Towards hot and dense hadronic matter
[DE94-007178] p 3938 N94-32638

FLUXES
Correlation of flux composition and inclusion characteristics with submerged arc weld metal properties in HY-100 steel
[AD-A277040] p 3726 N94-32261

FLYWHEELS
Flywheel Energy Storage Technology Workshop
[DE94-008064] p 3761 N94-32705

FOAMS
An investigation of the spin-coating process and a model for three-dimensional regular foams p 3649 N94-31206
Glutinous water: Protecting vertical and overhead surfaces from fire spread
[AD-A277280] p 3575 N94-32405

FOCAL PLANE DEVICES
Wavelet transform of fixed pattern noise in focal plane arrays
[AD-A276963] p 3712 N94-32393
A new high-speed IR camera system p 3713 N94-32459
Quantum well infrared photodetector FPA
[AD-A278010] p 3908 N94-33248

FOCUSING
Multi-line passive fiber optic slipring
[AD-D016092] p 3883 N94-32738

FOG
Drop size distributions and related properties of fog for five locations measured from aircraft
[NASA-CR-4585] p 3787 N94-33065

FOLDING STRUCTURES
MSAT boom joint testing and load absorber design p 3606 N94-33315
Deployable and retractable telescoping tubular structure development p 3607 N94-33317

FOOD PROCESSING
Novel ultrasonic method for food hydration
[AD-A277411] p 3804 N94-32580

FOOTPRINTS
The influence of the deorbit-burn manoeuvre on the footprint of a re-entry capsule
[LR-727] p 3609 N94-31705

FORCE DISTRIBUTION
Automatic analysis of force distribution in multi-fingered articulated hands
[ISBN-0-315-87205-5] p 3725 N94-31878

FORCED VIBRATION
Random vibrations of composite beams and plates p 3735 N94-31777

FORECASTING
Exploring phase space concepts in the forecasting of time series with artificial neural networks
[DE94-005810] p 3834 N94-32127
Simulation of a precipitation event in the western United States
[DE94-004835] p 3786 N94-32791
FAA aviation forecasts, fiscal years 1994-2005
[AD-A277808] p 3566 N94-33016
Snowmelt forecasting. Further cold regions development of operational hydrological forecasting, volume 2
[AD-A278123] p 3757 N94-33269

FOREST MANAGEMENT
Extraction of forests stand age parameters from airborne imaging spectroscopy data p 3745 N94-31867
Evaluation of GER- and FLI-data with reference to forest p 3746 N94-31868

FORESTS
Carbon balance in a forest ecosystem p 3770 N94-31007
Evaluation of Fluorescence Line Imager (FLI) airborne imaging spectrometer data for roadside tree damage assessment p 3745 N94-31866
Extraction of forests stand age parameters from airborne imaging spectroscopy data p 3745 N94-31867
Research and applications of a canopy reflectance model p 3747 N94-32492
Robust multisource classification method using the Markov random field methods p 3750 N94-32537
A case study comparing multi-temporal ERS-1 SAR data and SPOT data for tropical forest mapping p 3753 N94-32556
Comparing SPOT and SIR A for mapping superficial formations in tropical forest regions: Example of the Yaoundy Region (Cameroon) p 3755 N94-32562
Effects of long-term elevated atmospheric CO2 concentrations on Pinus ponderosa
[DE94-008832] p 3769 N94-32966

FORM FACTORS
The form factors of the nucleons
[DE94-007096] p 3872 N94-32630

FORMALDEHYDE
High-temperature study of O+H2CO yields OH+HCO
[DE94-006837] p 3864 N94-31321
Cometary molecules p 3935 N94-31869
Metal ion complexation by ionizable crown ethers
[DE94-008301] p 3661 N94-32847

FORMALISM
Informal introduction to the extended affix grammar formalism and its compiler
[TR-93-19] p 3817 N94-32287
Polarized lepton-nucleon scattering
[DE94-009027] p 3875 N94-33278

FORMAT
IRIG J asynchronous ASCII time code formats
[AD-A277244] p 3681 N94-32332

FORMING TECHNIQUES
Optimization of the forming parameters of PEEK/carbon fiber composite
[ISBN-0-315-86410-9] p 3620 N94-31716

FORTRAN
Varying execution discipline to increase performance
[DE94-007844] p 3819 N94-32651
Analytic formulation for the ac electrical conductivity in two-temperature, strongly coupled, overdense plasma: FORTRAN subroutine
[DE94-009466] p 3893 N94-32915
A software architecture for multidisciplinary applications: Integrating task and data parallelism
[NASA-CR-194896] p 3820 N94-32928

FORWARD SCATTERING
Analysis of the high energy behavior of the forward scattering parameters - sigma(tot), rho and B
[DE94-006537] p 3864 N94-31310
Photoelectron diffraction and holography: Present status and future prospects
[DE94-006298] p 3712 N94-31629
Surface forward-scattered acoustic measurements and analysis
[AD-A276998] p 3788 N94-32000

FOSSIL FUELS
Environmental issues related to biomass: An overview
[DE94-007226] p 3767 N94-32784
Climate effects of anthropogenic sulfate: Simulations from a coupled chemistry/climate model
[DE94-004352] p 3767 N94-32789
National US public policy on global warming derived from optimization of energy use and environmental impact studies
[DE94-004606] p 3768 N94-32790

FOUNDATIONS
Nonlinear vibration analysis of laminated plates on linear and nonlinear elastic foundations p 3737 N94-32079

FOUR-WAVE MIXING
Near resonant absorption by atoms in intense fluctuating laser fields
[DE94-005873] p 3714 N94-31200
Degenerate four-wave mixing as a diagnostic of plasma chemistry
[DE94-008588] p 3889 N94-31766

FOURIER ANALYSIS
Frames and stable bases for shift-invariant subspaces of L(sub 2)(IR(sup d))
[AD-A276470] p 3843 N94-31474

FOURIER TRANSFORMATION
Atmospheric structure simulation: An autoregressive model for smooth geophysical power spectra with known autocorrelation function
[AD-A276691] p 3773 N94-32118
System for monitoring and analyzing field energy exposure
[AD-D016115] p 3681 N94-32625
Laser and Fourier transform spectroscopy of novel propellant molecules
[AD-A277506] p 3667 N94-33013
An experimental study of pilot/vehicle dynamics using a tilt rotor flying machine
[AD-A277516] p 3805 N94-33349

FRACTALS
Fractal and spectral analysis
[ISBN-0-315-86460-5] p 3678 N94-31796

FRACTIONATION
Mars atmospheric loss and isotopic fractionation by solar-wind-induced sputtering and photochemical escape p 3947 N94-33208

FRACTOGRAPHY
Fatigue crack propagation and fractography of 3Y-TZP and ZTA
[ISBN-0-315-86561-X] p 3736 N94-31912

FRACTURE MECHANICS
A laboratory study of multiple site damage in fuselage lap splices
[AD-A276151] p 3578 N94-31078

Reliability analysis of structural ceramics subjected to biaxial flexure p 3650 N94-31454
Modeling of fracture and damage in quasibrittle materials p 3734 N94-31479
A cross-disciplinary report on the mathematical sciences applied to materials science, part 1
[AD-A276116] p 3843 N94-31529
On the constitutive response of transversely loaded fiber composites with compliant interphases p 3619 N94-31555
Multiple-site damage in aircraft fuselage structures
[LR-729] p 3578 N94-31675
Viscoelastic fracture characterization of polymeric solids p 3652 N94-31745
Acceptance criteria for weld defects in aluminium weldments
[PB94-138575] p 3735 N94-31841
Toughening mechanisms in fiber-reinforced ceramic-matrix composites p 3622 N94-31943
A fracture mechanics methodology for characterizing the performance of flawed polymeric dielectric materials p 3654 N94-31956
Influences of pressure-sensitive yielding and non-singular stress on plane-stress elastic-plastic crack-tip fields p 3737 N94-31965
Nonlinear effects in interfacial fracture p 3737 N94-31974
Fracture mechanics and micromechanisms in fiber-reinforced composites p 3622 N94-31986
Fatigue in single crystal nickel superalloys
[AD-A276662] p 3643 N94-32047
Mechanics of the single fiber pullout problem with several interface conditions p 3623 N94-32078
Finite element analysis of MB326H Macchi wing lower spar cap fatigue cracks
[AD-A277062] p 3580 N94-32264
Mechanics of failure of high temperature metal matrix composites
[AD-A277397] p 3624 N94-32342
The cyclic fatigue behaviour of adhesive joints
[AD-A277080] p 3738 N94-32351
The effect of ductile phase (Nb) reinforcement morphology on the mechanical behavior of an intermetallic matrix (MoSi2) p 3615 N94-32500
Mechanics of cracking for composite material p 3624 N94-32501
Stage 1 behavior in a stress corrosion study of Type 304 stainless steel
[DE94-008054] p 3645 N94-32614
Reactor pressure vessel structural integrity research in the US Nuclear Regulatory Commission HSST and HSSI Programs
[DE94-006550] p 3739 N94-32771
Fracture micromechanics of continuous fiber and textile reinforced metal and ceramic matrix composites
[AD-A277434] p 3627 N94-33008
Simpler J(sub Ic) test and data analysis procedures for high strength steels
[AD-A277731] p 3648 N94-33281

FRACTURE STRENGTH
Viscoelastic fracture characterization of polymeric solids p 3652 N94-31745
Toughening mechanisms in fiber-reinforced ceramic-matrix composites p 3622 N94-31943
High-temperature deformation and fracture toughness of duplex ceramic microstructures p 3653 N94-31945
A fracture mechanics methodology for characterizing the performance of flawed polymeric dielectric materials p 3654 N94-31956
Fracture mechanics and micromechanisms in fiber-reinforced composites p 3622 N94-31986
Development of high-pressure diaphragms for the AEDC impulse tunnel
[AD-A277053] p 3588 N94-32009
Fracture and fatigue strength evaluation of multiple site damaged aircraft fuselages - curved panel testing and analysis
[AD-A277100] p 3579 N94-32015
Joining of silicon nitrides using oxynitride glasses
[DE94-008517] p 3658 N94-32517
Mechanical properties of vacuum-sintered yttria ceramics
[DE94-008138] p 3659 N94-32617
Ceramic Technology Project database
[DE94-008494] p 3659 N94-32632
Influence of volume fraction of component materials and interlayer bond strength on fracture toughness of multi-layer Al 6090-25 volume percent SiCp and Al 5182 laminates
[DE94-007141] p 3626 N94-32665
Compliance measurements of chevron notched four point bend specimen
[NASA-TM-106538] p 3740 N94-32932
Interface engineering in oxide fiber/oxide matrix composites
[AD-A277672] p 3627 N94-33029
Simpler J(sub Ic) test and data analysis procedures for high strength steels
[AD-A277731] p 3648 N94-33281

FRACTURES (MATERIALS)
Fracture micromechanics of continuous fiber and textile reinforced metal and ceramic matrix composites
[AD-A277434] p 3627 N94-33008

FRACTURING
Modeling of fracture and damage in quasibrittle materials p 3734 N94-31479
Viscoelastic fracture characterization of polymeric solids p 3652 N94-31745
Irradiation-assisted stress corrosion cracking of materials from commercial BWRs: Role of grain-boundary microchemistry
[DE94-006542] p 3643 N94-32109
Tension fracture of laminates for transport fuselage. Part 1: Material screening p 3629 N94-33130

FRAGMENTATION
Using Monte Carlo techniques and parallel processing for debris hazard analysis of rocket systems
[DE94-007250] p 3609 N94-31382
Evolution of the interface properties with temperature in the T800H/ bismaleimide composites
[ONERA-NT-1993-14] p 3619 N94-31478
Experimental measurement of dynamic failure and fragmentation properties of metals
[DE94-007377] p 3737 N94-32135

FREE ATMOSPHERE
Turbulence structure of a premixed flame in a coaxial free air jet in the presence or absence of a base flow
[ISBN-0-315-78739-2] p 3633 N94-31471

FREE CONVECTION
Steady thermal convection in multiple liquid layers p 3705 N94-31844
Renormalization group theory of Bolgiano scaling in Boussinesq turbulence
[NASA-TM-106602] p 3710 N94-33070

FREE ELECTRON LASERS
Transverse mode analysis of hole-coupled free-electron lasers
[ETN-94-96019] p 3715 N94-31532
Free electrons as a versatile source of coherent radiation
[ETN-94-96011] p 3715 N94-31545
Two-gigawatt burst-mode operation of the Intense Microwave Prototype (IMP) Free-Electron Laser (FEL) for the Microwave Tokamak Experiment (MTX)
[DE94-006613] p 3715 N94-31580
Gyrotrons and free electron lasers for atmospheric sensing
[AD-A277281] p 3718 N94-32406
Selected applications of planar permanent magnet multipoles in FEL insertion device design
[DE94-009014] p 3721 N94-32845
International Free Electron Laser Conference
[AD-A277576] p 3721 N94-33000

FREE FLOW
Hypervelocity Tunnel 9 Mach 10/14 Calibration
[AD-A275960] p 3587 N94-31318
Six degree of freedom flight dynamic model of a Mk-82 store
[AD-A277065] p 3580 N94-32362
A critical evaluation of the Reynolds stress turbulence closure for the flow of a turbulent free-stream over a turbulent boundary layer
[ISBN-0-315-75792-2] p 3707 N94-32497

FREE JETS
Shear flow control of cold and heated rectangular jets by mechanical tabs. Volume 1: Results and discussion
[NASA-CR-182296-VOL-1] p 3708 N94-32867
Shear flow control of cold and heated rectangular jets by mechanical tabs. Volume 2: Tabulated data
[NASA-CR-182296-VOL-2] p 3709 N94-32869

FREE RADICALS
Infrared and near infrared transient absorption spectroscopy of molecular free radicals
[DE94-005446] p 3632 N94-31305
A visible light initiating system for free radical promoted cationic polymerization
[AD-A277164] p 3655 N94-32069

FREE VIBRATION
Vibration localization in dual-span axially moving elastic systems p 3736 N94-31964
Nonlinear vibration analysis of laminated plates on linear and nonlinear elastic foundations p 3737 N94-32079

FREE-PISTON ENGINES
A 1050 K Stirling space engine design
[NASA-CR-182149] p 3616 N94-32866

FRENCH GUIANA
Contribution of SAR ERS1 data to study the French Guiana tropical coast environment
[BRGM-93034] p 3748 N94-32527

FRENKEL DEFECTS
Point defect production, geometry, and stability in silicon: A molecular dynamics simulation study
[DE94-008292] p 3903 N94-32411

FREQUENCIES
Variable-resolution imagery for flight simulation
[AD-A276199] p 3586 N94-31058

FREQUENCY ASSIGNMENT
Economic analysis of the hertzian spectrum
[TELECOM-93-E-012] p 3670 N94-31171
Design, development, and testing of a Network Frequency Selection Service (NFSS)
[AD-A277362] p 3680 N94-32283

FREQUENCY DISTRIBUTION
DOME: Dynamic optimization on multiprocessor engines, a statistical approach p 3807 N94-31972

FREQUENCY DIVISION MULTIPLE ACCESS
Channel and terminal description of the ACTS mobile terminal p 3599 N94-31428

FREQUENCY DIVISION MULTIPLEXING
Advanced optical fiber communication systems
[AD-A276416] p 3878 N94-31330
Long distance transmission of 15 Gb/s digital using subcarrier multiplexing and external modulation
[DE94-008298] p 3682 N94-32756

FREQUENCY HOPPING
Spread-spectrum radio systems and networks
[AD-A276449] p 3671 N94-31260
Design, development, and testing of a Network Frequency Selection Service (NFSS)
[AD-A277362] p 3680 N94-32283

FREQUENCY MODULATION
Advanced optical fiber communication systems
[AD-A276416] p 3878 N94-31330
Hubless satellite communications networks p 3600 N94-31433
Pulse-splitting and AM-FM conversion in a nonlinear dispersive medium
[AD-A277041] p 3861 N94-32262
Fiber optic continuous true time-delay modulator
[AD-D016098] p 3883 N94-32720
An experimental compact Hi-Vision VCR using metal evaporated tape
[NHK-LABS-NOTE-423] p 3683 N94-33081

FREQUENCY MULTIPLIERS
Advanced material processing for integrated-optic frequency doubling systems
[AD-A278394] p 3698 N94-33163

FREQUENCY RANGES
Model updating of vibrating systems based on measured or calculated frequency response functions
[CTH-E-93-03] p 3732 N94-31091

FREQUENCY RESPONSE
Effective computational strategy for predicting the response of complex systems
[AD-A277452] p 3740 N94-33011

FRESNEL DIFFRACTION
Structure estimation of phase objects from the diffraction near field: Microwave and model calculations
[ETN-94-95737] p 3674 N94-31608

FRETTING
Cracking induced in small fretting: Application to the case of aeronautical aluminum alloys
[ECL-92-50] p 3735 N94-31870

FRICTION
Methodology for damage study of a tube-grill contact
[ECL-92-49] p 3734 N94-31562
Cracking induced in small fretting: Application to the case of aeronautical aluminum alloys
[ECL-92-50] p 3735 N94-31870
Computational methods for frictional contact with applications to the Space Shuttle orbiter nose-gear tire p 3608 N94-32295
New micro- and macroscopic models of contact and friction
[AD-A277240] p 3726 N94-32320
The effect of prolonged exposure to 750 C air on the tribological performance of PM212
[NASA-TM-106472] p 3617 N94-32941

FRICTION DRAG
Flight test results of riblets at supersonic speeds
[NASA-TM-4387] p 3572 N94-32880

FRICTION FACTOR
Computational methods for frictional contact with applications to the Space Shuttle orbiter nose-gear tire p 3608 N94-32295
Mechanics of failure of high temperature metal matrix composites
[AD-A277397] p 3624 N94-32342
Frictional behavior and adhesion of Ag and Au films applied to aluminum oxide by oxygen-ion assisted Screen Cage Ion Plating (SCIP)
[NASA-TM-106522] p 3647 N94-32931
Energy absorber for the CETA p 3604 N94-33303

FROST
One: Microphysics of frost metamorphism: Applications to Triton and Mars. Two: A global analysis of the ozone deficit in the upper stratosphere and lower mesosphere. Three: The diabatic circulation in the stratosphere as diagnosed from Microwave Limb Sounder data
p 3942 N94-31975
The influence of thermal inertia on Mars' seasonal pressure variation and the effect of the weather component p 3952 N94-33238
FUEL CELL POWER PLANTS
Economic feasibility analysis of distributed electric power generation based upon the natural gas fired fuel cell
[DE94-005795] p 3759 N94-31487
Detailed design of the 2MW Demonstration Plant
[DE94-000042] p 3762 N94-32823
FUEL CELLS
NEMO: Advanced energy systems and technologies
[DE94-721998] p 3760 N94-31767
Polymer electrolyte fuel cells
[DE94-007558] p 3761 N94-32762
FUEL COMBUSTION
Ignition studies in nonpremixed hydrogen/air combustion
[AD-A275954] p 3632 N94-31348
Emissions of greenhouse gases from the use of transportation fuels and electricity
[DE94-006166] p 3765 N94-31625
Soot and liquid-phase fuel distributions in a newly designed optically accessible DI diesel engine
[DE94-005648] p 3723 N94-31651
Climate effects of anthropogenic sulfate: Simulations from a coupled chemistry/climate model
[DE94-004352] p 3767 N94-32789
Ignition delays, heats of combustion, and reaction rates of aluminum alkyl derivatives used as ignition and combustion enhancers for supersonic combustion
[NASA-CR-189581] p 3638 N94-32868
FUEL CONSUMPTION
National US public policy on global warming derived from optimization of energy use and environmental impact studies
[DE94-004606] p 3768 N94-32790
FUEL INJECTION
Computational study of single-expansion-ramp nozzles with external burning
[NASA-TM-106550] p 3700 N94-31229
FUEL PRODUCTION
Development of a catalytic system for gasification of wet biomass
[DE94-006216] p 3759 N94-31762
FUEL SPRAYS
Soot and liquid-phase fuel distributions in a newly designed optically accessible DI diesel engine
[DE94-005648] p 3723 N94-31651
FUEL TANKS
Improved resealing procedures for the second deseal/reseal program in RAAF F111 aircraft fuel tanks
[AD-A277069] p 3580 N94-32378
FULLERENES
Theoretical studies of zirconium and carbon clusters with molecular dynamics simulations
[DE94-005276] p 3862 N94-31146
Occupied and unoccupied orbitals of C60 and C70
[DE94-008294] p 3873 N94-32755
FUNCTION SPACE
Comparing models of the non-extensional typed lambda-calculus
[ML-93-19] p 3842 N94-31409
FUNCTIONAL DESIGN SPECIFICATIONS
Modular Simulator System (MSS). System/segment specification for the generic modular simulator system-flight controls module, volume 3
[AD-A276970] p 3590 N94-32395
Modular Simulator System (MSS). System/segment specification for the generic modular simulator system-flight dynamics module, volume 4
[AD-A276971] p 3590 N94-32396
Modular Simulator System (MSS). System/segment specification for the generic modular simulator system-propulsion module propulsion module, volume 5
[AD-A276972] p 3590 N94-32397
Modular Simulator System (MSS). System/segment specification for the generic modular simulator system-navigation/communication module, volume 6
[AD-A276973] p 3590 N94-32398
Modular Simulator System (MSS). System/segment specification for the generic modular simulator system-weapons module, volume 7
[AD-A276974] p 3590 N94-32399
Development of a video fluorescence system for assessing burn depth
[AD-A278127] p 3798 N94-33092
Faultless software project
[AD-A278161] p 3822 N94-33188
Structuring Z specifications with views
[AD-A277618] p 3822 N94-33279
MODIS. Volume 1: MODIS level 1A software baseline requirements
[NASA-TM-104594-VOL-1] p 3823 N94-33287
FUNCTIONALS
The Laplace functional and Palm measure of a quasi-Cox process which is driven by a Markov chain
[REPT-93-82] p 3851 N94-31699
FUNCTIONS (MATHEMATICS)
Strictly positive definite functions on spheres
[AD-A276471] p 3855 N94-31244
The Cameron-Martin theorem
[W-9315] p 3844 N94-31676
Algebraic functions for recognition
[AD-A276803] p 3846 N94-32167
FURANS
The intramolecular cyclization of bis-2,5-dimethylene-2,5-dihydrofurans and bis-2,5-dimethylene-2,5-dihydrothiophenes: An approach to macrocycles
[DE94-007060] p 3657 N94-32377
FUSELAGES
A laboratory study of multiple site damage in fuselage lap splices
[AD-A276151] p 3578 N94-31078
Damage tolerance aspects of a full composite airplane fuselage: Requirements, modelling, predictions, experiments
[LR-728] p 3578 N94-31674
Multiple-site damage in aircraft fuselage structures
[LR-729] p 3578 N94-31675
Fracture and fatigue strength evaluation of multiple site damaged aircraft fuselages - curved panel testing and analysis
[AD-A277100] p 3579 N94-32015
Shearographic inspection of a DeHavilland DHC-7
[AD-A276716] p 3566 N94-32157
Improved resealing procedures for the second deseal/reseal program in RAAF F111 aircraft fuel tanks
[AD-A277069] p 3580 N94-32378
Application of a design-build-team approach to low cost and weight composite fuselage structure
[NASA-CR-4418] p 3626 N94-32863
Computation of three-dimensional compressible boundary layers to fourth-order accuracy on wings and fuselages
[NASA-CR-4269] p 3709 N94-32871
Composite fuselage shell structures research at NASA Langley Research Center p 3628 N94-33124
Resin transfer molding for advanced composite primary wing and fuselage structures p 3628 N94-33128
Test and analysis results for composite transport fuselage and wing structures p 3628 N94-33129
Tension fracture of laminates for transport fuselage. Part 1: Material screening p 3629 N94-33130
Local design optimization for composite transport fuselage crown panels p 3629 N94-33132
Composite fuselage crown panel manufacturing technology p 3629 N94-33133
Advanced textile applications for primary aircraft structures p 3629 N94-33135
Characterization and manufacture of braided composites for large commercial aircraft structures
p 3630 N94-33137
An experimental study of pilot/vehicle dynamics using a tilt rotor flying machine
[AD-A277516] p 3805 N94-33349
FUSION REACTORS
Spectroscopy and atomic physics in EBIT and SuperEBIT
[DE94-006050] p 3864 N94-31508
Magnetless magnetic fusion
[DE94-007114] p 3891 N94-32686
FUZZY SETS
Triangular norms and conorms: A general tool for generating fuzzy mathematical morphologies
[TELECOM-93-D-001] p 3839 N94-31092
FUZZY SYSTEMS
Fuzzy logic application for modeling man-in-the-loop space shuttle proximity operations
[NASA-CR-188283] p 3835 N94-32359
Refining fuzzy logic controllers with machine learning
p 3839 N94-32421
A fuzzy classifier system for process control
p 3839 N94-32422
Fuzzy-neural control of an aircraft tracking camera platform p 3839 N94-32423
Intelligent control of a multi-degree-of freedom reaction compensating platform system using fuzzy logic
p 3605 N94-33306

G

GADOLINIUM
Laser flash photolysis, EPR and Raman studies of liquids at elevated pressures
[DE94-008351] p 3718 N94-32413
GADOLINIUM-GALLIUM GARNET
Transient radiation-induced absorption in the materials for a GSGG laser
[DE94-005316] p 3714 N94-31148
GALACTIC BULGE
The chemical and dynamical evolution of the galaxy
p 3936 N94-31950
GALACTIC CLUSTERS
Theoretical studies of x ray emission from clusters of galaxies p 3954 N94-31103
The kinematics of dense clusters of galaxies
p 3937 N94-32029
GALACTIC COSMIC RAYS
Neutron measurements at the commercial aircraft altitudes
[ISBN-0-315-86201-7] p 3955 N94-31709
GALACTIC EVOLUTION
Fireworks in velocity and configuration space applied to cosmology
[USIP-93-90] p 3927 N94-31086
The stellar and gaseous content of massive low surface brightness disk galaxies p 3933 N94-31495
Gravitational effects of cosmic strings
[ISBN-0-315-75484-2] p 3934 N94-31789
Ionized gas in the halos of edge-on infrared-bright galaxies: Evidence for starburst-driven superwinds
p 3936 N94-31948
The chemical and dynamical evolution of the galaxy
p 3936 N94-31950
The role of galaxy type and environment in determining the properties of globular cluster systems
[ISBN-0-315-76447-3] p 3939 N94-33112
GALACTIC HALOS
Ionized gas in the halos of edge-on infrared-bright galaxies: Evidence for starburst-driven superwinds
p 3936 N94-31948
The chemical and dynamical evolution of the galaxy
p 3936 N94-31950
GALACTIC NUCLEI
The manifestations of energetic activity in the galactic center p 3937 N94-32028
GALACTIC RADIATION
Theoretical studies of x ray emission from clusters of galaxies p 3954 N94-31103
Line-strength gradients and kinematic profiles in elliptical galaxies p 3934 N94-31788
GALACTIC ROTATION
Line-strength gradients and kinematic profiles in elliptical galaxies p 3934 N94-31788
GALACTIC STRUCTURE
The chemical and dynamical evolution of the galaxy
p 3936 N94-31950
A study of the neutral hydrogen distribution of the Milky Way through 21 cm emission and Lyman alpha absorption p 3938 N94-32309
GALAXIES
A twisted disk equation that describes warped galaxy disks p 3928 N94-31118
The chemical and dynamical evolution of the galaxy
p 3936 N94-31950
The role of galaxy type and environment in determining the properties of globular cluster systems
[ISBN-0-315-76447-3] p 3939 N94-33112
GALERKIN METHOD
An adaptive finite element method for unsteady compressible rotor airfoil aerodynamics
p 3567 N94-31204
Penetrable wedge analysis
[AD-A277219] p 3845 N94-32022
GALILEO SPACECRAFT
The Galileo high gain antenna deployment anomaly
p 3607 N94-33319
GALLIUM ALLOYS
Phase relationships and stability of the (mu)- and (zeta)-phases in the Ag-Al-X (X=Zn, Ga, Ge) systems
[DE94-009391] p 3648 N94-33270
GALLIUM ARSENIDES
New material for high average power infrared generation: QPM-DB GaAs
[AD-A276389] p 3714 N94-31358
The relationship of the electronic structures of semiconductor surfaces and heterostructures to crystal growth
[AD-A276465] p 3896 N94-31473
High-performance GaAs/AlGaAs optical phase modulators for microwave/photonic integrated circuits
[DE94-006361] p 3688 N94-31483

GaAs/GaN strained layer superlattice materials for high temperature transistors, phase 1
[AD-A276115] p 3897 N94-31528
The effects of amorphous layer regrowth on carbon activation in GaAs and InP
[DE94-006290] p 3899 N94-31634
Photopyroelectric spectroscopy as a non-intrusive technique for the determination of the optical absorption spectra of multiple quantum well samples
[ISBN-0-315-87164-4] p 3833 N94-31875
Novel optoelectronic devices based on combining GaAs and InP on Si
[AD-A277018] p 3693 N94-32301
Radiation tolerant, high speed, low power, gallium arsenide logic
[AD-A277293] p 3694 N94-32509
Femtosecond probe-probe transmission studies of LT-grown GaAs near the band edge
[DE94-006660] p 3904 N94-32634
Research on high reliability refractory ohmic contacts for GaAs FETs and MODFETs
[AD-A276848] p 3697 N94-33034
Electrical characteristics of GaAs MESFET fabrication by ion implantation of Si or Se
[AD-A278416] p 3909 N94-33328

GALLIUM NITRIDES
GaAs/GaN strained layer superlattice materials for high temperature transistors, phase 1
[AD-A276115] p 3897 N94-31528

GAME THEORY
Effective truth
[ML-93-15] p 3856 N94-31416
Carbon dioxide abatement as a differential game
[DE94-722023] p 3765 N94-32590

GAMMA RAY ASTRONOMY
A search for 100 TeV gamma ray emission from the x ray binary pulsar 4U 0115+63 using the CYGNUS extensive air-shower array p 3955 N94-31900
BATSE data analysis
[NASA-CR-195818] p 3927 N94-32942

GAMMA RAY BURSTS
A search for 100 TeV gamma ray emission from the x ray binary pulsar 4U 0115+63 using the CYGNUS extensive air-shower array p 3955 N94-31900
Gamma-ray optical counterpart search experiment (GROCSE)
[DE94-007124] p 3955 N94-32129
BATSE data analysis
[NASA-CR-195818] p 3927 N94-32942
Nuclear physics and astrophysics
[DE94-007168] p 3939 N94-33147

GAMMA RAY TELESCOPES
Gamma Large Area Silicon Telescope (GLAST)
[DE94-006439] p 3925 N94-31786
Gamma-ray optical counterpart search experiment (GROCSE)
[DE94-007124] p 3955 N94-32129

GAMMA RAYS
Gamma Large Area Silicon Telescope (GLAST)
[DE94-006439] p 3925 N94-31786

GAS ANALYSIS
In-bed multiport sampling system
[AD-A275908] p 3763 N94-31339
The origin of neon-E: Neon-E in single interstellar silicon carbide and graphite grains p 3933 N94-31556
Rate coefficient for the reaction H + O2 yields OH + O: Results from 2000 to 5300 K
[DE94-008105] p 3871 N94-32615

GAS CHROMATOGRAPHY
In-bed multiport sampling system
[AD-A275908] p 3763 N94-31339
Group 12 thiolates: Syntheses, characterization and decomposition pathways
[AD-A277055] p 3900 N94-32011
New zinc-bis(dialkylamides) potentially usable as site-selective dopants for p-type ZnSe
[AD-A276947] p 3902 N94-32218

GAS COMPOSITION
The ozone and the physico-chemical processes in tropical regions p 3770 N94-31010
Photothermal laser deflection, an innovative technique to measure particles in exhausts
[AD-A277151] p 3718 N94-32366
Mexico City ozone concentrations as a function of readily-available meteorological parameters
[DE94-007576] p 3768 N94-32814

GAS DENSITY
Using laser absorption spectroscopy to monitor composition and physical properties of metal vapors
[DE94-001530] p 3716 N94-31599
CO observations in external galaxies and gas mass determination p 3925 N94-31790

GAS DISCHARGES
Time evolution and filamentation of KrF(star) laser gas discharges
[ETN-94-95758] p 3715 N94-31561

GAS DISSOCIATION
Production and detection of metastable atomic oxygen
[ISBN-0-315-87364-7] p 3868 N94-31915
Implementation of a vibrationally linked chemical reaction model for DSMC
[NASA-TM-109109] p 3710 N94-33020

GAS DYNAMICS
Gas dynamics for accretion disk simulations p 3932 N94-31144
Stability and instability criteria for magnetohydrodynamics
[PB94-148475] p 3889 N94-31772
Basic and applied studies of the ram accelerator as a hypervelocity projectile launcher
[AD-A277392] p 3602 N94-32288

GAS EXPANSION
Pulsed expansion of plasma in a magnetic thruster p 3889 N94-31776
Chemical vapor deposition fluid flow simulation modelling tool
[NASA-CR-189648] p 3707 N94-32480

GAS FLOW
The manifestations of energetic activity in the galactic center p 3937 N94-32028

GAS INJECTION
Control of hypersonic aerodynamic forces with surface blowing p 3567 N94-31216

GAS LASERS
DOE reactor-pumped laser program
[DE94-006372] p 3715 N94-31485

GAS MIXTURES
A numerical method for mixing/chemically reacting compressible flow with finite rate chemistry p 3634 N94-31824

GAS PRESSURE
Dynamics of flux tubes in accretion disks p 3932 N94-31142
Advanced thermally stable jet fuels
[DE94-006760] p 3667 N94-32150

GAS TRANSPORT
Computed potential energy surfaces for chemical reactions
[NASA-CR-195835] p 3639 N94-33036

GAS TUNGSTEN ARC WELDING
Development of an automated wire delivery system for robotic welding applications
[NASA-CR-194216] p 3727 N94-32479

GAS TURBINE ENGINES
Thermal-mechanical fatigue crack growth in aircraft engine materials
[ISBN-0-315-86543-1] p 3734 N94-31707
Photothermal laser deflection, an innovative technique to measure particles in exhausts
[AD-A277151] p 3718 N94-32366
Materials development program: Ceramic technology project bibliography, 1984-1992
[DE94-009297] p 3662 N94-32935

GAS TURBINES
Rotordynamic effects driven by fluid forces from a geometrically imperfect labyrinth
[AD-A276424] p 3722 N94-31333
Fatigue in single crystal nickel superalloys
[AD-A276662] p 3643 N94-32047
Materials development program: Ceramic technology project bibliography, 1984-1992
[DE94-009297] p 3662 N94-32935

GAS-METAL INTERACTIONS
Prediction of hydrogen entry and permeation in metals and alloys
[AD-A276637] p 3642 N94-31995
Chemisorbed-molecule potential-energy surfaces and electronically-stimulated processes
[DE94-007932] p 3719 N94-32603
Metal cluster-rare gas van der Waals complexes: Microscopic models of physisorption
[DE94-008134] p 3873 N94-32797

GASIFICATION
Development of a catalytic system for gasification of wet biomass
[DE94-006216] p 3759 N94-31762
Biological conversion of synthesis gas
[DE94-000094] p 3760 N94-31811

GASKETS
Compatibility of refrigerants and lubricants with elastomers
[DE94-008552] p 3658 N94-32518

GATES (CIRCUITS)
Advanced silicon technology for microwave circuits
[AD-A278039] p 3698 N94-33091
Design of free space interconnected signal processor
[AD-A278129] p 3683 N94-33093

GAUGE INVARIANCE
CP violation and the top quark
[DE94-008930] p 3874 N94-32841

GAUGE THEORY
High energy physics studies
[DE94-005970] p 3876 N94-31505
SU(2) WZNW model at higher genera from gauge field functional integral
[PB94-148467] p 3857 N94-31589
Perturbative aspects of lower-dimensional gauge theories
[ISBN-0-315-86269-6] p 3911 N94-31712
The Kaluza-Klein approach and gauge supersymmetry
[ISBN-0-315-86553-9] p 3912 N94-31911
Tensor gauge potentials in loop space formulation of Yang-Mills fields
[PB94-147147] p 3912 N94-31924
CP violation and the top quark
[DE94-008930] p 3874 N94-32841

GEAR TEETH
Manual for automatic generation of finite element models of spiral bevel gears in mesh
[NASA-CR-191009] p 3728 N94-32900
A procedure for 3-D contact stress analysis of spiral bevel gears
[NASA-CR-194472] p 3728 N94-32929

GEARS
Manual for automatic generation of finite element models of spiral bevel gears in mesh
[NASA-CR-191009] p 3728 N94-32900
Feed-forward control of gear mesh vibration using piezoelectric actuators
[NASA-TM-106366] p 3728 N94-32902
A procedure for 3-D contact stress analysis of spiral bevel gears
[NASA-CR-194472] p 3728 N94-32929
Spur, helical, and spiral bevel transmission life modeling
[NASA-TM-106552] p 3728 N94-32979

GELS
Vibration dampener and method for making same
[AD-D016094] p 3739 N94-32733

GENERAL OVERVIEWS
Summary of materials and hardware performance on LDEF p 3595 N94-31037
A comparison of product realization frameworks
[AD-A275992] p 3810 N94-31357
Mars: Five views on what is known
[NASA-TM-109751] p 3942 N94-31805
Recent developments in polymeric charge transfer complexes
[AD-A277108] p 3654 N94-31979
Sandia's photonic program and its changing national role
[DE94-008616] p 3883 N94-32878

GENETIC ALGORITHMS
On the use of genetic algorithms to solve the time-table problem
[REPT-90-060-REV] p 3829 N94-31176
A genetic algorithm based method for docking flexible molecules
[DE94-007525] p 3793 N94-32269

GENETICS
Laboratory Directed Research & Development Program
[DE94-005928] p 3956 N94-31523

GEOCENTRIC COORDINATES
World height system definition and implementation
[AD-A276725] p 3747 N94-32160

GEOCHEMISTRY
Origin and thermal evolution of Mars p 3940 N94-31109

GEODETIC SURVEYS
World height system definition and implementation
[AD-A276725] p 3747 N94-32160
Remote sensing and the Mississippi high accuracy reference network p 3758 N94-32466

GEODYNAMICS
The tectonic and volcanic evolution of Venus: Catastrophic or gradual? p 3940 N94-31111

GEOGRAPHIC INFORMATION SYSTEMS
Remote sensing for urban planning p 3758 N94-32465
Remote sensing and the Mississippi high accuracy reference network p 3758 N94-32466
The contribution of satellite data in communication infrastructure projects p 3749 N94-32530

GEOIDS
Filtering of satellite altimetry data with optimal smoothing cubic splines to compute geoid heights, along-tract geoid and gravity gradients in the Indonesian waters and its surroundings
[PB94-147527] p 3741 N94-31074
Application of radon transformation for improved analysis of sparsely sampled data: A feasibility study
[PB94-147535] p 3741 N94-31075
Geoid-to-topography ratios on Venus: A global perspective p 3940 N94-31110

GEOLOGICAL FAULTS
Tectonic History of the Terrestrial Planets
[NASA-CR-195696] p 3939 N94-31105
Patterns of deformation and volcanic flows associated with lithospheric loading by large volcanoes on Venus
p 3776 N94-31106
Aspects of modelling the tectonics of large volcanoes on the terrestrial planets p 3940 N94-31107
State of stress, faulting, and eruption characteristics of large volcanoes on Mars p 3940 N94-31108
Plains tectonism on Venus: The deformation belts of Lavinia Planitia p 3941 N94-31115
Respective contributions of VIS-PIR, SAR-ERS 1, and airborne radar data for morphostructural and morphoneotectonic analysis: Practical examples
p 3752 N94-32549
Use of SPOT and ERS-1 SAR data to study the tectonic and climatic history of arid regions p 3752 N94-32550

GEOLOGICAL SURVEYS
The effects of vegetation on the ability to map soils using GERIS data p 3744 N94-31860
Investigation on correction models for airborne imaging spectrometry data from the EISAC-campaign for geoscientific purposes p 3745 N94-31861
Contribution of SAR ERS1 data to study the French Guiana tropical coast environment
[BRGM-93034] p 3748 N94-32527
Comparison of SPOT, ERS-1, SEASAT, LANDSAT TM, and merged imagery for geological investigations
p 3752 N94-32547
Optimal geological data extraction from SPOT-radar synergism with samples from Djebel Amour (Algeria), Red Sea Hills (Sudan), Sirte Basin (Libya), and Magdalena Valley (Colombia) p 3752 N94-32548
Structural study in an alteritic region: Contribution of ERS-1 SAR data of the Mauges Plateau (Loire Atlantique, France)
[BRGM-93032] p 3752 N94-32551
The Lunar Scout Program: An international program to survey the Moon from orbit for geochemistry, mineralogy, imagery, geodesy, and gravity
[NASA-TM-104791] p 3943 N94-32923

GEOMAGNETISM
Magnetohydrodynamics of the Earth's core. 1: Steady, rotating magnetoconvection. 2: Magnetic Rossby waves
p 3770 N94-31104
Lightning-induced coupling of the radiation belts to geomagnetically conjugate ionospheric regions
p 3772 N94-31773

GEOMETRIC RECTIFICATION (IMAGERY)
Analysis of GER imaging spectrometry data for the identification of soil and vegetation parameters in land degradation studies p 3744 N94-31857
Optimal geological data extraction from SPOT-radar synergism with samples from Djebel Amour (Algeria), Red Sea Hills (Sudan), Sirte Basin (Libya), and Magdalena Valley (Colombia) p 3752 N94-32548

GEOMETRY
Interactive reconstruction of anatomical structures with free-form surfaces
[TELECOM-93-E-002] p 3794 N94-31195

GEOMORPHOLOGY
Plains tectonism on Venus: The deformation belts of Lavinia Planitia p 3941 N94-31115
Contribution of SAR ERS1 data to study the French Guiana tropical coast environment
[BRGM-93034] p 3748 N94-32527
Respective contributions of VIS-PIR, SAR-ERS 1, and airborne radar data for morphostructural and morphoneotectonic analysis: Practical examples
p 3752 N94-32549
Quantitative modeling of bottom morphology and subbottom properties
[AD-A278142] p 3790 N94-33062
Distribution and nature of UV absorbers on Triton's surface
[NASA-CR-195886] p 3943 N94-33104

GEOPHYSICAL FLUIDS
Magnetohydrodynamics of the Earth's core. 1: Steady, rotating magnetoconvection. 2: Magnetic Rossby waves
p 3770 N94-31104

GEOPHYSICS
Magnetohydrodynamics of the Earth's core. 1: Steady, rotating magnetoconvection. 2: Magnetic Rossby waves
p 3770 N94-31104
Origin and thermal evolution of Mars
p 3940 N94-31109
A tectonic resurfacing model for Venus
p 3941 N94-31113
Proceedings of the International Workshop on Artificial Intelligence Applications in Solar-Terrestrial Physics
[PB94-142064] p 3832 N94-31808
Atmospheric structure simulation: An autoregressive model for smooth geophysical power spectra with known autocorrelation function
[AD-A276691] p 3773 N94-32118

GEOPOTENTIAL HEIGHT
Filtering of satellite altimetry data with optimal smoothing cubic splines to compute geoid heights, along-tract geoid and gravity gradients in the Indonesian waters and its surroundings
[PB94-147527] p 3741 N94-31074

GEOSAT SATELLITES
Error analysis of real-time and post-processed orbit determination for the Geosat Follow-On altimetric satellite using GPS tracking p 3576 N94-31845
The effects of altimeter sampling characteristics: Some Geosat examples
[AD-A276899] p 3747 N94-32214

GEOTHERMAL ENERGY UTILIZATION
Renewable energy technology development at Sandia National Laboratories
[DE94-007734] p 3761 N94-32383

GERMANATES
Extended-range order in glasses
[DE94-008135] p 3661 N94-32798

GERMANIUM
An extended approach to oxidations and nitridations of Si and Ge(x)Si(1-x) materials
[AD-A276056] p 3631 N94-31282
Oriented Si and Ge nanocrystals formed in Al2O3 by ion implantation and annealing
[DE94-005593] p 3901 N94-32172
Lowering the Schottky barrier at metal or silicide/Si interfaces to extend the range of infrared detectors
[AD-A277253] p 3903 N94-32322
Intra-cascade surface recombination of point defects during ion bombardment of Ge(001)
[DE94-007740] p 3903 N94-32384
Ab initio study of the epitaxial growth of Ge on Si(100) surface
[DE94-007245] p 3904 N94-32724

GERMANIUM ALLOYS
Anomalous small angle x ray scattering studies of amorphous metal-germanium alloys
[DE94-007258] p 3900 N94-32065
Research on stable, high-efficiency amorphous silicon multijunction modules
[DE94-000298] p 3695 N94-32680
Anisotropic phase separation through the metal-insulator transition in amorphous Mo-Ge and Fe-Ge alloys
[DE94-007259] p 3646 N94-32795
Phase relationships and stability of the (mu)- and (zeta)-phases in the Ag-Al-X (X=Zn, Ga, Ge) systems
[DE94-009391] p 3648 N94-33270

GERMANIUM COMPOUNDS
Amorphous/crystalline structure and phase transformations in metastable semiconducting Ge(1-x)Sn(x)
[DE94-006659] p 3901 N94-32115

GERMANIUM OXIDES
Extended-range order in glasses
[DE94-008135] p 3661 N94-32798

GETTERS
Gettering of metal impurities by cavities in silicon
[DE94-005248] p 3645 N94-32672

GIANT STARS
A critical examination of stellar atmosphere theory for metal-poor K-giant stars p 3927 N94-32308

GIMBALS
High precision moving magnet chopper for variable operation conditions p 3605 N94-33307

GLACIERS
Estimation of visible and near-infrared reflectivity for Peyto Glacier Basin using satellite data
[ISBN-0-315-87039-7] p 3743 N94-31733
Feasibility in the use of satellite remote sensing data as a fast reaction tool for natural disaster relief
p 3748 N94-32526
Study of subpolar glaciers of Spitzbergen using SPOT, ERS-1, and hypsometric data: Results and perspectives
p 3753 N94-32553

GLACIOLOGY
A reassessment of the in-situ dielectric constant of polar firn
[AD-A276999] p 3773 N94-32154

GLASS
Physical properties of glasses exposed to Earth-facing and trailing-side environments on LDEF
p 3594 N94-31030
Analysis of leading edge and trailing edge cover glass samples before and after treatment with advanced satellite contamination removal techniques p 3596 N94-31041
Transient radiation-induced absorption in the materials for a GSGG laser
[DE94-005316] p 3714 N94-31148
Cost-effective ceramic machining: Summary of three-body wear experiments
[DE94-007757] p 3650 N94-31354
In-situ TEM crystallization of anorthite-glass films on (alpha)-Al2O3
[DE94-006317] p 3652 N94-31780
Elastic modulus measurements of LDEF glasses and glass-ceramics using a speckle technique
[NASA-CR-195911] p 3653 N94-31851
Toughening mechanisms in the high strain rate deformation of rubber-modified polymer glasses
p 3653 N94-31942
Determination of BPSG thin-film properties using IR reflection spectroscopy of product wafers
[DE94-006591] p 3634 N94-32110
Joining of silicon nitrides using oxynitride glasses
[DE94-008517] p 3658 N94-32517
Metal-ion spin-on glasses: Novel materials for active waveguides
[DE94-007738] p 3882 N94-32649
Inorganic polymer engineering materials
[DE94-008519] p 3659 N94-32655
Conductive paints
[DE94-008508] p 3661 N94-32788
Extended-range order in glasses
[DE94-008135] p 3661 N94-32798

GLASS FIBER REINFORCED PLASTICS
Micromechanical analysis of the interface and basic damage modes in glass fiber/epoxy resin model composites
[ONERA-NT-1993-4] p 3618 N94-31225
Fatigue behavior of unidirectional pultruded composite materials
[ISBN-0-315-86425-7] p 3621 N94-31719
Empirical optimization of the consolidation of thermoplastic prepregs
[ISBN-0-315-86455-9] p 3652 N94-31722
Bond stress-slip characteristics of FRP rebars
[AD-A277191] p 3623 N94-32070

GLASS FIBERS
Micromechanical analysis of the interface and basic damage modes in glass fiber/epoxy resin model composites
[ONERA-NT-1993-4] p 3618 N94-31225
Inorganic polymer engineering materials
[DE94-008519] p 3659 N94-32655

GLOBAL POSITIONING SYSTEM
Results of real-time testing and demonstration of the US Army Corps of Engineers real-time on-the-fly positioning system
[AD-A276160] p 3576 N94-31080
An investigation of airborne GPS/INS for high accuracy position and velocity determination
[DE94-006139] p 3576 N94-31306
Flight technical error for category B non-precision approaches and missed approaches using non-differential GPS for course guidance
[PB94-142734] p 3576 N94-31680
Error analysis of real-time and post-processed orbit determination for the Geosat Follow-On altimetric satellite using GPS tracking p 3576 N94-31845
Theoretical basis for state vector comparison, relative position display, and relative position/rendezvous prediction
[AD-A277216] p 3608 N94-32020
Remote sensing and the Mississippi high accuracy reference network p 3758 N94-32468
Performance analysis of an integrated GPS/inertial attitude determination system
[NASA-CR-188289] p 3577 N94-32864
Real-time centimeter positioning with GPS: A system developed by the US Army Corps of Engineers
[AD-A278152] p 3577 N94-33095
An evaluation of three GPS receivers for use in the GPS sounder
[AD-A278157] p 3577 N94-33253

GLOBAL WARMING
National US public policy on global warming derived from optimization of energy use and environmental impact studies
[DE94-004606] p 3768 N94-32790
Quantified estimates of total GWPs for greenhouse gases taking into account tropospheric chemistry
[DE94-007846] p 3768 N94-32817
Ocean variability and its influence on the detectability of greenhouse warming signals
[DE94-008670] p 3790 N94-32881
Current policies of the major countries coping with the global warming problem and the energy demand and supply
[DE94-757291] p 3769 N94-32920

GLOBULAR CLUSTERS
The role of galaxy type and environment in determining the properties of globular cluster systems
[ISBN-0-315-76447-3] p 3939 N94-33112

GLUCOSE
Perspectives of glucose sensing based on a charge-modulating competition reaction
[ISBN-9-09-005754-4] p 3795 N94-31652

Electrical communication between glucose oxidase and electrodes based on poly(vinylimidazole) complex of Os(bpy)2Cl2
[AD-A276585] p 3635 N94-32231

GLUONS
Transport properties of quark and gluon plasmas
[DE94-007043] p 3864 N94-31405

GOGGLES
Night vision camcorder system
[AD-A277004] p 3712 N94-32002
Assessment of interior modifications in C-130 and C-141 aircraft for night vision goggle operations
[AD-A276843] p 3582 N94-32223
Methods for measuring characteristics of night vision goggles
[AD-A277046] p 3804 N94-32302
An evaluation framework for designing a night vision, computer-based trainer
[AD-A278005] p 3590 N94-33139

GOLD
The adsorption of sulfate on gold(111) in acidic aqueous media: Adlayer structural inferences from infrared spectroscopy and scanning tunneling microscopy
[AD-A276643] p 3642 N94-31997
A new-type of long-range restructuring of ordered metal surfaces induced by lateral adsorbate interactions: Iodide on AU(110) electrodes
[AD-A276633] p 3643 N94-32060
Charge-dependent atomic-scale structures of high-index and (110) gold electrode surfaces as revealed by scanning tunneling microscopy
[AD-A276782] p 3869 N94-32170
Nanoscale structural changes upon electrooxidation of Au(111) as probed by potentiodynamic scanning tunneling microscopy
[AD-A276780] p 3909 N94-33275

GOLD ISOTOPES
Transverse energy production with Si and Au beams at AGS energy: Towards hot and dense hadronic matter
[DE94-007178] p 3938 N94-32638
A tandem microscopic-electrochemical examination of a charge-induced surface phase sequence: Ordered Au(110) in aqueous iodide electrolytes as probed by potentiodynamic scanning tunneling microscopy
[AD-A276905] p 3875 N94-33277

GOVERNMENT/INDUSTRY RELATIONS
Information resources for US Department of Energy pollution prevention programs
[DE94-006677] p 3763 N94-31582
NASA/DOD Aerospace Knowledge Diffusion Research Project. Paper 18: Scientific and Technical Information (STI) policy and the competitive position of the US aerospace industry
[NASA-TM-109782] p 3921 N94-32833

GRAIN BOUNDARIES
Defect-solute interactions near irradiation grain boundaries
[DE94-006215] p 3641 N94-31627
Irradiation-assisted stress corrosion cracking of materials from commercial BWRs: Role of grain-boundary microchemistry
[DE94-006542] p 3643 N94-32109
Attempts to model the generation of new grain boundaries during the deformation of polycrystals
[DE94-007527] p 3903 N94-32597
Effect of twin boundary density on the vortex melting transition in YBa2Cu3O(7-delta) single crystals
[DE94-007684] p 3904 N94-32601
Boron and hydrogen in Ni3Al. Part 2: Mechanical testing of bicrystals
[DE94-007441] p 3904 N94-32606
Characterization of nanoparticles and nanophase materials
[DE94-008348] p 3907 N94-32990
The path for long range conduction in high J(sub c) TlBa2Ca2Cu3O(8+x) spray-pyrolyzed deposits
[DE94-007211] p 3909 N94-33271

GRAIN SIZE
Work hardening behavior in aluminum alloy 2090
[DE94-007036] p 3643 N94-32064

GRAMMARS
On the equivalence of Lambek categorial grammars and basic categorial grammars
[LP-93-07] p 3842 N94-31451
Informal introduction to the extended affix grammar formalism and its compiler
[TR-93-19] p 3817 N94-32287

GRANULAR MATERIALS
Processing of novel nanoparticle dispersion strengthened ceramics for improved mechanical performance
[AD-A275965] p 3649 N94-31276
Contributions to the validation of the CJS model for granular materials
[ECL-92-56] p 3733 N94-31376

GRAPH THEORY
Scheduling techniques for multiple processor systems in real-time environments
[AD-A276149] p 3824 N94-31249
Polyhedric object recognition by indexing in a model base
[ETN-94-95913] p 3812 N94-31542
Some calculations on supersymmetric graphs as communication networks
[REPT-93-72] p 3824 N94-31641

GRAPHICAL USER INTERFACE
Automatic generation of context-sensitive textual help
[REPT-93-68] p 3812 N94-31646
Interactive graphical model building using telepresence and virtual reality
[DE94-001421] p 3818 N94-32353
Knowledge-based commodity distribution planning p 3915 N94-32427
On the implementation of error handling in dynamic interfaces to scientific codes
[DE94-006970] p 3818 N94-32585
The role of guideline-based design tools
[DE94-007482] p 3804 N94-32596
Design of graphic screens using Neuro Linguistic Programming
[DE94-007634] p 3819 N94-32599
Implementation and display of Computer Aided Design (CAD) models in Monte Carlo radiation transport and shielding applications
[DE94-007221] p 3819 N94-32641

GRAPHITE
Operation of D3-D with all-graphite walls
[DE94-004858] p 3886 N94-31304
The origin of neon-E: Neon-E in single interstellar silicon carbide and graphite grains p 3933 N94-31556
Stellar x ray polarimeter polarizer development and calibration at LEA/LLNL
[DE94-006400] p 3712 N94-31783
Occupied and unoccupied orbitals of C60 and C70
[DE94-008294] p 3873 N94-32755

GRAPHITE-EPOXY COMPOSITES
Atomic oxygen interaction at defect sights in protective coatings on polymers flown on LDEF p 3593 N94-31024
Assessment of impact damage in composite structures
[AD-A277063] p 3624 N94-32265
Comparison of the compressive strengths for stitched and toughened composite systems
[NASA-TM-109108] p 3627 N94-32939
Structural testing of the technology integration box beam p 3628 N94-33125

GRAPHS (CHARTS)
Selection of climate station data using clustering and triangulated irregular network techniques
[AD-A276658] p 3784 N94-32046
GRAFTED - GRAphical fault tree EDitor: A fault tree description program for target vulnerability/survivability analysis. User manual
[AD-A277067] p 3818 N94-32390

GRASSLANDS
Behavior and dynamics of tropical forests and savannas p 3757 N94-31004
Monitoring fertilizer application by imaging spectrometry (Somerset Levels test site) p 3745 N94-31863
ERS-1 SAR and optical data for land use/land cover mapping: A case study in a savannah zone of Guinea p 3755 N94-32565
Dry deposition of PAN to grassland vegetation
[DE94-005111] p 3768 N94-32894

GRATINGS (SPECTRA)
Observation of the traveling component of an x ray standing wave field
[DE94-007671] p 3672 N94-31317
Fast acting optical deflection
[AD-A276630] p 3879 N94-32037

GRAVITATION
Testing for preferred-frame effects in gravity with artificial Earth satellites
[PB94-148459] p 3610 N94-31771
New QCD results from string theory
[DE94-005226] p 3911 N94-31823
Defying gravity
[NASA-TM-109747] p 3667 N94-31884
World height system definition and implementation
[AD-A276725] p 3747 N94-32160

GRAVITATION THEORY
Testing for preferred-frame effects in gravity with artificial Earth satellites
[PB94-148459] p 3610 N94-31771
Research in theoretical high-energy physics
[DE94-008388] p 3876 N94-32407

GRAVITATIONAL COLLAPSE
Reactive flows in compact objects p 3934 N94-31567

GRAVITATIONAL EFFECTS
Numerical analysis of single-vortex/free-surface interaction
[AD-A276462] p 3701 N94-31241
General-relativistic celestial mechanics. 4: Theory of satellite motion
[PB94-147782] p 3601 N94-31769
Testing for preferred-frame effects in gravity with artificial Earth satellites
[PB94-148459] p 3610 N94-31771
Gravitational effects of cosmic strings
[ISBN-0-315-75484-2] p 3934 N94-31789
An experimental study of void formation during aluminum solidification in reduced gravity p 3667 N94-31944
Vibration Isolation Technology (VIT) ATD project
[NASA-TM-106496] p 3567 N94-33064

GRAVITATIONAL FIELDS
Topological conformal algebra in 2D gravity coupled to minimal matter
[DE94-008122] p 3910 N94-31052
Filtering of satellite altimetry data with optimal smoothing cubic splines to compute geoid heights, along-tract geoid and gravity gradients in the Indonesian waters and its surroundings
[PB94-147527] p 3741 N94-31074
Accretion disks around black holes p 3928 N94-31117
Research in theoretical high-energy physics
[DE94-008388] p 3876 N94-32407

GRAVITATIONAL WAVES
A study of angular momentum loss in binaries using the free Lagrange method p 3931 N94-31134

GRAVITY WAVES
On wave interactions of rotational and irrotational flows p 3700 N94-31219

GRAZING INCIDENCE
Dependence of x ray absorption magnetic circular dichroism on layer periodicity in iron-platinum multilayers
[DE94-008786] p 3647 N94-32892

GREASES
Silicone grease as a precursor to a pseudo crown-ether ligand: Crystal structure of (K(+)K(Me2SiO)7(+))(Hin(CH2CMe3)3(-))4)
[AD-A276343] p 3895 N94-31327
Status of developing a multifunctional aviation grease
[AD-A276755] p 3656 N94-32184
The preliminary evaluation of liquid lubricants for space applications by vacuum tribometry p 3606 N94-33313

GREAT PLAINS CORRIDOR (NORTH AMERICA)
Implementation of instruments and facilities at the SGP CART site
[DE94-006839] p 3781 N94-31322
Water vapor from sunradiometry in comparison with microwave and balloon-sonde measurements at the Southern Great Plains ARM Site
[DE94-007479] p 3786 N94-32759
Parameterizing atmosphere-land surface exchange for climate models with satellite data: A case study for the Southern Great Plains CART site
[DE94-005109] p 3775 N94-32874

GREEN'S FUNCTIONS
A Green's function approach to analysing the effects of random synaptic background activity in a model neural network
[MATHS-REPT-A-202] p 3828 N94-31157
Finite element solution to the Helmholtz equation with high wave number. Part 1: The h-version of the FEM
[AD-A277396] p 3848 N94-32341

GREENHOUSE EFFECT
The Earth's climate: Past, present, and future p 3777 N94-30982
Sources and wells of minor atmospheric constituents of climatic importance p 3770 N94-31008
Emissions of greenhouse gases from the use of transportation fuels and electricity
[DE94-006166] p 3765 N94-31625
Cumulus convection parameterization and numerical modelling of moist atmospheres p 3783 N94-31989
Carbon dioxide abatement as a differential game
[DE94-722023] p 3765 N94-32590
Fine resolution atmospheric sulfate model driven by operational meteorological data: Comparison with observations
[DE94-002994] p 3766 N94-32691
Diagnostic studies of climate variability
[DE94-003629] p 3767 N94-32711
Water vapor from sunradiometry in comparison with microwave and balloon-sonde measurements at the Southern Great Plains ARM Site
[DE94-007479] p 3786 N94-32759
National US public policy on global warming derived from optimization of energy use and environmental impact studies
[DE94-004606] p 3768 N94-32790

Quantified estimates of total GWPs for greenhouse gases taking into account tropospheric chemistry
[DE94-007846] p 3768 N94-32817
Ocean variability and its influence on the detectability of greenhouse warming signals
[DE94-008670] p 3790 N94-32881
A correlated k-distribution model of the heating rates for atmospheric mixtures of H2O, CO2, O3, CH4, and N2O in the 0-2500 cm(exp -1) wave number region at altitudes between 0 and 60 km
[DE94-005136] p 3775 N94-32895

GRID GENERATION (MATHEMATICS)
An adaptive finite element method for unsteady compressible rotor airfoil aerodynamics
p 3567 N94-31204
Grid sensitivity for aerodynamic optimization and flow analysis p 3568 N94-31287
Texture generation on irregular regions
[AD-A275999] p 3841 N94-31359
Cell-vertex discretisation of the driven cavity flow without artificial diffusion
[W-9317] p 3703 N94-31689
Polynomial interpolation and approximation of real functions. 2: Symmetrical interpolation for the triangle
[AD-A277345] p 3848 N94-32245
Eta percent-superconvergence in the interior of locally refined meshes of quadrilaterals: Superconvergence of the gradient in finite element solutions of Laplace's and Poisson's equations
[AD-A277242] p 3848 N94-32331
Additive turbulent decomposition of the incompressible and compressible Navier-Stokes equations
[AD-A277321] p 3708 N94-32511
New advances in the modeling of high-temperature superconductors
[DE94-007649] p 3905 N94-32815
Incremental triangulation by way of edge swapping and local optimization
[NASA-TM-103979] p 3709 N94-32946
Mesh optimization
[AD-A277644] p 3820 N94-32972
Transformation of two and three-dimensional regions by elliptic systems
[NASA-CR-195849] p 3821 N94-33049
Direct replacement of arbitrary grid-overlapping by non-structured grid
[NASA-TM-106601] p 3850 N94-33120

GRINDING (COMMINUTION)
On the formation of muon- and zets-phases in Ag-Al system by mechanical alloying
[DE94-007125] p 3845 N94-32836

GROOVES
Improved resealing procedures for the second deseal/reseal program in RAAF F111 aircraft fuel tanks
[AD-A277069] p 3580 N94-32378
Physics of heat pipe rewetting
[NASA-CR-195902] p 3913 N94-33148

GROUND CREWS
Aircraft communication and navigation systems and communication and navigation systems
[AD-A277309] p 3582 N94-32328

GROUND EFFECT (COMMUNICATIONS)
System analysis of ultra-wideband instrumentation radars: Impulse versus stepped-chirp approaches
[AD-A276624] p 3677 N94-32087

GROUND EFFECT MACHINES
Heave dynamics of an air cushion vehicle bag and finger skirt
[ISBN-0-315-87053-2] p 3568 N94-31734

GROUND STATE
Structural studies of photoinduced intramolecular electron transfer in cyclopentadienylnickelnitrosyl
[DE94-008467] p 3874 N94-32876
A quest for a new superconducting state
[DE94-008439] p 3908 N94-32991

GROUND SUPPORT EQUIPMENT
The 28th Aerospace Mechanisms Symposium
[NASA-CP-3260] p 3603 N94-33291

GROUND SUPPORT SYSTEMS
Development concept for Dutch user support
[PB94-125523] p 3598 N94-31208

GROUND TESTS
A large motion zero-gravity suspension system for experimental simulation of orbital construction and deployment
[NASA-CR-195881] p 3668 N94-33037

GROUND TRACKS
The effects of altimeter sampling characteristics: Some Geosat examples
[AD-A276899] p 3747 N94-32214

GROUND TRUTH
Ground based radiometric and atmospheric measurements p 3744 N94-31855
Feasibility evaluation of new data interpretation approaches for vegetation analysis from airborne imaging spectroscopy p 3745 N94-31862
Extraction of agricultural parameters from imaging-spectrometry data and simulated MERIS data through red edge analysis p 3745 N94-31865

GROUND WATER
Hydrologic Database user's manual
[DE94-003950] p 3743 N94-31603
Focused feasibility study final field sampling plan
[AD-A277445] p 3769 N94-33105
Temporal changes in the geographic distribution, elevation, and potential origin of the Martian outflow channels p 3951 N94-33235

GROUND WIND
Proceedings of the Ninth Annual Pacific Climate (PACLIM) Workshop
[DE94-003024] p 3766 N94-32693
Evolution of diurnal surface winds and surface currents for Monterey Bay
[AD-A277649] p 3790 N94-33057
Numerical simulation of thermally induced near-surface flows over Martian terrain p 3949 N94-33223
Polar sediment accumulation: Role of surface winds at the two poles p 3951 N94-33233

GROUP THEORY
Lambek calculus is L-complete
[LP-93-14] p 3841 N94-31388
A note on cocycles in a semidirect product
[REPT-93-65] p 3851 N94-31661
Multiparameter quantum groups and multiparameter R-matrices
[CWI-AM-R9307] p 3846 N94-32106
Quantum homogeneous spaces, duality, and quantum 2-spheres
[CWI-AM-R9309] p 3857 N94-32192

GROUP VELOCITY
Superluminous laser pulse in an active medium
[DE94-007110] p 3720 N94-32684

GUARDS (SHIELDS)
Design and performance of the telescope and detector covers on the Extreme Ultraviolet Explorer satellite
p 3605 N94-33309

GULF STREAM
Operations summary for the convection and moisture experiment (CAMEX)
[NASA-TM-108445] p 3786 N94-33004

GUN LAUNCHERS
Basic and applied studies of the ram accelerator as a hypervelocity projectile launcher
[AD-A277392] p 3602 N94-32288

GUN PROPELLANTS
Condensed-phase processes during solid propellant combustion. 3: Preliminary depth-profiling studies on XM39, JA2, M9, M30, and HMX2
[AD-A276595] p 3635 N94-32124

GYROSCOPES
An investigation of airborne GPS/INS for high accuracy position and velocity determination
[DE94-006139] p 3576 N94-31306

H

H ALPHA LINE
Multiwavelength search for protoplanetary disks
p 3599 N94-31430

H I REGIONS
A twisted disk equation that describes warped galaxy disks p 3928 N94-31118
Study of stellar associations located in the region contained between the Magellanic Clouds
[ISBN-0-315-86692-6] p 3935 N94-31913
A study of the neutral hydrogen distribution of the Milky Way through 21 cm emission and Lyman alpha absorption p 3938 N94-32309

H-INFINITY CONTROL
Digital state-feedback H(infinity) control of Pritchard-Salamon systems: A Popov function approach
[REPT-93-69] p 3830 N94-31647
Parametric robust control and system identification: Unified approach
[NASA-CR-195826] p 3836 N94-32080

H-60 HELICOPTER
Technical evaluation of the UH-60Q: Aircraft in typical aeromedical evacuation missions
[AD-A276944] p 3586 N94-32217
Technical evaluation of the UH-60Q: Medical oxygen system
[AD-A276983] p 3579 N94-32242

HADRONS
Particle identification in a segmented calorimeter (NUMASS test data, September 1991)
[USIP-93-08] p 3711 N94-31085
State of hadron collider physics
[DE94-005279] p 3863 N94-31147
The measurement of the hadronic energy flow and jet production with the ZEUS calorimeter in deep inelastic scattering events at HERA
[ETN-94-96021] p 3865 N94-31534
B lifetimes at CDF
[DE94-006850] p 3866 N94-31669
Perturbative and nonperturbative EM lepton pair production in relativistic heavy-ion collisions
[DE94-006315] p 3867 N94-31779
Probing lepton number violation via Majorana neutrinos at hadron supercolliders
[PB94-147055] p 3868 N94-31922
A search for rapidity gaps in jet events and a study of color coherence in multijet events at D0
[DE94-006849] p 3872 N94-32627
Transverse energy production with Si and Au beams at AGS energy: Towards hot and dense hadronic matter
[DE94-007178] p 3938 N94-32638
Proceedings of the Workshop on B Physics at Hadron Accelerators
[DE94-007961] p 3877 N94-32748
String-parton model description of relativistic heavy-ion collisions
[DE94-009164] p 3874 N94-32850

HAFNIUM OXIDES
Electrostatic reduction of particulates for laser resistant hafnia coatings
[DE94-005824] p 3651 N94-31557

HALF SPACES
Radiation from an aperture into an anisotropic plasma half-space p 3885 N94-31205
Penetrable wedge analysis
[AD-A277219] p 3845 N94-32022
Monoenergetic neutral particle transport in semi-infinite media
[AD-A277155] p 3870 N94-32368

HALLEY'S COMET
Composition and properties of dust from Comet Halley
p 3936 N94-31947

HALOS
A twisted disk equation that describes warped galaxy disks p 3928 N94-31118

HAMILTONIAN FUNCTIONS
A worst-case analysis of an approximate algorithm for finding the minimum hamiltonian cycle on paths
[REPT-93-042] p 3809 N94-31192
A brief introduction to symplectic integrators and recent results
[DE94-006225] p 3845 N94-31783
Quantum dynamics in dual spaces
[DE94-008303] p 3913 N94-32824

HAND (ANATOMY)
Minimization of carpal tunnel syndrome
[AD-A276409] p 3795 N94-31363
Digit-Eyes: Vision-based human hand tracking
[NASA-CR-195913] p 3803 N94-31447

HANDBOOKS
Cleanroom engineering handbook. Volume 1: Cleanroom engineering process introduction and overview
[AD-A275949] p 3587 N94-31356
Aircraft icing handbook (update)
[AD-A276499] p 3574 N94-31678
Typhoon havens handbook for the western Pacific and Indian Oceans, change 3
[AD-A277030] p 3784 N94-32260
Management of government quality assurance functions for NASA contracts
[NHB-5300.4(2B-2)] p 3731 N94-32387
Briefing and review meeting implementation of the military handbook 17 for polymer matrix and metal matrix composites
[AD-A277446] p 3663 N94-33010
Forecasters handbook for the Philippine Islands and surrounding waters
[AD-A277993] p 3787 N94-33089

HARBORS
Typhoon havens handbook for the western Pacific and Indian Oceans, change 3
[AD-A277030] p 3784 N94-32260

HARDNESS
Conductive paints
[DE94-008508] p 3661 N94-32788

HARDWARE
VME rollback hardware for time warp multiprocessor systems
[NASA-CR-191796] p 3826 N94-32483
A flexible IBM-PC based data acquisition system for nuclear physics experiments
[USIP-92-02] p 3922 N94-32856

HARDWARE DESCRIPTION LANGUAGES
Formal semantics for a subset of VHDL and its use in analysis of the FTPP scoreboard circuit
[NASA-CR-191577] p 3827 N94-32734

HARMONIC ANALYSIS
Applied harmonic analysis
[AD-A278384] p 3685 N94-33353
HARMONIC CONTROL
The analysis of wake-induced unsteady aerodynamics related to higher harmonic control
[AD-A277914] p 3573 N94-33108
HARMONIC EXCITATION
Doubly asymptotic approximations: Theoretical and numerical analyses
[ONERA-NT-1993-7] p 3840 N94-31231
HARMONIC GENERATIONS
Wavevector-frequency analysis with applications to acoustics
[AD-A276618] p 3861 N94-32125
High conversion efficiency pumped-cavity second harmonic generation of a diode laser
[DE94-006805] p 3717 N94-32134
New developments in second-order nonlinear optical polymeric materials
[AD-A277409] p 3658 N94-32578
Surface probes of porous toluene/water ices: Adsorption kinetics and annealing spectra measured by second harmonic generation
[DE94-007564] p 3637 N94-32743
Optical properties of lanthanide-doped RbTiOAsO4 and transition metal-doped KTiOPO4
[DE94-008433] p 3907 N94-32963
A relaxation study of poled nonlinear optical polymers by infrared reflection-absorption spectroscopy
[AD-A277513] p 3663 N94-33054
Second-order nonlinear optical polymers: From fundamentals to applications
[AD-A277514] p 3664 N94-33348
HARMONIC OSCILLATION
Field studies of raindrop oscillations with applications to radar meteorology p 3782 N94-31743
HARMONIC RADIATION
Second-order nonlinear optical polymers: From fundamentals to applications
[AD-A277514] p 3664 N94-33348
HARMONICS
Experimental and computational studies on propeller noise due to inflow distortion p 3860 N94-31846
Optimal adaptive estimation algorithm for harmonic current reduction using power limited active line conditioners
[AD-A277354] p 3693 N94-32336
HARRIER AIRCRAFT
Numerical simulation of combined external/internal transonic flow on the forebody/inlet of the AV-8B Harrier 2 p 3569 N94-31759
HARTREE APPROXIMATION
Nonlinearity as an origin of nonuniqueness in solution of Hartree's equation
[DE94-006538] p 3841 N94-31311
HAZARDS
Using Monte Carlo techniques and parallel processing for debris hazard analysis of rocket systems
[DE94-007250] p 3609 N94-31382
Typhoon havens handbook for the western Pacific and Indian Oceans, change 3
[AD-A277030] p 3784 N94-32260
Environmental issues related to biomass: An overview
[DE94-007226] p 3767 N94-32784
HEAD-UP DISPLAYS
Synthetic vision technology demonstration. Volume 1: Executive summary
[DOT/FAA/RD-93/40-VOL-1] p 3582 N94-33076
Synthetic vision technology demonstration. Volume 2: Sensor tower testing
[DOT/FAA/RD-93/40-VOL-2] p 3582 N94-33077
Synthetic vision technology demonstration. Volume 3: Flight tests
[DOT/FAA/RD-93/40-VOL-3] p 3582 N94-33078
Synthetic vision technology demonstration. Volume 4: Appendices
[DOT/FAA/RD-93/40-VOL-4] p 3583 N94-33079
HEALTH
Controlling hazardous energy sources (lockout/tagout)
[NASA-TM-105290] p 3669 N94-32861
HEAO 1
A multi-frequency study of an x ray selected sample of active galactic nuclei p 3937 N94-31987
HEARING
A silicon condenser microphone: Materials and technology
[ISBN-9-09-005899-0] p 3688 N94-31518
Three dimensional audio versus head down TCAS displays
[NASA-CR-177636] p 3576 N94-33063
HEAT AFFECTED ZONE
A review of weldment failure modes and weldability testing methods
[AD-A278096] p 3729 N94-33251
HEAT BUDGET
A model for the evolution of CO2 on Mars p 3946 N94-33205
HEAT ENGINES
Ceramic Technology Project database
[DE94-008494] p 3659 N94-32632
Materials development program: Ceramic technology project bibliography, 1984-1992
[DE94-009297] p 3662 N94-32935
HEAT EXCHANGERS
Heat transfer studies on a rectangular channel with offset plate fins
[AD-A277300] p 3912 N94-32043
Oscillating-flow loss test results in rectangular heat exchanger passages
[NASA-CR-185297] p 3615 N94-32792
HEAT FLUX
The prediction of convective transfer on the thermal insulation of a solid-propellant rocket motor
[ONERA-NT-1993-15] p 3614 N94-31423
Errors associated with the use of heat flow transducers p 3796 N94-31742
First-wall heat-flux measurements during ELMing H-mode plasma
[DE94-008310] p 3888 N94-31765
A long-term simulation of surface fluxes and soil moisture
[DE94-006661] p 3774 N94-32772
HEAT GENERATION
Numerical model of the thermal behavior of an extremity in a cold environment including counter-current heat exchange between the blood vessels
[AD-A278099] p 3798 N94-33040
HEAT MEASUREMENT
Errors associated with the use of heat flow transducers p 3796 N94-31742
First-wall heat-flux measurements during ELMing H-mode plasma
[DE94-008310] p 3888 N94-31765
Amorphous/crystalline structure and phase transformations in metastable semiconducting Ge(1-x)Sn(x)
[DE94-008659] p 3901 N94-32115
Ionization EM calorimetry with accordion electrodes and liquid krypton or argon
[DE94-009082] p 3713 N94-32821
HEAT PIPES
Space Station WP-2 application of LDEF MLI results p 3592 N94-31016
Development of lightweight radiators for lunar based power systems
[NASA-TM-106604] p 3726 N94-32272
Physics of heat pipe rewetting
[NASA-CR-195902] p 3913 N94-33148
HEAT PUMPS
Metal hydride heat pump engineering demonstration and evaluation model
[NASA-CR-188286] p 3669 N94-32857
HEAT RESISTANT ALLOYS
Fatigue in single crystal nickel superalloys
[AD-A276662] p 3643 N94-32047
HEAT SHIELDING
Electrical properties of double layer dielectric structures for space technology
[ISBN-0-315-86547-4] p 3610 N94-31910
Development of lightweight ceramic ablators and arc-jet test results
[NASA-TM-108798] p 3617 N94-33117
HEAT SINKS
Energetic and general circulation p 3777 N94-30983
HEAT SOURCES
Energetic and general circulation p 3777 N94-30983
HEAT TRANSFER
A preliminary investigation of high amplitude standing waves with laser Doppler anemometry
[AD-A276463] p 3860 N94-31242
Compressible convection with ionization p 3911 N94-31498
Chemical vapour deposition of tungsten for the application in integrated circuits
[ISBN-9-09-005151-1] p 3641 N94-31519
Solid surface
[NASA-TM-109746] p 3634 N94-31883
Heat transfer studies on a rectangular channel with offset plate fins
[AD-A277300] p 3912 N94-32043
The influence of cumulus parameterization on model forecasts of rapid oceanic cyclogenesis
[AD-A277207] p 3784 N94-32094
Numerical model of the thermal behavior of an extremity in a cold environment including counter-current heat exchange between the blood vessels
[AD-A278099] p 3798 N94-33040
HEAT TRANSMISSION
Computer implementation of Arnott's formulation of thermoacoustics using MATLAB
[AD-A276356] p 3860 N94-31257
HEAT TREATMENT
Acoustic emission from crack growth in 7050 aluminum and 7075 aluminum as a function of temperature and heat treatment
[DREP-CRS-93-15] p 3642 N94-31871
Sodium sulfate corrosion of silicon carbide fiber-reinforced lithium aluminosilicate glass-ceramic matrix composites
[AD-A277224] p 3623 N94-32023
Work hardening behavior in aluminum alloy 2090
[DE94-007036] p 3643 N94-32064
Continuous measurement of aging response in aluminum alloys by eddy current methods
[AD-A277233] p 3644 N94-32371
HEATERS
Electromagnetic wave reflection from irregular plasma layers
[AD-A276727] p 3678 N94-32161
Implementation of heaters on thermally actuated spacecraft mechanisms p 3607 N94-33320
HEATING
NATO Advanced Study Institute on Unsteady Combustion. Volume 2: Research papers, September 6-17, 1993
[AD-A276572] p 3634 N94-32033
HEAVING
Heave dynamics of an air cushion vehicle bag and finger skirt
[ISBN-0-315-87053-2] p 3568 N94-31734
HEAVY ELEMENTS
Control and monitoring of heavy metal emissions
[VTT-TIED-1508] p 3765 N94-31657
HEAVY IONS
Control heavy ion collisions in the systems Ar-40 + Ca-40 and Si-28 + Si-28, and the nature of particle emission in fusion-evaporation reactions
[ETN-94-95749] p 3866 N94-31614
Perturbative and nonperturbative EM lepton pair production in relativistic heavy-ion collisions
[DE94-006315] p 3867 N94-31779
Antiproton production in heavy ion collisions
[DE94-007552] p 3870 N94-32271
Transverse energy production with Si and Au beams at AGS energy: Towards hot and dense hadronic matter
[DE94-007178] p 3938 N94-32638
String-parton model description of relativistic heavy-ion collisions
[DE94-009164] p 3874 N94-32850
RHIC chromatic correction system
[DE94-008532] p 3883 N94-32994
HEAVY WATER
High resolution molecular spectroscopy of atmospheric species
[AD-A278382] p 3776 N94-33351
HEIGHT
World height system definition and implementation
[AD-A276725] p 3747 N94-32160
Apron heights around stepped massifs in the Cydonia Mensae region: Do they record the local paleobathymetry of Oceanus Borealis? p 3949 N94-33224
HELICAL ANTENNAS
Predicting antenna parameters from antenna physical dimensions
[AD-A276442] p 3672 N94-31300
HELICAL WINDINGS
Nonlinear analysis of springs using helical finite elements p 3859 N94-31906
HELICOPTER CONTROL
Controls design with crossfeeds for hovering rotorcraft using quantitative feedback theory
[NASA-CR-195765] p 3585 N94-31203
Development of a reconfigurable helicopter flight control system
[ISBN-0-315-87218-7] p 3585 N94-31837
The analysis of wake-induced unsteady aerodynamics related to higher harmonic control
[AD-A277914] p 3573 N94-33108
HELICOPTER DESIGN
Estimating the impact of crashworthiness standards on mortality and morbidity events in the US Army rotary-wing aircraft mishaps
[AD-A277121] p 3575 N94-32363
HELICOPTER PERFORMANCE
An analysis of the maintenance performance measurement system for LAMPS MK 3 helicopter squadrons
[AD-A276421] p 3565 N94-31332
HELICOPTER WAKES
Experimental and numerical simulation of helicopter rotor fuselage interaction
[ONERA-NT-1993-8] p 3568 N94-31421

User's guide for a flat wake rotor inflow/wake velocity prediction code, DOWN
[NASA-TM-104139] p 3572 N94-32873
The analysis of wake-induced unsteady aerodynamics related to higher harmonic control
[AD-A277914] p 3573 N94-33108

HELICOPTERS
Development of a reconfigurable helicopter flight control system
[ISBN-0-315-87218-7] p 3585 N94-31837
Evaluation of intensity distribution profiles for US. Army rotorcraft position lighting adapted for image intensifier operations
[AD-A276459] p 3804 N94-32171
Status of developing a multifunctional aviation grease
[AD-A276755] p 3656 N94-32184
Heliport Noise Model (HNM) version 2.2 (user's guide)
[AD-A277072] p 3861 N94-32418
A novel potential/viscous flow coupling technique for computing helicopter flow fields
[NASA-CR-193272] p 3571 N94-32476

HELIOSTATS
Operational experience and evaluation of a dual-element stretched-membrane heliostat
[DE94-008827] p 3763 N94-32965

HELIUM
Elimination of two atomic electrons by a single high energy photon
[DE94-006834] p 3864 N94-31320
Double photoionization of helium with synchrotron x rays: Proceedings
[DE94-006737] p 3866 N94-31668

HELIUM ATOMS
Diamagnetism in helium Rydberg atoms
[ETN-94-96015] p 3865 N94-31549

HELIUM COMPOUNDS
Wave packet studies of the vibrational predissociation of three and four-atom van der Waals complexes
[DE94-007623] p 3871 N94-32598

HELIUM ISOTOPES
Spin-structure function of the neutron He-3: SLAC results
[DE94-008927] p 3875 N94-33189

HELMHOLTZ EQUATIONS
Finite element solution to the Helmholtz equation with high wave number. Part 1: The h-version of the FEM
[AD-A277396] p 3848 N94-32341

HEMODYNAMICS
Incompressible viscous flow in tubes with occlusions
[ISBN-0-315-75467-2] p 3704 N94-31778

HEPTANES
Silicone grease as a precursor to a pseudo crown-ether ligand: Crystal structure of (K(+)K(Me2SiO)7(+))(Hln(CH2CMe3)3(-))4)
[AD-A276343] p 3895 N94-31327

HETEROCYCLIC COMPOUNDS
Isomeric poly(benzophenone)s: Synthesis of highly crystalline poly (4, 4 foot-benzophenone) and amorphous poly (2, 5-benzophenone), a soluble poly (p-phenylene) derivative
[AD-A277261] p 3655 N94-32017

HETERODYNING
Optically switched submillimeter-wave oscillator
[AD-A278014] p 3698 N94-33249

HETEROGENEITY
A heterogeneous computing environment for simulating astrophysical fluid flows p 3928 N94-31119
Effect of surface forces on the rheology of particle-liquid systems and the consolidation of ceramic powders
[AD-A277092] p 3657 N94-32391

HETEROJUNCTION DEVICES
Processing boron and boron carbide thin films for protective coatings and device fabrication
[AD-A277266] p 3900 N94-32041
Reconfigurable optical switches with monolithic electrical-to-optical interfaces
[DE94-007745] p 3881 N94-32385

HETEROJUNCTIONS
Passivation of III-V compound semiconductor based devices
[AD-A276178] p 3894 N94-31056
Ion beam synthesis of IrSi3 by 1-MeV Ir ion implantation into Si(111)
[DE94-006556] p 3896 N94-31501
Semiconductor microcavity lasers
[DE94-006143] p 3716 N94-31622

HEURISTIC METHODS
Simple Patch: A new heuristic for the product traveling salesman problem
[REPT-93-85] p 3845 N94-31702
On the convergence of stochastic iterative dynamic programming
[AD-A276517] p 3815 N94-31933
Varying execution discipline to increase performance
[DE94-007844] p 3819 N94-32651
Multiple-valued programmable logic array minimization by solution space search
[AD-A278033] p 3821 N94-33090
A heuristic multiple target tracker p 3686 N94-33346

HIBERNATION
Characterization and utilization of opiate-like hibernation factors
[AD-A278136] p 3794 N94-33098

HIERARCHIES
Detecting the erosion of hierarchic information structures
[RUU-CS-93-10] p 3916 N94-31385
A hierarchical approach to test generation for CMOS VLSI circuits
[ISBN-9-09-005449-9] p 3689 N94-31535
Report on implementing part relationships using VML metaclasses
[PB94-147485] p 3813 N94-31686
A brief introduction to symplectic integrators and recent results
[DE94-006225] p 3845 N94-31763
DTIC Thesaurus on diskette with dBase 4.1 runtime (computer diskette)
[AD-M000306] p 3922 N94-33256

HIGH ALTITUDE
Medical problems in high mountain environments. A handbook for medical officers
[AD-A278095] p 3798 N94-33268

HIGH ELECTRON MOBILITY TRANSISTORS
Characteristics of III-V semiconductor devices at high temperature
[NASA-TM-106574] p 3697 N94-33052

HIGH ENERGY INTERACTIONS
High energy physics program at the University of Alabama
[DE94-006544] p 3875 N94-31488
High energy physics studies
[DE94-005970] p 3876 N94-31505
RHIC spin physics
[DE94-005452] p 3876 N94-32099
The future of high energy physics in the US statement for the Science Subcommittee of the House Science, Space and Technology Committee
[DE94-008986] p 3876 N94-32586
The future of high-energy physics in the US: Statement for the 1994 HEPAP Subpanel
[DE94-008994] p 3876 N94-32588
A search for rapidity gaps in jet events and a study of color coherence in multijet events at D0
[DE94-006849] p 3872 N94-32627
Minimax: Multiparticle physics at the Tevatron collider
[DE94-007095] p 3873 N94-32689
String-parton model description of relativistic heavy-ion collisions
[DE94-009164] p 3874 N94-32850

HIGH FREQUENCIES
Atmospheric effects assessment program: Ionospheric sounding
[AD-A276447] p 3770 N94-31303
A multichannel architecture for Naval Task Force Communication
[AD-A276230] p 3673 N94-31446
Design, development, and testing of a Network Frequency Selection Service (NFSS)
[AD-A277362] p 3680 N94-32283
Broadband, high-power, 2-30 MHz, twin-whip antenna. Computer and 1/10-scale model design study
[AD-A277619] p 3682 N94-32971
High frequency active auroral research program (HAARP) imager
[AD-A277469] p 3775 N94-32999
High frequence and automatic link establishment (HF and ALE) radio propagation test to Antarctica
[AD-A277730] p 3682 N94-33001
Advanced high frequency partial discharge measuring system
[NASA-CR-195240] p 3697 N94-33044

HIGH GAIN
The Galileo high gain antenna deployment anomaly p 3607 N94-33319

HIGH POLYMERS
Novel sol-gel deposition for repair of conducting paths in polyceramic systems
[AD-A278381] p 3664 N94-33350

HIGH POWER LASERS
High-power CW diode-laser-array-pumped solid-state lasers and efficient nonlinear optical frequency conversion
[AD-A276126] p 3714 N94-31278
Inertial fusion with ultra-powerful lasers
[DE94-007242] p 3887 N94-31400
Automatic resonator alignment and power stabilization of high power C02 lasers
[ISBN-0-315-77217-4] p 3714 N94-31472
DOE reactor-pumped laser program
[DE94-006372] p 3715 N94-31485
Large-area conditioning of optics for high-power laser systems
[DE94-007028] p 3716 N94-31636
Sol-gel coatings for high power laser optics: Past, present, and future
[DE94-007240] p 3718 N94-32252
High power diode lasers for solid-state laser pumps p 3722 N94-32448
X ray imaging and x ray source development at Lawrence Livermore National Laboratory
[DE94-007077] p 3719 N94-32629
Short-pulse, high-intensity lasers at Los Alamos
[DE94-007545] p 3720 N94-32760
Ultrafast x ray sources
[AD-A277455] p 3721 N94-33012

HIGH PRESSURE
Development of high-pressure diaphragms for the AEDC impulse tunnel
[AD-A277053] p 3588 N94-32009

HIGH RESOLUTION
Concept, construction and testing of a high resolution QCLAM electron spectrometer with large solid angle and high impulse acceptance for the electron accelerator S-DALINAC
[ETN-94-95755] p 3711 N94-31515
High-resolution numerical methods for compressible multi-phase flow in hierarchical porous media
[DE94-008261] p 3707 N94-32410
Rapid estimates of crop acreage and production at European scale using high resolution imagery p 3754 N94-32557
High resolution molecular spectroscopy of atmospheric species
[AD-A278382] p 3776 N94-33351

HIGH REYNOLDS NUMBER
Control of hypersonic aerodynamic forces with surface blowing p 3567 N94-31216
Solution of the average-passage equations for the incompressible flow through multiple-blade-row turbomachinery
[AD-A276515] p 3583 N94-31931
The structure of high Reynolds number turbulent boundary layers, part A
[AD-A278392] p 3710 N94-33162

HIGH SPEED
A high-speed linear algebra library with automatic parallelism p 3828 N94-32440
High-speed data search p 3923 N94-32441

HIGH SPEED CAMERAS
A new high-speed IR camera system p 3713 N94-32459

HIGH SPEED PHOTOGRAPHY
Simultaneous pressure measurement and high-speed photography study of cavitation in a dynamically loaded journal bearing
[NASA-TM-106456] p 3728 N94-32893

HIGH STRENGTH
Evaluation of nondestructive inspection techniques for quality control of alumina-ceramic housing components
[AD-A276220] p 3730 N94-31065

HIGH STRENGTH STEELS
Simpler J(sub Ic) test and data analysis procedures for high strength steels
[AD-A277731] p 3648 N94-33281

HIGH TEMPERATURE
Atomic oxygen interaction at defect sights in protective coatings on polymers flown on LDEF p 3593 N94-31024
High-temperature study of O+H2CO yields OH+HCO
[DE94-006837] p 3864 N94-31321
High temperature ductility loss in titanium alloys: A review
[DE94-006606] p 3640 N94-31345
GaAs/GaN strained layer superlattice materials for high temperature transistors, phase 1
[AD-A276115] p 3897 N94-31528
In-situ TEM crystallization of anorthite-glass films on (alpha)-Al2O3
[DE94-006317] p 3652 N94-31780
High temperature NASP engine seal development
[NASA-TM-109750] p 3725 N94-31804
Creep-fatigue criteria and inelastic behavior of modified 9Cr-1Mo steel at elevated temperatures
[DE94-007915] p 3642 N94-31918
Computer modelling of cyclic deformation of high-temperature materials
[AD-A277056] p 3623 N94-32012
Fatigue in single crystal nickel superalloys
[AD-A276662] p 3643 N94-32047
Mechanics of failure of high temperature metal matrix composites
[AD-A277397] p 3624 N94-32342

Chemical vapor deposition fluid flow simulation modelling tool
[NASA-CR-189648] p 3707 N94-32480
Effect of elevated temperature and cyclic loading on properties and damage modes in ceramic composites
[DE94-008736] p 3662 N94-32891
Characteristics of III-V semiconductor devices at high temperature
[NASA-TM-106574] p 3697 N94-33052
Enhanced thermal capacity aerogels summary report, FY 1993
[DE94-008888] p 3639 N94-33260

HIGH TEMPERATURE AIR
Effect of elevated temperature and cyclic loading on properties and damage modes in ceramic composites
[DE94-008736] p 3662 N94-32891
Stabilized alumina/ethanol colloidal dispersion for seeding high temperature air flows
[NASA-TM-106591] p 3713 N94-32983

HIGH TEMPERATURE SUPERCONDUCTORS
Preliminary results from the CONCAP-2-01 and EIOM-3 experiments on STS-46 p 3596 N94-31042
Synthesis, characterization, phase diagrams and superconducting, and normal state magnetic properties of La(2-x)Sr(x)CuO4 (0 is less than or equal to x which is less than or equal to 0.08) and electrochemically oxidized La(2-x)Sr(x)CuO(4 + delta) (0 is less than or equal to x which is less than or equal to 0.33, 0 is less than or equal to delta which is less than or equal to 0.12)
[DE94-005260] p 3895 N94-31067
High-temperature superconducting transformer performance, cost, and market evaluation
[DE94-005494] p 3687 N94-31152
Electron spin resonance measurements of Er(3+) and Mn(2+) in the high temperature superconductor compounds La(2-x)Sr(x)CuO(4-delta)
[ETN-94-95746] p 3898 N94-31612
Short coherence length superconductors: Intermediate regime between BCS and bosons
[DE94-007694] p 3904 N94-32645
Strongly anisotropic s-wave versus d-wave gap in cuprate superconductors: Evidence and theory
[DE94-007579] p 3904 N94-32746
Quantum fluctuations of vortices in Josephson-coupled superconductors
[DE94-007609] p 3905 N94-32747
New advances in the modeling of high-temperature superconductors
[DE94-007649] p 3905 N94-32815
Proceedings, Strongly Correlated Electronic Materials: The 1993 Los Alamos Symposium
[DE94-009293] p 3906 N94-32913
Investigation of superconductivity and magnetism in d and f-electron materials
[DE94-008535] p 3907 N94-32933
Evidence for symmetry breaking local distortions in thallium barium copper oxide
[DE94-006149] p 3907 N94-32944
A quest for a new superconducting state
[DE94-008439] p 3908 N94-32991
High temperature superconducting Josephson junction array systems, phase 1
[AD-A277937] p 3908 N94-33246
The path for long range conduction in high J(sub c) TlBa2Ca2Cu3O(8+x) spray-pyrolyzed deposits
[DE94-007211] p 3909 N94-33271

HIGH TEMPERATURE TESTS
Evolution of the interface properties with temperature in the T800H/ bismaleimide composites
[ONERA-NT-1993-14] p 3619 N94-31478
The effect of prolonged exposure to 750 C air on the tribological performance of PM212
[NASA-TM-106472] p 3617 N94-32941

HIGH VOLTAGES
Modal analysis of multiterminal high voltage direct current transmission
[DE94-006426] p 3691 N94-31785
Advanced high frequency partial discharge measuring system
[NASA-CR-195240] p 3697 N94-33044
Time resolved measurements of light produced by onset of plasma formation on electrodes of fast pulsed high voltage diodes
[AD-A277974] p 3894 N94-33264

HIGHLY MANEUVERABLE AIRCRAFT
Installed F/A-18 inlet flow calculations at 30 degrees angle-of-attack: A comparative study
[NASA-CR-195297] p 3573 N94-33119

HILBERT SPACE
Frames and stable bases for shift-invariant subspaces of L(sub 2)(IR(sup d))
[AD-A276470] p 3843 N94-31474
The Cameron-Martin theorem
[W-9315] p 3844 N94-31676
Finite element solution to the Helmholtz equation with high wave number. Part 1: The h-version of the FEM
[AD-A277396] p 3848 N94-32341

HISTOGRAMS
Parallel processing for differencing and histogramming
[AD-A277060] p 3826 N94-32274

HISTORIES
Mars: Five views on what is known
[NASA-TM-109751] p 3942 N94-31805
A historical perspective on fifteen years of laser damage thresholds at LLNL
[DE94-007930] p 3719 N94-32613
Chronology of KSC and KSC related events for 1993
[NASA-TM-109196] p 3966 N94-33072

HMX
Condensed-phase processes during solid propellant combustion. 3: Preliminary depth-profiling studies on XM39, JA2, M9, M30, and HMX2
[AD-A276595] p 3635 N94-32124

HOLE BURNING
Development of materials for spectral hole burning applications
[AD-A278408] p 3909 N94-33324

HOLE DISTRIBUTION (ELECTRONICS)
Transverse mode analysis of hole-coupled free-electron lasers
[ETN-94-96019] p 3715 N94-31532

HOLE GEOMETRY (MECHANICS)
New thick film feedthrough configurations
[DE94-008706] p 3694 N94-32582

HOLES (ELECTRON DEFICIENCIES)
Transverse mode analysis of hole-coupled free-electron lasers
[ETN-94-96019] p 3715 N94-31532
High pressure experiments on the Y-Ba-Cu-O superconductors: A major role for holes
[ETN-94-96013] p 3897 N94-31547
Analytical solutions of minimum ionization particle induced current shapes of silicon detectors and simulation of charge collection properties
[DE94-007523] p 3870 N94-32355

HOLES (MECHANICS)
Finite element analysis of MB326H Macchi wing lower spar cap fatigue cracks
[AD-A277062] p 3580 N94-32264

HOLOGRAPHY
Photoelectron diffraction and holography: Present status and future prospects
[DE94-006298] p 3712 N94-31629
Millimeter wave, high-resolution, holographic surveillance system
[DE94-004289] p 3712 N94-31831
Reversible optical storage in azo polymers
[AD-A277109] p 3654 N94-31980
Ultra wide band radar holographic imaging of subsurface targets
[DE94-004271] p 3713 N94-32681
Imaging of surface structure with energy-dependent photoelectron diffraction
[DE94-009096] p 3907 N94-32934

HOMING DEVICES
Optical processing of MMW for agile beamsteering and beamforming
[AD-A277161] p 3880 N94-32068
Calibration and validation studies in the LENS facility
[AD-A278403] p 3591 N94-33167

HOMOGENEOUS TURBULENCE
Laser-induced fluorescence/particle tracking system for stratified flow research
[AD-A275917] p 3701 N94-31341

HOMOGENIZING
Competition between crystallization and mixing/demixing in polymer mixture
[ETN-94-95753] p 3651 N94-31513
Liquid-assisted diffusion bonding of NiAl
[DE94-008687] p 3645 N94-32522

HONEYCOMB STRUCTURES
Honeycomb sandwich structures: Vented versus unvented designs for space systems
[AD-A276713] p 3624 N94-32122
MSAT boom joint testing and load absorber design
p 3606 N94-33315

HORIZONTAL FLIGHT
The analysis of wake-induced unsteady aerodynamics related to higher harmonic control
[AD-A277914] p 3573 N94-33108

HORSESHOE VORTICES
Control of low-speed turbulent separated flow over a backward-facing ramp
[NASA-TM-109740] p 3573 N94-33071

HOT CORROSION
Sodium sulfate corrosion of silicon carbide fiber-reinforced lithium aluminosilicate glass-ceramic matrix composites
[AD-A277224] p 3623 N94-32023

HOT ELECTRONS
An extended approach to oxidations and nitridations of Si and Ge(x)Si(1-x) materials
[AD-A276056] p 3631 N94-31282

HOT PRESSING
Influence of volume fraction of component materials and interlayer bond strength on fracture toughness of multi-layer Al 6090-25 volume percent SiCp and Al 5182 laminates
[DE94-007141] p 3626 N94-32665

HOUSINGS
Evaluation of nondestructive inspection techniques for quality control of alumina-ceramic housing components
[AD-A276220] p 3730 N94-31065
Leveraging metal matrix composites to reduce costs in space mechanisms p 3604 N94-33301

HOVERING
The analysis of wake-induced unsteady aerodynamics related to higher harmonic control
[AD-A277914] p 3573 N94-33108

HOVERING STABILITY
Controls design with crossfeeds for hovering rotorcraft using quantitative feedback theory
[NASA-CR-195765] p 3585 N94-31203

HUBBLE CONSTANT
Measuring the Hubble constant and our Virgo-infall velocity independently p 3926 N94-31968

HUBBLE DIAGRAM
Fireworks in velocity and configuration space applied to cosmology
[USIP-93-90] p 3927 N94-31086

HULLS (STRUCTURES)
Evaluation of nondestructive inspection techniques for quality control of alumina-ceramic housing components
[AD-A276220] p 3730 N94-31065
Magnetohydrodynamic boundary layer control system
[AD-D016120] p 3710 N94-32958

HUMAN BEHAVIOR
An experimental study of pilot/vehicle dynamics using a tilt rotor flying machine
[AD-A277516] p 3805 N94-33349

HUMAN BODY
Minutes: Accredited Standards Committee on Bioacoustics, S3. US TAG for ISO/TC 43, acoustics, IEC/TC 29 electroacoustics, and ISO/TC 108/SC4 human exposure to mechanical vibration and shock
[AD-A276201] p 3795 N94-31490
Virtual reality in medical education and assessment
p 3798 N94-32471

HUMAN FACTORS ENGINEERING
AGARD highlights 94/1, April 1994
[AGARD-HIGHLIGHTS-94/1] p 3956 N94-31196
A review of microclimate cooling systems in the chemical, biological, radiological environment
[AD-A276446] p 3802 N94-31302
Minimization of carpal tunnel syndrome
[AD-A276409] p 3795 N94-31363
Assessment of interior modifications in C-130 and C-141 aircraft for night vision goggle operations
[AD-A276843] p 3582 N94-32223
THE VERTICAL p 3806 N94-32435
The relationship between integrative task design for information systems professionals and perceived information systems effectiveness p 3919 N94-32487
The role of guideline-based design tools
[DE94-007482] p 3804 N94-32596
Design of graphic screens using Neuro Linguistic Programming
[DE94-007634] p 3819 N94-32599
Aircrew Eye/Respiratory Protection (AERP): 16-hour extended wear evaluation of chemical protective equipment
[AD-A277288] p 3804 N94-32609
Aviation human factors research in US universities: Potential contributions to national needs
[NASA-TM-108814] p 3575 N94-32927
Use of a pitch adjustable foot restraint system: Operator strength capability and load requirements
[NASA-TP-3477] p 3805 N94-33050
Cockpit Electronic Display Workshop: Proceedings (computer diskette)
[AD-M000330] p 3805 N94-33171
Cockpit Electronic Display Workshop: A synopsis
[AD-A277728] p 3583 N94-33280

HUMAN PERFORMANCE
Development and enhancement of a model of performance and decision making under stress in a real life setting
[AD-A276029] p 3799 N94-31440
Effects of methamphetamine and fatigue on long- and short-term memory
[AD-A276452] p 3799 N94-32187
A systems approach to computer-based training
p 3823 N94-32436

HUMAN REACTIONS
Situational awareness: A feasibility investigation of near-threshold skills development
[AD-A276467] p 3798 N94-31243
HUMAN RESOURCES
European business confronted with the 21st century: Men, the essential risk
[ESA-SP-1167] p 3914 N94-31181
HUMAN TOLERANCES
Review of pharmacological approach to improve cold tolerance p 3796 N94-31740
Lipid metabolism in cold-exposed humans p 3796 N94-31741
Numerical model of the thermal behavior of an extremity in a cold environment including counter-current heat exchange between the blood vessels
[AD-A278099] p 3798 N94-33040
Exposure assessment of JAVELIN missile combustion products
[AD-A278128] p 3616 N94-33059
HUMAN-COMPUTER INTERFACE
Development concept for Dutch user support
[PB94-125523] p 3598 N94-31208
Extender's guide for artifacts and drafts
[AD-A276344] p 3810 N94-31328
Developing the Multimedia User Interface Component (MUSIC) for the Icarus Presentation System (IPS)
[AD-A276341] p 3810 N94-31335
Digit-Eyes: Vision-based human hand tracking
[NASA-CR-195913] p 3803 N94-31447
Automatic generation of context-sensitive textual help
[REPT-93-68] p 3812 N94-31646
GKS-9X: An experimental application
[PB94-147048] p 3813 N94-31685
Designing in virtual reality: Modelling Objects in a Virtual Environment (MOVE)
[REPT-93-91] p 3813 N94-31704
Beyond the read-eval loop: The artifacts system
[AD-A276589] p 3803 N94-32034
Human Computer Interface Specifications (HCIS) for the Integrated Maintenance Information System (IMIS)
[AD-A277184] p 3566 N94-32254
Modular Simulator System (MSS). Interface requirements specification for the generic MSS
[AD-A276965] p 3588 N94-32311
Interactive graphical model building using telepresence and virtual reality
[DE94-001421] p 3818 N94-32353
The intelligent monitoring system: Generic Database Interface (GDI). Revised user manual
[AD-A277131] p 3919 N94-32382
THE VERTICAL p 3806 N94-32435
Relationships between access and use in information systems: Remote access to and browsing of online catalogs p 3919 N94-32488
On the implementation of error handling in dynamic interfaces to scientific codes
[DE94-008970] p 3818 N94-32585
The role of guideline-based design tools
[DE94-007482] p 3804 N94-32596
Design of graphic screens using Neuro Linguistic Programming
[DE94-007634] p 3819 N94-32599
The hypermedia technology as front end to knowledge processing systems p 3854 N94-33343
HURRICANES
Remote sensing for hurricane Andrew impact assessment p 3758 N94-32464
HYBRID CIRCUITS
Superconducting and semiconducting hybrids and advance memory concepts for superconducting electronics
[AD-A277766] p 3907 N94-32988
HYBRID COMPUTERS
Real time simulation model for designing converter regulation
[ETN-94-95735] p 3689 N94-31576
HYBRID PROPELLANTS
Shock tube ignition and combustion of aluminum/magnesium alloy particles in oxygen at high pressure p 3631 N94-31286
HYBRID PROPULSION
Energy storage specification requirements for hybrid-electric vehicle
[DE94-008642] p 3694 N94-32521
HYDRATES
Gas hydrate detection and mapping on the US east coast
[DE94-005959] p 3742 N94-31504
HYDROCARBON COMBUSTION
Ignition studies in nonpremixed hydrogen/air combustion
[AD-A275954] p 3632 N94-31348
HYDROCARBON FUELS
Fuel property effects on engine combustion processes
[DE94-005529] p 3631 N94-31153
HYDROCARBONS
Dry deposition of PAN to grassland vegetation
[DE94-005111] p 3768 N94-32894
Development and preliminary evaluation of aryl ester boundary additives for perfluoropolyethers
[NASA-TM-106603] p 3663 N94-33024
HYDROCYANIC ACID
Time-resolved infrared absorption studies applied to the study of radical plus molecule reactions
[DE94-005921] p 3863 N94-31202
Cometary molecules p 3935 N94-31869
HYDRODYNAMICS
Workshop on advances in smooth particle hydrodynamics
[DE94-006221] p 3956 N94-31308
Fluid-structure interaction in case of water hammer with cavitation
[PB94-148277] p 3702 N94-31588
Studies in physico-chemical hydrodynamics of extended systems
[DE94-006752] p 3706 N94-32149
Boundary element analysis of three-dimensional nonlinear hydrodynamics in a reduced gravity environment p 3668 N94-32715
A study of near-surface and underwater explosions by computer simulations
[DE94-009038] p 3708 N94-32849
Convection in Type 2 supernovae
[DE94-009373] p 3938 N94-32914
HYDROGEN
Time-resolved infrared absorption studies applied to the study of radical plus molecule reactions
[DE94-005921] p 3863 N94-31202
Compressible convection with ionization p 3911 N94-31498
Hydrogen incorporation and radiation induced dynamics in metal-oxide-silicon structures: A study using nuclear reaction analysis
[ETN-94-95742] p 3898 N94-31610
Modern integral equation techniques for quantum reactive scattering theory
[DE94-007039] p 3857 N94-31639
Metal hydrides in hydrogen energy systems
[VTT-TIED-1407] p 3759 N94-31655
A study of the neutral hydrogen distribution of the Milky Way through 21 cm emission and Lyman alpha absorption p 3938 N94-32309
Boron and hydrogen in Ni3Al. Part 2: Mechanical testing of bicrystals
[DE94-007441] p 3904 N94-32606
HYDROGEN ATOMS
Rate coefficient for the reaction H + O2 yields OH + O: Results from 2000 to 5300 K
[DE94-008105] p 3871 N94-32615
HYDROGEN BONDS
Electric field-induced changes in odd-numbered nylons
[AD-A278003] p 3664 N94-33138
HYDROGEN COMPOUNDS
Time-resolved infrared absorption studies applied to the study of radical plus molecule reactions
[DE94-005921] p 3863 N94-31202
HYDROGEN EMBRITTLEMENT
Prediction of hydrogen entry and permeation in metals and alloys
[AD-A276637] p 3642 N94-31995
HYDROGEN ENGINES
The hydrogen hybrid option
[DE94-006733] p 3667 N94-32148
HYDROGEN FUELS
NEMO: Advanced energy systems and technologies
[DE94-721996] p 3760 N94-31767
Scenarios for multi-unit inertial fusion energy plants producing hydrogen fuel
[DE94-006614] p 3666 N94-32114
HYDROGEN IONS
Spectroscopic study of the molecular collisions (hydrogen-nitrogen and hydrogen-oxygen) at energies of several MeV
[ISBN-0-315-86794-9] p 3867 N94-31753
HYDROGEN OXYGEN ENGINES
The 7.5K lbf thrust engine preliminary design for Orbit Transfer Vehicle
[NASA-CR-189175] p 3614 N94-31618
HYDROGEN PEROXIDE
Hydrogen peroxide electrodes based on electrical connection of redox centers of various peroxidases to electrodes through a three-dimensional electron relaying polymer network
[AD-A276543] p 3691 N94-32056
Formation of gas-phase peroxides in a rural atmosphere: An interpretation of the recent SOS/SERON field results
[DE94-002995] p 3766 N94-32692
HYDROGEN PLASMA
Stark broadening of the 2S state of hydrogen and deuterium in arc plasmas of low density
[ETN-94-95731] p 3888 N94-31572
HYDROGEN PRODUCTION
Biological conversion of synthesis gas
[DE94-000094] p 3760 N94-31811
Scenarios for multi-unit inertial fusion energy plants producing hydrogen fuel
[DE94-006614] p 3666 N94-32114
HYDROGENATION
Experimental and theoretical studies of hydrogenated amorphous semiconductor alloys and superlattices
[AD-A276159] p 3686 N94-31079
Hydrogenated amorphous silicon (a-Si:H) based gamma camera: Monte Carlo simulations
[DE94-007042] p 3795 N94-31323
Electrochemical surface modification of silicon monocrystals: A surface analytic examination
[ETN-94-95733] p 3633 N94-31574
HYDROGRAPHY
Results of real-time testing and demonstration of the US Army Corps of Engineers real-time on-the-fly positioning system
[AD-A276160] p 3576 N94-31080
Hydrographic service Royal Australian Navy
[AD-A277134] p 3788 N94-32066
Three dimensional vorticity field in the California current system
[AD-A276951] p 3788 N94-32220
Real-time centimeter positioning with GPS: A system developed by the US Army Corps of Engineers
[AD-A278152] p 3577 N94-33095
Cruise report: Oceanus 250 leg 4 high resolution profiler survey for the North Atlantic Tracer Release Experiment, 25 March - 24 April, 1992
[AD-A277935] p 3791 N94-33245
HYDROLOGICAL CYCLE
Cumulus convection parameterization and numerical modelling of moist atmospheres p 3783 N94-31989
Development and testing of improved techniques for modeling the hydrologic cycle in a mesoscale weather prediction system
[AD-A277416] p 3786 N94-32921
HYDROLOGY
Hydrologic Database user's manual
[DE94-003950] p 3743 N94-31603
Application of ERS-1 SAR data for hydrological studies p 3754 N94-32558
Snowmelt forecasting. Further cold regions development of operational hydrological forecasting, volume 2
[AD-A278123] p 3757 N94-33269
HYDROLOGY MODELS
ADCIRC: An advanced three-dimensional circulation model for shelves, coasts, and estuaries. User's manual for ADCIRC-2DDI
[AD-A276150] p 3787 N94-31250
HYDROLYSIS
Preparation of catalyst particles using methods of colloid chemistry. Part 1: Preparation of silica particles from alcohol solutions
[PB94-135597] p 3634 N94-31679
Improved resealing procedures for the second deseal/reseal program in RAAF F111 aircraft fuel tanks
[AD-A277069] p 3580 N94-32378
HYDROPHONES
Prediction of the plane wave beamformed acoustic arrival structure for the 1992 Barents Sea coastal tomography test
[AD-A276741] p 3788 N94-32181
Long transect seafloor seismic array: A component of SAMSON (Sources of Ambient Micro Seismic Ocean ic Noise)
[AD-A277009] p 3789 N94-32401
HYDROSTATICS
Fermi surface instability at 0.4 K in a heavy-fermion YbBiPt: SDW?
[DE94-006224] p 3899 N94-31916
HYDROTHERMAL SYSTEMS
Light in Thermal Environments (LITE) Workshop
[NASA-CR-195851] p 3790 N94-32981
HYDROXYL EMISSION
Simulation of CO2 release at 800 km altitude
[AD-A276692] p 3776 N94-33272
HYDROXYL RADICALS
High-temperature study of O+H2CO yields OH+HCO
[DE94-006837] p 3864 N94-31321
Simulation of CO2 release at 800 km altitude
[AD-A276692] p 3776 N94-33272
HYPERBARIC CHAMBERS
Effects of combined breathing impediments on diver's respiratory performance
[AD-A277437] p 3805 N94-33084
HYPERBOLIC DIFFERENTIAL EQUATIONS
Fully discrete arbitrary-order schemes for a model hyperbolic conservation law
[CRANFIELD-AERO-9307] p 3843 N94-31539
A numerical method for mixing/chemically reacting compressible flow with finite rate chemistry p 3634 N94-31824

HYPERCUBE MULTIPROCESSORS
Spacecraft On-Board Information Extraction Computer (SOBIEC) p 3808 N94-32433
Development of a low-latency scalar communication routine on message-passing architectures [DE94-007061] p 3827 N94-32683
HYPERFINE STRUCTURE
Impact of observed hyperfine splitting on X-ray laser gain [DE94-005822] p 3717 N94-32128
HYPERONS
Hyperon polarization and magnetic moments [DE94-006041] p 3864 N94-31507
The Nijmegen hyperon-nucleon potentials [DE94-007557] p 3869 N94-32139
Hyperon polarization, crystal channeling, and E781 at Fermilab [DE94-008224] p 3877 N94-32802
HYPERSONIC AIRCRAFT
Hypervelocity Tunnel 9 Mach 10/14 Calibration [AD-A275960] p 3587 N94-31318
HYPERSONIC BOUNDARY LAYER
Boundary layer study on nozzle wall at hypersonic velocities p 3569 N94-31882
HYPERSONIC FLIGHT
Hypervelocity Tunnel 9 Mach 10/14 Calibration [AD-A275960] p 3587 N94-31318
HYPERSONIC FLOW
Analysis of the photodiode boundary layer transition indicator [DE94-005311] p 3701 N94-31268
Boundary layer study on nozzle wall at hypersonic velocities p 3569 N94-31882
Vibrational energy transfer of diatomic gases in hypersonic expanding flows p 3570 N94-31958
Surface boundary conditions and related technical issues concerning Burnett equations for 2-D hypersonic flow [AD-A277322] p 3706 N94-32256
Calibration and validation studies in the LENS facility [AD-A278403] p 3591 N94-33167
HYPERSONIC NOZZLES
Boundary layer study on nozzle wall at hypersonic velocities p 3569 N94-31882
HYPERSONIC SHOCK
Shock impingement near mild hypersonic expansion corners p 3569 N94-31879
HYPERSONIC SPEED
Hypervelocity Tunnel 9 Mach 10/14 Calibration [AD-A275960] p 3587 N94-31318
HYPERSONIC VEHICLES
A new inverse method for generating high-speed aerodynamic flows with application to waverider design p 3569 N94-31828
HYPERSONIC WIND TUNNELS
Boundary layer study on nozzle wall at hypersonic velocities p 3569 N94-31882
HYPERSONICS
Control of hypersonic aerodynamic forces with surface blowing p 3567 N94-31216
Hypervelocity Tunnel 9 Mach 10/14 Calibration [AD-A275960] p 3587 N94-31318
Computational radiative heat transfer in homogeneous and nonhomogeneous nonscattering media p 3702 N94-31563
A new inverse method for generating high-speed aerodynamic flows with application to waverider design p 3569 N94-31828
Vibrational energy transfer of diatomic gases in hypersonic expanding flows p 3570 N94-31958
HYPERVELOCITY IMPACT
Physical properties of glasses exposed to Earth-facing and trailing-side environments on LDEF p 3594 N94-31030
Morphology correlation of craters formed by hypervelocity impacts p 3594 N94-31031
Space hypervelocity microparticle impact damage in polymer matrix composites [ISBN-0-315-87057-5] p 3652 N94-31692
Development of high-pressure diaphragms for the AEDC impulse tunnel [AD-A277053] p 3588 N94-32009
Biospheric effects of a large extraterrestrial impact: Case study of the Cretaceous/Tertiary boundary crater [NASA-CR-195827] p 3942 N94-32740
HYPERVELOCITY LAUNCHERS
Development of high-pressure diaphragms for the AEDC impulse tunnel [AD-A277053] p 3588 N94-32009
Basic and applied studies of the ram accelerator as a hypervelocity projectile launcher [AD-A277392] p 3602 N94-32288
Design and evaluation of coils for a 50 mm diameter induction coilgun launcher [DE94-005244] p 3603 N94-32671
HYPERVELOCITY PROJECTILES
Basic and applied studies of the ram accelerator as a hypervelocity projectile launcher [AD-A277392] p 3602 N94-32288
HYPERVELOCITY WIND TUNNELS
Development of high-pressure diaphragms for the AEDC impulse tunnel [AD-A277053] p 3588 N94-32009
HYPOTHERMIA
Validation and sensitivity analysis of Texas human thermal model predictions during cold water immersion [AD-A275240] p 3797 N94-32156
HYPOTHESES
On the relationship between generalization error, hypothesis complexity, and sample complexity for radial basis functions [AD-A276802] p 3851 N94-32142
Varying execution discipline to increase performance [DE94-007844] p 3819 N94-32651
HYPSOMETERS
Study of subpolar glaciers of Spitzbergen using SPOT, ERS-1, and hypsometric data: Results and perspectives p 3753 N94-32553
HYSTERESIS
Element-specific magnetic hysteresis measurements, a new application of circularly polarized soft x-rays [DE94-007122] p 3858 N94-31397
The ferroelectric behavior of odd-numbered nylons [AD-A278126] p 3663 N94-33058

I

ICE
Satellite radar altimetry over the continental ice sheets p 3742 N94-31570
Microwave sensor for ice detection p 3583 N94-32457
Surface probes of porous toluene/water ices: Adsorption kinetics and annealing spectra measured by second harmonic generation [DE94-007564] p 3637 N94-32743
The distribution of Martian ground ice at other epochs p 3948 N94-33218
Temporal changes in the geographic distribution, elevation, and potential origin of the Martian outflow channels p 3951 N94-33235
ICE FLOES
Modeling of fracture and damage in quasibrittle materials p 3734 N94-31479
ICE FORMATION
Development of a three-dimensional icing model for predicting ice accretion on aircraft [ONERA-NT-1993-5] p 3574 N94-31230
Continuous measurement of aircraft wing icing p 3576 N94-32454
The distribution of Martian ground ice at other epochs p 3948 N94-33218
ICE PREVENTION
Aircraft icing handbook (update) [AD-A276499] p 3574 N94-31678
WHIPICE — computer program for analysis of aircraft deicing [NASA-TM-109749] p 3574 N94-31803
IDEAL FLUIDS
Stability and instability criteria for magnetohydrodynamics [PB94-148475] p 3889 N94-31772
IDENTIFYING
Particle identification in a segmented calorimeter (NUMASS test data, September 1991) [USIP-93-08] p 3711 N94-31085
IGNEOUS ROCKS
Evidence for ultramafic lavas on Syrtis Major p 3950 N94-33229
IGNITERS
A low cost igniter utilizing an SCB and titanium sub-hydride potassium perchlorate pyrotechnic [DE94-006467] p 3666 N94-31827
IGNITION
Ignition studies in nonpremixed hydrogen/air combustion [AD-A275954] p 3632 N94-31348
IGNITION SYSTEMS
Laser Diode Ignition (LDI) [DE94-006590] p 3666 N94-31579
IGNITRONS
High-power microwave-tube transmitters [DE94-005340] p 3686 N94-31150
High power switch design for the Nova upgrade laser (Project HERCULES: High Energy Research Concerning the Ultimate Lifetime of Experimental Switches) [DE94-007921] p 3719 N94-32654
ILLUMINANCE
The properties of sunflecks in a flexible plant canopy, and their relationship to turbulence p 3782 N94-31775
ILLUMINATING
Evaluation for the development of taxiway lighting intensity standards [AD-A276706] p 3588 N94-32120
Evaluation of intensity distribution profiles for US. Army rotorcraft position lighting adapted for image intensifier operations [AD-A276459] p 3804 N94-32171
Optical processing for semiconductor device fabrication p 3885 N94-32445
Temporal and spatial mapping of atmospheric dust opacity and surface albedo on Mars p 3947 N94-33211
IMAGE ANALYSIS
Computing the precision of localization in a plane using projective invariants [TELECOM-93-D-005] p 3840 N94-31095
Tracking roads in an aerial image by Kalman filtering [TELECOM-93-D-007] p 3711 N94-31096
Automatic extraction of cartographic objects by fusion of data extracted from satellite images [TELECOM-93-E-001] p 3742 N94-31165
Camera-space manipulation with natural visual information p 3829 N94-31207
Feature discovery in gray level imagery for one-class object recognition [DE94-005268] p 3671 N94-31267
Analytical applications of scanning tunneling microscopy [AD-A276066] p 3711 N94-31283
Radar image classification by texture measurements [ONERA-NT-1993-3] p 3673 N94-31419
Volumetric modelling of three dimensional scenes by octree decomposition of geometric models [ISBN-0-315-86866-X] p 3814 N94-31728
Safe navigation and active vision for autonomous vehicles: A purposive and direct solution p 3832 N94-31842
Feasibility evaluation of new data interpretation approaches for vegetation analysis from airborne imaging spectroscopy p 3745 N94-31862
The use of ERS-1 within an operational ice monitoring program p 3751 N94-32545
PSIDD: A Post-Scan Interactive Data Display system for ultrasonic scans [NASA-TM-4545] p 3732 N94-33038
IMAGE CLASSIFICATION
A neuron network for image classification: From algorithm to implantation [TELECOM-93-E-005] p 3687 N94-31168
Filtering and recognition of moving boats in radar images [REPT-93-039] p 3671 N94-31190
Radar image classification by texture measurements [ONERA-NT-1993-3] p 3673 N94-31419
Evaluation of GER- and FLI-data with reference to forest p 3746 N94-31868
A differential theory of learning for efficient statistical pattern recognition [AD-A277313] p 3800 N94-32277
An intelligent interactive visual database management system for Space Shuttle closeout image management p 3923 N94-32469
Monitoring land cover and crop types in Denmark using ERS-1 SAR and optical satellite images p 3748 N94-32528
SPOT imagery for updating land cover information of 1:50,000 numerical topographic maps p 3749 N94-32532
Assessment of region-based methods for automated SAR/optical registration, attribute extraction, and classification p 3750 N94-32536
Robust multisource classification method using the Markov random field methods p 3750 N94-32537
Technique of ERS-1 image processing in association with SPOT data p 3750 N94-32538
Airborne SAR as a complement to SPOT HRV in land-cover classification: The use of normalization and principal components analysis p 3750 N94-32539
Land cover change detection with ERS-1 data and data from other remote sensing satellites. Example: The delta of the River Ebro (Spain) p 3755 N94-32564
Statistical analysis and mapping of cotton and food crop cultivation surfaces in the west of Burkina Faso: Contribution of combined SPOT P and XS data p 3757 N94-32575
TRMM-related research: Tropical rainfall and energy analysis experiment [NASA-CR-195834] p 3787 N94-33288

IMAGE ENHANCEMENT
Digital image profilers for detecting faint sources which have bright companions
[NASA-CR-191348] p 3927 N94-32695
Theory and application of image enhancement
[AD-A277896] p 3821 N94-33031
IMAGE FILTERS
Filtering and recognition of moving boats in radar images
[REPT-93-039] p 3671 N94-31190
Morphological directional coding of images
[ISBN-0-315-86336-6] p 3814 N94-31715
IMAGE INTENSIFIERS
Variable-resolution imagery for flight simulation
[AD-A276199] p 3586 N94-31058
Evaluation of intensity distribution profiles for US. Army rotorcraft position lighting adapted for image intensifier operations
[AD-A276459] p 3804 N94-32171
IMAGE PROCESSING
Phase unwrapping problems in ISAR images
[TELECOM-93-D-008] p 3670 N94-31097
Entropy, information (and image), part 1
[TELECOM-93-D-009] p 3910 N94-31098
Regular wavelets: Application to fixed image compression
[TELECOM-93-E-004] p 3858 N94-31167
Interactive reconstruction of anatomical structures with free-form surfaces
[TELECOM-93-E-002] p 3794 N94-31195
Feature discovery in gray level imagery for one-class object recognition
[DE94-005268] p 3671 N94-31267
Hydrogenated amorphous silicon (a-Si:H) based gamma camera: Monte Carlo simulations
[DE94-007042] p 3795 N94-31323
Imaging AMS
[DE94-006662] p 3632 N94-31349
Concurrent architectures for VLSI signal and image processing
[AD-A276124] p 3688 N94-31445
Optical and image transmission through desert atmospheres
[AD-A276022] p 3742 N94-31496
Ultrasonic tomography in fiber-reinforced composite materials p 3620 N94-31565
Optimal detector strategies for the phase contrast imaging for scanning transmission electron microscopes
[ETN-94-95747] p 3866 N94-31613
Morphological directional coding of images
[ISBN-0-315-86336-6] p 3814 N94-31715
Linearly separable stack-like architecture for the design of weighted order statistic filters with application in image processing
[ISBN-0-315-87284-5] p 3675 N94-31731
Algorithms and parallel architectures for laser acoustic imaging
[ISBN-0-315-86466-4] p 3716 N94-31797
Texture library for 3-dimensional visualization systems
[AD-A276125] p 3917 N94-31829
Possibilities of GER data for soil surface characteristics in the Almaden area p 3744 N94-31859
A paraperspective factorization method for shape and motion recovery
[AD-A276513] p 3712 N94-31929
Alternatives to hierarchical techniques in stereo correlation
[AD-A276570] p 3746 N94-31938
Robot motion vision by fixation p 3833 N94-31991
High performance hardware and software for pattern recognition and image processing
[AD-A276405] p 3816 N94-32130
Algebraic functions for recognition
[AD-A276803] p 3846 N94-32167
Optical flow from 1D correlation: Application to a simple time-to-crash detector
[AD-A276777] p 3880 N94-32186
Real time character recognition for F-111C video tape records
[AD-A277061] p 3580 N94-32263
Neural models of spatial orientation in novel environments
[AD-A277383] p 3835 N94-32340
A visual detection model for DCT coefficient quantization p 3850 N94-32467
From Optics to Radar, SPOT and ERS Applications
[ISBN-2-85428-345-7] p 3747 N94-32523
Contribution of SAR ERS1 data to study the French Guiana tropical coast environment
[BRGM-93034] p 3748 N94-32527
The contribution of satellite data in communication infrastructure projects p 3749 N94-32530
Restoration of interferometric, polarimetric, radiometric, and textural information in SAR images p 3750 N94-32535
Technique of ERS-1 image processing in association with SPOT data p 3750 N94-32538
Production of terrain data: Optical radar complementarity p 3750 N94-32540
SAR image feature extraction system: A pre-operational application of ERS-1 SAR p 3751 N94-32543
Optimal geological data extraction from SPOT-radar synergism with samples from Djebel Amour (Algeria), Red Sea Hills (Sudan), Sirte Basin (Libya), and Magdalena Valley (Colombia) p 3752 N94-32548
The processing technology and some applications of Almaz-1 data p 3756 N94-32573
Ultra wide band radar holographic imaging of subsurface targets
[DE94-004271] p 3713 N94-32681
VLSI for high-speed digital signal processing
[AD-A277617] p 3697 N94-32957
High frequency active auroral research program (HAARP) imager
[AD-A277469] p 3775 N94-32999
Theory and application of image enhancement
[AD-A277896] p 3821 N94-33031
Fast nonsupervised 3D registration of PET and MR images of the brain
[TELECOM-93-C-006] p 3798 N94-33069
Global color views of Mars p 3948 N94-33217
IMAGE RECONSTRUCTION
Interactive reconstruction of anatomical structures with free-form surfaces
[TELECOM-93-E-002] p 3794 N94-31195
Ultrasonic tomography in fiber-reinforced composite materials p 3620 N94-31565
Stereoscopic correspondence based on the structure of shading
[ISBN-0-315-86418-4] p 3814 N94-31718
Volumetric modelling of three dimensional scenes by octree decomposition of geometric models
[ISBN-0-315-86866-X] p 3814 N94-31728
Linearly separable stack-like architecture for the design of weighted order statistic filters with application in image processing
[ISBN-0-315-87284-5] p 3675 N94-31731
A neural network model for the visual perception of the depth of a scene from stereoscopy and shading
[ISBN-0-315-86753-1] p 3831 N94-31750
IMAGE RESOLUTION
Incoherent imaging by Z-contrast stem: Towards 1 Angstrom resolution
[DE94-006551] p 3896 N94-31489
Regional sedimentological variations among dark crater floor features: Toward a model for modern eolian sand distribution on Mars p 3946 N94-33203
IMAGERY
Variable-resolution imagery for flight simulation
[AD-A276199] p 3586 N94-31058
Visual evaluation of computer-generated textures
[AD-A277201] p 3816 N94-32093
IMAGING RADAR
The development and testing of a backscatter absorption gas imaging (BAGI) system designed to image at a range of 300 m
[DE94-006192] p 3675 N94-31761
Comparing SPOT and SIR A for mapping superficial formations in tropical forest regions: Example of the Yaoundy Region (Cameroon) p 3755 N94-32562
ERS-1 SAR and optical data for land use/land cover mapping: A case study in a savannah zone of Guinea p 3755 N94-32565
IMAGING SPECTROMETERS
European Imaging Spectroscopy Aircraft Campaign
[ESA-SP-360] p 3743 N94-31853
The European Imaging Spectroscopy Airborne Campaign (EISAC). Data takes and evaluation programme: An overview p 3743 N94-31854
Ground based radiometric and atmospheric measurements p 3744 N94-31855
NORSMAP 1989: Norwegian remote sensing spectroscopy for mapping and monitoring or algal blooms and pollution p 3744 N94-31856
Analysis of GER imaging spectrometry data for the identification of soil and vegetation parameters in land degradation studies p 3744 N94-31857
Inflight calibration, preprocessing, and data evaluation of GER 2 imaging spectrometry data p 3744 N94-31858
Possibilities of GER data for soil surface characteristics in the Almaden area p 3744 N94-31859
The effects of vegetation on the ability to map soils using GERIS data p 3744 N94-31860
Investigation on correction models for airborne imaging spectrometry data from the EISAC-campaign for geoscientific purposes p 3745 N94-31861
Feasibility evaluation of new data interpretation approaches for vegetation analysis from airborne imaging spectroscopy p 3745 N94-31862
Monitoring fertilizer application by imaging spectrometry (Somerset Levels test site) p 3745 N94-31863
High resolution spectroscopy in agriculture: Results of the EISAC 1989 campaign p 3745 N94-31864
Extraction of agricultural parameters from imaging-spectrometry data and simulated MERIS data through red edge analysis p 3745 N94-31865
Evaluation of Fluorescence Line Imager (FLI) airborne imaging spectrometer data for roadside tree damage assessment p 3745 N94-31866
Extraction of forests stand age parameters from airborne imaging spectroscopy data p 3745 N94-31867
Evaluation of GER- and FLI-data with reference to forest p 3746 N94-31868
Earth observational research using multistage EOS-like data
[NASA-CR-195833] p 3757 N94-33019
MODIS. Volume 2: MODIS level 1 geolocation, characterization and calibration algorithm theoretical basis document, version 1
[NASA-TM-104594-VOL-2] p 3613 N94-33289
IMAGING TECHNIQUES
Studying transient mobility and energy loss using scanning tunneling microscopy
[AD-A276292] p 3877 N94-31256
New and emerging techniques for imaging surfaces
[AD-A276497] p 3878 N94-31262
Hydrogenated amorphous silicon (a-Si:H) based gamma camera: Monte Carlo simulations
[DE94-007042] p 3795 N94-31323
Imaging AMS
[DE94-006662] p 3632 N94-31349
Incoherent imaging by Z-contrast stem: Towards 1 Angstrom resolution
[DE94-006551] p 3896 N94-31489
Ultrasonic tomography in fiber-reinforced composite materials p 3620 N94-31565
Soot and liquid-phase fuel distributions in a newly designed optically accessible DI diesel engine
[DE94-005648] p 3723 N94-31651
The development and testing of a backscatter absorption gas imaging (BAGI) system designed to image at a range of 300 m
[DE94-006192] p 3675 N94-31761
Millimeter wave, high-resolution, holographic surveillance system
[DE94-004289] p 3712 N94-31831
Elastic modulus measurements of LDEF glasses and glass-ceramics using a speckle technique
[NASA-CR-195911] p 3653 N94-31851
A multi-frequency study of an x ray selected sample of active galactic nuclei p 3937 N94-31987
Robot motion vision by fixation p 3833 N94-31991
Night vision camcorder system
[AD-A277004] p 3712 N94-32002
Novel failure analysis techniques using photon probing with a scanning optical microscope
[DE94-006594] p 3692 N94-32112
Design and early results of the sodium-layer laser guide star adaptive optics experiment at the Lawrence Livermore National Laboratory
[DE94-006653] p 3926 N94-32189
Ocean optics, ocean imaging and optical tomography
[AD-A277010] p 3789 N94-32402
A versatile nondestructive evaluation imaging workstation p 3732 N94-32458
A new high-speed IR camera system p 3713 N94-32459
X ray imaging and x ray source development at Lawrence Livermore National Laboratory
[DE94-007077] p 3719 N94-32629
Dual-band infrared imaging to detect corrosion damage within airframes and concrete structures
[DE94-006047] p 3580 N94-32658
Ultra wide band radar holographic imaging of subsurface targets
[DE94-004271] p 3713 N94-32681
Digital image profilers for detecting faint sources which have bright companions
[NASA-CR-191348] p 3927 N94-32695
An electrical test system for conductor formation process analysis
[DE94-007291] p 3696 N94-32786
Imaging of surface structure with energy-dependent photoelectron diffraction
[DE94-009096] p 3907 N94-32934
High frequency active auroral research program (HAARP) imager
[AD-A277469] p 3775 N94-32999
Earth observational research using multistage EOS-like data
[NASA-CR-195833] p 3757 N94-33019
Fast nonsupervised 3D registration of PET and MR images of the brain
[TELECOM-93-C-006] p 3798 N94-33069

Synthetic vision technology demonstration. Volume 1: Executive summary
[DOT/FAA/RD-93/40-VOL-1] p 3582 N94-33076
Synthetic vision technology demonstration. Volume 2: Sensor tower testing
[DOT/FAA/RD-93/40-VOL-2] p 3582 N94-33077
Synthetic vision technology demonstration. Volume 3: Flight tests
[DOT/FAA/RD-93/40-VOL-3] p 3582 N94-33078
Synthetic vision technology demonstration. Volume 4: Appendices
[DOT/FAA/RD-93/40-VOL-4] p 3583 N94-33079
Scalar imaging velocimetry studies of turbulent flow structure and dynamics
[AD-A278395] p 3710 N94-33164
Nanoscale structural changes upon electrooxidation of Au(111) as probed by potentiodynamic scanning tunneling microscopy
[AD-A276780] p 3909 N94-33275
Simplified ultra-high resolution optic for soft x ray imaging
[AD-A278424] p 3885 N94-33331

IMPACT DAMAGE
Physical properties of glasses exposed to Earth-facing and trailing-side environments on LDEF p 3594 N94-31030
Morphology correlation of craters formed by hypervelocity impacts p 3594 N94-31031
Micrometeoroid/space debris effects on materials p 3595 N94-31032
Space environmental effects on polymer composites: Research needs and opportunities p 3595 N94-31035
Keeping that youthful look --- impact cratering of Venus p 3941 N94-31112
Space hypervelocity microparticle impact damage in polymer matrix composites
[ISBN-0-315-87057-5] p 3652 N94-31692
Evaluating in-plane elastic constants of damaged carbon-epoxy laminates using a quantitative ultrasonic technique p 3621 N94-31793
Location of impact damage sites in composite aircraft structures, task 3.4.1
[DSIS-94-01590] p 3621 N94-31892
Low velocity impact damage in carbon fiber/PEEK composite laminates
[ISBN-0-315-86546-6] p 3622 N94-31909
Experimental measurement of dynamic failure and fragmentation properties of metals
[DE94-007377] p 3737 N94-32135
Assessment of impact damage in composite structures
[AD-A277063] p 3624 N94-32265

IMPACT LOADS
Study of wave propagation and dynamic response of laminated composite structures
[AD-A276123] p 3619 N94-31444
Point-contact and point-impact dynamics for multibody chains
[ISBN-0-315-87056-7] p 3734 N94-31737
Toughening mechanisms in the high strain rate deformation of rubber-modified polymer glasses p 3653 N94-31942
Development of high-pressure diaphragms for the AEDC impulse tunnel
[AD-A277053] p 3588 N94-32009

IMPACT MELTS
Mineralogical diversity (spectral reflectance and Moessbauer data) in compositionally similar impact melt rocks from Manicouagan Crater, Canada p 3948 N94-33219

IMPACT PREDICTION
Planetesimal dynamics in the vicinity of a growing protoplanet p 3935 N94-31926

IMPACT STRENGTH
Development of stitched/RTM composite primary structures p 3628 N94-33127

IMPACT TESTS
Determining the bearing capacity of flexible airfield pavements using a heavy weight deflectometer
[ISBN-0-315-86210-6] p 3587 N94-31710
Toughening mechanisms in the high strain rate deformation of rubber-modified polymer glasses p 3653 N94-31942
Experimental measurement of dynamic failure and fragmentation properties of metals
[DE94-007377] p 3737 N94-32135
Test and analysis results for composite transport fuselage and wing structures p 3628 N94-33129

IMPINGEMENT
Shock impingement near mild hypersonic expansion corners p 3569 N94-31879

IMPLANTED ELECTRODES (BIOLOGY)
Perspectives of glucose sensing based on a charge-modulating competition reaction
[ISBN-9-09-005754-4] p 3795 N94-31652
Neostriatal neuronal activity and behavior
[AD-A278429] p 3802 N94-33333

IMPLOSIONS
Measurement of ICF fuel ion temperature on Nova
[DE94-006150] p 3892 N94-32730

IMPULSES
Development of high-pressure diaphragms for the AEDC impulse tunnel
[AD-A277053] p 3588 N94-32009
System analysis of ultra-wideband instrumentation radars: Impulse versus stepped-chirp approaches
[AD-A276624] p 3677 N94-32087
Limiting vibration in systems with constant amplitude actuators through command preshaping
[NASA-CR-188284] p 3739 N94-32907

IMPURITIES
Indium-vacancy complexes in mercury cadmium telluride
[AD-A276177] p 3894 N94-31055
Growth and characterization of III-V semiconductors with rare earth impurities for optoelectronic devices
[AD-A276021] p 3896 N94-31455
Impurities and conductivity in a D-wave superconductor
[DE94-006222] p 3898 N94-31628
The 4f heavy fermion photoelectron spectra do not exhibit the Kondo scale
[DE94-006252] p 3898 N94-31631
Development of sample charge compensation for characterization of impurities in semiconductor materials
[AD-A277113] p 3899 N94-31983
Characterization of atomic and molecular impurity sources and transport at the tokamak edge
[DE94-007212] p 3891 N94-32619
Gettering of metal impurities by cavities in silicon
[DE94-005248] p 3645 N94-32672

IN SITU MEASUREMENT
New and emerging techniques for imaging surfaces
[AD-A276497] p 3878 N94-31262
Characterization of the corrosion resistance of duplex stainless steels using local current density mapping techniques
[DE94-007980] p 3646 N94-32699
Scanning tunneling microscopy and infrared spectroscopy as combined in-situ probes of electrochemical adlayer structure: Cyanide on Pt(111)
[AD-A276715] p 3909 N94-33274

IN-FLIGHT MONITORING
OARE flight maneuvers and calibration measurements on STS-58
[NASA-TM-109093] p 3613 N94-32924

INCLUSIONS
Correlation of flux composition and inclusion characteristics with submerged arc weld metal properties in HY-100 steel
[AD-A277040] p 3726 N94-32261
Pressureless sintering of ceramic composites
[AD-A277274] p 3657 N94-32404

INCOMPRESSIBLE FLOW
Solution of the incompressible Navier-Stokes equations in general coordinates by Krylov subspace and multigrid methods
[REPT-93-64] p 3703 N94-31660
Simulations of the creation and motion of vortex rings
[W-9319] p 3703 N94-31691
Finite element numerical simulation of turbulent flows
[ISBN-0-315-86418-8] p 3703 N94-31717
Finite element vorticity-based methods for the solution of the incompressible and compressible Navier-Stokes equations
[ISBN-0-315-87265-9] p 3703 N94-31730
Incompressible viscous flow in tubes with occlusions
[ISBN-0-315-75467-2] p 3704 N94-31778
Tip effects on the vortex wake of an axisymmetric body at angle of attack p 3570 N94-31907
Solution of the average-passage equations for the incompressible flow through multiple-blade-row turbomachinery
[AD-A276515] p 3583 N94-31931
Chemical vapor deposition fluid flow simulation modelling tool
[NASA-CR-189648] p 3707 N94-32480
Additive turbulent decomposition of the incompressible and compressible Navier-Stokes equations
[AD-A277321] p 3708 N94-32511

INCONEL (TRADEMARK)
Operation of D3-D with all-graphite walls
[DE94-004858] p 3886 N94-31304

INDENTATION
Indentability of conventional and negative Poisson's ratio foams p 3629 N94-33131

INDEXES (DOCUMENTATION)
Aeronautical engineering: A continuing bibliography with indexes (supplement 302)
[NASA-SP-7037(302)] p 3565 N94-31342
Aeronautical engineering: A continuing bibliography with indexes (supplement 303)
[NASA-SP-7037(303)] p 3565 N94-31381
Aerospace medicine and biology: A continuing bibliography with indexes (supplement 388)
[NASA-SP-7011(388)] p 3795 N94-31414
Index to NASA news releases and speeches, 1993
[NASA-TM-109722] p 3917 N94-31688
The new Metals and Alloys Indexes, search manual: A phase diagram research tool
[DE94-005371] p 3643 N94-32098
A guide to experimental elementary particle physics literature, 1988-1992
[DE94-007445] p 3873 N94-32768
Aeronautical engineering: A continuing bibliography with indexes (supplement 304)
[NASA-SP-7037(304)] p 3566 N94-32853
Research and Technology Objectives and Plans Summary (RTOPS)
[NASA-TM-105441] p 3966 N94-32885
DTIC Thesaurus on diskette (ASC2) (computer diskette)
[AD-M000309] p 3922 N94-33257

INDIAN OCEAN
Typhoon havens handbook for the western Pacific and Indian Oceans, change 3
[AD-A277030] p 3784 N94-32260

INDIAN SPACECRAFT
INSAT-2A and 2B development mechanisms p 3603 N94-33293

INDIUM
Indium-vacancy complexes in mercury cadmium telluride
[AD-A276177] p 3894 N94-31055

INDIUM GALLIUM ARSENIDES
A 1-picosecond InGaAs photodetector for operation at 1300-1600 nm
[AD-A275959] p 3895 N94-31350
High speed, strained layer, multiquantum well, GaInAsP and GaAs lasers and heterostructures
[AD-A277287] p 3719 N94-32608
Large-diameter InGaAs/AlGaAs vertical-cavity surface-emitting lasers with low threshold current density fabricated using a simple chemical etch process
[AD-A277733] p 3721 N94-33003
Characteristics of III-V semiconductor devices at high temperature
[NASA-TM-106574] p 3697 N94-33052

INDIUM PHOSPHIDES
The effects of amorphous layer regrowth on carbon activation in GaAs and InP
[DE94-006290] p 3899 N94-31634
Novel growth technologies for in situ formation of semiconductor quantum wire structures
[AD-A277188] p 3902 N94-32255
Novel optoelectronic devices based on combining GaAs and InP on Si
[AD-A277018] p 3693 N94-32301
High speed, strained layer, multiquantum well, GaInAsP and GaAs lasers and heterostructures
[AD-A277287] p 3719 N94-32608

INDUCTION
Design and evaluation of coils for a 50 mm diameter induction coilgun launcher
[DE94-005244] p 3603 N94-32671

INDUCTION (MATHEMATICS)
Extensional realizability
[ML-93-18] p 3856 N94-31408

INDUSTRIAL SAFETY
Minimization of carpal tunnel syndrome
[AD-A276409] p 3795 N94-31363
Systems for the monitoring of working conditions relating to health and safety: Extensive description. Norway
[PB94-138542] p 3803 N94-31839

INDUSTRIES
Piezoelectric materials research in Europe
[AD-A276207] p 3648 N94-31059
Europe at the crossroads: The future of its satellite communications industry
[ESA-SP-1166] p 3670 N94-31182
Active matrix liquid crystal display. Industry survey results
[AD-A276415] p 3895 N94-31329
Satellite communications industry
[AD-A276685] p 3610 N94-32039
Strategies for survival in the new environmental era
[AD-A276827] p 3765 N94-32195
Sandia technology engineering and science accomplishments
[DE94-008312] p 3668 N94-32412
Biomass power industry: Assessment of key players and approaches for DOE and industry interaction
[DE94-000238] p 3761 N94-32725
LLNL casting technology
[DE94-008282] p 3669 N94-32839

INELASTIC COLLISIONS
Electron: Cluster interactions
[DE94-009089] p 3874 N94-32807
INELASTIC SCATTERING
The measurement of the hadronic energy flow and jet production with the ZEUS calorimeter in deep inelastic scattering events at HERA
[ETN-94-96021] p 3865 N94-31534
Results from the H1 experiment at HERA
[PB94-145174] p 3868 N94-32008
Strongly anisotropic s-wave versus d-wave gap in cuprate superconductors: Evidence and theory
[DE94-007579] p 3904 N94-32746
Electron: Cluster interactions
[DE94-009089] p 3874 N94-32807
Polarized lepton-nucleon scattering
[DE94-009027] p 3875 N94-33278
INERTIAL CONFINEMENT FUSION
Measurement of ICF fuel ion temperature on Nova
[DE94-006150] p 3892 N94-32730
Fusion with highly spin polarized HD and D2
[DE94-006209] p 3876 N94-32731
INERTIAL FUSION (REACTOR)
Scenarios for multi-unit inertial fusion energy plants producing hydrogen fuel
[DE94-006614] p 3666 N94-32114
INFECTIOUS DISEASES
Noninvasive spectroscopic diagnosis of superficial ocular lesions and corneal infections
[DE94-006231] p 3797 N94-32732
INFERENCE
Completeness and decidability of the mixed style of inference with composition
[LP-93-09] p 3842 N94-31453
Weaks vs. strong readings of donkey sentences and monotonicity inference in a dynamic setting
[LP-93-10] p 3856 N94-31468
Statistical inference for coherent systems from partial information and in resampling techniques in survival analysis
[AD-A277382] p 3852 N94-32339
A simulation of uncertain reasoning on parametric databases using data-dependency derived inference nets p 3919 N94-32499
Reading: Interaction with memory
[AD-A277547] p 3801 N94-32956
INFILTRATION
Improved oxidation resistance of 3-D carbon/carbon composites
[AD-A277349] p 3625 N94-32624
INFLUENCE COEFFICIENT
Design and initial testing of a facility to measure unsteady pressures on an oscillating cascade with supersonic leading edge locus p 3569 N94-31880
INFORMATION
On a formal approach to the methodology of information planning
[MEMO-INF-93-42] p 3917 N94-31415
Control of a random walk with noisy delayed information
[CWI-BS-R9316] p 3846 N94-32108
INFORMATION DISSEMINATION
LDEF materials special investigation group's data bases p 3596 N94-31038
An innovative approach to space education p 3600 N94-31436
Information resources for US Department of Energy pollution prevention programs
[DE94-006677] p 3783 N94-31582
Technology 2003: The Fourth National Technology Transfer Conference and Exposition, volume 2
[NASA-CP-3249] p 3956 N94-32420
Using the National Information Infrastructure for social science, education, and informed decision making
[DE94-005442] p 3920 N94-32676
Multimedia as a desktop and classroom tool
[DE94-009118] p 3807 N94-32766
Information systems to enhance technology exchange
[DE94-007744] p 3920 N94-32808
NASA/DOD Aerospace Knowledge Diffusion Research Project. Paper 5: Aerospace librarians and technical information specialists as information intermediaries: A report of phase 2 activities of the NASA/DOD Aerospace Knowledge Diffusion Research Project
[NASA-TM-109777] p 3921 N94-32829
NASA/DOD Aerospace Knowledge Diffusion Research Project. Paper 6: Aerospace knowledge diffusion in the academic community: A report of phase 3 activities of the NASA/DOD Aerospace Knowledge Diffusion Research Project
[NASA-TM-109771] p 3921 N94-32830
NASA/DOD Aerospace Knowledge Diffusion Research Project. Paper 10: The NASA/DOD Aerospace Knowledge Diffusion Research Project
[NASA-TM-109769] p 3921 N94-32831
NASA/DOD Aerospace Knowledge Diffusion Research Project. Paper 12: The diffusion of federally funded aerospace research and development (R/D) and the information seeking behavior of US aerospace engineers and scientists
[NASA-TM-109404] p 3921 N94-32832
NASA/DOD Aerospace Knowledge Diffusion Research Project. Paper 18: Scientific and Technical Information (STI) policy and the competitive position of the US aerospace industry
[NASA-TM-109782] p 3921 N94-32833
NASA/DOD Aerospace Knowledge Diffusion Research Project. Paper 11: The voice of the user: How US aerospace engineers and scientists view DOD technical reports
[NASA-TM-109348] p 3921 N94-32834
NASA/DOD Aerospace Knowledge Diffusion Research Project. Paper 1: The value of scientific and technical information (STI), its relationship to Research and Development (R/D), and its use by US aerospace engineers and scientists
[NASA-TM-109774] p 3922 N94-32835
NASA/DOD Aerospace Knowledge Diffusion Research Project. Report 25: The technical communications practices of British aerospace engineers and scientists: Results of the phase 4 RAeS mail survey
[NASA-TM-109098] p 3922 N94-32836
NASA/DOD Aerospace Knowledge Diffusion Research Project. Report 24: The technical communications practices of US aerospace engineers and scientists: Results of the phase 1 SAE mail survey
[NASA-TM-109088] p 3922 N94-32837
Opinion polls and the US civil space program
[NASA-TM-109700] p 3914 N94-33066
INFORMATION MANAGEMENT
Acquisition information management system telecommunication site survey results
[DE94-005688] p 3915 N94-31155
DoD information systems capacity management function
[AD-A275987] p 3916 N94-31355
Detecting the erosion of hierarchic information structures
[RUU-CS-93-10] p 3916 N94-31365
On a formal approach to the methodology of information planning
[MEMO-INF-93-42] p 3917 N94-31415
Information resources for US Department of Energy pollution prevention programs
[DE94-006677] p 3783 N94-31582
The Global Climatology Network precipitation data
[DE93-019199] p 3764 N94-31596
Application of Artificial Intelligence to the DoD Corporate Information Management (CIM) program
[AD-A276656] p 3834 N94-32061
Lifting the fog of corporate information management
[AD-A276680] p 3918 N94-32090
CIM in space: Corporate Information Management (CIM) implications for space-based information systems
[AD-A276882] p 3600 N94-32126
Untying the gordian data knot. A paper on Information Engineering (IE) and Corporate Information Management (CIM)
[AD-A276662] p 3918 N94-32210
Automated mainframe data collection in a network environment p 3923 N94-32443
Management of uncertainty in knowledge-based systems: A military perspective p 3854 N94-33341
INFORMATION PROCESSING (BIOLOGY)
Sensory sensitivities and discriminations and their roles in aviation
[AD-A277312] p 3800 N94-32276
Reading: Interaction with memory
[AD-A277547] p 3801 N94-32956
Workshop on Visual Perception: Computation and Psychophysics
[AD-A278412] p 3802 N94-33326
INFORMATION RETRIEVAL
An analysis of instruction-cached SIMD computer architecture
[AD-A276519] p 3806 N94-31934
High-speed data search p 3923 N94-32441
Database tomography for commercial application p 3923 N94-32442
Automated mainframe data collection in a network environment p 3923 N94-32443
An intelligent interactive visual database management system for Space Shuttle closeout image management p 3923 N94-32469
Relationships between access and use in information systems: Remote access to and browsing of online catalogs p 3919 N94-32488
A simulation of uncertain reasoning on parametric databases using data-dependency derived inference nets p 3919 N94-32499
Information disclosure in evolving information systems: Taking a shot at a moving target
[TR-93-22] p 3919 N94-32506
DTIC Thesaurus on diskette with dBase 4.1 runtime (computer diskette)
[AD-M000306] p 3922 N94-33256
DTIC Thesaurus on diskette (ASC2) (computer diskette)
[AD-M000309] p 3922 N94-33257
DTIC Thesaurus on diskette without runtime (computer diskette)
[AD-M000310] p 3923 N94-33258
DTIC Thesaurus on diskette without runtime (computer diskette)
[AD-M000312] p 3923 N94-33259
INFORMATION SYSTEMS
Discovery systems for manufacturing
[AD-A276216] p 3828 N94-31061
Acquisition information management system telecommunication site survey results
[DE94-005688] p 3915 N94-31155
A generic model for data acquisition: Connectionist methods of information processing
[TELECOM-93-E-003] p 3730 N94-31166
Putting the information infrastructure to work: Report of the Information Infrastructure Task Force Committee on Applications and Technology
[NIST/SP-857] p 3916 N94-31228
Covert channel analysis of trusted systems. A guide to understanding
[AD-A276418] p 3916 N94-31331
DoD information systems capacity management function
[AD-A275987] p 3916 N94-31355
On a formal approach to the methodology of information planning
[MEMO-INF-93-42] p 3917 N94-31415
Effective information modelling support
[PB94-148236] p 3917 N94-31586
Hydrologic Database user's manual
[DE94-003950] p 3743 N94-31603
On the validity of the BLP model
[REPT-93-70] p 3917 N94-31640
Current Research Information in Europe: Conference proceedings
[PB94-127933] p 3917 N94-31768
Systems for the monitoring of working conditions relating to health and safety: Extensive description. Norway
[PB94-138542] p 3803 N94-31839
The FELICIA bulletin board system and the IRBIS anonymous FTP server: Computer security information sources for the DOE community
[DE94-008219] p 3825 N94-31920
CIM in space: Corporate Information Management (CIM) implications for space-based information systems
[AD-A276882] p 3600 N94-32126
CMS Distribution Subsystem user's guide
[DE94-005328] p 3816 N94-32146
Untying the gordian data knot. A paper on Information Engineering (IE) and Corporate Information Management (CIM)
[AD-A276662] p 3918 N94-32210
Human Computer Interface Specifications (HCIS) for the Integrated Maintenance Information System (IMIS)
[AD-A277184] p 3566 N94-32254
An information system organized as stratified hypermedia
[TR-93-12] p 3918 N94-32289
EVORM: A conceptual modelling technique for evolving application domains
[TR-93-16] p 3918 N94-32290
Sandia technology engineering and science accomplishments
[DE94-008312] p 3668 N94-32412
A hypertext system that learns from user feedback p 3923 N94-32428
The relationship between integrative task design for information systems professionals and perceived information systems effectiveness p 3919 N94-32487
A simulation of uncertain reasoning on parametric databases using data-dependency derived inference nets p 3919 N94-32499
Information disclosure in evolving information systems: Taking a shot at a moving target
[TR-93-22] p 3919 N94-32506
Multidimensional scaling of user information satisfaction
[AD-A277230] p 3920 N94-32633
Using the National Information Infrastructure for social science, education, and informed decision making
[DE94-005442] p 3920 N94-32676
Information systems to enhance technology exchange
[DE94-007744] p 3920 N94-32808

NASA/DOD Aerospace Knowledge Diffusion Research Project. Paper 6: Aerospace knowledge diffusion in the academic community: A report of phase 3 activities of the NASA/DOD Aerospace Knowledge Diffusion Research Project
[NASA-TM-109771] p 3921 N94-32830

INFORMATION THEORY
Entropy, information (and image), part 1
[TELECOM-93-D-009] p 3910 N94-31098
Information acquisition from multi-agent resources; abstract
[LP-93-08] p 3917 N94-31452
Information theory for arm visuo-motor coordination p 3800 N94-32495
Molecular Science Research Center
[DE94-007464] p 3871 N94-32605
Ethics and rationality in information-enriched decisions: A model for technical communication
[DE93-040251] p 3681 N94-32679
Reliable communication in the presence of severe noise or jamming
[AD-A278410] p 3684 N94-33173
A theory of conditional information with applications
[AD-A278164] p 3850 N94-33255

INFORMATION TRANSFER
Satellite direct readout: Opportunities for science education
[AD-A276257] p 3609 N94-31292
Analysis of the effect of routing strategies for parallel implementations of a selected avionics application
[AD-A276069] p 3581 N94-31458
Automated mainframe data collection in a network environment p 3923 N94-32443
NASA/DOD Aerospace Knowledge Diffusion Research Project. Paper 5: Aerospace librarians and technical information specialists as information intermediaries: A report of phase 2 activities of the NASA/DOD Aerospace Knowledge Diffusion Research Project
[NASA-TM-109777] p 3921 N94-32829
NASA/DOD Aerospace Knowledge Diffusion Research Project. Paper 10: The NASA/DOD Aerospace Knowledge Diffusion Research Project
[NASA-TM-109769] p 3921 N94-32831
NASA/DOD Aerospace Knowledge Diffusion Research Project. Paper 12: The diffusion of federally funded aerospace research and development (R/D) and the information seeking behavior of US aerospace engineers and scientists
[NASA-TM-109404] p 3921 N94-32832
NASA/DOD Aerospace Knowledge Diffusion Research Project. Paper 11: The voice of the user: How US aerospace engineers and scientists view DOD technical reports
[NASA-TM-109348] p 3921 N94-32834
NASA/DOD Aerospace Knowledge Diffusion Research Project. Paper 1: The value of scientific and technical information (STI), its relationship to Research and Development (R/D), and its use by US aerospace engineers and scientists
[NASA-TM-109774] p 3922 N94-32835
NASA/DOD Aerospace Knowledge Diffusion Research Project. Report 25: The technical communications practices of British aerospace engineers and scientists: Results of the phase 4 RAeS mail survey
[NASA-TM-109098] p 3922 N94-32836
NASA/DOD Aerospace Knowledge Diffusion Research Project. Report 24: The technical communications practices of US aerospace engineers and scientists: Results of the phase 1 SAE mail survey
[NASA-TM-109088] p 3922 N94-32837

INFRARED ABSORPTION
Time-resolved infrared absorption studies applied to the study of radical plus molecule reactions
[DE94-005921] p 3863 N94-31202
Infrared and near infrared transient absorption spectroscopy of molecular free radicals
[DE94-005446] p 3632 N94-31305
Stability and precipitation kinetics in Si(1-y)C(y)/Si and Si(1-x-y)Ge(x)C(y)/Si heterostructures prepared by solid phase epitaxy
[DE94-006589] p 3902 N94-32296

INFRARED ASTRONOMY
Multiwavelength search for protoplanetary disks p 3599 N94-31430
Near infrared surveys of high mass star forming regions p 3925 N94-31898
Near and far infrared observations of protostars and dark clouds p 3926 N94-31969
High precision moving magnet chopper for variable operation conditions p 3605 N94-33307

INFRARED ASTRONOMY SATELLITE
Multiwavelength search for protoplanetary disks p 3599 N94-31430
Vibrational spectroscopy at metal-solution interfaces: Some perspectives and prospects for electrochemical surface science
[AD-A276781] p 3644 N94-32169

INFRARED DETECTORS
Chamber optics for testing passive remote sensing vapor detectors
[AD-A275909] p 3878 N94-31340
A 1-picosecond InGaAs photodetector for operation at 1300-1600 nm
[AD-A275959] p 3895 N94-31350
Remote infrared vapor detection of volatile organic compounds
[AD-A276982] p 3746 N94-31999
Advanced infrared photodetectors: Materials review
[AD-A277058] p 3879 N94-32013
Development of phase-only filters for sensor imagery
[AD-A276722] p 3880 N94-32151
Lowering the Schottky barrier at metal or silicide/Si interfaces to extend the range of infrared detectors
[AD-A277253] p 3903 N94-32322
Synthetic vision technology demonstration. Volume 1: Executive summary
[DOT/FAA/RD-93/40-VOL-1] p 3582 N94-33076
Synthetic vision technology demonstration. Volume 2: Sensor tower testing
[DOT/FAA/RD-93/40-VOL-2] p 3582 N94-33077
Synthetic vision technology demonstration. Volume 3: Flight tests
[DOT/FAA/RD-93/40-VOL-3] p 3582 N94-33078
Synthetic vision technology demonstration. Volume 4: Appendices
[DOT/FAA/RD-93/40-VOL-4] p 3583 N94-33079
Research in the optical sciences
[AD-A278271] p 3884 N94-33140
Proceedings SPIE: Conference Digest, volume 2104
[AD-A278107] p 3884 N94-33187

INFRARED FILTERS
Wavelet transform of fixed pattern noise in focal plane arrays
[AD-A276963] p 3712 N94-32393

INFRARED IMAGERY
Development of phase-only filters for sensor imagery
[AD-A276722] p 3880 N94-32151
Dual-band infrared imaging to detect corrosion damage within airframes and concrete structures
[DE94-006047] p 3580 N94-32658

INFRARED INSTRUMENTS
A new high-speed IR camera system p 3713 N94-32459

INFRARED LASERS
New material for high average power infrared generation: OPM-DB GaAs
[AD-A276389] p 3714 N94-31358
Methods for SBS threshold reduction
[AD-A276554] p 3717 N94-31936
Metal-ion spin-on glasses: Novel materials for active waveguides
[DE94-007738] p 3882 N94-32649

INFRARED RADAR
Synergy of thermal infrared and microwave remote sensing for evaporation estimation p 3754 N94-32559

INFRARED RADIATION
Infrared and near infrared transient absorption spectroscopy of molecular free radicals
[DE94-005446] p 3632 N94-31305
Free electrons as a versatile source of coherent radiation
[ETN-94-96011] p 3715 N94-31545
Advanced infrared photodetectors: Materials review
[AD-A277058] p 3879 N94-32013
The manifestations of energetic activity in the galactic center p 3937 N94-32028
Sensitivity analysis of the AVHRR infrared cirrus model
[AD-A276690] p 3784 N94-32117
Wavelet transform of fixed pattern noise in focal plane arrays
[AD-A276963] p 3712 N94-32393
A noncritically phase matched femtosecond optical parametric oscillator near 3 microns
[DE94-008050] p 3720 N94-32704
Microreflectance infrared study of electron-molecular vibrational coupling and lattice softness in BEDT-TTF salts
[DE94-008490] p 3907 N94-32989
Laser and Fourier transform spectroscopy of novel propellant molecules
[AD-A277506] p 3667 N94-33013
Quantum well infrared photodetector FPA
[AD-A278010] p 3908 N94-33248

INFRARED REFLECTION
Determination of BPSG thin-film properties using IR reflection spectroscopy of product wafers
[DE94-006591] p 3634 N94-32110

INFRARED SPECTRA
Infrared spectroelectrochemical study of cyanide adsorption and reactions at platinum electrodes in aqueous perchlorate electrolyte
[AD-A276402] p 3631 N94-31238
Infrared and near infrared transient absorption spectroscopy of molecular free radicals
[DE94-005446] p 3632 N94-31305
Nucleation and growth of cubic boron nitride films produced by ion-assisted pulsed laser deposition
[DE94-007295] p 3661 N94-32796
Structural studies of photoinduced intramolecular electron transfer in cyclopentadienylnickelnitrosyl
[DE94-008467] p 3874 N94-32876
Microreflectance infrared study of electron-molecular vibrational coupling and lattice softness in BEDT-TTF salts
[DE94-008490] p 3907 N94-32989
A relaxation study of poled nonlinear optical polymers by infrared reflection-absorption spectroscopy
[AD-A277513] p 3663 N94-33054
Thermal emission measurements (5-25 microns) of Hawaiian palagonitic soils with implications for Mars p 3944 N94-33193
Mars atmospheric dust properties: A synthesis of Mariner 9, Viking, and Phobos observations p 3945 N94-33200

INFRARED SPECTROSCOPY
Infrared and near infrared transient absorption spectroscopy of molecular free radicals
[DE94-005446] p 3632 N94-31305
Combustion-related studies using weakly-bonded complexes
[DE94-006632] p 3633 N94-31493
Free electrons as a versatile source of coherent radiation
[ETN-94-96011] p 3715 N94-31545
Near and far infrared observations of protostars and dark clouds p 3926 N94-31969
The adsorption of sulfate on gold(111) in acidic aqueous media: Adlayer structural inferences from infrared spectroscopy and scanning tunneling microscopy
[AD-A276643] p 3642 N94-31997
New molecular-based routes to binary main group metal sulfides
[AD-A277005] p 3900 N94-32003
Determination of BPSG thin-film properties using IR reflection spectroscopy of product wafers
[DE94-006591] p 3634 N94-32110
Vibrational spectroscopy at metal-solution interfaces: Some perspectives and prospects for electrochemical surface science
[AD-A276781] p 3644 N94-32169
Time-resolved IR spectroscopy, energy transfer, and state-to-state collision dynamics of atmospheric species
[AD-A277372] p 3773 N94-32338
Nucleation and growth of cubic boron nitride films produced by ion-assisted pulsed laser deposition
[DE94-007295] p 3661 N94-32796
A relaxation study of poled nonlinear optical polymers by infrared reflection-absorption spectroscopy
[AD-A277513] p 3663 N94-33054
Proceedings SPIE: Conference Digest, volume 2104
[AD-A278107] p 3884 N94-33187
Aerosols scattering and near-infrared observations of the Martian surface p 3946 N94-33204
Scanning tunneling microscopy and infrared spectroscopy as combined in-situ probes of electrochemical adlayer structure: Cyanide on Pt(111)
[AD-A276715] p 3909 N94-33274

INFRARED TELESCOPES
High precision moving magnet chopper for variable operation conditions p 3605 N94-33307

INHOMOGENEITY
Spectral inhomogeneity of the bacterial light-harvesting antennae: Causes and consequences
[ETN-94-96020] p 3792 N94-31533
Ultrasonic tomography in fiber-reinforced composite materials p 3620 N94-31565

INJURIES
THE VERTICAL p 3806 N94-32435
Controlling hazardous energy sources (lockout/tagout)
[NASA-TM-105290] p 3669 N94-32861

INLET AIRFRAME CONFIGURATIONS
Numerical simulation of combined external/internal transonic flow on the forebody/inlet of the AV-8B Harrier 2 p 3569 N94-31759
Installed F/A-18 inlet flow calculations at 30 degrees angle-of-attack: A comparative study
[NASA-CR-195297] p 3573 N94-33119

INLET FLOW
Numerical simulation of combined external/internal transonic flow on the forebody/inlet of the AV-8B Harrier 2 p 3569 N94-31759

Design of a two dimensional planer pressurized air labyrinth seal test rig
[AD-A277232] p 3726 N94-32370
Inlet distortion in engines on VSTOL aircraft
[NASA-CR-195841] p 3584 N94-33035
Installed F/A-18 inlet flow calculations at 30 degrees angle-of-attack: A comparative study
[NASA-CR-195297] p 3573 N94-33119

INLET PRESSURE
Design of a two dimensional planer pressurized air labyrinth seal test rig
[AD-A277232] p 3726 N94-32370

INORGANIC COMPOUNDS
Modification of semiconductor surface properties with chemically bound molecular films
[AD-A276162] p 3695 N94-31081

INPUT/OUTPUT ROUTINES
A redundant disk array architecture for efficient small writes
[AD-A276645] p 3815 N94-31940

INSOLATION
Modeling the interaction between solar radiation and terrestrial surfaces p 3779 N94-30999
Solar resource: Utility load-matching assessment
[DE94-000297] p 3758 N94-31264
Users manual for SERI QC software assessing the quality of solar radiation data
[DE93-018210] p 3953 N94-31491
Concentration system performance degradation in the aftermath of Mount Pinatubo
[DE94-001879] p 3764 N94-31602
Obliquity variation in a Mars climate evolution model p 3951 N94-33236
Simultaneous laboratory measurements of CO2 and H2O adsorption on palagonite: Implications for the Martian climate and volatile reservoir p 3952 N94-33240

INSPECTION
Millimeter wave, high-resolution, holographic surveillance system
[DE94-004289] p 3712 N94-31831
Shearographic inspection of a DeHavilland DHC-7
[AD-A276716] p 3566 N94-32157

INSTALLING
Implementation of instruments and facilities at the SGP CART site
[DE94-006839] p 3781 N94-31322
Gigabits to the Desktop: Installing tomorrow's networks today
[DE94-007701] p 3827 N94-32646

INSTRUCTORS
A facilitated mentoring process for engineers
[DE94-005823] p 3914 N94-32677

INSTRUMENT APPROACH
Flight technical error for category B non-precision approaches and missed approaches using non-differential GPS for course guidance
[PB94-142734] p 3576 N94-31680

INSTRUMENT COMPENSATION
NOAA-9 Earth Radiation Budget Experiment (ERBE) scanner offsets determination
[NASA-TM-109086] p 3785 N94-32737

INSTRUMENT ORIENTATION
High energy physics program at the University of Alabama
[DE94-006544] p 3875 N94-31488

INSULATORS
Anisotropic phase separation through the metal-insulator transition in amorphous Mo-Ge and Fe-Ge alloys
[DE94-007259] p 3646 N94-32795
Proceedings, Strongly Correlated Electronic Materials: The 1993 Los Alamos Symposium
[DE94-009293] p 3906 N94-32913

INTEGERS
Mixed 0-1 programming by lift-and-project in a branch-and-cut framework
[AD-A278045] p 3822 N94-33183

INTEGRAL EQUATIONS
Penetrable wedge analysis
[AD-A277219] p 3845 N94-32022

INTEGRALS
A survey of numerical cubature over triangles
[DE94-006810] p 3841 N94-31274
Finite-part integrals and the Euler-Maclaurin expansion
[DE94-006539] p 3844 N94-31665

INTEGRATED CIRCUITS
Passivation of III-V compound semiconductor based devices
[AD-A276178] p 3894 N94-31056
Study of continuous-time and mixed analog-digital operators
[TELECOM-93-E-010] p 3687 N94-31170
High-performance GaAs/AlGaAs optical phase modulators for microwave/photonic integrated circuits
[DE94-006361] p 3688 N94-31483
III-V compound semiconductor strip-loaded waveguide devices for PICs: Design for minimum crosstalk and high density
[DE94-006588] p 3897 N94-31502
Chemical vapour deposition of tungsten for the application in integrated circuits
[ISBN-9-09-005151-1] p 3641 N94-31519
Simulation of non-uniform transmission lines for weakly dispersive structures
[ISBN-0-315-86525-3] p 3690 N94-31726
Epitaxial liftoff technology onto processed silicon foundry wafers
[AD-A277116] p 3900 N94-31985
The advent of failure analysis software technology
[DE94-006593] p 3892 N94-32111
Novel failure analysis techniques using photon probing with a scanning optical microscope
[DE94-006594] p 3892 N94-32112
Novel optoelectronic devices based on combining GaAs and InP on Si
[AD-A277018] p 3693 N94-32301
WOCSDICE 1993 --- 17th European Workshop on Compound Semiconductor Devices and Integrated Circuits
[AD-A276766] p 3693 N94-32307
Radiation tolerant, high speed, low power, gallium arsenide logic
[AD-A277293] p 3694 N94-32509
Metal-ion spin-on glasses: Novel materials for active waveguides
[DE94-007738] p 3882 N94-32649
High-performance GaAs/AlGaAs optical phase modulators for microwave photonic integrated circuits
[DE94-007376] p 3696 N94-32809
Advanced silicon technology for microwave circuits
[AD-A278039] p 3698 N94-33091
Advanced material processing for integrated-optic frequency doubling systems
[AD-A278394] p 3698 N94-33163

INTEGRATED LIBRARY SYSTEMS
Relationships between access and use in information systems: Remote access to and browsing of online catalogs p 3919 N94-32488

INTEGRATED OPTICS
High-performance GaAs/AlGaAs optical phase modulators for microwave/photonic integrated circuits
[DE94-006361] p 3688 N94-31483
III-V compound semiconductor strip-loaded waveguide devices for PICs: Design for minimum crosstalk and high density
[DE94-006588] p 3897 N94-31502
Optimization of Y junctions in integrated optics
[ISBN-0-315-86782-5] p 3879 N94-31751
Epitaxial liftoff technology onto processed silicon foundry wafers
[AD-A277116] p 3900 N94-31985
Sandia's photonic program and its changing national role
[DE94-008616] p 3883 N94-32878
Advanced material processing for integrated-optic frequency doubling systems
[AD-A278394] p 3698 N94-33163

INTEGRATORS
Towards simplicity: Noise and cooperation in the perfect integrator
[AD-A276256] p 3799 N94-31291
A brief introduction to symplectic integrators and recent results
[DE94-006225] p 3845 N94-31763

INTELSAT SATELLITES
Two-axis antenna positioning mechanism p 3805 N94-33308

INTERACTIONAL AERODYNAMICS
Experimental and numerical simulation of helicopter rotor fuselage interaction
[ONERA-NT-1993-8] p 3568 N94-31421
Six degree of freedom flight dynamic model of a Mk-82 store
[AD-A277065] p 3580 N94-32362

INTERACTIVE CONTROL
Relationships between access and use in information systems: Remote access to and browsing of online catalogs p 3919 N94-32488

INTERCALATION
Synthesis, characterization, phase diagrams and superconducting, and normal state magnetic properties of La(2-x)Sr(x)CuO4 (0 is less than or equal to x which is less than or equal to 0.08) and electrochemically oxidized La(2-x)Sr(x)CuO(4 + delta) (0 is less than or equal to x which is less than or equal to 0.33, 0 is less than or equal to delta which is less than or equal to 0.12)
[DE94-005260] p 3895 N94-31067

INTERFACES
Micromechanical analysis of the interface and basic damage modes in glass fiber/epoxy resin model composites
[ONERA-NT-1993-4] p 3618 N94-31225
Molecular dynamics computer simulations of charged metal electrode-aqueous electrolyte interfaces
[AD-A276401] p 3863 N94-31237
Characterization of interface structure in multilayers using specular x ray reflectance
[DE94-007698] p 3657 N94-32358

INTERFACIAL ENERGY
Empirical and semi-empirical relationships of liquid-vapor, solid-vapor, and solid-liquid surface energies
[AD-A276480] p 3631 N94-31248
Molecular interactions at metal/polyimide interfaces: A correlation with adhesion and bond durability
[AD-A276301] p 3650 N94-31297

INTERFACIAL TENSION
Numerical analysis of single-vortex/free-surface interaction
[AD-A276462] p 3701 N94-31241
Empirical and semi-empirical relationships of liquid-vapor, solid-vapor, and solid-liquid surface energies
[AD-A276480] p 3631 N94-31248
Boundary element analysis of three-dimensional nonlinear hydrodynamics in a reduced gravity environment p 3668 N94-32715

INTERFEROMETERS
Performance analysis of an integrated GPS/inertial attitude determination system
[NASA-CR-188289] p 3577 N94-32864

INTERFEROMETRY
Phase unwrapping problems in ISAR images
[TELECOM-93-D-008] p 3670 N94-31097
Fiberoptisk magnetfaltsensor (fiber optic magnetometer)
[PB94-148061] p 3878 N94-31584
A technique for multiplexing 3x3-coupler terminated interferometric fiber-optic sensors
[AD-A276739] p 3680 N94-32180
SAR interferometry with ERS-1 p 3755 N94-32566
Techniques and applications of SAR interferometry for ERS-1 p 3756 N94-32568
Precision and level of artefacts in the computation of digital terrain models by interferometry p 3756 N94-32571
Fields of experiments in ERS-1 SAR interferometry in Bonn and Naples p 3756 N94-32572
The processing technology and some applications of Almaz-1 data p 3756 N94-32573

INTERGALACTIC MEDIA
Study of stellar associations located in the region contained between the Magellanic Clouds
[ISBN-0-315-86692-6] p 3935 N94-31913

INTERGRANULAR CORROSION
Irradiation-assisted stress corrosion cracking of materials from commercial BWRs: Role of grain-boundary microchemistry
[DE94-006542] p 3643 N94-32109
Modeling of residual stress mitigation in austenitic stainless steel pipe girth weldment
[DE94-007184] p 3738 N94-32639

INTERLAMINAR STRESS
An approximate solution for interlaminar stresses in laminated composites p 3621 N94-31901

INTERLAYERS
Influence of volume fraction of component materials and interlayer bond strength on fracture toughness of multi-layer Al 6090-25 volume percent SiCp and Al 5182 laminates
[DE94-007141] p 3626 N94-32665

INTERMETALLICS
The effect of ductile phase (Nb) reinforcement morphology on the mechanical behavior of an intermetallic matrix (MoSi2) p 3615 N94-32500
Structure, stability, and mechanical properties of intermetallic phases
[DE94-009178] p 3647 N94-32852
Investigation of superconductivity and magnetism in d and f-electron materials
[DE94-008535] p 3907 N94-32933

INTERMOLECULAR FORCES
Chemical interactions between protein molecules and polymer membrane materials
[DE94-006987] p 3651 N94-31672

INTERNAL ENERGY
Analytic properties of the OCP and ionic mixtures in the strongly coupled fluid state
[DE94-008216] p 3637 N94-32801

INTERNAL FRICTION
The 10th International Conference on Internal Friction and Ultrasonic Attenuation in Solids (ICIFUAS)
[AD-A276849] p 3902 N94-32209

INTERNAL PRESSURE
Composite fuselage shell structures research at NASA Langley Research Center p 3628 N94-33124
INTERNAL WAVES
Ocean acoustic propagation measurements and wave propagation in random media
[AD-A276165] p 3787 N94-31053
Laser-induced fluorescence/particle tracking system for stratified flow research
[AD-A275917] p 3701 N94-31341
Aeroacoustic sources in internal flows
[ISBN-9-03-86-0282-0] p 3860 N94-31653
Observations of turbulence, internal waves and background flows: An inquiry into the relationships between scales of motion p 3705 N94-31988
INTERNATIONAL COOPERATION
AGARD membership, 1994
[AGARD-MEMB-94] p 3914 N94-31197
Evaluating success levels of mega-projects p 3599 N94-31432
Coordination of mesoscale meteorological research between ASL and European group
[AD-A276730] p 3784 N94-32162
The complementary nature of the SPOT and ERS-1 systems and their place in major international programmes p 3748 N94-32524
Information systems to enhance technology exchange
[DE94-007744] p 3920 N94-32808
Current policies of the major countries coping with the global warming problem and the energy demand and supply
[DE94-757291] p 3769 N94-32920
INTERNATIONAL LAW
Legal regime of human activities in outer space law p 3599 N94-31431
INTERNATIONAL RELATIONS
NATO contributions to European environmental security
[AD-A275918] p 3763 N94-31275
INTERNATIONAL TRADE
Prospects for the French fighter industry in a post-cold war environment: Is the future more than a mirage? p 3565 N94-31959
INTERNETS
PEM public key certificate cache server
[DE94-006404] p 3675 N94-31784
INTERPLANETARY DUST
Composition and properties of dust from Comet Halley p 3936 N94-31947
INTERPLANETARY MAGNETIC FIELDS
Numerical simulation of interplanetary dynamics p 3933 N94-31566
Planetary magnetotails: Magnetic configuration and nonthermal plasma p 3942 N94-32326
INTERPLANETARY MEDIUM
Numerical simulation of interplanetary dynamics p 3933 N94-31566
INTERPOLATION
The High-Frequency Benchmark propagation program
[AD-A276323] p 3672 N94-31334
Recursive analysis of matrix scattering functions
[AD-A277264] p 3845 N94-32018
On interpolating random fields using a finite number of observations
[CWI-BS-R9314] p 3847 N94-32194
Polynomial interpolation and approximation of real functions. 2: Symmetrical interpolation for the triangle
[AD-A277345] p 3848 N94-32245
A new method for calculating wing along aerodynamics to angle of attack 180 deg
[AD-A277965] p 3574 N94-33263
INTERPROCESSOR COMMUNICATION
An efficient three-dimensional Poisson solver for SIMD high-performance-computing architectures p 3823 N94-31120
Study of structures of different complexity for the communication between two processors
[ETN-94-95750] p 3674 N94-31615
Some calculations on supersymmetric graphs as communication networks
[REPT-93-72] p 3824 N94-31641
Control and reliability of optical networks in multiprocessors
[AD-A277385] p 3881 N94-32285
Communication networks for autonomous mobile robot computer architectures and distributed real-time computing p 3680 N94-32310
INTERSTELLAR GAS
Ionized gas in the halos of edge-on infrared-bright galaxies: Evidence for starburst-driven superwinds p 3936 N94-31948
A study of physical conditions, radiative transfer and shocks in the interstellar medium p 3937 N94-31963
A study of the neutral hydrogen distribution of the Milky Way through 21 cm emission and Lyman alpha absorption p 3938 N94-32309
INTERSTELLAR MAGNETIC FIELDS
Dynamics of flux tubes in accretion disks p 3932 N94-31142
INTERSTELLAR MATTER
Odin aeronomy science: A phase-A report by the Aeronomy Science Working Group for the Odin satellite
[AP-31] p 3770 N94-31222
Physical chemistry of molecules and grains in space
[AD-A276037] p 3932 N94-31280
INTERSTITIALS
Tensile properties of commercially pure vanadium from room temperature to 1200 C
[DE94-006622] p 3641 N94-31581
INTERTROPICAL CONVERGENT ZONES
Dynamic climatology of West Africa p 3778 N94-30988
INVARIANCE
Multivariate spline approximation
[AD-A276034] p 3842 N94-31441
Frames and stable bases for shift-invariant subspaces of L(sub 2)(IR(sup d))
[AD-A276470] p 3843 N94-31474
Invariance of the generalized steady-state for 1-D distributed parameter systems
[REPT-93-66] p 3825 N94-31662
INVENTORY CONTROLS
Beginning the 21st century with advanced Automatic Parts Identification (API) p 3923 N94-32444
INVERSE KINEMATICS
Kinematic synthesis and analysis of a novel class of six-DOF parallel minimanipulators p 3723 N94-31568
Strategy for tracking and grabbing a moving object with the aid of a decouplable manipulator with six degrees of freedom general architecture, guided by a vision system
[ISBN-0-315-86864-3] p 3831 N94-31757
A new solution method for the inverse kinematic joint velocity calculations of redundant manipulators
[DE94-004427] p 3727 N94-32682
INVERSIONS
Photoelectron diffraction and holography: Present status and future prospects
[DE94-006298] p 3712 N94-31629
INVERTERS
Optimal planning of residential photovoltaic systems under various rate structure
[DE94-757272] p 3762 N94-32919
INVISCID FLOW
On the structure and stability of slender viscous vortices p 3700 N94-31218
On wave interactions of rotational and irrotational flows p 3700 N94-31219
Attitude dynamics of spinning rockets in space with internal mass motion p 3601 N94-31802
A study of the development and attenuation of wing-generated, vortical wakes p 3570 N94-31971
A critical evaluation of methods for imposing solid-wall boundary conditions in inviscid flow
[AD-A276959] p 3707 N94-32361
IODIDES
A new-type of long-range restructuring of ordered metal surfaces induced by lateral adsorbate interactions: Iodide on AU(110) electrodes
[AD-A276633] p 3643 N94-32060
Sensitivity of electrochemical adlayer structure to the metal crystallographic orientation: Potential-independent iodide adsorption on Au(100) in comparison with other low-index surfaces
[AD-A276714] p 3909 N94-33273
A tandem microscopic-electrochemical examination of a charge-induced surface phase sequence: Ordered Au(110) in aqueous iodide electrolytes as probed by potentiodynamic scanning tunneling microscopy
[AD-A276905] p 3875 N94-33277
IODINE COMPOUNDS
Wave packet studies of the vibrational predissociation of three and four-atom van der Waals complexes
[DE94-007623] p 3871 N94-32598
ION ACCELERATORS
Control heavy ion collisions in the systems Ar-40 + Ca-40 and Si-28 + Si-28, and the nature of particle emission in fusion-evaporation reactions
[ETN-94-95749] p 3866 N94-31614
ION BEAMS
Proceedings of the 37th international symposium on electron, ion, and photon beams
[AD-A276478] p 3875 N94-31247
Deposition of DLC via intense ion beam ablation
[DE94-005583] p 3651 N94-31650
Neutral ion sources in precision manufacturing p 3875 N94-32447
Transverse energy production with Si and Au beams at AGS energy: Towards hot and dense hadronic matter
[DE94-007178] p 3938 N94-32638
Potential applications of fusion neutral beam facilities for advanced material processing
[DE94-009167] p 3647 N94-32851
X ray absorption study of pulsed laser deposited boron nitride films
[DE94-008295] p 3662 N94-32855
Low energy ion beam assisted growth of homoepitaxial silicon films at low temperature
[AD-A278092] p 3908 N94-33039
ION CONCENTRATION
Inorganic materials for anomalous-dispersion phase-matched second harmonic generation: Rubidium titanyl arsenate isomorphs, Rb(Ti(1-2x)Ln(x)Nb(x))OAsO4
[DE94-006141] p 3899 N94-31847
ION CURRENTS
Conductivity measurements of ceria-based solid electrolytes using AC impedance
[DE94-007380] p 3694 N94-32593
Characteristics of ion flow in the quiet state of the inner plasma sheet
[AD-A277451] p 3894 N94-33106
ION CYCLOTRON RADIATION
ICRF heating and current drive in TFTR supershot plasmas: Data analysis and interpretation of ICRF/edge interactions
[DE94-008586] p 3890 N94-32520
ION DENSITY (CONCENTRATION)
Anomalous thermalization of fast ions in magnetized plasma
[DE94-007109] p 3891 N94-32631
ION EMISSION
Control heavy ion collisions in the systems Ar-40 + Ca-40 and Si-28 + Si-28, and the nature of particle emission in fusion-evaporation reactions
[ETN-94-95749] p 3866 N94-31614
ION EXCHANGE MEMBRANE ELECTROLYTES
Development of silver-zinc cells of improved cycle life and energy density
[AD-A277311] p 3693 N94-32329
Polymer electrolyte fuel cells
[DE94-007558] p 3761 N94-32762
Metal ion complexation by ionizable crown ethers
[DE94-008301] p 3661 N94-32847
ION EXCHANGE RESINS
An investigation of the radiolytic stability of a resorcinol-formaldehyde ion exchange resin
[DE94-007971] p 3660 N94-32698
Metal ion complexation by ionizable crown ethers
[DE94-008301] p 3661 N94-32847
ION EXCHANGING
Metal ion complexation by ionizable crown ethers
[DE94-008301] p 3661 N94-32847
ION IMPLANTATION
Enhancement of oxidation resistance of silicon carbide by high-dose and multi-energy aluminum implantation
[DE94-006560] p 3640 N94-31314
Ion beam synthesis of IrSi3 by 1-MeV Ir ion implantation into Si(111)
[DE94-006556] p 3896 N94-31501
Engineering of damage in ion implanted silicon
[ISBN-9-09-005097-3] p 3897 N94-31521
The effects of amorphous layer regrowth on carbon activation in GaAs and InP
[DE94-006290] p 3899 N94-31634
Oriented Si and Ge nanocrystals formed in Al2O3 by ion implantation and annealing
[DE94-005593] p 3901 N94-32172
Heteroepitaxial diamond growth
[AD-A277178] p 3902 N94-32306
Gettering of metal impurities by cavities in silicon
[DE94-005248] p 3645 N94-32672
Ultrahigh-current-density metal-ion implantation and diamondlike-hydrocarbon films for tribological applications
[DE94-008958] p 3906 N94-32843
Potential applications of fusion neutral beam facilities for advanced material processing
[DE94-009167] p 3647 N94-32851
Electrical characteristics of GaAs MESFET fabrication by ion implantation of Si or Se
[AD-A278416] p 3909 N94-33328
ION IRRADIATION
Ion-beam-driven amorphization of Ca2La8(Si4)6O2 single crystals
[DE94-006219] p 3895 N94-31307
Energy and angular distributions of secondary ions during electronic sputtering of nonconducting surfaces
[ETN-94-95756] p 3865 N94-31516
Ion-irradiation-induced densification of zirconia sol-gel thin films
[DE94-006248] p 3656 N94-32103
Intra-cascade surface recombination of point defects during ion bombardment of Ge(001)
[DE94-007740] p 3903 N94-32384
Formation mechanism and yield of molecules ejected from ZnS, CdS, and FeS2 during ion bombardment
[DE94-008487] p 3871 N94-32515

Irradiation-induced phase transformations in zirconium alloys
[DE94-008484] p 3648 N94-32993

ION PLATING
Frictional behavior and adhesion of Ag and Au films applied to aluminum oxide by oxygen-ion assisted Screen Cage Ion Plating (SCIP)
[NASA-TM-106522] p 3647 N94-32931

ION PROBES
The origin of neon-E: Neon-E in single interstellar silicon carbide and graphite grains p 3933 N94-31556

ION SOURCES
Neutral ion sources in precision manufacturing
p 3875 N94-32447
Potential applications of fusion neutral beam facilities for advanced material processing
[DE94-009167] p 3647 N94-32851

ION TEMPERATURE
Anomalous thermalization of fast ions in magnetized plasma
[DE94-007109] p 3891 N94-32631
Measurement of ICF fuel ion temperature on Nova
[DE94-006150] p 3892 N94-32730

ION TRAPS (INSTRUMENTATION)
Spectroscopy and atomic physics in EBIT and SuperEBIT
[DE94-006050] p 3864 N94-31508
Gettering of metal impurities by cavities in silicon
[DE94-005248] p 3645 N94-32672
Performance of an ion trap inductively coupled plasma mass spectrometer
[DE94-007470] p 3713 N94-32811

IONIC COLLISIONS
Control heavy ion collisions in the systems Ar-40 + Ca-40 and Si-28 + Si-28, and the nature of particle emission in fusion-evaporation reactions
[ETN-94-95749] p 3866 N94-31614
Antiproton production in heavy ion collisions
[DE94-007552] p 3870 N94-32271
String-parton model description of relativistic heavy-ion collisions
[DE94-009164] p 3874 N94-32850

IONIC CRYSTALS
Analytic properties of the OCP and ionic mixtures in the strongly coupled fluid state
[DE94-008216] p 3637 N94-32801

IONIC DIFFUSION
Electronic and nuclear factors in intramolecular charge and excitation transfer processes
[DE94-006598] p 3870 N94-32178

IONIC REACTIONS
A model of the ion chemistry of electrified convection
p 3868 N94-31993
Radiation and photochemistry section
[DE94-008880] p 3873 N94-32757

IONIZATION
Compressible convection with ionization
p 3911 N94-31498
Analytical solutions of minimum ionization particle induced current shapes of silicon detectors and simulation of charge collection properties
[DE94-007523] p 3870 N94-32355
Ionization probes of molecular structure and chemistry
[DE94-007605] p 3872 N94-32643
Analysis of Dietz's single, rectangular pulse theory for the generation of radiation via photoelectrons
[DE94-006131] p 3681 N94-32661
Ionization EM calorimetry with accordion electrodes and liquid krypton or argon
[DE94-009082] p 3713 N94-32821

IONIZATION CROSS SECTIONS
Theory, Image Simulation, and Data Analysis of Chemical Release Experiments
[NASA-CR-194865] p 3954 N94-31101

IONIZATION POTENTIALS
A polynomial representation of the valence orbital ionization potentials
[USIP-93-06] p 3640 N94-31083
Heteroepitaxial diamond growth
[AD-A277178] p 3902 N94-32306

IONIZED GASES
Ionized gas in the halos of edge-on infrared-bright galaxies: Evidence for starburst-driven superwinds
p 3936 N94-31948

IONIZING RADIATION
Ionizing radiation effects on silicon test structures
[DE94-006060] p 3865 N94-31607

IONOGRAMS
Eurocap program-ebre station
[AD-A277044] p 3772 N94-32007

IONOSONDES
Eurocap program-ebre station
[AD-A277044] p 3772 N94-32007

IONOSPHERIC DISTURBANCES
Atmospheric effects assessment program: Ionospheric sounding
[AD-A276447] p 3770 N94-31303
Analysis of ionospheric parameters in Europe and creation of the prediction algorithm
[AD-A276342] p 3771 N94-31326
Lightning-induced coupling of the radiation belts to geomagnetically conjugate ionospheric regions
p 3772 N94-31773
Theoretical studies on ionospheric irregularities and ion diode performance
[AD-A277115] p 3772 N94-31984
Performance statistics bulletin. High latitude meteor scatter propagation October, November, December 1990, January 1991
[AD-A276693] p 3676 N94-31998
Performance statistics bulletin. High latitude meteor scatter propagation February, March, April, May 1991
[AD-A276723] p 3678 N94-32158
Performance statistics bulletin. High latitude meteor scatter propagation October, November, December 1991, January 1992
[AD-A276724] p 3678 N94-32159
Electromagnetic wave reflection from irregular plasma layers
[AD-A276727] p 3678 N94-32161
Performance statistics bulletin. High latitude meteor scatter propagation
[AD-A276694] p 3680 N94-32298
Performance statistics bulletin. High latitude meteor scatter propagation
[AD-A276695] p 3680 N94-32299
Performance statistics bulletin. High latitude meteor scatter propagation
[AD-A276696] p 3680 N94-32300
Performance statistics bulletin. High latitude meteor scatter propagation, June, July, August, September 1992
[AD-A277508] p 3685 N94-33347

IONOSPHERIC ELECTRON DENSITY
An analysis of ionospheric dayglow from observations of the Naval Postgraduate School Middle Ultraviolet Spectrograph (MUSTANG)
[AD-A277351] p 3773 N94-32335

IONOSPHERIC HEATING
Ionospheric plasma outflow in response to transverse ion heating: Self-consistent macroscopic treatment
[NASA-CR-195820] p 3893 N94-33048

IONOSPHERIC PROPAGATION
Analysis of ionospheric parameters in Europe and creation of the prediction algorithm
[AD-A276342] p 3771 N94-31326
Performance statistics bulletin. High latitude metor scatter propagation, February, March, April, May 1992
[AD-A276667] p 3677 N94-32083
Performance statistics bulletin. High latitude meteor scatter propagation, November and December 1989, and January 1990
[AD-A276688] p 3680 N94-32297

IONOSPHERIC SOUNDING
Theory, Image Simulation, and Data Analysis of Chemical Release Experiments
[NASA-CR-194865] p 3954 N94-31101
Atmospheric effects assessment program: Ionospheric sounding
[AD-A276447] p 3770 N94-31303
Analysis of ionospheric parameters in Europe and creation of the prediction algorithm
[AD-A276342] p 3771 N94-31326
EUROCAP program
[AD-A278084] p 3776 N94-33184

IONS
Elimination of two atomic electrons by a single high energy photon
[DE94-006834] p 3864 N94-31320
Characterization of the rare earth orthophosphates and Ce-doped LaPO4 by x ray absorption spectroscopy
[DE94-006313] p 3898 N94-31630
Collective acceleration in solar flares
[DE94-006288] p 3953 N94-31632
Inorganic materials for anomalous-dispersion phase-matched second harmonic generation: Rubidium titanyl arsenate isomorphs, Rb(Ti(1-2x)Ln(x)Nb(x))OAsO4
[DE94-006141] p 3899 N94-31847
Combinatorial ion sensors
[AD-A276567] p 3825 N94-32032
Self-consistent effects of magnetospheric hydromagnetic waves on ring current ions
[AD-A277406] p 3774 N94-32346
Anomalous thermalization of fast ions in magnetized plasma
[DE94-007109] p 3891 N94-32631
Radiation and photochemistry section
[DE94-008880] p 3873 N94-32757
Progress in understanding and improving x ray lasers
[DE94-006048] p 3720 N94-32794
Optical properties of lanthanide-doped RbTiOAsO4 and transition metal-doped KTiOPO4
[DE94-008433] p 3907 N94-32963
Irradiation-induced phase transformations in zirconium alloys
[DE94-008484] p 3648 N94-32993
Ionospheric plasma outflow in response to transverse ion heating: Self-consistent macroscopic treatment
[NASA-CR-195820] p 3893 N94-33048

IRIDIUM COMPOUNDS
Ion beam synthesis of IrSi3 by 1-MeV Ir ion implantation into Si(111)
[DE94-006556] p 3896 N94-31501

IRON
Technology development for iron Fischer-Tropsch catalysts
[DE94-008723] p 3638 N94-32889
Thermal emission measurements (5-25 microns) of Hawaiian palagonitic soils with implications for Mars
p 3944 N94-33193
Deposition rates of oxidized iron on Mars
p 3945 N94-33198

IRON ALLOYS
Expandable pattern casting research
[DE94-004342] p 3668 N94-31604
Anisotropic phase separation through the metal-insulator transition in amorphous Mo-Ge and Fe-Ge alloys
[DE94-007259] p 3646 N94-32795
Structure, stability, and mechanical properties of intermetallic phases
[DE94-009178] p 3647 N94-32852

IRON COMPOUNDS
Molecular/polymeric magnetism
[DE94-005888] p 3649 N94-31201
Formation mechanism and yield of molecules ejected from ZnS, CdS, and FeS2 during ion bombardment
[DE94-008487] p 3871 N94-32515
Proceedings of the Ad Hoc Workshop on Ceramics for Li/FeS2 batteries
[DE94-007460] p 3694 N94-32607
The relative performance of FeS2 and CoS in long-life thermal-battery applications
[DE94-006145] p 3695 N94-32663
The development of precipitated iron catalysts with improved stability
[DE94-008711] p 3638 N94-32886

IRON OXIDES
Deposition rates of oxidized iron on Mars
p 3945 N94-33198

IRRADIATION
Disk irradiation and light curves of x ray novae
p 3929 N94-31124
Analysis of beam-on-target interaction in a neutron-source test facility
[DE94-005392] p 3863 N94-31151
Hydrogen incorporation and radiation induced dynamics in metal-oxide-silicon structures: A study using nuclear reaction analysis
[ETN-94-95742] p 3898 N94-31610
Defect-solute interactions near irradiation grain boundaries
[DE94-006215] p 3641 N94-31627
Irradiation-assisted stress corrosion cracking of materials from commercial BWRs: Role of grain-boundary microchemistry
[DE94-006542] p 3643 N94-32109
Electron energy dependence of amorphization in Zr3Fe
[DE94-008459] p 3906 N94-32875

ISING MODEL
Delft Ising computing engine
[PB94-148251] p 3806 N94-31587

ISOPROPYL COMPOUNDS
Tetraalkyldiarsines as potential precursors for electronic materials: Synthesis and characterization of various iso-propyl arsenic compounds
[AD-A277003] p 3900 N94-32001

ISOTOPES
AMS beyond 2000
[DE94-006666] p 3632 N94-31352
Mars atmospheric loss and isotopic fractionation by solar-wind-induced sputtering and photochemical escape
p 3947 N94-33208
SNC meteorites and their implications for reservoirs of Martian volatiles p 3947 N94-33209

ISOTOPIC SPIN
Collective and quasiparticle excitations in light Pb isotopes
[ETN-94-96014] p 3865 N94-31548

ISOTROPIC TURBULENCE
Renormalization group theory of Bolgiano scaling in Boussinesq turbulence
[NASA-TM-106602] p 3710 N94-33070

ITERATION
Techniques for increasing the robustness of iterative algorithms for multi-resources location problems
[REPT-93-037] p 3809 N94-31188
On the convergence of stochastic iterative dynamic programming
[AD-A276517] p 3815 N94-31933
Varying execution discipline to increase performance
[DE94-007844] p 3819 N94-32651
ITERATIVE SOLUTION
Doubly asymptotic approximations: Theoretical and numerical analyses
[ONERA-NT-1993-7] p 3840 N94-31231
Arnoldi code for computing selected eigenvalues of sparse real unsymmetric matrices
[PB94-145182] p 3813 N94-31682
A Gauss-Seidel type solver for special convex programs, with application to frictional contact mechanics
[REPT-93-77] p 3813 N94-31694
Nonlinear analysis of springs using helical finite elements p 3859 N94-31906
On an adaptation method for dense, 2D, C-type grids
[W-9321] p 3706 N94-32045
On the error committed by stopping the Newton iteration in Runge-Kutta methods and linear multistep methods
[TW-93-13] p 3847 N94-32206
Numerical transport theory
[DE94-009064] p 3857 N94-32589
Adjacent-cell Preconditioners for solving optically thick neutron transport problems
[DE94-007219] p 3872 N94-32666
Preconditioned time-difference methods for advection-diffusion-reaction equations
[DE94-006472] p 3638 N94-32840

J

J INTEGRAL
Simpler J(sub Ic) test and data analysis procedures for high strength steels
[AD-A277731] p 3648 N94-33281
JAMMING
Subspace estimation without eigenvectors for adaptive beamforming
[AD-A276287] p 3671 N94-31254
Low sidelobe reflector antenna design for communications
[AD-A276079] p 3673 N94-31463
Performance metrics for low probability of intercept-communication system
[AD-A277346] p 3677 N94-32073
JET ENGINE FUELS
Advanced thermally stable jet fuels
[DE94-006760] p 3667 N94-32150
Ignition delays, heats of combustion, and reaction rates of aluminum alkyl derivatives used as ignition and combustion enhancers for supersonic combustion
[NASA-CR-189581] p 3638 N94-32868
JET ENGINES
Analysis of intermediate level maintenance following F404-GE-400 engine component life reductions
[AD-A277918] p 3585 N94-33283
JET FLOW
The small-scale topology of a 2:1 aspect-ratio elliptic jet p 3699 N94-31184
Ignition studies in nonpremixed hydrogen/air combustion
[AD-A275954] p 3632 N94-31348
Jet physics and QCD tests at the Tevatron collider
[DE94-008987] p 3871 N94-32587
Shear flow control of cold and heated rectangular jets by mechanical tabs. Volume 1: Results and discussion
[NASA-CR-182296-VOL-1] p 3708 N94-32867
Shear flow control of cold and heated rectangular jets by mechanical tabs. Volume 2: Tabulated data
[NASA-CR-182296-VOL-2] p 3709 N94-32869
JET IMPINGEMENT
A six degree of freedom, plume-fuel optimal trajectory planner for spacecraft proximity operations using an A* node search
[NASA-CR-188285] p 3601 N94-32388
JET MIXING FLOW
Shear flow control of cold and heated rectangular jets by mechanical tabs. Volume 1: Results and discussion
[NASA-CR-182296-VOL-1] p 3708 N94-32867
Shear flow control of cold and heated rectangular jets by mechanical tabs. Volume 2: Tabulated data
[NASA-CR-182296-VOL-2] p 3709 N94-32869
Enhancement of mixing in a rectangular jet by mechanical tabs
[NASA-CR-185207] p 3709 N94-32872
JET PROPULSION
Modular Simulator System (MSS). System/segment specification for the generic modular simulator system-propulsion module propulsion module, volume 5
[AD-A276972] p 3590 N94-32397
JET STREAMS (METEOROLOGY)
Dynamics in the tropics and synoptic disturbances p 3778 N94-30990
The evolution of jet features during the 1993 east coast white hurricane: A case study using the global spectral model
[AD-A277217] p 3783 N94-32021
JETS
Studies of jet production with the D0 detector
[DE94-008271] p 3873 N94-32780
JOINING
Joining of silicon nitrides using oxynitride glasses
[DE94-008517] p 3658 N94-32517
JOINTS (JUNCTIONS)
Shearographic inspection of a DeHavilland DHC-7
[AD-A276716] p 3566 N94-32157
Influence of volume fraction of component materials and interlayer bond strength on fracture toughness of multi-layer Al 6090-25 volume percent SiCp and Al 5182 laminates
[DE94-007141] p 3626 N94-32665
Pip pin reliability and design p 3605 N94-33305
JOSEPHSON JUNCTIONS
Development, characterization, and applications of high temperature superconductor nanobridge Josephson junctions
[DE94-008113] p 3903 N94-32409
Quantum fluctuations of vortices in Josephson-coupled superconductors
[DE94-007609] p 3905 N94-32747
YBCO Josephson Junction arrays
[AD-A277426] p 3908 N94-33005
High temperature superconducting Josephson junction array systems, phase 1
[AD-A277937] p 3908 N94-33246
JOURNAL BEARINGS
Simultaneous pressure measurement and high-speed photography study of cavitation in a dynamically loaded journal bearing
[NASA-TM-106456] p 3728 N94-32893
JUDGMENTS
Visual perception of 3-dimensional structure from different types of optical deformation
[AD-A278272] p 3884 N94-33141
JUNCTION DIODES
Ionizing radiation effects on silicon test structures
[DE94-006060] p 3865 N94-31607

K

K STARS
A critical examination of stellar atmosphere theory for metal-poor K-giant stars p 3927 N94-32308
K-EPSILON TURBULENCE MODEL
Finite volume discretization of the k-epsilon turbulence model in general coordinates
[REPT-93-90] p 3703 N94-31703
An analysis of supersonic flows with low-Reynolds number compressible two-equation turbulence models using LU finite volume implicit numerical techniques
[NASA-CR-195302] p 3572 N94-32926
KALMAN FILTERS
Tracking roads in an aerial image by Kalman filtering
[TELECOM-93-D-007] p 3711 N94-31096
An adaptive Kalman filter excisor for suppressing narrowband interference
[AD-A276286] p 3671 N94-31253
Kalman filtering approach to blind equalization
[AD-A276320] p 3671 N94-31299
An investigation of airborne GPS/INS for high accuracy position and velocity determination
[DE94-006139] p 3576 N94-31306
Fault detection and isolation for the Bluebird test bed aircraft
[AD-A277979] p 3586 N94-33086
KAONS
BNL possibilities
[DE94-007179] p 3864 N94-31398
Medium energy measurements of N-N parameters
[DE94-006067] p 3869 N94-32173
Research program in particle physics
[DE94-008449] p 3871 N94-32512
KAPTON (TRADEMARK)
Space Station WP-2 application of LDEF MLI results p 3592 N94-31016
Atomic oxygen damage characterization by photothermal scanning p 3598 N94-31051
A fracture mechanics methodology for characterizing the performance of flawed polymeric dielectric materials p 3654 N94-31956
KAZAKHSTAN
Station climatic summaries: China, the former USSR, and Mongolia
[AD-A276548] p 3784 N94-32057
KERNEL FUNCTIONS
The Cameron-Martin theorem
[W-9315] p 3844 N94-31676
GKS-9X: An experimental application
[PB94-147048] p 3813 N94-31685
Varying execution discipline to increase performance
[DE94-007844] p 3819 N94-32651
KETONES
Low velocity impact damage in carbon fiber/PEEK composite laminates
[ISBN-0-315-86546-6] p 3622 N94-31909
Ligand intermediates in metal-catalyzed reactions
[DE94-008713] p 3638 N94-32887
KINEMATICS
Cometary molecules p 3935 N94-31869
High-speed path constrained manipulator operation using optimal-feedback combined controller p 3833 N94-31962
The kinematics of dense clusters of galaxies p 3937 N94-32029
Information theory for arm visuo-motor coordination p 3800 N94-32495
KINETIC ENERGY
Observations of turbulence, internal waves and background flows: An inquiry into the relationships between scales of motion p 3705 N94-31988
The evolution of jet features during the 1993 east coast white hurricane: A case study using the global spectral model
[AD-A277217] p 3783 N94-32021
A study of near-surface and underwater explosions by computer simulations
[DE94-009038] p 3708 N94-32849
KINETIC THEORY
Solvent diffusion coefficient concentration dependence in polymer solutions
[AD-A277023] p 3655 N94-32005
KINETICS
Some perspectives on solution-phase electron-transfer processes
[AD-A276906] p 3635 N94-32216
Dynamics and control of orbiting flexible systems: A formulation with applications
[ISBN-0-315-75390-0] p 3611 N94-32502
Surface probes of porous toluene/water ices: Adsorption kinetics and annealing spectra measured by second harmonic generation
[DE94-007564] p 3637 N94-32743
KLYSTRONS
High-power microwave-tube transmitters
[DE94-005340] p 3686 N94-31150
KNOWLEDGE BASED SYSTEMS
Hierarchical fault catalog process for diagnosis of analog circuits
[ETN-94-95730] p 3689 N94-31571
KNOWLEDGE BASES (ARTIFICIAL INTELLIGENCE)
Information acquisition from multi-agent resources; abstract
[LP-93-08] p 3917 N94-31452
LORE and reason maintenance
[REPT-93-88] p 3812 N94-31522
Hierarchical fault catalog process for diagnosis of analog circuits
[ETN-94-95730] p 3689 N94-31571
Knowledge-based commodity distribution planning p 3915 N94-32427
KNOWLEDGE REPRESENTATION
LORE and reason maintenance
[REPT-93-88] p 3812 N94-31522
An expert system architecture for heterogeneous domains: A case-study in the legal field
[ETN-94-96012] p 3830 N94-31546
Effective information modelling support
[PB94-148236] p 3917 N94-31586
KONDO EFFECT
The 4f heavy fermion photoelectron spectra do not exhibit the Kondo scale
[DE94-006252] p 3898 N94-31631
KRYPTON
Spectroscopy and atomic physics in EBIT and SuperEBIT
[DE94-006050] p 3864 N94-31508
KRYPTON FLUORIDE LASERS
Time evolution and filamentation of KrF(star) laser gas discharges
[ETN-94-95758] p 3715 N94-31561

L

LABORATORIES
Solar activities at Sandia National Laboratories
[DE94-007737] p 3761 N94-32648
LLNL casting technology
[DE94-008282] p 3669 N94-32839
LABRADOR
Common property resources and low-level flying in Labrador: Flight, fight or fancy?
[ISBN-0-315-87318-3] p 3924 N94-31732
LABYRINTH SEALS
Rotordynamic effects driven by fluid forces from a geometrically imperfect labyrinth
[AD-A276424] p 3722 N94-31333
Design of a two dimensional planer pressurized air labyrinth seal test rig
[AD-A277232] p 3726 N94-32370
LAGRANGE MULTIPLIERS
Tensor gauge potentials in loop space formulation of Yang-Mills fields
[PB94-147147] p 3912 N94-31924
LAGRANGIAN FUNCTION
Budget allocation and monopolistic pricing in a multiproduct firm
[REPT-93-86] p 3924 N94-31617
Computational methods for frictional contact with applications to the Space Shuttle orbiter nose-gear tire p 3608 N94-32295
Dynamics and control of orbiting flexible systems: A formulation with applications
[ISBN-0-315-75390-0] p 3611 N94-32502
Notes on the Langevin model for turbulent diffusion of marked particles
[DE94-007847] p 3708 N94-32652
Chiral symmetry and the threshold gamma(p) yields pi(sup 0)p reaction
[DE94-008117] p 3873 N94-32710
Fluid Dynamics Lagrangian Simulation Model
[AD-A277438] p 3710 N94-33009
An experimental study of pilot/vehicle dynamics using a tilt rotor flying machine
[AD-A277516] p 3805 N94-33349
LAMINAR BOUNDARY LAYER
Results for the hybrid laminar flow control experiment conducted in the NASA Langley 8-foot transonic pressure tunnel on a 7-foot chord model
[NASA-TM-107582] p 3601 N94-32870
The spatial development of the magnetospheric low-latitude boundary layer
[ISBN-0-315-77418-5] p 3776 N94-33111
LAMINAR FLOW
Control of hypersonic aerodynamic forces with surface blowing p 3567 N94-31216
Results for the hybrid laminar flow control experiment conducted in the NASA Langley 8-foot transonic pressure tunnel on a 7-foot chord model
[NASA-TM-107582] p 3601 N94-32870
LAMINATES
Vibration control and design of composite cantilevers taking into account structural uncertainties and damage p 3733 N94-31213
An efficient higher order theory for laminated composite plates and a finite element implementation p 3617 N94-31215
Reliability of multilayer copper/polyimide
[AD-A276228] p 3650 N94-31284
Inelastic deformation of metal matrix composites p 3618 N94-31285
Study of wave propagation and dynamic response of laminated composite structures
[AD-A276123] p 3619 N94-31444
Damage tolerance aspects of a full composite airplane fuselage: Requirements, modelling, predictions, experiments
[LR-728] p 3578 N94-31674
Random vibrations of composite beams and plates p 3735 N94-31777
Evaluating in-plane elastic constants of damaged carbon-epoxy laminates using a quantitative ultrasonic technique p 3621 N94-31793
Optimization of composite material failure loads
[ISBN-0-315-87214-4] p 3621 N94-31836
An approximate solution for interlaminar stresses in laminated composites p 3621 N94-31901
Theory of thick, laminated composite shallow shells p 3622 N94-31953
Nonlinear vibration analysis of laminated plates on linear and nonlinear elastic foundations p 3737 N94-32079
Computational methods for frictional contact with applications to the Space Shuttle orbiter nose-gear tire p 3608 N94-32295
Development of an advanced continuum theory for composite laminates, volume 1
[AD-A277275] p 3625 N94-32591
Development of an advanced continuum theory for composite laminates, volume 2
[AD-A277276] p 3625 N94-32592
A thermal viscoelastic analysis for thick-walled composite cylinders
[AD-A274143] p 3625 N94-32604
Influence of volume fraction of component materials and interlayer bond strength on fracture toughness of multi-layer Al 6090-25 volume percent SiCp and Al 5182 laminates
[DE94-007141] p 3626 N94-32665
Comparison of the compressive strengths for stitched and toughened composite systems
[NASA-TM-109108] p 3627 N94-32939
Effective computational strategy for predicting the response of complex systems
[AD-A277452] p 3740 N94-33011
Development of stitched/RTM composite primary structures p 3628 N94-33127
Tension fracture of laminates for transport fuselage. Part 1: Material screening p 3629 N94-33130
Structural integrity of intelligent materials and structures
[AD-A278397] p 3630 N94-33165
LAND ICE
A reassessment of the in-situ dielectric constant of polar firn
[AD-A276999] p 3773 N94-32154
LAND MANAGEMENT
Food security in the context of global environmental change
[DE94-007481] p 3768 N94-32812
LAND SURFACE TEMPERATURE
Numerical simulation of thermally induced near-surface flows over Martian terrain p 3949 N94-33223
LAND USE
Monitoring land cover and crop types in Denmark using ERS-1 SAR and optical satellite images p 3748 N94-32528
The contribution of satellite data in communication infrastructure projects p 3749 N94-32530
SPOT imagery for updating land cover information of 1:50,000 numerical topographic maps p 3749 N94-32532
The use of SPOT, and the contribution of ERS-1, in the assessment of urban pressure on agriculture land in Greater Tunis (Tunisia) p 3749 N94-32534
Airborne SAR as a complement to SPOT HRV in land-cover classification: The use of normalization and principal components analysis p 3750 N94-32539
Possible complementarity of SPOT/ERS in mapping land use: Study on agricultural land in Brittany (France) p 3755 N94-32563
Land cover change detection with ERS-1 data and data from other remote sensing satellites. Example: The delta of the River Ebro (Spain) p 3755 N94-32564
ERS-1 SAR and optical data for land use/land cover mapping: A case study in a savannah zone of Guinea p 3755 N94-32565
LANDAU FACTOR
Diamagnetism in helium Rydberg atoms
[ETN-94-96015] p 3865 N94-31549
LANDFORMS
Geologic controls of erosion and sedimentation on Mars p 3951 N94-33232
LANDING GEAR
Load-limiting landing gear footpad energy absorption system p 3607 N94-33323
LANDING SITES
MARSNET: A European network of stations on the surface of Mars p 3945 N94-33199
Dielectric properties of Mars' surface: Proposed measurement on a Mars lander p 3951 N94-33237
LANDSLIDES
Evaluation of the potential of SAR data for mapping of landslide risks
[BRGM-93033] p 3753 N94-32552
LANGEVIN FORMULA
Notes on the Langevin model for turbulent diffusion of marked particles
[DE94-007847] p 3708 N94-32652
Electron: Cluster interactions
[DE94-009089] p 3874 N94-32807
LANGMUIR-BLODGETT FILMS
Modification of semiconductor surface properties with chemically bound molecular films
[AD-A276162] p 3895 N94-31081
New developments in second-order nonlinear optical polymeric materials
[AD-A277409] p 3658 N94-32578
LANGUAGES
Resumptive quantifiers in exception sentences
[LP-93-11] p 3855 N94-31403
On the equivalence of Lambek categorial grammars and basic categorial grammars
[LP-93-07] p 3842 N94-31451
Compositionality of application oriented structuring mechanisms for algebraic specification languages with initial semantics
[ETN-94-95736] p 3812 N94-31577
Automatic translation among spoken languages p 3685 N94-32437
LANTHANUM
Inorganic materials for anomalous-dispersion phase-matched second harmonic generation: Rubidium titanyl arsenate isomorphs, Rb(Ti(1-2x)Ln(x)Nb(x))OAsO4
[DE94-006141] p 3899 N94-31847
LANTHANUM COMPOUNDS
Ion-beam-driven amorphization of Ca2La8(Si4)6O2 single crystals
[DE94-006219] p 3895 N94-31307
Electron spin resonance measurements of Er(3+) and Mn(2+) in the high temperature superconductor compounds La(2-x)Sr(x)CuO(4-delta)
[ETN-94-95746] p 3898 N94-31612
Thin-film decoupling capacitors for multi-chip modules
[DE94-007743] p 3695 N94-32650
LAPLACE EQUATION
The Laplace functional and Palm measure of a quasi-Cox process which is driven by a Markov chain
[REPT-93-82] p 3851 N94-31699
LAPLACE TRANSFORMATION
A cell-cycle model revisited
[CWI-AM-R9305] p 3851 N94-32229
Monoenergetic neutral particle transport in semi-infinite media
[AD-A277155] p 3870 N94-32368
A thermal viscoelastic analysis for thick-walled composite cylinders
[AD-A274143] p 3625 N94-32604
LARGE SPACE STRUCTURES
A study of the Space Station Freedom response to the disturbance environment p 3600 N94-31434
LASER ABLATION
Pump-probe method for investigating laser ablation and optical damage threshold mechanisms in optical materials
[DE94-008291] p 3720 N94-32753
LASER ANEMOMETERS
A preliminary investigation of high amplitude standing waves with laser Doppler anemometry
[AD-A276463] p 3860 N94-31242
LASER APPLICATIONS
Time-resolved infrared absorption studies applied to the study of radical plus molecule reactions
[DE94-005921] p 3863 N94-31202
DOE reactor-pumped laser program
[DE94-006372] p 3715 N94-31485
Diagnostics of high-brightness short-pulse lasers and the plasmas they generate
[DE94-006165] p 3716 N94-31624
The development and testing of a backscatter absorption gas imaging (BAGI) system designed to image at a range of 300 m
[DE94-006192] p 3675 N94-31761
Laser applications in wood processing
[PB94-138567] p 3717 N94-31840
Mechanical properties of acrylate networks formed by visible laser-induced polymerization. 2. Control of the mechanical properties
[AD-A277111] p 3655 N94-31982
Mechanisms of laser induced reactions in opaque heterogeneous environments
[AD-A276642] p 3717 N94-31996
The charging effect in high-Tc superconducting thin films
[AD-A277265] p 3900 N94-32040
Photothermal laser deflection, an innovative technique to measure particles in exhausts
[AD-A277151] p 3718 N94-32366
Laser flash photolysis, EPR and Raman studies of liquids at elevated pressures
[DE94-008351] p 3718 N94-32413
X ray imaging and x ray source development at Lawrence Livermore National Laboratory
[DE94-007077] p 3719 N94-32629
Progress in understanding and improving x ray lasers
[DE94-006048] p 3720 N94-32794
Development of a video fluorescence system for assessing burn depth
[AD-A278127] p 3798 N94-33092
Advanced release technologies program p 3607 N94-33322
LASER ARRAYS
High power diode lasers for solid-state laser pumps p 3722 N94-32448
LASER BEAMS
Laser safety manual for DREO
[AD-A276288] p 3714 N94-31255

The role of defects in laser damage of multilayer coatings
[DE94-006731] p 3714 N94-31269
Diagnostics of high-brightness short-pulse lasers and the plasmas they generate
[DE94-006165] p 3716 N94-31624
Statistics of time averaged atmospheric scintillation
[DE94-006998] p 3747 N94-32249
A historical perspective on fifteen years of laser damage thresholds at LLNL
[DE94-007930] p 3719 N94-32613
Short-pulse, high-intensity lasers at Los Alamos
[DE94-007545] p 3720 N94-32760
A miniaturized ASIC-based multichannel scaler instrument
[DE94-007222] p 3807 N94-32783
Coherent processes in atom in strong radiation fields
[AD-A278388] p 3874 N94-33144
Phase-only correction of scintillated laser beams: Downrange experimental results
[AD-A277778] p 3722 N94-33282

LASER CAVITIES
Semiconductor microcavity lasers
[DE94-006143] p 3716 N94-31622
Study of the dynamics of a nonlinear coupled-cavity laser system
[ISBN-0-315-86717-5] p 3716 N94-31748
A reliable low-maintenance flashlamp-pumped Ti:sapphire laser operating at 120 PPS
[DE94-009030] p 3721 N94-32848

LASER CUTTING
Laser applications in wood processing
[PB94-138567] p 3717 N94-31840
Thin EFG octagons
[DE94-006855] p 3905 N94-32764

LASER DAMAGE
Sol-gel metal oxide and metal oxide/polymer multilayers applied by meniscus coating
[DE94-005813] p 3649 N94-31199
Laser safety manual for DREO
[AD-A276288] p 3714 N94-31255
The role of defects in laser damage of multilayer coatings
[DE94-006731] p 3714 N94-31269
Large-area conditioning of optics for high-power laser systems
[DE94-007028] p 3716 N94-31636
A historical perspective on fifteen years of laser damage thresholds at LLNL
[DE94-007930] p 3719 N94-32613
Pump-probe method for investigating laser ablation and optical damage threshold mechanisms in optical materials
[DE94-008291] p 3720 N94-32753

LASER DEPOSITION
Reliability of multilayer copper/polyimide
[AD-A276228] p 3650 N94-31284
X ray absorption study of pulsed laser deposited boron nitride films
[DE94-008295] p 3662 N94-32855

LASER DOPPLER VELOCIMETERS
A preliminary investigation of high amplitude standing waves with laser Doppler anemometry
[AD-A276483] p 3860 N94-31242
Design of a two dimensional planer pressurized air labyrinth seal test rig
[AD-A277232] p 3726 N94-32370

LASER FUSION
Inertial fusion with ultra-powerful lasers
[DE94-007242] p 3887 N94-31400

LASER GUIDANCE
Design and early results of the sodium-layer laser guide star adaptive optics experiment at the Lawrence Livermore National Laboratory
[DE94-006653] p 3926 N94-32189

LASER INDUCED FLUORESCENCE
Laser-induced fluorescence of space-exposed polyurethane p 3593 N94-31026
Near resonant absorption by atoms in intense fluctuating laser fields
[DE94-005873] p 3714 N94-31200
Mechanisms of laser induced reactions in opaque heterogeneous environments
[AD-A276642] p 3717 N94-31996
Optical properties of doped sol-gel silica glasses
[AD-A278094] p 3884 N94-33267

LASER MATERIALS
Transient radiation-induced absorption in the materials for a GSGG laser
[DE94-005316] p 3714 N94-31148
New material for high average power infrared generation: QPM-DB GaAs
[AD-A276389] p 3714 N94-31358
Short-pulse, high-intensity lasers at Los Alamos
[DE94-007545] p 3720 N94-32760
Repetitively pulsed Cr:LiSAF laser for lidar applications
[DE94-007546] p 3720 N94-32761

LASER MICROSCOPY
X ray imaging and x ray source development at Lawrence Livermore National Laboratory
[DE94-007077] p 3719 N94-32629

LASER MODES
Transverse mode analysis of hole-coupled free-electron lasers
[ETN-94-96019] p 3715 N94-31532

LASER OUTPUTS
Near resonant absorption by atoms in intense fluctuating laser fields
[DE94-005873] p 3714 N94-31200
The role of defects in laser damage of multilayer coatings
[DE94-006731] p 3714 N94-31269
New material for high average power infrared generation: QPM-DB GaAs
[AD-A276389] p 3714 N94-31358
Diagnostics of high-brightness short-pulse lasers and the plasmas they generate
[DE94-006165] p 3716 N94-31624
Elastic modulus measurements of LDEF glasses and glass-ceramics using a speckle technique
[NASA-CR-195911] p 3653 N94-31851
Impact of observed hyperfine splitting on X-ray laser gain
[DE94-005822] p 3717 N94-32128
High conversion efficiency pumped-cavity second harmonic generation of a diode laser
[DE94-006805] p 3717 N94-32134
Ti:sapphire based ultrafast pump-probe laser source in the violet and ultraviolet
[DE94-007542] p 3718 N94-32270
High power diode lasers for solid-state laser pumps p 3722 N94-32448
Progress in understanding and improving x ray lasers
[DE94-008048] p 3720 N94-32794
A reliable low-maintenance flashlamp-pumped Ti:sapphire laser operating at 120 PPS
[DE94-009030] p 3721 N94-32848
Multifrequency, rapidly sequenced or simultaneous tunable laser
[AD-D016169] p 3721 N94-32968

LASER PLASMA INTERACTIONS
Inertial fusion with ultra-powerful lasers
[DE94-007242] p 3887 N94-31400

LASER PLASMAS
Diagnostics of high-brightness short-pulse lasers and the plasmas they generate
[DE94-006165] p 3716 N94-31624
Superluminous laser pulse in an active medium
[DE94-007110] p 3720 N94-32684
Molten metal analysis by laser produced plasmas
[DE94-007014] p 3646 N94-32782

LASER POWER BEAMING
DOE reactor-pumped laser program
[DE94-006372] p 3715 N94-31485

LASER PUMPING
Ti:sapphire based ultrafast pump-probe laser source in the violet and ultraviolet
[DE94-007542] p 3718 N94-32270
High power diode lasers for solid-state laser pumps p 3722 N94-32448
A noncritically phase matched femtosecond optical parametric oscillator near 3 microns
[DE94-008050] p 3720 N94-32704
A reliable low-maintenance flashlamp-pumped Ti:sapphire laser operating at 120 PPS
[DE94-009030] p 3721 N94-32848

LASER RANGE FINDERS
Synchronized laser scanning three dimensional acquisition system
[ISBN-0-315-86848-1] p 3879 N94-31756

LASER SPECTROSCOPY
Characterization of polymer decomposition products by laser desorption mass spectrometry p 3597 N94-31046
Stark broadening of the 2S state of hydrogen and deuterium in arc plasmas of low density
[ETN-94-95731] p 3888 N94-31572
Using laser absorption spectroscopy to monitor composition and physical properties of metal vapors
[DE94-001536] p 3716 N94-31599
Laser and Fourier transform spectroscopy of novel propellant molecules
[AD-A277506] p 3667 N94-33013

LASER STABILITY
Time evolution and filamentation of KrF(star) laser gas discharges
[ETN-94-95758] p 3715 N94-31561

LASER TARGET INTERACTIONS
Molten metal analysis by laser produced plasmas
[DE94-007014] p 3646 N94-32782
Coherent processes in atom in strong radiation fields
[AD-A278388] p 3874 N94-33144

LASER TARGETS
Inertial fusion with ultra-powerful lasers
[DE94-007242] p 3887 N94-31400
New polymer target-shell properties and characterizations
[DE94-008420] p 3890 N94-32415
Progress in understanding and improving x ray lasers
[DE94-008048] p 3720 N94-32794
Phase-only correction of scintillated laser beams: Downrange experimental results
[AD-A277778] p 3722 N94-33282

LASER WELDING
Nd-YAG laser welding of the fiber optic connector to the header shell on the 2SL actuator
[DE94-006104] p 3723 N94-31621

LASERS
High power switch design for the Nova upgrade laser (Project HERCULES: High Energy Research Concerning the Ultimate Lifetime of Experimental Switches)
[DE94-007921] p 3719 N94-32654
Comparison of coherent to incoherent detection at 2.09 micrometers using a solid state LADAR system
[AD-A277159] p 3721 N94-33102

LASING
Progress in understanding and improving x ray lasers
[DE94-008048] p 3720 N94-32794

LATCHES
Space Station Freedom solar array containment box mechanisms p 3603 N94-33292
Deployable and retractable telescoping tubular structure development p 3607 N94-33317

LATENT HEAT
The influence of cumulus parameterization on model forecasts of rapid oceanic cyclogenesis
[AD-A277207] p 3784 N94-32094
The influence of thermal inertia on Mars' seasonal pressure variation and the effect of the weather component p 3952 N94-33238

LATERAL CONTROL
Phase-lock roll control of inertially pointing spacecraft p 3609 N94-31470

LATTICE PARAMETERS
Inorganic materials for anomalous-dispersion phase-matched second harmonic generation: Rubidium titanyl arsenate isomorphs, Rb(Ti(1-2x)Ln(x)Nb(x))OAsO4
[DE94-006141] p 3899 N94-31847
Area-interaction point processes
[CWI-BS-R9318] p 3847 N94-32197
High temperature materials technology research for advanced thermionic systems
[DE94-008444] p 3644 N94-32416

LATTICE VIBRATIONS
The 10th International Conference on Internal Friction and Ultrasonic Attenuation in Solids (ICIFUAS)
[AD-A276849] p 3902 N94-32209

LATTICES (MATHEMATICS)
On the independent axiomatizability of modal and intermediate logics
[ML-93-17] p 3856 N94-31407
Lattice geometrodynamics p 3857 N94-31825

LAUNCH VEHICLE CONFIGURATIONS
Advanced transportation system study: Manned launch vehicle concepts for two way transportation system payloads to LEO
[NASA-CR-193951] p 3608 N94-33100

LAUNCH VEHICLES
On-line physical parameter identification and adaptive control of a launch vehicle p 3602 N94-31891
Access to space: The Space Shuttle's evolving rolee
[AD-A276785] p 3608 N94-32190
DOD space based requirements: Increasing DOD access to space
[AD-A276874] p 3601 N94-32211
Space flight risk data collection and analysis project: Risk and reliability database
[NASA-CR-195879] p 3603 N94-32494
Space Station evolution study
[NASA-CR-193937] p 3611 N94-32898
Aerospace sponsored research
[ATR-93(8498)-1] p 3966 N94-32949
Advanced transportation system study: Manned launch vehicle concepts for two way transportation system payloads to LEO
[NASA-CR-193951] p 3608 N94-33100

LAUNCHING BASES
DOD space based requirements: Increasing DOD access to space
[AD-A276874] p 3601 N94-32211

LAVA
Evidence for ultramafic lavas on Syrtis Major p 3950 N94-33229

LAW (JURISPRUDENCE)
Standardization and intellectual property control: A reflection on the informatics case
[TELECOM-93-E-016] p 3915 N94-31172
An expert system architecture for heterogeneous domains: A case-study in the legal field
[ETN-94-96012] p 3830 N94-31546
Analysis of Navy aircraft engine and engine component warranties
[AD-A276936] p 3584 N94-32238
LAY-UP
Comparison of the compressive strengths for stitched and toughened composite systems
[NASA-TM-109108] p 3627 N94-32939
LEAD (METAL)
Mass-loaded coating for reducing the resonant frequency of a ceramic disc
[AD-D016095] p 3660 N94-32739
LEAD ALLOYS
Electrooptic crystal growth and properties
[AD-A276023] p 3896 N94-31439
Aging effects on the microstructure, surface characteristics and wettability of Cu pretinned with Sn-Pb solders
[DE94-007033] p 3641 N94-31638
LEAD ISOTOPES
Collective and quasiparticle excitations in light Pb isotopes
[ETN-94-96014] p 3865 N94-31548
LEAD ZIRCONATE TITANATES
Passive vibration damping materials: Piezoelectric ceramic composites for vibration damping applications
[AD-A276550] p 3653 N94-31935
Thin-film decoupling capacitors for multi-chip modules
[DE94-007743] p 3695 N94-32650
LEADERSHIP
Space history, space policy, and executive leadership
[NASA-TM-109787] p 3924 N94-33067
LEADING EDGES
Design and initial testing of a facility to measure unsteady pressures on an oscillating cascade with supersonic leading edge locus p 3569 N94-31680
Hotwire measurements of the turbulent flow into a cascade of controlled-diffusion compressor blades
[AD-A277297] p 3706 N94-32042
LEAF AREA INDEX
High resolution spectroscopy in agriculture: Results of the EISAC 1989 campaign p 3745 N94-31864
Quantitative analysis of woody vegetation in Soudano-Sahalian region. Textural approach (application to a Burkina Faso region) p 3757 N94-32574
LEARNING
Reminding-based learning
[AD-A277424] p 3801 N94-32997
LEARNING THEORY
Concepts and environment
[REPT-93-032] p 3829 N94-31186
LEAST SQUARES METHOD
Identification of polynomial and rational NARMAX models
[RR-483] p 3842 N94-31413
Pairwise-comparison using the logarithmic least squares method and the generalized pseudoinverse
[REPT-93-84] p 3844 N94-31701
Model identification of a reconfigurable robot manipulator
[ISBN-0-315-87109-1] p 3725 N94-31874
Hierarchical mixtures of experts and the EM algorithm
[AD-A276516] p 3814 N94-31932
Least squares approximation by G1 piecewise parametric cubes
[AD-A277978] p 3850 N94-33265
LECTURES
Index to NASA news releases and speeches, 1993
[NASA-TM-109722] p 3917 N94-31888
Space history, space policy, and executive leadership
[NASA-TM-109787] p 3924 N94-33067
LENSES
Multi-line passive fiber optic slipring
[AD-D016092] p 3863 N94-32738
LEPTONS
Perturbative and nonperturbative EM lepton pair production in relativistic heavy-ion collisions
[DE94-006315] p 3867 N94-31779
Baryogenesis from a primordial lepton asymmetry
[PB94-145166] p 3868 N94-31921
Probing lepton number violation via Majorana neutrinos at hadron supercolliders
[PB94-147055] p 3868 N94-31922
Semileptonic decays of mesons in the SO(4) model
[DE94-008108] p 3873 N94-32708
LIAPUNOV FUNCTIONS
A Hyland-Bernstein approach to the digital control of Pritchard-Salamon systems
[REPT-93-76] p 3844 N94-31693
LIBRARIES
Texture library for 3-dimensional visualization systems
[AD-A276125] p 3917 N94-31829
A high-speed linear algebra library with automatic parallelism p 3828 N94-32440
NASA/DOD Aerospace Knowledge Diffusion Research Project. Paper 5: Aerospace librarians and technical information specialists as information intermediaries: A report of phase 2 activities of the NASA/DOD Aerospace Knowledge Diffusion Research Project
[NASA-TM-109777] p 3921 N94-32829
MDFF HELP library, version 2: On-line documentation for the map data formatting facility
[AD-A277763] p 3922 N94-32987
LIBRATION
Forced libration of Mercury and geodetic determination of a possible fluid core p 3774 N94-32493
LIE GROUPS
On wavelet representations of differential equations
[RR-482] p 3842 N94-31412
LIFE CYCLE COSTS
An analysis of non-integerizing the aircraft engines Cost Effectiveness Analysis Spreadsheet Model (CEAMOD version 2.0)
[AD-A276251] p 3583 N94-31290
Software reuse case study: TRILLIUM
[AD-A276108] p 3811 N94-31465
LIFE SCIENCES
Aerospace medicine and biology: A continuing bibliography with indexes (supplement 388)
[NASA-SP-7011(388)] p 3795 N94-31414
Aerospace medicine and biology: A continuing bibliography with indexes (supplement 389)
[NASA-SP-7011(389)] p 3797 N94-32347
Aerospace medicine and biology: A continuing bibliography with indexes (supplement 385)
[NASA-SP-7011(385)] p 3797 N94-32348
LIFE SUPPORT SYSTEMS
Technical assessment of Mir-1 life support hardware for the international space station
[NASA-TM-108441] p 3803 N94-31380
Design of a logistics model for building and supporting a lunar station
[ILR-MITT-282(1993)] p 3803 N94-31852
Aerospace medicine and biology: A continuing bibliography with indexes (supplement 389)
[NASA-SP-7011(389)] p 3797 N94-32347
Aerospace medicine and biology: A continuing bibliography with indexes (supplement 385)
[NASA-SP-7011(385)] p 3797 N94-32348
Catalytic methods using molecular oxygen for treatment of PMMS and ECLSS waste streams, volume 2
[NASA-CR-190299] p 3804 N94-32697
Characterization and utilization of opiate-like hibernation factors
[AD-A278136] p 3794 N94-33098
LIFTING BODIES
Aeroelastic vibrations of lifting surfaces
[ECL-91-01] p 3585 N94-31677
LIGANDS
Silicone grease as a precursor to a pseudo crown-ether ligand: Crystal structure of (K(+)K(Me2SiO)7(+))(HIn(CH2CMe3)3(-))4)
[AD-A276343] p 3895 N94-31327
Combinatorial ion sensors
[AD-A276567] p 3825 N94-32032
A genetic algorithm based method for docking flexible molecules
[DE94-007525] p 3793 N94-32269
Laser flash photolysis, EPR and Raman studies of liquids at elevated pressures
[DE94-008351] p 3718 N94-32413
Ligand intermediates in metal-catalyzed reactions
[DE94-008713] p 3638 N94-32887
LIGHT AMPLIFIERS
Short-pulse, high-intensity lasers at Los Alamos
[DE94-007545] p 3720 N94-32760
LIGHT BEAMS
Studies of optical beam phase conjugation and electromagnetic scattering process
[AD-A278389] p 3884 N94-33145
LIGHT ELEMENTS
Strongly coupled ionic mixtures and the H/He EOS
[DE94-006391] p 3934 N94-31782
LIGHT EMISSION
Matter-radiation interactions in the atmosphere p 3776 N94-30998
LIGHT EMITTING DIODES
Temperature dependence of the exciton-exciton annihilation rate constant in poly(di-n-hexylsilane)
[DE94-005584] p 3655 N94-32102
LIGHT MODULATION
Optical and image transmission through desert atmospheres
[AD-A276022] p 3742 N94-31496
Correlation filter synthesis using neural networks
[AD-A278124] p 3836 N94-33043
LIGHT SCATTERING
Single scattering of light by ensembles of particles with various shapes
[ETN-94-96016] p 3878 N94-31550
Methods for SBS threshold reduction
[AD-A276554] p 3717 N94-31936
Multiple size scale structures in silica/siloxane composites studied by small-angle scattering
[DE94-007300] p 3625 N94-32642
Light scattering studies of a model electrorheological fluid
[DE94-007860] p 3883 N94-32818
LIGHT SOURCES
Light in Thermal Environments (LITE) Workshop
[NASA-CR-195851] p 3790 N94-32981
LIGHT TRANSMISSION
Near resonant absorption by atoms in intense fluctuating laser fields
[DE94-005873] p 3714 N94-31200
Optical and image transmission through desert atmospheres
[AD-A276022] p 3742 N94-31496
Optimization of Y junctions in integrated optics
[ISBN-0-315-86782-5] p 3879 N94-31751
Fast acting optical deflection
[AD-A276830] p 3879 N94-32037
Statistics of time averaged atmospheric scintillation
[DE94-006996] p 3747 N94-32249
Ocean optics, ocean imaging and optical tomography
[AD-A277010] p 3789 N94-32402
Mathematical nonlinear optics
[AD-A277320] p 3882 N94-32510
Femtosecond probe-probe transmission studies of LT-grown GaAs near the band edge
[DE94-006660] p 3904 N94-32634
Structural studies of photoinduced intramolecular electron transfer in cyclopentadienylnickelnitrosyl
[DE94-008487] p 3874 N94-32876
Strain sensing using optical fibers
[NASA-CR-195807] p 3740 N94-32940
Studies of optical beam phase conjugation and electromagnetic scattering process
[AD-A278389] p 3884 N94-33145
LIGHTNING
Lightning-induced coupling of the radiation belts to geomagnetically conjugate ionospheric regions p 3772 N94-31773
LIGNIN
Towards a detailed understanding of the structural variability in lignins: A new approach
[DE94-007449] p 3793 N94-32267
LIKELIHOOD RATIO
Area-interaction point processes
[CWI-BS-R9318] p 3847 N94-32197
LIMITS (MATHEMATICS)
On wavelet representations of differential equations
[RR-482] p 3842 N94-31412
Stirling's formula and approximations for n(factorial) and the middle ratio
[REPT-93-73] p 3843 N94-31642
Qualitative properties of two-dimensional predator-prey systems
[REPT-93-75] p 3844 N94-31644
A predator-prey model with Iviev's functional response
[REPT-93-79] p 3844 N94-31696
Kaplan-Meier estimators of interpoint distance distributions for spatial point processes
[CWI-BS-R9315] p 3846 N94-32107
Multiserver queues with impatient customers
[CWI-BS-R9319] p 3835 N94-32198
LINE SPECTRA
Line-strength gradients and kinematic profiles in elliptical galaxies p 3934 N94-31788
LINEAR ACCELERATORS
Free electrons as a versatile source of coherent radiation
[ETN-94-96011] p 3715 N94-31545
Selected applications of planar permanent magnet multipoles in FEL insertion device design
[DE94-009014] p 3721 N94-32845
LINEAR CIRCUITS
Analysis and synthesis of MOS translinear circuits
[ISBN-9-09-005495-2] p 3690 N94-31616
LINEAR POLARIZATION
High-resolution synthetic aperture radar observations of the Moon p 3676 N94-31952
Post-calibration correction for rotating-analyzer ellipsometer with optical fiber bundle detection system
[AD-A277329] p 3881 N94-32260
LINEAR PROGRAMMING
Parallel structured optimization algorithms for inverse problems
[AD-A276053] p 3811 N94-31443

Perfect 0, +/- matrices
[AD-A277387] p 3848 N94-32286
A simple model for determining photoelectron-generated radiation scaling laws
[DE94-006130] p 3761 N94-32660
Optimal planning of residential photovoltaic systems under various rate structure
[DE94-757272] p 3762 N94-32919

LINEAR QUADRATIC GAUSSIAN CONTROL
A Hyland-Bernstein approach to the digital control of Pritchard-Salamon systems
[REPT-93-76] p 3844 N94-31693

LINEAR QUADRATIC REGULATOR
Approximation theory and computational methods for the identification and control of distributed parameter systems
[AD-A277335] p 3848 N94-32244

LINEAR SYSTEMS
Structural properties of inverse linear systems
[MATHS-REPT-A-200] p 3840 N94-31156
Wavevector-frequency analysis with applications to acoustics
[AD-A276618] p 3861 N94-32125

LINEAR TRANSFORMATIONS
Line transects, covariance functions and set approximation
[CWI-BS-R9311] p 3846 N94-32084

LINEARITY
On the linearity of fast atomic oxygen effects
p 3594 N94-31027

LINEARIZATION
Modeling and control of nonlinear systems
[AD-A277377] p 3834 N94-32095

LINGUISTICS
The interpretation of free focus
[CL-93-01] p 3855 N94-31390
An exploratory study of neuro linguistic programming and communication anxiety
[AD-A277756] p 3682 N94-32986

LIOUVILLE EQUATIONS
A general stochastic Liouville theory for sequential and superexchange electron-transfer reactions involving three Marcus potential surfaces
[DE94-007695] p 3869 N94-32141

LIPID METABOLISM
Lipid metabolism in cold-exposed humans
p 3796 N94-31741

LIQUEFIED GASES
Ionization EM calorimetry with accordion electrodes and liquid krypton or argon
[DE94-009082] p 3713 N94-32821

LIQUID ALLOYS
Structural ordering in liquid K-Te alloys
[DE94-008477] p 3645 N94-32514

LIQUID COOLING
A review of microclimate cooling systems in the chemical, biological, radiological environment
[AD-A276446] p 3802 N94-31302
Heat transfer studies on a rectangular channel with offset plate fins
[AD-A277300] p 3912 N94-32043

LIQUID CRYSTALS
Active matrix liquid crystal display. Industry survey results
[AD-A276415] p 3895 N94-31329
Thermotropic liquid crystals: A variable Clo material
p 3796 N94-31739
The sol-gel-xerogel transition
[AD-A276647] p 3616 N94-32038
Mathematical nonlinear optics
[AD-A277320] p 3882 N94-32510

LIQUID FUELS
Heterogeneous catalytic process for alcohol fuels from syngas
[DE94-008729] p 3667 N94-32583

LIQUID HYDROGEN
Computational modeling of convective heat transfer to liquid hydrogen coolant p 3707 N94-32485

LIQUID INJECTION
Analysis of strong acoustic excitation on the breakup and dispersion of a liquid jet
[ONERA-NT-1993-9] p 3701 N94-31422

LIQUID METALS
Solidification structure synthesis in undercooled liquids
[AD-A276166] p 3910 N94-31054
Metal induced embrittlement
[DE94-007450] p 3640 N94-31325
Control experiments in liquid metal combustion
[AD-A276918] p 3635 N94-32234
Molten metal analysis by laser produced plasmas
[DE94-007014] p 3646 N94-32782

LIQUID PHASES
Development of a catalytic system for gasification of wet biomass
[DE94-006216] p 3759 N94-31762

LIQUID-LIQUID INTERFACES
Steady thermal convection in multiple liquid layers
p 3705 N94-31844

LIQUID-SOLID INTERFACES
Interfacial behaviour: Wettability in SiC(sub p) metal matrix composites
[ISBN-0-315-87206-3] p 3621 N94-31835
Chemical structure and kinetics at liquid/solid interfaces
[AD-A277112] p 3636 N94-32304
Time-resolved analytical methods for liquid/solid interfaces
[DE94-008352] p 3637 N94-32826

LIQUIDS
Empirical and semi-empirical relationships of liquid-vapor, solid-vapor, and solid-liquid surface energies
[AD-A276480] p 3631 N94-31248

LISP (PROGRAMMING LANGUAGE)
Emacs Lisp in Edwin scheme
[AD-A276721] p 3818 N94-32504
Translating an AI application from Lisp to Ada: A case study
[NASA-TM-103845] p 3820 N94-32906

LITHIUM
Sodium sulfate corrosion of silicon carbide fiber-reinforced lithium aluminosilicate glass-ceramic matrix composites
[AD-A277224] p 3623 N94-32023
Status of developing a multifunctional aviation grease
[AD-A276755] p 3656 N94-32184
Performance of the Sony lithium-ion rechargeable battery
[AD-A277076] p 3693 N94-32303
Proceedings of the Ad Hoc Workshop on Ceramics for Li/FeS2 batteries
[DE94-007460] p 3694 N94-32607

LITHIUM ALLOYS
Calculations of nonspherically averaged charge densities for substitutionally disordered alloys
[DE94-008293] p 3646 N94-32754

LITHIUM NIOBATES
Manufacture of light-damage resistant, planar, single mode waveguide on lithium niobate
[DSIS-94-01503] p 3879 N94-31850

LITHOGRAPHY
Semiconductor microcavity lasers
[DE94-006143] p 3716 N94-31622
Development, characterization, and applications of high temperature superconductor nanobridge Josephson junctions
[DE94-008113] p 3903 N94-32409

LITHOLOGY
Analysis of deep seismic reflection and other data from the southern Washington Cascades
[DE94-005958] p 3771 N94-31525

LITHOSPHERE
Patterns of deformation and volcanic flows associated with lithospheric loading by large volcanoes on Venus
p 3776 N94-31106
State of stress, faulting, and eruption characteristics of large volcanoes on Mars p 3940 N94-31108
Origin and thermal evolution of Mars
p 3940 N94-31109
The tectonic and volcanic evolution of Venus: Catastrophic or gradual? p 3940 N94-31111

LOAD CARRYING CAPACITY
Mechanics of cracking for composite material
p 3624 N94-32501

LOAD TESTS
Determining the bearing capacity of flexible airfield pavements using a heavy weight deflectometer
[ISBN-0-315-86210-6] p 3587 N94-31710
Structural testing of the technology integration box beam p 3628 N94-33125
Technology integration box beam failure study
p 3628 N94-33126

LOADS (FORCES)
Patterns of deformation and volcanic flows associated with lithospheric loading by large volcanoes on Venus
p 3776 N94-31106
Energy absorber for the CETA p 3604 N94-33303

LOCAL THERMODYNAMIC EQUILIBRIUM
SOLGAS refined: A computerized thermodynamic equilibrium calculation tool
[DE94-009021] p 3913 N94-32848

LOCI
Design and initial testing of a facility to measure unsteady pressures on an oscillating cascade with supersonic leading edge locus p 3569 N94-31880

LOGARITHMS
Pairwise-comparison using the logarithmic least squares method and the generalized pseudoinverse
[REPT-93-84] p 3844 N94-31701

LOGIC
Correspondence theory for extended modal logics, version 3.0
[ML-93-16] p 3856 N94-31417

LOGIC CIRCUITS
Fault coverage measurement for digital microcircuits
[AD-A276226] p 3686 N94-31066
Formal verification of systolic multipliers with the Boyer-Moore theorem prover
[RR-897-M] p 3839 N94-31082
A neuron network for image classification: From algorithm to implantation
[TELECOM-93-E-005] p 3687 N94-31168
Study of continuous-time and mixed analog-digital operators
[TELECOM-93-E-010] p 3687 N94-31170
A hierarchical approach to test generation for CMOS VLSI circuits
[ISBN-9-09-005449-9] p 3689 N94-31535
Radiation tolerant, high speed, low power, gallium arsenide logic
[AD-A277293] p 3694 N94-32509
Multiple-valued programmable logic array minimization by solution space search
[AD-A278033] p 3821 N94-33090
A diagnostic expert system for digital circuits
p 3699 N94-33340

LOGIC DESIGN
Extension of the LUSTRE language and application to circuit design: The LUSTRE V4 language and the POLLUX system
[ETN-94-95918] p 3812 N94-31543
Radiation tolerant, high speed, low power, gallium arsenide logic
[AD-A277293] p 3694 N94-32509

LOGIC PROGRAMMING
LORE and reason maintenance
[REPT-93-88] p 3812 N94-31522

LOGISTICS
The Nomad Explorer assembly assist vehicle: An architecture for rapid global extraterrestrial base infrastructure establishment p 3599 N94-31429
Knowledge-based commodity distribution planning
p 3915 N94-32427
Space Station evolution study
[NASA-CR-193937] p 3611 N94-32898
Analysis of intermediate level maintenance following F404-GE-400 engine component life reductions
[AD-A277918] p 3585 N94-33283

LOGISTICS MANAGEMENT
A study of theoretical models for managing technology change and a comparison to a radio frequency identification implementation
[AD-A276012] p 3672 N94-31385
Modular Simulator System (MSS) management guide
[AD-A277098] p 3588 N94-32014

LONG DURATION EXPOSURE FACILITY
LDEF Materials Results for Spacecraft Applications
[NASA-CP-3257] p 3591 N94-31012
The performance of thermal control coatings on LDEF and implications to future spacecraft
p 3591 N94-31013
Performance of silvered Teflon (trademark) thermal control blankets on spacecraft p 3591 N94-31014
Space environment durability of beta cloth in LDEF thermal blankets p 3591 N94-31015
Space Station WP-2 application of LDEF MLI results
p 3592 N94-31016
Anodized aluminum on LDEF p 3592 N94-31017
Follow-up on the effects of the space environment on UHCRE thermal blankets p 3592 N94-31018
Modeling of LDEF contamination environment
p 3592 N94-31019
Spacecraft contamination issues from LDEF: Issues for design p 3592 N94-31020
Model of spacecraft atomic oxygen and solar exposure microenvironments p 3593 N94-31021
Atomic oxygen erosion considerations for spacecraft materials selection p 3593 N94-31022
Performance of selected polymeric materials on LDEF
p 3593 N94-31023
Atomic oxygen interaction at defect sights in protective coatings on polymers flown on LDEF
p 3593 N94-31024
Fluorescence observations of LDEF exposed materials as an indicator of induced material reactions
p 3593 N94-31025
Laser-induced fluorescence of space-exposed polyurethane p 3593 N94-31026
On the linearity of fast atomic oxygen effects
p 3594 N94-31027
Micrometeoroid/space debris effects on materials
p 3595 N94-31032
Thermal-vacuum response of polymer matrix composites in space p 3595 N94-31033

The impact of LDEF results on the space application of metal matrix composites p 3595 N94-31034
Low-Earth orbit effects on organic composite materials flown on LDEF p 3595 N94-31036
Summary of materials and hardware performance on LDEF p 3595 N94-31037
LDEF materials special investigation group's data bases p 3596 N94-31038
Analysis of leading edge and trailing edge cover glass samples before and after treatment with advanced satellite contamination removal techniques p 3596 N94-31041
Effects of orbital exposure on RTV during the LDEF mission p 3597 N94-31043
Spacecraft materials: Comparison between flight results obtained on LDEF and MIR p 3597 N94-31045
Characterization of polymer decomposition products by laser desorption mass spectrometry p 3597 N94-31046
Design application and development of spacecraft in LEO utilizing LDEF results p 3597 N94-31047
An overview of the on-orbit contamination of the Long Duration Exposure Facility (LDEF) p 3598 N94-31049
What LDEF means for development and testing of materials p 3598 N94-31050

LONG RANGE WEATHER FORECASTING
Thermospheric modeling accuracies using F10.7 and Ap
[AD-A277355] p 3773 N94-32337

LONG WAVE RADIATION
Development of a statistical method for estimating the downward longwave radiation at the surface from satellite observations p 3742 N94-31553

LOOPS
Varying execution discipline to increase performance
[DE94-007844] p 3819 N94-32651

LORENTZ FORCE
Magnetohydrodynamic boundary layer control system
[AD-D016120] p 3710 N94-32958

LOW COST
A low cost igniter utilizing an SCB and titanium sub-hydride potassium perchlorate pyrotechnic
[DE94-006467] p 3666 N94-31827

LOW DENSITY FLOW
Simulation of low-density nozzle plumes in non-zero ambient pressures
[NASA-TM-106501] p 3615 N94-32742

LOW GRAVITY MANUFACTURING
Design, characterization, and control of the NASA three degree of freedom reaction compensation platform p 3605 N94-33304

LOW PASS FILTERS
Variable-resolution imagery for flight simulation
[AD-A276199] p 3586 N94-31058

LOW REYNOLDS NUMBER
Aerodynamic drag of droplets in turbulent flow fields
[ISBN-0-315-75827-9] p 3571 N94-32491
An analysis of supersonic flows with low-Reynolds number compressible two-equation turbulence models using LU finite volume implicit numerical techniques
[NASA-CR-195302] p 3572 N94-32926
Backward-facing step measurements at low Reynolds number, Re(sub h)=5000
[NASA-TM-108807] p 3711 N94-33290

LOW SPEED
Control of low-speed turbulent separated flow over a backward-facing ramp
[NASA-TM-109740] p 3573 N94-33071

LOW TEMPERATURE
Performance of silvered Teflon (trademark) thermal control blankets on spacecraft p 3591 N94-31014
Metal cluster-rare gas van der Waals complexes: Microscopic models of physisorption
[DE94-008134] p 3873 N94-32797
Low energy ion beam assisted growth of homoepitaxial silicon films at low temperature
[AD-A278092] p 3908 N94-33039

LOW TEMPERATURE PHYSICS
Finite element analysis of time-independent superconductivity p 3691 N94-31905

LUBRICANTS
Measurement of viscosity, density, and gas solubility of refrigerant blends in selected synthetic lubricants
[DE94-007723] p 3653 N94-31917
Compatibility of refrigerants and lubricants with elastomers
[DE94-008552] p 3658 N94-32518
Perfluoropolyalkylether decomposition on catalytic aluminas
[NASA-TM-106547] p 3617 N94-33021
A comparison of the performance of solid and liquid lubricants in oscillating spacecraft ball bearings p 3606 N94-33311
The preliminary evaluation of liquid lubricants for space applications by vacuum tribometry p 3606 N94-33313

LUBRICATING OILS
Status of developing a multifunctional aviation grease
[AD-A276755] p 3656 N94-32184
Lubrication with binary mixtures: Liquid-liquid emulsion in elastohydrodynamics and metal forming p 3658 N94-32490

LUBRICATION
Lubrication with binary mixtures: Liquid-liquid emulsion in elastohydrodynamics and metal forming p 3658 N94-32490
Frictional behavior and adhesion of Ag and Au films applied to aluminum oxide by oxygen-ion assisted Screen Cage Ion Plating (SCIP)
[NASA-TM-106522] p 3647 N94-32931
Torque characteristics of solid lubricated precision bearings during oscillatory motion
[AD-A278133] p 3728 N94-33061

LUBRICATION SYSTEMS
Design of a high-speed reliable ball bearing p 3606 N94-33314

LUMINAIRES
An analysis of the maintenance performance measurement system for LAMPS MK 3 helicopter squadrons
[AD-A276421] p 3565 N94-31332
Evaluation for the development of taxiway lighting intensity standards
[AD-A276706] p 3588 N94-32120

LUMINESCENCE
A miniaturized ASIC-based multichannel scaler instrument
[DE94-007222] p 3807 N94-32783
Light in Thermal Environments (LITE) Workshop
[NASA-CR-195851] p 3790 N94-32981

LUMINOSITY
Can a variable alpha induce limit cycle behavior and exponential luminosity decay in transient soft x ray sources? p 3929 N94-31129
Thermal continua of AGN accretion disks p 3931 N94-31137

LUMINOUS INTENSITY
Radiation/remote sensing: Review of the principal definitions p 3757 N94-30996
Evaluation of intensity distribution profiles for US. Army rotorcraft position lighting adapted for image intensifier operations
[AD-A276459] p 3804 N94-32171
Bioluminescence bathyphotometer
[AD-D016102] p 3790 N94-32959

LUNAR BASED EQUIPMENT
Mitigation of adverse environmental effects on lunar-based astronomical instruments p 3598 N94-31426

LUNAR BASES
The Second Annual International Space University Alumni Conference
[NASA-CP-3253] p 3598 N94-31425
Solar lunar power p 3599 N94-31427
The Nomad Explorer assembly assist vehicle: An architecture for rapid global extraterrestrial base infrastructure establishment p 3599 N94-31429
Design of a logistics model for building and supporting a lunar station
[ILR-MITT-282(1993)] p 3803 N94-31852

LUNAR DUST
Mitigation of adverse environmental effects on lunar-based astronomical instruments p 3598 N94-31426

LUNAR EXPLORATION
The Nomad Explorer assembly assist vehicle: An architecture for rapid global extraterrestrial base infrastructure establishment p 3599 N94-31429
Apollo 11 highlights
[NASA-TM-109763] p 3600 N94-31820
A multitasking behavioral control system for the Robotic All Terrain Lunar Exploration Rover (RATLER)
[DE94-007293] p 3835 N94-32787

LUNAR GEOLOGY
The Lunar Scout Program: An international program to survey the Moon from orbit for geochemistry, mineralogy, imagery, geodesy, and gravity
[NASA-TM-104791] p 3943 N94-32923

LUNAR LANDING
Apollo 11 highlights
[NASA-TM-109763] p 3600 N94-31820
Load-limiting landing gear footpad energy absorption system p 3607 N94-33323

LUNAR LOGISTICS
Design of a logistics model for building and supporting a lunar station
[ILR-MITT-282(1993)] p 3803 N94-31852

LUNAR PROGRAMS
The Lunar Scout Program: An international program to survey the Moon from orbit for geochemistry, mineralogy, imagery, geodesy, and gravity
[NASA-TM-104791] p 3943 N94-32923

LUNAR SATELLITES
The Lunar Scout Program: An international program to survey the Moon from orbit for geochemistry, mineralogy, imagery, geodesy, and gravity
[NASA-TM-104791] p 3943 N94-32923

LUNAR SPACECRAFT
Load-limiting landing gear footpad energy absorption system p 3607 N94-33323

LUNAR SURFACE
The Nomad Explorer assembly assist vehicle: An architecture for rapid global extraterrestrial base infrastructure establishment p 3599 N94-31429
High-resolution synthetic aperture radar observations of the Moon p 3676 N94-31952
Load-limiting landing gear footpad energy absorption system p 3607 N94-33323

LUNGS
Effects of combined breathing impediments on diver's respiratory performance
[AD-A277437] p 3805 N94-33084

LYMAN ALPHA RADIATION
A study of the neutral hydrogen distribution of the Milky Way through 21 cm emission and Lyman alpha absorption p 3938 N94-32309

M

MACH NUMBER
Hypervelocity Tunnel 9 Mach 10/14 Calibration
[AD-A275960] p 3587 N94-31318
Hotwire measurements of the turbulent flow into a cascade of controlled-diffusion compressor blades
[AD-A277297] p 3706 N94-32042
A new method for calculating wing along aerodynamics to angle of attack 180 deg
[AD-A277965] p 3574 N94-33263

MACH-ZEHNDER INTERFEROMETERS
A technique for multiplexing 3x3-coupler terminated interferometric fiber-optic sensors
[AD-A276739] p 3880 N94-32180

MACHINE LEARNING
Report of the 'Mathematical Models for Neural Networks' course
[TELECOM-93-D-019] p 3828 N94-31100
Concepts and environment
[REPT-93-032] p 3829 N94-31186
Filtering and recognition of moving boats in radar images
[REPT-93-039] p 3671 N94-31190
A neural network methodology for engineering applications: The learning control of robotic systems
[RR-480] p 3830 N94-31500
Trajectory learning with a direct drive robotic manipulator p 3831 N94-31794
Neural network definitions of highly predictable protein secondary structure classes
[DE94-006234] p 3834 N94-32175
A differential theory of learning for efficient statistical pattern recognition
[AD-A277313] p 3800 N94-32277
Refining fuzzy logic controllers with machine learning p 3839 N94-32421
Analysis and synthesis of adaptive neural elements and assemblies
[AD-A277423] p 3836 N94-32996
Investigation of drive-reinforcement learning and application of learning to flight control
[AD-A277442] p 3801 N94-33053

MACHINE TRANSLATION
Automatic translation among spoken languages p 3685 N94-32437

MACHINING
Cost-effective ceramic machining: Summary of three-body wear experiments
[DE94-007757] p 3650 N94-31354
Neutral ion sources in precision manufacturing p 3875 N94-32447
Leveraging metal matrix composites to reduce costs in space mechanisms p 3604 N94-33301

MACROMOLECULES
Multifunctional macromolecules
[AD-A277347] p 3856 N94-32246

MAGELLANIC CLOUDS
Study of stellar associations located in the region contained between the Magellanic Clouds
[ISBN-0-315-86692-6] p 3935 N94-31913

MAGIC TEES
An investigation of a novel microstrip magic-T
[ISBN-0-315-86218-1] p 3690 N94-31711

MAGNESIUM
The magnesium chelation step in chlorophyll biosynthesis
[DE94-008727] p 3794 N94-32890

MAGNESIUM ALLOYS
Shock tube ignition and combustion of aluminum/magnesium alloy particles in oxygen at high pressure p 3631 N94-31286
MAGNESIUM ISOTOPES
Mechanisms of formation and of de-excitation in the reaction Mg-24 + C-12 yields 9 alpha at 35MeV per nucleon
[ISBN-0-315-86746-9] p 3867 N94-31749
MAGNET COILS
Structural design of the superconducting Poloidal Field coils for the Tokamak Physics Experiment
[DE94-007078] p 3887 N94-31406
Design and evaluation of coils for a 50 mm diameter induction coilgun launcher
[DE94-005244] p 3603 N94-32671
Coaxial slow source
[DE94-008191] p 3892 N94-32800
MAGNETIC ANOMALIES
Steps toward understanding the solar dynamo
[AD-A277398] p 3953 N94-32343
Surface conforming flexible eddy current probe for scanning varying surface contours
[AD-D016173] p 3627 N94-33018
MAGNETIC DISKS
Evolution of dynamo-generated magnetic fields in accretion disks around compact and young stars p 3931 N94-31138
Nonthermal accretion disk models around neutron stars p 3931 N94-31139
A redundant disk array architecture for efficient small writes
[AD-A276645] p 3815 N94-31940
Eurocap program-ebre station
[AD-A277044] p 3772 N94-32007
MAGNETIC EFFECTS
Evolution of protoplanetary disks with dynamo magnetic fields p 3931 N94-31135
Magnetless magnetic fusion
[DE94-007114] p 3891 N94-32686
Anomalous transport equations in toroidal plasmas
[DE94-009206] p 3893 N94-32922
MAGNETIC FIELD CONFIGURATIONS
Dynamics of flux tubes in accretion disks p 3932 N94-31142
Radiation from an aperture into an anisotropic plasma half-space p 3885 N94-31205
Planetary magnetotails: Magnetic configuration and nonthermal plasma p 3942 N94-32326
Magnetless magnetic fusion
[DE94-007114] p 3891 N94-32686
Stability of bootstrap current driven magnetic islands in stellarators
[DE94-009207] p 3893 N94-32912
MAGNETIC FIELD RECONNECTION
Nonthermal accretion disk models around neutron stars p 3931 N94-31139
MAGNETIC FIELDS
Laboratory and space experiments as a key to the plasma universe
[TRITA-ALP-1993-01] p 3885 N94-31088
Evolution of protoplanetary disks with dynamo magnetic fields p 3931 N94-31135
Evolution of dynamo-generated magnetic fields in accretion disks around compact and young stars p 3931 N94-31138
Toroidal pinch experiments
[DE94-005876] p 3887 N94-31558
Fiberoptisk magnetfaltsensor (fiber optic magnetometer)
[PB94-148061] p 3878 N94-31584
Collective acceleration in solar flares
[DE94-006288] p 3953 N94-31632
Fermi surface instability at 0.4 K in a heavy-fermion YbBiPt: SDW?
[DE94-006224] p 3899 N94-31916
Transport phenomena in the Earth's plasma sheet p 3772 N94-31970
Stability of bootstrap current driven magnetic islands in stellarators
[DE94-009207] p 3893 N94-32912
Anomalous transport equations in toroidal plasmas
[DE94-009206] p 3893 N94-32922
Investigation of superconductivity and magnetism in d and f-electron materials
[DE94-008535] p 3907 N94-32933
Electron acceleration system
[AD-D016143] p 3893 N94-32977
An approximate Riemann solver for magnetohydrodynamics (that works in more than one dimension)
[NASA-CR-194902] p 3649 N94-33033
MAGNETIC FLUX
Dynamics of flux tubes in accretion disks p 3932 N94-31142
Theoretical principles for designing long stator/linear motors with iron
[ETN-94-95741] p 3688 N94-31374
Transport phenomena in the Earth's plasma sheet p 3772 N94-31970
Steps toward understanding the solar dynamo
[AD-A277398] p 3953 N94-32343
MAGNETIC LEVITATION VEHICLES
Review and status of Maglev in the United States
[DE94-006832] p 3722 N94-31319
Theoretical principles for designing long stator/linear motors with iron
[ETN-94-95741] p 3688 N94-31374
Applicable dimensioning and measure and technological examination of long stator-linear motors for magnetic high-speed railways
[ETN-94-95734] p 3689 N94-31575
On the unsteady-motion theory of magnetic forces for maglev
[DE94-007765] p 3727 N94-32778
MAGNETIC MATERIALS
Piezoelectric materials research in Europe
[AD-A276207] p 3648 N94-31059
Correlations between micromagnetic, microstructural and microchemical properties in ultrathin epitaxial magnetic structures
[AD-A277200] p 3901 N94-32092
Surface conforming flexible eddy current probe for scanning varying surface contours
[AD-D016173] p 3627 N94-33018
MAGNETIC MEASUREMENT
Element-specific magnetic hysteresis measurements, a new application of circularly polarized soft x-rays
[DE94-007122] p 3858 N94-31397
Fiberoptisk magnetfaltsensor (fiber optic magnetometer)
[PB94-148061] p 3878 N94-31584
MAGNETIC MOMENTS
Molecular/polymeric magnetism
[DE94-005888] p 3649 N94-31201
Element-specific magnetic hysteresis measurements, a new application of circularly polarized soft x-rays
[DE94-007122] p 3858 N94-31397
Hyperon polarization and magnetic moments
[DE94-006041] p 3864 N94-31507
Hyperon polarization, crystal channeling, and E781 at Fermilab
[DE94-008224] p 3877 N94-32802
Dependence of x ray absorption magnetic circular dichroism on layer periodicity in iron-platinum multilayers
[DE94-008786] p 3647 N94-32892
MAGNETIC PERMEABILITY
Synthesis, characterization, phase diagrams and superconducting, and normal state magnetic properties of La(2-x)Sr(x)CuO4 (0 is less than or equal to x which is less than or equal to 0.08) and electrochemically oxidized La(2-x)Sr(x)CuO(4 + delta) (0 is less than or equal to x which is less than or equal to 0.33, 0 is less than or equal to delta which is less than or equal to 0.12)
[DE94-005260] p 3895 N94-31067
MAGNETIC PROPERTIES
Piezoelectric materials research in Europe
[AD-A276207] p 3648 N94-31059
Molecular/polymeric magnetism
[DE94-005888] p 3649 N94-31201
On the unsteady-motion theory of magnetic forces for maglev
[DE94-007765] p 3727 N94-32778
Investigation of superconductivity and magnetism in d and f-electron materials
[DE94-008535] p 3907 N94-32933
MAGNETIC RECORDING
An experimental compact Hi-Vision VCR using metal evaporated tape
[NHK-LABS-NOTE-423] p 3683 N94-33081
MAGNETIC RELAXATION
Low dispersion of the muon precession frequency in HTSC samples YBa2Cu3O(x) and EuBa2Cu3O(x)
[DE94-608388] p 3896 N94-31395
Experimental evidence for lattice effects in high temperature superconductors
[DE94-006250] p 3899 N94-31633
MAGNETIC RESONANCE
Fast nonsupervised 3D registration of PET and MR images of the brain
[TELECOM-93-C-006] p 3798 N94-33069
MAGNETIC SPECTROSCOPY
Concept, construction and testing of a high resolution QCLAM electron spectrometer with large solid angle and high impulse acceptance for the electron accelerator S-DALINAC
[ETN-94-95755] p 3711 N94-31515
MAGNETIC STORMS
Self-consistent effects of magnetospheric hydromagnetic waves on ring current ions
[AD-A277406] p 3774 N94-32346
MAGNETIC SURVEYS
Analysis of deep seismic reflection and other data from the southern Washington Cascades
[DE94-005958] p 3771 N94-31525
MAGNETIC SUSPENSION
On the unsteady-motion theory of magnetic forces for maglev
[DE94-007765] p 3727 N94-32778
Vibration Isolation Technology (VIT) ATD project
[NASA-TM-106496] p 3567 N94-33064
MAGNETIC VARIATIONS
Magnetohydrodynamics of the Earth's core. 1: Steady, rotating magnetoconvection. 2: Magnetic Rossby waves p 3770 N94-31104
A study of angular momentum loss in binaries using the free Lagrange method p 3931 N94-31134
MAGNETIZATION
Molecular/polymeric magnetism
[DE94-005888] p 3649 N94-31201
MAGNETOHYDRODYNAMIC FLOW
Transport suppression by shear flow generation in multihelicity resistive-g turbulence
[DE94-007108] p 3886 N94-31366
Hydrodynamics of neutron star interiors and laboratory superfluids p 3936 N94-31949
Characteristics of ion flow in the quiet state of the inner plasma sheet
[AD-A277451] p 3894 N94-33106
MAGNETOHYDRODYNAMIC GENERATORS
MHD seed recovery/regeneration, phase 2
[DE94-006772] p 3886 N94-31273
MAGNETOHYDRODYNAMIC STABILITY
Numerical method for the investigation of the magnetohydrodynamic stability of three dimensional plasma equilibria
[ETN-94-95752] p 3887 N94-31512
Toroidal pinch experiments
[DE94-005876] p 3887 N94-31558
High beta tokamak research
[DE94-006513] p 3888 N94-31664
Stability and instability criteria for magnetohydrodynamics
[PB94-148475] p 3889 N94-31772
Theoretical studies of magnetohydrodynamic equilibria and dynamics of a solar coronal loop p 3953 N94-31792
Instability heating of solid-fiber Z pinches
[DE94-007055] p 3889 N94-31809
Anomalous thermalization of fast ions in magnetized plasma
[DE94-007109] p 3891 N94-32631
Basic principles approach for studying nonlinear Alfven wave-alpha particle dynamics
[DE94-007112] p 3891 N94-32664
Cooperative program on D3-D (FY 1993)
[DE94-008343] p 3892 N94-32820
Stability of bootstrap current driven magnetic islands in stellarators
[DE94-009207] p 3893 N94-32912
Stabilization method of A.C. arc plasma
[DE94-757268] p 3893 N94-32916
The spatial development of the magnetospheric low-latitude boundary layer
[ISBN-0-315-77418-5] p 3776 N94-33111
MAGNETOHYDRODYNAMIC WAVES
Numerical simulation of interplanetary dynamics p 3933 N94-31566
Plasma confinement theory and transport simulation
[DE94-006065] p 3888 N94-31619
Self-consistent effects of magnetospheric hydromagnetic waves on ring current ions
[AD-A277406] p 3774 N94-32346
Basic principles approach for studying nonlinear Alfven wave-alpha particle dynamics
[DE94-007112] p 3891 N94-32664
MAGNETOHYDRODYNAMICS
Magnetohydrodynamics of the Earth's core. 1: Steady, rotating magnetoconvection. 2: Magnetic Rossby waves p 3770 N94-31104
Evolution of dynamo-generated magnetic fields in accretion disks around compact and young stars p 3931 N94-31138
Numerical simulation of interplanetary dynamics p 3933 N94-31566
High beta tokamak research
[DE94-006513] p 3888 N94-31664
Stability and instability criteria for magnetohydrodynamics
[PB94-148475] p 3889 N94-31772
Pulsed expansion of plasma in a magnetic thruster p 3889 N94-31776
Theoretical studies of magnetohydrodynamic equilibria and dynamics of a solar coronal loop p 3953 N94-31792
Computer modeling of active experiments in space plasmas p 3890 N94-31927

Hydrodynamics of neutron star interiors and laboratory superfluids p 3936 N94-31949
Theoretical studies on ionospheric irregularities and ion diode performance
[AD-A277115] p 3772 N94-31984
Scenarios for multi-unit inertial fusion energy plants producing hydrogen fuel
[DE94-006614] p 3666 N94-32114
Self-consistent effects of magnetospheric hydromagnetic waves on ring current ions
[AD-A277406] p 3774 N94-32346
Magnetohydrodynamic boundary layer control system
[AD-D016120] p 3710 N94-32958
An approximate Riemann solver for magnetohydrodynamics (that works in more than one dimension)
[NASA-CR-194902] p 3849 N94-33033
The spatial development of the magnetospheric low-latitude boundary layer
[ISBN-0-315-77418-5] p 3776 N94-33111

MAGNETOMETERS
Fiberoptisk magnetfaltsensor (fiber optic magnetometer)
[PB94-148061] p 3878 N94-31584

MAGNETOPAUSE
The spatial development of the magnetospheric low-latitude boundary layer
[ISBN-0-315-77418-5] p 3776 N94-33111

MAGNETOPLASMADYNAMICS
Performance of a quasi-steady, multi megawatt, coaxial plasma thruster
[NASA-CR-195311] p 3616 N94-32970

MAGNETORESISTIVITY
Effect of twin boundary density on the vortex melting transition in YBa2Cu3O(7-delta) single crystals
[DE94-007684] p 3904 N94-32601

MAGNETOSHEATH
The spatial development of the magnetospheric low-latitude boundary layer
[ISBN-0-315-77418-5] p 3776 N94-33111

MAGNETOSPHERE-IONOSPHERE COUPLING
Convection and electrodynamic signatures in the vicinity of a Sun-aligned arc: Results from the Polar Acceleration Regions and Convection Study (Polar ARCS)
p 3954 N94-31102

MAGNETOSTRICTION
Fiberoptisk magnetfaltsensor (fiber optic magnetometer)
[PB94-148061] p 3878 N94-31584

MAGNETRONS
Dependence of x ray absorption magnetic circular dichroism on layer periodicity in iron-platinum multilayers
[DE94-008786] p 3647 N94-32892

MAGNETS
Molecular/polymeric magnetism
[DE94-005888] p 3649 N94-31201
Magnetohydrodynamic boundary layer control system
[AD-D016120] p 3710 N94-32958

MAGNONS
Fermi surface instability at 0.4 K in a heavy-fermion YbBiPt: SDW?
[DE94-006224] p 3899 N94-31916

MAIN SEQUENCE STARS
The evolutionary status of PSR 1259-63
[DE94-007094] p 3938 N94-32503

MAINTENANCE
The maintenance of operational flight program
[AD-A276363] p 3565 N94-31367
Common modeling system for digital simulation
p 3823 N94-32429
Analysis of intermediate level maintenance following F404-GE-400 engine component life reductions
[AD-A277918] p 3585 N94-33283

MAN ENVIRONMENT INTERACTIONS
Fine resolution atmospheric sulfate model driven by operational meteorological data: Comparison with observations
[DE94-002994] p 3766 N94-32691

MAN MACHINE SYSTEMS
A real-time computer control and trajectory generation environment for Trussarm
[ISBN-0-315-87060-5] p 3832 N94-31833
Adaptive control of telerobotic systems worn by humans
[AD-A276608] p 3834 N94-32036
Aerospace medicine and biology: A continuing bibliography with indexes (supplement 389)
[NASA-SP-7011(389)] p 3797 N94-32347
Aerospace medicine and biology: A continuing bibliography with indexes (supplement 385)
[NASA-SP-7011(385)] p 3797 N94-32348
Technology transfer of operator-in-the-loop simulation
p 3802 N94-32472

MANAGEMENT ANALYSIS
An evaluation of aircraft maintenance performance factors in the objective wing
[AD-A276010] p 3565 N94-31362
Mapping analysis and planning system for the John F. Kennedy Space Center p 3757 N94-32463

MANAGEMENT INFORMATION SYSTEMS
Initial estimates of Integrated Maintenance Information System (IMIS) costs and benefits, volume 1
[AD-A276144] p 3565 N94-31830
Application of Artificial Intelligence to the DoD Corporate Information Management (CIM) program
[AD-A276656] p 3834 N94-32061
Lifting the fog of corporate information management
[AD-A276680] p 3918 N94-32090
Modular Simulator System (MSS). Executive report
[AD-A276966] p 3588 N94-32241
Managing performance of DB2 Ad Hoc Reports
[DE94-006669] p 3920 N94-32635
Developing a personal-computer-based records retention system using Paradox(tm)
[DE94-007984] p 3819 N94-32749

MANAGEMENT METHODS
Software reuse case study: TRILLIUM
[AD-A276108] p 3811 N94-31465
Process mapping: A user-friendly tool for process improvement
[DE94-004357] p 3730 N94-31605
Budget allocation and monopolistic pricing in a multiproduct firm
[REPT-93-86] p 3924 N94-31617
Lifting the fog of corporate information management
[AD-A276680] p 3918 N94-32090
CIM in space: Corporate Information Management (CIM) implications for space-based information systems
[AD-A276882] p 3600 N94-32126
Case studies of software process improvement methods
[AD-A277289] p 3818 N94-32508
Agile total quality guidelines for enhancing teamwork and success
[DE93-019972] p 3915 N94-32678
Total Quality Management implementation guidelines
[DE94-007232] p 3915 N94-32723

MANAGEMENT PLANNING
European business confronted with the 21st century: Men, the essential risk
[ESA-SP-1167] p 3914 N94-31181
Europe at the crossroads: The future of its satellite communications industry
[ESA-SP-1166] p 3670 N94-31182
An active computer supported medium for distributed planning in enterprises
[ETN-94-95738] p 3829 N94-31372
A study of theoretical models for managing technology change and a comparison to a radio frequency identification implementation
[AD-A276012] p 3672 N94-31385
NASCOM system development plan: System description, capabilities, and plans, FY 94-2
[NASA-TM-109744] p 3674 N94-31503
Modular Simulator System (MSS) management guide
[AD-A277098] p 3588 N94-32014
NASA strategic plan
[NASA-TM-109780] p 3915 N94-32222

MANAGEMENT SYSTEMS
Model borne data management system for wind tunnel testing, phase 2
[AD-A276296] p 3587 N94-31295
An analysis of the records management process to determine the impact of automation on productivity
[AD-A275923] p 3916 N94-31344
The development and use of an evaluation mechanism for the assessment of software configuration management tools
[AD-A275961] p 3810 N94-31383
A model and algorithms for a software evolution control system
[AD-A276431] p 3811 N94-31449

MANDRELS
Diamond turning in the production of x ray optics
p 3604 N94-33298

MANEUVERABILITY
Navy Omni-Directional Vehicle (ODV) development program p 3729 N94-32451

MANGANESE
Electron spin resonance measurements of Er(3+) and Mn(2+) in the high temperature superconductor compounds La(2-x)Sr(x)CuO(4-delta)
[ETN-94-95746] p 3898 N94-31612

MANGANESE COMPOUNDS
Molecular/polymeric magnetism
[DE94-005888] p 3649 N94-31201

MANIFOLDS (MATHEMATICS)
On the computation of simplical approximations of implicitly defined two-dimensional manifolds
[AD-A278132] p 3849 N94-33060

MANIPULATORS
A high-performance multi-arm environment: Theoretical aspects and practical implementation
[RR-479] p 3722 N94-31379
Kinematic synthesis and analysis of a novel class of six-DOF parallel minimanipulators p 3723 N94-31568
Remote robot manipulator coupled with remote-controlled guide vehicle for soil sampling in hazardous waste sites p 3723 N94-31569
Real-time control of the Trussarm variable-geometry-truss manipulator utilizing machine vision
[ISBN-0-315-87054-0] p 3830 N94-31735
Point-contact and point-impact dynamics for multibody chains
[ISBN-0-315-87056-7] p 3734 N94-31737
Development of a robotic simulator for studying interference and contact problems
[ISBN-0-315-86705-1] p 3588 N94-31747
Application of contact mechanics for the validation of robotized operations of grasping objects subjected to static and dynamic force fields
[ISBN-0-315-86831-7] p 3725 N94-31754
Strategy for tracking and grabbing a moving object with the aid of a decouplable manipulator with six degrees of freedom general architecture, guided by a vision system
[ISBN-0-315-86864-3] p 3831 N94-31757
Trajectory learning with a direct drive robotic manipulator p 3831 N94-31794
Development of a feedforward controller for a flexible manipulator
[ISBN-0-315-86515-6] p 3832 N94-31801
A real-time computer control and trajectory generation environment for Trussarm
[ISBN-0-315-87060-5] p 3832 N94-31833
Model identification of a reconfigurable robot manipulator
[ISBN-0-315-87109-1] p 3725 N94-31874
Automatic analysis of force distribution in multi-fingered articulated hands
[ISBN-0-315-87205-5] p 3725 N94-31878
High-speed path constrained manipulator operation using optimal-feedback combined controller
p 3833 N94-31962
Control of a flexible-link robotic arm manipulating an unknown dynamic payload p 3725 N94-31973
Parallel methods for synthesizing whole-hand grasps from generalized prototypes
[AD-A276798] p 3726 N94-32166
An experimental testbed for a free-floating manipulator
[AD-A277350] p 3726 N94-32334
Trajectory planning for space manipulators
[AD-A277229] p 3611 N94-32369
Applying robotics to HAZMAT p 3729 N94-32452
Technology transfer of operator-in-the-loop simulation
p 3802 N94-32472
Construction of a parallel processor for simulating manipulators and other mechanical systems
[NASA-CR-191327] p 3826 N94-32482
A new solution method for the inverse kinematic joint velocity calculations of redundant manipulators
[DE94-004427] p 3727 N94-32682
Development of an interchangeable end effector mechanism for the Ranger telerobotic vehicle
p 3604 N94-33297

MANNED SPACE FLIGHT
Atmosphere quality standards in manned space vehicles
[ESA-PSS-03-401-ISSUE-1] p 3802 N94-31224
Legal regime of human activities in outer space law
p 3599 N94-31431
Advanced transportation system study: Manned launch vehicle concepts for two way transportation system payloads to LEO
[NASA-CR-193951] p 3608 N94-33100
Load-limiting landing gear footpad energy absorption system p 3607 N94-33323

MANNED SPACECRAFT
Advanced transportation system study: Manned launch vehicle concepts for two way transportation system payloads to LEO
[NASA-CR-193951] p 3608 N94-33100

MANUALS
Laser safety manual for DREO
[AD-A276288] p 3714 N94-31255
CMS Distribution Subsystem user's guide
[DE94-005328] p 3816 N94-32146
Total Quality Management implementation guidelines
[DE94-007232] p 3915 N94-32723

MANUFACTURING
Automated solar cell assembly teamed process research
[DE94-000295] p 3759 N94-31279
The 18th annual electronics manufacturing seminar
[AD-A276038] p 3687 N94-31281
Fractional-factorial process development techniques
[DE94-005580] p 3690 N94-31593
The future of open architecture process control systems
[DE94-006163] p 3830 N94-31623
Laser applications in wood processing
[PB94-138567] p 3717 N94-31840
Advances in MOVPE compound semiconductor epitaxy manufacturing technology: From high throughput large area reactors to cluster tools
[DE94-006367] p 3901 N94-32104
Validation of the Environmentally Conscious Manufacturing Integrated Demonstration hardware
[DE94-003824] p 3765 N94-32144
Fiber optic chemical sensors
[AD-A277128] p 3881 N94-32380
From display and PWB to MCMs: Large panel manufacturing
[DE94-007855] p 3693 N94-32386
Empirical modeling for intelligent, real-time manufacture control p 3839 N94-32424
Neutral ion sources in precision manufacturing p 3875 N94-32447
Flexible manufacturing for photonics device assembly p 3669 N94-32449
LLNL casting technology
[DE94-008282] p 3669 N94-32839
Development of thermoplastic composite aircraft structures
[NASA-CR-189593] p 3626 N94-32860
Application of a design-build-team approach to low cost and weight composite fuselage structure
[NASA-CR-4418] p 3626 N94-32863
Second NASA Advanced Composites Technology Conference
[NASA-CP-3154] p 3627 N94-33121
Design, characterization, and control of the NASA three degree of freedom reaction compensation platform p 3605 N94-33304

MANY BODY PROBLEM
Micromechanics and effective properties of particulate composites and fluid suspensions p 3703 N94-31744
Numerical simulation of quantum many-body systems
[DE94-008451] p 3912 N94-32513
Near edge x ray spectroscopy theory
[DE94-008179] p 3905 N94-32799

MANY ELECTRON EFFECTS
Numerical simulation of quantum many-body systems
[DE94-008451] p 3912 N94-32513

MAPPING
NORSMAP 1989: Norwegian remote sensing spectroscopy for mapping and monitoring or algal blooms and pollution p 3744 N94-31856
Alternatives to hierarchical techniques in stereo correlation
[AD-A276570] p 3746 N94-31938
Optics and radar: Cohabitation, rivality or happy marriage. Towards new planning tools p 3748 N94-32529
The use of ERS images for mapping p 3749 N94-32531
The use of SPOT and ERS-1 images to map the eruption of Nevado Sabancaya (Province of Arequipa, South Peru) and evaluate associated risks p 3751 N94-32546
Evaluation of the potential of SAR data for mapping of landslide risks
[BRGM-93033] p 3753 N94-32552
Use of SPOT and ERS-1 to map tropical vegetation and mangrove dynamics in Guiana p 3753 N94-32555
Statistical analysis and mapping of cotton and food crop cultivation surfaces in the west of Burkina Faso: Contribution of combined SPOT P and XS data p 3757 N94-32575

MAPS
A brief introduction to symplectic integrators and recent results
[DE94-006225] p 3845 N94-31763
Techniques and applications of SAR interferometry for ERS-1 p 3756 N94-32568
MDFF HELP library, version 2: On-line documentation for the map data formatting facility
[AD-A277763] p 3922 N94-32987
Global color views of Mars p 3948 N94-33217

MARINE ENVIRONMENTS
High resolution properties of the marine atmospheric boundary layer
[DE94-006235] p 3774 N94-32736
SEASOAR and CTD observations during a COARE surveys cruise, W9211C, 22 January - 22 February, 1993
[AD-A277925] p 3791 N94-33244

MARINE METEOROLOGY
Hydrographic service Royal Australian Navy
[AD-A277134] p 3788 N94-32066
The influence of cumulus parameterization on model forecasts of rapid oceanic cyclogenesis
[AD-A277207] p 3784 N94-32094
Typhoon havens handbook for the western Pacific and Indian Oceans, change 3
[AD-A277030] p 3784 N94-32260
Evolution of diurnal surface winds and surface currents for Monterey Bay
[AD-A277649] p 3790 N94-33057

MARINE PROPULSION
Experimental and computational studies on propeller noise due to inflow distortion p 3860 N94-31846

MARITIME SATELLITES
An analysis of cellular telephone and INMARSAT systems for providing radio data link computer communications for US Navy vessels
[AD-A278143] p 3684 N94-33160

MARKET RESEARCH
Europe at the crossroads: The future of its satellite communications industry
[ESA-SP-1166] p 3670 N94-31182
Photovoltaics: Program overview, fiscal year 1993
[DE94-000246] p 3758 N94-31235
Current Research Information in Europe: Conference proceedings
[PB94-127933] p 3917 N94-31768
Environmental issues related to biomass: An overview
[DE94-007226] p 3767 N94-32784

MARKING
Beginning the 21st century with advanced Automatic Parts Identification (API) p 3923 N94-32444

MARKOV CHAINS
Dynamical entropy of generalized quantum Markov chains
[PB94-148483] p 3850 N94-31590
The Laplace functional and Palm measure of a quasi-Cox process which is driven by a Markov chain
[REPT-93-82] p 3851 N94-31699
Undiscounted Markov decision chains with partial information; an algorithm for computing a locally optimal periodic policy
[TW-93-10] p 3851 N94-32205
Adaptive control of nonlinear and stochastic systems
[AD-A278411] p 3839 N94-33325

MARKOV PROCESSES
Representation, prediction and identification of cyclostationary processes: A state-space approach
[REPT-93-041] p 3850 N94-31191
High-performance speech recognition using consistency modeling
[AD-A276775] p 3679 N94-32185
Area-interaction point processes
[CWI-BS-R9318] p 3847 N94-32197
Robust multisource classification method using the Markov random field methods p 3750 N94-32537
Hierarchical modeling for reliability analysis using Markov models
[NASA-CR-188288] p 3731 N94-32862

MARS (PLANET)
Origin and thermal evolution of Mars p 3940 N94-31109
Mars: Five views on what is known
[NASA-TM-109751] p 3942 N94-31805
Marsville: The cosmic village
[NASA-TM-109752] p 3913 N94-31806
Mars: Past, Present, and Future. Results from the MSATT Program, part 1
[NASA-CR-194279] p 3943 N94-33190
Depth-diameter ratios for Martian impact craters: Implications for target properties and episodes of degradation p 3943 N94-33191
Constraints on the Martian cratering rate imposed by the SNC meteorites and Vallis Marineris layered deposits p 3945 N94-33197
MARSNET: A European network of stations on the surface of Mars p 3945 N94-33199
Possible test of ancient dense Martian atmosphere p 3947 N94-33206
SNC meteorites and their implications for reservoirs of Martian volatiles p 3947 N94-33209
The Northern Plains MSATT Meeting, and a call for a field-oriented successor to MSATT p 3947 N94-33210
The effect of polar caps on obliquity p 3948 N94-33213
Might it be possible to predict the onset of major Martian dust storms? p 3948 N94-33215
The distribution of Martian ground ice at other epochs p 3948 N94-33218
Polar sediment accumulation: Role of surface winds at the two poles p 3951 N94-33233
The Martian sources of the SNC meteorites (two, not one), and what can and can't be learned from the SNC meteorites p 3951 N94-33234

MARS ATMOSPHERE
Mars: Past, Present, and Future. Results from the MSATT Program, part 1
[NASA-CR-194279] p 3943 N94-33190
Stationary eddies in the Mars general circulation as simulated by the NASA-Ames GCM p 3944 N94-33192
Deposition rates of oxidized iron on Mars p 3945 N94-33198
Mars atmospheric dust properties: A synthesis of Mariner 9, Viking, and Phobos observations p 3945 N94-33200
Magmatic volatiles and the weathering of Mars p 3946 N94-33201
Aerosols scattering and near-infrared observations of the Martian surface p 3946 N94-33204
A model for the evolution of CO2 on Mars p 3946 N94-33205
Possible test of ancient dense Martian atmosphere p 3947 N94-33206
Groundbased monitoring of Martian atmospheric opacity p 3947 N94-33207
Mars atmospheric loss and isotopic fractionation by solar-wind-induced sputtering and photochemical escape p 3947 N94-33208
SNC meteorites and their implications for reservoirs of Martian volatiles p 3947 N94-33209
How well was total ozone abundance inferred with Mariner 9 p 3947 N94-33212
Escape of Mars atmospheric carbon through time by photochemical means p 3948 N94-33214
Studies of atmospheric dust from Viking IR thermal mapper data p 3948 N94-33216
Eddy transport of water vapor in the Martian atmosphere p 3949 N94-33221
Numerical simulation of thermally induced near-surface flows over Martian terrain p 3949 N94-33223
The wavelength dependence of Martian atmospheric dust radiative properties p 3950 N94-33228
Carbonate formation on Mars: Latest experiments p 3950 N94-33231
Carbonates, surfates, phosphates, nitrates, and organic materials: Their association in a Martian meteorite p 3952 N94-33239
Simultaneous laboratory measurements of CO2 and H2O adsorption on palagonite: Implications for the Martian climate and volatile reservoir p 3952 N94-33240

MARS CRATERS
Depth-diameter ratios for Martian impact craters: Implications for target properties and episodes of degradation p 3943 N94-33191
Constraints on the Martian cratering rate imposed by the SNC meteorites and Vallis Marineris layered deposits p 3945 N94-33197
Regional sedimentological variations among dark crater floor features: Toward a model for modern eolian sand distribution on Mars p 3946 N94-33203
Possible test of ancient dense Martian atmosphere p 3947 N94-33206

MARS ENVIRONMENT
Fiber optic chemical sensors on Mars
[DE94-005251] p 3941 N94-31145
The importance of environmental conditions in reflectance spectroscopy of laboratory analogs for Mars surface materials p 3944 N94-33195
The effect of polar caps on obliquity p 3948 N94-33213
Might it be possible to predict the onset of major Martian dust storms? p 3948 N94-33215
Controls on the CO2 seasonal cycle p 3950 N94-33227
Obliquity variation in a Mars climate evolution model p 3951 N94-33236
The influence of thermal inertia on Mars' seasonal pressure variation and the effect of the weather component p 3952 N94-33238

MARS PHOTOGRAPHS
Regional sedimentological variations among dark crater floor features: Toward a model for modern eolian sand distribution on Mars p 3946 N94-33203

MARS PROBES
Mars: Five views on what is known
[NASA-TM-109751] p 3942 N94-31805

MARS SURFACE
State of stress, faulting, and eruption characteristics of large volcanoes on Mars p 3940 N94-31108
Origin and thermal evolution of Mars p 3940 N94-31109
Mars: Five views on what is known
[NASA-TM-109751] p 3942 N94-31805

One: Microphysics of frost metamorphism: Applications to Triton and Mars. Two: A global analysis of the ozone deficit in the upper stratosphere and lower mesosphere. Three: The diabatic circulation in the stratosphere as diagnosed from Microwave Limb Sounder data
p 3942 N94-31975
Mars: Past, Present, and Future. Results from the MSATT Program, part 1
[NASA-CR-194279] p 3943 N94-33190
Depth-diameter ratios for Martian impact craters: Implications for target properties and episodes of degradation p 3943 N94-33191
Thermal studies of Martian channels and valleys using Termoskan data: New results p 3944 N94-33194
The importance of environmental conditions in reflectance spectroscopy of laboratory analogs for Mars surface materials p 3944 N94-33195
Ferric sulfate montmorillonites as Mars soil analogs
p 3944 N94-33196
Constraints on the Martian cratering rate imposed by the SNC meteorites and Vallis Marineris layered deposits p 3945 N94-33197
Deposition rates of oxidized iron on Mars
p 3945 N94-33198
MARSNET: A European network of stations on the surface of Mars p 3945 N94-33199
Magmatic volatiles and the weathering of Mars
p 3946 N94-33201
Thermal and hydraulic considerations regarding the fate of water discharged by the outflow channels to the Martian northern plains p 3946 N94-33202
Regional sedimentological variations among dark crater floor features: Toward a model for modern eolian sand distribution on Mars p 3946 N94-33203
Aerosols scattering and near-infrared observations of the Martian surface p 3946 N94-33204
Groundbased monitoring of Martian atmospheric opacity p 3947 N94-33207
SNC meteorites and their implications for reservoirs of Martian volatiles p 3947 N94-33209
The Northern Plains MSATT Meeting, and a call for a field-oriented successor to MSATT
p 3947 N94-33210
Temporal and spatial mapping of atmospheric dust opacity and surface albedo on Mars
p 3947 N94-33211
The effect of polar caps on obliquity
p 3948 N94-33213
Might it be possible to predict the onset of major Martian dust storms? p 3948 N94-33215
Global color views of Mars p 3948 N94-33217
The distribution of Martian ground ice at other epochs
p 3948 N94-33218
Mineralogical diversity (spectral reflectance and Moessbauer data) in compositionally similar impact melt rocks from Manicouagan Crater, Canada
p 3948 N94-33219
Martian spectral units derived from ISM imaging spectrometer data p 3949 N94-33220
IRTM brightness temperature maps of the Martian south polar region during the polar night: The cold spots don't move p 3949 N94-33222
Numerical simulation of thermally induced near-surface flows over Martian terrain p 3949 N94-33223
Apron heights around stepped massifs in the Cydonia Mensae region: Do they record the local paleobathymetry of Oceanus Borealis? p 3949 N94-33224
The pH of Mars p 3950 N94-33225
The mineralogic evolution of the Martian surface through time: Implications from chemical reaction path modeling studies p 3950 N94-33226
Martian deltas: Morphology and distribution
p 3950 N94-33230
Geologic controls of erosion and sedimentation on Mars p 3951 N94-33232
Polar sediment accumulation: Role of surface winds at the two poles p 3951 N94-33233
The Martian sources of the SNC meteorites (two, not one), and what can and can't be learned from the SNC meteorites p 3951 N94-33234
Temporal changes in the geographic distribution, elevation, and potential origin of the Martian outflow channels p 3951 N94-33235
Obliquity variation in a Mars climate evolution model
p 3951 N94-33236
Dielectric properties of Mars' surface: Proposed measurement on a Mars lander p 3951 N94-33237
The influence of thermal inertia on Mars' seasonal pressure variation and the effect of the weather component p 3952 N94-33238
Carbonates, surfates, phosphates, nitrates, and organic materials: Their association in a Martian meteorite
p 3952 N94-33239

MARS VOLCANOES
Tectonic History of the Terrestrial Planets
[NASA-CR-195696] p 3939 N94-31105
State of stress, faulting, and eruption characteristics of large volcanoes on Mars p 3940 N94-31108
Evidence for ultramafic lavas on Syrtis Major
p 3950 N94-33229

MARTENSITIC STAINLESS STEELS
Characterization of the corrosion resistance of duplex stainless steels using local current density mapping techniques
[DE94-007980] p 3646 N94-32699

MARYLAND
Focused feasibility study final field sampling plan
[AD-A277445] p 3769 N94-33105

MASS
Evolution of vaporizing pulsars p 3929 N94-31128

MASS FLOW
Disk irradiation and light curves of x ray novae
p 3929 N94-31124

MASS FLOW RATE
Disk irradiation and light curves of x ray novae
p 3929 N94-31124
Control of hypersonic aerodynamic forces with surface blowing p 3567 N94-31216

MASS RATIOS
A study of angular momentum loss in binaries using the free Lagrange method p 3931 N94-31134
Gravitational instabilities in protostellar disks
p 3932 N94-31140
Double-lined pre-main-sequence binaries: A test of pre-main-sequence evolutionary theory
p 3933 N94-31497

MASS SPECTRA
Imaging AMS
[DE94-006662] p 3632 N94-31349
Composition and properties of dust from Comet Halley
p 3936 N94-31947
Performance of an ion trap inductively coupled plasma mass spectrometer
[DE94-007470] p 3713 N94-32811

MASS SPECTROMETERS
Imaging AMS
[DE94-006662] p 3632 N94-31349
Performance of an ion trap inductively coupled plasma mass spectrometer
[DE94-007470] p 3713 N94-32811

MASS SPECTROSCOPY
Characterization of polymer decomposition products by laser desorption mass spectrometry
p 3597 N94-31046
Imaging AMS
[DE94-006662] p 3632 N94-31349
AMS beyond 2000
[DE94-006666] p 3632 N94-31352
Development of sample charge compensation for characterization of impurities in semiconductor materials
[AD-A277113] p 3899 N94-31983
Group 12 thiolates: Syntheses, characterization and decomposition pathways
[AD-A277055] p 3900 N94-32011
New zinc-bis(dialkylamides) potentially usable as site-selective dopants for p-type ZnSe
[AD-A276947] p 3902 N94-32218
Organic analyses of the Murchison meteorite
p 3938 N94-32489
Performance of an ion trap inductively coupled plasma mass spectrometer
[DE94-007470] p 3713 N94-32811

MASS TRANSFER
Can a variable alpha induce limit cycle behavior and exponential luminosity decay in transient soft x ray sources? p 3929 N94-31129
The prediction of convective transfer on the thermal insulation of a solid-propellant rocket motor
[ONERA-NT-1993-15] p 3614 N94-31423
Cloud studies seen from a physical chemist's perspective
[DE94-006059] p 3771 N94-31527
Numerical simulations of monsoon rainfall with the NRL/NCSU regional nested grid model
p 3782 N94-31791
Computational study of simultaneous heat and mass transfer in turbulent separated flows
p 3704 N94-31843

MASSIVE STARS
Near infrared surveys of high mass star forming regions p 3925 N94-31898

MASSIVELY PARALLEL PROCESSORS
A heterogeneous computing environment for simulating astrophysical fluid flows p 3928 N94-31119
An efficient three-dimensional Poisson solver for SIMD high-performance-computing architectures
p 3823 N94-31120
Three-dimensional radiative transfer calculations on an SIMD machine applied to accretion disks
p 3932 N94-31141
Delft Ising computing engine
[PB94-148251] p 3806 N94-31587
Some calculations on supersymmetric graphs as communication networks
[REPT-93-72] p 3824 N94-31641
Massively parallel systems design for real-time embedded applications
[AD-A277256] p 3826 N94-32323
Spacecraft On-Board Information Extraction Computer (SOBIEC) p 3808 N94-32433
The Numerical Tokamak Project (NTP) simulation of turbulent transport in the core plasma: A grand challenge in plasma physics
[DE94-006279] p 3892 N94-32838
Overview of shock physics codes for armor analysis
[DE94-008948] p 3739 N94-32842
Parallel supercomputing: Advanced methods, algorithms, and software for large-scale linear and nonlinear problems
[DE94-008446] p 3836 N94-32992

MATCHING
Fast nonsupervised 3D registration of PET and MR images of the brain
[TELECOM-93-C-006] p 3798 N94-33069
Nearest-neighbour search in constant time: An alternative to neural networks for pattern matching applications p 3838 N94-33157

MATERIALS
Spacecraft materials: Comparison between flight results obtained on LDEF and MIR p 3597 N94-31045
Databases and demands for solar heating materials
[PB94-137494] p 3758 N94-31070

MATERIALS RECOVERY
MHD seed recovery/regeneration, phase 2
[DE94-006772] p 3686 N94-31273
Feasibility study for the recycling of nickel metal hydride electric vehicle batteries
[DE94-000268] p 3690 N94-31598

MATERIALS SCIENCE
Atomic oxygen erosion considerations for spacecraft materials selection p 3593 N94-31022
A cross-disciplinary report on the mathematical sciences applied to materials science, part 1
[AD-A276116] p 3843 N94-31529

MATERIALS TESTS
Performance of selected polymeric materials on LDEF
p 3593 N94-31023
Fluorescence observations of LDEF exposed materials as an indicator of induced material reactions
p 3593 N94-31025
Laser-induced fluorescence of space-exposed polyurethane p 3593 N94-31026
What LDEF means for development and testing of materials p 3598 N94-31050

MATHEMATICAL LOGIC
OTTER 3.0 reference manual and guide
[DE94-007457] p 3829 N94-31315
What comes first in dynamic semantics: A compositional, non-representational account of natural language presupposition
[LP-93-15] p 3855 N94-31389
The meaning of duplicates in the relational database model
[CT-93-04] p 3918 N94-31392
Binary quantifiers and relational semantics
[LP-93-13] p 3855 N94-31404
On the independent axiomatizability of modal and intermediate logics
[ML-93-17] p 3856 N94-31407
Extensional realizability
[ML-93-18] p 3856 N94-31408
The decidability of dependency in intuitionistic propositional logic
[ML-93-20] p 3856 N94-31410
Sums and quantifiers
[LP-93-05] p 3856 N94-31411
Effective truth
[ML-93-15] p 3856 N94-31416
Information acquisition from multi-agent resources; abstract
[LP-93-08] p 3917 N94-31452
Completeness and decidability of the mixed style of inference with composition
[LP-93-09] p 3842 N94-31453
Tractable deduction in some fragments of auto-epistemic logic
[REPT-93-89] p 3844 N94-31673
An epistemic proof system for parallel processes
[TR-93-17] p 3826 N94-32291
Fuzzy logic application for modeling man-in-the-loop space shuttle proximity operations
[NASA-CR-188283] p 3835 N94-32359

MATHEMATICAL MODELS
Model updating of vibrating systems based on measured or calculated frequency response functions
[CTH-E-93-03] p 3732 N94-31091

Report of the 'Mathematical Models for Neural Networks' course
[TELECOM-93-D-019] p 3826 N94-31100
Tectonic History of the Terrestrial Planets
[NASA-CR-195686] p 3939 N94-31105
Aspects of modelling the tectonics of large volcanoes on the terrestrial planets p 3940 N94-31107
Geoid-to-topography ratios on Venus: A global perspective p 3940 N94-31110
A tectonic resurfacing model for Venus p 3941 N94-31113
A Green's function approach to analysing the effects of random synaptic background activity in a model neural network
[MATHS-REPT-A-202] p 3828 N94-31157
Representation, prediction and identification of cyclostationary processes: A state-space approach
[REPT-93-041] p 3850 N94-31191
Interactive reconstruction of anatomical structures with free-form surfaces
[TELECOM-93-E-002] p 3794 N94-31195
An investigation of the spin-coating process and a model for three-dimensional regular foams p 3649 N94-31206
A comparison of predictors for first-guess wind speed errors
[AD-A276460] p 3781 N94-31239
Oscillations in piston-driven shear flow of a non-Newtonian fluid
[AD-A276472] p 3701 N94-31245
ADCIRC: An advanced three-dimensional circulation model for shelves, coasts, and estuaries. User's manual for ADCIRC-2DDI
[AD-A276150] p 3787 N94-31250
A study of theoretical models for managing technology change and a comparison to a radio frequency identification implementation
[AD-A276012] p 3672 N94-31385
An algebraic view on Rosetta
[CL-93-02] p 3841 N94-31391
Nonlinear model validation using correlation tests
[RR-463] p 3842 N94-31394
A review of sensitivity analysis techniques
[DE94-007192] p 3842 N94-31399
Identification of polynomial and rational NARMAX models
[RR-483] p 3842 N94-31413
Modeling of fracture and damage in quasibrittle materials p 3734 N94-31479
On the mechanics of stress analysis of fiber-reinforced composites p 3619 N94-31481
Fully discrete arbitrary-order schemes for a model hyperbolic conservation law
[CRANFIELD-AERO-9307] p 3843 N94-31539
A simplified Von Neumann method for linear stability analysis
[CRANFIELD-AERO-9310] p 3843 N94-31540
Two models solving the increasing energy problem of the continuous Hopfield network model
[REPT-93-87] p 3843 N94-31552
Development and implementation of a full-potential ASW method
[ETN-94-95757] p 3858 N94-31560
Numerical simulation of interplanetary dynamics p 3933 N94-31566
Evidence for a correct SiO2 voltage acceleration model
[DE94-006578] p 3690 N94-31594
Boundary-layer cumulus over land: Some observations and conceptual models
[DE93-040820] p 3781 N94-31597
Plasma confinement theory and transport simulation
[DE94-006065] p 3888 N94-31619
The influence of transmutation, void swelling, and flux/spectra uncertainties on the electrical properties of copper and copper alloys
[DE94-006213] p 3641 N94-31626
Impurities and conductivity in a D-wave superconductor
[DE94-006222] p 3898 N94-31628
On the validity of the BLP model
[REPT-93-70] p 3917 N94-31640
Aeroacoustic sources in internal flows
[ISBN-9-03-86-0282-0] p 3860 N94-31653
Aperture excitation of electrically large, lossy cavities
[PB94-145711] p 3675 N94-31683
Numerical modelling of turbulence
[ISBN-0-315-86439-7] p 3703 N94-31720
Micromechanics and effective properties of particulate composites and fluid suspensions p 3703 N94-31744
Stability and instability criteria for magnetohydrodynamics
[PB94-148475] p 3889 N94-31772
Numerical simulations of monsoon rainfall with the NRL/NCSU regional nested grid model p 3782 N94-31791
A model of concurrent flow flame spread over a thin solid fuel p 3634 N94-31795
Attitude dynamics of spinning rockets in space with internal mass motion p 3601 N94-31802
Cometary molecules p 3935 N94-31869
Seasons and chaos in population dynamics p 3912 N94-31897
A paraperspective factorization method for shape and motion recovery
[AD-A276513] p 3712 N94-31929
Cumulus convection parameterization and numerical modelling of moist atmospheres p 3783 N94-31989
Computer modelling of cyclic deformation of high-temperature materials
[AD-A277056] p 3623 N94-32012
Minimization of computational requirements in the hybrid stress finite element method
[AD-A277120] p 3846 N94-32048
Wavevector-frequency analysis with applications to acoustics
[AD-A276618] p 3861 N94-32125
A polling system with a dormant server
[CWI-BS-R9313] p 3835 N94-32193
Area-interaction point processes
[CWI-BS-R9318] p 3847 N94-32197
Multiple inheritance via intersection types
[TR-93-18] p 3848 N94-32292
Finite element solution to the Helmholtz equation with high wave number. Part 1: The h-version of the FEM
[AD-A277396] p 3848 N94-32341
Mechanics of failure of high temperature metal matrix composites
[AD-A277397] p 3624 N94-32342
Fuzzy logic application for modeling man-in-the-loop space shuttle proximity operations
[NASA-CR-188283] p 3835 N94-32359
Chemical vapor deposition fluid flow simulation modelling tool
[NASA-CR-189648] p 3707 N94-32480
The p-q-r-medial axis algorithm requires only local operations
[CWI-BS-R9317] p 3849 N94-32507
Numerical simulation of quantum many-body systems
[DE94-008451] p 3912 N94-32513
Molecular Science Research Center
[DE94-007464] p 3871 N94-32605
Modeling of residual stress mitigation in austenitic stainless steel pipe girth weldment
[DE94-007184] p 3738 N94-32639
Basic principles approach for studying nonlinear Alfven wave-alpha particle dynamics
[DE94-007112] p 3891 N94-32664
Arithmetic averaging: A versatile technique for smoothing and trend removal
[DE94-005274] p 3852 N94-32673
Ethics and rationality in information-enriched decisions: A model for technical communication
[DE93-040251] p 3681 N94-32679
A new solution method for the inverse kinematic joint velocity calculations of redundant manipulators
[DE94-004427] p 3727 N94-32682
Aspects of modeling uncertainty and prediction
[DE94-007565] p 3852 N94-32744
A long-term simulation of surface fluxes and soil moisture
[DE94-006661] p 3774 N94-32772
New advances in the modeling of high-temperature superconductors
[DE94-007649] p 3905 N94-32815
The Numerical Tokamak Project (NTP) simulation of turbulent transport in the core plasma: A grand challenge in plasma physics
[DE94-008279] p 3892 N94-32838
Hierarchical modeling for reliability analysis using Markov models
[NASA-CR-188288] p 3731 N94-32862
Manual for automatic generation of finite element models of spiral bevel gears in mesh
[NASA-CR-191009] p 3728 N94-32900
A mathematical model for simulating noise suppression of lined ejectors
[NASA-TP-3425] p 3861 N94-32930
Modeling of aircraft unsteady aerodynamic characteristics. Part 1: Postulated models
[NASA-TM-109120] p 3586 N94-32951
Fluid Dynamics Lagrangian Simulation Model
[AD-A277438] p 3710 N94-33009
Effective computational strategy for predicting the response of complex systems
[AD-A277452] p 3740 N94-33011
Fast nonsupervised 3D registration of PET and MR images of the brain
[TELECOM-93-C-006] p 3798 N94-33069
Statistical characteristics of bistatic surface scatter and mean bistatic surface scattering strengths
[AD-A278155] p 3862 N94-33096
Real-time sensor data validation
[NASA-CR-195295] p 3616 N94-33099
Designer's unified cost model p 3627 N94-33122
A comparison of rough surface parabolic equation models
[AD-A278090] p 3791 N94-33185
An approximate model for vertical polarization and surface roughness using the parabolic equation
[AD-A278091] p 3684 N94-33186

MATHEMATICAL PROGRAMMING
A new methodology of system parameter estimation
[MATHS-REPT-A-208] p 3808 N94-31163
A parallel implementation of the column subtraction algorithm
[AD-A275922] p 3810 N94-31343
On the computation of simplical approximations of implicitly defined two-dimensional manifolds
[AD-A278132] p 3849 N94-33060
Mixed 0-1 programming by lift-and-project in a branch-and-cut framework
[AD-A278045] p 3822 N94-33183

MATHEMATICS
A cross-disciplinary report on the mathematical sciences applied to materials science, part 1
[AD-A276116] p 3843 N94-31529
OPTIONS for systemic change in mathematics, science, and technology education: Scientist/teacher partnerships
[DE94-007472] p 3914 N94-32910

MATRICES (MATHEMATICS)
Structural properties of inverse linear systems
[MATHS-REPT-A-200] p 3840 N94-31156
Observations of the notion of minimality in the generalized state space
[MATHS-REPT-A-207] p 3840 N94-31162
Arnoldi code for computing selected eigenvalues of sparse real unsymmetric matrices
[PB94-145182] p 3813 N94-31682
Recursive analysis of matrix scattering functions
[AD-A277264] p 3845 N94-32018
Multiparameter quantum groups and multiparameter R-matrices
[CWI-AM-R9307] p 3846 N94-32106
Stability estimates for families of matrices of nonuniformly bounded order
[TW-93-14] p 3847 N94-32207
N(exp n(n-1)/2)-state R-matrix related with U(sub q)(si(n)) algebra at q(exp 2N) = 1
[DE94-608140] p 3902 N94-32247
Perfect 0, +/- matrices
[AD-A277387] p 3848 N94-32286

MATRIX MATERIALS
Characterization of polymer decomposition products by laser desorption mass spectrometry p 3597 N94-31046
Ultrasonic tomography in fiber-reinforced composite materials p 3620 N94-31565

MATRIX THEORY
Structural properties of inverse linear systems
[MATHS-REPT-A-200] p 3840 N94-31156
Observations of the notion of minimality in the generalized state space
[MATHS-REPT-A-207] p 3840 N94-31162
Pairwise-comparison using the logarithmic least squares method and the generalized pseudoinverse
[REPT-93-84] p 3844 N94-31701
Simple Patch: A new heuristic for the product traveling salesman problem
[REPT-93-85] p 3845 N94-31702
Stability estimates for families of matrices of nonuniformly bounded order
[TW-93-14] p 3847 N94-32207
Perfect 0, +/- matrices
[AD-A277387] p 3848 N94-32286

MAXIMA
Stability estimates for families of matrices of nonuniformly bounded order
[TW-93-14] p 3847 N94-32207

MAXIMUM ENTROPY METHOD
Probability distributions with given marginals and given correlation that have maximal entropy
[REPT-93-81] p 3851 N94-31698

MAXIMUM LIKELIHOOD ESTIMATES
Hierarchical mixtures of experts and the EM algorithm
[AD-A276516] p 3814 N94-31932
An experimental study of pilot/vehicle dynamics using a tilt rotor flying machine
[AD-A277516] p 3805 N94-33349

MAXIMUM USABLE FREQUENCY
Analysis of ionospheric parameters in Europe and creation of the prediction algorithm
[AD-A276342] p 3771 N94-31326

MAXWELL EQUATION
MOM3D method of moments code theory manual
[NASA-CR-189594] p 3682 N94-32897

MAXWELL-BOLTZMANN DENSITY FUNCTION
Atomic oxygen interaction at defect sights in protective coatings on polymers flown on LDEF
p 3593 N94-31024
MCDONNELL DOUGLAS AIRCRAFT
Aircraft incident report: In-flight turbulence encounter and loss of portions of the elevators, China Airlines Flight CI-012, McDonnell Douglas MD-11-P, Taiwan Registration B-150 about 20 miles east of Japan, 7 December 1992
[PB94-910403] p 3576 N94-32938
MEAN SQUARE VALUES
The generalized multi delay adaptive filter: Structure and convergence analysis
[TELECOM-93-D-004] p 3808 N94-31094
MEASURE AND INTEGRATION
A note on cocycles in a semidirect product
[REPT-93-65] p 3851 N94-31661
MEASURING INSTRUMENTS
Fiber optic chemical sensors on Mars
[DE94-005251] p 3941 N94-31145
Implementation of instruments and facilities at the SGP CART site
[DE94-006839] p 3781 N94-31322
Microwave dielectric behavior of soils. Report 2: A unique coaxial measurement apparatus
[AD-A275982] p 3771 N94-31353
Continuous measurement of aircraft wing icing
p 3576 N94-32454
Advanced high frequency partial discharge measuring system
[NASA-CR-195240] p 3697 N94-33044
Proceedings SPIE: Conference Digest, volume 2104
[AD-A278107] p 3884 N94-33187
MECHANICAL MEASUREMENT
Fluid mechanical measurements within the bottom boundary layer over the Northern California continental shelf during stress
[AD-A277916] p 3791 N94-33243
MECHANICAL PROPERTIES
Databases and demands for solar heating materials
[PB94-137494] p 3758 N94-31070
Performance predictions for composite materials
[AD-A276451] p 3618 N94-31261
Contributions to the validation of the CJS model for granular materials
[ECL-92-56] p 3733 N94-31376
On the constitutive response of transversely loaded fiber composites with compliant interphases
p 3619 N94-31555
An experimental and analytical investigation of a threaded fastener
[VTT-JULK-786] p 3724 N94-31654
Powder metallurgical processing of fibre reinforced aluminium composites
[PB94-148285] p 3620 N94-31688
Passive vibration damping materials: Piezoelectric ceramic composites for vibration damping applications
[AD-A276550] p 3653 N94-31935
Mechanical properties of acrylate networks formed by visible laser-induced polymerization. 2. Control of the mechanical properties
[AD-A277111] p 3655 N94-31982
Recent advances and developments in refractory alloys
[DE94-007929] p 3644 N94-32374
Multiple size scale structures in silica/siloxane composites studied by small-angle scattering
[DE94-007300] p 3625 N94-32642
Inorganic polymer engineering materials
[DE94-008519] p 3659 N94-32655
Influence of volume fraction of component materials and interlayer bond strength on fracture toughness of multi-layer Al 6090-25 volume percent SiCp and Al 5182 laminates
[DE94-007141] p 3626 N94-32665
Structure, stability, and mechanical properties of intermetallic phases
[DE94-009178] p 3647 N94-32852
Acoustic window
[AD-D016171] p 3862 N94-33017
Interface engineering in oxide fiber/oxide matrix composites
[AD-A277672] p 3627 N94-33029
MEDICAL EQUIPMENT
Hydrogenated amorphous silicon (a-Si:H) based gamma camera: Monte Carlo simulations
[DE94-007042] p 3795 N94-31323
Technical evaluation of the UH-60Q: Medical oxygen system
[AD-A276983] p 3579 N94-32242
MEDICAL PERSONNEL
Technical evaluation of the UH-60Q: Aircraft in typical aeromedical evacuation missions
[AD-A276944] p 3586 N94-32217
Medical problems in high mountain environments. A handbook for medical officers
[AD-A278095] p 3798 N94-33268
MEDICAL SCIENCE
Virtual reality in medical education and assessment
p 3798 N94-32471
MEDICAL SERVICES
Technical evaluation of the UH-60Q: Aircraft in typical aeromedical evacuation missions
[AD-A276944] p 3586 N94-32217
MEDITERRANEAN SEA
Some aspects of the drought in North Africa and in the Mediterranean basin p 3778 N94-30989
The climate of the Mediterranean basin: Its sensitivity to global change p 3778 N94-30993
The ocean-atmosphere interactions in the Mediterranean Sea p 3779 N94-30995
MELT SPINNING
Microstructures and mechanical properties of Al3Ti-based alloys: Analysis in single phase and multiphase systems
[ONERA-NT-1993-6] p 3640 N94-31420
MELTING
Effect of twin boundary density on the vortex melting transition in YBa2Cu3O(7-delta) single crystals
[DE94-007684] p 3904 N94-32601
Snowmelt forecasting. Further cold regions development of operational hydrological forecasting, volume 2
[AD-A278123] p 3757 N94-33269
MELTING POINTS
The ferroelectric behavior of odd-numbered nylons
[AD-A278126] p 3663 N94-33058
MEMORY
Effects of methamphetamine and fatigue on long- and short-term memory
[AD-A276452] p 3799 N94-32187
Reading: Interaction with memory
[AD-A277547] p 3801 N94-32956
Analysis and synthesis of adaptive neural elements and assemblies
[AD-A277423] p 3836 N94-32996
Reminding-based learning
[AD-A277424] p 3801 N94-32997
MEMORY (COMPUTERS)
A comparison of distributed memory and virtual shared memory parallel programming models
[DE94-005473] p 3825 N94-31663
Compiler techniques for managing data motion
[AD-A276514] p 3918 N94-31930
Interpreter composition issues in the formal verification of a processor-memory module
[NASA-CR-4594] p 3820 N94-32775
Toroidal computer memory for serial and parallel processors
[AD-D016144] p 3807 N94-32978
MENISCI
Sol-gel metal oxide and metal oxide/polymer multilayers applied by meniscus coating
[DE94-005813] p 3649 N94-31199
MERCURY (METAL)
Processable, chemical routes to binary metal sulfides
[AD-A277006] p 3642 N94-32004
MERCURY (PLANET)
Forced libration of Mercury and geodetic determination of a possible fluid core p 3774 N94-32493
MERCURY CADMIUM TELLURIDES
Indium-vacancy complexes in mercury cadmium telluride
[AD-A276177] p 3894 N94-31055
IR materials producibility
[AD-A277028] p 3879 N94-32006
MERCURY COMPOUNDS
High T(sub c) superconductor tunnel junctions for photon detectors
[DE94-007686] p 3904 N94-32602
MESOMETEOROLOGY
Coordination of mesoscale meteorological research between ASL and European group
[AD-A276730] p 3784 N94-32162
Use of cloud observations and mesoscale meteorology models to evaluate and improve cloud parameterizations
[DE94-003610] p 3785 N94-32717
Development and testing of improved techniques for modeling the hydrologic cycle in a mesoscale weather prediction system
[AD-A277416] p 3786 N94-32921
MESONS
Study of B(0) - bar-B(0) mixing in D0
[DE94-006000] p 3897 N94-31506
F0-975, A0-980 as eye-witnesses of confinement
[PB94-147105] p 3868 N94-31923
Semileptonic decays of mesons in the SO(4) model
[DE94-008108] p 3873 N94-32708
MESOSCALE PHENOMENA
Coordination of mesoscale meteorological research between ASL and European group
[AD-A276730] p 3784 N94-32162
Proceedings of the Ninth Annual Pacific Climate (PACLIM) Workshop
[DE94-003024] p 3766 N94-32693
Use of cloud observations and mesoscale meteorology models to evaluate and improve cloud parameterizations
[DE94-003610] p 3785 N94-32717
Development and testing of improved techniques for modeling the hydrologic cycle in a mesoscale weather prediction system
[AD-A277416] p 3786 N94-32921
Evolution of upwelling fronts off the coast of Portugal
[NASA-CR-195692] p 3790 N94-33045
MESOSPHERE
Odin aeronomy science: A phase-A report by the Aeronomy Science Working Group for the Odin satellite
[AP-31] p 3770 N94-31222
One: Microphysics of frost metamorphism: Applications to Triton and Mars. Two: A global analysis of the ozone deficit in the upper stratosphere and lower mesosphere. Three: The diabatic circulation in the stratosphere as diagnosed from Microwave Limb Sounder data
p 3942 N94-31975
Radar scattering from the summer polar mesosphere: Theory and observations p 3772 N94-32077
MESSAGE PROCESSING
Analysis of the effect of routing strategies for parallel implementations of a selected avionics application
[AD-A276069] p 3581 N94-31458
MICA, a facility to achieve portability for message-passing and dynamic memory management in FORTRAN
[DE94-006692] p 3807 N94-32147
MESSAGES
PEM public key certificate cache server
[DE94-006404] p 3675 N94-31784
METABOLISM
The organization of the suprachiasmatic circadian pacemaker of the rat and its regulation by neurotransmitters and modulators
[AD-A277324] p 3793 N94-32622
Numerical model of the thermal behavior of an extremity in a cold environment including counter-current heat exchange between the blood vessels
[AD-A278099] p 3798 N94-33040
METAL AIR BATTERIES
Promising future energy storage systems: Nanomaterial based systems, Zn-air, and electromechanical batteries
[DE94-007443] p 3692 N94-32136
Overview of Sandia's electric vehicle battery program
[DE94-008944] p 3696 N94-32806
METAL BONDING
Joining of alumina by vacuum brazing
[VTT-TIED-1495] p 3724 N94-31656
Soft x ray photoelectron spectroscopy study of the interaction of Cr with MoS2(0001)
[AD-A276916] p 3635 N94-32233
Liquid-assisted diffusion bonding of NiAl
[DE94-008687] p 3645 N94-32522
A review of weldment failure modes and weldability testing methods
[AD-A278096] p 3729 N94-33251
METAL CLUSTERS
Theoretical studies of zirconium and carbon clusters with molecular dynamics simulations
[DE94-005276] p 3862 N94-31146
Metal clusters: Dynamics and structure
[AD-A276842] p 3643 N94-32091
Metal cluster-rare gas van der Waals complexes: Microscopic models of physisorption
[DE94-008134] p 3873 N94-32797
METAL COATINGS
Atomic oxygen damage characterization by photothermal scanning p 3598 N94-31051
Robotic weld overlay coatings for erosion control
[DE94-008004] p 3658 N94-32408
METAL COMBUSTION
Shock tube ignition and combustion of aluminum/magnesium alloy particles in oxygen at high pressure p 3631 N94-31286
Control experiments in liquid metal combustion
[AD-A276918] p 3635 N94-32234
METAL CRYSTALS
High temperature materials technology research for advanced thermionic systems
[DE94-008341] p 3646 N94-32825
METAL FATIGUE
Multiple-site damage in aircraft fuselage structures
[LR-729] p 3578 N94-31675
Thermal-mechanical fatigue crack growth in aircraft engine materials
[ISBN-0-315-86543-1] p 3734 N94-31707

Acoustic emission from crack growth in 7050 aluminum and 7075 aluminum as a function of temperature and heat treatment
[DREP-CRS-93-15] p 3642 N94-31871
Creep-fatigue criteria and inelastic behavior of modified 9Cr-1Mo steel at elevated temperatures
[DE94-007915] p 3642 N94-31918
Fracture micromechanics of continuous fiber and textile reinforced metal and ceramic matrix composites
[AD-A277434] p 3627 N94-33008

METAL FILMS
Preliminary results from the CONCAP-2-01 and EIOM-3 experiments on STS-46 p 3596 N94-31042
Process parameter-growth environment-film property relationships for reactive sputter deposited metal (V, Nb, Zr, Y, Au) oxide, nitride, and oxynitride films
[AD-A276382] p 3640 N94-31258
Reliability of multilayer copper/polyimide
[AD-A276228] p 3650 N94-31284
Computerized Ultrasonic Testing System (CUTS) for in-process thickness determination
p 3662 N94-32456
Anisotropic phase separation through the metal-insulator transition in amorphous Mo-Ge and Fe-Ge alloys
[DE94-007259] p 3646 N94-32795

METAL FOAMS
Indentability of conventional and negative Poisson's ratio foams p 3629 N94-33131

METAL HYDRIDES
Feasibility study for the recycling of nickel metal hydride electric vehicle batteries
[DE94-000268] p 3690 N94-31598
Metal hydrides in hydrogen energy systems
[VTT-TIED-1407] p 3759 N94-31655
Metal hydride heat pump engineering demonstration and evaluation model
[NASA-CR-188286] p 3669 N94-32857
Development of nickel and metal hydride secondary battery
[DE94-757270] p 3697 N94-32917

METAL IONS
Enhancement of oxidation resistance of silicon carbide by high-dose and multi-energy aluminum implantation
[DE94-006560] p 3640 N94-31314
Performance of the Sony lithium-ion rechargeable battery
[AD-A277076] p 3693 N94-32303
Metal-ion spin-on glasses: Novel materials for active waveguides
[DE94-007738] p 3882 N94-32649
Performance of an ion trap inductively coupled plasma mass spectrometer
[DE94-007470] p 3713 N94-32811
Ultrahigh-current-density metal-ion implantation and diamondlike-hydrocarbon films for tribological applications
[DE94-008958] p 3906 N94-32843
Metal ion complexation by ionizable crown ethers
[DE94-008301] p 3661 N94-32847
Optical properties of lanthanide-doped RbTiOAsO4 and transition metal-doped KTiOPO4
[DE94-008433] p 3907 N94-32963
Rare Earth Doped Semiconductors and Materials Research Society Symposium Proceedings, Volume 301
[AD-A277517] p 3908 N94-33055

METAL JOINTS
Feasibility study of cold expansion processes modelling
[DSIS-94-01186] p 3735 N94-31849

METAL MATRIX COMPOSITES
The impact of LDEF results on the space application of metal matrix composites p 3595 N94-31034
Inelastic deformation of metal matrix composites
p 3618 N94-31285
Development and characterization of intermediary layers allowing the bond between a metal alloy and a plasma sprayed ceramic
[ECL-91-39] p 3619 N94-31377
Powder metallurgical processing of fibre reinforced aluminium composites
[PB94-148285] p 3620 N94-31688
Characterization and growth mechanisms of the MgAl2O4 phase in Al2O3-reinforced Al-Mg composites
[ISBN-0-315-86531-8] p 3620 N94-31706
Interfacial behaviour: Wettability in SiC(sub p) metal matrix composites
[ISBN-0-315-87206-3] p 3621 N94-31835
Mechanics of failure of high temperature metal matrix composites
[AD-A277397] p 3624 N94-32342
Influence of volume fraction of component materials and interlayer bond strength on fracture toughness of multi-layer Al 6090-25 volume percent SiCp and Al 5182 laminates
[DE94-007141] p 3626 N94-32665
METCAN demonstration manual, version 1.0
[NASA-TM-105607] p 3626 N94-32858
Fracture micromechanics of continuous fiber and textile reinforced metal and ceramic matrix composites
[AD-A277434] p 3627 N94-33008
Briefing and review meeting implementation of the military handbook 17 for polymer matrix and metal matrix composites
[AD-A277446] p 3663 N94-33010
On the mechanics of microballoon-reinforced metal matrix composites
[AD-A277928] p 3630 N94-33178
Leveraging metal matrix composites to reduce costs in space mechanisms p 3604 N94-33301

METAL OXIDE SEMICONDUCTORS
Process parameter-growth environment-film property relationships for reactive sputter deposited metal (V, Nb, Zr, Y, Au) oxide, nitride, and oxynitride films
[AD-A276382] p 3640 N94-31258
An extended approach to oxidations and nitridations of Si and Ge(x)Si(1-x) materials
[AD-A276056] p 3631 N94-31282
Hydrogen incorporation and radiation induced dynamics in metal-oxide-silicon structures: A study using nuclear reaction analysis
[ETN-94-95742] p 3898 N94-31610
Analysis and synthesis of MOS translinear circuits
[ISBN-9-09-005495-2] p 3690 N94-31616
Temperature dependence of single-event burnout in n-channel power MOSFET's
[AD-A277921] p 3698 N94-33177

METAL OXIDES
Sol-gel metal oxide and metal oxide/polymer multilayers applied by meniscus coating
[DE94-005813] p 3649 N94-31199
Experimental investigations and molecular dynamics simulations of radiation induced surface damage
[AD-A277323] p 3871 N94-32621

METAL PARTICLES
Oxidation resistant copper
[AD-D016099] p 3696 N94-32721

METAL PLATES
Effect of vibratory stress relief during welding of thick stainless steel plate
[DE94-006557] p 3733 N94-31312

METAL POWDER
The new Metals and Alloys Indexes, search manual: A phase diagram research tool
[DE94-005371] p 3643 N94-32098
On the formation of muon- and zeta-phases in Ag-Al system by mechanical alloying
[DE94-007125] p 3645 N94-32636
Development of nickel and metal hydride secondary battery
[DE94-757270] p 3697 N94-32917

METAL PROPELLANTS
Shock tube ignition and combustion of aluminum/magnesium alloy particles in oxygen at high pressure p 3631 N94-31286

METAL SURFACES
Interaction of water with metal surfaces
[AD-A276280] p 3632 N94-31293
Fiber optic sensors for the detection of surface acoustic waves on metals
[ISBN-0-315-87055-9] p 3878 N94-31736
A new-type of long-range restructuring of ordered metal surfaces induced by lateral adsorbate interactions: Iodide on AU(110) electrodes
[AD-A276633] p 3643 N94-32060
Vibrational spectroscopy at metal-solution interfaces: Some perspectives and prospects for electrochemical surface science
[AD-A276781] p 3644 N94-32169
Molten metal analysis by laser produced plasmas
[DE94-007014] p 3646 N94-32782
Metal cluster-rare gas van der Waals complexes: Microscopic models of physisorption
[DE94-008134] p 3873 N94-32797
Method and apparatus for inhibiting the disbonding of a paint from metal surfaces
[AD-D016106] p 3663 N94-32960

METAL VAPORS
Using laser absorption spectroscopy to monitor composition and physical properties of metal vapors
[DE94-001530] p 3716 N94-31599
Ultrahigh-current-density metal-ion implantation and diamondlike-hydrocarbon films for tribological applications
[DE94-008958] p 3906 N94-32843

METAL WORKING
Lubrication with binary mixtures: Liquid-liquid emulsion in elastohydrodynamics and metal forming
p 3658 N94-32490

METAL-GAS SYSTEMS
The 10th International Conference on Internal Friction and Ultrasonic Attenuation in Solids (ICIFUAS)
[AD-A276849] p 3902 N94-32209

METAL-METAL BONDING
Small cylindrical adhesive bonds
[PB94-148210] p 3651 N94-31585
Metal clusters: Dynamics and structure
[AD-A276842] p 3643 N94-32091

METALLICITY
Line-strength gradients and kinematic profiles in elliptical galaxies p 3934 N94-31788
The role of galaxy type and environment in determining the properties of globular cluster systems
[ISBN-0-315-76447-3] p 3939 N94-33112

METALLIZING
Research on high reliability refractory ohmic contacts for GaAs FETs and MODFETs
[AD-A276848] p 3697 N94-33034

METALLOGRAPHY
Nd-YAG laser welding of the fiber optic connector to the header shell on the 2SL actuator
[DE94-006104] p 3 N94-31621

METALORGANIC CHEMICAL VAPOR DEPOSITION
GaAs/GaN strained layer superlattice materials for high temperature transistors, phase 1
[AD-A276115] p 3897 N94-31528
Novel growth technologies for in situ formation of semiconductor quantum wire structures
[AD-A277188] p 3902 N94-32255

METALS
Metal induced embrittlement
[DE94-007450] p 3640 N94-31325
Control and monitoring of heavy metal emissions
[VTT-TIED-1508] p 3765 N94-31657
New molecular-based routes to binary main group metal sulfides
[AD-A277005] p 3900 N94-32003
The new Metals and Alloys Indexes, search manual: A phase diagram research tool
[DE94-005371] p 3643 N94-32098
Experimental measurement of dynamic failure and fragmentation properties of metals
[DE94-007377] p 3737 N94-32135
Characterization of nanoparticles and nanophase materials
[DE94-008348] p 3907 N94-32990
Ceramic and metal composite circuit-board-level technology for application specific electronic modules (ASEM)
[AD-A277961] p 3630 N94-33180

METASTABLE STATE
Production and detection of metastable atomic oxygen
[ISBN-0-315-87364-7] p 3868 N94-31915
NN-interaction in (1)S0-state: Virtual level or dibaryon resonance?
[DE94-606492] p 3869 N94-32097
Amorphous/crystalline structure and phase transformations in metastable semiconducting Ge(1-x)Sn(x)
[DE94-006659] p 3901 N94-32115
Stability and precipitation kinetics in Si(1-y)C(y)/Si and Si(1-x-y)Ge(x)C(y)/Si heterostructures prepared by solid phase epitaxy
[DE94-006589] p 3902 N94-32296
Structural studies of photoinduced intramolecular electron transfer in cyclopentadienylnickelnitrosyl
[DE94-008467] p 3874 N94-32876

METEOR TRAILS
Performance statistics bulletin. High latitude meteor scatter propagation October, November, December 1990, January 1991
[AD-A276693] p 3676 N94-31998
Performance statistics bulletin. High latitude metor scatter propagation, February, March, April, May 1992
[AD-A276667] p 3677 N94-32083
Performance statistics bulletin. High latitude meteor scatter propagation February, March, April, May 1991
[AD-A276723] p 3678 N94-32158
Performance statistics bulletin. High latitude meteor scatter propagation October, November, December 1991, January 1992
[AD-A276724] p 3678 N94-32159
Performance statistics bulletin. High latitude meteor scatter propagation, November and December 1989, and January 1990
[AD-A276688] p 3680 N94-32297
Performance statistics bulletin. High latitude meteor scatter propagation
[AD-A276694] p 3680 N94-32298
Performance statistics bulletin. High latitude meteor scatter propagation
[AD-A276695] p 3680 N94-32299
Performance statistics bulletin. High latitude meteor scatter propagation
[AD-A276696] p 3680 N94-32300

Performance statistics bulletin. High latitude meteor scatter propagation, June, July, August, September 1992
[AD-A277508] p 3685 N94-33347

METEORITE CRATERS
Keeping that youthful look --- impact cratering of Venus p 3941 N94-31112
Biospheric effects of a large extraterrestrial impact: Case study of the Cretaceous/Tertiary boundary crater
[NASA-CR-195827] p 3942 N94-32740
Constraints on the Martian cratering rate imposed by the SNC meteorites and Vallis Marineris layered deposits p 3945 N94-33197
Possible test of ancient dense Martian atmosphere p 3947 N94-33206
Mineralogical diversity (spectral reflectance and Moessbauer data) in compositionally similar impact melt rocks from Manicouagan Crater, Canada p 3948 N94-33219

METEORITES
Constraints on the Martian cratering rate imposed by the SNC meteorites and Vallis Marineris layered deposits p 3945 N94-33197
Carbonates, surfates, phosphates, nitrates, and organic materials: Their association in a Martian meteorite p 3952 N94-33239

METEORITIC COMPOSITION
The origin of neon-E: Neon-E in single interstellar silicon carbide and graphite grains p 3933 N94-31556
Organic analyses of the Murchison meteorite p 3938 N94-32489
SNC meteorites and their implications for reservoirs of Martian volatiles p 3947 N94-33209

METEORITIC DAMAGE
Morphology correlation of craters formed by hypervelocity impacts p 3594 N94-31031
Biospheric effects of a large extraterrestrial impact: Case study of the Cretaceous/Tertiary boundary crater
[NASA-CR-195827] p 3942 N94-32740

METEOROID SHOWERS
Performance statistics bulletin. High latitude meteor scatter propagation October, November, December 1990, January 1991
[AD-A276693] p 3676 N94-31998
Performance statistics bulletin. High latitude meteor scatter propagation February, March, April, May 1991
[AD-A276723] p 3678 N94-32158
Performance statistics bulletin. High latitude meteor scatter propagation October, November, December 1991, January 1992
[AD-A276724] p 3678 N94-32159
Performance statistics bulletin. High latitude meteor scatter propagation
[AD-A276694] p 3680 N94-32298
Performance statistics bulletin. High latitude meteor scatter propagation
[AD-A276695] p 3680 N94-32299
Performance statistics bulletin. High latitude meteor scatter propagation
[AD-A276696] p 3680 N94-32300
Performance statistics bulletin. High latitude meteor scatter propagation, June, July, August, September 1992
[AD-A277508] p 3685 N94-33347

METEOROIDS
Performance statistics bulletin. High latitude meteor scatter propagation October, November, December 1990, January 1991
[AD-A276693] p 3676 N94-31998
Performance statistics bulletin. High latitude meteor scatter propagation February, March, April, May 1991
[AD-A276723] p 3678 N94-32158
Performance statistics bulletin. High latitude meteor scatter propagation October, November, December 1991, January 1992
[AD-A276724] p 3678 N94-32159
Performance statistics bulletin. High latitude meteor scatter propagation
[AD-A276694] p 3680 N94-32298
Performance statistics bulletin. High latitude meteor scatter propagation
[AD-A276695] p 3680 N94-32299
Performance statistics bulletin. High latitude meteor scatter propagation
[AD-A276696] p 3680 N94-32300
Performance statistics bulletin. High latitude meteor scatter propagation, June, July, August, September 1992
[AD-A277508] p 3685 N94-33347

METEOROLOGICAL INSTRUMENTS
Implementation of instruments and facilities at the SGP CART site
[DE94-006839] p 3781 N94-31322
Low power, constant-flow air pump systems
[DE94-007463] p 3727 N94-32758

METEOROLOGICAL PARAMETERS
A comparison of predictors for first-guess wind speed errors
[AD-A276460] p 3781 N94-31239
Station climatic summaries: China, the former USSR, and Mongolia
[AD-A276548] p 3784 N94-32057
Recommendations for meteorological data collection during physiological field studies
[AD-A276834] p 3901 N94-32153
Recurvature dynamics of a typhoon
[AD-A276792] p 3784 N94-32164
Fine resolution atmospheric sulfate model driven by operational meteorological data: Comparison with observations
[DE94-002994] p 3766 N94-32691
Proceedings of the Ninth Annual Pacific Climate (PACLIM) Workshop
[DE94-003024] p 3766 N94-32693
Use of cloud observations and mesoscale meteorology models to evaluate and improve cloud parameterizations
[DE94-003610] p 3785 N94-32717
Mexico City ozone concentrations as a function of readily-available meteorological parameters
[DE94-007576] p 3768 N94-32814

METEOROLOGICAL RADAR
Radar measurements p 3685 N94-31002
Field studies of raindrop oscillations with applications to radar meteorology p 3782 N94-31743
Radar rainfall measurements from space p 3782 N94-31889
Gyrotrons and free electron lasers for atmospheric sensing
[AD-A277281] p 3718 N94-32406
An integrated cloud observation and modeling investigation in support of the ARM program
[DE94-003160] p 3785 N94-32716

METEOROLOGICAL SATELLITES
The use of meteorological satellite data for studying tropical atmospheric phenomena p 3779 N94-31000
Satellite direct readout: Opportunities for science education
[AD-A276257] p 3609 N94-31292
Use of Air Force cloud cover data to evaluate and improve cloud forecasts and parameterizations in mesocale meteorological models
[AD-A277384] p 3784 N94-32054

METEOROLOGY
Implementation of instruments and facilities at the SGP CART site
[DE94-006839] p 3781 N94-31322
Regional sources of error growth in the National Meteorological Center's medium-range forecast model p 3781 N94-31554
Use of Air Force cloud cover data to evaluate and improve cloud forecasts and parameterizations in mesocale meteorological models
[AD-A277384] p 3784 N94-32054
Recommendations for meteorological data collection during physiological field studies
[AD-A276834] p 3901 N94-32153
Proceedings of the Ninth Annual Pacific Climate (PACLIM) Workshop
[DE94-003024] p 3766 N94-32693
Development and testing of improved techniques for modeling the hydrologic cycle in a mesoscale weather prediction system
[AD-A277416] p 3786 N94-32921
Performance of a new wind updating system for a prognostic meteorological model in the environs of Mexico City
[DE94-006243] p 3786 N94-32937
Operations summary for the convection and moisture experiment (CAMEX)
[NASA-TM-108445] p 3786 N94-33004

METHAMPHETAMINE
Effects of methamphetamine and fatigue on long- and short-term memory
[AD-A276452] p 3799 N94-32187

METHANE
Feasibility study to evaluate plasma quench process for natural gas conversion applications
[DE94-000086] p 3758 N94-31234
Development of vanadium-phosphate catalysts for methanol production by selective oxidation of methane
[DE94-006759] p 3759 N94-31272
Volatiles combustion in fluidized beds
[DE94-008382] p 3636 N94-32414
Methyl chloride by way of oxyhydrochlorination of methane
[DE94-009129] p 3637 N94-32767
Direct aromatization of methane
[DE94-008719] p 3638 N94-32888
A correlated k-distribution model of the heating rates for atmospheric mixtures of H2O, CO2, O3, CH4, and N2O in the 0-2500 cm(exp -1) wave number region at altitudes between 0 and 60 km
[DE94-005136] p 3775 N94-32895

METHOD OF MOMENTS
Electromagnetic scattering through loaded aperture panels with nonzero contact impedance
[ONERA-NT-1993-2] p 3673 N94-31418
MOM3D method of moments code theory manual
[NASA-CR-189594] p 3682 N94-32897

METHYL ALCOHOL
Development of vanadium-phosphate catalysts for methanol production by selective oxidation of methane
[DE94-006759] p 3759 N94-31272
Novel approaches to the production of higher alcohols from synthesis gas
[DE94-006770] p 3666 N94-32132
High octane ethers from synthesis gas-derived alcohols
[DE94-006774] p 3667 N94-32133

METHYL CHLORIDE
Methyl chloride by way of oxyhydrochlorination of methane
[DE94-009129] p 3637 N94-32767

METHYL COMPOUNDS
High-temperature study of O+H2CO yields OH+HCO
[DE94-006837] p 3864 N94-31321
Solvent diffusion coefficient concentration dependence in polymer solutions
[AD-A277023] p 3655 N94-32005
Microstructure of copolymers containing disperse red 1 and methyl methacrylate
[AD-A277140] p 3660 N94-32722
Conversion of polymers of methyl- and vinylsilane to Si-C ceramics
[NASA-TM-106554] p 3662 N94-32945

METRIC SPACE
Line transects, covariance functions and set approximation
[CWI-BS-R9311] p 3846 N94-32084
The p-q-r-medial axis algorithm requires only local operations
[CWI-BS-R9317] p 3849 N94-32507

METROLOGY
Application of the modified voltage-dividing potentiometer to overlay metrology in a CMOS/bulk process
[DE94-007937] p 3695 N94-32700

MEXICO
Performance of a new wind updating system for a prognostic meteorological model in the environs of Mexico City
[DE94-006243] p 3786 N94-32937

MICHELSON INTERFEROMETERS
Fiber optic sensors for the detection of surface acoustic waves on metals
[ISBN-0-315-87055-9] p 3878 N94-31736
Coastal boundary layer and refractivity measurements using the ground-based high resolution interferometer sounder (GB-HIS)
[AD-A277980] p 3683 N94-33159
Development of long-life, low-noise linear bearings for atmospheric interferometry p 3606 N94-33312

MICROANALYSIS
Correlations between micromagnetic, microstructural and microchemical properties in ultrathin epitaxial magnetic structures
[AD-A277200] p 3901 N94-32092
Deuterium absorption and material phase characteristics of SAES St198 Zr-Fe alloy
[DE94-008275] p 3646 N94-32781

MICROBALANCES
Pre-flight testing of Thermoelectric Quartz Crystal Microbalances (TQCM) for midcourse space experiment (MSX) spacecraft
[AD-A277054] p 3610 N94-32010

MICROBALLOONS
On the mechanics of microballoon-reinforced metal matrix composites
[AD-A277928] p 3630 N94-33178

MICROCOMPUTERS
Design and Monte Carlo analysis of an unmanned aerial vehicle
[AD-A277648] p 3580 N94-33056

MICROCRYSTALS
Oriented Si and Ge nanocrystals formed in Al2O3 by ion implantation and annealing
[DE94-005593] p 3901 N94-32172

MICROELECTRONICS
Fault coverage measurement for digital microcircuits
[AD-A276226] p 3686 N94-31066
RF vacuum microelectronics
[AD-A276512] p 3691 N94-31928
Sandia technology engineering and science accomplishments
[DE94-008312] p 3668 N94-32412
Aerospace sponsored research
[ATR-93(8498)-1] p 3966 N94-32949

Silicon-Based Optoelectronic Materials Symposium and Materials Research Society Proceedings, volume 298
[AD-A277518] p 3662 N94-32952
The impact of ASIC devices on the SEU vulnerability of space-borne computers
[AD-A278134] p 3808 N94-33252

MICROGRAVITY
Space acceleration measurement system
[NASA-TM-109754] p 3913 N94-31807
Steady thermal convection in multiple liquid layers p 3705 N94-31844
Solid surface
[NASA-TM-109746] p 3634 N94-31883
Defying gravity
[NASA-TM-109747] p 3667 N94-31884
An experimental study of void formation during aluminum solidification in reduced gravity p 3667 N94-31944
Boundary element analysis of three-dimensional nonlinear hydrodynamics in a reduced gravity environment p 3668 N94-32715
Vibration Isolation Technology (VIT) ATD project
[NASA-TM-106496] p 3567 N94-33064
Design, characterization, and control of the NASA three degree of freedom reaction compensation platform p 3605 N94-33304

MICROGRAVITY APPLICATIONS
Vibration Isolation Technology (VIT) ATD project
[NASA-TM-106496] p 3567 N94-33064
Design, characterization, and control of the NASA three degree of freedom reaction compensation platform p 3605 N94-33304

MICROHARDNESS
Robotic weld overlay coatings for erosion control
[DE94-008004] p 3658 N94-32408

MICROMACHINING
RF vacuum microelectronics
[AD-A276512] p 3691 N94-31928

MICROMECHANICS
Micromechanical analysis of the interface and basic damage modes in glass fiber/epoxy resin model composites
[ONERA-NT-1993-4] p 3618 N94-31225
Unidirectional composites compressive behaviour: Test methods and micromechanical approach
[ONERA-NT-1993-10] p 3618 N94-31232
Inelastic deformation of metal matrix composites p 3618 N94-31285
On the constitutive response of transversely loaded fiber composites with compliant interphases p 3619 N94-31555
Micromechanics and effective properties of particulate composites and fluid suspensions p 3703 N94-31744
Toughening mechanisms in fiber-reinforced ceramic-matrix composites p 3622 N94-31943
Fracture mechanics and micromechanisms in fiber-reinforced composites p 3622 N94-31986
Finite element analysis of damage in fibrous composites using a micromechanical model
[AD-A277226] p 3623 N94-32024
Mechanics of the single fiber pullout problem with several interface conditions p 3623 N94-32078
New micro- and macroscopic models of contact and friction
[AD-A277240] p 3726 N94-32320
Development of an advanced continuum theory for composite laminates, volume 1
[AD-A277275] p 3625 N94-32591
Development of an advanced continuum theory for composite laminates, volume 2
[AD-A277276] p 3625 N94-32592
Fracture micromechanics of continuous fiber and textile reinforced metal and ceramic matrix composites
[AD-A277434] p 3627 N94-33008
Nonlocal theory for fracturing of quasibrittle materials
[AD-A278283] p 3740 N94-33143

MICROMETEOROIDS
Space Station WP-2 application of LDEF MLI results p 3592 N94-31016
Morphology correlation of craters formed by hypervelocity impacts p 3594 N94-31031
Micrometeoroid/space debris effects on materials p 3595 N94-31032

MICROPARTICLES
Space hypervelocity microparticle impact damage in polymer matrix composites
[ISBN-0-315-87057-5] p 3652 N94-31692
Stabilized alumina/ethanol colloidal dispersion for seeding high temperature air flows
[NASA-TM-106591] p 3713 N94-32983
Counting particles emitted by stratospheric aircraft and measuring size of particles emitted by stratospheric aircraft
[NASA-CR-195908] p 3769 N94-33170

MICROPHONES
A silicon condenser microphone: Modelling and electronic circuitry
[ISBN-9-09-005279-8] p 3688 N94-31517
A silicon condenser microphone: Materials and technology
[ISBN-9-09-005899-0] p 3688 N94-31518

MICROPROCESSORS
Interpreter composition issues in the formal verification of a processor-memory module
[NASA-CR-4594] p 3820 N94-32775

MICROSCOPES
X ray imaging and x ray source development at Lawrence Livermore National Laboratory
[DE94-007077] p 3719 N94-32629
Simplified ultra-high resolution optic for soft x ray imaging
[AD-A278424] p 3885 N94-33331

MICROSCOPY
Atomic oxygen damage characterization by photothermal scanning p 3598 N94-31051
New and emerging techniques for imaging surfaces
[AD-A276497] p 3878 N94-31262
Differential phase acoustic microscope for micro-NDE
[NASA-CR-189617] p 3731 N94-32481

MICROSEISMS
Long transect seafloor seismic array: A component of SAMSON (Sources of Ambient Micro Seismic Ocean ic Noise)
[AD-A277009] p 3789 N94-32401

MICROSTRIP ANTENNAS
The development of active integrated antennas and a design methodology
[ISBN-0-315-86119-3] p 3675 N94-31708
Proceedings of the 1993 Antenna Applications Symposium, volume 1
[AD-A277202] p 3676 N94-32049
Proceedings of the 1993 Antenna Applications Symposium, volume 2
[AD-A277203] p 3677 N94-32050
Microwave sensor for ice detection p 3583 N94-32457
COVICS: A covert video communications system
[DE94-007568] p 3682 N94-32745
Reconfigurable Array of Radiating Elements (RARE) controlled by light
[NASA-CR-195828] p 3884 N94-33073
The 20 GHz circularly polarized, high temperature superconducting microstrip antenna array
[NASA-CR-195097] p 3683 N94-33083

MICROSTRIP DEVICES
An investigation of a novel microstrip magic-T
[ISBN-0-315-86218-1] p 3690 N94-31711

MICROSTRIP TRANSMISSION LINES
Simulation of non-uniform transmission lines for weakly dispersive structures
[ISBN-0-315-86525-3] p 3690 N94-31726
Theoretical and experimental study of microstrip-to-slot line uniplanar transition
[NASA-TM-106566] p 3696 N94-32905
Reconfigurable Array of Radiating Elements (RARE) controlled by light
[NASA-CR-195828] p 3884 N94-33073

MICROSTRUCTURE
Microstructures and mechanical properties of Al3Ti-based alloys: Analysis in single phase and multiphase systems
[ONERA-NT-1993-6] p 3640 N94-31420
Structure and dynamics of microemulsions in bulk, at interfaces, and in confined geometries
[DE94-006043] p 3633 N94-31526
Aging effects on the microstructure, surface characteristics and wettability of Cu pretinned with Sn-Pb solders
[DE94-007033] p 3641 N94-31638
Effect of irradiation damage and helium on the swelling and structure of vanadium-base alloys
[DE94-006540] p 3641 N94-31666
High-temperature deformation and fracture toughness of duplex ceramic microstructures p 3653 N94-31945
Sodium sulfate corrosion of silicon carbide fiber-reinforced lithium aluminosilicate glass-ceramic matrix composites
[AD-A277224] p 3623 N94-32023
Work hardening behavior in aluminum alloy 2090
[DE94-007036] p 3643 N94-32064
Correlations between micromagnetic, microstructural and microchemical properties in ultrathin epitaxial magnetic structures
[AD-A277200] p 3901 N94-32092
Robotic weld overlay coatings for erosion control
[DE94-008004] p 3658 N94-32408
Mechanical properties of vacuum-sintered yttria ceramics
[DE94-008138] p 3659 N94-32617
Microstructure of copolymers containing disperse red 1 and methyl methacrylate
[AD-A277140] p 3660 N94-32722
Microanalytical study of defect formation in thin bismuth strontium calcium copper oxide films
[DE94-008217] p 3661 N94-32751
Isothermal sintering, microstructure, and superconducting properties of Y1Ba2Cu3O(7-x) compound
[DE94-008132] p 3905 N94-32779
NMR characterization of shocked quartz
[DE94-007733] p 3774 N94-32816
Light scattering studies of a model electrorheological fluid
[DE94-007860] p 3883 N94-32818
Phase behavior, structure, and properties of model block polymers
[AD-A277530] p 3662 N94-32954
Characterization of nanoparticles and nanophase materials
[DE94-008348] p 3907 N94-32990
Interface engineering in oxide fiber/oxide matrix composites
[AD-A277672] p 3627 N94-33029
Fine and microstructure observations at Fieberlin g Guyot R/V new horizon cruise report
[AD-A277917] p 3791 N94-33109
Cruise report: Oceanus 250 leg 4 high resolution profiler survey for the North Atlantic Tracer Release Experiment, 25 March - 24 April, 1992
[AD-A277935] p 3791 N94-33245
The path for long range conduction in high J(sub c) TlBa2Ca2Cu3O(8+x) spray-pyrolyzed deposits
[DE94-007211] p 3909 N94-33271
Microstructures and epitaxy in oxide superconductor thin films and devices
[AD-A278427] p 3910 N94-33332

MICROWAVE AMPLIFIERS
Design of a high power x-band magnicon amplifier
[AD-A277001] p 3692 N94-32199

MICROWAVE ANTENNAS
The development of active integrated antennas and a design methodology
[ISBN-0-315-86119-3] p 3675 N94-31708
SATCOM feasibility study for search and rescue aircraft
[DSIS-94-01083] p 3575 N94-31902
Reconfigurable Array of Radiating Elements (RARE) controlled by light
[NASA-CR-195828] p 3884 N94-33073
The 20 GHz circularly polarized, high temperature superconducting microstrip antenna array
[NASA-CR-195097] p 3683 N94-33083
Two-axis antenna positioning mechanism p 3605 N94-33308

MICROWAVE CIRCUITS
Microwave dielectric behavior of soils. Report 3: Measurement and modeling
[AD-A276060] p 3771 N94-31457
High-performance GaAs/AlGaAs optical phase modulators for microwave/photonic integrated circuits
[DE94-006361] p 3688 N94-31483
High performance YBCO films
[AD-A276493] p 3897 N94-31531
Simulation of non-uniform transmission lines for weakly dispersive structures
[ISBN-0-315-86525-3] p 3690 N94-31726
Design of a high power x-band magnicon amplifier
[AD-A277001] p 3692 N94-32199
High-performance GaAs/AlGaAs optical phase modulators for microwave photonic integrated circuits
[DE94-007376] p 3696 N94-32809
YBCO Josephson Junction arrays
[AD-A277426] p 3908 N94-33005
Advanced silicon technology for microwave circuits
[AD-A278039] p 3698 N94-33091

MICROWAVE COUPLING
An investigation of a novel microstrip magic-T
[ISBN-0-315-86218-1] p 3690 N94-31711

MICROWAVE EMISSION
High sensitivity and resolution decimetric spectroscope: Preliminary analysis of solar bursts
[INPE-5537-TDI/525] p 3954 N94-33080

MICROWAVE EQUIPMENT
Simulation of non-uniform transmission lines for weakly dispersive structures
[ISBN-0-315-86525-3] p 3690 N94-31726
Performance evaluation and operating characteristics of a waveguide microwave applicator for space propulsion applications p 3614 N94-31908
Division of Microwave Technology
[PB94-148079] p 3676 N94-31925
Estimation and analysis of climate-scale rainfall over the Tropical Pacific p 3783 N94-32030
Proceedings SPIE: Conference Digest, volume 2104
[AD-A278107] p 3884 N94-33187

MICROWAVE FREQUENCIES
Development of a frequency-domain electromagnetic scattering measurement system
[AD-A276738] p 3678 N94-32179
Processing and characterization of functionally gradient ceramic materials
[AD-A277154] p 3657 N94-32367
MICROWAVE IMAGERY
Estimation and analysis of climate-scale rainfall over the Tropical Pacific p 3783 N94-32030
MICROWAVE OSCILLATORS
Repetitively pulsed backward-wave oscillator investigations
[AD-A278281] p 3698 N94-33142
Optically switched submillimeter-wave oscillator
[AD-A278014] p 3698 N94-33249
MICROWAVE RADIOMETERS
An integrated cloud observation and modeling investigation in support of the ARM program
[DE94-003160] p 3785 N94-32716
Water vapor from sunradiometry in comparison with microwave and balloon-sonde measurements at the Southern Great Plains ARM Site
[DE94-007479] p 3786 N94-32759
MICROWAVE SENSORS
Radar rainfall measurements from space
p 3782 N94-31889
Microwave sensor for ice detection
p 3583 N94-32457
Application of ERS-1 SAR data for hydrological studies p 3754 N94-32558
Synergy of thermal infrared and microwave remote sensing for evaporation estimation p 3754 N94-32559
MICROWAVE SPECTRA
Cometary molecules p 3935 N94-31869
MICROWAVE TUBES
High-power microwave-tube transmitters
[DE94-005340] p 3686 N94-31150
MICROWAVES
Microwave dielectric behavior of soils. Report 1: Summary of related research and applications
[AD-A275980] p 3771 N94-31351
Microwave dielectric behavior of soils. Report 2: A unique coaxial measurement apparatus
[AD-A275982] p 3771 N94-31353
Two-gigawatt burst-mode operation of the Intense Microwave Prototype (IMP) Free-Electron Laser (FEL) for the Microwave Tokamak Experiment (MTX)
[DE94-006613] p 3715 N94-31580
Structure estimation of phase objects from the diffraction near field: Microwave and model calculations
[ETN-94-95737] p 3674 N94-31608
High peak power microwaves: A health hazard
[AD-A277168] p 3681 N94-32576
Water vapor from sunradiometry in comparison with microwave and balloon-sonde measurements at the Southern Great Plains ARM Site
[DE94-007479] p 3786 N94-32759
MID-OCEAN RIDGES
Light in Thermal Environments (LITE) Workshop
[NASA-CR-195851] p 3790 N94-32981
MILITARY AIRCRAFT
Unmanned Air Vehicle/Remotely Piloted Vehicle analysis for lethal UAV/RPV
[AD-A276052] p 3578 N94-31442
Aircraft weight prediction capability. Volume 1: Weight study and results
[AD-A277206] p 3579 N94-32062
A comparison of military and commercial aircraft development
[AD-A276830] p 3575 N94-32168
MILITARY HELICOPTERS
An analysis of the maintenance performance measurement system for LAMPS MK 3 helicopter squadrons
[AD-A276421] p 3565 N94-31332
Army scout/reconnaissance helicopters versus unmanned aerial vehicles
[AD-A276902] p 3579 N94-32232
Estimating the impact of crashworthiness standards on mortality and morbidity events in the US Army rotary-wing aircraft mishaps
[AD-A277121] p 3575 N94-32363
MILITARY OPERATIONS
Coordination of mesoscale meteorological research between ASL and European group
[AD-A276730] p 3784 N94-32162
DOD space based requirements: Increasing DOD access to space
[AD-A276874] p 3601 N94-32211
Medical problems in high mountain environments. A handbook for medical officers
[AD-A278095] p 3798 N94-33268
Proceedings of the Symposium/Workshop on Applications of Expert Systems in DND
[DSIS-93-00343] p 3853 N94-33335
Management of uncertainty in knowledge-based systems: A military perspective p 3854 N94-33341
MILITARY SPACECRAFT
CIM in space: Corporate Information Management (CIM) implications for space-based information systems
[AD-A276882] p 3600 N94-32126
MILITARY TECHNOLOGY
Automated detection of ship tracks in multispectral satellite data
[AD-A276697] p 3746 N94-32119
Common modeling system for digital simulation
p 3823 N94-32429
Interagency Advanced Power Group: Steering Group meeting minutes
[DE94-007951] p 3761 N94-32701
MILK
Hydrogen peroxide electrodes based on electrical connection of redox centers of various peroxidases to electrodes through a three-dimensional electron relaying polymer network
[AD-A276543] p 3691 N94-32056
MILKY WAY GALAXY
A study of the neutral hydrogen distribution of the Milky Way through 21 cm emission and Lyman alpha absorption p 3938 N94-32309
MILLIMETER WAVES
Millimeter wave, high-resolution, holographic surveillance system
[DE94-004289] p 3712 N94-31831
Optical processing of MMW for agile beamsteering and beamforming
[AD-A277161] p 3880 N94-32068
Fusion applications of high power millimeter wave sources
[DE94-007374] p 3718 N94-32202
YBCO Josephson Junction arrays
[AD-A277426] p 3908 N94-33005
Synthetic vision technology demonstration. Volume 1: Executive summary
[DOT/FAA/RD-93/40-VOL-1] p 3582 N94-33076
Synthetic vision technology demonstration. Volume 2: Sensor tower testing
[DOT/FAA/RD-93/40-VOL-2] p 3582 N94-33077
Synthetic vision technology demonstration. Volume 3: Flight tests
[DOT/FAA/RD-93/40-VOL-3] p 3582 N94-33078
Synthetic vision technology demonstration. Volume 4: Appendices
[DOT/FAA/RD-93/40-VOL-4] p 3583 N94-33079
Proceedings SPIE: Conference Digest, volume 2104
[AD-A278107] p 3884 N94-33187
High temperature superconducting Josephson junction array systems, phase 1
[AD-A277937] p 3908 N94-33246
MIMD (COMPUTERS)
Studies of an optical multi-processor interconnect
[AD-A277093] p 3881 N94-32392
MIMO (CONTROL SYSTEMS)
Antiwindup analysis and design approaches for MIMO systems
[NASA-CR-195304] p 3584 N94-32075
Control strategies for systems with limited actuators
[NASA-CR-195307] p 3727 N94-32741
MINERAL DEPOSITS
Thermal emission measurements (5-25 microns) of Hawaiian palagonitic soils with implications for Mars
p 3944 N94-33193
Deposition rates of oxidized iron on Mars
p 3945 N94-33198
Aerosols scattering and near-infrared observations of the Martian surface p 3946 N94-33204
MINERALOGY
Possibilities of GER data for soil surface characteristics in the Almaden area p 3744 N94-31859
Magmatic volatiles and the weathering of Mars
p 3946 N94-33201
Mineralogical diversity (spectral reflectance and Moessbauer data) in compositionally similar impact melt rocks from Manicouagan Crater, Canada
p 3948 N94-33219
The mineralogic evolution of the Martian surface through time: Implications from chemical reaction path modeling studies p 3950 N94-33226
Evidence for ultramafic lavas on Syrtis Major
p 3950 N94-33229
MINERALS
Inorganic polymer engineering materials
[DE94-008519] p 3659 N94-32655
The mineralogic evolution of the Martian surface through time: Implications from chemical reaction path modeling studies p 3950 N94-33226
MINES (EXCAVATIONS)
Emissions of greenhouse gases from the use of transportation fuels and electricity
[DE94-006166] p 3765 N94-31625
MINIATURIZATION
A miniaturized ASIC-based multichannel scaler instrument
[DE94-007222] p 3807 N94-32783
The ALEXIS mission recovery
[DE94-007549] p 3611 N94-32813
MINIMA
On the minimum of independent geometrically distributed random variables
[NASA-CR-194883] p 3821 N94-33075
MINORITY CARRIERS
Passivation of III-V compound semiconductor based devices
[AD-A276178] p 3894 N94-31056
Experimental and theoretical studies of hydrogenated amorphous semiconductor alloys and superlattices
[AD-A276159] p 3686 N94-31079
MIR SPACE STATION
Spacecraft materials: Comparison between flight results obtained on LDEF and MIR p 3597 N94-31045
Technical assessment of Mir-1 life support hardware for the international space station
[NASA-TM-108441] p 3803 N94-31380
MIRRORS
Degradation of optical components in space
p 3594 N94-31029
Automatic resonator alignment and power stabilization of high power C02 lasers
[ISBN-0-315-77217-4] p 3714 N94-31472
Fast acting optical deflection
[AD-A276630] p 3879 N94-32037
Electromagnetic wave reflection from irregular plasma layers
[AD-A276727] p 3678 N94-32161
Neutral ion sources in precision manufacturing
p 3875 N94-32447
X ray imaging and x ray source development at Lawrence Livermore National Laboratory
[DE94-007077] p 3719 N94-32629
Multi-line passive fiber optic slipring
[AD-D016092] p 3883 N94-32738
Operational experience and evaluation of a dual-element stretched-membrane heliostat
[DE94-008827] p 3763 N94-32965
Diamond turning in the production of x ray optics
p 3604 N94-33298
MIS (SEMICONDUCTORS)
Passivation of III-V compound semiconductor based devices
[AD-A276178] p 3894 N94-31056
MISSILE DEFENSE
Optical processing of MMW for agile beamsteering and beamforming
[AD-A277161] p 3880 N94-32068
MISSILE VIBRATION
Aeroelastic vibrations of lifting surfaces
[ECL-91-01] p 3585 N94-31677
MISSILES
Exposure assessment of JAVELIN missile combustion products
[AD-A278128] p 3616 N94-33059
MISSION PLANNING
NASA strategic plan
[NASA-TM-109780] p 3915 N94-32222
Forced libration of Mercury and geodetic determination of a possible fluid core p 3774 N94-32493
The Lunar Scout Program: An international program to survey the Moon from orbit for geochemistry, mineralogy, imagery, geodesy, and gravity
[NASA-TM-104791] p 3943 N94-32923
MARSNET: A European network of stations on the surface of Mars p 3945 N94-33199
Scheduling fighter missions using an expert system with an operations research module p 3853 N94-33337
MISSISSIPPI
Remote sensing and the Mississippi high accuracy reference network p 3758 N94-32466
MIXING
Competition between crystallization and mixing/demixing in polymer mixture
[ETN-94-95753] p 3651 N94-31513
MIXING LENGTH FLOW THEORY
Modification of the MML turbulence model for adverse pressure gradient flows
[NASA-TM-106544] p 3709 N94-32947
MIXTURES
Studies in physico-chemical hydrodynamics of extended systems
[DE94-006752] p 3706 N94-32149
MOBILE COMMUNICATION SYSTEMS
Fast autodidactic adaptive equalization algorithms
[TELECOM-93-E-018] p 3670 N94-31174
Communications networks in stressed environments
[AD-A275967] p 3672 N94-31384
Channel and terminal description of the ACTS mobile terminal p 3599 N94-31428

Multisatellite constellation configuration selection for multiregional highly elliptical orbit constellations
p 3600 N94-31437
A multichannel architecture for Naval Task Force Communication
[AD-A276230] p 3673 N94-31446

MOBILITY
Studying transient mobility and energy loss using scanning tunneling microscopy
[AD-A278292] p 3877 N94-31256

MODEL REFERENCE ADAPTIVE CONTROL
High-speed path constrained manipulator operation using optimal-feedback combined controller
p 3833 N94-31962

MODELS
On a formal approach to the methodology of information planning
[MEMO-INF-93-42] p 3917 N94-31415

MODULARITY
Modular Simulator System (MSS). Engineering design guide
[AD-A276967] p 3589 N94-32394

MODULATION
Modulation and coding for the Gaussian channel, possibly affected by fluctuations
[TELECOM-93-E-009] p 3840 N94-31169
A simple model for determining photoelectron-generated radiation scaling laws
[DE94-006130] p 3761 N94-32660
Long distance transmission of 15 Gb/s digital using subcarrier multiplexing and external modulation
[DE94-008298] p 3682 N94-32756
Automatic modulation recognition
p 3686 N94-33153

MODULATION TRANSFER FUNCTION
Optical and image transmission through desert atmospheres
[AD-A276022] p 3742 N94-31496

MODULATORS
High-performance GaAs/AlGaAs optical phase modulators for microwave/photonic integrated circuits
[DE94-006361] p 3688 N94-31483
Fiber optic continuous true time-delay modulator
[AD-D016098] p 3883 N94-32720
High-performance GaAs/AlGaAs optical phase modulators for microwave photonic integrated circuits
[DE94-007376] p 3696 N94-32809

MODULES
Modular Simulator System (MSS). System/segment specification for the generic modular simulator system-flight station module, volume 2
[AD-A276969] p 3588 N94-32313
Research on stable, high-efficiency amorphous silicon multijunction modules
[DE94-000298] p 3695 N94-32680

MODULUS OF ELASTICITY
Evaluation of nondestructive inspection techniques for quality control of alumina-ceramic housing components
[AD-A276220] p 3730 N94-31065
Considering ties elasticities in high frequency rail dynamics
[ILR-MITT-281(1993)] p 3733 N94-31375
Elastic modulus measurements of LDEF glasses and glass-ceramics using a speckle technique
[NASA-CR-195911] p 3653 N94-31851
Ceramic Technology Project database
[DE94-008494] p 3659 N94-32632

MOISTURE
Adsorption of water to the metal/polymer interface studied by neutron and x ray reflectivity
[DE94-005578] p 3651 N94-31649

MOISTURE CONTENT
Recurvature dynamics of a typhoon
[AD-A276792] p 3784 N94-32164
Effects of interphases on the mechanical, thermal and hygromechanical response of fiber-reinforced composites p 3624 N94-32496
Development and testing of improved techniques for modeling the hydrologic cycle in a mesoscale weather prediction system
[AD-A277416] p 3786 N94-32921
The importance of environmental conditions in reflectance spectroscopy of laboratory analogs for Mars surface materials p 3944 N94-33195

MOLECULAR BEAM EPITAXY
Growth and characterization of III-V semiconductors with rare earth impurities for optoelectronic devices
[AD-A276021] p 3896 N94-31455
Semiconductor microcavity lasers
[DE94-006143] p 3716 N94-31622
High speed, strained layer, multiquantum well, GaInAsP and GaAs lasers and heterostructures
[AD-A277287] p 3719 N94-32608
Compositions and chemical bonding in ceramics by quantitative electron energy-loss spectrometry
[DE94-007208] p 3659 N94-32640
Research in the optical sciences
[AD-A278271] p 3884 N94-33140

MOLECULAR BEAMS
Metal cluster-rare gas van der Waals complexes: Microscopic models of physisorption
[DE94-008134] p 3873 N94-32797

MOLECULAR BIOLOGY
Neural network definitions of highly predictable protein secondary structure classes
[DE94-006234] p 3834 N94-32175
Future directions of nonlinear dynamics in physical and biological systems. (Physica D nonlinear, volume 68, number 1)
[AD-A278085] p 3794 N94-33250

MOLECULAR CLOUDS
Circumstellar material around young stars in Orion
p 3930 N94-31133
Theory of protostellar accretion disks
p 3931 N94-31136
Evolution of dynamo-generated magnetic fields in accretion disks around compact and young stars
p 3931 N94-31138
CO observations in external galaxies and gas mass determination p 3925 N94-31790
A study of physical conditions, radiative transfer and shocks in the interstellar medium p 3937 N94-31963

MOLECULAR CLUSTERS
Molecular Science Research Center
[DE94-007464] p 3871 N94-32605

MOLECULAR COLLISIONS
Theoretical studies of zirconium and carbon clusters with molecular dynamics simulations
[DE94-005276] p 3862 N94-31146
Spectroscopic study of the molecular collisions (hydrogen-nitrogen and hydrogen-oxygen) at energies of several MeV
[ISBN-0-315-86794-9] p 3867 N94-31753
Analysis of forward and inverse problems in chemical dynamics and spectroscopy
[DE94-007607] p 3635 N94-32140
Time-resolved IR spectroscopy, energy transfer, and state-to-state collision dynamics of atmospheric species
[AD-A277372] p 3773 N94-32338
Energy transfer properties and mechanisms
[DE94-007403] p 3636 N94-32594

MOLECULAR DYNAMICS
Theoretical studies of zirconium and carbon clusters with molecular dynamics simulations
[DE94-005276] p 3862 N94-31146
Molecular dynamics computer simulations of charged metal electrode-aqueous electrolyte interfaces
[AD-A276401] p 3863 N94-31237
The threshold energy for defect production in SiC: A molecular dynamic study
[DE94-007123] p 3896 N94-31499
Modern integral equation techniques for quantum reactive scattering theory
[DE94-007039] p 3857 N94-31639
Atomic and molecular data needs for fusion
[DE94-006555] p 3870 N94-32177
Chemical structure and kinetics at liquid/solid interfaces
[AD-A277112] p 3636 N94-32304
Point defect production, geometry, and stability in silicon: A molecular dynamics simulation study
[DE94-008292] p 3903 N94-32411
Wave packet studies of the vibrational predissociation of three and four-atom van der Waals complexes
[DE94-007623] p 3871 N94-32598
Chemisorbed-molecule potential-energy surfaces and electronically-stimulated processes
[DE94-007932] p 3719 N94-32603
Experimental investigations and molecular dynamics simulations of radiation induced surface damage
[AD-A277323] p 3871 N94-32621
Molecular interactions in dilute supercritical mixtures: Molecular dynamics investigation
[DE94-007610] p 3872 N94-32644
Future directions of nonlinear dynamics in physical and biological systems. (Physica D nonlinear, volume 68, number 1)
[AD-A278085] p 3794 N94-33250
High resolution molecular spectroscopy of atmospheric species
[AD-A278382] p 3776 N94-33351

MOLECULAR EXCITATION
Cometary molecules p 3935 N94-31869
Electronic and nuclear factors in intramolecular charge and excitation transfer processes
[DE94-006598] p 3870 N94-32178
Energy transfer properties and mechanisms
[DE94-007403] p 3636 N94-32594

MOLECULAR GASES
CO observations in external galaxies and gas mass determination p 3925 N94-31790
The manifestations of energetic activity in the galactic center p 3937 N94-32028

MOLECULAR INTERACTIONS
Molecular interactions at metal/polyimide interfaces: A correlation with adhesion and bond durability
[AD-A276301] p 3650 N94-31297
High-temperature study of O+H2CO yields OH+HCO
[DE94-006837] p 3864 N94-31321
The 14th Annual West Coast Theoretical Chemistry/Statistical Mechanics Conference
[AD-A276942] p 3656 N94-32239
Molecular interactions in dilute supercritical mixtures: Molecular dynamics investigation
[DE94-007610] p 3872 N94-32644
Radiation and photochemistry section
[DE94-008880] p 3873 N94-32757
Implementation of a vibrationally linked chemical reaction model for DSMC
[NASA-TM-109109] p 3710 N94-33020
High resolution molecular spectroscopy of atmospheric species
[AD-A278382] p 3776 N94-33351

MOLECULAR RELAXATION
Vibrational energy transfer of diatomic gases in hypersonic expanding flows p 3570 N94-31958
Implementation of a vibrationally linked chemical reaction model for DSMC
[NASA-TM-109109] p 3710 N94-33020

MOLECULAR ROTATION
Collective and quasiparticle excitations in light Pb isotopes
[ETN-94-96014] p 3865 N94-31548

MOLECULAR SPECTRA
Summary of some data processing routines in the molecular physics group of Stockholm University
[USIP-93-05] p 3808 N94-31087

MOLECULAR SPECTROSCOPY
Summary of some data processing routines in the molecular physics group of Stockholm University
[USIP-93-05] p 3808 N94-31087
Laser and Fourier transform spectroscopy of novel propellant molecules
[AD-A277506] p 3667 N94-33013
High resolution molecular spectroscopy of atmospheric species
[AD-A278382] p 3776 N94-33351

MOLECULAR STRUCTURE
Summary of some data processing routines in the molecular physics group of Stockholm University
[USIP-93-05] p 3808 N94-31087
Theoretical studies of zirconium and carbon clusters with molecular dynamics simulations
[DE94-005276] p 3862 N94-31146
Analytical applications of scanning tunneling microscopy
[AD-A276066] p 3711 N94-31283
Infrared and near infrared transient absorption spectroscopy of molecular free radicals
[DE94-005446] p 3632 N94-31305
Collective and quasiparticle excitations in light Pb isotopes
[ETN-94-96014] p 3865 N94-31548
Double rotation NMR studies of zeolites and aluminophosphate molecular sieves
[DE94-007032] p 3866 N94-31637
Chemical interactions between protein molecules and polymer membrane materials
[DE94-006987] p 3651 N94-31672
Recent developments in polymeric charge transfer complexes
[AD-A277108] p 3654 N94-31979
New molecular-based routes to binary main group metal sulfides
[AD-A277005] p 3900 N94-32003
Neural network definitions of highly predictable protein secondary structure classes
[DE94-006234] p 3834 N94-32175
Towards a detailed understanding of the structural variability in lignins: A new approach
[DE94-007449] p 3793 N94-32267
Chemical structure and kinetics at liquid/solid interfaces
[AD-A277112] p 3636 N94-32304
Molecular Science Research Center
[DE94-007464] p 3871 N94-32605
Nonlinear optical polymers derived from organic/inorganic composites
[AD-A277408] p 3659 N94-32610
Ionization probes of molecular structure and chemistry
[DE94-007605] p 3872 N94-32643

MOLECULAR WEIGHT
Method and apparatus for inhibiting the disbonding of a paint from metal surfaces
[AD-D016106] p 3663 N94-32960

MOLECULES
Modification of semiconductor surface properties with chemically bound molecular films
[AD-A276162] p 3895 N94-31081
Physical chemistry of molecules and grains in space
[AD-A276037] p 3932 N94-31280
Positron-molecule interactions
[AD-A276542] p 3869 N94-32082
A genetic algorithm based method for docking flexible molecules
[DE94-007525] p 3793 N94-32269
MOLTEN SALT ELECTROLYTES
Room temperature molten salts for advanced energy conversion and storage
[AD-A277777] p 3763 N94-33015
MOLTEN SALTS
Room temperature molten salts for advanced energy conversion and storage
[AD-A277777] p 3763 N94-33015
MOLYBDENUM ALLOYS
Creep-fatigue criteria and inelastic behavior of modified 9Cr-1Mo steel at elevated temperatures
[DE94-007915] p 3642 N94-31918
MOLYBDENUM COMPOUNDS
Novel approaches to the production of higher alcohols from synthesis gas
[DE94-006770] p 3666 N94-32132
The effect of ductile phase (Nb) reinforcement morphology on the mechanical behavior of an intermetallic matrix (MoSi2) p 3615 N94-32500
MOLYBDENUM DISULFIDES
Soft x ray photoelectron spectroscopy study of the interaction of Cr with MoS2(0001)
[AD-A276916] p 3635 N94-32233
Torque characteristics of solid lubricated precision bearings during oscillatory motion
[AD-A278133] p 3728 N94-33061
MOLYBDENUM SULFIDES
Development of long-life, low-noise linear bearings for atmospheric interferometry p 3606 N94-33312
MOMENTS OF INERTIA
Forced libration of Mercury and geodetic determination of a possible fluid core p 3774 N94-32493
MOMENTUM
Gas dynamics for accretion disk simulations p 3932 N94-31144
MOMENTUM TRANSFER
The dynamical settling of warped disks and angular momentum transport in galaxies p 3928 N94-31121
Theory of protostellar accretion disks p 3931 N94-31136
A fully two-dimensional, non-oscillatory advection scheme for momentum and scalar transport equations
[DM-66] p 3700 N94-31221
MONATOMIC GASES
The stellar and gaseous content of massive low surface brightness disk galaxies p 3933 N94-31495
MONAURAL SIGNALS
Modelling the late part of room impulse responses using adaptive filtering: On the recreation of reality
[CTH-E-93-01] p 3859 N94-31076
MONGOLIA
Station climatic summaries: China, the former USSR, and Mongolia
[AD-A276548] p 3784 N94-32057
MONITORS
Pre-flight testing of Thermoelectric Quartz Crystal Microbalances (TQCM) for midcourse space experiment (MSX) spacecraft
[AD-A277054] p 3610 N94-32010
Continuous measurement of aging response in aluminum alloys by eddy current methods
[AD-A277233] p 3644 N94-32371
MONOMERS
Isomeric poly(benzophenone)s: Synthesis of highly crystalline poly (4, 4 foot-benzophenone) and amorphous poly (2, 5-benzophenone), a soluble poly (p-phenylene) derivative
[AD-A277261] p 3655 N94-32017
Recovery of carboxylic acids at pH greater than pKa
[DE94-007030] p 3636 N94-32376
Novel polydiacetylenes as materials for second and third order nonlinear optics
[AD-A277512] p 3664 N94-33082
MONOPOLE ANTENNAS
Time domain spectroscopy for studying a monopole antenna immersed in a plasma
[ISBN-0-315-86526-1] p 3888 N94-31727
MONSOONS
Numerical simulations of monsoon rainfall with the NRL/NCSU regional nested grid model p 3782 N94-31791
Forecasters handbook for the Philippine Islands and surrounding waters
[AD-A277993] p 3787 N94-33089
MONTE CARLO METHOD
Hydrogenated amorphous silicon (a-Si:H) based gamma camera: Monte Carlo simulations
[DE94-007042] p 3795 N94-31323
Using Monte Carlo techniques and parallel processing for debris hazard analysis of rocket systems
[DE94-007250] p 3609 N94-31382
Mixture model simulating reactive turbulent flows: Testing of Eulerian-Lagrangian probabilistic models
[ONERA-NT-1993-13] p 3702 N94-31477
Diagonal band probability distributions
[REPT-93-80] p 3851 N94-31697
Cometary molecules p 3935 N94-31869
ITS version 3.0: Powerful, user-friendly software for radiation modelling
[DE94-006607] p 3678 N94-32113
A comparison between two Monte Carlo codes on determination of transient chemical yields
[DE94-007224] p 3636 N94-32251
An algorithm for probabilistic, totally-ordered temporal projection
[AD-A277341] p 3817 N94-32257
Planetary magnetotails: Magnetic configuration and nonthermal plasma p 3942 N94-32326
Parallel Monte Carlo reactor neutronics
[DE94-007642] p 3826 N94-32357
Parallel particle simulations of low-density fluid flows
[DE94-007858] p 3707 N94-32373
Numerical simulation of quantum many-body systems
[DE94-008451] p 3912 N94-32513
Characterization of atomic and molecular impurity sources and transport at the tokamak edge
[DE94-007212] p 3891 N94-32619
Complete model description of an electron beam using ACCEPT Monte Carlo simulation code
[DE94-007063] p 3872 N94-32628
Implementation and display of Computer Aided Design (CAD) models in Monte Carlo radiation transport and shielding applications
[DE94-007221] p 3819 N94-32641
Simulation of low-density nozzle plumes in non-zero ambient pressures
[NASA-TM-106501] p 3615 N94-32742
Studies of jet production with the D0 detector
[DE94-008271] p 3873 N94-32780
Analytic properties of the OCP and ionic mixtures in the strongly coupled fluid state
[DE94-008216] p 3637 N94-32801
Implementation of a vibrationally linked chemical reaction model for DSMC
[NASA-TM-109109] p 3710 N94-33020
Design and Monte Carlo analysis of an unmanned aerial vehicle
[AD-A277648] p 3580 N94-33056
Simulation of CO2 release at 800 km altitude
[AD-A276692] p 3776 N94-33272
MONTEREY BAY (CA)
Evolution of diurnal surface winds and surface currents for Monterey Bay
[AD-A277649] p 3790 N94-33057
MONTMORILLONITE
Ferric sulfate montmorillonites as Mars soil analogs p 3944 N94-33196
Mars atmospheric dust properties: A synthesis of Mariner 9, Viking, and Phobos observations p 3945 N94-33200
MOON
Apollo 11 highlights
[NASA-TM-109763] p 3600 N94-31820
MORPHOLOGY
Morphological directional coding of images
[ISBN-0-315-86336-6] p 3814 N94-31715
The p-q-r-medial axis algorithm requires only local operations
[CWI-BS-R9317] p 3849 N94-32507
Martian deltas: Morphology and distribution p 3950 N94-33230
MORTALITY
Estimating the impact of crashworthiness standards on mortality and morbidity events in the US Army rotary-wing aircraft mishaps
[AD-A277121] p 3575 N94-32363
MOSAICS
Global color views of Mars p 3948 N94-33217
MOTION PERCEPTION
Sensory sensitivities and discriminations and their roles in aviation
[AD-A277312] p 3800 N94-32276
MOTION SICKNESS
Autogenic-feedback training as a treatment for airsickness in high-performance military aircraft: Two case studies
[NASA-TM-108810] p 3801 N94-33068
MOUNTAINS
Recommendations for meteorological data collection during physiological field studies
[AD-A276834] p 3901 N94-32153
Medical problems in high mountain environments. A handbook for medical officers
[AD-A278095] p 3798 N94-33268
MOUNTING
An analytical study of the vibration of beams fitted with neutralizers. Part 2: Assessment of the effects of mounting configurations
[ISVR-TR-225-PT-2] p 3740 N94-32982
MOVING TARGET INDICATORS
Some neural computing approaches to target tracking p 3837 N94-33151
MSAT
SATCOM feasibility study for search and rescue aircraft
[DSIS-94-01083] p 3575 N94-31902
MSAT boom joint testing and load absorber design p 3606 N94-33315
Special test equipment and fixturing for MSAT reflector assembly alignment p 3606 N94-33316
MULLITES
Enhancement of oxidation resistance of silicon carbide by high-dose and multi-energy aluminum implantation
[DE94-006560] p 3640 N94-31314
Interface engineering in oxide fiber/oxide matrix composites
[AD-A277672] p 3627 N94-33029
MULTIBEAM ANTENNAS
Proceedings of the 1993 Antenna Applications Symposium, volume 1
[AD-A277202] p 3676 N94-32049
Proceedings of the 1993 Antenna Applications Symposium, volume 2
[AD-A277203] p 3677 N94-32050
MULTICHANNEL COMMUNICATION
A multichannel architecture for Naval Task Force Communication
[AD-A276230] p 3673 N94-31446
Passive, multi-channel fiber optic rotary joint assembly
[AD-D016116] p 3682 N94-32626
Long distance transmission of 15 Gb/s digital using subcarrier multiplexing and external modulation
[DE94-008298] p 3682 N94-32756
MULTIGRID METHODS
Prediction of transonic potential flow with slipstreams around configurations
[FFA-TN-1992-15] p 3568 N94-31220
Development and application of a multimesh auto-adaptive finite element method for the calculation of an electric arc plasma
[ECL-89-03] p 3886 N94-31378
Solution of the incompressible Navier-Stokes equations in general coordinates by Krylov subspace and multigrid methods
[REPT-93-64] p 3703 N94-31660
Numerical simulation of combined external/internal transonic flow on the forebody/inlet of the AV-8B Harrier 2 p 3569 N94-31759
Multigrid diagonal implicit solutions for compressible turbulent flows and their evaluation p 3705 N94-31941
MULTILAYER INSULATION
Space environment durability of beta cloth in LDEF thermal blankets p 3591 N94-31015
Space Station WP-2 application of LDEF MLI results p 3592 N94-31016
MULTIMEDIA
Developing the Multimedia User Interface Component (MUSIC) for the Icarus Presentation System (IPS)
[AD-A276341] p 3810 N94-31335
The vision machines
[NASA-TM-109757] p 3806 N94-31816
Problems in survivable multi-media networks
[AD-A277370] p 3825 N94-32052
An information system organized as stratified hypermedia
[TR-93-12] p 3918 N94-32289
Literacity: A multimedia adult literacy package combining NASA technology, recursive ID theory, and authentic instruction theory p 3924 N94-32462
Voice and video transmission using XTP and FDDI p 3685 N94-32468
Long distance transmission of 15 Gb/s digital using subcarrier multiplexing and external modulation
[DE94-008298] p 3682 N94-32756
Multimedia as a desktop and classroom tool
[DE94-009118] p 3807 N94-32766
MADE: A Multiple Application Development Environment
[CWI-CS-R9360] p 3822 N94-33097

MULTIPATH TRANSMISSION
Direct-sequence spread-spectrum performance in a multipath fading environment
[AD-A276060] p 3673 N94-31464
The effects of a multipath channel and interference on coherent M-PSK digital communication systems
[AD-A278158] p 3684 N94-33254
MULTIPHASE FLOW
High-resolution numerical methods for compressible multi-phase flow in hierarchical porous media
[DE94-008261] p 3707 N94-32410
MULTIPLE ACCESS
Hubless satellite communications networks
p 3600 N94-31433
Applied harmonic analysis
[AD-A278384] p 3685 N94-33353
MULTIPLEXING
A technique for multiplexing 3x3-coupler terminated interferometric fiber-optic sensors
[AD-A276739] p 3880 N94-32180
MULTIPLICATION
A new tool for signal processing
[AD-A278385] p 3685 N94-33354
MULTIPLIERS
Formal verification of systolic multipliers with the Boyer-Moore theorem prover
[RR-897-M] p 3839 N94-31082
MULTIPOLES
General-relativistic celestial mechanics. 4: Theory of satellite motion
[PB94-147782] p 3601 N94-31769
Selected applications of planar permanent magnet multipoles in FEL insertion device design
[DE94-009014] p 3721 N94-32845
RHIC chromatic correction system
[DE94-008532] p 3883 N94-32994
MULTIPROCESSING (COMPUTERS)
Scheduling techniques for multiple processor systems in real-time environments
[AD-A276149] p 3824 N94-31249
List ranking and list scan on the CRAY C-90
[AD-A276411] p 3824 N94-31259
DOME: Dynamic optimization on multiprocessor engines, a statistical approach p 3807 N94-31972
VME rollback hardware for time warp multiprocessor systems
[NASA-CR-191796] p 3826 N94-32483
Development of a low-latency scalar communication routine on message-passing architectures
[DE94-007061] p 3827 N94-32683
Investigation of modularly configured attached processors with intelligent memories
[AD-A278418] p 3839 N94-33330
MULTISENSOR APPLICATIONS
Automatic extraction of cartographic objects by fusion of data extracted from satellite images
[TELECOM-93-E-001] p 3742 N94-31165
Chamber optics for testing passive remote sensing vapor detectors
[AD-A275909] p 3878 N94-31340
MULTISPECTRAL BAND SCANNERS
Analysis of GER imaging spectrometry data for the identification of soil and vegetation parameters in land degradation studies p 3744 N94-31857
Possibilities of GER data for soil surface characteristics in the Almaden area p 3744 N94-31859
The effects of vegetation on the ability to map soils using GERIS data p 3744 N94-31860
Extraction of forests stand age parameters from airborne imaging spectroscopy data p 3745 N94-31867
Remote sensing for hurricane Andrew impact assessment p 3758 N94-32464
MULTISPECTRAL PHOTOGRAPHY
Assessment of region-based methods for automated SAR/optical registration, attribute extraction, and classification p 3750 N94-32536
Earth observational research using multistage EOS-like data
[NASA-CR-195833] p 3757 N94-33019
MULTIVARIABLE CONTROL
A direct digital design for a multichannel structural test system using the characteristic locus method
[MATHS-REPT-A-206] p 3828 N94-31161
MULTIVARIATE STATISTICAL ANALYSIS
A radial basis function approach to financial time series analysis
[AD-A276408] p 3924 N94-31361
Multivariate spline approximation
[AD-A276034] p 3842 N94-31441
Probability distributions with given marginals and given correlation that have maximal entropy
[REPT-93-81] p 3851 N94-31698
MUON SPIN ROTATION
Low dispersion of the muon precession frequency in HTSC samples YBa2Cu3O(x) and EuBa2Cu3O(x)
[DE94-608386] p 3896 N94-31395
MUONS
Low dispersion of the muon precession frequency in HTSC samples YBa2Cu3O(x) and EuBa2Cu3O(x)
[DE94-608388] p 3896 N94-31395
Proceedings of the International Workshop on Low Energy Muon Science: LEMS 1993
[DE94-006495] p 3874 N94-32804
Ionization EM calorimetry with accordion electrodes and liquid krypton or argon
[DE94-009082] p 3713 N94-32821
MURCHISON METEORITE
Organic analyses of the Murchison meteorite
p 3938 N94-32489
MUSCLES
Muscle disuse through tail-suspension: Etiology and therapeutics p 3796 N94-31746
MUSCULOSKELETAL SYSTEM
Isolating strain parameters correlated to skeletal adaptation p 3797 N94-31960
MYOELECTRICITY
Application of dexterous space robotics technology to myoelectric prostheses p 3729 N94-32450

N

NAKHLITES
SNC meteorites and their implications for reservoirs of Martian volatiles p 3947 N94-33209
The Martian sources of the SNC meteorites (two, not one), and what can and can't be learned from the SNC meteorites p 3951 N94-33234
NARROWBAND
COVICS: A covert video communications system
[DE94-007568] p 3682 N94-32745
NASA PROGRAMS
Global change research and NASA's Earth Observing System
[PB94-126992] p 3741 N94-31068
NASCOM system development plan: System description, capabilities, and plans, FY 94-2
[NASA-TM-109744] p 3674 N94-31503
Marsville: The cosmic village
[NASA-TM-109752] p 3913 N94-31806
Aerospace test facilities at NASA LERC Plumbrook
[NASA-TM-109755] p 3602 N94-31814
Welcome to the Ohio Aerospace Institute
[NASA-TM-109756] p 3913 N94-31815
NASA select yearender review
[NASA-TM-109748] p 3956 N94-31885
The sky is your classroom
[NASA-TM-109759] p 3914 N94-31887
Index to NASA news releases and speeches, 1993
[NASA-TM-109722] p 3917 N94-31888
NASA strategic plan
[NASA-TM-109780] p 3915 N94-32222
Management of government quality assurance functions for NASA contracts
[NHB-5300.4(2B-2)] p 3731 N94-32387
NASA/DOD Aerospace Knowledge Diffusion Research Project. Paper 10: The NASA/DOD Aerospace Knowledge Diffusion Research Project
[NASA-TM-109769] p 3921 N94-32831
Research and Technology Objectives and Plans Summary (RTOPS)
[NASA-TM-105441] p 3966 N94-32885
Opinion polls and the US civil space program
[NASA-TM-109700] p 3914 N94-33066
Space history, space policy, and executive leadership
[NASA-TM-109787] p 3924 N94-33067
NASA SPACE PROGRAMS
NASA's space platform technology program and planning p 3597 N94-31044
MSFC orbital spacecraft development emphases for this decade p 3598 N94-31048
Chronology of KSC and KSC related events for 1993
[NASA-TM-109196] p 3966 N94-33072
NASCOM NETWORK
NASCOM system development plan: System description, capabilities, and plans, FY 94-2
[NASA-TM-109744] p 3674 N94-31503
NASTRAN
QUAD4 seminar
[AD-A277366] p 3818 N94-32330
NATIONAL AEROSPACE PLANE PROGRAM
Hypervelocity Tunnel 9 Mach 10/14 Calibration
[AD-A275960] p 3587 N94-31318
High temperature NASP engine seal development
[NASA-TM-109750] p 3725 N94-31804
Futurepath 3
[NASA-TM-109762] p 3735 N94-31819
The National Aerospace Plane (NASP): Development issues for the follow-on vehicle
[AD-A278417] p 3581 N94-33329
NATIONAL AIRSPACE SYSTEM
Civil tiltrotor market penetration: Effects on Northeast corridor airport delay
[AD-A277534] p 3576 N94-32955
NATIONAL AVIATION SYSTEM
FAA aviation forecasts, fiscal years 1994-2005
[AD-A277808] p 3566 N94-33016
NATURAL GAS
Feasibility study to evaluate plasma quench process for natural gas conversion applications
[DE94-000086] p 3758 N94-31234
Economic feasibility analysis of distributed electric power generation based upon the natural gas fired fuel cell
[DE94-005795] p 3759 N94-31487
Gas hydrate detection and mapping on the US east coast
[DE94-005959] p 3742 N94-31504
Analysis of deep seismic reflection and other data from the southern Washington Cascades
[DE94-005958] p 3771 N94-31525
Emissions of greenhouse gases from the use of transportation fuels and electricity
[DE94-006166] p 3765 N94-31625
NATURAL LANGUAGE (COMPUTERS)
What comes first in dynamic semantics: A compositional, non-representational account of natural language presupposition
[LP-93-15] p 3855 N94-31389
Methods for parallelizing search paths in phrasing
[AD-A276876] p 3817 N94-32212
High-speed data search p 3923 N94-32441
Finding all periods and initial palindromes of a string in parallel
[AD-B175069] p 3827 N94-33002
NATURAL LANGUAGE PROCESSING
Updates in dynamic semantics
[LP-93-06] p 3856 N94-31450
Weaks vs. strong readings of donkey sentences and monotonicity inference in a dynamic setting
[LP-93-10] p 3856 N94-31468
Finding all periods and initial palindromes of a string in parallel
[AD-B175069] p 3827 N94-33002
NAUTICAL CHARTS
MDFF HELP library, version 2: On-line documentation for the map data formatting facility
[AD-A277763] p 3922 N94-32987
NAVIER-STOKES EQUATION
CFD-based drag prediction: State-of-the-art, theory, prospects
[AD-B179297] p 3567 N94-31180
A priori tests of large eddy simulation of the compressible plane mixing layer
[MEMO-1152] p 3699 N94-31185
A solution adaptive structured-unstructured grid procedure for unsteady flows p 3700 N94-31217
On the structure and stability of slender viscous vortices p 3700 N94-31218
Solution of the incompressible Navier-Stokes equations in general coordinates by Krylov subspace and multigrid methods
[REPT-93-64] p 3703 N94-31660
Cell-vertex discretisation of the driven cavity flow without artificial diffusion
[W-9317] p 3703 N94-31689
Simulations of the creation and motion of vortex rings
[W-9319] p 3703 N94-31691
Finite volume discretization of the k-epsilon turbulence model in general coordinates
[REPT-93-90] p 3703 N94-31703
Finite element numerical simulation of turbulent flows
[ISBN-0-315-86416-8] p 3703 N94-31717
Numerical modelling of turbulence
[ISBN-0-315-86439-7] p 3703 N94-31720
Finite element vorticity-based methods for the solution of the incompressible and compressible Navier-Stokes equations
[ISBN-0-315-87265-9] p 3703 N94-31730
Multigrid diagonal implicit solutions for compressible turbulent flows and their evaluation
p 3705 N94-31941
Chemical vapor deposition fluid flow simulation modelling tool
[NASA-CR-189648] p 3707 N94-32480
Additive turbulent decomposition of the incompressible and compressible Navier-Stokes equations
[AD-A277321] p 3708 N94-32511
Advanced CFD methodology for fast transients encountered in nonlinear combustion instability problems. Volume 2: User's guide
[NASA-CR-191352] p 3637 N94-32694
Advanced CFD methodology for fast transients encountered in nonlinear combustion instability problems. Volume 1: Theory and validation
[NASA-CR-191351] p 3637 N94-32696

Study of dynamic stall phenomenon and its control using vorticity, stream function and circulation form of the unsteady Navier-Stokes equations p 3572 N94-32714
Modification of the MML turbulence model for adverse pressure gradient flows
[NASA-TM-106544] p 3709 N94-32947
Use of Navier-Stokes methods for the calculation of high-speed nozzle flow fields
[NASA-TM-106551] p 3573 N94-32984
A study of weak solutions and their regularizations by numerical methods
[AD-A277453] p 3850 N94-33175

NAVIGATION
Hydrographic service Royal Australian Navy
[AD-A277134] p 3788 N94-32066

NAVIGATION AIDS
Hydrographic service Royal Australian Navy
[AD-A277134] p 3788 N94-32066

NAVY
Procedures for computing site seismicity
[AD-A277666] p 3775 N94-33028

NEAR FIELDS
Formulation of time-domain planar near-field measurements without probe correction
[AD-A276380] p 3672 N94-31371
Structure estimation of phase objects from the diffraction near field: Microwave and model calculations
[ETN-94-95737] p 3674 N94-31608

NEAR INFRARED RADIATION
Infrared and near infrared transient absorption spectroscopy of molecular free radicals
[DE94-005446] p 3632 N94-31305
Near infrared surveys of high mass star forming regions p 3925 N94-31898
Aerosols scattering and near-infrared observations of the Martian surface p 3946 N94-33204

NEBULAE
Convective solar nebula p 3930 N94-31130

NEEDLE BEARINGS
Development of long-life, low-noise linear bearings for atmospheric interferometry p 3606 N94-33312

NEODYMIUM
Ion-beam-driven amorphization of Ca2La8(Si4)6O2 single crystals
[DE94-006219] p 3895 N94-31307

NEODYMIUM LASERS
High-power CW diode-laser-array-pumped solid-state lasers and efficient nonlinear optical frequency conversion
[AD-A276126] p 3714 N94-31278
High average power pulsed phase conjugate laser with birefringence correction
[DE94-006049] p 3719 N94-32659

NEON
Wave packet studies of the vibrational predissociation of three and four-atom van der Waals complexes
[DE94-007623] p 3871 N94-32598

NEON ISOTOPES
The origin of neon-E: Neon-E in single interstellar silicon carbide and graphite grains p 3933 N94-31556

NEPTUNE (PLANET)
Plasma and radio waves from Neptune: Source mechanisms and propagation
[NASA-CR-195877] p 3943 N94-33103

NETWORK ANALYSIS
A Green's function approach to analysing the effects of random synaptic background activity in a model neural network
[MATHS-REPT-A-202] p 3828 N94-31157
Some calculations on supersymmetric graphs as communication networks
[REPT-93-72] p 3824 N94-31641
Analysis and design of a formal neural network for filtering a dynamic signal
[ISBN-0-315-86932-1] p 3832 N94-31873
Multicast communication with guaranteed quality of service
[AD-A277650] p 3682 N94-33025
Assessing the vulnerability of multi-commodity networks with failing components
[AD-A278434] p 3684 N94-33334

NETWORK CONTROL
Communications networks in stressed environments
[AD-A275967] p 3672 N94-31384
The use of service limits for efficient operation of multi-station single-medium communication systems
[CWI-BS-R9312] p 3677 N94-32085
Undiscounted Markov decision chains with partial information; an algorithm for computing a locally optimal periodic policy
[TW-93-10] p 3851 N94-32205
Discrete-event-dynamic-system-based approaches for scheduling transmissions in multihop packet radio networks
[AD-A276566] p 3679 N94-32230
Voice and video transmission using XTP and FDDI p 3685 N94-32468
Use and administration of UNIX (tm) systems p 3821 N94-33051

NEUMANN PROBLEM
A simplified Von Neumann method for linear stability analysis
[CRANFIELD-AERO-9310] p 3843 N94-31540
Finite volume discretization of the k-epsilon turbulence model in general coordinates
[REPT-93-90] p 3703 N94-31703

NEURAL NETS
Machinery monitoring and diagnostics using pseudo Wigner-Ville distribution and backpropagation neural network
[AD-A276219] p 3828 N94-31064
Report of the 'Mathematical Models for Neural Networks' course
[TELECOM-93-D-019] p 3828 N94-31100
A Green's function approach to analysing the effects of random synaptic background activity in a model neural network
[MATHS-REPT-A-202] p 3828 N94-31157
A neuron network for image classification: From algorithm to implantation
[TELECOM-93-E-005] p 3687 N94-31168
Filtering and recognition of moving boats in radar images
[REPT-93-039] p 3671 N94-31190
ART: Adaptive Resonance Theory
[TELECOM-93-D-020] p 3829 N94-31193
Smart environmental monitor based on neural networks and multi-spectral pattern recognition
[AD-A276445] p 3829 N94-31301
A neural network methodology for engineering applications: The learning control of robotic systems
[RR-480] p 3830 N94-31500
Two models solving the increasing energy problem of the continuous Hopfield network model
[REPT-93-87] p 3843 N94-31552
A neural network model for the visual perception of the depth of a scene from stereoscopy and shading
[ISBN-0-315-86753-1] p 3831 N94-31750
The vision machines
[NASA-TM-109757] p 3806 N94-31816
Universal approximation in p-mean by neural networks
[W-9320] p 3832 N94-31821
Analysis and design of a formal neural network for filtering a dynamic signal
[ISBN-0-315-86932-1] p 3832 N94-31873
Hierarchical mixtures of experts and the EM algorithm
[AD-A276516] p 3814 N94-31932
Neural networks for model-based recognition
[AD-A277375] p 3834 N94-32053
Exploring phase space concepts in the forecasting of time series with artificial neural networks
[DE94-005810] p 3834 N94-32127
On the relationship between generalization error, hypothesis complexity, and sample complexity for radial basis functions
[AD-A276802] p 3851 N94-32142
Neural network definitions of highly predictable protein secondary structure classes
[DE94-006234] p 3834 N94-32175
Undergraduate robotics projects in support of research on neural networks
[AD-A277331] p 3835 N94-32281
Neural models of spatial orientation in novel environments
[AD-A277383] p 3835 N94-32340
Fuzzy-neural control of an aircraft tracking camera platform p 3839 N94-32423
Empirical modeling for intelligent, real-time manufacture control p 3839 N94-32424
Neural network wavelet technology: A frontier of automation p 3839 N94-32425
Analysis and synthesis of adaptive neural elements and assembles
[AD-A277423] p 3836 N94-32996
Proceedings of the NIPS 1993 Postconference Workshop on Pulling It All Together: Methods for Combining Neural Networks
[AD-A277507] p 3836 N94-33014
Correlation filter synthesis using neural networks
[AD-A278124] p 3836 N94-33043
CRAD Signal and Information Processing Working Group Workshop on Neural networks, volume 1
[DREA-TC-93-305-VOL-1] p 3836 N94-33149
The application of a radial basis function neural network for radar tracking over the sea p 3686 N94-33150
Some neural computing approaches to target tracking p 3837 N94-33151
Neural networks applied to the phonemic segmentation of speech p 3686 N94-33152
Automatic modulation recognition p 3686 N94-33153
Multi-sensor data fusion for target acquisition p 3837 N94-33154
Periodic and chaotic signal generation in a recursive artificial neural network p 3686 N94-33155
Modular neural network architectures p 3838 N94-33156
Nearest-neighbour search in constant time: An alternative to neural networks for pattern matching applications p 3838 N94-33157
Numerical optimization techniques in neural network training p 3838 N94-33158
A neural network application to search and rescue satellite aided tracking (SARSAT) p 3613 N94-33345

NEUROLOGY
Visual neural development and chromatic aberration
[AD-A277402] p 3800 N94-32345

NEURONS
Towards simplicity: Noise and cooperation in the perfect integrator
[AD-A276256] p 3799 N94-31291
Two models solving the increasing energy problem of the continuous Hopfield network model
[REPT-93-87] p 3843 N94-31552
Empirical modeling for intelligent, real-time manufacture control p 3839 N94-32424
The organization of the suprachiasmatic circadian pacemaker of the rat and its regulation by neurotransmitters and modulators
[AD-A277324] p 3793 N94-32622
Models of the neuronal mechanisms of target localization of the barn owl
[AD-A277332] p 3797 N94-32623
Analysis and synthesis of adaptive neural elements and assembles
[AD-A277423] p 3836 N94-32996
Neostriatal neuronal activity and behavior
[AD-A278429] p 3802 N94-33333

NEUROPHYSIOLOGY
Models of the neuronal mechanisms of target localization of the barn owl
[AD-A277332] p 3797 N94-32623
Analysis and synthesis of adaptive neural elements and assembles
[AD-A277423] p 3836 N94-32996
Neostriatal neuronal activity and behavior
[AD-A278429] p 3802 N94-33333

NEUROTRANSMITTERS
The organization of the suprachiasmatic circadian pacemaker of the rat and its regulation by neurotransmitters and modulators
[AD-A277324] p 3793 N94-32622

NEUTRAL ATOMS
Cooling and trapping of neutral atoms
[AD-A276957] p 3870 N94-32360

NEUTRAL BEAMS
Experimental survey of the L-H transition conditions in the D3-D tokamak
[DE94-007428] p 3891 N94-32595

NEUTRAL GASES
The manifestations of energetic activity in the galactic center p 3937 N94-32028

NEUTRAL PARTICLES
Monoenergetic neutral particle transport in semi-infinite media
[AD-A277155] p 3870 N94-32368

NEUTRALIZERS
An analytical study of the vibration of beams fitted with neutralizers. Part 2: Assessment of the effects of mounting configurations
[ISVR-TR-225-PT-2] p 3740 N94-32982

NEUTRINOS
Probing lepton number violation via Majorana neutrinos at hadron supercolliders
[PB94-147055] p 3868 N94-31922
Convection in Type 2 supernovae
[DE94-009373] p 3938 N94-32914

NEUTRON ABSORBERS
Irradiation-assisted stress corrosion cracking of materials from commercial BWRs: Role of grain-boundary microchemistry
[DE94-006542] p 3643 N94-32109

NEUTRON COUNTERS
Neutron measurements at the commercial aircraft altitudes
[ISBN-0-315-86201-7] p 3955 N94-31709
Resistivity measurements on the neutron irradiated detector grade silicon materials
[DE94-009083] p 3906 N94-32822

NEUTRON DIFFRACTION
Adsorption of water to the metal/polymer interface studied by neutron and x ray reflectivity
[DE94-005578] p 3651 N94-31649
Structural ordering in liquid K-Te alloys
[DE94-008477] p 3645 N94-32514
Extended-range order in glasses
[DE94-008135] p 3661 N94-32798

NEUTRON EMISSION
Control heavy ion collisions in the systems Ar-40 + Ca-40 and Si-28 + Si-28, and the nature of particle emission in fusion-evaporation reactions
[ETN-94-95749] p 3886 N94-31614
NEUTRON IRRADIATION
Effect of irradiation damage and helium on the swelling and structure of vanadium-base alloys
[DE94-006540] p 3641 N94-31666
Defect cascades produced by neutron irradiation in YBa2Cu3O(7-delta) superconductors
[DE94-007700] p 3903 N94-32372
Resistivity measurements on the neutron irradiated detector grade silicon materials
[DE94-009083] p 3906 N94-32822
NEUTRON RADIOGRAPHY
Practical neutron training course: Course notes
[PB94-145158] p 3867 N94-31681
NEUTRON SCATTERING
Structure and dynamics of microemulsions in bulk, at interfaces, and in confined geometries
[DE94-006043] p 3633 N94-31526
Practical neutron training course: Course notes
[PB94-145158] p 3867 N94-31681
Multiple size scale structures in silica/siloxane composites studied by small-angle scattering
[DE94-007300] p 3625 N94-32642
Strongly anisotropic s-wave versus d-wave gap in cuprate superconductors: Evidence and theory
[DE94-007579] p 3904 N94-32746
Investigation of superconductivity and magnetism in d and f-electron materials
[DE94-008535] p 3907 N94-32933
NEUTRON SOURCES
Analysis of beam-on-target interaction in a neutron-source test facility
[DE94-005392] p 3863 N94-31151
NEUTRON STARS
Nonthermal accretion disk models around neutron stars p 3931 N94-31139
Reactive flows in compact objects p 3934 N94-31567
Structure and stability of spherical accretion flows onto compact objects p 3935 N94-31946
Hydrodynamics of neutron star interiors and laboratory superfluids p 3936 N94-31949
NEUTRONS
Neutron measurements at the commercial aircraft altitudes
[ISBN-0-315-86201-7] p 3955 N94-31709
NN-interaction in (1)S0-state: Virtual level or dibaryon resonance?
[DE94-606492] p 3869 N94-32097
Parallel Monte Carlo reactor neutronics
[DE94-007642] p 3826 N94-32357
Adjacent-cell Preconditioners for solving optically thick neutron transport problems
[DE94-007219] p 3872 N94-32666
Irradiation-induced phase transformations in zirconium alloys
[DE94-008484] p 3648 N94-32993
Spin-structure function of the neutron He-3: SLAC results
[DE94-008927] p 3875 N94-33189
NEWS
Index to NASA news releases and speeches, 1993
[NASA-TM-109722] p 3917 N94-31888
NEWTON METHODS
Lattice geometrodynamics p 3857 N94-31825
On the error committed by stopping the Newton iteration in Runge-Kutta methods and linear multistep methods
[TW-93-13] p 3847 N94-32206
NICKEL
Interface controlled amorphization of crystalline Ni/Ti multilayers
[DE94-008685] p 3906 N94-32884
NICKEL ALLOYS
Transmissibility of nickel-titanium shape memory alloy springs
[AD-A276055] p 3640 N94-31456
Thermal-mechanical fatigue crack growth in aircraft engine materials
[ISBN-0-315-86543-1] p 3734 N94-31707
Fatigue in single crystal nickel superalloys
[AD-A276662] p 3643 N94-32047
Liquid-assisted diffusion bonding of NiAl
[DE94-008667] p 3645 N94-32522
Boron and hydrogen in Ni3Al. Part 2: Mechanical testing of bicrystals
[DE94-007441] p 3904 N94-32606
Structure, stability, and mechanical properties of intermetallic phases
[DE94-009178] p 3647 N94-32852
NICKEL CADMIUM BATTERIES
The 1988 Goddard Space Flight Center Battery Workshop
[NASA-CP-3237] p 3758 N94-31233
NICKEL COMPOUNDS
Development of nickel and metal hydride secondary battery
[DE94-757270] p 3697 N94-32917
NICKEL HYDROGEN BATTERIES
The 1988 Goddard Space Flight Center Battery Workshop
[NASA-CP-3237] p 3758 N94-31233
Development of nickel and metal hydride secondary battery
[DE94-757270] p 3697 N94-32917
NIGER
Monitoring landsurface characteristics in Niger using complementary SPOT and ERS-1 SAR data p 3754 N94-32560
NIGHT VISION
Night vision camcorder system
[AD-A277004] p 3712 N94-32002
Assessment of interior modifications in C-130 and C-141 aircraft for night vision goggle operations
[AD-A276843] p 3582 N94-32223
Methods for measuring characteristics of night vision goggles
[AD-A277046] p 3804 N94-32302
An evaluation framework for designing a night vision, computer-based trainer
[AD-A278005] p 3590 N94-33139
NIOBATES
Electrooptic crystal growth and properties
[AD-A276023] p 3896 N94-31439
On the nature of striae in strontium barium niobate
[DE94-006486] p 3901 N94-32176
NIOBIUM
Inorganic materials for anomalous-dispersion phase-matched second harmonic generation: Rubidium titanyl arsenate isomorphs, Rb(Ti(1-2x)Ln(x)Nb(x))OAsO4
[DE94-006141] p 3899 N94-31847
Characterization of interface structure in multilayers using specular x ray reflectance
[DE94-007698] p 3657 N94-32358
NITRAMINE PROPELLANTS
Condensed-phase processes during solid propellant combustion. 3: Preliminary depth-profiling studies on XM39, JA2, M9, M30, and HMX2
[AD-A276595] p 3635 N94-32124
NITRATE ESTERS
Condensed-phase processes during solid propellant combustion. 3: Preliminary depth-profiling studies on XM39, JA2, M9, M30, and HMX2
[AD-A276595] p 3635 N94-32124
NITRATES
Dry deposition of PAN to grassland vegetation
[DE94-005111] p 3768 N94-32894
Carbonates, surfates, phosphates, nitrates, and organic materials: Their association in a Martian meteorite p 3952 N94-33239
NITRIC OXIDE
Fuel property effects on engine combustion processes
[DE94-005529] p 3631 N94-31153
NITRIDES
Process parameter-growth environment-film property relationships for reactive sputter deposited metal (V, Nb, Zr, Y, Au) oxide, nitride, and oxynitride films
[AD-A276382] p 3640 N94-31258
Cost-effective ceramic machining: Summary of three-body wear experiments
[DE94-007757] p 3650 N94-31354
NITROGEN
Spectroscopic study of the molecular collisions (hydrogen-nitrogen and hydrogen-oxygen) at energies of several MeV
[ISBN-0-315-86794-9] p 3867 N94-31753
Vibrational energy transfer of diatomic gases in hypersonic expanding flows p 3570 N94-31958
Simulation of low-density nozzle plumes in non-zero ambient pressures
[NASA-TM-106501] p 3615 N94-32742
NITROGEN ATOMS
Enhanced thermal capacity aerogels summary report, FY 1993
[DE94-008888] p 3639 N94-33260
NITROGEN OXIDES
Identification of research relating to the critical loads concept and its potential application to the regulation of acidic deposition
[DE94-008234] p 3767 N94-32752
Dry deposition of PAN to grassland vegetation
[DE94-005111] p 3768 N94-32894
A correlated k-distribution model of the heating rates for atmospheric mixtures of H2O, CO2, O3, CH4, and N2O in the 0-2500 cm(exp -1) wave number region at altitudes between 0 and 60 km
[DE94-005136] p 3775 N94-32895
NITROGUANIDINE
Condensed-phase processes during solid propellant combustion. 3: Preliminary depth-profiling studies on XM39, JA2, M9, M30, and HMX2
[AD-A276595] p 3635 N94-32124
NITROUS OXIDES
A correlated k-distribution model of the heating rates for atmospheric mixtures of H2O, CO2, O3, CH4, and N2O in the 0-2500 cm(exp -1) wave number region at altitudes between 0 and 60 km
[DE94-005136] p 3775 N94-32895
NOAA SATELLITES
Development of a statistical method for estimating the downward longwave radiation at the surface from satellite observations p 3742 N94-31553
NOISE (SOUND)
An investigation of acoustic noise requirements for the Space Station centrifuge facility
[NASA-TM-108811] p 3805 N94-32936
NOISE INTENSITY
Investigation of sonic boom for the Space Shuttle: High cross-range orbiter
[NASA-TM-108238] p 3860 N94-31336
Investigation of sonic boom for the Space Shuttle: Low cross-range orbiter
[NASA-TM-108237] p 3860 N94-31337
Experimental and computational studies on propeller noise due to inflow distortion p 3860 N94-31846
NOISE MEASUREMENT
Long transect seafloor seismic array: A component of SAMSON (Sources of Ambient Micro Seismic Ocean ic Noise)
[AD-A277009] p 3789 N94-32401
NOISE POLLUTION
Common property resources and low-level flying in Labrador: Flight, fight or fancy?
[ISBN-0-315-87318-3] p 3924 N94-31732
NOISE PREDICTION
Scattering of a random acoustic field by an infinite cylinder: Application to the modelization of the acoustic environment of the 'Ariane 5' launcher scale-model using experimental data
[ONERA-NT-1993-11] p 3860 N94-31226
NOISE PROPAGATION
Reciprocity-based experimental determination of dynamic forces and moments: A feasibility study
[NASA-CR-194905] p 3862 N94-33023
NOISE REDUCTION
An adaptive Kalman filter excisor for suppressing narrowband interference
[AD-A276286] p 3671 N94-31253
Mitigation of adverse environmental effects on lunar-based astronomical instruments p 3598 N94-31426
A silicon condenser microphone: Modelling and electronic circuitry
[ISBN-9-09-005279-8] p 3688 N94-31517
A silicon condenser microphone: Materials and technology
[ISBN-9-09-005899-0] p 3688 N94-31518
Restoration of interferometric, polarimetric, radiometric, and textural information in SAR images p 3750 N94-32535
A mathematical model for simulating noise suppression of lined ejectors
[NASA-TP-3425] p 3861 N94-32930
An investigation of acoustic noise requirements for the Space Station centrifuge facility
[NASA-TM-108811] p 3805 N94-32936
Noise cancellation for CELP voice encoders in an F/A-18 noise environment
[AD-A277652] p 3683 N94-33026
NONDESTRUCTIVE TESTS
Evaluation of nondestructive inspection techniques for quality control of alumina-ceramic housing components
[AD-A276220] p 3730 N94-31065
Naval Surface Warfare Center Dahlgren Division Technical Digest: Advanced materials technology
[AD-A276448] p 3668 N94-31364
Determining the bearing capacity of flexible airfield pavements using a heavy weight deflectometer
[ISBN-0-315-86210-6] p 3587 N94-31710
Ultrasonic characterization of damage in a simulated CF-18 composite structure
[DREP-LN-93-26] p 3730 N94-31872
Location of impact damage sites in composite aircraft structures, task 3.4.1
[DSIS-94-01590] p 3621 N94-31892

Benchmarking of the state-of-the-art in nondestructive testing/evaluation for applicability in the Composite Armored Vehicle (CAV) Advanced Technology Demonstrator (ATD) program, phase 1
[AD-A276660] p 3730 N94-32088

Shearographic inspection of a DeHavilland DHC-7
[AD-A276716] p 3566 N94-32157

A versatile nondestructive evaluation imaging workstation p 3732 N94-32458

Differential phase acoustic microscope for micro-NDE
[NASA-CR-189617] p 3731 N94-32481

Dual-band infrared imaging to detect corrosion damage within airframes and concrete structures
[DE94-006047] p 3580 N94-32658

PSIDD: A Post-Scan Interactive Data Display system for ultrasonic scans
[NASA-TM-4545] p 3732 N94-33038

NONEQUILIBRIUM FLOW

Response of wall turbulence to high frequency streamwise and spanwise oscillations p 3700 N94-31211

NONHOLONOMIC EQUATIONS

Trajectory planning for space manipulators
[AD-A277229] p 3611 N94-32369

NONINTRUSIVE MEASUREMENT

Photopyroelectric spectroscopy as a non-intrusive technique for the determination of the optical absorption spectra of multiple quantum well samples
[ISBN-0-315-87164-4] p 3833 N94-31875

Design of a two dimensional planer pressurized air labyrinth seal test rig
[AD-A277232] p 3726 N94-32370

Scalar imaging velocimetry studies of turbulent flow structure and dynamics
[AD-A278395] p 3710 N94-33164

NONISOTHERMAL PROCESSES

Chemical vapour deposition of tungsten for the application in integrated circuits
[ISBN-9-09-005151-1] p 3641 N94-31519

NONLINEAR EQUATIONS

On wavelet representations of differential equations
[RR-482] p 3842 N94-31412

The finite element method with asymptotic self-similar solutions p 3736 N94-31904

Design and Monte Carlo analysis of an unmanned aerial vehicle
[AD-A277648] p 3580 N94-33056

NONLINEAR FILTERS

Linearly separable stack-like architecture for the design of weighted order statistic filters with application in image processing
[ISBN-0-315-87284-5] p 3675 N94-31731

NONLINEAR OPTICS

New material for high average power infrared generation: QPM-DB GaAs
[AD-A276389] p 3714 N94-31358

Compatibility studies of some azo polymer blends
[AD-A277141] p 3657 N94-32365

Mathematical nonlinear optics
[AD-A277320] p 3882 N94-32510

New developments in second-order nonlinear optical polymeric materials
[AD-A277409] p 3658 N94-32578

Stable second-order nonlinear optical materials based on interpenetrating polymer networks
[AD-A277410] p 3658 N94-32579

Nonlinear optical polymers derived from organic/inorganic composites
[AD-A277408] p 3659 N94-32610

Nonlinear optical properties of rigid-rod polymers
[NASA-CR-191349] p 3882 N94-32702

Low loss second-order nonlinear optical polymers based on all organic sol-gel materials
[AD-A277482] p 3663 N94-32985

A relaxation study of poled nonlinear optical polymers by infrared reflection-absorption spectroscopy
[AD-A277513] p 3663 N94-33054

Novel polydiacetylenes as materials for second and third order nonlinear optics
[AD-A277512] p 3664 N94-33082

Research in the optical sciences
[AD-A278271] p 3884 N94-33140

Studies of optical beam phase conjugation and electromagnetic scattering process
[AD-A278389] p 3884 N94-33145

Advanced material processing for integrated-optic frequency doubling systems
[AD-A278394] p 3698 N94-33163

Future directions of nonlinear dynamics in physical and biological systems. (Physica D nonlinear, volume 68, number 1)
[AD-A278085] p 3794 N94-33250

Optical properties of doped sol-gel silica glasses
[AD-A276094] p 3884 N94-33267

Second-order nonlinear optical polymers: From fundamentals to applications
[AD-A277514] p 3664 N94-33348

NONLINEAR PROGRAMMING

Optimal reactive power dispatch of power systems using nonlinear programming
[MATHS-REPT-A-209] p 3808 N94-31164

Parallel structured optimization algorithms for inverse problems
[AD-A276053] p 3811 N94-31443

A Gauss-Seidel type solver for special convex programs, with application to frictional contact mechanics
[REPT-93-77] p 3813 N94-31694

OPT++: An object-oriented class library for nonlinear optimization
[DE94-008890] p 3818 N94-32584

NONLINEAR SYSTEMS

A radial basis function approach to financial time series analysis
[AD-A276408] p 3924 N94-31361

Nonlinear model validation using correlation tests
[RR-463] p 3842 N94-31394

On wavelet representations of differential equations
[RR-482] p 3842 N94-31412

Adaptive nonlinear control of spacecraft p 3609 N94-31564

Chaotic attitude motion of satellites in the central gravitational field
[ISBN-0-315-78768-6] p 3610 N94-31723

Asymptotic behavior of dynamic systems p 3911 N94-31894

Structural stability and bifurcations p 3911 N94-31895

Deterministic chaos p 3912 N94-31896

Modeling and control of nonlinear systems
[AD-A277377] p 3834 N94-32095

Basic principles approach for studying nonlinear Alfven wave-alpha particle dynamics
[DE94-007112] p 3891 N94-32664

Advanced CFD methodology for fast transients encountered in nonlinear combustion instability problems. Volume 1: Theory and validation
[NASA-CR-191351] p 3637 N94-32696

State-space self-tuner for on-line adaptive control
[NASA-CR-195836] p 3835 N94-32943

RHIC chromatic correction system
[DE94-008532] p 3883 N94-32994

Investigation of drive-reinforcement learning and application of learning to flight control
[AD-A277442] p 3801 N94-33053

On the computation of simplical approximations of implicitly defined two-dimensional manifolds
[AD-A278132] p 3849 N94-33060

Future directions of nonlinear dynamics in physical and biological systems. (Physica D nonlinear, volume 68, number 1)
[AD-A278085] p 3794 N94-33250

Adaptive control of nonlinear and stochastic systems
[AD-A278411] p 3839 N94-33325

NONLINEARITY

Nonlinear calculations of the time evolution of black hole accretion disks p 3929 N94-31127

Taming chaotic circuits p 3910 N94-31289

Towards simplicity: Noise and cooperation in the perfect integrator
[AD-A276256] p 3799 N94-31291

Nonlinearity as an origin of nonuniqueness in solution of Hartree's equation
[DE94-006538] p 3841 N94-31311

On the relationship between generalization error, hypothesis complexity, and sample complexity for radial basis functions
[AD-A276802] p 3851 N94-32142

Advanced CFD methodology for fast transients encountered in nonlinear combustion instability problems. Volume 2: User's guide
[NASA-CR-191352] p 3637 N94-32694

Parallel supercomputing: Advanced methods, algorithms, and software for large-scale linear and nonlinear problems
[DE94-008446] p 3836 N94-32992

A relaxation study of poled nonlinear optical polymers by infrared reflection-absorption spectroscopy
[AD-A277513] p 3663 N94-33054

Novel polydiacetylenes as materials for second and third order nonlinear optics
[AD-A277512] p 3664 N94-33082

NONOSCILLATORY ACTION

A fully two-dimensional, non-oscillatory advection scheme for momentum and scalar transport equations
[DM-66] p 3700 N94-31221

NONPARAMETRIC STATISTICS

Stochastic models in reliability theory
[AD-A277529] p 3731 N94-32953

NONRESONANCE

Particle-In-Cell (PIC) code simulation results and comparison with theory scaling laws for photoelectron-generated radiation
[DE94-006132] p 3695 N94-32662

NONUNIFORM FLOW

Rotordynamic effects driven by fluid forces from a geometrically imperfect labyrinth
[AD-A276424] p 3722 N94-31333

Additional capabilities of the unified waves model
[AD-A276114] p 3702 N94-31467

Inlet distortion in engines on VSTOL aircraft
[NASA-CR-195841] p 3584 N94-33035

NONUNIFORMITY

Experimental and computational studies on propeller noise due to inflow distortion p 3860 N94-31846

Effect of surface forces on the rheology of particle-liquid systems and the consolidation of ceramic powders
[AD-A277092] p 3657 N94-32391

NORMALIZING (STATISTICS)

Airborne SAR as a complement to SPOT HRV in land-cover classification: The use of normalization and principal components analysis p 3750 N94-32539

NORMS

Triangular norms and conorms: A general tool for generating fuzzy mathematical morphologies
[TELECOM-93-D-001] p 3839 N94-31092

NORTH ATLANTIC TREATY ORGANIZATION (NATO)

AGARD highlights 94/1, April 1994
[AGARD-HIGHLIGHTS-94/1] p 3956 N94-31196

AGARD membership, 1994
[AGARD-MEMB-94] p 3914 N94-31197

NATO contributions to European environmental security
[AD-A275918] p 3763 N94-31275

NOSE CONES

Tip effects on the vortex wake of an axisymmetric body at angle of attack p 3570 N94-31907

Calibration and validation studies in the LENS facility
[AD-A278403] p 3591 N94-33167

NOSE WHEELS

Computational methods for frictional contact with applications to the Space Shuttle orbiter nose-gear tire p 3608 N94-32295

NOTCH SENSITIVITY

Tension fracture of laminates for transport fuselage. Part 1: Material screening p 3629 N94-33130

NOVAE

Disk instability and the spectral evolution of the 1992 outburst of the intermediate polar GK Persei p 3928 N94-31123

Disk irradiation and light curves of x ray novae p 3929 N94-31124

Observational constraints on black hole accretion disks p 3929 N94-31126

Can a variable alpha induce limit cycle behavior and exponential luminosity decay in transient soft x ray sources? p 3929 N94-31129

The physics of black hole x ray novae p 3932 N94-31143

NOZZLE DESIGN

Shear flow control of cold and heated rectangular jets by mechanical tabs. Volume 1: Results and discussion
[NASA-CR-182296-VOL-1] p 3708 N94-32867

Shear flow control of cold and heated rectangular jets by mechanical tabs. Volume 2: Tabulated data
[NASA-CR-182296-VOL-2] p 3709 N94-32869

Enhancement of mixing in a rectangular jet by mechanical tabs
[NASA-CR-185207] p 3709 N94-32872

NOZZLE FLOW

The small-scale topology of a 2:1 aspect-ratio elliptic jet p 3699 N94-31184

Boundary layer study on nozzle wall at hypersonic velocities p 3569 N94-31882

Simulation of low-density nozzle plumes in non-zero ambient pressures
[NASA-TM-106501] p 3615 N94-32742

Shear flow control of cold and heated rectangular jets by mechanical tabs. Volume 1: Results and discussion
[NASA-CR-182296-VOL-1] p 3708 N94-32867

Shear flow control of cold and heated rectangular jets by mechanical tabs. Volume 2: Tabulated data
[NASA-CR-182296-VOL-2] p 3709 N94-32869

Enhancement of mixing in a rectangular jet by mechanical tabs
[NASA-CR-185207] p 3709 N94-32872

Use of Navier-Stokes methods for the calculation of high-speed nozzle flow fields
[NASA-TM-106551] p 3573 N94-32984

NOZZLE GEOMETRY

Control experiments in liquid metal combustion
[AD-A276918] p 3635 N94-32234

NOZZLE INSERTS
Shear flow control of cold and heated rectangular jets by mechanical tabs. Volume 1: Results and discussion
[NASA-CR-182296-VOL-1] p 3708 N94-32867
Shear flow control of cold and heated rectangular jets by mechanical tabs. Volume 2: Tabulated data
[NASA-CR-182296-VOL-2] p 3709 N94-32869
NOZZLE WALLS
Boundary layer study on nozzle wall at hypersonic velocities p 3569 N94-31882
NUCLEAR ASTROPHYSICS
Reactive flows in compact objects
p 3934 N94-31567
NUCLEAR BINDING ENERGY
Indium-vacancy complexes in mercury cadmium telluride
[AD-A276177] p 3894 N94-31055
Nonthermal accretion disk models around neutron stars p 3931 N94-31139
IR materials producibility
[AD-A277028] p 3879 N94-32006
Gettering of metal impurities by cavities in silicon
[DE94-005248] p 3645 N94-32672
NUCLEAR ELECTRIC POWER GENERATION
Aerospace test facilities at NASA LERC Plumbrook
[NASA-TM-109755] p 3602 N94-31814
NUCLEAR ELECTRIC PROPULSION
Utilizing a Russian space nuclear reactor for a United States space mission: Flight qualification issues
[DE94-004674] p 3613 N94-31265
Integrated safety program for the Nuclear Electric Propulsion Space Test Program
[DE94-004670] p 3615 N94-32669
NUCLEAR FUELS
The development of CVR coatings for PBR fuels
[DE94-004233] p 3875 N94-31480
NUCLEAR FUSION
Plasma confinement theory and transport simulation
[DE94-006065] p 3888 N94-31619
Mechanisms of formation and of de-excitation in the reaction Mg-24 + C-12 yields 9 alpha at 35MeV per nucleon
[ISBN-0-315-86746-9] p 3867 N94-31749
Atomic and molecular data needs for fusion
[DE94-006555] p 3870 N94-32177
Fusion applications of high power millimeter wave sources
[DE94-007374] p 3718 N94-32202
Magnetless magnetic fusion
[DE94-007114] p 3891 N94-32686
Convection in Type 2 supernovae
[DE94-009373] p 3938 N94-32914
NUCLEAR HEAT
Development of lightweight radiators for lunar based power systems
[NASA-TM-106604] p 3726 N94-32272
NUCLEAR INTERACTIONS
Transverse energy production with Si and Au beams at AGS energy: Towards hot and dense hadronic matter
[DE94-007178] p 3938 N94-32638
NUCLEAR MAGNETIC RESONANCE
New molecular-based routes to binary main group metal sulfides
[AD-A277005] p 3900 N94-32003
NMR studies of organic thin films
[AD-A276953] p 3656 N94-32221
Advances and applications of dynamic-angle spinning nuclear magnetic resonance
[DE94-007031] p 3870 N94-32250
Dynamics of block poly(styrene-co-vinylpyridine) (SVP) in solution and on silica
[AD-A277139] p 3657 N94-32364
Strongly anisotropic s-wave versus d-wave gap in cuprate superconductors: Evidence and theory
[DE94-007579] p 3904 N94-32746
NMR characterization of shocked quartz
[DE94-007733] p 3774 N94-32816
A quest for a new superconducting state
[DE94-008439] p 3908 N94-32991
NUCLEAR MODELS
Influence of long-range correlations on the spectral functions and response of 48Ca and 90Zr
[ETN-94-96017] p 3865 N94-31537
NUCLEAR PHYSICS
Nuclear physics and astrophysics
[DE94-007168] p 3939 N94-33147
NUCLEAR POTENTIAL
Development and implementation of a full-potential ASW method
[ETN-94-95757] p 3858 N94-31560
NUCLEAR PROPULSION
Summary of particle bed reactor designs for the Space Nuclear Thermal Propulsion Program
[DE94-007434] p 3615 N94-32266
NUCLEAR PUMPED LASERS
DOE reactor-pumped laser program
[DE94-006372] p 3715 N94-31485
NUCLEAR REACTIONS
Reactive flows in compact objects
p 3934 N94-31567
Hydrogen incorporation and radiation induced dynamics in metal-oxide-silicon structures: A study using nuclear reaction analysis
[ETN-94-95742] p 3898 N94-31610
NUCLEAR REACTORS
Modeling of residual stress mitigation in austenitic stainless steel pipe girth weldment
[DE94-007184] p 3738 N94-32639
Integrated safety program for the Nuclear Electric Propulsion Space Test Program
[DE94-004670] p 3615 N94-32669
Reactor pressure vessel structural integrity research in the US Nuclear Regulatory Commission HSST and HSSI Programs
[DE94-006550] p 3739 N94-32771
NUCLEAR SCATTERING
The 14th Annual West Coast Theoretical Chemistry/Statistical Mechanics Conference
[AD-A276942] p 3656 N94-32239
NUCLEAR WEAPONS
The relative performance of FeS2 and CoS in long-life thermal-battery applications
[DE94-006145] p 3695 N94-32663
Vulnerability assessment of a space based weapon platform electronic system exposed to a thermonuclear weapon detonation
[DE94-007229] p 3611 N94-32667
NUCLEATION
Solidification structure synthesis in undercooled liquids
[AD-A276166] p 3910 N94-31054
Characterization and growth mechanisms of the MgAl2O4 phase in Al2O3-reinforced Al-Mg composites
[ISBN-0-315-86531-8] p 3620 N94-31706
A parameterization of cloud droplet nucleation
[DE94-007469] p 3785 N94-32268
Nucleation and growth of cubic boron nitride films produced by ion-assisted pulsed laser deposition
[DE94-007295] p 3661 N94-32796
Interface controlled amorphization of crystalline Ni/Ti multilayers
[DE94-006685] p 3906 N94-32884
NUCLEI (CYTOLOGY)
Stress-induced enhancement of the startle reflex
[AD-A278414] p 3802 N94-33327
NUCLEON-NUCLEON INTERACTIONS
The Nijmegen hyperon-nucleon potentials
[DE94-007557] p 3869 N94-32139
Medium energy measurements of N-N parameters
[DE94-006067] p 3869 N94-32173
NUCLEONS
The form factors of the nucleons
[DE94-007096] p 3872 N94-32630
Transverse energy production with Si and Au beams at AGS energy: Towards hot and dense hadronic matter
[DE94-007178] p 3938 N94-32638
Polarized lepton-nucleon scattering
[DE94-009027] p 3875 N94-33278
NUMERICAL ANALYSIS
Numerical detection and continuation of codimension-two homoclinic bifurcations
[CWI-AM-R9308] p 3847 N94-32191
Advanced CFD methodology for fast transients encountered in nonlinear combustion instability problems. Volume 2: User's guide
[NASA-CR-191352] p 3637 N94-32694
NUMERICAL CONTROL
ControlShell: A real-time software framework
[AD-A276481] p 3811 N94-31475
The future of open architecture process control systems
[DE94-006163] p 3830 N94-31623
Digital state-feedback H(infinity) control of Pritchard-Salamon systems: A Popov function approach
[REPT-93-69] p 3830 N94-31647
Quench detection and instrumentation for the Tokamak Physics Experiment magnets
[DE94-006656] p 3888 N94-31667
Real-time control and application to robotics: Hardware and software architectures
[ISBN-0-315-87192-X] p 3833 N94-31876
Evolving software reengineering technology for the emerging innovative-competitive era
p 3823 N94-32439
NUMERICAL INTEGRATION
Finite-part integrals and the Euler-Maclaurin expansion
[DE94-006539] p 3844 N94-31665
NUMERICAL STABILITY
A simplified Von Neumann method for linear stability analysis
[CRANFIELD-AERO-9310] p 3843 N94-31540
A stability estimate based on numerical ranges with application to a spectral discretization of a convection-diffusion equation
[TW-93-12] p 3847 N94-32200
Stability estimates for families of matrices of nonuniformly bounded order
[TW-93-14] p 3847 N94-32207
Eta percent-superconvergence in the interior of locally refined meshes of quadrilaterals: Superconvergence of the gradient in finite element solutions of Laplace's and Poisson's equations
[AD-A277242] p 3848 N94-32331
Finite element solution to the Helmholtz equation with high wave number. Part 1: The h-version of the FEM
[AD-A277396] p 3848 N94-32341
Preconditioned time-difference methods for advection-diffusion-reaction equations
[DE94-006472] p 3638 N94-32840
NUMERICAL WEATHER FORECASTING
A comparison of predictors for first-guess wind speed errors
[AD-A276460] p 3781 N94-31239
Regional sources of error growth in the National Meteorological Center's medium-range forecast model
p 3781 N94-31554
Numerical simulations of monsoon rainfall with the NRL/NCSU regional nested grid model
p 3782 N94-31791
Recurvature dynamics of a typhoon
[AD-A276792] p 3784 N94-32164
Tropical cyclone forecasters reference guide. 5: Numerical track forecast guidance
[AD-A277318] p 3785 N94-32278
NUTATION
Attitude dynamics of spinning rockets in space with internal mass motion p 3601 N94-31802
NUTATION DAMPERS
Attitude dynamics of spinning rockets in space with internal mass motion p 3601 N94-31802
NUTRITION
Food security in the context of global environmental change
[DE94-007481] p 3768 N94-32812
NUTS (FASTENERS)
An experimental and analytical investigation of a threaded fastener
[VTT-JULK-786] p 3724 N94-31654
NYLON (TRADEMARK)
The ferroelectric behavior of odd-numbered nylons
[AD-A278126] p 3663 N94-33058
Electric field-induced changes in odd-numbered nylons
[AD-A278003] p 3664 N94-33138

O

OBJECT-ORIENTED PROGRAMMING
A generic model for data acquisition: Connectionist methods of information processing
[TELECOM-93-E-003] p 3730 N94-31166
Design patterns mixing genericity and inheritance in the development of reusable components
[REPT-93-021] p 3808 N94-31178
A finite state machine model for object oriented systems
[REPT-93-040] p 3809 N94-31212
Real time simulation model for designing converter regulation
[ETN-94-95735] p 3689 N94-31576
Report on implementing part relationships using VML metaclasses
[PB94-147485] p 3813 N94-31686
EVORM: A conceptual modelling technique for evolving application domains
[TR-93-16] p 3918 N94-32290
Multiple inheritance via intersection types
[TR-93-18] p 3848 N94-32292
CONFIG: Integrated engineering of systems and their operation p 3823 N94-32432
OPT++: An object-oriented class library for nonlinear optimization
[DE94-008890] p 3818 N94-32584
A framework for developing and managing reusable avionics software
[AD-A276846] p 3582 N94-32909
OBLIQUENESS
The effect of polar caps on obliquity
p 3948 N94-33213
OBSERVATION
Aircraft weight prediction capability. Volume 1: Weight study and results
[AD-A277206] p 3579 N94-32062
OBSTACLE AVOIDANCE
Safe navigation and active vision for autonomous vehicles: A purposive and direct solution
p 3832 N94-31842

Tripping over obstacles: Biomechanical analyses of how young and old try to avoid it p 3803 N94-31954

OCCLUSION

Incompressible viscous flow in tubes with occlusions [ISBN-0-315-75467-2] p 3704 N94-31778

OCCUPATIONAL DISEASES

Minimization of carpal tunnel syndrome [AD-A276409] p 3795 N94-31363

OCEAN BOTTOM

Multi-scale studies of seafloor topography [AD-A277008] p 3789 N94-32400

Long transect seafloor seismic array: A component of SAMSON (Sources of Ambient Micro Seismic Ocean ic Noise) [AD-A277009] p 3789 N94-32401

Light in Thermal Environments (LITE) Workshop [NASA-CR-195851] p 3790 N94-32981

Quantitative modeling of bottom morphology and subbottom properties [AD-A278142] p 3790 N94-33062

OCEAN CURRENTS

General ocean circulation p 3777 N94-30984

Low frequency variability observed in the tropical Atlantic Ocean p 3778 N94-30991

The effect of westerly wind bursts on a tropical ocean general circulation model [AD-A276423] p 3788 N94-31448

Observations of turbulence, internal waves and background flows: An inquiry into the relationships between scales of motion p 3705 N94-31988

Three dimensional vorticity field in the California current system [AD-A276951] p 3788 N94-32220

Estimating subpycnocline density fluctuations in the California current region from upper ocean observations [AD-A277278] p 3789 N94-32325

Deep water studies of CTD data [AD-A277741] p 3791 N94-33176

Cruise report: Oceanus 250 leg 4 high resolution profiler survey for the North Atlantic Tracer Release Experiment, 25 March - 24 April, 1992 [AD-A277935] p 3791 N94-33245

OCEAN DATA ACQUISITIONS SYSTEMS

Profiling ALACE instruments [AD-A277246] p 3789 N94-32321

Long transect seafloor seismic array: A component of SAMSON (Sources of Ambient Micro Seismic Ocean ic Noise) [AD-A277009] p 3789 N94-32401

SEASOAR and CTD observations during a COARE surveys cruise, W9211C, 22 January - 22 February, 1993 [AD-A277925] p 3791 N94-33244

OCEAN DYNAMICS

General ocean circulation p 3777 N94-30984

Low frequence variability of the ocean atmosphere coupled system p 3777 N94-30986

The effect of westerly wind bursts on a tropical ocean general circulation model [AD-A276423] p 3788 N94-31448

Validation support of the ERIM ocean model [AD-A277364] p 3788 N94-32284

ENSO forced variations of the sea surface temperature and adjusted sea level along the west coast of the United States [AD-A277306] p 3789 N94-32327

OCEAN MODELS

Subtropical Climates and Their Evolution: From Space-Based Observation to Modelling [ISBN-2-85-428333-3] p 3776 N94-30981

General ocean circulation p 3777 N94-30984

Climatologic flux in tropical ocean p 3777 N94-30985

The effect of westerly wind bursts on a tropical ocean general circulation model [AD-A276423] p 3788 N94-31448

The influence of cumulus parameterization on model forecasts of rapid oceanic cyclogenesis [AD-A277207] p 3784 N94-32094

Validation support of the ERIM ocean model [AD-A277364] p 3788 N94-32284

Ocean variability and its influence on the detectability of greenhouse warming signals [DE94-008670] p 3790 N94-32881

Quantitative modeling of bottom morphology and subbottom properties [AD-A278142] p 3790 N94-33062

OCEAN SURFACE

The effects of altimeter sampling characteristics: Some Geosat examples [AD-A276899] p 3747 N94-32214

Validation support of the ERIM ocean model [AD-A277364] p 3788 N94-32284

Almaz marine applications p 3751 N94-32544

A comparison of rough surface parabolic equation models [AD-A278090] p 3791 N94-33185

An approximate model for vertical polarization and surface roughness using the parabolic equation [AD-A278091] p 3684 N94-33186

OCEAN TEMPERATURE

Profiling ALACE instruments [AD-A277246] p 3789 N94-32321

OCEANOGRAPHIC PARAMETERS

Application of radon transformation for improved analysis of sparsely sampled data: A feasibility study [PB94-147535] p 3741 N94-31075

Hydrographic service Royal Australian Navy [AD-A277134] p 3788 N94-32066

The effects of altimeter sampling characteristics: Some Geosat examples [AD-A276899] p 3747 N94-32214

Ocean variability and its influence on the detectability of greenhouse warming signals [DE94-008670] p 3790 N94-32881

Forecasters handbook for the Philippine Islands and surrounding waters [AD-A277993] p 3787 N94-33089

SEASOAR and CTD observations during a COARE surveys cruise, W9211C, 22 January - 22 February, 1993 [AD-A277925] p 3791 N94-33244

OCEANOGRAPHY

Ocean acoustic propagation measurements and wave propagation in random media [AD-A276165] p 3787 N94-31053

Evaluating success levels of mega-projects p 3599 N94-31432

The effects of altimeter sampling characteristics: Some Geosat examples [AD-A276899] p 3747 N94-32214

Almaz marine applications p 3751 N94-32544

Forecasters handbook for the Philippine Islands and surrounding waters [AD-A277993] p 3787 N94-33089

Fluid mechanical measurements within the bottom boundary layer over the Northern California continental shelf during stress [AD-A277916] p 3791 N94-33243

OCEANS

Ocean acoustic propagation measurements and wave propagation in random media [AD-A276165] p 3787 N94-31053

Observations of turbulence, internal waves and background flows: An inquiry into the relationships between scales of motion p 3705 N94-31988

OHMIC DISSIPATION

Time-resolved analytical methods for liquid/solid interfaces [DE94-008352] p 3637 N94-32826

OIL SLICKS

Ship traffic monitoring and oil spill detection using the ERS-1 SAR p 3751 N94-32542

OLIGOMERS

Conjugated polymer fluorescence: Interplay of correlations and alternation [DE94-005587] p 3660 N94-32729

ON-LINE SYSTEMS

Hierarchical mixtures of experts and the EM algorithm [AD-A276516] p 3814 N94-31932

A redundant disk array architecture for efficient small writes [AD-A276645] p 3815 N94-31940

Moving BASISplus and TECHLIBplus from VAX/VMS to UNIX [DE94-004696] p 3826 N94-32248

A hypertext system that learns from user feedback p 3923 N94-32428

Relationships between access and use in information systems: Remote access to and browsing of online catalogs p 3919 N94-32488

State-space self-tuner for on-line adaptive control [NASA-CR-195836] p 3835 N94-32943

MDFF HELP library, version 2: On-line documentation for the map data formatting facility [AD-A277763] p 3922 N94-32987

ONBOARD DATA PROCESSING

Error analysis of real-time and post-processed orbit determination for the Geosat Follow-On altimetric satellite using GPS tracking p 3576 N94-31845

Aerospace software engineering for advanced systems architectures [AD-A277101] p 3581 N94-31977

Aerospace sponsored research [ATR-93(8498)-1] p 3966 N94-32949

Data processing algorithms for on-board satellite event analysis [AD-A278406] p 3838 N94-33168

ONTARIO

The basement fracture pattern of southern Ontario: A tectonic interpretation based on Landsat TM imagery, airphotos and field data [ISBN-0-315-87086-9] p 3772 N94-31834

OPACITY

Groundbased monitoring of Martian atmospheric opacity p 3947 N94-33207

OPERATING SYSTEMS (COMPUTERS)

Adaptive operating systems concepts [ETN-94-95754] p 3830 N94-31514

Moving BASISplus and TECHLIBplus from VAX/VMS to UNIX [DE94-004696] p 3826 N94-32248

OPERATING TEMPERATURE

Performance of silvered Teflon (trademark) thermal control blankets on spacecraft p 3591 N94-31014

OPERATIONAL AMPLIFIERS

VLSI implementation of stray insensitive switched capacitor composite operational amplifiers [AD-A276461] p 3687 N94-31240

OPERATIONS RESEARCH

Mathematical research in materials science opportunities and perspectives, part 2 [AD-A276298] p 3852 N94-31296

A cross-disciplinary report on the mathematical sciences applied to materials science, part 1 [AD-A276116] p 3843 N94-31529

OPERATOR PERFORMANCE

Use of a pitch adjustable foot restraint system: Operator strength capability and load requirements [NASA-TP-3477] p 3805 N94-33050

OPERATORS (MATHEMATICS)

A cell-cycle model revisited [CWI-AM-R9305] p 3851 N94-32229

Conference on operator, wavelet and control theory [AD-A277429] p 3838 N94-33174

OPERATORS (PERSONNEL)

Modular Simulator System (MSS). System/segment specification for the generic modular simulator system-instructor/operator station module, volume 12 [AD-A276979] p 3589 N94-32318

OPTICAL COMMUNICATION

Advanced optical fiber communication systems [AD-A276416] p 3878 N94-31330

Pulse-splitting and AM-FM conversion in a nonlinear dispersive medium [AD-A277041] p 3861 N94-32262

Control and reliability of optical networks in multiprocessors [AD-A277385] p 3881 N94-32285

Passive, multi-channel fiber optic rotary joint assembly [AD-D016116] p 3882 N94-32626

Multi-line passive fiber optic slipring [AD-D016092] p 3883 N94-32738

Long distance transmission of 15 Gb/s digital using subcarrier multiplexing and external modulation [DE94-008298] p 3682 N94-32756

Pointing and tracking space mechanism for laser communication p 3606 N94-33310

OPTICAL COMPUTERS

Control and reliability of optical networks in multiprocessors [AD-A277385] p 3881 N94-32285

OPTICAL CONTROL

Reconfigurable Array of Radiating Elements (RARE) controlled by light [NASA-CR-195828] p 3884 N94-33073

OPTICAL CORRECTION PROCEDURE

High average power pulsed phase conjugate laser with birefringence correction [DE94-006049] p 3719 N94-32659

Phase-only correction of scintillated laser beams: Downrange experimental results [AD-A277778] p 3722 N94-33282

OPTICAL CORRELATORS

Development of phase-only filters for sensor imagery [AD-A276722] p 3880 N94-32151

Correlation filter synthesis using neural networks [AD-A278124] p 3836 N94-33043

A novel optoelectronic system for distortion-invariant ATR [AD-A277985] p 3884 N94-33087

OPTICAL COUNTERMEASURES

Atmospheric propagation effects through natural and man-made obscurants for visible to MM-wave radiation [AD-A276919] p 3679 N94-32235

OPTICAL COUPLING

Study of the dynamics of a nonlinear coupled-cavity laser system [ISBN-0-315-86717-5] p 3716 N94-31748

Optimization of Y junctions in integrated optics [ISBN-0-315-86782-5] p 3879 N94-31751

OPTICAL DATA PROCESSING

Correlation filter synthesis using neural networks [AD-A278124] p 3836 N94-33043

Design of free space interconnected signal processor [AD-A278129] p 3683 N94-33093

OPTICAL DATA STORAGE MATERIALS
Azo polymers for reversible optical storage. 4. Cooperative motion of rigid groups in semicrystalline polymers
[AD-A277107] p 3654 N94-31978
Reversible optical storage in azo polymers
[AD-A277109] p 3654 N94-31980
OPTICAL EQUIPMENT
Degradation of optical components in space
p 3594 N94-31029
Mitigation of adverse environmental effects on lunar-based astronomical instruments
p 3598 N94-31426
Neutral ion sources in precision manufacturing
p 3875 N94-32447
Proceedings SPIE: Conference Digest, volume 2104
[AD-A278107] p 3884 N94-33187
OPTICAL FIBERS
An axial approach to detection in capillary electrophoresis
[DE94-005556] p 3631 N94-31154
Advanced optical fiber communication systems
[AD-A276416] p 3878 N94-31330
Nd-YAG laser welding of the fiber optic connector to the header shell on the 2SL actuator
[DE94-006104] p 3723 N94-31621
Post-calibration correction for rotating-analyzer ellipsometer with optical fiber bundle detection system
[AD-A277329] p 3881 N94-32280
Studies of an optical multi-processor interconnect
[AD-A277093] p 3881 N94-32392
Flexible manufacturing for photonics device assembly
p 3669 N94-32449
Passive, multi-channel fiber optic rotary joint assembly
[AD-D016116] p 3882 N94-32626
Torque-balanced extendable fiber optic cable
[AD-D016097] p 3882 N94-32719
Fiber optic continuous true time-delay modulator
[AD-D016098] p 3883 N94-32720
Multi-line passive fiber optic slipring
[AD-D016092] p 3883 N94-32738
Strain sensing using optical fibers
[NASA-CR-195807] p 3740 N94-32940
OPTICAL FILTERS
Degradation of optical components in space
p 3594 N94-31029
Development of phase-only filters for sensor imagery
[AD-A276722] p 3880 N94-32151
Correlation filter synthesis using neural networks
[AD-A278124] p 3836 N94-33043
Analysis and design of a high speed, wide range stepwise tunable optical filter/amplifier
[PB94-149572] p 3698 N94-33169
OPTICAL FLOW (IMAGE ANALYSIS)
Safe navigation and active vision for autonomous vehicles: A purposive and direct solution
p 3832 N94-31842
Neural models of spatial orientation in novel environments
[AD-A277383] p 3835 N94-32340
OPTICAL MATERIALS
Transient radiation-induced absorption in the materials for a GSGG laser
[DE94-005316] p 3714 N94-31148
New material for high average power infrared generation: QPM-DB GaAs
[AD-A276389] p 3714 N94-31358
Large-area conditioning of optics for high-power laser systems
[DE94-007028] p 3716 N94-31636
Advanced infrared photodetectors: Materials review
[AD-A277058] p 3879 N94-32013
The sol-gel-xerogel transition
[AD-A276647] p 3616 N94-32038
Multifunctional macromolecules
[AD-A277347] p 3656 N94-32246
Sol-gel coatings for high power laser optics: Past, present, and future
[DE94-007240] p 3718 N94-32252
New developments in second-order nonlinear optical polymeric materials
[AD-A277409] p 3658 N94-32578
Stable second-order nonlinear optical materials based on interpenetrating polymer networks
[AD-A277410] p 3658 N94-32579
Nonlinear optical polymers derived from organic/inorganic composites
[AD-A277408] p 3659 N94-32610
A historical perspective on fifteen years of laser damage thresholds at LLNL
[DE94-007930] p 3719 N94-32613
Nonlinear optical properties of rigid-rod polymers
[NASA-CR-191349] p 3882 N94-32702
Pump-probe method for investigating laser ablation and optical damage threshold mechanisms in optical materials
[DE94-008291] p 3720 N94-32753
Silicon-Based Optoelectronic Materials Symposium and Materials Research Society Proceedings, volume 298
[AD-A277518] p 3662 N94-32952
Low loss second-order nonlinear optical polymers based on all organic sol-gel materials
[AD-A277482] p 3663 N94-32985
Novel polydiacetylenes as materials for second and third order nonlinear optics
[AD-A277512] p 3664 N94-33082
Research in the optical sciences
[AD-A278271] p 3884 N94-33140
Development of materials for spectral hole burning applications
[AD-A278408] p 3909 N94-33324
OPTICAL MEASUREMENT
Fiber optic chemical sensors on Mars
[DE94-005251] p 3941 N94-31145
Noninvasive spectral analysis and beam mapping of focused ultrasound, part 2
[AD-A276629] p 3861 N94-32059
Methods for measuring characteristics of night vision goggles
[AD-A277046] p 3804 N94-32302
Photothermal laser deflection, an innovative technique to measure particles in exhausts
[AD-A277151] p 3718 N94-32366
Calibration and validation studies in the LENS facility
[AD-A278403] p 3591 N94-33167
OPTICAL MEASURING INSTRUMENTS
Space equipment for Earth observations
p 3613 N94-30997
Correlation filter synthesis using neural networks
[AD-A278124] p 3836 N94-33043
Design, development, and testing of a lightweight optical sensor cover system p 3604 N94-33302
OPTICAL MEMORY (DATA STORAGE)
Azo polymers for reversible optical storage. 4. Cooperative motion of rigid groups in semicrystalline polymers
[AD-A277107] p 3654 N94-31978
Reversible optical storage in azo polymers
[AD-A277109] p 3654 N94-31980
High frequency active auroral research program (HAARP) imager
[AD-A277469] p 3775 N94-32999
OPTICAL MICROSCOPES
The conoscopic microscope
[TELECOM-93-E-017] p 3877 N94-31173
Novel failure analysis techniques using photon probing with a scanning optical microscope
[DE94-006594] p 3692 N94-32112
OPTICAL PATHS
A technique for multiplexing 3x3-coupler terminated interferometric fiber-optic sensors
[AD-A276739] p 3880 N94-32180
Phase-only correction of scintillated laser beams: Downrange experimental results
[AD-A277778] p 3722 N94-33282
OPTICAL POLARIZATION
Multiple scattering of polarized radiation in planetary atmospheres
[ETN-94-96018] p 3674 N94-31551
OPTICAL PROPERTIES
Matter-radiation interactions in the atmosphere
p 3776 N94-30998
Space environment durability of beta cloth in LDEF thermal blankets p 3591 N94-31015
Treatment of cloud radiative effects in general circulation models
[DE94-001864] p 3764 N94-31600
Inorganic materials for anomalous-dispersion phase-matched second harmonic generation: Rubidium titanyl arsenate isomorphs, Rb(Ti(1-2x)Ln(x)Nb(x))OAsO4
[DE94-006141] p 3899 N94-31847
Sensitivity analysis of the AVHRR infrared cirrus model
[AD-A276690] p 3784 N94-32117
Compatibility studies of some azo polymer blends
[AD-A277141] p 3657 N94-32365
Nonlinear optical properties of rigid-rod polymers
[NASA-CR-191349] p 3882 N94-32702
Short-pulse, high-intensity lasers at Los Alamos
[DE94-007545] p 3720 N94-32760
Optical properties of lanthanide-doped RbTiOAsO4 and transition metal-doped KTiOPO4
[DE94-008433] p 3907 N94-32963
Optical properties of doped sol-gel silica glasses
[AD-A278094] p 3884 N94-33267
OPTICAL PUMPING
High conversion efficiency pumped-cavity second harmonic generation of a diode laser
[DE94-006805] p 3717 N94-32134
Repetitively pulsed Cr:LiSAF laser for lidar applcations
[DE94-007546] p 3720 N94-32761
A reliable low-maintenance flashlamp-pumped Ti:sapphire laser operating at 120 PPS
[DE94-009030] p 3721 N94-32848
OPTICAL RADAR
The development and testing of a backscatter absorption gas imaging (BAGI) system designed to image at a range of 300 m
[DE94-006192] p 3675 N94-31761
Wind-speed measurements with a scanning elastic-backscatter lidar
[DE94-004974] p 3785 N94-32726
High resolution properties of the marine atmospheric boundary layer
[DE94-006235] p 3774 N94-32736
Water vapor from sunradiometry in comparison with microwave and balloon-sonde measurements at the Southern Great Plains ARM Site
[DE94-007479] p 3786 N94-32759
Repetitively pulsed Cr:LiSAF laser for lidar applcations
[DE94-007546] p 3720 N94-32761
Comparison of coherent to incoherent detection at 2.09 micrometers using a solid state LADAR system
[AD-A277159] p 3721 N94-33102
OPTICAL REFLECTION
Estimation of visible and near-infrared reflectivity for Peyto Glacier Basin using satellite data
[ISBN-0-315-87039-7] p 3743 N94-31733
OPTICAL RESONANCE
Near resonant absorption by atoms in intense fluctuating laser fields
[DE94-005873] p 3714 N94-31200
OPTICAL RESONATORS
Automatic resonator alignment and power stabilization of high power C02 lasers
[ISBN-0-315-77217-4] p 3714 N94-31472
Multifrequency, rapidly sequenced or simultaneous tunable laser
[AD-D016169] p 3721 N94-32968
OPTICAL SCANNERS
Synchronized laser scanning three dimensional acquisition system
[ISBN-0-315-86848-1] p 3879 N94-31756
Novel failure analysis techniques using photon probing with a scanning optical microscope
[DE94-006594] p 3692 N94-32112
A scanning defect mapping system for semiconductor characterization p 3885 N94-32446
OPTICAL SWITCHING
Advanced optical fiber communication systems
[AD-A276416] p 3878 N94-31330
Reconfigurable optical switches with monolithic electrical-to-optical interfaces
[DE94-007745] p 3881 N94-32385
Mathematical nonlinear optics
[AD-A277320] p 3882 N94-32510
Fiber optic continuous true time-delay modulator
[AD-D016098] p 3883 N94-32720
Design of free space interconnected signal processor
[AD-A278129] p 3683 N94-33093
Research in the optical sciences
[AD-A278271] p 3884 N94-33140
Optically switched submillimeter-wave oscillator
[AD-A278014] p 3698 N94-33249
OPTICAL THICKNESS
Matter-radiation interactions in the atmosphere
p 3776 N94-30998
Time-dependent behavior of Mount Pinatubo aerosol
[DE94-001877] p 3764 N94-31601
Evaluation of sulfate aerosol optical depths over the North Atlantic and comparison with satellite observations
[DE94-005457] p 3746 N94-32100
Sensitivity analysis of the AVHRR infrared cirrus model
[AD-A276690] p 3784 N94-32117
Adjacent-cell Preconditioners for solving optically thick neutron transport problems
[DE94-007219] p 3872 N94-32666
The wavelength dependence of Martian atmospheric dust radiative properties p 3950 N94-33228
OPTICAL TRACKING
Digit-Eyes: Vision-based human hand tracking
[NASA-CR-195913] p 3803 N94-31447
Strategy for tracking and grabbing a moving object with the aid of a decouplable manipulator with six degrees of freedom general architecture, guided by a vision system
[ISBN-0-315-06864-3] p 3831 N94-31757
Optical processing of MMW for agile beamsteering and beamforming
[AD-A277161] p 3880 N94-32068

Correlation filter synthesis using neural networks
[AD-A278124] p 3836 N94-33043
A novel optoelectronic system for distortion-invariant ATR
[AD-A277985] p 3884 N94-33087

OPTICAL TRANSFER FUNCTION
The conoscopic microscope
[TELECOM-93-E-017] p 3877 N94-31173

OPTICAL WAVEGUIDES
III-V compound semiconductor strip-loaded waveguide devices for PICs: Design for minimum crosstalk and high density
[DE94-006588] p 3897 N94-31502
Optimization of Y junctions in integrated optics
[ISBN-0-315-86782-5] p 3879 N94-31751
Low loss second-order nonlinear optical polymers based on all organic sol-gel materials
[AD-A277482] p 3663 N94-32985
Advanced material processing for integrated-optic frequency doubling systems
[AD-A278394] p 3698 N94-33163

OPTIMAL CONTROL
Feasibility and stability results for constrained stable generalized predictive control
[MATHS-REPT-A-203] p 3828 N94-31158
Optimal reactive power dispatch of power systems using nonlinear programming
[MATHS-REPT-A-209] p 3808 N94-31164
Vibration control and design of composite cantilevers taking into account structural uncertainties and damage p 3733 N94-31213
Motion and force control of coordinated robots
[ISBN-0-315-86323-4] p 3724 N94-31714
Control of a random walk with noisy delayed information
[CWI-BS-R9316] p 3846 N94-32108
Undiscounted Markov decision chains with partial information; an algorithm for computing a locally optimal periodic policy
[TW-93-10] p 3851 N94-32205
Investigation of drive-reinforcement learning and application of learning to flight control
[AD-A277442] p 3801 N94-33053

OPTIMIZATION
On the use of genetic algorithms to solve the time-table problem
[REPT-90-060-REV] p 3829 N94-31176
The ant system: An autocatalytic optimizing process
[REPT-91-016-REV] p 3824 N94-31177
Techniques for increasing the robustness of iterative algorithms for multi-resources location problems
[REPT-93-037] p 3809 N94-31188
A worst-case analysis of an approximate algorithm for finding the minimum hamiltonian cycle on paths
[REPT-93-042] p 3809 N94-31192
Two models solving the increasing energy problem of the continuous Hopfield network model
[REPT-93-87] p 3843 N94-31552
Optimization of the forming parameters of PEEK/carbon fiber composite
[ISBN-0-315-86410-9] p 3620 N94-31716
Multidisciplinary optimization of high-speed civil transport configurations using variable-complexity modeling p 3578 N94-31881
Principal component analysis with missing data and its application to object modeling
[AD-A276644] p 3845 N94-31939
Minimization of computational requirements in the hybrid stress finite element method
[AD-A277120] p 3846 N94-32048
Experiences with EDO: An Evolutionary Database Optimizer
[TR-93-23] p 3918 N94-32105
Mesh optimization
[AD-A277644] p 3820 N94-32972
Local design optimization for composite transport fuselage crown panels p 3629 N94-33132
Numerical optimization techniques in neural network training p 3838 N94-33158
Mixed 0-1 programming by lift-and-project in a branch-and-cut framework
[AD-A278045] p 3822 N94-33183

OPTOELECTRONIC DEVICES
Growth and characterization of III-V semiconductors with rare earth impurities for optoelectronic devices
[AD-A276021] p 3896 N94-31455
High-performance GaAs/AlGaAs optical phase modulators for microwave/photonic integrated circuits
[DE94-006361] p 3688 N94-31483
III-V compound semiconductor strip-loaded waveguide devices for PICs: Design for minimum crosstalk and high density
[DE94-006588] p 3897 N94-31502
Epitaxial liftoff technology onto processed silicon foundry wafers
[AD-A277116] p 3900 N94-31985
Novel optoelectronic devices based on combining GaAs and InP on Si
[AD-A277018] p 3693 N94-32301
WOCSDICE 1993 --- 17th European Workshop on Compound Semiconductor Devices and Integrated Circuits
[AD-A276766] p 3693 N94-32307
Flexible manufacturing for photonics device assembly p 3669 N94-32449
Automated fiber pigtailing technology
[DE94-007072] p 3695 N94-32688
Sandia's photonic program and its changing national role
[DE94-008616] p 3883 N94-32878
Silicon-Based Optoelectronic Materials Symposium and Materials Research Society Proceedings, volume 298
[AD-A277518] p 3662 N94-32952
Large-diameter InGaAs/AlGaAs vertical-cavity surface-emitting lasers with low threshold current density fabricated using a simple chemical etch process
[AD-A277733] p 3721 N94-33003
A novel optoelectronic system for distortion-invariant ATR
[AD-A277985] p 3884 N94-33087
Advanced material processing for integrated-optic frequency doubling systems
[AD-A278394] p 3698 N94-33163

ORBIT CALCULATION
Air Force Space Command satellite orbit predictor using parallel virtual machines
[AD-A276316] p 3601 N94-31298
Multisatellite constellation configuration selection for multiregional highly elliptical orbit constellations p 3600 N94-31437
Possible improvements of satellite ephemeris programs used in geodesy
[PB94-148681] p 3743 N94-31592
Testing for preferred-frame effects in gravity with artificial Earth satellites
[PB94-148459] p 3610 N94-31771
Semianalytic Satellite Theory (SST): Mathematical algorithms
[AD-A276836] p 3610 N94-32208

ORBIT TRANSFER VEHICLES
Computational radiative heat transfer in homogeneous and nonhomogeneous nonscattering media p 3702 N94-31563
The 7.5K lbf thrust engine preliminary design for Orbit Transfer Vehicle
[NASA-CR-189175] p 3614 N94-31618
Attitude dynamics of spinning rockets in space with internal mass motion p 3601 N94-31802

ORBITAL MANEUVERS
The influence of the deorbit-burn manoeuvre on the footprint of a re-entry capsule
[LR-727] p 3609 N94-31705

ORBITAL MECHANICS
Testing for preferred-frame effects in gravity with artificial Earth satellites
[PB94-148459] p 3610 N94-31771

ORBITAL POSITION ESTIMATION
Air Force Space Command satellite orbit predictor using parallel virtual machines
[AD-A276316] p 3601 N94-31298
Possible improvements of satellite ephemeris programs used in geodesy
[PB94-148681] p 3743 N94-31592
Error analysis of real-time and post-processed orbit determination for the Geosat Follow-On altimetric satellite using GPS tracking p 3576 N94-31845
Thermospheric modeling accuracies using F10.7 and Ap
[AD-A277355] p 3773 N94-32337
Aerospace sponsored research
[ATR-93(8498)-1] p 3966 N94-32949

ORBITAL WORKERS
Use of a pitch adjustable foot restraint system: Operator strength capability and load requirements
[NASA-TP-3477] p 3805 N94-33050

ORBITS
Numerical detection and continuation of codimension-two homoclinic bifurcations
[CWI-AM-R9308] p 3847 N94-32191

ORDER-DISORDER TRANSFORMATIONS
Experimental and theoretical studies of hydrogenated amorphous semiconductor alloys and superlattices
[AD-A276159] p 3686 N94-31079
Reversible optical storage in azo polymers
[AD-A277109] p 3654 N94-31980
Calculations of nonspherically averaged charge densities for substitutionally disordered alloys
[DE94-008293] p 3646 N94-32754
X ray absorption study of pulsed laser deposited boron nitride films
[DE94-008295] p 3662 N94-32855
Interface controlled amorphization of crystalline Ni/Ti multilayers
[DE94-008685] p 3906 N94-32884
Phase behavior, structure, and properties of model block polymers
[AD-A277530] p 3662 N94-32954

ORDNANCE
Advanced release technologies program p 3607 N94-33322

ORGANIC ALUMINUM COMPOUNDS
Ignition delays, heats of combustion, and reaction rates of aluminum alkyl derivatives used as ignition and combustion enhancers for supersonic combustion
[NASA-CR-189581] p 3638 N94-32868

ORGANIC CHEMISTRY
The intramolecular cyclization of bis-2,5-dimethylene-2,5-dihydrofurans and bis-2,5-dimethylene-2,5-dihydrothiophenes: An approach to macrocycles
[DE94-007060] p 3657 N94-32377
Organic analyses of the Murchison meteorite p 3938 N94-32489

ORGANIC COMPOUNDS
Remote infrared vapor detection of volatile organic compounds
[AD-A276982] p 3746 N94-31999
The sol-gel-xerogel transition
[AD-A276647] p 3616 N94-32038

ORGANIC MATERIALS
Low-Earth orbit effects on organic composite materials flown on LDEF p 3595 N94-31036
A compatibility study of FEFO with various containment materials
[DE94-005753] p 3649 N94-31198
NMR studies of organic thin films
[AD-A276953] p 3656 N94-32221
Development and application of photosensitive device systems to studies of biological and organic materials
[DE94-008503] p 3793 N94-32516

ORGANIC PEROXIDES
Formation of gas-phase peroxides in a rural atmosphere: An interpretation of the recent SOS/SERON field results
[DE94-002995] p 3766 N94-32692

ORGANIC SUPERCONDUCTORS
Microreflectance infrared study of electron-molecular vibrational coupling and lattice softness in BEDT-TTF salts
[DE94-008490] p 3907 N94-32989

ORGANISMS
Light utilization and photoinhibition of photosynthesis in marine phytoplankton
[DE94-005505] p 3794 N94-32896
Bioluminescence bathyphotometer
[AD-D016102] p 3790 N94-32959

ORGANIZATIONS
Piezoelectric materials research in Europe
[AD-A276207] p 3648 N94-31059
A redundant disk array architecture for efficient small writes
[AD-A276645] p 3815 N94-31940
Untying the gordian data knot. A paper on Information Engineering (IE) and Corporate Information Management (CIM)
[AD-A276662] p 3918 N94-32210

ORGANOMETALLIC COMPOUNDS
Molecular/polymeric magnetism
[DE94-005888] p 3649 N94-31201
Silicone grease as a precursor to a pseudo crown-ether ligand: Crystal structure of (K(+)K(Me2SiO)7(+))(HIn(CH2CMe3)3(-))4)
[AD-A276343] p 3895 N94-31327
Tetraalkyldiarsines as potential precursors for electronic materials: Synthesis and characterization of various iso-propyl arsenic compounds
[AD-A277003] p 3900 N94-32001
Advances in MOVPE compound semiconductor epitaxy manufacturing technology: From high throughput large area reactors to cluster tools
[DE94-006367] p 3901 N94-32104
New zinc-bis(dialkylamides) potentially usable as site-selective dopants for p-type ZnSe
[AD-A276947] p 3902 N94-32218

ORION CONSTELLATION
Theory of protostellar accretion disks p 3931 N94-31136

ORION NEBULA
Circumstellar material around young stars in Orion p 3930 N94-31133

ORTHOGONAL FUNCTIONS
Estimating subpycnocline density fluctuations in the California current region from upper ocean observations
[AD-A277278] p 3789 N94-32325

ORTHOGONALITY
Subspace estimation without eigenvectors for adaptive beamforming
[AD-A276287] p 3671 N94-31254

Combinatory reduction systems: Introduction and survey
[CWI-CS-R9362] p 3849 N94-32349

ORTHONORMAL FUNCTIONS

On interpolating random fields using a finite number of observations
[CWI-BS-R9314] p 3847 N94-32194
On constructing multi-variate orthonormal polynomials associated with spectral distribution functions
[CWI-BS-R9310] p 3851 N94-32225

ORTHOTROPISM

Mechanics of cracking for composite material p 3624 N94-32501

OSCILLATING FLOW

Response of wall turbulence to high frequency streamwise and spanwise oscillations p 3700 N94-31211
Design and initial testing of a facility to measure unsteady pressures on an oscillating cascade with supersonic leading edge locus p 3569 N94-31880
Oscillating-flow loss test results in rectangular heat exchanger passages
[NASA-CR-185297] p 3615 N94-32792
Flutter analysis of a supersonic cascade in time domain using an ADI Euler solver
[NASA-TM-105625] p 3739 N94-32883

OSCILLATIONS

Observational constraints on black hole accretion disks p 3929 N94-31126
Oscillations in piston-driven shear flow of a non-Newtonian fluid
[AD-A276472] p 3701 N94-31245
Considering ties elasticities in high frequency rail dynamics
[ILR-MITT-281(1993)] p 3733 N94-31375
Torque characteristics of solid lubricated precision bearings during oscillatory motion
[AD-A276133] p 3728 N94-33061
The analysis of wake-induced unsteady aerodynamics related to higher harmonic control
[AD-A277914] p 3573 N94-33108

OSCILLOGRAPHS

A 10 GHz bandwidth, single transient, digitized oscilloscope with 20 GHz capability
[DE94-005400] p 3713 N94-32728

OSCILLOSCOPES

A 10 GHz bandwidth, single transient, digitized oscilloscope with 20 GHz capability
[DE94-005400] p 3713 N94-32728

OSTWALD RIPENING

Experimental studies on the effect of coherency strains on coarsening kinetics: Current status and future outlook
[DE94-008480] p 3647 N94-32964

OUTGASSING

Thermal-vacuum response of polymer matrix composites in space p 3595 N94-31033
Origin and thermal evolution of Mars p 3940 N94-31109
Operation of D3-D with all-graphite walls
[DE94-004858] p 3886 N94-31304

OVERPRESSURE

Investigation of sonic boom for the Space Shuttle: High cross-range orbiter
[NASA-TM-108238] p 3860 N94-31336
Investigation of sonic boom for the Space Shuttle: Low cross-range orbiter
[NASA-TM-108237] p 3860 N94-31337

OVERVOLTAGE

The zinc electrode: Reactions and mechanisms
[DE94-007977] p 3691 N94-31919

OXAZOLE

Characterization of thermally stable dye-doped polyimide based electrooptic materials
[DE94-005309] p 3882 N94-32674

OXIDASE

Electrical communication between glucose oxidase and electrodes based on poly(vinylimidazole) complex of Os(bpy)2Cl2
[AD-A276585] p 3635 N94-32231

OXIDATION

Space environmental effects on polymer composites: Research needs and opportunities p 3595 N94-31035
Fuel property effects on engine combustion processes
[DE94-005529] p 3631 N94-31153
Development of vanadium-phosphate catalysts for methanol production by selective oxidation of methane
[DE94-006759] p 3759 N94-31272
An extended approach to oxidations and nitridations of Si and Ge(x)Si(1-x) materials
[AD-A276056] p 3631 N94-31282
Effects of oxidation and creep damage mechanisms on creep behavior in HIPed silicon nitrides
[DE94-006559] p 3618 N94-31313
Si/SiO2 interface studies by immersion ellipsometry
[AD-A277277] p 3881 N94-32324
Carbon cycle modeling calculations for the IPCC
[DE94-004332] p 3765 N94-32354
Catalytic methods using molecular oxygen for treatment of PMMS and ECLSS waste streams, volume 2
[NASA-CR-190299] p 3804 N94-32697
Oxidation resistant copper
[AD-D016099] p 3696 N94-32721
Electron cyclotron resonance plasma oxidation studies of InP
[AD-A277431] p 3893 N94-33007
Nanoscale structural changes upon electrooxidation of Au(111) as probed by potentiodynamic scanning tunneling microscopy
[AD-A276780] p 3909 N94-33275

OXIDATION RESISTANCE

Enhancement of oxidation resistance of silicon carbide by high-dose and multi-energy aluminum implantation
[DE94-006560] p 3640 N94-31314
Improved oxidation resistance of 3-D carbon/carbon composites
[AD-A277349] p 3625 N94-32624
Oxidation resistant copper
[AD-D016099] p 3696 N94-32721

OXIDATION-REDUCTION REACTIONS

Hydrogen peroxide electrodes based on electrical connection of redox centers of various peroxidases to electrodes through a three-dimensional electron relaying polymer network
[AD-A276543] p 3691 N94-32056

OXIDE FILMS

Process parameter-growth environment-film property relationships for reactive sputter deposited metal (V, Nb, Zr, Y, Au) oxide, nitride, and oxynitride films
[AD-A276382] p 3640 N94-31258
Chemical vapor deposition of metal nitrides, phosphides, and arsenides
[DE94-008096] p 3654 N94-31976
Sol-gel coatings for high power laser optics: Past, present, and future
[DE94-007240] p 3718 N94-32252
Si/SiO2 interface studies by immersion ellipsometry
[AD-A277277] p 3881 N94-32324
Energetics, bonding mechanism, and electronic structure of ceramic/ceramic and metal/ceramic interfaces
[DE94-008551] p 3659 N94-32656
Microanalytical study of defect formation in thin bismuth strontium calcium copper oxide films
[DE94-008217] p 3661 N94-32751
Evaluation of the Hughes conversion coating touch-up pen
[AD-A278398] p 3664 N94-33166
Nanoscale structural changes upon electrooxidation of Au(111) as probed by potentiodynamic scanning tunneling microscopy
[AD-A276780] p 3909 N94-33275
Microstructures and epitaxy in oxide superconductor thin films and devices
[AD-A278427] p 3910 N94-33332

OXIDES

Process parameter-growth environment-film property relationships for reactive sputter deposited metal (V, Nb, Zr, Y, Au) oxide, nitride, and oxynitride films
[AD-A276382] p 3640 N94-31258
Ionizing radiation effects on silicon test structures
[DE94-006060] p 3865 N94-31607
Photopolymerization of cyclohexene oxide: A visible light initiating system and mechanistic investigations
[AD-A277110] p 3654 N94-31981
Heterogeneous catalytic process for alcohol fuels from syngas
[DE94-008729] p 3667 N94-32583

OXIDIZERS

Control experiments in liquid metal combustion
[AD-A276918] p 3635 N94-32234
Formation of gas-phase peroxides in a rural atmosphere: An interpretation of the recent SOS/SERON field results
[DE94-002995] p 3766 N94-32692

OXYGEN

Spectroscopic study of the molecular collisions (hydrogen-nitrogen and hydrogen-oxygen) at energies of several MeV
[ISBN-0-315-86794-9] p 3867 N94-31753
Technical evaluation of the UH-60Q: Medical oxygen system
[AD-A276983] p 3579 N94-32242
Rate coefficient for the reaction H + O2 yields OH + O: Results from 2000 to 5300 K
[DE94-008105] p 3871 N94-32615

OXYGEN ATOMS

Space Station WP-2 application of LDEF MLI results p 3592 N94-31016
Follow-up on the effects of the space environment on UHCRE thermal blankets p 3592 N94-31018
Model of spacecraft atomic oxygen and solar exposure microenvironments p 3593 N94-31021
Atomic oxygen erosion considerations for spacecraft materials selection p 3593 N94-31022
Performance of selected polymeric materials on LDEF p 3593 N94-31023
Atomic oxygen interaction at defect sights in protective coatings on polymers flown on LDEF p 3593 N94-31024
Fluorescence observations of LDEF exposed materials as an indicator of induced material reactions p 3593 N94-31025
On the linearity of fast atomic oxygen effects p 3594 N94-31027
Low-Earth orbit effects on organic composite materials flown on LDEF p 3595 N94-31036
Ground-based simulation of LEO environment: Investigations of a select LDEF material: FEP Teflon (trademark) p 3596 N94-31039
An overview of the Evaluation of Oxygen Interaction with Materials-third phase (EOIM-3) experiment: Space Shuttle Mission 46 p 3596 N94-31040
Analysis of leading edge and trailing edge cover glass samples before and after treatment with advanced satellite contamination removal techniques p 3596 N94-31041
Spacecraft materials: Comparison between flight results obtained on LDEF and MIR p 3597 N94-31045
Atomic oxygen damage characterization by photothermal scanning p 3598 N94-31051
Production and detection of metastable atomic oxygen
[ISBN-0-315-87364-7] p 3868 N94-31915
Enhanced thermal capacity aerogels summary report, FY 1993
[DE94-008888] p 3639 N94-33260

OXYGEN IONS

Follow-up on the effects of the space environment on UHCRE thermal blankets p 3592 N94-31018
Frictional behavior and adhesion of Ag and Au films applied to aluminum oxide by oxygen-ion assisted Screen Cage Ion Plating (SCIP)
[NASA-TM-106522] p 3647 N94-32931

OXYGEN SUPPLY EQUIPMENT

Technical evaluation of the UH-60Q: Medical oxygen system
[AD-A276983] p 3579 N94-32242

OXYNITRIDES

Process parameter-growth environment-film property relationships for reactive sputter deposited metal (V, Nb, Zr, Y, Au) oxide, nitride, and oxynitride films
[AD-A276382] p 3640 N94-31258
Joining of silicon nitrides using oxynitride glasses
[DE94-008517] p 3658 N94-32517

OZONE

One: Microphysics of frost metamorphism: Applications to Triton and Mars. Two: A global analysis of the ozone deficit in the upper stratosphere and lower mesosphere. Three: The diabatic circulation in the stratosphere as diagnosed from Microwave Limb Sounder data p 3942 N94-31975
Formation of gas-phase peroxides in a rural atmosphere: An interpretation of the recent SOS/SERON field results
[DE94-002995] p 3766 N94-32692
Mexico City ozone concentrations as a function of readily-available meteorological parameters
[DE94-007576] p 3768 N94-32814
Quantified estimates of total GWPs for greenhouse gases taking into account tropospheric chemistry
[DE94-007846] p 3768 N94-32817
A correlated k-distribution model of the heating rates for atmospheric mixtures of H2O, CO2, O3, CH4, and N2O in the 0-2500 cm(exp -1) wave number region at altitudes between 0 and 60 km
[DE94-005136] p 3775 N94-32895
How well was total ozone abundance inferred with Mariner 9 p 3947 N94-33212

OZONE DEPLETION

The ozone and the physico-chemical processes in tropical regions p 3770 N94-31010
Odin aeronomy science: A phase-A report by the Aeronomy Science Working Group for the Odin satellite
[AP-31] p 3770 N94-31222
Ionization probes of molecular structure and chemistry
[DE94-007605] p 3872 N94-32643
Possible effect of the chlorine oxide dimer on transient ozone loss in rocket plumes
[AD-A278135] p 3616 N94-33094

P

P-I-N JUNCTIONS

Hydrogenated amorphous silicon (a-Si:H) based gamma camera: Monte Carlo simulations
[DE94-007042] p 3795 N94-31323

PACIFIC OCEAN
Investigation of carbon dioxide in the central South Pacific Ocean (WOCE Sections P-16C and P-17C) during the TUNES/2 expedition of the R/V Thomas Washington, July-August, 1991
[DE94-006638] p 3763 N94-31347
The effect of westerly wind bursts on a tropical ocean general circulation model
[AD-A276423] p 3788 N94-31448
Air-sea interaction patterns in the equatorial Pacific
[AD-A277305] p 3788 N94-32072
Typhoon havens handbook for the western Pacific and Indian Oceans, change 3
[AD-A277030] p 3784 N94-32260
ENSO forced variations of the sea surface temperature and adjusted sea level along the west coast of the United States
[AD-A277306] p 3789 N94-32327
Fine and microstructure observations at Fieberlin g Guyot R/V new horizon cruise report
[AD-A277917] p 3791 N94-33109
SEASOAR and CTD observations during a COARE surveys cruise, W9211C, 22 January - 22 February, 1993
[AD-A277925] p 3791 N94-33244
PACKET SWITCHING
Communications networks in stressed environments
[AD-A275967] p 3672 N94-31384
Discrete-event-dynamic-system-based approaches for scheduling transmissions in multihop packet radio networks
[AD-A276566] p 3679 N94-32230
Principles of ultradependability in chaotic routing
[AD-A277422] p 3827 N94-32995
Multicast communication with guaranteed quality of service
[AD-A277650] p 3682 N94-33025
PACKET TRANSMISSION
Discrete-event-dynamic-system-based approaches for scheduling transmissions in multihop packet radio networks
[AD-A276566] p 3679 N94-32230
PACKETS (COMMUNICATION)
Gigabits to the Desktop: Installing tomorrow's networks today
[DE94-007701] p 3827 N94-32646
Principles of ultradependability in chaotic routing
[AD-A277422] p 3827 N94-32995
PAINTS
Evaluation of corrosion protective organic coatings for steel structures in fresh water
[PB94-138484] p 3649 N94-31072
Oxide pigments in water: The colloid-chemical point of view
[PB94-148616] p 3633 N94-31591
Conductive paints
[DE94-008508] p 3661 N94-32788
Method and apparatus for inhibiting the disbonding of a paint from metal surfaces
[AD-D016106] p 3663 N94-32960
PAIR PRODUCTION
Time-dependent behavior of active galactic nuclei with pair production p 3929 N94-31125
A constraint on the pair-density ratio (Z+) in an electron-positron pair wind p 3930 N94-31132
Perturbative and nonperturbative EM lepton pair production in relativistic heavy-ion collisions
[DE94-006315] p 3867 N94-31779
Probing lepton number violation via Majorana neutrinos at hadron supercolliders
[PB94-147055] p 3868 N94-31922
PALEOCLIMATOLOGY
The Earth's climate: Past, present, and future p 3777 N94-30982
Biospheric effects of a large extraterrestrial impact: Case study of the Cretaceous/Tertiary boundary crater
[NASA-CR-195827] p 3942 N94-32740
Carbonate formation on Mars: Latest experiments p 3950 N94-33231
PALLADIUM
Chemisorbed-molecule potential-energy surfaces and electronically-stimulated processes
[DE94-007932] p 3719 N94-32603
PANELS
AGARD membership, 1994
[AGARD-MEMB-94] p 3914 N94-31197
Damage tolerance aspects of a full composite airplane fuselage: Requirements, modelling, predictions, experiments
[LR-728] p 3578 N94-31674
From display and PWB to MCMs: Large panel manufacturing
[DE94-007855] p 3693 N94-32386
Local design optimization for composite transport fuselage crown panels p 3629 N94-33132
Composite fuselage crown panel manufacturing technology p 3629 N94-33133
PARABOLIC DIFFERENTIAL EQUATIONS
Texture generation on irregular regions
[AD-A275999] p 3841 N94-31359
THERM3D: A boundary element computer program for transient heat conduction problems
[DE94-008112] p 3708 N94-32709
A comparison of rough surface parabolic equation models
[AD-A278090] p 3791 N94-33185
PARABOLIC REFLECTORS
Predicting antenna parameters from antenna physical dimensions
[AD-A276442] p 3672 N94-31300
Radar rainfall measurements from space p 3782 N94-31889
PARACHUTES
A novel CFD/structural analysis of a cross parachute
[DE94-005271] p 3568 N94-31578
PARALLEL COMPUTERS
Implanting algorithms on parallel machines
[TELECOM-93-D-017] p 3823 N94-31099
Analysis of the effect of routing strategies for parallel implementations of a selected avionics application
[AD-A276069] p 3581 N94-31458
Computational chemistry on parallel computers
[DE94-008106] p 3636 N94-32616
Toroidal computer memory for serial and parallel processors
[AD-D016144] p 3807 N94-32978
Principles of ultradependability in chaotic routing
[AD-A277422] p 3827 N94-32995
Investigation of modularly configured attached processors with intelligent memories
[AD-A278418] p 3839 N94-33330
PARALLEL FLOW
On wave interactions of rotational and irrotational flows p 3700 N94-31219
PARALLEL PROCESSING (COMPUTERS)
Implanting algorithms on parallel machines
[TELECOM-93-D-017] p 3823 N94-31099
A heterogeneous computing environment for simulating astrophysical fluid flows p 3928 N94-31119
A probabilistic view of Datalog parallelization
[TELECOM-93-D-021] p 3824 N94-31183
Design and analysis of scalable parallel algorithms
[AD-A276255] p 3809 N94-31251
List ranking and list scan on the CRAY C-90
[AD-A276411] p 3824 N94-31259
Proof of concept for the rewrite rule machine: Interensemble studies
[AD-A276506] p 3809 N94-31263
Air Force Space Command satellite orbit predictor using parallel virtual machines
[AD-A276316] p 3601 N94-31298
A parallel implementation of the column subtraction algorithm
[AD-A275922] p 3810 N94-31343
Using Monte Carlo techniques and parallel processing for debris hazard analysis of rocket systems
[DE94-007250] p 3609 N94-31382
Parallel structured optimization algorithms for inverse problems
[AD-A276053] p 3811 N94-31443
Analysis of the effect of routing strategies for parallel implementations of a selected avionics application
[AD-A276069] p 3581 N94-31458
Some calculations on supersymmetric graphs as communication networks
[REPT-93-72] p 3824 N94-31641
A comparison of distributed memory and virtual shared memory parallel programming models
[DE94-005473] p 3825 N94-31663
Generalized steady-state method for solving 2-D diffusion systems
[REPT-93-83] p 3825 N94-31700
Methods of implementing the Viterbi algorithm on a massively parallel computer of the SIMD (single instruction multiple data) type
[ISBN-0-315-86783-3] p 3814 N94-31752
Algorithms and parallel architectures for laser acoustic imaging
[ISBN-0-315-86466-4] p 3716 N94-31797
Large-scale shape optimization: Numerical methods, parallel algorithms, and applications to aerodynamic design p 3815 N94-31966
The named-state register file
[AD-A276796] p 3825 N94-32165
MULTIGRAPH: An architecture for model-based programming. Model-based program synthesis for parallel computing. PREMOS: Programming environment for model-based program synthesis, version 01.00.00
[AD-A276949] p 3817 N94-32219
Parallel and distributed computing combinatorial algorithms
[AD-A277333] p 3826 N94-32243
Parallel processing for differencing and histogramming
[AD-A277060] p 3826 N94-32274
An epistemic proof system for parallel processes
[TR-93-17] p 3826 N94-32291
Parallel Monte Carlo reactor neutronics
[DE94-007642] p 3826 N94-32357
Parallel particle simulations of low-density fluid flows
[DE94-007858] p 3707 N94-32373
Studies of an optical multi-processor interconnect
[AD-A277093] p 3881 N94-32392
A high-speed linear algebra library with automatic parallelism p 3828 N94-32440
Construction of a parallel processor for simulating manipulators and other mechanical systems
[NASA-CR-191327] p 3826 N94-32482
Computational chemistry on parallel computers
[DE94-008106] p 3636 N94-32616
Development of a low-latency scalar communication routine on message-passing architectures
[DE94-007061] p 3827 N94-32683
Overview of shock physics codes for armor analysis
[DE94-008948] p 3739 N94-32842
Toroidal computer memory for serial and parallel processors
[AD-D016144] p 3807 N94-32978
Principles of ultradependability in chaotic routing
[AD-A277422] p 3827 N94-32995
Investigation of modularly configured attached processors with intelligent memories
[AD-A278418] p 3839 N94-33330
PARALLEL PROGRAMMING
Implanting algorithms on parallel machines
[TELECOM-93-D-017] p 3823 N94-31099
The ant system: An autocatalytic optimizing process
[REPT-91-016-REV] p 3824 N94-31177
A probabilistic view of Datalog parallelization
[TELECOM-93-D-021] p 3824 N94-31183
A comparison of distributed memory and virtual shared memory parallel programming models
[DE94-005473] p 3825 N94-31663
The named-state register file
[AD-A276796] p 3825 N94-32165
Transformational derivation of (parallel) programs using skeletons
[TR-93-20] p 3825 N94-32196
Methods for parallelizing search paths in phrasing
[AD-A276876] p 3817 N94-32212
Computational chemistry on parallel computers
[DE94-008106] p 3636 N94-32616
A software architecture for multidisciplinary applications: Integrating task and data parallelism
[NASA-CR-194896] p 3820 N94-32928
Finding all periods and initial palindromes of a string in parallel
[AD-B175069] p 3827 N94-33002
PARAMAGNETISM
Molecular/polymeric magnetism
[DE94-005888] p 3649 N94-31201
PARAMETER IDENTIFICATION
A new methodology of system parameter estimation
[MATHS-REPT-A-208] p 3808 N94-31163
Identification of polynomial and rational NARMAX models
[RR-483] p 3842 N94-31413
A contribution to the repreaentation and identification of semi-flexible robots
[ISBN-0-315-86450-8] p 3724 N94-31721
Model identification of a reconfigurable robot manipulator
[ISBN-0-315-87109-1] p 3725 N94-31874
On-line physical parameter identification and adaptive control of a launch vehicle p 3602 N94-31891
Approximation theory and computational methods for the identification and control of distributed parameter systems
[AD-A277335] p 3848 N94-32244
PARAMETERIZATION
Use of Air Force cloud cover data to evaluate and improve cloud forecasts and parameterizations in mesocale meteorological models
[AD-A277384] p 3784 N94-32054
The influence of cumulus parameterization on model forecasts of rapid oceanic cyclogenesis
[AD-A277207] p 3784 N94-32094
A parameterization of cloud droplet nucleation
[DE94-007469] p 3785 N94-32268
PARAMETRIC AMPLIFIERS
A noncritically phase matched femtosecond optical parametric oscillator near 3 microns
[DE94-008050] p 3720 N94-32704
PARSING ALGORITHMS
Methods for parallelizing search paths in phrasing
[AD-A276876] p 3817 N94-32212
Informal introduction to the extended affix grammar formalism and its compiler
[TR-93-19] p 3817 N94-32287

PARTIAL DIFFERENTIAL EQUATIONS
Large-scale shape optimization: Numerical methods, parallel algorithms, and applications to aerodynamic design p 3815 N94-31966
Control and stabilization of distributed parameter systems; theoretical and computational aspects [AD-A277239] p 3738 N94-32275
Coherent processes in atom in strong radiation fields [AD-A278388] p 3874 N94-33144
PARTIAL PRESSURE
Simultaneous laboratory measurements of CO2 and H2O adsorption on palagonite: Implications for the Martian climate and volatile reservoir p 3952 N94-33240
PARTICLE ACCELERATION
Collective acceleration in solar flares [DE94-006268] p 3953 N94-31632
PARTICLE ACCELERATOR TARGETS
Transverse energy production with Si and Au beams at AGS energy: Towards hot and dense hadronic matter [DE94-007178] p 3938 N94-32638
Spin-structure function of the neutron He-3: SLAC results [DE94-008927] p 3875 N94-33189
PARTICLE ACCELERATORS
AMS beyond 2000 [DE94-006666] p 3632 N94-31352
The D0 upgrade [DE94-006953] p 3867 N94-31671
Probing lepton number violation via Majorana neutrinos at hadron supercolliders [PB94-147055] p 3868 N94-31922
Jet physics and QCD tests at the Tevatron collider [DE94-008987] p 3871 N94-32587
The future of high-energy physics in the US: Statement for the 1994 HEPAP Subpanel [DE94-008994] p 3876 N94-32588
A search for rapidity gaps in jet events and a study of color coherence in multijet events at D0 [DE94-006849] p 3872 N94-32627
Minimax: Multiparticle physics at the Tevatron collider [DE94-007095] p 3873 N94-32689
PARTICLE BEAMS
BNL possibilities [DE94-007179] p 3864 N94-31398
PARTICLE COLLISIONS
The measurement of the hadronic energy flow and jet production with the ZEUS calorimeter in deep inelastic scattering events at HERA [ETN-94-96021] p 3865 N94-31534
Perturbative and nonperturbative EM lepton pair production in relativistic heavy-ion collisions [DE94-006315] p 3867 N94-31779
Collisional and chaotic transport of energetic particles in toroidal plasma [DE94-006504] p 3889 N94-31787
Monoenergetic neutral particle transport in semi-infinite media [AD-A277155] p 3870 N94-32368
Jet physics and QCD tests at the Tevatron collider [DE94-008987] p 3871 N94-32587
Transverse energy production with Si and Au beams at AGS energy: Towards hot and dense hadronic matter [DE94-007178] p 3938 N94-32638
Electron: Cluster interactions [DE94-009089] p 3874 N94-32807
PARTICLE DECAY
B lifetimes at CDF [DE94-006850] p 3866 N94-31669
Medium energy measurements of N-N parameters [DE94-006067] p 3869 N94-32173
Semileptonic decays of mesons in the SO(4) model [DE94-008108] p 3873 N94-32708
PARTICLE DIFFUSION
Notes on the Langevin model for turbulent diffusion of marked particles [DE94-007847] p 3708 N94-32652
Particle diffusion from the beam-beam interaction in synchrotron colliders [DE94-007111] p 3876 N94-32685
PARTICLE EMISSION
Counting particles emitted by stratospheric aircraft and measuring size of particles emitted by stratospheric aircraft [NASA-CR-195908] p 3769 N94-33170
PARTICLE ENERGY
Influence of long-range correlations on the spectral functions and response of 48Ca and 90Zr [ETN-94-96017] p 3865 N94-31537
PARTICLE FLUX DENSITY
Surface fluxes of trace gases derived from convective-layer profiles p 3704 N94-31774
PARTICLE IMAGE VELOCIMETRY
Stabilized alumina/ethanol colloidal dispersion for seeding high temperature air flows [NASA-TM-106591] p 3713 N94-32983
PARTICLE IN CELL TECHNIQUE
Pulsed expansion of plasma in a magnetic thruster p 3889 N94-31776
PARTICLE INTERACTIONS
Analysis of the high energy behavior of the forward scattering parameters - sigma(tot), rho and B [DE94-006537] p 3864 N94-31310
The measurement of the hadronic energy flow and jet production with the ZEUS calorimeter in deep inelastic scattering events at HERA [ETN-94-96021] p 3865 N94-31534
PARTICLE MASS
Attitude dynamics of spinning rockets in space with internal mass motion p 3601 N94-31802
PARTICLE MOTION
X ray pulse considerations and electron flow in high voltage diodes [AD-A277301] p 3868 N94-32044
PARTICLE PRODUCTION
State of hadron collider physics [DE94-005279] p 3863 N94-31147
Elimination of two atomic electrons by a single high energy photon [DE94-006834] p 3864 N94-31320
Study of B(0) - bar-B(0) mixing in D0 [DE94-006000] p 3897 N94-31506
Elementary particle physics [DE94-006071] p 3866 N94-31620
Study of associated gauge boson production at D0: W gamma production [DE94-006951] p 3866 N94-31670
Perturbative and nonperturbative EM lepton pair production in relativistic heavy-ion collisions [DE94-006315] p 3867 N94-31779
Baryogenesis from a primordial lepton asymmetry [PB94-145166] p 3868 N94-31921
Medium energy measurements of N-N parameters [DE94-006067] p 3869 N94-32173
Antiproton production in heavy ion collisions [DE94-007552] p 3870 N94-32271
Jet physics and QCD tests at the Tevatron collider [DE94-008987] p 3871 N94-32587
A search for rapidity gaps in jet events and a study of color coherence in multijet events at D0 [DE94-006849] p 3872 N94-32627
Proceedings of the Workshop on B Physics at Hadron Accelerators [DE94-007961] p 3877 N94-32748
Studies of jet production with the D0 detector [DE94-008271] p 3873 N94-32780
Hyperon polarization, crystal channeling, and E781 at Fermilab [DE94-008224] p 3877 N94-32802
PARTICLE SIZE DISTRIBUTION
Combustor and nozzle effects on particulate behavior in solid rocket motors [AD-A277304] p 3614 N94-32071
Drop size distributions and related properties of fog for five locations measured from aircraft [NASA-CR-4585] p 3787 N94-33065
Counting particles emitted by stratospheric aircraft and measuring size of particles emitted by stratospheric aircraft [NASA-CR-195908] p 3769 N94-33170
The wavelength dependence of Martian atmospheric dust radiative properties p 3950 N94-33228
PARTICLE SPIN
RHIC spin physics [DE94-005452] p 3876 N94-32099
PARTICLE THEORY
Semileptonic decays of mesons in the SO(4) model [DE94-008108] p 3873 N94-32708
PARTICLE TRACKS
Proceedings of the Workshop on B Physics at Hadron Accelerators [DE94-007961] p 3877 N94-32748
PARTICLE TRAJECTORIES
Monoenergetic neutral particle transport in semi-infinite media [AD-A277155] p 3870 N94-32368
PARTICLES
Single scattering of light by ensembles of particles with various shapes [ETN-94-96016] p 3878 N94-31550
PARTICULATE REINFORCED COMPOSITES
Processing of novel nanoparticle dispersion strengthened ceramics for improved mechanical performance [AD-A275965] p 3649 N94-31276
PARTICULATE SAMPLING
Remote robot manipulator coupled with remote-controlled guide vehicle for soil sampling in hazardous waste sites p 3723 N94-31569
Counting particles emitted by stratospheric aircraft and measuring size of particles emitted by stratospheric aircraft [NASA-CR-195908] p 3769 N94-33170
PARTICULATES
Electrostatic reduction of particulates for laser resistant hafnia coatings [DE94-005824] p 3651 N94-31557
Micromechanics and effective properties of particulate composites and fluid suspensions p 3703 N94-31744
Combustor and nozzle effects on particulate behavior in solid rocket motors [AD-A277304] p 3614 N94-32071
Photothermal laser deflection, an innovative technique to measure particles in exhausts [AD-A277151] p 3718 N94-32366
PARTITIONS (MATHEMATICS)
SU(2) WZNW model at higher genera from gauge field functional integral [PB94-148467] p 3857 N94-31589
PARTONS
String-parton model description of relativistic heavy-ion collisions [DE94-009164] p 3874 N94-32850
PASSENGER AIRCRAFT
Fracture and fatigue strength evaluation of multiple site damaged aircraft fuselages - curved panel testing and analysis [AD-A277100] p 3579 N94-32015
A comparison of military and commercial aircraft development [AD-A276830] p 3575 N94-32168
PASSIVITY
Passivation of III-V compound semiconductor based devices [AD-A276178] p 3894 N94-31056
Modification of semiconductor surface properties with chemically bound molecular films [AD-A276162] p 3895 N94-31081
Determination of BPSG thin-film properties using IR reflection spectroscopy of product wafers [DE94-006591] p 3634 N94-32110
PATHOLOGY
High peak power microwaves: A health hazard [AD-A277168] p 3681 N94-32576
PATTERN RECOGNITION
Tracking roads in an aerial image by Kalman filtering [TELECOM-93-D-007] p 3711 N94-31096
Automatic extraction of cartographic objects by fusion of data extracted from satellite images [TELECOM-93-E-001] p 3742 N94-31165
Filtering and recognition of moving boats in radar images [REPT-93-039] p 3671 N94-31190
Feature discovery in gray level imagery for one-class object recognition [DE94-005268] p 3671 N94-31267
Smart environmental monitor based on neural networks and multi-spectral pattern recognition [AD-A276445] p 3829 N94-31301
Digit-Eyes: Vision-based human hand tracking [NASA-CR-195913] p 3803 N94-31447
Polyhedric object recognition by indexing in a model base [ETN-94-95913] p 3812 N94-31542
CAD-based off-line planning for an active-vision system [ISBN-0-315-86317-X] p 3813 N94-31713
Morphological directional coding of images [ISBN-0-315-86336-6] p 3814 N94-31715
Neural networks for model-based recognition [AD-A277375] p 3834 N94-32053
High performance hardware and software for pattern recognition and image processing [AD-A276405] p 3816 N94-32130
Development of phase-only filters for sensor imagery [AD-A276722] p 3880 N94-32151
Algebraic functions for recognition [AD-A276803] p 3846 N94-32167
A differential theory of learning for efficient statistical pattern recognition [AD-A277313] p 3800 N94-32277
Wavelet transform of fixed pattern noise in focal plane arrays [AD-A276963] p 3712 N94-32393
SAR image feature extraction system: A pre-operational application of ERS-1 SAR p 3751 N94-32543
Mechanisms of temporal pattern discrimination by human observers [AD-A277407] p 3801 N94-32577
Correlation filter synthesis using neural networks [AD-A278124] p 3836 N94-33043
A novel optoelectronic system for distortion-invariant ATR [AD-A277985] p 3884 N94-33087

CRAD Signal and Information Processing Working Group Workshop on Neural networks, volume 1
[DREA-TC-93-305-VOL-1] p 3836 N94-33149
Neural networks applied to the phonemic segmentation of speech p 3686 N94-33152
Automatic modulation recognition p 3686 N94-33153
Nearest-neighbour search in constant time: An alternative to neural networks for pattern matching applications p 3838 N94-33157

PATTERN REGISTRATION
Fast nonsupervised 3D registration of PET and MR images of the brain
[TELECOM-93-C-006] p 3798 N94-33069

PAVEMENTS
Determining the bearing capacity of flexible airfield pavements using a heavy weight deflectometer
[ISBN-0-315-86210-6] p 3587 N94-31710

PAYLOAD INTEGRATION
Payload holddown and release mechanism p 3607 N94-33321

PAYLOAD INTEGRATION PLAN
Development concept for Dutch user support
[PB94-125523] p 3598 N94-31208

PAYLOADS
Theoretical basis for state vector comparison, relative position display, and relative position/rendezvous prediction
[AD-A277216] p 3608 N94-32020
DOD space based requirements: Increasing DOD access to space
[AD-A276874] p 3601 N94-32211
Pip pin reliability and design p 3605 N94-33305
Payload holddown and release mechanism p 3607 N94-33321

PEBBLE BED REACTORS
Summary of particle bed reactor designs for the Space Nuclear Thermal Propulsion Program
[DE94-007434] p 3615 N94-32266

PEEK
Optimization of the forming parameters of PEEK/carbon fiber composite
[ISBN-0-315-86410-9] p 3620 N94-31716
Low velocity impact damage in carbon fiber/PEEK composite laminates
[ISBN-0-315-86546-6] p 3622 N94-31909

PENDULUMS
Modeling and control of nonlinear systems
[AD-A277377] p 3834 N94-32095

PENETRATION
Tearing resistance of a thin shell against projectile penetration: Material property effects
[DE94-007466] p 3733 N94-31316
Low dispersion of the muon precession frequency in HTSC samples YBa2Cu3O(x) and EuBa2Cu3O(x)
[DE94-608388] p 3896 N94-31395

PERCEPTUAL TIME CONSTANT
The effects of Above Real-Time Training (ARTT) in an F-16 simulator p 3591 N94-32474

PERCHLORATES
Infrared spectroelectrochemical study of cyanide adsorption and reactions at platinum electrodes in aqueous perchlorate electrolyte
[AD-A276402] p 3631 N94-31238

PERCHLORIC ACID
Charge-dependent atomic-scale structures of high-index and (110) gold electrode surfaces as revealed by scanning tunneling microscopy
[AD-A276782] p 3869 N94-32170

PERFLUORO COMPOUNDS
Perfluoropolyalkylether decomposition on catalytic aluminas
[NASA-TM-106547] p 3617 N94-33021
Development and preliminary evaluation of aryl ester boundary additives for perfluoropolyethers
[NASA-TM-106603] p 3663 N94-33024

PERFORMANCE PREDICTION
Performance predictions for composite materials
[AD-A276451] p 3618 N94-31261
Predicting antenna parameters from antenna physical dimensions
[AD-A276442] p 3672 N94-31300
An analysis of the maintenance performance measurement system for LAMPS MK 3 helicopter squadrons
[AD-A276421] p 3565 N94-31332
Communications networks in stressed environments
[AD-A275967] p 3672 N94-31384
Compiler techniques for managing data motion
[AD-A276514] p 3918 N94-31930
Civil tiltrotor market penetration: Effects on Northeast corridor airport delay
[AD-A277534] p 3576 N94-32955

PERFORMANCE TESTS
Testing Operational Flight Programs (OFP's)
[AD-A276361] p 3578 N94-31387
Technical evaluation of the UH-60Q: Medical oxygen system
[AD-A276983] p 3579 N94-32242
Performance of the Sony lithium-ion rechargeable battery
[AD-A277076] p 3693 N94-32303
A low-cost, CCD solid state star tracker
[NASA-CR-192722] p 3882 N94-32417
Aircrew Eye/Respiratory Protection (AERP): 16-hour extended wear evaluation of chemical protective equipment
[AD-A277288] p 3804 N94-32609
The relative performance of FeS2 and CoS in long-life thermal-battery applications
[DE94-006145] p 3695 N94-32663
Design and evaluation of coils for a 50 mm diameter induction coilgun launcher
[DE94-005244] p 3603 N94-32671
Temperature-humidity-bias aging technique to identify defective surface mount capacitors
[DE94-005354] p 3660 N94-32727
A 10 GHz bandwidth, single transient, digitized oscilloscope with 20 GHz capability
[DE94-005400] p 3713 N94-32728
Polymer electrolyte fuel cells
[DE94-007558] p 3761 N94-32762
EDD-7 Electric Charge Point Meter test results
[DE94-008515] p 3696 N94-32828
Enhancement of mixing in a rectangular jet by mechanical tabs
[NASA-CR-185207] p 3709 N94-32872
Operational experience and evaluation of a dual-element stretched-membrane heliostat
[DE94-008827] p 3763 N94-32965
Two-axis antenna positioning mechanism p 3605 N94-33308

PERIODIC FUNCTIONS
Representation, prediction and identification of cyclostationary processes: A state-space approach
[REPT-93-041] p 3850 N94-31191
Remarks on a result of LAV Carvalho
[AD-A276404] p 3841 N94-31360

PERIODIC VARIATIONS
Oscillations in piston-driven shear flow of a non-Newtonian fluid
[AD-A276472] p 3701 N94-31245
ENSO forced variations of the sea surface temperature and adjusted sea level along the west coast of the United States
[AD-A277306] p 3789 N94-32327
Dependence of x ray absorption magnetic circular dichroism on layer periodicity in iron-platinum multilayers
[DE94-008786] p 3647 N94-32892

PERIPHERAL EQUIPMENT (COMPUTERS)
Pen-based computers: Computers without keys p 3808 N94-32434
THE VERTICAL p 3806 N94-32435

PERMAFROST
Thermal and hydraulic considerations regarding the fate of water discharged by the outflow channels to the Martian northern plains p 3946 N94-33202
Temporal changes in the geographic distribution, elevation, and potential origin of the Martian outflow channels p 3951 N94-33235

PERMANENT MAGNETS
Selected applications of planar permanent magnet multipoles in FEL insertion device design
[DE94-009014] p 3721 N94-32845

PERMEABILITY
New polymer target-shell properties and characterizations
[DE94-008420] p 3890 N94-32415

PERMEATING
Prediction of hydrogen entry and permeation in metals and alloys
[AD-A276637] p 3642 N94-31995

PERMITTIVITY
Microwave dielectric behavior of soils. Report 1: Summary of related research and applications
[AD-A275980] p 3771 N94-31351
Microwave dielectric behavior of soils. Report 2: A unique coaxial measurement apparatus
[AD-A275982] p 3771 N94-31353
A study of areas of low radio-thermal emissivity on Venus p 3942 N94-31992
A reassessment of the in-situ dielectric constant of polar firn
[AD-A276999] p 3773 N94-32154
Electromagnetic probe technique for fluid flow measurements p 3711 N94-32455
Inorganic polymer engineering materials
[DE94-008519] p 3659 N94-32655
Dielectric properties of Mars' surface: Proposed measurement on a Mars lander p 3951 N94-33237

PEROVSKITES
Energetics, bonding mechanism, and electronic structure of ceramic/ceramic and metal/ceramic interfaces
[DE94-008551] p 3659 N94-32656

PEROXIDES
Hydrogen peroxide electrodes based on electrical connection of redox centers of various peroxidases to electrodes through a three-dimensional electron relaying polymer network
[AD-A276543] p 3691 N94-32056

PERSONAL COMPUTERS
A PC program to optimize system configuration for desired reliability at minimum cost p 3823 N94-32438
Multimedia as a desktop and classroom tool
[DE94-009118] p 3807 N94-32766

PERSONNEL DEVELOPMENT
European business confronted with the 21st century: Men, the essential risk
[ESA-SP-1167] p 3914 N94-31181
Aircraft communication and navigation systems and communication and navigation systems
[AD-A277309] p 3582 N94-32328

PERSONNEL MANAGEMENT
European business confronted with the 21st century: Men, the essential risk
[ESA-SP-1167] p 3914 N94-31181
Drug-related problems in the workplace
[CRANFIELD-AERO-9306] p 3914 N94-31538

PERTURBATION
Vibration control and design of composite cantilevers taking into account structural uncertainties and damage p 3733 N94-31213
Gravitational effects of cosmic strings
[ISBN-0-315-75484-2] p 3934 N94-31789
Effective computational strategy for predicting the response of complex systems
[AD-A277452] p 3740 N94-33011

PERTURBATION THEORY
Development and implementation of a full-potential ASW method
[ETN-94-95757] p 3858 N94-31560
Perturbative aspects of lower-dimensional gauge theories
[ISBN-0-315-86269-6] p 3911 N94-31712
Electromagnetic wave reflection from irregular plasma layers
[AD-A276727] p 3678 N94-32161
Semianalytic Satellite Theory (SST): Mathematical algorithms
[AD-A276836] p 3610 N94-32208
A cell-cycle model revisited
[CWI-AM-R9305] p 3851 N94-32229
Quantum dynamics in dual spaces
[DE94-008303] p 3913 N94-32824

PETRI NETS
Performability modelling using DyQNtool+
[MEMO-INF-93-45] p 3812 N94-31659
Design Methods based On Nets: DEMON
[PB94-147493] p 3813 N94-31687

PH
Recovery of carboxylic acids at pH greater than pKa
[DE94-007030] p 3636 N94-32376
A fuzzy classifier system for process control p 3839 N94-32422
Studies of the fundamental nature of catalytic acidity, sites and intermediates
[DE94-006999] p 3646 N94-32805
The pH of Mars p 3950 N94-33225

PHARMACOLOGY
International Journal of Quantum Chemistry. Quantum Biology Symposium number 20. Proceedings of the International Symposium on the Application of Fundamental Theory to Problems of Biology and Pharmacology
[AD-A276294] p 3792 N94-31294
Review of pharmacological approach to improve cold tolerance p 3796 N94-31740

PHASE COHERENCE
Incoherent imaging by Z-contrast stem: Towards 1 Angstrom resolution
[DE94-006551] p 3896 N94-31489
Evaluation of surface phase change on large zones p 3755 N94-32567
Techniques and applications of SAR interferometry for ERS-1 p 3756 N94-32568

PHASE CONJUGATION
Methods for SBS threshold reduction
[AD-A276554] p 3717 N94-31936
High average power pulsed phase conjugate laser with birefringence correction
[DE94-006049] p 3719 N94-32659
Studies of optical beam phase conjugation and electromagnetic scattering process
[AD-A278389] p 3884 N94-33145

PHASE CONTRAST
Optimal detector strategies for the phase contrast imaging for scanning transmission electron microscopes
[ETN-94-95747] p 3866 N94-31613
PHASE DIAGRAMS
Synthesis, characterization, phase diagrams and superconducting, and normal state magnetic properties of La(2-x)Sr(x)CuO4 (0 is less than or equal to x which is less than or equal to 0.08) and electrochemically oxidized La(2-x)Sr(x)CuO(4 + delta) (0 is less than or equal to x which is less than or equal to 0.33, 0 is less than or equal to delta which is less than or equal to 0.12)
[DE94-005260] p 3895 N94-31067
The new Metals and Alloys Indexes, search manual: A phase diagram research tool
[DE94-005371] p 3643 N94-32098
Phase behavior, structure, and properties of model block polymers
[AD-A277530] p 3662 N94-32954
PHASE LOCKED SYSTEMS
Development, characterization, and applications of high temperature superconductor nanobridge Josephson junctions
[DE94-008113] p 3903 N94-32409
YBCO Josephson Junction arrays
[AD-A277426] p 3908 N94-33005
PHASE MODULATION
Advanced optical fiber communication systems
[AD-A276416] p 3878 N94-31330
High-performance GaAs/AlGaAs optical phase modulators for microwave/photonic integrated circuits
[DE94-006361] p 3688 N94-31483
Analysis of key performance parameters of phase sampling digital RF memories
[AD-A276019] p 3688 N94-31494
High-performance GaAs/AlGaAs optical phase modulators for microwave photonic integrated circuits
[DE94-007376] p 3696 N94-32809
PHASE SHIFT
Phase unwrapping problems in ISAR images
[TELECOM-93-D-006] p 3670 N94-31097
Field studies of raindrop oscillations with applications to radar meteorology p 3782 N94-31743
Fiber optic continuous true time-delay modulator
[AD-D016098] p 3883 N94-32720
High-performance GaAs/AlGaAs optical phase modulators for microwave photonic integrated circuits
[DE94-007376] p 3696 N94-32809
Effective computational strategy for predicting the response of complex systems
[AD-A277452] p 3740 N94-33011
PHASE SHIFT KEYING
Modulation and coding for the Gaussian channel, possibly affected by fluctuations
[TELECOM-93-E-009] p 3840 N94-31169
Advanced optical fiber communication systems
[AD-A276416] p 3878 N94-31330
PHASE STABILITY (MATERIALS)
Structure, stability, and mechanical properties of intermetallic phases
[DE94-009178] p 3647 N94-32852
The distribution of Martian ground ice at other epochs p 3948 N94-33218
Phase relationships and stability of the (mu)- and (zeta)-phases in the Ag-Al-X (X=Zn, Ga, Ge) systems
[DE94-009391] p 3648 N94-33270
PHASE TRANSFORMATIONS
Structure and dynamics of microemulsions in bulk, at interfaces, and in confined geometries
[DE94-006043] p 3633 N94-31526
Fermi surface instability at 0.4 K in a heavy-fermion YbBiPt: SDW?
[DE94-006224] p 3899 N94-31916
Amorphous/crystalline structure and phase transformations in metastable semiconducting Ge(1-x)Sn(x)
[DE94-006659] p 3901 N94-32115
The 10th International Conference on Internal Friction and Ultrasonic Attenuation in Solids (ICIFUAS)
[AD-A276849] p 3902 N94-32209
Fabrication, phase transformation studies and characterization of SiC-AlN-Al2OC ceramics
[DE94-008587] p 3659 N94-32657
Surface probes of porous toluene/water ices: Adsorption kinetics and annealing spectra measured by second harmonic generation
[DE94-007564] p 3637 N94-32743
Interface controlled amorphization of crystalline Ni/Ti multilayers
[DE94-008685] p 3906 N94-32884
Irradiation-induced phase transformations in zirconium alloys
[DE94-008484] p 3648 N94-32993
A tandem microscopic-electrochemical examination of a charge-induced surface phase sequence: Ordered Au(110) in aqueous iodide electrolytes as probed by potentiodynamic scanning tunneling microscopy
[AD-A276905] p 3875 N94-33277
PHASE VELOCITY
Superluminous laser pulse in an active medium
[DE94-007110] p 3720 N94-32684
PHASED ARRAYS
The development of active integrated antennas and a design methodology
[ISBN-0-315-86119-3] p 3675 N94-31708
Proceedings of the 1993 Antenna Applications Symposium, volume 1
[AD-A277202] p 3676 N94-32049
Proceedings of the 1993 Antenna Applications Symposium, volume 2
[AD-A277203] p 3677 N94-32050
Processing and characterization of functionally gradient ceramic materials
[AD-A277154] p 3657 N94-32367
PHENYLS
A relaxation study of poled nonlinear optical polymers by infrared reflection-absorption spectroscopy
[AD-A277513] p 3663 N94-33054
PHILIPPINES
Forecasters handbook for the Philippine Islands and surrounding waters
[AD-A277993] p 3787 N94-33089
PHONEMICS
Neural networks applied to the phonemic segmentation of speech p 3686 N94-33152
PHONONS
Experimental investigation of phonon eigenvectors using x ray interference fields
[ETN-94-95751] p 3865 N94-31511
PHOSPHATES
Development of vanadium-phosphate catalysts for methanol production by selective oxidation of methane
[DE94-006759] p 3759 N94-31272
Carbonates, surfates, phosphates, nitrates, and organic materials: Their association in a Martian meteorite p 3952 N94-33239
PHOSPHAZENE
Inorganic polymer engineering materials
[DE94-008519] p 3659 N94-32655
PHOSPHORUS
Determination of BPSG thin-film properties using IR reflection spectroscopy of product wafers
[DE94-006591] p 3634 N94-32110
PHOTOACOUSTIC MICROSCOPY
Atomic oxygen damage characterization by photothermal scanning p 3598 N94-31051
PHOTOCHEMICAL REACTIONS
Proceedings of the Seventeenth DOE Solar Photochemistry Research Conference
[DE94-005552] p 3759 N94-31648
Photopolymerization of cyclohexene oxide: A visible light initiating system and mechanistic investigations
[AD-A277110] p 3654 N94-31981
Mechanical properties of acrylate networks formed by visible laser-induced polymerization. 2. Control of the mechanical properties
[AD-A277111] p 3655 N94-31982
A model of the ion chemistry of electrified convection p 3868 N94-31993
Mechanisms of laser induced reactions in opaque heterogeneous environments
[AD-A276642] p 3717 N94-31996
The Sixth Symposium on Unconventional Photoactive Solids. Abstracts
[AD-A277198] p 3655 N94-32016
A visible light initiating system for free radical promoted cationic polymerization
[AD-A277164] p 3655 N94-32069
Radiation and photochemistry section
[DE94-008880] p 3873 N94-32757
Structural studies of photoinduced intramolecular electron transfer in cyclopentadienylnickelnitrosyl
[DE94-008467] p 3874 N94-32876
Dry deposition of PAN to grassland vegetation
[DE94-005111] p 3768 N94-32894
Mars atmospheric loss and isotopic fractionation by solar-wind-induced sputtering and photochemical escape p 3947 N94-33208
How well was total ozone abundance inferred with Mariner 9 p 3947 N94-33212
Escape of Mars atmospheric carbon through time by photochemical means p 3948 N94-33214
PHOTOCONDUCTIVITY
Multifunctional macromolecules
[AD-A277347] p 3656 N94-32246
PHOTOCONDUCTORS
The Sixth Symposium on Unconventional Photoactive Solids. Abstracts
[AD-A277198] p 3655 N94-32016
Fast acting optical deflection
[AD-A276630] p 3879 N94-32037
PHOTODECOMPOSITION
High-energy chemical processes: Laser irradiation of aromatic hydrocarbons
[DE94-008107] p 3720 N94-32707
PHOTODIODES
Analysis of the photodiode boundary layer transition indicator
[DE94-005311] p 3701 N94-31268
PHOTOELECTRIC EFFECT
Imaging of surface structure with energy-dependent photoelectron diffraction
[DE94-009096] p 3907 N94-32934
PHOTOELECTRIC EMISSION
The 4f heavy fermion photoelectron spectra do not exhibit the Kondo scale
[DE94-006252] p 3898 N94-31631
Analysis of Dietz's single, rectangular pulse theory for the generation of radiation via photoelectrons
[DE94-006131] p 3681 N94-32661
Particle-In-Cell (PIC) code simulation results and comparison with theory scaling laws for photoelectron-generated radiation
[DE94-006132] p 3695 N94-32662
Strongly anisotropic s-wave versus d-wave gap in cuprate superconductors: Evidence and theory
[DE94-007579] p 3904 N94-32746
Investigation of superconductivity and magnetism in d and f-electron materials
[DE94-008535] p 3907 N94-32933
PHOTOELECTROCHEMISTRY
Proceedings of the Seventeenth DOE Solar Photochemistry Research Conference
[DE94-005552] p 3759 N94-31648
PHOTOELECTRON SPECTROSCOPY
Electron cyclotron resonance plasma oxidation studies of InP
[AD-A277431] p 3893 N94-33007
PHOTOELECTRONS
Photoelectron diffraction and holography: Present status and future prospects
[DE94-006298] p 3712 N94-31629
The 4f heavy fermion photoelectron spectra do not exhibit the Kondo scale
[DE94-006252] p 3898 N94-31631
A simple model for determining photoelectron-generated radiation scaling laws
[DE94-006130] p 3761 N94-32660
Analysis of Dietz's single, rectangular pulse theory for the generation of radiation via photoelectrons
[DE94-006131] p 3681 N94-32661
Particle-In-Cell (PIC) code simulation results and comparison with theory scaling laws for photoelectron-generated radiation
[DE94-006132] p 3695 N94-32662
Near edge x ray spectroscopy theory
[DE94-008179] p 3905 N94-32799
Imaging of surface structure with energy-dependent photoelectron diffraction
[DE94-009096] p 3907 N94-32934
PHOTOGEOLOGY
A model geophysics program
[DE94-007415] p 3747 N94-32203
PHOTOGRAMMETRY
Apron heights around stepped massifs in the Cydonia Mensae region: Do they record the local paleobathymetry of Oceanus Borealis? p 3949 N94-33224
PHOTOGRAPHIC EQUIPMENT
Imaging devices for satellite remote sensing
[VTT-TIED-1517] p 3743 N94-31658
PHOTOGRAPHIC PROCESSING
The trustworthy digital camera: Restoring credibility to the photographic image p 3714 N94-32470
PHOTOGRAPHS
A paraperspective factorization method for shape and motion recovery
[AD-A276513] p 3712 N94-31929
The trustworthy digital camera: Restoring credibility to the photographic image p 3714 N94-32470
PHOTOINTERPRETATION
Radar image classification by texture measurements
[ONERA-NT-1993-3] p 3673 N94-31419
Assessment of region-based methods for automated SAR/optical registration, attribute extraction, and classification p 3750 N94-32536
Almaz marine applications p 3751 N94-32544
Statistical analysis and mapping of cotton and food crop cultivation surfaces in the west of Burkina Faso: Contribution of combined SPOT P and XS data p 3757 N94-32575
PHOTOIONIZATION
Elimination of two atomic electrons by a single high energy photon
[DE94-006834] p 3864 N94-31320

Double photoionization of helium with synchrotron x rays: Proceedings
[DE94-006737] p 3866 N94-31668
High-energy chemical processes: Laser irradiation of aromatic hydrocarbons
[DE94-008107] p 3720 N94-32707

PHOTOLUMINESCENCE
Fluorescence observations of LDEF exposed materials as an indicator of induced material reactions p 3593 N94-31025
Femtosecond probe-probe transmission studies of LT-grown GaAs near the band edge
[DE94-006660] p 3904 N94-32634
Material engineering of the novel semiconductor structures
[AD-A278386] p 3910 N94-33355

PHOTOLYSIS
Time-resolved infrared absorption studies applied to the study of radical plus molecule reactions
[DE94-005921] p 3863 N94-31202
Mechanisms of laser induced reactions in opaque heterogeneous environments
[AD-A276642] p 3717 N94-31996
Laser flash photolysis, EPR and Raman studies of liquids at elevated pressures
[DE94-008351] p 3718 N94-32413
Dry deposition of PAN to grassland vegetation
[DE94-005111] p 3768 N94-32894

PHOTOMAPPING
A model geophysics program
[DE94-007415] p 3747 N94-32203
Ultra wide band radar holographic imaging of subsurface targets
[DE94-004271] p 3713 N94-32681

PHOTOMETERS
Hydrogenated amorphous silicon (a-Si:H) based gamma camera: Monte Carlo simulations
[DE94-007042] p 3795 N94-31323
A 1-picosecond InGaAs photodetector for operation at 1300-1600 nm
[AD-A275959] p 3895 N94-31350
Advanced infrared photodetectors: Materials review
[AD-A277058] p 3879 N94-32013
High T(sub c) superconductor tunnel junctions for photon detectors
[DE94-007686] p 3904 N94-32602
Bioluminescence bathyphotometer
[AD-D016102] p 3790 N94-32959
Quantum well infrared photodetector FPA
[AD-A278010] p 3908 N94-33248

PHOTOMULTIPLIER TUBES
Hydrogenated amorphous silicon (a-Si:H) based gamma camera: Monte Carlo simulations
[DE94-007042] p 3795 N94-31323

PHOTON BEAMS
Proceedings of the 37th international symposium on electron, ion, and photon beams
[AD-A276478] p 3875 N94-31247

PHOTONICS
Photonic bandgaps in periodic dielectric structures
[ISBN-0-315-86902-X] p 3899 N94-31729
Photonic band gap materials
[DE94-005566] p 3677 N94-32101
Flexible manufacturing for photonics device assembly p 3669 N94-32449
Automated fiber pigtailing technology
[DE94-007072] p 3695 N94-32688
Sandia's photonic program and its changing national role
[DE94-008616] p 3883 N94-32878

PHOTONS
Time-dependent behavior of active galactic nuclei with pair production p 3929 N94-31125
Elimination of two atomic electrons by a single high energy photon
[DE94-006834] p 3864 N94-31320
Transport properties of quark and gluon plasmas
[DE94-007043] p 3864 N94-31405
Novel failure analysis techniques using photon probing with a scanning optical microscope
[DE94-006594] p 3692 N94-32112
ITS version 3.0: Powerful, user-friendly software for radiation modelling
[DE94-006607] p 3678 N94-32113
A quest for a new superconducting state
[DE94-008439] p 3908 N94-32991

PHOTONUCLEAR REACTIONS
NN-interaction in (1)S0-state: Virtual level or dibaryon resonance?
[DE94-606492] p 3869 N94-32097

PHOTOPRODUCTION
Results from the H1 experiment at HERA
[PB94-145174] p 3868 N94-32008
Chiral symmetry and the threshold gamma(p) yields pi(sup 0)p reaction
[DE94-008117] p 3873 N94-32710

PHOTOSPHERE
Observations of accretion and angular momentum regulation in young circumstellar disks and the implications for planetary formation p 3928 N94-31122

PHOTOSYNTHESIS
Spectral inhomogeneity of the bacterial light-harvesting antennae: Causes and consequences
[ETN-94-96020] p 3792 N94-31533
Light utilization and photoinhibition of photosynthesis in marine phytoplankton
[DE94-005505] p 3794 N94-32896

PHOTOTRANSISTORS
Reconfigurable optical switches with monolithic electrical-to-optical interfaces
[DE94-007745] p 3881 N94-32385

PHOTOVOLTAIC CELLS
Draft minutes of IAPG Mechanical Working Group meeting
[DE94-004954] p 3759 N94-31266
Solar lunar power p 3599 N94-31427
Field operation test of utility interactive load conditioner with photovoltaic cells at a demonstration house
[DE94-757271] p 3762 N94-32918

PHOTOVOLTAIC CONVERSION
Solar energy in China
[PB94-137502] p 3758 N94-31071
Photovoltaics: Program overview, fiscal year 1993
[DE94-000246] p 3758 N94-31235
Solar resource: Utility load-matching assessment
[DE94-000297] p 3758 N94-31264
Silicon-Film(tm) photovoltaic manufacturing technology
[DE94-000202] p 3760 N94-32143
Renewable energy technology development at Sandia National Laboratories
[DE94-007734] p 3761 N94-32383
Solar activities at Sandia National Laboratories
[DE94-007737] p 3761 N94-32648
Development of a computer model for polycrystalline thin-film CuInSe2 and CdTe solar cells
[DE94-006853] p 3762 N94-32763
Optimal planning of residential photovoltaic systems under various rate structure
[DE94-757272] p 3762 N94-32919

PHOTOVOLTAIC EFFECT
Impact of LDEF photovoltaic experiment findings upon spacecraft solar array design and development requirements p 3594 N94-31028

PHYSICAL CHEMISTRY
Physical chemistry of molecules and grains in space
[AD-A276037] p 3932 N94-31280
Studies in physico-chemical hydrodynamics of extended systems
[DE94-006752] p 3706 N94-32149

PHYSICAL EXAMINATIONS
Hydrogenated amorphous silicon (a-Si:H) based gamma camera: Monte Carlo simulations
[DE94-007042] p 3795 N94-31323

PHYSICAL OPTICS
The conoscopic microscope
[TELECOM-93-E-017] p 3877 N94-31173
An approximate model for vertical polarization and surface roughness using the parabolic equation
[AD-A278091] p 3684 N94-33186

PHYSIOLOGICAL EFFECTS
Review of pharmacological approach to improve cold tolerance p 3796 N94-31740
Muscle disuse through tail-suspension: Etiology and therapeutics p 3796 N94-31746
Exposure assessment of JAVELIN missile combustion products
[AD-A278128] p 3616 N94-33059
Characterization and utilization of opiate-like hibernation factors
[AD-A278136] p 3794 N94-33098

PHYSIOLOGICAL RESPONSES
Isolating strain parameters correlated to skeletal adaptation p 3797 N94-31960
Autogenic-feedback training as a treatment for airsickness in high-performance military aircraft: Two case studies
[NASA-TM-108810] p 3801 N94-33068

PHYSIOLOGICAL TESTS
Tripping over obstacles: Biomechanical analyses of how young and old try to avoid it p 3803 N94-31954
Exposure assessment of JAVELIN missile combustion products
[AD-A278128] p 3616 N94-33059

PHYSIOLOGY
Recommendations for meteorological data collection during physiological field studies
[AD-A276834] p 3901 N94-32153

PHYTOPLANKTON
Interaction processes between the ocean and the atmosphere p 3777 N94-30987
Light utilization and photoinhibition of photosynthesis in marine phytoplankton
[DE94-005505] p 3794 N94-32896
Bioluminescence bathyphotometer
[AD-D016102] p 3790 N94-32959

PICOSECOND PULSES
Pump-probe method for investigating laser ablation and optical damage threshold mechanisms in optical materials
[DE94-008291] p 3720 N94-32753

PIEZOELECTRIC CERAMICS
Passive vibration damping materials: Piezoelectric ceramic composites for vibration damping applications
[AD-A276550] p 3653 N94-31935

PIEZOELECTRIC TRANSDUCERS
PVDF pressure transducers for shock wave and explosives research
[AD-A277319] p 3712 N94-32051

PIEZOELECTRICITY
Piezoelectric materials research in Europe
[AD-A276207] p 3648 N94-31059
Electric field-induced changes in odd-numbered nylons
[AD-A278003] p 3664 N94-33138

PIGMENTS
Oxide pigments in water: The colloid-chemical point of view
[PB94-148616] p 3633 N94-31591
Evolution of upwelling fronts off the coast of Portugal
[NASA-CR-195692] p 3790 N94-33045

PILOT ERROR
Flight technical error for category B non-precision approaches and missed approaches using non-differential GPS for course guidance
[PB94-142734] p 3576 N94-31680

PILOT PERFORMANCE
Aircraft simulation and pilot proficiency: From surrogate flying towards effective training
[AD-B179300] p 3587 N94-31179
Situational awareness: A feasibility investigation of near-threshold skills development
[AD-A276467] p 3798 N94-31243
Flight technical error for category B non-precision approaches and missed approaches using non-differential GPS for course guidance
[PB94-142734] p 3576 N94-31680
Fuzzy logic application for modeling man-in-the-loop space shuttle proximity operations
[NASA-CR-188283] p 3835 N94-32359
The effects of Above Real-Time Training (ARTT) in an F-16 simulator p 3591 N94-32474

PILOT TRAINING
Aircraft simulation and pilot proficiency: From surrogate flying towards effective training
[AD-B179300] p 3587 N94-31179
Situational awareness: A feasibility investigation of near-threshold skills development
[AD-A276467] p 3798 N94-31243
The effects of Above Real-Time Training (ARTT) in an F-16 simulator p 3591 N94-32474
Autogenic-feedback training as a treatment for airsickness in high-performance military aircraft: Two case studies
[NASA-TM-108810] p 3801 N94-33068

PILOTLESS AIRCRAFT
Army scout/reconnaissance helicopters versus unmanned aerial vehicles
[AD-A276902] p 3579 N94-32232
Design and Monte Carlo analysis of an unmanned aerial vehicle
[AD-A277648] p 3580 N94-33056

PINCH EFFECT
Pinched propagation of high-power, pulsed electron beams for welding and materials processing applications
[AD-A276925] p 3726 N94-32236

PINNING
Effect of twin boundary density on the vortex melting transition in YBa2Cu3O(7-delta) single crystals
[DE94-007684] p 3904 N94-32601

PINS
Pip pin reliability and design p 3605 N94-33305

PION BEAMS
BNL possibilities
[DE94-007179] p 3864 N94-31398

PIONS
Medium energy measurements of N-N parameters
[DE94-006067] p 3869 N94-32173
Chiral symmetry and the threshold gamma(p) yields pi(sup 0)p reaction
[DE94-008117] p 3873 N94-32710

PIPE FLOW
Fluid-structure interaction in case of water hammer with cavitation
[PB94-148277] p 3702 N94-31588
Incompressible viscous flow in tubes with occlusions
[ISBN-0-315-75467-2] p 3704 N94-31778

Electromagnetic probe technique for fluid flow measurements p 3711 N94-32455

PIPELINING (COMPUTERS)

Investigation of modularly configured attached processors with intelligent memories [AD-A278418] p 3839 N94-33330

PIPES (TUBES)

Methodology for damage study of a tube-grill contact [ECL-92-49] p 3734 N94-31562

Fluid-structure interaction in case of water hammer with cavitation [PB94-148277] p 3702 N94-31588

Modeling of residual stress mitigation in austenitic stainless steel pipe girth weldment [DE94-007184] p 3738 N94-32639

PISTON ENGINES

The hydrogen hybrid option [DE94-006733] p 3667 N94-32148

PIVOTS

High precision moving magnet chopper for variable operation conditions p 3605 N94-33307

An experimental study of pilot/vehicle dynamics using a tilt rotor flying machine [AD-A277516] p 3805 N94-33349

PLAINS

Thermal and hydraulic considerations regarding the fate of water discharged by the outflow channels to the Martian northern plains p 3946 N94-33202

PLANE STRESS

Influences of pressure-sensitive yielding and non-singular stress on plane-stress elastic-plastic crack-tip fields p 3737 N94-31965

Nonlinear effects in interfacial fracture p 3737 N94-31974

BUCKY instruction manual, version 3.3 [NASA-TM-104793] p 3820 N94-32899

PLANE WAVES

On wave interactions of rotational and irrotational flows p 3700 N94-31219

Boundary control of scattering p 3861 N94-31899

Penetrable wedge analysis [AD-A277219] p 3845 N94-32022

Sound scattering by cylinders of noncircular cross section [AD-A276663] p 3861 N94-32089

Prediction of the plane wave beamformed acoustic arrival structure for the 1992 Barents Sea coastal tomography test [AD-A276741] p 3788 N94-32181

PLANETARY COMPOSITION

Magmatic volatiles and the weathering of Mars p 3946 N94-33201

The pH of Mars p 3950 N94-33225

The mineralogic evolution of the Martian surface through time: Implications from chemical reaction path modeling studies p 3950 N94-33226

PLANETARY CORES

Forced libration of Mercury and geodetic determination of a possible fluid core p 3774 N94-32493

PLANETARY CRATERS

The tectonic and volcanic evolution of Venus: Catastrophic or gradual? p 3940 N94-31111

Keeping that youthful look --- impact cratering of Venus p 3941 N94-31112

A tectonic resurfacing model for Venus p 3941 N94-31113

The resurfacing controversy for Venus: An overview and a mechanistic perspective p 3941 N94-31114

PLANETARY CRUSTS

The tectonic and volcanic evolution of Venus: Catastrophic or gradual? p 3940 N94-31111

The resurfacing controversy for Venus: An overview and a mechanistic perspective p 3941 N94-31114

Plains tectonism on Venus: The deformation belts of Lavinia Planitia p 3941 N94-31115

Thermal and hydraulic considerations regarding the fate of water discharged by the outflow channels to the Martian northern plains p 3946 N94-33202

The Martian sources of the SNC meteorites (two, not one), and what can and can't be learned from the SNC meteorites p 3951 N94-33234

Temporal changes in the geographic distribution, elevation, and potential origin of the Martian outflow channels p 3951 N94-33235

PLANETARY EVOLUTION

Tectonic History of the Terrestrial Planets [NASA-CR-195696] p 3939 N94-31105

The tectonic and volcanic evolution of Venus: Catastrophic or gradual? p 3940 N94-31111

Keeping that youthful look --- impact cratering of Venus p 3941 N94-31112

A tectonic resurfacing model for Venus p 3941 N94-31113

The resurfacing controversy for Venus: An overview and a mechanistic perspective p 3941 N94-31114

Plains tectonism on Venus: The deformation belts of Lavinia Planitia p 3941 N94-31115

Observations of accretion and angular momentum regulation in young circumstellar disks and the implications for planetary formation p 3928 N94-31122

Evolution of protoplanetary disks with dynamo magnetic fields p 3931 N94-31135

Theory of protostellar accretion disks p 3931 N94-31136

Planetesimal dynamics in the vicinity of a growing protoplanet p 3935 N94-31926

A model for the evolution of CO2 on Mars p 3946 N94-33205

The effect of polar caps on obliquity p 3948 N94-33213

The distribution of Martian ground ice at other epochs p 3948 N94-33218

The mineralogic evolution of the Martian surface through time: Implications from chemical reaction path modeling studies p 3950 N94-33226

Geologic controls of erosion and sedimentation on Mars p 3951 N94-33232

PLANETARY GEOLOGY

Tectonic History of the Terrestrial Planets [NASA-CR-195696] p 3939 N94-31105

Aspects of modelling the tectonics of large volcanoes on the terrestrial planets p 3940 N94-31107

State of stress, faulting, and eruption characteristics of large volcanoes on Mars p 3940 N94-31108

Origin and thermal evolution of Mars p 3940 N94-31109

Geoid-to-topography ratios on Venus: A global perspective p 3940 N94-31110

The tectonic and volcanic evolution of Venus: Catastrophic or gradual? p 3940 N94-31111

Keeping that youthful look --- impact cratering of Venus p 3941 N94-31112

A tectonic resurfacing model for Venus p 3941 N94-31113

The resurfacing controversy for Venus: An overview and a mechanistic perspective p 3941 N94-31114

Quantitative modeling of bottom morphology and subbottom properties [AD-A278142] p 3790 N94-33062

Fine and microstructure observations at Fieberlin g Guyot R/V new horizon cruise report [AD-A277917] p 3791 N94-33109

Mars: Past, Present, and Future. Results from the MSATT Program, part 1 [NASA-CR-194279] p 3943 N94-33190

Deposition rates of oxidized iron on Mars p 3945 N94-33198

Thermal and hydraulic considerations regarding the fate of water discharged by the outflow channels to the Martian northern plains p 3946 N94-33202

The Northern Plains MSATT Meeting, and a call for a field-oriented successor to MSATT p 3947 N94-33210

Mineralogical diversity (spectral reflectance and Moessbauer data) in compositionally similar impact melt rocks from Manicouagan Crater, Canada p 3948 N94-33219

Martian spectral units derived from ISM imaging spectrometer data p 3949 N94-33220

Apron heights around stepped massifs in the Cydonia Mensae region: Do they record the local paleobathymetry of Oceanus Borealis? p 3949 N94-33224

The mineralogic evolution of the Martian surface through time: Implications from chemical reaction path modeling studies p 3950 N94-33226

Martian deltas: Morphology and distribution p 3950 N94-33230

Geologic controls of erosion and sedimentation on Mars p 3951 N94-33232

The Martian sources of the SNC meteorites (two, not one), and what can and can't be learned from the SNC meteorites p 3951 N94-33234

Temporal changes in the geographic distribution, elevation, and potential origin of the Martian outflow channels p 3951 N94-33235

PLANETARY MAGNETOSPHERES

Plasma and radio waves from Neptune: Source mechanisms and propagation [NASA-CR-195877] p 3943 N94-33103

PLANETARY MAGNETOTAILS

Planetary magnetotails: Magnetic configuration and nonthermal plasma p 3942 N94-32326

PLANETARY MAPPING

Geoid-to-topography ratios on Venus: A global perspective p 3940 N94-31110

Mars: Five views on what is known [NASA-TM-109751] p 3942 N94-31805

The Lunar Scout Program: An international program to survey the Moon from orbit for geochemistry, mineralogy, imagery, geodesy, and gravity [NASA-TM-104791] p 3943 N94-32923

Mars: Past, Present, and Future. Results from the MSATT Program, part 1 [NASA-CR-194279] p 3943 N94-33190

Thermal studies of Martian channels and valleys using Termoskan data: New results p 3944 N94-33194

Global color views of Mars p 3948 N94-33217

Apron heights around stepped massifs in the Cydonia Mensae region: Do they record the local paleobathymetry of Oceanus Borealis? p 3949 N94-33224

PLANETARY METEOROLOGY

Eddy transport of water vapor in the Martian atmosphere p 3949 N94-33221

Numerical simulation of thermally induced near-surface flows over Martian terrain p 3949 N94-33223

Controls on the CO2 seasonal cycle p 3950 N94-33227

The wavelength dependence of Martian atmospheric dust radiative properties p 3950 N94-33228

PLANETARY ORBITS

The distribution of Martian ground ice at other epochs p 3948 N94-33218

PLANETARY RADIATION

Plasma and radio waves from Neptune: Source mechanisms and propagation [NASA-CR-195877] p 3943 N94-33103

PLANETARY ROTATION

Planetesimal dynamics in the vicinity of a growing protoplanet p 3935 N94-31926

PLANETARY STRUCTURE

Forced libration of Mercury and geodetic determination of a possible fluid core p 3774 N94-32493

PLANETARY SURFACES

Tectonic History of the Terrestrial Planets [NASA-CR-195696] p 3939 N94-31105

PLANETARY SYSTEMS

Evolution of protoplanetary disks with dynamo magnetic fields p 3931 N94-31135

PLANETARY TEMPERATURE

IRTM brightness temperature maps of the Martian south polar region during the polar night: The cold spots don't move p 3949 N94-33222

PLANETARY WAVES

Magnetohydrodynamics of the Earth's core. 1: Steady, rotating magnetoconvection. 2: Magnetic Rossby waves p 3770 N94-31104

Stationary eddies in the Mars general circulation as simulated by the NASA-Ames GCM p 3944 N94-33192

PLANKTON

Light utilization and photoinhibition of photosynthesis in marine phytoplankton [DE94-005505] p 3794 N94-32896

PLANNING

On a formal approach to the methodology of information planning [MEMO-INF-93-42] p 3917 N94-31415

Planning of air crew schedules [ISBN-0-315-86506-7] p 3914 N94-32074

Utility-based planning [NASA-CR-195878] p 3816 N94-32086

An algorithm for probabilistic, totally-ordered temporal projection [AD-A277341] p 3817 N94-32257

PLANTS (BOTANY)

Ninth International Workshop on Plant Membrane Biology [DE94-005690] p 3794 N94-32769

PLASMA ARC WELDING

Robotic weld overlay coatings for erosion control [DE94-008004] p 3658 N94-32408

Development of an automated wire delivery system for robotic welding applications [NASA-CR-194216] p 3727 N94-32479

PLASMA CHEMISTRY

Feasibility study to evaluate plasma quench process for natural gas conversion applications [DE94-000086] p 3758 N94-31234

Degenerate four-wave mixing as a diagnostic of plasma chemistry [DE94-008588] p 3889 N94-31766

PLASMA CLOUDS

Theory, Image Simulation, and Data Analysis of Chemical Release Experiments [NASA-CR-194865] p 3954 N94-31101

Computer modeling of active experiments in space plasmas p 3890 N94-31927

PLASMA COMPOSITION

Characterization of atomic and molecular impurity sources and transport at the tokamak edge [DE94-007212] p 3891 N94-32619

Analysis of data from the plasma composition experiment on the International Sun-Earth Explorer (ISEE 1) [NASA-CR-195880] p 3893 N94-33074

PLASMA CONTROL
L-H confinement mode dynamics in three-dimensional state space
[DE94-007113] p 3887 N94-31396
Toroidal pinch experiments
[DE94-005876] p 3887 N94-31558
Plasma confinement theory and transport simulation
[DE94-006065] p 3888 N94-31619
High beta tokamak research
[DE94-006513] p 3888 N94-31664
First-wall heat-flux measurements during ELMing H-mode plasma
[DE94-008310] p 3888 N94-31765
Collisional and chaotic transport of energetic particles in toroidal plasma
[DE94-006504] p 3889 N94-31787
FWCD and ECCD experiments on D3-D
[DE94-007371] p 3890 N94-32201
Experimental survey of the L-H transition conditions in the D3-D tokamak
[DE94-007428] p 3891 N94-32595
Recent VH-mode results on D3-D
[DE94-007429] p 3891 N94-32611
Overview of H-mode studies in D3-D
[DE94-007430] p 3891 N94-32612
Anomalous thermalization of fast ions in magnetized plasma
[DE94-007109] p 3891 N94-32631
Coaxial slow source
[DE94-008191] p 3892 N94-32800
Divertor pumping and other reactor application issues for H-mode
[DE94-007431] p 3892 N94-32810
Cooperative program on D3-D (FY 1993)
[DE94-008343] p 3892 N94-32820
Anomalous transport equations in toroidal plasmas
[DE94-009206] p 3893 N94-32922

PLASMA CURRENTS
First-wall heat-flux measurements during ELMing H-mode plasma
[DE94-008310] p 3888 N94-31765
FWCD and ECCD experiments on D3-D
[DE94-007371] p 3890 N94-32201

PLASMA DENSITY
An edge density fluctuation diagnostic for D3-D using lithium beams
[DE94-008554] p 3890 N94-32519
Divertor pumping and other reactor application issues for H-mode
[DE94-007431] p 3892 N94-32810

PLASMA DIAGNOSTICS
Spectroscopy and atomic physics in EBIT and SuperEBIT
[DE94-006050] p 3864 N94-31508
Plasma confinement theory and transport simulation
[DE94-006065] p 3888 N94-31619
Diagnostics of high-brightness short-pulse lasers and the plasmas they generate
[DE94-006165] p 3716 N94-31624
High beta tokamak research
[DE94-006513] p 3888 N94-31664
Degenerate four-wave mixing as a diagnostic of plasma chemistry
[DE94-008588] p 3889 N94-31766
An edge density fluctuation diagnostic for D3-D using lithium beams
[DE94-008554] p 3890 N94-32519
Characterization of atomic and molecular impurity sources and transport at the tokamak edge
[DE94-007212] p 3891 N94-32619
Measurement of ICF fuel ion temperature on Nova
[DE94-006150] p 3892 N94-32730
Performance of a quasi-steady, multi megawatt, coaxial plasma thruster
[NASA-CR-195311] p 3616 N94-32970
Ultrafast x ray sources
[AD-A277455] p 3721 N94-33012
Millstone Hill radar studies of plasma waves and turbulence
[AD-A278409] p 3684 N94-33172

PLASMA DIFFUSION
Anomalous transport equations in toroidal plasmas
[DE94-009206] p 3893 N94-32922

PLASMA DYNAMICS
Convection and electrodynamic signatures in the vicinity of a Sun-aligned arc: Results from the Polar Acceleration Regions and Convection Study (Polar ARCS)
p 3954 N94-31102
L-H confinement mode dynamics in three-dimensional state space
[DE94-007113] p 3887 N94-31396
Plasma confinement theory and transport simulation
[DE94-006065] p 3888 N94-31619
Pulsed expansion of plasma in a magnetic thruster
p 3889 N94-31776
Computer modeling of active experiments in space plasmas p 3890 N94-31927
Basic principles approach for studying nonlinear Alfven wave-alpha particle dynamics
[DE94-007112] p 3891 N94-32664
Analytic formulation for the ac electrical conductivity in two-temperature, strongly coupled, overdense plasma: FORTRAN subroutine
[DE94-009466] p 3893 N94-32915

PLASMA ELECTRODES
Time resolved measurements of light produced by onset of plasma formation on electrodes of fast pulsed high voltage diodes
[AD-A277974] p 3894 N94-33264

PLASMA ENGINES
Pulsed expansion of plasma in a magnetic thruster
p 3889 N94-31776
Performance evaluation and operating characteristics of a waveguide microwave applicator for space propulsion applications p 3614 N94-31908
Performance of a quasi-steady, multi megawatt, coaxial plasma thruster
[NASA-CR-195311] p 3616 N94-32970

PLASMA ETCHING
Electron cyclotron resonance plasma oxidation studies of InP
[AD-A277431] p 3893 N94-33007

PLASMA FOCUS
Studies of the plasma triggering mechanism of inverse pinch switch
[AD-A276117] p 3887 N94-31530

PLASMA HEATING
Instability heating of solid-fiber Z pinches
[DE94-007055] p 3889 N94-31809
Performance evaluation and operating characteristics of a waveguide microwave applicator for space propulsion applications p 3614 N94-31908
ICRF heating and current drive in TFTR supershot plasmas: Data analysis and interpretation of ICRF/edge interactions
[DE94-008586] p 3890 N94-32520
Experimental survey of the L-H transition conditions in the D3-D tokamak
[DE94-007428] p 3891 N94-32595
Anomalous thermalization of fast ions in magnetized plasma
[DE94-007109] p 3891 N94-32631
A comprehensive analysis of electron conical distributions from multi-satellite databases
[NASA-CR-195848] p 3953 N94-33047
Ionospheric plasma outflow in response to transverse ion heating: Self-consistent macroscopic treatment
[NASA-CR-195820] p 3893 N94-33048
Time resolved measurements of light produced by onset of plasma formation on electrodes of fast pulsed high voltage diodes
[AD-A277974] p 3894 N94-33264

PLASMA INTERACTIONS
High sensitivity and resolution decimetric spectroscope: Preliminary analysis of solar bursts
[INPE-5537-TDI/525] p 3954 N94-33080

PLASMA JETS
Development and application of a multimesh auto-adaptive finite element method for the calculation of an electric arc plasma
[ECL-89-03] p 3886 N94-31378
The measurement of the hadronic energy flow and jet production with the ZEUS calorimeter in deep inelastic scattering events at HERA
[ETN-94-96021] p 3865 N94-31534
Stark broadening of the 2S state of hydrogen and deuterium in arc plasmas of low density
[ETN-94-95731] p 3888 N94-31572
Ultrahigh-current-density metal-ion implantation and diamondlike-hydrocarbon films for tribological applications
[DE94-008958] p 3906 N94-32843

PLASMA LAYERS
Transport phenomena in the Earth's plasma sheet
p 3772 N94-31970
Electromagnetic wave reflection from irregular plasma layers
[AD-A276727] p 3678 N94-32161
Planetary magnetotails: Magnetic configuration and nonthermal plasma p 3942 N94-32326
Analysis of data from the plasma composition experiment on the International Sun-Earth Explorer (ISEE 1)
[NASA-CR-195880] p 3893 N94-33074
Characteristics of ion flow in the quiet state of the inner plasma sheet
[AD-A277451] p 3894 N94-33106

PLASMA OSCILLATIONS
Simultaneous excitation of parametric decay cascades and the OTSI in 1D numerical simulations based on Aakarov's equations
[AD-A278108] p 3893 N94-33042

PLASMA PHYSICS
Laboratory and space experiments as a key to the plasma universe
[TRITA-ALP-1993-01] p 3885 N94-31088
The double probe electric field experiment on Freja: Description and first results
[TRITA-ALP-1993-02] p 3885 N94-31089
Studies of the plasma triggering mechanism of inverse pinch switch
[AD-A276117] p 3887 N94-31530
Stability and instability criteria for magnetohydrodynamics
[PB94-148475] p 3889 N94-31772
Workshop on Models for Plasma Spectroscopy
[AD-A276565] p 3890 N94-32031
Atomic and molecular data needs for fusion
[DE94-006555] p 3870 N94-32177
Analytic properties of the OCP and ionic mixtures in the strongly coupled fluid state
[DE94-008216] p 3637 N94-32801
Cooperative program on D3-D (FY 1993)
[DE94-008343] p 3892 N94-32820
The Numerical Tokamak Project (NTP) simulation of turbulent transport in the core plasma: A grand challenge in plasma physics
[DE94-008279] p 3892 N94-32838
Stability of tearing modes in tokamak plasmas
[DE94-009205] p 3892 N94-32911
Electron cyclotron resonance plasma oxidation studies of InP
[AD-A277431] p 3893 N94-33007
Simultaneous excitation of parametric decay cascades and the OTSI in 1D numerical simulations based on Aakarov's equations
[AD-A278108] p 3893 N94-33042

PLASMA PINCH
Studies of the plasma triggering mechanism of inverse pinch switch
[AD-A276117] p 3887 N94-31530

PLASMA PRESSURE
Magnetless magnetic fusion
[DE94-007114] p 3891 N94-32686

PLASMA PROPULSION
Performance evaluation and operating characteristics of a waveguide microwave applicator for space propulsion applications p 3614 N94-31908
Performance of a quasi-steady, multi megawatt, coaxial plasma thruster
[NASA-CR-195311] p 3616 N94-32970

PLASMA RADIATION
Radiation from an aperture into an anisotropic plasma half-space p 3885 N94-31205
Spacecraft environmental anomalies expert system
[AD-A277962] p 3612 N94-33262

PLASMA RESONANCE
Time domain spectroscopy for studying a monopole antenna immersed in a plasma
[ISBN-0-315-86526-1] p 3888 N94-31727

PLASMA SHEATHS
Time domain spectroscopy for studying a monopole antenna immersed in a plasma
[ISBN-0-315-86526-1] p 3888 N94-31727
Dispersion relations for a plasma-filled helix-loaded-waveguide
[DE94-006333] p 3675 N94-31781
ICRF heating and current drive in TFTR supershot plasmas: Data analysis and interpretation of ICRF/edge interactions
[DE94-008586] p 3890 N94-32520
The spatial development of the magnetospheric low-latitude boundary layer
[ISBN-0-315-77418-5] p 3776 N94-33111

PLASMA SPECTRA
Workshop on Models for Plasma Spectroscopy
[AD-A276565] p 3890 N94-32031

PLASMA SPRAYING
Development and characterization of intermediary layers allowing the bond between a metal alloy and a plasma sprayed ceramic
[ECL-91-39] p 3619 N94-31377

PLASMA TORCHES
Stabilization method of A.C. arc plasma
[DE94-757268] p 3893 N94-32916

PLASMA TURBULENCE
Dynamics of flux tubes in accretion disks
p 3932 N94-31142
Transport suppression by shear flow generation in multihelicity resistive-g turbulence
[DE94-007108] p 3886 N94-31366

L-H confinement mode dynamics in three-dimensional state space
[DE94-007113] p 3887 N94-31396
An edge density fluctuation diagnostic for D3-D using lithium beams
[DE94-008554] p 3890 N94-32519
Recent VH-mode results on D3-D
[DE94-007429] p 3891 N94-32611
The Numerical Tokamak Project (NTP) simulation of turbulent transport in the core plasma: A grand challenge in plasma physics
[DE94-008279] p 3892 N94-32638
Millstone Hill radar studies of plasma waves and turbulence
[AD-A278409] p 3684 N94-33172

PLASMA WAVES
Collective acceleration in solar flares
[DE94-006288] p 3953 N94-31632
Time domain spectroscopy for studying a monopole antenna immersed in a plasma
[ISBN-0-315-86526-1] p 3888 N94-31727
Basic principles approach for studying nonlinear Alfven wave-alpha particle dynamics
[DE94-007112] p 3891 N94-32664
Simultaneous excitation of parametric decay cascades and the OTSI in 1D numerical simulations based on Aakarov's equations
[AD-A278108] p 3893 N94-33042
Plasma and radio waves from Neptune: Source mechanisms and propagation
[NASA-CR-195877] p 3943 N94-33103
Participation in the scientific activities of the Waves in Space Plasma (WISP) project
[NASA-CR-195903] p 3894 N94-33113
Millstone Hill radar studies of plasma waves and turbulence
[AD-A278409] p 3684 N94-33172

PLASMAS (PHYSICS)
Dynamics of flux tubes in accretion disks
p 3932 N94-31142
Radiation from an aperture into an anisotropic plasma half-space p 3885 N94-31205
Theoretical studies on ionospheric irregularities and ion diode performance
[AD-A277115] p 3772 N94-31984
Analytic properties of the OCP and ionic mixtures in the strongly coupled fluid state
[DE94-008215] p 3637 N94-32601
The 1994 International Sherwood Fusion Theory Conference
[DE94-008961] p 3877 N94-32844
Potential applications of fusion neutral beam facilities for advanced material processing
[DE94-009167] p 3647 N94-32851
Stabilization method of A.C. arc plasma
[DE94-757268] p 3893 N94-32916
Ultrafast x ray sources
[AD-A277455] p 3721 N94-33012
Time resolved measurements of light produced by onset of plasma formation on electrodes of fast pulsed high voltage diodes
[AD-A277974] p 3894 N94-33264

PLASTIC COATINGS
Follow-up on the effects of the space environment on UHCRE thermal blankets p 3592 N94-31018

PLASTIC DEFORMATION
Inelastic deformation of metal matrix composites
p 3618 N94-31285
Toughening mechanisms in the high strain rate deformation of rubber-modified polymer glasses
p 3653 N94-31942
High-temperature deformation and fracture toughness of duplex ceramic microstructures p 3653 N94-31945
A state variable material model for superplastic titanium-6 percent Al-4 percent V p 3644 N94-32498

PLASTIC PROPERTIES
On the mechanics of microballoon-reinforced metal matrix composites
[AD-A277928] p 3630 N94-33178

PLASTICIZERS
Electrostrictive response of elastomeric polymers
[AD-A277983] p 3664 N94-33247

PLATE THEORY
An efficient higher order theory for laminated composite plates and a finite element implementation
p 3617 N94-31215

PLATEAUS
Electron energy dependence of amorphization in Zr3Fe
[DE94-008459] p 3906 N94-32875

PLATES
Response of a cantilevered plate in supersonic flow
[AD-A277487] p 3580 N94-33107

PLATES (STRUCTURAL MEMBERS)
An efficient higher order theory for laminated composite plates and a finite element implementation
p 3617 N94-31215
Random vibrations of composite beams and plates
p 3735 N94-31777
QUAD4 seminar
[AD-A277366] p 3818 N94-32330
Effective computational strategy for predicting the response of complex systems
[AD-A277452] p 3740 N94-33011

PLATES (TECTONICS)
The tectonic and volcanic evolution of Venus: Catastrophic or gradual? p 3940 N94-31111

PLATINUM
Infrared spectroelectrochemical study of cyanide adsorption and reactions at platinum electrodes in aqueous perchlorate electrolyte
[AD-A276402] p 3631 N94-31238
Lowering the Schottky barrier at metal or silicide/Si interfaces to extend the range of infrared detectors
[AD-A277253] p 3903 N94-32322
Induced adsorption of chloride and bromide by submonolayer amounts of copper underpotentially deposited on Pt(111)
[AD-A278023] p 3648 N94-33182
Scanning tunneling microscopy and infrared spectroscopy as combined in-situ probes of electrochemical adlayer structure: Cyanide on Pt(111)
[AD-A276715] p 3909 N94-33274

PLATINUM ALLOYS
Fermi surface instability at 0.4 K in a heavy-fermion YbBiPt: SDW?
[DE94-006224] p 3899 N94-31916

PLAYBACKS
An experimental compact Hi-Vision VCR using metal evaporated tape
[NHK-LABS-NOTE-423] p 3683 N94-33081

PLOTTING
Description of a package for the analysis and display of the results of numerical simulations
[AD-A276285] p 3841 N94-31252

PNEUMATICS
Controlling hazardous energy sources (lockout/tagout)
[NASA-TM-105290] p 3669 N94-32861

POINT DEFECTS
Indium-vacancy complexes in mercury cadmium telluride
[AD-A276177] p 3894 N94-31055
Defect-solute interactions near irradiation grain boundaries
[DE94-006215] p 3641 N94-31627
IR materials producibility
[AD-A277028] p 3879 N94-32006
The 10th International Conference on Internal Friction and Ultrasonic Attenuation in Solids (ICIFUAS)
[AD-A276849] p 3902 N94-32209
Intra-cascade surface recombination of point defects during ion bombardment of Ge(001)
[DE94-007740] p 3903 N94-32384
Structure, stability, and mechanical properties of intermetallic phases
[DE94-009178] p 3647 N94-32852

POINT IMPACT
Point-contact and point-impact dynamics for multibody chains
[ISBN-0-315-87056-7] p 3734 N94-31737

POINTING CONTROL SYSTEMS
Pointing and tracking space mechanism for laser communication p 3606 N94-33310

POINTS (MATHEMATICS)
Kaplan-Meier estimators of interpoint distance distributions for spatial point processes
[CWI-BS-R9315] p 3846 N94-32107

POISSON DENSITY FUNCTIONS
The Laplace functional and Palm measure of a quasi-Cox process which is driven by a Markov chain
[REPT-93-82] p 3851 N94-31699
Light-traffic analysis for queues with spatially distributed arrivals
[MEMO-1150] p 3832 N94-31826
Kaplan-Meier estimators of interpoint distance distributions for spatial point processes
[CWI-BS-R9315] p 3846 N94-32107

POISSON EQUATION
An efficient three-dimensional Poisson solver for SIMD high-performance-computing architectures
p 3823 N94-31120
Eta percent-superconvergence in the interior of locally refined meshes of quadrilaterals: Superconvergence of the gradient in finite element solutions of Laplace's and Poisson's equations
[AD-A277242] p 3848 N94-32331

POISSON RATIO
Ceramic Technology Project database
[DE94-008494] p 3659 N94-32632
Indentability of conventional and negative Poisson's ratio foams p 3629 N94-33131

POLAR CAP ABSORPTION
Performance statistics bulletin. High latitude meteor scatter propagation, February, March, April, May 1992
[AD-A276667] p 3677 N94-32083
Performance statistics bulletin. High latitude meteor scatter propagation February, March, April, May 1991
[AD-A276723] p 3678 N94-32158
Performance statistics bulletin. High latitude meteor scatter propagation October, November, December 1991, January 1992
[AD-A276724] p 3678 N94-32159
Performance statistics bulletin. High latitude meteor scatter propagation, November and December 1989, and January 1990
[AD-A276688] p 3680 N94-32297
Performance statistics bulletin. High latitude meteor scatter propagation
[AD-A276694] p 3680 N94-32298
Performance statistics bulletin. High latitude meteor scatter propagation
[AD-A276695] p 3680 N94-32299
Performance statistics bulletin. High latitude meteor scatter propagation
[AD-A276696] p 3680 N94-32300
Performance statistics bulletin. High latitude meteor scatter propagation, June, July, August, September 1992
[AD-A277508] p 3685 N94-33347

POLAR CAPS
A reassessment of the in-situ dielectric constant of polar firn
[AD-A276999] p 3773 N94-32154
The effect of polar caps on obliquity
p 3948 N94-33213

POLAR REGIONS
Convection and electrodynamic signatures in the vicinity of a Sun-aligned arc: Results from the Polar Acceleration Regions and Convection Study (Polar ARCS)
p 3954 N94-31102
Radar scattering from the summer polar mesosphere: Theory and observations p 3772 N94-32077
IRTM brightness temperature maps of the Martian south polar region during the polar night: The cold spots don't move p 3949 N94-33222
Polar sediment accumulation: Role of surface winds at the two poles p 3951 N94-33233
Obliquity variation in a Mars climate evolution model
p 3951 N94-33238

POLARIMETERS
Stellar x ray polarimeter polarizer development and calibration at LEA/LLNL
[DE94-006400] p 3712 N94-31783

POLARIMETRY
Multiple scattering of polarized radiation in planetary atmospheres
[ETN-94-96018] p 3674 N94-31551

POLARIZATION (SPIN ALIGNMENT)
Hyperon polarization and magnetic moments
[DE94-006041] p 3864 N94-31507
Fusion with highly spin polarized HD and D2
[DE94-006209] p 3876 N94-32731
Hyperon polarization, crystal channeling, and E781 at Fermilab
[DE94-008224] p 3877 N94-32802

POLARIZATION (WAVES)
Structure estimation of phase objects from the diffraction near field: Microwave and model calculations
[ETN-94-95737] p 3674 N94-31608
An approximate model for vertical polarization and surface roughness using the parabolic equation
[AD-A278091] p 3684 N94-33186

POLARIZED LIGHT
Post-calibration correction for rotating-analyzer ellipsometer with optical fiber bundle detection system
[AD-A277329] p 3881 N94-32280
Microreflectance infrared study of electron-molecular vibrational coupling and lattice softness in BEDT-TTF salts
[DE94-008490] p 3907 N94-32989
Coherent processes in atom in strong radiation fields
[AD-A278388] p 3874 N94-33144

POLARIZED RADIATION
Multiple scattering of polarized radiation in planetary atmospheres
[ETN-94-96018] p 3674 N94-31551
RHIC spin physics
[DE94-005452] p 3876 N94-32099

POLARIZERS
Large-area conditioning of optics for high-power laser systems
[DE94-007028] p 3716 N94-31636
Stellar x ray polarimeter polarizer development and calibration at LEA/LLNL
[DE94-006400] p 3712 N94-31783

POLARONS
Theoretical studies of electron transfer and optical spectroscopy
[DE94-006985] p 3871 N94-32375
POLICIES
Europe at the crossroads: The future of its satellite communications industry
[ESA-SP-1166] p 3670 N94-31182
Satellite communications industry
[AD-A276685] p 3610 N94-32039
Interagency Advanced Power Group: Steering Group meeting minutes
[DE94-007951] p 3761 N94-32701
National US public policy on global warming derived from optimization of energy use and environmental impact studies
[DE94-004606] p 3768 N94-32790
NASA/DOD Aerospace Knowledge Diffusion Research Project. Paper 18: Scientific and Technical Information (STI) policy and the competitive position of the US aerospace industry
[NASA-TM-109782] p 3921 N94-32833
Current policies of the major countries coping with the global warming problem and-the energy demand and supply
[DE94-757291] p 3769 N94-32920
Opinion polls and the US civil space program
[NASA-TM-109700] p 3914 N94-33066
Space history, space policy, and executive leadership
[NASA-TM-109787] p 3924 N94-33067
POLISHING
Neutral ion sources in precision manufacturing
p 3875 N94-32447
POLLEN
Backscatter and transmission of aerosol at UV through middle IR wavelengths
[AD-A277127] p 3718 N94-32305
POLLUTION CONTROL
Information resources for US Department of Energy pollution prevention programs
[DE94-006677] p 3763 N94-31582
Control and monitoring of heavy metal emissions
[VTT-TIED-1508] p 3765 N94-31657
Carbon dioxide abatement as a differential game
[DE94-722023] p 3765 N94-32590
Removal of CO2 from flue gases by algae
[DE94-008039] p 3766 N94-32703
Identification of research relating to the critical loads concept and its potential application to the regulation of acidic deposition
[DE94-008234] p 3767 N94-32752
Evaluation of the Hughes conversion coating touch-up pen
[AD-A278398] p 3664 N94-33166
POLLUTION MONITORING
Control and monitoring of heavy metal emissions
[VTT-TIED-1508] p 3765 N94-31657
NORSMAP 1989: Norwegian remote sensing spectroscopy for mapping and monitoring or algal blooms and pollution p 3744 N94-31856
Evaluation of Fluorescence Line Imager (FLI) airborne imaging spectrometer data for roadside tree damage assessment p 3745 N94-31866
Focused feasibility study final field sampling plan
[AD-A277445] p 3769 N94-33105
POLLUTION TRANSPORT
Temporal and spatial mapping of atmospheric dust opacity and surface albedo on Mars
p 3947 N94-33211
POLYATOMIC MOLECULES
Energy transfer properties and mechanisms
[DE94-007403] p 3636 N94-32594
Wave packet studies of the vibrational predissociation of three and four-atom van der Waals complexes
[DE94-007623] p 3871 N94-32598
POLYCARBOSILANES
Conversion of polymers of methyl- and vinylsilane to Si-C ceramics
[NASA-TM-106554] p 3662 N94-32945
POLYCRYSTALS
Piezoelectric materials research in Europe
[AD-A276207] p 3648 N94-31059
Synthesis, characterization, phase diagrams and superconducting, and normal state magnetic properties of La(2-x)Sr(x)CuO4 (0 is less than or equal to x which is less than or equal to 0.08) and electrochemically oxidized La(2-x)Sr(x)CuO(4 + delta) (0 is less than or equal to x which is less than or equal to 0.33, 0 is less than or equal to delta which is less than or equal to 0.12)
[DE94-005260] p 3895 N94-31067
Role of polycrystallinity in CdTe and CuInSe2 photovoltaic cells
[DE94-000293] p 3758 N94-31236
A scanning defect mapping system for semiconductor characterization p 3885 N94-32446
Attempts to model the generation of new grain boundaries during the deformation of polycrystals
[DE94-007527] p 3903 N94-32597
Development of a computer model for polycrystalline thin-film CuInSe2 and CdTe solar cells
[DE94-006853] p 3762 N94-32763
Isothermal sintering, microstructure, and superconducting properties of Y1Ba2Cu3O(7-x) compound
[DE94-008132] p 3905 N94-32779
Nucleation and growth of cubic boron nitride films produced by ion-assisted pulsed laser deposition
[DE94-007295] p 3661 N94-32796
The path for long range conduction in high J(sub c) TiBa2Ca2Cu3O(8+x) spray-pyrolyzed deposits
[DE94-007211] p 3909 N94-33271
POLYESTERS
Improved resealing procedures for the second deseal/reseal program in RAAF F111 aircraft fuel tanks
[AD-A277069] p 3580 N94-32378
POLYETHYLENE TEREPHTHALATE
Electrical properties of double layer dielectric structures for space technology
[ISBN-0-315-86547-4] p 3610 N94-31910
POLYHEDRONS
Polyhedric object recognition by indexing in a model base
[ETN-94-95913] p 3812 N94-31542
POLYIMIDES
Performance of selected polymeric materials on LDEF
p 3593 N94-31023
Reliability of multilayer copper/polyimide
[AD-A276228] p 3650 N94-31284
Molecular interactions at metal/polyimide interfaces: A correlation with adhesion and bond durability
[AD-A276301] p 3650 N94-31297
Electrical properties of double layer dielectric structures for space technology
[ISBN-0-315-86547-4] p 3610 N94-31910
Characterization of thermally stable dye-doped polyimide based electrooptic materials
[DE94-005309] p 3882 N94-32674
Characterization of crosslinked electrooptic polyimides
[DE94-007934] p 3661 N94-32819
POLYMER BLENDS
Recent developments in polymeric charge transfer complexes
[AD-A277108] p 3654 N94-31979
Solvent diffusion coefficient concentration dependence in polymer solutions
[AD-A277023] p 3655 N94-32005
Compatibility studies of some azo polymer blends
[AD-A277141] p 3657 N94-32365
POLYMER CHEMISTRY
Reactions of electrophilic maleic anhydride and epoxy groups with nucleophilic functionalities such as carboxyl, hydroxyl, and amine groups. Polymer Technology Publication series no. 16
[PB94-135589] p 3648 N94-31069
Novel electroactive polymers and block copolymers
[AD-A276119] p 3650 N94-31509
Competition between crystallization and mixing/demixing in polymer mixture
[ETN-94-95753] p 3651 N94-31513
Mechanical properties of acrylate networks formed by visible laser-induced polymerization. 2. Control of the mechanical properties
[AD-A277111] p 3655 N94-31982
Multifunctional macromolecules
[AD-A277347] p 3656 N94-32246
Nonlinear optical polymers derived from organic/inorganic composites
[AD-A277408] p 3659 N94-32610
Nonlinear optical properties of rigid-rod polymers
[NASA-CR-191349] p 3882 N94-32702
Novel precursor approached for CMC derived by polymer pyrolysis
[AD-A278383] p 3665 N94-33352
POLYMER MATRIX COMPOSITES
Thermal-vacuum response of polymer matrix composites in space p 3595 N94-31033
Space environmental effects on polymer composites: Research needs and opportunities p 3595 N94-31035
Characterization of polymer decomposition products by laser desorption mass spectrometry
p 3597 N94-31046
Space hypervelocity microparticle impact damage in polymer matrix composites
[ISBN-0-315-87057-5] p 3652 N94-31692
Briefing and review meeting implementation of the military handbook 17 for polymer matrix and metal matrix composites
[AD-A277446] p 3663 N94-33010
POLYMER PHYSICS
Competition between crystallization and mixing/demixing in polymer mixture
[ETN-94-95753] p 3651 N94-31513
Influence of trace components on the viscoelastic properties of a polymer solution
[AD-A277171] p 3656 N94-32253
Stable second-order nonlinear optical materials based on interpenetrating polymer networks
[AD-A277410] p 3658 N94-32579
Conjugated polymer fluorescence: Interplay of correlations and alternation
[DE94-005587] p 3660 N94-32729
POLYMERIC FILMS
Fluorescence observations of LDEF exposed materials as an indicator of induced material reactions
p 3593 N94-31025
On the linearity of fast atomic oxygen effects
p 3594 N94-31027
Adsorption of water to the metal/polymer interface studied by neutron and x ray reflectivity
[DE94-005578] p 3651 N94-31649
Chemical interactions between protein molecules and polymer membrane materials
[DE94-006987] p 3651 N94-31672
Reversible optical storage in azo polymers
[AD-A277109] p 3654 N94-31980
Electrical communication between glucose oxidase and electrodes based on poly(vinylimidazole) complex of Os(bpy)2Cl2
[AD-A276585] p 3635 N94-32231
New developments in second-order nonlinear optical polymeric materials
[AD-A277409] p 3658 N94-32578
Stable second-order nonlinear optical materials based on interpenetrating polymer networks
[AD-A277410] p 3658 N94-32579
Electrostrictive response of elastomeric polymers
[AD-A277983] p 3664 N94-33247
POLYMERIZATION
Photopolymerization of cyclohexene oxide: A visible light initiating system and mechanistic investigations
[AD-A277110] p 3654 N94-31981
Mechanical properties of acrylate networks formed by visible laser-induced polymerization. 2. Control of the mechanical properties
[AD-A277111] p 3655 N94-31982
Isomeric poly(benzophenone)s: Synthesis of highly crystalline poly (4, 4 foot-benzophenone) and amorphous poly (2, 5-benzophenone), a soluble poly (p-phenylene) derivative
[AD-A277261] p 3655 N94-32017
A visible light initiating system for free radical promoted cationic polymerization
[AD-A277164] p 3655 N94-32069
Multifunctional macromolecules
[AD-A277347] p 3656 N94-32246
Intramolecular charge transfer complexes as fluorescence probes for UV and visible light induced acrylate polymerization
[AD-A277129] p 3657 N94-32381
Structure-property relationships of carbon aerogels
[DE94-007120] p 3660 N94-32687
Metal ion complexation by ionizable crown ethers
[DE94-006301] p 3661 N94-32847
Interpenetrating polymer network acoustic damping material
[AD-D016141] p 3663 N94-32975
Novel polydiacetylenes as materials for second and third order nonlinear optics
[AD-A277512] p 3664 N94-33082
POLYMERS
Performance of selected polymeric materials on LDEF
p 3593 N94-31023
Molecular/polymeric magnetism
[DE94-005888] p 3649 N94-31201
Nonlinear optical properties of rigid-rod polymers
[NASA-CR-191349] p 3882 N94-32702
Low loss second-order nonlinear optical polymers based on all organic sol-gel materials
[AD-A277482] p 3663 N94-32985
Fundamental studies in crack initiation
[AD-A278387] p 3741 N94-33356
POLYMETHYL METHACRYLATE
Compatibility studies of some azo polymer blends
[AD-A277141] p 3657 N94-32365
A relaxation study of poled nonlinear optical polymers by infrared reflection-absorption spectroscopy
[AD-A277513] p 3663 N94-33054
POLYNOMIALS
A polynomial representation of the valence orbital ionization potentials
[USIP-93-06] p 3640 N94-31083
A fully two-dimensional, non-oscillatory advection scheme for momentum and scalar transport equations
[DM-66] p 3700 N94-31221

Identification of polynomial and rational NARMAX models
[RR-483] p 3842 N94-31413
Penetrable wedge analysis
[AD-A277219] p 3845 N94-32022
On interpolating random fields using a finite number of observations
[CWI-BS-R9314] p 3847 N94-32194
On constructing multi-variate orthonormal polynomials associated with spectral distribution functions
[CWI-BS-R9310] p 3851 N94-32225
Polynomial interpolation and approximation of real functions. 2: Symmetrical interpolation for the triangle
[AD-A277345] p 3848 N94-32245
Least squares approximation by G1 piecewise parametric cubes
[AD-A277978] p 3850 N94-33265

POLYSILANES
Temperature dependence of the exciton-exciton annihilation rate constant in poly(di-n-hexylsilane)
[DE94-005584] p 3655 N94-32102
Conversion of polymers of methyl- and vinylsilane to Si-C ceramics
[NASA-TM-106554] p 3662 N94-32945

POLYSILOXANES
Metal-ion spin-on glasses: Novel materials for active waveguides
[DE94-007738] p 3882 N94-32649

POLYSTYRENE
Performance of selected polymeric materials on LDEF p 3593 N94-31023
Toughening mechanisms in the high strain rate deformation of rubber-modified polymer glasses p 3653 N94-31942
Solvent diffusion coefficient concentration dependence in polymer solutions
[AD-A277023] p 3655 N94-32005
New polymer target-shell properties and characterizations
[DE94-008420] p 3890 N94-32415

POLYSULFIDES
Improved resealing procedures for the second deseal/reseal program in RAAF F111 aircraft fuel tanks
[AD-A277069] p 3580 N94-32378

POLYTETRAFLUOROETHYLENE
Custom uniform source system
[NASA-CR-189332] p 3711 N94-31492
Evaluation of pyrolysis and arc tracking on candidate wire insulation designs for space applications
[NASA-CR-195332] p 3731 N94-32901

POLYURETHANE RESINS
Fluorescence observations of LDEF exposed materials as an indicator of induced material reactions p 3593 N94-31025
Laser-induced fluorescence of space-exposed polyurethane p 3593 N94-31026
Mass-loaded coating for reducing the resonant frequency of a ceramic disc
[AD-D016095] p 3660 N94-32739
Acoustic window
[AD-D016171] p 3862 N94-33017
Electrostrictive response of elastomeric polymers
[AD-A277983] p 3664 N94-33247

POPULATION THEORY
Bifurcation and deterministic chaos in dynamic systems
[REPT-93-047] p 3911 N94-31893
On the reciprocal relationship between life histories and population dynamics
[CWI-AM-R9302] p 3793 N94-32226

POPULATIONS
Seasons and chaos in population dynamics p 3912 N94-31897
On the reciprocal relationship between life histories and population dynamics
[CWI-AM-R9302] p 3793 N94-32226
Food security in the context of global environmental change
[DE94-007481] p 3768 N94-32812

POROSITY
Surface probes of porous toluene/water ices: Adsorption kinetics and annealing spectra measured by second harmonic generation
[DE94-007564] p 3637 N94-32743
Characterization of nanoparticles and nanophase materials
[DE94-008348] p 3907 N94-32990

POROUS MATERIALS
The sol-gel-xerogel transition
[AD-A276647] p 3616 N94-32038
High-resolution numerical methods for compressible multi-phase flow in hierarchical porous media
[DE94-008261] p 3707 N94-32410

PORTABLE LIFE SUPPORT SYSTEMS
Metal hydride heat pump engineering demonstration and evaluation model
[NASA-CR-188286] p 3669 N94-32857

PORTUGAL
Evolution of upwelling fronts off the coast of Portugal
[NASA-CR-195692] p 3790 N94-33045

POSEIDON SATELLITE
Lessons learned from selecting and testing spaceflight potentiometers p 3607 N94-33318

POSITION (LOCATION)
Computing the precision of localization in a plane using projective invariants
[TELECOM-93-D-005] p 3840 N94-31095
Shiptrack database analysis
[AD-A277228] p 3746 N94-32025
Selection of climate station data using clustering and triangulated irregular network techniques
[AD-A276658] p 3784 N94-32046
MODIS. Volume 2: MODIS level 1 geolocation, characterization and calibration algorithm theoretical basis document, version 1
[NASA-TM-104594-VOL-2] p 3613 N94-33289

POSITION ERRORS
Error analysis of real-time and post-processed orbit determination for the Geosat Follow-On altimetric satellite using GPS tracking p 3576 N94-31845

POSITION SENSING
Hydrogenated amorphous silicon (a-Si:H) based gamma camera: Monte Carlo simulations
[DE94-007042] p 3795 N94-31323
Digit-Eyes: Vision-based human hand tracking
[NASA-CR-195913] p 3803 N94-31447
CAD-based off-line planning for an active-vision system
[ISBN-0-315-86317-X] p 3813 N94-31713

POSITIONING DEVICES (MACHINERY)
Two-axis antenna positioning mechanism p 3605 N94-33308

POSITIVE IONS
Performance of an ion trap inductively coupled plasma mass spectrometer
[DE94-007470] p 3713 N94-32811

POSITRON ANNIHILATION
A constraint on the pair-density ratio (Z+) in an electron-positron pair wind p 3930 N94-31132
High energy physics program at the University of Alabama
[DE94-006544] p 3875 N94-31488
Production of charginos and neutralinos for the reaction positron electron yields Z' boson yields chargino(+) (sub i) chargino(-) (sub j) or neutralino (sub i) neutralino (sub j) in SU(2) (sub L) x SU(2) (sub R) x U(1) (sub B-L)
[ISBN-0-315-87316-7] p 3867 N94-31832
Positron-molecule interactions
[AD-A276542] p 3869 N94-32082

POSITRONS
Positron-molecule interactions
[AD-A276542] p 3869 N94-32082
Isothermal sintering, microstructure, and superconducting properties of Y1Ba2Cu3O(7-x) compound
[DE94-008132] p 3905 N94-32779

POTASSIUM
Silicone grease as a precursor to a pseudo crown-ether ligand: Crystal structure of (K(+)K(Me2SiO)7(+)) (HIn(CH2CMe3)3(-))4
[AD-A276343] p 3895 N94-31327

POTASSIUM ALLOYS
Electrooptic crystal growth and properties
[AD-A276023] p 3896 N94-31439
Structural ordering in liquid K-Te alloys
[DE94-008477] p 3645 N94-32514

POTASSIUM HYDROXIDES
Development of nickel and metal hydride secondary battery
[DE94-757270] p 3697 N94-32917

POTASSIUM OXIDES
High T(sub c) superconductor tunnel junctions for photon detectors
[DE94-007686] p 3904 N94-32602

POTASSIUM PERCHLORATES
A low cost igniter utilizing an SCB and titanium sub-hydride potassium perchlorate pyrotechnic
[DE94-006467] p 3666 N94-31827

POTASSIUM PHOSPHATES
Optical properties of lanthanide-doped RbTiOAsO4 and transition metal-doped KTiOPO4
[DE94-008433] p 3907 N94-32963

POTENTIAL ENERGY
Interaction of water with metal surfaces
[AD-A276260] p 3632 N94-31293
Chemisorbed-molecule potential-energy surfaces and electronically-stimulated processes
[DE94-007932] p 3719 N94-32603
Computed potential energy surfaces for chemical reactions
[NASA-CR-195835] p 3639 N94-33036

POTENTIAL FLOW
Prediction of transonic potential flow with slipstreams around configurations
[FFA-TN-1992-15] p 3568 N94-31220
A novel potential/viscous flow coupling technique for computing helicopter flow fields
[NASA-CR-193272] p 3571 N94-32476

POTENTIAL THEORY
A general stochastic Liouville theory for sequential and superexchange electron-transfer reactions involving three Marcus potential surfaces
[DE94-007695] p 3869 N94-32141

POTENTIOMETERS
Lessons learned from selecting and testing spaceflight potentiometers p 3607 N94-33318

POWDER (PARTICLES)
Effect of surface forces on the rheology of particle-liquid systems and the consolidation of ceramic powders
[AD-A277092] p 3657 N94-32391
SUNY beamline facilities at the National Synchrotron Light Source
[DE94-006343] p 3905 N94-32770
Isothermal sintering, microstructure, and superconducting properties of Y1Ba2Cu3O(7-x) compound
[DE94-008132] p 3905 N94-32779
Deuterium absorption and material phase characteristics of SAES St198 Zr-Fe alloy
[DE94-008275] p 3646 N94-32781
X ray absorption study of pulsed laser deposited boron nitride films
[DE94-008295] p 3662 N94-32855
Optical properties of lanthanide-doped RbTiOAsO4 and transition metal-doped KTiOPO4
[DE94-008433] p 3907 N94-32963
Characterization of nanoparticles and nanophase materials
[DE94-008348] p 3907 N94-32990

POWDER METALLURGY
Powder metallurgical processing of fibre reinforced aluminium composites
[PB94-148285] p 3620 N94-31688
Pressureless sintering of ceramic composites
[AD-A277274] p 3657 N94-32404
On the formation of muon- and zeta-phases in Ag-Al system by mechanical alloying
[DE94-007125] p 3645 N94-32636

POWDERED ALUMINUM
On the formation of muon- and zeta-phases in Ag-Al system by mechanical alloying
[DE94-007125] p 3645 N94-32636

POWER AMPLIFIERS
Design of a high power x-band magnicon amplifier
[AD-A277001] p 3692 N94-32199
Design, characterization and control of the Unique Mobility Corporation robot p 3603 N94-33296

POWER CONDITIONING
Optimal adaptive estimation algorithm for harmonic current reduction using power limited active line conditioners
[AD-A277354] p 3693 N94-32336
Universal signal conditioning amplifier p 3699 N94-32460
The constant current loop: A new paradigm for resistance signal conditioning p 3685 N94-32461
Field operation test of utility interactive load conditioner with photovoltaic cells at a demonstration house
[DE94-757271] p 3762 N94-32918

POWER CONVERTERS
Real time simulation model for designing converter regulation
[ETN-94-95735] p 3689 N94-31576

POWER EFFICIENCY
Optimal reactive power dispatch of power systems using nonlinear programming
[MATHS-REPT-A-209] p 3808 N94-31164

POWER LINES
Optimal adaptive estimation algorithm for harmonic current reduction using power limited active line conditioners
[AD-A277354] p 3693 N94-32336

POWER SPECTRA
Analysis using bi-spectral related technique
[AD-A276017] p 3672 N94-31386
Atmospheric structure simulation: An autoregressive model for smooth geophysical power spectra with known autocorrelation function
[AD-A276691] p 3773 N94-32118
Note on the variance of autospectral density processed using Welch's method
[DE94-005352] p 3849 N94-32675

POWER TRANSMISSION
High-temperature superconducting transformer performance, cost, and market evaluation
[DE94-005494] p 3687 N94-31152
Roll ring assemblies for the Space Station
p 3603 N94-33294
PRE-MAIN SEQUENCE STARS
Circumstellar material around young stars in Orion
p 3930 N94-31133
Double-lined pre-main-sequence binaries: A test of pre-main-sequence evolutionary theory
p 3933 N94-31497
Radio emission from pre-main-sequence stars
p 3955 N94-31890
PRECESSION
A twisted disk equation that describes warped galaxy disks p 3928 N94-31118
The dynamical settling of warped disks and angular momentum transport in galaxies p 3928 N94-31121
Hyperon polarization, crystal channeling, and E781 at Fermilab
[DE94-008224] p 3877 N94-32802
PRECIPITATES
Indium-vacancy complexes in mercury cadmium telluride
[AD-A276177] p 3894 N94-31055
Irradiation-induced phase transformations in zirconium alloys
[DE94-008484] p 3648 N94-32993
PRECIPITATION (CHEMISTRY)
Preparation of catalyst particles using methods of colloid chemistry. Part 1: Preparation of silica particles from alcohol solutions
[PB94-135597] p 3634 N94-31679
PRECIPITATION (METEOROLOGY)
Some aspects of the drought in North Africa and in the Mediterranean basin p 3778 N94-30989
Tropical squall lines p 3778 N94-30992
The ocean-atmosphere interactions in the Mediterranean Sea p 3779 N94-30995
The Global Climatology Network precipitation data
[DE93-019199] p 3764 N94-31596
Diagnostic studies of climate variability
[DE94-003629] p 3767 N94-32711
PRECIPITATION HARDENING
Continuous measurement of aging response in aluminum alloys by eddy current methods
[AD-A277233] p 3644 N94-32371
Experimental studies on the effect of coherency strains on coarsening kinetics: Current status and future outlook
[DE94-008480] p 3647 N94-32964
PRECIPITATION PARTICLE MEASUREMENT
Drop size distributions and related properties of fog for five locations measured from aircraft
[NASA-CR-4585] p 3787 N94-33065
PRECISION
Computing the precision of localization in a plane using projective invariants
[TELECOM-93-D-005] p 3840 N94-31095
PRECONDITIONING
Preconditioned time-difference methods for advection-diffusion-reaction equations
[DE94-006472] p 3638 N94-32840
PREDATORS
Qualitative properties of two-dimensional predator-prey systems
[REPT-93-75] p 3844 N94-31644
A predator-prey model with Ivlev's functional response
[REPT-93-79] p 3844 N94-31698
PREDICATE LOGIC
Updates in dynamic semantics
[LP-93-06] p 3856 N94-31450
Weaks vs. strong readings of donkey sentences and monotonicity inference in a dynamic setting
[LP-93-10] p 3856 N94-31468
PREDICTION ANALYSIS TECHNIQUES
Feasibility and stability results for constrained stable generalized predictive control
[MATHS-REPT-A-203] p 3828 N94-31158
Prediction of transonic potential flow with slipstreams around configurations
[FFA-TN-1992-15] p 3568 N94-31220
Development of a three-dimensional icing model for predicting ice accretion on aircraft
[ONERA-NT-1993-5] p 3574 N94-31230
Analysis of ionospheric parameters in Europe and creation of the prediction algorithm
[AD-A276342] p 3771 N94-31326
The prediction of convective transfer on the thermal insulation of a solid-propellant rocket motor
[ONERA-NT-1993-15] p 3614 N94-31423
Viscoelastic fracture characterization of polymeric solids p 3652 N94-31745
Computer modelling of cyclic deformation of high-temperature materials
[AD-A277056] p 3623 N94-32012
Fracture and fatigue strength evaluation of multiple site damaged aircraft fuselages - curved panel testing and analysis
[AD-A277100] p 3579 N94-32015
Aircraft weight prediction capability. Volume 1: Weight study and results
[AD-A277206] p 3579 N94-32062
Exploring phase space concepts in the forecasting of time series with artificial neural networks
[DE94-005810] p 3834 N94-32127
Analysis of Dietz's single, rectangular pulse theory for the generation of radiation via photoelectrons
[DE94-006131] p 3681 N94-32661
Aspects of modeling uncertainty and prediction
[DE94-007565] p 3852 N94-32744
User's guide for a flat wake rotor inflow/wake velocity prediction code, DOWN
[NASA-TM-104139] p 3572 N94-32873
Development and testing of improved techniques for modeling the hydrologic cycle in a mesoscale weather prediction system
[AD-A277416] p 3786 N94-32921
Effective computational strategy for predicting the response of complex systems
[AD-A277452] p 3740 N94-33011
Reciprocity-based experimental determination of dynamic forces and moments: A feasibility study
[NASA-CR-194905] p 3862 N94-33023
Statistical characteristics of bistatic surface scatter and mean bistatic surface scattering strengths
[AD-A278155] p 3862 N94-33096
PREDICTIONS
Contribution to the study of multiaxial fatigue under periodic or random stresses
[ISAL-92-0004] p 3734 N94-31544
PREDICTOR-CORRECTOR METHODS
Effective computational strategy for predicting the response of complex systems
[AD-A277452] p 3740 N94-33011
PREFORMS
Second NASA Advanced Composites Technology Conference
[NASA-CP-3154] p 3627 N94-33121
Recent progress in NASA Langley Research Center textile reinforced composites program
p 3629 N94-33134
Advanced textile applications for primary aircraft structures p 3629 N94-33135
Comparison of resin film infusion, resin transfer molding, and consolidation of textile preforms for primary aircraft structure p 3630 N94-33136
PREMIXED FLAMES
Turbulence structure of a premixed flame in a coaxial free air jet in the presence or absence of a base flow
[ISBN-0-315-78739-2] p 3633 N94-31471
PREPREGS
Empirical optimization of the consolidation of thermoplastic prepregs
[ISBN-0-315-86455-9] p 3652 N94-31722
PREPROCESSING
Extension of the LUSTRE language and application to circuit design: The LUSTRE V4 language and the POLLUX system
[ETN-94-95918] p 3812 N94-31543
Inflight calibration, preprocessing, and data evaluation of GER 2 imaging spectrometry data
p 3744 N94-31858
CMS Preprocessing Subsystem user's guide: Software version 2.0
[DE94-005327] p 3816 N94-32145
CMS Distribution Subsystem user's guide
[DE94-005328] p 3816 N94-32146
An analog preprocessing architecture for high-speed analog-to-digital conversion
[AD-A276737] p 3807 N94-32163
A novel optoelectronic system for distortion-invariant ATR
[AD-A277985] p 3884 N94-33087
PRESIDENTIAL REPORTS
Aeronautics and space report of the President: Fiscal year 1993 activities p 3966 N94-32854
PRESSURE BROADENING
High resolution molecular spectroscopy of atmospheric species
[AD-A278382] p 3776 N94-33351
PRESSURE DEPENDENCE
High pressure experiments on the Y-Ba-Cu-O superconductors: A major role for holes
[ETN-94-96013] p 3897 N94-31547
PRESSURE DISTRIBUTION
Dynamics of flux tubes in accretion disks
p 3932 N94-31142
Rotordynamic effects driven by fluid forces from a geometrically imperfect labyrinth
[AD-A276424] p 3722 N94-31333
Shock impingement near mild hypersonic expansion corners p 3569 N94-31879
Design of a two dimensional planer pressurized air labyrinth seal test rig
[AD-A277232] p 3726 N94-32370
In flight measurement of steady and unsteady blade surface pressure of a single rotation large scale advanced prop-fan installed on the PTA aircraft
[NASA-CR-187096] p 3584 N94-32859
PRESSURE EFFECTS
Computational study of single-expansion-ramp nozzles with external burning
[NASA-TM-106550] p 3700 N94-31229
A model of the ion chemistry of electrified convection
p 3868 N94-31993
Advanced thermally stable jet fuels
[DE94-006760] p 3667 N94-32150
Simulation of low-density nozzle plumes in non-zero ambient pressures
[NASA-TM-106501] p 3615 N94-32742
Composite fuselage shell structures research at NASA Langley Research Center p 3628 N94-33124
The influence of thermal inertia on Mars' seasonal pressure variation and the effect of the weather component p 3952 N94-33238
PRESSURE GRADIENTS
Modification of the MML turbulence model for adverse pressure gradient flows
[NASA-TM-106544] p 3709 N94-32947
PRESSURE MEASUREMENT
Research in marine boundary layer intermittency
[AD-A276076] p 3701 N94-31460
Development of a cascade simulation of fan-passage flow
[AD-A277234] p 3584 N94-32026
In flight measurement of steady and unsteady blade surface pressure of a single rotation large scale advanced prop-fan installed on the PTA aircraft
[NASA-CR-187096] p 3584 N94-32859
Simultaneous pressure measurement and high-speed photography study of cavitation in a dynamically loaded journal bearing
[NASA-TM-106456] p 3728 N94-32893
PRESSURE OSCILLATIONS
Shock impingement near mild hypersonic expansion corners p 3569 N94-31879
PRESSURE SENSORS
PVDF pressure transducers for shock wave and explosives research
[AD-A277319] p 3712 N94-32051
PRESSURE VESSELS
Development of high-pressure diaphragms for the AEDC impulse tunnel
[AD-A277053] p 3588 N94-32009
Reactor pressure vessel structural integrity research in the US Nuclear Regulatory Commission HSST and HSSI Programs
[DE94-006550] p 3739 N94-32771
PRESSURIZING
Control experiments in liquid metal combustion
[AD-A276918] p 3635 N94-32234
PRETREATMENT
Technology development for iron Fischer-Tropsch catalysts
[DE94-008723] p 3638 N94-32889
Evaluation of the Hughes conversion coating touch-up pen
[AD-A278398] p 3664 N94-33166
PRINCIPAL COMPONENTS ANALYSIS
Principal component analysis with missing data and its application to object modeling
[AD-A276644] p 3845 N94-31939
Airborne SAR as a complement to SPOT HRV in land-cover classification: The use of normalization and principal components analysis p 3750 N94-32539
Statistical intercomparison of global climate models: A common principal component approach
[DE94-008671] p 3768 N94-32882
PRINTED CIRCUITS
From display and PWB to MCMs: Large panel manufacturing
[DE94-007855] p 3693 N94-32386
An electrical test system for conductor formation process analysis
[DE94-007291] p 3696 N94-32786
Space flight printed wiring board measling investigation
[NASA-TM-104602] p 3732 N94-33101
PRIVACY
PEM public key certificate cache server
[DE94-006404] p 3675 N94-31784
PROBABILITY DENSITY FUNCTIONS
Detection of a chi-square fluctuating target in Gaussian noise
[AD-A276078] p 3850 N94-31462

Mixture model simulating reactive turbulent flows: Testing of Eulerian-Lagrangian probabilistic models
[ONERA-NT-1993-13] p 3702 N94-31477
Diagonal band probability distributions
[REPT-93-80] p 3851 N94-31697
A non-local model for prediction of the probability density function of turbulent fluctuations in boundary-layer flows
p 3706 N94-32076
High-performance speech recognition using consistency modeling
[AD-A276775] p 3679 N94-32185

PROBABILITY DISTRIBUTION FUNCTIONS
Diagonal band probability distributions
[REPT-93-80] p 3851 N94-31697
Probability distributions with given marginals and given correlation that have maximal entropy
[REPT-93-81] p 3851 N94-31698
On the relationship between generalization error, hypothesis complexity, and sample complexity for radial basis functions
[AD-A276802] p 3851 N94-32142

PROBABILITY THEORY
A probabilistic view of Datalog parallelization
[TELECOM-93-D-021] p 3824 N94-31183
Study of B(0) - bar-B(0) mixing in D0
[DE94-006000] p 3897 N94-31506
The Laplace functional and Palm measure of a quasi-Cox process which is driven by a Markov chain
[REPT-93-82] p 3851 N94-31699
Performance metrics for low probability of intercept-communication system
[AD-A277346] p 3677 N94-32073
High-performance speech recognition using consistency modeling
[AD-A276775] p 3679 N94-32185
Multiserver queues with impatient customers
[CWI-BS-R9319] p 3835 N94-32198
An algorithm for probabilistic, totally-ordered temporal projection
[AD-A277341] p 3817 N94-32257
Structural probability concepts adapted to electrical engineering
[NASA-TM-106499] p 3739 N94-32735
Aspects of modeling uncertainty and prediction
[DE94-007565] p 3852 N94-32744
Visual processing of object velocity and acceleration
[AD-A277425] p 3801 N94-32998

PROBLEM SOLVING
On the use of genetic algorithms to solve the time-table problem
[REPT-90-060-REV] p 3829 N94-31176
Techniques for increasing the robustness of iterative algorithms for multi-resources location problems
[REPT-93-037] p 3809 N94-31188
Exact solution of the single machine scheduling problem with earliness and flow time penalties
[REPT-93-038] p 3809 N94-31189
A hypertext system that learns from user feedback
p 3923 N94-32428
Reminding-based learning
[AD-A277424] p 3801 N94-32997

PROCESS CONTROL (INDUSTRY)
Managing customer order driven engineering. An interdisciplinary and design oriented approach
[PB94-145083] p 3917 N94-31583
The future of open architecture process control systems
[DE94-006163] p 3830 N94-31623
Powder metallurgical processing of fibre reinforced aluminium composites
[PB94-148285] p 3620 N94-31688
A fuzzy classifier system for process control
p 3839 N94-32422

PROCUREMENT
Estimating the impact of crashworthiness standards on mortality and morbidity events in the US Army rotary-wing aircraft mishaps
[AD-A277121] p 3575 N94-32363

PRODUCT DEVELOPMENT
A comparison of product realization frameworks
[AD-A275992] p 3810 N94-31357
An application reference model for layered manufacturing
[DE94-006368] p 3811 N94-31484
Concept, construction and testing of a high resolution QCLAM electron spectrometer with large solid angle and high impulse acceptance for the electron accelerator S-DALINAC
[ETN-94-95755] p 3711 N94-31515
Managing customer order driven engineering. An interdisciplinary and design oriented approach
[PB94-145083] p 3917 N94-31583
Effective information modelling support
[PB94-148236] p 3917 N94-31586
Case studies of software process improvement methods
[AD-A277289] p 3818 N94-32508

PRODUCTION COSTS
Budget allocation and monopolistic pricing in a multiproduct firm
[REPT-93-86] p 3924 N94-31617
Recovery of carboxylic acids at pH greater than pKa
[DE94-007030] p 3636 N94-32376
Leveraging metal matrix composites to reduce costs in space mechanisms p 3604 N94-33301

PRODUCTION ENGINEERING
Managing customer order driven engineering. An interdisciplinary and design oriented approach
[PB94-145083] p 3917 N94-31583
Fractional-factorial process development techniques
[DE94-005580] p 3690 N94-31593
Flexible manufacturing for photonics device assembly
p 3669 N94-32449

PRODUCTION MANAGEMENT
An application reference model for layered manufacturing
[DE94-006368] p 3811 N94-31484
Managing customer order driven engineering. An interdisciplinary and design oriented approach
[PB94-145083] p 3917 N94-31583
Process mapping: A user-friendly tool for process improvement
[DE94-004357] p 3730 N94-31605

PRODUCTIVITY
An analysis of the records management process to determine the impact of automation on productivity
[AD-A275923] p 3916 N94-31344
Drug-related problems in the workplace
[CRANFIELD-AERO-9306] p 3914 N94-31538

PROGRAM VERIFICATION (COMPUTERS)
Cleanroom engineering handbook. Volume 6: Certification team practices
[AD-A275951] p 3587 N94-31346
The maintenance of operational flight program
[AD-A276363] p 3565 N94-31367
Testing Operational Flight Programs (OFP's)
[AD-A276361] p 3578 N94-31387
Consistency checks for SCR-style requirements specifications
[AD-A276077] p 3811 N94-31461
An epistemic proof system for parallel processes
[TR-93-17] p 3826 N94-32291
SynRGen: An extensible file reference generator
[AD-A277678] p 3821 N94-33030
Faultless software project
[AD-A278161] p 3822 N94-33188
Ada support for the mathematical foundations of software engineering
[AD-A278031] p 3822 N94-33284

PROGRAMMABLE LOGIC DEVICES
Extension of the LUSTRE language and application to circuit design: The LUSTRE V4 language and the POLLUX system
[ETN-94-95918] p 3812 N94-31543

PROGRAMMING ENVIRONMENTS
E-L user's manual
[AD-A276378] p 3810 N94-31370
LORE and reason maintenance
[REPT-93-88] p 3812 N94-31522
Automatic generation of context-sensitive textual help
[REPT-93-68] p 3812 N94-31646
Incremental recompilation for Standard ML of New Jersey
[AD-A276522] p 3815 N94-32080
Integrated Trusted System Development Environment Process
[AD-A276414] p 3816 N94-32131
MULTIGRAPH: An architecture for model-based programming. Model-based program synthesis for parallel computing. PREMOS: Programming environment for model-based program synthesis, version 01.00.00
[AD-A276949] p 3817 N94-32219
Evolving software reengineering technology for the emerging innovative-competitive era
p 3823 N94-32439
MADE: A Multiple Application Development Environment
[CWI-CS-R9360] p 3822 N94-33097

PROGRAMMING LANGUAGES
LORE and reason maintenance
[REPT-93-88] p 3812 N94-31522
Extension of the LUSTRE language and application to circuit design: The LUSTRE V4 language and the POLLUX system
[ETN-94-95918] p 3812 N94-31543
Methods for parallelizing search paths in phrasing
[AD-A276876] p 3817 N94-32212
Translucent procedures, abstraction without opacity
[AD-A276877] p 3817 N94-32213
Information disclosure in evolving information systems: Taking a shot at a moving target
[TR-93-22] p 3919 N94-32506
Machine assisted implementation of complex algorithms and labor intensive software, closing report
[AD-A277662] p 3821 N94-33027

PROJECT MANAGEMENT
An active computer supported medium for distributed planning in enterprises
[ETN-94-95738] p 3829 N94-31372
Evaluating success levels of mega-projects
p 3599 N94-31432

PROJECT PLANNING
NASA's space platform technology program and planning p 3597 N94-31044
NASCOM system development plan: System description, capabilities, and plans, FY 94-2
[NASA-TM-109744] p 3674 N94-31503

PROJECT SETI
The quest for contact
[NASA-TM-109778] p 3806 N94-32389

PROJECTILES
Tearing resistance of a thin shell against projectile penetration: Material property effects
[DE94-007466] p 3733 N94-31316
Using Monte Carlo techniques and parallel processing for debris hazard analysis of rocket systems
[DE94-007250] p 3609 N94-31382

PROJECTIVE GEOMETRY
Computing the precision of localization in a plane using projective invariants
[TELECOM-93-D-005] p 3840 N94-31095
Algebraic functions for recognition
[AD-A276803] p 3846 N94-32167

PROJECTORS
A paraperspective factorization method for shape and motion recovery
[AD-A276513] p 3712 N94-31929

PROKARYOTES
Light utilization and photoinhibition of photosynthesis in marine phytoplankton
[DE94-005505] p 3794 N94-32896

PROLATE SPHEROIDS
Three-dimensional velocity measurements on a 6:1 prolate spheroid at 10 deg angle of attack
[AD-A276485] p 3702 N94-31476

PROP-FAN TECHNOLOGY
In flight measurement of steady and unsteady blade surface pressure of a single rotation large scale advanced prop-fan installed on the PTA aircraft
[NASA-CR-187096] p 3584 N94-32859

PROPAGATION VELOCITY
Superluminous laser pulse in an active medium
[DE94-007110] p 3720 N94-32684

PROPANE
Volatiles combustion in fluidized beds
[DE94-008382] p 3636 N94-32414

PROPELLANT ADDITIVES
A compatibility study of FEFO with various containment materials
[DE94-005753] p 3649 N94-31198

PROPELLANT COMBUSTION
Photothermal laser deflection, an innovative technique to measure particles in exhausts
[AD-A277151] p 3718 N94-32366

PROPELLANT GRAINS
Condensed-phase processes during solid propellant combustion. 3: Preliminary depth-profiling studies on XM39, JA2, M9, M30, and HMX2
[AD-A276595] p 3635 N94-32124

PROPELLANT STORABILITY
A compatibility study of FEFO with various containment materials
[DE94-005753] p 3649 N94-31198

PROPELLANT STORAGE
A compatibility study of FEFO with various containment materials
[DE94-005753] p 3649 N94-31198

PROPELLER BLADES
In flight measurement of steady and unsteady blade surface pressure of a single rotation large scale advanced prop-fan installed on the PTA aircraft
[NASA-CR-187096] p 3584 N94-32859

PROPELLER FANS
In flight measurement of steady and unsteady blade surface pressure of a single rotation large scale advanced prop-fan installed on the PTA aircraft
[NASA-CR-187096] p 3584 N94-32859

PROPELLER NOISE
A pilot study of comfort criteria and sound quality metrics for sound inside cabins of propeller-driven aircraft
[CTH-F-93-03] p 3859 N94-31090
Experimental and computational studies on propeller noise due to inflow distortion p 3860 N94-31846

PROPELLERS
Experimental and computational studies on propeller noise due to inflow distortion p 3860 N94-31846
PROPORTIONAL CONTROL
Development of a reconfigurable helicopter flight control system
[ISBN-0-315-87218-7] p 3585 N94-31837
PROPULSION
Institute for Computational Mechanics in Propulsion (ICOMP)
[NASA-TM-106542] p 3710 N94-32969
PROPULSION SYSTEM CONFIGURATIONS
Futurepath 3
[NASA-TM-109762] p 3735 N94-31819
PROPULSION SYSTEM PERFORMANCE
Futurepath 3
[NASA-TM-109762] p 3735 N94-31819
Performance of a quasi-steady, multi megawatt, coaxial plasma thruster
[NASA-CR-195311] p 3616 N94-32970
PROPULSIVE EFFICIENCY
Pulsed expansion of plasma in a magnetic thruster p 3889 N94-31776
PROSTHETIC DEVICES
Application of dexterous space robotics technology to myoelectric prostheses p 3729 N94-32450
PROTECTION
Controlling hazardous energy sources (lockout/tagout)
[NASA-TM-105290] p 3669 N94-32861
PROTECTIVE CLOTHING
A review of microclimate cooling systems in the chemical, biological, radiological environment
[AD-A276446] p 3802 N94-31302
Proceedings of the DCIEM Diver Thermal Protection Workshop
[DCIEM-92-10] p 3795 N94-31738
Thermotropic liquid crystals: A variable Clo material p 3796 N94-31739
Validation and sensitivity analysis of Texas human thermal model predictions during cold water immersion
[AD-A275240] p 3797 N94-32156
Aerospace medicine and biology: A continuing bibliography with indexes (supplement 389)
[NASA-SP-7011(389)] p 3797 N94-32347
Aerospace medicine and biology: A continuing bibliography with indexes (supplement 385)
[NASA-SP-7011(385)] p 3797 N94-32348
Aircrew Eye/Respiratory Protection (AERP): 16-hour extended wear evaluation of chemical protective equipment
[AD-A277288] p 3804 N94-32609
PROTECTIVE COATINGS
Atomic oxygen interaction at defect sights in protective coatings on polymers flown on LDEF p 3593 N94-31024
Low-Earth orbit effects on organic composite materials flown on LDEF p 3595 N94-31036
Evaluation of corrosion protective organic coatings for steel structures in fresh water
[PB94-138484] p 3649 N94-31072
Sol-gel metal oxide and metal oxide/polymer multilayers applied by meniscus coating
[DE94-005813] p 3649 N94-31199
Electrostatic reduction of particulates for laser resistant hafnia coatings
[DE94-005824] p 3651 N94-31557
Processing boron and boron carbide thin films for protective coatings and device fabrication
[AD-A277266] p 3900 N94-32041
Compilation of diamond-like carbon properties for barriers and hard coatings
[DE94-008231] p 3661 N94-32803
Method and apparatus for inhibiting the disbonding of a paint from metal surfaces
[AD-D016106] p 3663 N94-32960
Interface engineering in oxide fiber/oxide matrix composites
[AD-A277672] p 3627 N94-33029
Evaluation of the Hughes conversion coating touch-up pen
[AD-A278398] p 3664 N94-33166
PROTEINS
Employment of a porous gold actuator in ISFET-based coulometric sensor-actuator systems with application to protein characterization
[ISBN-9-09-005887-7] p 3689 N94-31536
Chemical interactions between protein molecules and polymer membrane materials
[DE94-006987] p 3651 N94-31672
Neural network definitions of highly predictable protein secondary structure classes
[DE94-006234] p 3834 N94-32175
A genetic algorithm based method for docking flexible molecules
[DE94-007525] p 3793 N94-32269
Development and application of photosensitive device systems to studies of biological and organic materials
[DE94-008503] p 3793 N94-32516
The magnesium chelation step in chlorophyll biosynthesis
[DE94-008727] p 3794 N94-32890
PROTOCOL (COMPUTERS)
Communications networks in stressed environments
[AD-A275967] p 3672 N94-31384
Using atomic actions in replica groups to simplify the replication implementation
[REPT-93-78] p 3813 N94-31695
The FELICIA bulletin board system and the IRBIS anonymous FTP server: Computer security information sources for the DOE community
[DE94-008219] p 3825 N94-31920
The use of service limits for efficient operation of multi-station single-medium communication systems
[CWI-BS-R9312] p 3677 N94-32085
IRIG J asynchronous ASCII time code formats
[AD-A277244] p 3681 N94-32332
Voice and video transmission using XTP and FDDI p 3685 N94-32468
Multicast communication with guaranteed quality of service
[AD-A277650] p 3682 N94-33025
PROTON BEAMS
RHIC spin physics
[DE94-005452] p 3876 N94-32099
PROTON BELTS
Self-consistent effects of magnetospheric hydromagnetic waves on ring current ions
[AD-A277406] p 3774 N94-32346
PROTON-PROTON REACTIONS
Analysis of the high energy behavior of the forward scattering parameters - sigma(tot), rho and B
[DE94-006537] p 3864 N94-31310
PROTONS
State of hadron collider physics
[DE94-005279] p 3863 N94-31147
F0-975, A0-980 as eye-witnesses of confinement
[PB94-147105] p 3868 N94-31923
NN-interaction in (1)S0-state: Virtual level or dibaryon resonance?
[DE94-606492] p 3869 N94-32097
Self-consistent effects of magnetospheric hydromagnetic waves on ring current ions
[AD-A277406] p 3774 N94-32346
Studies of jet production with the D0 detector
[DE94-008271] p 3873 N94-32780
PROTOPLANETS
Observations of accretion and angular momentum regulation in young circumstellar disks and the implications for planetary formation p 3928 N94-31122
Evolution of protoplanetary disks with dynamo magnetic fields p 3931 N94-31135
Multiwavelength search for protoplanetary disks p 3599 N94-31430
Planetesimal dynamics in the vicinity of a growing protoplanet p 3935 N94-31926
PROTOSTARS
Theory of protostellar accretion disks p 3931 N94-31136
Gravitational instabilities in protostellar disks p 3932 N94-31140
Near and far infrared observations of protostars and dark clouds p 3926 N94-31969
PROTOTYPES
Results of real-time testing and demonstration of the US Army Corps of Engineers real-time on-the-fly positioning system
[AD-A276160] p 3576 N94-31080
Model borne data management system for wind tunnel testing, phase 2
[AD-A276296] p 3587 N94-31295
Study of virtual prototyping of aircraft instruments
[CMC-0687-1090] p 3581 N94-31903
Parallel methods for synthesizing whole-hand grasps from generalized prototypes
[AD-A276798] p 3726 N94-32166
Technical evaluation of the UH-60Q: Aircraft in typical aeromedical evacuation missions
[AD-A276944] p 3586 N94-32217
Airborne Trailblazer: Two decades with NASA Langley's 737 flying laboratory
[NASA-SP-4216] p 3566 N94-32793
Design, development, and testing of a lightweight optical sensor cover system p 3604 N94-33302
PSEUDOPOTENTIALS
Theoretical studies of electron transfer and optical spectroscopy
[DE94-006985] p 3871 N94-32375
PSYCHOACOUSTICS
Quality of sound in large rooms: Alteration of room impulse responses
[CTH-E-93-02] p 3859 N94-31077
Complex auditory signals
[AD-A278391] p 3862 N94-33146
PSYCHOPHYSICS
Sensory sensitivities and discriminations and their roles in aviation
[AD-A277312] p 3800 N94-32276
Visual encoding of spatial relations
[AD-A277400] p 3800 N94-32344
Workshop on Visual Perception: Computation and Psychophysics
[AD-A278412] p 3802 N94-33326
PSYCHOPHYSIOLOGY
Determination of multiple sound sources
[AD-A277379] p 3799 N94-32096
From animals to animats
[AD-A277427] p 3802 N94-33241
PUBLIC HEALTH
Systems for the monitoring of working conditions relating to health and safety: Extensive description. Norway
[PB94-138542] p 3803 N94-31839
PUBLIC SPEAKING
An exploratory study of neuro linguistic programming and communication anxiety
[AD-A277756] p 3682 N94-32986
PULMONARY FUNCTIONS
Medical problems in high mountain environments. A handbook for medical officers
[AD-A278095] p 3798 N94-33268
PULSARS
Evolution of vaporizing pulsars p 3929 N94-31128
A study of angular momentum loss in binaries using the free Lagrange method p 3931 N94-31134
A search for 100 TeV gamma ray emission from the x ray binary pulsar 4U 0115+63 using the CYGNUS extensive air-shower array p 3955 N94-31900
The evolutionary status of PSR 1259-63
[DE94-007094] p 3938 N94-32503
PULSE AMPLITUDE
A miniaturized ASIC-based multichannel scaler instrument
[DE94-007222] p 3807 N94-32783
PULSE COMMUNICATION
Channel equalization for block transmission systems
[TELECOM-93-D-002] p 3670 N94-31093
Kalman filtering approach to blind equalization
[AD-A276320] p 3671 N94-31299
The effects of a multipath channel and interference on coherent M-PSK digital communication systems
[AD-A278158] p 3684 N94-33254
PULSE DURATION
Limiting vibration in systems with constant amplitude actuators through command preshaping
[NASA-CR-188284] p 3739 N94-32907
PULSE DURATION MODULATION
Real time simulation model for designing converter regulation
[ETN-94-95735] p 3689 N94-31576
Examination of fast semiconductor diodes (recovery) with respect to switching valves in PWM and resonance devices
[ETN-94-95740] p 3690 N94-31609
Design, characterization and control of the Unique Mobility Corporation robot p 3603 N94-33296
PULSE GENERATORS
Waveform generation for ultra-wideband radar system
[AD-A276352] p 3673 N94-31401
A noncritically phase matched femtosecond optical parametric oscillator near 3 microns
[DE94-008050] p 3720 N94-32704
PULSE MODULATION
Workshop on Commercialization of Pulsed Power Science and Technology Proceedings
[AD-A276987] p 3692 N94-32258
PULSED JET ENGINES
Pulsed expansion of plasma in a magnetic thruster p 3889 N94-31776
PULSED LASER DEPOSITION
In-situ TEM crystallization of anorthite-glass films on (alpha)-Al2O3
[DE94-006317] p 3652 N94-31780
Properties of doped and undoped (Ca,Sr)CuO2 thin films
[DE94-007230] p 3905 N94-32785
Nucleation and growth of cubic boron nitride films produced by ion-assisted pulsed laser deposition
[DE94-007295] p 3661 N94-32796
X ray absorption study of pulsed laser deposited boron nitride films
[DE94-008295] p 3662 N94-32855
PULSED LASERS
Time-resolved infrared absorption studies applied to the study of radical plus molecule reactions
[DE94-005921] p 3863 N94-31202
Workshop on Commercialization of Pulsed Power Science and Technology Proceedings
[AD-A276987] p 3692 N94-32258

Ti:sapphire based ultrafast pump-probe laser source in the violet and ultraviolet
[DE94-007542] p 3716 N94-32270
High average power pulsed phase conjugate laser with birefringence correction
[DE94-006049] p 3719 N94-32659
Superluminous laser pulse in an active medium
[DE94-007110] p 3720 N94-32684
Repetitively pulsed Cr:LiSAF laser for lidar applications
[DE94-007546] p 3720 N94-32761
Progress in understanding and improving x ray lasers
[DE94-006048] p 3720 N94-32794
A reliable low-maintenance flashlamp-pumped Ti:sapphire laser operating at 120 PPS
[DE94-009030] p 3721 N94-32848
X ray absorption study of pulsed laser deposited boron nitride films
[DE94-008295] p 3662 N94-32855
Ultrafast x ray sources
[AD-A277455] p 3721 N94-33012

PULSED RADIATION
Free electrons as a versatile source of coherent radiation
[ETN-94-96011] p 3715 N94-31545
Design and characterization of a pulsed x ray source for fluorescent lifetime measurements
[DE94-007495] p 3880 N94-32138
A historical perspective on fifteen years of laser damage thresholds at LLNL
[DE94-007930] p 3719 N94-32613

PULTRUSION
Fatigue behavior of unidirectional pultruded composite materials
[ISBN-0-315-86425-7] p 3621 N94-31719

PUMPS
Low power, constant-flow air pump systems
[DE94-007463] p 3727 N94-32758

PURSUIT TRACKING
Analysis of pursuit tracking eye movements in pilots and nonfliers
[AD-A276597] p 3799 N94-32035

PUSHBROOM SENSOR MODES
Airborne SAR as a complement to SPOT HRV in land-cover classification: The use of normalization and principal components analysis p 3750 N94-32539

PYRIDINES
Hydrogen peroxide electrodes based on electrical connection of redox centers of various peroxidases to electrodes through a three-dimensional electron relaying polymer network
[AD-A276543] p 3691 N94-32056
Dynamics of block poly(styrene-co-vinylpyridine) (SVP) in solution and on silica
[AD-A277139] p 3657 N94-32364
Laser flash photolysis, EPR and Raman studies of liquids at elevated pressures
[DE94-008351] p 3718 N94-32413

PYROELECTRICITY
Photopyroelectric spectroscopy as a non-intrusive technique for the determination of the optical absorption spectra of multiple quantum well samples
[ISBN-0-315-87164-4] p 3833 N94-31875

PYROLYSIS
The intramolecular cyclization of bis-2,5-dimethylene-2,5-dihydrofurans and bis-2,5-dimethylene-2,5-dihydrothiophenes: An approach to macrocycles
[DE94-007060] p 3657 N94-32377
Improved oxidation resistance of 3-D carbon/carbon composites
[AD-A277349] p 3625 N94-32624
Structure-property relationships of carbon aerogels
[DE94-007120] p 3660 N94-32687
Direct aromatization of methane
[DE94-008719] p 3638 N94-32888
Evaluation of pyrolysis and arc tracking on candidate wire insulation designs for space applications
[NASA-CR-195332] p 3731 N94-32901
Conversion of polymers of methyl- and vinylsilane to Si-C ceramics
[NASA-TM-106554] p 3662 N94-32945
Novel precursor approached for CMC derived by polymer pyrolysis
[AD-A278383] p 3665 N94-33352

PYROPHORIC MATERIALS
Ignition delays, heats of combustion, and reaction rates of aluminum alkyl derivatives used as ignition and combustion enhancers for supersonic combustion
[NASA-CR-189581] p 3638 N94-32868

PYROTECHNICS
A low cost igniter utilizing an SCB and titanium sub-hydride potassium perchlorate pyrotechnic
[DE94-006467] p 3666 N94-31827

PYROXENES
Evidence for ultramafic lavas on Syrtis Major
p 3950 N94-33229

Q

Q FACTORS
Aperture excitation of electrically large, lossy cavities
[PB94-145711] p 3675 N94-31683

Q SWITCHED LASERS
Repetitively pulsed Cr:LiSAF laser for lidar applications
[DE94-007546] p 3720 N94-32761

QUADRATIC PROGRAMMING
Large-scale shape optimization: Numerical methods, parallel algorithms, and applications to aerodynamic design p 3815 N94-31966

QUADRATURES
A survey of numerical cubature over triangles
[DE94-006810] p 3841 N94-31274

QUADRUPOLES
General-relativistic celestial mechanics. 4: Theory of satellite motion
[PB94-147782] p 3601 N94-31769
RHIC chromatic correction system
[DE94-008532] p 3883 N94-32994

QUALIFICATIONS
Utilizing a Russian space nuclear reactor for a United States space mission: Flight qualification issues
[DE94-004674] p 3613 N94-31265

QUALITATIVE ANALYSIS
Tetraalkyldiarsines as potential precursors for electronic materials: Synthesis and characterization of various iso-propyl arsenic compounds
[AD-A277003] p 3900 N94-32001

QUALITY
Quality of sound in large rooms: Alteration of room impulse responses
[CTH-E-93-02] p 3859 N94-31077

QUALITY CONTROL
Evaluation of nondestructive inspection techniques for quality control of alumina-ceramic housing components
[AD-A276220] p 3730 N94-31065
Guide to software quality assurance
[ESA-PSS-05-11-ISSUE-1] p 3809 N94-31223
Cleanroom engineering handbook. Volume 6: Certification team practices
[AD-A275951] p 3587 N94-31346
Determination of BPSG thin-film properties using IR reflection spectroscopy of product wafers
[DE94-006591] p 3634 N94-32110
Management of government quality assurance functions for NASA contracts
[NHB-5300.4(2B-2)] p 3731 N94-32387
A facilitated mentoring process for engineers
[DE94-005823] p 3914 N94-32677
Pip pin reliability and design p 3605 N94-33305

QUANTITATIVE ANALYSIS
Development of sample charge compensation for characterization of impurities in semiconductor materials
[AD-A277113] p 3899 N94-31983
Rate coefficient for the reaction H + O2 yields OH + O: Results from 2000 to 5300 K
[DE94-008105] p 3871 N94-32615
Molten metal analysis by laser produced plasmas
[DE94-007014] p 3646 N94-32782

QUANTUM CHEMISTRY
International Journal of Quantum Chemistry. Quantum Biology Symposium number 20. Proceedings of the International Symposium on the Application of Fundamental Theory to Problems of Biology and Pharmacology
[AD-A276294] p 3792 N94-31294

QUANTUM CHROMODYNAMICS
The measurement of the hadronic energy flow and jet production with the ZEUS calorimeter in deep inelastic scattering events at HERA
[ETN-94-96021] p 3865 N94-31534
Non-equilibrium electrodynamics in the large N expansion
[DE94-006156] p 3911 N94-31760
New QCD results from string theory
[DE94-005226] p 3911 N94-31823
F0-975, A0-980 as eye-witnesses of confinement
[PB94-147105] p 3868 N94-31923
Research in theoretical high-energy physics
[DE94-008388] p 3876 N94-32407
Jet physics and QCD tests at the Tevatron collider
[DE94-008987] p 3871 N94-32587
The form factors of the nucleons
[DE94-007096] p 3872 N94-32630

QUANTUM EFFICIENCY
Quantum well infrared photodetector FPA
[AD-A278010] p 3908 N94-33248

QUANTUM ELECTRODYNAMICS
Spectroscopy and atomic physics in EBIT and SuperEBIT
[DE94-006050] p 3864 N94-31508
Perturbative aspects of lower-dimensional gauge theories
[ISBN-0-315-86269-6] p 3911 N94-31712
Non-equilibrium electrodynamics in the large N expansion
[DE94-006156] p 3911 N94-31760

QUANTUM ELECTRONICS
Novel growth technologies for in situ formation of semiconductor quantum wire structures
[AD-A277188] p 3902 N94-32255

QUANTUM MECHANICS
Modern integral equation techniques for quantum reactive scattering theory
[DE94-007039] p 3857 N94-31639
Cometary molecules p 3935 N94-31869
Research program in particle physics
[DE94-008449] p 3871 N94-32512
Quantum dynamics in dual spaces
[DE94-008303] p 3913 N94-32824
Computed potential energy surfaces for chemical reactions
[NASA-CR-195835] p 3639 N94-33036

QUANTUM NUMBERS
Baryogenesis from a primordial lepton asymmetry
[PB94-145166] p 3868 N94-31921

QUANTUM THEORY
Dynamical entropy of generalized quantum Markov chains
[PB94-148483] p 3850 N94-31590
Multiparameter quantum groups and multiparameter R-matrices
[CWI-AM-R9307] p 3846 N94-32106
Quantum homogeneous spaces, duality, and quantum 2-spheres
[CWI-AM-R9309] p 3857 N94-32192
Research in theoretical high-energy physics
[DE94-008388] p 3876 N94-32407
Research program in particle physics
[DE94-008449] p 3871 N94-32512
Quantum fluctuations of vortices in Josephson-coupled superconductors
[DE94-007609] p 3905 N94-32747

QUANTUM WELL LASERS
High speed, strained layer, multiquantum well, GaInAsP and GaAs lasers and heterostructures
[AD-A277287] p 3719 N94-32608

QUANTUM WELLS
Photopyroelectric spectroscopy as a non-intrusive technique for the determination of the optical absorption spectra of multiple quantum well samples
[ISBN-0-315-87164-4] p 3833 N94-31875
Cooling and trapping of neutral atoms
[AD-A276957] p 3870 N94-32360
High speed, strained layer, multiquantum well, GaInAsP and GaAs lasers and heterostructures
[AD-A277287] p 3719 N94-32608
The 6th International Conference on Modulated Semiconductor Structures
[AD-A276815] p 3906 N94-32908
Large-diameter InGaAs/AlGaAs vertical-cavity surface-emitting lasers with low threshold current density fabricated using a simple chemical etch process
[AD-A277733] p 3721 N94-33003
Research in the optical sciences
[AD-A278271] p 3884 N94-33140
Quantum well infrared photodetector FPA
[AD-A278010] p 3908 N94-33248
Material engineering of the novel semiconductor structures
[AD-A278386] p 3910 N94-33355

QUARK MODELS
Polarized lepton-nucleon scattering
[DE94-009027] p 3875 N94-33278

QUARK PARTON MODEL
Spin-structure function of the neutron He-3: SLAC results
[DE94-008927] p 3875 N94-33189

QUARKS
Transport properties of quark and gluon plasmas
[DE94-007043] p 3864 N94-31405
F0-975, A0-980 as eye-witnesses of confinement
[PB94-147105] p 3868 N94-31923
The form factors of the nucleons
[DE94-007096] p 3872 N94-32630
CP violation and the top quark
[DE94-008930] p 3874 N94-32841
Nuclear physics and astrophysics
[DE94-007168] p 3939 N94-33147

QUARTZ
NMR characterization of shocked quartz
[DE94-007733] p 3774 N94-32816

QUARTZ CRYSTALS
Pre-flight testing of Thermoelectric Quartz Crystal Microbalances (TQCM) for midcourse space experiment (MSX) spacecraft
[AD-A277054] p 3610 N94-32010

QUERY LANGUAGES
A probabilistic view of Datalog parallelization
[TELECOM-93-D-021] p 3824 N94-31183
The meaning of duplicates in the relational database model
[CT-93-04] p 3916 N94-31392
A simulation of uncertain reasoning on parametric databases using data-dependency derived inference nets p 3919 N94-32499
Information disclosure in evolving information systems: Taking a shot at a moving target
[TR-93-22] p 3919 N94-32506
QUEUEING THEORY
Performability modelling using DyQNtool+
[MEMO-INF-93-45] p 3812 N94-31659
Light-traffic analysis for queues with spatially distributed arrivals
[MEMO-1150] p 3832 N94-31826
The use of service limits for efficient operation of multi-station single-medium communication systems
[CWI-BS-R9312] p 3677 N94-32085
A polling system with a dormant server
[CWI-BS-R9313] p 3835 N94-32193
Multiserver queues with impatient customers
[CWI-BS-R9319] p 3835 N94-32198
Undiscounted Markov decision chains with partial information; an algorithm for computing a locally optimal periodic policy
[TW-93-10] p 3851 N94-32205

R

RADAR
System analysis of ultra-wideband instrumentation radars: Impulse versus stepped-chirp approaches
[AD-A276624] p 3677 N94-32087
RADAR ANTENNAS
Proceedings of the 1993 Antenna Applications Symposium, volume 1
[AD-A277202] p 3676 N94-32049
Proceedings of the 1993 Antenna Applications Symposium, volume 2
[AD-A277203] p 3677 N94-32050
Development of a frequency-domain electromagnetic scattering measurement system
[AD-A276738] p 3678 N94-32179
Generation of the ambiguity function for ultra wideband radar waveforms
[AD-A277913] p 3684 N94-33261
RADAR ATTENUATION
Low altitude near-the-horizon propagation: A comparison between RPO and M-layer
[AD-A277358] p 3679 N94-32282
RADAR BEAMS
Subspace estimation without eigenvectors for adaptive beamforming
[AD-A276287] p 3671 N94-31254
RADAR CROSS SECTIONS
Development of a frequency-domain electromagnetic scattering measurement system
[AD-A276738] p 3678 N94-32179
MOM3D method of moments code theory manual
[NASA-CR-189594] p 3682 N94-32897
RADAR DATA
Radar measurements p 3685 N94-31002
Patterns of deformation and volcanic flows associated with lithospheric loading by large volcanoes on Venus p 3776 N94-31106
RADAR DETECTION
Peak detection of Swerling type targets. Part 1: Detection probabilities in white noise
[AD-A276217] p 3670 N94-31062
Proceedings of the 4th Tunnel Detection Symposium on Subsurface Exploration Technology
[AD-A276372] p 3771 N94-31369
Waveform generation for ultra-wideband radar system
[AD-A276352] p 3673 N94-31401
The development and testing of a backscatter absorption gas imaging (BAGI) system designed to image at a range of 300 m
[DE94-006192] p 3675 N94-31761
Some problems of applied algebra
[CWI-AM-R9306] p 3847 N94-32204
RADAR ECHOES
Radar scattering from the summer polar mesosphere: Theory and observations p 3772 N94-32077
RADAR EQUIPMENT
Modular Simulator System (MSS). System/segment specification for the generic modular simulator system-radar module, volume 8
[AD-A276975] p 3589 N94-32314
Assembly flow simulation of a radar p 3823 N94-32431
RADAR IMAGERY
Phase unwrapping problems in ISAR images
[TELECOM-93-D-008] p 3670 N94-31097
Patterns of deformation and volcanic flows associated with lithospheric loading by large volcanoes on Venus p 3776 N94-31106
Radar image classification by texture measurements
[ONERA-NT-1993-3] p 3673 N94-31419
Real time character recognition for F-111C video tape records
[AD-A277061] p 3580 N94-32263
Validation support of the ERIM ocean model
[AD-A277364] p 3788 N94-32284
Restoration of interferometric, polarimetric, radiometric, and textural information in SAR images p 3750 N94-32535
Fusion of multispectral (XS) and Panchromatic (P) SPOT images and radar images p 3750 N94-32541
Almaz marine applications p 3751 N94-32544
Structural study in an alteritic region: Contribution of ERS-1 SAR data of the Mauges Plateau (Loire Atlantique, France)
[BRGM-93032] p 3752 N94-32551
Synergy of thermal infrared and microwave remote sensing for evaporation estimation p 3754 N94-32559
European MARS project: The potential integration of SPOT and air- and satellite-borne radar data over two pilot areas for agricultural statistics. PROSPER programme and ERS-1 pilot project
[BRGM-93035] p 3754 N94-32561
Land cover change detection with ERS-1 data and data from other remote sensing satellites. Example: The delta of the River Ebro (Spain) p 3755 N94-32564
The processing technology and some applications of Almaz-1 data p 3756 N94-32573
Synthetic vision technology demonstration. Volume 1: Executive summary
[DOT/FAA/RD-93/40-VOL-1] p 3582 N94-33076
Synthetic vision technology demonstration. Volume 2: Sensor tower testing
[DOT/FAA/RD-93/40-VOL-2] p 3582 N94-33077
Synthetic vision technology demonstration. Volume 3: Flight tests
[DOT/FAA/RD-93/40-VOL-3] p 3582 N94-33078
Synthetic vision technology demonstration. Volume 4: Appendices
[DOT/FAA/RD-93/40-VOL-4] p 3583 N94-33079
RADAR MEASUREMENT
Radar measurements p 3685 N94-31002
Microwave dielectric behavior of soils. Report 1: Summary of related research and applications
[AD-A275980] p 3771 N94-31351
Satellite radar altimetry over the continental ice sheets p 3742 N94-31570
Radar rainfall measurements from space p 3782 N94-31889
High-resolution synthetic aperture radar observations of the Moon p 3676 N94-31952
A reassessment of the in-situ dielectric constant of polar firn
[AD-A276999] p 3773 N94-32154
Gyrotrons and free electron lasers for atmospheric sensing
[AD-A277281] p 3718 N94-32406
The use of ERS images for mapping p 3749 N94-32531
RADAR RECEIVERS
An evaluation of three GPS receivers for use in the GPS sounder
[AD-A278157] p 3577 N94-33253
Generation of the ambiguity function for ultra wideband radar waveforms
[AD-A277913] p 3684 N94-33261
RADAR SCATTERING
Radar scattering from the summer polar mesosphere: Theory and observations p 3772 N94-32077
Millstone Hill radar studies of plasma waves and turbulence
[AD-A278409] p 3684 N94-33172
RADAR SIGNATURES
Precision and level of artefacts in the computation of digital terrain models by interferometry p 3756 N94-32571
RADAR TARGETS
Ultra wide band radar holographic imaging of subsurface targets
[DE94-004271] p 3713 N94-32681
RADAR TRACKING
CRAD Signal and Information Processing Working Group Workshop on Neural networks, volume 1
[DREA-TC-93-305-VOL-1] p 3836 N94-33149
The application of a radial basis function neural network for radar tracking over the sea p 3686 N94-33150
Some neural computing approaches to target tracking p 3837 N94-33151
A heuristic multiple target tracker p 3686 N94-33346
RADAR TRANSMISSION
Waveform generation for ultra-wideband radar system
[AD-A276352] p 3673 N94-31401
Low altitude near-the-horizon propagation: A comparison between RPO and M-layer
[AD-A277358] p 3679 N94-32282
A new tool for signal processing
[AD-A278385] p 3685 N94-33354
RADAR TRANSMITTERS
The CF-18 diagnostic and maintenance expert system project p 3567 N94-33338
RADIAL DISTRIBUTION
Structural ordering in liquid K-Te alloys
[DE94-008477] p 3645 N94-32514
RADIANCE
Custom uniform source system
[NASA-CR-189332] p 3711 N94-31492
Development of a statistical method for estimating the downward longwave radiation at the surface from satellite observations p 3742 N94-31553
RADIANT HEATING
Optical processing for semiconductor device fabrication p 3885 N94-32445
RADIATION ABSORPTION
A comprehensive analysis of electron conical distributions from multi-satellite databases
[NASA-CR-195848] p 3953 N94-33047
RADIATION BELTS
Lightning-induced coupling of the radiation belts to geomagnetically conjugate ionospheric regions p 3772 N94-31773
Self-consistent effects of magnetospheric hydromagnetic waves on ring current ions
[AD-A277406] p 3774 N94-32346
RADIATION CHEMISTRY
Radiation and photochemistry section
[DE94-008880] p 3873 N94-32757
RADIATION COUNTERS
The D0 upgrade
[DE94-006953] p 3867 N94-31671
Gamma Large Area Silicon Telescope (GLAST)
[DE94-006439] p 3925 N94-31786
Studies of jet production with the D0 detector
[DE94-008271] p 3873 N94-32780
RADIATION DAMAGE
Atomic oxygen damage characterization by photothermal scanning p 3598 N94-31051
The threshold energy for defect production in SiC: A molecular dynamic study
[DE94-007123] p 3896 N94-31499
Effect of irradiation damage and helium on the swelling and structure of vanadium-base alloys
[DE94-006540] p 3641 N94-31666
Experimental investigations and molecular dynamics simulations of radiation induced surface damage
[AD-A277323] p 3871 N94-32621
Vulnerability assessment of a space based weapon platform electronic system exposed to a thermonuclear weapon detonation
[DE94-007229] p 3611 N94-32667
Irradiation-induced phase transformations in zirconium alloys
[DE94-008484] p 3648 N94-32993
The impact of ASIC devices on the SEU vulnerability of space-borne computers
[AD-A278134] p 3808 N94-33252
RADIATION DETECTORS
Implementation of instruments and facilities at the SGP CART site
[DE94-006839] p 3781 N94-31322
High energy physics program at the University of Alabama
[DE94-006544] p 3875 N94-31488
Minimax: Multiparticle physics at the Tevatron collider
[DE94-007095] p 3873 N94-32689
Studies of jet production with the D0 detector
[DE94-008271] p 3873 N94-32780
RADIATION DISTRIBUTION
A study of physical conditions, radiative transfer and shocks in the interstellar medium p 3937 N94-31963
RADIATION DOSAGE
Model of spacecraft atomic oxygen and solar exposure microenvironments p 3593 N94-31021
Ionizing radiation effects on silicon test structures
[DE94-006060] p 3865 N94-31607
Neutron measurements at the commercial aircraft altitudes
[ISBN-0-315-86201-7] p 3955 N94-31709
Ion-irradiation-induced densification of zirconia sol-gel thin films
[DE94-006248] p 3656 N94-32103
Complete model description of an electron beam using ACCEPT Monte Carlo simulation code
[DE94-007063] p 3872 N94-32628

Vulnerability assessment of a space based weapon platform electronic system exposed to a thermonuclear weapon detonation
[DE94-007229] p 3611 N94-32667
An investigation of the radiolytic stability of a resorcinol-formaldehyde ion exchange resin
[DE94-007971] p 3660 N94-32698
Controlling hazardous energy sources (lockout/tagout)
[NASA-TM-105290] p 3669 N94-32861
Electron energy dependence of amorphization in Zr3Fe
[DE94-008459] p 3906 N94-32875
Spacecraft environmental anomalies expert system
[AD-A277962] p 3612 N94-33262

RADIATION EFFECTS
Model of spacecraft atomic oxygen and solar exposure microenvironments p 3593 N94-31021
Performance of selected polymeric materials on LDEF p 3593 N94-31023
Fluorescence observations of LDEF exposed materials as an indicator of induced material reactions p 3593 N94-31025
Laser-induced fluorescence of space-exposed polyurethane p 3593 N94-31026
Degradation of optical components in space p 3594 N94-31029
Physical properties of glasses exposed to Earth-facing and trailing-side environments on LDEF p 3594 N94-31030
Space environmental effects on polymer composites: Research needs and opportunities p 3595 N94-31035
Spacecraft materials: Comparison between flight results obtained on LDEF and MIR p 3597 N94-31045
Transient radiation-induced absorption in the materials for a GSGG laser
[DE94-005316] p 3714 N94-31148
Analysis of beam-on-target interaction in a neutron-source test facility
[DE94-005392] p 3863 N94-31151
The role of defects in laser damage of multilayer coatings
[DE94-006731] p 3714 N94-31269
Ion-beam-driven amorphization of Ca2La8(Si4)6O2 single crystals
[DE94-006219] p 3895 N94-31307
Mitigation of adverse environmental effects on lunar-based astronomical instruments p 3598 N94-31426
The threshold energy for defect production in SiC: A molecular dynamic study
[DE94-007123] p 3896 N94-31499
Ionizing radiation effects on silicon test structures
[DE94-006060] p 3865 N94-31607
The influence of transmutation, void swelling, and flux/spectra uncertainties on the electrical properties of copper and copper alloys
[DE94-006213] p 3641 N94-31626
Defect-solute interactions near irradiation grain boundaries
[DE94-006215] p 3641 N94-31627
Design of new polymers to improve radiation stability of plastic scintillators
[DE94-008220] p 3652 N94-31764
ITS version 3.0: Powerful, user-friendly software for radiation modelling
[DE94-006607] p 3678 N94-32113
A comparison between two Monte Carlo codes on determination of transient chemical yields
[DE94-007224] p 3636 N94-32251
Analytical solutions of minimum ionization particle induced current shapes of silicon detectors and simulation of charge collection properties
[DE94-007523] p 3870 N94-32355
Intra-cascade surface recombination of point defects during ion bombardment of Ge(001)
[DE94-007740] p 3903 N94-32384
Point defect production, geometry, and stability in silicon: A molecular dynamics simulation study
[DE94-008292] p 3903 N94-32411
Vulnerability assessment of a space based weapon platform electronic system exposed to a thermonuclear weapon detonation
[DE94-007229] p 3611 N94-32667
Electron energy dependence of amorphization in Zr3Fe
[DE94-008459] p 3906 N94-32875
Irradiation-induced phase transformations in zirconium alloys
[DE94-008484] p 3648 N94-32993
Spacecraft environmental anomalies expert system
[AD-A277962] p 3612 N94-33262

RADIATION HARDENING
Radiation tolerant, high speed, low power, gallium arsenide logic
[AD-A277293] p 3694 N94-32509
Spacecraft environmental anomalies expert system
[AD-A277962] p 3612 N94-33262

RADIATION HAZARDS
Laser safety manual for DREO
[AD-A276288] p 3714 N94-31255
High peak power microwaves: A health hazard
[AD-A277168] p 3681 N94-32576
Independent safety assessment of the Topaz-2 space nuclear reactor power system
[DE94-008653] p 3877 N94-32879

RADIATION INJURIES
High peak power microwaves: A health hazard
[AD-A277168] p 3681 N94-32576

RADIATION LAWS
A simple model for determining photoelectron-generated radiation scaling laws
[DE94-006130] p 3761 N94-32660

RADIATION MEASUREMENT
Neutron measurements at the commercial aircraft altitudes
[ISBN-0-315-86201-7] p 3955 N94-31709
Investigation of scintillator and fibre light in plastic scintillation dosimetry
[ISBN-0-315-87190-3] p 3879 N94-31877
System for monitoring and analyzing field energy exposure
[AD-D016115] p 3681 N94-32625
Water vapor from sunradiometry in comparison with microwave and balloon-sonde measurements at the Southern Great Plains ARM Site
[DE94-007479] p 3786 N94-32759
Radiometry spot measurement system
[NASA-TM-106561] p 3883 N94-32777

RADIATION MEASURING INSTRUMENTS
Evidence of solar oscillations in Rayleigh-scattered light p 3952 N94-31214

RADIATION PROTECTION
Design of new polymers to improve radiation stability of plastic scintillators
[DE94-008220] p 3652 N94-31764
Integrated safety program for the Nuclear Electric Propulsion Space Test Program
[DE94-004670] p 3615 N94-32669

RADIATION SHIELDING
Mitigation of adverse environmental effects on lunar-based astronomical instruments p 3598 N94-31426
Complete model description of an electron beam using ACCEPT Monte Carlo simulation code
[DE94-007063] p 3872 N94-32628
Implementation and display of Computer Aided Design (CAD) models in Monte Carlo radiation transport and shielding applications
[DE94-007221] p 3819 N94-32641

RADIATION THERAPY
Laboratory Directed Research & Development Program
[DE94-005928] p 3956 N94-31523

RADIATION TRANSPORT
ITS version 3.0: Powerful, user-friendly software for radiation modelling
[DE94-006607] p 3678 N94-32113
Implementation and display of Computer Aided Design (CAD) models in Monte Carlo radiation transport and shielding applications
[DE94-007221] p 3819 N94-32641
The 2D deterministic radiation transport with the discontinuous finite element method
[DE94-004687] p 3849 N94-32670

RADIATIVE HEAT TRANSFER
Computational radiative heat transfer in homogeneous and nonhomogeneous nonscattering media p 3702 N94-31563
Chemical vapor deposition fluid flow simulation modelling tool
[NASA-CR-189648] p 3707 N94-32480
An evaluation of RAMS radiation schemes by field measurements
[DE94-008053] p 3767 N94-32750

RADIATIVE LIFETIME
B lifetimes at CDF
[DE94-006850] p 3866 N94-31669

RADIATIVE RECOMBINATION
Material engineering of the novel semiconductor structures
[AD-A278386] p 3910 N94-33355

RADIATIVE TRANSFER
Thermal continua of AGN accretion disks p 3931 N94-31137
Three-dimensional radiative transfer calculations on an SIMD machine applied to accretion disks p 3932 N94-31141
A study of physical conditions, radiative transfer and shocks in the interstellar medium p 3937 N94-31963
Sensitivity analysis of the AVHRR infrared cirrus model
[AD-A276690] p 3784 N94-32117
Temporal and spatial mapping of atmospheric dust opacity and surface albedo on Mars p 3947 N94-33211
How well was total ozone abundance inferred with Mariner 9 p 3947 N94-33212
The wavelength dependence of Martian atmospheric dust radiative properties p 3950 N94-33228

RADICALS
Time-resolved infrared absorption studies applied to the study of radical plus molecule reactions
[DE94-005921] p 3863 N94-31202
A comparison between two Monte Carlo codes on determination of transient chemical yields
[DE94-007224] p 3636 N94-32251

RADIO ANTENNAS
Broadband, high-power, 2-30 MHz, twin-whip antenna. Computer and 1/10-scale model design study
[AD-A277619] p 3682 N94-32971

RADIO ASTRONOMY
Plasma and radio waves from Neptune: Source mechanisms and propagation
[NASA-CR-195877] p 3943 N94-33103

RADIO COMMUNICATION
Fast autodidactic adaptive equalization algorithms
[TELECOM-93-E-018] p 3670 N94-31174
Atmospheric effects assessment program: Ionospheric sounding
[AD-A276447] p 3770 N94-31303
Analysis of ionospheric parameters in Europe and creation of the prediction algorithm
[AD-A276342] p 3771 N94-31326
A multichannel architecture for Naval Task Force Communication
[AD-A276230] p 3673 N94-31446
Performance statistics bulletin. High latitude meteor scatter propagation October, November, December 1990, January 1991
[AD-A276693] p 3676 N94-31998
Design, development, and testing of a Network Frequency Selection Service (NFSS)
[AD-A277362] p 3680 N94-32283
High frequence and automatic link establishment (HF and ALE) radio propagation test to Antarctica
[AD-A277730] p 3682 N94-33001
An analysis of cellular telephone and INMARSAT systems for providing radio data link computer communications for US Navy vessels
[AD-A278143] p 3684 N94-33160
High temperature superconducting Josephson junction array systems, phase 1
[AD-A277937] p 3908 N94-33246

RADIO CONTROL
Remote robot manipulator coupled with remote-controlled guide vehicle for soil sampling in hazardous waste sites p 3723 N94-31569

RADIO EMISSION
Radio emission from pre-main-sequence stars p 3955 N94-31890
Plasma and radio waves from Neptune: Source mechanisms and propagation
[NASA-CR-195877] p 3943 N94-33103

RADIO EQUIPMENT
Low sidelobe reflector antenna design for communications
[AD-A276079] p 3673 N94-31463
High frequence and automatic link establishment (HF and ALE) radio propagation test to Antarctica
[AD-A277730] p 3682 N94-33001

RADIO FREQUENCIES
Noninductive current drive experiments on D3-D, and future plans
[DE94-007373] p 3886 N94-31324
Advanced optical fiber communication systems
[AD-A276416] p 3878 N94-31330
RF vacuum microelectronics
[AD-A276512] p 3691 N94-31928
High frequency active auroral research program (HAARP) imager
[AD-A277469] p 3775 N94-32999

RADIO FREQUENCY HEATING
FWCD and ECCD experiments on D3-D
[DE94-007371] p 3890 N94-32201
ICRF heating and current drive in TFTR supershot plasmas: Data analysis and interpretation of ICRF/edge interactions
[DE94-008586] p 3890 N94-32520

RADIO FREQUENCY INTERFERENCE
Aperture excitation of electrically large, lossy cavities
[PB94-145711] p 3675 N94-31683
The effects of a multipath channel and interference on coherent M-PSK digital communication systems
[AD-A278158] p 3684 N94-33254

RADIO FREQUENCY SHIELDING
Aperture excitation of electrically large, lossy cavities
[PB94-145711] p 3675 N94-31683
RADIO HORIZONS
Low altitude near-the-horizon propagation: A comparison between RPO and M-layer
[AD-A277358] p 3679 N94-32282
RADIO METEOROLOGY
Field studies of raindrop oscillations with applications to radar meteorology p 3782 N94-31743
RADIO RECEIVERS
Design, performance, and test standards for flight termination receivers/decoders. Volume 1: Design and performance requirements
[AD-A277245] p 3602 N94-32333
RADIO SIGNALS
Performance statistics bulletin. High latitude metor scatter propagation, February, March, April, May 1992
[AD-A276667] p 3677 N94-32083
Performance statistics bulletin. High latitude meteor scatter propagation February, March, April, May 1991
[AD-A276723] p 3678 N94-32158
Performance statistics bulletin. High latitude meteor scatter propagation October, November, December 1991, January 1992
[AD-A276724] p 3678 N94-32159
Performance statistics bulletin. High latitude meteor scatter propagation, November and December 1989, and January 1990
[AD-A276688] p 3680 N94-32297
Performance statistics bulletin. High latitude meteor scatter propagation
[AD-A276694] p 3680 N94-32298
Performance statistics bulletin. High latitude meteor scatter propagation
[AD-A276695] p 3680 N94-32299
Performance statistics bulletin. High latitude meteor scatter propagation
[AD-A276696] p 3680 N94-32300
Automatic modulation recognition
p 3686 N94-33153
RADIO SPECTROSCOPY
High sensitivity and resolution decimetric spectroscope: Preliminary analysis of solar bursts
[INPE-5537-TDI/525] p 3954 N94-33080
RADIO TELESCOPES
The quest for contact
[NASA-TM-109778] p 3806 N94-32389
RADIO TRANSMISSION
Discrete-event-dynamic-system-based approaches for scheduling transmissions in multihop packet radio networks
[AD-A276566] p 3679 N94-32230
High frequence and automatic link establishment (HF and ALE) radio propagation test to Antarctica
[AD-A277730] p 3682 N94-33001
A comparison of rough surface parabolic equation models
[AD-A278090] p 3791 N94-33185
An approximate model for vertical polarization and surface roughness using the parabolic equation
[AD-A278091] p 3684 N94-33186
RADIO TRANSMITTERS
High-power microwave-tube transmitters
[DE94-005340] p 3686 N94-31150
RADIO WAVES
Low altitude near-the-horizon propagation: A comparison between RPO and M-layer
[AD-A277358] p 3679 N94-32282
RADIOACTIVE DECAY
Collective and quasiparticle excitations in light Pb isotopes
[ETN-94-96014] p 3865 N94-31548
RADIOACTIVE WASTES
Surface chemistry and durability of borosilicate glass
[DE94-006734] p 3656 N94-32116
RADIOLYSIS
A comparison between two Monte Carlo codes on determination of transient chemical yields
[DE94-007224] p 3636 N94-32251
An investigation of the radiolytic stability of a resorcinol-formaldehyde ion exchange resin
[DE94-007971] p 3660 N94-32698
High-energy chemical processes: Laser irradiation of aromatic hydrocarbons
[DE94-008107] p 3720 N94-32707
RADIOMETERS
A study of areas of low radio-thermal emissivity on Venus p 3942 N94-31992
NOAA-9 Earth Radiation Budget Experiment (ERBE) scanner offsets determination
[NASA-TM-109086] p 3785 N94-32737
Radiometry spot measurement system
[NASA-TM-106561] p 3883 N94-32777
Studies of atmospheric dust from Viking IR thermal mapper data p 3948 N94-33216
RADIOMETRIC CORRECTION
European Imaging Spectroscopy Aircraft Campaign
[ESA-SP-360] p 3743 N94-31853
The European Imaging Spectroscopy Airborne Campaign (EISAC). Data takes and evaluation programme: An overview p 3743 N94-31854
Ground based radiometric and atmospheric measurements p 3744 N94-31855
Investigation on correction models for airborne imaging spectrometry data from the EISAC-campaign for geoscientific purposes p 3745 N94-31861
Extraction of agricultural parameters from imaging-spectrometry data and simulated MERIS data through red edge analysis p 3745 N94-31865
Restoration of interferometric, polarimetric, radiometric, and textural information in SAR images
p 3750 N94-32535
RADIOSONDES
Coastal boundary layer and refractivity measurements using the ground-based high resolution interferometer sounder (GB-HIS)
[AD-A277980] p 3683 N94-33159
RADIOTELEPHONES
An analysis of cellular telephone and INMARSAT systems for providing radio data link computer communications for US Navy vessels
[AD-A278143] p 3684 N94-33160
RAIL TRANSPORTATION
Theoretical principles for designing long stator/linear motors with iron
[ETN-94-95741] p 3688 N94-31374
Applicable dimensioning and measure and technological examination of long stator-linear motors for magnetic high-speed railways
[ETN-94-95734] p 3689 N94-31575
RAILGUN ACCELERATORS
Design and evaluation of coils for a 50 mm diameter induction coilgun launcher
[DE94-005244] p 3603 N94-32671
RAILS
Considering ties elasticities in high frequency rail dynamics
[ILR-MITT-281(1993)] p 3733 N94-31375
RAIN
Numerical simulations of monsoon rainfall with the NRL/NCSU regional nested grid model
p 3782 N94-31791
Radar rainfall measurements from space
p 3782 N94-31889
Estimation and analysis of climate-scale rainfall over the Tropical Pacific p 3783 N94-32030
Simulation of a precipitation event in the western United States
[DE94-004835] p 3786 N94-32791
TRMM-related research: Tropical rainfall and energy analysis experiment
[NASA-CR-195834] p 3787 N94-33288
RAIN FORESTS
Behavior and dynamics of tropical forests and savannas p 3757 N94-31004
RAINDROPS
Field studies of raindrop oscillations with applications to radar meteorology p 3782 N94-31743
RAMAN SPECTROSCOPY
Vibrational spectroscopy at metal-solution interfaces: Some perspectives and prospects for electrochemical surface science
[AD-A276781] p 3644 N94-32169
RANDOM ACCESS MEMORY
Design of free space interconnected signal processor
[AD-A278129] p 3683 N94-33093
RANDOM ERRORS
Regional sources of error growth in the National Meteorological Center's medium-range forecast model
p 3781 N94-31554
Bounds on least-squares four-parameter sine-fit errors due to harmonic distortion and noise
[DE94-007859] p 3849 N94-32653
RANDOM LOADS
Random vibrations of composite beams and plates
p 3735 N94-31777
RANDOM NOISE
Modulation and coding for the Gaussian channel, possibly affected by fluctuations
[TELECOM-93-E-009] p 3840 N94-31169
An adaptive Kalman filter excisor for suppressing narrowband interference
[AD-A276286] p 3671 N94-31253
Analysis using bi-spectral related technique
[AD-A276017] p 3672 N94-31386
Detection of a chi-square fluctuating target in Gaussian noise
[AD-A276078] p 3850 N94-31462
Control of a random walk with noisy delayed information
[CWI-BS-R9316] p 3846 N94-32108
Stochastic realization of a Gaussian stochastic control system
[CWI-BS-R9320] p 3852 N94-32350
The effects of a multipath channel and interference on coherent M-PSK digital communication systems
[AD-A278158] p 3684 N94-33254
RANDOM PROCESSES
On interpolating random fields using a finite number of observations
[CWI-BS-R9314] p 3847 N94-32194
Area-interaction point processes
[CWI-BS-R9318] p 3847 N94-32197
Robust multisource classification method using the Markov random field methods p 3750 N94-32537
RANDOM VARIABLES
Probability distributions with given marginals and given correlation that have maximal entropy
[REPT-93-81] p 3851 N94-31698
On the minimum of independent geometrically distributed random variables
[NASA-CR-194883] p 3821 N94-33075
RANDOM VIBRATION
Random vibrations of composite beams and plates
p 3735 N94-31777
RANDOM WALK
Control of a random walk with noisy delayed information
[CWI-BS-R9316] p 3846 N94-32108
RANGE SAFETY
Design, performance, and test standards for flight termination receivers/decoders. Volume 1: Design and performance requirements
[AD-A277245] p 3602 N94-32333
Integrated safety program for the Nuclear Electric Propulsion Space Test Program
[DE94-004670] p 3615 N94-32669
Independent safety assessment of the Topaz-2 space nuclear reactor power system
[DE94-008653] p 3877 N94-32879
RANKING
List ranking and list scan on the CRAY C-90
[AD-A276411] p 3824 N94-31259
RAPID QUENCHING (METALLURGY)
Solidification structure synthesis in undercooled liquids
[AD-A276166] p 3910 N94-31054
Microstructures and mechanical properties of Al3Ti-based alloys: Analysis in single phase and multiphase systems
[ONERA-NT-1993-6] p 3640 N94-31420
RAPID TRANSIT SYSTEMS
Applicable dimensioning and measure and technological examination of long stator-linear motors for magnetic high-speed railways
[ETN-94-95734] p 3689 N94-31575
RARE EARTH COMPOUNDS
Conductivity measurements of ceria-based solid electrolytes using AC impedance
[DE94-007380] p 3694 N94-32593
RARE EARTH ELEMENTS
Metal-ion spin-on glasses: Novel materials for active waveguides
[DE94-007738] p 3862 N94-32649
Rare Earth Doped Semiconductors and Materials Research Society Symposium Proceedings, Volume 301
[AD-A277517] p 3908 N94-33055
RARE GASES
Metal cluster-rare gas van der Waals complexes: Microscopic models of physisorption
[DE94-008134] p 3873 N94-32797
RAREFIED GAS DYNAMICS
Surface boundary conditions and related technical issues concerning Burnett equations for 2-D hypersonic flow
[AD-A277322] p 3706 N94-32256
Analysis and computation for vortex dynamics and rarefied gases
[AD-A277415] p 3708 N94-32581
Simulation of CO2 release at 800 km altitude
[AD-A276692] p 3776 N94-33272
RAREFIED GASES
Analysis and computation for vortex dynamics and rarefied gases
[AD-A277415] p 3708 N94-32581
RASTER SCANNING
Optimal detector strategies for the phase contrast imaging for scanning transmission electron microscopes
[ETN-94-95747] p 3866 N94-31613
Differential phase acoustic microscope for micro-NDE
[NASA-CR-189617] p 3731 N94-32481
RAWINSONDES
Development and testing of improved techniques for modeling the hydrologic cycle in a mesoscale weather prediction system
[AD-A277416] p 3786 N94-32921

RAY TRACING
The High-Frequency Benchmark propagation program
[AD-A276323] p 3672 N94-31334
Ultrasonic tomography in fiber-reinforced composite materials p 3620 N94-31565
Prediction of the plane wave beamformed acoustic arrival structure for the 1992 Barents Sea coastal tomography test
[AD-A276741] p 3788 N94-32181

RAYLEIGH SCATTERING
Evidence of solar oscillations in Rayleigh-scattered light p 3952 N94-31214

RDX
Condensed-phase processes during solid propellant combustion. 3: Preliminary depth-profiling studies on XM39, JA2, M9, M30, and HMX2
[AD-A276595] p 3635 N94-32124

REACTING FLOW
Mixture model simulating reactive turbulent flows: Testing of Eulerian-Lagrangian probabilistic models
[ONERA-NT-1993-13] p 3702 N94-31477
Reactive flows in compact objects p 3934 N94-31567
A numerical method for mixing/chemically reacting compressible flow with finite rate chemistry p 3634 N94-31824
Computed potential energy surfaces for chemical reactions
[NASA-CR-195835] p 3639 N94-33036
Turbulent reacting flows and supersonic combustion
[AD-A277462] p 3639 N94-33242

REACTION KINETICS
High-temperature study of O+H2CO yields OH+HCO
[DE94-006837] p 3864 N94-31321
Combustion-related studies using weakly-bonded complexes
[DE94-006632] p 3633 N94-31493
Cloud studies seen from a physical chemist's perspective
[DE94-006059] p 3771 N94-31527
Modern integral equation techniques for quantum reactive scattering theory
[DE94-007039] p 3857 N94-31639
A numerical method for mixing/chemically reacting compressible flow with finite rate chemistry p 3634 N94-31824
Analysis of forward and inverse problems in chemical dynamics and spectroscopy
[DE94-007607] p 3635 N94-32140
Stability and precipitation kinetics in Si(1-y)C(y)/Si and Si(1-x-y)Ge(x)C(y)/Si heterostructures prepared by solid phase epitaxy
[DE94-006589] p 3902 N94-32296
Chemical structure and kinetics at liquid/solid interfaces
[AD-A277112] p 3636 N94-32304
Time-resolved IR spectroscopy, energy transfer, and state-to-state collision dynamics of atmospheric species
[AD-A277372] p 3773 N94-32338
Volatiles combustion in fluidized beds
[DE94-008382] p 3636 N94-32414
Chemical vapor deposition fluid flow simulation modelling tool
[NASA-CR-189648] p 3707 N94-32480
Formation mechanism and yield of molecules ejected from ZnS, CdS, and FeS2 during ion bombardment
[DE94-008487] p 3871 N94-32515
Molecular Science Research Center
[DE94-007464] p 3871 N94-32605
Rate coefficient for the reaction H + O2 yields OH + O: Results from 2000 to 5300 K
[DE94-008105] p 3871 N94-32615
Time-resolved analytical methods for liquid/solid interfaces
[DE94-008352] p 3637 N94-32826
Ignition delays, heats of combustion, and reaction rates of aluminum alkyl derivatives used as ignition and combustion enhancers for supersonic combustion
[NASA-CR-189581] p 3638 N94-32868
Experimental studies on the effect of coherency strains on coarsening kinetics: Current status and future outlook
[DE94-008480] p 3647 N94-32964
Computed potential energy surfaces for chemical reactions
[NASA-CR-195835] p 3639 N94-33036

REACTION PRODUCTS
Ground-based simulation of LEO environment: Investigations of a select LDEF material: FEP Teflon (trademark) p 3596 N94-31039

REACTIVITY
An overview of the Evaluation of Oxygen Interaction with Materials-third phase (EOIM-3) experiment: Space Shuttle Mission 46 p 3596 N94-31040
Process parameter-growth environment-film property relationships for reactive sputter deposited metal (V, Nb, Zr, Y, Au) oxide, nitride, and oxynitride films
[AD-A276382] p 3640 N94-31258
Cloud studies seen from a physical chemist's perspective
[DE94-006059] p 3771 N94-31527

REACTOR DESIGN
Summary of particle bed reactor designs for the Space Nuclear Thermal Propulsion Program
[DE94-007434] p 3615 N94-32266
Overview of H-mode studies in D3-D
[DE94-007430] p 3891 N94-32612

REACTOR MATERIALS
Analysis of beam-on-target interaction in a neutron-source test facility
[DE94-005392] p 3863 N94-31151
Creep properties of vanadium-base alloys
[DE94-006541] p 3641 N94-31486
The influence of transmutation, void swelling, and flux/spectra uncertainties on the electrical properties of copper and copper alloys
[DE94-006213] p 3641 N94-31626
Effect of irradiation damage and helium on the swelling and structure of vanadium-base alloys
[DE94-006540] p 3641 N94-31666
Creep-fatigue criteria and inelastic behavior of modified 9Cr-1Mo steel at elevated temperatures
[DE94-007915] p 3642 N94-31918
Irradiation-assisted stress corrosion cracking of materials from commercial BWRs: Role of grain-boundary microchemistry
[DE94-006542] p 3643 N94-32109

REACTOR SAFETY
Quench detection and instrumentation for the Tokamak Physics Experiment magnets
[DE94-006656] p 3888 N94-31667
Integrated safety program for the Nuclear Electric Propulsion Space Test Program
[DE94-004670] p 3615 N94-32669
Independent safety assessment of the Topaz-2 space nuclear reactor power system
[DE94-008653] p 3877 N94-32879

READING
Literacity: A multimedia adult literacy package combining NASA technology, recursive ID theory, and authentic instruction theory p 3924 N94-32462
Reading: Interaction with memory
[AD-A277547] p 3801 N94-32956

REAGENTS
Time-resolved analytical methods for liquid/solid interfaces
[DE94-008352] p 3637 N94-32826

REAL TIME OPERATION
Results of real-time testing and demonstration of the US Army Corps of Engineers real-time on-the-fly positioning system
[AD-A276160] p 3576 N94-31080
Scheduling techniques for multiple processor systems in real-time environments
[AD-A276149] p 3824 N94-31249
New and emerging techniques for imaging surfaces
[AD-A276497] p 3878 N94-31262
Algorithms and structures for real-time signal processing
[AD-A276101] p 3810 N94-31277
ControlShell: A real-time software framework
[AD-A276481] p 3811 N94-31475
A neural network methodology for engineering applications: The learning control of robotic systems
[RR-480] p 3830 N94-31500
The future of open architecture process control systems
[DE94-006163] p 3830 N94-31623
The development and testing of a backscatter absorption gas imaging (BAGI) system designed to image at a range of 300 m
[DE94-006192] p 3675 N94-31761
A theory of distributed time
[AD-A276631] p 3815 N94-31994
Theoretical basis for state vector comparison, relative position display, and relative position/rendezvous prediction
[AD-A277216] p 3608 N94-32020
Gamma-ray optical counterpart search experiment (GROCSE)
[DE94-007124] p 3955 N94-32129
Real time character recognition for F-111C video tape records
[AD-A277061] p 3580 N94-32263
Communication networks for autonomous mobile robot computer architectures and distributed real-time computing p 3680 N94-32310
Photothermal laser deflection, an innovative technique to measure particles in exhausts
[AD-A277151] p 3718 N94-32366
Empirical modeling for intelligent, real-time manufacture control p 3839 N94-32424
New approaches for real time decision support systems p 3915 N94-32426
Construction of a parallel processor for simulating manipulators and other mechanical systems
[NASA-CR-191327] p 3826 N94-32482
Model-based reconfiguration: Diagnosis and recovery
[NASA-CR-4596] p 3820 N94-32776
A multitasking behavioral control system for the Robotic All Terrain Lunar Exploration Rover (RATLER)
[DE94-007293] p 3835 N94-32787
High frequency active auroral research program (HAARP) imager
[AD-A277469] p 3775 N94-32999
Theory and application of image enhancement
[AD-A277896] p 3821 N94-33031
Real-time centimeter positioning with GPS: A system developed by the US Army Corps of Engineers
[AD-A278152] p 3577 N94-33095
Real-time sensor data validation
[NASA-CR-195295] p 3616 N94-33099
An experimental study of pilot/vehicle dynamics using a tilt rotor flying machine
[AD-A277516] p 3805 N94-33349

RECEIVERS
Development of a frequency-domain electromagnetic scattering measurement system
[AD-A276738] p 3678 N94-32179
Operational experience and evaluation of a dual-element stretched-membrane heliostat
[DE94-008827] p 3763 N94-32965

RECIRCULATIVE FLUID FLOW
Computational study of simultaneous heat and mass transfer in turbulent separated flows p 3704 N94-31843
An experimental study of the flowfield on a semispan rectangular wing with a simulated glaze ice accretion
[NASA-CR-195301] p 3571 N94-32475

RECOMBINATION REACTIONS
High-temperature study of O+H2CO yields OH+HCO
[DE94-006837] p 3864 N94-31321
Material engineering of the novel semiconductor structures
[AD-A278386] p 3910 N94-33355

RECONNAISSANCE AIRCRAFT
Army scout/reconnaissance helicopters versus unmanned aerial vehicles
[AD-A276902] p 3579 N94-32232

RECORDS MANAGEMENT
An analysis of the records management process to determine the impact of automation on productivity
[AD-A275923] p 3916 N94-31344
Developing a personal-computer-based records retention system using Paradox(tm)
[DE94-007984] p 3819 N94-32749

RECRYSTALLIZATION
Work hardening behavior in aluminum alloy 2090
[DE94-007036] p 3643 N94-32064
Attempts to model the generation of new grain boundaries during the deformation of polycrystals
[DE94-007527] p 3903 N94-32597

RECTANGULAR PANELS
Response of a cantilevered plate in supersonic flow
[AD-A277487] p 3580 N94-33107

RECTANGULAR PLATES
Nonlinear vibration analysis of laminated plates on linear and nonlinear elastic foundations p 3737 N94-32079

RECTANGULAR WAVEGUIDES
Performance evaluation and operating characteristics of a waveguide microwave applicator for space propulsion applications p 3614 N94-31908

RECTANGULAR WINGS
An experimental study of the flowfield on a semispan rectangular wing with a simulated glaze ice accretion
[NASA-CR-195301] p 3571 N94-32475

RECURSIVE FUNCTIONS
Formal verification of systolic multipliers with the Boyer-Moore theorem prover
[RR-897-M] p 3839 N94-31082

RECYCLING
Feasibility study for the recycling of nickel metal hydride electric vehicle batteries
[DE94-000268] p 3690 N94-31598

RED SHIFT
A constraint on the pair-density ratio (Z+) in an electron-positron pair wind p 3930 N94-31132
The kinematics of dense clusters of galaxies p 3937 N94-32029

REDUNDANCY
A PC program to optimize system configuration for desired reliability at minimum cost p 3823 N94-32438
A new solution method for the inverse kinematic joint velocity calculations of redundant manipulators
[DE94-004427] p 3727 N94-32682

REDUNDANT COMPONENTS
A PC program to optimize system configuration for desired reliability at minimum cost p 3823 N94-32438
Hierarchical modeling for reliability analysis using Markov models
[NASA-CR-188288] p 3731 N94-32862
Fault detection and isolation for the Bluebird test bed aircraft
[AD-A277979] p 3586 N94-33086
REED-SOLOMON CODES
Modulation and coding for the Gaussian channel, possibly affected by fluctuations
[TELECOM-93-E-009] p 3840 N94-31169
REFERENCE STARS
Design and early results of the sodium-layer laser guide star adaptive optics experiment at the Lawrence Livermore National Laboratory
[DE94-006653] p 3926 N94-32189
REFLECTANCE
Modeling the interaction between solar radiation and terrestrial surfaces p 3779 N94-30999
Shiptrack database analysis
[AD-A277228] p 3746 N94-32025
Electromagnetic wave reflection from irregular plasma layers
[AD-A276727] p 3678 N94-32161
Research and applications of a canopy reflectance model p 3747 N94-32492
A quest for a new superconducting state
[DE94-008439] p 3908 N94-32991
REFLECTOR ANTENNAS
Low sidelobe reflector antenna design for communications
[AD-A276079] p 3673 N94-31463
Proceedings of the 1993 Antenna Applications Symposium, volume 1
[AD-A277202] p 3676 N94-32049
Proceedings of the 1993 Antenna Applications Symposium, volume 2
[AD-A277203] p 3677 N94-32050
INSAT-2A and 2B development mechanisms p 3603 N94-33293
Special test equipment and fixturing for MSAT reflector assembly alignment p 3606 N94-33316
REFLECTORS
Sol-gel metal oxide and metal oxide/polymer multilayers applied by meniscus coating
[DE94-005813] p 3649 N94-31199
Electromagnetic wave reflection from irregular plasma layers
[AD-A276727] p 3678 N94-32161
Special test equipment and fixturing for MSAT reflector assembly alignment p 3606 N94-33316
REFLEXES
Analysis of pursuit tracking eye movements in pilots and nonfliers
[AD-A276597] p 3799 N94-32035
REFRACTED WAVES
Ocean acoustic propagation measurements and wave propagation in random media
[AD-A276165] p 3787 N94-31053
REFRACTIVITY
Ocean acoustic propagation measurements and wave propagation in random media
[AD-A276165] p 3787 N94-31053
Multifunctional macromolecules
[AD-A277347] p 3656 N94-32246
Coastal boundary layer and refractivity measurements using the ground-based high resolution interferometer sounder (GB-HIS)
[AD-A277980] p 3683 N94-33159
REFRACTORIES
High temperature materials technology research for advanced thermionic systems
[DE94-008341] p 3646 N94-32825
REFRACTORY COATINGS
The development of CVR coatings for PBR fuels
[DE94-004233] p 3875 N94-31480
REFRACTORY MATERIALS
High temperature NASP engine seal development
[NASA-TM-109750] p 3725 N94-31804
Computer modelling of cyclic deformation of high-temperature materials
[AD-A277056] p 3623 N94-32012
High temperature materials technology research for advanced thermionic systems
[DE94-008341] p 3646 N94-32825
Research on high reliability refractory ohmic contacts for GaAs FETs and MODFETs
[AD-A276848] p 3697 N94-33034
REFRACTORY METAL ALLOYS
Recent advances and developments in refractory alloys
[DE94-007929] p 3644 N94-32374
High temperature materials technology research for advanced thermionic systems
[DE94-008444] p 3644 N94-32416
High temperature materials technology research for advanced thermionic systems
[DE94-008341] p 3646 N94-32825
REFRACTORY METALS
Recent advances and developments in refractory alloys
[DE94-007929] p 3644 N94-32374
High temperature materials technology research for advanced thermionic systems
[DE94-008341] p 3646 N94-32825
REFRIGERANTS
Application of natural refrigerants: A rational solution to a pressing problem
[PB94-138781] p 3668 N94-31073
Measurement of viscosity, density, and gas solubility of refrigerant blends in selected synthetic lubricants
[DE94-007723] p 3653 N94-31917
Compatibility of refrigerants and lubricants with elastomers
[DE94-008552] p 3658 N94-32518
REFRIGERATING
Application of natural refrigerants: A rational solution to a pressing problem
[PB94-138781] p 3668 N94-31073
REGENERATIVE COOLING
The 4 K Stirling cryocooler demonstration
[NASA-CR-191792] p 3669 N94-32484
REGENERATORS
The 4 K Stirling cryocooler demonstration
[NASA-CR-191792] p 3669 N94-32484
REGOLITH
The pH of Mars p 3950 N94-33225
Temporal changes in the geographic distribution, elevation, and potential origin of the Martian outflow channels p 3951 N94-33235
Simultaneous laboratory measurements of CO2 and H2O adsorption on palagonite: Implications for the Martian climate and volatile reservoir p 3952 N94-33240
REGRESSION ANALYSIS
Representation, prediction and identification of cyclostationary processes: A state-space approach
[REPT-93-041] p 3850 N94-31191
A review of sensitivity analysis techniques
[DE94-007192] p 3842 N94-31399
Diagonal band probability distributions
[REPT-93-80] p 3851 N94-31697
Multiple regression and measurement errors: Relative efficiency of two models, the standard model and Fuller's model, for estimating structural relationships
[ISBN-0-315-86834-1] p 3845 N94-31755
Feasibility evaluation of new data interpretation approaches for vegetation analysis from airborne imaging spectroscopy p 3745 N94-31862
Hierarchical mixtures of experts and the EM algorithm
[AD-A276516] p 3814 N94-31932
Proceedings of the NIPS 1993 Postconference Workshop on Pulling It All Together: Methods for Combining Neural Networks
[AD-A277507] p 3836 N94-33014
REINFORCED PLATES
Vibrational and acoustic response of ribbed plates p 3736 N94-31955
REINFORCEMENT (STRUCTURES)
Test and analysis results for composite transport fuselage and wing structures p 3628 N94-33129
REINFORCING FIBERS
On the mechanics of stress analysis of fiber-reinforced composites p 3619 N94-31481
Toughening mechanisms in fiber-reinforced ceramic-matrix composites p 3622 N94-31943
Mechanics of the single fiber pullout problem with several interface conditions p 3623 N94-32078
The effect of ductile phase (Nb) reinforcement morphology on the mechanical behavior of an intermetallic matrix (MoSi2) p 3615 N94-32500
Engineering scale development of the Vapor-Liquid-Solid (VLS) process for the production of silicon carbide fibrils
[DE94-007132] p 3659 N94-32618
Comparison of resin film infusion, resin transfer molding, and consolidation of textile preforms for primary aircraft structure p 3630 N94-33136
REINFORCING MATERIALS
Leveraging metal matrix composites to reduce costs in space mechanisms p 3604 N94-33301
RELATIVISTIC EFFECTS
General-relativistic celestial mechanics. 4: Theory of satellite motion
[PB94-147782] p 3601 N94-31769
RELATIVISTIC ELECTRON BEAMS
Pinched propagation of high-power, pulsed electron beams for welding and materials processing applications
[AD-A276925] p 3726 N94-32236
RELATIVISTIC PARTICLES
Perturbative and nonperturbative EM lepton pair production in relativistic heavy-ion collisions
[DE94-006315] p 3867 N94-31779
RELATIVISTIC PLASMAS
Transport properties of quark and gluon plasmas
[DE94-007043] p 3864 N94-31405
Non-equilibrium electrodynamics in the large N expansion
[DE94-006156] p 3911 N94-31760
RELATIVISTIC THEORY
General-relativistic celestial mechanics. 4: Theory of satellite motion
[PB94-147782] p 3601 N94-31769
RELATIVITY
Lattice geometrodynamics p 3857 N94-31825
RELAXATION (MECHANICS)
Viscoelastic fracture characterization of polymeric solids p 3652 N94-31745
RELAXATION METHOD (MATHEMATICS)
Exact solution of the single machine scheduling problem with earliness and flow time penalties
[REPT-93-038] p 3809 N94-31189
RELIABILITY
Reliability of multilayer copper/polyimide
[AD-A276228] p 3650 N94-31284
Validation of the Environmentally Conscious Manufacturing Integrated Demonstration hardware
[DE94-003824] p 3765 N94-32144
Effect of surface forces on the rheology of particle-liquid systems and the consolidation of ceramic powders
[AD-A277092] p 3657 N94-32391
A PC program to optimize system configuration for desired reliability at minimum cost p 3823 N94-32438
Space flight risk data collection and analysis project: Risk and reliability database
[NASA-CR-195879] p 3603 N94-32494
Temperature-humidity-bias aging technique to identify defective surface mount capacitors
[DE94-005354] p 3660 N94-32727
Implementing software safety in the NASA environment
[NASA-TM-106597] p 3731 N94-33032
Pip pin reliability and design p 3605 N94-33305
RELIABILITY ANALYSIS
An evaluation of aircraft maintenance performance factors in the objective wing
[AD-A276010] p 3565 N94-31362
Reliability analysis of structural ceramics subjected to biaxial flexure p 3650 N94-31454
Statistical inference for coherent systems from partial information and in resampling techniques in survival analysis
[AD-A277382] p 3852 N94-32339
A PC program to optimize system configuration for desired reliability at minimum cost p 3823 N94-32438
Automatic contact in DYNA3D for vehicle crashworthiness
[DE94-007143] p 3738 N94-32637
Hierarchical modeling for reliability analysis using Markov models
[NASA-CR-188288] p 3731 N94-32862
Stochastic models in reliability theory
[AD-A277529] p 3731 N94-32953
Spur, helical, and spiral bevel transmission life modeling
[NASA-TM-106552] p 3728 N94-32979
Accelerated reliability testing utilizing design of experiments
[AD-A277989] p 3732 N94-33088
Advanced release technologies program p 3607 N94-33322
Assessing the vulnerability of multi-commodity networks with failing components
[AD-A278434] p 3684 N94-33334
RELIABILITY ENGINEERING
Engineering of damage in ion implanted silicon
[ISBN-9-09-005097-3] p 3897 N94-31521
RELIEF MAPS
SPOT imagery for updating land cover information of 1:50,000 numerical topographic maps p 3749 N94-32532
Example of SPOT/ERS-1 complementarity p 3749 N94-32533
REMOTE CONSOLES
Relationships between access and use in information systems: Remote access to and browsing of online catalogs p 3919 N94-32488
REMOTE CONTROL
Development of a frequency-domain electromagnetic scattering measurement system
[AD-A276738] p 3678 N94-32179
A low-cost, CCD solid state star tracker
[NASA-CR-192722] p 3682 N94-32417
Applying robotics to HAZMAT p 3729 N94-32452

Technology transfer of operator-in-the-loop simulation p 3802 N94-32472

REMOTE SENSING

Subtropical Climates and Their Evolution: From Space-Based Observation to Modelling
[ISBN-2-85-428333-3] p 3776 N94-30981

Radiation/remote sensing: Review of the principal definitions p 3757 N94-30996

Modeling the interaction between solar radiation and terrestrial surfaces p 3779 N94-30999

Radar measurements p 3685 N94-31002

Airborne instruments p 3757 N94-31006

Global change research and NASA's Earth Observing System
[PB94-126992] p 3741 N94-31068

Chamber optics for testing passive remote sensing vapor detectors
[AD-A275909] p 3878 N94-31340

Gas hydrate detection and mapping on the US east coast
[DE94-005959] p 3742 N94-31504

Development of a statistical method for estimating the downward longwave radiation at the surface from satellite observations p 3742 N94-31553

Imaging devices for satellite remote sensing
[VTT-TIED-1517] p 3743 N94-31658

The development and testing of a backscatter absorption gas imaging (BAGI) system designed to image at a range of 300 m
[DE94-006192] p 3675 N94-31761

European Imaging Spectroscopy Aircraft Campaign
[ESA-SP-360] p 3743 N94-31853

The European Imaging Spectroscopy Airborne Campaign (EISAC). Data takes and evaluation programme: An overview p 3743 N94-31854

NORSMAP 1989: Norwegian remote sensing spectroscopy for mapping and monitoring or algal blooms and pollution p 3744 N94-31856

Analysis of GER imaging spectrometry data for the identification of soil and vegetation parameters in land degradation studies p 3744 N94-31857

Inflight calibration, preprocessing, and data evaluation of GER 2 imaging spectrometry data p 3744 N94-31858

Possibilities of GER data for soil surface characteristics in the Almaden area p 3744 N94-31859

The effects of vegetation on the ability to map soils using GERIS data p 3744 N94-31860

Investigation on correction models for airborne imaging spectrometry data from the EISAC-campaign for geoscientific purposes p 3745 N94-31861

Feasibility evaluation of new data interpretation approaches for vegetation analysis from airborne imaging spectroscopy p 3745 N94-31862

Monitoring fertilizer application by imaging spectrometry (Somerset Levels test site) p 3745 N94-31863

High resolution spectroscopy in agriculture: Results of the EISAC 1989 campaign p 3745 N94-31864

Extraction of agricultural parameters from imaging-spectrometry data and simulated MERIS data through red edge analysis p 3745 N94-31865

Remote infrared vapor detection of volatile organic compounds
[AD-A276982] p 3746 N94-31999

Estimation and analysis of climate-scale rainfall over the Tropical Pacific p 3783 N94-32030

Gyrotrons and free electron lasers for atmospheric sensing
[AD-A277281] p 3718 N94-32406

Remote sensing for urban planning p 3758 N94-32465

Remote sensing and the Mississippi high accuracy reference network p 3758 N94-32466

Assessment of region-based methods for automated SAR/optical registration, attribute extraction, and classification p 3750 N94-32536

Ship traffic monitoring and oil spill detection using the ERS-1 SAR p 3751 N94-32542

SAR image feature extraction system: A pre-operational application of ERS-1 SAR p 3751 N94-32543

Almaz marine applications p 3751 N94-32544

Evaluation of the potential of SAR data for mapping of landslide risks
[BRGM-93033] p 3753 N94-32552

A case study comparing multi-temporal ERS-1 SAR data and SPOT data for tropical forest mapping p 3753 N94-32556

Synergy of thermal infrared and microwave remote sensing for evaporation estimation p 3754 N94-32559

Monitoring landsurface characteristics in Niger using complementary SPOT and ERS-1 SAR data p 3754 N94-32560

European MARS project: The potential integration of SPOT and air- and satellite-borne radar data over two pilot areas for agricultural statistics. PROSPER programme and ERS-1 pilot project
[BRGM-93035] p 3754 N94-32561

Evaluation of surface phase change on large zones p 3755 N94-32567

Quantitative analysis of woody vegetation in Soudano-Sahalian region. Textural approach (application to a Burkina Faso region) p 3757 N94-32574

Statistical analysis and mapping of cotton and food crop cultivation surfaces in the west of Burkina Faso: Contribution of combined SPOT P and XS data p 3757 N94-32575

An integrated cloud observation and modeling investigation in support of the ARM program
[DE94-003160] p 3785 N94-32716

Water vapor from sunradiometry in comparison with microwave and balloon-sonde measurements at the Southern Great Plains ARM Site
[DE94-007479] p 3786 N94-32759

Repetitively pulsed Cr:LiSAF laser for lidar applcations
[DE94-007546] p 3720 N94-32761

Evolution of diurnal surface winds and surface currents for Monterey Bay
[AD-A277649] p 3790 N94-33057

REMOTE SENSORS

Space equipment for Earth observations p 3613 N94-30997

Airborne instruments p 3757 N94-31006

Imaging devices for satellite remote sensing
[VTT-TIED-1517] p 3743 N94-31658

The processing technology and some applications of Almaz-1 data p 3756 N94-32573

REMOTELY PILOTED VEHICLES

Unmanned Air Vehicle/Remotely Piloted Vehicle analysis for lethal UAV/RPV
[AD-A276052] p 3578 N94-31442

A model geophysics program
[DE94-007415] p 3747 N94-32203

Army scout/reconnaissance helicopters versus unmanned aerial vehicles
[AD-A276902] p 3579 N94-32232

RENDEZVOUS GUIDANCE

Theoretical basis for state vector comparison, relative position display, and relative position/rendezvous prediction
[AD-A277216] p 3608 N94-32020

RENDEZVOUS TRAJECTORIES

A six degree of freedom, plume-fuel optimal trajectory planner for spacecraft proximity operations using an A* node search
[NASA-CR-188285] p 3601 N94-32388

RENORMALIZATION GROUP METHODS

Renormalization group theory of Bolgiano scaling in Boussinesq turbulence
[NASA-TM-106602] p 3710 N94-33070

REPEATERS

Advanced satellite communication system
[NASA-CR-194211] p 3681 N94-32477

REPLACING

Enhanced thermal capacity aerogels summary report, FY 1993
[DE94-008888] p 3639 N94-33260

REPORTS

NASA/DOD Aerospace Knowledge Diffusion Research Project. Paper 11: The voice of the user: How US aerospace engineers and scientists view DOD technical reports
[NASA-TM-109348] p 3921 N94-32834

NASA/DOD Aerospace Knowledge Diffusion Research Project. Report 25: The technical communications practices of British aerospace engineers and scientists: Results of the phase 4 RAeS mail survey
[NASA-TM-109098] p 3922 N94-32836

NASA/DOD Aerospace Knowledge Diffusion Research Project. Report 24: The technical communications practices of US aerospace engineers and scientists: Results of the phase 1 SAE mail survey
[NASA-TM-109088] p 3922 N94-32837

REPRODUCTION (BIOLOGY)

The legacy of Kermack and McKendrick
[CWI-AM-R9304] p 3793 N94-32228

REQUIREMENTS

MODIS. Volume 1: MODIS level 1A software baseline requirements
[NASA-TM-104594-VOL-1] p 3823 N94-33287

RESCUE OPERATIONS

SATCOM feasibility study for search and rescue aircraft
[DSIS-94-01083] p 3575 N94-31902

The ALEXIS mission recovery
[DE94-007549] p 3611 N94-32813

RESEARCH

Aviation human factors research in US universities: Potential contributions to national needs
[NASA-TM-108814] p 3575 N94-32927

RESEARCH AIRCRAFT

Fault detection and isolation for the Bluebird test bed aircraft
[AD-A277979] p 3586 N94-33086

RESEARCH AND DEVELOPMENT

Naval Surface Warfare Center Dahlgren Division Technical Digest: Advanced materials technology
[AD-A276448] p 3668 N94-31364

Laboratory Directed Research & Development Program
[DE94-005928] p 3956 N94-31523

The contribution of aeronautics and astronautics to the quality of life on Earth
[ILR-MITT-283(1993)] p 3764 N94-31611

Aerospace test facilities at NASA LERC Plumbrook
[NASA-TM-109755] p 3602 N94-31814

NASA select yearender review
[NASA-TM-109748] p 3956 N94-31885

Division of Microwave Technology
[PB94-148079] p 3676 N94-31925

Advances in MOVPE compound semiconductor epitaxy manufacturing technology: From high throughput large area reactors to cluster tools
[DE94-006367] p 3901 N94-32104

X ray optics for science and technology
[AD-A277369] p 3880 N94-32155

The future of high energy physics in the US statement for the Science Subcommittee of the House Science, Space and Technology Committee
[DE94-008986] p 3876 N94-32586

The future of high-energy physics in the US: Statement for the 1994 HEPAP Subpanel
[DE94-008994] p 3876 N94-32588

Research on stable, high-efficiency amorphous silicon multijunction modules
[DE94-000298] p 3695 N94-32680

NASA/DOD Aerospace Knowledge Diffusion Research Project. Paper 5: Aerospace librarians and technical information specialists as information intermediaries: A report of phase 2 activities of the NASA/DOD Aerospace Knowledge Diffusion Research Project
[NASA-TM-109777] p 3921 N94-32829

NASA/DOD Aerospace Knowledge Diffusion Research Project. Paper 10: The NASA/DOD Aerospace Knowledge Diffusion Research Project
[NASA-TM-109769] p 3921 N94-32831

NASA/DOD Aerospace Knowledge Diffusion Research Project. Paper 12: The diffusion of federally funded aerospace research and development (R/D) and the information seeking behavior of US aerospace engineers and scientists
[NASA-TM-109404] p 3921 N94-32832

NASA/DOD Aerospace Knowledge Diffusion Research Project. Paper 18: Scientific and Technical Information (STI) policy and the competitive position of the US aerospace industry
[NASA-TM-109782] p 3921 N94-32833

NASA/DOD Aerospace Knowledge Diffusion Research Project. Paper 1: The value of scientific and technical information (STI), its relationship to Research and Development (R/D), and its use by US aerospace engineers and scientists
[NASA-TM-109774] p 3922 N94-32835

LLNL casting technology
[DE94-008282] p 3669 N94-32839

Sandia's photonic program and its changing national role
[DE94-008616] p 3883 N94-32878

Research and Technology Objectives and Plans Summary (RTOPS)
[NASA-TM-105441] p 3966 N94-32885

Aerospace sponsored research
[ATR-93(8498)-1] p 3966 N94-32949

Novel sol-gel deposition for repair of conducting paths in polyceramic systems
[AD-A278381] p 3664 N94-33350

RESEARCH FACILITIES

BNL possibilities
[DE94-007179] p 3864 N94-31398

Free electrons as a versatile source of coherent radiation
[ETN-94-96011] p 3715 N94-31545

Aerospace test facilities at NASA LERC Plumbrook
[NASA-TM-109755] p 3602 N94-31814

NASA select yearender review
[NASA-TM-109748] p 3956 N94-31885

Airborne Trailblazer: Two decades with NASA Langley's 737 flying laboratory
[NASA-SP-4216] p 3566 N94-32793

RESEARCH MANAGEMENT

NASA select yearender review
[NASA-TM-109748] p 3956 N94-31885

Construction of visual representations and time-space organization of resources in astronomy
[ISBN-0-315-86694-2] p 3925 N94-31914
Advances in MOVPE compound semiconductor epitaxy manufacturing technology: From high throughput large area reactors to cluster tools
[DE94-006367] p 3901 N94-32104
Research and Technology Objectives and Plans Summary (RTOPS)
[NASA-TM-105441] p 3966 N94-32885
Aviation human factors research in US universities: Potential contributions to national needs
[NASA-TM-108814] p 3575 N94-32927

RESEARCH PROJECTS
State of hadron collider physics
[DE94-005279] p 3863 N94-31147
Aerospace test facilities at NASA LERC Plumbrook
[NASA-TM-109755] p 3602 N94-31814

RESEARCH VEHICLES
Benchmarking of the state-of-the-art in nondestructive testing/evaluation for applicability in the Composite Armored Vehicle (CAV) Advanced Technology Demonstrator (ATD) program, phase 1
[AD-A276660] p 3730 N94-32088
Airborne Trailblazer: Two decades with NASA Langley's 737 flying laboratory
[NASA-SP-4216] p 3566 N94-32793
Installed F/A-18 inlet flow calculations at 30 degrees angle-of-attack: A comparative study
[NASA-CR-195297] p 3573 N94-33119

RESERVOIRS
SNC meteorites and their implications for reservoirs of Martian volatiles p 3947 N94-33209

RESIDENTIAL AREAS
Remote sensing for urban planning p 3758 N94-32465

RESIDUAL STRESS
Processing of novel nanoparticle dispersion strengthened ceramics for improved mechanical performance
[AD-A275965] p 3649 N94-31276
Inelastic deformation of metal matrix composites p 3618 N94-31285
Effect of vibratory stress relief during welding of thick stainless steel plate
[DE94-006557] p 3733 N94-31312
Feasibility study of cold expansion processes modelling
[DSIS-94-01186] p 3735 N94-31849
Mechanics of failure of high temperature metal matrix composites
[AD-A277397] p 3624 N94-32342
Modeling of residual stress mitigation in austenitic stainless steel pipe girth weldment
[DE94-007184] p 3738 N94-32639

RESIN TRANSFER MOLDING
Development of stitched/RTM composite primary structures p 3628 N94-33127
Resin transfer molding for advanced composite primary wing and fuselage structures p 3628 N94-33128
Test and analysis results for composite transport fuselage and wing structures p 3628 N94-33129
Composite fuselage crown panel manufacturing technology p 3629 N94-33133
Advanced textile applications for primary aircraft structures p 3629 N94-33135
Comparison of resin film infusion, resin transfer molding, and consolidation of textile preforms for primary aircraft structure p 3630 N94-33136

RESINS
Development of stitched/RTM composite primary structures p 3628 N94-33127

RESISTANCE HEATING
Solid-state resistance upset welding: A process with unique advantages for advanced materials
[DE94-005941] p 3723 N94-31524
Time-resolved analytical methods for liquid/solid interfaces
[DE94-008352] p 3637 N94-32826

RESONANCE FLUORESCENCE
Particle-In-Cell (PIC) code simulation results and comparison with theory scaling laws for photoelectron-generated radiation
[DE94-006132] p 3695 N94-32662

RESONANT FREQUENCIES
A series resonant converter in half bridge circuits with combined serial and parallel charge coupling and several output circuits
[ETN-94-95739] p 3687 N94-31373
Considering ties elasticities in high frequency rail dynamics
[ILR-MITT-281(1993)] p 3733 N94-31375
Vibration localization in dual-span axially moving elastic systems p 3736 N94-31964
Mass-loaded coating for reducing the resonant frequency of a ceramic disc
[AD-D016095] p 3660 N94-32739

RESOURCE ALLOCATION
NEMO: Advanced energy systems and technologies
[DE94-721996] p 3760 N94-31767
Construction of visual representations and time-space organization of resources in astronomy
[ISBN-0-315-86694-2] p 3925 N94-31914

RESOURCES MANAGEMENT
Techniques for increasing the robustness of iterative algorithms for multi-resources location problems
[REPT-93-037] p 3809 N94-31188
Common property resources and low-level flying in Labrador: Flight, fight or fancy?
[ISBN-0-315-87318-3] p 3924 N94-31732
Food security in the context of global environmental change
[DE94-007481] p 3768 N94-32812

RESPIRATION
Effects of combined breathing impediments on diver's respiratory performance
[AD-A277437] p 3805 N94-33084
Characterization and utilization of opiate-like hibernation factors
[AD-A278136] p 3794 N94-33098

RETICLES
Application of the modified voltage-dividing potentiometer to overlay metrology in a CMOS/bulk process
[DE94-007937] p 3695 N94-32700

RETINA
High peak power microwaves: A health hazard
[AD-A277168] p 3681 N94-32576

RETRACTABLE EQUIPMENT
Deployable and retractable telescoping tubular structure development p 3607 N94-33317

REVERBERATION
Modelling the late part of room impulse responses using adaptive filtering: On the recreation of reality
[CTH-E-93-01] p 3859 N94-31076
Quality of sound in large rooms: Alteration of room impulse responses
[CTH-E-93-02] p 3859 N94-31077
Surface forward-scattered acoustic measurements and analysis
[AD-A276998] p 3788 N94-32000

REVERSE FIELD PINCH
Toroidal pinch experiments
[DE94-005876] p 3887 N94-31558
Coaxial slow source
[DE94-008191] p 3892 N94-32800

REYNOLDS NUMBER
Hypervelocity Tunnel 9 Mach 10/14 Calibration
[AD-A275960] p 3587 N94-31318
Heat transfer studies on a rectangular channel with offset plate fins
[AD-A277300] p 3912 N94-32043
Design of a two dimensional planer pressurized air labyrinth seal test rig
[AD-A277232] p 3726 N94-32370

REYNOLDS STRESS
Transport suppression by shear flow generation in multihelicity resistive-g turbulence
[DE94-007108] p 3886 N94-31366
Three-dimensional velocity measurements on a 6:1 prolate spheroid at 10 deg angle of attack
[AD-A276485] p 3702 N94-31476
A critical evaluation of the Reynolds stress turbulence closure for the flow of a turbulent free-stream over a turbulent boundary layer
[ISBN-0-315-75792-2] p 3707 N94-32497
Backward-facing step measurements at low Reynolds number, Re(sub h)=5000
[NASA-TM-108807] p 3711 N94-33290

RHENIUM COMPOUNDS
Novel approaches to the production of higher alcohols from synthesis gas
[DE94-006770] p 3666 N94-32132
Ligand intermediates in metal-catalyzed reactions
[DE94-008713] p 3638 N94-32887

RHEOLOGY
Influence of trace components on the viscoelastic properties of a polymer solution
[AD-A277171] p 3656 N94-32253
Effect of surface forces on the rheology of particle-liquid systems and the consolidation of ceramic powders
[AD-A277092] p 3657 N94-32391

RHODIUM COMPOUNDS
Novel approaches to the production of higher alcohols from synthesis gas
[DE94-006770] p 3666 N94-32132

RHOMBOHEDRONS
X ray absorption study of pulsed laser deposited boron nitride films
[DE94-008295] p 3662 N94-32855

RIBLETS
Flight test results of riblets at supersonic speeds
[NASA-TM-4387] p 3572 N94-32880

RIBONUCLEIC ACIDS
Employment of a porous gold actuator in ISFET-based coulometric sensor-actuator systems with application to protein characterization
[ISBN-9-09-005887-7] p 3689 N94-31536

RIBS (SUPPORTS)
Vibrational and acoustic response of ribbed plates p 3736 N94-31955

RICCATI EQUATION
Digital state-feedback H(infinity) control of Pritchard-Salamon systems: A Popov function approach
[REPT-93-69] p 3830 N94-31647
A Hyland-Bernstein approach to the digital control of Pritchard-Salamon systems
[REPT-93-76] p 3844 N94-31693

RIEMANN MANIFOLD
SU(2) WZNW model at higher genera from gauge field functional integral
[PB94-148467] p 3857 N94-31589
Conformal field theory and geometry of strings
[PB94-148442] p 3857 N94-31770

RIEMANN WAVES
An approximate Riemann solver for magnetohydrodynamics (that works in more than one dimension)
[NASA-CR-194902] p 3849 N94-33033

RING LASERS
High-power CW diode-laser-array-pumped solid-state lasers and efficient nonlinear optical frequency conversion
[AD-A276126] p 3714 N94-31278
An investigation of airborne GPS/INS for high accuracy position and velocity determination
[DE94-006139] p 3576 N94-31306

RING STRUCTURES
Roll ring assemblies for the Space Station p 3603 N94-33294
International Space Station Alpha's bearing, motor, and roll ring module developmental testing and results p 3603 N94-33295

RISK
Space flight risk data collection and analysis project: Risk and reliability database
[NASA-CR-195879] p 3603 N94-32494
Evaluation of the potential of SAR data for mapping of landslide risks
[BRGM-93033] p 3753 N94-32552

RIVETED JOINTS
Multiple-site damage in aircraft fuselage structures
[LR-729] p 3578 N94-31675

RLC CIRCUITS
Broadband, high-power, 2-30 MHz, twin-whip antenna. Computer and 1/10-scale model design study
[AD-A277619] p 3682 N94-32971

ROADS
Tracking roads in an aerial image by Kalman filtering
[TELECOM-93-D-007] p 3711 N94-31096
The contribution of satellite data in communication infrastructure projects p 3749 N94-32530

ROBOT ARMS
A high-performance multi-arm environment: Theoretical aspects and practical implementation
[RR-479] p 3722 N94-31379
Control of a flexible space robot tracking a moving target p 3722 N94-31469
Point-contact and point-impact dynamics for multibody chains
[ISBN-0-315-87056-7] p 3734 N94-31737
Trajectory learning with a direct drive robotic manipulator p 3831 N94-31794
Model identification of a reconfigurable robot manipulator
[ISBN-0-315-87109-1] p 3725 N94-31874
Control of a flexible-link robotic arm manipulating an unknown dynamic payload p 3725 N94-31973
Parallel methods for synthesizing whole-hand grasps from generalized prototypes
[AD-A276798] p 3726 N94-32166
Information theory for arm visuo-motor coordination p 3800 N94-32495
Design, characterization and control of the Unique Mobility Corporation robot p 3603 N94-33296

ROBOT CONTROL
Camera-space manipulation with natural visual information p 3829 N94-31207
A high-performance multi-arm environment: Theoretical aspects and practical implementation
[RR-479] p 3722 N94-31379
Control of a flexible space robot tracking a moving target p 3722 N94-31469
ControlShell: A real-time software framework
[AD-A276481] p 3811 N94-31475

Contingency-tolerant robot motion planning and control p 3830 N94-31482
A neural network methodology for engineering applications: The learning control of robotic systems [RR-480] p 3830 N94-31500
Motion and force control of coordinated robots [ISBN-0-315-86323-4] p 3724 N94-31714
Strategy for tracking and grabbing a moving object with the aid of a decouplable manipulator with six degrees of freedom general architecture, guided by a vision system [ISBN-0-315-86864-3] p 3831 N94-31757
Trajectory learning with a direct drive robotic manipulator p 3831 N94-31794
Adaptive control of a robot in Cartesian coordinates: Analysis and implementation [ISBN-0-315-86493-1] p 3831 N94-31798
Development of a feedforward controller for a flexible manipulator [ISBN-0-315-86515-6] p 3832 N94-31801
Real-time control and application to robotics: Hardware and software architectures [ISBN-0-315-87192-X] p 3833 N94-31876
High-speed path constrained manipulator operation using optimal-feedback combined controller p 3833 N94-31962
Control of a flexible-link robotic arm manipulating an unknown dynamic payload p 3725 N94-31973
Parallel methods for synthesizing whole-hand grasps from generalized prototypes [AD-A276798] p 3726 N94-32166
An experimental testbed for a free-floating manipulator [AD-A277350] p 3726 N94-32334
Applying robotics to HAZMAT p 3729 N94-32452
Information theory for arm visuo-motor coordination p 3800 N94-32495
A multitasking behavioral control system for the Robotic All Terrain Lunar Exploration Rover (RATLER) [DE94-007293] p 3835 N94-32787
Identification and control of structures in space [NASA-CR-195910] p 3612 N94-33115
Design, characterization and control of the Unique Mobility Corporation robot p 3603 N94-33296

ROBOT DYNAMICS
Camera-space manipulation with natural visual information p 3829 N94-31207
A high-performance multi-arm environment: Theoretical aspects and practical implementation [RR-479] p 3722 N94-31379
Control of a flexible space robot tracking a moving target p 3722 N94-31469
Kinematic synthesis and analysis of a novel class of six-DOF parallel minimanipulators p 3723 N94-31568
Remote robot manipulator coupled with remote-controlled guide vehicle for soil sampling in hazardous waste sites p 3723 N94-31569
Penetration distances and their applications to path planning p 3858 N94-31725
Point-contact and point-impact dynamics for multibody chains [ISBN-0-315-87056-7] p 3734 N94-31737
Application of contact mechanics for the validation of robotized operations of grasping objects subjected to static and dynamic force fields [ISBN-0-315-86831-7] p 3725 N94-31754
Trajectory learning with a direct drive robotic manipulator p 3831 N94-31794
Study of a path planning and tracking system for an articulated mobile robot [ISBN-0-315-86502-4] p 3831 N94-31800
Automatic analysis of force distribution in multi-fingered articulated hands [ISBN-0-315-87205-5] p 3725 N94-31878
Hierarchical mixtures of experts and the EM algorithm [AD-A276516] p 3814 N94-31932
High-speed path constrained manipulator operation using optimal-feedback combined controller p 3833 N94-31962
Robot motion vision by fixation p 3833 N94-31991
An experimental testbed for a free-floating manipulator [AD-A277350] p 3726 N94-32334
Construction of a parallel processor for simulating manipulators and other mechanical systems [NASA-CR-191327] p 3826 N94-32482
Dynamic error compensation in robotic trusses p 3738 N94-32486
Identification and control of structures in space [NASA-CR-195910] p 3612 N94-33115

ROBOT SENSORS
Synchronized laser scanning three dimensional acquisition system [ISBN-0-315-86848-1] p 3879 N94-31756
Undergraduate robotics projects in support of research on neural networks [AD-A277331] p 3835 N94-32281

ROBOTICS
ControlShell: A real-time software framework [AD-A276481] p 3811 N94-31475
Kinematic synthesis and analysis of a novel class of six-DOF parallel minimanipulators p 3723 N94-31568
A contribution to the representation and identification of semi-flexible robots [ISBN-0-315-86450-8] p 3724 N94-31721
Robot grasping: Stability and optimization issues p 3724 N94-31724
Real-time control and application to robotics: Hardware and software architectures [ISBN-0-315-87192-X] p 3833 N94-31876
Adaptive control of telerobotic systems worn by humans [AD-A276608] p 3834 N94-32036
Parallel methods for synthesizing whole-hand grasps from generalized prototypes [AD-A276798] p 3726 N94-32166
Undergraduate robotics projects in support of research on neural networks [AD-A277331] p 3835 N94-32281
Application of dexterous space robotics technology to myoelectric prostheses p 3729 N94-32450
Navy Omni-Directional Vehicle (ODV) development program p 3729 N94-32451
Development of an automated wire delivery system for robotic welding applications [NASA-CR-194216] p 3727 N94-32479
Dynamic error compensation in robotic trusses p 3738 N94-32486
A new solution method for the inverse kinematic joint velocity calculations of redundant manipulators [DE94-004427] p 3727 N94-32682
A multitasking behavioral control system for the Robotic All Terrain Lunar Exploration Rover (RATLER) [DE94-007293] p 3835 N94-32787
Identification and control of structures in space [NASA-CR-195910] p 3612 N94-33115
The 28th Aerospace Mechanisms Symposium [NASA-CP-3260] p 3603 N94-33291
Innovative mechanism for measuring the mass properties of an object p 3604 N94-33299

ROBOTS
Concepts and environment [REPT-93-032] p 3829 N94-31186
A high-performance multi-arm environment: Theoretical aspects and practical implementation [RR-479] p 3722 N94-31379
Control of a flexible space robot tracking a moving target p 3722 N94-31469
Remote robot manipulator coupled with remote-controlled guide vehicle for soil sampling in hazardous waste sites p 3723 N94-31569
CAD-based off-line planning for an active-vision system [ISBN-0-315-86317-X] p 3813 N94-31713
Motion and force control of coordinated robots [ISBN-0-315-86323-4] p 3724 N94-31714
A contribution to the representation and identification of semi-flexible robots [ISBN-0-315-86450-8] p 3724 N94-31721
Development of a robotic simulator for studying interference and contact problems [ISBN-0-315-86705-1] p 3588 N94-31747
Application of contact mechanics for the validation of robotized operations of grasping objects subjected to static and dynamic force fields [ISBN-0-315-86831-7] p 3725 N94-31754
Adaptive control of a robot in Cartesian coordinates: Analysis and implementation [ISBN-0-315-86493-1] p 3831 N94-31798
Study of a path planning and tracking system for an articulated mobile robot [ISBN-0-315-86502-4] p 3831 N94-31800
Development of a feedforward controller for a flexible manipulator [ISBN-0-315-86515-6] p 3832 N94-31801
Control of a flexible-link robotic arm manipulating an unknown dynamic payload p 3725 N94-31973
Communication networks for autonomous mobile robot computer architectures and distributed real-time computing p 3680 N94-32310
An experimental testbed for a free-floating manipulator [AD-A277350] p 3726 N94-32334
Applying robotics to HAZMAT p 3729 N94-32452
Identification and control of structures in space [NASA-CR-195910] p 3612 N94-33115
From animals to animats [AD-A277427] p 3802 N94-33241

ROBUSTNESS (MATHEMATICS)
Robust multisource classification method using the Markov random field methods p 3750 N94-32537
Limiting vibration in systems with constant amplitude actuators through command preshaping [NASA-CR-188284] p 3739 N94-32907

ROCHE LIMIT
Evolution of vaporizing pulsars p 3929 N94-31128

ROCKET ENGINE DESIGN
The 7.5K lbf thrust engine preliminary design for Orbit Transfer Vehicle [NASA-CR-189175] p 3614 N94-31618
Performance evaluation and operating characteristics of a waveguide microwave applicator for space propulsion applications p 3614 N94-31908
Design of a cold-flow test facility for the high pressure fuel turbopump turbine of the Space Shuttle main engine [AD-A276743] p 3615 N94-32182
Summary of particle bed reactor designs for the Space Nuclear Thermal Propulsion Program [DE94-007434] p 3615 N94-32266

ROCKET ENGINES
Using Monte Carlo techniques and parallel processing for debris hazard analysis of rocket systems [DE94-007250] p 3609 N94-31382

ROCKET EXHAUST
A six degree of freedom, plume-fuel optimal trajectory planner for spacecraft proximity operations using an A* node search [NASA-CR-188285] p 3601 N94-32388
Simulation of low-density nozzle plumes in non-zero ambient pressures [NASA-TM-106501] p 3615 N94-32742
Possible effect of the chlorine oxide dimer on transient ozone loss in rocket plumes [AD-A278135] p 3616 N94-33094

ROCKET PROPELLANTS
Laser and Fourier transform spectroscopy of novel propellant molecules [AD-A277506] p 3667 N94-33013

ROCKS
Nonlocal theory for fracturing of quasibrittle materials [AD-A278283] p 3740 N94-33143

ROLL
Phase-lock roll control of inertially pointing spacecraft p 3609 N94-31470

ROLL FORMING
Development of thermoplastic composite aircraft structures [NASA-CR-189593] p 3626 N94-32860

ROLLER BEARINGS
Development of long-life, low-noise linear bearings for atmospheric interferometry p 3606 N94-33312

ROOM TEMPERATURE
Molecular/polymeric magnetism [DE94-005888] p 3649 N94-31201
Room temperature molten salts for advanced energy conversion and storage [AD-A277777] p 3763 N94-33015

ROOT-MEAN-SQUARE ERRORS
Development of a statistical method for estimating the downward longwave radiation at the surface from satellite observations p 3742 N94-31553

ROSAT MISSION
Multiwavelength search for protoplanetary disks p 3599 N94-31430

ROSS ICE SHELF
A reassessment of the in-situ dielectric constant of polar firn [AD-A276999] p 3773 N94-32154

ROSSBY REGIMES
Rotational effects in turbulence driven by convection p 3930 N94-31131

ROTARY WING AIRCRAFT
Controls design with crossfeeds for hovering rotorcraft using quantitative feedback theory [NASA-CR-195765] p 3585 N94-31203
Rotorcraft ditchings and water-related impacts that occurred from 1982 - 1989, phase 2 [AD-A276473] p 3574 N94-31246

ROTARY WINGS
Experimental and numerical simulation of helicopter rotor fuselage interaction [ONERA-NT-1993-8] p 3568 N94-31421
A critical assessment of UH-60 main rotor blade airfoil data [NASA-TM-103985] p 3571 N94-32063
User's guide for a flat wake rotor inflow/wake velocity prediction code, DOWN [NASA-TM-104139] p 3572 N94-32873
The analysis of wake-induced unsteady aerodynamics related to higher harmonic control [AD-A277914] p 3573 N94-33108

ROTATING ENVIRONMENTS
Autogenic-feedback training as a treatment for airsickness in high-performance military aircraft: Two case studies [NASA-TM-108810] p 3801 N94-33068

ROTATING FLUIDS
Magnetohydrodynamics of the Earth's core. 1: Steady, rotating magnetoconvection. 2: Magnetic Rossby waves p 3770 N94-31104

On the structure and stability of slender viscous vortices p 3700 N94-31218
ROTATION
Theory of protostellar accretion disks p 3931 N94-31136
Optical flow from 1D correlation: Application to a simple time-to-crash detector [AD-A276777] p 3880 N94-32186
Unit specific crew rest strategies: Phase 1 evaluation of the 1/212th Aviation Battalion during shiftwork transitions [AD-A277122] p 3804 N94-32379
ROTATIONAL SPECTRA
Degenerate four-wave mixing as a diagnostic of plasma chemistry [DE94-008588] p 3889 N94-31766
ROTOR AERODYNAMICS
An adaptive finite element method for unsteady compressible rotor airfoil aerodynamics p 3567 N94-31204
Experimental and numerical simulation of helicopter rotor fuselage interaction [ONERA-NT-1993-8] p 3568 N94-31421
ROTOR BLADES (TURBOMACHINERY)
Development of a cascade simulation of fan-passage flow [AD-A277234] p 3584 N94-32026
ROTOR BODY INTERACTIONS
Experimental and numerical simulation of helicopter rotor fuselage interaction [ONERA-NT-1993-8] p 3568 N94-31421
ROTOR DYNAMICS
Rotordynamic effects driven by fluid forces from a geometrically imperfect labyrinth [AD-A276424] p 3722 N94-31333
ROTORS
Rotordynamic effects driven by fluid forces from a geometrically imperfect labyrinth [AD-A276424] p 3722 N94-31333
RUBBER
Toughening mechanisms in the high strain rate deformation of rubber-modified polymer glasses p 3653 N94-31942
RUBIDIUM
Optical properties of lanthanide-doped RbTiOAsO4 and transition metal-doped KTiOPO4 [DE94-008433] p 3907 N94-32963
RUBIDIUM COMPOUNDS
Inorganic materials for anomalous-dispersion phase-matched second harmonic generation: Rubidium titanyl arsenate isomorphs, Rb(Ti(1-2x)Ln(x)Nb(x))OAsO4 [DE94-006141] p 3899 N94-31847
Advances and applications of dynamic-angle spinning nuclear magnetic resonance [DE94-007031] p 3870 N94-32250
Extended-range order in glasses [DE94-008135] p 3681 N94-32798
RUBY LASERS
A reliable low-maintenance flashlamp-pumped Ti:sapphire laser operating at 120 PPS [DE94-009030] p 3721 N94-32848
RUNGE-KUTTA METHOD
Symplectic Runge-Kutta schemes 3: Canonical elementary differentials [MATHS-REPT-A-204] p 3840 N94-31159
Symbolic derivation of Runge-Kutta methods [MATHS-REPT-A-205] p 3840 N94-31160
A brief introduction to symplectic integrators and recent results [DE94-006225] p 3845 N94-31763
Solution of the average-passage equations for the incompressible flow through multiple-blade-row turbomachinery [AD-A276515] p 3583 N94-31931
On the error committed by stopping the Newton iteration in Runge-Kutta methods and linear multistep methods [TW-93-13] p 3847 N94-32206
Fourth-order 2N-storage Runge-Kutta schemes [NASA-TM-109112] p 3573 N94-32950
RUNWAYS
Determining the bearing capacity of flexible airfield pavements using a heavy weight deflectometer [ISBN-0-315-86210-6] p 3587 N94-31710
Evaluation for the development of taxiway lighting intensity standards [AD-A276706] p 3588 N94-32120
RURAL LAND USE
Common property resources and low-level flying in Labrador: Flight, fight or fancy? [ISBN-0-315-87318-3] p 3924 N94-31732
RUSSIAN FEDERATION
Station climatic summaries: China, the former USSR, and Mongolia [AD-A276548] p 3784 N94-32057
Information systems to enhance technology exchange [DE94-007744] p 3920 N94-32808
RYDBERG SERIES
Diamagnetism in helium Rydberg atoms [ETN-94-96015] p 3865 N94-31549

S

S MATRIX THEORY
Single scattering of light by ensembles of particles with various shapes [ETN-94-96016] p 3878 N94-31550
S WAVES
On wave interactions of rotational and irrotational flows p 3700 N94-31219
SADDLE POINTS
Heteroclinic attractors: Time averages and moduli of topological conjugacy [W-9318] p 3844 N94-31690
Steepest descent paths for integrals defining the modified Bessel functions of imaginary order [CWI-AM-R9303] p 3848 N94-32227
SAFETY
Laser safety manual for DREO [AD-A276288] p 3714 N94-31255
Scientific basis for safety science [PB94-138534] p 3668 N94-31838
Systems for the monitoring of working conditions relating to health and safety: Extensive description. Norway [PB94-138542] p 3803 N94-31839
Controlling hazardous energy sources (lockout/tagout) [NASA-TM-105290] p 3669 N94-32861
Implementing software safety in the NASA environment [NASA-TM-106597] p 3731 N94-33032
SAFETY MANAGEMENT
Scientific basis for safety science [PB94-138534] p 3668 N94-31838
Integrated safety program for the Nuclear Electric Propulsion Space Test Program [DE94-004670] p 3615 N94-32669
Independent safety assessment of the Topaz-2 space nuclear reactor power system [DE94-008653] p 3877 N94-32879
SAMPLING
Analysis of key performance parameters of phase sampling digital RF memories [AD-A276019] p 3688 N94-31494
The effects of altimeter sampling characteristics: Some Geosat examples [AD-A276899] p 3747 N94-32214
Focused feasibility study final field sampling plan [AD-A277445] p 3769 N94-33105
SANDSTONES
NMR characterization of shocked quartz [DE94-007733] p 3774 N94-32816
SANDWICH STRUCTURES
Damage tolerance aspects of a full composite airplane fuselage: Requirements, modelling, predictions, experiments [LR-728] p 3578 N94-31674
Honeycomb sandwich structures: Vented versus unvented designs for space systems [AD-A276713] p 3624 N94-32122
SARSAT
A neural network application to search and rescue satellite aided tracking (SARSAT) p 3613 N94-33345
SATELLITE ALTIMETRY
Filtering of satellite altimetry data with optimal smoothing cubic splines to compute geoid heights, along-tract geoid and gravity gradients in the Indonesian waters and its surroundings [PB94-147527] p 3741 N94-31074
Application of radon transformation for improved analysis of sparsely sampled data: A feasibility study [PB94-147535] p 3741 N94-31075
Satellite radar altimetry over the continental ice sheets p 3742 N94-31570
Error analysis of real-time and post-processed orbit determination for the Geosat Follow-On altimetric satellite using GPS tracking p 3576 N94-31845
The effects of altimeter sampling characteristics: Some Geosat examples [AD-A276899] p 3747 N94-32214
Fields of experiments in ERS-1 SAR interferometry in Bonn and Naples p 3756 N94-32572
SATELLITE ANTENNAS
Proceedings of the 1993 Antenna Applications Symposium, volume 1 [AD-A277202] p 3676 N94-32049
Proceedings of the 1993 Antenna Applications Symposium, volume 2 [AD-A277203] p 3677 N94-32050
Two-axis antenna positioning mechanism p 3605 N94-33308
Special test equipment and fixturing for MSAT reflector assembly alignment p 3606 N94-33316
SATELLITE ATTITUDE CONTROL
Chaotic attitude motion of satellites in the central gravitational field [ISBN-0-315-78768-6] p 3610 N94-31723
Trajectory planning for space manipulators [AD-A277229] p 3611 N94-32369
Performance analysis of an integrated GPS/inertial attitude determination system [NASA-CR-188289] p 3577 N94-32864
SATELLITE COMMUNICATION
Europe at the crossroads: The future of its satellite communications industry [ESA-SP-1166] p 3670 N94-31182
Channel and terminal description of the ACTS mobile terminal p 3599 N94-31428
Hubless satellite communications networks p 3600 N94-31433
Multisatellite constellation configuration selection for multiregional highly elliptical orbit constellations p 3600 N94-31437
SATCOM feasibility study for search and rescue aircraft [DSIS-94-01083] p 3575 N94-31902
Satellite communications industry [AD-A276685] p 3610 N94-32039
CIM in space: Corporate Information Management (CIM) implications for space-based information systems [AD-A276882] p 3600 N94-32126
Advanced satellite communication system [NASA-CR-194211] p 3681 N94-32477
COVICS: A covert video communications system [DE94-007568] p 3682 N94-32745
Aerospace sponsored research [ATR-93(8498)-1] p 3966 N94-32949
Pointing and tracking space mechanism for laser communication p 3606 N94-33310
SATELLITE CONSTELLATIONS
Multisatellite constellation configuration selection for multiregional highly elliptical orbit constellations p 3600 N94-31437
SATELLITE CONTROL
Aerospace sponsored research [ATR-93(8498)-1] p 3966 N94-32949
SATELLITE DESIGN
Automated detection of ship tracks in multispectral satellite data [AD-A276697] p 3746 N94-32119
Design and performance of the telescope and detector covers on the Extreme Ultraviolet Explorer satellite p 3605 N94-33309
Pointing and tracking space mechanism for laser communication p 3606 N94-33310
MSAT boom joint testing and load absorber design p 3606 N94-33315
SATELLITE DOPPLER POSITIONING
A neural network application to search and rescue satellite aided tracking (SARSAT) p 3613 N94-33345
SATELLITE GUIDANCE
The ALEXIS mission recovery [DE94-007549] p 3611 N94-32813
SATELLITE IMAGERY
Desert aerosols: Sources, transports, and impacts determined by remote sensing p 3770 N94-31003
Automatic extraction of cartographic objects by fusion of data extracted from satellite images [TELECOM-93-E-001] p 3742 N94-31165
Estimation of visible and near-infrared reflectivity for Peyto Glacier Basin using satellite data [ISBN-0-315-87039-7] p 3743 N94-31733
The basement fracture pattern of southern Ontario: A tectonic interpretation based on Landsat TM imagery, airphotos and field data [ISBN-0-315-87086-9] p 3772 N94-31834
Shiptrack database analysis [AD-A277228] p 3746 N94-32025
Sensitivity analysis of the AVHRR infrared cirrus model [AD-A276690] p 3784 N94-32117
Automated detection of ship tracks in multispectral satellite data [AD-A276697] p 3746 N94-32119
Research and applications of a canopy reflectance model p 3747 N94-32492
From Optics to Radar, SPOT and ERS Applications [ISBN-2-85428-345-7] p 3747 N94-32523
Monitoring land cover and crop types in Denmark using ERS-1 SAR and optical satellite images p 3748 N94-32528
Optics and radar: Cohabitation, rivality or happy marriage. Towards new planning tools p 3748 N94-32529
The contribution of satellite data in communication infrastructure projects p 3749 N94-32530

The use of ERS images for mapping
p 3749 N94-32531
SPOT imagery for updating land cover information of 1:50,000 numerical topographic maps
p 3749 N94-32532
Example of SPOT/ERS-1 complementarity
p 3749 N94-32533
The use of SPOT, and the contribution of ERS-1, in the assessment of urban pressure on agriculture land in Greater Tunis (Tunisia) p 3749 N94-32534
Restoration of interferometric, polarimetric, radiometric, and textural information in SAR images
p 3750 N94-32535
Assessment of region-based methods for automated SAR/optical registration, attribute extraction, and classification p 3750 N94-32536
Technique of ERS-1 image processing in association with SPOT data p 3750 N94-32538
Production of terrain data: Optical radar complementarity p 3750 N94-32540
Fusion of multispectral (XS) and Panchromatic (P) SPOT images and radar images p 3750 N94-32541
Integration of ERS-1 images into the European Agriculture Statistics project Action 4: Thematic aspect
p 3753 N94-32554
Rapid estimates of crop acreage and production at European scale using high resolution imagery
p 3754 N94-32557
Differential interferometry study of an earthquake
p 3756 N94-32570
Quantitative analysis of woody vegetation in Soudano-Sahalian region. Textural approach (application to a Burkina Faso region) p 3757 N94-32574
Evolution of upwelling fronts off the coast of Portugal
[NASA-CR-195692] p 3790 N94-33045

SATELLITE INSTRUMENTS
MODIS. Volume 1: MODIS level 1A software baseline requirements
[NASA-TM-104594-VOL-1] p 3823 N94-33287

SATELLITE NETWORKS
The Second Annual International Space University Alumni Conference
[NASA-CP-3253] p 3598 N94-31425

SATELLITE OBSERVATION
Subtropical Climates and Their Evolution: From Space-Based Observation to Modelling
[ISBN-2-85-428333-3] p 3776 N94-30981
Space equipment for Earth observations
p 3613 N94-30997
The use of meteorological satellite data for studying tropical atmospheric phenomena p 3779 N94-31000
The surface parameters: Remote sensing observations and climatology applications p 3779 N94-31001
Desert aerosols: Sources, transports, and impacts determined by remote sensing p 3770 N94-31003
Airborne instruments p 3757 N94-31006
Development of a statistical method for estimating the downward longwave radiation at the surface from satellite observations p 3742 N94-31553
Imaging devices for satellite remote sensing
[VTT-TIED-1517] p 3743 N94-31658
Radar rainfall measurements from space
p 3782 N94-31889
Sensitivity analysis of the AVHRR infrared cirrus model
[AD-A276690] p 3784 N94-32117
Remote sensing and the Mississippi high accuracy reference network p 3758 N94-32466
Research and applications of a canopy reflectance model p 3747 N94-32492
From Optics to Radar, SPOT and ERS Applications
[ISBN-2-85428-345-7] p 3747 N94-32523
The complementary nature of the SPOT and ERS-1 systems and their place in major international programmes p 3748 N94-32524
From optics to radar: Environmental problems and the SPOT/ERS systems p 3748 N94-32525
Feasibility in the use of satellite remote sensing data as a fast reaction tool for natural disaster relief
p 3748 N94-32526
Contribution of SAR ERS1 data to study the French Guiana tropical coast environment
[BRGM-93034] p 3748 N94-32527
Monitoring land cover and crop types in Denmark using ERS-1 SAR and optical satellite images
p 3748 N94-32528
Optics and radar: Cohabitation, rivality or happy marriage. Towards new planning tools
p 3748 N94-32529
The contribution of satellite data in communication infrastructure projects p 3749 N94-32530
The use of ERS images for mapping
p 3749 N94-32531
SPOT imagery for updating land cover information of 1:50,000 numerical topographic maps
p 3749 N94-32532
Example of SPOT/ERS-1 complementarity
p 3749 N94-32533
The use of SPOT, and the contribution of ERS-1, in the assessment of urban pressure on agriculture land in Greater Tunis (Tunisia) p 3749 N94-32534
Almaz marine applications p 3751 N94-32544
The use of SPOT and ERS-1 images to map the eruption of Nevado Sabancaya (Province of Arequipa, South Peru) and evaluate associated risks p 3751 N94-32546
A case study comparing multi-temporal ERS-1 SAR data and SPOT data for tropical forest mapping
p 3753 N94-32556
Land cover change detection with ERS-1 data and data from other remote sensing satellites. Example: The delta of the River Ebro (Spain) p 3755 N94-32564
ERS-1 SAR and optical data for land use/land cover mapping: A case study in a savannah zone of Guinea
p 3755 N94-32565
Statistical analysis and mapping of cotton and food crop cultivation surfaces in the west of Burkina Faso: Contribution of combined SPOT P and XS data
p 3757 N94-32575
Parameterizing atmosphere-land surface exchange for climate models with satellite data: A case study for the Southern Great Plains CART site
[DE94-005109] p 3775 N94-32874
Evolution of upwelling fronts off the coast of Portugal
[NASA-CR-195692] p 3790 N94-33045
Stationary eddies in the Mars general circulation as simulated by the NASA-Ames GCM
p 3944 N94-33192
TRMM-related research: Tropical rainfall and energy analysis experiment
[NASA-CR-195834] p 3787 N94-33288
MODIS. Volume 2: MODIS level 1 geolocation, characterization and calibration algorithm theoretical basis document, version 1
[NASA-TM-104594-VOL-2] p 3613 N94-33289

SATELLITE ORBITS
Multisatellite constellation configuration selection for multiregional highly elliptical orbit constellations
p 3600 N94-31437
Possible improvements of satellite ephemeris programs used in geodesy
[PB94-148681] p 3743 N94-31592
General-relativistic celestial mechanics. 4: Theory of satellite motion
[PB94-147782] p 3601 N94-31769
Testing for preferred-frame effects in gravity with artificial Earth satellites
[PB94-148459] p 3610 N94-31771
Semianalytic Satellite Theory (SST): Mathematical algorithms
[AD-A276836] p 3610 N94-32208

SATELLITE ORIENTATION
The ALEXIS mission recovery
[DE94-007549] p 3611 N94-32813
Performance analysis of an integrated GPS/inertial attitude determination system
[NASA-CR-188289] p 3577 N94-32864

SATELLITE PERTURBATION
Semianalytic Satellite Theory (SST): Mathematical algorithms
[AD-A276836] p 3610 N94-32208

SATELLITE SOUNDING
The use of meteorological satellite data for studying tropical atmospheric phenomena p 3779 N94-31000
Development of a statistical method for estimating the downward longwave radiation at the surface from satellite observations p 3742 N94-31553

SATELLITE TRACKING
Air Force Space Command satellite orbit predictor using parallel virtual machines
[AD-A276316] p 3801 N94-31298

SATELLITE-BORNE INSTRUMENTS
Space equipment for Earth observations
p 3613 N94-30997
Imaging devices for satellite remote sensing
[VTT-TIED-1517] p 3743 N94-31658

SATELLITE-TO-SATELLITE TRACKING
Pointing and tracking space mechanism for laser communication p 3606 N94-33310

SCALARS
Notes on the Langevin model for turbulent diffusion of marked particles
[DE94-007847] p 3708 N94-32652

SCALE EFFECT
Multiple size scale structures in silica/siloxane composites studied by small-angle scattering
[DE94-007300] p 3625 N94-32642

SCALERS
A miniaturized ASIC-based multichannel scaler instrument
[DE94-007222] p 3807 N94-32783

SCALING LAWS
Computer modelling of cyclic deformation of high-temperature materials
[AD-A277056] p 3623 N94-32012
Electromagnetic wave reflection from irregular plasma layers
[AD-A276727] p 3678 N94-32161
A simple model for determining photoelectron-generated radiation scaling laws
[DE94-006130] p 3761 N94-32660
Analysis of Dietz's single, rectangular pulse theory for the generation of radiation via photoelectrons
[DE94-006131] p 3681 N94-32661
Particle-In-Cell (PIC) code simulation results and comparison with theory scaling laws for photoelectron-generated radiation
[DE94-006132] p 3695 N94-32662

SCANNERS
Millimeter wave, high-resolution, holographic surveillance system
[DE94-004289] p 3712 N94-31831
COVICS: A covert video communications system
[DE94-007568] p 3682 N94-32745
PSIDD: A Post-Scan Interactive Data Display system for ultrasonic scans
[NASA-TM-4545] p 3732 N94-33038

SCANNING ELECTRON MICROSCOPY
Optimal detector strategies for the phase contrast imaging for scanning transmission electron microscopes
[ETN-94-95747] p 3866 N94-31613
Deuterium absorption and material phase characteristics of SAES St198 Zr-Fe alloy
[DE94-008275] p 3646 N94-32781

SCANNING TUNNELING MICROSCOPY
Studying transient mobility and energy loss using scanning tunneling microscopy
[AD-A276292] p 3877 N94-31256
Analytical applications of scanning tunneling microscopy
[AD-A276066] p 3711 N94-31283
The adsorption of sulfate on gold(111) in acidic aqueous media: Adlayer structural inferences from infrared spectroscopy and scanning tunneling microscopy
[AD-A276643] p 3642 N94-31997
Vibrational spectroscopy at metal-solution interfaces: Some perspectives and prospects for electrochemical surface science
[AD-A276781] p 3644 N94-32169
Charge-dependent atomic-scale structures of high-index and (110) gold electrode surfaces as revealed by scanning tunneling microscopy
[AD-A276782] p 3869 N94-32170
The 14th Annual West Coast Theoretical Chemistry/Statistical Mechanics Conference
[AD-A276942] p 3656 N94-32239
Sensitivity of electrochemical adlayer structure to the metal crystallographic orientation: Potential-independent iodide adsorption on Au(100) in comparison with other low-index surfaces
[AD-A276714] p 3909 N94-33273
Scanning tunneling microscopy and infrared spectroscopy as combined in-situ probes of electrochemical adlayer structure: Cyanide on Pt(111)
[AD-A276715] p 3909 N94-33274
Nanoscale structural changes upon electrooxidation of Au(111) as probed by potentiodynamic scanning tunneling microscopy
[AD-A276780] p 3909 N94-33275

SCATTER PROPAGATION
Performance statistics bulletin. High latitude meteor scatter propagation October, November, December 1990, January 1991
[AD-A276693] p 3676 N94-31998
Performance statistics bulletin. High latitude metor scatter propagation, February, March, April, May 1992
[AD-A276667] p 3677 N94-32083
Performance statistics bulletin. High latitude meteor scatter propagation February, March, April, May 1991
[AD-A276723] p 3678 N94-32158
Performance statistics bulletin. High latitude meteor scatter propagation October, November, December 1991, January 1992
[AD-A276724] p 3678 N94-32159
Performance statistics bulletin. High latitude meteor scatter propagation, November and December 1989, and January 1990
[AD-A276688] p 3680 N94-32297
Performance statistics bulletin. High latitude meteor scatter propagation
[AD-A276694] p 3680 N94-32298
Performance statistics bulletin. High latitude meteor scatter propagation
[AD-A276695] p 3680 N94-32299
Performance statistics bulletin. High latitude meteor scatter propagation
[AD-A276696] p 3680 N94-32300

Performance statistics bulletin. High latitude meteor scatter propagation, June, July, August, September 1992
[AD-A277508] p 3685 N94-33347

SCATTERING
Impurities and conductivity in a D-wave superconductor
[DE94-006222] p 3898 N94-31628
Modern integral equation techniques for quantum reactive scattering theory
[DE94-007039] p 3857 N94-31639
Stellar x ray polarimeter polarizer development and calibration at LEA/LLNL
[DE94-006400] p 3712 N94-31783
Penetrable wedge analysis
[AD-A277219] p 3845 N94-32022

SCATTERING COEFFICIENTS
Backscatter and transmission of aerosol at UV through middle IR wavelengths
[AD-A277127] p 3718 N94-32305

SCATTERING CROSS SECTIONS
Production of charginos and neutralinos for the reaction positron electron yields Z' boson yields chargino(+) (sub i) chargino(-) (sub j) or neutralino (sub i) neutralino (sub j) in SU(2) (sub L) x SU(2) (sub R) x U(1) (sub B-L)
[ISBN-0-315-87316-7] p 3867 N94-31832
Scatterometer wind-speed exponents: A review and SAXON 35-GHz measurements
[AD-A276568] p 3783 N94-31937
Development of a frequency-domain electromagnetic scattering measurement system
[AD-A276738] p 3678 N94-32179
Time-resolved IR spectroscopy, energy transfer, and state-to-state collision dynamics of atmospheric species
[AD-A277372] p 3773 N94-32338
Quantum dynamics in dual spaces
[DE94-008303] p 3913 N94-32824

SCATTERING FUNCTIONS
Single scattering of light by ensembles of particles with various shapes
[ETN-94-96016] p 3878 N94-31550
Recursive analysis of matrix scattering functions
[AD-A277264] p 3845 N94-32018

SCATTEROMETERS
Scatterometer wind-speed exponents: A review and SAXON 35-GHz measurements
[AD-A276568] p 3783 N94-31937

SCENE ANALYSIS
Automatic extraction of cartographic objects by fusion of data extracted from satellite images
[TELECOM-93-E-001] p 3742 N94-31165
Volumetric modelling of three dimensional scenes by octree decomposition of geometric models
[ISBN-0-315-86866-X] p 3814 N94-31728
A neural network model for the visual perception of the depth of a scene from stereoscopy and shading
[ISBN-0-315-86753-1] p 3831 N94-31750
Safe navigation and active vision for autonomous vehicles: A purposive and direct solution
p 3832 N94-31842
Neural models of spatial orientation in novel environments
[AD-A277383] p 3835 N94-32340

SCHEDULES
Unit specific crew rest strategies: Phase 1 evaluation of the 1/212th Aviation Battalion during shiftwork transitions
[AD-A277122] p 3804 N94-32379

SCHEDULING
On the use of genetic algorithms to solve the time-table problem
[REPT-90-060-REV] p 3829 N94-31176
Exact solution of the single machine scheduling problem with earliness and flow time penalties
[REPT-93-038] p 3809 N94-31189
Scheduling techniques for multiple processor systems in real-time environments
[AD-A276149] p 3824 N94-31249
A model and algorithms for a software evolution control system
[AD-A276431] p 3811 N94-31449
Planning of air crew schedules
[ISBN-0-315-86506-7] p 3914 N94-32074
Discrete-event-dynamic-system-based approaches for scheduling transmissions in multihop packet radio networks
[AD-A276566] p 3679 N94-32230
Scheduling fighter missions using an expert system with an operations research module p 3853 N94-33337

SCHLIEREN PHOTOGRAPHY
Noninvasive spectral analysis and beam mapping of focused ultrasound, part 1
[AD-A276211] p 3859 N94-31060

SCHOTTKY DIODES
Modification of semiconductor surface properties with chemically bound molecular films
[AD-A276162] p 3895 N94-31081
Lowering the Schottky barrier at metal or silicide/Si interfaces to extend the range of infrared detectors
[AD-A277253] p 3903 N94-32322

SCHROEDINGER EQUATION
Coherent processes in atom in strong radiation fields
[AD-A278388] p 3874 N94-33144

SCIENCE
OPTIONS for systemic change in mathematics, science, and technology education: Scientist/teacher partnerships
[DE94-007472] p 3914 N94-32910

SCIENTIFIC SATELLITES
MSFC orbital spacecraft development emphases for this decade p 3598 N94-31048
Odin aeronomy science: A phase-A report by the Aeronomy Science Working Group for the Odin satellite
[AP-31] p 3770 N94-31222

SCIENTIFIC VISUALIZATION
Applications of data compression to 3-D scalar field visualization p 3817 N94-32294
Virtual reality in medical education and assessment
p 3798 N94-32471
On the use of computers for teaching fluid mechanics
[NASA-TM-106587] p 3820 N94-32773

SCIENTISTS
Construction of visual representations and time-space organization of resources in astronomy
[ISBN-0-315-86694-2] p 3925 N94-31914
NASA/DOD Aerospace Knowledge Diffusion Research Project. Paper 12: The diffusion of federally funded aerospace research and development (R/D) and the information seeking behavior of US aerospace engineers and scientists
[NASA-TM-109404] p 3921 N94-32832
NASA/DOD Aerospace Knowledge Diffusion Research Project. Paper 11: The voice of the user: How US aerospace engineers and scientists view DOD technical reports
[NASA-TM-109348] p 3921 N94-32834
NASA/DOD Aerospace Knowledge Diffusion Research Project. Paper 1: The value of scientific and technical information (STI), its relationship to Research and Development (R/D), and its use by US aerospace engineers and scientists
[NASA-TM-109774] p 3922 N94-32835
NASA/DOD Aerospace Knowledge Diffusion Research Project. Report 25: The technical communications practices of British aerospace engineers and scientists: Results of the phase 4 RAeS mail survey
[NASA-TM-109098] p 3922 N94-32836
NASA/DOD Aerospace Knowledge Diffusion Research Project. Report 24: The technical communications practices of US aerospace engineers and scientists: Results of the phase 1 SAE mail survey
[NASA-TM-109088] p 3922 N94-32837

SCINTILLATING FIBERS
Final results from the SDC dopant search for new green wavelength shifting (WLS) fibers, volume 1
[DE94-006744] p 3878 N94-31271
Investigation of scintillator and fibre light in plastic scintillation dosimetry
[ISBN-0-315-87190-3] p 3879 N94-31877

SCINTILLATION
Final results from the SDC dopant search for new green wavelength shifting (WLS) fibers, volume 1
[DE94-006744] p 3878 N94-31271
Design of new polymers to improve radiation stability of plastic scintillators
[DE94-008220] p 3652 N94-31764
Statistics of time averaged atmospheric scintillation
[DE94-006998] p 3747 N94-32249
Phase-only correction of scintillated laser beams: Downrange experimental results
[AD-A277778] p 3722 N94-33282

SCINTILLATION COUNTERS
Particle identification in a segmented calorimeter (NUMASS test data, September 1991)
[USIP-93-08] p 3711 N94-31085
Final results from the SDC dopant search for new green wavelength shifting (WLS) fibers, volume 1
[DE94-006744] p 3878 N94-31271
Mechanisms of formation and of de-excitation in the reaction Mg-24 + C-12 yields 9 alpha at 35MeV per nucleon
[ISBN-0-315-86746-9] p 3867 N94-31749
Design of new polymers to improve radiation stability of plastic scintillators
[DE94-008220] p 3652 N94-31764
Investigation of scintillator and fibre light in plastic scintillation dosimetry
[ISBN-0-315-87190-3] p 3879 N94-31877

SCREWS
An experimental and analytical investigation of a threaded fastener
[VTT-JULK-786] p 3724 N94-31654

SEA BREEZE
Evolution of diurnal surface winds and surface currents for Monterey Bay
[AD-A277649] p 3790 N94-33057

SEA FLOOR SPREADING
Light in Thermal Environments (LITE) Workshop
[NASA-CR-195851] p 3790 N94-32981

SEA ICE
The use of ERS-1 within an operational ice monitoring program p 3751 N94-32545

SEA LEVEL
World height system definition and implementation
[AD-A276725] p 3747 N94-32160
ENSO forced variations of the sea surface temperature and adjusted sea level along the west coast of the United States
[AD-A277306] p 3789 N94-32327

SEA STATES
The application of a radial basis function neural network for radar tracking over the sea p 3686 N94-33150

SEA SURFACE TEMPERATURE
General ocean circulation p 3777 N94-30984
Low frequency variability observed in the tropical Atlantic Ocean p 3778 N94-30991
Air-sea interaction patterns in the equatorial Pacific
[AD-A277305] p 3788 N94-32072
ENSO forced variations of the sea surface temperature and adjusted sea level along the west coast of the United States
[AD-A277306] p 3789 N94-32327

SEA WATER
Investigation of carbon dioxide in the central South Pacific Ocean (WOCE Sections P-16C and P-17C) during the TUNES/2 expedition of the R/V Thomas Washington, July-August, 1991
[DE94-008638] p 3763 N94-31347
Magnetohydrodynamic boundary layer control system
[AD-D016120] p 3710 N94-32958

SEALERS
Improved resealing procedures for the second deseal/reseal program in RAAF F111 aircraft fuel tanks
[AD-A277069] p 3580 N94-32378
Compatibility of refrigerants and lubricants with elastomers
[DE94-008552] p 3658 N94-32518

SEALING
Compatibility of refrigerants and lubricants with elastomers
[DE94-008552] p 3658 N94-32518

SEALS (STOPPERS)
High temperature NASP engine seal development
[NASA-TM-109750] p 3725 N94-31804

SEAMOUNTS
Fine and microstructure observations at Fieberlin g Guyot R/V new horizon cruise report
[AD-A277917] p 3791 N94-33109

SEARCH PROFILES
Methods for parallelizing search paths in phrasing
[AD-A276876] p 3817 N94-32212

SEASAT SATELLITES
Comparison of SPOT, ERS-1, SEASAT, LANDSAT TM, and merged imagery for geological investigations
p 3752 N94-32547
Evaluation of surface phase change on large zones
p 3755 N94-32567

SECONDARY EMISSION
Elimination of two atomic electrons by a single high energy photon
[DE94-006834] p 3864 N94-31320
Energy and angular distributions of secondary ions during electronic sputtering of nonconducting surfaces
[ETN-94-95756] p 3865 N94-31516

SECONDARY FLOW
Incorporating radial mixing in axisymmetric streamline curvature through-flow analysis
[AD-A277325] p 3706 N94-32279

SECURITY
NATO contributions to European environmental security
[AD-A275918] p 3763 N94-31275
Millimeter wave, high-resolution, holographic surveillance system
[DE94-004289] p 3712 N94-31831

SEDIMENT TRANSPORT
Temporal and spatial mapping of atmospheric dust opacity and surface albedo on Mars
p 3947 N94-33211
Fluid mechanical measurements within the bottom boundary layer over the Northern California continental shelf during stress
[AD-A277916] p 3791 N94-33243

SEDIMENTARY ROCKS
Analysis of deep seismic reflection and other data from the southern Washington Cascades
[DE94-005958] p 3771 N94-31525

SEDIMENTS
Gas hydrate detection and mapping on the US east coast
[DE94-005959] p 3742 N94-31504
Geologic controls of erosion and sedimentation on Mars p 3951 N94-33232
Polar sediment accumulation: Role of surface winds at the two poles p 3951 N94-33233
Fluid mechanical measurements within the bottom boundary layer over the Northern California continental shelf during stress
[AD-A277916] p 3791 N94-33243

SEISMIC ENERGY
Finite-element modeling of the blockage and scattering of LG propagation
[AD-A277430] p 3775 N94-33006

SEISMIC WAVES
Finite-element modeling of the blockage and scattering of LG propagation
[AD-A277430] p 3775 N94-33006

SEISMOGRAPHS
Long transect seafloor seismic array: A component of SAMSON (Sources of Ambient Micro Seismic Ocean ic Noise)
[AD-A277009] p 3789 N94-32401

SEISMOLOGY
Proceedings of the 4th Tunnel Detection Symposium on Subsurface Exploration Technology
[AD-A276372] p 3771 N94-31369
Gas hydrate detection and mapping on the US east coast
[DE94-005959] p 3742 N94-31504
Differential interferometry study of an earthquake p 3756 N94-32570
Procedures for computing site seismicity
[AD-A277666] p 3775 N94-33028

SELENIUM
Electrical characteristics of GaAs MESFET fabrication by ion implantation of Si or Se
[AD-A278416] p 3909 N94-33328

SELF LUBRICATING MATERIALS
The effect of prolonged exposure to 750 C air on the tribological performance of PM212
[NASA-TM-106472] p 3617 N94-32941

SELF LUBRICATION
Torque characteristics of solid lubricated precision bearings during oscillatory motion
[AD-A278133] p 3728 N94-33061

SELF ORGANIZING SYSTEMS
A generic model for data acquisition: Connectionist methods of information processing
[TELECOM-93-E-003] p 3730 N94-31166
ART: Adaptive Resonance Theory
[TELECOM-93-D-020] p 3829 N94-31193
Numerical optimization techniques in neural network training p 3838 N94-33158

SELF TESTS
Module generation for self-testing integrated systems
[ISBN-9-09-004570-8] p 3688 N94-31520

SEMANTICS
What comes first in dynamic semantics: A compositional, non-representational account of natural language presupposition
[LP-93-15] p 3855 N94-31389
The interpretation of free focus
[CL-93-01] p 3855 N94-31390
Resumptive quantifiers in exception sentences
[LP-93-11] p 3855 N94-31403
Binary quantifiers and relational semantics
[LP-93-13] p 3855 N94-31404
Sums and quantifiers
[LP-93-05] p 3856 N94-31411
Effective truth
[ML-93-15] p 3856 N94-31416
Correspondence theory for extended modal logics, version 3.0
[ML-93-16] p 3856 N94-31417
Updates in dynamic semantics
[LP-93-06] p 3856 N94-31450
Completeness and decidability of the mixed style of inference with composition
[LP-93-09] p 3842 N94-31453
Weaks vs. strong readings of donkey sentences and monotonicity inference in a dynamic setting
[LP-93-10] p 3856 N94-31468
Compositionality of application oriented structuring mechanisms for algebraic specification languages with initial semantics
[ETN-94-95736] p 3812 N94-31577
Report on implementing part relationships using VML metaclasses
[PB94-147485] p 3813 N94-31686
Translucent procedures, abstraction without opacity
[AD-A276877] p 3817 N94-32213
An epistemic proof system for parallel processes
[TR-93-17] p 3826 N94-32291
Multiple inheritance via intersection types
[TR-93-18] p 3848 N94-32292
Formal semantics for a subset of VHDL and its use in analysis of the FTPP scoreboard circuit
[NASA-CR-191577] p 3827 N94-32734

SEMICONDUCTOR DEVICES
III-V compound semiconductor strip-loaded waveguide devices for PICs: Design for minimum crosstalk and high density
[DE94-006588] p 3897 N94-31502
Examination of fast semiconductor diodes (recovery) with respect to switching valves in PWM and resonance devices
[ETN-94-95740] p 3690 N94-31609
Advanced infrared photodetectors: Materials review
[AD-A277058] p 3879 N94-32013
Novel growth technologies for in situ formation of semiconductor quantum wire structures
[AD-A277188] p 3902 N94-32255
WOCSDICE 1993 --- 17th European Workshop on Compound Semiconductor Devices and Integrated Circuits
[AD-A276766] p 3693 N94-32307
Optical processing for semiconductor device fabrication p 3885 N94-32445
Sandia's photonic program and its changing national role
[DE94-008616] p 3883 N94-32878
The 6th International Conference on Modulated Semiconductor Structures
[AD-A276815] p 3906 N94-32908
Superconducting and semiconducting hybrids and advance memory concepts for superconducting electronics
[AD-A277766] p 3907 N94-32988
Optically switched submillimeter-wave oscillator
[AD-A278014] p 3698 N94-33249
Material engineering of the novel semiconductor structures
[AD-A278386] p 3910 N94-33355

SEMICONDUCTOR DIODES
Examination of fast semiconductor diodes (recovery) with respect to switching valves in PWM and resonance devices
[ETN-94-95740] p 3690 N94-31609
High power diode lasers for solid-state laser pumps p 3722 N94-32448

SEMICONDUCTOR JUNCTIONS
Lowering the Schottky barrier at metal or silicide/Si interfaces to extend the range of infrared detectors
[AD-A277253] p 3903 N94-32322

SEMICONDUCTOR LASERS
Laser Diode Ignition (LDI)
[DE94-006590] p 3666 N94-31579
Semiconductor microcavity lasers
[DE94-006143] p 3716 N94-31622
High conversion efficiency pumped-cavity second harmonic generation of a diode laser
[DE94-006805] p 3717 N94-32134
Control and reliability of optical networks in multiprocessors
[AD-A277385] p 3881 N94-32285
High power diode lasers for solid-state laser pumps p 3722 N94-32448
Flexible manufacturing for photonics device assembly p 3669 N94-32449
Rare Earth Doped Semiconductors and Materials Research Society Symposium Proceedings, Volume 301
[AD-A277517] p 3908 N94-33055
Research in the optical sciences
[AD-A278271] p 3884 N94-33140
Advanced release technologies program p 3607 N94-33322

SEMICONDUCTORS (MATERIALS)
Indium-vacancy complexes in mercury cadmium telluride
[AD-A276177] p 3894 N94-31055
Passivation of III-V compound semiconductor based devices
[AD-A276178] p 3894 N94-31056
Electron-beam controlled semiconductor switches
[AD-A276198] p 3686 N94-31057
Modification of semiconductor surface properties with chemically bound molecular films
[AD-A276162] p 3895 N94-31081
Growth and characterization of III-V semiconductors with rare earth impurities for optoelectronic devices
[AD-A276021] p 3896 N94-31455
Semiconductor microcavity lasers
[DE94-006143] p 3716 N94-31622
A low cost igniter utilizing an SCB and titanium sub-hydride potassium perchlorate pyrotechnic
[DE94-006467] p 3666 N94-31827
Development of sample charge compensation for characterization of impurities in semiconductor materials
[AD-A277113] p 3899 N94-31983
IR materials producibility
[AD-A277028] p 3879 N94-32006
Advanced infrared photodetectors: Materials review
[AD-A277058] p 3879 N94-32013
Anomalous small angle x ray scattering studies of amorphous metal-germanium alloys
[DE94-007258] p 3900 N94-32065
Advances in MOVPE compound semiconductor epitaxy manufacturing technology: From high throughput large area reactors to cluster tools
[DE94-006367] p 3901 N94-32104
Amorphous/crystalline structure and phase transformations in metastable semiconducting Ge(1-x)Sn(x)
[DE94-008659] p 3901 N94-32115
The 10th International Conference on Internal Friction and Ultrasonic Attenuation in Solids (ICIFUAS)
[AD-A276849] p 3902 N94-32209
Novel growth technologies for in situ formation of semiconductor quantum wire structures
[AD-A277188] p 3902 N94-32255
Proceedings of the International Workshop on Computational Electronics
[AD-A277020] p 3692 N94-32259
WOCSDICE 1993 --- 17th European Workshop on Compound Semiconductor Devices and Integrated Circuits
[AD-A276766] p 3693 N94-32307
Theoretical studies of electron transfer and optical spectroscopy
[DE94-006985] p 3871 N94-32375
A scanning defect mapping system for semiconductor characterization p 3885 N94-32446
Ionization probes of molecular structure and chemistry
[DE94-007605] p 3872 N94-32643
Metal-ion spin-on glasses: Novel materials for active waveguides
[DE94-007738] p 3882 N94-32649
Research on stable, high-efficiency amorphous silicon multijunction modules
[DE94-000298] p 3695 N94-32680
Application of the modified voltage-dividing potentiometer to overlay metrology in a CMOS/bulk process
[DE94-007937] p 3695 N94-32700
The 6th International Conference on Modulated Semiconductor Structures
[AD-A276815] p 3906 N94-32908
Silicon-Based Optoelectronic Materials Symposium and Materials Research Society Proceedings, volume 298
[AD-A277518] p 3662 N94-32952
Rare Earth Doped Semiconductors and Materials Research Society Symposium Proceedings, Volume 301
[AD-A277517] p 3908 N94-33055
Spacecraft environmental anomalies expert system
[AD-A277962] p 3612 N94-33262
Electrical characteristics of GaAs MESFET fabrication by ion implantation of Si or Se
[AD-A278416] p 3909 N94-33328
Material engineering of the novel semiconductor structures
[AD-A278386] p 3910 N94-33355

SENSITIVITY
A review of sensitivity analysis techniques
[DE94-007192] p 3842 N94-31399
Sensitivity analysis of the AVHRR infrared cirrus model
[AD-A276690] p 3784 N94-32117
Sensitivity of electrochemical adlayer structure to the metal crystallographic orientation: Potential-independent iodide adsorption on Au(100) in comparison with other low-index surfaces
[AD-A276714] p 3909 N94-33273

SENSORIMOTOR PERFORMANCE
Concepts and environment
[REPT-93-032] p 3829 N94-31186
Situational awareness: A feasibility investigation of near-threshold skills development
[AD-A276467] p 3798 N94-31243
Tripping over obstacles: Biomechanical analyses of how young and old try to avoid it p 3803 N94-31954
Information theory for arm visuo-motor coordination p 3800 N94-32495

SENSORS
Fiber optic chemical sensors on Mars
[DE94-005251] p 3941 N94-31145

SENSORY DISCRIMINATION
Mechanisms of temporal pattern discrimination by human observers
[AD-A277407] p 3801 N94-32577
Complex auditory signals
[AD-A278391] p 3862 N94-33146

SENTENCES
Resumptive quantifiers in exception sentences
[LP-93-11] p 3855 N94-31403

Sums and quantifiers
[LP-93-05] p 3856 N94-31411
Updates in dynamic semantics
[LP-93-06] p 3856 N94-31450
Completeness and decidability of the mixed style of inference with composition
[LP-93-09] p 3842 N94-31453
Weaks vs. strong readings of donkey sentences and monotonicity inference in a dynamic setting
[LP-93-10] p 3856 N94-31468

SEPARATED FLOW
Computational study of simultaneous heat and mass transfer in turbulent separated flows
p 3704 N94-31843
Computational prediction of stall flutter in spanwise-finite blade cascades p 3584 N94-31967
Control of low-speed turbulent separated flow over a backward-facing ramp
[NASA-TM-109740] p 3573 N94-33071
Backward-facing step measurements at low Reynolds number, Re(sub h)=5000
[NASA-TM-108807] p 3711 N94-33290

SEPARATORS
Electrostatic reduction of particulates for laser resistant hafnia coatings
[DE94-005824] p 3651 N94-31557
Development of silver-zinc cells of improved cycle life and energy density
[AD-A277311] p 3693 N94-32329
Fabrication, phase transformation studies and characterization of SiC-AlN-Al2OC ceramics
[DE94-008587] p 3659 N94-32657

SEQUENTIAL CONTROL
Novel failure analysis techniques using photon probing with a scanning optical microscope
[DE94-006594] p 3692 N94-32112

SERIES EXPANSION
Symplectic Runge-Kutta schemes 3: Canonical elementary differentials
[MATHS-REPT-A-204] p 3840 N94-31159
Stirling's formula and approximations for n(factorial) and the middle ratio
[REPT-93-73] p 3843 N94-31642
Generalization of a theorem of Kusmin
[REPT-93-74] p 3844 N94-31643
Finite-part integrals and the Euler-Maclaurin expansion
[DE94-006539] p 3844 N94-31665
Probability distributions with given marginals and given correlation that have maximal entropy
[REPT-93-81] p 3851 N94-31698

SERVICE LIFE
Model of spacecraft atomic oxygen and solar exposure microenvironments p 3593 N94-31021
Design application and development of spacecraft in LEO utilizing LDEF results p 3597 N94-31047
Shearographic inspection of a DeHavilland DHC-7
[AD-A276716] p 3566 N94-32157
Development of silver-zinc cells of improved cycle life and energy density
[AD-A277311] p 3693 N94-32329
Spur, helical, and spiral bevel transmission life modeling
[NASA-TM-106552] p 3728 N94-32979
Analysis of intermediate level maintenance following F404-GE-400 engine component life reductions
[AD-A277918] p 3585 N94-33283
Design of a high-speed reliable ball bearing
p 3606 N94-33314

SERVOMECHANISMS
Design, characterization and control of the Unique Mobility Corporation robot p 3603 N94-33296

SET THEORY
Triangular norms and conorms: A general tool for generating fuzzy mathematical morphologies
[TELECOM-93-D-001] p 3839 N94-31092
Frames and stable bases for shift-invariant subspaces of L(sub 2)(IR(sup d))
[AD-A276470] p 3843 N94-31474
Line transects, covariance functions and set approximation
[CWI-BS-R9311] p 3846 N94-32084
Multiple inheritance via intersection types
[TR-93-18] p 3848 N94-32292

SEWING
Development of stitched/RTM composite primary structures p 3628 N94-33127
Test and analysis results for composite transport fuselage and wing structures p 3628 N94-33129

SHAFTS (MACHINE ELEMENTS)
Flexible drive shaft coupling
[AD-D016096] p 3727 N94-32718
The analysis of wake-induced unsteady aerodynamics related to higher harmonic control
[AD-A277914] p 3573 N94-33108

SHAKING
Procedures for computing site seismicity
[AD-A277666] p 3775 N94-33028

SHALLOW SHELLS
Theory of thick, laminated composite shallow shells
p 3622 N94-31953

SHAPE MEMORY ALLOYS
Transmissibility of nickel-titanium shape memory alloy springs
[AD-A276055] p 3640 N94-31456
Implementation of heaters on thermally actuated spacecraft mechanisms p 3607 N94-33320

SHAPES
Interactive reconstruction of anatomical structures with free-form surfaces
[TELECOM-93-E-002] p 3794 N94-31195
A paraperspective factorization method for shape and motion recovery
[AD-A276513] p 3712 N94-31929
Principal component analysis with missing data and its application to object modeling
[AD-A276644] p 3845 N94-31939
Large-scale shape optimization: Numerical methods, parallel algorithms, and applications to aerodynamic design p 3815 N94-31966
Visual encoding of spatial relations
[AD-A277400] p 3800 N94-32344
Visual neural development and chromatic aberration
[AD-A277402] p 3800 N94-32345

SHEAR FLOW
On wave interactions of rotational and irrotational flows p 3700 N94-31219
Oscillations in piston-driven shear flow of a non-Newtonian fluid
[AD-A276472] p 3701 N94-31245
Transport suppression by shear flow generation in multihelicity resistive-g turbulence
[DE94-007108] p 3886 N94-31366
Shear flow control of cold and heated rectangular jets by mechanical tabs. Volume 1: Results and discussion
[NASA-CR-182296-VOL-1] p 3708 N94-32867
Shear flow control of cold and heated rectangular jets by mechanical tabs. Volume 2: Tabulated data
[NASA-CR-182296-VOL-2] p 3709 N94-32869
The structure of high Reynolds number turbulent boundary layers, part A
[AD-A278392] p 3710 N94-33162

SHEAR LAYERS
Control of hypersonic aerodynamic forces with surface blowing p 3567 N94-31216

SHEAR PROPERTIES
Ceramic Technology Project database
[DE94-008494] p 3659 N94-32632
Analysis of new composite architectures
[NASA-CR-195303] p 3626 N94-32904

SHEAR STRENGTH
Joining of alumina by vacuum brazing
[VTT-TIED-1495] p 3724 N94-31656

SHEAR STRESS
An efficient higher order theory for laminated composite plates and a finite element implementation
p 3617 N94-31215
Considering ties elasticities in high frequency rail dynamics
[ILR-MITT-281(1993)] p 3733 N94-31375
Fatigue in single crystal nickel superalloys
[AD-A276662] p 3643 N94-32047
Shearographic inspection of a DeHavilland DHC-7
[AD-A276716] p 3566 N94-32157

SHELL STABILITY
A separation technique for asymptotic-numeric solution for general shells of revolution p 3736 N94-31961

SHELL THEORY
Theory of thick, laminated composite shallow shells
p 3622 N94-31953
Development of an advanced continuum theory for composite laminates, volume 2
[AD-A277276] p 3625 N94-32592

SHELLS (STRUCTURAL FORMS)
A separation technique for asymptotic-numeric solution for general shells of revolution p 3736 N94-31961
Effective computational strategy for predicting the response of complex systems
[AD-A277452] p 3740 N94-33011

SHERGOTTITES
SNC meteorites and their implications for reservoirs of Martian volatiles p 3947 N94-33209
The Martian sources of the SNC meteorites (two, not one), and what can and can't be learned from the SNC meteorites p 3951 N94-33234

SHIFT REGISTERS
Some problems of applied algebra
[CWI-AM-R9306] p 3847 N94-32204

SHIP TO SHORE COMMUNICATION
An analysis of cellular telephone and INMARSAT systems for providing radio data link computer communications for US Navy vessels
[AD-A278143] p 3684 N94-33160

SHIPS
Shiptrack database analysis
[AD-A277228] p 3746 N94-32025
Automated detection of ship tracks in multispectral satellite data
[AD-A276697] p 3746 N94-32119
Ship traffic monitoring and oil spill detection using the ERS-1 SAR p 3751 N94-32542

SHOCK ABSORBERS
MSAT boom joint testing and load absorber design
p 3606 N94-33315

SHOCK DISCONTINUITY
An adaptive method for the exact resolution of shock waves and contact discontinuities
[ISBN-0-315-86498-2] p 3704 N94-31799

SHOCK LAYERS
Development of a cascade simulation of fan-passage flow
[AD-A277234] p 3584 N94-32026

SHOCK RESISTANCE
Mechanical properties of vacuum-sintered yttria ceramics
[DE94-008138] p 3659 N94-32617

SHOCK TUBES
Development of high-pressure diaphragms for the AEDC impulse tunnel
[AD-A277053] p 3588 N94-32009

SHOCK TUNNELS
Calibration and validation studies in the LENS facility
[AD-A278403] p 3591 N94-33167

SHOCK WAVE INTERACTION
Development of a cascade simulation of fan-passage flow
[AD-A277234] p 3584 N94-32026
Numerical analysis of transonic wing buffet
p 3586 N94-32713
An analysis of supersonic flows with low-Reynolds number compressible two-equation turbulence models using LU fir:te volume implicit numerical techniques
[NASA-CR-195302] p 3572 N94-32926

SHOCK WAVE PROPAGATION
Advanced CFD methodology for fast transients encountered in nonlinear combustion instability problems. Volume 1: Theory and validation
[NASA-CR-191351] p 3637 N94-32696
Convection in Type 2 supernovae
[DE94-009373] p 3938 N94-32914

SHOCK WAVES
Control of hypersonic aerodynamic forces with surface blowing p 3567 N94-31216
Numerical simulation of interplanetary dynamics
p 3933 N94-31566
An adaptive method for the exact resolution of shock waves and contact discontinuities
[ISBN-0-315-86498-2] p 3704 N94-31799
A new inverse method for generating high-speed aerodynamic flows with application to waverider design
p 3569 N94-31828
Shock impingement near mild hypersonic expansion corners p 3569 N94-31879
A study of physical conditions, radiative transfer and shocks in the interstellar medium p 3937 N94-31963
PVDF pressure transducers for shock wave and explosives research
[AD-A277319] p 3712 N94-32051
Elastic as limit of viscoelastic response, in a context of self-similar viscous limits
[AD-A277043] p 3738 N94-32273
Overview of shock physics codes for armor analysis
[DE94-008948] p 3739 N94-32842
Analysis of data from the plasma composition experiment on the International Sun-Earth Explorer (ISEE 1)
[NASA-CR-195880] p 3893 N94-33074

SHOT NOISE
Wavelet transform of fixed pattern noise in focal plane arrays
[AD-A276963] p 3712 N94-32393

SHUTTLE IMAGING RADAR
Optimal geological data extraction from SPOT-radar synergism with samples from Djebel Amour (Algeria), Red Sea Hills (Sudan), Sirte Basin (Libya), and Magdalena Valley (Colombia) p 3752 N94-32548

SIALON
Compositions and chemical bonding in ceramics by quantitative electron energy-loss spectrometry
[DE94-007208] p 3659 N94-32640

SIDELOBES
Low sidelobe reflector antenna design for communications
[AD-A276079] p 3673 N94-31463

SIGNAL ANALYSIS
Automatic modulation recognition
p 3686 N94-33153
SIGNAL ANALYZERS
Surface forward-scattered acoustic measurements and analysis
[AD-A276998] p 3788 N94-32000
Design of free space interconnected signal processor
[AD-A278129] p 3683 N94-33093
SIGNAL DETECTION
Optimal detector strategies for the phase contrast imaging for scanning transmission electron microscopes
[ETN-94-95747] p 3866 N94-31613
Auditory perception
[AD-A277414] p 3800 N94-32419
Mechanisms of temporal pattern discrimination by human observers
[AD-A277407] p 3801 N94-32577
SIGNAL DISTORTION
Kalman filtering approach to blind equalization
[AD-A276320] p 3671 N94-31299
SIGNAL GENERATORS
Periodic and chaotic signal generation in a recursive artificial neural network p 3686 N94-33155
SIGNAL PROCESSING
The generalized multi delay adaptive filter: Structure and convergence analysis
[TELECOM-93-D-004] p 3808 N94-31094
Modulation and coding for the Gaussian channel, possibly affected by fluctuations
[TELECOM-93-E-009] p 3840 N94-31169
Fast autodidactic adaptive equalization algorithms
[TELECOM-93-E-018] p 3670 N94-31174
Scheduling techniques for multiple processor systems in real-time environments
[AD-A276149] p 3824 N94-31249
Algorithms and structures for real-time signal processing
[AD-A276101] p 3810 N94-31277
Kalman filtering approach to blind equalization
[AD-A276320] p 3671 N94-31299
Smart environmental monitor based on neural networks and multi-spectral pattern recognition
[AD-A276445] p 3829 N94-31301
Analysis using bi-spectral related technique
[AD-A276017] p 3672 N94-31386
Concurrent architectures for VLSI signal and image processing
[AD-A276124] p 3688 N94-31445
Analysis of the effect of routing strategies for parallel implementations of a selected avionics application
[AD-A276069] p 3581 N94-31458
Analysis of key performance parameters of phase sampling digital RF memories
[AD-A276019] p 3688 N94-31494
Linearly separable stack-like architecture for the design of weighted order statistic filters with application in image processing
[ISBN-0-315-87284-5] p 3675 N94-31731
Algorithms and parallel architectures for laser acoustic imaging
[ISBN-0-315-86466-4] p 3716 N94-31797
Analysis and design of a formal neural network for filtering a dynamic signal
[ISBN-0-315-86932-1] p 3832 N94-31873
Pulse-splitting and AM-FM conversion in a nonlinear dispersive medium
[AD-A277041] p 3861 N94-32262
Empirical modeling for intelligent, real-time manufacture control p 3839 N94-32424
A new high-speed IR camera system
p 3713 N94-32459
Universal signal conditioning amplifier
p 3699 N94-32460
The constant current loop: A new paradigm for resistance signal conditioning p 3685 N94-32461
Bounds on least-squares four-parameter sine-fit errors due to harmonic distortion and noise
[DE94-007859] p 3849 N94-32653
Arithmetic averaging: A versatile technique for smoothing and trend removal
[DE94-005274] p 3852 N94-32673
COVICS: A covert video communications system
[DE94-007568] p 3682 N94-32745
Noise cancellation for CELP voice encoders in an F/A-18 noise environment
[AD-A277652] p 3683 N94-33026
Design of free space interconnected signal processor
[AD-A278129] p 3683 N94-33093
High temperature superconducting Josephson junction array systems, phase 1
[AD-A277937] p 3908 N94-33246
Design, characterization and control of the Unique Mobility Corporation robot p 3603 N94-33296
Applied harmonic analysis
[AD-A278384] p 3685 N94-33353
A new tool for signal processing
[AD-A278385] p 3685 N94-33354
SIGNAL RECEPTION
An evaluation of three GPS receivers for use in the GPS sounder
[AD-A278157] p 3577 N94-33253
SIGNAL TO NOISE RATIOS
Performance statistics bulletin. High latitude meteor scatter propagation February, March, April, May 1991
[AD-A276723] p 3678 N94-32158
Performance statistics bulletin. High latitude meteor scatter propagation October, November, December 1991, January 1992
[AD-A276724] p 3678 N94-32159
Performance statistics bulletin. High latitude meteor scatter propagation
[AD-A276695] p 3680 N94-32299
Performance statistics bulletin. High latitude meteor scatter propagation
[AD-A276696] p 3680 N94-32300
Performance statistics bulletin. High latitude meteor scatter propagation, June, July, August, September 1992
[AD-A277508] p 3685 N94-33347
SIGNAL TRANSMISSION
Channel equalization for block transmission systems
[TELECOM-93-D-002] p 3670 N94-31093
Multi-line passive fiber optic slipring
[AD-D016092] p 3883 N94-32738
Digital beamforming and filtering circuit
[AD-D016142] p 3697 N94-32976
Roll ring assemblies for the Space Station
p 3603 N94-33294
International Space Station Alpha's bearing, motor, and roll ring module developmental testing and results
p 3603 N94-33295
SIGNATURES
The trustworthy digital camera: Restoring credibility to the photographic image p 3714 N94-32470
SILICA GEL
Surface chemistry and durability of borosilicate glass
[DE94-006734] p 3656 N94-32116
Time-resolved analytical methods for liquid/solid interfaces
[DE94-008352] p 3637 N94-32826
SILICA GLASS
Oriented Si and Ge nanocrystals formed in Al2O3 by ion implantation and annealing
[DE94-005593] p 3901 N94-32172
Interface engineering in oxide fiber/oxide matrix composites
[AD-A277672] p 3627 N94-33029
Optical properties of doped sol-gel silica glasses
[AD-A278094] p 3884 N94-33267
SILICATES
Advances and applications of dynamic-angle spinning nuclear magnetic resonance
[DE94-007031] p 3870 N94-32250
SILICIDES
Ion beam synthesis of IrSi3 by 1-MeV Ir ion implantation into Si(111)
[DE94-006556] p 3896 N94-31501
The effect of ductile phase (Nb) reinforcement morphology on the mechanical behavior of an intermetallic matrix (MoSi2) p 3615 N94-32500
Gettering of metal impurities by cavities in silicon
[DE94-005248] p 3645 N94-32672
SILICON
An extended approach to oxidations and nitridations of Si and Ge(x)Si(1-x) materials
[AD-A276056] p 3631 N94-31282
Ion beam synthesis of IrSi3 by 1-MeV Ir ion implantation into Si(111)
[DE94-006556] p 3896 N94-31501
A silicon condenser microphone: Modelling and electronic circuitry
[ISBN-9-09-005279-8] p 3688 N94-31517
A silicon condenser microphone: Materials and technology
[ISBN-9-09-005899-0] p 3688 N94-31518
Engineering of damage in ion implanted silicon
[ISBN-9-09-005097-3] p 3897 N94-31521
Electrochemical surface modification of silicon monocrystals: A surface analytic examination
[ETN-94-95733] p 3633 N94-31574
Ionizing radiation effects on silicon test structures
[DE94-006060] p 3865 N94-31607
Silicon-Film(tm) photovoltaic manufacturing technology
[DE94-000202] p 3760 N94-32143
Oriented Si and Ge nanocrystals formed in Al2O3 by ion implantation and annealing
[DE94-005593] p 3901 N94-32172
Novel optoelectronic devices based on combining GaAs and InP on Si
[AD-A277018] p 3693 N94-32301
Lowering the Schottky barrier at metal or silicide/Si interfaces to extend the range of infrared detectors
[AD-A277253] p 3903 N94-32322
Si/SiO2 interface studies by immersion ellipsometry
[AD-A277277] p 3881 N94-32324
Analytical solutions of minimum ionization particle induced current shapes of silicon detectors and simulation of charge collection properties
[DE94-007523] p 3870 N94-32355
Characterization of interface structure in multilayers using specular x ray reflectance
[DE94-007698] p 3657 N94-32358
Point defect production, geometry, and stability in silicon: A molecular dynamics simulation study
[DE94-008292] p 3903 N94-32411
A scanning defect mapping system for semiconductor characterization p 3885 N94-32446
Femtosecond probe-probe transmission studies of LT-grown GaAs near the band edge
[DE94-006660] p 3904 N94-32634
Gettering of metal impurities by cavities in silicon
[DE94-005248] p 3645 N94-32672
Ab initio study of the epitaxial growth of Ge on Si(100) surface
[DE94-007245] p 3904 N94-32724
Thin EFG octagons
[DE94-006855] p 3905 N94-32764
Silicon-Based Optoelectronic Materials Symposium and Materials Research Society Proceedings, volume 298
[AD-A277518] p 3662 N94-32952
Low energy ion beam assisted growth of homoepitaxial silicon films at low temperature
[AD-A278092] p 3908 N94-33039
Reconfigurable Array of Radiating Elements (RARE) controlled by light
[NASA-CR-195828] p 3884 N94-33073
Electrical characteristics of GaAs MESFET fabrication by ion implantation of Si or Se
[AD-A278416] p 3909 N94-33328
SILICON ALLOYS
In-situ characterization of growth and interfaces in a-Si:H devices
[DE94-000291] p 3760 N94-31812
Research on the stability, electronic properties, and structure of a-Si:H and its alloys
[DE94-000292] p 3899 N94-31813
Research on stable, high-efficiency amorphous silicon multijunction modules
[DE94-000298] p 3695 N94-32680
Large-area, triple-junction a-Si alloy production scale-up
[DE94-006856] p 3762 N94-32785
SILICON CARBIDES
Processing of novel nanoparticle dispersion strengthened ceramics for improved mechanical performance
[AD-A275965] p 3649 N94-31276
Enhancement of oxidation resistance of silicon carbide by high-dose and multi-energy aluminum implantation
[DE94-006560] p 3640 N94-31314
The threshold energy for defect production in SiC: A molecular dynamic study
[DE94-007123] p 3896 N94-31499
The origin of neon-E: Neon-E in single interstellar silicon carbide and graphite grains p 3933 N94-31556
Interfacial behaviour: Wettability in SiC(sub p) metal matrix composites
[ISBN-0-315-87206-3] p 3621 N94-31835
Sodium sulfate corrosion of silicon carbide fiber-reinforced lithium aluminosilicate glass-ceramic matrix composites
[AD-A277224] p 3623 N94-32023
Pressureless sintering of ceramic composites
[AD-A277274] p 3657 N94-32404
Engineering scale development of the Vapor-Liquid-Solid (VLS) process for the production of silicon carbide fibrils
[DE94-007132] p 3659 N94-32618
Improved oxidation resistance of 3-D carbon/carbon composites
[AD-A277349] p 3625 N94-32624
Compositions and chemical bonding in ceramics by quantitative electron energy-loss spectrometry
[DE94-007208] p 3659 N94-32640
Conversion of polymers of methyl- and vinylsilane to Si-C ceramics
[NASA-TM-106554] p 3662 N94-32945
Novel precursor approached for CMC derived by polymer pyrolysis
[AD-A278383] p 3665 N94-33352
SILICON DIOXIDE
Evidence for a correct SiO2 voltage acceleration model
[DE94-006578] p 3690 N94-31594

Hydrogen incorporation and radiation induced dynamics in metal-oxide-silicon structures: A study using nuclear reaction analysis
[ETN-94-95742] p 3898 N94-31610
Preparation of catalyst particles using methods of colloid chemistry. Part 1: Preparation of silica particles from alcohol solutions
[PB94-135597] p 3634 N94-31679
Electrical properties of double layer dielectric structures for space technology
[ISBN-0-315-86547-4] p 3610 N94-31910
Chemical vapor deposition of metal nitrides, phosphides, and arsenides
[DE94-008096] p 3654 N94-31976
Sol-gel coatings for high power laser optics: Past, present, and future
[DE94-007240] p 3718 N94-32252
Si/SiO2 interface studies by immersion ellipsometry
[AD-A277277] p 3881 N94-32324
Dynamics of block poly(styrene-co-vinylpyridine) (SVP) in solution and on silica
[AD-A277139] p 3657 N94-32364
Multiple size scale structures in silica/siloxane composites studied by small-angle scattering
[DE94-007300] p 3625 N94-32642
Enhanced thermal capacity aerogels summary report, FY 1993
[DE94-008888] p 3639 N94-33260

SILICON FILMS
Low energy ion beam assisted growth of homoepitaxial silicon films at low temperature
[AD-A278092] p 3908 N94-33039

SILICON JUNCTIONS
Si/SiO2 interface studies by immersion ellipsometry
[AD-A277277] p 3881 N94-32324
Resistivity measurements on the neutron irradiated detector grade silicon materials
[DE94-009083] p 3906 N94-32822

SILICON NITRIDES
Effects of oxidation and creep damage mechanisms on creep behavior in HIPed silicon nitrides
[DE94-006559] p 3618 N94-31313
Reliability analysis of structural ceramics subjected to biaxial flexure p 3650 N94-31454
Electrical properties of double layer dielectric structures for space technology
[ISBN-0-315-86547-4] p 3610 N94-31910
Chemical vapor deposition of metal nitrides, phosphides, and arsenides
[DE94-008096] p 3654 N94-31976
Joining of silicon nitrides using oxynitride glasses
[DE94-008517] p 3658 N94-32517
Novel precursor approached for CMC derived by polymer pyrolysis
[AD-A278383] p 3665 N94-33352

SILICON RADIATION DETECTORS
Gamma Large Area Silicon Telescope (GLAST)
[DE94-006439] p 3925 N94-31786
Resistivity measurements on the neutron irradiated detector grade silicon materials
[DE94-009083] p 3906 N94-32822

SILICONE RUBBER
Effects of orbital exposure on RTV during the LDEF mission p 3597 N94-31043

SILICONES
Silicone grease as a precursor to a pseudo crown-ether ligand: Crystal structure of (K(+)K(Me2SiO)7(+))(HIn(CH2CMe3)3(-))4)
[AD-A276343] p 3895 N94-31327

SILOXANES
Multiple size scale structures in silica/siloxane composites studied by small-angle scattering
[DE94-007300] p 3625 N94-32642

SILVER
High performance YBCO films
[AD-A276493] p 3897 N94-31531
On the formation of muon- and zeta-phases in Ag-Al system by mechanical alloying
[DE94-007125] p 3645 N94-32636

SILVER ALLOYS
On the formation of muon- and zeta-phases in Ag-Al system by mechanical alloying
[DE94-007125] p 3645 N94-32636
Phase relationships and stability of the (mu)- and (zeta)-phases in the Ag-Al-X (X=Zn, Ga, Ge) systems
[DE94-009391] p 3648 N94-33270

SILVER ZINC BATTERIES
Development of silver-zinc cells of improved cycle life and energy density
[AD-A277311] p 3693 N94-32329

SIMD (COMPUTERS)
An efficient three-dimensional Poisson solver for SIMD high-performance-computing architectures
p 3823 N94-31120
Three-dimensional radiative transfer calculations on an SIMD machine applied to accretion disks
p 3932 N94-31141
Proof of concept for the rewrite rule machine: Interensemble studies
[AD-A276506] p 3809 N94-31263
Methods of implementing the Viterbi algorithm on a massively parallel computer of the SIMD (single instruction multiple data) type
[ISBN-0-315-86783-3] p 3814 N94-31752
An analysis of instruction-cached SIMD computer architecture
[AD-A276519] p 3806 N94-31934
Transformational derivation of (parallel) programs using skeletons
[TR-93-20] p 3825 N94-32196

SIMULATION
Plasma confinement theory and transport simulation
[DE94-006065] p 3888 N94-31619
Modular Simulator System (MSS) management guide
[AD-A277098] p 3588 N94-32014
Basic principles approach for studying nonlinear Alfven wave-alpha particle dynamics
[DE94-007112] p 3891 N94-32664

SIMULATORS
Modular Simulator System (MSS) management guide
[AD-A277098] p 3588 N94-32014

SINE WAVES
Visual evaluation of computer-generated textures
[AD-A277201] p 3816 N94-32093
Cooling and trapping of neutral atoms
[AD-A276957] p 3870 N94-32360
Bounds on least-squares four-parameter sine-fit errors due to harmonic distortion and noise
[DE94-007859] p 3849 N94-32653
Generation of the ambiguity function for ultra wideband radar waveforms
[AD-A277913] p 3684 N94-33261

SINGLE CRYSTALS
Ion-beam-driven amorphization of Ca2La8(Si4)6O2 single crystals
[DE94-006219] p 3895 N94-31307
Electrooptic crystal growth and properties
[AD-A276023] p 3896 N94-31439
GaAs/GaN strained layer superlattice materials for high temperature transistors, phase 1
[AD-A276115] p 3897 N94-31528
Characterization of the rare earth orthophosphates and Ce-doped LaPO4 by x ray absorption spectroscopy
[DE94-006313] p 3898 N94-31630
The 4f heavy fermion photoelectron spectra do not exhibit the Kondo scale
[DE94-006252] p 3898 N94-31631
In-situ TEM crystallization of anorthite-glass films on (alpha)-Al2O3
[DE94-006317] p 3652 N94-31780
Thermocapillary convection in evaporating sessile drops
[NASA-TM-109758] p 3705 N94-31886
Group 12 thiolates: Syntheses, characterization and decomposition pathways
[AD-A277055] p 3900 N94-32011
Fatigue in single crystal nickel superalloys
[AD-A276662] p 3643 N94-32047
Effect of twin boundary density on the vortex melting transition in YBa2Cu3O(7-delta) single crystals
[DE94-007684] p 3904 N94-32601
SUNY beamline facilities at the National Synchrotron Light Source
[DE94-006343] p 3905 N94-32770
Hyperon polarization, crystal channeling, and E781 at Fermilab
[DE94-008224] p 3877 N94-32802
High temperature materials technology research for advanced thermionic systems
[DE94-008341] p 3646 N94-32825
Novel polydiacetylenes as materials for second and third order nonlinear optics
[AD-A277512] p 3664 N94-33082

SINGLE EVENT UPSETS
Radiation tolerant, high speed, low power, gallium arsenide logic
[AD-A277293] p 3694 N94-32509
Temperature dependence of single-event burnout in n-channel power MOSFET's
[AD-A277921] p 3698 N94-33177
The impact of ASIC devices on the SEU vulnerability of space-borne computers
[AD-A278134] p 3808 N94-33252
Spacecraft environmental anomalies expert system
[AD-A277962] p 3612 N94-33262

SINGLE STAGE TO ORBIT VEHICLES
The National Aerospace Plane (NASP): Development issues for the follow-on vehicle
[AD-A278417] p 3581 N94-33329

SINGULARITY (MATHEMATICS)
Finite-part integrals and the Euler-Maclaurin expansion
[DE94-006539] p 3844 N94-31665

SINKS
Defect-solute interactions near irradiation grain boundaries
[DE94-006215] p 3641 N94-31627

SINTERING
Pressureless sintering of ceramic composites
[AD-A277274] p 3657 N94-32404
Isothermal sintering, microstructure, and superconducting properties of Y1Ba2Cu3O(7-x) compound
[DE94-008132] p 3905 N94-32779
Enhanced thermal capacity aerogels summary report, FY 1993
[DE94-008888] p 3639 N94-33260

SIS (SUPERCONDUCTORS)
High T(sub c) superconductor tunnel junctions for photon detectors
[DE94-007686] p 3904 N94-32602

SKIN (ANATOMY)
Development of a video fluorescence system for assessing burn depth
[AD-A278127] p 3798 N94-33092

SKIN FRICTION
Flight test results of riblets at supersonic speeds
[NASA-TM-4387] p 3572 N94-32880

SKIN TEMPERATURE (BIOLOGY)
Errors associated with the use of heat flow transducers p 3796 N94-31742

SKIRTS
Heave dynamics of an air cushion vehicle bag and finger skirt
[ISBN-0-315-87053-2] p 3568 N94-31734

SKY SURVEYS (ASTRONOMY)
Multiwavelength search for protoplanetary disks
p 3599 N94-31430
Near infrared surveys of high mass star forming regions p 3925 N94-31898
A multi-frequency study of an x ray selected sample of active galactic nuclei p 3937 N94-31987

SKY WAVES
Atmospheric effects assessment program: Ionospheric sounding
[AD-A276447] p 3770 N94-31303

SLEEP
Unit specific crew rest strategies: Phase 1 evaluation of the 1/212th Aviation Battalion during shiftwork transitions
[AD-A277122] p 3804 N94-32379

SLEEP DEPRIVATION
Effects of methamphetamine and fatigue on long- and short-term memory
[AD-A276452] p 3799 N94-32187

SLENDER BODIES
A new method for calculating wing along aerodynamics to angle of attack 180 deg
[AD-A277965] p 3574 N94-33263

SLIDING FRICTION
Mechanics of failure of high temperature metal matrix composites
[AD-A277397] p 3624 N94-32342

SLIP CASTING
Pressureless sintering of ceramic composites
[AD-A277274] p 3657 N94-32404

SLIPSTREAMS
Prediction of transonic potential flow with slipstreams around configurations
[FFA-TN-1992-15] p 3568 N94-31220

SLOT ANTENNAS
Analysis of a slot coupled coplanar waveguide fed patch antenna
[NASA-TM-106567] p 3698 N94-33116

SLOTS
Applied Computational Electromagnetics Society Journal, volume 9, number 1, March 1994
[AD-A276753] p 3679 N94-32183

SLURRIES
Development of a catalytic system for gasification of wet biomass
[DE94-006216] p 3759 N94-31762
Effect of surface forces on the rheology of particle-liquid systems and the consolidation of ceramic powders
[AD-A277092] p 3657 N94-32391
Technology development for iron Fischer-Tropsch catalysts
[DE94-008723] p 3638 N94-32889

SMALL SCIENTIFIC SATELLITES
The ALEXIS mission recovery
[DE94-007549] p 3611 N94-32813

SMART STRUCTURES
Control and stabilization of distributed parameter systems; theoretical and computational aspects
[AD-A277239] p 3738 N94-32275

Structural integrity of intelligent materials and structures
[AD-A278397] p 3630 N94-33165
SMOOTHING
Filtering of satellite altimetry data with optimal smoothing cubic splines to compute geoid heights, along-tract geoid and gravity gradients in the Indonesian waters and its surroundings
[PB94-147527] p 3741 N94-31074
SNOW
Satellite radar altimetry over the continental ice sheets p 3742 N94-31570
The evolution of jet features during the 1993 east coast white hurricane: A case study using the global spectral model
[AD-A277217] p 3783 N94-32021
Simulation of a precipitation event in the western United States
[DE94-004835] p 3786 N94-32791
SNOW COVER
Snowmelt forecasting. Further cold regions development of operational hydrological forecasting, volume 2
[AD-A278123] p 3757 N94-33269
SOCIAL FACTORS
Using the National Information Infrastructure for social science, education, and informed decision making
[DE94-005442] p 3920 N94-32676
SOCIOLOGY
The contribution of aeronautics and astronautics to the quality of life on Earth
[ILR-MITT-283(1993)] p 3764 N94-31611
Using the National Information Infrastructure for social science, education, and informed decision making
[DE94-005442] p 3920 N94-32676
SODIUM
Near resonant absorption by atoms in intense fluctuating laser fields
[DE94-005873] p 3714 N94-31200
SODIUM SULFATES
Sodium sulfate corrosion of silicon carbide fiber-reinforced lithium aluminosilicate glass-ceramic matrix composites
[AD-A277224] p 3623 N94-32023
SODIUM SULFUR BATTERIES
Overview of Sandia's electric vehicle battery program
[DE94-008944] p 3696 N94-32806
SOFTWARE ENGINEERING
Design patterns mixing genericity and inheritance in the development of reusable components
[REPT-93-021] p 3808 N94-31178
Guide to software quality assurance
[ESA-PSS-05-11-ISSUE-1] p 3809 N94-31223
Cleanroom engineering handbook. Volume 6: Certification team practices
[AD-A275951] p 3587 N94-31346
Cleanroom engineering handbook. Volume 1: Cleanroom engineering process introduction and overview
[AD-A275949] p 3587 N94-31356
E-L user's manual
[AD-A276378] p 3810 N94-31370
The development and use of an evaluation mechanism for the assessment of software configuration management tools
[AD-A275961] p 3810 N94-31383
A model and algorithms for a software evolution control system
[AD-A276431] p 3811 N94-31449
Software reuse case study: TRILLIUM
[AD-A276108] p 3811 N94-31465
Overview of megaprogramming course: Lectures and exercises
[AD-A276169] p 3814 N94-31810
Aerospace software engineering for advanced systems architectures
[AD-A277101] p 3581 N94-31977
Getting a handle on designing for avionics software supportability and maintainability
[AD-A276362] p 3581 N94-32055
The advent of failure analysis software technology
[DE94-006593] p 3692 N94-32111
Integrated Trusted System Development Environment Process
[AD-A276414] p 3816 N94-32131
Modular Simulator System (MSS). Engineering design guide
[AD-A276967] p 3589 N94-32394
Modular Simulator System (MSS): Interface design document for the generic MSS
[AD-A277270] p 3590 N94-32403
Evolving software reengineering technology for the emerging innovative-competitive era p 3823 N94-32439
Emacs Lisp in Edwin scheme
[AD-A276721] p 3818 N94-32504
Case studies of software process improvement methods
[AD-A277289] p 3818 N94-32508
OPT++: An object-oriented class library for nonlinear optimization
[DE94-008890] p 3818 N94-32584
The role of guideline-based design tools
[DE94-007482] p 3804 N94-32596
A framework for developing and managing reusable avionics software
[AD-A276846] p 3582 N94-32909
Machine assisted implementation of complex algorithms and labor intensive software, closing report
[AD-A277662] p 3821 N94-33027
Implementing software safety in the NASA environment
[NASA-TM-106597] p 3731 N94-33032
Increasing the practical impact of formal methods for computer-aided software development: Software slicing, merging and integration
[AD-A277929] p 3822 N94-33179
Faultless software project
[AD-A278161] p 3822 N94-33188
Structuring Z specifications with views
[AD-A277618] p 3822 N94-33279
Ada support for the mathematical foundations of software engineering
[AD-A278031] p 3822 N94-33284
MODIS. Volume 1: MODIS level 1A software baseline requirements
[NASA-TM-104594-VOL-1] p 3823 N94-33287
A problem-solving approach to knowledge acquisition p 3854 N94-33344
SOFTWARE RELIABILITY
Guide to software quality assurance
[ESA-PSS-05-11-ISSUE-1] p 3809 N94-31223
Cleanroom engineering handbook. Volume 6: Certification team practices
[AD-A275951] p 3587 N94-31346
Consistency checks for SCR-style requirements specifications
[AD-A276077] p 3811 N94-31461
Getting a handle on designing for avionics software supportability and maintainability
[AD-A276362] p 3581 N94-32055
A framework for developing and managing reusable avionics software
[AD-A276846] p 3582 N94-32909
Increasing the practical impact of formal methods for computer-aided software development: Software slicing, merging and integration
[AD-A277929] p 3822 N94-33179
SOFTWARE REUSE
Design patterns mixing genericity and inheritance in the development of reusable components
[REPT-93-021] p 3808 N94-31178
Software reuse case study: TRILLIUM
[AD-A276108] p 3811 N94-31465
Evolving software reengineering technology for the emerging innovative-competitive era p 3823 N94-32439
A framework for developing and managing reusable avionics software
[AD-A276846] p 3582 N94-32909
SOFTWARE TOOLS
Discovery systems for manufacturing
[AD-A276216] p 3828 N94-31061
A comparison of product realization frameworks
[AD-A275992] p 3810 N94-31357
The development and use of an evaluation mechanism for the assessment of software configuration management tools
[AD-A275961] p 3810 N94-31383
Consistency checks for SCR-style requirements specifications
[AD-A276077] p 3811 N94-31461
A hierarchical approach to test generation for CMOS VLSI circuits
[ISBN-9-09-005449-9] p 3689 N94-31535
DOME: Dynamic optimization on multiprocessor engines, a statistical approach p 3807 N94-31972
Incremental recompilation for Standard ML of New Jersey
[AD-A276522] p 3815 N94-32080
Experiences with EDO: An Evolutionary Database Optimizer
[TR-93-23] p 3918 N94-32105
The advent of failure analysis software technology
[DE94-006593] p 3692 N94-32111
Analytical Design Package (ADP2): A computer aided engineering tool for aircraft transparency design p 3823 N94-32430
CONFIG: Integrated engineering of systems and their operation p 3823 N94-32432
Spacecraft On-Board Information Extraction Computer (SOBIEC) p 3808 N94-32433
Emacs Lisp in Edwin scheme
[AD-A276721] p 3818 N94-32504
Production of terrain data: Optical radar complementarity p 3750 N94-32540
MADE: A Multiple Application Development Environment
[CWI-CS-R9360] p 3822 N94-33097
Selection criteria and facilitation training for the study of groupware
[NASA-CR-195906] p 3822 N94-33114
The hypermedia technology as front end to knowledge processing systems p 3854 N94-33343
SOI (SEMICONDUCTORS)
Advanced silicon technology for microwave circuits
[AD-A278039] p 3698 N94-33091
SOIL EROSION
Arid regions and wind erosion p 3780 N94-31005
SOIL MAPPING
Possible complementarity of SPOT/ERS in mapping land use: Study on agricultural land in Brittany (France) p 3755 N94-32563
SOIL MECHANICS
Microwave dielectric behavior of soils. Report 3: Measurement and modeling
[AD-A276060] p 3771 N94-31457
SOIL MOISTURE
Microwave dielectric behavior of soils. Report 1: Summary of related research and applications
[AD-A275980] p 3771 N94-31351
Microwave dielectric behavior of soils. Report 2: A unique coaxial measurement apparatus
[AD-A275982] p 3771 N94-31353
Application of ERS-1 SAR data for hydrological studies p 3754 N94-32558
A long-term simulation of surface fluxes and soil moisture
[DE94-006661] p 3774 N94-32772
SOIL SCIENCE
Microwave dielectric behavior of soils. Report 1: Summary of related research and applications
[AD-A275980] p 3771 N94-31351
Microwave dielectric behavior of soils. Report 2: A unique coaxial measurement apparatus
[AD-A275982] p 3771 N94-31353
SOILS
Fiber optic chemical sensors on Mars
[DE94-005251] p 3941 N94-31145
Microwave dielectric behavior of soils. Report 1: Summary of related research and applications
[AD-A275980] p 3771 N94-31351
Microwave dielectric behavior of soils. Report 2: A unique coaxial measurement apparatus
[AD-A275982] p 3771 N94-31353
Microwave dielectric behavior of soils. Report 3: Measurement and modeling
[AD-A276060] p 3771 N94-31457
Analysis of GER imaging spectrometry data for the identification of soil and vegetation parameters in land degradation studies p 3744 N94-31857
Possibilities of GER data for soil surface characteristics in the Almaden area p 3744 N94-31859
The effects of vegetation on the ability to map soils using GERIS data p 3744 N94-31860
Procedures for computing site seismicity
[AD-A277666] p 3775 N94-33028
Mars: Past, Present, and Future. Results from the MSATT Program, part 1
[NASA-CR-194279] p 3943 N94-33190
Thermal emission measurements (5-25 microns) of Hawaiian palagonitic soils with implications for Mars p 3944 N94-33193
The importance of environmental conditions in reflectance spectroscopy of laboratory analogs for Mars surface materials p 3944 N94-33195
Ferric sulfate montmorillonites as Mars soil analogs p 3944 N94-33196
Magmatic volatiles and the weathering of Mars p 3946 N94-33201
Martian spectral units derived from ISM imaging spectrometer data p 3949 N94-33220
SOL-GEL PROCESSES
Sol-gel metal oxide and metal oxide/polymer multilayers applied by meniscus coating
[DE94-005813] p 3649 N94-31199
Passive vibration damping materials: Piezoelectric ceramic composites for vibration damping applications
[AD-A276550] p 3653 N94-31935
The sol-gel-xerogel transition
[AD-A276647] p 3616 N94-32038
Ion-irradiation-induced densification of zirconia sol-gel thin films
[DE94-006248] p 3656 N94-32103
Sol-gel coatings for high power laser optics: Past, present, and future
[DE94-007240] p 3718 N94-32252

Nonlinear optical polymers derived from organic/inorganic composites
[AD-A277408] p 3659 N94-32610
Structure-property relationships of carbon aerogels
[DE94-007120] p 3660 N94-32687
Low loss second-order nonlinear optical polymers based on all organic sol-gel materials
[AD-A277482] p 3663 N94-32985
Optical properties of doped sol-gel silica glasses
[AD-A278094] p 3884 N94-33267
Novel sol-gel deposition for repair of conducting paths in polyceramic systems
[AD-A278381] p 3664 N94-33350

SOLAR ACTIVITY
Proceedings of the International Workshop on Artificial Intelligence Applications in Solar-Terrestrial Physics
[PB94-142064] p 3832 N94-31808
Steps toward understanding the solar dynamo
[AD-A277398] p 3953 N94-32343
Solar activities at Sandia National Laboratories
[DE94-007737] p 3761 N94-32648
Diurnal, seasonal and solar activity variations of F-region parameters
[AD-A278106] p 3776 N94-33285

SOLAR ACTIVITY EFFECTS
Evidence of solar oscillations in Rayleigh-scattered light p 3952 N94-31214

SOLAR ARRAYS
Atomic oxygen erosion considerations for spacecraft materials selection p 3593 N94-31022
Impact of LDEF photovoltaic experiment findings upon spacecraft solar array design and development requirements p 3594 N94-31028
Solar lunar power p 3599 N94-31427
A solar array module fabrication process for HALE solar electric UAVs
[DE94-006212] p 3760 N94-32174
Arcing in space structures in low Earth orbit
[NASA-CR-194223] p 3694 N94-32478
INSAT-2A and 2B development mechanisms p 3603 N94-33293
Space Station Freedom Solar Array tension mechanism development p 3604 N94-33300
Lessons learned from selecting and testing spaceflight potentiometers p 3607 N94-33318
Implementation of heaters on thermally actuated spacecraft mechanisms p 3607 N94-33320

SOLAR BLANKETS
Space Station Freedom solar array containment box mechanisms p 3603 N94-33292

SOLAR CELLS
Impact of LDEF photovoltaic experiment findings upon spacecraft solar array design and development requirements p 3594 N94-31028
Role of polycrystallinity in CdTe and CuInSe2 photovoltaic cells
[DE94-000293] p 3758 N94-31236
Automated solar cell assembly teamed process research
[DE94-000295] p 3759 N94-31279
Solar lunar power p 3599 N94-31427
In-situ characterization of growth and interfaces in a-Si:H devices
[DE94-000291] p 3760 N94-31812
Research on the stability, electronic properties, and structure of a-Si:H and its alloys
[DE94-000292] p 3899 N94-31813
Silicon-Film(tm) photovoltaic manufacturing technology
[DE94-000202] p 3760 N94-32143
A solar array module fabrication process for HALE solar electric UAVs
[DE94-006212] p 3760 N94-32174
A scanning defect mapping system for semiconductor characterization p 3885 N94-32446
Arcing in space structures in low Earth orbit
[NASA-CR-194223] p 3694 N94-32478
Research on stable, high-efficiency amorphous silicon multijunction modules
[DE94-000298] p 3695 N94-32680
Development of a computer model for polycrystalline thin-film CuInSe2 and CdTe solar cells
[DE94-006853] p 3762 N94-32763
Thin EFG octagons
[DE94-006855] p 3905 N94-32764
Large-area, triple-junction a-Si alloy production scale-up
[DE94-006856] p 3762 N94-32765
Combined contamination and space environmental effects on solar cells and thermal control surfaces
[NASA-TM-106592] p 3617 N94-33022
Space Station Freedom solar array containment box mechanisms p 3603 N94-33292
Space Station Freedom Solar Array tension mechanism development p 3604 N94-33300

SOLAR COLLECTORS
Databases and demands for solar heating materials
[PB94-137494] p 3758 N94-31070
Solar energy in China
[PB94-137502] p 3758 N94-31071
Concentration system performance degradation in the aftermath of Mount Pinatubo
[DE94-001879] p 3764 N94-31602
Operational experience and evaluation of a dual-element stretched-membrane heliostat
[DE94-008827] p 3763 N94-32965

SOLAR ENERGY
Solar resource: Utility load-matching assessment
[DE94-000297] p 3758 N94-31264
Solar lunar power p 3599 N94-31427
NEMO: Advanced energy systems and technologies
[DE94-721996] p 3760 N94-31767
Renewable energy technology development at Sandia National Laboratories
[DE94-007734] p 3761 N94-32383
Solar activities at Sandia National Laboratories
[DE94-007737] p 3761 N94-32648

SOLAR ENERGY CONVERSION
Solar energy in China
[PB94-137502] p 3758 N94-31071
Proceedings of the Seventeenth DOE Solar Photochemistry Research Conference
[DE94-005552] p 3759 N94-31648
NEMO: Advanced energy systems and technologies
[DE94-721996] p 3760 N94-31767

SOLAR FLARES
Collective acceleration in solar flares
[DE94-006288] p 3953 N94-31632
Steps toward understanding the solar dynamo
[AD-A277398] p 3953 N94-32343
BATSE data analysis
[NASA-CR-195818] p 3927 N94-32942
Spatial correlation of ionospheric variability
[AD-A278105] p 3776 N94-33041

SOLAR FLUX
An evaluation of RAMS radiation schemes by field measurements
[DE94-008053] p 3767 N94-32750

SOLAR GENERATORS
Metal hydrides in hydrogen energy systems
[VTT-TIED-1407] p 3759 N94-31655
Optimal planning of residential photovoltaic systems under various rate structure
[DE94-757272] p 3762 N94-32919

SOLAR HEATING
Databases and demands for solar heating materials
[PB94-137494] p 3758 N94-31070
Solar energy in China
[PB94-137502] p 3758 N94-31071

SOLAR INSTRUMENTS
Evidence of solar oscillations in Rayleigh-scattered light p 3952 N94-31214

SOLAR MAGNETIC FIELD
Theoretical studies of magnetohydrodynamic equilibria and dynamics of a solar coronal loop p 3953 N94-31792
Steps toward understanding the solar dynamo
[AD-A277398] p 3953 N94-32343

SOLAR NEUTRINOS
Nuclear physics and astrophysics
[DE94-007168] p 3939 N94-33147

SOLAR OSCILLATIONS
Evidence of solar oscillations in Rayleigh-scattered light p 3952 N94-31214

SOLAR PHYSICS
Solar physics and terrestrial effects. A curriculum guide for teachers, grade 7-12
[PB94-142247] p 3953 N94-31595
Theoretical studies of magnetohydrodynamic equilibria and dynamics of a solar coronal loop p 3953 N94-31792
Proceedings of the International Workshop on Artificial Intelligence Applications in Solar-Terrestrial Physics
[PB94-142064] p 3832 N94-31808
High sensitivity and resolution decimetric spectroscope: Preliminary analysis of solar bursts
[INPE-5537-TDI/525] p 3954 N94-33080

SOLAR POWERED AIRCRAFT
A solar array module fabrication process for HALE solar electric UAVs
[DE94-006212] p 3760 N94-32174

SOLAR RADIATION
Model of spacecraft atomic oxygen and solar exposure microenvironments p 3593 N94-31021
Fluorescence observations of LDEF exposed materials as an indicator of induced material reactions p 3593 N94-31025
Laser-induced fluorescence of space-exposed polyurethane p 3593 N94-31026
Evidence of solar oscillations in Rayleigh-scattered light p 3952 N94-31214
Users manual for SERI QC software assessing the quality of solar radiation data
[DE93-018210] p 3953 N94-31491
Recommendations for meteorological data collection during physiological field studies
[AD-A276834] p 3901 N94-32153
Steps toward understanding the solar dynamo
[AD-A277398] p 3953 N94-32343

SOLAR RADIO BURSTS
High sensitivity and resolution decimetric spectroscope: Preliminary analysis of solar bursts
[INPE-5537-TDI/525] p 3954 N94-33080

SOLAR TERRESTRIAL INTERACTIONS
Solar physics and terrestrial effects. A curriculum guide for teachers, grade 7-12
[PB94-142247] p 3953 N94-31595
Proceedings of the International Workshop on Artificial Intelligence Applications in Solar-Terrestrial Physics
[PB94-142064] p 3832 N94-31808
Analysis of data from the plasma composition experiment on the International Sun-Earth Explorer (ISEE 1)
[NASA-CR-195880] p 3893 N94-33074

SOLAR THERMAL ELECTRIC POWER PLANTS
Renewable energy technology development at Sandia National Laboratories
[DE94-007734] p 3761 N94-32383

SOLAR WIND
Analysis of data from the plasma composition experiment on the International Sun-Earth Explorer (ISEE 1)
[NASA-CR-195880] p 3893 N94-33074

SOLDERING
Automated solar cell assembly teamed process research
[DE94-000295] p 3759 N94-31279
The 18th annual electronics manufacturing seminar
[AD-A276038] p 3687 N94-31281
Aging effects on the microstructure, surface characteristics and wettability of Cu pretinned with Sn-Pb solders
[DE94-007033] p 3641 N94-31638
Automated fiber pigtailing technology
[DE94-007072] p 3695 N94-32688
Space flight printed wiring board measling investigation
[NASA-TM-104602] p 3732 N94-33101

SOLDERS
Aging effects on the microstructure, surface characteristics and wettability of Cu pretinned with Sn-Pb solders
[DE94-007033] p 3641 N94-31638

SOLID ELECTROLYTES
Novel electroactive polymers and block copolymers
[AD-A276119] p 3650 N94-31509
Conductivity measurements of ceria-based solid electrolytes using AC impedance
[DE94-007380] p 3694 N94-32593

SOLID LUBRICANTS
Soft x ray photoelectron spectroscopy study of the interaction of Cr with MoS2(0001)
[AD-A276916] p 3635 N94-32233
The effect of prolonged exposure to 750 C air on the tribological performance of PM212
[NASA-TM-106472] p 3617 N94-32941
Torque characteristics of solid lubricated precision bearings during oscillatory motion
[AD-A278133] p 3728 N94-33061
Development of long-life, low-noise linear bearings for atmospheric interferometry p 3606 N94-33312

SOLID PHASES
Strongly coupled ionic mixtures and the H/He EOS
[DE94-006391] p 3934 N94-31782
Stability and precipitation kinetics in Si(1-y)C(y)/Si and Si(1-x-y)Ge(x)C(y)/Si heterostructures prepared by solid phase epitaxy
[DE94-006589] p 3902 N94-32296

SOLID PROPELLANT COMBUSTION
Condensed-phase processes during solid propellant combustion. 3: Preliminary depth-profiling studies on XM39, JA2, M9, M30, and HMX2
[AD-A276595] p 3635 N94-32124

SOLID PROPELLANT IGNITION
Shock tube ignition and combustion of aluminum/magnesium alloy particles in oxygen at high pressure p 3631 N94-31286

SOLID PROPELLANT ROCKET ENGINES
The prediction of convective transfer on the thermal insulation of a solid-propellant rocket motor
[ONERA-NT-1993-15] p 3614 N94-31423
Combustor and nozzle effects on particulate behavior in solid rocket motors
[AD-A277304] p 3614 N94-32071

SOLID PROPELLANTS
A model of concurrent flow flame spread over a thin solid fuel p 3634 N94-31795

NATO Advanced Study Institute on Unsteady Combustion. Volume 2: Research papers, September 6-17, 1993
[AD-A276572] p 3634 N94-32033
SOLID SOLUTIONS
On the formation of muon- and zeta-phases in Ag-Al system by mechanical alloying
[DE94-007125] p 3645 N94-32636
Phase relationships and stability of the (mu)- and (zeta)-phases in the Ag-Al-X (X=Zn, Ga, Ge) systems
[DE94-009391] p 3648 N94-33270
SOLID STATE
Summary of the 1993 Winter ACP Workshop on Collective Dynamics in Disordered System
[AD-A276355] p 3664 N94-31402
Solid-state resistance upset welding: A process with unique advantages for advanced materials
[DE94-005941] p 3723 N94-31524
Isothermal sintering, microstructure, and superconducting properties of Y1Ba2Cu3O(7-x) compound
[DE94-006132] p 3905 N94-32779
SOLID STATE DEVICES
Proceedings of the International Workshop on Computational Electronics
[AD-A277020] p 3692 N94-32259
SOLID STATE LASERS
Transient radiation-induced absorption in the materials for a GSGG laser
[DE94-005316] p 3714 N94-31148
High-power CW diode-laser-array-pumped solid-state lasers and efficient nonlinear optical frequency conversion
[AD-A276126] p 3714 N94-31278
Scenarios for multi-unit inertial fusion energy plants producing hydrogen fuel
[DE94-006614] p 3666 N94-32114
High conversion efficiency pumped-cavity second harmonic generation of a diode laser
[DE94-006805] p 3717 N94-32134
Ti:sapphire based ultrafast pump-probe laser source in the violet and ultraviolet
[DE94-007542] p 3718 N94-32270
Repetitively pulsed Cr:LiSAF laser for lidar applcations
[DE94-007546] p 3720 N94-32761
Multifrequency, rapidly sequenced or simultaneous tunable laser
[AD-D016169] p 3721 N94-32968
SOLID SURFACES
Solid surface
[NASA-TM-109746] p 3634 N94-31883
SOLID-SOLID INTERFACES
Adsorption of water to the metal/polymer interface studied by neutron and x ray reflectivity
[DE94-005578] p 3651 N94-31649
New micro- and macroscopic models of contact and friction
[AD-A277240] p 3726 N94-32320
SOLIDIFICATION
Solidification structure synthesis in undercooled liquids
[AD-A276166] p 3910 N94-31054
Microstructures and mechanical properties of Al3Ti-based alloys: Analysis in single phase and multiphase systems
[ONERA-NT-1993-6] p 3640 N94-31420
SOLIDS
Empirical and semi-empirical relationships of liquid-vapor, solid-vapor, and solid-liquid surface energies
[AD-A276480] p 3631 N94-31248
The Sixth Symposium on Unconventional Photoactive Solids. Abstracts
[AD-A277198] p 3655 N94-32016
The 10th International Conference on Internal Friction and Ultrasonic Attenuation in Solids (ICIFUAS)
[AD-A276849] p 3902 N94-32209
Advances and applications of dynamic-angle spinning nuclear magnetic resonance
[DE94-007031] p 3870 N94-32250
SOLITARY WAVES
Future directions of nonlinear dynamics in physical and biological systems. (Physica D nonlinear, volume 68, number 1)
[AD-A278085] p 3794 N94-33250
SOLUBILITY
Cloud studies seen from a physical chemist's perspective
[DE94-006059] p 3771 N94-31527
Inorganic materials for anomalous-dispersion phase-matched second harmonic generation: Rubidium titanyl arsenate isomorphs, Rb(Ti(1-2x)Ln(x)Nb(x))OAsO4
[DE94-006141] p 3899 N94-31847
Measurement of viscosity, density, and gas solubility of refrigerant blends in selected synthetic lubricants
[DE94-007723] p 3653 N94-31917
Phase relationships and stability of the (mu)- and (zeta)-phases in the Ag-Al-X (X=Zn, Ga, Ge) systems
[DE94-009391] p 3648 N94-33270
SOLUTES
Defect-solute interactions near irradiation grain boundaries
[DE94-006215] p 3641 N94-31627
SOLUTIONS
Solvent diffusion coefficient concentration dependence in polymer solutions
[AD-A277023] p 3655 N94-32005
Influence of trace components on the viscoelastic properties of a polymer solution
[AD-A277171] p 3656 N94-32253
Dynamics of block poly(styrene-co-vinylpyridine) (SVP) in solution and on silica
[AD-A277139] p 3657 N94-32364
SOLVATION
Radiation and photochemistry section
[DE94-008880] p 3873 N94-32757
SOLVENT EXTRACTION
Recovery of carboxylic acids at pH greater than pKa
[DE94-007030] p 3636 N94-32376
SOLVENTS
Solvent diffusion coefficient concentration dependence in polymer solutions
[AD-A277023] p 3655 N94-32005
Dynamics of block poly(styrene-co-vinylpyridine) (SVP) in solution and on silica
[AD-A277139] p 3657 N94-32364
Radiation and photochemistry section
[DE94-008880] p 3873 N94-32757
SONAR
Analysis using bi-spectral related technique
[AD-A276017] p 3672 N94-31386
Multi-scale studies of seafloor topography
[AD-A277008] p 3789 N94-32400
SONDES
Water vapor from sunradiometry in comparison with microwave and balloon-sonde measurements at the Southern Great Plains ARM Site
[DE94-007479] p 3786 N94-32759
SONIC BOOMS
Investigation of sonic boom for the Space Shuttle: High cross-range orbiter
[NASA-TM-108238] p 3860 N94-31336
Investigation of sonic boom for the Space Shuttle: Low cross-range orbiter
[NASA-TM-108237] p 3860 N94-31337
SOOT
Soot and liquid-phase fuel distributions in a newly designed optically accessible DI diesel engine
[DE94-005648] p 3723 N94-31651
Photothermal laser deflection, an innovative technique to measure particles in exhausts
[AD-A277151] p 3718 N94-32366
SORBENTS
Recovery of carboxylic acids at pH greater than pKa
[DE94-007030] p 3636 N94-32376
SOUND FIELDS
Scattering of a random acoustic field by an infinite cylinder: Application to the modelization of the acoustic environment of the 'Ariane 5' launcher scale-model using experimental data
[ONERA-NT-1993-11] p 3860 N94-31226
Computer implementation of Arnott's formulation of thermoacoustics using MATLAB
[AD-A276356] p 3860 N94-31257
Wavevector-frequency analysis with applications to acoustics
[AD-A276618] p 3861 N94-32125
SOUND PRESSURE
Investigation of sonic boom for the Space Shuttle: High cross-range orbiter
[NASA-TM-108238] p 3860 N94-31336
Investigation of sonic boom for the Space Shuttle: Low cross-range orbiter
[NASA-TM-108237] p 3860 N94-31337
SOUND RANGING
Multi-scale studies of seafloor topography
[AD-A277008] p 3789 N94-32400
SOUND TRANSMISSION
Vibrations of a heavy truck diesel engine and gearbox unit: Examining structure-borne sound transmission with statistical energy analysis
[CTH-E-93-04] p 3722 N94-31194
Acoustic window
[AD-D016171] p 3862 N94-33017
SOUND WAVES
Ocean acoustic propagation measurements and wave propagation in random media
[AD-A276165] p 3787 N94-31053
Quality of sound in large rooms: Alteration of room impulse responses
[CTH-E-93-02] p 3859 N94-31077
A preliminary investigation of high amplitude standing waves with laser Doppler anemometry
[AD-A276463] p 3860 N94-31242
Aeroacoustic sources in internal flows
[ISBN-9-03-86-0282-0] p 3860 N94-31653
Fiber optic sensors for the detection of surface acoustic waves on metals
[ISBN-0-315-87055-9] p 3878 N94-31736
Experimental and computational studies on propeller noise due to inflow distortion p 3860 N94-31846
Boundary control of scattering p 3861 N94-31899
Wavevector-frequency analysis with applications to acoustics
[AD-A276618] p 3861 N94-32125
Pulse-splitting and AM-FM conversion in a nonlinear dispersive medium
[AD-A277041] p 3861 N94-32262
Auditory perception
[AD-A277414] p 3800 N94-32419
Advanced satellite communication system
[NASA-CR-194211] p 3681 N94-32477
Digital beamforming and filtering circuit
[AD-D016142] p 3697 N94-32976
Acoustic window
[AD-D016171] p 3862 N94-33017
SOURCE PROGRAMS
Incremental recompilation for Standard ML of New Jersey
[AD-A276522] p 3815 N94-32080
SOUTHERN OSCILLATION
Air-sea interaction patterns in the equatorial Pacific
[AD-A277305] p 3788 N94-32072
ENSO forced variations of the sea surface temperature and adjusted sea level along the west coast of the United States
[AD-A277306] p 3789 N94-32327
SPACE BASED RADAR
Radar rainfall measurements from space p 3782 N94-31889
SPACE CHARGE
Development of a 3D numerical code to calculate the trajectories of the blow off electrons emitted by a vacuum surface discharge: Application to the study of the electromagnetic interference induced on a spacecraft
[ONERA-NT-1993-12] p 3863 N94-31227
Resistivity measurements on the neutron irradiated detector grade silicon materials
[DE94-009083] p 3906 N94-32822
SPACE COLONIES
Marsville: The cosmic village
[NASA-TM-109752] p 3913 N94-31806
SPACE COMMERCIALIZATION
Access to space: The Space Shuttle's evolving rolee
[AD-A276785] p 3608 N94-32190
SPACE DEBRIS
Space environment durability of beta cloth in LDEF thermal blankets p 3591 N94-31015
Morphology correlation of craters formed by hypervelocity impacts p 3594 N94-31031
Micrometeoroid/space debris effects on materials p 3595 N94-31032
SPACE ENVIRONMENT SIMULATION
Ground-based simulation of LEO environment: Investigations of a select LDEF material: FEP Teflon (trademark) p 3596 N94-31039
What LDEF means for development and testing of materials p 3598 N94-31050
Aerospace test facilities at NASA LERC Plumbrook
[NASA-TM-109755] p 3602 N94-31814
SPACE ERECTABLE STRUCTURES
MSAT boom joint testing and load absorber design p 3606 N94-33315
SPACE EXPLORATION
Evaluating success levels of mega-projects p 3599 N94-31432
NASA report to education, volume 9
[NASA-TM-109760] p 3913 N94-31817
NASA strategic plan
[NASA-TM-109780] p 3915 N94-32222
SPACE INDUSTRIALIZATION
Space industrialization: A guide to government information
[RELEASE-1.2] p 3916 N94-31338
DOD space based requirements: Increasing DOD access to space
[AD-A276874] p 3601 N94-32211
SPACE LAW
Legal regime of human activities in outer space law p 3599 N94-31431
Space history, space policy, and executive leadership
[NASA-TM-109787] p 3924 N94-33067
SPACE LOGISTICS
Advanced transportation system study: Manned launch vehicle concepts for two way transportation system payloads to LEO
[NASA-CR-193951] p 3608 N94-33100

SPACE MAINTENANCE
Use of a pitch adjustable foot restraint system: Operator strength capability and load requirements
[NASA-TP-3477] p 3805 N94-33050
SPACE MANUFACTURING
A large motion zero-gravity suspension system for experimental simulation of orbital construction and deployment
[NASA-CR-195881] p 3668 N94-33037
Design, characterization, and control of the NASA three degree of freedom reaction compensation platform
p 3605 N94-33304
SPACE MISSIONS
The double probe electric field experiment on Freja: Description and first results
[TRITA-ALP-1993-02] p 3885 N94-31089
Participation in the scientific activities of the Waves in Space Plasma (WISP) project
[NASA-CR-195903] p 3894 N94-33113
SPACE NAVIGATION
The contribution of aeronautics and astronautics to the quality of life on Earth
[ILR-MITT-283(1993)] p 3764 N94-31611
SPACE PERCEPTION
A neural network model for the visual perception of the depth of a scene from stereoscopy and shading
[ISBN-0-315-86753-1] p 3831 N94-31750
Sensory sensitivities and discriminations and their roles in aviation
[AD-A277312] p 3800 N94-32276
Neural models of spatial orientation in novel environments
[AD-A277383] p 3835 N94-32340
Visual neural development and chromatic aberration
[AD-A277402] p 3800 N94-32345
SPACE PLASMAS
Laboratory and space experiments as a key to the plasma universe
[TRITA-ALP-1993-01] p 3885 N94-31088
Dispersion relations for a plasma-filled helix-loaded-waveguide
[DE94-006333] p 3675 N94-31781
Computer modeling of active experiments in space plasmas p 3890 N94-31927
Planetary magnetotails: Magnetic configuration and nonthermal plasma p 3942 N94-32326
Ionospheric plasma outflow in response to transverse ion heating: Self-consistent macroscopic treatment
[NASA-CR-195820] p 3893 N94-33048
Characteristics of ion flow in the quiet state of the inner plasma sheet
[AD-A277451] p 3894 N94-33106
The spatial development of the magnetospheric low-latitude boundary layer
[ISBN-0-315-77418-5] p 3776 N94-33111
Participation in the scientific activities of the Waves in Space Plasma (WISP) project
[NASA-CR-195903] p 3894 N94-33113
SPACE PLATFORMS
NASA's space platform technology program and planning p 3597 N94-31044
SPACE POWER REACTORS
Utilizing a Russian space nuclear reactor for a United States space mission: Flight qualification issues
[DE94-004674] p 3613 N94-31265
Draft minutes of IAPG Mechanical Working Group meeting
[DE94-004954] p 3759 N94-31266
The development of CVR coatings for PBR fuels
[DE94-004233] p 3875 N94-31480
Development of lightweight radiators for lunar based power systems
[NASA-TM-106604] p 3726 N94-32272
A 1050 K Stirling space engine design
[NASA-CR-182149] p 3616 N94-32866
Independent safety assessment of the Topaz-2 space nuclear reactor power system
[DE94-008653] p 3877 N94-32879
SPACE PROBES
The double probe electric field experiment on Freja: Description and first results
[TRITA-ALP-1993-02] p 3885 N94-31089
SPACE PROCESSING
Design, characterization, and control of the NASA three degree of freedom reaction compensation platform
p 3605 N94-33304
SPACE PROGRAMS
Aeronautics and space report of the President: Fiscal year 1993 activities p 3966 N94-32854
SPACE RENDEZVOUS
Fuzzy logic application for modeling man-in-the-loop space shuttle proximity operations
[NASA-CR-188283] p 3835 N94-32359
A six degree of freedom, plume-fuel optimal trajectory planner for spacecraft proximity operations using an A* node search
[NASA-CR-188285] p 3601 N94-32388
SPACE SHUTTLE MAIN ENGINE
Design of a cold-flow test facility for the high pressure fuel turbopump turbine of the Space Shuttle main engine
[AD-A276743] p 3615 N94-32182
Real-time sensor data validation
[NASA-CR-195295] p 3616 N94-33099
SPACE SHUTTLE MISSIONS
OARE flight maneuvers and calibration measurements on STS-58
[NASA-TM-109093] p 3613 N94-32924
Chronology of KSC and KSC related events for 1993
[NASA-TM-109196] p 3966 N94-33072
SPACE SHUTTLE ORBITERS
Investigation of sonic boom for the Space Shuttle: High cross-range orbiter
[NASA-TM-108238] p 3860 N94-31336
Investigation of sonic boom for the Space Shuttle: Low cross-range orbiter
[NASA-TM-108237] p 3860 N94-31337
Computational methods for frictional contact with applications to the Space Shuttle orbiter nose-gear tire
p 3608 N94-32295
SPACE SHUTTLES
Theoretical basis for state vector comparison, relative position display, and relative position/rendezvous prediction
[AD-A277216] p 3608 N94-32020
Access to space: The Space Shuttle's evolving rolee
[AD-A276785] p 3608 N94-32190
Fuzzy logic application for modeling man-in-the-loop space shuttle proximity operations
[NASA-CR-188283] p 3835 N94-32359
Limiting vibration in systems with constant amplitude actuators through command preshaping
[NASA-CR-188284] p 3739 N94-32907
Pip pin reliability and design p 3605 N94-33305
SPACE STATION FREEDOM
A study of the Space Station Freedom response to the disturbance environment p 3600 N94-31434
Solar connection
[NASA-TM-109761] p 3614 N94-31818
A hypertext system that learns from user feedback
p 3923 N94-32428
Catalytic methods using molecular oxygen for treatment of PMMS and ECLSS waste streams, volume 2
[NASA-CR-190299] p 3804 N94-32697
Space Station evolution study
[NASA-CR-193937] p 3611 N94-32898
An investigation of acoustic noise requirements for the Space Station centrifuge facility
[NASA-TM-108811] p 3805 N94-32936
Space Station Freedom solar array containment box mechanisms p 3603 N94-33292
Roll ring assemblies for the Space Station
p 3603 N94-33294
Space Station Freedom Solar Array tension mechanism development p 3604 N94-33300
Energy absorber for the CETA p 3604 N94-33303
SPACE STATION PAYLOADS
Space Station evolution study
[NASA-CR-193937] p 3611 N94-32898
SPACE STATION POWER SUPPLIES
Solar lunar power p 3599 N94-31427
Solar connection
[NASA-TM-109761] p 3614 N94-31818
SPACE STATION STRUCTURES
A study of the Space Station Freedom response to the disturbance environment p 3600 N94-31434
SPACE STATIONS
Space Station WP-2 application of LDEF MLI results
p 3592 N94-31016
The Second Annual International Space University Alumni Conference
[NASA-CP-3253] p 3598 N94-31425
Access to space: The Space Shuttle's evolving rolee
[AD-A276785] p 3608 N94-32190
Fuzzy logic application for modeling man-in-the-loop space shuttle proximity operations
[NASA-CR-188283] p 3835 N94-32359
Research and technology, 1993
[NASA-TM-106376] p 3567 N94-33046
SPACE TRANSPORTATION
Design of a logistics model for building and supporting a lunar station
[ILR-MITT-282(1993)] p 3803 N94-31852
Access to space: The Space Shuttle's evolving rolee
[AD-A276785] p 3608 N94-32190
SPACE TRANSPORTATION SYSTEM
Access to space: The Space Shuttle's evolving rolee
[AD-A276785] p 3608 N94-32190
Pen-based computers: Computers without keys
p 3808 N94-32434
Advanced transportation system study: Manned launch vehicle concepts for two way transportation system payloads to LEO
[NASA-CR-193951] p 3608 N94-33100
SPACE TRANSPORTATION SYSTEM FLIGHTS
Fuzzy logic application for modeling man-in-the-loop space shuttle proximity operations
[NASA-CR-188283] p 3835 N94-32359
SPACE WEAPONS
Vulnerability assessment of a space based weapon platform electronic system exposed to a thermonuclear weapon detonation
[DE94-007229] p 3611 N94-32667
SPACE-TIME FUNCTIONS
Research in theoretical high-energy physics
[DE94-008388] p 3876 N94-32407
SPACEBORNE EXPERIMENTS
Spacecraft contamination issues from LDEF: Issues for design p 3592 N94-31020
Impact of LDEF photovoltaic experiment findings upon spacecraft solar array design and development requirements p 3594 N94-31028
Space environmental effects on polymer composites: Research needs and opportunities p 3595 N94-31035
Spacecraft materials: Comparison between flight results obtained on LDEF and MIR p 3597 N94-31045
Design application and development of spacecraft in LEO utilizing LDEF results p 3597 N94-31047
What LDEF means for development and testing of materials p 3598 N94-31050
Laboratory and space experiments as a key to the plasma universe
[TRITA-ALP-1993-01] p 3885 N94-31088
Development concept for Dutch user support
[PB94-125523] p 3596 N94-31208
Various magnet options for Delta launched version of ASTROMAG
[DE94-006292] p 3955 N94-31635
Space acceleration measurement system
[NASA-TM-109754] p 3913 N94-31807
Steady thermal convection in multiple liquid layers
p 3705 N94-31844
Computer modeling of active experiments in space plasmas p 3890 N94-31927
Pre-flight testing of Thermoelectric Quartz Crystal Microbalances (TQCM) for midcourse space experiment (MSX) spacecraft
[AD-A277054] p 3610 N94-32010
Implementation of heaters on thermally actuated spacecraft mechanisms p 3607 N94-33320
SPACEBORNE PHOTOGRAPHY
An intelligent interactive visual database management system for Space Shuttle closeout image management
p 3923 N94-32469
SPACECRAFT ANTENNAS
The 20 GHz circularly polarized, high temperature superconducting microstrip antenna array
[NASA-CR-195097] p 3683 N94-33083
The Galileo high gain antenna deployment anomaly
p 3607 N94-33319
SPACECRAFT CABIN ATMOSPHERES
Atmosphere quality standards in manned space vehicles
[ESA-PSS-03-401-ISSUE-1] p 3802 N94-31224
Technical assessment of Mir-1 life support hardware for the international space station
[NASA-TM-108441] p 3803 N94-31380
SPACECRAFT CHARGING
Development of a 3D numerical code to calculate the trajectories of the blow off electrons emitted by a vacuum surface discharge: Application to the study of the electromagnetic interference induced on a spacecraft
[ONERA-NT-1993-12] p 3863 N94-31227
Arcing in space structures in low Earth orbit
[NASA-CR-194223] p 3694 N94-32478
Spacecraft environmental anomalies expert system
[AD-A277962] p 3612 N94-33262
SPACECRAFT COMMUNICATION
Communications networks in stressed environments
[AD-A275967] p 3672 N94-31384
SPACECRAFT COMPONENTS
The 28th Aerospace Mechanisms Symposium
[NASA-CP-3260] p 3603 N94-33291
SPACECRAFT CONFIGURATIONS
Dynamics and control of orbiting flexible systems: A formulation with applications
[ISBN-0-315-75390-0] p 3611 N94-32502
SPACECRAFT CONSTRUCTION MATERIALS
LDEF Materials Results for Spacecraft Applications
[NASA-CP-3257] p 3591 N94-31012
Model of spacecraft atomic oxygen and solar exposure microenvironments p 3593 N94-31021
Atomic oxygen erosion considerations for spacecraft materials selection p 3593 N94-31022
Performance of selected polymeric materials on LDEF
p 3593 N94-31023

Fluorescence observations of LDEF exposed materials as an indicator of induced material reactions p 3593 N94-31025
On the linearity of fast atomic oxygen effects p 3594 N94-31027
Summary of materials and hardware performance on LDEF p 3595 N94-31037
LDEF materials special investigation group's data bases p 3596 N94-31038
An overview of the Evaluation of Oxygen Interaction with Materials-third phase (EOIM-3) experiment: Space Shuttle Mission 46 p 3596 N94-31040
Analysis of leading edge and trailing edge cover glass samples before and after treatment with advanced satellite contamination removal techniques p 3596 N94-31041
Preliminary results from the CONCAP-2-01 and EIOM-3 experiments on STS-46 p 3596 N94-31042
Design application and development of spacecraft in LEO utilizing LDEF results p 3597 N94-31047
What LDEF means for development and testing of materials p 3598 N94-31050
Computer modelling of cyclic deformation of high-temperature materials
[AD-A277056] p 3623 N94-32012

SPACECRAFT CONTAMINATION
Spacecraft contamination issues from LDEF: Issues for design p 3592 N94-31020
Analysis of leading edge and trailing edge cover glass samples before and after treatment with advanced satellite contamination removal techniques p 3596 N94-31041
Preliminary results from the CONCAP-2-01 and EIOM-3 experiments on STS-46 p 3596 N94-31042
An overview of the on-orbit contamination of the Long Duration Exposure Facility (LDEF) p 3598 N94-31049
Pre-flight testing of Thermoelectric Quartz Crystal Microbalances (TQCM) for midcourse space experiment (MSX) spacecraft
[AD-A277054] p 3610 N94-32010
Combined contamination and space environmental effects on solar cells and thermal control surfaces
[NASA-TM-106592] p 3617 N94-33022
Design and performance of the telescope and detector covers on the Extreme Ultraviolet Explorer satellite p 3605 N94-33309

SPACECRAFT CONTROL
Phase-lock roll control of inertially pointing spacecraft p 3609 N94-31470
Adaptive nonlinear control of spacecraft p 3609 N94-31564
Dynamics and control of orbiting flexible systems: A formulation with applications
[ISBN-0-315-75390-0] p 3611 N94-32502

SPACECRAFT DESIGN
LDEF Materials Results for Spacecraft Applications
[NASA-CP-3257] p 3591 N94-31012
Spacecraft contamination issues from LDEF: Issues for design p 3592 N94-31020
Model of spacecraft atomic oxygen and solar exposure microenvironments p 3593 N94-31021
The Second Annual International Space University Alumni Conference
[NASA-CP-3253] p 3598 N94-31425
Honeycomb sandwich structures: Vented versus unvented designs for space systems
[AD-A276713] p 3624 N94-32122

SPACECRAFT DOCKING
Fuzzy logic application for modeling man-in-the-loop space shuttle proximity operations
[NASA-CR-188283] p 3835 N94-32359
A six degree of freedom, plume-fuel optimal trajectory planner for spacecraft proximity operations using an A* node search
[NASA-CR-188285] p 3601 N94-32388

SPACECRAFT ELECTRONIC EQUIPMENT
Characteristics of III-V semiconductor devices at high temperature
[NASA-TM-106574] p 3697 N94-33052

SPACECRAFT ENVIRONMENTS
Modeling of LDEF contamination environment p 3592 N94-31019
Atmosphere quality standards in manned space vehicles
[ESA-PSS-03-401-ISSUE-1] p 3802 N94-31224
Technical assessment of Mir-1 life support hardware for the international space station
[NASA-TM-108441] p 3803 N94-31380
Spacecraft environmental anomalies expert system
[AD-A277962] p 3612 N94-33262

SPACECRAFT EQUIPMENT
Implementation of heaters on thermally actuated spacecraft mechanisms p 3607 N94-33320
Payload holddown and release mechanism p 3607 N94-33321
Advanced release technologies program p 3607 N94-33322

SPACECRAFT INSTRUMENTS
Space acceleration measurement system
[NASA-TM-109754] p 3913 N94-31807

SPACECRAFT LAUNCHING
Scattering of a random acoustic field by an infinite cylinder: Application to the modelization of the acoustic environment of the 'Ariane 5' launcher scale-model using experimental data
[ONERA-NT-1993-11] p 3860 N94-31226
DOD space based requirements: Increasing DOD access to space
[AD-A276874] p 3601 N94-32211
Independent safety assessment of the Topaz-2 space nuclear reactor power system
[DE94-008653] p 3877 N94-32879
Chronology of KSC and KSC related events for 1993
[NASA-TM-109196] p 3966 N94-33072
Advanced transportation system study: Manned launch vehicle concepts for two way transportation system payloads to LEO
[NASA-CR-193951] p 3608 N94-33100
Design, development, and testing of a lightweight optical sensor cover system p 3604 N94-33302

SPACECRAFT LUBRICATION
Soft x ray photoelectron spectroscopy study of the interaction of Cr with MoS2(0001)
[AD-A276916] p 3635 N94-32233
A comparison of the performance of solid and liquid lubricants in oscillating spacecraft ball bearings p 3606 N94-33311
Development of long-life, low-noise linear bearings for atmospheric interferometry p 3606 N94-33312
The preliminary evaluation of liquid lubricants for space applications by vacuum tribometry p 3606 N94-33313

SPACECRAFT MAINTENANCE
Development of an interchangeable end effector mechanism for the Ranger telerobotic vehicle p 3604 N94-33297

SPACECRAFT MANEUVERS
OARE flight maneuvers and calibration measurements on STS-58
[NASA-TM-109093] p 3613 N94-32924

SPACECRAFT MODELS
Attitude dynamics of spinning rockets in space with internal mass motion p 3601 N94-31802

SPACECRAFT ORBITS
Combined contamination and space environmental effects on solar cells and thermal control surfaces
[NASA-TM-106592] p 3617 N94-33022

SPACECRAFT PERFORMANCE
Spacecraft contamination issues from LDEF: Issues for design p 3592 N94-31020
Space flight risk data collection and analysis project: Risk and reliability database
[NASA-CR-195879] p 3603 N94-32494

SPACECRAFT POWER SUPPLIES
Room temperature molten salts for advanced energy conversion and storage
[AD-A277777] p 3763 N94-33015
The 28th Aerospace Mechanisms Symposium
[NASA-CP-3260] p 3603 N94-33291
Roll ring assemblies for the Space Station p 3603 N94-33294
International Space Station Alpha's bearing, motor, and roll ring module developmental testing and results p 3603 N94-33295

SPACECRAFT PROPULSION
The 7.5K lbf thrust engine preliminary design for Orbit Transfer Vehicle
[NASA-CR-189175] p 3614 N94-31618
Aerospace test facilities at NASA LERC Plumbrook
[NASA-TM-109755] p 3602 N94-31814
Performance evaluation and operating characteristics of a waveguide microwave applicator for space propulsion applications p 3614 N94-31908
Summary of particle bed reactor designs for the Space Nuclear Thermal Propulsion Program
[DE94-007434] p 3615 N94-32266

SPACECRAFT RADIATORS
Thermocapillary convection in evaporating sessile drops
[NASA-TM-109758] p 3705 N94-31886
Development of lightweight radiators for lunar based power systems
[NASA-TM-106604] p 3726 N94-32272

SPACECRAFT REENTRY
The influence of the deorbit-burn manoeuvre on the footprint of a re-entry capsule
[LR-727] p 3609 N94-31705
Implementation of a vibrationally linked chemical reaction model for DSMC
[NASA-TM-109109] p 3710 N94-33020

SPACECRAFT SHIELDING
Electrical properties of double layer dielectric structures for space technology
[ISBN-0-315-86547-4] p 3610 N94-31910

SPACECRAFT STERILIZATION
Analysis of leading edge and trailing edge cover glass samples before and after treatment with advanced satellite contamination removal techniques p 3596 N94-31041

SPACECRAFT STRUCTURES
Anodized aluminum on LDEF p 3592 N94-31017
Trajectory planning for space manipulators
[AD-A277229] p 3611 N94-32369
Arcing in space structures in low Earth orbit
[NASA-CR-194223] p 3694 N94-32478

SPACECRAFT SURVIVABILITY
NASA report to education, volume 9
[NASA-TM-109760] p 3913 N94-31817

SPACECRAFT TEMPERATURE
Physics of heat pipe rewetting
[NASA-CR-195902] p 3913 N94-33148

SPACECRAFT TRAJECTORIES
Trajectory planning for space manipulators
[AD-A277229] p 3611 N94-32369
A six degree of freedom, plume-fuel optimal trajectory planner for spacecraft proximity operations using an A* node search
[NASA-CR-188285] p 3601 N94-32388

SPACECREWS
Legal regime of human activities in outer space law p 3599 N94-31431

SPALLING
Micrometeoroid/space debris effects on materials p 3595 N94-31032

SPATIAL DISTRIBUTION
A comparison between two Monte Carlo codes on determination of transient chemical yields
[DE94-007224] p 3636 N94-32251
A study of the neutral hydrogen distribution of the Milky Way through 21 cm emission and Lyman alpha absorption p 3938 N94-32309
Visual encoding of spatial relations
[AD-A277400] p 3800 N94-32344
A scanning defect mapping system for semiconductor characterization p 3885 N94-32446
Spatial correlation of ionospheric variability
[AD-A278105] p 3776 N94-33041
Martian spectral units derived from ISM imaging spectrometer data p 3949 N94-33220
Martian deltas: Morphology and distribution p 3950 N94-33230

SPECKLE PATTERNS
Elastic modulus measurements of LDEF glasses and glass-ceramics using a speckle technique
[NASA-CR-195911] p 3653 N94-31851
Restoration of interferometric, polarimetric, radiometric, and textural information in SAR images p 3750 N94-32535

SPECTRA
Quantum dynamics in dual spaces
[DE94-008303] p 3913 N94-32824

SPECTRAL BANDS
Characterization of the rare earth orthophosphates and Ce-doped LaPO4 by x ray absorption spectroscopy
[DE94-006313] p 3898 N94-31630

SPECTRAL EMISSION
Computational radiative heat transfer in homogeneous and nonhomogeneous nonscattering media p 3702 N94-31563

SPECTRAL ENERGY DISTRIBUTION
Multiwavelength search for protoplanetary disks p 3599 N94-31430
Radio emission from pre-main-sequence stars p 3955 N94-31890
Near and far infrared observations of protostars and dark clouds p 3926 N94-31969
Note on the variance of autospectral density processed using Welch's method
[DE94-005352] p 3849 N94-32675

SPECTRAL LINE WIDTH
Impact of observed hyperfine splitting on X-ray laser gain
[DE94-005822] p 3717 N94-32128

SPECTRAL METHODS
Spectral analysis method and sample generation for real time visualization of speech
[ETN-94-95732] p 3674 N94-31573
A stability estimate based on numerical ranges with application to a spectral discretization of a convection-diffusion equation
[TW-93-12] p 3847 N94-32200
Analysis of a slot coupled coplanar waveguide fed patch antenna
[NASA-TM-106567] p 3698 N94-33116

SPECTRAL RECONNAISSANCE
Remote sensing for hurricane Andrew impact assessment p 3758 N94-32464
Developments in ERS-1 SAR interferometry: Use of the spectral shift p 3756 N94-32569

SPECTRAL REFLECTANCE
Radiation/remote sensing: Review of the principal definitions p 3757 N94-30996
Modeling the interaction between solar radiation and terrestrial surfaces p 3779 N94-30999
Estimation of visible and near-infrared reflectivity for Peyto Glacier Basin using satellite data [ISBN-0-315-87039-7] p 3743 N94-31733
Feasibility evaluation of new data interpretation approaches for vegetation analysis from airborne imaging spectroscopy p 3745 N94-31862
Monitoring fertilizer application by imaging spectrometry (Somerset Levels test site) p 3745 N94-31863
High resolution spectroscopy in agriculture: Results of the EISAC 1989 campaign p 3745 N94-31864
Evaluation of Fluorescence Line Imager (FLI) airborne imaging spectrometer data for roadside tree damage assessment p 3745 N94-31866
Parameterizing atmosphere-land surface exchange for climate models with satellite data: A case study for the Southern Great Plains CART site [DE94-005109] p 3775 N94-32874
The importance of environmental conditions in reflectance spectroscopy of laboratory analogs for Mars surface materials p 3944 N94-33195
Ferric sulfate montmorillonites as Mars soil analogs p 3944 N94-33196
Mineralogical diversity (spectral reflectance and Moessbauer data) in compositionally similar impact melt rocks from Manicouagan Crater, Canada p 3948 N94-33219
Martian spectral units derived from ISM imaging spectrometer data p 3949 N94-33220

SPECTRAL RESOLUTION
Evaluation of GER- and FLI-data with reference to forest p 3746 N94-31868

SPECTRAL SIGNATURES
Convection and electrodynamic signatures in the vicinity of a Sun-aligned arc: Results from the Polar Acceleration Regions and Convection Study (Polar ARCS) p 3954 N94-31102
Smart environmental monitor based on neural networks and multi-spectral pattern recognition [AD-A276445] p 3829 N94-31301
European Imaging Spectroscopy Aircraft Campaign [ESA-SP-360] p 3743 N94-31853
Inflight calibration, preprocessing, and data evaluation of GER 2 imaging spectrometry data p 3744 N94-31858
Extraction of agricultural parameters from imaging-spectrometry data and simulated MERIS data through red edge analysis p 3745 N94-31865
Near and far infrared observations of protostars and dark clouds p 3926 N94-31969
Mineralogical diversity (spectral reflectance and Moessbauer data) in compositionally similar impact melt rocks from Manicouagan Crater, Canada p 3948 N94-33219

SPECTRAL THEORY
The evolution of jet features during the 1993 east coast white hurricane: A case study using the global spectral model [AD-A277217] p 3783 N94-32021

SPECTROMETERS
Instrumentation for EXELFS measurements using convergent beam diffraction coupling to the electron energy loss spectrometer [USIP-93-07] p 3858 N94-31084
Odin aeronomy science: A phase-A report by the Aeronomy Science Working Group for the Odin satellite [AP-31] p 3770 N94-31222
Elementary particle physics [DE94-006071] p 3866 N94-31620
Varicus magnet options for Delta launched version of ASTROMAG [DE94-006292] p 3955 N94-31635
Time domain spectroscopy for studying a monopole antenna immersed in a plasma [ISBN-0-315-86526-1] p 3888 N94-31727
The Los Alamos National Laboratory precision double crystal spectrometer [DE94-008075] p 3713 N94-32706

SPECTROPHOTOMETRY
Digital image profilers for detecting faint sources which have bright companions [NASA-CR-191348] p 3927 N94-32695

SPECTRORADIOMETERS
Chamber optics for testing passive remote sensing vapor detectors [AD-A275909] p 3878 N94-31340
MODIS. Volume 1: MODIS level 1A software baseline requirements [NASA-TM-104594-VOL-1] p 3823 N94-33287

SPECTROSCOPIC ANALYSIS
Summary of some data processing routines in the molecular physics group of Stockholm University [USIP-93-05] p 3808 N94-31087
Infrared spectroelectrochemical study of cyanide adsorption and reactions at platinum electrodes in aqueous perchlorate electrolyte [AD-A276402] p 3631 N94-31238
Compositions and chemical bonding in ceramics by quantitative electron energy-loss spectrometry [DE94-007208] p 3659 N94-32640
Ionization probes of molecular structure and chemistry [DE94-007605] p 3872 N94-32643
Gettering of metal impurities by cavities in silicon [DE94-005248] p 3645 N94-32672
Characterization of thermally stable dye-doped polyimide based electrooptic materials [DE94-005309] p 3882 N94-32674
Ferric sulfate montmorillonites as Mars soil analogs p 3944 N94-33196
Aerosols scattering and near-infrared observations of the Martian surface p 3946 N94-33204
Material engineering of the novel semiconductor structures [AD-A278386] p 3910 N94-33355

SPECTROSCOPY
Time domain spectroscopy for studying a monopole antenna immersed in a plasma [ISBN-0-315-86526-1] p 3888 N94-31727
Photopyroelectric spectroscopy as a non-intrusive technique for the determination of the optical absorption spectra of multiple quantum well samples [ISBN-0-315-87164-4] p 3833 N94-31875
Workshop on Models for Plasma Spectroscopy [AD-A276565] p 3890 N94-32031
Cooling and trapping of neutral atoms [AD-A276957] p 3870 N94-32360
Theoretical studies of electron transfer and optical spectroscopy [DE94-006985] p 3871 N94-32375
A miniaturized ASIC-based multichannel scaler instrument [DE94-007222] p 3807 N94-32783
Technology development for iron Fischer-Tropsch catalysts [DE94-008723] p 3638 N94-32889
Electron cyclotron resonance plasma oxidation studies of InP [AD-A277431] p 3893 N94-33007

SPECTRUM ANALYSIS
Noninvasive spectral analysis and beam mapping of focused ultrasound, part 1 [AD-A276211] p 3859 N94-31060
Analysis using bi-spectral related technique [AD-A276017] p 3672 N94-31386
Influence of long-range correlations on the spectral functions and response of 48Ca and 90Zr [ETN-94-96017] p 3865 N94-31537
Impurities and conductivity in a D-wave superconductor [DE94-006222] p 3898 N94-31628
Fractal and spectral analysis [ISBN-0-315-86460-5] p 3676 N94-31796
Inflight calibration, preprocessing, and data evaluation of GER 2 imaging spectrometry data p 3744 N94-31858
Noninvasive spectral analysis and beam mapping of focused ultrasound, part 2 [AD-A276629] p 3861 N94-32059
Atmospheric structure simulation: An autoregressive model for smooth geophysical power spectra with known autocorrelation function [AD-A276691] p 3773 N94-32118
Development, characterization, and applications of high temperature superconductor nanobridge Josephson junctions [DE94-008113] p 3903 N94-32409
Noninvasive spectroscopic diagnosis of superficial ocular lesions and corneal infections [DE94-006231] p 3797 N94-32732
Index and bulk parameters for frequency-direction spectra measured at CERC Field Research Facility [AD-A277759] p 3791 N94-33085
Distribution and nature of UV absorbers on Triton's surface [NASA-CR-195886] p 3943 N94-33104

SPECULAR REFLECTION
Characterization of interface structure in multilayers using specular x ray reflectance [DE94-007698] p 3657 N94-32358

SPEECH
Automatic translation among spoken languages p 3685 N94-32437

SPEECH RECOGNITION
Application of the wavelet transform for speech processing p 3600 N94-31435
Segment-based acoustic models for continuous speech recognition [AD-A276109] p 3673 N94-31466
Spectral analysis method and sample generation for real time visualization of speech [ETN-94-95732] p 3674 N94-31573
High-performance speech recognition using consistency modeling [AD-A276775] p 3679 N94-32185
Automatic translation among spoken languages p 3685 N94-32437
Neural networks applied to the phonemic segmentation of speech p 3686 N94-33152
Modular neural network architectures p 3838 N94-33156

SPHERES
Strictly positive definite functions on spheres [AD-A276471] p 3855 N94-31244
Custom uniform source system [NASA-CR-189332] p 3711 N94-31492
Quantum homogeneous spaces, duality, and quantum 2-spheres [CWI-AM-R9309] p 3857 N94-32192

SPHERICAL HARMONICS
Geoid-to-topography ratios on Venus: A global perspective p 3940 N94-31110

SPHERICAL WAVES
Development and implementation of a full-potential ASW method [ETN-94-95757] p 3858 N94-31560

SPHEROIDS
Single scattering of light by ensembles of particles with various shapes [ETN-94-96016] p 3878 N94-31550

SPIN
Spin-structure function of the neutron He-3: SLAC results [DE94-008927] p 3875 N94-33189

SPINEL
Characterization and growth mechanisms of the MgAl2O4 phase in Al2O3-reinforced Al-Mg composites [ISBN-0-315-86531-8] p 3620 N94-31706

SPIRAL ANTENNAS
Predicting antenna parameters from antenna physical dimensions [AD-A276442] p 3672 N94-31300

SPIRAL GALAXIES
The dynamical settling of warped disks and angular momentum transport in galaxies p 3928 N94-31121

SPLINE FUNCTIONS
Filtering of satellite altimetry data with optimal smoothing cubic splines to compute geoid heights, along-tract geoid and gravity gradients in the Indonesian waters and its surroundings [PB94-147527] p 3741 N94-31074
Multivariate spline approximation [AD-A276034] p 3842 N94-31441

SPORES
Backscatter and transmission of aerosol at UV through middle IR wavelengths [AD-A277127] p 3718 N94-32305

SPOT (FRENCH SATELLITE)
From Optics to Radar, SPOT and ERS Applications [ISBN-2-85428-345-7] p 3747 N94-32523
The complementary nature of the SPOT and ERS-1 systems and their place in major international programmes p 3748 N94-32524
From optics to radar: Environmental problems and the SPOT/ERS systems p 3748 N94-32525
Optics and radar: Cohabitation, rivality or happy marriage. Towards new planning tools p 3748 N94-32529
Assessment of region-based methods for automated SAR/optical registration, attribute extraction, and classification p 3750 N94-32536
Robust multisource classification method using the Markov random field methods p 3750 N94-32537
Technique of ERS-1 image processing in association with SPOT data p 3750 N94-32538
Airborne SAR as a complement to SPOT HRV in land-cover classification: The use of normalization and principal components analysis p 3750 N94-32539
Production of terrain data: Optical radar complementarity p 3750 N94-32540
Fusion of multispectral (XS) and Panchromatic (P) SPOT images and radar images p 3750 N94-32541
The use of SPOT and ERS-1 images to map the eruption of Nevado Sabancaya (Province of Arequipa, South Peru) and evaluate associated risks p 3751 N94-32546
Comparison of SPOT, ERS-1, SEASAT, LANDSAT TM, and merged imagery for geological investigations p 3752 N94-32547
Optimal geological data extraction from SPOT-radar synergism with samples from Djebel Amour (Algeria), Red Sea Hills (Sudan), Sirte Basin (Libya), and Magdalena Valley (Colombia) p 3752 N94-32548

Use of SPOT and ERS-1 SAR data to study the tectonic and climatic history of arid regions p 3752 N94-32550
Study of subpolar glaciers of Spitzbergen using SPOT, ERS-1, and hypsometric data: Results and perspectives p 3753 N94-32553
Use of SPOT and ERS-1 to map tropical vegetation and mangrove dynamics in Guiana p 3753 N94-32555
A case study comparing multi-temporal ERS-1 SAR data and SPOT data for tropical forest mapping p 3753 N94-32556
Rapid estimates of crop acreage and production at European scale using high resolution imagery p 3754 N94-32557
Monitoring landsurface characteristics in Niger using complementary SPOT and ERS-1 SAR data p 3754 N94-32560
European MARS project: The potential integration of SPOT and air- and satellite-borne radar data over two pilot areas for agricultural statistics. PROSPER programme and ERS-1 pilot project
[BRGM-93035] p 3754 N94-32561
Comparing SPOT and SIR A for mapping superficial formations in tropical forest regions: Example of the Yaoundy Region (Cameroon) p 3755 N94-32562
Possible complementarity of SPOT/ERS in mapping land use: Study on agricultural land in Brittany (France) p 3755 N94-32563
Land cover change detection with ERS-1 data and data from other remote sensing satellites. Example: The delta of the River Ebro (Spain) p 3755 N94-32564
ERS-1 SAR and optical data for land use/land cover mapping: A case study in a savannah zone of Guinea p 3755 N94-32565
Quantitative analysis of woody vegetation in Soudano-Sahalian region. Textural approach (application to a Burkina Faso region) p 3757 N94-32574
Statistical analysis and mapping of cotton and food crop cultivation surfaces in the west of Burkina Faso: Contribution of combined SPOT P and XS data p 3757 N94-32575

SPRAYERS
Thermocapillary convection in evaporating sessile drops
[NASA-TM-109758] p 3705 N94-31886

SPRAYING
Analysis of strong acoustic excitation on the breakup and dispersion of a liquid jet
[ONERA-NT-1993-9] p 3701 N94-31422

SPREAD SPECTRUM TRANSMISSION
Spread-spectrum radio systems and networks
[AD-A276449] p 3671 N94-31260
Communications networks in stressed environments
[AD-A275967] p 3672 N94-31384
Direct-sequence spread-spectrum performance in a multipath fading environment
[AD-A276080] p 3673 N94-31464
Applied harmonic analysis
[AD-A278384] p 3685 N94-33353
A new tool for signal processing
[AD-A278385] p 3685 N94-33354

SPRINGS (ELASTIC)
Transmissibility of nickel-titanium shape memory alloy springs
[AD-A276055] p 3640 N94-31456
Nonlinear analysis of springs using helical finite elements p 3859 N94-31906

SPUTTERING
Process parameter-growth environment-film property relationships for reactive sputter deposited metal (V, Nb, Zr, Y, Au) oxide, nitride, and oxynitride films
[AD-A276382] p 3640 N94-31258
Energy and angular distributions of secondary ions during electronic sputtering of nonconducting surfaces
[ETN-94-95756] p 3865 N94-31516
Amorphous/crystalline structure and phase transformations in metastable semiconducting Ge(1-x)Sn(x)
[DE94-006659] p 3901 N94-32115
Formation mechanism and yield of molecules ejected from ZnS, CdS, and FeS2 during ion bombardment
[DE94-008487] p 3871 N94-32515
Dependence of x ray absorption magnetic circular dichroism on layer periodicity in iron-platinum multilayers
[DE94-008786] p 3647 N94-32892
Mars atmospheric loss and isotopic fractionation by solar-wind-induced sputtering and photochemical escape p 3947 N94-33208

SQUALLS
Tropical squall lines p 3778 N94-30992

STABILITY
The performance of thermal control coatings on LDEF and implications to future spacecraft p 3591 N94-31013
Nonlinear calculations of the time evolution of black hole accretion disks p 3929 N94-31127
Gravitational instabilities in protostellar disks p 3932 N94-31140
Multidimensional WAF-type schemes for model conservation laws
[CRANFIELD-AERO-9312] p 3843 N94-31541
Design of new polymers to improve radiation stability of plastic scintillators
[DE94-008220] p 3652 N94-31764
Modal analysis of multiterminal high voltage direct current transmission
[DE94-006426] p 3691 N94-31785
Stability and precipitation kinetics in Si(1-y)C(y)/Si and Si(1-x-y)Ge(x)C(y)/Si heterostructures prepared by solid phase epitaxy
[DE94-006589] p 3902 N94-32296
Research on stable, high-efficiency amorphous silicon multijunction modules
[DE94-000298] p 3695 N94-32680
Stability of tearing modes in tokamak plasmas
[DE94-009205] p 3892 N94-32911

STABILITY TESTS
A simplified Von Neumann method for linear stability analysis
[CRANFIELD-AERO-9310] p 3843 N94-31540
Attitude dynamics of spinning rockets in space with internal mass motion p 3601 N94-31802

STABILIZATION
Automatic resonator alignment and power stabilization of high power C02 lasers
[ISBN-0-315-77217-4] p 3714 N94-31472
Stabilization method of A.C. arc plasma
[DE94-757268] p 3893 N94-32916

STABILIZERS (AGENTS)
Oxide pigments in water: The colloid-chemical point of view
[PB94-148616] p 3633 N94-31591

STABILIZERS (FLUID DYNAMICS)
Active control for fin buffet alleviation
[AD-A276844] p 3586 N94-32224

STACKS
Detailed design of the 2MW Demonstration Plant
[DE94-000042] p 3762 N94-32823

STAINLESS STEELS
Effect of vibratory stress relief during welding of thick stainless steel plate
[DE94-006557] p 3733 N94-31312
Solid-state resistance upset welding: A process with unique advantages for advanced materials
[DE94-005941] p 3723 N94-31524
Irradiation-assisted stress corrosion cracking of materials from commercial BWRs: Role of grain-boundary microchemistry
[DE94-006542] p 3643 N94-32109
Stage 1 behavior in a stress corrosion study of Type 304 stainless steel
[DE94-008054] p 3645 N94-32614
Modeling of residual stress mitigation in austenitic stainless steel pipe girth weldment
[DE94-007184] p 3738 N94-32639

STANDARD DEVIATION
Development of a statistical method for estimating the downward longwave radiation at the surface from satellite observations p 3742 N94-31553

STANDARDIZATION
Standardization and intellectual property control: A reflection on the informatics case
[TELECOM-93-E-016] p 3915 N94-31172
Untying the gordian data knot. A paper on Information Engineering (IE) and Corporate Information Management (CIM)
[AD-A276862] p 3918 N94-32210

STANDARDS
Guide to software quality assurance
[ESA-PSS-05-11-ISSUE-1] p 3809 N94-31223
Minutes: Accredited Standards Committee on Bioacoustics, S3. US TAG for ISO/TC 43, acoustics, IEC/TC 29 electroacoustics, and ISO/TC 108/SC4 human exposure to mechanical vibration and shock
[AD-A276201] p 3795 N94-31490
Evaluation for the development of taxiway lighting intensity standards
[AD-A276706] p 3588 N94-32120

STANDING WAVES
A preliminary investigation of high amplitude standing waves with laser Doppler anemometry
[AD-A276463] p 3860 N94-31242
Observation of the traveling component of an x ray standing wave field
[DE94-007671] p 3672 N94-31317
Cooling and trapping of neutral atoms
[AD-A276957] p 3870 N94-32360

STAR CLUSTERS
Circumstellar material around young stars in Orion p 3930 N94-31133
Near infrared surveys of high mass star forming regions p 3925 N94-31898

STAR DISTRIBUTION
Nonthermal accretion disk models around neutron stars p 3931 N94-31139

STAR FORMATION
Circumstellar material around young stars in Orion p 3930 N94-31133
Gravitational instabilities in protostellar disks p 3932 N94-31140
The stellar and gaseous content of massive low surface brightness disk galaxies p 3933 N94-31495
Double-lined pre-main-sequence binaries: A test of pre-main-sequence evolutionary theory p 3933 N94-31497
Evolution of stars and winds in the starburst galaxy M82 p 3934 N94-31758
Near infrared surveys of high mass star forming regions p 3925 N94-31898
Near and far infrared observations of protostars and dark clouds p 3926 N94-31969

STAR FORMATION RATE
Evolution of stars and winds in the starburst galaxy M82 p 3934 N94-31758
Ionized gas in the halos of edge-on infrared-bright galaxies: Evidence for starburst-driven superwinds p 3936 N94-31948

STAR TRACKERS
Design and early results of the sodium-layer laser guide star adaptive optics experiment at the Lawrence Livermore National Laboratory
[DE94-006653] p 3926 N94-32189

STARBURST GALAXIES
Evolution of stars and winds in the starburst galaxy M82 p 3934 N94-31758
Ionized gas in the halos of edge-on infrared-bright galaxies: Evidence for starburst-driven superwinds p 3936 N94-31948

STARK EFFECT
Stark broadening of the 2S state of hydrogen and deuterium in arc plasmas of low density
[ETN-94-95731] p 3888 N94-31572

STATE ESTIMATION
Representation, prediction and identification of cyclostationary processes: A state-space approach
[REPT-93-041] p 3850 N94-31191

STATE VECTORS
Observations of the notion of minimality in the generalized state space
[MATHS-REPT-A-207] p 3840 N94-31162
A separation technique for asymptotic-numeric solution for general shells of revolution p 3736 N94-31961
Theoretical basis for state vector comparison, relative position display, and relative position/rendezvous prediction
[AD-A277216] p 3608 N94-32020

STATIC CHARACTERISTICS
METCAN demonstration manual, version 1.0
[NASA-TM-105607] p 3626 N94-32858

STATIC PRESSURE
Development of a cascade simulation of fan-passage flow
[AD-A277234] p 3584 N94-32026

STATIC STABILITY
Robot grasping: Stability and optimization issues p 3724 N94-31724

STATISTICAL ANALYSIS
Vibrations of a heavy truck diesel engine and gearbox unit: Examining structure-borne sound transmission with statistical energy analysis
[CTH-E-93-04] p 3722 N94-31194
Development of a statistical method for estimating the downward longwave radiation at the surface from satellite observations p 3742 N94-31553
DOME: Dynamic optimization on multiprocessor engines, a statistical approach p 3807 N94-31972
Development of phase-only filters for sensor imagery
[AD-A276722] p 3880 N94-32151
Area-interaction point processes
[CWI-BS-R9318] p 3847 N94-32197
European MARS project: The potential integration of SPOT and air- and satellite-borne radar data over two pilot areas for agricultural statistics. PROSPER programme and ERS-1 pilot project
[BRGM-93035] p 3754 N94-32561
Arithmetic averaging: A versatile technique for smoothing and trend removal
[DE94-005274] p 3852 N94-32673
Using the National Information Infrastructure for social science, education, and informed decision making
[DE94-005442] p 3920 N94-32676
Faultless software project
[AD-A278161] p 3822 N94-33188

STATISTICAL CORRELATION
Analysis of ionospheric parameters in Europe and creation of the prediction algorithm
[AD-A276342] p 3771 N94-31326

Selection of climate station data using clustering and triangulated irregular network techniques
[AD-A276658] p 3784 N94-32046

STATISTICAL DISTRIBUTIONS
Machinery monitoring and diagnostics using pseudo Wigner-Ville distribution and backpropagation neural network
[AD-A276219] p 3828 N94-31064
On the minimum of independent geometrically distributed random variables
[NASA-CR-194883] p 3821 N94-33075

STATISTICAL MECHANICS
A cross-disciplinary report on the mathematical sciences applied to materials science, part 1
[AD-A276116] p 3843 N94-31529
The 14th Annual West Coast Theoretical Chemistry/Statistical Mechanics Conference
[AD-A276942] p 3656 N94-32239

STATISTICAL TESTS
Nonlinear model validation using correlation tests
[RR-463] p 3842 N94-31394
Statistical inference for coherent systems from partial information and in resampling techniques in survival analysis
[AD-A277382] p 3852 N94-32339
Multidimensional scaling of user information satisfaction
[AD-A277230] p 3920 N94-32633
Fault detection and isolation for the Bluebird test bed aircraft
[AD-A277979] p 3586 N94-33086
Statistical characteristics of bistatic surface scatter and mean bistatic surface scattering strengths
[AD-A278155] p 3862 N94-33096

STATORS
Theoretical principles for designing long stator/linear motors with iron
[ETN-94-95741] p 3688 N94-31374
Hotwire measurements of the turbulent flow into a cascade of controlled-diffusion compressor blades
[AD-A277297] p 3706 N94-32042

STEADY FLOW
CFD-based drag prediction: State-of-the-art, theory, prospects
[AD-B179297] p 3567 N94-31180
Additional capabilities of the unified waves model
[AD-A276114] p 3702 N94-31467

STEADY STATE
Invariance of the generalized steady-state for 1-D distributed parameter systems
[REPT-93-66] p 3825 N94-31662
Generalized steady-state method for solving 2-D diffusion systems
[REPT-93-83] p 3825 N94-31700

STEADY STATE CREEP
Creep properties of vanadium-base alloys
[DE94-006541] p 3641 N94-31486

STEEL STRUCTURES
Evaluation of corrosion protective organic coatings for steel structures in fresh water
[PB94-138484] p 3649 N94-31072

STEELS
Correlation of flux composition and inclusion characteristics with submerged arc weld metal properties in HY-100 steel
[AD-A277040] p 3726 N94-32261
Reactor pressure vessel structural integrity research in the US Nuclear Regulatory Commission HSST and HSSI Programs
[DE94-006550] p 3739 N94-32771
Method and apparatus for inhibiting the disbonding of a paint from metal surfaces
[AD-D016106] p 3663 N94-32960

STEERING
Optical processing of MMW for agile beamsteering and beamforming
[AD-A277161] p 3880 N94-32068

STELLAR ATMOSPHERES
A critical examination of stellar atmosphere theory for metal-poor K-giant stars p 3927 N94-32308

STELLAR COLOR
Near infrared surveys of high mass star forming regions p 3925 N94-31898

STELLAR COMPOSITION
Line-strength gradients and kinematic profiles in elliptical galaxies p 3934 N94-31788
A critical examination of stellar atmosphere theory for metal-poor K-giant stars p 3927 N94-32308

STELLAR ENVELOPES
Observations of accretion and angular momentum regulation in young circumstellar disks and the implications for planetary formation p 3928 N94-31122
Circumstellar material around young stars in Orion p 3930 N94-31133
Multiwavelength search for protoplanetary disks p 3599 N94-31430

STELLAR EVOLUTION
Observations of accretion and angular momentum regulation in young circumstellar disks and the implications for planetary formation p 3928 N94-31122

STELLAR LUMINOSITY
Near infrared surveys of high mass star forming regions p 3925 N94-31898

STELLAR MAGNETIC FIELDS
Dynamics of flux tubes in accretion disks p 3932 N94-31142
Hydrodynamics of neutron star interiors and laboratory superfluids p 3936 N94-31949

STELLAR MAGNITUDE
Near infrared surveys of high mass star forming regions p 3925 N94-31898

STELLAR MASS
Near infrared surveys of high mass star forming regions p 3925 N94-31898
A chemical analysis of solar neighborhood dwarfs p 3926 N94-31951

STELLAR MASS ACCRETION
Reactive flows in compact objects p 3934 N94-31567
Structure and stability of spherical accretion flows onto compact objects p 3935 N94-31946

STELLAR MODELS
Evolution of vaporizing pulsars p 3929 N94-31128
Double-lined pre-main-sequence binaries: A test of pre-main-sequence evolutionary theory p 3933 N94-31497
Theoretical studies of magnetohydrodynamic equilibria and dynamics of a solar coronal loop p 3953 N94-31792
Structure and stability of spherical accretion flows onto compact objects p 3935 N94-31946
A critical examination of stellar atmosphere theory for metal-poor K-giant stars p 3927 N94-32308
Convection in Type 2 supernovae
[DE94-009373] p 3938 N94-32914

STELLAR RADIATION
A search for 100 TeV gamma ray emission from the x ray binary pulsar 4U 0115+63 using the CYGNUS extensive air-shower array p 3955 N94-31900

STELLAR ROTATION
The evolutionary status of PSR 1259-63
[DE94-007094] p 3938 N94-32503

STELLAR SPECTRA
Extreme ultraviolet opacity sources in the DA white dwarf G191-B2B p 3924 N94-31210
A chemical analysis of solar neighborhood dwarfs p 3926 N94-31951

STELLAR SYSTEMS
Study of stellar associations located in the region contained between the Magellanic Clouds
[ISBN-0-315-86692-6] p 3935 N94-31913

STELLAR WINDS
Evolution of stars and winds in the starburst galaxy M82 p 3934 N94-31758
Winds from disks in compact binaries
[DE94-007452] p 3938 N94-32137
The evolutionary status of PSR 1259-63
[DE94-007094] p 3938 N94-32503

STELLARATORS
L-H confinement mode dynamics in three-dimensional state space
[DE94-007113] p 3887 N94-31396
Collisional and chaotic transport of energetic particles in toroidal plasma
[DE94-006504] p 3889 N94-31787
Stability of bootstrap current driven magnetic islands in stellarators
[DE94-009207] p 3893 N94-32912

STEPPES
Parameterizing atmosphere-land surface exchange for climate models with satellite data: A case study for the Southern Great Plains CART site
[DE94-005109] p 3775 N94-32874

STEREOSCOPIC VISION
Stereoscopic correspondence based on the structure of shading
[ISBN-0-315-86418-4] p 3814 N94-31718
A neural network model for the visual perception of the depth of a scene from stereoscopy and shading
[ISBN-0-315-86753-1] p 3831 N94-31750

STEREOSCOPY
Alternatives to hierarchical techniques in stereo correlation
[AD-A276570] p 3746 N94-31938

STIFFENING
Test and analysis results for composite transport fuselage and wing structures p 3628 N94-33129

STIFFNESS
Effect of elevated temperature and cyclic loading on properties and damage modes in ceramic composites
[DE94-008736] p 3662 N94-32891

STIFFNESS MATRIX
Minimization of computational requirements in the hybrid stress finite element method
[AD-A277120] p 3846 N94-32048

STIMULANTS
Effects of methamphetamine and fatigue on long- and short-term memory
[AD-A276452] p 3799 N94-32187

STIRLING CYCLE
The 4 K Stirling cryocooler demonstration
[NASA-CR-191792] p 3669 N94-32484

STIRLING ENGINES
Oscillating-flow loss test results in rectangular heat exchanger passages
[NASA-CR-185297] p 3615 N94-32792
A 1050 K Stirling space engine design
[NASA-CR-182149] p 3616 N94-32866

STOCHASTIC PROCESSES
The ant system: An autocatalytic optimizing process
[REPT-91-016-REV] p 3824 N94-31177
Representation, prediction and identification of cyclostationary processes: A state-space approach
[REPT-93-041] p 3850 N94-31191
Near resonant absorption by atoms in intense fluctuating laser fields
[DE94-005873] p 3714 N94-31200
Towards simplicity: Noise and cooperation in the perfect integrator
[AD-A276256] p 3799 N94-31291
Identification of polynomial and rational NARMAX models
[RR-483] p 3842 N94-31413
Light-traffic analysis for queues with spatially distributed arrivals
[MEMO-1150] p 3832 N94-31826
On the convergence of stochastic iterative dynamic programming
[AD-A276517] p 3815 N94-31933
Utility-based planning
[NASA-CR-195878] p 3816 N94-32086
Modeling and control of nonlinear systems
[AD-A277377] p 3834 N94-32095
Kaplan-Meier estimators of interpoint distance distributions for spatial point processes
[CWI-BS-R9315] p 3846 N94-32107
Atmospheric structure simulation: An autoregressive model for smooth geophysical power spectra with known autocorrelation function
[AD-A276691] p 3773 N94-32118
Multiserver queues with impatient customers
[CWI-BS-R9319] p 3835 N94-32198
Stochastic realization of a Gaussian stochastic control system
[CWI-BS-R9320] p 3852 N94-32350
Notes on the Langevin model for turbulent diffusion of marked particles
[DE94-007847] p 3708 N94-32652
State-space self-tuner for on-line adaptive control
[NASA-CR-195836] p 3835 N94-32943
Stochastic models in reliability theory
[AD-A277529] p 3731 N94-32953
SynRGen: An extensible file reference generator
[AD-A277678] p 3821 N94-33030
On the minimum of independent geometrically distributed random variables
[NASA-CR-194883] p 3821 N94-33075
Adaptive control of nonlinear and stochastic systems
[AD-A278411] p 3839 N94-33325

STOICHIOMETRY
Properties of doped and undoped (Ca,Sr)CuO2 thin films
[DE94-007230] p 3905 N94-32785

STORAGE BATTERIES
NEMO: Advanced energy systems and technologies
[DE94-721996] p 3760 N94-31767
Performance of the Sony lithium-ion rechargeable battery
[AD-A277076] p 3693 N94-32303
Development of nickel and metal hydride secondary battery
[DE94-757270] p 3697 N94-32917
Field operation test of utility interactive load conditioner with photovoltaic cells at a demonstration house
[DE94-757271] p 3762 N94-32918
Optimal planning of residential photovoltaic systems under various rate structure
[DE94-757272] p 3762 N94-32919

STORAGE RINGS (PARTICLE ACCELERATORS)
The measurement of the hadronic energy flow and jet production with the ZEUS calorimeter in deep inelastic scattering events at HERA
[ETN-94-96021] p 3865 N94-31534
Results from the H1 experiment at HERA
[PB94-145174] p 3868 N94-32008

STORAGE STABILITY
An investigation of the radiolytic stability of a resorcinol-formaldehyde ion exchange resin
[DE94-007971] p 3660 N94-32698
STORM DAMAGE
Remote sensing for hurricane Andrew impact assessment p 3758 N94-32464
STORMS
The evolution of jet features during the 1993 east coast white hurricane: A case study using the global spectral model
[AD-A277217] p 3783 N94-32021
STORMS (METEOROLOGY)
Tropical squall lines p 3778 N94-30992
STOVL AIRCRAFT
Antiwindup analysis and design approaches for MIMO systems
[NASA-CR-195304] p 3584 N94-32075
STRAIN DISTRIBUTION
Isolating strain parameters correlated to skeletal adaptation p 3797 N94-31960
STRAIN ENERGY METHODS
Development of thermoplastic composite aircraft structures
[NASA-CR-189593] p 3626 N94-32860
STRAIN ENERGY RELEASE RATE
Acoustic emission from crack growth in 7050 aluminum and 7075 aluminum as a function of temperature and heat treatment
[DREP-CRS-93-15] p 3642 N94-31871
STRAIN GAGES
A laboratory study of multiple site damage in fuselage lap splices
[AD-A276151] p 3578 N94-31078
Strain sensing using optical fibers
[NASA-CR-195807] p 3740 N94-32940
STRAIN MEASUREMENT
Fiber optic sensors for the detection of surface acoustic waves on metals
[ISBN-0-315-87055-9] p 3878 N94-31736
Strain sensing using optical fibers
[NASA-CR-195807] p 3740 N94-32940
STRAIN RATE
Tensile properties of commercially pure vanadium from room temperature to 1200 C
[DE94-006622] p 3641 N94-31581
Isolating strain parameters correlated to skeletal adaptation p 3797 N94-31960
STRANGE ATTRACTORS
Heteroclinic attractors: Time averages and moduli of topological conjugacy
[W-9318] p 3844 N94-31690
Deterministic chaos p 3912 N94-31896
STRATIFICATION
Steady thermal convection in multiple liquid layers p 3705 N94-31844
STRATIFIED FLOW
Laser-induced fluorescence/particle tracking system for stratified flow research
[AD-A275917] p 3701 N94-31341
Effects of buoyancy on fluid flows and turbulence
[AD-A276586] p 3706 N94-32123
STRATIGRAPHY
Analysis of deep seismic reflection and other data from the southern Washington Cascades
[DE94-005958] p 3771 N94-31525
STRATOCUMULUS CLOUDS
An integrated cloud observation and modeling investigation in support of the ARM program
[DE94-003160] p 3785 N94-32716
STRATOSPHERE
Odin aeronomy science: A phase-A report by the Aeronomy Science Working Group for the Odin satellite
[AP-31] p 3770 N94-31222
One: Microphysics of frost metamorphism: Applications to Triton and Mars. Two: A global analysis of the ozone deficit in the upper stratosphere and lower mesosphere. Three: The diabatic circulation in the stratosphere as diagnosed from Microwave Limb Sounder data p 3942 N94-31975
Quantified estimates of total GWPs for greenhouse gases taking into account tropospheric chemistry
[DE94-007846] p 3768 N94-32817
Counting particles emitted by stratospheric aircraft and measuring size of particles emitted by stratospheric aircraft
[NASA-CR-195908] p 3769 N94-33170
STREAM FUNCTIONS (FLUIDS)
Finite element vorticity-based methods for the solution of the incompressible and compressible Navier-Stokes equations
[ISBN-0-315-87265-9] p 3703 N94-31730
STRESS (PHYSIOLOGY)
Muscle disuse through tail-suspension: Etiology and therapeutics p 3796 N94-31746
STRESS (PSYCHOLOGY)
Development and enhancement of a model of performance and decision making under stress in a real life setting
[AD-A276029] p 3799 N94-31440
Stress-induced enhancement of the startle reflex
[AD-A278414] p 3802 N94-33327
STRESS ANALYSIS
Aspects of modelling the tectonics of large volcanoes on the terrestrial planets p 3940 N94-31107
State of stress, faulting, and eruption characteristics of large volcanoes on Mars p 3940 N94-31108
On the mechanics of stress analysis of fiber-reinforced composites p 3619 N94-31481
Contribution to the study of multiaxial fatigue under periodic or random stresses
[ISAL-92-0004] p 3734 N94-31544
A novel CFD/structural analysis of a cross parachute
[DE94-005271] p 3568 N94-31578
An approximate solution for interlaminar stresses in laminated composites p 3621 N94-31901
Finite element analysis of damage in fibrous composites using a micromechanical model
[AD-A277226] p 3623 N94-32024
Bond stress-slip characteristics of FRP rebars
[AD-A277191] p 3623 N94-32070
Mechanics of the single fiber pullout problem with several interface conditions p 3623 N94-32078
Finite element analysis of MB326H Macchi wing lower spar cap fatigue cracks
[AD-A277062] p 3580 N94-32264
A critical evaluation of the Reynolds stress turbulence closure for the flow of a turbulent free-stream over a turbulent boundary layer
[ISBN-0-315-75792-2] p 3707 N94-32497
Development of an advanced continuum theory for composite laminates, volume 1
[AD-A277275] p 3625 N94-32591
Development of an advanced continuum theory for composite laminates, volume 2
[AD-A277276] p 3625 N94-32592
A thermal viscoelastic analysis for thick-walled composite cylinders
[AD-A274143] p 3625 N94-32604
Design and evaluation of coils for a 50 mm diameter induction coilgun launcher
[DE94-005244] p 3603 N94-32671
METCAN demonstration manual, version 1.0
[NASA-TM-105607] p 3626 N94-32858
A procedure for 3-D contact stress analysis of spiral bevel gears
[NASA-CR-194472] p 3728 N94-32929
STRESS CONCENTRATION
Physical properties of glasses exposed to Earth-facing and trailing-side environments on LDEF p 3594 N94-31030
Micromechanical analysis of the interface and basic damage modes in glass fiber/epoxy resin model composites
[ONERA-NT-1993-4] p 3618 N94-31225
Reliability analysis of structural ceramics subjected to biaxial flexure p 3650 N94-31454
Tension fracture of laminates for transport fuselage. Part 1: Material screening p 3629 N94-33130
Structural integrity of intelligent materials and structures
[AD-A278397] p 3630 N94-33165
Fundamental studies in crack initiation
[AD-A278387] p 3741 N94-33356
STRESS CORROSION CRACKING
Irradiation-assisted stress corrosion cracking of materials from commercial BWRs: Role of grain-boundary microchemistry
[DE94-006542] p 3643 N94-32109
Stage 1 behavior in a stress corrosion study of Type 304 stainless steel
[DE94-008054] p 3645 N94-32614
Modeling of residual stress mitigation in austenitic stainless steel pipe girth weldment
[DE94-007184] p 3738 N94-32639
STRESS DISTRIBUTION
State of stress, faulting, and eruption characteristics of large volcanoes on Mars p 3940 N94-31108
Influences of pressure-sensitive yielding and non-singular stress on plane-stress elastic-plastic crack-tip fields p 3737 N94-31965
Minimization of computational requirements in the hybrid stress finite element method
[AD-A277120] p 3846 N94-32048
Mechanics of the single fiber pullout problem with several interface conditions p 3623 N94-32078
Analysis of new composite architectures
[NASA-CR-195303] p 3626 N94-32904
A procedure for 3-D contact stress analysis of spiral bevel gears
[NASA-CR-194472] p 3728 N94-32929
Tension fracture of laminates for transport fuselage. Part 1: Material screening p 3629 N94-33130
STRESS INTENSITY FACTORS
A fracture mechanics methodology for characterizing the performance of flawed polymeric dielectric materials p 3654 N94-31956
Effects of interphases on the mechanical, thermal and hygromechanical response of fiber-reinforced composites p 3624 N94-32496
Stage 1 behavior in a stress corrosion study of Type 304 stainless steel
[DE94-008054] p 3645 N94-32614
Compliance measurements of chevron notched four point bend specimen
[NASA-TM-106538] p 3740 N94-32932
STRESS MEASUREMENT
Shearographic inspection of a DeHavilland DHC-7
[AD-A276716] p 3566 N94-32157
Compilation of diamond-like carbon properties for barriers and hard coatings
[DE94-008231] p 3661 N94-32803
STRESS RELAXATION
Processing of novel nanoparticle dispersion strengthened ceramics for improved mechanical performance
[AD-A275965] p 3649 N94-31276
Effect of vibratory stress relief during welding of thick stainless steel plate
[DE94-006557] p 3733 N94-31312
STRESS-STRAIN RELATIONSHIPS
Boron and hydrogen in Ni3Al. Part 2: Mechanical testing of bicrystals
[DE94-007441] p 3904 N94-32606
On the mechanics of microballoon-reinforced metal matrix composites
[AD-A277928] p 3630 N94-33178
STRIATION
On the nature of striae in strontium barium niobate
[DE94-006486] p 3901 N94-32176
STRING THEORY
Gravitational effects of cosmic strings
[ISBN-0-315-75484-2] p 3934 N94-31789
New QCD results from string theory
[DE94-005226] p 3911 N94-31823
The Kaluza-Klein approach and gauge supersymmetry
[ISBN-0-315-86553-9] p 3912 N94-31911
Tensor gauge potentials in loop space formulation of Yang-Mills fields
[PB94-147147] p 3912 N94-31924
String-parton model description of relativistic heavy-ion collisions
[DE94-009164] p 3874 N94-32850
STRONG INTERACTIONS (FIELD THEORY)
The D0 upgrade
[DE94-006953] p 3867 N94-31671
Baryogenesis from a primordial lepton asymmetry
[PB94-145166] p 3868 N94-31921
STRONGLY COUPLED PLASMAS
Analytic formulation for the ac electrical conductivity in two-temperature, strongly coupled, overdense plasma: FORTRAN subroutine
[DE94-009466] p 3893 N94-32915
STRONTIUM OXIDES
On the nature of striae in strontium barium niobate
[DE94-006486] p 3901 N94-32176
STRUCTURAL ANALYSIS
A novel CFD/structural analysis of a cross parachute
[DE94-005271] p 3568 N94-31578
Nonlinear analysis of springs using helical finite elements p 3859 N94-31906
Theory of thick, laminated composite shallow shells p 3622 N94-31953
Prediction of hydrogen entry and permeation in metals and alloys
[AD-A276637] p 3642 N94-31995
Finite element analysis of damage in fibrous composites using a micromechanical model
[AD-A277226] p 3623 N94-32024
QUAD4 seminar
[AD-A277366] p 3818 N94-32330
Structural study in an alteritic region: Contribution of ERS-1 SAR data of the Mauges Plateau (Loire Atlantique, France)
[BRGM-93032] p 3752 N94-32551
Molecular Science Research Center
[DE94-007464] p 3871 N94-32605
Innovative fabrication processing of advanced composite materials concepts for primary aircraft structures
[NASA-CR-189558] p 3626 N94-32877
A case study of analysis methods for large deflections of a cantilever beam
[NASA-TM-108454] p 3739 N94-32903
Institute for Computational Mechanics in Propulsion (ICOMP)
[NASA-TM-106542] p 3710 N94-32969

STRUCTURAL BASINS
Thermal studies of Martian channels and valleys using Termoskan data: New results p 3944 N94-33194
Apron heights around stepped massifs in the Cydonia Mensae region: Do they record the local paleobathymetry of Oceanus Borealis? p 3949 N94-33224

STRUCTURAL DESIGN
Structural design of the superconducting Poloidal Field coils for the Tokamak Physics Experiment
[DE94-007078] p 3887 N94-31406
Multidisciplinary optimization of high-speed civil transport configurations using variable-complexity modeling p 3578 N94-31881
Fracture and fatigue strength evaluation of multiple site damaged aircraft fuselages - curved panel testing and analysis
[AD-A277100] p 3579 N94-32015
Inorganic polymer engineering materials
[DE94-008519] p 3659 N94-32655
Structural probability concepts adapted to electrical engineering
[NASA-TM-106499] p 3739 N94-32735
Local design optimization for composite transport fuselage crown panels p 3629 N94-33132
Leveraging metal matrix composites to reduce costs in space mechanisms p 3604 N94-33301

STRUCTURAL FAILURE
Deformation and rupture of cylindrical shells under dynamic loading p 3733 N94-31288
Reactor pressure vessel structural integrity research in the US Nuclear Regulatory Commission HSST and HSSI Programs
[DE94-006550] p 3739 N94-32771
Structural integrity of intelligent materials and structures
[AD-A278397] p 3630 N94-33165
Design, development, and testing of a lightweight optical sensor cover system p 3604 N94-33302

STRUCTURAL PROPERTIES (GEOLOGY)
The basement fracture pattern of southern Ontario: A tectonic interpretation based on Landsat TM imagery, airphotos and field data
[ISBN-0-315-87086-9] p 3772 N94-31834
Procedures for computing site seismicity
[AD-A277666] p 3775 N94-33028

STRUCTURAL RELIABILITY
Structural probability concepts adapted to electrical engineering
[NASA-TM-106499] p 3739 N94-32735
Structural integrity of intelligent materials and structures
[AD-A278397] p 3630 N94-33165

STRUCTURAL STABILITY
Structural stability and bifurcations p 3911 N94-31895

STRUCTURAL STRAIN
Deformation and rupture of cylindrical shells under dynamic loading p 3733 N94-31288

STRUCTURAL VIBRATION
Vibrations of a heavy truck diesel engine and gearbox unit: Examining structure-borne sound transmission with statistical energy analysis
[CTH-E-93-04] p 3722 N94-31194
Effect of vibratory stress relief during welding of thick stainless steel plate
[DE94-006557] p 3733 N94-31312
Rotordynamic effects driven by fluid forces from a geometrically imperfect labyrinth
[AD-A276424] p 3722 N94-31333
Study of wave propagation and dynamic response of laminated composite structures
[AD-A276123] p 3619 N94-31444
Random vibrations of composite beams and plates p 3735 N94-31777
Vibrational and acoustic response of ribbed plates p 3736 N94-31955
Nonlinear vibration analysis of laminated plates on linear and nonlinear elastic foundations p 3737 N94-32079
Feed-forward control of gear mesh vibration using piezoelectric actuators
[NASA-TM-106366] p 3728 N94-32902
An analytical study of the vibration of beams fitted with neutralizers. Part 2: Assessment of the effects of mounting configurations
[ISVR-TR-225-PT-2] p 3740 N94-32982
Reciprocity-based experimental determination of dynamic forces and moments: A feasibility study
[NASA-CR-194905] p 3862 N94-33023
Vibration Isolation Technology (VIT) ATD project
[NASA-TM-106496] p 3567 N94-33064
Response of a cantilevered plate in supersonic flow
[AD-A277487] p 3580 N94-33107
Structural damping studies at cryogenic temperatures
[NASA-TM-109073] p 3740 N94-33118

STRUCTURAL WEIGHT
Aircraft weight prediction capability. Volume 1: Weight study and results
[AD-A277206] p 3579 N94-32062

STRUCTURED PROGRAMMING
Compositionality of application oriented structuring mechanisms for algebraic specification languages with initial semantics
[ETN-94-95736] p 3812 N94-31577

STUDENTS
Ada support for the mathematical foundations of software engineering
[AD-A278031] p 3822 N94-33284

STYRENES
Design of new polymers to improve radiation stability of plastic scintillators
[DE94-008220] p 3652 N94-31764
Dynamics of block poly(styrene-co-vinylpyridine) (SVP) in solution and on silica
[AD-A277139] p 3857 N94-32364

SUBDUCTION (GEOLOGY)
The tectonic and volcanic evolution of Venus: Catastrophic or gradual? p 3940 N94-31111
Cruise report: Oceanus 250 leg 4 high resolution profiler survey for the North Atlantic Tracer Release Experiment, 25 March - 24 April, 1992
[AD-A277935] p 3791 N94-33245

SUBGROUPS
A note on cocycles in a semidirect product
[REPT-93-65] p 3851 N94-31661
Quantum homogeneous spaces, duality, and quantum 2-spheres
[CWI-AM-R9309] p 3857 N94-32192

SUBLIMATION
Obliquity variation in a Mars climate evolution model p 3951 N94-33236

SUBMILLIMETER WAVES
Optically switched submillimeter-wave oscillator
[AD-A278014] p 3698 N94-33249
High precision moving magnet chopper for variable operation conditions p 3605 N94-33307

SUBREFLECTORS
High precision moving magnet chopper for variable operation conditions p 3605 N94-33307

SUBROUTINES
Arnoldi code for computing selected eigenvalues of sparse real unsymmetric matrices
[PB94-145182] p 3813 N94-31682
Analytic formulation for the ac electrical conductivity in two-temperature, strongly coupled, overdense plasma: FORTRAN subroutine
[DE94-009466] p 3893 N94-32915

SUBSONIC FLOW
An experimental study of the flowfield on a semispan rectangular wing with a simulated glaze ice accretion
[NASA-CR-195301] p 3571 N94-32475
Shear flow control of cold and heated rectangular jets by mechanical tabs. Volume 1: Results and discussion
[NASA-CR-182296-VOL-1] p 3708 N94-32867
Shear flow control of cold and heated rectangular jets by mechanical tabs. Volume 2: Tabulated data
[NASA-CR-182296-VOL-2] p 3709 N94-32869

SUBSONIC FLUTTER
Aeroelastic vibrations of lifting surfaces
[ECL-91-01] p 3585 N94-31677

SUBSONIC SPEED
installed F/A-18 inlet flow calculations at 30 degrees angle-of-attack: A comparative study
[NASA-CR-195297] p 3573 N94-33119

SUBSONIC WIND TUNNELS
Hotwire measurements of the turbulent flow into a cascade of controlled-diffusion compressor blades
[AD-A277297] p 3706 N94-32042

SUBSTRATES
A new mechanism for surface diffusion: Motion of a substrate-adsorbate complex
[AD-A276072] p 3632 N94-31459
In-situ TEM crystallization of anorthite-glass films on (alpha)-Al2O3
[DE94-006317] p 3652 N94-31780
Epitaxial liftoff technology onto processed silicon foundry wafers
[AD-A277116] p 3900 N94-31985
Materials processing and manufacturing technologies for diamond substrates multichip modules
[AD-A276904] p 3692 N94-32215
Stability and precipitation kinetics in Si(1-y)C(y)/Si and Si(1-x-y)Ge(x)C(y)/Si heterostructures prepared by solid phase epitaxy
[DE94-006589] p 3902 N94-32296
An electrical test system for conductor formation process analysis
[DE94-007291] p 3696 N94-32786
Conductive paints
[DE94-008508] p 3661 N94-32788
Ultrahigh-current-density metal-ion implantation and diamondlike-hydrocarbon films for tribological applications
[DE94-008958] p 3906 N94-32843

SUBSTRUCTURES
Transport phenomena in the Earth's plasma sheet p 3772 N94-31970

SUCTION
Results for the hybrid laminar flow control experiment conducted in the NASA Langley 8-foot transonic pressure tunnel on a 7-foot chord model
[NASA-TM-107582] p 3601 N94-32870

SULFATES
The adsorption of sulfate on gold(111) in acidic aqueous media: Adlayer structural inferences from infrared spectroscopy and scanning tunneling microscopy
[AD-A276643] p 3642 N94-31997
Evaluation of sulfate aerosol optical depths over the North Atlantic and comparison with satellite observations
[DE94-005457] p 3746 N94-32100
Fine resolution atmospheric sulfate model driven by operational meteorological data: Comparison with observations
[DE94-002994] p 3766 N94-32691
Climate effects of anthropogenic sulfate: Simulations from a coupled chemistry/climate model
[DE94-004352] p 3767 N94-32789
Ferric sulfate montmorillonites as Mars soil analogs p 3944 N94-33196

SULFIDES
New molecular-based routes to binary main group metal sulfides
[AD-A277005] p 3900 N94-32003
Processable, chemical routes to binary metal sulfides
[AD-A277006] p 3642 N94-32004
Group 12 thiolates: Syntheses, characterization and decomposition pathways
[AD-A277055] p 3900 N94-32011
The relative performance of FeS2 and CoS in long-life thermal-battery applications
[DE94-006145] p 3695 N94-32663

SULFONIC ACID
Metal ion complexation by ionizable crown ethers
[DE94-008301] p 3661 N94-32847

SULFUR
The intramolecular cyclization of bis-2,5-dimethylene-2,5-dihydrofurans and bis-2,5-dimethylene-2,5-dihydrothiophenes: An approach to macrocycles
[DE94-007060] p 3657 N94-32377
Fine resolution atmospheric sulfate model driven by operational meteorological data: Comparison with observations
[DE94-002994] p 3766 N94-32691

SULFUR COMPOUNDS
Processable, chemical routes to binary metal sulfides
[AD-A277006] p 3642 N94-32004

SULFUR DIOXIDES
Cloud studies seen from a physical chemist's perspective
[DE94-006059] p 3771 N94-31527
Time-dependent behavior of Mount Pinatubo aerosol
[DE94-001877] p 3764 N94-31601
Concentration system performance degradation in the aftermath of Mount Pinatubo
[DE94-001879] p 3764 N94-31602

SULFUR OXIDES
Identification of research relating to the critical loads concept and its potential application to the regulation of acidic deposition
[DE94-008234] p 3767 N94-32752

SULFURIC ACID
Anodized aluminum on LDEF p 3592 N94-31017
Climate effects of anthropogenic sulfate: Simulations from a coupled chemistry/climate model
[DE94-004352] p 3767 N94-32789

SUM RULES
Spin-structure function of the neutron He-3: SLAC results
[DE94-008927] p 3875 N94-33189

SUNLIGHT
Spectral inhomogeneity of the bacterial light-harvesting antennae: Causes and consequences
[ETN-94-96020] p 3792 N94-31533
The properties of sunflecks in a flexible plant canopy, and their relationship to turbulence p 3782 N94-31775

SUPERCOMPUTERS
Sandia's research network for Supercomputing 1993: A demonstration of advanced technologies for building high-performance networks
[DE94-005319] p 3823 N94-31149
Parallel supercomputing: Advanced methods, algorithms, and software for large-scale linear and nonlinear problems
[DE94-008446] p 3836 N94-32992

SUPERCONDUCTING DEVICES
Future directions of nonlinear dynamics in physical and biological systems. (Physica D nonlinear, volume 68, number 1)
[AD-A278085] p 3794 N94-33250
Microstructures and epitaxy in oxide superconductor thin films and devices
[AD-A278427] p 3910 N94-33332
SUPERCONDUCTING FILMS
Preliminary results from the CONCAP-2-01 and EIOM-3 experiments on STS-46 p 3596 N94-31042
High performance YBCO films
[AD-A276493] p 3897 N94-31531
The charging effect in high-Tc superconducting thin films
[AD-A277265] p 3900 N94-32040
Microanalytical study of defect formation in thin bismuth strontium calcium copper oxide films
[DE94-008217] p 3661 N94-32751
Microstructures and epitaxy in oxide superconductor thin films and devices
[AD-A278427] p 3910 N94-33332
SUPERCONDUCTING MAGNETS
Structural design of the superconducting Poloidal Field coils for the Tokamak Physics Experiment
[DE94-007078] p 3887 N94-31406
Various magnet options for Delta launched version of ASTROMAG
[DE94-006292] p 3955 N94-31635
Quench detection and instrumentation for the Tokamak Physics Experiment magnets
[DE94-006656] p 3888 N94-31667
On the unsteady-motion theory of magnetic forces for maglev
[DE94-007765] p 3727 N94-32778
RHIC chromatic correction system
[DE94-008532] p 3883 N94-32994
SUPERCONDUCTIVITY
Synthesis, characterization, phase diagrams and superconducting, and normal state magnetic properties of La(2-x)Sr(x)CuO4 (0 is less than or equal to x which is less than or equal to 0.08) and electrochemically oxidized La(2-x)Sr(x)CuO(4 + delta) (0 is less than or equal to x which is less than or equal to 0.33, 0 is less than or equal to delta which is less than or equal to 0.12)
[DE94-005260] p 3895 N94-31067
Experimental evidence for lattice effects in high temperature superconductors
[DE94-006250] p 3899 N94-31633
Finite element analysis of time-independent superconductivity p 3691 N94-31905
Isothermal sintering, microstructure, and superconducting properties of Y1Ba2Cu3O(7-x) compound
[DE94-008132] p 3905 N94-32779
Investigation of superconductivity and magnetism in d and f-electron materials
[DE94-008535] p 3907 N94-32933
Superconducting and semiconducting hybrids and advance memory concepts for superconducting electronics
[AD-A277766] p 3907 N94-32988
A quest for a new superconducting state
[DE94-008439] p 3908 N94-32991
SUPERCONDUCTORS
Various magnet options for Delta launched version of ASTROMAG
[DE94-006292] p 3955 N94-31635
Finite element analysis of time-independent superconductivity p 3691 N94-31905
The 10th International Conference on Internal Friction and Ultrasonic Attenuation in Solids (ICIFUAS)
[AD-A276849] p 3902 N94-32209
Strongly anisotropic s-wave versus d-wave gap in cuprate superconductors: Evidence and theory
[DE94-007579] p 3904 N94-32746
Superconducting and semiconducting hybrids and advance memory concepts for superconducting electronics
[AD-A277766] p 3907 N94-32988
SUPERCOOLING
Solidification structure synthesis in undercooled liquids
[AD-A276166] p 3910 N94-31054
SUPERCRITICAL FLUIDS
Biocatalytic processing polymers in supercritical fluids
[AD-A276120] p 3651 N94-31510
Improved oxidation resistance of 3-D carbon/carbon composites
[AD-A277349] p 3625 N94-32624
SUPERFLUIDITY
Hydrodynamics of neutron star interiors and laboratory superfluids p 3936 N94-31949
SUPERHIGH FREQUENCIES
Design of a high power x-band magnicon amplifier
[AD-A277001] p 3892 N94-32199
YBCO Josephson Junction arrays
[AD-A277426] p 3908 N94-33005
The 20 GHz circularly polarized, high temperature superconducting microstrip antenna array
[NASA-CR-195097] p 3683 N94-33083
SUPERLATTICES
Experimental and theoretical studies of hydrogenated amorphous semiconductor alloys and superlattices
[AD-A276159] p 3686 N94-31079
A 1-picosecond InGaAs photodetector for operation at 1300-1600 nm
[AD-A275959] p 3895 N94-31350
The relationship of the electronic structures of semiconductor surfaces and heterostructures to crystal growth
[AD-A276465] p 3896 N94-31473
Ion beam synthesis of IrSi3 by 1-MeV Ir ion implantation into Si(111)
[DE94-006556] p 3896 N94-31501
GaAs/GaN strained layer superlattice materials for high temperature transistors, phase 1
[AD-A276115] p 3897 N94-31528
Energetics, bonding mechanism, and electronic structure of ceramic/ceramic and metal/ceramic interfaces
[DE94-008551] p 3659 N94-32656
Microanalytical study of defect formation in thin bismuth strontium calcium copper oxide films
[DE94-008217] p 3661 N94-32751
Interface controlled amorphization of crystalline Ni/Ti multilayers
[DE94-008685] p 3906 N94-32884
SUPERNOVA REMNANTS
Structure and stability of spherical accretion flows onto compact objects p 3935 N94-31946
SUPERNOVAE
Reactive flows in compact objects p 3934 N94-31567
Evolution of stars and winds in the starburst galaxy M82 p 3934 N94-31758
Convection in Type 2 supernovae
[DE94-009373] p 3938 N94-32914
SUPERPLASTICITY
A state variable material model for superplastic titanium-6 percent Al-4 percent V p 3644 N94-32498
SUPERSONIC AIRCRAFT
Development of a cascade simulation of fan-passage flow
[AD-A277234] p 3584 N94-32026
SUPERSONIC COMBUSTION
Ignition delays, heats of combustion, and reaction rates of aluminum alkyl derivatives used as ignition and combustion enhancers for supersonic combustion
[NASA-CR-189581] p 3638 N94-32868
Turbulent reacting flows and supersonic combustion
[AD-A277462] p 3639 N94-33242
SUPERSONIC COMBUSTION RAMJET ENGINES
A numerical method for mixing/chemically reacting compressible flow with finite rate chemistry p 3634 N94-31824
SUPERSONIC FLOW
Shock-dependent, optimum thrust wings in supersonic flow p 3570 N94-32027
Shear flow control of cold and heated rectangular jets by mechanical tabs. Volume 1: Results and discussion
[NASA-CR-182296-VOL-1] p 3708 N94-32867
Shear flow control of cold and heated rectangular jets by mechanical tabs. Volume 2: Tabulated data
[NASA-CR-182296-VOL-2] p 3709 N94-32869
Flutter analysis of a supersonic cascade in time domain using an ADI Euler solver
[NASA-TM-105625] p 3739 N94-32883
An analysis of supersonic flows with low-Reynolds number compressible two-equation turbulence models using LU finite volume implicit numerical techniques
[NASA-CR-195302] p 3572 N94-32926
A mathematical model for simulating noise suppression of lined ejectors
[NASA-TP-3425] p 3861 N94-32930
Response of a cantilevered plate in supersonic flow
[AD-A277487] p 3580 N94-33107
Turbulent reacting flows and supersonic combustion
[AD-A277462] p 3639 N94-33242
SUPERSONIC FLUTTER
Aeroelastic vibrations of lifting surfaces
[ECL-91-01] p 3585 N94-31677
SUPERSONIC SPEED
Investigation of sonic boom for the Space Shuttle: High cross-range orbiter
[NASA-TM-108238] p 3860 N94-31336
Flight test results of riblets at supersonic speeds
[NASA-TM-4387] p 3572 N94-32880
SUPERSONIC TRANSPORTS
Multidisciplinary optimization of high-speed civil transport configurations using variable-complexity modeling p 3578 N94-31881
Use of Navier-Stokes methods for the calculation of high-speed nozzle flow fields
[NASA-TM-106551] p 3573 N94-32984
SUPERSYMMETRY
High energy physics studies
[DE94-005970] p 3876 N94-31505
Some calculations on supersymmetric graphs as communication networks
[REPT-93-72] p 3824 N94-31641
Conformal field theory and geometry of strings
[PB94-148442] p 3857 N94-31770
Production of charginos and neutralinos for the reaction positron electron yields Z° boson yields chargino(+) (sub i) chargino(-) (sub j) or neutralino (sub i) neutralino (sub j) in SU(2) (sub L) x SU(2) (sub R) x U(1) (sub B-L)
[ISBN-0-315-87316-7] p 3867 N94-31832
The Kaluza-Klein approach and gauge supersymmetry
[ISBN-0-315-86553-9] p 3912 N94-31911
Baryogenesis from a primordial lepton asymmetry
[PB94-145166] p 3868 N94-31921
Tensor gauge potentials in loop space formulation of Yang-Mills fields
[PB94-147147] p 3912 N94-31924
SUPPORT SYSTEMS
New approaches for real time decision support systems p 3915 N94-32426
Knowledge-based commodity distribution planning p 3915 N94-32427
Selection criteria and facilitation training for the study of groupware
[NASA-CR-195906] p 3822 N94-33114
A decision support system for electronic warfare analysts p 3853 N94-33336
SUPPRESSORS
An adaptive Kalman filter excisor for suppressing narrowband interference
[AD-A276286] p 3671 N94-31253
SURFACE CRACKS
Temperature-humidity-bias aging technique to identify defective surface mount capacitors
[DE94-005354] p 3660 N94-32727
Fundamental studies in crack initiation
[AD-A278387] p 3741 N94-33356
SURFACE DEFECTS
Reliability analysis of structural ceramics subjected to biaxial flexure p 3650 N94-31454
Intra-cascade surface recombination of point defects during ion bombardment of Ge(001)
[DE94-007740] p 3903 N94-32384
Reactor pressure vessel structural integrity research in the US Nuclear Regulatory Commission HSST and HSSI Programs
[DE94-006550] p 3739 N94-32771
SURFACE DIFFUSION
Synthesis, characterization, phase diagrams and superconducting, and normal state magnetic properties of La(2-x)Sr(x)CuO4 (0 is less than or equal to x which is less than or equal to 0.08) and electrochemically oxidized La(2-x)Sr(x)CuO(4 + delta) (0 is less than or equal to x which is less than or equal to 0.33, 0 is less than or equal to delta which is less than or equal to 0.12)
[DE94-005260] p 3895 N94-31067
A new mechanism for surface diffusion: Motion of a substrate-adsorbate complex
[AD-A276072] p 3632 N94-31459
SURFACE EMITTING LASERS
Passivation of III-V compound semiconductor based devices
[AD-A276178] p 3894 N94-31056
Large-diameter InGaAs/AlGaAs vertical-cavity surface-emitting lasers with low threshold current density fabricated using a simple chemical etch process
[AD-A277733] p 3721 N94-33003
SURFACE ENERGY
Empirical and semi-empirical relationships of liquid-vapor, solid-vapor, and solid-liquid surface energies
[AD-A276480] p 3631 N94-31248
SURFACE FINISHING
Analysis of leading edge and trailing edge cover glass samples before and after treatment with advanced satellite contamination removal techniques p 3596 N94-31041
Neutral ion sources in precision manufacturing p 3875 N94-32447
SURFACE LAYERS
Adsorption of water to the metal/polymer interface studied by neutron and x ray reflectivity
[DE94-005578] p 3651 N94-31649
High-resolution synthetic aperture radar observations of the Moon p 3676 N94-31952
Dielectric properties of Mars' surface: Proposed measurement on a Mars lander p 3951 N94-33237
SURFACE PROPERTIES
The surface parameters: Remote sensing observations and climatology applications p 3779 N94-31001

Modification of semiconductor surface properties with chemically bound molecular films
[AD-A276162] p 3895 N94-31081
Molecular dynamics computer simulations of charged metal electrode-aqueous electrolyte interfaces
[AD-A276401] p 3863 N94-31237
Electromagnetic scattering through loaded aperture panels with nonzero contact impedance
[ONERA-NT-1993-2] p 3673 N94-31418
A new mechanism for surface diffusion: Motion of a substrate-adsorbate complex
[AD-A276072] p 3632 N94-31459
The relationship of the electronic structures of semiconductor surfaces and heterostructures to crystal growth
[AD-A276485] p 3896 N94-31473
Satellite radar altimetry over the continental ice sheets p 3742 N94-31570
Prediction of hydrogen entry and permeation in metals and alloys
[AD-A276637] p 3642 N94-31995
Metal clusters: Dynamics and structure
[AD-A276842] p 3643 N94-32091
Visual neural development and chromatic aberration
[AD-A277402] p 3800 N94-32345
SUNY beamline facilities at the National Synchrotron Light Source
[DE94-006343] p 3905 N94-32770
Parameterizing atmosphere-land surface exchange for climate models with satellite data: A case study for the Southern Great Plains CART site
[DE94-005109] p 3775 N94-32874
Imaging of surface structure with energy-dependent photoelectron diffraction
[DE94-009096] p 3907 N94-32934
Surface conforming flexible eddy current probe for scanning varying surface contours
[AD-D016173] p 3627 N94-33018
Distribution and nature of UV absorbers on Triton's surface
[NASA-CR-195886] p 3943 N94-33104
The importance of environmental conditions in reflectance spectroscopy of laboratory analogs for Mars surface materials p 3944 N94-33195
Martian spectral units derived from ISM imaging spectrometer data p 3949 N94-33220

SURFACE REACTIONS
Ground-based simulation of LEO environment: Investigations of a select LDEF material: FEP Teflon (trademark) p 3596 N94-31039
An overview of the Evaluation of Oxygen Interaction with Materials-third phase (EOIM-3) experiment: Space Shuttle Mission 46 p 3596 N94-31040
Effects of orbital exposure on RTV during the LDEF mission p 3597 N94-31043
Solidification structure synthesis in undercooled liquids
[AD-A276166] p 3910 N94-31054
Mechanisms of laser induced reactions in opaque heterogeneous environments
[AD-A276642] p 3717 N94-31996
A new-type of long-range restructuring of ordered metal surfaces induced by lateral adsorbate interactions: Iodide on AU(110) electrodes
[AD-A276633] p 3643 N94-32060
Surface chemistry and durability of borosilicate glass
[DE94-006734] p 3656 N94-32116
Soft x ray photoelectron spectroscopy study of the interaction of Cr with MoS2(0001)
[AD-A276916] p 3635 N94-32233
Chemical structure and kinetics at liquid/solid interfaces
[AD-A277112] p 3636 N94-32304
Chemisorbed-molecule potential-energy surfaces and electronically-stimulated processes
[DE94-007932] p 3719 N94-32603
Surface probes of porous toluene/water ices: Adsorption kinetics and annealing spectra measured by second harmonic generation
[DE94-007564] p 3637 N94-32743
Time-resolved analytical methods for liquid/solid interfaces
[DE94-008352] p 3637 N94-32826
Induced adsorption of chloride and bromide by submonolayer amounts of copper underpotentially deposited on Pt(111)
[AD-A278023] p 3648 N94-33182

SURFACE ROUGHNESS
New micro- and macroscopic models of contact and friction
[AD-A277240] p 3726 N94-32320
Almaz marine applications p 3751 N94-32544
Metal cluster-rare gas van der Waals complexes: Microscopic models of physisorption
[DE94-008134] p 3873 N94-32797
Interface engineering in oxide fiber/oxide matrix composites
[AD-A277672] p 3627 N94-33029

SURFACE ROUGHNESS EFFECTS
A comparison of rough surface parabolic equation models
[AD-A278090] p 3791 N94-33185
An approximate model for vertical polarization and surface roughness using the parabolic equation
[AD-A278091] p 3684 N94-33186

SURFACE STABILITY
Fermi surface instability at 0.4 K in a heavy-fermion YbBiPt: SDW?
[DE94-006224] p 3899 N94-31916

SURFACE TEMPERATURE
Heat transfer studies on a rectangular channel with offset plate fins
[AD-A277300] p 3912 N94-32043
Sensitivity analysis of the AVHRR infrared cirrus model
[AD-A276690] p 3784 N94-32117
Synergy of thermal infrared and microwave remote sensing for evaporation estimation p 3754 N94-32559
Dual-band infrared imaging to detect corrosion damage within airframes and concrete structures
[DE94-006047] p 3580 N94-32658
Development of lightweight ceramic ablators and arc-jet test results
[NASA-TM-108798] p 3617 N94-33117

SURFACE TREATMENT
Operation of D3-D with all-graphite walls
[DE94-004858] p 3886 N94-31304
Large-area conditioning of optics for high-power laser systems
[DE94-007028] p 3716 N94-31636
Fatigue testing of 2024-T3 material after four cycles of PMB stripping
[AD-A276926] p 3644 N94-32237
Evaluation of the Hughes conversion coating touch-up pen
[AD-A278398] p 3664 N94-33166

SURFACE VEHICLES
Navy Omni-Directional Vehicle (ODV) development program p 3729 N94-32451

SURFACES
Aeroelastic vibrations of lifting surfaces
[ECL-91-01] p 3585 N94-31677

SURVEILLANCE
Millimeter wave, high-resolution, holographic surveillance system
[DE94-004289] p 3712 N94-31831

SURVEYS
Results of real-time testing and demonstration of the US Army Corps of Engineers real-time on-the-fly positioning system
[AD-A276160] p 3576 N94-31080
Active matrix liquid crystal display. Industry survey results
[AD-A276415] p 3895 N94-31329
Hydrographic service Royal Australian Navy
[AD-A277134] p 3788 N94-32066
Aircraft communication and navigation systems and communication and navigation systems
[AD-A277309] p 3582 N94-32328
The relationship between integrative task design for information systems professionals and perceived information systems effectiveness p 3919 N94-32487
Relationships between access and use in information systems: Remote access to and browsing of online catalogs p 3919 N94-32488
Multidimensional scaling of user information satisfaction
[AD-A277230] p 3920 N94-32633

SURVIVAL
NASA report to education, volume 9
[NASA-TM-109760] p 3913 N94-31817

SUSPENDING (HANGING)
A large motion zero-gravity suspension system for experimental simulation of orbital construction and deployment
[NASA-CR-195881] p 3668 N94-33037

SUSPENSIONS
Micromechanics and effective properties of particulate composites and fluid suspensions p 3703 N94-31744

SWELLING
The influence of transmutation, void swelling, and flux/spectra uncertainties on the electrical properties of copper and copper alloys
[DE94-006213] p 3641 N94-31626
Effect of irradiation damage and helium on the swelling and structure of vanadium-base alloys
[DE94-006540] p 3641 N94-31666

SWEPT WINGS
Numerical analysis of transonic wing buffet p 3586 N94-32713

SWITCHES
Electron-beam controlled semiconductor switches
[AD-A276198] p 3686 N94-31057
Studies of the plasma triggering mechanism of inverse pinch switch
[AD-A276117] p 3887 N94-31530
The named-state register file
[AD-A276796] p 3825 N94-32165
Reconfigurable optical switches with monolithic electrical-to-optical interfaces
[DE94-007745] p 3881 N94-32385
High power switch design for the Nova upgrade laser (Project HERCULES: High Energy Research Concerning the Ultimate Lifetime of Experimental Switches)
[DE94-007921] p 3719 N94-32654
Optically switched submillimeter-wave oscillator
[AD-A278014] p 3698 N94-33249

SWITCHING
Studies of the plasma triggering mechanism of inverse pinch switch
[AD-A276117] p 3887 N94-31530
High power switch design for the Nova upgrade laser (Project HERCULES: High Energy Research Concerning the Ultimate Lifetime of Experimental Switches)
[DE94-007921] p 3719 N94-32654

SWITCHING CIRCUITS
Electron-beam controlled semiconductor switches
[AD-A276198] p 3686 N94-31057
Examination of fast semiconductor diodes (recovery) with respect to switching valves in PWM and resonance devices
[ETN-94-95740] p 3690 N94-31609
The named-state register file
[AD-A276796] p 3825 N94-32165
Characterization of thermally stable dye-doped polyimide based electrooptic materials
[DE94-005309] p 3882 N94-32674
Fiber optic continuous true time-delay modulator
[AD-D016098] p 3883 N94-32720
Buffered feedthrough crossbar switch
[AD-D016145] p 3697 N94-32967

SYMBOLS
Beginning the 21st century with advanced Automatic Parts Identification (API) p 3923 N94-32444

SYMMETRY
N(exp n(n-1)/2)-state R-matrix related with U(sub q)(sl(n)) algebra at q(exp 2N) = 1
[DE94-608140] p 3902 N94-32247
Fabrication, phase transformation studies and characterization of SiC-AlN-Al2OC ceramics
[DE94-008587] p 3659 N94-32657

SYNCHRONISM
Extension of the LUSTRE language and application to circuit design: The LUSTRE V4 language and the POLLUX system
[ETN-94-95918] p 3812 N94-31543

SYNCHRONOUS MOTORS
Theoretical principles for designing long stator/linear motors with iron
[ETN-94-95741] p 3688 N94-31374
Applicable dimensioning and measure and technological examination of long stator-linear motors for magnetic high-speed railways
[ETN-94-95734] p 3689 N94-31575

SYNCHROTRON RADIATION
Characterization of the rare earth orthophosphates and Ce-doped LaPO4 by x ray absorption spectroscopy
[DE94-006313] p 3898 N94-31630
Double photoionization of helium with synchrotron x rays: Proceedings
[DE94-006737] p 3866 N94-31668
Near edge x ray spectroscopy theory
[DE94-008179] p 3905 N94-32799

SYNCHROTRONS
Time-dependent behavior of active galactic nuclei with pair production p 3929 N94-31125
Particle diffusion from the beam-beam interaction in synchrotron colliders
[DE94-007111] p 3876 N94-32b95

SYNOPTIC METEOROLOGY
Dynamics in the tropics and synoptic disturbances p 3778 N94-30990

SYNTAX
Correspondence theory for extended modal logics, version 3.0
[ML-93-16] p 3856 N94-31417
Compositionality of application oriented structuring mechanisms for algebraic specification languages with initial semantics
[ETN-94-95736] p 3812 N94-31577
Informal introduction to the extended affix grammar formalism and its compiler
[TR-93-19] p 3817 N94-32287
An epistemic proof system for parallel processes
[TR-93-17] p 3826 N94-32291

SYNTHESIS (CHEMISTRY)
Feasibility study to evaluate plasma quench process for natural gas conversion applications
[DE94-000086] p 3758 N94-31234
Novel electroactive polymers and block copolymers
[AD-A276119] p 3650 N94-31509
Biocatalytic processing polymers in supercritical fluids
[AD-A276120] p 3651 N94-31510
Inorganic materials for anomalous-dispersion phase-matched second harmonic generation: Rubidium titanyl arsenate isomorphs, Rb(Ti(1-2x)Ln(x)Nb(x))OAsO4
[DE94-006141] p 3899 N94-31847
Tetraalkyldiarsines as potential precursors for electronic materials: Synthesis and characterization of various iso-propyl arsenic compounds
[AD-A277003] p 3900 N94-32001
Processable, chemical routes to binary metal sulfides
[AD-A277006] p 3642 N94-32004
Group 12 thiolates: Syntheses, characterization and decomposition pathways
[AD-A277055] p 3900 N94-32011
High octane ethers from synthesis gas-derived alcohols
[DE94-006774] p 3667 N94-32133
Towards a detailed understanding of the structural variability in lignins: A new approach
[DE94-007449] p 3793 N94-32267
SYNTHESIZERS
Modelling the late part of room impulse responses using adaptive filtering: On the recreation of reality
[CTH-E-93-01] p 3859 N94-31076
SYNTHETIC APERTURE RADAR
Phase unwrapping problems in ISAR images
[TELECOM-93-D-008] p 3670 N94-31097
High-resolution synthetic aperture radar observations of the Moon p 3676 N94-31952
Validation support of the ERIM ocean model
[AD-A277364] p 3788 N94-32284
From Optics to Radar, SPOT and ERS Applications
[ISBN-2-85428-345-7] p 3747 N94-32523
Contribution of SAR ERS1 data to study the French Guiana tropical coast environment
[BRGM-93034] p 3748 N94-32527
Monitoring land cover and crop types in Denmark using ERS-1 SAR and optical satellite images p 3748 N94-32528
The use of ERS images for mapping p 3749 N94-32531
Example of SPOT/ERS-1 complementarity p 3749 N94-32533
Restoration of interferometric, polarimetric, radiometric, and textural information in SAR images p 3750 N94-32535
Assessment of region-based methods for automated SAR/optical registration, attribute extraction, and classification p 3750 N94-32536
Airborne SAR as a complement to SPOT HRV in land-cover classification: The use of normalization and principal components analysis p 3750 N94-32539
Ship traffic monitoring and oil spill detection using the ERS-1 SAR p 3751 N94-32542
SAR image feature extraction system: A pre-operational application of ERS-1 SAR p 3751 N94-32543
Almaz marine applications p 3751 N94-32544
The use of ERS-1 within an operational ice monitoring program p 3751 N94-32545
The use of SPOT and ERS-1 images to map the eruption of Nevado Sabancaya (Province of Arequipa, South Peru) and evaluate associated risks p 3751 N94-32546
Respective contributions of VIS-PIR, SAR-ERS 1, and airborne radar data for morphostructural and morphoneotectonic analysis: Practical examples p 3752 N94-32549
Use of SPOT and ERS-1 SAR data to study the tectonic and climatic history of arid regions p 3752 N94-32550
Structural study in an alteritic region: Contribution of ERS-1 SAR data of the Mauges Plateau (Loire Atlantique, France)
[BRGM-93032] p 3752 N94-32551
Evaluation of the potential of SAR data for mapping of landslide risks
[BRGM-93033] p 3753 N94-32552
Use of SPOT and ERS-1 to map tropical vegetation and mangrove dynamics in Guiana p 3753 N94-32555
A case study comparing multi-temporal ERS-1 SAR data and SPOT data for tropical forest mapping p 3753 N94-32556
Application of ERS-1 SAR data for hydrological studies p 3754 N94-32558
Synergy of thermal infrared and microwave remote sensing for evaporation estimation p 3754 N94-32559
Monitoring landsurface characteristics in Niger using complementary SPOT and ERS-1 SAR data p 3754 N94-32560
Possible complementarity of SPOT/ERS in mapping land use: Study on agricultural land in Brittany (France) p 3755 N94-32563
ERS-1 SAR and optical data for land use/land cover mapping: A case study in a savannah zone of Guinea p 3755 N94-32565
SAR interferometry with ERS-1 p 3755 N94-32566
Techniques and applications of SAR interferometry for ERS-1 p 3756 N94-32568
Developments in ERS-1 SAR interferometry: Use of the spectral shift p 3756 N94-32569
Fields of experiments in ERS-1 SAR interferometry in Bonn and Naples p 3756 N94-32572
The processing technology and some applications of Almaz-1 data p 3756 N94-32573
Ultra wide band radar holographic imaging of subsurface targets
[DE94-004271] p 3713 N94-32681
SYNTHETIC APERTURES
Ultra wide band radar holographic imaging of subsurface targets
[DE94-004271] p 3713 N94-32681
SYNTHETIC FUELS
Heterogeneous catalytic process for alcohol fuels from syngas
[DE94-008729] p 3667 N94-32583
SYSTEM EFFECTIVENESS
The relationship between integrative task design for information systems professionals and perceived information systems effectiveness p 3919 N94-32487
Multidimensional scaling of user information satisfaction
[AD-A277230] p 3920 N94-32633
SYSTEM FAILURES
Spacecraft contamination issues from LDEF: Issues for design p 3592 N94-31020
Principles of ultradependability in chaotic routing
[AD-A277422] p 3827 N94-32995
SYSTEM IDENTIFICATION
A new methodology of system parameter estimation
[MATHS-REPT-A-208] p 3808 N94-31163
Optimal adaptive estimation algorithm for harmonic current reduction using power limited active line conditioners
[AD-A277354] p 3693 N94-32336
Stochastic realization of a Gaussian stochastic control system
[CWI-BS-R9320] p 3852 N94-32350
Parametric robust control and system identification: Unified approach
[NASA-CR-195826] p 3836 N94-32980
SYSTEMS ANALYSIS
A new methodology of system parameter estimation
[MATHS-REPT-A-208] p 3808 N94-31163
Covert channel analysis of trusted systems. A guide to understanding
[AD-A276418] p 3916 N94-31331
On a formal approach to the methodology of information planning
[MEMO-INF-93-42] p 3917 N94-31415
Modal analysis of multiterminal high voltage direct current transmission
[DE94-006426] p 3691 N94-31785
System analysis of ultra-wideband instrumentation radars: Impulse versus stepped-chirp approaches
[AD-A276624] p 3677 N94-32087
World height system definition and implementation
[AD-A276725] p 3747 N94-32160
A polling system with a dormant server
[CWI-BS-R9313] p 3835 N94-32193
Hierarchical modeling for reliability analysis using Markov models
[NASA-CR-188288] p 3731 N94-32862
SYSTEMS ENGINEERING
A new methodology of system parameter estimation
[MATHS-REPT-A-208] p 3808 N94-31163
A neural network methodology for engineering applications: The learning control of robotic systems
[RR-480] p 3830 N94-31500
Effective information modelling support
[PB94-148236] p 3917 N94-31586
Modular Simulator System (MSS). System/segment specification for the generic modular simulator system-flight station module, volume 2
[AD-A276969] p 3588 N94-32313
A PC program to optimize system configuration for desired reliability at minimum cost p 3823 N94-32438
Research and technology, 1993
[NASA-TM-106376] p 3567 N94-33046
Real-time centimeter positioning with GPS: A system developed by the US Army Corps of Engineers
[AD-A278152] p 3577 N94-33095
SYSTEMS INTEGRATION
Channel and terminal description of the ACTS mobile terminal p 3599 N94-31428
An information system organized as stratified hypermedia
[TR-93-12] p 3918 N94-32289
Modular Simulator System (MSS). System/segment specification for the generic MSS-system integration, volume 1
[AD-A276968] p 3588 N94-32312
Modular Simulator System (MSS): Interface design document for the generic MSS
[AD-A277270] p 3590 N94-32403
SYSTEMS MANAGEMENT
DoD information systems capacity management function
[AD-A275987] p 3916 N94-31355
SYSTEMS SIMULATION
A finite state machine model for object oriented systems
[REPT-93-040] p 3809 N94-31212
SYSTEMS STABILITY
Structural stability and bifurcations p 3911 N94-31895

T

T TAURI STARS
Observations of accretion and angular momentum regulation in young circumstellar disks and the implications for planetary formation p 3928 N94-31122
Evolution of dynamo-generated magnetic fields in accretion disks around compact and young stars p 3931 N94-31138
Multiwavelength search for protoplanetary disks p 3599 N94-31430
TABS (CONTROL SURFACES)
Shear flow control of cold and heated rectangular jets by mechanical tabs. Volume 1: Results and discussion
[NASA-CR-182296-VOL-1] p 3708 N94-32867
Shear flow control of cold and heated rectangular jets by mechanical tabs. Volume 2: Tabulated data
[NASA-CR-182296-VOL-2] p 3709 N94-32869
Enhancement of mixing in a rectangular jet by mechanical tabs
[NASA-CR-185207] p 3709 N94-32872
TAKEOFF
Scattering of a random acoustic field by an infinite cylinder: Application to the modelization of the acoustic environment of the 'Ariane 5' launcher scale-model using experimental data
[ONERA-NT-1993-11] p 3860 N94-31226
TALKING
Spectral analysis method and sample generation for real time visualization of speech
[ETN-94-95732] p 3674 N94-31573
TANTALUM ALLOYS
Electrooptic crystal growth and properties
[AD-A276023] p 3896 N94-31439
TARGET ACQUISITION
Peak detection of Swerling type targets. Part 1: Detection probabilities in white noise
[AD-A276217] p 3670 N94-31062
Analysis using bi-spectral related technique
[AD-A276017] p 3672 N94-31386
Waveform generation for ultra-wideband radar system
[AD-A276352] p 3673 N94-31401
Detection of a chi-square fluctuating target in Gaussian noise
[AD-A276078] p 3850 N94-31462
Visual processing of object velocity and acceleration
[AD-A277425] p 3801 N94-32998
The application of a radial basis function neural network for radar tracking over the sea p 3686 N94-33150
Some neural computing approaches to target tracking p 3837 N94-33151
Multi-sensor data fusion for target acquisition p 3837 N94-33154
TARGET RECOGNITION
Atmospheric propagation effects through natural and man-made obscurants for visible to MM-wave radiation
[AD-A276919] p 3679 N94-32235
Correlation filter synthesis using neural networks
[AD-A278124] p 3836 N94-33043
A novel optoelectronic system for distortion-invariant ATR
[AD-A277985] p 3884 N94-33087
Multi-sensor data fusion for target acquisition p 3837 N94-33154
TASK PLANNING (ROBOTICS)
A high-performance multi-arm environment: Theoretical aspects and practical implementation
[RR-479] p 3722 N94-31379
Contingency-tolerant robot motion planning and control p 3830 N94-31482
Advanced teleoperation: Technology innovations and applications p 3806 N94-32453

TAXIING
Evaluation for the development of taxiway lighting intensity standards
[AD-A276706] p 3588 N94-32120
TAYLOR SERIES
Probability distributions with given marginals and given correlation that have maximal entropy
[REPT-93-81] p 3851 N94-31698
Light-traffic analysis for queues with spatially distributed arrivals
[MEMO-1150] p 3832 N94-31826
TEARING
Tearing resistance of a thin shell against projectile penetration: Material property effects
[DE94-007486] p 3733 N94-31316
TEARING MODES (PLASMAS)
Stability of tearing modes in tokamak plasmas
[DE94-009205] p 3892 N94-32911
TECHNOLOGIES
OPTIONS for systemic change in mathematics, science, and technology education: Scientist/teacher partnerships
[DE94-007472] p 3914 N94-32910
TECHNOLOGY ASSESSMENT
High-temperature superconducting transformer performance, cost, and market evaluation
[DE94-005494] p 3687 N94-31152
Active matrix liquid crystal display. Industry survey results
[AD-A276415] p 3895 N94-31329
Technical assessment of Mir-1 life support hardware for the international space station
[NASA-TM-108441] p 3803 N94-31380
Semiconductor microcavity lasers
[DE94-006143] p 3716 N94-31622
Benchmarking of the state-of-the-art in nondestructive testing/evaluation for applicability in the Composite Armored Vehicle (CAV) Advanced Technology Demonstrator (ATD) program, phase 1
[AD-A276660] p 3730 N94-32088
LLNL casting technology
[DE94-008282] p 3669 N94-32839
Application of a design-build-team approach to low cost and weight composite fuselage structure
[NASA-CR-4418] p 3626 N94-32863
TECHNOLOGY TRANSFER
Photovoltaics: Program overview, fiscal year 1993
[DE94-000246] p 3758 N94-31235
Cleanroom engineering handbook. Volume 1: Cleanroom engineering process introduction and overview
[AD-A275949] p 3587 N94-31356
Naval Surface Warfare Center Dahlgren Division Technical Digest: Advanced materials technology
[AD-A276448] p 3668 N94-31364
Renewable energy technology development at Sandia National Laboratories
[DE94-007734] p 3761 N94-32383
Technology 2003: The Fourth National Technology Transfer Conference and Exposition, volume 2
[NASA-CP-3249] p 3956 N94-32420
Information systems to enhance technology exchange
[DE94-007744] p 3920 N94-32808
Sandia's photonic program and its changing national role
[DE94-008616] p 3883 N94-32878
Research and technology, 1993
[NASA-TM-106376] p 3567 N94-33046
TECHNOLOGY UTILIZATION
High-temperature superconducting transformer performance, cost, and market evaluation
[DE94-005494] p 3687 N94-31152
Putting the information infrastructure to work: Report of the Information Infrastructure Task Force Committee on Applications and Technology
[NIST/SP-857] p 3916 N94-31228
AMS beyond 2000
[DE94-006666] p 3632 N94-31352
A study of theoretical models for managing technology change and a comparison to a radio frequency identification implementation
[AD-A276012] p 3672 N94-31385
The contribution of aeronautics and astronautics to the quality of life on Earth
[ILR-MITT-283(1993)] p 3764 N94-31611
Workshop on Commercialization of Pulsed Power Science and Technology Proceedings
[AD-A276987] p 3692 N94-32258
Advanced teleoperation: Technology innovations and applications p 3806 N94-32453
Research and technology, 1993
[NASA-TM-106376] p 3567 N94-33046
Spacecraft environmental anomalies expert system
[AD-A277962] p 3612 N94-33262
Advanced release technologies program p 3607 N94-33322
TECTONICS
Tectonic History of the Terrestrial Planets
[NASA-CR-195696] p 3939 N94-31105
Patterns of deformation and volcanic flows associated with lithospheric loading by large volcanoes on Venus p 3776 N94-31106
Aspects of modelling the tectonics of large volcanoes on the terrestrial planets p 3940 N94-31107
State of stress, faulting, and eruption characteristics of large volcanoes on Mars p 3940 N94-31108
Geoid-to-topography ratios on Venus: A global perspective p 3940 N94-31110
The tectonic and volcanic evolution of Venus: Catastrophic or gradual? p 3940 N94-31111
A tectonic resurfacing model for Venus p 3941 N94-31113
The resurfacing controversy for Venus: An overview and a mechanistic perspective p 3941 N94-31114
Plains tectonism on Venus: The deformation belts of Lavinia Planitia p 3941 N94-31115
Respective contributions of VIS-PIR, SAR-ERS 1, and airborne radar data for morphostructural and morphoneotectonic analysis: Practical examples p 3752 N94-32549
Use of SPOT and ERS-1 SAR data to study the tectonic and climatic history of arid regions p 3752 N94-32550
TEFLON (TRADEMARK)
Performance of silvered Teflon (trademark) thermal control blankets on spacecraft p 3591 N94-31014
Follow-up on the effects of the space environment on UHCRE thermal blankets p 3592 N94-31018
Ground-based simulation of LEO environment: Investigations of a select LDEF material: FEP Teflon (trademark) p 3596 N94-31039
TELECOMMUNICATION
The Nomad Explorer assembly assist vehicle: An architecture for rapid global extraterrestrial base infrastructure establishment p 3599 N94-31429
TELECONNECTIONS (METEOROLOGY)
Short term teleconnections associated with an individual tropical cyclone
[AD-A277210] p 3783 N94-32019
TELEMETRY
Data processing algorithms for on-board satellite event analysis
[AD-A278406] p 3838 N94-33168
TELEOPERATORS
Adaptive control of telerobotic systems worn by humans
[AD-A276608] p 3834 N94-32036
Advanced teleoperation: Technology innovations and applications p 3806 N94-32453
Technology transfer of operator-in-the-loop simulation p 3802 N94-32472
Development of an interchangeable end effector mechanism for the Ranger telerobotic vehicle p 3604 N94-33297
TELEPHONES
Remote sensing for urban planning p 3758 N94-32465
TELEPHONY
Remote sensing for urban planning p 3758 N94-32465
Reliable communication in the presence of severe noise or jamming
[AD-A278410] p 3684 N94-33173
TELEROBOTICS
Remote robot manipulator coupled with remote-controlled guide vehicle for soil sampling in hazardous waste sites p 3723 N94-31569
Applying robotics to HAZMAT p 3729 N94-32452
Advanced teleoperation: Technology innovations and applications p 3806 N94-32453
Technology transfer of operator-in-the-loop simulation p 3802 N94-32472
Development of an interchangeable end effector mechanism for the Ranger telerobotic vehicle p 3604 N94-33297
TELESCOPES
Design and early results of the sodium-layer laser guide star adaptive optics experiment at the Lawrence Livermore National Laboratory
[DE94-006653] p 3926 N94-32189
Digital image profilers for detecting faint sources which have bright companions
[NASA-CR-191348] p 3927 N94-32695
TELEVISION SYSTEMS
The development and testing of a backscatter absorption gas imaging (BAGI) system designed to image at a range of 300 m
[DE94-006192] p 3675 N94-31761
Welcome to the Ohio Aerospace Institute
[NASA-TM-109756] p 3913 N94-31815
TELLURIUM ALLOYS
Structural ordering in liquid K-Te alloys
[DE94-008477] p 3645 N94-32514
TEMPERATURE CONTROL
Performance of silvered Teflon (trademark) thermal control blankets on spacecraft p 3591 N94-31014
Space environment durability of beta cloth in LDEF thermal blankets p 3591 N94-31015
Draft minutes of IAPG Mechanical Working Group meeting
[DE94-004954] p 3759 N94-31266
Metal hydride heat pump engineering demonstration and evaluation model
[NASA-CR-188286] p 3669 N94-32857
Combined contamination and space environmental effects on solar cells and thermal control surfaces
[NASA-TM-106592] p 3617 N94-33022
TEMPERATURE DEPENDENCE
The 4f heavy fermion photoelectron spectra do not exhibit the Kondo scale
[DE94-006252] p 3898 N94-31631
Acoustic emission from crack growth in 7050 aluminum and 7075 aluminum as a function of temperature and heat treatment
[DREP-CRS-93-15] p 3642 N94-31871
Fermi surface instability at 0.4 K in a heavy-fermion YbBiPt: SDW?
[DE94-006224] p 3899 N94-31916
Creep-fatigue criteria and inelastic behavior of modified 9Cr-1Mo steel at elevated temperatures
[DE94-007915] p 3642 N94-31918
Temperature dependence of the exciton-exciton annihilation rate constant in poly(di-n-hexylsilane)
[DE94-005584] p 3655 N94-32102
Computerized Ultrasonic Testing System (CUTS) for in-process thickness determination p 3862 N94-32456
Computational modeling of convective heat transfer to liquid hydrogen coolant p 3707 N94-32485
Rate coefficient for the reaction H + O2 yields OH + O: Results from 2000 to 5300 K
[DE94-008105] p 3871 N94-32615
The relative performance of FeS2 and CoS in long-life thermal-battery applications
[DE94-006145] p 3695 N94-32663
Temperature dependence of single-event burnout in n-channel power MOSFET's
[AD-A277921] p 3698 N94-33177
TEMPERATURE DISTRIBUTION
Atomic oxygen interaction at defect sights in protective coatings on polymers flown on LDEF p 3593 N94-31024
CO observations in external galaxies and gas mass determination p 3925 N94-31790
Computational modeling of convective heat transfer to liquid hydrogen coolant p 3707 N94-32485
IRTM brightness temperature maps of the Martian south polar region during the polar night: The cold spots don't move p 3949 N94-33222
TEMPERATURE EFFECTS
Computational study of single-expansion-ramp nozzles with external burning
[NASA-TM-106550] p 3700 N94-31229
Tensile properties of commercially pure vanadium from room temperature to 1200 C
[DE94-006822] p 3641 N94-31581
Experimental evidence for lattice effects in high temperature superconductors
[DE94-006250] p 3899 N94-31633
A model of the ion chemistry of electrified convection p 3868 N94-31993
Effects of interphases on the mechanical, thermal and hygromechanical response of fiber-reinforced composites p 3624 N94-32496
Temperature-humidity-bias aging technique to identify defective surface mount capacitors
[DE94-005354] p 3660 N94-32727
Deuterium absorption and material phase characteristics of SAES St198 Zr-Fe alloy
[DE94-008275] p 3646 N94-32781
Effect of elevated temperature and cyclic loading on properties and damage modes in ceramic composites
[DE94-008736] p 3662 N94-32891
Numerical model of the thermal behavior of an extremity in a cold environment including counter-current heat exchange between the blood vessels
[AD-A278099] p 3798 N94-33040
Advanced high frequency partial discharge measuring system
[NASA-CR-195240] p 3697 N94-33044
Space flight printed wiring board measling investigation
[NASA-TM-104602] p 3732 N94-33101
Development of lightweight ceramic ablators and arc-jet test results
[NASA-TM-108798] p 3617 N94-33117
Structural damping studies at cryogenic temperatures
[NASA-TM-109073] p 3740 N94-33118

Physics of heat pipe rewetting
[NASA-CR-195902] p 3913 N94-33148
Implementation of heaters on thermally actuated spacecraft mechanisms p 3607 N94-33320

TEMPERATURE MEASUREMENT
Profiling ALACE instruments
[AD-A277246] p 3789 N94-32321
Design of a two dimensional planer pressurized air labyrinth seal test rig
[AD-A277232] p 3726 N94-32370
Homogeneous global mean temperature time series
[DE94-002194] p 3766 N94-32690
Radiometry spot measurement system
[NASA-TM-106561] p 3883 N94-32777
High resolution molecular spectroscopy of atmospheric species
[AD-A278382] p 3776 N94-33351

TEMPERATURE MEASURING INSTRUMENTS
Radiometry spot measurement system
[NASA-TM-106561] p 3883 N94-32777

TEMPERATURE PROFILES
Effects of the deep tropical convection in the large scale atmospheric flow p 3778 N94-30994
Multiwavelength search for protoplanetary disks p 3599 N94-31430
Profiling ALACE instruments
[AD-A277246] p 3789 N94-32321
Mars atmospheric dust properties: A synthesis of Mariner 9, Viking, and Phobos observations p 3945 N94-33200

TEMPORAL RESOLUTION
A case study comparing multi-temporal ERS-1 SAR data and SPOT data for tropical forest mapping p 3753 N94-32556

TENDONS
Minimization of carpal tunnel syndrome
[AD-A276409] p 3795 N94-31363

TENSILE CREEP
Toughening mechanisms in the high strain rate deformation of rubber-modified polymer glasses p 3653 N94-31942
High-temperature deformation and fracture toughness of duplex ceramic microstructures p 3653 N94-31945

TENSILE DEFORMATION
An approximate solution for interlaminar stresses in laminated composites p 3621 N94-31901
Bond stress-slip characteristics of FRP rebars
[AD-A277191] p 3623 N94-32070

TENSILE PROPERTIES
Tensile properties of commercially pure vanadium from room temperature to 1200 C
[DE94-006622] p 3641 N94-31581
Evaluating in-plane elastic constants of damaged carbon-epoxy laminates using a quantitative ultrasonic technique p 3621 N94-31793
Boron and hydrogen in Ni3Al. Part 2: Mechanical testing of bicrystals
[DE94-007441] p 3904 N94-32606
Influence of volume fraction of component materials and interlayer bond strength on fracture toughness of multi-layer Al 6090-25 volume percent SiCp and Al 5182 laminates
[DE94-007141] p 3626 N94-32665

TENSILE STRENGTH
Ceramic Technology Project database
[DE94-008494] p 3659 N94-32632
Development of stitched/RTM composite primary structures p 3628 N94-33127

TENSILE STRESS
Torque-balanced extendable fiber optic cable
[AD-D016097] p 3882 N94-32719

TENSILE TESTS
Tensile properties of commercially pure vanadium from room temperature to 1200 C
[DE94-006622] p 3641 N94-31581
Irradiation-assisted stress corrosion cracking of materials from commercial BWRs: Role of grain-boundary microchemistry
[DE94-006542] p 3643 N94-32109
Boron and hydrogen in Ni3Al. Part 2: Mechanical testing of bicrystals
[DE94-007441] p 3904 N94-32606

TENSION
Space Station Freedom Solar Array tension mechanism development p 3604 N94-33300

TENSORS
Tensor gauge potentials in loop space formulation of Yang-Mills fields
[PB94-147147] p 3912 N94-31924

TERMINAL BALLISTICS
Tearing resistance of a thin shell against projectile penetration: Material property effects
[DE94-007466] p 3733 N94-31316
Experimental measurement of dynamic failure and fragmentation properties of metals
[DE94-007377] p 3737 N94-32135

TERMINAL FACILITIES
Cockpit Electronic Display Workshop: A synopsis
[AD-A277728] p 3583 N94-33280

TERMINOLOGY
Total Quality Management implementation guidelines
[DE94-007232] p 3915 N94-32723

TERMS
DTIC Thesaurus on diskette with dBase 4.1 runtime (computer diskette)
[AD-M000306] p 3922 N94-33256
DTIC Thesaurus on diskette (ASC2) (computer diskette)
[AD-M000309] p 3922 N94-33257
DTIC Thesaurus on diskette without runtime (computer diskette)
[AD-M000310] p 3923 N94-33258
DTIC Thesaurus on diskette without runtime (computer diskette)
[AD-M000312] p 3923 N94-33259

TERNARY SYSTEMS
Phase relationships and stability of the (mu)- and (zeta)-phases in the Ag-Al-X (X=Zn, Ga, Ge) systems
[DE94-009391] p 3648 N94-33270

TERRAIN
A paraperspective factorization method for shape and motion recovery
[AD-A276513] p 3712 N94-31929
Alternatives to hierarchical techniques in stereo correlation
[AD-A276570] p 3746 N94-31938
Monitoring landsurface characteristics in Niger using complementary SPOT and ERS-1 SAR data p 3754 N94-32560
A multitasking behavioral control system for the Robotic All Terrain Lunar Exploration Rover (RATLER)
[DE94-007293] p 3835 N94-32787
Numerical simulation of thermally induced near-surface flows over Martian terrain p 3949 N94-33223

TERRAIN ANALYSIS
Example of SPOT/ERS-1 complementarity p 3749 N94-32533
Production of terrain data: Optical radar complementarity p 3750 N94-32540
Evaluation of the potential of SAR data for mapping of landslide risks
[BRGM-93033] p 3753 N94-32552
Study of subpolar glaciers of Spitzbergen using SPOT, ERS-1, and hypsometric data: Results and perspectives p 3753 N94-32553
Comparing SPOT and SIR A for mapping superficial formations in tropical forest regions: Example of the Yaoundy Region (Cameroon) p 3755 N94-32562
Evaluation of surface phase change on large zones p 3755 N94-32567
Precision and level of artefacts in the computation of digital terrain models by interferometry p 3756 N94-32571
Fields of experiments in ERS-1 SAR interferometry in Bonn and Naples p 3756 N94-32572

TERRESTRIAL PLANETS
Tectonic History of the Terrestrial Planets
[NASA-CR-195696] p 3939 N94-31105
Aspects of modelling the tectonics of large volcanoes on the terrestrial planets p 3940 N94-31107

TEST CHAMBERS
Design of a two dimensional planer pressurized air labyrinth seal test rig
[AD-A277232] p 3726 N94-32370

TEST EQUIPMENT
Design of a two dimensional planer pressurized air labyrinth seal test rig
[AD-A277232] p 3726 N94-32370

TEST FACILITIES
Analysis of beam-on-target interaction in a neutron-source test facility
[DE94-005392] p 3863 N94-31151
Implementation of instruments and facilities at the SGP CART site
[DE94-006839] p 3781 N94-31322
Aerospace test facilities at NASA LERC Plumbrook
[NASA-TM-109755] p 3602 N94-31814
Real-time control and application to robotics: Hardware and software architectures
[ISBN-0-315-87192-X] p 3833 N94-31876
Design of a cold-flow test facility for the high pressure fuel turbopump turbine of the Space Shuttle main engine
[AD-A276743] p 3615 N94-32182
High power switch design for the Nova upgrade laser (Project HERCULES: High Energy Research Concerning the Ultimate Lifetime of Experimental Switches)
[DE94-007921] p 3719 N94-32654
The preliminary evaluation of liquid lubricants for space applications by vacuum tribometry p 3606 N94-33313

TEST PATTERN GENERATORS
A hierarchical approach to test generation for CMOS VLSI circuits
[ISBN-9-09-005449-9] p 3689 N94-31535

TEST RANGES
Hydrologic Database user's manual
[DE94-003950] p 3743 N94-31603

TEST STANDS
Implementation of instruments and facilities at the SGP CART site
[DE94-006839] p 3781 N94-31322
An experimental testbed for a free-floating manipulator
[AD-A277350] p 3726 N94-32334

TETRAETHYL ORTHOSILICATE
Preparation of catalyst particles using methods of colloid chemistry. Part 1: Preparation of silica particles from alcohol solutions
[PB94-135597] p 3634 N94-31679

TETRAGONS
Eta percent-superconvergence in the interior of locally refined meshes of quadrilaterals: Superconvergence of the gradient in finite element solutions of Laplace's and Poisson's equations
[AD-A277242] p 3848 N94-32331

TETRAHEDRONS
Rare Earth Doped Semiconductors and Materials Research Society Symposium Proceedings, Volume 301
[AD-A277517] p 3908 N94-33055

TEXTBOOKS
Solar physics and terrestrial effects. A curriculum guide for teachers, grade 7-12
[PB94-142247] p 3953 N94-31595

TEXTILES
Analysis of new composite architectures
[NASA-CR-195303] p 3626 N94-32904
Fracture micromechanics of continuous fiber and textile reinforced metal and ceramic matrix composites
[AD-A277434] p 3627 N94-33008
Second NASA Advanced Composites Technology Conference
[NASA-CP-3154] p 3627 N94-33121
Recent progress in NASA Langley Research Center textile reinforced composites program p 3629 N94-33134
Advanced textile applications for primary aircraft structures p 3629 N94-33135
Comparison of resin film infusion, resin transfer molding, and consolidation of textile preforms for primary aircraft structure p 3630 N94-33136
Characterization and manufacture of braided composites for large commercial aircraft structures p 3630 N94-33137

TEXTS
Detecting the erosion of hierarchic information structures
[RUU-CS-93-10] p 3916 N94-31365
High-speed data search p 3923 N94-32441
Emacs Lisp in Edwin scheme
[AD-A276721] p 3818 N94-32504
Finding all periods and initial palindromes of a string in parallel
[AD-B175069] p 3827 N94-33002

TEXTURES
Texture generation on irregular regions
[AD-A275999] p 3841 N94-31359
Radar image classification by texture measurements
[ONERA-NT-1993-3] p 3673 N94-31419
Visual evaluation of computer-generated textures
[AD-A277201] p 3816 N94-32093
Quantitative analysis of woody vegetation in Soudano-Sahalian region. Textural approach (application to a Burkina Faso region) p 3757 N94-32574

THALLIUM COMPOUNDS
The path for long range conduction in high J(sub c) TlBa2Ca2Cu3O(8+x) spray-pyrolyzed deposits
[DE94-007211] p 3909 N94-33271

THEMATIC MAPPERS (LANDSAT)
Comparison of SPOT, ERS-1, SEASAT, LANDSAT TM, and merged imagery for geological investigations p 3752 N94-32547
Optimal geological data extraction from SPOT-radar synergism with samples from Djebel Amour (Algeria), Red Sea Hills (Sudan), Sirte Basin (Libya), and Magdalena Valley (Colombia) p 3752 N94-32548
Rapid estimates of crop acreage and production at European scale using high resolution imagery p 3754 N94-32557
ERS-1 SAR and optical data for land use/land cover mapping: A case study in a savannah zone of Guinea p 3755 N94-32565

THEMATIC MAPPING
The effects of vegetation on the ability to map soils using GERIS data p 3744 N94-31860
A case study comparing multi-temporal ERS-1 SAR data and SPOT data for tropical forest mapping p 3753 N94-32556

Comparing SPOT and SIR A for mapping superficial formations in tropical forest regions: Example of the Yaoundy Region (Cameroon) p 3755 N94-32562
ERS-1 SAR and optical data for land use/land cover mapping: A case study in a savannah zone of Guinea p 3755 N94-32565

THEOREM PROVING
Formal verification of systolic multipliers with the Boyer-Moore theorem prover
[RR-897-M] p 3839 N94-31082
OTTER 3.0 reference manual and guide
[DE94-007457] p 3829 N94-31315
Proving theorems of the Lambek calculus of order 2 in polynomial time
[CT-93-05] p 3842 N94-31393
The p-q-r-medial axis algorithm requires only local operations
[CWI-BS-R9317] p 3849 N94-32507
Interpreter composition issues in the formal verification of a processor-memory module
[NASA-CR-4594] p 3820 N94-32775

THEOREMS
Remarks on a result of LAV Carvalho
[AD-A276404] p 3841 N94-31360
Generalization of a theorem of Kusmin
[REPT-93-74] p 3844 N94-31643
The Cameron-Martin theorem
[W-9315] p 3844 N94-31676
The p-q-r-medial axis algorithm requires only local operations
[CWI-BS-R9317] p 3849 N94-32507

THEORETICAL PHYSICS
Conformal field theory and geometry of strings
[PB94-148442] p 3857 N94-31770
New QCD results from string theory
[DE94-005226] p 3911 N94-31823
The 14th Annual West Coast Theoretical Chemistry/Statistical Mechanics Conference
[AD-A276942] p 3656 N94-32239
Research program in particle physics
[DE94-008449] p 3871 N94-32512

THERMAL ANALYSIS
A thermal viscoelastic analysis for thick-walled composite cylinders
[AD-A274143] p 3625 N94-32604
THERM3D: A boundary element computer program for transient heat conduction problems
[DE94-008112] p 3708 N94-32709
Novel precursor approached for CMC derived by polymer pyrolysis
[AD-A278383] p 3665 N94-33352

THERMAL BATTERIES
The relative performance of FeS2 and CoS in long-life thermal-battery applications
[DE94-006145] p 3695 N94-32663

THERMAL BUCKLING
Effective computational strategy for predicting the response of complex systems
[AD-A277452] p 3740 N94-33011

THERMAL CONDUCTIVITY
The impact of LDEF results on the space application of metal matrix composites p 3595 N94-31034
Materials processing and manufacturing technologies for diamond substrates multichip modules
[AD-A276904] p 3692 N94-32215
Ceramic Technology Project database
[DE94-008494] p 3659 N94-32632
Snowmelt forecasting. Further cold regions development of operational hydrological forecasting, volume 2
[AD-A278123] p 3757 N94-33269

THERMAL CONTROL COATINGS
The performance of thermal control coatings on LDEF and implications to future spacecraft p 3591 N94-31013
Anodized aluminum on LDEF p 3592 N94-31017
Fluorescence observations of LDEF exposed materials as an indicator of induced material reactions p 3593 N94-31025

THERMAL CYCLING TESTS
Laser-induced fluorescence of space-exposed polyurethane p 3593 N94-31026
Space environmental effects on polymer composites: Research needs and opportunities p 3595 N94-31035
Pre-flight testing of Thermoelectric Quartz Crystal Microbalances (TQCM) for midcourse space experiment (MSX) spacecraft
[AD-A277054] p 3610 N94-32010

THERMAL DEGRADATION
Fatigue in single crystal nickel superalloys
[AD-A276662] p 3643 N94-32047

THERMAL DIFFUSIVITY
Ceramic Technology Project database
[DE94-008494] p 3659 N94-32632

THERMAL EMISSION
Dual-band infrared imaging to detect corrosion damage within airframes and concrete structures
[DE94-006047] p 3580 N94-32658
Thermal emission measurements (5-25 microns) of Hawaiian palagonitic soils with implications for Mars p 3944 N94-33193
Thermal studies of Martian channels and valleys using Termoskan data: New results p 3944 N94-33194
Regional sedimentological variations among dark crater floor features: Toward a model for modern eolian sand distribution on Mars p 3946 N94-33203
Temporal and spatial mapping of atmospheric dust opacity and surface albedo on Mars p 3947 N94-33211

THERMAL ENERGY
Thermal continua of AGN accretion disks p 3931 N94-31137
Stability and precipitation kinetics in Si(1-y)C(y)/Si and Si(1-x-y)Ge(x)C(y)/Si heterostructures prepared by solid phase epitaxy
[DE94-006589] p 3902 N94-32296

THERMAL ENVIRONMENTS
Light in Thermal Environments (LITE) Workshop
[NASA-CR-195851] p 3790 N94-32981

THERMAL EXPANSION
Thermal-vacuum response of polymer matrix composites in space p 3595 N94-31033
The impact of LDEF results on the space application of metal matrix composites p 3595 N94-31034
Chemical vapor deposition fluid flow simulation modelling tool
[NASA-CR-189648] p 3707 N94-32480
Mechanics of cracking for composite material p 3624 N94-32501
Inorganic polymer engineering materials
[DE94-008519] p 3659 N94-32655
Interface engineering in oxide fiber/oxide matrix composites
[AD-A277672] p 3627 N94-33029

THERMAL FATIGUE
The impact of LDEF results on the space application of metal matrix composites p 3595 N94-31034
Development and characterization of intermediary layers allowing the bond between a metal alloy and a plasma sprayed ceramic
[ECL-91-39] p 3619 N94-31377
Thermal-mechanical fatigue crack growth in aircraft engine materials
[ISBN-0-315-86543-1] p 3734 N94-31707
Fatigue in single crystal nickel superalloys
[AD-A276662] p 3643 N94-32047

THERMAL INSTABILITY
Disk instability and the spectral evolution of the 1992 outburst of the intermediate polar GK Persei p 3928 N94-31123
Disk irradiation and light curves of x ray novae p 3929 N94-31124
Can a variable alpha induce limit cycle behavior and exponential luminosity decay in transient soft x ray sources? p 3929 N94-31129
The physics of black hole x ray novae p 3932 N94-31143

THERMAL INSULATION
Space environment durability of beta cloth in LDEF thermal blankets p 3591 N94-31015
Follow-up on the effects of the space environment on UHCRE thermal blankets p 3592 N94-31018
The prediction of convective transfer on the thermal insulation of a solid-propellant rocket motor
[ONERA-NT-1993-15] p 3614 N94-31423
Proceedings of the DCIEM Diver Thermal Protection Workshop
[DCIEM-92-10] p 3795 N94-31738
Thermotropic liquid crystals: A variable Clo material p 3796 N94-31739

THERMAL MAPPING
Thermal studies of Martian channels and valleys using Termoskan data: New results p 3944 N94-33194
Regional sedimentological variations among dark crater floor features: Toward a model for modern eolian sand distribution on Mars p 3946 N94-33203
Temporal and spatial mapping of atmospheric dust opacity and surface albedo on Mars p 3947 N94-33211
Studies of atmospheric dust from Viking IR thermal mapper data p 3948 N94-33216
IRTM brightness temperature maps of the Martian south polar region during the polar night: The cold spots don't move p 3949 N94-33222

THERMAL NOISE
Computer implementation of Arnott's formulation of thermoacoustics using MATLAB
[AD-A276356] p 3860 N94-31257

THERMAL PROTECTION
Development and characterization of intermediary layers allowing the bond between a metal alloy and a plasma sprayed ceramic
[ECL-91-39] p 3619 N94-31377
Proceedings of the DCIEM Diver Thermal Protection Workshop
[DCIEM-92-10] p 3795 N94-31738
Thermotropic liquid crystals: A variable Clo material p 3796 N94-31739

THERMAL RADIATION
Thermal continua of AGN accretion disks p 3931 N94-31137
Radiometry spot measurement system
[NASA-TM-106561] p 3883 N94-32777
Light in Thermal Environments (LITE) Workshop
[NASA-CR-195851] p 3790 N94-32981

THERMAL SHOCK
Mechanical properties of vacuum-sintered yttria ceramics
[DE94-008138] p 3659 N94-32617

THERMAL STABILITY
Advanced thermally stable jet fuels
[DE94-006760] p 3667 N94-32150
Characterization of thermally stable dye-doped polyimide based electrooptic materials
[DE94-005309] p 3882 N94-32674
An investigation of the radiolytic stability of a resorcinol-formaldehyde ion exchange resin
[DE94-007971] p 3660 N94-32698
The development of precipitated iron catalysts with improved stability
[DE94-008711] p 3638 N94-32886
The effect of prolonged exposure to 750 C air on the tribological performance of PM212
[NASA-TM-106472] p 3617 N94-32941
Novel polydiacetylenes as materials for second and third order nonlinear optics
[AD-A277512] p 3664 N94-33082

THERMAL STRESSES
Evolution of the interface properties with temperature in the T800H/ bismaleimide composites
[ONERA-NT-1993-14] p 3619 N94-31478
Validation and sensitivity analysis of Texas human thermal model predictions during cold water immersion
[AD-A275240] p 3797 N94-32156

THERMAL VACUUM TESTS
Thermal-vacuum response of polymer matrix composites in space p 3595 N94-31033

THERMIONIC CONVERTERS
High temperature materials technology research for advanced thermionic systems
[DE94-008341] p 3646 N94-32825

THERMISTORS
Automatic resonator alignment and power stabilization of high power C02 lasers
[ISBN-0-315-77217-4] p 3714 N94-31472

THERMOCHEMICAL PROPERTIES
Ignition delays, heats of combustion, and reaction rates of aluminum alkyl derivatives used as ignition and combustion enhancers for supersonic combustion
[NASA-CR-189581] p 3638 N94-32868

THERMODYNAMIC CYCLES
Application of natural refrigerants: A rational solution to a pressing problem
[PB94-138781] p 3668 N94-31073

THERMODYNAMIC EQUILIBRIUM
Non-equilibrium electrodynamics in the large N expansion
[DE94-006156] p 3911 N94-31760
SOLGAS refined: A computerized thermodynamic equilibrium calculation tool
[DE94-009021] p 3913 N94-32846

THERMODYNAMIC PROPERTIES
A numerical method for mixing/chemically reacting compressible flow with finite rate chemistry p 3634 N94-31824
Group 12 thiolates: Syntheses, characterization and decomposition pathways
[AD-A277055] p 3900 N94-32011
Isomeric poly(benzophenone)s: Synthesis of highly crystalline poly (4, 4 foot-benzophenone) and amorphous poly (2, 5-benzophenone), a soluble poly (p-phenylene) derivative
[AD-A277261] p 3655 N94-32017
Some perspectives on solution-phase electron-transfer processes
[AD-A276906] p 3635 N94-32216
Inorganic polymer engineering materials
[DE94-008519] p 3659 N94-32655
Investigation of superconductivity and magnetism in d and f-electron materials
[DE94-008535] p 3907 N94-32933

CET93 and CETPC: An interim updated version of the NASA Lewis computer program for calculating complex chemical equilibria with applications
[NASA-TM-4557] p 3636 N94-32948
Regional sedimentological variations among dark crater floor features: Toward a model for modern eolian sand distribution on Mars p 3946 N94-33203

THERMODYNAMICS
Reactive flows in compact objects
p 3934 N94-31567
Strongly coupled ionic mixtures and the H/He EOS
[DE94-006391] p 3934 N94-31782
Numerical simulations of monsoon rainfall with the NRL/NCSU regional nested grid model
p 3782 N94-31791
SOLGAS refined: A computerized thermodynamic equilibrium calculation tool
[DE94-009021] p 3913 N94-32846

THERMOELECTRICITY
Pre-flight testing of Thermoelectric Quartz Crystal Microbalances (TQCM) for midcourse space experiment (MSX) spacecraft
[AD-A277054] p 3610 N94-32010

THERMOGRAVIMETRY
New molecular-based routes to binary main group metal sulfides
[AD-A277005] p 3900 N94-32003

THERMOMECHANICAL TREATMENT
A state variable material model for superplastic titanium-6 percent Al-4 percent V p 3644 N94-32498
Influence of volume fraction of component materials and interlayer bond strength on fracture toughness of multi-layer Al 6090-25 volume percent SiCp and Al 5182 laminates
[DE94-007141] p 3626 N94-32665

THERMONUCLEAR EXPLOSIONS
Vulnerability assessment of a space based weapon platform electronic system exposed to a thermonuclear weapon detonation
[DE94-007229] p 3611 N94-32667

THERMONUCLEAR REACTIONS
Anomalous thermalization of fast ions in magnetized plasma
[DE94-007109] p 3891 N94-32631

THERMOPHYSICAL PROPERTIES
Computational modeling of convective heat transfer to liquid hydrogen coolant p 3707 N94-32485

THERMOPILES
Radiometry spot measurement system
[NASA-TM-106561] p 3883 N94-32777

THERMOPLASTIC RESINS
Empirical optimization of the consolidation of thermoplastic prepregs
[ISBN-0-315-86455-9] p 3652 N94-31722
Development of thermoplastic composite aircraft structures
[NASA-CR-189593] p 3626 N94-32660
Characterization and manufacture of braided composites for large commercial aircraft structures
p 3630 N94-33137

THERMOSETTING RESINS
Evolution of the interface properties with temperature in the T800H/ bismaleimide composites
[ONERA-NT-1993-14] p 3619 N94-31478

THERMOSPHERE
Thermospheric modeling accuracies using F10.7 and Ap
[AD-A277355] p 3773 N94-32337

THESAURI
DTIC Thesaurus on diskette with dBase 4.1 runtime (computer diskette)
[AD-M000306] p 3922 N94-33256
DTIC Thesaurus on diskette (ASC2) (computer diskette)
[AD-M000309] p 3922 N94-33257
DTIC Thesaurus on diskette without runtime (computer diskette)
[AD-M000310] p 3923 N94-33258
DTIC Thesaurus on diskette without runtime (computer diskette)
[AD-M000312] p 3923 N94-33259

THETA PINCH
Coaxial slow source
[DE94-008191] p 3892 N94-32800

THICK FILMS
New thick film feedthrough configurations
[DE94-008706] p 3694 N94-32582

THICK PLATES
An efficient higher order theory for laminated composite plates and a finite element implementation
p 3617 N94-31215

THICKNESS
Materials processing and manufacturing technologies for diamond substrates multichip modules
[AD-A276904] p 3692 N94-32215
Computerized Ultrasonic Testing System (CUTS) for in-process thickness determination
p 3862 N94-32456

THIN FILMS
Sol-gel metal oxide and metal oxide/polymer multilayers applied by meniscus coating
[DE94-005813] p 3649 N94-31199
Adsorption of water to the metal/polymer interface studied by neutron and x ray reflectivity
[DE94-005578] p 3651 N94-31649
Degenerate four-wave mixing as a diagnostic of plasma chemistry
[DE94-008588] p 3889 N94-31766
Electrical properties of double layer dielectric structures for space technology
[ISBN-0-315-86547-4] p 3610 N94-31910
RF vacuum microelectronics
[AD-A276512] p 3691 N94-31928
A fracture mechanics methodology for characterizing the performance of flawed polymeric dielectric materials
p 3654 N94-31956
Chemical vapor deposition of metal nitrides, phosphides, and arsenides
[DE94-008096] p 3654 N94-31976
The charging effect in high-Tc superconducting thin films
[AD-A277265] p 3900 N94-32040
Processing boron and boron carbide thin films for protective coatings and device fabrication
[AD-A277266] p 3900 N94-32041
Anomalous small angle x ray scattering studies of amorphous metal-germanium alloys
[DE94-007258] p 3900 N94-32065
Metal clusters: Dynamics and structure
[AD-A276842] p 3643 N94-32091
Correlations between micromagnetic, microstructural and microchemical properties in ultrathin epitaxial magnetic structures
[AD-A277200] p 3901 N94-32092
Ion-irradiation-induced densification of zirconia sol-gel thin films
[DE94-006248] p 3656 N94-32103
Determination of BPSG thin-film properties using IR reflection spectroscopy of product wafers
[DE94-006591] p 3634 N94-32110
Materials processing and manufacturing technologies for diamond substrates multichip modules
[AD-A276904] p 3692 N94-32215
NMR studies of organic thin films
[AD-A276953] p 3656 N94-32221
Si/SiO2 interface studies by immersion ellipsometry
[AD-A277277] p 3881 N94-32324
Stable second-order nonlinear optical materials based on interpenetrating polymer networks
[AD-A277410] p 3658 N94-32579
Femtosecond probe-probe transmission studies of LT-grown GaAs near the band edge
[DE94-006660] p 3904 N94-32634
Thin-film decoupling capacitors for multi-chip modules
[DE94-007743] p 3695 N94-32650
Energetics, bonding mechanism, and electronic structure of ceramic/ceramic and metal/ceramic interfaces
[DE94-008551] p 3659 N94-32656
Microanalytical study of defect formation in thin bismuth strontium calcium copper oxide films
[DE94-008217] p 3661 N94-32751
Development of a computer model for polycrystalline thin-film CuInSe2 and CdTe solar cells
[DE94-006853] p 3762 N94-32763
Thin EFG octagons
[DE94-006855] p 3905 N94-32764
Properties of doped and undoped (Ca,Sr)CuO2 thin films
[DE94-007230] p 3905 N94-32785
Nucleation and growth of cubic boron nitride films produced by ion-assisted pulsed laser deposition
[DE94-007295] p 3661 N94-32796
Ultrahigh-current-density metal-ion implantation and diamondlike-hydrocarbon films for tribological applications
[DE94-008958] p 3906 N94-32843
X ray absorption study of pulsed laser deposited boron nitride films
[DE94-008295] p 3662 N94-32855
Frictional behavior and adhesion of Ag and Au films applied to aluminum oxide by oxygen-ion assisted Screen Cage Ion Plating (SCIP)
[NASA-TM-106522] p 3647 N94-32931
Low energy ion beam assisted growth of homoepitaxial silicon films at low temperature
[AD-A276092] p 3908 N94-33039
Rare Earth Doped Semiconductors and Materials Research Society Symposium Proceedings, Volume 301
[AD-A277517] p 3908 N94-33055
Ceramic and metal composite circuit-board-level technology for application specific electronic modules (ASEM)
[AD-A277961] p 3630 N94-33180
Microstructures and epitaxy in oxide superconductor thin films and devices
[AD-A278427] p 3910 N94-33332

THIN PLATES
Nonlinear vibration analysis of laminated plates on linear and nonlinear elastic foundations p 3737 N94-32079

THIN WALLED SHELLS
Tearing resistance of a thin shell against projectile penetration: Material property effects
[DE94-007466] p 3733 N94-31316

THIOLS
Group 12 thiolates: Syntheses, characterization and decomposition pathways
[AD-A277055] p 3900 N94-32011

THREADS
An experimental and analytical investigation of a threaded fastener
[VTT-JULK-786] p 3724 N94-31654

THREE DIMENSIONAL BODIES
Visual perception of 3-dimensional structure from different types of optical deformation
[AD-A278272] p 3884 N94-33141

THREE DIMENSIONAL BOUNDARY LAYER
Computation of three-dimensional compressible boundary layers to fourth-order accuracy on wings and fuselages
[NASA-CR-4269] p 3709 N94-32871

THREE DIMENSIONAL COMPOSITES
A thermal viscoelastic analysis for thick-walled composite cylinders
[AD-A274143] p 3625 N94-32604

THREE DIMENSIONAL FLOW
A heterogeneous computing environment for simulating astrophysical fluid flows p 3928 N94-31119
Three-dimensional velocity measurements on a 6:1 prolate spheroid at 10 deg angle of attack
[AD-A276485] p 3702 N94-31476
A new inverse method for generating high-speed aerodynamic flows with application to waverider design
p 3569 N94-31828
Solution of the average-passage equations for the incompressible flow through multiple-blade-row turbomachinery
[AD-A276515] p 3583 N94-31931
A study of the development and attenuation of wing-generated, vortical wakes p 3570 N94-31971
An experimental study of the flowfield on a semispan rectangular wing with a simulated glaze ice accretion
[NASA-CR-195301] p 3571 N94-32475
Boundary element analysis of three-dimensional nonlinear hydrodynamics in a reduced gravity environment p 3668 N94-32715
Inlet distortion in engines on VSTOL aircraft
[NASA-CR-195841] p 3584 N94-33035

THREE DIMENSIONAL MODELS
The dynamical settling of warped disks and angular momentum transport in galaxies p 3928 N94-31121
An investigation of the spin-coating process and a model for three-dimensional regular foams
p 3649 N94-31206
Development of a 3D numerical code to calculate the trajectories of the blow off electrons emitted by a vacuum surface discharge: Application to the study of the electromagnetic interference induced on a spacecraft
[ONERA-NT-1993-12] p 3863 N94-31227
Development of a three-dimensional icing model for predicting ice accretion on aircraft
[ONERA-NT-1993-5] p 3574 N94-31230
ADCIRC: An advanced three-dimensional circulation model for shelves, coasts, and estuaries. User's manual for ADCIRC-2DDI
[AD-A276150] p 3787 N94-31250
Multidimensional WAF-type schemes for model conservation laws
[CRANFIELD-AERO-9312] p 3843 N94-31541
Finite element analysis of damage in fibrous composites using a micromechanical model
[AD-A277226] p 3623 N94-32024
Complete model description of an electron beam using ACCEPT Monte Carlo simulation code
[DE94-007063] p 3872 N94-32628
Climate effects of anthropogenic sulfate: Simulations from a coupled chemistry/climate model
[DE94-004352] p 3767 N94-32789
Fast nonsupervised 3D registration of PET and MR images of the brain
[TELECOM-93-C-006] p 3798 N94-33069

THREE DIMENSIONAL MOTION
Identification and control of structures in space
[NASA-CR-195910] p 3612 N94-33115

THRESHOLD CURRENTS
Large-diameter InGaAs/AlGaAs vertical-cavity surface-emitting lasers with low threshold current density fabricated using a simple chemical etch process
[AD-A277733] p 3721 N94-33003
THRUST
Shock-dependent, optimum thrust wings in supersonic flow p 3570 N94-32027
THRUST CONTROL
A six degree of freedom, plume-fuel optimal trajectory planner for spacecraft proximity operations using an A* node search
[NASA-CR-188285] p 3601 N94-32388
TILT ROTOR AIRCRAFT
Civil tiltrotor market penetration: Effects on Northeast corridor airport delay
[AD-A277534] p 3576 N94-32955
An experimental study of pilot/vehicle dynamics using a tilt rotor flying machine
[AD-A277516] p 3805 N94-33349
TIME DEPENDENCE
Time-dependent behavior of active galactic nuclei with pair production p 3929 N94-31125
The physics of black hole x ray novae p 3932 N94-31143
A theory of distributed time
[AD-A276631] p 3815 N94-31994
Prediction of the plane wave beamformed acoustic arrival structure for the 1992 Barents Sea coastal tomography test
[AD-A276741] p 3788 N94-32181
Arithmetic averaging: A versatile technique for smoothing and trend removal
[DE94-005274] p 3852 N94-32673
Deuterium absorption and material phase characteristics of SAES St198 Zr-Fe alloy
[DE94-008275] p 3646 N94-32781
Space flight printed wiring board measling investigation
[NASA-TM-104602] p 3732 N94-33101
TIME DISCRIMINATION
Mechanisms of temporal pattern discrimination by human observers
[AD-A277407] p 3801 N94-32577
TIME DIVISION MULTIPLE ACCESS
Reliable communication in the presence of severe noise or jamming
[AD-A278410] p 3684 N94-33173
TIME LAG
A theory of distributed time
[AD-A276631] p 3815 N94-31994
Fiber optic continuous true time-delay modulator
[AD-D016098] p 3883 N94-32720
TIME MARCHING
Preconditioned time-difference methods for advection-diffusion-reaction equations
[DE94-006472] p 3638 N94-32840
TIME MEASUREMENT
VME rollback hardware for time warp multiprocessor systems
[NASA-CR-191796] p 3826 N94-32483
Time resolved measurements of light produced by onset of plasma formation on electrodes of fast pulsed high voltage diodes
[AD-A277974] p 3894 N94-33264
TIME OF FLIGHT SPECTROMETERS
Production and detection of metastable atomic oxygen
[ISBN-0-315-87364-7] p 3868 N94-31915
TIME RESPONSE
The Second International Workshop on Discrete Time Domain Modelling of Electromagnetic Fields and Networks. Program and information
[AD-A277136] p 3677 N94-32067
TIME SERIES ANALYSIS
A radial basis function approach to financial time series analysis
[AD-A276408] p 3924 N94-31361
Exploring phase space concepts in the forecasting of time series with artificial neural networks
[DE94-005810] p 3834 N94-32127
Arithmetic averaging: A versatile technique for smoothing and trend removal
[DE94-005274] p 3852 N94-32673
Homogeneous global mean temperature time series
[DE94-002194] p 3766 N94-32690
SEASOAR and CTD observations during a COARE surveys cruise, W9211C, 22 January - 22 February, 1993
[AD-A277925] p 3791 N94-33244
TIME SIGNALS
Machinery monitoring and diagnostics using pseudo Wigner-Ville distribution and backpropagation neural network
[AD-A276219] p 3828 N94-31064
IRIG J asynchronous ASCII time code formats
[AD-A277244] p 3681 N94-32332
TIME TEMPERATURE PARAMETER
Deuterium absorption and material phase characteristics of SAES St198 Zr-Fe alloy
[DE94-008275] p 3646 N94-32781
TIN
Lowering the Schottky barrier at metal or silicide/Si interfaces to extend the range of infrared detectors
[AD-A277253] p 3903 N94-32322
Interface engineering in oxide fiber/oxide matrix composites
[AD-A277672] p 3627 N94-33029
TIN ALLOYS
Aging effects on the microstructure, surface characteristics and wettability of Cu pretinned with Sn-Pb solders
[DE94-007033] p 3641 N94-31638
TIN COMPOUNDS
Amorphous/crystalline structure and phase transformations in metastable semiconducting Ge(1-x)Sn(x)
[DE94-006659] p 3901 N94-32115
TIN OXIDES
Chemical vapor deposition of metal nitrides, phosphides, and arsenides
[DE94-008096] p 3654 N94-31976
TITANIUM
A low cost igniter utilizing an SCB and titanium sub-hydride potassium perchlorate pyrotechnic
[DE94-006467] p 3666 N94-31827
Interface controlled amorphization of crystalline Ni/Ti multilayers
[DE94-008685] p 3906 N94-32884
TITANIUM ALLOYS
High temperature ductility loss in titanium alloys: A review
[DE94-006606] p 3640 N94-31345
Microstructures and mechanical properties of Al3Ti-based alloys: Analysis in single phase and multiphase systems
[ONERA-NT-1993-6] p 3640 N94-31420
Transmissibility of nickel-titanium shape memory alloy springs
[AD-A276055] p 3640 N94-31456
Creep properties of vanadium-base alloys
[DE94-006541] p 3641 N94-31486
Thermal-mechanical fatigue crack growth in aircraft engine materials
[ISBN-0-315-86543-1] p 3734 N94-31707
A state variable material model for superplastic titanium-6 percent Al-4 percent V p 3644 N94-32498
Structure, stability, and mechanical properties of intermetallic phases
[DE94-009178] p 3647 N94-32852
TITANIUM COMPOUNDS
Inorganic materials for anomalous-dispersion phase-matched second harmonic generation: Rubidium titanyl arsenate isomorphs, Rb(Ti(1-2x)Ln(x)Nb(x))OAsO4
[DE94-006141] p 3899 N94-31847
TITANIUM OXIDES
Oxide pigments in water: The colloid-chemical point of view
[PB94-148616] p 3633 N94-31591
Processing and characterization of functionally gradient ceramic materials
[AD-A277154] p 3657 N94-32367
TITRATION
A fuzzy classifier system for process control p 3839 N94-32422
Isothermal sintering, microstructure, and superconducting properties of Y1Ba2Cu3O(7-x) compound
[DE94-008132] p 3905 N94-32779
TOKAMAK DEVICES
Operation of D3-D with all-graphite walls
[DE94-004858] p 3886 N94-31304
Noninductive current drive experiments on D3-D, and future plans
[DE94-007373] p 3886 N94-31324
L-H confinement mode dynamics in three-dimensional state space
[DE94-007113] p 3887 N94-31396
Structural design of the superconducting Poloidal Field coils for the Tokamak Physics Experiment
[DE94-007078] p 3887 N94-31406
Spectroscopy and atomic physics in EBIT and SuperEBIT
[DE94-006050] p 3864 N94-31508
Two-gigawatt burst-mode operation of the Intense Microwave Prototype (IMP) Free-Electron Laser (FEL) for the Microwave Tokamak Experiment (MTX)
[DE94-006613] p 3715 N94-31580
Plasma confinement theory and transport simulation
[DE94-006065] p 3888 N94-31619
High beta tokamak research
[DE94-006513] p 3888 N94-31664
Quench detection and instrumentation for the Tokamak Physics Experiment magnets
[DE94-006656] p 3888 N94-31667
First-wall heat-flux measurements during ELMing H-mode plasma
[DE94-008310] p 3888 N94-31765
Collisional and chaotic transport of energetic particles in toroidal plasma
[DE94-006504] p 3889 N94-31787
FWCD and ECCD experiments on D3-D
[DE94-007371] p 3890 N94-32201
Fusion applications of high power millimeter wave sources
[DE94-007374] p 3718 N94-32202
An edge density fluctuation diagnostic for D3-D using lithium beams
[DE94-008554] p 3890 N94-32519
Experimental survey of the L-H transition conditions in the D3-D tokamak
[DE94-007428] p 3891 N94-32595
Recent VH-mode results on D3-D
[DE94-007429] p 3891 N94-32611
Overview of H-mode studies in D3-D
[DE94-007430] p 3891 N94-32612
Characterization of atomic and molecular impurity sources and transport at the tokamak edge
[DE94-007212] p 3891 N94-32619
Basic principles approach for studying nonlinear Alfven wave-alpha particle dynamics
[DE94-007112] p 3891 N94-32664
Cooperative program on D3-D (FY 1993)
[DE94-008343] p 3892 N94-32820
The Numerical Tokamak Project (NTP) simulation of turbulent transport in the core plasma: A grand challenge in plasma physics
[DE94-008279] p 3892 N94-32838
Stability of tearing modes in tokamak plasmas
[DE94-009205] p 3892 N94-32911
TOLERANCES (MECHANICS)
Assessment of impact damage in composite structures
[AD-A277063] p 3624 N94-32265
Tension fracture of laminates for transport fuselage. Part 1: Material screening p 3629 N94-33130
TOLUENE
Energy transfer properties and mechanisms
[DE94-007403] p 3636 N94-32594
Surface probes of porous toluene/water ices: Adsorption kinetics and annealing spectra measured by second harmonic generation
[DE94-007564] p 3637 N94-32743
TOMOGRAPHY
Ultrasonic tomography in fiber-reinforced composite materials p 3620 N94-31565
Prediction of the plane wave beamformed acoustic arrival structure for the 1992 Barents Sea coastal tomography test
[AD-A276741] p 3788 N94-32181
Ocean optics, ocean imaging and optical tomography
[AD-A277010] p 3789 N94-32402
TOOLING
Analytical Design Package (ADP2): A computer aided engineering tool for aircraft transparency design p 3823 N94-32430
Innovative fabrication processing of advanced composite materials concepts for primary aircraft structures
[NASA-CR-189558] p 3626 N94-32877
TOPEX
Lessons learned from selecting and testing spaceflight potentiometers p 3607 N94-33318
TOPOGRAPHY
Patterns of deformation and volcanic flows associated with lithospheric loading by large volcanoes on Venus p 3776 N94-31106
Geoid-to-topography ratios on Venus: A global perspective p 3940 N94-31110
Three dimensional vorticity field in the California current system
[AD-A276951] p 3788 N94-32220
Modular Simulator System (MSS). System/segment specification for the generic modular simulator system-environment module, volume 13
[AD-A276980] p 3589 N94-32319
Multi-scale studies of seafloor topography
[AD-A277008] p 3789 N94-32400
The use of ERS images for mapping p 3749 N94-32531
Use of SPOT and ERS-1 SAR data to study the tectonic and climatic history of arid regions p 3752 N94-32550
Monitoring landsurface characteristics in Niger using complementary SPOT and ERS-1 SAR data p 3754 N94-32560
Comparing SPOT and SIR A for mapping superficial formations in tropical forest regions: Example of the Yaoundy Region (Cameroon) p 3755 N94-32562

SAR interferometry with ERS-1 p 3755 N94-32566
Techniques and applications of SAR interferometry for ERS-1 p 3756 N94-32568
Developments in ERS-1 SAR interferometry: Use of the spectral shift p 3756 N94-32569
Differential interferometry study of an earthquake p 3756 N94-32570
Simulation of a precipitation event in the western United States
[DE94-004835] p 3786 N94-32791
Quantitative modeling of bottom morphology and subbottom properties
[AD-A278142] p 3790 N94-33062
Fine and microstructure observations at Fieberlin g Guyot R/V new horizon cruise report
[AD-A277917] p 3791 N94-33109

TOPOLOGY
The small-scale topology of a 2:1 aspect-ratio elliptic jet p 3699 N94-31184
Strictly positive definite functions on spheres
[AD-A276471] p 3855 N94-31244
SU(2) WZNW model at higher genera from gauge field functional integral
[PB94-148467] p 3857 N94-31589
Heteroclinic attractors: Time averages and moduli of topological conjugacy
[W-9318] p 3844 N94-31690

TOROIDAL PLASMAS
Numerical method for the investigation of the magnetohydrodynamic stability of three dimensional plasma equilibria
[ETN-94-95752] p 3887 N94-31512
Toroidal pinch experiments
[DE94-005876] p 3887 N94-31558
First-wall heat-flux measurements during ELMing H-mode plasma
[DE94-008310] p 3888 N94-31765
Collisional and chaotic transport of energetic particles in toroidal plasma
[DE94-008504] p 3889 N94-31787
Experimental survey of the L-H transition conditions in the D3-D tokamak
[DE94-007428] p 3891 N94-32595
The Numerical Tokamak Project (NTP) simulation of turbulent transport in the core plasma: A grand challenge in plasma physics
[DE94-008279] p 3892 N94-32838
Stability of tearing modes in tokamak plasmas
[DE94-009205] p 3892 N94-32911
Anomalous transport equations in toroidal plasmas
[DE94-009206] p 3893 N94-32922

TORQUE
Flexible drive shaft coupling
[AD-D016096] p 3727 N94-32718
Torque-balanced extendable fiber optic cable
[AD-D016097] p 3882 N94-32719
Torque characteristics of solid lubricated precision bearings during oscillatory motion
[AD-A278133] p 3728 N94-33061
A comparison of the performance of solid and liquid lubricants in oscillating spacecraft ball bearings p 3606 N94-33311

TORQUE MOTORS
International Space Station Alpha's bearing, motor, and roll ring module developmental testing and results p 3603 N94-33295

TORSION
Flexible drive shaft coupling
[AD-D016096] p 3727 N94-32718
Technology integration box beam failure study p 3628 N94-33126

TOTAL QUALITY MANAGEMENT
Process mapping: A user-friendly tool for process improvement
[DE94-004357] p 3730 N94-31605
Application of Artificial Intelligence to the DoD Corporate Information Management (CIM) program
[AD-A276656] p 3834 N94-32061
CIM in space: Corporate Information Management (CIM) implications for space-based information systems
[AD-A276882] p 3600 N94-32126
Case studies of software process improvement methods
[AD-A277289] p 3818 N94-32508
Agile total quality guidelines for enhancing teamwork and success
[DE93-019972] p 3915 N94-32678
Total Quality Management implementation guidelines
[DE94-007232] p 3915 N94-32723

TOUGHNESS
Toughening mechanisms in the high strain rate deformation of rubber-modified polymer glasses p 3653 N94-31942
Toughening mechanisms in fiber-reinforced ceramic-matrix composites p 3622 N94-31943
Correlation of flux composition and inclusion characteristics with submerged arc weld metal properties in HY-100 steel
[AD-A277040] p 3726 N94-32261
The effect of ductile phase (Nb) reinforcement morphology on the mechanical behavior of an intermetallic matrix (MoSi2) p 3615 N94-32500

TOXIC HAZARDS
Applying robotics to HAZMAT p 3729 N94-32452
Controlling hazardous energy sources (lockout/tagout)
[NASA-TM-105290] p 3669 N94-32861

TOXICITY
Formation of gas-phase peroxides in a rural atmosphere: An interpretation of the recent SOS/SERON field results
[DE94-002995] p 3766 N94-32692

TRACE CONTAMINANTS
Control and monitoring of heavy metal emissions
[VTT-TIED-1508] p 3765 N94-31657

TRACE ELEMENTS
Control and monitoring of heavy metal emissions
[VTT-TIED-1508] p 3765 N94-31657
Surface fluxes of trace gases derived from convective-layer profiles p 3704 N94-31774
Development of sample charge compensation for characterization of impurities in semiconductor materials
[AD-A277113] p 3899 N94-31983

TRACERS
Cruise report: Oceanus 250 leg 4 high resolution profiler survey for the North Atlantic Tracer Release Experiment, 25 March - 24 April, 1992
[AD-A277935] p 3791 N94-33245

TRACKING (POSITION)
Tracking roads in an aerial image by Kalman filtering
[TELECOM-93-D-007] p 3711 N94-31096
Study of a path planning and tracking system for an articulated mobile robot
[ISBN-0-315-86502-4] p 3831 N94-31800
A paraperspective factorization method for shape and motion recovery
[AD-A276513] p 3712 N94-31929
Automated detection of ship tracks in multispectral satellite data
[AD-A276697] p 3746 N94-32119
Fuzzy-neural control of an aircraft tracking camera platform p 3839 N94-32423

TRACKING FILTERS
Some neural computing approaches to target tracking p 3837 N94-33151

TRACKING PROBLEM
Feasibility and stability results for constrained stable generalized predictive control
[MATHS-REPT-A-203] p 3828 N94-31158
Strategy for tracking and grabbing a moving object with the aid of a decouplable manipulator with six degrees of freedom general architecture, guided by a vision system
[ISBN-0-315-86864-3] p 3831 N94-31757
The application of a radial basis function neural network for radar tracking over the sea p 3686 N94-33150
Some neural computing approaches to target tracking p 3837 N94-33151

TRAILERS
Implementation of instruments and facilities at the SGP CART site
[DE94-006839] p 3781 N94-31322

TRAINING ANALYSIS
The effects of Above Real-Time Training (ARTT) in an F-16 simulator p 3591 N94-32474

TRAINING DEVICES
Modular Simulator System (MSS) management guide
[AD-A277098] p 3588 N94-32014
Modular Simulator System (MSS). Executive report
[AD-A276966] p 3588 N94-32241
Modular Simulator System (MSS). System/segment specification for the generic MSS-system integration, volume 1
[AD-A276968] p 3588 N94-32312
Modular Simulator System (MSS). System/segment specification for the generic modular simulator system-flight station module, volume 2
[AD-A276969] p 3588 N94-32313
Modular Simulator System (MSS). System/segment specification for the generic modular simulator system-radar module, volume 8
[AD-A276975] p 3589 N94-32314
Modular Simulator System (MSS). System/segment specification for the generic modular simulator system-electronic warfare module, volume 9
[AD-A276976] p 3589 N94-32315
Modular Simulator System (MSS). System/segment specification for the generic modular simulator system-physical cues module, volume 10
[AD-A276977] p 3589 N94-32316
Modular Simulator System (MSS). System/segment specification for the generic modular simulator system-visual module, volume 11
[AD-A276978] p 3589 N94-32317
Modular Simulator System (MSS). System/segment specification for the generic modular simulator system-instructor/operator station module, volume 12
[AD-A276979] p 3589 N94-32318
Modular Simulator System (MSS). System/segment specification for the generic modular simulator system-environment module, volume 13
[AD-A276980] p 3589 N94-32319
Modular Simulator System (MSS). System/segment specification for the generic modular simulator system-flight controls module, volume 3
[AD-A276970] p 3590 N94-32395
Modular Simulator System (MSS). System/segment specification for the generic modular simulator system-flight dynamics module, volume 4
[AD-A276971] p 3590 N94-32396
Modular Simulator System (MSS). System/segment specification for the generic modular simulator system-propulsion module propulsion module, volume 5
[AD-A276972] p 3590 N94-32397
Modular Simulator System (MSS). System/segment specification for the generic modular simulator system-navigation/communication module, volume 6
[AD-A276973] p 3590 N94-32398
Modular Simulator System (MSS). System/segment specification for the generic modular simulator system-weapons module, volume 7
[AD-A276974] p 3590 N94-32399
Modular Simulator System (MSS): Interface design document for the generic MSS
[AD-A277270] p 3590 N94-32403
A systems approach to computer-based training p 3823 N94-32436
An evaluation framework for designing a night vision, computer-based trainer
[AD-A278005] p 3590 N94-33139

TRAINING EVALUATION
Aircraft simulation and pilot proficiency: From surrogate flying towards effective training
[AD-B179300] p 3587 N94-31179

TRAINING SIMULATORS
Aircraft simulation and pilot proficiency: From surrogate flying towards effective training
[AD-B179300] p 3587 N94-31179

TRAJECTORIES
Visual processing of object velocity and acceleration
[AD-A277425] p 3801 N94-32998

TRAJECTORY ANALYSIS
Using Monte Carlo techniques and parallel processing for debris hazard analysis of rocket systems
[DE94-007250] p 3609 N94-31382
A paraperspective factorization method for shape and motion recovery
[AD-A276513] p 3712 N94-31929
Self-consistent effects of magnetospheric hydromagnetic waves on ring current ions
[AD-A277406] p 3774 N94-32346

TRAJECTORY CONTROL
ControlShell: A real-time software framework
[AD-A276481] p 3811 N94-31475
Trajectory learning with a direct drive robotic manipulator p 3831 N94-31794
Adaptive control of a robot in Cartesian coordinates: Analysis and implementation
[ISBN-0-315-86493-1] p 3831 N94-31798
On-line physical parameter identification and adaptive control of a launch vehicle p 3602 N94-31891
High-speed path constrained manipulator operation using optimal-feedback combined controller p 3833 N94-31962
Trajectory planning for space manipulators
[AD-A277229] p 3611 N94-32369

TRAJECTORY PLANNING
ControlShell: A real-time software framework
[AD-A276481] p 3811 N94-31475
Abstracts of the Workshop on Computational Geometry (CG 1992)
[PB94-147022] p 3844 N94-31684
Penetration distances and their applications to path planning p 3858 N94-31725
Strategy for tracking and grabbing a moving object with the aid of a decouplable manipulator with six degrees of freedom general architecture, guided by a vision system
[ISBN-0-315-86864-3] p 3831 N94-31757
Study of a path planning and tracking system for an articulated mobile robot
[ISBN-0-315-86502-4] p 3831 N94-31800
Trajectory planning for space manipulators
[AD-A277229] p 3611 N94-32369
A six degree of freedom, plume-fuel optimal trajectory planner for spacecraft proximity operations using an A* node search
[NASA-CR-188285] p 3601 N94-32388

TRANSATMOSPHERIC VEHICLES
The National Aerospace Plane (NASP): Development issues for the follow-on vehicle
[AD-A278417] p 3581 N94-33329
TRANSDUCERS
Errors associated with the use of heat flow transducers p 3796 N94-31742
Universal signal conditioning amplifier p 3699 N94-32460
The constant current loop: A new paradigm for resistance signal conditioning p 3685 N94-32461
Acoustic window
[AD-D016171] p 3862 N94-33017
TRANSFER FUNCTIONS
Structural properties of inverse linear systems
[MATHS-REPT-A-200] p 3840 N94-31156
Observations of the notion of minimality in the generalized state space
[MATHS-REPT-A-207] p 3840 N94-31162
Analysis and synthesis of MOS translinear circuits
[ISBN-9-09-005495-2] p 3690 N94-31616
Performance statistics bulletin. High latitude meteor scatter propagation October, November, December 1991, January 1992
[AD-A276724] p 3678 N94-32159
Performance statistics bulletin. High latitude meteor scatter propagation, June, July, August, September 1992
[AD-A277508] p 3685 N94-33347
TRANSFORMATIONS (MATHEMATICS)
Application of radon transformation for improved analysis of sparsely sampled data: A feasibility study
[PB94-147535] p 3741 N94-31075
Structural properties of inverse linear systems
[MATHS-REPT-A-200] p 3840 N94-31156
An algebraic view on Rosetta
[CL-93-02] p 3841 N94-31391
Minimization of computational requirements in the hybrid stress finite element method
[AD-A277120] p 3846 N94-32048
Modeling and control of nonlinear systems
[AD-A277377] p 3834 N94-32095
Transformational derivation of (parallel) programs using skeletons
[TR-93-20] p 3825 N94-32196
Steepest descent paths for integrals defining the modified Bessel functions of imaginary order
[CWI-AM-R9303] p 3848 N94-32227
TRANSFORMERS
High-temperature superconducting transformer performance, cost, and market evaluation
[DE94-005494] p 3687 N94-31152
TRANSIENT OSCILLATIONS
Advanced CFD methodology for fast transients encountered in nonlinear combustion instability problems. Volume 1: Theory and validation
[NASA-CR-191351] p 3637 N94-32696
TRANSIENT RESPONSE
Study of wave propagation and dynamic response of laminated composite structures
[AD-A276123] p 3619 N94-31444
TRANSISTOR CIRCUITS
Analysis and synthesis of MOS translinear circuits
[ISBN-9-09-005495-2] p 3690 N94-31616
TRANSISTOR LOGIC
Novel failure analysis techniques using photon probing with a scanning optical microscope
[DE94-006594] p 3692 N94-32112
TRANSISTORS
GaAs/GaN strained layer superlattice materials for high temperature transistors, phase 1
[AD-A276115] p 3897 N94-31528
Analysis and synthesis of MOS translinear circuits
[ISBN-9-09-005495-2] p 3690 N94-31616
RF vacuum microelectronics
[AD-A276512] p 3691 N94-31928
Application of the modified voltage-dividing potentiometer to overlay metrology in a CMOS/bulk process
[DE94-007937] p 3695 N94-32700
TRANSITION FLOW
Analysis of the photodiode boundary layer transition indicator
[DE94-005311] p 3701 N94-31268
TRANSITION METALS
A polynomial representation of the valence orbital ionization potentials
[USIP-93-06] p 3640 N94-31083
Combinatorial ion sensors
[AD-A276567] p 3825 N94-32032
Vibrational spectroscopy at metal-solution interfaces: Some perspectives and prospects for electrochemical surface science
[AD-A276781] p 3644 N94-32169
Experimental investigations and molecular dynamics simulations of radiation induced surface damage
[AD-A277323] p 3871 N94-32621
Optical properties of lanthanide-doped RbTiOAsO4 and transition metal-doped KTiOPO4
[DE94-008433] p 3907 N94-32963
TRANSITION TEMPERATURE
Fermi surface instability at 0.4 K in a heavy-fermion YbBiPt: SDW?
[DE94-006224] p 3899 N94-31916
Short coherence length superconductors: Intermediate regime between BCS and bosons
[DE94-007694] p 3904 N94-32645
A quest for a new superconducting state
[DE94-008439] p 3908 N94-32991
TRANSLATING
Combinatory reduction systems: Introduction and survey
[CWI-CS-R9362] p 3849 N94-32349
Automatic translation among spoken languages p 3685 N94-32437
Translating an AI application from Lisp to Ada: A case study
[NASA-TM-103845] p 3820 N94-32906
Energy absorber for the CETA p 3604 N94-33303
TRANSLATIONAL MOTION
A paraperspective factorization method for shape and motion recovery
[AD-A276513] p 3712 N94-31929
Vibration localization in dual-span axially moving elastic systems p 3736 N94-31964
TRANSMISSION ELECTRON MICROSCOPY
Incoherent imaging by Z-contrast stem: Towards 1 Angstrom resolution
[DE94-006551] p 3896 N94-31489
Engineering of damage in ion implanted silicon
[ISBN-9-09-005097-3] p 3897 N94-31521
Optimal detector strategies for the phase contrast imaging for scanning transmission electron microscopes
[ETN-94-95747] p 3866 N94-31613
Gettering of metal impurities by cavities in silicon
[DE94-005248] p 3645 N94-32672
Nucleation and growth of cubic boron nitride films produced by ion-assisted pulsed laser deposition
[DE94-007295] p 3661 N94-32796
TRANSMISSION LINES
Studies of an optical multi-processor interconnect
[AD-A277093] p 3881 N94-32392
Torque-balanced extendable fiber optic cable
[AD-D016097] p 3882 N94-32719
TRANSMISSION LOSS
Optimal reactive power dispatch of power systems using nonlinear programming
[MATHS-REPT-A-209] p 3808 N94-31164
Low altitude near-the-horizon propagation: A comparison between RPO and M-layer
[AD-A277358] p 3679 N94-32282
TRANSMISSIONS (MACHINE ELEMENTS)
Spur, helical, and spiral bevel transmission life modeling
[NASA-TM-106552] p 3728 N94-32979
TRANSMISSIVITY
Development of a statistical method for estimating the downward longwave radiation at the surface from satellite observations p 3742 N94-31553
TRANSMITTANCE
Degradation of optical components in space p 3594 N94-31029
Fast acting optical deflection
[AD-A276630] p 3879 N94-32037
TRANSMITTER RECEIVERS
Advanced optical fiber communication systems
[AD-A276416] p 3878 N94-31330
Analysis and design of a high speed, wide range stepwise tunable optical filter/amplifier
[PB94-149572] p 3698 N94-33169
High temperature superconducting Josephson junction array systems, phase 1
[AD-A277937] p 3908 N94-33246
TRANSMITTERS
Multicast communication with guaranteed quality of service
[AD-A277650] p 3682 N94-33025
TRANSMUTATION
The influence of transmutation, void swelling, and flux/spectra uncertainties on the electrical properties of copper and copper alloys
[DE94-006213] p 3641 N94-31626
TRANSONIC FLOW
Prediction of transonic potential flow with slipstreams around configurations
[FFA-TN-1992-15] p 3568 N94-31220
Numerical simulation of combined external/internal transonic flow on the forebody/inlet of the AV-8B Harrier 2 p 3569 N94-31759
An adaptive method for the exact resolution of shock waves and contact discontinuities
[ISBN-0-315-86498-2] p 3704 N94-31799
Numerical analysis of transonic wing buffet p 3586 N94-32713
A finite-difference approximate-factorization algorithm for solution of the unsteady transonic small-disturbance equation
[NASA-TP-3129] p 3572 N94-32865
TRANSONIC FLUTTER
Numerical analysis of transonic wing buffet p 3586 N94-32713
TRANSONIC WIND TUNNELS
Results for the hybrid laminar flow control experiment conducted in the NASA Langley 8-foot transonic pressure tunnel on a 7-foot chord model
[NASA-TM-107582] p 3601 N94-32870
TRANSPIRATION
A long-term simulation of surface fluxes and soil moisture
[DE94-006661] p 3774 N94-32772
TRANSPORT AIRCRAFT
CFD-based drag prediction: State-of-the-art, theory, prospects
[AD-B179297] p 3567 N94-31180
Airborne Trailblazer: Two decades with NASA Langley's 737 flying laboratory
[NASA-SP-4216] p 3566 N94-32793
Application of a design-build-team approach to low cost and weight composite fuselage structure
[NASA-CR-4418] p 3626 N94-32863
Designer's unified cost model p 3627 N94-33122
COINS: A composites information database system p 3627 N94-33123
Composite fuselage shell structures research at NASA Langley Research Center p 3628 N94-33124
Structural testing of the technology integration box beam p 3628 N94-33125
Local design optimization for composite transport fuselage crown panels p 3629 N94-33132
Recent progress in NASA Langley Research Center textile reinforced composites program p 3629 N94-33134
TRANSPORT PROPERTIES
Studying transient mobility and energy loss using scanning tunneling microscopy
[AD-A276292] p 3877 N94-31256
Transport properties of quark and gluon plasmas
[DE94-007043] p 3864 N94-31405
Compressible convection with ionization p 3911 N94-31498
Adjacent-cell Preconditioners for solving optically thick neutron transport problems
[DE94-007219] p 3872 N94-32666
Anomalous transport equations in toroidal plasmas
[DE94-009206] p 3893 N94-32922
CET93 and CETPC: An interim updated version of the NASA Lewis computer program for calculating complex chemical equilibria with applications
[NASA-TM-4557] p 3638 N94-32948
Computed potential energy surfaces for chemical reactions
[NASA-CR-195835] p 3639 N94-33036
Transport and diffusion in turbulent fields modeling and measurements techniques
[AD-A278114] p 3769 N94-33110
TRANSPORT THEORY
Transport suppression by shear flow generation in multihelicity resistive-g turbulence
[DE94-007108] p 3886 N94-31366
Plasma confinement theory and transport simulation
[DE94-006065] p 3888 N94-31619
Non-equilibrium electrodynamics in the large N expansion
[DE94-006156] p 3911 N94-31760
Parallel Monte Carlo reactor neutronics
[DE94-007642] p 3826 N94-32357
Monoenergetic neutral particle transport in semi-infinite media
[AD-A277155] p 3870 N94-32368
Numerical transport theory
[DE94-009064] p 3857 N94-32589
Characterization of atomic and molecular impurity sources and transport at the tokamak edge
[DE94-007212] p 3891 N94-32619
Adjacent-cell Preconditioners for solving optically thick neutron transport problems
[DE94-007219] p 3872 N94-32666
Analytic formulation for the ac electrical conductivity in two-temperature, strongly coupled, overdense plasma: FORTRAN subroutine
[DE94-009466] p 3893 N94-32915
Anomalous transport equations in toroidal plasmas
[DE94-009206] p 3893 N94-32922
TRANSPORTATION
Review and status of Maglev in the United States
[DE94-006832] p 3722 N94-31319

Sandia technology engineering and science accomplishments
[DE94-008312] p 3668 N94-32412

TRANSVERSE LOADS
On the constitutive response of transversely loaded fiber composites with compliant interphases
p 3619 N94-31555

TRANSVERSE OSCILLATION
Study of wave propagation and dynamic response of laminated composite structures
[AD-A276123] p 3619 N94-31444
Transverse mode analysis of hole-coupled free-electron lasers
[ETN-94-96019] p 3715 N94-31532
Vibration localization in dual-span axially moving elastic systems p 3736 N94-31964

TRAPEZOIDS
Transformational derivation of (parallel) programs using skeletons
[TR-93-20] p 3825 N94-32196

TRAPPED PARTICLES
Collisional and chaotic transport of energetic particles in toroidal plasma
[DE94-006504] p 3889 N94-31787

TRAPPING
Cooling and trapping of neutral atoms
[AD-A276957] p 3870 N94-32360

TRAVELING SALESMAN PROBLEM
The ant system: An autocatalytic optimizing process
[REPT-91-016-REV] p 3824 N94-31177
A worst-case analysis of two approximate algorithms for the symmetric travelling salesman problem
[REPT-93-036] p 3840 N94-31187
Simple Patch: A new heuristic for the product traveling salesman problem
[REPT-93-85] p 3845 N94-31702

TRAVELING WAVES
Observation of the traveling component of an x ray standing wave field
[DE94-007671] p 3672 N94-31317

TREES (MATHEMATICS)
Symplectic Runge-Kutta schemes 3: Canonical elementary differentials
[MATHS-REPT-A-204] p 3840 N94-31159
Symbolic derivation of Runge-Kutta methods
[MATHS-REPT-A-205] p 3840 N94-31160
A worst-case analysis of two approximate algorithms for the symmetric travelling salesman problem
[REPT-93-036] p 3840 N94-31187
A worst-case analysis of an approximate algorithm for finding the minimum hamiltonian cycle on paths
[REPT-93-042] p 3809 N94-31192

TRIANGLES
A survey of numerical cubature over triangles
[DE94-006810] p 3841 N94-31274

TRIANGULATION
Abstracts of the Workshop on Computational Geometry (CG 1992)
[PB94-147022] p 3844 N94-31684
Selection of climate station data using clustering and triangulated irregular network techniques
[AD-A276656] p 3784 N94-32046
Incremental triangulation by way of edge swapping and local optimization
[NASA-TM-103979] p 3709 N94-32946

TRIBOLOGY
Cracking induced in small fretting: Application to the case of aeronautical aluminum alloys
[ECL-92-50] p 3735 N94-31870
New micro- and macroscopic models of contact and friction
[AD-A277240] p 3726 N94-32320
Lubrication with binary mixtures: Liquid-liquid emulsion in elastohydrodynamics and metal forming
p 3658 N94-32490
Ultrahigh-current-density metal-ion implantation and diamondlike-hydrocarbon films for tribological applications
[DE94-008958] p 3906 N94-32843
The effect of prolonged exposure to 750 C air on the tribological performance of PM212
[NASA-TM-106472] p 3617 N94-32941
A comparison of the performance of solid and liquid lubricants in oscillating spacecraft ball bearings
p 3606 N94-33311
Development of long-life, low-noise linear bearings for atmospheric interferometry p 3606 N94-33312
The preliminary evaluation of liquid lubricants for space applications by vacuum tribometry p 3606 N94-33313

TRIODES
RF vacuum microelectronics
[AD-A276512] p 3691 N94-31928

TRITON
One: Microphysics of frost metamorphism: Applications to Triton and Mars. Two: A global analysis of the ozone deficit in the upper stratosphere and lower mesosphere. Three: The diabatic circulation in the stratosphere as diagnosed from Microwave Limb Sounder data
p 3942 N94-31975
Distribution and nature of UV absorbers on Triton's surface
[NASA-CR-195886] p 3943 N94-33104

TROPICAL METEOROLOGY
The use of meteorological satellite data for studying tropical atmospheric phenomena p 3779 N94-31000
Air-sea interaction patterns in the equatorial Pacific
[AD-A277305] p 3788 N94-32072
Tropical cyclone forecasters reference guide. 5: Numerical track forecast guidance
[AD-A277318] p 3785 N94-32278
TRMM-related research: Tropical rainfall and energy analysis experiment
[NASA-CR-195834] p 3787 N94-33288

TROPICAL REGIONS
Subtropical Climates and Their Evolution: From Space-Based Observation to Modelling
[ISBN-2-85-428333-3] p 3776 N94-30981
Dynamics in the tropics and synoptic disturbances
p 3778 N94-30990
Low frequency variability observed in the tropical Atlantic Ocean p 3778 N94-30991
Tropical squall lines p 3778 N94-30992
Effects of the deep tropical convection in the large scale atmospheric flow p 3778 N94-30994
Behavior and dynamics of tropical forests and savannas p 3757 N94-31004
The ozone and the physico-chemical processes in tropical regions p 3770 N94-31010
The effect of westerly wind bursts on a tropical ocean general circulation model
[AD-A276423] p 3788 N94-31448
Use of SPOT and ERS-1 to map tropical vegetation and mangrove dynamics in Guiana p 3753 N94-32555
A case study comparing multi-temporal ERS-1 SAR data and SPOT data for tropical forest mapping
p 3753 N94-32556
Comparing SPOT and SIR A for mapping superficial formations in tropical forest regions: Example of the Yaoundy Region (Cameroon) p 3755 N94-32562

TROPICAL STORMS
Short term teleconnections associated with an individual tropical cyclone
[AD-A277210] p 3783 N94-32019
Tropical cyclone forecasters reference guide. 5: Numerical track forecast guidance
[AD-A277318] p 3785 N94-32278
Forecasters handbook for the Philippine Islands and surrounding waters
[AD-A277993] p 3787 N94-33089

TROPOSPHERE
The ozone and the physico-chemical processes in tropical regions p 3770 N94-31010
Quantified estimates of total GWPs for greenhouse gases taking into account tropospheric chemistry
[DE94-007846] p 3768 N94-32817
Dry deposition of PAN to grassland vegetation
[DE94-005111] p 3768 N94-32894

TRUSSES
Real-time control of the Trussarm variable-geometry-truss manipulator utilizing machine vision
[ISBN-0-315-87054-0] p 3830 N94-31735
A real-time computer control and trajectory generation environment for Trussarm
[ISBN-0-315-87060-5] p 3832 N94-31833
Dynamic error compensation in robotic trusses
p 3738 N94-32486

TUNABLE LASERS
Ionization probes of molecular structure and chemistry
[DE94-007605] p 3872 N94-32643
A reliable low-maintenance flashlamp-pumped Ti:sapphire laser operating at 120 PPS
[DE94-009030] p 3721 N94-32848
Multifrequency, rapidly sequenced or simultaneous tunable laser
[AD-D016169] p 3721 N94-32968

TUNGSTEN
Chemical vapour deposition of tungsten for the application in integrated circuits
[ISBN-9-09-005151-1] p 3641 N94-31519
High temperature materials technology research for advanced thermionic systems
[DE94-008444] p 3644 N94-32416

TUNGSTEN COMPOUNDS
Laser flash photolysis, EPR and Raman studies of liquids at elevated pressures
[DE94-008351] p 3718 N94-32413

TUNISIA
The use of SPOT, and the contribution of ERS-1, in the assessment of urban pressure on agriculture land in Greater Tunis (Tunisia) p 3749 N94-32534

TUNNEL JUNCTIONS
High T(sub c) superconductor tunnel junctions for photon detectors
[DE94-007686] p 3904 N94-32602

TUNNELS
Proceedings of the 4th Tunnel Detection Symposium on Subsurface Exploration Technology
[AD-A276372] p 3771 N94-31369

TURBINE BLADES
Computational study of simultaneous heat and mass transfer in turbulent separated flows
p 3704 N94-31843

TURBINE PUMPS
The 7.5K lbf thrust engine preliminary design for Orbit Transfer Vehicle
[NASA-CR-189175] p 3614 N94-31618
Solution of the average-passage equations for the incompressible flow through multiple-blade-row turbomachinery
[AD-A276515] p 3583 N94-31931
Design of a cold-flow test facility for the high pressure fuel turbopump turbine of the Space Shuttle main engine
[AD-A276743] p 3615 N94-32182

TURBOCOMPRESSORS
Inlet distortion in engines on VSTOL aircraft
[NASA-CR-195841] p 3584 N94-33035

TURBOFAN ENGINES
Development of a cascade simulation of fan-passage flow
[AD-A277234] p 3584 N94-32026
Analysis of intermediate level maintenance following F404-GE-400 engine component life reductions
[AD-A277918] p 3585 N94-33283

TURBOMACHINE BLADES
Computational prediction of stall flutter in spanwise-finite blade cascades p 3584 N94-31967
Hotwire measurements of the turbulent flow into a cascade of controlled-diffusion compressor blades
[AD-A277297] p 3706 N94-32042

TURBOMACHINERY
A solution adaptive structured-unstructured grid procedure for unsteady flows p 3700 N94-31217
Solution of the average-passage equations for the incompressible flow through multiple-blade-row turbomachinery
[AD-A276515] p 3583 N94-31931
Incorporating radial mixing in axisymmetric streamline curvature through-flow analysis
[AD-A277325] p 3706 N94-32279

TURBULENCE
Rotational effects in turbulence driven by convection
p 3930 N94-31131
A priori tests of large eddy simulation of the compressible plane mixing layer
[MEMO-1152] p 3699 N94-31185
Response of wall turbulence to high frequency streamwise and spanwise oscillations
p 3700 N94-31211
Turbulence structure of a premixed flame in a coaxial free air jet in the presence or absence of a base flow
[ISBN-0-315-78739-2] p 3633 N94-31471
Three-dimensional velocity measurements on a 6:1 prolate spheroid at 10 deg angle of attack
[AD-A276485] p 3702 N94-31476
Observations of turbulence, internal waves and background flows: An inquiry into the relationships between scales of motion p 3705 N94-31988
Hotwire measurements of the turbulent flow into a cascade of controlled-diffusion compressor blades
[AD-A277297] p 3706 N94-32042
A non-local model for prediction of the probability density function of turbulent fluctuations in boundary-layer flows
p 3706 N94-32076
Effects of buoyancy on fluid flows and turbulence
[AD-A276586] p 3706 N94-32123
A critical evaluation of the Reynolds stress turbulence closure for the flow of a turbulent free-stream over a turbulent boundary layer
[ISBN-0-315-75792-2] p 3707 N94-32497
Transport and diffusion in turbulent fields modeling and measurements techniques
[AD-A278114] p 3769 N94-33110
The structure of high Reynolds number turbulent boundary layers, part A
[AD-A278392] p 3710 N94-33162
Scalar imaging velocimetry studies of turbulent flow structure and dynamics
[AD-A278395] p 3710 N94-33164

TURBULENCE EFFECTS
Phase-only correction of scintillated laser beams: Downrange experimental results
[AD-A277778] p 3722 N94-33282

TURBULENCE MODELS
A critical evaluation of the Reynolds stress turbulence closure for the flow of a turbulent free-stream over a turbulent boundary layer
[ISBN-0-315-75792-2] p 3707 N94-32497
Additive turbulent decomposition of the incompressible and compressible Navier-Stokes equations
[AD-A277321] p 3708 N94-32511
Performance of a new wind updating system for a prognostic meteorological model in the environs of Mexico City
[DE94-006243] p 3786 N94-32937
Modification of the MML turbulence model for adverse pressure gradient flows
[NASA-TM-106544] p 3709 N94-32947
Use of Navier-Stokes methods for the calculation of high-speed nozzle flow fields
[NASA-TM-106551] p 3573 N94-32984
Renormalization group theory of Bolgiano scaling in Boussinesq turbulence
[NASA-TM-106602] p 3710 N94-33070
TURBULENT BOUNDARY LAYER
Shock impingement near mild hypersonic expansion corners p 3569 N94-31879
A non-local model for prediction of the probability density function of turbulent fluctuations in boundary-layer flows p 3706 N94-32076
A critical evaluation of the Reynolds stress turbulence closure for the flow of a turbulent free-stream over a turbulent boundary layer
[ISBN-0-315-75792-2] p 3707 N94-32497
Flight test results of riblets at supersonic speeds
[NASA-TM-4387] p 3572 N94-32880
An analysis of supersonic flows with low-Reynolds number compressible two-equation turbulence models using LU finite volume implicit numerical techniques
[NASA-CR-195302] p 3572 N94-32926
Modification of the MML turbulence model for adverse pressure gradient flows
[NASA-TM-106544] p 3709 N94-32947
The spatial development of the magnetospheric low-latitude boundary layer
[ISBN-0-315-77418-5] p 3776 N94-33111
The structure of high Reynolds number turbulent boundary layers, part A
[AD-A278392] p 3710 N94-33162
TURBULENT DIFFUSION
Incorporating radial mixing in axisymmetric streamline curvature through-flow analysis
[AD-A277325] p 3706 N94-32279
Notes on the Langevin model for turbulent diffusion of marked particles
[DE94-007847] p 3708 N94-32652
TURBULENT FLOW
Convective solar nebula p 3930 N94-31130
The small-scale topology of a 2:1 aspect-ratio elliptic jet p 3699 N94-31184
Response of wall turbulence to high frequency streamwise and spanwise oscillations p 3700 N94-31211
Research in marine boundary layer intermittency
[AD-A276076] p 3701 N94-31460
Mixture model simulating reactive turbulent flows: Testing of Eulerian-Lagrangian probabilistic models
[ONERA-NT-1993-13] p 3702 N94-31477
Finite volume discretization of the k-epsilon turbulence model in general coordinates
[REPT-93-90] p 3703 N94-31703
Finite element numerical simulation of turbulent flows
[ISBN-0-315-86416-8] p 3703 N94-31717
Numerical modelling of turbulence
[ISBN-0-315-86439-7] p 3703 N94-31720
Computational study of simultaneous heat and mass transfer in turbulent separated flows p 3704 N94-31843
Multigrid diagonal implicit solutions for compressible turbulent flows and their evaluation p 3705 N94-31941
NATO Advanced Study Institute on Unsteady Combustion. Volume 2: Research papers, September 6-17, 1993
[AD-A276572] p 3634 N94-32033
Hotwire measurements of the turbulent flow into a cascade of controlled-diffusion compressor blades
[AD-A277297] p 3706 N94-32042
A non-local model for prediction of the probability density function of turbulent fluctuations in boundary-layer flows p 3706 N94-32076
Effects of buoyancy on fluid flows and turbulence
[AD-A276586] p 3706 N94-32123
Wavevector-frequency analysis with applications to acoustics
[AD-A276618] p 3861 N94-32125
Aerodynamic drag of droplets in turbulent flow fields
[ISBN-0-315-75827-9] p 3571 N94-32491
A critical evaluation of the Reynolds stress turbulence closure for the flow of a turbulent free-stream over a turbulent boundary layer
[ISBN-0-315-75792-2] p 3707 N94-32497
Additive turbulent decomposition of the incompressible and compressible Navier-Stokes equations
[AD-A277321] p 3708 N94-32511
Notes on the Langevin model for turbulent diffusion of marked particles
[DE94-007847] p 3708 N94-32652
Numerical analysis of transonic wing buffet p 3586 N94-32713
An analysis of supersonic flows with low-Reynolds number compressible two-equation turbulence models using LU finite volume implicit numerical techniques
[NASA-CR-195302] p 3572 N94-32926
Control of low-speed turbulent separated flow over a backward-facing ramp
[NASA-TM-109740] p 3573 N94-33071
Scalar imaging velocimetry studies of turbulent flow structure and dynamics
[AD-A278395] p 3710 N94-33164
Turbulent reacting flows and supersonic combustion
[AD-A277462] p 3639 N94-33242
TURBULENT HEAT TRANSFER
Mixture model simulating reactive turbulent flows: Testing of Eulerian-Lagrangian probabilistic models
[ONERA-NT-1993-13] p 3702 N94-31477
TURBULENT MIXING
A priori tests of large eddy simulation of the compressible plane mixing layer
[MEMO-1152] p 3699 N94-31185
Laser-induced fluorescence/particle tracking system for stratified flow research
[AD-A275917] p 3701 N94-31341
Observations of turbulence, internal waves and background flows: An inquiry into the relationships between scales of motion p 3705 N94-31988
Use of Navier-Stokes methods for the calculation of high-speed nozzle flow fields
[NASA-TM-106551] p 3573 N94-32984
Turbulent reacting flows and supersonic combustion
[AD-A277462] p 3639 N94-33242
Cruise report: Oceanus 250 leg 4 high resolution profiler survey for the North Atlantic Tracer Release Experiment, 25 March - 24 April, 1992
[AD-A277935] p 3791 N94-33245
TURING MACHINES
A finite state machine model for object oriented systems
[REPT-93-040] p 3809 N94-31212
TVD SCHEMES
Viscous limiter functions for model convection-diffusion equations
[CRANFIELD-AERO-9103] p 3702 N94-31559
TWINNING
Effect of twin boundary density on the vortex melting transition in YBa2Cu3O(7-delta) single crystals
[DE94-007684] p 3904 N94-32601
TWO DIMENSIONAL FLOW
A solution adaptive structured-unstructured grid procedure for unsteady flows p 3700 N94-31217
A fully two-dimensional, non-oscillatory advection scheme for momentum and scalar transport equations
[DM-66] p 3700 N94-31221
Multigrid diagonal implicit solutions for compressible turbulent flows and their evaluation p 3705 N94-31941
On an adaptation method for dense, 2D, C-type grids
[W-9321] p 3706 N94-32045
Surface boundary conditions and related technical issues concerning Burnett equations for 2-D hypersonic flow
[AD-A277322] p 3706 N94-32256
TWO DIMENSIONAL MODELS
A fully two-dimensional, non-oscillatory advection scheme for momentum and scalar transport equations
[DM-66] p 3700 N94-31221
Multidimensional WAF-type schemes for model conservation laws
[CRANFIELD-AERO-9312] p 3843 N94-31541
Qualitative properties of two-dimensional predator-prey systems
[REPT-93-75] p 3844 N94-31644
A predator-prey model with Ivlev's functional response
[REPT-93-79] p 3844 N94-31696
Perturbative aspects of lower-dimensional gauge theories
[ISBN-0-315-86269-6] p 3911 N94-31712
On an adaptation method for 2-dimensional C-type grids
[W-9322] p 3569 N94-31822
The 2D deterministic radiation transport with the discontinuous finite element method
[DE94-004687] p 3849 N94-32670
TYPHOONS
Recurvature dynamics of a typhoon
[AD-A276792] p 3784 N94-32164
Typhoon havens handbook for the western Pacific and Indian Oceans, change 3
[AD-A277030] p 3784 N94-32260
Forecasters handbook for the Philippine Islands and surrounding waters
[AD-A277993] p 3787 N94-33089

U

U.S.S.R.
Station climatic summaries: China, the former USSR, and Mongolia
[AD-A276548] p 3784 N94-32057
Information systems to enhance technology exchange
[DE94-007744] p 3920 N94-32808
UH-60A HELICOPTER
A critical assessment of UH-60 main rotor blade airfoil data
[NASA-TM-103985] p 3571 N94-32063
ULTRAHIGH FREQUENCIES
A multichannel architecture for Naval Task Force Communication
[AD-A276230] p 3673 N94-31446
System analysis of ultra-wideband instrumentation radars: Impulse versus stepped-chirp approaches
[AD-A276624] p 3677 N94-32087
Millstone Hill radar studies of plasma waves and turbulence
[AD-A278409] p 3684 N94-33172
ULTRASHORT PULSED LASERS
Study of the dynamics of a nonlinear coupled-cavity laser system
[ISBN-0-315-86717-5] p 3716 N94-31748
ULTRASONIC AGITATION
Novel ultrasonic method for food hydration
[AD-A277411] p 3804 N94-32580
ULTRASONIC FLAW DETECTION
Evaluating in-plane elastic constants of damaged carbon-epoxy laminates using a quantitative ultrasonic technique p 3621 N94-31793
Ultrasonic characterization of damage in a simulated CF-18 composite structure
[DREP-LN-93-26] p 3730 N94-31872
ULTRASONIC RADIATION
Noninvasive spectral analysis and beam mapping of focused ultrasound, part 2
[AD-A276629] p 3861 N94-32059
ULTRASONIC SCANNERS
Ultrasonic characterization of damage in a simulated CF-18 composite structure
[DREP-LN-93-26] p 3730 N94-31872
A versatile nondestructive evaluation imaging workstation p 3732 N94-32458
ULTRASONIC TESTS
Computerized Ultrasonic Testing System (CUTS) for in-process thickness determination p 3862 N94-32456
Differential phase acoustic microscope for micro-NDE
[NASA-CR-189617] p 3731 N94-32481
PSIDD: A Post-Scan Interactive Data Display system for ultrasonic scans
[NASA-TM-4545] p 3732 N94-33038
ULTRASONIC WAVE TRANSDUCERS
Fiber optic sensors for the detection of surface acoustic waves on metals
[ISBN-0-315-87055-9] p 3878 N94-31736
ULTRASONICS
Noninvasive spectral analysis and beam mapping of focused ultrasound, part 1
[AD-A276211] p 3859 N94-31060
Ultrasonic tomography in fiber-reinforced composite materials p 3620 N94-31565
Noninvasive spectral analysis and beam mapping of focused ultrasound, part 2
[AD-A276629] p 3861 N94-32059
Novel ultrasonic method for food hydration
[AD-A277411] p 3804 N94-32580
ULTRAVIOLET ABSORPTION
Laser and Fourier transform spectroscopy of novel propellant molecules
[AD-A277506] p 3667 N94-33013
Distribution and nature of UV absorbers on Triton's surface
[NASA-CR-195886] p 3943 N94-33104
ULTRAVIOLET ASTRONOMY
Extreme ultraviolet opacity sources in the DA white dwarf G191-B2B p 3924 N94-31210
ULTRAVIOLET EMISSION
Laser and Fourier transform spectroscopy of novel propellant molecules
[AD-A277506] p 3667 N94-33013

ULTRAVIOLET LASERS
Ti:sapphire based ultrafast pump-probe laser source in the violet and ultraviolet
[DE94-007542] p 3718 N94-32270
ULTRAVIOLET RADIATION
Model of spacecraft atomic oxygen and solar exposure microenvironments p 3593 N94-31021
Fluorescence observations of LDEF exposed materials as an indicator of induced material reactions p 3593 N94-31025
Laser-induced fluorescence of space-exposed polyurethane p 3593 N94-31026
ULTRAVIOLET SPECTRA
Disk instability and the spectral evolution of the 1992 outburst of the intermediate polar GK Persei p 3928 N94-31123
The 4f heavy fermion photoelectron spectra do not exhibit the Kondo scale
[DE94-006252] p 3898 N94-31631
An analysis of ionospheric dayglow from observations of the Naval Postgraduate School Middle Ultraviolet Spectrograph (MUSTANG)
[AD-A277351] p 3773 N94-32335
Distribution and nature of UV absorbers on Triton's surface
[NASA-CR-195886] p 3943 N94-33104
How well was total ozone abundance inferred with Mariner 9 p 3947 N94-33212
ULTRAVIOLET SPECTROSCOPY
An analysis of ionospheric dayglow from observations of the Naval Postgraduate School Middle Ultraviolet Spectrograph (MUSTANG)
[AD-A277351] p 3773 N94-32335
Fiber optic chemical sensors
[AD-A277128] p 3881 N94-32380
UNDERGROUND STRUCTURES
Proceedings of the 4th Tunnel Detection Symposium on Subsurface Exploration Technology
[AD-A276372] p 3771 N94-31369
UNDERWATER ACOUSTICS
Ocean acoustic propagation measurements and wave propagation in random media
[AD-A276165] p 3787 N94-31053
Vibrational and acoustic response of ribbed plates p 3736 N94-31955
Surface forward-scattered acoustic measurements and analysis
[AD-A276998] p 3788 N94-32000
Sound scattering by cylinders of noncircular cross section
[AD-A276663] p 3861 N94-32089
Long transect seafloor seismic array: A component of SAMSON (Sources of Ambient Micro Seismic Ocean ic Noise)
[AD-A277009] p 3789 N94-32401
Acoustic window
[AD-D016171] p 3862 N94-33017
Statistical characteristics of bistatic surface scatter and mean bistatic surface scattering strengths
[AD-A278155] p 3862 N94-33096
UNDERWATER EXPLOSIONS
A study of near-surface and underwater explosions by computer simulations
[DE94-009038] p 3708 N94-32849
UNDERWATER OPTICS
Ocean optics, ocean imaging and optical tomography
[AD-A277010] p 3789 N94-32402
UNDERWATER PHYSIOLOGY
Proceedings of the DCIEM Diver Thermal Protection Workshop
[DCIEM-92-10] p 3795 N94-31738
UNIFORM FLOW
Hypervelocity Tunnel 9 Mach 10/14 Calibration
[AD-A275960] p 3587 N94-31318
UNIQUENESS
Qualitative properties of two-dimensional predator-prey systems
[REPT-93-75] p 3844 N94-31644
UNIQUENESS THEOREM
A predator-prey model with Iviev's functional response
[REPT-93-79] p 3844 N94-31696
UNITED KINGDOM
NASA/DOD Aerospace Knowledge Diffusion Research Project. Report 25: The technical communications practices of British aerospace engineers and scientists: Results of the phase 4 RAeS mail survey
[NASA-TM-109098] p 3922 N94-32836
UNITED STATES
Review and status of Maglev in the United States
[DE94-006832] p 3722 N94-31319
Aeronautics and space report of the President: Fiscal year 1993 activities p 3966 N94-32854
UNIVERSE
Testing for preferred-frame effects in gravity with artificial Earth satellites
[PB94-148459] p 3610 N94-31771
UNIVERSITIES
ISU in an era of partial reconvergence --- International Space University p 3600 N94-31438
NASA/DOD Aerospace Knowledge Diffusion Research Project. Paper 6: Aerospace knowledge diffusion in the academic community: A report of phase 3 activities of the NASA/DOD Aerospace Knowledge Diffusion Research Project
[NASA-TM-109771] p 3921 N94-32830
Aviation human factors research in US universities: Potential contributions to national needs
[NASA-TM-108814] p 3575 N94-32927
UNIVERSITY PROGRAM
Welcome to the Ohio Aerospace Institute
[NASA-TM-109756] p 3913 N94-31815
UNIX (OPERATING SYSTEM)
Extender's guide for artifacts and drafts
[AD-A276344] p 3810 N94-31328
An MS-DOS file system for UNIX
[AD-A276523] p 3816 N94-32081
Moving BASISplus and TECHLIBplus from VAX/VMS to UNIX
[DE94-004696] p 3826 N94-32248
Use and administration of UNIX (tm) systems p 3821 N94-33051
UNSTEADY AERODYNAMICS
An adaptive finite element method for unsteady compressible rotor airfoil aerodynamics p 3567 N94-31204
Aeroelastic vibrations of lifting surfaces
[ECL-91-01] p 3585 N94-31677
Experimental and computational studies on propeller noise due to inflow distortion p 3860 N94-31846
Computational prediction of stall flutter in spanwise-finite blade cascades p 3584 N94-31967
Numerical analysis of transonic wing buffet p 3586 N94-32713
Study of dynamic stall phenomenon and its control using vorticity, stream function and circulation form of the unsteady Navier-Stokes equations p 3572 N94-32714
In flight measurement of steady and unsteady blade surface pressure of a single rotation large scale advanced prop-fan installed on the PTA aircraft
[NASA-CR-187096] p 3584 N94-32859
A finite-difference approximate-factorization algorithm for solution of the unsteady transonic small-disturbance equation
[NASA-TP-3129] p 3572 N94-32865
Flutter analysis of a supersonic cascade in time domain using an ADI Euler solver
[NASA-TM-105625] p 3739 N94-32883
Modeling of aircraft unsteady aerodynamic characteristics. Part 1: Postulated models
[NASA-TM-109120] p 3586 N94-32951
The analysis of wake-induced unsteady aerodynamics related to higher harmonic control
[AD-A277914] p 3573 N94-33108
UNSTEADY FLOW
An adaptive finite element method for unsteady compressible rotor airfoil aerodynamics p 3567 N94-31204
A solution adaptive structured-unstructured grid procedure for unsteady flows p 3700 N94-31217
Simulations of the creation and motion of vortex rings
[W-9319] p 3703 N94-31691
NATO Advanced Study Institute on Unsteady Combustion. Volume 2: Research papers, September 6-17, 1993
[AD-A276572] p 3634 N94-32033
Study of dynamic stall phenomenon and its control using vorticity, stream function and circulation form of the unsteady Navier-Stokes equations p 3572 N94-32714
UPPER ATMOSPHERE
Theory, Image Simulation, and Data Analysis of Chemical Release Experiments
[NASA-CR-194865] p 3954 N94-31101
UPWELLING WATER
Evolution of upwelling fronts off the coast of Portugal
[NASA-CR-195692] p 3790 N94-33045
UPWIND SCHEMES (MATHEMATICS)
Multidimensional WAF-type schemes for model conservation laws
[CRANFIELD-AERO-9312] p 3843 N94-31541
URANIUM
Spectroscopy and atomic physics in EBIT and SuperEBIT
[DE94-006050] p 3864 N94-31508
URANIUM ALLOYS
Investigation of superconductivity and magnetism in d and f-electron materials
[DE94-008535] p 3907 N94-32933
URANIUM CARBIDES
The development of CVR coatings for PBR fuels
[DE94-004233] p 3875 N94-31480
URANUS (PLANET)
Planetary magnetotails: Magnetic configuration and nonthermal plasma p 3942 N94-32326
URBAN DEVELOPMENT
The use of SPOT, and the contribution of ERS-1, in the assessment of urban pressure on agriculture land in Greater Tunis (Tunisia) p 3749 N94-32534
URBAN PLANNING
Remote sensing for urban planning p 3758 N94-32465
The contribution of satellite data in communication infrastructure projects p 3749 N94-32530
URBAN TRANSPORTATION
Greenhouse gas emission impacts of electric vehicles under varying driving cycles in various countries and US cities
[DE94-007647] p 3765 N94-32600
USER MANUALS (COMPUTER PROGRAMS)
ADCIRC: An advanced three-dimensional circulation model for shelves, coasts, and estuaries. User's manual for ADCIRC-2DDI
[AD-A276150] p 3787 N94-31250
Predicting antenna parameters from antenna physical dimensions
[AD-A276442] p 3672 N94-31300
OTTER 3.0 reference manual and guide
[DE94-007457] p 3829 N94-31315
Extender's guide for artifacts and drafts
[AD-A276344] p 3810 N94-31328
Developing the Multimedia User Interface Component (MUSIC) for the Icarus Presentation System (IPS)
[AD-A276341] p 3810 N94-31335
E-L user's manual
[AD-A276378] p 3810 N94-31370
Users manual for SERI QC software assessing the quality of solar radiation data
[DE93-018210] p 3953 N94-31491
Hydrologic Database user's manual
[DE94-003950] p 3743 N94-31603
Arnoldi code for computing selected eigenvalues of sparse real unsymmetric matrices
[PB94-145182] p 3813 N94-31682
Noninvasive spectral analysis and beam mapping of focused ultrasound, part 2
[AD-A276629] p 3861 N94-32059
MICA, a facility to achieve portability for message-passing and dynamic memory management in FORTRAN
[DE94-006692] p 3807 N94-32147
The intelligent monitoring system: Generic Database Interface (GDI). Revised user manual
[AD-A277131] p 3919 N94-32382
GRAFTED - GRAphical fault tree EDitor: A fault tree description program for target vulnerability/survivability analysis. User manual
[AD-A277067] p 3818 N94-32390
Heliport Noise Model (HNM) version 2.2 (user's guide)
[AD-A277072] p 3861 N94-32418
THERM3D: A boundary element computer program for transient heat conduction problems
[DE94-008112] p 3708 N94-32709
METCAN demonstration manual, version 1.0
[NASA-TM-105607] p 3626 N94-32858
User's guide for a flat wake rotor inflow/wake velocity prediction code, DOWN
[NASA-TM-104139] p 3572 N94-32873
MOM3D method of moments code theory manual
[NASA-CR-189594] p 3682 N94-32897
BUCKY instruction manual, version 3.3
[NASA-TM-104793] p 3820 N94-32899
Incremental triangulation by way of edge swapping and local optimization
[NASA-TM-103979] p 3709 N94-32946
CET93 and CETPC: An interim updated version of the NASA Lewis computer program for calculating complex chemical equilibria with applications
[NASA-TM-4557] p 3638 N94-32948
Spur, helical, and spiral bevel transmission life modeling
[NASA-TM-106552] p 3728 N94-32979
Use and administration of UNIX (tm) systems p 3821 N94-33051
USER REQUIREMENTS
Automatic generation of context-sensitive textual help
[REPT-93-68] p 3812 N94-31646
A hypertext system that learns from user feedback p 3923 N94-32428
From optics to radar: Environmental problems and the SPOT/ERS systems p 3748 N94-32525
On the implementation of error handling in dynamic interfaces to scientific codes
[DE94-008970] p 3818 N94-32585
UTILITIES
Solar resource: Utility load-matching assessment
[DE94-000297] p 3758 N94-31264

Remote sensing for urban planning
p 3758 N94-32465

V

V-22 AIRCRAFT
V-22: Dual-use technology or red herring?
[AD-A276577] p 3579 N94-32058
V/STOL AIRCRAFT
Inlet distortion in engines on VSTOL aircraft
[NASA-CR-195841] p 3584 N94-33035
VACANCIES (CRYSTAL DEFECTS)
Indium-vacancy complexes in mercury cadmium telluride
[AD-A276177] p 3894 N94-31055
VACUUM
Space environment durability of beta cloth in LDEF thermal blankets p 3591 N94-31015
Vibrational spectroscopy at metal-solution interfaces: Some perspectives and prospects for electrochemical surface science
[AD-A276781] p 3644 N94-32169
Pinched propagation of high-power, pulsed electron beams for welding and materials processing applications
[AD-A276925] p 3726 N94-32236
VACUUM APPARATUS
RF vacuum microelectronics
[AD-A276512] p 3691 N94-31928
VACUUM ARC SWITCHES
Theoretical studies on ionospheric irregularities and ion diode performance
[AD-A277115] p 3772 N94-31984
VACUUM EFFECTS
Dispersion relations for a plasma-filled helix-loaded-waveguide
[DE94-006333] p 3675 N94-31781
VALENCE
A polynomial representation of the valence orbital ionization potentials
[USIP-93-06] p 3640 N94-31083
Characterization of the rare earth orthophosphates and Ce-doped LaPO4 by x ray absorption spectroscopy
[DE94-006313] p 3898 N94-31630
VAN DE GRAAFF ACCELERATORS
Knowledge engineering for PACES, the particle accelerator control expert system p 3854 N94-33342
VAN DER WAALS FORCES
Wave packet studies of the vibrational predissociation of three and four-atom van der Waals complexes
[DE94-007623] p 3871 N94-32598
Metal cluster-rare gas van der Waals complexes: Microscopic models of physisorption
[DE94-008134] p 3873 N94-32797
VANADIUM
Tensile properties of commercially pure vanadium from room temperature to 1200 C
[DE94-006622] p 3641 N94-31581
VANADIUM ALLOYS
Creep properties of vanadium-base alloys
[DE94-006541] p 3641 N94-31486
Effect of irradiation damage and helium on the swelling and structure of vanadium-base alloys
[DE94-006540] p 3641 N94-31666
A state variable material model for superplastic titanium-6 percent Al-4 percent V p 3644 N94-32498
VANADIUM COMPOUNDS
Molecular/polymeric magnetism
[DE94-005888] p 3649 N94-31201
Development of vanadium-phosphate catalysts for methanol production by selective oxidation of methane
[DE94-006759] p 3759 N94-31272
VAPOR DEPOSITION
The development of CVR coatings for PBR fuels
[DE94-004233] p 3875 N94-31480
A silicon condenser microphone: Materials and technology
[ISBN-9-09-005899-0] p 3688 N94-31518
Chemical vapour deposition of tungsten for the application in integrated circuits
[ISBN-9-09-005151-1] p 3641 N94-31519
Degenerate four-wave mixing as a diagnostic of plasma chemistry
[DE94-008588] p 3889 N94-31766
Chemical vapor deposition of metal nitrides, phosphides, and arsenides
[DE94-008096] p 3654 N94-31976
Chemical vapor deposition fluid flow simulation modelling tool
[NASA-CR-189648] p 3707 N94-32480
Engineering scale development of the Vapor-Liquid-Solid (VLS) process for the production of silicon carbide fibrils
[DE94-007132] p 3659 N94-32618
Anisotropic phase separation through the metal-insulator transition in amorphous Mo-Ge and Fe-Ge alloys
[DE94-007259] p 3646 N94-32795
VAPOR PHASE EPITAXY
Advances in MOVPE compound semiconductor epitaxy manufacturing technology: From high throughput large area reactors to cluster tools
[DE94-006367] p 3901 N94-32104
New zinc-bis(dialkylamides) potentially usable as site-selective dopants for p-type ZnSe
[AD-A276947] p 3902 N94-32218
Research on high reliability refractory ohmic contacts for GaAs FETs and MODFETs
[AD-A276848] p 3697 N94-33034
VAPOR PHASES
Modern integral equation techniques for quantum reactive scattering theory
[DE94-007039] p 3857 N94-31639
Metal clusters: Dynamics and structure
[AD-A276842] p 3643 N94-32091
Vibrational spectroscopy at metal-solution interfaces: Some perspectives and prospects for electrochemical surface science
[AD-A276781] p 3644 N94-32169
New zinc-bis(dialkylamides) potentially usable as site-selective dopants for p-type ZnSe
[AD-A276947] p 3902 N94-32218
Formation of gas-phase peroxides in a rural atmosphere: An interpretation of the recent SOS/SERON field results
[DE94-002995] p 3766 N94-32692
VAPOR PRESSURE
New zinc-bis(dialkylamides) potentially usable as site-selective dopants for p-type ZnSe
[AD-A276947] p 3902 N94-32218
VAPORIZING
Ultrahigh-current-density metal-ion implantation and diamondlike-hydrocarbon films for tribological applications
[DE94-008958] p 3906 N94-32843
VAPORS
Empirical and semi-empirical relationships of liquid-vapor, solid-vapor, and solid-liquid surface energies
[AD-A276480] p 3631 N94-31248
Using laser absorption spectroscopy to monitor composition and physical properties of metal vapors
[DE94-001530] p 3716 N94-31599
Measurement of viscosity, density, and gas solubility of refrigerant blends in selected synthetic lubricants
[DE94-007723] p 3653 N94-31917
Remote infrared vapor detection of volatile organic compounds
[AD-A276982] p 3746 N94-31999
VARIABILITY
Diagnostic studies of climate variability
[DE94-003629] p 3767 N94-32711
Aspects of modeling uncertainty and prediction
[DE94-007565] p 3852 N94-32744
Spatial correlation of ionospheric variability
[AD-A278105] p 3776 N94-33041
VARIABLE GEOMETRY STRUCTURES
Real-time control of the Trussarm variable-geometry-truss manipulator utilizing machine vision
[ISBN-0-315-87054-0] p 3830 N94-31735
VARIATIONAL PRINCIPLES
Finite element analysis of time-independent superconductivity p 3691 N94-31905
VECTOR ANALYSIS
Theoretical basis for state vector comparison, relative position display, and relative position/rendezvous prediction
[AD-A277216] p 3608 N94-32020
VECTOR DOMINANCE MODEL
The form factors of the nucleons
[DE94-007096] p 3872 N94-32630
VECTOR MESONS
The form factors of the nucleons
[DE94-007096] p 3872 N94-32630
VECTOR PROCESSING (COMPUTERS)
Parallel processing for differencing and histogramming
[AD-A277060] p 3826 N94-32274
VECTOR QUANTIZATION
Applications of data compression to 3-D scalar field visualization p 3817 N94-32294
VECTOR SPACES
The Cameron-Martin theorem
[W-9315] p 3844 N94-31676
Stability and instability criteria for magnetohydrodynamics
[PB94-148475] p 3889 N94-31772
VEGETATION
Modeling of the continental biosphere
p 3770 N94-31011
Analysis of GER imaging spectrometry data for the identification of soil and vegetation parameters in land degradation studies p 3744 N94-31857
Inflight calibration, preprocessing, and data evaluation of GER 2 imaging spectrometry data
p 3744 N94-31858
The effects of vegetation on the ability to map soils using GERIS data p 3744 N94-31860
Feasibility evaluation of new data interpretation approaches for vegetation analysis from airborne imaging spectroscopy p 3745 N94-31862
Monitoring fertilizer application by imaging spectrometry (Somerset Levels test site) p 3745 N94-31863
High resolution spectroscopy in agriculture: Results of the EISAC 1989 campaign p 3745 N94-31864
Extraction of agricultural parameters from imaging-spectrometry data and simulated MERIS data through red edge analysis p 3745 N94-31865
Use of SPOT and ERS-1 to map tropical vegetation and mangrove dynamics in Guiana p 3753 N94-32555
Dry deposition of PAN to grassland vegetation
[DE94-005111] p 3768 N94-32894
VEGETATIVE INDEX
Synergy of thermal infrared and microwave remote sensing for evaporation estimation p 3754 N94-32559
Quantitative analysis of woody vegetation in Soudano-Sahalian region. Textural approach (application to a Burkina Faso region) p 3757 N94-32574
VEHICLES
Automatic contact in DYNA3D for vehicle crashworthiness
[DE94-007143] p 3738 N94-32637
VELOCITY DISTRIBUTION
Atomic oxygen interaction at defect sights in protective coatings on polymers flown on LDEF
p 3593 N94-31024
Three-dimensional velocity measurements on a 6:1 prolate spheroid at 10 deg angle of attack
[AD-A276485] p 3702 N94-31476
The kinematics of dense clusters of galaxies
p 3937 N94-32029
Scalar imaging velocimetry studies of turbulent flow structure and dynamics
[AD-A278395] p 3710 N94-33164
VELOCITY MEASUREMENT
A preliminary investigation of high amplitude standing waves with laser Doppler anemometry
[AD-A276463] p 3860 N94-31242
Three-dimensional velocity measurements on a 6:1 prolate spheroid at 10 deg angle of attack
[AD-A276485] p 3702 N94-31476
Measuring the Hubble constant and our Virgo-infall velocity independently p 3926 N94-31968
Scalar imaging velocimetry studies of turbulent flow structure and dynamics
[AD-A278395] p 3710 N94-33164
VENTING
Honeycomb sandwich structures: Vented versus unvented designs for space systems
[AD-A276713] p 3624 N94-32122
VENTS
Light in Thermal Environments (LITE) Workshop
[NASA-CR-195851] p 3790 N94-32981
VENUS (PLANET)
Tectonic History of the Terrestrial Planets
[NASA-CR-195696] p 3939 N94-31105
Patterns of deformation and volcanic flows associated with lithospheric loading by large volcanoes on Venus
p 3776 N94-31106
Geoid-to-topography ratios on Venus: A global perspective p 3940 N94-31110
The tectonic and volcanic evolution of Venus: Catastrophic or gradual? p 3940 N94-31111
Keeping that youthful look --- impact cratering of Venus p 3941 N94-31112
A tectonic resurfacing model for Venus
p 3941 N94-31113
The resurfacing controversy for Venus: An overview and a mechanistic perspective p 3941 N94-31114
Plains tectonism on Venus: The deformation belts of Lavinia Planitia p 3941 N94-31115
A study of areas of low radio-thermal emissivity on Venus p 3942 N94-31992
VENUS ATMOSPHERE
Multiple scattering of polarized radiation in planetary atmospheres
[ETN-94-96018] p 3674 N94-31551
VENUS SURFACE
Patterns of deformation and volcanic flows associated with lithospheric loading by large volcanoes on Venus
p 3776 N94-31106
Geoid-to-topography ratios on Venus: A global perspective p 3940 N94-31110
Keeping that youthful look --- impact cratering of Venus p 3941 N94-31112

The resurfacing controversy for Venus: An overview and a mechanistic perspective p 3941 N94-31114
Plains tectonism on Venus: The deformation belts of Lavinia Planitia p 3941 N94-31115
A study of areas of low radio-thermal emissivity on Venus p 3942 N94-31992

VERBAL COMMUNICATION
Virtual annotation: Verbal communication in virtual reality
[REPT-93-67] p 3674 N94-31645

VERSATILITY
Design patterns mixing genericity and inheritance in the development of reusable components
[REPT-93-021] p 3808 N94-31178

VERTICAL MOTION
Three dimensional vorticity field in the California current system
[AD-A276951] p 3788 N94-32220
Simulation of a precipitation event in the western United States
[DE94-004835] p 3786 N94-32791

VERY LARGE SCALE INTEGRATION
A neuron network for image classification: From algorithm to implantation
[TELECOM-93-E-005] p 3687 N94-31168
VLSI implementation of stray insensitive switched capacitor composite operational amplifiers
[AD-A276461] p 3687 N94-31240
Module generation for self-testing integrated systems
[ISBN-9-09-004570-8] p 3688 N94-31520
A hierarchical approach to test generation for CMOS VLSI circuits
[ISBN-9-09-005449-9] p 3689 N94-31535
An analysis of instruction-cached SIMD computer architecture
[AD-A276519] p 3806 N94-31934
Application of the modified voltage-dividing potentiometer to overlay metrology in a CMOS/bulk process
[DE94-007937] p 3695 N94-32700
VLSI for high-speed digital signal processing
[AD-A277617] p 3697 N94-32957

VERY LOW FREQUENCIES
Lightning-induced coupling of the radiation belts to geomagnetically conjugate ionospheric regions p 3772 N94-31773
Applied Computational Electromagnetics Society Journal, volume 9, number 1, March 1994
[AD-A276753] p 3679 N94-32183

VESTIBULAR TESTS
Model-based scientific discovery: A study in space bioengineering p 3799 N94-31990

VHSIC (CIRCUITS)
Formal semantics for a subset of VHDL and its use in analysis of the FTPP scoreboard circuit
[NASA-CR-191577] p 3827 N94-32734

VIBRATION
Vibration control and design of composite cantilevers taking into account structural uncertainties and damage p 3733 N94-31213
Vibration dampener and method for making same
[AD-D016094] p 3739 N94-32733
Limiting vibration in systems with constant amplitude actuators through command preshaping
[NASA-CR-188284] p 3739 N94-32907
Microreflectance infrared study of electron-molecular vibrational coupling and lattice softness in BEDT-TTF salts
[DE94-008490] p 3907 N94-32989
Design, development, and testing of a lightweight optical sensor cover system p 3604 N94-33302
Intelligent control of a multi-degree-of freedom reaction compensating platform system using fuzzy logic p 3605 N94-33306

VIBRATION DAMPING
Vibration control and design of composite cantilevers taking into account structural uncertainties and damage p 3733 N94-31213
Transmissibility of nickel-titanium shape memory alloy springs
[AD-A276055] p 3640 N94-31456
Control of a flexible space robot tracking a moving target p 3722 N94-31469
Passive vibration damping materials: Piezoelectric ceramic composites for vibration damping applications
[AD-A276550] p 3653 N94-31935
The 10th International Conference on Internal Friction and Ultrasonic Attenuation in Solids (ICIFUAS)
[AD-A276849] p 3902 N94-32209
Vibration dampener and method for making same
[AD-D016094] p 3739 N94-32733
Feed-forward control of gear mesh vibration using piezoelectric actuators
[NASA-TM-106366] p 3728 N94-32902
Limiting vibration in systems with constant amplitude actuators through command preshaping
[NASA-CR-188284] p 3739 N94-32907
Structural damping studies at cryogenic temperatures
[NASA-TM-109073] p 3740 N94-33118
Intelligent control of a multi-degree-of freedom reaction compensating platform system using fuzzy logic p 3605 N94-33306

VIBRATION ISOLATORS
Transmissibility of nickel-titanium shape memory alloy springs
[AD-A276055] p 3640 N94-31456
Vibration Isolation Technology (VIT) ATD project
[NASA-TM-106496] p 3567 N94-33064

VIBRATION MODE
Vibration control and design of composite cantilevers taking into account structural uncertainties and damage p 3733 N94-31213
Nonlinear vibration analysis of laminated plates on linear and nonlinear elastic foundations p 3737 N94-32079

VIBRATION SIMULATORS
A direct digital design for a multichannel structural test system using the characteristic locus method
[MATHS-REPT-A-206] p 3828 N94-31161

VIBRATION TESTS
A direct digital design for a multichannel structural test system using the characteristic locus method
[MATHS-REPT-A-206] p 3828 N94-31161

VIBRATIONAL SPECTRA
Degenerate four-wave mixing as a diagnostic of plasma chemistry
[DE94-008588] p 3889 N94-31766
Vibrational spectroscopy at metal-solution interfaces: Some perspectives and prospects for electrochemical surface science
[AD-A276781] p 3644 N94-32169

VIBRATIONAL STATES
Time-resolved infrared absorption studies applied to the study of radical plus molecule reactions
[DE94-005921] p 3863 N94-31202
Vibrational energy transfer of diatomic gases in hypersonic expanding flows p 3570 N94-31958
Electronic and nuclear factors in intramolecular charge and excitation transfer processes
[DE94-006598] p 3870 N94-32178
Cooling and trapping of neutral atoms
[AD-A276957] p 3870 N94-32360
Wave packet studies of the vibrational predissociation of three and four-atom van der Waals complexes
[DE94-007623] p 3871 N94-32598

VIDEO COMMUNICATION
Voice and video transmission using XTP and FDDI p 3685 N94-32468
COVICS: A covert video communications system
[DE94-007568] p 3682 N94-32745

VIDEO COMPRESSION
A visual detection model for DCT coefficient quantization p 3850 N94-32467

VIDEO DATA
First-wall heat-flux measurements during ELMing H-mode plasma
[DE94-008310] p 3888 N94-31765

VIDEO EQUIPMENT
Development of a video fluorescence system for assessing burn depth
[AD-A278127] p 3798 N94-33092

VIDEO SIGNALS
An experimental compact Hi-Vision VCR using metal evaporated tape
[NHK-LABS-NOTE-423] p 3683 N94-33081

VIDEO TAPE RECORDERS
Night vision camcorder system
[AD-A277004] p 3712 N94-32002
An experimental compact Hi-Vision VCR using metal evaporated tape
[NHK-LABS-NOTE-423] p 3683 N94-33081

VIDEO TAPES
An experimental compact Hi-Vision VCR using metal evaporated tape
[NHK-LABS-NOTE-423] p 3683 N94-33081

VIEWING
Visual perception of 3-dimensional structure from different types of optical deformation
[AD-A278272] p 3884 N94-33141

VINYL COPOLYMERS
Dynamics of block poly(styrene-co-vinylpyridine) (SVP) in solution and on silica
[AD-A277139] p 3657 N94-32364

VINYL POLYMERS
PVDF pressure transducers for shock wave and explosives research
[AD-A277319] p 3712 N94-32051
Hydrogen peroxide electrodes based on electrical connection of redox centers of various peroxidases to electrodes through a three-dimensional electron relaying polymer network
[AD-A276543] p 3691 N94-32056
Electrical communication between glucose oxidase and electrodes based on poly(vinylimidazole) complex of Os(bpy)2Cl2
[AD-A276585] p 3835 N94-32231
Conversion of polymers of methyl- and vinylsilane to Si-C ceramics
[NASA-TM-106554] p 3662 N94-32945

VINYL RADICAL
Design of new polymers to improve radiation stability of plastic scintillators
[DE94-008220] p 3652 N94-31764

VINYLIDENE
PVDF pressure transducers for shock wave and explosives research
[AD-A277319] p 3712 N94-32051

VIRGO GALACTIC CLUSTER
Measuring the Hubble constant and our Virgo-infall velocity independently p 3926 N94-31968

VIRTUAL MEMORY SYSTEMS
A comparison of distributed memory and virtual shared memory parallel programming models
[DE94-005473] p 3825 N94-31663
Compiler techniques for managing data motion
[AD-A276514] p 3918 N94-31930

VIRTUAL REALITY
Virtual annotation: Verbal communication in virtual reality
[REPT-93-67] p 3674 N94-31645
Designing in virtual reality: Modelling Objects in a Virtual Environment (MOVE)
[REPT-93-91] p 3813 N94-31704
Interactive graphical model building using telepresence and virtual reality
[DE94-001421] p 3818 N94-32353
Virtual reality in medical education and assessment p 3798 N94-32471

VISCOELASTICITY
State of stress, faulting, and eruption characteristics of large volcanoes on Mars p 3940 N94-31108
Viscoelastic fracture characterization of polymeric solids p 3652 N94-31745
Influence of trace components on the viscoelastic properties of a polymer solution
[AD-A277171] p 3656 N94-32253
Elastic as limit of viscoelastic response, in a context of self-similar viscous limits
[AD-A277043] p 3738 N94-32273
A thermal viscoelastic analysis for thick-walled composite cylinders
[AD-A274143] p 3625 N94-32604

VISCOMETERS
Dielectric viscometer including fixed and variable cells
[AD-D016139] p 3639 N94-32973

VISCOPLASTICITY
Inelastic deformation of metal matrix composites p 3618 N94-31285
Micromechanics and effective properties of particulate composites and fluid suspensions p 3703 N94-31744
New micro- and macroscopic models of contact and friction
[AD-A277240] p 3726 N94-32320
A state variable material model for superplastic titanium-6 percent Al-4 percent V p 3644 N94-32498

VISCOSITY
Nonlinear calculations of the time evolution of black hole accretion disks p 3929 N94-31127
Convective solar nebula p 3930 N94-31130
Rotational effects in turbulence driven by convection p 3930 N94-31131
Measurement of viscosity, density, and gas solubility of refrigerant blends in selected synthetic lubricants
[DE94-007723] p 3653 N94-31917
Status of developing a multifunctional aviation grease
[AD-A276755] p 3656 N94-32184
Influence of trace components on the viscoelastic properties of a polymer solution
[AD-A277171] p 3656 N94-32253
Dielectric viscometer including fixed and variable cells
[AD-D016139] p 3639 N94-32973

VISCOUS FLOW
A solution adaptive structured-unstructured grid procedure for unsteady flows p 3700 N94-31217
Numerical analysis of single-vortex/free-surface interaction
[AD-A276462] p 3701 N94-31241
Viscous limiter functions for model convection-diffusion equations
[CRANFIELD-AERO-9103] p 3702 N94-31559

Finite element vorticity-based methods for the solution of the incompressible and compressible Navier-Stokes equations
[ISBN-0-315-87265-9] p 3703 N94-31730
Incompressible viscous flow in tubes with occlusions
[ISBN-0-315-75467-2] p 3704 N94-31778
Attitude dynamics of spinning rockets in space with internal mass motion p 3601 N94-31802
On an adaptation method for dense, 2D, C-type grids
[W-9321] p 3706 N94-32045
Incorporating radial mixing in axisymmetric streamline curvature through-flow analysis
[AD-A277325] p 3706 N94-32279
A novel potential/viscous flow coupling technique for computing helicopter flow fields
[NASA-CR-193272] p 3571 N94-32476

VISCOUS FLUIDS
Oscillations in piston-driven shear flow of a non-Newtonian fluid
[AD-A276472] p 3701 N94-31245
Attitude dynamics of spinning rockets in space with internal mass motion p 3601 N94-31802

VISIBILITY
Synthetic vision technology demonstration. Volume 1: Executive summary
[DOT/FAA/RD-93/40-VOL-1] p 3582 N94-33076
Synthetic vision technology demonstration. Volume 2: Sensor tower testing
[DOT/FAA/RD-93/40-VOL-2] p 3582 N94-33077
Synthetic vision technology demonstration. Volume 3: Flight tests
[DOT/FAA/RD-93/40-VOL-3] p 3582 N94-33078
Synthetic vision technology demonstration. Volume 4: Appendices
[DOT/FAA/RD-93/40-VOL-4] p 3583 N94-33079

VISIBLE SPECTRUM
A historical perspective on fifteen years of laser damage thresholds at LLNL
[DE94-007930] p 3719 N94-32613

VISION
Sensory sensitivities and discriminations and their roles in aviation
[AD-A277312] p 3800 N94-32276
Workshop on Visual Perception: Computation and Psychophysics
[AD-A278412] p 3802 N94-33326

VISUAL AIDS
Variable-resolution imagery for flight simulation
[AD-A276199] p 3586 N94-31058

VISUAL CONTROL
Technology transfer of operator-in-the-loop simulation p 3802 N94-32472

VISUAL DISCRIMINATION
Variable-resolution imagery for flight simulation
[AD-A276199] p 3586 N94-31058
Sensory sensitivities and discriminations and their roles in aviation
[AD-A277312] p 3800 N94-32276
A visual detection model for DCT coefficient quantization p 3850 N94-32467

VISUAL FIELDS
Variable-resolution imagery for flight simulation
[AD-A276199] p 3586 N94-31058

VISUAL OBSERVATION
Construction of visual representations and time-space organization of resources in astronomy
[ISBN-0-315-86694-2] p 3925 N94-31914
Use of Air Force cloud cover data to evaluate and improve cloud forecasts and parameterizations in mesocale meteorological models
[AD-A277384] p 3784 N94-32054
An integrated cloud observation and modeling investigation in support of the ARM program
[DE94-003160] p 3785 N94-32716
Use of cloud observations and mesoscale meteorology models to evaluate and improve cloud parameterizations
[DE94-003610] p 3785 N94-32717

VISUAL PERCEPTION
Morphological directional coding of images
[ISBN-0-315-86336-6] p 3814 N94-31715
Analysis of pursuit tracking eye movements in pilots and nonfliers
[AD-A276597] p 3799 N94-32035
Algebraic functions for recognition
[AD-A276803] p 3846 N94-32167
Modular Simulator System (MSS). System/segment specification for the generic modular simulator system-visual module, volume 11
[AD-A276978] p 3589 N94-32317
Visual encoding of spatial relations
[AD-A277400] p 3800 N94-32344
Visual neural development and chromatic aberration
[AD-A277402] p 3800 N94-32345
Information theory for arm visuo-motor coordination p 3800 N94-32495
Mechanisms of temporal pattern discrimination by human observers
[AD-A277407] p 3801 N94-32577
Models of the neuronal mechanisms of target localization of the barn owl
[AD-A277332] p 3797 N94-32623
Visual processing of object velocity and acceleration
[AD-A277425] p 3801 N94-32998
Synthetic vision technology demonstration. Volume 2: Sensor tower testing
[DOT/FAA/RD-93/40-VOL-2] p 3582 N94-33077
Synthetic vision technology demonstration. Volume 3: Flight tests
[DOT/FAA/RD-93/40-VOL-3] p 3582 N94-33078
Visual perception of 3-dimensional structure from different types of optical deformation
[AD-A278272] p 3884 N94-33141
Workshop on Visual Perception: Computation and Psychophysics
[AD-A278412] p 3802 N94-33326

VISUAL SIGNALS
Visual processing of object velocity and acceleration
[AD-A277425] p 3801 N94-32998

VISUAL TASKS
Optical flow from 1D correlation: Application to a simple time-to-crash detector
[AD-A276777] p 3880 N94-32186

VITERBI DECODERS
Methods of implementing the Viterbi algorithm on a massively parallel computer of the SIMD (single instruction multiple data) type
[ISBN-0-315-86783-3] p 3814 N94-31752

VOICE COMMUNICATION
Virtual annotation: Verbal communication in virtual reality
[REPT-93-67] p 3674 N94-31645
Voice and video transmission using XTP and FDDI p 3685 N94-32468
An exploratory study of neuro linguistic programming and communication anxiety
[AD-A277756] p 3682 N94-32986

VOICE CONTROL
Application of the wavelet transform for speech processing p 3600 N94-31435

VOICE DATA PROCESSING
Application of the wavelet transform for speech processing p 3600 N94-31435
Spectral analysis method and sample generation for real time visualization of speech
[ETN-94-95732] p 3674 N94-31573

VOIDS
The influence of transmutation, void swelling, and flux/spectra uncertainties on the electrical properties of copper and copper alloys
[DE94-006213] p 3641 N94-31626
An experimental study of void formation during aluminum solidification in reduced gravity p 3667 N94-31944

VOLATILITY
Remote infrared vapor detection of volatile organic compounds
[AD-A276982] p 3746 N94-31999
Volatiles combustion in fluidized beds
[DE94-008382] p 3636 N94-32414
Magmatic volatiles and the weathering of Mars p 3946 N94-33201

VOLCANOES
Tectonic History of the Terrestrial Planets
[NASA-CR-195696] p 3939 N94-31105
Patterns of deformation and volcanic flows associated with lithospheric loading by large volcanoes on Venus p 3776 N94-31106
Aspects of modelling the tectonics of large volcanoes on the terrestrial planets p 3940 N94-31107
State of stress, faulting, and eruption characteristics of large volcanoes on Mars p 3940 N94-31108
The tectonic and volcanic evolution of Venus: Catastrophic or gradual? p 3940 N94-31111
Keeping that youthful look --- impact cratering of Venus p 3941 N94-31112
A tectonic resurfacing model for Venus p 3941 N94-31113
The resurfacing controversy for Venus: An overview and a mechanistic perspective p 3941 N94-31114
Plains tectonism on Venus: The deformation belts of Lavinia Planitia p 3941 N94-31115
Time-dependent behavior of Mount Pinatubo aerosol
[DE94-001877] p 3764 N94-31601
Concentration system performance degradation in the aftermath of Mount Pinatubo
[DE94-001879] p 3764 N94-31602
The use of SPOT and ERS-1 images to map the eruption of Nevado Sabancaya (Province of Arequipa, South Peru) and evaluate associated risks p 3751 N94-32546

VOLCANOLOGY
Aspects of modelling the tectonics of large volcanoes on the terrestrial planets p 3940 N94-31107
State of stress, faulting, and eruption characteristics of large volcanoes on Mars p 3940 N94-31108
The tectonic and volcanic evolution of Venus: Catastrophic or gradual? p 3940 N94-31111
Keeping that youthful look --- impact cratering of Venus p 3941 N94-31112
A tectonic resurfacing model for Venus p 3941 N94-31113
The resurfacing controversy for Venus: An overview and a mechanistic perspective p 3941 N94-31114
Evidence for ultramafic lavas on Syrtis Major p 3950 N94-33229

VOLTAGE CONVERTERS (DC TO DC)
A series resonant converter in half bridge circuits with combined serial and parallel charge coupling and several output circuits
[ETN-94-95739] p 3687 N94-31373
Examination of fast semiconductor diodes (recovery) with respect to switching valves in PWM and resonance devices
[ETN-94-95740] p 3690 N94-31609

VOLUME
Apron heights around stepped massifs in the Cydonia Mensae region: Do they record the local paleobathymetry of Oceanus Borealis? p 3949 N94-33224

VORTEX ALLEVIATION
A study of the development and attenuation of wing-generated, vortical wakes p 3570 N94-31971

VORTEX BREAKDOWN
On the structure and stability of slender viscous vortices p 3700 N94-31218

VORTEX GENERATORS
Control of low-speed turbulent separated flow over a backward-facing ramp
[NASA-TM-109740] p 3573 N94-33071

VORTEX RINGS
Simulations of the creation and motion of vortex rings
[W-9319] p 3703 N94-31691

VORTEX SHEDDING
The effect of an axial flow component on a circular cylinder wake p 3699 N94-31209
Field studies of raindrop oscillations with applications to radar meteorology p 3782 N94-31743
Control of low-speed turbulent separated flow over a backward-facing ramp
[NASA-TM-109740] p 3573 N94-33071

VORTEX SHEETS
A study of weak solutions and their regularizations by numerical methods
[AD-A277453] p 3850 N94-33175

VORTICES
Rotational effects in turbulence driven by convection p 3930 N94-31131
The small-scale topology of a 2:1 aspect-ratio elliptic jet p 3699 N94-31184
A priori tests of large eddy simulation of the compressible plane mixing layer
[MEMO-1152] p 3699 N94-31185
On the structure and stability of slender viscous vortices p 3700 N94-31218
Numerical analysis of single-vortex/free-surface interaction
[AD-A276462] p 3701 N94-31241
Field studies of raindrop oscillations with applications to radar meteorology p 3782 N94-31743
Tip effects on the vortex wake of an axisymmetric body at angle of attack p 3570 N94-31907
A study of the development and attenuation of wing-generated, vortical wakes p 3570 N94-31971
Analysis and computation for vortex dynamics and rarefied gases
[AD-A277415] p 3708 N94-32581
Notes on the Langevin model for turbulent diffusion of marked particles
[DE94-007847] p 3708 N94-32652
Quantum fluctuations of vortices in Josephson-coupled superconductors
[DE94-007609] p 3905 N94-32747
New advances in the modeling of high-temperature superconductors
[DE94-007649] p 3905 N94-32815
Active vortex control for a high performance wing
[AD-D016140] p 3573 N94-32974
Control of low-speed turbulent separated flow over a backward-facing ramp
[NASA-TM-109740] p 3573 N94-33071
Installed F/A-18 inlet flow calculations at 30 degrees angle-of-attack: A comparative study
[NASA-CR-195297] p 3573 N94-33119
Stationary eddies in the Mars general circulation as simulated by the NASA-Ames GCM p 3944 N94-33192
Eddy transport of water vapor in the Martian atmosphere p 3949 N94-33221

VORTICITY
Convective solar nebula p 3930 N94-31130

The small-scale topology of a 2:1 aspect-ratio elliptic jet p 3699 N94-31184
The effect of an axial flow component on a circular cylinder wake p 3699 N94-31209
On wave interactions of rotational and irrotational flows p 3700 N94-31219
A study of the development and attenuation of wing-generated, vortical wakes p 3570 N94-31971
Three dimensional vorticity field in the California current system
[AD-A276951] p 3788 N94-32220

VORTICITY EQUATIONS
On wave interactions of rotational and irrotational flows p 3700 N94-31219
Finite element vorticity-based methods for the solution of the incompressible and compressible Navier-Stokes equations
[ISBN-0-315-87265-9] p 3703 N94-31730

VSAT (NETWORK)
Hubless satellite communications networks p 3600 N94-31433

VULNERABILITY
GRAFTED - GRAphical fault tree EDitor: A fault tree description program for target vulnerability/survivability analysis. User manual
[AD-A277067] p 3818 N94-32390
Vulnerability assessment of a space based weapon platform electronic system exposed to a thermonuclear weapon detonation
[DE94-007229] p 3611 N94-32667

W

WAFERS
Epitaxial liftoff technology onto processed silicon foundry wafers
[AD-A277116] p 3900 N94-31985
Determination of BPSG thin-film properties using IR reflection spectroscopy of product wafers
[DE94-006591] p 3634 N94-32110
Silicon-Film(tm) photovoltaic manufacturing technology
[DE94-000202] p 3760 N94-32143
A scanning defect mapping system for semiconductor characterization p 3865 N94-32446
Metal-ion spin-on glasses: Novel materials for active waveguides
[DE94-007738] p 3882 N94-32649
Application of the modified voltage-dividing potentiometer to overlay metrology in a CMOS/bulk process
[DE94-007937] p 3695 N94-32700

WAKES
The effect of an axial flow component on a circular cylinder wake p 3699 N94-31209
Gravitational effects of cosmic strings
[ISBN-0-315-75484-2] p 3934 N94-31789
Tip effects on the vortex wake of an axisymmetric body at angle of attack p 3570 N94-31907
Ship traffic monitoring and oil spill detection using the ERS-1 SAR p 3751 N94-32542
Superluminous laser pulse in an active medium
[DE94-007110] p 3720 N94-32684

WALKING
Tripping over obstacles: Biomechanical analyses of how young and old try to avoid it p 3803 N94-31954

WALL FLOW
Response of wall turbulence to high frequency streamwise and spanwise oscillations p 3700 N94-31211
Control of hypersonic aerodynamic forces with surface blowing p 3567 N94-31216
Oscillations in piston-driven shear flow of a non-Newtonian fluid
[AD-A276472] p 3701 N94-31245

WALLOPS ISLAND
Operations summary for the convection and moisture experiment (CAMEX)
[NASA-TM-108445] p 3786 N94-33004

WALLS
Operation of D3-D with all-graphite walls
[DE94-004858] p 3886 N94-31304

WARFARE
Naval Surface Warfare Center Dahlgren Division Technical Digest: Advanced materials technology
[AD-A276448] p 3668 N94-31364

WARNING SYSTEMS
Covert channel analysis of trusted systems. A guide to understanding
[AD-A276418] p 3916 N94-31331

WASTE DISPOSAL
Sandia technology engineering and science accomplishments
[DE94-008312] p 3668 N94-32412

WASTE ENERGY UTILIZATION
Detailed design of the 2MW Demonstration Plant
[DE94-000042] p 3762 N94-32823

WASTE WATER
Catalytic methods using molecular oxygen for treatment of PMMS and ECLSS waste streams, volume 2
[NASA-CR-190299] p 3804 N94-32697

WATER
Interaction of water with metal surfaces
[AD-A276260] p 3632 N94-31293
Development of a catalytic system for gasification of wet biomass
[DE94-006216] p 3759 N94-31762
Glutinous water: Protecting vertical and overhead surfaces from fire spread
[AD-A277280] p 3575 N94-32405
Surface probes of porous toluene/water ices: Adsorption kinetics and annealing spectra measured by second harmonic generation
[DE94-007564] p 3637 N94-32743
Simulation of a precipitation event in the western United States
[DE94-004835] p 3786 N94-32791
Thermal and hydraulic considerations regarding the fate of water discharged by the outflow channels to the Martian northern plains p 3946 N94-33202
Geologic controls of erosion and sedimentation on Mars p 3951 N94-33232
Simultaneous laboratory measurements of CO2 and H2O adsorption on palagonite: Implications for the Martian climate and volatile reservoir p 3952 N94-33240

WATER CURRENTS
ADCIRC: An advanced three-dimensional circulation model for shelves, coasts, and estuaries. User's manual for ADCIRC-2DDI
[AD-A276150] p 3787 N94-31250

WATER HAMMER
Fluid-structure interaction in case of water hammer with cavitation
[PB94-148277] p 3702 N94-31588

WATER IMMERSION
Validation and sensitivity analysis of Texas human thermal model predictions during cold water immersion
[AD-A275240] p 3797 N94-32156

WATER POLLUTION
Focused feasibility study final field sampling plan
[AD-A277445] p 3769 N94-33105

WATER RECLAMATION
Catalytic methods using molecular oxygen for treatment of PMMS and ECLSS waste streams, volume 2
[NASA-CR-190299] p 3804 N94-32697

WATER RESOURCES
Possible complementarity of SPOT/ERS in mapping land use: Study on agricultural land in Brittany (France) p 3755 N94-32563
Simulation of a precipitation event in the western United States
[DE94-004835] p 3786 N94-32791
Food security in the context of global environmental change
[DE94-007481] p 3768 N94-32812

WATER SPLITTING
Scenarios for multi-unit inertial fusion energy plants producing hydrogen fuel
[DE94-006614] p 3666 N94-32114

WATER TREATMENT
Catalytic methods using molecular oxygen for treatment of PMMS and ECLSS waste streams, volume 2
[NASA-CR-190299] p 3804 N94-32697

WATER VAPOR
High resolution properties of the marine atmospheric boundary layer
[DE94-006235] p 3774 N94-32736
Water vapor from sunradiometry in comparison with microwave and balloon-sonde measurements at the Southern Great Plains ARM Site
[DE94-007479] p 3786 N94-32759
A correlated k-distribution model of the heating rates for atmospheric mixtures of H2O, CO2, O3, CH4, and N2O in the 0-2500 cm(exp -1) wave number region at altitudes between 0 and 60 km
[DE94-005136] p 3775 N94-32895
Eddy transport of water vapor in the Martian atmosphere p 3949 N94-33221

WATER WAVES
On wave interactions of rotational and irrotational flows p 3700 N94-31219
Additional capabilities of the unified waves model
[AD-A276114] p 3702 N94-31467
Observations of turbulence, internal waves and background flows: An inquiry into the relationships between scales of motion p 3705 N94-31988
The effects of altimeter sampling characteristics: Some Geosat examples
[AD-A276899] p 3747 N94-32214
Index and bulk parameters for frequency-direction spectra measured at CERC Field Research Facility
[AD-A277759] p 3791 N94-33085

WATERSHEDS
Snowmelt forecasting. Further cold regions development of operational hydrological forecasting, volume 2
[AD-A278123] p 3757 N94-33269

WATERWAYS
Real-time centimeter positioning with GPS: A system developed by the US Army Corps of Engineers
[AD-A278152] p 3577 N94-33095

WAVE ATTENUATION
Strain sensing using optical fibers
[NASA-CR-195807] p 3740 N94-32940
PSIDD: A Post-Scan Interactive Data Display system for ultrasonic scans
[NASA-TM-4545] p 3732 N94-33038

WAVE DISPERSION
Dispersion relations for a plasma-filled helix-loaded-waveguide
[DE94-006333] p 3675 N94-31781

WAVE EQUATIONS
Aeroacoustic sources in internal flows
[ISBN-9-03-86-0282-0] p 3860 N94-31653
Boundary control of scattering p 3861 N94-31899
Finite element solution to the Helmholtz equation with high wave number. Part 1: The h-version of the FEM
[AD-A277396] p 3848 N94-32341

WAVE EXCITATION
Dispersion relations for a plasma-filled helix-loaded-waveguide
[DE94-006333] p 3675 N94-31781
MOM3D method of moments code theory manual
[NASA-CR-189594] p 3682 N94-32897
Material engineering of the novel semiconductor structures
[AD-A278386] p 3910 N94-33355

WAVE FUNCTIONS
Development and implementation of a full-potential ASW method
[ETN-94-95757] p 3858 N94-31560
The form factors of the nucleons
[DE94-007096] p 3872 N94-32630

WAVE INTERACTION
On wave interactions of rotational and irrotational flows p 3700 N94-31219

WAVE PROPAGATION
Observation of the traveling component of an x ray standing wave field
[DE94-007671] p 3672 N94-31317
Study of wave propagation and dynamic response of laminated composite structures
[AD-A276123] p 3619 N94-31444
Additional capabilities of the unified waves model
[AD-A276114] p 3702 N94-31467
Dispersion relations for a plasma-filled helix-loaded-waveguide
[DE94-006333] p 3675 N94-31781
Self-consistent effects of magnetospheric hydromagnetic waves on ring current ions
[AD-A277406] p 3774 N94-32346
Superluminous laser pulse in an active medium
[DE94-007110] p 3720 N94-32684
A study of near-surface and underwater explosions by computer simulations
[DE94-009038] p 3708 N94-32849
Finite-element modeling of the blockage and scattering of LG propagation
[AD-A277430] p 3775 N94-33006
A comparison of rough surface parabolic equation models
[AD-A278090] p 3791 N94-33185
An approximate model for vertical polarization and surface roughness using the parabolic equation
[AD-A278091] p 3684 N94-33186

WAVE REFLECTION
Electromagnetic wave reflection from irregular plasma layers
[AD-A276727] p 3678 N94-32161

WAVE SCATTERING
On wave interactions of rotational and irrotational flows p 3700 N94-31219
Electromagnetic wave reflection from irregular plasma layers
[AD-A276727] p 3678 N94-32161
Finite-element modeling of the blockage and scattering of LG propagation
[AD-A277430] p 3775 N94-33006

WAVEFORMS
Waveform generation for ultra-wideband radar system
[AD-A276352] p 3673 N94-31401
Performance metrics for low probability of intercept-communication system
[AD-A277346] p 3677 N94-32073

Development of a frequency-domain electromagnetic scattering measurement system
[AD-A276738] p 3678 N94-32179
Generation of the ambiguity function for ultra wideband radar waveforms
[AD-A277913] p 3684 N94-33261

WAVEGUIDE ANTENNAS
Analysis of a slot coupled coplanar waveguide fed patch antenna
[NASA-TM-106567] p 3698 N94-33116

WAVEGUIDES
Manufacture of light-damage resistant, planar, single mode waveguide on lithium niobate
[DSIS-94-01503] p 3879 N94-31850
Applied Computational Electromagnetics Society Journal, volume 9, number 1, March 1994
[AD-A276753] p 3679 N94-32183
Metal-ion spin-on glasses: Novel materials for active waveguides
[DE94-007738] p 3882 N94-32649

WAVELENGTH DIVISION MULTIPLEXING
Advanced optical fiber communication systems
[AD-A276416] p 3878 N94-31330

WAVELET ANALYSIS
Regular wavelets: Application to fixed image compression
[TELECOM-93-E-004] p 3858 N94-31167
On wavelet representations of differential equations
[RR-482] p 3842 N94-31412
Application of the wavelet transform for speech processing p 3600 N94-31435
Wavelet transform of fixed pattern noise in focal plane arrays
[AD-A276963] p 3712 N94-32393
Neural network wavelet technology: A frontier of automation p 3839 N94-32425
Conference on operator, wavelet and control theory
[AD-A277429] p 3838 N94-33174

WAVERIDERS
A new inverse method for generating high-speed aerodynamic flows with application to waverider design p 3569 N94-31828

WEAK INTERACTIONS (FIELD THEORY)
Baryogenesis from a primordial lepton asymmetry
[PB94-145166] p 3868 N94-31921
Proceedings of the International Workshop on Low Energy Muon Science: LEMS 1993
[DE94-006495] p 3874 N94-32804

WEAPON SYSTEMS
Naval Surface Warfare Center Dahlgren Division Technical Digest: Advanced materials technology
[AD-A276448] p 3668 N94-31364
Unmanned Air Vehicle/Remotely Piloted Vehicle analysis for lethal UAV/RPV
[AD-A276052] p 3578 N94-31442
Modular Simulator System (MSS) management guide
[AD-A277098] p 3588 N94-32014
Getting a handle on designing for avionics software supportability and maintainability
[AD-A276362] p 3581 N94-32055
Analysis of Navy aircraft engine and engine component warranties
[AD-A276936] p 3584 N94-32238
Modular Simulator System (MSS). System/segment specification for the generic modular simulator system-weapons module, volume 7
[AD-A276974] p 3590 N94-32399
Vulnerability assessment of a space based weapon platform electronic system exposed to a thermonuclear weapon detonation
[DE94-007229] p 3611 N94-32667
Accelerated reliability testing utilizing design of experiments
[AD-A277989] p 3732 N94-33088

WEAR
Cost-effective ceramic machining: Summary of three-body wear experiments
[DE94-007757] p 3650 N94-31354

WEAR RESISTANCE
The effect of prolonged exposure to 750 C air on the tribological performance of PM212
[NASA-TM-106472] p 3617 N94-32941

WEAR TESTS
Cracking induced in small fretting: Application to the case of aeronautical aluminum alloys
[ECL-92-50] p 3735 N94-31870
The effect of prolonged exposure to 750 C air on the tribological performance of PM212
[NASA-TM-106472] p 3617 N94-32941
The preliminary evaluation of liquid lubricants for space applications by vacuum tribometry p 3606 N94-33313

WEATHER
Satellite direct readout: Opportunities for science education
[AD-A276257] p 3609 N94-31292
The evolution of jet features during the 1993 east coast white hurricane: A case study using the global spectral model
[AD-A277217] p 3783 N94-32021
Recommendations for meteorological data collection during physiological field studies
[AD-A276834] p 3901 N94-32153
Technical evaluation of the UH-60Q: Aircraft in typical aeromedical evacuation missions
[AD-A276944] p 3586 N94-32217
The influence of thermal inertia on Mars' seasonal pressure variation and the effect of the weather component p 3952 N94-33238

WEATHER FORECASTING
The climate of the Mediterranean basin: Its sensitivity to global change p 3778 N94-30993
Estimation and analysis of climate-scale rainfall over the Tropical Pacific p 3783 N94-32030
Use of Air Force cloud cover data to evaluate and improve cloud forecasts and parameterizations in mesocale meteorological models
[AD-A277384] p 3784 N94-32054
The influence of cumulus parameterization on model forecasts of rapid oceanic cyclogenesis
[AD-A277207] p 3784 N94-32094
Coordination of mesoscale meteorological research between ASL and European group
[AD-A276730] p 3784 N94-32162
Development and testing of improved techniques for modeling the hydrologic cycle in a mesoscale weather prediction system
[AD-A277416] p 3786 N94-32921
Forecasters handbook for the Philippine Islands and surrounding waters
[AD-A277993] p 3787 N94-33089
Might it be possible to predict the onset of major Martian dust storms? p 3948 N94-33215

WEATHER STATIONS
Selection of climate station data using clustering and triangulated irregular network techniques
[AD-A276658] p 3784 N94-32046
Station climatic summaries: China, the former USSR, and Mongolia
[AD-A276548] p 3784 N94-32057
Recommendations for meteorological data collection during physiological field studies
[AD-A276834] p 3901 N94-32153

WEATHERING
Deposition rates of oxidized iron on Mars p 3945 N94-33198
Magmatic volatiles and the weathering of Mars p 3946 N94-33201

WEAVING
Characterization and manufacture of braided composites for large commercial aircraft structures p 3630 N94-33137

WEDGES
Control of hypersonic aerodynamic forces with surface blowing p 3567 N94-31216
Penetrable wedge analysis
[AD-A277219] p 3845 N94-32022

WEIGHT ANALYSIS
Aircraft weight prediction capability. Volume 1: Weight study and results
[AD-A277206] p 3579 N94-32062

WEIGHT MEASUREMENT
Innovative mechanism for measuring the mass properties of an object p 3604 N94-33299

WEIGHTLESSNESS
Muscle disuse through tail-suspension: Etiology and therapeutics p 3796 N94-31746
An experimental testbed for a free-floating manipulator
[AD-A277350] p 3726 N94-32334
A large motion zero-gravity suspension system for experimental simulation of orbital construction and deployment
[NASA-CR-195881] p 3668 N94-33037

WEIGHTLESSNESS SIMULATION
A large motion zero-gravity suspension system for experimental simulation of orbital construction and deployment
[NASA-CR-195881] p 3668 N94-33037

WELD TESTS
A review of weldment failure modes and weldability testing methods
[AD-A278096] p 3729 N94-33251

WELDABILITY
A review of weldment failure modes and weldability testing methods
[AD-A278096] p 3729 N94-33251

WELDED JOINTS
Nd-YAG laser welding of the fiber optic connector to the header shell on the 2SL actuator
[DE94-006104] p 3723 N94-31621
Acceptance criteria for weld defects in aluminium weldments
[PB94-138575] p 3735 N94-31641
Correlation of flux composition and inclusion characteristics with submerged arc weld metal properties in HY-100 steel
[AD-A277040] p 3726 N94-32261
Modeling of residual stress mitigation in austenitic stainless steel pipe girth weldment
[DE94-007184] p 3738 N94-32639
A review of weldment failure modes and weldability testing methods
[AD-A278096] p 3729 N94-33251

WELDING
Effect of vibratory stress relief during welding of thick stainless steel plate
[DE94-006557] p 3733 N94-31312
Solid-state resistance upset welding: A process with unique advantages for advanced materials
[DE94-005941] p 3723 N94-31524
Pinched propagation of high-power, pulsed electron beams for welding and materials processing applications
[AD-A276925] p 3726 N94-32236
Empirical modeling for intelligent, real-time manufacture control p 3839 N94-32424
Modeling of residual stress mitigation in austenitic stainless steel pipe girth weldment
[DE94-007184] p 3738 N94-32639

WELDING MACHINES
Development of an automated wire delivery system for robotic welding applications
[NASA-CR-194216] p 3727 N94-32479

WETTABILITY
Aging effects on the microstructure, surface characteristics and wettability of Cu pretinned with Sn-Pb solders
[DE94-007033] p 3641 N94-31638

WETTING
Interfacial behaviour: Wettability in SiC(sub p) metal matrix composites
[ISBN-0-315-87206-3] p 3621 N94-31835
Physics of heat pipe rewetting
[NASA-CR-195902] p 3913 N94-33148

WHEATSTONE BRIDGES
The constant current loop: A new paradigm for resistance signal conditioning p 3685 N94-32461

WHIP ANTENNAS
Broadband, high-power, 2-30 MHz, twin-whip antenna. Computer and 1/10-scale model design study
[AD-A277619] p 3682 N94-32971

WHISTLERS
Lightning-induced coupling of the radiation belts to geomagnetically conjugate ionospheric regions p 3772 N94-31773
Dispersion relations for a plasma-filled helix-loaded-waveguide
[DE94-006333] p 3675 N94-31781
Plasma and radio waves from Neptune: Source mechanisms and propagation
[NASA-CR-195877] p 3943 N94-33103

WHITE DWARF STARS
Extreme ultraviolet opacity sources in the DA white dwarf G191-B2B p 3924 N94-31210

WHITE NOISE
Peak detection of Swerling type targets. Part 1: Detection probabilities in white noise
[AD-A276217] p 3670 N94-31062
Stochastic realization of a Gaussian stochastic control system
[CWI-BS-R9320] p 3852 N94-32350
The effects of a multipath channel and interference on coherent M-PSK digital communication systems
[AD-A278158] p 3684 N94-33254

WIND (METEOROLOGY)
A comparison of predictors for first-guess wind speed errors
[AD-A276460] p 3781 N94-31239
An integrated cloud observation and modeling investigation in support of the ARM program
[DE94-003160] p 3785 N94-32716
Evolution of diurnal surface winds and surface currents for Monterey Bay
[AD-A277649] p 3790 N94-33057

WIND DIRECTION
Wind-speed measurements with a scanning elastic-backscatter lidar
[DE94-004974] p 3785 N94-32726
Mexico City ozone concentrations as a function of readily-available meteorological parameters
[DE94-007576] p 3768 N94-32814
Polar sediment accumulation: Role of surface winds at the two poles p 3951 N94-33233

WIND EFFECTS
The effect of westerly wind bursts on a tropical ocean general circulation model
[AD-A276423] p 3788 N94-31448

The properties of sunflecks in a flexible plant canopy, and their relationship to turbulence p 3782 N94-31775
Regional sedimentological variations among dark crater floor features: Toward a model for modern eolian sand distribution on Mars p 3946 N94-33203

WIND EROSION
Arid regions and wind erosion p 3780 N94-31005

WIND MEASUREMENT
Three dimensional vorticity field in the California current system
[AD-A276951] p 3788 N94-32220
Wind-speed measurements with a scanning elastic-backscatter lidar
[DE94-004974] p 3785 N94-32726
Evolution of upwelling fronts off the coast of Portugal
[NASA-CR-195692] p 3790 N94-33045

WIND TUNNEL MODELS
Model borne data management system for wind tunnel testing, phase 2
[AD-A276296] p 3587 N94-31295

WIND TUNNEL TESTS
Model borne data management system for wind tunnel testing, phase 2
[AD-A276296] p 3587 N94-31295
Hypervelocity Tunnel 9 Mach 10/14 Calibration
[AD-A275960] p 3587 N94-31318
Investigation of sonic boom for the Space Shuttle: High cross-range orbiter
[NASA-TM-108238] p 3860 N94-31336
Investigation of sonic boom for the Space Shuttle: Low cross-range orbiter
[NASA-TM-108237] p 3860 N94-31337
Research in marine boundary layer intermittency
[AD-A276076] p 3701 N94-31460
Three-dimensional velocity measurements on a 6:1 prolate spheroid at 10 deg angle of attack
[AD-A276485] p 3702 N94-31476
Boundary layer study on nozzle wall at hypersonic velocities p 3569 N94-31882
A critical assessment of UH-60 main rotor blade airfoil data
[NASA-TM-103985] p 3571 N94-32063
A non-local model for prediction of the probability density function of turbulent fluctuations in boundary-layer flows p 3706 N94-32076
Six degree of freedom flight dynamic model of a Mk-82 store
[AD-A277065] p 3580 N94-32362
An experimental study of the flowfield on a semispan rectangular wing with a simulated glaze ice accretion
[NASA-CR-195301] p 3571 N94-32475
Aerodynamic drag of droplets in turbulent flow fields
[ISBN-0-315-75827-9] p 3571 N94-32491
Results for the hybrid laminar flow control experiment conducted in the NASA Langley 8-foot transonic pressure tunnel on a 7-foot chord model
[NASA-TM-107582] p 3601 N94-32870
Control of low-speed turbulent separated flow over a backward-facing ramp
[NASA-TM-109740] p 3573 N94-33071
Structural damping studies at cryogenic temperatures
[NASA-TM-109073] p 3740 N94-33118
Calibration and validation studies in the LENS facility
[AD-A278403] p 3591 N94-33167
Backward-facing step measurements at low Reynolds number, Re(sub h)=5000
[NASA-TM-108807] p 3711 N94-33290

WIND VARIATIONS
Low frequency variability observed in the tropical Atlantic Ocean p 3778 N94-30991

WIND VELOCITY
A comparison of predictors for first-guess wind speed errors
[AD-A276460] p 3781 N94-31239
Scatterometer wind-speed exponents: A review and SAXON 35-GHz measurements
[AD-A276568] p 3783 N94-31937
Recurvature dynamics of a typhoon
[AD-A276792] p 3784 N94-32164
Wind-speed measurements with a scanning elastic-backscatter lidar
[DE94-004974] p 3785 N94-32726
Mexico City ozone concentrations as a function of readily-available meteorological parameters
[DE94-007576] p 3768 N94-32814

WIND VELOCITY MEASUREMENT
Scatterometer wind-speed exponents: A review and SAXON 35-GHz measurements
[AD-A276568] p 3783 N94-31937

WINDPOWER UTILIZATION
NEMO: Advanced energy systems and technologies
[DE94-721996] p 3760 N94-31767
Renewable energy technology development at Sandia National Laboratories
[DE94-007734] p 3761 N94-32383

WING NACELLE CONFIGURATIONS
Multidisciplinary optimization of high-speed civil transport configurations using variable-complexity modeling p 3578 N94-31881

WING PANELS
Active vortex control for a high performance wing
[AD-D016140] p 3573 N94-32974

WING PROFILES
Computation of three-dimensional compressible boundary layers to fourth-order accuracy on wings and fuselages
[NASA-CR-4269] p 3709 N94-32871

WINGS
Grid sensitivity for aerodynamic optimization and flow analysis p 3568 N94-31287
Finite element analysis of MB326H Macchi wing lower spar cap fatigue cracks
[AD-A277062] p 3580 N94-32264
Active vortex control for a high performance wing
[AD-D016140] p 3573 N94-32974
Structural testing of the technology integration box beam p 3628 N94-33125
Resin transfer molding for advanced composite primary wing and fuselage structures p 3628 N94-33128
Test and analysis results for composite transport fuselage and wing structures p 3628 N94-33129
A new method for calculating wing along aerodynamics to angle of attack 180 deg
[AD-A277965] p 3574 N94-33263

WINTER
Simulation of a precipitation event in the western United States
[DE94-004835] p 3786 N94-32791

WIRE
Novel growth technologies for in situ formation of semiconductor quantum wire structures
[AD-A277188] p 3902 N94-32255
Development of an automated wire delivery system for robotic welding applications
[NASA-CR-194216] p 3727 N94-32479

WOOD
Laser applications in wood processing
[PB94-138567] p 3717 N94-31840

WORK CAPACITY
Drug-related problems in the workplace
[CRANFIELD-AERO-9306] p 3914 N94-31538

WORK HARDENING
Work hardening behavior in aluminum alloy 2090
[DE94-007036] p 3643 N94-32064

WORKING FLUIDS
Application of natural refrigerants: A rational solution to a pressing problem
[PB94-138781] p 3668 N94-31073

WORKLOADS (PSYCHOPHYSIOLOGY)
Unit specific crew rest strategies: Phase 1 evaluation of the 1/212th Aviation Battalion during shiftwork transitions
[AD-A277122] p 3804 N94-32379
The effects of Above Real-Time Training (ARTT) in an F-16 simulator p 3591 N94-32474

WORKSTATIONS
Minimization of carpal tunnel syndrome
[AD-A276409] p 3795 N94-31363
Modular Simulator System (MSS). System/segment specification for the generic modular simulator system-instructor/operator station module, volume 12
[AD-A276979] p 3589 N94-32318
A high-speed linear algebra library with automatic parallelism p 3828 N94-32440
Gigabits to the Desktop: Installing tomorrow's networks today
[DE94-007701] p 3827 N94-32646
Overview of shock physics codes for armor analysis
[DE94-008948] p 3739 N94-32842
Design and Monte Carlo analysis of an unmanned aerial vehicle
[AD-A277648] p 3580 N94-33056

WOVEN COMPOSITES
Analysis of new composite architectures
[NASA-CR-195303] p 3626 N94-32904
Comparison of the compressive strengths for stitched and toughened composite systems
[NASA-TM-109108] p 3627 N94-32939

WRIST
Minimization of carpal tunnel syndrome
[AD-A276409] p 3795 N94-31363

WURTZITE
Pump-probe method for investigating laser ablation and optical damage threshold mechanisms in optical materials
[DE94-008291] p 3720 N94-32753

X

X RAY ABSORPTION
Characterization of the rare earth orthophosphates and Ce-doped LaPO4 by x ray absorption spectroscopy
[DE94-006313] p 3898 N94-31630
The zinc electrode: Reactions and mechanisms
[DE94-007977] p 3691 N94-31919
Near edge x ray spectroscopy theory
[DE94-008179] p 3905 N94-32799
X ray absorption study of pulsed laser deposited boron nitride films
[DE94-008295] p 3662 N94-32855
Dependence of x ray absorption magnetic circular dichroism on layer periodicity in iron-platinum multilayers
[DE94-008786] p 3647 N94-32892
Evidence for symmetry breaking local distortions in thallium barium copper oxide
[DE94-006149] p 3907 N94-32944

X RAY ANALYSIS
Element-specific magnetic hysteresis measurements, a new application of circularly polarized soft x-rays
[DE94-007122] p 3858 N94-31397
X ray imaging and x ray source development at Lawrence Livermore National Laboratory
[DE94-007077] p 3719 N94-32629
Simplified ultra-high resolution optic for soft x ray imaging
[AD-A278424] p 3885 N94-33331

X RAY ASTRONOMY
Workshop on Physics of Accretion Disks Around Compact and Young Stars
[NASA-CR-195756] p 3927 N94-31116

X RAY BINARIES
Evolution of vaporizing pulsars p 3929 N94-31128
Can a variable alpha induce limit cycle behavior and exponential luminosity decay in transient soft x ray sources? p 3929 N94-31129
A study of angular momentum loss in binaries using the free Lagrange method p 3931 N94-31134
A search for 100 TeV gamma ray emission from the x ray binary pulsar 4U 0115+63 using the CYGNUS extensive air-shower array p 3955 N94-31900
Winds from disks in compact binaries
[DE94-007452] p 3938 N94-32137
The evolutionary status of PSR 1259-63
[DE94-007094] p 3938 N94-32503

X RAY DETECTORS
Development and application of photosensitive device systems to studies of biological and organic materials
[DE94-008503] p 3793 N94-32516

X RAY DIFFRACTION
Observation of the traveling component of an x ray standing wave field
[DE94-007671] p 3672 N94-31317
Adsorption of water to the metal/polymer interface studied by neutron and x ray reflectivity
[DE94-005578] p 3651 N94-31649
Group 12 thiolates: Syntheses, characterization and decomposition pathways
[AD-A277055] p 3900 N94-32011
The new Metals and Alloys Indexes, search manual: A phase diagram research tool
[DE94-005371] p 3643 N94-32098
SUNY beamline facilities at the National Synchrotron Light Source
[DE94-006343] p 3905 N94-32770
Deuterium absorption and material phase characteristics of SAES St198 Zr-Fe alloy
[DE94-008275] p 3646 N94-32781
Extended-range order in glasses
[DE94-008135] p 3661 N94-32798
Near edge x ray spectroscopy theory
[DE94-008179] p 3905 N94-32799

X RAY IMAGERY
A multi-frequency study of an x ray selected sample of active galactic nuclei p 3937 N94-31987
X ray imaging and x ray source development at Lawrence Livermore National Laboratory
[DE94-007077] p 3719 N94-32629

X RAY INSPECTION
Characterization of interface structure in multilayers using specular x ray reflectance
[DE94-007698] p 3657 N94-32358

X RAY LASERS
Impact of observed hyperfine splitting on X-ray laser gain
[DE94-005822] p 3717 N94-32128
X ray imaging and x ray source development at Lawrence Livermore National Laboratory
[DE94-007077] p 3719 N94-32629
Quantum fluctuations of vortices in Josephson-coupled superconductors
[DE94-007609] p 3905 N94-32747

Progress in understanding and improving x ray lasers
[DE94-006048] p 3720 N94-32794
Ultrafast x ray sources
[AD-A277455] p 3721 N94-33012

X RAY OPTICS
X ray optics for science and technology
[AD-A277369] p 3880 N94-32155
Diamond turning in the production of x ray optics
p 3604 N94-33298
Simplified ultra-high resolution optic for soft x ray imaging
[AD-A278424] p 3885 N94-33331

X RAY SCATTERING
Experimental investigation of phonon eigenvectors using x ray interference fields
[ETN-94-95751] p 3865 N94-31511
Anomalous small angle x ray scattering studies of amorphous metal-germanium alloys
[DE94-007258] p 3900 N94-32065
X ray optics for science and technology
[AD-A277369] p 3880 N94-32155
Anisotropic phase separation through the metal-insulator transition in amorphous Mo-Ge and Fe-Ge alloys
[DE94-007259] p 3646 N94-32795
Dependence of x ray absorption magnetic circular dichroism on layer periodicity in iron-platinum multilayers
[DE94-008786] p 3647 N94-32892

X RAY SOURCES
Theoretical studies of x ray emission from clusters of galaxies p 3954 N94-31103
The physics of black hole x ray novae
p 3932 N94-31143
A multi-frequency study of an x ray selected sample of active galactic nuclei p 3937 N94-31987
X ray imaging and x ray source development at Lawrence Livermore National Laboratory
[DE94-007077] p 3719 N94-32629
Near edge x ray spectroscopy theory
[DE94-008179] p 3905 N94-32799
Ultrafast x ray sources
[AD-A277455] p 3721 N94-33012

X RAY SPECTROSCOPY
Spectroscopy and atomic physics in EBIT and SuperEBIT
[DE94-006050] p 3864 N94-31508
The Los Alamos National Laboratory precision double crystal spectrometer
[DE94-008075] p 3713 N94-32706
Near edge x ray spectroscopy theory
[DE94-008179] p 3905 N94-32799
Structural studies of photoinduced intramolecular electron transfer in cyclopentadienylnickelnitrosyl
[DE94-008467] p 3874 N94-32876
Evidence for symmetry breaking local distortions in thallium barium copper oxide
[DE94-006149] p 3907 N94-32944
Electron cyclotron resonance plasma oxidation studies of InP
[AD-A277431] p 3893 N94-33007

X RAY STARS
Workshop on Physics of Accretion Disks Around Compact and Young Stars
[NASA-CR-195756] p 3927 N94-31116
Disk irradiation and light curves of x ray novae
p 3929 N94-31124
Observational constraints on black hole accretion disks p 3929 N94-31126
Stellar x ray polarimeter polarizer development and calibration at LEA/LLNL
[DE94-006400] p 3712 N94-31783

X RAY TUBES
Design and characterization of a pulsed x ray source for fluorescent lifetime measurements
[DE94-007495] p 3880 N94-32138

X RAYS
Theoretical studies of x ray emission from clusters of galaxies p 3954 N94-31103
Observation of the traveling component of an x ray standing wave field
[DE94-007671] p 3672 N94-31317
Double photoionization of helium with synchrotron x rays: Proceedings
[DE94-006737] p 3866 N94-31668
X ray pulse considerations and electron flow in high voltage diodes
[AD-A277301] p 3868 N94-32044
X ray optics for science and technology
[AD-A277369] p 3880 N94-32155
Simplified ultra-high resolution optic for soft x ray imaging
[AD-A278424] p 3885 N94-33331

X-30 VEHICLE
The National Aerospace Plane (NASP): Development issues for the follow-on vehicle
[AD-A278417] p 3581 N94-33329

XENON CHLORIDE LASERS
Diagnostics of high-brightness short-pulse lasers and the plasmas they generate
[DE94-006165] p 3716 N94-31624

Y

YAG LASERS
High-power CW diode-laser-array-pumped solid-state lasers and efficient nonlinear optical frequency conversion
[AD-A276126] p 3714 N94-31278
Methods for SBS threshold reduction
[AD-A276554] p 3717 N94-31936
Backscatter and transmission of aerosol at UV through middle IR wavelengths
[AD-A277127] p 3718 N94-32305
High average power pulsed phase conjugate laser with birefringence correction
[DE94-006049] p 3719 N94-32659

YANG-MILLS FIELDS
The Kaluza-Klein approach and gauge supersymmetry
[ISBN-0-315-86553-9] p 3912 N94-31911
Tensor gauge potentials in loop space formulation of Yang-Mills fields
[PB94-147147] p 3912 N94-31924

YANG-MILLS THEORY
Tensor gauge potentials in loop space formulation of Yang-Mills fields
[PB94-147147] p 3912 N94-31924

YBCO SUPERCONDUCTORS
Low dispersion of the muon precession frequency in HTSC samples YBa2Cu3O(x) and EuBa2Cu3O(x)
[DE94-608388] p 3896 N94-31395
High performance YBCO films
[AD-A276493] p 3897 N94-31531
High pressure experiments on the Y-Ba-Cu-O superconductors: A major role for holes
[ETN-94-96013] p 3897 N94-31547
Impurities and conductivity in a D-wave superconductor
[DE94-006222] p 3898 N94-31628
Experimental evidence for lattice effects in high temperature superconductors
[DE94-006250] p 3899 N94-31633
The charging effect in high-Tc superconducting thin films
[AD-A277265] p 3900 N94-32040
Defect cascades produced by neutron irradiation in YBa2Cu3O(7-delta) superconductors
[DE94-007700] p 3903 N94-32372
Development, characterization, and applications of high temperature superconductor nanobridge Josephson junctions
[DE94-008113] p 3903 N94-32409
Effect of twin boundary density on the vortex melting transition in YBa2Cu3O(7-delta) single crystals
[DE94-007684] p 3904 N94-32601
YBCO Josephson Junction arrays
[AD-A277426] p 3908 N94-33005
The 20 GHz circularly polarized, high temperature superconducting microstrip antenna array
[NASA-CR-195097] p 3683 N94-33083
Microstructures and epitaxy in oxide superconductor thin films and devices
[AD-A278427] p 3910 N94-33332

YIELD STRENGTH
Tearing resistance of a thin shell against projectile penetration: Material property effects
[DE94-007466] p 3733 N94-31316
Influence of volume fraction of component materials and interlayer bond strength on fracture toughness of multi-layer Al 6090-25 volume percent SiCp and Al 5182 laminates
[DE94-007141] p 3626 N94-32665
Indentability of conventional and negative Poisson's ratio foams p 3629 N94-33131

YTTERBIUM COMPOUNDS
Fermi surface instability at 0.4 K in a heavy-fermion YbBiPt: SDW?
[DE94-006224] p 3899 N94-31916

YTTRIA-STABILIZED ZIRCONIA
High-temperature deformation and fracture toughness of duplex ceramic microstructures p 3653 N94-31945

YTTRIUM OXIDES
Mechanical properties of vacuum-sintered yttria ceramics
[DE94-008138] p 3659 N94-32617

YTTRIUM-ALUMINUM GARNET
High-temperature deformation and fracture toughness of duplex ceramic microstructures p 3653 N94-31945
Development of materials for spectral hole burning applications
[AD-A278408] p 3909 N94-33324

Z

ZEOLITES
Double rotation NMR studies of zeolites and aluminophosphate molecular sieves
[DE94-007032] p 3866 N94-31637
Studies of the fundamental nature of catalytic acidity, sites and intermediates
[DE94-006999] p 3646 N94-32805

ZETA PINCH
Instability heating of solid-fiber Z pinches
[DE94-007055] p 3889 N94-31809

ZINC
The zinc electrode: Reactions and mechanisms
[DE94-007977] p 3691 N94-31919

ZINC ALLOYS
Phase relationships and stability of the (mu)- and (zeta)-phases in the Ag-Al-X (X=Zn, Ga, Ge) systems
[DE94-009391] p 3648 N94-33270

ZINC COMPOUNDS
Lightweight zinc electrode
[AD-D016181] p 3698 N94-33181

ZINC OXIDES
The zinc electrode: Reactions and mechanisms
[DE94-007977] p 3691 N94-31919

ZINC SELENIDES
The relationship of the electronic structures of semiconductor surfaces and heterostructures to crystal growth
[AD-A276465] p 3896 N94-31473

ZINC SULFIDES
Formation mechanism and yield of molecules ejected from ZnS, CdS, and FeS2 during ion bombardment
[DE94-008487] p 3871 N94-32515

ZIRCONIUM
Theoretical studies of zirconium and carbon clusters with molecular dynamics simulations
[DE94-005276] p 3862 N94-31146
A low cost igniter utilizing an SCB and titanium sub-hydride potassium perchlorate pyrotechnic
[DE94-006467] p 3666 N94-31827

ZIRCONIUM ALLOYS
Irradiation-induced phase transformations in zirconium alloys
[DE94-008484] p 3648 N94-32993

ZIRCONIUM ISOTOPES
Influence of long-range correlations on the spectral functions and response of 48Ca and 90Zr
[ETN-94-96017] p 3865 N94-31537

ZIRCONIUM OXIDES
Sol-gel metal oxide and metal oxide/polymer multilayers applied by meniscus coating
[DE94-005813] p 3649 N94-31199
Cost-effective ceramic machining: Summary of three-body wear experiments
[DE94-007757] p 3650 N94-31354
Fatigue crack propagation and fractography of 3Y-TZP and ZTA
[ISBN-0-315-86561-X] p 3736 N94-31912
Ion-irradiation-induced densification of zirconia sol-gel thin films
[DE94-006248] p 3656 N94-32103
Sol-gel coatings for high power laser optics: Past, present, and future
[DE94-007240] p 3718 N94-32252
Interface engineering in oxide fiber/oxide matrix composites
[AD-A277672] p 3627 N94-33029

ZONAL FLOW (METEOROLOGY)
Dynamic climatology of West Africa
p 3778 N94-30988

ZOOPLANKTON
Bioluminescence bathyphotometer
[AD-D016102] p 3790 N94-32959

PERSONAL AUTHOR INDEX

Typical Personal Author Index Listing

ALEXOPOULOS, JIM S. ..... p 436 N94-12023

PERSONAL AUTHOR | PAGE NUMBER | ACCESSION NUMBER

Listings in this index are arranged alphabetically by personal author. The page number helps you locate the citation in the abstract section. The accession number denotes the number by which the citation is identified.

A

AAMODT, R. E. ..... p 3890 N94-32520
AARTS, ERIK ..... p 3842 N94-31393
ABBATE, A. ..... p 3862 N94-32456
ABBE, B. S. ..... p 3599 N94-31428
ABBOTT, BEN ..... p 3817 N94-32219
ABBOTT, R. T. ..... p 3648 N94-33281
ABDELNASER, AHMAD SHEHADEH ..... p 3735 N94-31777
ABEL, P. B. ..... p 3606 N94-33313
ABEL, PHILIP B. ..... p 3728 N94-32893
ABEL, S. A. ..... p 3868 N94-31921
ABNEY, DARRELL T. ..... p 3883 N94-32738
ABOURAHMA, AHMED A. ..... p 3573 N94-33108
ABRAHAM, M. M. ..... p 3898 N94-31630
ABRAMO, R. S. ..... p 3682 N94-32971
ABRAMOWICZ, M. A. ..... p 3928 N94-31117
ABRAMS, M. J. ..... p 3877 N94-31256
ABREVAYA, H. ..... p 3638 N94-32886
ABRUNA, H. D. ..... p 3648 N94-33182
ACEVES, R. C. ..... p 3760 N94-32174
ACKERMAN, S. ..... p 3787 N94-33288
ACOHEN, JAAP ..... p 3917 N94-31415
ADAMS, A. C. ..... p 3881 N94-32385
ADAMS, J. T. ..... p 3723 N94-31621
ADAMS, J. W. ..... p 3675 N94-31683
ADIMI, MOHAMED REDA ..... p 3621 N94-31719
ADLER, JOHN J. ..... p 3773 N94-32337
ADRAGNA, F. ..... p 3756 N94-32570
AEM, G. ..... p 3668 N94-31838
AGAN, M. J. ..... p 3599 N94-31428
AGARWAL, A. K. ..... p 3698 N94-33091
AGER, J. W., III ..... p 3899 N94-31634
AHLBRANDT, T. S. ..... p 3742 N94-31504
AHUJA, K. K. ..... p 3708 N94-32867
p 3709 N94-32869
p 3709 N94-32872
AHUMADA, ALBERT J., JR. ..... p 3850 N94-32467
AICHER, WINFRIED ..... p 3605 N94-33307
AITA, CAROLYN R. ..... p 3640 N94-31258
AITAMRANE, O. ..... p 3808 N94-31094
AKERLOF, C. ..... p 3955 N94-32129
AKHRAS, GEORGES ..... p 3853 N94-33335
AKIN, C. ..... p 3766 N94-32703
AKIN, DAVID L. ..... p 3604 N94-33297
AKITT, DALE RICHARD ..... p 3714 N94-31472
AKKERMAN, G. J. ..... p 3844 N94-31673
AKSE, JAMES R. ..... p 3804 N94-32697
ALAPATI, KIRANKUMAR VENKATA ..... p 3782 N94-31791
ALBERCA, LUIS F. ..... p 3772 N94-32007
ALBERT, BRIAN ..... p 3727 N94-32758
ALBERT, STEPHEN L. ..... p 3806 N94-32435
ALDER, LAWRENCE JOHN ..... p 3725 N94-31973
ALDYKIEWICZ, A. ..... p 3646 N94-32699
ALECHINA, NATASHA ..... p 3855 N94-31404
ALEKHIN, S. I. ..... p 3873 N94-32768
ALEXANDER, N. ..... p 3890 N94-32415
ALEXANDER, TIMOTHY M. ..... p 3758 N94-32466
ALEXANDER, YEHUDAH ..... p 3769 N94-33110
ALEXANDREAS, DIMITRIS E. ..... p 3955 N94-31900
ALIPPI, CESARE ..... p 3671 N94-31190
ALJAWI, ABDULGHAFFAR AZHARI NAWAWI ..... p 3736 N94-31984
ALLAN, LAWRENCE W. ..... p 3804 N94-32379
ALLAN, W. D. E. ..... p 3585 N94-33339
ALLARA, D. L. ..... p 3632 N94-31459
ALLARA, DAVID L. ..... p 3895 N94-31081
ALLEN, JAMES W. ..... p 3784 N94-32094
ALLEN, JOHN H. ..... p 3712 N94-32002
ALLEN, PATRICK G. ..... p 3907 N94-32944
ALLEN, R. A. ..... p 3695 N94-32700
ALLEN, S. ..... p 3715 N94-31580
ALLEN, S. L. ..... p 3888 N94-31765
p 3891 N94-32612
p 3892 N94-32810
ALLER, RAJU ..... p 3603 N94-33293
ALLMON, CURTIS ..... p 3604 N94-33300
ALMAN, DAVID E. ..... p 3615 N94-32500
ALPERT, YAKOV L. ..... p 3894 N94-33113
ALTEROVITZ, SAMUEL A. ..... p 3697 N94-33052
ALTMAN, EITHAN ..... p 3846 N94-32108
ALVISO, C. T. ..... p 3660 N94-32687
AMANI, MAHYAR ..... p 3725 N94-31878
AMBROSE, D. ..... p 3869 N94-32173
AMBUR, D. R. ..... p 3628 N94-33126
AMES, GREGORY ..... p 3882 N94-32626
AMUSIA, M. Y. ..... p 3864 N94-31320
AMUSIA, M. YA. ..... p 3841 N94-31311
AN, I. ..... p 3760 N94-31812
ANCELLET, GERARD ..... p 3770 N94-31010
ANCEY, H. ..... p 3750 N94-32540
ANCONA, NICOLA ..... p 3880 N94-32186
ANDERSON, BIANCA T. ..... p 3572 N94-32880
ANDERSON, E. ..... p 3719 N94-32629
ANDERSON, GRANT ..... p 3603 N94-33292
ANDERSON, JEAN ..... p 3919 N94-32382
ANDERSON, K. D. ..... p 3577 N94-33253
ANDERSON, KARL F. ..... p 3685 N94-32461
ANDERSON, M. G. ..... p 3757 N94-33269
ANDERSON, M. T. ..... p 3899 N94-31847
p 3907 N94-32963
ANDERSON, SCOTT D. ..... p 3625 N94-32624
ANDERSON, W. E. ..... p 3738 N94-32639
ANDERSON, W. T. ..... p 3697 N94-33034
ANDERSSEN, TOM ..... p 3751 N94-32542
ANDREOLI, G. ..... p 3744 N94-31855
ANDREWS, A. B. ..... p 3898 N94-31631
ANDREWS, L. A. ..... p 3666 N94-31579
ANDREWS, MELISSA S. ..... p 3584 N94-32238
ANGELOPOULOS, V. ..... p 3894 N94-33106
ANGELOPOULOS, VASSILIS ..... p 3772 N94-31970
ANNIS, CHARLES ..... p 3643 N94-32047
ANUTA, PAUL ..... p 3613 N94-33289
AOUNI, L. ..... p 3749 N94-32534
APPELQUIST, G. ..... p 3922 N94-32856
ARAMAS, NELSON A. ..... p 3673 N94-31463
ARAPOSTATHIS, ARISTOTLE ..... p 3839 N94-33325
ARAS, CAGLAN MEHMET ..... p 3680 N94-32310
ARCH, D. K. ..... p 3691 N94-31928
ARCHER, CHARLES A., SR. ..... p 3916 N94-31355
ARDANUY, PHILIP ..... p 3823 N94-33287
ARENDALE, W. F. ..... p 3881 N94-32380
ARIGONI, ANIO O. ..... p 3829 N94-31186
ARKO, A. J. ..... p 3898 N94-31631
ARMENDARIZ, M. G. ..... p 3688 N94-31483
p 3696 N94-32809
ARMSTRONG, T. ..... p 3611 N94-32813
ARMSTRONG, T. W. ..... p 3598 N94-31426
ARNDT, G. D. ..... p 3711 N94-32455
p 3583 N94-32457
ARNOLD, J. E. ..... p 3786 N94-33004
ARO, C. ..... p 3638 N94-32840
ARVIDSON, M. ..... p 3691 N94-31848
ARVIDSON, R. ..... p 3950 N94-33228
ASANO, H. ..... p 3762 N94-32919
ASHBY, CAROL I. H. ..... p 3882 N94-32649
ASHENFELTER, W. ..... p 3762 N94-32765
ASHLEY, HOLT ..... p 3586 N94-32224
ASHLEY, KEVIN ..... p 3631 N94-31238
ASHOK, S. ..... p 3895 N94-31081
ASKNE, J. ..... p 3770 N94-31222
ASSINK, R. A. ..... p 3774 N94-32816
ATHERTON, L. J. ..... p 3719 N94-32613
ATKESON, CHRISTOPHER ..... p 3835 N94-32281
ATKINS, STEPHEN C. ..... p 3801 N94-33053
ATTERIDGE, D. G. ..... p 3738 N94-32639
ATTEWELL, PAUL ..... p 3678 N94-32121
ATTWOOD, DAVID T. ..... p 3880 N94-32155
ATWOOD, D. ..... p 3874 N94-32841
AU, GEORGE ..... p 3693 N94-32303
AUDET, P. ..... p 3654 N94-31978
AUDETTE, MICHEL ALBERT ..... p 3814 N94-31718
AUER, BRUCE M. ..... p 3593 N94-31024
AUERBACH, S. M. ..... p 3857 N94-31639
AUGENSTEIN, B. W. ..... p 3581 N94-33329
AUMAN, N. ..... p 3717 N94-31840
AUNELA, LEENA ..... p 3765 N94-31657
AUSLANDER, LOUIS ..... p 3685 N94-33353
p 3685 N94-33354
AUSTIN, J. C. ..... p 3894 N94-31055
AUSTIN, M. E. ..... p 3886 N94-31324
p 3890 N94-32201
AUSTIN, THOMAS ROBERT ..... p 3699 N94-31184
AVERY, W. B. ..... p 3629 N94-33130
AVICOLA, K. ..... p 3926 N94-32189
AVIS, LEE M. ..... p 3785 N94-32737
AVNIR, D. ..... p 3616 N94-32038
AXFORD, R. A. ..... p 3684 N94-33254
AZMY, Y. Y. ..... p 3872 N94-32666

B

BAART, DOUGLAS ..... p 3576 N94-32955
BABU, S. V. ..... p 3650 N94-31284
BABUSKA, I. ..... p 3848 N94-32331
BABUSKA, IVO ..... p 3848 N94-32245
p 3848 N94-32341
BACH, HEIKE ..... p 3745 N94-31865
BACHMAN, M. ..... p 3869 N94-32173
BACKLUND, R. W. ..... p 3699 N94-33340
BADDELEY, A. J. ..... p 3846 N94-32084
p 3847 N94-32197
BADDELEY, ADRIAN J. ..... p 3846 N94-32107
BADR, SALAH E. ..... p 3811 N94-31449
BAGDIGIAN, R. M. ..... p 3803 N94-31380
BAGGAG, ABDELKADER ..... p 3703 N94-31717
BAGLEY, J. B., JR. ..... p 3834 N94-32036
BAGOT, KEITH W. ..... p 3588 N94-32120
BAILEY, A. D. ..... p 3676 N94-31998
BAILEY, ALAN D. ..... p 3677 N94-32083
p 3678 N94-32158
p 3678 N94-32159
p 3680 N94-32297
p 3680 N94-32298
p 3680 N94-32299
p 3680 N94-32300
p 3685 N94-33347
BAILEY, SHEILA G. ..... p 3599 N94-31427
BAIRD, LEEMON C., III ..... p 3801 N94-33053
BAITY, F. W. ..... p 3886 N94-31324
p 3890 N94-32201
BAKER, D. R. ..... p 3891 N94-32612
BAKER, DENNIS J. ..... p 3673 N94-31446
p 3680 N94-32283
BAKER, S. ..... p 3651 N94-31649
BAKER, WALTER L. ..... p 3801 N94-33053
BAKHLE, M. A. ..... p 3739 N94-32883
BAKKER, RENE JOHAN ..... p 3715 N94-31545
BAKSAY, L. ..... p 3875 N94-31488
BALACHANDRAN, U. ..... p 3905 N94-32779
BALAN, K. S. ..... p 3603 N94-33293
BALAS, EGON ..... p 3822 N94-33183
BALASUBRAMANIA, NAGARAJAN ..... p 3747 N94-32160
BALATSKY, A. V. ..... p 3898 N94-31628
BALAZS, G. B. ..... p 3694 N94-32593
BALCOM, JOHN L. ..... p 3711 N94-31492
BALHORN, R. ..... p 3719 N94-32629
BALLANCE, JOHN ..... p 3662 N94-32952
p 3908 N94-33055
BALTISBERGER, J. H. ..... p 3870 N94-32250

BANKS, BRUCE A. p 3593 N94-31024
BANKS, S. P. p 3842 N94-31412
BANNINGER, C. p 3745 N94-31866
BARASHKOV, N. p 3652 N94-31764
BARB, FLORIN DAN p 3830 N94-31647
p 3844 N94-31693
BARCLAY, REBECCA O. p 3921 N94-32831
p 3921 N94-32832
p 3922 N94-32835
p 3922 N94-32836
p 3922 N94-32837
BARINAGA, C. J. p 3713 N94-32811
BARK, LINDLEY W. p 3574 N94-31246
BARKASZI, M. J. p 3757 N94-32463
BARKER, J. R. p 3836 N94-32594
BARKER, JOHN L. p 3613 N94-33289
BARKER, K. p 3928 N94-31118
BARLETTA, R. E. p 3875 N94-31480
BARLETTA, W. p 3953 N94-31632
BARLOS, FOTIOS N. p 3807 N94-31972
BARLOW, N. G. p 3943 N94-33191
BARMAK, K. p 3901 N94-32115
BARNARD, R. D. p 3692 N94-32111
BARNES, J. R. p 3944 N94-33192
BARNETT, A. M. p 3760 N94-32143
BARNETT, B. M. p 3690 N94-31598
BARRETTE, J. p 3938 N94-32638
BARRIE, RONALD E. p 3629 N94-33135
BARRIOS, A. E. p 3791 N94-33185
BARRY, B. p 3755 N94-32565
BARTEL, T. p 3707 N94-32373
BARTHELMY, S. p 3955 N94-32129
BARTHOLOME, PIERRE p 3670 N94-31182
BARTLETT, R. J. p 3898 N94-31631
BARTLETT, RODNEY J. p 3792 N94-31294
BARTNIK, INGRID p 3810 N94-31335
BARTON, D. L. p 3692 N94-32112
BARTON, SIMON A. p 3686 N94-33155
BARTSCH, R. A. p 3661 N94-32847
BASU, R. p 3760 N94-31811
BATES, FRANK S. p 3662 N94-32954
BATINA, JOHN T. p 3572 N94-32865
BATISTA, J. p 3603 N94-33294
BATSON, R. M. p 3948 N94-33217
BATTEN, S. p 3580 N94-32378
BATTRICK, B. p 3670 N94-31182
BAUER, REINHOLD p 3728 N94-33061
BAUER, ROBERT A. p 3597 N94-31043
BAXTER, LAURENCE p 3731 N94-32953
BAZANT, ZDENEK P. p 3740 N94-33143
BAZOW, TERENCE JOHN p 3861 N94-31899
BEACHLY, O. T., JR. p 3895 N94-31327
BEASLEY, M. R. p 3907 N94-32988
BEAUCAGE, G. p 3625 N94-32642
BEAUCHEMIN, PATRICK p 3703 N94-31720
BEAUDET, R. A. p 3633 N94-31493
BEAUDOIN, A. J. p 3903 N94-32597
BEAUPERE, ANNE p 3673 N94-31419
BEAUPRE, J. C. F. p 3686 N94-33346
BEAVER, DAVID IAN p 3855 N94-31389
BECKEDAHL, D. p 3682 N94-32756
BECKER, T. L. p 3948 N94-33217
BEDELL, K. S. p 3906 N94-32913
BEDFORD, TIM p 3851 N94-31698
BEGAULT, DURAND R. p 3576 N94-33063
BEIDLER, JOHN p 3822 N94-33284
BEIERSDORFER, P. p 3864 N94-31508
BEJCZY, ANTAL K. p 3806 N94-32453
BEKLEMISHEV, A. D. p 3891 N94-32686
BELFORT, G. p 3651 N94-31672
BELL, ANN F. p 3799 N94-32035
BELL, BRAD p 3798 N94-32471
BELL, H. p 3715 N94-31580
BELL, J. F., III p 3944 N94-33193
p 3948 N94-33219
BELLO, A. F. p 3904 N94-32634
BELMANS, P. F. R. p 3727 N94-32682
BEMIS, KIRK p 3617 N94-32941
BENAOUN, ZINE EL ABIDINE p 3737 N94-31965
BENBAOUCHE, LAHCENE p 3689 N94-31576
BENCH, P. M. p 3676 N94-31998
BENCH, PATRICIA M. p 3677 N94-32083
p 3678 N94-32158
p 3678 N94-32159
p 3680 N94-32298
p 3680 N94-32299
p 3680 N94-32300
p 3685 N94-33347
BENDA, LESLIE P. p 3577 N94-32961
BENDALY, HACHMI p 3620 N94-31716
BENDRIEM, BERNARD p 3798 N94-33069
BENECKE, J. D. p 3695 N94-32700
BENEMANN, J. p 3766 N94-32703
BENGTSSON, J. P. p 3878 N94-31584
BENKOVITZ, C. M. p 3746 N94-32100
p 3766 N94-32691
BENNAHMIAS, M. J. p 3904 N94-32634
BENNETT, GARY L. p 3597 N94-31044
BENNING, P. J. p 3898 N94-31631
BENNINGTON, S. M. p 3867 N94-31681
BENSON, K. E. C. p 3868 N94-31921
BENSON, THOMAS J. p 3820 N94-32773
BENTLEY, J. p 3652 N94-31780
p 3659 N94-32640
BENZEL, TERRY C. p 3816 N94-32131
BERDING, M. A. p 3879 N94-32006
BERENJI, HAMID R. p 3839 N94-32421
BERG, WESLEY KEITH p 3783 N94-32030
BERGAMETTI, G. p 3780 N94-31005
BERGMAN, MICHAEL I. p 3770 N94-31104
BERINSTAIN, ALAIN B. p 3600 N94-31436
BERK, H. L. p 3891 N94-32664
BERKOWITZ, C. M. p 3746 N94-32100
p 3766 N94-32691
BERN, Z. p 3911 N94-31823
BERNARD, MARIE p 3735 N94-31849
BERNATH, PETER F. p 3667 N94-33013
BERNER, JOSEPH M. p 3623 N94-32024
BERNSTEIN, STEVEN A. p 3790 N94-32959
BERTELRUD, ARILD p 3572 N94-32880
BERTRAND, W. T. p 3610 N94-32010
BERZINS, L. V. p 3716 N94-31599
BERZINS, VALDIS p 3822 N94-33179
BESJES, J. G. p 3843 N94-31642
BESNUS, Y. p 3752 N94-32547
BEST, E. p 3813 N94-31687
BEST, R. C. p 3585 N94-33339
BETHARDY, G. A. p 3863 N94-31202
BETHOUX, J. P. p 3779 N94-30995
BETTS, B. H. p 3944 N94-33194
BEUERMANN, K. p 3928 N94-31123
BEUHLER, A. J. p 3882 N94-32674
p 3661 N94-32819
BEUKERS, A. p 3578 N94-31674
BEUTTENMULLER, R. p 3865 N94-31607
BEYENE, KASSAHUN p 3662 N94-32945
BHATIA, N. P. p 3841 N94-31360
BHATTI, N. p 3767 N94-32752
BI, YUBAI p 3654 N94-31981
p 3655 N94-32069
BIANCHI, J. p 3595 N94-31035
BIBEL, G. p 3728 N94-32929
BIBEL, G. D. p 3728 N94-32900
BIBLER, J. P. p 3660 N94-32698
BIBLER, N. E. p 3660 N94-32698
BICKES, R. W., JR. p 3666 N94-31827
BICKFORD, MARK p 3827 N94-32734
BICKMORE, TIMOTHY W. p 3616 N94-33099
BIEZAD, DANIEL J. p 3585 N94-31203
BIGGERS, RAND R. p 3796 N94-31739
BIGGS, P. M. p 3823 N94-32431
BIGIO, I. J. p 3797 N94-32732
BIHARI, B. p 3658 N94-32578
p 3664 N94-33082
BILLETT, S. J. p 3843 N94-31541
BILLINGE, S. J. L. p 3899 N94-31633
BILLINGS, S. A. p 3842 N94-31394
p 3842 N94-31413
BIONTA, R. p 3955 N94-32129
BIRCH, JAMES R. p 3884 N94-33187
BIRD, GRAEME A. p 3710 N94-33020
BIRKHIMER, CRAIG p 3605 N94-33304
BIRKHOLZ, MATTHEW p 3818 N94-32504
BIRNER, R. p 3606 N94-33312
BISCHOF, C. H. p 3841 N94-31309
BISHOP, D. M. p 3645 N94-32672
BISHOP, J. p 3944 N94-33195
BISHOP, J. L. p 3944 N94-33196
p 3950 N94-33225
BISSINGER, H. D. p 3926 N94-32189
BITTANTI, SERGIO p 3850 N94-31191
BITTER, M. p 3864 N94-31508
BITZER, THOMAS p 3633 N94-31574
BJORKEN, J. D. p 3873 N94-32689
BLACK, DORWIN C. p 3616 N94-32970
BLACK, E. p 3625 N94-32642
BLACKLOCK, DAVID p 3923 N94-32469
BLAIN, C. A. p 3787 N94-31250
BLAIR, J. p 3682 N94-32756
BLANCHARD, ROBERT C. p 3613 N94-32924
BLANKESPOOR, S. C. p 3880 N94-32138
BLASCO, F. p 3753 N94-32555
BLELLOCH, GUY E. p 3824 N94-31259
BLOCH, ISABELLE p 3839 N94-31092
p 3798 N94-33069
BLOCH, J. p 3611 N94-32813
BLOCH, J. C. p 3632 N94-31305
BLOCK, M. M. p 3864 N94-31310
BLOMBERG, L. G. p 3885 N94-31089
BLOMQUIST, J. p 3640 N94-31083
BLOMQUIST, R. N. p 3826 N94-32357
BLONDA, P. p 3745 N94-31862
BLOOMFIELD, HARVEY S. p 3726 N94-32272
BLUE, M. D. p 3594 N94-31029
BLUM, FRANK D. p 3655 N94-32005
p 3656 N94-32221
p 3657 N94-32364
BLYTH, R. I. R. p 3898 N94-31631
BOATNER, L. A. p 3898 N94-31630
BOBBITT, PERCY J. p 3601 N94-32870
BOBO, STEPHEN N. p 3566 N94-32157
BODECHTEL, J. p 3743 N94-31854
BOEHME, D. R. p 3661 N94-32796
p 3661 N94-32803
BOER, W. P. p 3587 N94-31179
BOGDANSKI, MICHAEL S. p 3617 N94-32941
BOHM, C. p 3922 N94-32856
BOHON, HERMAN L. p 3627 N94-33121
BOITEN, EERKE A. p 3825 N94-32196
BOKAIE, MICHAEL D. p 3607 N94-33320
BOLDEN, WILLIAM C. p 3785 N94-32737
BOLDI, ROBERT A. p 3868 N94-31993
BOLLENS, ROSS JOHN p 3890 N94-31927
BOLTER, JAY DAVID p 3674 N94-31645
BOLZERN, PAOLO p 3850 N94-31191
BONEY, C. M. p 3666 N94-31579
BORAH, BOLINDRA N. p 3859 N94-33161
BORCHERDING, F. p 3872 N94-32627
BORN, GEORGE p 3747 N94-32214
BORONKAY, ALLEN R. p 3738 N94-32486
BORST, S. C. p 3677 N94-32085
p 3835 N94-32193
BORZAKOV, S. B. p 3869 N94-32097
BOSLOUGH, M. B. p 3774 N94-32816
BOSSE, ELOI p 3686 N94-33150
BOTSIS, JOHN p 3741 N94-33356
BOTTENBERG, W. R. p 3760 N94-32143
BOTTON, GIANLUIGI p 3620 N94-31706
BOUASSIDA, L. p 3749 N94-32534
BOUCHER, MICHAEL L. p 3828 N94-32440
BOUGEAULT, P. p 3778 N94-30994
BOURASSA, R. J. p 3593 N94-31021
BOURCIER, W. L. p 3656 N94-32116
BOURN, STEPHEN p 3580 N94-32263
BOUWMEESTER, L. H. A. p 3813 N94-31695
BOWERS, J. S. p 3690 N94-31593
BOWERS, JOHN p 3719 N94-32608
BOWERS, M. W. p 3719 N94-32659
BOWMAN, C. T. p 3639 N94-33242
BOWMAN, J. p 3715 N94-31580
BOWMAN, M. K. p 3874 N94-32876
BOXMA, O. J. p 3677 N94-32085
p 3835 N94-32198
BOYD, L. p 3584 N94-32859
BOYER, ERIC B. p 3682 N94-33025
BOYLE, J. S. p 3768 N94-32882
BRACHT, ROGER p 3682 N94-32745
BRADLEY, ELIZABETH p 3910 N94-31289
BRADLEY, R. S. p 3767 N94-32711
BRADSHAW, JOHN L. p 3721 N94-33003
BRADSHAW, PHILIP C. p 3862 N94-33017
BRANDENBURG, J. E. p 3945 N94-33197
BRANDOW, BAIRD p 3904 N94-32746
BRANNON, P. J. p 3714 N94-31148
BRASE, J. M. p 3926 N94-32189
BRASSEUR, JAMES G. p 3710 N94-33162
BRAYTON, D. D. p 3915 N94-32678
BREEN, W. F. p 3759 N94-31279
BREIZMAN, B. N. p 3891 N94-32664
BRENNAN, T. M. p 3716 N94-31622
BRESLAUER, DANY p 3827 N94-33002
BRESSLOFF, PAUL C. p 3828 N94-31157
BREWE, DAVID E. p 3728 N94-32893
BREWER, SUSAN K. p 3601 N94-31298
BRICE, D. K. p 3903 N94-32384
BRICOUT, RICARDO p 3690 N94-31726
BRIDGES, DAVID HENRY p 3570 N94-31907
BRIDGES, TERRY JAMES p 3939 N94-33112
BRIERE, M. A. p 3898 N94-31610
BRIGGS, ROGER P. p 3953 N94-31595
BRIGGS, S. A. p 3745 N94-31863
BRIJS, P. A. J. p 3813 N94-31704
BRINKKEMPER, SJAAK N. p 3917 N94-31415
BRINSMEAD, M. D. p 3567 N94-33338
BRITTEN, J. A. p 3649 N94-31199
BRODZIK, MONICA L. p 3849 N94-33060
BROENSTAD, B. M. p 3717 N94-31840
BROOKS, K. N. p 3646 N94-32781
BROOKS, N. H. p 3892 N94-32810
BROOKS, R. D. p 3892 N94-32800
BROSSE, J. M. p 3752 N94-32551
BROUGH, LAWRENCE F. p 3900 N94-32001
BROUSSEAU, N. p 3714 N94-31255
BROWER, WILLIAM E., JR. p 3597 N94-31043
BROWN-VANHOOZER, S. ALENKA p 3819 N94-32599
BROWN, D. p 3654 N94-31978
BROWN, F. B. p 3826 N94-32357

BROWN, J. p 3588 N94-32014
p 3588 N94-32241
p 3588 N94-32311
p 3588 N94-32312
p 3588 N94-32313
p 3589 N94-32314
p 3589 N94-32315
p 3589 N94-32316
p 3589 N94-32317
p 3589 N94-32318
p 3589 N94-32319
p 3589 N94-32394
p 3590 N94-32395
p 3590 N94-32396
p 3590 N94-32397
p 3590 N94-32398
p 3590 N94-32399
p 3590 N94-32403
BROWN, J. C. p 3807 N94-32147
BROWN, JAMES H. p 3773 N94-32118
BROWN, JAY C. p 3862 N94-33017
BROWN, M. J. p 3768 N94-32814
BROWN, MICHAEL JOHN p 3706 N94-32076
BROWN, ROBERT B. p 3835 N94-32359
BROWN, T. p 3629 N94-33133
BROWN, W. H. p 3708 N94-32867
p 3709 N94-32869
p 3709 N94-32872
BROWNING, J. p 3651 N94-31649
BRUCKART, JAMES E. p 3586 N94-32217
p 3579 N94-32242
BRUCKNER, ADAM P. p 3602 N94-32288
BRUCKNER, ERIC J. p 3617 N94-33022
BRUEGGEMANN, W. p 3790 N94-32881
BRUEMMER, S. M. p 3641 N94-31627
BRUHWEILER, F. C. p 3928 N94-31123
BRUNER, DAVID ALLEN p 3859 N94-31906
BRUNNER, LOIS M. p 3682 N94-32986
BRUNSCHVIG, A. p 3606 N94-33310
BRUZA, P. D. p 3916 N94-31365
BRYAN, D. p 3684 N94-33254
BRYANT, TOM p 3613 N94-33289
BRYSON, R. J. p 3610 N94-32010
BU, XIN-YA p 3662 N94-32945
BUA, DOMINIC p 3798 N94-33092
BUBSEY, RAYMOND p 3740 N94-32932
BUCKLAND, MICHAEL E. p 3818 N94-32390
BUCKLEY, DONALD JOSEPH, JR. p 3653 N94-31942
BUDAI, J. D. p 3901 N94-32172
p 3905 N94-32785
BUEHRLE, RALPH D. p 3740 N94-33118
BUEKER, C. p 3745 N94-31864
BUETTNER, L. C. p 3763 N94-31339
BULAEVSKII, L. N. p 3905 N94-32747
BULLAT, DAVID M. p 3862 N94-33017
BULLISTER, EDWARD T. p 3707 N94-32480
BULSARA, A. R. p 3799 N94-31291
BUNCE, G. p 3876 N94-32099
BURBECK, CHRISTINA A. p 3800 N94-32344
BURGERS, C. A. J. p 3918 N94-32289
BURGESS, BRYAN p 3758 N94-32465
BURGESS, MALCOLM A. p 3582 N94-33076
p 3582 N94-33077
p 3582 N94-33078
p 3583 N94-33079
BURGESS, WILLIAM CARGILL p 3772 N94-31773
BURKE, A. F. p 3694 N94-32521
BURNS, A. R. p 3719 N94-32603
BURNS, R. G. p 3944 N94-33196
p 3945 N94-33198
BURNS, T. J. p 3819 N94-32641
BURPO, STEVEN J. p 3626 N94-32860
BURRELL, K. H. p 3891 N94-32611
BURTON, REGINA M. p 3680 N94-32297
BURTON, ROBERT M. p 3832 N94-31821
BUSCH, JOHN D. p 3607 N94-33320
BUSENITZ, J. K. p 3875 N94-31488
BUSSEY, ALLAN J. p 3784 N94-32117
BUSZKOWSKI, WOJCIEH p 3842 N94-31451
BUTLER, DAVID W. p 3732 N94-32458
BUTLER, ELIZABETH PATRICIA p 3622 N94-31943
BUTLER, M. A. p 3941 N94-31145
BUTMAN, BRADFORD p 3791 N94-33243
BUTNER, R. S. p 3763 N94-31582
BUTTLER, W. T. p 3785 N94-32726
BUTTS, KENT H. p 3763 N94-31275
BUZZELL, CALVIN A. p 3826 N94-32483
BYER, ROBERT L. p 3714 N94-31278
p 3714 N94-31358
BYLUND, HOWARD E., JR. p 3834 N94-32061
BYRNE, JOHN H. p 3836 N94-32996

C

CABO, A. J. p 3846 N94-32084
CADET, DANIEL L. p 3778 N94-30990
CAFLISCH, RUSSEL E. p 3708 N94-32581
CAHILL, P. A. p 3682 N94-32674
p 3661 N94-32819
CAI, Y. p 3727 N94-32778
CAILTON, JEAN-GUILHEM p 3750 N94-32538
CALABRESE, P. G. p 3850 N94-33255
CALAWAY, W. F. p 3871 N94-32515
CALLAHAN, MICHAEL O. p 3868 N94-32044
CALLEN, J. D. p 3892 N94-32911
p 3893 N94-32912
p 3893 N94-32922
CALLIS, R. W. p 3886 N94-31324
p 3890 N94-32201
CALOGERO, A. B. p 3565 N94-31830
CALOMINO, ANTHONY p 3740 N94-32932
CAMPBELL, E. M. p 3887 N94-31400
CAMPBELL, P. L. p 3819 N94-32651
CAMPBELL, ROY L., JR. p 3821 N94-33031
CANCES, M. p 3757 N94-32575
CANDELARIA, J. p 3902 N94-32296
CANFIELD, P. C. p 3898 N94-31631
p 3899 N94-31916
CANN, C. p 3755 N94-32563
CANNON, M. E. p 3576 N94-31306
CANNON, R. H. p 3811 N94-31475
CAPORASO, G. J. p 3863 N94-31270
CAREY, G. F. p 3836 N94-32992
CAREY, P. G. p 3760 N94-32174
CARHART, HOMER W. p 3575 N94-32405
CARIM, ALTAF H. p 3910 N94-33332
CARL, J. R. p 3711 N94-32455
CARLETON, K. L. p 3694 N94-32478
CARLISLE, J. A. p 3873 N94-32755
CARLISLE, ROBERT GEORGE p 3707 N94-32485
CARLISLE, ROBERT J. p 3953 N94-31595
CARLSON, A. B. p 3710 N94-33020
CARLSON, D. D. p 3727 N94-32682
CARLSON, P. p 3681 N94-32679
CARLSTROM, T. N. p 3891 N94-32595
p 3891 N94-32611
CARMONA, C. p 3755 N94-32567
p 3756 N94-32570
CARNEC, CLAUDIE p 3753 N94-32552
CAROPPO, C. p 3745 N94-31862
CARPENTER, LLOYD p 3823 N94-33287
CARPENTER, MARK H. p 3573 N94-32950
CARR, LESTER E., III p 3785 N94-32278
CARR, M. H. p 3951 N94-33232
CARRASQUILLO, R. L. p 3803 N94-31380
CARRIERES, THOMAS p 3751 N94-32545
CARRILLO, GERARDO p 3742 N94-31496
CARRILLO, LUIS p 3742 N94-31496
CARRIVEAU, GARY W. p 3730 N94-32088
CARROLL, S. A. p 3656 N94-32116
CARRON, B. p 3750 N94-32540
CARRUTH, M. RALPH, JR. p 3592 N94-31019
CARSON, M. L. p 3730 N94-31605
CARSON, R. F. p 3688 N94-31483
p 3696 N94-32809
p 3883 N94-32878
CARTER, C. B. p 3652 N94-31780
p 3659 N94-32640
CARTER, D. L. p 3803 N94-31380
CARTER, EMILY A. p 3643 N94-32091
CARTER, JASON L. p 3581 N94-31458
CARTER, R. D. p 3765 N94-32144
CARY, J. R. p 3889 N94-31787
CASAS, L. M. p 3640 N94-31314
CASE, JAMES F. p 3790 N94-32959
CASEY, SEAN C. p 3713 N94-32459
CASSANDRAS, C. G. p 3825 N94-32052
CASSANDRAS, CHRISTOS G. p 3679 N94-32230
CASTELLANO, TIMOTHY p 3805 N94-32936
CATURLA, M. J. p 3903 N94-32411
CAUBLE, R. p 3893 N94-32915
CAUDLE, ERIC W. p 3590 N94-33139
CAUTRU, J. P. p 3748 N94-32527
CAVESTRI, R. C. p 3653 N94-31917
CAZECA, MARIO p 3864 N94-33348
CAZES, J. p 3928 N94-31119
CECIL, JIM p 3699 N94-32460
CECOT, W. p 3726 N94-32320
CERIA, SEBASTIAN p 3822 N94-33183
CERNANSKY, N. P. p 3631 N94-31153
CHAGROV, ALEXANDER p 3856 N94-31407
CHAGROVA, L. A. p 3856 N94-31410
CHAIKEN, A. p 3858 N94-31397
p 3661 N94-32751
p 3662 N94-32855
CHAKOUMAKOS, B. C. p 3905 N94-32785
CHAMIS, CHRISTOS C. p 3739 N94-32735
CHAMPMAN, J. B. p 3743 N94-31603
CHAMPNEYS, A. R. p 3847 N94-32191
CHAN, HELEN M. p 3649 N94-31278
CHAN, S. H. p 3913 N94-33148
CHANCHANI, R. p 3660 N94-32727
CHANEY, KENNETH p 3586 N94-32224
CHANG, B. C. p 3632 N94-31305
CHANG, C. P. p 3595 N94-31035
CHANG, JIN-DER PAUL p 3622 N94-31953
CHANG, TERENCE p 3582 N94-33076
p 3582 N94-33078
p 3583 N94-33079
CHANG, YI-CHIEH p 3839 N94-33330
CHANG, YIA-CHUNG p 3896 N94-31473
CHANNELL, P. J. p 3845 N94-31763
CHAO, LUEN-YUAN p 3650 N94-31454
CHAO, SUN-HUA L. p 3895 N94-31327
CHAPLIN, M. R. p 3888 N94-31667
CHAPMAN, BARBARA p 3820 N94-32928
CHAPUT, DALE p 3607 N94-33321
CHAR, K. p 3903 N94-32409
p 3908 N94-33246
CHARRON, C. p 3748 N94-32527
CHARY, M. LAXMANA p 3603 N94-33293
CHASE, L. L. p 3720 N94-32753
CHASON, E. p 3903 N94-32384
CHATAIN, MARTINE p 3749 N94-32530
CHATTERJEE, A. p 3636 N94-32251
CHAWLA, K. K. p 3627 N94-33029
CHEN, C. T. p 3858 N94-31397
CHEN, DONG p 3793 N94-32622
CHEN, H. p 3647 N94-32964
CHEN, HARRY H. p 3883 N94-32777
CHEN, HSIEH-CHING p 3803 N94-31954
CHEN, J. I. p 3658 N94-32579
p 3659 N94-32610
p 3663 N94-32985
CHEN, JENG I. p 3663 N94-33054
p 3664 N94-33348
CHEN, JONG p 3659 N94-32657
CHEN, JUN p 3904 N94-32602
CHEN, K. R. p 3891 N94-32631
CHEN, L. X. p 3874 N94-32876
CHEN, M. p 3864 N94-31508
CHEN, QI p 3848 N94-32245
CHEN, S. R. p 3903 N94-32597
CHEN, S. S. p 3727 N94-32778
CHEN, TSONG-HSIN p 3584 N94-31967
CHEN, TSUNG-MUH p 3703 N94-31744
CHEN, VICTOR L. p 3628 N94-33129
CHEN, W. p 3865 N94-31607
p 3870 N94-32355
CHEN, Y. M. p 3663 N94-33054
CHEN, YI-FENG p 3722 N94-31489
CHENEAU-HENRY, PERRINE p 3619 N94-31478
CHENG, EDWIN p 3685 N94-32468
CHENG, J. p 3881 N94-32385
CHENG, JUI-CHING p 3698 N94-33116
CHENG, P. Y. p 3917 N94-31829
CHEONG, D. W. p 3658 N94-32578
CHERN, E. JAMES p 3732 N94-32458
CHESNAKAS, CHRISTOPHER J. p 3702 N94-31476
CHEUNG, ANNY S. p 3576 N94-32955
CHEUNG, T. p 3675 N94-31784
CHIANG, HSIAO-FENG p 3673 N94-31401
CHIARAMONTE, FRANCIS PAUL, III p 3667 N94-31944
CHIARAMONTE, JAMES A. p 3804 N94-32379
CHICARRO, A. F. p 3945 N94-33199
CHIEN, LARRY S. p 3625 N94-32604
CHIPMAN, D. W. p 3763 N94-31347
CHIU, S. C. p 3886 N94-31324
p 3890 N94-32201
CHMIELOWSKI, M. p 3882 N94-32417
CHO, JOHN YUNGDO NAGAMICHI p 3772 N94-32077
CHO, MAENG-HYO p 3617 N94-31215
CHOI, BENJAMIN p 3605 N94-33304
CHOI, BENJAMIN B. p 3605 N94-33306
CHOI, HEUNG SOAP p 3624 N94-32496
CHOI, JIN SEONG p 3652 N94-31745
CHOI, WONYUN p 3830 N94-31482
CHOINSKI, THOMAS C. p 3826 N94-32323
CHOROWICZ, J. p 3751 N94-32546
p 3753 N94-32553
CHOROWICZ, JEAN p 3752 N94-32549
CHOU, F. p 3895 N94-31067
CHOU, I. p 3649 N94-31276
CHOU, JACK C. p 3626 N94-32877
CHOW, A. p 3920 N94-32635
CHOW, R. p 3714 N94-31269
p 3651 N94-31557
CHOW, WENG W. p 3666 N94-31579
CHRIEN, R. E. p 3892 N94-32730
CHRISTEN, D. K. p 3905 N94-32785
CHRISTENSEN, P. R. p 3946 N94-33203
p 3950 N94-33229

CHRISTIANSEN, P. L. p 3794 N94-33250
CHRISTIANSEN, SCOTT p 3604 N94-33302
CHRISTOPH, G. p 3826 N94-32356
CHRZAS, J. p 3672 N94-31317
CHU, A. p 3583 N94-32457
CHU, JAN-HWA p 3785 N94-32278
CHUANG, C. C. p 3785 N94-32268
p 3767 N94-32789
CHUNG, CHAN-HONG p 3615 N94-32742
CHUNG, H. M. p 3641 N94-31486
p 3641 N94-31666
p 3643 N94-32109
CHUNG, JOON p 3568 N94-31734
CHUNG, KUNG-MING p 3569 N94-31879
CHURCHILL, J. K. p 3666 N94-31827
CHURCHILL, MELVYN R. p 3895 N94-31327
CIARDO, GIANFRANCO p 3821 N94-33075
CLANCY, R. T. p 3945 N94-33200
p 3947 N94-33211
CLARIDGE, REX p 3604 N94-33301
CLARK, B. C. p 3946 N94-33201
CLARK, C. W. p 3874 N94-33144
CLARK, E. L. p 3852 N94-32673
CLARK, M. p 3914 N94-32677
CLARK, P. p 3740 N94-32982
CLARK, R. P. p 3696 N94-32806
CLARKSON, VAUGHAN p 3826 N94-32274
CLASSEN, INGO p 3812 N94-31577
CLAUSEN, E. C. p 3760 N94-31811
CLEMENTS, J. W. p 3666 N94-31579
CLEROUX, LOUISE p 3724 N94-31721
CLEVELAND, JEFF I., II p 3591 N94-32473
CLEVERS, J. G. P. W. p 3745 N94-31864
CLIFFORD, S. M. p 3946 N94-33202
p 3951 N94-33235
CLIFT, W. M. p 3661 N94-32803
CLINE, T. p 3955 N94-32129
CLOSE, F. E. p 3868 N94-31923
COBBLE, J. A. p 3716 N94-31624
COCKROFT, NIGEL J. p 3720 N94-32761
COE, HAROLD H. p 3728 N94-32979
COENRADIE, B. p 3746 N94-31868
COFFEY, H. T. p 3722 N94-31319
COFFEY, MICHAEL P. p 3625 N94-32624
COFFEY, P. p 3869 N94-32173
COHEN, BRIAN S. p 3810 N94-31357
COHEN, GERALD C. p 3820 N94-32775
COHEN, MARION F. p 3800 N94-32419
COHEN, ROBERT p 3604 N94-33297
COHL, H. p 3823 N94-31120
COLACOT, THOMAS J. p 3900 N94-32001
COLBERT, MALCOLM N. p 3804 N94-32171
COLBORN, B. L. p 3598 N94-31426
COLDREN, LARRY p 3719 N94-32608
COLE, E. I., JR. p 3692 N94-32112
COLELLA, N. J. p 3760 N94-32174
COLEMAN, H. H. p 3931 N94-31137
COLEMAN, J. T. p 3690 N94-31598
COLEMAN, M. M. p 3667 N94-32150
COLEMAN, WILLIAM F. p 3861 N94-32262
COLLINS, CURTIS A. p 3789 N94-32325
COLLINS, H. D. p 3712 N94-31831
p 3713 N94-32681
COLLINS, R. W. p 3760 N94-31812
COLLMAN, J. P. p 3908 N94-32991
COLORNI, ALBERTO p 3829 N94-31176
p 3824 N94-31177
COMBS, R. J. p 3746 N94-31999
COMFORT, W. J., III p 3669 N94-32839
COMINSKY, L. p 3938 N94-32503
COMPAGNONI, ADRIANA B. p 3848 N94-32292
COMPERATORE, CARLOS A. p 3804 N94-32379
CONFORTI, MICHELE p 3848 N94-32286
CONKLIN, CHERYL L. p 3808 N94-32434
CONLEY, JULIANNE M. p 3709 N94-32947
CONRAD, J. p 3766 N94-32703
CONRADSON, STEVEN D. p 3907 N94-32944
CONWAY, J. A. p 3753 N94-32556
COOK, D. R. p 3768 N94-32894
COOKE, C. p 3818 N94-32353
COOLS, R. p 3841 N94-31274
COOPER, D. p 3774 N94-32736
COOPER, DAVID L., JR. p 3684 N94-33160
COOPER, GEORGE p 3938 N94-32489
COPPENS, P. p 3905 N94-32770
CORNUEJOLS, GERARD p 3848 N94-32286
p 3822 N94-33183
CORONADO, P. R. p 3639 N94-33260
CORONITI, F. V. p 3894 N94-33106
CORRIGAN, TIMOTHY J. p 3860 N94-31242
CORWIN, W. R. p 3739 N94-32771
COSTIGAN, KELLY p 3685 N94-32437
COTE, JEAN p 3831 N94-31757
COTTINGAME, W. p 3774 N94-32736
COTTON, J. D. p 3903 N94-32597
COULSON, S. N. p 3755 N94-32566
COURTRIGHT, WILLIAM V., II p 3815 N94-31940
COUSINS, T. p 3854 N94-33342
COWEN, DAVE J. p 3758 N94-32465
COWINGS, PATRICIA S. p 3801 N94-33068
COX, M. R. p 3690 N94-31598
COY, JOHN J. p 3728 N94-32979
CRABTREE, G. W. p 3904 N94-32601
CRAIG, JEFFREY L. p 3582 N94-32223
CRAIG, L. D. p 3739 N94-32903
CRAIN, W. R. p 3808 N94-33252
CRAVES, A. p 3755 N94-32563
CRAWFORD, C. L. p 3660 N94-32698
CRAWFORD, GARY D. p 3594 N94-31031
CRAWFORD, K. B. p 3808 N94-33252
CRERIE, JEFFREY ROGER p 3609 N94-31470
CRESSWELL, M. W. p 3695 N94-32700
CRISP, D. p 3949 N94-33222
CRISWICK, JOHN p 3600 N94-31436
CROCKER, STEPHEN D. p 3816 N94-32131
CROSS, JON B. p 3596 N94-31039
CROW, JUDY p 3820 N94-32776
CROWELL, R. A. p 3720 N94-32704
CRUTCHER, RUSS p 3592 N94-31020
CSILLAG, STEFAN p 3858 N94-31084
CUBASCH, U. p 3790 N94-32881
CULICK, F. E. p 3634 N94-32033
CULIOLI, J. C. p 3727 N94-32682
CULLEN, D. E. p 3698 N94-33163
CULVER, R. L. p 3862 N94-33096
CURRIE, J. W. p 3687 N94-31152
CURTIS, CARLTON H. p 3680 N94-32297
CURTIS, JOHN O. p 3771 N94-31351
p 3771 N94-31353
p 3771 N94-31457
CUSWORTH, ROLAND ALAN p 3633 N94-31471
CYGAN, R. T. p 3774 N94-32816
CYKOSKI, RUSSELL C. p 3597 N94-31044
CYMERMAN, ALLEN p 3798 N94-33268

D

DABNEY, PHILIP W. p 3713 N94-32459
DABROWSKA-ZIELINSKA, K. p 3754 N94-32558
DAGLE, J. E. p 3687 N94-31152
p 3691 N94-31785
DAHM, WERNER J. p 3710 N94-33164
DAI, XINGDE p 3838 N94-33174
DAI, YI p 3734 N94-31707
DAINTON, J. p 3868 N94-32008
DAJANI, KARMA p 3844 N94-31643
p 3851 N94-31661
DALLEMAND, J. F. p 3755 N94-32565
DALLEORE, CRISTINA MOREA p 3927 N94-32308
DAMKROGER, B. K. p 3640 N94-31345
DAMNJANOVIC, L. B. p 3813 N94-31685
DAMOUR, T. p 3601 N94-31769
p 3610 N94-31771
DANIELSON, D. A. p 3610 N94-32208
DANN, J. N. p 3643 N94-32098
DANSAERT, FRANK p 3750 N94-32537
DAPP, TIMOTHY L. p 3663 N94-32975
DARKAZALLI, G. p 3759 N94-31279
DAS-GUPTA, D. K. p 3879 N94-32037
DASILVA, CHRISTINE ALISON p 3833 N94-31875
DASILVA, L. B. p 3717 N94-32128
p 3720 N94-32794
DASTIN, S. p 3630 N94-33136
DATTA, A. p 3868 N94-31922
DAVID, S. A. p 3733 N94-31312
DAVIDSON, D. L. p 3627 N94-33008
DAVIS, B. H. p 3638 N94-32889
DAVIS, BRUCE A. p 3758 N94-32464
p 3758 N94-32465
DAVIS, CURT H. p 3742 N94-31570
DAVIS, D. D., JR. p 3628 N94-33126
DAVIS, G. D. p 3650 N94-31297
DAVIS, GLORIA J. p 3820 N94-32906
DAVIS, H. A. p 3651 N94-31650
DAVIS, J. C. p 3632 N94-31352
DAVIS, JOHN G., JR. p 3627 N94-33121
DAVIS, JOHN M. p 3596 N94-31038
DAVIS, KENNETH J. p 3704 N94-31774
DAVIS, MICHAEL p 3802 N94-33327
DAVIS, RANDALL C. p 3628 N94-33126
DAVIS, W. L. p 3946 N94-33205
DAVY, JACQUES p 3822 N94-33097
DEAN, D. J. p 3874 N94-32850
DEANGELIS, D. L. p 3741 N94-31606
DEATON, JERRY W. p 3628 N94-33129
DEBANY, WARREN H., JR. p 3686 N94-31066
DEBENEDETTI, P. G. p 3872 N94-32644
DEBOER, STEVEN FRANCIS p 3879 N94-31877
DEBOISANGER, M. p 3606 N94-33310
DEBOISSEZON, H. p 3754 N94-32557
DEBOOR, CARL R. p 3842 N94-31441
DEBRAAL, J. D. p 3950 N94-33226
DEC, J. E. p 3723 N94-31651
DECAMPOS, TARCISIO PASSOS RIBEIRO p 3800 N94-32495
DECARO, ROBERT E. p 3808 N94-32433
DECASTRO, MANUEL p 3778 N94-30993
DECAUX, V. p 3864 N94-31508
DEDIEU, G. p 3757 N94-30996
DEFELICE, P. p 3778 N94-30988
DEFFONTAINES, B. p 3748 N94-32527
DEFFONTAINES, BENOIT p 3752 N94-32549
DEFRAIPONT, P. p 3752 N94-32547
DEGOEDE, M. J. p 3917 N94-31768
DEGRAAFF, JOHANNES J. p 3812 N94-31646
DEGRASSIE, J. S. p 3886 N94-31324
p 3890 N94-32201
DEGROH, KIM K. p 3593 N94-31024
DEHLING, HEROLD G. p 3832 N94-31821
DEHOOP, D. p 3598 N94-31208
DEITZEL, JOHN p 3664 N94-33166
DEJESUSGONZALEZ-GONZALEZ, JOSE p 3934 N94-31788
DEJONG, PAULUS JOHANNES p 3865 N94-31534
DEJONG, T. p 3578 N94-31674
DEJONGH, DICK p 3856 N94-31410
DEKKER, L. p 3825 N94-31662
p 3825 N94-31700
DEKKER, PAUL p 3856 N94-31450
DEKONING, WILLEM p 3830 N94-31647
p 3844 N94-31693
DELARUBIA, T. D. p 3903 N94-32411
DELECLUSE, P. p 3777 N94-30984
p 3777 N94-30986
DELGRANDE, N. K. p 3580 N94-32658
DELL, F. p 3883 N94-32994
DELLACORTE, CHRISTOPHER p 3617 N94-32941
DELLAMICO, MAURO p 3809 N94-31189
DELMAS, ROBERT p 3770 N94-31008
DELONG, M. p 3715 N94-31580
p 3675 N94-31761
DELUCA, DANIEL P. p 3643 N94-32047
DELUCA, J. A. p 3909 N94-33271
DELUCHI, M. A. p 3765 N94-31625
DEMARCKEN, CARL p 3817 N94-32212
DEMARCO, F. P. p 3719 N94-32613
DEMARCO, GEORGE p 3811 N94-31465
DEMARCO, STEVEN p 3793 N94-32622
DEMEESTER, P. p 3693 N94-32301
DEMPSEY, J. F. p 3603 N94-32671
DENBAARS, S. P. p 3902 N94-32255
DENICOLAO, GIUSEPPE p 3850 N94-31191
DENLINGER, EDGAR J. p 3897 N94-31531
DENNIS, JOHN E., JR. p 3811 N94-31443
DENNIS, R. F. p 3771 N94-31369
DENTREMONT, ROBERT P. p 3784 N94-32117
DERIJKE, MAARTEN p 3856 N94-31417
DERION, T. p 3802 N94-31302
DERMER, C. D. p 3929 N94-31125
DEROIN, J. P. p 3748 N94-32527
DEROOVER, BOUDEWIJN P. p 3745 N94-31867
DEROSE, TONY p 3820 N94-32972
DESBOIS, MICHEL p 3779 N94-31000
DESCHENEAU, WAYNE M. p 3810 N94-31383
DESIMONE, J. M. p 3655 N94-32017
DESPRATS, J. F. p 3752 N94-32551
p 3754 N94-32561
DESTEESE, J. G. p 3687 N94-31152
DETERING, B. A. p 3758 N94-31234
DEVER, JOYCE A. p 3617 N94-33022
DEWAAL, P. R. p 3835 N94-32198
DEWITT, H. E. p 3934 N94-31782
p 3637 N94-32801
DEWITT, J. R. p 3588 N94-32009
DEWITT, KENNETH J. p 3615 N94-32742
DEWULF, ROBERT R. p 3745 N94-31867
DEXTER, H. BENSON p 3629 N94-33134
DEYST, J. P. p 3849 N94-32653
DHINGRA, JASTEJ p 3680 N94-32283
DIABY, N. p 3755 N94-32565
DIAZ, H. F. p 3767 N94-32711
DIAZDELARUBIA, T. p 3896 N94-31499
DIB, NIHAD I. p 3696 N94-32905
p 3698 N94-33116
DICKSON, B. C. p 3686 N94-33152
DICUS, D. A. p 3871 N94-32512
DIDIER, B. T. p 3816 N94-32145
DIDZIULIS, STEPHEN V. p 3635 N94-32233
DIEKMANN, O. p 3793 N94-32228
DIEKMANN, ODO p 3793 N94-32226
p 3851 N94-32229
DIEQIAN, WANG p 3568 N94-31220
DIETZ, KURTIS L. p 3598 N94-31426
DIGILAKIS, VASSILIOS p 3679 N94-32185
DIGUMARTHI, RAMARAO p 3586 N94-32224
DIJKHUIZEN, MARHIJS S. p 3857 N94-32192
DIKEL, DAVID p 3811 N94-31465

DILLON, W. P. ..... p 3742 N94-31504
DIMOS, D. ..... p 3695 N94-32650
DINAR, NATHAN ..... p 3769 N94-33110
DING, JIAN ..... p 3793 N94-32622
DINGLER, B. ..... p 3611 N94-32813
DINH, L. N. ..... p 3904 N94-32634
DINICOLA, AL J. ..... p 3626 N94-32877
DION, MARC ..... p 3670 N94-31063
p 3841 N94-31252
DIPERNA, DANIEL T. ..... p 3861 N94-32089
DIPLAS, ATHANASSIOS ..... p 3938 N94-32309
DIPP, T. M. ..... p 3761 N94-32660
p 3681 N94-32661
p 3695 N94-32662
DIPPOLITO, D. A. ..... p 3890 N94-32520
DIRKS, J. A. ..... p 3687 N94-31152
DISMUKES, R. KEY ..... p 3575 N94-32927
DITMIRE, T. R. ..... p 3904 N94-32634
DIXON, L. ..... p 3911 N94-31823
DJAROUDIB, K. ..... p 3757 N94-32574
DOANE, JAY SCOTT ..... p 3934 N94-31758
DODDS, G. I. ..... p 3722 N94-31379
DOHM, J. M. ..... p 3951 N94-33232
DOKSHITZER, V. L. ..... p 3868 N94-31923
DOLL, G. L. ..... p 3682 N94-32855
DOMAN, DAVID B. ..... p 3805 N94-33349
DOMINGUEZ, MANUEL B. ..... p 3669 N94-32861
DOMINIAK, R. ..... p 3826 N94-32248
DONALD, L. ..... p 3914 N94-32677
DONNELLAN, THOMAS M. ..... p 3639 N94-32973
DORAN, J. C. ..... p 3767 N94-32750
DORIGO, MARCO ..... p 3829 N94-31176
p 3824 N94-31177
DOSKEY, P. V. ..... p 3768 N94-32894
DOSS, HANI ..... p 3852 N94-32339
DOTY, KEITH L. ..... p 3604 N94-33299
DOU, L. ..... p 3865 N94-31607
DOUGLAS, G. M. ..... p 3603 N94-32671
DOW, MARVIN B. ..... p 3628 N94-33127
DOWBEN, PETER ..... p 3900 N94-32041
DOWELL, M. B. ..... p 3875 N94-31480
DOXBECK, M. ..... p 3862 N94-32456
DRAKE, M. J. ..... p 3940 N94-31109
DRAPE, GAYLEN W. ..... p 3823 N94-32436
DRESSEL, S. B. ..... p 3681 N94-32679
DREWERY, J. S. ..... p 3795 N94-31323
DREYER, J. J. ..... p 3583 N94-31931
DRISCOLL, JAMES N. ..... p 3923 N94-32441
DRIVER, DAVID M. ..... p 3711 N94-33290
DROPPO, J. G., JR. ..... p 3712 N94-31831
DROSOPOULOS, ANASTASIOS ..... p 3670 N94-31062
DROZHKO, EUGENE ..... p 3920 N94-32808
DRUCKER, J. S. ..... p 3901 N94-32092
DRUEDING, THOMAS W. ..... p 3875 N94-32447
DRUILHET, A. ..... p 3757 N94-31006
DRUMHELLER, DAVID M. ..... p 3850 N94-31462
DRUMMOND, JOHN ..... p 3685 N94-32468
DU, H. ..... p 3640 N94-31314
DU, HONG ..... p 3864 N94-31321
p 3871 N94-32615
DUCE, D. A. ..... p 3813 N94-31685
DUCHAMP, TOM ..... p 3820 N94-32972
DUCHARME, M. B. ..... p 3796 N94-31742
DUCROT-GAMBART, D. ..... p 3753 N94-32555
DUESBERY, M. S. ..... p 3623 N94-32012
DUFF, J. ..... p 3926 N94-32189
DUFFY, JAMES B. ..... p 3608 N94-33100
DUGINOV, V. N. ..... p 3896 N94-31395
DUIGNAN, M. T. ..... p 3717 N94-31936
DUMAIS, J. G. ..... p 3854 N94-33344
DUMOUCHE, J. G. L. ..... p 3853 N94-33336
DUNCAN, R. C. ..... p 3932 N94-31142
DUNFORD, DALE E. ..... p 3582 N94-33076
p 3582 N94-33078
p 3583 N94-33079
DUNSTER, S. B. ..... p 3751 N94-32543
DUPLESSY, J. C. ..... p 3777 N94-30982
DUPONT, J. N. ..... p 3658 N94-32408
DURBIN, P. F. ..... p 3580 N94-32658
DURBIN, THOMAS D. ..... p 3635 N94-32233
DURGAPAL, PRABHA ..... p 3912 N94-32774
DURSCH, HARRY ..... p 3595 N94-31037
DURSCH, HARRY W. ..... p 3595 N94-31036
DUSSAULT, HEATHER B. ..... p 3686 N94-31066
DUTTA, JYOTSNA M. ..... p 3776 N94-33351
DUTTRY, STEVEN R. ..... p 3608 N94-32190
DYE, RAYMOND ..... p 3799 N94-32096
DZHAPARIDZE, G. K. ..... p 3856 N94-31416
DZHAPARIDZE, KACHA O. ..... p 3847 N94-32194
p 3851 N94-32225

E

EARLY, JAMES W. ..... p 3720 N94-32761
EARLY, L. W. ..... p 3610 N94-32208
EAST, A. J. ..... p 3656 N94-32246
EASTER, R. C. ..... p 3766 N94-32691
EASTERLING, D. R. ..... p 3764 N94-31596
p 3766 N94-32690
EATHER, ROBERT ..... p 3775 N94-32999
EBEL, RENE ..... p 3794 N94-31195
EBERHART, HENRY J. ..... p 3923 N94-32442
EBLING, MARIA R. ..... p 3821 N94-33030
EBY-FREDERICK, SCOTT WALTER
p 3867 N94-31832
ECKLUND, EARL ..... p 3810 N94-31357
EDELSTEIN, ALAN S. ..... p 3696 N94-32721
EDENS, GREGORY J. ..... p 3642 N94-31997
p 3869 N94-32170
p 3909 N94-33273
p 3875 N94-33277
EDGETT, K. S. ..... p 3946 N94-33203
EDLOW, RALPH ..... p 3627 N94-33123
EDMONDS, GARY O. ..... p 3729 N94-32452
EDWARDS, D. J. ..... p 3641 N94-31626
EDWARDS, G. R. ..... p 3640 N94-31345
EDWARDS, J. O. ..... p 3950 N94-33225
EDWARDS, MICHAEL ..... p 3607 N94-33321
EEK, ROBERT E. ..... p 3919 N94-32499
EGAMI, T. ..... p 3661 N94-32798
EGERLAND, W. O. ..... p 3841 N94-31360
EGGERS, ALFRED J., JR. ..... p 3586 N94-32224
EHRLICH, JACQUES ..... p 3730 N94-31166
EICHINGER, W. ..... p 3774 N94-32736
EICHINGER, W. E. ..... p 3785 N94-32726
EILBECK, J. C. ..... p 3794 N94-33250
EISCHEID, J. K. ..... p 3764 N94-31596
p 3766 N94-32690
EISENMAN, DAVID ..... p 3808 N94-32433
EISNER, E. ..... p 3888 N94-31664
EK, M. ..... p 3774 N94-32772
EKHOLM, A. ..... p 3922 N94-32856
ELAMRANI, KHADIJA ..... p 3733 N94-31376
ELDHUSET, KNUT ..... p 3751 N94-32542
ELIZAVETIN, I. V. ..... p 3756 N94-32573
ELLENWOOD, C. H. ..... p 3695 N94-32700
ELLIOTT, D. C. ..... p 3759 N94-31762
ELLIOTT, S. ..... p 3864 N94-31508
ELLIS, MICHAEL G., SR. ..... p 3821 N94-33031
ELLISON, A. J. G. ..... p 3661 N94-32798
ELMS, K. ..... p 3629 N94-33131
ELUSZKIEWICZ, JANUSZ BRONISTAW
p 3942 N94-31975
EMBURY, J. D. ..... p 3903 N94-32597
EMRETSSON, BO-GOERAN ..... p 3722 N94-31194
ENDERBY, J. E. ..... p 3645 N94-32514
ENDERLE, JACK D. ..... p 3799 N94-32035
ENEMARK, D. ..... p 3611 N94-32813
ENGEL, B. A. ..... p 3757 N94-32463
ENGEL, S. ..... p 3947 N94-33206
ENGELBRECHT, JAN R. ..... p 3904 N94-32645
ENGELKEN, EDWARD J. ..... p 3799 N94-32035
ENGELMANN, B. E. ..... p 3738 N94-32637
ENGLEBRETSON, RONALD E. ..... p 3784 N94-32260
p 3787 N94-33089
ENGMANN, ROLF ..... p 3917 N94-31415
ENNAJI, M. ABDERRAHIM ..... p 3832 N94-31873
EPEMA, G. F. ..... p 3744 N94-31859
EPEMA, GERRIT F. ..... p 3754 N94-32560
EPPERSON, J. E. ..... p 3647 N94-32964
EPSTEIN, GEORGE ..... p 3624 N94-32122
ERARD, S. ..... p 3946 N94-33204
EREMIN, V. ..... p 3870 N94-32355
ERICSON, M. N. ..... p 3807 N94-32783
ERSKINE, D. J. ..... p 3904 N94-32634
ERWIN, DANIEL EUGENE ..... p 3569 N94-31880
ESER, S. ..... p 3667 N94-32150
ESMAN, RONALD D. ..... p 3883 N94-32720
ESPARZA, JORGE A. ..... p 3807 N94-32163
ESPEY, C. ..... p 3723 N94-31651
ESPOSITO-FARESE, G. ..... p 3610 N94-31771
ESTES, T. A. ..... p 3696 N94-32786
ETEMAD, S. ..... p 3660 N94-32729
EVANS, DAVID B. ..... p 3611 N94-32898
EVERETT, T. ..... p 3881 N94-32380
EVIATAR, A. ..... p 3771 N94-31326
EWART, TERRY E. ..... p 3787 N94-31053
EYERT, VOLKER ..... p 3858 N94-31560
EYRING, E. M. ..... p 3718 N94-32413
EZHELA, V. V. ..... p 3873 N94-32768

F

FAATZ, BART ..... p 3715 N94-31532
FADLEY, C. S. ..... p 3712 N94-31629
FAELTHAMMAR, C.-G. ..... p 3885 N94-31089
FAELTHAMMAR, CARL-GUNNE ..... p 3885 N94-31088
FAGUNDO, ARTURO ..... p 3731 N94-32862
FAIMAN, LIA ..... p 3793 N94-32622
FALCONE, ROGER W. ..... p 3721 N94-33012
FALKOWSKI, P. G. ..... p 3794 N94-32896
FAN, Q. ..... p 3890 N94-32415
FANG, J. ..... p 3649 N94-31276
FARBER, R. ..... p 3834 N94-32175
FARIDANI, J. ..... p 3912 N94-31924
FARLEY, G. L. ..... p 3628 N94-33126
FARMER, J. ..... p 3903 N94-32372
FAROOQ, M. ..... p 3686 N94-33346
FARR, TOM G. ..... p 3752 N94-32550
FARRY, KRISTIN A. ..... p 3729 N94-32450
FATHY, ALY ..... p 3897 N94-31531
FATUZZO, M. ..... p 3955 N94-32129
FAWCETT, RICHARD K. ..... p 3565 N94-31332
FAWCETT, STEVEN C. ..... p 3875 N94-32447
p 3604 N94-33298
FAYETTE, L. ..... p 3914 N94-32910
FEAGA, ADAM C. ..... p 3681 N94-32625
FEDRO, MARK J. ..... p 3630 N94-33137
FEELEY, O. C. ..... p 3667 N94-32133
FEILER, CHARLES E. ..... p 3710 N94-32969
FEILLARD, PASCAL ..... p 3618 N94-31225
FEJER, J. A. ..... p 3893 N94-33042
FELDHEIM, DANIEL L. ..... p 3631 N94-31238
FELIU, J. M. ..... p 3648 N94-33182
FELKER, B. ..... p 3715 N94-31580
FELTY, J. R. ..... p 3715 N94-31485
FENDRICH, J. ..... p 3904 N94-32601
FENG, SHECHAO ..... p 3618 N94-31261
FENSKE, DAVID ALLAN ..... p 3830 N94-31735
FENSTERMACHER, M. ..... p 3715 N94-31580
FENTON, R. E. ..... p 3587 N94-31710
FERBER, M. K. ..... p 3618 N94-31313
FERER, KENNETH M. ..... p 3790 N94-32959
FERGUSON, J. A. ..... p 3672 N94-31334
FERGUSON, S. W. ..... p 3715 N94-31580
FERKUL, PAUL VINCENT ..... p 3634 N94-31795
FERNANDES, FRANCISCO CARLOS ROCHA
p 3954 N94-33080
FERNANDO, H. J. ..... p 3701 N94-31341
FERNANDO, M. ..... p 3738 N94-32351
FERNSLER, RICHARD F. ..... p 3726 N94-32236
FERRANDO, WILLIAM A. ..... p 3698 N94-33181
FERRARO, J. R. ..... p 3907 N94-32989
FERRIS, JAMES C. ..... p 3601 N94-32870
FERRITTO, JOHN ..... p 3775 N94-33028
FEUCHTER, D. ..... p 3606 N94-33313
FEUCHTER, DEBRA K. ..... p 3663 N94-33024
FIELD, E. L. ..... p 3690 N94-31598
FIELD, R. W. ..... p 3632 N94-31305
FIELDS, W. F., IV ..... p 3715 N94-31580
FIFER, ROBERT A. ..... p 3635 N94-32124
FILIMONOV, B. B. ..... p 3873 N94-32768
FINCKENOR, MIRIA M. ..... p 3591 N94-31015
p 3595 N94-31032
FINDAKLY, T. ..... p 3656 N94-32246
FINLAYSON, R. D. ..... p 3730 N94-31872
FISHER, D. L. ..... p 3720 N94-32684
FISHER, P. ..... p 3928 N94-31121
FISK, MARK ..... p 3746 N94-32119
FISK, Z. ..... p 3898 N94-31631
p 3899 N94-31916
FITZURKA, M. ..... p 3928 N94-31123
FLANIGAN, DENNIS F. ..... p 3878 N94-31340
FLANNERY, DAVID L. ..... p 3836 N94-33043
FLEIG, ALBERT ..... p 3823 N94-33287
FLEISCHAUER, PAUL D. ..... p 3728 N94-33061
FLEISCHBEIN, J. ..... p 3791 N94-33244
FLEMING, GREGG G. ..... p 3861 N94-32418
FLEMING, LAND ..... p 3823 N94-32432
FLESHLER, S. ..... p 3904 N94-32601
FLINT, GRAHAM ..... p 3927 N94-32695
FLORO, J. A. ..... p 3903 N94-32384
FOG, BJARNE ..... p 3748 N94-32528
FOLLSTAEDT, D. M. ..... p 3645 N94-32672
FONK, Y. ..... p 3806 N94-31587
FORBES, JERRY ..... p 3712 N94-32051
FORDHAM, JOSEPH P. ..... p 3580 N94-33056
FOREST, C. B. ..... p 3886 N94-31324
p 3890 N94-32201
FORGET, F. ..... p 3950 N94-33227
FORGUES, SYLVAIN ..... p 3735 N94-31849
FORIN, ALESSANDRO ..... p 3816 N94-32081
FORMAN, P. ..... p 3774 N94-32736
FORSYTH, J. B. ..... p 3867 N94-31681
FORTNER, J. ..... p 3645 N94-32514
FOSTER, G. ..... p 3652 N94-31764
FOSTER, G. W. ..... p 3878 N94-31271
FOSTER, JOHN C. ..... p 3684 N94-33172
FOSTER, MICHAEL D. ..... p 3790 N94-33057
FOSTER, P. ..... p 3649 N94-31198
FOUQUART, Y. ..... p 3776 N94-30998
FOWLER, BRYCE L. ..... p 3630 N94-33165
FOWLER, T. K. ..... p 3892 N94-32820
FOX, J. A. ..... p 3804 N94-32596
FOX, J. L. ..... p 3947 N94-33208
FRAME, MICHAEL ..... p 3810 N94-31357

FRANCESCO, CARLA DE ..... p 3848 N94-32286
FRANKE, HUBERTUS ..... p 3817 N94-32219
FRANKE, J. E. ..... p 3634 N94-32110
FRANKEL, J. ..... p 3862 N94-32456
FRANKS, G. D. ..... p 3803 N94-31380
FRANKS, L. A. ..... p 3901 N94-32176
FRANSSON, K. ..... p 3922 N94-32856
FRATERNALI, PIERO ..... p 3808 N94-31178
FRAZIER, WILLIAM E. ..... p 3631 N94-31248
FREDERICKS, J. J. ..... p 3791 N94-33243
FREEMAN, A. J. ..... p 3659 N94-32656
FREEMAN, R. L. ..... p 3886 N94-31324
p 3890 N94-32201
p 3718 N94-32202
FREEMAN, S. P. H. T. ..... p 3632 N94-31349
FREEMAN, WILLIAM T. ..... p 3627 N94-33122
FREITAG, L. ..... p 3905 N94-32815
FRENCH, JONATHAN DAVID ..... p 3653 N94-31945
FRETTE, OEYVIND ..... p 3744 N94-31856
FRETWURST, E. ..... p 3865 N94-31607
FRIDAY, D. K. ..... p 3763 N94-31339
FRIEDLANDER, S. ..... p 3889 N94-31772
FRIEDMAN, GARY L. ..... p 3714 N94-32470
FRIEDMAN, H. W. ..... p 3926 N94-32189
FRIEDMANN, T. A. ..... p 3661 N94-32796
FRIES, SYLVIA DOUGHTY ..... p 3914 N94-33066
FRIESNER, R. A. ..... p 3871 N94-32375
FRIM, J. ..... p 3796 N94-31742
FRISCH, H. P. ..... p 3802 N94-32472
FRISCHHERZ, M. C. ..... p 3903 N94-32372
FRITSCHE, C. T. ..... p 3694 N94-32582
FRODGE, SALLY L. ..... p 3576 N94-31080
p 3577 N94-33095
FROEHLICH, J. ..... p 3857 N94-31770
FROGER, ETIENNE ..... p 3863 N94-31227
FROMARD, F. ..... p 3753 N94-32555
FROUIN, VINCENT ..... p 3798 N94-33069
FUEHRER, PERRY LEE ..... p 3702 N94-31563
FUERST, RUEDIGER ..... p 3689 N94-31575
FUGERE, J. ..... p 3854 N94-33341
FULLERTON, E. E. ..... p 3657 N94-32358
FULTON, R. D. ..... p 3716 N94-31624
FULTON, ROBERT D. ..... p 3720 N94-32760
FUNK, JOAN G. ..... p 3596 N94-31038
FURA, DAVID A. ..... p 3820 N94-32775

G

GADDY, J. L. ..... p 3760 N94-31811
GAERDHAGEN, BO ..... p 3722 N94-31194
GAINES, DAVID A. ..... p 3916 N94-31344
GALASSI, MARK CORRADO ..... p 3857 N94-31825
GALAUP, M. ..... p 3749 N94-32534
GALAUP, MAYLIS ..... p 3750 N94-32538
p 3753 N94-32554
GALEA, S. C. ..... p 3624 N94-32265
GALIL, ZVI ..... p 3827 N94-33002
GALLOWAY, K. F. ..... p 3698 N94-33177
GALTIER, BERTRAND ..... p 3748 N94-32529
GALVAO, D. S. ..... p 3660 N94-32729
GAMALETSOS, ARGIRIOS L. ..... p 3860 N94-31257
GAMBILL, STANLEY E. ..... p 3919 N94-32487
GAMBOA, RICK ..... p 3742 N94-31496
GANAPOL, BARRY D. ..... p 3870 N94-32368
GANG, LIU ..... p 3900 N94-32001
GANGARAJ, S. K. ..... p 3848 N94-32331
GAO, W. ..... p 3775 N94-32874
p 3768 N94-32894
GAO, XIAO-PING ..... p 3642 N94-31997
GAO, XIAOPING ..... p 3643 N94-32060
p 3869 N94-32170
p 3909 N94-33273
p 3909 N94-33275
p 3875 N94-33277
GARCIA, JOSE A. ..... p 3616 N94-32970
GARLINGTON, Y. ..... p 3881 N94-32380
GARNER, F. A. ..... p 3641 N94-31626
GAROFALO, A. ..... p 3888 N94-31664
GARVIS, D. ..... p 3675 N94-31761
GARY, MOLLY J. ..... p 3582 N94-33077
GASH, J. D. ..... p 3816 N94-32145
p 3816 N94-32146
GATELLI, F. ..... p 3756 N94-32569
GATES, D. ..... p 3888 N94-31664
GAUTHIER, LUC ..... p 3925 N94-31914
GAVEL, D. T. ..... p 3926 N94-32189
GAVER, DONALD P. ..... p 3781 N94-31239
GAWEDZKI, K. ..... p 3857 N94-31589
p 3857 N94-31770
GAYLES, ELLIS CALVIN ..... p 3796 N94-31746
GE, WEIGUO ..... p 3935 N94-31869
GEBAUER, LINDA ..... p 3593 N94-31024
GEBHARDT, HAGEN ..... p 3690 N94-31609
GEERLING, A. MAX ..... p 3825 N94-32196
GEHRELS, N. ..... p 3955 N94-32129
GEHRKE, K. ..... p 3905 N94-32779
GELBART, WILLIAM M. ..... p 3618 N94-31261
GELLER, J. ..... p 3813 N94-31686
GELOTTE, ERIK ..... p 3606 N94-33314
GENDRON, M. L. ..... p 3922 N94-32987
GENEST, J. ..... p 3853 N94-33337
GEORGE, PETE E. ..... p 3595 N94-31036
GEORGE, T. V. ..... p 3718 N94-32202
GEORGIADIS, NICHOLAS J. ..... p 3573 N94-32984
GERI, GEORGE A. ..... p 3586 N94-31058
p 3816 N94-32093
GERMAIN, MARVIN EDWARD ..... p 3952 N94-31214
GERSHTEIN, S. S. ..... p 3953 N94-31632
GERSTELL, M. ..... p 3767 N94-32712
GERWIN, RICHARD A. ..... p 3616 N94-32970
GEUBELLE, PHILIPPE HUBERT ..... p 3737 N94-31974
GEURTS, BERNARD J. ..... p 3699 N94-31185
GEURTS, MARIANNE ..... p 3917 N94-31415
GEX, WILL ..... p 3685 N94-32468
GHAN, S. J. ..... p 3746 N94-32100
p 3785 N94-32268
GHANIMATI, G. R. ..... p 3625 N94-32591
p 3625 N94-32592
GHOSN, LOUIS J. ..... p 3740 N94-32932
GIANNELIS, E. P. ..... p 3656 N94-32103
GIBSON, GARTH A. ..... p 3815 N94-31940
GIBSON, GLENN ..... p 3839 N94-33330
GIBSON, ROY ..... p 3748 N94-32525
GIBSON, WARREN C. ..... p 3630 N94-33165
GIERASCH, P. J. ..... p 3951 N94-33233
GIERULL, CHRISTOPH ..... p 3671 N94-31254
GIESSELMANN, MICHAEL ..... p 3719 N94-32654
GIGORD, PATRICK ..... p 3749 N94-32531
GILL, RICHARD D. ..... p 3846 N94-32107
GILL, S. ..... p 3606 N94-33311
p 3606 N94-33312
GILLES, P. E. ..... p 3682 N94-33001
GILLETTE, MARTHA U. ..... p 3793 N94-32622
GILLIAM, MICHAEL ..... p 3923 N94-32469
GILMER, G. H. ..... p 3903 N94-32411
GILMORE, RICHARD E. ..... p 3784 N94-32260
GINDI, GENE ..... p 3834 N94-32053
GIRARD, ISABELLE ..... p 3831 N94-31800
GIRARDEY, C. C. ..... p 3599 N94-31428
GIRAULT, FRANCOIS ..... p 3753 N94-32552
GIRAULT, FRANCOIS M. ..... p 3752 N94-32551
GIROSI, FEDERICO ..... p 3851 N94-32142
GLADSTONE, G. R. ..... p 3945 N94-33200
p 3947 N94-33211
GLADYSZ, J. A. ..... p 3638 N94-32887
GLANTZ, C. S. ..... p 3914 N94-32910
GLASS, G. ..... p 3869 N94-32173
GLASS, R. S. ..... p 3694 N94-32593
GLASSMAN, MYRON ..... p 3922 N94-32835
GLENNIE, DEREK JOHN ..... p 3876 N94-31736
GLIGOR, VIRGIL ..... p 3916 N94-31331
GLINSKY, M. ..... p 3887 N94-31400
GLOSLI, JAMES N. ..... p 3863 N94-31237
GODDARD, J. G. ..... p 3763 N94-31347
GODFREY, G. L. ..... p 3925 N94-31786
GOEDHART, BOB ..... p 3812 N94-31522
GOEDKEN, VIRGIL L. ..... p 3900 N94-32011
GOETZ, M. ..... p 3733 N94-31375
GOFF, THOMAS ..... p 3823 N94-33287
GOHIL, P. ..... p 3891 N94-32595
GOLD, S. H. ..... p 3692 N94-32199
GOLDA, CARLO ..... p 3599 N94-31431
GOLDEN, D. C. ..... p 3948 N94-33219
GOLDEN, JOHNNY L. ..... p 3592 N94-31017
GOLUB, S. V. ..... p 3597 N94-31043
GOMEZ, MANUEL ..... p 3686 N94-31079
GOMEZ, R. ..... p 3648 N94-33182
GONGLEWSKI, J. D. ..... p 3722 N94-33282
GONIS, A. ..... p 3904 N94-32606
p 3646 N94-32754
GONZALES, G. ..... p 3754 N94-32557
GONZALES, RICHARD R. ..... p 3798 N94-33040
GOODS, S. H. ..... p 3649 N94-31198
GOODY, R. ..... p 3767 N94-32712
GOOSSENS, ROLAND E. ..... p 3745 N94-31867
GORADIA, SURESH H. ..... p 3601 N94-32870
GORDON, SANFORD ..... p 3638 N94-32948
GORDON, TIM ..... p 3592 N94-31019
GORE, R. A. ..... p 3830 N94-31623
GORNIAK, MARK J. ..... p 3686 N94-31066
GORSLINE, D. S. ..... p 3949 N94-33224
GOSSAGE, S. A. ..... p 3823 N94-31149
GOSSNER, J. R. ..... p 3828 N94-31158
GOSZ, MICHAEL RICHARD ..... p 3619 N94-31555
GOTTESFELD, S. ..... p 3761 N94-32762
GOUINAUD, C. ..... p 3749 N94-32534
GOULDING, R. H. ..... p 3886 N94-31324
p 3890 N94-32201
GOURDIN, W. ..... p 3904 N94-32606
GOURLEY, P. L. ..... p 3716 N94-31622
GOW, ANTHONY J. ..... p 3773 N94-32154
GOWDA, RAGHAVA G. ..... p 3582 N94-32909
GOYAL, A. ..... p 3909 N94-33271
GOZA, STEWART MICHAEL ..... p 3798 N94-32471
GRABOWSKA, D. G. ..... p 3706 N94-32279
GRADY, D. E. ..... p 3737 N94-32135
GRADY, M. M. ..... p 3952 N94-33239
GRAESSER, D. ..... p 3629 N94-33132
GRAESSER, EDWARD J. ..... p 3640 N94-31456
GRAHAM, TODD A. ..... p 3604 N94-33299
GRAN, M. ..... p 3823 N94-32430
GRANDSIRE-VINCON, ISABELLE ..... p 3618 N94-31232
GRANICA, KLAUS ..... p 3748 N94-32526
GRANNIS, P. D. ..... p 3863 N94-31147
GRANT, A. J. ..... p 3825 N94-31663
GRANT, C. ..... p 3629 N94-33133
GRANT, K. E. ..... p 3775 N94-32895
GRARD, R. ..... p 3951 N94-33237
GRAY, J. L. ..... p 3762 N94-32763
GRAY, K. E. ..... p 3904 N94-32602
GRAY, K. J. ..... p 3743 N94-31603
GRAY, MARK A. ..... p 3565 N94-31362
GRAY, S. K. ..... p 3871 N94-32598
GREBINNIK, V. G. ..... p 3896 N94-31395
GREEN, DAVID M. ..... p 3862 N94-33146
GREEN, I. J. ..... p 3751 N94-32543
GREEN, M. A. ..... p 3955 N94-31635
GREENE, R. ..... p 3794 N94-32896
GREENSITE, J. P. ..... p 3876 N94-32407
GREENWOOD, L. R. ..... p 3641 N94-31626
GREGORY, J. C. ..... p 3594 N94-31027
GREGORY, JOHN ..... p 3591 N94-31012
GREGORY, JOHN C. ..... p 3596 N94-31042
GREITZER, EDWARD M. ..... p 3584 N94-33035
GREITZER, F. L. ..... p 3816 N94-32145
p 3816 N94-32146
GRENIER, Y. ..... p 3808 N94-31094
GRIBBLE, R. P. ..... p 3713 N94-32681
GRIBBLE, ROBERT F. ..... p 3616 N94-32970
GRIBOV, V. N. ..... p 3868 N94-31923
GRIEWANK, A. ..... p 3841 N94-31309
GRIFFIN, C. F. ..... p 3628 N94-33125
GRIFFIN, V. L. ..... p 3786 N94-33004
GRIFFITH, L. V. ..... p 3650 N94-31354
GRIFFITHS, C. L. ..... p 3903 N94-32322
GRITZ, D. C. ..... p 3797 N94-32732
GRODSINSKY, CARLOS M. ..... p 3567 N94-33064
GROEBNER, R. J. ..... p 3891 N94-32612
GROENEWEG, J. ..... p 3847 N94-32206
GROLEAU, NICOLAS ..... p 3799 N94-31990
GRONDIN, LUC ..... p 3935 N94-31913
GRONEY, DAVID J. ..... p 3612 N94-33262
GROSS, DAVID L. ..... p 3923 N94-32443
GROSS, TED S. ..... p 3797 N94-31960
GROSSAN, BRUCE ALAN ..... p 3937 N94-31987
GROSSBERG, STEPHEN ..... p 3835 N94-32340
GROSSI, MARIO D. ..... p 3894 N94-33113
GROSSMAN, A. S. ..... p 3775 N94-32895
GRUBELICH, M. C. ..... p 3666 N94-31827
GRUEN, D. M. ..... p 3871 N94-32515
GRUENENDAHL, S. ..... p 3867 N94-31671
GRUNER, S. M. ..... p 3793 N94-32516
GRUNTHANER, F. J. ..... p 3941 N94-31145
GRUSZCZYNSKA, M. ..... p 3754 N94-32558
GU, Z.-Q. ..... p 3896 N94-31473
GUARINO, THOMAS J. ..... p 3565 N94-31830
GUCHAIT, M. ..... p 3868 N94-31922
GUCKENBERGER, DUTCH ..... p 3591 N94-32474
GUEVREMONT, GRANT ..... p 3703 N94-31730
GUHA, S. ..... p 3695 N94-32680
GUIDOTTI, R. A. ..... p 3695 N94-32663
GUILHEM, D. ..... p 3891 N94-32619
GUILLANDE, R. ..... p 3751 N94-32546
GUILLAUMON, JEAN-CLAUDE ..... p 3597 N94-31045
GUILLORY, A. R. ..... p 3786 N94-33004
GUINAN, M. W. ..... p 3896 N94-31499
GUNNING, DAVID R. ..... p 3566 N94-32254
GUNZBURGER ..... p 3839 N94-33325
GUPPY, A. ..... p 3914 N94-31538
GUSTAFSON, STEVEN C. ..... p 3836 N94-33043
GUSTAVSON, PAUL ..... p 3712 N94-32051
GUTOWSKI, T. ..... p 3627 N94-33122
GUYENNE, T. D. ..... p 3914 N94-31181
p 3743 N94-31853
GWINN, K. W. ..... p 3568 N94-31578
GYLLENBERG, MATS ..... p 3851 N94-32229

H

HAALAND, D. M. ..... p 3634 N94-32110
HABER, WILLIAM J. ..... p 3697 N94-32967
HABERLE, R. M. ..... p 3943 N94-33190
HABERLE, ROBERT M. ..... p 3944 N94-33192
p 3946 N94-33205
p 3949 N94-33221
p 3950 N94-33227
p 3951 N94-33236

HACKETT, MICHAEL p 3956 N94-32420
HADLEY, G. R. p 3697 N94-31502
HADLEY, G. RONALD p 3882 N94-32649
HAERENDEL, G. p 3885 N94-31089
HAFICH, M. J. p 3719 N94-32608
HAFIZI, B. p 3692 N94-32199
HAGENIERS, OMER L. p 3621 N94-31892
HAGER, BRADFORD H. p 3941 N94-31115
HAIR, D. CHARLES p 3915 N94-32426
HAKE, K. A. p 3915 N94-31155
HALBLEIB, J. A. p 3678 N94-32113
HALE, ROBERT A. p 3789 N94-32325
HALL, C. R. p 3757 N94-32463
HALL, G. E. p 3632 N94-31305
HALL, R. B. p 3760 N94-32143
HALL, T. E. p 3712 N94-31831
HALLBERG, CARL p 3699 N94-32460
HALLER, E. E. p 3899 N94-31634
HALLS, JOANNE p 3758 N94-32465
HALPER, M. p 3813 N94-31686
HALSEY, T. C. p 3883 N94-32818
HALSTENBERG, BERND p 3674 N94-31615
HALZEN, F. p 3864 N94-31310
HAMBY, D. M. p 3842 N94-31399
HAMED, G. R. p 3658 N94-32518
HAMELIN, ANTOINETTE p 3869 N94-32170
HAMM, R. N. p 3636 N94-32251
HAMMEL, MICHAEL p 3866 N94-31613
HAMMER, J. p 3887 N94-31400
HAMMOND, CARL MAX, JR. p 3942 N94-32326
HAMMONS, B. E. p 3716 N94-31622
HAMMOUD, AHMAD p 3731 N94-32901
HAMPSHIRE, JOHN p 3800 N94-32277
HAN, KWANG S. p 3887 N94-31530
HAND, BRIAN JOHN p 3911 N94-31712
HANES, M. H. p 3698 N94-33091
HANEY, ROBERT L. p 3789 N94-32325
HANKLA, A. K. p 3719 N94-32659
HANNA, CHARLES L. p 3565 N94-31830
HANNAUER, GEORGE p 3826 N94-32482
HANNON, A. C. p 3867 N94-31681
HANOTEL, ROLAND p 3568 N94-31421
HANSEL, S. J. p 3808 N94-33252
HANSEN, CHRIS p 3607 N94-33323
HANSEN, J. C. p 3804 N94-32580
HANSEN, THORKILD B. p 3672 N94-31371
HANSFORD, G. p 3632 N94-31305
HANSON, R. K. p 3639 N94-33242
HANSSEN, R. F. p 3741 N94-31075
HARLAN, CHARLENE p 3920 N94-32808
HARLOWE, W. W. p 3638 N94-32868
HARMER, MARTIN P. p 3649 N94-31276
HARMS, JOCHEN p 3750 N94-32538
p 3753 N94-32554
p 3755 N94-32564
HARNDEN, JOANN M. K. p 3613 N94-33289
HARPER, ROBERT p 3815 N94-32080
HARRINGTON, MARK p 3920 N94-32808
HARRIS, C. E. p 3629 N94-33130
HARRIS, CHARLES E. p 3629 N94-33134
HARRIS, D. B. p 3892 N94-32730
HARRIS, E. D. p 3581 N94-33329
HARRIS, J. M. p 3637 N94-32826
HARRIS, JOEL M. p 3636 N94-32304
HARRIS, K. p 3895 N94-31329
HARRIS, R. R. p 3915 N94-32678
HARRIS, VINCENT G. p 3696 N94-32721
HARRISON, L. C. p 3786 N94-32759
HARRISON, R. J. p 3636 N94-32616
HART, T. R. p 3759 N94-31762
HARTE, J. p 3849 N94-32670
HARTIGAN, P. p 3928 N94-31122
HARTL, P. p 3755 N94-32566
HARTL, PHILIPP p 3756 N94-32572
HARTMAN, BRYCE O. p 3798 N94-31243
HARTMAN, J. K. p 3666 N94-31827
HARTMAN, RICHARD T. p 3804 N94-32302
HARTMANN, W. K. p 3947 N94-33206
HARVEY, R. W. p 3886 N94-31324
p 3890 N94-32201
HARVEY, WILLIAM D. p 3601 N94-32870
HARWELL, J. p 3881 N94-32380
HARY, STEPHEN L. p 3581 N94-31458
HASEGAWA, MARK M. p 3592 N94-31016
HASLAM, GEORGE p 3670 N94-31062
HASPER, ALBERT p 3641 N94-31519
HASSANEIN, A. p 3863 N94-31151
HASSELMANN, K. p 3790 N94-32881
HASSENZAHL, W. V. p 3888 N94-31667
HASTI, DAVID E. p 3761 N94-32648
HATCHER, P. G. p 3667 N94-32150
HATCHER, R. p 3881 N94-32380
HATFIELD, L. D. p 3816 N94-32146
HATHAWAY, D. p 3715 N94-31580
HAUGEN, BERT p 3603 N94-33292
p 3604 N94-33300
HAUSER, JOHN E. p 3834 N94-32095
HAVERKORT, BOUDEWIJN R. p 3812 N94-31659
HAVRE, S. L. p 3816 N94-32145
HAYDEN, WARREN R. p 3614 N94-31618
HAYES, J. P. p 3906 N94-32684
HAYTON, G. E. p 3840 N94-31156
p 3840 N94-31162
HAZEWINKEL, MICHIEL p 3846 N94-32106
p 3847 N94-32204
HE, M. Y. p 3630 N94-33178
HE, XIAOYU p 3813 N94-31713
HEADLEY, T. J. p 3661 N94-32803
HEBB, RICHARD C. p 3712 N94-32002
HECK, ANDREAS p 3830 N94-31514
HEDDE, THIERRY p 3574 N94-31230
HEDGES, R. E. M. p 3632 N94-31349
HEDMAN, SVEN G. p 3568 N94-31220
HEEG, R. S. p 3703 N94-31691
HEESTERBEEK, J. A. P. p 3793 N94-32228
HEGNA, C. C. p 3892 N94-32911
p 3893 N94-32912
HEIDE, DAVID A. p 3683 N94-33026
HEIJMAN, S. G. J. p 3633 N94-31591
HEIKINHEIMO, LIISA p 3724 N94-31656
HEIMANN, PAULA J. p 3662 N94-32945
HEINISCH, H. L. p 3641 N94-31627
HEISELBERG, H. p 3864 N94-31405
HEITMEYER, CONSTANCE L. p 3811 N94-31461
HEITOR, M. V. p 3634 N94-32033
HELD, T. W. p 3823 N94-32430
HELLER, ADAM p 3691 N94-32056
p 3635 N94-32231
HELLINGER, ROLF p 3688 N94-31374
HELLWARTH, ROBERT W. p 3884 N94-33145
HEMBREE, D. M. p 3901 N94-32172
HEMBREE, G. G. p 3901 N94-32092
HEMMINGER, CAROL p 3591 N94-31014
HENDERSON, C. L. p 3692 N94-32111
p 3692 N94-32112
HENINS, IVARS p 3616 N94-32970
HENKEL, J. p 3745 N94-31861
HENRY, WENDELL A. p 3816 N94-32130
HENSHALL, G. A. p 3641 N94-31581
p 3645 N94-32522
HENSLEY, SCOTT p 3756 N94-32568
HENSON, BRYAN F. p 3637 N94-32743
HERALD, MICHELLE p 3605 N94-33308
HERKENHOFF, K. E. p 3947 N94-33207
HERMAN, IVAN p 3822 N94-33097
HERMAN, R. G. p 3667 N94-32133
HERNON, PETER p 3921 N94-32833
HERRERA-FIERRO, P. p 3606 N94-33313
HERY, P. p 3753 N94-32555
HESKETH, R. P. p 3636 N94-32414
HESS, CECIL F. p 3718 N94-32366
HESS, CLIFFORD p 3729 N94-32450
HESS, N. J. p 3895 N94-31307
HESS, W. R. p 3891 N94-32619
HESSLER, J. P. p 3864 N94-31321
p 3871 N94-32615
HEWER, GARY A. p 3712 N94-32393
HICKEY, SUZANNE C. p 3584 N94-32238
HICKS, RAYMOND M. p 3860 N94-31336
p 3860 N94-31337
HIETALA, V. M. p 3688 N94-31483
p 3903 N94-32409
p 3696 N94-32809
HIETAOJA, P. p 3648 N94-31069
HILAL, KATIA p 3670 N94-31174
HILES, STEVEN p 3740 N94-32940
HILL, D. A. p 3675 N94-31683
HILL, D. N. p 3888 N94-31765
HILL, ED p 3795 N94-31363
HILL, JOACHIM p 3744 N94-31857
HILL, RALPH H., JR. p 3593 N94-31026
HILL, T. A. p 3695 N94-32700
HILLER, J. M. p 3807 N94-32783
HILLS, STEVEN W. p 3823 N94-32438
HINKLE, C. R. p 3757 N94-32463
HINKLE, L. R. p 3666 N94-31579
HINKS, D. G. p 3904 N94-32602
HINNEBERG, H.-J. p 3896 N94-31501
HINS, A. G. p 3643 N94-32109
HINTON, B. p 3787 N94-33288
HIPPENSTIEL, RALPH p 3672 N94-31386
HIROSE, A. p 3893 N94-32922
HITNEY, HERBERT V. p 3684 N94-33186
HO, G. H. p 3858 N94-31397
HO, SHRWAI p 3624 N94-32501
HOADLEY, D. p 3579 N94-32015
HOAGLAND, R. G. p 3640 N94-31325
HOBOHM, KLAUS p 3674 N94-31573
HOECK, H. p 3790 N94-32881
HOEFEL, ALBERT p 3689 N94-31571
HOEK, T. S. p 3813 N94-31704
HOFFHEINS, B. S. p 3807 N94-32783
HOFFMAN, D. M. p 3654 N94-31978
HOGAN, J. T. p 3891 N94-32619
HOGAN, S. J. p 3759 N94-31279
HOH, ROGER H. p 3582 N94-33076
p 3582 N94-33078
p 3583 N94-33079
HOHIMER, JOHN P. p 3882 N94-32649
HOLDEN, D. p 3611 N94-32813
HOLDEN, MICHAEL p 3591 N94-33167
HOLDEN, T. M. p 3733 N94-31312
HOLDER, D. W., JR. p 3803 N94-31380
HOLDER, J. S. p 3646 N94-32781
HOLLAND, MARK p 3815 N94-31940
HOLLAR, W. E., JR. p 3659 N94-32618
HOLLERBACH, M. p 3886 N94-31304
HOLLOWAY, GLENN p 3810 N94-31328
HOLM, ELIAS VALUR p 3700 N94-31221
HOLMES, C. L. p 3863 N94-31270
HOLMES, MARION R. p 3850 N94-33265
HOLSTI-MIETTINEN, R. p 3648 N94-31069
HOLTOM, G. R. p 3720 N94-32704
HOLTROP, K. L. p 3886 N94-31304
HONEY, W. E. p 3603 N94-32671
HONG-MO, C. p 3912 N94-31924
HONG, SEOK H. p 3656 N94-32253
HONG, W. S. p 3795 N94-31323
HONG, Y. p 3642 N94-31871
HONIG, A. p 3890 N94-32415
p 3876 N94-32731
HOOFATT, MICHELLE S. p 3733 N94-31288
HOOFMAN, RAYMOND p 3842 N94-31409
HOOPER, E. B. p 3715 N94-31580
p 3675 N94-31781
HOPKINS, MARK A. p 3580 N94-33107
HOPPE, HUGHES p 3820 N94-32972
HORAIN, PATRICK p 3840 N94-31095
HORDIJK, A. p 3851 N94-32205
HORN, K. M. p 3903 N94-32384
HORNE, WALTER F. p 3582 N94-33076
p 3582 N94-33078
p 3583 N94-33079
HOROWITZ, M. p 3907 N94-32988
HORTON, L. L. p 3659 N94-32640
HORTON, W. p 3886 N94-31366
p 3887 N94-31396
HOSGOOD, B. p 3744 N94-31855
HOTALING, S. P. p 3596 N94-31041
HOUCK, JOHN CHARLES p 3935 N94-31946
HOUGHTON, RICHARD p 3740 N94-32940
HOUZELLE, STEPHANE p 3742 N94-31165
HOVANDER, B. p 3922 N94-32856
HOWARD, A. D. p 3949 N94-33223
HOWDEN, WILLIAM p 3822 N94-33188
HOWE, L. M. p 3906 N94-32875
p 3648 N94-32993
HOWE, MICHAEL S. p 3862 N94-33023
HOWELL, D. p 3761 N94-32705
HOWELL, R. H. p 3661 N94-32751
HOWELLS, W. S. p 3661 N94-32798
HOYT, R. W. p 3901 N94-32153
HOYT, ROBERT P. p 3616 N94-32970
HROVAT, KENNETH p 3731 N94-32901
HRUBESH, L. W. p 3639 N94-33260
HSIUE, G. H. p 3663 N94-32985
HSU, WEN L. p 3661 N94-32803
HU, RUI-ZHONG p 3661 N94-32798
HU, Y. Z. p 3893 N94-33007
HU, YAN-RU p 3724 N94-31714
HUAMAN, D. p 3751 N94-32546
HUANG, HUAXIONG p 3704 N94-31778
HUANG, R. H. p 3580 N94-32378
HUANG, S. R. p 3731 N94-32481
HUANG, T. C. p 3643 N94-32098
HUANG, ZHISHENG p 3917 N94-31452
HUBBARD, C. R. p 3733 N94-31312
HUBBARD, RICHARD F. p 3726 N94-32236
HUBER, H. D. p 3687 N94-31152
HUDSON, BRIAN H. p 3582 N94-33077
p 3583 N94-33079
HUDSON, C. L. p 3713 N94-32728
HUDSON, E. S. p 3873 N94-32755
HUDSON, G. p 3902 N94-32306
HUDSON, MARY p 3774 N94-32346
HUFF, D. L. p 3739 N94-32883
HUGENBERG, K. p 3682 N94-32756
HUGES, WILLIAM C. p 3894 N94-31055
HUGHES, E. p 3875 N94-33278
HUGHES, M. p 3767 N94-32784
HUHN, RICHARD p 3803 N94-31852
HUIBERS, T. W. C. p 3916 N94-31365
HUNDSDORFER, W. p 3847 N94-32200
HUNTER, TOM p 3920 N94-32808
HUNTLEY, M. S. p 3576 N94-31680
HUNTLEY, M. S., JR. p 3583 N94-33280
HUNTON, DONALD p 3596 N94-31040
HUPP, JOSEPH T. p 3635 N94-32216

HURLEY, MIKE p 3604 N94-33302
HURWITZ, FRANCES I. p 3662 N94-32945
HUTCHENS, C. F. p 3803 N94-31380
HUTCHINSON, JAMES M. p 3924 N94-31361
HUTCHISON, MATTHEW GERRY p 3578 N94-31881
HUYER, A. p 3791 N94-33244
HVAL, M. p 3735 N94-31841
HWANG, JAMES p 3621 N94-31835
HWANG, PHILLIP Q. p 3823 N94-32439
HYMAN, ELLIS p 3710 N94-33009

I

IACHELLO, F. p 3873 N94-32708
IANNO, N. J. p 3661 N94-32788
IDZERDA, Y. U. p 3858 N94-31397
IGA, J. p 3762 N94-32918
IGARASHI, S. p 3897 N94-31506
IHLENBURG, FRANK p 3848 N94-32341
IINOYA, FUJIO p 3889 N94-31776
IKEUCHI, KATSUSHI p 3845 N94-31939
IKEYA, T. p 3697 N94-32917
ILCEWICZ, L. B. p 3626 N94-32863
p 3627 N94-33122
p 3629 N94-33130
p 3629 N94-33132
ILIAS, N. p 3733 N94-31375
IMAM, M. A. p 3640 N94-31345
IMAMURA, E. p 3762 N94-32919
IMBAULT, M. p 3752 N94-32551
INEICHEN, P. p 3764 N94-31602
INGBER, M. S. p 3708 N94-32709
IOFFE, A. F. p 3841 N94-31311
p 3864 N94-31320
IONESCU, VLAD p 3830 N94-31647
IRENE, E. A. p 3881 N94-32280
p 3881 N94-32324
p 3893 N94-33007
IRWIN, G. W. p 3722 N94-31379
ISAACS, H. S. p 3646 N94-32699
ISHIHARA, K. p 3762 N94-32918
ISKENDERIAN, T. p 3607 N94-33318
IVERS, T. H. p 3888 N94-31664
IWAHORI, T. p 3697 N94-32917
p 3762 N94-32918
IWATA, M. p 3893 N94-32916
IYER, VENKIT p 3709 N94-32871
IZEN, J. M. p 3866 N94-31620

J

JAAKKOLA, TOMMI p 3815 N94-31933
JACAK, B. V. p 3870 N94-32271
JACCODINE, RALPH J. p 3631 N94-31282
JACKSON, ANTHONY C. p 3629 N94-33135
JACKSON, DANIEL p 3822 N94-33279
JACKSON, E. L. p 3760 N94-32143
JACKSON, G. L. p 3886 N94-31304
JACKSON, KEVIN p 3924 N94-32462
JACKSON, MARK CHARLES p 3601 N94-32388
JACKSON, W. B. p 3899 N94-31813
JACOBS, I. p 3796 N94-31740
p 3796 N94-31741
JACOBS, PATRICIA A. p 3781 N94-31239
JACOBS, ROBERT A. p 3814 N94-31932
JACOBSON, G. F. p 3719 N94-32659
JAEGER, E. P. p 3793 N94-32269
JAFFE, JULES S. p 3789 N94-32402
JAHN, RALPH RAINER p 3734 N94-31737
JAIN, A. K. p 3765 N94-32354
JAKOSKY, B. M. p 3947 N94-33208
p 3948 N94-33218
JAMES, P. B. p 3948 N94-33215
JAMES, STANLEY D. p 3693 N94-32329
JANG, BOR Z. p 3595 N94-31035
JANG, GUANG-WAY p 3664 N94-33350
JANKOWIAK, I. p 3770 N94-31003
JANKOWSKI, A. F. p 3906 N94-32884
p 3647 N94-32892
JANKOWSKI, DAVID G. p 3941 N94-31115
JANOWSKA, M. p 3754 N94-32558
JANSSEN, RENE H. P. p 3847 N94-32194
p 3851 N94-32225
JANSSEN, THEO M. V. p 3841 N94-31391
JARBOE, T. R. p 3892 N94-32800
JASKOLLA, F. p 3745 N94-31861
JAYNE, D. T. p 3606 N94-33313
JEDREY, T. C. p 3599 N94-31428
JEFFRIES, RICHARD A. p 3785 N94-32278
JELINEK, R. p 3866 N94-31637
JELONEK, M. P. p 3722 N94-33282
JENG, R. J. p 3658 N94-32579
p 3659 N94-32610
p 3663 N94-32985
JENKINS, A. L. p 3853 N94-33336
p 3854 N94-33344
JENNISON, D. R. p 3719 N94-32603
JENSEN, JOHN R. p 3758 N94-32465
JERATH, MAYA p 3798 N94-33092
JESSON, D. E. p 3896 N94-31489
p 3904 N94-32724
JHA, M. C. p 3759 N94-31272
JHABVALA, MURZY D. p 3713 N94-32459
JI, Y. p 3859 N94-33161
JIA, SHIYI p 3725 N94-31874
JIANG, X. p 3644 N94-32169
JIANG, X. L. p 3658 N94-32579
JING, T. p 3795 N94-31323
JIRASEK, MILAN p 3734 N94-31479
JOBST, B. p 3869 N94-32173
JODOGNE, J. C. p 3776 N94-33184
JOHANNESSEN, OLA M. p 3744 N94-31856
JOHANNSEN, C. J. p 3757 N94-33019
JOHANSSON, A. p 3922 N94-32856
JOHANSSON, M. p 3908 N94-33246
JOHANSSON, M. A. p 3667 N94-32133
JOHANSSON, M. E. p 3903 N94-32409
JOHNSEN, H. A. p 3661 N94-32796
p 3661 N94-32803
JOHNSON, E. R. p 3760 N94-31811
JOHNSON, G. H. p 3698 N94-33177
JOHNSON, IVAN p 3915 N94-32427
JOHNSON, J. O. p 3611 N94-32667
JOHNSON, LES p 3598 N94-31425
p 3598 N94-31426
JOHNSON, MARK E. p 3603 N94-33292
JOHNSON, MICHAEL R. p 3607 N94-33319
JOHNSON, N. p 3899 N94-31813
JOHNSON, P. E. p 3904 N94-32606
JOHNSON, P. M. p 3872 N94-32643
JOHNSON, R. E. p 3947 N94-33208
JOHNSON, R. P. p 3730 N94-31065
JOHNSON, S. Y. p 3771 N94-31525
JOHNSON, T. p 3797 N94-32732
JOHNSTON, G. P. p 3651 N94-31650
JOHNSTON, NORMAN J. p 3629 N94-33134
JONES, A. R. p 3745 N94-31863
JONES, CHARLES R. p 3776 N94-33351
JONES, CHARLIE E. p 3565 N94-31830
JONES, CHERIE A. p 3592 N94-31016
JONES, E. C. p 3905 N94-32785
JONES, J. H. p 3610 N94-32010
p 3947 N94-33209
JONES, KENNETH MORRIS p 3569 N94-31882
JONES, KEVIN DANIEL p 3569 N94-31828
JONES, LLOYD H. p 3828 N94-31064
JONES, M. p 3905 N94-32815
JONES, R. p 3624 N94-32265
JONES, R. H. p 3645 N94-32614
JONES, SYNTHIA S. p 3920 N94-32633
JONES, W. R., JR. p 3606 N94-33313
JONES, WILLIAM R., JR. p 3663 N94-33024
JONSSON, JONAS p 3808 N94-31087
JORDAN, MICHAEL I. p 3614 N94-31932
p 3815 N94-31933
p 3852 N94-33276
JORDAN, THOMAS H. p 3790 N94-33062
JORNA, P. G. A. M. p 3587 N94-31179
JOSELYN, J. p 3832 N94-31808
JOSEPH, J. p 3893 N94-33007
JOVIC, SRBA p 3711 N94-33290
JOYCE, J. J. p 3898 N94-31631
JUANG, TEN-BIN p 3736 N94-31955
JUDSON, R. S. p 3793 N94-32269
JUHASZ, ALBERT J. p 3726 N94-32272
JULIEN, DENIS p 3735 N94-31849
JUNG, GLENN H. p 3787 N94-33089
JUNG, WEN-JE p 3700 N94-31211
JURASEK, DAVID W. p 3808 N94-32433
JUST, OLIVER p 3902 N94-32218

K

KAATZ, FORREST H. p 3696 N94-32721
KACIK, TERRANCE A. p 3662 N94-32945
KADI, MOHAMMED p 3778 N94-30989
KADUWELA, A. P. p 3712 N94-31629
KAEMPFER, N. p 3770 N94-31222
KAIPA, RAVI C. p 3713 N94-32459
KALEJS, J. P. p 3905 N94-32764
KALMAN, EVA p 3670 N94-31171
KALMAN, LASZLO p 3855 N94-31390
KALOKITIS, DAVID p 3897 N94-31531
KALTENBERGER, BURKE R. p 3578 N94-31442
KAMEGAI, M. p 3708 N94-32849
KAMENETZKY, RACHEL R. p 3593 N94-31022
p 3593 N94-31025
KAMIJO, KOJI p 3683 N94-33081
KAMSICKAS, G. p 3588 N94-32014
p 3588 N94-32241
p 3588 N94-32311
p 3588 N94-32312
p 3588 N94-32313
p 3589 N94-32314
p 3589 N94-32315
p 3589 N94-32316
p 3589 N94-32317
p 3589 N94-32318
p 3589 N94-32319
p 3589 N94-32394
p 3590 N94-32395
p 3590 N94-32396
p 3590 N94-32397
p 3590 N94-32398
p 3590 N94-32399
p 3590 N94-32403
KAN, LEI p 3698 N94-31612
KANADE, TAKEO p 3803 N94-31447
p 3712 N94-31929
KANAZAWA, MAKOTO p 3842 N94-31453
p 3856 N94-31468
KANNE, W. R., JR. p 3723 N94-31524
KAO, KAI-HSIUNG p 3850 N94-33120
KAPANIA, RAKESH K. p 3619 N94-31444
KAPLAN, HADASSAH p 3769 N94-33110
KAPLAN, S. N. p 3795 N94-31323
KARADY, GEORGE G. p 3697 N94-33044
KARAMPETAKIS, N. P. p 3840 N94-31156
p 3840 N94-31162
KARGEL, J. S. p 3947 N94-33210
KARPALA, FRANK p 3621 N94-31892
KARR, C. L. p 3839 N94-32422
KARR, MICHAEL p 3810 N94-31328
KARR, MIKE p 3803 N94-32034
KARY, DAVID MICHAEL p 3935 N94-31926
KASCAK, ALBERT F. p 3728 N94-32902
KASHAEV, R. M. p 3902 N94-32247
KASS, W. J. p 3666 N94-31579
KASSAPOGLOU, CHRISTOS p 3626 N94-32877
KASSNER, T. F. p 3643 N94-32109
KASTEN, MICHAEL S. p 3713 N94-32459
KATAN, J. R. p 3682 N94-33001
KATEHI, LINDA P. B. p 3696 N94-32905
p 3698 N94-33116
KATSUBE, M. W. p 3690 N94-31711
KATZ, N. p 3838 N94-33168
KAUFMAN, JONATHAN W. p 3797 N94-32156
KAUFMANN, V. p 3755 N94-32565
KAUPPINEN, PENTTI p 3724 N94-31656
KAVANAGH, P. p 3706 N94-32279
KAWASKALEH, GHASSAN p 3670 N94-31093
KAYE, R. J. p 3603 N94-32671
KAZOVSKY, LEONID G. p 3878 N94-31330
KEANE, J. A. p 3825 N94-31663
KEEL, LEEHYUN p 3836 N94-32980
KEELING, S. L. p 3707 N94-32361
KEICHER, D. M. p 3717 N94-32134
KELLER, BRIAN SCOTT p 3602 N94-31891
KELLERMAN, B. K. p 3903 N94-32384
KELLMAN, A. G. p 3886 N94-31304
KELLOGG, KENNETH G. p 3621 N94-31793
KELLY, K. p 3588 N94-32014
p 3588 N94-32241
p 3588 N94-32311
p 3588 N94-32312
p 3588 N94-32313
p 3589 N94-32314
p 3589 N94-32315
p 3589 N94-32316
p 3589 N94-32317
p 3589 N94-32318
p 3589 N94-32319
p 3589 N94-32394
p 3590 N94-32395
p 3590 N94-32396
p 3590 N94-32397
p 3590 N94-32398
p 3590 N94-32399
p 3590 N94-32403
KELLY, MARY D. p 3601 N94-32211
KENDIG, MARTIN W. p 3663 N94-32960
KENGOR, PAUL p 3811 N94-31465
KENNEDY, CHRISTOPHER A. p 3573 N94-32950
KENNEDY, JOHN M. p 3921 N94-32829
p 3921 N94-32830
p 3921 N94-32831
p 3921 N94-32832
p 3921 N94-32834
p 3922 N94-32836
p 3922 N94-32837
KENNEDY, R. p 3675 N94-31761
KENNEL, C. F. p 3894 N94-33106
KENNICOTT, P. R. p 3811 N94-31484
KENSEK, R. P. p 3678 N94-32113
p 3872 N94-32628
KENT, JOHN E. p 3788 N94-32072

KENT, M. S. p 3651 N94-31649
KEPLER, R. G. p 3655 N94-32102
p 3660 N94-32729
KERCHER, J. R. p 3769 N94-32966
KERN, STEVEN B. p 3573 N94-32974
KERSHAW, D. p 3849 N94-32670
KETTELL, KENT W. p 3726 N94-32261
KEY, B. G. p 3915 N94-31155
KEYES, B. L. P. p 3659 N94-32632
KEYSER, L. F. p 3950 N94-33231
KHADEMI, P. M. p 3841 N94-31309
KHALI, HAKIM p 3716 N94-31797
KHAN, ISHRAT M. p 3650 N94-31509
KHATTAK, CHANDRA P. p 3909 N94-33324
KHODADOUST, ABDOLLAH p 3571 N94-32475
KHOZE, V. A. p 3868 N94-31923
KHURGIN, JACOB p 3910 N94-33355
KIERSTEAD, J. A. p 3865 N94-31607
KIEU, DUC CONG p 3782 N94-31889
KILLINGSWORTH, M. J. p 3681 N94-32679
KIM, H. J. p 3626 N94-32860
KIM, J. p 3774 N94-32772
p 3948 N94-33214
KIM, JINWON p 3786 N94-32791
KIM, KIHO p 3723 N94-31569
KIM, S. Y. p 3881 N94-32280
KIM, S.-W. p 3928 N94-31123
p 3929 N94-31124
p 3932 N94-31143
KIM, W. H. p 3664 N94-33082
KIM, W. K. p 3658 N94-32578
KIM, WON S. p 3806 N94-32453
KIM, YONG W. p 3646 N94-32782
KING, C. p 3754 N94-32561
KING, JERI S. p 3585 N94-33283
KING, TERENCE A. p 3884 N94-33267
KINGSBURY, E. p 3606 N94-33313
KINLOCH, A. J. p 3738 N94-32351
KINSER, D. L. p 3653 N94-31851
KINSER, DONALD L. p 3594 N94-31030
KIOUSSIS, N. p 3904 N94-32606
KIPP, M. E. p 3737 N94-32135
KIRK, M. A. p 3903 N94-32372
KIRKLAND, T. P. p 3618 N94-31313
KIRKPATRICK, R. J. p 3774 N94-32816
KISER, D. M. p 3920 N94-32827
KIVELSON, DANIEL p 3618 N94-31261
KIVELSON, M. G. p 3894 N94-33106
KIZHAKEVARIAM, N. p 3644 N94-32169
KJAELL, P. p 3640 N94-31083
KLARER, P. p 3835 N94-32787
KLASSON, K. T. p 3760 N94-31811
KLAUS, E. J. p 3661 N94-32796
KLEIN, VLADISLAV p 3586 N94-32951
KLEINER, MENDEL p 3859 N94-31090
KLEMETTI, W. I. p 3676 N94-31998
KLEMETTI, WAYNE I. p 3677 N94-32083
p 3678 N94-32158
p 3678 N94-32159
p 3680 N94-32297
p 3680 N94-32298
p 3680 N94-32299
p 3680 N94-32300
p 3685 N94-33347
KLEPPER, C. C. p 3891 N94-32619
KLERSY, R. p 3748 N94-32524
KLIER, K. p 3667 N94-32133
KLIMAS, P. C. p 3761 N94-32383
KLIMAS, PAUL C. p 3761 N94-32648
KLINKER, D. H. p 3606 N94-33315
KLOP, JAN WILLEM p 3849 N94-32349
KLUIT, P. G. p 3824 N94-31641
p 3813 N94-31695
KLUMPP, D. A. p 3657 N94-32377
KLUTE, GLENN K. p 3805 N94-33050
KNAPP, D. p 3864 N94-31508
KNAPP, R. B. p 3746 N94-31999
KNEZEK, PATRICIA MARIE p 3933 N94-31495
KNICKELBEIN, M. B. p 3873 N94-32797
KNIGHT, ED p 3613 N94-33289
KNIGHT, W. D. p 3874 N94-32807
KNILL, DAVID C. p 3802 N94-33326
KNIRSCH, MARTIN p 3711 N94-31515
KNOTEK, M. L. p 3871 N94-32605
KNOTHE, K. p 3733 N94-31375
KNOWLEN, CARL p 3602 N94-32288
KNOWLES, DAN, JR. p 3613 N94-33289
KOBIERSKI, R. D. p 3581 N94-31903
KOCH, B. p 3746 N94-31868
KOCH, J. A. p 3717 N94-32128
p 3720 N94-32794
KOCH, M. W. p 3671 N94-31267
KOCIMSKI, S. M. p 3713 N94-32728
KOCKS, U. F. p 3903 N94-32597
KODALI, P. p 3656 N94-32103
KOEHLER, J. p 3651 N94-31672
KOELLE, HEINZ-HERMANN p 3764 N94-31611
KOENIG, MARK A. p 3801 N94-33053
KOENIG, SVEN p 3816 N94-32086
KOGA, J. K. p 3876 N94-32685
KOGA, R. p 3838 N94-33168
p 3698 N94-33177
p 3808 N94-33252
KOHL, HANS p 3753 N94-32554
KOLBAS, ROBERT M. p 3896 N94-31455
KOLBER, Z. p 3794 N94-32896
KOLMODIN, CARL-OVE p 3732 N94-31091
KOMBARGI, R. p 3888 N94-31664
KOMPANIETZ, G. p 3615 N94-32669
KONG, F. M. p 3660 N94-32687
KONG, P. C. p 3758 N94-31234
KONICKI, JOSEPH S. p 3726 N94-32370
KOOIJ, R. E. p 3844 N94-31644
p 3844 N94-31696
KOOLE, GER p 3846 N94-32108
KOONEN, A. M. J. p 3698 N94-33169
KOONS, HARRY C. p 3612 N94-33262
KOONTZ, STEVEN L. p 3596 N94-31039
p 3596 N94-31040
KOOPMAN, N. p 3598 N94-31208
KOOPMAN, R. p 3692 N94-32136
KOOPMANS, B. N. p 3752 N94-32548
KOORNWINDER, TOM H. p 3857 N94-32192
KOPF, CARLO p 3603 N94-33296
KOPPENAAL, D. W. p 3713 N94-32811
KORDE, UMESH ARVIND p 3829 N94-31207
KOROTKIKH, N. p 3652 N94-31764
KOSC, T. Z. p 3661 N94-32819
KOSIERB, RICHARD p 3955 N94-31709
KOSOWER, D. A. p 3911 N94-31823
KOSRO, P. M. p 3791 N94-33244
KOSTOFF, RONALD N. p 3923 N94-32442
KOURIS, DEMITRIS A. p 3624 N94-32342
KOUVARITAKIS, B. p 3828 N94-31158
KOVACS, AUSTIN p 3773 N94-32154
KOVACS, G. p 3916 N94-31175
KOWALCZYK, T. C. p 3661 N94-32819
KOZAITIS, SAMUEL P. p 3880 N94-32151
KOZLOWSKI, L. p 3908 N94-33248
KOZLOWSKI, M. R. p 3714 N94-31269
p 3716 N94-31636
p 3719 N94-32613
KOZMINCHUK, BRIAN W. p 3671 N94-31253
KRAAIKAMP, COR p 3844 N94-31643
KRAEMER, SYLVIA K. p 3924 N94-33067
KRAEUTER, GERTRUD p 3900 N94-32003
p 3642 N94-32004
KRAFT, ANTON J. p 3783 N94-32021
KRANER, H. W. p 3865 N94-31607
KRAUT, ROBERT E. p 3678 N94-32121
KRAUTER, GERTRUD p 3900 N94-32011
KRAVITZ, S. H. p 3688 N94-31483
p 3696 N94-32809
KRESIN, V. V. p 3874 N94-32807
KREUTZ, THOMAS G. p 3632 N94-31348
KRISHAN, V. p 3953 N94-31632
KRISHNAMURTI, T. N. p 3784 N94-32164
KROEGER, D. M. p 3909 N94-33271
KROESE, DIRK P. p 3832 N94-31826
KROUTIL, R. T. p 3746 N94-31999
KRUER, W. p 3887 N94-31400
KRUISE, JANS p 3795 N94-31652
KRUKONIS, VAL p 3625 N94-32624
KRUMBUEGEL, MARCO ALEXANDER p 3674 N94-31608
KUCKERTZ, TOM p 3682 N94-32745
KUERTEN, J. G. M. p 3699 N94-31185
KUES, HENRY A. p 3681 N94-32576
KUHFUSS, TIMOTHY C. p 3827 N94-32646
KUIK, FOEKE p 3878 N94-31550
KULLERD, SUSAN M. p 3628 N94-33127
p 3628 N94-33129
KULP, T. J. p 3675 N94-31761
KUMAGAI, AKIHIKO p 3833 N94-31962
KUMAI, K. p 3697 N94-32917
KUMAR, A. p 3728 N94-32900
p 3728 N94-32929
KUMAR, A. H. p 3630 N94-33180
KUMAR, B. V. p 3800 N94-32277
KUMAR, H. N. SURESHA p 3603 N94-33293
KUMAR, J. p 3658 N94-32578
p 3659 N94-32610
p 3663 N94-33054
p 3664 N94-33082
KUMAR, VIPIN p 3809 N94-31251
KUMARASWAMY, MOHAN M. p 3599 N94-31432
KUNTZ, D. W. p 3701 N94-31268
KUO, WEI p 3712 N94-32393
KURKCHUBASCHE, R. R. p 3730 N94-31065
KUROSE, J. F. p 3825 N94-32052
KUTLU, MEHMET p 3671 N94-31299
KUZNETSOV, Y. A. p 3847 N94-32191
KUZNIA, JONATHAN N. p 3897 N94-31528
KVARAN, GEIR p 3613 N94-33289
KWA, TECK-SENG p 3627 N94-33123
KWAST, KAREN L. p 3916 N94-31392
KWEI, G. H. p 3899 N94-31633
KWIAT, KEVIN A. p 3686 N94-31066
KWIATKOWSKI, J. J. p 3723 N94-31621
KWIESIELEWICZ, M. p 3844 N94-31701
KWOK, W. K. p 3904 N94-32601
KYRALA, G. A. p 3716 N94-31624
KYRALA, GEORGE A. p 3720 N94-32760
KYRILLIDIS, A. p 3859 N94-33161

L

LAARHUIS, J. H. p 3698 N94-33169
LABAW, BRUCE G. p 3811 N94-31461
LABEGORRE, BERNARD p 3701 N94-31422
LABONTE, BARRY p 3953 N94-32343
LABOUR, SHERRI p 3924 N94-31732
LACERDA, A. p 3899 N94-31916
LACH, J. p 3864 N94-31507
p 3877 N94-32802
LACHMAN, MOISES p 3915 N94-31172
LACSER, AVI p 3769 N94-33110
LAFARGE, R. A. p 3609 N94-31382
p 3568 N94-31578
LAGOUARDE, JEAN-PIERRE p 3779 N94-31001
LAGUETTE, S. p 3754 N94-32559
LAI, B. p 3672 N94-31317
LAINE, G. p 3757 N94-32575
LAKE, CHARLES H. p 3895 N94-31327
LAKES, R. S. p 3629 N94-33131
LAM, P. p 3738 N94-32351
LAMONTAGNE, RENE p 3686 N94-33153
LAMOREAUX, CYNTHIA p 3593 N94-31024
LAMPE, MARTIN p 3726 N94-32236
LAMPO, S. p 3760 N94-32143
LANCE, CYRIL p 3775 N94-32999
LANCTO, R. p 3657 N94-32367
LANDGREBE, D. A. p 3757 N94-33019
LANDIS, GEOFFREY A. p 3599 N94-31427
LANDSTROEM, SVEN p 3859 N94-31076
LANE, A. L. p 3941 N94-31145
LANE, NORMAN E. p 3591 N94-32474
LANG, K. p 3871 N94-32512
LANGE, FRED F. p 3657 N94-32391
LANGE, G. p 3606 N94-33312
LANGFORD, ROLAND E. p 3616 N94-33059
LAPEDES, A. p 3834 N94-32175
LAPUCHA, DARIUSZ p 3576 N94-31080
p 3577 N94-33095
LAREAU, R. T. p 3640 N94-31314
LARJAVA, KARI p 3765 N94-31657
LARMAN, KEVIN T. p 3613 N94-32924
LAROCHELLE, YVES p 3867 N94-31749
LARSEN, EDWARD W. p 3857 N94-32589
LARSON, N. p 3764 N94-31601
LASIECKA, I. p 3738 N94-32275
LASNIER, C. J. p 3868 N94-31765
LATHAM, ROY p 3917 N94-31829
LATOMBE, J. C. p 3811 N94-31475
LAUER, E. J. p 3863 N94-31270
LAUER, H. V., JR. p 3948 N94-33219
LAUNILA, OLLI p 3808 N94-31087
LAURORE, L. p 3749 N94-32534
LAURORE, LIONEL p 3749 N94-32530
LAW, CHUNG K. p 3632 N94-31348
LAWHORN, KATHY L. p 3804 N94-32379
LAWLER, MARK E. p 3936 N94-31947
LAWN, STEPHEN J. p 3883 N94-32777
LAWRENCE, CHARLES p 3605 N94-33304
p 3605 N94-33306
LAWRENCE, D. W. p 3650 N94-31284
LE, TUYEN D. p 3595 N94-31034
LEAR, K. L. p 3881 N94-32385
LEAVITT, RICHARD P. p 3721 N94-33003
LEBEDA, C. p 3774 N94-32736
LECLAIR, LANCE RICHARD p 3868 N94-31915
LEDEBUHR, A. p 3955 N94-32129
LEDESMA, ROY R. p 3683 N94-33159
LEE, B. p 3955 N94-32129
LEE, CHI-WAI p 3933 N94-31497
LEE, CHIN-HWA p 3826 N94-32323
LEE, E. M. p 3948 N94-33217
LEE, H. p 3795 N94-31323
p 3950 N94-33227
LEE, H.-J. p 3626 N94-32858
LEE, HAI-TIEN p 3742 N94-31553
LEE, J. p 3572 N94-32926
LEE, J. H. p 3766 N94-32692
LEE, J. W. p 3664 N94-33247
LEE, PETER p 3815 N94-32080
LEE, R. L. p 3886 N94-31304
p 3774 N94-32772

LEE, RICHARD Q. p 3698 N94-33116
LEE, ROBERT B., III p 3785 N94-32737
LEE, S. M. p 3901 N94-32115
LEE, S. R. p 3902 N94-32296
LEE, S. S. p 3662 N94-32891
LEE, S. W. p 3945 N94-33200
p 3947 N94-33211
LEE, T. S. H. p 3873 N94-32708
p 3873 N94-32710
LEE, VEN-GEN p 3619 N94-31481
LEE, Y. J. p 3762 N94-32763
LEEMIS, LAWRENCE M. p 3821 N94-33075
LEFAHLER, ERIC p 3877 N94-31173
LEFAUCONNIER, B. p 3753 N94-32553
LEFEBVRE, L. p 3853 N94-33337
LEFEVRE, MIREILLE p 3828 N94-31100
p 3829 N94-31193
LEGER, LUBERT J. p 3596 N94-31040
LEGUERN, F. p 3751 N94-32546
LEHMANN, F. p 3744 N94-31858
LEHMANN, K. p 3744 N94-31856
LEHNERT, MATTHEW DAVID p 3936 N94-31948
LEHOUEROU, H. N. p 3780 N94-31009
LEIBENGUTH, R. E. p 3688 N94-31483
p 3881 N94-32385
LEIGHTON, TOM p 3826 N94-32243
LEITNAKER, J. M. p 3913 N94-32846
LEMASTER, PAUL S. p 3591 N94-31013
LEMIEUX, MARKO p 3676 N94-31796
LENKO, DANIEL S. p 3681 N94-32625
LENNARTSSON, O. W. p 3893 N94-33074
LENNARTZ, J. A. p 3875 N94-31480
LEON, EFRAIN p 3684 N94-33261
LEON, M. p 3874 N94-32804
LEONARD, A. W. p 3888 N94-31765
LEPAGE, RICHARD p 3831 N94-31750
LEROY, MARC p 3613 N94-30997
LESICZKA, JOHN A. p 3909 N94-33324
LESTER, CHARLES S. p 3720 N94-32761
LESUER, D. R. p 3626 N94-32665
LETREUT, H. p 3777 N94-30987
LETZRING, S. p 3876 N94-32731
LEUNG, HENRY p 3686 N94-33150
LEVADOU, FRANCOIS p 3592 N94-31018
LEVESQUE, MARIO J. p 3586 N94-33086
LEVIN, B. F. p 3658 N94-32408
LEVINE, L. O. p 3730 N94-31605
LEVINE, T. E. p 3656 N94-32103
LEVY, H. p 3677 N94-32085
LEVY, LIONEL L., JR. p 3860 N94-31336
p 3860 N94-31337
LEVY, MILTON p 3644 N94-32240
LEWIS, CHRISTINE GLADDING p 3699 N94-31209
LEWIS, N. G. p 3793 N94-32267
LEYSEN, M. M. p 3753 N94-32556
LEYSEN, MARC M. p 3745 N94-31867
LI, GUONGUANG p 3907 N94-32944
LI, H. p 3929 N94-31125
LI, HUA p 3907 N94-32934
LI, L. p 3658 N94-32579
p 3663 N94-32985
LI, LARRY C. H. p 3729 N94-32450
LI, LIAN p 3664 N94-33348
LI, M. p 3738 N94-32639
LI, S. Y. p 3719 N94-32603
LI, SHUH-HUEI p 3622 N94-31986
LI, YONG p 3651 N94-31513
LI, Z. p 3865 N94-31607
p 3870 N94-32355
LI, ZHENG p 3906 N94-32822
LIAN, ANQING p 3610 N94-31910
LIANG, EDISON P. p 3927 N94-31116
p 3929 N94-31126
p 3929 N94-31129
p 3931 N94-31139
LIBERA, M. p 3640 N94-31314
LICHTENEGGER, J. p 3755 N94-32565
LICHTENSTEIN, JONATHAN p 3811 N94-31465
LICINA, JOSEPH R. p 3586 N94-32217
p 3579 N94-32242
LIE, SEN p 3681 N94-32477
LIECHTI, K. M. p 3650 N94-31297
LIEFIELD, R. J. p 3713 N94-32706
LIEFTING, JAN REINDER p 3897 N94-31521
LIESCH, D. S. p 3730 N94-31872
LIFSCHITZ, SERGIO p 3824 N94-31183
LILJEGREN, J. C. p 3786 N94-32759
LIN, H. C. p 3802 N94-32472
LIN, H.-J. p 3858 N94-31397
LIN, JOHN C. p 3573 N94-33071
LIN, T. C. p 3802 N94-32472
LIN, YUEH-JAW p 3605 N94-33306
LINCE, JEFFREY R. p 3635 N94-32233
LINCH, H. S. p 3641 N94-31638
LINCOLN, KENNETH A. p 3597 N94-31046
LIND, P. C. p 3854 N94-33342
LINDBERG, R. p 3634 N94-31679
LINDEN, KURT J. p 3722 N94-32448
LINDGREEN, EDO ROOS p 3917 N94-31640
LINDNER, B. L. p 3947 N94-33212
p 3948 N94-33213
LINDQVIST, P.-A. p 3885 N94-31089
LINDSTROEM, G. p 3865 N94-31607
LINHOLM, L. W. p 3695 N94-32700
LINTON, ROGER C. p 3591 N94-31015
p 3593 N94-31025
LINTZ, STEVEN J. p 3791 N94-33243
LINUSSON, PER p 3859 N94-31077
LIOU, MENG-SING p 3850 N94-33120
LIPINSKI, R. J. p 3715 N94-31485
LIPKOVICH, MATTHEW A. p 3900 N94-32001
LISSENDEN, CLIFFORD JESSE p 3618 N94-31285
LITTLE, C. p 3611 N94-32813
LITTLE, W. A. p 3908 N94-32991
LIU, A. D. p 3720 N94-32707
LIU, C. T. p 3647 N94-32852
LIU, FAN-CHEN p 3909 N94-33273
LIU, JOHN M. p 3627 N94-33018
LIU, Q. p 3881 N94-32324
LIU, Y. M. p 3595 N94-31035
LIU, YU-CHENG p 3839 N94-33330
LOCK, EVAN p 3823 N94-32439
LOCKWOOD, S. J. p 3695 N94-32650
LOENVIK, L. E. p 3918 N94-32293
LOERCHER, G. p 3745 N94-31861
LOEVE, J. A. p 3851 N94-32205
LOFFREDO, D. M. p 3720 N94-32707
LOGAN, B. G. p 3666 N94-32114
LOGSDON, KIRK A. p 3567 N94-33064
LOHRENZ, M. C. p 3922 N94-32987
LOINTIER, M. p 3748 N94-32527
p 3753 N94-32555
LOIZZO, R. p 3745 N94-31862
LONG, CHARLES E. p 3791 N94-33085
LONG, STUART A. p 3683 N94-33083
LONGCOPE, DANA WARFIELD p 3953 N94-31792
LOOMIS, B. A. p 3641 N94-31486
p 3641 N94-31666
LOOMIS, G. E. p 3651 N94-31557
LOPES, A. p 3750 N94-32535
p 3753 N94-32555
LOPEZ-KRAHE, JAIME p 3798 N94-33069
LORENTZEN, G. p 3668 N94-31073
LOTTS, C. G. p 3628 N94-33126
LOUAHALA, S. p 3755 N94-32563
LOUMAGNE, C. p 3755 N94-32563
LOWE, ANDREW TIMOTHY p 3743 N94-31733
LOWENSTINE, MARK p 3790 N94-32959
LOWNDES, D. H. p 3905 N94-32785
LOWRY, M. p 3682 N94-32756
LOWRY, M. E. p 3695 N94-32688
LU, NANYAO p 3926 N94-31968
LU, QINGYUAN p 3700 N94-31219
LU, S. Y. p 3695 N94-32688
LU, SHIN-YEE p 3669 N94-32449
LU, TAI-WEI p 3829 N94-31301
LU, Y. p 3760 N94-31812
LUBOMSKI, JOSEPH F. p 3567 N94-33064
LUDEWIG, H. p 3615 N94-32266
LUERS, PHILIP J. p 3713 N94-32459
LUETTICH, R. A., JR. p 3787 N94-31250
LUHMANN, J. G. p 3948 N94-33214
LUKE, MARVIN p 3736 N94-31904
LUMB, C. C. p 3567 N94-33338
LUND, A. L. p 3645 N94-32614
LUND, P. p 3760 N94-31767
LUNDGREN, CLAES p 3605 N94-33084
LUNDHOLM, STEVEN E. p 3672 N94-31300
LUNDSTEDT, H. p 3832 N94-31808
LUNDY, DONALD O. p 3616 N94-33059
LUNEL, SJOERD M. VERDUYN p 3851 N94-32229
LUO, C. p 3929 N94-31127
p 3930 N94-31131
LUO, JIANG p 3689 N94-31536
LUXEY, PASCAL p 3752 N94-32549
LYBERIS, N. p 3753 N94-32553
LYNCH, FRANKLIN E. p 3669 N94-32857
LYNESS, J. N. p 3841 N94-31274
p 3844 N94-31665
LYON, DON R. p 3816 N94-32093
LYU, CHENG-HSUAN p 3937 N94-31963

M

MA, J. T. p 3808 N94-31163
p 3808 N94-31164
MA, M. T. p 3675 N94-31683
MA, Z. Y. p 3664 N94-33247
MAASS, ANNE-MARIE p 3812 N94-31659
MACCABE, A. B. p 3819 N94-32651
MACDONALD, R. G. p 3863 N94-31202
MACELROY, J. M. p 3655 N94-32005
MACERA, ANTHONY R. p 3686 N94-31066
MACGOWAN, B. J. p 3717 N94-32128
p 3720 N94-32794
MACIEJEWSKI, WENDELL p 3739 N94-32733
MACKENZIE, COLIN F. p 3799 N94-31440
MACKINNON, JOHN C. p 3707 N94-32497
MACRITCHIE, BONNIE p 3919 N94-32382
MADAN, RAM C. p 3628 N94-33129
MADDEN, MICHAEL M. p 3702 N94-31476
MADDOX, DOUGLAS L. p 3726 N94-32334
MAES, STEPHANE p 3600 N94-31435
MAGRUDER, R. H. p 3901 N94-32172
MAHLE, J. J. p 3763 N94-31339
MAIER-REIMER, E. p 3790 N94-32881
MAITRE, HENRI p 3910 N94-31098
MAJDA, GEORGE p 3850 N94-33175
MAKA, A. p 3766 N94-32703
MAKEPEACE, LESTER B., III p 3608 N94-32020
MAKOWSKI, M. A. p 3675 N94-31781
MAKSYM, JOSEPH N. p 3837 N94-33151
MALAN, GERALD R. p 3816 N94-32081
MALDIA, LEOPOLDO C. p 3623 N94-32023
MALEY, M. P. p 3905 N94-32747
MALHOTRA, V. p 3894 N94-31056
MALIK, JOHN p 3603 N94-33296
MALIN, JANE T. p 3823 N94-32432
MALKUS, DAVID S. p 3701 N94-31245
MALLAMACI, M. P. p 3652 N94-31780
MALONEY, LAURENCE T. p 3800 N94-32345
MALVAR, L. J. p 3623 N94-32070
MANCHALA, DANIEL p 3728 N94-32902
MANGAZEEV, V. V. p 3902 N94-32247
MANGIN, JEAN-FRANCOIS p 3798 N94-33069
MANGOLINI, MARC p 3750 N94-32541
MANNHEIMER, WALLACE M. p 3718 N94-32406
MANIEZZO, VITTORIO p 3829 N94-31176
p 3824 N94-31177
p 3829 N94-31186
MANNERSKOG, G. p 3878 N94-31584
MANUEL, JOHN R. p 3776 N94-33111
MANUELPILLAI, GERALD N. p 3652 N94-31692
MARACCI, G. p 3744 N94-31855
MARANVILLE, MARK S. p 3610 N94-32039
MARASCO, PETER L. p 3804 N94-32302
MARCOPOLI, VINCENT R. p 3584 N94-32075
p 3727 N94-32741
MARDER, A. R. p 3658 N94-32408
MAREAN, MICHAEL W. p 3810 N94-31357
MARGOLIN, LEN G. p 3774 N94-32647
MARGOLIS, B. p 3864 N94-31310
MARIELLA, R. P., JR. p 3904 N94-32634
MARINELLI, W. J. p 3694 N94-32478
MARITON, M. p 3750 N94-32540
MARKLEY, F. p 3652 N94-31764
MARKLUND, G. T. p 3885 N94-31089
MARKS, L. D. p 3878 N94-31262
p 3871 N94-32621
MARKUNAS, R. J. p 3902 N94-32306
MARKUS, ALAN p 3628 N94-33128
MARR, WILLIAM W. p 3765 N94-32600
MARREN, DAN p 3587 N94-31318
MARRON, ANTONY C. p 3773 N94-32335
MARRS, R. p 3864 N94-31508
MARSH, DAVE p 3917 N94-31829
MARSHALL, A. C. p 3615 N94-32669
MARTELLO, SILVANO p 3809 N94-31189
MARTENS, J. p 3908 N94-33246
MARTENS, J. S. p 3903 N94-32409
MARTIN, D. p 3787 N94-33288
MARTIN, FRANCOIS p 3716 N94-31748
MARTIN, J. E. p 3883 N94-32818
MARTIN, L. J. p 3947 N94-33207
p 3948 N94-33215
MARTIN, L. R. p 3616 N94-33094
MARTIN, PHILIPPE p 3770 N94-31011
MARTIN, T. Z. p 3947 N94-33211
p 3948 N94-33216
MARTON, CHRISTINE p 3600 N94-31436
MARTURUNKAKUL, S. p 3658 N94-32579
p 3659 N94-32610
p 3663 N94-32985
MARTURUNKAKUL, SUTIYAO p 3663 N94-33054
p 3664 N94-33348
MARTY, G. p 3753 N94-32555
MASNOVI, JOHN p 3662 N94-32945
MASON, R. p 3887 N94-31400
MASSALASKI, T. B. p 3648 N94-33270
MASSALSKI, T. B. p 3645 N94-32636
MASSE, C. E. p 3664 N94-33082
MASSONNET, D. p 3755 N94-32567
p 3756 N94-32570
p 3756 N94-32571
MASTERSON, JEFFREY M. p 3912 N94-32043
MASTIN, C. WAYNE p 3821 N94-33049
MASUD, A. p 3625 N94-32591
p 3625 N94-32592

MASUOKA, EDWARD p 3823 N94-33287
MATA, SILVESTER G. p 3644 N94-32371
MATARRESE, MICHAEL DAVID p 3567 N94-31216
MATHE, NATHALIE p 3923 N94-32428
MATHUR, SANJAY R. p 3700 N94-31217
MATOSSIAN, MARK G. p 3600 N94-31437
MATSUI, TOSHIYUKI p 3683 N94-33081
MATTHEWS, R. p 3595 N94-31033
MAUCHE, C. W. p 3938 N94-32137
MAUEL, M. E. p 3888 N94-31664
MAURER, D. p 3888 N94-31664
MAUSER, WOLFRAM p 3745 N94-31865
MAX, C. E. p 3926 N94-32189
MAYER, ERNST WILHELM p 3700 N94-31218
MAYER, J. W. p 3658 N94-32103
p 3902 N94-32296
MAYER, WALTER p 3859 N94-31060
p 3861 N94-32059
MAYES, PAUL p 3676 N94-32049
p 3677 N94-32050
MAYO, ROBERT M. p 3616 N94-32970
MAYS, DOUGLAS E. p 3746 N94-32025
MAYVILLE, R. p 3578 N94-31078
MCALLISTER, LOUISA H. p 3765 N94-32195
MCARTHUR, B. A. p 3836 N94-33149
MCARTHUR, D. A. p 3715 N94-31485
MCBRAYER, J. D. p 3690 N94-31593
MCBREEN, J. p 3691 N94-31919
MCBRIDE, BONNIE J. p 3638 N94-32948
MCBRIDE, P. p 3877 N94-32748
MCBRIDE, S. L. p 3642 N94-31871
MCCAMPBELL, C. B. p 3666 N94-31827
MCCARDIE, A. H. p 3799 N94-32187
MCCARTEN, DAVID R. p 3606 N94-33316
MCCARTY, K. F. p 3661 N94-32796
MCCORMICK, P. p 3929 N94-31128
MCCORMICK, R. L. p 3759 N94-31272
MCCUNE, W. W. p 3829 N94-31315
MCDANIEL, FLOYD D. p 3899 N94-31983
MCDANIEL, S. T. p 3788 N94-32000
MCDERMOTT, DREW p 3817 N94-32257
MCDONALD, CARLOS p 3742 N94-31496
MCDONALD, JOHN p 3820 N94-32972
MCDONNELL, PATRICK N. p 3722 N94-32448
MCDONOUGH, J. M. p 3708 N94-32511
MCELIECE, ROBERT J. p 3684 N94-33173
MCEWEN, A. S. p 3948 N94-33217
MCGIBBON, A. J. p 3896 N94-31489
MCGILL, GEORGE E. p 3941 N94-31115
MCGLAUN, M. p 3739 N94-32842
MCGOVERN, LAWRENCE K. p 3713 N94-32459
MCGOVERN, PATRICK J. p 3776 N94-31106
p 3940 N94-31107
p 3940 N94-31108
MCGOWEN, HILLERY p 3729 N94-32451
MCGRATH, DENNIS p 3839 N94-32423
MCGREGOR, DENNIS N. p 3673 N94-31446
MCHARGUE, C. J. p 3659 N94-32640
MCILRATH, T. J. p 3874 N94-33144
MCINTYRE, D. C. p 3651 N94-31649
MCINVILLE, ROY M. p 3574 N94-33263
MCKAY, AL p 3613 N94-33289
MCKAY, C. P. p 3946 N94-33205
MCKAY, MICHAEL D. p 3852 N94-32744
MCKEAN, M. C. p 3854 N94-33341
MCKEE, SUZANNE p 3801 N94-32998
MCKERNAN, S. p 3659 N94-32640
MCKINNEY, BARRY T. p 3732 N94-33088
MCKOON, GAIL p 3801 N94-32956
MCLAUGHLIN, DAVID W. p 3882 N94-32510
MCMACKIN, L. p 3722 N94-33282
MCMAKIN, D. L. p 3712 N94-31831
MCMANN, M. p 3659 N94-32617
MCMILLAN, D. E. p 3807 N94-32783
MCNAUGHTON, K. H. p 3869 N94-32173
MCRAE, K. I. p 3730 N94-31872
MEDELIUS, PEDRO J. p 3699 N94-32460
MEDERNACH, J. W. p 3645 N94-32672
MEDLIN, D. L. p 3661 N94-32796
MEEUWISSEN, ADRIANUS M. H. p 3851 N94-31697
p 3851 N94-31698
MEGEATH, SAMUEL THOMAS p 3925 N94-31898
MEGIE, GERARD p 3770 N94-31010
MEGIER, JACQUES p 3744 N94-31857
MEHL, WOLFGANG p 3744 N94-31857
MEHLMAN, W. F. p 3615 N94-32669
MEHLMANN, OLAF F. p 3829 N94-31372
MEHROTRA, PIYUSH p 3820 N94-32928
MEI, B. Z. p 3663 N94-33058
MEIGS, G. p 3858 N94-31397
MEINDL, M. A. p 3576 N94-31306
MEINHARDT, M. B. p 3882 N94-32674
p 3661 N94-32819
MEIRELLESFILHO, C. p 3929 N94-31129
p 3930 N94-31130
p 3930 N94-31131
MEIROVITCH, LEONARD p 3612 N94-33115
MEISSNER, W. p 3584 N94-32859
MELL, RICHARD J. p 3591 N94-31013
MELLON, M. T. p 3948 N94-33218
MENAUT, J. C. p 3757 N94-31004
MENDENHALL, MARCUS H. p 3594 N94-31030
MENDOZA, JOEL P. p 3860 N94-31336
p 3860 N94-31337
MENDOZA, M. M. p 3567 N94-33338
MENEZES, W. J. C. p 3873 N94-32797
MENG, JAMES C. p 3710 N94-32958
MENIETTI, J. DOUGLAS p 3953 N94-33047
MERING, C. p 3753 N94-32553
MEROT, P. p 3755 N94-32563
MERRICK, S. B. p 3687 N94-31152
MERRILL, CRAIG F. p 3701 N94-31241
MERSMAN, C. R. p 3696 N94-32828
MERSON, J. A. p 3666 N94-31579
MESEGUER, JOSE p 3809 N94-31263
MESSICK, C. p 3690 N94-31594
MESSIER, DOUGLAS M. p 3600 N94-31438
METCALF, HAROLD p 3870 N94-32360
METSCHAN, S. p 3629 N94-33133
METSCHAN, S. L. p 3626 N94-32863
METZ, J. A. J. p 3793 N94-32226
p 3793 N94-32228
MEWE, R. p 3770 N94-31222
MEYER, J.-J. C. p 3826 N94-32291
MEYER, W. J. p 3883 N94-32878
MEZA, J. C. p 3818 N94-32584
MEZIANI, Z. E. p 3875 N94-33189
MICHALSKY, J. p 3764 N94-31601
MICHALSKY, J. J. p 3764 N94-31602
p 3786 N94-32759
MICHAUD, GAETAN p 3588 N94-31747
MICK, MARK p 3758 N94-32466
MICSIK, A. p 3916 N94-31175
MIELKE, MICHAEL p 3764 N94-31611
MIGLIONICO, CHARLES J. p 3597 N94-31046
MIHALIK, G. B. p 3901 N94-32176
MIKKELSEN, I. S. p 3954 N94-31102
MIKOLAJEWICZ, U. p 3790 N94-32881
MILLER, CHARLES D. p 3918 N94-32090
MILLER, D. S. p 3938 N94-32914
MILLER, EDGAR R. p 3591 N94-31013
MILLER, M. D. p 3651 N94-31557
MILLER, MARTIN S. p 3635 N94-32124
MILLER, NEAL E. p 3801 N94-33068
MILLER, R. M. p 3771 N94-31369
MILLER, W. A. p 3956 N94-31308
MILLER, W. M. p 3690 N94-31594
MILLINGTON, PETER J. p 3801 N94-33053
MILLS, M. J. p 3661 N94-32796
MILLS, W. H. p 3659 N94-32618
MILMAN, V. p 3904 N94-32724
MINESHIGE, S. p 3928 N94-31123
p 3929 N94-31124
p 3932 N94-31143
MIRESHGHI, A. p 3795 N94-31323
MIRIN, A. A. p 3807 N94-32147
MIRKARIMI, P. B. p 3661 N94-32796
MISHRA, C. S. p 3877 N94-32748
MITA, Y. p 3762 N94-32918
MITCHELL, K. L. p 3803 N94-31380
MOCK, RICHARD V. p 3600 N94-32126
MODI, V. J. p 3600 N94-31434
MOLENKAMP, JAN BERTUS p 3924 N94-31617
p 3845 N94-31702
p 3899 N94-31634
MOLL, A. J. p 3855 N94-31403
MOLTMANN, FRIEDERIKE p 3679 N94-32185
MONACO, PETER p 3660 N94-32739
MONAHAN, PATRICK p 3901 N94-32176
MONCHAMP, R. R. p 3728 N94-32902
MONTAGUE, GERALD T. p 3874 N94-32876
MONTANO, P. A. p 3788 N94-32220
MONTENEGRO, GONZALO p 3791 N94-33109
MONTGOMERY, ELLYN T. p 3791 N94-33245
MONTGOMERY, HARRY p 3613 N94-33289
MONTI-GUARNIERI, A. p 3755 N94-32566
p 3756 N94-32569
MOOIJ, E. p 3609 N94-31705
MOORE, FRANK G. p 3574 N94-33263
MOORMAN, LAURA L. p 3566 N94-32254
MORALES, W. p 3606 N94-33313
MORALES, WILFREDO p 3617 N94-33021
MORAN, TOM p 3607 N94-33321
MORENCY, ROGER L. p 3882 N94-32626
MORENO, J. C. p 3717 N94-32128
p 3720 N94-32794
MOREY, REXFORD M. p 3773 N94-32154
MORGAN, D. V. p 3713 N94-32706
MORLIERE, ALAIN p 3778 N94-30991
MORRIS, ELENA p 3927 N94-32695
MORRIS, J. R. p 3926 N94-32189
MORRIS, R. V. p 3948 N94-33219
MORRIS, TIMOTHY B. p 3727 N94-32479
MORRISON, DONALD A. p 3943 N94-32923
MORRISON, ROWENA p 3583 N94-33280
MORROW, JARRETT D. p 3683 N94-33083
MORTELL, MARI p 3919 N94-32382
MOSCOSO, M. D. p 3930 N94-31132
p 3932 N94-31143
MOSELEY, SAMUEL H. p 3713 N94-32459
MOSER, A. p 3842 N94-31412
MOSES, RONALD W., JR. p 3616 N94-32970
MOSHAMMER, ROBERT p 3865 N94-31516
MOSHER, DANIEL ABBOTT p 3644 N94-32498
MOSLEY, W. C. p 3646 N94-32781
MOTTA, A. T. p 3906 N94-32875
p 3648 N94-32993
MOTTOLA, E. p 3911 N94-31760
MOUGIN, E. p 3753 N94-32555
MOULINES, E. p 3808 N94-31094
MOURANT, J. R. p 3797 N94-32732
MOVSHOVICH, R. p 3899 N94-31916
MOY, K. p 3901 N94-32104
MOYA, M. M. p 3671 N94-31267
MOZER, F. S. p 3885 N94-31089
MUELLER, JUERGEN p 3614 N94-31908
MUELLER, M. H. p 3643 N94-32096
MUELLER, THOMAS p 3715 N94-31561
MUENCHAUSEN, R. E. p 3651 N94-31650
MULLER, M. W. p 3879 N94-32006
MULLER, MARK p 3574 N94-31246
MULLIGAN, W. P. p 3760 N94-32143
MULLIS, CLIFFORD T. p 3810 N94-31277
MUNGAL, M. G. p 3639 N94-33242
MUNSON, C. p 3611 N94-32813
MUNTSLAG, D. R. p 3917 N94-31583
MURACH, J. M. p 3759 N94-31279
MURALIDHARAN, G. p 3647 N94-32964
MURCHIE, S. p 3944 N94-33195
p 3949 N94-33220
MURDOCCA, MILES p 3683 N94-33093
MURPHY, J. R. p 3949 N94-33221
MURPHY, R. J. p 3744 N94-31860
MURPHY, TIMOTHY p 3924 N94-32462
MURRAY, B. C. p 3944 N94-33194
MURTAGH, D. P. p 3770 N94-31222
MURTHY, P. L. N. p 3626 N94-32858
MURTHY, V. SRIDHARA p 3603 N94-33293
MURVEIT, HY p 3679 N94-32185
MUSKET, R. G. p 3661 N94-32751
MUSSA-IVALDI, FERDINANDO p 3834 N94-32152
MUSTARD, J. p 3944 N94-33195
p 3949 N94-33220
MUSTREDELEON, JOSE p 3907 N94-32944
MUTOU, KAZUTOSHI p 3683 N94-33081
MUTTY, MICHAEL S. p 3575 N94-32168
MYERS, S. M. p 3645 N94-32672
MYKYTA, JOHN L. p 3788 N94-32181
MYRA, J. R. p 3890 N94-32520
MYRICK, S. A. p 3922 N94-32987
MYSKO, STEPHEN JOHN, III p 3569 N94-31759

N

NACKEN, PETER F. M. p 3849 N94-32507
NADLE, D. p 3888 N94-31664
NAGY, A. F. p 3948 N94-33214
NAIL, KEN, JR. p 3966 N94-33072
NARUMALANI, SUNIL p 3758 N94-32465
NASTASI, M. p 3656 N94-32103
NATANSOHN, A. p 3654 N94-31978
p 3654 N94-31979
p 3654 N94-31980
NATANSOHN, ALMERIA p 3657 N94-32365
p 3660 N94-32722
NATARAJU, B. S. p 3603 N94-33293
NAVARRA, ANNA p 3829 N94-31186
NAVRATIL, G. A. p 3888 N94-31664
NEAL, DANIEL R. p 3882 N94-32649
NEBERGALL, TERRY D. p 3673 N94-31464
NECKERS, D. C. p 3654 N94-31981
p 3655 N94-31982
p 3655 N94-32069
p 3657 N94-32381
NEIGHBORS, THOMAS p 3859 N94-31060
p 3861 N94-32059
NELSEN, J. M. p 3568 N94-31578
NELSON, D. C. p 3695 N94-32688
NELSON, S. p 3807 N94-32766
NELSON, TREVOR J. p 3916 N94-31344
NEMESURE, S. p 3746 N94-32100
NERI, D. F. p 3799 N94-32187
NESBITT, DAVID J. p 3773 N94-32338
NETA, B. p 3610 N94-32208
NEUENSCHWANDER, G. G. p 3759 N94-31762
NEUHAEUSER, RALPH p 3599 N94-31430
NEUMAN, M. p 3826 N94-32356

NEUMANN, P. D.	p 3862	N94-33096
NEUMULLER, BERNHARD	p 3900	N94-32011
NEWMAN, B. A.	p 3663	N94-33058
	p 3664	N94-33138
NEWMAN, BRIAN A.	p 3664	N94-33247
NEWMAN, WYATT	p 3605	N94-33304
NEWMAN, WYATT S.	p 3603	N94-33296
NEWTON, CRYSTAL H.	p 3663	N94-33010
NEZHEVENKO, O. A.	p 3692	N94-32199
NG, CHUN-KI ALFRED	p 3611	N94-32502
NGO, E.	p 3657	N94-32367
NGUYEN, C.	p 3869	N94-32173
NGUYEN, H. V.	p 3760	N94-31812
NICHOLS, ROBERT HILL, JR.	p 3933	N94-31556
NICHOLSON, JOHN Y.	p 3613	N94-32924
NICKEL, JANIS H.	p 3907	N94-32944
NICKEL, N.	p 3899	N94-31813
NICOL, DAVID	p 3821	N94-33075
NICOUD, FRANCK	p 3614	N94-31423
NIEH, T. G.	p 3644	N94-32374
NIEM, L.	p 3854	N94-33341
NIEMCZYK, T. M.	p 3634	N94-32110
NIKKEL, D. J.	p 3695	N94-32688
NIKOLIC, VOJIN RADE	p 3570	N94-31971
NIKZAD, S.	p 3871	N94-32515
NILSEN, J.	p 3717	N94-32128
	p 3720	N94-32794
NING, PAUL	p 3817	N94-32294
NISHI, R. Y.	p 3795	N94-31738
NISHIOKA, NORMAN S.	p 3798	N94-33092
NIYOGI, PARTHA	p 3851	N94-32142
NOBILE, A.	p 3648	N94-32781
NODERER, KEITH D.	p 3586	N94-32951
NOEL, J.	p 3755	N94-32562
NOEL, JEAN	p 3886	N94-31378
NOHEL, JOHN A.	p 3701	N94-31245
NOOR, AHMED K.	p 3740	N94-33011
NORMAND, M.	p 3755	N94-32563
NORRIS, J. R.	p 3874	N94-32876
NORTH, R. C.	p 3684	N94-33254
NORTH, W.	p 3686	N94-31150
NORTHRUP, F. J.	p 3863	N94-31202
NORTON, D. P.	p 3905	N94-32785
NORVELLE, F. R.	p 3746	N94-31938
NOVIKOVA, T.	p 3652	N94-31764
NOWLAN, M. J.	p 3759	N94-31279
NUNEZ, MIGUEL	p 3742	N94-31496
NUNNELEY, SARAH A.	p 3804	N94-32609
NUTH, PETER R.	p 3825	N94-32165
NYE, TED	p 3604	N94-33301
NYITRAY, A.	p 3651	N94-31649
NYQUIST, J. E.	p 3747	N94-32203

O

OBERACKER, V. E.	p 3867	N94-31779
OBERSTEDT, ANDREAS	p 3866	N94-31614
OBRIEN, DAVID L.	p 3603	N94-33295
OBRIEN, M. H.	p 3658	N94-32517
OCKERT-BELL, M. E.	p 3950	N94-33228
OCONNOR, T. G.	p 3887	N94-31406
ODAY, M. E.	p 3657	N94-32367
ODDY, C. J.	p 3750	N94-32536
ODELL, C. R.	p 3930	N94-31133
ODELL, DOUGLAS L.	p 3697	N94-32976
ODEN, J. T.	p 3726	N94-32320
ODIJK, M. A.	p 3843	N94-31552
ODOWD, J.	p 3762	N94-32765
OELTGEN, PETER R.	p 3794	N94-33098
OEVEL, W.	p 3840	N94-31159
OGATA, T.	p 3642	N94-31918
OGDEN, T. R.	p 3635	N94-32234
OGEKA, G. J.	p 3956	N94-31523
OGLE, K. Y.	p 3803	N94-31380
OGREN, P. J.	p 3864	N94-31321
OH, DONGHOON	p 3733	N94-31213
OH, KENNETH K.	p 3678	N94-32179
OHARA, TIMOTHY J.	p 3635	N94-32231
OKAIN, D.	p 3761	N94-32705
OKAMOTO, P. R.	p 3906	N94-32875
	p 3648	N94-32993
OLEKSUK, L.	p 3662	N94-32891
OLINTO, A. V.	p 3939	N94-33147
OLIU, WALTER E.	p 3922	N94-32835
OLIVIER, P.	p 3755	N94-32563
OLIVIER, S. S.	p 3926	N94-32189
OLSEN, JAMES J.	p 3881	N94-32285
OLSON, C. G.	p 3898	N94-31631
OLSON, STANLEY	p 3727	N94-32718
OMALLEY, R.	p 3791	N94-33244
ONDREJKA, A. R.	p 3675	N94-31683
ONG, CHONG JIN	p 3858	N94-31725
OOLE, THOMAS E.	p 3579	N94-32062
OPSTAD, K.	p 3918	N94-32293
OROZCO, CARLOS EDUARDO	p 3815	N94-31966
ORTOLA, SOPHIE	p 3840	N94-31231
ORVIS, W. J.	p 3825	N94-31920
ORWIG, GARY	p 3923	N94-32469
OSBORNE, T. H.	p 3891	N94-32611
OSTENDORF, MARI	p 3673	N94-31466
OSTERGAARD, JEN C.	p 3680	N94-32297
OSTERHELD, A.	p 3864	N94-31508
OSWALD, R.	p 3762	N94-32765
OTTESEN, D. K.	p 3661	N94-32796
	p 3661	N94-32803
OTTLE, C.	p 3755	N94-32563
OUTKA, D. A.	p 3661	N94-32803
OVERBECK, JAY A.	p 3721	N94-33102
OWEN, J. C., III	p 3695	N94-32700
OWEN, T. E.	p 3576	N94-31306
OZARD, JOHN M.	p 3838	N94-33157

P

PACIESAS, WILLIAM S.	p 3927	N94-32942
PADEN, JACK	p 3785	N94-32737
PAI, R.	p 3827	N94-32683
PAIGE, D. A.	p 3949	N94-33222
	p 3952	N94-33238
PAIGE, ROBERT A.	p 3821	N94-33027
PAIGE, T. S.	p 3587	N94-31295
PAILLOUS, ALAIN	p 3597	N94-31045
PAINTER, RICK	p 3823	N94-32429
PALAGANAS, MARVILYN P.	p 3750	N94-32539
PALAZZOLO, ALAN	p 3728	N94-32902
PALLIX, JOAN B.	p 3597	N94-31046
PALMER, D. W.	p 3693	N94-32386
PALMER, N.	p 3890	N94-32415
PALMER, R.	p 3576	N94-31680
PANAHANDEH, M.	p 3625	N94-32591
	p 3625	N94-32592
PANCE, A.	p 3908	N94-33246
PANDA, S.	p 3910	N94-31052
PANDEY, DHIRENDRA K.	p 3785	N94-32737
PANDITPAGWIWOKO, COSMAS	p 3585	N94-31677
PANDOLF, KENT B.	p 3798	N94-33040
PAPADOPOULOS, DENNIS	p 3678	N94-32161
PAPAMICHAEL, K.	p 3819	N94-32668
PARABOSCHI, STEFANO	p 3809	N94-31212
PARASCHIVOIU, MARIUS	p 3704	N94-31799
PARE, JEAN-PIERRE	p 3912	N94-31911
PARE, S.	p 3757	N94-32575
PARHI, KESHAB K.	p 3688	N94-31445
PARIKH, A. N.	p 3632	N94-31459
PARISH, T. R.	p 3949	N94-33223
PARIZZI, F.	p 3756	N94-32569
PARK, H. S.	p 3955	N94-32129
PARK, Y. M.	p 3850	N94-31590
PARKE, MICHAEL E.	p 3747	N94-32214
PARKER, T. J.	p 3949	N94-33224
PARKER, TERENCE J.	p 3884	N94-33187
PARKS, ALLEN D.	p 3807	N94-32978
PARKS, JACK	p 3828	N94-31061
PARMENTIER, R. D.	p 3794	N94-33250
PARMES, E.	p 3749	N94-32532
PARNELL, L. A.	p 3635	N94-32234
PARRISH, JOHN A.	p 3798	N94-33092
PARROT, J.-F.	p 3753	N94-32553
PARRY, DIANE B.	p 3631	N94-31238
PARTSCH, HELMUT A.	p 3825	N94-32196
PARUCHURI, M. R.	p 3645	N94-32636
	p 3648	N94-33270
PARZYCH, D.	p 3584	N94-32859
PASQUALI, P.	p 3756	N94-32569
PASQUARIELLO, G.	p 3745	N94-31862
PATEL, S.	p 3766	N94-32703
PATTEN, K. O.	p 3768	N94-32817
PAUL, A. K.	p 3776	N94-33285
PAUL, J. J.	p 3624	N94-32265
PAULISH, DANIEL J.	p 3818	N94-32508
PAULSON, ANDREW DANTON	p 3578	N94-31957
PAXTON, A. T.	p 3879	N94-32006
PAYER, ANDREW F.	p 3798	N94-32471
PAYNE, J. L.	p 3701	N94-31268
PAYNE, M. C.	p 3904	N94-32724
PEARCE, B. C.	p 3873	N94-32710
PEARCE, R. P.	p 3784	N94-32162
PEARSON, JOHN	p 3797	N94-32623
PEASE, B. L.	p 3682	N94-33001
PEDERSEN, A.	p 3885	N94-31089
PEGGS, S.	p 3883	N94-32994
PEKALA, R. W.	p 3660	N94-32687
PEKKER, M.	p 3891	N94-32664
PELISSIER, CHRISTIAN	p 3821	N94-33051
PELLAT, R.	p 3894	N94-33106
PELLIN, M. J.	p 3871	N94-32515
PELTZER, GILLES F.	p 3752	N94-32550
PENDERGRASS, R. A.	p 3636	N94-32414
PENKO, PAUL F.	p 3615	N94-32742
PENNELL, W. E.	p 3739	N94-32771
PENNER, J. E.	p 3785	N94-32268
	p 3767	N94-32789
PENNOCK, S. T.	p 3679	N94-32188
PENNYCOOK, S. J.	p 3896	N94-31489
	p 3901	N94-32172
	p 3904	N94-32724
PENSWICK, L. BARRY	p 3616	N94-32866
PENTUS, MATI	p 3841	N94-31388
PEOPLES, J., JR.	p 3876	N94-32586
	p 3876	N94-32588
PEPIN, R. O.	p 3947	N94-33208
PEPPER, S. V.	p 3606	N94-33313
PEREPEZKO, J. H.	p 3910	N94-31054
PEREZ-MENDEZ, V.	p 3795	N94-31323
PEREZ, A. S.	p 3896	N94-31499
PEREZ, C. L.	p 3611	N94-32667
PEREZ, R.	p 3758	N94-31264
	p 3764	N94-31602
PERL, Y.	p 3813	N94-31686
PERLADO, J. M.	p 3896	N94-31499
PERLANT, F.	p 3749	N94-32533
	p 3756	N94-32571
PERRONE, MICHAEL P.	p 3836	N94-33014
PERRY, D.	p 3898	N94-31630
PERRY, J. L.	p 3803	N94-31380
PERRY, JAMES C.	p 3807	N94-32978
PERRY, M. D.	p 3887	N94-31400
	p 3904	N94-32634
PERRYMAN, DENNIS C.	p 3784	N94-32260
PERSSON, H.	p 3691	N94-31848
PESCE-RODRIGUEZ, ROSE A.	p 3635	N94-32124
PETERS, MARINUS CAROLUS ADRIANUS M.	p 3860	N94-31653
PETERSON, K. L.	p 3763	N94-31582
PETERSON, T. C.	p 3764	N94-31596
	p 3766	N94-32690
PETRATOS, G. G.	p 3872	N94-32630
PETRIE, T. W.	p 3888	N94-31765
PETTERSSON, LASSE H.	p 3744	N94-31853
PEYTAVIN, LAURENT	p 3750	N94-32537
PEZOLET, M.	p 3654	N94-31978
PFAHL, C. L.	p 3626	N94-32863
PFENNING, FRANK	p 3815	N94-32080
PHAM, JOHN T.	p 3721	N94-33003
PHELPS, M. R.	p 3759	N94-31762
PHILIPPE, RONY	p 3837	N94-33154
PHILLIPS, B. L.	p 3656	N94-32116
PHILLIPS, D.	p 3648	N94-32993
PHILLIPS, J. C.	p 3839	N94-32422
PHILLIPS, M. L. F.	p 3839	N94-31847
	p 3907	N94-32963
PHILLIPS, PAUL T.	p 3827	N94-32646
PHILLIPS, R. W.	p 3655	N94-32017
PHILLIPS, STEPHEN M.	p 3584	N94-32075
	p 3727	N94-32741
PHILPOTT, MICHAEL R.	p 3863	N94-31237
	p 3631	N94-31238
	p 3632	N94-31293
PICCARDI, CARLO	p 3911	N94-31893
	p 3912	N94-31897
PICKARD, P. S.	p 3715	N94-31485
PICKERING, H. W.	p 3642	N94-31995
PICKSLAY, KENT	p 3915	N94-32426
PICONE, PHILIP J.	p 3879	N94-32013
PICRAUX, S. T.	p 3902	N94-32296
	p 3903	N94-32384
PIEPER, JOHN S.	p 3918	N94-31930
PIERCE, BENJAMIN C.	p 3848	N94-32292
PIERRE, LAURENCE	p 3839	N94-31082
PIERSON, KIM W.	p 3908	N94-33039
PIETERS, C.	p 3944	N94-33195
PIETERS, C. M.	p 3944	N94-33196
PILAFTSIS, A.	p 3868	N94-31922
PILE, P. H.	p 3864	N94-31398
PILLINGER, C. T.	p 3952	N94-33239
PIN, F. G.	p 3727	N94-32682
PINDERA, M. Z.	p 3637	N94-32694
	p 3637	N94-32696
PINELLI, THOMAS E.	p 3921	N94-32829
	p 3921	N94-32830
	p 3921	N94-32831
	p 3921	N94-32832
	p 3921	N94-32833
	p 3921	N94-32834
	p 3922	N94-32835
	p 3922	N94-32836
	p 3922	N94-32837
PINKERTON, S. D.	p 3838	N94-33168
	p 3808	N94-33252
PINTY, BERNARD	p 3779	N94-30999
PION, J.	p 3752	N94-32547
PION, J. C.	p 3752	N94-32547
PIOTROWIAK, P.	p 3870	N94-32178
PIPPIN, GARY	p 3591	N94-31014
	p 3592	N94-31020
	p 3595	N94-31037

PIPPIN, H. G. ..... p 3593 N94-31021
PIRODDI, LUIGI ..... p 3850 N94-31191
PIT, FABIENNE ..... p 3702 N94-31477
PITTMAN, JAMES LEE ..... p 3570 N94-32027
PITTMAN, MARC T. ..... p 3576 N94-33063
PLA-DALMAU, A. ..... p 3878 N94-31271
p 3652 N94-31764
PLANTE, JACINTHE ..... p 3867 N94-31753
PLANTON, S. ..... p 3777 N94-30985
PLASSMANN, P. ..... p 3905 N94-32815
PLIMPTON, S. ..... p 3707 N94-32373
PLOHR, BRADLEY J. ..... p 3701 N94-31245
PLOMPEN, ADRIANUS JOHANNES MARIA
p 3865 N94-31548
PLUMB, R. C. ..... p 3950 N94-33225
PLUMLEE, G. S. ..... p 3950 N94-33226
PLUNKETT, R. ..... p 3871 N94-32587
PLUT, T. A. ..... p 3903 N94-32409
POCHA, M. D. ..... p 3695 N94-32688
POCHA, MICHAEL D. ..... p 3669 N94-32449
POCHIRAJU, KISHORE VENKATESWARA
p 3623 N94-32078
POCO, J. F. ..... p 3639 N94-33260
PODLESKI, STEVE D. ..... p 3573 N94-33119
POE, C. C., JR. ..... p 3629 N94-33130
POEHLMAN, W. F. S. ..... p 3854 N94-33342
POELMAN, CONRAD J. ..... p 3712 N94-31929
POEPPEL, R. B. ..... p 3659 N94-32617
POGGIO, TOMASO ..... p 3880 N94-32186
POIRIER, D. M. ..... p 3898 N94-31631
POLANSKY, G. F. ..... p 3613 N94-31265
POLINER, JEFFREY ..... p 3805 N94-33050
POLING, D. ..... p 3774 N94-32736
POLITO, MICHAEL D. ..... p 3727 N94-32758
POLLACK, J. B. ..... p 3944 N94-33192
p 3950 N94-33227
p 3950 N94-33228
POLLARD, NANCY S. ..... p 3726 N94-32166
POLZIN, KURT LEWIS ..... p 3705 N94-31988
POPE, KEVIN O. ..... p 3942 N94-32740
POPELAR, SCOTT FREDERICK . p 3654 N94-31956
POPPE, BARBARA B. ..... p 3953 N94-31595
PORCHIER, J. C. ..... p 3754 N94-32561
PORTWOOD, M. H. ..... p 3816 N94-32146
POSSELT, W. ..... p 3606 N94-33312
POSTHILL, J. B. ..... p 3902 N94-32306
POTEZ, LAURENCE ..... p 3640 N94-31420
POUJADE, VERONIQUE ..... p 3749 N94-32530
POULIS, H. ..... p 3651 N94-31585
POULSEN, JAN NYHOLM ..... p 3748 N94-32528
POUS, B. ..... p 3754 N94-32557
POWELL, J. R. ..... p 3615 N94-32266
POWELL, KENNETH G. ..... p 3849 N94-33033
POWELL, ROBERT C. ..... p 3884 N94-33140
POZOS, R. S. ..... p 3802 N94-31302
PRABHU, A. N. ..... p 3630 N94-33180
PRAKASH, AJAY ..... p 3705 N94-31844
PRATER, R. ..... p 3886 N94-31324
p 3890 N94-32201
PRATI, C. ..... p 3755 N94-32566
p 3756 N94-32569
PRATT, R. W. ..... p 3828 N94-31161
PRATT, S. ..... p 3944 N94-33195
PRESCOTT, GLEN ..... p 3677 N94-32073
PRICE, D. L. ..... p 3661 N94-32798
PRICE, JERRY ..... p 3924 N94-32462
PRIEDHORSKY, B. ..... p 3611 N94-32813
PRIMDAHL, F. ..... p 3954 N94-31102
PRINZ, G. A. ..... p 3858 N94-31397
PRONK, C. N. A. ..... p 3598 N94-31208
PROPER, H. A. ..... p 3918 N94-32289
p 3918 N94-32290
p 3919 N94-32506
PROSNITZ, D. ..... p 3863 N94-31270
PROST, M. T. ..... p 3748 N94-32527
p 3753 N94-32555
PROTZEN, J. P. ..... p 3819 N94-32668
PROVANCHA, M. J. ..... p 3757 N94-32463
PRYWES, NOAH ..... p 3823 N94-32439
PRZEKWAS, A. J. ..... p 3637 N94-32694
p 3637 N94-32696
PUGH, A. C. ..... p 3840 N94-31156
p 3840 N94-31162
PURDY, BILL ..... p 3607 N94-33322
PURSLEY, MICHAEL B. ..... p 3671 N94-31260
PUSATERI, T. L. ..... p 3731 N94-32481

Q

QUIGG, JOHN H. ..... p 3824 N94-31249
QUILL, LAURIE L. ..... p 3566 N94-32254
QUINN, J. M. ..... p 3676 N94-31998
QUINN, JOHN M. ..... p 3677 N94-32083
p 3678 N94-32158
p 3678 N94-32159
p 3680 N94-32298
p 3680 N94-32299
p 3680 N94-32300
p 3685 N94-33347
QUINN, R. ..... p 3952 N94-33240

R

RABAUTE, T. ..... p 3756 N94-32571
RABITZ, H. ..... p 3635 N94-32140
RADEKA, V. ..... p 3713 N94-32821
RADIGAN, K. J. ..... p 3634 N94-32110
RADLEY, CHARLES F. ..... p 3731 N94-33032
RADOUSKY, H. B. ..... p 3904 N94-32634
RAFFANTI, M. ..... p 3712 N94-31783
RAGUSA, JAMES M. ..... p 3923 N94-32489
RAHMAN, F. ..... p 3754 N94-32559
RAIKAR, GANESH N. ..... p 3596 N94-31042
RAINER, F. ..... p 3716 N94-31636
p 3719 N94-32613
RAISTRICK, IAN D. ..... p 3907 N94-32944
RAJAGOPAL, PAVAN ..... p 3585 N94-31837
RAJAGOPALAN, RAVI ..... p 3635 N94-32231
RAJASEKHAR, A. M. ..... p 3931 N94-31134
RAKOTOARIVONY, L. ..... p 3754 N94-32559
RALSTON, JAMES ..... p 3677 N94-32087
RAMACHANDRAN, N. ..... p 3567 N94-33064
RAMASMAY, S. ..... p 3905 N94-32779
RAMSDELL, J. V. ..... p 3816 N94-32145
RAMSEY, C. B. ..... p 3632 N94-31349
RAMSEY, P. B. ..... p 3906 N94-32884
RANALLI, MARGARET M. ..... p 3565 N94-31362
RANCHIN, THIERRY ..... p 3750 N94-32541
RANDERIA, MOHIT ..... p 3904 N94-32645
RANNEY, J. W. ..... p 3767 N94-32784
RANTANEN, RAY ..... p 3592 N94-31019
RAO, M. NAGESWARA ..... p 3603 N94-33293
RAPP, D. A. ..... p 3926 N94-32189
RAPP, RICHARD H. ..... p 3747 N94-32160
RAPPAPORT, STEPHEN S. ..... p 3672 N94-31384
RASH, CLARENCE E. ..... p 3804 N94-32171
RASMUSSEN, D. H. ..... p 3650 N94-31284
RAST, MARK PETER ..... p 3911 N94-31498
RATH, B. B. ..... p 3640 N94-31345
RAU, KARL F. ..... p 3583 N94-31290
RAUCH, GEORGE B., JR. ..... p 3597 N94-31047
RAY, C. D. ..... p 3803 N94-31380
RAY, PINAKI S. ..... p 3826 N94-32274
RAYMOND, D. ..... p 3748 N94-32527
RAYMOND, DANIEL ..... p 3752 N94-32549
REBOULET, MARK S. ..... p 3672 N94-31385
RECK, R. ..... p 3768 N94-32790
REDDICK, N. A. ..... p 3757 N94-32463
REDDY, J. N. ..... p 3619 N94-31444
REDDY, RAJ ..... p 3845 N94-31939
REDDY, S. ..... p 3728 N94-32900
REDDY, T. S. R. ..... p 3739 N94-32883
REDELSPERGER, J.-L. ..... p 3778 N94-30992
REDMOND, K. T. ..... p 3766 N94-32693
REED, M. H. ..... p 3950 N94-33226
REEDER, JAMES R. ..... p 3627 N94-32939
REES, B. J. ..... p 3650 N94-31297
REES, D. ..... p 3580 N94-32264
REES, WILLIAM S., JR. ..... p 3900 N94-32003
p 3642 N94-32004
p 3900 N94-32011
p 3902 N94-32218
REEVES, ROSS R. ..... p 3585 N94-33266
REGAN, DAVID M. ..... p 3800 N94-32278
REGAN, M. J. ..... p 3646 N94-32795
REHG, JAMES M. ..... p 3803 N94-31447
REICH, M. ..... p 3755 N94-32566
REICHERT, P. ..... p 3755 N94-32565
REID-MILLER, MARGARET ..... p 3824 N94-31259
REID, GREGORY J. ..... p 3880 N94-32180
REIFF, P. H. ..... p 3954 N94-31102
REIFSNIDER, K. L. ..... p 3662 N94-32891
REINHARDT, F. W. ..... p 3695 N94-32663
REINSCH, K. ..... p 3928 N94-31123
REISENEGGER, TASSILO ANDREAS
p 3936 N94-31949
REISER, M. ..... p 3953 N94-31632
REISS, HOWARD ..... p 3618 N94-31261
REJ, D. J. ..... p 3651 N94-31650
REMONDI, BENJAMIN ..... p 3577 N94-33095
REMONDI, BENJAMIN W. ..... p 3576 N94-31080
REN, S.-F. ..... p 3896 N94-31473
RENAUD, PIERRE-RICHARD ..... p 3888 N94-31727
RENIERI, MICHAEL P. ..... p 3626 N94-32860
RENNO, NILTON DE OLIVEIRA .. p 3783 N94-31989
RENO, MARTIN A. ..... p 3638 N94-32948
REYERS, WILLIAM F. ..... p 3918 N94-32210
REYES-RUIZ, M. ..... p 3930 N94-31130
p 3930 N94-31131
p 3931 N94-31135
REYES, D. P. ..... p 3950 N94-33229
REYNOLDS, CAROLYN A. ..... p 3781 N94-31554
REYNOLDS, E. L. ..... p 3613 N94-31265
REYNOLDS, G. T. ..... p 3793 N94-32516
REYNOLDS, GRAHAM J. ..... p 3822 N94-33097
REYNOLDS, STEPHEN A. ..... p 3787 N94-31053
REYNOLDS, W. C. ..... p 3639 N94-33242
REYNOSO, SAMUEL ..... p 3801 N94-33068
RHEE, IN-SIK ..... p 3656 N94-32184
RHEINBOLDT, WERNER C. ..... p 3849 N94-33060
RHODES, R. J. ..... p 3696 N94-32786
RICCHETTI, E. ..... p 3752 N94-32548
RICCO, A. J. ..... p 3941 N94-31145
RICE, J. W., JR. ..... p 3950 N94-33230
RICE, M. ..... p 3900 N94-32065
RICHARDS, WHITMAN ..... p 3802 N94-33326
RICHARDSON, J. ..... p 3692 N94-32136
RICHARDSON, J. F. ..... p 3841 N94-31359
RICHARDSON, M. I. ..... p 3949 N94-33222
RICHARDSON, R. A. ..... p 3920 N94-32827
RICHTER, R. ..... p 3744 N94-31858
RICKLEY, EDWARD J. ..... p 3861 N94-32418
RIDDLE, B. F. ..... p 3675 N94-31683
RIDLEY, W. I. ..... p 3950 N94-33226
RIFE, J. L. ..... p 3692 N94-32112
RIGHINI, GIOVANNI ..... p 3840 N94-31187
p 3809 N94-31188
p 3809 N94-31192
RIGLEY, JACK ..... p 3575 N94-31902
RIJSDIJK, GUESTL ADONIS ..... p 3865 N94-31537
RILEY, P. J. ..... p 3869 N94-32173
RILEY, R. A., JR. ..... p 3889 N94-31809
RINALDI, SERGIO ..... p 3911 N94-31893
p 3911 N94-31894
p 3911 N94-31895
p 3912 N94-31896
p 3912 N94-31897
RIOUL, OLIVIER ..... p 3858 N94-31167
RIPKE, B. ..... p 3733 N94-31375
RISTIC, VELIMIR M. ..... p 3879 N94-31850
RITCHIE, J. L. ..... p 3871 N94-32512
RITTER, JAMES R. ..... p 3613 N94-32924
RIVARD, M. ..... p 3652 N94-31764
ROBB, MICHAEL J. ..... p 3826 N94-32483
ROBERGE, P. R. ..... p 3854 N94-33343
ROBERGE, PIERRE ..... p 3853 N94-33335
ROBERT, JEAN-LOUIS ..... p 3734 N94-31544
ROBERT, SYLVAIN ..... p 3831 N94-31798
ROBERTAZZI, T. G. ..... p 3672 N94-31384
ROBERTS, D. ..... p 3659 N94-32617
ROBERTS, E. W. ..... p 3606 N94-33312
ROBERTS, J. P. ..... p 3718 N94-32270
ROBERTS, JEFFREY P. ..... p 3720 N94-32760
ROBERTS, TED ANTHONY ..... p 3631 N94-31286
ROBERTSON, S. ..... p 3887 N94-31558
ROBICHAUX, BARRY P. ..... p 3822 N94-33114
ROBINSOLN, ALAN R. ..... p 3684 N94-33334
ROBINSON, GARY Y. ..... p 3719 N94-32608
ROBINSON, JEANNE M. ..... p 3637 N94-32743
ROBINSON, NEIL W. ..... p 3810 N94-31383
ROBINSON, PAUL A. ..... p 3598 N94-31425
ROBINSON, PETER ALAN ..... p 3800 N94-31433
ROBINSON, PHILLIP L. ..... p 3872 N94-31385
ROCCA, F. ..... p 3755 N94-32566
p 3756 N94-32569
ROCHETEAU, FREDERIC ..... p 3812 N94-31543
ROCHON, P. ..... p 3654 N94-31978
p 3654 N94-31980
ROCHON, PAUL ..... p 3657 N94-32365
p 3660 N94-32722
ROCK, PAUL B. ..... p 3798 N94-33268
ROCK, STEPHEN M. ..... p 3586 N94-32224
ROCKOFF, TODD E. ..... p 3806 N94-31934
RODEAN, H. C. ..... p 3708 N94-32652
RODRIGUE, G. ..... p 3638 N94-32840
RODRIGUEZ, G. ..... p 3718 N94-32270
RODRIGUEZ, GEORGE ..... p 3720 N94-32760
ROGERS, KEITH ERIC ..... p 3739 N94-32907
ROGERS, M. S. ..... p 3695 N94-32650
ROGERS, R. D. ..... p 3834 N94-32127
ROGRON, B. ..... p 3755 N94-32567
ROHLICEK, J. R. ..... p 3673 N94-31466
ROHN, DOUGLAS A. ..... p 3567 N94-33064
p 3603 N94-33291
ROITBLAT, HERBERT L. ..... p 3802 N94-33241
ROLLETT, A. D. ..... p 3903 N94-32597
ROLLINS, EUGENE ..... p 3815 N94-32080
ROMANO, A. J. ..... p 3956 N94-31523
RON, AMOS ..... p 3855 N94-31244
p 3842 N94-31441
p 3843 N94-31474
ROOT, J. H. ..... p 3733 N94-31312
ROSCOE, DAVID J. ..... p 3675 N94-31708
ROSE, CHERYL ANGELINE ..... p 3621 N94-31901
ROSE, M. F. ..... p 3644 N94-32416
p 3646 N94-32825
ROSE, M. FRANK ..... p 3594 N94-31031

ROSEN, I. G. p 3848 N94-32244
ROSEN, PAUL A. p 3756 N94-32568
ROSEN, STEVE p 3810 N94-31328
ROSENBERG, N. J. p 3768 N94-32812
ROSOFF, JONATHAN p 3811 N94-31465
ROSS, BRIAN H. p 3801 N94-32997
ROSS, D. W. p 3888 N94-31619
ROSSI, M. p 3756 N94-32570
ROSSITER, J. A. p 3828 N94-31158
p 3828 N94-31161
ROSSMAN, G. R. p 3950 N94-33231
ROTH, DON J. p 3732 N94-33038
ROTHFUSS, H. p 3744 N94-31858
ROTHNIE, DOUGLAS W. p 3816 N94-32131
ROUND, WILLIAM H. p 3579 N94-32058
ROUNDY, LANCE M. p 3626 N94-32860
ROUSH, T. L. p 3944 N94-33193
ROUSSEL-DUPRE, D. p 3611 N94-32813
ROUX, FRANK p 3685 N94-31002
ROUZEAU, OLLIVIER p 3753 N94-32552
ROXBY, DON p 3923 N94-32444
ROY, J. M. J. p 3686 N94-33346
ROY, LOUIS p 3879 N94-31751
ROY, S. p 3910 N94-31052
ROY, SEBASTIEN p 3814 N94-31752
ROYBAL, ROBERT E. p 3597 N94-31046
ROZAS, GUILLERMO J. p 3817 N94-32213
ROZMUS, W. p 3893 N94-32915
RUBADEUX, KELLY L. p 3728 N94-32979
RUBIN, S. p 3763 N94-31347
RUBINO, R. A. p 3698 N94-33163
RUBINSTEIN, ROBERT p 3710 N94-33070
RUDANT, J. P. p 3748 N94-32527
p 3753 N94-32555
RUDANT, J.-P. p 3753 N94-32553
RUDANT, JEAN-PAUL p 3752 N94-32549
RUDDER, R. A. p 3902 N94-32306
RUDEN, S. p 3931 N94-31136
RUF, HERBERT p 3859 N94-31060
p 3861 N94-32059
RUFFIN, STEPHEN MERRICK p 3570 N94-31958
RUGGLES, M. B. p 3642 N94-31918
RUMMEL, R. p 3741 N94-31074
RUSHBY, JOHN p 3820 N94-32776
RUSSELL, ALAN J. p 3651 N94-31510
RUSSELL, ROBERTA L. p 3804 N94-32609
RUTH, SUSAN p 3624 N94-32122
RUTHER, W. E. p 3643 N94-32109
RUTHERFORD, W. C. p 3823 N94-32431
RUTTY, ANDREA LOY p 3772 N94-31834
RYAN, DAN p 3823 N94-32432
RYAN, THOMAS W., III p 3638 N94-32868
RYE, A. J. p 3750 N94-32536
RYSKIN, M. G. p 3868 N94-31923

S

SABATINI, J. C. p 3690 N94-31598
SABIERS, RALPH p 3614 N94-31618
SABOUNGI, M. L. p 3645 N94-32514
p 3661 N94-32798
SADEMELO, CARLOS A. R. p 3904 N94-32645
SADOURNY, ROBERT p 3777 N94-30983
SADOVNIK, LEV p 3880 N94-32068
p 3884 N94-33073
p 3884 N94-33087
SADREHAGHIGHI, IDEEN p 3568 N94-31287
SAETHER, ERIK p 3846 N94-32048
SAIF, GAUSSEEM p 3619 N94-31377
SAKS, VICTOR p 3915 N94-32427
SALAS, F. J. p 3666 N94-31579
SALEM, NABEEL H. p 3831 N94-31794
SALLMEN, JOSEPH P. p 3832 N94-31833
SAMANT, MAHESH G. p 3631 N94-31238
SAMAVEDAM, G. p 3579 N94-32015
SAMBLES, K. M. p 3757 N94-33269
SAMPAYAN, S. E. p 3883 N94-31270
SAMPSON, CHARLES R. p 3785 N94-32278
SAMPSONIONS, JOHN A. p 3648 N94-31059
SAMULSKI, E. T. p 3655 N94-32017
SANCHEZ, JESUS p 3823 N94-31099
SANDHOLT, INGE p 3748 N94-32528
SANECKI, J. E. p 3643 N94-32109
SANKAR, M. K. V. p 3888 N94-31664
SANSONE, LOUIS E. p 3882 N94-32719
SANSONE, M. J. p 3656 N94-32246
SANTEE, M. L. p 3949 N94-33222
SANTEE, W. R. p 3901 N94-32153
SANTER, B. D. p 3790 N94-32881
SANZ, J. p 3896 N94-31499
SARWATE, DILIP V. p 3671 N94-31260
SATHYANARAYAN, M. N. p 3603 N94-33293
SATO, T. p 3662 N94-32855
SATOGATA, T. p 3883 N94-32994
SATTERTHWAITE, CHARLES P. p 3565 N94-31367
p 3581 N94-31368
SATYANARAYANAN, M. p 3578 N94-31387
p 3581 N94-32055
SAUER, JON R. p 3821 N94-33030
SAUGIER, BERNARD p 3881 N94-32392
SAVAGE, MICHAEL p 3770 N94-31007
SAVARD, DENIS p 3728 N94-32979
SAVARD, G. p 3845 N94-31755
SAVIN, CHRISTIAN EMANUEL p 3853 N94-33337
SAWYER, F. G. p 3675 N94-31731
SAYLOR, R. p 3751 N94-32543
SCALAPINO, D. J. p 3949 N94-33220
SCANVIC, JEAN-YVES p 3912 N94-32513
p 3752 N94-32551
p 3753 N94-32552
SCARSTEIN, ROBERT W. p 3845 N94-32022
SCARZELLO, JOHN F. p 3681 N94-32625
SCHADE, NICHOLAS F. p 3697 N94-32962
SCHAEFER, D. W. p 3625 N94-32642
SCHAEFER, E. D. p 3613 N94-31265
SCHAEFFER, J. p 3950 N94-33227
SCHAMILOGLU, EDL p 3698 N94-33142
SCHAPER, W. p 3905 N94-32779
SCHAPPERT, G. T. p 3716 N94-31624
SCHAPPERT, GOTTFRIED T. p 3720 N94-32760
SCHEEPER, PATRICK RICHARD p 3688 N94-31518
SCHEFFNER, NORMAN W. p 3787 N94-31250
SCHEIDEMANN, A. A. p 3874 N94-32807
SCHEIMAN, DAVID A. p 3617 N94-33022
SCHEINBEIM, J. I. p 3663 N94-33058
p 3664 N94-33138
SCHEINBEIM, JERRY I. p 3664 N94-33247
SCHEINFEIN, M. R. p 3901 N94-32092
SCHENKER, PAUL S. p 3806 N94-32453
SCHEPS, RICHARD p 3721 N94-32968
SCHEUER, JAY T. p 3616 N94-32970
SCHIJVE, J. p 3578 N94-31675
SCHLENK, MANFRED p 3687 N94-31373
SCHMID, FREDERICK p 3909 N94-33324
SCHMID, MANFRED p 3605 N94-33307
SCHMIDT-KALER, THEODOR p 3599 N94-31430
SCHMIDT, G. L. p 3613 N94-31265
SCHMIDT, NICHOLAS p 3758 N94-32464
p 3758 N94-32465
SCHMIDT, VOLKER p 3832 N94-31826
SCHMIDT, WAYDE R. p 3665 N94-33352
SCHMITT, RAYMOND W., JR. p 3791 N94-33245
SCHMITT, URSULA p 3748 N94-32526
SCHNEIBEL, J. H. p 3647 N94-32852
SCHNEIDER, JUDY p 3614 N94-31618
SCHNEIDER, S. A. p 3811 N94-31475
SCHOBERT, H. H. p 3667 N94-32150
SCHOENBACH, KARL p 3686 N94-31057
SCHOENBERG, KURT F. p 3616 N94-32970
SCHOENMAKERS, JOHN G. M. p 3851 N94-31699
SCHRAMM, D. N. p 3939 N94-33147
SCHRAMM, FRED p 3923 N94-32444
SCHREINER, WILLIAM STEVEN p 3576 N94-31845
SCHRIMPF, R. D. p 3698 N94-33177
SCHROEDER, MICHAEL A. p 3635 N94-32124
SCHROEDER, S. C. p 3862 N94-32456
SCHUBERT, G. p 3940 N94-31109
SCHULER, JAMES JOSEPH p 3691 N94-31905
SCHULTZ, D. R. p 3870 N94-32177
SCHULTZ, J. H. p 3888 N94-31667
SCHWAB, CAROLIN p 3887 N94-31512
SCHWAB, F. C. p 3657 N94-32364
SCHWAB, S. T. p 3638 N94-32868
SCHWARTZ, R. J. p 3762 N94-32763
SCHWARTZ, R. W. p 3695 N94-32650
SCHWARTZ, S. E. p 3771 N94-31527
p 3746 N94-32100
p 3766 N94-32691
SCHWINGHAMER, ROBERT J. p 3598 N94-31048
SCOFIELD, J. H. p 3717 N94-32128
p 3720 N94-32794
SCOTT, A. M. p 3717 N94-31936
SCOTT, D. H. p 3950 N94-33230
SCOTT, J. A. p 3813 N94-31682
SEAGER, C. H. p 3882 N94-32674
p 3661 N94-32819
SEALOCK, L. J. p 3759 N94-31762
SEALS, R. p 3758 N94-31264
p 3764 N94-31602
SEARS, T. J. p 3632 N94-31305
SECRIST, GRANT E. p 3798 N94-31243
SEIBER, F. L. p 3610 N94-32010
SEIDMAN, D. p 3871 N94-32621
SEIFRING, C. p 3954 N94-31102
SEIPLE, R. H. p 3658 N94-32518
SELAWSKI, CLAIRE J. p 3635 N94-32124
SENGUPTA, L. C. p 3657 N94-32367
SENGUPTA, S. K. p 3768 N94-32882
SENGUPYA, SANDIP p 3664 N94-33348
SEPHTON, A. J. p 3750 N94-32536
p 3750 N94-32537
SERENYI, ROBERTO p 3693 N94-32329
SESSLER, A. M. p 3953 N94-31632
SETAYESH, A. p 3776 N94-33272
SEUTTER, M. p 3817 N94-32287
SEVILLANON, EVELIO p 3692 N94-32215
SEYLER, F. p 3755 N94-32562
SHAD, KHALIQ UR-REHMAN p 3736 N94-31961
SHADMEHR, REZA p 3834 N94-32152
SHAEFFER, JOHN F. p 3682 N94-32897
SHAH, BHARAT M. p 3629 N94-33135
SHANAHAN, DENNIS F. p 3575 N94-32363
SHANKARLINGHAM, S. p 3859 N94-33161
SHANNON, SAMUEL G. p 3575 N94-32363
SHANNY, RAMY p 3678 N94-32161
SHAPIRO, A. B. p 3669 N94-32839
SHARBER, J. R. p 3954 N94-31102
SHARMAN, M. p 3754 N94-32557
SHASHARINA, S. G. p 3889 N94-31787
SHASHUA, AMNON p 3846 N94-32167
SHAYKHIAN, ALI p 3923 N94-32469
SHEARES, V. V. p 3655 N94-32017
SHEEHAN, L. M. p 3716 N94-31636
p 3719 N94-32613
SHEEN, D. M. p 3712 N94-31831
SHEEN, JYH-JONG p 3609 N94-31564
SHEFT, STANLEY p 3799 N94-32096
SHELLMAN, C. H. p 3672 N94-31334
SHEN, ZUOWEI p 3843 N94-31474
SHENDER, BARRY S. p 3797 N94-32156
SHEPARD, CHARLES E. p 3912 N94-32774
SHEPARD, M. p 3950 N94-33228
SHEPARD, R. p 3636 N94-32616
SHEPODD, T. J. p 3649 N94-31198
SHER, A. p 3879 N94-32006
SHERBY, O. D. p 3626 N94-32665
SHERMAN, JEFF p 3789 N94-32321
SHI, J. p 3843 N94-31539
SHI, JIAN p 3843 N94-31540
SHIBUYA, M. p 3893 N94-32916
SHIDELER, J. A. p 3690 N94-31594
SHIEH, L. S. p 3835 N94-32943
SHIELDS, G. A. p 3931 N94-31137
SHIH, YAN-SHIN p 3737 N94-32079
SHILO, M. A. p 3580 N94-32362
SHIMADA, T. p 3797 N94-32732
SHIMADA, TSUTOMU p 3720 N94-32761
SHIMP, K. J. p 3603 N94-32671
SHIRANI, A. p 3650 N94-31297
SHITZER, AVRAHAM p 3798 N94-33040
SHIVELY, JON H. p 3597 N94-31046
SHOKAIR, I. R. p 3603 N94-32671
SHORT, ROBERT D. p 3678 N94-32161
SHU, PETER K. p 3713 N94-32459
SHUART, MARK J. p 3628 N94-33124
p 3628 N94-33126
SHUELY, WENDEL J. p 3656 N94-32253
SHUEY, K. p 3606 N94-33315
SHUH, D. K. p 3898 N94-31630
SHUH, DAVID K. p 3635 N94-32233
SHUKLA, JAY G. p 3629 N94-33135
SHUM, HEUNG-YEUNG p 3845 N94-31939
SIAHPUSH, ALI S. p 3823 N94-32438
SIBIRI, TRAORE p 3725 N94-31754
SIDDIQI, SHAHID p 3627 N94-33123
SIEBER, A. J. p 3753 N94-32556
SIEGEL, R. W. p 3907 N94-32990
SIGELMANN, M. p 3578 N94-31078
SIGMON, T. W. p 3909 N94-33328
SILFVAST, W. T. p 3885 N94-33331
SILVER, E. p 3712 N94-31783
SILVER, GEOFFREY p 3798 N94-33092
SILVERNAGEL, GREGORY A. p 3687 N94-31240
SIMMONS, REID G. p 3816 N94-32086
SIMON, RANDY p 3908 N94-33005
SIMON, YOLANDE MARIE p 3565 N94-31959
SIMONDS, GREGORY p 3882 N94-32719
SIMONEN, E. P. p 3641 N94-31627
SIMONIS, GEORGE J. p 3721 N94-33003
SIMONS, MARK p 3940 N94-31110
p 3941 N94-31115
SIMONS, RAINEE N. p 3696 N94-32905
p 3697 N94-33052
p 3698 N94-33116
SIMPSON, ROGER L. p 3702 N94-31476
SINCLAIR, M. B. p 3907 N94-32963
SINGER, HERBERT B. p 3606 N94-33314
SINGER, K. D. p 3661 N94-32819
SINGH, N. p 3893 N94-33048
SINGH, P. P. p 3646 N94-32754
SINGH, SANJAY p 3839 N94-33330
SINGH, SATINDER P. p 3815 N94-31933
SINGH, VIJAY p 3839 N94-33330
SINHA, B. R. p 3657 N94-32364
SIPILAE, SISKO p 3724 N94-31654
SIRAT, J. A. p 3750 N94-32540
SIREN, MIKA p 3724 N94-31656
SISTERSON, D. L. p 3781 N94-31322

SITES, J. R. p 3758 N94-31236
SIVASHINSKY, G. I. p 3706 N94-32149
SJOREEN, T. P. p 3896 N94-31501
SKARHA, J. E. p 3866 N94-31669
SKILLMAN, JOHN B. p 3789 N94-32327
SKINNER, D. M. p 3759 N94-31266
SKINNER, STEPHEN LEE p 3955 N94-31890
SKLET, S. p 3803 N94-31839
SKOEELV, AAGE p 3751 N94-32542
SKOGLUND, JAN p 3859 N94-31076
SKRIVER, HENNING p 3748 N94-32528
SKUPSKY, S. p 3876 N94-32731
SKYLES, LANE P. p 3605 N94-33305
SLAVEY, ROBERT p 3927 N94-32695
SLEEP, N. H. p 3940 N94-31109
SLEMP, WAYNE S. p 3593 N94-31023
SLINEY, HAROLD E. p 3647 N94-32931
p 3617 N94-32941
SLOCUM, KEVIN R. p 3784 N94-32046
SLOOFF, J. W. p 3567 N94-31180
SMALL, DAVID L. p 3756 N94-32568
SMALL, G. W. p 3746 N94-31999
SMALLWOOD, D. O. p 3849 N94-32675
SMECKER-HANE, TAMMY ANN p 3936 N94-31950
SMETS, G. J. F. p 3813 N94-31704
SMID, JON p 3613 N94-33289
SMITH, B. p 3611 N94-32813
SMITH, C. FREDERIC p 3573 N94-33119
SMITH, CHARLES A. p 3592 N94-31016
SMITH, D. p 3663 N94-31151
SMITH, D. L. p 3641 N94-31486
p 3641 N94-31666
SMITH, G. S. p 3651 N94-31649
SMITH, HENRY I. p 3875 N94-31247
SMITH, J. R. p 3667 N94-32148
SMITH, JAMES P. p 3820 N94-32899
SMITH, K. J. p 3828 N94-31161
SMITH, M. R. p 3713 N94-32811
SMITH, N. F. p 3690 N94-31594
SMITH, R. R. p 3712 N94-31831
SMITH, S. A. p 3687 N94-31152
SMITH, S. J. p 3714 N94-31200
SMITH, SEAN W. p 3815 N94-31994
SMITH, T. H. p 3810 N94-31343
SMITH, T. J. p 3698 N94-33091
SMITH, WENDY L. p 3791 N94-33085
SMOLARKIEWICZ, PIOTR K. p 3774 N94-32647
SMOLYAKOV, A. I. p 3893 N94-32922
SNELL, ROY C. p 3686 N94-33152
p 3838 N94-33158
SNELSON, PAMELA p 3919 N94-32488
SNOOK, ELLEN H. p 3804 N94-32171
SNOWDEN-SWAN, L. J. p 3763 N94-31582
SNYDER, LAWRENCE p 3827 N94-32995
SOBOLEWSKI, ROMAN p 3845 N94-32018
p 3900 N94-32040
SODEN, J. M. p 3692 N94-32112
SODERBLOM, L. A. p 3948 N94-33217
SOFFEL, M. p 3601 N94-31769
SOFRONIOU, M. p 3840 N94-31159
p 3840 N94-31160
SOLAAS, G. A. p 3755 N94-32566
SOLOMON, C. J. p 3818 N94-32585
SOLOMON, CARL p 3823 N94-33287
SOLOMON, O. M. p 3849 N94-32653
SOLOMON, SEAN C. p 3939 N94-31105
p 3776 N94-31106
p 3940 N94-31107
p 3940 N94-31108
p 3940 N94-31109
p 3940 N94-31110
p 3940 N94-31111
p 3941 N94-31112
p 3941 N94-31113
p 3941 N94-31114
p 3941 N94-31115
SOMMER, S. p 3743 N94-31854
SONG, C. p 3667 N94-32150
SONG, JIANCHENG p 3657 N94-32381
SOONG, S. T. p 3786 N94-32791
SOOS, Z. G. p 3655 N94-32102
p 3660 N94-32729
SOPIRA, M. M. p 3698 N94-33091
SOPORI, BHUSHAN L. p 3885 N94-32445
SOPORI, BUSHNAN L. p 3885 N94-32446
SORATHIA, USMAN A. p 3663 N94-32975
SORKIN, ROBERT D. p 3801 N94-32577
SOSSA, HUMBERTO p 3812 N94-31542
SOUDERS, T. M. p 3849 N94-32653
SOUKOULIS, C. M. p 3677 N94-32101
SOUKUP, R. J. p 3661 N94-32788
SPAANG, MARTIN p 3732 N94-31091
SPADAFORA, A. L. p 3866 N94-31670
SPADAFORA, STEPHEN J. p 3864 N94-33166
SPALVINS, TALIVALDIS p 3647 N94-32931
SPANOS, L. p 3881 N94-32280
SPECHT, E. D. p 3909 N94-33271
SPECTOR, J. p 3713 N94-32728
SPENCER, JEFFREY B. p 3806 N94-32435
SPENCER, MICHAEL G. p 3698 N94-33249
SPIESMAN, WILLIAM JOHN p 3926 N94-31951
SPIESS, FRED N. p 3789 N94-32400
SPIJKER, M. N. p 3847 N94-32207
SPINHERNE, J. M. p 3722 N94-33282
SPOONER, S. p 3733 N94-31312
SPRAGUE, LAURIE A. p 3798 N94-32471
SPRAGUE, R. A. p 3770 N94-31303
p 3776 N94-33041
p 3893 N94-33042
SPROUSE, B. p 3819 N94-32749
SQUYRES, STEVEN W. p 3941 N94-31115
SRIKASEM, SUTHUM p 3885 N94-31205
ST.CLAIR, D. R. p 3606 N94-33315
STACHIW, J. D. p 3730 N94-31065
STACY, NICHOLAS JOHN SHOLTO p 3676 N94-31952
STACY, W. DODD p 3669 N94-32484
STAGGS, M. C. p 3716 N94-31636
p 3719 N94-32613
STAHOVEC, J. p 3675 N94-31761
STAIR, P. C. p 3871 N94-32621
STALLARD, B. W. p 3675 N94-31781
STAMBAUGH, R. D. p 3892 N94-32810
STANLEY, W. D. p 3771 N94-31525
STANNEY, KAY p 3591 N94-32474
STANNY, R. R. p 3799 N94-32187
STANSFIELD, S. p 3818 N94-32353
STAPLES, EDWARD J. p 3681 N94-32477
STARK, J. W. p 3854 N94-33342
STARNES, JAMES H., JR. p 3628 N94-33124
STASSI, JOSEPH C. p 3785 N94-32737
STAUNTON, BRIAN DOUGLAS p 3601 N94-31802
STAVNES, MARK W. p 3731 N94-32901
STECHEL, E. B. p 3719 N94-32603
STECKEL, GARY L. p 3595 N94-31034
STEEG, E. p 3834 N94-32175
STEIGER, ANDREAS p 3888 N94-31572
STEIN, BLAND A. p 3593 N94-31023
p 3598 N94-31050
STEIN, CHARLES p 3597 N94-31046
STEIN, H. J. p 3902 N94-32296
STEINBERG, ERIC P. p 3739 N94-32735
STEINETZ, BRUCE p 3603 N94-33296
STEINSMO, U. p 3649 N94-31072
STEPHENS, ELIZABETH p 3924 N94-32462
STEPHENS, S. K. p 3950 N94-33231
STEPINSKI, TOMASZ F. p 3927 N94-31116
p 3931 N94-31135
p 3931 N94-31138
STERN, S. ALAN p 3943 N94-33104
STERNBERG, MARC p 3673 N94-31418
STEVENS, C. J. p 3713 N94-32706
STEVENS, KENNITH W. p 3799 N94-32035
STEVENS, WILLIAM p 3924 N94-32462
STEVENSON, D. J. p 3950 N94-33231
STEWART, H. D. p 3695 N94-32700
STEWART, R. p 3758 N94-31264
STICH, I. p 3904 N94-32724
STIDHAM, CURTIS R. p 3617 N94-33022
STILL, W. C. p 3825 N94-32032
STINCHCOMB, W. W. p 3662 N94-32891
STINTON, D. P. p 3662 N94-32891
STIRLING, W. L. p 3647 N94-32851
STJERNHOLM, MICHAEL p 3748 N94-32528
STODOLSKY, DANIEL p 3815 N94-31940
STOLARCZYK, G. L. p 3583 N94-32457
STOLARCZYK, L. G. p 3583 N94-32457
STONE, M. L. p 3659 N94-32655
STONE, THOMAS p 3683 N94-33093
STONER, S. p 3626 N94-32665
STOREY-HELD, K. p 3797 N94-32732
STOREY, JAMES p 3823 N94-33287
STOUT, P. p 3907 N94-32989
STOWELL, S. p 3657 N94-32367
STRACHAN, J. W. p 3763 N94-32965
STRAETEMANS, F. A. J. p 3847 N94-32207
STRAND, O. T. p 3695 N94-32688
STRAND, OLIVER T. p 3669 N94-32449
STRANE, J. W. p 3902 N94-32296
STRANICK, S. J. p 3632 N94-31459
STRASH, DANIEL J. p 3571 N94-32476
STRAUBE, TIMOTHY MILTON p 3668 N94-33037
STRAWDERMAN, WAYNE A. p 3861 N94-32125
STRAYER, p 3874 N94-32850
STRAYER, M. R. p 3867 N94-31779
STREIMER, GARY E. p 3577 N94-32961
STREUBER, R. D. p 3759 N94-31272
STRICKLAND, JOHN W. p 3596 N94-31038
STROSCHEIN, LEANDER A. p 3798 N94-33040
STROUBOULIS, T. p 3848 N94-32331
STROUD, P. p 3747 N94-32249
STRUM, M. J. p 3645 N94-32522
STUBBS, ROBERT M. p 3615 N94-32742
STUCKEY, W. K. p 3598 N94-31049
STUCKEY, WAYNE p 3591 N94-31014
STUCKEY, WAYNE K. p 3598 N94-31050
STUCKY, G. D. p 3899 N94-31847
STUDEVAN, COLIN C. p 3615 N94-32182
STUEBER, THOMAS J. p 3731 N94-32901
STUETZLE, WERNER p 3820 N94-32972
STUHLMANN, C. p 3644 N94-32169
STUHLMANN, CHRISTOPHER p 3909 N94-33274
STULL, R. B. p 3781 N94-31597
STURROCK, W. R. p 3730 N94-31872
SU, SHEN-JWU p 3586 N94-32713
SUAREZ, J. p 3630 N94-33136
SUBRAMANIAN, SRINIVASAN p 3860 N94-31846
SUDAN, R. N. p 3772 N94-31984
SUDARSHAN, E. C. G. p 3871 N94-32512
SUDARSHAN, E. C.G. p 3913 N94-32824
SUDDUTH, RICHARD D. p 3597 N94-31047
SUGAMA, H. p 3886 N94-31366
p 3887 N94-31396
SUGAR, R. L. p 3912 N94-32513
SUKAVIRIYA, PIYAWADEE NOI p 3812 N94-31646
SULEMAN, AFZAL p 3600 N94-31434
SULKES, MARTIN p 3693 N94-32303
SULLIVAN, CHARLES T. p 3882 N94-32649
SULLIVAN, TIM p 3798 N94-32471
SULLIVAN, WENDY I. p 3577 N94-32864
SUMMA, J. MICHAEL p 3571 N94-32476
SUMMERFIELD, B. R. p 3757 N94-32463
SUN, D. C. p 3728 N94-32893
SUN, H. p 3576 N94-31306
SUN, XINGPING p 3855 N94-31244
SUOMI, VERNER E. p 3787 N94-33288
SURANO, K. A. p 3769 N94-32966
SURATWALA, T. p 3659 N94-32617
SURKO, CLIFFORD M. p 3869 N94-32082
SUSKO, M. p 3786 N94-33004
SUSSMAN, A. p 3630 N94-33180
SUTERS, MARK GERARD p 3926 N94-31969
SUTHERLAND, S. C. p 3763 N94-31347
SUTHERLAND, S. F. p 3759 N94-31279
SUTHERLAND, STEPHEN HOLBROOK p 3668 N94-32715
SUTLIFF, J. A. p 3909 N94-33271
SVEDIN, J. p 3676 N94-31925
SWANSON, G. D. p 3626 N94-32863
p 3627 N94-33122
p 3629 N94-33132
SWANSON, M. L. p 3894 N94-31055
SYDOR, JOHN p 3575 N94-31902
SYN, C. K. p 3626 N94-32665
SZATMARY, STEVEN A. p 3732 N94-33038
SZEDON, J. R. p 3698 N94-33091
SZTIPANOVITS, JANOS p 3817 N94-32219
SZU, HAROLD p 3839 N94-32425

T

TAALAS, P. p 3770 N94-31222
TAALEBINEZHAAD, M. ALI p 3833 N94-31991
TABAK, M. p 3887 N94-31400
TACONET, O. p 3754 N94-32559
TAEHTINEN, SEPPO p 3759 N94-31655
TAFRESHI, MOHAMMED A. p 3858 N94-31084
TAHMASEBI, FARHAD p 3723 N94-31568
TAHVANAINEN, JARI p 3743 N94-31658
TAHVONEN, O. p 3765 N94-32590
TAIKUM, ORAWAN p 3658 N94-32518
TAJIMA, T. p 3720 N94-32684
p 3876 N94-32685
p 3891 N94-32686
TAKAHASHI, T. p 3763 N94-31347
TAKENS, FLORIS p 3844 N94-31690
TAKRIFF, M. p 3760 N94-31811
TAMARESIS, J. S. p 3768 N94-32817
TAN, CHOON S. p 3584 N94-33035
TAN, I. S. L. p 3567 N94-33338
TANAKA, K. L. p 3951 N94-33232
TANG, I. N. p 3766 N94-32692
TANG, J. p 3869 N94-32141
TANG, XIAO p 3698 N94-33249
TANNER, JOHN A. p 3606 N94-32295
TANRE, D. p 3770 N94-31003
TANSKANEN, P. p 3885 N94-31089
TAPIA, RICHARD A. p 3811 N94-31443
TAPP, ERIC A. p 3584 N94-32026
TASK, HARRY L. p 3804 N94-32302
TASKER, DOUGLAS p 3712 N94-32051
TATCHYN, R. p 3721 N94-32845
TAUB, SUSAN R. p 3696 N94-32905
p 3697 N94-33052
TAUD, H. p 3753 N94-32553
TAVANI, M. p 3931 N94-31139
TAYLOR, A. J. p 3716 N94-31624
p 3718 N94-32270

TAYLOR, ANTOINETTE J. p 3720 N94-32760
TAYLOR, IVAN W. p 3613 N94-33345
TAYLOR, J. A. p 3631 N94-31154
TAYLOR, K. E. p 3767 N94-32789
TAYLOR, S. R. p 3804 N94-32580
TCHEUNE, RAPHAEL p 3914 N94-32074
TEICHMAN, LOU p 3595 N94-31037
TEMME, N. M. p 3848 N94-32227
TENG, YU-CHIUNG p 3775 N94-33006
TENNYSON, R. C. p 3595 N94-31033
TEPIKIAN, S. p 3883 N94-32994
TERHAAR, J. H. p 3620 N94-31688
TERMINELLO, L. J. p 3898 N94-31630
p 3873 N94-32755
p 3662 N94-32855
TERRES, J. M. p 3754 N94-32561
TESMER, J. p 3656 N94-32103
THALER, B. J. p 3630 N94-33180
THANG, BUI-QUOC p 3735 N94-31849
THANGAVELU, MADHU p 3599 N94-31429
THARP, V. L. p 3766 N94-32693
THEODORE, D. p 3902 N94-32296
THEVUTHASAN, S. p 3712 N94-31629
THIEL, KARL-HEINZ p 3756 N94-32572
THIEME, HORST p 3851 N94-32229
THOET, WILLIAM A. p 3673 N94-31446
THOMAS, C. P. p 3758 N94-31234
THOMAS, D. M. p 3890 N94-32519
THOMAS, ERIK G. F. p 3844 N94-31676
THOMAS, ERWIN p 3728 N94-32902
THOMAS, I. M. p 3649 N94-31199
p 3718 N94-32252
THOMAS, J p 3713 N94-32728
THOMAS, P. C. p 3951 N94-33233
THOMAS, R. E. p 3902 N94-32306
THOMAS, WALTER B., III p 3732 N94-33101
THOMPSON, C. B. p 3743 N94-31603
THOMPSON, J. B. p 3760 N94-32174
THOMPSON, J. D. p 3899 N94-31633
p 3899 N94-31916
THOMPSON, M. p 3649 N94-31276
THOMSON, M. W. p 3607 N94-33317
THORTON, R. p 3774 N94-32736
THOURET, J. C. p 3751 N94-32546
TIAN, QIANG p 3659 N94-32657
TIGGES, C. P. p 3903 N94-32409
TIJSSELING, A. S. p 3702 N94-31588
TIMMERMANS, R. p 3869 N94-32139
TIMMES, FRANCIS XAVIER p 3934 N94-31567
TISCHLER, VICTORIA A. p 3818 N94-32330
TIWARI, P. p 3651 N94-31650
TKACZYK, J. E. p 3909 N94-33271
TKALCEVIC, FRANK J. p 3818 N94-32390
TOBIN, J. G. p 3647 N94-32892
p 3907 N94-32934
TOBIN, M. p 3896 N94-31499
TODD, JAMES T. p 3684 N94-33141
TODD, R. A. p 3807 N94-32783
TODD, STEPHANIE A. p 3626 N94-32860
TODDY, T. J. p 3606 N94-33313
TODOSOW, M. p 3615 N94-32266
TOENNESSEN, K. p 3717 N94-31840
TOHLINE, J. E. p 3932 N94-31140
TOKAY, ALI p 3782 N94-31743
TOLLET, A. p 3757 N94-32575
TOLSON, CAROL J. p 3785 N94-32737
TOM, JAMES L. p 3605 N94-33309
TOMASETTI, ROBERT J. p 3565 N94-31830
TOMBRELLO, T. A. p 3871 N94-32515
TOMPA, G. S. p 3901 N94-32104
TON, VINH THAT p 3634 N94-31824
TONG, HONGLIANG p 3782 N94-31775
TONG, S. Y. p 3907 N94-32934
TONG, XIAOHUA p 3610 N94-31723
TONN, B. E. p 3920 N94-32676
TOOKER, WILLIAM M. p 3585 N94-33283
TOOLE, JOHN M. p 3791 N94-33109
TORO, E. F. p 3843 N94-31539
p 3843 N94-31541
p 3702 N94-31559
TORRES-FILHO, AFRANIO p 3655 N94-31982
p 3657 N94-32381
TORRES, S. G. p 3641 N94-31581
TOSCANO, WILLIAM B. p 3801 N94-33088
TOTAH, JOSEPH p 3571 N94-32063
TOULGOAT, MYLENE p 3671 N94-31254
TOWERS, G. H. N. p 3793 N94-32267
TOWNLEY, JUDY G. p 3810 N94-31370
TOWSLEY, D. p 3825 N94-32052
TRABOCCO, RONALD E. p 3639 N94-32973
TRAN, HUY K. p 3617 N94-33117
TRANGENSTEIN, J. A. p 3707 N94-32410
TRAVIS, JEFFREY W. p 3713 N94-32459
TRBOJEVIC, D. p 3883 N94-32994
TREASURYWALA, A. M. p 3793 N94-32269
TREBES, J. p 3719 N94-32629
TREFNY, CHARLES J. p 3700 N94-31229
TREIMAN, A. H. p 3951 N94-33234
TREMBLAY, JEAN-FRANCOIS p 3879 N94-31756
TRENCHARD, M. E. p 3922 N94-32987
TREURNIET, WILLIAM C. p 3838 N94-33156
TRIBE, S. p 3951 N94-33235
TRIFUNAC, A. D. p 3720 N94-32707
TRIGGIANI, R. p 3738 N94-32275
TRIMBLE, D. O. p 3863 N94-31270
TRIMMER, MARK S. p 3882 N94-32702
TRINH, K. V. p 3733 N94-31316
TRIPATHY, S. K. p 3658 N94-32578
p 3659 N94-32610
TRIPATHY, SUKANY K. p 3663 N94-33054
p 3664 N94-33082
TROIANO, E. J. p 3648 N94-33281
TROLINGER, J. p 3832 N94-31808
TROTIN, ANNE p 3687 N94-31168
TROWBRIDGE, JOHN H. p 3791 N94-33243
TROWBRIDGE, L. D. p 3913 N94-32846
TRUBIAN, MARCO p 3840 N94-31187
p 3809 N94-31192
TRUE, M. A. p 3788 N94-32284
TRUSLOVE, G. p 3626 N94-32863
TSAI, C. C. p 3647 N94-32851
TSAI, JOHN C. p 3954 N94-31103
TSAI, TED p 3607 N94-33323
TSEDILINA, E. E. p 3771 N94-31326
TSENG, C. p 3643 N94-32064
TSUN, T. S. p 3912 N94-31924
TUBMAN, J. B. p 3567 N94-33338
TUCKER, JOHN R. p 3843 N94-31529
TUCKER, RICHARD F. p 3582 N94-33076
p 3582 N94-33078
p 3583 N94-33079
TUCKER, W. p 3588 N94-32014
p 3588 N94-32241
p 3588 N94-32311
p 3588 N94-32312
p 3588 N94-32313
p 3589 N94-32314
p 3589 N94-32315
p 3589 N94-32316
p 3589 N94-32317
p 3589 N94-32318
p 3589 N94-32319
p 3589 N94-32394
p 3590 N94-32395
p 3590 N94-32396
p 3590 N94-32397
p 3590 N94-32398
p 3590 N94-32399
p 3590 N94-32403
TULLOCH, F. A. p 3727 N94-32682
TUNG, L. A. p 3636 N94-32376
TURCOTTE, D. L. p 3940 N94-31109
TURNER, G. W. p 3807 N94-32783
TURNER, HOWARD p 3919 N94-32382
TURNER, J. E. p 3636 N94-32251
TURNER, J. W. p 3576 N94-31680
TURNER, M. p 3864 N94-31402
TURNER, ROSS M. p 3671 N94-31254
TURNEY, C. R. p 3816 N94-32145
p 3816 N94-32146
TUTTLE, M. p 3629 N94-33132
TWORZYDLO, W. W. p 3726 N94-32320
TYLER, D. p 3946 N94-33205
p 3951 N94-33236
TZAVARAS, ANTHANASIOS E. p 3738 N94-32273
TZENG, JEROME T. p 3625 N94-32604

U

UCHIDA, KEVEN ISAO p 3937 N94-32028
UHM, HAN S. p 3893 N94-32977
ULAMEC, S. p 3951 N94-33237
ULIBARRI, T. p 3625 N94-32642
UMAR, A. S. p 3867 N94-31779
p 3874 N94-32850
UNDERWOOD, J. H. p 3648 N94-33281
UPADHYAY, C. S. p 3848 N94-32331
UPSCHULTE, B. L. p 3694 N94-32478

V

VACHON, M. p 3853 N94-33337
VACHON, PIERRE p 3814 N94-31728
VAHLE, M. O. p 3823 N94-31149
VALDEZ, G. D. p 3678 N94-32113
VALLERAND, A. L. p 3796 N94-31740
p 3796 N94-31741
VALTEN, R. J. p 3743 N94-31592
VANACKEN, GREGOR A. p 3845 N94-31702
VANATTA, CHARLES W. p 3706 N94-32123
VANBEIJNEN, M. N. p 3578 N94-31674
VANBOMMEL, P. p 3916 N94-31175
VANBOMMEL, PATRICK p 3918 N94-32105
VANDAL, RENE p 3845 N94-31702
VANDEKAMP, ILSE p 3917 N94-31415
VANDENNEHEUVEL, SIEGER p 3916 N94-31392
VANDER, GEEST, J. p 3763 N94-32965
VANDERDOES, JAAP p 3856 N94-31411
VANDERDONK, ARMAND GIJSBERTUS H. p 3688 N94-31517
VANDERLINDEN, J. p 3916 N94-31365
VANDERMAST, C. A. P. G. p 3813 N94-31704
VANDERMAST, CHARLES p 3674 N94-31645
VANDERMAST, CHARLES A. P. G. p 3812 N94-31646
VANDERVELDT, TONNY p 3865 N94-31549
VANDERVOOREN, J. p 3567 N94-31180
VANDERWEIDE, T. P. p 3918 N94-32289
p 3918 N94-32290
p 3919 N94-32506
VANDERWOERD, H. p 3770 N94-31222
VANDORSSELAER, J. L. M. p 3847 N94-32200
VANEENIGE, ENGELINA NIESKE p 3897 N94-31547
VANEESBEEK, MARC p 3592 N94-31018
VANEMDEBOAS, PETER p 3917 N94-31452
VANHENGEL, P. W. J. p 3569 N94-31822
VANHORSSEN, W. J. p 3843 N94-31642
VANHULST, M. p 3826 N94-32291
VANIER, P. E. p 3875 N94-31480
VANKLEEF, E. R. A. p 3587 N94-31179
VANLEUSEN, NOOR p 3855 N94-31390
VANLIESHOUT, M. N. M. p 3847 N94-32197
VANMAAREN, HANS p 3924 N94-31617
VANMOURIK, FRANK p 3792 N94-31533
VANOEVELEN, PETER J. p 3754 N94-32560
VANOOSTEN, JAAP p 3856 N94-31408
VANOOSTROM, VINCENT p 3849 N94-32349
VANOPSTAL, T. p 3916 N94-31365
VANRAAMSDONK, FEMKE p 3849 N94-32349
VANRIESSEN, RONALD PIETER p 3688 N94-31520
VANROSENDALE, JOHN p 3820 N94-32928
VANSCHUPPEN, J. H. p 3852 N94-32350
VANTOOREN, M. J. L. p 3578 N94-31674
VANYSEK, PETR p 3636 N94-32352
VARDULAKIS, A. I. p 3840 N94-31162
VARDULAKIS, A. I. G. p 3840 N94-31156
VARMA, K. VENUGOPAL p 3724 N94-31724
VARMA, RAMA RAJARAJA p 3705 N94-31941
VARNIER, JEAN p 3860 N94-31226
VATH, H. p 3932 N94-31141
VATN, J. p 3668 N94-31838
VAUDIN, M. p 3904 N94-32606
VAWTER, G. A. p 3688 N94-31483
p 3897 N94-31502
p 3716 N94-31622
p 3881 N94-32385
p 3696 N94-32809
VAWTER, G. ALLEN p 3882 N94-32649
VELASCO, VIRGILIO B., JR. p 3803 N94-33296
VEMURI, V. p 3834 N94-32127
VENET, B. p 3722 N94-33282
VENKAYYA, V. B. p 3600 N94-31434
VENKAYYA, VIPPERLA B. p 3818 N94-32330
VER, ISTVAN L. p 3862 N94-33023
VERAN, JEAN-PIERRE p 3711 N94-31096
p 3670 N94-31097
VERHOEF, T. F. p 3917 N94-31586
VERLINDEN, JOUKE C. p 3674 N94-31645
VERNON, SUSAN N. p 3627 N94-33018
VERSTRAETE, MICHEL M. p 3779 N94-30999
VERVERS, F. p 3813 N94-31695
VETRANO, J. S. p 3641 N94-31627
VIANU, VICTOR p 3824 N94-31183
VICCARO, P. J. p 3672 N94-31317
VIDAL-MADJAR, D. p 3754 N94-32559
p 3755 N94-32563
VIDAL, A. p 3754 N94-32559
p 3755 N94-32563
VIGNEAULT, MICHEL O. p 3613 N94-33345
VIGO, DANIELE p 3809 N94-31189
VILLAREAL, JAMES A. p 3924 N94-32462
VILLEGAS, I. p 3644 N94-32169
VILLEGAS, IGNACIO p 3909 N94-33274
VILLENEUVE, PIERRE R. p 3899 N94-31729
VIRDEN, MARK D. p 3688 N94-31494
VIRKAR, A. V. p 3659 N94-32657
VIS, M. A. p 3569 N94-31822
p 3706 N94-32045
VISCONTI, MARK p 3607 N94-33321
VISE, J. p 3603 N94-33294
VISENTINE, JAMES T. p 3596 N94-31040
VISHIK, M. M. p 3889 N94-31772
VISHNIAC, E. T. p 3932 N94-31142
VISWANATH, R. N. p 3905 N94-32779
VISWANATHA, N. p 3603 N94-33293
VITAL, PAUL p 3798 N94-33040

VO-DINH, T. p 3901 N94-32172
VOISIN, JEAN-MARC p 3734 N94-31562
VOLK, S. R. p 3695 N94-32700
VOLLEBREGT, E. A. H. p 3813 N94-31694
VOLLICK, DANIEL p 3934 N94-31789
VOSE, R. S. p 3764 N94-31596
p 3766 N94-32690
VOSS, MARK p 3798 N94-32471
VOSTEEN, LOUIS F. p 3627 N94-33123
VOVOR, TSEVI M. G. p 3652 N94-31722
VRANA, CRAIG A. p 3586 N94-31058
VREEKE, MARK S. p 3691 N94-32056
VREMAN, A. W. p 3699 N94-31185
VUIK, C. p 3703 N94-31660

W

WADDILL, G. D. p 3647 N94-32892
p 3907 N94-32934
WADGE, G. p 3744 N94-31860
WADSWORTH, J. p 3644 N94-32374
WAGANAAR, W. J. p 3651 N94-31650
WAGENER, F. O. O. p 3703 N94-31689
WAGENER, R. p 3746 N94-32100
WAGES, S. p 3651 N94-31649
WAGGONER, R. A. p 3655 N94-32005
WAGH, A. S. p 3659 N94-32617
WAGNER, A. F. p 3636 N94-32616
WAGNER, THOMAS W. p 3609 N94-31292
WAHL, TERJE p 3751 N94-32542
WAI, LEILANI C. p 3605 N94-33308
WAKE, L. V. p 3580 N94-32378
WAKEFIELD, BRYCE E. p 3706 N94-32042
WALCEK, C. J. p 3785 N94-32717
WALCEK, CHRIS p 3784 N94-32054
WALCH, STEPHEN P. p 3639 N94-33036
WALD, LUCIEN p 3750 N94-32541
WALKER, IAN D. p 3729 N94-32450
WALKER, JIM p 3604 N94-33301
WALKER, ROBERT FREDERIK p 3830 N94-31546
WALKER, T. H. p 3626 N94-32863
p 3629 N94-33130
p 3629 N94-33132
WALLACE, LANE E. p 3566 N94-32793
WALLACE, P. L. p 3643 N94-32098
WALSH, CLARE p 3924 N94-32462
WALSH, P. M. p 3667 N94-32150
WALTER, SHARON M. p 3685 N94-32437
WALTERS, MARVIN M. p 3573 N94-32974
WALTON, J. J. p 3767 N94-32789
WALUKIEWICZ, W. p 3899 N94-31634
WAMPLER, JEFFREY L. p 3566 N94-32254
WANG, H. H. p 3907 N94-32989
WANG, HAO p 3622 N94-31909
WANG, J. T. p 3628 N94-33126
WANG, L. M. p 3895 N94-31307
WANG, MICHAEL Q. p 3765 N94-32600
WANG, SONGHAO p 3658 N94-32490
WANG, W. C. p 3764 N94-31600
WANG, X. L. p 3733 N94-31312
WANG, XIAO-PING p 3783 N94-31937
WANG, YING p 3882 N94-32702
WANG, YUQIN p 3620 N94-31565
WANG, Z. J. p 3637 N94-32694
p 3637 N94-32696
WANG, Z. L. p 3909 N94-33271
WANG, ZHI-YU p 3874 N94-32876
WARGOWSKI, D. A. p 3882 N94-32674
p 3661 N94-32819
WARNER, THOMAS T. p 3786 N94-32921
WARNICA, WILLIAM DAVID p 3571 N94-32491
WARREN, BRUCE A. p 3791 N94-33176
WARREN, M. E. p 3716 N94-31622
WATERS, DAVID D. p 3731 N94-32481
WATKINS, J. C. p 3891 N94-32595
WATSON, ANDREW B. p 3850 N94-32467
WATSON, WILLIE R. p 3861 N94-32930
WATTERS, R. B. p 3606 N94-33312
WAUBEN, WILLEM MARIA FRANS p 3674 N94-31551
WAVRIK, R. W. p 3603 N94-32671
WAY, BOB p 3924 N94-32462
WEAVER, MICHAEL J. p 3642 N94-31997
p 3643 N94-32060
p 3644 N94-32169
p 3669 N94-32170
p 3635 N94-32216
p 3909 N94-33273
p 3909 N94-33274
p 3909 N94-33275
p 3875 N94-33277
WEAVER, ROBERT T., JR. p 3916 N94-31338
WEBB, SPAHR C. p 3789 N94-32401
WEBER, E. J. p 3954 N94-31102
WEBER, W. J. p 3895 N94-31307
WEBSTER, BRUCE EUGENE p 3567 N94-31204
WEBSTER, LEE F. p 3587 N94-31295
WEBSTER, MARK p 3818 N94-32390
WEDDLE, CHARLES A. p 3788 N94-31448
WEEKS, ROBERT A. p 3594 N94-31030
WEENING, EDWARD CHRISTIAAN p 3689 N94-31535
WEERTS, H. p 3873 N94-32780
WEI, J. p 3883 N94-32994
WEI, X. p 3890 N94-32415
WEINSTEIN-LLOYD, J. B. p 3766 N94-32692
WEINSTEIN, J. p 3794 N94-32890
WEINTRAUB, MITCHEL p 3679 N94-32185
WEISER, MARTIN W. p 3657 N94-32404
WEISS, D. E. p 3872 N94-32628
WEISS, L. A. p 3954 N94-31102
WEISS, P. S. p 3877 N94-31256
p 3711 N94-31283
p 3632 N94-31459
WEISZ, ZVI S. p 3686 N94-31079
WEITZ, E. p 3871 N94-32621
WELCH, RICHARD V. p 3729 N94-32452
WELLER, ROBERT A. p 3594 N94-31030
WELLS, J. C. p 3867 N94-31779
WELLS, PETER M. p 3581 N94-31903
WELLS, STUART p 3917 N94-31829
WELP, U. p 3904 N94-32601
WENDT, CHARLES G. p 3821 N94-33090
WENDT, J. R. p 3716 N94-31622
p 3903 N94-32409
WENNERHOLM, H. p 3758 N94-31070
p 3758 N94-31071
WERESZCZAK, A. A. p 3618 N94-31313
WERNER, C. p 3755 N94-32566
WERNER, CHARLES L. p 3756 N94-32568
WERNET, JUDITH H. p 3713 N94-32983
WERNET, MARK P. p 3713 N94-32983
WESCOTT, EUGENE M. p 3954 N94-31101
p 3954 N94-31102
WESELY, M. L. p 3781 N94-31322
p 3768 N94-32894
WESSELING, P. p 3703 N94-31660
WESSELSKI, CLARENCE J. p 3604 N94-33303
WEST, S. L. p 3738 N94-32639
WESTENSKOW, G. A. p 3863 N94-31270
WESTERINK, J. J. p 3787 N94-31250
WETHERHOLT, MARTHA S. p 3731 N94-33032
WEYL, G. p 3694 N94-32478
WHANGBO, MYUNG-HWAN p 3907 N94-32989
WHEALTON, J. H. p 3647 N94-32851
WHEELER, D. R. p 3606 N94-33313
WHEELER, J. C. p 3928 N94-31123
p 3929 N94-31124
p 3930 N94-31132
p 3932 N94-31143
WHIRLEY, R. G. p 3738 N94-32637
WHISNANT, P. L. p 3650 N94-31297
WHITAKER, ANN F. p 3591 N94-31012
p 3591 N94-31015
p 3593 N94-31022
p 3593 N94-31025
p 3598 N94-31050
WHITCOMB, JOHN D. p 3626 N94-32904
WHITE, A. R. p 3864 N94-31310
WHITE, C. W. p 3901 N94-32172
WHITE, J. W. p 3708 N94-32849
WHITE, R. G. p 3740 N94-32982
WHITE, ROBERT E. p 3859 N94-33161
WHITEHURST, R. p 3932 N94-31144
WHITELAW, J. H. p 3634 N94-32033
WHITELEY, S. p 3908 N94-33246
WHITNEY, W. T. p 3717 N94-31936
WIDDER, EDITH A. p 3790 N94-32959
WIDLUND, LENNARD p 3927 N94-31086
WIDMANN, K. p 3864 N94-31508
WIEDLOCHER, D. E. p 3653 N94-31851
WIEDLOCHER, DAVID E. p 3594 N94-31030
WIEGERINK, REMCO JOHN p 3690 N94-31616
WIELOGORSKA, A. p 3754 N94-32558
WILBUR, P. J. p 3906 N94-32843
WILKEN, A. C. p 3701 N94-31268
WILKES, DONALD R. p 3591 N94-31013
WILKES, JOHN S. p 3763 N94-33015
WILKINSON, ERIK p 3924 N94-31210
WILKINSON, F. p 3717 N94-31996
WILKS, S. p 3887 N94-31400
WILLDEN, K. S. p 3626 N94-32863
WILLDEN, KURTIS p 3629 N94-33133
p 3630 N94-33137
WILLIAMS, A. J., III p 3791 N94-33243
WILLIAMS, A. W. p 3598 N94-31051
WILLIAMS, ELLEN D. p 3878 N94-31262
WILLIAMS, FORREST R. p 3787 N94-33089
WILLIAMS, J. M. p 3647 N94-32851
WILLIAMS, JEFFERY T. p 3683 N94-33083
WILLIAMS, JOHN G. p 3639 N94-32973
WILLIAMS, JOHN R. p 3663 N94-33024
WILLIAMS, K. A. p 3760 N94-32174
WILLIAMS, M. D. p 3786 N94-32937
WILLIAMS, R. J. p 3666 N94-31579
WILLIAMS, T. A. p 3687 N94-31152
WILLIAMSON, DENNIS A. p 3579 N94-32232
WILLIS, DEE ANNA p 3924 N94-32462
WILLIS, JERRY p 3924 N94-32462
WILLISTON, WILLIAM C., JR. p 3722 N94-31333
WILLSON, ALAN N., JR. p 3697 N94-32957
WILMINGTON, ROBERT P. p 3805 N94-33050
WILSON, A. K. p 3745 N94-31863
WILSON, J. D. p 3699 N94-33340
WILSON, JAMES CHARLES p 3769 N94-33170
WILSON, JOHN C. p 3572 N94-32873
WILSON, M. p 3788 N94-32000
WILSON, ROBERT S. p 3785 N94-32737
WILT, ROBERT JOSEPH p 3942 N94-31992
WILTBERGER, N. LYN p 3709 N94-32946
WINGATE, C. A. p 3956 N94-31308
WINNBERG, A. p 3770 N94-31222
WINNINGHAM, J. D. p 3954 N94-31102
WISCHOW, P. W. p 3922 N94-32987
WITHROW, S. P. p 3640 N94-31314
p 3901 N94-32172
WITT, G. p 3770 N94-31222
WITTE, K. H. p 3721 N94-32848
WITTING, J. M. p 3702 N94-31467
WOLCOTT, KEDRON R. p 3604 N94-33299
WOLF, JOHN p 3859 N94-31060
p 3861 N94-32059
WOLFE, JOHN C. p 3683 N94-33083
WOLFE, KURT A. p 3694 N94-32509
WOLITZER, D. p 3638 N94-32840
WOLL, STEPHEN C. p 3783 N94-32019
WONG, ALOYSIUS p 3621 N94-31836
WONG, H. K. p 3943 N94-33103
WONG, J. p 3896 N94-31499
p 3662 N94-32855
WOOD, B. E. p 3610 N94-32010
WOOD, J. p 3651 N94-31672
WOOD, J. GARY p 3615 N94-32792
WOOD, N. J. p 3598 N94-31051
WOOD, S. E. p 3952 N94-33238
WOODS, DAN p 3828 N94-31061
WOODSTRA, R. R. p 3713 N94-32728
WOODWARD, DONALD J. p 3802 N94-33333
WOODWORTH, J. p 3887 N94-31400
WOOLLEY, STAN p 3758 N94-32466
WOROBEY, W. p 3693 N94-32386
WRAY, S. p 3819 N94-32749
WRIGHT, CHARLES M. p 3894 N94-33264
WRIGHT, I. P. p 3952 N94-33239
WRIGHT, S. I. p 3903 N94-32597
WRONSKI, C. R. p 3760 N94-31812
WU, CHI-WEI p 3679 N94-32282
WU, CHIN-CHUN p 3933 N94-31566
WU, I. C. p 3690 N94-31598
WU, M. p 3632 N94-31305
WU, Q. H. p 3808 N94-31163
p 3808 N94-31164
WU, XIAOPING p 3774 N94-32493
WU, YECHENG p 3747 N94-32492
WUEBBLES, D. J. p 3765 N94-32354
p 3768 N94-32817
WUERER, J. E. p 3823 N94-32430
WYNGAARD, JOHN C. p 3701 N94-31480
WYNKOOP, CHER E. p 3566 N94-32254
WYNNE, D. p 3882 N94-32417
WYROSTEK, A. p 3584 N94-32859

X

XENOFONTOV, E. p 3751 N94-32544
XIE, M. p 3953 N94-31632
p 3657 N94-32364
XIE, SHUANG p 3657 N94-32365
p 3660 N94-32722
XIE, SHUDING p 3925 N94-31790
XIE, X. S. p 3720 N94-32704
XU, C. p 3601 N94-31789
XU, LEI p 3852 N94-33276
XU, M.-Q. p 3825 N94-31663
XU, XIAOSHU p 3839 N94-32424

Y

YABLONOVITCH, ELI p 3900 N94-31985
YAE, K. H. p 3802 N94-32472
YAGHJIAN, ARTHUR D. p 3672 N94-31371
YAKIN, BULENT p 3614 N94-32071
YAKOVLEV, V. P. p 3692 N94-32199
YANG, FUJI p 3687 N94-31170
YANG, H. Q. p 3637 N94-32694
p 3637 N94-32696

YANG, JUNHO ..... p 3572 N94-32714
YANG, N. Y. C. ..... p 3661 N94-32803
YANG, Y. ..... p 3708 N94-32511
YANG, Z. ..... p 3640 N94-31314
YAO, STEPHEN S. C. ..... p 3576 N94-32454
YARMOFF, JORY A. ..... p 3635 N94-32233
YASUI, S. ..... p 3893 N94-32916
YEAGER, WILLIAM L. ..... p 3663 N94-32975
YENCHO, STEPHEN ..... p 3810 N94-31357
YESOU, H. ..... p 3752 N94-32547
YEW, C. H. ..... p 3726 N94-32320
YI, THOMAS Y. ..... p 3758 N94-31233
YODER, DENNIS A. ..... p 3573 N94-32984
YOERGER, E. J. ..... p 3788 N94-32000
YOO, SUNGYUL ..... p 3571 N94-32476
YOOK, JONG-GWAN ..... p 3696 N94-32905
YOSHIKAWA, SHOKO ..... p 3653 N94-31935
YOST, WILLIAM A. ..... p 3799 N94-32096
YOUNG, C. E. ..... p 3871 N94-32515
YOUNG, CLARENCE P., JR. ..... p 3740 N94-33118
YOUNG, D. M. ..... p 3836 N94-32992
YOUNG, DONALD R. ..... p 3631 N94-31282
YOUNG, GEORGE ..... p 3729 N94-33251
YOUNG, GIN-SHU ..... p 3832 N94-31842
YOUNG, JEFFREY A. ..... p 3606 N94-33316
YOUNG, K. ..... p 3603 N94-33294
YOUNG, K. D. ..... p 3695 N94-32688
YOUNG, K. DAVID ..... p 3669 N94-32449
YOUNG, LEIGHTON E. ..... p 3594 N94-31028
YOUNG, PAUL G. ..... p 3697 N94-33052
YOUNG, PHILIP R. ..... p 3593 N94-31023
YOUNGSON, GORDON ..... p 3581 N94-31903
YU, K. M. ..... p 3899 N94-31634
YUAN, ZOU WEI ..... p 3858 N94-31084
YUN, W. B. ..... p 3672 N94-31317
YUNGSTER, SHAYE ..... p 3700 N94-31229
YURUR, TEKIN ..... p 3752 N94-32549

Z

ZABIELSKI, CHESTER V. ..... p 3644 N94-32240
ZABINSKY, Z. ..... p 3629 N94-33132
ZABLUDOFF, ANN I. ..... p 3937 N94-32029
ZAK, J. ALLEN ..... p 3787 N94-33065
p 3582 N94-33077
p 3582 N94-33078
ZAKARAUSKAS, PIERRE ..... p 3838 N94-33157
ZAKARIA, A. B. ..... p 3598 N94-31051
ZAKHARYASCHEV, MICHAEL ..... p 3856 N94-31407
ZALZALA, A. M. S. ..... p 3722 N94-31379
ZALZALA, ALI M. S. ..... p 3830 N94-31500
ZARE, R. N. ..... p 3889 N94-31766
ZASADZINSKI, JOHN ..... p 3904 N94-32602
ZAWADZKI, P. A. ..... p 3901 N94-32104
ZBASNIK, J. P. ..... p 3887 N94-31406
ZEBKER, HOWARD A. ..... p 3756 N94-32568
ZEE, R. H. ..... p 3644 N94-32416
p 3646 N94-32825
ZEE, RALPH H. ..... p 3594 N94-31031
ZEEVI, YEHOSHUA Y. ..... p 3586 N94-31058
p 3816 N94-32093
ZEGELING, A. ..... p 3844 N94-31696
ZEGELING, Z. ..... p 3844 N94-31644
ZENG, S. ..... p 3703 N94-31660
ZENT, A. P. ..... p 3952 N94-33240
ZHANG, B. ..... p 3862 N94-31146
ZHANG, D. L. ..... p 3645 N94-32636
ZHANG, G. ..... p 3878 N94-31271
ZHANG, LIZ-HONG ..... p 3634 N94-32110
ZHANG, Q.-P. ..... p 3711 N94-31085
ZHANG, WEIDONG ..... p 3840 N94-31169
ZHANG, Y. ..... p 3865 N94-31607
ZHONG, S. ..... p 3767 N94-32750
ZHONG, X. ..... p 3708 N94-32511
ZHONG, XIAO-LIN ..... p 3706 N94-32256
ZHOU, CHANGZUN ..... p 3736 N94-31912
ZHOU, CHIN ..... p 3833 N94-31876
ZHOU, D. S. ..... p 3901 N94-32172
ZHOU, P. ..... p 3881 N94-32385
ZHOU, SAMUEL ZIHENG ..... p 3814 N94-31715
ZHOU, WEIQUN ..... p 3649 N94-31206
ZHOU, ZHONG RONG ..... p 3735 N94-31870
ZHU, Q. M. ..... p 3842 N94-31394
p 3842 N94-31413
ZHU, QICAO ..... p 3859 N94-31060
p 3861 N94-32059
ZHU, S. ..... p 3727 N94-32778
ZHU, SHENG-BAI ..... p 3632 N94-31293
ZHUKOV, V. A. ..... p 3896 N94-31395
ZIARATI, KOORUSH ..... p 3832 N94-31801
ZIERKE, W. C. ..... p 3583 N94-31931
ZIGH, ABDELGHANI ..... p 3704 N94-31843
ZIJLEMA, M. ..... p 3703 N94-31703
ZIMA, HANS ..... p 3820 N94-32928
ZINN, MICHAEL R. ..... p 3606 N94-33316
ZIOCK, K. ..... p 3712 N94-31783
ZOBEL, ANNETTE R. ..... p 3804 N94-32302
ZOK, F. W. ..... p 3630 N94-33178
ZOLPER, J. C. ..... p 3881 N94-32385
ZOUNEK, ALEXIS N. ..... p 3865 N94-31511
ZUNIGA, FANNY A. ..... p 3572 N94-32680
ZUPFER, JOEL E. ..... p 3693 N94-32336
ZUREK, R. W. ..... p 3948 N94-33215
ZUROWSKI, MARY M. ..... p 3611 N94-32369
ZWIENER, JAMES M. ..... p 3591 N94-31013
p 3595 N94-31032
ZYRA, S. ..... p 3878 N94-31584

Typical Corporate Source Index Listing

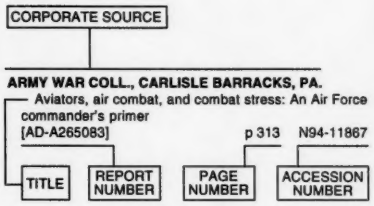

Listings in this index are arranged alphabetically by corporate source. The title of the document provides the user with a brief description of the subject matter. The report number helps to indicate the type of document cited (e.g., NASA report, translation, NASA contractor report). The accession number denotes the number by which the citation is identified. The page number helps you locate the citation in the abstract section. The titles are arranged under each corporate source in ascending accession number order.

A

ABERDEEN PROVING GROUND, MD.
In-bed multiport sampling system
[AD-A275908] p 3763 N94-31339

Chamber optics for testing passive remote sensing vapor detectors
[AD-A275909] p 3878 N94-31340

Focused feasibility study final field sampling plan
[AD-A277445] p 3769 N94-33105

ACADEMY OF SCIENCES (USSR), SAINT PETERSBURG.
F0-975, A0-980 as eye-witnesses of confinement
[PB94-147105] p 3868 N94-31923

ACOUSTICAL SOCIETY OF AMERICA, NEW YORK, NY.
Minutes: Accredited Standards Committee on Bioacoustics, S3. US TAG for ISO/TC 43, acoustics, IEC/TC 29 electroacoustics, and ISO/TC 108/SC4 human exposure to mechanical vibration and shock
[AD-A276201] p 3795 N94-31490

ADAPTIVE SOLUTIONS, INC., BEAVERTON, OR.
High performance hardware and software for pattern recognition and image processing
[AD-A276405] p 3816 N94-32130

ADVISORY GROUP FOR AEROSPACE RESEARCH AND DEVELOPMENT, NEUILLY-SUR-SEINE (FRANCE).
AGARD highlights 94/1, April 1994
[AGARD-HIGHLIGHTS-94/1] p 3956 N94-31196

AGARD membership, 1994
[AGARD-MEMB-94] p 3914 N94-31197

Aerospace software engineering for advanced systems architectures
[AD-A277101] p 3581 N94-31977

Atmospheric propagation effects through natural and man-made obscurants for visible to MM-wave radiation
[AD-A276919] p 3679 N94-32235

AEROJET SOLID PROPULSION CO., SACRAMENTO, CA.
The 7.5K lbf thrust engine preliminary design for Orbit Transfer Vehicle
[NASA-CR-189175] p 3614 N94-31618

AERONAUTICAL RADIO, INC., ANNAPOLIS, MD.
Active matrix liquid crystal display. Industry survey results
[AD-A276415] p 3895 N94-31329

AERONAUTICAL RESEARCH INST. OF SWEDEN, STOCKHOLM.
Prediction of transonic potential flow with slipstreams around configurations
[FFA-TN-1992-15] p 3568 N94-31220

AERONAUTICAL RESEARCH LABS., MELBOURNE (AUSTRALIA).
Finite element analysis of MB326H Macchi wing lower spar cap fatigue cracks
[AD-A277062] p 3580 N94-32264

Assessment of impact damage in composite structures
[AD-A277063] p 3624 N94-32265

Six degree of freedom flight dynamic model of a Mk-82 store
[AD-A277065] p 3580 N94-32362

AERONAUTICAL SYSTEMS DIV., WRIGHT-PATTERSON AFB, OH.
Aircraft weight prediction capability. Volume 1: Weight study and results
[AD-A277206] p 3579 N94-32062

AEROSPACE CORP., EL SEGUNDO, CA.
The impact of LDEF results on the space application of metal matrix composites p 3595 N94-31034

An overview of the on-orbit contamination of the Long Duration Exposure Facility (LDEF) p 3598 N94-31049

Honeycomb sandwich structures: Vented versus unvented designs for space systems
[AD-A276713] p 3624 N94-32122

Soft x ray photoelectron spectroscopy study of the interaction of Cr with MoS2(0001)
[AD-A276916] p 3635 N94-32233

Aerospace sponsored research
[ATR-93(8498)-1] p 3966 N94-32949

Torque characteristics of solid lubricated precision bearings during oscillatory motion
[AD-A278133] p 3728 N94-33061

Possible effect of the chlorine oxide dimer on transient ozone loss in rocket plumes
[AD-A278135] p 3616 N94-33094

Characteristics of ion flow in the quiet state of the inner plasma sheet
[AD-A277451] p 3894 N94-33106

Data processing algorithms for on-board satellite event analysis
[AD-A278406] p 3838 N94-33168

Temperature dependence of single-event burnout in n-channel power MOSFET's
[AD-A277921] p 3698 N94-33177

The impact of ASIC devices on the SEU vulnerability of space-borne computers
[AD-A278134] p 3808 N94-33252

Spacecraft environmental anomalies expert system
[AD-A277962] p 3612 N94-33262

AEROSPACE MEDICAL RESEARCH LABS., BROOKS AFB, TX.
Analysis of pursuit tracking eye movements in pilots and nonfliers
[AD-A276597] p 3799 N94-32035

Aircrew Eye/Respiratory Protection (AERP): 16-hour extended wear evaluation of chemical protective equipment
[AD-A277288] p 3804 N94-32609

AEROSPACE MEDICAL RESEARCH LABS., WRIGHT-PATTERSON AFB, OH.
Human Computer Interface Specifications (HCIS) for the Integrated Maintenance Information System (IMIS)
[AD-A277184] p 3566 N94-32254

AEROSPATIALE, CANNES (FRANCE).
Fusion of multispectral (XS) and Panchromatic (P) SPOT images and radar images p 3750 N94-32541

AIR FORCE ACADEMY, CO.
Room temperature molten salts for advanced energy conversion and storage
[AD-A277777] p 3763 N94-33015

AIR FORCE ENVIRONMENTAL TECHNICAL APPLICATIONS CENTER, SCOTT AFB, IL.
Station climatic summaries: China, the former USSR, and Mongolia
[AD-A276548] p 3784 N94-32057

AIR FORCE INST. OF TECH., WRIGHT-PATTERSON AFB, OH.
An analysis of the records management process to determine the impact of automation on productivity
[AD-A275923] p 3916 N94-31344

An evaluation of aircraft maintenance performance factors in the objective wing
[AD-A276010] p 3565 N94-31362

The development and use of an evaluation mechanism for the assessment of software configuration management tools
[AD-A275961] p 3810 N94-31383

A study of theoretical models for managing technology change and a comparison to a radio frequency identification implementation
[AD-A276012] p 3672 N94-31385

Assessing the vulnerability of multi-commodity networks with failing components
[AD-A278434] p 3684 N94-33334

AIR FORCE OCCUPATIONAL MEASUREMENT CENTER, RANDOLPH AFB, TX.
Aircraft communication and navigation systems and communication and navigation systems
[AD-A277309] p 3582 N94-32328

AIR TRANSPORT GROUP HEADQUARTERS, ASTRA (ONTARIO).
A neural network application to search and rescue satellite aided tracking (SARSAT) p 3613 N94-33345

AKRON UNIV., OH.
Compatibility of refrigerants and lubricants with elastomers
[DE94-008552] p 3658 N94-32518

A procedure for 3-D contact stress analysis of spiral bevel gears
[NASA-CR-194472] p 3728 N94-32929

ALABAMA UNIV., HUNTSVILLE.
On the linearity of fast atomic oxygen effects p 3594 N94-31027

Preliminary results from the CONCAP-2-01 and EIOM-3 experiments on STS-46 p 3596 N94-31042

Numerical simulation of interplanetary dynamics p 3933 N94-31566

Fiber optic chemical sensors
[AD-A277128] p 3881 N94-32380

BATSE data analysis
[NASA-CR-195818] p 3927 N94-32942

Ionospheric plasma outflow in response to transverse ion heating: Self-consistent macroscopic treatment
[NASA-CR-195820] p 3893 N94-33048

ALABAMA UNIV., UNIVERSITY.
High energy physics program at the University of Alabama
[DE94-006544] p 3875 N94-31488

Penetrable wedge analysis
[AD-A277219] p 3845 N94-32022

ALASKA UNIV., FAIRBANKS.
Theory, Image Simulation, and Data Analysis of Chemical Release Experiments
[NASA-CR-194865] p 3954 N94-31101

ALBERTA RESEARCH COUNCIL, EDMONTON.
The CF-18 diagnostic and maintenance expert system project p 3567 N94-33338

ALBERTA UNIV., EDMONTON.
Automatic resonator alignment and power stabilization of high power C02 lasers
[ISBN-0-315-77217-4] p 3714 N94-31472

The spatial development of the magnetospheric low-latitude boundary layer
[ISBN-0-315-77418-5] p 3776 N94-33111

ALLIED-SIGNAL AEROSPACE CO., KANSAS CITY, MO.
Validation of the Environmentally Conscious Manufacturing Integrated Demonstration hardware
[DE94-003824] p 3765 N94-32144

New thick film feedthrough configurations
[DE94-008706] p 3694 N94-32582

ALLIED-SIGNAL CORP., KANSAS CITY, MO.
Assembly flow simulation of a radar
p 3823 N94-32431

ALTAMIRA INSTRUMENTS, INC., PITTSBURGH, PA.
Direct aromatization of methane
[DE94-008719] p 3638 N94-32888

AMAX RESEARCH AND DEVELOPMENT CENTER, GOLDEN, CO.
Development of vanadium-phosphate catalysts for methanol production by selective oxidation of methane
[DE94-006759] p 3759 N94-31272

AMERASIA TECHNOLOGY, INC., WESTLAKE VILLAGE, CA.
Advanced satellite communication system
[NASA-CR-194211] p 3681 N94-32477

AMERICAN FOUNDREYMENS' SOCIETY, DES PLAINES, IL.
Expandable pattern casting research
[DE94-004342] p 3668 N94-31604

AMERICAN WELDING INST., LOUISVILLE, TN.
Empirical modeling for intelligent, real-time manufacture control p 3839 N94-32424

AMES LAB., IA.
Synthesis, characterization, phase diagrams and superconducting, and normal state magnetic properties of La(2-x)Sr(x)CuO4 (0 is less than or equal to x which is less than or equal to 0.08) and electrochemically oxidized La(2-x)Sr(x)CuO(4 + delta) (0 is less than or equal to x which is less than or equal to 0.33, 0 is less than or equal to delta which is less than or equal to 0.12)
[DE94-005260] p 3895 N94-31067
Proceedings of the Seventeenth DOE Solar Photochemistry Research Conference
[DE94-005552] p 3759 N94-31648
Photonic band gap materials
[DE94-005566] p 3677 N94-32101
The intramolecular cyclization of bis-2,5-dimethylene-2,5-dihydrofurans and bis-2,5-dimethylene-2,5-dihydrothiophenes: An approach to macrocycles
[DE94-007060] p 3657 N94-32377
Development of a low-latency scalar communication routine on message-passing architectures
[DE94-007061] p 3827 N94-32683

AMSTERDAM UNIV. (NETHERLANDS).
Lambek calculus is L-complete
[LP-93-14] p 3841 N94-31388
What comes first in dynamic semantics: A compositional, non-representational account of natural language presupposition
[LP-93-15] p 3855 N94-31389
The interpretation of free focus
[CL-93-01] p 3855 N94-31390
An algebraic view on Rosetta
[CL-93-02] p 3841 N94-31391
The meaning of duplicates in the relational database model
[CT-93-04] p 3916 N94-31392
Proving theorems of the Lambek calculus of order 2 in polynomial time
[CT-93-05] p 3842 N94-31393
Resumptive quantifiers in exception sentences
[LP-93-11] p 3855 N94-31403
Binary quantifiers and relational semantics
[LP-93-13] p 3855 N94-31404
On the independent axiomatizability of modal and intermediate logics
[ML-93-17] p 3856 N94-31407
Extensional realizability
[ML-93-18] p 3856 N94-31408
Comparing models of the non-extensional typed lambda-calculus
[ML-93-19] p 3842 N94-31409
The decidability of dependency in intuitionistic propositional logic
[ML-93-20] p 3856 N94-31410
Sums and quantifiers
[LP-93-05] p 3856 N94-31411
Effective truth
[ML-93-15] p 3856 N94-31416
Correspondence theory for extended modal logics, version 3.0
[ML-93-16] p 3856 N94-31417
Updates in dynamic semantics
[LP-93-06] p 3856 N94-31450
On the equivalence of Lambek categorial grammars and basic categorial grammars
[LP-93-07] p 3842 N94-31451
Information acquisition from multi-agent resources; abstract
[LP-93-08] p 3917 N94-31452
Completeness and decidability of the mixed style of inference with composition
[LP-93-09] p 3842 N94-31453
Weaks vs. strong readings of donkey sentences and monotonicity inference in a dynamic setting
[LP-93-10] p 3856 N94-31468
Spectral inhomogeneity of the bacterial light-harvesting antennae: Causes and consequences
[ETN-94-96020] p 3792 N94-31533
The measurement of the hadronic energy flow and jet production with the ZEUS calorimeter in deep inelastic scattering events at HERA
[ETN-94-96021] p 3865 N94-31534

ANALEX SPACE SYSTEMS, INC., COCOA BEACH, FL.
Pen-based computers: Computers without keys
p 3808 N94-32434
Automated mainframe data collection in a network environment p 3923 N94-32443

ANALYTICAL METHODS, INC., REDMOND, WA.
A novel potential/viscous flow coupling technique for computing helicopter flow fields
[NASA-CR-193272] p 3571 N94-32476

ANALYTICAL SERVICES AND MATERIALS, INC., HAMPTON, VA.
COINS: A composites information database system
p 3627 N94-33123

APA OPTICS, INC., BLAINE, MN.
GaAs/GaN strained layer superlattice materials for high temperature transistors, phase 1
[AD-A276115] p 3897 N94-31528

APPLIED EXPERTISE, INC., ARLINGTON, VA.
Software reuse case study: TRILLIUM
[AD-A276108] p 3811 N94-31465

APPLIED RESEARCH CORP., LANDOVER, MD.
A low-cost, CCD solid state star tracker
[NASA-CR-192722] p 3882 N94-32417

APPLIED SCIENCE AND TECHNOLOGY, INC., WOBURN, MA.
Materials processing and manufacturing technologies for diamond substrates multichip modules
[AD-A276904] p 3692 N94-32215

ARCO POWER TECHNOLOGIES, INC., WASHINGTON, DC.
Electromagnetic wave reflection from irregular plasma layers
[AD-A276727] p 3678 N94-32161

ARGONNE NATIONAL LAB., IDAHO FALLS, ID.
Observation of the traveling component of an x ray standing wave field
[DE94-007671] p 3672 N94-31317
Design of graphic screens using Neuro Linguistic Programming
[DE94-007634] p 3719 N94-32599

ARGONNE NATIONAL LAB., IL.
Analysis of beam-on-target interaction in a neutron-source test facility
[DE94-005392] p 3863 N94-31151
Time-resolved infrared absorption studies applied to the study of radical plus molecule reactions
[DE94-005921] p 3863 N94-31202
A survey of numerical cubature over triangles
[DE94-006810] p 3841 N94-31274
First theory institute on computational differentiation
[DE94-006491] p 3841 N94-31309
Analysis of the high energy behavior of the forward scattering parameters - sigma(tot), rho and B
[DE94-006537] p 3864 N94-31310
Nonlinearity as an origin of nonuniqueness in solution of Hartree's equation
[DE94-006538] p 3841 N94-31311
OTTER 3.0 reference manual and guide
[DE94-007457] p 3829 N94-31315
Review and status of Maglev in the United States
[DE94-006832] p 3722 N94-31319
Elimination of two atomic electrons by a single high energy photon
[DE94-006834] p 3864 N94-31320
High-temperature study of O+H2CO yields OH+HCO
[DE94-006837] p 3864 N94-31321
Implementation of instruments and facilities at the SGP CART site
[DE94-006839] p 3781 N94-31322
Creep properties of vanadium-base alloys
[DE94-006541] p 3641 N94-31486
Emissions of greenhouse gases from the use of transportation fuels and electricity
[DE94-006166] p 3765 N94-31625
A comparison of distributed memory and virtual shared memory parallel programming models
[DE94-005473] p 3825 N94-31663
Finite-part integrals and the Euler-Maclaurin expansion
[DE94-006539] p 3844 N94-31665
Effect of irradiation damage and helium on the swelling and structure of vanadium-base alloys
[DE94-006540] p 3641 N94-31666
Double photoionization of helium with synchrotron x rays: Proceedings
[DE94-006737] p 3866 N94-31668
The new Metals and Alloys Indexes, search manual: A phase diagram research tool
[DE94-005371] p 3643 N94-32098
Irradiation-assisted stress corrosion cracking of materials from commercial BWRs: Role of grain-boundary microchemistry
[DE94-006542] p 3643 N94-32109
A general stochastic Liouville theory for sequential and superexchange electron-transfer reactions involving three Marcus potential surfaces
[DE94-007695] p 3869 N94-32141
Moving BASISplus and TECHLIBplus from VAX/VMS to UNIX
[DE94-004696] p 3826 N94-32248
Parallel Monte Carlo reactor neutronics
[DE94-007642] p 3826 N94-32357
Characterization of interface structure in multilayers using specular x ray reflectance
[DE94-007698] p 3657 N94-32358
Defect cascades produced by neutron irradiation in YBa2Cu3O(7-delta) superconductors
[DE94-007700] p 3903 N94-32372
Structural ordering in liquid K-Te alloys
[DE94-008477] p 3645 N94-32514
Formation mechanism and yield of molecules ejected from ZnS, CdS, and FeS2 during ion bombardment
[DE94-008487] p 3871 N94-32515
Wave packet studies of the vibrational predissociation of three and four-atom van der Waals complexes
[DE94-007623] p 3871 N94-32598
Greenhouse gas emission impacts of electric vehicles under varying driving cycles in various countries and US cities
[DE94-007647] p 3765 N94-32600
Effect of twin boundary density on the vortex melting transition in YBa2Cu3O(7-delta) single crystals
[DE94-007684] p 3904 N94-32601
High T(sub c) superconductor tunnel junctions for photon detectors
[DE94-007686] p 3904 N94-32602
Proceedings of the Ad Hoc Workshop on Ceramics for Li/FeS2 batteries
[DE94-007460] p 3694 N94-32607
Rate coefficient for the reaction H + O2 yields OH + O: Results from 2000 to 5300 K
[DE94-008105] p 3871 N94-32615
Computational chemistry on parallel computers
[DE94-008106] p 3636 N94-32616
Mechanical properties of vacuum-sintered yttria ceramics
[DE94-008138] p 3659 N94-32617
Short coherence length superconductors: Intermediate regime between BCS and bosons
[DE94-007694] p 3904 N94-32645
Gigabits to the Desktop: Installing tomorrow's networks today
[DE94-007701] p 3827 N94-32646
High-energy chemical processes: Laser irradiation of aromatic hydrocarbons
[DE94-008107] p 3720 N94-32707
Semileptonic decays of mesons in the SQ(4) model
[DE94-008108] p 3873 N94-32708
Chiral symmetry and the threshold gamma(p) yields pi(sup 0)p reaction
[DE94-008117] p 3873 N94-32710
Identification of research relating to the critical loads concept and its potential application to the regulation of acidic deposition
[DE94-008234] p 3767 N94-32752
Radiation and photochemistry section
[DE94-008880] p 3873 N94-32757
On the unsteady-motion theory of magnetic forces for maglev
[DE94-007765] p 3727 N94-32778
Isothermal sintering, microstructure, and superconducting properties of Y1Ba2Cu3O(7-x) compound
[DE94-008132] p 3905 N94-32779
National US public policy on global warming derived from optimization of energy use and environmental impact studies
[DE94-004606] p 3768 N94-32790
Metal cluster-rare gas van der Waals complexes: Microscopic models of physisorption
[DE94-008134] p 3873 N94-32797
Extended-range order in glasses
[DE94-008135] p 3661 N94-32798
New advances in the modeling of high-temperature superconductors
[DE94-007649] p 3905 N94-32815
Ultrahigh-current-density metal-ion implantation and diamondlike-hydrocarbon films for tribological applications
[DE94-008958] p 3906 N94-32843

Parameterizing atmosphere-land surface exchange for climate models with satellite data: A case study for the Southern Great Plains CART site
[DE94-005109] p 3775 N94-32874
Electron energy dependence of amorphization in Zr3Fe
[DE94-008459] p 3906 N94-32875
Structural studies of photoinduced intramolecular electron transfer in cyclopentadienylnickelnitrosyl
[DE94-008467] p 3874 N94-32876
Dry deposition of PAN to grassland vegetation
[DE94-005111] p 3768 N94-32894
Experimental studies on the effect of coherency strains on coarsening kinetics: Current status and future outlook
[DE94-008480] p 3647 N94-32964
Microreflectance infrared study of electron-molecular vibrational coupling and lattice softness in BEDT-TTF salts
[DE94-008490] p 3907 N94-32989
Characterization of nanoparticles and nanophase materials
[DE94-008348] p 3907 N94-32990
Irradiation-induced phase transformations in zirconium alloys
[DE94-008484] p 3648 N94-32993

ARIZONA STATE UNIV., TEMPE.
Laser-induced fluorescence/particle tracking system for stratified flow research
[AD-A275917] p 3701 N94-31341
Correlations between micromagnetic, microstructural and microchemical properties in ultrathin epitaxial magnetic structures
[AD-A277200] p 3901 N94-32092
Mechanics of failure of high temperature metal matrix composites
[AD-A277397] p 3624 N94-32342
Organic analyses of the Murchison meteorite p 3938 N94-32489
Advanced high frequency partial discharge measuring system
[NASA-CR-195240] p 3697 N94-33044
Regional sedimentological variations among dark crater floor features: Toward a model for modern eolian sand distribution on Mars p 3946 N94-33203
Evidence for ultramafic lavas on Syrtis Major p 3950 N94-33229
Martian deltas: Morphology and distribution p 3950 N94-33230

ARIZONA UNIV., TUCSON.
Evidence of solar oscillations in Rayleigh-scattered light p 3952 N94-31214
Research in the optical sciences
[AD-A278271] p 3884 N94-33140

ARKANSAS UNIV., FAYETTEVILLE.
Biological conversion of synthesis gas
[DE94-000094] p 3760 N94-31811

ARMY AEROMEDICAL RESEARCH LAB., FORT RUCKER, AL.
Evaluation of intensity distribution profiles for US. Army rotorcraft position lighting adapted for image intensifier operations
[AD-A276459] p 3804 N94-32171
Technical evaluation of the UH-60Q: Aircraft in typical aeromedical evacuation missions
[AD-A276944] p 3586 N94-32217
Technical evaluation of the UH-60Q: Medical oxygen system
[AD-A276983] p 3579 N94-32242
Estimating the impact of crashworthiness standards on mortality and morbidity events in the US Army rotary-wing aircraft mishaps
[AD-A277121] p 3575 N94-32363
Unit specific crew rest strategies: Phase 1 evaluation of the 1/212th Aviation Battalion during shiftwork transitions
[AD-A277122] p 3804 N94-32379

ARMY ARMAMENT MUNITIONS AND CHEMICAL COMMAND, WATERVLIET, NY.
Computerized Ultrasonic Testing System (CUTS) for in-process thickness determination p 3862 N94-32456

ARMY ARMAMENT RESEARCH, DEVELOPMENT AND ENGINEERING CENTER, WATERVLIET, NY.
A review of weldment failure modes and weldability testing methods
[AD-A278096] p 3729 N94-33251
Simpler J(sub Ic) test and data analysis procedures for high strength steels
[AD-A277731] p 3648 N94-33281

ARMY BELVOIR RESEARCH AND DEVELOPMENT CENTER, FORT BELVOIR, VA.
Status of developing a multifunctional aviation grease
[AD-A276755] p 3656 N94-32184

ARMY COLD REGIONS RESEARCH AND ENGINEERING LAB., HANOVER, NH.
A reassessment of the in-situ dielectric constant of polar firn
[AD-A276999] p 3773 N94-32154

ARMY ENGINEER WATERWAYS EXPERIMENT STATION, VICKSBURG, MS.
ADCIRC: An advanced three-dimensional circulation model for shelves, coasts, and estuaries. User's manual for ADCIRC-2DDI
[AD-A276150] p 3787 N94-31250
Microwave dielectric behavior of soils. Report 1: Summary of related research and applications
[AD-A275980] p 3771 N94-31351
Microwave dielectric behavior of soils. Report 2: A unique coaxial measurement apparatus
[AD-A275982] p 3771 N94-31353
Microwave dielectric behavior of soils. Report 3: Measurement and modeling
[AD-A276060] p 3771 N94-31457
Theory and application of image enhancement
[AD-A277896] p 3821 N94-33031

ARMY RESEARCH INST. OF ENVIRONMENTAL MEDICINE, NATICK, MA.
Recommendations for meteorological data collection during physiological field studies
[AD-A276834] p 3901 N94-32153
Numerical model of the thermal behavior of an extremity in a cold environment including counter-current heat exchange between the blood vessels
[AD-A278099] p 3798 N94-33040
Medical problems in high mountain environments. A handbook for medical officers
[AD-A278095] p 3798 N94-33268

ARMY RESEARCH LAB., ABERDEEN PROVING GROUND, MD.
Remarks on a result of LAV Carvalho
[AD-A276404] p 3841 N94-31360
Condensed-phase processes during solid propellant combustion. 3: Preliminary depth-profiling studies on XM39, JA2, M9, M30, and HMX2
[AD-A276595] p 3635 N94-32124
A thermal viscoelastic analysis for thick-walled composite cylinders
[AD-A274143] p 3625 N94-32604

ARMY RESEARCH LAB., ADELPHI, MD.
Processing and characterization of functionally gradient ceramic materials
[AD-A277154] p 3657 N94-32367
Large-diameter InGaAs/AlGaAs vertical-cavity surface-emitting lasers with low threshold current density fabricated using a simple chemical etch process
[AD-A277733] p 3721 N94-33003

ARMY RESEARCH LAB., FORT MONMOUTH, NJ.
Performance of the Sony lithium-ion rechargeable battery
[AD-A277076] p 3693 N94-32303

ARMY RESEARCH LAB., WATERTOWN, MA.
Minimization of computational requirements in the hybrid stress finite element method
[AD-A277120] p 3846 N94-32048
Study of type 2 and 3 anodized Al 5052-0 in aqueous DS2 solutions
[AD-A276960] p 3644 N94-32240

ARMY TOPOGRAPHIC ENGINEERING CENTER, FORT BELVOIR, VA.
Results of real-time testing and demonstration of the US Army Corps of Engineers real-time on-the-fly positioning system
[AD-A276160] p 3576 N94-31080
Alternatives to hierarchical techniques in stereo correlation
[AD-A276570] p 3746 N94-31938
Selection of climate station data using clustering and triangulated irregular network techniques
[AD-A276658] p 3784 N94-32046
Real-time centimeter positioning with GPS: A system developed by the US Army Corps of Engineers
[AD-A278152] p 3577 N94-33095

ARMY WAR COLL., CARLISLE BARRACKS, PA.
NATO contributions to European environmental security
[AD-A275918] p 3763 N94-31275

ARNOLD ENGINEERING DEVELOPMENT CENTER, ARNOLD AFS, TN.
Development of high-pressure diaphragms for the AEDC impulse tunnel
[AD-A277053] p 3588 N94-32009
Pre-flight testing of Thermoelectric Quartz Crystal Microbalances (TQCM) for midcourse space experiment (MSX) spacecraft
[AD-A277054] p 3610 N94-32010
A critical evaluation of methods for imposing solid-wall boundary conditions in inviscid flow
[AD-A276959] p 3707 N94-32361

ARTIFICIAL INTELLIGENCE MANAGEMENT AND DEVELOPMENT CORP., TORONTO (ONTARIO).
Plan recognition for an air traffic control simulation
[DSIS-94-01221] p 3577 N94-32505

ASPEN CENTER FOR PHYSICS, CO.
Summary of the 1993 Winter ACP Workshop on Collective Dynamics in Disordered System
[AD-A276355] p 3864 N94-31402

ASTRO AEROSPACE CORP., CARPINTERIA, CA.
Deployable and retractable telescoping tubular structure development p 3607 N94-33317

ASTROPOWER, INC., NEWARK, DE.
Silicon-Film(tm) photovoltaic manufacturing technology
[DE94-000202] p 3760 N94-32143

ATMOSPHERIC AND ENVIRONMENTAL RESEARCH, INC., CAMBRIDGE, MA.
How well was total ozone abundance inferred with Mariner 9 p 3947 N94-33212
The effect of polar caps on obliquity p 3948 N94-33213

AUBURN UNIV., AL.
Morphology correlation of craters formed by hypervelocity impacts p 3594 N94-31031
Space environmental effects on polymer composites: Research needs and opportunities p 3595 N94-31035
High temperature materials technology research for advanced thermionic systems
[DE94-008444] p 3644 N94-32416
High temperature materials technology research for advanced thermionic systems
[DE94-008341] p 3646 N94-32825

AXIOMATICS CORP., WOBURN, MA.
Continuous measurement of aircraft wing icing p 3576 N94-32454

B

BBN SYSTEMS AND TECHNOLOGIES CORP., CAMBRIDGE, MA.
Reciprocity-based experimental determination of dynamic forces and moments: A feasibility study
[NASA-CR-194905] p 3662 N94-33023

BERKELEY APPLIED SCIENCE AND ENGINEERING, INC., SAN FRANCISCO, CA.
Development of an advanced continuum theory for composite laminates, volume 1
[AD-A277275] p 3625 N94-32591
Development of an advanced continuum theory for composite laminates, volume 2
[AD-A277276] p 3625 N94-32592

BIO-IMAGING RESEARCH, INC., LINCOLNSHIRE, IL.
Differential phase acoustic microscope for micro-NDE
[NASA-CR-189617] p 3731 N94-32481

BOEING CO., RENTON, WA.
Application of a design-build-team approach to low cost and weight composite fuselage structure
[NASA-CR-4418] p 3626 N94-32863

BOEING CO., SEATTLE, WA.
Interpreter composition issues in the formal verification of a processor-memory module
[NASA-CR-4594] p 3820 N94-32775
Characterization and manufacture of braided composites for large commercial aircraft structures p 3630 N94-33137

BOEING COMMERCIAL AIRPLANE CO., SEATTLE, WA.
Local design optimization for composite transport fuselage crown panels p 3629 N94-33132
Composite fuselage crown panel manufacturing technology p 3629 N94-33133

BOEING DEFENSE AND SPACE GROUP, HUNTSVILLE, AL.
Design application and development of spacecraft in LEO utilizing LDEF results p 3597 N94-31047
Modular Simulator System (MSS) management guide
[AD-A277098] p 3588 N94-32014
Modular Simulator System (MSS). Executive report
[AD-A276966] p 3588 N94-32241
Modular Simulator System (MSS). Interface requirements specification for the generic MSS
[AD-A276965] p 3588 N94-32311
Modular Simulator System (MSS). System/segment specification for the generic MSS-system integration, volume 1
[AD-A276968] p 3588 N94-32312
Modular Simulator System (MSS). System/segment specification for the generic modular simulator system-flight station module, volume 2
[AD-A276969] p 3588 N94-32313
Modular Simulator System (MSS). System/segment specification for the generic modular simulator system-radar module, volume 8
[AD-A276975] p 3589 N94-32314

Modular Simulator System (MSS). System/segment specification for the generic modular simulator system-electronic warfare module, volume 9
[AD-A276976] p 3589 N94-32315
Modular Simulator System (MSS). System/segment specification for the generic modular simulator system-physical cues module, volume 10
[AD-A276977] p 3589 N94-32316
Modular Simulator System (MSS). System/segment specification for the generic modular simulator system-visual module, volume 11
[AD-A276978] p 3589 N94-32317
Modular Simulator System (MSS). System/segment specification for the generic modular simulator system-instructor/operator station module, volume 12
[AD-A276979] p 3589 N94-32318
Modular Simulator System (MSS). System/segment specification for the generic modular simulator system-environment module, volume 13
[AD-A276980] p 3589 N94-32319
Modular Simulator System (MSS). Engineering design guide
[AD-A276967] p 3589 N94-32394
Modular Simulator System (MSS). System/segment specification for the generic modular simulator system-flight controls module, volume 3
[AD-A276970] p 3590 N94-32395
Modular Simulator System (MSS). System/segment specification for the generic modular simulator system-flight dynamics module, volume 4
[AD-A276971] p 3590 N94-32396
Modular Simulator System (MSS). System/segment specification for the generic modular simulator system-propulsion module propulsion module, volume 5
[AD-A276972] p 3590 N94-32397
Modular Simulator System (MSS). System/segment specification for the generic modular simulator system-navigation/communication module, volume 6
[AD-A276973] p 3590 N94-32398
Modular Simulator System (MSS). System/segment specification for the generic modular simulator system-weapons module, volume 7
[AD-A276974] p 3590 N94-32399
Modular Simulator System (MSS): Interface design document for the generic MSS
[AD-A277270] p 3590 N94-32403
Space Station evolution study
[NASA-CR-193937] p 3611 N94-32898

BOEING DEFENSE AND SPACE GROUP, SEATTLE, WA.
Performance of silvered Teflon (trademark) thermal control blankets on spacecraft p 3591 N94-31014
Anodized aluminum on LDEF p 3592 N94-31017
Spacecraft contamination issues from LDEF: Issues for design p 3592 N94-31020
Model of spacecraft atomic oxygen and solar exposure microenvironments p 3593 N94-31021
Low-Earth orbit effects on organic composite materials flown on LDEF p 3595 N94-31036

BOSTON UNIV., MA.
Segment-based acoustic models for continuous speech recognition
[AD-A276109] p 3673 N94-31466
Neural models of spatial orientation in novel environments
[AD-A277383] p 3835 N94-32340
Research and applications of a canopy reflectance model p 3747 N94-32492

BOWLING GREEN STATE UNIV., OH.
Photopolymerization of cyclohexene oxide: A visible light initiating system and mechanistic investigations
[AD-A277110] p 3654 N94-31981
Mechanical properties of acrylate networks formed by visible laser-induced polymerization. 2. Control of the mechanical properties
[AD-A277111] p 3655 N94-31982
A visible light initiating system for free radical promoted cationic polymerization
[AD-A277164] p 3655 N94-32069
Intramolecular charge transfer complexes as fluorescence probes for UV and visible light induced acrylate polymerization
[AD-A277129] p 3657 N94-32381

BP AMERICA, INC., CLEVELAND, OH.
Engineering scale development of the Vapor-Liquid-Solid (VLS) process for the production of silicon carbide fibrils
[DE94-007132] p 3659 N94-32618

BRISTOL UNIV. (ENGLAND).
Snowmelt forecasting. Further cold regions development of operational hydrological forecasting, volume 2
[AD-A278123] p 3757 N94-33269

BRITISH COLUMBIA UNIV., VANCOUVER.
Incompressible viscous flow in tubes with occlusions
[ISBN-0-315-75467-2] p 3704 N94-31778
Gravitational effects of cosmic strings
[ISBN-0-315-75484-2] p 3934 N94-31789
Dynamics and control of orbiting flexible systems: A formulation with applications
[ISBN-0-315-75390-0] p 3611 N94-32502
Temporal changes in the geographic distribution, elevation, and potential origin of the Martian outflow channels p 3951 N94-33235

BRITISH NATIONAL SPACE CENTRE, HUNTINGDON (ENGLAND).
Monitoring fertilizer application by imaging spectrometry (Somerset Levels test site) p 3745 N94-31863

BROOKHAVEN NATIONAL LAB., UPTON, NY.
Infrared and near infrared transient absorption spectroscopy of molecular free radicals
[DE94-005446] p 3632 N94-31305
BNL possibilities
[DE94-007179] p 3864 N94-31398
The development of CVR coatings for PBR fuels
[DE94-004233] p 3875 N94-31480
Laboratory Directed Research & Development Program
[DE94-005928] p 3956 N94-31523
Cloud studies seen from a physical chemist's perspective
[DE94-006059] p 3771 N94-31527
Ionizing radiation effects on silicon test structures
[DE94-006060] p 3865 N94-31607
The zinc electrode: Reactions and mechanisms
[DE94-007977] p 3691 N94-31919
RHIC spin physics
[DE94-005452] p 3876 N94-32099
Evaluation of sulfate aerosol optical depths over the North Atlantic and comparison with satellite observations
[DE94-005457] p 3746 N94-32100
Summary of particle bed reactor designs for the Space Nuclear Thermal Propulsion Program
[DE94-007434] p 3615 N94-32266
Analytical solutions of minimum ionization particle induced current shapes of silicon detectors and simulation of charge collection properties
[DE94-007523] p 3870 N94-32355
Transverse energy production with Si and Au beams at AGS energy: Towards hot and dense hadronic matter
[DE94-007178] p 3938 N94-32638
Fine resolution atmospheric sulfate model driven by operational meteorological data: Comparison with observations
[DE94-002994] p 3766 N94-32691
Formation of gas-phase peroxides in a rural atmosphere: An interpretation of the recent SOS/SERON field results
[DE94-002995] p 3766 N94-32692
Characterization of the corrosion resistance of duplex stainless steels using local current density mapping techniques
[DE94-007980] p 3646 N94-32699
Ionization EM calorimetry with accordion electrodes and liquid krypton or argon
[DE94-009082] p 3713 N94-32821
Resistivity measurements on the neutron irradiated detector grade silicon materials
[DE94-009083] p 3906 N94-32822
Light utilization and photoinhibition of photosynthesis in marine phytoplankton
[DE94-005505] p 3794 N94-32896
RHIC chromatic correction system
[DE94-008532] p 3883 N94-32994

BROWN UNIV., PROVIDENCE, RI.
Proceedings of the NIPS 1993 Postconference Workshop on Pulling It All Together: Methods for Combining Neural Networks
[AD-A277507] p 3836 N94-33014
The importance of environmental conditions in reflectance spectroscopy of laboratory analogs for Mars surface materials p 3944 N94-33195
Ferric sulfate montmorillonites as Mars soil analogs p 3944 N94-33196

BUREAU DE RECHERCHES GEOLOGIQUES ET MINIERES, ORLEANS (FRANCE).
Structural study in an alteritic region: Contribution of ERS-1 SAR data of the Mauges Plateau (Loire Atlantique, France)
[BRGM-93032] p 3752 N94-32551
Evaluation of the potential of SAR data for mapping of landslide risks
[BRGM-93033] p 3753 N94-32552
European MARS project: The potential integration of SPOT and air- and satellite-borne radar data over two pilot areas for agricultural statistics. PROSPER programme and ERS-1 pilot project
[BRGM-93035] p 3754 N94-32561

BUREAU OF MINES, TUSCALOOSA, AL.
A fuzzy classifier system for process control p 3839 N94-32422

C

CALGARY UNIV. (ALBERTA).
Introduction to electrochemical impedance
[AD-A277081] p 3636 N94-32352

CALIFORNIA INST. OF TECH., PASADENA.
Pulsed expansion of plasma in a magnetic thruster p 3889 N94-31776
Tip effects on the vortex wake of an axisymmetric body at angle of attack p 3570 N94-31907
Hydrodynamics of neutron star interiors and laboratory superfluids p 3936 N94-31949
Nonlinear effects in interfacial fracture p 3737 N94-31974
One: Microphysics of frost metamorphism: Applications to Triton and Mars. Two: A global analysis of the ozone deficit in the upper stratosphere and lower mesosphere. Three: The diabatic circulation in the stratosphere as diagnosed from Microwave Limb Sounder data p 3942 N94-31975
Reliable communication in the presence of severe noise or jamming
[AD-A278410] p 3684 N94-33173
Thermal studies of Martian channels and valleys using Termoskan data: New results p 3944 N94-33194
Carbonate formation on Mars: Latest experiments p 3950 N94-33231

CALIFORNIA POLYTECHNIC STATE UNIV., SAN LUIS OBISPO.
Controls design with crossfeeds for hovering rotorcraft using quantitative feedback theory
[NASA-CR-195765] p 3585 N94-31203

CALIFORNIA UNIV., BERKELEY.
Cooperative program on D3-D (FY 1993)
[DE94-008343] p 3892 N94-32820
Ultrafast x ray sources
[AD-A277455] p 3721 N94-33012
Design and performance of the telescope and detector covers on the Extreme Ultraviolet Explorer satellite p 3605 N94-33309

CALIFORNIA UNIV., BERKELEY. LAWRENCE BERKELEY LAB.
Hydrogenated amorphous silicon (a-Si:H) based gamma camera: Monte Carlo simulations
[DE94-007042] p 3795 N94-31323
Transport properties of quark and gluon plasmas
[DE94-007043] p 3864 N94-31405
Photoelectron diffraction and holography: Present status and future prospects
[DE94-006298] p 3712 N94-31629
Collective acceleration in solar flares
[DE94-006288] p 3953 N94-31632
The effects of amorphous layer regrowth on carbon activation in GaAs and InP
[DE94-006290] p 3899 N94-31634
Various magnet options for Delta launched version of ASTROMAG
[DE94-006292] p 3955 N94-31635
Double rotation NMR studies of zeolites and aluminophosphate molecular sieves
[DE94-007032] p 3866 N94-31637
Aging effects on the microstructure, surface characteristics and wettability of Cu pretinned with Sn-Pb solders
[DE94-007033] p 3641 N94-31638
Modern integral equation techniques for quantum reactive scattering theory
[DE94-007039] p 3857 N94-31639
Work hardening behavior in aluminum alloy 2090
[DE94-007036] p 3643 N94-32064
Design and characterization of a pulsed x ray source for fluorescent lifetime measurements
[DE94-007495] p 3880 N94-32138
X ray optics for science and technology
[AD-A277369] p 3880 N94-32155
Advances and applications of dynamic-angle spinning nuclear magnetic resonance
[DE94-007031] p 3870 N94-32250
Recovery of carboxylic acids at pH greater than pKa
[DE94-007030] p 3636 N94-32376
The limits of intelligence in design
[DE94-004668] p 3819 N94-32668
A guide to experimental elementary particle physics literature, 1988-1992
[DE94-007445] p 3873 N94-32768

CALIFORNIA UNIV., DAVIS.
Proceedings of the Ninth Annual Pacific Climate (PACLIM) Workshop
[DE94-003024] p 3766 N94-32693

CALIFORNIA UNIV., IRVINE.
Theory of protostellar accretion disks p 3931 N94-31136
Computational radiative heat transfer in homogeneous and nonhomogeneous nonscattering media p 3702 N94-31563

A search for 100 TeV gamma ray emission from the x ray binary pulsar 4U 0115+63 using the CYGNUS extensive air-shower array p 3955 N94-31900

CALIFORNIA UNIV., LOS ANGELES.

Origin and thermal evolution of Mars p 3940 N94-31109

Performance predictions for composite materials [AD-A276451] p 3618 N94-31261

Attitude dynamics of spinning rockets in space with internal mass motion p 3601 N94-31802

A numerical method for mixing/chemically reacting compressible flow with finite rate chemistry p 3634 N94-31824

Computer modeling of active experiments in space plasmas p 3890 N94-31927

Transport phenomena in the Earth's plasma sheet p 3772 N94-31970

The manifestations of energetic activity in the galactic center p 3937 N94-32028

Metal clusters: Dynamics and structure [AD-A276842] p 3643 N94-32091

The 14th Annual West Coast Theoretical Chemistry/Statistical Mechanics Conference [AD-A276942] p 3656 N94-32239

Surface boundary conditions and related technical issues concerning Burnett equations for 2-D hypersonic flow [AD-A277322] p 3706 N94-32256

Planetary magnetotails: Magnetic configuration and nonthermal plasma p 3942 N94-32326

Analysis and computation for vortex dynamics and rarefied gases [AD-A277415] p 3708 N94-32581

Recent VH-mode results on D3-D [DE94-007429] p 3891 N94-32611

VLSI for high-speed digital signal processing [AD-A277617] p 3697 N94-32957

Escape of Mars atmospheric carbon through time by photochemical means p 3948 N94-33214

IRTM brightness temperature maps of the Martian south polar region during the polar night: The cold spots don't move p 3949 N94-33222

The influence of thermal inertia on Mars' seasonal pressure variation and the effect of the weather component p 3952 N94-33238

CALIFORNIA UNIV., SAN DIEGO.

The effect of an axial flow component on a circular cylinder wake p 3699 N94-31209

CALIFORNIA UNIV., SAN DIEGO, LA JOLLA.

Positron-molecule interactions [AD-A276542] p 3869 N94-32082

Effects of buoyancy on fluid flows and turbulence [AD-A276586] p 3706 N94-32123

Investigation of superconductivity and magnetism in d and f-electron materials [DE94-008535] p 3907 N94-32933

Faultless software project [AD-A278161] p 3822 N94-33188

CALIFORNIA UNIV., SANTA BARBARA.

Novel growth technologies for in situ formation of semiconductor quantum wire structures [AD-A277188] p 3902 N94-32255

Effect of surface forces on the rheology of particle-liquid systems and the consolidation of ceramic powders [AD-A277092] p 3657 N94-32391

Mechanics of cracking for composite material p 3624 N94-32501

Numerical simulation of quantum many-body systems [DE94-008451] p 3912 N94-32513

High speed, strained layer, multiquantum well, GaInAsP and GaAs lasers and heterostructures [AD-A277287] p 3719 N94-32608

On the mechanics of microballoon-reinforced metal matrix composites [AD-A277928] p 3630 N94-33178

CALIFORNIA UNIV., SANTA CRUZ.

Reactive flows in compact objects p 3934 N94-31567

Evolution of stars and winds in the starburst galaxy M82 p 3934 N94-31758

Line-strength gradients and kinematic profiles in elliptical galaxies p 3934 N94-31788

A critical examination of stellar atmosphere theory for metal-poor K-giant stars p 3927 N94-32308

Ninth International Workshop on Plant Membrane Biology [DE94-005690] p 3794 N94-32769

CALSPAN-BUFFALO UNIV. RESEARCH CENTER, NY.

Calibration and validation studies in the LENS facility [AD-A278403] p 3591 N94-33167

CALSPAN CORP., ARNOLD AFS, TN.

Development of high-pressure diaphragms for the AEDC impulse tunnel [AD-A277053] p 3588 N94-32009

Pre-flight testing of Thermoelectric Quartz Crystal Microbalances (TQCM) for midcourse space experiment (MSX) spacecraft [AD-A277054] p 3610 N94-32010

CALSPAN CORP., BUFFALO, NY.

Monoenergetic neutral particle transport in semi-infinite media [AD-A277155] p 3870 N94-32368

CANADIAN FORCES BASE TRENTON, ASTRA (ONTARIO).

An expert system application for troubleshooting the CF18 F404 engine p 3585 N94-33339

CANADIAN MARCONI CO. LTD., KANATA (ONTARIO).

Study of virtual prototyping of aircraft instruments [CMC-0687-1090] p 3581 N94-31903

CARBORUNDUM CO., NIAGARA FALLS, NY.

Engineering scale development of the Vapor-Liquid-Solid (VLS) process for the production of silicon carbide fibrils [DE94-007132] p 3659 N94-32618

CARNEGIE GROUP, INC., PITTSBURGH, PA.

Knowledge-based commodity distribution planning p 3915 N94-32427

CARNEGIE INSTITUTION OF WASHINGTON, DC.

The tectonic and volcanic evolution of Venus: Catastrophic or gradual? p 3940 N94-31111

Keeping that youthful look p 3941 N94-31112

A tectonic resurfacing model for Venus p 3941 N94-31113

The resurfacing controversy for Venus: An overview and a mechanistic perspective p 3941 N94-31114

CARNEGIE-MELLON UNIV., PITTSBURGH, PA.

List ranking and list scan on the CRAY C-90 [AD-A276411] p 3824 N94-31259

A parallel implementation of the column subtraction algorithm [AD-A275922] p 3810 N94-31343

Digit-Eyes: Vision-based human hand tracking [NASA-CR-195913] p 3803 N94-31447

A paraperspective factorization method for shape and motion recovery [AD-A276513] p 3712 N94-31929

Compiler techniques for managing data motion [AD-A276514] p 3918 N94-31930

An analysis of instruction-cached SIMD computer architecture [AD-A276519] p 3806 N94-31934

Principal component analysis with missing data and its application to object modeling [AD-A276644] p 3845 N94-31939

A redundant disk array architecture for efficient small writes [AD-A276645] p 3815 N94-31940

Large-scale shape optimization: Numerical methods, parallel algorithms, and applications to aerodynamic design p 3815 N94-31966

A theory of distributed time [AD-A276631] p 3815 N94-31994

Incremental recompilation for Standard ML of New Jersey [AD-A276522] p 3815 N94-32080

An MS-DOS file system for UNIX [AD-A276523] p 3816 N94-32081

Utility-based planning [NASA-CR-195878] p 3816 N94-32086

Electronic mail and organizational knowledge: Media use in a global corporation [AD-A276707] p 3678 N94-32121

A differential theory of learning for efficient statistical pattern recognition [AD-A277313] p 3800 N94-32277

Perfect 0, +/- matrices [AD-A277387] p 3848 N94-32286

Case studies of software process improvement methods [AD-A277289] p 3818 N94-32508

SynRGen: An extensible file reference generator [AD-A277678] p 3821 N94-33030

Mixed 0-1 programming by lift-and-project in a branch-and-cut framework [AD-A278045] p 3822 N94-33183

Structuring Z specifications with views [AD-A277618] p 3822 N94-33279

CASE WESTERN RESERVE UNIV., CLEVELAND, OH.

A model of concurrent flow flame spread over a thin solid fuel p 3634 N94-31795

Antiwindup analysis and design approaches for MIMO systems [NASA-CR-195304] p 3584 N94-32075

Control strategies for systems with limited actuators [NASA-CR-195307] p 3727 N94-32741

CATHOLIC UNIV. OF AMERICA, WASHINGTON, DC.

Boundary control of scattering p 3861 N94-31899

A study of physical conditions, radiative transfer and shocks in the interstellar medium p 3937 N94-31963

CENTER FOR MATHEMATICS AND COMPUTER SCIENCE, AMSTERDAM (NETHERLANDS).

Line transects, covariance functions and set approximation [CWI-BS-R9311] p 3846 N94-32084

The use of service limits for efficient operation of multi-station single-medium communication systems [CWI-BS-R9312] p 3677 N94-32085

Multiparameter quantum groups and multiparameter R-matrices [CWI-AM-R9307] p 3846 N94-32106

Kaplan-Meier estimators of interpoint distance distributions for spatial point processes [CWI-BS-R9315] p 3846 N94-32107

Control of a random walk with noisy delayed information [CWI-BS-R9316] p 3846 N94-32108

Numerical detection and continuation of codimension-two homoclinic bifurcations [CWI-AM-R9308] p 3847 N94-32191

Quantum homogeneous spaces, duality, and quantum 2-spheres [CWI-AM-R9309] p 3857 N94-32192

A polling system with a dormant server [CWI-BS-R9313] p 3835 N94-32193

On interpolating random fields using a finite number of observations [CWI-BS-R9314] p 3847 N94-32194

Area-interaction point processes [CWI-BS-R9318] p 3847 N94-32197

Multiserver queues with impatient customers [CWI-BS-R9319] p 3835 N94-32198

Some problems of applied algebra [CWI-AM-R9306] p 3847 N94-32204

On constructing multi-variate orthonormal polynomials associated with spectral distribution functions [CWI-BS-R9310] p 3851 N94-32225

On the reciprocal relationship between life histories and population dynamics [CWI-AM-R9302] p 3793 N94-32226

Steepest descent paths for integrals defining the modified Bessel functions of imaginary order [CWI-AM-R9303] p 3848 N94-32227

The legacy of Kermack and McKendrick [CWI-AM-R9304] p 3793 N94-32228

A cell-cycle model revisited [CWI-AM-R9305] p 3851 N94-32229

Combinatory reduction systems: Introduction and survey [CWI-CS-R9362] p 3849 N94-32349

Stochastic realization of a Gaussian stochastic control system [CWI-BS-R9320] p 3852 N94-32350

The p-q-r-medial axis algorithm requires only local operations [CWI-BS-R9317] p 3849 N94-32507

Finding all periods and initial palindromes of a string in parallel [AD-B175069] p 3827 N94-33002

MADE: A Multiple Application Development Environment [CWI-CS-R9360] p 3822 N94-33097

CENTRAL RESEARCH INST. OF ELECTRIC POWER INDUSTRY, TOKYO (JAPAN).

Stabilization method of A.C. arc plasma [DE94-757268] p 3893 N94-32916

Development of nickel and metal hydride secondary battery [DE94-757270] p 3697 N94-32917

Field operation test of utility interactive load conditioner with photovoltaic cells at a demonstration house [DE94-757271] p 3762 N94-32918

Optimal planning of residential photovoltaic systems under various rate structure [DE94-757272] p 3762 N94-32919

CENTRE D'ETUDE SPATIALE DES RAYONNEMENTS, TOULOUSE (FRANCE).

Restoration of interferometric, polarimetric, radiometric, and textural information in SAR images p 3750 N94-32535

Use of SPOT and ERS-1 to map tropical vegetation and mangrove dynamics in Guiana p 3753 N94-32555

CENTRE D'ETUDES TECHNIQUES DE L'EQUIPMENT, LYON (FRANCE).

The contribution of satellite data in communication infrastructure projects p 3749 N94-32530

CENTRE DE COOPERATION INTERNATIONALE EN RECHERCHE AGRONOMIQUE POUR LE DEVELOPPEMENT, MONTPELLIER (FRANCE).

Statistical analysis and mapping of cotton and food crop cultivation surfaces in the west of Burkina Faso: Contribution of combined SPOT P and XS data p 3757 N94-32575

CENTRE DE RECHERCHES EN PHYSIQUE DE L'ENVIRONNEMENT, VELIZY (FRANCE).
Synergy of thermal infrared and microwave remote sensing for evaporation estimation p 3754 N94-32559
CENTRE DE RECHERCHES EN PHYSIQUE DE L'ENVIRONNEMENT, ISSY-LES-MOULINEAUX (FRANCE).
Radar measurements p 3685 N94-31002
CENTRE NATIONAL D'ETUDES SPATIALES, TOULOUSE (FRANCE).
Subtropical Climates and Their Evolution: From Space-Based Observation to Modelling
[ISBN-2-85-428333-3] p 3776 N94-30981
Radiation/remote sensing: Review of the principal definitions p 3757 N94-30996
Space equipment for Earth observations p 3613 N94-30997
Modeling of the continental biosphere p 3770 N94-31011
Spacecraft materials: Comparison between flight results obtained on LDEF and MIR p 3597 N94-31045
From Optics to Radar, SPOT and ERS Applications
[ISBN-2-85428-345-7] p 3747 N94-32523
From optics to radar: Environmental problems and the SPOT/ERS systems p 3748 N94-32525
Evaluation of surface phase change on large zones p 3755 N94-32567
Differential interferometry study of an earthquake p 3756 N94-32570
Precision and level of artefacts in the computation of digital terrain models by interferometry p 3756 N94-32571
CENTRE NATIONAL DE LA RECHERCHE SCIENTIFIQUE, GIF-SUR-YVETTE (FRANCE).
The Earth's climate: Past, present, and future p 3777 N94-30982
CENTRE NATIONAL DE LA RECHERCHE SCIENTIFIQUE, MONTPELLIER (FRANCE).
Climatic evolution and desertization p 3780 N94-31009
CENTRE NATIONAL DE LA RECHERCHE SCIENTIFIQUE, PALAISEAU (FRANCE).
Dynamic climatology of West Africa p 3778 N94-30988
Dynamics in the tropics and synoptic disturbances p 3778 N94-30990
The use of meteorological satellite data for studying tropical atmospheric phenomena p 3779 N94-31000
CENTRE NATIONAL DE LA RECHERCHE SCIENTIFIQUE, PARIS (FRANCE).
Energetic and general circulation p 3777 N94-30983
General ocean circulation p 3777 N94-30984
Low frequence variability of the ocean atmosphere coupled system p 3777 N94-30986
Interaction processes between the ocean and the atmosphere p 3777 N94-30987
CENTRE NATIONAL DE LA RECHERCHE SCIENTIFIQUE, TOULOUSE (FRANCE).
Effects of the deep tropical convection in the large scale atmospheric flow p 3778 N94-30994
CENTRE NATIONAL DE LA RECHERCHE SCIENTIFIQUE, VERRIERES-LE BUISSON (FRANCE).
The ozone and the physico-chemical processes in tropical regions p 3770 N94-31010
CENTRE NATIONAL DE RECHERCHES METEOROLOGIQUES, TOULOUSE (FRANCE).
Climatologic flux in tropical ocean p 3777 N94-30985
Tropical squall lines p 3778 N94-30992
CENTRE NATIONAL DE TELEDETECTION, TUNIS (TUNISIA).
The use of SPOT, and the contribution of ERS-1, in the assessment of urban pressure on agriculture land in Greater Tunis (Tunisia) p 3749 N94-32534
CENTRE NATIONAL DES TECHNIQUES SPATIALES (ALGERIA).
Quantitative analysis of woody vegetation in Soudano-Sahalian region. Textural approach (application to a Burkina Faso region) p 3757 N94-32574
CHALMERS UNIV. OF TECHNOLOGY, GOETEBORG (SWEDEN).
Modelling the late part of room impulse responses using adaptive filtering: On the recreation of reality
[CTH-E-93-01] p 3859 N94-31076
Quality of sound in large rooms: Alteration of room impulse responses
[CTH-E-93-02] p 3859 N94-31077
A pilot study of comfort criteria and sound quality metrics for sound inside cabins of propeller-driven aircraft
[CTH-F-93-03] p 3859 N94-31090
Model updating of vibrating systems based on measured or calculated frequency response functions
[CTH-E-93-03] p 3732 N94-31091
Vibrations of a heavy truck diesel engine and gearbox unit: Examining structure-borne sound transmission with statistical energy analysis
[CTH-E-93-04] p 3722 N94-31194
CHICAGO UNIV., IL.
Nuclear physics and astrophysics
[DE94-007168] p 3939 N94-33147
CINCINNATI UNIV., OH.
Study of dynamic stall phenomenon and its control using vorticity, stream function and circulation form of the unsteady Navier-Stokes equations p 3572 N94-32714
CITY COLL. OF THE CITY UNIV. OF NEW YORK, NY.
Studies in physico-chemical hydrodynamics of extended systems
[DE94-006752] p 3706 N94-32149
CITY UNIV. OF NEW YORK, NY.
Applied harmonic analysis
[AD-A278384] p 3685 N94-33353
A new tool for signal processing
[AD-A278385] p 3685 N94-33354
CLARK-ATLANTA UNIV., GA.
Novel electroactive polymers and block copolymers
[AD-A276119] p 3650 N94-31509
CLARKSON UNIV., POTSDAM, NY.
Reliability of multilayer copper/polyimide
[AD-A276228] p 3650 N94-31284
Trajectory learning with a direct drive robotic manipulator p 3831 N94-31794
CLEMSON APPAREL RESEARCH, PENGLETON, SC.
Minimization of carpal tunnel syndrome
[AD-A276409] p 3795 N94-31363
CLEMSON UNIV., SC.
The magnesium chelation step in chlorophyll biosynthesis
[DE94-008727] p 3794 N94-32890
COASTAL ENGINEERING RESEARCH CENTER, VICKSBURG, MS.
Index and bulk parameters for frequency-direction spectra measured at CERC Field Research Facility
[AD-A277759] p 3791 N94-33085
COLORADO SCHOOL OF MINES, GOLDEN.
Proceedings of the 4th Tunnel Detection Symposium on Subsurface Exploration Technology
[AD-A276372] p 3771 N94-31369
COLORADO UNIV., BOULDER.
Near resonant absorption by atoms in intense fluctuating laser fields
[DE94-005873] p 3714 N94-31200
Extreme ultraviolet opacity sources in the DA white dwarf G191-B2B p 3924 N94-31210
Algorithms and structures for real-time signal processing
[AD-A276101] p 3810 N94-31277
Compressible convection with ionization p 3911 N94-31498
Toroidal pinch experiments
[DE94-005876] p 3887 N94-31558
Muscle disuse through tail-suspension: Etiology and therapeutics p 3796 N94-31746
Numerical simulation of combined external/internal transonic flow on the forebody/inlet of the AV-8B Harrier 2 p 3569 N94-31759
Surface fluxes of trace gases derived from convective-layer profiles p 3704 N94-31774
Collisional and chaotic transport of energetic particles in toroidal plasma
[DE94-006504] p 3889 N94-31787
A new inverse method for generating high-speed aerodynamic flows with application to waverider design p 3569 N94-31828
Steady thermal convection in multiple liquid layers p 3705 N94-31844
Error analysis of real-time and post-processed orbit determination for the Geosat Follow-On altimetric satellite using GPS tracking p 3576 N94-31845
Radio emission from pre-main-sequence stars p 3955 N94-31890
Finite element analysis of time-independent superconductivity p 3691 N94-31905
Estimation and analysis of climate-scale rainfall over the Tropical Pacific p 3783 N94-32030
The effects of altimeter sampling characteristics: Some Geosat examples
[AD-A276899] p 3747 N94-32214
Time-resolved IR spectroscopy, energy transfer, and state-to-state collision dynamics of atmospheric species
[AD-A277372] p 3773 N94-32338
Studies of an optical multi-processor interconnect
[AD-A277093] p 3861 N94-32392
Forced libration of Mercury and geodetic determination of a possible fluid core p 3774 N94-32493
Numerical analysis of transonic wing buffet p 3586 N94-32713
Boundary element analysis of three-dimensional nonlinear hydrodynamics in a reduced gravity environment p 3668 N94-32715
A large motion zero-gravity suspension system for experimental simulation of orbital construction and deployment
[NASA-CR-195881] p 3668 N94-33037
Mars atmospheric dust properties: A synthesis of Mariner 9, Viking, and Phobos observations p 3945 N94-33200
Mars atmospheric loss and isotopic fractionation by solar-wind-induced sputtering and photochemical escape p 3947 N94-33208
Temporal and spatial mapping of atmospheric dust opacity and surface albedo on Mars p 3947 N94-33211
The distribution of Martian ground ice at other epochs p 3948 N94-33218
COLUMBIA UNIV., NEW YORK, NY.
High beta tokamak research
[DE94-006513] p 3888 N94-31664
Combinatorial ion sensors
[AD-A276567] p 3825 N94-32032
Theoretical studies of electron transfer and optical spectroscopy
[DE94-006985] p 3871 N94-32375
Finite-element modeling of the blockage and scattering of LG propagation
[AD-A277430] p 3775 N94-33006
COLUMBIA UNIV., PALISADES, NY.
Investigation of carbon dioxide in the central South Pacific Ocean (WOCE Sections P-16C and P-17C) during the TUNES/2 expedition of the R/V Thomas Washington, July-August, 1991
[DE94-006638] p 3763 N94-31347
Evolution of upwelling fronts off the coast of Portugal
[NASA-CR-195692] p 3790 N94-33045
COMMUNICATIONS RESEARCH CENTRE, OTTAWA (ONTARIO).
SATCOM feasibility study for search and rescue aircraft
[DSIS-94-01083] p 3575 N94-31902
Modular neural network architectures p 3838 N94-33156
COMPUTATIONAL FLUID DYNAMICS RESEARCH CORP., HUNTSVILLE, AL.
Advanced CFD methodology for fast transients encountered in nonlinear combustion instability problems. Volume 2: User's guide
[NASA-CR-191352] p 3637 N94-32694
Advanced CFD methodology for fast transients encountered in nonlinear combustion instability problems. Volume 1: Theory and validation
[NASA-CR-191351] p 3637 N94-32696
COMPUTATIONAL MECHANICS CO., AUSTIN, TX.
New micro- and macroscopic models of contact and friction
[AD-A277240] p 3726 N94-32320
COMPUTER GRAPHICS SYSTEMS DEVELOPMENT CORP., MOUNTAIN VIEW, CA.
Texture library for 3-dimensional visualization systems
[AD-A276125] p 3917 N94-31829
CONCORDIA UNIV., LOYOLA CAMPUS, MONTREAL (QUEBEC).
Finite element vorticity-based methods for the solution of the incompressible and compressible Navier-Stokes equations
[ISBN-0-315-87265-9] p 3703 N94-31730
Linearly separable stack-like architecture for the design of weighted order statistic filters with application in image processing
[ISBN-0-315-87284-5] p 3675 N94-31731
Common property resources and low-level flying in Labrador: Flight, fight or fancy?
[ISBN-0-315-87318-3] p 3924 N94-31732
CONCORDIA UNIV., MONTREAL (QUEBEC).
Production of charginos and neutralinos for the reaction positron electron yields Z' boson yields chargino(+) (sub i) chargino(-) (sub j) or neutralino (sub i) neutralino (sub j) in SU(2) (sub L) x SU(2) (sub R) x U(1) (sub B-L)
[ISBN-0-315-87316-7] p 3867 N94-31832
CONDUCTUS, INC., SUNNYVALE, CA.
YBCO Josephson Junction arrays
[AD-A277426] p 3908 N94-33005
High temperature superconducting Josephson junction array systems, phase 1
[AD-A277937] p 3908 N94-33246
CONNECTICUT UNIV., STORRS.
Auditory perception
[AD-A277414] p 3800 N94-32419
CONSIGLIO NAZIONALE DELLE RICERCHE, BARI (ITALY).
Feasibility evaluation of new data interpretation approaches for vegetation analysis from airborne imaging spectroscopy p 3745 N94-31862
COPENHAGEN UNIV. (DENMARK).
Monitoring land cover and crop types in Denmark using ERS-1 SAR and optical satellite images p 3748 N94-32528

CORNELL UNIV., ITHACA, NY.
Plains tectonism on Venus: The deformation belts of Lavinia Planitia p 3941 N94-31115
Theoretical studies of magnetohydrodynamic equilibria and dynamics of a solar coronal loop p 3953 N94-31792
Near infrared surveys of high mass star forming regions p 3925 N94-31898
Multigrid diagonal implicit solutions for compressible turbulent flows and their evaluation p 3705 N94-31941
Toughening mechanisms in the high strain rate deformation of rubber-modified polymer glasses p 3653 N94-31942
High-resolution synthetic aperture radar observations of the Moon p 3676 N94-31952
Measuring the Hubble constant and our Virgo-infall velocity independently p 3926 N94-31968
Theoretical studies on ionospheric irregularities and ion diode performance
[AD-A277115] p 3772 N94-31984
Radar scattering from the summer polar mesosphere: Theory and observations p 3772 N94-32077
A state variable material model for superplastic titanium-6 percent Al-4 percent V p 3644 N94-32498
Induced adsorption of chloride and bromide by submonolayer amounts of copper underpotentially deposited on Pt(111)
[AD-A278023] p 3648 N94-33182
Polar sediment accumulation: Role of surface winds at the two poles p 3951 N94-33233
CRANFIELD INST. OF TECH., BEDFORD (ENGLAND).
Drug-related problems in the workplace
[CRANFIELD-AERO-9306] p 3914 N94-31538
Fully discrete arbitrary-order schemes for a model hyperbolic conservation law
[CRANFIELD-AERO-9307] p 3843 N94-31539
A simplified Von Neumann method for linear stability analysis
[CRANFIELD-AERO-9310] p 3843 N94-31540
Multidimensional WAF-type schemes for model conservation laws
[CRANFIELD-AERO-9312] p 3843 N94-31541
Viscous limiter functions for model convection-diffusion equations
[CRANFIELD-AERO-9103] p 3702 N94-31559
CREARE, INC., HANOVER, NH.
The 4 K Stirling cryocooler demonstration
[NASA-CR-191792] p 3669 N94-32484
CRYSTAL SYSTEMS, INC., SALEM, MA.
Development of materials for spectral hole burning applications
[AD-A278408] p 3909 N94-33324
CSA ENGINEERING, INC., PALO ALTO, CA.
Structural integrity of intelligent materials and structures
[AD-A278397] p 3630 N94-33165

D

DAKOTA SCIENTIFIC SOFTWARE, INC., RAPID CITY, SD.
A high-speed linear algebra library with automatic parallelism p 3828 N94-32440
DARTMOUTH COLL., HANOVER, NH.
Self-consistent effects of magnetospheric hydromagnetic waves on ring current ions
[AD-A277406] p 3774 N94-32346
DAVID SARNOFF RESEARCH CENTER, PRINCETON, NJ.
High performance YBCO films
[AD-A276493] p 3897 N94-31531
Models of the neuronal mechanisms of target localization of the barn owl
[AD-A277332] p 3797 N94-32623
Ceramic and metal composite circuit-board-level technology for application specific electronic modules (ASEM)
[AD-A277961] p 3630 N94-33180
DAYTON UNIV., OH.
Visual evaluation of computer-generated textures
[AD-A277201] p 3816 N94-32093
Correlation filter synthesis using neural networks
[AD-A278124] p 3836 N94-33043
DAYTON UNIV. RESEARCH INST., OH.
Variable-resolution imagery for flight simulation
[AD-A276199] p 3586 N94-31058
DEFENCE AND CIVIL INST. OF ENVIRONMENTAL MEDICINE, NORTH YORK (ONTARIO).
Proceedings of the DCIEM Diver Thermal Protection Workshop
[DCIEM-92-10] p 3795 N94-31738
DEFENCE AND CIVIL INST. OF ENVIRONMENTAL MEDICINE, TORONTO (ONTARIO).
Review of pharmacological approach to improve cold tolerance p 3796 N94-31740
Lipid metabolism in cold-exposed humans p 3796 N94-31741
DEFENCE RESEARCH ESTABLISHMENT ATLANTIC, DARTMOUTH (NOVA SCOTIA).
CRAD Signal and Information Processing Working Group Workshop on Neural networks, volume 1
[DREA-TC-93-305-VOL-1] p 3836 N94-33149
Some neural computing approaches to target tracking p 3837 N94-33151
Multi-sensor data fusion for target acquisition p 3837 N94-33154
Numerical optimization techniques in neural network training p 3838 N94-33158
DEFENCE RESEARCH ESTABLISHMENT, OTTAWA (ONTARIO).
Peak detection of Swerling type targets. Part 1: Detection probabilities in white noise
[AD-A276217] p 3670 N94-31062
Evaluation of HardSys/HardDraw, an expert system for electromagnetic interactions modelling
[AD-A276218] p 3670 N94-31063
Description of a package for the analysis and display of the results of numerical simulations
[AD-A276285] p 3841 N94-31252
An adaptive Kalman filter excisor for suppressing narrowband interference
[AD-A276286] p 3671 N94-31253
Subspace estimation without eigenvectors for adaptive beamforming
[AD-A276287] p 3671 N94-31254
Laser safety manual for DREO
[AD-A276288] p 3714 N94-31255
The application of a radial basis function neural network for radar tracking over the sea p 3686 N94-33150
Automatic modulation recognition p 3686 N94-33153
DEFENCE RESEARCH ESTABLISHMENT PACIFIC, VICTORIA (BRITISH COLUMBIA).
Ultrasonic characterization of damage in a simulated CF-18 composite structure
[DREP-LN-93-26] p 3730 N94-31872
Nearest-neighbour search in constant time: An alternative to neural networks for pattern matching applications p 3838 N94-33157
DEFENCE RESEARCH ESTABLISHMENT SUFFIELD, RALSTON (ALBERTA).
Periodic and chaotic signal generation in a recursive artificial neural network p 3686 N94-33155
DEFENSE INFORMATION SYSTEMS AGENCY, ARLINGTON, VA.
DoD information systems capacity management function
[AD-A275987] p 3916 N94-31355
DEFENSE MAPPING AGENCY SYSTEMS CENTER, FAIRFAX, VA.
Evolving software reengineering technology for the emerging innovative-competitive era p 3823 N94-32439
DEFENSE TECHNICAL INFORMATION CENTER, ALEXANDRIA, VA.
DTIC Thesaurus on diskette with dBase 4.1 runtime (computer diskette)
[AD-M000306] p 3922 N94-33256
DTIC Thesaurus on diskette (ASC2) (computer diskette)
[AD-M000309] p 3922 N94-33257
DTIC Thesaurus on diskette without runtime (computer diskette)
[AD-M000310] p 3923 N94-33258
DTIC Thesaurus on diskette without runtime (computer diskette)
[AD-M000312] p 3923 N94-33259
DELAWARE UNIV., NEWARK.
Performance metrics for low probability of intercept-communication system
[AD-A277346] p 3677 N94-32073
DENMAR, INC., MARIETTA, GA.
MOM3D method of moments code theory manual
[NASA-CR-189594] p 3682 N94-32897
DENVER UNIV., CO.
Counting particles emitted by stratospheric aircraft and measuring size of particles emitted by stratospheric aircraft
[NASA-CR-195908] p 3769 N94-33170
DEPARTMENT OF ENERGY, NEW YORK, NY.
Low power, constant-flow air pump systems
[DE94-007463] p 3727 N94-32758
DEPARTMENT OF ENERGY, WASHINGTON, DC.
Total Quality Management implementation guidelines
[DE94-007232] p 3915 N94-32723

Independent safety assessment of the Topaz-2 space nuclear reactor power system
[DE94-008653] p 3877 N94-32879
DEPARTMENT OF THE NAVY, WASHINGTON, DC.
System for monitoring and analyzing field energy exposure
[AD-D016115] p 3681 N94-32625
Passive, multi-channel fiber optic rotary joint assembly
[AD-D016116] p 3882 N94-32626
Flexible drive shaft coupling
[AD-D016095] p 3727 N94-32718
Torque-balanced extendable fiber optic cable
[AD-D016097] p 3882 N94-32719
Fiber optic continuous true time-delay modulator
[AD-D016098] p 3883 N94-32720
Oxidation resistant copper
[AD-D016099] p 3696 N94-32721
Vibration dampener and method for making same
[AD-D016094] p 3739 N94-32733
Multi-line passive fiber optic slipring
[AD-D016092] p 3883 N94-32738
Mass-loaded coating for reducing the resonant frequency of a ceramic disc
[AD-D016095] p 3660 N94-32739
Magnetohydrodynamic boundary layer control system
[AD-D016120] p 3710 N94-32958
Bioluminescence bathyphotometer
[AD-D016102] p 3790 N94-32959
Method and apparatus for inhibiting the disbonding of a paint from metal surfaces
[AD-D016106] p 3663 N94-32960
Relative motion pinwheel
[AD-D016107] p 3577 N94-32961
Grounding ring for ground adapters
[AD-D016118] p 3697 N94-32962
Buffered feedthrough crossbar switch
[AD-D016145] p 3697 N94-32967
Multifrequency, rapidly sequenced or simultaneous tunable laser
[AD-D016169] p 3721 N94-32968
Dielectric viscometer including fixed and variable cells
[AD-D016139] p 3639 N94-32973
Active vortex control for a high performance wing
[AD-D016140] p 3573 N94-32974
Interpenetrating polymer network acoustic damping material
[AD-D016141] p 3663 N94-32975
Digital beamforming and filtering circuit
[AD-D016142] p 3697 N94-32976
Electron acceleration system
[AD-D016143] p 3893 N94-32977
Toroidal computer memory for serial and parallel processors
[AD-D016144] p 3807 N94-32978
Acoustic window
[AD-D016171] p 3862 N94-33017
Surface conforming flexible eddy current probe for scanning varying surface contours
[AD-D016173] p 3627 N94-33018
Lightweight zinc electrode
[AD-D016181] p 3698 N94-33181
DEUTSCHE FORSCHUNGSANSTALT FUER LUFT- UND RAUMFAHRT, OBERPFAFFENHOFEN (GERMANY).
Inflight calibration, preprocessing, and data evaluation of GER 2 imaging spectrometry data p 3744 N94-31858
DIFFRACTO LTD., WINDSOR (ONTARIO).
Location of impact damage sites in composite aircraft structures, task 3.4.1
[DSIS-94-01590] p 3621 N94-31892
DIMENSIONS INTERNATIONAL, INC., ALEXANDRIA, VA.
Space flight risk data collection and analysis project: Risk and reliability database
[NASA-CR-195879] p 3603 N94-32494
DORNIER SYSTEM G.M.B.H., FRIEDRICHSHAFEN (GERMANY).
High precision moving magnet chopper for variable operation conditions p 3605 N94-33307
DOUGLAS AIRCRAFT CO., INC., LONG BEACH, CA.
Resin transfer molding for advanced composite primary wing and fuselage structures p 3628 N94-33128
DOW CORNING CORP., CARROLLTON, KY.
Methyl chloride by way of oxyhydrochlorination of methane
[DE94-009129] p 3637 N94-32767
DRAPER (CHARLES STARK) LAB., INC., CAMBRIDGE, MA.
Fuzzy logic application for modeling man-in-the-loop space shuttle proximity operations
[NASA-CR-188283] p 3835 N94-32359
A six degree of freedom, plume-fuel optimal trajectory planner for spacecraft proximity operations using an A* node search
[NASA-CR-188285] p 3601 N94-32388

Hierarchical modeling for reliability analysis using Markov models
[NASA-CR-188288] p 3731 N94-32862
Performance analysis of an integrated GPS/inertial attitude determination system
[NASA-CR-188289] p 3577 N94-32864
Limiting vibration in systems with constant amplitude actuators through command preshaping
[NASA-CR-188284] p 3739 N94-32907
Investigation of drive-reinforcement learning and application of learning to flight control
[AD-A277442] p 3801 N94-33053
Design of a high-speed reliable ball bearing
p 3606 N94-33314

DREXEL UNIV., PHILADELPHIA, PA.
Fuel property effects on engine combustion processes
[DE94-005529] p 3631 N94-31153
Mechanics of the single fiber pullout problem with several interface conditions p 3623 N94-32078

DUKE UNIV., DURHAM, NC.
High-resolution numerical methods for compressible multi-phase flow in hierarchical porous media
[DE94-008261] p 3707 N94-32410

DURHAM UNIV. (ENGLAND).
F0-975, A0-980 as eye-witnesses of confinement
[PB94-147105] p 3868 N94-31923

E

ECC INTERNATIONAL CORP., ORLANDO, FL.
The effects of Above Real-Time Training (ARTT) in an F-16 simulator p 3591 N94-32474

ECOLE CENTRALE DE LYON (FRANCE).
Contributions to the validation of the CJS model for granular materials
[ECL-92-56] p 3733 N94-31376
Development and characterization of intermediary layers allowing the bond between a metal alloy and a plasma sprayed ceramic
[ECL-91-39] p 3619 N94-31377
Development and application of a multimesh auto-adaptive finite element method for the calculation of an electric arc plasma
[ECL-89-03] p 3886 N94-31378
Methodology for damage study of a tube-grill contact
[ECL-92-49] p 3734 N94-31562
Aeroelastic vibrations of lifting surfaces
[ECL-91-01] p 3585 N94-31677
Cracking induced in small fretting: Application to the case of aeronautical aluminum alloys
[ECL-92-50] p 3735 N94-31870

ECOLE NATIONALE SUPERIEURE DES TELECOMMUNICATIONS, PARIS (FRANCE).
Triangular norms and conorms: A general tool for generating fuzzy mathematical morphologies
[TELECOM-93-D-001] p 3839 N94-31092
Channel equalization for block transmission systems
[TELECOM-93-D-002] p 3670 N94-31093
The generalized multi delay adaptive filter: Structure and convergence analysis
[TELECOM-93-D-004] p 3808 N94-31094
Computing the precision of localization in a plane using projective invariants
[TELECOM-93-D-005] p 3840 N94-31095
Tracking roads in an aerial image by Kalman filtering
[TELECOM-93-D-007] p 3711 N94-31096
Phase unwrapping problems in ISAR images
[TELECOM-93-D-008] p 3670 N94-31097
Entropy, information (and image), part 1
[TELECOM-93-D-009] p 3910 N94-31098
Implanting algorithms on parallel machines
[TELECOM-93-D-017] p 3823 N94-31099
Report of the 'Mathematical Models for Neural Networks' course
[TELECOM-93-D-019] p 3828 N94-31100
Automatic extraction of cartographic objects by fusion of data extracted from satellite images
[TELECOM-93-E-001] p 3742 N94-31165
A generic model for data acquisition: Connectionist methods of information processing
[TELECOM-93-E-003] p 3730 N94-31166
Regular wavelets: Application to fixed image compression
[TELECOM-93-E-004] p 3858 N94-31167
A neuron network for image classification: From algorithm to implantation
[TELECOM-93-E-005] p 3687 N94-31168
Modulation and coding for the Gaussian channel, possibly affected by fluctuations
[TELECOM-93-E-009] p 3840 N94-31169
Study of continuous-time and mixed analog-digital operators
[TELECOM-93-E-010] p 3687 N94-31170
Economic analysis of the hertzian spectrum
[TELECOM-93-E-012] p 3670 N94-31171
Standardization and intellectual property control: A reflection on the informatics case
[TELECOM-93-E-016] p 3915 N94-31172
The conoscopic microscope
[TELECOM-93-E-017] p 3877 N94-31173
Fast autodidactic adaptive equalization algorithms
[TELECOM-93-E-018] p 3670 N94-31174
A probabilistic view of Datalog parallelization
[TELECOM-93-D-021] p 3824 N94-31183
ART: Adaptive Resonance Theory
[TELECOM-93-D-020] p 3829 N94-31193
Interactive reconstruction of anatomical structures with free-form surfaces
[TELECOM-93-E-002] p 3794 N94-31195
Fast nonsupervised 3D registration of PET and MR images of the brain
[TELECOM-93-C-006] p 3798 N94-33069

ECOLE NORMALE SUPERIEURE, PARIS (FRANCE).
Behavior and dynamics of tropical forests and savannas p 3757 N94-31004

ECOLE POLYTECHNIQUE, MONTREAL (QUEBEC).
Feasibility study of cold expansion processes modelling
[DSIS-94-01186] p 3735 N94-31849

EDGERTON, GERMESHAUSEN AND GRIER, INC., IDAHO FALLS, ID.
Feasibility study to evaluate plasma quench process for natural gas conversion applications
[DE94-000086] p 3758 N94-31234
Inorganic polymer engineering materials
[DE94-008519] p 3659 N94-32655
Preliminary evaluation of the University of South Florida Mobile Data Acquisition System, the Idaho National Engineering Laboratory Versatile Data Acquisition System, and the Autologger Vehicle User Survey System produced by Instrumental Solutions of Ottawa, Canada for the Site Operator Program Field Data Collection
[DE94-008514] p 3920 N94-32827
EDD-7 Electric Charge Point Meter test results
[DE94-008515] p 3696 N94-32828

EDGEWOOD ARSENAL, ABERDEEN PROVING GROUND, MD.
Remote infrared vapor detection of volatile organic compounds
[AD-A276982] p 3746 N94-31999
Influence of trace components on the viscoelastic properties of a polymer solution
[AD-A277171] p 3656 N94-32253

EG AND G ENERGY MEASUREMENTS, INC., GOLETA, CA.
On the nature of striae in strontium barium niobate
[DE94-006486] p 3901 N94-32176

EG AND G ENERGY MEASUREMENTS, INC., IDAHO FALLS.
Joining of silicon nitrides using oxynitride glasses
[DE94-008517] p 3658 N94-32517
Energy storage specification requirements for hybrid-electric vehicle
[DE94-008642] p 3694 N94-32521

EG AND G ENERGY MEASUREMENTS, INC., LAS VEGAS, NV.
A 10 GHz bandwidth, single transient, digitized oscilloscope with 20 GHz capability
[DE94-005400] p 3713 N94-32728

EG AND G MOUND APPLIED TECHNOLOGIES, MIAMISBURG, OH.
Nd-YAG laser welding of the fiber optic connector to the header shell on the 2SL actuator
[DE94-006104] p 3723 N94-31621

ELECTRIC POWER RESEARCH INST., PALO ALTO, CA.
Creep-fatigue criteria and inelastic behavior of modified 9Cr-1Mo steel at elevated temperatures
[DE94-007915] p 3642 N94-31918

ELECTRONIC ASSOCIATES, INC., LONG BRANCH, NJ.
Construction of a parallel processor for simulating manipulators and other mechanical systems
[NASA-CR-191327] p 3826 N94-32482

ELECTRONICS RESEARCH LAB., ADELAIDE (AUSTRALIA).
Real time character recognition for F-111C video tape records
[AD-A277061] p 3580 N94-32263
Parallel processing for differencing and histogramming
[AD-A277060] p 3826 N94-32274

ELORET CORP., PALO ALTO, CA.
Arc-heater performance research
[NASA-CR-195821] p 3912 N94-32774
Computed potential energy surfaces for chemical reactions
[NASA-CR-195835] p 3639 N94-33036

ENSCO, INC., MELBOURNE, FL.
A systems approach to computer-based training
p 3823 N94-32436

ENVIRONMENTAL RESEARCH INST. OF MICHIGAN, ANN ARBOR.
Satellite direct readout: Opportunities for science education
[AD-A276257] p 3609 N94-31292
Validation support of the ERIM ocean model
[AD-A277364] p 3788 N94-32284

ERGONOMIC-INTERFACE KEYBOARD SYSTEMS, INC., LA JOLLA, CA.
THE VERTICAL p 3806 N94-32435

EUROPEAN OFFICE OF AEROSPACE RESEARCH AND DEVELOPMENT, FPO NEW YORK, NY.
Workshop on Models for Plasma Spectroscopy
[AD-A276565] p 3890 N94-32031

EUROPEAN SPACE AGENCY, PARIS (FRANCE).
European business confronted with the 21st century: Men, the essential risk
[ESA-SP-1167] p 3914 N94-31181
Guide to software quality assurance
[ESA-PSS-05-11-ISSUE-1] p 3809 N94-31223

EUROPEAN SPACE AGENCY. ESRIN, FRASCATI (ITALY).
SAR interferometry with ERS-1 p 3755 N94-32566

EUROPEAN SPACE AGENCY. EUROPEAN SPACE RESEARCH AND TECHNOLOGY CENTER, ESTEC, NOORDWIJK (NETHERLANDS).
Follow-up on the effects of the space environment on UHCRE thermal blankets p 3592 N94-31018
Europe at the crossroads: The future of its satellite communications industry
[ESA-SP-1166] p 3670 N94-31182
Atmosphere quality standards in manned space vehicles
[ESA-PSS-03-401-ISSUE-1] p 3802 N94-31224
European Imaging Spectroscopy Aircraft Campaign
[ESA-SP-360] p 3743 N94-31853
MARSNET: A European network of stations on the surface of Mars p 3945 N94-33199
Dielectric properties of Mars' surface: Proposed measurement on a Mars lander p 3951 N94-33237

EUROPEAN SPACE TRIBOLOGY LAB., RISLEY (ENGLAND).
A comparison of the performance of solid and liquid lubricants in oscillating spacecraft ball bearings
p 3606 N94-33311
Development of long-life, low-noise linear bearings for atmospheric interferometry p 3606 N94-33312

EXECUTIVE OFFICE OF THE PRESIDENT, WASHINGTON, DC.
Aeronautics and space report of the President: Fiscal year 1993 activities p 3966 N94-32854

F

FAIRFAX MATERIALS RESEARCH, INC., ALEXANDRIA, VA.
Computer modelling of cyclic deformation of high-temperature materials
[AD-A277056] p 3623 N94-32012

FEDERAL AVIATION ADMINISTRATION, ATLANTIC CITY, NJ.
Evaluation for the development of taxiway lighting intensity standards
[AD-A276706] p 3588 N94-32120
Shearographic inspection of a DeHavilland DHC-7
[AD-A276716] p 3566 N94-32157
Civil tiltrotor market penetration: Effects on Northeast corridor airport delay
[AD-A277534] p 3576 N94-32955

FEDERAL AVIATION ADMINISTRATION, CAMBRIDGE, MA.
Flight technical error for category B non-precision approaches and missed approaches using non-differential GPS for course guidance
[PB94-142734] p 3576 N94-31680
Heliport Noise Model (HNM) version 2.2 (user's guide)
[AD-A277072] p 3861 N94-32418
Cockpit Electronic Display Workshop: Proceedings (computer diskette)
[AD-M000330] p 3805 N94-33171
Cockpit Electronic Display Workshop: A synopsis
[AD-A277728] p 3583 N94-33280

FEDERAL AVIATION ADMINISTRATION, WASHINGTON, DC.
FAA aviation forecasts, fiscal years 1994-2005
[AD-A277808] p 3566 N94-33016
Synthetic vision technology demonstration. Volume 1: Executive summary
[DOT/FAA/RD-93/40-VOL-1] p 3582 N94-33076
Synthetic vision technology demonstration. Volume 2: Sensor tower testing
[DOT/FAA/RD-93/40-VOL-2] p 3582 N94-33077
Synthetic vision technology demonstration. Volume 3: Flight tests
[DOT/FAA/RD-93/40-VOL-3] p 3582 N94-33078

Synthetic vision technology demonstration. Volume 4: Appendices
[DOT/FAA/RD-93/40-VOL-4] p 3583 N94-33079

FERMI NATIONAL ACCELERATOR LAB., BATAVIA, IL.
State of hadron collider physics
[DE94-005279] p 3863 N94-31147
Final results from the SDC dopant search for new green wavelength shifting (WLS) fibers, volume 1
[DE94-006744] p 3878 N94-31271
Study of B(0) - bar-B(0) mixing in D0
[DE94-006000] p 3897 N94-31506
Hyperon polarization and magnetic moments
[DE94-006041] p 3864 N94-31507
B lifetimes at CDF
[DE94-006850] p 3866 N94-31669
Study of associated gauge boson production at D0: W gamma production
[DE94-006951] p 3866 N94-31670
The D0 upgrade
[DE94-006953] p 3867 N94-31671
Design of new polymers to improve radiation stability of plastic scintillators
[DE94-008220] p 3652 N94-31764
The future of high energy physics in the US statement for the Science Subcommittee of the House Science, Space and Technology Committee
[DE94-008986] p 3876 N94-32586
Jet physics and QCD tests at the Tevatron collider
[DE94-008987] p 3871 N94-32587
The future of high-energy physics in the US: Statement for the 1994 HEPAP Subpanel
[DE94-008994] p 3876 N94-32588
A search for rapidity gaps in jet events and a study of color coherence in multijet events at D0
[DE94-006849] p 3872 N94-32627
Proceedings of the Workshop on B Physics at Hadron Accelerators
[DE94-007961] p 3877 N94-32748
Studies of jet production with the D0 detector
[DE94-008271] p 3873 N94-32780
Hyperon polarization, crystal channeling, and E781 at Fermilab
[DE94-008224] p 3877 N94-32802

FLORIDA INST. OF TECH., MELBOURNE.
Development of phase-only filters for sensor imagery
[AD-A276722] p 3880 N94-32151

FLORIDA STATE UNIV., TALLAHASSEE.
Recurvature dynamics of a typhoon
[AD-A276792] p 3784 N94-32164
Statistical inference for coherent systems from partial information and in resampling techniques in survival analysis
[AD-A277382] p 3852 N94-32339

FLORIDA UNIV., GAINESVILLE.
International Journal of Quantum Chemistry. Quantum Biology Symposium number 20. Proceedings of the International Symposium on the Application of Fundamental Theory to Problems of Biology and Pharmacology
[AD-A276294] p 3792 N94-31294
Mechanisms of temporal pattern discrimination by human observers
[AD-A277407] p 3801 N94-32577
Complex auditory signals
[AD-A278391] p 3862 N94-33146

FOM-INST. VOOR PLASMAFYSICA, RIJNHUIZEN, JUTPHAAS (NETHERLANDS).
Free electrons as a versatile source of coherent radiation
[ETN-94-96011] p 3715 N94-31545
International Free Electron Laser Conference
[AD-A277576] p 3721 N94-33000

FOOD AND AGRICULTURE ORGANIZATION OF THE UNITED NATIONS, ROME (ITALY).
ERS-1 SAR and optical data for land use/land cover mapping: A case study in a savannah zone of Guinea
p 3755 N94-32565

FOSTER-MILLER ASSOCIATES, INC., WALTHAM, MA.
Fracture and fatigue strength evaluation of multiple site damaged aircraft fuselages - curved panel testing and analysis
[AD-A277100] p 3579 N94-32015

FUEL CELL ENGINEERING CORP., DANBURY, CT.
Detailed design of the 2MW Demonstration Plant
[DE94-000042] p 3762 N94-32823

FUTUREVISION, BUCHANAN, GA.
Space industrialization: A guide to government information
[RELEASE-1.2] p 3916 N94-31338

G

G AND H TECHNOLOGY, INC., CAMARILLO, CA.
Payload holddown and release mechanism
p 3607 N94-33321

GALAXY SCIENTIFIC CORP., PLEASANTVILLE, NJ.
Rotorcraft ditchings and water-related impacts that occurred from 1982 - 1989, phase 2
[AD-A276473] p 3574 N94-31246
Fatigue testing of 2024-T3 material after four cycles of PMB stripping
[AD-A276926] p 3644 N94-32237

GATES LEARJET CORP., WICHITA, KS.
Aircraft icing handbook (update)
[AD-A276499] p 3574 N94-31678

GEC-MARCONI RESEARCH CENTRE, CHELMSFORD (ENGLAND).
Assessment of region-based methods for automated SAR/optical registration, attribute extraction, and classification p 3750 N94-32536

GENCORP AEROJET, SACRAMENTO, CA.
Real-time sensor data validation
[NASA-CR-195295] p 3616 N94-33099

GENERAL ATOMIC CO., SAN DIEGO, CA.
Operation of D3-D with all-graphite walls
[DE94-004858] p 3886 N94-31304
Noninductive current drive experiments on D3-D, and future plans
[DE94-007373] p 3886 N94-31324
FWCD and ECCD experiments on D3-D
[DE94-007371] p 3890 N94-32201
Fusion applications of high power millimeter wave sources
[DE94-007374] p 3718 N94-32202
An edge density fluctuation diagnostic for D3-D using lithium beams
[DE94-008554] p 3890 N94-32519
Experimental survey of the L-H transition conditions in the D3-D tokamak
[DE94-007428] p 3891 N94-32595
Overview of H-mode studies in D3-D
[DE94-007430] p 3891 N94-32612
Divertor pumping and other reactor application issues for H-mode
[DE94-007431] p 3892 N94-32810

GENERAL ATOMICS TECHNOLOGIES CORP., SAN DIEGO, CA.
Recent VH-mode results on D3-D
[DE94-007429] p 3891 N94-32611

GEO ECO ARC RESEARCH, LA CANADA, CA.
Biospheric effects of a large extraterrestrial impact: Case study of the Cretaceous/Tertiary boundary crater
[NASA-CR-195827] p 3942 N94-32740

GEOLOGICAL SURVEY, DENVER, CO.
Analysis of deep seismic reflection and other data from the southern Washington Cascades
[DE94-005958] p 3771 N94-31525
The mineralogic evolution of the Martian surface through time: Implications from chemical reaction path modeling studies p 3950 N94-33226

GEOLOGICAL SURVEY, FLAGSTAFF, AZ.
The Northern Plains MSATT Meeting, and a call for a field-oriented successor to MSATT
p 3947 N94-33210
Global color views of Mars p 3948 N94-33217
Geologic controls of erosion and sedimentation on Mars p 3951 N94-33232

GEOLOGICAL SURVEY, RESTON, VA.
Gas hydrate detection and mapping on the US east coast
[DE94-005959] p 3742 N94-31504

GEORGE MASON UNIV., FAIRFAX, VA.
DOME: Dynamic optimization on multiprocessor engines, a statistical approach p 3807 N94-31972
A simulation of uncertain reasoning on parametric databases using data-dependency derived inference nets p 3919 N94-32499

GEORGE WASHINGTON UNIV., WASHINGTON, DC.
ISU in an era of partial reconvergence
p 3600 N94-31438
Shock-dependent, optimum thrust wings in supersonic flow p 3570 N94-32027
Computational methods for frictional contact with applications to the Space Shuttle orbiter nose-gear tire
p 3608 N94-32295

GEORGETOWN UNIV., WASHINGTON, DC.
Noninvasive spectral analysis and beam mapping of focused ultrasound, part 1
[AD-A276211] p 3859 N94-31060
Noninvasive spectral analysis and beam mapping of focused ultrasound, part 2
[AD-A276629] p 3861 N94-32059

GEORGIA INST. OF TECH., ATLANTA.
Tetraalkyldiarsines as potential precursors for electronic materials: Synthesis and characterization of various iso-propyl arsenic compounds
[AD-A277003] p 3900 N94-32001
New molecular-based routes to binary main group metal sulfides
[AD-A277005] p 3900 N94-32003
Processable, chemical routes to binary metal sulfides
[AD-A277006] p 3642 N94-32004
Group 12 thiolates: Syntheses, characterization and decomposition pathways
[AD-A277055] p 3900 N94-32011
New zinc-bis(dialkylamides) potentially usable as site-selective dopants for p-type ZnSe
[AD-A276947] p 3902 N94-32218
Enhancement of mixing in a rectangular jet by mechanical tabs
[NASA-CR-185207] p 3709 N94-32872
Reciprocity-based experimental determination of dynamic forces and moments: A feasibility study
[NASA-CR-194905] p 3862 N94-33023

GEORGIA TECH RESEARCH INST., ATLANTA.
Degradation of optical components in space
p 3594 N94-31029

GEOSCIENCE CONSULTANTS, PARIS (FRANCE).
The use of SPOT and ERS-1 images to map the eruption of Nevado Sabancaya (Province of Arequipa, South Peru) and evaluate associated risks p 3751 N94-32546

GEOSYS, RAMONVILLE (FRANCE).
Possible complementarity of SPOT/ERS in mapping land use: Study on agricultural land in Brittany (France)
p 3755 N94-32563

GESELLSCHAFT FUER MATHEMATIK UND DATENVERARBEITUNG, BONN (GERMANY).
Report on implementing part relationships using VML metaclasses
[PB94-147485] p 3813 N94-31686

GESELLSCHAFT FUER MATHEMATIK UND DATENVERARBEITUNG, SAINT AUGUSTIN (GERMANY).
Design Methods based On Nets: DEMON
[PB94-147493] p 3813 N94-31687

GHENT UNIV. (BELGIUM).
Extraction of forests stand age parameters from airborne imaging spectroscopy data p 3745 N94-31867
Novel optoelectronic devices based on combining GaAs and InP on Si
[AD-A277018] p 3693 N94-32301

GOSUDARSTVENNYI KOMITET PO ISPOLZOVANIYU ATOMNOI ENERGII, SERPUKHOV (USSR).
N(exp n(n-1)/2)-state R-matrix related with U(sub q)(sl(n)) algebra at q(exp 2N) = 1
[DE94-608140] p 3902 N94-32247

GOTHENBURG UNIV. (SWEDEN).
Accretion disks around black holes
p 3928 N94-31117

GRENOBLE-1 UNIV. (FRANCE).
Formal verification of systolic multipliers with the Boyer-Moore theorem prover
[RR-897-M] p 3839 N94-31082

GRONINGEN RIJKSUNIV. (NETHERLANDS).
The Cameron-Martin theorem
[W-9315] p 3844 N94-31676
Cell-vertex discretisation of the driven cavity flow without artificial diffusion
[W-9317] p 3703 N94-31689
Heteroclinic attractors: Time averages and moduli of topological conjugacy
[W-9318] p 3844 N94-31690
Simulations of the creation and motion of vortex rings
[W-9319] p 3703 N94-31691
Universal approximation in p-mean by neural networks
[W-9320] p 3832 N94-31821
On an adaptation method for 2-dimensional C-type grids
[W-9322] p 3569 N94-31822
On an adaptation method for dense, 2D, C-type grids
[W-9321] p 3706 N94-32045

GROUPEMENT SCIENTIFIQUE DE TELEDETECTION DE STRASBOURG (FRANCE).
Comparison of SPOT, ERS-1, SEASAT, LANDSAT TM, and merged imagery for geological investigations
p 3752 N94-32547

GRUMMAN AEROSPACE CORP., BETHPAGE, NY.
Comparison of resin film infusion, resin transfer molding, and consolidation of textile preforms for primary aircraft structure p 3630 N94-33136

GUMBS (R.) ASSOCIATES, EAST BRUNSWICK, NJ.
Novel sol-gel deposition for repair of conducting paths in polyceramic systems
[AD-A278381] p 3664 N94-33350

H

HAMPTON UNIV., VA.
Studies of the plasma triggering mechanism of inverse pinch switch
[AD-A276117] p 3887 N94-31530

HARVARD UNIV., BOSTON, MA.
The kinematics of dense clusters of galaxies
p 3937 N94-32029

HARVARD UNIV., CAMBRIDGE, MA.
Physical basis for climate change models
[DE94-003827] p 3767 N94-32712
HAWAII UNIV., HONOLULU.
Passivation of III-V compound semiconductor based devices
[AD-A276178] p 3894 N94-31056
Steps toward understanding the solar dynamo
[AD-A277396] p 3953 N94-32343
From animals to animats
[AD-A277427] p 3802 N94-33241
HCC SCIENCE AND TECHNOLOGY CO., SUMMIT, NJ.
Multifunctional macromolecules
[AD-A277347] p 3656 N94-32246
HEBREW UNIV., JERUSALEM (ISRAEL).
The sol-gel-xerogel transition
[AD-A276647] p 3616 N94-32038
HELSINKI UNIV. OF TECHNOLOGY, ESPOO (FINLAND).
Reactions of electrophilic maleic anhydride and epoxy groups with nucleophilic functionalities such as carboxyl, hydroxyl, and amine groups. Polymer Technology Publication series no. 16
[PB94-135589] p 3648 N94-31069
Preparation of catalyst particles using methods of colloid chemistry. Part 1: Preparation of silica particles from alcohol solutions
[PB94-135597] p 3634 N94-31679
HONEYWELL, INC., PHOENIX, AZ.
Roll ring assemblies for the Space Station
p 3603 N94-33294
HONG KONG UNIV.
Evaluating success levels of mega-projects
p 3599 N94-31432
HORIZON DATA CORP., RESTON, VA.
Draft minutes of IAPG Mechanical Working Group meeting
[DE94-004954] p 3759 N94-31266
Interagency Advanced Power Group: Steering Group meeting minutes
[DE94-007951] p 3761 N94-32701
HOUSTON UNIV., TX.
Chemical vapor deposition of metal nitrides, phosphides, and arsenides
[DE94-008096] p 3654 N94-31976
State-space self-tuner for on-line adaptive control
[NASA-CR-195836] p 3835 N94-32943
The 20 GHz circularly polarized, high temperature superconducting microstrip antenna array
[NASA-CR-195097] p 3683 N94-33083
HOWARD UNIV., WASHINGTON, DC.
Optically switched submillimeter-wave oscillator
[AD-A278014] p 3698 N94-33249
HYDROGEN CONSULTANTS, INC., LITTLETON, CO.
Metal hydride heat pump engineering demonstration and evaluation model
[NASA-CR-188286] p 3669 N94-32857

I

IBM FEDERAL SYSTEMS DIV., GAITHERSBURG, MD.
Cleanroom engineering handbook. Volume 6: Certification team practices
[AD-A275951] p 3587 N94-31346
Cleanroom engineering handbook. Volume 1: Cleanroom engineering process introduction and overview
[AD-A275949] p 3587 N94-31356
Software reuse case study: TRILLIUM
[AD-A276108] p 3811 N94-31465
IBM RESEARCH LAB., SAN JOSE, CA.
Interaction of water with metal surfaces
[AD-A276260] p 3632 N94-31293
ICE CENTRE ENVIRONMENT CANADA, OTTAWA (ONTARIO).
The use of ERS-1 within an operational ice monitoring program p 3751 N94-32545
IDAHO NATIONAL ENGINEERING LAB., IDAHO FALLS.
A PC program to optimize system configuration for desired reliability at minimum cost p 3823 N94-32438
ILLINOIS DEPT. OF ENERGY AND NATURAL RESOURCES, SPRINGFIELD.
Removal of CO2 from flue gases by algae
[DE94-008039] p 3766 N94-32703
ILLINOIS UNIV., CHICAGO.
Fundamental studies in crack initiation
[AD-A278387] p 3741 N94-33356
ILLINOIS UNIV., URBANA.
Spread-spectrum radio systems and networks
[AD-A276449] p 3671 N94-31260
The relationship of the electronic structures of semiconductor surfaces and heterostructures to crystal growth
[AD-A276465] p 3896 N94-31473
An experimental study of the flowfield on a semispan rectangular wing with a simulated glaze ice accretion
[NASA-CR-195301] p 3571 N94-32475
The organization of the suprachiasmatic circadian pacemaker of the rat and its regulation by neurotransmitters and modulators
[AD-A277324] p 3793 N94-32622
Reminding-based learning
[AD-A277424] p 3801 N94-32997
ILLINOIS UNIV., URBANA-CHAMPAIGN.
An investigation of the spin-coating process and a model for three-dimensional regular foams
p 3649 N94-31206
Shock tube ignition and combustion of aluminum/magnesium alloy particles in oxygen at high pressure p 3631 N94-31286
Field studies of raindrop oscillations with applications to radar meteorology p 3782 N94-31743
Information theory for arm visuo-motor coordination
p 3800 N94-32495
IMAGINATION RESOURCES, INC., DUBLIN, OH.
Measurement of viscosity, density, and gas solubility of refrigerant blends in selected synthetic lubricants
[DE94-007723] p 3653 N94-31917
IMPERIAL COLL. OF SCIENCE AND TECHNOLOGY, LONDON (ENGLAND).
The cyclic fatigue behaviour of adhesive joints
[AD-A277080] p 3738 N94-32351
INDUSTRIAL COLL. OF THE ARMED FORCES, WASHINGTON, DC.
Satellite communications industry
[AD-A276685] p 3610 N94-32039
V-22: Dual-use technology or red herring?
[AD-A276577] p 3579 N94-32058
Application of Artificial Intelligence to the DoD Corporate Information Management (CIM) program
[AD-A276656] p 3834 N94-32061
Lifting the fog of corporate information management
[AD-A276680] p 3918 N94-32090
CIM in space: Corporate Information Management (CIM) implications for space-based information systems
[AD-A276882] p 3600 N94-32126
A comparison of military and commercial aircraft development
[AD-A276830] p 3575 N94-32168
Access to space: The Space Shuttle's evolving rolee
[AD-A276785] p 3608 N94-32190
Strategies for survival in the new environmental era
[AD-A276827] p 3765 N94-32195
Untying the gordian data knot. A paper on Information Engineering (IE) and Corporate Information Management (CIM)
[AD-A276862] p 3918 N94-32210
DOD space based requirements: Increasing DOD access to space
[AD-A276874] p 3601 N94-32211
Army scout/reconnaissance helicopters versus unmanned aerial vehicles
[AD-A276902] p 3579 N94-32232
INSTITUT DES HAUTES ETUDES SCIENTIFIQUES, BURES-SUR-YVETTE (FRANCE).
SU(2) WZNW model at higher genera from gauge field functional integral
[PB94-148467] p 3857 N94-31589
Dynamical entropy of generalized quantum Markov chains
[PB94-148483] p 3850 N94-31590
General-relativistic celestial mechanics. 4: Theory of satellite motion
[PB94-147782] p 3601 N94-31769
Conformal field theory and geometry of strings
[PB94-148442] p 3857 N94-31770
Testing for preferred-frame effects in gravity with artificial Earth satellites
[PB94-148459] p 3610 N94-31771
Stability and instability criteria for magnetohydrodynamics
[PB94-148475] p 3889 N94-31772
INSTITUT FUER KOSMOSFORSCHUNG, BERLIN (GERMANY).
The Second International Workshop on Discrete Time Domain Modelling of Electromagnetic Fields and Networks. Program and information
[AD-A277136] p 3677 N94-32067
INSTITUT GEOGRAPHIQUE NATIONAL ESPACE, TOULOSE (FRANCE).
Optics and radar: Cohabitation, rivality or happy marriage. Towards new planning tools
p 3748 N94-32529
The use of ERS images for mapping
p 3749 N94-32531
INSTITUT NATIONAL DE LA RECHERCHE AGRONOMIQUE, VILLENAVE D'ORNON (FRANCE).
The surface parameters: Remote sensing observations and climatology applications p 3779 N94-31001
INSTITUT NATIONAL DES SCIENCES APPLIQUEES, LYON (FRANCE).
Contribution to the study of multiaxial fatigue under periodic or random stresses
[ISAL-92-0004] p 3734 N94-31544
INSTITUT NATIONAL POLYTECHNIQUE, GRENOBLE (FRANCE).
Polyhedric object recognition by indexing in a model base
[ETN-94-95913] p 3812 N94-31542
Extension of the LUSTRE language and application to circuit design: The LUSTRE V4 language and the POLLUX system
[ETN-94-95918] p 3812 N94-31543
INSTITUT ROYAL METEOROLOGIQUE DE BELGIQUE, DOURBES.
EUROCAP program
[AD-A278084] p 3776 N94-33184
INSTITUTE FOR COMPUTER APPLICATIONS IN SCIENCE AND ENGINEERING, HAMPTON, VA.
A software architecture for multidisciplinary applications: Integrating task and data parallelism
[NASA-CR-194896] p 3820 N94-32928
An approximate Riemann solver for magnetohydrodynamics (that works in more than one dimension)
[NASA-CR-194902] p 3849 N94-33033
On the minimum of independent geometrically distributed random variables
[NASA-CR-194883] p 3821 N94-33075
Cumulative reports and publications through December 31, 1993
[NASA-CR-194889] p 3806 N94-33286
INSTITUTE FOR DEFENSE ANALYSES, ALEXANDRIA, VA.
A comparison of product realization frameworks
[AD-A275992] p 3810 N94-31357
System analysis of ultra-wideband instrumentation radars: Impulse versus stepped-chirp approaches
[AD-A276624] p 3677 N94-32087
INSTITUTE FOR IMAGE PROCESSING COMPUTER MAPPING, GRAZ (AUSTRIA).
Feasibility in the use of satellite remote sensing data as a fast reaction tool for natural disaster relief
p 3748 N94-32526
INSTITUTE OF ENERGY ECONOMICS OF JAPAN.
Current policies of the major countries coping with the global warming problem and-the energy demand and supply
[DE94-757291] p 3769 N94-32920
INSTITUTE OF GEODESY AND CARTOGRAPHY, WARSAW (POLAND).
Application of ERS-1 SAR data for hydrological studies p 3754 N94-32558
INSTITUTO DE PESQUISAS ESPACIAIS, SAO JOSE DOS CAMPOS (BRAZIL).
High sensitivity and resolution decimetric spectroscope: Preliminary analysis of solar bursts
[INPE-5537-TDI/525] p 3954 N94-33080
INSTITUTO SUPERIOR TECNICO, LISBON (PORTUGAL).
NATO Advanced Study Institute on Unsteady Combustion. Volume 2: Research papers, September 6-17, 1993
[AD-A276572] p 3634 N94-32033
INSTITUTO TECNOLOGICO DE AERONAUTICA, SAO PAULO (BRAZIL).
Legal regime of human activities in outer space law
p 3599 N94-31431
INTEGRATED PARALLEL TECHNOLOGY, PLEASANTON, CA.
VME rollback hardware for time warp multiprocessor systems
[NASA-CR-191796] p 3826 N94-32483
INTERNATIONAL BUSINESS MACHINES CORP., SAN JOSE, CA.
Molecular dynamics computer simulations of charged metal electrode-aqueous electrolyte interfaces
[AD-A276401] p 3863 N94-31237
Infrared spectroelectrochemical study of cyanide adsorption and reactions at platinum electrodes in aqueous perchlorate electrolyte
[AD-A276402] p 3631 N94-31238
INTERNATIONAL CENTRE FOR THEORETICAL PHYSICS, TRIESTE (ITALY).
Topological conformal algebra in 2D gravity coupled to minimal matter
[DE94-608122] p 3910 N94-31052
INTERNATIONAL INST. FOR AEROSPACE SURVEY AND EARTH SCIENCES, ENSCHEDE (NETHERLANDS).
Optimal geological data extraction from SPOT-radar synergism with samples from Djebel Amour (Algeria), Red Sea Hills (Sudan), Sirte Basin (Libya), and Magdalena Valley (Colombia) p 3752 N94-32548

INTERNATIONAL SOCIETY FOR OPTICAL ENGINEERING, BELLINGHAM, WA.
Proceedings SPIE: Conference Digest, volume 2104
[AD-A278107] p 3884 N94-33187
INTERNATIONAL SPACE UNIV., INC., TORONTO (ONTARIO).
An innovative approach to space education
p 3600 N94-31436
IOWA STATE UNIV. OF SCIENCE AND TECHNOLOGY, AMES.
Theoretical studies of zirconium and carbon clusters with molecular dynamics simulations
[DE94-005276] p 3862 N94-31146
An axial approach to detection in capillary electrophoresis
[DE94-005556] p 3631 N94-31154
A solution adaptive structured-unstructured grid procedure for unsteady flows p 3700 N94-31217
Remote robot manipulator coupled with remote-controlled guide vehicle for soil sampling in hazardous waste sites p 3723 N94-31569
Vibrational and acoustic response of ribbed plates
p 3736 N94-31955
Incorporating radial mixing in axisymmetric streamline curvature through-flow analysis
[AD-A277325] p 3706 N94-32279
IOWA UNIV., IOWA CITY.
A comprehensive analysis of electron conical distributions from multi-satellite databases
[NASA-CR-195848] p 3953 N94-33047
Indentability of conventional and negative Poisson's ratio foams p 3629 N94-33131
ISRAEL INST. FOR BIOLOGICAL RESEARCH, NESS-ZIONA.
Transport and diffusion in turbulent fields modeling and measurements techniques
[AD-A278114] p 3769 N94-33110
ISRO SATELLITE CENTRE, PEENYA, BANGALORE (INDIA).
INSAT-2A and 2B development mechanisms
p 3603 N94-33293
ISTAR, VALBONNE (FRANCE).
Example of SPOT/ERS-1 complementarity
p 3749 N94-32533

J

JADAVPUR UNIV., CALCUTTA (INDIA).
Probing lepton number violation via Majorana neutrinos at hadron supercolliders
[PB94-147055] p 3868 N94-31922
JAPAN BROADCASTING CORP., TOKYO.
An experimental compact Hi-Vision VCR using metal evaporated tape
[NHK-LABS-NOTE-423] p 3683 N94-33081
JET PROPULSION LAB., CALIFORNIA INST. OF TECH., PASADENA.
Channel and terminal description of the ACTS mobile terminal p 3599 N94-31428
Spacecraft On-Board Information Extraction Computer (SOBIEC) p 3808 N94-32433
Applying robotics to HAZMAT p 3729 N94-32452
Advanced teleoperation: Technology innovations and applications p 3806 N94-32453
The trustworthy digital camera: Restoring credibility to the photographic image p 3714 N94-32470
Use of SPOT and ERS-1 SAR data to study the tectonic and climatic history of arid regions p 3752 N94-32550
Techniques and applications of SAR interferometry for ERS-1 p 3756 N94-32568
Groundbased monitoring of Martian atmospheric opacity p 3947 N94-33207
Studies of atmospheric dust from Viking IR thermal mapper data p 3948 N94-33216
Lessons learned from selecting and testing spaceflight potentiometers p 3607 N94-33318
The Galileo high gain antenna deployment anomaly
p 3607 N94-33319
JIL SYSTEMS, INC., ARLINGTON, VA.
The 1993 aviation system capacity plan
[AD-A276958] p 3575 N94-32620
JOANNEUM RESEARCH CENTRE, GRAZ (AUSTRIA).
Evaluation of Fluorescence Line Imager (FLI) airborne imaging spectrometer data for roadside tree damage assessment p 3745 N94-31866
JOHNS HOPKINS UNIV., BALTIMORE, MD.
Ionized gas in the halos of edge-on infrared-bright galaxies: Evidence for starburst-driven superwinds
p 3936 N94-31948
The chemical and dynamical evolution of the galaxy
p 3936 N94-31950
Material engineering of the novel semiconductor structures
[AD-A278386] p 3910 N94-33355
JOHNS HOPKINS UNIV., LAUREL, MD.
High peak power microwaves: A health hazard
[AD-A277168] p 3681 N94-32576
JOINT INST. FOR NUCLEAR RESEARCH, DUBNA (USSR).
Low dispersion of the muon precession frequency in HTSC samples YBa2Cu3O(x) and EuBa2Cu3O(x)
[DE94-608388] p 3896 N94-31395
NN-interaction in (1)S0-state: Virtual level or dibaryon resonance?
[DE94-606492] p 3869 N94-32097
JOINT RESEARCH CENTRE OF THE EUROPEAN COMMUNITIES, ISPRA (ITALY).
Modeling the interaction between solar radiation and terrestrial surfaces p 3779 N94-30999
Ground based radiometric and atmospheric measurements p 3744 N94-31855
Analysis of GER imaging spectrometry data for the identification of soil and vegetation parameters in land degradation studies p 3744 N94-31857
The complementary nature of the SPOT and ERS-1 systems and their place in major international programmes p 3748 N94-32524
A case study comparing multi-temporal ERS-1 SAR data and SPOT data for tropical forest mapping
p 3753 N94-32556

K

KANSAS UNIV., LAWRENCE.
Satellite radar altimetry over the continental ice sheets
p 3742 N94-31570
Radar rainfall measurements from space
p 3782 N94-31889
KANSAS UNIV. CENTER FOR RESEARCH, INC., LAWRENCE.
Scatterometer wind-speed exponents: A review and SAXON 35-GHz measurements
[AD-A276568] p 3783 N94-31937
KATHOLIEKE UNIV. TE LEUVEN (BELGIUM).
The Sixth Symposium on Unconventional Photoactive Solids. Abstracts
[AD-A277198] p 3655 N94-32016
KAUPPA-JA TEOLLISUUSMINISTERIO, HELSINKI (FINLAND).
NEMO: Advanced energy systems and technologies
[DE94-721996] p 3760 N94-31767
KENTUCKY UNIV., LEXINGTON.
Nonlinear analysis of springs using helical finite elements p 3859 N94-31906
Additive turbulent decomposition of the incompressible and compressible Navier-Stokes equations
[AD-A277321] p 3708 N94-32511
Technology development for iron Fischer-Tropsch catalysts
[DE94-008723] p 3638 N94-32869
Characterization and utilization of opiate-like hibernation factors
[AD-A278136] p 3794 N94-33098
KEO CONSULTANTS, BROOKLINE, MA.
High frequency active auroral research program (HAARP) imager
[AD-A277469] p 3775 N94-32999
KOZPONTI FIZIKAI KUTATO INTEZET, BUDAPEST (HUNGARY).
F0-975, A0-980 as eye-witnesses of confinement
[PB94-147105] p 3868 N94-31923

L

LABSPHERE, INC., NORTH SUTTON, NH.
Custom uniform source system
[NASA-CR-189332] p 3711 N94-31492
LASER POWER RESEARCH, SAN DIEGO, CA.
Digital image profilers for detecting faint sources which have bright companions
[NASA-CR-191348] p 3927 N94-32695
LAVAL UNIV. (QUEBEC).
Volumetric modelling of three dimensional scenes by octree decomposition of geometric models
[ISBN-0-315-86866-X] p 3814 N94-31728
Photonic bandgaps in periodic dielectric structures
[ISBN-0-315-86902-X] p 3899 N94-31729
Development of a robotic simulator for studying interference and contact problems
[ISBN-0-315-86705-1] p 3588 N94-31747
Study of the dynamics of a nonlinear coupled-cavity laser system
[ISBN-0-315-86717-5] p 3716 N94-31748
Mechanisms of formation and of de-excitation in the reaction Mg-24 + C-12 yields 9 alpha at 35MeV per nucleon
[ISBN-0-315-86746-9] p 3867 N94-31749
A neural network model for the visual perception of the depth of a scene from stereoscopy and shading
[ISBN-0-315-86753-1] p 3831 N94-31750
Optimization of Y junctions in integrated optics
[ISBN-0-315-86782-5] p 3879 N94-31751
Methods of implementing the Viterbi algorithm on a massively parallel computer of the SIMD (single instruction multiple data) type
[ISBN-0-315-86783-3] p 3814 N94-31752
Spectroscopic study of the molecular collisions (hydrogen-nitrogen and hydrogen-oxygen) at energies of several MeV
[ISBN-0-315-86794-9] p 3867 N94-31753
Application of contact mechanics for the validation of robotized operations of grasping objects subjected to static and dynamic force fields
[ISBN-0-315-86831-7] p 3725 N94-31754
Multiple regression and measurement errors: Relative efficiency of two models, the standard model and Fuller's model, for estimating structural relationships
[ISBN-0-315-86834-1] p 3845 N94-31755
Synchronized laser scanning three dimensional acquisition system
[ISBN-0-315-86848-1] p 3879 N94-31756
Strategy for tracking and grabbing a moving object with the aid of a decouplable manipulator with six degrees of freedom general architecture, guided by a vision system
[ISBN-0-315-86864-3] p 3831 N94-31757
LAWRENCE LIVERMORE NATIONAL LAB., CA.
Sol-gel metal oxide and metal oxide/polymer multilayers applied by meniscus coating
[DE94-005813] p 3649 N94-31199
The role of defects in laser damage of multilayer coatings
[DE94-006731] p 3714 N94-31269
Emission from ferroelectric cathodes
[DE94-006732] p 3863 N94-31270
Imaging AMS
[DE94-006662] p 3632 N94-31349
AMS beyond 2000
[DE94-006666] p 3632 N94-31352
Cost-effective ceramic machining: Summary of three-body wear experiments
[DE94-007757] p 3650 N94-31354
Element-specific magnetic hysteresis measurements, a new application of circularly polarized soft x-rays
[DE94-007122] p 3858 N94-31397
Inertial fusion with ultra-powerful lasers
[DE94-007242] p 3887 N94-31400
Structural design of the superconducting Poloidal Field coils for the Tokamak Physics Experiment
[DE94-007078] p 3887 N94-31406
The threshold energy for defect production in SiC: A molecular dynamic study
[DE94-007123] p 3896 N94-31499
Spectroscopy and atomic physics in EBIT and SuperEBIT
[DE94-006050] p 3864 N94-31508
Electrostatic reduction of particulates for laser resistant hafnia coatings
[DE94-005824] p 3651 N94-31557
Two-gigawatt burst-mode operation of the Intense Microwave Prototype (IMP) Free-Electron Laser (FEL) for the Microwave Tokamak Experiment (MTX)
[DE94-006613] p 3715 N94-31580
Tensile properties of commercially pure vanadium from room temperature to 1200 C
[DE94-006622] p 3641 N94-31581
Using laser absorption spectroscopy to monitor composition and physical properties of metal vapors
[DE94-001530] p 3716 N94-31599
Large-area conditioning of optics for high-power laser systems
[DE94-007028] p 3716 N94-31636
Quench detection and instrumentation for the Tokamak Physics Experiment magnets
[DE94-006656] p 3888 N94-31667
The development and testing of a backscatter absorption gas imaging (BAGI) system designed to image at a range of 300 m
[DE94-006192] p 3675 N94-31761
First-wall heat-flux measurements during ELMing H-mode plasma
[DE94-008310] p 3888 N94-31765
Dispersion relations for a plasma-filled helix-loaded-waveguide
[DE94-006333] p 3675 N94-31781
Strongly coupled ionic mixtures and the H/He EOS
[DE94-006391] p 3934 N94-31782
Stellar x ray polarimeter polarizer development and calibration at LEA/LLNL
[DE94-006400] p 3712 N94-31783
PEM public key certificate cache server
[DE94-006404] p 3675 N94-31784

The FELICIA bulletin board system and the IRBIS anonymous FTP server: Computer security information sources for the DOE community
[DE94-008219] p 3825 N94-31920
Scenarios for multi-unit inertial fusion energy plants producing hydrogen fuel
[DE94-006614] p 3666 N94-32114
Amorphous/crystalline structure and phase transformations in metastable semiconducting Ge(1-x)Sn(x)
[DE94-006659] p 3901 N94-32115
Surface chemistry and durability of borosilicate glass
[DE94-006734] p 3656 N94-32116
Exploring phase space concepts in the forecasting of time series with artificial neural networks
[DE94-005810] p 3834 N94-32127
Impact of observed hyperfine splitting on X-ray laser gain
[DE94-005822] p 3717 N94-32128
Gamma-ray optical counterpart search experiment (GROCSE)
[DE94-007124] p 3955 N94-32129
Promising future energy storage systems: Nanomaterial based systems, Zn-air, and electromechanical batteries
[DE94-007443] p 3692 N94-32136
Winds from disks in compact binaries
[DE94-007452] p 3938 N94-32137
MICA, a facility to achieve portability for message-passing and dynamic memory management in FORTRAN
[DE94-006692] p 3807 N94-32147
The hydrogen hybrid option
[DE94-006733] p 3667 N94-32148
A solar array module fabrication process for HALE solar electric UAVs
[DE94-006212] p 3760 N94-32174
Using TSAR with the post-processing far-field option
[DE94-006615] p 3679 N94-32188
Design and early results of the sodium-layer laser guide star adaptive optics experiment at the Lawrence Livermore National Laboratory
[DE94-006653] p 3926 N94-32189
Sol-gel coatings for high power laser optics: Past, present, and future
[DE94-007240] p 3718 N94-32252
Carbon cycle modeling calculations for the IPCC
[DE94-004332] p 3765 N94-32354
Recent advances and developments in refractory alloys
[DE94-007929] p 3644 N94-32374
Point defect production, geometry, and stability in silicon: A molecular dynamics simulation study
[DE94-008292] p 3903 N94-32411
Flexible manufacturing for photonics device assembly p 3669 N94-32449
Liquid-assisted diffusion bonding of NiAl
[DE94-008687] p 3645 N94-32522
On the implementation of error handling in dynamic interfaces to scientific codes
[DE94-008970] p 3818 N94-32585
Conductivity measurements of ceria-based solid electrolytes using AC impedance
[DE94-007380] p 3694 N94-32593
Boron and hydrogen in Ni3Al. Part 2: Mechanical testing of bicrystals
[DE94-007441] p 3904 N94-32606
X ray imaging and x ray source development at Lawrence Livermore National Laboratory
[DE94-007077] p 3719 N94-32629
Femtosecond probe-probe transmission studies of LT-grown GaAs near the band edge
[DE94-006660] p 3904 N94-32634
On the formation of muon- and zeta-phases in Ag-Al system by mechanical alloying
[DE94-007125] p 3645 N94-32636
Automatic contact in DYNA3D for vehicle crashworthiness
[DE94-007143] p 3738 N94-32637
Notes on the Langevin model for turbulent diffusion of marked particles
[DE94-007847] p 3708 N94-32652
Dual-band infrared imaging to detect corrosion damage within airframes and concrete structures
[DE94-008047] p 3580 N94-32658
High average power pulsed phase conjugate laser with birefringence correction
[DE94-006049] p 3719 N94-32659
Influence of volume fraction of component materials and interlayer bond strength on fracture toughness of multi-layer Al 6090-25 volume percent SiCp and Al 5182 laminates
[DE94-007141] p 3626 N94-32665
The 2D deterministic radiation transport with the discontinuous finite element method
[DE94-004687] p 3849 N94-32670
A facilitated mentoring process for engineers
[DE94-005823] p 3914 N94-32677
Structure-property relationships of carbon aerogels
[DE94-007120] p 3660 N94-32687
Automated fiber pigtailing technology
[DE94-007072] p 3695 N94-32688
Microanalytical study of defect formation in thin bismuth strontium calcium copper oxide films
[DE94-008217] p 3661 N94-32751
Pump-probe method for investigating laser ablation and optical damage threshold mechanisms in optical materials
[DE94-008291] p 3720 N94-32753
Calculations of nonspherically averaged charge densities for substitutionally disordered alloys
[DE94-008293] p 3646 N94-32754
Occupied and unoccupied orbitals of C60 and C70
[DE94-008294] p 3873 N94-32755
Long distance transmission of 15 Gb/s digital using subcarrier multiplexing and external modulation
[DE94-008298] p 3682 N94-32756
A long-term simulation of surface fluxes and soil moisture
[DE94-006661] p 3774 N94-32772
Climate effects of anthropogenic sulfate: Simulations from a coupled chemistry/climate model
[DE94-004352] p 3767 N94-32789
Simulation of a precipitation event in the western United States
[DE94-004835] p 3786 N94-32791
Progress in understanding and improving x ray lasers
[DE94-006048] p 3720 N94-32794
Analytic properties of the OCP and ionic mixtures in the strongly coupled fluid state
[DE94-008216] p 3637 N94-32801
Electron: Cluster interactions
[DE94-009089] p 3874 N94-32807
Quantified estimates of total GWPs for greenhouse gases taking into account tropospheric chemistry
[DE94-007846] p 3768 N94-32817
The Numerical Tokamak Project (NTP) simulation of turbulent transport in the core plasma: A grand challenge in plasma physics
[DE94-008279] p 3892 N94-32838
LLNL casting technology
[DE94-008282] p 3669 N94-32839
Preconditioned time-difference methods for advection-diffusion-reaction equations
[DE94-006472] p 3638 N94-32840
A study of near-surface and underwater explosions by computer simulations
[DE94-009038] p 3708 N94-32849
X ray absorption study of pulsed laser deposited boron nitride films
[DE94-008295] p 3662 N94-32855
Ocean variability and its influence on the detectability of greenhouse warming signals
[DE94-008670] p 3790 N94-32881
Statistical intercomparison of global climate models: A common principal component approach
[DE94-008671] p 3768 N94-32882
Interface controlled amorphization of crystalline Ni/Ti multilayers
[DE94-008685] p 3906 N94-32884
Dependence of x ray absorption magnetic circular dichroism on layer periodicity in iron-platinum multilayers
[DE94-008786] p 3647 N94-32892
A correlated k-distribution model of the heating rates for atmospheric mixtures of H2O, CO2, O3, CH4, and N2O in the 0-2500 cm(exp -1) wave number region at altitudes between 0 and 60 km
[DE94-005136] p 3775 N94-32895
Convection in Type 2 supernovae
[DE94-009373] p 3938 N94-32914
Analytic formulation for the ac electrical conductivity in two-temperature, strongly coupled, overdense plasma: FORTRAN subroutine
[DE94-009466] p 3893 N94-32915
Imaging of surface structure with energy-dependent photoelectron diffraction
[DE94-009096] p 3907 N94-32934
Effects of long-term elevated atmospheric CO2 concentrations on Pinus ponderosa
[DE94-008832] p 3769 N94-32966
Enhanced thermal capacity aerogels summary report, FY 1993
[DE94-008868] p 3639 N94-33260
Phase relationships and stability of the (mu)- and (zeta)-phases in the Ag-Al-X (X=Zn, Ga, Ge) systems
[DE94-009391] p 3648 N94-33270

LEEDS UNIV. (ENGLAND).
Proceedings of the International Workshop on Computational Electronics
[AD-A277020] p 3692 N94-32259

LEHIGH UNIV., BETHLEHEM, PA.
Processing of novel nanoparticle dispersion strengthened ceramics for improved mechanical performance
[AD-A275965] p 3649 N94-31276
An extended approach to oxidations and nitridations of Si and Ge(x)Si(1-x) materials
[AD-A276056] p 3631 N94-31282
Toughening mechanisms in fiber-reinforced ceramic-matrix composites p 3622 N94-31943
High-temperature deformation and fracture toughness of duplex ceramic microstructures p 3653 N94-31945
High octane ethers from synthesis gas-derived alcohols
[DE94-006774] p 3667 N94-32133
Robotic weld overlay coatings for erosion control
[DE94-008004] p 3658 N94-32408
Molten metal analysis by laser produced plasmas
[DE94-007014] p 3646 N94-32782

LEIDEN UNIV. (NETHERLANDS).
A stability estimate based on numerical ranges with application to a spectral discretization of a convection-diffusion equation
[TW-93-12] p 3847 N94-32200
Undiscounted Markov decision chains with partial information; an algorithm for computing a locally optimal periodic policy
[TW-93-10] p 3851 N94-32205
On the error committed by stopping the Newton iteration in Runge-Kutta methods and linear multistep methods
[TW-93-13] p 3847 N94-32206
Stability estimates for families of matrices of nonuniformly bounded order
[TW-93-14] p 3847 N94-32207

LITTLE (ARTHUR D.), INC., CAMBRIDGE, MA.
A laboratory study of multiple site damage in fuselage lap splices
[AD-A276151] p 3578 N94-31078
Feasibility study for the recycling of nickel metal hydride electric vehicle batteries
[DE94-000268] p 3690 N94-31598

LOCKHEED ADVANCED DEVELOPMENT CO., SUNLAND, CA.
MOM3D method of moments code theory manual
[NASA-CR-189594] p 3682 N94-32897

LOCKHEED AERONAUTICAL SYSTEMS CO., MARIETTA, GA.
Shear flow control of cold and heated rectangular jets by mechanical tabs. Volume 1: Results and discussion
[NASA-CR-182296-VOL-1] p 3708 N94-32867
Shear flow control of cold and heated rectangular jets by mechanical tabs. Volume 2: Tabulated data
[NASA-CR-182296-VOL-2] p 3709 N94-32869
Structural testing of the technology integration box beam p 3628 N94-33125
Advanced textile applications for primary aircraft structures p 3629 N94-33135

LOCKHEED ENGINEERING AND SCIENCES CO., HOUSTON, TX.
The Martian sources of the SNC meteorites (two, not one), and what can and can't be learned from the SNC meteorites p 3951 N94-33234
Energy absorber for the CETA p 3604 N94-33303
Pip pin reliability and design p 3605 N94-33305

LOCKHEED MISSILES AND SPACE CO., PALO ALTO, CA.
Analysis of data from the plasma composition experiment on the International Sun-Earth Explorer (ISEE 1)
[NASA-CR-195880] p 3893 N94-33074

LOCKHEED MISSILES AND SPACE CO., SUNNYVALE, CA.
Space Station Freedom solar array containment box mechanisms p 3603 N94-33292
Space Station Freedom Solar Array tension mechanism development p 3604 N94-33300
MSAT boom joint testing and load absorber design p 3606 N94-33315
Special test equipment and fixturing for MSAT reflector assembly alignment p 3606 N94-33316

LODESTAR RESEARCH CORP., BOULDER, CO.
ICRF heating and current drive in TFTR supershot plasmas: Data analysis and interpretation of ICRF/edge interactions
[DE94-008586] p 3890 N94-32520

LOGICON TECHNICAL SERVICES, INC., DAYTON, OH.
Assessment of interior modifications in C-130 and C-141 aircraft for night vision goggle operations
[AD-A276843] p 3582 N94-32223
Methods for measuring characteristics of night vision goggles
[AD-A277046] p 3804 N94-32302

LOS ALAMOS NATIONAL LAB., NM.
High-power microwave-tube transmitters
[DE94-005340] p 3686 N94-31150

Workshop on advances in smooth particle hydrodynamics
[DE94-006221] p 3956 N94-31308
The future of open architecture process control systems
[DE94-006163] p 3830 N94-31623
Diagnostics of high-brightness short-pulse lasers and the plasmas they generate
[DE94-006165] p 3716 N94-31624
Impurities and conductivity in a D-wave superconductor
[DE94-006222] p 3898 N94-31628
The 4f heavy fermion photoelectron spectra do not exhibit the Kondo scale
[DE94-006252] p 3898 N94-31631
Experimental evidence for lattice effects in high temperature superconductors
[DE94-006250] p 3899 N94-31633
Non-equilibrium electrodynamics in the large N expansion
[DE94-006156] p 3911 N94-31760
A brief introduction to symplectic integrators and recent results
[DE94-006225] p 3845 N94-31763
Instability heatino of solid-fiber Z pinches
[DE94-007055] p 3889 N94-31809
Fermi surface instability at 0.4 K in a heavy-fermion YbBiPt: SDW?
[DE94-006224] p 3899 N94-31916
Chemical vapor deposition of metal nitrides, phosphides, and arsenides
[DE94-008096] p 3654 N94-31976
Ion-irradiation-induced densification of zirconia sol-gel thin films
[DE94-006248] p 3656 N94-32103
The Nijmegen hyperon-nucleon potentials
[DE94-007557] p 3869 N94-32139
Neural network definitions of highly predictable protein secondary structure classes
[DE94-006234] p 3834 N94-32175
Statistics of time averaged atmospheric scintillation
[DE94-006998] p 3747 N94-32249
Ti:sapphire based ultrafast pump-probe laser source in the violet and ultraviolet
[DE94-007542] p 3718 N94-32270
Antiproton production in heavy ion collisions
[DE94-007552] p 3870 N94-32271
The Operator Shell: A means of privilege distribution under Unix
[DE94-007566] p 3826 N94-32356
Numerical transport theory
[DE94-009064] p 3857 N94-32589
Attempts to model the generation of new grain boundaries during the deformation of polycrystals
[DE94-007527] p 3903 N94-32597
A historical perspective on fifteen years of laser damage thresholds at LLNL
[DE94-007930] p 3719 N94-32613
Variational elliptic solver for atmospheric applications
[DE94-007725] p 3774 N94-32647
High power switch design for the Nova upgrade laser (Project HERCULES: High Energy Research Concerning the Ultimate Lifetime of Experimental Switches)
[DE94-007921] p 3719 N94-32654
A simple model for determining photoelectron-generated radiation scaling laws
[DE94-006130] p 3761 N94-32660
Analysis of Dietz's single, rectangular pulse theory for the generation of radiation via photoelectrons
[DE94-006131] p 3681 N94-32661
Particle-In-Cell (PIC) code simulation results and comparison with theory scaling laws for photoelectron-generated radiation
[DE94-006132] p 3695 N94-32662
Ethics and rationality in information-enriched decisions: A model for technical communication
[DE93-040251] p 3681 N94-32679
The Los Alamos National Laboratory precision double crystal spectrometer
[DE94-008075] p 3713 N94-32706
Wind-speed measurements with a scanning elastic-backscatter lidar
[DE94-004974] p 3785 N94-32726
Measurement of ICF fuel ion temperature on Nova
[DE94-006150] p 3892 N94-32730
Noninvasive spectroscopic diagnosis of superficial ocular lesions and corneal infections
[DE94-006231] p 3797 N94-32732
High resolution properties of the marine atmospheric boundary layer
[DE94-006235] p 3774 N94-32736
Surface probes of porous toluene/water ices: Adsorption kinetics and annealing spectra measured by second harmonic generation
[DE94-007564] p 3637 N94-32743
Aspects of modeling uncertainty and prediction
[DE94-007565] p 3852 N94-32744
COVICS: A covert video communications system
[DE94-007568] p 3682 N94-32745
Strongly anisotropic s-wave versus d-wave gap in cuprate superconductors: Evidence and theory
[DE94-007579] p 3904 N94-32746
Quantum fluctuations of vortices in Josephson-coupled superconductors
[DE94-007609] p 3905 N94-32747
Short-pulse, high-intensity lasers at Los Alamos
[DE94-007545] p 3720 N94-32760
Repetitively pulsed Cr:LiSAF laser for lidar applcations
[DE94-007546] p 3720 N94-32761
Polymer electrolyte fuel cells
[DE94-007558] p 3761 N94-32762
Proceedings of the International Workshop on Low Energy Muon Science: LEMS 1993
[DE94-006495] p 3874 N94-32804
The ALEXIS mission recovery
[DE94-007549] p 3611 N94-32813
Mexico City ozone concentrations as a function of readily-available meteorological parameters
[DE94-007576] p 3768 N94-32814
Proceedings, Strongly Correlated Electronic Materials: The 1993 Los Alamos Symposium
[DE94-009293] p 3906 N94-32913
Performance of a new wind updating system for a prognostic meteorological model in the environs of Mexico City
[DE94-006243] p 3786 N94-32937
Evidence for symmetry breaking local distortions in thallium barium copper oxide
[DE94-006149] p 3907 N94-32944
Performance of a quasi-steady, multi megawatt, coaxial plasma thruster
[NASA-CR-195311] p 3616 N94-32970

LOUGHBOROUGH UNIV. OF TECHNOLOGY (ENGLAND).
Structural properties of inverse linear systems
[MATHS-REPT-A-200] p 3840 N94-31156
A Green's function approach to analysing the effects of random synaptic background activity in a model neural network
[MATHS-REPT-A-202] p 3828 N94-31157
Feasibility and stability results for constrained stable generalized predictive control
[MATHS-REPT-A-203] p 3828 N94-31158
Symplectic Runge-Kutta schemes 3: Canonical elementary differentials
[MATHS-REPT-A-204] p 3840 N94-31159
Symbolic derivation of Runge-Kutta methods
[MATHS-REPT-A-205] p 3840 N94-31160
A direct digital design for a multichannel structural test system using the characteristic locus method
[MATHS-REPT-A-206] p 3828 N94-31161
Observations of the notion of minimality in the generalized state space
[MATHS-REPT-A-207] p 3840 N94-31162
A new methodology of system parameter estimation
[MATHS-REPT-A-208] p 3808 N94-31163
Optimal reactive power dispatch of power systems using nonlinear programming
[MATHS-REPT-A-209] p 3808 N94-31164
Mechanisms of laser induced reactions in opaque heterogeneous environments
[AD-A276642] p 3717 N94-31996

LOUISIANA STATE UNIV., BATON ROUGE.
A twisted disk equation that describes warped galaxy disks p 3928 N94-31118
A heterogeneous computing environment for simulating astrophysical fluid flows p 3928 N94-31119
An efficient three-dimensional Poisson solver for SIMD high-performance-computing architectures p 3823 N94-31120
The dynamical settling of warped disks and angular momentum transport in galaxies p 3928 N94-31121
Evolution of vaporizing pulsars p 3929 N94-31128
A study of angular momentum loss in binaries using the free Lagrange method p 3931 N94-31134
Gravitational instabilities in protostellar disks p 3932 N94-31140
Three-dimensional radiative transfer calculations on an SIMD machine applied to accretion disks p 3932 N94-31141
Gas dynamics for accretion disk simulations p 3932 N94-31144

LOUVAIN UNIV. (BELGIUM).
Quantitative analysis of woody vegetation in Soudano-Sahalian region. Textural approach (application to a Burkina Faso region) p 3757 N94-32574

LOWELL OBSERVATORY, FLAGSTAFF, AZ.
Might it be possible to predict the onset of major Martian dust storms? p 3948 N94-33215

LOYOLA UNIV., CHICAGO, IL.
Determination of multiple sound sources
[AD-A277379] p 3799 N94-32096

LUDWIG-MAXIMILIANS-UNIV., MUNICH (GERMANY).
The European Imaging Spectroscopy Airborne Campaign (EISAC). Data takes and evaluation programme: An overview p 3743 N94-31854
Evaluation of GER- and FLI-data with reference to forest p 3746 N94-31868

LUNAR AND PLANETARY INST., HOUSTON, TX.
Workshop on Physics of Accretion Disks Around Compact and Young Stars
[NASA-CR-195756] p 3927 N94-31116
Evolution of dynamo-generated magnetic fields in accretion disks around compact and young stars p 3931 N94-31138
Mars: Past, Present, and Future. Results from the MSATT Program, part 1
[NASA-CR-194279] p 3943 N94-33190
Depth-diameter ratios for Martian impact craters: Implications for target properties and episodes of degradation p 3943 N94-33191
Thermal and hydraulic considerations regarding the fate of water discharged by the outflow channels to the Martian northern plains p 3946 N94-33202
Martian spectral units derived from ISM imaging spectrometer data p 3949 N94-33220

LUND UNIV. (SWEDEN).
F0-975, A0-980 as eye-witnesses of confinement
[PB94-147105] p 3868 N94-31923

M

MANCHESTER UNIV. (ENGLAND).
Optical properties of doped sol-gel silica glasses
[AD-A278094] p 3884 N94-33267

MANES ASSOCIATES, INC., HUNTINGTON BEACH, CA.
Economic feasibility analysis of distributed electric power generation based upon the natural gas fired fuel cell
[DE94-005795] p 3759 N94-31487

MANITOBA UNIV., WINNIPEG.
The development of active integrated antennas and a design methodology
[ISBN-0-315-86119-3] p 3675 N94-31708

MARQUETTE UNIV., MILWAUKEE, WI.
Effects of orbital exposure on RTV during the LDEF mission p 3597 N94-31043

MARTIN MARIETTA CORP., DENVER, CO.
Magmatic volatiles and the weathering of Mars p 3946 N94-33201

MARTIN MARIETTA LABS., BALTIMORE, MD.
Molecular interactions at metal/polyimide interfaces: A correlation with adhesion and bond durability
[AD-A276301] p 3650 N94-31297

MARYLAND UNIV., BALTIMORE.
Development and enhancement of a model of performance and decision making under stress in a real life setting
[AD-A276029] p 3799 N94-31440

MARYLAND UNIV., COLLEGE PARK.
Development of a statistical method for estimating the downward longwave radiation at the surface from satellite observations p 3742 N94-31553
Kinematic synthesis and analysis of a novel class of six-DOF parallel minimanipulators p 3723 N94-31568
Robot grasping: Stability and optimization issues p 3724 N94-31724
Safe navigation and active vision for autonomous vehicles: A purposive and direct solution p 3832 N94-31842
Polynomial interpolation and approximation of real functions. 2: Symmetrical interpolation for the triangle
[AD-A277345] p 3848 N94-32245
Eta percent-superconvergence in the interior of locally refined meshes of quadrilaterals: Superconvergence of the gradient in finite element solutions of Laplace's and Poisson's equations
[AD-A277242] p 3848 N94-32331
Finite element solution to the Helmholtz equation with high wave number. Part 1: The h-version of the FEM
[AD-A277396] p 3848 N94-32341
Coherent processes in atom in strong radiation fields
[AD-A278388] p 3874 N94-33144
Development of an interchangeable end effector mechanism for the Ranger telerobotic vehicle p 3604 N94-33297

MASHINSTROYENIYE, MOSCOW (USSR).
Almaz marine applications p 3751 N94-32544
The processing technology and some applications of Almaz-1 data p 3756 N94-32573

MASSACHUSETTS GENERAL HOSPITAL, BOSTON.
Development of a video fluorescence system for assessing burn depth
[AD-A278127] p 3798 N94-33092

MASSACHUSETTS INST. OF TECH., CAMBRIDGE.
Theoretical studies of x ray emission from clusters of galaxies p 3954 N94-31103
Magnetohydrodynamics of the Earth's core. 1: Steady, rotating magnetoconvection. 2: Magnetic Rossby waves p 3770 N94-31104
Tectonic History of the Terrestrial Planets [NASA-CR-195696] p 3939 N94-31105
Patterns of deformation and volcanic flows associated with lithospheric loading by large volcanoes on Venus p 3776 N94-31106
Aspects of modelling the tectonics of large volcanoes on the terrestrial planets p 3940 N94-31107
State of stress, faulting, and eruption characteristics of large volcanoes on Mars p 3940 N94-31108
Geoid-to-topography ratios on Venus: A global perspective p 3940 N94-31110
On wave interactions of rotational and irrotational flows p 3700 N94-31219
Proceedings of the 37th international symposium on electron, ion, and photon beams [AD-A276478] p 3875 N94-31247
Deformation and rupture of cylindrical shells under dynamic loading p 3733 N94-31288
Taming chaotic circuits p 3910 N94-31289
A radial basis function approach to financial time series analysis [AD-A276408] p 3924 N94-31361
Structure and dynamics of microemulsions in bulk, at interfaces, and in confined geometries [DE94-006043] p 3633 N94-31526
Hierarchical mixtures of experts and the EM algorithm [AD-A276516] p 3814 N94-31932
On the convergence of stochastic iterative dynamic programming [AD-A276517] p 3815 N94-31933
A multi-frequency study of an x ray selected sample of active galactic nuclei p 3937 N94-31987
Observations of turbulence, internal waves and background flows: An inquiry into the relationships between scales of motion p 3705 N94-31988
Cumulus convection parameterization and numerical modelling of moist atmospheres p 3783 N94-31989
Model-based scientific discovery: A study in space bioengineering p 3799 N94-31990
Robot motion vision by fixation p 3833 N94-31991
A study of areas of low radio-thermal emissivity on Venus p 3942 N94-31992
A model of the ion chemistry of electrified convection p 3868 N94-31993
On the relationship between generalization error, hypothesis complexity, and sample complexity for radial basis functions [AD-A276802] p 3851 N94-32142
Geometric structure of the adaptive controller of the human arm [AD-A276797] p 3834 N94-32152
The named-state register file [AD-A276796] p 3825 N94-32165
Parallel methods for synthesizing whole-hand grasps from generalized prototypes [AD-A276798] p 3726 N94-32166
Algebraic functions for recognition [AD-A276803] p 3846 N94-32167
Optical flow from 1D correlation: Application to a simple time-to-crash detector [AD-A276777] p 3880 N94-32186
Methods for parallelizing search paths in phrasing [AD-A276876] p 3817 N94-32212
Translucent procedures, abstraction without opacity [AD-A276877] p 3817 N94-32213
Parallel and distributed computing combinatorial algorithms [AD-A277333] p 3826 N94-32243
Undergraduate robotics projects in support of research on neural networks [AD-A277331] p 3835 N94-32281
Emacs Lisp in Edwin scheme [AD-A276721] p 3818 N94-32504
Inlet distortion in engines on VSTOL aircraft [NASA-CR-195841] p 3584 N94-33035
Quantitative modeling of bottom morphology and subbottom properties [AD-A278142] p 3790 N94-33062
Deposition rates of oxidized iron on Mars p 3945 N94-33198
Convergence results for the EM approach to mixtures of experts architectures [AD-A276801] p 3852 N94-33276

MASSACHUSETTS INST. OF TECH., LEXINGTON.
Control and reliability of optical networks in multiprocessors [AD-A277385] p 3881 N94-32285

MASSACHUSETTS UNIV., AMHERST.
Observations of accretion and angular momentum regulation in young circumstellar disks and the implications for planetary formation p 3928 N94-31122
The stellar and gaseous content of massive low surface brightness disk galaxies p 3933 N94-31495
CO observations in external galaxies and gas mass determination p 3925 N94-31790
Cometary molecules p 3935 N94-31869
Problems in survivable multi-media networks [AD-A277370] p 3825 N94-32052
Discrete-event-dynamic-system-based approaches for scheduling transmissions in multihop packet radio networks [AD-A276566] p 3679 N94-32230

MASSACHUSETTS UNIV., BOSTON.
Diagnostic studies of climate variability [DE94-003629] p 3767 N94-32711

MASSACHUSETTS UNIV., LOWELL.
New developments in second-order nonlinear optical polymeric materials [AD-A277409] p 3658 N94-32578
Stable second-order nonlinear optical materials based on interpenetrating polymer networks [AD-A277410] p 3658 N94-32579
Nonlinear optical polymers derived from organic/inorganic composites [AD-A277408] p 3659 N94-32610
Low loss second-order nonlinear optical polymers based on all organic sol-gel materials [AD-A277482] p 3663 N94-32985
A relaxation study of poled nonlinear optical polymers by infrared reflection-absorption spectroscopy [AD-A277513] p 3663 N94-33054
Novel polydiacetylenes as materials for second and third order nonlinear optics [AD-A277512] p 3664 N94-33082
Second-order nonlinear optical polymers: From fundamentals to applications [AD-A277514] p 3664 N94-33348

MATERIALS RESEARCH LABS., ASCOT VALE (AUSTRALIA).
Improved resealing procedures for the second deseal/reseal program in RAAF F111 aircraft fuel tanks [AD-A277069] p 3580 N94-32378
GRAFTED - GRAphical fault tree EDitor: A fault tree description program for target vulnerability/survivability analysis. User manual [AD-A277067] p 3818 N94-32390

MATERIALS RESEARCH SOCIETY, PITTSBURG, PA.
Silicon-Based Optoelectronic Materials Symposium and Materials Research Society Proceedings, volume 298 [AD-A277518] p 3662 N94-32952
Rare Earth Doped Semiconductors and Materials Research Society Symposium Proceedings, Volume 301 [AD-A277517] p 3908 N94-33055

MATERIALS SCIENCES CORP., FORT WASHINGTON, PA.
Briefing and review meeting implementation of the military handbook 17 for polymer matrix and metal matrix composites [AD-A277446] p 3663 N94-33010

MATRA MARCONI SPACE (ENGLAND).
SAR image feature extraction system: A pre-operational application of ERS-1 SAR p 3751 N94-32543

MATRA MARCONI SPACE, TOULOUSE (FRANCE).
Pointing and tracking space mechanism for laser communication p 3606 N94-33310

MATRA SEP IMAGERIE ET INFORMATIQUE, SAINT QUENTIN EN YVELINES (FRANCE).
Assessment of region-based methods for automated SAR/optical registration, attribute extraction, and classification p 3750 N94-32536
Robust multisource classification method using the Markov random field methods p 3750 N94-32537
Production of terrain data: Optical radar complementarity p 3750 N94-32540

MAX-PLANCK-INST. FUER EXTRATERRESTRISCHE PHYSIK, GARCHING (GERMANY).
Multiwavelength search for protoplanetary disks p 3599 N94-31430

MAXDEM, INC., SAN DIMAS, CA.
Nonlinear optical properties of rigid-rod polymers [NASA-CR-191349] p 3882 N94-32702

MCDONNELL AIRCRAFT CO., SAINT LOUIS, MO.
Development of thermoplastic composite aircraft structures [NASA-CR-189593] p 3626 N94-32860

MCDONNELL-DOUGLAS AEROSPACE, HUNTINGTON BEACH, CA.
Space Station WP-2 application of LDEF MLI results p 3592 N94-31016

MCMASTER UNIV., HAMILTON (ONTARIO).
Knowledge engineering for PACES, the particle accelerator control expert system p 3854 N94-33342

MEMPHIS STATE UNIV., TN.
The relationship between integrative task design for information systems professionals and perceived information systems effectiveness p 3919 N94-32487

METROLASER, IRVINE, CA.
Photothermal laser deflection, an innovative technique to measure particles in exhausts [AD-A277151] p 3718 N94-32366

MICHIGAN UNIV., ANN ARBOR.
Response of wall turbulence to high frequency streamwise and spanwise oscillations p 3700 N94-31211
Control of hypersonic aerodynamic forces with surface blowing p 3567 N94-31216
On the structure and stability of slender viscous vortices p 3700 N94-31218
Penetration distances and their applications to path planning p 3858 N94-31725
Tripping over obstacles: Biomechanical analyses of how young and old try to avoid it p 3803 N94-31954
Vibration localization in dual-span axially moving elastic systems p 3736 N94-31964
Influences of pressure-sensitive yielding and non-singular stress on plane-stress elastic-plastic crack-tip fields p 3737 N94-31965
Energy transfer properties and mechanisms [DE94-007403] p 3636 N94-32594
Scalar imaging velocimetry studies of turbulent flow structure and dynamics [AD-A278395] p 3710 N94-33164

MIDWEST RESEARCH INST., GOLDEN, CO.
Photovoltaics: Program overview, fiscal year 1993 [DE94-000246] p 3758 N94-31235
Role of polycrystallinity in CdTe and CuInSe2 photovoltaic cells [DE94-000293] p 3758 N94-31236
Solar resource: Utility load-matching assessment [DE94-000297] p 3758 N94-31264
Automated solar cell assembly teamed process research [DE94-000295] p 3759 N94-31279
Users manual for SERI QC software assessing the quality of solar radiation data [DE93-018210] p 3953 N94-31491
Feasibility study for the recycling of nickel metal hydride electric vehicle batteries [DE94-000268] p 3690 N94-31598
In-situ characterization of growth and interfaces in a-Si:H devices [DE94-000291] p 3760 N94-31812
Research on the stability, electronic properties, and structure of a-Si:H and its alloys [DE94-000292] p 3899 N94-31813
Silicon-Film(tm) photovoltaic manufacturing technology [DE94-000202] p 3760 N94-32143
Optical processing for semiconductor device fabrication p 3885 N94-32445
A scanning defect mapping system for semiconductor characterization p 3885 N94-32446
Research on stable, high-efficiency amorphous silicon multijunction modules [DE94-000298] p 3695 N94-32680
Biomass power industry: Assessment of key players and approaches for DOE and industry interaction [DE94-000238] p 3761 N94-32725
Development of a computer model for polycrystalline thin-film CuInSe2 and CdTe solar cells [DE94-006853] p 3762 N94-32763
Thin EFG octagons [DE94-006855] p 3905 N94-32764
Large-area, triple-junction a-Si alloy production scale-up [DE94-006856] p 3762 N94-32765

MINNESOTA UNIV., MINNEAPOLIS.
Design and analysis of scalable parallel algorithms [AD-A276255] p 3809 N94-31251
Concurrent architectures for VLSI signal and image processing [AD-A276124] p 3688 N94-31445
Phase behavior, structure, and properties of model block polymers [AD-A277530] p 3662 N94-32954
Workshop on Visual Perception: Computation and Psychophysics [AD-A278412] p 3802 N94-33326

MISSION RESEARCH CORP., SANTA BARBARA, CA.
Automated detection of ship tracks in multispectral satellite data [AD-A276697] p 3746 N94-32119

MISSISSIPPI STATE UNIV., MISSISSIPPI STATE.
Transformation of two and three-dimensional regions by elliptic systems [NASA-CR-195849] p 3821 N94-33049

MISSOURI UNIV., ROLLA.
Solvent diffusion coefficient concentration dependence in polymer solutions
[AD-A277023] p 3655 N94-32005
NMR studies of organic thin films
[AD-A276953] p 3656 N94-32221
Dynamics of block poly(styrene-co-vinylpyridine) (SVP) in solution and on silica
[AD-A277139] p 3657 N94-32364
MITECH, INC., ROCKVILLE, MD.
The 1993 aviation system capacity plan
[AD-A276958] p 3575 N94-32620
MITRE CORP., MCLEAN, VA.
The 1993 aviation system capacity plan
[AD-A276958] p 3575 N94-32620
MOBIL TYCO SOLAR ENERGY CORP., BILLERICA, MA.
Thin EFG octagons
[DE94-006855] p 3905 N94-32764
MONTREAL UNIV. (QUEBEC).
Characterization and growth mechanisms of the MgAl2O4 phase in Al2O3-reinforced Al-Mg composites
[ISBN-0-315-86531-8] p 3620 N94-31706
Thermal-mechanical fatigue crack growth in aircraft engine materials
[ISBN-0-315-86543-1] p 3734 N94-31707
Optimization of the forming parameters of PEEK/carbon fiber composite
[ISBN-0-315-86410-9] p 3620 N94-31716
Finite element numerical simulation of turbulent flows
[ISBN-0-315-86416-8] p 3703 N94-31717
Stereoscopic correspondence based on the structure of shading
[ISBN-0-315-86418-4] p 3814 N94-31718
Fatigue behavior of unidirectional pultruded composite materials
[ISBN-0-315-86425-7] p 3621 N94-31719
Numerical modelling of turbulence
[ISBN-0-315-86439-7] p 3703 N94-31720
A contribution to the representation and identification of semi-flexible robots
[ISBN-0-315-86450-8] p 3724 N94-31721
Empirical optimization of the consolidation of thermoplastic prepregs
[ISBN-0-315-86455-9] p 3652 N94-31722
Simulation of non-uniform transmission lines for weakly dispersive structures
[ISBN-0-315-86525-3] p 3690 N94-31726
Time domain spectroscopy for studying a monopole antenna immersed in a plasma
[ISBN-0-315-86526-1] p 3888 N94-31727
Fractal and spectral analysis
[ISBN-0-315-86460-5] p 3676 N94-31796
Algorithms and parallel architectures for laser acoustic imaging
[ISBN-0-315-86466-4] p 3716 N94-31797
Adaptive control of a robot in Cartesian coordinates: Analysis and implementation
[ISBN-0-315-86493-1] p 3831 N94-31798
An adaptive method for the exact resolution of shock waves and contact discontinuities
[ISBN-0-315-86498-2] p 3704 N94-31799
Study of a path planning and tracking system for an articulated mobile robot
[ISBN-0-315-86502-4] p 3831 N94-31800
Development of a feedforward controller for a flexible manipulator
[ISBN-0-315-86515-6] p 3832 N94-31801
Low velocity impact damage in carbon fiber/PEEK composite laminates
[ISBN-0-315-86546-6] p 3622 N94-31909
Electrical properties of double layer dielectric structures for space technology
[ISBN-0-315-86547-4] p 3610 N94-31910
The Kaluza-Klein approach and gauge supersymmetry
[ISBN-0-315-86553-9] p 3912 N94-31911
Fatigue crack propagation and fractography of 3Y-TZP and ZTA
[ISBN-0-315-86561-X] p 3736 N94-31912
Study of stellar associations located in the region contained between the Magellanic Clouds
[ISBN-0-315-86692-6] p 3935 N94-31913
Construction of visual representations and time-space organization of resources in astronomy
[ISBN-0-315-86694-2] p 3925 N94-31914
Planning of air crew schedules
[ISBN-0-315-86506-7] p 3914 N94-32074

N

NANSEN ENVIRONMENTAL AND REMOTE SENSING CENTER, SOLHEIMSVIK (NORWAY).
NORSMAP 1989: Norwegian remote sensing spectroscopy for mapping and monitoring or algal blooms and pollution p 3744 N94-31856
NATIONAL ACADEMY OF SCIENCES - NATIONAL RESEARCH COUNCIL, WASHINGTON, DC.
Mathematical research in materials science opportunities and perspectives, part 2
[AD-A276298] p 3852 N94-31296
A cross-disciplinary report on the mathematical sciences applied to materials science, part 1
[AD-A276116] p 3843 N94-31529
NATIONAL AERONAUTICS AND SPACE ADMINISTRATION, WASHINGTON, DC.
NASA's space platform technology program and planning p 3597 N94-31044
Aeronautical engineering: A continuing bibliography with indexes (supplement 302)
[NASA-SP-7037(302)] p 3565 N94-31342
Aeronautical engineering: A continuing bibliography with indexes (supplement 303)
[NASA-SP-7037(303)] p 3565 N94-31381
Aerospace medicine and biology: A continuing bibliography with indexes (supplement 388)
[NASA-SP-7011(388)] p 3795 N94-31414
Apollo 11 highlights
[NASA-TM-109763] p 3600 N94-31820
Index to NASA news releases and speeches, 1993
[NASA-TM-109722] p 3917 N94-31888
NASA strategic plan
[NASA-TM-109780] p 3915 N94-32222
Aerospace medicine and biology: A continuing bibliography with indexes (supplement 389)
[NASA-SP-7011(389)] p 3797 N94-32347
Aerospace medicine and biology: A continuing bibliography with indexes (supplement 385)
[NASA-SP-7011(385)] p 3797 N94-32348
Management of government quality assurance functions for NASA contracts
[NHB-5300.4(2B-2)] p 3731 N94-32387
Technology 2003: The Fourth National Technology Transfer Conference and Exposition, volume 2
[NASA-CP-3249] p 3956 N94-32420
Airborne Trailblazer: Two decades with NASA Langley's 737 flying laboratory
[NASA-SP-4216] p 3566 N94-32793
Aeronautical engineering: A continuing bibliography with indexes (supplement 304)
[NASA-SP-7037(304)] p 3566 N94-32853
Research and Technology Objectives and Plans Summary (RTOPS)
[NASA-TM-105441] p 3966 N94-32885
Opinion polls and the US civil space program
[NASA-TM-109700] p 3914 N94-33066
Space history, space policy, and executive leadership
[NASA-TM-109787] p 3924 N94-33067
NATIONAL AERONAUTICS AND SPACE ADMINISTRATION. AMES RESEARCH CENTER, MOFFETT FIELD, CA.
Characterization of polymer decomposition products by laser desorption mass spectrometry p 3597 N94-31046
Investigation of sonic boom for the Space Shuttle: High cross-range orbiter
[NASA-TM-108238] p 3860 N94-31336
Investigation of sonic boom for the Space Shuttle: Low cross-range orbiter
[NASA-TM-108237] p 3860 N94-31337
A critical assessment of UH-60 main rotor blade airfoil data
[NASA-TM-103985] p 3571 N94-32063
The quest for contact
[NASA-TM-109778] p 3806 N94-32389
Refining fuzzy logic controllers with machine learning p 3839 N94-32421
A hypertext system that learns from user feedback p 3923 N94-32428
A visual detection model for DCT coefficient quantization p 3850 N94-32467
Translating an AI application from Lisp to Ada: A case study
[NASA-TM-103845] p 3820 N94-32906
Aviation human factors research in US universities: Potential contributions to national needs
[NASA-TM-108814] p 3575 N94-32927
An investigation of acoustic noise requirements for the Space Station centrifuge facility
[NASA-TM-108811] p 3805 N94-32936
Incremental triangulation by way of edge swapping and local optimization
[NASA-TM-103979] p 3709 N94-32946
Autogenic-feedback training as a treatment for airsickness in high-performance military aircraft: Two case studies
[NASA-TM-108810] p 3801 N94-33068
Development of lightweight ceramic ablators and arc-jet test results
[NASA-TM-108798] p 3617 N94-33117
Stationary eddies in the Mars general circulation as simulated by the NASA-Ames GCM p 3944 N94-33192
Thermal emission measurements (5-25 microns) of Hawaiian palagonitic soils with implications for Mars p 3944 N94-33193
A model for the evolution of CO2 on Mars p 3946 N94-33205
Eddy transport of water vapor in the Martian atmosphere p 3949 N94-33221
Controls on the CO2 seasonal cycle p 3950 N94-33227
The wavelength dependence of Martian atmospheric dust radiative properties p 3950 N94-33228
Obliquity variation in a Mars climate evolution model p 3951 N94-33236
Simultaneous laboratory measurements of CO2 and H2O adsorption on palagonite: Implications for the Martian climate and volatile reservoir p 3952 N94-33240
Backward-facing step measurements at low Reynolds number, Re(sub h)=5000
[NASA-TM-108807] p 3711 N94-33290
NATIONAL AERONAUTICS AND SPACE ADMINISTRATION. GODDARD SPACE FLIGHT CENTER, GREENBELT, MD.
The 1988 Goddard Space Flight Center Battery Workshop
[NASA-CP-3237] p 3758 N94-31233
NASCOM system development plan: System description, capabilities, and plans, FY 94-2
[NASA-TM-109744] p 3674 N94-31503
A versatile nondestructive evaluation imaging workstation p 3732 N94-32458
A new high-speed IR camera system p 3713 N94-32459
Technology transfer of operator-in-the-loop simulation p 3802 N94-32472
Space flight printed wiring board measling investigation
[NASA-TM-104602] p 3732 N94-33101
MODIS. Volume 1: MODIS level 1A software baseline requirements
[NASA-TM-104594-VOL-1] p 3823 N94-33287
MODIS. Volume 2: MODIS level 1 geolocation, characterization and calibration algorithm theoretical basis document, version 1
[NASA-TM-104594-VOL-2] p 3613 N94-33289
NATIONAL AERONAUTICS AND SPACE ADMINISTRATION. HUGH L. DRYDEN FLIGHT RESEARCH FACILITY, EDWARDS, CA.
The constant current loop: A new paradigm for resistance signal conditioning p 3685 N94-32461
Flight test results of riblets at supersonic speeds
[NASA-TM-4387] p 3572 N94-32880
NATIONAL AERONAUTICS AND SPACE ADMINISTRATION. JOHN C. STENNIS SPACE CENTER, BAY SAINT LOUIS, MS.
Remote sensing for hurricane Andrew impact assessment p 3758 N94-32464
Remote sensing for urban planning p 3758 N94-32465
Remote sensing and the Mississippi high accuracy reference network p 3758 N94-32466
NATIONAL AERONAUTICS AND SPACE ADMINISTRATION. JOHN F. KENNEDY SPACE CENTER, COCOA BEACH, FL.
Universal signal conditioning amplifier p 3699 N94-32460
Mapping analysis and planning system for the John F. Kennedy Space Center p 3757 N94-32463
Chronology of KSC and KSC related events for 1993
[NASA-TM-109196] p 3966 N94-33072
Innovative mechanism for measuring the mass properties of an object p 3604 N94-33299
NATIONAL AERONAUTICS AND SPACE ADMINISTRATION. LYNDON B. JOHNSON SPACE CENTER, HOUSTON, TX.
Ground-based simulation of LEO environment: Investigations of a select LDEF material: FEP Teflon (trademark) p 3596 N94-31039
An overview of the Evaluation of Oxygen Interaction with Materials-third phase (EOIM-3) experiment: Space Shuttle Mission 46 p 3596 N94-31040
CONFIG: Integrated engineering of systems and their operation p 3823 N94-32432
Application of dexterous space robotics technology to myoelectric prostheses p 3729 N94-32450
Electromagnetic probe technique for fluid flow measurements p 3711 N94-32455
Microwave sensor for ice detection p 3583 N94-32457
Literacy: A multimedia adult literacy package combining NASA technology, recursive ID theory, and authentic instruction theory p 3924 N94-32482
Virtual reality in medical education and assessment p 3798 N94-32471

BUCKY instruction manual, version 3.3
[NASA-TM-104793] p 3820 N94-32899
The Lunar Scout Program: An international program to survey the Moon from orbit for geochemistry, mineralogy, imagery, geodesy, and gravity
[NASA-TM-104791] p 3943 N94-32923
Use of a pitch adjustable foot restraint system: Operator strength capability and load requirements
[NASA-TP-3477] p 3805 N94-33050
SNC meteorites and their implications for reservoirs of Martian volatiles p 3947 N94-33209
Mineralogical diversity (spectral reflectance and Moessbauer data) in compositionally similar impact melt rocks from Manicouagan Crater, Canada p 3948 N94-33219
Load-limiting landing gear footpad energy absorption system p 3607 N94-33323

NATIONAL AERONAUTICS AND SPACE ADMINISTRATION. LANGLEY RESEARCH CENTER, HAMPTON, VA.
Performance of selected polymeric materials on LDEF p 3593 N94-31023
Summary of materials and hardware performance on LDEF p 3595 N94-31037
High performance real-time flight simulation at NASA Langley p 3591 N94-32473
NOAA-9 Earth Radiation Budget Experiment (ERBE) scanner offsets determination
[NASA-TM-109086] p 3785 N94-32737
NASA/DOD Aerospace Knowledge Diffusion Research Project. Paper 5: Aerospace librarians and technical information specialists as information intermediaries: A report of phase 2 activities of the NASA/DOD Aerospace Knowledge Diffusion Research Project
[NASA-TM-109777] p 3921 N94-32829
NASA/DOD Aerospace Knowledge Diffusion Research Project. Paper 6: Aerospace knowledge diffusion in the academic community: A report of phase 3 activities of the NASA/DOD Aerospace Knowledge Diffusion Research Project
[NASA-TM-109771] p 3921 N94-32830
NASA/DOD Aerospace Knowledge Diffusion Research Project. Paper 10: The NASA/DOD Aerospace Knowledge Diffusion Research Project
[NASA-TM-109769] p 3921 N94-32831
NASA/DOD Aerospace Knowledge Diffusion Research Project. Paper 12: The diffusion of federally funded aerospace research and development (R/D) and the information seeking behavior of US aerospace engineers and scientists
[NASA-TM-109404] p 3921 N94-32832
NASA/DOD Aerospace Knowledge Diffusion Research Project. Paper 18: Scientific and Technical Information (STI) policy and the competitive position of the US aerospace industry
[NASA-TM-109782] p 3921 N94-32833
NASA/DOD Aerospace Knowledge Diffusion Research Project. Paper 11: The voice of the user: How US aerospace engineers and scientists view DOD technical reports
[NASA-TM-109348] p 3921 N94-32834
NASA/DOD Aerospace Knowledge Diffusion Research Project. Paper 1: The value of scientific and technical information (STI), its relationship to Research and Development (R/D), and its use by US aerospace engineers and scientists
[NASA-TM-109774] p 3922 N94-32835
NASA/DOD Aerospace Knowledge Diffusion Research Project. Report 25: The technical communications practices of British aerospace engineers and scientists: Results of the phase 4 RAeS mail survey
[NASA-TM-109098] p 3922 N94-32836
NASA/DOD Aerospace Knowledge Diffusion Research Project. Report 24: The technical communications practices of US aerospace engineers and scientists: Results of the phase 1 SAE mail survey
[NASA-TM-109088] p 3922 N94-32837
A finite-difference approximate-factorization algorithm for solution of the unsteady transonic small-disturbance equation
[NASA-TP-3129] p 3572 N94-32865
Results for the hybrid laminar flow control experiment conducted in the NASA Langley 8-foot transonic pressure tunnel on a 7-foot chord model
[NASA-TM-107582] p 3601 N94-32870
User's guide for a flat wake rotor inflow/wake velocity prediction code, DOWN
[NASA-TM-104139] p 3572 N94-32873
OARE flight maneuvers and calibration measurements on STS-58
[NASA-TM-109093] p 3613 N94-32924
A mathematical model for simulating noise suppression of lined ejectors
[NASA-TP-3425] p 3861 N94-32930
Comparison of the compressive strengths for stitched and toughened composite systems
[NASA-TM-109108] p 3627 N94-32939
Fourth-order 2N-storage Runge-Kutta schemes
[NASA-TM-109112] p 3573 N94-32950
Modeling of aircraft unsteady aerodynamic characteristics. Part 1: Postulated models
[NASA-TM-109120] p 3586 N94-32951
Implementation of a vibrationally linked chemical reaction model for DSMC
[NASA-TM-109109] p 3710 N94-33020
Structural damping studies at cryogenic temperatures
[NASA-TM-109073] p 3740 N94-33118
Second NASA Advanced Composites Technology Conference
[NASA-CP-3154] p 3627 N94-33121
Designer's unified cost model p 3627 N94-33122
Composite fuselage shell structures research at NASA Langley Research Center p 3628 N94-33124
Technology integration box beam failure study p 3628 N94-33126
Development of stitched/RTM composite primary structures p 3628 N94-33127
Test and analysis results for composite transport fuselage and wing structures p 3628 N94-33129
Tension fracture of laminates for transport fuselage. Part 1: Material screening p 3629 N94-33130
Recent progress in NASA Langley Research Center textile reinforced composites program p 3629 N94-33134

NATIONAL AERONAUTICS AND SPACE ADMINISTRATION. LEWIS RESEARCH CENTER, CLEVELAND, OH.
Atomic oxygen interaction at defect sights in protective coatings on polymers flown on LDEF p 3593 N94-31024
Computational study of single-expansion-ramp nozzles with external burning
[NASA-TM-106550] p 3700 N94-31229
Solar lunar power p 3599 N94-31427
WHIPICE
[NASA-TM-109749] p 3574 N94-31803
High temperature NASP engine seal development
[NASA-TM-109750] p 3725 N94-31804
Mars: Five views on what is known
[NASA-TM-109751] p 3942 N94-31805
Marsville: The cosmic village
[NASA-TM-109752] p 3913 N94-31806
Space acceleration measurement system
[NASA-TM-109754] p 3913 N94-31807
Aerospace test facilities at NASA LERC Plumbrook
[NASA-TM-109755] p 3602 N94-31814
Welcome to the Ohio Aerospace Institute
[NASA-TM-109756] p 3913 N94-31815
The vision machines
[NASA-TM-109757] p 3806 N94-31816
NASA report to education, volume 9
[NASA-TM-109760] p 3913 N94-31817
Solar connection
[NASA-TM-109761] p 3614 N94-31818
Futurepath 3
[NASA-TM-109762] p 3735 N94-31819
Solid surface
[NASA-TM-109746] p 3634 N94-31883
Defying gravity
[NASA-TM-109747] p 3667 N94-31884
NASA select yearender review
[NASA-TM-109748] p 3956 N94-31885
Thermocapillary convection in evaporating sessile drops
[NASA-TM-109758] p 3705 N94-31886
The sky is your classroom
[NASA-TM-109759] p 3914 N94-31887
Development of lightweight radiators for lunar based power systems
[NASA-TM-106604] p 3726 N94-32272
Structural probability concepts adapted to electrical engineering
[NASA-TM-106499] p 3739 N94-32735
Simulation of low-density nozzle plumes in non-zero ambient pressures
[NASA-TM-106501] p 3615 N94-32742
On the use of computers for teaching fluid mechanics
[NASA-TM-106587] p 3820 N94-32773
Radiometry spot measurement system
[NASA-TM-106561] p 3883 N94-32777
METCAN demonstration manual, version 1.0
[NASA-TM-105607] p 3626 N94-32858
Controlling hazardous energy sources (lockout/tagout)
[NASA-TM-105290] p 3669 N94-32861
Flutter analysis of a supersonic cascade in time domain using an ADI Euler solver
[NASA-TM-105625] p 3739 N94-32883
Simultaneous pressure measurement and high-speed photography study of cavitation in a dynamically loaded journal bearing
[NASA-TM-106456] p 3728 N94-32893
Feed-forward control of gear mesh vibration using piezoelectric actuators
[NASA-TM-106366] p 3728 N94-32902
Theoretical and experimental study of microstrip-to-slot line uniplanar transition
[NASA-TM-106566] p 3696 N94-32905
Frictional behavior and adhesion of Ag and Au films applied to aluminum oxide by oxygen-ion assisted Screen Cage Ion Plating (SCIP)
[NASA-TM-106522] p 3647 N94-32931
Compliance measurements of chevron notched four point bend specimen
[NASA-TM-106538] p 3740 N94-32932
The effect of prolonged exposure to 750 C air on the tribological performance of PM212
[NASA-TM-106472] p 3617 N94-32941
Conversion of polymers of methyl- and vinylsilane to Si-C ceramics
[NASA-TM-106554] p 3662 N94-32945
Modification of the MML turbulence model for adverse pressure gradient flows
[NASA-TM-106544] p 3709 N94-32947
CET93 and CETPC: An interim updated version of the NASA Lewis computer program for calculating complex chemical equilibria with applications
[NASA-TM-4557] p 3638 N94-32948
Institute for Computational Mechanics in Propulsion (ICOMP)
[NASA-TM-106542] p 3710 N94-32969
Spur, helical, and spiral bevel transmission life modeling
[NASA-TM-106552] p 3728 N94-32979
Stabilized alumina/ethanol colloidal dispersion for seeding high temperature air flows
[NASA-TM-106591] p 3713 N94-32983
Use of Navier-Stokes methods for the calculation of high-speed nozzle flow fields
[NASA-TM-106551] p 3573 N94-32984
Perfluoropolyalkylether decomposition on catalytic aluminas
[NASA-TM-106547] p 3617 N94-33021
Combined contamination and space environmental effects on solar cells and thermal control surfaces
[NASA-TM-106592] p 3617 N94-33022
Development and preliminary evaluation of aryl ester boundary additives for perfluoropolyethers
[NASA-TM-106603] p 3663 N94-33024
Implementing software safety in the NASA environment
[NASA-TM-106597] p 3731 N94-33032
PSIDD: A Post-Scan Interactive Data Display system for ultrasonic scans
[NASA-TM-4545] p 3732 N94-33038
Research and technology, 1993
[NASA-TM-106376] p 3567 N94-33046
Characteristics of III-V semiconductor devices at high temperature
[NASA-TM-106574] p 3697 N94-33052
Vibration Isolation Technology (VIT) ATD project
[NASA-TM-106496] p 3567 N94-33064
Renormalization group theory of Bolgiano scaling in Boussinesq turbulence
[NASA-TM-106602] p 3710 N94-33070
Analysis of a slot coupled coplanar waveguide fed patch antenna
[NASA-TM-106567] p 3698 N94-33116
Direct replacement of arbitrary grid-overlapping by non-structured grid
[NASA-TM-106601] p 3850 N94-33120
The 28th Aerospace Mechanisms Symposium
[NASA-CP-3260] p 3603 N94-33291
Design, characterization and control of the Unique Mobility Corporation robot p 3603 N94-33296
Design, characterization, and control of the NASA three degree of freedom reaction compensation platform p 3605 N94-33304
Intelligent control of a multi-degree-of freedom reaction compensating platform system using fuzzy logic p 3605 N94-33306
The preliminary evaluation of liquid lubricants for space applications by vacuum tribometry p 3606 N94-33313

NATIONAL AERONAUTICS AND SPACE ADMINISTRATION. MARSHALL SPACE FLIGHT CENTER, HUNTSVILLE, AL.
LDEF Materials Results for Spacecraft Applications
[NASA-CP-3257] p 3591 N94-31012
The performance of thermal control coatings on LDEF and implications to future spacecraft p 3591 N94-31013
Space environment durability of beta cloth in LDEF thermal blankets p 3591 N94-31015

Modeling of LDEF contamination environment
p 3592 N94-31019
Atomic oxygen erosion considerations for spacecraft materials selection p 3593 N94-31022
Fluorescence observations of LDEF exposed materials as an indicator of induced material reactions
p 3593 N94-31025
Impact of LDEF photovoltaic experiment findings upon spacecraft solar array design and development requirements p 3594 N94-31028
Micrometeoroid/space debris effects on materials
p 3595 N94-31032
LDEF materials special investigation group's data bases p 3596 N94-31038
MSFC orbital spacecraft development emphases for this decade p 3598 N94-31048
What LDEF means for development and testing of materials p 3598 N94-31050
Technical assessment of Mir-1 life support hardware for the international space station
[NASA-TM-108441] p 3803 N94-31380
The Second Annual International Space University Alumni Conference
[NASA-CP-3253] p 3598 N94-31425
Mitigation of adverse environmental effects on lunar-based astronomical instruments
p 3598 N94-31426
Beginning the 21st century with advanced Automatic Parts Identification (API) p 3923 N94-32444
Neutral ion sources in precision manufacturing
p 3875 N94-32447
A case study of analysis methods for large deflections of a cantilever beam
[NASA-TM-108454] p 3739 N94-32903
Operations summary for the convection and moisture experiment (CAMEX)
[NASA-TM-108445] p 3786 N94-33004
Diamond turning in the production of x ray optics
p 3604 N94-33298

NATIONAL AEROSPACE LAB., AMSTERDAM (NETHERLANDS).
Aircraft simulation and pilot proficiency: From surrogate flying towards effective training
[AD-B179300] p 3587 N94-31179
CFD-based drag prediction: State-of-the-art, theory, prospects
[AD-B179297] p 3567 N94-31180
Development concept for Dutch user support
[PB94-125523] p 3598 N94-31208
On an adaptation method for 2-dimensional C-type grids
[W-9322] p 3569 N94-31822
On an adaptation method for dense, 2D, C-type grids
[W-9321] p 3706 N94-32045

NATIONAL DEFENCE HEADQUARTERS, OTTAWA (ONTARIO).
A decision support system for electronic warfare analysts p 3853 N94-33336

NATIONAL DEFENCE RESEARCH ESTABLISHMENT, LINKOEPING (SWEDEN).
Fiberoptisk magnetfaltsensor (fiber optic magnetometer)
[PB94-148061] p 3878 N94-31584

NATIONAL INST. OF STANDARDS AND TECHNOLOGY, BOULDER, CO.
Aperture excitation of electrically large, lossy cavities
[PB94-145711] p 3675 N94-31683

NATIONAL INST. OF STANDARDS AND TECHNOLOGY, GAITHERSBURG, MD.
Putting the information infrastructure to work: Report of the Information Infrastructure Task Force Committee on Applications and Technology
[NIST/SP-857] p 3916 N94-31228

NATIONAL MAPPING AND RESOURCE INFORMATION AUTHORITY (PHILIPPINES).
Airborne SAR as a complement to SPOT HRV in land-cover classification: The use of normalization and principal components analysis p 3750 N94-32539

NATIONAL OCEANIC AND ATMOSPHERIC ADMINISTRATION, BOULDER, CO.
Solar physics and terrestrial effects. A curriculum guide for teachers, grade 7-12
[PB94-142247] p 3953 N94-31595
Proceedings of the International Workshop on Artificial Intelligence Applications in Solar-Terrestrial Physics
[PB94-142064] p 3832 N94-31808

NATIONAL TRANSPORTATION SAFETY BOARD, WASHINGTON, DC.
Annual review of aircraft accident data: US air carrier operations, calendar year 1991
[PB94-158847] p 3575 N94-32925
Aircraft incident report: In-flight turbulence encounter and loss of portions of the elevators, China Airlines Flight CI-012, McDonnell Douglas MD-11-P, Taiwan Registration B-150 about 20 miles east of Japan, 7 December 1992
[PB94-910403] p 3576 N94-32938

NAVAL AEROSPACE MEDICAL RESEARCH LAB., PENSACOLA, FL.
Effects of methamphetamine and fatigue on long- and short-term memory
[AD-A276452] p 3799 N94-32187

NAVAL AIR WARFARE CENTER, CHINA LAKE, CA.
The 18th annual electronics manufacturing seminar
[AD-A276038] p 3687 N94-31281
Wavelet transform of fixed pattern noise in focal plane arrays
[AD-A276963] p 3712 N94-32393

NAVAL AIR WARFARE CENTER, LAKEHURST, NJ.
Fuzzy-neural control of an aircraft tracking camera platform p 3839 N94-32423

NAVAL AIR WARFARE CENTER, ORLANDO, FL.
Night vision camcorder system
[AD-A277004] p 3712 N94-32002

NAVAL AIR WARFARE CENTER, WARMINSTER, PA.
Empirical and semi-empirical relationships of liquid-vapor, solid-vapor, and solid-liquid surface energies
[AD-A276480] p 3631 N94-31248
Validation and sensitivity analysis of Texas human thermal model predictions during cold water immersion
[AD-A275240] p 3797 N94-32156
Evaluation of the Hughes conversion coating touch-up pen
[AD-A278398] p 3664 N94-33166

NAVAL CIVIL ENGINEERING LAB., PORT HUENEME, CA.
Procedures for computing site seismicity
[AD-A277666] p 3775 N94-33028

NAVAL COASTAL SYSTEMS CENTER, PANAMA CITY, FL.
Covert channel analysis of trusted systems. A guide to understanding
[AD-A276418] p 3916 N94-31331
Thermotropic liquid crystals: A variable Clo material
p 3796 N94-31739

NAVAL COMMAND, CONTROL AND OCEAN SURVEILLANCE CENTER, SAN DIEGO, CA.
Evaluation of nondestructive inspection techniques for quality control of alumina-ceramic housing components
[AD-A276220] p 3730 N94-31065
Towards simplicity: Noise and cooperation in the perfect integrator
[AD-A276256] p 3799 N94-31291
Atmospheric effects assessment program: Ionospheric sounding
[AD-A276447] p 3770 N94-31303
The High-Frequency Benchmark propagation program
[AD-A276323] p 3672 N94-31334
Texture generation on irregular regions
[AD-A275999] p 3841 N94-31359
Control experiments in liquid metal combustion
[AD-A276918] p 3635 N94-32234
New approaches for real time decision support systems p 3915 N94-32426
Voice and video transmission using XTP and FDDI
p 3685 N94-32468
Broadband, high-power, 2-30 MHz, twin-whip antenna. Computer and 1/10-scale model design study
[AD-A277619] p 3682 N94-32971
Spatial correlation of ionospheric variability
[AD-A278105] p 3776 N94-33041
Simultaneous excitation of parametric decay cascades and the OTSI in 1D numerical simulations based on Aakarov's equations
[AD-A278108] p 3893 N94-33042
A comparison of rough surface parabolic equation models
[AD-A278090] p 3791 N94-33185
An approximate model for vertical polarization and surface roughness using the parabolic equation
[AD-A278091] p 3684 N94-33186
An evaluation of three GPS receivers for use in the GPS sounder
[AD-A278157] p 3577 N94-33253
The effects of a multipath channel and interference on coherent M-PSK digital communication systems
[AD-A278158] p 3684 N94-33254
A theory of conditional information with applications
[AD-A278164] p 3850 N94-33255
Diurnal, seasonal and solar activity variations of F-region parameters
[AD-A278106] p 3776 N94-33285

NAVAL ENERGY AND ENVIRONMENTAL SUPPORT ACTIVITY, PORT HUENEME, CA.
Bond stress-slip characteristics of FRP rebars
[AD-A277191] p 3623 N94-32070

NAVAL HEALTH RESEARCH CENTER, SAN DIEGO, CA.
A review of microclimate cooling systems in the chemical, biological, radiological environment
[AD-A276446] p 3802 N94-31302

NAVAL POSTGRADUATE SCHOOL, MONTEREY, CA.
Machinery monitoring and diagnostics using pseudo Wigner-Ville distribution and backpropagation neural network
[AD-A276219] p 3828 N94-31064
A comparison of predictors for first-guess wind speed errors
[AD-A276460] p 3781 N94-31239
VLSI implementation of stray insensitive switched capacitor composite operational amplifiers
[AD-A276461] p 3687 N94-31240
Numerical analysis of single-vortex/free-surface interaction
[AD-A276462] p 3701 N94-31241
A preliminary investigation of high amplitude standing waves with laser Doppler anemometry
[AD-A276463] p 3860 N94-31242
Scheduling techniques for multiple processor systems in real-time environments
[AD-A276149] p 3824 N94-31249
Computer implementation of Arnott's formulation of thermoacoustics using MATLAB
[AD-A276356] p 3860 N94-31257
An analysis of non-integerizing the aircraft engines Cost Effectiveness Analysis Spreadsheet Model (CEAMOD version 2.0)
[AD-A276251] p 3583 N94-31290
Air Force Space Command satellite orbit predictor using parallel virtual machines
[AD-A276316] p 3801 N94-31298
Kalman filtering approach to blind equalization
[AD-A276320] p 3671 N94-31299
Predicting antenna parameters from antenna physical dimensions
[AD-A276442] p 3672 N94-31300
An analysis of the maintenance performance measurement system for LAMPS MK 3 helicopter squadrons
[AD-A276421] p 3565 N94-31332
Rotordynamic effects driven by fluid forces from a geometrically imperfect labyrinth
[AD-A276424] p 3722 N94-31333
Analysis using bi-spectral related technique
[AD-A276017] p 3672 N94-31386
Waveform generation for ultra-wideband radar system
[AD-A276352] p 3673 N94-31401
Unmanned Air Vehicle/Remotely Piloted Vehicle analysis for lethal UAV/RPV
[AD-A276052] p 3578 N94-31442
The effect of westerly wind bursts on a tropical ocean general circulation model
[AD-A276423] p 3788 N94-31448
A model and algorithms for a software evolution control system
[AD-A276431] p 3811 N94-31449
Low sidelobe reflector antenna design for communications
[AD-A276079] p 3673 N94-31463
Short term teleconnections associated with an individual tropical cyclone
[AD-A277210] p 3783 N94-32019
Theoretical basis for state vector comparison, relative position display, and relative position/rendezvous prediction
[AD-A277216] p 3608 N94-32020
The evolution of jet features during the 1993 east coast white hurricane: A case study using the global spectral model
[AD-A277217] p 3783 N94-32021
Sodium sulfate corrosion of silicon carbide fiber-reinforced lithium aluminosilicate glass-ceramic matrix composites
[AD-A277224] p 3623 N94-32023
Finite element analysis of damage in fibrous composites using a micromechanical model
[AD-A277226] p 3623 N94-32024
Shiptrack database analysis
[AD-A277228] p 3746 N94-32025
Development of a cascade simulation of fan-passage flow
[AD-A277234] p 3584 N94-32026
Hotwire measurements of the turbulent flow into a cascade of controlled-diffusion compressor blades
[AD-A277297] p 3706 N94-32042
Heat transfer studies on a rectangular channel with offset plate fins
[AD-A277300] p 3912 N94-32043
X ray pulse considerations and electron flow in high voltage diodes
[AD-A277301] p 3868 N94-32044
Combustor and nozzle effects on particulate behavior in solid rocket motors
[AD-A277304] p 3614 N94-32071
Air-sea interaction patterns in the equatorial Pacific
[AD-A277305] p 3788 N94-32072

The influence of cumulus parameterization on model forecasts of rapid oceanic cyclogenesis
[AD-A277207] p 3784 N94-32094
An analog preprocessing architecture for high-speed analog-to-digital conversion
[AD-A276737] p 3807 N94-32163
Development of a frequency-domain electromagnetic scattering measurement system
[AD-A276738] p 3678 N94-32179
A technique for multiplexing 3x3-coupler terminated interferometric fiber-optic sensors
[AD-A276739] p 3880 N94-32180
Prediction of the plane wave beamformed acoustic arrival structure for the 1992 Barents Sea coastal tomography test
[AD-A276741] p 3788 N94-32181
Design of a cold-flow test facility for the high pressure fuel turbopump turbine of the Space Shuttle main engine
[AD-A276743] p 3615 N94-32182
Applied Computational Electromagnetics Society Journal, volume 9, number 1, March 1994
[AD-A276753] p 3679 N94-32183
Semianalytic Satellite Theory (SST): Mathematical algorithms
[AD-A276836] p 3610 N94-32208
Three dimensional vorticity field in the California current system
[AD-A276951] p 3788 N94-32220
Analysis of Navy aircraft engine and engine component warranties
[AD-A276936] p 3584 N94-32238
Correlation of flux composition and inclusion characteristics with submerged arc weld metal properties in HY-100 steel
[AD-A277040] p 3726 N94-32261
Pulse-splitting and AM-FM conversion in a nonlinear dispersive medium
[AD-A277041] p 3861 N94-32262
Low altitude near-the-horizon propagation: A comparison between RPO and M-layer
[AD-A277358] p 3679 N94-32282
Estimating subpycnocline density fluctuations in the California current region from upper ocean observations
[AD-A277278] p 3789 N94-32325
ENSO forced variations of the sea surface temperature and adjusted sea level along the west coast of the United States
[AD-A277306] p 3789 N94-32327
An experimental testbed for a free-floating manipulator
[AD-A277350] p 3726 N94-32334
An analysis of ionospheric dayglow from observations of the Naval Postgraduate School Middle Ultraviolet Spectrograph (MUSTANG)
[AD-A277351] p 3773 N94-32335
Optimal adaptive estimation algorithm for harmonic current reduction using power limited active line conditioners
[AD-A277354] p 3693 N94-32336
Thermospheric modeling accuracies using F10.7 and Ap
[AD-A277355] p 3773 N94-32337
Trajectory planning for space manipulators
[AD-A277229] p 3611 N94-32369
Design of a two dimensional planer pressurized air labyrinth seal test rig
[AD-A277232] p 3726 N94-32370
Continuous measurement of aging response in aluminum alloys by eddy current methods
[AD-A277233] p 3644 N94-32371
Radiation tolerant, high speed, low power, gallium arsenide logic
[AD-A277293] p 3694 N94-32509
Multidimensional scaling of user information satisfaction
[AD-A277230] p 3920 N94-32633
An exploratory study of neuro linguistic programming and communication anxiety
[AD-A277756] p 3682 N94-32986
Multicast communication with guaranteed quality of service
[AD-A277650] p 3682 N94-33025
Design and Monte Carlo analysis of an unmanned aerial vehicle
[AD-A277648] p 3580 N94-33056
Evolution of diurnal surface winds and surface currents for Monterey Bay
[AD-A277649] p 3790 N94-33057
Fault detection and isolation for the Bluebird test bed aircraft
[AD-A277979] p 3586 N94-33086
Multiple-valued programmable logic array minimization by solution space search
[AD-A278033] p 3821 N94-33090
The analysis of wake-induced unsteady aerodynamics related to higher harmonic control
[AD-A277914] p 3573 N94-33108
An evaluation framework for designing a night vision, computer-based trainer
[AD-A278005] p 3590 N94-33139
Coastal boundary layer and refractivity measurements using the ground-based high resolution interferometer sounder (GB-HIS)
[AD-A277980] p 3683 N94-33159
An analysis of cellular telephone and INMARSAT systems for providing radio data link computer communications for US Navy vessels
[AD-A278143] p 3684 N94-33160
Increasing the practical impact of formal methods for computer-aided software development: Software slicing, merging and integration
[AD-A277929] p 3822 N94-33179
Generation of the ambiguity function for ultra wideband radar waveforms
[AD-A277913] p 3684 N94-33261
Time resolved measurements of light produced by onset of plasma formation on electrodes of fast pulsed high voltage diodes
[AD-A277974] p 3894 N94-33264
Least squares approximation by G1 piecewise parametric cubes
[AD-A277978] p 3850 N94-33265
A user's manual for the cost effectiveness analysis spreadsheet model for aircraft engines (CEAMOD version 2.0)
[AD-A278042] p 3585 N94-33266
Analysis of intermediate level maintenance following F404-GE-400 engine component life reductions
[AD-A277918] p 3585 N94-33283

NAVAL RESEARCH LAB., BAY SAINT LOUIS, MS.
Surface forward-scattered acoustic measurements and analysis
[AD-A276998] p 3788 N94-32000
MDFF HELP library, version 2: On-line documentation for the map data formatting facility
[AD-A277763] p 3922 N94-32987

NAVAL RESEARCH LAB., MONTEREY, CA.
Typhoon havens handbook for the western Pacific and Indian Oceans, change 3
[AD-A277030] p 3784 N94-32260
Tropical cyclone forecasters reference guide. 5: Numerical track forecast guidance
[AD-A277318] p 3785 N94-32278
Forecasters handbook for the Philippine islands and surrounding waters
[AD-A277993] p 3787 N94-33089

NAVAL RESEARCH LAB., WASHINGTON, DC.
A multichannel architecture for Naval Task Force Communication
[AD-A276230] p 3673 N94-31446
Consistency checks for SCR-style requirements specifications
[AD-A276077] p 3811 N94-31461
Detection of a chi-square fluctuating target in Gaussian noise
[AD-A276078] p 3850 N94-31462
Additional capabilities of the unified waves model
[AD-A276114] p 3702 N94-31467
Analysis of key performance parameters of phase sampling digital RF memories
[AD-A276019] p 3688 N94-31494
Methods for SBS threshold reduction
[AD-A276554] p 3717 N94-31936
Design of a high power x-band magnicon amplifier
[AD-A277001] p 3692 N94-32199
Pinched propagation of high-power, pulsed electron beams for welding and materials processing applications
[AD-A276925] p 3726 N94-32236
Design, development, and testing of a Network Frequency Selection Service (NFSS)
[AD-A277362] p 3680 N94-32283
Glutinous water: Protecting vertical and overhead surfaces from fire spread
[AD-A277280] p 3575 N94-32405
Gyrotrons and free electron lasers for atmospheric sensing
[AD-A277281] p 3718 N94-32406
Noise cancellation for CELP voice encoders in an F/A-18 noise environment
[AD-A277652] p 3683 N94-33026
Design, development, and testing of a lightweight optical sensor cover system p 3604 N94-33302
Advanced release technologies program
p 3607 N94-33322

NAVAL SURFACE WARFARE CENTER, BETHESDA, MD.
Transmissibility of nickel-titanium shape memory alloy springs
[AD-A276055] p 3640 N94-31456

NAVAL SURFACE WARFARE CENTER, DAHLGREN, VA.
Naval Surface Warfare Center Dahlgren Division Technical Digest: Advanced materials technology
[AD-A276448] p 3668 N94-31364
A new method for calculating wing along aerodynamics to angle of attack 180 deg
[AD-A277965] p 3574 N94-33263

NAVAL SURFACE WARFARE CENTER, PANAMA CITY, FL.
Navy Omni-Directional Vehicle (ODV) development program p 3729 N94-32451

NAVAL SURFACE WARFARE CENTER, SILVER SPRING, MD.
PVDF pressure transducers for shock wave and explosives research
[AD-A277319] p 3712 N94-32051
Neural network wavelet technology: A frontier of automation p 3839 N94-32425

NAVAL SURFACE WEAPONS CENTER, SILVER SPRING, MD.
Hypervelocity Tunnel 9 Mach 10/14 Calibration
[AD-A275960] p 3587 N94-31318

NAVAL UNDERSEA WARFARE CENTER, NEWPORT, RI.
Adaptive control of telerobotic systems worn by humans
[AD-A276608] p 3834 N94-32036
Wavevector-frequency analysis with applications to acoustics
[AD-A276618] p 3861 N94-32125
Massively parallel systems design for real-time embedded applications
[AD-A277256] p 3826 N94-32323

NAVAL UNDERWATER ORDNANCE STATION, NEWPORT, RI.
High frequence and automatic link establishment (HF and ALE) radio propagation test to Antarctica
[AD-A277730] p 3682 N94-33001

NEBRASKA UNIV., LINCOLN.
Conductive paints
[DE94-008508] p 3661 N94-32788

NEKTONICS, INC., CAMBRIDGE, MA.
Chemical vapor deposition fluid flow simulation modelling tool
[NASA-CR-189648] p 3707 N94-32480

NETHERLANDS BIBLIOGRAPHICAL AND DOCUMENTARY COMMITTEE, AMSTERDAM.
Current Research Information in Europe: Conference proceedings
[PB94-127933] p 3917 N94-31768

NEVADA UNIV., RENO.
Hydrologic Database user's manual
[DE94-003950] p 3743 N94-31603

NEW JERSEY INST. OF TECH., NEWARK.
Report on implementing part relationships using VML metaclasses
[PB94-147485] p 3813 N94-31686

NEW MEXICO INST. OF MINING AND TECHNOLOGY, SOCORRO.
Interface engineering in oxide fiber/oxide matrix composites
[AD-A277672] p 3627 N94-33029

NEW MEXICO STATE UNIV., LAS CRUCES.
The Los Alamos National Laboratory precision double crystal spectrometer
[DE94-008075] p 3713 N94-32706

NEW MEXICO UNIV., ALBUQUERQUE.
Pressureless sintering of ceramic composites
[AD-A277274] p 3657 N94-32404
Repetitively pulsed backward-wave oscillator investigations
[AD-A278281] p 3698 N94-33142

NEW ORLEANS UNIV., LA.
Electronic and nuclear factors in intramolecular charge and excitation transfer processes
[DE94-006598] p 3870 N94-32178

NEW YORK UNIV., NEW YORK.
Visual neural development and chromatic aberration
[AD-A277402] p 3800 N94-32345
Machine assisted implementation of complex algorithms and labor intensive software, closing report
[AD-A277662] p 3821 N94-33027

NICHOLS RESEARCH CORP., HUNTSVILLE, AL.
Development of an automated wire delivery system for robotic welding applications
[NASA-CR-194216] p 3727 N94-32479

NIJMEGEN UNIV. (NETHERLANDS).
Transformation of database populations and operations from the conceptual to the internal level
[TR-92-27] p 3916 N94-31175
Experiences with EDO: An Evolutionary Database Optimizer
[TR-93-23] p 3918 N94-32105

Transformational derivation of (parallel) programs using skeletons
[TR-93-20] p 3825 N94-32196
Informal introduction to the extended affix grammar formalism and its compiler
[TR-93-19] p 3817 N94-32287
An information system organized as stratified hypermedia
[TR-93-12] p 3918 N94-32289
EVORM: A conceptual modelling technique for evolving application domains
[TR-93-16] p 3918 N94-32290
An epistemic proof system for parallel processes
[TR-93-17] p 3826 N94-32291
Multiple inheritance via intersection types
[TR-93-18] p 3848 N94-32292
Information disclosure in evolving information systems: Taking a shot at a moving target
[TR-93-22] p 3919 N94-32506

NONDESTRUCTIVE TESTING INFORMATION ANALYSIS CENTER, SAN ANTONIO, TX.
Benchmarking of the state-of-the-art in nondestructive testing/evaluation for applicability in the Composite Armored Vehicle (CAV) Advanced Technology Demonstrator (ATD) program, phase 1
[AD-A276660] p 3730 N94-32088

NORGES TEKNISKE HOEGSKOLE, TRONDHEIM.
Laser applications in wood processing
[PB94-138567] p 3717 N94-31840

NORTH CAROLINA AGRICULTURAL AND TECHNICAL STATE UNIV., GREENSBORO.
Computational methods in continuum mechanics
[AD-A278144] p 3859 N94-33161

NORTH CAROLINA CENTRAL UNIV., DURHAM.
High resolution molecular spectroscopy of atmospheric species
[AD-A278382] p 3776 N94-33351

NORTH CAROLINA STATE UNIV., RALEIGH.
Numerical simulations of monsoon rainfall with the NRL/NCSU regional nested grid model
p 3782 N94-31791
Boundary layer study on nozzle wall at hypersonic velocities p 3569 N94-31882
A non-local model for prediction of the probability density function of turbulent fluctuations in boundary-layer flows
p 3706 N94-32076
Novel approaches to the production of higher alcohols from synthesis gas
[DE94-006770] p 3666 N94-32132
Communication networks for autonomous mobile robot computer architectures and distributed real-time computing p 3680 N94-32310

NORTH CAROLINA UNIV., CHAPEL HILL.
Indium-vacancy complexes in mercury cadmium telluride
[AD-A276177] p 3894 N94-31055
Isomeric poly(benzophenone)s: Synthesis of highly crystalline poly (4, 4 foot-benzophenone) and amorphous poly (2, 5-benzophenone), a soluble poly (p-phenylene) derivative
[AD-A277261] p 3655 N94-32017
Post-calibration correction for rotating-analyzer ellipsometer with optical fiber bundle detection system
[AD-A277329] p 3881 N94-32280
Si/SiO2 interface studies by immersion ellipsometry
[AD-A277277] p 3881 N94-32324
Visual encoding of spatial relations
[AD-A277400] p 3800 N94-32344
Electron cyclotron resonance plasma oxidation studies of InP
[AD-A277431] p 3893 N94-33007

NORTH CAROLINA UNIV., CHARLOTTE.
Conference on operator, wavelet and control theory
[AD-A277429] p 3838 N94-33174

NORTH CAROLINA UNIV., RALEIGH.
Growth and characterization of III-V semiconductors with rare earth impurities for optoelectronic devices
[AD-A276021] p 3896 N94-31455

NORTH DAKOTA UNIV., GRAND FORKS.
Manual for automatic generation of finite element models of spiral bevel gears in mesh
[NASA-CR-191009] p 3728 N94-32900

NORTHEAST RADIO OBSERVATORY CORP., WESTFORD, MASS. HAYSTACK OBSERVATORY.
Millstone Hill radar studies of plasma waves and turbulence
[AD-A278409] p 3684 N94-33172

NORTHWESTERN UNIV., CHICAGO, IL.
Modeling of fracture and damage in quasibrittle materials p 3734 N94-31479
On the mechanics of stress analysis of fiber-reinforced composites p 3619 N94-31481
On the constitutive response of transversely loaded fiber composites with compliant interphases
p 3619 N94-31555

NORTHWESTERN UNIV., EVANSTON, IL.
New and emerging techniques for imaging surfaces
[AD-A276497] p 3878 N94-31262
Fracture mechanics and micromechanisms in fiber-reinforced composites p 3622 N94-31986
Effects of interphases on the mechanical, thermal and hygromechanical response of fiber-reinforced composites p 3624 N94-32496
Experimental investigations and molecular dynamics simulations of radiation induced surface damage
[AD-A277323] p 3871 N94-32621
Energetics, bonding mechanism, and electronic structure of ceramic/ceramic and metal/ceramic interfaces
[DE94-008551] p 3659 N94-32656
Reading: Interaction with memory
[AD-A277547] p 3801 N94-32956
Nonlocal theory for fracturing of quasibrittle materials
[AD-A278283] p 3740 N94-33143

NORWEGIAN DEFENCE RESEARCH ESTABLISHMENT, KJELLER.
Ship traffic monitoring and oil spill detection using the ERS-1 SAR p 3751 N94-32542

NOTRE DAME UNIV., IN.
Camera-space manipulation with natural visual information p 3829 N94-31207
Experimental and computational studies on propeller noise due to inflow distortion p 3860 N94-31846
A study of the development and attenuation of wing-generated, vortical wakes p 3570 N94-31971

NYMA, INC., BROOK PARK, OH.
Evaluation of pyrolysis and arc tracking on candidate wire insulation designs for space applications
[NASA-CR-195332] p 3731 N94-32901

O

OAK RIDGE K-25 SITE, TN.
SOLGAS refined: A computerized thermodynamic equilibrium calculation tool
[DE94-009021] p 3913 N94-32846

OAK RIDGE NATIONAL LAB., TN.
Acquisition information management system telecommunication site survey results
[DE94-005688] p 3915 N94-31155
Effect of vibratory stress relief during welding of thick stainless steel plate
[DE94-006557] p 3733 N94-31312
Effects of oxidation and creep damage mechanisms on creep behavior in HIPed silicon nitrides
[DE94-006559] p 3618 N94-31313
Enhancement of oxidation resistance of silicon carbide by high-dose and multi-energy aluminum implantation
[DE94-006560] p 3640 N94-31314
Incoherent imaging by Z-contrast stem: Towards 1 Angstrom resolution
[DE94-006551] p 3896 N94-31489
Ion beam synthesis of IrSi3 by 1-MeV Ir ion implantation into Si(111)
[DE94-006556] p 3896 N94-31501
The Global Climatology Network precipitation data
[DE93-019199] p 3764 N94-31596
Proceedings of a Joint US-Japan Seminar in the Environmental Sciences
[DE94-004727] p 3741 N94-31606
Characterization of the rare earth orthophosphates and Ce-doped LaPO4 by x ray absorption spectroscopy
[DE94-006313] p 3898 N94-31630
Perturbative and nonperturbative EM lepton pair production in relativistic heavy-ion collisions
[DE94-006315] p 3867 N94-31779
In-situ TEM crystallization of anorthite-glass films on (alpha)-Al2O3
[DE94-006317] p 3652 N94-31780
Creep-fatigue criteria and inelastic behavior of modified 9Cr-1Mo steel at elevated temperatures
[DE94-007915] p 3642 N94-31918
Oriented Si and Ge nanocrystals formed in Al2O3 by ion implantation and annealing
[DE94-005593] p 3901 N94-32172
Atomic and molecular data needs for fusion
[DE94-006555] p 3870 N94-32177
A model geophysics program
[DE94-007415] p 3747 N94-32203
A comparison between two Monte Carlo codes on determination of transient chemical yields
[DE94-007224] p 3636 N94-32251
Characterization of atomic and molecular impurity sources and transport at the tokamak edge
[DE94-007212] p 3891 N94-32619
Ceramic Technology Project database
[DE94-008494] p 3659 N94-32632
Compositions and chemical bonding in ceramics by quantitative electron energy-loss spectrometry
[DE94-007208] p 3659 N94-32640
Implementation and display of Computer Aided Design (CAD) models in Monte Carlo radiation transport and shielding applications
[DE94-007221] p 3819 N94-32641
Adjacent-cell Preconditioners for solving optically thick neutron transport problems
[DE94-007219] p 3872 N94-32666
Vulnerability assessment of a space based weapon platform electronic system exposed to a thermonuclear weapon detonation
[DE94-007229] p 3611 N94-32667
Using the National Information Infrastructure for social science, education, and informed decision making
[DE94-005442] p 3920 N94-32676
A new solution method for the inverse kinematic joint velocity calculations of redundant manipulators
[DE94-004427] p 3727 N94-32682
Homogeneous global mean temperature time series
[DE94-002194] p 3766 N94-32690
Flywheel Energy Storage Technology Workshop
[DE94-008064] p 3761 N94-32705
Ab initio study of the epitaxial growth of Ge on Si(100) surface
[DE94-007245] p 3904 N94-32724
Reactor pressure vessel structural integrity research in the US Nuclear Regulatory Commission HSST and HSSI Programs
[DE94-006550] p 3739 N94-32771
A miniaturized ASIC-based multichannel scaler instrument
[DE94-007222] p 3807 N94-32783
Environmental issues related to biomass: An overview
[DE94-007226] p 3767 N94-32784
Properties of doped and undoped (Ca,Sr)CuO2 thin films
[DE94-007230] p 3905 N94-32785
String-parton model description of relativistic heavy-ion collisions
[DE94-009164] p 3874 N94-32850
Potential applications of fusion neutral beam facilities for advanced material processing
[DE94-009167] p 3647 N94-32851
Structure, stability, and mechanical properties of intermetallic phases
[DE94-009178] p 3647 N94-32852
Effect of elevated temperature and cyclic loading on properties and damage modes in ceramic composites
[DE94-008736] p 3662 N94-32891
Materials development program: Ceramic technology project bibliography, 1984-1992
[DE94-009297] p 3662 N94-32935
The path for long range conduction in high J(sub c) TlBa2Ca2Cu3O(8+x) spray-pyrolyzed deposits
[DE94-007211] p 3909 N94-33271

OBSERVATORIO DEL EBRO, ROQUETAS (SPAIN).
Eurocap program-ebre station
[AD-A277044] p 3772 N94-32007

ODYSSEY RESEARCH ASSOCIATES, INC., ITHACA, NY.
Formal semantics for a subset of VHDL and its use in analysis of the FTPP scoreboard circuit
[NASA-CR-191577] p 3827 N94-32734

OFFICE DE LA RECHERCHE SCIENTIFIQUE ET TECHNIQUE OUTRE-MER, MONTPELLIER (FRANCE).
Contribution of SAR ERS1 data to study the French Guiana tropical coast environment
[BRGM-93034] p 3748 N94-32527

OFFICE DE LA RECHERCHE SCIENTIFIQUE ET TECHNIQUE OUTRE-MER, PARIS (FRANCE).
General ocean circulation p 3777 N94-30984
Low frequence variability of the ocean atmosphere coupled system p 3777 N94-30986
Low frequency variability observed in the tropical Atlantic Ocean p 3778 N94-30991
Study of subpolar glaciers of Spitzbergen using SPOT, ERS-1, and hypsometric data: Results and perspectives
p 3753 N94-32553

OFFICE DE LA RECHERCHE SCIENTIFIQUE ET TECHNIQUE OUTRE-MER, YAOUNDE (CAMEROON).
Comparing SPOT and SIR A for mapping superficial formations in tropical forest regions: Example of the Yaoundy Region (Cameroon) p 3755 N94-32562

OFFICE NATIONAL D'ETUDES ET DE RECHERCHES AEROSPATIALES, PARIS (FRANCE).
Micromechanical analysis of the interface and basic damage modes in glass fiber/epoxy resin model composites
[ONERA-NT-1993-4] p 3618 N94-31225
Scattering of a random acoustic field by an infinite cylinder: Application to the modelization of the acoustic environment of the 'Ariane 5' launcher scale-model using experimental data
[ONERA-NT-1993-11] p 3860 N94-31226

Development of a 3D numerical code to calculate the trajectories of the blow off electrons emitted by a vacuum surface discharge: Application to the study of the electromagnetic interference induced on a spacecraft
[ONERA-NT-1993-12] p 3863 N94-31227
Development of a three-dimensional icing model for predicting ice accretion on aircraft
[ONERA-NT-1993-5] p 3574 N94-31230
Doubly asymptotic approximations: Theoretical and numerical analyses
[ONERA-NT-1993-7] p 3840 N94-31231
Unidirectional composites compressive behaviour: Test methods and micromechanical approach
[ONERA-NT-1993-10] p 3618 N94-31232
Electromagnetic scattering through loaded aperture panels with nonzero contact impedance
[ONERA-NT-1993-2] p 3673 N94-31418
Radar image classification by texture measurements
[ONERA-NT-1993-3] p 3673 N94-31419
Microstructures and mechanical properties of Al3Ti-based alloys: Analysis in single phase and multiphase systems
[ONERA-NT-1993-6] p 3640 N94-31420
Experimental and numerical simulation of helicopter rotor fuselage interaction
[ONERA-NT-1993-8] p 3568 N94-31421
Analysis of strong acoustic excitation on the breakup and dispersion of a liquid jet
[ONERA-NT-1993-9] p 3701 N94-31422
The prediction of convective transfer on the thermal insulation of a solid-propellant rocket motor
[ONERA-NT-1993-15] p 3614 N94-31423
Mixture model simulating reactive turbulent flows: Testing of Eulerian-Lagrangian probabilistic models
[ONERA-NT-1993-13] p 3702 N94-31477
Evolution of the interface properties with temperature in the T800H/ bismaleimide composites
[ONERA-NT-1993-14] p 3619 N94-31478
Use and administration of UNIX (tm) systems
p 3821 N94-33051

OFFICE NATIONAL DE LA METEOROLOGIE, ALGIERS (ALGERIA).
Some aspects of the drought in North Africa and in the Mediterranean basin p 3778 N94-30989

OFFICE OF NAVAL RESEARCH, ARLINGTON, VA.
Workshop on Commercialization of Pulsed Power Science and Technology Proceedings
[AD-A276987] p 3692 N94-32258
Database tomography for commercial application
p 3923 N94-32442

OFFICE OF NAVAL RESEARCH EUROPEAN OFFICE, FPO NEW YORK, NY.
Piezoelectric materials research in Europe
[AD-A276207] p 3648 N94-31059

OFFICE OF TECHNOLOGY ASSESSMENT, WASHINGTON, DC.
Global change research and NASA's Earth Observing System
[PB94-126992] p 3741 N94-31068

OHIO STATE UNIV., COLUMBUS.
Molecular/polymeric magnetism
[DE94-005888] p 3649 N94-31201
High energy physics studies
[DE94-005970] p 3876 N94-31505
Design and initial testing of a facility to measure unsteady pressures on an oscillating cascade with supersonic leading edge locus p 3569 N94-31880
Theory of thick, laminated composite shallow shells
p 3622 N94-31953
A fracture mechanics methodology for characterizing the performance of flawed polymeric dielectric materials
p 3654 N94-31956
World height system definition and implementation
[AD-A276725] p 3747 N94-32160
Visual perception of 3-dimensional structure from different types of optical deformation
[AD-A276272] p 3884 N94-33141
A study of weak solutions and their regularizations by numerical methods
[AD-A277453] p 3850 N94-33175

OHIO UNIV., ATHENS.
Radiation from an aperture into an anisotropic plasma half-space p 3885 N94-31205
Remote infrared vapor detection of volatile organic compounds
[AD-A276982] p 3746 N94-31999

OKLAHOMA UNIV., NORMAN.
Ultrasonic tomography in fiber-reinforced composite materials p 3620 N94-31565

OLD DOMINION UNIV., NORFOLK, VA.
Electron-beam controlled semiconductor switches
[AD-A276198] p 3686 N94-31057
Grid sensitivity for aerodynamic optimization and flow analysis p 3568 N94-31287
Control of low-speed turbulent separated flow over a backward-facing ramp
[NASA-TM-109740] p 3573 N94-33071

OPEN UNIV., MILTON (ENGLAND).
Carbonates, surfates, phosphates, nitrates, and organic materials: Their association in a Martian meteorite
p 3952 N94-33239

OREGON STATE UNIV., CORVALLIS.
SEASOAR and CTD observations during a COARE surveys cruise, W9211C, 22 January - 22 February, 1993
[AD-A277925] p 3791 N94-33244

OULU UNIV. (FINLAND).
Carbon dioxide abatement as a differential game
[DE94-722023] p 3765 N94-32590

OXFORD UNIV. (ENGLAND).
Baryogenesis from a primordial lepton asymmetry
[PB94-145166] p 3868 N94-31921
Tensor gauge potentials in loop space formulation of Yang-Mills fields
[PB94-147147] p 3912 N94-31924

P

PACIFIC NORTHWEST LAB., RICHLAND, WA.
High-temperature superconducting transformer performance, cost, and market evaluation
[DE94-005494] p 3687 N94-31152
Ion-beam-driven amorphization of Ca2La8(Si4)6O2 single crystals
[DE94-006219] p 3895 N94-31307
Information resources for US Department of Energy pollution prevention programs
[DE94-006677] p 3763 N94-31582
Process mapping: A user-friendly tool for process improvement
[DE94-004357] p 3730 N94-31605
The influence of transmutation, void swelling, and flux/spectra uncertainties on the electrical properties of copper and copper alloys
[DE94-006213] p 3641 N94-31626
Defect-solute interactions near irradiation grain boundaries
[DE94-006215] p 3641 N94-31627
Development of a catalytic system for gasification of wet biomass
[DE94-006216] p 3759 N94-31762
Modal analysis of multiterminal high voltage direct current transmission
[DE94-006426] p 3691 N94-31785
Millimeter wave, high-resolution, holographic surveillance system
[DE94-004289] p 3712 N94-31831
CMS Preprocessing Subsystem user's guide: Software version 2.0
[DE94-005327] p 3816 N94-32145
CMS Distribution Subsystem user's guide
[DE94-005328] p 3816 N94-32146
A parameterization of cloud droplet nucleation
[DE94-007469] p 3785 N94-32268
The role of guideline-based design tools
[DE94-007482] p 3804 N94-32596
Molecular Science Research Center
[DE94-007464] p 3871 N94-32605
Stage 1 behavior in a stress corrosion study of Type 304 stainless steel
[DE94-008054] p 3645 N94-32614
Ultra wide band radar holographic imaging of subsurface targets
[DE94-004271] p 3713 N94-32681
A noncritically phase matched femtosecond optical parametric oscillator near 3 microns
[DE94-008050] p 3720 N94-32704
An evaluation of RAMS radiation schemes by field measurements
[DE94-008053] p 3767 N94-32750
Water vapor from sunradiometry in comparison with microwave and balloon-sonde measurements at the Southern Great Plains ARM Site
[DE94-007479] p 3786 N94-32759
Performance of an ion trap inductively coupled plasma mass spectrometer
[DE94-007470] p 3713 N94-32811
Food security in the context of global environmental change
[DE94-007481] p 3768 N94-32812
OPTIONS for systemic change in mathematics, science, and technology education: Scientist/teacher partnerships
[DE94-007472] p 3914 N94-32910

PARIS-SUD UNIV., ORSAY (FRANCE).
Carbon balance in a forest ecosystem
p 3770 N94-31007

PARIS VI UNIV. (FRANCE).
General ocean circulation p 3777 N94-30984
Low frequence variability of the ocean atmosphere coupled system p 3777 N94-30986
Respective contributions of VIS-PIR, SAR-ERS 1, and airborne radar data for morphostructural and morphoneotectonic analysis: Practical examples
p 3752 N94-32549

PARIS VI UNIV., VILLEFRANCHE-SUR-MER (FRANCE).
The ocean-atmosphere interactions in the Mediterranean Sea p 3779 N94-30995

PARIS VII UNIV. (FRANCE).
Arid regions and wind erosion p 3780 N94-31005

PARMA UNIV. (ITALY).
WOCSDICE 1993
[AD-A276766] p 3693 N94-32307

PDA ENGINEERING, SANTA ANA, CA.
Analytical Design Package (ADP2): A computer aided engineering tool for aircraft transparency design
p 3823 N94-32430

PENNSYLVANIA STATE UNIV., UNIVERSITY PARK.
Modification of semiconductor surface properties with chemically bound molecular films
[AD-A276162] p 3895 N94-31081
Studying transient mobility and energy loss using scanning tunneling microscopy
[AD-A276292] p 3877 N94-31256
Analytical applications of scanning tunneling microscopy
[AD-A276066] p 3711 N94-31283
A new mechanism for surface diffusion: Motion of a substrate-adsorbate complex
[AD-A276072] p 3632 N94-31459
Research in marine boundary layer intermittency
[AD-A276076] p 3701 N94-31460
Regional sources of error growth in the National Meteorological Center's medium-range forecast model
p 3781 N94-31554
In-situ characterization of growth and interfaces in a-Si:H devices
[DE94-000291] p 3760 N94-31812
Performance evaluation and operating characteristics of a waveguide microwave applicator for space propulsion applications p 3614 N94-31908
Solution of the average-passage equations for the incompressible flow through multiple-blade-row turbomachinery
[AD-A276515] p 3583 N94-31931
Passive vibration damping materials: Piezoelectric ceramic composites for vibration damping applications
[AD-A276550] p 3653 N94-31935
Prediction of hydrogen entry and permeation in metals and alloys
[AD-A276637] p 3642 N94-31995
Advanced thermally stable jet fuels
[DE94-006760] p 3667 N94-32150
An integrated cloud observation and modeling investigation in support of the ARM program
[DE94-003160] p 3785 N94-32716
Development and testing of improved techniques for modeling the hydrologic cycle in a mesoscale weather prediction system
[AD-A277416] p 3786 N94-32921
Statistical characteristics of bistatic surface scatter and mean bistatic surface scattering strengths
[AD-A278155] p 3862 N94-33096
The structure of high Reynolds number turbulent boundary layers, part A
[AD-A278392] p 3710 N94-33162
Microstructures and epitaxy in oxide superconductor thin films and devices
[AD-A278427] p 3910 N94-33332

PHASEX CORP., LAWRENCE, MA.
Improved oxidation resistance of 3-D carbon/carbon composites
[AD-A277349] p 3625 N94-32624

PHILLIPS LAB., HANSCOM AFB, MA.
Performance statistics bulletin. High latitude meteor scatter propagation October, November, December 1990, January 1991
[AD-A276693] p 3676 N94-31998
Performance statistics bulletin. High latitude metor scatter propagation, February, March, April, May 1992
[AD-A276667] p 3677 N94-32083
Sensitivity analysis of the AVHRR infrared cirrus model
[AD-A276690] p 3784 N94-32117
Atmospheric structure simulation: An autoregressive model for smooth geophysical power spectra with known autocorrelation function
[AD-A276691] p 3773 N94-32118
Performance statistics bulletin. High latitude meteor scatter propagation February, March, April, May 1991
[AD-A276723] p 3678 N94-32158
Performance statistics bulletin. High latitude meteor scatter propagation October, November, December 1991, January 1992
[AD-A276724] p 3678 N94-32159

Performance statistics bulletin. High latitude meteor scatter propagation, November and December 1989, and January 1990
[AD-A276688] p 3680 N94-32297
Performance statistics bulletin. High latitude meteor scatter propagation
[AD-A276694] p 3680 N94-32298
Performance statistics bulletin. High latitude meteor scatter propagation
[AD-A276695] p 3680 N94-32299
Performance statistics bulletin. High latitude meteor scatter propagation
[AD-A276696] p 3680 N94-32300
Performance statistics bulletin. High latitude meteor scatter propagation, June, July, August, September 1992
[AD-A277508] p 3685 N94-33347

PHILLIPS LAB., KIRTLAND AFB, NM.
Phase-only correction of scintillated laser beams: Downrange experimental results
[AD-A277778] p 3722 N94-33282

PHYSICAL OPTICS CORP., TORRANCE, CA.
Smart environmental monitor based on neural networks and multi-spectral pattern recognition
[AD-A276445] p 3829 N94-31301
Optical processing of MMW for agile beamsteering and beamforming
[AD-A277161] p 3880 N94-32068
Reconfigurable Array of Radiating Elements (RARE) controlled by light
[NASA-CR-195828] p 3884 N94-33073
A novel optoelectronic system for distortion-invariant ATR
[AD-A277985] p 3884 N94-33087

PHYSICAL SCIENCES, INC., ANDOVER, MA.
Arcing in space structures in low Earth orbit
[NASA-CR-194223] p 3694 N94-32478

PICOTRONIX, INC., ANN ARBOR, MI.
A 1-picosecond InGaAs photodetector for operation at 1300-1600 nm
[AD-A275959] p 3895 N94-31350

PITTSBURGH UNIV., PA.
Biocatalytic processing polymers in supercritical fluids
[AD-A276120] p 3651 N94-31510
Lubrication with binary mixtures: Liquid-liquid emulsion in elastohydrodynamics and metal forming
p 3658 N94-32490
Studies of the fundamental nature of catalytic acidity, sites and intermediates
[DE94-006999] p 3646 N94-32805
On the computation of simplical approximations of implicitly defined two-dimensional manifolds
[AD-A278132] p 3849 N94-33060

PLANETARY SCIENCE INST., TUCSON, AZ.
Possible test of ancient dense Martian atmosphere
p 3947 N94-33206

POLITECNICO DI MILANO (ITALY).
On the use of genetic algorithms to solve the time-table problem
[REPT-90-060-REV] p 3829 N94-31176
The ant system: An autocatalytic optimizing process
[REPT-91-016-REV] p 3824 N94-31177
Design patterns mixing genericity and inheritance in the development of reusable components
[REPT-93-021] p 3808 N94-31178
Concepts and environment
[REPT-93-032] p 3829 N94-31186
A worst-case analysis of two approximate algorithms for the symmetric travelling salesman problem
[REPT-93-036] p 3840 N94-31187
Techniques for increasing the robustness of iterative algorithms for multi-resources location problems
[REPT-93-037] p 3809 N94-31188
Exact solution of the single machine scheduling problem with earliness and flow time penalties
[REPT-93-038] p 3809 N94-31189
Filtering and recognition of moving boats in radar images
[REPT-93-039] p 3671 N94-31190
Representation, prediction and identification of cyclostationary processes: A state-space approach
[REPT-93-041] p 3850 N94-31191
A worst-case analysis of an approximate algorithm for finding the minimum hamiltonian cycle on paths
[REPT-93-042] p 3809 N94-31192
A finite state machine model for object oriented systems
[REPT-93-040] p 3809 N94-31212
Bifurcation and deterministic chaos in dynamic systems
[REPT-93-047] p 3911 N94-31893
Asymptotic behavior of dynamic systems
p 3911 N94-31894
Structural stability and bifurcations
p 3911 N94-31895
Deterministic chaos p 3912 N94-31896
Seasons and chaos in population dynamics
p 3912 N94-31897
Developments in ERS-1 SAR interferometry: Use of the spectral shift p 3756 N94-32569

PRATT AND WHITNEY AIRCRAFT, WEST PALM BEACH, FL.
Fatigue in single crystal nickel superalloys
[AD-A276662] p 3643 N94-32047

PRINCETON UNIV., NJ.
Nonthermal accretion disk models around neutron stars p 3931 N94-31139
Ignition studies in nonpremixed hydrogen/air combustion
[AD-A275954] p 3632 N94-31348
Micromechanics and effective properties of particulate composites and fluid suspensions p 3703 N94-31744
Analysis of forward and inverse problems in chemical dynamics and spectroscopy
[DE94-007607] p 3635 N94-32140
Mathematical nonlinear optics
[AD-A277320] p 3882 N94-32510
Development and application of photosensitive device systems to studies of biological and organic materials
[DE94-008503] p 3793 N94-32516
Molecular interactions in dilute supercritical mixtures: Molecular dynamics investigation
[DE94-007610] p 3872 N94-32644

PUERTO RICO UNIV., RIO PIEDRAS.
Experimental and theoretical studies of hydrogenated amorphous semiconductor alloys and superlattices
[AD-A276159] p 3686 N94-31079

PURDUE UNIV., WEST LAFAYETTE, IN.
The adsorption of sulfate on gold(111) in acidic aqueous media: Adlayer structural inferences from infrared spectroscopy and scanning tunneling microscopy
[AD-A276643] p 3642 N94-31997
A new-type of long-range restructuring of ordered metal surfaces induced by lateral adsorbate interactions: Iodide on AU(110) electrodes
[AD-A276633] p 3643 N94-32060
Vibrational spectroscopy at metal-solution interfaces: Some perspectives and prospects for electrochemical surface science
[AD-A276781] p 3644 N94-32169
Charge-dependent atomic-scale structures of high-index and (110) gold electrode surfaces as revealed by scanning tunneling microscopy
[AD-A276782] p 3869 N94-32170
Some perspectives on solution-phase electron-transfer processes
[AD-A276906] p 3635 N94-32216
Development of a computer model for polycrystalline thin-film CuInSe2 and CdTe solar cells
[DE94-006853] p 3762 N94-32763
Earth observational research using multistage EOS-like data
[NASA-CR-195833] p 3757 N94-33019
Sensitivity of electrochemical adlayer structure to the metal crystallographic orientation: Potential-independent iodide adsorption on Au(100) in comparison with other low-index surfaces
[AD-A276714] p 3909 N94-33273
Scanning tunneling microscopy and infrared spectroscopy as combined in-situ probes of electrochemical adlayer structure: Cyanide on Pt(111)
[AD-A276715] p 3909 N94-33274
Nanoscale structural changes upon electrooxidation of Au(111) as probed by potentiodynamic scanning tunneling microscopy
[AD-A276780] p 3909 N94-33275
A tandem microscopic-electrochemical examination of a charge-induced surface phase sequence: Ordered Au(110) in aqueous iodide electrolytes as probed by potentiodynamic scanning tunneling microscopy
[AD-A276905] p 3875 N94-33277

Q

QUEBEC UNIV., CHICOUTIMI.
Analysis and design of a formal neural network for filtering a dynamic signal
[ISBN-0-315-86932-1] p 3832 N94-31873

QUEENS UNIV., KINGSTON (ONTARIO).
Azo polymers for reversible optical storage. 4. Cooperative motion of rigid groups in semicrystalline polymers
[AD-A277107] p 3654 N94-31978
Recent developments in polymeric charge transfer complexes
[AD-A277108] p 3654 N94-31979
Reversible optical storage in azo polymers
[AD-A277109] p 3654 N94-31980
Compatibility studies of some azo polymer blends
[AD-A277141] p 3657 N94-32365
Microstructure of copolymers containing disperse red 1 and methyl methacrylate
[AD-A277140] p 3660 N94-32722
The role of galaxy type and environment in determining the properties of globular cluster systems
[ISBN-0-315-76447-3] p 3939 N94-33112

R

RADEX, INC., BEDFORD, MA.
Simulation of CO2 release at 800 km altitude
[AD-A276692] p 3776 N94-33272

RAND CORP., SANTA MONICA, CA.
The National Aerospace Plane (NASP): Development issues for the follow-on vehicle
[AD-A278417] p 3581 N94-33329

RAND GRADUATE INST. FOR POLICIES STUDY, SANTA MONICA, CA.
Prospects for the French fighter industry in a post-cold war environment: Is the future more than a mirage?
p 3565 N94-31959

RANGE COMMANDERS COUNCIL, WHITE SANDS MISSILE RANGE, NM.
IRIG J asynchronous ASCII time code formats
[AD-A277244] p 3681 N94-32332
Design, performance, and test standards for flight termination receivers/decoders. Volume 1: Design and performance requirements
[AD-A277245] p 3602 N94-32333

RANN, INC., PALO ALTO, CA.
Active control for fin buffet alleviation
[AD-A276844] p 3586 N94-32224

RAYTHEON CO., LEXINGTON, MA.
RF vacuum microelectronics
[AD-A276512] p 3691 N94-31928

READING UNIV. (ENGLAND).
The effects of vegetation on the ability to map soils using GERIS data p 3744 N94-31860
Coordination of mesoscale meteorological research between ASL and European group
[AD-A276730] p 3784 N94-32162

RENSSELAER POLYTECHNIC INST., TROY, NY.
An adaptive finite element method for unsteady compressible rotor airfoil aerodynamics
p 3567 N94-31204
Chemical interactions between protein molecules and polymer membrane materials
[DE94-006987] p 3651 N94-31672
The effect of ductile phase (Nb) reinforcement morphology on the mechanical behavior of an intermetallic matrix (MoSi2) p 3615 N94-32500

RESEARCH INST. FOR COMPUTING AND INFORMATION SYSTEMS, HOUSTON, TX.
Selection criteria and facilitation training for the study of groupware
[NASA-CR-195906] p 3822 N94-33114

RESEARCH INST. OF NATIONAL DEFENCE, LINKOEPING (SWEDEN).
Division of Microwave Technology
[PB94-148079] p 3676 N94-31925

RESEARCH SUPPORT INSTRUMENTS, INC., ALEXANDRIA, VA.
Constraints on the Martian cratering rate imposed by the SNC meteorites and Vallis Marineris layered deposits p 3945 N94-33197

RESEARCH TRIANGLE INST., RESEARCH TRIANGLE PARK, NC.
Heteroepitaxial diamond growth
[AD-A277178] p 3902 N94-32306

RICE UNIV., HOUSTON, TX.
Convection and electrodynamic signatures in the vicinity of a Sun-aligned arc: Results from the Polar Acceleration Regions and Convection Study (Polar ARCS)
p 3954 N94-31102
Time-dependent behavior of active galactic nuclei with pair production p 3929 N94-31125
Observational constraints on black hole accretion disks p 3929 N94-31126
Nonlinear calculations of the time evolution of black hole accretion disks p 3929 N94-31127
Can a variable alpha induce limit cycle behavior and exponential luminosity decay in transient soft x ray sources? p 3929 N94-31129
Convective solar nebula p 3930 N94-31130
Rotational effects in turbulence driven by convection
p 3930 N94-31131
Circumstellar material around young stars in Orion
p 3930 N94-31133
Evolution of protoplanetary disks with dynamo magnetic fields p 3931 N94-31135
Parallel structured optimization algorithms for inverse problems
[AD-A276053] p 3811 N94-31443

ROBBINS-GIOIA, INC., ALEXANDRIA, VA.
Initial estimates of Integrated Maintenance Information System (IMIS) costs and benefits, volume 1
[AD-A276144] p 3565 N94-31830
ROCHESTER UNIV., NY.
The charging effect in high-Tc superconducting thin films
[AD-A277265] p 3900 N94-32040
ROCKWELL INTERNATIONAL CORP., CANOGA PARK, CA.
International Space Station Alpha's bearing, motor, and roll ring module developmental testing and results
p 3603 N94-33295
ROCKWELL INTERNATIONAL CORP., HUNTSVILLE, AL.
Advanced transportation system study: Manned launch vehicle concepts for two way transportation system payloads to LEO
[NASA-CR-193951] p 3608 N94-33100
ROCKWELL INTERNATIONAL CORP., THOUSAND OAKS, CA.
Quantum well infrared photodetector FPA
[AD-A278010] p 3908 N94-33248
ROME LAB., GRIFFISS AFB, NY.
Analysis of leading edge and trailing edge cover glass samples before and after treatment with advanced satellite contamination removal techniques p 3596 N94-31041
Fault coverage measurement for digital microcircuits
[AD-A276226] p 3686 N94-31066
Developing the Multimedia User Interface Component (MUSIC) for the Icarus Presentation System (IPS)
[AD-A276341] p 3810 N94-31335
Automatic translation among spoken languages
p 3685 N94-32437
Accelerated reliability testing utilizing design of experiments
[AD-A277989] p 3732 N94-33088
ROME LAB., HANSCOM AFB, MA.
Formulation of time-domain planar near-field measurements without probe correction
[AD-A276380] p 3672 N94-31371
Proceedings of the 1993 Antenna Applications Symposium, volume 1
[AD-A277202] p 3676 N94-32049
Proceedings of the 1993 Antenna Applications Symposium, volume 2
[AD-A277203] p 3677 N94-32050
ROME UNIV. (ITALY).
The 10th International Conference on Internal Friction and Ultrasonic Attenuation in Solids (ICIFUAS)
[AD-A276849] p 3902 N94-32209
ROYAL AUSTRALIAN NAVY HYDROGRAPHIC SERVICE, CANBERRA.
Hydrographic service Royal Australian Navy
[AD-A277134] p 3788 N94-32066
ROYAL INST. OF TECH., STOCKHOLM (SWEDEN).
Laboratory and space experiments as a key to the plasma universe
[TRITA-ALP-1993-01] p 3885 N94-31088
The double probe electric field experiment on Freja: Description and first results
[TRITA-ALP-1993-02] p 3885 N94-31089
ROYAL MILITARY COLL. OF CANADA, KINGSTON (ONTARIO).
Neutron measurements at the commercial aircraft altitudes
[ISBN-0-315-86201-7] p 3955 N94-31709
Determining the bearing capacity of flexible airfield pavements using a heavy weight deflectometer
[ISBN-0-315-86210-6] p 3587 N94-31710
An investigation of a novel microstrip magic-T
[ISBN-0-315-86218-1] p 3690 N94-31711
Acoustic emission from crack growth in 7050 aluminum and 7075 aluminum as a function of temperature and heat treatment
[DREP-CRS-93-15] p 3642 N94-31871
Proceedings of the Symposium/Workshop on Applications of Expert Systems in DND
[DSIS-93-00343] p 3853 N94-33335
A diagnostic expert system for digital circuits
p 3699 N94-33340
Management of uncertainty in knowledge-based systems: A military perspective p 3854 N94-33341
The hypermedia technology as front end to knowledge processing systems p 3854 N94-33343
A problem-solving approach to knowledge acquisition
p 3854 N94-33344
A heuristic multiple target tracker
p 3686 N94-33346
ROYAL MILITARY COLL. OF SAINT-JEAN, RICHELAIN (QUEBEC).
Scheduling fighter missions using an expert system with an operations research module p 3853 N94-33337
RUTGERS - THE STATE UNIV., NEW BRUNSWICK, NJ.
Relationships between access and use in information systems: Remote access to and browsing of online catalogs p 3919 N94-32488
Design of free space interconnected signal processor
[AD-A278129] p 3683 N94-33093
RUTGERS - THE STATE UNIV., PISCATAWAY, NJ.
The ferroelectric behavior of odd-numbered nylons
[AD-A278126] p 3663 N94-33058
Electric field-induced changes in odd-numbered nylons
[AD-A278003] p 3664 N94-33138
Electrostrictive response of elastomeric polymers
[AD-A277983] p 3664 N94-33247
RUTGERS UNIV., PISCATAWAY, NJ.
Application of the wavelet transform for speech processing p 3600 N94-31435
RUTHERFORD APPLETON LAB., CHILTON (ENGLAND).
Practical neutron training course: Course notes
[PB94-145158] p 3867 N94-31681
Arnoldi code for computing selected eigenvalues of sparse real unsymmetric matrices
[PB94-145182] p 3813 N94-31682
GKS-9X: An experimental application
[PB94-147048] p 3813 N94-31685
Baryogenesis from a primordial lepton asymmetry
[PB94-145166] p 3868 N94-31921
Probing lepton number violation via Majorana neutrinos at hadron supercolliders
[PB94-147055] p 3868 N94-31922
F0-975, A0-980 as eye-witnesses of confinement
[PB94-147105] p 3868 N94-31923
Tensor gauge potentials in loop space formulation of Yang-Mills fields
[PB94-147147] p 3912 N94-31924
Results from the H1 experiment at HERA
[PB94-145174] p 3868 N94-32008

S

SAN FRANCISCO STATE UNIV., CA.
Research in theoretical high-energy physics
[DE94-008388] p 3876 N94-32407
SAN JOSE STATE UNIV., CA.
Three dimensional audio versus head down TCAS displays
[NASA-CR-177636] p 3576 N94-33063
SANDIA NATIONAL LABS., ALBUQUERQUE, NM.
Fiber optic chemical sensors on Mars
[DE94-005251] p 3941 N94-31145
Transient radiation-induced absorption in the materials for a GSGG laser
[DE94-005316] p 3714 N94-31148
Sandia's research network for Supercomputing 1993: A demonstration of advanced technologies for building high-performance networks
[DE94-005319] p 3823 N94-31149
Utilizing a Russian space nuclear reactor for a United States space mission: Flight qualification issues
[DE94-004674] p 3613 N94-31265
Feature discovery in gray level imagery for one-class object recognition
[DE94-005268] p 3671 N94-31267
Analysis of the photodiode boundary layer transition indicator
[DE94-005311] p 3701 N94-31268
An investigation of airborne GPS/INS for high accuracy position and velocity determination
[DE94-006139] p 3576 N94-31306
Tearing resistance of a thin shell against projectile penetration: Material property effects
[DE94-007466] p 3733 N94-31316
High temperature ductility loss in titanium alloys: A review
[DE94-006606] p 3640 N94-31345
Using Monte Carlo techniques and parallel processing for debris hazard analysis of rocket systems
[DE94-007250] p 3609 N94-31382
High-performance GaAs/AlGaAs optical phase modulators for microwave/photonic integrated circuits
[DE94-006361] p 3688 N94-31483
An application reference model for layered manufacturing
[DE94-006368] p 3811 N94-31484
DOE reactor-pumped laser program
[DE94-006372] p 3715 N94-31485
III-V compound semiconductor strip-loaded waveguide devices for PICs: Design for minimum crosstalk and high density
[DE94-006588] p 3897 N94-31502
A novel CFD/structural analysis of a cross parachute
[DE94-005271] p 3568 N94-31578
Laser Diode Ignition (LDI)
[DE94-006590] p 3666 N94-31579
Fractional-factorial process development techniques
[DE94-005580] p 3690 N94-31593
Evidence for a correct SiO2 voltage acceleration model
[DE94-006578] p 3690 N94-31594
Semiconductor microcavity lasers
[DE94-006143] p 3716 N94-31622
Adsorption of water to the metal/polymer interface studied by neutron and x ray reflectivity
[DE94-005578] p 3651 N94-31649
Deposition of DLC via intense ion beam ablation
[DE94-005583] p 3651 N94-31650
A low cost igniter utilizing an SCB and titanium sub-hydride potassium perchlorate pyrotechnic
[DE94-006467] p 3666 N94-31827
Inorganic materials for anomalous-dispersion phase-matched second harmonic generation: Rubidium titanyl arsenate isomorphs, Rb(Ti(1-2x)Ln(x)Nb(x))OAsO4
[DE94-006141] p 3899 N94-31847
Temperature dependence of the exciton-exciton annihilation rate constant in poly(di-n-hexylsilane)
[DE94-005584] p 3655 N94-32102
Advances in MOVPE compound semiconductor epitaxy manufacturing technology: From high throughput large area reactors to cluster tools
[DE94-006367] p 3901 N94-32104
Determination of BPSG thin-film properties using IR reflection spectroscopy of product wafers
[DE94-006591] p 3634 N94-32110
The advent of failure analysis software technology
[DE94-006593] p 3692 N94-32111
Novel failure analysis techniques using photon probing with a scanning optical microscope
[DE94-006594] p 3692 N94-32112
ITS version 3.0: Powerful, user-friendly software for radiation modelling
[DE94-006607] p 3678 N94-32113
High conversion efficiency pumped-cavity second harmonic generation of a diode laser
[DE94-006805] p 3717 N94-32134
Experimental measurement of dynamic failure and fragmentation properties of metals
[DE94-007377] p 3737 N94-32135
Stability and precipitation kinetics in Si(1-y)C(y)/Si and Si(1-x-y)Ge(x)C(y)/Si heterostructures prepared by solid phase epitaxy
[DE94-006589] p 3902 N94-32296
Interactive graphical model building using telepresence and virtual reality
[DE94-001421] p 3818 N94-32353
Parallel particle simulations of low-density fluid flows
[DE94-007858] p 3707 N94-32373
Renewable energy technology development at Sandia National Laboratories
[DE94-007734] p 3761 N94-32383
Intra-cascade surface recombination of point defects during ion bombardment of Ge(001)
[DE94-007740] p 3903 N94-32384
Reconfigurable optical switches with monolithic electrical-to-optical interfaces
[DE94-007745] p 3881 N94-32385
From display and PWB to MCMs: Large panel manufacturing
[DE94-007855] p 3693 N94-32386
Development, characterization, and applications of high temperature superconductor nanobridge Josephson junctions
[DE94-008113] p 3903 N94-32409
Sandia technology engineering and science accomplishments
[DE94-008312] p 3668 N94-32412
Chemisorbed-molecule potential-energy surfaces and electronically-stimulated processes
[DE94-007932] p 3719 N94-32603
Complete model description of an electron beam using ACCEPT Monte Carlo simulation code
[DE94-007063] p 3872 N94-32628
Multiple size scale structures in silica/siloxane composites studied by small-angle scattering
[DE94-007300] p 3625 N94-32642
Solar activities at Sandia National Laboratories
[DE94-007737] p 3761 N94-32648
Metal-ion spin-on glasses: Novel materials for active waveguides
[DE94-007738] p 3882 N94-32649
Thin-film decoupling capacitors for multi-chip modules
[DE94-007743] p 3695 N94-32650
Varying execution discipline to increase performance
[DE94-007844] p 3819 N94-32651
Bounds on least-squares four-parameter sine-fit errors due to harmonic distortion and noise
[DE94-007859] p 3849 N94-32653
The relative performance of FeS2 and CoS in long-life thermal-battery applications
[DE94-006145] p 3695 N94-32663

Integrated safety program for the Nuclear Electric Propulsion Space Test Program
[DE94-004670] p 3615 N94-32669
Design and evaluation of coils for a 50 mm diameter induction coilgun launcher
[DE94-005244] p 3603 N94-32671
Gettering of metal impurities by cavities in silicon
[DE94-005248] p 3645 N94-32672
Arithmetic averaging: A versatile technique for smoothing and trend removal
[DE94-005274] p 3852 N94-32673
Characterization of thermally stable dye-doped polyimide based electrooptic materials
[DE94-005309] p 3882 N94-32674
Note on the variance of autospectral density processed using Welch's method
[DE94-005352] p 3849 N94-32675
Application of the modified voltage-dividing potentiometer to overlay metrology in a CMOS/bulk process
[DE94-007937] p 3695 N94-32700
THERM3D: A boundary element computer program for transient heat conduction problems
[DE94-008112] p 3708 N94-32709
Temperature-humidity-bias aging technique to identify defective surface mount capacitors
[DE94-005354] p 3660 N94-32727
Conjugated polymer fluorescence: Interplay of correlations and alternation
[DE94-005587] p 3660 N94-32729
Multimedia as a desktop and classroom tool
[DE94-009118] p 3807 N94-32766
An electrical test system for conductor formation process analysis
[DE94-007291] p 3696 N94-32786
A multitasking behavioral control system for the Robotic All Terrain Lunar Exploration Rover (RATLER)
[DE94-007293] p 3835 N94-32787
Nucleation and growth of cubic boron nitride films produced by ion-assisted pulsed laser deposition
[DE94-007295] p 3661 N94-32796
Overview of Sandia's electric vehicle battery program
[DE94-008944] p 3696 N94-32806
Information systems to enhance technology exchange
[DE94-007744] p 3920 N94-32808
High-performance GaAs/AlGaAs optical phase modulators for microwave photonic integrated circuits
[DE94-007376] p 3696 N94-32809
NMR characterization of shocked quartz
[DE94-007733] p 3774 N94-32816
Light scattering studies of a model electrorheological fluid
[DE94-007860] p 3883 N94-32818
Characterization of crosslinked electrooptic polyimides
[DE94-007934] p 3661 N94-32819
Overview of shock physics codes for armor analysis
[DE94-008948] p 3739 N94-32842
Sandia's photonic program and its changing national role
[DE94-008616] p 3883 N94-32878
Optical properties of lanthanide-doped RbTiOAsO4 and transition metal-doped KTiOPO4
[DE94-008433] p 3907 N94-32963
Operational experience and evaluation of a dual-element stretched-membrane heliostat
[DE94-008827] p 3763 N94-32965

SANDIA NATIONAL LABS., LIVERMORE, CA.
A compatibility study of FEFO with various containment materials
[DE94-005753] p 3649 N94-31198
Soot and liquid-phase fuel distributions in a newly designed optically accessible DI diesel engine
[DE94-005648] p 3723 N94-31651
A genetic algorithm based method for docking flexible molecules
[DE94-007525] p 3793 N94-32269
OPT++: An object-oriented class library for nonlinear optimization
[DE94-008890] p 3818 N94-32584
Compilation of diamond-like carbon properties for barriers and hard coatings
[DE94-008231] p 3661 N94-32803

SCIENCE APPLICATIONS INTERNATIONAL CORP., MCLEAN, VA.
Fluid Dynamics Lagrangian Simulation Model
[AD-A277438] p 3710 N94-33009

SCIENCE APPLICATIONS INTERNATIONAL CORP., NEW YORK, NY.
Space flight risk data collection and analysis project: Risk and reliability database
[NASA-CR-195879] p 3603 N94-32494

SCIENCE APPLICATIONS INTERNATIONAL CORP., SAN DIEGO, CA.
The intelligent monitoring system: Generic Database Interface (GDI). Revised user manual
[AD-A277131] p 3919 N94-32382

SCOT CONSEIL, RAMONVILLE (FRANCE).
Technique of ERS-1 image processing in association with SPOT data p 3750 N94-32538
Integration of ERS-1 images into the European Agriculture Statistics project Action 4: Thematic aspect p 3753 N94-32554
Land cover change detection with ERS-1 data and data from other remote sensing satellites. Example: The delta of the River Ebro (Spain) p 3755 N94-32564

SCRANTON UNIV., PA.
Ada support for the mathematical foundations of software engineering
[AD-A278031] p 3822 N94-33284

SCRIPPS INSTITUTION OF OCEANOGRAPHY, LA JOLLA, CA.
Profiling ALACE instruments
[AD-A277246] p 3789 N94-32321
Multi-scale studies of seafloor topography
[AD-A277008] p 3789 N94-32400
Long transect seafloor seismic array: A component of SAMSON (Sources of Ambient Micro Seismic Ocean ic Noise)
[AD-A277009] p 3789 N94-32401
Ocean optics, ocean imaging and optical tomography
[AD-A277010] p 3789 N94-32402

SELSKAPET FOR INDUSTRIELL OG TEKNISK FORSKNING, TRONDHEIM (NORWAY).
Evaluation of corrosion protective organic coatings for steel structures in fresh water
[PB94-138484] p 3649 N94-31072
Application of natural refrigerants: A rational solution to a pressing problem
[PB94-138781] p 3668 N94-31073
Scientific basis for safety science
[PB94-138534] p 3668 N94-31838
Systems for the monitoring of working conditions relating to health and safety: Extensive description. Norway
[PB94-138542] p 3803 N94-31839
Laser applications in wood processing
[PB94-138567] p 3717 N94-31840
Acceptance criteria for weld defects in aluminium weldments
[PB94-138575] p 3735 N94-31841
Description of DCS (Data Converting System) and CT (Cone Tool). A reprint of a note published in Fire and Materials titled Fire Test Data Available for Your Purpose
[PB94-138559] p 3918 N94-32293

SHEFFIELD UNIV. (ENGLAND).
A high-performance multi-arm environment: Theoretical aspects and practical implementation
[RR-479] p 3722 N94-31379
Nonlinear model validation using correlation tests
[RR-463] p 3842 N94-31394
On wavelet representations of differential equations
[RR-482] p 3842 N94-31412
Identification of polynomial and rational NARMAX models
[RR-483] p 3842 N94-31413
A neural network methodology for engineering applications: The learning control of robotic systems
[RR-480] p 3830 N94-31500

SHERIKON SPACE SYSTEMS, INC., KENNEDY SPACE CENTER, FL.
Chronology of KSC and KSC related events for 1993
[NASA-TM-109196] p 3966 N94-33072

SIKORSKY AIRCRAFT, STRATFORD, CT.
Innovative fabrication processing of advanced composite materials concepts for primary aircraft structures
[NASA-CR-189558] p 3626 N94-32877

SMITH-KETTLEWELL INST. OF VISUAL SCIENCES, SAN FRANCISCO, CA.
Visual processing of object velocity and acceleration
[AD-A277425] p 3801 N94-32998

SMITHSONIAN ASTROPHYSICAL OBSERVATORY, CAMBRIDGE, MA.
Participation in the scientific activities of the Waves in Space Plasma (WISP) project
[NASA-CR-195903] p 3894 N94-33113

SOCIETE FRANCAISE DE CHIMIE-PHYSIQUE, PARIS.
Physical chemistry of molecules and grains in space
[AD-A276037] p 3932 N94-31280

SOFTWARE OPTIONS, INC., CAMBRIDGE, MA.
Extender's guide for artifacts and drafts
[AD-A276344] p 3810 N94-31328
E-L user's manual
[AD-A276378] p 3810 N94-31370
Beyond the read-eval loop: The artifacts system
[AD-A276589] p 3803 N94-32034

SOFTWARE PRODUCTIVITY CONSORTIUM, HERNDON, VA.
Overview of megaprogramming course: Lectures and exercises
[AD-A276169] p 3814 N94-31810

SOLAREX CORP., NEWTOWN, PA.
Large-area, triple-junction a-Si alloy production scale-up
[DE94-006856] p 3762 N94-32765

SOTEMA, RAMONVILLE SAINT-AGNE (FRANCE).
Rapid estimates of crop acreage and production at European scale using high resolution imagery p 3754 N94-32557

SOUTHAMPTON UNIV. (ENGLAND).
An analytical study of the vibration of beams fitted with neutralizers. Part 2: Assessment of the effects of mounting configurations
[ISVR-TR-225-PT-2] p 3740 N94-32982

SOUTHEASTERN CENTER FOR ELECTRICAL ENGINEERING EDUCATION, INC., SAINT CLOUD, FL.
Situational awareness: A feasibility investigation of near-threshold skills development
[AD-A276467] p 3798 N94-31243

SOUTHERN CALIFORNIA GAS CO., LOS ANGELES.
Economic feasibility analysis of distributed electric power generation based upon the natural gas fired fuel cell
[DE94-005795] p 3759 N94-31487

SOUTHERN RESEARCH INST., BIRMINGHAM, AL.
Expandable pattern casting research
[DE94-004342] p 3868 N94-31604

SOUTHWEST RESEARCH INST., SAN ANTONIO, TX.
Laser-induced fluorescence of space-exposed polyurethane p 3593 N94-31026
Ignition delays, heats of combustion, and reaction rates of aluminum alkyl derivatives used as ignition and combustion enhancers for supersonic combustion
[NASA-CR-189581] p 3638 N94-32868
Fracture micromechanics of continuous fiber and textile reinforced metal and ceramic matrix composites
[AD-A277434] p 3627 N94-33008
Plasma and radio waves from Neptune: Source mechanisms and propagation
[NASA-CR-195877] p 3943 N94-33103
Distribution and nature of UV absorbers on Triton's surface
[NASA-CR-195886] p 3943 N94-33104

SPACE SYSTEMS/LORAL, PALO ALTO, CA.
Two-axis antenna positioning mechanism p 3605 N94-33308

SPEECH TECHNOLOGY RESEARCH LTD., VICTORIA (BRITISH COLUMBIA).
Neural networks applied to the phonemic segmentation of speech p 3686 N94-33152

SPIRE CORP., BEDFORD, MA.
High power diode lasers for solid-state laser pumps p 3722 N94-32448

SRI INTERNATIONAL CORP., MENLO PARK, CA.
Proof of concept for the rewrite rule machine: Interensemble studies
[AD-A276506] p 3809 N94-31263
IR materials producibility
[AD-A277028] p 3879 N94-32006
High-performance speech recognition using consistency modeling
[AD-A276775] p 3679 N94-32185
Model-based reconfiguration: Diagnosis and recovery
[NASA-CR-4596] p 3820 N94-32776

STANFORD LINEAR ACCELERATOR CENTER, CA.
New QCD results from string theory
[DE94-005226] p 3911 N94-31823
Anomalous small angle x ray scattering studies of amorphous metal-germanium alloys
[DE94-007258] p 3900 N94-32065
The form factors of the nucleons
[DE94-007096] p 3872 N94-32630
Minimax: Multiparticle physics at the Tevatron collider
[DE94-007095] p 3873 N94-32689
Anisotropic phase separation through the metal-insulator transition in amorphous Mo-Ge and Fe-Ge alloys
[DE94-007259] p 3646 N94-32795

STANFORD RESEARCH INST., MENLO PARK, CA.
Gamma Large Area Silicon Telescope (GLAST)
[DE94-006439] p 3925 N94-31786
The evolutionary status of PSR 1259-63
[DE94-007094] p 3938 N94-32503
CP violation and the top quark
[DE94-008930] p 3874 N94-32841
Selected applications of planar permanent magnet multipoles in FEL insertion device design
[DE94-009014] p 3721 N94-32845
A reliable low-maintenance flashlamp-pumped Ti:sapphire laser operating at 120 PPS
[DE94-009030] p 3721 N94-32848
Spin-structure function of the neutron He-3: SLAC results
[DE94-008927] p 3875 N94-33189
Polarized lepton-nucleon scattering
[DE94-009027] p 3875 N94-33278

STANFORD UNIV., CA.
High-power CW diode-laser-array-pumped solid-state lasers and efficient nonlinear optical frequency conversion
[AD-A276126] p 3714 N94-31278
Advanced optical fiber communication systems
[AD-A276416] p 3878 N94-31330
New material for high average power infrared generation: QPM-DB GaAs
[AD-A276389] p 3714 N94-31358
Phase-lock roll control of inertially pointing spacecraft p 3609 N94-31470
ControlShell: A real-time software framework
[AD-A276481] p 3811 N94-31475
Contingency-tolerant robot motion planning and control p 3830 N94-31482
Degenerate four-wave mixing as a diagnostic of plasma chemistry
[DE94-008588] p 3889 N94-31766
Lightning-induced coupling of the radiation belts to geomagnetically conjugate ionospheric regions p 3772 N94-31773
On-line physical parameter identification and adaptive control of a launch vehicle p 3602 N94-31891
Vibrational energy transfer of diatomic gases in hypersonic expanding flows p 3570 N94-31958
A separation technique for asymptotic-numeric solution for general shells of revolution p 3736 N94-31961
Control of a flexible-link robotic arm manipulating an unknown dynamic payload p 3725 N94-31973
Recursive analysis of matrix scattering functions
[AD-A277264] p 3845 N94-32018
Applications of data compression to 3-D scalar field visualization p 3817 N94-32294
Dynamic error compensation in robotic trusses p 3738 N94-32486
Superconducting and semiconducting hybrids and advance memory concepts for superconducting electronics
[AD-A277766] p 3907 N94-32988
A quest for a new superconducting state
[DE94-008439] p 3908 N94-32991
Turbulent reacting flows and supersonic combustion
[AD-A277462] p 3639 N94-33242
Electrical characteristics of GaAs MESFET fabrication by ion implantation of Si or Se
[AD-A278416] p 3909 N94-33328

STATE UNIV. COLL. OF NEW YORK, BUFFALO.
Silicone grease as a precursor to a pseudo crown-ether ligand: Crystal structure of (K(+)K(Me2SiO)7(+)) (HIn(CH2CMe3)3(-))4)
[AD-A276343] p 3895 N94-31327

STATE UNIV. OF NEW YORK, ALBANY.
Treatment of cloud radiative effects in general circulation models
[DE94-001864] p 3764 N94-31600
Time-dependent behavior of Mount Pinatubo aerosol
[DE94-001877] p 3764 N94-31601
Concentration system performance degradation in the aftermath of Mount Pinatubo
[DE94-001879] p 3764 N94-31602
Use of Air Force cloud cover data to evaluate and improve cloud forecasts and parameterizations in mesocale meteorological models
[AD-A277384] p 3784 N94-32054
Use of cloud observations and mesoscale meteorology models to evaluate and improve cloud parameterizations
[DE94-003610] p 3785 N94-32717

STATE UNIV. OF NEW YORK, BUFFALO.
SUNY beamline facilities at the National Synchrotron Light Source
[DE94-006343] p 3905 N94-32770
Effects of combined breathing impediments on diver's respiratory performance
[AD-A277437] p 3805 N94-33084

STATE UNIV. OF NEW YORK, STONY BROOK.
Communications networks in stressed environments
[AD-A275967] p 3672 N94-31384
Lattice geometrodynamics p 3857 N94-31825
Planetesimal dynamics in the vicinity of a growing protoplanet p 3935 N94-31926
Isolating strain parameters correlated to skeletal adaptation p 3797 N94-31960
Cooling and trapping of neutral atoms
[AD-A276957] p 3870 N94-32360
Ionization probes of molecular structure and chemistry
[DE94-007605] p 3872 N94-32643
Stochastic models in reliability theory
[AD-A277529] p 3731 N94-32953

STEVENS INST. OF TECH., HOBOKEN, NJ.
Computational study of simultaneous heat and mass transfer in turbulent separated flows p 3704 N94-31843
Computational prediction of stall flutter in spanwise-finite blade cascades p 3584 N94-31967

STOCKHOLM UNIV. (SWEDEN).
A polynomial representation of the valence orbital ionization potentials
[USIP-93-06] p 3640 N94-31083
Instrumentation for EXELFS measurements using convergent beam diffraction coupling to the electron energy loss spectrometer
[USIP-93-07] p 3858 N94-31084
Particle identification in a segmented calorimeter (NUMASS test data, September 1991)
[USIP-93-08] p 3711 N94-31085
Fireworks in velocity and configuration space applied to cosmology
[USIP-93-90] p 3927 N94-31086
Summary of some data processing routines in the molecular physics group of Stockholm University
[USIP-93-05] p 3808 N94-31087
A fully two-dimensional, non-oscillatory advection scheme for momentum and scalar transport equations
[DM-66] p 3700 N94-31221
Odin aeronomy science: A phase-A report by the Aeronomy Science Working Group for the Odin satellite
[AP-31] p 3770 N94-31222
A flexible IBM-PC based data acquisition system for nuclear physics experiments
[USIP-92-02] p 3922 N94-32856

STUTTGART UNIV. (GERMANY).
Fields of experiments in ERS-1 SAR interferometry in Bonn and Naples p 3756 N94-32572

SUNPOWER, INC., ATHENS, OH.
Oscillating-flow loss test results in rectangular heat exchanger passages
[NASA-CR-185297] p 3615 N94-32792
A 1050 K Stirling space engine design
[NASA-CR-182149] p 3616 N94-32866

SURVEILLANCE RESEARCH LAB., SALISBURY (AUSTRALIA).
Advanced infrared photodetectors: Materials review
[AD-A277058] p 3879 N94-32013

SVERDRUP TECHNOLOGY, INC., BROOK PARK, OH.
An analysis of supersonic flows with low-Reynolds number compressible two-equation turbulence models using LU finite volume implicit numerical techniques
[NASA-CR-195302] p 3572 N94-32926
Installed F/A-18 inlet flow calculations at 30 degrees angle-of-attack: A comparative study
[NASA-CR-195297] p 3573 N94-33119

SWEDISH INST. FOR MATERIALS TESTING, BORAS.
Databases and demands for solar heating materials
[PB94-137494] p 3758 N94-31070
Solar energy in China
[PB94-137502] p 3758 N94-31071
Influence of carbon dioxide on electronic equipment: Fire extinguishing with low concentration
[PB94-148749] p 3691 N94-31848

SYRACUSE UNIV., NY.
Processing boron and boron carbide thin films for protective coatings and device fabrication
[AD-A277266] p 3900 N94-32041
New polymer target-shell properties and characterizations
[DE94-008420] p 3890 N94-32415
Fusion with highly spin polarized HD and D2
[DE94-006209] p 3876 N94-32731

T

TAYLOR (S. R.) AND ASSOCIATES, BARTLESVILLE, OK.
Novel ultrasonic method for food hydration
[AD-A277411] p 3804 N94-32580

TECHNICAL RESEARCH CENTRE OF FINLAND, ESPOO.
An experimental and analytical investigation of a threaded fastener
[VTT-JULK-786] p 3724 N94-31654
Metal hydrides in hydrogen energy systems
[VTT-TIED-1407] p 3759 N94-31655
Joining of alumina by vacuum brazing
[VTT-TIED-1495] p 3724 N94-31656
Control and monitoring of heavy metal emissions
[VTT-TIED-1508] p 3765 N94-31657
Imaging devices for satellite remote sensing
[VTT-TIED-1517] p 3743 N94-31658
SPOT imagery for updating land cover information of 1:50,000 numerical topographic maps p 3749 N94-32532

TECHNICAL UNIV. OF DENMARK, LYNGBY.
Future directions of nonlinear dynamics in physical and biological systems. (Physica D nonlinear, volume 68, number 1)
[AD-A278085] p 3794 N94-33250

TECHNISCHE UNIV., BERLIN (GERMANY).
An active computer supported medium for distributed planning in enterprises
[ETN-94-95738] p 3829 N94-31372
A series resonant converter in half bridge circuits with combined serial and parallel charge coupling and several output circuits
[ETN-94-95739] p 3687 N94-31373
Theoretical principles for designing long stator/linear motors with iron
[ETN-94-95741] p 3688 N94-31374
Considering ties elasticities in high frequency rail dynamics
[ILR-MITT-281(1993)] p 3733 N94-31375
Hierarchical fault catalog process for diagnosis of analog circuits
[ETN-94-95730] p 3689 N94-31571
Stark broadening of the 2S state of hydrogen and deuterium in arc plasmas of low density
[ETN-94-95731] p 3888 N94-31572
Spectral analysis method and sample generation for real time visualization of speech
[ETN-94-95732] p 3674 N94-31573
Electrochemical surface modification of silicon monocrystals: A surface analytic examination
[ETN-94-95733] p 3633 N94-31574
Applicable dimensioning and measure and technological examination of long stator-linear motors for magnetic high-speed railways
[ETN-94-95734] p 3689 N94-31575
Real time simulation model for designing converter regulation
[ETN-94-95735] p 3689 N94-31576
Compositionality of application oriented structuring mechanisms for algebraic specification languages with initial semantics
[ETN-94-95736] p 3812 N94-31577
Structure estimation of phase objects from the diffraction near field: Microwave and model calculations
[ETN-94-95737] p 3674 N94-31608
Examination of fast semiconductor diodes (recovery) with respect to switching valves in PWM and resonance devices
[ETN-94-95740] p 3690 N94-31609
Hydrogen incorporation and radiation induced dynamics in metal-oxide-silicon structures: A study using nuclear reaction analysis
[ETN-94-95742] p 3898 N94-31610
The contribution of aeronautics and astronautics to the quality of life on Earth
[ILR-MITT-283(1993)] p 3764 N94-31611
Design of a logistics model for building and supporting a lunar station
[ILR-MITT-282(1993)] p 3803 N94-31852

TECHNISCHE UNIV., DARMSTADT (GERMANY).
Experimental investigation of phonon eigenvectors using x ray interference fields
[ETN-94-95751] p 3865 N94-31511
Numerical method for the investigation of the magnetohydrodynamic stability of three dimensional plasma equilibria
[ETN-94-95752] p 3887 N94-31512
Competition between crystallization and mixing/demixing in polymer mixture
[ETN-94-95753] p 3651 N94-31513
Adaptive operating systems concepts
[ETN-94-95754] p 3830 N94-31514
Concept, construction and testing of a high resolution QCLAM electron spectrometer with large solid angle and high impulse acceptance for the electron accelerator S-DALINAC
[ETN-94-95755] p 3711 N94-31515
Energy and angular distributions of secondary ions during electronic sputtering of nonconducting surfaces
[ETN-94-95756] p 3865 N94-31516
Development and implementation of a full-potential ASW method
[ETN-94-95757] p 3858 N94-31560
Time evolution and filamentation of KrF(star) laser gas discharges
[ETN-94-95758] p 3715 N94-31561
Electron spin resonance measurements of Er(3+) and Mn(2+) in the high temperature superconductor compounds La(2-x)Sr(x)CuO(4-delta)
[ETN-94-95746] p 3898 N94-31612
Optimal detector strategies for the phase contrast imaging for scanning transmission electron microscopes
[ETN-94-95747] p 3866 N94-31613
Control heavy ion collisions in the systems Ar-40 + Ca-40 and Si-28 + Si-28, and the nature of particle emission in fusion-evaporation reactions
[ETN-94-95749] p 3866 N94-31614
Study of structures of different complexity for the communication between two processors
[ETN-94-95750] p 3674 N94-31615

TECHNISCHE UNIV., DELFT (NETHERLANDS).
Filtering of satellite altimetry data with optimal smoothing cubic splines to compute geoid heights, along-tract geoid and gravity gradients in the Indonesian waters and its surroundings
[PB94-147527] p 3741 N94-31074
Application of radon transformation for improved analysis of sparsely sampled data: A feasibility study
[PB94-147535] p 3741 N94-31075
LORE and reason maintenance
[REPT-93-88] p 3812 N94-31522
Two models solving the increasing energy problem of the continuous Hopfield network model
[REPT-93-87] p 3843 N94-31552
Small cylindrical adhesive bonds
[PB94-148210] p 3651 N94-31585
Effective information modelling support
[PB94-148236] p 3917 N94-31586
Delft Ising computing engine
[PB94-148251] p 3806 N94-31587
Fluid-structure interaction in case of water hammer with cavitation
[PB94-148277] p 3702 N94-31588
Possible improvements of satellite ephemeris programs used in geodesy
[PB94-148681] p 3743 N94-31592
Budget allocation and monopolistic pricing in a multiproduct firm
[REPT-93-86] p 3924 N94-31617
On the validity of the BLP model
[REPT-93-70] p 3917 N94-31640
Some calculations on supersymmetric graphs as communication networks
[REPT-93-72] p 3824 N94-31641
Stirling's formula and approximations for n(factorial) and the middle ratio
[REPT-93-73] p 3843 N94-31642
Generalization of a theorem of Kusmin
[REPT-93-74] p 3844 N94-31643
Qualitative properties of two-dimensional predator-prey systems
[REPT-93-75] p 3844 N94-31644
Virtual annotation: Verbal communication in virtual reality
[REPT-93-67] p 3674 N94-31645
Automatic generation of context-sensitive textual help
[REPT-93-68] p 3812 N94-31646
Digital state-feedback H(infinity) control of Pritchard-Salamon systems: A Popov function approach
[REPT-93-69] p 3830 N94-31647
Solution of the incompressible Navier-Stokes equations in general coordinates by Krylov subspace and multigrid methods
[REPT-93-64] p 3703 N94-31660
A note on cocycles in a semidirect product
[REPT-93-65] p 3851 N94-31661
Invariance of the generalized steady-state for 1-D distributed parameter systems
[REPT-93-66] p 3825 N94-31662
Tractable deduction in some fragments of auto-epistemic logic
[REPT-93-89] p 3844 N94-31673
Damage tolerance aspects of a full composite airplane fuselage: Requirements, modelling, predictions, experiments
[LR-728] p 3578 N94-31674
Multiple-site damage in aircraft fuselage structures
[LR-729] p 3578 N94-31675
Powder metallurgical processing of fibre reinforced aluminium composites
[PB94-148285] p 3620 N94-31688
A Hyland-Bernstein approach to the digital control of Pritchard-Salamon systems
[REPT-93-76] p 3844 N94-31693
A Gauss-Seidel type solver for special convex programs, with application to frictional contact mechanics
[REPT-93-77] p 3813 N94-31694
Using atomic actions in replica groups to simplify the replication implementation
[REPT-93-78] p 3813 N94-31695
A predator-prey model with Ivlev's functional response
[REPT-93-79] p 3844 N94-31696
Diagonal band probability distributions
[REPT-93-80] p 3851 N94-31697
Probability distributions with given marginals and given correlation that have maximal entropy
[REPT-93-81] p 3851 N94-31698
The Laplace functional and Palm measure of a quasi-Cox process which is driven by a Markov chain
[REPT-93-82] p 3851 N94-31699
Generalized steady-state method for solving 2-D diffusion systems
[REPT-93-83] p 3825 N94-31700
Pairwise-comparison using the logarithmic least squares method and the generalized pseudoinverse
[REPT-93-84] p 3844 N94-31701
Simple Patch: A new heuristic for the product traveling salesman problem
[REPT-93-85] p 3845 N94-31702
Finite volume discretization of the k-epsilon turbulence model in general coordinates
[REPT-93-90] p 3703 N94-31703
Designing in virtual reality: Modelling Objects in a Virtual Environment (MOVE)
[REPT-93-91] p 3813 N94-31704
The influence of the deorbit-burn manoeuvre on the footprint of a re-entry capsule
[LR-727] p 3609 N94-31705
TECHNISCHE UNIV., EINDHOVEN (NETHERLANDS).
Managing customer order driven engineering. An interdisciplinary and design oriented approach
[PB94-145083] p 3917 N94-31583
Oxide pigments in water: The colloid-chemical point of view
[PB94-148616] p 3633 N94-31591
Aeroacoustic sources in internal flows
[ISBN-9-03-86-0282-0] p 3860 N94-31653
TECHNISCHE UNIV., MUNICH (GERMANY).
Investigation on correction models for airborne imaging spectrometry data from the EISAC-campaign for geoscientific purposes p 3745 N94-31861
Extraction of agricultural parameters from imaging-spectrometry data and simulated MERIS data through red edge analysis p 3745 N94-31865
The 6th International Conference on Modulated Semiconductor Structures
[AD-A276815] p 3906 N94-32908
TEL-AVIV UNIV. (ISRAEL).
Analysis of ionospheric parameters in Europe and creation of the prediction algorithm
[AD-A276342] p 3771 N94-31326
TELSTRA CORP. LTD., SYDNEY (AUSTRALIA).
Hubless satellite communications networks
p 3600 N94-31433
TENNESSEE STATE UNIV., NASHVILLE.
Parametric robust control and system identification: Unified approach
[NASA-CR-195826] p 3836 N94-32980
TENNESSEE TECHNOLOGICAL UNIV., COOKEVILLE.
Strain sensing using optical fibers
[NASA-CR-195807] p 3740 N94-32940
TESCO, INC., TULLAHOMA, TN.
Model borne data management system for wind tunnel testing, phase 2
[AD-A276296] p 3587 N94-31295
TEXAS A&M UNIV., COLLEGE STATION.
Electrooptic crystal growth and properties
[AD-A276023] p 3896 N94-31439
Viscoelastic fracture characterization of polymeric solids p 3652 N94-31745
Analysis of new composite architectures
[NASA-CR-195303] p 3626 N94-32904
TEXAS TECHNOLOGICAL UNIV., LUBBOCK.
High power switch design for the Nova upgrade laser (Project HERCULES: High Energy Research Concerning the Ultimate Lifetime of Experimental Switches)
[DE94-007921] p 3719 N94-32654
Metal ion complexation by ionizable crown ethers
[DE94-008301] p 3661 N94-32847
TEXAS UNIV., ARLINGTON.
Shock impingement near mild hypersonic expansion corners p 3569 N94-31879
TEXAS UNIV., AUSTIN.
Disk instability and the spectral evolution of the 1992 outburst of the intermediate polar GK Persei p 3928 N94-31123
Disk irradiation and light curves of x ray novae p 3929 N94-31124
A constraint on the pair-density ratio (Z+) in an electron-positron pair wind p 3930 N94-31132
Thermal continua of AGN accretion disks p 3931 N94-31137
Dynamics of flux tubes in accretion disks p 3932 N94-31142
The physics of black hole x ray novae p 3932 N94-31143
Transport suppression by shear flow generation in multihelicity resistive-g turbulence
[DE94-007108] p 3886 N94-31366
L-H confinement mode dynamics in three-dimensional state space
[DE94-007113] p 3887 N94-31396
Adaptive nonlinear control of spacecraft p 3609 N94-31564
Plasma confinement theory and transport simulation
[DE94-006065] p 3888 N94-31619
Hydrogen peroxide electrodes based on electrical connection of redox centers of various peroxidases to electrodes through a three-dimensional electron relaying polymer network
[AD-A276543] p 3691 N94-32056
Medium energy measurements of N-N parameters
[DE94-006067] p 3869 N94-32173
Electrical communication between glucose oxidase and electrodes based on poly(vinylimidazole) complex of Os(bpy)2Cl2
[AD-A276585] p 3635 N94-32231
Research program in particle physics
[DE94-008449] p 3871 N94-32512
Anomalous thermalization of fast ions in magnetized plasma
[DE94-007109] p 3891 N94-32631
Basic principles approach for studying nonlinear Alfven wave-alpha particle dynamics
[DE94-007112] p 3891 N94-32664
Superluminous laser pulse in an active medium
[DE94-007110] p 3720 N94-32684
Particle diffusion from the beam-beam interaction in synchrotron colliders
[DE94-007111] p 3876 N94-32685
Magnetless magnetic fusion
[DE94-007114] p 3891 N94-32686
Quantum dynamics in dual spaces
[DE94-008303] p 3913 N94-32824
The 1994 International Sherwood Fusion Theory Conference
[DE94-008961] p 3877 N94-32844
Parallel supercomputing: Advanced methods, algorithms, and software for large-scale linear and nonlinear problems
[DE94-008446] p 3836 N94-32992
Adaptive control of nonlinear and stochastic systems
[AD-A278411] p 3839 N94-33325
TEXAS UNIV., EL PASO.
Optical and image transmission through desert atmospheres
[AD-A276022] p 3742 N94-31496
Investigation of modularly configured attached processors with intelligent memories
[AD-A278418] p 3839 N94-33330
TEXAS UNIV., HOUSTON.
Analysis and synthesis of adaptive neural elements and assemblies
[AD-A277423] p 3836 N94-32996
TEXAS UNIV. AT DALLAS, RICHARDSON.
Elementary particle physics
[DE94-006071] p 3866 N94-31620
THINKALONG SOFTWARE, INC., BROWNSVILLE, CA.
Discovery systems for manufacturing
[AD-A276216] p 3828 N94-31061
TINI ALLOY CO., SAN LEANDRO, CA.
Implementation of heaters on thermally actuated spacecraft mechanisms p 3607 N94-33320
TOLEDO UNIV., OH.
An experimental study of void formation during aluminum solidification in reduced gravity p 3667 N94-31944
TORONTO UNIV., NORTH YORK (ONTARIO).
Thermal-vacuum response of polymer matrix composites in space p 3595 N94-31033
TORONTO UNIV. (ONTARIO).
Turbulence structure of a premixed flame in a coaxial free air jet in the presence or absence of a base flow
[ISBN-0-315-78739-2] p 3633 N94-31471
Space hypervelocity microparticle impact damage in polymer matrix composites
[ISBN-0-315-87057-5] p 3652 N94-31692
Perturbative aspects of lower-dimensional gauge theories
[ISBN-0-315-86269-6] p 3911 N94-31712
CAD-based off-line planning for an active-vision system
[ISBN-0-315-86317-X] p 3813 N94-31713
Motion and force control of coordinated robots
[ISBN-0-315-86323-4] p 3724 N94-31714
Morphological directional coding of images
[ISBN-0-315-86336-6] p 3814 N94-31715
Chaotic attitude motion of satellites in the central gravitational field
[ISBN-0-315-78768-6] p 3610 N94-31723
Estimation of visible and near-infrared reflectivity for Peyto Glacier Basin using satellite data
[ISBN-0-315-87039-7] p 3743 N94-31733
Heave dynamics of an air cushion vehicle bag and finger skirt
[ISBN-0-315-87053-2] p 3568 N94-31734
Real-time control of the Trussarm variable-geometry-truss manipulator utilizing machine vision
[ISBN-0-315-87054-0] p 3830 N94-31735
Fiber optic sensors for the detection of surface acoustic waves on metals
[ISBN-0-315-87055-9] p 3878 N94-31736
Point-contact and point-impact dynamics for multibody chains
[ISBN-0-315-87056-7] p 3734 N94-31737
Errors associated with the use of heat flow transducers p 3796 N94-31742

A real-time computer control and trajectory generation environment for Trussarm
[ISBN-0-315-87060-5] p 3632 N94-31833
The basement fracture pattern of southern Ontario: A tectonic interpretation based on Landsat TM imagery, airphotos and field data
[ISBN-0-315-87086-9] p 3772 N94-31834
Interfacial behaviour: Wettability in SiC(sub p) metal matrix composites
[ISBN-0-315-87206-3] p 3621 N94-31835
Optimization of composite material failure loads
[ISBN-0-315-87214-4] p 3621 N94-31836
Development of a reconfigurable helicopter flight control system
[ISBN-0-315-87218-7] p 3585 N94-31837
Manufacture of light-damage resistant, planar, single mode waveguide on lithium niobate
[DSIS-94-01503] p 3879 N94-31850
Model identification of a reconfigurable robot manipulator
[ISBN-0-315-87109-1] p 3725 N94-31874
Photopyroelectric spectroscopy as a non-intrusive technique for the determination of the optical absorption spectra of multiple quantum well samples
[ISBN-0-315-87164-4] p 3833 N94-31875
Real-time control and application to robotics: Hardware and software architectures
[ISBN-0-315-87192-X] p 3833 N94-31876
Investigation of scintillator and fibre light in plastic scintillation dosimetry
[ISBN-0-315-87190-3] p 3879 N94-31877
Automatic analysis of force distribution in multi-fingered articulated hands
[ISBN-0-315-87205-5] p 3725 N94-31878

TOULOUSE UNIV. (FRANCE).
Airborne instruments p 3757 N94-31006
Sources and wells of minor atmospheric constituents of climatic importance p 3770 N94-31008

TRUSTED INFORMATION SYSTEMS, INC., LOS ANGELES, CA.
Integrated Trusted System Development Environment Process
[AD-A276414] p 3816 N94-32131

TRW, INC., REDONDO BEACH, CA.
MHD seed recovery/regeneration, phase 2
[DE94-006772] p 3886 N94-31273

TRW SYSTEMS GROUP, REDONDO BEACH, CA.
Leveraging metal matrix composites to reduce costs in space mechanisms p 3604 N94-33301

TSUKUBA SPACE CENTER (JAPAN).
Multisatellite constellation configuration selection for multiregional highly elliptical orbit constellations p 3600 N94-31437

TULSA UNIV., OK.
Volatiles combustion in fluidized beds
[DE94-008382] p 3636 N94-32414

U

UMPQUA RESEARCH CO., MYRTLE CREEK, OR.
Catalytic methods using molecular oxygen for treatment of PMMS and ECLSS waste streams, volume 2
[NASA-CR-190299] p 3804 N94-32697

UNION CARBIDE CORP., SOUTH CHARLESTON, WV.
Heterogeneous catalytic process for alcohol fuels from syngas
[DE94-008729] p 3667 N94-32583

UNITED SOLAR SYSTEMS CORP., TROY, MI.
Research on stable, high-efficiency amorphous silicon multijunction modules
[DE94-000298] p 3695 N94-32680

UNITED TECHNOLOGIES CORP., WINDSOR LOCKS, CT.
In flight measurement of steady and unsteady blade surface pressure of a single rotation large scale advanced prop-fan installed on the PTA aircraft
[NASA-CR-187096] p 3584 N94-32859

UNITED TECHNOLOGIES RESEARCH CENTER, EAST HARTFORD, CT.
Advanced material processing for integrated-optic frequency doubling systems
[AD-A278394] p 3698 N94-33163
Novel precursor approached for CMC derived by polymer pyrolysis
[AD-A278383] p 3665 N94-33352

UNIVERSIDAD COMPLUTENSE, MADRID (SPAIN).
The climate of the Mediterranean basin: Its sensitivity to global change p 3778 N94-30993

UNIVERSITE DES SCIENCES ET TECHNIQUES DE LILLE (FRANCE).
Matter-radiation interactions in the atmosphere p 3776 N94-30998
Desert aerosols: Sources, transports, and impacts determined by remote sensing p 3770 N94-31003

UNIVERSITEIT TWENTE, ENSCHEDE (NETHERLANDS).
A priori tests of large eddy simulation of the compressible plane mixing layer
[MEMO-1152] p 3699 N94-31185
On a formal approach to the methodology of information planning
[MEMO-INF-93-42] p 3917 N94-31415
A silicon condenser microphone: Modelling and electronic circuitry
[ISBN-9-09-005279-8] p 3688 N94-31517
A silicon condenser microphone: Materials and technology
[ISBN-9-09-005899-0] p 3688 N94-31518
Chemical vapour deposition of tungsten for the application in integrated circuits
[ISBN-9-09-005151-1] p 3641 N94-31519
Module generation for self-testing integrated systems
[ISBN-9-09-004570-8] p 3688 N94-31520
Engineering of damage in ion implanted silicon
[ISBN-9-09-005097-3] p 3897 N94-31521
A hierarchical approach to test generation for CMOS VLSI circuits
[ISBN-9-09-005449-9] p 3689 N94-31535
Employment of a porous gold actuator in ISFET-based coulometric sensor-actuator systems with application to protein characterization
[ISBN-9-09-005887-7] p 3689 N94-31536
Analysis and synthesis of MOS translinear circuits
[ISBN-9-09-005495-2] p 3690 N94-31616
Perspectives of glucose sensing based on a charge-modulating competition reaction
[ISBN-9-09-005754-4] p 3795 N94-31652
Performability modelling using DyQNtool+
[MEMO-INF-93-45] p 3812 N94-31659
Light-traffic analysis for queues with spatially distributed arrivals
[MEMO-1150] p 3832 N94-31826
Analysis and design of a high speed, wide range stepwise tunable optical filter/amplifier
[PB94-149572] p 3698 N94-33169

UNIVERSITY COLL., GALWAY (IRELAND).
Backscatter and transmission of aerosol at UV through middle IR wavelengths
[AD-A277127] p 3718 N94-32305

UNIVERSITY COLL. OF NORTH WALES, BANGOR.
Fast acting optical deflection
[AD-A276630] p 3879 N94-32037

UNIVERSITY OF CENTRAL FLORIDA, ORLANDO.
High-speed data search p 3923 N94-32441
An intelligent interactive visual database management system for Space Shuttle closeout image management p 3923 N94-32469
Simplified ultra-high resolution optic for soft x ray imaging
[AD-A278424] p 3885 N94-33331

UNIVERSITY OF NORTH TEXAS, DENTON.
Development of sample charge compensation for characterization of impurities in semiconductor materials
[AD-A277113] p 3899 N94-31983

UNIVERSITY OF SOUTHERN CALIFORNIA, LOS ANGELES.
The small-scale topology of a 2:1 aspect-ratio elliptic jet p 3699 N94-31184
The Nomad Explorer assembly assist vehicle: An architecture for rapid global extraterrestrial base infrastructure establishment p 3599 N94-31429
Combustion-related studies using weakly-bonded complexes
[DE94-006632] p 3633 N94-31493
Epitaxial liftoff technology onto processed silicon foundry wafers
[AD-A277116] p 3900 N94-31985
Modeling and control of nonlinear systems
[AD-A277377] p 3834 N94-32095
Approximation theory and computational methods for the identification and control of distributed parameter systems
[AD-A277335] p 3848 N94-32244
Studies of optical beam phase conjugation and electromagnetic scattering process
[AD-A278389] p 3884 N94-33145
Apron heights around stepped massifs in the Cydonia Mensae region: Do they record the local paleobathymetry of Oceanus Borealis? p 3949 N94-33224

UOP, INC., DES PLAINES, IL.
The development of precipitated iron catalysts with improved stability
[DE94-008711] p 3638 N94-32886

UTAH STATE UNIV., LOGAN.
The properties of sunflecks in a flexible plant canopy, and their relationship to turbulence p 3782 N94-31775
Evaluating in-plane elastic constants of damaged carbon-epoxy laminates using a quantitative ultrasonic technique p 3621 N94-31793
Nonlinear vibration analysis of laminated plates on linear and nonlinear elastic foundations p 3737 N94-32079

UTAH UNIV., SALT LAKE CITY.
Reliability analysis of structural ceramics subjected to biaxial flexure p 3650 N94-31454
Effects of frequency and amplitude variations of superimposed minor loading sequences on the corrosion fatigue behavior of aircraft structural aluminum alloys p 3578 N94-31957
Chemical structure and kinetics at liquid/solid interfaces
[AD-A277112] p 3636 N94-32304
Laser flash photolysis, EPR and Raman studies of liquids at elevated pressures
[DE94-008351] p 3718 N94-32413
Fabrication, phase transformation studies and characterization of SiC-AlN-Al2OC ceramics
[DE94-008587] p 3659 N94-32657
Time-resolved analytical methods for liquid/solid interfaces
[DE94-008352] p 3637 N94-32826
Ligand intermediates in metal-catalyzed reactions
[DE94-008713] p 3638 N94-32887

UTRECHT STATE UNIV. (NETHERLANDS).
Detecting the erosion of hierarchic information structures
[RUU-CS-93-10] p 3916 N94-31365
Abstracts of the Workshop on Computational Geometry (CG 1992)
[PB94-147022] p 3844 N94-31684

V

VANDERBILT UNIV., NASHVILLE, TN.
Physical properties of glasses exposed to Earth-facing and trailing-side environments on LDEF p 3594 N94-31030
Elastic modulus measurements of LDEF glasses and glass-ceramics using a speckle technique
[NASA-CR-195911] p 3653 N94-31851

VIALE UNIV., ROME (ITALY).
Aerosols scattering and near-infrared observations of the Martian surface p 3946 N94-33204

VIGYAN RESEARCH ASSOCIATES, INC., HAMPTON, VA.
Computation of three-dimensional compressible boundary layers to fourth-order accuracy on wings and fuselages
[NASA-CR-4269] p 3709 N94-32871
Drop size distributions and related properties of fog for five locations measured from aircraft
[NASA-CR-4585] p 3787 N94-33065

VIRGINIA CENTER OF EXCELLANCE FOR SOFTWARE REUSE AND TECHNOLOGY TRANSFER, HERNDON.
Overview of megaprogramming course: Lectures and exercises
[AD-A276169] p 3814 N94-31810
MULTIGRAPH: An architecture for model-based programming. Model-based program synthesis for parallel computing. PREMOS: Programming environment for model-based program synthesis, version 01.00.00
[AD-A276949] p 3817 N94-32219

VIRGINIA POLYTECHNIC INST. AND STATE UNIV., BLACKSBURG.
Vibration control and design of composite cantilevers taking into account structural uncertainties and damage p 3733 N94-31213
Study of wave propagation and dynamic response of laminated composite structures
[AD-A276123] p 3619 N94-31444
Control of a flexible space robot tracking a moving target p 3722 N94-31469
Three-dimensional velocity measurements on a 6:1 prolate spheroid at 10 deg angle of attack
[AD-A276485] p 3702 N94-31476
Random vibrations of composite beams and plates p 3735 N94-31777
Multidisciplinary optimization of high-speed civil transport configurations using variable-complexity modeling p 3578 N94-31881
Effect of elevated temperature and cyclic loading on properties and damage modes in ceramic composites
[DE94-008736] p 3662 N94-32891
Identification and control of structures in space
[NASA-CR-195910] p 3612 N94-33115

VIRGINIA UNIV., CHARLOTTESVILLE.
Inelastic deformation of metal matrix composites p 3618 N94-31285
An approximate solution for interlaminar stresses in laminated composites p 3621 N94-31901
Structure and stability of spherical accretion flows onto compact objects p 3935 N94-31946
Control and stabilization of distributed parameter systems; theoretical and computational aspects
[AD-A277239] p 3738 N94-32275

Computational modeling of convective heat transfer to liquid hydrogen coolant p 3707 N94-32485
Effective computational strategy for predicting the response of complex systems
[AD-A277452] p 3740 N94-33011
Research on high reliability refractory ohmic contacts for GaAs FETs and MODFETs
[AD-A276848] p 3697 N94-33034

VRIJE UNIV., AMSTERDAM (NETHERLANDS).
Transverse mode analysis of hole-coupled free-electron lasers
[ETN-94-96019] p 3715 N94-31532
Influence of long-range correlations on the spectral functions and response of 48Ca and 90Zr
[ETN-94-96017] p 3865 N94-31537
Free electrons as a versatile source of coherent radiation
[ETN-94-96011] p 3715 N94-31545
An expert system architecture for heterogeneous domains: A case-study in the legal field
[ETN-94-96012] p 3830 N94-31546
High pressure experiments on the Y-Ba-Cu-O superconductors: A major role for holes
[ETN-94-96013] p 3897 N94-31547
Collective and quasiparticle excitations in light Pb isotopes
[ETN-94-96014] p 3865 N94-31548
Diamagnetism in helium Rydberg atoms
[ETN-94-96015] p 3865 N94-31549
Single scattering of light by ensembles of particles with various shapes
[ETN-94-96016] p 3878 N94-31550
Multiple scattering of polarized radiation in planetary atmospheres
[ETN-94-96018] p 3674 N94-31551

W

WAGENINGEN AGRICULTURAL UNIV. (NETHERLANDS).
Possibilities of GER data for soil surface characteristics in the Almaden area p 3744 N94-31859
High resolution spectroscopy in agriculture: Results of the EISAC 1989 campaign p 3745 N94-31864
Monitoring landsurface characteristics in Niger using complementary SPOT and ERS-1 SAR data p 3754 N94-32560

WAKE FOREST UNIV., WINSTON-SALEM, NC.
Neostriatal neuronal activity and behavior
[AD-A278429] p 3802 N94-33333

WALES UNIV., SWANSEA.
Atomic oxygen damage characterization by photothermal scanning p 3598 N94-31051

WALES UNIV. INST. OF SCIENCE AND TECHNOLOGY, CARDIFF.
Lowering the Schottky barrier at metal or silicide/Si interfaces to extend the range of infrared detectors
[AD-A277253] p 3903 N94-32322

WALTER REED ARMY INST. OF RESEARCH, WASHINGTON, DC.
Exposure assessment of JAVELIN missile combustion products
[AD-A278128] p 3616 N94-33059

WASHINGTON STATE UNIV., PULLMAN.
Metal induced embrittlement
[DE94-007450] p 3640 N94-31325
Towards a detailed understanding of the structural variability in lignins: A new approach
[DE94-007449] p 3793 N94-32267

WASHINGTON UNIV., SEATTLE.
Ocean acoustic propagation measurements and wave propagation in random media
[AD-A276165] p 3787 N94-31053
An efficient higher order theory for laminated composite plates and a finite element implementation p 3617 N94-31215
The origin of neon-E: Neon-E in single interstellar silicon carbide and graphite grains p 3933 N94-31556
The finite element method with asymptotic self-similar solutions p 3736 N94-31904
Composition and properties of dust from Comet Halley p 3936 N94-31947
A chemical analysis of solar neighborhood dwarfs p 3926 N94-31951
Basic and applied studies of the ram accelerator as a hypervelocity projectile launcher
[AD-A277392] p 3602 N94-32288
Near edge x ray spectroscopy theory
[DE94-008179] p 3905 N94-32799
Coaxial slow source
[DE94-008191] p 3892 N94-32800
Mesh optimization
[AD-A277644] p 3820 N94-32972
Principles of ultradependability in chaotic routing
[AD-A277422] p 3827 N94-32995

WATERLOO UNIV. (ONTARIO).
Aerodynamic drag of droplets in turbulent flow fields
[ISBN-0-315-75827-9] p 3571 N94-32491
A critical evaluation of the Reynolds stress turbulence closure for the flow of a turbulent free-stream over a turbulent boundary layer
[ISBN-0-315-75792-2] p 3707 N94-32497
Laser and Fourier transform spectroscopy of novel propellant molecules
[AD-A277506] p 3667 N94-33013

WESTINGHOUSE HANFORD CO., RICHLAND, WA.
Agile total quality guidelines for enhancing teamwork and success
[DE93-019972] p 3915 N94-32678
Developing a personal-computer-based records retention system using Paradox(tm)
[DE94-007984] p 3819 N94-32749

WESTINGHOUSE SAVANNAH RIVER CO., AIKEN, SC.
A review of sensitivity analysis techniques
[DE94-007192] p 3842 N94-31399
Solid-state resistance upset welding: A process with unique advantages for advanced materials
[DE94-005941] p 3723 N94-31524
Managing performance of DB2 Ad Hoc Reports
[DE94-006669] p 3920 N94-32635
Modeling of residual stress mitigation in austenitic stainless steel pipe girth weldment
[DE94-007184] p 3738 N94-32639
An investigation of the radiolytic stability of a resorcinol-formaldehyde ion exchange resin
[DE94-007971] p 3660 N94-32698
Deuterium absorption and material phase characteristics of SAES St198 Zr-Fe alloy
[DE94-008275] p 3646 N94-32781

WESTINGHOUSE SCIENCE AND TECHNOLOGY CENTER, PITTSBURGH, PA.
Advanced silicon technology for microwave circuits
[AD-A278039] p 3698 N94-33091

WILMER OPHTHALMOLOGICAL INST., BALTIMORE, MD.
High peak power microwaves: A health hazard
[AD-A277168] p 3681 N94-32576

WINDSOR UNIV. (ONTARIO).
Production and detection of metastable atomic oxygen
[ISBN-0-315-87364-7] p 3868 N94-31915

WISCONSIN UNIV., MADISON.
Solidification structure synthesis in undercooled liquids
[AD-A276166] p 3910 N94-31054
Strictly positive definite functions on spheres
[AD-A276471] p 3855 N94-31244
Oscillations in piston-driven shear flow of a non-Newtonian fluid
[AD-A276472] p 3701 N94-31245
Multivariate spline approximation
[AD-A276034] p 3842 N94-31441
Frames and stable bases for shift-invariant subspaces of L(sub 2)(IR(sup d))
[AD-A276470] p 3843 N94-31474
Double-lined pre-main-sequence binaries: A test of pre-main-sequence evolutionary theory p 3933 N94-31497
Boundary-layer cumulus over land: Some observations and conceptual models
[DE93-040820] p 3781 N94-31597
Elastic as limit of viscoelastic response, in a context of self-similar viscous limits
[AD-A277043] p 3738 N94-32273
A study of the neutral hydrogen distribution of the Milky Way through 21 cm emission and Lyman alpha absorption p 3938 N94-32309
Stability of tearing modes in tokamak plasmas
[DE94-009205] p 3892 N94-32911
Stability of bootstrap current driven magnetic islands in stellarators
[DE94-009207] p 3893 N94-32912
Anomalous transport equations in toroidal plasmas
[DE94-009206] p 3893 N94-32922
Low energy ion beam assisted growth of homoepitaxial silicon films at low temperature
[AD-A278092] p 3908 N94-33039
TRMM-related research: Tropical rainfall and energy analysis experiment
[NASA-CR-195834] p 3787 N94-33288

WISCONSIN UNIV., MILWAUKEE.
Process parameter-growth environment-film property relationships for reactive sputter deposited metal (V, Nb, Zr, Y, Au) oxide, nitride, and oxynitride films
[AD-A276382] p 3640 N94-31258
High-speed path constrained manipulator operation using optimal-feedback combined controller p 3833 N94-31962
Physics of heat pipe rewetting
[NASA-CR-195902] p 3913 N94-33148

WOLLONGONG UNIV. (AUSTRALIA).
Near and far infrared observations of protostars and dark clouds p 3926 N94-31969

WOODS HOLE OCEANOGRAPHIC INST., MA.
Sound scattering by cylinders of noncircular cross section
[AD-A276663] p 3861 N94-32089
Light in Thermal Environments (LITE) Workshop
[NASA-CR-195851] p 3790 N94-32981
Fine and microstructure observations at Fieberlin g Guyot R/V new horizon cruise report
[AD-A277917] p 3791 N94-33109
Deep water studies of CTD data
[AD-A277741] p 3791 N94-33176
Fluid mechanical measurements within the bottom boundary layer over the Northern California continental shelf during stress
[AD-A277916] p 3791 N94-33243
Cruise report: Oceanus 250 leg 4 high resolution profiler survey for the North Atlantic Tracer Release Experiment, 25 March - 24 April, 1992
[AD-A277935] p 3791 N94-33245

WORCESTER POLYTECHNIC INST., MA.
The pH of Mars p 3950 N94-33225

WRIGHT LAB., WRIGHT-PATTERSON AFB, OH.
The maintenance of operational flight program
[AD-A276363] p 3565 N94-31367
Technologies for avionics embedded computer systems
[AD-A276364] p 3581 N94-31368
Testing Operational Flight Programs (OFP's)
[AD-A276361] p 3578 N94-31387
A study of the Space Station Freedom response to the disturbance environment p 3600 N94-31434
Analysis of the effect of routing strategies for parallel implementations of a selected avionics application
[AD-A276069] p 3581 N94-31458
Direct-sequence spread-spectrum performance in a multipath fading environment
[AD-A276080] p 3673 N94-31464
Getting a handle on designing for avionics software supportability and maintainability
[AD-A276362] p 3581 N94-32055
Common modeling system for digital simulation p 3823 N94-32429
A framework for developing and managing reusable avionics software
[AD-A276846] p 3582 N94-32909
Comparison of coherent to incoherent detection at 2.09 micrometers using a solid state LADAR system
[AD-A277159] p 3721 N94-33102
Response of a cantilevered plate in supersonic flow
[AD-A277487] p 3580 N94-33107
An experimental study of pilot/vehicle dynamics using a tilt rotor flying machine
[AD-A277516] p 3805 N94-33349

WRIGHT RESEARCH DEVELOPMENT CENTER, WRIGHT-PATTERSON AFB, OH.
QUAD4 seminar
[AD-A277366] p 3818 N94-32330

WYOMING UNIV., LARAMIE.
Numerical simulation of thermally induced near-surface flows over Martian terrain p 3949 N94-33223

X

XEROX PALO ALTO RESEARCH CENTER, CA.
Research on the stability, electronic properties, and structure of a-Si:H and its alloys
[DE94-000292] p 3899 N94-31813

Y

YALE UNIV., NEW HAVEN, CT.
Neural networks for model-based recognition
[AD-A277375] p 3834 N94-32053
An algorithm for probabilistic, totally-ordered temporal projection
[AD-A277341] p 3817 N94-32257
Stress-induced enhancement of the startle reflex
[AD-A278414] p 3802 N94-33327

YARDNEY TECHNICAL PRODUCTS, INC., PAWCATUCK, CT.
Development of silver-zinc cells of improved cycle life and energy density
[AD-A277311] p 3693 N94-32329

YORK UNIV. (ONTARIO).
Sensory sensitivities and discriminations and their roles in aviation
[AD-A277312] p 3800 N94-32276

Typical Contract Number Index Listing

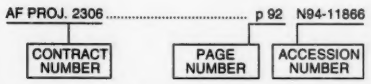

Listings in this index are arranged alphanumerically by contract number. Under each contract number the accession numbers denoting documents that have been produced as a result of research done under that contract are arranged in ascending order. The page number helps to locate the citation in the abstract section. The accession number denotes the number by which the citation is identified.

AF PROJ. ILIR ..... p 3799 N94-32035
AF PROJ. 0100 ..... p 3721 N94-33102
AF PROJ. 2003 ..... p 3581 N94-31458
AF PROJ. 2304 ..... p 3672 N94-31371
AF PROJ. 2338 ..... p 3732 N94-33088
AF PROJ. 2401 ..... p 3580 N94-33107
AF PROJ. 4594 ..... p 3810 N94-31335
AF PROJ. 4643 ..... p 3676 N94-31998
p 3677 N94-32083
p 3680 N94-32298
p 3680 N94-32299
p 3680 N94-32300
p 3685 N94-33347
AF PROJ. 7184 ..... p 3804 N94-32302
AF PROJ. 7755 ..... p 3799 N94-32035
AF PROJ. 9993 ..... p 3722 N94-33282
AF PROJ. 9994 ..... p 3565 N94-31367
p 3581 N94-31368
p 3578 N94-31387
p 3673 N94-31464
p 3581 N94-32055
p 3582 N94-32909
AF-AFOSR-0003-90 ..... p 3708 N94-32581
AF-AFOSR-0018-91 ..... p 3677 N94-32073
AF-AFOSR-0027-91 ..... p 3836 N94-32996
AF-AFOSR-0035-91 ..... p 3802 N94-33327
AF-AFOSR-0037-91 ..... p 3684 N94-33173
AF-AFOSR-0055-90 ..... p 3773 N94-32338
AF-AFOSR-0060-91 ..... p 3845 N94-32018
AF-AFOSR-0065-91 ..... p 3801 N94-32577
AF-AFOSR-0076-91 ..... p 3848 N94-32244
AF-AFOSR-0080-91 ..... p 3800 N94-32276
AF-AFOSR-0109-91 ..... p 3874 N94-33144
AF-AFOSR-0113-90 ..... p 3710 N94-33162
AF-AFOSR-0116-90 ..... p 3953 N94-32343
AF-AFOSR-0129-90 ..... p 3880 N94-32155
AF-AFOSR-0140-91 ..... p 3740 N94-33143
AF-AFOSR-0151-90 ..... p 3639 N94-33242
AF-AFOSR-0161-90 ..... p 3882 N94-32510
AF-AFOSR-0183-91 ..... p 3910 N94-33355
AF-AFOSR-0202-90 ..... p 3852 N94-32339
AF-AFOSR-0203-87 ..... p 3954 N94-31102
AF-AFOSR-0205-90 ..... p 3793 N94-32622
AF-AFOSR-0207-90 ..... p 3662 N94-32954
AF-AFOSR-0224-90 ..... p 3834 N94-32053
AF-AFOSR-0235-90 ..... p 3624 N94-32342
AF-AFOSR-0246-90 ..... p 3801 N94-32956
AF-AFOSR-0255-91 ..... p 3834 N94-32095
AF-AFOSR-0265-90 ..... p 3657 N94-32404
AF-AFOSR-0303-91 ..... p 3871 N94-32621
AF-AFOSR-0309-91 ..... p 3850 N94-33175
AF-AFOSR-0342-90 ..... p 3903 N94-32322
AF-AFOSR-0369-90 ..... p 3740 N94-33011
AF-AFOSR-0447-89 ..... p 3801 N94-32997
AF-AFOSR-0476-89 ..... p 3721 N94-33012
AF-AFOSR-0511-89 ..... p 3738 N94-32275
AF-AFOSR-0551-89 ..... p 3800 N94-32277
ARPA ORDER A840 ..... p 3630 N94-33180
ARPA ORDER 6266 ..... p 3919 N94-32382
ARPA ORDER 6860 ..... p 3909 N94-33328
ARPA ORDER 7144 ..... p 3719 N94-32608
ARPA ORDER 7330 ..... p 3918 N94-31930
p 3815 N94-31940
ARPA ORDER 7597 ..... p 3712 N94-31929
p 3806 N94-31934
ARPA ORDER 7781 ..... p 3726 N94-32236
ARPA ORDER 8100 ..... p 3897 N94-31531
ARPA ORDER 8313 ..... p 3815 N94-32080
ARPA ORDER 8557 ..... p 3879 N94-32006
BBN PROJ. 621697 ..... p 3862 N94-33023
BMFT-TV8202/8406 ..... p 3689 N94-31575
BMFT-06-DA-184-I ..... p 3866 N94-31614
BMWF-GZ-308.9281-IV/3/93 ..... p 3820 N94-32928
BRGM-CB47-73 ..... p 3754 N94-32561
CAPES/MEC-1245/90-13 ..... p 3824 N94-31183
CNES/92/0393 ..... p 3753 N94-32555
DA PROJ. MP9-2 ..... p 3791 N94-33185
p 3684 N94-33186
DA PROJ. RM-3-3-T-24 ..... p 3712 N94-32002
DA PROJ. RM3-3-F-60 ..... p 3775 N94-33028
DA PROJ. S13-37 ..... p 3682 N94-32971
DA PROJ. 1L1-61102-AH-43 ..... p 3635 N94-32124
DA PROJ. 1L1-61102-AH-45 ..... p 3728 N94-32893
p 3728 N94-32902
DA PROJ. 1L1-61102-BH-57 ..... p 3879 N94-32037
DA PROJ. 1L1-62211-A-47-A ..... p 3728 N94-32900
p 3728 N94-32929
p 3728 N94-32979
DA PROJ. 101-62622-A-553 ..... p 3763 N94-31339
DA PROJ. 104-63806-D-601 ..... p 3878 N94-31340
DA PROJ. 3M1-62787-A-874 ..... p 3794 N94-33098
DA PROJ. 3M1-62787-A-878 ..... p 3575 N94-32363
DA PROJ. 3M1-62787-A-879 ..... p 3804 N94-32171
p 3804 N94-32379
DA PROJ. 3M2-63004-D-805 ..... p 3798 N94-33092
DA PROJ. 4A1-62784-A-855 ..... p 3784 N94-32046
DAAB07-94-C-C009 ..... p 3630 N94-33180
DAAH04-93-C-0072 ..... p 3792 N94-31294
DAAH04-94-G-0006 ..... p 3845 N94-31939
DAAK60-93-C-0020 ..... p 3804 N94-32580
DAAK70-92-C-0015 ..... p 3771 N94-31369
DAAL01-93-C-4064 ..... p 3663 N94-33010
DAAL03-88-K-0058 ..... p 3810 N94-31277
DAAL03-89-G-0087 ..... p 3650 N94-31509
DAAL03-89-G-0108 ..... p 3742 N94-31496
DAAL03-89-G-0113 ..... p 3887 N94-31530
DAAL03-89-G-0114 ..... p 3686 N94-31079
DAAL03-89-K-0022 ..... p 3640 N94-31258
DAAL03-89-K-0144 ..... p 3618 N94-31261
DAAL03-90-C-0026 ..... p 3714 N94-31278
DAAL03-90-G-0018 ..... p 3686 N94-31057
DAAL03-90-G-0042 ..... p 3910 N94-31054
DAAL03-90-G-0063 ..... p 3688 N94-31445
DAAL03-90-G-0090 ..... p 3855 N94-31244
p 3842 N94-31441
p 3843 N94-31474
DAAL03-90-G-0093 ..... p 3811 N94-31443
DAAL03-90-G-0134 ..... p 3619 N94-31444
DAAL03-90-G-0145 ..... p 3651 N94-31510
DAAL03-90-G-0201 ..... p 3809 N94-31251
DAAL03-90-G-0209 ..... p 3894 N94-31056
DAAL03-90-G-0216 ..... p 3859 N94-33161
DAAL03-90-G-0222 ..... p 3632 N94-31348
DAAL03-91-C-0027 ..... p 3701 N94-31245
DAAL03-91-G-0080 ..... p 3894 N94-31055
DAAL03-91-G-0154 ..... p 3671 N94-31260
DAAL03-92-C-0036 ..... p 3897 N94-31528
DAAL03-92-G-0013 ..... p 3852 N94-31296
p 3843 N94-31529
DAAL03-92-G-0150 ..... p 3895 N94-31081
DAAL03-92-G-0185 ..... p 3701 N94-31245
DAAL03-92-G-0224 ..... p 3631 N94-31282
DAAL03-92-G-0257 ..... p 3698 N94-33249
DAAL03-92-G-0400 ..... p 3714 N94-31358
DAAL03-92-G-0410 ..... p 3822 N94-33284
DABT63-93-C-0054 ..... p 3816 N94-32081
DACA76-93-C-0004 ..... p 3829 N94-31301
DACA76-93-C-0010 ..... p 3917 N94-31829
DAHA45-93-M-0293 ..... p 3902 N94-32209
DAJA45-89-C-0024 ..... p 3616 N94-32038
DAJA45-89-C-0028 ..... p 3757 N94-33269
DAJA45-90-C-0003 ..... p 3693 N94-32301
DAJA45-90-C-0005 ..... p 3879 N94-32037
DAJA45-90-C-0021 ..... p 3784 N94-32162
DAJA45-90-C-0022 ..... p 3717 N94-31996
DAJA45-92-C-0005 ..... p 3884 N94-33267
DAJA45-92-C-0006 ..... p 3771 N94-31326
DAJA45-92-C-0024 ..... p 3718 N94-32305
DAJA45-92-M-0163 ..... p 3794 N94-33250
DAJA45-93-C-0008 ..... p 3738 N94-32351
DAJA45-93-C-0041 ..... p 3772 N94-32007
DAJA45-93-C-0042 ..... p 3776 N94-33184
DAJA45-93-M-0151 ..... p 3634 N94-32033
DAJA45-93-M-0162 ..... p 3692 N94-32259
DAJA45-93-M-0211 ..... p 3693 N94-32307
DAJA45-93-M-0294 ..... p 3906 N94-32908
DAJA45-93-M-0434 ..... p 3721 N94-33000
DAJA45-93-M-0440 ..... p 3655 N94-32016
DAMD17-92-C-2026 ..... p 3794 N94-33098
DAMD17-92-J-2019 ..... p 3798 N94-33092
DASG60-91-C-1043 ..... p 3881 N94-32392
DE-AC01-90CE-90053 ..... p 3759 N94-31266
p 3761 N94-32701
DE-AC02-76CH-00016 ..... p 3632 N94-31305
p 3864 N94-31398
p 3875 N94-31480
p 3956 N94-31523
p 3771 N94-31527
p 3865 N94-31607
p 3691 N94-31919
p 3876 N94-32099
p 3746 N94-32100
p 3615 N94-32266
p 3870 N94-32355
p 3938 N94-32638
p 3766 N94-32691
p 3766 N94-32692
p 3646 N94-32699
p 3713 N94-32821
p 3906 N94-32822
p 3794 N94-32896
p 3883 N94-32994
DE-AC02-76CH-03000 ..... p 3863 N94-31147
p 3878 N94-31271
p 3897 N94-31506
p 3864 N94-31507
p 3866 N94-31669
p 3866 N94-31670
p 3867 N94-31671
p 3652 N94-31764
p 3876 N94-32586
p 3871 N94-32587
p 3876 N94-32588
p 3872 N94-32627
p 3877 N94-32748
p 3873 N94-32780
p 3877 N94-32802
DE-AC02-76CH-03073 ..... p 3887 N94-31406
p 3888 N94-31667
DE-AC02-76ER-00881 ..... p 3864 N94-31310
DE-AC02-76ER-02289 ..... p 3864 N94-31310
DE-AC02-78ET-51013 ..... p 3891 N94-32595
DE-AC02-83CH-10093 ..... p 3758 N94-31235
p 3758 N94-31236
p 3758 N94-31264
p 3759 N94-31279
p 3953 N94-31491
p 3690 N94-31598
p 3760 N94-31812
p 3899 N94-31813
p 3760 N94-32143
p 3695 N94-32680
p 3761 N94-32725
p 3762 N94-32763
p 3905 N94-32764
p 3762 N94-32765
DE-AC03-76DP-00789 ..... p 3891 N94-32612
DE-AC03-76SF-00098 ..... p 3795 N94-31323
p 3864 N94-31405
p 3712 N94-31629
p 3898 N94-31630
p 3953 N94-31632
p 3899 N94-31634
p 3955 N94-31635
p 3866 N94-31637
p 3641 N94-31638
p 3857 N94-31639

p 3643 N94-32064
p 3880 N94-32138
p 3870 N94-32250
p 3636 N94-32376
p 3819 N94-32668
p 3873 N94-32768
DE-AC03-76SF-00515 ..... p 3925 N94-31786
p 3911 N94-31823
p 3900 N94-32065
p 3938 N94-32503
p 3872 N94-32630
p 3873 N94-32689
p 3646 N94-32795
p 3874 N94-32841
p 3721 N94-32845
p 3721 N94-32848
p 3875 N94-33189
p 3875 N94-33278
DE-AC03-84ER-51044 ..... p 3888 N94-31765
DE-AC03-89ER-51114 ..... p 3886 N94-31304
p 3886 N94-31324
p 3890 N94-32201
p 3891 N94-32595
p 3891 N94-32611
p 3891 N94-32612
p 3892 N94-32810
DE-AC03-89ER-52153 ..... p 3718 N94-32202
DE-AC04-76DP-00613 ..... p 3765 N94-32144
p 3823 N94-32431
p 3694 N94-32582
DE-AC04-76DP-00789 ..... p 3764 N94-31602
p 3891 N94-32595
p 3892 N94-32810
DE-AC04-76DR-00789 ..... p 3733 N94-31316
p 3723 N94-31651
p 3793 N94-32269
p 3818 N94-32584
p 3661 N94-32803
DE-AC04-88DP-43495 ..... p 3723 N94-31621
DE-AC04-94AL-85000 ..... p 3941 N94-31145
p 3714 N94-31148
p 3823 N94-31149
p 3649 N94-31198
p 3613 N94-31265
p 3671 N94-31267
p 3701 N94-31268
p 3576 N94-31306
p 3640 N94-31345
p 3609 N94-31382
p 3688 N94-31483
p 3811 N94-31484
p 3715 N94-31485
p 3897 N94-31502
p 3568 N94-31578
p 3666 N94-31579
p 3690 N94-31593
p 3690 N94-31594
p 3716 N94-31622
p 3651 N94-31649
p 3651 N94-31650
p 3666 N94-31827
p 3899 N94-31847
p 3655 N94-32102
p 3901 N94-32104
p 3634 N94-32110
p 3692 N94-32111
p 3692 N94-32112
p 3678 N94-32113
p 3717 N94-32134
p 3737 N94-32135
p 3902 N94-32296
p 3818 N94-32353
p 3707 N94-32373
p 3761 N94-32383
p 3903 N94-32384
p 3881 N94-32385
p 3693 N94-32386
p 3903 N94-32409
p 3668 N94-32412
p 3719 N94-32603
p 3872 N94-32628
p 3625 N94-32642
p 3761 N94-32648
p 3882 N94-32649
p 3695 N94-32650
p 3819 N94-32651
p 3849 N94-32653
p 3695 N94-32663
p 3615 N94-32669
p 3603 N94-32671
p 3645 N94-32672
p 3852 N94-32673
p 3882 N94-32674
p 3849 N94-32675
p 3695 N94-32700
p 3708 N94-32709

DE-AC05-76OR-00033 ..... p 3652 N94-31780
p 3659 N94-32640
p 3727 N94-32682
DE-AC05-84OR-21400 ..... p 3915 N94-31155
p 3733 N94-31312
p 3618 N94-31313
p 3640 N94-31314
p 3886 N94-31324
p 3896 N94-31489
p 3896 N94-31501
p 3764 N94-31596
p 3741 N94-31606
p 3898 N94-31630
p 3867 N94-31779
p 3652 N94-31780
p 3642 N94-31918
p 3901 N94-32172
p 3870 N94-32177
p 3890 N94-32201
p 3747 N94-32203
p 3636 N94-32251
p 3891 N94-32611
p 3891 N94-32612
p 3659 N94-32618
p 3891 N94-32619
p 3659 N94-32632
p 3659 N94-32640
p 3819 N94-32641
p 3872 N94-32666
p 3611 N94-32667
p 3920 N94-32676
p 3727 N94-32682
p 3766 N94-32690
p 3761 N94-32705
p 3904 N94-32724
p 3739 N94-32771
p 3807 N94-32783
p 3767 N94-32784
p 3905 N94-32785
p 3892 N94-32810
p 3874 N94-32850
p 3647 N94-32851
p 3647 N94-32852
p 3662 N94-32891
p 3662 N94-32935
p 3909 N94-33271
DE-AC06-76RL-01830 ..... p 3687 N94-31152
p 3895 N94-31307
p 3763 N94-31582
p 3764 N94-31601
p 3730 N94-31605
p 3641 N94-31626
p 3641 N94-31627
p 3759 N94-31762
p 3691 N94-31785
p 3712 N94-31831
p 3746 N94-32100
p 3816 N94-32145
p 3816 N94-32146
p 3785 N94-32268
p 3804 N94-32596
p 3871 N94-32605
p 3645 N94-32614
p 3713 N94-32681
p 3766 N94-32691
p 3720 N94-32704
p 3767 N94-32750
p 3786 N94-32759
p 3713 N94-32811
p 3768 N94-32812
p 3914 N94-32910
DE-AC06-87RL-10930 ..... p 3915 N94-32678
p 3819 N94-32749
DE-AC07-76ID-01570 ..... p 3658 N94-32517
p 3694 N94-32521
p 3659 N94-32655
p 3920 N94-32827
p 3696 N94-32828
DE-AC08-90NV-10845 ..... p 3743 N94-31603
DE-AC08-93NV-11265 ..... p 3901 N94-32176

p 3660 N94-32727
p 3660 N94-32729
p 3807 N94-32766
p 3696 N94-32786
p 3835 N94-32787
p 3661 N94-32796
p 3696 N94-32806
p 3920 N94-32808
p 3696 N94-32809
p 3774 N94-32816
p 3883 N94-32818
p 3661 N94-32819
p 3739 N94-32842
p 3883 N94-32878
p 3907 N94-32963
p 3763 N94-32965

DE-AC09-89SR-18035 ..... p 3713 N94-32728
p 3842 N94-31399
p 3723 N94-31524
p 3920 N94-32635
p 3738 N94-32639
p 3660 N94-32698
p 3646 N94-32781

DE-AC22-87PC-79672 ..... p 3886 N94-31273
DE-AC22-87PC-79812 ..... p 3638 N94-32886
DE-AC22-90PC-90043 ..... p 3666 N94-32132
DE-AC22-90PC-90044 ..... p 3667 N94-32133
DE-AC22-91PC-90046 ..... p 3667 N94-32583
DE-AC22-91PC-90056 ..... p 3638 N94-32889
DE-AC22-91PC-91030 ..... p 3637 N94-32767
DE-AC22-92PC-92109 ..... p 3638 N94-32888
DE-AC22-92PC-92110 ..... p 3759 N94-31272
DE-AI05-90ER-60952 ..... p 3764 N94-31596
DE-AI05-90OR-21956 ..... p 3764 N94-31596
DE-AI21-83MC-20422 ..... p 3742 N94-31504
DE-AT21-92MC-29267 ..... p 3771 N94-31525
DE-A101-91CE-50306 ..... p 3617 N94-32941
DE-FC03-90ER-61010 ..... p 3766 N94-32693
p 3767 N94-32712
DE-FC07-89ID-12869 ..... p 3668 N94-31604
DE-FC07-91ID-13103 ..... p 3646 N94-32782
DE-FC21-92MC-29227 ..... p 3759 N94-31487
DE-FC21-92MC-29237 ..... p 3762 N94-32823
DE-FC22-92PC-92521 ..... p 3766 N94-32703
DE-FG01-92CE-15974 ..... p 3661 N94-32788
DE-FG02-85ER-13421 ..... p 3714 N94-31200
DE-FG02-85ER-13442 ..... p 3636 N94-32594
DE-FG02-85ER-53207 ..... p 3889 N94-31787
DE-FG02-86ER-13480 ..... p 3635 N94-32140
DE-FG02-86ER-13590 ..... p 3872 N94-32643
DE-FG02-86ER-45231 ..... p 3905 N94-32770
DE-FG02-86ER-45271 ..... p 3649 N94-31201
DE-FG02-86ER-53218 ..... p 3892 N94-32911
p 3893 N94-32912
p 3893 N94-32922
DE-FG02-86ER-53222 ..... p 3888 N94-31664
DE-FG02-87ER-13714 ..... p 3872 N94-32644
DE-FG02-87ER-13774 ..... p 3646 N94-32805
DE-FG02-87ER-53244 ..... p 3887 N94-31558
DE-FG02-87ER-60522 ..... p 3793 N94-32516
DE-FG02-88ER-13822 ..... p 3706 N94-32149
DE-FG02-88ER-45372 ..... p 3659 N94-32656
DE-FG02-89ER-69017 ..... p 3767 N94-32711
DE-FG02-90ER-14114 ..... p 3651 N94-31672
DE-FG02-90ER-14162 ..... p 3871 N94-32375
DE-FG02-90ER-45429 ..... p 3633 N94-31526
DE-FG02-90ER-60983 ..... p 3763 N94-31347
DE-FG02-90ER-61071 ..... p 3785 N94-32716
DE-FG02-90ER-61072 ..... p 3764 N94-31601
p 3764 N94-31602
DE-FG02-90ER-61073 ..... p 3764 N94-31600
DE-FG02-91CE-23810 ..... p 3653 N94-31917
p 3658 N94-32518
DE-FG02-91ER-40606 ..... p 3939 N94-33147
DE-FG02-91ER-40608 ..... p 3873 N94-32708
DE-FG02-91ER-40690 ..... p 3876 N94-31505
DE-FG02-91ER-45439 ..... p 3647 N94-32964
DE-FG02-91ER-61206 ..... p 3766 N94-32692
DE-FG02-92ER-45465 ..... p 3652 N94-31780
DE-FG02-92ER-61361 ..... p 3781 N94-31597
DE-FG02-92ER-61364 ..... p 3785 N94-32717
DE-FG03-85ER-45197 ..... p 3912 N94-32513
DE-FG03-86ER-45230 ..... p 3907 N94-32933
DE-FG03-86ER-45245 ..... p 3908 N94-32991
DE-FG03-86ER-53225 ..... p 3891 N94-32611
p 3891 N94-32612
DE-FG03-88ER-40439 ..... p 3875 N94-33189
DE-FG03-89ER-14053 ..... p 3633 N94-31493
DE-FG03-89ER-51116 ..... p 3892 N94-32820
DE-FG03-89ER-51121 ..... p 3891 N94-32595
p 3891 N94-32612
p 3892 N94-32810
DE-FG03-90ER-54081 ..... p 3890 N94-32519
DE-FG03-91ER-40662 ..... p 3911 N94-31823
DE-FG03-91SF-18862 ..... p 3890 N94-32415
p 3876 N94-32731
DE-FG03-92ER-14304 ..... p 3889 N94-31766
DE-FG03-92ER-20081 ..... p 3794 N94-32769
DE-FG03-92ER-40711 ..... p 3876 N94-32407
DE-FG03-93ER-14321 ..... p 3638 N94-32887
DE-FG03-93ER-14333 ..... p 3637 N94-32826
DE-FG03-93ER-14340 ..... p 3718 N94-32413
DE-FG03-93ER-40757 ..... p 3871 N94-32512
p 3913 N94-32824
DE-FG03-93ER-45482 ..... p 3659 N94-32657
DE-FG03-93ER-54212 ..... p 3890 N94-32520
DE-FG03-93SF-19645 ..... p 3644 N94-32416
p 3646 N94-32825
DE-FG04-87AL-44658 ..... p 3631 N94-31153
DE-FG05-80ET-53088 ..... p 3886 N94-31366
p 3887 N94-31396
p 3891 N94-32631

	p 3891	N94-32664
	p 3720	N94-32684
	p 3876	N94-32685
	p 3891	N94-32686
DE-FG05-84ER-40141	p 3875	N94-31488
DE-FG05-85ER-40200	p 3871	N94-32512
DE-FG05-86ER-45259	p 3907	N94-32989
DE-FG05-87ER-25048	p 3836	N94-32992
DE-FG05-87ER-40376	p 3874	N94-32850
DE-FG05-88ER-13832	p 3661	N94-32847
DE-FG05-88ER-40446	p 3869	N94-32173
DE-FG05-88ER-53266	p 3888	N94-31619
	p 3877	N94-32844
DE-FG05-89ER-45384	p 3691	N94-31919
DE-FG05-92ER-14310	p 3870	N94-32178
DE-FG05-92ER-25145	p 3707	N94-32410
DE-FG05-92ER-40736	p 3866	N94-31620
DE-FG06-85ER-25006	p 3820	N94-32972
DE-FG06-87ER-45287	p 3640	N94-31325
DE-FG06-87ER-53243	p 3892	N94-32800
DE-FG06-90ER-45415	p 3905	N94-32799
DE-FG06-91ER-20022	p 3793	N94-32267
DE-FG09-89ER-13989	p 3794	N94-32890
DE-FG21-90MC-27225	p 3760	N94-31811
DE-FG22-92PC-92104	p 3667	N94-32150
DE-FG22-92PC-92539	p 3636	N94-32414
DE-FG22-92PC-92542	p 3658	N94-32408
DFG-MA-875/2-2	p 3745	N94-31865
DLA900-87-D-0017	p 3795	N94-31363
DLA900-88-D-0392	p 3609	N94-31292
DLA900-90-D-0123	p 3730	N94-32088
DTFA03-89-C-00043	p 3574	N94-31246
	p 3644	N94-32237
DTRS57-89-D-0009	p 3579	N94-32015
EEC-SC1-0004-C	p 3792	N94-31533
ETN-71.1403	p 3860	N94-31653
FWF-P8989-PHY	p 3820	N94-32928
F04701-88-C-0089	p 3595	N94-31034
	p 3624	N94-32122
	p 3635	N94-32233
	p 3894	N94-33106
	p 3698	N94-33177
F04701-93-C-0094	p 3728	N94-33061
	p 3616	N94-33094
	p 3838	N94-33168
	p 3808	N94-33252
	p 3612	N94-33262
F08635-89-C-0288	p 3881	N94-32380
F08635-89-C-0350	p 3718	N94-32366
F19628-88-D-0032	p 3587	N94-31346
	p 3587	N94-31356
F19628-89-C-0174	p 3678	N94-32161
F19628-89-K-0042	p 3719	N94-32608
F19628-90-C-0002	p 3881	N94-32285
F19628-90-C-0003	p 3818	N94-32508
F19628-90-C-0191	p 3776	N94-33272
F19628-91-C-0141	p 3775	N94-32999
F19628-91-C-0168	p 3815	N94-32080
F19628-91-K-0014	p 3836	N94-33043
F19628-92-K-0026	p 3747	N94-32160
F19628-93-C-0129	p 3811	N94-31465
F19628-93-C-0193	p 3821	N94-33030
F29601-91-C-0100	p 3667	N94-33013
F30602-88-D-0026	p 3870	N94-32368
F30602-88-D-0028	p 3650	N94-31284
	p 3683	N94-33093
F30602-91-C-0049	p 3816	N94-32131
F30602-93-C-0024	p 3880	N94-32151
F33600-85-D-7002	p 3565	N94-31830
F33615-87-C-0614	p 3798	N94-31243
F33615-88-C-0024	p 3566	N94-32254
F33615-88-C-1740	p 3801	N94-33053
F33615-89-C-0532	p 3582	N94-32223
F33615-90-C-0005	p 3586	N94-31058
	p 3816	N94-32093
F33615-90-C-1465	p 3712	N94-31929
	p 3806	N94-31934
	p 3845	N94-31939
	p 3821	N94-33030
F33615-90-C-3200	p 3604	N94-33301
F33615-91-C-3007	p 3587	N94-31295
F33615-92-C-3605	p 3586	N94-32224
F33615-92-C-5802	p 3828	N94-31061
F33615-93-D-3800	p 3895	N94-31329
F33615-93-1-1330	p 3824	N94-31259
	p 3815	N94-31994
	p 3822	N94-33279
F33657-86-C-0149	p 3588	N94-32014
	p 3588	N94-32241
	p 3588	N94-32311
	p 3588	N94-32312
	p 3588	N94-32313
	p 3589	N94-32314
	p 3589	N94-32315
	p 3589	N94-32316
	p 3589	N94-32317
F33733-89-C-1011	p 3589	N94-32318
F49620-89-C-0020	p 3589	N94-32319
F49620-89-C-0080	p 3589	N94-32394
F49620-89-C-0094	p 3590	N94-32395
F49620-89-C-0131	p 3590	N94-32396
F49620-91-C-0009	p 3590	N94-32397
F49620-91-C-0011	p 3590	N94-32398
F49620-91-C-0017	p 3590	N94-32399
F49620-91-C-0018	p 3590	N94-32403
F49620-91-C-0019	p 3604	N94-33301
	p 3685	N94-33353
F49620-91-C-0022	p 3776	N94-33351
F49620-91-C-0062	p 3909	N94-33328
F49620-91-C-0085	p 3797	N94-32623
F49620-92-C-0036	p 3884	N94-33140
F49620-92-C-0048	p 3726	N94-32320
F49620-92-J-0025	p 3665	N94-33352
F49620-92-J-0075	p 3884	N94-33145
F49620-92-J-0083	p 3625	N94-32591
F49620-92-J-0090	p 3625	N94-32592
F49620-92-J-0101	p 3698	N94-33163
F49620-92-J-0113	p 3656	N94-32246
F49620-92-J-0114	p 3591	N94-33167
F49620-92-J-0118	p 3625	N94-32624
F49620-92-J-0125	p 3908	N94-33005
F49620-92-J-0139	p 3710	N94-33164
F49620-92-J-0156	p 3900	N94-32040
F49620-92-J-0157	p 3839	N94-33325
F49620-92-J-0159	p 3706	N94-32256
F49620-92-J-0187	p 3731	N94-32953
F49620-92-J-0226	p 3708	N94-32511
F49620-92-J-0301	p 3800	N94-32344
F49620-92-J-0375	p 3786	N94-32921
F49620-92-J-0405	p 3826	N94-32243
F49620-92-J-0412	p 3862	N94-33146
F49620-92-J-0489	p 3801	N94-32998
F49620-92-J-0493	p 3698	N94-33142
F49620-92-J-0499	p 3910	N94-33332
F49620-92-J-0503	p 3800	N94-32345
F49620-92-J-0530	p 3706	N94-32279
F49620-93-C-0026	p 3802	N94-33333
F49620-93-C-0035	p 3602	N94-32288
F49620-93-C-0041	p 3885	N94-33331
F49620-93-C-0048	p 3685	N94-33354
F49620-93-1-0019	p 3799	N94-32096
F49620-93-1-0070	p 3741	N94-33356
F49620-93-1-0073	p 3835	N94-32340
F49620-93-1-0101	p 3900	N94-32041
F49620-93-1-0104	p 3802	N94-33241
F49620-93-1-0116	p 3630	N94-33165
F49620-93-1-0124	p 3909	N94-33324
F49620-93-1-0156	p 3908	N94-33246
F49620-93-1-0180	p 3664	N94-33350
F49620-93-1-0383	p 3684	N94-33172
F49621-92-J-0018	p 3800	N94-32419
L-17761D	p 3775	N94-33006
MDA903-89-C-0003	p 3774	N94-32346
	p 3835	N94-32281
MDA972-90-C-0035	p 3884	N94-33141
	p 3802	N94-33326
MDA972-91-C-0030	p 3908	N94-33055
MDA972-92-C-0026	p 3838	N94-33174
MDA972-92-C-0053	p 3662	N94-32952
MDA972-92-J-1018	p 3784	N94-32054
	p 3594	N94-31030
MIPR-92MM2600	p 3810	N94-31357
NAGW-1175	p 3677	N94-32087
NAGW-1388	p 3918	N94-31930
NAGW-1655	p 3815	N94-31940
NAGW-1937	p 3691	N94-31928
NAGW-2058	p 3919	N94-32382
NAGW-2220	p 3879	N94-32006
	p 3814	N94-31810
NAGW-2257	p 3817	N94-32219
NAGW-2412	p 3681	N94-32576
NAGW-2447	p 3816	N94-32086
	p 3668	N94-33037
	p 3954	N94-31102
	p 3939	N94-31105
	p 3790	N94-33045
	p 3944	N94-33196
	p 3945	N94-33198
NAGW-28	p 3948	N94-33215
	p 3943	N94-33103
NAGW-2903	p 3928	N94-31118
NAGW-3311	p 3928	N94-31119
	p 3823	N94-31120
	p 3928	N94-31121
	p 3929	N94-31128
	p 3931	N94-31134
	p 3932	N94-31140
	p 3932	N94-31141
	p 3944	N94-33195
	p 3944	N94-33196
	p 3893	N94-33048
NAGW-3402	p 3948	N94-33215
NAGW-3452	p 3943	N94-33104
NAGW-748	p 3790	N94-32981
	p 3944	N94-33195
	p 3944	N94-33196
NAGW-925	p 3757	N94-33019
NAG1-1490	p 3668	N94-33037
NAG1-225	p 3612	N94-33115
NAG10-0058	p 3923	N94-32469
NAG3-1062	p 3709	N94-32872
NAG3-1134	p 3571	N94-32475
NAG3-1139	p 3697	N94-33044
NAG3-1232	p 3584	N94-32075
	p 3727	N94-32741
NAG3-1270	p 3626	N94-32904
NAG3-1476	p 3728	N94-32900
	p 3728	N94-32929
NAG3-1567	p 3584	N94-33035
NAG5-1586	p 3787	N94-33288
NAG5-1925	p 3894	N94-33113
NAG5-2102	p 3953	N94-33047
NAG5-2109	p 3836	N94-32980
NAG6-1	p 3954	N94-31101
NAG8-156	p 3594	N94-31030
	p 3653	N94-31851
NAG9-380	p 3835	N94-32943
NAG9-525	p 3913	N94-33148
NAG9-593	p 3683	N94-33083
NASA ORDER C-30065-A	p 3616	N94-32970
NASA ORDER L-17761-D	p 3653	N94-31851
NASW-4574	p 3927	N94-31116
	p 3943	N94-33190
NASW-4614	p 3948	N94-33213
NASW-4776	p 3603	N94-32494
NASW-4812	p 3942	N94-32740
NAS1-18191	p 3638	N94-32868
NAS1-18224	p 3592	N94-31017
	p 3592	N94-31020
	p 3595	N94-31036
	p 3595	N94-31037
NAS1-18226	p 3820	N94-32778
NAS1-18585	p 3709	N94-32871
NAS1-18586	p 3820	N94-32775
NAS1-18603	p 3682	N94-32897
NAS1-18660	p 3722	N94-32448
NAS1-18799	p 3626	N94-32877
NAS1-18862	p 3626	N94-32860
NAS1-18888	p 3629	N94-33135
NAS1-18889	p 3626	N94-32863
	p 3629	N94-33130
	p 3629	N94-33132
	p 3629	N94-33133
	p 3630	N94-33137
NAS1-18972	p 3827	N94-32734
NAS1-19061	p 3862	N94-33023
NAS1-19099	p 3731	N94-32481
NAS1-19102	p 3707	N94-32480
NAS1-19247	p 3592	N94-31017
	p 3592	N94-31020
	p 3593	N94-31021
	p 3595	N94-31036
	p 3595	N94-31037
NAS1-19301	p 3722	N94-32448
NAS1-19341	p 3787	N94-33065
NAS1-19480	p 3820	N94-32928
	p 3849	N94-33033
	p 3821	N94-33075
	p 3806	N94-33286
NAS10-11675	p 3808	N94-32434
NAS2-13194	p 3571	N94-32478
NAS3-23051	p 3584	N94-32859
NAS3-23772	p 3614	N94-31618
NAS3-23885	p 3615	N94-32792
	p 3616	N94-32866
NAS3-25266	p 3572	N94-32926
	p 3697	N94-33052
	p 3573	N94-33119
NAS3-25409	p 3708	N94-32867
	p 3709	N94-32869
NAS3-25685	p 3663	N94-33024
NAS3-25797	p 3694	N94-32478
NAS3-25862	p 3681	N94-32477
NAS3-25883	p 3616	N94-33099
NAS3-26285	p 3603	N94-33296
NAS3-26764	p 3731	N94-33032
NAS3-27186	p 3731	N94-32901
	p 3696	N94-32905
	p 3617	N94-33022
	p 3698	N94-33116
NAS5-29298	p 3605	N94-33309
NAS5-30905	p 3826	N94-32482
NAS5-31169	p 3882	N94-32417
NAS5-31331	p 3823	N94-33287
	p 3613	N94-33289
NAS5-32349	p 3711	N94-31492
NAS5-33047	p 3893	N94-33074
NAS5-38039	p 3884	N94-33073

NAS7-1102 p 3826 N94-32483
NAS7-1103 p 3927 N94-32695
NAS7-1104 p 3882 N94-32702
NAS7-1111 p 3669 N94-32484
NAS8-32695 p 3594 N94-31030
p 3653 N94-31851
NAS8-38477 p 3727 N94-32479
NAS8-38489 p 3637 N94-32694
p 3637 N94-32696
NAS8-38490 p 3804 N94-32697
NAS8-38609 p 3927 N94-32942
NAS8-38783 p 3611 N94-32898
NAS8-39207 p 3608 N94-33100
NAS9-17819 p 3669 N94-32857
NAS9-18426 p 3835 N94-32359
p 3601 N94-32388
p 3731 N94-32862
p 3577 N94-32864
p 3739 N94-32907
NAS9-18800 p 3805 N94-33050
NCC2-327 p 3576 N94-33063
NCC2-478 p 3639 N94-33036
NCC2-666 p 3769 N94-33170
NCC2-688 p 3912 N94-32774
NCC2-833 p 3585 N94-31203
NCC3-171 p 3615 N94-32742
NCC3-233 p 3700 N94-31229
p 3710 N94-32969
p 3710 N94-33070
p 3850 N94-33120
NCC3-63 p 3662 N94-32945
NCC8-8 p 3740 N94-32940
NCC9-16 p 3822 N94-33114
NERC-F60/G6/12 p 3744 N94-31860
NERC-GT4/88/GT/99 p 3744 N94-31860
NF-102/62-356 p 3842 N94-31393
NF-63/62-518 p 3825 N94-32196
NGT-50559 p 3803 N94-31447
NR PROJ. M33-P-30 p 3802 N94-31302
NR PROJ. RR0-3204 p 3702 N94-31467
NR PROJ. R03-GE-81 p 3770 N94-31303
NR PROJ. R03-5-B-03 p 3850 N94-31462
NR PROJ. SC3-97 p 3730 N94-31065
NSF ASC-92-17041 p 3814 N94-31932
p 3815 N94-31933
p 3834 N94-32152
p 3817 N94-32212
p 3852 N94-33276
NSF AST-90-08166 p 3928 N94-31118
p 3928 N94-31119
p 3823 N94-31120
p 3928 N94-31121
p 3932 N94-31140
NSF AST-90-20855 p 3929 N94-31128
p 3931 N94-31134
NSF ATM-91-03440 p 3954 N94-31102
NSF CCR-88-20279 p 3848 N94-32331
NSF CCR-88-58087 p 3815 N94-31994
NSF CCR-89-57323 p 3820 N94-32972
NSF CCR-90-14605 p 3827 N94-33002
NSF CCR-92-03488 p 3849 N94-33060
NSF CCR-92-58525 p 3824 N94-31259
NSF CCR-93-08726 p 3822 N94-33279
NSF DDM-92-01340 p 3822 N94-33183
NSF DMS-90-00053 p 3843 N94-31474
NSF DMS-91-01979 p 3851 N94-32229
NSF DMS-91-02857 p 3843 N94-31474
NSF DMS-91-23946 p 3889 N94-31772
NSF DMS-92-09049 p 3738 N94-32273
NSF DMS-92-24748 p 3855 N94-31244
p 3843 N94-31474
NSF ECD-89-07068 p 3815 N94-31940
NSF ECS-92-16531 p 3814 N94-31932
p 3815 N94-31933
NSF INT-90-02363 p 3764 N94-31602
NSF IRI-90-13991 p 3814 N94-31932
p 3815 N94-31933
NSF IRI-92-21268 p 3824 N94-31183
NSF IRI-92-24521 p 3845 N94-31939
NSF MIP-90-01651 p 3817 N94-32213
p 3818 N94-32504
NSF MSS-90-25110 p 3848 N94-32331
NSG-1577 p 3821 N94-33049
NUTEK-5623-92-01540 p 3568 N94-31220
NUTEK-92-05162P p 3859 N94-31090
NWO-B-80-61 p 3847 N94-32191
N00014-84-K-0656 p 3648 N94-33182
N00014-85-C-0710 p 3810 N94-31370
p 3803 N94-32034
N00014-85-K-0198 p 3810 N94-31343
N00014-88-K-0738 p 3825 N94-32165
N00014-89-C-2106 p 3710 N94-33009
N00014-89-C-6014 p 3789 N94-32321
N00014-89-J-1058 p 3791 N94-33243
N00014-89-J-1063 p 3848 N94-32286
p 3822 N94-33183
N00014-89-J-1067 p 3791 N94-33243
N00014-89-J-1073 p 3791 N94-33109
N00014-89-J-1076 p 3791 N94-33176
N00014-89-J-1088 p 3789 N94-32401
N00014-89-J-1178 p 3881 N94-32280
p 3881 N94-32324
p 3893 N94-33007
N00014-89-J-1412 p 3636 N94-32304
N00014-89-J-1419 p 3789 N94-32402
N00014-89-J-1459 p 3627 N94-33029
N00014-89-J-1492 p 3643 N94-32091
N00014-89-J-1729 p 3861 N94-32089
N00014-89-J-1751 p 3822 N94-33188
N00014-89-J-1769 p 3869 N94-32082
N00014-89-J-1770 p 3772 N94-31984
N00014-89-J-1795 p 3859 N94-31060
p 3861 N94-32059
N00014-89-J-3221 p 3783 N94-31937
N00014-90-C-0024 p 3803 N94-32034
N00014-90-C-0210 p 3809 N94-31263
N00014-90-J-1012 p 3870 N94-32360
N00014-90-J-1025 p 3849 N94-33060
N00014-90-J-1030 p 3848 N94-32331
N00014-90-J-1148 p 3658 N94-32578
p 3658 N94-32579
p 3659 N94-32610
p 3663 N94-32985
p 3663 N94-33054
p 3664 N94-33082
p 3664 N94-33348
N00014-90-J-1260 p 3787 N94-31053
N00014-90-J-1267 p 3896 N94-31473
N00014-90-J-1293 p 3825 N94-32052
N00014-90-J-1441 p 3657 N94-32391
N00014-90-J-1530 p 3895 N94-31327
N00014-90-J-1584 p 3790 N94-33062
N00014-90-J-1691 p 3899 N94-31983
N00014-90-J-1890 p 3821 N94-33027
N00014-90-J-1942 p 3814 N94-31932
p 3815 N94-31933
p 3852 N94-33276
N00014-90-J-1946 p 3834 N94-32152
N00014-91-C-0067 p 3623 N94-32012
N00014-91-C-0163 p 3908 N94-33248
N00014-91-C-0216 p 3897 N94-31531
N00014-91-C-2313 p 3698 N94-33091
N00014-91-J-1007 p 3827 N94-32995
N00014-91-J-1078 p 3663 N94-33058
p 3664 N94-33138
p 3664 N94-33247
N00014-91-J-1095 p 3789 N94-32400
N00014-91-J-1189 p 3642 N94-31995
N00014-91-J-1270 p 3846 N94-32167
p 3880 N94-32186
N00014-91-J-1274 p 3655 N94-32005
p 3656 N94-32221
p 3657 N94-32364
N00014-91-J-1316 p 3836 N94-33014
N00014-91-J-1409 p 3642 N94-31997
p 3643 N94-32060
p 3644 N94-32169
p 3869 N94-32170
p 3635 N94-32216
p 3909 N94-33273
p 3909 N94-33274
p 3909 N94-33275
p 3875 N94-33277
N00014-91-J-1540 p 3799 N94-31440
N00014-91-J-1577 p 3817 N94-32257
N00014-91-J-1630 p 3877 N94-31256
p 3711 N94-31283
p 3632 N94-31459
N00014-91-J-1732 p 3702 N94-31476
N00014-91-J-1852 p 3697 N94-32957
N00014-91-J-1857 p 3878 N94-31330
N00014-91-J-1921 p 3654 N94-31981
p 3655 N94-31982
p 3655 N94-32069
p 3657 N94-32381
N00014-91-J-2025 p 3679 N94-32230
N00014-91-J-4038 p 3924 N94-31361
p 3726 N94-32166
p 3817 N94-32212
N00014-91-J-4063 p 3672 N94-31384
N00014-91-P-2037 p 3697 N94-33034
N00014-91-1-0243 p 3784 N94-32164
N00014-92-C-0081 p 3902 N94-32306
N00014-92-C-0173 p 3863 N94-31237
p 3631 N94-31238
p 3632 N94-31293
N00014-92-J-1121 p 3706 N94-32123
N00014-92-J-1374 p 3655 N94-32017
N00014-92-J-1391 p 3653 N94-31935
N00014-92-J-1635 p 3649 N94-31276
N00014-92-J-1694 p 3902 N94-32255
N00014-92-J-1778 p 3673 N94-31466
N00014-92-J-1809 p 3811 N94-31475
N00014-92-J-1814 p 3726 N94-32166
N00014-92-J-1820 p 3902 N94-32218
N00014-92-J-1828 p 3900 N94-32001
p 3900 N94-32003
p 3642 N94-32004
p 3900 N94-32011
N00014-92-J-1879 p 3924 N94-31361
p 3851 N94-32142
p 3846 N94-32167
p 3880 N94-32186
N00014-92-J-1886 p 3907 N94-32988
N00014-92-J-4097 p 3817 N94-32213
p 3818 N94-32504
N00014-92-J-4101 p 3701 N94-31341
N00014-92-J-6004 p 3747 N94-32214
N00014-92-1323 p 3791 N94-33245
N00014-93-C-0004 p 3650 N94-31297
N00014-93-C-0015 p 3738 N94-32273
N00014-93-C-0040 p 3627 N94-33008
N00014-93-C-0135 p 3884 N94-33087
N00014-93-C-0136 p 3880 N94-32068
N00014-93-C-0139 p 3895 N94-31350
N00014-93-C-0197 p 3746 N94-32119
N00014-93-C-0234 p 3816 N94-32130
N00014-93-C-2019 p 3768 N94-32284
N00014-93-C-2026 p 3692 N94-32215
N00014-93-I-0131 p 3848 N94-32245
p 3848 N94-32341
N00014-93-I-0224 p 3630 N94-33178
N00014-93-1-0099 p 3901 N94-32092
N00014-93-1-0195 p 3906 N94-33039
N00014-93-1-0271 p 3864 N94-31402
N00014-93-1-0288 p 3825 N94-32032
N00014-93-1-0311 p 3900 N94-31985
N00014-93-1-0363 p 3878 N94-31262
N00014-93-1-0385 p 3924 N94-31361
p 3851 N94-32142
N00014-93-1-0474 p 3875 N94-31247
N00014-93-1-0509 p 3805 N94-33084
N00014-93-1-0615 p 3654 N94-31978
p 3654 N94-31979
p 3654 N94-31980
N00014-93-1-0665 p 3896 N94-31455
N00014-93-1-0920 p 3896 N94-31439
N00014-93-1-1343 p 3839 N94-33330
N00014-93-1-6014 p 3845 N94-32022
N00039-92-C-0100 p 3583 N94-31931
p 3862 N94-33096
N60921-91-C-0205 p 3693 N94-32329
ONR PROJ. RC32W11 p 3684 N94-33254
ONR PROJ. R035S83 p 3577 N94-33253
ONR PROJ. ZW82 p 3776 N94-33041
p 3776 N94-33285
RICIS PROJ. IR-01B p 3822 N94-33114
RTOP 199-70-12-14 p 3801 N94-33068
RTOP 232-01-04-04 p 3710 N94-33020
RTOP 233-02-0B p 3726 N94-32272
RTOP 233-02-0D p 3663 N94-33024
RTOP 237-02-02-11 p 3613 N94-32924
RTOP 312-00-00 p 3732 N94-33101
RTOP 323-57-4A p 3731 N94-32901
RTOP 323-88-03 p 3731 N94-33032
RTOP 324-02-00 p 3731 N94-32481
RTOP 324-02-02 p 3707 N94-32480
RTOP 474-46-10 p 3617 N94-33022
RTOP 505-59-36-01 p 3572 N94-32873
RTOP 505-59-36 p 3571 N94-32063
RTOP 505-59-50 p 3709 N94-32946
p 3711 N94-33290
RTOP 505-59-52-02 p 3861 N94-32930
RTOP 505-59-54-01 p 3740 N94-33118
RTOP 505-60-21 p 3572 N94-32880
RTOP 505-60-31-05 p 3709 N94-32871
RTOP 505-62-00 p 3709 N94-32869
p 3709 N94-32872
RTOP 505-62-06 p 3728 N94-32902
RTOP 505-62-10 p 3626 N94-32904
p 3728 N94-32929
p 3728 N94-32979
RTOP 505-62-36 p 3728 N94-32900
RTOP 505-62-40-01 p 3638 N94-32868
RTOP 505-62-40 p 3572 N94-32926
RTOP 505-62-50 p 3584 N94-32075
p 3727 N94-32741
p 3713 N94-32983
RTOP 505-62-52 p 3615 N94-32742
p 3820 N94-32773
p 3709 N94-32947
p 3638 N94-32948
RTOP 505-63-12 p 3740 N94-32932
RTOP 505-63-5A p 3728 N94-32893
p 3647 N94-32931
p 3617 N94-33021
RTOP 505-63-5B p 3728 N94-32902
RTOP 505-63-50-04 p 3627 N94-32939

RTOP 505-63-50-12 ..... p 3572 N94-32865
RTOP 505-63-51 ..... p 3662 N94-32945
RTOP 505-64-10-13 ..... p 3827 N94-32734
RTOP 505-64-13-67 ..... p 3787 N94-33065
RTOP 505-64-13 ..... p 3575 N94-32927
RTOP 505-64-50-04 ..... p 3820 N94-32775
p 3820 N94-32776
RTOP 505-64-52-01 ..... p 3586 N94-32951
RTOP 505-68-10 ..... p 3571 N94-32475
RTOP 505-68-30 ..... p 3573 N94-33119
RTOP 505-69-20-01 ..... p 3601 N94-32870
RTOP 505-69-30-01 ..... p 3682 N94-32897
RTOP 505-70-62-13 ..... p 3573 N94-32950
RTOP 505-90-00 ..... p 3922 N94-32836
p 3922 N94-32837
RTOP 505-90-5K ..... p 3710 N94-32969
p 3710 N94-33070
p 3850 N94-33120
RTOP 505-90-5R ..... p 3700 N94-31229
RTOP 505-90-52-01 ..... p 3820 N94-32928
p 3849 N94-33033
p 3821 N94-33075
p 3806 N94-33286
RTOP 506-42-31 ..... p 3616 N94-32970
RTOP 506-43-41 ..... p 3603 N94-33291
RTOP 506-44-2C ..... p 3696 N94-32905
p 3697 N94-33052
p 3698 N94-33116
RTOP 506-46-31 ..... p 3617 N94-33117
RTOP 510-01-50 ..... p 3626 N94-32858
p 3732 N94-33038
RTOP 510-02-11 ..... p 3626 N94-32877
RTOP 510-02-13-01 ..... p 3626 N94-32863
p 3627 N94-33121
RTOP 535-03-01 ..... p 3739 N94-32683
RTOP 535-03-10 ..... p 3584 N94-32859
RTOP 537-02-23 ..... p 3573 N94-32984
RTOP 538-03-14-01 ..... p 3862 N94-33023
RTOP 549-03-61 ..... p 3820 N94-32906
RTOP 584-03-11 ..... p 3739 N94-32735
p 3616 N94-33099
RTOP 586-01-11 ..... p 3616 N94-32866
RTOP 590-13-11 ..... p 3615 N94-32792
RTOP 593-12-21 ..... p 3614 N94-31618
RTOP 665-45-20-01 ..... p 3785 N94-32737
RTOP 694-03-0C ..... p 3567 N94-33064
RTOP 920-00-00 ..... p 3823 N94-33287
p 3613 N94-33289
RTOP 960-60-90 ..... p 3805 N94-32936
RTOP 963-10-0F ..... p 3883 N94-32777
SBIR-02.09-9090 ..... p 3571 N94-32476
SBIR-04.08-5224 ..... p 3882 N94-32702
SBIR-04.09-6425A ..... p 3731 N94-32481
SBIR-05.03-1100 ..... p 3826 N94-32482
SBIR-05.05-2200 ..... p 3727 N94-32479
SBIR-06.08-4448 ..... p 3826 N94-32483
SBIR-08.12-3800 ..... p 3669 N94-32484
SBIR-08.18-0700 ..... p 3927 N94-32695
SBIR-09.12-8442 ..... p 3882 N94-32417
SBIR-10.01-9030 ..... p 3694 N94-32478
SBIR-11.04-6576A(VOL-1) ..... p 3637 N94-32696
SBIR-11.04-6576A(VOL-2) ..... p 3637 N94-32694
SBIR-12.02-5201(VOL-2) ..... p 3804 N94-32697
SBIR-14.05-9388 ..... p 3681 N94-32477
SBIR-15.03-5777 ..... p 3707 N94-32480
SC1-CT92-0779 ..... p 3852 N94-32350
SERC-GR/G59990 ..... p 3828 N94-31161
SERC-GR/H3528.6 ..... p 3842 N94-31394
p 3842 N94-31413
SION-612-317-404 ..... p 3817 N94-32287
ST79 ..... p 3722 N94-31379
SWRI PROJ. 01-1302 ..... p 3638 N94-32868
SWRI PROJ. 15-4167 ..... p 3943 N94-33103
SWRI PROJ. 15-5653 ..... p 3943 N94-33104
TGP92037 ..... p 3917 N94-31640
U-OF-I PROJ. 14251600 ..... p 3953 N94-33047
USECHQ-93-C-0001 ..... p 3913 N94-32846
W-31-109-ENG-38 ..... p 3863 N94-31151
p 3863 N94-31202
p 3841 N94-31274
p 3841 N94-31309
p 3864 N94-31310
p 3841 N94-31311
p 3829 N94-31315
p 3672 N94-31317
p 3722 N94-31319
p 3864 N94-31320
p 3864 N94-31321
p 3781 N94-31322
p 3641 N94-31486
p 3765 N94-31625
p 3825 N94-31663
p 3844 N94-31665
p 3641 N94-31666
p 3866 N94-31668
p 3643 N94-32098
W-7405-ENG-36 ..... p 3643 N94-32109
p 3869 N94-32141
p 3826 N94-32248
p 3826 N94-32357
p 3657 N94-32358
p 3903 N94-32372
p 3645 N94-32514
p 3871 N94-32515
p 3871 N94-32598
p 3819 N94-32599
p 3765 N94-32600
p 3904 N94-32601
p 3904 N94-32602
p 3694 N94-32607
p 3871 N94-32615
p 3636 N94-32616
p 3659 N94-32617
p 3904 N94-32645
p 3827 N94-32646
p 3720 N94-32707
p 3873 N94-32708
p 3873 N94-32710
p 3767 N94-32752
p 3873 N94-32757
p 3727 N94-32778
p 3905 N94-32779
p 3768 N94-32790
p 3873 N94-32797
p 3661 N94-32798
p 3905 N94-32815
p 3906 N94-32843
p 3775 N94-32874
p 3906 N94-32875
p 3874 N94-32876
p 3768 N94-32894
p 3647 N94-32964
p 3907 N94-32989
p 3907 N94-32990
p 3648 N94-32993
p 3686 N94-31150
p 3956 N94-31308
p 3830 N94-31623
p 3716 N94-31624
p 3898 N94-31628
p 3898 N94-31631
p 3899 N94-31633
p 3911 N94-31760
p 3845 N94-31763
p 3889 N94-31809
p 3899 N94-31916
p 3654 N94-31976
p 3656 N94-32103
p 3869 N94-32139
p 3834 N94-32175
p 3747 N94-32249
p 3718 N94-32270
p 3870 N94-32271
p 3826 N94-32356
p 3857 N94-32589
p 3903 N94-32597
p 3774 N94-32647
p 3761 N94-32660
p 3681 N94-32661
p 3695 N94-32662
p 3681 N94-32679
p 3713 N94-32706
p 3785 N94-32726
p 3892 N94-32730
p 3797 N94-32732
p 3774 N94-32736
p 3637 N94-32743
p 3852 N94-32744
p 3682 N94-32745
p 3904 N94-32746
p 3905 N94-32747
p 3720 N94-32760
p 3720 N94-32761
p 3761 N94-32762
p 3874 N94-32804
p 3611 N94-32813
p 3768 N94-32814
p 3906 N94-32913
p 3786 N94-32937
p 3907 N94-32944
W-7405-ENG-48 ..... p 3649 N94-31199
p 3714 N94-31269
p 3863 N94-31270
p 3886 N94-31324
p 3632 N94-31349
p 3632 N94-31352
p 3650 N94-31354
p 3858 N94-31397
p 3887 N94-31400
p 3887 N94-31406
p 3896 N94-31499
p 3864 N94-31508
p 3651 N94-31557
p 3715 N94-31580
p 3641 N94-31581
p 3716 N94-31599
p 3898 N94-31630
p 3716 N94-31636
p 3868 N94-31667
p 3675 N94-31761
p 3888 N94-31765
p 3675 N94-31781
p 3934 N94-31782
p 3712 N94-31783
p 3675 N94-31784
p 3825 N94-31920
p 3666 N94-32114
p 3901 N94-32115
p 3656 N94-32116
p 3834 N94-32127
p 3717 N94-32128
p 3955 N94-32129
p 3692 N94-32136
p 3938 N94-32137
p 3807 N94-32147
p 3667 N94-32148
p 3760 N94-32174
p 3679 N94-32188
p 3926 N94-32189
p 3890 N94-32201
p 3718 N94-32252
p 3765 N94-32354
p 3644 N94-32374
p 3903 N94-32411
p 3645 N94-32522
p 3818 N94-32585
p 3694 N94-32593
p 3904 N94-32606
p 3891 N94-32611
p 3719 N94-32613
p 3719 N94-32629
p 3904 N94-32634
p 3645 N94-32636
p 3738 N94-32637
p 3708 N94-32652
p 3719 N94-32654
p 3580 N94-32658
p 3719 N94-32659
p 3626 N94-32665
p 3849 N94-32670
p 3914 N94-32677
p 3660 N94-32687
p 3695 N94-32688
p 3661 N94-32751
p 3720 N94-32753
p 3646 N94-32754
p 3873 N94-32755
p 3682 N94-32756
p 3774 N94-32772
p 3767 N94-32789
p 3786 N94-32791
p 3720 N94-32794
p 3637 N94-32801
p 3874 N94-32807
p 3892 N94-32810
p 3768 N94-32817
p 3892 N94-32838
p 3669 N94-32839
p 3638 N94-32840
p 3708 N94-32849
p 3662 N94-32855
p 3790 N94-32881
p 3768 N94-32882
p 3906 N94-32884
p 3647 N94-32892
p 3775 N94-32895
p 3938 N94-32914
p 3893 N94-32915
p 3907 N94-32934
p 3769 N94-32966
p 3639 N94-33260
p 3648 N94-33270
W-7405-ENG-82 ..... p 3895 N94-31067
p 3862 N94-31146
p 3631 N94-31154
p 3759 N94-31648
p 3677 N94-32101
p 3657 N94-32377
p 3827 N94-32683
W-745-ENG-48 ..... p 3669 N94-32449

Typical Report Number Index Listing

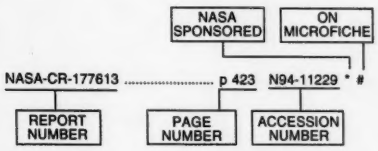

Listings in this index are arranged alphanumerically by report number. The accession number denotes the number by which the citation is identified. The page number helps to locate the citation in the abstract section. An asterisk (*) indicates that the item is a NASA report. A pound sign (#) indicates that the item is available on microfiche.

A-8402 ..... p 3709 N94-32872 * #
A-91094 ..... p 3820 N94-32906 * #
A-92196 ..... p 3709 N94-32946 * #
A-93004 ..... p 3571 N94-32063 * #
A-94017 ..... p 3617 N94-33117 * #
A-94043 ..... p 3711 N94-33290 * #
A-94048 ..... p 3801 N94-33068 * #
A-94050 ..... p 3805 N94-32936 * #
A-94060 ..... p 3575 N94-32927 * #
A-94066 ..... p 3576 N94-33063 * #

AD-A252152 ..... p 3921 N94-32831 * #
AD-A252563 ..... p 3921 N94-32830 * #
AD-A252565 ..... p 3922 N94-32835 * #
AD-A252566 ..... p 3921 N94-32834 * #
AD-A274143 ..... p 3625 N94-32604 #
AD-A275240 ..... p 3797 N94-32156 #
AD-A275908 ..... p 3763 N94-31339 #
AD-A275909 ..... p 3878 N94-31340 #
AD-A275917 ..... p 3701 N94-31341 #
AD-A275918 ..... p 3763 N94-31275 #
AD-A275922 ..... p 3810 N94-31343 #
AD-A275923 ..... p 3916 N94-31344 #
AD-A275949 ..... p 3587 N94-31356 #
AD-A275951 ..... p 3587 N94-31346 #
AD-A275954 ..... p 3632 N94-31348
AD-A275959 ..... p 3895 N94-31350
AD-A275960 ..... p 3587 N94-31318
AD-A275961 ..... p 3810 N94-31383 #
AD-A275965 ..... p 3649 N94-31276
AD-A275967 ..... p 3672 N94-31384 #
AD-A275980 ..... p 3771 N94-31351 #
AD-A275982 ..... p 3771 N94-31353 #
AD-A275987 ..... p 3916 N94-31355 #
AD-A275992 ..... p 3810 N94-31357 #
AD-A275999 ..... p 3841 N94-31359 #
AD-A276010 ..... p 3565 N94-31362 #
AD-A276012 ..... p 3672 N94-31385 #
AD-A276017 ..... p 3672 N94-31386 #
AD-A276019 ..... p 3688 N94-31494 #
AD-A276021 ..... p 3896 N94-31455 #
AD-A276022 ..... p 3742 N94-31496 #
AD-A276023 ..... p 3896 N94-31439 #
AD-A276029 ..... p 3799 N94-31440 #
AD-A276034 ..... p 3842 N94-31441 #
AD-A276037 ..... p 3932 N94-31280
AD-A276038 ..... p 3687 N94-31281
AD-A276052 ..... p 3578 N94-31442 #
AD-A276053 ..... p 3811 N94-31443 #
AD-A276055 ..... p 3640 N94-31456 #
AD-A276056 ..... p 3631 N94-31282 #
AD-A276060 ..... p 3771 N94-31457 #
AD-A276066 ..... p 3711 N94-31283 #
AD-A276069 ..... p 3581 N94-31458 #
AD-A276072 ..... p 3632 N94-31459 #

AD-A276076 ..... p 3701 N94-31460 #
AD-A276077 ..... p 3811 N94-31461 #
AD-A276078 ..... p 3850 N94-31462 #
AD-A276079 ..... p 3673 N94-31463 #
AD-A276080 ..... p 3673 N94-31464 #
AD-A276101 ..... p 3810 N94-31277 #
AD-A276108 ..... p 3811 N94-31465 #
AD-A276109 ..... p 3673 N94-31466 #
AD-A276114 ..... p 3702 N94-31467 #
AD-A276115 ..... p 3897 N94-31528 #
AD-A276116 ..... p 3843 N94-31529 #
AD-A276117 ..... p 3887 N94-31530 #
AD-A276119 ..... p 3650 N94-31509 #
AD-A276120 ..... p 3651 N94-31510 #
AD-A276123 ..... p 3619 N94-31444 #
AD-A276124 ..... p 3688 N94-31445 #
AD-A276125 ..... p 3917 N94-31829 #
AD-A276126 ..... p 3714 N94-31278 #
AD-A276144 ..... p 3565 N94-31830 #
AD-A276149 ..... p 3824 N94-31249 #
AD-A276150 ..... p 3787 N94-31250 #
AD-A276151 ..... p 3578 N94-31078 #
AD-A276159 ..... p 3686 N94-31079 #
AD-A276160 ..... p 3576 N94-31080 #
AD-A276162 ..... p 3895 N94-31081 #
AD-A276165 ..... p 3787 N94-31053 #
AD-A276166 ..... p 3910 N94-31054 #
AD-A276169 ..... p 3814 N94-31810 #
AD-A276177 ..... p 3894 N94-31055 #
AD-A276178 ..... p 3894 N94-31056 #
AD-A276198 ..... p 3686 N94-31057 #
AD-A276199 ..... p 3586 N94-31058 #
AD-A276201 ..... p 3795 N94-31490 #
AD-A276207 ..... p 3648 N94-31059 #
AD-A276211 ..... p 3859 N94-31060 #
AD-A276216 ..... p 3828 N94-31061 #
AD-A276217 ..... p 3670 N94-31062 #
AD-A276218 ..... p 3670 N94-31063 #
AD-A276219 ..... p 3828 N94-31064 #
AD-A276220 ..... p 3730 N94-31065 #
AD-A276226 ..... p 3686 N94-31066 #
AD-A276228 ..... p 3650 N94-31284 #
AD-A276230 ..... p 3673 N94-31446
AD-A276251 ..... p 3583 N94-31290 #
AD-A276255 ..... p 3809 N94-31251
AD-A276256 ..... p 3799 N94-31291 #
AD-A276257 ..... p 3609 N94-31292 #
AD-A276260 ..... p 3632 N94-31293 #
AD-A276285 ..... p 3841 N94-31252
AD-A276286 ..... p 3671 N94-31253
AD-A276287 ..... p 3671 N94-31254
AD-A276288 ..... p 3714 N94-31255
AD-A276292 ..... p 3877 N94-31256
AD-A276294 ..... p 3792 N94-31294 #
AD-A276296 ..... p 3587 N94-31295 #
AD-A276298 ..... p 3852 N94-31296 #
AD-A276301 ..... p 3650 N94-31297 #
AD-A276316 ..... p 3601 N94-31298 #
AD-A276320 ..... p 3671 N94-31299 #
AD-A276323 ..... p 3672 N94-31334 #
AD-A276341 ..... p 3810 N94-31335 #
AD-A276342 ..... p 3771 N94-31326 #
AD-A276343 ..... p 3895 N94-31327 #
AD-A276344 ..... p 3810 N94-31328 #
AD-A276352 ..... p 3673 N94-31401 #
AD-A276355 ..... p 3864 N94-31402 #
AD-A276356 ..... p 3860 N94-31257
AD-A276361 ..... p 3578 N94-31387 #
AD-A276362 ..... p 3581 N94-32055 #
AD-A276363 ..... p 3565 N94-31367 #
AD-A276364 ..... p 3581 N94-31368 #
AD-A276372 ..... p 3771 N94-31369 #
AD-A276378 ..... p 3810 N94-31370 #
AD-A276380 ..... p 3672 N94-31371 #
AD-A276382 ..... p 3640 N94-31258
AD-A276389 ..... p 3714 N94-31358 #
AD-A276401 ..... p 3863 N94-31237
AD-A276402 ..... p 3631 N94-31238
AD-A276404 ..... p 3841 N94-31360 #
AD-A276405 ..... p 3816 N94-32130 #
AD-A276408 ..... p 3924 N94-31361 #
AD-A276409 ..... p 3795 N94-31363 #
AD-A276411 ..... p 3824 N94-31259

AD-A276414 ..... p 3816 N94-32131 #
AD-A276415 ..... p 3895 N94-31329 #
AD-A276416 ..... p 3878 N94-31330 #
AD-A276417 ..... p 3803 N94-31447 *
AD-A276418 ..... p 3916 N94-31331 #
AD-A276421 ..... p 3565 N94-31332 #
AD-A276423 ..... p 3788 N94-31448 #
AD-A276424 ..... p 3722 N94-31333 #
AD-A276431 ..... p 3811 N94-31449 #
AD-A276442 ..... p 3672 N94-31300 #
AD-A276445 ..... p 3829 N94-31301 #
AD-A276446 ..... p 3802 N94-31302 #
AD-A276447 ..... p 3770 N94-31303 #
AD-A276448 ..... p 3668 N94-31304 #
AD-A276449 ..... p 3671 N94-31260 #
AD-A276451 ..... p 3618 N94-31261 #
AD-A276452 ..... p 3799 N94-32187 #
AD-A276459 ..... p 3804 N94-32171 #
AD-A276460 ..... p 3781 N94-31239 #
AD-A276461 ..... p 3687 N94-31240 #
AD-A276462 ..... p 3701 N94-31241 #
AD-A276463 ..... p 3860 N94-31242 #
AD-A276465 ..... p 3896 N94-31473 #
AD-A276467 ..... p 3798 N94-31243 #
AD-A276470 ..... p 3843 N94-31474 #
AD-A276471 ..... p 3855 N94-31244 #
AD-A276472 ..... p 3701 N94-31245 #
AD-A276473 ..... p 3574 N94-31246 #
AD-A276478 ..... p 3875 N94-31247 #
AD-A276480 ..... p 3631 N94-31248 #
AD-A276481 ..... p 3811 N94-31475 #
AD-A276485 ..... p 3702 N94-31476 #
AD-A276493 ..... p 3897 N94-31531 #
AD-A276497 ..... p 3878 N94-31262 #
AD-A276499 ..... p 3574 N94-31678 #
AD-A276506 ..... p 3809 N94-31263 #
AD-A276512 ..... p 3691 N94-31928 #
AD-A276513 ..... p 3712 N94-31929 #
AD-A276514 ..... p 3918 N94-31930 #
AD-A276515 ..... p 3583 N94-31931
AD-A276516 ..... p 3814 N94-31932 #
AD-A276517 ..... p 3815 N94-31933 #
AD-A276519 ..... p 3806 N94-31934 #
AD-A276521 ..... p 3816 N94-32086 * #
AD-A276522 ..... p 3815 N94-32080 #
AD-A276523 ..... p 3816 N94-32081 #
AD-A276542 ..... p 3869 N94-32082 #
AD-A276543 ..... p 3691 N94-32056 #
AD-A276548 ..... p 3784 N94-32057 #
AD-A276550 ..... p 3653 N94-31935 #
AD-A276554 ..... p 3717 N94-31936 #
AD-A276565 ..... p 3890 N94-32031
AD-A276566 ..... p 3679 N94-32230 #
AD-A276567 ..... p 3825 N94-32032 #
AD-A276568 ..... p 3783 N94-31937 #
AD-A276570 ..... p 3746 N94-31938 #
AD-A276572 ..... p 3634 N94-32033
AD-A276577 ..... p 3579 N94-32058 #
AD-A276585 ..... p 3635 N94-32231
AD-A276586 ..... p 3706 N94-32123
AD-A276589 ..... p 3803 N94-32034
AD-A276595 ..... p 3635 N94-32124 #
AD-A276597 ..... p 3799 N94-32035
AD-A276608 ..... p 3834 N94-32036
AD-A276618 ..... p 3861 N94-32125 #
AD-A276624 ..... p 3677 N94-32087 #
AD-A276629 ..... p 3861 N94-32059 #
AD-A276630 ..... p 3879 N94-32037
AD-A276631 ..... p 3815 N94-31994
AD-A276633 ..... p 3643 N94-32060 #
AD-A276637 ..... p 3642 N94-31995
AD-A276642 ..... p 3717 N94-31996
AD-A276643 ..... p 3642 N94-31997
AD-A276644 ..... p 3845 N94-31939 #
AD-A276645 ..... p 3815 N94-31940
AD-A276647 ..... p 3616 N94-32038
AD-A276656 ..... p 3834 N94-32061 #
AD-A276658 ..... p 3784 N94-32046 #
AD-A276660 ..... p 3730 N94-32088 #
AD-A276662 ..... p 3643 N94-32047 #
AD-A276663 ..... p 3861 N94-32089 #
AD-A276667 ..... p 3677 N94-32083 #
AD-A276680 ..... p 3918 N94-32090 #

AD-A276685 ..... p 3610 N94-32039 #
AD-A276688 ..... p 3680 N94-32297 #
AD-A276690 ..... p 3784 N94-32117 #
AD-A276691 ..... p 3773 N94-32118
AD-A276692 ..... p 3776 N94-33272 #
AD-A276693 ..... p 3676 N94-31998 #
AD-A276694 ..... p 3680 N94-32298 #
AD-A276695 ..... p 3680 N94-32299 #
AD-A276696 ..... p 3680 N94-32300 #
AD-A276697 ..... p 3746 N94-32119 #
AD-A276706 ..... p 3588 N94-32120 #
AD-A276707 ..... p 3678 N94-32121 #
AD-A276713 ..... p 3624 N94-32122 #
AD-A276714 ..... p 3909 N94-33273
AD-A276715 ..... p 3909 N94-33274 #
AD-A276716 ..... p 3566 N94-32157 #
AD-A276721 ..... p 3818 N94-32504 #
AD-A276722 ..... p 3680 N94-32151 #
AD-A276723 ..... p 3678 N94-32158 #
AD-A276724 ..... p 3678 N94-32159
AD-A276725 ..... p 3747 N94-32160 #
AD-A276727 ..... p 3678 N94-32161 #
AD-A276730 ..... p 3784 N94-32162
AD-A276737 ..... p 3807 N94-32163
AD-A276738 ..... p 3678 N94-32179 #
AD-A276739 ..... p 3880 N94-32180 #
AD-A276741 ..... p 3788 N94-32181 #
AD-A276743 ..... p 3615 N94-32182 #
AD-A276753 ..... p 3679 N94-32183 #
AD-A276755 ..... p 3656 N94-32184 #
AD-A276766 ..... p 3693 N94-32307 #
AD-A276775 ..... p 3679 N94-32185 #
AD-A276777 ..... p 3880 N94-32186 #
AD-A276780 ..... p 3909 N94-33275 #
AD-A276781 ..... p 3644 N94-32169 #
AD-A276782 ..... p 3869 N94-32170 #
AD-A276785 ..... p 3608 N94-32190 #
AD-A276792 ..... p 3784 N94-32164 #
AD-A276796 ..... p 3825 N94-32165 #
AD-A276797 ..... p 3834 N94-32152 #
AD-A276798 ..... p 3726 N94-32166 #
AD-A276801 ..... p 3852 N94-33276 #
AD-A276802 ..... p 3851 N94-32142 #
AD-A276803 ..... p 3846 N94-32167 #
AD-A276815 ..... p 3906 N94-32908
AD-A276827 ..... p 3765 N94-32195 #
AD-A276830 ..... p 3575 N94-32168 #
AD-A276834 ..... p 3901 N94-32153 #
AD-A276836 ..... p 3610 N94-32208 #
AD-A276842 ..... p 3643 N94-32091 #
AD-A276843 ..... p 3582 N94-32223 #
AD-A276844 ..... p 3586 N94-32224 #
AD-A276846 ..... p 3582 N94-32909 #
AD-A276848 ..... p 3697 N94-33034 #
AD-A276849 ..... p 3902 N94-32209
AD-A276862 ..... p 3918 N94-32210 #
AD-A276874 ..... p 3601 N94-32211
AD-A276876 ..... p 3817 N94-32212
AD-A276877 ..... p 3817 N94-32213
AD-A276882 ..... p 3600 N94-32126 #
AD-A276899 ..... p 3747 N94-32214
AD-A276902 ..... p 3579 N94-32232 #
AD-A276904 ..... p 3692 N94-32215 #
AD-A276905 ..... p 3875 N94-33277
AD-A276906 ..... p 3635 N94-32216 #
AD-A276916 ..... p 3635 N94-32233 #
AD-A276918 ..... p 3635 N94-32234 #
AD-A276919 ..... p 3679 N94-32235
AD-A276925 ..... p 3726 N94-32236 #
AD-A276926 ..... p 3644 N94-32237 #
AD-A276936 ..... p 3584 N94-32238
AD-A276942 ..... p 3656 N94-32239 #
AD-A276944 ..... p 3586 N94-32217 #
AD-A276947 ..... p 3902 N94-32218 #
AD-A276949 ..... p 3817 N94-32219
AD-A276951 ..... p 3788 N94-32220 #
AD-A276953 ..... p 3656 N94-32221 #
AD-A276957 ..... p 3870 N94-32360
AD-A276958 ..... p 3575 N94-32620 #
AD-A276959 ..... p 3707 N94-32361
AD-A276960 ..... p 3644 N94-32240 #
AD-A276963 ..... p 3712 N94-32393 #
AD-A276965 ..... p 3588 N94-32311
AD-A276966 ..... p 3588 N94-32241
AD-A276967 ..... p 3589 N94-32394 #
AD-A276968 ..... p 3588 N94-32312
AD-A276969 ..... p 3588 N94-32313
AD-A276970 ..... p 3590 N94-32395 #
AD-A276971 ..... p 3590 N94-32396 #
AD-A276972 ..... p 3590 N94-32397 #
AD-A276973 ..... p 3590 N94-32398 #
AD-A276974 ..... p 3590 N94-32399 #
AD-A276975 ..... p 3589 N94-32314 #
AD-A276976 ..... p 3589 N94-32315
AD-A276977 ..... p 3589 N94-32316
AD-A276978 ..... p 3589 N94-32317
AD-A276979 ..... p 3589 N94-32318 #
AD-A276980 ..... p 3589 N94-32319
AD-A276982 ..... p 3746 N94-31999 #
AD-A276983 ..... p 3579 N94-32242
AD-A276987 ..... p 3692 N94-32258 #
AD-A276998 ..... p 3788 N94-32000 #
AD-A276999 ..... p 3773 N94-32154
AD-A277001 ..... p 3692 N94-32199
AD-A277003 ..... p 3900 N94-32001 #
AD-A277004 ..... p 3712 N94-32002 #
AD-A277005 ..... p 3900 N94-32003 #
AD-A277006 ..... p 3642 N94-32004 #
AD-A277008 ..... p 3789 N94-32400
AD-A277009 ..... p 3789 N94-32401
AD-A277010 ..... p 3789 N94-32402
AD-A277018 ..... p 3693 N94-32301
AD-A277020 ..... p 3692 N94-32259
AD-A277023 ..... p 3655 N94-32005 #
AD-A277028 ..... p 3879 N94-32006 #
AD-A277030 ..... p 3784 N94-32260
AD-A277040 ..... p 3726 N94-32261 #
AD-A277041 ..... p 3861 N94-32262 #
AD-A277043 ..... p 3738 N94-32273 #
AD-A277044 ..... p 3772 N94-32007
AD-A277046 ..... p 3804 N94-32302
AD-A277053 ..... p 3588 N94-32009
AD-A277054 ..... p 3610 N94-32010
AD-A277055 ..... p 3900 N94-32011
AD-A277056 ..... p 3623 N94-32012
AD-A277058 ..... p 3879 N94-32013
AD-A277060 ..... p 3826 N94-32274
AD-A277061 ..... p 3580 N94-32263
AD-A277062 ..... p 3580 N94-32264
AD-A277063 ..... p 3624 N94-32265
AD-A277065 ..... p 3580 N94-32362
AD-A277067 ..... p 3818 N94-32390
AD-A277069 ..... p 3580 N94-32378
AD-A277072 ..... p 3861 N94-32418 #
AD-A277076 ..... p 3693 N94-32303
AD-A277080 ..... p 3736 N94-32351
AD-A277081 ..... p 3636 N94-32352
AD-A277092 ..... p 3657 N94-32391 #
AD-A277093 ..... p 3881 N94-32392 #
AD-A277098 ..... p 3588 N94-32014 #
AD-A277100 ..... p 3579 N94-32015 #
AD-A277101 ..... p 3581 N94-31977
AD-A277107 ..... p 3654 N94-31978
AD-A277108 ..... p 3654 N94-31979
AD-A277109 ..... p 3654 N94-31980
AD-A277110 ..... p 3654 N94-31981
AD-A277111 ..... p 3655 N94-31982
AD-A277112 ..... p 3636 N94-32304
AD-A277113 ..... p 3899 N94-31983
AD-A277115 ..... p 3772 N94-31984
AD-A277116 ..... p 3900 N94-31985
AD-A277120 ..... p 3846 N94-32048 #
AD-A277121 ..... p 3575 N94-32363 #
AD-A277122 ..... p 3804 N94-32379 #
AD-A277127 ..... p 3718 N94-32305
AD-A277128 ..... p 3881 N94-32380 #
AD-A277129 ..... p 3657 N94-32381 #
AD-A277131 ..... p 3919 N94-32382 #
AD-A277134 ..... p 3768 N94-32066
AD-A277136 ..... p 3677 N94-32067
AD-A277139 ..... p 3657 N94-32364 #
AD-A277140 ..... p 3660 N94-32722 #
AD-A277141 ..... p 3657 N94-32365 #
AD-A277151 ..... p 3718 N94-32366 #
AD-A277154 ..... p 3657 N94-32367 #
AD-A277155 ..... p 3870 N94-32368 #
AD-A277159 ..... p 3721 N94-33102
AD-A277161 ..... p 3880 N94-32068
AD-A277164 ..... p 3655 N94-32069
AD-A277168 ..... p 3681 N94-32576 #
AD-A277171 ..... p 3656 N94-32253
AD-A277178 ..... p 3902 N94-32306 #
AD-A277184 ..... p 3566 N94-32254 #
AD-A277188 ..... p 3902 N94-32255 #
AD-A277191 ..... p 3623 N94-32070 #
AD-A277198 ..... p 3655 N94-32016 #
AD-A277200 ..... p 3901 N94-32092
AD-A277201 ..... p 3816 N94-32093
AD-A277202 ..... p 3676 N94-32049
AD-A277203 ..... p 3677 N94-32050
AD-A277206 ..... p 3579 N94-32062
AD-A277207 ..... p 3784 N94-32094 #
AD-A277210 ..... p 3783 N94-32019 #
AD-A277216 ..... p 3608 N94-32020
AD-A277217 ..... p 3783 N94-32021
AD-A277219 ..... p 3845 N94-32022 #
AD-A277224 ..... p 3623 N94-32023
AD-A277226 ..... p 3623 N94-32024
AD-A277228 ..... p 3746 N94-32025
AD-A277229 ..... p 3611 N94-32369
AD-A277230 ..... p 3920 N94-32633
AD-A277232 ..... p 3726 N94-32370
AD-A277233 ..... p 3644 N94-32371
AD-A277234 ..... p 3584 N94-32026
AD-A277239 ..... p 3738 N94-32275
AD-A277240 ..... p 3726 N94-32320
AD-A277242 ..... p 3848 N94-32331
AD-A277244 ..... p 3681 N94-32332
AD-A277245 ..... p 3602 N94-32333
AD-A277246 ..... p 3789 N94-32321
AD-A277253 ..... p 3903 N94-32322
AD-A277256 ..... p 3826 N94-32323 #
AD-A277261 ..... p 3655 N94-32017
AD-A277264 ..... p 3845 N94-32018
AD-A277265 ..... p 3900 N94-32040
AD-A277266 ..... p 3900 N94-32041
AD-A277270 ..... p 3590 N94-32403
AD-A277274 ..... p 3657 N94-32404
AD-A277275 ..... p 3625 N94-32591
AD-A277276 ..... p 3625 N94-32592 #
AD-A277277 ..... p 3881 N94-32324 #
AD-A277278 ..... p 3789 N94-32325 #
AD-A277280 ..... p 3575 N94-32405
AD-A277281 ..... p 3718 N94-32406
AD-A277287 ..... p 3719 N94-32608
AD-A277288 ..... p 3804 N94-32609
AD-A277289 ..... p 3818 N94-32508
AD-A277293 ..... p 3694 N94-32509
AD-A277297 ..... p 3706 N94-32042 #
AD-A277300 ..... p 3912 N94-32043 #
AD-A277301 ..... p 3868 N94-32044 #
AD-A277304 ..... p 3614 N94-32071 #
AD-A277305 ..... p 3788 N94-32072 #
AD-A277306 ..... p 3789 N94-32327
AD-A277309 ..... p 3582 N94-32328
AD-A277311 ..... p 3693 N94-32329
AD-A277312 ..... p 3800 N94-32276
AD-A277313 ..... p 3800 N94-32277
AD-A277318 ..... p 3785 N94-32278
AD-A277319 ..... p 3712 N94-32051 #
AD-A277320 ..... p 3882 N94-32510
AD-A277321 ..... p 3708 N94-32511
AD-A277322 ..... p 3706 N94-32256 #
AD-A277323 ..... p 3871 N94-32621
AD-A277324 ..... p 3793 N94-32622
AD-A277325 ..... p 3706 N94-32279 #
AD-A277329 ..... p 3881 N94-32280 #
AD-A277331 ..... p 3835 N94-32281 #
AD-A277332 ..... p 3797 N94-32623
AD-A277333 ..... p 3826 N94-32243
AD-A277335 ..... p 3848 N94-32244
AD-A277341 ..... p 3817 N94-32257
AD-A277345 ..... p 3848 N94-32245 #
AD-A277346 ..... p 3677 N94-32073
AD-A277347 ..... p 3656 N94-32246 #
AD-A277349 ..... p 3625 N94-32624
AD-A277350 ..... p 3726 N94-32334
AD-A277351 ..... p 3773 N94-32335
AD-A277354 ..... p 3693 N94-32336
AD-A277355 ..... p 3773 N94-32337
AD-A277358 ..... p 3679 N94-32282
AD-A277362 ..... p 3680 N94-32283 #
AD-A277364 ..... p 3788 N94-32284 #
AD-A277366 ..... p 3818 N94-32330 #
AD-A277369 ..... p 3880 N94-32155
AD-A277370 ..... p 3825 N94-32052
AD-A277372 ..... p 3773 N94-32338 #
AD-A277375 ..... p 3834 N94-32053
AD-A277377 ..... p 3834 N94-32095
AD-A277379 ..... p 3799 N94-32096
AD-A277382 ..... p 3852 N94-32339 #
AD-A277383 ..... p 3835 N94-32340 #
AD-A277384 ..... p 3784 N94-32054
AD-A277385 ..... p 3881 N94-32285
AD-A277387 ..... p 3848 N94-32286
AD-A277392 ..... p 3602 N94-32268
AD-A277396 ..... p 3848 N94-32341 #
AD-A277397 ..... p 3624 N94-32342
AD-A277398 ..... p 3953 N94-32343
AD-A277400 ..... p 3800 N94-32344
AD-A277402 ..... p 3800 N94-32345 #
AD-A277406 ..... p 3774 N94-32346
AD-A277407 ..... p 3801 N94-32577 #
AD-A277408 ..... p 3659 N94-32610
AD-A277409 ..... p 3658 N94-32578
AD-A277410 ..... p 3658 N94-32579 #
AD-A277411 ..... p 3804 N94-32580
AD-A277414 ..... p 3800 N94-32419
AD-A277415 ..... p 3708 N94-32581 #
AD-A277416 ..... p 3786 N94-32921 #
AD-A277422 ..... p 3827 N94-32995 #
AD-A277423 ..... p 3836 N94-32996 #
AD-A277424 ..... p 3801 N94-32997 #
AD-A277425 ..... p 3801 N94-32998 #
AD-A277426 ..... p 3908 N94-33005 #
AD-A277427 ..... p 3802 N94-33241
AD-A277429 ..... p 3838 N94-33174
AD-A277430 ..... p 3775 N94-33006 #

AD-A277431 ..... p 3893 N94-33007 #
AD-A277434 ..... p 3627 N94-33008 #
AD-A277437 ..... p 3805 N94-33084
AD-A277438 ..... p 3710 N94-33009 #
AD-A277442 ..... p 3801 N94-33053
AD-A277445 ..... p 3769 N94-33105
AD-A277446 ..... p 3663 N94-33010 #
AD-A277451 ..... p 3894 N94-33106
AD-A277452 ..... p 3740 N94-33011 #
AD-A277453 ..... p 3850 N94-33175
AD-A277455 ..... p 3721 N94-33012 #
AD-A277462 ..... p 3639 N94-33242
AD-A277469 ..... p 3775 N94-32999
AD-A277482 ..... p 3663 N94-32985
AD-A277487 ..... p 3580 N94-33107
AD-A277506 ..... p 3667 N94-33013 #
AD-A277507 ..... p 3836 N94-33014 #
AD-A277508 ..... p 3685 N94-33347
AD-A277512 ..... p 3664 N94-33082 #
AD-A277513 ..... p 3663 N94-33054 #
AD-A277514 ..... p 3664 N94-33348
AD-A277516 ..... p 3805 N94-33349
AD-A277517 ..... p 3908 N94-33055 #
AD-A277518 ..... p 3662 N94-32952 #
AD-A277529 ..... p 3731 N94-32953 #
AD-A277530 ..... p 3662 N94-32954 #
AD-A277534 ..... p 3576 N94-32955 #
AD-A277547 ..... p 3801 N94-32956 #
AD-A277576 ..... p 3721 N94-33000 #
AD-A277617 ..... p 3697 N94-32957 #
AD-A277618 ..... p 3822 N94-33279 #
AD-A277619 ..... p 3682 N94-32971 #
AD-A277644 ..... p 3820 N94-32972 #
AD-A277648 ..... p 3580 N94-33056 #
AD-A277649 ..... p 3790 N94-33057 #
AD-A277650 ..... p 3682 N94-33025 #
AD-A277652 ..... p 3683 N94-33026 #
AD-A277662 ..... p 3821 N94-33027 #
AD-A277666 ..... p 3775 N94-33028 #
AD-A277672 ..... p 3627 N94-33029 #
AD-A277678 ..... p 3821 N94-33030 #
AD-A277696 ..... p 3727 N94-32778
AD-A277728 ..... p 3583 N94-33280 #
AD-A277730 ..... p 3682 N94-33001 #
AD-A277731 ..... p 3648 N94-33281 #
AD-A277733 ..... p 3721 N94-33003
AD-A277741 ..... p 3791 N94-33176 #
AD-A277756 ..... p 3682 N94-32986 #
AD-A277759 ..... p 3791 N94-33085 #
AD-A277763 ..... p 3922 N94-32987 #
AD-A277766 ..... p 3907 N94-32988 #
AD-A277777 ..... p 3763 N94-33015 #
AD-A277778 ..... p 3722 N94-33282 #
AD-A277808 ..... p 3566 N94-33016 #
AD-A277896 ..... p 3821 N94-33031 #
AD-A277913 ..... p 3684 N94-33261 #
AD-A277914 ..... p 3573 N94-33108 #
AD-A277916 ..... p 3791 N94-33243 #
AD-A277917 ..... p 3791 N94-33109 #
AD-A277918 ..... p 3585 N94-33283
AD-A277921 ..... p 3698 N94-33177
AD-A277925 ..... p 3791 N94-33244
AD-A277928 ..... p 3630 N94-33178
AD-A277929 ..... p 3822 N94-33179
AD-A277935 ..... p 3791 N94-33245
AD-A277937 ..... p 3908 N94-33246
AD-A277961 ..... p 3630 N94-33180
AD-A277962 ..... p 3612 N94-33262
AD-A277965 ..... p 3574 N94-33263
AD-A277974 ..... p 3894 N94-33264 #
AD-A277978 ..... p 3850 N94-33265 #
AD-A277979 ..... p 3586 N94-33086 #
AD-A277980 ..... p 3683 N94-33159 #
AD-A277983 ..... p 3664 N94-33247 #
AD-A277985 ..... p 3884 N94-33087 #
AD-A277989 ..... p 3732 N94-33088 #
AD-A277993 ..... p 3787 N94-33089
AD-A278003 ..... p 3664 N94-33138 #
AD-A278005 ..... p 3590 N94-33139
AD-A278010 ..... p 3908 N94-33248 #
AD-A278014 ..... p 3698 N94-33249 #
AD-A278023 ..... p 3648 N94-33182
AD-A278031 ..... p 3822 N94-33284
AD-A278033 ..... p 3821 N94-33090
AD-A278039 ..... p 3698 N94-33091
AD-A278042 ..... p 3585 N94-33266
AD-A278045 ..... p 3822 N94-33183
AD-A278084 ..... p 3776 N94-33184
AD-A278085 ..... p 3794 N94-33250
AD-A278090 ..... p 3791 N94-33185
AD-A278091 ..... p 3684 N94-33186
AD-A278092 ..... p 3908 N94-33039 #
AD-A278094 ..... p 3884 N94-33267
AD-A278095 ..... p 3798 N94-33268
AD-A278096 ..... p 3729 N94-33251
AD-A278099 ..... p 3798 N94-33040 #
AD-A278105 ..... p 3776 N94-33041 #
AD-A278106 ..... p 3776 N94-33265 #
AD-A278107 ..... p 3884 N94-33187
AD-A278108 ..... p 3893 N94-33042 #
AD-A278114 ..... p 3769 N94-33110
AD-A278123 ..... p 3757 N94-33269
AD-A278124 ..... p 3836 N94-33043 #
AD-A278126 ..... p 3663 N94-33058 #
AD-A278127 ..... p 3798 N94-33092
AD-A278128 ..... p 3616 N94-33059 #
AD-A278129 ..... p 3683 N94-33093 #
AD-A278132 ..... p 3849 N94-33060
AD-A278133 ..... p 3728 N94-33061 #
AD-A278134 ..... p 3808 N94-33252 #
AD-A278135 ..... p 3616 N94-33094 #
AD-A278136 ..... p 3794 N94-33098 #
AD-A278142 ..... p 3790 N94-33062 #
AD-A278143 ..... p 3684 N94-33160 #
AD-A278144 ..... p 3859 N94-33161 #
AD-A278152 ..... p 3577 N94-33095 #
AD-A278155 ..... p 3862 N94-33096 #
AD-A278157 ..... p 3577 N94-33253
AD-A278158 ..... p 3684 N94-33254 #
AD-A278161 ..... p 3822 N94-33188
AD-A278164 ..... p 3850 N94-33255 #
AD-A278271 ..... p 3884 N94-33140 #
AD-A278272 ..... p 3884 N94-33141 #
AD-A278281 ..... p 3698 N94-33142 #
AD-A278283 ..... p 3740 N94-33143
AD-A278381 ..... p 3664 N94-33350
AD-A278382 ..... p 3776 N94-33351 #
AD-A278383 ..... p 3665 N94-33352 #
AD-A278384 ..... p 3685 N94-33353 #
AD-A278385 ..... p 3685 N94-33354
AD-A278386 ..... p 3910 N94-33355
AD-A278387 ..... p 3741 N94-33356 #
AD-A278388 ..... p 3874 N94-33144
AD-A278389 ..... p 3884 N94-33145 #
AD-A278391 ..... p 3862 N94-33146
AD-A278392 ..... p 3710 N94-33162
AD-A278394 ..... p 3698 N94-33163
AD-A278395 ..... p 3710 N94-33164
AD-A278397 ..... p 3630 N94-33165
AD-A278398 ..... p 3664 N94-33166
AD-A278403 ..... p 3591 N94-33167
AD-A278406 ..... p 3838 N94-33168 #
AD-A278408 ..... p 3909 N94-33324 #
AD-A278409 ..... p 3684 N94-33172
AD-A278410 ..... p 3684 N94-33173
AD-A278411 ..... p 3839 N94-33325
AD-A278412 ..... p 3802 N94-33326
AD-A278414 ..... p 3802 N94-33327 #
AD-A278416 ..... p 3909 N94-33328 #
AD-A278417 ..... p 3581 N94-33329
AD-A278418 ..... p 3839 N94-33330
AD-A278424 ..... p 3885 N94-33331
AD-A278427 ..... p 3910 N94-33332
AD-A278429 ..... p 3802 N94-33333
AD-A278434 ..... p 3684 N94-33334
AD-B161021L ..... p 3572 N94-32873 * #
AD-B175069 ..... p 3827 N94-33002
AD-B175123L ..... p 3921 N94-32829 * #
AD-B175124L ..... p 3921 N94-32833 * #
AD-B179297 ..... p 3567 N94-31180
AD-B179300 ..... p 3587 N94-31179 #
AD-D016092 ..... p 3883 N94-32738 #
AD-D016094 ..... p 3739 N94-32733 #
AD-D016095 ..... p 3660 N94-32739 #
AD-D016096 ..... p 3727 N94-32718 #
AD-D016097 ..... p 3882 N94-32719 #
AD-D016098 ..... p 3883 N94-32720 #
AD-D016099 ..... p 3696 N94-32721 #
AD-D016102 ..... p 3790 N94-32959
AD-D016106 ..... p 3663 N94-32960
AD-D016107 ..... p 3577 N94-32961
AD-D016115 ..... p 3681 N94-32625 #
AD-D016116 ..... p 3882 N94-32626
AD-D016118 ..... p 3697 N94-32962
AD-D016120 ..... p 3710 N94-32958
AD-D016139 ..... p 3639 N94-32973
AD-D016140 ..... p 3573 N94-32974
AD-D016141 ..... p 3663 N94-32975
AD-D016142 ..... p 3697 N94-32976
AD-D016143 ..... p 3893 N94-32977
AD-D016144 ..... p 3807 N94-32978
AD-D016145 ..... p 3697 N94-32967
AD-D016169 ..... p 3721 N94-32968
AD-D016171 ..... p 3862 N94-33017
AD-D016173 ..... p 3627 N94-33018
AD-D016181 ..... p 3698 N94-33181
AD-E201753 ..... p 3680 N94-32297 #
AD-E201756 ..... p 3784 N94-32117 #
AD-E201761 ..... p 3687 N94-33013 #
AD-E201762 ..... p 3773 N94-32118
AD-E201774 ..... p 3678 N94-32161 #
AD-E201777 ..... p 3747 N94-32160 #
AD-E201778 ..... p 3678 N94-32159
AD-E201779 ..... p 3678 N94-32158 #
AD-E201780 ..... p 3680 N94-32300 #
AD-E201781 ..... p 3676 N94-31998 #
AD-E201782 ..... p 3680 N94-32299 #
AD-E201783 ..... p 3680 N94-32296 #
AD-E201796 ..... p 3685 N94-33347
AD-E201833 ..... p 3775 N94-32999
AD-E201838 ..... p 3722 N94-33262 #
AD-E501747 ..... p 3810 N94-31357 #
AD-E501749 ..... p 3677 N94-32067 #
AD-M000306 ..... p 3922 N94-33256
AD-M000309 ..... p 3922 N94-33257
AD-M000310 ..... p 3923 N94-33258
AD-M000312 ..... p 3923 N94-33259
AD-M000330 ..... p 3805 N94-33171
AEDC-TR-93-23 ..... p 3707 N94-32361
AEDC-TR-93-24 ..... p 3610 N94-32010
AEDC-TR-93-28 ..... p 3588 N94-32009
AFESC/ESL-TR-90-16 ..... p 3718 N94-32366 #
AFESC/ESL-TR-91-08 ..... p 3881 N94-32380 #
AFIT/GLM/LA/93S-22 ..... p 3565 N94-31362 #
AFIT/GLM/LA/93S-36 ..... p 3672 N94-31385 #
AFIT/GOR/ENS/94M-12 ..... p 3684 N94-33334
AFIT/GSS/LAR/93D-4 ..... p 3916 N94-31344 #
AFIT/GSS/LAS/93D-3 ..... p 3810 N94-31383 #
AFOSR-94-0041TR ..... p 3662 N94-32952 #
AFOSR-94-0042TR ..... p 3908 N94-33055 #
AFOSR-94-0043TR-VOL-1 ..... p 3625 N94-32591
AFOSR-94-0043TR-VOL-2 ..... p 3625 N94-32592 #
AFOSR-94-0045TR ..... p 3726 N94-32320
AFOSR-94-0047TR ..... p 3793 N94-32622
AFOSR-94-0048TR ..... p 3834 N94-32053
AFOSR-94-0051TR ..... p 3826 N94-32243
AFOSR-94-0052TR ..... p 3834 N94-32095
AFOSR-94-0053TR ..... p 3848 N94-32244
AFOSR-94-0054TR ..... p 3738 N94-32275
AFOSR-94-0055TR ..... p 3845 N94-32018
AFOSR-94-0056TR ..... p 3657 N94-32404
AFOSR-94-0057TR ..... p 3773 N94-32338 #
AFOSR-94-0058TR ..... p 3900 N94-32040
AFOSR-94-0059TR ..... p 3900 N94-32041
AFOSR-94-0061 ..... p 3797 N94-32623
AFOSR-94-0062TR ..... p 3882 N94-32510
AFOSR-94-0063TR ..... p 3721 N94-33012 #
AFOSR-94-0065TR ..... p 3850 N94-33175
AFOSR-94-0071TR ..... p 3802 N94-33241
AFOSR-94-0072TR ..... p 3624 N94-32342
AFOSR-94-0073TR ..... p 3800 N94-32277
AFOSR-94-0074TR ..... p 3706 N94-32256 #
AFOSR-94-0075TR ..... p 3908 N94-33005 #
AFOSR-94-0076TR ..... p 3708 N94-32511
AFOSR-94-0077TR ..... p 3880 N94-32155
AFOSR-94-0078TR ..... p 3800 N94-32276
AFOSR-94-0079TR ..... p 3706 N94-32279 #
AFOSR-94-0080TR ..... p 3639 N94-33242
AFOSR-94-0081TR ..... p 3625 N94-32624
AFOSR-94-0082TR ..... p 3658 N94-32248 #
AFOSR-94-0083TR ..... p 3871 N94-32621
AFOSR-94-0085TR ..... p 3677 N94-32073
AFOSR-94-0087TR ..... p 3731 N94-32953 #
AFOSR-94-0088TR ..... p 3835 N94-32281 #
AFOSR-94-0089TR ..... p 3838 N94-33174
AFOSR-94-0092TR ..... p 3852 N94-32339 #
AFOSR-94-0093TR ..... p 3708 N94-32581 #
AFOSR-94-0094TR ..... p 3662 N94-32954 #
AFOSR-94-0095TR ..... p 3836 N94-32996 #
AFOSR-94-0096TR ..... p 3740 N94-33011 #
AFOSR-94-0097TR ..... p 3801 N94-32956 #
AFOSR-94-0098TR ..... p 3953 N94-32343
AFOSR-94-0099TR ..... p 3775 N94-33006 #
AFOSR-94-0100TR ..... p 3602 N94-32288
AFOSR-94-0102TR ..... p 3801 N94-32998 #
AFOSR-94-0105TR ..... p 3800 N94-32419
AFOSR-94-0109TR ..... p 3800 N94-32345 #
AFOSR-94-0112TR ..... p 3784 N94-32054
AFOSR-94-0113TR ..... p 3774 N94-32346
AFOSR-94-0115TR ..... p 3800 N94-32344
AFOSR-94-0116TR ..... p 3835 N94-32340 #
AFOSR-94-0126TR ..... p 3801 N94-32997 #
AFOSR-94-0127TR ..... p 3799 N94-32096
AFOSR-94-0129TR ..... p 3801 N94-32577 #
AFOSR-94-0130TR ..... p 3786 N94-32921 #
AFOSR-94-0132TR ..... p 3908 N94-33246
AFOSR-94-0139TR ..... p 3685 N94-33354

AFOSR-94-0140TR ..... p 3685 N94-33353 #
AFOSR-94-0161TR ..... p 3591 N94-33167
AFOSR-94-0164TR ..... p 3710 N94-33164
AFOSR-94-0166TR ..... p 3630 N94-33165
AFOSR-94-0173TR ..... p 3802 N94-33327 #
AFOSR-94-0175TR ..... p 3802 N94-33333
AFOSR-94-0184TR ..... p 3776 N94-33351 #
AFOSR-94-0187TR ..... p 3664 N94-33350
AFOSR-94-0191TR ..... p 3910 N94-33332
AFOSR-94-0192TR ..... p 3885 N94-33331
AFOSR-94-0198TR ..... p 3665 N94-33352 #
AFOSR-94-0204TR ..... p 3740 N94-33143
AFOSR-94-0207TR ..... p 3710 N94-33162
AFOSR-94-0210TR ..... p 3684 N94-33173
AFOSR-94-0213TR ..... p 3862 N94-33146
AFOSR-94-0215TR ..... p 3874 N94-33144
AFOSR-94-0218TR ..... p 3839 N94-33325
AFOSR-94-0219TR ..... p 3802 N94-33326
AFOSR-94-0222TR ..... p 3884 N94-33141 #
AFOSR-94-0223TR ..... p 3684 N94-33172
AFOSR-94-0227TR ..... p 3741 N94-33356 #
AFOSR-94-0228TR ..... p 3909 N94-33328 #
AFOSR-94-0230TR ..... p 3910 N94-33355
AFOSR-94-0232TR ..... p 3698 N94-33142 #
AFOSR-94-0234TR ..... p 3884 N94-33145 #
AFOSR-94-0237TR ..... p 3698 N94-33163
AFOSR-94-0238TR ..... p 3884 N94-33140 #
AFOSR-94-0242TR ..... p 3909 N94-33324 #

AFPT-90-455-876 ..... p 3582 N94-32328

AGARD-CP-542 ..... p 3679 N94-32235
AGARD-CP-545 ..... p 3581 N94-31977

AGARD-HIGHLIGHTS-94/1 ..... p 3956 N94-31196 #

AGARD-MEMB-94 ..... p 3914 N94-31197 #

AI-TR-1427 ..... p 3817 N94-32213
AI-TR-1451 ..... p 3818 N94-32504 #
AI-TR-1453 ..... p 3817 N94-32212
AI-TR-1457 ..... p 3924 N94-31361 #
AI-TR-1459 ..... p 3825 N94-32165 #
AI-TR-1464 ..... p 3726 N94-32166 #

AI-1437 ..... p 3834 N94-32152 #

AIAA PAPER 92-0796 ..... p 3921 N94-32833 * #
AIAA PAPER 94-0024 ..... p 3700 N94-31229 * #
AIAA PAPER 94-0193 ..... p 3572 N94-32926 * #
AIAA PAPER 94-0357 ..... p 3615 N94-32742 * #
AIAA PAPER 94-0454 ..... p 3701 N94-31268 #
AIAA PAPER 94-1383 ..... p 3739 N94-32735 * #
AIAA PAPER 94-2627 ..... p 3617 N94-33022 * #
AIAA PAPER 94-3079 ..... p 3728 N94-32979 * #
AIAA PAPER 94-3212 ..... p 3573 N94-32984 * #

AIM-1375 ..... p 3880 N94-32186 #
AIM-1440 ..... p 3814 N94-31932 #
AIM-1441 ..... p 3815 N94-31933 #
AIM-1452 ..... p 3846 N94-32167 #
AIM-1458 ..... p 3852 N94-33276 #
AIM-1467 ..... p 3851 N94-32142 #

AL-TP-1993-0014 ..... p 3804 N94-32609

AL/AO-PC-1994-0003 ..... p 3799 N94-32035

AL/AO-TR-1994-0002 ..... p 3798 N94-31243 #

AL/CF-TR-1993-0095 ..... p 3582 N94-32223 #
AL/CF-TR-1993-0177 ..... p 3804 N94-32302

AL/HR-TP-1993-0035 ..... p 3566 N94-32254 #

AL/HR-TR-1993-0178-VOL-1 ..... p 3565 N94-31830 #
AL/HR-TR-1993-0180 ..... p 3586 N94-31058 #
AL/HR-TR-1993-0189 ..... p 3816 N94-32093

AMI-9304 ..... p 3571 N94-32476 * #

ANL-HEP-CP-94-9 ..... p 3864 N94-31310 #

ANL-93/39 ..... p 3727 N94-32778
ANL-94/6 ..... p 3829 N94-31315 #

ANL/APS/PP-73889 ..... p 3672 N94-31317 #

ANL/CHM/CP-81226 ..... p 3864 N94-31321 #
ANL/CHM/CP-81637 ..... p 3871 N94-32598
ANL/CHM/CP-81658 ..... p 3863 N94-31202 #

ANL/CHM/PP-73485 ..... p 3636 N94-32616
ANL/CHM/PP-74824 ..... p 3907 N94-32989 #
ANL/CHM/PP-74944 ..... p 3720 N94-32707 #
ANL/CHM/PP-75156 ..... p 3871 N94-32615

ANL/CHM/PP-75637 ..... p 3873 N94-32797 #
ANL/CHM/PP-76357 ..... p 3871 N94-32515 #
ANL/CHM/PP-80246 ..... p 3869 N94-32141 #
ANL/CHM/PP-80920 ..... p 3874 N94-32876 #

ANL/CMT/PP-75501 ..... p 3645 N94-32514 #

ANL/CMT/PROC-81920 ..... p 3694 N94-32607

ANL/DIS/TM-4 ..... p 3767 N94-32752 #

ANL/ECT/CP-82125 ..... p 3827 N94-32646 #

ANL/EP/CP-79740-REV. ..... p 3863 N94-31151 #

ANL/ER/CP-80342 ..... p 3768 N94-32894 #
ANL/ER/CP-80451 ..... p 3781 N94-31322 #
ANL/ER/CP-80788 ..... p 3775 N94-32874
ANL/ER/CP-81397 ..... p 3768 N94-32790 #

ANL/ES/CP-82064 ..... p 3722 N94-31319 #
ANL/ES/CP-82079 ..... p 3765 N94-32600 #

ANL/ESD/TM-22-VOL-2 ..... p 3765 N94-31625 #

ANL/ET/CP-80141 ..... p 3643 N94-32109
ANL/ET/CP-81785 ..... p 3641 N94-31486 #
ANL/ET/CP-81786 ..... p 3641 N94-31666 #

ANL/FE/CP-81703 ..... p 3643 N94-32098 #

ANL/IFR/CP-80791 ..... p 3819 N94-32599 #

ANL/IPD/CP-81274 ..... p 3826 N94-32248 #

ANL/IPNS/CP-82301 ..... p 3647 N94-32964 #

ANL/MCS-TM-183 ..... p 3841 N94-31309 #

ANL/MCS/CP-81645 ..... p 3825 N94-31663 #
ANL/MCS/CP-81883 ..... p 3841 N94-31274 #
ANL/MCS/CP-81897 ..... p 3844 N94-31665
ANL/MCS/CP-82091 ..... p 3905 N94-32815 #

ANL/MCT/PP-71579 ..... p 3659 N94-32617
ANL/MCT/PP-72124 ..... p 3905 N94-32779 #

ANL/MSD/CP-80658 ..... p 3907 N94-32990
ANL/MSD/CP-82054 ..... p 3904 N94-32645 #
ANL/MSD/CP-82067 ..... p 3903 N94-32372 #
ANL/MSD/CP-82073 ..... p 3657 N94-32358 #
ANL/MSD/CP-82165 ..... p 3904 N94-32602 #
ANL/MSD/CP-82175 ..... p 3904 N94-32601 #
ANL/MSD/CP-82234 ..... p 3906 N94-32875
ANL/MSD/CP-82244 ..... p 3648 N94-32993 #

ANL/MSD/PP-77692 ..... p 3661 N94-32798 #

ANL/OTM/CR-4 ..... p 3906 N94-32843 #

ANL/PHY-94/1 ..... p 3866 N94-31668 #

ANL/PHY/CP-81852 ..... p 3864 N94-31320 #
ANL/PHY/CP-81870 ..... p 3841 N94-31311 #

ANL/PHY/PP-71811 ..... p 3873 N94-32710 #
ANL/PHY/PP-73096 ..... p 3873 N94-32708 #

ANL/RA/CP-81815 ..... p 3826 N94-32357 #

ANL/RPG-94/1 ..... p 3873 N94-32757 #

AP-31 ..... p 3770 N94-31222 #

ARCCB-TR-94001 ..... p 3648 N94-33281 #
ARCCB-TR-94003 ..... p 3729 N94-33251

ARL-CR-121 ..... p 3728 N94-32900 * #
ARL-CR-72 ..... p 3728 N94-32929 * #

ARL-TN-25 ..... p 3580 N94-32362
ARL-TN-32 ..... p 3721 N94-33003
ARL-TN-63 ..... p 3580 N94-32264

ARL-TR-10 ..... p 3728 N94-32893 * #
ARL-TR-23 ..... p 3624 N94-32265
ARL-TR-310 ..... p 3625 N94-32604 #
ARL-TR-335 ..... p 3644 N94-32240 #
ARL-TR-336 ..... p 3846 N94-32048 #
ARL-TR-337 ..... p 3657 N94-32367 #
ARL-TR-346 ..... p 3635 N94-32124 #
ARL-TR-351 ..... p 3841 N94-31360 #
ARL-TR-390 ..... p 3728 N94-32979 * #
ARL-TR-416 ..... p 3728 N94-32902 * #
ARL-TR-71 ..... p 3693 N94-32303
ARL-TR-94-07 ..... p 3862 N94-33096 #

ARO-25470.9-EL ..... p 3810 N94-31277 #
ARO-25715.6-MS-SAH ..... p 3686 N94-31079 #
ARO-26427.12-MS ..... p 3640 N94-31258
ARO-26499.3-PH-SAH ..... p 3887 N94-31530 #
ARO-26821.8-PH ..... p 3686 N94-31057 #
ARO-26891.7-MS-A ..... p 3618 N94-31261 #
ARO-26908.14-EG ..... p 3619 N94-31444 #
ARO-26932.28-MA-SDI ..... p 3811 N94-31443 #
ARO-27076.39-EL ..... p 3688 N94-31445 #
ARO-27141.7-CH-SM ..... p 3650 N94-31509 #
ARO-27259.2-GS-SAH ..... p 3742 N94-31496 #
ARO-27472.6-MS ..... p 3910 N94-31054 #
ARO-27565.3-EG ..... p 3632 N94-31348
ARO-27690.22-MA ..... p 3842 N94-31441 #
ARO-27770.1-CH ..... p 3895 N94-31081 #
ARO-27846.8-MS ..... p 3894 N94-31055 #
ARO-27994.10-EL ..... p 3671 N94-31260 #
ARO-28043.13-LS ..... p 3651 N94-31510 #
ARO-28214.10-EL-SAH ..... p 3894 N94-31056 #
ARO-28348.4-PH-A ..... p 3714 N94-31278 #
ARO-28408.1-MA-SDI ..... p 3809 N94-31251
ARO-29282.1-MS ..... p 3631 N94-31282 #
ARO-29397.1-MA-PT-1 ..... p 3843 N94-31529 #
ARO-29397.2-MA-PT-2 ..... p 3852 N94-31296 #
ARO-30481.1-EL-SBI-PHASE-1 ... p 3897 N94-31528 #
ARO-30708.2-PH ..... p 3714 N94-31358 #
ARO-31084.1-PH-CF ..... p 3792 N94-31294 #

ASC-TR-93-5022-VOL-1 ..... p 3579 N94-32062
ASC-TR-94-5005 ..... p 3588 N94-32311
ASC-TR-94-5006 ..... p 3588 N94-32241
ASC-TR-94-5007 ..... p 3589 N94-32394 #
ASC-TR-94-5008 ..... p 3588 N94-32014 #
ASC-TR-94-5009 ..... p 3590 N94-32403
ASC-TR-94-5010 ..... p 3588 N94-32312
ASC-TR-94-5011 ..... p 3588 N94-32313
ASC-TR-94-5013 ..... p 3590 N94-32395 #
ASC-TR-94-5014 ..... p 3590 N94-32396 #
ASC-TR-94-5015 ..... p 3590 N94-32397 #
ASC-TR-94-5016 ..... p 3590 N94-32398 #
ASC-TR-94-5017 ..... p 3590 N94-32399 #
ASC-TR-94-5018 ..... p 3589 N94-32314 #
ASC-TR-94-5019 ..... p 3589 N94-32315
ASC-TR-94-5020 ..... p 3589 N94-32316
ASC-TR-94-5021 ..... p 3589 N94-32317
ASC-TR-94-5022 ..... p 3589 N94-32318 #
ASC-TR-94-5023 ..... p 3589 N94-32319

ASU-DWA-0080 ..... p 3697 N94-33044 * #

ATR-93(8498)-1 ..... p 3966 N94-32949 #

AVSCOM-TR-91-B-016 ..... p 3572 N94-32873 * #

BBN-7967 ..... p 3862 N94-33023 * #

BIR-2380 ..... p 3731 N94-32481 * #

BN-1158 ..... p 3848 N94-32245 #
BN-1159-PT-1 ..... p 3848 N94-32341 #
BN-1161 ..... p 3848 N94-32331

BNL-49536 ..... p 3766 N94-32691 #
BNL-49600 ..... p 3766 N94-32692 #
BNL-49656 ..... p 3883 N94-32994 #
BNL-49703 ..... p 3875 N94-31480
BNL-49719 ..... p 3876 N94-32099 #
BNL-49744 ..... p 3771 N94-31527
BNL-49758 ..... p 3746 N94-32100 #
BNL-49806 ..... p 3713 N94-32821 #
BNL-49816 ..... p 3870 N94-32355
BNL-49821 ..... p 3794 N94-32896 #
BNL-49822 ..... p 3906 N94-32822 #
BNL-49823 ..... p 3865 N94-31607 #
BNL-49888 ..... p 3632 N94-31305 #
BNL-49921 ..... p 3864 N94-31398 #
BNL-49968 ..... p 3938 N94-32638
BNL-52351-REV-12/93 ..... p 3956 N94-31523 #
BNL-52408 ..... p 3615 N94-32266
BNL-60038 ..... p 3691 N94-31919 #
BNL-60099 ..... p 3646 N94-32699 #

BRDEC-2546 ..... p 3656 N94-32184 #

BRGM-93032 ..... p 3752 N94-32551
BRGM-93033 ..... p 3753 N94-32552
BRGM-93034 ..... p 3748 N94-32527
BRGM-93035 ..... p 3754 N94-32561

CARDEROCKDIV-MRD-93/25 ..... p 3640 N94-31456 #

CBCL-MEMO-74 ..... p 3880 N94-32186 #
CBCL-MEMO-83 ..... p 3814 N94-31932 #
CBCL-MEMO-84 ..... p 3815 N94-31933 #
CBCL-MEMO-87 ..... p 3852 N94-33276 #
CBCL-MEMO-88 ..... p 3851 N94-32142 #

CBCL-MEMO-90 ..... p 3846 N94-32167 #

CCMS-93-18 ..... p 3662 N94-32891

CERC-94-2 ..... p 3791 N94-33085 #

CFDRC-4110/2-VOL-1 ..... p 3637 N94-32696 * #
CFDRC-4110/2-VOL-2 ..... p 3637 N94-32694 * #

CL-93-01 ..... p 3855 N94-31390
CL-93-02 ..... p 3841 N94-31391

CMC-0687-1090 ..... p 3581 N94-31903
CMC-93-09 ..... p 3848 N94-32331

CMOTT-94-2 ..... p 3710 N94-33070 * #

CMS-TSR-94-6 ..... p 3855 N94-31244 #
CMS-TSR-94-7 ..... p 3843 N94-31474 #
CMS-TSR-94-8 ..... p 3701 N94-31245 #

CMU-CS-93-196 ..... p 3816 N94-32081 #
CMU-CS-93-200 ..... p 3815 N94-31940
CMU-CS-93-208 ..... p 3678 N94-32121 #
CMU-CS-93-213 ..... p 3845 N94-31939 #
CMU-CS-93-217 ..... p 3918 N94-31930 #
CMU-CS-93-218 ..... p 3806 N94-31934 #
CMU-CS-93-219 ..... p 3712 N94-31929 #
CMU-CS-93-220 ..... p 3803 N94-31447 *
CMU-CS-93-222 ..... p 3816 N94-32086 * #
CMU-CS-93-231 ..... p 3815 N94-31994
CMU-CS-94-101 ..... p 3824 N94-31259
CMU-CS-94-116 ..... p 3815 N94-32080 #
CMU-CS-94-119 ..... p 3821 N94-33030 #
CMU-CS-94-126 ..... p 3822 N94-33279 #

CMU/SEI-93-TR-26 ..... p 3818 N94-32508

CONF-8804344 ..... p 3741 N94-31606 #
CONF-9204273-SUMM ..... p 3766 N94-32693 #
CONF-9207229 ..... p 3794 N94-32769
CONF-930159-59 ..... p 3632 N94-31305 #
CONF-930346-4 ..... p 3764 N94-31601 #
CONF-9304145 ..... p 3874 N94-32804 #
CONF-9304148-2 ..... p 3636 N94-32251 #
CONF-9304227-1 ..... p 3825 N94-31663 #
CONF-9304229-1 ..... p 3874 N94-32841 #
CONF-930435-10 ..... p 3764 N94-31602 #
CONF-930445-28 ..... p 3675 N94-31761 #
CONF-9305155-3-REV-1 ..... p 3863 N94-31270 #
CONF-9305285 ..... p 3841 N94-31309 #
CONF-9305317-1 ..... p 3911 N94-31823 #
CONF-9306113-2 ..... p 3870 N94-32178 #
CONF-9306113 ..... p 3759 N94-31648 #
CONF-9306223-4 ..... p 3677 N94-32101 #
CONF-9306251-3 ..... p 3871 N94-32587 #
CONF-9306252-1 ..... p 3781 N94-31597 #
CONF-9306258 ..... p 3877 N94-32748
CONF-9306287-2 ..... p 3934 N94-31782 #
CONF-9306304-1 ..... p 3671 N94-31267 #
CONF-930636-12 ..... p 3938 N94-32638
CONF-930703-43 ..... p 3955 N94-31635
CONF-9307127-1-APP-A ..... p 3890 N94-32415 #
CONF-9307145-3 ..... p 3872 N94-32630 #
CONF-9307715-2 ..... p 3874 N94-32807 #
CONF-9307163-1 ..... p 3865 N94-31607 #
CONF-9307163-2 ..... p 3906 N94-32822 #
CONF-9307164-1 ..... p 3723 N94-31651 #
CONF-9307166-1 ..... p 3925 N94-31786 #
CONF-9307167-1 ..... p 3938 N94-32137 #
CONF-9307174-1 ..... p 3883 N94-32818
CONF-930722-58 ..... p 3712 N94-31783 #
CONF-930722-59 ..... p 3858 N94-31397 #
CONF-930759-7 ..... p 3646 N94-32754
CONF-930764-1 ..... p 3712 N94-31629 #
CONF-930767-2 ..... p 3875 N94-33278
CONF-9308106-3 ..... p 3759 N94-31762 #
CONF-9308106-4 ..... p 3767 N94-32784 #
CONF-9308116-1 ..... p 3841 N94-31274 #
CONF-9308154-4 ..... p 3907 N94-32934
CONF-9308156-3 ..... p 3647 N94-32851
CONF-9308164-8 ..... p 3875 N94-33189 #
CONF-9308167-6 ..... p 3713 N94-32681
CONF-9308181-2 ..... p 3864 N94-31405 #
CONF-9308203-1 ..... p 3819 N94-32668
CONF-9308206-2 ..... p 3953 N94-31632 #
CONF-9308210-1 ..... p 3864 N94-31507 #
CONF-9308211-1 ..... p 3911 N94-31760 #
CONF-9308215-1 ..... p 3926 N94-32189 #
CONF-930855-9 ..... p 3721 N94-32845 #
CONF-930888-1 ..... p 3891 N94-32664 #
CONF-9309119-3 ..... p 3864 N94-31508 #
CONF-9309119-4 ..... p 3891 N94-32619 #
CONF-9309119-5 ..... p 3870 N94-32177 #
CONF-9309148-1 ..... p 3637 N94-32801 #
CONF-9309166-4 ..... p 3713 N94-32821 #
CONF-9309168-4 ..... p 3730 N94-31605 #
CONF-9309199-8 ..... p 3716 N94-31599 #
CONF-9309203 ..... p 3694 N94-32607
CONF-9309223-1 ..... p 3764 N94-31596 #
CONF-9309251-2 ..... p 3648 N94-32993 #
CONF-9309259-5 ..... p 3720 N94-32753 #
CONF-9309928-25 ..... p 3641 N94-31626 #
CONF-9309928-26 ..... p 3641 N94-31666 #
CONF-9309928-27 ..... p 3641 N94-31486 #
CONF-9309928-28 ..... p 3896 N94-31499 #
CONF-9309928-3-REV. ..... p 3863 N94-31151 #
CONF-9309290-2 ..... p 3719 N94-32629 #
CONF-9309297-4 ..... p 3864 N94-31310 #
CONF-9309297-5 ..... p 3873 N94-32689
CONF-9309300-1 ..... p 3765 N94-32354 #
CONF-9309312-1 ..... p 3794 N94-32896 #
CONF-9309323-1 ..... p 3876 N94-32099 #
CONF-9309337-1 ..... p 3956 N94-31308 #
CONF-930960-8 ..... p 3632 N94-31352 #
CONF-930960-9 ..... p 3632 N94-31349 #
CONF-930999-6 ..... p 3867 N94-31779 #
CONF-930999-9 ..... p 3874 N94-32850 #
CONF-931009-19 ..... p 3643 N94-32098 #
CONF-931009-20 ..... p 3909 N94-33271 #
CONF-931009-21 ..... p 3903 N94-32597
CONF-931009-22 ..... p 3647 N94-32852
CONF-9310100-8 ..... p 3804 N94-32596
CONF-9310147-2 ..... p 3690 N94-31594
CONF-9310164-8 ..... p 3712 N94-31831
CONF-9310169-2 ..... p 3696 N94-32806 #
CONF-931018-79 ..... p 3888 N94-31667 #
CONF-931018-83 ..... p 3715 N94-31580 #
CONF-931018-84 ..... p 3887 N94-31406 #
CONF-9310190 ..... p 3866 N94-31668 #
CONF-9310225-2 ..... p 3713 N94-32728 #
CONF-9310247-10 ..... p 3897 N94-31506 #
CONF-9310247-11 ..... p 3866 N94-31669 #
CONF-9310247-12 ..... p 3872 N94-32627
CONF-9310247-14 ..... p 3866 N94-31670 #
CONF-9310247-16 ..... p 3867 N94-31671 #
CONF-9310247-21 ..... p 3873 N94-32780 #
CONF-9310247-4 ..... p 3863 N94-31147 #
CONF-9310249-1 ..... p 3768 N94-32790 #
CONF-9310252-5 ..... p 3955 N94-32129 #
CONF-9310259-2 ..... p 3864 N94-31398 #
CONF-9310259-3 ..... p 3869 N94-32139 #
CONF-9310259-4 ..... p 3877 N94-32802 #
CONF-9310268-1 ..... p 3771 N94-31527
CONF-9310269-1 ..... p 3845 N94-31763 #
CONF-9310281-1 ..... p 3864 N94-31320 #
CONF-9310282-1 ..... p 3667 N94-32148 #
CONF-9310282-2 ..... p 3692 N94-32136 #
CONF-9310283-1 ..... p 3938 N94-32503 #
CONF-9310287-1 ..... p 3907 N94-32990
CONF-9310293-1 ..... p 3870 N94-32271 #
CONF-9310294-1 ..... p 3852 N94-32744 #
CONF-9310300-1 ..... p 3819 N94-32749 #
CONF-931048-10 ..... p 3720 N94-32760 #
CONF-931048-11 ..... p 3892 N94-32730 #
CONF-931048-6 ..... p 3666 N94-32114
CONF-931054-10 ..... p 3719 N94-32613 #
CONF-931054-3 ..... p 3651 N94-31557 #
CONF-931054-5 ..... p 3649 N94-31199 #
CONF-931054-7 ..... p 3714 N94-31269 #
CONF-931054-8 ..... p 3716 N94-31636 #
CONF-931054-9 ..... p 3718 N94-32252 #
CONF-931079-17 ..... p 3643 N94-32109
CONF-931102-3 ..... p 3722 N94-31319 #
CONF-931107-34 ..... p 3807 N94-32783 #
CONF-931107-35 ..... p 3870 N94-32355
CONF-931108-17 ..... p 3875 N94-31480
CONF-931108-51 ..... p 3651 N94-31650 #
CONF-931108-52 ..... p 3901 N94-32172 #
CONF-931108-55 ..... p 3655 N94-32102 #
CONF-931108-59 ..... p 3899 N94-31634 #
CONF-931108-60 ..... p 3652 N94-31780 #
CONF-931108-61 ..... p 3641 N94-31627 #
CONF-931108-62 ..... p 3896 N94-31489 #
CONF-931108-63 ..... p 3902 N94-32296 #
CONF-931108-67 ..... p 3895 N94-31307 #
CONF-931108-70 ..... p 3640 N94-31314 #
CONF-931108-73 ..... p 3898 N94-31630 #
CONF-931108-76 ..... p 3896 N94-31501 #
CONF-931108-77 ..... p 3634 N94-32110
CONF-931108-78 ..... p 3882 N94-32674
CONF-931108-79 ..... p 3901 N94-32115
CONF-931108-80 ..... p 3656 N94-32116
CONF-931108-83 ..... p 3904 N94-32724 #
CONF-931108-84-PT-2 ..... p 3904 N94-32606 #
CONF-931108-85 ..... p 3661 N94-32796 #
CONF-931108-87 ..... p 3656 N94-32103 #
CONF-931108-89 ..... p 3660 N94-32729 #
CONF-931108-90 ..... p 3644 N94-32374 #
CONF-931108-91 ..... p 3662 N94-32855 #
CONF-931108-92 ..... p 3903 N94-32411 #
CONF-931108-93 ..... p 3906 N94-32875
CONF-931108-95 ..... p 3906 N94-32884
CONF-9311104-15 ..... p 3886 N94-31304 #
CONF-9311104-20 ..... p 3647 N94-32892 #
CONF-9311115-2 ..... p 3691 N94-31919 #
CONF-9311140-2 ..... p 3890 N94-32201 #
CONF-9311147-3 ..... p 3892 N94-32810 #
CONF-9311147-4 ..... p 3891 N94-32612 #
CONF-9311147-5 ..... p 3891 N94-32611 #
CONF-9311147-6 ..... p 3891 N94-32595 #
CONF-9311149-SUMM ..... p 3759 N94-31266 #
CONF-9311152-1 ..... p 3826 N94-32248 #
CONF-9311153-2 ..... p 3659 N94-32640
CONF-9311153-3 ..... p 3903 N94-32384 #
CONF-9311155 ..... p 3761 N94-32705 #
CONF-9311168-1 ..... p 3717 N94-32128 #
CONF-9311171-2 ..... p 3834 N94-32175 #
CONF-9311191-1 ..... p 3768 N94-32812 #
CONF-931121-38 ..... p 3738 N94-32637
CONF-931132-2 ..... p 3887 N94-31400 #
CONF-931142-6 ..... p 3899 N94-31847 #
CONF-931156-15 ..... p 3742 N94-31504 #
CONF-931156-16 ..... p 3771 N94-31525 #
CONF-931156-21 ..... p 3758 N94-31234 #
CONF-931160-40 ..... p 3834 N94-32127 #
CONF-931178-1 ..... p 3886 N94-31324 #
CONF-931234-6 ..... p 3733 N94-31312 #
CONF-931234-8 ..... p 3738 N94-32639
CONF-931237-6 ..... p 3720 N94-32794 #
CONF-931237-7 ..... p 3907 N94-32963
CONF-931237-9 ..... p 3721 N94-32848
CONF-931247-1 ..... p 3898 N94-31631 #
CONF-931247-2 ..... p 3899 N94-31916 #
CONF-931247-3 ..... p 3898 N94-31628 #
CONF-931247-4 ..... p 3899 N94-31633 #
CONF-931247-7 ..... p 3904 N94-32645 #
CONF-931247-8 ..... p 3904 N94-32746 #
CONF-931247-9 ..... p 3907 N94-32944 #
CONF-931247 ..... p 3906 N94-32913 #
CONF-931249-1 ..... p 3844 N94-31665
CONF-931251-1 ..... p 3786 N94-32937 #
CONF-931252-1 ..... p 3841 N94-31311 #
CONF-931254-4 ..... p 3883 N94-32994 #
CONF-931255-1 ..... p 3660 N94-32687
CONF-931257-1 ..... p 3905 N94-32785 #
CONF-940101-28 ..... p 3613 N94-31265 #
CONF-940101-29 ..... p 3615 N94-32669
CONF-940113-7 ..... p 3830 N94-31623 #
CONF-940114-2 ..... p 3716 N94-31622 #
CONF-940114-3 ..... p 3637 N94-32743 #
CONF-940115-10 ..... p 3766 N94-32690 #
CONF-940115-11 ..... p 3766 N94-32691 #
CONF-940115-12 ..... p 3766 N94-32692 #
CONF-940115-15 ..... p 3767 N94-32789 #
CONF-940115-17 ..... p 3768 N94-32894 #
CONF-940115-18 ..... p 3775 N94-32895 #
CONF-940115-22 ..... p 3746 N94-32100 #
CONF-940115-23 ..... p 3786 N94-32791 #
CONF-940115-24 ..... p 3774 N94-32772 #
CONF-940115-30 ..... p 3914 N94-32910 #
CONF-940115-31 ..... p 3785 N94-32268 #
CONF-940121-3 ..... p 3905 N94-32747 #
CONF-940122-2 ..... p 3904 N94-32601 #
CONF-940122-3 ..... p 3903 N94-32372 #
CONF-940131-2 ..... p 3775 N94-32874
CONF-940131-5 ..... p 3786 N94-32759 #
CONF-940132-1 ..... p 3718 N94-32202 #
CONF-940132-2 ..... p 3904 N94-32602 #
CONF-940135-3 ..... p 3618 N94-31313 #
CONF-940142-10 ..... p 3863 N94-31202 #
CONF-940142-11 ..... p 3715 N94-31485 #
CONF-940142-18 ..... p 3897 N94-31502 #
CONF-940142-22 ..... p 3719 N94-32603 #
CONF-940142-23 ..... p 3661 N94-32819 #
CONF-940142-24 ..... p 3882 N94-32649 #
CONF-940142-25 ..... p 3661 N94-32751
CONF-940142-26 ..... p 3718 N94-32270 #
CONF-940142-27 ..... p 3881 N94-32385 #
CONF-940142-29 ..... p 3883 N94-32878
CONF-940142-3 ..... p 3716 N94-31624 #
CONF-940142-7 ..... p 3688 N94-31483 #
CONF-940142-8 ..... p 3797 N94-32732 #
CONF-940152-1 ..... p 3568 N94-31578 #
CONF-940152-2 ..... p 3701 N94-31268 #
CONF-940154-1 ..... p 3811 N94-31484 #
CONF-940158-1 ..... p 3576 N94-31306 #
CONF-940167-1 ..... p 3713 N94-32811 #
CONF-940204-5 ..... p 3626 N94-32665 #
CONF-940210-1 ..... p 3761 N94-32762 #
CONF-940214-6 ..... p 3941 N94-31145 #
CONF-940221-3 ..... p 3640 N94-31345 #
CONF-940222-13 ..... p 3645 N94-32614
CONF-940225-52 ..... p 3920 N94-32808 #
CONF-940225-67 ..... p 3660 N94-32698 #
CONF-940226-4 ..... p 3720 N94-32761 #
CONF-940226-5 ..... p 3720 N94-32704 #
CONF-940244-1 ..... p 3651 N94-31649 #

CONF-940245-1 ..... p 3666 N94-31827 #
CONF-940245-2 ..... p 3666 N94-31579 #
CONF-940254-1 ..... p 3795 N94-31323 #
CONF-940255-1 ..... p 3739 N94-32842
CONF-940256-1 ..... p 3737 N94-32135
CONF-940259-1 ..... p 3611 N94-32813
CONF-940262-2 ..... p 3873 N94-32755 #
CONF-940265-1 ..... p 3767 N94-32750 #
CONF-940266-1 ..... p 3768 N94-32814
CONF-940301-19 ..... p 3625 N94-32642 #
CONF-940301-9 ..... p 3864 N94-31321 #
CONF-940328 ..... p 3877 N94-32844 #
CONF-940337-1 ..... p 3690 N94-31593
CONF-940337-2 ..... p 3660 N94-32727 #
CONF-940348-2 ..... p 3649 N94-31198 #
CONF-940353-3 ..... p 3747 N94-32203 #
CONF-940362-1 ..... p 3785 N94-32726 #
CONF-940363-3 ..... p 3682 N94-32756 #
CONF-940365-3 ..... p 3835 N94-32787 #
CONF-940367-1 ..... p 3723 N94-31524 #
CONF-940367-2 ..... p 3645 N94-32522 #
CONF-940368-1 ..... p 3774 N94-32736 #
CONF-940369-2 ..... p 3695 N94-32700 #
CONF-940373-1 ..... p 3781 N94-31322 #
CONF-940377-1 ..... p 3827 N94-32646 #
CONF-940378-1 ..... p 3682 N94-32745 #
CONF-940379-1 ..... p 3657 N94-32358 #
CONF-940380-1 ..... p 3774 N94-32816 #
CONF-940383-1 ..... p 3647 N94-32964 #
CONF-9404103-1 ..... p 3638 N94-32840 #
CONF-9404106-1 ..... p 3871 N94-32598
CONF-9404107-4 ..... p 3761 N94-32383 #
CONF-940411-1 ..... p 3904 N94-32634 #
CONF-9404110-1 ..... p 3826 N94-32356 #
CONF-9404112-1 ..... p 3696 N94-32786 #
CONF-9404118-1 ..... p 3693 N94-32386 #
CONF-940422-1 ..... p 3765 N94-32600 #
CONF-940424-16 ..... p 3611 N94-32667 #
CONF-940424-20 ..... p 3872 N94-32666 #
CONF-940424-22 ..... p 3819 N94-32641
CONF-940428-2 ..... p 3707 N94-32373 #
CONF-940443-1 ..... p 3761 N94-32648 #
CONF-940449-1 ..... p 3747 N94-32249
CONF-940453-2 ..... p 3692 N94-32111 #
CONF-940453-3 ..... p 3692 N94-32112
CONF-940456-11 ..... p 3819 N94-32599 #
CONF-940456-12 ..... p 3826 N94-32357 #
CONF-940456-13 ..... p 3905 N94-32815 #
CONF-940467-2 ..... p 3914 N94-32677 #
CONF-940481-1 ..... p 3603 N94-32671 #
CONF-940483-1 ..... p 3580 N94-32658
CONF-940510-1 ..... p 3849 N94-32675 #
CONF-9405112-1 ..... p 3696 N94-32809 #
CONF-940529-1 ..... p 3694 N94-32593 #
CONF-940529-2 ..... p 3695 N94-32663 #
CONF-940534-2 ..... p 3681 N94-32679 #
CONF-940537-1 ..... p 3645 N94-32672
CONF-940538-1 ..... p 3915 N94-32678 #
CONF-940550-10 ..... p 3727 N94-32682
CONF-940550-2 ..... p 3818 N94-32353 #
CONF-940557-1 ..... p 3849 N94-32653 #
CONF-940566-1 ..... p 3678 N94-32113
CONF-940566-2 ..... p 3872 N94-32628 #
CONF-940581-1 ..... p 3852 N94-32673 #
CONF-940582-1 ..... p 3719 N94-32659 #
CONF-940588-1 ..... p 3901 N94-32104 #
CONF-940594-1 ..... p 3739 N94-32771
CONF-940595-1 ..... p 3920 N94-32635 #
CONF-940596-1 ..... p 3695 N94-32688
CONF-940596-2 ..... p 3695 N94-32650 #

CRANFIELD-AERO-9103 ..... p 3702 N94-31559 #
CRANFIELD-AERO-9306 ..... p 3914 N94-31538 #
CRANFIELD-AERO-9307 ..... p 3843 N94-31539 #
CRANFIELD-AERO-9310 ..... p 3843 N94-31540 #
CRANFIELD-AERO-9312 ..... p 3843 N94-31541 #

CRIE-T-92089 ..... p 3697 N94-32917
CRIE-T-92090 ..... p 3762 N94-32918

CRIE-W-92016 ..... p 3893 N94-32916 #

CRIE-Y-93001 ..... p 3762 N94-32919

CRINC/RSL-TR-8621-2 ..... p 3783 N94-31937 #

CRREL-93-26 ..... p 3773 N94-32154

CSC-93-34 ..... p 3668 N94-33037 * #

CSDL-R-2575 ..... p 3801 N94-33053

CSDL-T-1205 ..... p 3835 N94-32359 * #
CSDL-T-1214 ..... p 3739 N94-32907 * #
CSDL-T-1220 ..... p 3731 N94-32862 * #
CSDL-T-1221 ..... p 3601 N94-32388 * #
CSDL-T-1227 ..... p 3577 N94-32864 * #

CSTM-USS-4000 ..... p 3711 N94-31492 * #

CT-93-04 ..... p 3916 N94-31392
CT-93-05 ..... p 3842 N94-31393

CTH-E-93-01 ..... p 3859 N94-31076
CTH-E-93-02 ..... p 3859 N94-31077
CTH-E-93-03 ..... p 3732 N94-31091
CTH-E-93-04 ..... p 3722 N94-31194

CTH-F-93-03 ..... p 3859 N94-31090

CTN-94-61181 ..... p 3795 N94-31738
CTN-94-61182 ..... p 3853 N94-33335
CTN-94-61183 ..... p 3836 N94-33149
CTN-94-61184 ..... p 3675 N94-31708 #
CTN-94-61185 ..... p 3955 N94-31709 #
CTN-94-61186 ..... p 3587 N94-31710 #
CTN-94-61187 ..... p 3690 N94-31711 #
CTN-94-61188 ..... p 3911 N94-31712 #
CTN-94-61189 ..... p 3813 N94-31713 #
CTN-94-61190 ..... p 3724 N94-31714 #
CTN-94-61191 ..... p 3814 N94-31715 #
CTN-94-61192 ..... p 3620 N94-31716 #
CTN-94-61193 ..... p 3703 N94-31717 #
CTN-94-61194 ..... p 3814 N94-31718 #
CTN-94-61195 ..... p 3621 N94-31719 #
CTN-94-61196 ..... p 3703 N94-31720 #
CTN-94-61197 ..... p 3724 N94-31721 #
CTN-94-61198 ..... p 3652 N94-31722 #
CTN-94-61199 ..... p 3676 N94-31796 #
CTN-94-61200 ..... p 3716 N94-31797 #
CTN-94-61201 ..... p 3831 N94-31798 #
CTN-94-61202 ..... p 3704 N94-31799 #
CTN-94-61203 ..... p 3831 N94-31800 #
CTN-94-61204 ..... p 3914 N94-32074 #
CTN-94-61205 ..... p 3832 N94-31801 #
CTN-94-61206 ..... p 3690 N94-31726 #
CTN-94-61207 ..... p 3888 N94-31727 #
CTN-94-61208 ..... p 3620 N94-31706 #
CTN-94-61209 ..... p 3734 N94-31707 #
CTN-94-61210 ..... p 3622 N94-31909 #
CTN-94-61211 ..... p 3610 N94-31910 #
CTN-94-61212 ..... p 3912 N94-31911 #
CTN-94-61213 ..... p 3736 N94-31912 #
CTN-94-61214 ..... p 3575 N94-31902
CTN-94-61215 ..... p 3581 N94-31903
CTN-94-61216 ..... p 3735 N94-31849
CTN-94-61217 ..... p 3577 N94-32505
CTN-94-61218 ..... p 3642 N94-31871
CTN-94-61219 ..... p 3730 N94-31872
CTN-94-61220 ..... p 3832 N94-31873 #
CTN-94-61221 ..... p 3935 N94-31913 #
CTN-94-61222 ..... p 3925 N94-31914 #
CTN-94-61223 ..... p 3868 N94-31915 #
CTN-94-61224 ..... p 3588 N94-31747 #
CTN-94-61225 ..... p 3716 N94-31748 #
CTN-94-61226 ..... p 3867 N94-31749 #
CTN-94-61227 ..... p 3831 N94-31750 #
CTN-94-61228 ..... p 3879 N94-31751 #
CTN-94-61229 ..... p 3814 N94-31752 #
CTN-94-61230 ..... p 3867 N94-31753 #
CTN-94-61231 ..... p 3725 N94-31754 #
CTN-94-61232 ..... p 3845 N94-31755 #
CTN-94-61233 ..... p 3879 N94-31756 #
CTN-94-61234 ..... p 3831 N94-31757 #
CTN-94-61235 ..... p 3814 N94-31728 #
CTN-94-61236 ..... p 3899 N94-31729 #
CTN-94-61237 ..... p 3703 N94-31730 #
CTN-94-61238 ..... p 3675 N94-31731 #
CTN-94-61239 ..... p 3867 N94-31832 #
CTN-94-61240 ..... p 3924 N94-31732 #
CTN-94-61241 ..... p 3743 N94-31733 #
CTN-94-61242 ..... p 3568 N94-31734 #
CTN-94-61243 ..... p 3830 N94-31735 #
CTN-94-61244 ..... p 3878 N94-31736 #
CTN-94-61245 ..... p 3734 N94-31737 #
CTN-94-61246 ..... p 3652 N94-31692 #
CTN-94-61247 ..... p 3832 N94-31833 #
CTN-94-61248 ..... p 3772 N94-31834 #
CTN-94-61249 ..... p 3725 N94-31874 #
CTN-94-61250 ..... p 3833 N94-31875 #
CTN-94-61251 ..... p 3833 N94-31876 #
CTN-94-61252 ..... p 3879 N94-31877 #
CTN-94-61253 ..... p 3725 N94-31878 #
CTN-94-61254 ..... p 3621 N94-31835 #
CTN-94-61255 ..... p 3621 N94-31836 #
CTN-94-61256 ..... p 3585 N94-31837 #
CTN-94-61257 ..... p 3879 N94-31850
CTN-94-61258 ..... p 3621 N94-31892

CU-153-6951 ..... p 3810 N94-31277 #

CWI-AM-R9302 ..... p 3793 N94-32226
CWI-AM-R9303 ..... p 3848 N94-32227
CWI-AM-R9304 ..... p 3793 N94-32228
CWI-AM-R9305 ..... p 3851 N94-32229
CWI-AM-R9306 ..... p 3847 N94-32204
CWI-AM-R9307 ..... p 3846 N94-32106
CWI-AM-R9308 ..... p 3847 N94-32191
CWI-AM-R9309 ..... p 3857 N94-32192

CWI-BS-R9310 ..... p 3851 N94-32225
CWI-BS-R9311 ..... p 3846 N94-32084
CWI-BS-R9312 ..... p 3677 N94-32085
CWI-BS-R9313 ..... p 3835 N94-32193
CWI-BS-R9314 ..... p 3847 N94-32194
CWI-BS-R9315 ..... p 3846 N94-32107
CWI-BS-R9316 ..... p 3846 N94-32108
CWI-BS-R9317 ..... p 3849 N94-32507
CWI-BS-R9318 ..... p 3847 N94-32197
CWI-BS-R9319 ..... p 3835 N94-32198
CWI-BS-R9320 ..... p 3852 N94-32350

CWI-CS-R9248 ..... p 3827 N94-33002
CWI-CS-R9360 ..... p 3822 N94-33097 #
CWI-CS-R9362 ..... p 3849 N94-32349

DCIEM-92-10 ..... p 3795 N94-31738

DE93-018210 ..... p 3953 N94-31491 #
DE93-019199 ..... p 3764 N94-31596 #
DE93-019972 ..... p 3915 N94-32678 #
DE93-040251 ..... p 3681 N94-32679 #
DE93-040820 ..... p 3781 N94-31597 #
DE94-000042 ..... p 3762 N94-32823 #
DE94-000086 ..... p 3758 N94-31234 #
DE94-000094 ..... p 3760 N94-31811 #
DE94-000202 ..... p 3760 N94-32143 #
DE94-000238 ..... p 3761 N94-32725 #
DE94-000246 ..... p 3758 N94-31235
DE94-000268 ..... p 3690 N94-31598 #
DE94-000291 ..... p 3760 N94-31812
DE94-000292 ..... p 3899 N94-31813
DE94-000293 ..... p 3758 N94-31236 #
DE94-000295 ..... p 3759 N94-31279 #
DE94-000297 ..... p 3758 N94-31264 #
DE94-000298 ..... p 3695 N94-32680 #
DE94-001421 ..... p 3818 N94-32353 #
DE94-001530 ..... p 3716 N94-31599 #
DE94-001864 ..... p 3764 N94-31600
DE94-001877 ..... p 3764 N94-31601 #
DE94-001879 ..... p 3764 N94-31602 #
DE94-002194 ..... p 3766 N94-32690 #
DE94-002994 ..... p 3766 N94-32691 #
DE94-002995 ..... p 3766 N94-32692 #
DE94-003024 ..... p 3766 N94-32693 #
DE94-003160 ..... p 3785 N94-32716 #
DE94-003610 ..... p 3785 N94-32717 #
DE94-003629 ..... p 3767 N94-32711 #
DE94-003824 ..... p 3765 N94-32144
DE94-003827 ..... p 3767 N94-32712 #
DE94-003950 ..... p 3743 N94-31603 #
DE94-004233 ..... p 3875 N94-31480
DE94-004271 ..... p 3713 N94-32681
DE94-004289 ..... p 3712 N94-31831
DE94-004332 ..... p 3765 N94-32354 #
DE94-004342 ..... p 3668 N94-31604 #
DE94-004352 ..... p 3767 N94-32789 #
DE94-004357 ..... p 3730 N94-31605 #
DE94-004427 ..... p 3727 N94-32682
DE94-004606 ..... p 3768 N94-32790 #
DE94-004668 ..... p 3819 N94-32668
DE94-004670 ..... p 3615 N94-32669
DE94-004674 ..... p 3613 N94-31265 #
DE94-004687 ..... p 3849 N94-32670
DE94-004696 ..... p 3826 N94-32248 #
DE94-004727 ..... p 3741 N94-31606 #
DE94-004835 ..... p 3786 N94-32791 #
DE94-004858 ..... p 3886 N94-31304 #
DE94-004954 ..... p 3759 N94-31266 #
DE94-004974 ..... p 3785 N94-32726 #
DE94-005109 ..... p 3775 N94-32874
DE94-005111 ..... p 3768 N94-32894 #
DE94-005136 ..... p 3775 N94-32895 #
DE94-005226 ..... p 3911 N94-31823 #
DE94-005244 ..... p 3603 N94-32671 #
DE94-005248 ..... p 3645 N94-32672
DE94-005251 ..... p 3941 N94-31145 #
DE94-005260 ..... p 3895 N94-31067 #
DE94-005268 ..... p 3671 N94-31267 #
DE94-005271 ..... p 3568 N94-31578 #
DE94-005274 ..... p 3852 N94-32673 #
DE94-005276 ..... p 3862 N94-31146 #
DE94-005279 ..... p 3863 N94-31147 #
DE94-005309 ..... p 3882 N94-32674
DE94-005311 ..... p 3701 N94-31268 #
DE94-005316 ..... p 3714 N94-31148 #
DE94-005319 ..... p 3823 N94-31149 #
DE94-005327 ..... p 3816 N94-32145 #

DE94-005328 ..... p 3816 N94-32146 #
DE94-005340 ..... p 3686 N94-31150 #
DE94-005352 ..... p 3849 N94-32675 #
DE94-005354 ..... p 3660 N94-32727 #
DE94-005371 ..... p 3643 N94-32098 #
DE94-005392 ..... p 3863 N94-31151 #
DE94-005400 ..... p 3713 N94-32728 #
DE94-005442 ..... p 3920 N94-32676 #
DE94-005446 ..... p 3632 N94-31305 #
DE94-005452 ..... p 3876 N94-32099 #
DE94-005457 ..... p 3746 N94-32100 #
DE94-005473 ..... p 3825 N94-31663 #
DE94-005494 ..... p 3687 N94-31152 #
DE94-005505 ..... p 3794 N94-32896 #
DE94-005529 ..... p 3631 N94-31153 #
DE94-005552 ..... p 3759 N94-31648 #
DE94-005556 ..... p 3631 N94-31154 #
DE94-005566 ..... p 3677 N94-32101 #
DE94-005578 ..... p 3651 N94-31649 #
DE94-005580 ..... p 3690 N94-31593
DE94-005583 ..... p 3651 N94-31650 #
DE94-005584 ..... p 3655 N94-32102 #
DE94-005587 ..... p 3660 N94-32729 #
DE94-005593 ..... p 3901 N94-32172 #
DE94-005648 ..... p 3723 N94-31651 #
DE94-005688 ..... p 3915 N94-31155 #
DE94-005690 ..... p 3794 N94-32769
DE94-005753 ..... p 3649 N94-31198 #
DE94-005795 ..... p 3759 N94-31487 #
DE94-005810 ..... p 3834 N94-32127 #
DE94-005813 ..... p 3649 N94-31199 #
DE94-005822 ..... p 3717 N94-32128 #
DE94-005823 ..... p 3914 N94-32677 #
DE94-005824 ..... p 3651 N94-31557 #
DE94-005873 ..... p 3714 N94-31200 #
DE94-005876 ..... p 3887 N94-31558 #
DE94-005888 ..... p 3649 N94-31201 #
DE94-005921 ..... p 3863 N94-31202 #
DE94-005928 ..... p 3956 N94-31523 #
DE94-005941 ..... p 3723 N94-31524 #
DE94-005958 ..... p 3771 N94-31525 #
DE94-005959 ..... p 3742 N94-31504 #
DE94-005970 ..... p 3876 N94-31505 #
DE94-006000 ..... p 3897 N94-31506 #
DE94-006041 ..... p 3864 N94-31507 #
DE94-006043 ..... p 3633 N94-31526 #
DE94-006047 ..... p 3580 N94-32658
DE94-006048 ..... p 3720 N94-32794 #
DE94-006049 ..... p 3719 N94-32659 #
DE94-006050 ..... p 3864 N94-31508 #
DE94-006059 ..... p 3771 N94-31527
DE94-006060 ..... p 3865 N94-31607 #
DE94-006065 ..... p 3888 N94-31619 #
DE94-006067 ..... p 3869 N94-32173 #
DE94-006071 ..... p 3866 N94-31620 #
DE94-006104 ..... p 3723 N94-31621 #
DE94-006130 ..... p 3761 N94-32660
DE94-006131 ..... p 3681 N94-32661
DE94-006132 ..... p 3695 N94-32662
DE94-006139 ..... p 3576 N94-31306 #
DE94-006141 ..... p 3899 N94-31847 #
DE94-006143 ..... p 3716 N94-31622 #
DE94-006145 ..... p 3695 N94-32663 #
DE94-006149 ..... p 3907 N94-32944 #
DE94-006150 ..... p 3892 N94-32730 #
DE94-006156 ..... p 3911 N94-31760 #
DE94-006163 ..... p 3830 N94-31623 #
DE94-006165 ..... p 3716 N94-31624 #
DE94-006166 ..... p 3765 N94-31625 #
DE94-006192 ..... p 3675 N94-31761 #
DE94-006209 ..... p 3876 N94-32731 #
DE94-006212 ..... p 3760 N94-32174 #
DE94-006213 ..... p 3641 N94-31626 #
DE94-006215 ..... p 3641 N94-31627 #
DE94-006216 ..... p 3759 N94-31762 #
DE94-006219 ..... p 3895 N94-31307 #
DE94-006221 ..... p 3956 N94-31308 #
DE94-006222 ..... p 3898 N94-31628 #
DE94-006224 ..... p 3899 N94-31916 #
DE94-006225 ..... p 3845 N94-31763 #
DE94-006231 ..... p 3797 N94-32732 #
DE94-006234 ..... p 3834 N94-32175 #
DE94-006235 ..... p 3774 N94-32736 #
DE94-006243 ..... p 3786 N94-32937 #
DE94-006248 ..... p 3656 N94-32103 #
DE94-006250 ..... p 3899 N94-31633 #
DE94-006252 ..... p 3898 N94-31631 #
DE94-006288 ..... p 3953 N94-31632 #
DE94-006290 ..... p 3899 N94-31634 #
DE94-006292 ..... p 3955 N94-31635
DE94-006298 ..... p 3712 N94-31629 #
DE94-006313 ..... p 3898 N94-31630 #
DE94-006315 ..... p 3867 N94-31779 #
DE94-006317 ..... p 3652 N94-31780 #
DE94-006333 ..... p 3675 N94-31781 #
DE94-006343 ..... p 3905 N94-32770
DE94-006361 ..... p 3688 N94-31483 #
DE94-006367 ..... p 3901 N94-32104 #
DE94-006368 ..... p 3811 N94-31484 #
DE94-006372 ..... p 3715 N94-31485 #
DE94-006391 ..... p 3934 N94-31782 #
DE94-006400 ..... p 3712 N94-31783 #
DE94-006404 ..... p 3675 N94-31784 #
DE94-006426 ..... p 3691 N94-31785 #
DE94-006439 ..... p 3925 N94-31788 #
DE94-006467 ..... p 3666 N94-31827 #
DE94-006472 ..... p 3638 N94-32840 #
DE94-006486 ..... p 3901 N94-32176 #
DE94-006491 ..... p 3841 N94-31309 #
DE94-006495 ..... p 3874 N94-32804 #
DE94-006504 ..... p 3889 N94-31787 #
DE94-006513 ..... p 3888 N94-31664 #
DE94-006537 ..... p 3864 N94-31310 #
DE94-006538 ..... p 3841 N94-31311 #
DE94-006539 ..... p 3844 N94-31665
DE94-006540 ..... p 3641 N94-31666 #
DE94-006541 ..... p 3641 N94-31486 #
DE94-006542 ..... p 3643 N94-32109
DE94-006544 ..... p 3875 N94-31488 #
DE94-006550 ..... p 3739 N94-32771
DE94-006551 ..... p 3896 N94-31489 #
DE94-006555 ..... p 3870 N94-32177 #
DE94-006556 ..... p 3896 N94-31501 #
DE94-006557 ..... p 3733 N94-31312 #
DE94-006559 ..... p 3618 N94-31313 #
DE94-006560 ..... p 3640 N94-31314 #
DE94-006578 ..... p 3690 N94-31594
DE94-006588 ..... p 3897 N94-31502 #
DE94-006589 ..... p 3902 N94-32296 #
DE94-006590 ..... p 3666 N94-31579 #
DE94-006591 ..... p 3634 N94-32110
DE94-006593 ..... p 3692 N94-32111 #
DE94-006594 ..... p 3692 N94-32112
DE94-006598 ..... p 3870 N94-32178 #
DE94-006606 ..... p 3640 N94-31345 #
DE94-006607 ..... p 3678 N94-32113
DE94-006613 ..... p 3715 N94-31580 #
DE94-006614 ..... p 3666 N94-32114
DE94-006615 ..... p 3679 N94-32188 #
DE94-006622 ..... p 3641 N94-31581 #
DE94-006632 ..... p 3633 N94-31493 #
DE94-006638 ..... p 3763 N94-31347 #
DE94-006653 ..... p 3926 N94-32189 #
DE94-006656 ..... p 3888 N94-31667 #
DE94-006659 ..... p 3901 N94-32115
DE94-006660 ..... p 3904 N94-32634 #
DE94-006661 ..... p 3774 N94-32772 #
DE94-006662 ..... p 3632 N94-31349 #
DE94-006666 ..... p 3632 N94-31352 #
DE94-006669 ..... p 3920 N94-32635 #
DE94-006677 ..... p 3763 N94-31582 #
DE94-006692 ..... p 3807 N94-32147 #
DE94-006731 ..... p 3714 N94-31269 #
DE94-006732 ..... p 3863 N94-31270 #
DE94-006733 ..... p 3667 N94-32148 #
DE94-006734 ..... p 3656 N94-32116
DE94-006737 ..... p 3866 N94-31668 #
DE94-006744 ..... p 3878 N94-31271 #
DE94-006752 ..... p 3706 N94-32149 #
DE94-006759 ..... p 3759 N94-31272 #
DE94-006760 ..... p 3667 N94-32150 #
DE94-006770 ..... p 3668 N94-32132 #
DE94-006772 ..... p 3886 N94-31273 #
DE94-006774 ..... p 3667 N94-32133 #
DE94-006805 ..... p 3717 N94-32134 #
DE94-006810 ..... p 3841 N94-31274 #
DE94-006832 ..... p 3722 N94-31319 #
DE94-006834 ..... p 3864 N94-31320 #
DE94-006837 ..... p 3864 N94-31321 #
DE94-006839 ..... p 3781 N94-31322 #
DE94-006849 ..... p 3872 N94-32627
DE94-006850 ..... p 3866 N94-31669 #
DE94-006853 ..... p 3762 N94-32763 #
DE94-006855 ..... p 3905 N94-32764 #
DE94-006856 ..... p 3762 N94-32765 #
DE94-006951 ..... p 3868 N94-31670 #
DE94-006953 ..... p 3867 N94-31671 #
DE94-006985 ..... p 3871 N94-32375 #
DE94-006987 ..... p 3651 N94-31672 #
DE94-006998 ..... p 3747 N94-32249
DE94-006999 ..... p 3646 N94-32805 #
DE94-007014 ..... p 3646 N94-32782 #
DE94-007028 ..... p 3716 N94-31636 #
DE94-007030 ..... p 3636 N94-32376 #
DE94-007031 ..... p 3870 N94-32250 #
DE94-007032 ..... p 3866 N94-31637 #
DE94-007033 ..... p 3641 N94-31638 #
DE94-007036 ..... p 3643 N94-32064
DE94-007039 ..... p 3857 N94-31639 #
DE94-007042 ..... p 3795 N94-31323 #
DE94-007043 ..... p 3864 N94-31405 #
DE94-007055 ..... p 3889 N94-31809 #
DE94-007060 ..... p 3657 N94-32377 #
DE94-007061 ..... p 3827 N94-32683
DE94-007063 ..... p 3872 N94-32628 #
DE94-007072 ..... p 3695 N94-32688
DE94-007077 ..... p 3719 N94-32629 #
DE94-007078 ..... p 3887 N94-31406 #
DE94-007094 ..... p 3938 N94-32503 #
DE94-007095 ..... p 3873 N94-32689
DE94-007096 ..... p 3872 N94-32630 #
DE94-007108 ..... p 3886 N94-31366 #
DE94-007109 ..... p 3891 N94-32631 #
DE94-007110 ..... p 3720 N94-32684
DE94-007111 ..... p 3876 N94-32685
DE94-007112 ..... p 3891 N94-32664 #
DE94-007113 ..... p 3887 N94-31396 #
DE94-007114 ..... p 3891 N94-32686
DE94-007120 ..... p 3660 N94-32687
DE94-007122 ..... p 3858 N94-31397 #
DE94-007123 ..... p 3896 N94-31499 #
DE94-007124 ..... p 3955 N94-32129 #
DE94-007125 ..... p 3645 N94-32636
DE94-007132 ..... p 3659 N94-32618 #
DE94-007141 ..... p 3626 N94-32665 #
DE94-007143 ..... p 3738 N94-32637
DE94-007168 ..... p 3939 N94-33147
DE94-007178 ..... p 3938 N94-32638
DE94-007179 ..... p 3864 N94-31398 #
DE94-007184 ..... p 3738 N94-32639
DE94-007192 ..... p 3842 N94-31399 #
DE94-007208 ..... p 3659 N94-32640
DE94-007211 ..... p 3909 N94-33271 #
DE94-007212 ..... p 3891 N94-32619 #
DE94-007219 ..... p 3872 N94-32666 #
DE94-007221 ..... p 3819 N94-32641
DE94-007222 ..... p 3807 N94-32783 #
DE94-007224 ..... p 3636 N94-32251 #
DE94-007226 ..... p 3767 N94-32784 #
DE94-007229 ..... p 3611 N94-32667 #
DE94-007230 ..... p 3905 N94-32785 #
DE94-007232 ..... p 3915 N94-32723 #
DE94-007240 ..... p 3718 N94-32252 #
DE94-007242 ..... p 3887 N94-31400 #
DE94-007245 ..... p 3904 N94-32724 #
DE94-007250 ..... p 3609 N94-31382 #
DE94-007258 ..... p 3900 N94-32065 #
DE94-007259 ..... p 3646 N94-32795 #
DE94-007291 ..... p 3696 N94-32786 #
DE94-007293 ..... p 3835 N94-32787 #
DE94-007295 ..... p 3661 N94-32796 #
DE94-007300 ..... p 3625 N94-32642 #
DE94-007371 ..... p 3890 N94-32201 #
DE94-007373 ..... p 3886 N94-31324 #
DE94-007374 ..... p 3718 N94-32202 #
DE94-007376 ..... p 3696 N94-32809 #
DE94-007377 ..... p 3737 N94-32135
DE94-007380 ..... p 3694 N94-32593 #
DE94-007403 ..... p 3636 N94-32594
DE94-007415 ..... p 3747 N94-32203 #
DE94-007428 ..... p 3891 N94-32595 #
DE94-007429 ..... p 3891 N94-32611 #
DE94-007430 ..... p 3891 N94-32612 #
DE94-007431 ..... p 3892 N94-32810 #
DE94-007434 ..... p 3615 N94-32266
DE94-007441 ..... p 3904 N94-32606 #
DE94-007443 ..... p 3692 N94-32136 #
DE94-007445 ..... p 3873 N94-32768 #
DE94-007449 ..... p 3793 N94-32267 #
DE94-007450 ..... p 3640 N94-31325 #
DE94-007452 ..... p 3938 N94-32137 #
DE94-007457 ..... p 3829 N94-31315 #
DE94-007460 ..... p 3694 N94-32607
DE94-007463 ..... p 3727 N94-32758 #
DE94-007464 ..... p 3871 N94-32605
DE94-007466 ..... p 3733 N94-31316 #
DE94-007469 ..... p 3785 N94-32268 #
DE94-007470 ..... p 3713 N94-32811 #
DE94-007472 ..... p 3914 N94-32910 #
DE94-007479 ..... p 3786 N94-32759 #
DE94-007481 ..... p 3768 N94-32812 #
DE94-007482 ..... p 3804 N94-32596
DE94-007495 ..... p 3880 N94-32138
DE94-007523 ..... p 3870 N94-32355
DE94-007525 ..... p 3793 N94-32269 #
DE94-007527 ..... p 3903 N94-32597
DE94-007542 ..... p 3718 N94-32270 #
DE94-007545 ..... p 3720 N94-32760 #
DE94-007546 ..... p 3720 N94-32761 #
DE94-007549 ..... p 3611 N94-32813
DE94-007552 ..... p 3870 N94-32271 #
DE94-007557 ..... p 3869 N94-32139 #
DE94-007558 ..... p 3761 N94-32762 #
DE94-007564 ..... p 3637 N94-32743 #
DE94-007565 ..... p 3852 N94-32744 #
DE94-007566 ..... p 3826 N94-32356 #
DE94-007568 ..... p 3682 N94-32745 #
DE94-007576 ..... p 3768 N94-32814

DE94-007579 ..... p 3904 N94-32746 #
DE94-007605 ..... p 3872 N94-32643
DE94-007607 ..... p 3635 N94-32140 #
DE94-007609 ..... p 3905 N94-32747 #
DE94-007610 ..... p 3872 N94-32644
DE94-007623 ..... p 3871 N94-32598
DE94-007634 ..... p 3819 N94-32599 #
DE94-007642 ..... p 3826 N94-32357 #
DE94-007647 ..... p 3765 N94-32600 #
DE94-007649 ..... p 3905 N94-32815 #
DE94-007671 ..... p 3672 N94-31317 #
DE94-007684 ..... p 3904 N94-32601 #
DE94-007686 ..... p 3904 N94-32602 #
DE94-007694 ..... p 3904 N94-32645 #
DE94-007695 ..... p 3869 N94-32141 #
DE94-007698 ..... p 3657 N94-32358 #
DE94-007700 ..... p 3903 N94-32372 #
DE94-007701 ..... p 3827 N94-32646 #
DE94-007723 ..... p 3653 N94-31917
DE94-007725 ..... p 3774 N94-32647 #
DE94-007733 ..... p 3774 N94-32816 #
DE94-007734 ..... p 3761 N94-32383 #
DE94-007737 ..... p 3761 N94-32648 #
DE94-007738 ..... p 3882 N94-32649 #
DE94-007740 ..... p 3903 N94-32384 #
DE94-007743 ..... p 3695 N94-32650 #
DE94-007744 ..... p 3920 N94-32808 #
DE94-007745 ..... p 3881 N94-32385 #
DE94-007757 ..... p 3650 N94-31354 #
DE94-007765 ..... p 3727 N94-32778
DE94-007844 ..... p 3819 N94-32651
DE94-007846 ..... p 3768 N94-32817
DE94-007847 ..... p 3708 N94-32652
DE94-007855 ..... p 3693 N94-32386 #
DE94-007858 ..... p 3707 N94-32373 #
DE94-007859 ..... p 3849 N94-32653 #
DE94-007860 ..... p 3883 N94-32818
DE94-007915 ..... p 3642 N94-31918 #
DE94-007921 ..... p 3719 N94-32654 #
DE94-007929 ..... p 3644 N94-32374 #
DE94-007930 ..... p 3719 N94-32613 #
DE94-007932 ..... p 3719 N94-32603 #
DE94-007934 ..... p 3661 N94-32819 #
DE94-007937 ..... p 3695 N94-32700 #
DE94-007951 ..... p 3761 N94-32701 #
DE94-007961 ..... p 3877 N94-32748
DE94-007971 ..... p 3660 N94-32698 #
DE94-007977 ..... p 3691 N94-31919 #
DE94-007980 ..... p 3646 N94-32699 #
DE94-007984 ..... p 3819 N94-32749 #
DE94-008004 ..... p 3658 N94-32408 #
DE94-008039 ..... p 3766 N94-32703 #
DE94-008050 ..... p 3720 N94-32704 #
DE94-008053 ..... p 3767 N94-32750 #
DE94-008054 ..... p 3645 N94-32614
DE94-008064 ..... p 3761 N94-32705 #
DE94-008075 ..... p 3713 N94-32706 #
DE94-008096 ..... p 3654 N94-31976 #
DE94-008105 ..... p 3871 N94-32615
DE94-008106 ..... p 3636 N94-32616
DE94-008107 ..... p 3720 N94-32707 #
DE94-008108 ..... p 3873 N94-32708 #
DE94-008112 ..... p 3708 N94-32709 #
DE94-008113 ..... p 3903 N94-32409 #
DE94-008117 ..... p 3873 N94-32710 #
DE94-008132 ..... p 3905 N94-32779 #
DE94-008134 ..... p 3873 N94-32797 #
DE94-008135 ..... p 3661 N94-32798 #
DE94-008138 ..... p 3659 N94-32617
DE94-008179 ..... p 3905 N94-32799 #
DE94-008191 ..... p 3892 N94-32800 #
DE94-008216 ..... p 3637 N94-32801 #
DE94-008217 ..... p 3661 N94-32751
DE94-008219 ..... p 3825 N94-31920 #
DE94-008220 ..... p 3652 N94-31764 #
DE94-008224 ..... p 3877 N94-32802 #
DE94-008231 ..... p 3661 N94-32803 #
DE94-008234 ..... p 3767 N94-32752 #
DE94-008261 ..... p 3707 N94-32410 #
DE94-008271 ..... p 3873 N94-32780 #
DE94-008275 ..... p 3646 N94-32781 #
DE94-008279 ..... p 3892 N94-32838 #
DE94-008282 ..... p 3669 N94-32839 #
DE94-008291 ..... p 3720 N94-32753 #
DE94-008292 ..... p 3903 N94-32411 #
DE94-008293 ..... p 3646 N94-32754
DE94-008294 ..... p 3873 N94-32755 #
DE94-008295 ..... p 3662 N94-32855 #
DE94-008298 ..... p 3682 N94-32756 #
DE94-008301 ..... p 3661 N94-32847 #
DE94-008303 ..... p 3913 N94-32824 #
DE94-008310 ..... p 3888 N94-31765 #
DE94-008312 ..... p 3668 N94-32412
DE94-008341 ..... p 3646 N94-32825 #
DE94-008343 ..... p 3892 N94-32820 #
DE94-008348 ..... p 3907 N94-32990
DE94-008351 ..... p 3718 N94-32413 #
DE94-008352 ..... p 3637 N94-32826 #
DE94-008382 ..... p 3636 N94-32414 #
DE94-008388 ..... p 3876 N94-32407 #
DE94-008420 ..... p 3890 N94-32415 #
DE94-008433 ..... p 3907 N94-32963
DE94-008439 ..... p 3908 N94-32991 #
DE94-008444 ..... p 3644 N94-32416 #
DE94-008446 ..... p 3836 N94-32992 #
DE94-008449 ..... p 3871 N94-32512 #
DE94-008451 ..... p 3912 N94-32513 #
DE94-008459 ..... p 3906 N94-32875
DE94-008467 ..... p 3874 N94-32876 #
DE94-008477 ..... p 3645 N94-32514 #
DE94-008480 ..... p 3647 N94-32964 #
DE94-008484 ..... p 3648 N94-32993 #
DE94-008487 ..... p 3871 N94-32515 #
DE94-008490 ..... p 3907 N94-32989 #
DE94-008494 ..... p 3659 N94-32632
DE94-008503 ..... p 3793 N94-32516 #
DE94-008508 ..... p 3661 N94-32788 #
DE94-008514 ..... p 3920 N94-32827 #
DE94-008515 ..... p 3696 N94-32828 #
DE94-008517 ..... p 3658 N94-32517 #
DE94-008519 ..... p 3659 N94-32655
DE94-008532 ..... p 3883 N94-32994 #
DE94-008535 ..... p 3907 N94-32933 #
DE94-008551 ..... p 3659 N94-32656
DE94-008552 ..... p 3658 N94-32518 #
DE94-008554 ..... p 3890 N94-32519 #
DE94-008586 ..... p 3890 N94-32520 #
DE94-008587 ..... p 3659 N94-32657
DE94-008588 ..... p 3889 N94-31766 #
DE94-008616 ..... p 3883 N94-32878
DE94-008642 ..... p 3694 N94-32521 #
DE94-008653 ..... p 3877 N94-32879 #
DE94-008670 ..... p 3790 N94-32881
DE94-008671 ..... p 3768 N94-32882
DE94-008685 ..... p 3906 N94-32884
DE94-008687 ..... p 3645 N94-32522 #
DE94-008706 ..... p 3694 N94-32582 #
DE94-008711 ..... p 3638 N94-32886
DE94-008713 ..... p 3638 N94-32887 #
DE94-008719 ..... p 3638 N94-32888 #
DE94-008723 ..... p 3638 N94-32889 #
DE94-008727 ..... p 3794 N94-32890 #
DE94-008729 ..... p 3667 N94-32583 #
DE94-008736 ..... p 3662 N94-32891
DE94-008786 ..... p 3647 N94-32892 #
DE94-008827 ..... p 3763 N94-32965
DE94-008832 ..... p 3769 N94-32966 #
DE94-008880 ..... p 3873 N94-32757 #
DE94-008888 ..... p 3639 N94-33260 #
DE94-008890 ..... p 3818 N94-32584 #
DE94-008927 ..... p 3875 N94-33189 #
DE94-008930 ..... p 3874 N94-32841 #
DE94-008944 ..... p 3696 N94-32806 #
DE94-008948 ..... p 3739 N94-32842
DE94-008958 ..... p 3906 N94-32843 #
DE94-008961 ..... p 3877 N94-32844 #
DE94-008970 ..... p 3818 N94-32585 #
DE94-008986 ..... p 3876 N94-32586 #
DE94-008987 ..... p 3871 N94-32587 #
DE94-008994 ..... p 3876 N94-32588 #
DE94-009014 ..... p 3721 N94-32845 #
DE94-009021 ..... p 3913 N94-32846
DE94-009027 ..... p 3875 N94-33278
DE94-009030 ..... p 3721 N94-32848
DE94-009038 ..... p 3708 N94-32849
DE94-009064 ..... p 3857 N94-32589 #
DE94-009082 ..... p 3713 N94-32821 #
DE94-009083 ..... p 3906 N94-32822 #
DE94-009089 ..... p 3874 N94-32807 #
DE94-009096 ..... p 3907 N94-32934
DE94-009118 ..... p 3807 N94-32766 #
DE94-009129 ..... p 3637 N94-32767
DE94-009164 ..... p 3874 N94-32850 #
DE94-009167 ..... p 3647 N94-32851
DE94-009178 ..... p 3647 N94-32852
DE94-009205 ..... p 3892 N94-32911 #
DE94-009206 ..... p 3893 N94-32922
DE94-009207 ..... p 3893 N94-32912 #
DE94-009293 ..... p 3906 N94-32913 #
DE94-009297 ..... p 3662 N94-32935
DE94-009373 ..... p 3938 N94-32914 #
DE94-009391 ..... p 3648 N94-33270
DE94-009466 ..... p 3893 N94-32915 #
DE94-606492 ..... p 3869 N94-32097 #
DE94-608122 ..... p 3910 N94-31052
DE94-608140 ..... p 3902 N94-32247
DE94-608388 ..... p 3896 N94-31395
DE94-721996 ..... p 3760 N94-31767 #
DE94-722023 ..... p 3765 N94-32590 #
DE94-757268 ..... p 3893 N94-32916 #
DE94-757270 ..... p 3697 N94-32917
DE94-757271 ..... p 3762 N94-32918
DE94-757272 ..... p 3762 N94-32919
DE94-757291 ..... p 3769 N94-32920

DM-66 ..... p 3700 N94-31221 #

DODA-AR-006-666 ..... p 3580 N94-32362
DODA-AR-006-924 ..... p 3580 N94-32263
DODA-AR-008-135 ..... p 3826 N94-32274
DODA-AR-008-157 ..... p 3879 N94-32013
DODA-AR-008-409 ..... p 3624 N94-32265
DODA-AR-008-410 ..... p 3580 N94-32264
DODA-AR-008-614 ..... p 3818 N94-32390
DODA-AR-008-616 ..... p 3580 N94-32378
DODA-AR-008-886 ..... p 3788 N94-32066

DOE/AL-44658/T2 ..... p 3631 N94-31153 #

DOE/CE-15974/T7 ..... p 3661 N94-32788 #
DOE/CE-23810/14 ..... p 3658 N94-32518 #
DOE/CE-23810/33C ..... p 3653 N94-31917
DOE/CE-90053/T62 ..... p 3761 N94-32701 #

DOE/CH-10093/257 ..... p 3761 N94-32725 #
DOE/CH-10093/264 ..... p 3758 N94-31235

DOE/ER-13421/10 ..... p 3714 N94-31200 #
DOE/ER-13442/8 ..... p 3636 N94-32594
DOE/ER-13480/4 ..... p 3635 N94-32140 #
DOE/ER-13590/13 ..... p 3872 N94-32643
DOE/ER-13714/T2 ..... p 3872 N94-32644
DOE/ER-13774/4 ..... p 3646 N94-32805 #
DOE/ER-13822/7 ..... p 3706 N94-32149 #
DOE/ER-13832/36 ..... p 3661 N94-32847 #
DOE/ER-13989/4 ..... p 3794 N94-32890 #
DOE/ER-14053/T5 ..... p 3633 N94-31493 #
DOE/ER-14114/3 ..... p 3651 N94-31672 #
DOE/ER-14162/3 ..... p 3871 N94-32375 #
DOE/ER-14304/1 ..... p 3889 N94-31766 #
DOE/ER-14321/T2 ..... p 3638 N94-32887 #
DOE/ER-14333/1 ..... p 3637 N94-32826 #
DOE/ER-14340/1 ..... p 3718 N94-32413 #
DOE/ER-20022/T1 ..... p 3793 N94-32267 #
DOE/ER-25048/T8 ..... p 3836 N94-32992 #
DOE/ER-25145/T1 ..... p 3707 N94-32410 #
DOE/ER-40141/T1 ..... p 3875 N94-31488 #
DOE/ER-40446/6 ..... p 3869 N94-32173 #
DOE/ER-40606/3 ..... p 3939 N94-33147
DOE/ER-40690/2 ..... p 3876 N94-31505 #
DOE/ER-40711/T1 ..... p 3876 N94-32407 #
DOE/ER-40736/1 ..... p 3866 N94-31620 #
DOE/ER-40757/020 ..... p 3913 N94-32824 #
DOE/ER-40757/322 ..... p 3871 N94-32512 #
DOE/ER-45197/8 ..... p 3912 N94-32513 #
DOE/ER-45230/T2 ..... p 3907 N94-32933 #
DOE/ER-45231/8 ..... p 3905 N94-32770
DOE/ER-45245/T2 ..... p 3908 N94-32991 #
DOE/ER-45271/T7 ..... p 3649 N94-31201 #
DOE/ER-45287/6 ..... p 3640 N94-31325 #
DOE/ER-45372/6 ..... p 3659 N94-32656
DOE/ER-45415/T1 ..... p 3905 N94-32799 #
DOE/ER-45429/T1 ..... p 3633 N94-31526 #
DOE/ER-45482/1 ..... p 3659 N94-32657
DOE/ER-51116/T4 ..... p 3892 N94-32820 #
DOE/ER-53207/10 ..... p 3889 N94-31787 #
DOE/ER-53222/T3 ..... p 3888 N94-31664 #
DOE/ER-53243/5 ..... p 3892 N94-32800 #
DOE/ER-53244/20 ..... p 3887 N94-31558 #
DOE/ER-53266/46 ..... p 3888 N94-31619 #
DOE/ER-54212/1 ..... p 3890 N94-32520 #
DOE/ER-60522/7 ..... p 3793 N94-32516 #
DOE/ER-60983/3 ..... p 3763 N94-31347 #
DOE/ER-61010/T22 ..... p 3767 N94-32712 #
DOE/ER-61071/3 ..... p 3785 N94-32716 #
DOE/ER-61072/6 ..... p 3764 N94-31601 #
DOE/ER-61072/8 ..... p 3764 N94-31602 #
DOE/ER-61073/3 ..... p 3764 N94-31600
DOE/ER-61364/2 ..... p 3785 N94-32717 #
DOE/ER-69017/5 ..... p 3767 N94-32711 #

DOE/ET-53088/631 ..... p 3886 N94-31366 #
DOE/ET-53088/634 ..... p 3891 N94-32631 #
DOE/ET-53088/635 ..... p 3720 N94-32684
DOE/ET-53088/636 ..... p 3876 N94-32685
DOE/ET-53088/637 ..... p 3891 N94-32664 #
DOE/ET-53088/639 ..... p 3887 N94-31396 #
DOE/ET-53088/646 ..... p 3891 N94-32686

DOE/HR-0066 ..... p 3915 N94-32723 #

DOE/ID-12869/3 ..... p 3668 N94-31604 #
DOE/ID-13103/T1 ..... p 3646 N94-32782 #

DOE/MC-20422/94/C0315 ..... p 3742 N94-31504 #
DOE/MC-27225/3625 ..... p 3760 N94-31811 #
DOE/MC-29227/3588 ..... p 3759 N94-31487 #
DOE/MC-29237/3512 ..... p 3762 N94-32823 #

DOE/MC-29267/94/C0314 ..... p 3771 N94-31525 #

DOE/NASA/50306-4 ..... p 3617 N94-32941 * #

DOE/NE-0001P ..... p 3877 N94-32879 #

DOE/NV-10845/31 ..... p 3743 N94-31603 #

DOE/PC-79672/T8 ..... p 3886 N94-31273 #
DOE/PC-79812/T17 ..... p 3638 N94-32886
DOE/PC-90043/T12 ..... p 3666 N94-32132 #
DOE/PC-90044/12 ..... p 3667 N94-32133 #
DOE/PC-90046/T8 ..... p 3667 N94-32583 #
DOE/PC-90056/T13 ..... p 3638 N94-32889 #
DOE/PC-91030/T7 ..... p 3637 N94-32767
DOE/PC-92104/T3 ..... p 3667 N94-32150 #
DOE/PC-92109/T3 ..... p 3638 N94-32888 #
DOE/PC-92110/T4 ..... p 3759 N94-31272 #
DOE/PC-92521/T97 ..... p 3766 N94-32703 #
DOE/PC-92539/5 ..... p 3636 N94-32414 #
DOE/PC-92542/T4 ..... p 3658 N94-32408 #

DOE/SF-18862/T2-APP-A ..... p 3890 N94-32415 #
DOE/SF-18862/T2 ..... p 3876 N94-32731 #
DOE/SF-19645/T3 ..... p 3646 N94-32825 #
DOE/SF-19645/T4 ..... p 3644 N94-32416 #

DOT-VNTSC-FAA-93-12 ..... p 3578 N94-31078 #
DOT-VNTSC-FAA-93-17 ..... p 3576 N94-31680
DOT-VNTSC-FAA-93-21-CD ..... p 3805 N94-33171
DOT-VNTSC-FAA-93-21 ..... p 3583 N94-33280 #
DOT-VNTSC-FAA-93-8 ..... p 3579 N94-32015 #
DOT-VNTSC-FAA-94-3 ..... p 3861 N94-32418 #

DOT/FAA/ASC-93-1 ..... p 3575 N94-32620 #

DOT/FAA/CT-TN92/39 ..... p 3566 N94-32157 #
DOT/FAA/CT-TN93/50 ..... p 3588 N94-32120 #
DOT/FAA/CT-TN94/1 ..... p 3576 N94-32955 #

DOT/FAA/CT-92/14 ..... p 3574 N94-31246 #
DOT/FAA/CT-93/43 ..... p 3644 N94-32237 #
DOT/FAA/CT-93/74 ..... p 3578 N94-31078 #
DOT/FAA/CT-94/02 ..... p 3787 N94-33065 * #
DOT/FAA/CT-94/10 ..... p 3579 N94-32015 #

DOT/FAA/EE-94-01 ..... p 3861 N94-32418 #

DOT/FAA/RD-93/17 ..... p 3576 N94-31680
DOT/FAA/RD-93/40-VOL-1 ..... p 3582 N94-33076 #
DOT/FAA/RD-93/40-VOL-2 ..... p 3582 N94-33077 #
DOT/FAA/RD-93/40-VOL-3 ..... p 3582 N94-33078 #
DOT/FAA/RD-93/40-VOL-4 ..... p 3583 N94-33079 #
DOT/FAA/RD-93/42-CD ..... p 3805 N94-33171
DOT/FAA/RD-93/42 ..... p 3583 N94-33280 #

DREA-TC-93-305-VOL-1 ..... p 3836 N94-33149

DREO-TN-93-20 ..... p 3671 N94-31253
DREO-TN-93-21 ..... p 3841 N94-31252
DREO-TN-93-36 ..... p 3714 N94-31255

DREO-1175 ..... p 3670 N94-31063 #
DREO-1193-PT-2 ..... p 3670 N94-31062 #
DREO-1194 ..... p 3671 N94-31254

DREP-CRS-93-15 ..... p 3642 N94-31871

DREP-LN-93-26 ..... p 3730 N94-31872

DSIS-92-03143 ..... p 3795 N94-31738
DSIS-93-00343 ..... p 3853 N94-33335
DSIS-93-02664-VOL-1 ..... p 3836 N94-33149
DSIS-94-01061 ..... p 3730 N94-31872
DSIS-94-01083 ..... p 3575 N94-31902
DSIS-94-01128 ..... p 3642 N94-31871
DSIS-94-01186 ..... p 3735 N94-31849
DSIS-94-01221 ..... p 3577 N94-32505
DSIS-94-01381 ..... p 3581 N94-31903
DSIS-94-01503 ..... p 3879 N94-31850
DSIS-94-01590 ..... p 3621 N94-31892

D495-69756-1 ..... p 3611 N94-32898 * #

E-6627 ..... p 3669 N94-32861 * #
E-6834 ..... p 3728 N94-32893 * #
E-6944 ..... p 3626 N94-32858 * #
E-6966 ..... p 3739 N94-32883 * #
E-8167 ..... p 3732 N94-33038 * #
E-8168 ..... p 3728 N94-32902 * #
E-8187 ..... p 3567 N94-33046 * #
E-8297 ..... p 3638 N94-32948 * #
E-8341 ..... p 3617 N94-32941 * #
E-8401 ..... p 3614 N94-31618 * #
E-8487 ..... p 3567 N94-33064 * #
E-8493 ..... p 3739 N94-32735 * #
E-8514 ..... p 3615 N94-32742 * #
E-8613 ..... p 3728 N94-32929 * #
E-8645 ..... p 3647 N94-32931 * #
E-8667 ..... p 3603 N94-33291 * #
E-8671 ..... p 3728 N94-32900 * #
E-8672 ..... p 3616 N94-33099 * #
E-8678 ..... p 3573 N94-33119 * #
E-8679 ..... p 3740 N94-32932 * #
E-8686 ..... p 3710 N94-32969 * #
E-8690 ..... p 3709 N94-32947 * #
E-8693 ..... p 3571 N94-32475 * #
E-8697 ..... p 3617 N94-33021 * #
E-8701 ..... p 3572 N94-32926 * #
E-8702 ..... p 3700 N94-31229 * #
E-8703 ..... p 3573 N94-32984 * #
E-8704 ..... p 3662 N94-32945 * #
E-8705 ..... p 3626 N94-32904 * #
E-8706 ..... p 3584 N94-32075 * #
E-8707 ..... p 3728 N94-32979 * #
E-8714 ..... p 3727 N94-32741 * #
E-8723 ..... p 3616 N94-32970 * #
E-8727 ..... p 3883 N94-32777 * #
E-8743 ..... p 3696 N94-32905 * #
E-8749 ..... p 3698 N94-33116 * #
E-8801 ..... p 3697 N94-33052 * #
E-8849 ..... p 3731 N94-32901 * #
E-8851 ..... p 3820 N94-32773 * #
E-8858 ..... p 3713 N94-32983 * #
E-8859 ..... p 3617 N94-33022 * #
E-8870 ..... p 3731 N94-33032 * #
E-8875 ..... p 3850 N94-33120 * #
E-8877 ..... p 3710 N94-33070 * #
E-8878 ..... p 3663 N94-33024 * #
E-8880 ..... p 3726 N94-32272 * #

ECL-89-03 ..... p 3886 N94-31378
ECL-91-01 ..... p 3585 N94-31677 #
ECL-91-39 ..... p 3619 N94-31377 #
ECL-92-49 ..... p 3734 N94-31562 #
ECL-92-50 ..... p 3735 N94-31870
ECL-92-56 ..... p 3733 N94-31376

ECS-LFCS-93-275 ..... p 3848 N94-32292

EFD-003 ..... p 3701 N94-31341 #

EGG-EP-10948 ..... p 3920 N94-32827 #
EGG-EP-10949 ..... p 3694 N94-32521 #
EGG-EP-10999 ..... p 3696 N94-32828 #

EGG-SCM-10713 ..... p 3658 N94-32517 #
EGG-SCM-10804 ..... p 3659 N94-32655

EGG-11265-2021 ..... p 3713 N94-32728 #
EGG-11265-2040 ..... p 3901 N94-32176 #

EML-558 ..... p 3727 N94-32758 #

EOARD-TR-94-03 ..... p 3903 N94-32322

ERDEC-TR-086 ..... p 3656 N94-32253
ERDEC-TR-111 ..... p 3746 N94-31999 #
ERDEC-TR-127 ..... p 3878 N94-31340 #
ERDEC-TR-134 ..... p 3763 N94-31339 #

ERIM-251600-4-F ..... p 3788 N94-32284 #
ERIM-253860-1-X(R) ..... p 3609 N94-31292 #

ERL-0593-RN ..... p 3580 N94-32263
ERL-0692-RR ..... p 3826 N94-32274

ERP-1126 ..... p 3784 N94-32117 #
ERP-1128 ..... p 3773 N94-32118
ERP-1133 ..... p 3680 N94-32297 #
ERP-1139 ..... p 3678 N94-32159
ERP-1140 ..... p 3678 N94-32158 #
ERP-1141 ..... p 3680 N94-32300 #
ERP-1142 ..... p 3676 N94-31998 #
ERP-1143 ..... p 3680 N94-32299 #
ERP-1144 ..... p 3680 N94-32298 #
ERP-1145 ..... p 3685 N94-33347
ERP-1146 ..... p 3677 N94-32083 #

ESA-PSS-03-401-ISSUE-1 ..... p 3802 N94-31224 #
ESA-PSS-05-11-ISSUE-1 ..... p 3809 N94-31223 #

ESA-SP-1166 ..... p 3670 N94-31182 #
ESA-SP-1167 ..... p 3914 N94-31181 #
ESA-SP-360 ..... p 3743 N94-31853 #

ESC-TR-93-200 ..... p 3818 N94-32508
ESC-TR-93-237 ..... p 3681 N94-32285

ESDP-4124344 ..... p 3741 N94-31606 #

ETN-93-94691 ..... p 3698 N94-33169

ETN-93-94845 ..... p 3922 N94-32856 #
ETN-94-94728 ..... p 3827 N94-33002
ETN-94-95568 ..... p 3598 N94-31208
ETN-94-95615 ..... p 3916 N94-31175
ETN-94-95647 ..... p 3916 N94-31365 #
ETN-94-95716 ..... p 3917 N94-31415 #
ETN-94-95724 ..... p 3832 N94-31826 #
ETN-94-95726 ..... p 3699 N94-31185
ETN-94-95730 ..... p 3689 N94-31571
ETN-94-95731 ..... p 3888 N94-31572
ETN-94-95732 ..... p 3674 N94-31573
ETN-94-95733 ..... p 3633 N94-31574
ETN-94-95734 ..... p 3689 N94-31575
ETN-94-95735 ..... p 3689 N94-31576
ETN-94-95736 ..... p 3812 N94-31577
ETN-94-95737 ..... p 3674 N94-31608
ETN-94-95738 ..... p 3829 N94-31372 #
ETN-94-95739 ..... p 3687 N94-31373
ETN-94-95740 ..... p 3690 N94-31609
ETN-94-95741 ..... p 3688 N94-31374
ETN-94-95742 ..... p 3898 N94-31610
ETN-94-95743 ..... p 3733 N94-31375 #
ETN-94-95744 ..... p 3803 N94-31852
ETN-94-95745 ..... p 3764 N94-31611
ETN-94-95746 ..... p 3898 N94-31612
ETN-94-95747 ..... p 3866 N94-31613 #
ETN-94-95749 ..... p 3866 N94-31614 #
ETN-94-95750 ..... p 3674 N94-31615 #
ETN-94-95751 ..... p 3865 N94-31511 #
ETN-94-95752 ..... p 3887 N94-31512
ETN-94-95753 ..... p 3851 N94-31513
ETN-94-95754 ..... p 3830 N94-31514 #
ETN-94-95755 ..... p 3711 N94-31515 #
ETN-94-95756 ..... p 3865 N94-31516 #
ETN-94-95757 ..... p 3858 N94-31560 #
ETN-94-95758 ..... p 3715 N94-31561 #
ETN-94-95799 ..... p 3776 N94-30981
ETN-94-95800 ..... p 3743 N94-31853 #
ETN-94-95801 ..... p 3829 N94-31176
ETN-94-95802 ..... p 3824 N94-31177
ETN-94-95803 ..... p 3808 N94-31178
ETN-94-95804 ..... p 3829 N94-31186
ETN-94-95805 ..... p 3840 N94-31187
ETN-94-95806 ..... p 3809 N94-31188
ETN-94-95807 ..... p 3809 N94-31189
ETN-94-95808 ..... p 3671 N94-31190
ETN-94-95809 ..... p 3809 N94-31212
ETN-94-95810 ..... p 3850 N94-31191
ETN-94-95811 ..... p 3809 N94-31192
ETN-94-95814 ..... p 3911 N94-31893
ETN-94-95852 ..... p 3747 N94-32523
ETN-94-95859 ..... p 3914 N94-31181 #
ETN-94-95860 ..... p 3670 N94-31182 #
ETN-94-95861 ..... p 3840 N94-31156 #
ETN-94-95862 ..... p 3828 N94-31157 #
ETN-94-95863 ..... p 3828 N94-31158 #
ETN-94-95864 ..... p 3840 N94-31159 #
ETN-94-95865 ..... p 3840 N94-31160 #
ETN-94-95866 ..... p 3828 N94-31161 #
ETN-94-95867 ..... p 3840 N94-31162 #
ETN-94-95868 ..... p 3808 N94-31163 #
ETN-94-95869 ..... p 3808 N94-31164 #
ETN-94-95872 ..... p 3802 N94-31224 #
ETN-94-95873 ..... p 3618 N94-31225 #
ETN-94-95874 ..... p 3574 N94-31230 #
ETN-94-95875 ..... p 3840 N94-31231 #
ETN-94-95876 ..... p 3618 N94-31232 #
ETN-94-95877 ..... p 3860 N94-31226 #
ETN-94-95878 ..... p 3863 N94-31227 #
ETN-94-95879 ..... p 3568 N94-31220 #
ETN-94-95880 ..... p 3700 N94-31221 #
ETN-94-95881 ..... p 3770 N94-31222 #
ETN-94-95883 ..... p 3809 N94-31223 #
ETN-94-95884 ..... p 3839 N94-31092
ETN-94-95885 ..... p 3670 N94-31093
ETN-94-95886 ..... p 3808 N94-31094
ETN-94-95887 ..... p 3840 N94-31095
ETN-94-95888 ..... p 3711 N94-31096
ETN-94-95889 ..... p 3670 N94-31097
ETN-94-95890 ..... p 3910 N94-31098
ETN-94-95891 ..... p 3823 N94-31099
ETN-94-95892 ..... p 3828 N94-31100
ETN-94-95893 ..... p 3829 N94-31193
ETN-94-95894 ..... p 3824 N94-31183
ETN-94-95895 ..... p 3742 N94-31165
ETN-94-95896 ..... p 3730 N94-31166
ETN-94-95897 ..... p 3858 N94-31167
ETN-94-95898 ..... p 3687 N94-31168
ETN-94-95899 ..... p 3840 N94-31169
ETN-94-95900 ..... p 3687 N94-31170
ETN-94-95901 ..... p 3670 N94-31171
ETN-94-95902 ..... p 3915 N94-31172
ETN-94-95903 ..... p 3877 N94-31173
ETN-94-95904 ..... p 3670 N94-31174
ETN-94-95906 ..... p 3735 N94-31870
ETN-94-95908 ..... p 3733 N94-31376

ETN-94-95909 ..... p 3619 N94-31377 #
ETN-94-95910 ..... p 3886 N94-31378
ETN-94-95911 ..... p 3734 N94-31562 #
ETN-94-95913 ..... p 3812 N94-31542 #
ETN-94-95918 ..... p 3812 N94-31543 #
ETN-94-95919 ..... p 3734 N94-31544 #
ETN-94-95937 ..... p 3839 N94-31082
ETN-94-95938 ..... p 3640 N94-31083
ETN-94-95939 ..... p 3858 N94-31084
ETN-94-95940 ..... p 3711 N94-31085
ETN-94-95941 ..... p 3927 N94-31086
ETN-94-95942 ..... p 3808 N94-31087
ETN-94-95943 ..... p 3885 N94-31088
ETN-94-95944 ..... p 3885 N94-31089
ETN-94-95948 ..... p 3859 N94-31090
ETN-94-95949 ..... p 3859 N94-31076
ETN-94-95950 ..... p 3859 N94-31077
ETN-94-95951 ..... p 3732 N94-31091
ETN-94-95952 ..... p 3722 N94-31194
ETN-94-95973 ..... p 3587 N94-31179 #
ETN-94-95974 ..... p 3567 N94-31180
ETN-94-95979 ..... p 3798 N94-33069
ETN-94-95980 ..... p 3794 N94-31195 #
ETN-94-95985 ..... p 3585 N94-31677 #
ETN-94-95991 ..... p 3856 N94-31416
ETN-94-95992 ..... p 3856 N94-31417
ETN-94-95993 ..... p 3856 N94-31407
ETN-94-95994 ..... p 3856 N94-31408
ETN-94-95995 ..... p 3842 N94-31409
ETN-94-95996 ..... p 3856 N94-31410
ETN-94-95997 ..... p 3856 N94-31411
ETN-94-95998 ..... p 3856 N94-31450
ETN-94-95999 ..... p 3842 N94-31451
ETN-94-96000 ..... p 3917 N94-31452
ETN-94-96001 ..... p 3842 N94-31453
ETN-94-96002 ..... p 3856 N94-31468
ETN-94-96003 ..... p 3855 N94-31403
ETN-94-96004 ..... p 3855 N94-31404
ETN-94-96005 ..... p 3841 N94-31388
ETN-94-96006 ..... p 3855 N94-31389
ETN-94-96007 ..... p 3855 N94-31390
ETN-94-96008 ..... p 3841 N94-31391
ETN-94-96009 ..... p 3916 N94-31392
ETN-94-96010 ..... p 3842 N94-31393
ETN-94-96011 ..... p 3715 N94-31545 #
ETN-94-96012 ..... p 3830 N94-31546 #
ETN-94-96013 ..... p 3897 N94-31547 #
ETN-94-96014 ..... p 3865 N94-31548 #
ETN-94-96015 ..... p 3865 N94-31549 #
ETN-94-96016 ..... p 3878 N94-31550 #
ETN-94-96017 ..... p 3865 N94-31537 #
ETN-94-96018 ..... p 3674 N94-31551 #
ETN-94-96019 ..... p 3715 N94-31532 #
ETN-94-96020 ..... p 3792 N94-31533 #
ETN-94-96021 ..... p 3865 N94-31534 #
ETN-94-96022 ..... p 3689 N94-31535 #
ETN-94-96023 ..... p 3689 N94-31536 #
ETN-94-96024 ..... p 3688 N94-31517 #
ETN-94-96025 ..... p 3688 N94-31518 #
ETN-94-96026 ..... p 3641 N94-31519 #
ETN-94-96027 ..... p 3688 N94-31520 #
ETN-94-96028 ..... p 3897 N94-31521 #
ETN-94-96029 ..... p 3690 N94-31616 #
ETN-94-96030 ..... p 3795 N94-31652 #
ETN-94-96031 ..... p 3860 N94-31653 #
ETN-94-96036 ..... p 3724 N94-31654 #
ETN-94-96037 ..... p 3759 N94-31655 #
ETN-94-96039 ..... p 3724 N94-31656 #
ETN-94-96040 ..... p 3765 N94-31657 #
ETN-94-96041 ..... p 3743 N94-31658 #
ETN-94-96055 ..... p 3842 N94-31394
ETN-94-96056 ..... p 3722 N94-31379
ETN-94-96057 ..... p 3830 N94-31500
ETN-94-96058 ..... p 3842 N94-31412
ETN-94-96059 ..... p 3842 N94-31413
ETN-94-96060 ..... p 3673 N94-31418 #
ETN-94-96061 ..... p 3673 N94-31419 #
ETN-94-96062 ..... p 3640 N94-31420 #
ETN-94-96063 ..... p 3568 N94-31421 #
ETN-94-96064 ..... p 3701 N94-31422 #
ETN-94-96065 ..... p 3702 N94-31477 #
ETN-94-96066 ..... p 3619 N94-31478 #
ETN-94-96067 ..... p 3614 N94-31423 #
ETN-94-96068 ..... p 3702 N94-31559 #
ETN-94-96069 ..... p 3914 N94-31538 #
ETN-94-96070 ..... p 3843 N94-31539 #
ETN-94-96071 ..... p 3843 N94-31540 #
ETN-94-96072 ..... p 3843 N94-31541 #
ETN-94-96107 ..... p 3812 N94-31659 #
ETN-94-96109 ..... p 3703 N94-31660 #
ETN-94-96110 ..... p 3851 N94-31661 #
ETN-94-96111 ..... p 3825 N94-31662 #
ETN-94-96112 ..... p 3674 N94-31645 #
ETN-94-96113 ..... p 3812 N94-31646 #
ETN-94-96114 ..... p 3830 N94-31647 #
ETN-94-96115 ..... p 3917 N94-31640 #
ETN-94-96117 ..... p 3824 N94-31641 #
ETN-94-96118 ..... p 3843 N94-31642 #
ETN-94-96119 ..... p 3844 N94-31643 #
ETN-94-96120 ..... p 3844 N94-31644 #
ETN-94-96121 ..... p 3844 N94-31693 #
ETN-94-96122 ..... p 3813 N94-31694 #
ETN-94-96123 ..... p 3613 N94-31695 #
ETN-94-96124 ..... p 3844 N94-31696 #
ETN-94-96125 ..... p 3851 N94-31697 #
ETN-94-96126 ..... p 3851 N94-31698 #
ETN-94-96127 ..... p 3851 N94-31699 #
ETN-94-96128 ..... p 3825 N94-31700 #
ETN-94-96129 ..... p 3844 N94-31701 #
ETN-94-96130 ..... p 3845 N94-31702 #
ETN-94-96131 ..... p 3924 N94-31617 #
ETN-94-96132 ..... p 3843 N94-31552 #
ETN-94-96133 ..... p 3812 N94-31522 #
ETN-94-96134 ..... p 3844 N94-31673 #
ETN-94-96135 ..... p 3703 N94-31703 #
ETN-94-96136 ..... p 3813 N94-31704 #
ETN-94-96137 ..... p 3609 N94-31705 #
ETN-94-96138 ..... p 3578 N94-31674 #
ETN-94-96139 ..... p 3578 N94-31675 #
ETN-94-96154 ..... p 3822 N94-33097 #
ETN-94-96156 ..... p 3849 N94-32349
ETN-94-96165 ..... p 3851 N94-32225
ETN-94-96166 ..... p 3793 N94-32226
ETN-94-96167 ..... p 3848 N94-32227
ETN-94-96168 ..... p 3793 N94-32228
ETN-94-96169 ..... p 3851 N94-32229
ETN-94-96170 ..... p 3847 N94-32204
ETN-94-96177 ..... p 3844 N94-31676 #
ETN-94-96178 ..... p 3703 N94-31689 #
ETN-94-96179 ..... p 3844 N94-31690 #
ETN-94-96180 ..... p 3703 N94-31691 #
ETN-94-96181 ..... p 3832 N94-31821 #
ETN-94-96182 ..... p 3706 N94-32045 #
ETN-94-96183 ..... p 3569 N94-31822 #
ETN-94-96200 ..... p 3851 N94-32205
ETN-94-96201 ..... p 3847 N94-32200
ETN-94-96202 ..... p 3847 N94-32206
ETN-94-96203 ..... p 3847 N94-32207
ETN-94-96209 ..... p 3918 N94-32289
ETN-94-96210 ..... p 3918 N94-32290
ETN-94-96211 ..... p 3826 N94-32291
ETN-94-96212 ..... p 3848 N94-32292
ETN-94-96213 ..... p 3817 N94-32287
ETN-94-96214 ..... p 3825 N94-32196
ETN-94-96215 ..... p 3919 N94-32506
ETN-94-96216 ..... p 3918 N94-32105
ETN-94-96217 ..... p 3846 N94-32106
ETN-94-96218 ..... p 3847 N94-32191
ETN-94-96219 ..... p 3857 N94-32192
ETN-94-96220 ..... p 3846 N94-32084
ETN-94-96221 ..... p 3677 N94-32085
ETN-94-96222 ..... p 3835 N94-32193
ETN-94-96223 ..... p 3847 N94-32194
ETN-94-96224 ..... p 3846 N94-32107
ETN-94-96225 ..... p 3846 N94-32108
ETN-94-96226 ..... p 3849 N94-32507
ETN-94-96227 ..... p 3847 N94-32197
ETN-94-96228 ..... p 3835 N94-32198
ETN-94-96229 ..... p 3852 N94-32350

F-254279 ..... p 3893 N94-33074 * #

FAA-AOR-100-94-001 ..... p 3576 N94-32955 #

FAA-APR-94-1 ..... p 3566 N94-33016 #

FFA-TN-1992-15 ..... p 3568 N94-31220 #

FNAL-TM-1868 ..... p 3652 N94-31764 #
FNAL-TM-1873-VOL-1 ..... p 3878 N94-31271 #
FNAL-TM-1876 ..... p 3876 N94-32586 #
FNAL-TM-1877 ..... p 3876 N94-32588 #

FNAL/C-93/381 ..... p 3864 N94-31507 #
FNAL/C-93/384 ..... p 3863 N94-31147 #
FNAL/C-93/386-E ..... p 3897 N94-31506 #
FNAL/C-93/388-E ..... p 3872 N94-32627
FNAL/C-93/402-E ..... p 3866 N94-31669 #
FNAL/C-94/016-E ..... p 3866 N94-31670 #
FNAL/C-94/023-E ..... p 3867 N94-31671 #
FNAL/C-94/031 ..... p 3877 N94-32802 #
FNAL/C-94/035-E ..... p 3873 N94-32780 #
FNAL/C-94/045-E ..... p 3871 N94-32587 #

FOA-C-30726-3.2 ..... p 3676 N94-31925
FOA-C-30730-3.1 ..... p 3878 N94-31584

FRCR-440 ..... p 3868 N94-31619 #

GA-A-21487 ..... p 3886 N94-31304 #
GA-A-21517 ..... p 3718 N94-32202 #
GA-A-21518 ..... p 3890 N94-32201 #
GA-A-21520 ..... p 3891 N94-32612 #
GA-A-21525 ..... p 3886 N94-31324 #
GA-A-21541 ..... p 3891 N94-32595 #
GA-A-21542 ..... p 3892 N94-32810 #
GA-A-21554 ..... p 3891 N94-32611 #
GA-A-21584 ..... p 3890 N94-32519 #

GL-5129 ..... p 3714 N94-31278 #

GMD-217 ..... p 3813 N94-31687
GMD-224 ..... p 3813 N94-31686

H-1774 ..... p 3572 N94-32880 * #

IBM-05021-002 ..... p 3811 N94-31465 #

IC-93/307 ..... p 3910 N94-31052

ICASE-94-12 ..... p 3821 N94-33075 * #
ICASE-94-18 ..... p 3820 N94-32928 * #
ICASE-94-24 ..... p 3849 N94-33033 * #

ICMA-94-187 ..... p 3849 N94-33060

ICOMP-94-01 ..... p 3710 N94-32969 * #
ICOMP-94-5 ..... p 3700 N94-31229 * #
ICOMP-94-7 ..... p 3850 N94-33120 * #
ICOMP-94-8 ..... p 3710 N94-33070 * #

IDA-D-1439 ..... p 3810 N94-31357 #

IDA-P-2831 ..... p 3677 N94-32087 #

IDA/HQ-93-43524 ..... p 3677 N94-32087 #
IDA/HQ-93-44605 ..... p 3810 N94-31357 #

IEE-SR-248 ..... p 3769 N94-32920

IFSR-631 ..... p 3886 N94-31366 #
IFSR-634 ..... p 3891 N94-32631 #
IFSR-635 ..... p 3720 N94-32684
IFSR-636 ..... p 3876 N94-32685
IFSR-637 ..... p 3891 N94-32664 #
IFSR-639 ..... p 3887 N94-31396 #
IFSR-646 ..... p 3891 N94-32686

IHEP-TD-92-32 ..... p 3902 N94-32247

IHES/P/93/41 ..... p 3889 N94-31772
IHES/P/93/47 ..... p 3601 N94-31769 #
IHES/P/93/48 ..... p 3610 N94-31771
IHES/P/93/59 ..... p 3857 N94-31770
IHES/P/93/60 ..... p 3850 N94-31590
IHES/P/93/66 ..... p 3857 N94-31589

ILR-MITT-281(1993) ..... p 3733 N94-31375 #
ILR-MITT-282(1993) ..... p 3803 N94-31852
ILR-MITT-283(1993) ..... p 3764 N94-31611

INPE-5537-TDI/525 ..... p 3954 N94-33080 #

IS-M-751 ..... p 3677 N94-32101 #

IS-T-1627 ..... p 3657 N94-32377 #
IS-T-1658 ..... p 3631 N94-31154 #
IS-T-1661 ..... p 3895 N94-31067 #
IS-T-1662 ..... p 3862 N94-31146 #
IS-T-1704 ..... p 3827 N94-32683

IS-5097 ..... p 3759 N94-31648 #

ISAL-92-0004 ..... p 3734 N94-31544 #

ISBN-0-16-043188-3 ..... p 3916 N94-31228 #
ISBN-0-315-75390-0 ..... p 3611 N94-32502
ISBN-0-315-75467-2 ..... p 3704 N94-31778
ISBN-0-315-75484-2 ..... p 3934 N94-31789
ISBN-0-315-75792-2 ..... p 3707 N94-32497
ISBN-0-315-75827-9 ..... p 3571 N94-32491
ISBN-0-315-76447-3 ..... p 3939 N94-33112
ISBN-0-315-77217-4 ..... p 3714 N94-31472
ISBN-0-315-77418-5 ..... p 3776 N94-33111
ISBN-0-315-78739-2 ..... p 3633 N94-31471
ISBN-0-315-78768-6 ..... p 3610 N94-31723
ISBN-0-315-86119-3 ..... p 3675 N94-31708 #
ISBN-0-315-86201-7 ..... p 3955 N94-31709 #
ISBN-0-315-86210-6 ..... p 3587 N94-31710 #
ISBN-0-315-86218-1 ..... p 3690 N94-31711 #
ISBN-0-315-86269-6 ..... p 3911 N94-31712 #
ISBN-0-315-86317-X ..... p 3813 N94-31713 #
ISBN-0-315-86323-4 ..... p 3724 N94-31714 #
ISBN-0-315-86336-6 ..... p 3814 N94-31715 #
ISBN-0-315-86410-9 ..... p 3620 N94-31716 #
ISBN-0-315-86416-8 ..... p 3703 N94-31717 #
ISBN-0-315-86418-4 ..... p 3814 N94-31718 #
ISBN-0-315-86425-7 ..... p 3621 N94-31719 #

ISBN-0-315-86439-7 ..... p 3703 N94-31720 #
ISBN-0-315-86450-8 ..... p 3724 N94-31721 #
ISBN-0-315-86455-9 ..... p 3652 N94-31722 #
ISBN-0-315-86460-5 ..... p 3676 N94-31796 #
ISBN-0-315-86466-4 ..... p 3716 N94-31797 #
ISBN-0-315-86493-1 ..... p 3831 N94-31798 #
ISBN-0-315-86498-2 ..... p 3704 N94-31799 #
ISBN-0-315-86502-4 ..... p 3831 N94-31800 #
ISBN-0-315-86506-7 ..... p 3914 N94-32074 #
ISBN-0-315-86515-6 ..... p 3832 N94-31801 #
ISBN-0-315-86525-3 ..... p 3690 N94-31726 #
ISBN-0-315-86526-1 ..... p 3888 N94-31727 #
ISBN-0-315-86531-8 ..... p 3620 N94-31706 #
ISBN-0-315-86543-1 ..... p 3734 N94-31707 #
ISBN-0-315-86546-6 ..... p 3622 N94-31909 #
ISBN-0-315-86547-4 ..... p 3610 N94-31910 #
ISBN-0-315-86553-9 ..... p 3912 N94-31911 #
ISBN-0-315-86561-X ..... p 3736 N94-31912 #
ISBN-0-315-86692-6 ..... p 3935 N94-31913 #
ISBN-0-315-86694-2 ..... p 3925 N94-31914 #
ISBN-0-315-86705-1 ..... p 3588 N94-31747 #
ISBN-0-315-86717-5 ..... p 3716 N94-31748 #
ISBN-0-315-86746-9 ..... p 3867 N94-31749 #
ISBN-0-315-86753-1 ..... p 3831 N94-31750 #
ISBN-0-315-86782-5 ..... p 3879 N94-31751 #
ISBN-0-315-86783-3 ..... p 3814 N94-31752 #
ISBN-0-315-86794-9 ..... p 3867 N94-31753 #
ISBN-0-315-86831-7 ..... p 3725 N94-31754 #
ISBN-0-315-86834-1 ..... p 3845 N94-31755 #
ISBN-0-315-86848-1 ..... p 3879 N94-31756 #
ISBN-0-315-86864-3 ..... p 3831 N94-31757 #
ISBN-0-315-86866-X ..... p 3814 N94-31728 #
ISBN-0-315-86902-X ..... p 3899 N94-31729 #
ISBN-0-315-86932-1 ..... p 3832 N94-31873 #
ISBN-0-315-87039-7 ..... p 3743 N94-31733 #
ISBN-0-315-87053-2 ..... p 3568 N94-31734 #
ISBN-0-315-87054-0 ..... p 3830 N94-31735 #
ISBN-0-315-87055-9 ..... p 3878 N94-31736 #
ISBN-0-315-87056-7 ..... p 3734 N94-31737 #
ISBN-0-315-87057-5 ..... p 3652 N94-31692 #
ISBN-0-315-87060-5 ..... p 3832 N94-31833 #
ISBN-0-315-87086-9 ..... p 3772 N94-31834 #
ISBN-0-315-87109-1 ..... p 3725 N94-31874 #
ISBN-0-315-87164-4 ..... p 3833 N94-31875 #
ISBN-0-315-87190-3 ..... p 3879 N94-31877 #
ISBN-0-315-87192-X ..... p 3833 N94-31876 #
ISBN-0-315-87205-5 ..... p 3725 N94-31878 #
ISBN-0-315-87206-3 ..... p 3621 N94-31835 #
ISBN-0-315-87214-4 ..... p 3621 N94-31836 #
ISBN-0-315-87218-7 ..... p 3585 N94-31837 #
ISBN-0-315-87265-9 ..... p 3703 N94-31730 #
ISBN-0-315-87284-5 ..... p 3675 N94-31731 #
ISBN-0-315-87316-7 ..... p 3867 N94-31832 #
ISBN-0-315-87318-3 ..... p 3924 N94-31732 #
ISBN-0-315-87364-7 ..... p 3868 N94-31915 #
ISBN-0-8330-1842-4 ..... p 3581 N94-33329
ISBN-1-871564-60-3 ..... p 3702 N94-31559 #
ISBN-1-871564-61-1 ..... p 3914 N94-31538 #
ISBN-1-871564-62-X ..... p 3843 N94-31540 #
ISBN-1-871564-63-8 ..... p 3843 N94-31539 #
ISBN-1-871564-65-4 ..... p 3843 N94-31541 #
ISBN-2-85-428333-3 ..... p 3776 N94-30981
ISBN-2-85428-345-7 ..... p 3747 N94-32523
ISBN-82-595-7449-7 ..... p 3717 N94-31840
ISBN-9-03-86-0282-0 ..... p 3860 N94-31653 #
ISBN-9-06-275906-8 ..... p 3609 N94-31705 #
ISBN-9-09-004570-8 ..... p 3688 N94-31520 #
ISBN-9-09-005097-3 ..... p 3897 N94-31521 #
ISBN-9-09-005151-1 ..... p 3641 N94-31519 #
ISBN-9-09-005279-8 ..... p 3688 N94-31517 #
ISBN-9-09-005449-9 ..... p 3689 N94-31535 #
ISBN-9-09-005495-2 ..... p 3690 N94-31616 #
ISBN-9-09-005754-4 ..... p 3795 N94-31652 #
ISBN-9-09-005887-7 ..... p 3689 N94-31536 #
ISBN-9-09-005899-0 ..... p 3688 N94-31518 #
ISBN-9-29-092101-3 ..... p 3670 N94-31182 #
ISBN-9-29-092105-6 ..... p 3914 N94-31181 #
ISBN-9-51-384134-0 ..... p 3724 N94-31654 #
ISBN-9-51-384301-7 ..... p 3759 N94-31655 #
ISBN-9-51-384429-3 ..... p 3724 N94-31656 #
ISBN-9-51-384442-0 ..... p 3765 N94-31657 #
ISBN-9-51-384451-X ..... p 3743 N94-31658 #
ISBN-90-386-0251-0 ..... p 3917 N94-31583
ISBN-90-9006176-2 ..... p 3917 N94-31586
ISBN-92-835-0727-4 ..... p 3679 N94-32235
ISBN-92-9092-282-6 ..... p 3743 N94-31853 #
ISBN-951-22-1712-0 ..... p 3648 N94-31069
ISBN-951-22-1761-9 ..... p 3634 N94-31679 #

ISRN-KTH/ALP/R-93/01-SE ..... p 3885 N94-31088
ISRN-KTH/ALP/R-93/02-SE ..... p 3885 N94-31089

ISU-ERI-AMES-94-088 ..... p 3706 N94-32279 #

ISVR-TR-225-PT-2 ..... p 3740 N94-32982

JINR-R-14-92-345 ..... p 3896 N94-31395
JINR-R-15-93-29 ..... p 3869 N94-32097 #

JRC-RR-91-08 ..... p 3881 N94-32380 #

K/ETO-140 ..... p 3913 N94-32846

KCP-613-5307 ..... p 3765 N94-32144
KCP-613-5330 ..... p 3694 N94-32582 #

KSC-KHR-18 ..... p 3966 N94-33072 * #

KTM/E-B-150 ..... p 3760 N94-31767 #

L-16781 ..... p 3572 N94-32865 * #
L-17106 ..... p 3627 N94-33121 * #
L-17283 ..... p 3861 N94-32930 * #

LA-SUB-94-39 ..... p 3713 N94-32706 #
LA-SUB-94-3 ..... p 3857 N94-32589 #
LA-SUB-94-41 ..... p 3654 N94-31976 #

LA-UR-93-2864 ..... p 3681 N94-32679 #
LA-UR-93-4375 ..... p 3956 N94-31308 #
LA-UR-93-4520 ..... p 3903 N94-32597
LA-UR-93-4526 ..... p 3785 N94-32726 #
LA-UR-94-0063 ..... p 3845 N94-31763 #
LA-UR-94-0274 ..... p 3830 N94-31623 #
LA-UR-94-0277 ..... p 3899 N94-31633 #
LA-UR-94-101 ..... p 3774 N94-32736 #
LA-UR-94-110 ..... p 3834 N94-32175 #
LA-UR-94-1148 ..... p 3906 N94-32913 #
LA-UR-94-16 ..... p 3797 N94-32732 #
LA-UR-94-217 ..... p 3898 N94-31631 #
LA-UR-94-229 ..... p 3786 N94-32937 #
LA-UR-94-271 ..... p 3716 N94-31624 #
LA-UR-94-310 ..... p 3656 N94-32103 #
LA-UR-94-343 ..... p 3907 N94-32944 #
LA-UR-94-345 ..... p 3892 N94-32730 #
LA-UR-94-381 ..... p 3911 N94-31760 #
LA-UR-94-502 ..... p 3718 N94-32270 #
LA-UR-94-503 ..... p 3611 N94-32813
LA-UR-94-526 ..... p 3720 N94-32761 #
LA-UR-94-528 ..... p 3720 N94-32760 #
LA-UR-94-538 ..... p 3905 N94-32747 #
LA-UR-94-563 ..... p 3904 N94-32746 #
LA-UR-94-572 ..... p 3768 N94-32814
LA-UR-94-597 ..... p 3682 N94-32745 #
LA-UR-94-604 ..... p 3826 N94-32356 #
LA-UR-94-605 ..... p 3852 N94-32744 #
LA-UR-94-606 ..... p 3637 N94-32743 #
LA-UR-94-659 ..... p 3761 N94-32762 #
LA-UR-94-676 ..... p 3869 N94-32139 #
LA-UR-94-691 ..... p 3747 N94-32249
LA-UR-94-713 ..... p 3870 N94-32271 #
LA-UR-94-73 ..... p 3899 N94-31916 #
LA-UR-94-96 ..... p 3898 N94-31628 #

LA-12628-MS ..... p 3695 N94-32662
LA-12629-MS ..... p 3681 N94-32661
LA-12674 ..... p 3761 N94-32660
LA-12687-MS ..... p 3686 N94-31150 #
LA-12698-C ..... p 3874 N94-32804 #
LA-12712-MS ..... p 3774 N94-32647 #
LA-12722-T ..... p 3889 N94-31809 #

LAB-RP-10717-1 ..... p 3711 N94-31492 * #

LBL-31742 ..... p 3819 N94-32668
LBL-34289 ..... p 3899 N94-31634 #
LBL-34669 ..... p 3636 N94-32376 #
LBL-34842 ..... p 3953 N94-31632 #
LBL-34881 ..... p 3866 N94-31637 #
LBL-34883 ..... p 3870 N94-32250 #
LBL-34911 ..... p 3864 N94-31405 #
LBL-34923 ..... p 3857 N94-31639 #
LBL-34991 ..... p 3641 N94-31638 #
LBL-35003 ..... p 3955 N94-31635
LBL-35050 ..... p 3795 N94-31323 #
LBL-35054 ..... p 3712 N94-31629 #
LBL-35057 ..... p 3643 N94-32064
LBL-35092 ..... p 3880 N94-32138
LBL-90-REV ..... p 3873 N94-32768 #

LC-94-5874 ..... p 3566 N94-32793 * #

LG89ER0059-VOL-1 ..... p 3708 N94-32867 * #
LG89ER0059-VOL-2 ..... p 3709 N94-32869 * #

LP-93-05 ..... p 3856 N94-31411
LP-93-06 ..... p 3856 N94-31450
LP-93-07 ..... p 3842 N94-31451
LP-93-08 ..... p 3917 N94-31452
LP-93-09 ..... p 3842 N94-31453
LP-93-10 ..... p 3856 N94-31468
LP-93-11 ..... p 3855 N94-31403

LP-93-13 ..... p 3855 N94-31404
LP-93-14 ..... p 3841 N94-31388
LP-93-15 ..... p 3855 N94-31389

LPI-TR-93-06-PT-1 ..... p 3943 N94-33190 * #
LPI-TR-94-03-PT-1 ..... p 3927 N94-31116 * #

LR-727 ..... p 3609 N94-31705 #
LR-728 ..... p 3578 N94-31674 #
LR-729 ..... p 3578 N94-31675 #

LRC-93-43 ..... p 3890 N94-32520 #

M-738 ..... p 3598 N94-31425 * #
M-742 ..... p 3591 N94-31012 * #

MATHS-REPT-A-200 ..... p 3840 N94-31156 #
MATHS-REPT-A-202 ..... p 3828 N94-31157 #
MATHS-REPT-A-203 ..... p 3828 N94-31158 #
MATHS-REPT-A-204 ..... p 3840 N94-31159 #
MATHS-REPT-A-205 ..... p 3840 N94-31160 #
MATHS-REPT-A-206 ..... p 3828 N94-31161 #
MATHS-REPT-A-207 ..... p 3840 N94-31162 #
MATHS-REPT-A-208 ..... p 3808 N94-31163 #
MATHS-REPT-A-209 ..... p 3808 N94-31164 #

MEMO-INF-93-18 ..... p 3698 N94-33169
MEMO-INF-93-42 ..... p 3917 N94-31415 #
MEMO-INF-93-45 ..... p 3812 N94-31659 #

MEMO-1150 ..... p 3832 N94-31826 #
MEMO-1152 ..... p 3699 N94-31185

ML-93-15 ..... p 3856 N94-31416
ML-93-16 ..... p 3856 N94-31417
ML-93-17 ..... p 3856 N94-31407
ML-93-18 ..... p 3856 N94-31408
ML-93-19 ..... p 3842 N94-31409
ML-93-20 ..... p 3856 N94-31410

MLM-3790 ..... p 3723 N94-31621 #

MML-TR-94-08 ..... p 3650 N94-31297 #

MPL-U-1/94 ..... p 3789 N94-32402
MPL-U-10/94 ..... p 3789 N94-32401
MPL-U-2/94 ..... p 3789 N94-32400

MRL-GD-0057 ..... p 3818 N94-32390

MRL-TR-93-64 ..... p 3580 N94-32378

MSRR-596 ..... p 3810 N94-31343 #
MSRR-603 ..... p 3822 N94-33183

NAMRL-1387 ..... p 3799 N94-32187 #

NAS 1.15:103845 ..... p 3820 N94-32906 * #
NAS 1.15:103979 ..... p 3709 N94-32946 * #
NAS 1.15:103985 ..... p 3571 N94-32063 * #
NAS 1.15:104139 ..... p 3572 N94-32873 * #
NAS 1.15:104594-VOL-1 ..... p 3823 N94-33287 * #
NAS 1.15:104594-VOL-2 ..... p 3613 N94-33289 * #
NAS 1.15:104602 ..... p 3732 N94-33101 * #
NAS 1.15:104791 ..... p 3943 N94-32923 * #
NAS 1.15:104793 ..... p 3820 N94-32899 * #
NAS 1.15:105290 ..... p 3669 N94-32861 * #
NAS 1.15:105441 ..... p 3966 N94-32885 * #
NAS 1.15:105607 ..... p 3626 N94-32858 * #
NAS 1.15:105625 ..... p 3739 N94-32883 * #
NAS 1.15:106366 ..... p 3728 N94-32902 * #
NAS 1.15:106376 ..... p 3567 N94-33046 * #
NAS 1.15:106456 ..... p 3728 N94-32893 * #
NAS 1.15:106472 ..... p 3617 N94-32941 * #
NAS 1.15:106496 ..... p 3567 N94-33064 * #
NAS 1.15:106499 ..... p 3739 N94-32735 * #
NAS 1.15:106501 ..... p 3615 N94-32742 * #
NAS 1.15:106522 ..... p 3647 N94-32931 * #
NAS 1.15:106538 ..... p 3740 N94-32932 * #
NAS 1.15:106542 ..... p 3710 N94-32969 * #
NAS 1.15:106544 ..... p 3709 N94-32947 * #
NAS 1.15:106547 ..... p 3617 N94-33021 * #
NAS 1.15:106550 ..... p 3700 N94-31229 * #
NAS 1.15:106551 ..... p 3573 N94-32984 * #
NAS 1.15:106552 ..... p 3728 N94-32979 * #
NAS 1.15:106554 ..... p 3662 N94-32945 * #
NAS 1.15:106561 ..... p 3883 N94-32777 * #
NAS 1.15:106566 ..... p 3696 N94-32905 * #
NAS 1.15:106567 ..... p 3698 N94-33116 * #
NAS 1.15:106574 ..... p 3897 N94-33052 * #
NAS 1.15:106587 ..... p 3820 N94-32773 * #
NAS 1.15:106591 ..... p 3713 N94-32983 * #
NAS 1.15:106592 ..... p 3617 N94-33022 * #
NAS 1.15:106597 ..... p 3731 N94-33032 * #
NAS 1.15:106601 ..... p 3850 N94-33120 * #
NAS 1.15:106602 ..... p 3710 N94-33070 * #

NAS 1.15:106603 ..... p 3663 N94-33024 * #
NAS 1.15:106604 ..... p 3726 N94-32272 * #
NAS 1.15:107582 ..... p 3601 N94-32870 * #
NAS 1.15:108237 ..... p 3860 N94-31337 * #
NAS 1.15:108238 ..... p 3860 N94-31336 * #
NAS 1.15:108441 ..... p 3803 N94-31380 * #
NAS 1.15:108445 ..... p 3786 N94-33004 * #
NAS 1.15:108454 ..... p 3739 N94-32903 * #
NAS 1.15:108798 ..... p 3617 N94-33117 * #
NAS 1.15:108807 ..... p 3711 N94-33290 * #
NAS 1.15:108810 ..... p 3801 N94-33068 * #
NAS 1.15:108811 ..... p 3805 N94-32936 * #
NAS 1.15:108814 ..... p 3575 N94-32927 * #
NAS 1.15:109073 ..... p 3740 N94-33118 * #
NAS 1.15:109086 ..... p 3785 N94-32737 * #
NAS 1.15:109088 ..... p 3922 N94-32837 * #
NAS 1.15:109093 ..... p 3613 N94-32924 * #
NAS 1.15:109098 ..... p 3922 N94-32836 * #
NAS 1.15:109108 ..... p 3627 N94-32939 * #
NAS 1.15:109109 ..... p 3710 N94-33020 * #
NAS 1.15:109112 ..... p 3573 N94-32950 * #
NAS 1.15:109120 ..... p 3586 N94-32951 * #
NAS 1.15:109196 ..... p 3966 N94-33072 * #
NAS 1.15:109348 ..... p 3921 N94-32834 * #
NAS 1.15:109404 ..... p 3921 N94-32832 * #
NAS 1.15:109700 ..... p 3914 N94-33066 * #
NAS 1.15:109722 ..... p 3917 N94-31888 * #
NAS 1.15:109740 ..... p 3573 N94-33071 * #
NAS 1.15:109744 ..... p 3674 N94-31503 * #
NAS 1.15:109769 ..... p 3921 N94-32831 * #
NAS 1.15:109771 ..... p 3921 N94-32830 * #
NAS 1.15:109774 ..... p 3922 N94-32835 * #
NAS 1.15:109777 ..... p 3921 N94-32829 * #
NAS 1.15:109780 ..... p 3915 N94-32222 * #
NAS 1.15:109782 ..... p 3921 N94-32833 * #
NAS 1.15:109787 ..... p 3924 N94-33067 * #
NAS 1.15:4387 ..... p 3572 N94-32880 * #
NAS 1.15:4545 ..... p 3732 N94-33038 * #
NAS 1.15:4557 ..... p 3638 N94-32948 * #
NAS 1.18:5300.4(2B-2) ..... p 3731 N94-32387 * #
NAS 1.21:4216 ..... p 3566 N94-32793 * #
NAS 1.21:7011(385) ..... p 3797 N94-32348 *
NAS 1.21:7011(388) ..... p 3795 N94-31414 *
NAS 1.21:7011(389) ..... p 3797 N94-32347 *
NAS 1.21:7037(302) ..... p 3565 N94-31342 *
NAS 1.21:7037(303) ..... p 3565 N94-31381 *
NAS 1.21:7037(304) ..... p 3566 N94-32853 *
NAS 1.26:177636 ..... p 3576 N94-33063 * #
NAS 1.26:182149 ..... p 3616 N94-32866 * #
NAS 1.26:182296-VOL-1 ..... p 3708 N94-32867 * #
NAS 1.26:182296-VOL-2 ..... p 3709 N94-32869 * #
NAS 1.26:185207 ..... p 3709 N94-32872 * #
NAS 1.26:185297 ..... p 3615 N94-32792 * #
NAS 1.26:187096 ..... p 3584 N94-32859 * #
NAS 1.26:188283 ..... p 3835 N94-32359 * #
NAS 1.26:188284 ..... p 3739 N94-32907 * #
NAS 1.26:188285 ..... p 3601 N94-32388 * #
NAS 1.26:188286 ..... p 3669 N94-32857 * #
NAS 1.26:188288 ..... p 3731 N94-32862 * #
NAS 1.26:188289 ..... p 3577 N94-32864 * #
NAS 1.26:189175 ..... p 3614 N94-31618 * #
NAS 1.26:189332 ..... p 3711 N94-31492 * #
NAS 1.26:189558 ..... p 3626 N94-32877 * #
NAS 1.26:189581 ..... p 3638 N94-32868 * #
NAS 1.26:189593 ..... p 3626 N94-32860 * #
NAS 1.26:189594 ..... p 3682 N94-32897 * #
NAS 1.26:189617 ..... p 3731 N94-32481 * #
NAS 1.26:189648 ..... p 3707 N94-32480 * #
NAS 1.26:190299 ..... p 3804 N94-32697 * #
NAS 1.26:191009 ..... p 3728 N94-32900 * #
NAS 1.26:191327 ..... p 3826 N94-32482 * #
NAS 1.26:191348 ..... p 3927 N94-32695 * #
NAS 1.26:191349 ..... p 3882 N94-32702 * #
NAS 1.26:191351 ..... p 3637 N94-32696 * #
NAS 1.26:191352 ..... p 3637 N94-32694 * #
NAS 1.26:191577 ..... p 3827 N94-32734 * #
NAS 1.26:191792 ..... p 3669 N94-32484 *
NAS 1.26:191796 ..... p 3826 N94-32483 * #
NAS 1.26:192722 ..... p 3882 N94-32417 * #
NAS 1.26:193272 ..... p 3571 N94-32476 * #
NAS 1.26:193937 ..... p 3611 N94-32898 * #
NAS 1.26:193951 ..... p 3608 N94-33100 * #
NAS 1.26:194211 ..... p 3681 N94-32477 * #
NAS 1.26:194216 ..... p 3727 N94-32479 * #
NAS 1.26:194223 ..... p 3694 N94-32478 * #
NAS 1.26:194279 ..... p 3943 N94-33190 * #
NAS 1.26:194472 ..... p 3728 N94-32929 * #
NAS 1.26:194865 ..... p 3954 N94-31101 * #
NAS 1.26:194883 ..... p 3821 N94-33075 * #
NAS 1.26:194889 ..... p 3806 N94-33286 * #
NAS 1.26:194896 ..... p 3820 N94-32928 * #
NAS 1.26:194902 ..... p 3849 N94-33033 * #
NAS 1.26:194905 ..... p 3862 N94-33023 * #
NAS 1.26:195097 ..... p 3683 N94-33083 * #
NAS 1.26:195240 ..... p 3697 N94-33044 * #
NAS 1.26:195295 ..... p 3616 N94-33099 * #
NAS 1.26:195297 ..... p 3573 N94-33119 * #
NAS 1.26:195301 ..... p 3571 N94-32475 * #
NAS 1.26:195302 ..... p 3572 N94-32926 * #
NAS 1.26:195303 ..... p 3626 N94-32904 * #
NAS 1.26:195304 ..... p 3584 N94-32075 * #
NAS 1.26:195307 ..... p 3727 N94-32741 * #
NAS 1.26:195311 ..... p 3616 N94-32970 * #
NAS 1.26:195332 ..... p 3731 N94-32901 * #
NAS 1.26:195692 ..... p 3790 N94-33045 * #
NAS 1.26:195696 ..... p 3939 N94-31105 * #
NAS 1.26:195756 ..... p 3927 N94-31116 * #
NAS 1.26:195765 ..... p 3585 N94-31203 * #
NAS 1.26:195807 ..... p 3740 N94-32940 * #
NAS 1.26:195818 ..... p 3927 N94-32942 * #
NAS 1.26:195820 ..... p 3893 N94-33048 * #
NAS 1.26:195821 ..... p 3912 N94-32774 * #
NAS 1.26:195826 ..... p 3836 N94-32980 * #
NAS 1.26:195827 ..... p 3942 N94-32740 * #
NAS 1.26:195828 ..... p 3884 N94-33073 * #
NAS 1.26:195833 ..... p 3757 N94-33019 * #
NAS 1.26:195834 ..... p 3787 N94-33288 * #
NAS 1.26:195835 ..... p 3639 N94-33036 * #
NAS 1.26:195836 ..... p 3835 N94-32943 * #
NAS 1.26:195841 ..... p 3584 N94-33035 * #
NAS 1.26:195848 ..... p 3953 N94-33047 * #
NAS 1.26:195849 ..... p 3821 N94-33049 * #
NAS 1.26:195851 ..... p 3790 N94-32981 * #
NAS 1.26:195877 ..... p 3943 N94-33103 * #
NAS 1.26:195878 ..... p 3816 N94-32086 * #
NAS 1.26:195879 ..... p 3603 N94-32494 * #
NAS 1.26:195880 ..... p 3893 N94-33074 * #
NAS 1.26:195881 ..... p 3668 N94-33037 * #
NAS 1.26:195886 ..... p 3943 N94-33104 * #
NAS 1.26:195902 ..... p 3913 N94-33148 * #
NAS 1.26:195903 ..... p 3894 N94-33113 * #
NAS 1.26:195906 ..... p 3822 N94-33114 * #
NAS 1.26:195908 ..... p 3769 N94-33170 * #
NAS 1.26:195910 ..... p 3612 N94-33115 * #
NAS 1.26:195911 ..... p 3653 N94-31851 * #
NAS 1.26:195913 ..... p 3803 N94-31447 *
NAS 1.26:4269 ..... p 3709 N94-32871 * #
NAS 1.26:4418 ..... p 3626 N94-32863 * #
NAS 1.26:4585 ..... p 3787 N94-33065 * #
NAS 1.26:4594 ..... p 3820 N94-32775 * #
NAS 1.26:4596 ..... p 3820 N94-32776 * #
NAS 1.55:3154 ..... p 3627 N94-33121 * #
NAS 1.55:3237 ..... p 3758 N94-31233 * #
NAS 1.55:3249 ..... p 3956 N94-32420 * #
NAS 1.55:3253 ..... p 3598 N94-31425 * #
NAS 1.55:3257 ..... p 3591 N94-31012 * #
NAS 1.55:3260 ..... p 3603 N94-33291 * #
NAS 1.60:3129 ..... p 3572 N94-32865 * #
NAS 1.60:3425 ..... p 3861 N94-32930 * #
NAS 1.60:3477 ..... p 3805 N94-33050 * #

NASA-CP-3154 ..... p 3627 N94-33121 * #
NASA-CP-3237 ..... p 3758 N94-31233 * #
NASA-CP-3249 ..... p 3956 N94-32420 * #
NASA-CP-3253 ..... p 3598 N94-31425 * #
NASA-CP-3257 ..... p 3591 N94-31012 * #
NASA-CP-3260 ..... p 3603 N94-33291 * #

NASA-CR-177636 ..... p 3576 N94-33063 * #
NASA-CR-182149 ..... p 3616 N94-32866 * #
NASA-CR-182296-VOL-1 ..... p 3708 N94-32867 * #
NASA-CR-182296-VOL-2 ..... p 3709 N94-32869 * #
NASA-CR-185207 ..... p 3709 N94-32872 * #
NASA-CR-185297 ..... p 3615 N94-32792 * #
NASA-CR-187096 ..... p 3584 N94-32859 * #
NASA-CR-188283 ..... p 3835 N94-32359 * #
NASA-CR-188284 ..... p 3739 N94-32907 * #
NASA-CR-188285 ..... p 3601 N94-32388 * #
NASA-CR-188286 ..... p 3669 N94-32857 * #
NASA-CR-188288 ..... p 3731 N94-32862 * #
NASA-CR-188289 ..... p 3577 N94-32864 * #
NASA-CR-189175 ..... p 3614 N94-31618 * #
NASA-CR-189332 ..... p 3711 N94-31492 * #
NASA-CR-189558 ..... p 3626 N94-32877 * #
NASA-CR-189581 ..... p 3638 N94-32868 * #
NASA-CR-189593 ..... p 3626 N94-32860 * #
NASA-CR-189594 ..... p 3682 N94-32897 * #
NASA-CR-189617 ..... p 3731 N94-32481 * #
NASA-CR-189648 ..... p 3707 N94-32480 * #
NASA-CR-190299 ..... p 3804 N94-32697 * #
NASA-CR-191009 ..... p 3728 N94-32900 * #
NASA-CR-191327 ..... p 3826 N94-32482 * #
NASA-CR-191348 ..... p 3927 N94-32695 * #
NASA-CR-191349 ..... p 3882 N94-32702 * #
NASA-CR-191351 ..... p 3637 N94-32696 * #
NASA-CR-191352 ..... p 3637 N94-32694 * #
NASA-CR-191577 ..... p 3827 N94-32734 * #
NASA-CR-191792 ..... p 3669 N94-32484 *
NASA-CR-191796 ..... p 3826 N94-32483 * #
NASA-CR-192722 ..... p 3882 N94-32417 * #
NASA-CR-193272 ..... p 3571 N94-32476 * #
NASA-CR-193937 ..... p 3611 N94-32898 * #
NASA-CR-193951 ..... p 3608 N94-33100 * #
NASA-CR-194211 ..... p 3681 N94-32477 * #
NASA-CR-194216 ..... p 3727 N94-32479 * #
NASA-CR-194223 ..... p 3694 N94-32478 * #
NASA-CR-194279 ..... p 3943 N94-33190 * #
NASA-CR-194472 ..... p 3728 N94-32929 * #
NASA-CR-194865 ..... p 3954 N94-31101 * #
NASA-CR-194883 ..... p 3821 N94-33075 * #
NASA-CR-194889 ..... p 3806 N94-33286 * #
NASA-CR-194896 ..... p 3820 N94-32928 * #
NASA-CR-194902 ..... p 3849 N94-33033 * #
NASA-CR-194905 ..... p 3862 N94-33023 * #
NASA-CR-195097 ..... p 3683 N94-33083 * #
NASA-CR-195240 ..... p 3697 N94-33044 * #
NASA-CR-195295 ..... p 3616 N94-33099 * #
NASA-CR-195297 ..... p 3573 N94-33119 * #
NASA-CR-195301 ..... p 3571 N94-32475 * #
NASA-CR-195302 ..... p 3572 N94-32926 * #
NASA-CR-195303 ..... p 3626 N94-32904 * #
NASA-CR-195304 ..... p 3584 N94-32075 * #
NASA-CR-195307 ..... p 3727 N94-32741 * #
NASA-CR-195311 ..... p 3616 N94-32970 * #
NASA-CR-195332 ..... p 3731 N94-32901 * #
NASA-CR-195692 ..... p 3790 N94-33045 * #
NASA-CR-195696 ..... p 3939 N94-31105 * #
NASA-CR-195756 ..... p 3927 N94-31116 * #
NASA-CR-195765 ..... p 3585 N94-31203 * #
NASA-CR-195807 ..... p 3740 N94-32940 * #
NASA-CR-195818 ..... p 3927 N94-32942 * #
NASA-CR-195820 ..... p 3893 N94-33048 * #
NASA-CR-195821 ..... p 3912 N94-32774 * #
NASA-CR-195826 ..... p 3836 N94-32980 * #
NASA-CR-195827 ..... p 3942 N94-32740 * #
NASA-CR-195828 ..... p 3884 N94-33073 * #
NASA-CR-195833 ..... p 3757 N94-33019 * #
NASA-CR-195834 ..... p 3787 N94-33288 * #
NASA-CR-195835 ..... p 3639 N94-33036 * #
NASA-CR-195836 ..... p 3835 N94-32943 * #
NASA-CR-195841 ..... p 3584 N94-33035 * #
NASA-CR-195848 ..... p 3953 N94-33047 * #
NASA-CR-195849 ..... p 3821 N94-33049 * #
NASA-CR-195851 ..... p 3790 N94-32981 * #
NASA-CR-195877 ..... p 3943 N94-33103 * #
NASA-CR-195878 ..... p 3816 N94-32086 * #
NASA-CR-195879 ..... p 3603 N94-32494 * #
NASA-CR-195880 ..... p 3893 N94-33074 * #
NASA-CR-195881 ..... p 3668 N94-33037 * #
NASA-CR-195886 ..... p 3943 N94-33104 * #
NASA-CR-195902 ..... p 3913 N94-33148 * #
NASA-CR-195903 ..... p 3894 N94-33113 * #
NASA-CR-195906 ..... p 3822 N94-33114 * #
NASA-CR-195908 ..... p 3769 N94-33170 * #
NASA-CR-195910 ..... p 3612 N94-33115 * #
NASA-CR-195911 ..... p 3653 N94-31851 * #
NASA-CR-195913 ..... p 3803 N94-31447 *
NASA-CR-4269 ..... p 3709 N94-32871 * #
NASA-CR-4418 ..... p 3626 N94-32863 * #
NASA-CR-4585 ..... p 3787 N94-33065 * #
NASA-CR-4594 ..... p 3820 N94-32775 * #
NASA-CR-4596 ..... p 3820 N94-32776 * #

NASA-SP-4216 ..... p 3566 N94-32793 * #
NASA-SP-7011(385) ..... p 3797 N94-32348 *
NASA-SP-7011(388) ..... p 3795 N94-31414 *
NASA-SP-7011(389) ..... p 3797 N94-32347 *
NASA-SP-7037(302) ..... p 3565 N94-31342 *
NASA-SP-7037(303) ..... p 3565 N94-31381 *
NASA-SP-7037(304) ..... p 3566 N94-32853 *

NASA-TM-103845 ..... p 3820 N94-32906 * #
NASA-TM-103979 ..... p 3709 N94-32946 * #
NASA-TM-103985 ..... p 3571 N94-32063 * #
NASA-TM-104139 ..... p 3572 N94-32873 * #
NASA-TM-104594-VOL-1 ..... p 3823 N94-33287 * #
NASA-TM-104594-VOL-2 ..... p 3613 N94-33289 * #
NASA-TM-104602 ..... p 3732 N94-33101 * #
NASA-TM-104791 ..... p 3943 N94-32923 * #
NASA-TM-104793 ..... p 3820 N94-32899 * #
NASA-TM-105280 ..... p 3669 N94-32861 * #
NASA-TM-105441 ..... p 3966 N94-32885 * #
NASA-TM-105607 ..... p 3626 N94-32858 * #
NASA-TM-105625 ..... p 3739 N94-32883 * #
NASA-TM-106366 ..... p 3728 N94-32902 * #
NASA-TM-106376 ..... p 3567 N94-33046 * #
NASA-TM-106456 ..... p 3728 N94-32893 * #
NASA-TM-106472 ..... p 3617 N94-32941 * #
NASA-TM-106496 ..... p 3567 N94-33064 * #
NASA-TM-106499 ..... p 3739 N94-32735 * #
NASA-TM-106501 ..... p 3615 N94-32742 * #
NASA-TM-106522 ..... p 3647 N94-32931 * #
NASA-TM-106538 ..... p 3740 N94-32932 * #
NASA-TM-106542 ..... p 3710 N94-32969 * #
NASA-TM-106544 ..... p 3709 N94-32947 * #
NASA-TM-106547 ..... p 3617 N94-33021 * #
NASA-TM-106550 ..... p 3700 N94-31229 * #
NASA-TM-106551 ..... p 3573 N94-32984 * #

NASA-TM-106552 ..... p 3728 N94-32979 * #
NASA-TM-106554 ..... p 3662 N94-32945 * #
NASA-TM-106561 ..... p 3883 N94-32777 * #
NASA-TM-106566 ..... p 3696 N94-32905 * #
NASA-TM-106567 ..... p 3698 N94-33116 * #
NASA-TM-106574 ..... p 3697 N94-33052 * #
NASA-TM-106587 ..... p 3820 N94-32773 * #
NASA-TM-106591 ..... p 3713 N94-32983 * #
NASA-TM-106592 ..... p 3617 N94-33022 * #
NASA-TM-106597 ..... p 3731 N94-33032 * #
NASA-TM-106601 ..... p 3850 N94-33120 * #
NASA-TM-106602 ..... p 3710 N94-33070 * #
NASA-TM-106603 ..... p 3663 N94-33024 * #
NASA-TM-106604 ..... p 3726 N94-32272 * #
NASA-TM-107582 ..... p 3601 N94-32870 * #
NASA-TM-108237 ..... p 3860 N94-31337 * #
NASA-TM-108238 ..... p 3860 N94-31336 * #
NASA-TM-108441 ..... p 3803 N94-31380 * #
NASA-TM-108445 ..... p 3786 N94-33004 * #
NASA-TM-108454 ..... p 3739 N94-32903 * #
NASA-TM-108798 ..... p 3617 N94-33117 * #
NASA-TM-108807 ..... p 3711 N94-33290 * #
NASA-TM-108810 ..... p 3801 N94-33068 * #
NASA-TM-108811 ..... p 3805 N94-32936 * #
NASA-TM-108814 ..... p 3575 N94-32927 * #
NASA-TM-109073 ..... p 3740 N94-33118 * #
NASA-TM-109086 ..... p 3785 N94-32737 * #
NASA-TM-109088 ..... p 3922 N94-32837 * #
NASA-TM-109093 ..... p 3613 N94-32924 * #
NASA-TM-109098 ..... p 3922 N94-32836 * #
NASA-TM-109108 ..... p 3627 N94-32939 * #
NASA-TM-109109 ..... p 3710 N94-33020 * #
NASA-TM-109112 ..... p 3573 N94-32950 * #
NASA-TM-109120 ..... p 3586 N94-32951 * #
NASA-TM-109196 ..... p 3966 N94-33072 * #
NASA-TM-109348 ..... p 3921 N94-32834 * #
NASA-TM-109404 ..... p 3921 N94-32832 * #
NASA-TM-109700 ..... p 3914 N94-33066 * #
NASA-TM-109722 ..... p 3917 N94-31888 * #
NASA-TM-109740 ..... p 3573 N94-33071 * #
NASA-TM-109744 ..... p 3674 N94-31503 * #
NASA-TM-109746 ..... p 3634 N94-31883 *
NASA-TM-109747 ..... p 3667 N94-31884 *
NASA-TM-109748 ..... p 3956 N94-31885 *
NASA-TM-109749 ..... p 3574 N94-31803 *
NASA-TM-109750 ..... p 3725 N94-31804 *
NASA-TM-109751 ..... p 3942 N94-31805 *
NASA-TM-109752 ..... p 3913 N94-31806 *
NASA-TM-109754 ..... p 3913 N94-31807 *
NASA-TM-109755 ..... p 3602 N94-31814 *
NASA-TM-109756 ..... p 3913 N94-31815 *
NASA-TM-109757 ..... p 3806 N94-31816 *
NASA-TM-109758 ..... p 3705 N94-31886 *
NASA-TM-109759 ..... p 3914 N94-31887 *
NASA-TM-109760 ..... p 3913 N94-31817 *
NASA-TM-109761 ..... p 3614 N94-31818 *
NASA-TM-109762 ..... p 3735 N94-31819 *
NASA-TM-109763 ..... p 3600 N94-31820 *
NASA-TM-109769 ..... p 3921 N94-32831 * #
NASA-TM-109771 ..... p 3921 N94-32830 * #
NASA-TM-109774 ..... p 3922 N94-32835 * #
NASA-TM-109777 ..... p 3921 N94-32829 * #
NASA-TM-109778 ..... p 3806 N94-32389 *
NASA-TM-109780 ..... p 3915 N94-32222 * #
NASA-TM-109782 ..... p 3921 N94-32833 * #
NASA-TM-109787 ..... p 3924 N94-33067 * #
NASA-TM-4387 ..... p 3572 N94-32880 * #
NASA-TM-4545 ..... p 3732 N94-33038 * #
NASA-TM-4557 ..... p 3638 N94-32948 * #

NASA-TP-3129 ..... p 3572 N94-32865 * #
NASA-TP-3425 ..... p 3861 N94-32930 * #
NASA-TP-3477 ..... p 3805 N94-33050 * #

NATICK-TR-94/014 ..... p 3804 N94-32580

NAVSWC-TR-91-506 ..... p 3712 N94-32051 #

NAVY-CASE-70935 ..... p 3882 N94-32626
NAVY-CASE-75176 ..... p 3681 N94-32625 #

NAWC-WPNS-TP-8183 ..... p 3687 N94-31281
NAWC-WPNS-TP-8185 ..... p 3712 N94-32393 #

NAWCADWAR-93050-60 ..... p 3664 N94-33166
NAWCADWAR-93053-60 ..... p 3631 N94-31248 #
NAWCADWAR-93069-60 ..... p 3797 N94-32156 #

NAWCTSD-TR-93-021 ..... p 3712 N94-32002 #

NCCOSC/RDT/E-TD-2608 ..... p 3672 N94-31334 #
NCCOSC/RDT/E-TD-2609 ..... p 3770 N94-31303 #

NCCOSC/RDT/E-TR-1588 ..... p 3730 N94-31065 #
NCCOSC/RDT/E-TR-1636 ..... p 3684 N94-33254 #
NCCOSC/RDT/E-TR-1637 ..... p 3577 N94-33253

NCSC-TG-030 ..... p 3916 N94-31331 #

NDU-ICAF-93-DIS ..... p 3610 N94-32039 #
NDU-ICAF-93-F22A ..... p 3918 N94-32090 #
NDU-ICAF-93-F22B ..... p 3600 N94-32126 #
NDU-ICAF-93-F22 ..... p 3918 N94-32210 #
NDU-ICAF-93-F27 ..... p 3608 N94-32190 #
NDU-ICAF-93-F39 ..... p 3579 N94-32058 #
NDU-ICAF-93-F40 ..... p 3834 N94-32061 #
NDU-ICAF-93-S40 ..... p 3601 N94-32211
NDU-ICAF-93-S83 ..... p 3579 N94-32232 #

NDU/ICAF-93-F3 ..... p 3575 N94-32168 #
NDU/ICAF-93-RS1 ..... p 3765 N94-32195 #

NFESC-TR-2013-SHR ..... p 3623 N94-32070 #
NFESC-TR-2016-SHR ..... p 3775 N94-33028 #

NHB-5300.4(2B-2) ..... p 3731 N94-32387 * #

NHK-LABS-NOTE-423 ..... p 3683 N94-33081

NHRC-93-23 ..... p 3802 N94-31302 #

NIST/SP-857 ..... p 3916 N94-31228 #

NIST/TN-1361 ..... p 3675 N94-31683 #

NLR-TP-90247-U ..... p 3567 N94-31180
NLR-TP-91489-U ..... p 3587 N94-31179 #
NLR-TP-92272-U ..... p 3598 N94-31208

NONP-DTIC-DK-94-11178 ..... p 3805 N94-33171
NONP-DTIC-DK-94-2360 ..... p 3922 N94-33256
NONP-DTIC-DK-94-2362 ..... p 3922 N94-33257
NONP-DTIC-DK-94-2365 ..... p 3923 N94-33259

NONP-NASA-VT-94-9946 ..... p 3634 N94-31883 *
NONP-NASA-VT-94-9947 ..... p 3667 N94-31884 *
NONP-NASA-VT-94-9948 ..... p 3956 N94-31885 *
NONP-NASA-VT-94-9949 ..... p 3574 N94-31803 *
NONP-NASA-VT-94-9950 ..... p 3725 N94-31804 *
NONP-NASA-VT-94-9951 ..... p 3942 N94-31805 *
NONP-NASA-VT-94-9952 ..... p 3913 N94-31806 *
NONP-NASA-VT-94-9954 ..... p 3913 N94-31807 *
NONP-NASA-VT-94-9955 ..... p 3602 N94-31814 *
NONP-NASA-VT-94-9956 ..... p 3913 N94-31815 *
NONP-NASA-VT-94-9957 ..... p 3806 N94-31816 *
NONP-NASA-VT-94-9958 ..... p 3705 N94-31886 *
NONP-NASA-VT-94-9959 ..... p 3914 N94-31887 *
NONP-NASA-VT-94-9960 ..... p 3913 N94-31817 *
NONP-NASA-VT-94-9961 ..... p 3614 N94-31818 *
NONP-NASA-VT-94-9962 ..... p 3735 N94-31819 *
NONP-NASA-VT-94-9963 ..... p 3600 N94-31820 *
NONP-NASA-VT-94-9978 ..... p 3806 N94-32389 *

NPS-EC-93-020 ..... p 3672 N94-31386 #
NPS-EC-93-022 ..... p 3679 N94-32282

NPS-MA-94-001 ..... p 3610 N94-32208 #

NPS-MR-94-001 ..... p 3789 N94-32325 #

NPS-OR-93-020 ..... p 3781 N94-31239 #

NRAD-TD-2597 ..... p 3682 N94-32971 #

NRC-TR-92-143 ..... p 3727 N94-32479 * #

NREL/TP-411-5815 ..... p 3760 N94-32143 #
NREL/TP-411-6264 ..... p 3759 N94-31279 #
NREL/TP-411-6292 ..... p 3758 N94-31264 #
NREL/TP-411-6396 ..... p 3695 N94-32680 #
NREL/TP-411-6397 ..... p 3762 N94-32765 #
NREL/TP-411-6399 ..... p 3905 N94-32764 #
NREL/TP-451-6135 ..... p 3760 N94-31812
NREL/TP-451-6192 ..... p 3899 N94-31813
NREL/TP-451-6215 ..... p 3758 N94-31236 #
NREL/TP-451-6398 ..... p 3762 N94-32763 #
NREL/TP-463-5608 ..... p 3953 N94-31491 #
NREL/TP-463-6153 ..... p 3690 N94-31598 #

NRL-CR-7181-94-0004 ..... p 3845 N94-32022 #

NRL-CR/7320-93-0004 ..... p 3747 N94-32214
NRL-CR/7330-93-0001 ..... p 3789 N94-32321

NRL-MR-5194 ..... p 3702 N94-31467 #

NRL/FR/5520-94-9703 ..... p 3673 N94-31446
NRL/FR/5530-94-9712 ..... p 3683 N94-33026 #
NRL/FR/5540-93-9586 ..... p 3811 N94-31461 #
NRL/FR/5640-94-9704 ..... p 3717 N94-31936 #
NRL/FR/5742-94-9705 ..... p 3688 N94-31494 #
NRL/FR/7140-94-9700 ..... p 3850 N94-31462 #

NRL/MR/5520-94-7442 ..... p 3680 N94-32283 #
NRL/MR/6180-94-7431 ..... p 3575 N94-32405
NRL/MR/6707-94-7444 ..... p 3718 N94-32406
NRL/MR/6790-93-7403 ..... p 3726 N94-32236 #
NRL/MR/6790-94-7408 ..... p 3692 N94-32199
NRL/MR/7441-93-7071 ..... p 3922 N94-32967 #

NRL/PP/7174-93-0034 ..... p 3788 N94-32000 #

NRL/PU/7515-93-0011 ..... p 3785 N94-32278
NRL/PU/7541-92-0001 ..... p 3787 N94-33089
NRL/PU/7541-93-0014 ..... p 3784 N94-32260

NSWCDD-TR-92/296 ..... p 3693 N94-32329

NSWCDD/MP-93/200 ..... p 3668 N94-31364 #

NSWCDD/TR-92/160 ..... p 3587 N94-31318
NSWCDD/TR-94/3 ..... p 3574 N94-33263

NTIAC-7304-103 ..... p 3730 N94-32068 #

NTSB/AAR-94/02 ..... p 3576 N94-32938 #

NTSB/ARC-94/01 ..... p 3575 N94-32925 #

NUWC-NPT-TD-10212 ..... p 3834 N94-32036

NUWC-NPT-TR-10427 ..... p 3682 N94-33001 #

NUWC-NPT-10591 ..... p 3826 N94-32323 #

ONERA-NT-1993-10 ..... p 3618 N94-31232 #
ONERA-NT-1993-11 ..... p 3860 N94-31226 #
ONERA-NT-1993-12 ..... p 3863 N94-31227 #
ONERA-NT-1993-13 ..... p 3702 N94-31477 #
ONERA-NT-1993-14 ..... p 3619 N94-31478 #
ONERA-NT-1993-15 ..... p 3614 N94-31423 #
ONERA-NT-1993-2 ..... p 3673 N94-31418 #
ONERA-NT-1993-3 ..... p 3673 N94-31419 #
ONERA-NT-1993-4 ..... p 3618 N94-31225 #
ONERA-NT-1993-5 ..... p 3574 N94-31230 #
ONERA-NT-1993-6 ..... p 3640 N94-31420 #
ONERA-NT-1993-7 ..... p 3840 N94-31231 #
ONERA-NT-1993-8 ..... p 3568 N94-31421 #
ONERA-NT-1993-9 ..... p 3701 N94-31422 #

ONREUR-93-7-R ..... p 3648 N94-31059 #

ORNL/M-3155 ..... p 3659 N94-32632
ORNL/M-3198 ..... p 3642 N94-31918 #
ORNL/M-3201 ..... p 3662 N94-32935

ORNL/SUB-86-SD861/01 ..... p 3659 N94-32618 #
ORNL/SUB-87-SA946/03 ..... p 3662 N94-32891

ORNL/TM-12112 ..... p 3915 N94-31155 #
ORNL/TM-12392 ..... p 3741 N94-31606 #
ORNL/TM-12651 ..... p 3920 N94-32676 #

OTA-BP-ISC-122 ..... p 3741 N94-31068

OY/TTO-DP-4 ..... p 3765 N94-32590 #

PB94-125523 ..... p 3598 N94-31208
PB94-126992 ..... p 3741 N94-31068
PB94-127933 ..... p 3917 N94-31768 #
PB94-135589 ..... p 3648 N94-31069
PB94-135597 ..... p 3634 N94-31679 #
PB94-137494 ..... p 3758 N94-31070
PB94-137502 ..... p 3758 N94-31071
PB94-138484 ..... p 3649 N94-31072
PB94-138534 ..... p 3668 N94-31838
PB94-138542 ..... p 3803 N94-31839
PB94-138559 ..... p 3918 N94-32293
PB94-138567 ..... p 3717 N94-31840
PB94-138575 ..... p 3735 N94-31841
PB94-138781 ..... p 3668 N94-31073
PB94-142064 ..... p 3832 N94-31808
PB94-142247 ..... p 3953 N94-31595
PB94-142734 ..... p 3576 N94-31680
PB94-145083 ..... p 3917 N94-31583
PB94-145158 ..... p 3867 N94-31681
PB94-145166 ..... p 3868 N94-31921
PB94-145174 ..... p 3868 N94-32008
PB94-145182 ..... p 3813 N94-31682
PB94-145711 ..... p 3675 N94-31683 #
PB94-147022 ..... p 3844 N94-31684 #
PB94-147048 ..... p 3813 N94-31685
PB94-147055 ..... p 3868 N94-31922
PB94-147105 ..... p 3868 N94-31923
PB94-147147 ..... p 3912 N94-31924
PB94-147485 ..... p 3813 N94-31686
PB94-147493 ..... p 3813 N94-31687
PB94-147527 ..... p 3741 N94-31074
PB94-147535 ..... p 3741 N94-31075

PB94-147782 ..... p 3601 N94-31769 #
PB94-148061 ..... p 3878 N94-31584
PB94-148079 ..... p 3676 N94-31925
PB94-148210 ..... p 3651 N94-31585
PB94-148236 ..... p 3917 N94-31586
PB94-148251 ..... p 3806 N94-31587
PB94-148277 ..... p 3702 N94-31588
PB94-148285 ..... p 3620 N94-31688
PB94-148442 ..... p 3857 N94-31770
PB94-148459 ..... p 3610 N94-31771
PB94-148467 ..... p 3857 N94-31589
PB94-148475 ..... p 3889 N94-31772
PB94-148483 ..... p 3850 N94-31590
PB94-148616 ..... p 3633 N94-31591
PB94-148681 ..... p 3743 N94-31592
PB94-148749 ..... p 3691 N94-31848
PB94-149572 ..... p 3698 N94-33169
PB94-158847 ..... p 3575 N94-32925 #
PB94-910403 ..... p 3576 N94-32938 #

PCMDI-13 ..... p 3768 N94-32882
PCMDI-14 ..... p 3790 N94-32881

PL-TR-93-1058 ..... p 3722 N94-33282 #
PL-TR-93-2166 ..... p 3784 N94-32117 #
PL-TR-93-2177 ..... p 3776 N94-33272 #
PL-TR-93-2185 ..... p 3773 N94-32118
PL-TR-93-2204 ..... p 3678 N94-32161 #
PL-TR-93-2219 ..... p 3775 N94-32999
PL-TR-93-2234 ..... p 3680 N94-32297 #
PL-TR-93-3088 ..... p 3667 N94-33013 #
PL-TR-94-2001 ..... p 3747 N94-32160 #
PL-TR-94-2020 ..... p 3678 N94-32159
PL-TR-94-2021 ..... p 3678 N94-32158 #
PL-TR-94-2022 ..... p 3680 N94-32300 #
PL-TR-94-2023 ..... p 3676 N94-31998 #
PL-TR-94-2024 ..... p 3680 N94-32299 #
PL-TR-94-2025 ..... p 3680 N94-32298 #
PL-TR-94-2026 ..... p 3685 N94-33347
PL-TR-94-2027 ..... p 3677 N94-32083 #

PNL-SA-21969 ..... p 3804 N94-32596
PNL-SA-22151 ..... p 3712 N94-31831
PNL-SA-22168 ..... p 3730 N94-31605 #
PNL-SA-22301 ..... p 3713 N94-32681
PNL-SA-22452 ..... p 3641 N94-31626 #
PNL-SA-22582 ..... p 3759 N94-31762 #
PNL-SA-22700 ..... p 3713 N94-32811 #
PNL-SA-22718 ..... p 3895 N94-31307 #
PNL-SA-22751 ..... p 3746 N94-32100 #
PNL-SA-22766 ..... p 3641 N94-31627 #
PNL-SA-23042 ..... p 3785 N94-32268 #
PNL-SA-23229 ..... p 3786 N94-32759 #
PNL-SA-23410 ..... p 3645 N94-32614
PNL-SA-23576 ..... p 3914 N94-32910 #
PNL-SA-23581 ..... p 3767 N94-32750 #
PNL-SA-23676 ..... p 3720 N94-32704 #
PNL-SA-23709 ..... p 3768 N94-32812 #

PNL-7318 ..... p 3687 N94-31152 #
PNL-8994 ..... p 3816 N94-32146 #
PNL-8995 ..... p 3816 N94-32145 #
PNL-8999 ..... p 3871 N94-32605
PNL-9002 ..... p 3763 N94-31582 #
PNL-9011 ..... p 3691 N94-31785 #

POC-3225 ..... p 3884 N94-33087 #

PSI-2123/TR-1153 ..... p 3694 N94-32478 * #

PSU/ARL-TR-94-05 ..... p 3583 N94-31931

PW/GESP-FR21998-22 ..... p 3643 N94-32047 #

R-223 ..... p 3577 N94-33095 #
R-3878/1-AF ..... p 3581 N94-33329

R/D-5548-MS-01 ..... p 3616 N94-32038
R/D-6194-EN-01-VOL-2 ..... p 3757 N94-33269
R/D-6291-EE-01 ..... p 3693 N94-32301
R/D-6294-CH-01 ..... p 3717 N94-31996
R/D-6310-MS-01 ..... p 3879 N94-32037
R/D-6323-EN-01 ..... p 3784 N94-32162
R/D-6709-EE-01 ..... p 3884 N94-33267
R/D-6798-EN-01 ..... p 3718 N94-32305
R/D-6869-MS-01 ..... p 3738 N94-32351
R/D-6891-MA-02 ..... p 3794 N94-33250
R/D-7051-EE-02-VOL-2104 ..... p 3884 N94-33187
R/D-7071-EE-03 ..... p 3692 N94-32259
R/D-7096-EE-03 ..... p 3693 N94-32307 #
R/D-7110-CH-02 ..... p 3721 N94-33000 #
R/D-7121-EE-03 ..... p 3677 N94-32067
R/D-7125-EE-02 ..... p 3906 N94-32908
R/D-7131-EE-0041 ..... p 3772 N94-32007
R/D-7150-EE-01 ..... p 3776 N94-33184
R/D-7211-CH-02 ..... p 3655 N94-32016 #

RAL-93-049 ..... p 3868 N94-31923
RAL-93-074 ..... p 3868 N94-31922
RAL-93-080 ..... p 3912 N94-31924
RAL-93-083 ..... p 3867 N94-31681
RAL-93-088 ..... p 3813 N94-31685
RAL-93-097 ..... p 3813 N94-31682
RAL-93-103 ..... p 3868 N94-31921
RAL-94-012 ..... p 3868 N94-32008

RCC-212-94 ..... p 3681 N94-32332

RCC/RSG-313-94-VOL-1 ..... p 3602 N94-32333

RELEASE-1.2 ..... p 3916 N94-31338

REPT-0650-350-0457 ..... p 3740 N94-33143
REPT-1148-94-05 ..... p 3663 N94-33054 #
REPT-1148-94-06 ..... p 3663 N94-32985
REPT-1148-94-08 ..... p 3664 N94-33348
REPT-1148-94-09 ..... p 3664 N94-33082 #
REPT-3256 ..... p 3884 N94-33073 * #
REPT-540-030 ..... p 3674 N94-31503 * #
REPT-90-060-REV ..... p 3829 N94-31176
REPT-91-016-REV ..... p 3824 N94-31177
REPT-93-021 ..... p 3808 N94-31178
REPT-93-032 ..... p 3829 N94-31186
REPT-93-036 ..... p 3840 N94-31187
REPT-93-037 ..... p 3809 N94-31188
REPT-93-038 ..... p 3809 N94-31189
REPT-93-039 ..... p 3671 N94-31190
REPT-93-040 ..... p 3809 N94-31212
REPT-93-041 ..... p 3850 N94-31191
REPT-93-042 ..... p 3809 N94-31192
REPT-93-047 ..... p 3911 N94-31893
REPT-93-64 ..... p 3703 N94-31660 #
REPT-93-65 ..... p 3851 N94-31661 #
REPT-93-66 ..... p 3825 N94-31662 #
REPT-93-67 ..... p 3674 N94-31645 #
REPT-93-68 ..... p 3812 N94-31646 #
REPT-93-69 ..... p 3830 N94-31647 #
REPT-93-70 ..... p 3917 N94-31640 #
REPT-93-72 ..... p 3824 N94-31641 #
REPT-93-73 ..... p 3843 N94-31642 #
REPT-93-74 ..... p 3844 N94-31643 #
REPT-93-75 ..... p 3844 N94-31644 #
REPT-93-76 ..... p 3844 N94-31693 #
REPT-93-77 ..... p 3813 N94-31694 #
REPT-93-78 ..... p 3813 N94-31695 #
REPT-93-79 ..... p 3844 N94-31696 #
REPT-93-80 ..... p 3851 N94-31697 #
REPT-93-81 ..... p 3851 N94-31698 #
REPT-93-82 ..... p 3851 N94-31699 #
REPT-93-83 ..... p 3825 N94-31700 #
REPT-93-84 ..... p 3844 N94-31701 #
REPT-93-85 ..... p 3845 N94-31702 #
REPT-93-86 ..... p 3924 N94-31617 #
REPT-93-87 ..... p 3843 N94-31552 #
REPT-93-88 ..... p 3812 N94-31522 #
REPT-93-89 ..... p 3844 N94-31673 #
REPT-93-90 ..... p 3703 N94-31703 #
REPT-93-91 ..... p 3813 N94-31704 #
REPT-94B00058-VOL-1 ..... p 3823 N94-33287 * #
REPT-94B00069-VOL-2 ..... p 3613 N94-33289 * #
REPT-94B00071 ..... p 3732 N94-33101 * #
REPT-94001-SBIR-1-F ..... p 3908 N94-33246

RL-TM-93-6 ..... p 3810 N94-31335 #

RL-TR-93-176 ..... p 3870 N94-32368 #
RL-TR-93-193 ..... p 3816 N94-32131 #
RL-TR-93-210 ..... p 3672 N94-31371 #
RL-TR-93-215 ..... p 3650 N94-31284 #
RL-TR-93-217 ..... p 3686 N94-31066 #
RL-TR-93-239 ..... p 3836 N94-33043 #
RL-TR-93-241 ..... p 3719 N94-32608
RL-TR-93-248 ..... p 3880 N94-32151 #
RL-TR-93-249 ..... p 3732 N94-33088 #
RL-TR-93-260 ..... p 3683 N94-33093 #
RL-TR-94-20-VOL-1 ..... p 3676 N94-32049
RL-TR-94-20-VOL-2 ..... p 3677 N94-32050

RR-463 ..... p 3842 N94-31394
RR-479 ..... p 3722 N94-31379
RR-480 ..... p 3830 N94-31500
RR-482 ..... p 3842 N94-31412
RR-483 ..... p 3842 N94-31413
RR-897-M ..... p 3839 N94-31082

RTI-83U-5294 ..... p 3902 N94-32306 #

RTI/5294/94-QUARTERLY ..... p 3902 N94-32306 #

RUU-CS-92-10 ..... p 3844 N94-31684 #
RUU-CS-93-10 ..... p 3916 N94-31365 #

RXR-93081 ..... p 3776 N94-33272 #

R92-204 ..... p 3882 N94-32417 * #
R94-970051-3 ..... p 3665 N94-33352 #

S-762 ..... p 3943 N94-32923 * #
S-764 ..... p 3805 N94-33050 * #
S-766 ..... p 3820 N94-32899 * #

SAIC-93/1001 ..... p 3919 N94-32382 #
SAIC-94/1017 ..... p 3710 N94-33009 #

SAND-93-0092C ..... p 3603 N94-32671 #
SAND-93-0909 ..... p 3717 N94-32134 #
SAND-93-1274C ..... p 3701 N94-31268 #
SAND-93-1473C ..... p 3902 N94-32296 #
SAND-93-1544C ..... p 3651 N94-31650 #
SAND-93-1545C ..... p 3882 N94-32674
SAND-93-1587C ..... p 3660 N94-32729 #
SAND-93-1590C ..... p 3688 N94-31483 #
SAND-93-1601C ..... p 3941 N94-31145 #
SAND-93-1635C ..... p 3634 N94-32110
SAND-93-1734C ..... p 3666 N94-31827 #
SAND-93-1752C ..... p 3661 N94-32819 #
SAND-93-1785C ..... p 3882 N94-32649 #
SAND-93-1816C ..... p 3897 N94-31502 #
SAND-93-1830C ..... p 3690 N94-31594
SAND-93-1977C ..... p 3818 N94-32353 #
SAND-93-2047C ..... p 3645 N94-32672
SAND-93-2073 ..... p 3609 N94-31382 #
SAND-93-2077C ..... p 3678 N94-32113
SAND-93-2084C ..... p 3872 N94-32628 #
SAND-93-2112C ..... p 3907 N94-32963
SAND-93-2124C ..... p 3615 N94-32669
SAND-93-2128C ..... p 3690 N94-31593
SAND-93-2204C ..... p 3613 N94-31265 #
SAND-93-2413C ..... p 3576 N94-31306 #
SAND-93-2417 ..... p 3714 N94-31148 #
SAND-93-2429C ..... p 3692 N94-32112
SAND-93-2453 ..... p 3763 N94-32965
SAND-93-2474C ..... p 3625 N94-32642 #
SAND-93-2552C ..... p 3739 N94-32842
SAND-93-2556C ..... p 3707 N94-32373 #
SAND-93-2679C ..... p 3737 N94-32135
SAND-93-2687 ..... p 3668 N94-32412
SAND-93-2702C ..... p 3901 N94-32104 #
SAND-93-2719C ..... p 3715 N94-31485 #
SAND-93-2743C ..... p 3899 N94-31847 #
SAND-93-3807 ..... p 3823 N94-31149 #
SAND-93-3863C ..... p 3651 N94-31649 #
SAND-93-3865C ..... p 3695 N94-32663 #
SAND-93-3872C ..... p 3661 N94-32796 #
SAND-93-3895C ..... p 3568 N94-31578 #
SAND-93-3967C ..... p 3920 N94-32808 #
SAND-93-3979C ..... p 3852 N94-32673 #
SAND-93-4040C ..... p 3671 N94-31267 #
SAND-93-4088 ..... p 3819 N94-32651
SAND-93-4104C ..... p 3849 N94-32675 #
SAND-93-7072 ..... p 3708 N94-32709 #
SAND-93-8221 ..... p 3733 N94-31316 #
SAND-93-8688 ..... p 3793 N94-32269 #
SAND-93-8690C ..... p 3723 N94-31651 #
SAND-94-0009C ..... p 3693 N94-32386 #
SAND-94-0054C ..... p 3660 N94-32727 #
SAND-94-0056C ..... p 3655 N94-32102 #
SAND-94-0123C ..... p 3811 N94-31484 #
SAND-94-0147C ..... p 3716 N94-31622 #
SAND-94-0158 ..... p 3903 N94-32409 #
SAND-94-0163C ..... p 3695 N94-32650 #
SAND-94-0249 ..... p 3807 N94-32766 #
SAND-94-0254C ..... p 3849 N94-32653 #
SAND-94-0259C ..... p 3666 N94-31579 #
SAND-94-0277C ..... p 3883 N94-32878
SAND-94-0283C ..... p 3640 N94-31345 #
SAND-94-0317C ..... p 3719 N94-32603 #
SAND-94-0328C ..... p 3774 N94-32816 #
SAND-94-0357C ..... p 3903 N94-32384 #
SAND-94-0393C ..... p 3883 N94-32818
SAND-94-0402C ..... p 3692 N94-32111 #
SAND-94-0405C ..... p 3695 N94-32700 #
SAND-94-0408C ..... p 3835 N94-32787 #
SAND-94-0477C ..... p 3696 N94-32809 #
SAND-94-0497C ..... p 3761 N94-32383 #
SAND-94-0524C ..... p 3881 N94-32385 #
SAND-94-0552C ..... p 3761 N94-32648 #
SAND-94-0597C ..... p 3696 N94-32786 #
SAND-94-0630C ..... p 3696 N94-32806 #
SAND-94-8219 ..... p 3661 N94-32803 #
SAND-94-8225 ..... p 3818 N94-32584 #
SAND-94-8508C ..... p 3649 N94-31198 #

SC71061.FR ..... p 3908 N94-33248 #

SLAC-PUB-6393 ..... p 3875 N94-33189 #

SLAC/SSRL-0049 ..... p 3721 N94-32845 #

SMC-TR-94-02 ..... p 3624 N94-32122 #

SMC-TR-94-04 ..... p 3894 N94-33106
SMC-TR-94-06 ..... p 3635 N94-32233 #
SMC-TR-94-07 ..... p 3612 N94-33262
SMC-TR-94-11 ..... p 3698 N94-33177
SMC-TR-94-13 ..... p 3728 N94-33061 #
SMC-TR-94-14 ..... p 3616 N94-33094 #
SMC-TR-94-16 ..... p 3838 N94-33168 #
SMC-TR-94-17 ..... p 3808 N94-33252 #

SP-RAPP-1993:16 ..... p 3758 N94-31070
SP-RAPP-1993:20 ..... p 3691 N94-31848
SP-RAPP-1993:36 ..... p 3758 N94-31071

SPC-93026-CMC ..... p 3814 N94-31810 #
SPC-93154-CMC ..... p 3817 N94-32219

SR-7 ..... p 3776 N94-33272 #

SRL-0117-RR ..... p 3879 N94-32013

SSCL-SR-1225 ..... p 3877 N94-32748

SSD93M0025-1 ..... p 3608 N94-33100 * #

STF11-A93032 ..... p 3668 N94-31073
STF20-A93124 ..... p 3735 N94-31841
STF25-A93026 ..... p 3918 N94-32293
STF34-A93158 ..... p 3649 N94-31072
STF75-A93038 ..... p 3668 N94-31838
STF75-A93042 ..... p 3803 N94-31839

SU-GL-5133 ..... p 3714 N94-31358 #

SU-SLAC-PUB-6320 ..... p 3721 N94-32845 #
SU-SLAC-PUB-6328 ..... p 3872 N94-32630 #
SU-SLAC-PUB-6388 ..... p 3911 N94-31823 #
SU-SLAC-PUB-6390 ..... p 3925 N94-31786 #
SU-SLAC-PUB-6405 ..... p 3938 N94-32503 #
SU-SLAC-PUB-6430 ..... p 3873 N94-32689
SU-SLAC-PUB-6434 ..... p 3874 N94-32841 #
SU-SLAC-PUB-6439 ..... p 3875 N94-33278
SU-SLAC-PUB-6443 ..... p 3721 N94-32848

SU-SLAC-427 ..... p 3646 N94-32795 #
SU-SLAC-434 ..... p 3900 N94-32065 #

SU-SLAC/SSRL-0061 ..... p 3646 N94-32795 #
SU-SLAC/SSRL-0065 ..... p 3900 N94-32065 #

SUNYBUF/DC/TR-38 ..... p 3895 N94-31327 #

SWRI-06-5555/1 ..... p 3627 N94-33008 #

S495-10400D-VOL-10 ..... p 3589 N94-32316
S495-10400D-VOL-11 ..... p 3589 N94-32317
S495-10400D-VOL-12 ..... p 3589 N94-32318 #
S495-10400D-VOL-13 ..... p 3589 N94-32319
S495-10400D-VOL-1 ..... p 3588 N94-32312
S495-10400D-VOL-2 ..... p 3588 N94-32313
S495-10400D-VOL-3 ..... p 3590 N94-32395 #
S495-10400D-VOL-4 ..... p 3590 N94-32396 #
S495-10400D-VOL-5 ..... p 3590 N94-32397 #
S495-10400D-VOL-6 ..... p 3590 N94-32398 #
S495-10400D-VOL-7 ..... p 3590 N94-32399 #
S495-10400D-VOL-8 ..... p 3589 N94-32314 #
S495-10400D-VOL-9 ..... p 3589 N94-32315
S495-10440-1 ..... p 3589 N94-32394 #
S495-10441-1 ..... p 3588 N94-32241
S495-10459-1 ..... p 3588 N94-32014 #
S495-10734-1 ..... p 3588 N94-32311
S495-10735-1 ..... p 3590 N94-32403

TARDEC-TR-13604 ..... p 3730 N94-32088 #

TEC-R-215 ..... p 3576 N94-31080 #
TEC-R-217 ..... p 3746 N94-31938 #

TEC-0041 ..... p 3784 N94-32046 #
TEC-0048 ..... p 3829 N94-31301 #

TELECOM-93-C-006 ..... p 3798 N94-33069
TELECOM-93-D-001 ..... p 3839 N94-31092
TELECOM-93-D-002 ..... p 3670 N94-31093
TELECOM-93-D-004 ..... p 3808 N94-31094
TELECOM-93-D-005 ..... p 3840 N94-31095
TELECOM-93-D-007 ..... p 3711 N94-31096
TELECOM-93-D-008 ..... p 3670 N94-31097
TELECOM-93-D-009 ..... p 3910 N94-31098
TELECOM-93-D-017 ..... p 3823 N94-31099
TELECOM-93-D-019 ..... p 3828 N94-31100
TELECOM-93-D-020 ..... p 3829 N94-31193
TELECOM-93-D-021 ..... p 3824 N94-31183
TELECOM-93-E-001 ..... p 3742 N94-31165
TELECOM-93-E-002 ..... p 3794 N94-31195 #
TELECOM-93-E-003 ..... p 3730 N94-31166
TELECOM-93-E-004 ..... p 3858 N94-31167
TELECOM-93-E-005 ..... p 3687 N94-31168
TELECOM-93-E-009 ..... p 3840 N94-31169
TELECOM-93-E-010 ..... p 3687 N94-31170
TELECOM-93-E-012 ..... p 3670 N94-31171
TELECOM-93-E-016 ..... p 3915 N94-31172
TELECOM-93-E-017 ..... p 3877 N94-31173
TELECOM-93-E-018 ..... p 3670 N94-31174

TESCO-TR-93-1-PHASE-2 ..... p 3587 N94-31295 #

TIOS-93-10 ..... p 3698 N94-33169
TIOS-93-27 ..... p 3812 N94-31659 #

TM-1563 ..... p 3669 N94-32484 *
TM-92-0045 ..... p 3827 N94-32734 * #

TR-MCTR-0594-07 ..... p 3740 N94-32940 * #

TR-009-1993 ..... p 3691 N94-32056 #
TR-0091(6940-05)-6 ..... p 3808 N94-33252 #
TR-0091(6940-05)-8 ..... p 3838 N94-33168 #
TR-07 ..... p 3631 N94-31238
TR-08 ..... p 3632 N94-31293 #
TR-09 ..... p 3863 N94-31237
TR-10 ..... p 3632 N94-31459 #
TR-10 ..... p 3657 N94-32365 #
TR-10 ..... p 3657 N94-32391 #
TR-11 ..... p 3877 N94-31256
TR-11 ..... p 3657 N94-32391 #
TR-11 ..... p 3660 N94-32722 #
TR-12 ..... p 3654 N94-31979
TR-12 ..... p 3657 N94-32391 #
TR-13 ..... p 3654 N94-31978
TR-143 ..... p 3644 N94-32169 #
TR-145 ..... p 3635 N94-32216 #
TR-146 ..... p 3909 N94-33275 #
TR-147 ..... p 3909 N94-33274 #
TR-148 ..... p 3642 N94-31997
TR-149 ..... p 3869 N94-32170 #
TR-14 ..... p 3655 N94-32017
TR-150 ..... p 3643 N94-32060 #
TR-152 ..... p 3875 N94-33277
TR-153 ..... p 3909 N94-33273
TR-28 ..... p 3864 N94-33138 #
TR-29-ONR ..... p 3663 N94-33058 #
TR-3-ONR ..... p 3655 N94-32069
TR-3-ONR ..... p 3869 N94-32082 #
TR-30 ..... p 3864 N94-33247 #
TR-35 ..... p 3648 N94-33182
TR-3 ..... p 3902 N94-32218 #
TR-4 ..... p 3657 N94-32381 #
TR-5 ..... p 3655 N94-31982
TR-5 ..... p 3900 N94-32011
TR-61 ..... p 3893 N94-33007 #
TR-64 ..... p 3881 N94-32280 #
TR-6 ..... p 3654 N94-31981
TR-8 ..... p 3657 N94-32391 #
TR-92(2940)-16 ..... p 3698 N94-33177
TR-92-27 ..... p 3916 N94-31175
TR-93(3904)-1 ..... p 3624 N94-32122 #
TR-93(3935)-11 ..... p 3728 N94-33061 #
TR-93(3935)-2 ..... p 3635 N94-32233 #
TR-93(3940)-11 ..... p 3612 N94-33262
TR-93(3940)-7 ..... p 3894 N94-33106
TR-93-01-01 ..... p 3820 N94-32972 #
TR-93-10 ..... p 3726 N94-32320
TR-93-12 ..... p 3918 N94-32289
TR-93-16 ..... p 3918 N94-32290
TR-93-17 ..... p 3826 N94-32291
TR-93-18 ..... p 3848 N94-32292
TR-93-19 ..... p 3817 N94-32287
TR-93-20 ..... p 3825 N94-32196
TR-93-22 ..... p 3919 N94-32506
TR-93-23 ..... p 3918 N94-32105
TR-94(4231)-1 ..... p 3616 N94-33094 #
TR-94-0002 ..... p 3616 N94-33059 #
TR-94-06-ONR ..... p 3663 N94-32985
TR-94-07 ..... p 3658 N94-32579 #
TR-94-10 ..... p 3659 N94-32610
TR-94-11 ..... p 3658 N94-32578
TR-94-13 ..... p 3683 N94-33083 * #
TR-985 ..... p 3881 N94-32285
TR-9 ..... p 3711 N94-31283 #
TR-9 ..... p 3654 N94-31980
TR-9 ..... p 3657 N94-32391 #

TRITA-ALP-1993-01 ..... p 3885 N94-31088
TRITA-ALP-1993-02 ..... p 3885 N94-31089

TTU-124-894-83 ..... p 3740 N94-32940 * #

TW-93-10 ..... p 3851 N94-32205
TW-93-12 ..... p 3847 N94-32200
TW-93-13 ..... p 3847 N94-32206
TW-93-14 ..... p 3847 N94-32207

UAH-94-429 ..... p 3893 N94-33048 * #

UCRL-CR-114777 ..... p 3645 N94-32636
UCRL-CR-114778 ..... p 3648 N94-33270
UCRL-CR-115799-SUMM ..... p 3639 N94-33260 #
UCRL-CR-116290 ..... p 3719 N94-32654 #

UCRL-ID-114591 ..... p 3641 N94-31581 #
UCRL-ID-115268 ..... p 3760 N94-32174 #
UCRL-ID-115325 ..... p 3893 N94-32915 #
UCRL-ID-115329 ..... p 3790 N94-32881
UCRL-ID-115525 ..... p 3849 N94-32670
UCRL-ID-115638 ..... p 3769 N94-32966 #
UCRL-ID-115678 ..... p 3650 N94-31354 #
UCRL-ID-115850 ..... p 3768 N94-32817
UCRL-ID-115869 ..... p 3708 N94-32652
UCRL-ID-115962 ..... p 3892 N94-32838 #
UCRL-ID-115969 ..... p 3675 N94-31781 #
UCRL-ID-115975 ..... p 3807 N94-32147 #
UCRL-ID-116155 ..... p 3768 N94-32882
UCRL-ID-116271 ..... p 3888 N94-31765 #
UCRL-ID-116320 ..... p 3669 N94-32839 #
UCRL-ID-116360 ..... p 3708 N94-32849

UCRL-JC-112646-REV-1 ..... p 3863 N94-31270 #
UCRL-JC-112889 ..... p 3907 N94-32934
UCRL-JC-112979 ..... p 3716 N94-31599 #
UCRL-JC-113493 ..... p 3714 N94-31269 #
UCRL-JC-113900 ..... p 3901 N94-32115
UCRL-JC-114078 ..... p 3767 N94-32789 #
UCRL-JC-114133 ..... p 3662 N94 32855 #
UCRL-JC-114145 ..... p 3632 N94-31352 #
UCRL-JC-114159-PT-2 ..... p 3904 N94-32606 #
UCRL-JC-114168 ..... p 3906 N94-32884
UCRL-JC-114260 ..... p 3715 N94-31590 #
UCRL-JC-114261 ..... p 3888 N94-31667 #
UCRL-JC-114266 ..... p 3887 N94-31406 #
UCRL-JC-114373 ..... p 3864 N94-31508 #
UCRL-JC-114411 ..... p 3774 N94-32772 #
UCRL-JC-114412 ..... p 3786 N94-32791 #
UCRL-JC-114495 ..... p 3666 N94-32114
UCRL-JC-114568 ..... p 3717 N94-32128 #
UCRL-JC-114598 ..... p 3738 N94-32637
UCRL-JC-114730 ..... p 3649 N94-31199 #
UCRL-JC-114770 ..... p 3720 N94-32753 #
UCRL-JC-114787 ..... p 3660 N94-32687
UCRL-JC-114789 ..... p 3896 N94-31499 #
UCRL-JC-114794 ..... p 3858 N94-31397 #
UCRL-JC-114837 ..... p 3926 N94-32189 #
UCRL-JC-114845 ..... p 3651 N94-31557 #
UCRL-JC-114984 ..... p 3955 N94-32129 #
UCRL-JC-114997 ..... p 3719 N94-32613 #
UCRL-JC-114998 ..... p 3716 N94-31636 #
UCRL-JC-115032 ..... p 3675 N94-31761 #
UCRL-JC-115044 ..... p 3775 N94-32895 #
UCRL-JC-115072 ..... p 3834 N94-32127 #
UCRL-JC-115120 ..... p 3718 N94-32252 #
UCRL-JC-115163 ..... p 3719 N94-32629 #
UCRL-JC-115262 ..... p 3712 N94-31783 #
UCRL-JC-115337 ..... p 3765 N94-32354 #
UCRL-JC-115359 ..... p 3647 N94-32892 #
UCRL-JC-115382 ..... p 3692 N94-32136 #
UCRL-JC-115425 ..... p 3667 N94-32148 #
UCRL-JC-115464 ..... p 3938 N94-32137 #
UCRL-JC-115500 ..... p 3887 N94-31400 #
UCRL-JC-115625 ..... p 3904 N94-32634 #
UCRL-JC-115687 ..... p 3719 N94-32659 #
UCRL-JC-115698 ..... p 3626 N94-32665 #
UCRL-JC-115706 ..... p 3914 N94-32677 #
UCRL-JC-115711 ..... p 3682 N94-32756 #
UCRL-JC-115737 ..... p 3645 N94-32522 #
UCRL-JC-115791 ..... p 3632 N94-31349 #
UCRL-JC-115805 ..... p 3934 N94-31782 #
UCRL-JC-115806 ..... p 3637 N94-32801 #
UCRL-JC-115840 ..... p 3638 N94-32840 #
UCRL-JC-115842 ..... p 3661 N94-32751
UCRL-JC-115950 ..... p 3580 N94-32658
UCRL-JC-116080 ..... p 3720 N94-32794 #
UCRL-JC-116104 ..... p 3656 N94-32116
UCRL-JC-116117 ..... p 3644 N94-32374 #
UCRL-JC-116148 ..... p 3695 N94-32688
UCRL-JC-116364 ..... p 3903 N94-32411 #
UCRL-JC-116372 ..... p 3646 N94-32754
UCRL-JC-116378 ..... p 3694 N94-32593 #
UCRL-JC-116383 ..... p 3874 N94-32807 #
UCRL-JC-116395 ..... p 3873 N94-32755 #

UCRL-LR-115467 ..... p 3938 N94-32914 #
UCRL-LR-116004 ..... p 3818 N94-32585 #

UCRL-MA-115257 ..... p 3679 N94-32188 #
UCRL-MA-115651 ..... p 3675 N94-31784 #
UCRL-MA-115837 ..... p 3825 N94-31920 #

UMR-FDB-33 ..... p 3655 N94-32005 #
UMR-FDB-34 ..... p 3656 N94-32221 #

UMR-FDB-35 ..... p 3657 N94-32364 #

US-PATENT-APPL-SN-016325 ..... p 3710 N94-32958
US-PATENT-APPL-SN-089915 ..... p 3727 N94-32718 #
US-PATENT-APPL-SN-102924 ..... p 3883 N94-32720 #
US-PATENT-APPL-SN-127178 ..... p 3660 N94-32739 #
US-PATENT-APPL-SN-129725 ..... p 3883 N94-32738 #
US-PATENT-APPL-SN-134192 ..... p 3882 N94-32719 #
US-PATENT-APPL-SN-151396 ..... p 3882 N94-32626
US-PATENT-APPL-SN-151693 ..... p 3696 N94-32721 #
US-PATENT-APPL-SN-155606 ..... p 3739 N94-32733 #
US-PATENT-APPL-SN-186711 ..... p 3681 N94-32625 #
US-PATENT-APPL-SN-546595 ..... p 3807 N94-32978
US-PATENT-APPL-SN-685588 ..... p 3697 N94-32967
US-PATENT-APPL-SN-725719 ..... p 3697 N94-32962
US-PATENT-APPL-SN-751352 ..... p 3663 N94-32975
US-PATENT-APPL-SN-758978 ..... p 3893 N94-32977
US-PATENT-APPL-SN-880824 ..... p 3697 N94-32976
US-PATENT-APPL-SN-896695 ..... p 3663 N94-32960
US-PATENT-APPL-SN-902138 ..... p 3639 N94-32973
US-PATENT-APPL-SN-910378 ..... p 3790 N94-32959
US-PATENT-APPL-SN-956327 ..... p 3577 N94-32961
US-PATENT-APPL-SN-970328 ..... p 3721 N94-32968
US-PATENT-APPL-SN-97181 ..... p 3698 N94-33181
US-PATENT-APPL-SN-972341 ..... p 3627 N94-33018
US-PATENT-APPL-SN-987497 ..... p 3862 N94-33017
US-PATENT-APPL-SN-994229 ..... p 3573 N94-32974

US-PATENT-CLASS-174-65 ..... p 3697 N94-32962
US-PATENT-CLASS-244-199 ..... p 3573 N94-32974
US-PATENT-CLASS-324-234 ..... p 3627 N94-33018
US-PATENT-CLASS-328-233 ..... p 3893 N94-32977
US-PATENT-CLASS-33-1-SB ..... p 3577 N94-32961
US-PATENT-CLASS-340-825.79 .. p 3697 N94-32967
US-PATENT-CLASS-356-28 ..... p 3790 N94-32959
US-PATENT-CLASS-367-103 ..... p 3697 N94-32976
US-PATENT-CLASS-367-174 ..... p 3862 N94-33017
US-PATENT-CLASS-372-20 ..... p 3721 N94-32968
US-PATENT-CLASS-395-425 ..... p 3807 N94-32978
US-PATENT-CLASS-429-217 ..... p 3698 N94-33181
US-PATENT-CLASS-440-6 ..... p 3710 N94-32958
US-PATENT-CLASS-524-236 ..... p 3663 N94-32960
US-PATENT-CLASS-525-454 ..... p 3663 N94-32975
US-PATENT-CLASS-73-54.01 ..... p 3639 N94-32973

US-PATENT-5,237,018 ..... p 3663 N94-32975
US-PATENT-5,264,906 ..... p 3790 N94-32959
US-PATENT-5,266,623 ..... p 3663 N94-32960
US-PATENT-5,268,877 ..... p 3697 N94-32976
US-PATENT-5,273,465 ..... p 3710 N94-32958
US-PATENT-5,276,658 ..... p 3862 N94-33017
US-PATENT-5,276,695 ..... p 3721 N94-32968
US-PATENT-5,278,352 ..... p 3697 N94-32962
US-PATENT-5,278,498 ..... p 3627 N94-33018
US-PATENT-5,278,548 ..... p 3697 N94-32967
US-PATENT-5,278,966 ..... p 3807 N94-32978
US-PATENT-5,279,149 ..... p 3639 N94-32973
US-PATENT-5,282,591 ..... p 3573 N94-32974
US-PATENT-5,283,138 ..... p 3698 N94-33181
US-PATENT-5,283,530 ..... p 3893 N94-32977

USAARL-93-36 ..... p 3804 N94-32171 #
USAARL-93-37 ..... p 3575 N94-32363 #
USAARL-94-10 ..... p 3586 N94-32217 #
USAARL-94-3 ..... p 3804 N94-32379 #
USAARL-94-9 ..... p 3579 N94-32242

USAFETAC/DS-94/037 ..... p 3784 N94-32057 #

USARIEM-TN94-2 ..... p 3798 N94-33268

USARIEM-T94-10 ..... p 3798 N94-33040 #
USARIEM-T94-9 ..... p 3901 N94-32153 #

USIP-92-02 ..... p 3922 N94-32856 #
USIP-93-05 ..... p 3808 N94-31087
USIP-93-06 ..... p 3640 N94-31083
USIP-93-07 ..... p 3858 N94-31084
USIP-93-08 ..... p 3711 N94-31085
USIP-93-90 ..... p 3927 N94-31086

UTRC-R94-970053-1 ..... p 3698 N94-33163

UVA/525469/EE94/101 ..... p 3697 N94-33034 #
UVA/525714/AM94/101 ..... p 3738 N94-32275
UVA/525733/CEAM94/101 ..... p 3740 N94-33011 #

UW-CPTC-94-1 ..... p 3892 N94-32911 #
UW-CPTC-94-2 ..... p 3893 N94-32922
UW-CPTC-94-3 ..... p 3893 N94-32912 #

UWAERP-42 ..... p 3892 N94-32800 #

VPI-AOE-202-REV ..... p 3702 N94-31476 #

VTT-JULK-786 ..... p 3724 N94-31654 #
VTT-TIED-1407 ..... p 3759 N94-31655 #
VTT-TIED-1495 ..... p 3724 N94-31656 #
VTT-TIED-1508 ..... p 3765 N94-31657 #
VTT-TIED-1517 ..... p 3743 N94-31658 #

W-9315 ..... p 3844 N94-31676 #
W-9317 ..... p 3703 N94-31689 #
W-9318 ..... p 3844 N94-31690 #
W-9319 ..... p 3703 N94-31691 #
W-9320 ..... p 3832 N94-31821 #
W-9321 ..... p 3706 N94-32045 #
W-9322 ..... p 3569 N94-31822 #

WES/TR/DRP-92-6-2 ..... p 3787 N94-31250 #

WES/TR/EL-93-25-REPT-1 ..... p 3771 N94-31351 #
WES/TR/EL-93-25-REPT-2 ..... p 3771 N94-31353 #
WES/TR/EL-93-25-REPT-3 ..... p 3771 N94-31457 #

WES/TR/ITL-94-1 ..... p 3821 N94-33031 #

WHC-SA-1705 ..... p 3819 N94-32749 #
WHC-SA-2050 ..... p 3915 N94-32678 #

WHOI-93-32 ..... p 3791 N94-33243 #
WHOI-93-39 ..... p 3791 N94-33245
WHOI-93-47 ..... p 3861 N94-32089 #
WHOI-93-51 ..... p 3791 N94-33109 #

WL-TM-94-3031 ..... p 3580 N94-33107

WL-TR-93-1135 ..... p 3673 N94-31464 #
WL-TR-93-1153 ..... p 3801 N94-33053
WL-TR-93-1173 ..... p 3581 N94-31458 #
WL-TR-93-1176 ..... p 3895 N94-31329 #
WL-TR-93-3063 ..... p 3805 N94-33349
WL-TR-93-3099 ..... p 3586 N94-32224 #
WL-TR-93-3125-PHASE-2 ..... p 3587 N94-31295 #
WL-TR-94-1007 ..... p 3578 N94-31387 #
WL-TR-94-1008 ..... p 3581 N94-32055 #
WL-TR-94-1009 ..... p 3565 N94-31367 #
WL-TR-94-1010 ..... p 3581 N94-31368 #
WL-TR-94-1033 ..... p 3582 N94-32909 #
WL-TR-94-1038 ..... p 3721 N94-33102
WL-TR-94-4008 ..... p 3828 N94-31061 #

WRDC-TR-89-3046 ..... p 3818 N94-32330 #

WSRC-MS-93-305 ..... p 3723 N94-31524 #
WSRC-MS-93-550 ..... p 3660 N94-32698 #
WSRC-MS-93-576 ..... p 3842 N94-31399 #
WSRC-MS-94-029 ..... p 3920 N94-32635 #
WSRC-MS-94-080 ..... p 3738 N94-32639

WSRC-TR-92-557-REV-1 ..... p 3646 N94-32781 #

X5-XD ..... p 3670 N94-31063 #

YALEU/DCS/RR-1014 ..... p 3817 N94-32257

APPENDIX

NASA SCIENTIFIC AND TECHNICAL INFORMATION PROGRAM PRODUCTS AND SERVICES

The NASA Scientific and Technical Information (STI) Program provides for the collection and announcement of aerospace-related reports and literature obtained worldwide through agreements and exchanges. The result of the collection is the comprehensive NASA STI Database that covers aeronautics, space, and supporting disciplines.

The STI Database, documents generated or obtained by NASA, and products and services derived from or supporting the database are made available to the NASA research community and to the public. Descriptions and sources of these items are presented in the following pages.

Scientific and Technical Aerospace Reports (STAR) is an abstract journal, listing citations with abstracts for aerospace-related reports obtained from worldwide sources. *STAR* is issued on the first of each month, and announces current documents that have been entered into the NASA STI Database during the previous month. The reports are of the following types:

- NASA, NASA contractor, and NASA grantee reports;
- Reports issued by other U.S. Government agencies, domestic and foreign institutions, universities, and private firms;
- Translations in report form;
- NASA-owned patents and patent applications
- Other U.S. Government agency and foreign patents and patent applications
- Domestic and foreign dissertations and theses.

Journal, book, and conference literature, journal translations, and certain foreign dissertations having the same subject scope as *STAR* are announced in a companion journal, *NASA Open Volumes on Aerospace (NOVA). NOVA* is issued on the 15th of each month and is available from the NASA Center for AeroSpace Information, at the address below.

ELIGIBILITY AND REGISTRATION FOR NASA STI PRODUCTS AND SERVICES

Organizations of the type listed below that have registered with NASA can receive products and services.

- NASA offices and installations, contractors, subcontractors, grantees, and consultants;
- Other U.S. Government agencies and their contractors;
- Libraries in the United States that have arrangements with NASA to maintain collections of NASA documents for public reference;
- Other organizations in the United States having a need for NASA documents in work related to aeronautics and space research;
- Organizations abroad that have established reciprocal documents exchange arrangements with NASA.

The central service points—central points of document acquisition and control within qualified organizations—or individuals are eligible to register for NASA STI products and services. Domestic organizations or individuals may be eligible to receive various classes of NASA publications and services and should address their requests for registration or further information to:

ATTN: Registration Services
NASA Center for AeroSpace Information
800 Elkridge Landing Road
Linthicum Heights, MD 21090-2934
301-621-0390

Organizations abroad should direct requests to:

National Aeronautics and Space Administration
Scientific and Technical Information Program (JTT)
International STI Program
Washington, DC 20546-0001
USA
703-271-5640

SUBJECT SCOPE

The subject scope of *STAR* and *NOVA* includes all aspects of aeronautics and space research and development, supporting basic and applied research, and applications. Aerospace aspects of Earth resources, energy development, conservation, oceanography, environmental protection, urban transportation, and other topics of high national priority are also covered.

HOW TO USE *STAR* SUBJECT CATEGORIES

Abstracts in *STAR* are categorized by 10 major subject divisions that are divided further into 76 specific subject categories. The subject divisions and categories are listed in the Table of Contents together with a note for each that defines its scope and provides any cross-references. For example:

16 SPACE TRANSPORTATION

Includes passenger and cargo space transportation, e.g., shuttle operations; and space rescue techniques. For related information see also *03 Air Transportation and Safety* and *18 Spacecraft Design, Testing and Performance*. For space suits see *54 Man/System Technology and Life Support*.

CROSS-REFERENCES

Individual *STAR* abstracts are not ordinarily cross-referenced, except for certain conference reports or book translations that have had separate abstracts written for their component papers or chapters. Citations and abstracts of the components follow immediately after those of the parent document. When the subject content of a component differs sufficiently from the general content of the parent, a cross-reference citation also is printed at the end of the category to which it normally would have been assigned if it were independent.

DOCUMENTS ON MICROFICHE

Documents available on microfiche are designated by a pound sign (#) following the accession number.

LIMITED REPRODUCIBILITY

A note of limited reproducibility appears in the citation, if there are factors affecting the reproducibility of more than 20% of the document. These factors include faint or broken type, color photographs, black and white photographs, foldouts, dot matrix print, or some other factor that limits the reproducibility of the document. This notation also appears on the microfiche header.

NASA PATENTS AND PATENT APPLICATIONS

Patents and patent applications owned by NASA are announced in *STAR* under appropriate subject categories and are referenced in the *STAR* indexes. In the Report Number Index, patents are indexed by the NASA Case Number, and the U.S. Patent Class. Patent applications are indexed by the NASA Case Number and the U.S. Patent Application Serial Number.

Printed copies of patents (which are not microfiched) are available for purchase from the U.S. Patent and Trademark Office.

When ordering patents, the U.S. Patent Number should be used, and payment must be remitted in advance, by money order or check payable to the Commissioner of Patents and Trademarks. Prepaid purchase coupons for ordering are also available from the U.S. Patent and Trademark Office.

NASA patent application specifications are sold in both paper copy and microfiche by the NASA Center for AeroSpace Information (CASI). The N accession number should be used in ordering either paper copy or microfiche from CASI.

The patents and patent applications announced in *STAR* are owned by NASA and are available for royalty-free licensing. Requests for licensing terms and further information should be addressed to:

National Aeronautics and Space Administration
Associate General Counsel for Intellectual Property
Code GP
Washington, DC 20546-0001

SOURCES FOR DOCUMENTS

One or more sources from which a document announced in *STAR* is available to the public is ordinarily given on the last line of the citation. The most commonly indicated sources and their acronyms or abbreviations are listed below, and their addresses are listed on page A-6. If the publication is available from a source other than those listed, the publisher and his address will be displayed on the availability line or in combination with the corporate source line.

Avail: CASI. Sold by the NASA Center for AeroSpace Information. Prices for hard copy (HC) and microfiche (MF) are indicated by a price code following the letters HC or MF in the *STAR* citation. Current values for the price codes are given in the tables on page A-7.

NOTE ON ORDERING DOCUMENTS: When ordering publications from CASI, use the N accession number or other report number. It is also advisable to cite the title and other bibliographic identification.

Avail: SOD (or GPO). Sold by the Superintendent of Documents, U.S. Government Printing Office, in hard copy.

Avail: BLL (formerly NLL): British Library Lending Division, Boston Spa, Wetherby, Yorkshire, England. Photocopies available from this organization at the price shown. (If none is given, inquiry should be addressed to the BLL.)

Avail: DOE Depository Libraries. Organizations in U.S. cities and abroad that maintain collections of Department of Energy reports, usually in microfiche form, are listed in *Energy Research Abstracts*. Services available from the DOE and its depositories are described in a booklet, *DOE Technical Information Center - Its Functions and Services* (TID-4660), which may be obtained without charge from the DOE Technical Information Center.

Avail: ESDU. Pricing information on specific data, computer programs, and details on Engineering Sciences Data Unit (ESDU) topic categories can be obtained from ESDU International Ltd. Requesters in North America should use the Virginia address while all other requesters should use the London address, both of which are on page A-6.

Avail: Fachinformationszentrum Karlsruhe. Gesellschaft für wissenschaftlich-technische Information mbH 76344 Eggenstein-Leopoldshafen, Germany.

Avail: HMSO. Publications of Her Majesty's Stationery Office are sold in the U.S. by Pendragon House, Inc. (PHI), Redwood City, CA. The U.S. price (including a service and mailing charge) is given, or a conversion table may be obtained from PHI.

Avail: Issuing Activity, or Corporate Author, or no indication of availability. Inquiries as to the availability of these documents should be addressed to the organization shown in the citation as the corporate author of the document.

Avail: NASA Public Document Rooms. Documents so indicated may be examined at or purchased from the National Aeronautics and Space Administration (JBD-4), Public Documents Room (Room 1H23), Washington, DC 20546-0001, or public document rooms located at NASA installations, and the NASA Pasadena Office at the Jet Propulsion Laboratory.

Avail: NTIS. Sold by the National Technical Information Service. Initially distributed microfiche under the NTIS SRIM (Selected Research in Microfiche) are available. For information concerning this service, consult the NTIS Subscription Section, Springfield, VA 22161.

Avail: Univ. Microfilms. Documents so indicated are dissertations selected from *Dissertation Abstracts* and are sold by University Microfilms as xerographic copy (HC) and microfilm. All requests should cite the author and the Order Number as they appear in the citation.

Avail: US Patent and Trademark Office. Sold by Commissioner of Patents and Trademarks, U.S. Patent and Trademark Office, at the standard price of $1.50 each, postage free. (See discussion of NASA patents and patent applications on page A-3.)

Avail: (US Sales Only). These foreign documents are available to users within the United States from the National Technical Information Service (NTIS). They are available to users outside the United States through the International Nuclear Information Service (INIS) representative in their country, or by applying directly to the issuing organization.

Avail: USGS. Originals of many reports from the U.S. Geological Survey, which may contain color illustrations, or otherwise may not have the quality of illustrations preserved in the microfiche or facsimile reproduction, may be examined by the public at the libraries of the USGS field offices whose addresses are listed on page A-6. The libraries may be queried concerning the availability of specific documents and the possible utilization of local copying services, such as color reproduction.

FEDERAL DEPOSITORY LIBRARY PROGRAM

In order to provide the general public with greater access to U.S. Government publications, Congress established the Federal Depository Library Program under the Government Printing Office (GPO), with 53 regional depositories responsible for permanent retention of material, inter-library loan, and reference services. At least one copy of nearly every NASA and NASA-sponsored publication, either in printed or microfiche format, is received and retained by the 53 regional depositories. A list of the regional GPO libraries, arranged alphabetically by state, appears on page A-8. These libraries are *not* sales outlets. A local library can contact a regional depository to help locate specific reports, or direct contact may be made by an individual.

PUBLIC COLLECTION OF NASA DOCUMENTS

An extensive collection of NASA and NASA-sponsored publications is maintained by the British Library Lending Division, Boston Spa, Wetherby, Yorkshire, England for public access. The British Library Lending Division also has available many of the non-NASA publications cited in *STAR.* European requesters may purchase facsimile copy or microfiche of NASA and NASA-sponsored documents, those identified by both the symbols # and * from ESA — Information Retrieval Service European Space Agency, 8-10 rue Mario-Nikis, 75738 CEDEX 15, France.

SUBMITTING DOCUMENTS

All users of this abstract service are urged to forward reports to be considered for announcement in *STAR.* This will aid NASA in its efforts to provide the fullest possible coverage of all scientific and technical publications that might support aeronautics and space research and development. If you have prepared relevant reports (other than those you will transmit to NASA, DOD, or DOE through the

usual contract- or grant-reporting channels), please send them for consideration to the NASA Center for AeroSpace Information, 800 Elkridge Landing Road, Linthicum Heights, MD 21090-2934.

Reprints of journal articles, book chapters, and conference papers are also welcome. These will be considered for announcement in *STAR's* companion journal, *NOVA.*

You may specify a particular source to be included in a report announcement if you wish; otherwise the report will be placed on a public sale at the NASA Center for AeroSpace Information. Copyrighted publications will be announced but not distributed or sold.

PURCHASE OF *STAR*

STAR is publicly available on annual subscription from the NASA Center for AeroSpace Information (CASI). The 1994 subscription price of $94.00/domestic, $117.00/foreign will be applied on a prorated basis, through 1994. 1995 *STAR* subscription prices are $100.00/domestic and $125.00/foreign. Single copy prices: $33.00/domestic, $41.00/foreign.

An annual, cumulative *STAR Index* is also available at $54.00/domestic, $65.00/foreign.

STAR is available to registered users on annual subscription from the NASA Center for AeroSpace Information, ATTN: Registration Services, 800 Elkridge Landing Road, Linthicum Heights, MD 21090-2934.

ADDRESSES OF ORGANIZATIONS

British Library Lending Division
Boston Spa, Wetherby, Yorkshire
England

Commissioner of Patents and Trademarks
U.S. Patent and Trademark Office
Washington, DC 20231

Department of Energy
Technical Information Center
P.O. Box 62
Oak Ridge, TN 37830

European Space Agency-
Information Retrieval Service ESRIN
Via Galileo Galilei
00044 Frascati (Rome) Italy

Engineering Sciences Data Unit International
P.O. Box 1633
Manassas, VA 22110

Engineering Sciences Data Unit
International, Ltd.
251-259 Regent Street
London, W1R 7AD, England

Fachinformationszentrum Karlsruhe
Gesellschaft für wissenschaftlich-technische
Information mbH
76344 Eggenstein-Leopoldshafen, Germany

Her Majesty's Stationery Office
P.O. Box 569, S.E. 1
London, England

NASA Center for AeroSpace Information
800 Elkridge Landing Road
Linthicum Heights, MD 21090-2934

National Aeronautics and Space Administration
Scientific and Technical Information Program
(JTT)
Washington, DC 20546-0001

National Technical Information Service
5285 Port Royal Road
Springfield, VA 22161

Pendragon House, Inc.
899 Broadway Avenue
Redwood City, CA 94063

Superintendent of Documents
U.S. Government Printing Office
Washington, DC 20402

University Microfilms
A Xerox Company
300 North Zeeb Road
Ann Arbor, MI 48106

University Microfilms, Ltd.
Tylers Green
London, England

U.S. Geological Survey Library National Center
MS 950
12201 Sunrise Valley Drive
Reston, VA 22092

U.S. Geological Survey Library
2255 North Gemini Drive
Flagstaff, AZ 86001

U.S. Geological Survey
345 Middlefield Road
Menlo Park, CA 94025

U.S. Geological Survey Library
Box 25046
Denver Federal Center, MS914
Denver, CO 80225

CASI PRICE TABLES

(Effective August 1, 1993)

STANDARD PRICE DOCUMENTS

PRICE CODE	NORTH AMERICAN PRICE	FOREIGN PRICE
A01	$ 9.00	$ 18.00
A02	12.50	25.00
A03	17.50	35.00
A04-A05	19.50	39.00
A06-A09	27.00	54.00
A10-A13	36.50	73.00
A14-A17	44.50	89.00
A18-A21	52.00	104.00
A22-A25	61.00	122.00
A99	Call For Price	Call For Price

MICROFICHE

PRICE CODE	NORTH AMERICAN PRICE	FOREIGN PRICE
A01	$ 9.00	$ 18.00
A02	12.50	25.00
A03	17.50	35.00
A04	19.50	39.00
A06	27.00	54.00
A10	36.50	73.00

IMPORTANT NOTICE

CASI Shipping and Handling Charges
U.S.—ADD $3.00 per TOTAL ORDER
Canada and Mexico—ADD $3.50 per TOTAL ORDER
All Other Countries—ADD $7.50 per TOTAL ORDER
Does NOT apply to orders
requesting CASI RUSH HANDLING.
CASI accepts most credit/charge cards.

NASA Center for AeroSpace Information
800 Elkridge Landing Road
Linthicum Heights, MD 21090-2934
Telephone: (301) 621-0390
E-mail: help@sti.nasa.gov
Fax: (301) 621-0134

FEDERAL REGIONAL DEPOSITORY LIBRARIES

ALABAMA

AUBURN UNIV. AT MONTGOMERY LIBRARY
Documents Dept.
7300 University Dr.
Montgomery, AL 36117-3596
(205) 244-3650 Fax: (205) 244-0678

UNIV. OF ALABAMA
Amelia Gayle Gorgas Library
Govt. Documents
Box 870266
Tuscaloosa, AL 35487-0266
(205) 348-6046 Fax: (205) 348-8833

ARIZONA

DEPT. OF LIBRARY, ARCHIVES, AND PUBLIC RECORDS
Federal Documents
Third Floor State Capitol
1700 West Washington
Phoenix, AZ 85007
(602) 542-4121 Fax: (602) 542-4400, 542-4500

ARKANSAS

ARKANSAS STATE LIBRARY
State Library Services
One Capitol Mall
Little Rock, AR 72201
(501) 682-2869

CALIFORNIA

CALIFORNIA STATE LIBRARY
Govt. Publications Section
914 Capitol Mall - P.O. Box 942837
Sacramento, CA 94237-0001
(916) 322-4572 Fax: (916) 324-8120

COLORADO

UNIV. OF COLORADO - BOULDER
Norlin Library
Govt. Publications
Campus Box 184
Boulder, CO 83309-0184
(303) 492-8834 Fax: (303) 492-2185

DENVER PUBLIC LIBRARY
Govt. Publications Dept. BS/GPD
1357 Broadway
Denver, CO 80203
(303) 571-2135

CONNECTICUT

CONNECTICUT STATE LIBRARY
231 Capitol Avenue
Hartford, CT 06106
(203) 566-4971 Fax: (203) 566-3322

FLORIDA

UNIV. OF FLORIDA LIBRARIES
Documents Dept.
Library West
Gainesville, FL 32611-2048
(904) 392-0366 Fax: (904) 392-7251

GEORGIA

UNIV. OF GEORGIA LIBRARIES
Govt. Documents Dept.
Jackson Street
Athens, GA 30602
(404) 542-8949 Fax: (404) 542-6522

HAWAII

UNIV. OF HAWAII
Hamilton Library
Govt. Documents Collection
2550 The Mall
Honolulu, HI 96822
(808) 948-8230 Fax: (808) 956-5968

IDAHO

UNIV. OF IDAHO LIBRARY
Documents Section
Moscow, ID 83843
(208) 885-6344 Fax: (208) 885-6817

ILLINOIS

ILLINOIS STATE LIBRARY
Reference Dept.
300 South Second
Springfield, IL 62701-1796
(217) 782-7596 Fax: (217) 524-0041

INDIANA

INDIANA STATE LIBRARY
Serials/Documents Section
140 North Senate Avenue
Indianapolis, IN 46204
(317) 232-3678 Fax: (317) 232-3728

IOWA

UNIV. OF IOWA LIBRARIES
Govt. Publications Dept.
Washington & Madison Streets
Iowa City, IA 52242
(319) 335-5926 Fax: (319) 335-5830

KANSAS

UNIV. OF KANSAS
Govt. Documents & Map Library
6001 Malatt Hall
Lawrence, KS 66045-2800
(913) 864-4660 Fax: (913) 864-5380

KENTUCKY

UNIV. OF KENTUCKY LIBRARIES
Govt. Publications/Maps Dept.
Lexington, KY 40506-0039
(606) 257-3139 Fax: (606) 257-1563, 257-8379

LOUISIANA

LOUISIANA STATE UNIV.
Middleton Library
Govt. Documents Dept.
Baton Rouge, LA 70803
(504) 388-2570 Fax: (504) 388-6992

LOUISIANA TECHNICAL UNIV.
Prescott Memorial Library
Govt. Documents Dept.
305 Wisteria Street
Ruston, LA 71270-9985
(318) 257-4962 Fax: (318) 257-2447

MAINE

TRI-STATE DOCUMENTS DEPOS.
Raymond H. Fogler Library
Govt. Documents & Microforms Dept.
Univ. of Maine
Orono, ME 04469
(207) 581-1680

MARYLAND

UNIV. OF MARYLAND
Hornbake Library
Govt. Documents/Maps Unit
College Park, MD 20742
(301) 454-3034 Fax: (301) 454-4985

MASSACHUSETTS

BOSTON PUBLIC LIBRARY
Govt. Documents Dept.
666 Boylston Street
Boston, MA 02117
(617) 536-5400 ext. 226
Fax: (617) 267-8273, 267-8248

MICHIGAN

DETROIT PUBLIC LIBRARY
5201 Woodward Avenue
Detroit, MI 48202-4093
(313) 833-1440, 833-1409
Fax: (313) 833-5039

LIBRARY OF MICHIGAN
Govt. Documents Unit
P.O. Box 30007
Lansing, MI 48909
(517) 373-0640 Fax: (517) 373-3381

MINNESOTA

UNIV. OF MINNESOTA
Wilson Library
Govt. Publications Library
309 19th Avenue South
Minneapolis, MN 55455
(612) 624-5073 Fax: (612) 626-9353

MISSISSIPPI

UNIV. OF MISSISSIPPI
J.D. Williams Library
Federal Documents Dept.
106 Old Gym Bldg.
University, MS 38677
(601) 232-5857 Fax: (601) 232-5453

MISSOURI

UNIV. OF MISSOURI - COLUMBIA
Ellis Library
Govt. Documents
Columbia, MO 65201
(314) 882-6733 Fax: (314) 882-8044

MONTANA

UNIV. OF MONTANA
Maureen & Mike Mansfield Library
Documents Div.
Missoula, MT 59812-1195
(406)243-6700 Fax: (406) 243-2060

NEBRASKA

UNIV. OF NEBRASKA - LINCOLN
D.L. Love Memorial Library
Documents Dept.
Lincoln, NE 68588
(402) 472-2562

NEVADA

UNIV. OF NEVADA
Reno Library
Govt. Publications Dept.
Reno, NV 89557
(702) 784-6579 Fax: (702) 784-1751

NEW JERSEY

NEWARK PUBLIC LIBRARY
U.S. Documents Div.
5 Washington Street -
P.O. Box 630
Newark, NJ 07101-0630
(201) 733-7812 Fax: (201) 733-5648

NEW MEXICO

UNIV. OF NEW MEXICO
General Library
Govt. Publications Dept.
Albuquerque, NM 87131-1466
(505) 277-5441 Fax: (505) 277-6019

NEW MEXICO STATE LIBRARY
325 Don Gaspar Avenue
Santa Fe, NM 87503
(505) 827-3826 Fax: (505) 827-3820

NEW YORK

NEW YORK STATE LIBRARY
Documents/Gift & Exchange Section
Federal Depository Program
Cultural Education Center
Albany, NY 12230
(518) 474-5563 Fax: (518) 474-5786

NORTH CAROLINA

UNIV. OF NORTH CAROLINA - CHAPEL HILL
CB#3912, Davis Library
BA/SS Dept. - Documents
Chapel Hill, NC 27599
(919) 962-1151 Fax: (919) 962-0484

NORTH DAKOTA

NORTH DAKOTA STATE UNIV. LIB.
Documents Office
Fargo, ND 58105
(701) 237-8886 Fax: (701) 237-7138
In cooperation with Univ. of North Dakota, Chester Fritz Library
Grand Forks

OHIO

STATE LIBRARY OF OHIO
Documents Dept.
65 South Front Street
Columbus, OH 43266
(614) 644-7051 Fax: (614) 752-9178

OKLAHOMA

OKLAHOMA DEPT. OF LIBRARIES
U.S. Govt. information Div.
200 NE 18th Street
Oklahoma City, OK 73105-3298
(405) 521-2502, ext. 252, 253
Fax: (405) 525-7804

OKLAHOMA STATE UNIV.
Edmon Low Library
Documents Dept.
Stillwater, OK 74078
(405) 744-6546 Fax: (405) 744-5183

OREGON

PORTLAND STATE UNIV.
Millar Library
934 SW Harrison - P.O. Box 1151
Portland, OR 97207
(503) 725-3673 Fax: (503) 725-4527

PENNSYLVANIA

STATE LIBRARY OF PENN.
Govt. Publications Section
Walnut St. & Commonwealth Ave. -
P.O. Box 1601
Harrisburg, PA 17105
(717) 787-3752

SOUTH CAROLINA

CLEMSON UNIV.
Cooper Library
Public Documents Unit
Clemson, SC 29634-3001
(803) 656-5174 Fax: (803) 656-3025
In cooperation with Univ. of South Carolina, Thomas Cooper Library, Columbia

TENNESSEE

MEMPHIS STATE UNIV. LIBRARIES
Govt. Documents
Memphis, TN 38152
(901) 678-2586 Fax: (901) 678-2511

TEXAS

TEXAS STATE LIBRARY
United States Documents
P.O. Box 12927 - 1201 Brazos
Austin, TX 78711
(512) 463-5455 Fax: (512) 463-5436

TEXAS TECH. UNIV. LIBRARY
Documents Dept.
Lubbock, TX 79409
(806) 742-2268 Fax: (806) 742-1920

UTAH

UTAH STATE UNIV.
Merrill Library & Learning Resources Center, UMC-3000
Documents Dept.
Logan, UT 84322-3000
(801) 750-2684 Fax: (801) 750-2677

VIRGINIA

UNIV. OF VIRGINIA
Alderman Library
Govt. Documents
Charlottesville, VA 22903-2498
(804) 824-3133 Fax: (804) 924-4337

WASHINGTON

WASHINGTON STATE LIBRARY
Document Section
MS AJ-11
Olympia, WA 98504-0111
(206) 753-4027 Fax: (206) 753-3546

WEST VIRGINIA

WEST VIRGINIA UNIV. LIBRARY
Govt. Documents Section
P.O. Box 6069
Morgantown, WV 26506
(304) 293-3640

WISCONSIN

ST. HIST. SOC. OF WISCONSIN LIBRARY
Govt. Publications Section
816 State Street
Madison, WI 53706
(608) 262-2781 Fax: (608) 262-4711
In cooperation with Univ. of Wisconsin - Madison, Memorial Library

MILWAUKEE PUBLIC LIBRARY
Documents Div.
814 West Wisconsin Avenue
Milwaukee, WI 53233
(414) 278-2167 Fax: (414) 278-2137

• U.S. GOVERNMENT PRINTING OFFICE: 1994-301-249/00008

SCAN Goes Electronic!

*I*f you have NASA Mail or if you can access the Internet you can get biweekly issues of *SCAN* delivered to your desktop — absolutely *free*!

Electronic SCAN takes advantage of computer technology to alert you to the latest aerospace-related, worldwide scientific and technical information that has been published.

*N*o more waiting while the paper copy is printed and mailed to you. You can review *Electronic SCAN* the same day it is released! And you get all 191 — or any combination of — subject areas of announcements with abstracts to browse at your leisure. When you locate a publication of interest, you can print the announcement or electronically add it to your publication order list.

*S*tart your free access to *Electronic SCAN* today. Over 1,000 announcements of new reports, books, conference proceedings, journal articles . . . and more — delivered to your computer every two weeks.

Electronic SCAN.
Timely.
Flexible.
Complete.
Free!

*F*or instant access via Internet:

ftp.sti.nasa.gov
gopher.sti.nasa.gov
listserv@sti.nasa.gov

*F*or additional information:

e-mail: help@sti.nasa.gov
scan@sti.nasa.gov
(Enter this address on the "To" line. Leave the subject line blank and send. You will receive an automatic reply with instructions in minutes.)

phone: 301-621-0390

fax: 301-621-0134

write: NASA Access Help Desk
NASA STI Program
NASA Center for AeroSpace Information
800 Elkridge Landing Road
Linthicum Heights, MD 21090-2934

NASA STI PROGRAM
SCIENTIFIC & TECHNICAL INFORMATION

SCAN *and* Electronic SCAN *are products of the NASA Scientific & Technical Information Program.*

9/93

POSTMASTER
Address Correction Requested
(Sections 137 and 159 Post Manual)

National Aeronautics and
Space Administration
Code JTT
Washington, DC 20546-0001

Official Business
Penalty for Private Use, $300

BULK RATE
POSTAGE & FEES PAID
NASA
PERMIT No. G-27

NASA

POSTMASTER: If Undeliverable (Section 158
Postal Manual) Do Not Return

Please circulate this publication to other colleagues within your organization.

NASA STI PROGRAM
SCIENTIFIC &
TECHNICAL
INFORMATION